



*A National Center of Excellence in Advanced Technology Applications*

ISSN 1520-295X

# Experimental Study of Seismic Isolation Systems with Emphasis on Secondary System Response and Verification of Accuracy of Dynamic Response History Analysis Methods

by

Eric D. Wolff and Michael C. Constantinou

University at Buffalo, State University of New York  
Department of Civil, Structural and Environmental Engineering  
Ketter Hall  
Buffalo, New York 14260

Technical Report MCEER-04-0001

January 16, 2004

This research was conducted at the University at Buffalo, State University of New York and was supported primarily by the Earthquake Engineering Research Centers Program of the National Science Foundation under award number EEC-9701471.

## NOTICE

This report was prepared by the University at Buffalo, State University of New York as a result of research sponsored by the Multidisciplinary Center for Earthquake Engineering Research (MCEER) through a grant from the Earthquake Engineering Research Centers Program of the National Science Foundation under NSF award number EEC-9701471 and other sponsors. Neither MCEER, associates of MCEER, its sponsors, the University at Buffalo, State University of New York, nor any person acting on their behalf:

- a. makes any warranty, express or implied, with respect to the use of any information, apparatus, method, or process disclosed in this report or that such use may not infringe upon privately owned rights; or
- b. assumes any liabilities of whatsoever kind with respect to the use of, or the damage resulting from the use of, any information, apparatus, method, or process disclosed in this report.

Any opinions, findings, and conclusions or recommendations expressed in this publication are those of the author(s) and do not necessarily reflect the views of MCEER, the National Science Foundation, or other sponsors.

## **DISCLAIMER**

- ❖ This document has been reproduced from the best copy furnished by the sponsoring agency. It is being released in the interest of making available as much information as possible.





---

# Experimental Study of Seismic Isolation Systems with Emphasis on Secondary System Response and Verification of Accuracy of Dynamic Response History Analysis

by

Eric D. Wolff<sup>1</sup> and Michael C. Constantinou<sup>2</sup>

Publication Date: January 16, 2004

Submittal Date: September 3, 2003

Technical Report MCEER-04-0001

Task Numbers 01-2041a, 01-2043c, 02-2041a, 02-2043c and Year 6 Task 3.2

NSF Master Contract Number EEC-9701471

- 1 Project Leader, Southwest Division, Naval Facilities Engineering Command, Department of the Navy, San Diego, CA; former Research Assistant, Department of Civil, Structural and Environmental Engineering, University at Buffalo, State University of New York
- 2 Professor and Chair, Department of Civil, Structural and Environmental Engineering, University at Buffalo, State University of New York

MULTIDISCIPLINARY CENTER FOR EARTHQUAKE ENGINEERING RESEARCH  
University at Buffalo, State University of New York  
Red Jacket Quadrangle, Buffalo, NY 14261

---



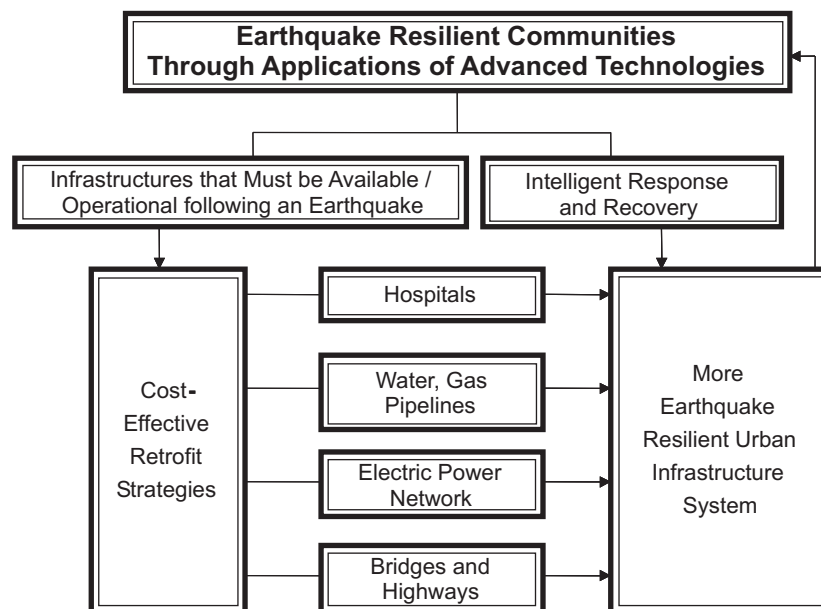
## Preface

The Multidisciplinary Center for Earthquake Engineering Research (MCEER) is a national center of excellence in advanced technology applications that is dedicated to the reduction of earthquake losses nationwide. Headquartered at the University at Buffalo, State University of New York, the Center was originally established by the National Science Foundation in 1986, as the National Center for Earthquake Engineering Research (NCEER).

Comprising a consortium of researchers from numerous disciplines and institutions throughout the United States, the Center's mission is to reduce earthquake losses through research and the application of advanced technologies that improve engineering, pre-earthquake planning and post-earthquake recovery strategies. Toward this end, the Center coordinates a nationwide program of multidisciplinary team research, education and outreach activities.

MCEER's research is conducted under the sponsorship of two major federal agencies: the National Science Foundation (NSF) and the Federal Highway Administration (FHWA), and the State of New York. Significant support is derived from the Federal Emergency Management Agency (FEMA), other state governments, academic institutions, foreign governments and private industry.

MCEER's NSF-sponsored research objectives are twofold: to increase resilience by developing seismic evaluation and rehabilitation strategies for the post-disaster facilities and systems (hospitals, electrical and water lifelines, and bridges and highways) that society expects to be operational following an earthquake; and to further enhance resilience by developing improved emergency management capabilities to ensure an effective response and recovery following the earthquake (see the figure below).



A cross-program activity focuses on the establishment of an effective experimental and analytical network to facilitate the exchange of information between researchers located in various institutions across the country. These are complemented by, and integrated with, other MCEER activities in education, outreach, technology transfer, and industry partnerships.

*This combined experimental and analytical study provides an assessment of the validity and accuracy of analysis methods commonly used for seismically isolated structures, emphasizing secondary system response, contemporary seismic isolation systems, and strong and/or near-fault seismic excitation. A six-story steel model was used in three configurations: flexible moment-frame, asymmetrically braced-frame and stiff braced-frame. Eight isolation systems were studied, namely, low damping elastomeric bearings with and without linear and nonlinear viscous dampers, Friction Pendulum (FP) bearings with and without linear and nonlinear viscous dampers, low damping elastomeric bearings with lead cores, and low damping elastomeric bearings in conjunction with flat sliding bearings. Over 300 experiments were conducted. The various experimental results were compared with analytical results obtained using the SAP2000 and 3D-BASIS-ME computer programs. The vast database of experimental results on secondary system response provided the opportunity to assess the performance of various seismic isolation systems.*



## **ABSTRACT**

This report consists of two main parts: an experimental study of seismic isolation systems with emphasis on secondary system response, and verification of the accuracy of dynamic response-history analysis programs. Tests were performed on a single bearing test machine to determine isolation system properties for analytical modeling. Earthquake simulator tests were performed on a quarter-scale, six story, building model. A total of eight different isolation systems were studied, namely, low damping elastomeric bearings with and without linear and nonlinear viscous dampers, Friction Pendulum (FP) bearings with and without linear and nonlinear viscous dampers, low damping elastomeric bearings with lead cores, and low damping elastomeric bearings in conjunction with flat sliding bearings. Each configuration was modeled in two dynamic analysis computer programs: SAP2000 and 3D-BASIS-ME.



## ACKNOWLEDGMENTS

Financial support for this project was provided by the Multidisciplinary Center for Earthquake Engineering Research (Project Nos. 01-2041a, 01-2043c, 02-2041a, 02-2043c and Year 6/task 3.2), Earthquake Protection Systems, Inc., R. J. Watson, Inc. and Taylor Devices, Inc. Taylor Devices, Inc., North Tonawanda, NY, manufactured and donated the fluid viscous damping devices. Scougal Rubber Corporation, Seattle, WA, manufactured and donated the elastomeric bearings and lead-core bearings. Earthquake Protection Systems, Richmond, CA, manufactured and donated the Friction Pendulum bearings. The flat sliding bearings were assembled with parts salvaged from hardware from previous testing in the laboratory that included a FP slider from Earthquake Protection Systems, and a flat sliding surface from R. J. Watson, Inc. This report is nearly identical to the doctoral dissertation of Eric D. Wolff. The dissertation committee consisted of Dr. Michael C. Constantinou (advisor), Dr. Andrew S. Whittaker, Dr. Andrei Reinhorn, Dr. Gary Dargush, and Dr. Constantin Christopoulos (outside reader, University of Toronto).



# TABLE OF CONTENTS

SEC.	TITLE	PAGE
<b>1</b>	<b>INTRODUCTION</b>	1
1.1	Background	1
1.2	Report Organization	2
<b>2</b>	<b>NON-STRUCTURAL COMPONENT RESPONSE AND SEISMIC ISOLATION SYSTEMS</b>	3
<b>3</b>	<b>COMPONENT AND SYSTEM EVALUATION</b>	9
3.1	Introduction	9
3.2	Testing Machine Description	9
3.3	Viscous Damping Devices	11
3.4	Bearing Testing	11
3.4.1	Friction Pendulum (FP) Bearings	15
3.4.2	Low Damping Elastomeric Bearings	16
3.4.3	Lead-Core Bearings	21
3.4.4	Flat Sliding Bearings	24
3.5	Six-Story Model	26
3.6	Tested Configurations	29
3.7	Identification of Properties of Tested Configurations	33
3.8	Instrumentation	38
3.9	Testing Program	38
<b>4</b>	<b>RESULTS OF EARTHQUAKE SIMULATOR TESTING</b>	61
4.1	Introduction	61
4.2	Moment Frame Test Results	61
4.3	Braced Frame Test Results	66
4.4	Asymmetrically Braced Frame Test Results	70
4.5	Interpretation of Results	74
4.5.1	Impact of Added Viscous Damping Devices	75
4.5.2	Primary and Secondary System Response	78
4.5.3	Torsional Response in Asymmetric Seismically Isolated Buildings	89
4.5.4	Variation of Axial Load on Bearings	92
<b>5</b>	<b>ANALYTICAL PREDICTION OF RESPONSE</b>	97
5.1	Introduction	97
5.2	Analytical Model of Bearings	97
5.2.1	Low Damping Elastomeric Bearings	97
5.2.2	Friction Pendulum (FP) Bearings	100
5.2.3	Lead-Core Bearings	100
5.2.4	Flat Sliding Bearings	100
5.3	Analytical Model of Damping Devices	102

## TABLE OF CONTENTS (CONTD.)

SEC.	TITLE	PAGE
5.4	Analytical Model of Tested Structure	102
5.5	Comparison of Analytical and Experimental Results	106
<b>6</b>	<b>CONCLUSIONS</b>	<b>115</b>
<b>7</b>	<b>REFERENCES</b>	<b>117</b>
<b>APPENDIX A</b>	<b>EXPERIMENTAL RESULTS</b>	<b>*</b>
<b>APPENDIX B</b>	<b>COMPUTER PROGRAM SAMPLE INPUT FILES</b>	<b>*</b>
<b>APPENDIX C</b>	<b>ANALYTICAL (SAP2000) VS. EXPERIMENTAL RESPONSE</b>	<b>*</b>
<b>APPENDIX D</b>	<b>ANALYTICAL (3D-BASIS-ME) VS. EXPERIMENTAL RESPONSE</b>	<b>*</b>

\* The appendices are provided after the original report.

## LIST OF FIGURES

FIGURE	TITLE	PAGE
2-1	Logic Tree Diagram for Medical Gas Supply Equipment (Zhu, 1998)	5
2-2	Logic Tree Diagram for San Francisco High Rise Fire Suppression System (Grigoriu, 1998)	6
3-1	Schematic of Machine Used to Test Individual Isolators	10
3-2	Photograph of Machine Used to Test Individual Isolators	10
3-3	Recorded Force-Displacement Loops of Linear Fluid Viscous Damper (adapted from Kasalanati and Constantinou, 1999)	12
3-4	Recorded Force-Displacement Loops of Nonlinear Fluid Viscous Damper (adapted from Kasalanati and Constantinou, 1999)	13
3-5	Relation Between Peak Damping Force and Peak Velocity (adapted from Kasalanati and Constantinou, 1999)	14
3-6	FP Bearing Section	15
3-7	Recorded Normalized Force-Displacement Loops of a FP Bearing	16
3-8	Coefficient of Sliding Friction Versus Velocity for a FP Bearing	17
3-9	Schematic of Tested Low Damping Rubber Bearings	18
3-10	Recorded Lateral Force-Displacement Loops for Elastomeric Bearing Nos. 1,2 and 3 under Three Different Axial Loads	19
3-11	Recorded Lateral Force-Displacement Loops for Elastomeric Bearing Nos. 1 and 4 under Varying Shear Strain and Temperature Conditions	20
3-12	Schematic of Tested Lead-Core Bearing	22
3-13	Force-Displacement Relation of Lead-Core Bearing	23
3-14	Recorded Force-Displacement Loops of Lead-Core Bearings	23
3-15	Schematic of Flat Sliding Bearing	24
3-16	Recorded Normalized Force-Displacement Loops of a Flat Sliding Bearing	25
3-17	Coefficient of Sliding Friction Versus Velocity in a Flat Sliding Bearing	26
3-18	Schematic of Tested Six-Story Isolated Model Structure	27
3-19	Photograph of Tested Six-Story Isolated Model Structure on the University at Buffalo Earthquake Simulator	28
3-20	Illustration of Tested Configurations	30
3-21	Installation Geometry for Fluid Viscous Dampers	31
3-22	Transfer Function Amplitudes Obtained from White Noise Excitation of Moment Frame Structure	35
3-23	Transfer Function Amplitudes Obtained from White Noise Excitation of Asymmetrically Braced Frame Structure	36

## LIST OF FIGURES (CONTD.)

FIGURE	TITLE	PAGE
3-24	Transfer Function Amplitudes Obtained from White Noise Excitation of Symmetrically Braced Frame Structure	37
3-25	Instrumentation Diagram	39
3-26	Histories of Displacement, Velocity and Acceleration and the Acceleration Response Spectrum of Earthquake Simulator Motion for the El Centro S00E 200% Excitation	46
3-27	Histories of Displacement, Velocity and Acceleration and the Acceleration Response Spectrum of Earthquake Simulator Motion for the Taft N21E 500% Excitation	47
3-28	Histories of Displacement, Velocity and Acceleration and the Acceleration Response Spectrum of Earthquake Simulator Motion for the Northridge-Newhall 90° 100% Excitation	48
3-29	Histories of Displacement, Velocity and Acceleration and the Acceleration Response Spectrum of Earthquake Simulator Motion for the Northridge-Newhall 360° 100% Excitation	49
3-30	Histories of Displacement, Velocity and Acceleration and the Acceleration Response Spectrum of Earthquake Simulator Motion for the Northridge-Sylmar 90° 100% Excitation	50
3-31	Histories of Displacement, Velocity and Acceleration and the Acceleration Response Spectrum of Earthquake Simulator Motion for the 1995 Kobe N-S 100% Excitation	51
3-32	Histories of Displacement, Velocity and Acceleration and the Acceleration Response Spectrum of Earthquake Simulator Motion for the YPT 330 100% Excitation	52
3-33	Histories of Displacement, Velocity and Acceleration and the Acceleration Response Spectrum of Earthquake Simulator Motion for the YPT 060 100% Excitation	53
3-34	Histories of Displacement, Velocity and Acceleration and the Acceleration Response Spectrum of Earthquake Simulator Motion for the Mexico N90W 100% Excitation	54
3-35	Histories of Displacement, Velocity and Acceleration and the Acceleration Response Spectrum of Earthquake Simulator Motion for the Pacoima S74W 100% Excitation	55
3-36	Histories of Displacement, Velocity and Acceleration and the Acceleration Response Spectrum of Earthquake Simulator Motion for the Pacoima S16E 100% Excitation	56
3-37	Histories of Displacement, Velocity and Acceleration and the Acceleration Response Spectrum of Earthquake Simulator Motion for the Chi-Chi TCU 129 E-W 100% Excitation	57
3-38	Histories of Displacement, Velocity and Acceleration and the Acceleration Response Spectrum of Earthquake Simulator Motion for the Miyagiken Oki 500% Excitation	58



## LIST OF FIGURES (CONTD.)

FIGURE	TITLE	PAGE
3-39	Histories of Displacement, Velocity and Acceleration and the Acceleration Response Spectrum of Earthquake Simulator Motion for the Hachinohe N-S 300% Excitation	59
4-1	Comparison of Load Cell Readings with Processed Acceleration Records for El Centro S00E 200%	66
4-2	Comparison of Peak Responses of Isolated Moment Frame Structure with Friction Pendulum Bearings and Viscous Dampers	76
4-3	Comparison of Peak Responses of Isolated Braced Frame Structure with Friction Pendulum Bearings and Viscous Dampers	76
4-4	Comparison of Peak Responses of Isolated Moment Frame Structure with Elastomeric Bearings and Viscous Dampers	77
4-5	Comparison of Peak Responses of Isolated Braced Frame Structure with Elastomeric Bearings and Viscous Dampers	77
4-6	Floor Response Spectra of Isolated Moment Frame Structure for the El Centro S00E 200% Excitation	80
4-7	Floor Response Spectra of Isolated Moment Frame Structure for the Sylmar 90° 100% Excitation	81
4-8	Floor Response Spectra of Isolated Braced Frame Structure for the El Centro S00E 200% Excitation	82
4-9	Floor Response Spectra of Isolated Braced Frame Structure for the Sylmar 90° 100% Excitation	83
4-10	Experimental Corner Displacement Magnification Ratios for FP Bearings with and without Linear and Nonlinear Viscous Damping Devices Bearings for the Asymmetrically Braced Frame Structure	90
4-11	Experimental Corner Displacement Magnification Ratios for Low Damping Elastomeric Bearings with and without Linear and Nonlinear Viscous Damping Devices for the Asymmetrically Braced Frame Structure	91
4-12	Experimental Corner Displacement Magnification Ratios for Lead-Core Bearings and Low Damping Elastomeric Bearings in Combination with Flat Sliding Bearings for the Asymmetrically Braced Frame Structure	92
4-13	History of Recorded Axial Force of the FP Bearing Isolated Moment Frame Structure in Sylmar 90° 100%	93
4-14	History of Recorded Axial Force of the FP Bearing Isolated Moment Frame Structure with Nonlinear Fluid Viscous Damping Devices in Sylmar 90° 100%	94

## LIST OF FIGURES (CONTD.)

FIGURE	TITLE	PAGE
4-15	History of Recorded Axial Force of the Low Damping Elastomeric Bearing Isolated Moment Frame Structure in Sylmar 90° 100%	94
4-16	History of Recorded Axial Force of the Low Damping Elastomeric Bearing Isolated Moment Frame Structure with Linear Fluid Viscous Damping Devices in Sylmar 90° 100%	95
5-1	Stiffening Hysteretic Element in Program 3D-BASIS-ME (adapted from Tsopelas et al., 1994)	98
5-2	Experimental and Analytical Low Damping Bearing Force-Displacement Loops Generated by Programs SAP2000 and 3D-BASIS-ME	99
5-3	Experimental and Analytical Lead-Core Bearing Force-Displacement Loops Generated by Programs SAP2000 and 3D-BASIS-ME	101
5-4	Model of One Frame of the Six-Story Isolated Structure in SAP2000	103
5-5	Comparison of Experimental and SAP2000 Generated Results for the FP Isolated Moment Frame in the Sylmar 90° 100% Excitation	108
5-6	Comparison of Experimental and 3D-BASIS Generated Results for the FP Isolated Moment Frame in the Sylmar 90° 100% Excitation	109
5-7	Comparison of Experimental and SAP2000 Generated Results for the Elastomeric Bearing with Linear Viscous Damper Isolated Moment Frame in the Sylmar 90° 100% Excitation	110
5-8	Comparison of Experimental and 3D-BASIS Generated Results for the Elastomeric Bearing with Linear Viscous Damper Isolated Moment Frame in the Sylmar 90° 100% Excitation	111
5-9	Comparison of Experimental and SAP2000 Generated Results for the Combined FP-Nonlinear Fluid Viscous Damper Isolated Moment Frame in the Sylmar 90° 100% Excitation	112
5-10	Comparison of Experimental and SAP2000 Generated Uplift Response for the Combined FP-Nonlinear Fluid Viscous Damper Isolated Moment Frame in the Sylmar 90° 100% Excitation	113

## LIST OF TABLES

TABLE	TITLE	PAGE
3-1	Summary of Bearing Testing Machine Capabilities	11
3-2	Scale Factors Used in Model Structure	29
3-3	Characteristics of Fixed Base Moment Frame Structure	34
3-4	Characteristics of Asymmetrically and Symmetrically Braced Fixed Base Structure	34
3-5	List of Data Acquisition Channels	40
3-6	List of Earthquake Motions and Characteristics in Prototype Scale	42
3-7	List of Earthquake Simulation Tests Conducted on Six-Story Model	43
4-1	Peak Response of Non-isolated Moment Frame Structure	62
4-2	Peak Response of Isolated Moment Frame Structure with Lead-Core Bearings	62
4-3	Peak Response of Isolated Moment Frame Structure with Low Damping Elastomeric Bearings	63
4-4	Peak Response of Isolated Moment Frame Structure with Friction Pendulum Bearings	64
4-5	Peak Response of Isolated Moment Frame Structure with Combined Low Damping Elastomeric and Flat Sliding Bearings	65
4-6	Peak Response of Non-isolated Braced Frame Structure	66
4-7	Peak Response of Isolated Braced Frame Structure with Low Damping Elastomeric Bearings	67
4-8	Peak Response of Isolated Braced Frame Structure with Friction Pendulum Bearings	68
4-9	Peak Response of Isolated Braced Frame Structure with Lead-Core Bearings	70
4-10	Peak Response of Isolated Braced Frame Structure with Combined Low Damping Elastomeric and Flat Sliding Bearings	70
4-11	Peak Response of Non-isolated Asymmetrically Braced Frame Structure	71
4-12	Peak Response of Isolated Asymmetrically Braced Frame Structure with Friction Pendulum Bearings	71
4-13	Peak Response of Isolated Asymmetrically Braced Frame Structure with Low Damping Elastomeric Bearings	73
4-14	Peak Response of Isolated Asymmetrically Braced Frame Structure with Lead-Core Bearings	74
4-15	Peak Response of Isolated Asymmetrically Braced Frame Structure with Combined Low Damping Elastomeric and Flat Sliding Bearings	74
4-16	Comparison of Peak Response Quantities of Isolated Moment Frame Structure in El Centro S00E 200%	85
4-17	Comparison of Peak Response Quantities of Isolated Moment Frame Structure in Sylmar 90° 100%	86

## LIST OF TABLES (CONTD.)

<b>TABLE</b>	<b>TITLE</b>	<b>PAGE</b>
4-18	Comparison of Peak Response Quantities of Isolated Braced Frame Structure in El Centro S00E 200%	87
4-19	Comparison of Peak Response Quantities of Isolated Braced Frame Structure in Sylmar 90° 100%	88
5-1	Comparison of Experimentally and Analytically Determined Characteristics of Fixed Base Moment Frame Structure	104
5-2	Comparison of Experimentally and Analytically Determined Characteristics of Asymmetrically and Symmetrically Braced Fixed Base Structure	105

# SECTION 1

## INTRODUCTION

### 1.1 Background

Recent building codes accept that earthquake induced forces can be absorbed by the structural system through inelastic action which lengthens the period of the system and increases its energy dissipation capabilities (e.g., structural components are detailed for increased deformability and hysteretic damping). This action involves damage to the structural system; this damage is acceptable because it is not economically feasible with standard construction methods to construct a facility that will not sustain damage. However, earthquakes have other cost impacts such as repair and disruption costs after the earthquake, and emotional costs from personal losses and injuries.

Seismic isolation is a design technique for reducing the effects of earthquakes on structures by using a mechanism that provides flexibility and energy absorption while simultaneously supporting the weight of the structure. This is achieved by building the structure on devices that serve to substantially decouple the structure from the damaging horizontal components of the earthquake motions. This not only prevents the structural system from experiencing the full effects of the earthquake, but also damage to contents and non-structural components is significantly reduced or eliminated.

Currently more than 1000 structures worldwide have been constructed or are being constructed on seismic isolation. The first application of seismic isolation in the United States in a building structure was the use of high damping elastomeric bearings in the Foothill Communities Law and Justice Center in California in 1985. Since then there have been several more applications in new construction and retrofit of historic structures. The damage caused by the 1989 Loma Prieta and 1994 Northridge earthquakes greatly increased the demand for base isolated structures on the west coast of the United States. The number of new and retrofitted projects using seismic isolation demonstrates the increasing acceptance of this design technique and is also reflected in the new seismic isolation code provisions and specifications in the IBC 2000, FEMA 273 & 274 and AASHTO 2000.

The application of new technologies (specifically energy dissipation and seismic isolation systems) in important construction (particularly hospitals, emergency operation centers, buildings housing sensitive equipment and historic buildings with fragile ornaments) has very recently reached an interesting development. Guidelines for performance-based design now include statements on the performance of secondary systems. This performance is quantified in terms of a single parameter: the peak value of structural acceleration. However, it is well understood now that non-structural components and secondary systems are affected by several structural system response parameters, such as structural drift (e.g., piping systems, cladding, etc.), peak floor acceleration (e.g., rigidly attached equipment), spectral floor acceleration (e.g., flexibly attached equipment), and combination of response parameters (e.g., cabinets and equipment that are allowed to rock, and complex systems such as sprinkler systems, gas supply systems, etc.). Applied Technology Council – ATC (1998) has addressed many issues with non-structural components. While the ATC document identifies structural

response parameters that affect non-structural system response, it does not define response limits for specific performance objectives.

Apart from the fact that peak acceleration cannot adequately describe the potential for damage to secondary systems, there are concerns that current methods of analysis, whether simplified or sophisticated response-history methods, are capable of providing accurate information for assessing the potential for damage to secondary systems. Particularly, there has been little work to date on assessing the validity and accuracy of methods of analysis of seismically isolated structures with emphasis on secondary system response. Apart from the study of Juhn et al. (1992), which was very limited in scope, there is no work done on the verification of accuracy of methods of dynamic analysis of secondary systems in seismically isolated structures by comparison with experimental data.

Given the current emphasis on high performance structures and the interest in the behavior of non-structural components, there is a need to assess the validity and accuracy of methods of analysis of seismically isolated structures with emphasis on:

- (a) secondary system response,
- (b) contemporary seismic isolation systems, and
- (c) seismic excitation that is characteristic of strong seismicity and near-fault effects.

A number of seismic isolation and energy dissipation systems in configurations not previously tested but which are now often envisioned for applications in areas of high seismicity and near-fault excitation were designed and manufactured for this purpose. They include highly flexible and highly damped systems. While such systems are effective in reducing the response of the structural system, they are likely less effective in the protection of secondary (non-structural) components and systems.

The scope of this research is to acquire data on displacements, velocities and accelerations, as well as forces relevant to design of the structural system and utilize these data both to study the effectiveness of these systems and to investigate the accuracy of analytical prediction by the commonly utilized dynamic analysis programs. An existing six-story steel model was used in three configurations: flexible moment-frame, asymmetrically braced-frame and stiff braced-frame.

## **1.2 Report Organization**

Section 2 provides current information on non-structural component response to seismic excitation and seismic isolation systems. Section 3 provides information on the isolator testing machine, isolation system properties, the six-story structural model, tested configurations, instrumentation, and the simulator used for earthquake testing. Section 4 provides a summary of test results and interpretation of results. Analytical models of the isolation systems and the six-story structural system are developed and comparisons of response history analysis with experimental results are provided in Section 5. Section 6 includes a summary of key findings and conclusions drawn from this research project. The full results of experimental testing are presented in Appendix A. Appendix B provides sample computer input files used in analytical modeling. Appendices C and D provide analytical vs. experimental response results for computer programs SAP2000 and 3D-BASIS-ME, respectively.

## SECTION 2

### NON-STRUCTURAL COMPONENT RESPONSE AND SEISMIC ISOLATION SYSTEMS

Recent earthquakes, such as the 1989 Loma Prieta and 1994 Northridge earthquakes, have shown that code-designed buildings can suffer serious damage to their structural and non-structural systems when subjected to moderate and severe earthquake excitations. In particular, non-structural and secondary systems have sustained heavy damage, which in some cases have rendered the structures unusable. Since 1994, particular attention has been focused on the economic consequences of damage to non-structural components and systems. ATC (1997a) presents a historical review of the seismic design and construction practices of non-structural components in the U.S.

Recent seismic retrofit guidelines distinguish between non-structural components whose failure represents life hazard, those whose failure represents loss of building function, and those whose failure represents economic loss (ATC 33, 1997a,b). Building codes, seismic provisions and guidelines, such as the SEAOC (1999), IBC (2000), ATC (1997a,b) and FEMA (2001), contain some provisions for the seismic design of non-structural components. Other equipment and components installed in the building after completion (i.e. computer systems, furniture and art) are excluded. The failure or damage of such equipment and components could have a significant impact on building safety or function. Moreover, apart from ATC (1997a,b), there is no attempt in any building code or seismic provision to relate the seismic design criteria to performance-based design and there is no information on the expected state of damage (Arnold, 1998).

The ATC (1997a,b) has the first comprehensive guideline for performance-based seismic design. FEMA 273/274 provides design criteria for non-structural components to achieve the performance levels of Life Safety and Immediate Occupancy. No specific criteria are included for the performance levels of Operational. Moreover, no criteria are provided for complex non-structural systems, such as those that are essential for the operation of hospitals, or complex telecommunication systems that are essential for emergency, post-earthquake operations.

Seismic protective systems and particularly seismic isolation systems are generally presented as the systems most likely to achieve Operational Performance Level and to be useful for application in hospitals, emergency centers, museums and structures of architectural significance where damage to non-structural components is unacceptable (ATC 33, 1997a). Actually, the vast majority of seismically isolated buildings in the U.S. and Japan are structures of architectural significance, hospitals, emergency operations centers and buildings containing sensitive equipment or artifacts. This is to a certain extent a paradox given that there are no established procedures for achieving Operational performance – the level of performance contemplated for the seismically isolated structures.

Over the last decade a number of researchers have sought to identify what variables are important to the design of different types of non-structural components and systems. Some limit states have been established for various components, but to test all components in every type of structure in every orientation is impractical. It is possible to set criteria for some non-structural components that have a relatively small pool of

commercially available products, like architectural glass and windows, which seem to be controlled by drift, and possibly out-of-plane acceleration. For example, Behr and Worrell (1998) studied limit stages for architectural glass under simulated seismic loading. Many different types of glass with different types of laminates and prestressing were tested in plane. The glass did not start cracking until about 2% story drift in these tests.

For other non-structural components, like suspended ceilings, is more difficult to choose a critical structural response parameter. If the ceiling is braced in plane, it could be considered rigid and thus the peak floor acceleration might be critical. On the other hand, if the ceiling system is flexible in plane, the response of the ceiling system might depend on how close the natural frequency of the ceiling is to the peaks in the floor acceleration spectrum. In addition to acceleration, drift and bay deformation due to torsion may necessitate a gap between the ceiling system and the walls.

After the 1994 Northridge earthquake, the Olive View Medical Center was rendered unusable due to flooding from a failed fire sprinkler line that resulted from interaction between the ceiling system and the fire sprinkler heads (McGavin et al. 1998). These two non-structural systems had a joint boundary at the sprinkler head, and since their motions did not match, some heads were ruptured causing significant flooding. The hospital was then evacuated despite the complete lack of structural damage.

Many components in a building structure are dependant upon a specific single criterion for proper design, and some, like block type elements subject to sliding and overturning, depend on a combination of many variables. Upon first glance, the aspect ratio would appear to vastly affect the probability of overturning a block type element (i.e. filing cabinet, computer server, printer, copy machine, etc.). However, recent work by Zhu and Soong (1998) has shown that aspect ratio has relatively little effect on overturning. Instead, the general size of the object, the duration of excitation, the peak floor acceleration (the combination of the latter two parameters denotes the significance of floor velocity), vertical acceleration, and the restitution coefficient matter most. The aspect ratio and coefficient of friction determine whether the object is subject to sliding or rocking possibly leading to overturning. However, the probability of overturning is markedly affected by the restitution coefficient, leading to the conclusion that simply softer floor tiles may reduce the overturning effects by 50 to 90 percent. On the other hand, research by Agbabian et al. (1990) for the J. Paul Getty Museum contains experimental data which portrays a vastly different view. Instead, their results reinforce the logical assumption that the aspect ratio of the object plays a dominant role in the prediction of overturning. These two differing conclusions point to the fact that secondary system response parameters require much more research.

The plotting of probability of failure or damage to a non-structural system or component versus a particular input parameter is usually referred to as a fragility curve. Grigoriu and Waisman (1998), as well as Zhu and Soong (1998), have recently presented the idea of evaluation of system reliability using fragility data and a logic tree. Figures 2-1 and 2-2 present sample logic trees for two non-structural systems. Note that each system is made up of components, which in turn could be made up of sub-systems of components, and the trees can quickly branch out to a substantial number of components and variables. Every component in Figures 2-1 and 2-2 have different response characteristics, which are dependent on different primary structural responses. Piping that



runs vertically is likely dependent on story drifts, while valves and piping running horizontally are likely more affected by acceleration, but probably the full floor acceleration spectrum is needed to characterize damage rather than the peak floor acceleration. Peak acceleration or peak displacement alone is not sufficient information to assess the performance of secondary components and systems. Rather, the components and systems should probably be broken down to components with known fragility curves and an overall system fragility created. One can optimize the overall structural system by concentrating design effort on the limiting the probability of failure of specific components or subsystems that are critical for the operation of the facility.

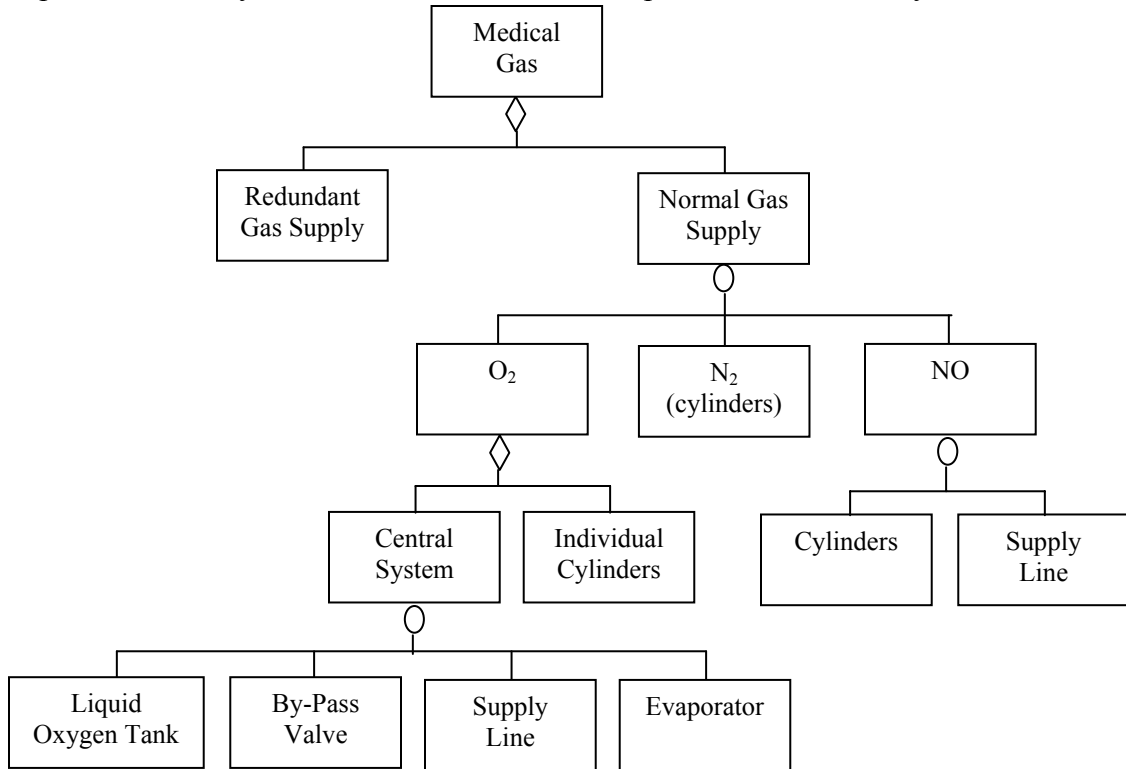


**FIGURE 2-1 Logic Tree Diagram for Medical Gas Supply Equipment (Zhu, 1998)**

It is thus indeed a severe problem that single-parameter statements on the performance of secondary components and systems in seismically isolated structures have been included in performance specifications, and oversimplification by some researchers has led to general conclusions that certain isolation systems may have significant and harmful impacts on the contents of isolated buildings. For example, Skinner et al. (1993) mistakenly conclude that isolation systems with high non-linearity are harmful to building contents. This observation is based entirely on analysis of a simple four-degree-of-freedom system subjected to the 1940 El Centro NS input and by using the top floor acceleration response as the parameter for assessing the performance of secondary systems. This will be visited again in Section 4.5.

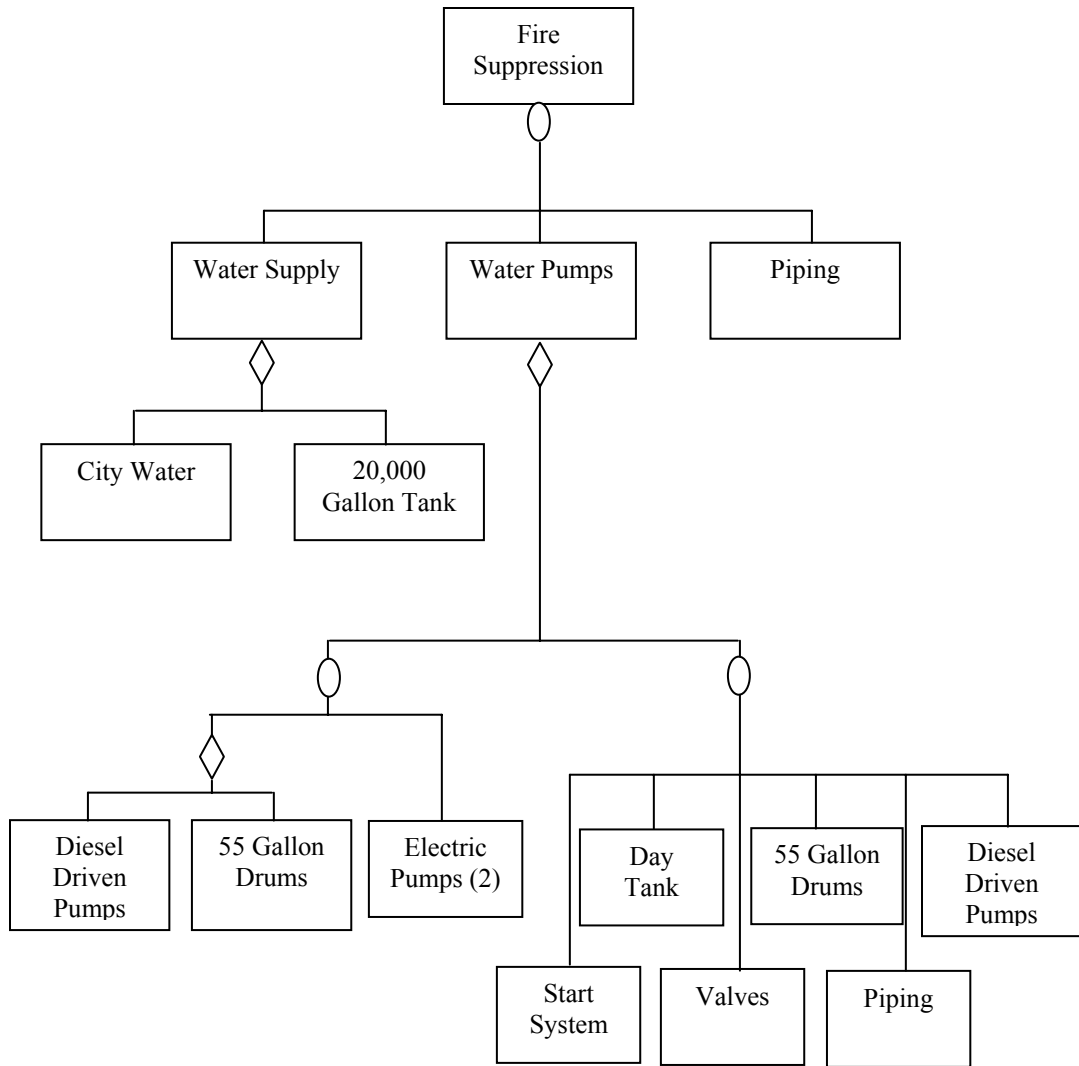


**FIGURE 2-2 Logic Tree Diagram for San Francisco High Rise Fire Suppression System (Grigoriu, 1998)**

It should be noted that it is generally accepted that properly designed seismic isolation systems reduce demands on non-structural components and systems by comparison with conventional fixed base structures. This conclusion is based on limited analytical studies such as those reported in Fan and Ahmadi (1990) and Skinner et al. (1993), and the experimental studies of Kelly and Tsai (1985) and Juhn et al. (1992).

The experimental studies of Kelly and Tsai (1985) and Juhn et al. (1992) concentrated on elastomeric and sliding isolation systems, respectively, both however of design and construction that do not correspond to those of isolation systems in use today. Nevertheless, both studies attempted analytical predictions of the response of secondary systems, with Kelly and Tsai (1985) presenting a simplified method applicable only to linear systems (such as low-damped elastomeric systems). While the studies correctly predicted trends in the response of secondary systems, peak values of interest in design could not be accurately predicted.

Accurate prediction of the response of secondary systems in seismically isolated structures is important in performance-based design. The available tools for analysis of

seismically isolated structures have not been evaluated for accuracy in the prediction of the dynamic response of secondary systems. Moreover, the evaluation of accuracy of these tools in the prediction of the dynamic response of the primary system has been limited. The study reported herein presents such an evaluation by (a) generating experimental results on six contemporary seismic isolation systems, and (b) comparing the experimental responses to analytically obtained results using currently available computer software.



## **SECTION 3**

### **COMPONENT AND SYSTEM EVALUATION**

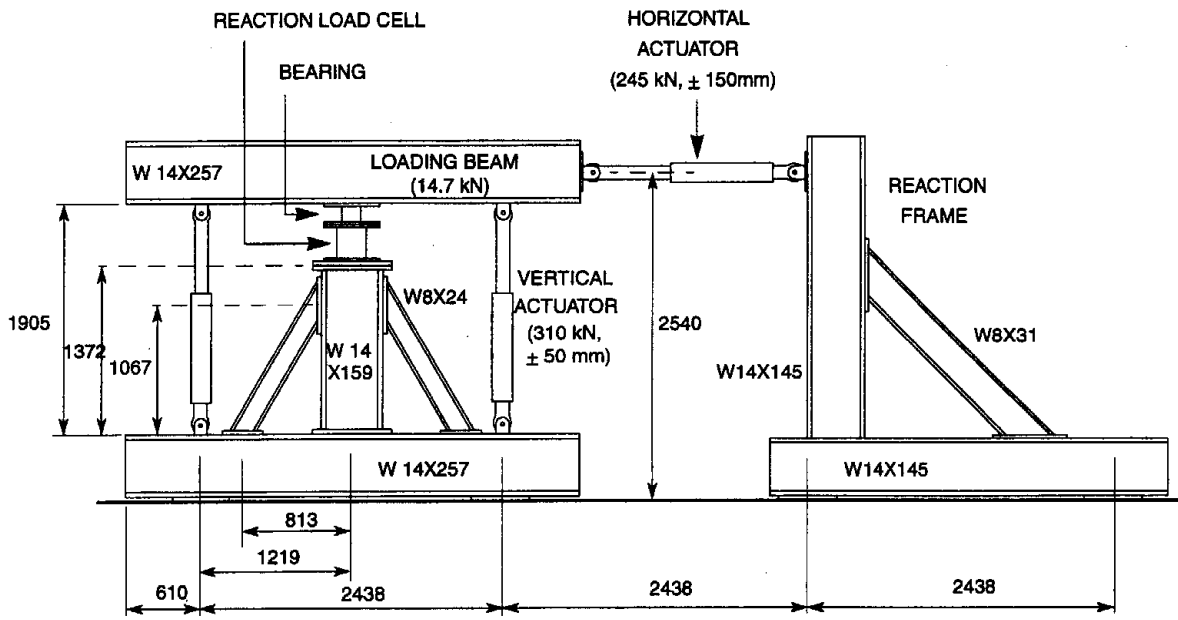
#### **3.1 Introduction**

The building model used in the earthquake simulator test program is the one used in numerous experiments at the University at Buffalo over the last 15 years. The model was originally tested in its fixed base configuration by Reinhorn et al. (1989), and the properties of the model were identified at that time by dynamic testing. The properties of the model were then verified and presented later in this section. Moreover, all seismic isolation and energy dissipation hardware was tested and its characteristics and properties are reported herein. FP and lead-core bearings were chosen since these systems represent the types of isolation systems used in the United States. Furthermore, elastomeric bearings, and FP bearings combined with viscous damping devices were studied because of their perceived usefulness in near fault applications. The combined elastomeric and flat sliding bearing system was tested because it is viewed as a competitor to the FP system in applications of large displacement demand and low bearing loads where purely elastomeric systems are ineffective due to inability to be designed with low stiffness.

#### **3.2 Testing Machine Description**

The single bearing test machine at the University at Buffalo was used to test the seismic isolation bearings. A schematic and a photograph of the bearing testing machine are presented in Figures 3-1 and 3-2 respectively. It was designed by Kasalanati and Constantinou (1999) to be a versatile, small-scale bearing test machine. Its capabilities are listed in Table 3-1. These capabilities are currently limited by the available reaction load cell and neither the strength of the support framing nor the capacity of the hydraulic actuators

The machine is capable of applying high-speed horizontal movement of the loading beam while controlling the axial load on the specimen to either a fixed value or to a prescribed history. A multi-component reaction load cell measures the forces in the isolator. The use of the reaction load cell and the overall construction of the machine greatly improve the accuracy of measurement since they eliminate the necessity for corrections due to dynamic and frictional losses that result from indirect measurement of forces.



ALL DIMENSIONS IN mm

FIGURE 3-1 Schematic of Machine Used to Test Individual Isolators



FIGURE 3-2 Photograph of Machine Used to Test Individual Isolators

**TABLE 3-1 Summary of Bearing Testing Machine Capabilities**

Vertical Load Capacity	220 kN
Horizontal Load Capacity	90 kN
Vertical Displacement Capacity	± 50 mm
Horizontal Displacement Capacity	± 150 mm
Specimen Plan Dimensions	Within 300 mm x 300 mm square
Specimen Height	Adjustable from 6mm to 230 mm

### 3.3 Viscous Damping Devices

Damping devices were added between the earthquake simulator and the rigid base of the model for selected tests to increase the effective damping of the isolation system. Linear and nonlinear fluid viscous damping devices were used in conjunction with both the Friction Pendulum and low damping elastomeric isolation systems. The properties of the damping devices were determined previously by Kasalanati and Constantinou (1999). Sinusoidal tests of varying amplitude and frequency (up to 10 Hz) were imposed on the dampers using the MTS test machine, and the force in the load cell directly connected to each damper was recorded. Figures 3-3 and 3-4 present the force-displacement loops from the testing of one linear and one nonlinear damper, respectively.

The dampers exhibited nearly pure viscous behavior. Figure 3-5 presents graphs of the peak damping force (at zero displacement) versus the peak velocity (amplitude times circular frequency). The force in the linear dampers can be described by

$$F_D = C_0 \dot{U}_D \quad (3-1)$$

where  $\dot{U}_D$  is the velocity of the piston in the damper and the damping constant  $C_0 = 0.0664$  kN-s/mm, which was determined in previous testing. The force in the nonlinear dampers is given by

$$F_D = C_N |\dot{U}_D|^\delta \cdot \text{sgn}(\dot{U}_D) \quad (3-2)$$

where the damping constant  $C_N = 2.226$  kN (s/mm)<sup>0.397</sup>, the velocity exponent  $\delta = 0.397$ , also determined by previous testing, and  $\text{sgn}(V_D)$ , the signum function, is the sign of the force is dependent on the direction of motion in the bearing (sign of relative velocity  $\dot{U}$ ).

### 3.4 Bearing Testing

The isolation systems were designed to result in an effective period of about 1 second in the 233 kN weight of the model structure for a displacement of 50 mm. FP bearings were supplied with a radius of 762 mm and coefficient of friction of 0.077, resulting in an effective period of 1.19 seconds at the displacement of 50 mm. The low damping elastomeric bearings had an effective period of 0.87 seconds. The lead-core bearings were designed identical to the low damping elastomeric but with the addition of a 25 mm lead plug. The lead plug caused a marked increase in strength (approximately 0.17 of the model weight on each bearing). The resulting increase in the effective stiffness of these bearings resulted in an effective period of 0.68 seconds for the displacement of 50 mm

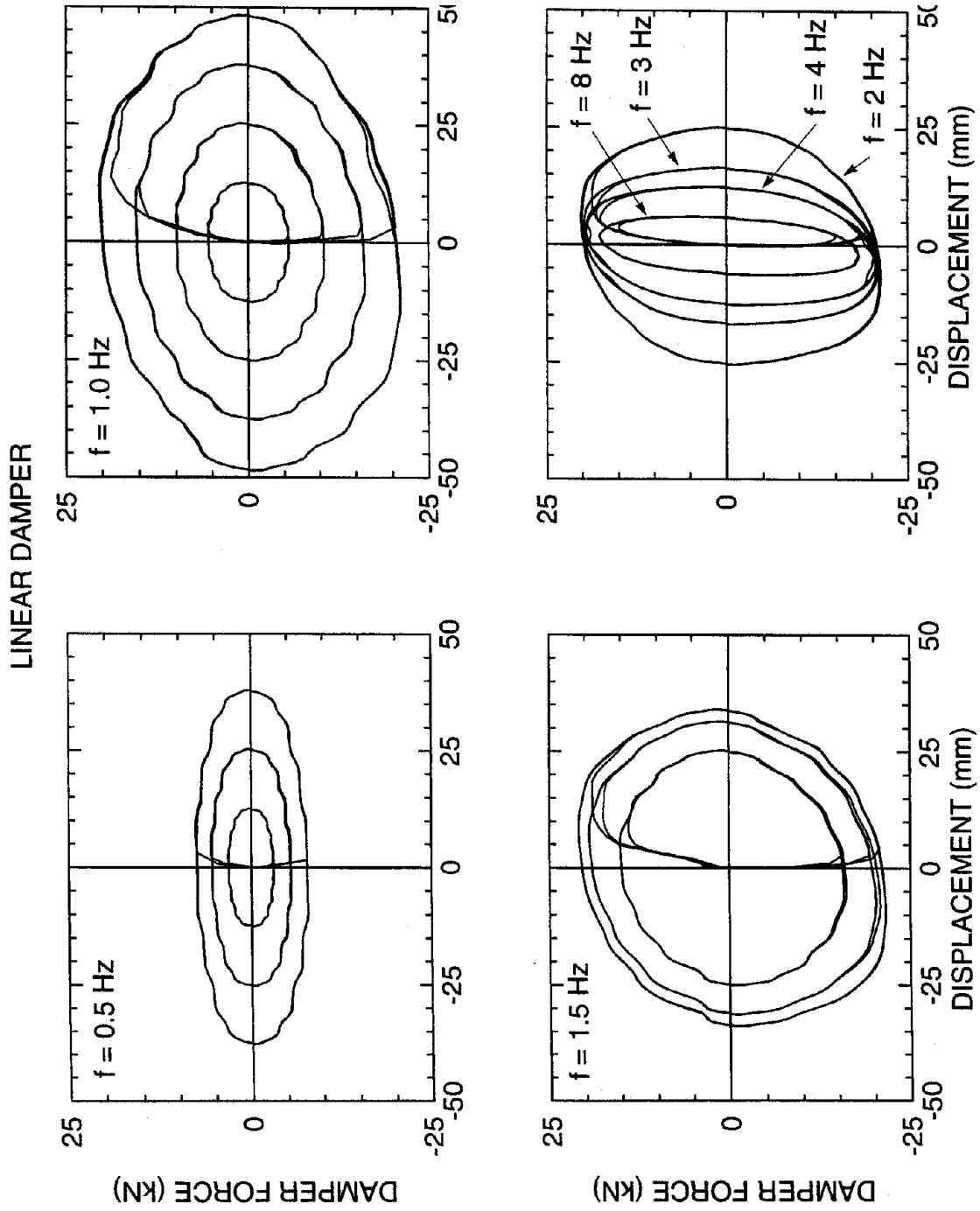


**FIGURE 3-3** Recorded Force-Displacement Loops of Linear Fluid Viscous Damper. (adapted from Kasalanati and Constantinou, 1999)



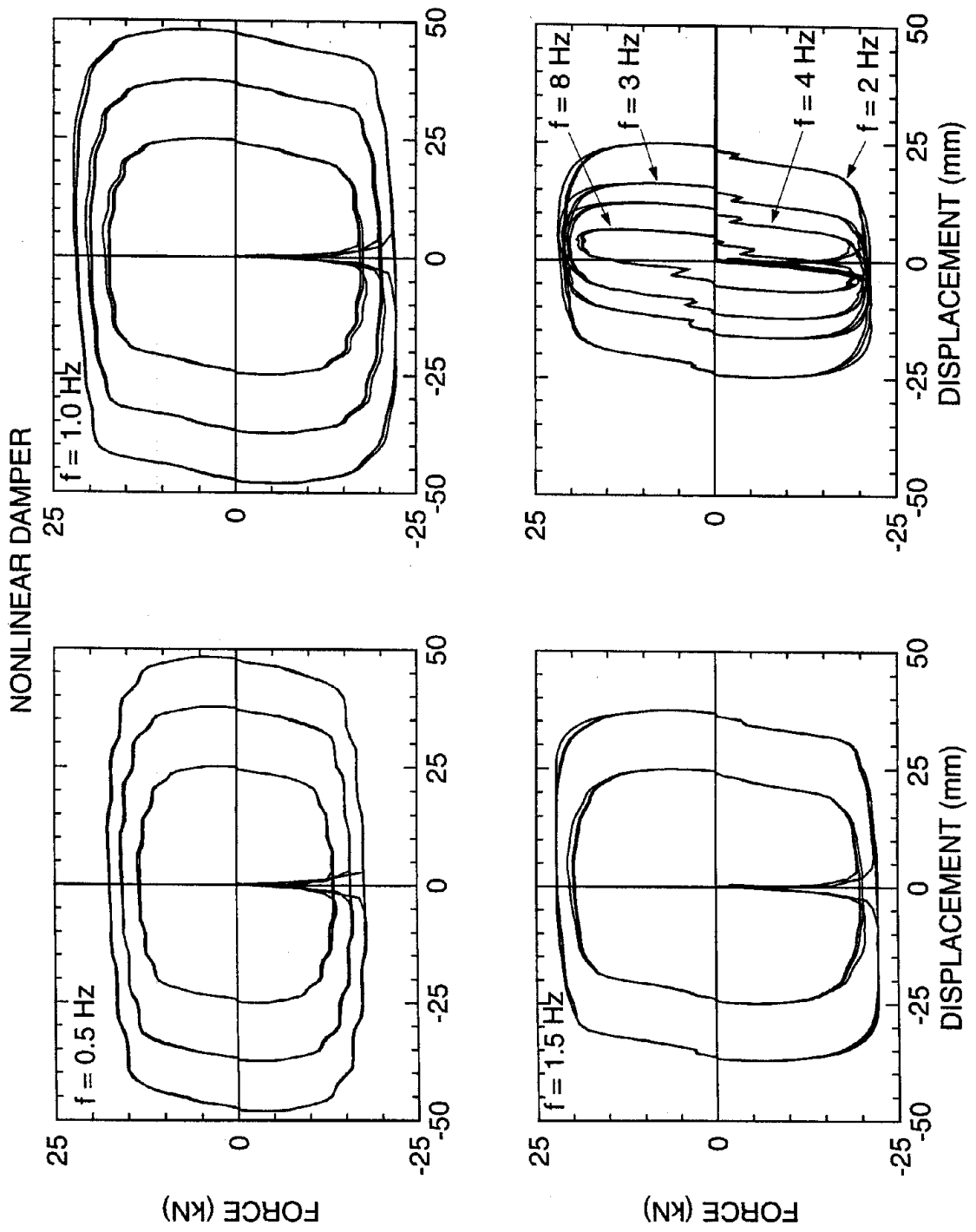
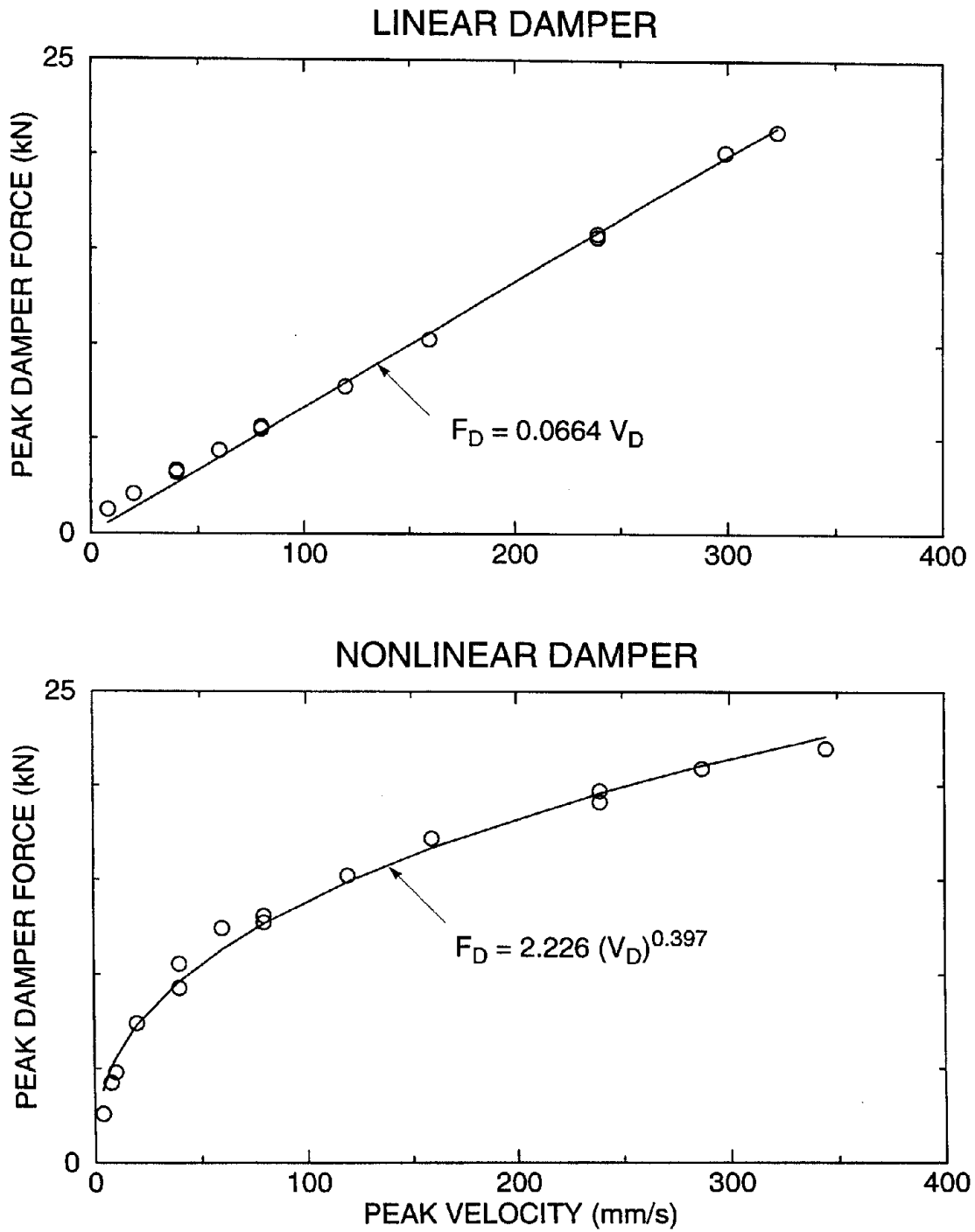


FIGURE 3-4 Recorded Force-Displacement Loops of Nonlinear Fluid Viscous Damper. (adapted from Kasalanati and Constantinou, 1999)



**FIGURE 3-5 Relationship Between Peak Damping Force and Peak Velocity for Two Dampers. (adapted from Kasalanati and Constantinou, 1999)**

### 3.4.1 Friction Pendulum (FP) Bearings

The principles of operation of the FP bearing have been established by Zayas et al. (1987), Mokha et al. (1990), Constantinou et al. (1993) and Tsopelas et al. (1993). An exploded cross-section view of the FP bearings used in this research project is shown in Figure 3-6. The bearing consists of a spherical sliding surface and an articulated slider, which is faced with a PTFE-based composite identical to that described in Constantinou et al. (1999). The force-displacement relation of a FP bearing in any direction is given by

$$F = \frac{N}{R}U + \mu_s N \operatorname{sgn}(\dot{U}) \quad (3-3)$$

where  $R$  is the radius of curvature of the sliding surface,  $N$  is the normal load,  $U$  is the displacement,  $\dot{U}$  is the velocity and  $\mu_s$  is the coefficient of sliding friction as given by Mokha and Constantinou (1990) as

$$\mu = f_{\max} - (f_{\max} - f_{\min}) \exp(-\alpha|\dot{U}|) \quad (3-4)$$

where  $f_{\max}$  and  $f_{min}$  are the maximum and minimum friction coefficients, respectively,  $\alpha$  is a parameter which controls the variation of friction with velocity, and other terms have been defined previously.

To identify the variables needed to properly model the FP bearings, several tests were conducted on a single FP bearing. All tests were conducted under constant normal load and three cycles of sinusoidal lateral displacement. Sample results are presented in Figure 3-7.

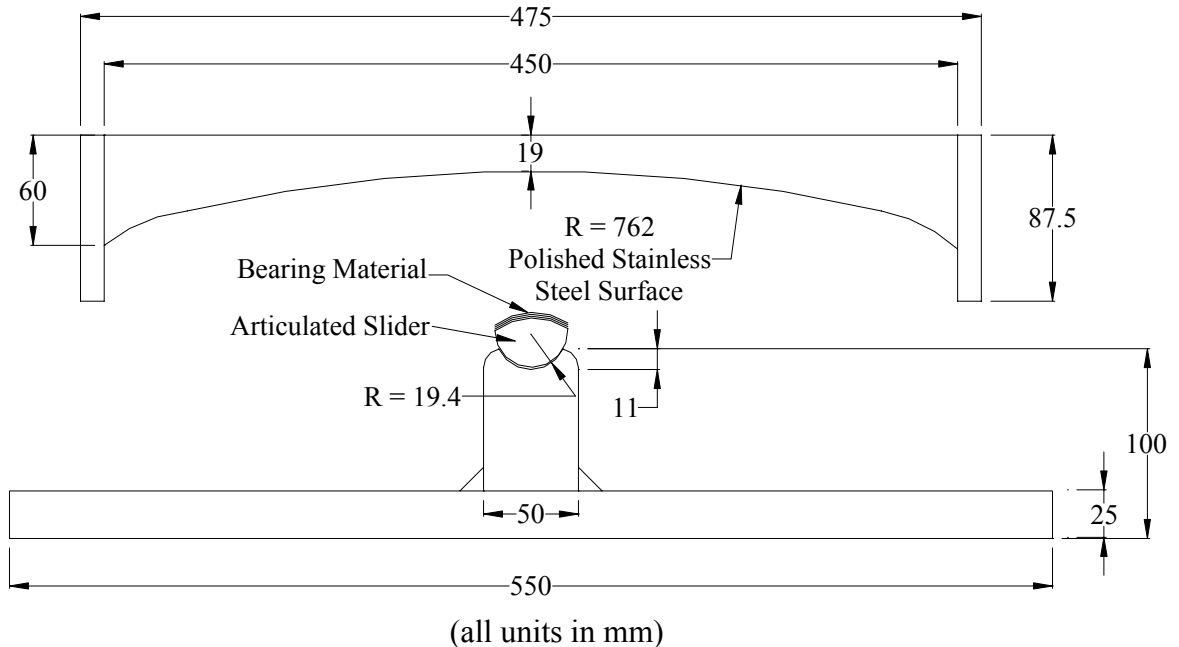


**FIGURE 3-6 FP Bearing Section**

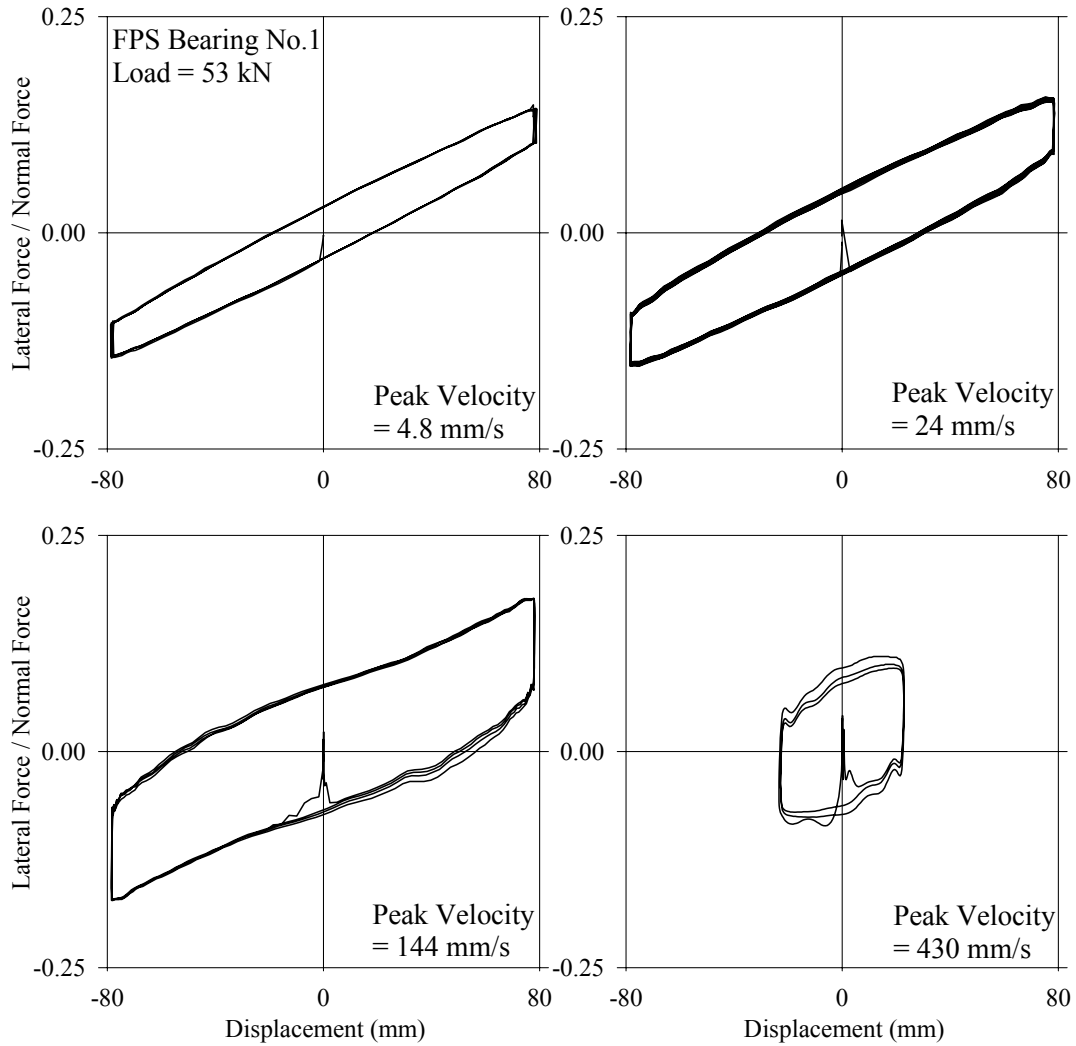


**FIGURE 3-7 Recorded Normalized Force-Displacement Loops of a FP Bearing**

The loops in Figure 3-7 reveal the dependency of the coefficient of friction on the velocity of sliding, which is depicted in Figure 3-8 together with predictions of the calibrated equation (3-4). Also, the loops of Figure 3-7 show waviness in the high velocity tests. This waviness is the result of fluctuating normal load due to inability of the test machine to accommodate the changes in the height of the bearing during high speed testing. For example, in the test at a peak velocity of 430 mm/sec, the normal load varied between 36 and 77 kN. The problem is more pronounced in the combined large amplitude-large velocity (144 mm/sec) test where the normal load varied between 22 and 85 kN.

### 3.4.2 Low Damping Elastomeric Bearings

Figure 3-9 presents a schematic of the low damping rubber bearings used in this research project. The bearings were made of natural rubber of grade 5 and hardness 50. The shear modulus for this material is typically in the range of 0.6 to 0.7 MPa. Assuming a shear modulus,  $G$ , of 0.7 MPa, the effective stiffness of the bearings can be predicted by

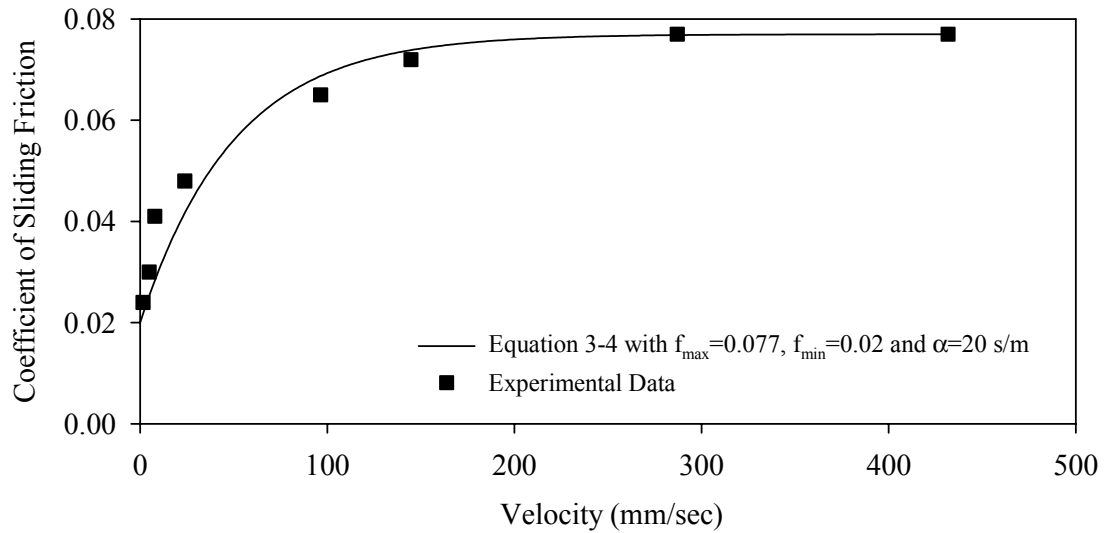


**FIGURE 3-8 Coefficient of Sliding Friction Versus Velocity for a FP Bearings**

$$K_{eff} = \frac{GA_r}{T_r} \quad (3-5)$$

where  $A_r$  is the bonded rubber area, and  $T_r$  is the total rubber thickness. For  $A_r = 24280 \text{ mm}^2$  and  $T_r = 57 \text{ mm}$ ,  $K_{eff}$  is 0.30 kN/mm. Thus for four bearings supporting a weight of 233 kN, these bearing would provide a period of about 1.0 sec in the scale of the experiment and 2.0 sec in the prototype scale.

After receiving the bearings, they were tested in the bearing test machine to determine their actual properties before being utilized for earthquake simulator testing. Figures 3-10 and 3-11 present recorded lateral force-displacement loops of the four elastomeric bearings tested under a variety of conditions, including

- a) Axial loads of about 25% (13.3 kN) to about 235% (124.5 kN) of the gravity load on the bearings during the earthquake simulator testing,
- b) Rubber shear strain in the range of 50 to 150%, and
- c) Temperature in the range of 20 to 55 °C.

The bearings exhibited stable properties, which for all practical purposes may be described by an effective stiffness of 0.32 kN/mm and an effective damping of 0.045. Thus, the effective shear modulus of the rubber is 0.75 MPa. However, it may be noted in the loops of Figures 3-10 and 3-11 that the bearings exhibit a reduced stiffness for displacements exceeding about 25 mm (which corresponds to a shear strain in the rubber of about 50%). The origin of this phenomenon is not known but appeared important for the analytical prediction of the response of the isolated model structure.

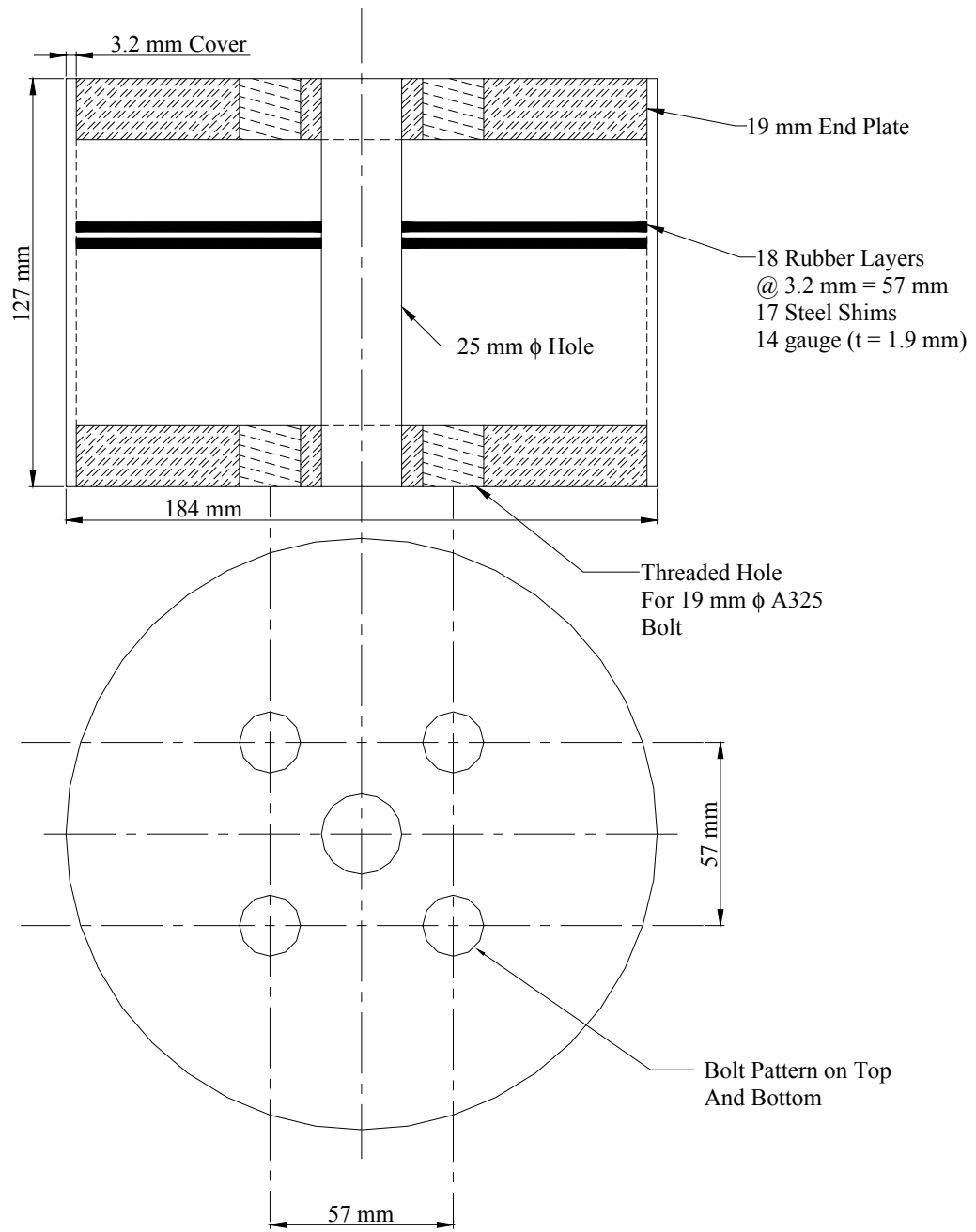


**FIGURE 3-9 Schematic of Tested Low Damping Rubber Bearings**

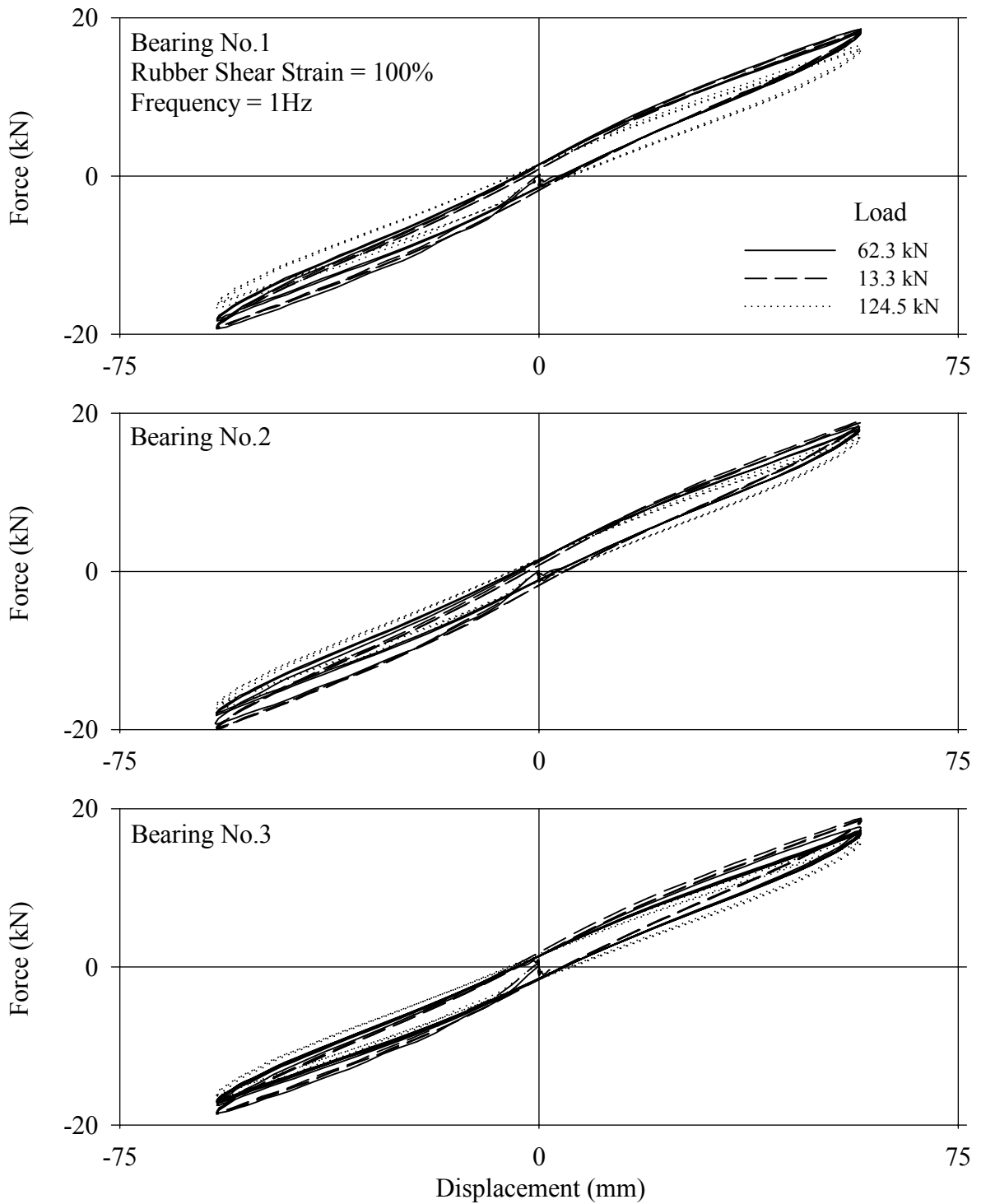


**FIGURE 3-10 Recorded Lateral Force-Displacement Loops for Elastomeric Bearing Nos. 1,2 and 3 under Three Different Axial Loads**

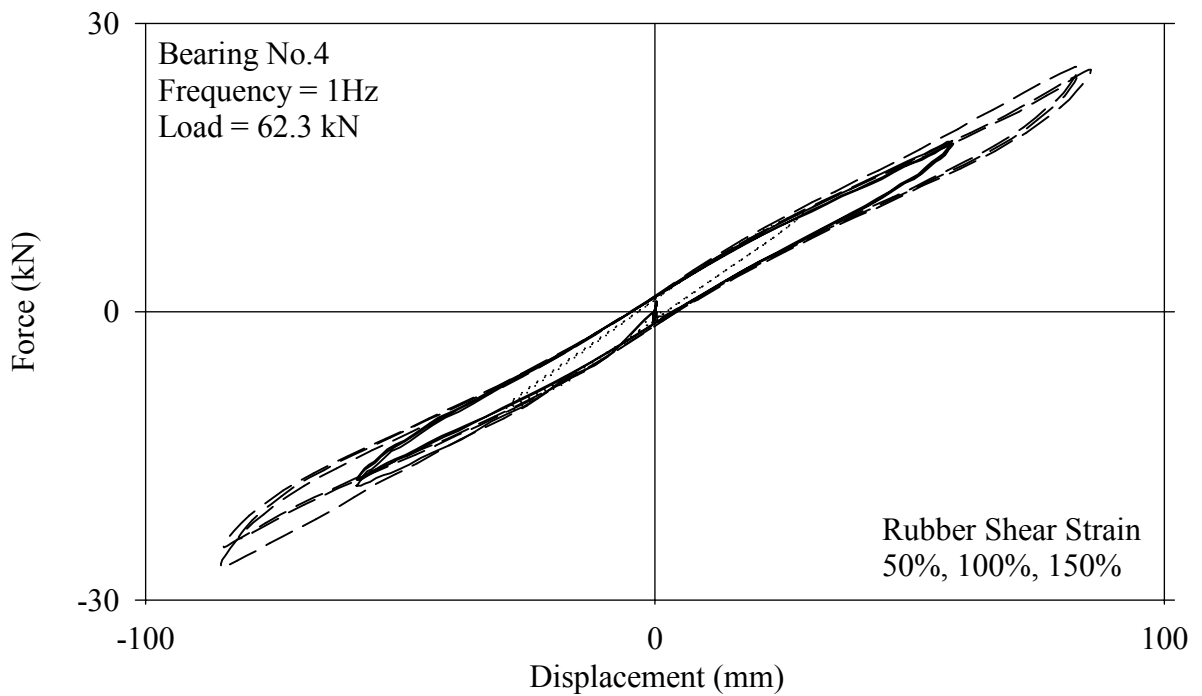
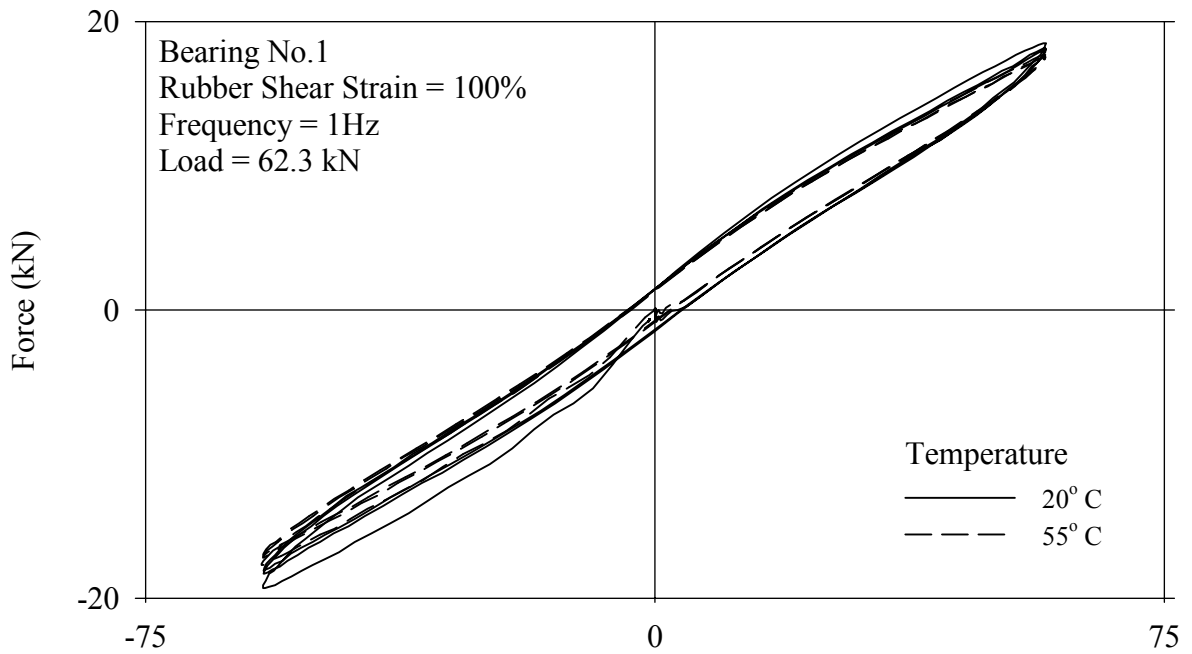


**FIGURE 3-11 Recorded Lateral Force-Displacement Loops for Elastomeric Bearing Nos. 1 and 4 under Varying Shear Strain and Temperature Conditions**



### 3.4.3 Lead-Core Bearings

The lead-core bearing consists of an elastomeric bearing (in this case, identical to the low damping elastomeric bearings described in Section 3.4.2) with a lead plug fitted in a central hole. The addition of the lead core substantially increases the capability for energy absorption due to yielding of the lead core and provides a large horizontal stiffness at very low displacements, which may be advantageous for resisting service loads. Figure 3-12 is a schematic of the lead-core (or lead-rubber) bearings used in this research project.

The lateral force-displacement relation of the lead-core bearing is shown, in idealized form, in Figure 3-13. In this figure,  $K_e$  is the elastic stiffness,  $K_p$  is the post-elastic stiffness,  $D_y$  is the yield displacement,  $F_y$  is the yield force and  $Q$  is the characteristic strength (or zero-displacement intercept).

After receiving the four lead-core bearings, they were all tested in the single bearing test machine to determine the actual properties before being utilized in earthquake simulator testing. Figure 3-14 presents lateral force-displacement loops for the four lead core bearings, recorded in tests under load of 62.3 kN, frequency of 1Hz and rubber shear strain of 100%. The loops in Figure 3-14 demonstrate minimal variability of properties among the four bearings and a small reduction of strength with increasing number of cycles. This is very good performance given the large energy dissipation capacity of the bearings, the high speed of testing (peak velocity of 358 mm/s) and the generated heat (see Constantinou et al., 1999 for discussion). The following average properties for the four bearings and over the three cycles of testing parameters were calculated from the loops of Figure 3-13:

- a) Characteristic strength  $Q = 9.75$  kN,
- b) Post-elastic stiffness  $K_p = 0.37$  kN/mm,
- c) Elastic stiffness  $K_e = 5.25$  kN/mm, and
- d) Yield displacement  $D_y = 2.0$  mm.

Two characteristics of the lead core bearings were important to assess the performance of the isolation system in the earthquake simulator tests. The first is characteristic strength. At 9.75 kN, this value is 17% of the gravity load on the bearings (=58 kN) in the earthquake simulator testing, and uncharacteristically high for lead core bearings in actual applications. Given the very large strength of the bearings, the effective stiffness is high leading to low effective period of the isolated model. The lead-core bearings could not be designed for larger flexibility for reasons of isolator stability at the quarter length scale used for earthquake simulator testing.

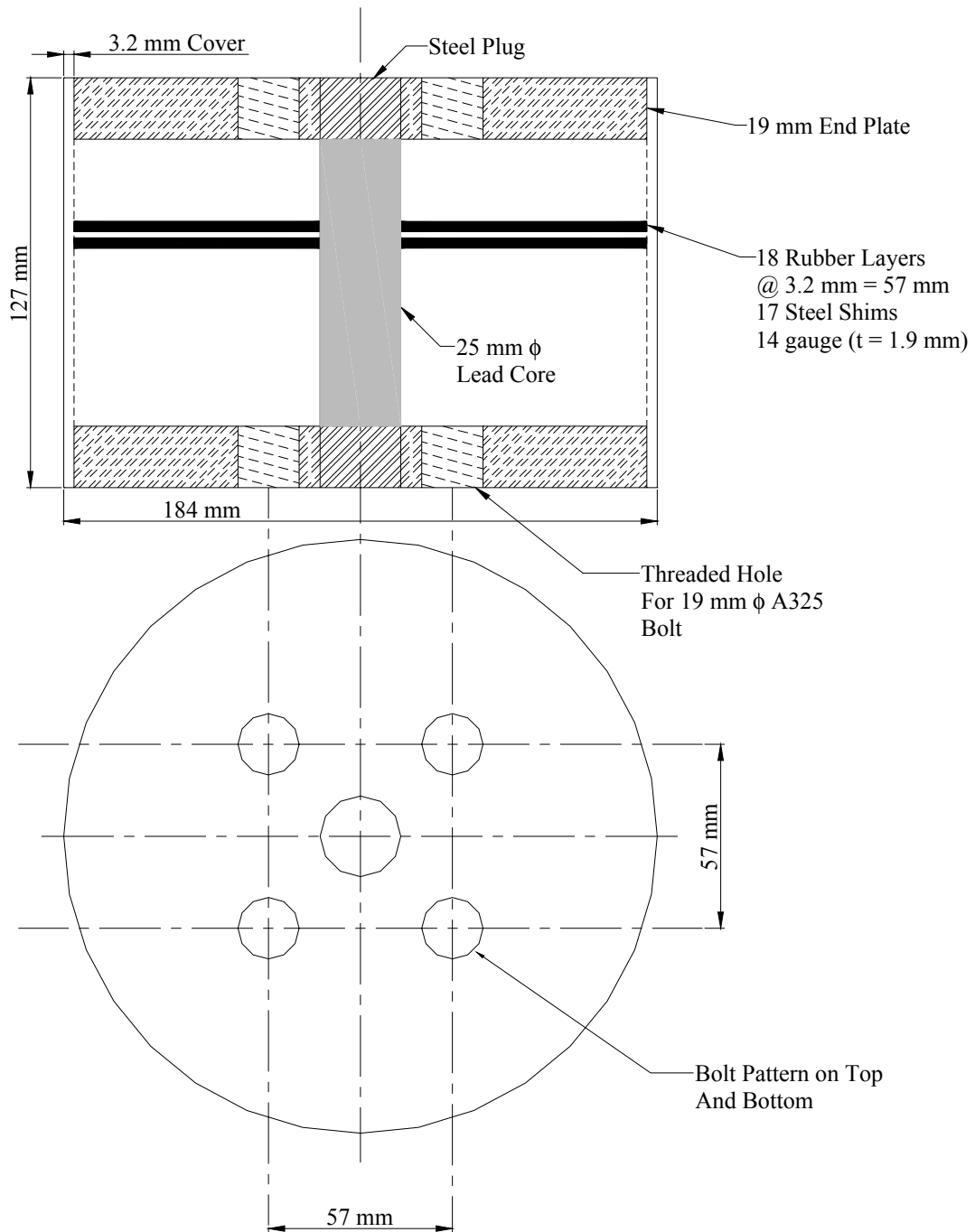


**FIGURE 3-12 Schematic of Tested Lead-Core Bearing**

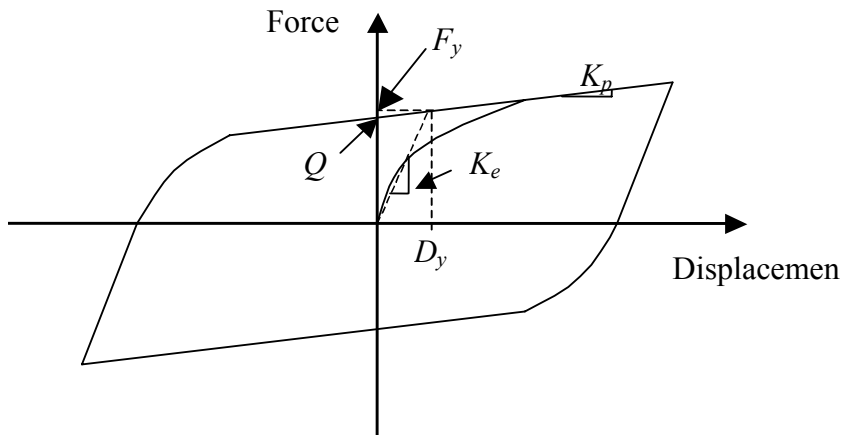


**FIGURE 3-13 Force-Displacement Relation of Lead Core Bearing**

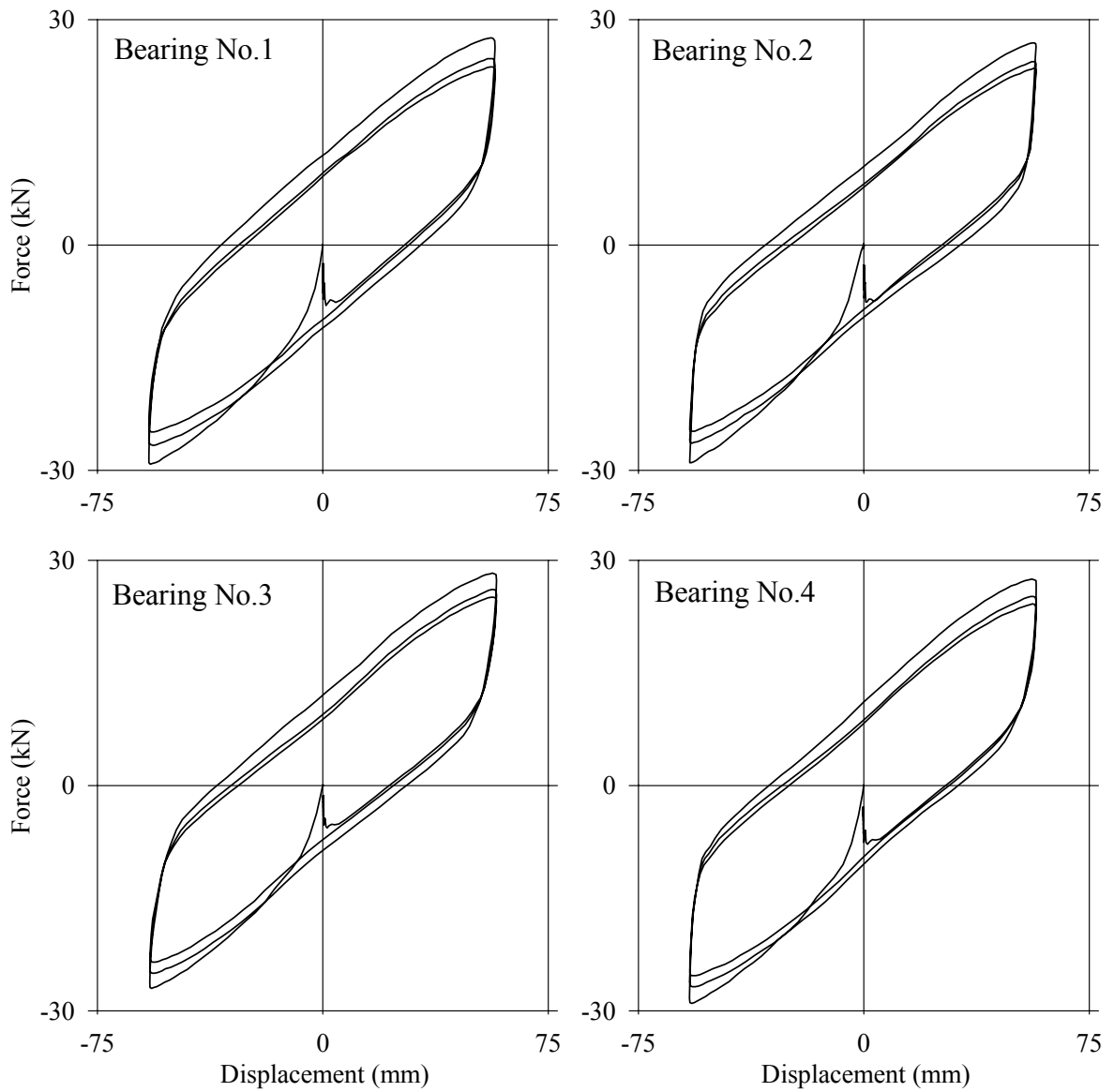


**FIGURE 3-14 Recorded Force-Displacement Loops of Lead-Core Bearings**

### 3.4.4 Flat Sliding Bearings

In this research project, flat sliding bearings were used in combination with low damping elastomeric bearings to create an isolation system with low effective stiffness and moderate characteristic strength. Figure 3-15 presents a schematic of the sliding bearings utilized in the experiments described herein. The force-displacement relationship for flat sliding bearings is

$$F = \mu_s N \cdot \text{sgn}(\dot{U}) \quad (3-6)$$

where  $F$  is the force,  $\mu_s$  is the coefficient of sliding friction and given by equation (3-4),  $N$  is the normal force on the bearing, and  $\text{sgn}(\dot{U})$  is the signum function.

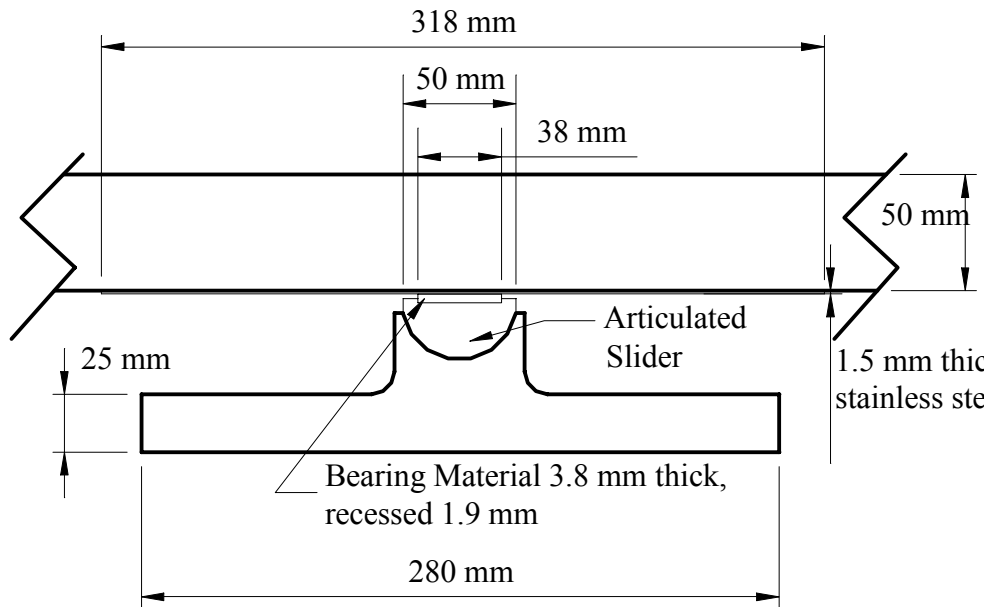


**FIGURE 3-15 Schematic of Tested Flat Sliding Bearing**

Testing was performed on one flat sliding bearing. Sample results are shown in Figure 3-16 in which four representative normalized force-displacement loops are presented. On the basis of these test results, the coefficient of friction was determined and plotted versus the velocity of sliding in Figure 3-17. Also plotted in the figure is the prediction of equation (3-4) following calibration and using the parameters shown in the figure. Of interest is to note in Figure 3-16 is the substantial breakaway friction in the test at velocity of 2.4 mm/sec. This was the first test to be conducted on the bearing. This behavior has been described in Constantinou et al. (1999), where physical explanations for this behavior are presented. The breakaway friction, approximately 0.06, is ignored in the analytical modeling because it is much less than the maximum friction of 0.11 that occurs at high velocities.

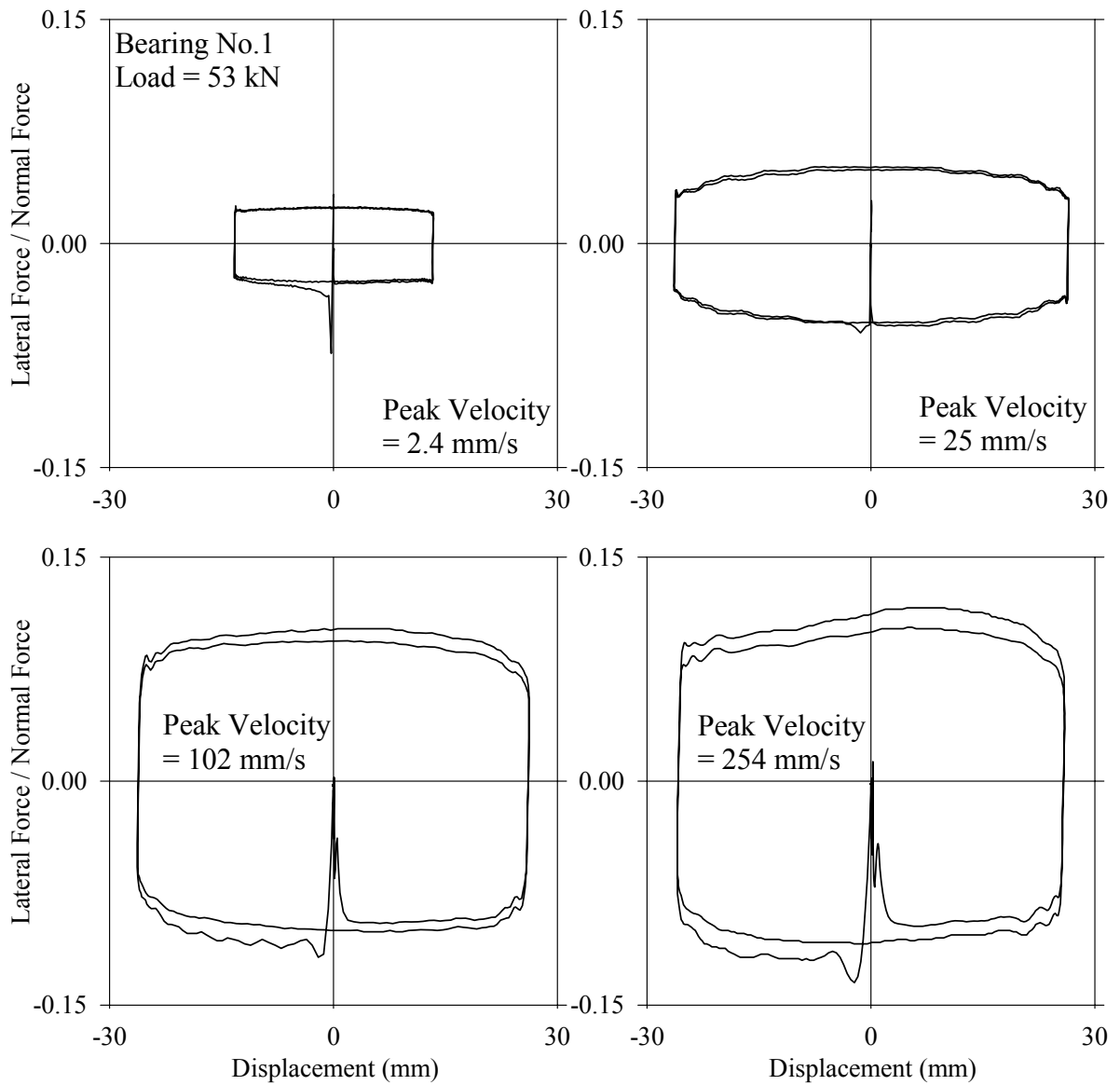


**FIGURE 3-16 Recorded Normalized Force-Displacement Loops of a Flat Sliding Bearing**

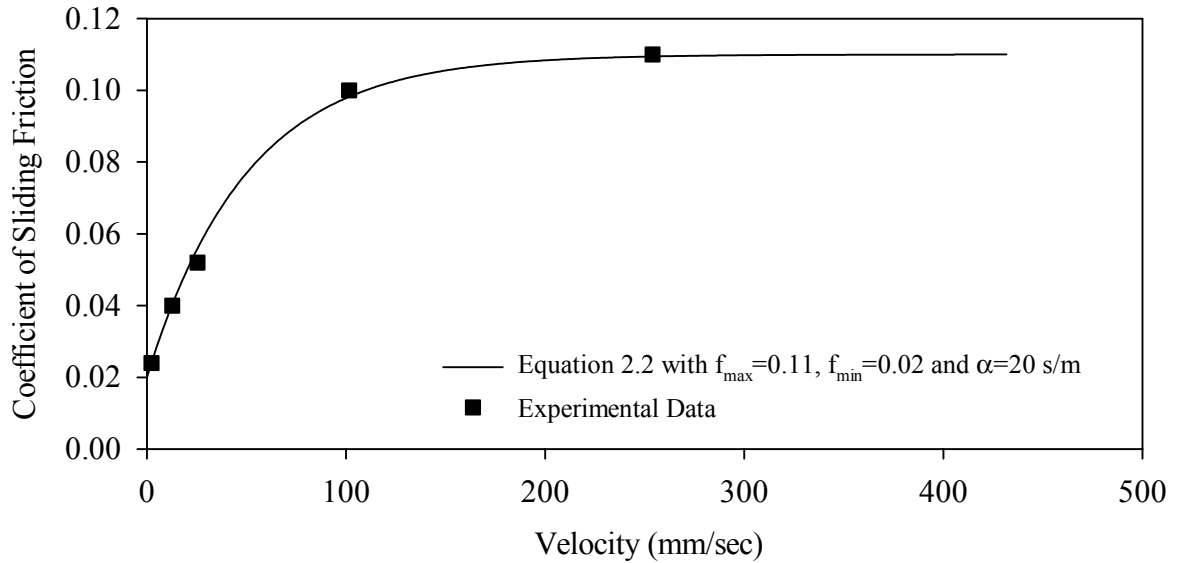
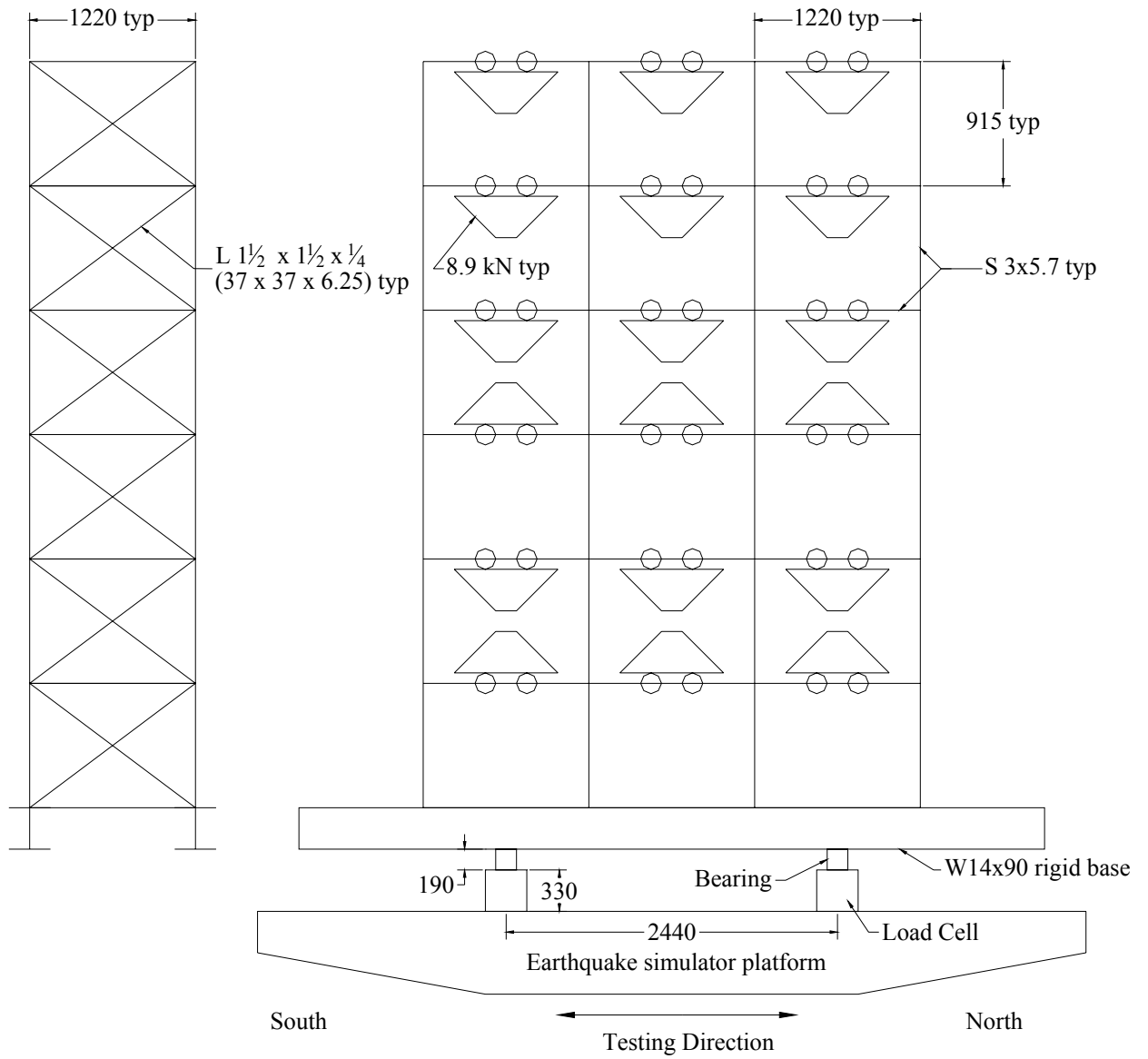


**FIGURE 3-17 Coefficient of Sliding Friction Versus Velocity in a Flat Sliding Bearing**

### 3.5 Six-Story Model

The six-story model used in the earthquake simulator testing is identical to that used in previous testing of energy dissipation and seismic isolation systems at the University at Buffalo (Reinhorn et al., 1989; Mokha et al., 1990; Constantinou et al., 1990). It represents a section in the weak direction of a steel moment-resisting frame.

The structure is shown in Figures 3-18 and 3-19. All column and beam sections are S3x5.7, and all out-of-plane braces are L 1½x1½x¼ (37x37x6.25). The structure is attached to a rigid base comprised of two AISC W14x90 sections, 5.2 m long with six transversely connected beams. The model has six stories of 0.914 m height each, giving a total height of 5.486 m above the base. The model is three bays by one bay in plan, each bay being 1.22 m wide, for total plan dimensions of 1.22 m by 3.66 m. Concrete blocks were used to add mass to satisfy similitude requirements, bringing the total weight, including the base, to 233 kN. The structure was constructed to have a length scale of 4. Other scale factors used in the testing are presented in Table 3-2.



(all units in mm)

**FIGURE 3-18 Schematic of Tested Six-Story Isolated Model Structure**

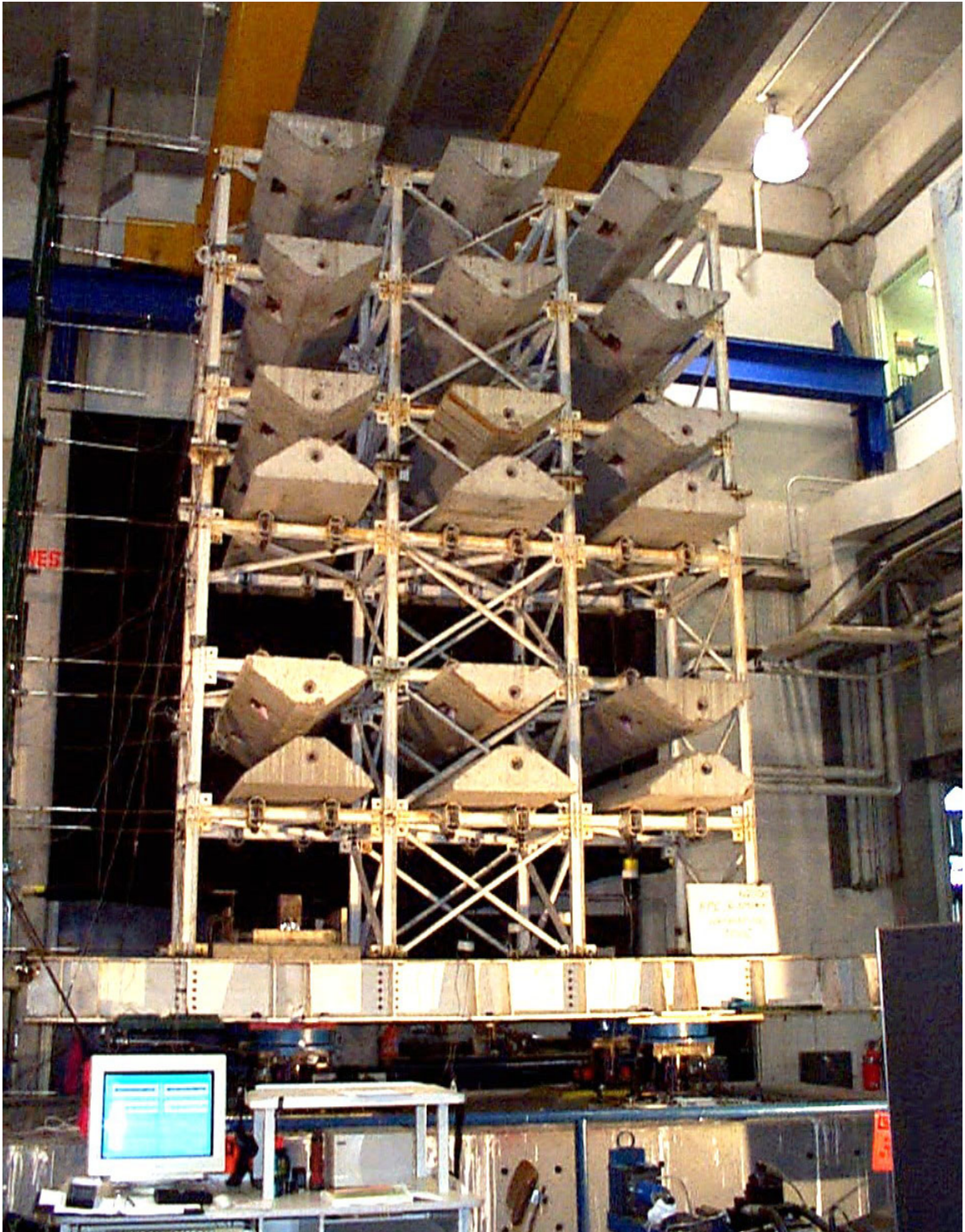


**FIGURE 3-19** Photograph of Tested Six-Story Isolated Model Structure on the University at Buffalo Earthquake Simulator



**TABLE 3-2 Scale Factors Used in Model Structure**

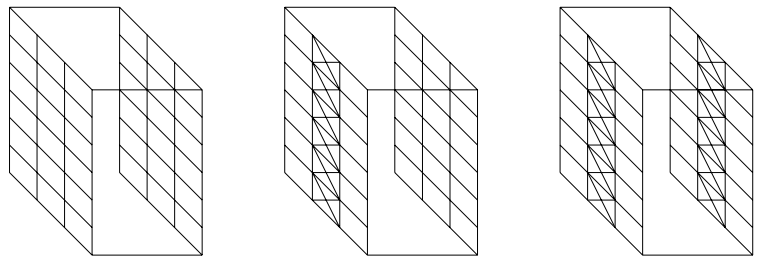
QUANTITY	DIMENSION <sup>1</sup>	SCALE FACTOR
Linear Dimension	L	4
Displacement	L	4
Time	T	2
Velocity	LT <sup>-1</sup>	2
Acceleration	LT <sup>-2</sup>	1
Frequency	T <sup>-1</sup>	½
Stress / Pressure	ML <sup>-1</sup> T <sup>-2</sup>	1
Force	MLT <sup>-2</sup>	16
Strain	-	1

1. L = length, T = time, M = mass

### 3.6 Tested Configurations

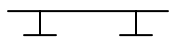
A total of 27 configurations of the six-story model were tested as listed below. Figure 3-20 presents a schematic description of these configurations.

1. Non-isolated Six-story Moment Frame (FBMF): The six-story steel moment frame structure was tested with the bearings locked and additional L 6x6x½ (152x152x12) angle braces between the rigid base and the simulator platform to ensure fixed base conditions; fundamental period was 2.34 Hz.
2. Non-isolated Six-story Asymmetrically Braced Frame (FBAB): The six-story FBMF steel moment frame structure was altered by adding L 1½x1½x¼ (37x37x6.25) braces on one side of the middle bay on each floor to induce torsion; fundamental period was 3.32 Hz.
3. Non-isolated Six-story Symmetrically Braced Frame (FBSB): The six-story FBMF steel moment frame structure was altered by adding L 1½x1½x¼ (37x37x6.25) braces to both sides of the middle bay on each floor to create a fully braced structure; fundamental period was 4.0 Hz.
4. FP-isolated Six-story Moment Frame (FPMF): The six-story moment frame of configuration 1 isolated from the earthquake simulator with four FP bearings.
5. FP-isolated Six-story Asymmetrically Braced Frame (FPAB): The six-story asymmetrically braced frame of configuration 2 isolated from the earthquake simulator with four FP bearings.
6. FP-isolated Six-story Symmetrically Braced Frame (FPSB): The six-story symmetrically braced frame of configuration 3 isolated from the earthquake simulator with four FP bearings.



Non Isolated	FBMF	FBAB	FBSB
FP Isolated no Dampers	FPMF	FPAB	FPSB
FP Isolated Linear Dampers	FPML	FPAL	FPSL
FP Isolated Non-Lin Damper	FPMN	FPAN	FPSN
Elastomeric no Dampers	LDMF	LDAB	LDSB
Elastomeric Linear Dampers	LDML	LDAL	LDSL
Elastomeric Non-Lin Dampers	LDMN	LDAN	LDSN
Lead Core no Dampers	LCMF	LCAB	LCSB
Elastomeric + Flat Sliding	EFMF	EFAB	EFBS

**FIGURE 3-20 Illustration of Tested Configurations**



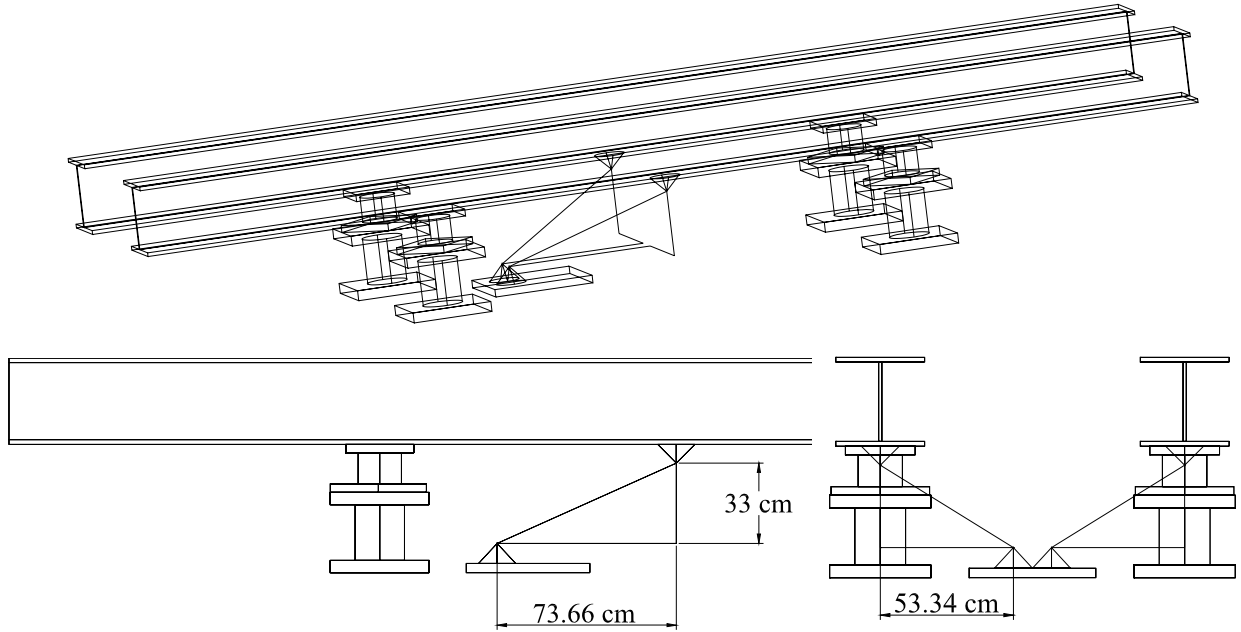


**FIGURE 3-21 Installation Geometry for Fluid Viscous Dampers**

7. FP-isolated Six-story Moment Frame with Linear Dampers (FPML): Linear viscous dampers were added between the rigid base and the simulation platform to the six-story FP-isolated moment frame of configuration 4. The dampers were connected
8. from the earthquake simulator to the center of the underside of the W14x90 beams as shown in Figure 3-21. The total length of the installed damper assemblage was 96.75 cm, and the angle between the damper axis and the longitudinal base direction was 40.4 degrees. However, since the dampers could move  $\pm 5$  cm along the axis of the damper ( $\pm 6.5$  cm along the longitudinal axis of the base) the angle between the damper axis, and the direction of motion axis varied from 38 to 43 degrees.
9. FP-isolated Six-story Asymmetrically Braced Frame with Linear Dampers (FPAL): Linear viscous dampers were added between the rigid base and the simulator platform to the six-story FP-isolated asymmetrically braced frame of configuration 5.
10. FP-isolated Six-story Symmetrically Braced Frame with Linear Dampers (FPSL): Linear viscous dampers were added between the rigid base and the simulator platform to the six-story FP-isolated symmetrically braced frame of configuration 6.
11. FP-isolated Six-story Moment Frame with Nonlinear Dampers (FPMN): Nonlinear viscous dampers were added between the rigid base and the simulator platform to the six-story FP-isolated moment frame of configuration 4. The nonlinear dampers were connected per configuration 7.
12. FP-isolated Six-story Asymmetrically Braced Frame with Nonlinear Dampers (FPAN): Nonlinear viscous dampers were added between the rigid base and the simulator platform to the six-story FP-isolated asymmetrically braced frame of configuration 5.

13. FP-isolated Six-story Symmetrically Braced Frame with Nonlinear Dampers (FPSN): Nonlinear viscous dampers were added between the rigid base and the simulator platform to the six-story FP-isolated symmetrically braced frame of configuration 6.
14. Low Damping Elastomeric Bearing isolated Six-story Moment Frame (LDMF): The six-story moment frame of configuration 1 isolated from the earthquake simulator with four low damping elastomeric bearings.
15. Low Damping Elastomeric Bearing isolated Six-story Asymmetrically Braced Frame (LDAB): The six-story asymmetrically braced frame of configuration 2 isolated from the earthquake simulator with four low damping elastomeric bearings.
16. Low Damping Elastomeric Bearing isolated Six-story Symmetrically Braced Frame (LDSB): The six-story symmetrically braced frame of configuration 3 isolated from the earthquake simulator with four low damping elastomeric bearings.
17. Low Damping Elastomeric Bearing isolated Six-story Moment Frame with Linear Dampers (LDML): Linear viscous dampers were added between the rigid base and the simulator platform to the six-story low damping elastomeric bearing isolated moment frame of configuration 13. The dampers were connected per configuration 7.
18. Low Damping Elastomeric Bearing isolated Six-story Asymmetrically Braced Frame with Linear Dampers (LDAL): Linear viscous dampers were added between the rigid base and the simulator platform to the six-story low damping elastomeric bearing isolated asymmetrically braced frame of configuration 14.
19. Low Damping Elastomeric Bearing isolated Six-story Symmetrically Braced Frame with Linear Dampers (LDSL): Linear viscous dampers were added between the rigid base and the simulator platform to the six-story low damping elastomeric bearing isolated symmetrically braced frame of configuration 15.
20. Low Damping Elastomeric Bearing isolated Six-story Moment Frame with Nonlinear Dampers (LDMN): Nonlinear viscous dampers were added between the rigid base and the simulator platform to the six-story low damping elastomeric bearing isolated moment frame of configuration 13. The dampers were connected per configuration 7.
21. Low Damping Elastomeric Bearing isolated Six-story Asymmetrically Braced Frame with Nonlinear Dampers (LDAN): Nonlinear viscous dampers were added between the rigid base and the simulator platform to the six-story low damping elastomeric bearing isolated asymmetrically braced frame of configuration 14.
22. Low Damping Elastomeric Bearing isolated Six-story Symmetrically Braced Frame with Nonlinear Dampers (LDSN): Nonlinear viscous dampers were added between the rigid base and the simulator platform to the six-story low damping elastomeric bearing isolated symmetrically braced frame of configuration 15.
23. Lead-core Bearing isolated Six-story Moment Frame (LCMF): The six-story moment frame of configuration 1 isolated from the simulator platform with four lead-core bearings.
24. Lead-core Bearing isolated Six-story Asymmetrically Braced Frame (LCAB): The six-story asymmetrically braced frame of configuration 2 isolated from the simulator platform with four lead-core bearings.
25. Lead-core Bearing isolated Six-story Symmetrically Braced Frame (LCSB): The six-story symmetrically braced frame of configuration 3 isolated from the simulator platform with four lead-core bearings.

26. Low Damping Elastomeric Bearing with Flat Slider isolated Six-story Moment Frame (EFMF): The six-story moment frame of configuration 1 isolated from the simulator platform with two low damping elastomeric and two flat sliding bearings.
27. Low Damping Elastomeric Bearing with Flat Slider isolated Six-story Asymmetrically Braced Frame (EFAB): The six-story asymmetrically braced frame of configuration 2 isolated from the simulator platform with two low damping elastomeric and two flat sliding bearings.
28. Low Damping Elastomeric Bearing with Flat Slider isolated Six-story Symmetrically Braced Frame (EFSB): The six-story symmetrically braced frame of configuration 3 isolated from the simulator platform with two low damping elastomeric and two flat sliding bearings.

### **3.7 Identification of Properties of Tested Configurations**

Prior to testing the isolated six-story model structure, fixed base testing was performed to determine the characteristic modes and mode shapes of the six-story superstructure. The tests for each structure, moment frame, braced frame and asymmetrically braced frame, were conducted with a banded white noise (0 to 40 Hz) excitation with acceleration amplitude of 0.05 g.

Transfer functions were obtained as the ratio of the Fourier transform of the horizontal acceleration of each floor (average of accelerations recorded on east and west sides of model) of the structure to the Fourier transform of the base horizontal acceleration (average of east and west sides, measured at the W14x90 sections) while the isolation system was fixed. These transfer functions were used to identify the frequencies, damping ratios and mode shapes of the model. The procedure followed in the identification of the model properties is described in Reinhorn et al. (1989). Table 3-3 shows the results of this analysis for the first six significant modes of the moment frame.

Identification of the asymmetrically braced frame presented difficulties in determining the correct damping ratio for the torsional mode. By following the same procedures as for the other two frames, information is lost by averaging the two, east and west, acceleration time histories. The damping ratio of the torsional mode was approximately determined by examination of free vibration records of the difference of the accelerations recorded on east and west sides of model. A damping ratio on the order of 0.02 was determined. This value was utilized in the analysis (described in Section 5.4), which resulted in predictions of dynamic response that were in good agreement with the experimental results.

Tables 3-4 a and b present the results of this analysis for the first three modes of the asymmetrically braced and symmetrically braced frame configurations, respectively. The first and third modes of the asymmetrically braced frame structure are the first two modes that are predominantly in the direction of testing, correspondingly, the first two modes of the symmetrically braced structure. The second mode of the asymmetrically braced frame structure is a torsional mode.

Figures 3-22 thru 3-24 present the plots of transfer function amplitude versus frequency for the three different configurations. In some cases the true peak was likely missing, and had to be extrapolated from the slopes on either side of the peak to perform the identification. In all three figures, the frequency content is presented in the range of 0 to 35 Hz. This range contains the first six modes for the moment frame, and the first three modes for the other two configurations.

**TABLE 3-3 Characteristics of Fixed Base Moment Frame Structure**

Experimental

Mode	Frequency (Hz)	Damping Ratio	Mode Shape					
			Floor 1	Floor 2	Floor 3	Floor 4	Floor 5	Floor 6
1	2.34	0.048	0.22	0.43	0.60	0.77	0.94	1.00
2	7.90	0.019	-0.52	-1.05	-0.98	-0.41	0.40	1.00
3	13.65	0.011	0.98	1.02	-0.27	-1.27	-0.59	1.00
4	19.79	0.003	-2.21	0.48	1.99	-0.28	-1.67	1.00
5	25.45	0.014	2.51	-1.66	0.14	2.40	-2.86	1.00
6	29.54	0.018	-2.16	4.94	-4.96	4.22	-2.50	1.00

**TABLE 3-4 Characteristics of Asymmetrically and Symmetrically Braced Fixed Base Structure**

a. Asymmetrically Braced Experimental

Mode	Frequency (Hz)	Damping Ratio	Mode Shape					
			Floor 1	Floor 2	Floor 3	Floor 4	Floor 5	Floor 6
1	3.32	0.042	0.20	0.39	0.55	0.73	0.91	1.00
2	5.32	0.020 <sup>1</sup>	0.26	0.38	0.50	0.63	0.86	1.00
3	12.80	0.016	-0.62	-1.11	-0.97	-0.41	0.38	1.00

1. See comments in text.

b. Symmetrically Braced Experimental

Mode	Frequency (Hz)	Damping Ratio	Mode Shape					
			Floor 1	Floor 2	Floor 3	Floor 4	Floor 5	Floor 6
1	4.00	0.040	0.17	0.34	0.49	0.67	0.87	1.00
2	17.09	0.017	-0.67	-1.16	-0.96	-0.43	0.38	1.00
3	30.70	0.009	1.00	1.06	-0.71	-1.38	-0.63	1.00

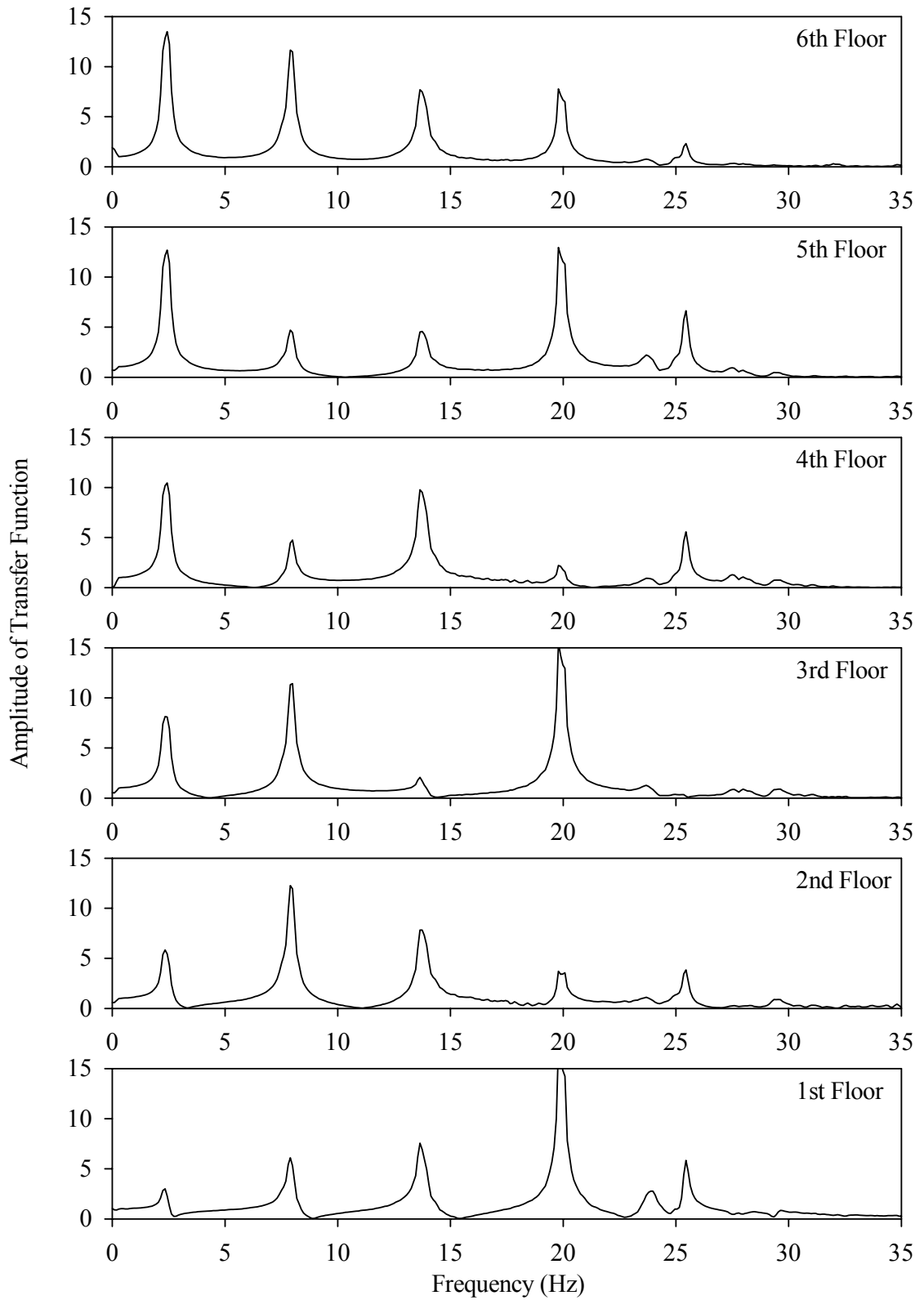


**FIGURE 3-22 Transfer Function Amplitudes Obtained from White Noise Excitation of Moment Frame Structure**

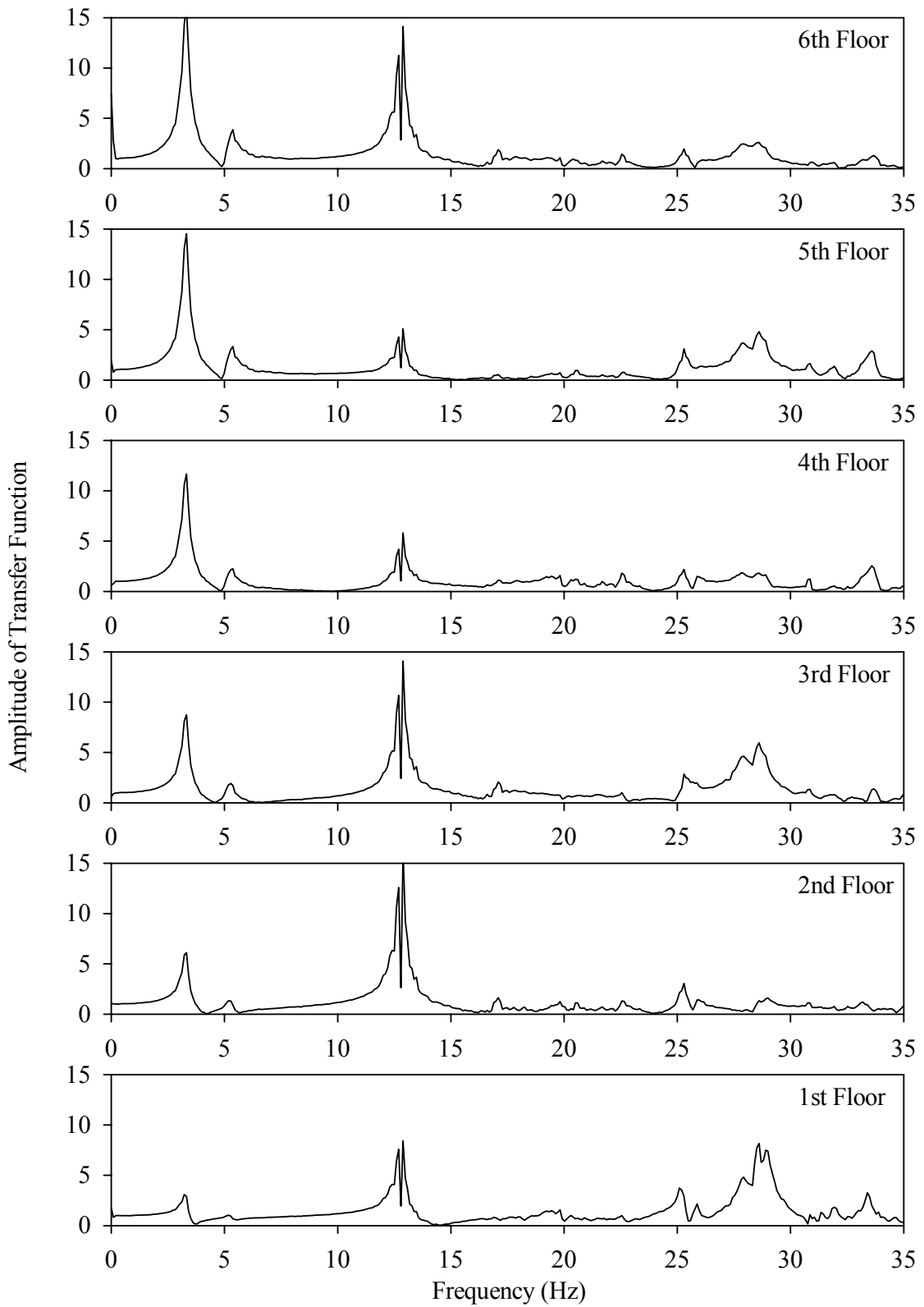


**FIGURE 3-23** Transfer Function Amplitudes Obtained from White Noise Excitation of Asymmetrically Braced Frame Structure



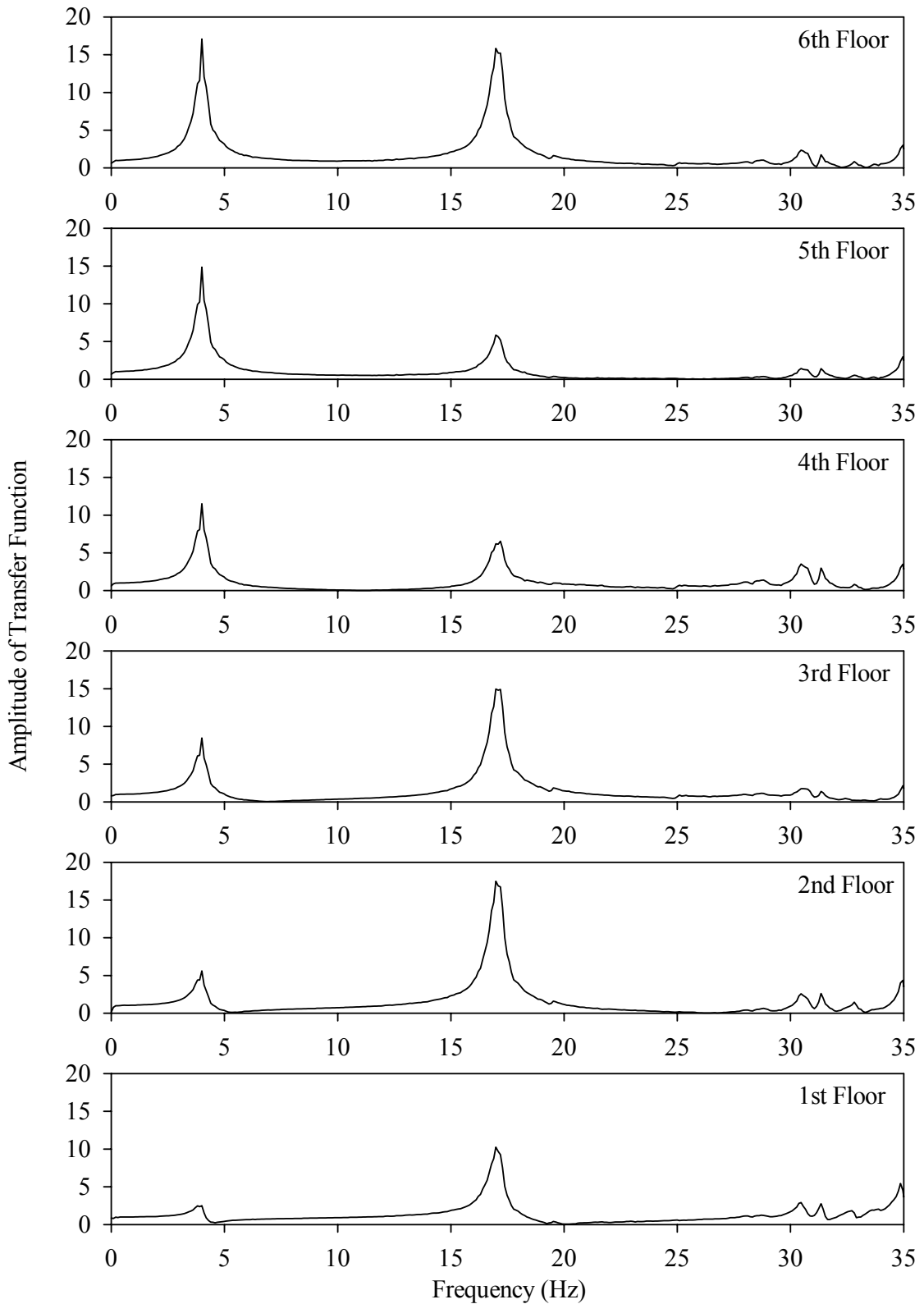


**FIGURE 3-24 Transfer Function Amplitudes Obtained from White Noise Excitation of Symmetrically Braced Frame Structure**

### 3.8 Instrumentation

The instrumentation of the six-story model structure consisted of load cells, accelerometers, and displacement transducers. Accelerations and absolute displacements were recorded on the east and west side at each floor level, the base, and the simulator platform in the horizontal direction (see Figure 3-25). In addition, the vertical acceleration above and below the southeast bearing and the vertical acceleration of two beams on the sixth floor were recorded. Four load cells at the base of the structure measured vertical and shear forces in the four bearings. Table 3-5 contains a list of channels for all the instruments.

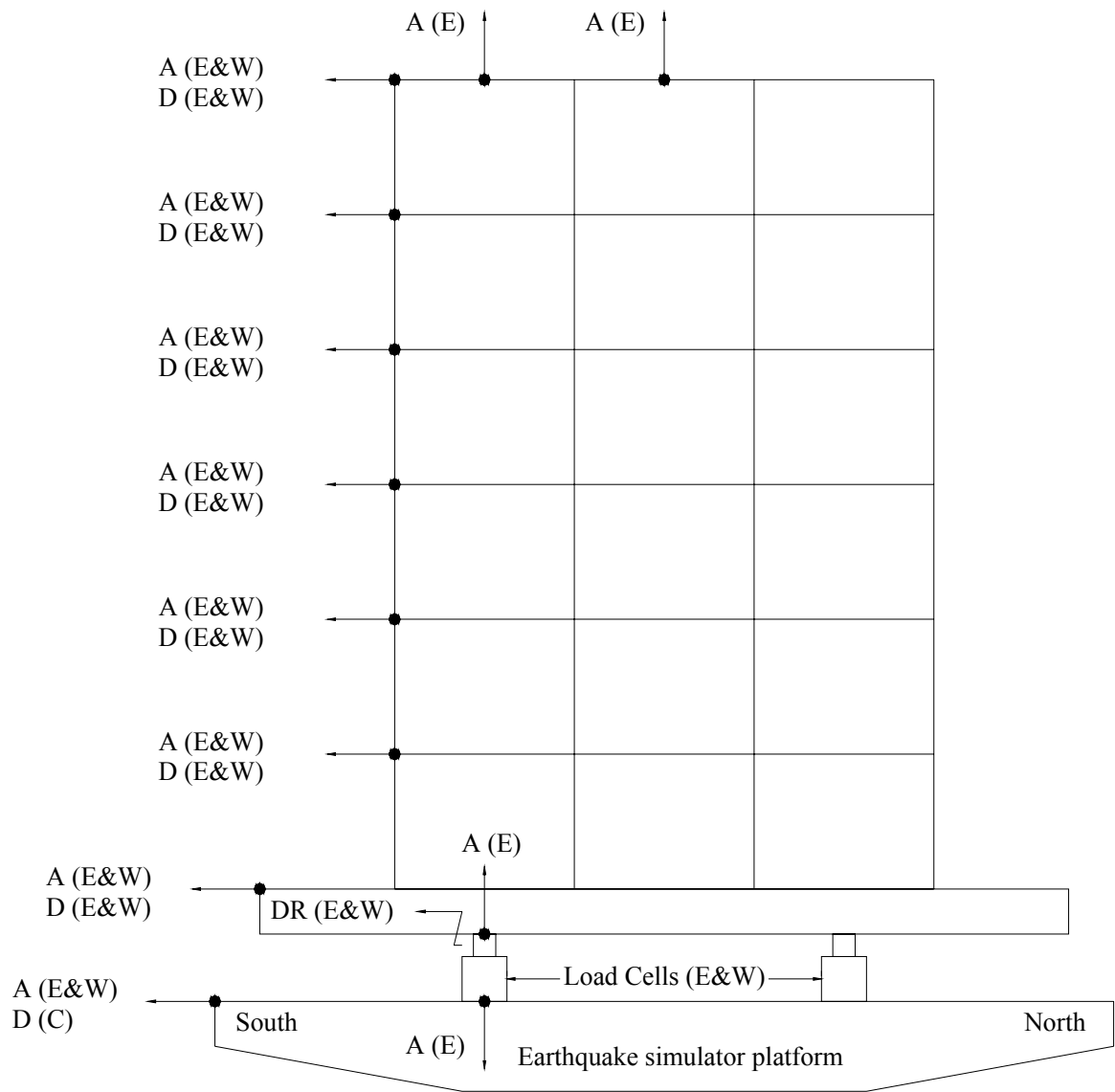
Important response quantities were measured by both direct and indirect means to provide redundancy for checking the accuracy of important measurements. To check accelerations, the absolute displacement at that location was double differentiated to obtain the history of acceleration. To check shear forces in the load cells, the base shear was calculated by summing up the inertial forces at each floor level. Each floor's inertial force was calculated by multiplying the recorded average acceleration (from the two instruments on the east and west sides of the floor) by the mass of that floor.

### 3.9 Testing Program

The six-story model structure was tested with several different earthquake motions. Table 3-6 lists the motions utilized in testing and their peak ground motion characteristics in prototype scale. Of the earthquakes listed, El Centro, Miyagiken and Taft, are generally considered "standard", "high frequency-content", benchmark motions, while most of the other motions were chosen for their near fault characteristics, such as the motions recorded in the 1994 Northridge earthquake, the 1999 Chi-Chi, the 1995 Kobe, and the 1971 Pacoima earthquakes. The 1985 Mexico City and 1968 Hachinohe earthquakes were chosen for their content in long period components. The 1999 Kocaeli earthquake was added because of its catastrophic nature and because data became available during testing. Each record was compressed in time by a factor of two to conform to similitude requirements.

Table 3-7 lists the tests that were conducted on the six-story model. Each earthquake excitation was applied with an intensity identified in Table 3-7 with a percentage figure. For example, a figure of 200% denotes an excitation twice as strong as the actual record, but with the time scale compressed by a factor of 2 as noted above. Vertical excitation was attempted for one configuration (denoted in Table 3-7 as H+V), however, the earthquake simulator was unable to correctly simulate the vertical component of El Centro and the table hydraulics actually failed during the El Centro 200% H+V test. Furthermore, testing was cut short during the FP isolated symmetrically braced testing with linear dampers because one of the dampers failed during the Pacoima S16E test. A total of 304 tests were performed.

Figures 3-26 to 3-39 present the recorded histories of the table motion in fourteen tests with these earthquake inputs. The acceleration and displacements records were directly measured, whereas the velocity record was calculated by differentiating the displacement record. The figures also show the 5-percent damped response spectra of the platform motion, which are plotted against the spectra of the target records. It can be seen that the earthquake simulator produced motions that are in acceptable agreement with the spectra of the target motions in the period range of the isolated model structure.



A- Acceleration      D- Absolute Displacement      DR- Relative Displacement  
 E- East                  W- West                                  C- Center

**FIGURE 3-25 Instrumentation Diagram**

**TABLE 3-5 List of Data Acquisition Channels**

Output Channel	Input Channel	Notation	Instrument <sup>1</sup>	Unit	Response Quantity
1		Time	CLOCK	sec	Time
2	8	LC1SY	20 kip LC	kips	Bearing Shear Force - Transverse - North East
3	9	LC1SX	20 kip LC	kips	Bearing Shear Force - Longitudinal - North East
4	10	LC1N	50 kip LC	kips	Bearing Axial Force - North East
5	11	LC2SY	20 kip LC	kips	Bearing Shear Force - Transverse - South West
6	12	LC2SX	20 kip LC	kips	Bearing Shear Force - Longitudinal - South West
7	13	LC2N	50 kip LC	kips	Bearing Axial Force - South West
8	14	LC3SY	20 kip LC	kips	Bearing Shear Force - Transverse - South East
9	15	LC3SX	20 kip LC	kips	Bearing Shear Force - Longitudinal - South East
10	16	LC3N	50 kip LC	kips	Bearing Axial Force - South East
11	17	LC4SY	20 kip LC	kips	Bearing Shear Force - Transverse - North West
12	18	LC4SX	20 kip LC	kips	Bearing Shear Force - Longitudinal - North West
13	19	LC4N	50 kip LC	kips	Bearing Axial Force - North West
14		Sum_Fn		kips	Sum of All Bearing Axial Forces
15	76	DHBE	DT	inch	Base Displacement - South East Corner
16	77	DHBW	DT	inch	Base Displacement - South West Corner
17	65	DH1E	DT	inch	First Floor Displacement - South East Corner
18	66	DH1W	DT	inch	First Floor Displacement - South West Corner
19	67	DH2E	DT	inch	Second Floor Displacement - South East Corner
20	68	DH2W	DT	inch	Second Floor Displacement - South West Corner
21	64	DH3E	DT	inch	Third Floor Displacement - South East Corner
22	69	DH3W	DT	inch	Third Floor Displacement - South West Corner
23	70	DH4E	DT	inch	Fourth Floor Displacement - South East Corner
24	71	DH4W	DT	inch	Fourth Floor Displacement - South West Corner
25	72	DH5E	DT	inch	Fifth Floor Displacement - South East Corner
26	73	DH5W	DT	inch	Fifth Floor Displacement - South West Corner
27	74	DH6E	DT	inch	Sixth Floor Displacement - South East Corner
28	75	DH6W	DT	inch	Sixth Floor Displacement - South West Corner
29	80	DHTC	DT	inch	Table Displacement - Center
30	78	DRSE	DT	inch	Relative Displacement in Bearing - South East

**TABLE 3-5 Continued**

Output Channel	Input Channel	Notation	Instrument <sup>1</sup>	Unit	Response Quantity
31	79	DRSW	DT	inch	Relative Displacement in Bearing - South West
32	20	AHTE	ACCL	g	Table Horizontal Acceleration - South East
33	21	AHTW	ACCL	g	Table Horizontal Acceleration - South West
34	22	AHBE	ACCL	g	Base Horizontal Acceleration - South East
35	23	AHBW	ACCL	g	Base Horizontal Acceleration - South West
36	24	AH1E	ACCL	g	First Floor Horizontal Acceleration - South East
37	25	AH1W	ACCL	g	First Floor Horizontal Acceleration - South West
38	26	AH2E	ACCL	g	Second Floor Horizontal Acceleration - South East
39	27	AH2W	ACCL	g	Second Floor Horizontal Acceleration - South West
40	28	AH3E	ACCL	g	Third Floor Horizontal Acceleration - South East
41	29	AH3W	ACCL	g	Third Floor Horizontal Acceleration - South West
42	30	AH4E	ACCL	g	Fourth Floor Horizontal Acceleration - South East
43	31	AH4W	ACCL	g	Fourth Floor Horizontal Acceleration - South West
44	32	AH5E	ACCL	g	Fifth Floor Horizontal Acceleration - South East
45	33	AH5W	ACCL	g	Fifth Floor Horizontal Acceleration - South West
46	34	AH6E	ACCL	g	Sixth Floor Horizontal Acceleration - South East
47	35	AH6W	ACCL	g	Sixth Floor Horizontal Acceleration - South West
48	36	AVFS	ACCL	g	Table Vertical Acceleration - South East
49	38	AVBS	ACCL	g	Base Vertical Acceleration - South East
50	40	AVTS	ACCL	g	Sixth Floor Vertical Acceleration - South East
51	37	AVTM	ACCL	g	Sixth Floor Vertical Acceleration - Middle East
52	6	WestDamp	10 kip LC	kips	Axial Force in West Damper
53	7	EastDamp	10 kip LC	kips	Axial Force in East Damper
54	85	DRDE	DT	inch	Relative Displacement in East Damper
55	84	DRDW	DT	inch	Relative Displacement in West Damper
56	0	P1	ACCL	g	Acceleration of Pendulum 1 (1.85 Hz)
57	1	P2	ACCL	g	Acceleration of Pendulum 2 (5.17 Hz)
58	2	P3	ACCL	g	Acceleration of Pendulum 3 (10.33 Hz)
59	3	P4	ACCL	g	Acceleration of Pendulum 4 (16.27 Hz)
60		DRFT_4_3		inch	Fouth Floor Story Drift East Side

1. ACCL = Accelerometer; DT = Displacement Transducer; LC = Load Cell

**TABLE 3-6 List of Earthquake Motions and Characteristics in Prototype Scale**

Notation	Excitation	Peak Ground Motion		
		Disp (mm)	Velocity (mm/s)	Accel (g)
El Centro S00E	Imperial Valley, May 18, 1940, Component S00E	109	335	0.34
Taft N21E	Kern County, July 21, 1952, Component N21E	67	157	0.16
NR Newhall 90°	Northridge-Newhall, LA County Fire Station, January 17, 1994, Component 90°	176	748	0.58
NR Newhall 360°	Northridge-Newhall, LA County Fire Station, January 17, 1994, Component 360°	305	947	0.59
NR Sylmar 90°	Northridge-Sylmar, Parking Lot, January 17, 1994, Component 90°	152	769	0.60
Kobe N-S	Kobe Station, Japan, January 17, 1995, Component N-S	207	914	0.83
Mexico N90W	Mexico City, September 19, 1985, SCT Building, Component N90W	212	605	0.17
Pacoima S74W	San Fernando, February 9, 1971, Pacoima Dam, Component S74W	108	568	1.08
Pacoima S16E	San Fernando, February 9, 1971, Pacoima Dam, Component S16E	365	1132	1.17
Chi-Chi (Taiwan)	Taiwan, September 21, 1999, Station TCU 129, Component E-W	502	600	0.98
Miyagiken Oki	Miyagi, Japan, June 12, 1978, Ofunato-Bochi, Component E-W	51	141	0.16
Hachinohe N-S	Tokachi, Japan, May 16, 1968, Hachinohe, Component N-S	119	357	0.23
YPT 060	Kocaeli, Turkey, August 17, 1999, Yarimça, Component E-W	570	657	0.27
YPT 330	Kocaeli, Turkey, August 17, 1999, Yarimça, Component N-S	510	621	0.35

**TABLE 3-7 List of Earthquake Simulation Tests Conducted on the Six-Story Model**

Earthquake	Intensity	Fixed Base			Lead Core			Elastomeric and Flat Sliding		
		FBMF	FBAB	FBSB	LCMF	LCAB	LCSB	EFMF	EFAB	EFSB
El Centro S00E	30%	√	√	√	-	-	-	-	-	-
	50%	-	-	-	√	-	-	√	-	-
	100%	-	-	-	√	-	-	√	√	√
	150%	-	-	-	√	-	-	√	-	-
	200%	-	-	-	√	√	√	√	√	√
	100% H+V	-	-	-	-	-	-	-	-	-
	200% H+V	-	-	-	-	-	-	-	-	-
Taft N21E	50%	√	√	√	-	-	-	-	-	-
	100%	√	-	-	-	-	-	-	-	-
	200%	-	-	-	√	√	√	√	√	√
	300%	-	-	-	-	-	-	√	-	-
	400%	-	-	-	√	√	√	√	√	√
	500%	-	-	-	-	-	-	-	-	-
Newhall 90°	15%	√	√	√	-	-	-	-	-	-
	75%	-	-	-	-	-	-	√	√	√
	100%	-	-	-	√	√	√	-	-	-
Newhall 360°	15%	√	√	√	-	-	-	-	-	-
	50%	-	-	-	-	-	-	√	√	√
	75%	-	-	-	√	-	-	-	-	√
	100%	-	-	-	√	√	√	-	-	-
Sylmar 90°	50%	-	-	-	-	-	-	√	√	√
	100%	-	-	-	√	√	√	-	√	√
Kobe	15%	√	√	√	-	-	-	-	-	-
	50%	-	-	-	-	-	-	√	√	√
	100%	-	-	-	√	√	√	-	-	-
YPT 330	33%	√	√	√	-	-	-	-	-	-
	100%	-	-	-	-	-	-	-	-	-
YPT 060	33%	√	√	√	-	-	-	-	-	-
	100%	-	-	-	-	-	-	-	-	-
Mexico	100%	-	-	-	-	-	-	-	-	-
Pacoima S74W	100%	-	-	-	-	-	-	-	-	-
Pacoima S16E	50%	-	-	-	-	-	-	-	-	-
	75%	-	-	-	-	-	-	-	-	-
	100%	-	-	-	-	-	-	-	-	-
Chi-Chi	100%	-	-	-	-	-	-	-	-	-
Miyagiken-Okii	300%	-	-	-	-	-	-	-	-	-
	500%	-	-	-	-	-	-	-	-	-
Hachinohe N-S	100%	-	-	-	-	-	-	-	-	-
	200%	-	-	-	-	-	-	-	-	-
	300%	-	-	-	-	-	-	-	-	-
Total Number of Experiments		8	7	7	11	7	7	11	9	10

**TABLE 3-7 Continued**

Earthquake	Intensity	Elastomeric								
		No Dampers			Linear Dampers			Nonlinear Dampers		
		LDMF	LDAB	LDSB	LDML	LDAL	LDSL	LDMN	LDAN	LDSN
El Centro S00E	30%	-	-	-	-	-	-	-	-	-
	50%	-	-	-	-	-	-	-	-	-
	100%	√	√	√	√	√	√	√	√	√
	150%	-	-	√	-	-	-	-	-	-
	200%	√	√	√	√	√	√	√	√	√
	100% H+V	-	-	-	-	-	-	-	-	-
	200% H+V	-	-	-	-	-	-	-	-	-
Taft N21E	50%	-	-	-	-	-	-	-	-	-
	100%	-	-	-	-	-	-	-	-	-
	200%	√	√	√	√	√	√	√	√	√
	300%	-	-	-	-	-	-	-	-	-
	400%	√	√	√	√	√	√	√	√	√
	500%	-	-	-	-	-	-	-	-	-
Newhall 90°	15%	-	-	-	-	-	-	-	-	-
	75%	√	√	√	√	√	√	√	√	√
	100%	-	-	-	-	-	-	-	-	-
Newhall 360°	15%	-	-	-	-	-	-	-	-	-
	50%	√	√	√	√	√	√	√	√	√
	75%	-	-	-	-	-	-	-	-	-
	100%	-	-	-	-	-	-	-	-	-
Sylmar 90°	50%	√	√	√	√	√	√	√	√	√
	100%	√	√	√	√	√	√	√	√	√
Kobe	15%	-	-	-	-	-	-	-	-	-
	50%	√	√	√	√	√	√	√	√	√
	100%	-	-	-	-	-	-	-	-	-
YPT 330	33%	-	-	-	-	-	-	-	-	-
	100%	-	-	-	-	-	-	-	-	-
YPT 060	33%	-	-	-	-	-	-	-	-	-
	100%	-	-	-	-	-	-	-	-	-
Mexico	100%	-	-	-	-	-	-	-	-	-
Pacoima S74W	100%	-	-	-	-	-	-	-	-	-
Pacoima S16E	50%	-	-	-	-	-	-	-	-	-
	75%	-	-	-	-	-	-	-	-	-
	100%	-	-	-	-	-	-	-	-	-
Chi-Chi	100%	-	-	-	-	-	-	-	-	-
Miyagiken- Oki	300%	-	-	-	-	-	-	-	-	-
	500%	-	-	-	-	-	-	-	-	-
Hachinohe N-S	100%	-	-	-	-	-	-	-	-	-
	200%	-	-	-	-	-	-	-	-	-
	300%	-	-	-	-	-	-	-	-	-
Total Number of Experiments		9	9	10	9	9	9	9	9	9



**TABLE 3-7 Continued**

Earthquake	Intensity	FPS								
		No Dampers			Linear Dampers			Nonlinear Dampers		
		FPMF	FPAB	FPSB	FPML	FPAL	FPSL	FPMN	FPAN	FPSN
El Centro S00E	30%	-	-	-	-	-	-	-	-	-
	50%	-	√	-	-	-	-	-	-	-
	100%	-	√	√	-	-	√	-	-	-
	150%	-	-	-	-	-	-	-	-	-
	200%	√	√	√	√	√	√	√	√	√
	100% H+V	-	-	√	-	-	-	-	-	-
	200% H+V	-	-	√	-	-	-	-	-	-
Taft N21E	50%	-	-	-	-	-	-	-	-	-
	100%	-	√	√	-	-	-	-	-	-
	200%	-	-	√	-	-	-	-	-	-
	300%	-	√	√	-	-	-	-	-	-
	400%	-	-	√	-	-	-	-	-	-
	500%	√	√	√	√	√	√	√	√	√
Newhall 90°	15%	-	-	-	-	-	-	-	-	-
	75%	-	-	-	-	-	-	-	-	-
	100%	√	√	√	√	√	-	√	√	√
Newhall 360°	15%	-	-	-	-	-	-	-	-	-
	50%	-	-	-	-	-	-	-	-	-
	75%	-	-	-	-	-	-	-	-	-
	100%	√	√	√	√	√	√	√	√	√
Sylmar 90°	50%	-	-	-	-	-	-	-	-	-
	100%	√	√	√	√	√	√	√	√	√
Kobe	15%	-	-	-	-	-	-	-	-	-
	50%	-	-	-	-	-	-	-	-	-
	100%	√	√	√	√	√	√	√	√	√
YPT 330	33%	-	-	-	-	-	-	-	-	-
	100%	√	√	√	√	√	-	√	√	√
YPT 060	33%	-	-	-	-	-	-	-	-	-
	100%	√	√	√	√	√	√	√	√	√
Mexico	100%	√	√	√	√	√	-	√	√	√
Pacoima S74W	100%	√	√	√	√	√	√	√	√	√
Pacoima S16E	50%	-	-	-	√	-	-	-	-	-
	75%	√	√	√	√	-	-	√	√	√
	100%	√	√	√	√	√	√	√	√	√
Chi-Chi	100%	√	√	√	√	√	-	√	√	√
Miyagiken-Okii	300%	-	-	√	-	-	-	-	-	-
	500%	√	√	√	√	√	√	√	√	√
Hachinohe N-S	100%	-	√	√	-	-	-	-	-	-
	200%	-	-	√	-	-	-	-	-	-
	300%	√	√	√	√	√	-	√	√	√
Total Number of Experiments		15	20	25	16	14	10	15	15	15

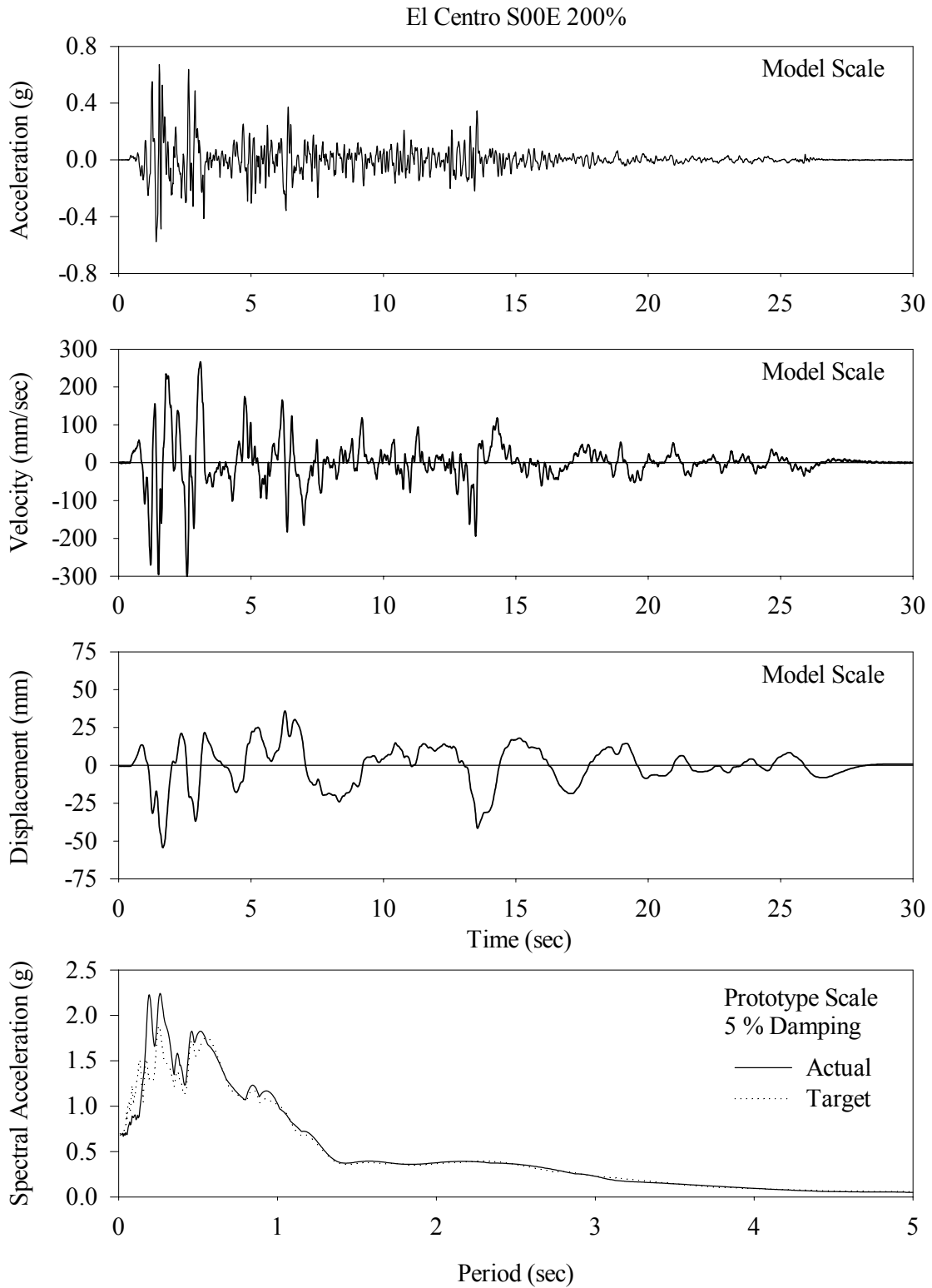


**FIGURE 3-26 Histories of Displacement, Velocity and Acceleration and the Acceleration Response Spectrum of Earthquake Simulator Motion for the El Centro S00E 200% Excitation**

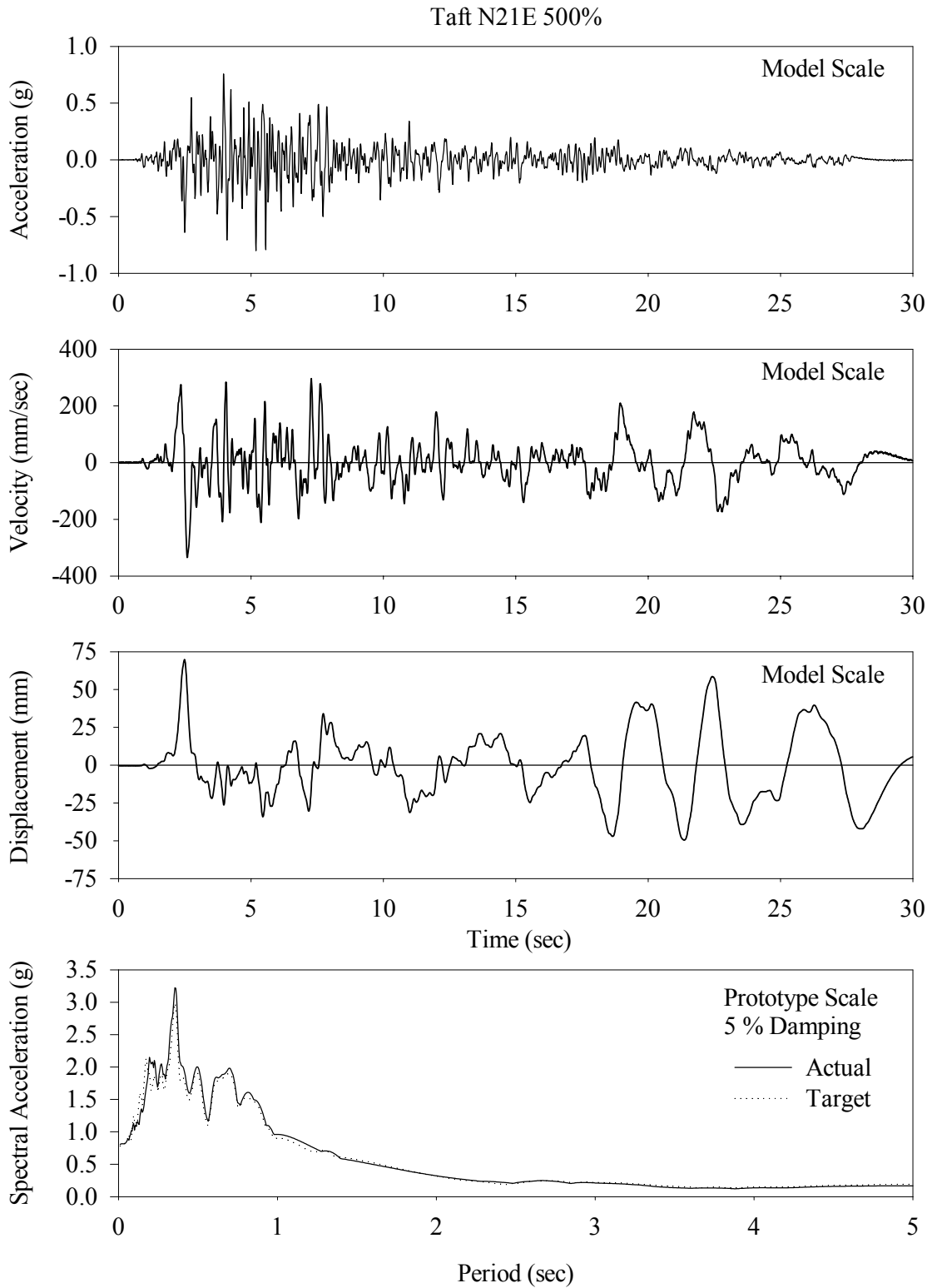


**FIGURE 3-27 Histories of Displacement, Velocity and Acceleration and the Acceleration Response Spectrum of Earthquake Simulator Motion for the Taft N21E 500% Excitation**

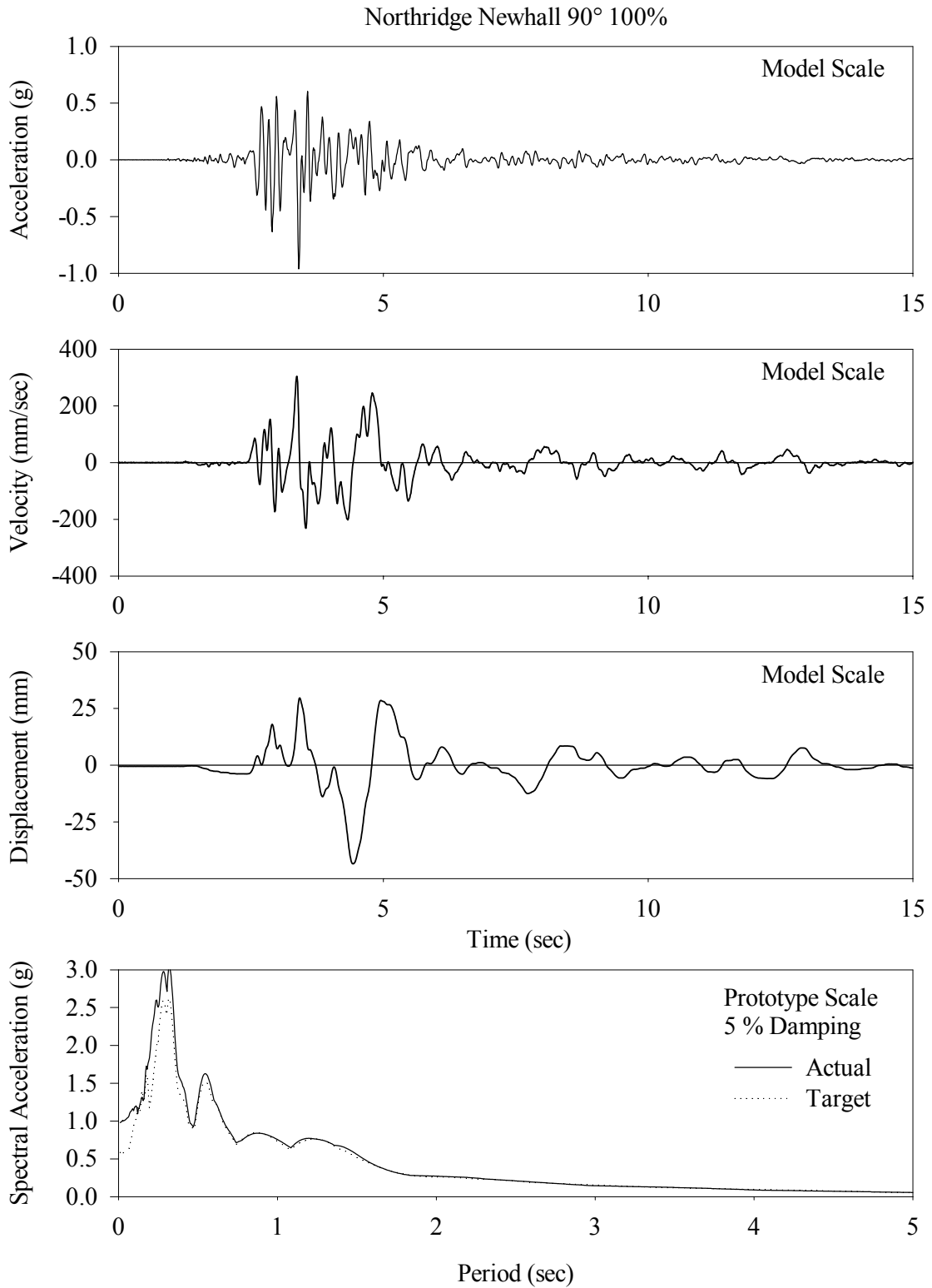


**FIGURE 3-28 Histories of Displacement, Velocity and Acceleration and the Acceleration Response Spectrum of Earthquake Simulator Motion for the Northridge-Newhall 90° 100% Excitation**

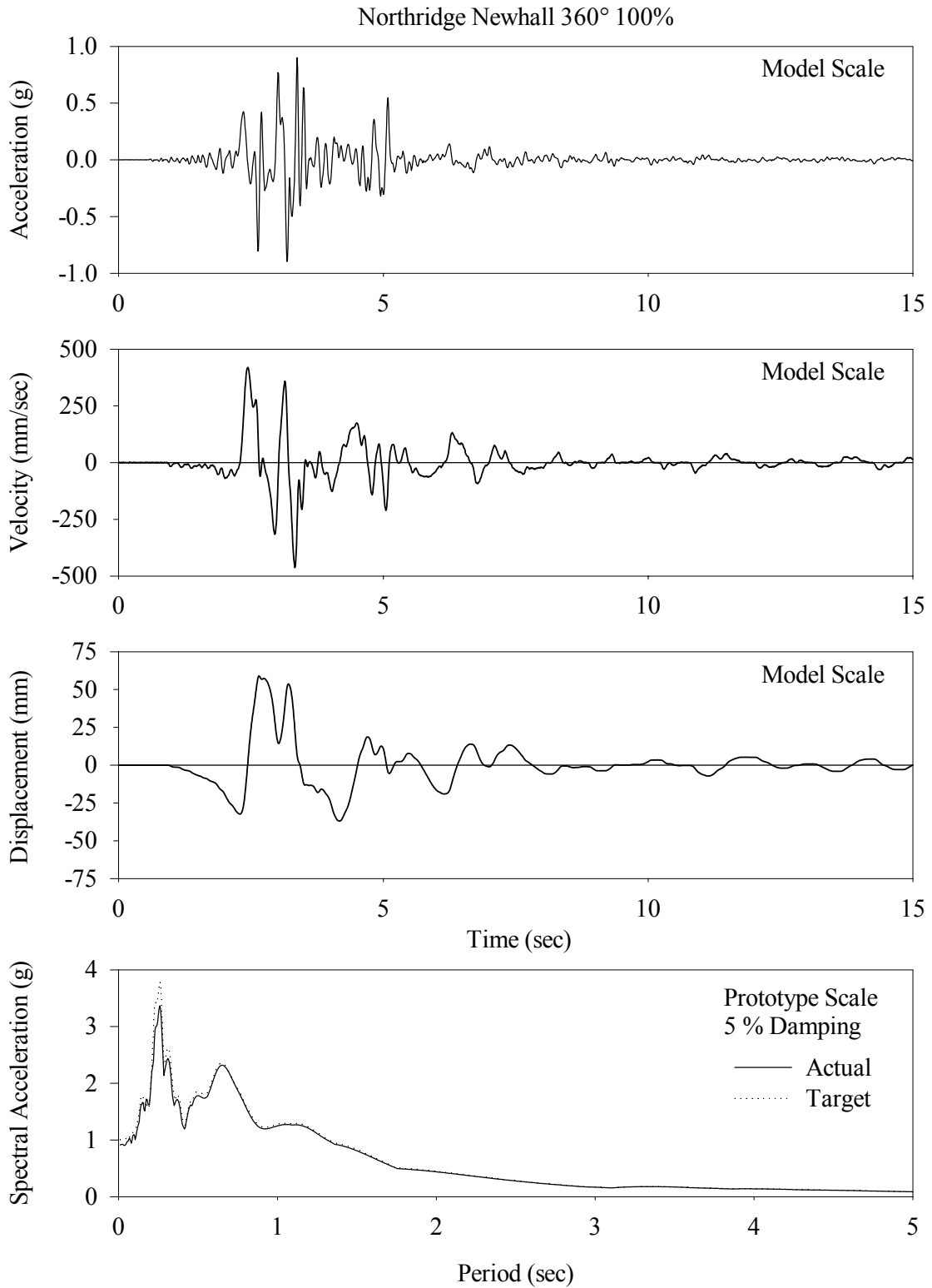


**FIGURE 3-29 Histories of Displacement, Velocity and Acceleration and the Acceleration Response Spectrum of Earthquake Simulator Motion for the Northridge-Newhall 360° 100% Excitation**

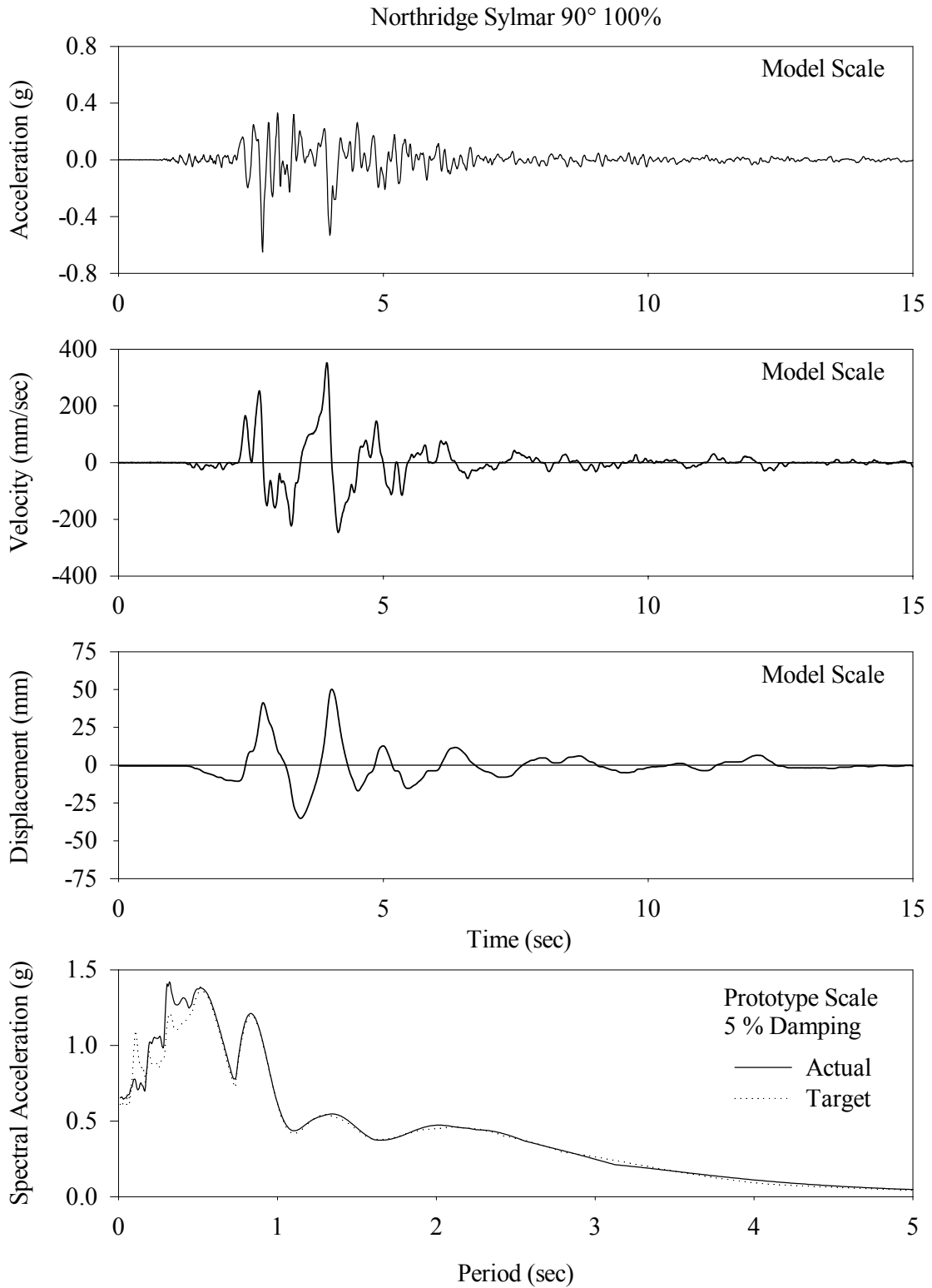


**FIGURE 3-30 Histories of Displacement, Velocity and Acceleration and the Acceleration Response Spectrum of Earthquake Simulator Motion for the Northridge-Sylmar 90° 100% Excitation**

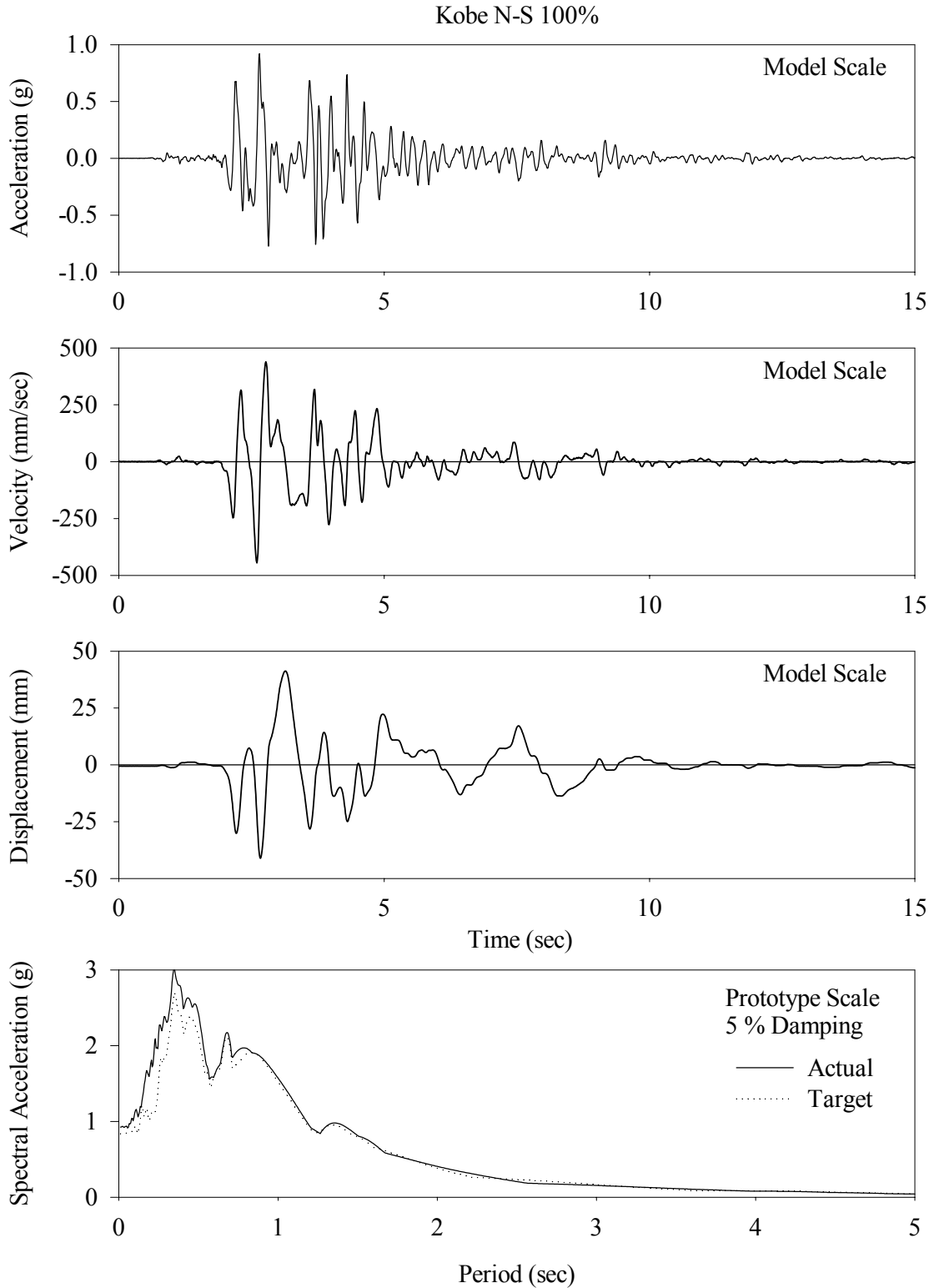


**FIGURE 3-31 Histories of Displacement, Velocity and Acceleration and the Acceleration Response Spectrum of Earthquake Simulator Motion for the Kobe N-S 100% Excitation**

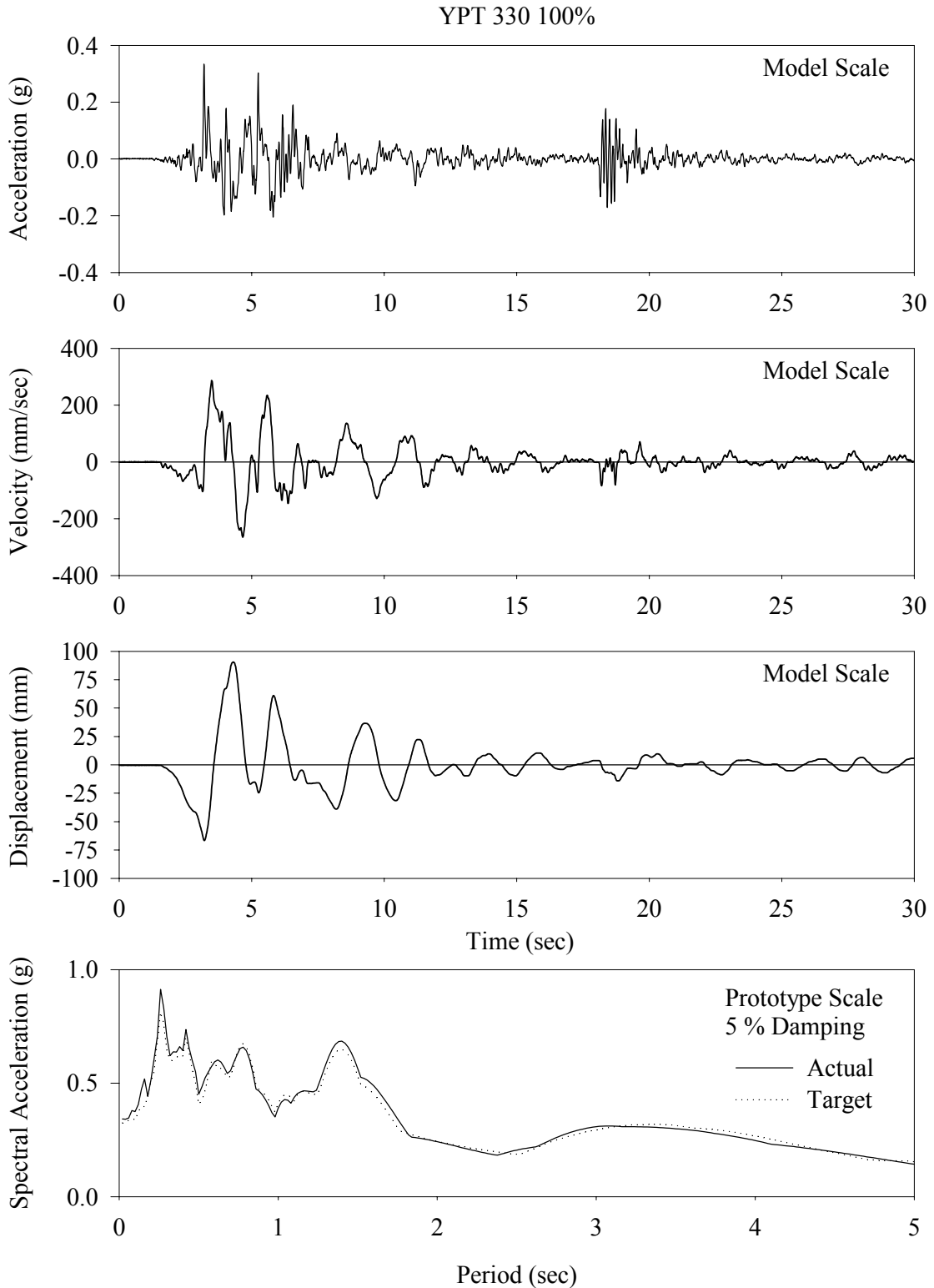


**FIGURE 3-32 Histories of Displacement, Velocity and Acceleration and the Acceleration Response Spectrum of Earthquake Simulator Motion for the YPT 330 100% Excitation**



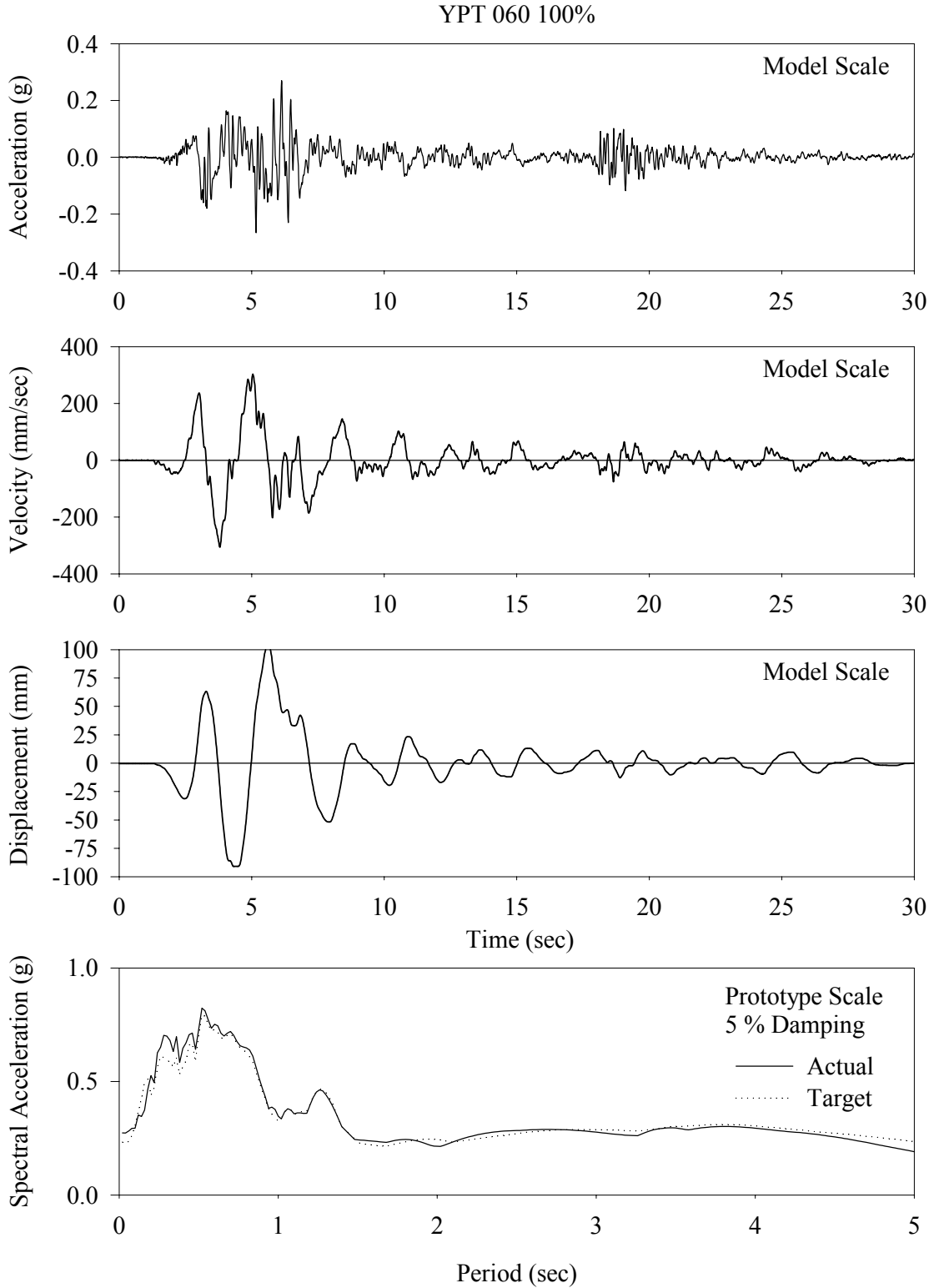


**FIGURE 3-33 Histories of Displacement, Velocity and Acceleration and the Acceleration Response Spectrum of Earthquake Simulator Motion for the YPT 060 100% Excitation**

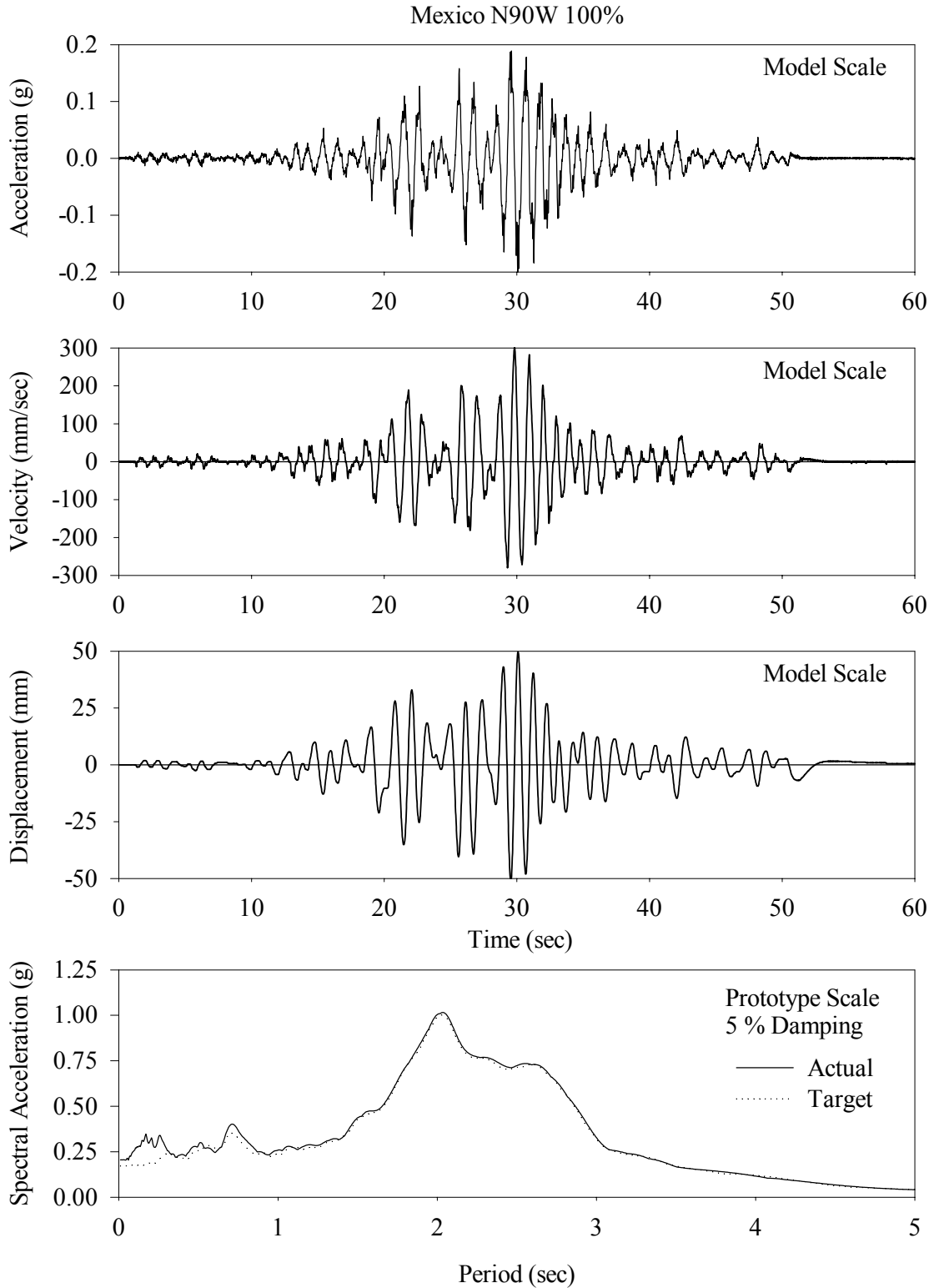


**FIGURE 3-34 Histories of Displacement, Velocity and Acceleration and the Acceleration Response Spectrum of Earthquake Simulator Motion for the Mexico N90W 100% Excitation**

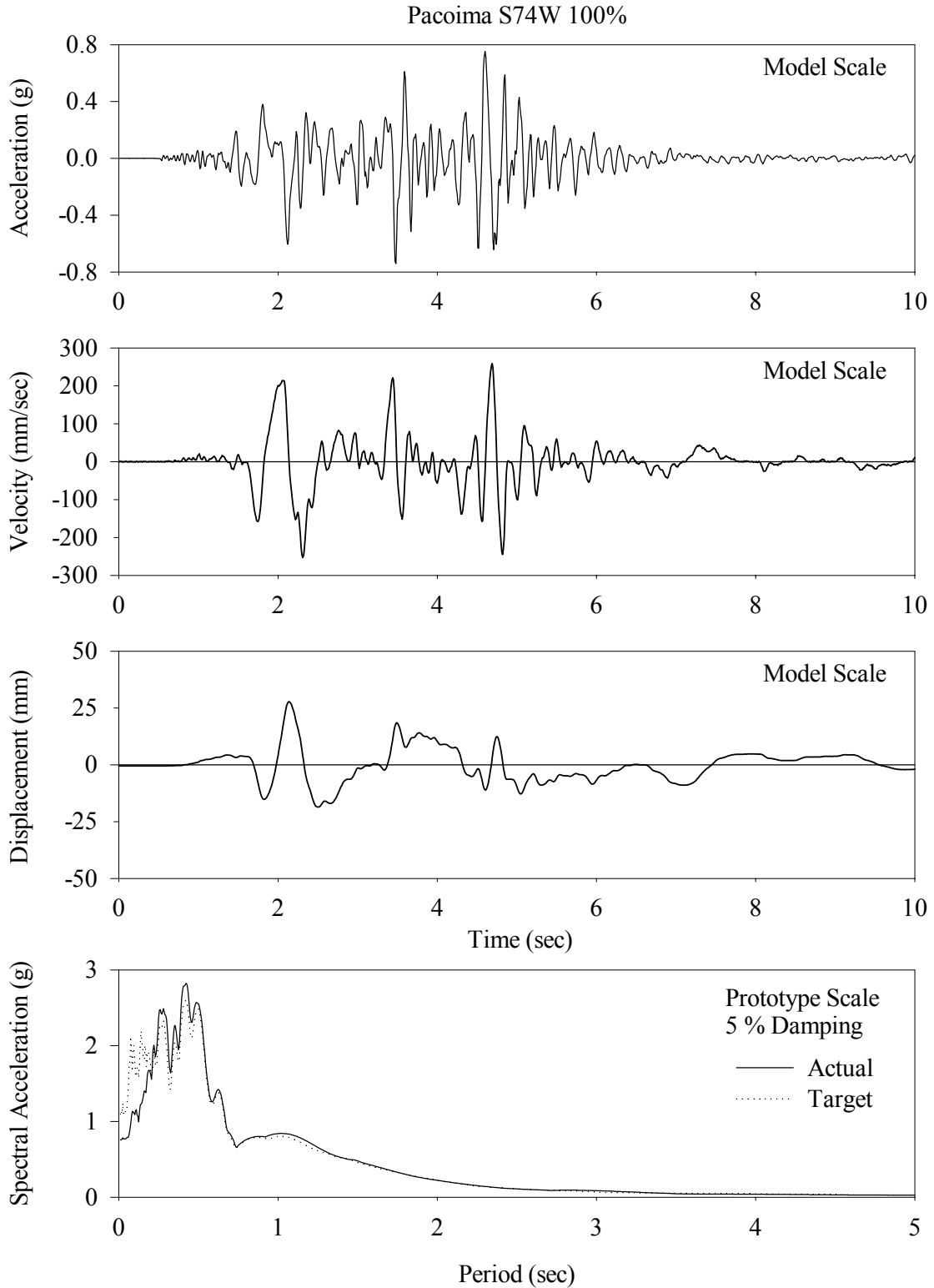


**FIGURE 3-35 Histories of Displacement, Velocity and Acceleration and the Acceleration Response Spectrum of Earthquake Simulator Motion for the Pacoima S74W 100% Excitation**

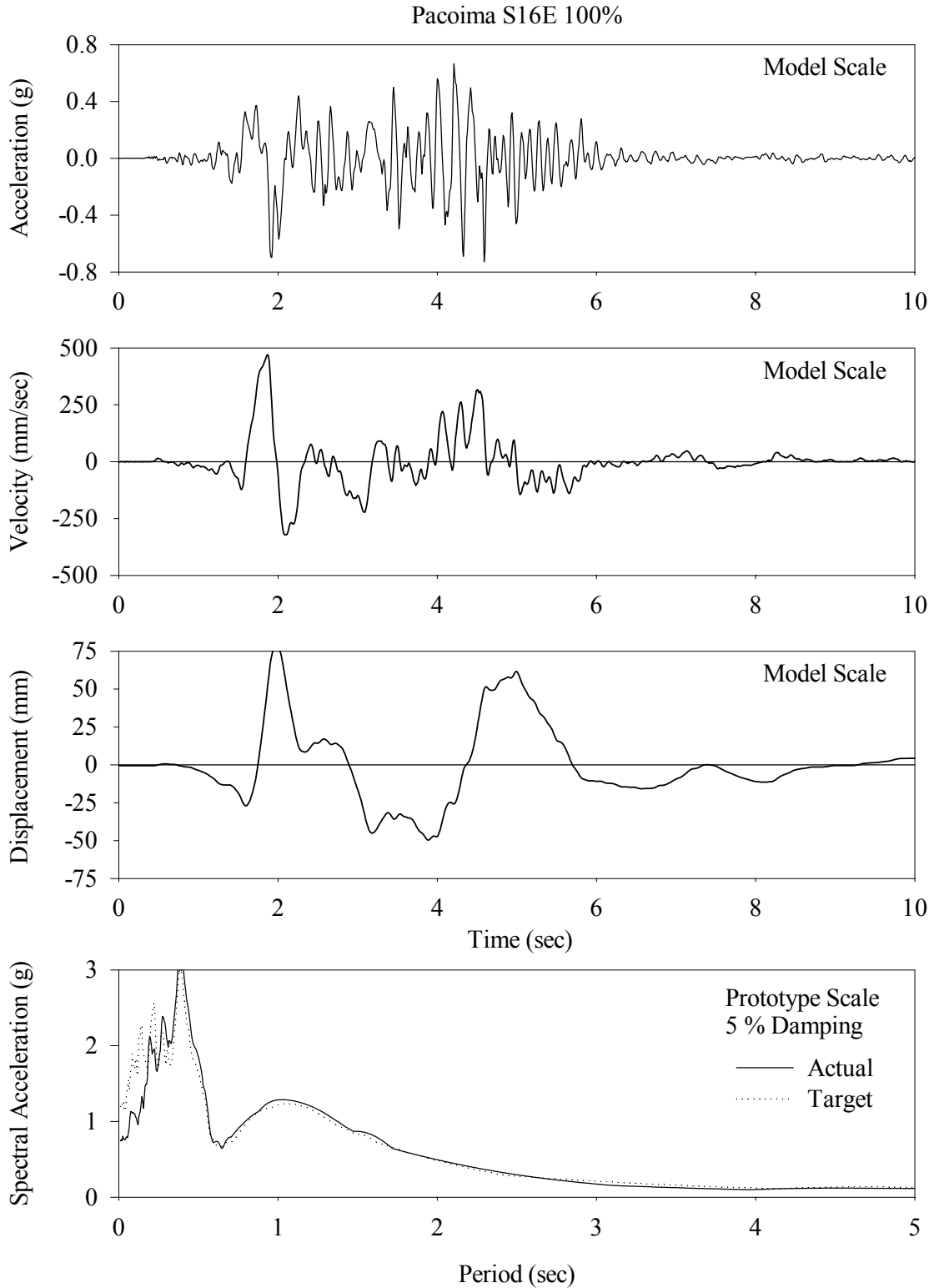


**FIGURE 3-36 Histories of Displacement, Velocity and Acceleration and the Acceleration Response Spectrum of Earthquake Simulator Motion for the Pacoima S16E 100% Excitation**

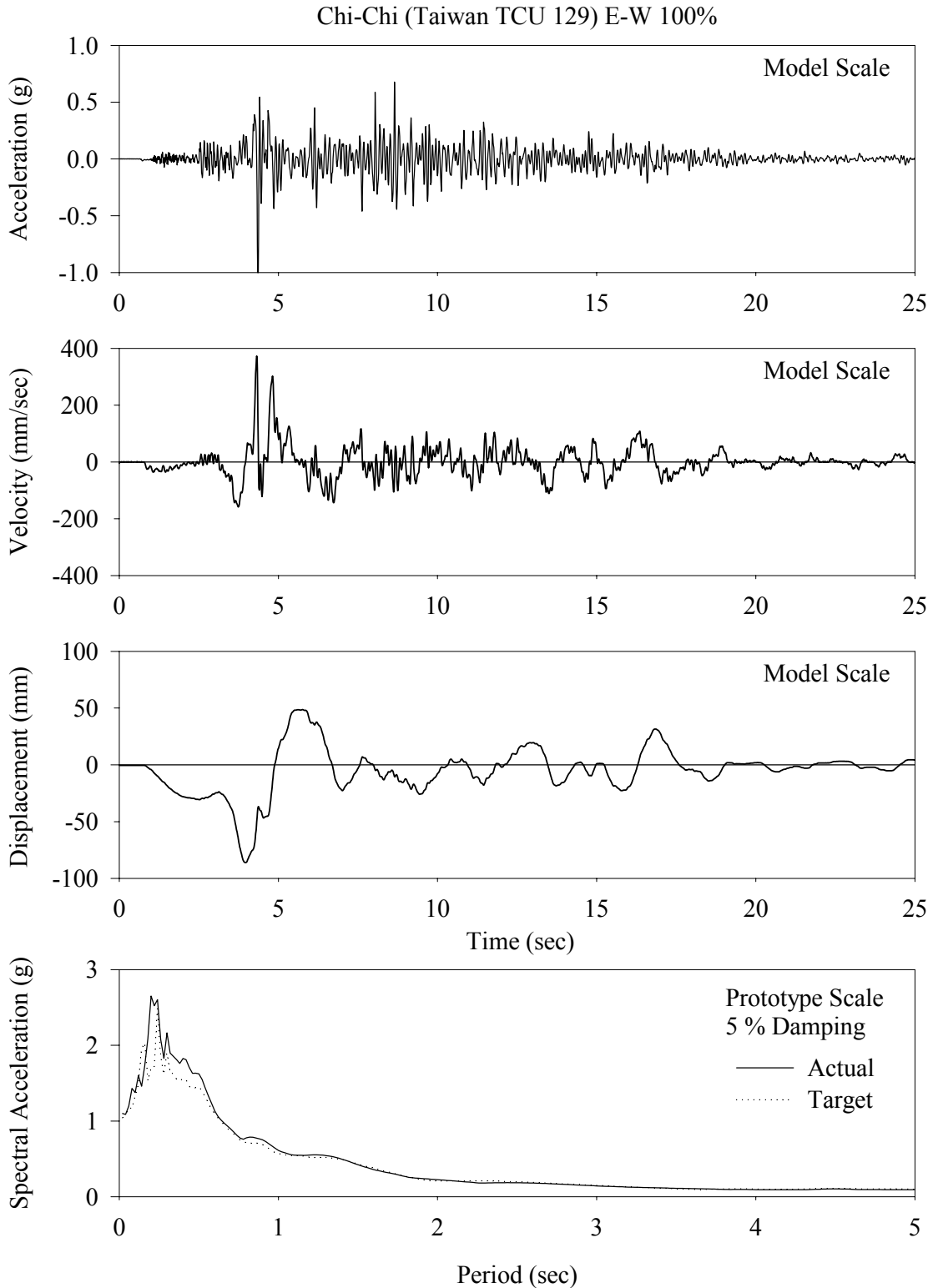


**FIGURE 3-37 Histories of Displacement, Velocity and Acceleration and the Acceleration Response Spectrum of Earthquake Simulator Motion for the Chi-Chi TCU 129 E-W 100% Excitation**

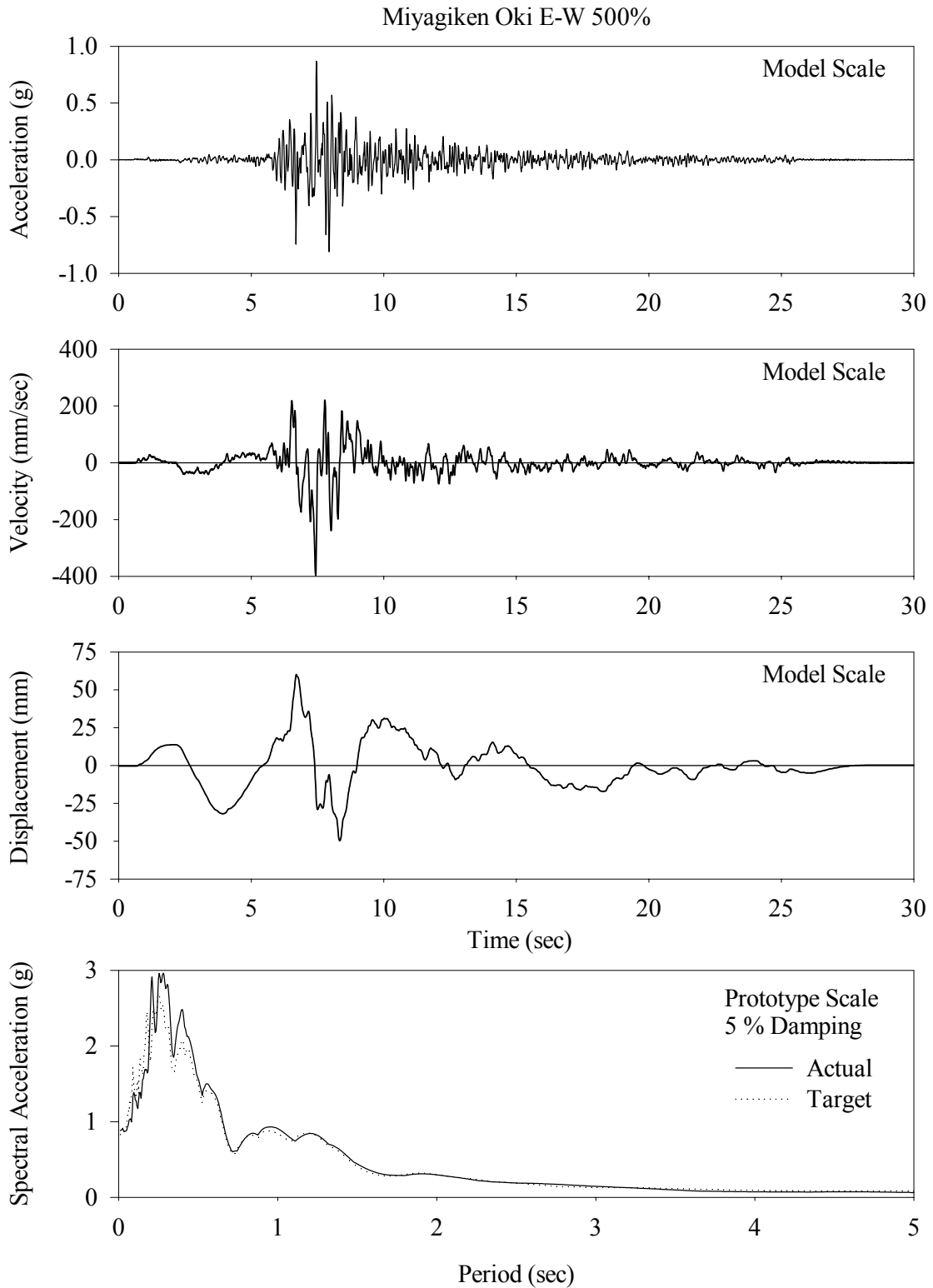


**FIGURE 3-38 Histories of Displacement, Velocity and Acceleration and the Acceleration Response Spectrum of Earthquake Simulator Motion for the Miyagiken Oki 500% Excitation**

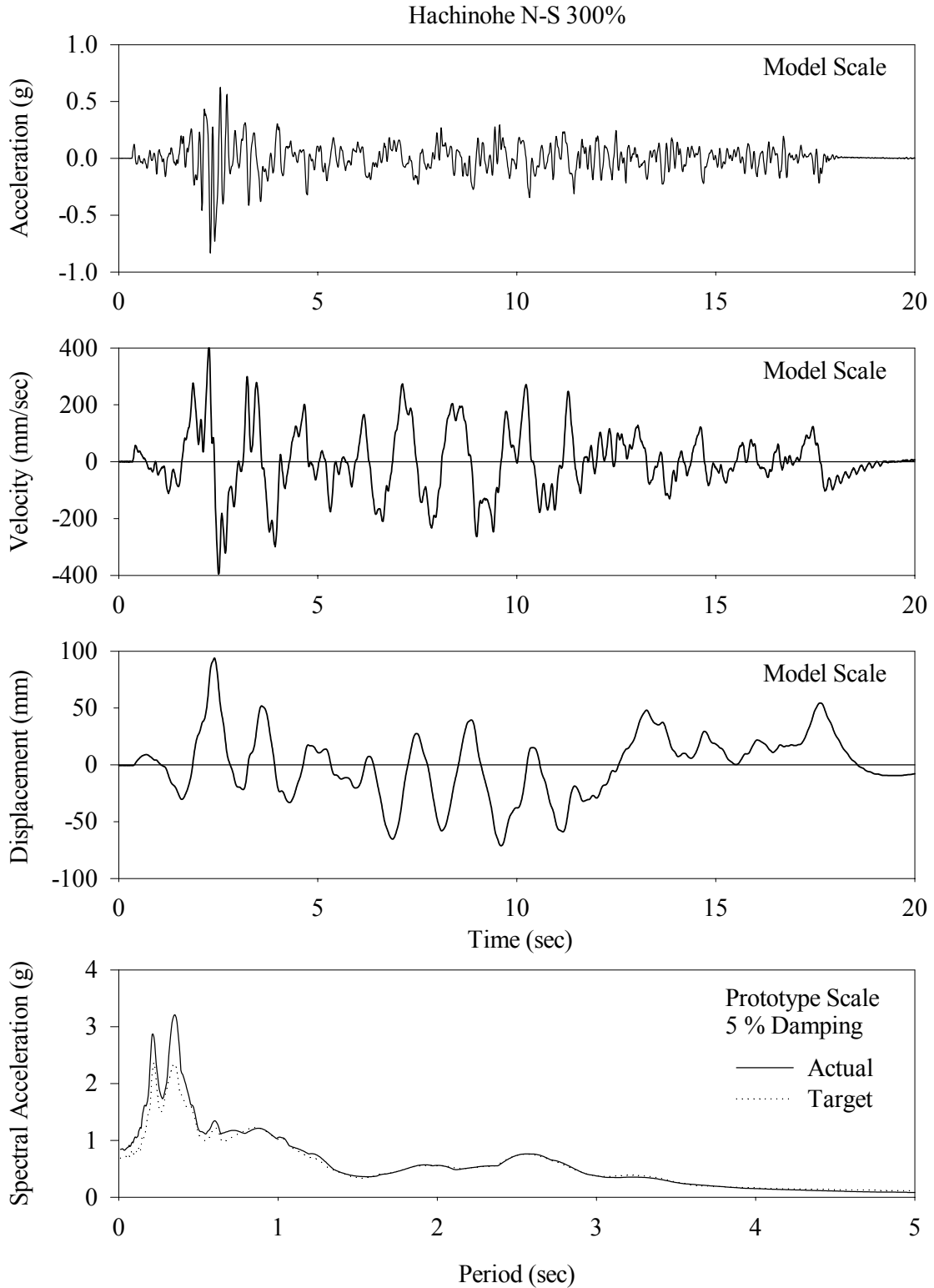


**FIGURE 3-39 Histories of Displacement, Velocity and Acceleration and the Acceleration Response Spectrum of Earthquake Simulator Motion for the Hachinohe N-S 300% Excitation**





## SECTION 4

### RESULTS OF EARTHQUAKE SIMULATOR TESTING

#### 4.1 Introduction

The results of the earthquake simulator tests are presented in this section, divided into subsections based on the structural system configuration. The summary results presented in the following sections contain selected peak values only. A more detailed presentation of results is included in Appendix A, where histories of response, bearing force-displacement hysteresis loops and floor response spectra are presented for each test.

#### 4.2 Moment Frame Test Results

The moment frame tests are divided into five sections based on the isolation system used. Tables 4-1 thru 4-5 present the results for the moment frame configuration of the tested structure for non-isolated conditions (fixed base), and for isolated conditions using lead-core, low damping elastomeric, Friction Pendulum and combined low damping elastomeric and flat sliding bearings, respectively.

The response quantities for all tests are:

1. The peak values of displacement (mm), velocity (mm/sec) and acceleration (g) of the earthquake simulator. Of these, the displacement and acceleration were directly measured, whereas the velocity was obtained by numerical differentiation of the displacement record.
2. The initial isolation system displacement. The initial displacement was measured just prior to conducting the test.
3. The peak isolation system response. The isolation system displacement, base acceleration and residual displacement were measured directly. The residual displacement was measured at the conclusion of each test (residual displacements had the tendency to reduce over time due to micro-vibrations of the shake table). The absolute base velocity was obtained by numerical differentiation of the absolute base displacement record. The base shear was calculated as the sum of each average floor acceleration times the mass of that floor, and was compared with the sum of the shear forces in the four load cells divided by the total weight, see Figure 4-1 and Appendix A. The base shear is presented normalized by the total weight,  $W$ , which is equal to 233 kN.
4. The peak superstructure response. The maximum story shear was calculated by the same means as the base shear, and is presented with the story at which it occurred. The maximum inter-story drift was calculated as the difference of measured horizontal displacement between the two floors divided by the story height, and is presented with the story at which it occurred. The sixth floor acceleration was directly measured.
5. The peak force, displacement and velocity measured in the dampers. The force and displacement were directly measured by a load cell and an LVDT attached inline with the damper. The relative velocity along the damper was obtained by numerical differentiation of the relative displacement history.

**TABLE 4-1 Peak Response of Non-isolated Moment Frame Structure** (values are in units of g for acceleration, mm/s for velocity and mm for displacement)

Test	Excitation*	Peak Table Motion			Peak Base Response						Peak Superstructure Response				
		Accel	Vel.	Disp.	Initial Disp.	Isol. Disp.	Base Accel.	Base Shear/W	Base Vel.	Res. <sup>1</sup> Disp.	Story Shear/W	Drift / Height (%)		Floor Accel.	
FBMFE30.1	EI Centro S00E 30%	0.11	52.8	8.1	N/A	N/A	0.15	0.13	56.4	N/A	0.13	1	0.25	2	0.31
FBMFK15.1	Kobe - Kobe 15%	0.12	67.5	6.5	N/A	N/A	0.15	0.16	57.5	N/A	0.16	2	0.34	2	0.31
FBMFN10.1	NR Newhall 360° 15%	0.11	65.8	8.5	N/A	N/A	0.11	0.13	55.8	N/A	0.13	2	0.25	2	0.24
FBMFNH1.1	NR Newhall 90° 15%	0.09	41.1	6.8	N/A	N/A	0.10	0.09	48.0	N/A	0.10	2	0.20	2	0.25
FBMFT50.1	Taft N21E 50%	0.07	37.1	6.6	N/A	N/A	0.08	0.10	35.6	N/A	0.10	2	0.21	2	0.23

1. Residual Displacement

\* The excitations were reduced for the non-isolated configuration to ensure the model remained elastic.

**TABLE 4-2 Peak Response of Isolated Moment Frame Structure with Lead-Core Bearings** (values are in units of g for acceleration, mm/s for velocity and mm for displacement)

Test	Excitation	Peak Table Motion			Peak Isolation System Response						Peak Superstructure Response				
		Accel	Vel.	Disp.	Initial Disp.	Isol. Disp.	Base Accel.	Base Shear/W	Base Vel.	Res. <sup>1</sup> Disp.	Story Shear/W	Drift / Height (%)		Floor Accel.	
LCMFE50.1	EI Centro S00E 50%	0.15	85	14	-1.5	-6	0.19	0.12	90	-1.8	0.12	2	0.27	2	0.26
LCMFE10.1	EI Centro S00E 100%	0.32	171	27	-1.8	-13	0.33	0.19	163	-2.3	0.17	1,2	0.37	2	0.38
LCMFE15.1	EI Centro S00E 150%	0.50	258	41	-2.3	-21	0.47	0.25	248	-2.5	0.23	1	0.43	2	0.51
LCMFE20.1	EI Centro S00E 200%	0.70	327	56	-2.5	-30	0.66	0.31	341	-2.5	0.28	1	0.54	2	0.71
LCMFT20.1	Taft N21E 200%	0.36	126	28	-2.5	-16	0.43	0.19	175	-2.3	0.17	1	0.34	2	0.37
LCMFT40.1	Taft N21E 400%	0.69	268	57	-2.3	-36	0.78	0.33	394	-1.8	0.31	1	0.65	2	0.71
LCMFK10.1	Kobe - Kobe 100%	0.97	459	43	-1.8	-37	0.87	0.36	413	-2.5	0.36	2	0.89	2	1.11
LCMFS10.1	NR Sylmar 90° 100%	0.66	348	51	-2.5	-40	0.60	0.35	417	-2.8	0.30	1	0.63	2	0.64
LCMFNH1.1	NR Newhall 90° 100%	1.09	306	39	-2.8	-30	0.67	0.30	416	-3.0	0.26	1	0.57	2	0.66
LCMFN75.1	NR Newhall 360° 75%	0.65	336	46	-3.0	35	0.58	0.37	290	-2.5	0.33	1	0.66	2	0.56
LCMFN10.1	NR Newhall 360° 100%	0.91	463	61	-1.0	47	0.75	0.43	394	-0.8	0.38	1	0.78	2	0.66

1. Residual Displacement

**TABLE 4-3 Peak Response of Isolated Moment Frame Structure with Low Damping Elastomeric Bearings** (values are in units of g for acceleration, mm/s for velocity, mm for displacement and kN for force)

Test	Excitation	Peak Table Motion			Peak Isolation System Response							Peak Superstructure Response				Damper Response		
		Accel	Vel.	Disp.	Initial Disp.	Isol. Disp.	Base Accel.	Base Shear/W	Base Vel.	Res. <sup>1</sup> Disp.	Story Shear/W	Drift / Height (%)	Floor Accel.	Force	Disp.	Vel.		
LDMFE10.1	EI Centro S00E 100%	0.35	166	27	-0.8	-29	0.29	0.17	221	-0.8	0.16	1	0.31	2	0.29	N/A	N/A	N/A
LDMFE20.1	EI Centro S00E 200%	0.71	319	60	-0.8	-60	0.54	0.32	409	-0.8	0.29	1	0.67	2	0.54	N/A	N/A	N/A
LDMFT20.1	Taft N21E 200%	0.35	124	28	-0.8	-27	0.21	0.17	217	-0.8	0.15	1	0.32	2	0.26	N/A	N/A	N/A
LDMFT40.1	Taft N21E 400%	0.75	253	56	-0.8	-55	0.38	0.30	434	-0.8	0.27	1	0.58	2	0.46	N/A	N/A	N/A
LDMFK50.1	Kobe - Kobe 50%	0.37	220	21	-0.8	41	0.29	0.24	259	-0.8	0.21	1	0.44	2	0.38	N/A	N/A	N/A
LDMFS50.1	NR Sylmar 90° 50%	0.32	177	25	-0.8	-34	0.22	0.20	263	-0.8	0.18	1	0.38	2	0.26	N/A	N/A	N/A
LDMFS10.1	NR Sylmar 90° 100%	0.69	354	54	-0.8	65	0.48	0.36	473	-0.8	0.33	1	1.03	2	0.54	N/A	N/A	N/A
LDMFNH7.1	NR Newhall 90° 75%	0.79	231	29	-0.8	36	0.38	0.21	308	-0.8	0.19	1	0.40	2	0.39	N/A	N/A	N/A
LDMFN50.1	NR Newhall 360° 50%	0.41	218	29	-0.8	-40	0.32	0.23	247	-0.8	0.20	1	0.42	2	0.37	N/A	N/A	N/A
LDMLE10.1	EI Centro S00E 100%	0.31	165	27	-0.8	-18	0.25	0.14	165	-0.8	0.13	1	0.26	2	0.30	6.7	13	104
LDMLE20.1	EI Centro S00E 200%	0.68	318	59	-0.8	-36	0.45	0.26	312	-0.8	0.24	1	0.49	2	0.52	14.0	27	219
LDMLT20.1	Taft N21E 200%	0.34	122	28	-0.8	-20	0.22	0.15	165	-0.8	0.15	1	0.29	2	0.24	7.1	14	115
LDMLT40.1	Taft N21E 400%	0.75	252	56	-0.8	-41	0.41	0.28	338	-0.8	0.27	1	0.55	2	0.46	13.7	31	229
LDMLK50.1	Kobe - Kobe 50%	0.36	211	21	-0.8	24	0.29	0.19	202	-0.8	0.18	1	0.41	2	0.43	11.0	18	186
LDMLS50.1	NR Sylmar 90° 50%	0.32	174	25	-0.8	-20	0.25	0.16	171	-0.8	0.15	1	0.28	2	0.30	6.4	14	103
LDMLS10.1	NR Sylmar 90° 100%	0.66	348	53	-0.8	-42	0.45	0.29	354	-0.8	0.27	1	0.55	2	0.54	14.3	31	209
LDMLNH7.1	NR Newhall 90° 75%	0.78	228	29	-0.8	-24	0.32	0.18	249	-0.8	0.17	1	0.32	2	0.35	10.0	18	150
LDMLN50.1	NR Newhall 360° 50%	0.40	214	29	-0.8	-25	0.29	0.20	220	-0.8	0.21	1	0.45	2	0.37	13.3	19	198
LDMNE10.1	EI Centro S00E 100%	0.29	161	27	-0.8	-10	0.38	0.17	154	-0.8	0.17	1	0.33	2	0.48	14.0	7	79
LDMNE20.1	EI Centro S00E 200%	0.72	318	59	-0.8	-25	0.66	0.26	296	-0.8	0.25	2	0.56	2	0.78	18.8	17	201
LDMNT20.1	Taft N21E 200%	0.36	126	28	-0.8	-13	0.43	0.17	147	-0.8	0.16	1	0.31	2	0.46	14.1	9	87
LDMNT40.1	Taft N21E 400%	0.77	265	56	-0.8	-31	0.73	0.29	285	-0.8	0.28	1	0.57	2	0.77	19.9	23	215
LDMNK50.1	Kobe - Kobe 50%	0.38	212	21	-0.8	-16	0.45	0.21	185	-0.8	0.22	1	0.44	3	0.62	17.2	11	157
LDMNS50.1	NR Sylmar 90° 50%	0.32	172	25	-0.8	-13	0.35	0.18	156	-0.8	0.18	1	0.34	2	0.45	13.2	9	79
LDMNS10.1	NR Sylmar 90° 100%	0.69	346	53	-0.8	-32	0.61	0.31	315	-0.8	0.30	1	0.61	2	0.76	19.7	24	217
LDMNNH7.1	NR Newhall 90° 75%	0.75	223	30	-0.8	14	0.55	0.21	275	-0.8	0.24	2	0.50	2	0.70	16.6	11	133
LDMNN50.1	NR Newhall 360° 50%	0.42	211	30	-0.8	15	0.34	0.23	202	-0.8	0.22	1	0.45	2	0.47	16.7	11	157

1. Residual Displacement

**TABLE 4-4 Peak Response of Isolated Moment Frame Structure with Friction Pendulum Bearings** (values are in units of g for acceleration, mm/s for velocity, mm for displacement, and kN for force)

Test	Excitation	Peak Table Motion			Peak Isolation System Response						Peak Superstructure Response				Damper Response			
		Accel	Vel.	Disp.	Initial Disp.	Isol. Disp.	Base Accel.	Base Shear/W	Base Vel.	Res. <sup>1</sup> Disp.	Story Shear/W	Drift / Height (%)	Floor Accel.	Force	Disp.	Vel.		
FPMFE20.1	El Centro S00E 200%	0.67	300	54	-0.8	40	0.55	0.14	237	0.3	0.20	3,4	0.42	4	0.80	N/A	N/A	N/A
FPMFT50.1	Taft N21E 500%	0.80	335	70	0.3	-54	0.61	0.15	284	-1.3	0.19	2	0.40	2	0.75	N/A	N/A	N/A
FPMFK10.1	Kobe - Kobe 100%	0.92	445	41	-1.3	37	0.66	0.14	201	0.0	0.21	3,4	0.43	4	0.81	N/A	N/A	N/A
FPMFH30.1	Hachinohe NS 300%	0.83	410	94	0.0	-72	0.63	0.19	370	-10.2	0.22	2	0.48	2	0.70	N/A	N/A	N/A
FPMFM50.1	Miyagiken-Oki EW 500%	0.87	398	60	-10.2	-32	0.69	0.13	343	0.5	0.22	2	0.45	2	0.79	N/A	N/A	N/A
FPMFN10.1	NR Newhall 360° 100%	0.90	463	59	0.5	-54	0.44	0.16	288	0.3	0.17	1,2	0.35	2	0.60	N/A	N/A	N/A
FPMFNH1.1	NR Newhall 90° 100%	0.96	304	43	0.3	33	0.55	0.14	215	-1.0	0.17	2	0.32	2	0.72	N/A	N/A	N/A
FPMFS10.1	NR Sylmar 90° 100%	0.65	352	50	-1.0	-61	0.65	0.17	286	-0.3	0.24	3	0.48	3	0.84	N/A	N/A	N/A
FPMFPS1.1	Pacoima S74W 100%	0.75	259	28	-0.3	28	0.70	0.12	210	1.5	0.23	3	0.44	3	0.72	N/A	N/A	N/A
FPMFPE7.1	Pacoima S16E 75%	0.61	356	59	1.0	-42	0.52	0.14	297	-2.0	0.19	3	0.41	2	0.68	N/A	N/A	N/A
FPMFPE1.1	Pacoima S16E 100%	0.73	471	78	-2.0	-59	0.65	0.16	392	-2.5	0.24	3	0.49	2,3	0.76	N/A	N/A	N/A
FPMFYN1.1	Marmara YPT NS 100%	0.33	287	90	-2.0	-33	0.31	0.12	283	0.0	0.14	2	0.30	2	0.39	N/A	N/A	N/A
FPMFYE1.1	Marmara YPT EW 100%	0.27	306	103	0.0	-24	0.23	0.11	303	-0.3	0.11	1	0.25	2	0.32	N/A	N/A	N/A
FPMFM10.1	Mexico N90W 100%	0.20	302	51	-0.3	71	0.36	0.17	338	0.8	0.16	1	0.34	2	0.37	N/A	N/A	N/A
FPMFTW1.1	Taiwan TCU 129 EW 100%	1.06	373	86	0.8	19	0.89	0.12	292	-0.5	0.21	5	0.46	5	0.96	N/A	N/A	N/A
FPMNE20.1	El Centro S00E 200%	0.65	307	54	-0.8	23	0.56	0.26	240	-0.5	0.31	3	0.66	3	0.95	20	18	183
FPMNT50.1	Taft N21E 500%	0.86	344	70	-0.5	-41	0.70	0.28	275	0.0	0.28	1	0.55	2,3	0.97	22	30	296
FPMNK10.1	Kobe - Kobe 100%	0.98	455	42	0.0	-31	0.77	0.29	241	-1.8	0.34	3	0.77	2,3	0.89	22	22	311
FPMNH30.1	Hachinohe NS 300%	0.88	412	94	-1.8	-59	0.73	0.30	384	-4.3	0.33	1	0.67	2	0.77	25	42	432
FPMNM50.1	Miyagiken-Oki EW 500%	0.98	406	60	-4.3	-24	0.86	0.25	384	-0.8	0.29	1	0.61	2	1.05	19	14	240
FPMNN10.1	NR Newhall 360° 100%	0.98	456	59	-0.8	-30	0.52	0.28	327	0.0	0.31	1,2	0.69	2	0.90	22	21	357
FPMNNH1.1	NR Newhall 90° 100%	0.99	300	44	0.0	-19	0.90	0.24	263	-0.5	0.33	2	0.74	2	1.13	18	14	171
FPMNS10.1	NR Sylmar 90° 100%	0.65	346	50	-0.5	-37	0.65	0.26	287	-8.9	0.29	2	0.68	2	0.86	22	27	314
FPMNPS1.1	Pacoima S74W 100%	0.78	274	28	-8.6	-29	0.83	0.26	276	-2.3	0.27	2	0.60	2	0.93	20	14	217
FPMNPE7.1	Pacoima S16E 75%	0.65	366	60	-2.3	-41	0.82	0.28	343	-5.1	0.29	1,2	0.66	2	0.89	23	28	368
FPMNYN1.1	Marmara YPT NS 100%	0.33	283	90	-5.1	-13	0.33	0.22	279	0.0	0.22	1	0.44	2	0.47	15	10	119
FPMNYE1.1	Marmara YPT EW 100%	0.28	311	103	0.0	-12	0.27	0.20	317	-2.3	0.20	1	0.37	2	0.51	13	10	84
FPMNM10.1	Mexico N90W 100%	0.19	305	51	-2.3	-17	0.27	0.19	304	-2.3	0.17	1	0.34	2	0.29	14	11	88
FPMNTW1.1	Taiwan TCU 129 EW 100%	1.06	370	86	-2.3	-14	1.06	0.27	309	-0.5	0.35	2	0.67	2	1.22	19	8	191
FPMNPE1.1	Pacoima S16E 100%	0.86	487	79	-0.5	-60	0.82	0.32	442	-5.8	0.29	1,2	0.74	2	0.96	26	44	465

1. Residual Displacement

**TABLE 4-4 Continued**

Test	Excitation	Peak Table Motion			Peak Isolation System Response							Peak Superstructure Response			Damper Response			
		Accel	Vel.	Disp.	Initial Disp.	Isol. Disp.	Base Accel.	Base Shear/W	Base Vel.	Res. <sup>1</sup> Disp.	Story Shear/W	Drift / Height (%)	Floor Accel.	Force	Disp.	Vel.		
FPMLE20.1	EI Centro S00E 200%	0.65	307	54	-0.8	29	0.56	0.12	241	0.5	0.25	2	0.53	2	0.81	10	22	174
FPMLT50.1	Taft N21E 500%	0.84	339	70	0.5	-42	0.69	0.26	261	-0.3	0.24	1	0.44	2	0.88	20	32	305
FPMLK10.1	Kobe - Kobe 100%	0.94	447	41	-0.3	28	0.69	0.25	231	-0.3	0.29	3	0.61	2	0.87	21	20	311
FPMLH30.1	Hachinohe NS 300%	0.84	407	94	-0.3	-55	0.57	0.30	356	-6.4	0.30	1	0.53	2	0.64	27	41	369
FPMLM50.1	Miyagiken-Oki EW 500%	0.94	399	60	-6.4	-26	0.78	0.22	355	0.0	0.24	2	0.49	2	0.91	16	14	244
FPMLN10.1	NR Newhall 360° 100%	0.90	458	41	0.0	-36	0.58	0.26	303	0.0	0.29	1	0.58	2	0.81	21	27	299
FPMLNH1.1	NR Newhall 90° 100%	0.97	303	59	0.0	-18	0.68	0.19	255	-0.5	0.28	2	0.57	2	0.96	11	14	178
FPMLS10.1	NR Sylmar 90° 100%	0.64	349	44	-0.5	-41	0.60	0.26	286	-4.1	0.26	3	0.55	2,3	0.87	20	31	306
FPMLPS1.1	Pacoima S74W 100%	0.76	264	28	-4.1	-23	0.75	0.21	246	0.0	0.25	3	0.49	3	0.84	14	17	218
FPMLPE5.1	Pacoima S16E 50%	0.45	241	39	0.0	-23	0.39	0.21	226	-2.8	0.21	1	0.44	2	0.65	13	18	221
FPMLPE7.1	Pacoima S16E 75%	0.64	364	59	-2.8	-37	0.49	0.26	312	-2.5	0.26	1	0.53	2	0.78	22	25	323
FPMLYN1.1	Marmara YPT NS 100%	0.34	283	90	-2.5	19	0.32	0.17	263	0.0	0.16	1	0.33	2	0.38	8	17	138
FPMLYE1.1	Marmara YPT EW 100%	0.27	309	103	0.0	-17	0.27	0.15	309	-0.5	0.14	1	0.34	2	0.41	6	13	96
FPMLM10.1	Mexico N90W 100%	0.18	304	52	-0.5	-35	0.23	0.17	291	0.8	0.15	1	0.33	2	0.26	11	26	174
FPMLTW1.1	Taiwan TCU 129 EW 100%	1.08	373	86	0.8	-13	1.00	0.23	294	-0.5	0.29	2	0.58	2	1.15	13	10	221
FPMLPE1.1	Pacoima S16E 100%	0.81	487	79	-4.8	-52	0.61	0.34	385	-2.5	0.33	1	0.63	2	0.86	33	34	401

1. Residual Displacement

**TABLE 4-5 Peak Response of Isolated Moment Frame Structure with Combined Low Damping Elastomeric and Flat Sliding Bearings (values are in units of g for acceleration, mm/s for velocity and mm for displacement)**

Test	Excitation	Peak Table Motion			Peak Isolation System Response							Peak Superstructure Response			
		Accel	Vel.	Disp.	Initial Disp.	Isol. Disp.	Base Accel.	Base Shear/W	Base Vel.	Res. <sup>1</sup> Disp.	Story Shear/W	Drift / Height (%)	Floor Accel.		
EFMFE50.1	EI Centro S00E 50%	0.17	88	14	0.5	-6	0.20	0.06	68	-1.3	0.07	2	0.14	2,3	0.27
EFMFE10.1	EI Centro S00E 100%	0.35	167	27	-1.3	14	0.26	0.09	147	-1.8	0.11	2	0.22	2	0.37
EFMFE15.1	EI Centro S00E 150%	0.55	263	42	-1.8	33	0.43	0.15	245	-1.8	0.14	2	0.28	2	0.53
EFMFT20.1	Taft N21E 200%	0.33	126	27	-1.8	-19	0.35	0.11	161	-1.8	0.10	1	0.20	2	0.43
EFMFT30.1	Taft N21E 300%	0.52	192	42	-1.8	-33	0.47	0.15	279	-1.5	0.15	1,2	0.31	2	0.53
EFMFK50.1	Kobe - Kobe 50%	0.39	219	21	-1.5	18	0.37	0.11	136	-1.8	0.13	3	0.28	4	0.43
EFMFS50.1	NR Sylmar 90° 50%	0.32	172	25	-1.8	-24	0.38	0.12	158	-2.5	0.13	3	0.27	2	0.46
EFMFNH7.1	NR Newhall 90° 75%	0.75	231	29	-1.5	-25	0.43	0.13	211	-1.3	0.13	1,2	0.24	2	0.47
EFMFN50.1	NR Newhall 360° 50%	0.40	212	29	-1.3	-26	0.35	0.14	167	-0.5	0.12	1	0.22	2	0.38
EFMFE20.1	EI Centro S00E 200%	0.78	315	54	-0.5	57	0.55	0.21	344	-1.0	0.17	1	0.36	2	0.64
EFMFT40.1	Taft N21E 400%	0.70	249	56	-1.0	-46	0.56	0.19	353	-0.5	0.20	1	0.40	2	0.64

1. Residual Displacement

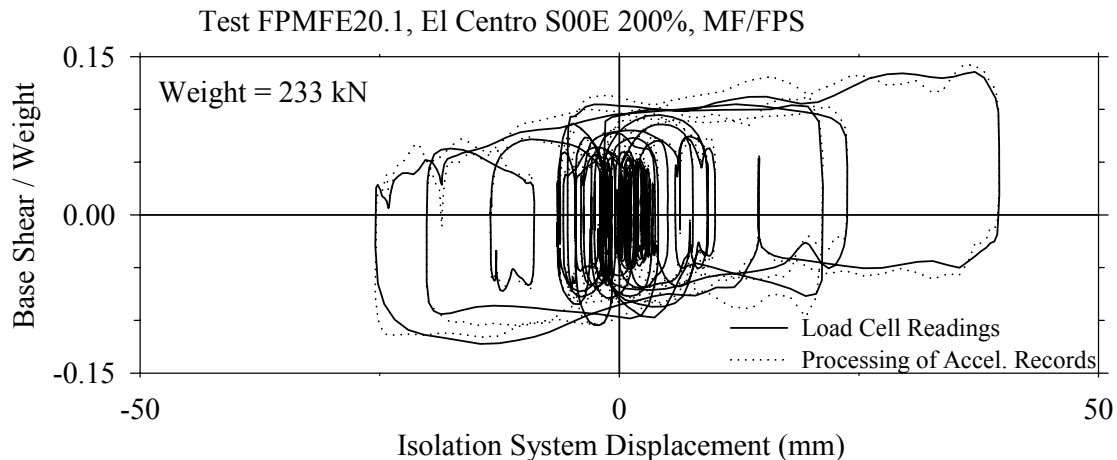


**FIGURE 4-1 Comparison of Load Cell Readings with Processed Acceleration Records for El Centro S00E 200%**

### 4.3 Braced Frame Test Results

The braced frame tests are divided into five sections based on the isolation system used. Tables 4-6 thru 4-10 present the results for the braced frame configuration of the tested structure for the non-isolated condition (fixed base), and for isolated conditions using lead-core, low damping elastomeric, Friction Pendulum and combined low damping elastomeric and flat sliding bearings, respectively. The response quantities for all tests are the same as those presented for the moment frame test results.

**TABLE 4-6 Peak Response of Non-isolated Braced Frame Structure** (values are in units of g for acceleration, mm/s for velocity and mm for displacement)

Test	Excitation*	Peak Table Motion			Peak Base Response						Peak Superstructure Response				
		Accel	Vel.	Disp.	Initial Disp.	Isol. Disp.	Base Accel.	Base Shear/W	Base Vel.	Res. <sup>1</sup> Disp.	Story Shear/W	Drift / Height (%)	Floor Accel.		
FBSBE30.1	El Centro S00E 30%	0.12	51.2	8.7	N/A	N/A	0.20	0.22	57.7	N/A	0.21	1	0.16	4	0.41
FBSBT50.1	Taft N21E 50%	0.09	38.4	6.8	N/A	N/A	0.11	0.13	39.1	N/A	0.12	1	0.08	3	0.21
FBSBK15.1	Kobe - Kobe 15%	0.14	68.6	6.4	N/A	N/A	0.14	0.19	76.2	N/A	0.19	1	0.14	4	0.36
FBSBN15.1	NR Newhall 360° 15%	0.12	79.5	8.6	N/A	N/A	0.16	0.23	93.1	N/A	0.22	1	0.17	3	0.36

1. Residual Displacement

\* The excitations were reduced for the non-isolated configuration to ensure the model remained elastic.

**TABLE 4-7 Peak Response of Isolated Braced Frame Structure with Low Damping Elastomeric Bearings** (values are in units of g for acceleration, mm/s for velocity, mm for displacement and kN for force)

Test	Excitation	Peak Table Motion			Peak Isolation System Response						Peak Superstructure Response				Damper Response			
		Accel	Vel.	Disp.	Initial Disp.	Isol. Disp.	Base Accel.	Base Shear/W	Base Vel.	Res. <sup>1</sup> Disp.	Story Shear/W	Drift / Height (%)	Floor Accel.	Force	Disp.	Vel.		
LDSBE10.1	EI Centro S00E 100%	0.34	165	27	-0.8	-28	0.21	0.18	240	-0.8	0.16	1	0.12	5	0.21	N/A	N/A	N/A
LDSBE15.1	EI Centro S00E 150%	0.52	243	41	-0.8	-46	0.28	0.26	358	-0.8	0.24	1	0.20	5	0.34	N/A	N/A	N/A
LDSBE20.1	EI Centro S00E 200%	0.68	324	53	-0.8	-60	0.38	0.33	445	-0.8	0.30	1	0.35	2.5	0.38	N/A	N/A	N/A
LDSBT20.1	Taft N21E 200%	0.33	128	28	-0.8	-29	0.19	0.18	252	-0.8	0.16	1	0.13	2.5	0.22	N/A	N/A	N/A
LDSBT40.1	Taft N21E 400%	0.73	247	56	-0.8	-60	0.21	0.31	466	-0.8	0.29	1	0.29	2.5	0.41	N/A	N/A	N/A
LDSBK50.1	Kobe - Kobe 50%	0.36	226	21	-0.8	45	0.30	0.26	304	-0.8	0.23	1	0.24	2	0.36	N/A	N/A	N/A
LDSBS10.1	NR Sylmar 90° 50%	0.31	173	25	-0.8	-32	0.18	0.19	250	-0.8	0.17	1	0.14	2.5	0.21	N/A	N/A	N/A
LDSBS90.1	NR Sylmar 90° 90%	0.60	318	45	-0.8	-61	0.34	0.33	436	-0.8	0.29	1	0.34	2.5	0.38	N/A	N/A	N/A
LDSBS10.2	NR Sylmar 90° 100%	0.68	354	51	-0.8	-67	0.41	0.36	481	-0.8	0.31	1	0.48	5	0.43	N/A	N/A	N/A
LDSBNH7.1	NR Newhall 90° 75%	0.76	227	32	-0.8	-42	0.22	0.23	338	-0.8	0.21	1	0.19	2	0.27	N/A	N/A	N/A
LDSBN50.1	NR Newhall 360° 50%	0.40	233	29	-0.8	-41	0.26	0.24	328	-0.8	0.21	1	0.19	2.5	0.29	N/A	N/A	N/A
LDSLE10.1	EI Centro S00E 100%	0.31	161	25	-0.8	-17	0.21	0.13	175	-0.8	0.12	1	0.10	2	0.23	8.2	13	128
LDSLE20.1	EI Centro S00E 200%	0.68	316	53	-0.8	-35	0.39	0.24	349	-0.8	0.21	1	0.18	2	0.41	17.0	26	257
LDSL20.1	Taft N21E 200%	0.34	129	28	-0.8	-21	0.18	0.16	176	-0.8	0.14	1	0.10	2.5	0.23	8.0	15	132
LDSL40.1	Taft N21E 400%	0.71	240	55	-0.8	-42	0.32	0.28	333	-0.8	0.27	1	0.22	2.5	0.44	15.7	33	237
LDSLK50.1	Kobe - Kobe 50%	0.35	221	20	-0.8	22	0.26	0.20	197	-0.8	0.19	1	0.17	2	0.33	12.9	17	208
LDSL50.1	NR Sylmar 90° 50%	0.33	182	26	-0.8	-21	0.16	0.17	189	-0.8	0.15	1	0.11	5	0.21	7.4	15	123
LDSL10.1	NR Sylmar 90° 100%	0.69	354	50	-0.8	-43	0.33	0.29	362	-0.8	0.27	1	0.25	2	0.37	14.6	32	242
LDSLNH7.1	NR Newhall 90° 75%	0.76	228	32	-0.8	-23	0.35	0.18	264	-0.8	0.17	1	0.15	5	0.38	12.3	17	205
LDSL50.1	NR Newhall 360° 50%	0.40	234	30	-0.8	-23	0.25	0.22	223	-0.8	0.21	1	0.18	2.5	0.34	15.0	17	228
LDSNE10.1	EI Centro S00E 100%	0.31	160	25	-0.8	-10	0.32	0.17	166	-0.8	0.16	2	0.13	5	0.41	15.3	7	109
LDSNE20.1	EI Centro S00E 200%	0.69	317	54	-0.8	-25	0.51	0.26	319	-0.8	0.23	1	0.20	2	0.54	19.2	19	238
LDSNT20.1	Taft N21E 200%	0.33	129	27	-0.8	-13	0.24	0.17	175	-0.8	0.16	1	0.14	5	0.34	14.3	9	99
LDSNT40.1	Taft N21E 400%	0.70	241	55	-0.8	-32	0.44	0.29	305	-0.8	0.28	1	0.23	5	0.52	19.4	24	232
LDSNK50.1	Kobe - Kobe 50%	0.36	222	21	-0.8	-17	0.24	0.23	167	-0.8	0.21	1	0.16	2	0.34	18.9	12	222
LDSNS50.1	NR Sylmar 90° 50%	0.34	182	27	-0.8	-16	0.23	0.21	166	-0.8	0.19	1	0.12	5	0.33	15.5	12	115
LDSNS10.1	NR Sylmar 90° 100%	0.71	355	51	-0.8	-36	0.47	0.32	331	-0.8	0.30	1	0.33	5	0.52	20.3	27	258
LDSNNH7.1	NR Newhall 90° 75%	0.76	227	31	-0.8	-17	0.46	0.24	236	-0.8	0.20	1	0.18	2	0.53	18.9	12	204
LDSNN50.1	NR Newhall 360° 50%	0.39	233	29	-0.8	16	0.28	0.23	215	-0.8	0.21	1	0.18	5	0.37	18.4	12	212

1. Residual Displacement

**TABLE 4-8 Peak Response of Isolated Braced Frame Structure with Friction Pendulum Bearings** (values are in units of g for acceleration, mm/s for velocity, mm for displacement and kN for force)

Test	Excitation	Peak Table Motion			Peak Isolation System Response							Peak Superstructure Response				Damper Response		
		Accel	Vel.	Disp.	Initial Disp.	Isol. Disp.	Base Accel.	Base Shear/W	Base Vel.	Res. <sup>1</sup> Disp.	Story Shear/W	Drift / Height (%)		Floor Accel.	Force	Disp.	Vel.	
FPSBE10.1	EI Centro S00E 100%	0.38	161	27	N/A	-15	0.24	0.07	97	-4.0	0.08	2	0.10	2	0.27	N/A	N/A	N/A
FPSBE20.1	EI Centro S00E 200%	0.79	317	54	N/A	49	0.50	0.12	194	0.0	0.12	1,2	0.11	4	0.45	N/A	N/A	N/A
FPSBE20.2	EI Centro S00E 200%	0.80	316	54	N/A	47	0.53	0.12	197	0.0	0.13	1,2	0.11	4	0.48	N/A	N/A	N/A
FPSBT10.1	Taft N21E 100%	0.17	72	14	N/A	-6	0.14	0.07	61	-2.0	0.07	2	0.08	4,5	0.20	N/A	N/A	N/A
FPSBT20.1	Taft N21E 200%	0.38	127	28	N/A	-18	0.26	0.08	112	0.0	0.11	3	0.09	4	0.31	N/A	N/A	N/A
FPSBT30.1	Taft N21E 300%	0.58	186	42	N/A	-34	0.35	0.10	149	0.5	0.13	3	0.11	4	0.37	N/A	N/A	N/A
FPSBT40.1	Taft N21E 400%	0.80	247	56	N/A	-49	0.39	0.12	184	0.3	0.13	3	0.10	4	0.42	N/A	N/A	N/A
FPSBT50.1	Taft N21E 500%	1.03	318	70	N/A	-63	0.41	0.14	210	0.0	0.14	1	0.12	4	0.45	N/A	N/A	N/A
FPSBH10.1	Hachinohe NS 100%	0.27	137	31	N/A	-11	0.21	0.08	102	-0.3	0.08	1,2	0.07	3	0.21	N/A	N/A	N/A
FPSBH20.1	Hachinohe NS 200%	0.58	287	62	N/A	-41	0.28	0.12	183	-4.3	0.12	3	0.12	6	0.34	N/A	N/A	N/A
FPSBM30.1	Miyagiken-Oki EW 300%	0.62	246	36	N/A	20	0.37	0.09	150	7.3	0.13	3	0.09	4	0.38	N/A	N/A	N/A
FPSBH30.1	Hachinohe NS 300%	0.92	422	93	N/A	-85	0.40	0.19	298	-11.8	0.18	1,2	0.16	3	0.40	N/A	N/A	N/A
FPSBM50.1	Miyagiken-Oki EW 500%	1.03	398	60	N/A	48	0.55	0.12	253	10.7	0.16	3	0.13	4	0.57	N/A	N/A	N/A
FPSBN10.1	NR Newhall 360° 100%	1.01	469	58	N/A	-62	0.38	0.15	316	-0.7	0.16	1	0.15	2	0.51	N/A	N/A	N/A
FPSBK10.1	Kobe - Kobe 100%	0.89	458	41	N/A	-39	0.33	0.12	212	-0.3	0.13	2	0.11	4	0.39	N/A	N/A	N/A
FPSBYN1.1	Marmara YPT NS 100%	0.34	280	90	N/A	-39	0.27	0.11	278	-0.3	0.12	2	0.11	4	0.30	N/A	N/A	N/A
FPSBYE1.1	Marmara YPT EW 100%	0.35	307	103	N/A	-31	0.27	0.10	304	0.6	0.10	2,3	0.10	4	0.25	N/A	N/A	N/A
FPSBNH1.1	NR Newhall 90° 100%	1.14	302	42	N/A	33	0.44	0.11	205	0.3	0.16	3	0.13	4	0.51	N/A	N/A	N/A
FPSBS10.1	NR Sylmar 90° 100%	0.68	346	50	N/A	-65	0.35	0.15	290	-0.3	0.15	1	0.13	5	0.33	N/A	N/A	N/A
FPSBPS1.1	Pacoima S74W 100%	0.91	255	28	N/A	32	0.49	0.11	131	1.8	0.19	3	0.15	3	0.48	N/A	N/A	N/A
FPSBPE1.1	Pacoima S16E 75%	0.91	373	59	N/A	-53	0.40	0.13	265	-4.3	0.14	3	0.11	5	0.39	N/A	N/A	N/A
FPSBPE2.1	Pacoima S16E 100%	1.00	479	78	N/A	70	0.37	0.16	328	0.8	0.16	1	0.13	4,5	0.47	N/A	N/A	N/A
FPSBM10.1	Mexico N90W 100%	0.19	295	51	N/A	85	0.23	0.17	298	4.2	0.16	1	0.14	2	0.22	N/A	N/A	N/A
FPSBTW1.1	Taiwan TCU 129 EW 100%	1.21	380	86	N/A	30	0.59	0.12	201	-0.5	0.15	4	0.14	4	0.53	N/A	N/A	N/A

1. Residual Displacement



**TABLE 4-8 Continued**

Test	Excitation	Peak Table Motion			Peak Isolation System Response							Peak Superstructure Response				Damper Response		
		Accel	Vel.	Disp.	Initial Disp.	Isol. Disp.	Base Accel.	Base Shear/W	Base Vel.	Res. <sup>1</sup> Disp.	Story Shear/W	Drift / Height (%)	Floor Accel.	Force	Disp.	Vel.		
FPSLE10.1	EI Centro S00E 100%	0.33	162	27	N/A	14	0.21	0.13	119	2.8	0.13	2	0.12	2	0.34	6.9	N/A <sup>2</sup>	N/A <sup>2</sup>
FPSLE10.2	EI Centro S00E 100%	0.33	164	27	N/A	11	0.21	0.14	121	0.0	0.14	2	0.11	2	0.36	6.6	N/A <sup>2</sup>	N/A <sup>2</sup>
FPSLE20.1	EI Centro S00E 200%	0.67	305	54	N/A	27	0.53	0.18	199	-0.8	0.18	2	0.15	2	0.49	12.5	N/A <sup>2</sup>	N/A <sup>2</sup>
FPSLE10.3	EI Centro S00E 100%	0.32	161	27	-0.01	12	0.21	0.13	122	1.5	0.14	2	0.13	2	0.36	6.9	9	107
FPSLE20.2	EI Centro S00E 200%	0.67	306	54	0.06	29	0.46	0.19	200	1.0	0.17	2	0.16	2	0.48	12.9	21	206
FPSLT50.1	Taft N21E 500%	0.85	324	70	0.04	-46	0.48	0.22	247	-0.3	0.22	3	0.20	4	0.54	17.7	34	249
FPSLH30.1	Hachinohe NS 300%	0.80	412	93	-0.01	-44	0.45	0.25	320	-9.7	0.24	1	0.19	4	0.47	18.8	32	294
FPSLN31.1	NR Newhall 360° 100%	1.06	464	58	-0.38	-35	0.44	0.23	298	-1.0	0.20	1	0.15	4	0.51	23.3	26	347
FPSLM50.1	Miyagiken-Oki EW 500%	0.90	394	60	-0.04	-23	0.57	0.16	243	0.8	0.20	2,3	0.20	4	0.53	12.3	17	193
FPSLK10.1	Kobe - Kobe 100%	0.93	446	42	0.03	31	0.46	0.28	199	-1.5	0.25	1	0.20	4	0.56	24.3	23	335
FPSLS10.1	NR Sylmar 90° 100%	0.67	351	50	-0.06	-41	0.39	0.21	267	-2.5	0.19	2	0.15	2	0.45	16.9	29	273
FPSLPS1.1	Pacoima S74W 100%	0.85	259	28	-0.10	-24	0.46	0.18	186	1.0	0.23	3	0.20	4	0.62	14.4	18	234
FPSLPE1.1	Pacoima S16E 100%	1.00	477	78	0.04	-59	0.50	0.23	392	-2.3	0.21	1	0.18	2	0.45	22.7	47	457
FPSNE20.1	EI Centro S00E 200%	0.65	301	54	-0.12	24	0.57	0.24	242	1.3	0.25	2	0.21	4	0.64	18.7	21	210
FPSNE20.2	EI Centro S00E 200%	0.69	305	54	-0.05	26	0.60	0.24	237	1.3	0.25	2	0.22	5	0.64	18.6	21	211
FPSNT50.1	Taft N21E 500%	0.87	328	70	0.05	-38	0.58	0.25	275	-0.5	0.25	1,2	0.22	2	0.68	19.6	29	268
FPSNH30.1	Hachinohe NS 300%	0.76	409	94	-0.02	-40	0.57	0.27	345	-7.6	0.26	2	0.21	3	0.58	19.8	29	265
FPSNN10.1	NR Newhall 360° 100%	1.04	480	59	-0.30	34	0.55	0.27	339	1.3	0.25	1,2	0.23	4	0.67	20.7	31	351
FPSNNH1.1	NR Newhall 90° 100%	0.95	297	44	0.05	-25	0.51	0.26	237	-0.8	0.27	3	0.23	2	0.73	20.4	19	261
FPSNM50.1	Miyagiken-Oki EW 500%	0.84	388	60	-0.03	-17	0.68	0.23	291	1.0	0.28	2	0.22	4	0.71	19.3	13	228
FPSNK10.1	Kobe - Kobe 100%	0.90	453	42	0.04	40	0.54	0.29	241	-2.3	0.28	2	0.28	4	0.68	21.0	28	378
FPSNS10.1	NR Sylmar 90° 100%	0.66	353	50	-0.09	-41	0.51	0.25	289	-5.8	0.24	1	0.21	2	0.61	20.1	29	267
FPSNPS1.1	Pacoima S74W 100%	0.78	253	28	-0.23	-24	0.49	0.23	229	-2.3	0.28	2	0.22	2	0.70	19.7	14	237
FPSNPE7.1	Pacoima S16E 75%	0.78	373	59	-0.08	-39	0.49	0.25	364	-6.4	0.23	1	0.19	2	0.59	20.5	26	270
FPSNPE1.1	Pacoima S16E 100%	0.97	487	78	-0.25	-61	0.58	0.28	450	-5.6	0.26	1	0.24	2	0.73	22.0	39	401
FPSNYN1.1	Marmara YPT NS 100%	0.32	285	90	-0.24	-15	0.26	0.18	282	-0.5	0.17	1	0.17	2	0.34	15.1	10	109
FPSNYE1.1	Marmara YPT EW 100%	0.33	308	103	-0.02	-11	0.23	0.19	299	-1.8	0.18	1	0.14	4	0.34	14.9	8	103
FPSNM10.1	Mexico N90W 100%	0.19	305	51	-0.07	13	0.20	0.17	307	-2.0	0.15	1	0.14	2	0.20	12.7	12	66
FPSNTW.1	Taiwan TCU 129 EW 100%	1.09	377	86	-0.08	14	0.56	0.23	247	-0.8	0.28	3	0.22	4	0.73	20.1	12	219

1. Residual Displacement

2. The displacement transducer (LVDT) was not functioning.

**TABLE 4-9 Peak Response of Isolated Braced Frame Structure with Lead-Core Bearings** (values are in units of g for acceleration, mm/s for velocity and mm for displacement)

Test	Excitation	Peak Table Motion			Peak Isolation System Response						Peak Superstructure Response				
		Accel	Vel.	Disp.	Initial Disp.	Isol. Disp.	Base Accel.	Base Shear/W	Base Vel.	Res. <sup>1</sup> Disp.	Story Shear/W	Drift / Height (%)		Floor Accel.	
LCSBE20.1	EI Centro S00E 200%	0.69	360	52	-0.5	-30	0.54	0.30	374	-0.3	0.28	1	0.23	5	0.61
LCSBT40.1	Taft N21E 400%	0.68	283	59	-0.3	-36	0.49	0.33	387	-0.8	0.31	1	0.24	5	0.50
LCSBK10.1	Kobe - Kobe 100%	0.94	460	43	-0.8	-38	0.62	0.36	378	-1.3	0.34	1	0.31	5	0.66
LCSBS10.1	NR Sylmar 90° 100%	0.68	351	50	-1.3	-42	0.50	0.37	373	-1.0	0.35	1	0.32	5	0.55
LCSBNH1.1	NR Newhall 90° 100%	1.04	301	43	-1.0	27	0.55	0.29	364	-0.3	0.26	1	0.25	3	0.58
LCSBN10.1	NR Newhall 360° 100%	1.01	464	59	-0.3	51	0.55	0.44	445	0.5	0.40	1	0.45	5	0.76

1. Residual Displacement

**TABLE 4-10 Peak Response of Isolated Braced Frame Structure with Combined Low Damping Elastomeric and Flat Sliding Bearings** (values are in units of g for acceleration, mm/s for velocity and mm for displacement)

Test	Excitation	Peak Table Motion			Peak Isolation System Response						Peak Superstructure Response				
		Accel	Vel.	Disp.	Initial Disp.	Isol. Disp.	Base Accel.	Base Shear/W	Base Vel.	Res. <sup>1</sup> Disp.	Story Shear/W	Drift / Height (%)		Floor Accel.	
EFSBE10.1	EI Centro S00E 100%	0.34	163	27	-0.8	14	0.27	0.10	161	-0.3	0.10	1	0.08	2	0.31
EFSBE20.1	EI Centro S00E 200%	0.72	311	53	-0.3	55	0.47	0.20	330	-0.8	0.18	1	0.15	2	0.43
EFSBT20.1	Taft N21E 200%	0.34	126	28	-0.8	-18	0.28	0.11	135	-1.3	0.11	3	0.08	5	0.29
EFSBT40.1	Taft N21E 400%	0.74	254	56	-1.3	-50	0.38	0.20	280	-0.5	0.18	1	0.12	4	0.36
EFSBK50.1	Kobe - Kobe 50%	0.39	220	21	-0.5	17	0.31	0.11	123	-1.3	0.12	2	0.10	4	0.31
EFSBS50.1	NR Sylmar 90° 50%	0.29	166	24	-1.3	-26	0.26	0.13	146	-1.0	0.12	1	0.09	2	0.24
EFSBS10.1	NR Sylmar 90° 100%	0.67	355	51	-1.0	-72	0.44	0.26	381	-1.0	0.23	1	0.22	5	0.38
EFSBNH7.1	NR Newhall 90° 75%	0.71	230	29	-1.0	-25	0.32	0.12	230	-0.3	0.12	3	0.10	5	0.41
EFSBN50.1	NR Newhall 360° 50%	0.39	210	29	-0.3	-24	0.31	0.13	187	-0.8	0.12	2	0.10	5	0.31
EFSBN75.1	NR Newhall 360° 75%	0.64	333	44	-0.8	-49	0.34	0.20	262	-1.0	0.18	1	0.12	4	0.30

1. Residual Displacement

#### 4.4 Asymmetrically Braced Frame Test Results

The asymmetrically braced frame tests are divided into five sections based on the isolation system used. Tables 4-11 thru 4-15 present the results for the moment frame configuration of the tested structure for non-isolated conditions (fixed base), and for isolated conditions using lead-core, combined low damping elastomeric and flat sliding bearings, low damping elastomeric and Friction Pendulum bearings respectively. The response quantities for all tests are the same as those presented for the moment frame test results, with the exception that split cells present the individual results of the east and west (braced and unbraced moment) frames separately whereas previously these values were averaged together as both frames were either braced or unbraced.

**TABLE 4-11 Peak Response of Non-isolated Asymmetrically Braced Frame Structure** (values are in units of g for acceleration, mm/s for velocity and mm for displacement)

Test	Excitation*	Peak Table Motion			Peak Base Response							Peak Superstructure Response			
		Accel	Vel.	Disp.	Initial Disp.	Isol. Disp.	Base Accel.	Base Shear/W	Base Vel.	Res. <sup>1</sup> Disp.	Story Shear/W	Drift / Height (%)		Floor Accel.	
FBABE30.1	El Centro S00E 30%	0.11	50.0	8.4	N/A	N/A	0.13	0.13	59.1	N/A	0.14	3	0.26	3	0.28
					N/A	N/A	0.14			N/A			0.28	4	0.39
FBABT50.1	Taft N21E 50%	0.09	38.9	6.7	N/A	N/A	0.09	0.15	28.7	N/A	0.14	1	0.23	2	0.26
					N/A	N/A	0.09			N/A			0.27	3	0.30
FBABK15.1	Kobe - Kobe 15%	0.14	70.1	6.6	N/A	N/A	0.15	0.22	82.3	N/A	0.21	1	0.35	3	0.33
					N/A	N/A	0.15			N/A			0.42	4	0.41
FBABN15.1	NR Newhall 360° 15%	0.13	67.8	8.5	N/A	N/A	0.14	0.26	49.0	N/A	0.25	1	0.38	2	0.35
					N/A	N/A	0.14			N/A			0.50	3	0.44

1. Residual Displacement

\* The excitations were reduced for the non-isolated configuration to ensure the model remained elastic.

**TABLE 4-12 Peak Response of Isolated Asymmetrically Braced Frame Structure with Friction Pendulum Bearings** (values are in units of g for acceleration, mm/s for velocity, mm for displacement and kN for force)

Test	Excitation	Peak Table Motion			Peak Isolation System Response							Peak Superstructure Response				Damper Response		
		Accel	Vel.	Disp.	Initial Disp.	Isol. Disp.	Base Accel.	Base Shear/W	Base Vel.	Res. <sup>1</sup> Disp.	Story Shear/W	Drift / Height (%)		Floor Accel.	Force	Disp.	Vel.	
FPABE50.1	El Centro S00E 50%	0.20	85	14	-9.9	-10	0.14	0.10	78	-2.8	0.10	2	0.11	3,4	0.26	N/A	N/A	N/A
					-7.9	-8	0.19			1.8			0.12	2	0.30			
FPABE10.1	El Centro S00E 100%	0.36	167	27	-2.8	11	0.25	0.10	128	0.5	0.12	3	0.12	3	0.31	N/A	N/A	N/A
					1.8	16	0.33			3.3			0.19	2	0.40			
FPABE20.1	El Centro S00E 200%	0.72	312	55	0.5	38	0.44	0.14	223	4.1	0.15	4	0.16	3,4	0.50	N/A	N/A	N/A
					3.3	42	0.48			3.6			0.28	2	0.57			
FPABT10.1	Taft N21E 100%	0.15	70	14	4.1	5	0.09	0.10	65	-1.3	0.10	2	0.13	4	0.25	N/A	N/A	N/A
					3.6	5	0.17			-1.5			0.15	5	0.28			
FPABT30.1	Taft N21E 300%	0.49	192	42	-1.3	-29	0.28	0.12	164	-3.3	0.14	3	0.16	4	0.42	N/A	N/A	N/A
					-1.5	-30	0.46			-1.3			0.18	2	0.50			
FPABT50.1	Taft N21E 500%	0.87	332	70	-3.3	-64	0.43	0.16	230	-1.3	0.16	1	0.20	3	0.47	N/A	N/A	N/A
					-1.3	-64	0.64			-0.8			0.25	2	0.55			
FPABH10.1	Hachinohe NS 100%	0.28	134	31	-1.3	-11	0.17	0.11	124	-3.0	0.11	1,2	0.12	3	0.35	N/A	N/A	N/A
					-0.8	-12	0.27			-3.0			0.15	4,5	0.36			
FPABH30.1	Hachinohe NS 300%	0.84	421	94	-3.0	-69	0.37	0.17	320	-11.9	0.18	2	0.25	3	0.50	N/A	N/A	N/A
					-3.0	-71	0.55			-9.7			0.26	2	0.58			
FPABM50.1	Miyagiken-Oki EW 500%	0.87	398	60	-11.9	29	0.49	0.13	284	-1.0	0.16	4	0.17	3,4	0.58	N/A	N/A	N/A
					-9.7	37	0.59			0.3			0.27	4	0.74			
FPABN10.1	NR Newhall 360° 100%	0.91	464	59	-1.0	-57	0.40	0.15	313	-2.8	0.14	1	0.19	3	0.38	N/A	N/A	N/A
					0.3	-58	0.57			0.5			0.24	2	0.48			
FPABNH1.1	NR Newhall 90° 100%	0.98	300	44	-2.8	28	0.46	0.14	239	-1.8	0.15	2,3	0.17	3,4	0.52	N/A	N/A	N/A
					0.5	33	0.69			0.0			0.27	2	0.55			
FPABS10.1	NR Sylmar 90° 100%	0.62	353	51	-1.8	-68	0.37	0.17	289	-3.8	0.17	1	0.26	3	0.48	N/A	N/A	N/A
					0.0	-66	0.48			-0.3			0.28	2	0.56			
FPABPS1.1	Pacoima S74W 100%	0.79	264	28	-3.8	-30	0.54	0.13	188	2.0	0.16	3	0.18	3,4	0.49	N/A	N/A	N/A
					-0.3	-30	0.64			2.0			0.26	2	0.59			
FPABPE7.1	Pacoima S16E 75%	0.68	369	59	1.8	-56	0.37	0.15	279	-5.6	0.16	3	0.21	3	0.46	N/A	N/A	N/A
					1.8	-55	0.47			-4.3			0.29	2	0.55			
FPABPE1.1	Pacoima S16E 100%	0.89	483	78	-5.6	-68	0.44	0.17	311	-6.4	0.19	3	0.22	3	0.52	N/A	N/A	N/A
					-4.1	-66	0.61			-4.1			0.32	2	0.64			
FPABK10.1	Kobe - Kobe 100%	0.88	459	42	-5.8	38	0.42	0.14	210	-5.8	0.17	2,3	0.20	3	0.50	N/A	N/A	N/A
					-3.8	38	0.63			-0.8			0.27	2	0.61			
FPABYN1.1	Marmara YPT NS 100%	0.34	282	91	-5.8	-30	0.23	0.12	259	-3.3	0.12	2	0.18	3	0.27	N/A	N/A	N/A
					-0.8	-30	0.29			1.0			0.19	2	0.33			
FPABYE1.1	Marmara YPT EW 100%	0.30	304	103	-3.3	-21	0.25	0.11	304	-2.5	0.11	2,3	0.15	3,4	0.30	N/A	N/A	N/A
					1.0	-18	0.28			0.3			0.20	2	0.40			
FPABM10.1	Mexico N90W 100%	0.20	304	51	-2.5	-70	0.25	0.16	303	0.0	0.15	1	0.20	3	0.25	N/A	N/A	N/A
					0.3	-70	0.28			1.3			0.22	2	0.31			
FPABTW1.1	Taiwan TCU 129 EW 100%	1.14	380	86	0.0	22	0.44	0.13	217	-0.8	0.18	4	0.18	3,4	0.61	N/A	N/A	N/A
					1.3	23	0.57			-0.3			0.24	2,4	0.76			

1. Residual Displacement



**TABLE 4-13 Peak Response of Isolated Asymmetrically Braced Frame Structure with Low Damping Elastomeric Bearings** (values are in units of g for acceleration, mm/s for velocity, mm for displacement and kN for force)

Test	Excitation	Peak Table Motion			Peak Isolation System Response						Peak Superstructure Response				Damper Response			
		Accel	Vel.	Disp.	Initial Disp.	Isol. Disp.	Base Accel.	Base Shear/W	Base Vel.	Res. <sup>1</sup> Disp.	Story Shear/W	Drift / Height (%)		Floor Accel.	Force	Disp.	Vel.	
LDABE10.1	El Centro S00E 100%	0.35	166	27	0.5	-28	0.19	0.18	235	0.5	0.16	1	0.19	2	0.19	N/A	N/A	N/A
					-2.0	-31	0.22			0.23			1	0.24				
LDABE20.1	El Centro S00E 200%	0.70	326	58	0.5	-59	0.34	0.33	435	0.5	0.29	1	0.40	2	0.39	N/A	N/A	N/A
					-2.0	-62	0.36			0.48			2	0.41				
LDABT20.1	Taft N21E 200%	0.35	126	28	0.5	-28	0.17	0.17	228	0.5	0.15	1	0.21	2	0.22	N/A	N/A	N/A
					-2.0	-30	0.20			0.20			2	0.23				
LDABT40.1	Taft N21E 400%	0.75	251	56	0.5	-58	0.34	0.32	455	0.5	0.28	1	0.35	2	0.41	N/A	N/A	N/A
					-2.0	-60	0.35			0.43			2	0.45				
LDABK50.1	Kobe - Kobe 50%	0.37	219	21	0.5	46	0.29	0.25	285	0.5	0.22	1	0.27	2	0.33	N/A	N/A	N/A
					-2.0	42	0.32			0.33			2	0.36				
LDABS50.1	NR Sylmar 90° 50%	0.32	173	25	0.5	-30	0.18	0.18	240	0.5	0.16	1	0.19	2,3	0.21	N/A	N/A	N/A
					-2.0	-33	0.18			0.21			2	0.22				
LDABS10.1	NR Sylmar 90° 100%	0.67	357	53	0.5	-64	0.36	0.35	479	0.5	0.31	1	0.59	2	0.43	N/A	N/A	N/A
					-2.0	-67	0.36			0.69			2	0.44				
LDABNH7.1	NR Newhall 90° 75%	0.78	232	30	0.5	-39	0.24	0.22	316	0.5	0.19	1	0.24	2	0.27	N/A	N/A	N/A
					-2.0	-40	0.32			0.28			1	0.31				
LDABN50.1	NR Newhall 360° 50%	0.41	212	29	0.5	-39	0.26	0.22	302	0.5	0.21	1	0.23	3	0.29	N/A	N/A	N/A
					-2.0	-42	0.25			0.28			2	0.33				
LDALE10.1	El Centro S00E 100%	0.32	160	27	0.5	-16	0.18	0.14	172	0.5	0.12	1	0.13	5	0.23	7.7	12	124
					-2.0	-18	0.22			0.18			2	0.28	7.8	12	123	
LDALE20.1	El Centro S00E 200%	0.68	325	58	0.5	-34	0.30	0.24	325	0.5	0.21	1	0.25	3	0.38	15.7	25	257
					-2.0	-37	0.35			0.32			2	0.43	16.7	27	263	
LDALE20.1	Taft N21E 200%	0.33	123	28	0.5	-19	0.16	0.15	167	0.5	0.14	1	0.14	3	0.23	7.7	14	123
					-2.0	-21	0.20			0.19			2	0.26	7.9	15	127	
LDALE40.1	Taft N21E 400%	0.72	260	56	0.5	-40	0.29	0.27	318	0.5	0.25	1	0.32	3	0.43	14.4	30	233
					-2.0	-43	0.38			0.41			2	0.47	14.9	31	238	
LDALK50.1	Kobe - Kobe 50%	0.37	215	21	0.5	23	0.27	0.19	207	0.5	0.19	1	0.21	5	0.36	12.1	16	188
					-2.0	21	0.31			0.28			2	0.39	12.4	19	184	
LDALS50.1	NR Sylmar 90° 50%	0.32	174	25	0.5	-20	0.17	0.16	188	0.5	0.15	1	0.13	3	0.19	7.0	15	118
					-2.0	-21	0.22			0.17			2	0.23	7.9	16	126	
LDALS10.1	NR Sylmar 90° 100%	0.67	347	53	0.5	-42	0.34	0.30	353	0.5	0.26	1	0.32	3	0.35	13.7	31	220
					-2.0	-43	0.41			0.38			2	0.40	14.9	33	246	
LDALNH7.1	NR Newhall 90° 75%	0.78	229	29	0.5	-22	0.29	0.17	239	0.5	0.16	1	0.20	5	0.36	11.5	17	192
					-2.0	-24	0.36			0.24			2,5	0.45	11.7	18	191	
LDALN50.1	NR Newhall 360° 50%	0.40	205	29	0.5	-22	0.22	0.22	226	0.5	0.21	1	0.23	2,5	0.32	13.9	17	213
					-2.0	-25	0.25			0.29			2	0.32	15.0	18	216	
LDANE10.1	El Centro S00E 100%	0.32	158	27	0.5	-9	0.25	0.18	169	0.5	0.17	1	0.18	3,5	0.42	15.4	8	103
					-2.0	-11	0.36			0.29			2	0.47	14.3	8	120	
LDANE20.1	El Centro S00E 200%	0.70	325	57	0.5	-24	0.38	0.27	320	0.5	0.25	1	0.27	3	0.58	19.7	17	234
					-2.0	-26	0.57			0.43			2	0.73	19.3	20	244	
LDANT20.1	Taft N21E 200%	0.34	130	28	0.5	-11	0.25	0.17	168	0.5	0.16	2	0.21	5	0.36	14.8	8	98
					-2.0	-14	0.39			0.24			2	0.42	14.8	10	111	
LDANT40.1	Taft N21E 400%	0.71	261	56	0.5	-30	0.40	0.30	301	0.5	0.27	1	0.30	3	0.55	20.1	22	236
					-2.0	-33	0.59			0.39			2	0.60	19.4	25	238	
LDANK50.1	Kobe - Kobe 50%	0.35	218	21	0.5	-16	0.27	0.22	187	0.5	0.21	1	0.23	5	0.47	18.7	12	200
					-2.0	-18	0.37			0.29			2	0.44	17.8	12	201	
LDANS50.1	NR Sylmar 90° 50%	0.30	171	25	0.5	-15	0.26	0.21	165	0.5	0.18	1	0.18	3	0.36	16.0	11	123
					-2.0	-17	0.31			0.24			2	0.43	15.3	12	122	
LDANS10.1	NR Sylmar 90° 100%	0.68	341	51	0.5	-35	0.46	0.33	340	0.5	0.29	1	0.36	3	0.49	20.7	25	250
					-2.0	-36	0.63			0.44			2	0.65	20.5	28	275	
LDANNH7.1	NR Newhall 90° 75%	0.75	227	29	0.5	-15	0.43	0.23	241	0.5	0.22	1	0.24	3	0.50	19.1	11	179
					-2.0	-16	0.70			0.39			2	0.69	18.4	14	191	
LDANN50.1	NR Newhall 360° 50%	0.39	207	29	0.5	17	0.26	0.23	219	0.5	0.21	1	0.23	3	0.39	18.1	11	174
					-2.0	15	0.38			0.27			2	0.45	17.6	13	191	

1. Residual Displacement

**TABLE 4-14 Peak Response of Isolated Asymmetrically Braced Frame Structure with Lead-Core Bearings** (values are in units of g for acceleration, mm/s for velocity and mm for displacement)

Test	Excitation	Peak Table Motion			Peak Isolation System Response						Peak Superstructure Response				
		Accel	Vel.	Disp.	Initial Disp.	Isol. Disp.	Base Accel.	Base Shear/W	Base Vel.	Res. <sup>1</sup> Disp.	Story Shear/W	Drift / Height (%)		Floor Accel.	
LCABE20.1	El Centro S00E 200%	0.71	334	56	-1.5	-31	0.41	0.31	329	-1.3	0.28	1	0.29	3	0.48
					0.0	-29	0.50			-0.3			0.37	2	0.58
LCABT40.1	Taft N21E 400%	0.68	265	56	-1.3	-36	0.39	0.33	377	-1.3	0.31	1	0.32	3	0.49
					-0.3	-36	0.52			0.3			0.41	2	0.63
LCABK10.1	Kobe - Kobe 100%	0.95	459	42	-1.3	-39	0.57	0.37	379	-2.0	0.33	1	0.42	2	0.61
					0.3	-38	0.71			-0.5			0.51	2	0.82
LCABS10.1	NR Sylmar 90° 100%	0.69	349	50	-2.0	-42	0.46	0.37	392	-2.3	0.32	1	0.36	3	0.53
					-0.5	-40	0.50			-0.8			0.43	2	0.64
LCABNH1.1	NR Newhall 90° 100%	1.07	313	46	-2.3	23	0.47	0.28	366	-1.5	0.27	1	0.31	2	0.56
					-0.8	26	0.69			0.0			0.41	2	0.71
LCABN10.1	NR Newhall 360° 100%	0.97	460	59	-1.5	49	0.50	0.43	425	-0.5	0.40	1	0.53	5	0.62
					0.0	50	0.62			-0.3			0.65	5	0.89

1. Residual Displacement

**TABLE 4-15 Peak Response of Isolated Asymmetrically Braced Frame Structure with Combined Low Damping Elastomeric and Flat Sliding Bearings** (values are in units of g for acceleration, mm/s for velocity and mm for displacement)

Test	Excitation	Peak Table Motion			Peak Isolation System Response						Peak Superstructure Response				
		Accel	Vel.	Disp.	Initial Disp.	Isol. Disp.	Base Accel.	Base Shear/W	Base Vel.	Res. <sup>1</sup> Disp.	Story Shear/W	Drift / Height (%)		Floor Accel.	
EFABE10.1	El Centro S00E 100%	0.34	165	27	-1.0	16	0.33	0.10	153	1.3	0.09	2,3	0.13	3,4	0.34
					-2.3	16	0.24			-0.3			0.11	2	0.29
EFABE20.1	El Centro S00E 200%	0.73	311	54	1.3	57	0.46	0.20	328	1.8	0.18	1	0.20	1,3	0.43
					-0.3	57	0.33			0.5			0.20	2	0.41
EFABT30.1	Taft N21E 300%	0.54	195	43	1.8	-34	0.44	0.16	230	-0.5	0.16	1	0.18	3	0.40
					0.5	-34	0.25			-1.3			0.16	2	0.36
EFABT20.1	Taft N21E 200%	0.34	127	27	-0.5	-17	0.30	0.11	150	0.0	0.11	3	0.14	3	0.32
					-1.3	-17	0.24			-1.3			0.11	2	0.34
EFABT40.1	Taft N21E 400%	0.72	253	56	0.0	-50	0.48	0.21	273	-0.3	0.19	1	0.22	3	0.43
					-1.3	-50	0.30			-1.3			0.20	2	0.38
EFABK50.1	Kobe - Kobe 50%	0.37	217	21	-0.3	18	0.33	0.11	131	0.3	0.12	2	0.14	3	0.37
					-1.3	18	0.28			-1.3			0.12	2	0.36
EFABS50.1	NR Sylmar 90° 50%	0.30	167	24	0.3	-24	0.26	0.13	162	-0.3	0.13	1	0.15	3	0.33
					-1.3	-24	0.20			-1.8			0.13	2	0.28
EFABS10.1	NR Sylmar 90° 100%	0.64	350	50	-0.3	-68	0.43	0.26	366	-0.3	0.24	1	0.29	3	0.43
					-1.8	-70	0.32			-1.3			0.31	2	0.38
EFABNH7.1	NR Newhall 90° 75%	0.76	234	30	-0.3	-22	0.48	0.12	225	0.5	0.11	2	0.15	3	0.43
					-1.3	-24	0.37			-0.8			0.13	2	0.39
EFABN50.1	NR Newhall 360° 50%	0.41	213	29	0.5	-22	0.30	0.13	173	-1.0	0.11	1	0.13	4	0.32
					-0.8	-22	0.20			0.0			0.11	2	0.28

1. Residual Displacement

## 4.5 Interpretation of Results

The experimental results in the preceding tables and in Appendix A contain a large amount of information that will be used in this section to assess the performance of the seismic isolation systems tested herein. Certain aspects of behavior of the tested isolation systems have been selected for further presentation and discussion. From these findings, some general conclusions of the performance of isolation systems may be drawn.

#### 4.5.1 Impact of Added Viscous Damping Devices

The elastomeric bearing and the Friction Pendulum systems were tested without and with added linear or nonlinear viscous damping devices. Damping devices have been used in isolation systems for reducing the displacement demand, although this may result in increased response of the superstructure, including the response of secondary systems. A comparison of peak response parameters that are relevant for the design of the isolation system and superstructure are presented in Figures 4-2 through 4-5 for each of the conducted tests. In these figures, the response is presented against the peak table velocity in each of the conducted tests. This single parameter describes well the intensity of the seismic input given that the isolated structural system is highly flexible (with period that falls in the velocity-controlled domain of the spectrum).

Figures 4-2 and 4-3 present the results for the Friction Pendulum system. The linear and nonlinear fluid viscous dampers provided the expected reduction in isolation system displacement, however, due to the high inherent damping of the FP system, the addition of damping devices also produced a substantial adverse effect on story drifts and shear forces. In general, the nonlinear damping devices resulted in a larger increase in story drifts and shear forces as compared with the linear viscous devices. It should be noted that use of damping devices in seismic isolation systems has been so far limited to nonlinear devices and to application of strong seismicity with near-fault effects. To the contrary, experimental results in Figures 4-2 and 4-3 indicate that the FP system without damping devices may provide better response characteristics than the same system with damping devices and with comparable isolation displacements in near-fault cases, which in Figures 4-2 through 4-5 are those with large table velocities (e.g., see cases with excitation of Kobe, Newhall 360°, or Pacoima S16E in Tables 4-4 and 4-9). It should be noted that these observations are based on results with FP bearings having rather high friction (about 0.08). It is likely that the addition of damping devices in low friction FP systems may prove to be beneficial.

The results in Figures 4-4 and 4-5 for the elastomeric bearing system with viscous dampers again demonstrate that the addition of dampers results in substantial reduction of isolation system displacement (this was expected given that the elastomeric bearing system was lightly damped). However, the addition of damping devices to the elastomeric bearing system also generated a reduction of story drifts and shear forces. This is also explained by the low damping capacity of the elastomeric bearings.

Based on the results of Figures 4-2 through 4-5, some general conclusions may be drawn on the effects of linear and nonlinear damping devices on systems of various inherent damping. It would appear that linear damping devices, in general, provide better response characteristics than nonlinear damping devices. However, in the case of a lightly damped system, like the low damping elastomeric bearing system in Figures 4-4 and 4-5, the nonlinear dampers provided markedly better performance than the linear dampers at reducing isolation displacements without an increased penalty in structural response. Furthermore, the addition of dampers to highly damped systems, like the tested FP system, provides for a small reduction of isolation displacements with a substantial increase in structural response.

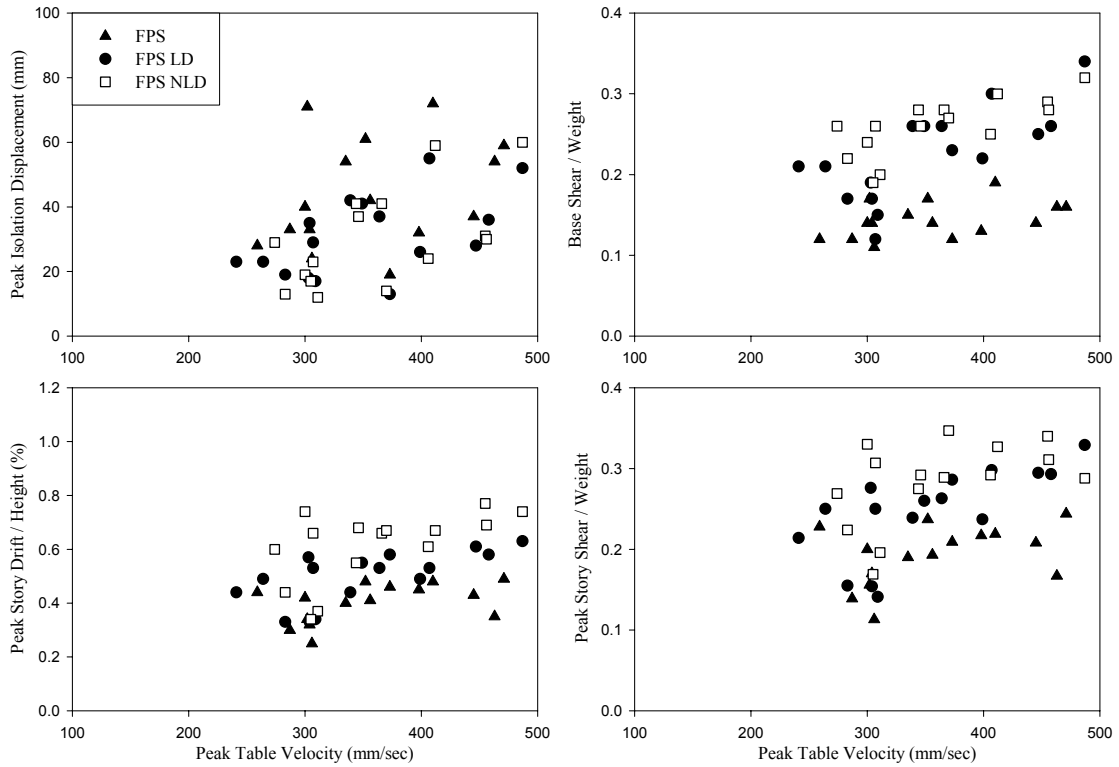


**FIGURE 4-2 Comparison of Peak Response Values of Isolated Moment Frame Structure with Friction Pendulum Bearings and Viscous Dampers**

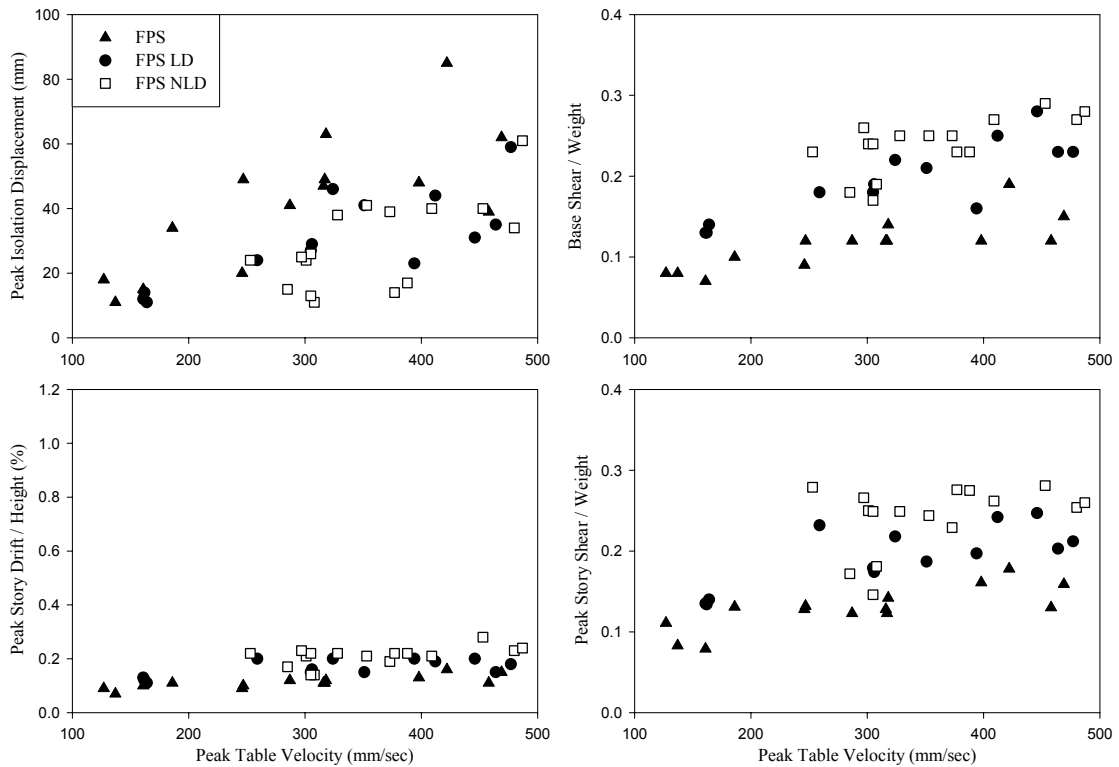


**FIGURE 4-3 Comparison of Peak Response Values of Isolated Braced Frame Structure with Friction Pendulum Bearings and Viscous Dampers**



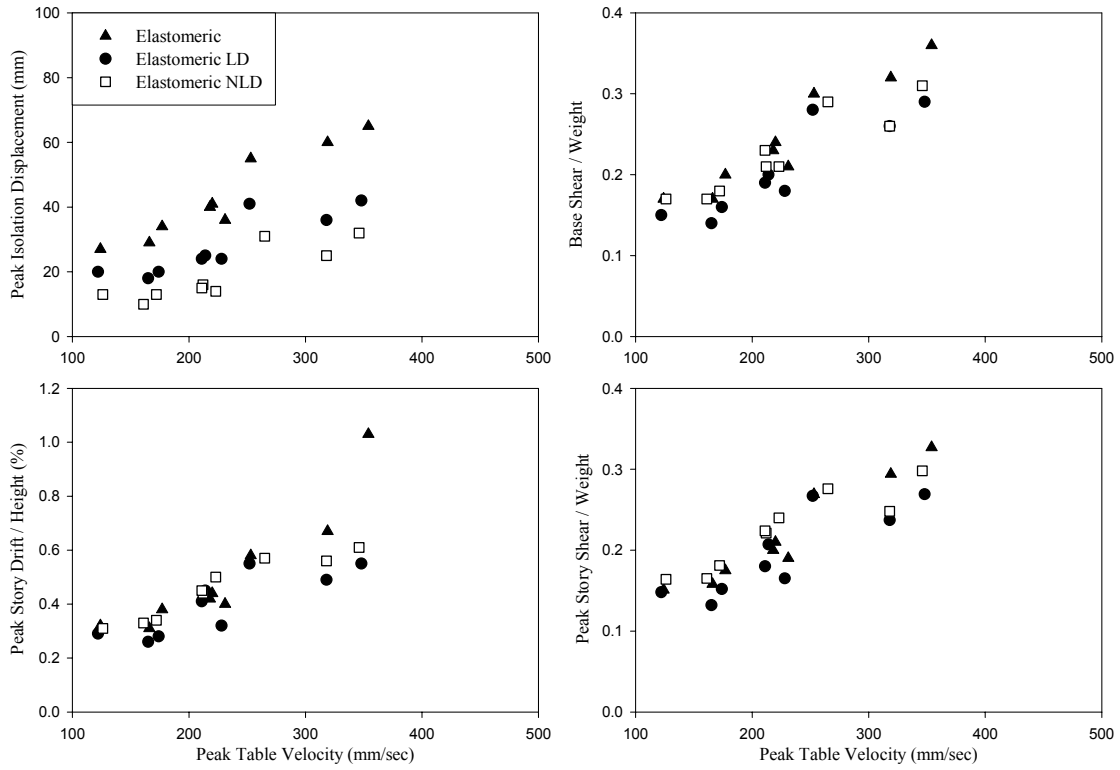


**FIGURE 4-4 Comparison of Peak Response Values of Isolated Moment Frame Structure with Elastomeric Bearings and Viscous Dampers**

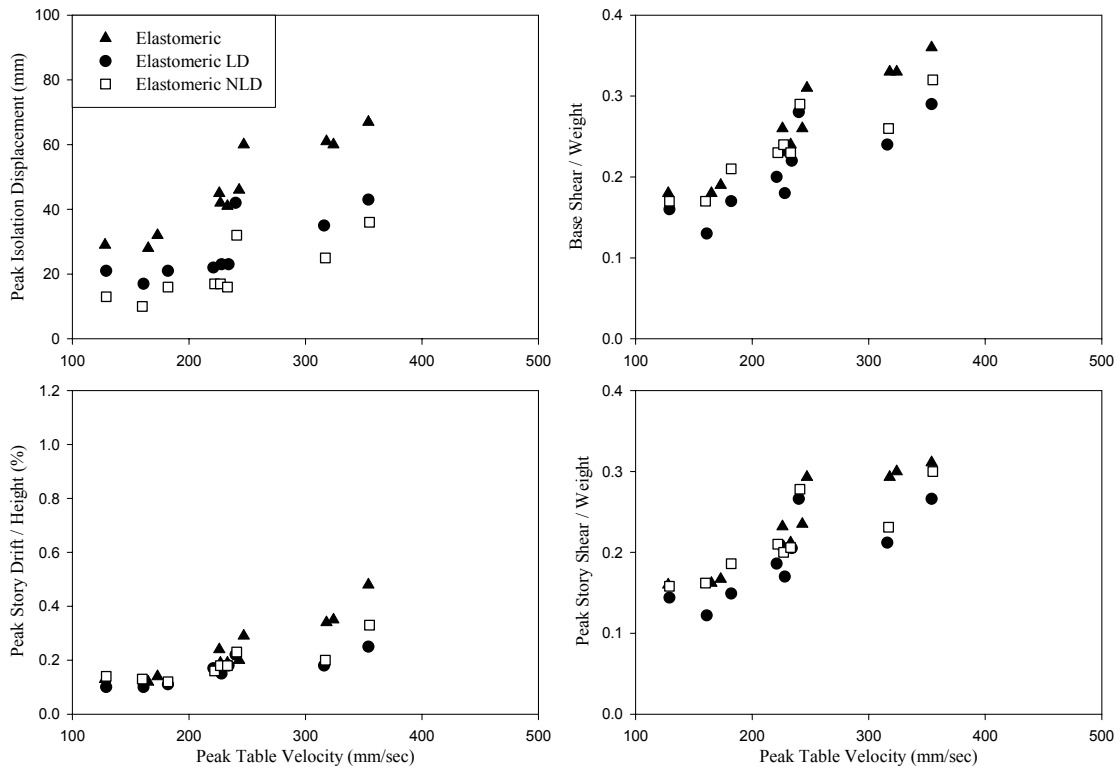


**FIGURE 4-5 Comparison of Peak Response Values of Isolated Braced Frame Structure with Elastomeric Bearings and Viscous Dampers**

#### 4.5.2 Primary and Secondary System Response

The response of secondary systems is affected by a variety of parameters, including story drifts, floor velocities and floor accelerations. As discussed in Section 2, there is no single parameter that can be used to assess the performance of secondary systems. On the other hand, the design of the primary system is dependent on a few parameters such as the base shear force and the story drifts.

Herein we look at both the response of the primary and secondary systems in the tested isolated structures. For the primary system response, the isolation system displacement, base shear force and story drifts are used as the key parameters. For the secondary systems, the story drifts, peak total floor velocity, peak total floor acceleration and the floor spectral accelerations over the range of 0.1 to 20 Hz are used as key response parameters.

Figures 4-6 through 4-9 present 5%-damped floor response spectra of the isolated moment frame and symmetrically braced frame structures in the El Centro S00E 200% and Sylmar 90° 100% tests. El Centro represents a strong far-field motion with high frequency content, while the Sylmar motion is a very strong near-field motion. The floor spectra were derived from the recorded floor acceleration histories for four isolation systems that are identified in the figures. The combined system of elastomeric and flat sliding bearings was not tested for the moment frame condition with the Sylmar 100% excitation, and is therefore not presented. All other plots compare the response spectra of the base, third and fifth floor for the following isolation systems: Friction Pendulum, elastomeric bearings, combined flat sliding and elastomeric bearings, and elastomeric bearings with linear dampers. All of the isolation systems shown have basically the same effective period, in the range of about 0.9 to 1.2 seconds. Furthermore, Figure 4-6 also contains the floor spectra of the fixed base response of the moment frame structure to the El Centro S00E 30% excitation scaled up by a factor of 3.3 to the 100% level. It was determined by analysis that, approximately, the 100% El Centro motion would have induced only minor inelastic action in the non-isolated frame, so that the presented floor response spectra are valid.

Figures 4-6 through 4-9 present the experimental results so as to evaluate how different isolation systems affect different secondary system response quantities. The plots demonstrate large differences in the floor spectral response for frequencies in the neighborhood of the effective frequency of the isolated structure. Of interest is to observe the substantially smaller floor spectral values in the neighborhood of the fundamental frequency for the two sliding systems. It should be noted that the elastomeric system with linear dampers has a larger effective damping than the combined flat sliding and elastomeric system, but yet it has larger floor spectral response. This leads to the conclusion that the degree of nonlinearity of the isolation system may be as important as the effective damping of the system in reducing the floor spectral response in the neighborhood of the fundamental frequency. For example, in Figure 4-6, there is an expected reduction in response of the elastomeric system when linear dampers are added, increasing the effective damping, however, the combined flat sliding and elastomeric system with less effective damping but a higher degree of nonlinearity provided even lesser response. Furthermore, the FP system with an even higher degree of nonlinearity and a larger effective damping produced the least response of all the systems.

Figures 4-6 through 4-9 also present information on the floor spectral acceleration response in the high frequency range. For flexible structural systems, as shown in Figures 4-6 and 4-7, the purely elastomeric system provides a slightly better response as compared to the other systems, but it should be noted that the difference is small and at higher frequencies (i.e., approaching conditions of rigidly attached components) the responses of various systems tend to converge. Furthermore, for stiff structural systems, as shown in Figure 4-8 and 4-9, the elastomeric systems provide nearly identical response as the highly nonlinear systems. These results tend to disprove the generally accepted view that highly nonlinear systems, such as those presented here, “have very high attack on building contents” by affecting a larger response in the higher modes of the structure (Skinner et al., 1993). Instead, the nonlinear systems tend to cause a lesser response at the fundamental frequency with comparable response at higher modes, eventually converging with elastomeric systems.

On the basis of the results in these figures and considering the performance of numerous secondary systems in a building structure, which are affected by spectral accelerations over a wide range of frequencies, the Friction Pendulum and the combined elastomeric/sliding isolation systems are likely to have the least impact on the contents of the building. Interestingly, these two systems are highly nonlinear, whereas the other two are typically presumed to be linear elastic and linear viscous.

In addition to the information presented on Figures 4-7 through 4-9, Figure 4-6 presents the fixed base response to the El Centro 30% excitation scaled up to 100%. Even though this excitation is only half that of the isolated system excitation, the dramatic reduction in floor spectral response is evident.

Tables 4-16 thru 4-19 present a comparison of peak response quantities, derived from experimental data, relevant to both primary and secondary system performance assessment. The tables include information on the isolation system, its effective properties (period and damping per the definitions of the 2000 International Building Code (ICC, 2001), for the isolation system displacement recorded in the experiment), the isolation system peak response, the superstructure peak story shear force and inter-story drift and secondary system response parameters for the base, 3<sup>rd</sup> floor and 5<sup>th</sup> floors. These response parameters are the peak acceleration recorded at that floor, the peak value of the spectral acceleration for a 5%-damped attachment to the floor and for the frequency range of 0.1 to 20 Hz, and the peak total floor velocity.

The data in these tables lead to a number of interesting observations:

- a) The addition of fluid viscous damping devices to already highly damped hysteretic systems, such as the tested FP system, provides little benefit to the structural response. While the isolator displacements are substantially reduced, there were penalties in terms of increased forces, drifts, accelerations and velocities, all of which impact primary and secondary system performance.

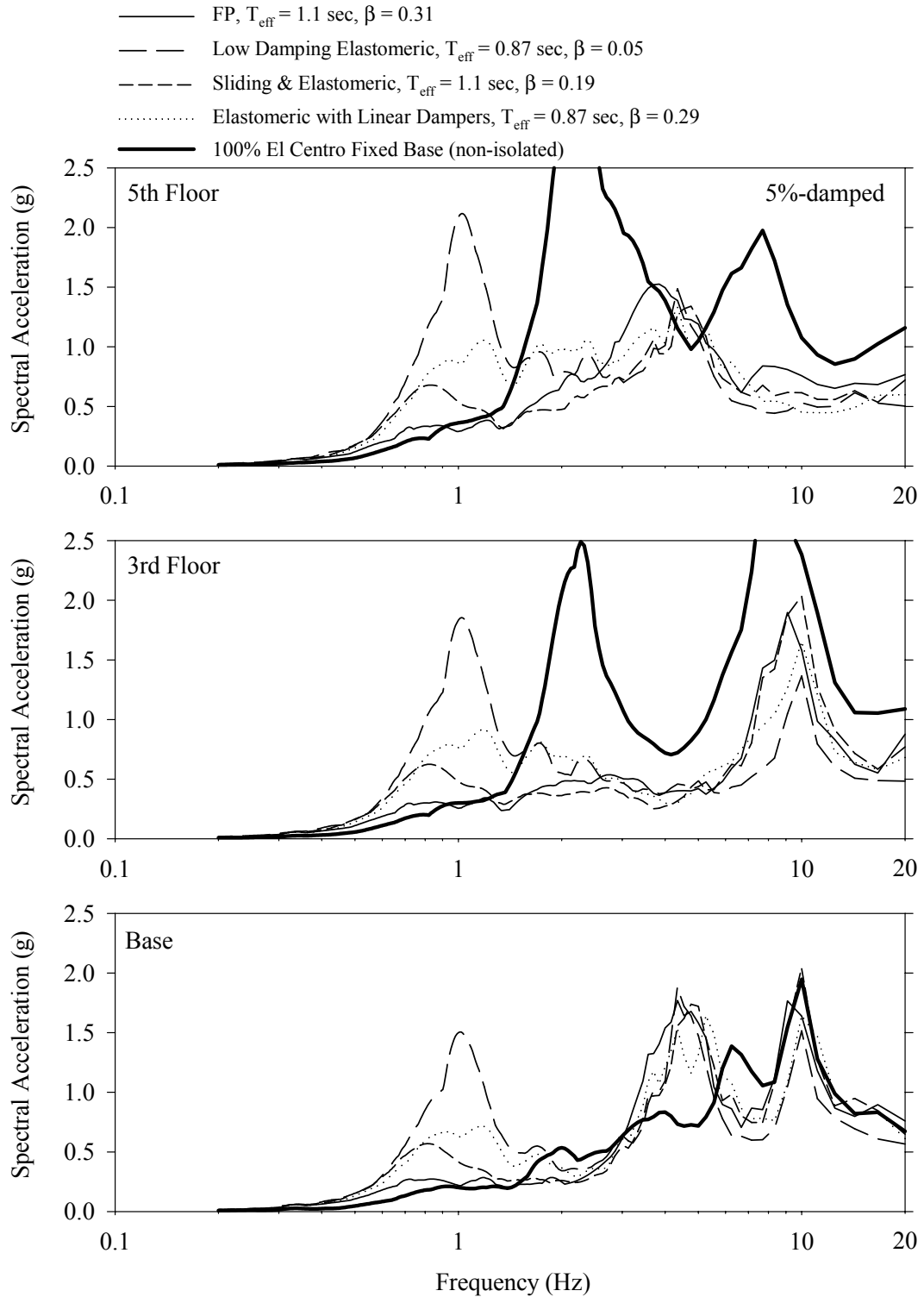


**FIGURE 4-6 Floor Response Spectra of Isolated Moment Frame Structure for the El Centro S00E 200% Excitation**

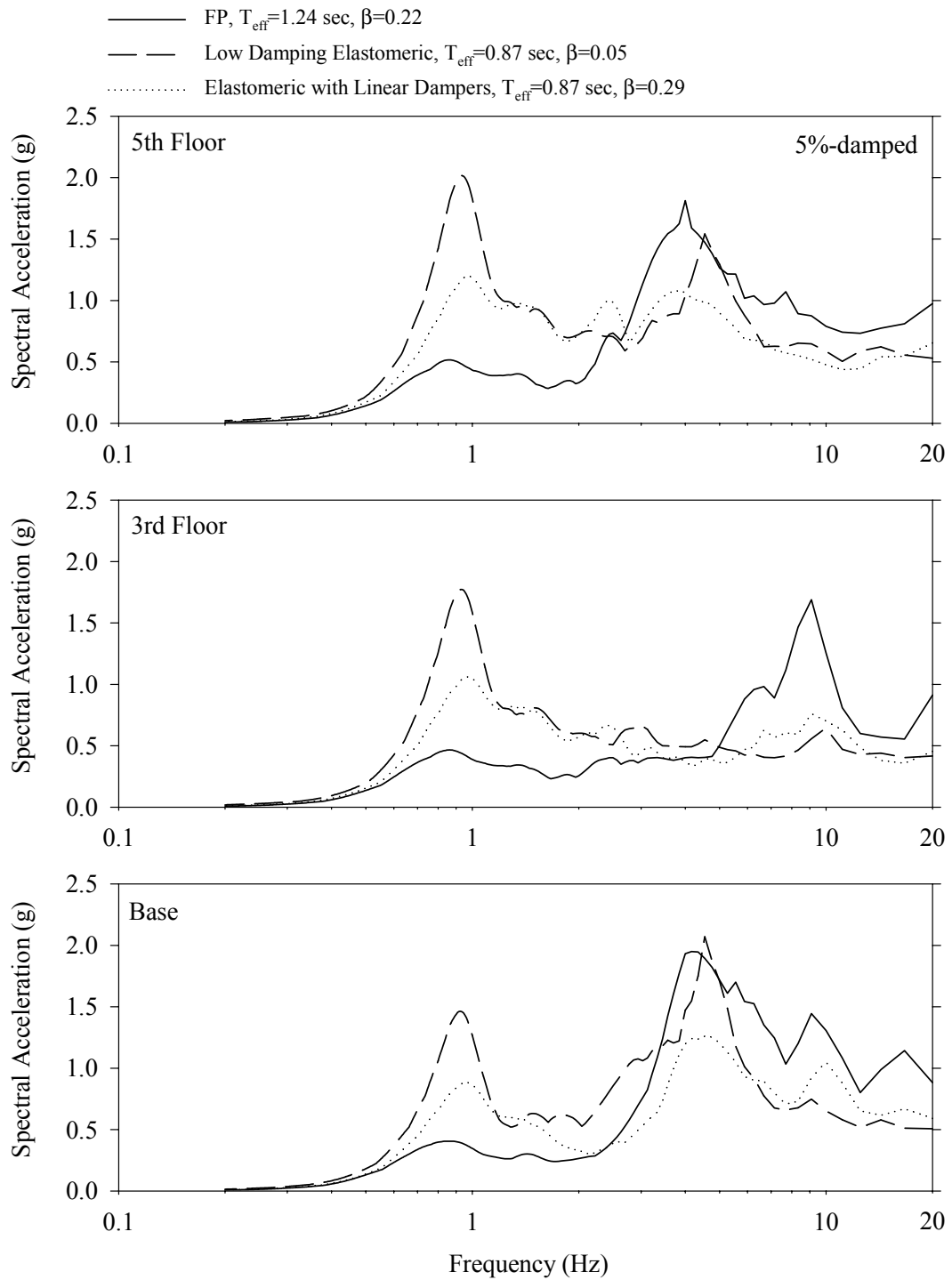


**FIGURE 4-7 Floor Response Spectra of Isolated Moment Frame Structure for the Sylmar 90° 100% Excitation**

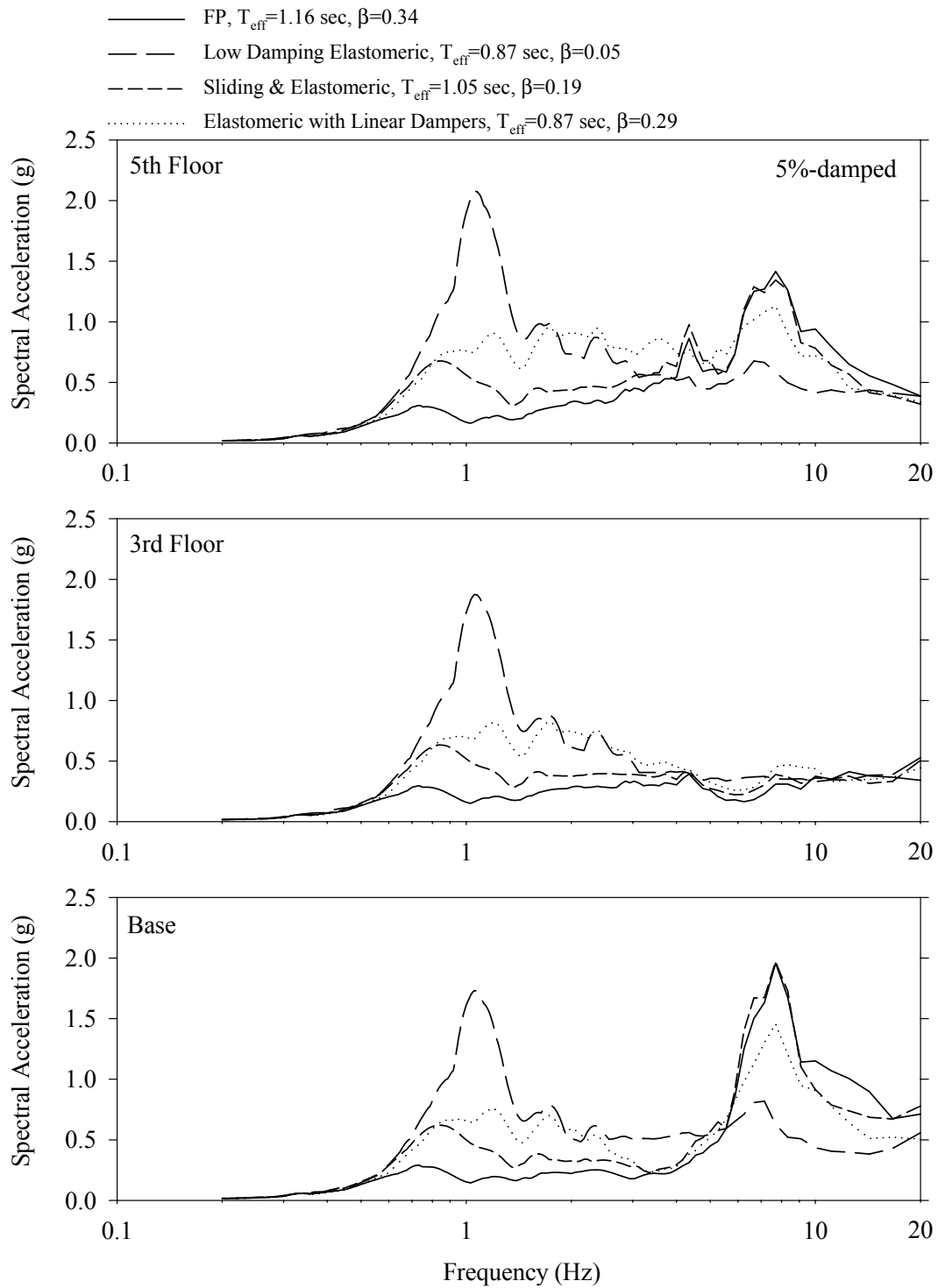


**FIGURE 4-8 Floor Response Spectra of Isolated Braced Frame Structure for the El Centro S00E 200% Excitation**

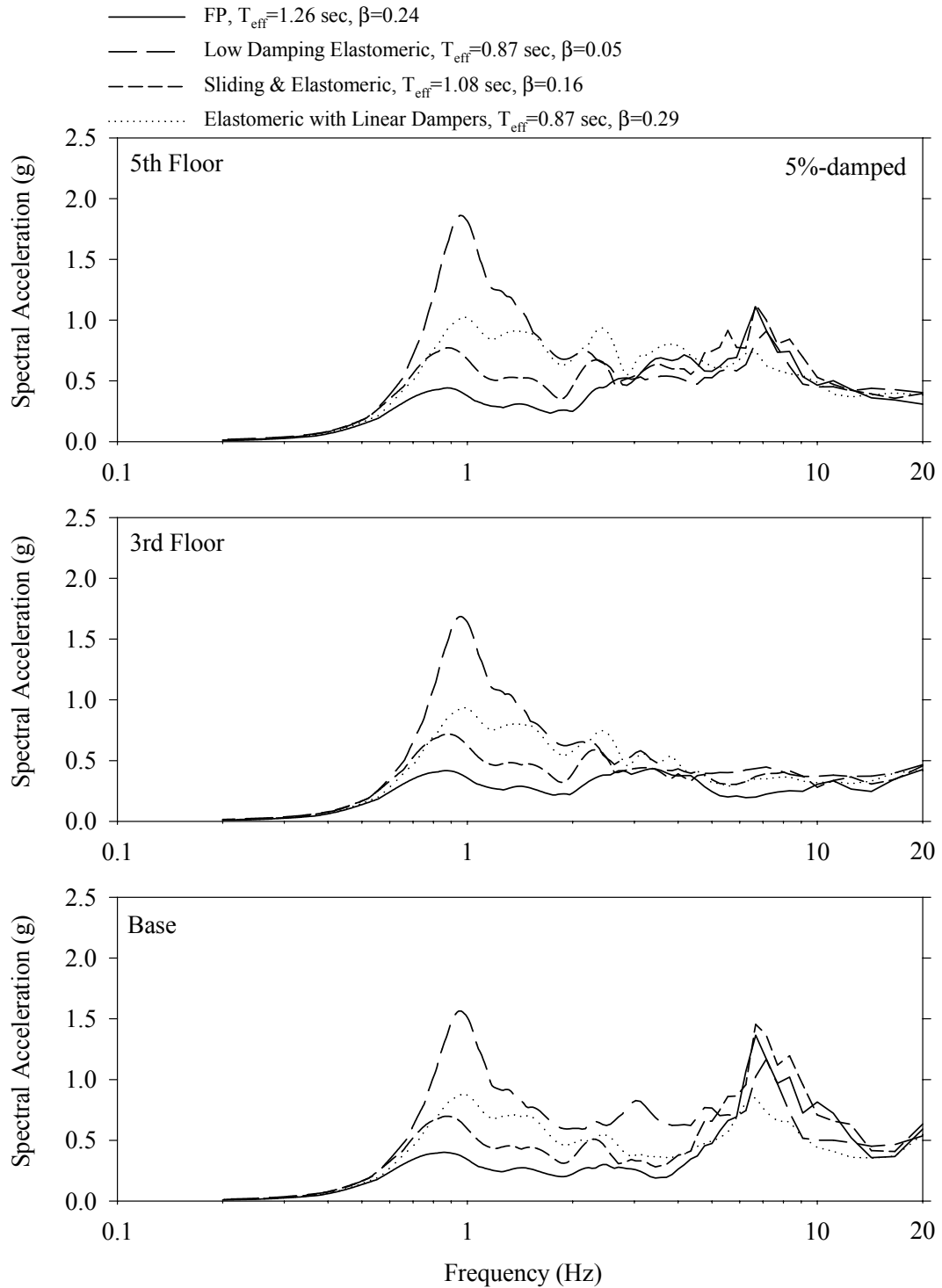


**FIGURE 4-9 Floor Response Spectra of Isolated Braced Frame Structure for the Sylmar 90° 100% Excitation**

- b) The peak floor acceleration varies over the height of the building. In general, the acceleration is magnified from the base above the isolators to the roof and the magnification depends on the degree of nonlinearity of the isolation system and the stiffness of the structural system. For example, in the case of the flexible moment frame, the magnification of acceleration over the height (roof to base) is 1.0 for the low damping elastomeric system, and between 1.16 and 1.45 for the sliding systems, depending on the value of the friction coefficient (friction coefficient of about 0.05 for the amplification factor of 1.16 and friction coefficient of about 0.08 for the amplification factor of 1.45). Such behavior is well understood and typically conveyed in comparisons of seismic isolation systems (e.g., Skinner et al., 1993; Naeim and Kelly, 1999). It should be noted that the fixed-base period of the moment-frame model is 0.43 sec (or 0.86 sec in prototype scale), whereas the effective period of the isolation system is of the order of 1.0 sec (or 2.0 sec in prototype scale).
- c) A very different picture emerges when the floor acceleration response in the braced frame model is investigated. The braced frame in its fixed-base condition had a fundamental period of 0.25 sec (or 0.5 sec in prototype scale). In this case, the ratio of effective period of the isolated structure to the fixed-base period is equal to about 4, whereas in the case of the moment frame the ratio is equal to about 2.3. As seen in the results of Tables 4-18 and 4-19 there is very little amplification of acceleration over the height of the model for all tested isolation systems. Interestingly, the two tested sliding systems without damping devices show even a reduction of acceleration over the height.
- d) The peak floor acceleration values in units of g are typically larger, and in highly nonlinear systems substantially larger, than the peak base shear normalized by the weight. This demonstrates that the dynamic response is strongly affected by higher mode contributions so that the peak floor accelerations occur at different times. This is true even for the low damping elastomeric system.
- e) The peak total floor velocity has been shown to affect the response of high profile objects that are not rigidly attached to the floor (see Section 2). Values of this velocity vary dramatically for the various tested isolation systems. The smallest velocity was typically recorded for the FP isolation system, whereas the largest velocities were recorded for the low damping elastomeric system. The ratio of highest to lowest velocity was typically of the order of 1.5 for the flexible superstructure and over 2.0 for the stiff superstructure. Such substantial differences in velocity response should not be disregarded in the assessment of performance of secondary systems.
- f) Drift is a response quantity of importance in the assessment of performance of secondary systems such as vertical pipes, conduits and wall attachments. Drift in the tested isolation systems was systematically least (and often substantially less) in the FP and the combined elastomeric-sliding system.



**TABLE 4-16 Comparison of Peak Response Quantities of Isolated Moment Frame Structure in El Centro S00E 200%**

Isolation System	Effective Period (sec)	Effective Damping	Peak Isolator Disp. (mm)	Peak Base Shear/Weight	Peak Story Shear/Weight	Peak Drift/Height (%)	Peak Base Response			Peak 3 <sup>rd</sup> Floor Response			Peak 5 <sup>th</sup> Floor Response			Peak Roof Accel (g)
							Accel (g)	Spectral Accel. (g)	Vel. (mm/s)	Accel (g)	Spectral Accel. (g)	Vel. (mm/s)	Accel (g)	Spectral Accel. (g)	Vel. (mm/s)	
Low Damping Elastomeric	0.87	0.05	60	0.32	0.29	0.67	0.54	1.88	409	0.45	1.85	506	0.41	2.12	585	0.54
Low Damping Elastomeric-Linear Dampers	0.87	0.29	36	0.26	0.24	0.49	0.45	1.64	312	0.35	1.65	406	0.40	1.33	480	0.52
Low Damping Elastomeric-Nonlinear Dampers	0.87	0.27	25	0.26	0.25	0.56	0.66	2.36	296	0.45	1.64	368	0.63	1.57	453	0.78
Low Damping Elastomeric-Flat Sliding Bearing	1.05	0.19	57	0.21	0.17	0.36	0.55	2.04	344	0.37	2.03	314	0.38	1.34	354	0.64
FPS	1.10	0.31	40	0.14	0.20	0.42	0.55	1.77	237	0.35	1.90	227	0.51	1.52	302	0.80
FPS-Linear Dampers	0.99	0.60	29	0.12	0.25	0.53	0.56	1.88	241	0.54	1.95	286	0.64	1.81	313	0.81
FPS-Nonlinear Dampers	0.92	0.67	23	0.26	0.31	0.66	0.56	2.03	240	0.64	2.21	337	0.79	2.07	377	0.95
Lead-Core	0.59	0.28	30	0.31	0.28	0.54	0.66	2.45	341	0.51	1.83	402	0.47	1.80	480	0.71

**TABLE 4-17 Comparison of Peak Response Quantities of Isolated Moment Frame Structure in Sylmar 90°**

Isolation System	Effective Period (sec)	Effective Damping	Peak Isolator Disp. (mm)	Peak Base Shear/Weight	Peak Story Shear/Weight	Peak Drift/Height (%)	Peak Base Response			Peak 3 <sup>rd</sup> Floor Response			Peak 5 <sup>th</sup> Floor Response			Peak Roof Accel (g)
							Accel (g)	Spectral Accel. (g)	Vel. (mm/s)	Accel (g)	Spectral Accel. (g)	Vel. (mm/s)	Accel (g)	Spectral Accel. (g)	Vel. (mm/s)	
Low Damping Elastomeric	0.87	0.05	65	0.36	0.33	1.03	0.48	2.07	473	0.39	1.77	581	0.52	2.02	656	0.54
Low Damping Elastomeric-Linear Dampers	0.87	0.29	42	0.29	0.27	0.55	0.45	1.26	354	0.33	1.06	417	0.46	1.20	472	0.54
Low Damping Elastomeric-Nonlinear Dampers	0.87	0.24	32	0.31	0.30	0.61	0.61	1.49	315	0.46	1.36	373	0.60	1.40	436	0.76
Low Damping Elastomeric-Flat Sliding Bearing	N/A	N/A	N/A	N/A	N/A	N/A	N/A	N/A	N/A	N/A	N/A	N/A	N/A	N/A	N/A	N/A
FPS	1.24	0.22	61	0.17	0.24	0.48	0.65	1.95	286	0.39	1.69	314	0.59	1.81	382	0.84
FPS-Linear Dampers	1.11	0.49	41	0.26	0.26	0.55	0.60	1.79	286	0.41	1.64	303	0.63	1.67	399	0.87
FPS-Nonlinear Dampers	1.07	0.49	37	0.26	0.29	0.68	0.65	1.71	287	0.48	1.63	296	0.65	1.98	433	0.86
Lead-Core	0.63	0.28	40	0.35	0.30	0.63	0.60	2.16	417	0.46	1.66	393	0.50	1.70	463	0.64

**TABLE 4-18 Comparison of Peak Response Quantities of Isolated Braced Frame Structure in El Centro S00E 200%**

Isolation System	Effective Period (sec)	Effective Damping	Peak Isolator Disp. (mm)	Peak Base Shear/Weight	Peak Story Shear/Weight	Peak Drift/Height (%)	Peak Base Response			Peak 3 <sup>rd</sup> Floor Response			Peak 5 <sup>th</sup> Floor Response			Peak Roof Accel (g)
							Accel (g)	Spectral Accel. (g)	Vel. (mm/s)	Accel (g)	Spectral Accel. (g)	Vel. (mm/s)	Accel (g)	Spectral Accel. (g)	Vel. (mm/s)	
Low Damping Elastomeric	0.87	0.05	60	0.33	0.30	0.35	0.38	1.73	445	0.34	1.87	485	0.37	2.08	521	0.38
Low Damping Elastomeric-Linear Dampers	0.87	0.29	35	0.24	0.21	0.18	0.39	1.46	349	0.25	0.82	388	0.28	1.13	419	0.41
Low Damping Elastomeric-Nonlinear Dampers	0.87	0.27	25	0.26	0.23	0.20	0.51	2.39	319	0.32	1.04	363	0.46	1.75	413	0.54
Low Damping Elastomeric-Flat Sliding Bearing	1.05	0.19	55	0.20	0.18	0.15	0.47	1.97	330	0.31	0.63	380	0.41	1.34	432	0.43
FPS	1.16	0.34	49	0.12	0.12	0.11	0.50	1.96	194	0.14	0.41	171	0.28	1.42	185	0.45
FPS-Linear Dampers	0.97	0.64	27	0.18	0.18	0.15	0.53	1.85	199	0.25	0.72	225	0.38	1.39	256	0.49
FPS-Nonlinear Dampers	0.93	0.65	24	0.24	0.25	0.21	0.57	2.32	242	0.32	1.08	296	0.48	1.72	338	0.64
Lead-Core	0.62	0.30	30	0.30	0.28	0.23	0.54	2.65	374	0.21	1.10	313	0.29	1.77	333	0.61

**TABLE 4-19 Comparison of Peak Response Quantities of Isolated Braced Frame Structure in Sylmar 90° 100%**

Isolation System	Effective Period (sec)	Effective Damping	Peak Isolator Disp. (mm)	Peak Base Shear/Weight	Peak Story Shear/Weight	Peak Drift/Height (%)	Peak Base Response			Peak 3 <sup>rd</sup> Floor Response			Peak 5 <sup>th</sup> Floor Response			Peak Roof Accel (g)
							Accel (g)	Spectral Accel. (g)	Vel. (mm/s)	Accel (g)	Spectral Accel. (g)	Vel. (mm/s)	Accel (g)	Spectral Accel. (g)	Vel. (mm/s)	
Low Damping Elastomeric	0.87	0.05	67	0.36	0.31	0.48	0.41	1.56	481	0.37	1.68	506	0.40	1.86	550	0.48
Low Damping Elastomeric-Linear Dampers	0.87	0.29	43	0.29	0.27	0.25	0.33	0.88	362	0.30	0.93	399	0.36	1.02	433	0.37
Low Damping Elastomeric-Nonlinear Dampers	0.87	0.22	36	0.32	0.30	0.33	0.47	1.33	331	0.35	1.09	356	0.43	1.38	400	0.52
Low Damping Elastomeric-Flat Sliding Bearing	1.08	0.16	72	0.26	0.23	0.22	0.44	1.45	381	0.37	0.72	388	0.50	1.13	407	0.38
FPS	1.26	0.24	65	0.15	0.15	0.13	0.35	1.36	290	0.18	0.46	286	0.26	1.10	326	0.33
FPS-Linear Dampers	1.11	0.49	41	0.21	0.19	0.15	0.39	1.06	267	0.28	0.78	294	0.37	1.10	338	0.45
FPS-Nonlinear Dampers	1.11	0.50	41	0.25	0.24	0.21	0.51	0.82	289	0.34	1.10	323	0.49	1.48	381	0.61
Lead-Core	0.64	0.32	42	0.37	0.35	0.32	0.50	1.57	373	0.29	1.23	352	0.33	1.52	394	0.55

### **4.5.3 Torsional Response in Asymmetric Seismically Isolated Buildings**

Experimental studies of asymmetric seismically isolated buildings are limited to the work of Zayas et al. (1987) on the FP isolation system. Eccentricities in the structural system were created by shifting the mass, which did not have any adverse effect on the response because of the unique property of FP bearings to produce a lateral force that is proportional to the vertical load.

Other work, such as Jangid and Dutta (1994) and Nagarajaiah et al. (1993a, 1993b) dealt with the effects of torsional coupling in analytical studies. These studies conclude that eccentricity in the superstructure may have a substantial effect on the response of the isolation system, particularly in isolated structures with a torsionally flexible superstructure.

The tested asymmetric seismically isolated model did not exhibit the torsional flexibility identified in Nagarajaiah et al. (1993a, 1993b), which is a highly unlikely situation, but had a substantial eccentricity between the center of mass (which was aligned with the center of rigidity of the isolation system) and the center of rigidity of the superstructure. The superstructure consisted of two frames at a distance of 1220 mm, with the braced frame having a stiffness approximately 2.5 times larger than the stiffness of the unbraced frame. Effectively, the center of rigidity was at a distance of about 260 mm from the center of mass, creating an eccentricity of 21% of the plan dimension perpendicular to the direction of seismic excitation. The eccentricity was purely due to asymmetry in the structural stiffness and not due to the distribution of mass.

Eccentricities of this order would have induced a substantial torsional response in a fixed base structure. However, for seismically isolated structures the torsional response is expected to be small as demonstrated by analysis by Eisenberger and Rutenberg (1986). Indeed, the experimental results confirm this. For each tested configuration, the ratio of the peak corner bearing displacement to the average bearing displacement is calculated for all tested excitations and plotted in Figures 4-10 to 4-12 versus the peak table velocity for the corresponding excitation. This ratio, which represents the magnification of the isolation system displacement due to the eccentricity, is plotted against the peak table velocity for each conducted test. The ratio is in the range of 1.0 to 1.1 and the torsional response is minimal despite the large eccentricity.

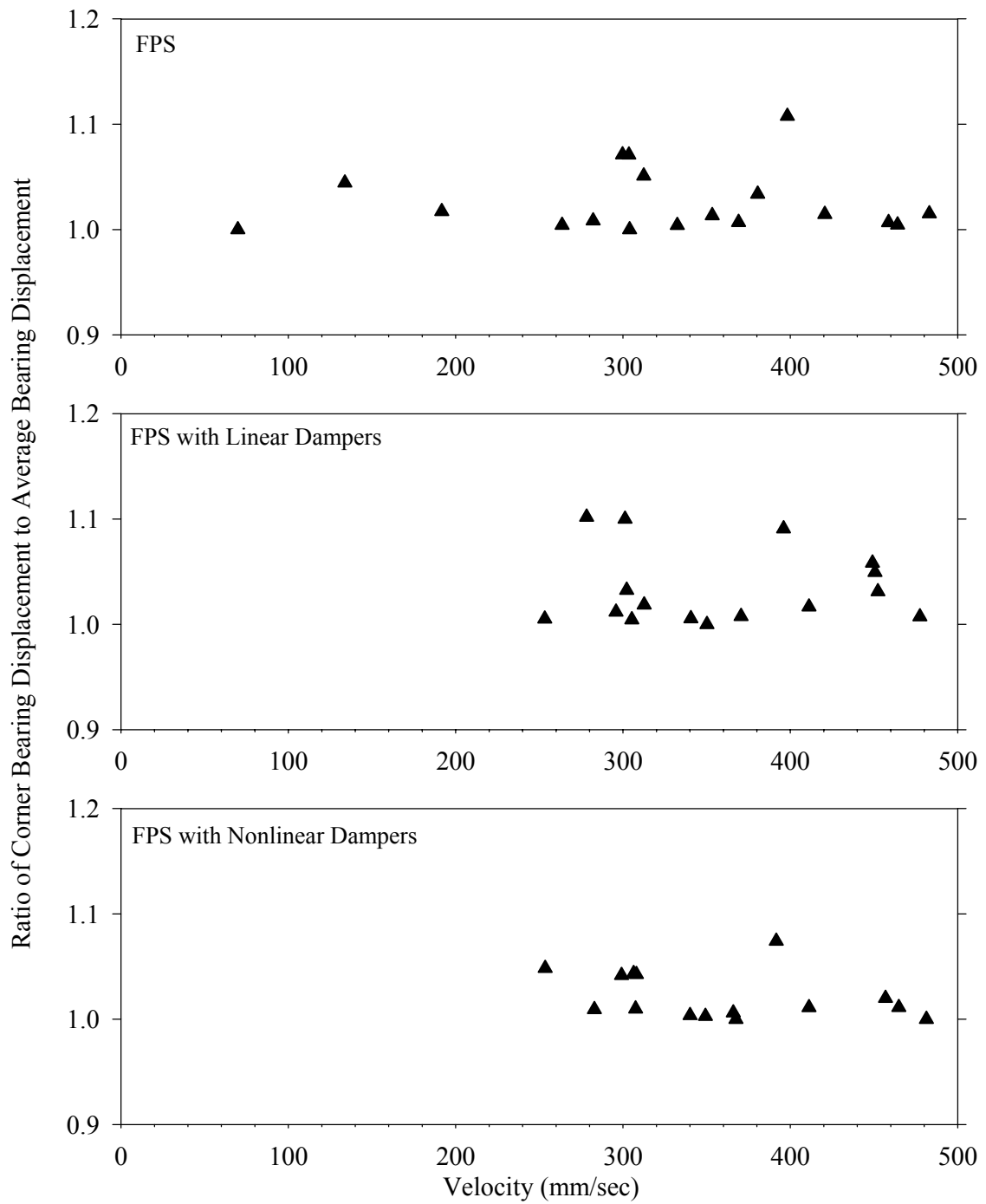


**FIGURE 4-10 Experimental Corner Displacement Magnification Ratios for FP Bearings with and without Linear and Nonlinear Viscous Damping Devices Bearings for the Asymmetrically Braced Frame Structure**

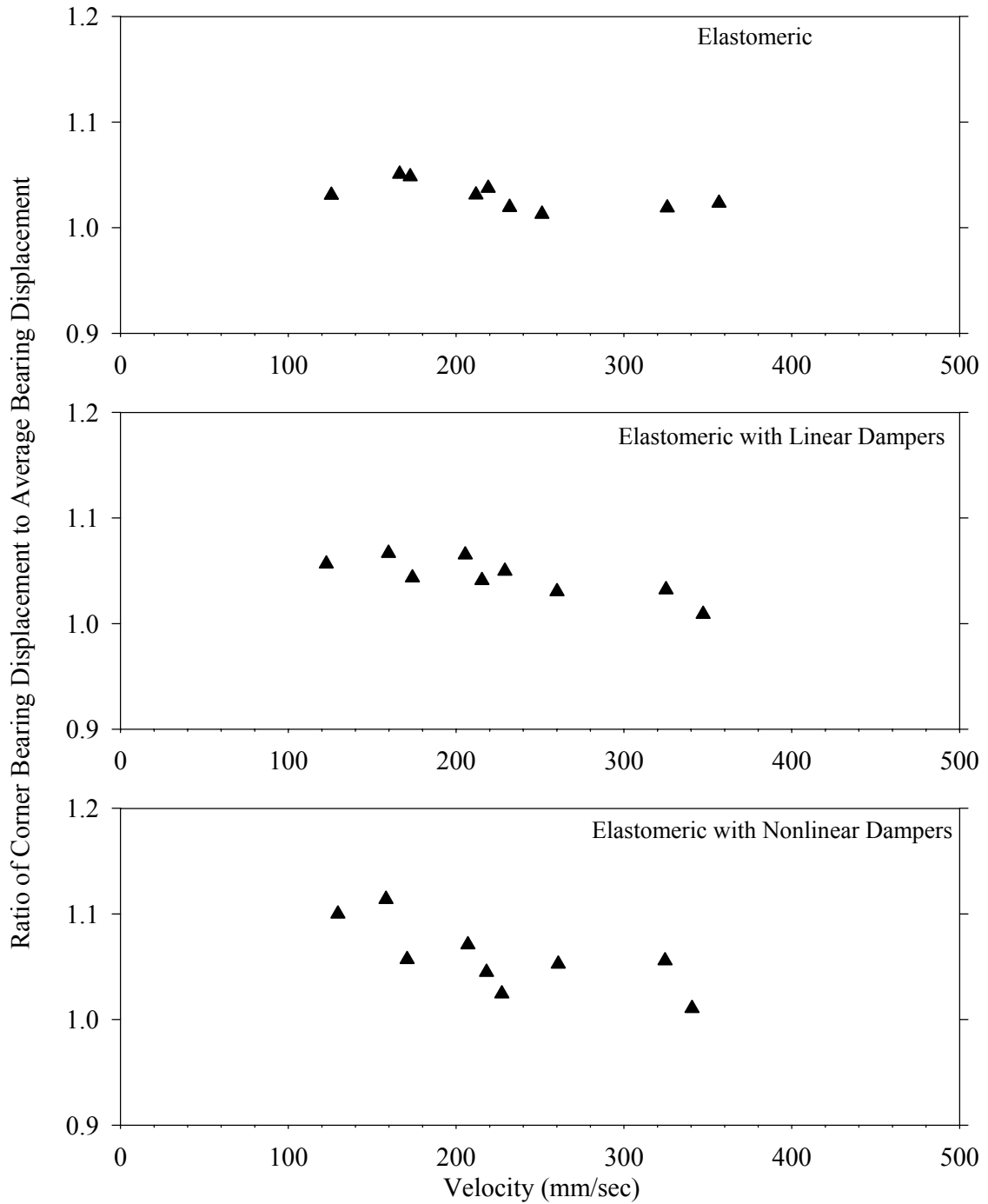


**FIGURE 4-11 Experimental Corner Displacement Magnification Ratios for Low Damping Elastomeric Bearings with and without Linear and Nonlinear Viscous Damping Devices for the Asymmetrically Braced Frame Structure**

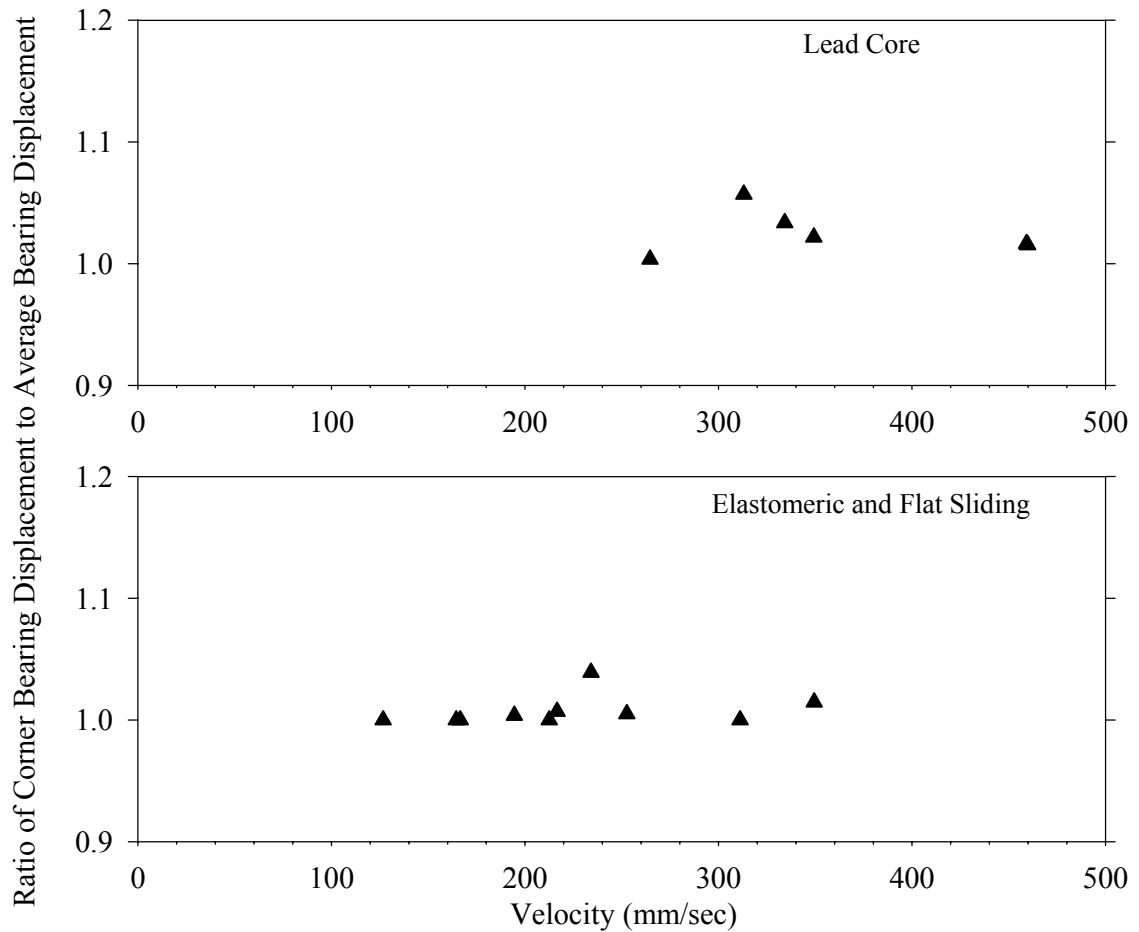


**FIGURE 4-12 Experimental Corner Displacement Magnification Ratios for Lead-Core Bearings and Elastomeric Bearings in Combination with Flat Sliding Bearings for the Asymmetrically Braced Frame Structure**

#### 4.5.4 Variation of Axial Load on Bearings

The results in Appendix A reveal that the variation of axial load on bearings due to the overturning moment effect was substantial. In a few cases, there was either uplift of sliding bearings or tension in the elastomeric bearings. Figures 4-13 through 4-16 present histories of axial force on the bearings for the moment frame configuration subjected to the Sylmar 90° 100% excitation. For all figures, the top graph is the history of the sum of the axial forces on all four bearings. The small variation in total axial force on all four bearings indicates that there is little vertical acceleration on the model. By contrast, the histories of the sum of the axial force in the two north or south bearings show large variations in axial force, on the order of 100%. This considerable variation in axial force demonstrates that large overturning moment is present.

Of interest is to observe that while there is no uplift (indicated by a zero value in the axial force history) shown for the FP system in Figure 4-13, the history in Figure 4-14 for the FP system with added nonlinear viscous damping devices shows that the bearing



experienced uplift. The experimental results with conditions of uplift or near uplift in sliding systems provides an excellent case for testing the accuracy of analysis tools under extreme dynamic conditions

In Figure 4-15, the bearing axial force history for the low damping elastomeric system with no damping devices, subjected to the Sylmar 90° 100% excitation, shows tension (a value less than zero), while the bearing axial force history for the low damping elastomeric system with linear viscous dampers, shown in Figure 4-16, demonstrates that uplift did not occur. The reason for this behavior is that the addition of damping devices in the already highly damped FP system caused a noticeable increase in the base shear and overturning moment. The opposite was true for the low damping elastomeric system, in which the displacement, base shear and overturning responses were markedly reduced with the addition of fluid viscous dampers. Tension in the elastomeric bearings was too small to cause either cavitation of rubber or fracture. Tensile force per bearing was approximately 3 kN and negative pressure was about 0.12 MPa, whereas cavitation pressures are typically over 0.7 MPa (Skinner et al., 1993).

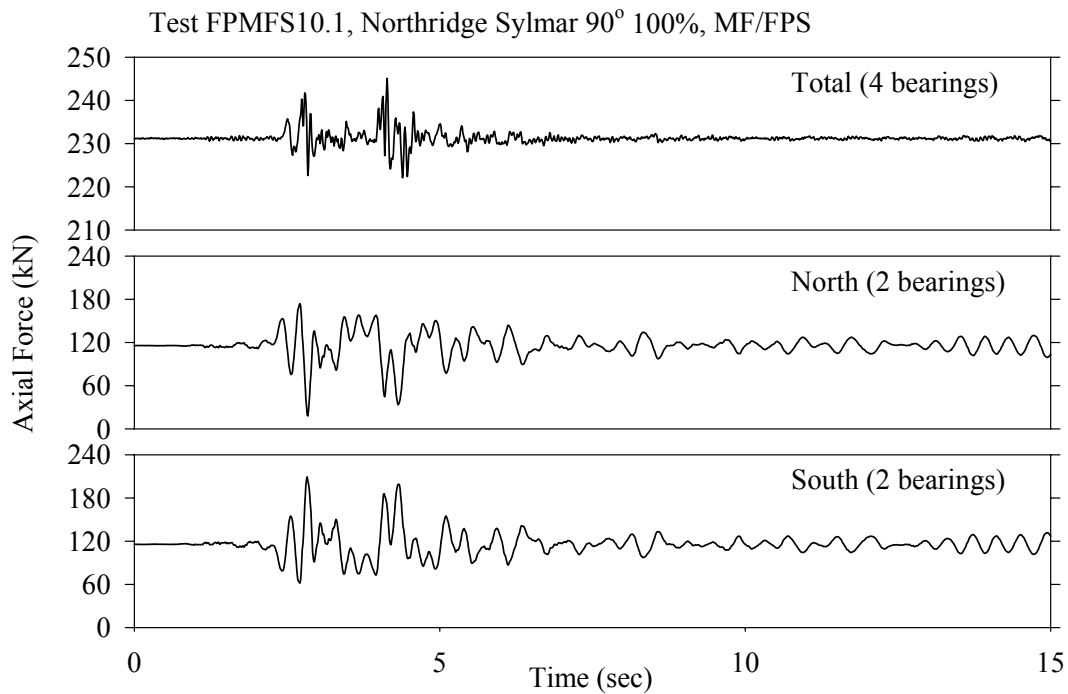


**FIGURE 4-13 History of Recorded Axial Force of the FP Bearing Isolated Moment Frame Structure in Sylmar 90° 100%**

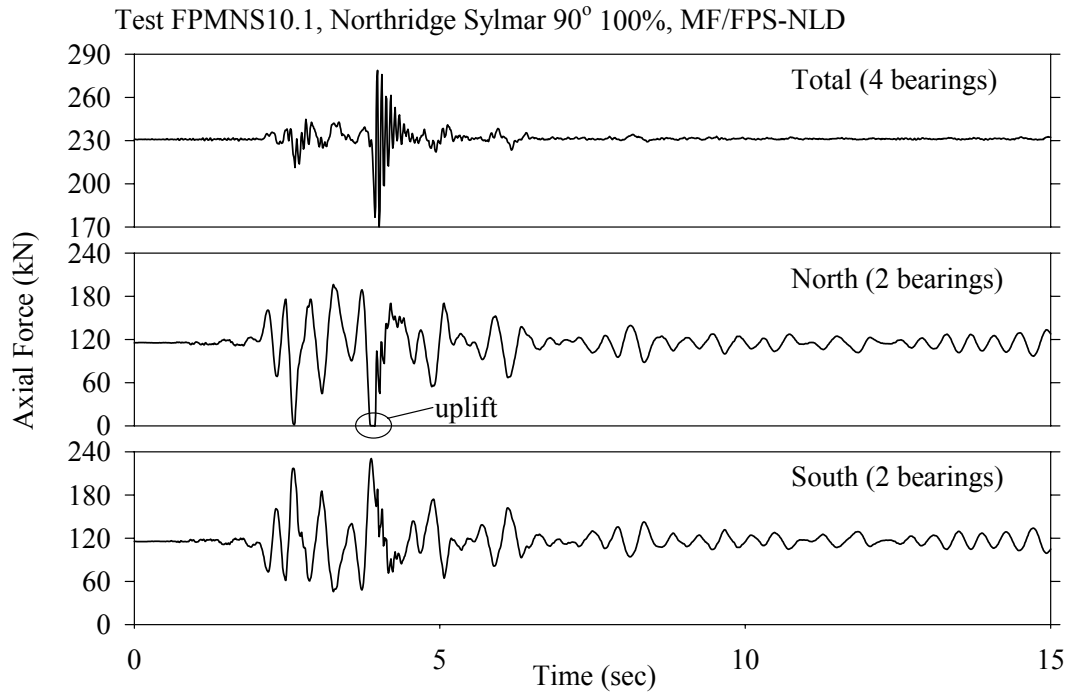


**FIGURE 4-14 History of Recorded Axial Force of the FP Bearing Isolated Moment Frame Structure with Nonlinear Fluid Viscous Damping Devices in Sylmar 90° 100%**

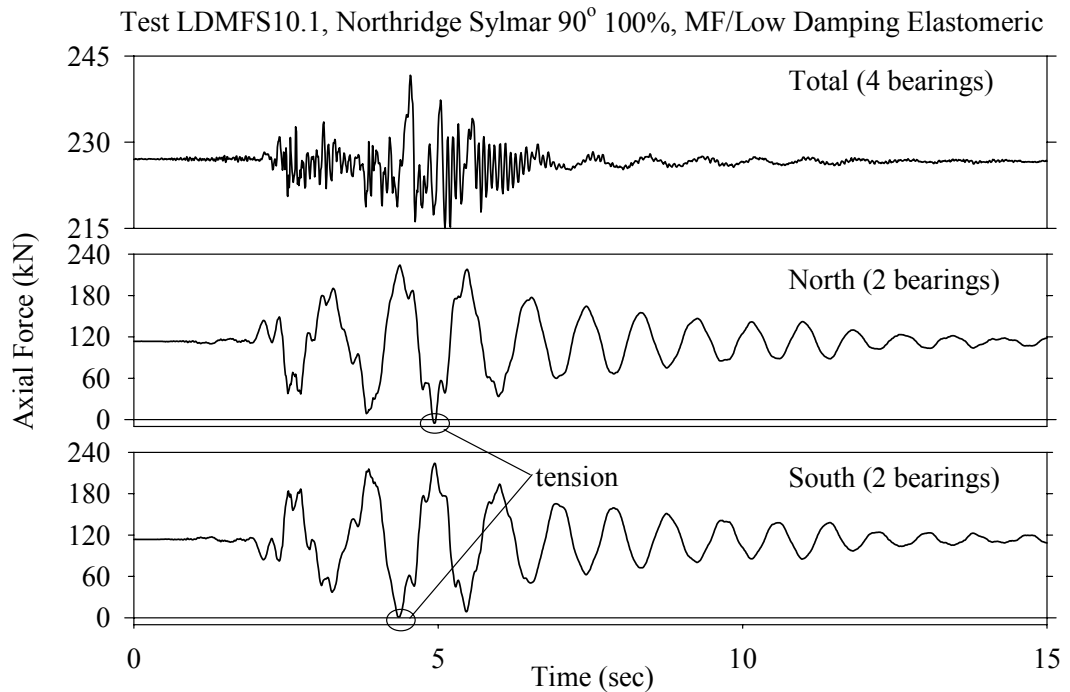


**FIGURE 4-15 History of Recorded Axial Force of the Low Damping Elastomeric Bearing Isolated Moment Frame Structure in Sylmar 90° 100%**

Test LDMLS10.1, Northridge Sylmar 90° 100%, MF/Low Damping Elastomeric-Linear Dampers

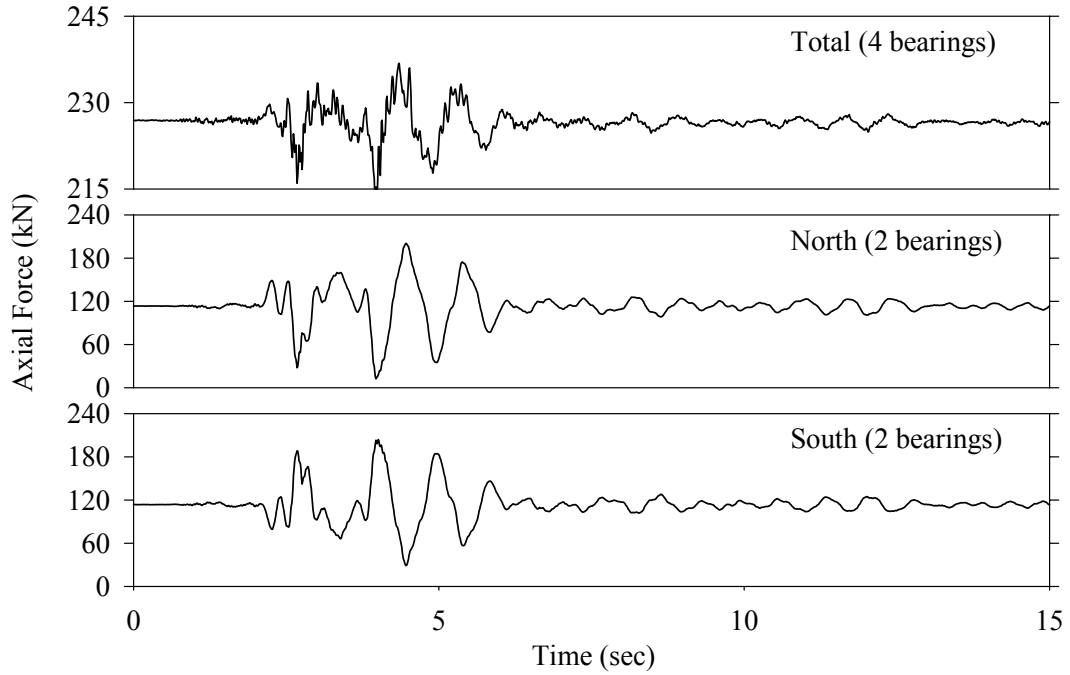


**FIGURE 4-16 History of Recorded Axial Force of the Low Damping Elastomeric Bearing Isolated Moment Frame Structure with Linear Fluid Viscous Damping Devices in Sylmar 90° 100%**



## SECTION 5

### ANALYTICAL PREDICTION OF RESPONSE

#### 5.1 Introduction

There is a variety of computer software that can be used for the prediction of the dynamic response of seismically isolated structures. Software used so far in seismic isolation projects analysis include 3D-BASIS (Nagarajaiah et al., 1989), SAP2000 (Computers & Structures, 1998), ANSYS (Swanson Analysis Systems 1996) and ABAQUS (Hibbitt et al., 1997). Herein we use two of the most commonly used computer programs to perform analysis of the tested isolated model structures: SAP2000, Version 7.44 and the 3D-BASIS-ME (Tsopelas et al. 1994) version of the 3D-BASIS class of programs.

A large number of analyses are performed, covering all of the tested isolation systems and seismic excitations with far-field and near-field characteristics. Calculated response quantities include histories of displacements, velocities, accelerations and shear forces, and floor response spectra in the range of 0.1 to 20 Hz. These calculated response quantities are compared to those obtained experimentally and conclusions are derived on the accuracy of the analysis methods. Moreover, the methods used to model the seismic isolation hardware are described.

#### 5.2 Analytical Model of Bearings

##### 5.2.1 Low Damping Elastomeric Bearings

The properties of the low damping elastomeric bearings were previously determined from testing in the single bearing test machine. There are many choices for modeling low damping elastomeric bearings depending on the computer program used. For example, in both SAP2000 and 3D-BASIS they can be simply modeled as linear elastic spring elements with stiffness equal to  $K_{eff} = 0.32$  kN/mm in conjunction with a viscous damping element that results in a damping ratio  $\beta = 0.045$  for the isolated system. This corresponds to a damping element with constant  $C = 3.92$  kN-s/m for each bearing location. However, this tends to provide incorrect results for high velocity motions where the viscous damping element becomes more pronounced, resulting in a larger total force than the bearings are truly capable of delivering.

Elastomeric bearings should, more appropriately, be modeled as bilinear hysteretic elements. In SAP2000 the NLLINK element Isolator1 property was used to model the low damping elastomeric bearings with an initial (elastic) stiffness  $K_i = 0.55$  kN/mm, a yield force  $F_y = 3.1$  kN, and a ratio of post-to-pre-yield stiffness = 0.55.

In 3D-BASIS-ME, the bilinear hysteretic stiffening element was utilized. This element consists of an elastoplastic hysteretic element and a stiffening elastic element as shown in Figure 5-1 (Tsopelas et al., 1994). The element can also be used to model softening behavior by specifying stiffness  $K_2$  to be less than stiffness  $K_1$ . This feature was used in modeling the low damping elastomeric bearings because they exhibited some noticeable reduction in stiffness for displacements beyond about 20 mm. Accordingly, the bearings were modeled using the following parameters:  $K_1 = 0.34$  kN/mm,  $K_2 = 0.26$  kN/mm, characteristic strength  $Q = 1.4$  kN,  $D_1 = 20.8$  mm and  $D_2 = 20.9$  mm.

Figure 5-2 presents experimental and analytical force-displacement loops for the low damping elastomeric bearing using the aforementioned parameters in programs 3D-BASIS-ME and SAP2000. These analytical loops were obtained by exciting the analytical model of the tested structure with harmonic ground motion of 1Hz frequency until the desired amplitude of bearing motion was reached.

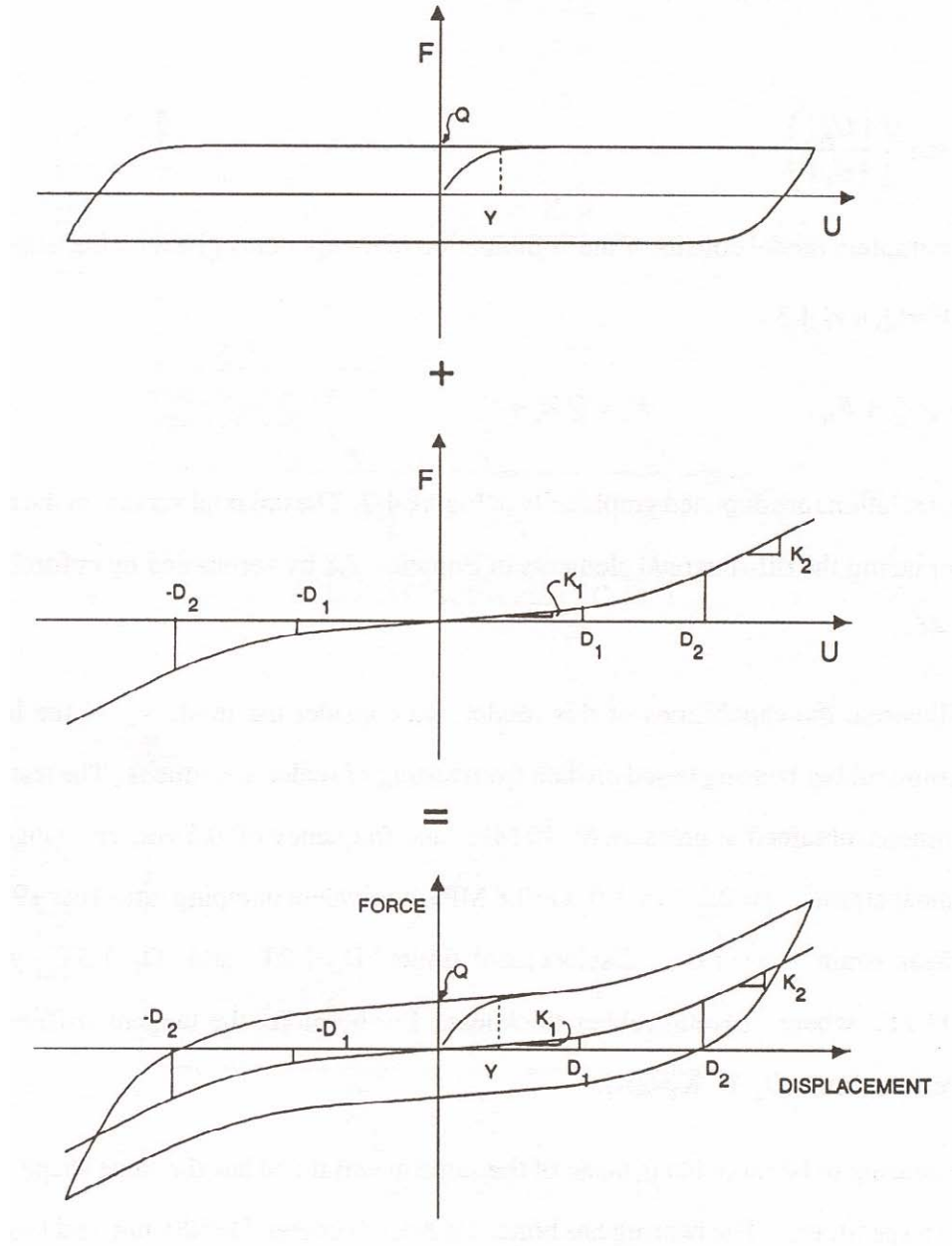


**FIGURE 5-1 Stiffening Hysteretic Element in Program 3D-BASIS-ME (adapted from Tsopelas et al., 1994)**

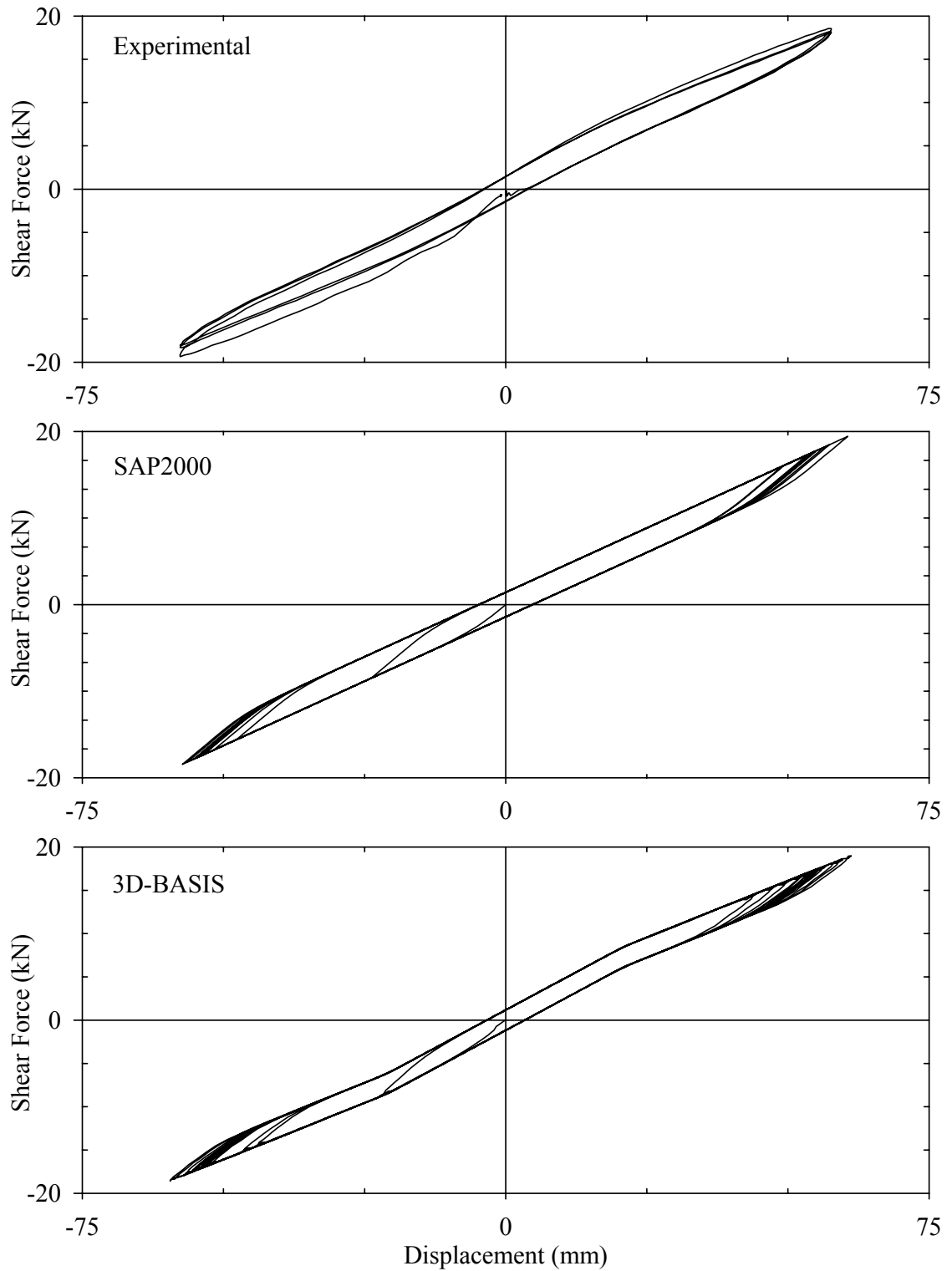


**FIGURE 5-2 Experimental and Analytical Low Damping Bearing Force-Displacement Loops Generated by Programs SAP2000 and 3D-BASIS-ME**

## 5.2.2 Friction Pendulum (FP) Bearings

The FP bearings shown in Figure 3-6 were modeled in SAP2000 using the NLLINK element Isolator2 property with the following parameters for the shear deformation degree of freedom: radius of sliding surface  $R = 762$  mm, friction coefficient fast  $f_{max} = 0.08$ , friction coefficient slow  $f_{min} = 0.02$ , rate parameter  $\alpha = 20$  s/m and an initial stiffness of 175 kN/mm. Although program 3D-BASIS-ME has an FP element with pressure dependent frictional properties and axial load effects, the simpler bilinear hysteretic element for sliding bearings, element No. 4, was used for modeling frictional behavior combined with a global spring of stiffness  $k = W/R = 233/762 = 0.305$  kN/mm ( $W = 233$  kN is the weight of the structure and  $R = 762$  mm is the FP bearing radius of curvature). The four sliding bearings were each modeled using the following parameters:  $f_{max} = 0.08$ ,  $f_{min} = 0.02$ ,  $\alpha = 20$  s/m, initial normal load = 58.3 kN and yield displacement = 0.03 mm.

## 5.2.3 Lead-Core Bearings

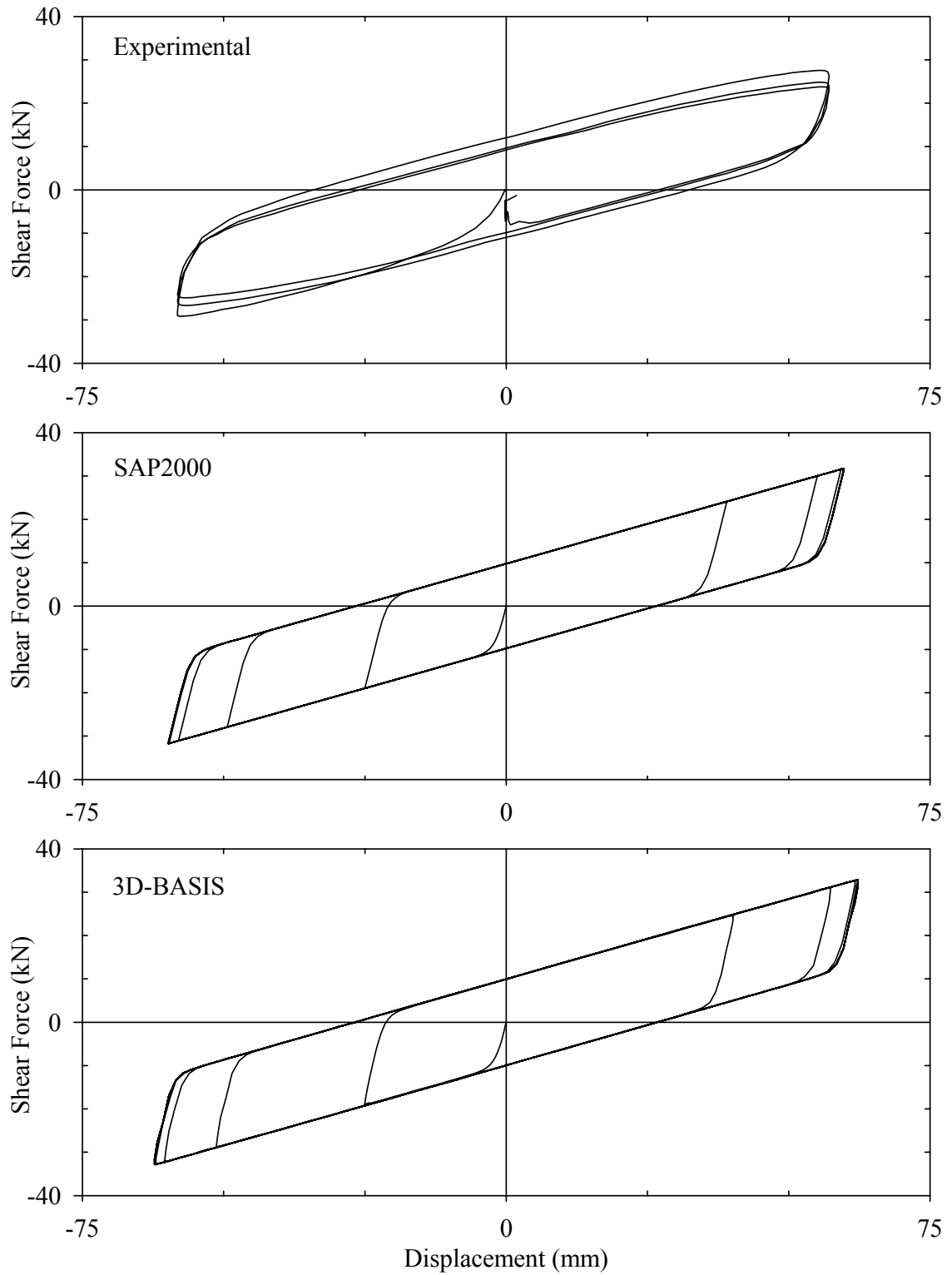
In SAP2000, the lead-core bearings were modeled using the NLLINK element Isolator1 with the following parameters: initial stiffness  $K_i = 5.25$  kN/mm, yield force  $F_y = 10.7$  kN, and a ratio of post-to-pre-yield stiffness  $r = 0.07$ . In 3D-BASIS-ME, the lead-core bearings were modeled using the bilinear hysteretic element, element No. 3, with the following parameters: yield force  $F_y = 10.7$  kN, yield displacement  $D_y = 2.0$  mm, and a ratio of post to pre-yield stiffness equal to 0.07.

Figure 5-3 presents the experimental and analytical force-displacement loops generated by SAP2000 and 3D-BASIS-ME for one lead-core bearing. The analytical loops were obtained by the procedure described in Section 5.2.1.

## 5.2.4 Flat Sliding Bearings

The flat sliding bearings were modeled in SAP2000 using the NLLINK element Isolator2 property with the following parameters for the shear deformation degree of freedom: a large radius of sliding surface  $R = 250,000$  mm to model a flat sliding surface, friction coefficient fast  $f_{max} = 0.11$ , friction coefficient slow  $f_{min} = 0.02$ , rate parameter  $\alpha = 20$  s/m and an initial stiffness of 175 kN/mm. In program 3D-BASIS-ME, the bilinear hysteretic element for sliding bearings, element No. 4, was used with parameters identical to those specified in SAP2000 except that instead of the initial stiffness, the yield displacement was specified. The yield displacement was specified as 0.03 mm. The initial normal load was specified as 58.3 kN in both programs.





**FIGURE 5-3 Experimental and Analytical Lead-Core Bearing Force-Displacement Loops Generated by Programs SAP2000 and 3D-BASIS-ME**

### 5.3 Analytical Model of Damping Devices

In program SAP2000, linear and nonlinear viscous damping devices can be directly modeled as elements extending between two given points. This approach was followed by specifying the correct damper orientation in space and using a damping coefficient

$C = 0.066 \text{ kN} \frac{\text{s}}{\text{mm}}$  for each of the linear dampers, and a damping coefficient  $C_N = 2.226 \text{ kN} \left( \frac{\text{s}}{\text{mm}} \right)^{0.397}$  and power of velocity  $\delta = 0.397$  for each of the nonlinear dampers.

In program 3D-BASIS-ME, the damping element is assumed to extend in the two principle directions ( $X$  and  $Y$ ) and to have a zero vertical inclination. Accordingly, the dampers were specified to be oriented in the testing direction with a damping coefficient given by  $C_o \cos^{1+\delta} \theta$  where  $C_o$  = damping coefficient of the device (either  $C$  or  $C_N$ ),  $\theta$  = angle of damper axis to the testing direction axis,  $\delta = 1$  for the linear dampers and  $\delta = 0.397$  for the nonlinear dampers. Since angle  $\theta = 40^\circ$  (see Section 3.6), the damping coefficient for each of the linear dampers was  $C = 0.039 \text{ kN} \frac{\text{s}}{\text{mm}}$  and

$C_N = 1.534 \text{ kN} \left( \frac{\text{s}}{\text{mm}} \right)^{0.397}$  for each nonlinear damper.

### 5.4 Analytical Model of Tested Structure

The three dimensional analytical model of the 6-story superstructure was constructed utilizing the members and connection details of the actual model (see Figures 3-18 and 3-19 for details). Figure 5-4 presents one frame section of the computer model in SAP2000 for the moment frame structure. No special constraints were utilized, and end offsets with rigid-end factors were used to represent the web stiffeners welded to the columns and beams of the structure at every joint. Additionally, the splices in the 4<sup>th</sup> story columns were modeled as accurately as possible. The concrete blocks were represented as lumped masses at the joints. The gravity load was developed utilizing a ramp function from 0 to 1 over 5 seconds with the self-weight multiplier set to 1. Thus the vertical load on the bearings was calculated during each time step from the nodal masses. For verification of the superstructure analytical model, the mode shapes from SAP2000 were compared with the experimental mode shapes. As can be seen in Tables 5-1 and 5-2, the analytical fixed base superstructure model constructed in SAP2000 produces mode shapes with very good correlation to those determined experimentally. Based on the SAP 2000 model output, only the first three modes were necessary to achieve 95 percent of the mass modal participation for the symmetrically and asymmetrically braced frame models.

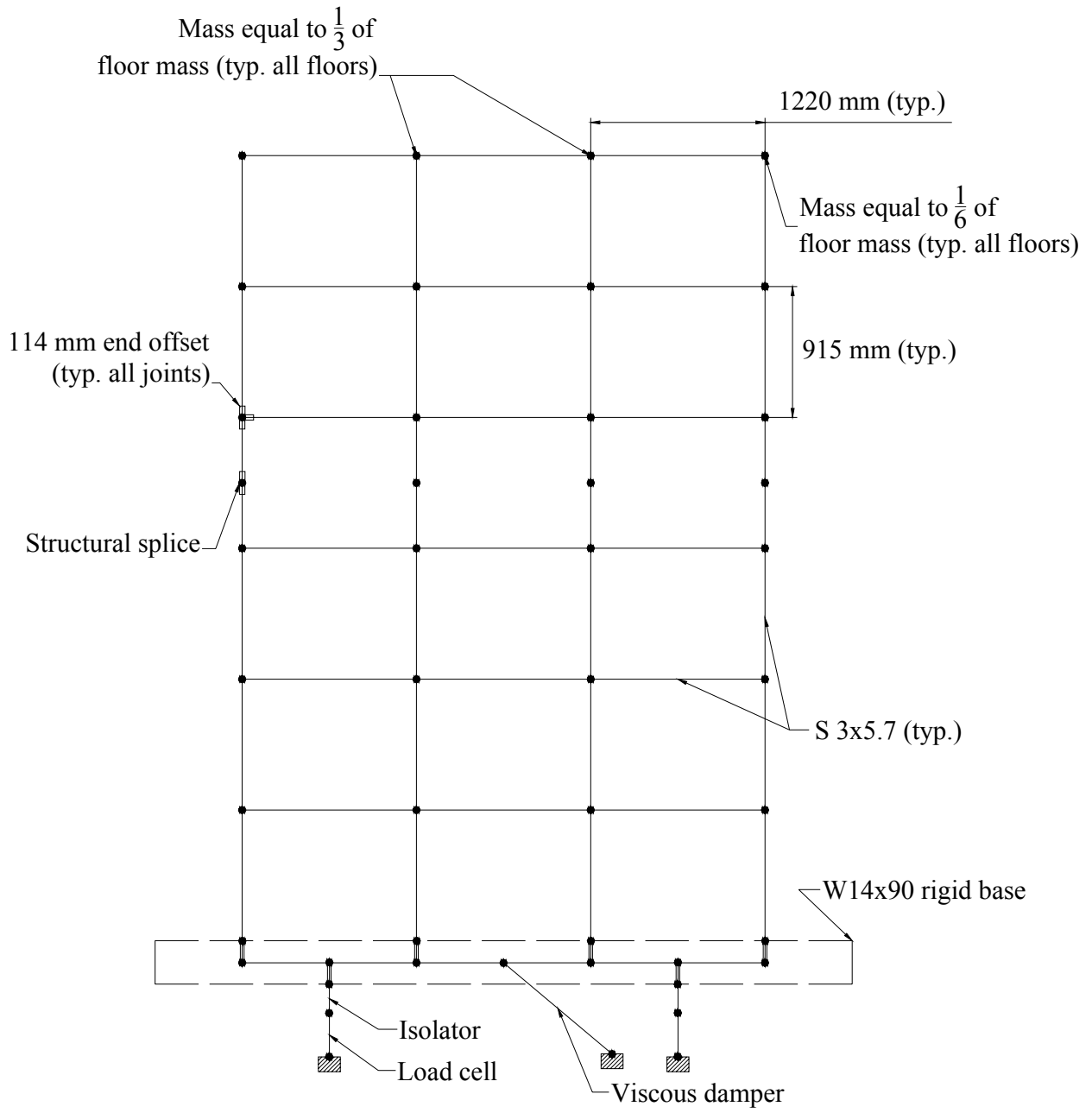


**FIGURE 5-4 Model of One Frame of the Six-Story Isolated Structure in SAP2000**

**TABLE 5-1 Comparison of Experimentally and Analytically Determined Characteristics of Fixed Base Moment Frame Structure**

Experimental

Mode	Frequency (Hz)	Damping Ratio	Mode Shape					
			Floor 1	Floor 2	Floor 3	Floor 4	Floor 5	Floor 6
1	2.34	0.048	0.22	0.43	0.60	0.77	0.94	1.00
2	7.90	0.019	-0.52	-1.05	-0.98	-0.41	0.40	1.00
3	13.65	0.011	0.98	1.02	-0.27	-1.27	-0.59	1.00
4	19.79	0.003	-2.21	0.48	1.99	-0.28	-1.67	1.00
5	25.45	0.014	2.51	-1.66	0.14	2.40	-2.86	1.00
6	29.54	0.018	-2.16	4.94	-4.96	4.22	-2.50	1.00

Analytical

Mode	Frequency (Hz)	Damping Ratio	Mode Shape					
			Floor 1	Floor 2	Floor 3	Floor 4	Floor 5	Floor 6
1	2.38	NA	0.19	0.43	0.64	0.80	0.93	1.00
2	7.41		-0.57	-0.98	-0.87	-0.36	0.42	1.00
3	13.07		1.13	1.01	-0.45	-1.20	-0.42	1.00
4	19.60		-1.43	0.17	1.34	-0.39	-1.44	1.00
5	25.58		2.57	-2.46	0.38	1.82	-2.30	1.00
6	32.25		-2.27	3.99	-5.51	5.22	-3.12	1.00

**TABLE 5-2 Comparison of Experimentally and Analytically Determined Characteristics of Asymmetrically and Symmetrically Braced Fixed Base Structure**

Asymmetrically Braced Experimental

Mode	Frequency (Hz)	Damping Ratio	Mode Shape					
			Floor 1	Floor 2	Floor 3	Floor 4	Floor 5	Floor 6
1	3.32	0.042	0.20	0.39	0.55	0.73	0.91	1.00
2	5.32	0.020 <sup>1</sup>	0.26	0.38	0.50	0.63	0.86	1.00
3	12.80	0.016	-0.62	-1.11	-0.97	-0.41	0.38	1.00

1. See comments in Section 3.7.

Asymmetrically Braced Analytical

Mode	Frequency (Hz)	Damping Ratio	Mode Shape					
			Floor 1	Floor 2	Floor 3	Floor 4	Floor 5	Floor 6
1	3.67		0.16	0.33	0.51	0.69	0.86	1.00
2	6.06	N/A	0.08	0.28	0.50	0.70	0.87	1.00
3	12.29		-0.72	-1.09	-0.99	-0.47	0.29	1.00

Symmetrically Braced Experimental

Mode	Frequency (Hz)	Damping Ratio	Mode Shape					
			Floor 1	Floor 2	Floor 3	Floor 4	Floor 5	Floor 6
1	4.00	0.040	0.17	0.34	0.49	0.67	0.87	1.00
2	17.09	0.017	-0.67	-1.16	-0.96	-0.43	0.38	1.00
3	30.70	0.009	1.00	1.06	-0.71	-1.38	-0.63	1.00

Symmetrically Braced Analytical

Mode	Frequency (Hz)	Damping Ratio	Mode Shape					
			Floor 1	Floor 2	Floor 3	Floor 4	Floor 5	Floor 6
1	4.89		0.12	0.28	0.47	0.65	0.84	1.00
2	17.61	N/A	-0.64	-1.07	-1.06	-0.58	0.20	1.00
3	34.60		1.29	1.12	-0.32	-1.27	-0.56	1.00

In program 3D-BASIS-ME, coupled lateral-torsional response is accounted for by maintaining three degrees of freedom per floor, that is two translational and one torsional degrees of freedom. 3D-BASIS-ME has two options for superstructure data input:

1. shear-type representation in which the stiffness matrix of the superstructure is internally constructed by the program, and
2. full three dimensional representation in which the eigenvalues and eigenvectors, determined by SAP2000 and verified experimentally, are imported into the program 3D-BASIS-ME.

To ensure the results of both programs would be comparable, the frequencies and mode shapes from SAP2000 were used to create the eigenvalues and eigenvectors that represent the superstructure model in 3D-BASIS-ME (in lieu of using the experimental eigenvectors and eigenvalues). The inherent damping of the structure is modeled differently in the two programs. In program 3D-BASIS-ME, the superstructure damping is specified in terms of the modal damping ratios for the fixed base superstructure (given in Tables 5-1 and 5-2) separate from the damping in the isolation system. Conversely, in program SAP2000, the damping ratios entered are applied to the isolated model. In general, a damping ratio of 0.04 was used for the first mode, and 0.02 for all other modes. Six modes were used to model the moment frame structure, and three modes were used to model both the symmetrically braced and asymmetrically braced frame structure.

## **5.5 Comparison of Analytical and Experimental Results**

The dynamic response of the six-story structure was analytically predicted using both the SAP2000 and 3D-BASIS-ME computer programs. Appendix B provides samples of SAP2000 and 3D-BASIS input files. Appendices C and D present comparisons of experimental and analytical results produced by programs SAP2000 and 3D-BASIS-ME, respectively. A representative sample of results from Appendices C and D are presented in Figures 5-5 through 5-10, including a case in which bearing uplift occurred.

An examination of the results of Appendices C and D reveals the following:

1. Both programs generate results in good agreement with the experimental results. The maximum differences observed between peak experimental and analytical response quantities was on the order of 15% or less. Such differences are not great but they should be viewed in the light of the fact that the development of the analytical models was based on extensive experimental data and that the tested structures lacked the complexity of real structures. For real building structures, in which knowledge of mass and stiffness properties is incomplete, errors in the analytical prediction of response will likely much exceed 15%.
2. The global response of the isolated structure (floor acceleration histories, story shear force and drift histories and floor response spectra) is predicted equally well by the two programs for the FP isolation system. Figures 5-5 and 5-6 show specifically the FP isolated moment frame response to the Sylmar 90° 100% excitation. Although this is just one example, it is representative of the quality of the analytical results produced by both programs presented in Appendices C and D. It should be noted that the modeling of the isolation bearings in the two programs differed in the following:
  - a. Explicit representation of FP bearing behavior with variable axial load effects in SAP2000, and

- b. Implicit representation consisting of a global spring and frictional elements without variable axial load effects in 3D-BASIS-ME.

The reason for the good prediction of response by 3D-BASIS-ME despite the use of an incomplete bearing model is that the four bearings collectively exhibited the correct behavior. This was also reported in Al-Hussaini et al. (1994).

3. Scheller et al. (1999) provide a verification study of SAP2000 Version 7.4. It was shown that SAP2000 Version 7.4 was problematic when modeling FP bearings with significant variations in axial load. Furthermore, the use of the axial linear effective stiffness for the NLLINK Isolator2 element has been corrected in SAP2000 Version 7.44. In previous research, it was found that only very small values of the elastic stiffness,  $k_e$ , yielded good results. In the new version of SAP2000, the actual value of the elastic stiffness will allow the analysis to be executed without problems and with good results as shown in Appendix D. In particular, the case of the moment frame superstructure with FP bearings and nonlinear viscous fluid dampers excited by the Kobe N-S 100% motion clearly demonstrates the ability of SAP2000 Version 7.44 to adequately model the FP bearings at extreme dynamic conditions that include bearing uplift. This particular analysis included over a 100% variation in axial load and achieved uplift for a prolonged period of time at two instances. In particular, as shown in Figure 4-14, the FP bearing with nonlinear viscous damper isolated moment frame structure excited by the Sylmar 90° 100% motion experienced uplift, furthermore, as can be seen in Figure 5-10, SAP2000 was able to capture the response even with uplift of the FP bearing element.

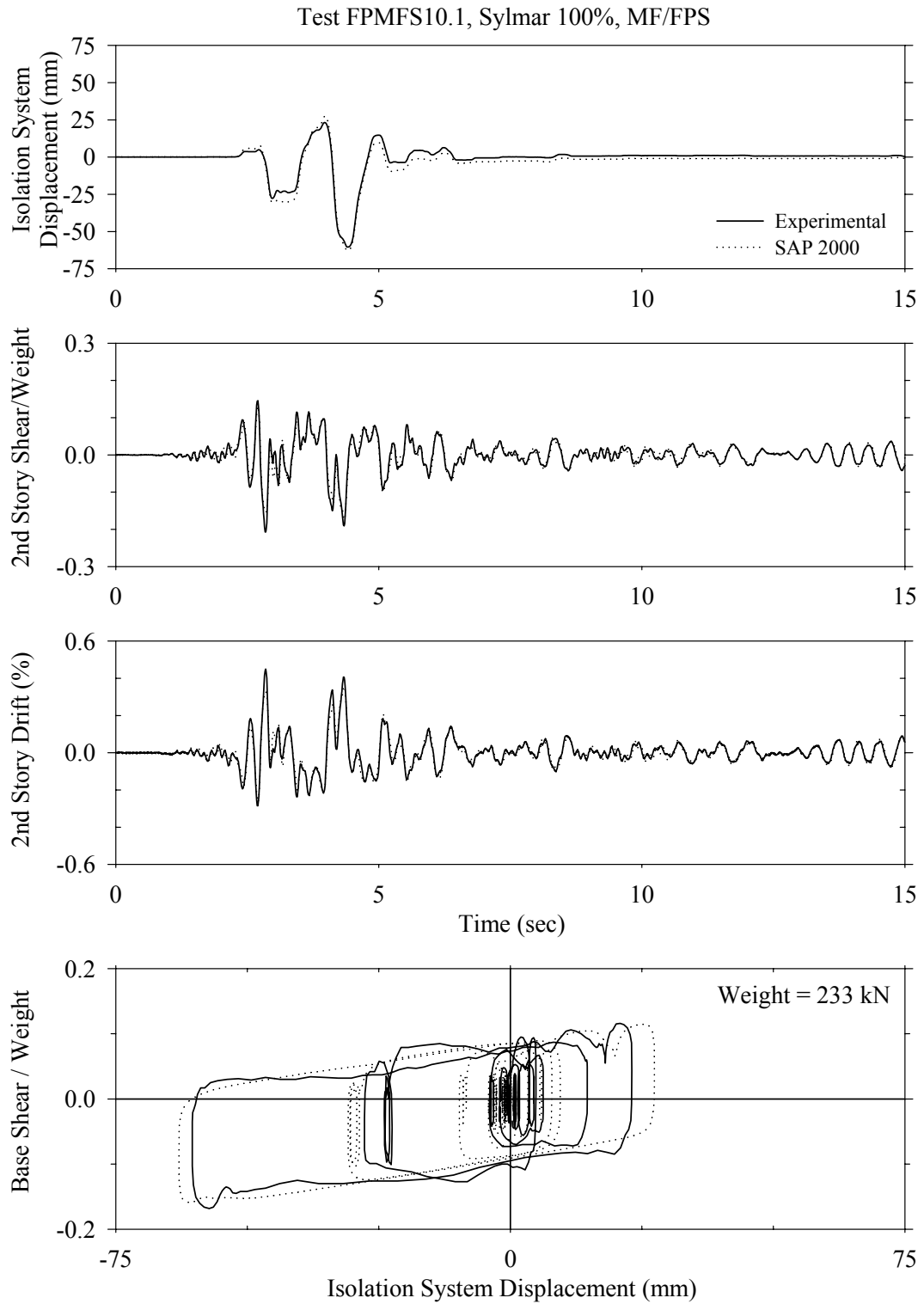


**FIGURE 5-5 Comparison of Experimental and SAP2000 Generated Results for the FP Isolated Moment Frame in the Sylmar 90° 100% Excitation**



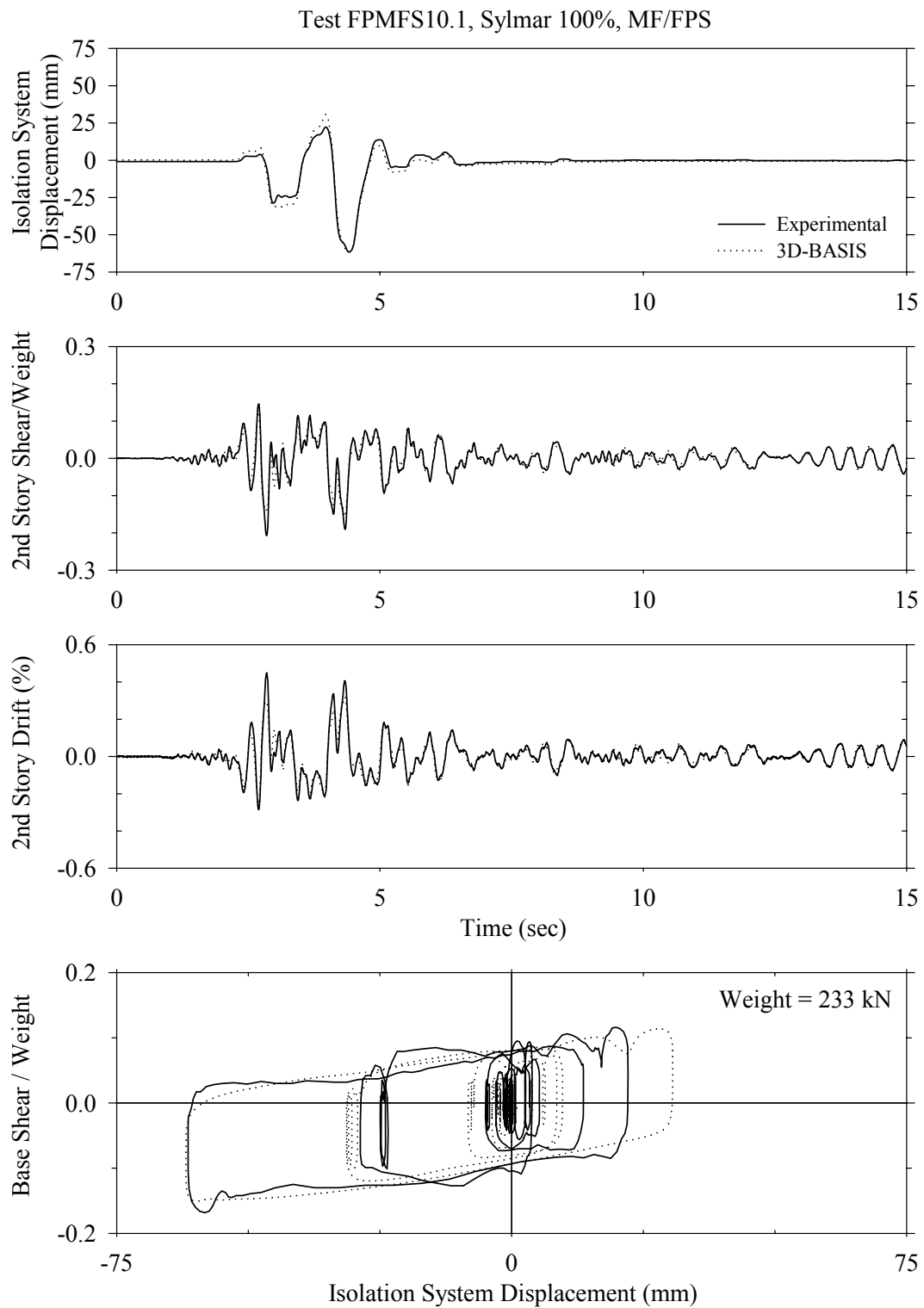


**FIGURE 5-6 Comparison of Experimental and 3D-BASIS Generated Results for the FP Isolated Moment Frame in the Sylmar 90° 100% Excitation**

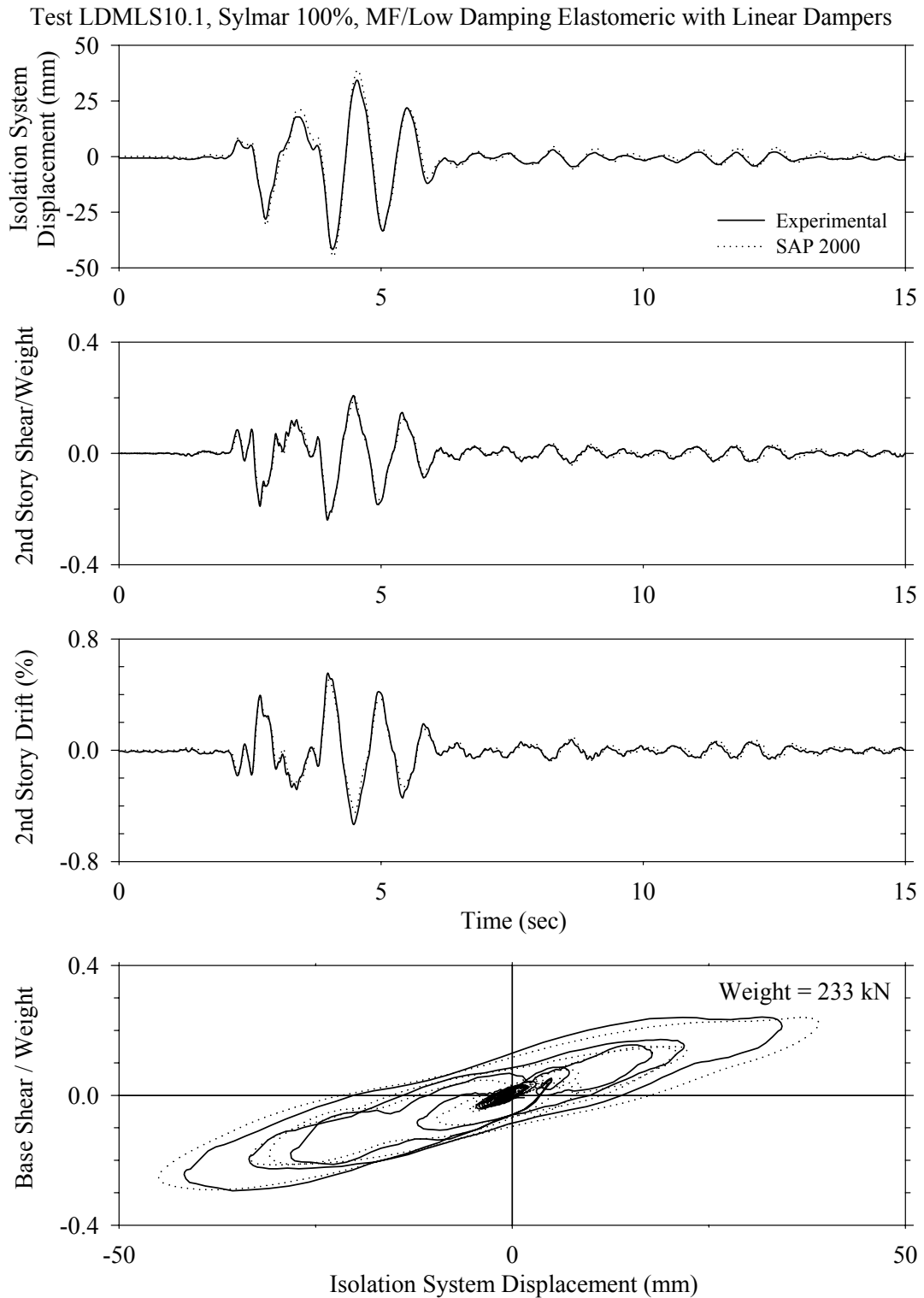


**FIGURE 5-7 Comparison of Experimental and SAP2000 Generated Results for the Elastomeric Bearing with Linear Viscous Damper Isolated Moment Frame in the Sylmar 90° 100% Excitation**

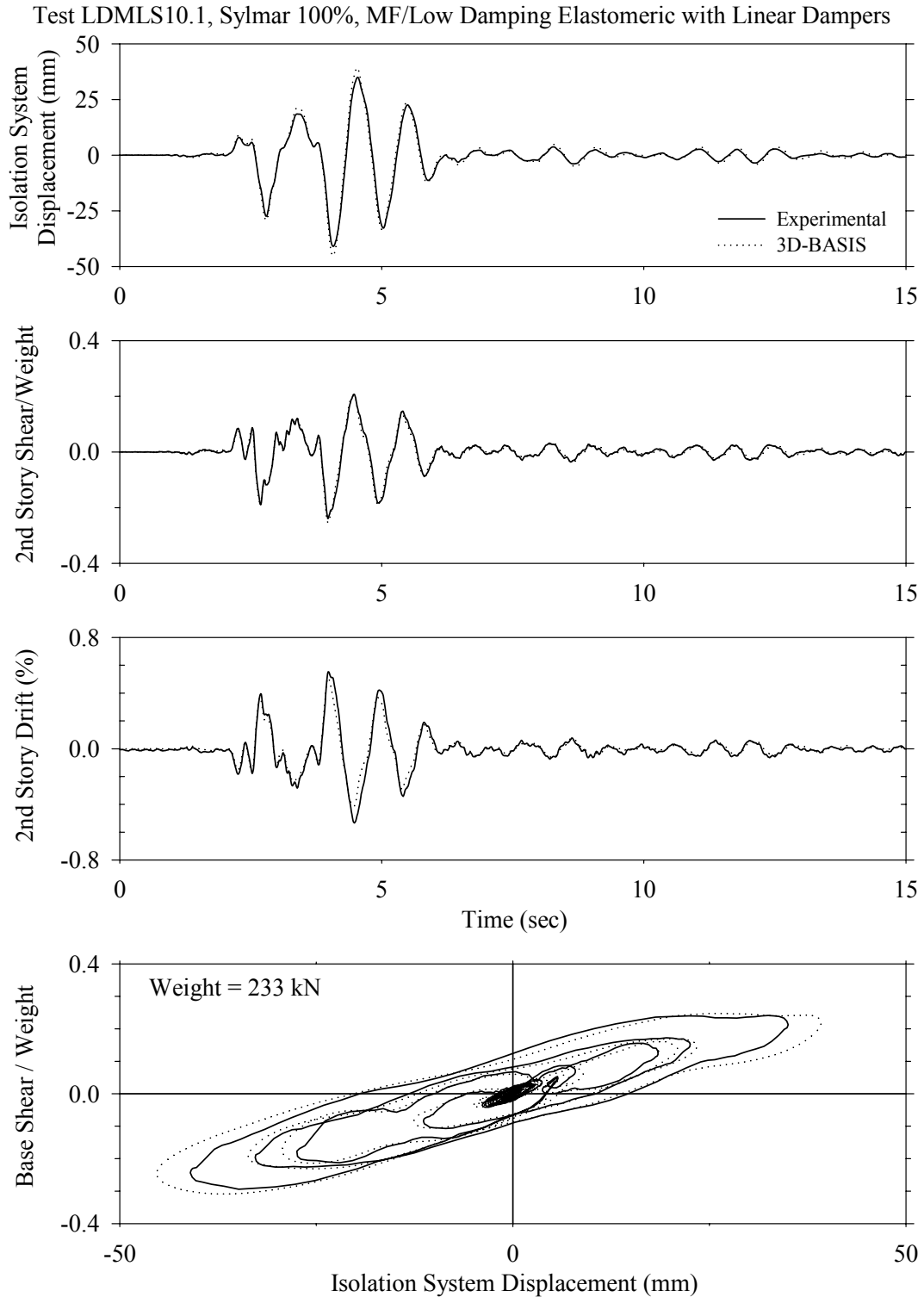


**FIGURE 5-8 Comparison of Experimental and 3D-BASIS Generated Results for the Elastomeric Bearing with Linear Viscous Damper Isolated Moment Frame in the Sylmar 90° 100% Excitation**

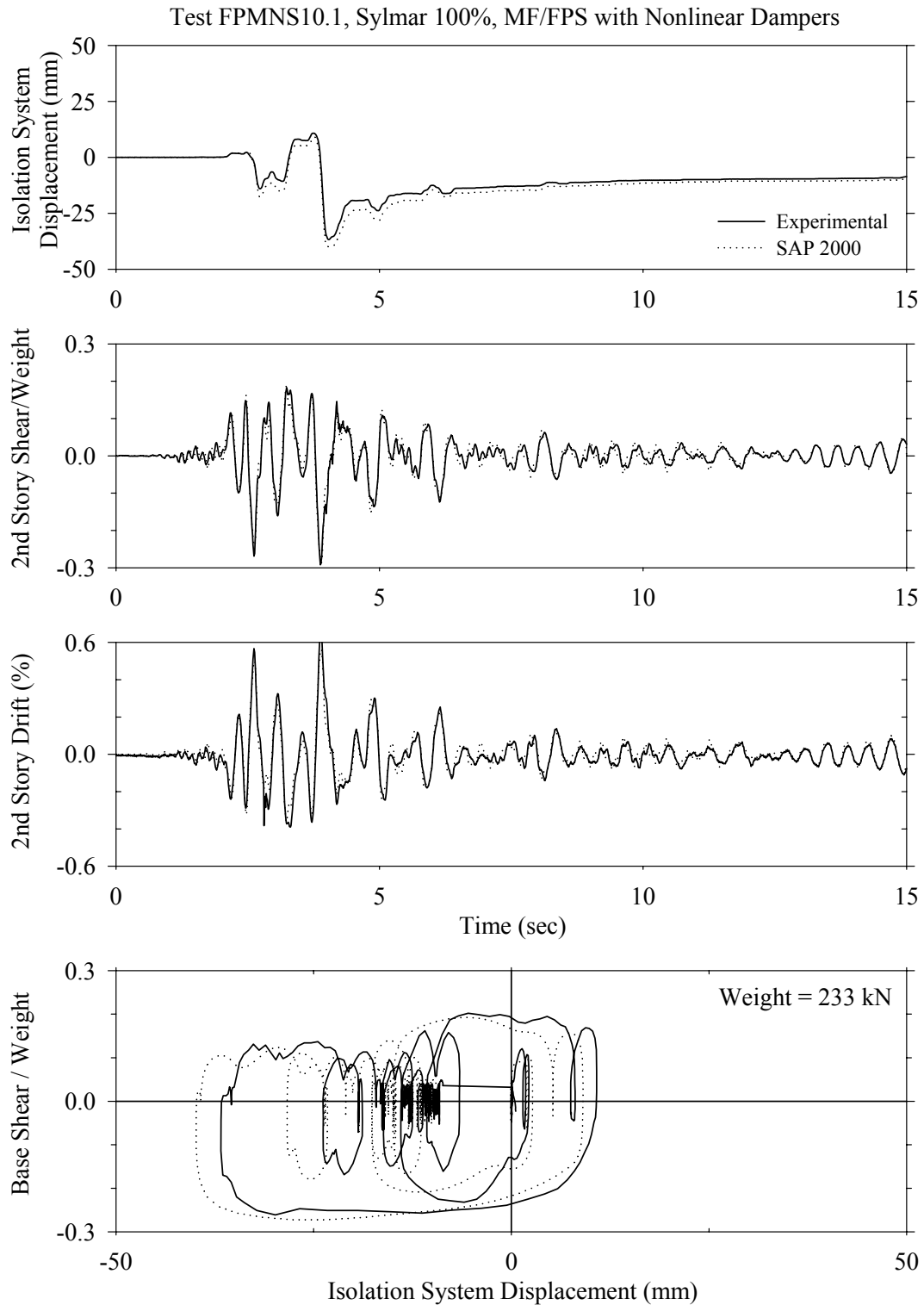


**FIGURE 5-9 Comparison of Experimental and SAP2000 Generated Results for the Combined FP-Nonlinear Fluid Viscous Damper Isolated Moment Frame in the Sylmar 90° 100% Excitation**

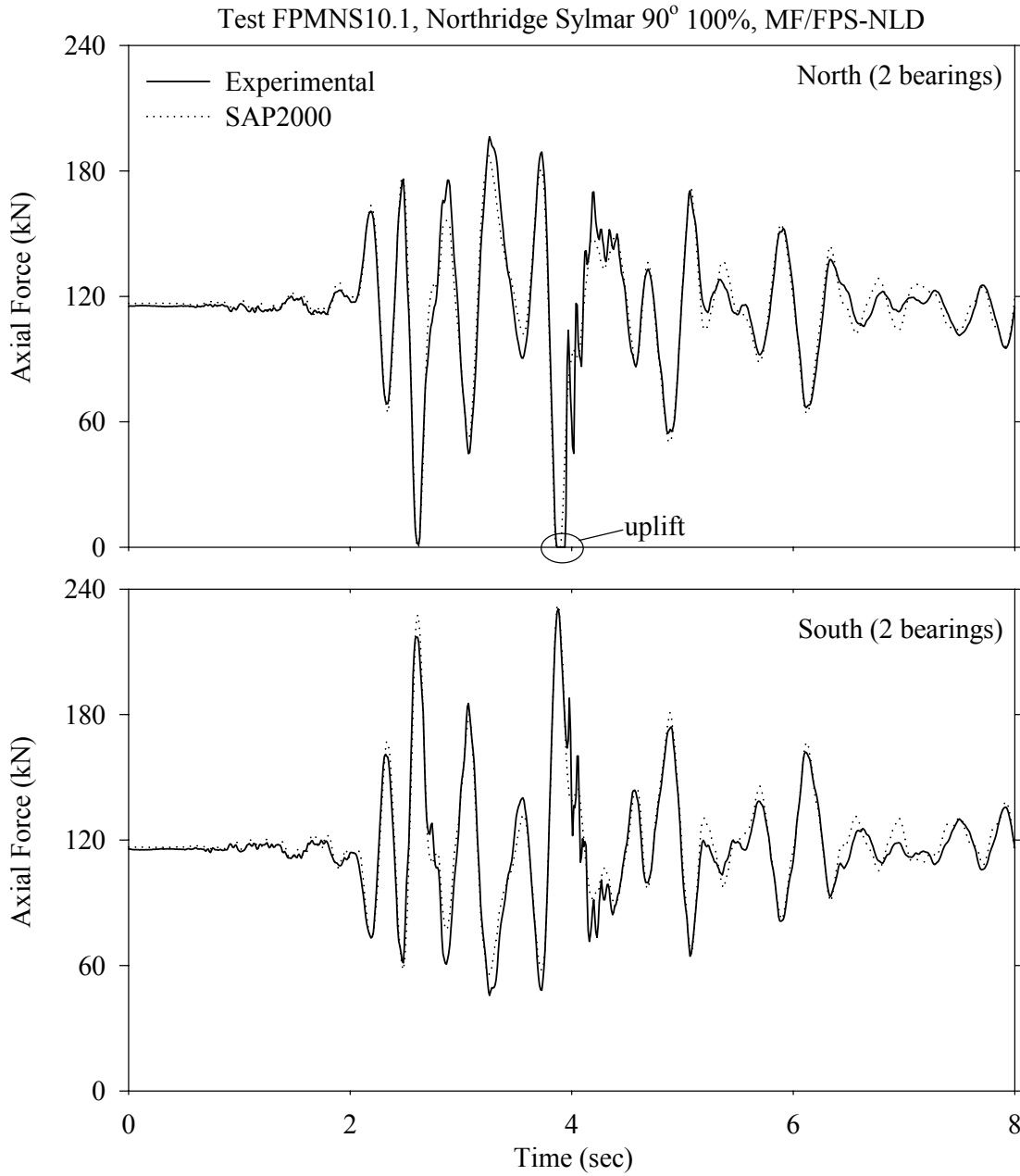


**FIGURE 5-10 Comparison of Experimental and SAP2000 Generated Uplift Response for the Combined FP-Nonlinear Fluid Viscous Damper Isolated Moment Frame in the Sylmar 90° 100% Excitation**



## SECTION 6

### SUMMARY AND CONCLUSIONS

Earthquake simulator tests were conducted on a six-story building model in moment frame and braced frame configurations in conjunction with several isolation systems. The building models included an unbraced moment frame, a braced frame and an asymmetrically braced frame. The isolation systems utilized were Friction Pendulum (FP), low damping elastomeric bearing, lead-core bearing, and flat slider in combination with low damping elastomeric bearings. Damping devices were also used in combination with the FP and low damping elastomeric bearings. The experimental results were compared with analytical results obtained using computer programs SAP2000 and 3D-BASIS-ME. The capability of these programs to adequately predict primary and secondary system response was evaluated. The generated large database will be useful in assessing the validity and accuracy of other dynamic analysis software. The main conclusions of this study are:

1. The addition of damping devices to a lightly damped system, like the tested elastomeric bearing system, resulted in a reduction in isolation displacement, but also a reduction in primary and secondary response quantities, such as story drifts, shear forces, floor accelerations, floor velocities and floor spectral accelerations.
2. The addition of damping devices to a highly damped system, like the tested FP system (with friction of 0.08), resulted in the expected reduction in isolation displacement, however, at the expense of significant increase in primary and secondary response quantities.
3. In general, whether added to highly damped or lightly damped isolation systems, nonlinear viscous damping devices resulted in a larger increase in story drifts and shear forces than the linear viscous devices.
4. The response of secondary systems affected by floor spectral accelerations, such as flexibly attached components (e.g., fire sprinkler systems, drop ceilings, computer floors etc.) exhibits a complex relation with the type of isolation system and flexibility of the superstructure. Particularly:
  - a. In the frequency range around the fundamental frequency of the isolated structure, highly nonlinear systems, such as the tested FP system and the combined elastomeric-sliding bearing system, resulted in much smaller floor spectral accelerations than the tested elastomeric and combined elastomeric-viscous damper systems.
  - b. In the very high frequency range, corresponding to components which are rigidly attached to the floors, the floor spectral acceleration response was (i) basically the same for all tested isolation systems with a stiff superstructure, and (ii) slightly higher for the tested highly nonlinear systems (such as the tested FP system and the combined elastomeric-sliding bearing system) with a flexible superstructure.
  - c. In the high frequency range, there is no systematic behavior that can be described in a general statement. Rather, depending on the type of excitation and the flexibility of the superstructure, either the highly nonlinear systems exhibit higher floor spectral response than the effectively linear systems or

vice versa. However, more often the highly nonlinear systems exhibited higher floor spectral response.

5. The total floor velocities recorded for the highly nonlinear systems, were typically much smaller than the velocities recorded for the low damping elastomeric system. This also supports the statement that the sliding systems are likely to have a lesser impact on secondary systems that are affected by velocity, such as unbraced equipment, cabinets, and art objects.
6. The experimental results presented herein tend to disprove the view that highly nonlinear systems, such as the tested FP system and the combined elastomeric-sliding bearing system, have a very high impact on building contents (Skinner et al., 1993). Rather, these highly nonlinear systems tend to provide for a lesser impact on contents when considering all relevant response quantities, which include story drifts, floor velocities and floor spectral accelerations over a wide frequency range.
7. The analytical predicted peak primary and secondary system response in terms of isolator displacements, base shear forces, story shear forces, story drifts, floor accelerations, floor velocities and floor spectral accelerations, was within approximately 15% of the experimentally obtained response. Such differences are not great but they should be viewed in the light of the fact that the development of the analytical models was based on extensive experimental data and that the tested structures lacked the complexity of real structures. For real building structures, in which knowledge of mass and stiffness properties is incomplete, errors in the analytical prediction of response will likely much exceed 15%.



## SECTION 7

### REFERENCES

1. Al-Hussaini, T. M., Zayas, V. A. and Constantinou, M. C., (1994), “Seismic Isolation of Multi-Story Frame Structures Using Spherical Sliding Isolation Systems”, **NCEER-94-0007**, National Center for Earthquake Engineering Research, State University of New York, Buffalo, New York.
2. Agbabian, M. S., Masri, S. F. and Nigbor, R. L., (1990), “Evaluation of Seismic Mitigation Measures for Art Objects”, **Getty Conservation Institute Scientific Program Report**, J. Paul Getty Museum, Santa Monica, California.
3. American Association of State Highway and Transportation Officials – AASHTO (1999), **Guide Specifications for Seismic Isolation Design**, Washington, D.C.
4. Applied Technology Council, (1997a), **NEHRP Commentary on the Guidelines for the Seismic Rehabilitation of Buildings (FEMA 274)**, ATC-33, Redwood City, CA.
5. Applied Technology Council, (1997b), **NEHRP Guidelines for the Seismic Rehabilitation of Buildings (FEMA 273)**, ATC-33, Redwood City, CA.
6. Applied Technology Council, (1998), **Proceedings of Seminar on Seismic Design, Retrofit and Performance of Nonstructural Components**, ATC 29-1, Redwood City, CA.
7. Arnold, C., (1998), “The Requirements for Non-Structural Components for the NEHRP Guidelines for the Seismic Rehabilitation of Buildings”, **Proceedings of Seminar on Seismic Design, Retrofit and Performance of Nonstructural Components, ATC 29-1**, Applied Technology Council, Redwood City, CA.
8. Behr, R. A. and Worrell, C. L., (1998), “Limit States for Architectural Glass Under Simulated Seismic Loadings”, **Proceedings of Seminar on Seismic Design, Retrofit and Performance of Nonstructural Components, ATC 29-1**, Applied Technology Council, Redwood City, CA.
9. Computers and Structures, Inc., (1998), SAP2000, **Integrated Finite Element Analysis and Design of Structures**, Version 7.44, Berkeley, CA.
10. Constantinou, M. C., Mokha, A. S. and Reinhorn, A. M., (1991), “Study of a Sliding Bearing and Helical Steel Spring Isolation System”, **Journal of Structural Engineering**, 117(4), 1259-1277, ASCE, Reston VA.
11. Constantinou, M. C., Tsopelas, P. C., Kasalanati, A. and Wolff, E., (1999), “Property Modification Factors for Seismic Isolation Bearings”, **Report No. MCEER-99-0012**, Multidisciplinary Center for Earthquake Engineering Research, State University of New York, Buffalo, New York.

12. Constantinou, M. C., Tsopelas, P. C., Kim, Y-S and Okamoto, S., (1993), "NCEER-TAISEI Corporation Research Program on Sliding Seismic Isolation Systems for Bridges: Experimental and Analytical Study of Friction Pendulum System (FPS)" **Report No. NCEER-93-0020**, National Center for Earthquake Engineering Research, State University of New York, Buffalo, New York.
13. Eisenberger, M., and Rutenberg, A., (1986), "Seismic Base Isolation of Asymmetric Shear Buildings", **Engineering Structures**, 8(1), 2-8.
14. Fan, F. G. and Ahmadi, G., (1990), "Floor Response Spectra for Base-Isolated Multistory Structures", **Earthquake Engineering & Structural Dynamics**, 19(3), 377-388.
15. Grigoriu, M., and Waisman, F., (1998), "Seismic Reliability and Performance of Nonstructural Components", **Proceedings of Seminar on Seismic Design, Retrofit and Performance of Nonstructural Components, ATC 29-1**, Applied Technology Council, Redwood City, CA.
16. Hibbitt, Karlsson and Sorenson, Inc., (1997), **ABAQUS/Standard, User's Manual**, Version 5.7, Pawtucket, Rhode Island.
17. International Building Code – **IBC** (2000), International Code Council, Falls Creek, VA.
18. Jangid, R.S., and Datta, T. K., (1994), "Non-linear Response of Torsionally Coupled Base Isolated Structures," **Journal of Structural Engineering**, 120(1), ASCE, Reston VA.
19. Juhn, G., Manolis, G. D., Constantinou, M.C., and Reinhorn, A. M., (1992), "Experimental Study of Secondary Systems in Base-Isolated Structures", **Journal of Structural Engineering**, 118(8), ASCE, Reston VA.
20. Kasalanati, A. and Constantinou, M. C., (1999), "Experimental Study of Bridge Elastomeric and Other Isolation and Energy Dissipation Systems with Emphasis on Uplift Prevention and High Velocity Near-source Seismic Excitation", **Report No. MCEER-99-0004**, Multidisciplinary Center for Earthquake Engineering Research, State University of New York, Buffalo, New York.
21. Kelly, J. M. and Tsai, H. C., (1985), "Seismic Response of Light Internal Equipment in Base-Isolated Structures", **Earthquake Engineering & Structural Dynamics**, 13(6), 711-732.
22. McGavin, G. L., Lai, J., and Ikkanda, S., (1998), "City of LA Proposed Ordinance Changes for Suspended Ceiling Systems Prompted by the 1994 Northridge Earthquakes", **Proceedings of Seminar on Seismic Design, Retrofit and Performance of Nonstructural Components, ATC 29-1**, Applied Technology Council, Redwood City, CA.

23. Mokha, A. S., Constantinou, M. C. and Reinhorn, A. M., (1990), "Experimental Study and Analytical Prediction of Earthquake Response of a Sliding Isolation System with Spherical Surface", **Report No. NCEER-90-0020**, National Center for Earthquake Engineering Research, State University of New York, Buffalo, New York.
24. Naeim, F., Kelly, J. M., (1999), **Design of Seismic Isolated Structures – From Theory to Practice**, John Wiley & Sons Inc., NY.
25. Nagarajaiah, S., Reinhorn, A. M., Constantinou, M. C., (1989), "Nonlinear Dynamic Analysis of Three-Dimensional Base Isolated Structures (3D-BASIS)", **Report No. NCEER-89-0019**, National Center for Earthquake Engineering Research, State University of New York, Buffalo, New York.
26. Nagarajaiah, S., Reinhorn, A. M., and Constantinou, M. C., (1993a), "Torsional Coupling in Sliding Base Isolated Structures," **Journal of Structural Engineering**, 119(1), 130-149, ASCE, Reston VA.
27. Nagarajaiah, S., Reinhorn, A. M., and Constantinou, M. C., (1993b), "Torsion in Base Isolated Structures with Elastomeric Isolation Systems," **Journal of Structural Engineering**, 119(10), 2932-2951, ASCE, Reston VA.
28. Reinhorn, A. M. et al. (1989), "1:4 Scale Model Studies of Active Tendon Systems and Active Mass Dampers for Aseismic Protection", **Report No. NCEER-89-0026**, National Center for Earthquake Engineering Research, State University of New York, Buffalo, New York
29. Skinner, R. I., Robinson, W. H. and McVerry, G. H., (1993), **An Introduction to Seismic Isolation**, John Wiley & Sons Inc., NY.
30. Soong, T. T. and Constantinou, M. C., (1994), **Passive and Active Structural Vibration Control in Civil Engineering**, Springer-Verlag, Wein, New York.
31. Structural Engineers Association of California – SEAOC (1999), **Recommended Lateral Force Requirements and Commentary**, Sacramento, CA.
32. Swanson Analysis Systems IP, Inc., (1996), **ANSYS, Finite Element Program and User's Manual**, Version 5.3, Houston, PA.
33. Tsopelas, P. C., Constantinou, M. C., Kim, Y-S and Okamoto, S., (1993), "Experimental Study of (FPS) System in Bridge Seismic Isolation", **Earthquake Engineering & Structural Dynamics**, Vol. 25, 65-78
34. Tsopelas, P. C., Constantinou, M. C. and Reinhorn, A. M., (1994), "3D-BASIS-ME: Computer Program for Nonlinear Dynamic Analysis of Seismically Isolated Single and Multiple Structures and Liquid Storage Tanks", **Report No. MCEER-94-0010**, Multidisciplinary Center for Earthquake Engineering Research, State University of New York, Buffalo, New York.

35. Zayas, V., Low, S. S. and Mahin, S. A. (1987), "The FPS Earthquake Resisting System, Experimental Report", **Report No. UBC/EERC-87/01**, Earthquake Engineering Research Center, University of California, Berkeley, CA.
36. Zhu, Z. Y. and Soong, T. T., (1998), "Toppling Fragility of Unrestrained Equipment", **Proceedings of Seminar on Seismic Design, Retrofit and Performance of Nonstructural Components, ATC 29-1**, Applied Technology Council, Redwood City, CA.

## **Multidisciplinary Center for Earthquake Engineering Research List of Technical Reports**

The Multidisciplinary Center for Earthquake Engineering Research (MCEER) publishes technical reports on a variety of subjects related to earthquake engineering written by authors funded through MCEER. These reports are available from both MCEER Publications and the National Technical Information Service (NTIS). Requests for reports should be directed to MCEER Publications, Multidisciplinary Center for Earthquake Engineering Research, State University of New York at Buffalo, Red Jacket Quadrangle, Buffalo, New York 14261. Reports can also be requested through NTIS, 5285 Port Royal Road, Springfield, Virginia 22161. NTIS accession numbers are shown in parenthesis, if available.

- NCEER-87-0001 "First-Year Program in Research, Education and Technology Transfer," 3/5/87, (PB88-134275, A04, MF-A01).
- NCEER-87-0002 "Experimental Evaluation of Instantaneous Optimal Algorithms for Structural Control," by R.C. Lin, T.T. Soong and A.M. Reinhorn, 4/20/87, (PB88-134341, A04, MF-A01).
- NCEER-87-0003 "Experimentation Using the Earthquake Simulation Facilities at University at Buffalo," by A.M. Reinhorn and R.L. Ketter, to be published.
- NCEER-87-0004 "The System Characteristics and Performance of a Shaking Table," by J.S. Hwang, K.C. Chang and G.C. Lee, 6/1/87, (PB88-134259, A03, MF-A01). This report is available only through NTIS (see address given above).
- NCEER-87-0005 "A Finite Element Formulation for Nonlinear Viscoplastic Material Using a Q Model," by O. Gyebi and G. Dasgupta, 11/2/87, (PB88-213764, A08, MF-A01).
- NCEER-87-0006 "Symbolic Manipulation Program (SMP) - Algebraic Codes for Two and Three Dimensional Finite Element Formulations," by X. Lee and G. Dasgupta, 11/9/87, (PB88-218522, A05, MF-A01).
- NCEER-87-0007 "Instantaneous Optimal Control Laws for Tall Buildings Under Seismic Excitations," by J.N. Yang, A. Akbarpour and P. Ghaemmaghami, 6/10/87, (PB88-134333, A06, MF-A01). This report is only available through NTIS (see address given above).
- NCEER-87-0008 "IDARC: Inelastic Damage Analysis of Reinforced Concrete Frame - Shear-Wall Structures," by Y.J. Park, A.M. Reinhorn and S.K. Kunnath, 7/20/87, (PB88-134325, A09, MF-A01). This report is only available through NTIS (see address given above).
- NCEER-87-0009 "Liquefaction Potential for New York State: A Preliminary Report on Sites in Manhattan and Buffalo," by M. Budhu, V. Vijayakumar, R.F. Giese and L. Baumgras, 8/31/87, (PB88-163704, A03, MF-A01). This report is available only through NTIS (see address given above).
- NCEER-87-0010 "Vertical and Torsional Vibration of Foundations in Inhomogeneous Media," by A.S. Veletsos and K.W. Dotson, 6/1/87, (PB88-134291, A03, MF-A01). This report is only available through NTIS (see address given above).
- NCEER-87-0011 "Seismic Probabilistic Risk Assessment and Seismic Margins Studies for Nuclear Power Plants," by Howard H.M. Hwang, 6/15/87, (PB88-134267, A03, MF-A01). This report is only available through NTIS (see address given above).
- NCEER-87-0012 "Parametric Studies of Frequency Response of Secondary Systems Under Ground-Acceleration Excitations," by Y. Yong and Y.K. Lin, 6/10/87, (PB88-134309, A03, MF-A01). This report is only available through NTIS (see address given above).
- NCEER-87-0013 "Frequency Response of Secondary Systems Under Seismic Excitation," by J.A. HoLung, J. Cai and Y.K. Lin, 7/31/87, (PB88-134317, A05, MF-A01). This report is only available through NTIS (see address given above).
- NCEER-87-0014 "Modelling Earthquake Ground Motions in Seismically Active Regions Using Parametric Time Series Methods," by G.W. Ellis and A.S. Cakmak, 8/25/87, (PB88-134283, A08, MF-A01). This report is only available through NTIS (see address given above).

- NCEER-87-0015 "Detection and Assessment of Seismic Structural Damage," by E. DiPasquale and A.S. Cakmak, 8/25/87, (PB88-163712, A05, MF-A01). This report is only available through NTIS (see address given above).
- NCEER-87-0016 "Pipeline Experiment at Parkfield, California," by J. Isenberg and E. Richardson, 9/15/87, (PB88-163720, A03, MF-A01). This report is available only through NTIS (see address given above).
- NCEER-87-0017 "Digital Simulation of Seismic Ground Motion," by M. Shinozuka, G. Deodatis and T. Harada, 8/31/87, (PB88-155197, A04, MF-A01). This report is available only through NTIS (see address given above).
- NCEER-87-0018 "Practical Considerations for Structural Control: System Uncertainty, System Time Delay and Truncation of Small Control Forces," J.N. Yang and A. Akbarpour, 8/10/87, (PB88-163738, A08, MF-A01). This report is only available through NTIS (see address given above).
- NCEER-87-0019 "Modal Analysis of Nonclassically Damped Structural Systems Using Canonical Transformation," by J.N. Yang, S. Sarkani and F.X. Long, 9/27/87, (PB88-187851, A04, MF-A01).
- NCEER-87-0020 "A Nonstationary Solution in Random Vibration Theory," by J.R. Red-Horse and P.D. Spanos, 11/3/87, (PB88-163746, A03, MF-A01).
- NCEER-87-0021 "Horizontal Impedances for Radially Inhomogeneous Viscoelastic Soil Layers," by A.S. Veletsos and K.W. Dotson, 10/15/87, (PB88-150859, A04, MF-A01).
- NCEER-87-0022 "Seismic Damage Assessment of Reinforced Concrete Members," by Y.S. Chung, C. Meyer and M. Shinozuka, 10/9/87, (PB88-150867, A05, MF-A01). This report is available only through NTIS (see address given above).
- NCEER-87-0023 "Active Structural Control in Civil Engineering," by T.T. Soong, 11/11/87, (PB88-187778, A03, MF-A01).
- NCEER-87-0024 "Vertical and Torsional Impedances for Radially Inhomogeneous Viscoelastic Soil Layers," by K.W. Dotson and A.S. Veletsos, 12/87, (PB88-187786, A03, MF-A01).
- NCEER-87-0025 "Proceedings from the Symposium on Seismic Hazards, Ground Motions, Soil-Liquefaction and Engineering Practice in Eastern North America," October 20-22, 1987, edited by K.H. Jacob, 12/87, (PB88-188115, A23, MF-A01). This report is available only through NTIS (see address given above).
- NCEER-87-0026 "Report on the Whittier-Narrows, California, Earthquake of October 1, 1987," by J. Pantelic and A. Reinhorn, 11/87, (PB88-187752, A03, MF-A01). This report is available only through NTIS (see address given above).
- NCEER-87-0027 "Design of a Modular Program for Transient Nonlinear Analysis of Large 3-D Building Structures," by S. Srivastav and J.F. Abel, 12/30/87, (PB88-187950, A05, MF-A01). This report is only available through NTIS (see address given above).
- NCEER-87-0028 "Second-Year Program in Research, Education and Technology Transfer," 3/8/88, (PB88-219480, A04, MF-A01).
- NCEER-88-0001 "Workshop on Seismic Computer Analysis and Design of Buildings With Interactive Graphics," by W. McGuire, J.F. Abel and C.H. Conley, 1/18/88, (PB88-187760, A03, MF-A01). This report is only available through NTIS (see address given above).
- NCEER-88-0002 "Optimal Control of Nonlinear Flexible Structures," by J.N. Yang, F.X. Long and D. Wong, 1/22/88, (PB88-213772, A06, MF-A01).
- NCEER-88-0003 "Substructuring Techniques in the Time Domain for Primary-Secondary Structural Systems," by G.D. Manolis and G. Juhn, 2/10/88, (PB88-213780, A04, MF-A01).
- NCEER-88-0004 "Iterative Seismic Analysis of Primary-Secondary Systems," by A. Singhal, L.D. Lutes and P.D. Spanos, 2/23/88, (PB88-213798, A04, MF-A01).

- NCEER-88-0005 "Stochastic Finite Element Expansion for Random Media," by P.D. Spanos and R. Ghanem, 3/14/88, (PB88-213806, A03, MF-A01).
- NCEER-88-0006 "Combining Structural Optimization and Structural Control," by F.Y. Cheng and C.P. Pantelides, 1/10/88, (PB88-213814, A05, MF-A01).
- NCEER-88-0007 "Seismic Performance Assessment of Code-Designed Structures," by H.H-M. Hwang, J-W. Jaw and H-J. Shau, 3/20/88, (PB88-219423, A04, MF-A01). This report is only available through NTIS (see address given above).
- NCEER-88-0008 "Reliability Analysis of Code-Designed Structures Under Natural Hazards," by H.H-M. Hwang, H. Ushiba and M. Shinozuka, 2/29/88, (PB88-229471, A07, MF-A01). This report is only available through NTIS (see address given above).
- NCEER-88-0009 "Seismic Fragility Analysis of Shear Wall Structures," by J-W Jaw and H.H-M. Hwang, 4/30/88, (PB89-102867, A04, MF-A01).
- NCEER-88-0010 "Base Isolation of a Multi-Story Building Under a Harmonic Ground Motion - A Comparison of Performances of Various Systems," by F-G Fan, G. Ahmadi and I.G. Tadjbakhsh, 5/18/88, (PB89-122238, A06, MF-A01). This report is only available through NTIS (see address given above).
- NCEER-88-0011 "Seismic Floor Response Spectra for a Combined System by Green's Functions," by F.M. Lavelle, L.A. Bergman and P.D. Spanos, 5/1/88, (PB89-102875, A03, MF-A01).
- NCEER-88-0012 "A New Solution Technique for Randomly Excited Hysteretic Structures," by G.Q. Cai and Y.K. Lin, 5/16/88, (PB89-102883, A03, MF-A01).
- NCEER-88-0013 "A Study of Radiation Damping and Soil-Structure Interaction Effects in the Centrifuge," by K. Weissman, supervised by J.H. Prevost, 5/24/88, (PB89-144703, A06, MF-A01).
- NCEER-88-0014 "Parameter Identification and Implementation of a Kinematic Plasticity Model for Frictional Soils," by J.H. Prevost and D.V. Griffiths, to be published.
- NCEER-88-0015 "Two- and Three- Dimensional Dynamic Finite Element Analyses of the Long Valley Dam," by D.V. Griffiths and J.H. Prevost, 6/17/88, (PB89-144711, A04, MF-A01).
- NCEER-88-0016 "Damage Assessment of Reinforced Concrete Structures in Eastern United States," by A.M. Reinhorn, M.J. Seidel, S.K. Kunnath and Y.J. Park, 6/15/88, (PB89-122220, A04, MF-A01). This report is only available through NTIS (see address given above).
- NCEER-88-0017 "Dynamic Compliance of Vertically Loaded Strip Foundations in Multilayered Viscoelastic Soils," by S. Ahmad and A.S.M. Israil, 6/17/88, (PB89-102891, A04, MF-A01).
- NCEER-88-0018 "An Experimental Study of Seismic Structural Response With Added Viscoelastic Dampers," by R.C. Lin, Z. Liang, T.T. Soong and R.H. Zhang, 6/30/88, (PB89-122212, A05, MF-A01). This report is available only through NTIS (see address given above).
- NCEER-88-0019 "Experimental Investigation of Primary - Secondary System Interaction," by G.D. Manolis, G. Juhn and A.M. Reinhorn, 5/27/88, (PB89-122204, A04, MF-A01).
- NCEER-88-0020 "A Response Spectrum Approach For Analysis of Nonclassically Damped Structures," by J.N. Yang, S. Sarkani and F.X. Long, 4/22/88, (PB89-102909, A04, MF-A01).
- NCEER-88-0021 "Seismic Interaction of Structures and Soils: Stochastic Approach," by A.S. Veletsos and A.M. Prasad, 7/21/88, (PB89-122196, A04, MF-A01). This report is only available through NTIS (see address given above).
- NCEER-88-0022 "Identification of the Serviceability Limit State and Detection of Seismic Structural Damage," by E. DiPasquale and A.S. Cakmak, 6/15/88, (PB89-122188, A05, MF-A01). This report is available only through NTIS (see address given above).

- NCEER-88-0023 "Multi-Hazard Risk Analysis: Case of a Simple Offshore Structure," by B.K. Bhartia and E.H. Vanmarcke, 7/21/88, (PB89-145213, A05, MF-A01).
- NCEER-88-0024 "Automated Seismic Design of Reinforced Concrete Buildings," by Y.S. Chung, C. Meyer and M. Shinozuka, 7/5/88, (PB89-122170, A06, MF-A01). This report is available only through NTIS (see address given above).
- NCEER-88-0025 "Experimental Study of Active Control of MDOF Structures Under Seismic Excitations," by L.L. Chung, R.C. Lin, T.T. Soong and A.M. Reinhorn, 7/10/88, (PB89-122600, A04, MF-A01).
- NCEER-88-0026 "Earthquake Simulation Tests of a Low-Rise Metal Structure," by J.S. Hwang, K.C. Chang, G.C. Lee and R.L. Ketter, 8/1/88, (PB89-102917, A04, MF-A01).
- NCEER-88-0027 "Systems Study of Urban Response and Reconstruction Due to Catastrophic Earthquakes," by F. Kozin and H.K. Zhou, 9/22/88, (PB90-162348, A04, MF-A01).
- NCEER-88-0028 "Seismic Fragility Analysis of Plane Frame Structures," by H.H-M. Hwang and Y.K. Low, 7/31/88, (PB89-131445, A06, MF-A01).
- NCEER-88-0029 "Response Analysis of Stochastic Structures," by A. Kardara, C. Bucher and M. Shinozuka, 9/22/88, (PB89-174429, A04, MF-A01).
- NCEER-88-0030 "Nonnormal Accelerations Due to Yielding in a Primary Structure," by D.C.K. Chen and L.D. Lutes, 9/19/88, (PB89-131437, A04, MF-A01).
- NCEER-88-0031 "Design Approaches for Soil-Structure Interaction," by A.S. Veletsos, A.M. Prasad and Y. Tang, 12/30/88, (PB89-174437, A03, MF-A01). This report is available only through NTIS (see address given above).
- NCEER-88-0032 "A Re-evaluation of Design Spectra for Seismic Damage Control," by C.J. Turkstra and A.G. Tallin, 11/7/88, (PB89-145221, A05, MF-A01).
- NCEER-88-0033 "The Behavior and Design of Noncontact Lap Splices Subjected to Repeated Inelastic Tensile Loading," by V.E. Sagan, P. Gergely and R.N. White, 12/8/88, (PB89-163737, A08, MF-A01).
- NCEER-88-0034 "Seismic Response of Pile Foundations," by S.M. Mamoon, P.K. Banerjee and S. Ahmad, 11/1/88, (PB89-145239, A04, MF-A01).
- NCEER-88-0035 "Modeling of R/C Building Structures With Flexible Floor Diaphragms (IDARC2)," by A.M. Reinhorn, S.K. Kunnath and N. Panahshahi, 9/7/88, (PB89-207153, A07, MF-A01).
- NCEER-88-0036 "Solution of the Dam-Reservoir Interaction Problem Using a Combination of FEM, BEM with Particular Integrals, Modal Analysis, and Substructuring," by C-S. Tsai, G.C. Lee and R.L. Ketter, 12/31/88, (PB89-207146, A04, MF-A01).
- NCEER-88-0037 "Optimal Placement of Actuators for Structural Control," by F.Y. Cheng and C.P. Pantelides, 8/15/88, (PB89-162846, A05, MF-A01).
- NCEER-88-0038 "Teflon Bearings in Aseismic Base Isolation: Experimental Studies and Mathematical Modeling," by A. Mokha, M.C. Constantinou and A.M. Reinhorn, 12/5/88, (PB89-218457, A10, MF-A01). This report is available only through NTIS (see address given above).
- NCEER-88-0039 "Seismic Behavior of Flat Slab High-Rise Buildings in the New York City Area," by P. Weidlinger and M. Ettouney, 10/15/88, (PB90-145681, A04, MF-A01).
- NCEER-88-0040 "Evaluation of the Earthquake Resistance of Existing Buildings in New York City," by P. Weidlinger and M. Ettouney, 10/15/88, to be published.
- NCEER-88-0041 "Small-Scale Modeling Techniques for Reinforced Concrete Structures Subjected to Seismic Loads," by W. Kim, A. El-Attar and R.N. White, 11/22/88, (PB89-189625, A05, MF-A01).



- NCEER-88-0042 "Modeling Strong Ground Motion from Multiple Event Earthquakes," by G.W. Ellis and A.S. Cakmak, 10/15/88, (PB89-174445, A03, MF-A01).
- NCEER-88-0043 "Nonstationary Models of Seismic Ground Acceleration," by M. Grigoriu, S.E. Ruiz and E. Rosenblueth, 7/15/88, (PB89-189617, A04, MF-A01).
- NCEER-88-0044 "SARCF User's Guide: Seismic Analysis of Reinforced Concrete Frames," by Y.S. Chung, C. Meyer and M. Shinozuka, 11/9/88, (PB89-174452, A08, MF-A01).
- NCEER-88-0045 "First Expert Panel Meeting on Disaster Research and Planning," edited by J. Pantelic and J. Stoyke, 9/15/88, (PB89-174460, A05, MF-A01).
- NCEER-88-0046 "Preliminary Studies of the Effect of Degrading Infill Walls on the Nonlinear Seismic Response of Steel Frames," by C.Z. Chrysostomou, P. Gergely and J.F. Abel, 12/19/88, (PB89-208383, A05, MF-A01).
- NCEER-88-0047 "Reinforced Concrete Frame Component Testing Facility - Design, Construction, Instrumentation and Operation," by S.P. Pessiki, C. Conley, T. Bond, P. Gergely and R.N. White, 12/16/88, (PB89-174478, A04, MF-A01).
- NCEER-89-0001 "Effects of Protective Cushion and Soil Compliancy on the Response of Equipment Within a Seismically Excited Building," by J.A. HoLung, 2/16/89, (PB89-207179, A04, MF-A01).
- NCEER-89-0002 "Statistical Evaluation of Response Modification Factors for Reinforced Concrete Structures," by H.H-M. Hwang and J-W. Jaw, 2/17/89, (PB89-207187, A05, MF-A01).
- NCEER-89-0003 "Hysteretic Columns Under Random Excitation," by G-Q. Cai and Y.K. Lin, 1/9/89, (PB89-196513, A03, MF-A01).
- NCEER-89-0004 "Experimental Study of 'Elephant Foot Bulge' Instability of Thin-Walled Metal Tanks," by Z-H. Jia and R.L. Ketter, 2/22/89, (PB89-207195, A03, MF-A01).
- NCEER-89-0005 "Experiment on Performance of Buried Pipelines Across San Andreas Fault," by J. Isenberg, E. Richardson and T.D. O'Rourke, 3/10/89, (PB89-218440, A04, MF-A01). This report is available only through NTIS (see address given above).
- NCEER-89-0006 "A Knowledge-Based Approach to Structural Design of Earthquake-Resistant Buildings," by M. Subramani, P. Gergely, C.H. Conley, J.F. Abel and A.H. Zaghaw, 1/15/89, (PB89-218465, A06, MF-A01).
- NCEER-89-0007 "Liquefaction Hazards and Their Effects on Buried Pipelines," by T.D. O'Rourke and P.A. Lane, 2/1/89, (PB89-218481, A09, MF-A01).
- NCEER-89-0008 "Fundamentals of System Identification in Structural Dynamics," by H. Imai, C-B. Yun, O. Maruyama and M. Shinozuka, 1/26/89, (PB89-207211, A04, MF-A01).
- NCEER-89-0009 "Effects of the 1985 Michoacan Earthquake on Water Systems and Other Buried Lifelines in Mexico," by A.G. Ayala and M.J. O'Rourke, 3/8/89, (PB89-207229, A06, MF-A01).
- NCEER-89-R010 "NCEER Bibliography of Earthquake Education Materials," by K.E.K. Ross, Second Revision, 9/1/89, (PB90-125352, A05, MF-A01). This report is replaced by NCEER-92-0018.
- NCEER-89-0011 "Inelastic Three-Dimensional Response Analysis of Reinforced Concrete Building Structures (IDARC-3D), Part I - Modeling," by S.K. Kunnath and A.M. Reinhorn, 4/17/89, (PB90-114612, A07, MF-A01). This report is available only through NTIS (see address given above).
- NCEER-89-0012 "Recommended Modifications to ATC-14," by C.D. Poland and J.O. Malley, 4/12/89, (PB90-108648, A15, MF-A01).
- NCEER-89-0013 "Repair and Strengthening of Beam-to-Column Connections Subjected to Earthquake Loading," by M. Corazao and A.J. Durrani, 2/28/89, (PB90-109885, A06, MF-A01).

- NCEER-89-0014 "Program EXKAL2 for Identification of Structural Dynamic Systems," by O. Maruyama, C-B. Yun, M. Hoshiya and M. Shinozuka, 5/19/89, (PB90-109877, A09, MF-A01).
- NCEER-89-0015 "Response of Frames With Bolted Semi-Rigid Connections, Part I - Experimental Study and Analytical Predictions," by P.J. DiCorso, A.M. Reinhorn, J.R. Dickerson, J.B. Radzinski and W.L. Harper, 6/1/89, to be published.
- NCEER-89-0016 "ARMA Monte Carlo Simulation in Probabilistic Structural Analysis," by P.D. Spanos and M.P. Mignolet, 7/10/89, (PB90-109893, A03, MF-A01).
- NCEER-89-P017 "Preliminary Proceedings from the Conference on Disaster Preparedness - The Place of Earthquake Education in Our Schools," Edited by K.E.K. Ross, 6/23/89, (PB90-108606, A03, MF-A01).
- NCEER-89-0017 "Proceedings from the Conference on Disaster Preparedness - The Place of Earthquake Education in Our Schools," Edited by K.E.K. Ross, 12/31/89, (PB90-207895, A012, MF-A02). This report is available only through NTIS (see address given above).
- NCEER-89-0018 "Multidimensional Models of Hysteretic Material Behavior for Vibration Analysis of Shape Memory Energy Absorbing Devices, by E.J. Graesser and F.A. Cozzarelli, 6/7/89, (PB90-164146, A04, MF-A01).
- NCEER-89-0019 "Nonlinear Dynamic Analysis of Three-Dimensional Base Isolated Structures (3D-BASIS)," by S. Nagarajaiah, A.M. Reinhorn and M.C. Constantinou, 8/3/89, (PB90-161936, A06, MF-A01). This report has been replaced by NCEER-93-0011.
- NCEER-89-0020 "Structural Control Considering Time-Rate of Control Forces and Control Rate Constraints," by F.Y. Cheng and C.P. Pantelides, 8/3/89, (PB90-120445, A04, MF-A01).
- NCEER-89-0021 "Subsurface Conditions of Memphis and Shelby County," by K.W. Ng, T-S. Chang and H-H.M. Hwang, 7/26/89, (PB90-120437, A03, MF-A01).
- NCEER-89-0022 "Seismic Wave Propagation Effects on Straight Jointed Buried Pipelines," by K. Elhadi and M.J. O'Rourke, 8/24/89, (PB90-162322, A10, MF-A02).
- NCEER-89-0023 "Workshop on Serviceability Analysis of Water Delivery Systems," edited by M. Grigoriu, 3/6/89, (PB90-127424, A03, MF-A01).
- NCEER-89-0024 "Shaking Table Study of a 1/5 Scale Steel Frame Composed of Tapered Members," by K.C. Chang, J.S. Hwang and G.C. Lee, 9/18/89, (PB90-160169, A04, MF-A01).
- NCEER-89-0025 "DYNA1D: A Computer Program for Nonlinear Seismic Site Response Analysis - Technical Documentation," by Jean H. Prevost, 9/14/89, (PB90-161944, A07, MF-A01). This report is available only through NTIS (see address given above).
- NCEER-89-0026 "1:4 Scale Model Studies of Active Tendon Systems and Active Mass Dampers for Aseismic Protection," by A.M. Reinhorn, T.T. Soong, R.C. Lin, Y.P. Yang, Y. Fukao, H. Abe and M. Nakai, 9/15/89, (PB90-173246, A10, MF-A02). This report is available only through NTIS (see address given above).
- NCEER-89-0027 "Scattering of Waves by Inclusions in a Nonhomogeneous Elastic Half Space Solved by Boundary Element Methods," by P.K. Hadley, A. Askar and A.S. Cakmak, 6/15/89, (PB90-145699, A07, MF-A01).
- NCEER-89-0028 "Statistical Evaluation of Deflection Amplification Factors for Reinforced Concrete Structures," by H.H.M. Hwang, J-W. Jaw and A.L. Ch'ng, 8/31/89, (PB90-164633, A05, MF-A01).
- NCEER-89-0029 "Bedrock Accelerations in Memphis Area Due to Large New Madrid Earthquakes," by H.H.M. Hwang, C.H.S. Chen and G. Yu, 11/7/89, (PB90-162330, A04, MF-A01).
- NCEER-89-0030 "Seismic Behavior and Response Sensitivity of Secondary Structural Systems," by Y.Q. Chen and T.T. Soong, 10/23/89, (PB90-164658, A08, MF-A01).
- NCEER-89-0031 "Random Vibration and Reliability Analysis of Primary-Secondary Structural Systems," by Y. Ibrahim, M. Grigoriu and T.T. Soong, 11/10/89, (PB90-161951, A04, MF-A01).

- NCEER-89-0032 "Proceedings from the Second U.S. - Japan Workshop on Liquefaction, Large Ground Deformation and Their Effects on Lifelines, September 26-29, 1989," Edited by T.D. O'Rourke and M. Hamada, 12/1/89, (PB90-209388, A22, MF-A03).
- NCEER-89-0033 "Deterministic Model for Seismic Damage Evaluation of Reinforced Concrete Structures," by J.M. Bracci, A.M. Reinhorn, J.B. Mander and S.K. Kunnath, 9/27/89, (PB91-108803, A06, MF-A01).
- NCEER-89-0034 "On the Relation Between Local and Global Damage Indices," by E. DiPasquale and A.S. Cakmak, 8/15/89, (PB90-173865, A05, MF-A01).
- NCEER-89-0035 "Cyclic Undrained Behavior of Nonplastic and Low Plasticity Silts," by A.J. Walker and H.E. Stewart, 7/26/89, (PB90-183518, A10, MF-A01).
- NCEER-89-0036 "Liquefaction Potential of Surficial Deposits in the City of Buffalo, New York," by M. Budhu, R. Giese and L. Baumgrass, 1/17/89, (PB90-208455, A04, MF-A01).
- NCEER-89-0037 "A Deterministic Assessment of Effects of Ground Motion Incoherence," by A.S. Veletsos and Y. Tang, 7/15/89, (PB90-164294, A03, MF-A01).
- NCEER-89-0038 "Workshop on Ground Motion Parameters for Seismic Hazard Mapping," July 17-18, 1989, edited by R.V. Whitman, 12/1/89, (PB90-173923, A04, MF-A01).
- NCEER-89-0039 "Seismic Effects on Elevated Transit Lines of the New York City Transit Authority," by C.J. Costantino, C.A. Miller and E. Heymsfield, 12/26/89, (PB90-207887, A06, MF-A01).
- NCEER-89-0040 "Centrifugal Modeling of Dynamic Soil-Structure Interaction," by K. Weissman, Supervised by J.H. Prevost, 5/10/89, (PB90-207879, A07, MF-A01).
- NCEER-89-0041 "Linearized Identification of Buildings With Cores for Seismic Vulnerability Assessment," by I-K. Ho and A.E. Aktan, 11/1/89, (PB90-251943, A07, MF-A01).
- NCEER-90-0001 "Geotechnical and Lifeline Aspects of the October 17, 1989 Loma Prieta Earthquake in San Francisco," by T.D. O'Rourke, H.E. Stewart, F.T. Blackburn and T.S. Dickerman, 1/90, (PB90-208596, A05, MF-A01).
- NCEER-90-0002 "Nonnormal Secondary Response Due to Yielding in a Primary Structure," by D.C.K. Chen and L.D. Lutes, 2/28/90, (PB90-251976, A07, MF-A01).
- NCEER-90-0003 "Earthquake Education Materials for Grades K-12," by K.E.K. Ross, 4/16/90, (PB91-251984, A05, MF-A05). This report has been replaced by NCEER-92-0018.
- NCEER-90-0004 "Catalog of Strong Motion Stations in Eastern North America," by R.W. Busby, 4/3/90, (PB90-251984, A05, MF-A01).
- NCEER-90-0005 "NCEER Strong-Motion Data Base: A User Manual for the GeoBase Release (Version 1.0 for the Sun3)," by P. Friberg and K. Jacob, 3/31/90 (PB90-258062, A04, MF-A01).
- NCEER-90-0006 "Seismic Hazard Along a Crude Oil Pipeline in the Event of an 1811-1812 Type New Madrid Earthquake," by H.H.M. Hwang and C-H.S. Chen, 4/16/90, (PB90-258054, A04, MF-A01).
- NCEER-90-0007 "Site-Specific Response Spectra for Memphis Sheahan Pumping Station," by H.H.M. Hwang and C.S. Lee, 5/15/90, (PB91-108811, A05, MF-A01).
- NCEER-90-0008 "Pilot Study on Seismic Vulnerability of Crude Oil Transmission Systems," by T. Ariman, R. Dobry, M. Grigoriu, F. Kozin, M. O'Rourke, T. O'Rourke and M. Shinozuka, 5/25/90, (PB91-108837, A06, MF-A01).
- NCEER-90-0009 "A Program to Generate Site Dependent Time Histories: EQGEN," by G.W. Ellis, M. Srinivasan and A.S. Cakmak, 1/30/90, (PB91-108829, A04, MF-A01).
- NCEER-90-0010 "Active Isolation for Seismic Protection of Operating Rooms," by M.E. Talbott, Supervised by M. Shinozuka, 6/8/9, (PB91-110205, A05, MF-A01).

- NCEER-90-0011 "Program LINEARID for Identification of Linear Structural Dynamic Systems," by C-B. Yun and M. Shinozuka, 6/25/90, (PB91-110312, A08, MF-A01).
- NCEER-90-0012 "Two-Dimensional Two-Phase Elasto-Plastic Seismic Response of Earth Dams," by A.N. Yiagos, Supervised by J.H. Prevost, 6/20/90, (PB91-110197, A13, MF-A02).
- NCEER-90-0013 "Secondary Systems in Base-Isolated Structures: Experimental Investigation, Stochastic Response and Stochastic Sensitivity," by G.D. Manolis, G. Juhn, M.C. Constantinou and A.M. Reinhorn, 7/1/90, (PB91-110320, A08, MF-A01).
- NCEER-90-0014 "Seismic Behavior of Lightly-Reinforced Concrete Column and Beam-Column Joint Details," by S.P. Pessiki, C.H. Conley, P. Gergely and R.N. White, 8/22/90, (PB91-108795, A11, MF-A02).
- NCEER-90-0015 "Two Hybrid Control Systems for Building Structures Under Strong Earthquakes," by J.N. Yang and A. Danielians, 6/29/90, (PB91-125393, A04, MF-A01).
- NCEER-90-0016 "Instantaneous Optimal Control with Acceleration and Velocity Feedback," by J.N. Yang and Z. Li, 6/29/90, (PB91-125401, A03, MF-A01).
- NCEER-90-0017 "Reconnaissance Report on the Northern Iran Earthquake of June 21, 1990," by M. Mehrain, 10/4/90, (PB91-125377, A03, MF-A01).
- NCEER-90-0018 "Evaluation of Liquefaction Potential in Memphis and Shelby County," by T.S. Chang, P.S. Tang, C.S. Lee and H. Hwang, 8/10/90, (PB91-125427, A09, MF-A01).
- NCEER-90-0019 "Experimental and Analytical Study of a Combined Sliding Disc Bearing and Helical Steel Spring Isolation System," by M.C. Constantinou, A.S. Mokha and A.M. Reinhorn, 10/4/90, (PB91-125385, A06, MF-A01). This report is available only through NTIS (see address given above).
- NCEER-90-0020 "Experimental Study and Analytical Prediction of Earthquake Response of a Sliding Isolation System with a Spherical Surface," by A.S. Mokha, M.C. Constantinou and A.M. Reinhorn, 10/11/90, (PB91-125419, A05, MF-A01).
- NCEER-90-0021 "Dynamic Interaction Factors for Floating Pile Groups," by G. Gazetas, K. Fan, A. Kaynia and E. Kausel, 9/10/90, (PB91-170381, A05, MF-A01).
- NCEER-90-0022 "Evaluation of Seismic Damage Indices for Reinforced Concrete Structures," by S. Rodriguez-Gomez and A.S. Cakmak, 9/30/90, PB91-171322, A06, MF-A01).
- NCEER-90-0023 "Study of Site Response at a Selected Memphis Site," by H. Desai, S. Ahmad, E.S. Gazetas and M.R. Oh, 10/11/90, (PB91-196857, A03, MF-A01).
- NCEER-90-0024 "A User's Guide to Strongmo: Version 1.0 of NCEER's Strong-Motion Data Access Tool for PCs and Terminals," by P.A. Friberg and C.A.T. Susch, 11/15/90, (PB91-171272, A03, MF-A01).
- NCEER-90-0025 "A Three-Dimensional Analytical Study of Spatial Variability of Seismic Ground Motions," by L-L. Hong and A.H.-S. Ang, 10/30/90, (PB91-170399, A09, MF-A01).
- NCEER-90-0026 "MUMOID User's Guide - A Program for the Identification of Modal Parameters," by S. Rodriguez-Gomez and E. DiPasquale, 9/30/90, (PB91-171298, A04, MF-A01).
- NCEER-90-0027 "SARCF-II User's Guide - Seismic Analysis of Reinforced Concrete Frames," by S. Rodriguez-Gomez, Y.S. Chung and C. Meyer, 9/30/90, (PB91-171280, A05, MF-A01).
- NCEER-90-0028 "Viscous Dampers: Testing, Modeling and Application in Vibration and Seismic Isolation," by N. Makris and M.C. Constantinou, 12/20/90 (PB91-190561, A06, MF-A01).
- NCEER-90-0029 "Soil Effects on Earthquake Ground Motions in the Memphis Area," by H. Hwang, C.S. Lee, K.W. Ng and T.S. Chang, 8/2/90, (PB91-190751, A05, MF-A01).

- NCEER-91-0001 "Proceedings from the Third Japan-U.S. Workshop on Earthquake Resistant Design of Lifeline Facilities and Countermeasures for Soil Liquefaction, December 17-19, 1990," edited by T.D. O'Rourke and M. Hamada, 2/1/91, (PB91-179259, A99, MF-A04).
- NCEER-91-0002 "Physical Space Solutions of Non-Proportionally Damped Systems," by M. Tong, Z. Liang and G.C. Lee, 1/15/91, (PB91-179242, A04, MF-A01).
- NCEER-91-0003 "Seismic Response of Single Piles and Pile Groups," by K. Fan and G. Gazetas, 1/10/91, (PB92-174994, A04, MF-A01).
- NCEER-91-0004 "Damping of Structures: Part 1 - Theory of Complex Damping," by Z. Liang and G. Lee, 10/10/91, (PB92-197235, A12, MF-A03).
- NCEER-91-0005 "3D-BASIS - Nonlinear Dynamic Analysis of Three Dimensional Base Isolated Structures: Part II," by S. Nagarajaiah, A.M. Reinhorn and M.C. Constantinou, 2/28/91, (PB91-190553, A07, MF-A01). This report has been replaced by NCEER-93-0011.
- NCEER-91-0006 "A Multidimensional Hysteretic Model for Plasticity Deforming Metals in Energy Absorbing Devices," by E.J. Graesser and F.A. Cozzarelli, 4/9/91, (PB92-108364, A04, MF-A01).
- NCEER-91-0007 "A Framework for Customizable Knowledge-Based Expert Systems with an Application to a KBES for Evaluating the Seismic Resistance of Existing Buildings," by E.G. Ibarra-Anaya and S.J. Fenves, 4/9/91, (PB91-210930, A08, MF-A01).
- NCEER-91-0008 "Nonlinear Analysis of Steel Frames with Semi-Rigid Connections Using the Capacity Spectrum Method," by G.G. Deierlein, S-H. Hsieh, Y-J. Shen and J.F. Abel, 7/2/91, (PB92-113828, A05, MF-A01).
- NCEER-91-0009 "Earthquake Education Materials for Grades K-12," by K.E.K. Ross, 4/30/91, (PB91-212142, A06, MF-A01). This report has been replaced by NCEER-92-0018.
- NCEER-91-0010 "Phase Wave Velocities and Displacement Phase Differences in a Harmonically Oscillating Pile," by N. Makris and G. Gazetas, 7/8/91, (PB92-108356, A04, MF-A01).
- NCEER-91-0011 "Dynamic Characteristics of a Full-Size Five-Story Steel Structure and a 2/5 Scale Model," by K.C. Chang, G.C. Yao, G.C. Lee, D.S. Hao and Y.C. Yeh," 7/2/91, (PB93-116648, A06, MF-A02).
- NCEER-91-0012 "Seismic Response of a 2/5 Scale Steel Structure with Added Viscoelastic Dampers," by K.C. Chang, T.T. Soong, S-T. Oh and M.L. Lai, 5/17/91, (PB92-110816, A05, MF-A01).
- NCEER-91-0013 "Earthquake Response of Retaining Walls; Full-Scale Testing and Computational Modeling," by S. Alampalli and A-W.M. Elgamal, 6/20/91, to be published.
- NCEER-91-0014 "3D-BASIS-M: Nonlinear Dynamic Analysis of Multiple Building Base Isolated Structures," by P.C. Tsopelas, S. Nagarajaiah, M.C. Constantinou and A.M. Reinhorn, 5/28/91, (PB92-113885, A09, MF-A02).
- NCEER-91-0015 "Evaluation of SEAOC Design Requirements for Sliding Isolated Structures," by D. Theodossiou and M.C. Constantinou, 6/10/91, (PB92-114602, A11, MF-A03).
- NCEER-91-0016 "Closed-Loop Modal Testing of a 27-Story Reinforced Concrete Flat Plate-Core Building," by H.R. Somaprasad, T. Toksoy, H. Yoshiyuki and A.E. Aktan, 7/15/91, (PB92-129980, A07, MF-A02).
- NCEER-91-0017 "Shake Table Test of a 1/6 Scale Two-Story Lightly Reinforced Concrete Building," by A.G. El-Attar, R.N. White and P. Gergely, 2/28/91, (PB92-222447, A06, MF-A02).
- NCEER-91-0018 "Shake Table Test of a 1/8 Scale Three-Story Lightly Reinforced Concrete Building," by A.G. El-Attar, R.N. White and P. Gergely, 2/28/91, (PB93-116630, A08, MF-A02).
- NCEER-91-0019 "Transfer Functions for Rigid Rectangular Foundations," by A.S. Veletsos, A.M. Prasad and W.H. Wu, 7/31/91, to be published.

- NCEER-91-0020 "Hybrid Control of Seismic-Excited Nonlinear and Inelastic Structural Systems," by J.N. Yang, Z. Li and A. Daniellians, 8/1/91, (PB92-143171, A06, MF-A02).
- NCEER-91-0021 "The NCEER-91 Earthquake Catalog: Improved Intensity-Based Magnitudes and Recurrence Relations for U.S. Earthquakes East of New Madrid," by L. Seeber and J.G. Armbruster, 8/28/91, (PB92-176742, A06, MF-A02).
- NCEER-91-0022 "Proceedings from the Implementation of Earthquake Planning and Education in Schools: The Need for Change - The Roles of the Changemakers," by K.E.K. Ross and F. Winslow, 7/23/91, (PB92-129998, A12, MF-A03).
- NCEER-91-0023 "A Study of Reliability-Based Criteria for Seismic Design of Reinforced Concrete Frame Buildings," by H.H.M. Hwang and H-M. Hsu, 8/10/91, (PB92-140235, A09, MF-A02).
- NCEER-91-0024 "Experimental Verification of a Number of Structural System Identification Algorithms," by R.G. Ghanem, H. Gavin and M. Shinozuka, 9/18/91, (PB92-176577, A18, MF-A04).
- NCEER-91-0025 "Probabilistic Evaluation of Liquefaction Potential," by H.H.M. Hwang and C.S. Lee," 11/25/91, (PB92-143429, A05, MF-A01).
- NCEER-91-0026 "Instantaneous Optimal Control for Linear, Nonlinear and Hysteretic Structures - Stable Controllers," by J.N. Yang and Z. Li, 11/15/91, (PB92-163807, A04, MF-A01).
- NCEER-91-0027 "Experimental and Theoretical Study of a Sliding Isolation System for Bridges," by M.C. Constantinou, A. Kartoum, A.M. Reinhorn and P. Bradford, 11/15/91, (PB92-176973, A10, MF-A03).
- NCEER-92-0001 "Case Studies of Liquefaction and Lifeline Performance During Past Earthquakes, Volume 1: Japanese Case Studies," Edited by M. Hamada and T. O'Rourke, 2/17/92, (PB92-197243, A18, MF-A04).
- NCEER-92-0002 "Case Studies of Liquefaction and Lifeline Performance During Past Earthquakes, Volume 2: United States Case Studies," Edited by T. O'Rourke and M. Hamada, 2/17/92, (PB92-197250, A20, MF-A04).
- NCEER-92-0003 "Issues in Earthquake Education," Edited by K. Ross, 2/3/92, (PB92-222389, A07, MF-A02).
- NCEER-92-0004 "Proceedings from the First U.S. - Japan Workshop on Earthquake Protective Systems for Bridges," Edited by I.G. Buckle, 2/4/92, (PB94-142239, A99, MF-A06).
- NCEER-92-0005 "Seismic Ground Motion from a Haskell-Type Source in a Multiple-Layered Half-Space," A.P. Theoharis, G. Deodatis and M. Shinozuka, 1/2/92, to be published.
- NCEER-92-0006 "Proceedings from the Site Effects Workshop," Edited by R. Whitman, 2/29/92, (PB92-197201, A04, MF-A01).
- NCEER-92-0007 "Engineering Evaluation of Permanent Ground Deformations Due to Seismically-Induced Liquefaction," by M.H. Baziar, R. Dobry and A-W.M. Elgamel, 3/24/92, (PB92-222421, A13, MF-A03).
- NCEER-92-0008 "A Procedure for the Seismic Evaluation of Buildings in the Central and Eastern United States," by C.D. Poland and J.O. Malley, 4/2/92, (PB92-222439, A20, MF-A04).
- NCEER-92-0009 "Experimental and Analytical Study of a Hybrid Isolation System Using Friction Controllable Sliding Bearings," by M.Q. Feng, S. Fujii and M. Shinozuka, 5/15/92, (PB93-150282, A06, MF-A02).
- NCEER-92-0010 "Seismic Resistance of Slab-Column Connections in Existing Non-Ductile Flat-Plate Buildings," by A.J. Durrani and Y. Du, 5/18/92, (PB93-116812, A06, MF-A02).
- NCEER-92-0011 "The Hysteretic and Dynamic Behavior of Brick Masonry Walls Upgraded by Ferrocement Coatings Under Cyclic Loading and Strong Simulated Ground Motion," by H. Lee and S.P. Prawl, 5/11/92, to be published.
- NCEER-92-0012 "Study of Wire Rope Systems for Seismic Protection of Equipment in Buildings," by G.F. Demetriades, M.C. Constantinou and A.M. Reinhorn, 5/20/92, (PB93-116655, A08, MF-A02).

- NCEER-92-0013 "Shape Memory Structural Dampers: Material Properties, Design and Seismic Testing," by P.R. Witting and F.A. Cozzarelli, 5/26/92, (PB93-116663, A05, MF-A01).
- NCEER-92-0014 "Longitudinal Permanent Ground Deformation Effects on Buried Continuous Pipelines," by M.J. O'Rourke, and C. Nordberg, 6/15/92, (PB93-116671, A08, MF-A02).
- NCEER-92-0015 "A Simulation Method for Stationary Gaussian Random Functions Based on the Sampling Theorem," by M. Grigoriu and S. Balopoulou, 6/11/92, (PB93-127496, A05, MF-A01).
- NCEER-92-0016 "Gravity-Load-Designed Reinforced Concrete Buildings: Seismic Evaluation of Existing Construction and Detailing Strategies for Improved Seismic Resistance," by G.W. Hoffmann, S.K. Kunnath, A.M. Reinhorn and J.B. Mander, 7/15/92, (PB94-142007, A08, MF-A02).
- NCEER-92-0017 "Observations on Water System and Pipeline Performance in the Limón Area of Costa Rica Due to the April 22, 1991 Earthquake," by M. O'Rourke and D. Ballantyne, 6/30/92, (PB93-126811, A06, MF-A02).
- NCEER-92-0018 "Fourth Edition of Earthquake Education Materials for Grades K-12," Edited by K.E.K. Ross, 8/10/92, (PB93-114023, A07, MF-A02).
- NCEER-92-0019 "Proceedings from the Fourth Japan-U.S. Workshop on Earthquake Resistant Design of Lifeline Facilities and Countermeasures for Soil Liquefaction," Edited by M. Hamada and T.D. O'Rourke, 8/12/92, (PB93-163939, A99, MF-E11).
- NCEER-92-0020 "Active Bracing System: A Full Scale Implementation of Active Control," by A.M. Reinhorn, T.T. Soong, R.C. Lin, M.A. Riley, Y.P. Wang, S. Aizawa and M. Higashino, 8/14/92, (PB93-127512, A06, MF-A02).
- NCEER-92-0021 "Empirical Analysis of Horizontal Ground Displacement Generated by Liquefaction-Induced Lateral Spreads," by S.F. Bartlett and T.L. Youd, 8/17/92, (PB93-188241, A06, MF-A02).
- NCEER-92-0022 "IDARC Version 3.0: Inelastic Damage Analysis of Reinforced Concrete Structures," by S.K. Kunnath, A.M. Reinhorn and R.F. Lobo, 8/31/92, (PB93-227502, A07, MF-A02).
- NCEER-92-0023 "A Semi-Empirical Analysis of Strong-Motion Peaks in Terms of Seismic Source, Propagation Path and Local Site Conditions, by M. Kamiyama, M.J. O'Rourke and R. Flores-Berrones, 9/9/92, (PB93-150266, A08, MF-A02).
- NCEER-92-0024 "Seismic Behavior of Reinforced Concrete Frame Structures with Nonductile Details, Part I: Summary of Experimental Findings of Full Scale Beam-Column Joint Tests," by A. Beres, R.N. White and P. Gergely, 9/30/92, (PB93-227783, A05, MF-A01).
- NCEER-92-0025 "Experimental Results of Repaired and Retrofitted Beam-Column Joint Tests in Lightly Reinforced Concrete Frame Buildings," by A. Beres, S. El-Borgi, R.N. White and P. Gergely, 10/29/92, (PB93-227791, A05, MF-A01).
- NCEER-92-0026 "A Generalization of Optimal Control Theory: Linear and Nonlinear Structures," by J.N. Yang, Z. Li and S. Vongchavalitkul, 11/2/92, (PB93-188621, A05, MF-A01).
- NCEER-92-0027 "Seismic Resistance of Reinforced Concrete Frame Structures Designed Only for Gravity Loads: Part I - Design and Properties of a One-Third Scale Model Structure," by J.M. Bracci, A.M. Reinhorn and J.B. Mander, 12/1/92, (PB94-104502, A08, MF-A02).
- NCEER-92-0028 "Seismic Resistance of Reinforced Concrete Frame Structures Designed Only for Gravity Loads: Part II - Experimental Performance of Subassemblages," by L.E. Aycaardi, J.B. Mander and A.M. Reinhorn, 12/1/92, (PB94-104510, A08, MF-A02).
- NCEER-92-0029 "Seismic Resistance of Reinforced Concrete Frame Structures Designed Only for Gravity Loads: Part III - Experimental Performance and Analytical Study of a Structural Model," by J.M. Bracci, A.M. Reinhorn and J.B. Mander, 12/1/92, (PB93-227528, A09, MF-A01).

- NCEER-92-0030 "Evaluation of Seismic Retrofit of Reinforced Concrete Frame Structures: Part I - Experimental Performance of Retrofitted Subassemblages," by D. Choudhuri, J.B. Mander and A.M. Reinhorn, 12/8/92, (PB93-198307, A07, MF-A02).
- NCEER-92-0031 "Evaluation of Seismic Retrofit of Reinforced Concrete Frame Structures: Part II - Experimental Performance and Analytical Study of a Retrofitted Structural Model," by J.M. Bracci, A.M. Reinhorn and J.B. Mander, 12/8/92, (PB93-198315, A09, MF-A03).
- NCEER-92-0032 "Experimental and Analytical Investigation of Seismic Response of Structures with Supplemental Fluid Viscous Dampers," by M.C. Constantinou and M.D. Symans, 12/21/92, (PB93-191435, A10, MF-A03). This report is available only through NTIS (see address given above).
- NCEER-92-0033 "Reconnaissance Report on the Cairo, Egypt Earthquake of October 12, 1992," by M. Khater, 12/23/92, (PB93-188621, A03, MF-A01).
- NCEER-92-0034 "Low-Level Dynamic Characteristics of Four Tall Flat-Plate Buildings in New York City," by H. Gavin, S. Yuan, J. Grossman, E. Pekelis and K. Jacob, 12/28/92, (PB93-188217, A07, MF-A02).
- NCEER-93-0001 "An Experimental Study on the Seismic Performance of Brick-Infilled Steel Frames With and Without Retrofit," by J.B. Mander, B. Nair, K. Wojtkowski and J. Ma, 1/29/93, (PB93-227510, A07, MF-A02).
- NCEER-93-0002 "Social Accounting for Disaster Preparedness and Recovery Planning," by S. Cole, E. Pantoja and V. Razak, 2/22/93, (PB94-142114, A12, MF-A03).
- NCEER-93-0003 "Assessment of 1991 NEHRP Provisions for Nonstructural Components and Recommended Revisions," by T.T. Soong, G. Chen, Z. Wu, R-H. Zhang and M. Grigoriu, 3/1/93, (PB93-188639, A06, MF-A02).
- NCEER-93-0004 "Evaluation of Static and Response Spectrum Analysis Procedures of SEAOC/UBC for Seismic Isolated Structures," by C.W. Winters and M.C. Constantinou, 3/23/93, (PB93-198299, A10, MF-A03).
- NCEER-93-0005 "Earthquakes in the Northeast - Are We Ignoring the Hazard? A Workshop on Earthquake Science and Safety for Educators," edited by K.E.K. Ross, 4/2/93, (PB94-103066, A09, MF-A02).
- NCEER-93-0006 "Inelastic Response of Reinforced Concrete Structures with Viscoelastic Braces," by R.F. Lobo, J.M. Bracci, K.L. Shen, A.M. Reinhorn and T.T. Soong, 4/5/93, (PB93-227486, A05, MF-A02).
- NCEER-93-0007 "Seismic Testing of Installation Methods for Computers and Data Processing Equipment," by K. Kosar, T.T. Soong, K.L. Shen, J.A. HoLung and Y.K. Lin, 4/12/93, (PB93-198299, A07, MF-A02).
- NCEER-93-0008 "Retrofit of Reinforced Concrete Frames Using Added Dampers," by A. Reinhorn, M. Constantinou and C. Li, to be published.
- NCEER-93-0009 "Seismic Behavior and Design Guidelines for Steel Frame Structures with Added Viscoelastic Dampers," by K.C. Chang, M.L. Lai, T.T. Soong, D.S. Hao and Y.C. Yeh, 5/1/93, (PB94-141959, A07, MF-A02).
- NCEER-93-0010 "Seismic Performance of Shear-Critical Reinforced Concrete Bridge Piers," by J.B. Mander, S.M. Waheed, M.T.A. Chaudhary and S.S. Chen, 5/12/93, (PB93-227494, A08, MF-A02).
- NCEER-93-0011 "3D-BASIS-TABS: Computer Program for Nonlinear Dynamic Analysis of Three Dimensional Base Isolated Structures," by S. Nagarajaiah, C. Li, A.M. Reinhorn and M.C. Constantinou, 8/2/93, (PB94-141819, A09, MF-A02).
- NCEER-93-0012 "Effects of Hydrocarbon Spills from an Oil Pipeline Break on Ground Water," by O.J. Helweg and H.H.M. Hwang, 8/3/93, (PB94-141942, A06, MF-A02).
- NCEER-93-0013 "Simplified Procedures for Seismic Design of Nonstructural Components and Assessment of Current Code Provisions," by M.P. Singh, L.E. Suarez, E.E. Matheu and G.O. Maldonado, 8/4/93, (PB94-141827, A09, MF-A02).
- NCEER-93-0014 "An Energy Approach to Seismic Analysis and Design of Secondary Systems," by G. Chen and T.T. Soong, 8/6/93, (PB94-142767, A11, MF-A03).



- NCEER-93-0015 "Proceedings from School Sites: Becoming Prepared for Earthquakes - Commemorating the Third Anniversary of the Loma Prieta Earthquake," Edited by F.E. Winslow and K.E.K. Ross, 8/16/93, (PB94-154275, A16, MF-A02).
- NCEER-93-0016 "Reconnaissance Report of Damage to Historic Monuments in Cairo, Egypt Following the October 12, 1992 Dahshur Earthquake," by D. Sykora, D. Look, G. Croci, E. Karaesmen and E. Karaesmen, 8/19/93, (PB94-142221, A08, MF-A02).
- NCEER-93-0017 "The Island of Guam Earthquake of August 8, 1993," by S.W. Swan and S.K. Harris, 9/30/93, (PB94-141843, A04, MF-A01).
- NCEER-93-0018 "Engineering Aspects of the October 12, 1992 Egyptian Earthquake," by A.W. Elgamal, M. Amer, K. Adalier and A. Abul-Fadl, 10/7/93, (PB94-141983, A05, MF-A01).
- NCEER-93-0019 "Development of an Earthquake Motion Simulator and its Application in Dynamic Centrifuge Testing," by I. Krstelj, Supervised by J.H. Prevost, 10/23/93, (PB94-181773, A-10, MF-A03).
- NCEER-93-0020 "NCEER-Taisei Corporation Research Program on Sliding Seismic Isolation Systems for Bridges: Experimental and Analytical Study of a Friction Pendulum System (FPS)," by M.C. Constantinou, P. Tsopelas, Y-S. Kim and S. Okamoto, 11/1/93, (PB94-142775, A08, MF-A02).
- NCEER-93-0021 "Finite Element Modeling of Elastomeric Seismic Isolation Bearings," by L.J. Billings, Supervised by R. Shepherd, 11/8/93, to be published.
- NCEER-93-0022 "Seismic Vulnerability of Equipment in Critical Facilities: Life-Safety and Operational Consequences," by K. Porter, G.S. Johnson, M.M. Zadeh, C. Scawthorn and S. Eder, 11/24/93, (PB94-181765, A16, MF-A03).
- NCEER-93-0023 "Hokkaido Nansei-oki, Japan Earthquake of July 12, 1993, by P.I. Yanev and C.R. Scawthorn, 12/23/93, (PB94-181500, A07, MF-A01).
- NCEER-94-0001 "An Evaluation of Seismic Serviceability of Water Supply Networks with Application to the San Francisco Auxiliary Water Supply System," by I. Markov, Supervised by M. Grigoriu and T. O'Rourke, 1/21/94, (PB94-204013, A07, MF-A02).
- NCEER-94-0002 "NCEER-Taisei Corporation Research Program on Sliding Seismic Isolation Systems for Bridges: Experimental and Analytical Study of Systems Consisting of Sliding Bearings, Rubber Restoring Force Devices and Fluid Dampers," Volumes I and II, by P. Tsopelas, S. Okamoto, M.C. Constantinou, D. Ozaki and S. Fujii, 2/4/94, (PB94-181740, A09, MF-A02 and PB94-181757, A12, MF-A03).
- NCEER-94-0003 "A Markov Model for Local and Global Damage Indices in Seismic Analysis," by S. Rahman and M. Grigoriu, 2/18/94, (PB94-206000, A12, MF-A03).
- NCEER-94-0004 "Proceedings from the NCEER Workshop on Seismic Response of Masonry Infills," edited by D.P. Abrams, 3/1/94, (PB94-180783, A07, MF-A02).
- NCEER-94-0005 "The Northridge, California Earthquake of January 17, 1994: General Reconnaissance Report," edited by J.D. Goltz, 3/11/94, (PB193943, A10, MF-A03).
- NCEER-94-0006 "Seismic Energy Based Fatigue Damage Analysis of Bridge Columns: Part I - Evaluation of Seismic Capacity," by G.A. Chang and J.B. Mander, 3/14/94, (PB94-219185, A11, MF-A03).
- NCEER-94-0007 "Seismic Isolation of Multi-Story Frame Structures Using Spherical Sliding Isolation Systems," by T.M. Al-Hussaini, V.A. Zayas and M.C. Constantinou, 3/17/94, (PB193745, A09, MF-A02).
- NCEER-94-0008 "The Northridge, California Earthquake of January 17, 1994: Performance of Highway Bridges," edited by I.G. Buckle, 3/24/94, (PB94-193851, A06, MF-A02).
- NCEER-94-0009 "Proceedings of the Third U.S.-Japan Workshop on Earthquake Protective Systems for Bridges," edited by I.G. Buckle and I. Friedland, 3/31/94, (PB94-195815, A99, MF-A06).

- NCEER-94-0010 "3D-BASIS-ME: Computer Program for Nonlinear Dynamic Analysis of Seismically Isolated Single and Multiple Structures and Liquid Storage Tanks," by P.C. Tsopelas, M.C. Constantinou and A.M. Reinhorn, 4/12/94, (PB94-204922, A09, MF-A02).
- NCEER-94-0011 "The Northridge, California Earthquake of January 17, 1994: Performance of Gas Transmission Pipelines," by T.D. O'Rourke and M.C. Palmer, 5/16/94, (PB94-204989, A05, MF-A01).
- NCEER-94-0012 "Feasibility Study of Replacement Procedures and Earthquake Performance Related to Gas Transmission Pipelines," by T.D. O'Rourke and M.C. Palmer, 5/25/94, (PB94-206638, A09, MF-A02).
- NCEER-94-0013 "Seismic Energy Based Fatigue Damage Analysis of Bridge Columns: Part II - Evaluation of Seismic Demand," by G.A. Chang and J.B. Mander, 6/1/94, (PB95-18106, A08, MF-A02).
- NCEER-94-0014 "NCEER-Taisei Corporation Research Program on Sliding Seismic Isolation Systems for Bridges: Experimental and Analytical Study of a System Consisting of Sliding Bearings and Fluid Restoring Force/Damping Devices," by P. Tsopelas and M.C. Constantinou, 6/13/94, (PB94-219144, A10, MF-A03).
- NCEER-94-0015 "Generation of Hazard-Consistent Fragility Curves for Seismic Loss Estimation Studies," by H. Hwang and J-R. Huo, 6/14/94, (PB95-181996, A09, MF-A02).
- NCEER-94-0016 "Seismic Study of Building Frames with Added Energy-Absorbing Devices," by W.S. Pong, C.S. Tsai and G.C. Lee, 6/20/94, (PB94-219136, A10, A03).
- NCEER-94-0017 "Sliding Mode Control for Seismic-Excited Linear and Nonlinear Civil Engineering Structures," by J. Yang, J. Wu, A. Agrawal and Z. Li, 6/21/94, (PB95-138483, A06, MF-A02).
- NCEER-94-0018 "3D-BASIS-TABS Version 2.0: Computer Program for Nonlinear Dynamic Analysis of Three Dimensional Base Isolated Structures," by A.M. Reinhorn, S. Nagarajaiah, M.C. Constantinou, P. Tsopelas and R. Li, 6/22/94, (PB95-182176, A08, MF-A02).
- NCEER-94-0019 "Proceedings of the International Workshop on Civil Infrastructure Systems: Application of Intelligent Systems and Advanced Materials on Bridge Systems," Edited by G.C. Lee and K.C. Chang, 7/18/94, (PB95-252474, A20, MF-A04).
- NCEER-94-0020 "Study of Seismic Isolation Systems for Computer Floors," by V. Lambrou and M.C. Constantinou, 7/19/94, (PB95-138533, A10, MF-A03).
- NCEER-94-0021 "Proceedings of the U.S.-Italian Workshop on Guidelines for Seismic Evaluation and Rehabilitation of Unreinforced Masonry Buildings," Edited by D.P. Abrams and G.M. Calvi, 7/20/94, (PB95-138749, A13, MF-A03).
- NCEER-94-0022 "NCEER-Taisei Corporation Research Program on Sliding Seismic Isolation Systems for Bridges: Experimental and Analytical Study of a System Consisting of Lubricated PTFE Sliding Bearings and Mild Steel Dampers," by P. Tsopelas and M.C. Constantinou, 7/22/94, (PB95-182184, A08, MF-A02).
- NCEER-94-0023 "Development of Reliability-Based Design Criteria for Buildings Under Seismic Load," by Y.K. Wen, H. Hwang and M. Shinozuka, 8/1/94, (PB95-211934, A08, MF-A02).
- NCEER-94-0024 "Experimental Verification of Acceleration Feedback Control Strategies for an Active Tendon System," by S.J. Dyke, B.F. Spencer, Jr., P. Quast, M.K. Sain, D.C. Kaspari, Jr. and T.T. Soong, 8/29/94, (PB95-212320, A05, MF-A01).
- NCEER-94-0025 "Seismic Retrofitting Manual for Highway Bridges," Edited by I.G. Buckle and I.F. Friedland, published by the Federal Highway Administration (PB95-212676, A15, MF-A03).
- NCEER-94-0026 "Proceedings from the Fifth U.S.-Japan Workshop on Earthquake Resistant Design of Lifeline Facilities and Countermeasures Against Soil Liquefaction," Edited by T.D. O'Rourke and M. Hamada, 11/7/94, (PB95-220802, A99, MF-E08).

- NCEER-95-0001 “Experimental and Analytical Investigation of Seismic Retrofit of Structures with Supplemental Damping: Part I - Fluid Viscous Damping Devices,” by A.M. Reinhorn, C. Li and M.C. Constantinou, 1/3/95, (PB95-266599, A09, MF-A02).
- NCEER-95-0002 “Experimental and Analytical Study of Low-Cycle Fatigue Behavior of Semi-Rigid Top-And-Seat Angle Connections,” by G. Pekcan, J.B. Mander and S.S. Chen, 1/5/95, (PB95-220042, A07, MF-A02).
- NCEER-95-0003 “NCEER-ATC Joint Study on Fragility of Buildings,” by T. Anagnos, C. Rojahn and A.S. Kiremidjian, 1/20/95, (PB95-220026, A06, MF-A02).
- NCEER-95-0004 “Nonlinear Control Algorithms for Peak Response Reduction,” by Z. Wu, T.T. Soong, V. Gattulli and R.C. Lin, 2/16/95, (PB95-220349, A05, MF-A01).
- NCEER-95-0005 “Pipeline Replacement Feasibility Study: A Methodology for Minimizing Seismic and Corrosion Risks to Underground Natural Gas Pipelines,” by R.T. Eguchi, H.A. Seligson and D.G. Honegger, 3/2/95, (PB95-252326, A06, MF-A02).
- NCEER-95-0006 “Evaluation of Seismic Performance of an 11-Story Frame Building During the 1994 Northridge Earthquake,” by F. Naeim, R. DiSulio, K. Benuska, A. Reinhorn and C. Li, to be published.
- NCEER-95-0007 “Prioritization of Bridges for Seismic Retrofitting,” by N. Basöz and A.S. Kiremidjian, 4/24/95, (PB95-252300, A08, MF-A02).
- NCEER-95-0008 “Method for Developing Motion Damage Relationships for Reinforced Concrete Frames,” by A. Singhal and A.S. Kiremidjian, 5/11/95, (PB95-266607, A06, MF-A02).
- NCEER-95-0009 “Experimental and Analytical Investigation of Seismic Retrofit of Structures with Supplemental Damping: Part II - Friction Devices,” by C. Li and A.M. Reinhorn, 7/6/95, (PB96-128087, A11, MF-A03).
- NCEER-95-0010 “Experimental Performance and Analytical Study of a Non-Ductile Reinforced Concrete Frame Structure Retrofitted with Elastomeric Spring Dampers,” by G. Pekcan, J.B. Mander and S.S. Chen, 7/14/95, (PB96-137161, A08, MF-A02).
- NCEER-95-0011 “Development and Experimental Study of Semi-Active Fluid Damping Devices for Seismic Protection of Structures,” by M.D. Symans and M.C. Constantinou, 8/3/95, (PB96-136940, A23, MF-A04).
- NCEER-95-0012 “Real-Time Structural Parameter Modification (RSPM): Development of Innervated Structures,” by Z. Liang, M. Tong and G.C. Lee, 4/11/95, (PB96-137153, A06, MF-A01).
- NCEER-95-0013 “Experimental and Analytical Investigation of Seismic Retrofit of Structures with Supplemental Damping: Part III - Viscous Damping Walls,” by A.M. Reinhorn and C. Li, 10/1/95, (PB96-176409, A11, MF-A03).
- NCEER-95-0014 “Seismic Fragility Analysis of Equipment and Structures in a Memphis Electric Substation,” by J-R. Huo and H.H.M. Hwang, 8/10/95, (PB96-128087, A09, MF-A02).
- NCEER-95-0015 “The Hanshin-Awaji Earthquake of January 17, 1995: Performance of Lifelines,” Edited by M. Shinozuka, 11/3/95, (PB96-176383, A15, MF-A03).
- NCEER-95-0016 “Highway Culvert Performance During Earthquakes,” by T.L. Youd and C.J. Beckman, available as NCEER-96-0015.
- NCEER-95-0017 “The Hanshin-Awaji Earthquake of January 17, 1995: Performance of Highway Bridges,” Edited by I.G. Buckle, 12/1/95, to be published.
- NCEER-95-0018 “Modeling of Masonry Infill Panels for Structural Analysis,” by A.M. Reinhorn, A. Madan, R.E. Valles, Y. Reichmann and J.B. Mander, 12/8/95, (PB97-110886, MF-A01, A06).
- NCEER-95-0019 “Optimal Polynomial Control for Linear and Nonlinear Structures,” by A.K. Agrawal and J.N. Yang, 12/11/95, (PB96-168737, A07, MF-A02).

- NCEER-95-0020 "Retrofit of Non-Ductile Reinforced Concrete Frames Using Friction Dampers," by R.S. Rao, P. Gergely and R.N. White, 12/22/95, (PB97-133508, A10, MF-A02).
- NCEER-95-0021 "Parametric Results for Seismic Response of Pile-Supported Bridge Bents," by G. Mylonakis, A. Nikolaou and G. Gazetas, 12/22/95, (PB97-100242, A12, MF-A03).
- NCEER-95-0022 "Kinematic Bending Moments in Seismically Stressed Piles," by A. Nikolaou, G. Mylonakis and G. Gazetas, 12/23/95, (PB97-113914, MF-A03, A13).
- NCEER-96-0001 "Dynamic Response of Unreinforced Masonry Buildings with Flexible Diaphragms," by A.C. Costley and D.P. Abrams, 10/10/96, (PB97-133573, MF-A03, A15).
- NCEER-96-0002 "State of the Art Review: Foundations and Retaining Structures," by I. Po Lam, to be published.
- NCEER-96-0003 "Ductility of Rectangular Reinforced Concrete Bridge Columns with Moderate Confinement," by N. Wehbe, M. Saiidi, D. Sanders and B. Douglas, 11/7/96, (PB97-133557, A06, MF-A02).
- NCEER-96-0004 "Proceedings of the Long-Span Bridge Seismic Research Workshop," edited by I.G. Buckle and I.M. Friedland, to be published.
- NCEER-96-0005 "Establish Representative Pier Types for Comprehensive Study: Eastern United States," by J. Kulicki and Z. Prucz, 5/28/96, (PB98-119217, A07, MF-A02).
- NCEER-96-0006 "Establish Representative Pier Types for Comprehensive Study: Western United States," by R. Imbsen, R.A. Schamber and T.A. Osterkamp, 5/28/96, (PB98-118607, A07, MF-A02).
- NCEER-96-0007 "Nonlinear Control Techniques for Dynamical Systems with Uncertain Parameters," by R.G. Ghanem and M.I. Bujakov, 5/27/96, (PB97-100259, A17, MF-A03).
- NCEER-96-0008 "Seismic Evaluation of a 30-Year Old Non-Ductile Highway Bridge Pier and Its Retrofit," by J.B. Mander, B. Mahmoodzadegan, S. Bhadra and S.S. Chen, 5/31/96, (PB97-110902, MF-A03, A10).
- NCEER-96-0009 "Seismic Performance of a Model Reinforced Concrete Bridge Pier Before and After Retrofit," by J.B. Mander, J.H. Kim and C.A. Ligozio, 5/31/96, (PB97-110910, MF-A02, A10).
- NCEER-96-0010 "IDARC2D Version 4.0: A Computer Program for the Inelastic Damage Analysis of Buildings," by R.E. Valles, A.M. Reinhorn, S.K. Kunnath, C. Li and A. Madan, 6/3/96, (PB97-100234, A17, MF-A03).
- NCEER-96-0011 "Estimation of the Economic Impact of Multiple Lifeline Disruption: Memphis Light, Gas and Water Division Case Study," by S.E. Chang, H.A. Seligson and R.T. Eguchi, 8/16/96, (PB97-133490, A11, MF-A03).
- NCEER-96-0012 "Proceedings from the Sixth Japan-U.S. Workshop on Earthquake Resistant Design of Lifeline Facilities and Countermeasures Against Soil Liquefaction, Edited by M. Hamada and T. O'Rourke, 9/11/96, (PB97-133581, A99, MF-A06).
- NCEER-96-0013 "Chemical Hazards, Mitigation and Preparedness in Areas of High Seismic Risk: A Methodology for Estimating the Risk of Post-Earthquake Hazardous Materials Release," by H.A. Seligson, R.T. Eguchi, K.J. Tierney and K. Richmond, 11/7/96, (PB97-133565, MF-A02, A08).
- NCEER-96-0014 "Response of Steel Bridge Bearings to Reversed Cyclic Loading," by J.B. Mander, D-K. Kim, S.S. Chen and G.J. Premus, 11/13/96, (PB97-140735, A12, MF-A03).
- NCEER-96-0015 "Highway Culvert Performance During Past Earthquakes," by T.L. Youd and C.J. Beckman, 11/25/96, (PB97-133532, A06, MF-A01).
- NCEER-97-0001 "Evaluation, Prevention and Mitigation of Pounding Effects in Building Structures," by R.E. Valles and A.M. Reinhorn, 2/20/97, (PB97-159552, A14, MF-A03).
- NCEER-97-0002 "Seismic Design Criteria for Bridges and Other Highway Structures," by C. Rojahn, R. Mayes, D.G. Anderson, J. Clark, J.H. Hom, R.V. Nutt and M.J. O'Rourke, 4/30/97, (PB97-194658, A06, MF-A03).

- NCEER-97-0003 "Proceedings of the U.S.-Italian Workshop on Seismic Evaluation and Retrofit," Edited by D.P. Abrams and G.M. Calvi, 3/19/97, (PB97-194666, A13, MF-A03).
- NCEER-97-0004 "Investigation of Seismic Response of Buildings with Linear and Nonlinear Fluid Viscous Dampers," by A.A. Seleemah and M.C. Constantinou, 5/21/97, (PB98-109002, A15, MF-A03).
- NCEER-97-0005 "Proceedings of the Workshop on Earthquake Engineering Frontiers in Transportation Facilities," edited by G.C. Lee and I.M. Friedland, 8/29/97, (PB98-128911, A25, MR-A04).
- NCEER-97-0006 "Cumulative Seismic Damage of Reinforced Concrete Bridge Piers," by S.K. Kunnath, A. El-Bahy, A. Taylor and W. Stone, 9/2/97, (PB98-108814, A11, MF-A03).
- NCEER-97-0007 "Structural Details to Accommodate Seismic Movements of Highway Bridges and Retaining Walls," by R.A. Imbsen, R.A. Schamber, E. Thorkildsen, A. Kartoum, B.T. Martin, T.N. Rosser and J.M. Kulicki, 9/3/97, (PB98-108996, A09, MF-A02).
- NCEER-97-0008 "A Method for Earthquake Motion-Damage Relationships with Application to Reinforced Concrete Frames," by A. Singhal and A.S. Kiremidjian, 9/10/97, (PB98-108988, A13, MF-A03).
- NCEER-97-0009 "Seismic Analysis and Design of Bridge Abutments Considering Sliding and Rotation," by K. Fishman and R. Richards, Jr., 9/15/97, (PB98-108897, A06, MF-A02).
- NCEER-97-0010 "Proceedings of the FHWA/NCEER Workshop on the National Representation of Seismic Ground Motion for New and Existing Highway Facilities," edited by I.M. Friedland, M.S. Power and R.L. Mayes, 9/22/97, (PB98-128903, A21, MF-A04).
- NCEER-97-0011 "Seismic Analysis for Design or Retrofit of Gravity Bridge Abutments," by K.L. Fishman, R. Richards, Jr. and R.C. Divito, 10/2/97, (PB98-128937, A08, MF-A02).
- NCEER-97-0012 "Evaluation of Simplified Methods of Analysis for Yielding Structures," by P. Tsopelas, M.C. Constantinou, C.A. Kircher and A.S. Whittaker, 10/31/97, (PB98-128929, A10, MF-A03).
- NCEER-97-0013 "Seismic Design of Bridge Columns Based on Control and Repairability of Damage," by C-T. Cheng and J.B. Mander, 12/8/97, (PB98-144249, A11, MF-A03).
- NCEER-97-0014 "Seismic Resistance of Bridge Piers Based on Damage Avoidance Design," by J.B. Mander and C-T. Cheng, 12/10/97, (PB98-144223, A09, MF-A02).
- NCEER-97-0015 "Seismic Response of Nominally Symmetric Systems with Strength Uncertainty," by S. Balopoulou and M. Grigoriu, 12/23/97, (PB98-153422, A11, MF-A03).
- NCEER-97-0016 "Evaluation of Seismic Retrofit Methods for Reinforced Concrete Bridge Columns," by T.J. Wipf, F.W. Klaiber and F.M. Russo, 12/28/97, (PB98-144215, A12, MF-A03).
- NCEER-97-0017 "Seismic Fragility of Existing Conventional Reinforced Concrete Highway Bridges," by C.L. Mullen and A.S. Cakmak, 12/30/97, (PB98-153406, A08, MF-A02).
- NCEER-97-0018 "Loss Assessment of Memphis Buildings," edited by D.P. Abrams and M. Shinozuka, 12/31/97, (PB98-144231, A13, MF-A03).
- NCEER-97-0019 "Seismic Evaluation of Frames with Infill Walls Using Quasi-static Experiments," by K.M. Mosalam, R.N. White and P. Gergely, 12/31/97, (PB98-153455, A07, MF-A02).
- NCEER-97-0020 "Seismic Evaluation of Frames with Infill Walls Using Pseudo-dynamic Experiments," by K.M. Mosalam, R.N. White and P. Gergely, 12/31/97, (PB98-153430, A07, MF-A02).
- NCEER-97-0021 "Computational Strategies for Frames with Infill Walls: Discrete and Smeared Crack Analyses and Seismic Fragility," by K.M. Mosalam, R.N. White and P. Gergely, 12/31/97, (PB98-153414, A10, MF-A02).

- NCEER-97-0022 "Proceedings of the NCEER Workshop on Evaluation of Liquefaction Resistance of Soils," edited by T.L. Youd and I.M. Idriss, 12/31/97, (PB98-155617, A15, MF-A03).
- MCEER-98-0001 "Extraction of Nonlinear Hysteretic Properties of Seismically Isolated Bridges from Quick-Release Field Tests," by Q. Chen, B.M. Douglas, E.M. Maragakis and I.G. Buckle, 5/26/98, (PB99-118838, A06, MF-A01).
- MCEER-98-0002 "Methodologies for Evaluating the Importance of Highway Bridges," by A. Thomas, S. Eshenaur and J. Kulicki, 5/29/98, (PB99-118846, A10, MF-A02).
- MCEER-98-0003 "Capacity Design of Bridge Piers and the Analysis of Overstrength," by J.B. Mander, A. Dutta and P. Goel, 6/1/98, (PB99-118853, A09, MF-A02).
- MCEER-98-0004 "Evaluation of Bridge Damage Data from the Loma Prieta and Northridge, California Earthquakes," by N. Basoz and A. Kiremidjian, 6/2/98, (PB99-118861, A15, MF-A03).
- MCEER-98-0005 "Screening Guide for Rapid Assessment of Liquefaction Hazard at Highway Bridge Sites," by T. L. Youd, 6/16/98, (PB99-118879, A06, not available on microfiche).
- MCEER-98-0006 "Structural Steel and Steel/Concrete Interface Details for Bridges," by P. Ritchie, N. Kauh and J. Kulicki, 7/13/98, (PB99-118945, A06, MF-A01).
- MCEER-98-0007 "Capacity Design and Fatigue Analysis of Confined Concrete Columns," by A. Dutta and J.B. Mander, 7/14/98, (PB99-118960, A14, MF-A03).
- MCEER-98-0008 "Proceedings of the Workshop on Performance Criteria for Telecommunication Services Under Earthquake Conditions," edited by A.J. Schiff, 7/15/98, (PB99-118952, A08, MF-A02).
- MCEER-98-0009 "Fatigue Analysis of Unconfined Concrete Columns," by J.B. Mander, A. Dutta and J.H. Kim, 9/12/98, (PB99-123655, A10, MF-A02).
- MCEER-98-0010 "Centrifuge Modeling of Cyclic Lateral Response of Pile-Cap Systems and Seat-Type Abutments in Dry Sands," by A.D. Gadre and R. Dobry, 10/2/98, (PB99-123606, A13, MF-A03).
- MCEER-98-0011 "IDARC-BRIDGE: A Computational Platform for Seismic Damage Assessment of Bridge Structures," by A.M. Reinhorn, V. Simeonov, G. Mylonakis and Y. Reichman, 10/2/98, (PB99-162919, A15, MF-A03).
- MCEER-98-0012 "Experimental Investigation of the Dynamic Response of Two Bridges Before and After Retrofitting with Elastomeric Bearings," by D.A. Wendichansky, S.S. Chen and J.B. Mander, 10/2/98, (PB99-162927, A15, MF-A03).
- MCEER-98-0013 "Design Procedures for Hinge Restrainers and Hinge Sear Width for Multiple-Frame Bridges," by R. Des Roches and G.L. Fenves, 11/3/98, (PB99-140477, A13, MF-A03).
- MCEER-98-0014 "Response Modification Factors for Seismically Isolated Bridges," by M.C. Constantinou and J.K. Quarshie, 11/3/98, (PB99-140485, A14, MF-A03).
- MCEER-98-0015 "Proceedings of the U.S.-Italy Workshop on Seismic Protective Systems for Bridges," edited by I.M. Friedland and M.C. Constantinou, 11/3/98, (PB2000-101711, A22, MF-A04).
- MCEER-98-0016 "Appropriate Seismic Reliability for Critical Equipment Systems: Recommendations Based on Regional Analysis of Financial and Life Loss," by K. Porter, C. Scawthorn, C. Taylor and N. Blais, 11/10/98, (PB99-157265, A08, MF-A02).
- MCEER-98-0017 "Proceedings of the U.S. Japan Joint Seminar on Civil Infrastructure Systems Research," edited by M. Shinozuka and A. Rose, 11/12/98, (PB99-156713, A16, MF-A03).
- MCEER-98-0018 "Modeling of Pile Footings and Drilled Shafts for Seismic Design," by I. PoLam, M. Kapuskar and D. Chaudhuri, 12/21/98, (PB99-157257, A09, MF-A02).

- MCEER-99-0001 "Seismic Evaluation of a Masonry Infilled Reinforced Concrete Frame by Pseudodynamic Testing," by S.G. Buonopane and R.N. White, 2/16/99, (PB99-162851, A09, MF-A02).
- MCEER-99-0002 "Response History Analysis of Structures with Seismic Isolation and Energy Dissipation Systems: Verification Examples for Program SAP2000," by J. Scheller and M.C. Constantinou, 2/22/99, (PB99-162869, A08, MF-A02).
- MCEER-99-0003 "Experimental Study on the Seismic Design and Retrofit of Bridge Columns Including Axial Load Effects," by A. Dutta, T. Kokorina and J.B. Mander, 2/22/99, (PB99-162877, A09, MF-A02).
- MCEER-99-0004 "Experimental Study of Bridge Elastomeric and Other Isolation and Energy Dissipation Systems with Emphasis on Uplift Prevention and High Velocity Near-source Seismic Excitation," by A. Kasalanati and M. C. Constantinou, 2/26/99, (PB99-162885, A12, MF-A03).
- MCEER-99-0005 "Truss Modeling of Reinforced Concrete Shear-flexure Behavior," by J.H. Kim and J.B. Mander, 3/8/99, (PB99-163693, A12, MF-A03).
- MCEER-99-0006 "Experimental Investigation and Computational Modeling of Seismic Response of a 1:4 Scale Model Steel Structure with a Load Balancing Supplemental Damping System," by G. Pekcan, J.B. Mander and S.S. Chen, 4/2/99, (PB99-162893, A11, MF-A03).
- MCEER-99-0007 "Effect of Vertical Ground Motions on the Structural Response of Highway Bridges," by M.R. Button, C.J. Cronin and R.L. Mayes, 4/10/99, (PB2000-101411, A10, MF-A03).
- MCEER-99-0008 "Seismic Reliability Assessment of Critical Facilities: A Handbook, Supporting Documentation, and Model Code Provisions," by G.S. Johnson, R.E. Sheppard, M.D. Quilici, S.J. Eder and C.R. Scawthorn, 4/12/99, (PB2000-101701, A18, MF-A04).
- MCEER-99-0009 "Impact Assessment of Selected MCEER Highway Project Research on the Seismic Design of Highway Structures," by C. Rojahn, R. Mayes, D.G. Anderson, J.H. Clark, D'Appolonia Engineering, S. Gloyd and R.V. Nutt, 4/14/99, (PB99-162901, A10, MF-A02).
- MCEER-99-0010 "Site Factors and Site Categories in Seismic Codes," by R. Dobry, R. Ramos and M.S. Power, 7/19/99, (PB2000-101705, A08, MF-A02).
- MCEER-99-0011 "Restrainer Design Procedures for Multi-Span Simply-Supported Bridges," by M.J. Randall, M. Saiidi, E. Maragakis and T. Isakovic, 7/20/99, (PB2000-101702, A10, MF-A02).
- MCEER-99-0012 "Property Modification Factors for Seismic Isolation Bearings," by M.C. Constantinou, P. Tsopelas, A. Kasalanati and E. Wolff, 7/20/99, (PB2000-103387, A11, MF-A03).
- MCEER-99-0013 "Critical Seismic Issues for Existing Steel Bridges," by P. Ritchie, N. Kauh and J. Kulicki, 7/20/99, (PB2000-101697, A09, MF-A02).
- MCEER-99-0014 "Nonstructural Damage Database," by A. Kao, T.T. Soong and A. Vender, 7/24/99, (PB2000-101407, A06, MF-A01).
- MCEER-99-0015 "Guide to Remedial Measures for Liquefaction Mitigation at Existing Highway Bridge Sites," by H.G. Cooke and J. K. Mitchell, 7/26/99, (PB2000-101703, A11, MF-A03).
- MCEER-99-0016 "Proceedings of the MCEER Workshop on Ground Motion Methodologies for the Eastern United States," edited by N. Abrahamson and A. Becker, 8/11/99, (PB2000-103385, A07, MF-A02).
- MCEER-99-0017 "Quindío, Colombia Earthquake of January 25, 1999: Reconnaissance Report," by A.P. Asfura and P.J. Flores, 10/4/99, (PB2000-106893, A06, MF-A01).
- MCEER-99-0018 "Hysteretic Models for Cyclic Behavior of Deteriorating Inelastic Structures," by M.V. Sivaselvan and A.M. Reinhorn, 11/5/99, (PB2000-103386, A08, MF-A02).

- MCEER-99-0019 "Proceedings of the 7<sup>th</sup> U.S.- Japan Workshop on Earthquake Resistant Design of Lifeline Facilities and Countermeasures Against Soil Liquefaction," edited by T.D. O'Rourke, J.P. Bardet and M. Hamada, 11/19/99, (PB2000-103354, A99, MF-A06).
- MCEER-99-0020 "Development of Measurement Capability for Micro-Vibration Evaluations with Application to Chip Fabrication Facilities," by G.C. Lee, Z. Liang, J.W. Song, J.D. Shen and W.C. Liu, 12/1/99, (PB2000-105993, A08, MF-A02).
- MCEER-99-0021 "Design and Retrofit Methodology for Building Structures with Supplemental Energy Dissipating Systems," by G. Pekcan, J.B. Mander and S.S. Chen, 12/31/99, (PB2000-105994, A11, MF-A03).
- MCEER-00-0001 "The Marmara, Turkey Earthquake of August 17, 1999: Reconnaissance Report," edited by C. Scawthorn; with major contributions by M. Bruneau, R. Eguchi, T. Holzer, G. Johnson, J. Mander, J. Mitchell, W. Mitchell, A. Papageorgiou, C. Scaethorn, and G. Webb, 3/23/00, (PB2000-106200, A11, MF-A03).
- MCEER-00-0002 "Proceedings of the MCEER Workshop for Seismic Hazard Mitigation of Health Care Facilities," edited by G.C. Lee, M. Ettouney, M. Grigoriu, J. Hauer and J. Nigg, 3/29/00, (PB2000-106892, A08, MF-A02).
- MCEER-00-0003 "The Chi-Chi, Taiwan Earthquake of September 21, 1999: Reconnaissance Report," edited by G.C. Lee and C.H. Loh, with major contributions by G.C. Lee, M. Bruneau, I.G. Buckle, S.E. Chang, P.J. Flores, T.D. O'Rourke, M. Shinozuka, T.T. Soong, C-H. Loh, K-C. Chang, Z-J. Chen, J-S. Hwang, M-L. Lin, G-Y. Liu, K-C. Tsai, G.C. Yao and C-L. Yen, 4/30/00, (PB2001-100980, A10, MF-A02).
- MCEER-00-0004 "Seismic Retrofit of End-Sway Frames of Steel Deck-Truss Bridges with a Supplemental Tendon System: Experimental and Analytical Investigation," by G. Pekcan, J.B. Mander and S.S. Chen, 7/1/00, (PB2001-100982, A10, MF-A02).
- MCEER-00-0005 "Sliding Fragility of Unrestrained Equipment in Critical Facilities," by W.H. Chong and T.T. Soong, 7/5/00, (PB2001-100983, A08, MF-A02).
- MCEER-00-0006 "Seismic Response of Reinforced Concrete Bridge Pier Walls in the Weak Direction," by N. Abo-Shadi, M. Saiidi and D. Sanders, 7/17/00, (PB2001-100981, A17, MF-A03).
- MCEER-00-0007 "Low-Cycle Fatigue Behavior of Longitudinal Reinforcement in Reinforced Concrete Bridge Columns," by J. Brown and S.K. Kunnath, 7/23/00, (PB2001-104392, A08, MF-A02).
- MCEER-00-0008 "Soil Structure Interaction of Bridges for Seismic Analysis," I. PoLam and H. Law, 9/25/00, (PB2001-105397, A08, MF-A02).
- MCEER-00-0009 "Proceedings of the First MCEER Workshop on Mitigation of Earthquake Disaster by Advanced Technologies (MEDAT-1), edited by M. Shinozuka, D.J. Inman and T.D. O'Rourke, 11/10/00, (PB2001-105399, A14, MF-A03).
- MCEER-00-0010 "Development and Evaluation of Simplified Procedures for Analysis and Design of Buildings with Passive Energy Dissipation Systems," by O.M. Ramirez, M.C. Constantinou, C.A. Kircher, A.S. Whittaker, M.W. Johnson, J.D. Gomez and C. Chrysostomou, 11/16/01, (PB2001-105523, A23, MF-A04).
- MCEER-00-0011 "Dynamic Soil-Foundation-Structure Interaction Analyses of Large Caissons," by C-Y. Chang, C-M. Mok, Z-L. Wang, R. Settgast, F. Waggoner, M.A. Ketchum, H.M. Gonnermann and C-C. Chin, 12/30/00, (PB2001-104373, A07, MF-A02).
- MCEER-00-0012 "Experimental Evaluation of Seismic Performance of Bridge Restrainers," by A.G. Vlassis, E.M. Maragakis and M. Saiid Saiidi, 12/30/00, (PB2001-104354, A09, MF-A02).
- MCEER-00-0013 "Effect of Spatial Variation of Ground Motion on Highway Structures," by M. Shinozuka, V. Saxena and G. Deodatis, 12/31/00, (PB2001-108755, A13, MF-A03).
- MCEER-00-0014 "A Risk-Based Methodology for Assessing the Seismic Performance of Highway Systems," by S.D. Werner, C.E. Taylor, J.E. Moore, II, J.S. Walton and S. Cho, 12/31/00, (PB2001-108756, A14, MF-A03).



- MCEER-01-0001 "Experimental Investigation of P-Delta Effects to Collapse During Earthquakes," by D. Vian and M. Bruneau, 6/25/01, (PB2002-100534, A17, MF-A03).
- MCEER-01-0002 "Proceedings of the Second MCEER Workshop on Mitigation of Earthquake Disaster by Advanced Technologies (MEDAT-2)," edited by M. Bruneau and D.J. Inman, 7/23/01, (PB2002-100434, A16, MF-A03).
- MCEER-01-0003 "Sensitivity Analysis of Dynamic Systems Subjected to Seismic Loads," by C. Roth and M. Grigoriu, 9/18/01, (PB2003-100884, A12, MF-A03).
- MCEER-01-0004 "Overcoming Obstacles to Implementing Earthquake Hazard Mitigation Policies: Stage 1 Report," by D.J. Alesch and W.J. Petak, 12/17/01, (PB2002-107949, A07, MF-A02).
- MCEER-01-0005 "Updating Real-Time Earthquake Loss Estimates: Methods, Problems and Insights," by C.E. Taylor, S.E. Chang and R.T. Eguchi, 12/17/01, (PB2002-107948, A05, MF-A01).
- MCEER-01-0006 "Experimental Investigation and Retrofit of Steel Pile Foundations and Pile Bents Under Cyclic Lateral Loadings," by A. Shama, J. Mander, B. Blabac and S. Chen, 12/31/01, (PB2002-107950, A13, MF-A03).
- MCEER-02-0001 "Assessment of Performance of Bolu Viaduct in the 1999 Duzce Earthquake in Turkey" by P.C. Roussis, M.C. Constantinou, M. Erdik, E. Durukal and M. Dicleli, 5/8/02, (PB2003-100883, A08, MF-A02).
- MCEER-02-0002 "Seismic Behavior of Rail Counterweight Systems of Elevators in Buildings," by M.P. Singh, Rildova and L.E. Suarez, 5/27/02. (PB2003-100882, A11, MF-A03).
- MCEER-02-0003 "Development of Analysis and Design Procedures for Spread Footings," by G. Mylonakis, G. Gazetas, S. Nikolaou and A. Chauncey, 10/02/02, (PB2004-101636, A13, MF-A03, CD-A13).
- MCEER-02-0004 "Bare-Earth Algorithms for Use with SAR and LIDAR Digital Elevation Models," by C.K. Huyck, R.T. Eguchi and B. Houshmand, 10/16/02, (PB2004-101637, A07, CD-A07).
- MCEER-02-0005 "Review of Energy Dissipation of Compression Members in Concentrically Braced Frames," by K.Lee and M. Bruneau, 10/18/02, (PB2004-101638, A10, CD-A10).
- MCEER-03-0001 "Experimental Investigation of Light-Gauge Steel Plate Shear Walls for the Seismic Retrofit of Buildings" by J. Berman and M. Bruneau, 5/2/03, (PB2004-101622, A10, MF-A03, CD-A10).
- MCEER-03-0002 "Statistical Analysis of Fragility Curves," by M. Shinozuka, M.Q. Feng, H. Kim, T. Uzawa and T. Ueda, 6/16/03, (PB2004-101849, A09, CD-A09).
- MCEER-03-0003 "Proceedings of the Eighth U.S.-Japan Workshop on Earthquake Resistant Design of Lifeline Facilities and Countermeasures Against Liquefaction," edited by M. Hamada, J.P. Bardet and T.D. O'Rourke, 6/30/03.
- MCEER-03-0004 "Proceedings of the PRC-US Workshop on Seismic Analysis and Design of Special Bridges," edited by L.C. Fan and G.C. Lee, 7/15/03.
- MCEER-03-0005 "Urban Disaster Recovery: A Framework and Simulation Model," by S.B. Miles and S.E. Chang, 7/25/03.
- MCEER-03-0006 "Behavior of Underground Piping Joints Due to Static and Dynamic Loading," by R.D. Meis, M. Maragakis and R. Siddharthan, 11/17/03.
- MCEER-03-0007 "Seismic Vulnerability of Timber Bridges and Timber Substructures," by A.A. Shama, J.B. Mander, I.M. Friedland and D.R. Allcock, 12/15/03.
- MCEER-04-0001 "Experimental Study of Seismic Isolation Systems with Emphasis on Secondary System Response and Verification of Accuracy of Dynamic Response History Analysis Methods," by E. Wolff and M. Constantinou, 1/16/04.



**Experimental Study of Seismic  
Isolation Systems with Emphasis on  
Secondary System Response and  
Verification of Accuracy of Dynamic  
Response History Analysis Methods**



**MCEER-04-0001**

**E.D. Wolff, M.C. Constantinou**

**Appendices A, B, C and D**

**1/16/2004**

**Experimental Study of Seismic  
Isolation Systems with Emphasis on  
Secondary System Response and  
Verification of Accuracy of Dynamic  
Response History Analysis Methods**



**MCEER-04-0001**

**E.D. Wolff, M.C. Constantinou**

**Appendices A, B, C and D**

**1/16/2004**



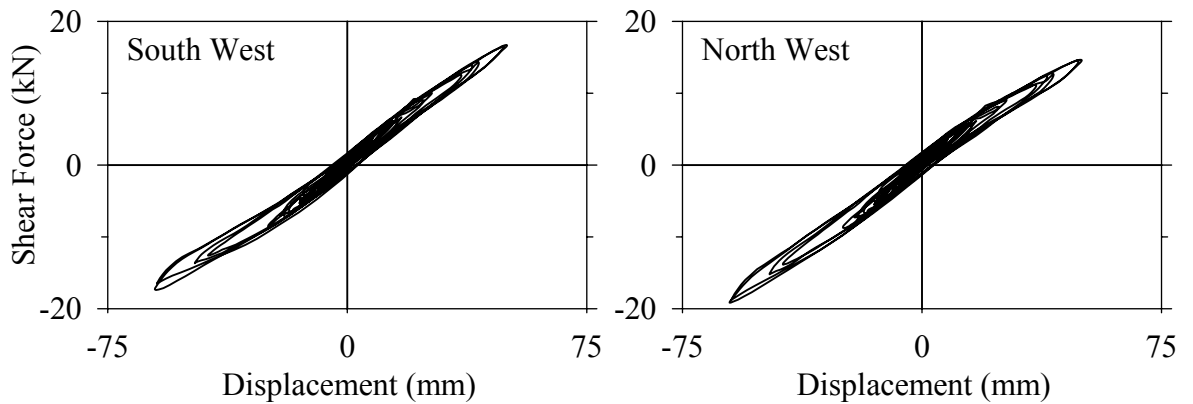
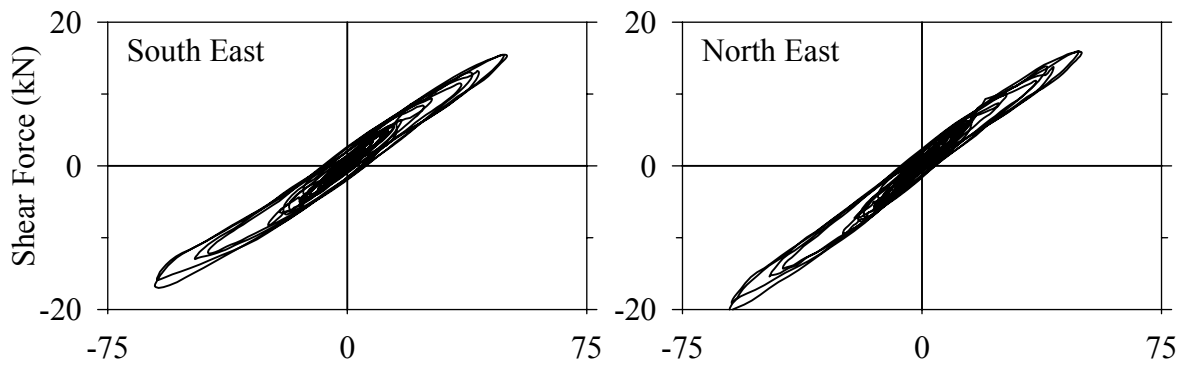
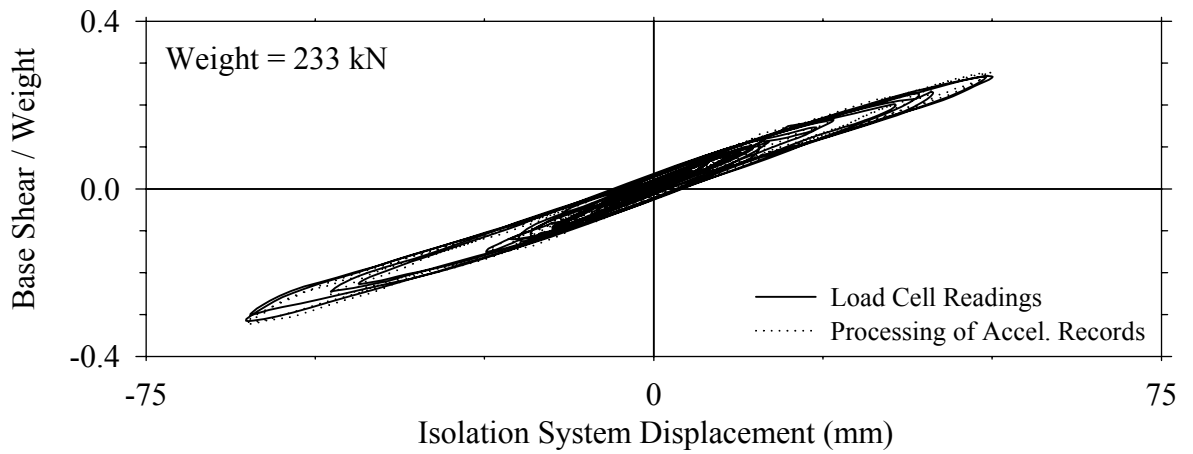
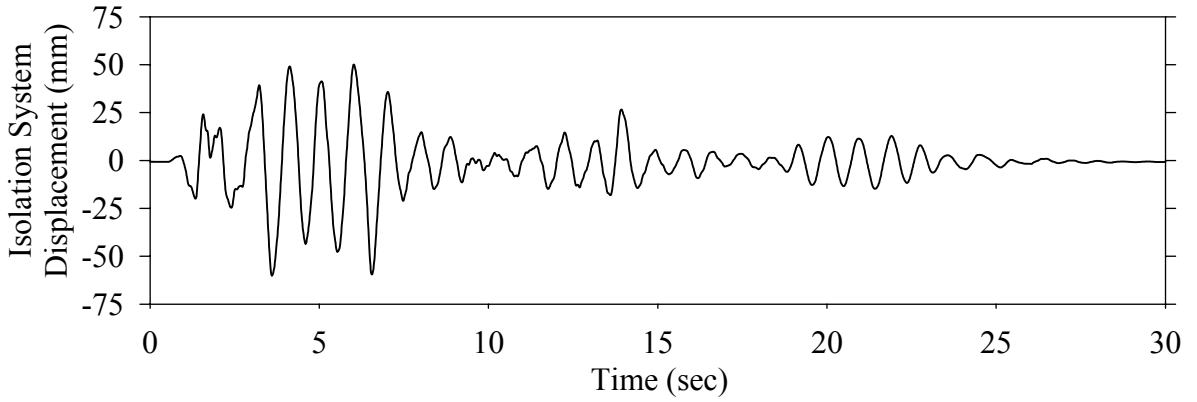
**APPENDIX A**  
**EXPERIMENTAL RESULTS**

This appendix presents results in graphical form for four excitations of each configuration tested. The presented results include:

1. Isolation system displacement history.
2. Base shear divided by weight versus isolation system displacement loop. Two independent measurements of base shear force are presented, one directly from the load cells supporting the bearings, and one indirectly by summing up the floor inertia forces (floor mass times acceleration). The two measurements compare well, thus confirming the fidelity of the measurements.
3. Individual bearing force displacement loops as recorded by each individual load cell. The variation in shear force of sliding bearings due to varying axial loads is evident.
4. Load cell axial force time history. The first plot is the sum of all four load cells. The next two plots are the sum of the north two and south two load cells respectively. The large variation in axial load due to overturning moment effects can be seen in these plots, while the total sum of axial force tends to remain constant.
5. Base shear divided by weight versus isolation system displacement containing:
  - a. For FPS bearings without damping devices: the sum of the south two load cell shear forces and the sum of the north two load cell shear forces.
  - b. For FPS bearings with damping devices: the first plot contains the sum of the four load cell shear forces, and the second contains the total base shear including the horizontal component of force from the damping devices.
  - c. For lead core bearings these plots are blank.

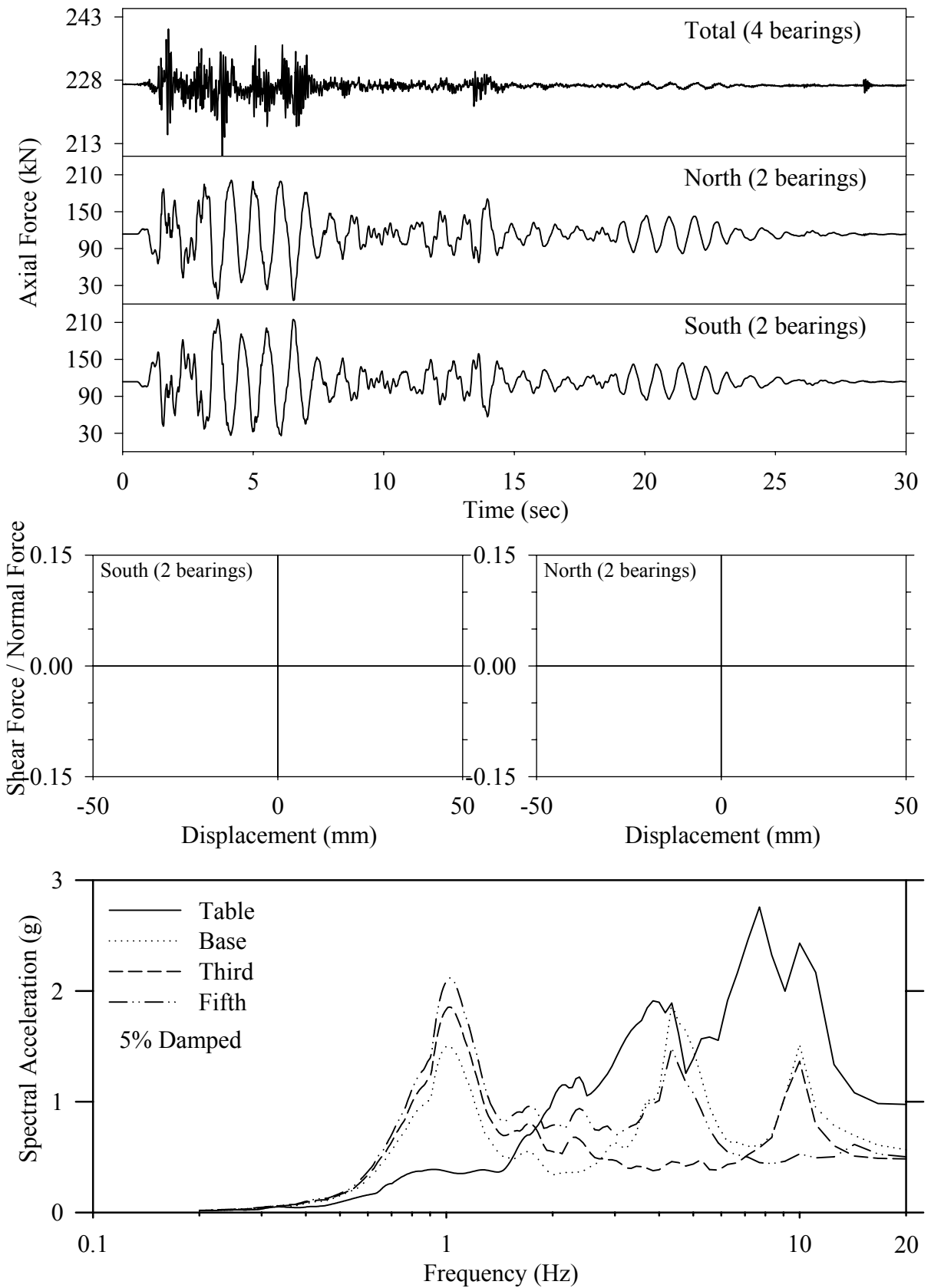
- d. For low damping elastomeric bearings without damping devices these plots are blank.
  - e. For low damping elastomeric bearings with damping devices: the first plot contains the sum of the four load cell shear forces, and the second contains the total base shear including the horizontal component of force from the damping devices.
6. The 5% damped spectra calculated from the recorded acceleration time histories of the table, the base, the 3<sup>rd</sup> floor and the 5<sup>th</sup> floor.

Test LDMFE20.1, El Centro S00E 200%, MF/Low Damping Elastomeric

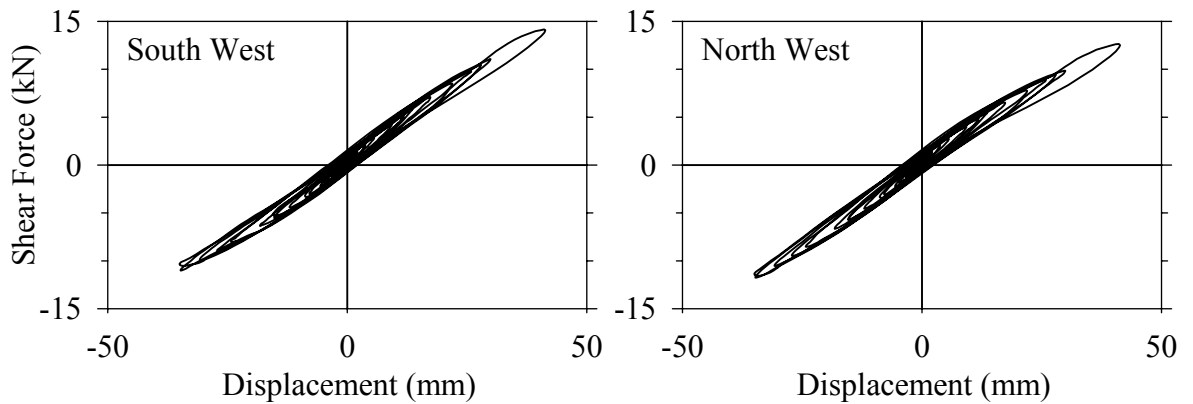
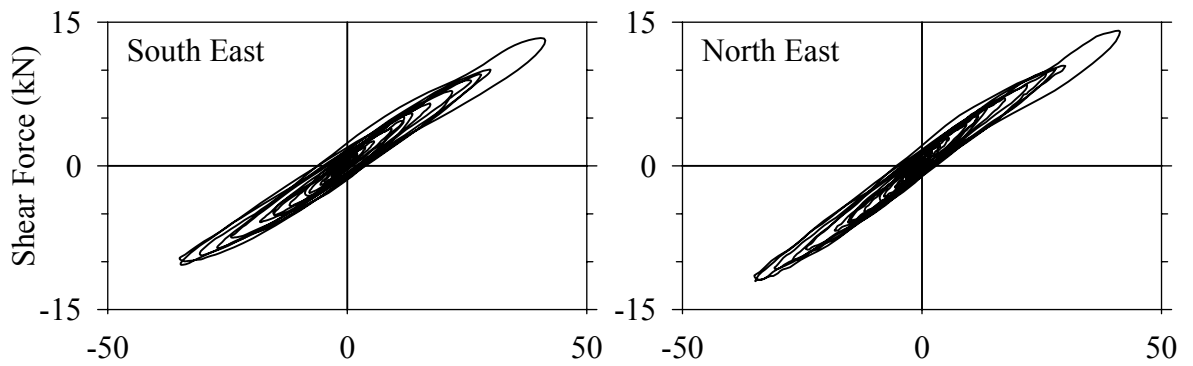
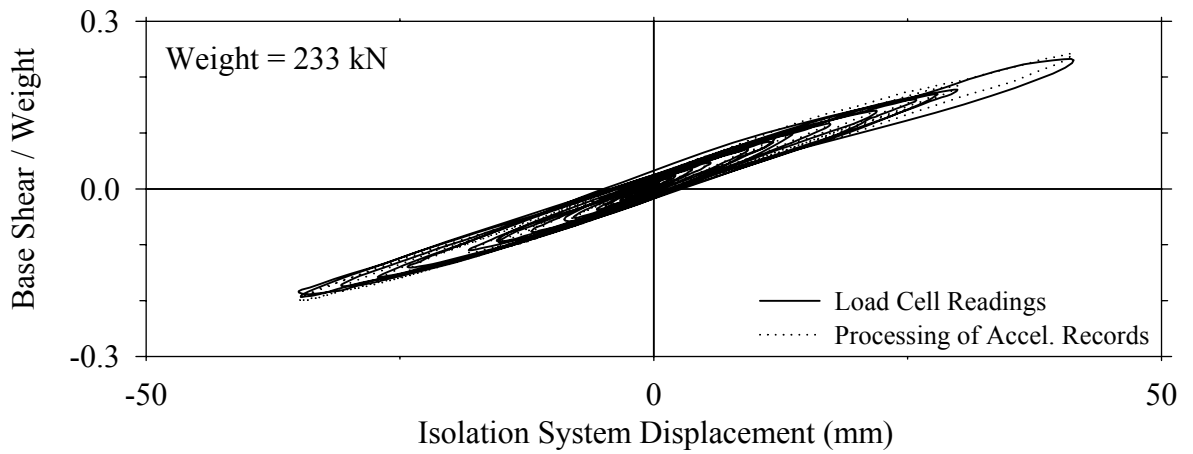
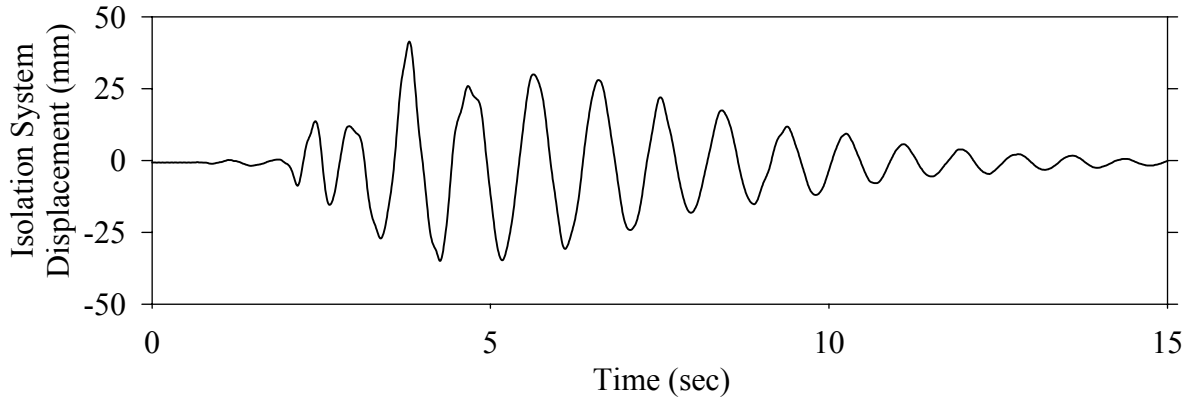




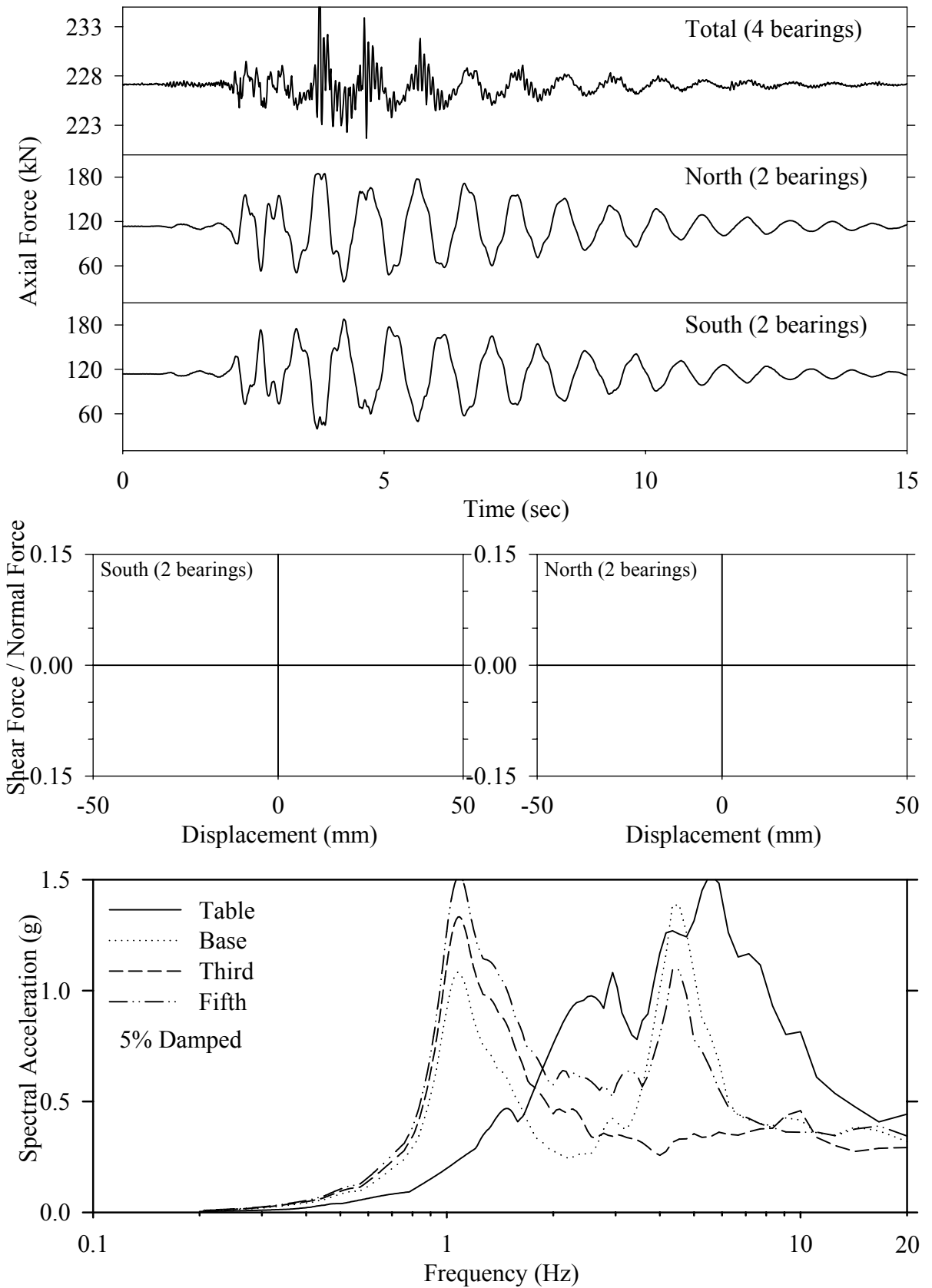
Test LDMFE20.1, El Centro S00E 200%, MF/Low Damping Elastomeric



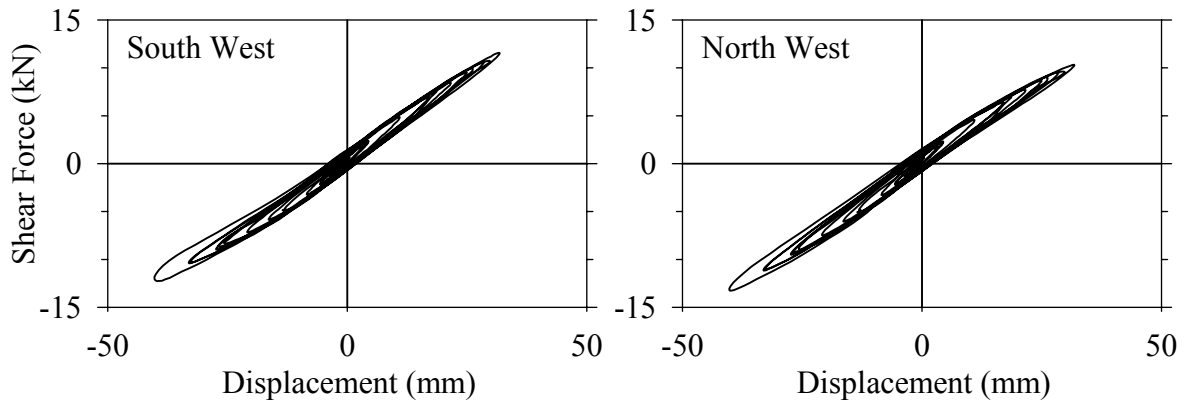
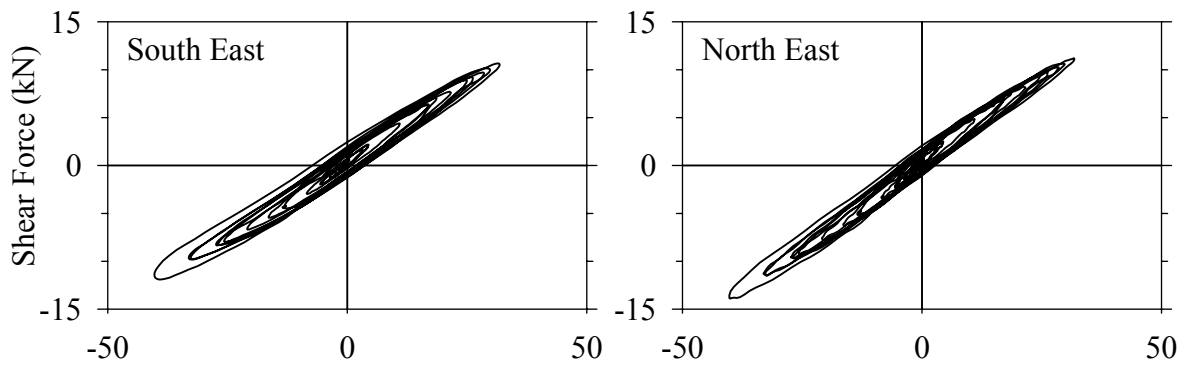
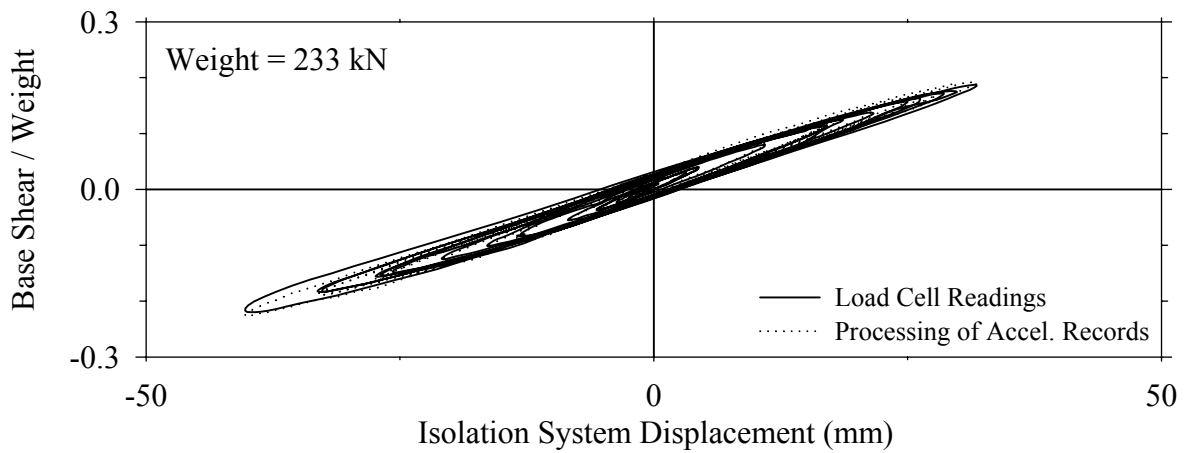
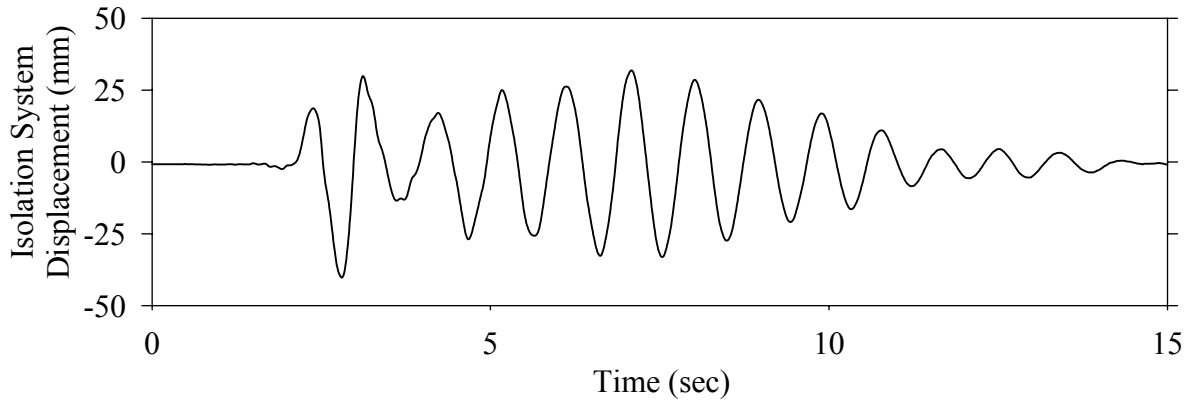
Test LDMFK50.1, Kobe N-S 50%, MF/Low Damping Elastomeric



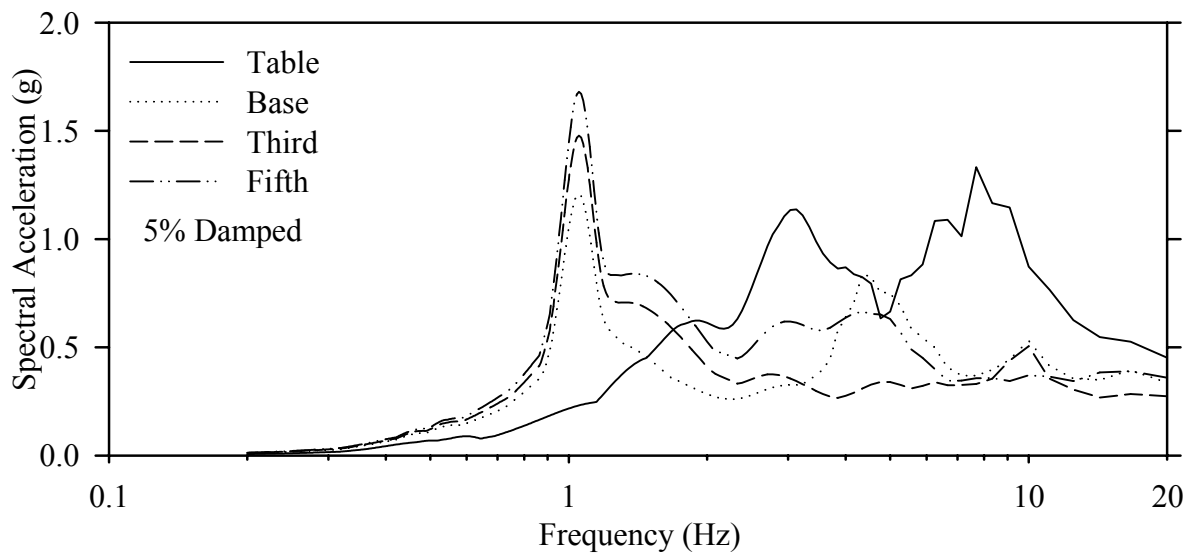
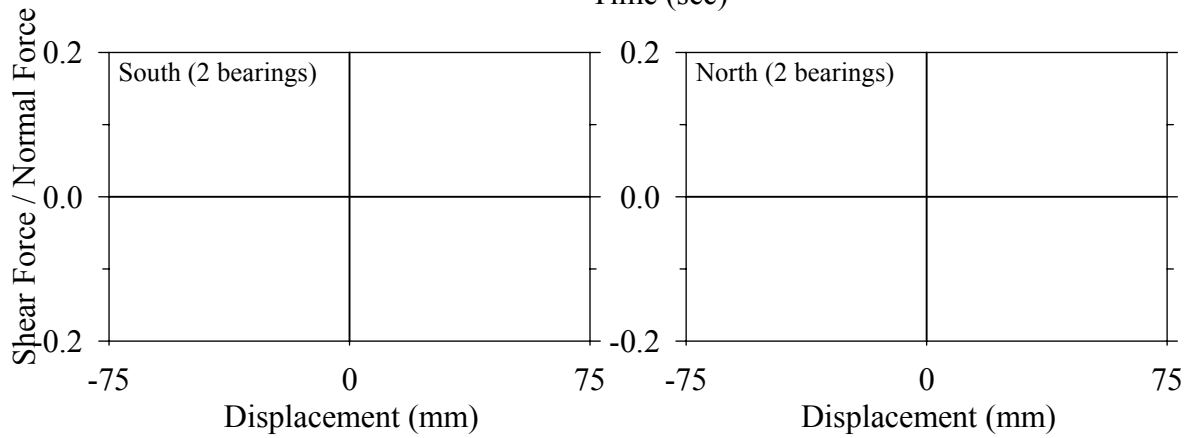
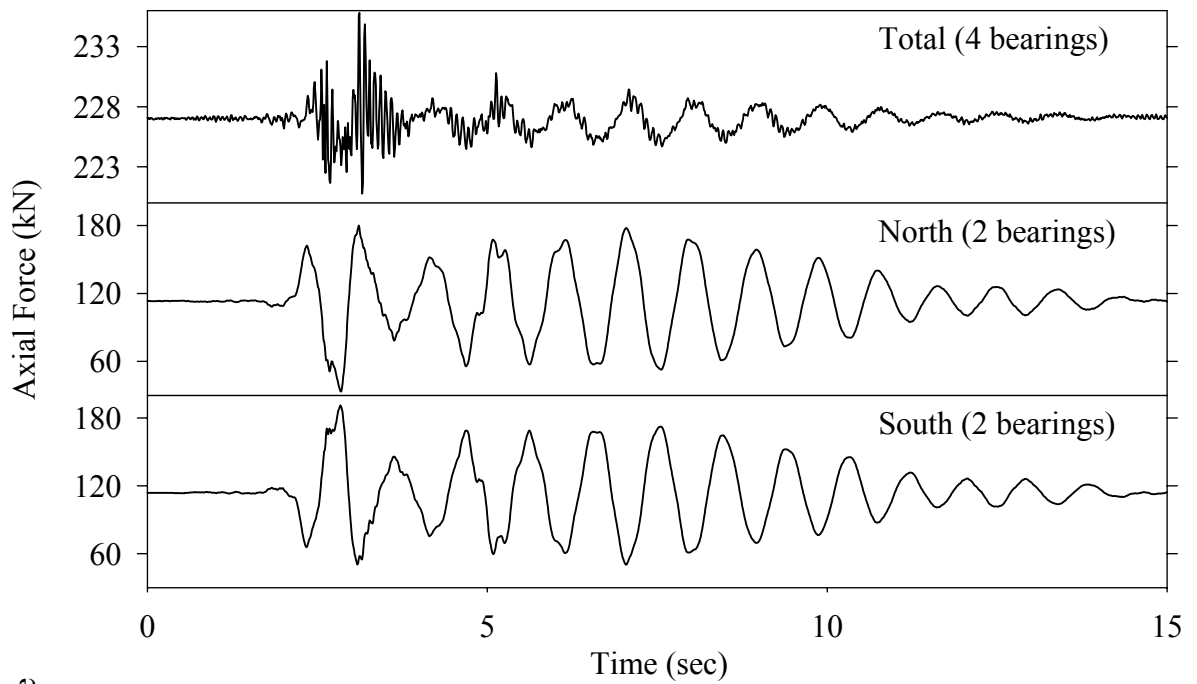
Test LDMFK50.1, Kobe N-S 50%, MF/Low Damping Elastomeric



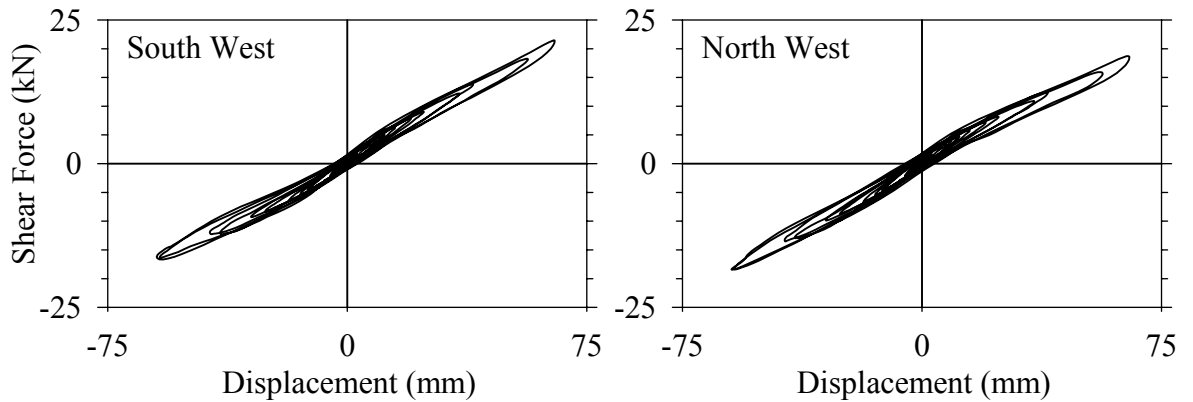
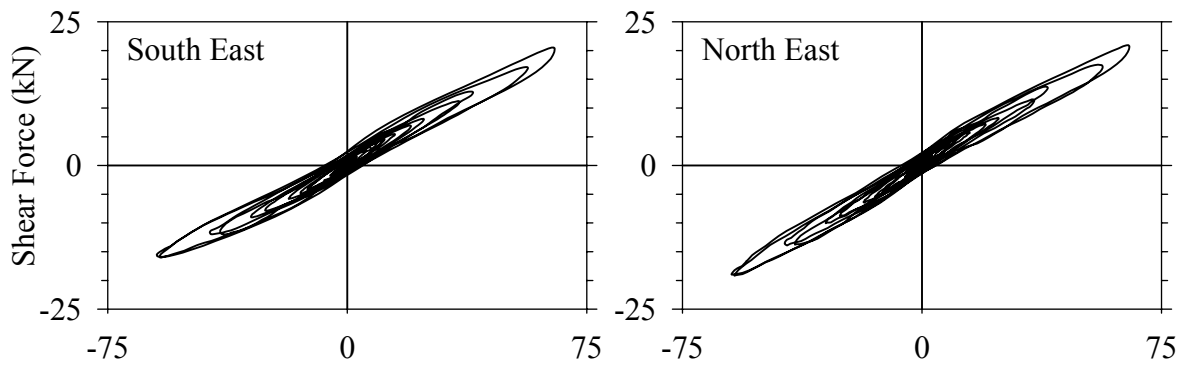
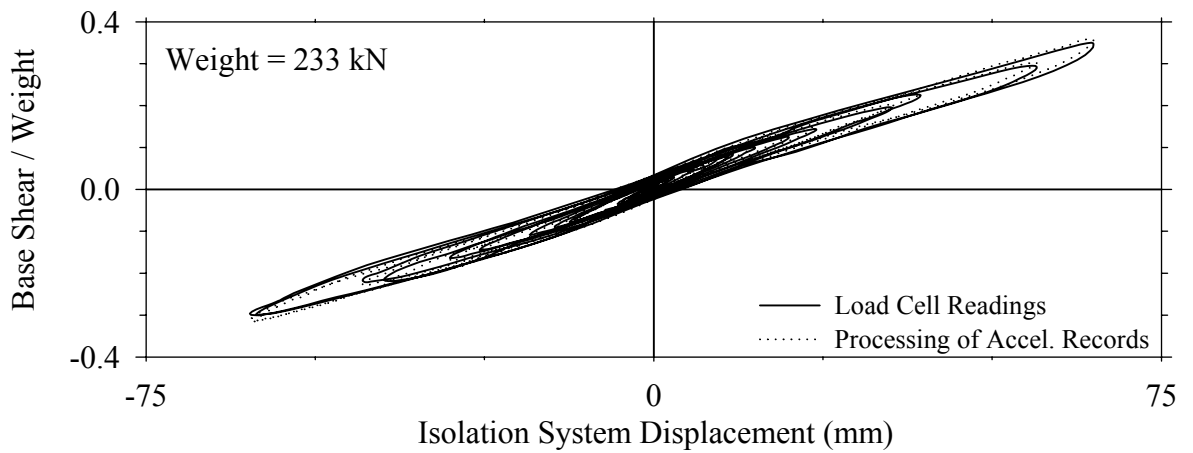
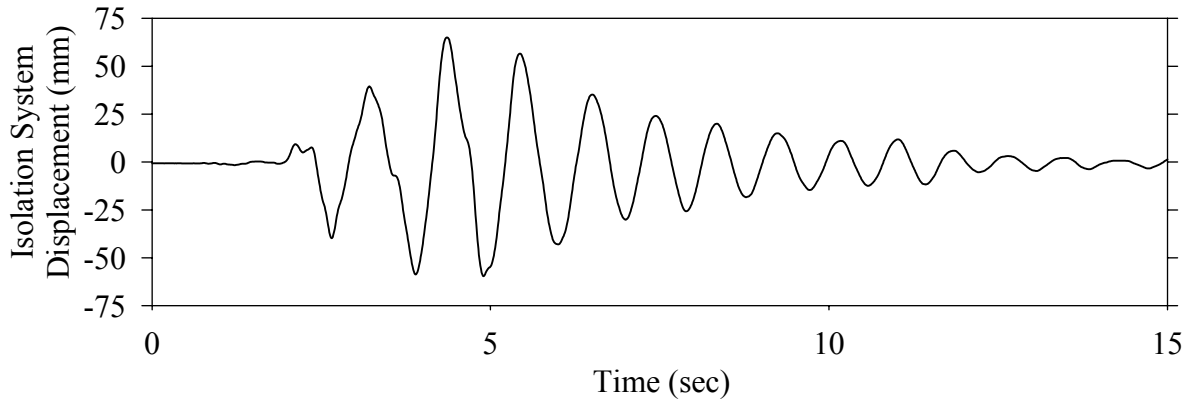
Test LDMFN50.1, Northridge Newhall 360° 50%, MF/Low Damping Elastomeric



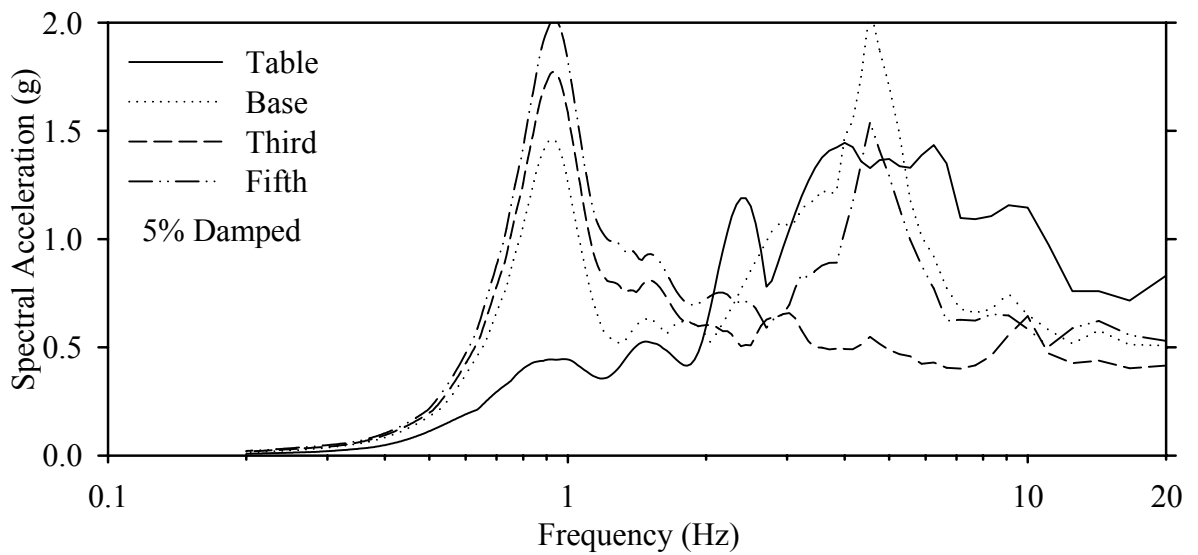
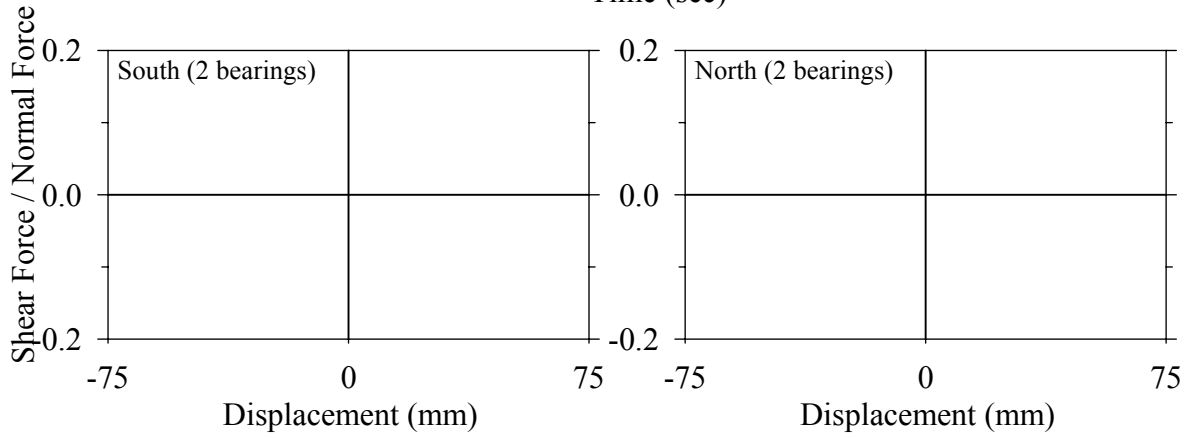
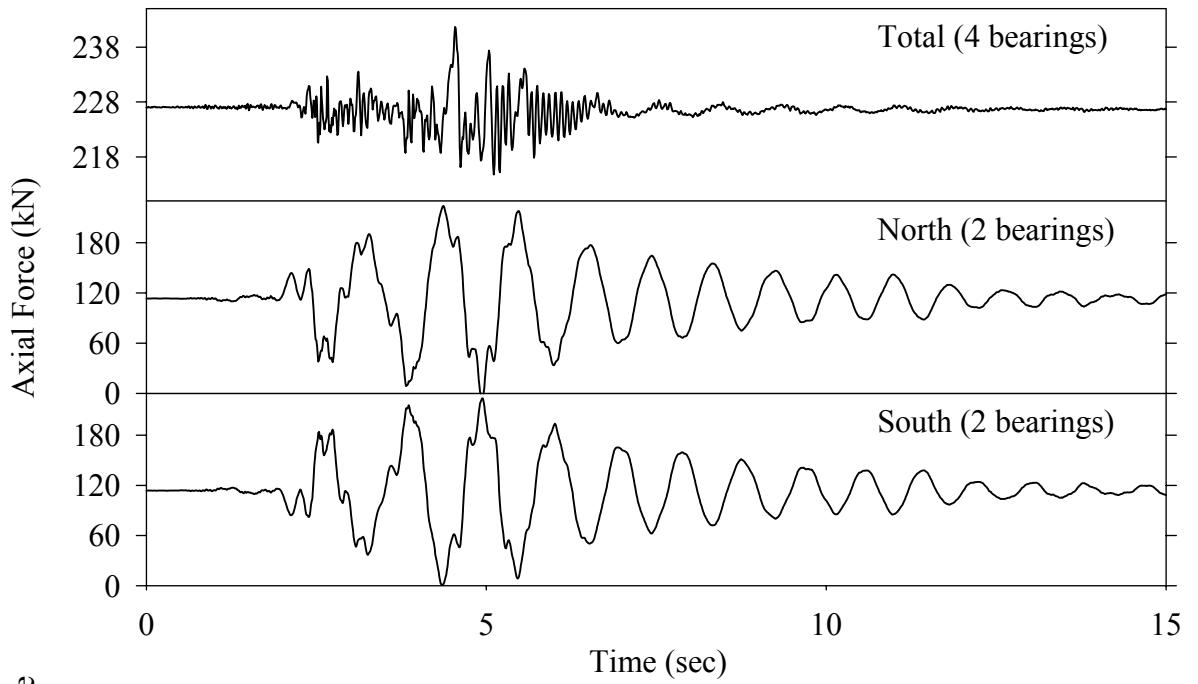
Test LDMFN50.1, Northridge Newhall 360° 50%, MF/Low Damping Elastomeric



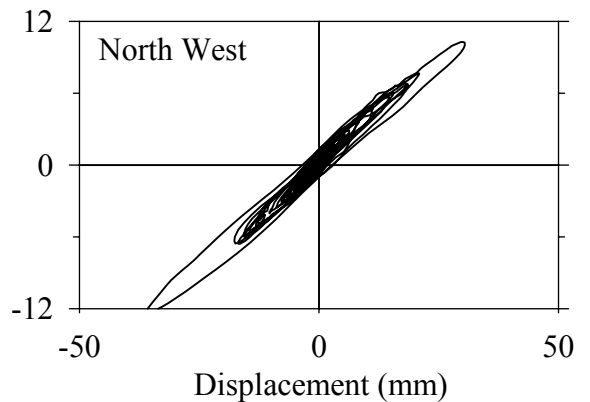
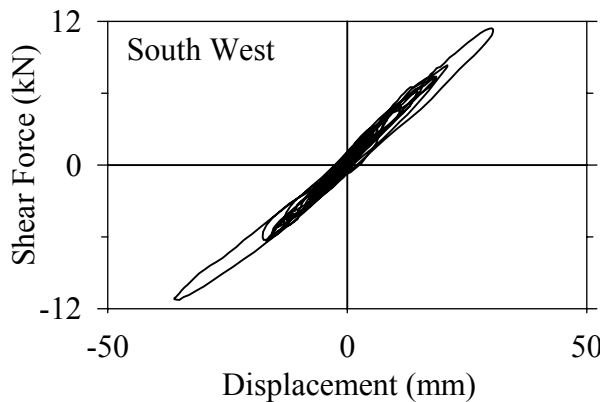
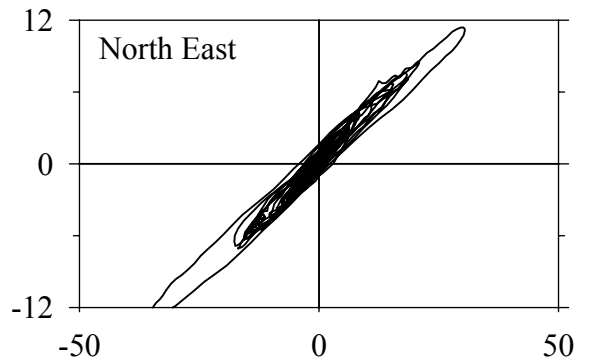
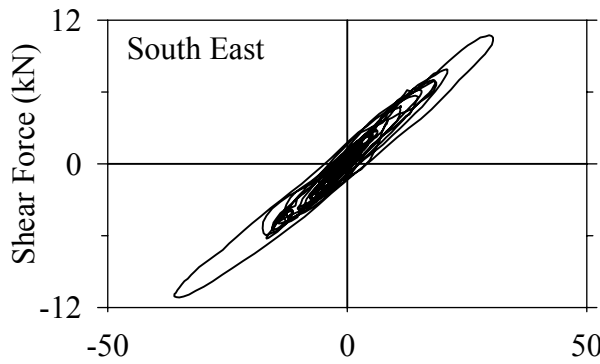
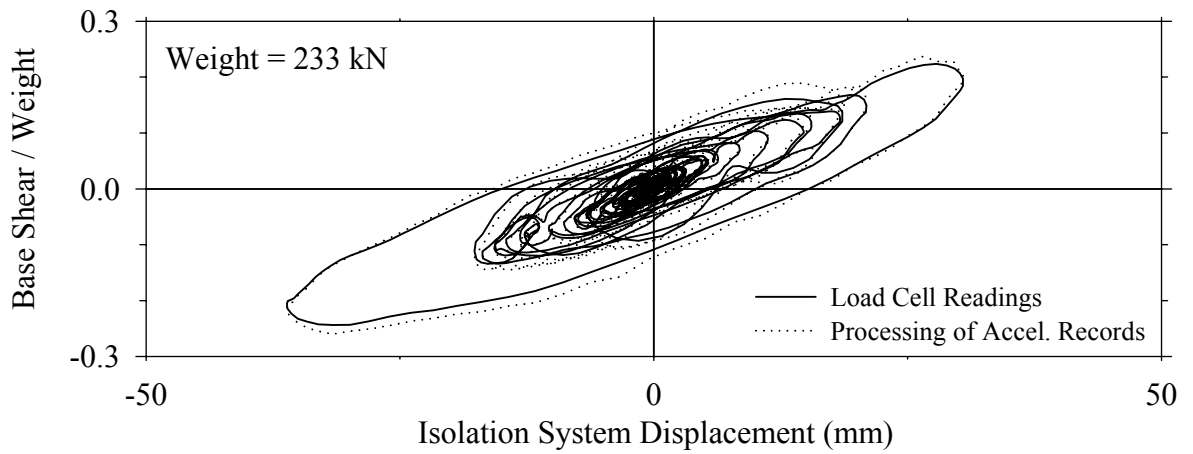
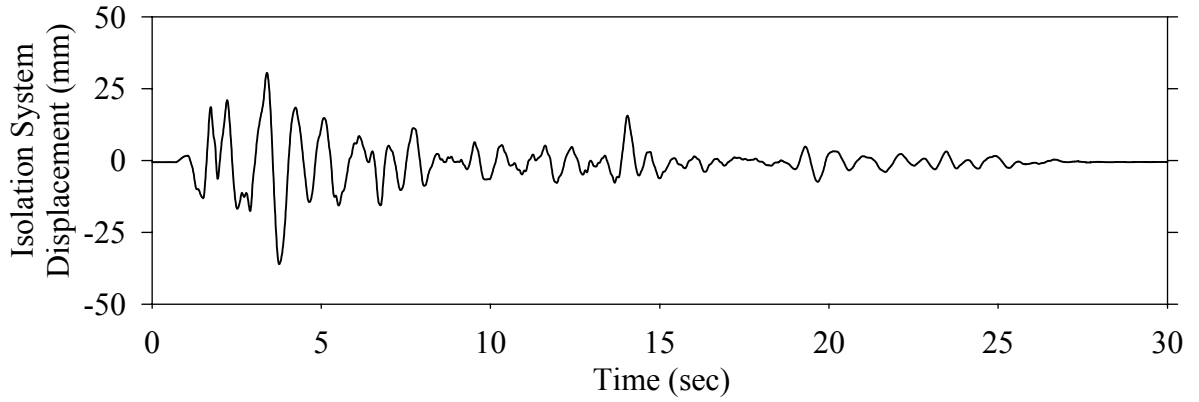
Test LDMFS10.1, Northridge Sylmar 90° 100%, MF/Low Damping Elastomeric



Test LDMFS10.1, Northridge Sylmar 90° 100%, MF/Low Damping Elastomeric

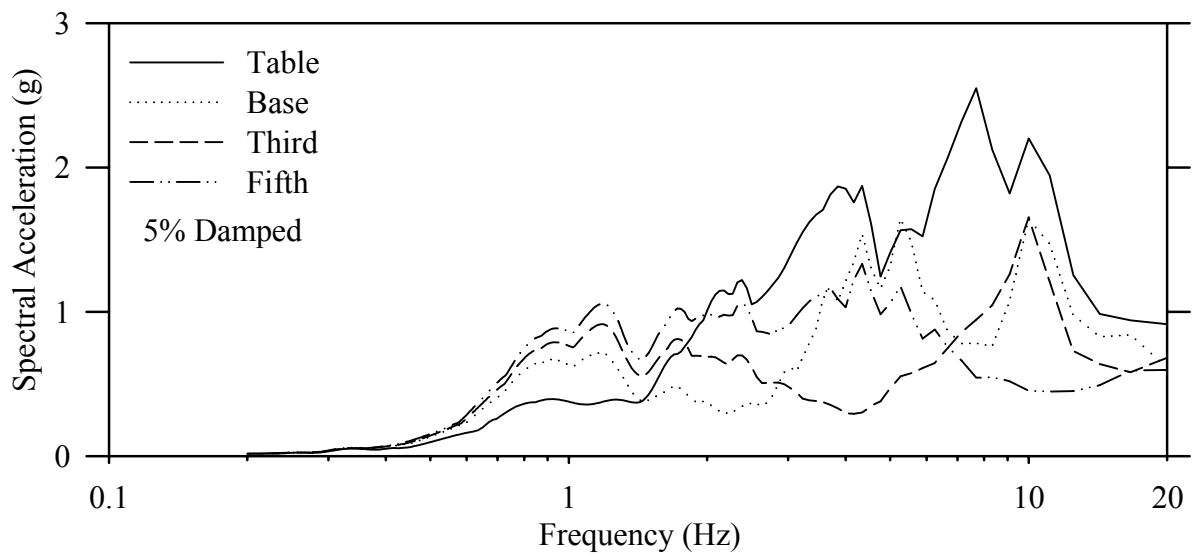
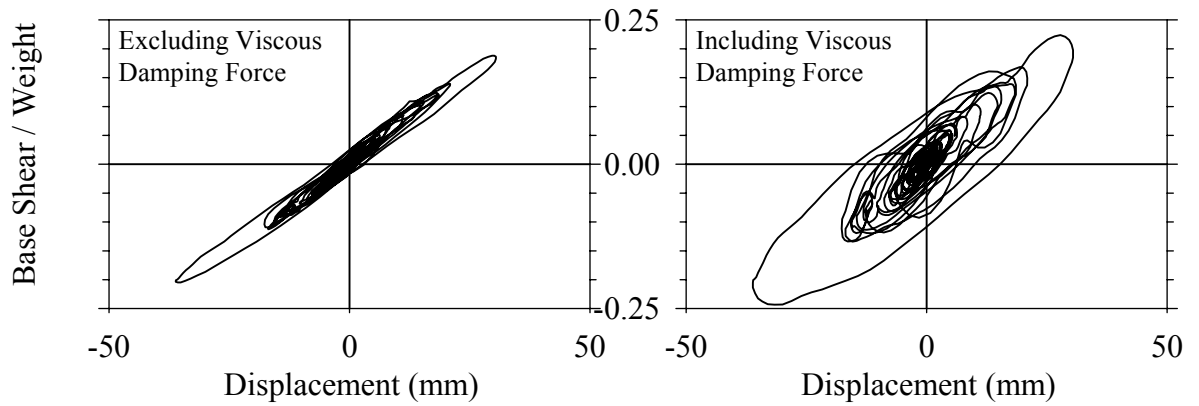
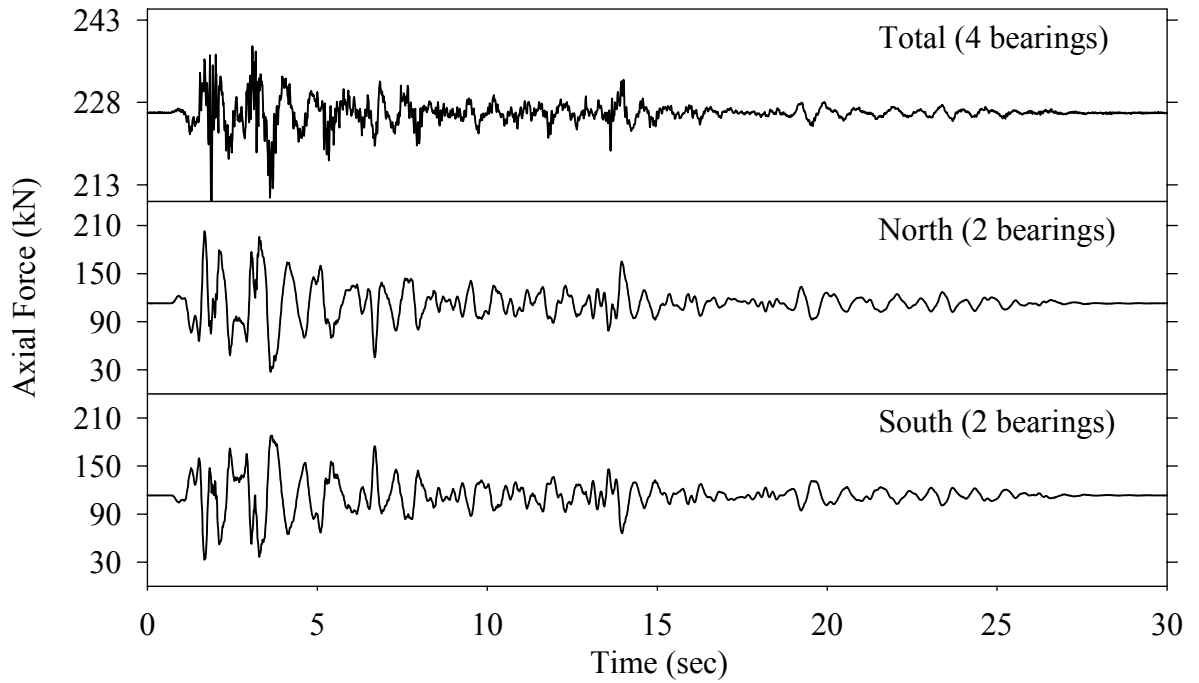


Test LDMLE20.1, El Centro S00E 200%, MF/Low Damping Elastomeric-Linear Dampers

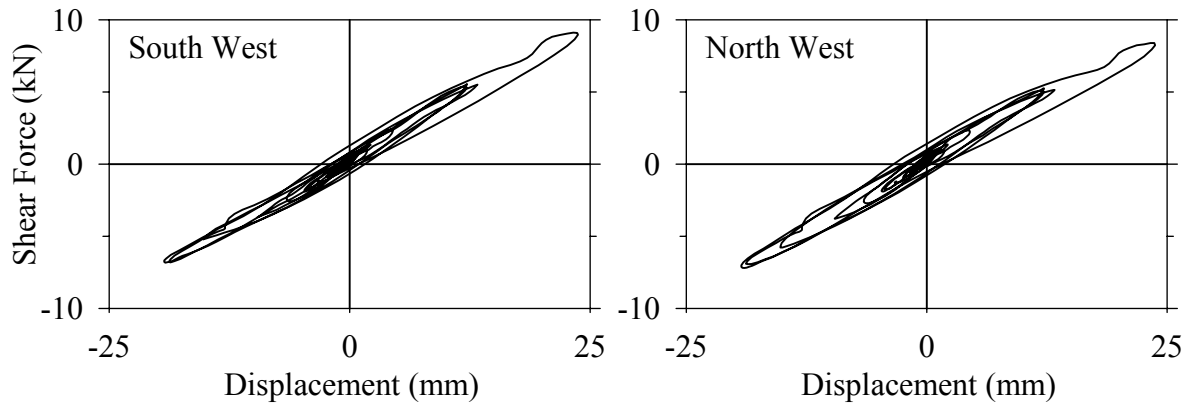
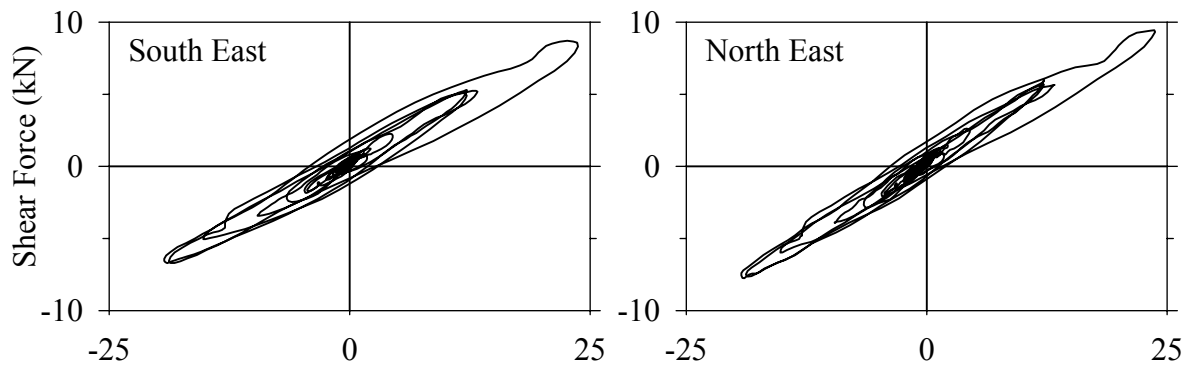
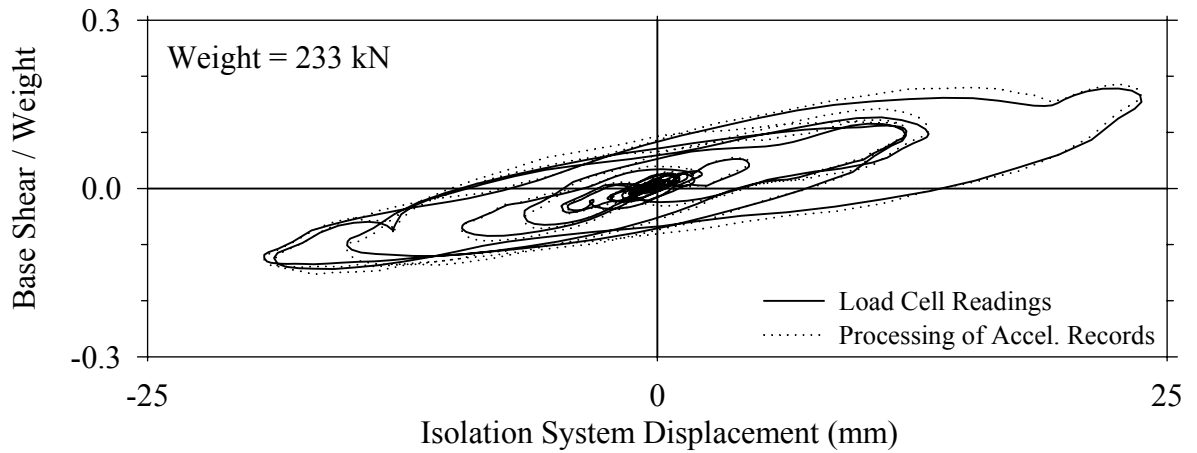
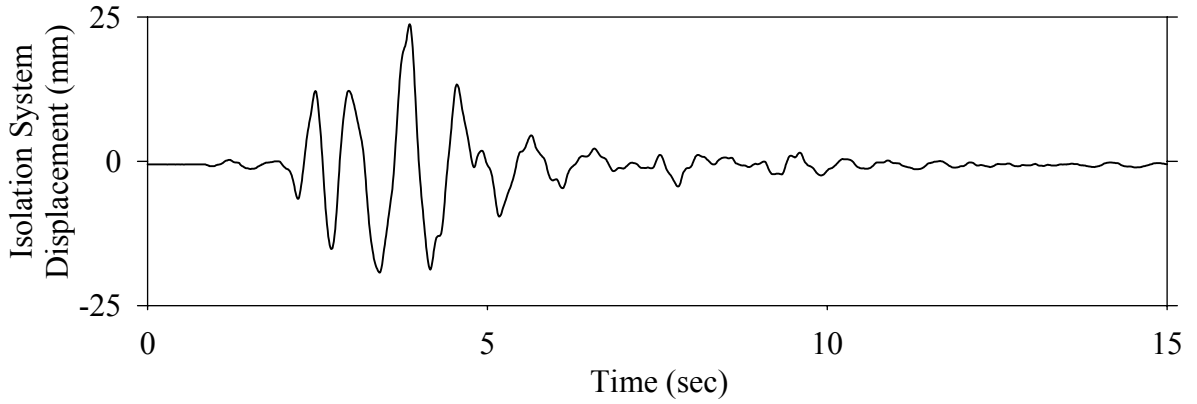




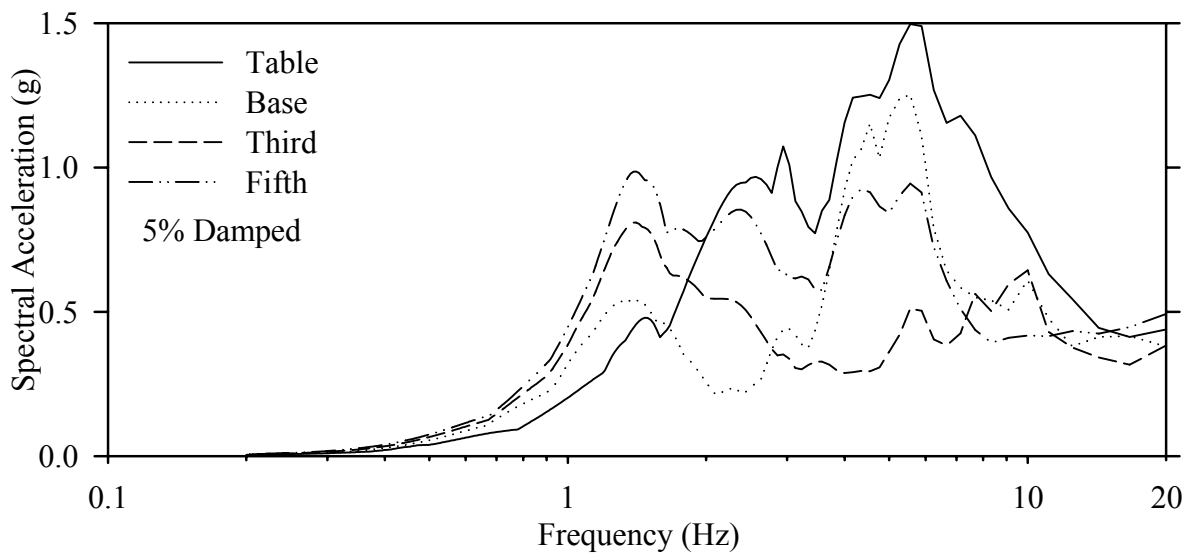
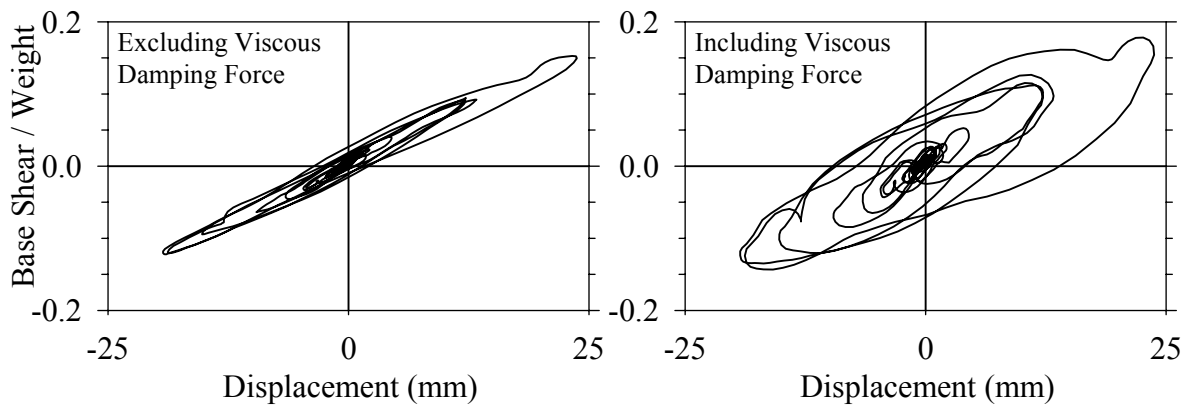
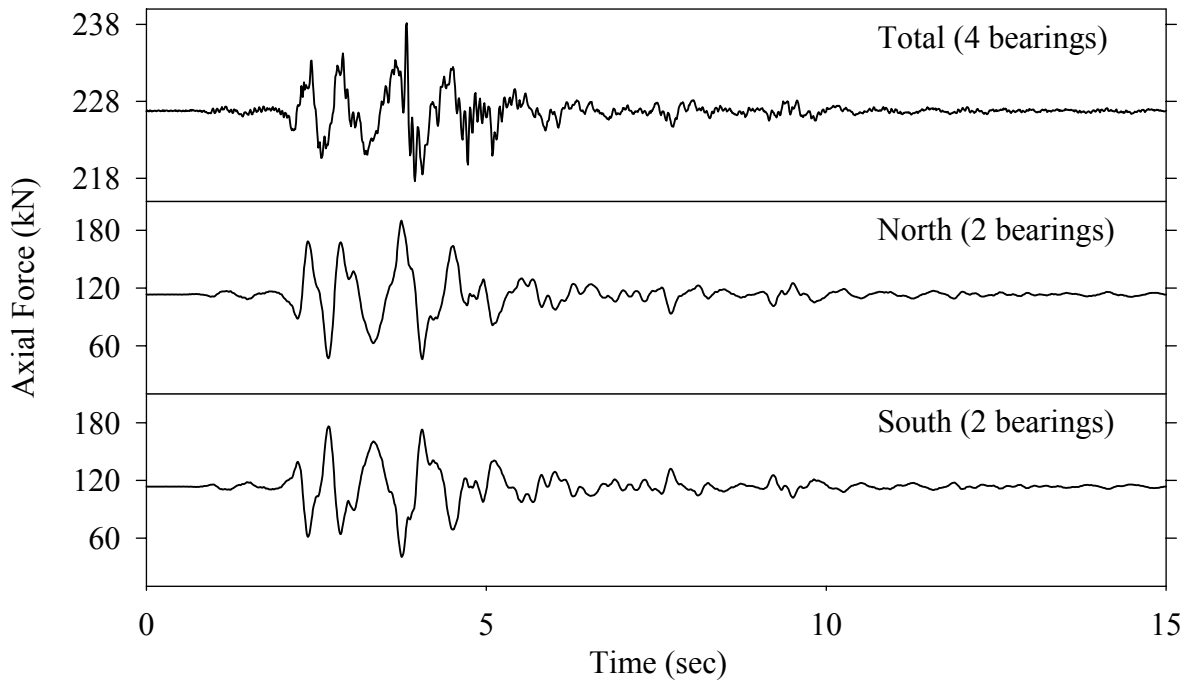
Test LDMLE20.1, El Centro S00E 200%, MF/Low Damping Elastomeric-Linear Dampers



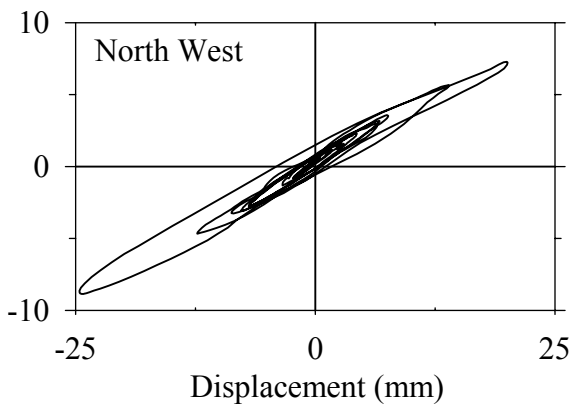
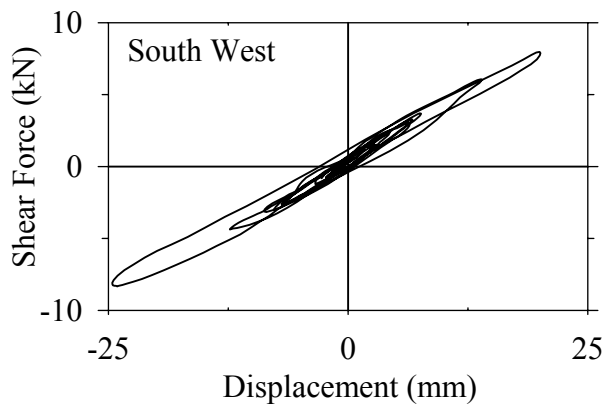
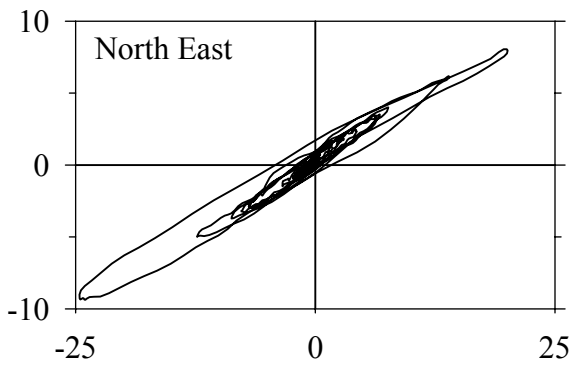
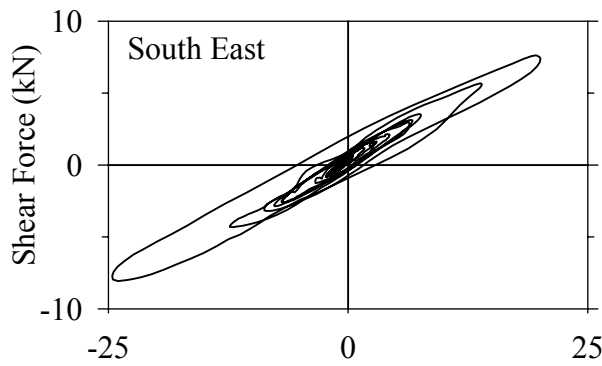
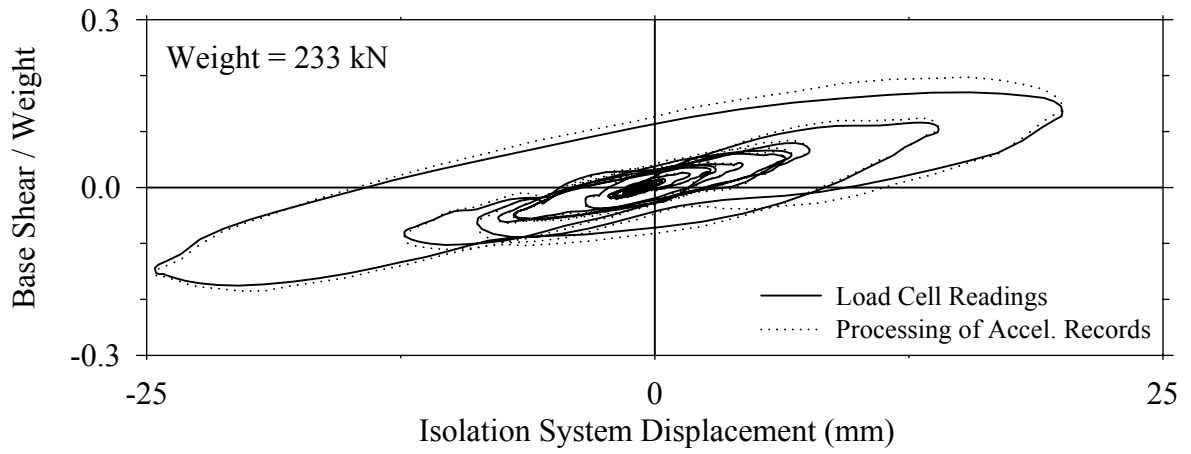
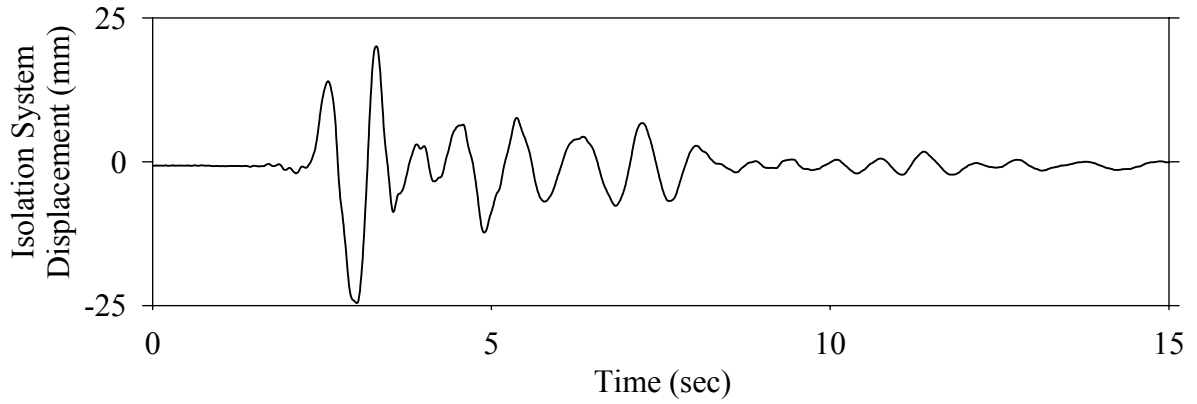
Test LDMLK50.1, Kobe N-S 50%, MF/Low Damping Elastomeric-Linear Dampers



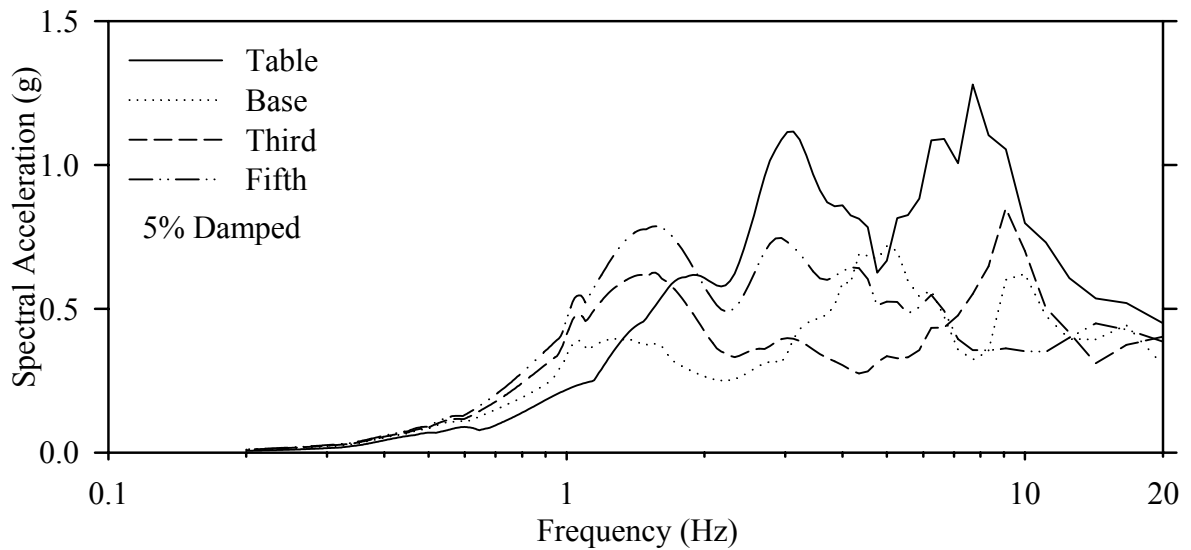
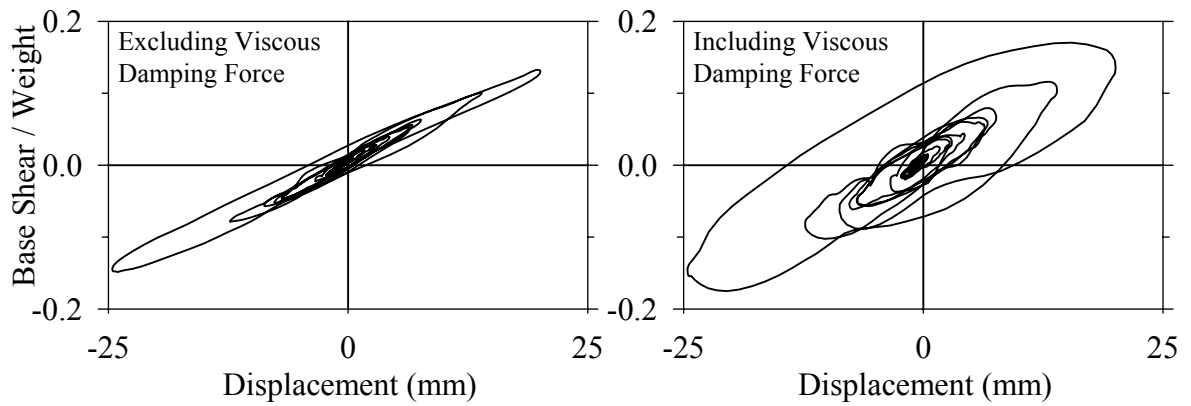
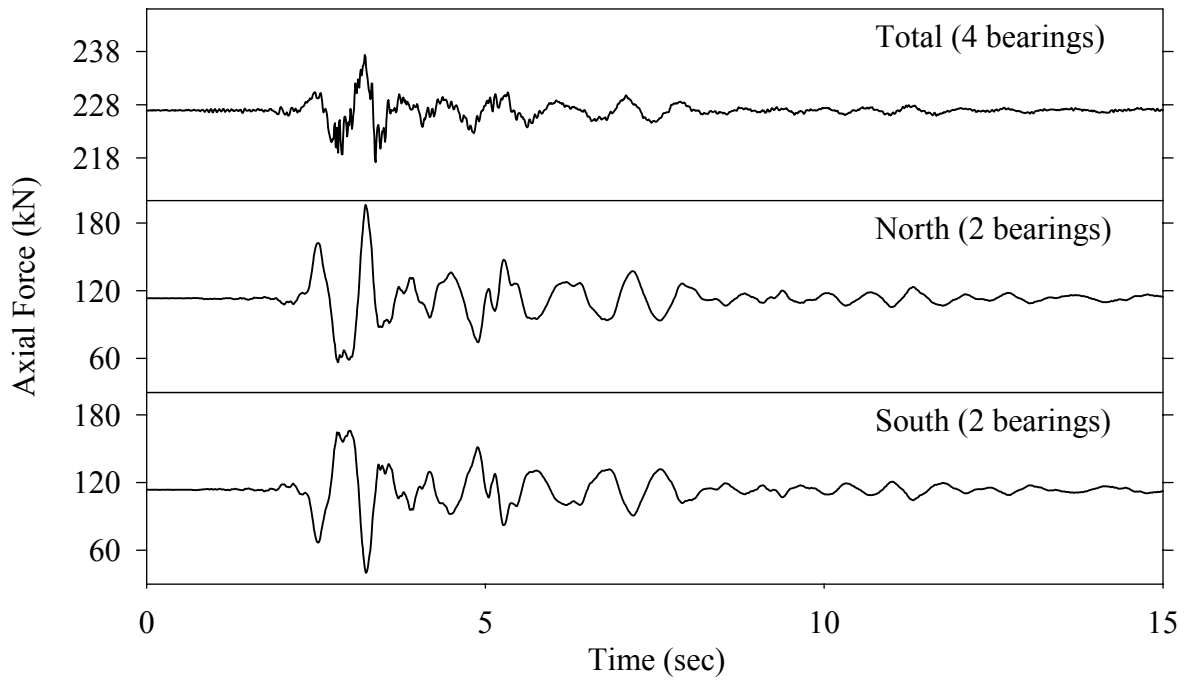
Test LDMLK50.1, Kobe N-S 50%, MF/Low Damping Elastomeric-Linear Dampers



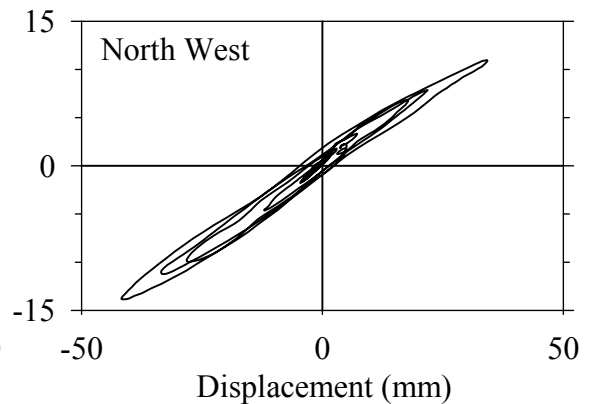
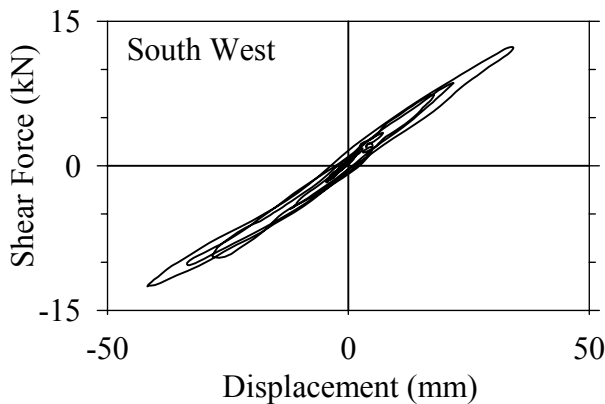
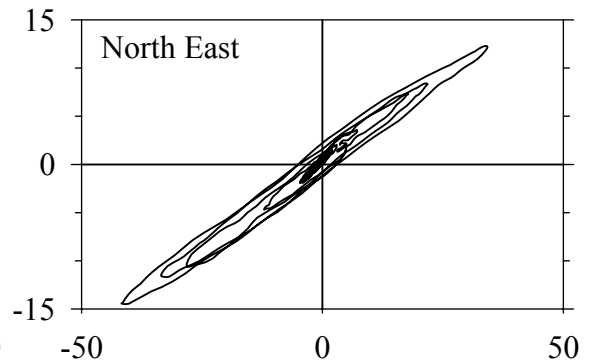
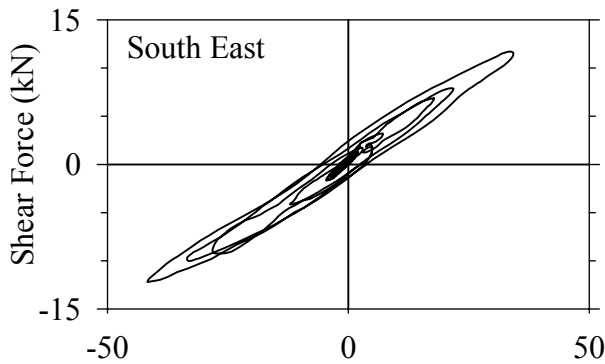
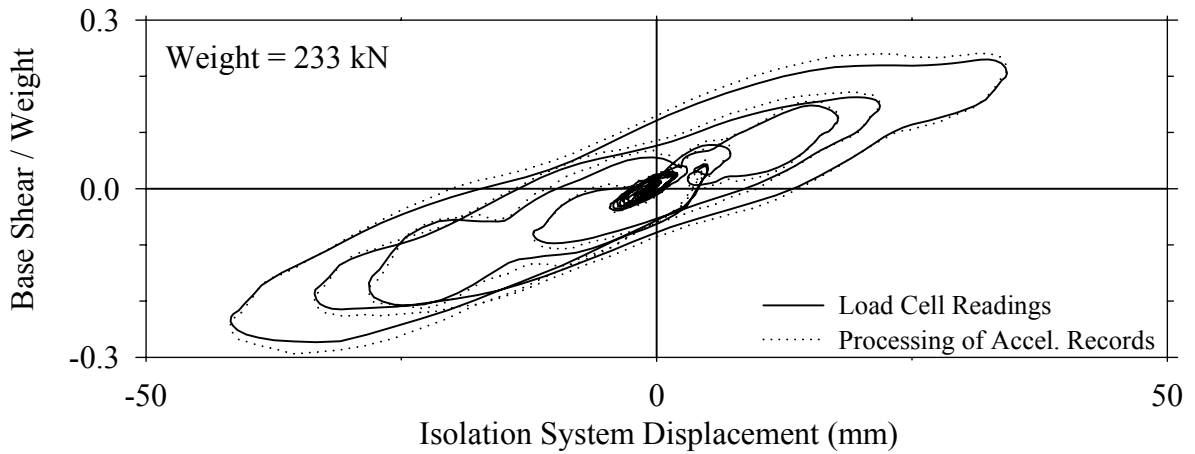
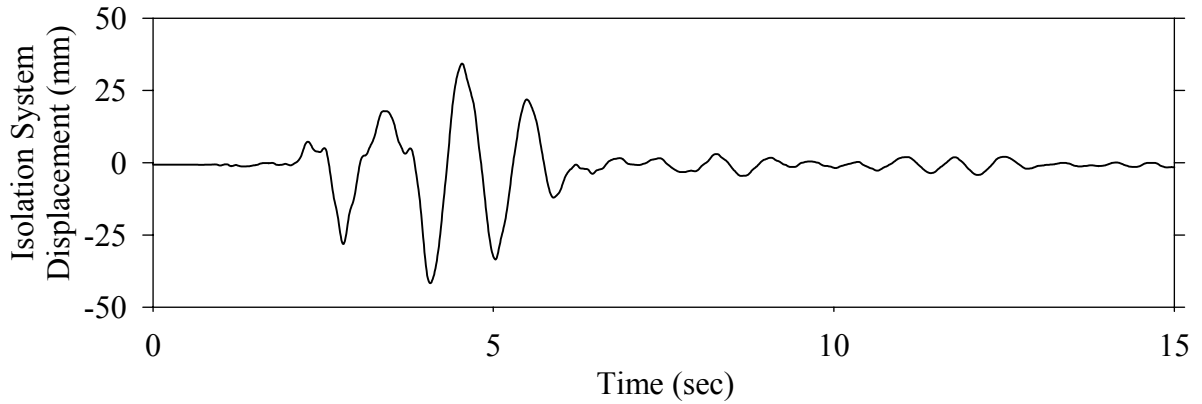
Test LDMLN50.1, Northridge Newhall 360° 50%, MF/Low Damping Elastomeric-Linear Dampers



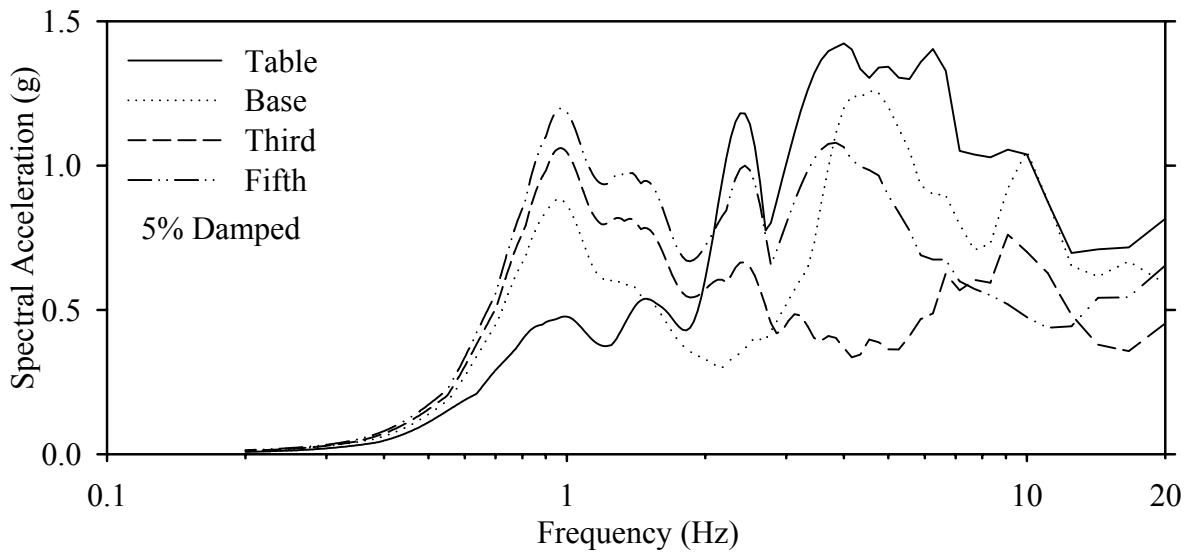
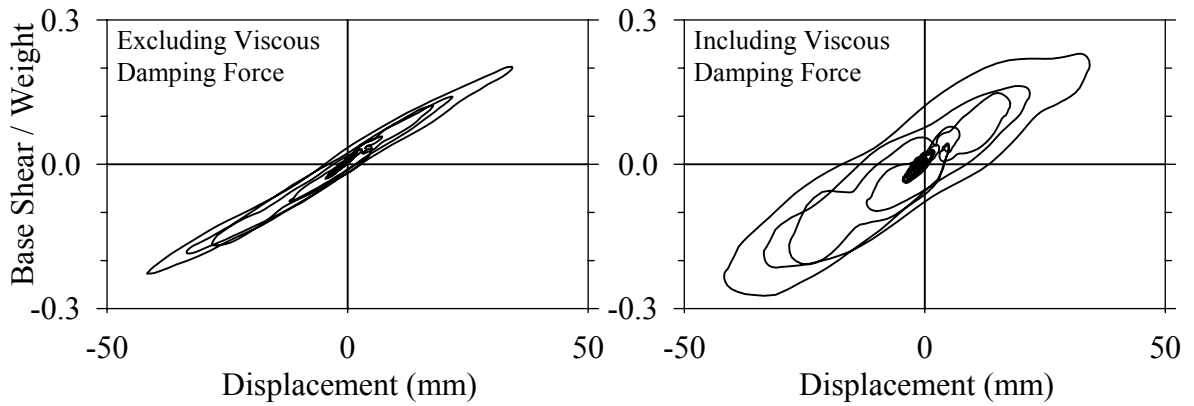
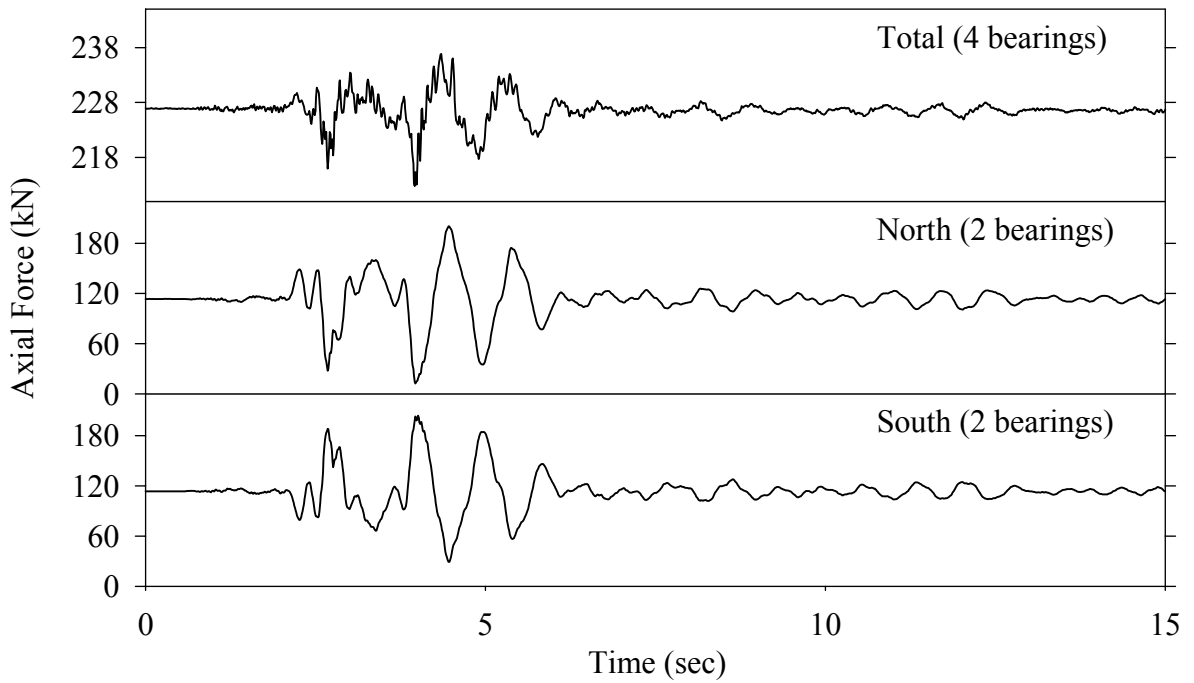
Test LDMLN50.1, Northridge Newhall 360° 50%, MF/Low Damping Elastomeric-Linear Dampers



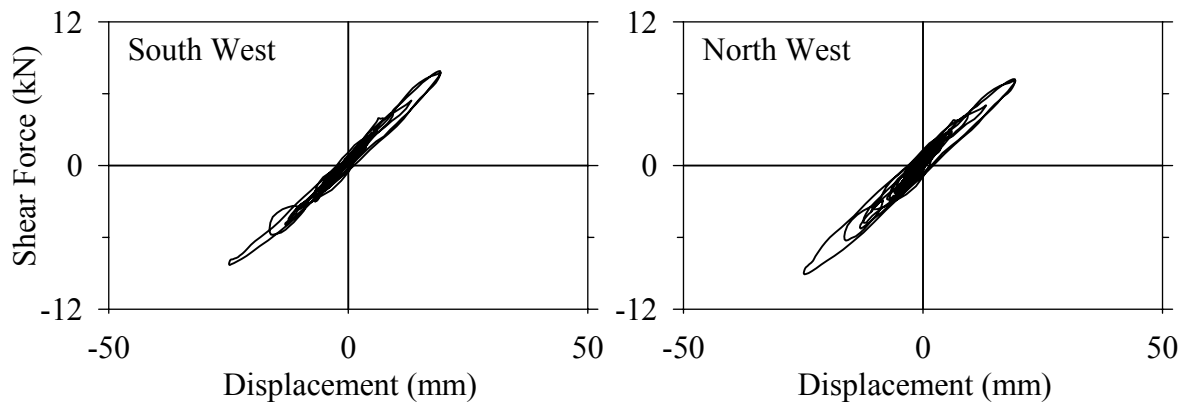
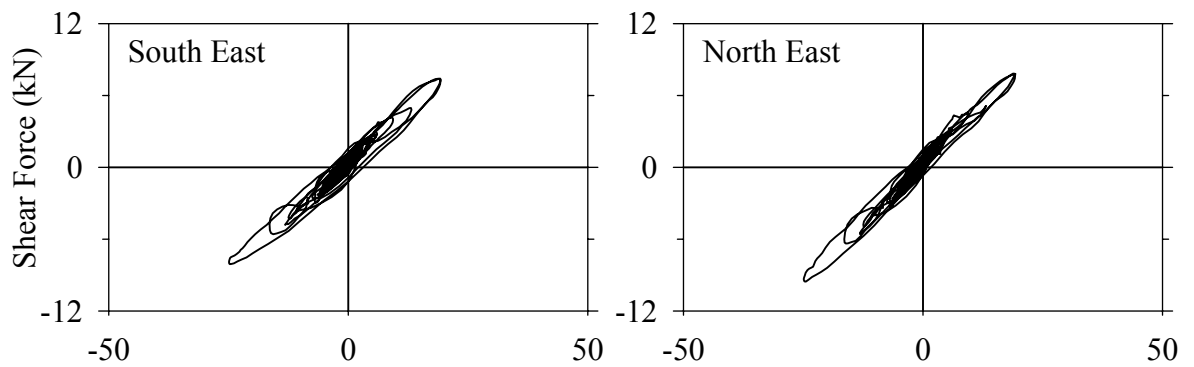
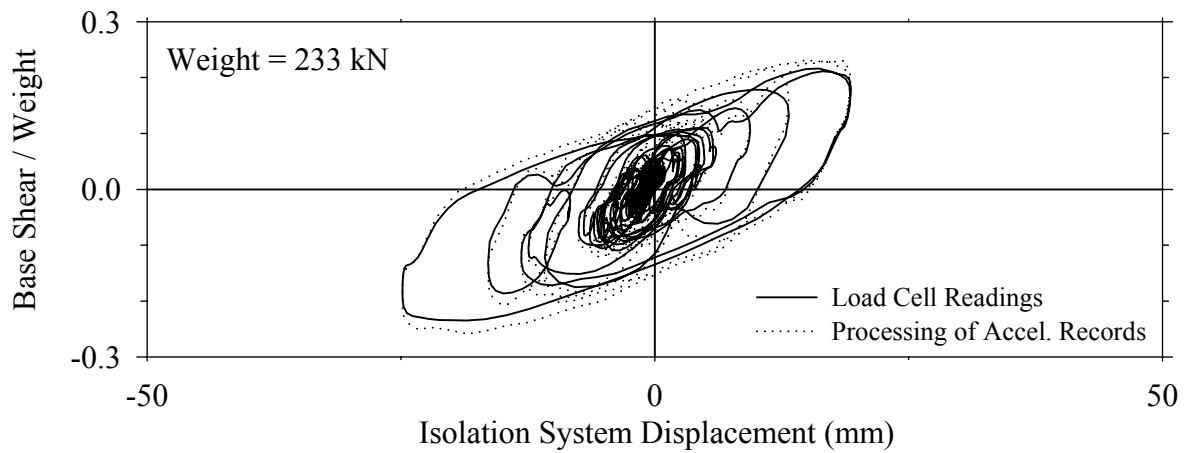
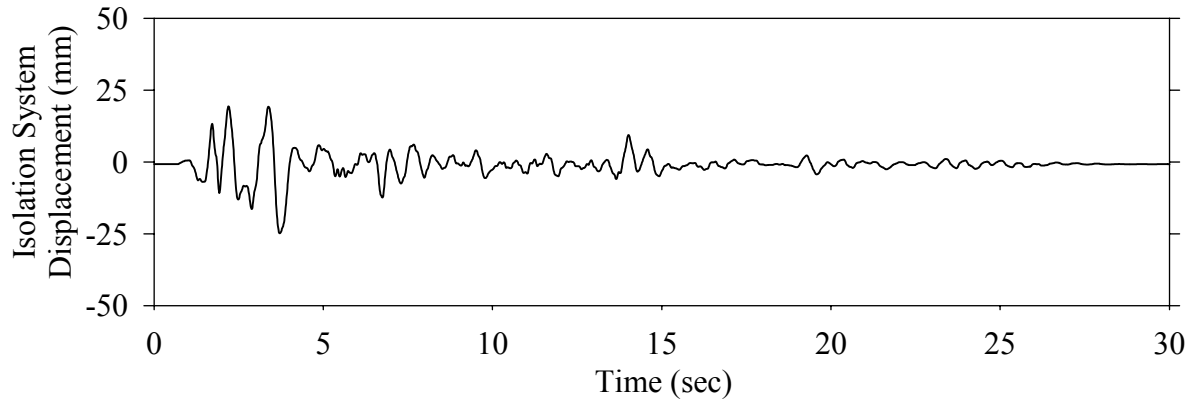
Test LDMLS10.1, Northridge Sylmar 90° 100%, MF/Low Damping Elastomeric-Linear Dampers



Test LDMLS10.1, Northridge Sylmar 90° 100%, MF/Low Damping Elastomeric-Linear Dampers

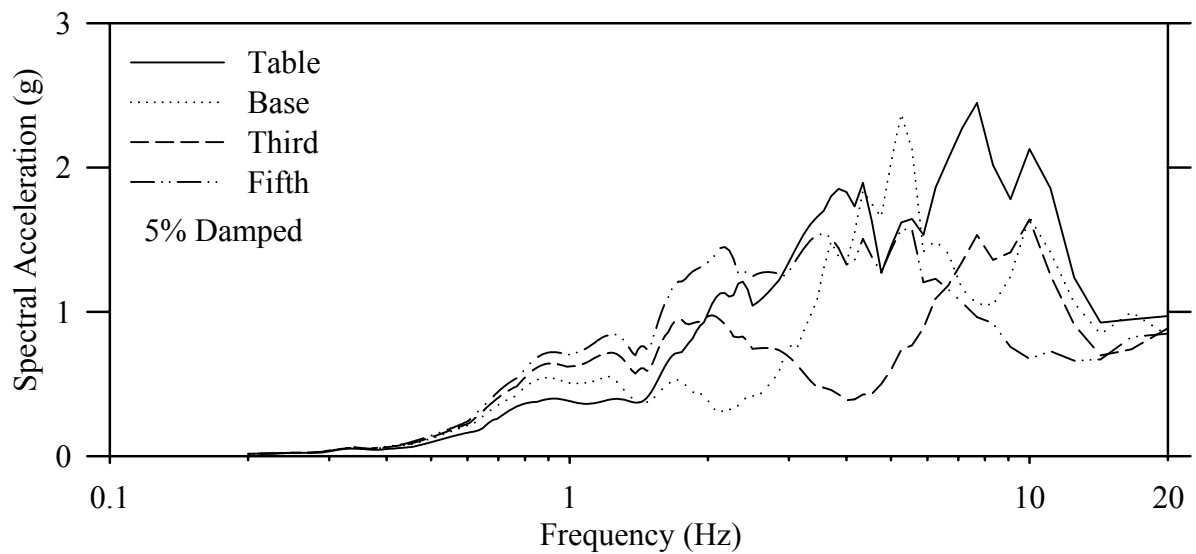
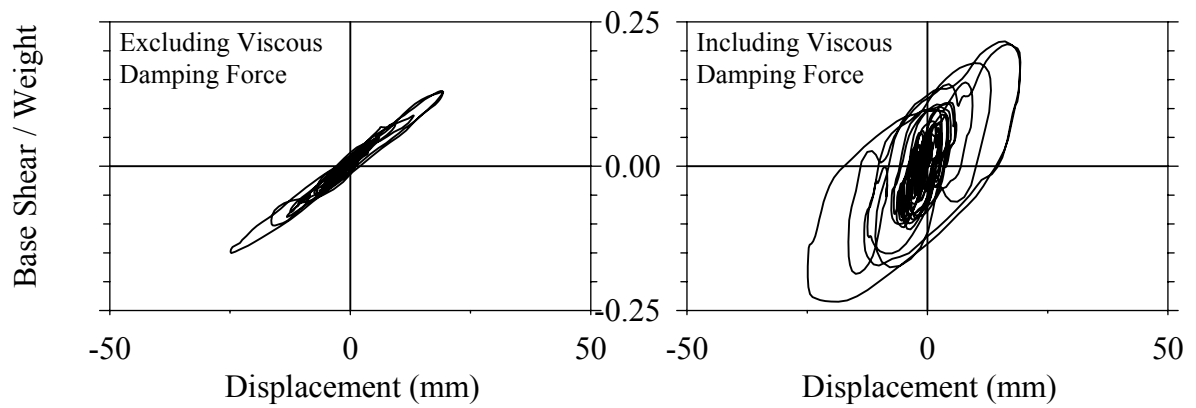
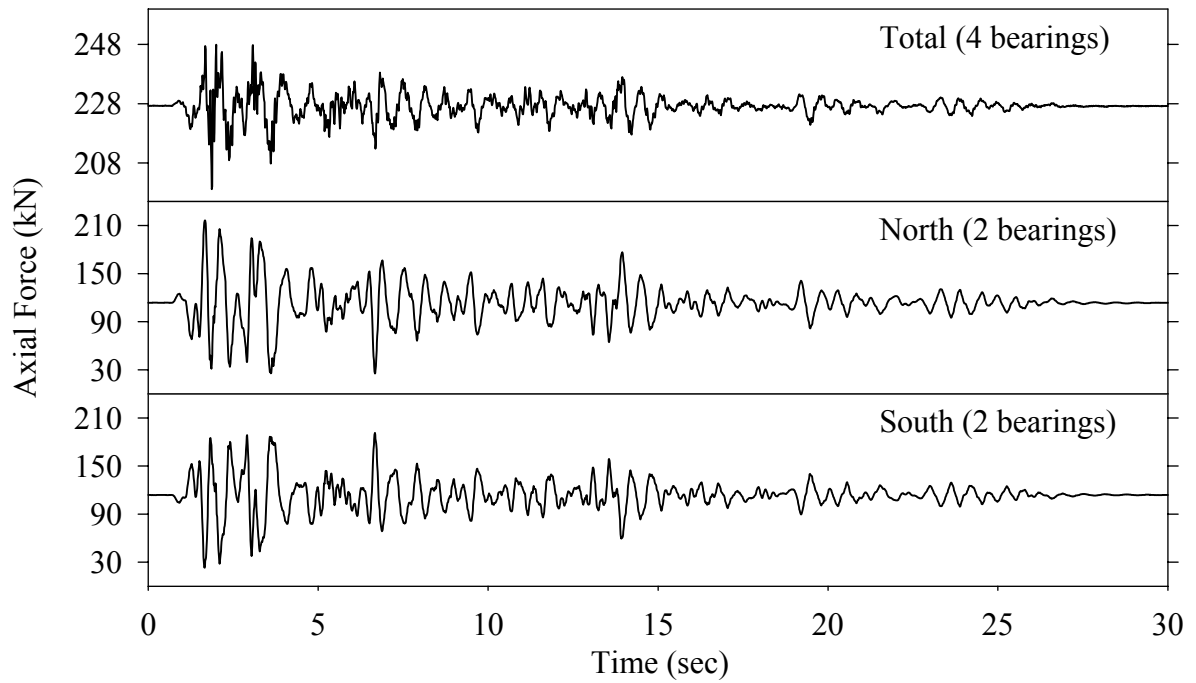


Test LDMNE20.1, El Centro S00E 200%, MF/Low Damping Elastomeric-Nonlinear Dampers

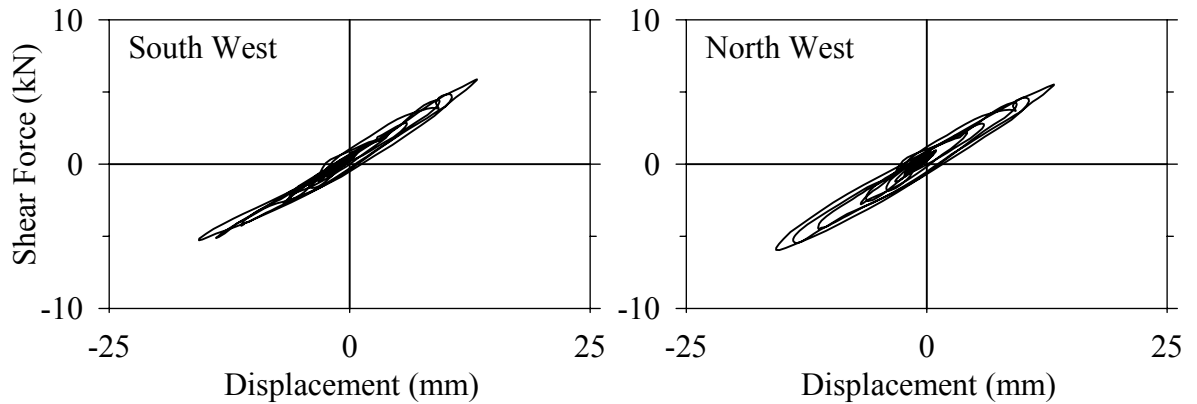
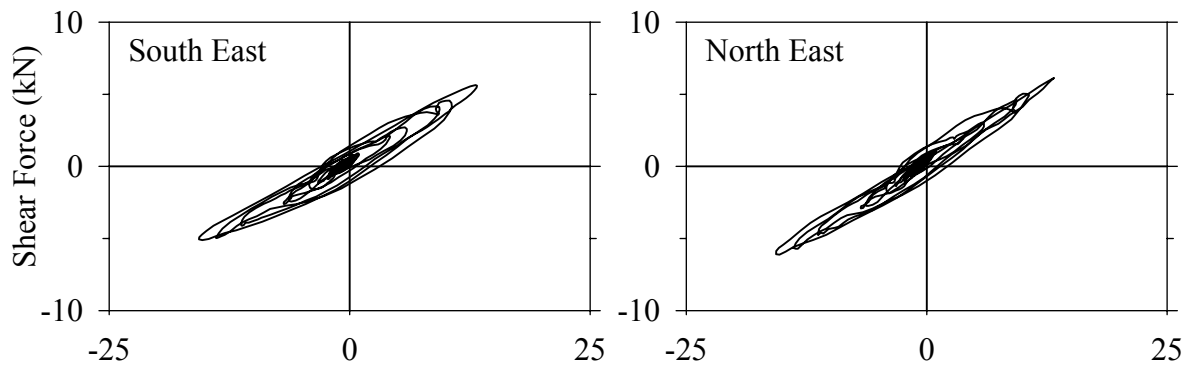
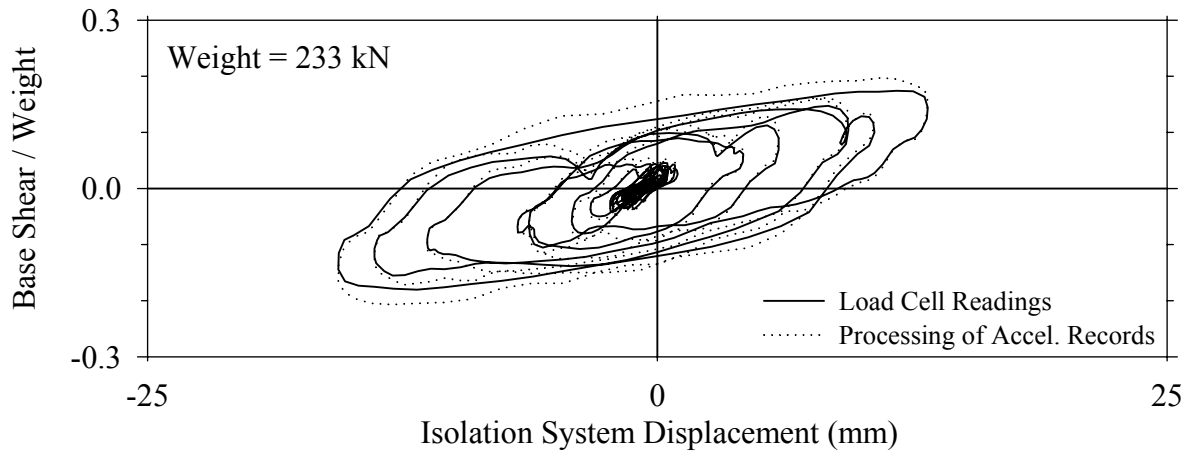
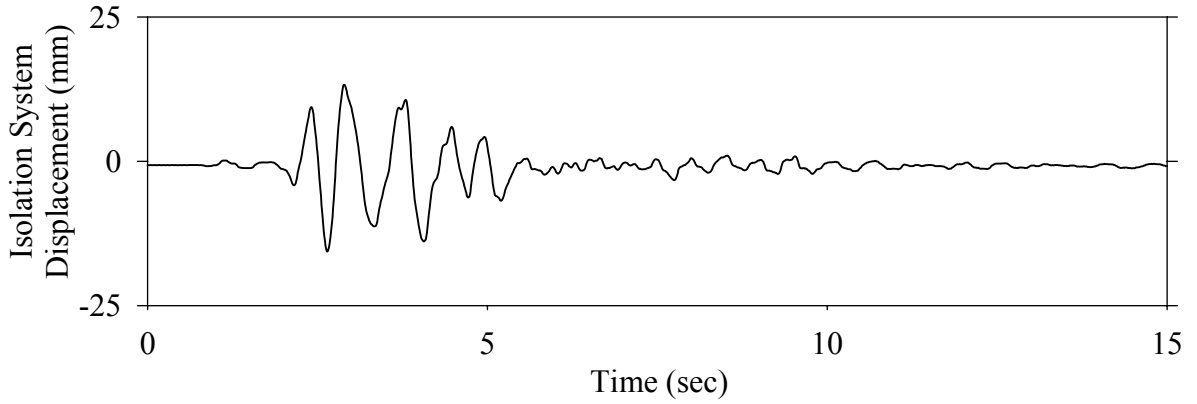




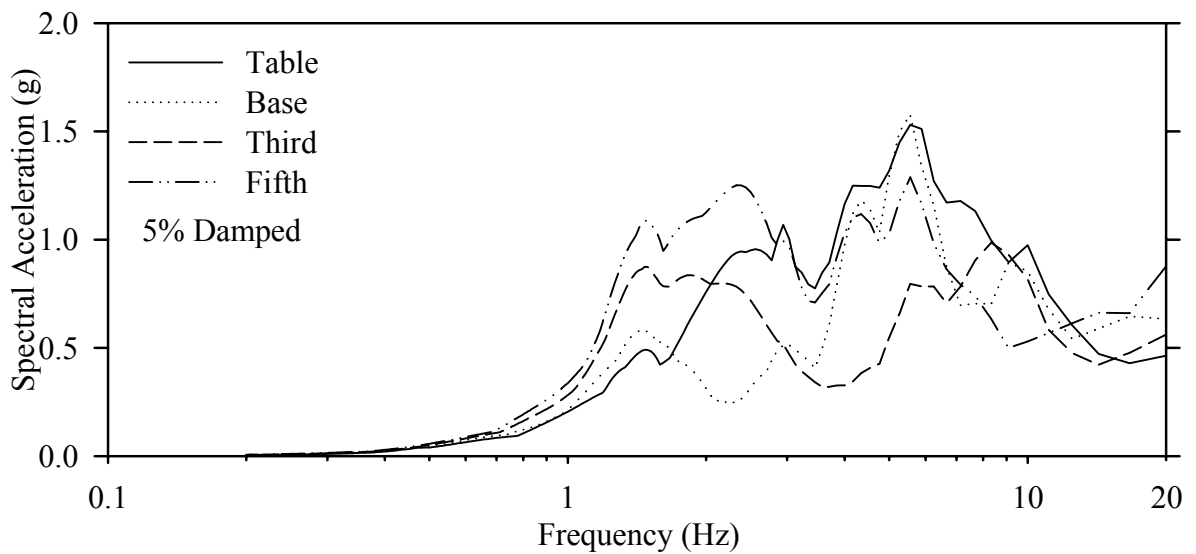
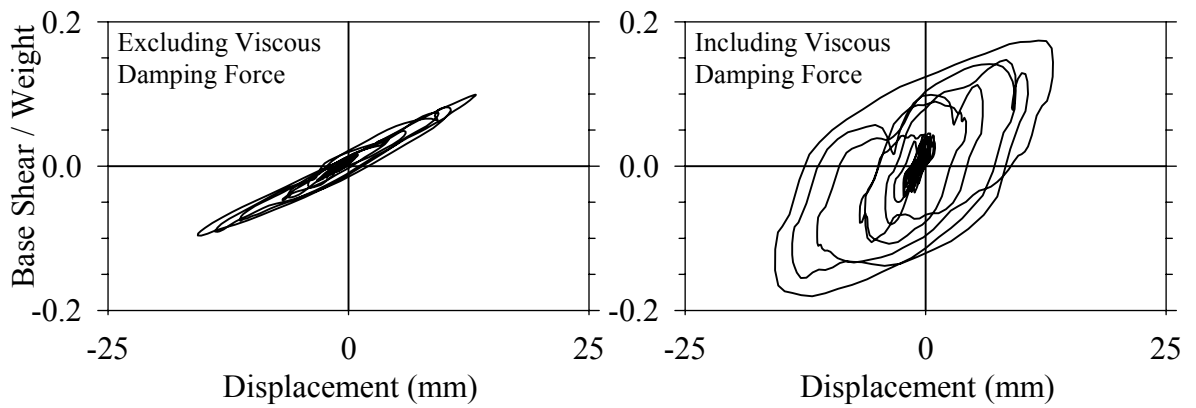
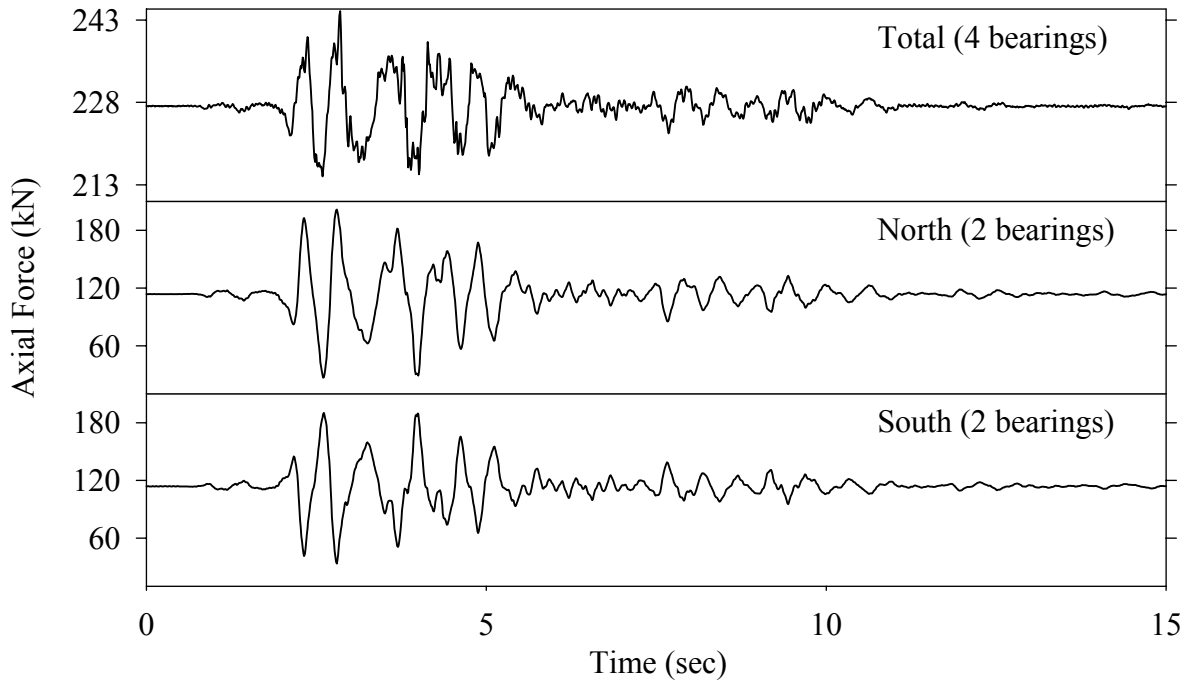
Test LDMNE20.1, El Centro S00E 200%, MF/Low Damping Elastomeric-Nonlinear Dampers



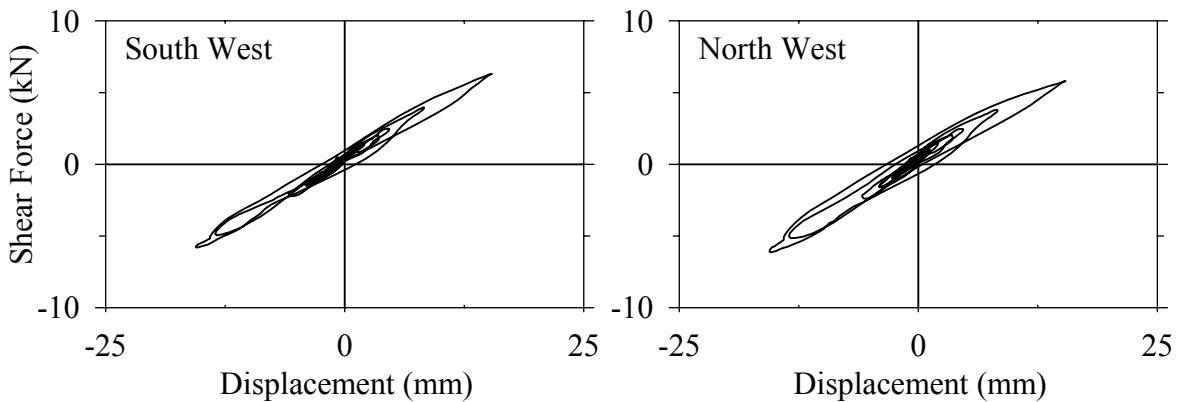
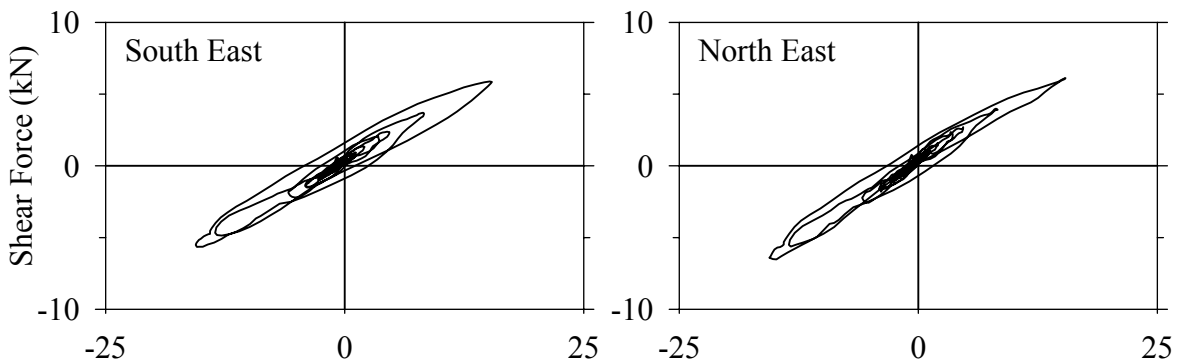
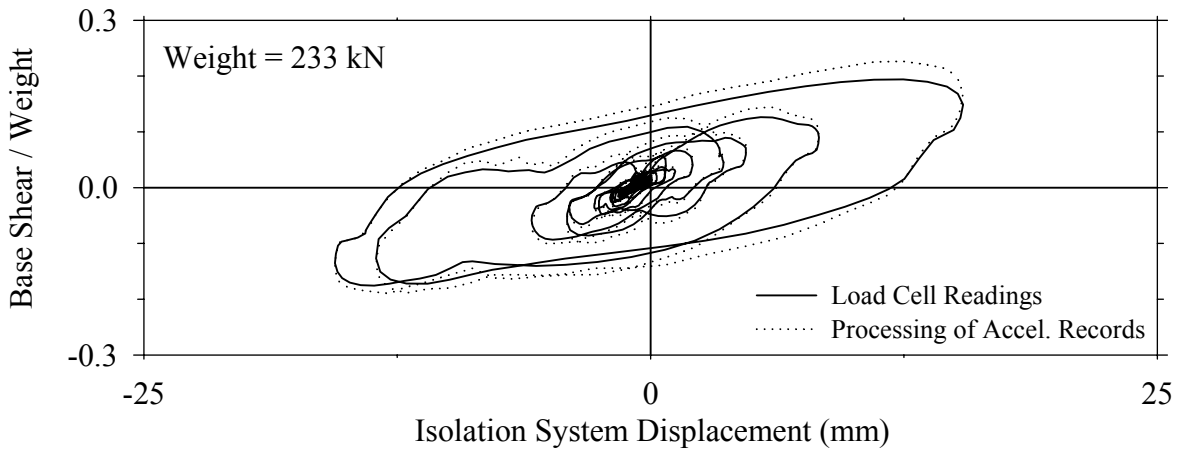
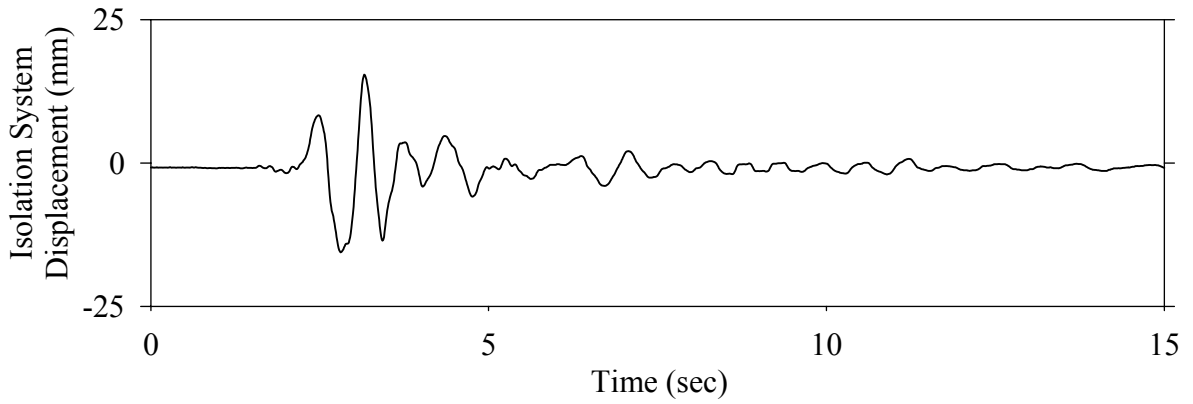
Test LDMNK50.1, Kobe N-S 50%, MF/Low Damping Elastomeric-Nonlinear Dampers



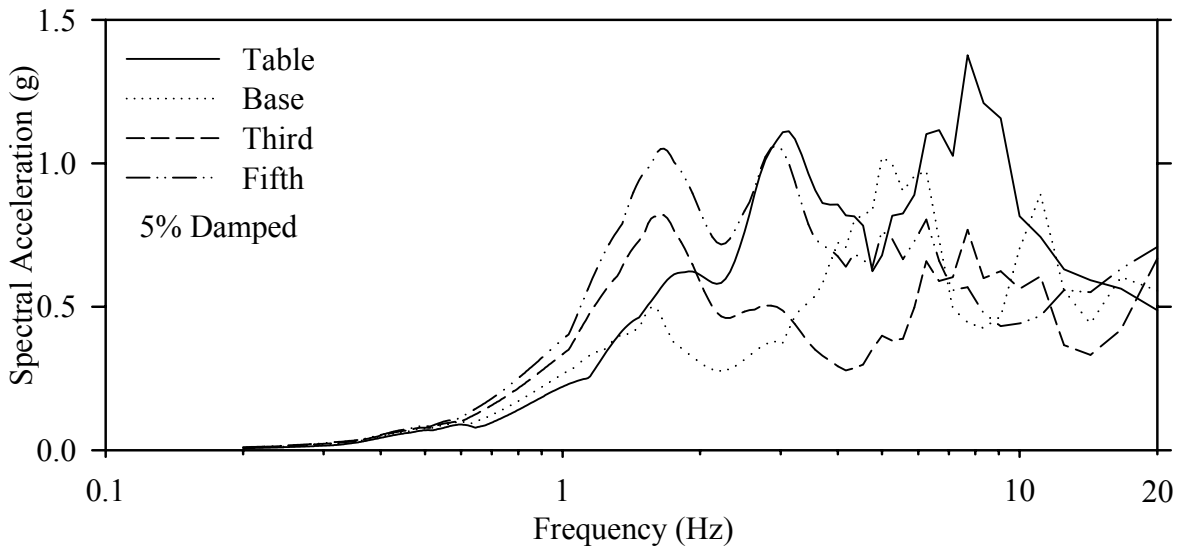
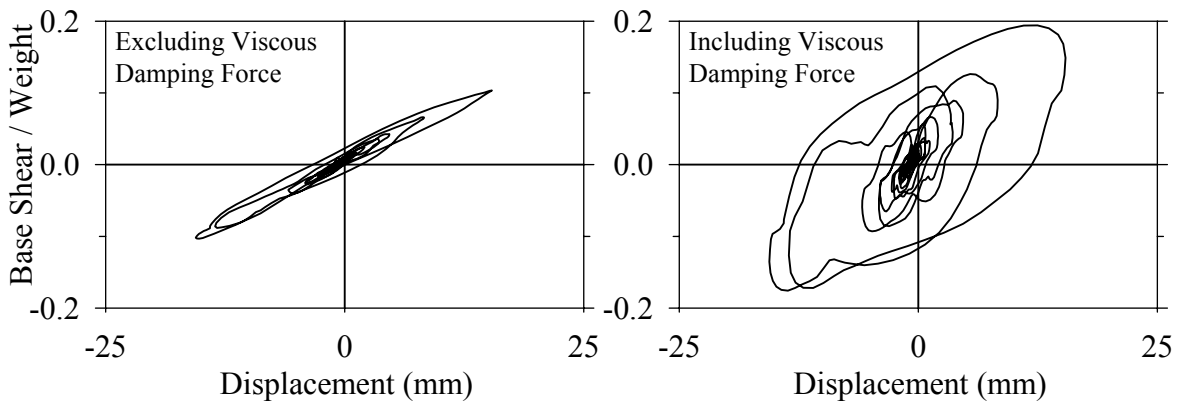
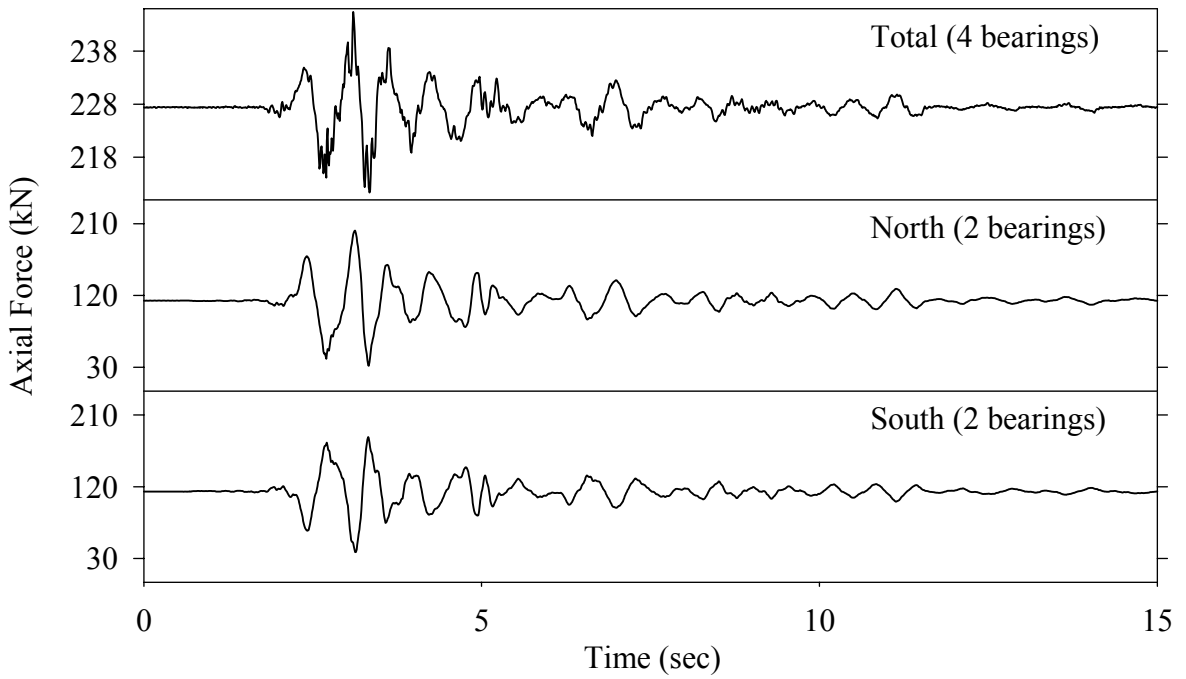
Test LDMNK50.1, Kobe N-S 50%, MF/Low Damping Elastomeric-Nonlinear Dampers



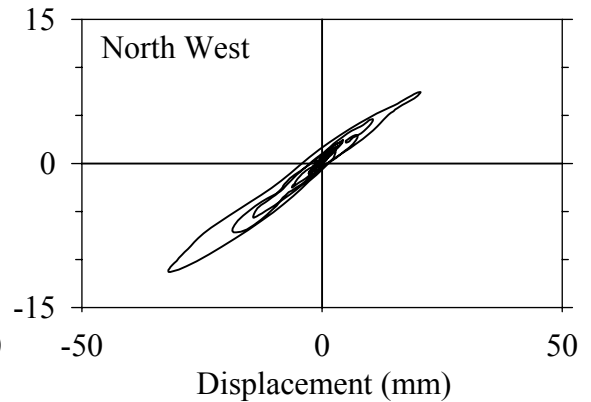
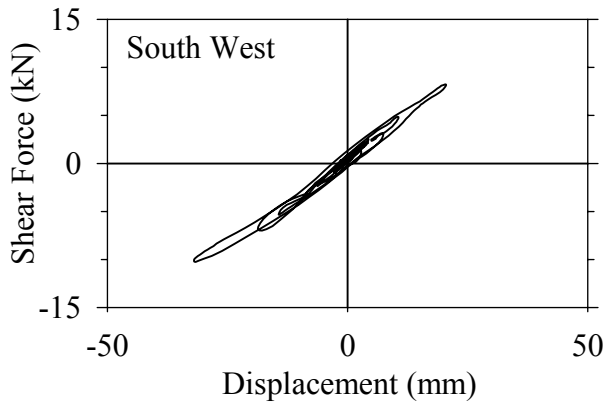
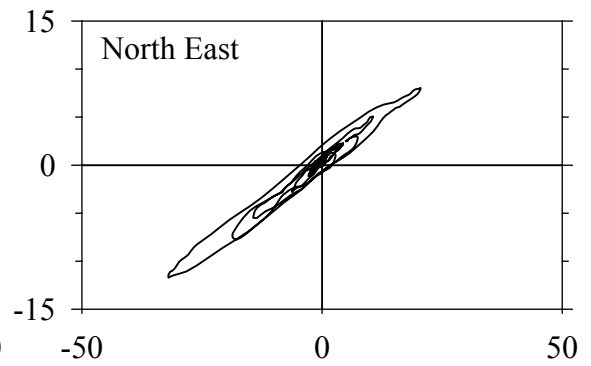
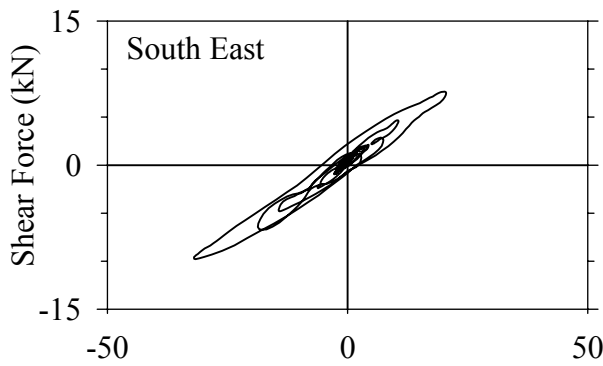
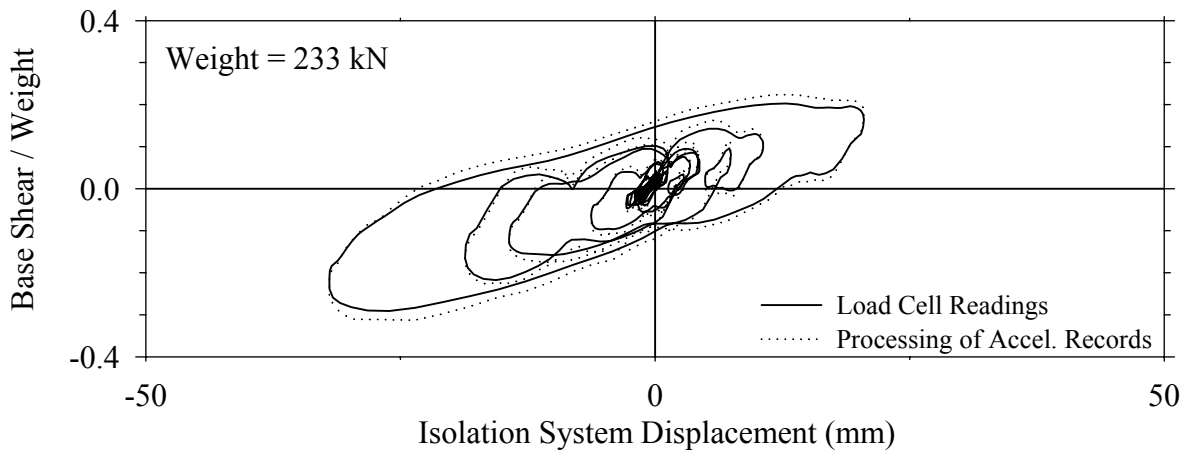
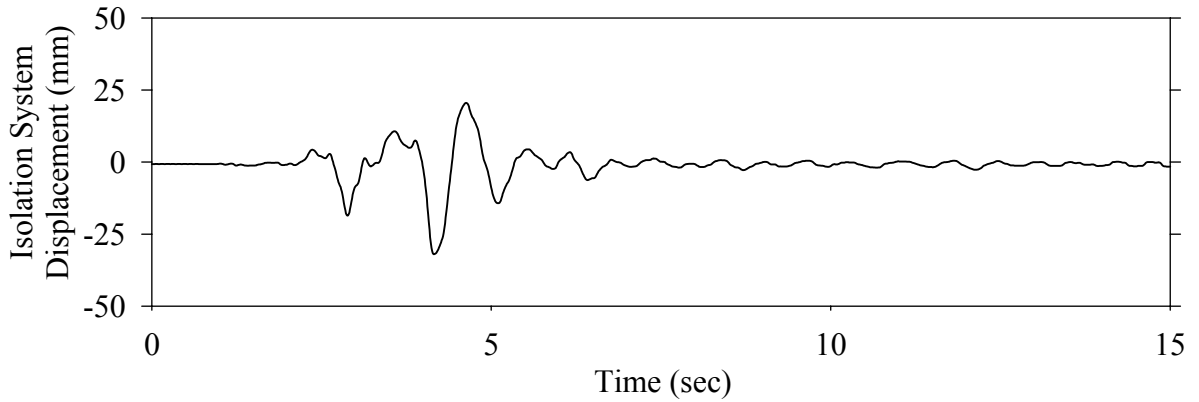
Test LDMNN50.1, Northridge Newhall 360° 50%, MF/Low Damping Elastomeric-Nonlinear Dampers



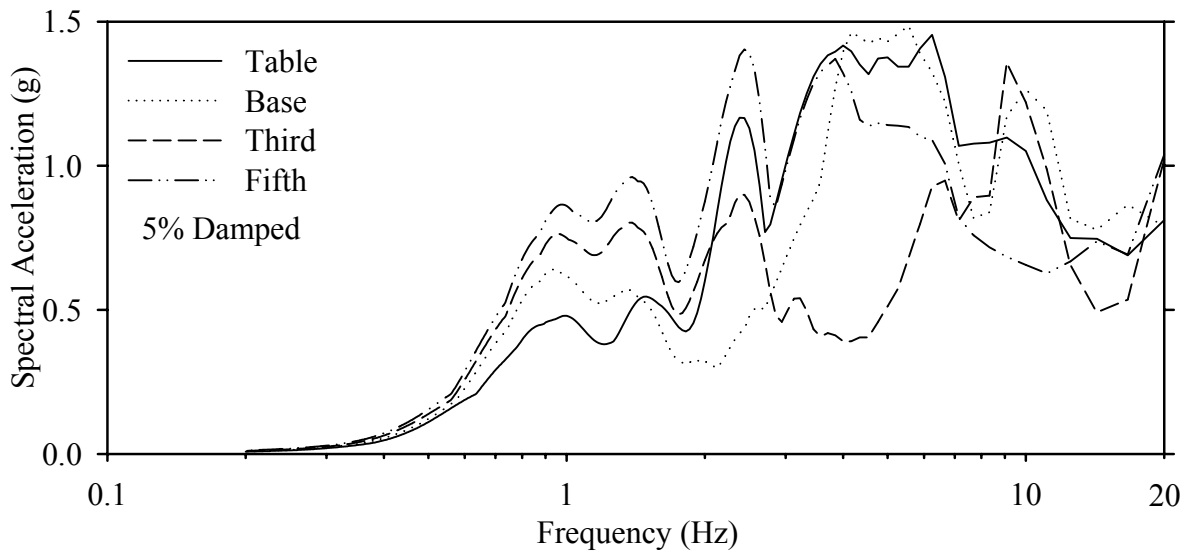
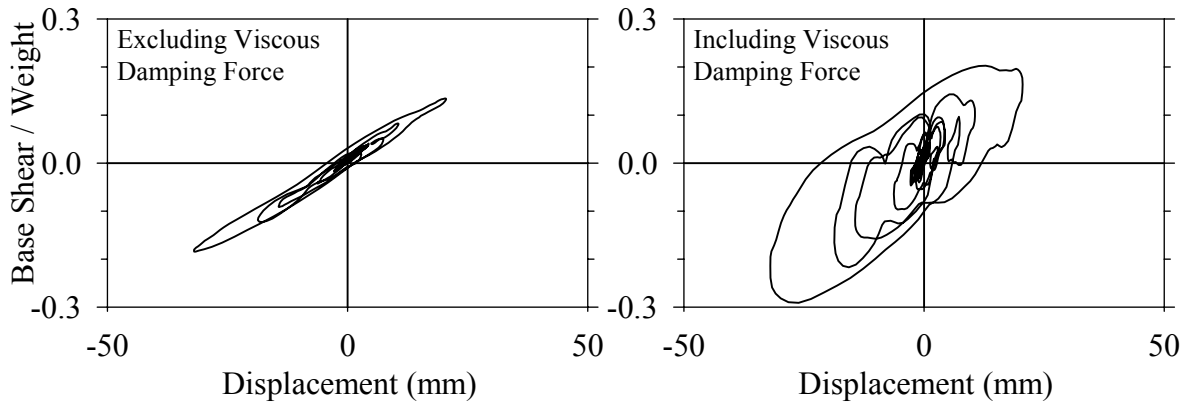
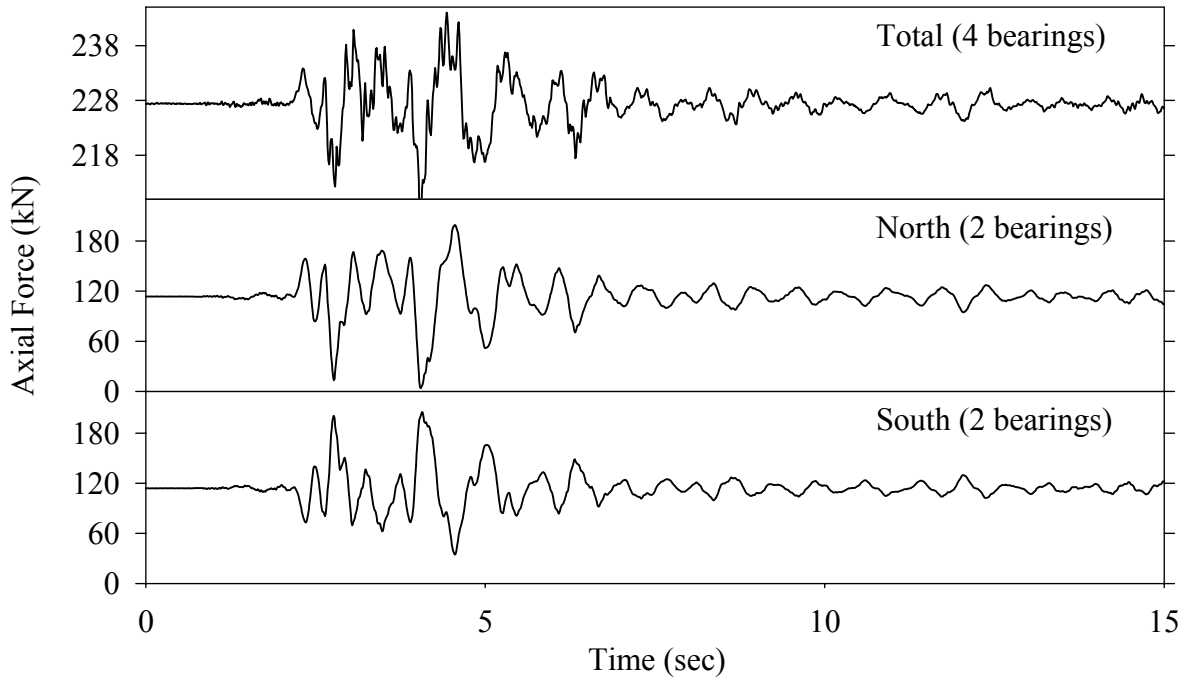
Test LDMNN50.1, Northridge Newhall 360° 50%, MF/Low Damping Elastomeric-Nonlinear Dampers



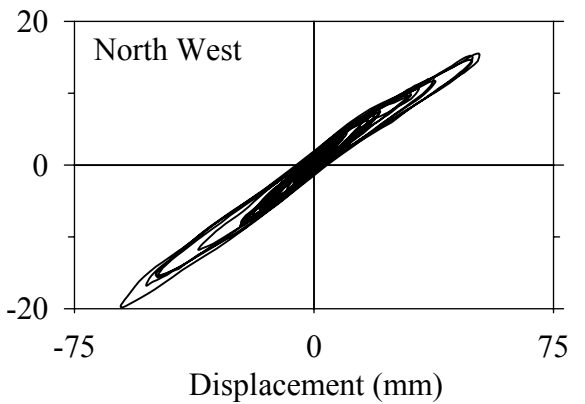
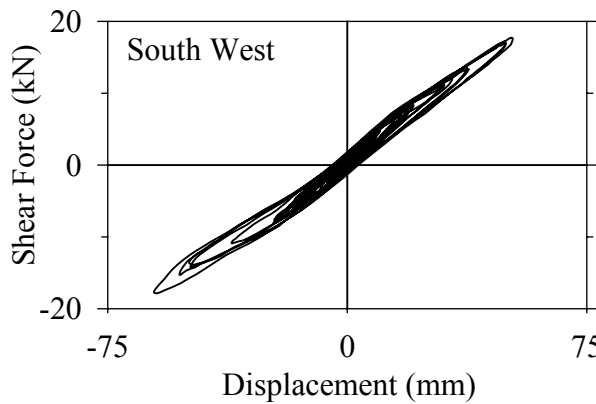
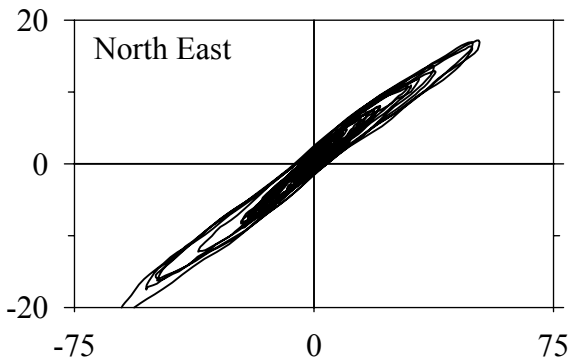
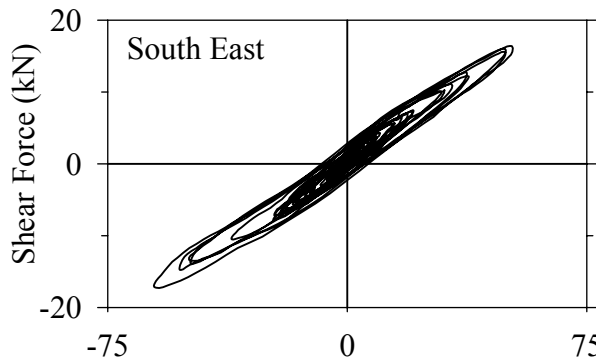
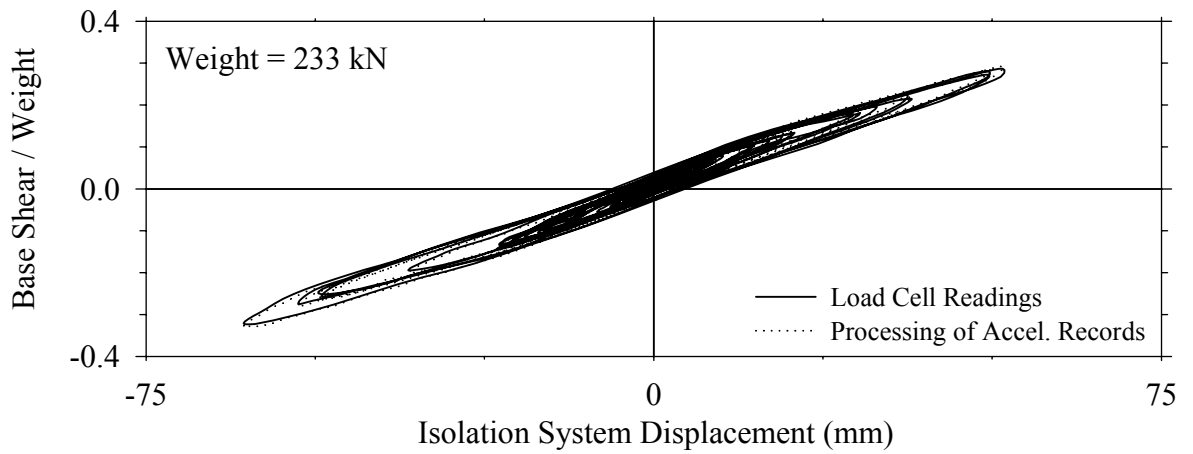
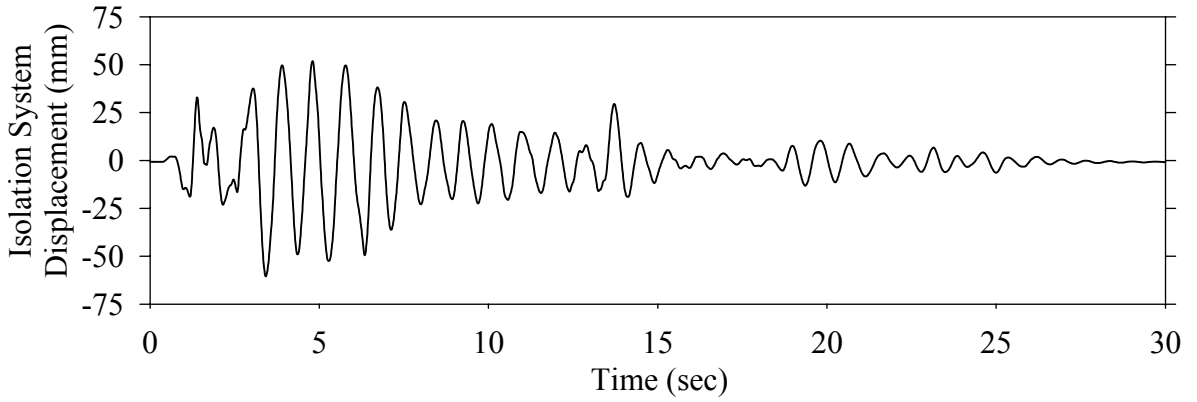
Test LDMNS10.1, Northridge Sylmar 90° 100%, MF/Low Damping Elastomeric-Nonlinear Dampers



Test LDMNS10.1, Northridge Sylmar 90° 100%, MF/Low Damping Elastomeric-Nonlinear Dampers

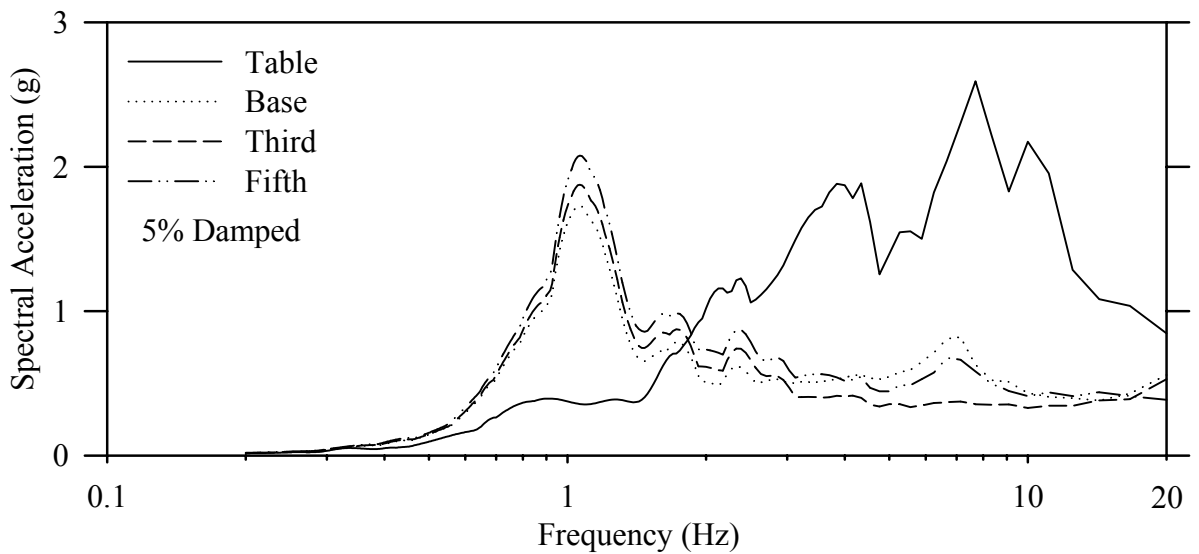
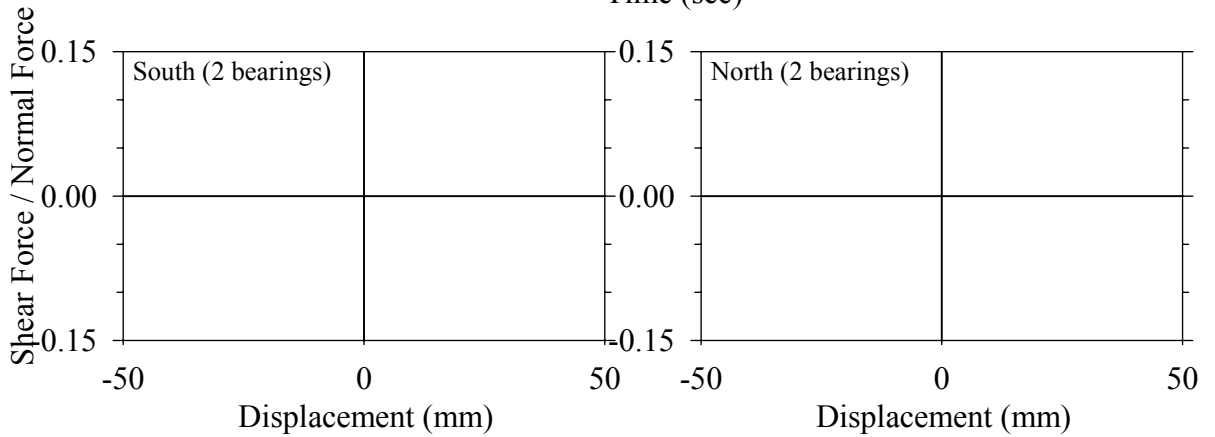
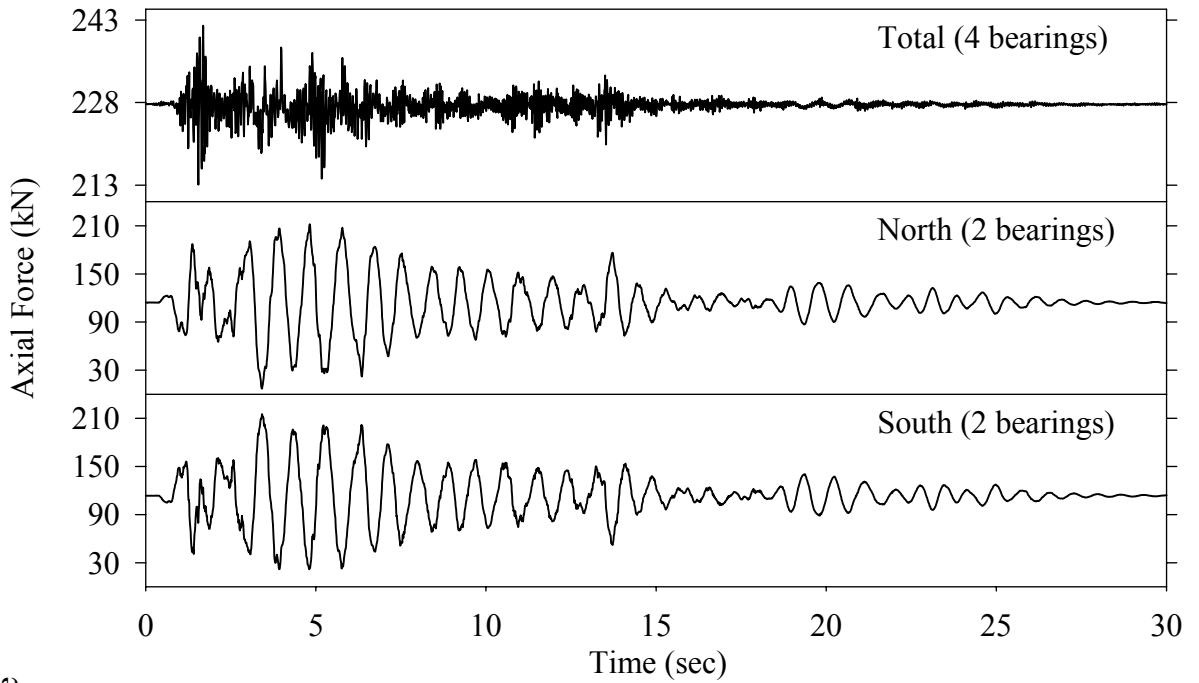


Test LDSBE20.1, El Centro S00E 200%, SB/Low Damping Elastomeric

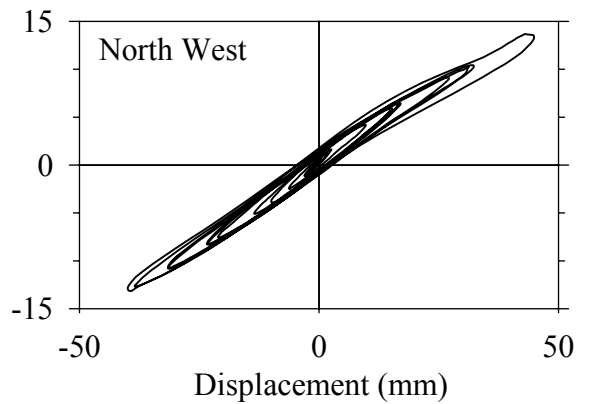
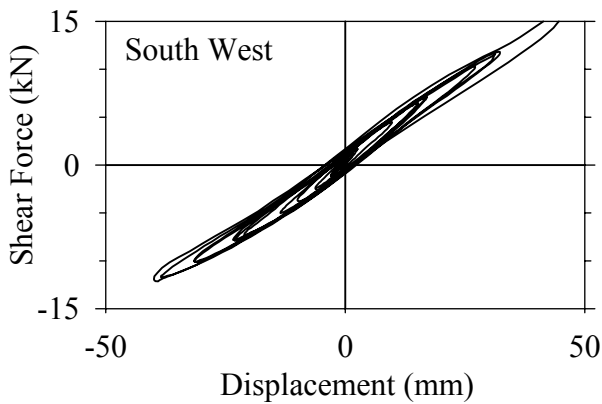
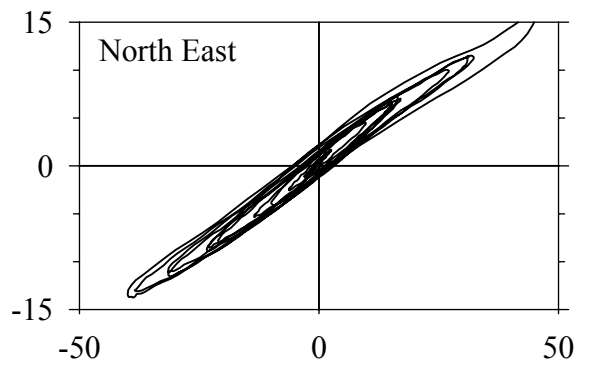
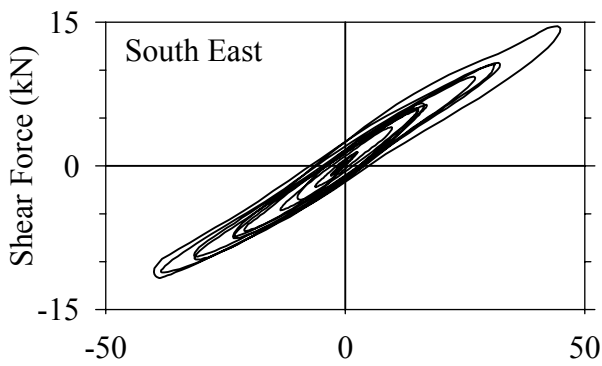
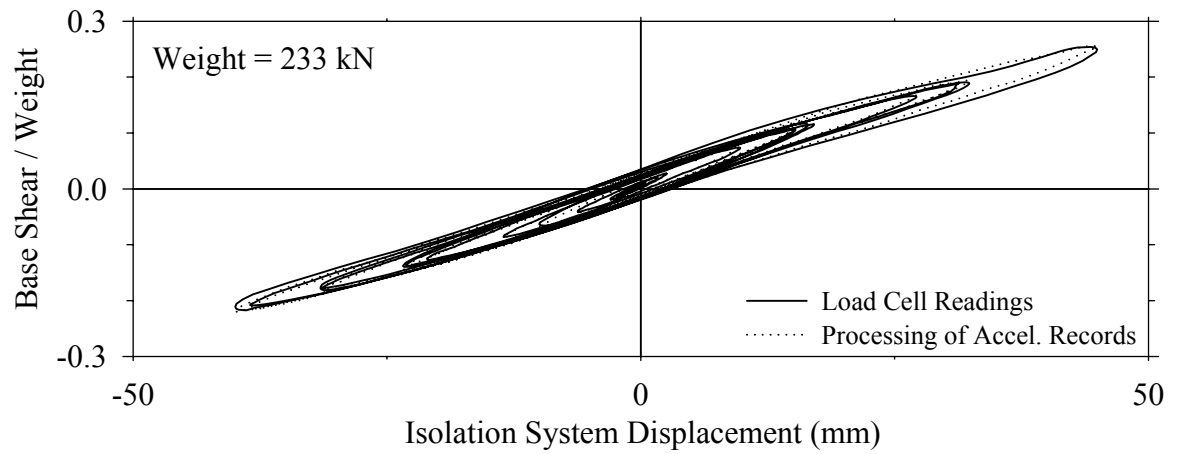
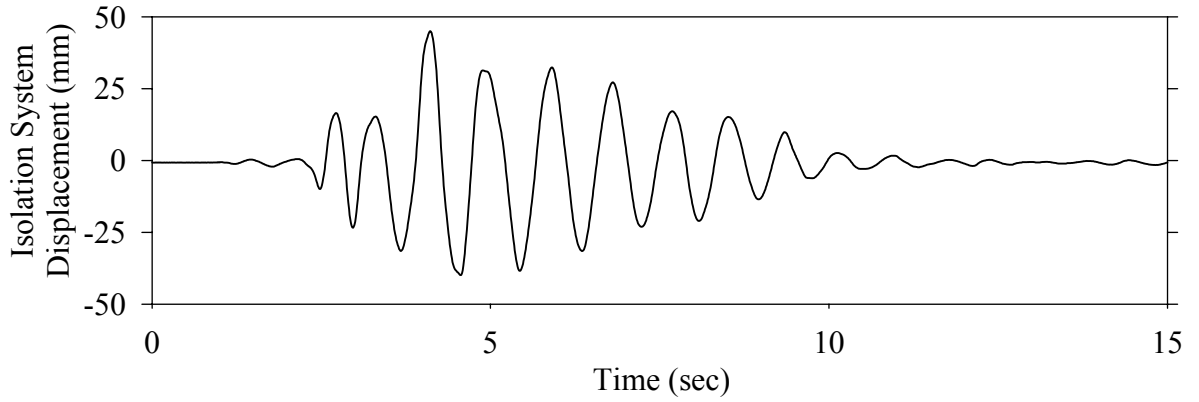




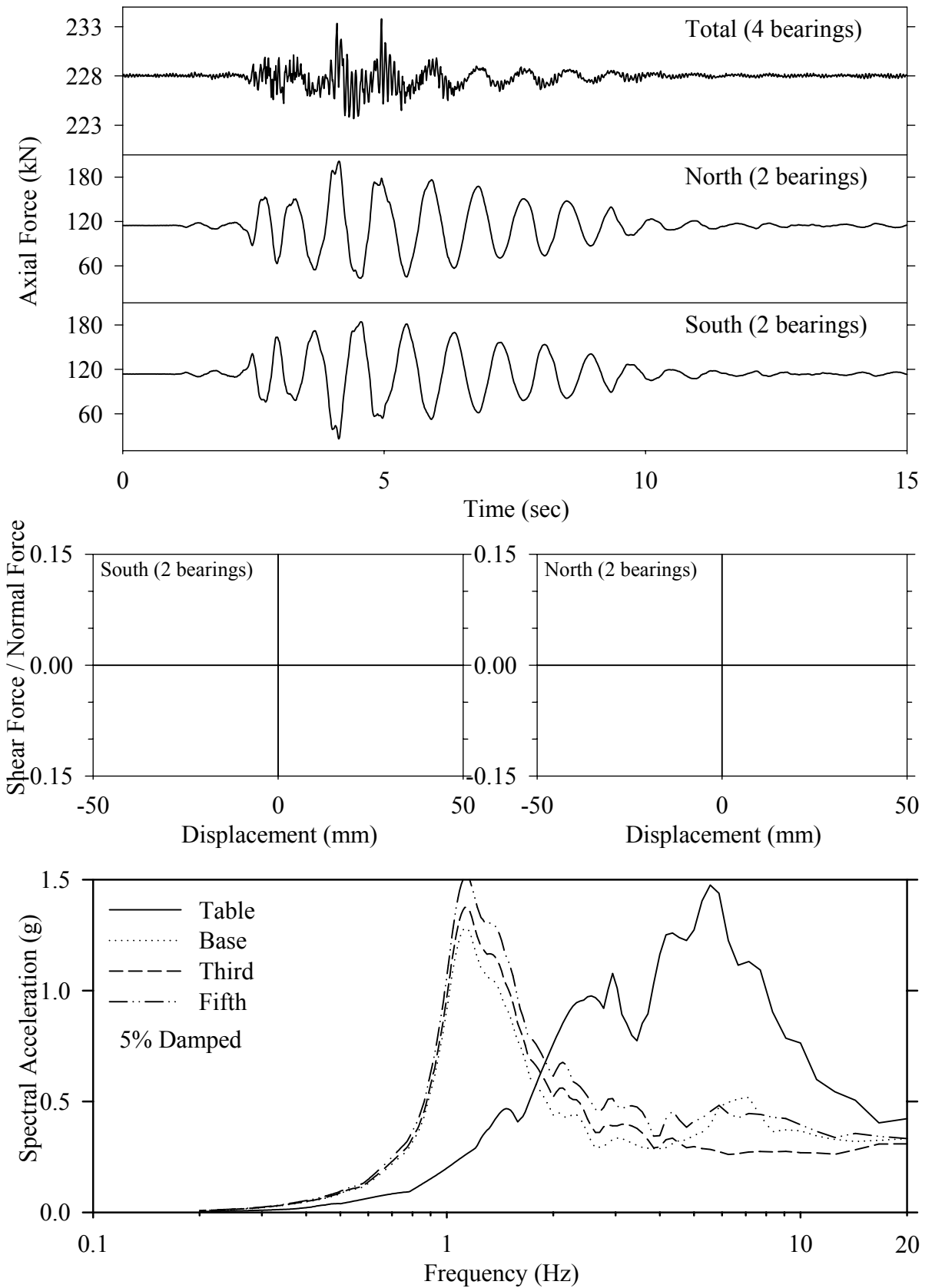
Test LDSBE20.1, El Centro S00E 200%, SB/Low Damping Elastomeric



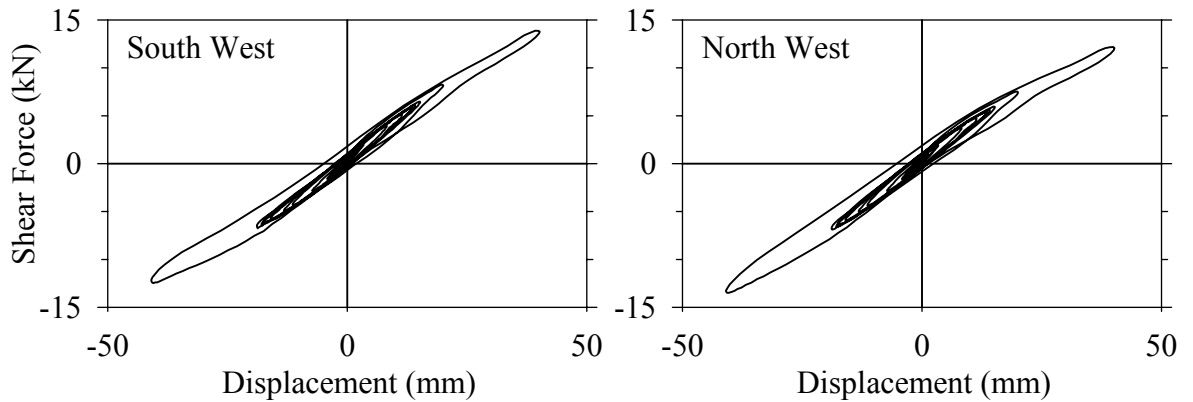
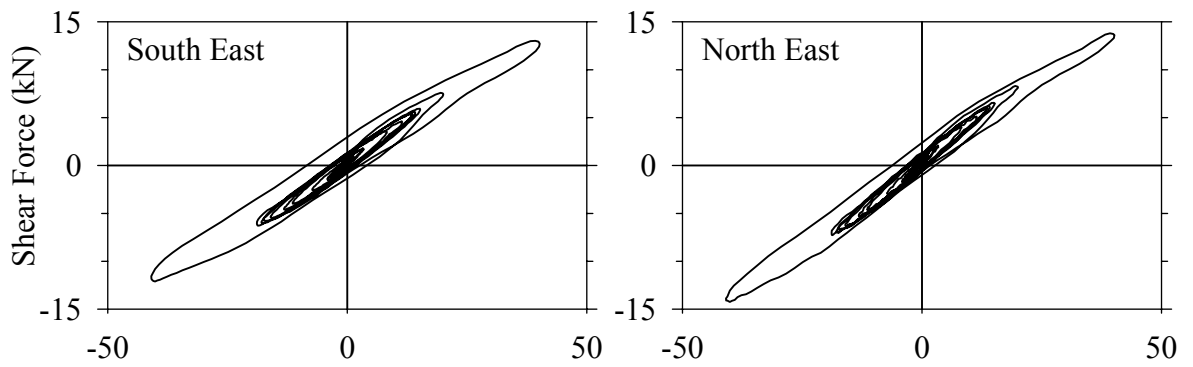
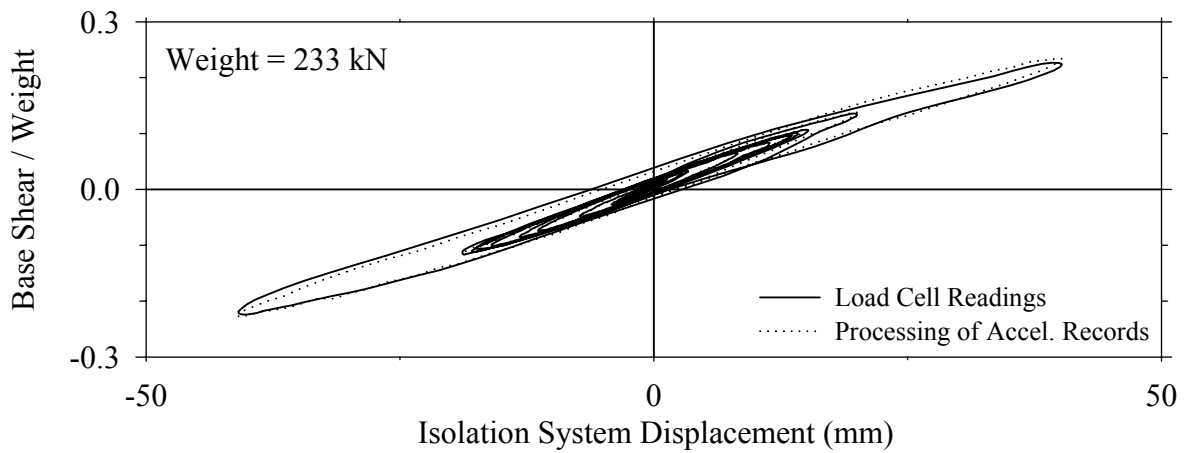
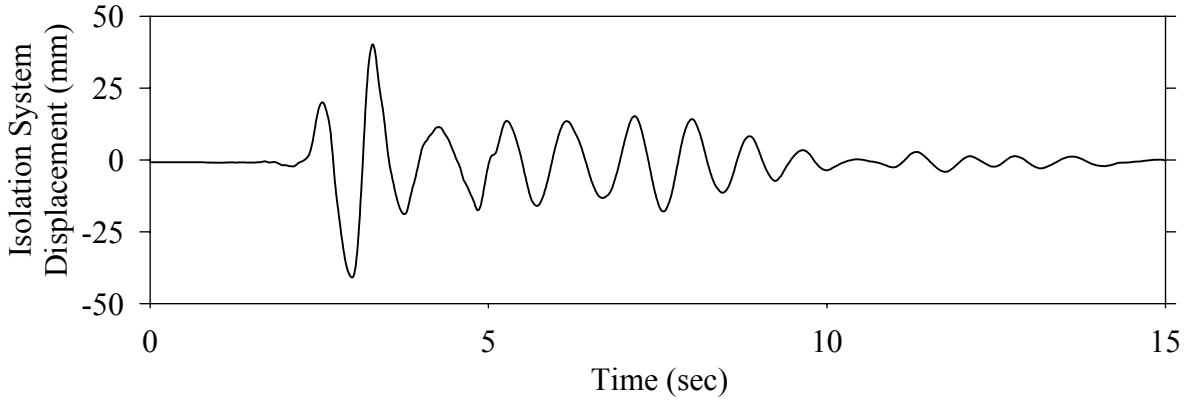
Test LDSBK50.1, Kobe N-S 50%, SB/Low Damping Elastomeric



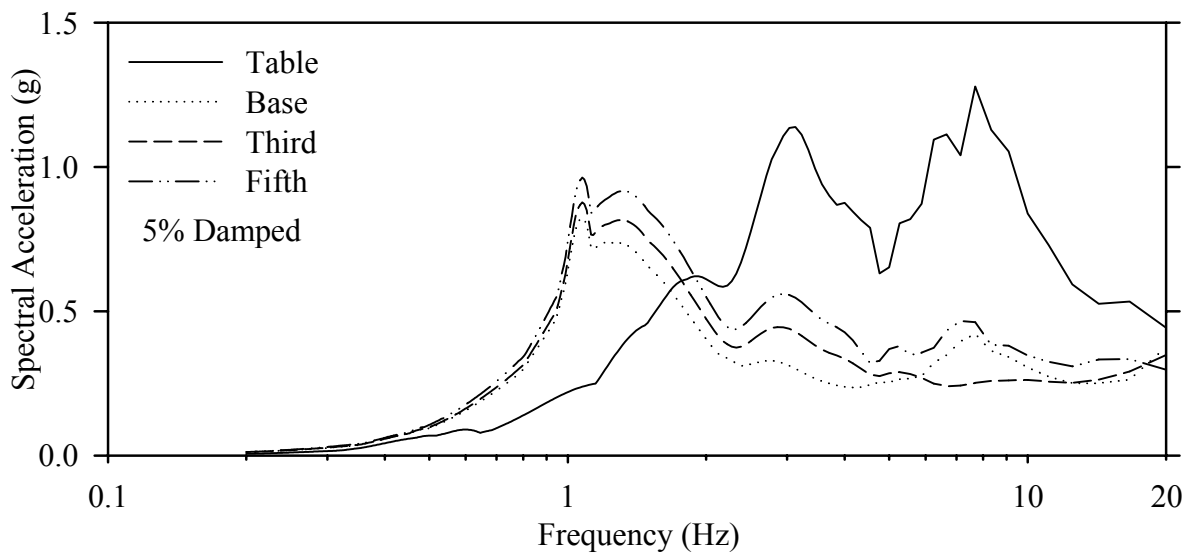
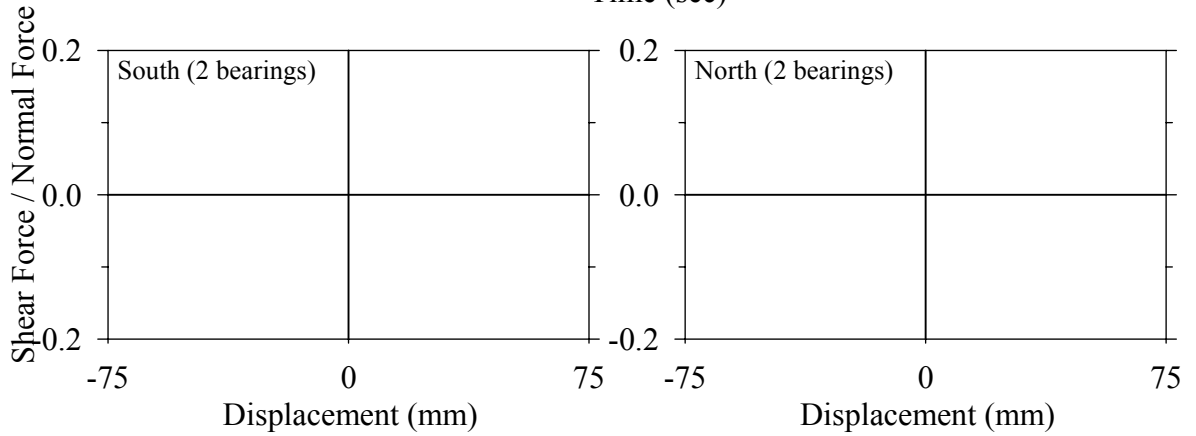
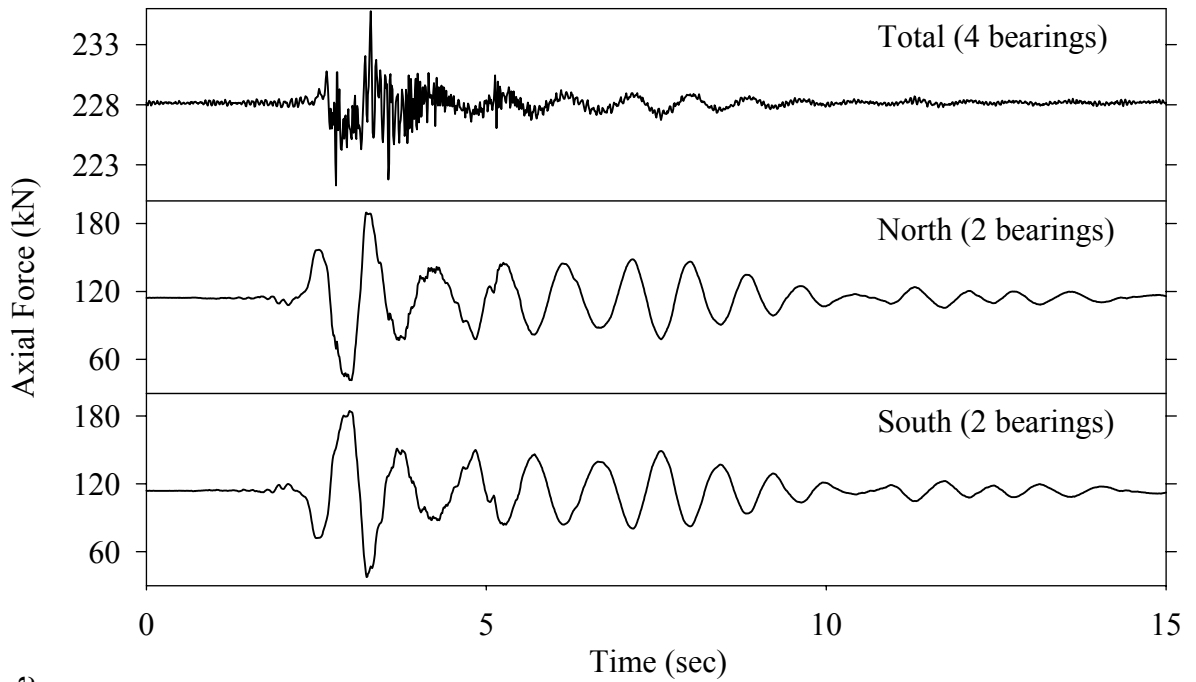
Test LDSBK50.1, Kobe N-S 50%, SB/Low Damping Elastomeric



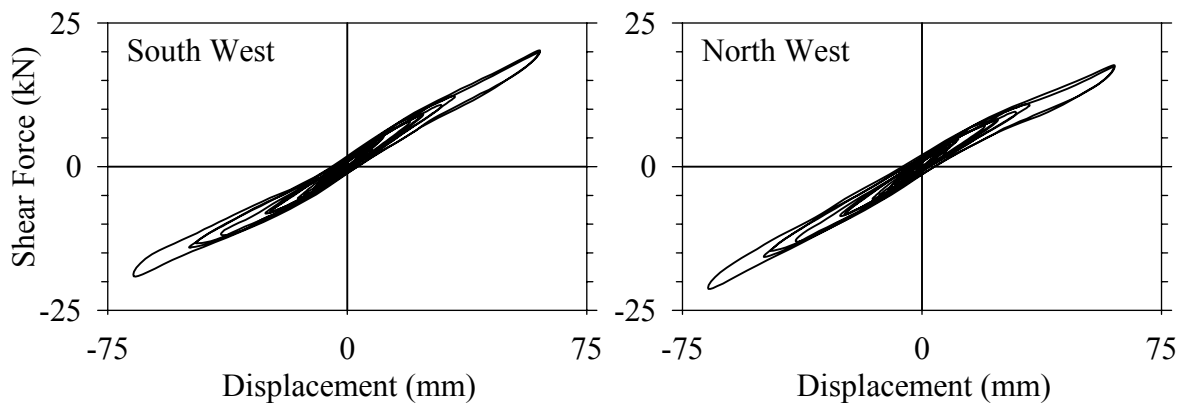
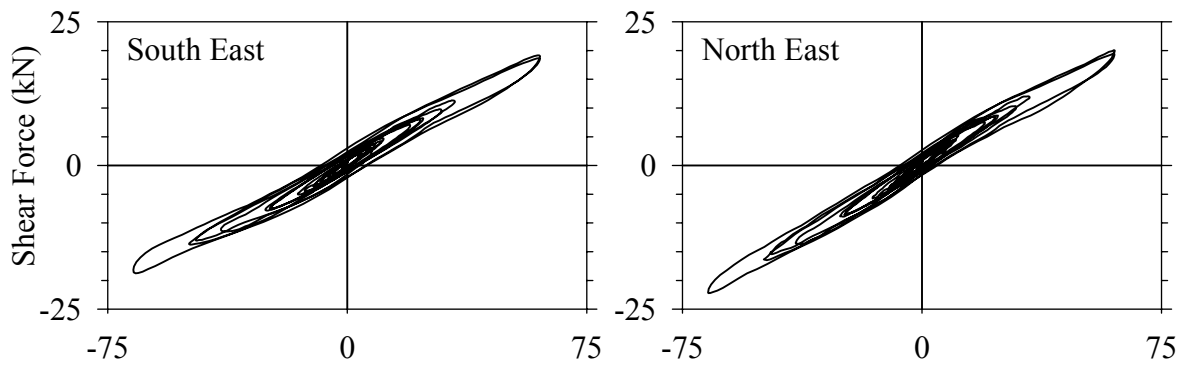
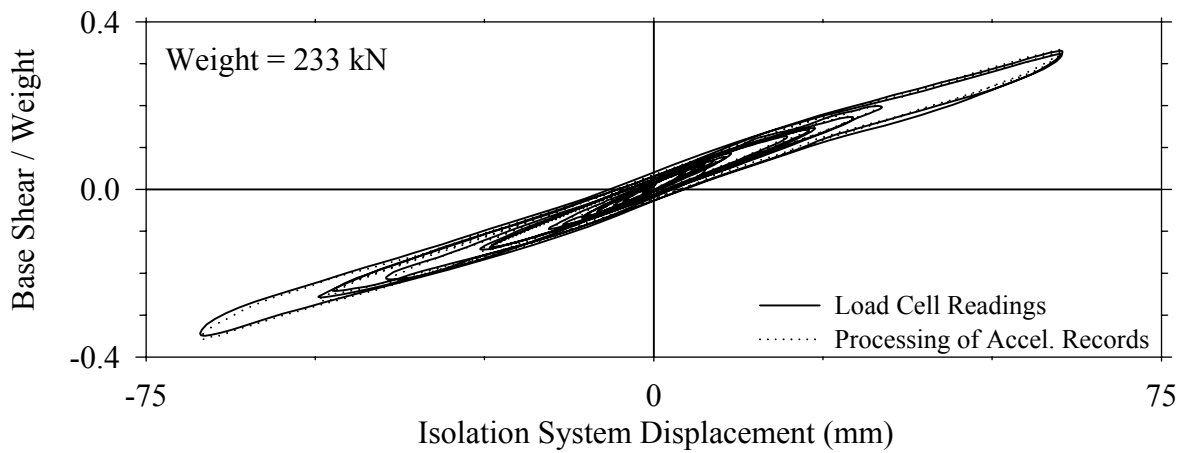
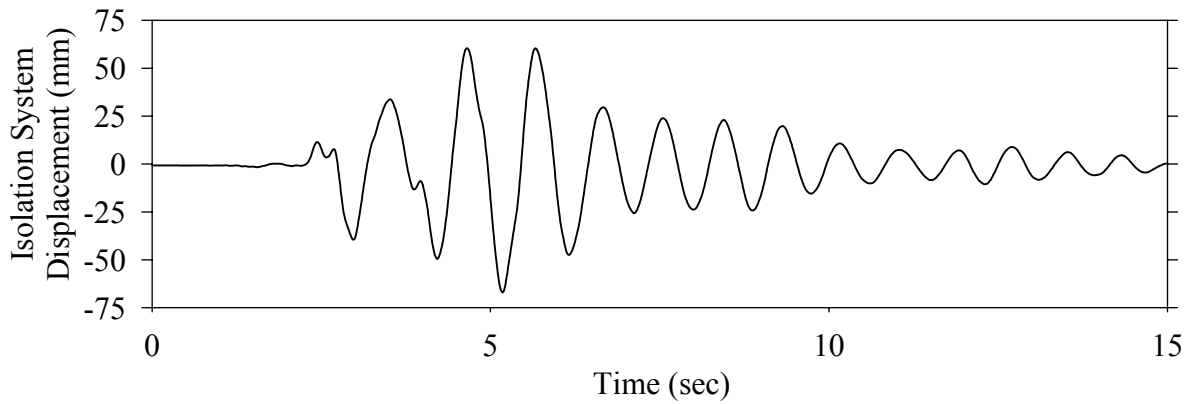
Test LDSBN50.1, Northridge Newhall 360° 50%, SB/Low Damping Elastomeric



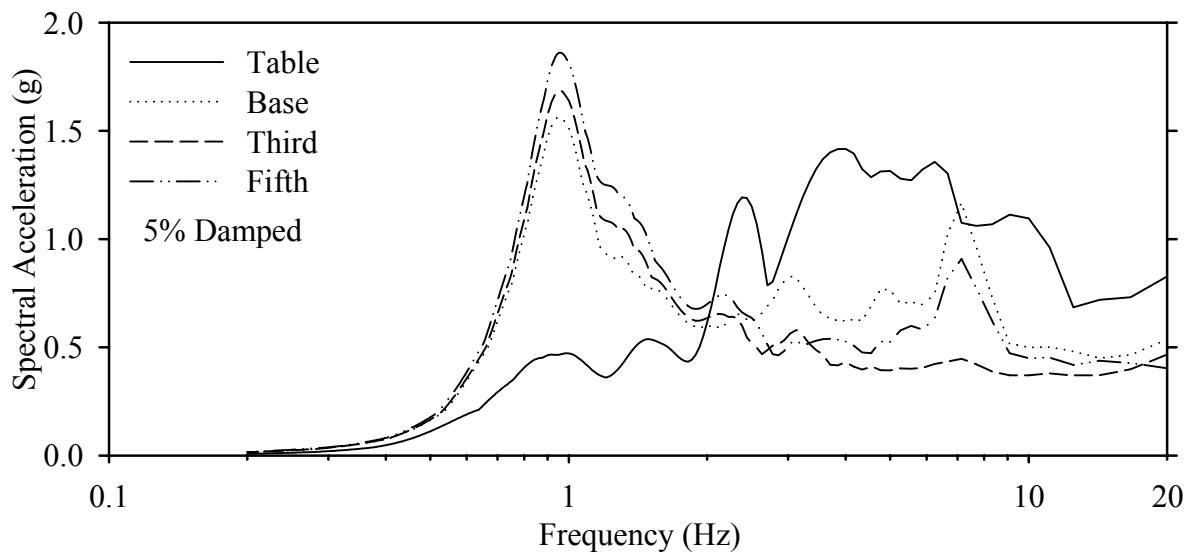
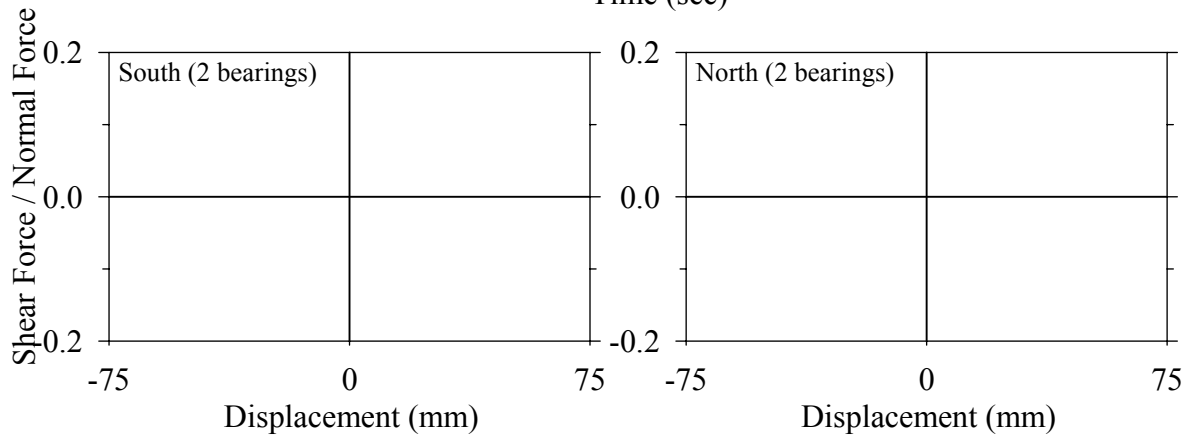
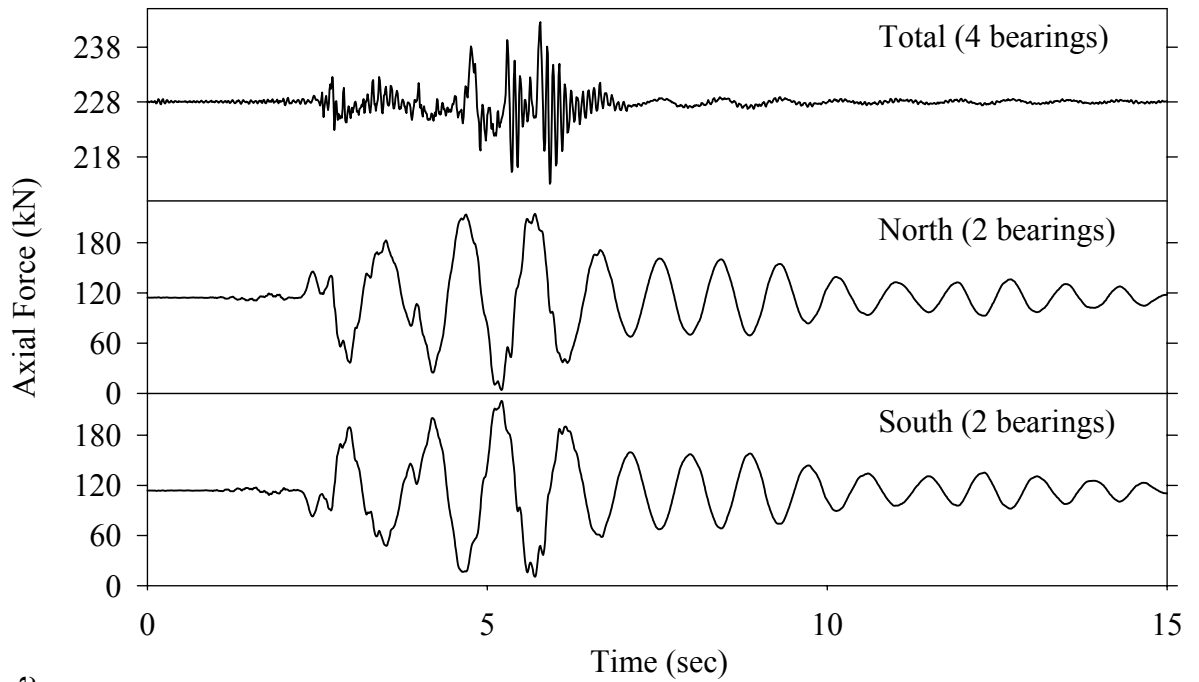
Test LDSBN50.1, Northridge Newhall 360° 50%, SB/Low Damping Elastomeric



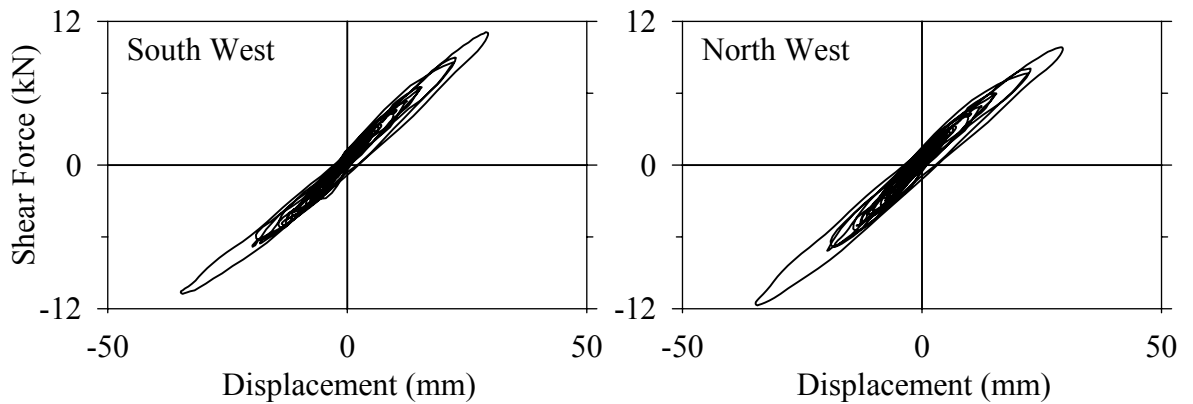
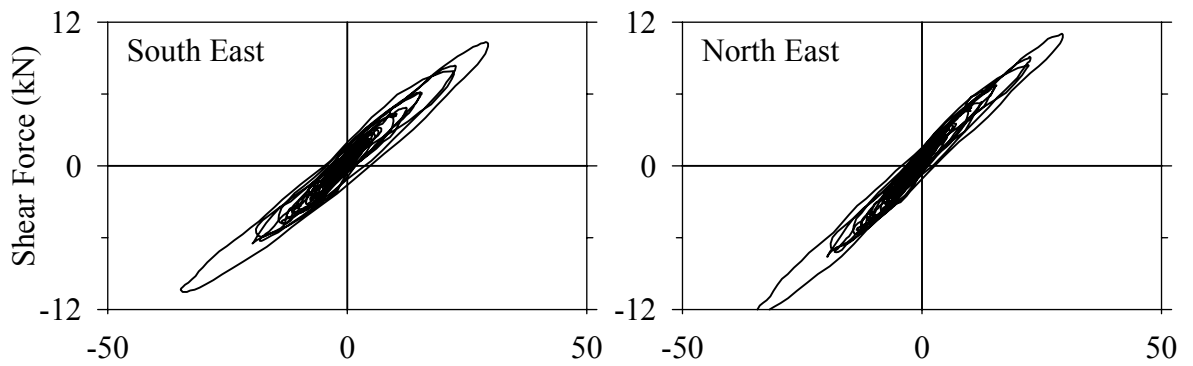
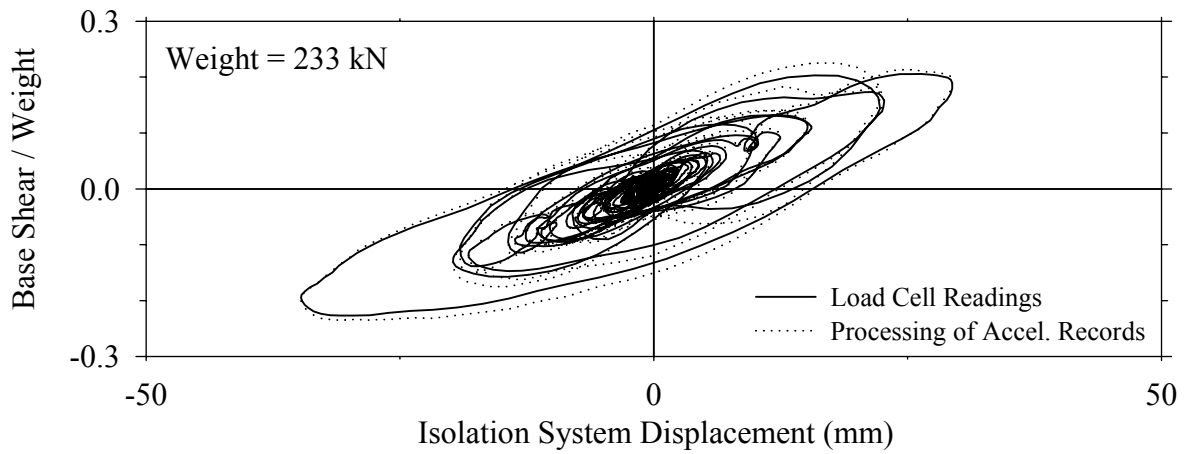
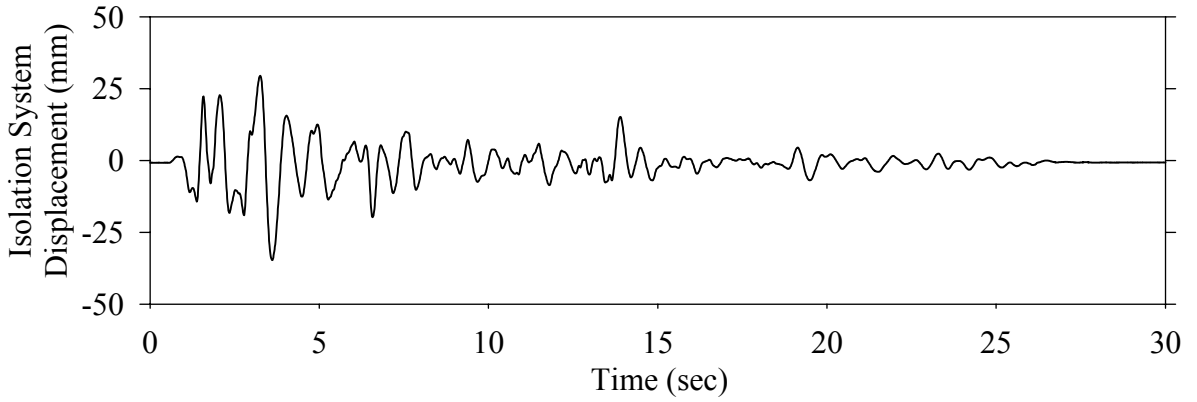
Test LDSBS10.2, Northridge Sylmar 90° 100%, SB/Low Damping Elastomeric



Test LDSBS10.2, Northridge Sylmar 90° 100%, SB/Low Damping Elastomeric

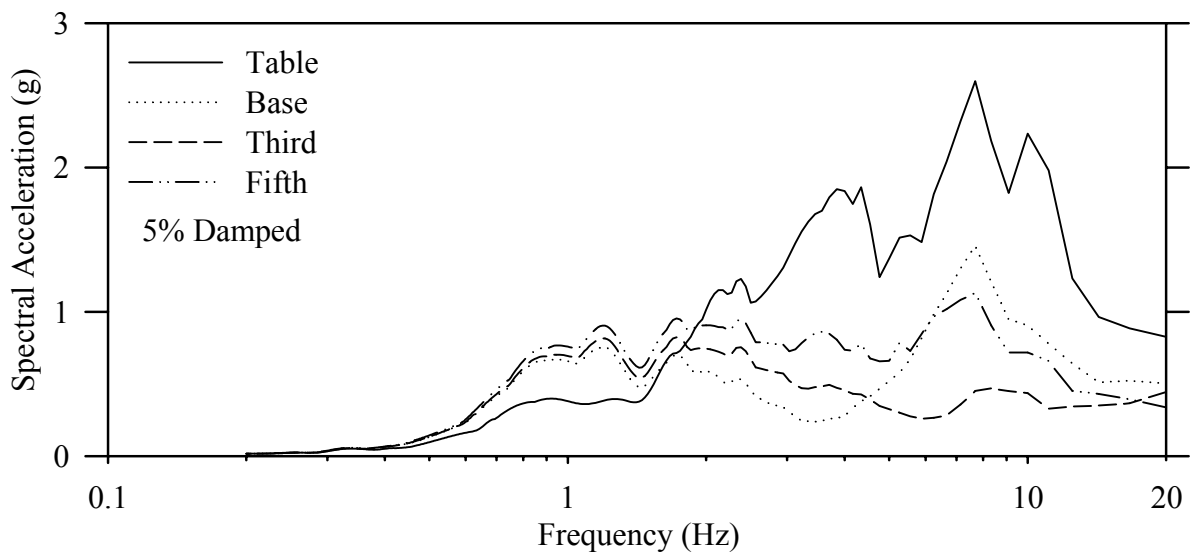
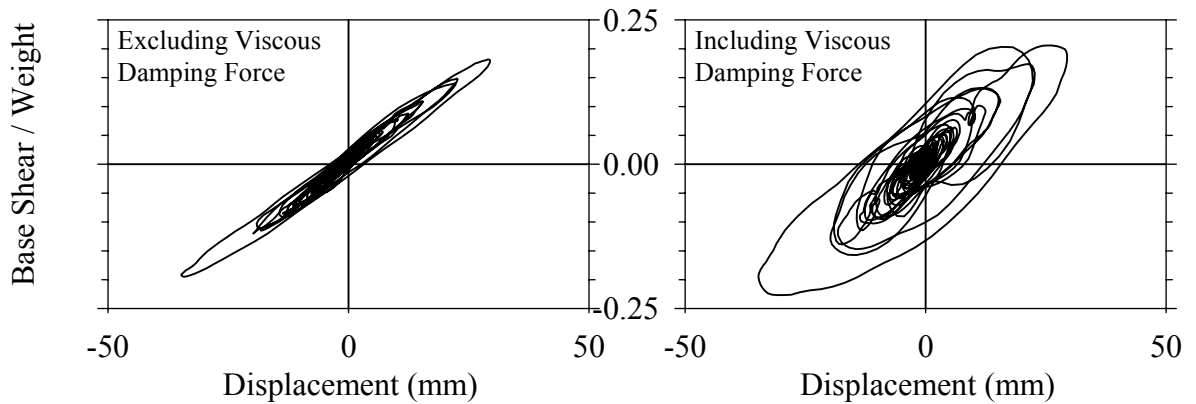
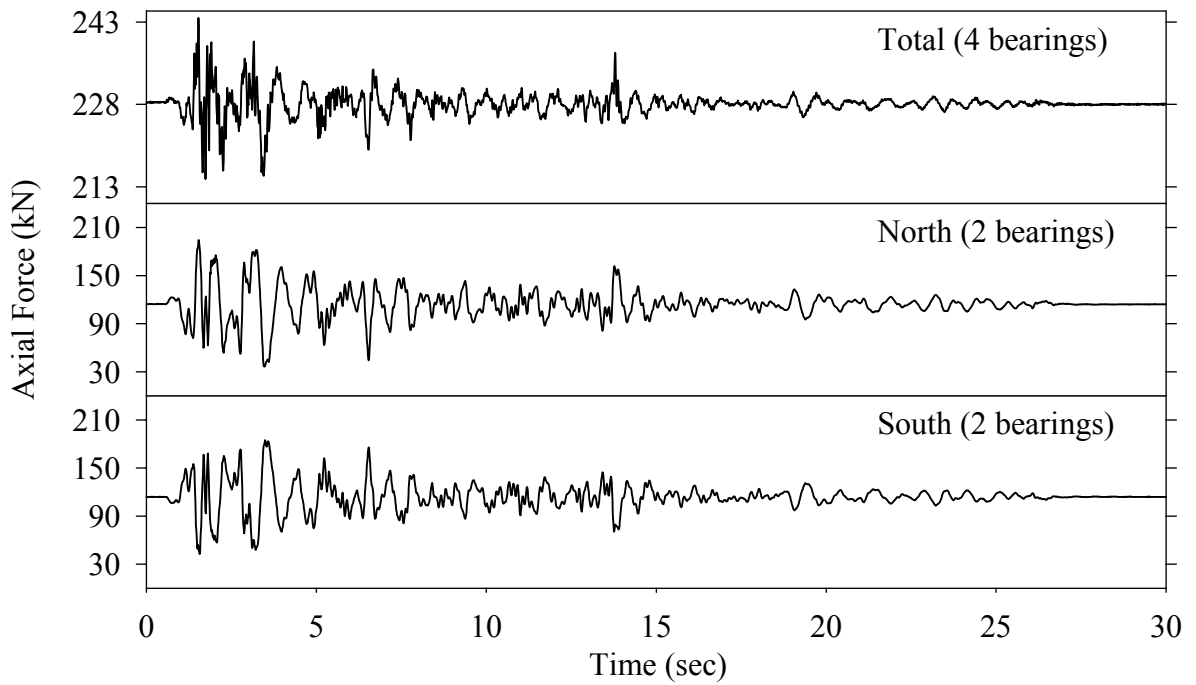


Test LDSLE20.1, El Centro S00E 200%, SB/Low Damping Elastomeric-Linear Dampers

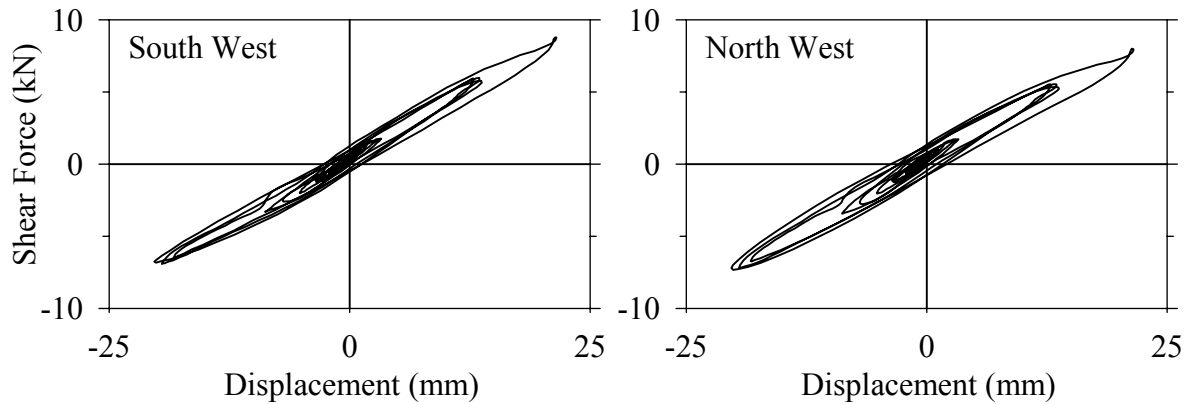
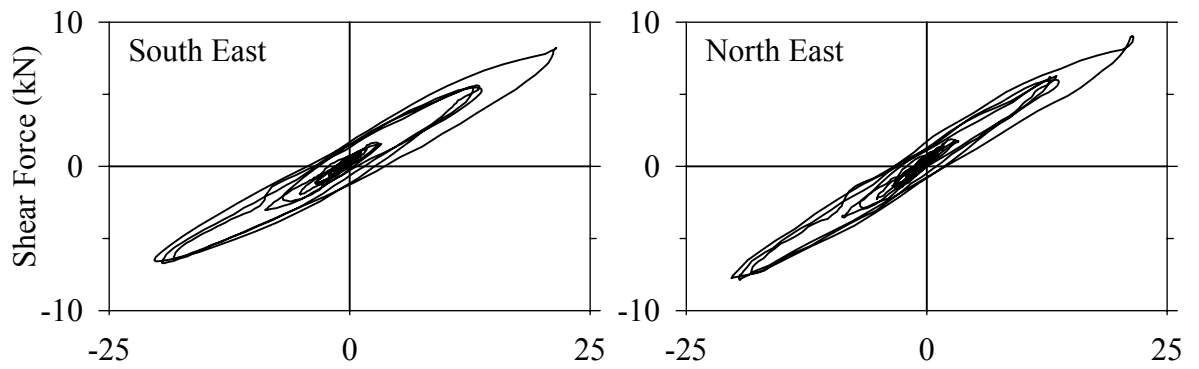
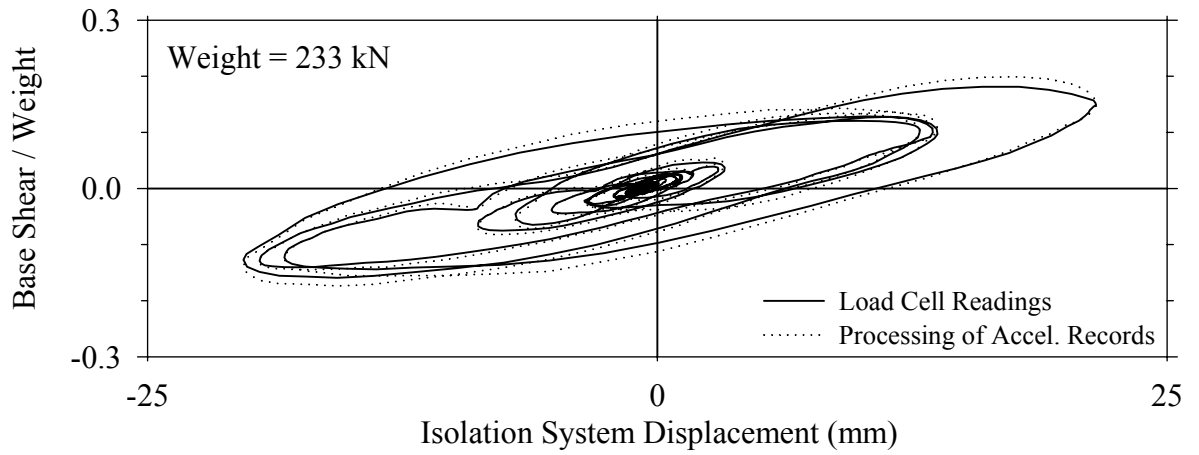
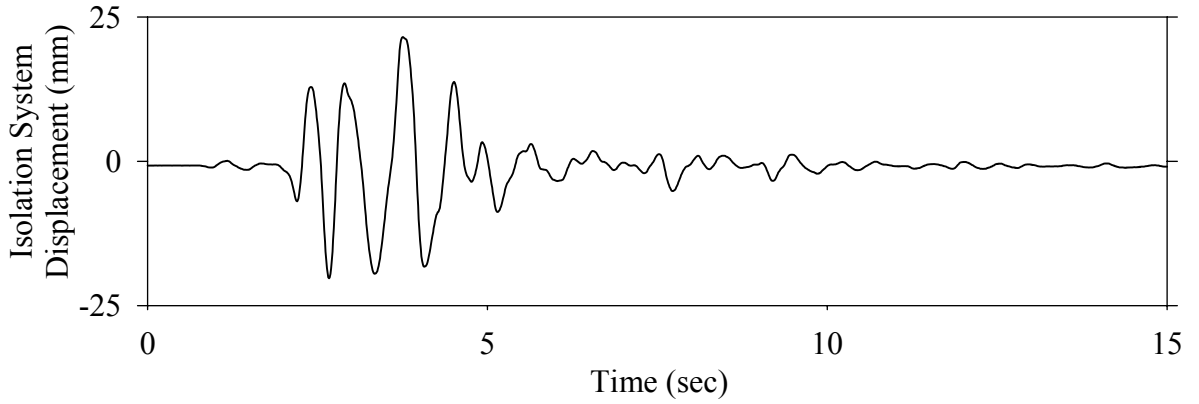




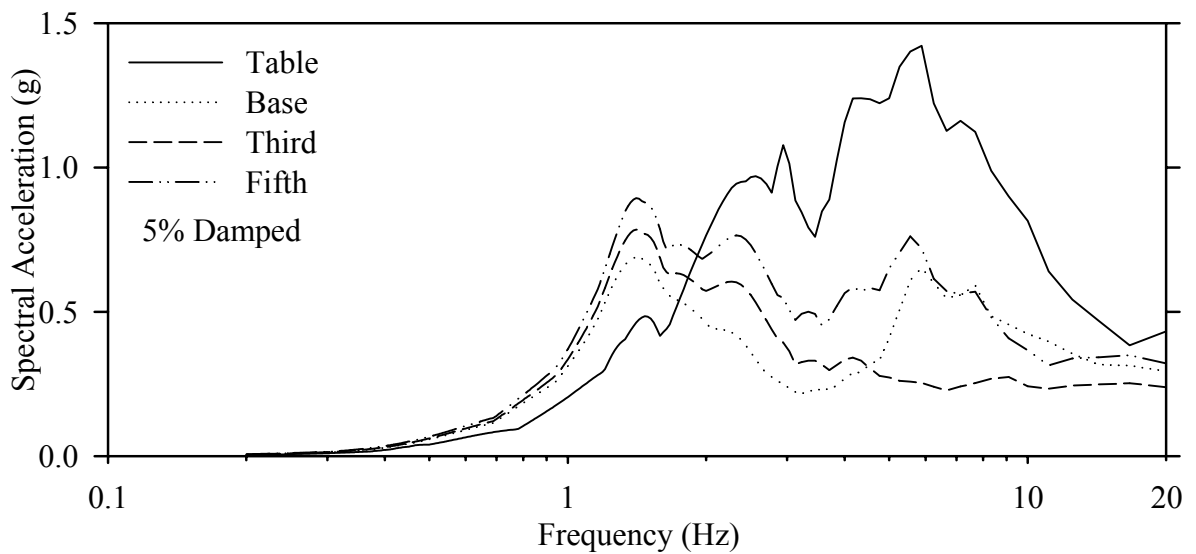
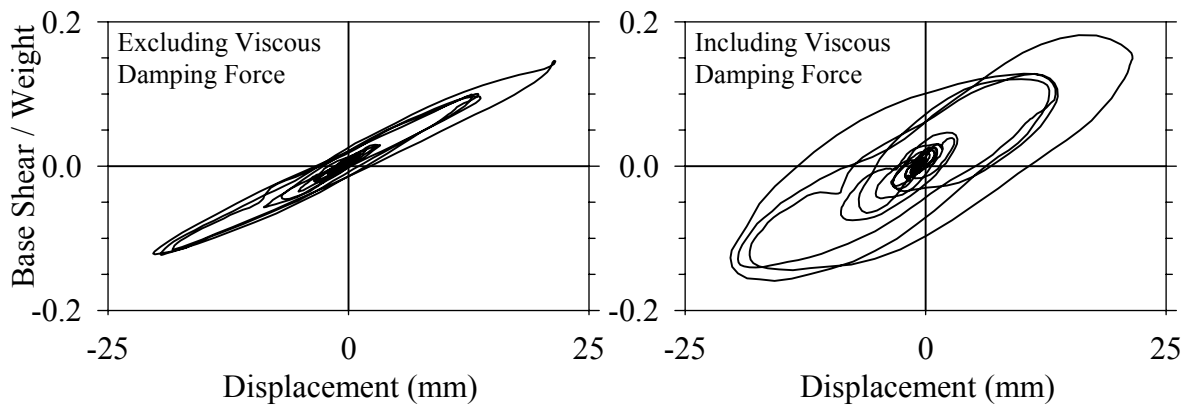
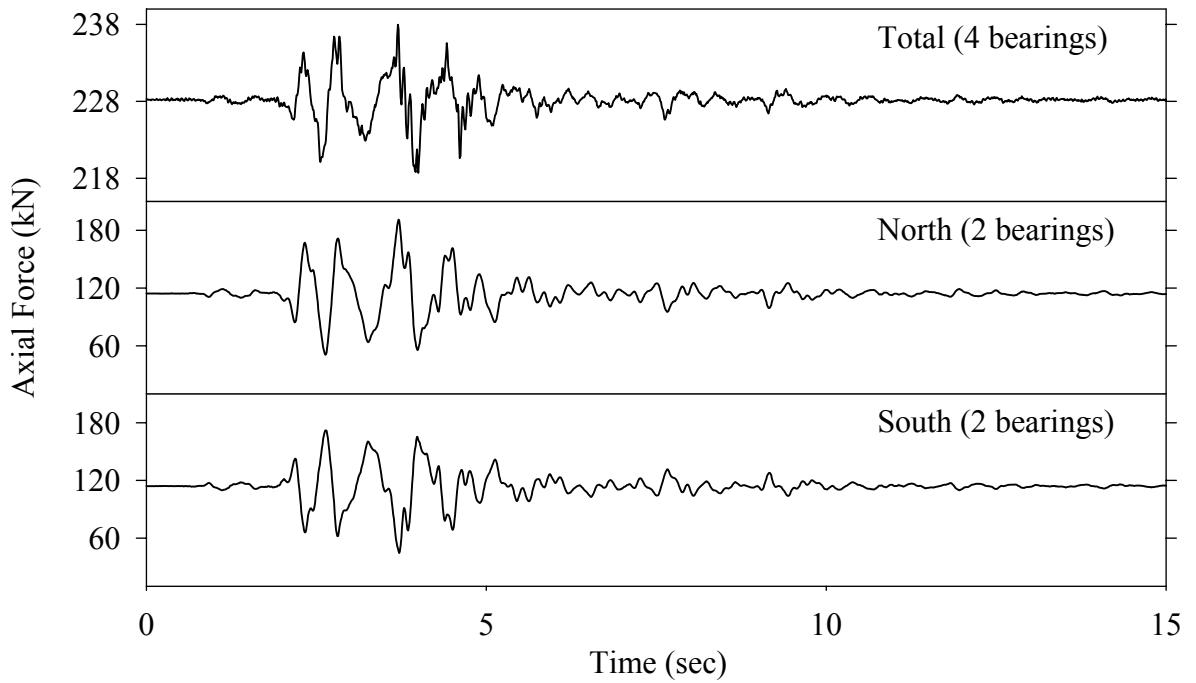
Test LDSLE20.1, El Centro S00E 200%, SB/Low Damping Elastomeric-Linear Dampers



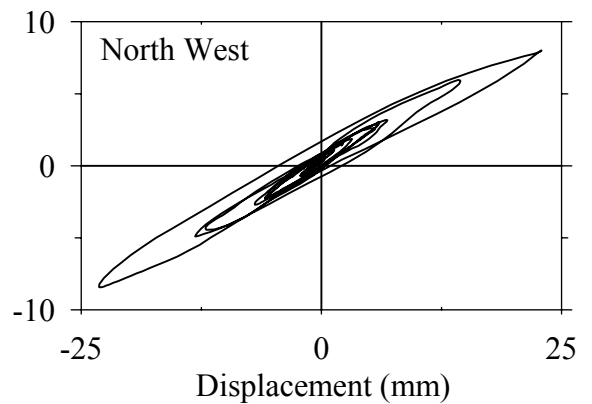
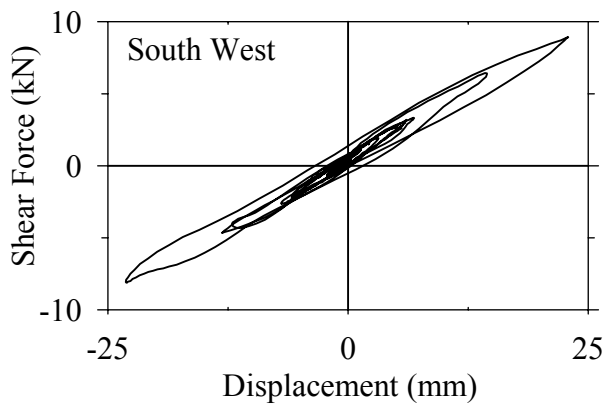
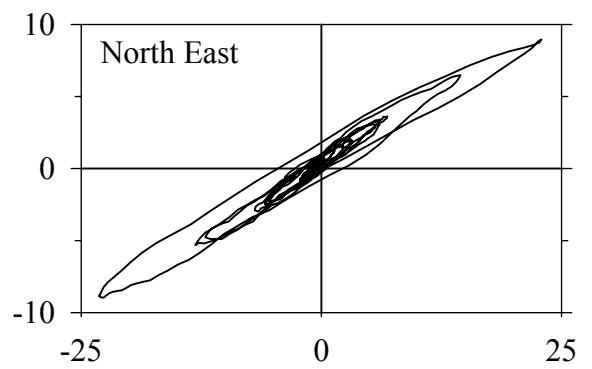
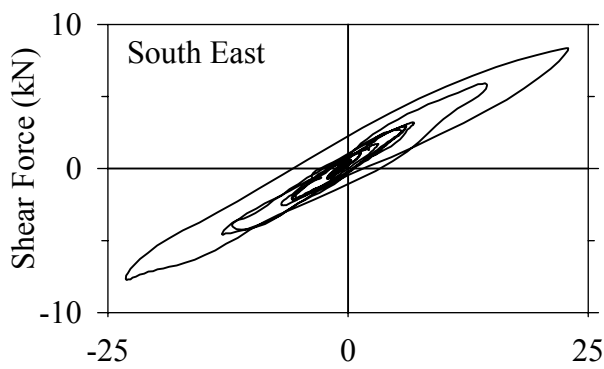
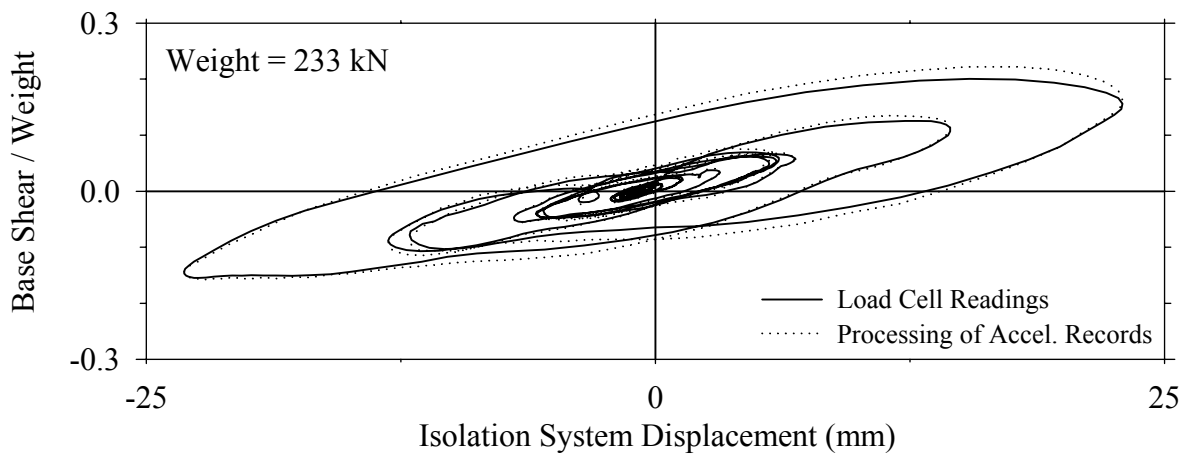
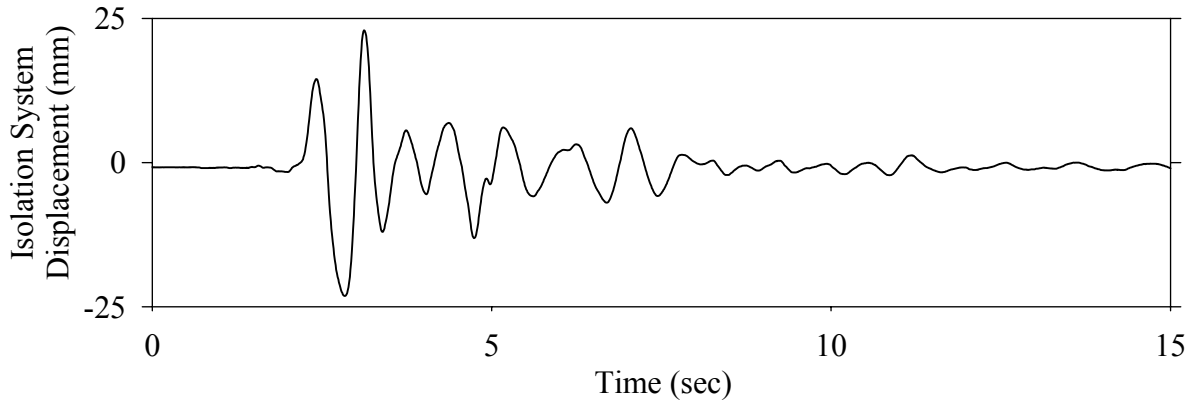
Test LDSLK50.1, Kobe N-S 50%, SB/Low Damping Elastomeric-Linear Dampers



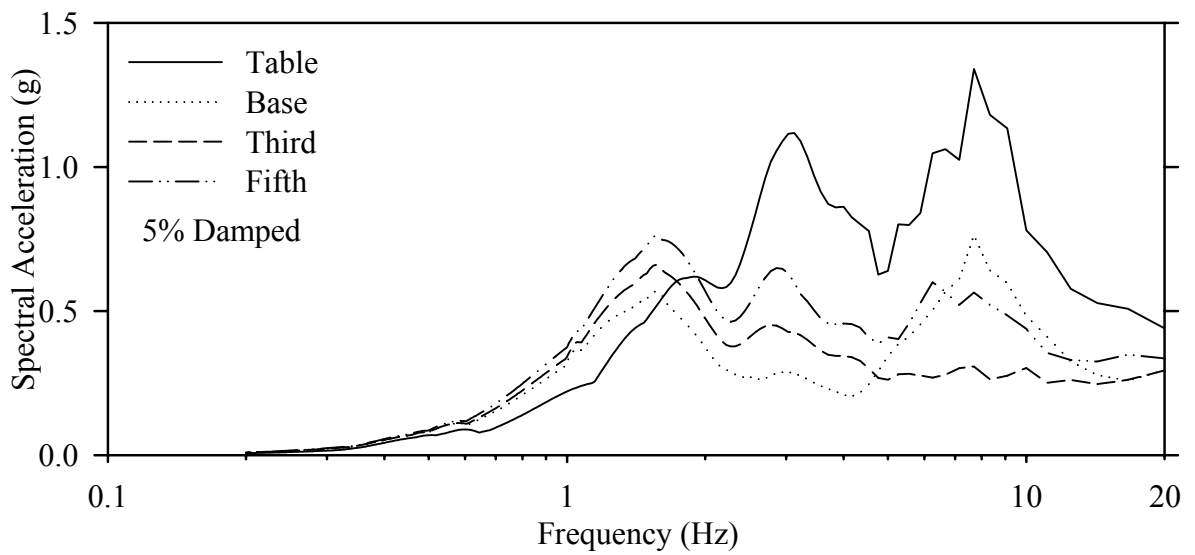
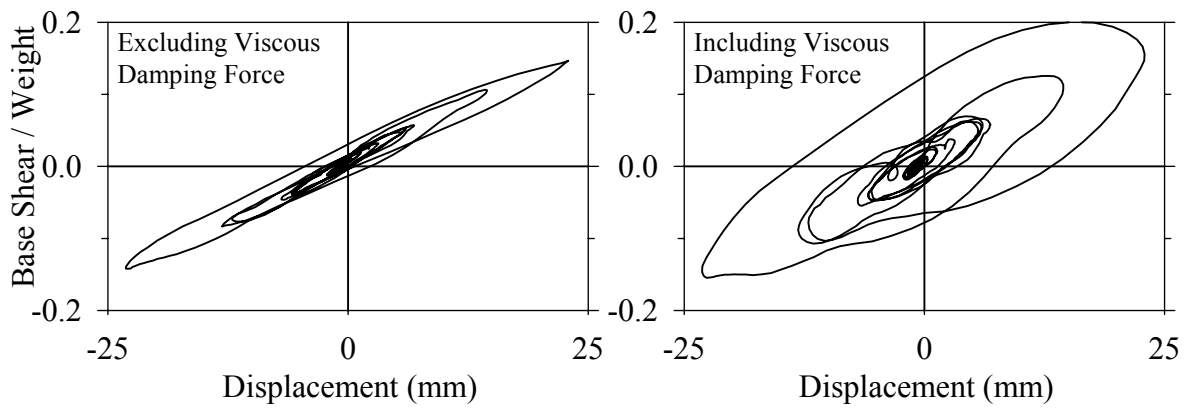
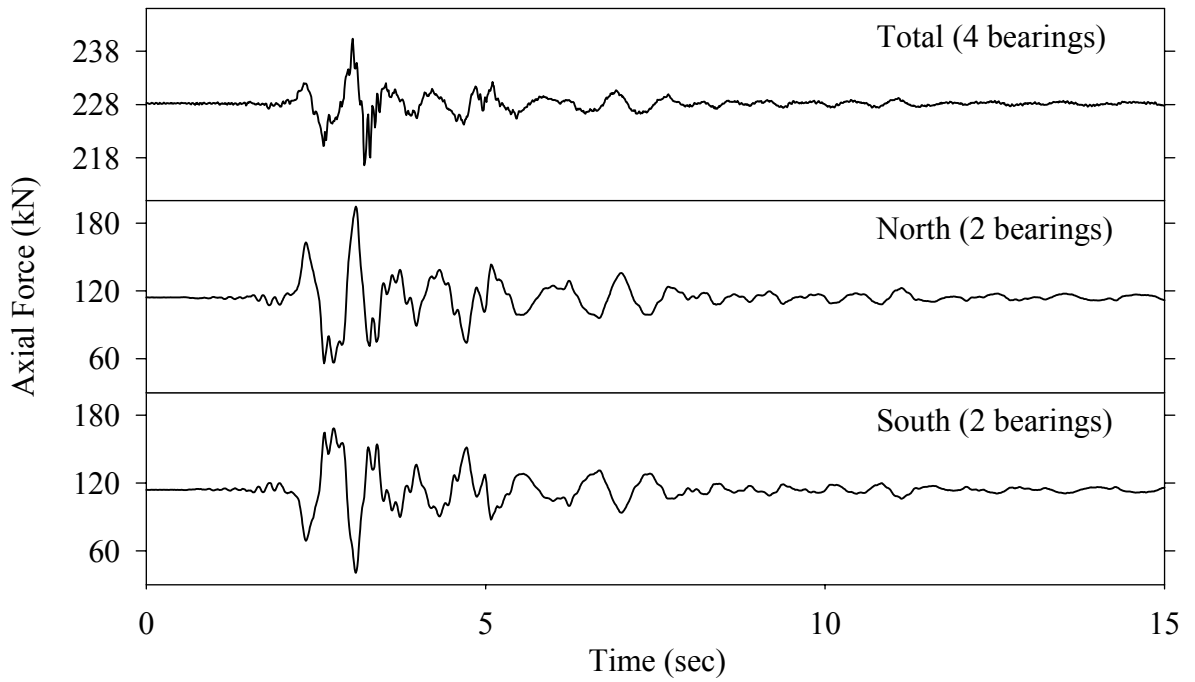
Test LDSLK50.1, Kobe N-S 50%, SB/Low Damping Elastomeric-Linear Dampers



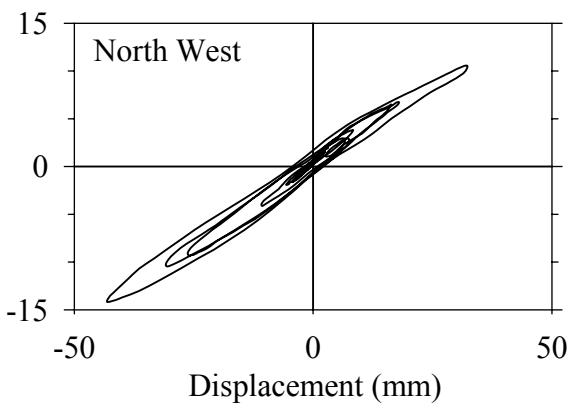
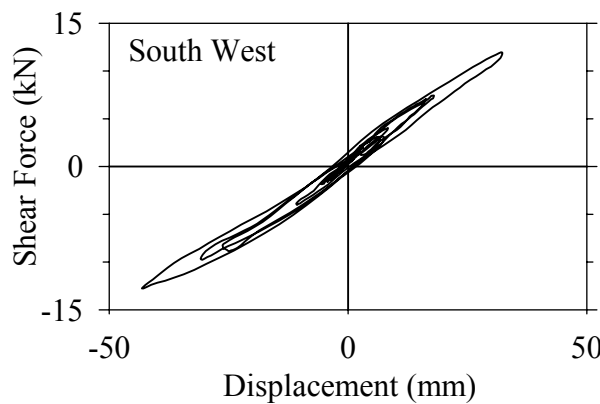
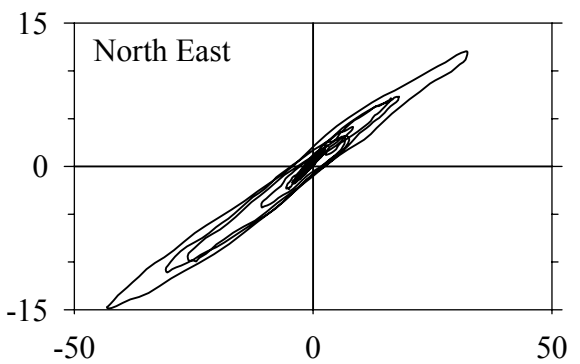
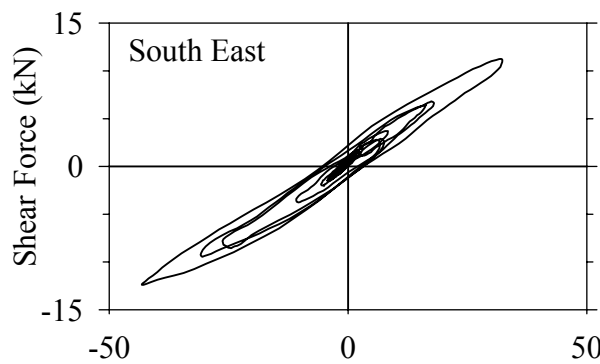
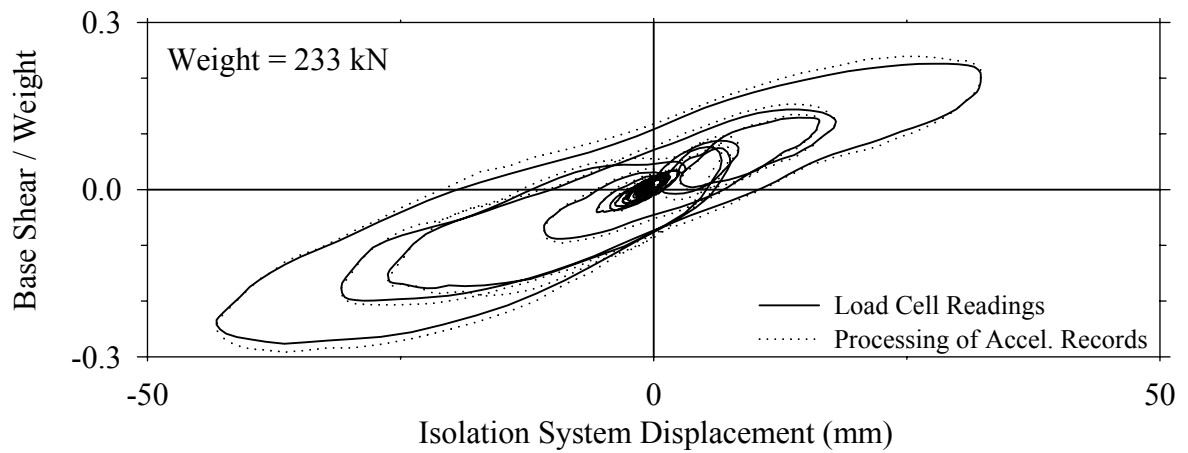
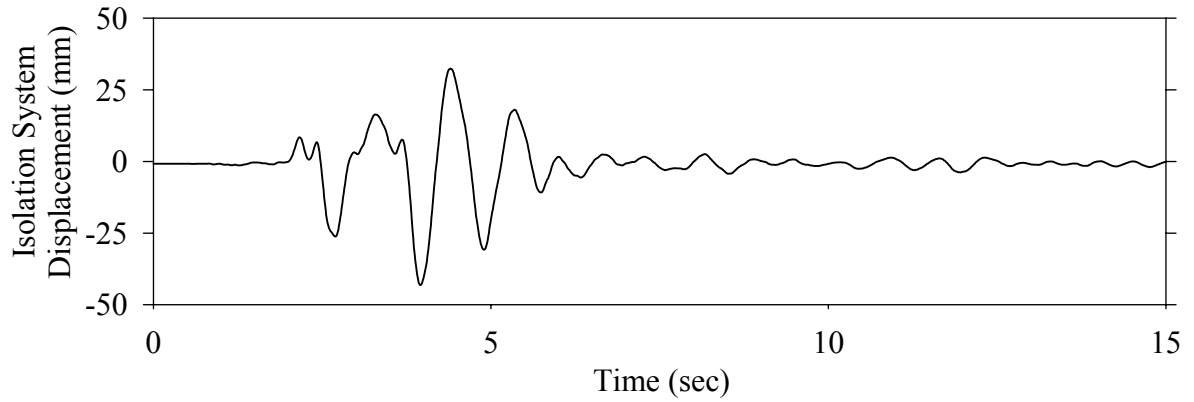
Test LDSLN50.1, Northridge Newhall 360° 50%, SB/Low Damping Elastomeric-Linear Dampers



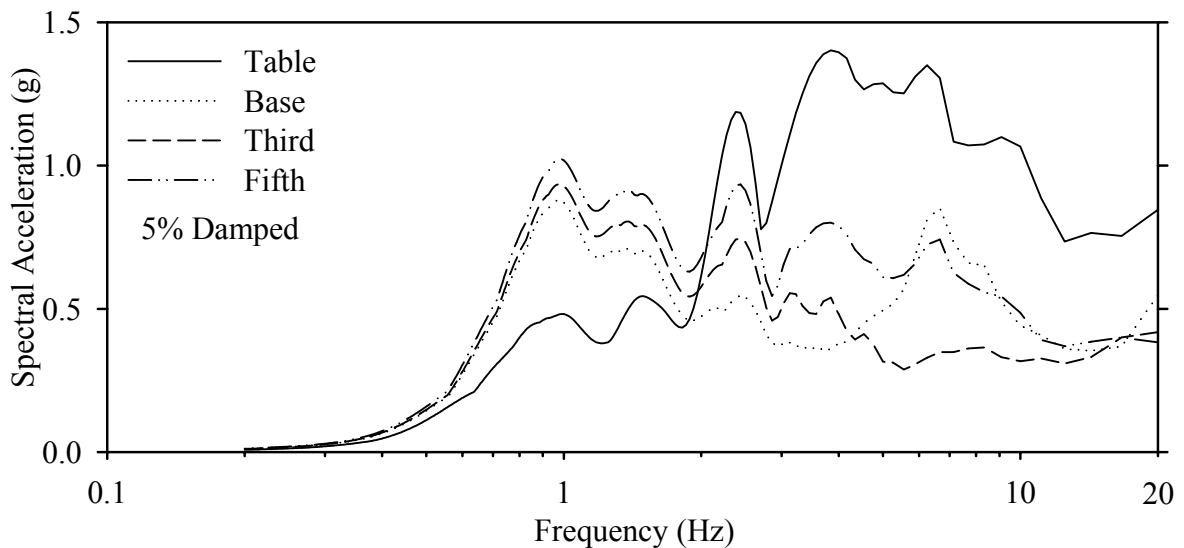
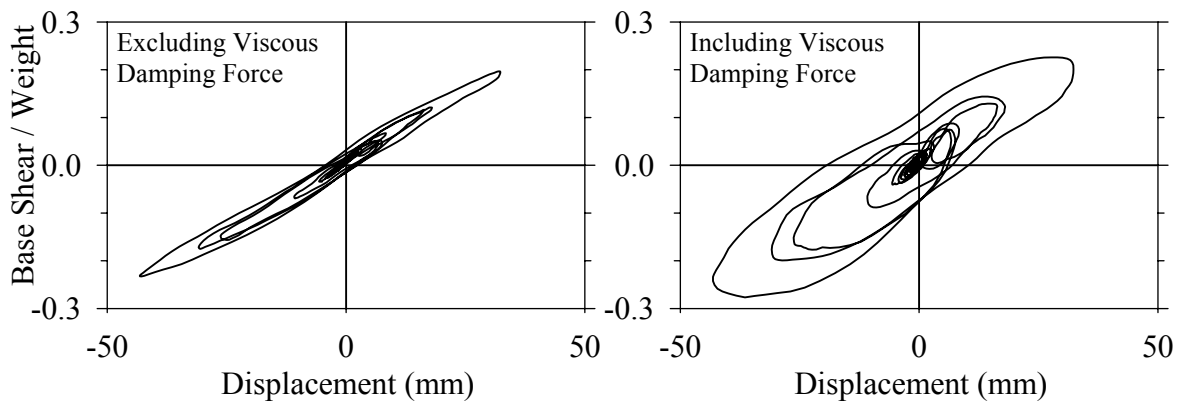
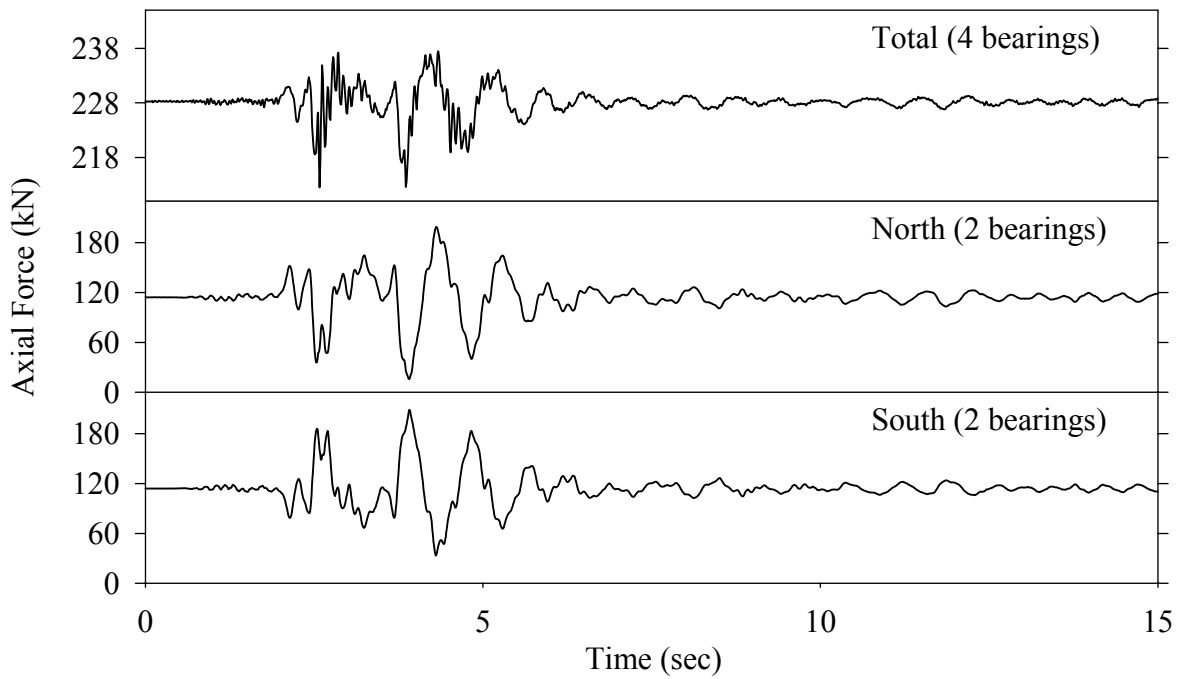
Test LDSLN50.1, Northridge Newhall 360° 50%, SB/Low Damping Elastomeric-Linear Dampers



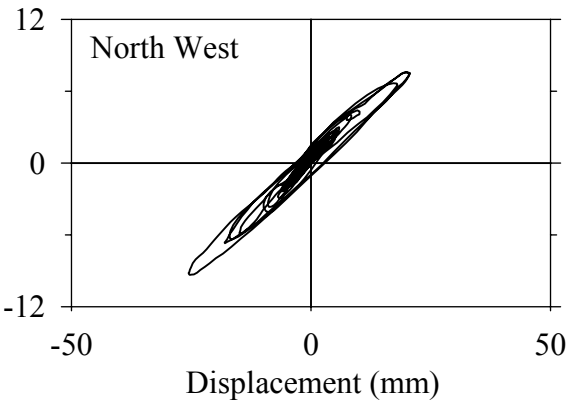
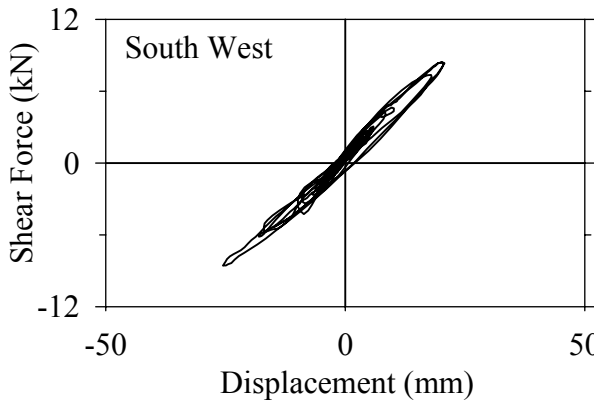
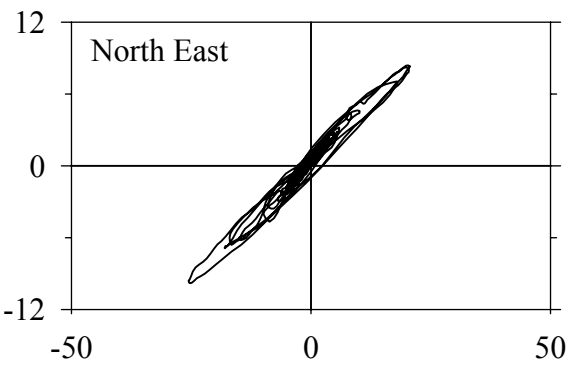
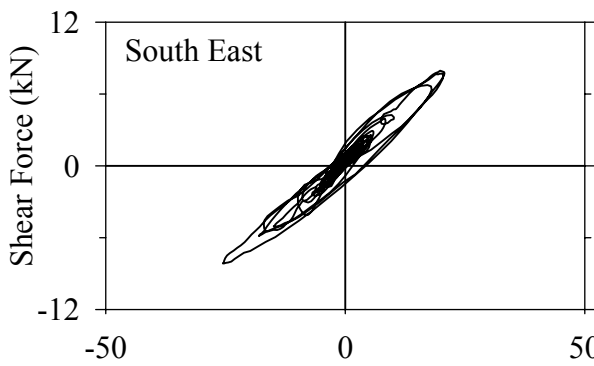
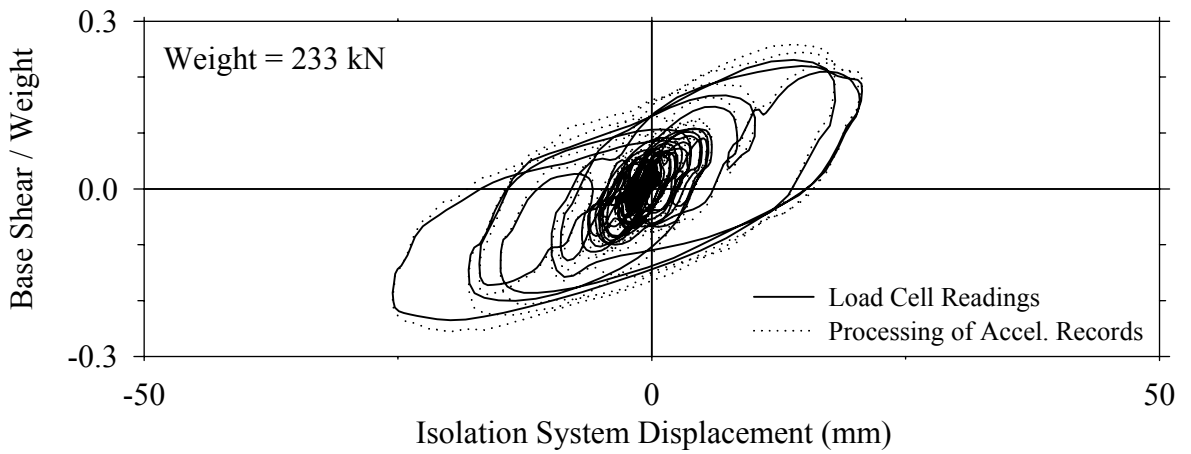
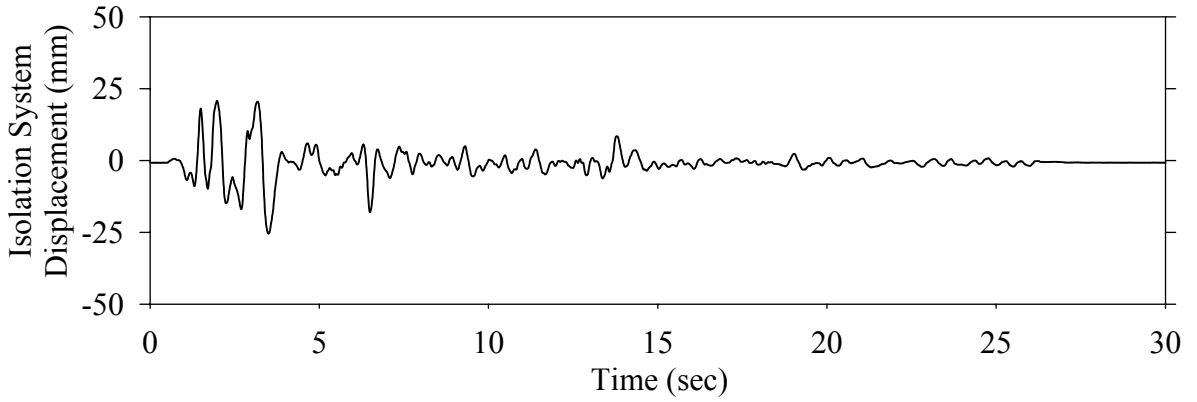
Test LDSLS10.1, Northridge Sylmar 90° 100%, SB/Low Damping Elastomeric-Linear Dampers



Test LDSLS10.1, Northridge Sylmar 90° 100%, SB/Low Damping Elastomeric-Linear Dampers

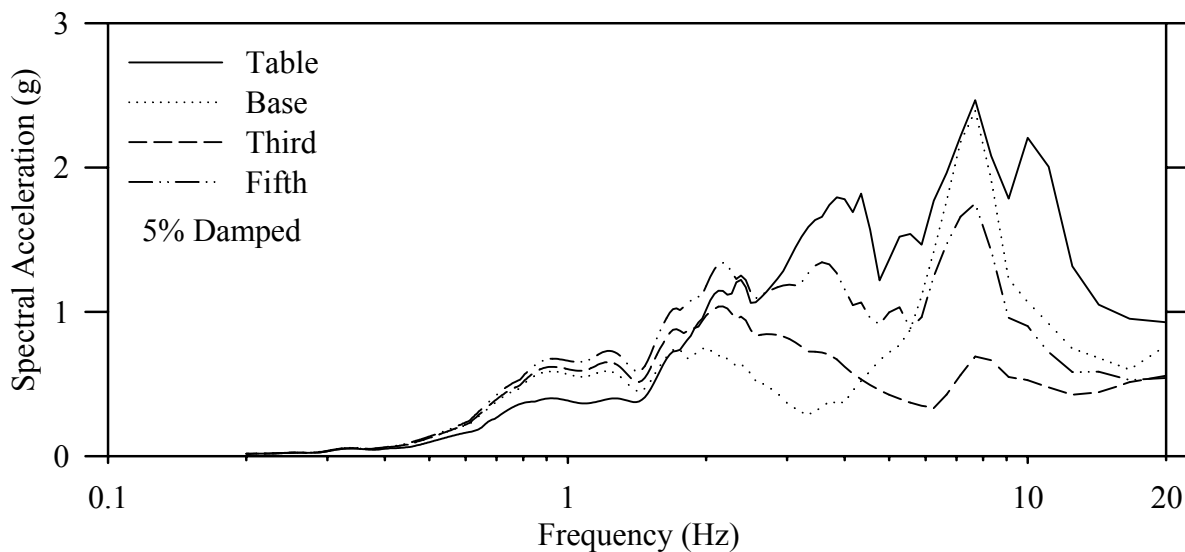
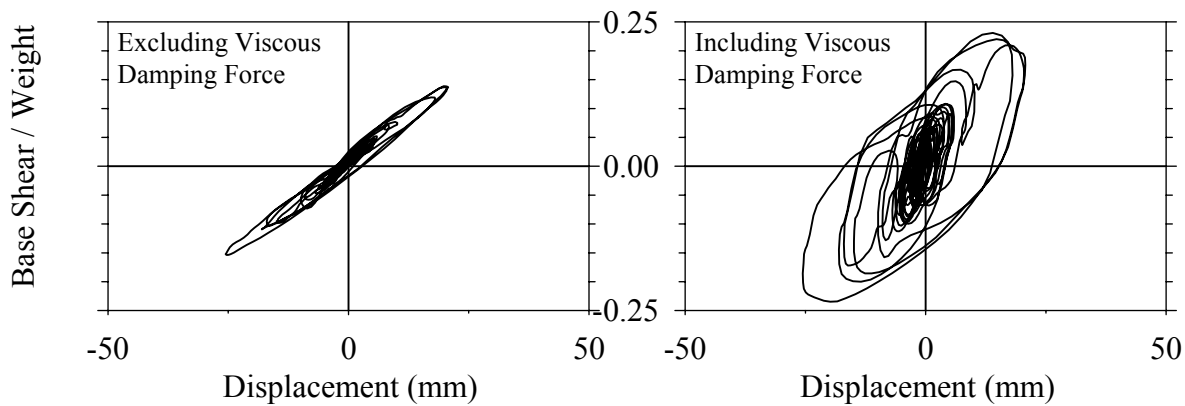
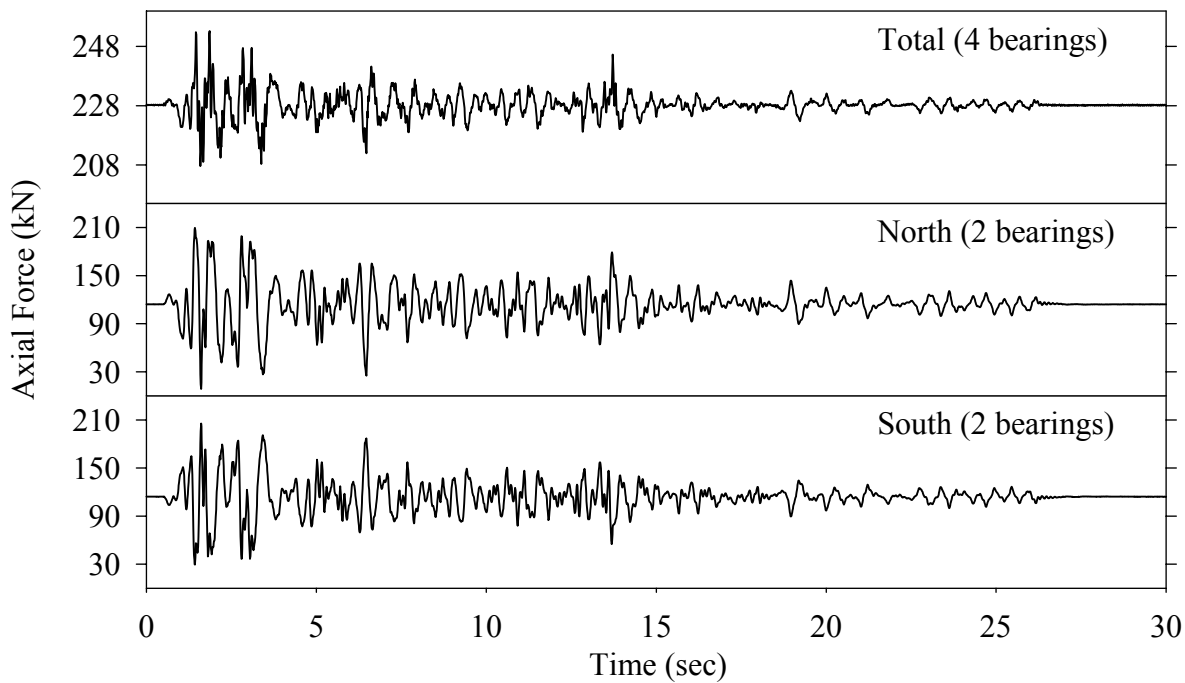


Test LDSNE20.1, El Centro S00E 200%, SB/Low Damping Elastomeric-Nonlinear Dampers

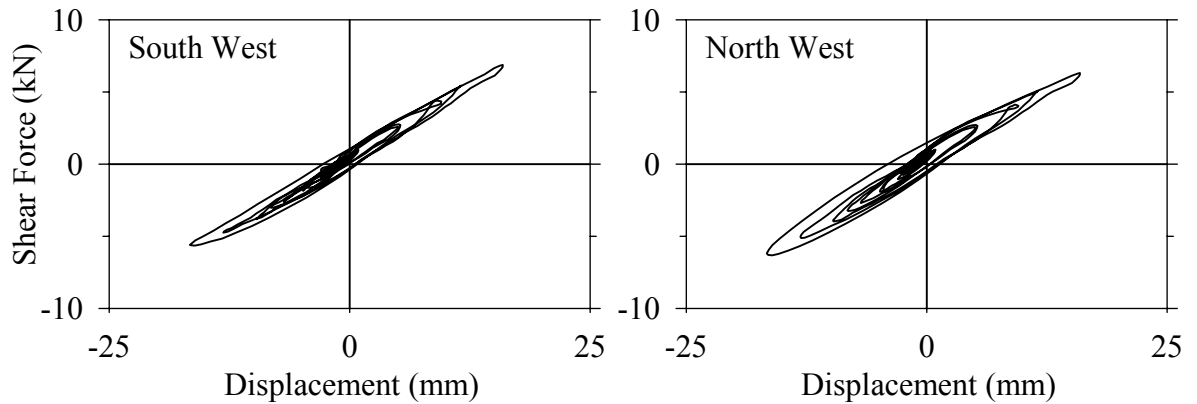
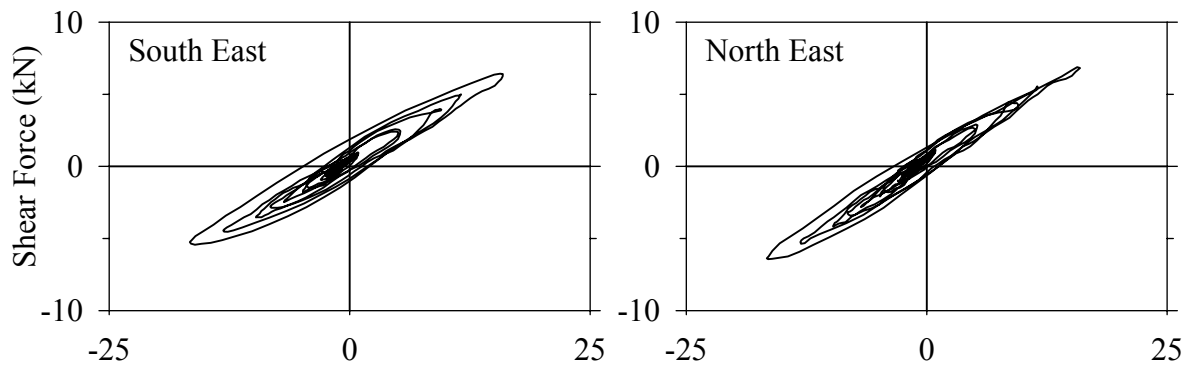
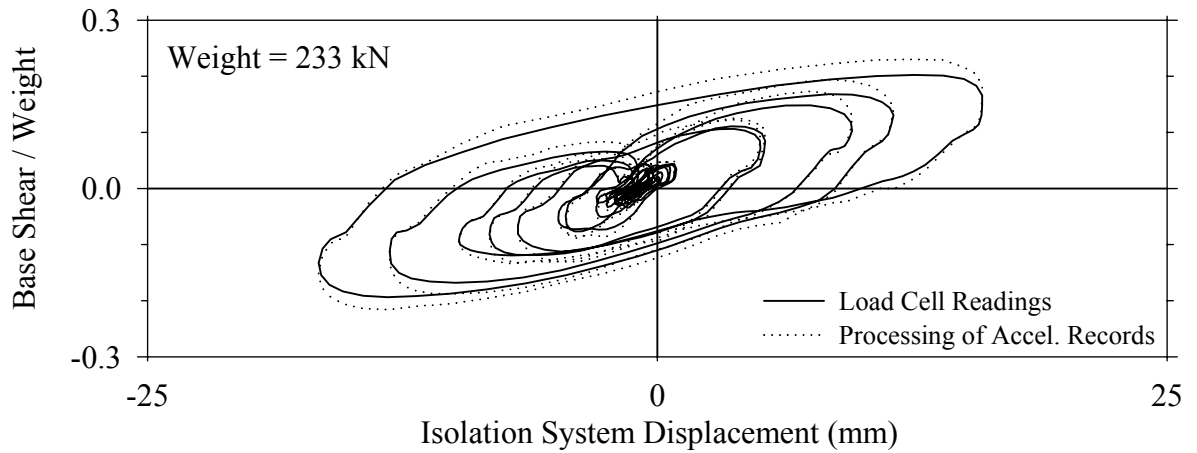
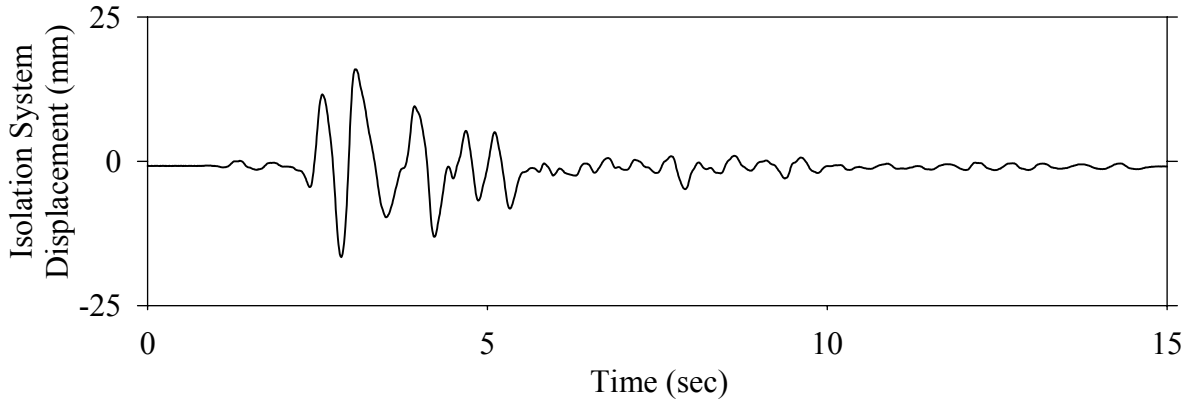




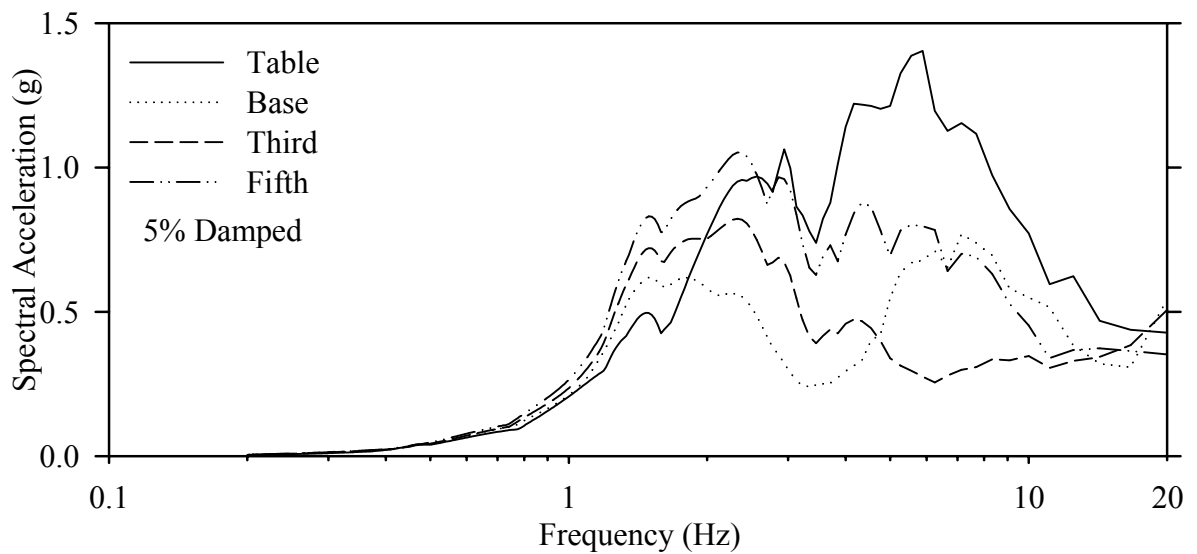
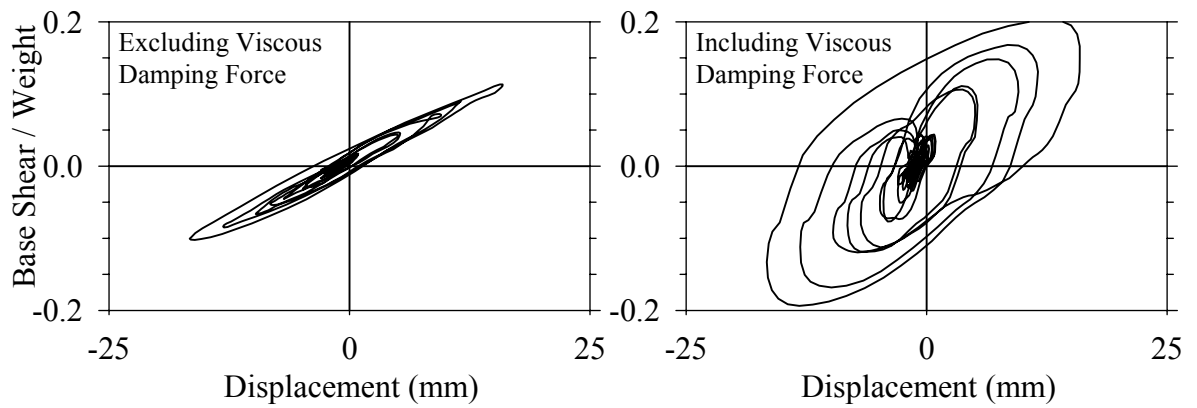
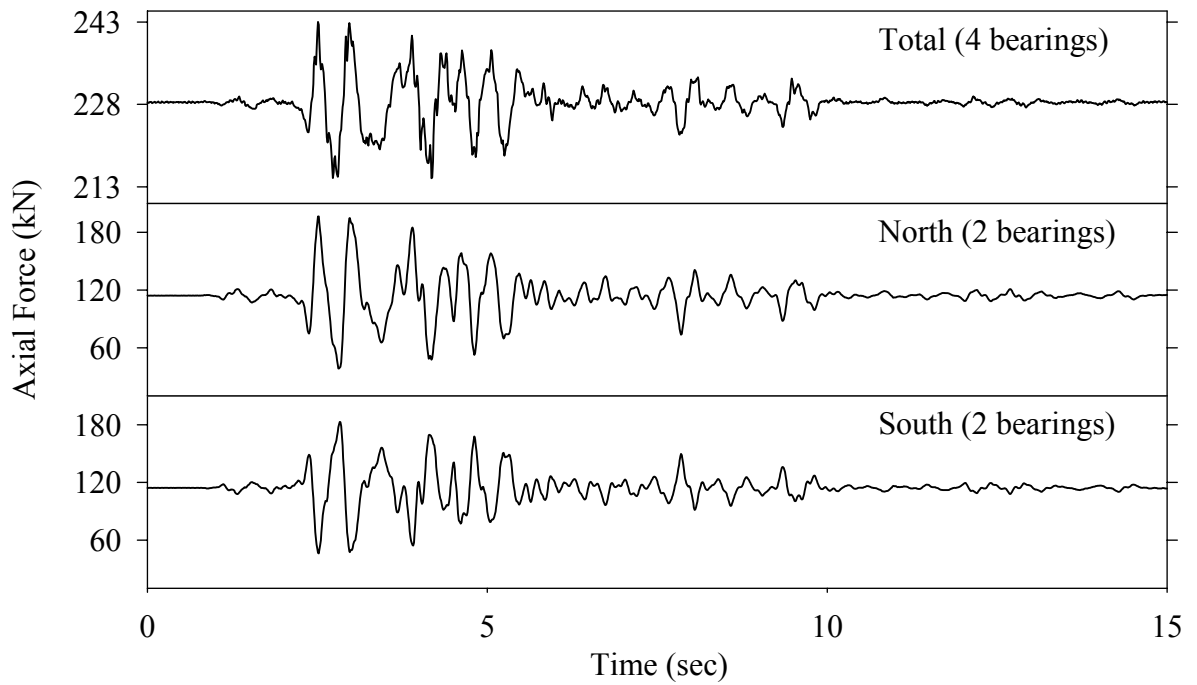
Test LDSNE20.1, El Centro S00E 200%, SB/Low Damping Elastomeric-Nonlinear Dampers



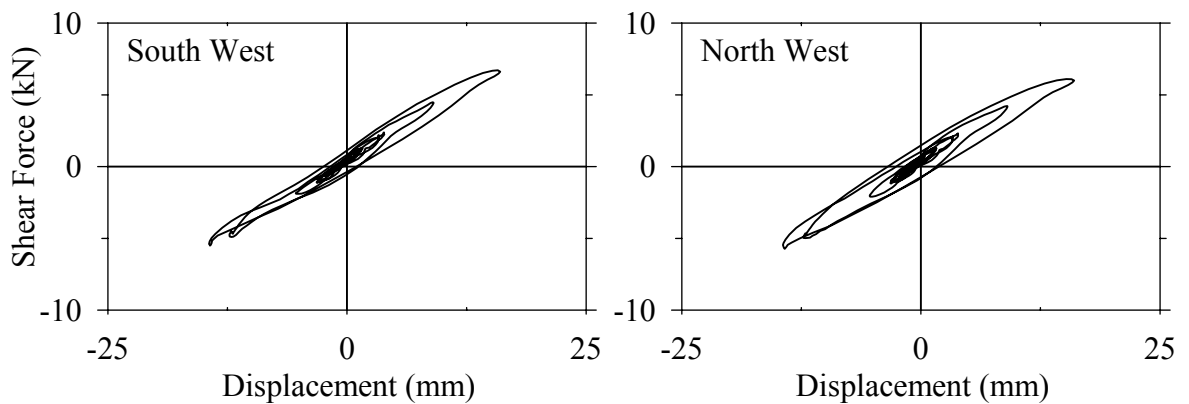
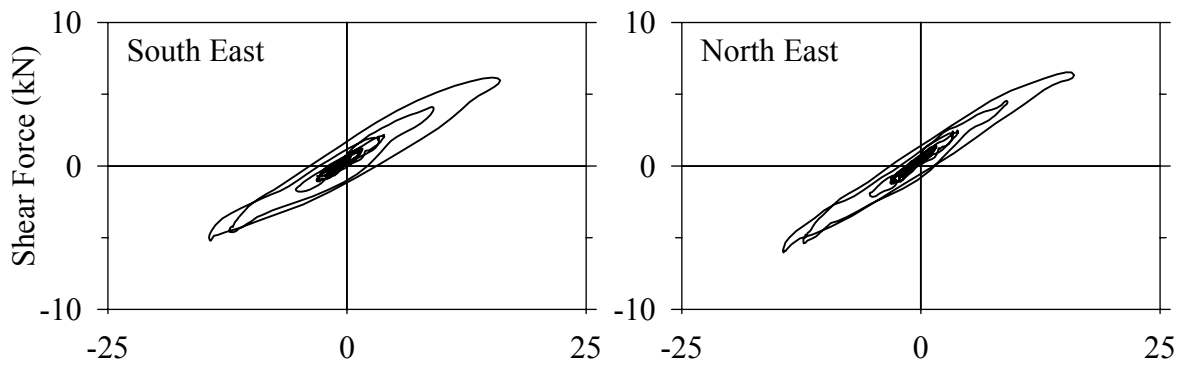
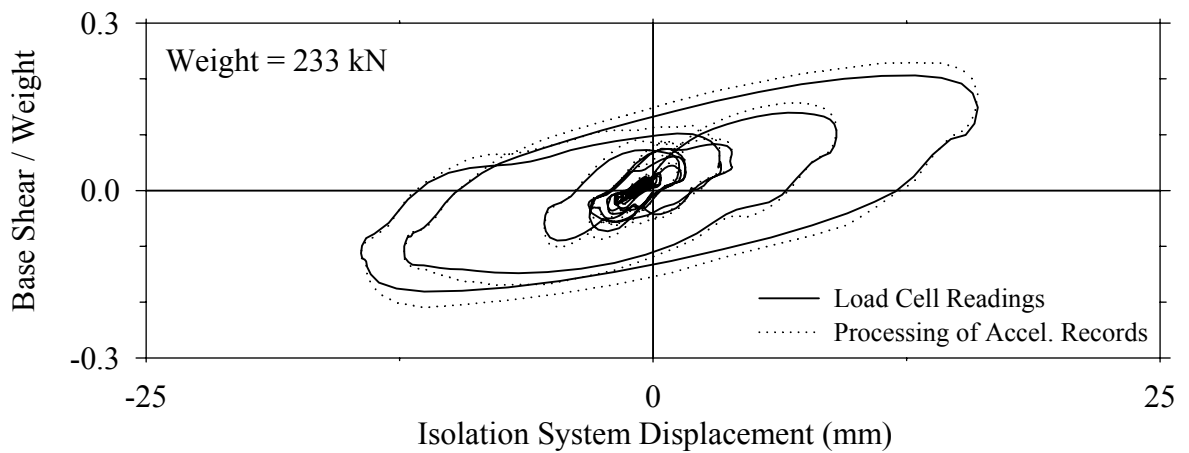
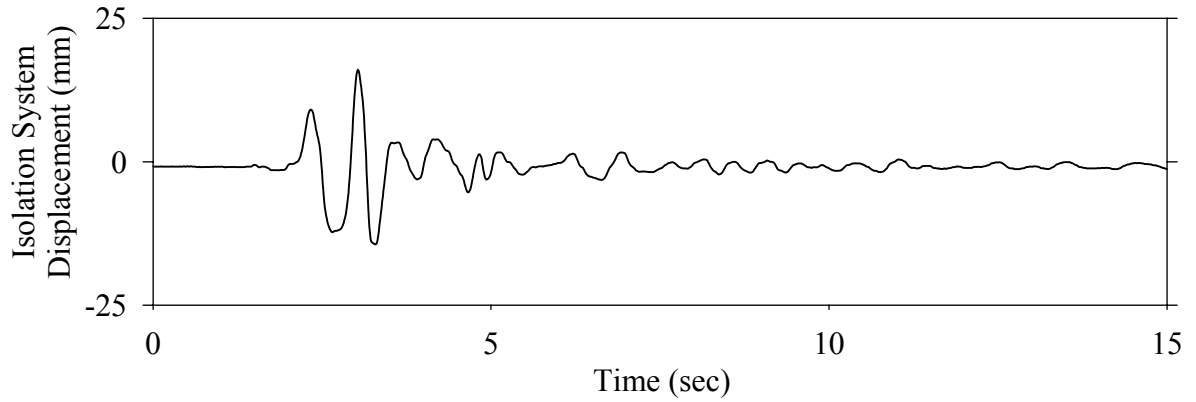
Test LDSNK50.1, Kobe N-S 50%, SB/Low Damping Elastomeric-Nonlinear Dampers



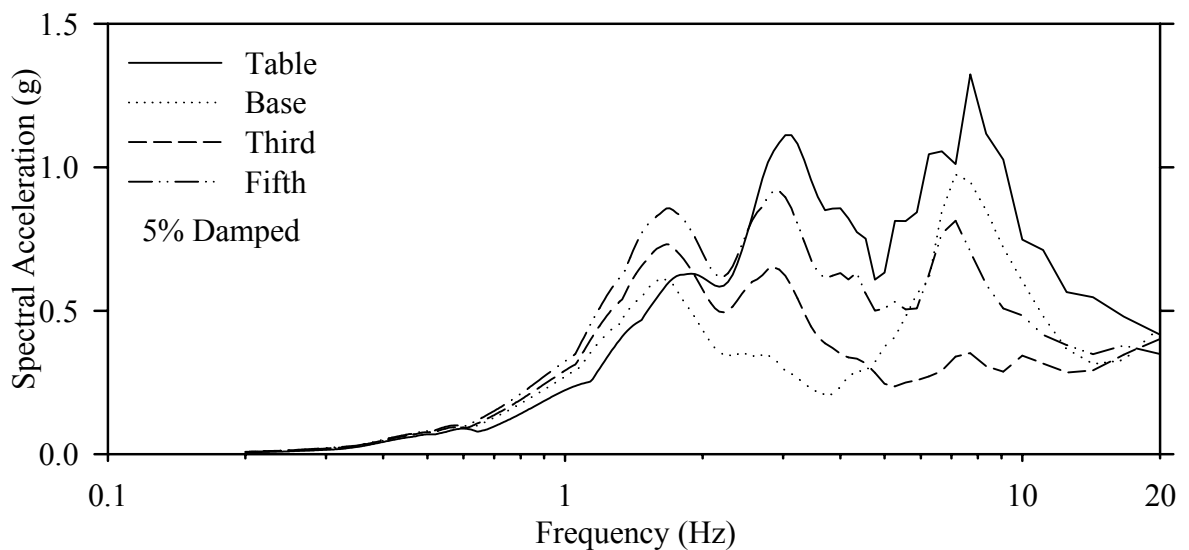
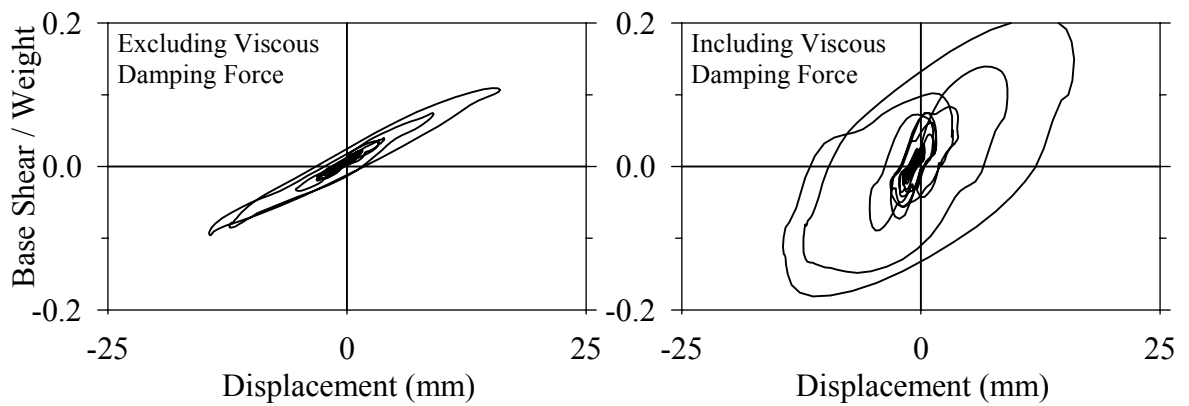
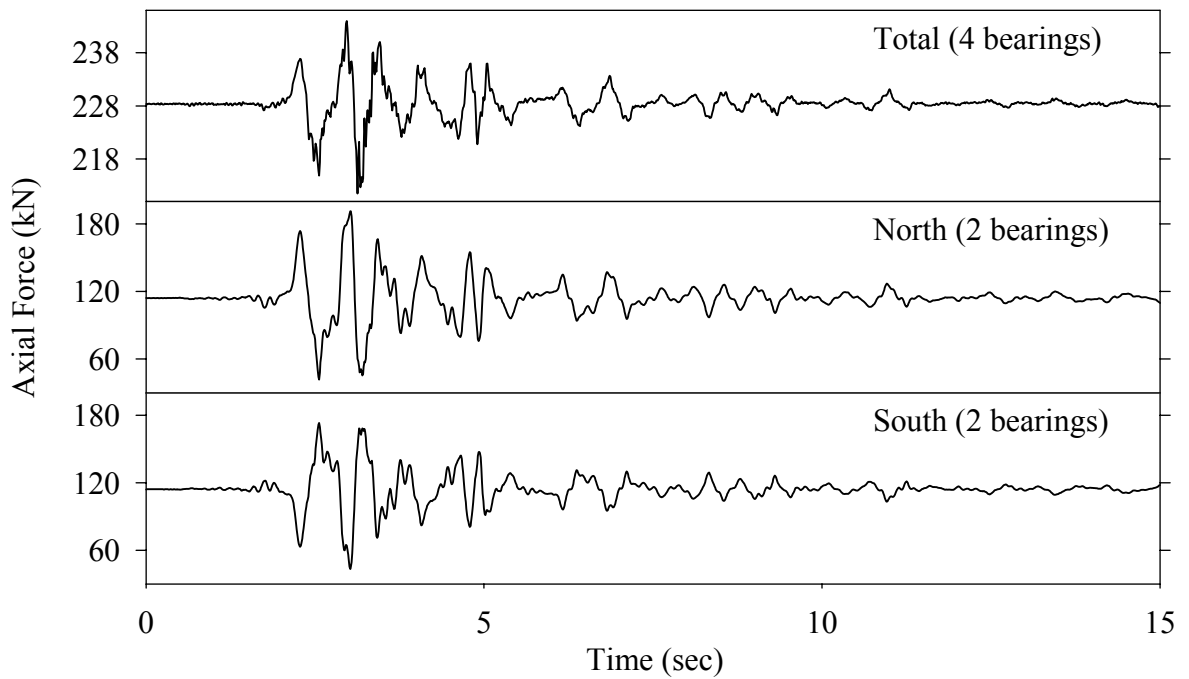
Test LDSNK50.1, Kobe N-S 50%, SB/Low Damping Elastomeric-Nonlinear Dampers



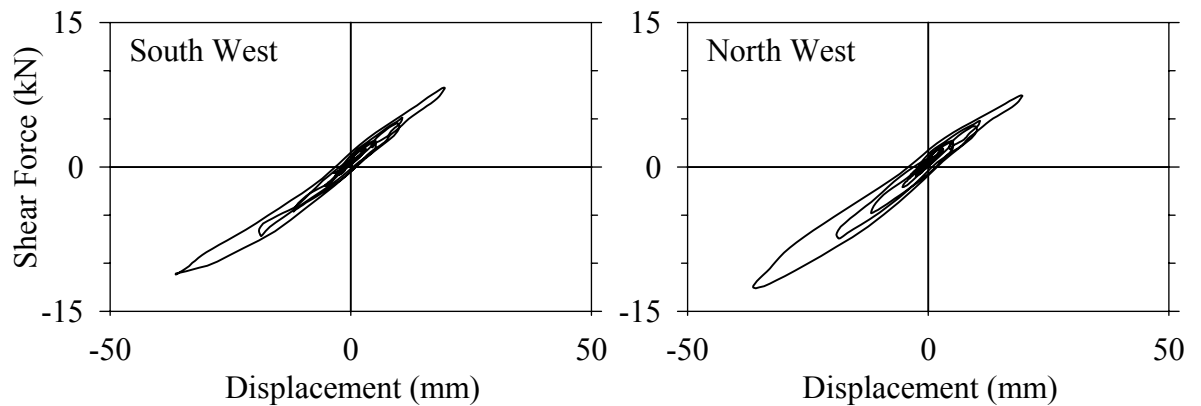
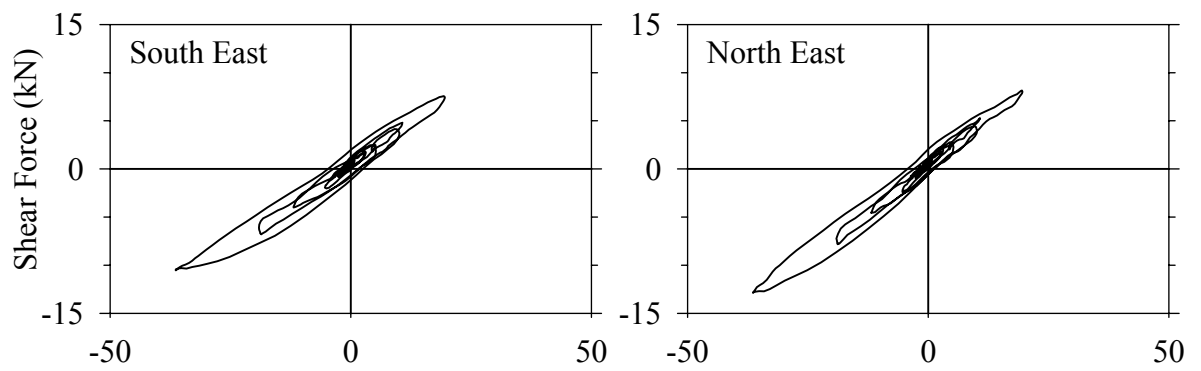
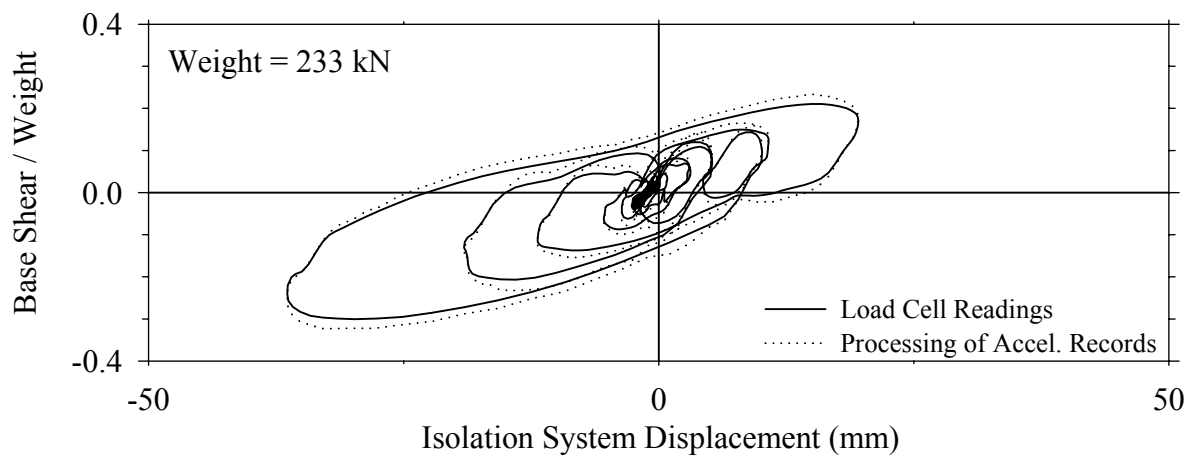
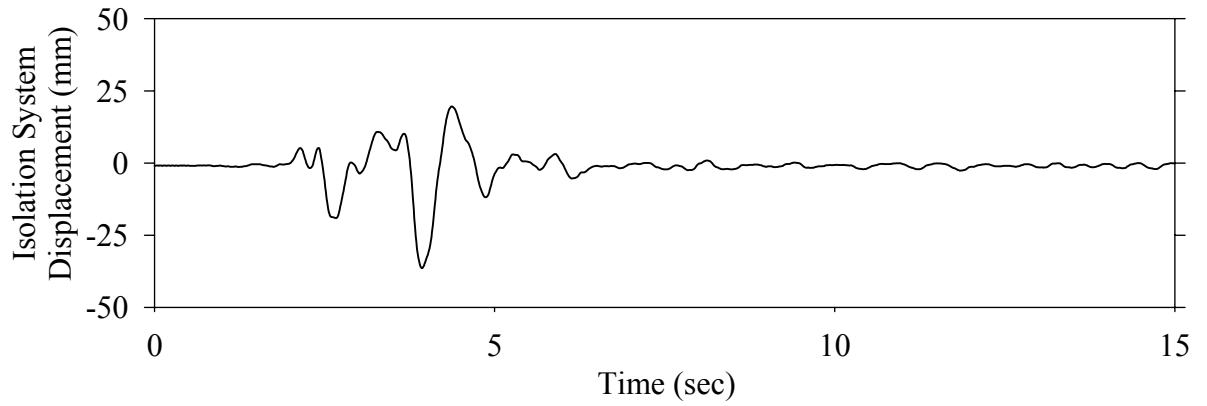
Test LDSNN50.1, Northridge Newhall 360° 50%, SB/Low Damping Elastomeric-Nonlinear Dampers



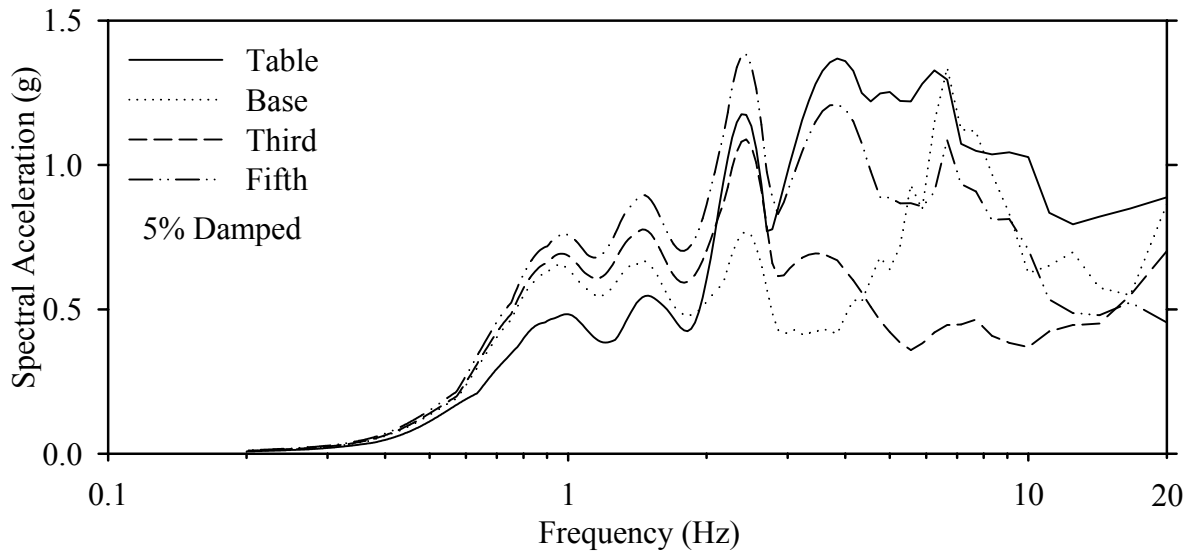
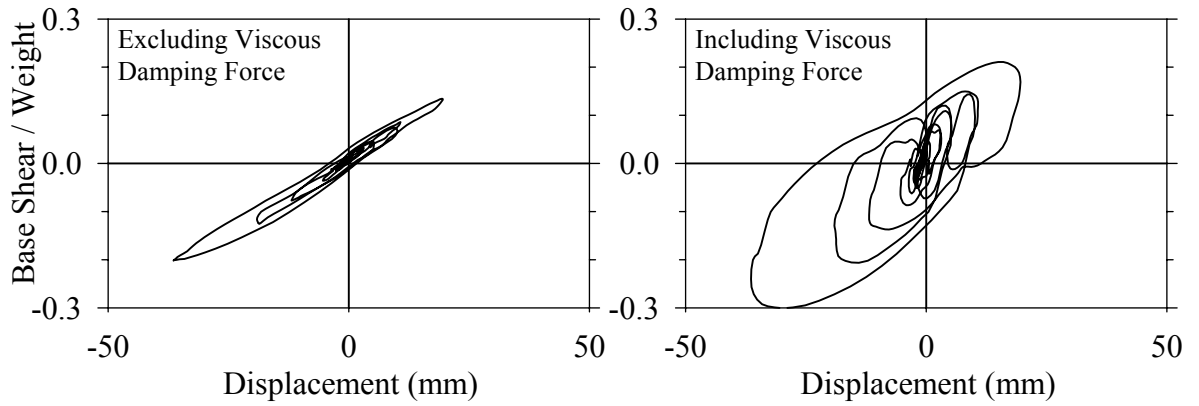
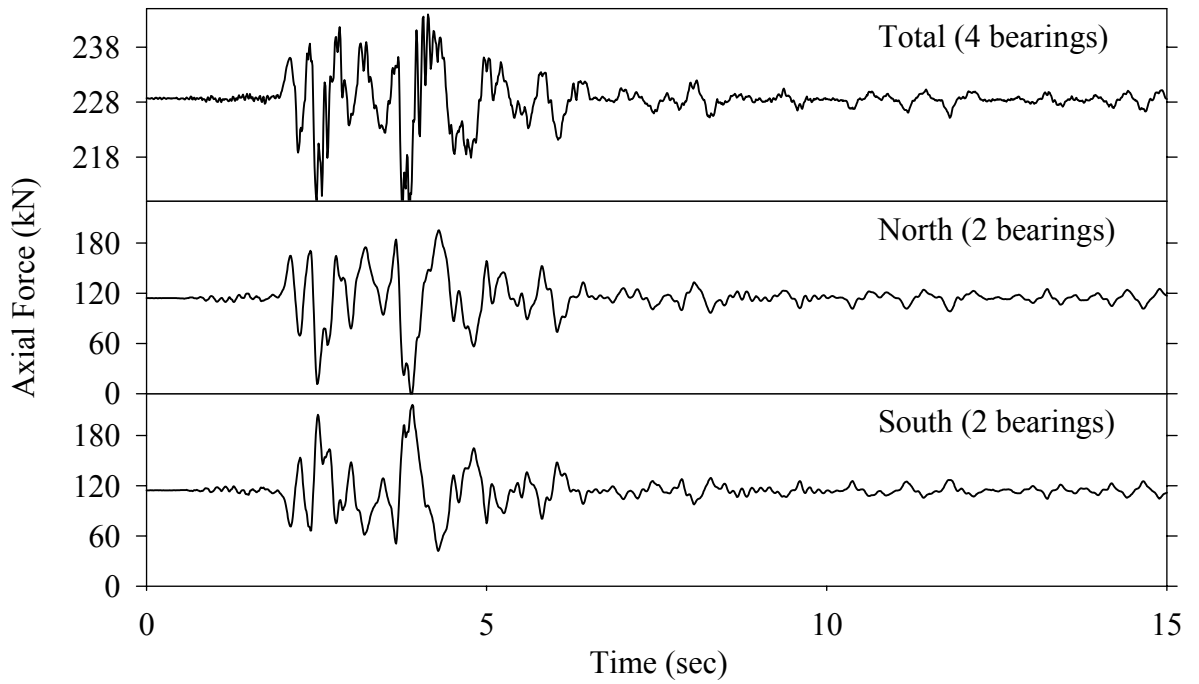
Test LDSNN50.1, Northridge Newhall 360° 50%, SB/Low Damping Elastomeric-Nonlinear Dampers



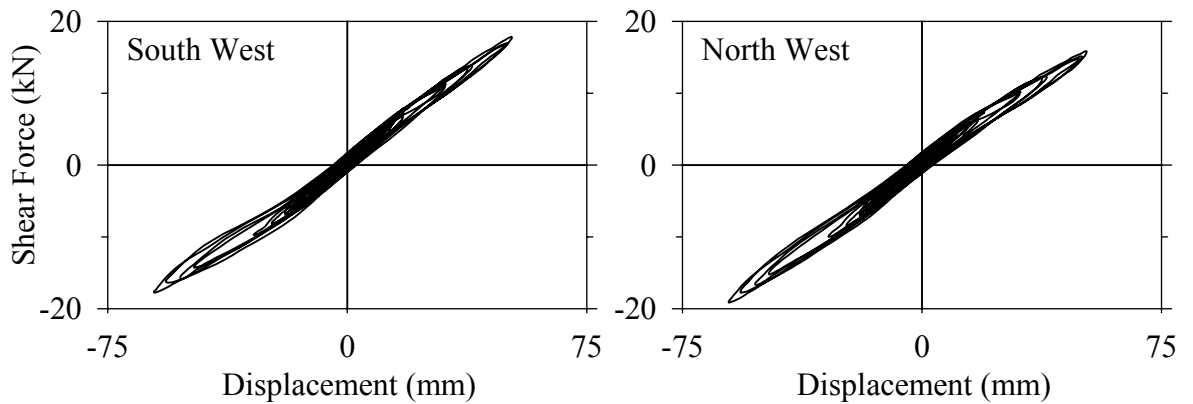
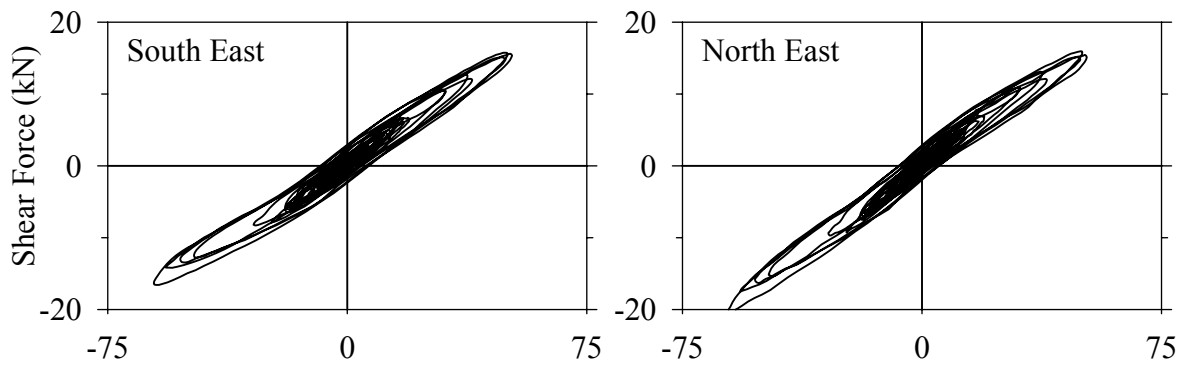
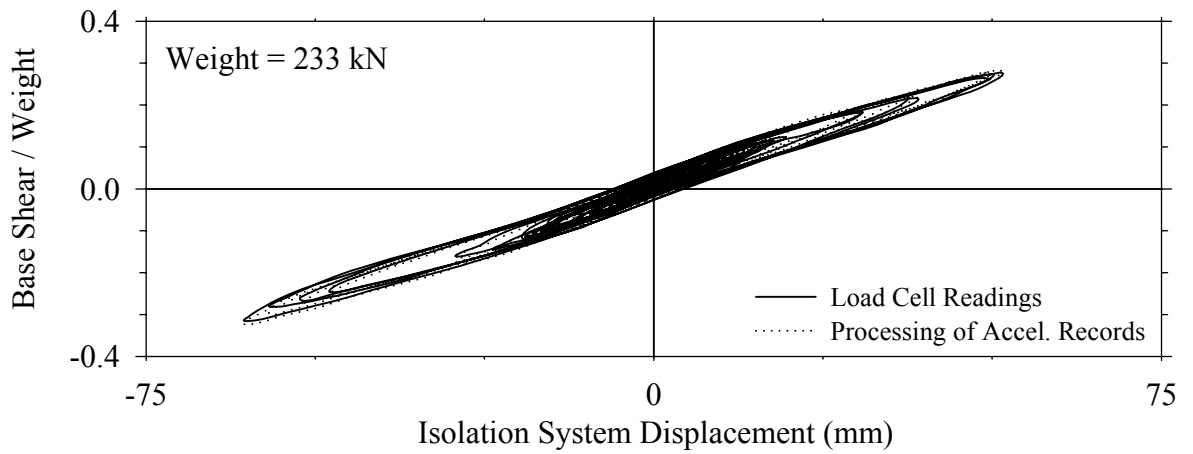
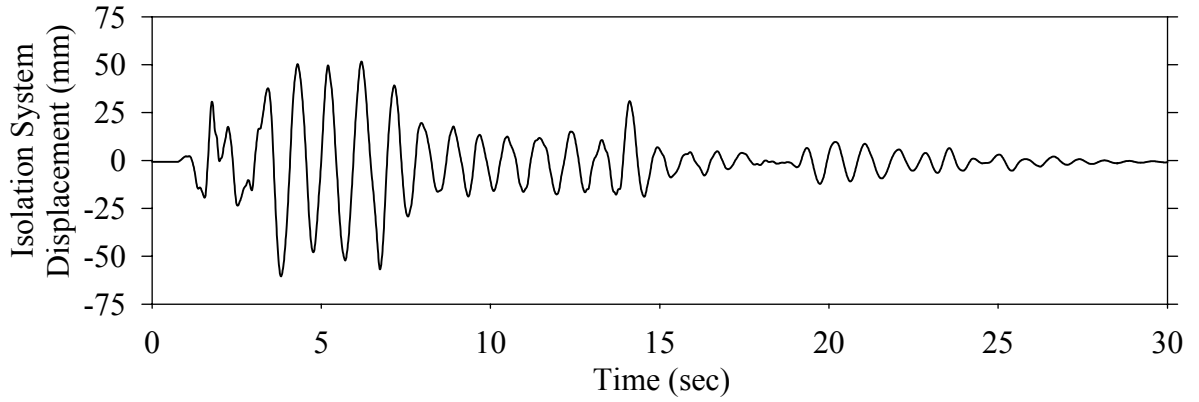
Test LDSNS10.1, Northridge Sylmar 90° 100%, SB/Low Damping Elastomeric-Nonlinear Dampers



Test LDSNS10.1, Northridge Sylmar 90° 100%, SB/Low Damping Elastomeric-Nonlinear Dampers

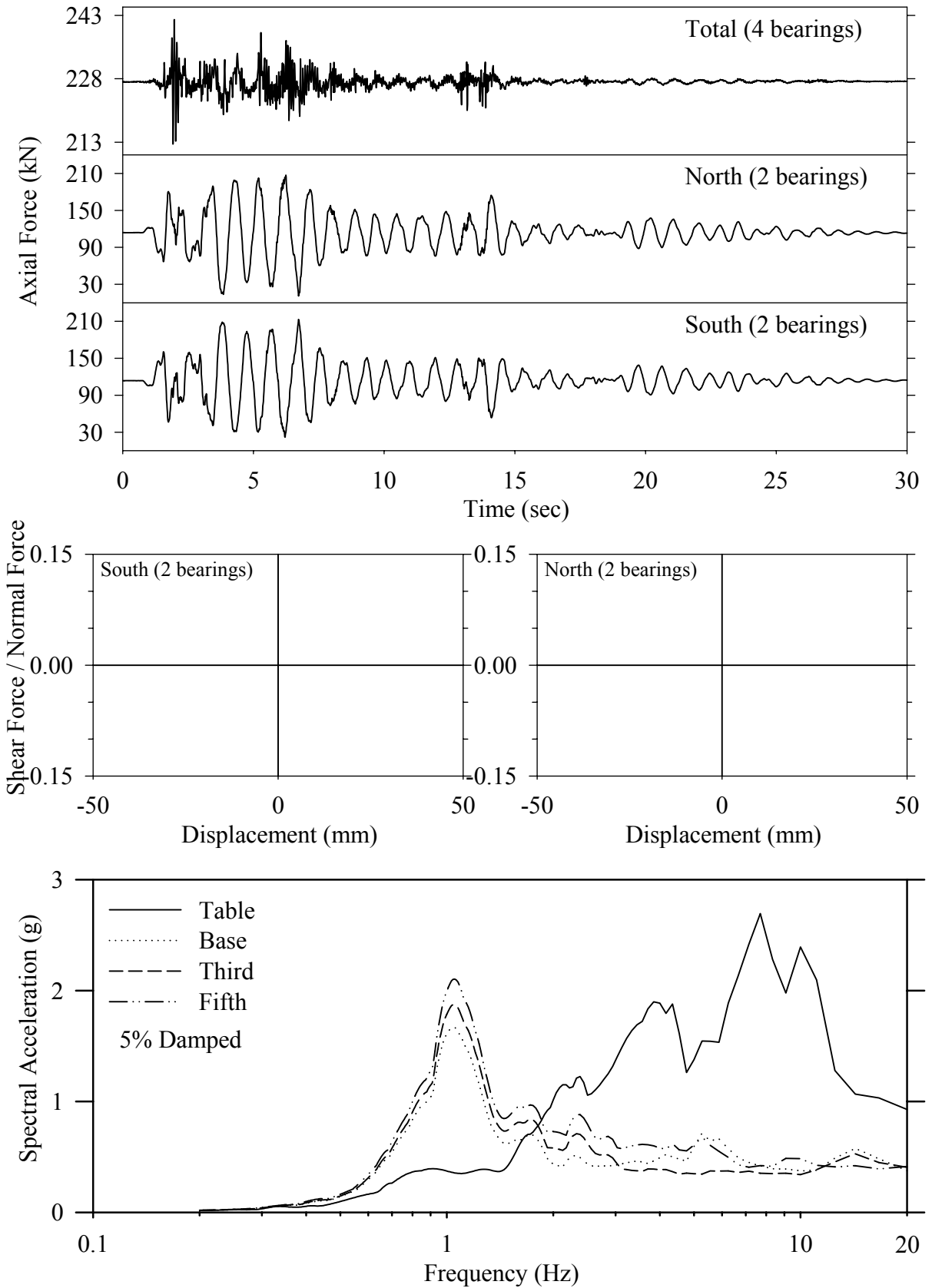


Test LDABE20.1, El Centro S00E 200%, AB/Low Damping Elastomeric

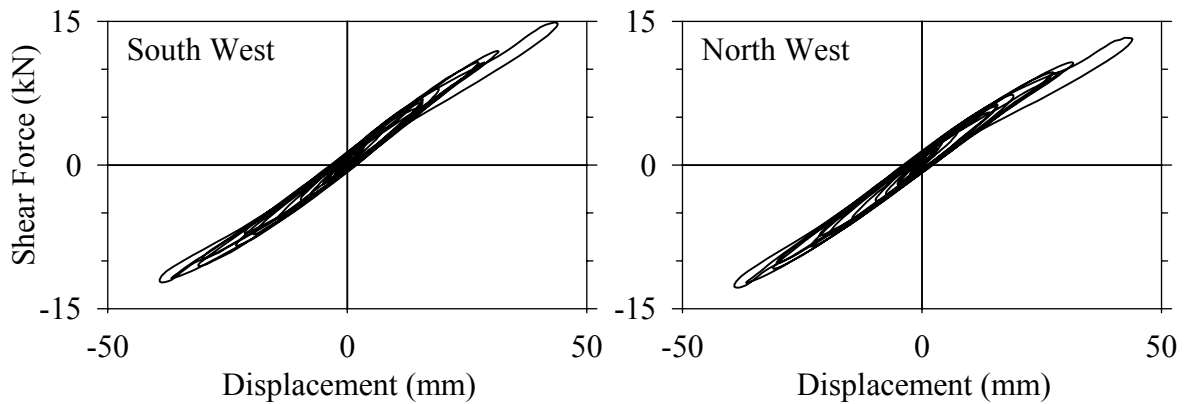
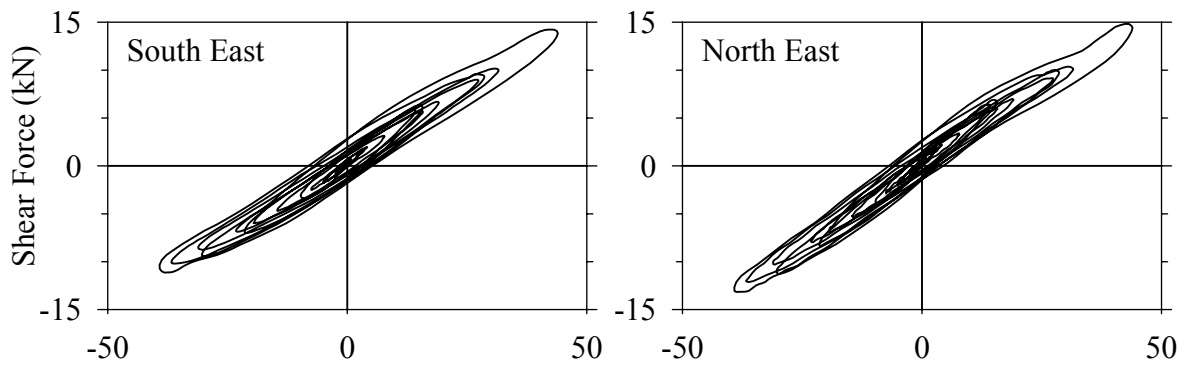
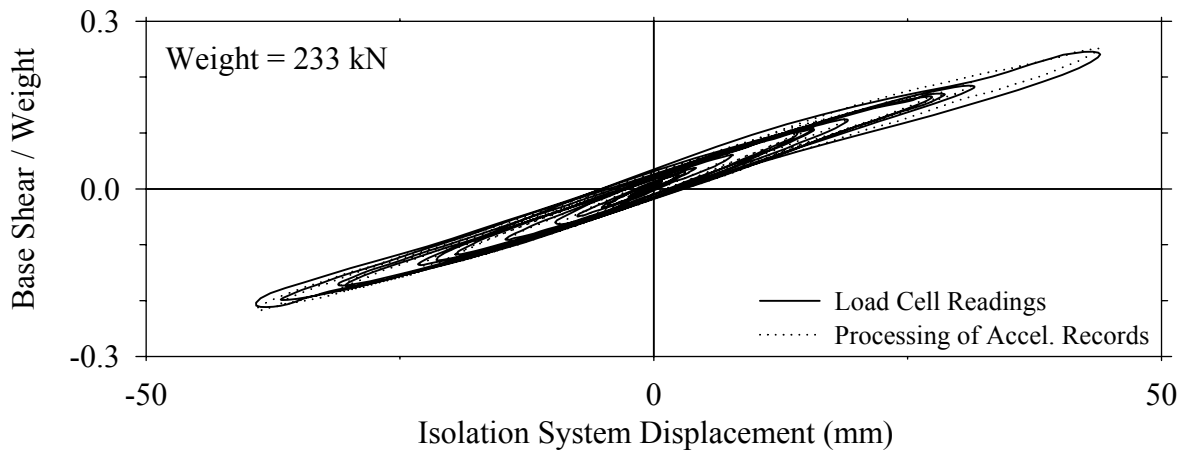
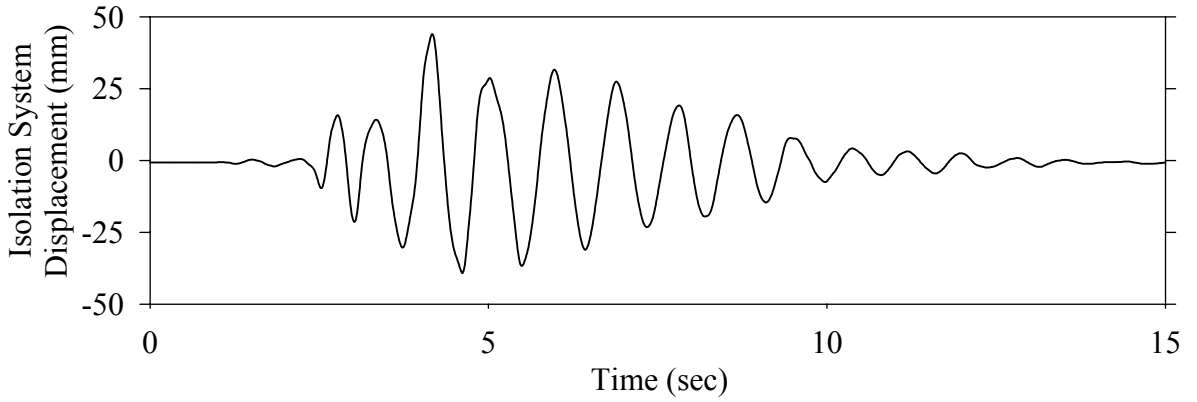




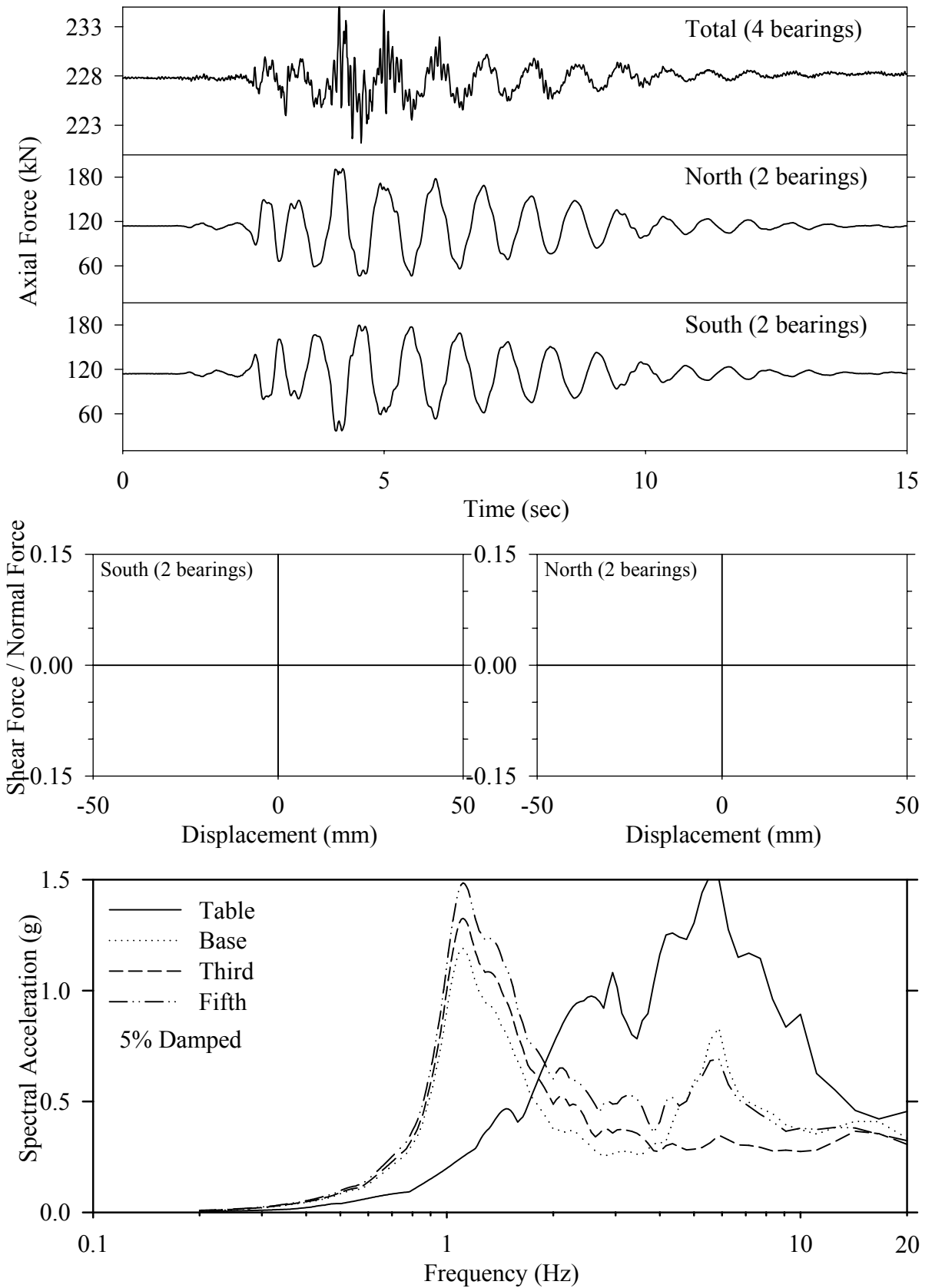
Test LDABE20.1, El Centro S00E 200%, AB/Low Damping Elastomeric



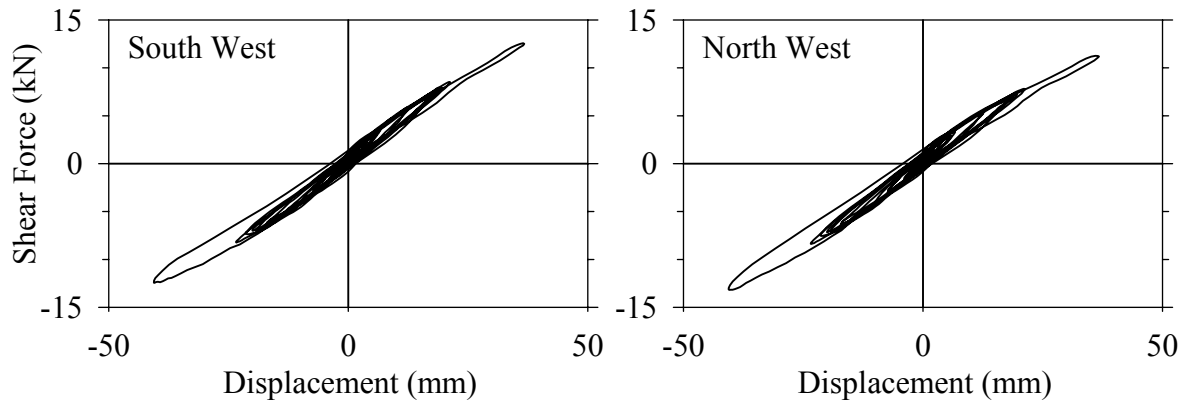
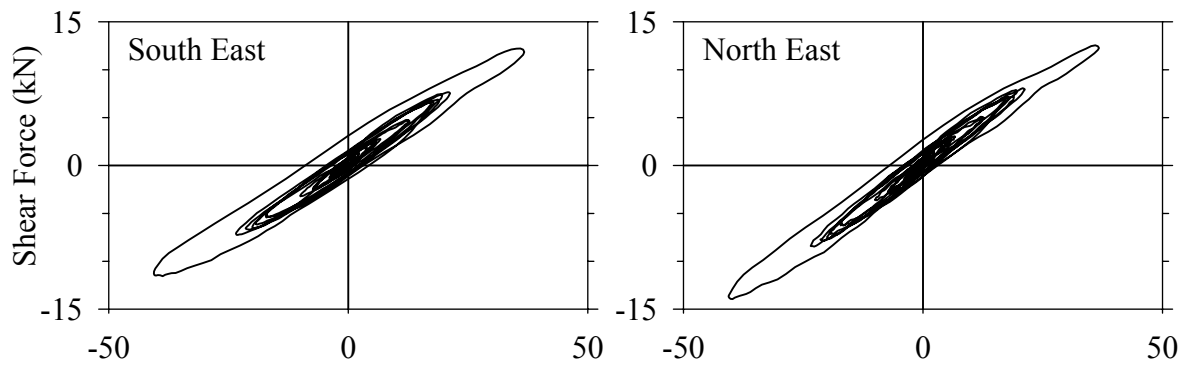
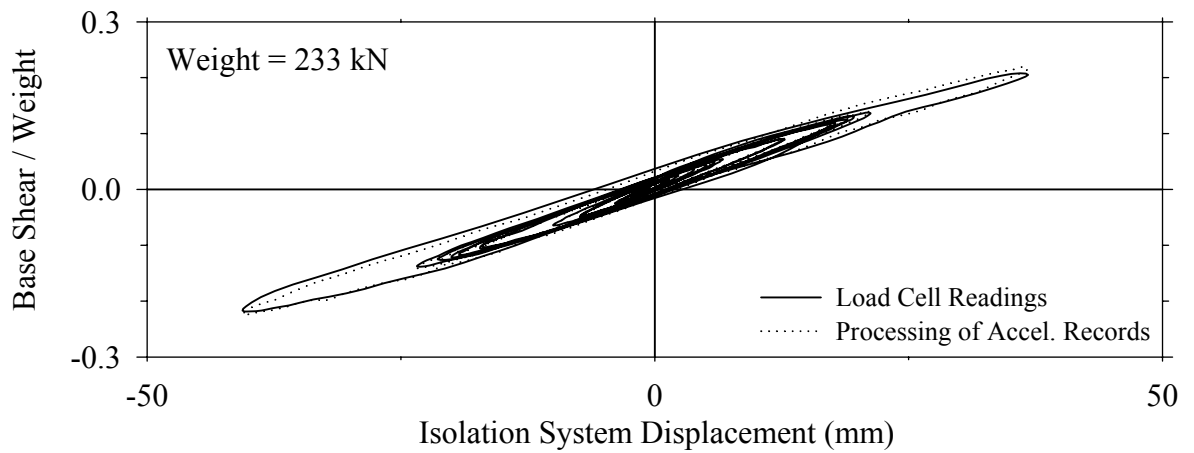
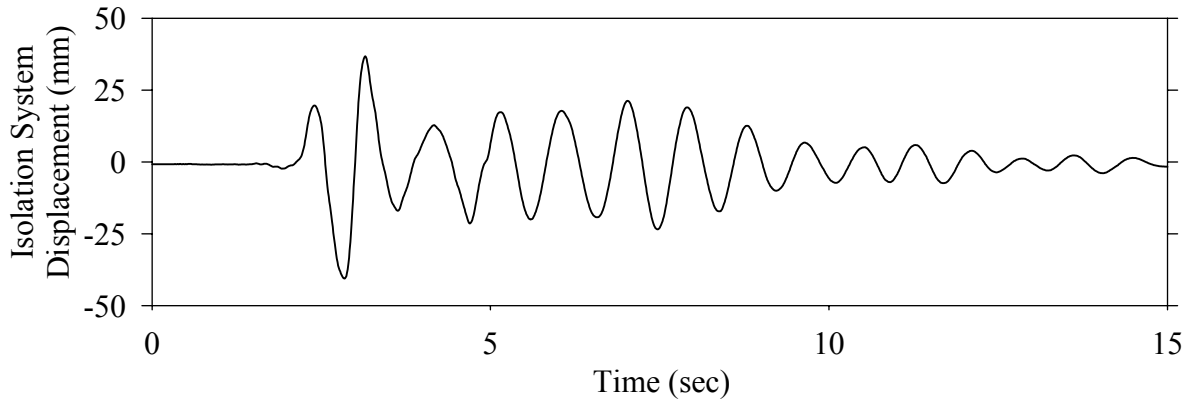
Test LDABK50.1, Kobe N-S 50%, AB/Low Damping Elastomeric



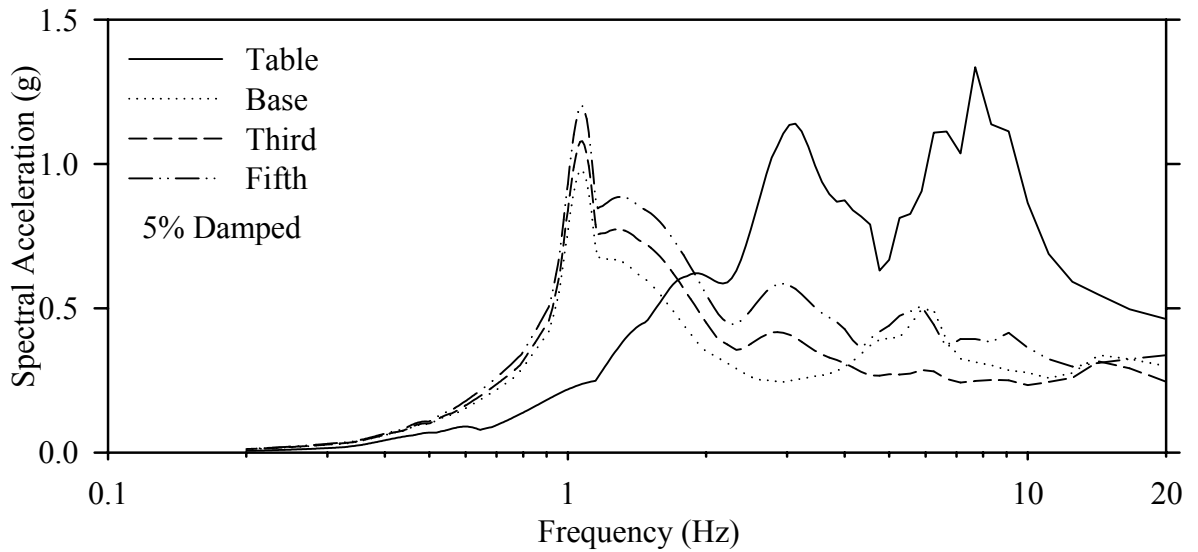
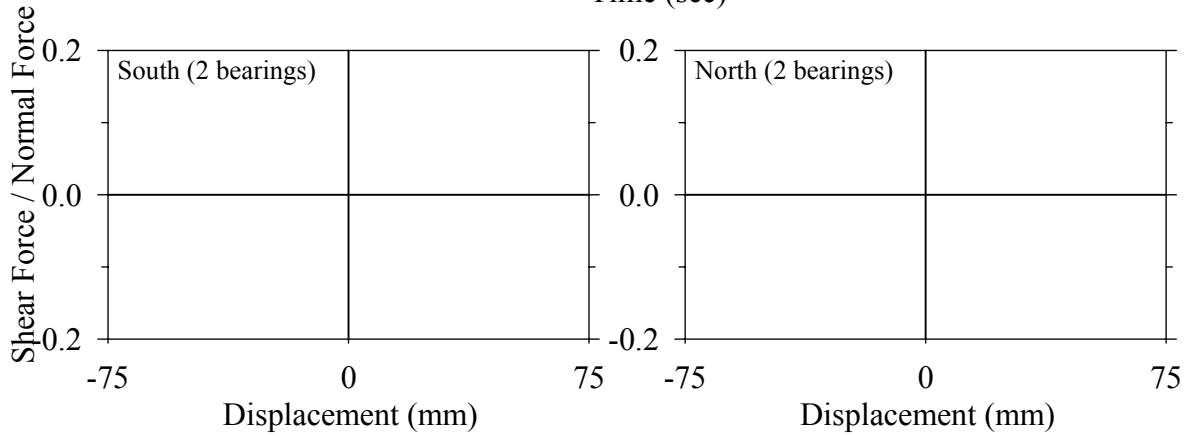
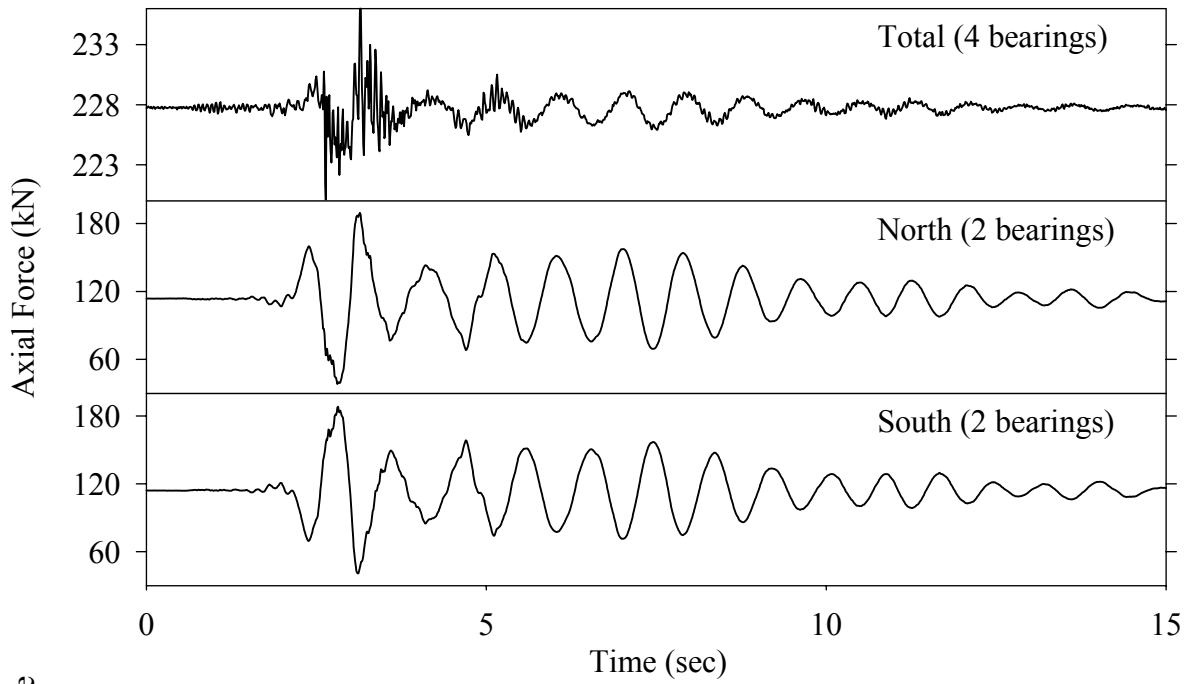
Test LDABK50.1, Kobe N-S 50%, AB/Low Damping Elastomeric



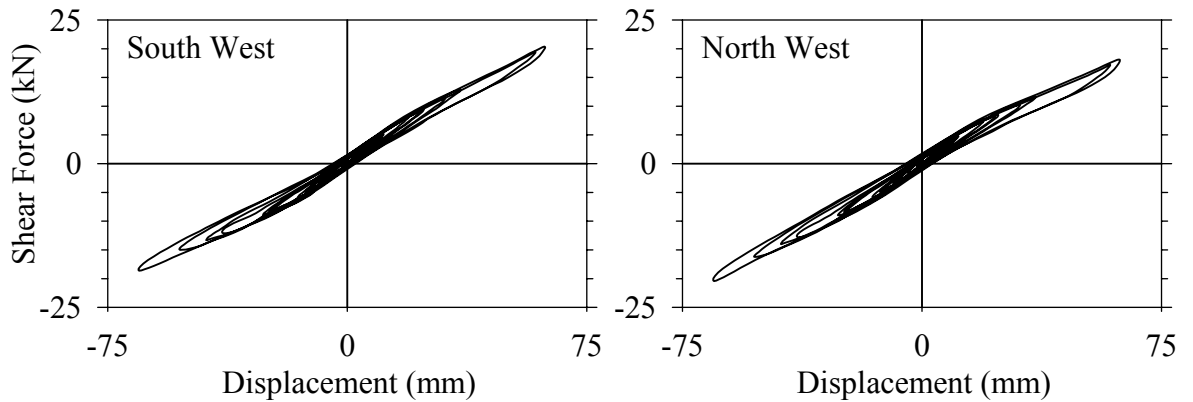
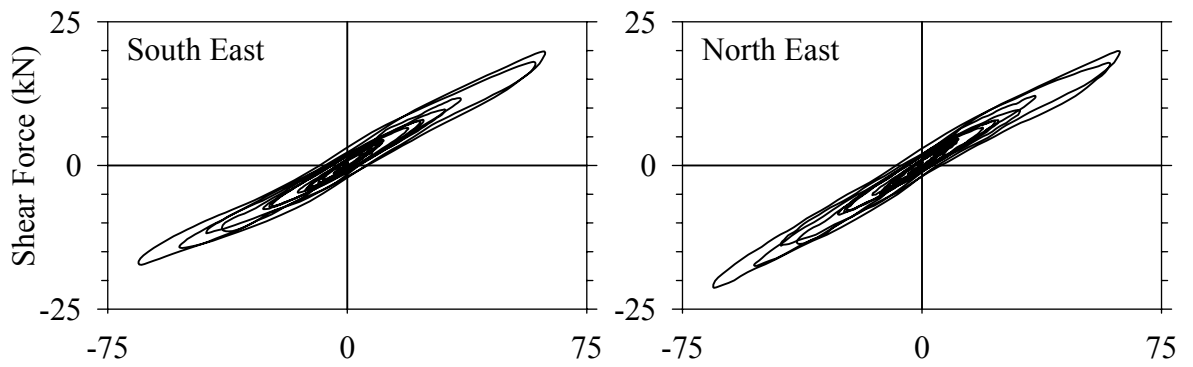
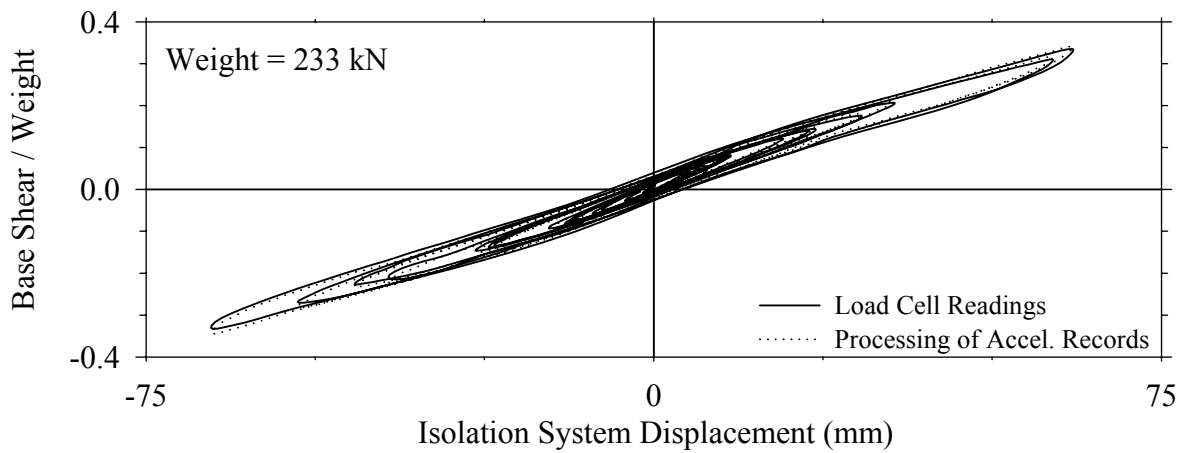
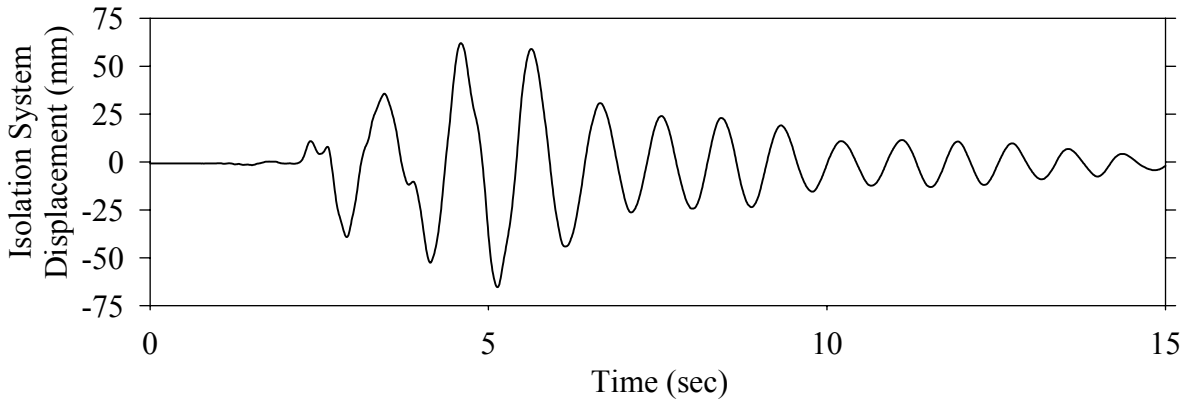
Test LDABN50.1, Northridge Newhall 360° 50%, AB/Low Damping Elastomeric



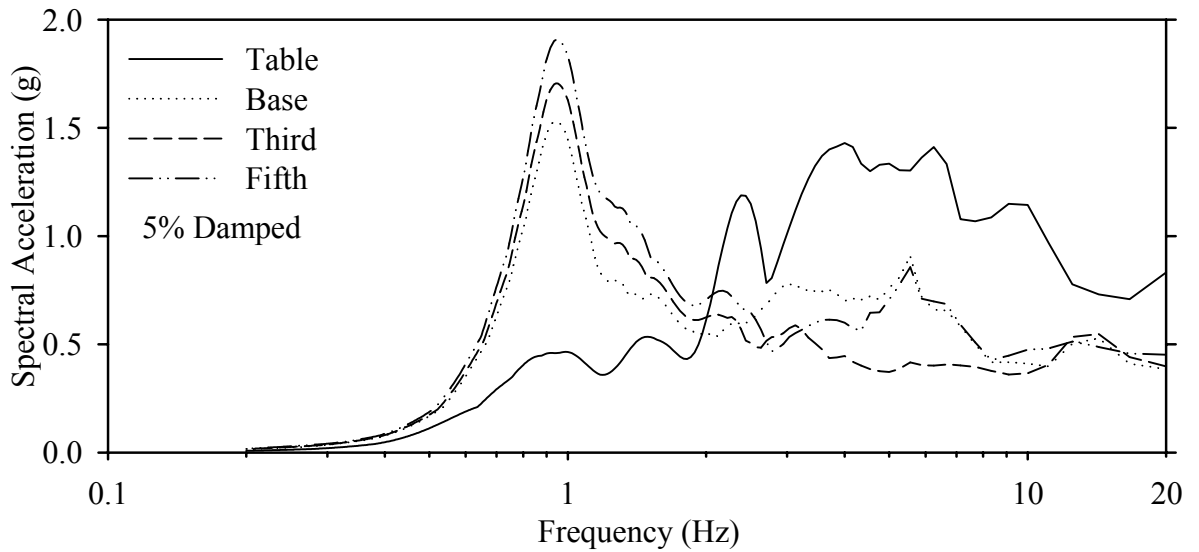
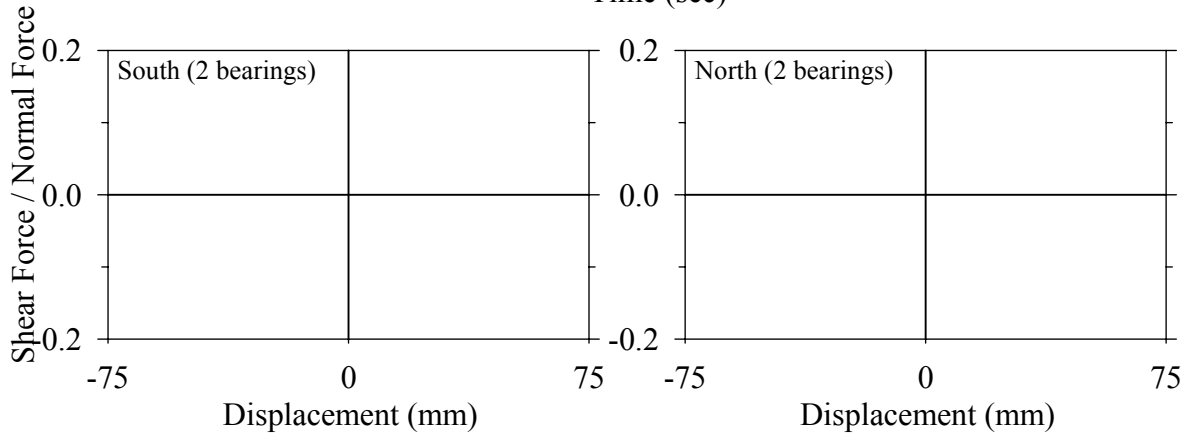
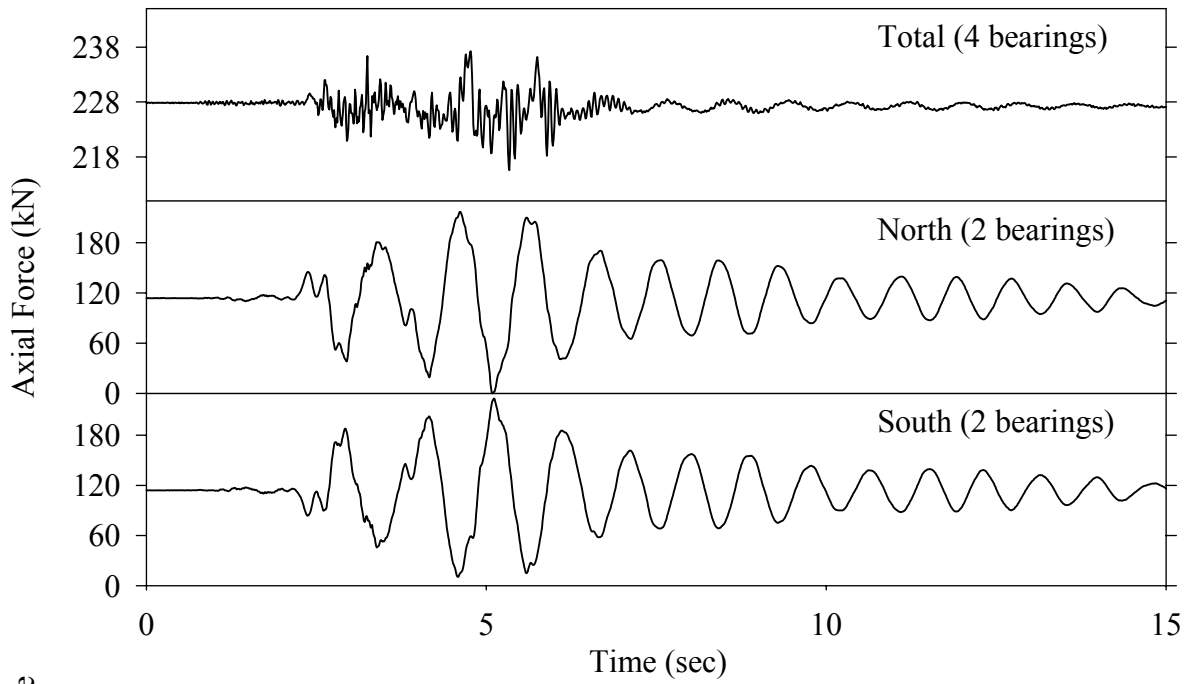
Test LDABN50.1, Northridge Newhall 360° 50%, AB/Low Damping Elastomeric



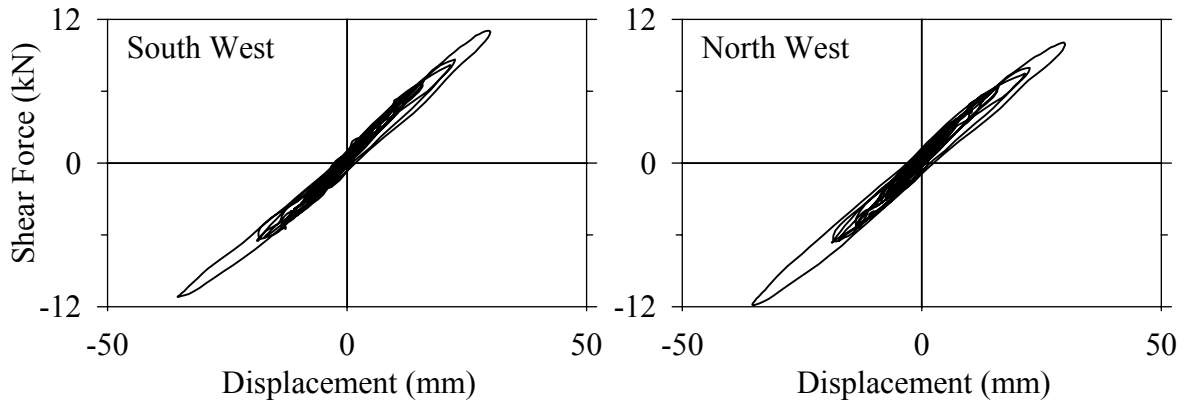
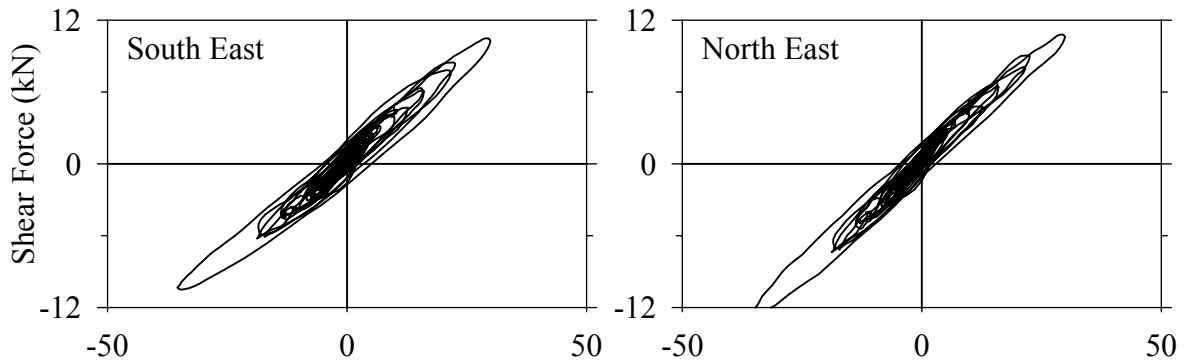
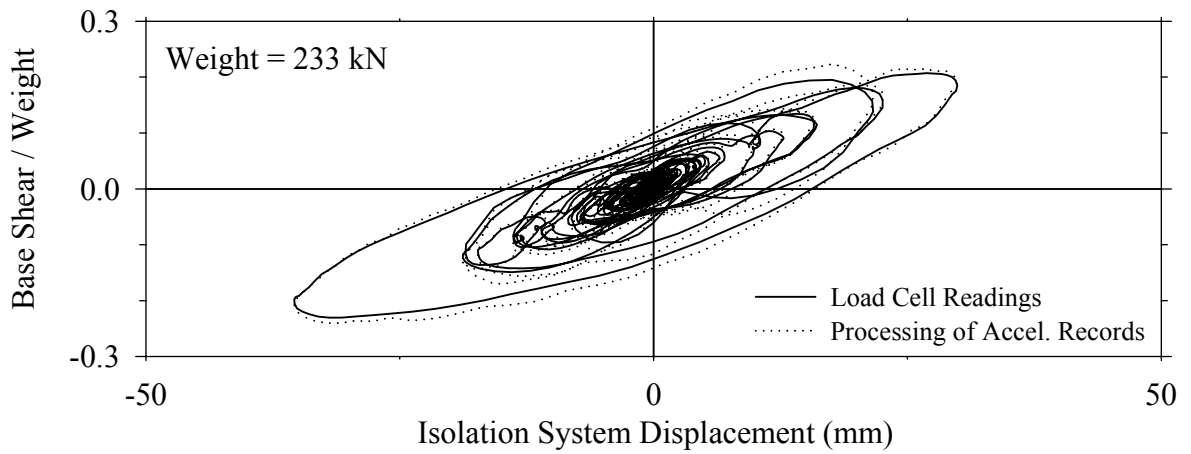
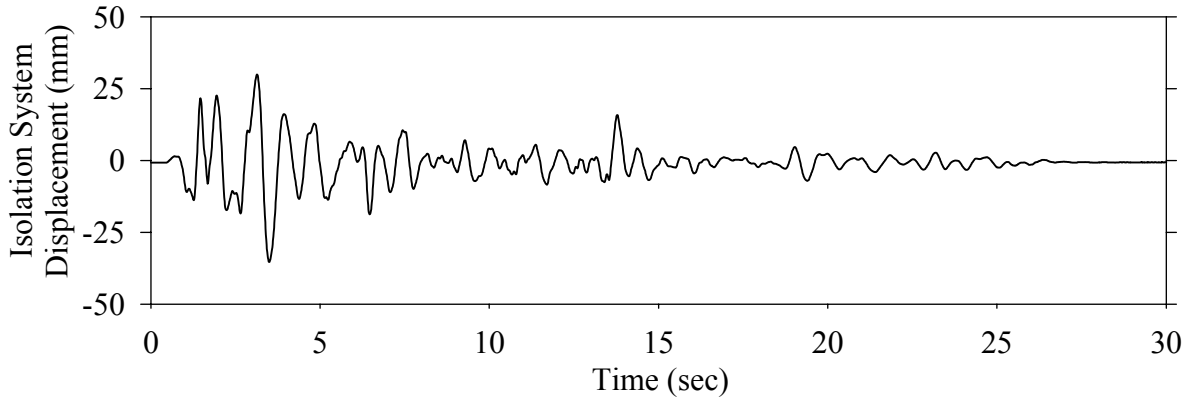
Test LDABS10.1, Northridge Sylmar 90° 100%, AB/Low Damping Elastomeric



Test LDABS10.1, Northridge Sylmar 90° 100%, AB/Low Damping Elastomeric

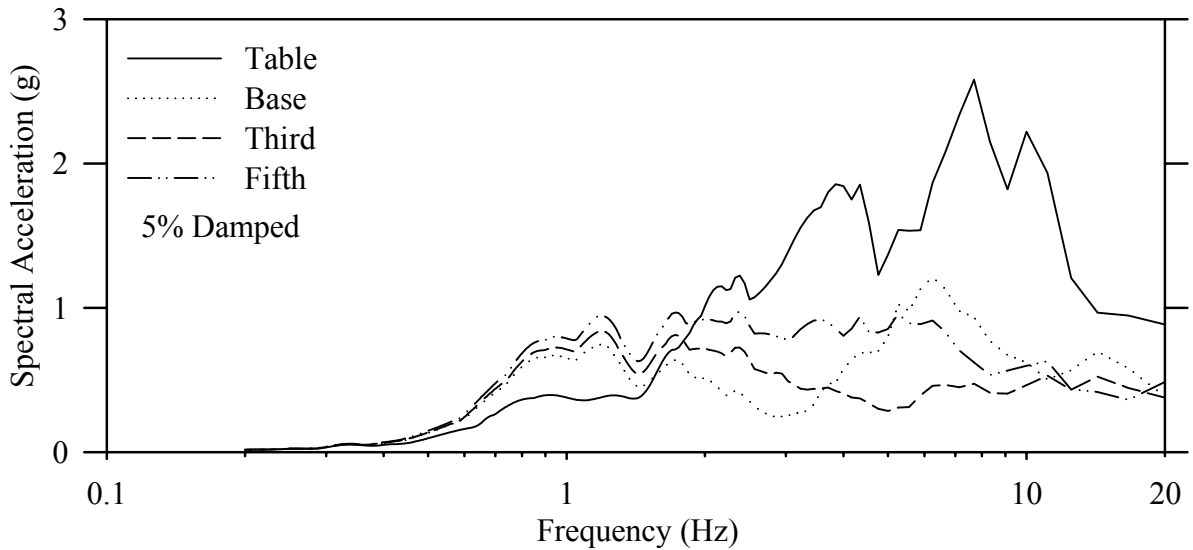
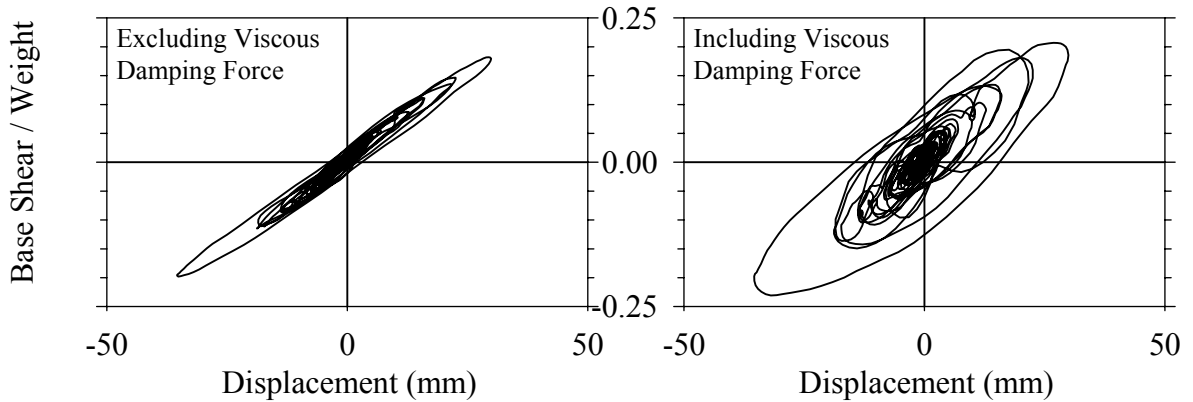
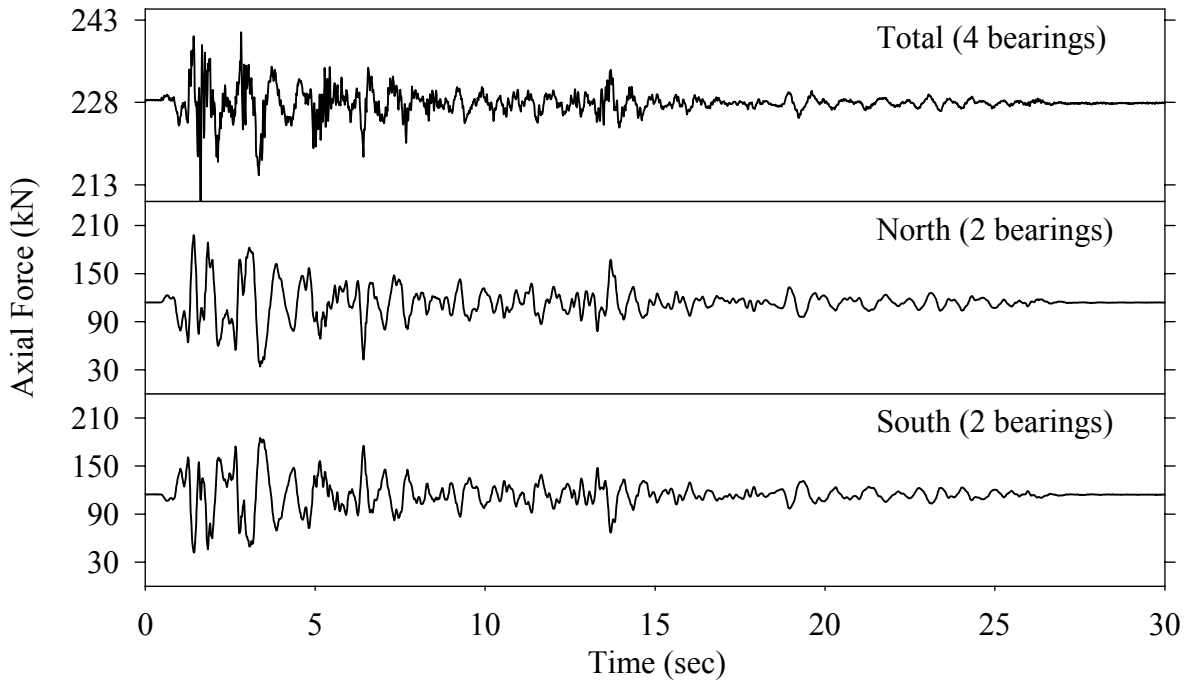


Test LDALE20.1, El Centro S00E 200%, AB/Low Damping Elastomeric-Linear Dampers

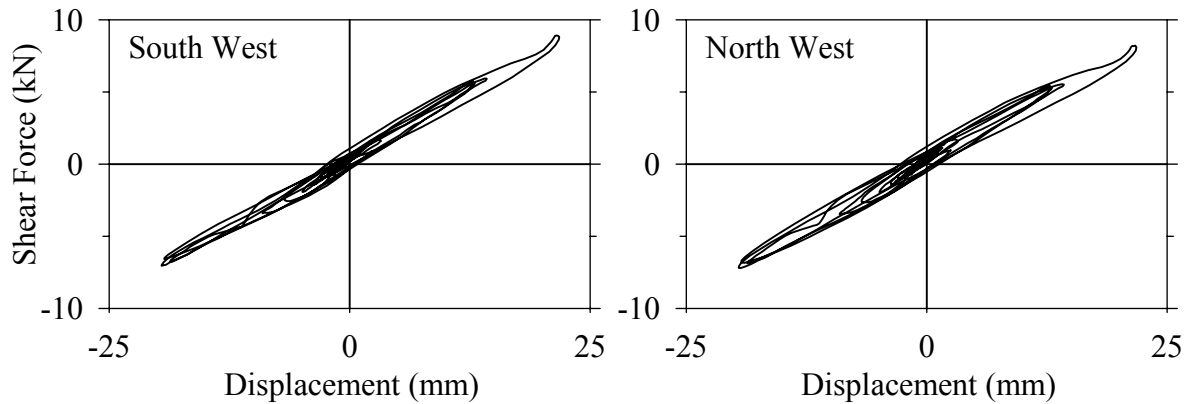
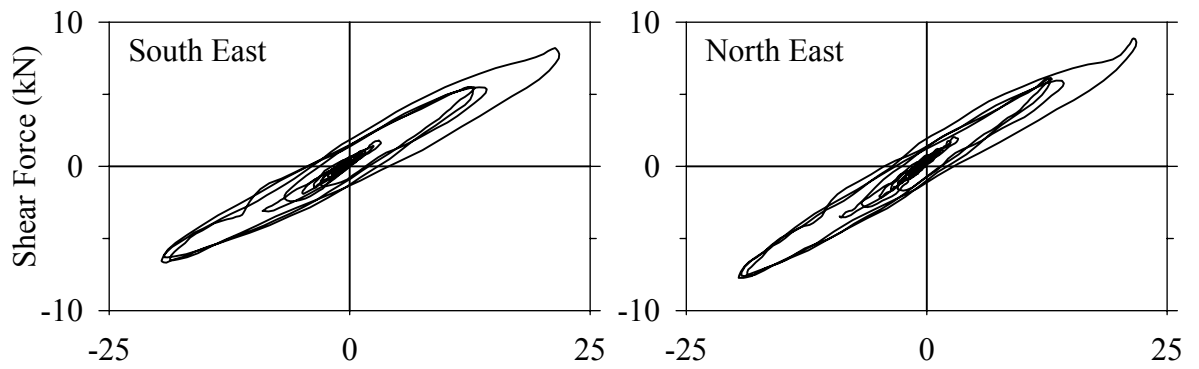
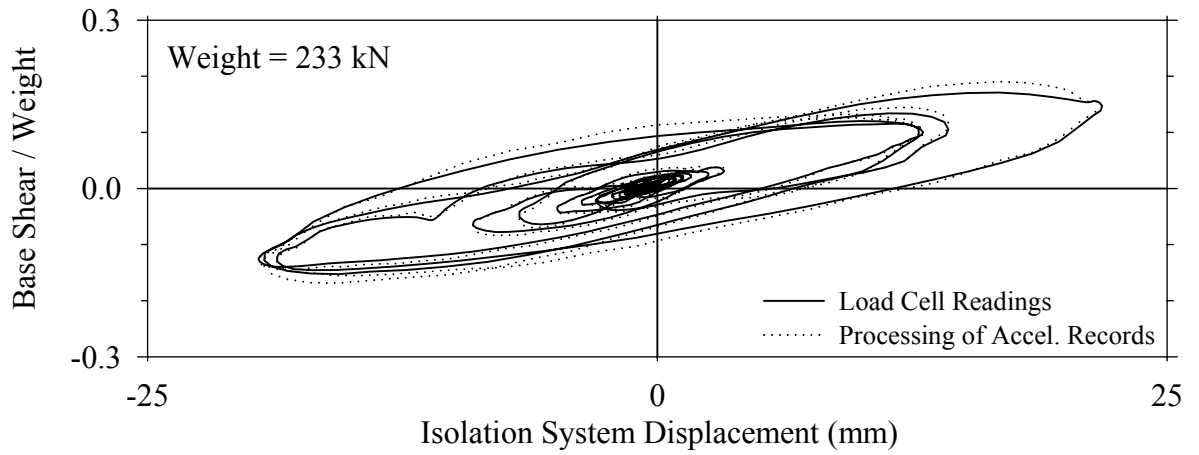
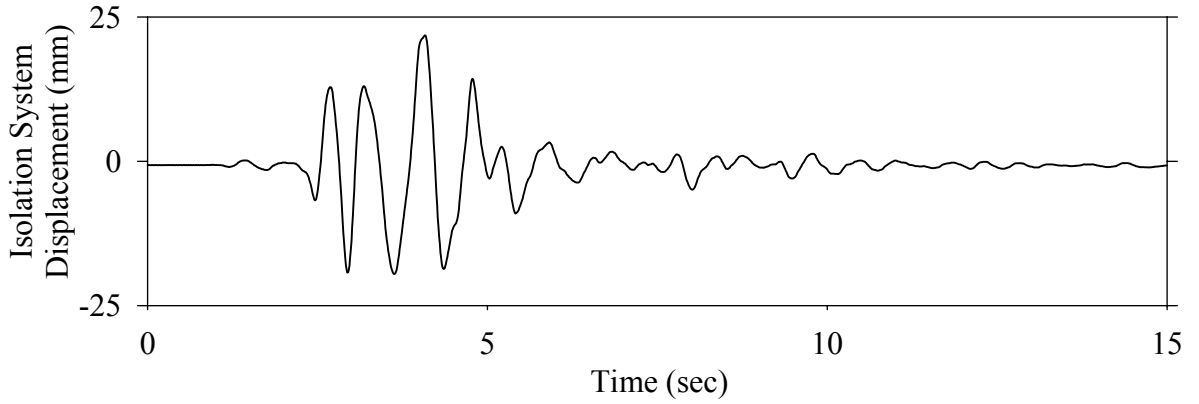




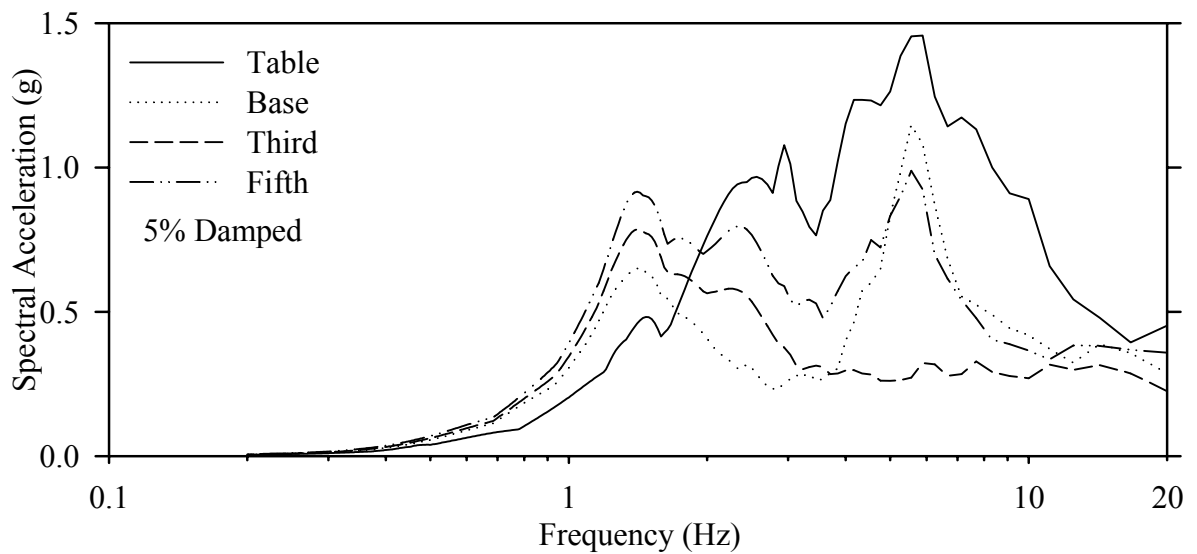
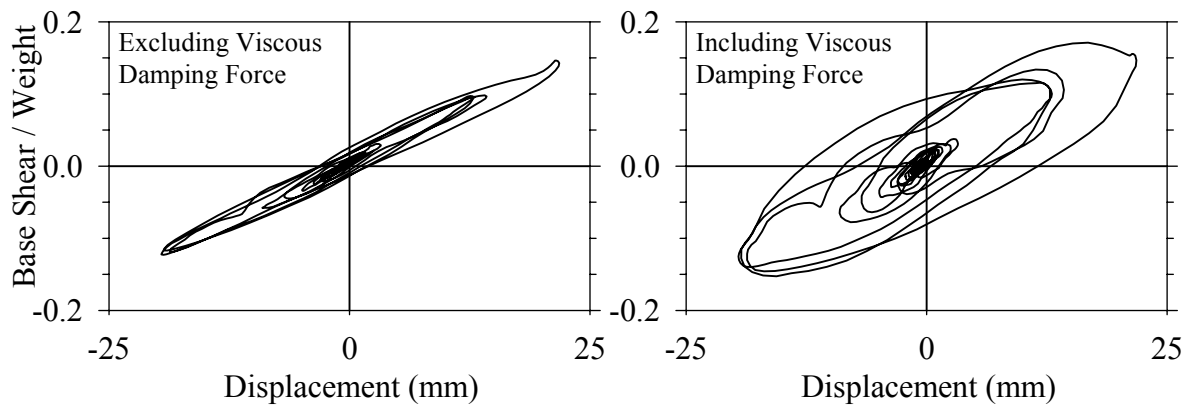
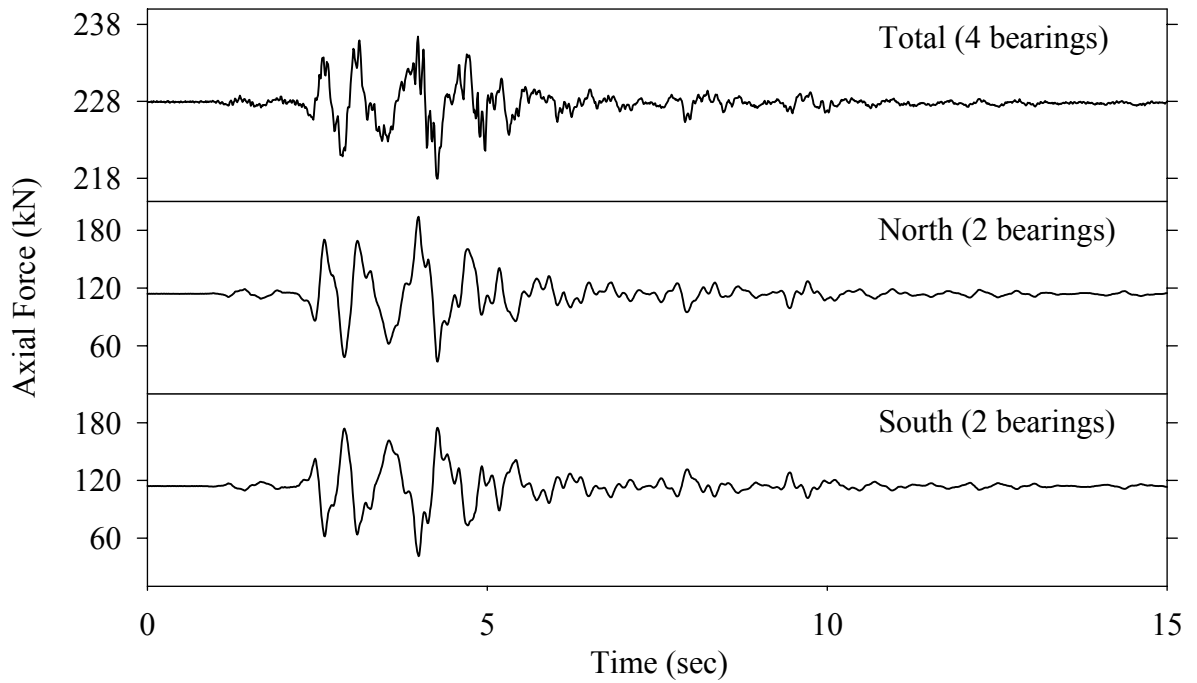
Test LDALE20.1, El Centro S00E 200%, AB/Low Damping Elastomeric-Linear Dampers



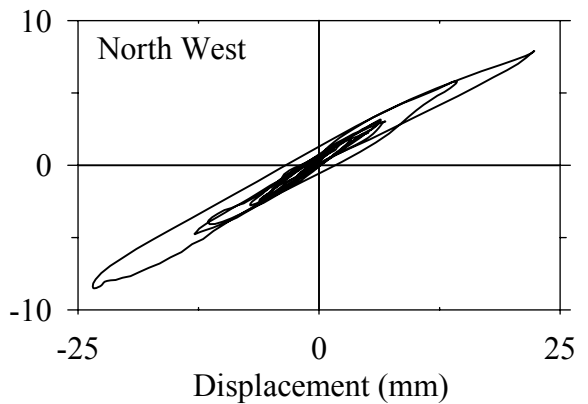
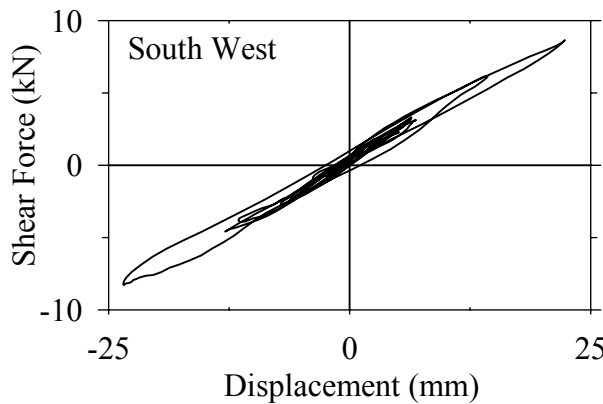
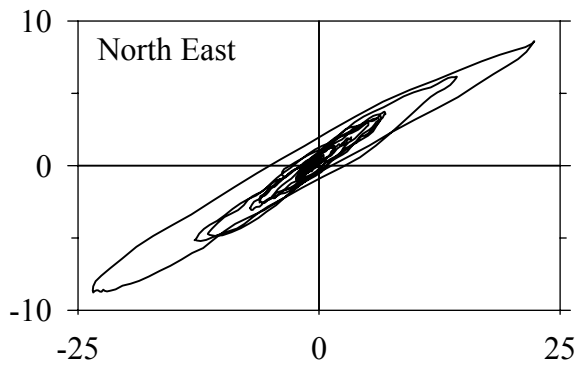
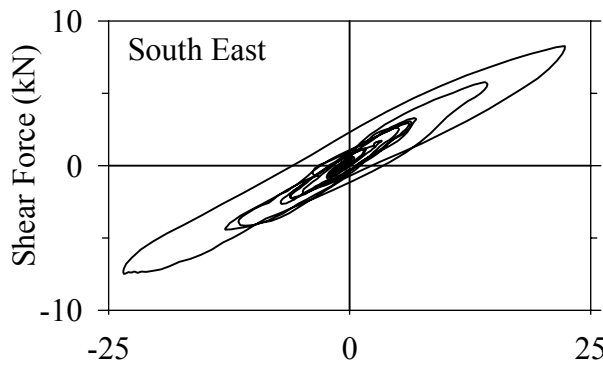
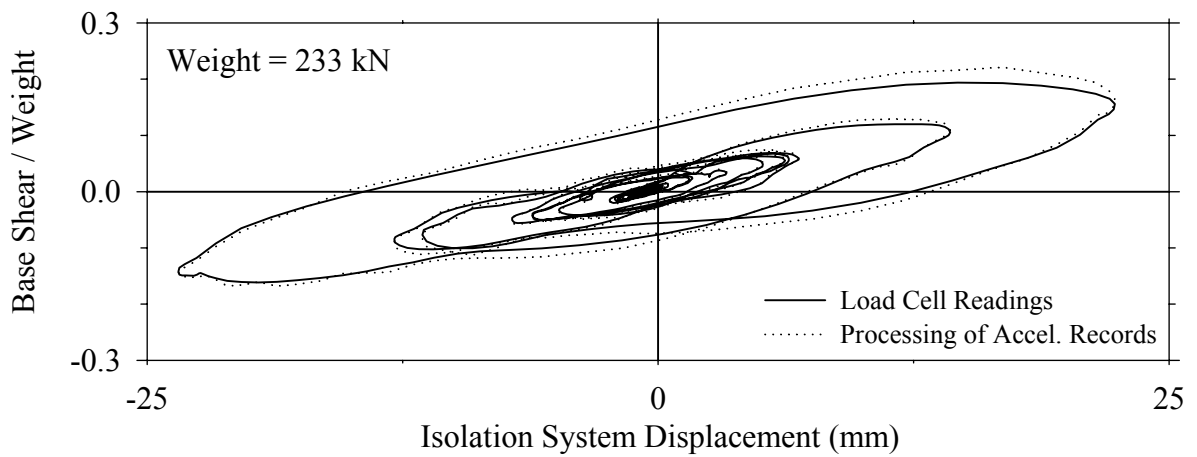
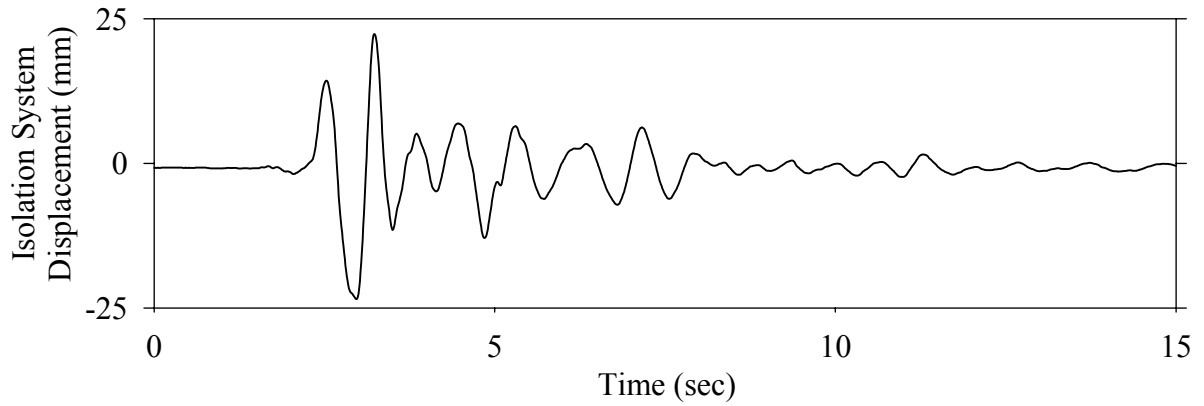
Test LDALK50.1, Kobe N-S 50%, AB/Low Damping Elastomeric-Linear Dampers



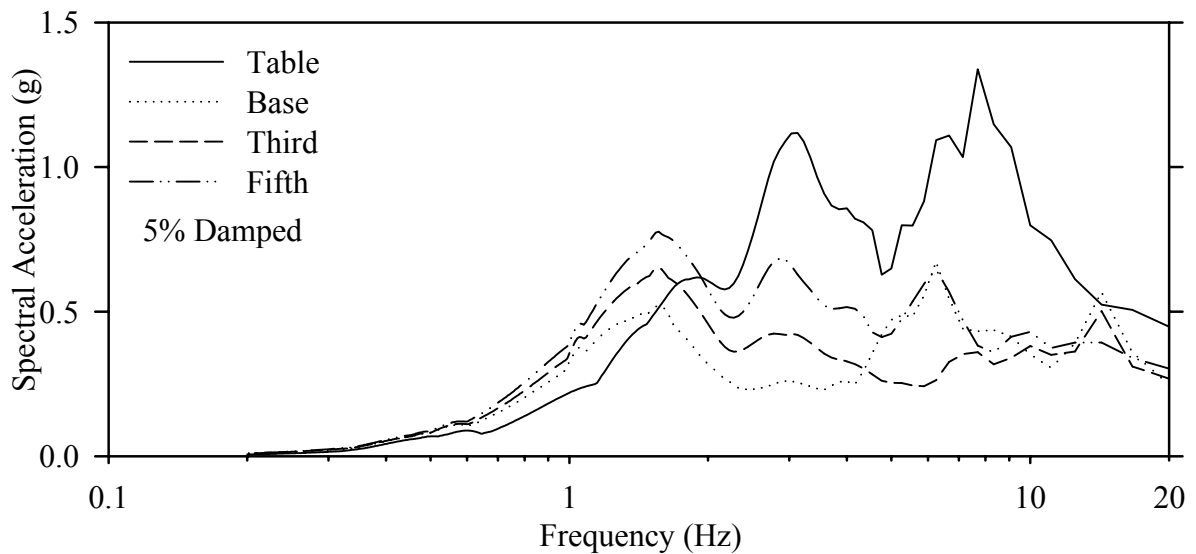
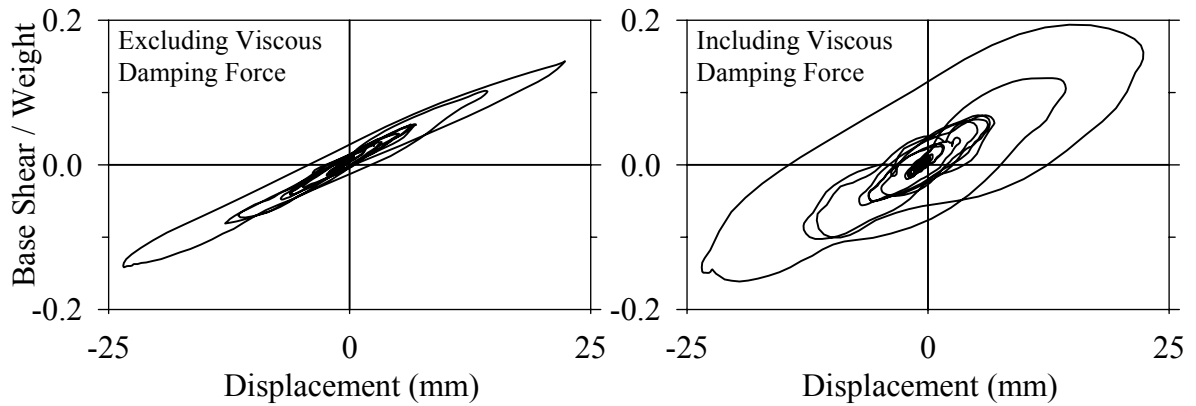
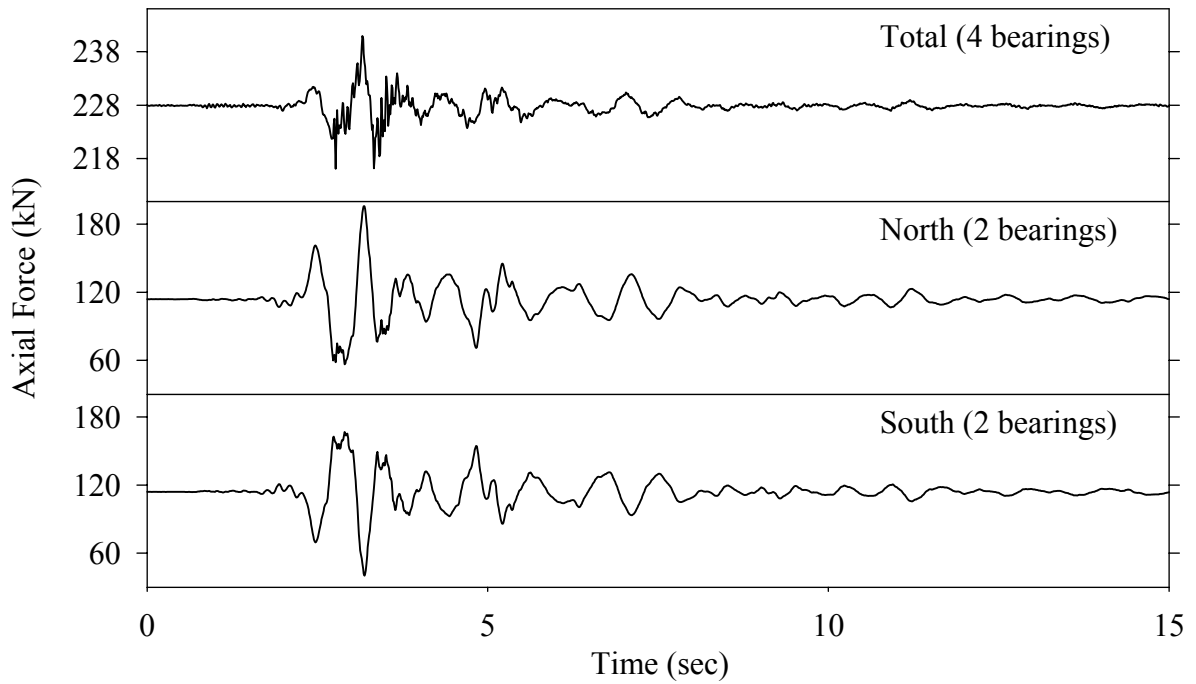
Test LDALK50.1, Kobe N-S 50%, AB/Low Damping Elastomeric-Linear Dampers



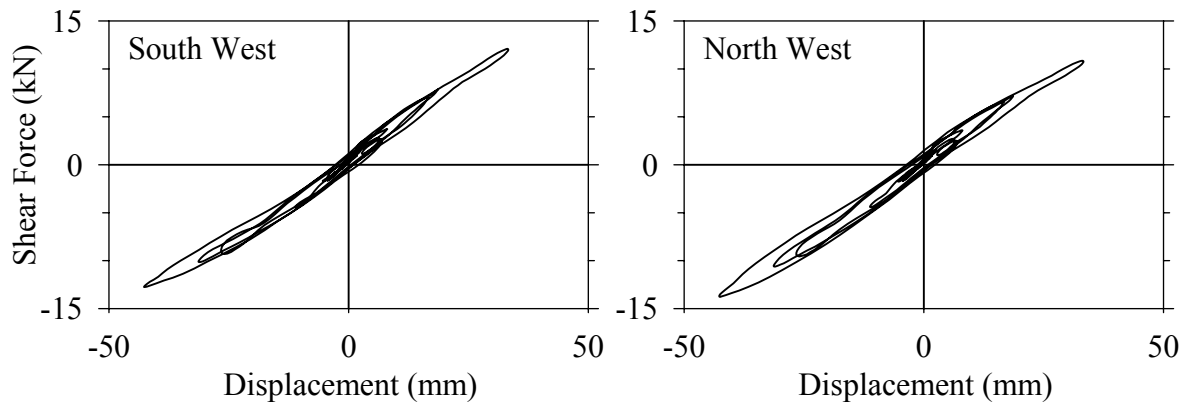
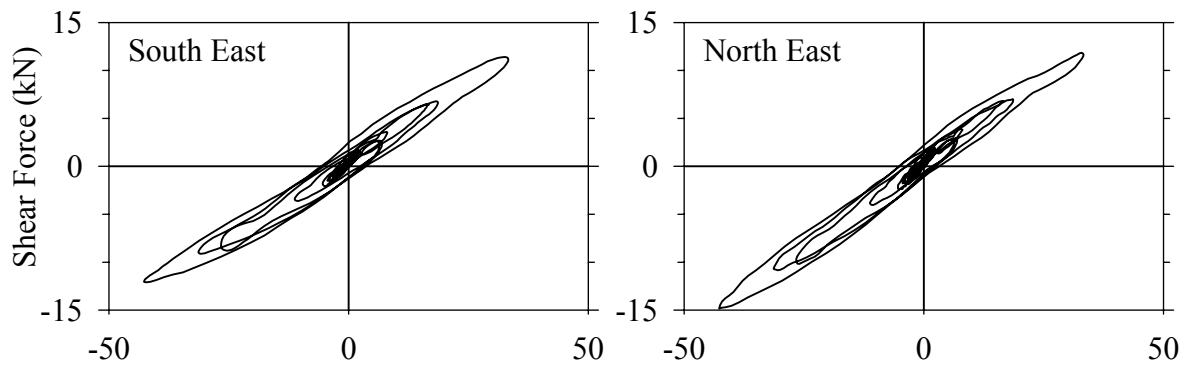
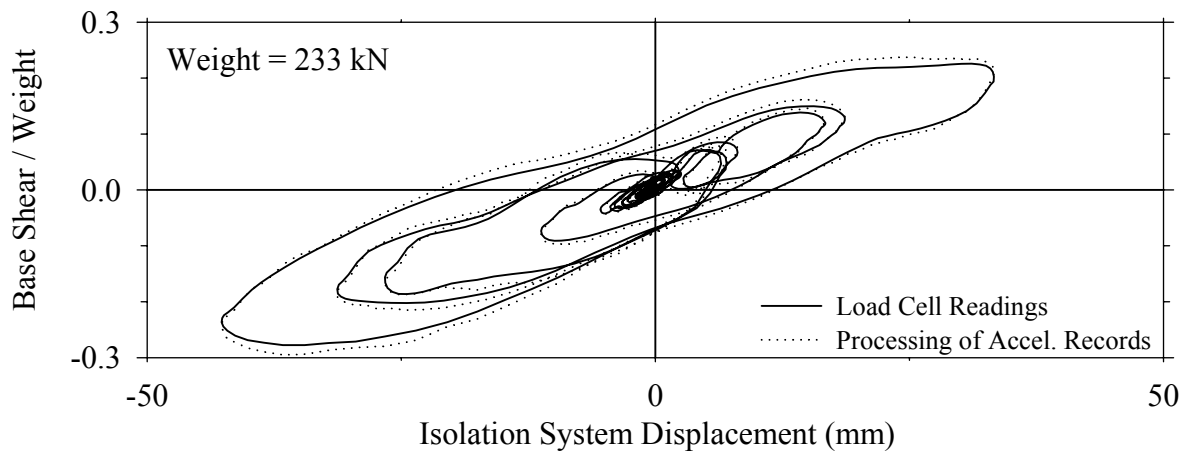
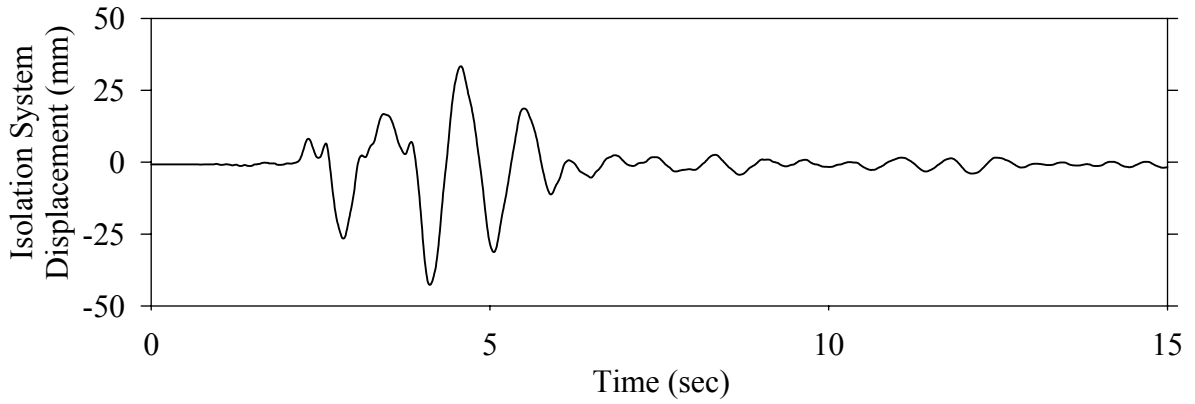
Test LDALN50.1, Northridge Newhall 360° 50%, AB/Low Damping Elastomeric-Linear Dampers



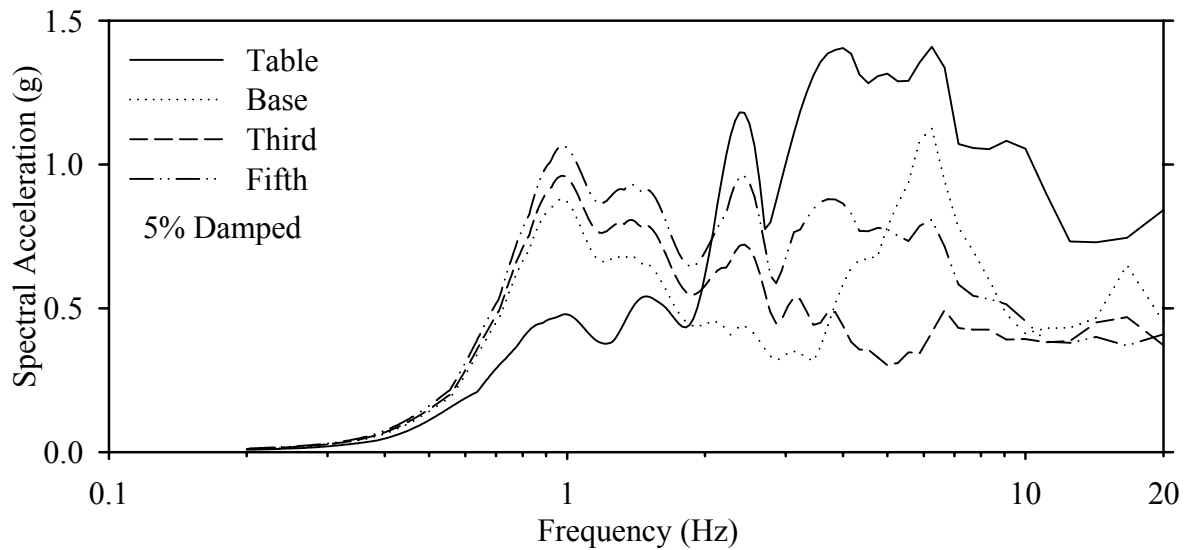
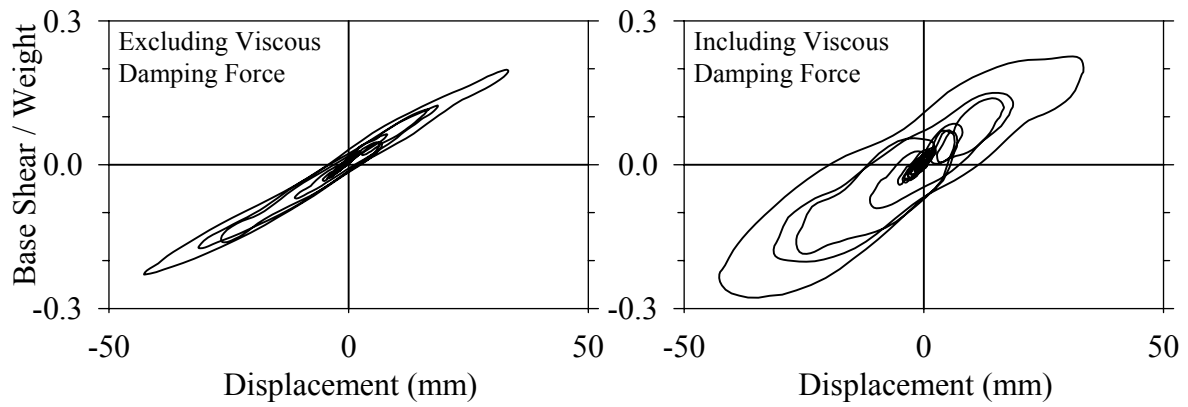
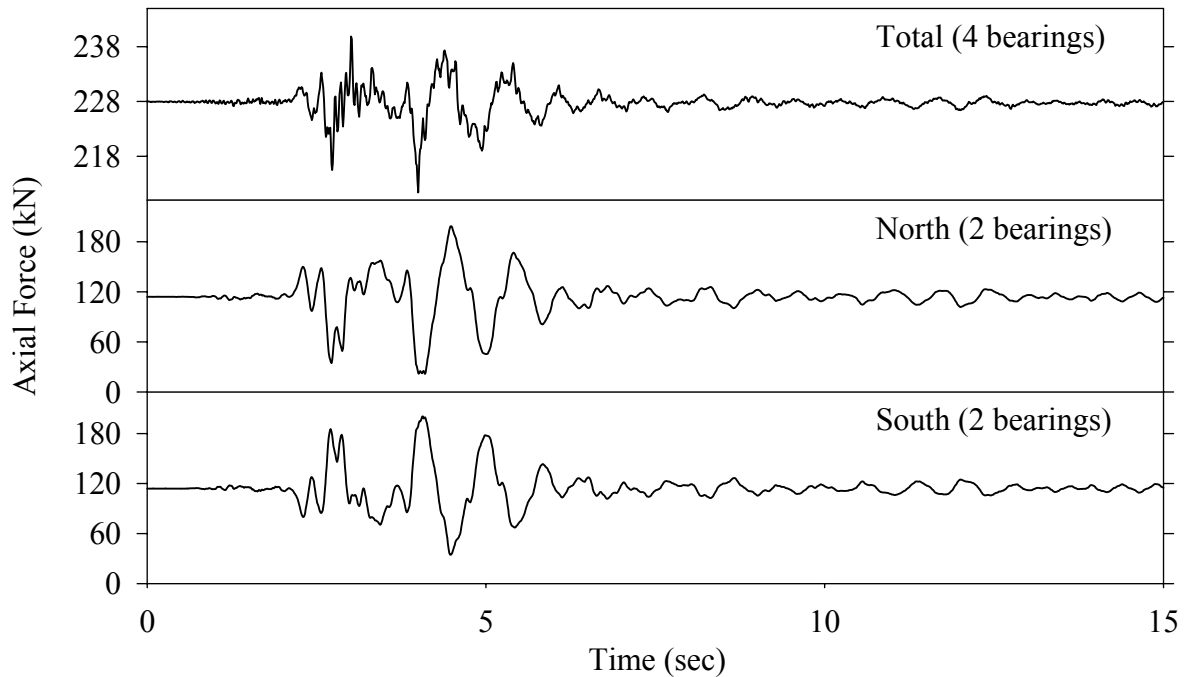
Test LDALN50.1, Northridge Newhall 360° 50%, AB/Low Damping Elastomeric-Linear Dampers



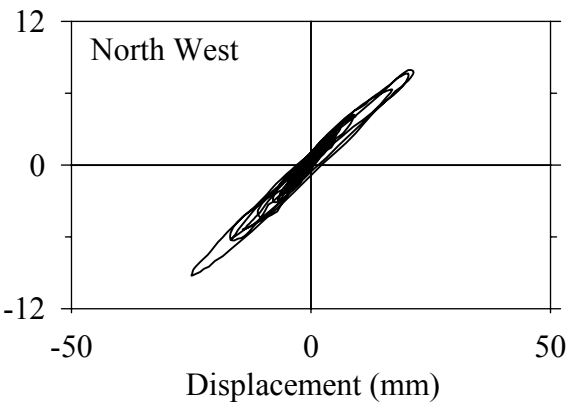
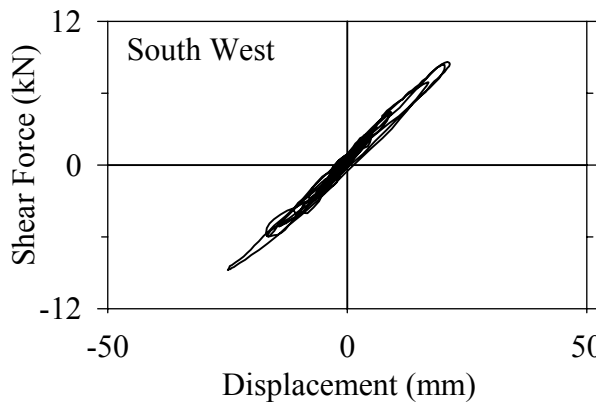
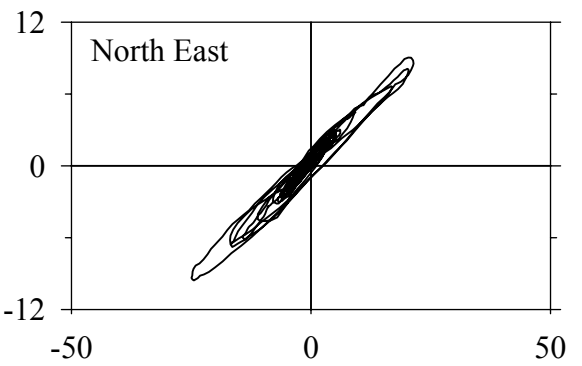
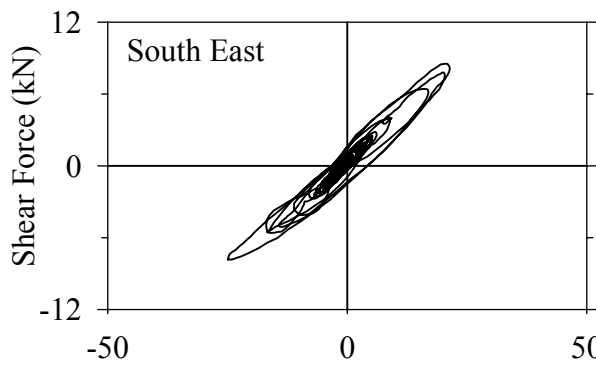
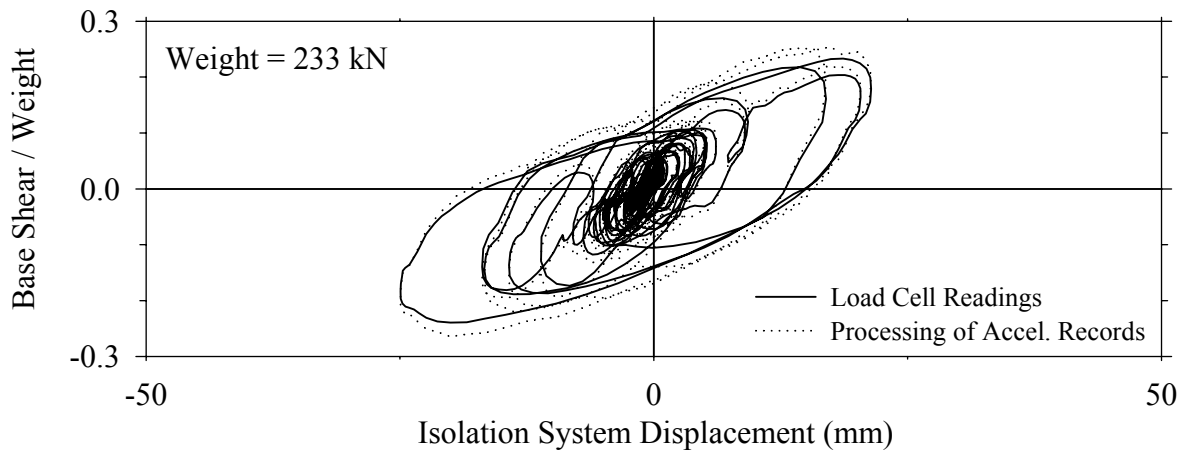
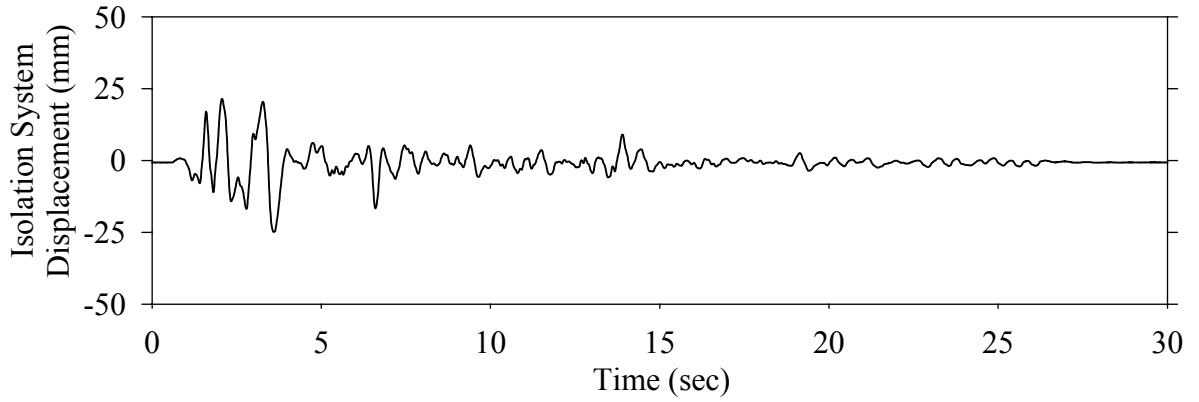
Test LDALS10.1, Northridge Sylmar 90° 100%, AB/Low Damping Elastomeric-Linear Dampers



Test LDALS10.1, Northridge Sylmar 90° 100%, AB/Low Damping Elastomeric-Linear Dampers

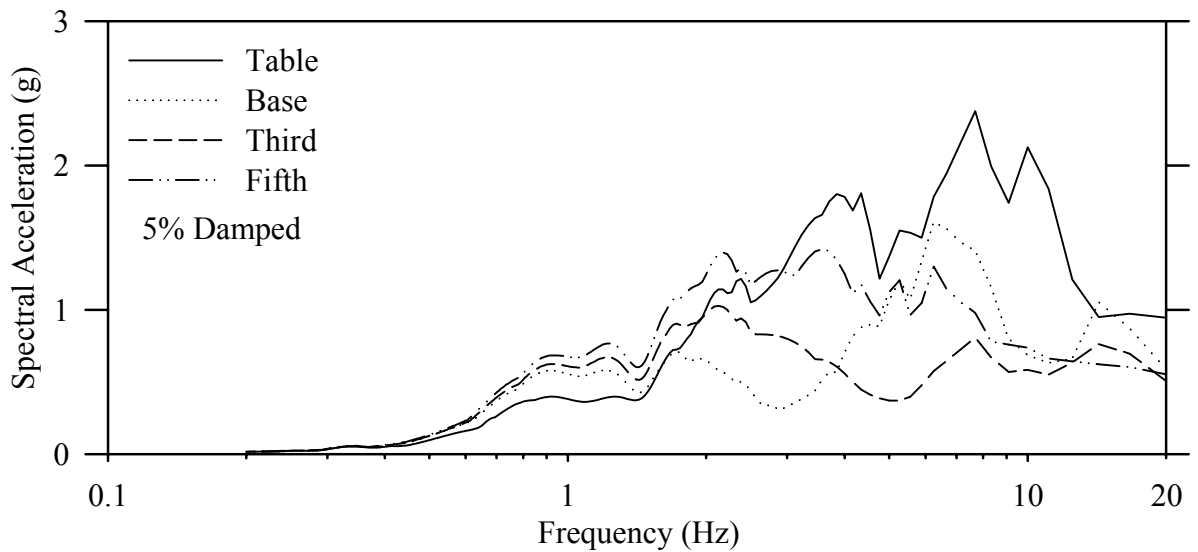
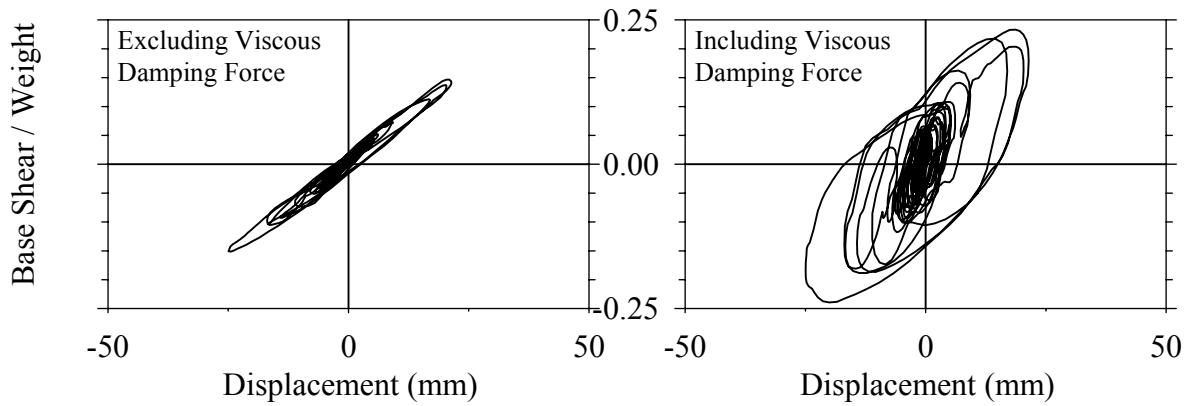
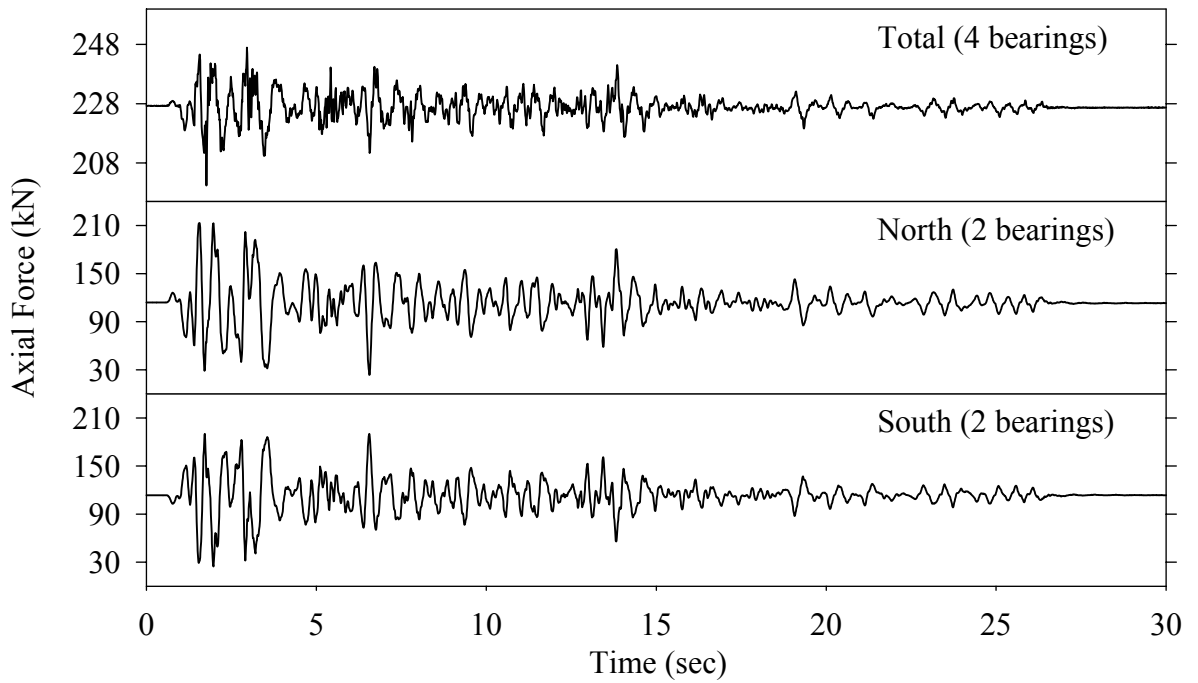


Test LDANE20.1, El Centro S00E 200%, AB/Low Damping Elastomeric-Nonlinear Dampers

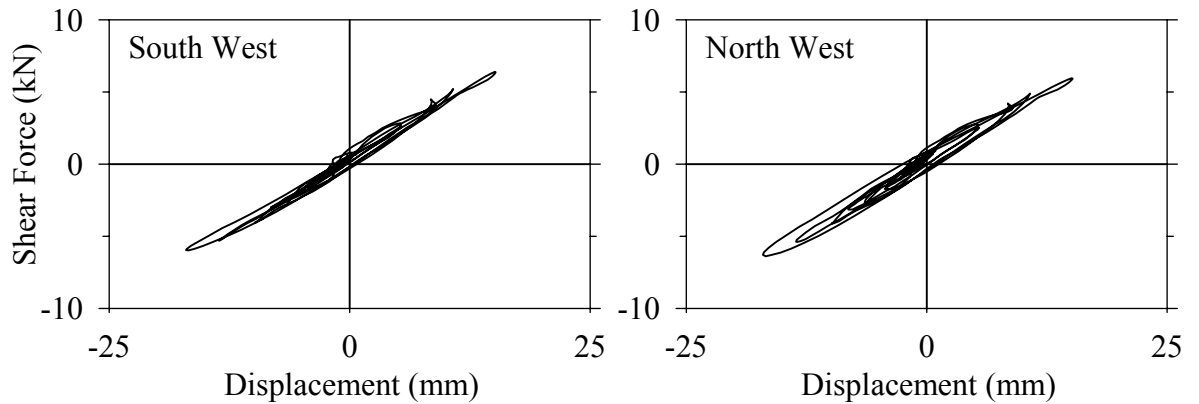
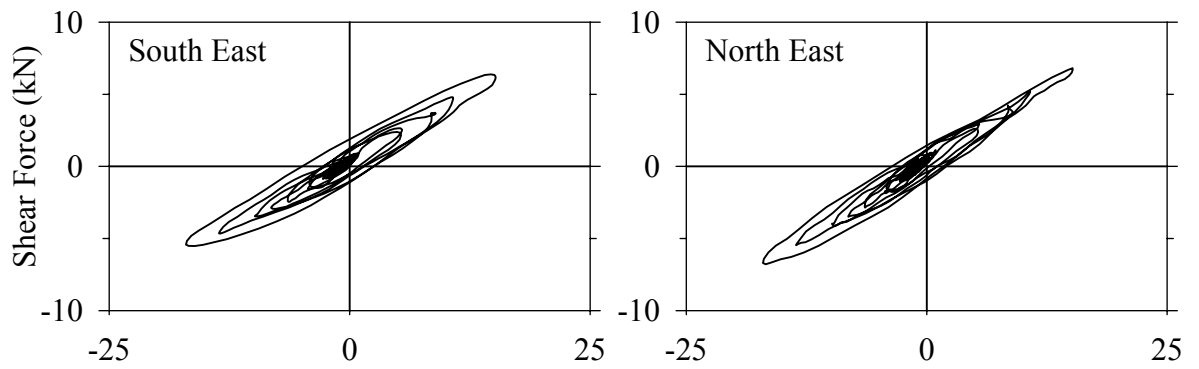
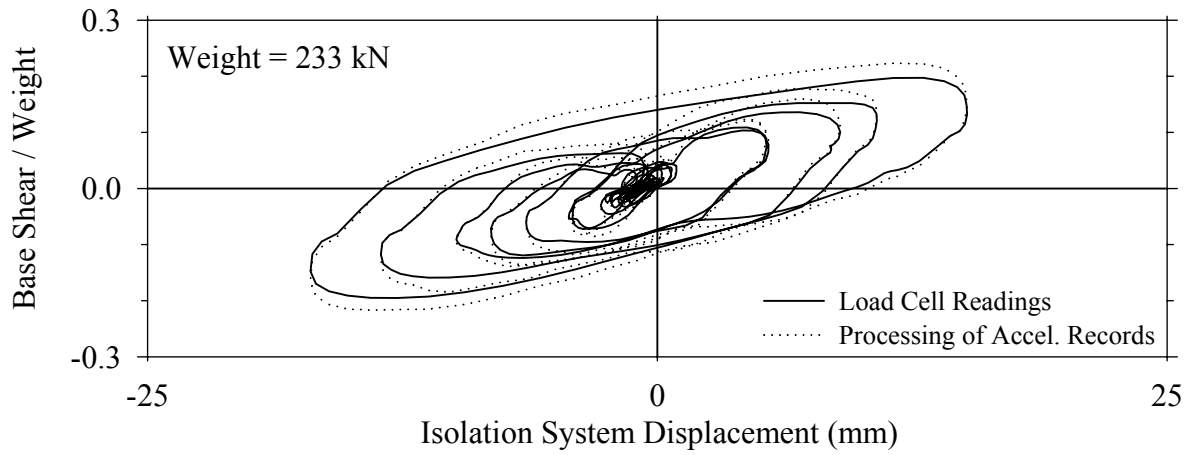
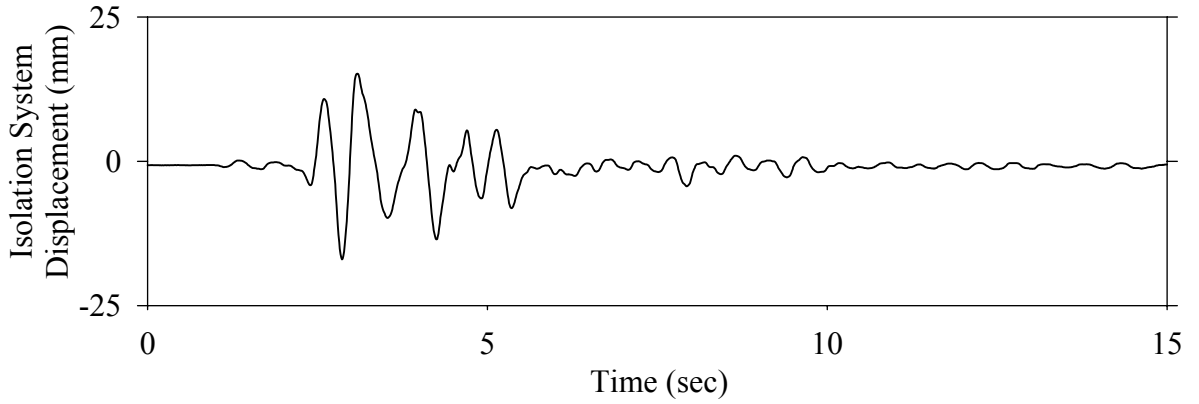




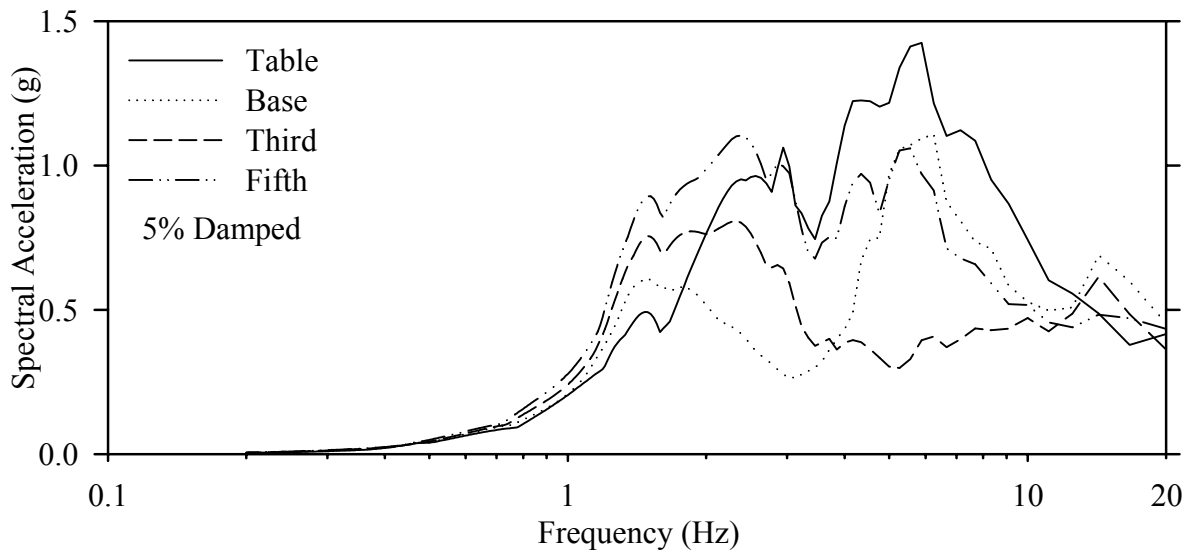
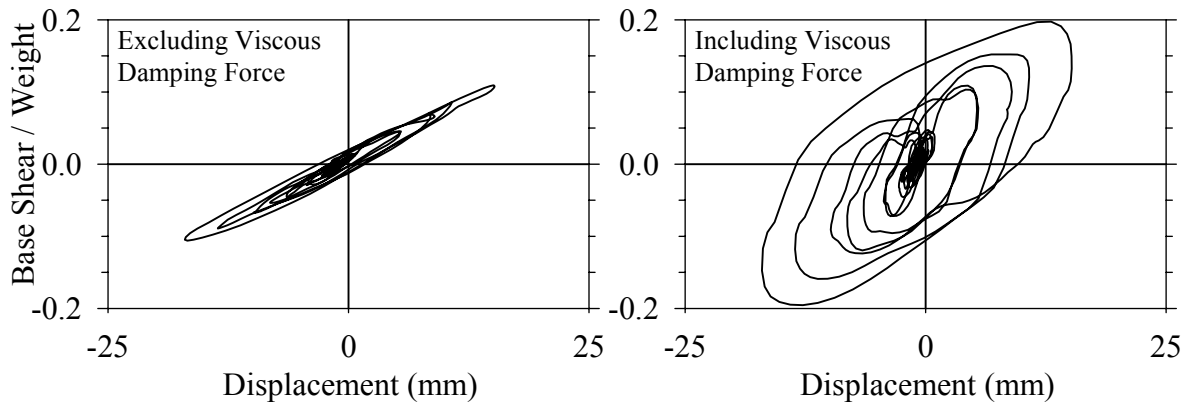
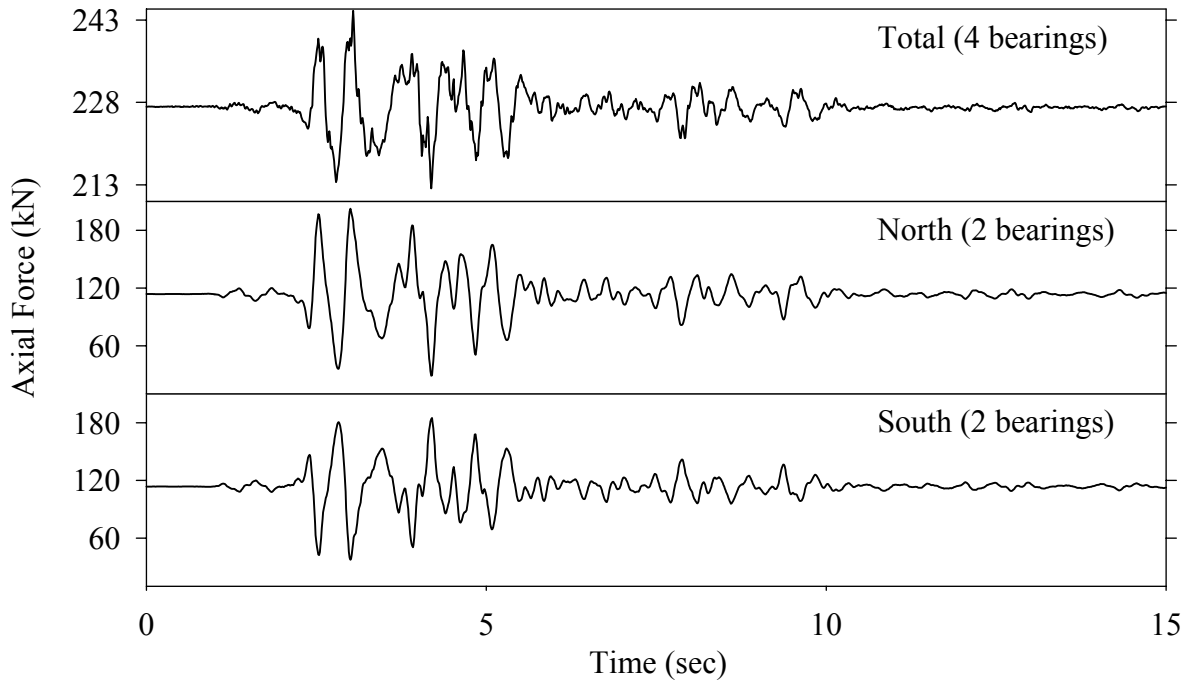
Test LDANE20.1, El Centro S00E 200%, AB/Low Damping Elastomeric-Nonlinear Dampers



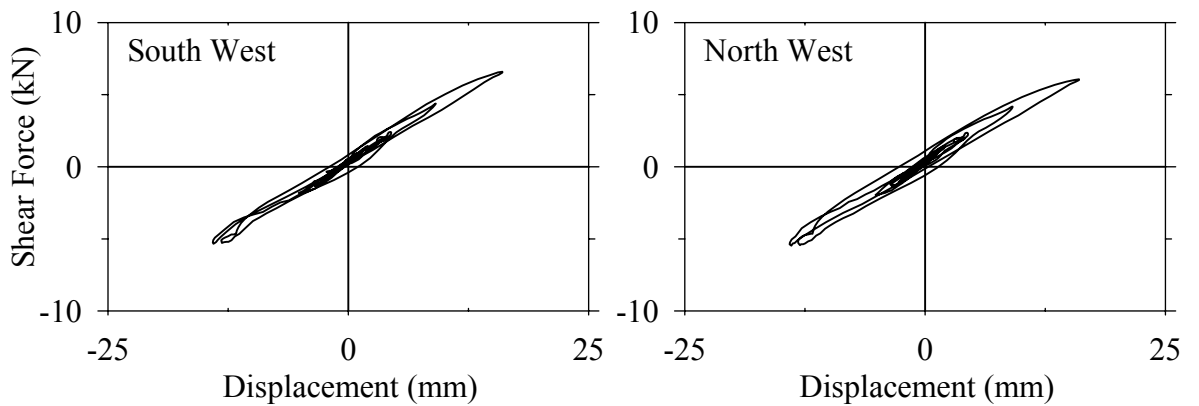
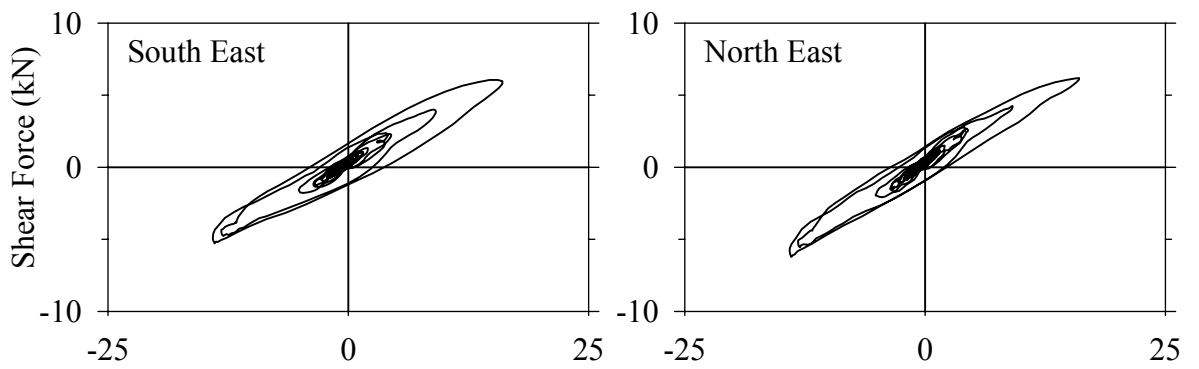
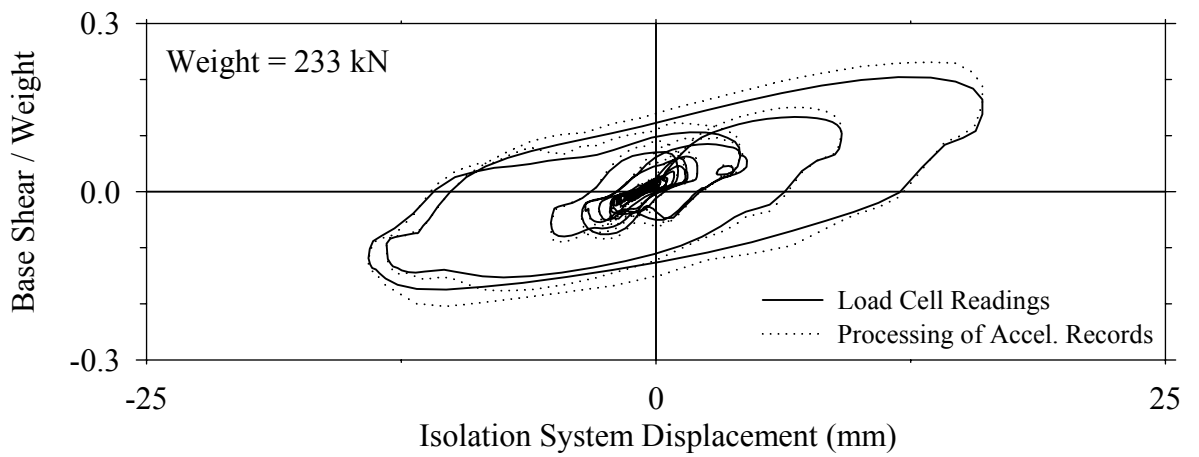
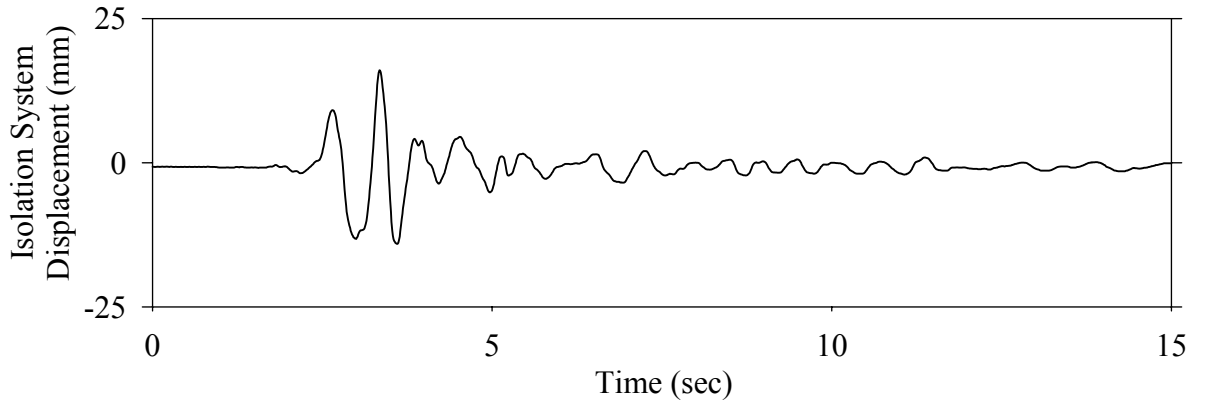
Test LDANK50.1, Kobe N-S 50%, AB/Low Damping Elastomeric-Nonlinear Dampers



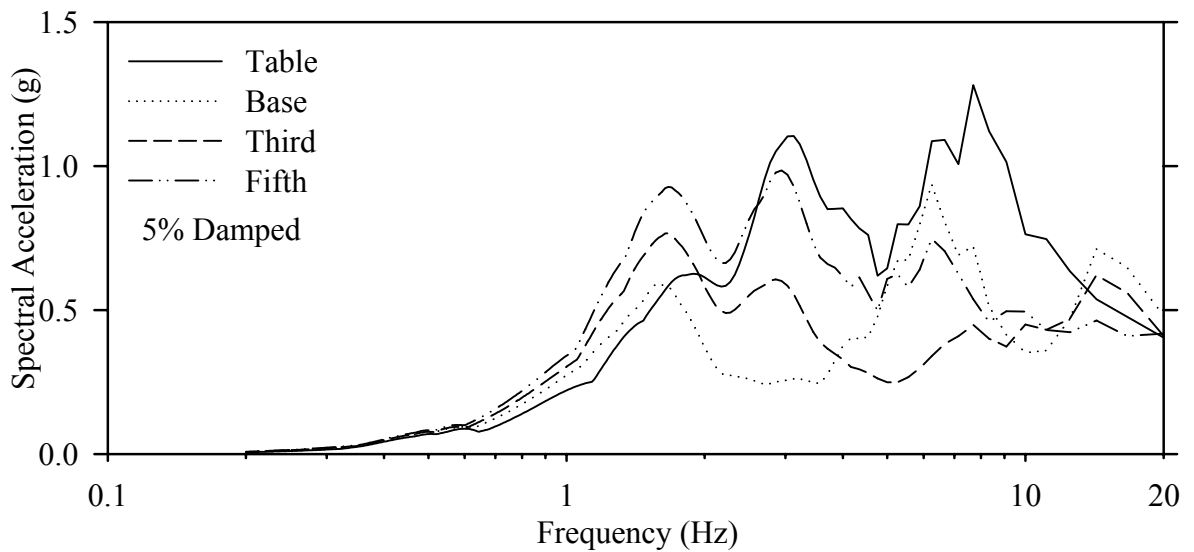
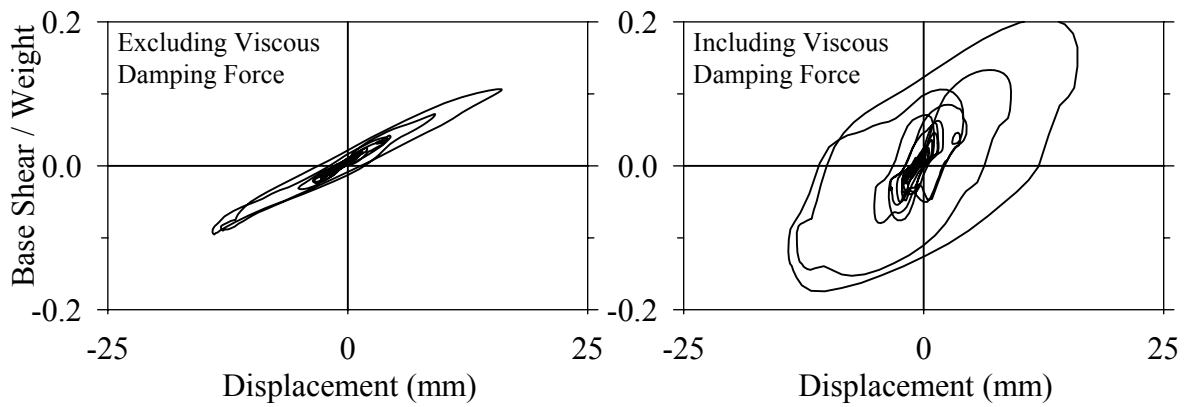
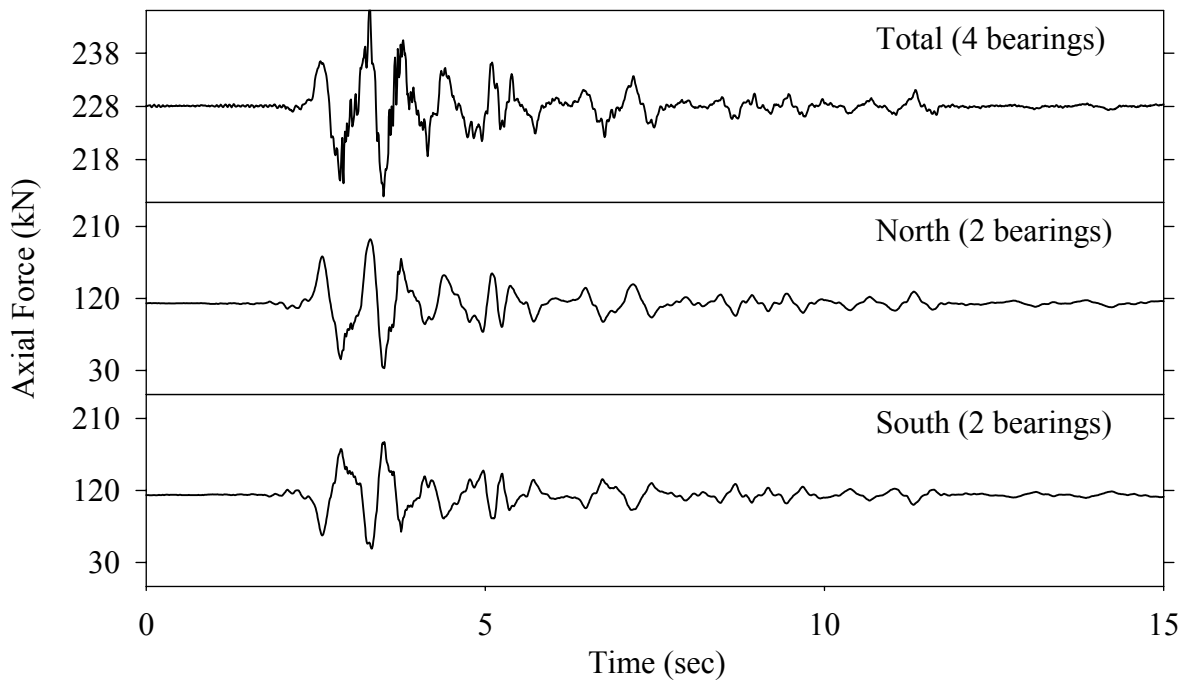
Test LDANK50.1, Kobe N-S 50%, AB/Low Damping Elastomeric-Nonlinear Dampers



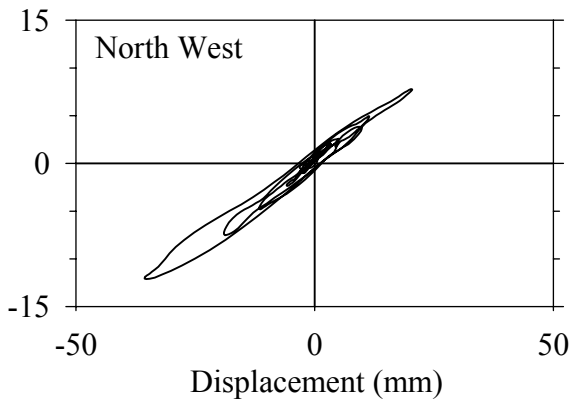
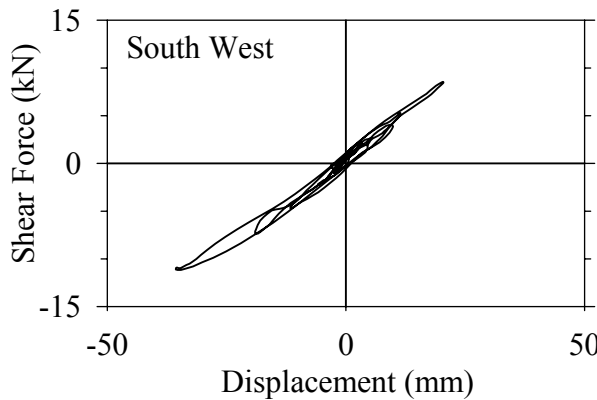
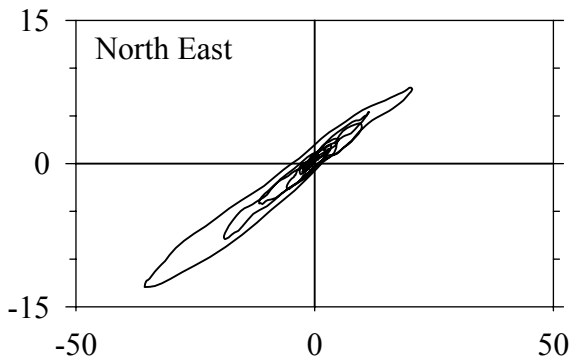
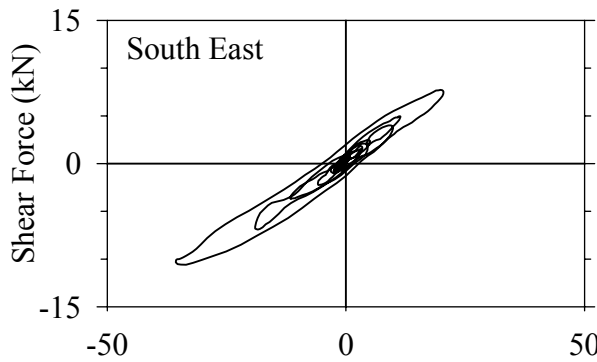
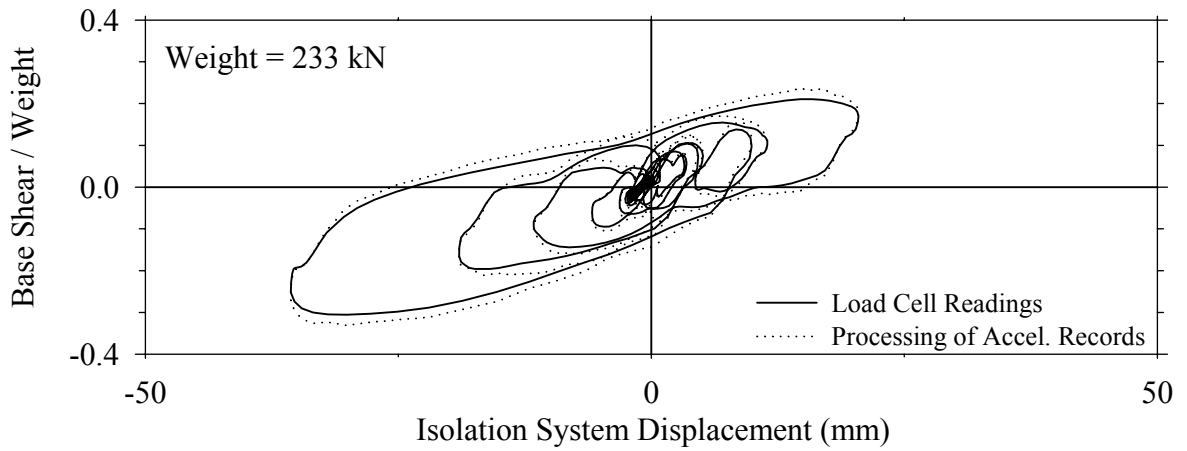
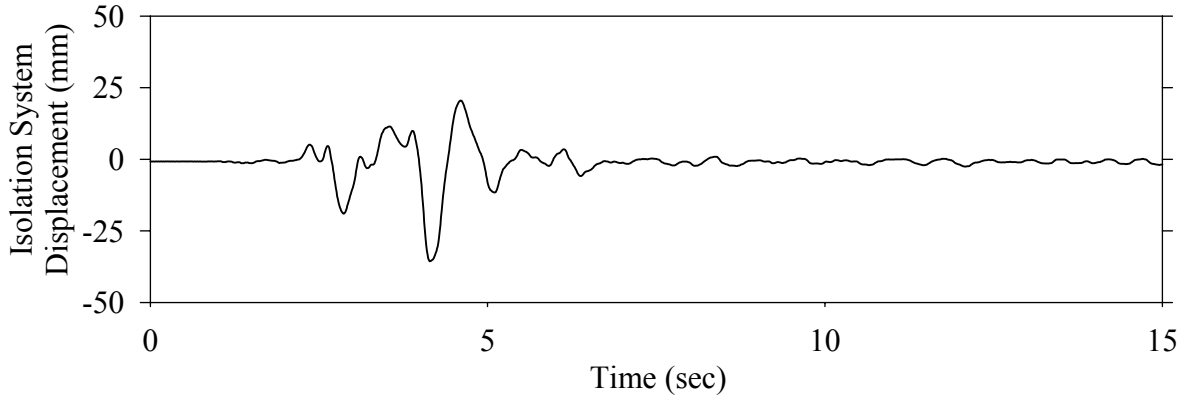
Test LDANN50.1, Northridge Newhall 360° 50%, AB/Low Damping Elastomeric-Nonlinear Dampers



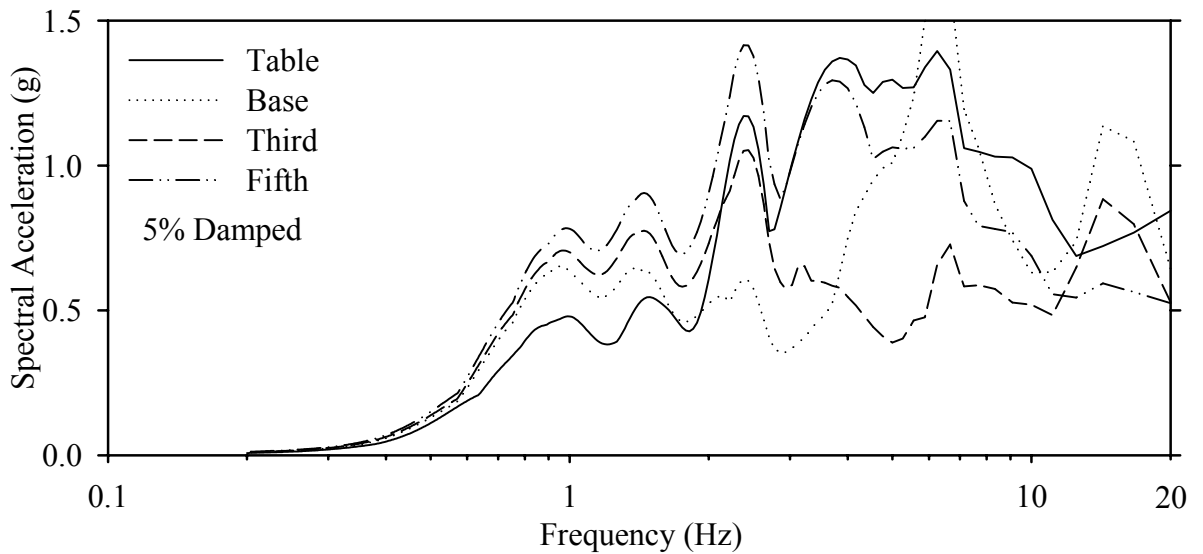
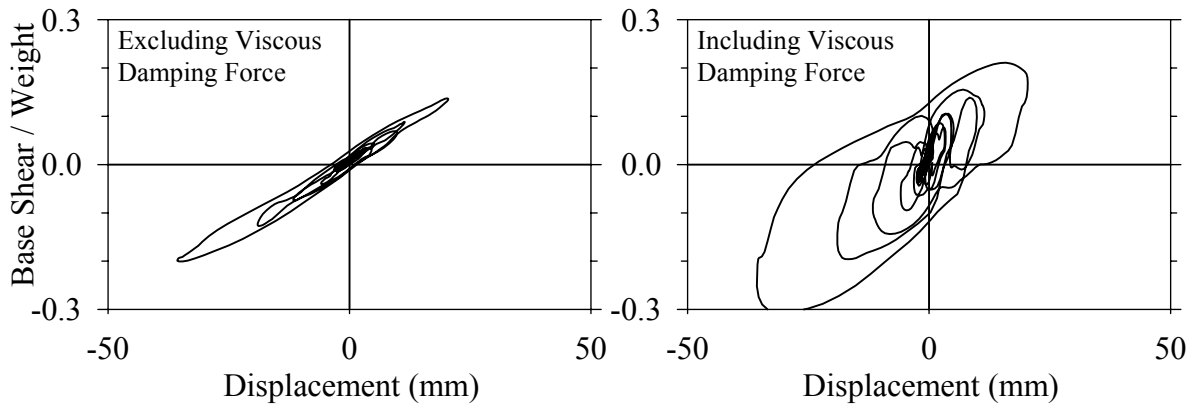
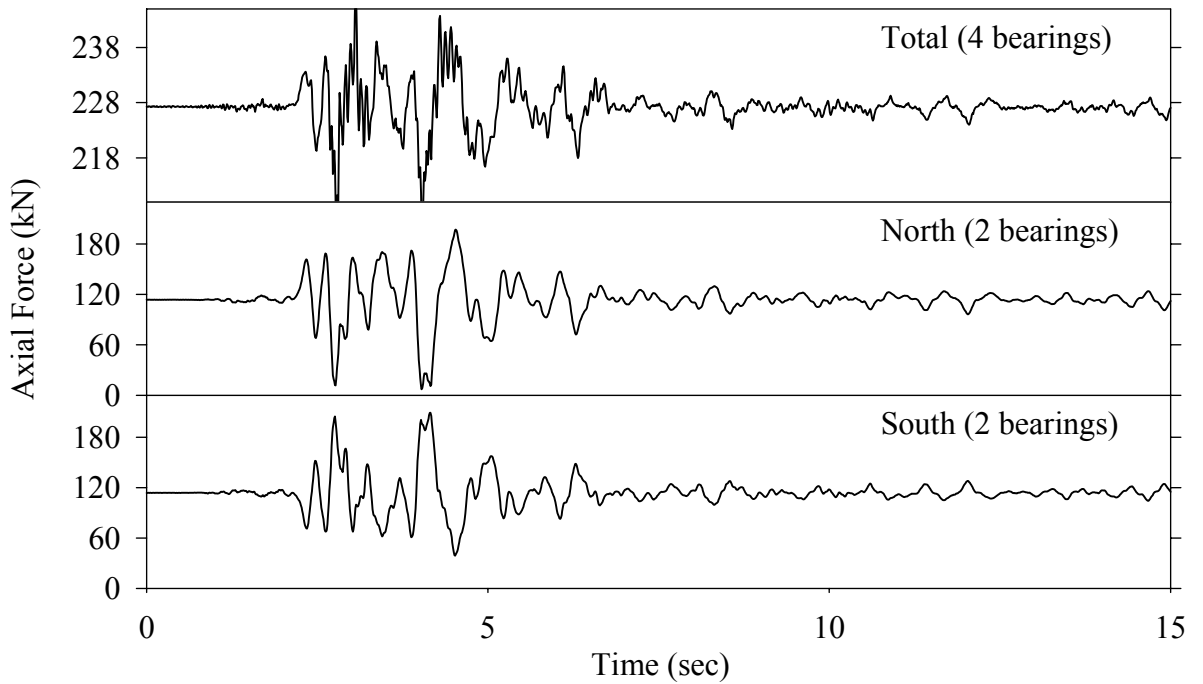
Test LDANN50.1, Northridge Newhall 360° 50%, AB/Low Damping Elastomeric-Nonlinear Dampers



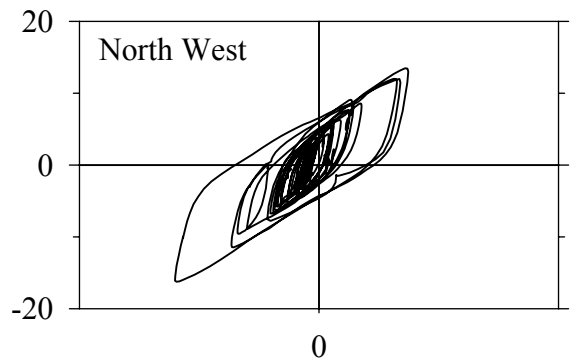
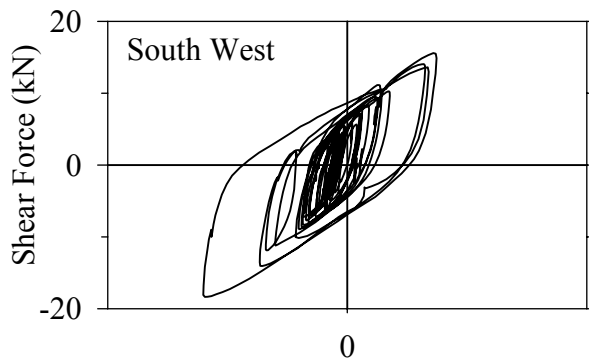
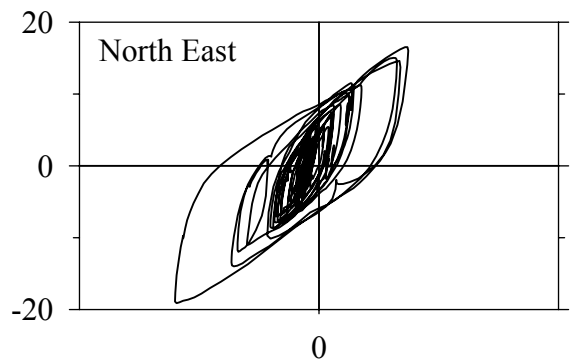
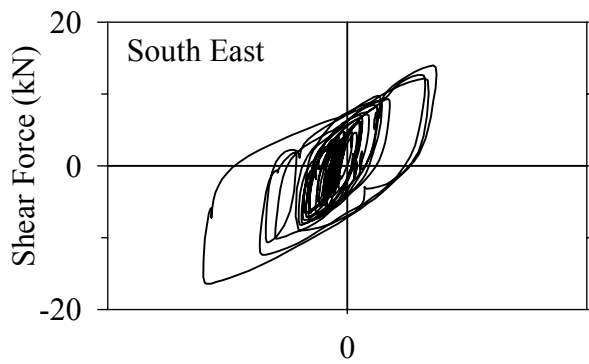
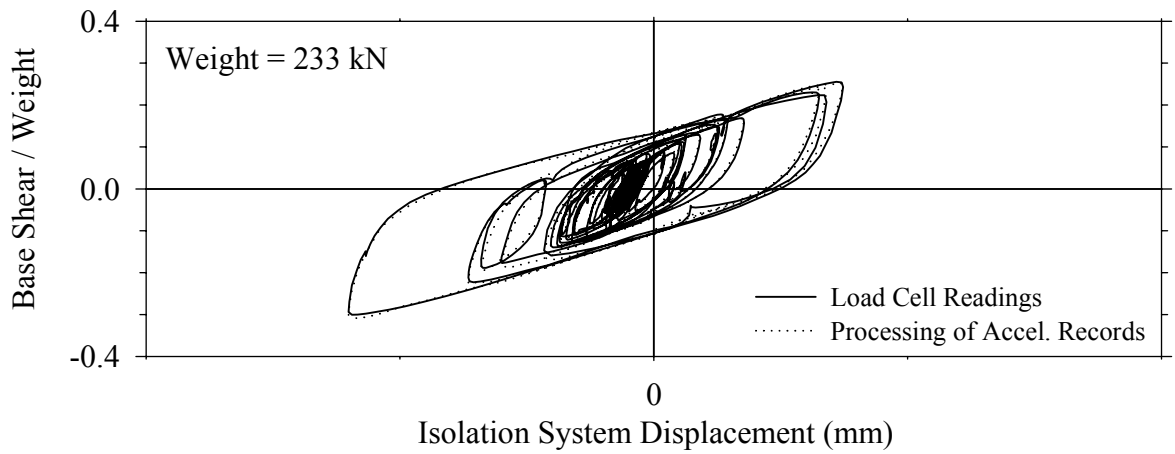
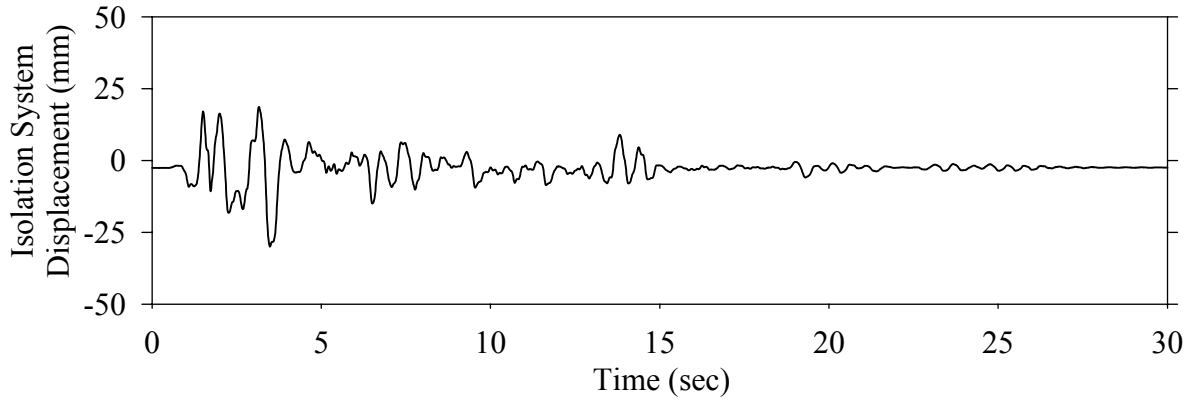
Test LDANS10.1, Northridge Sylmar 90° 100%, AB/Low Damping Elastomeric-Nonlinear Dampers



Test LDANS10.1, Northridge Sylmar 90° 100%, AB/Low Damping Elastomeric-Nonlinear Dampers

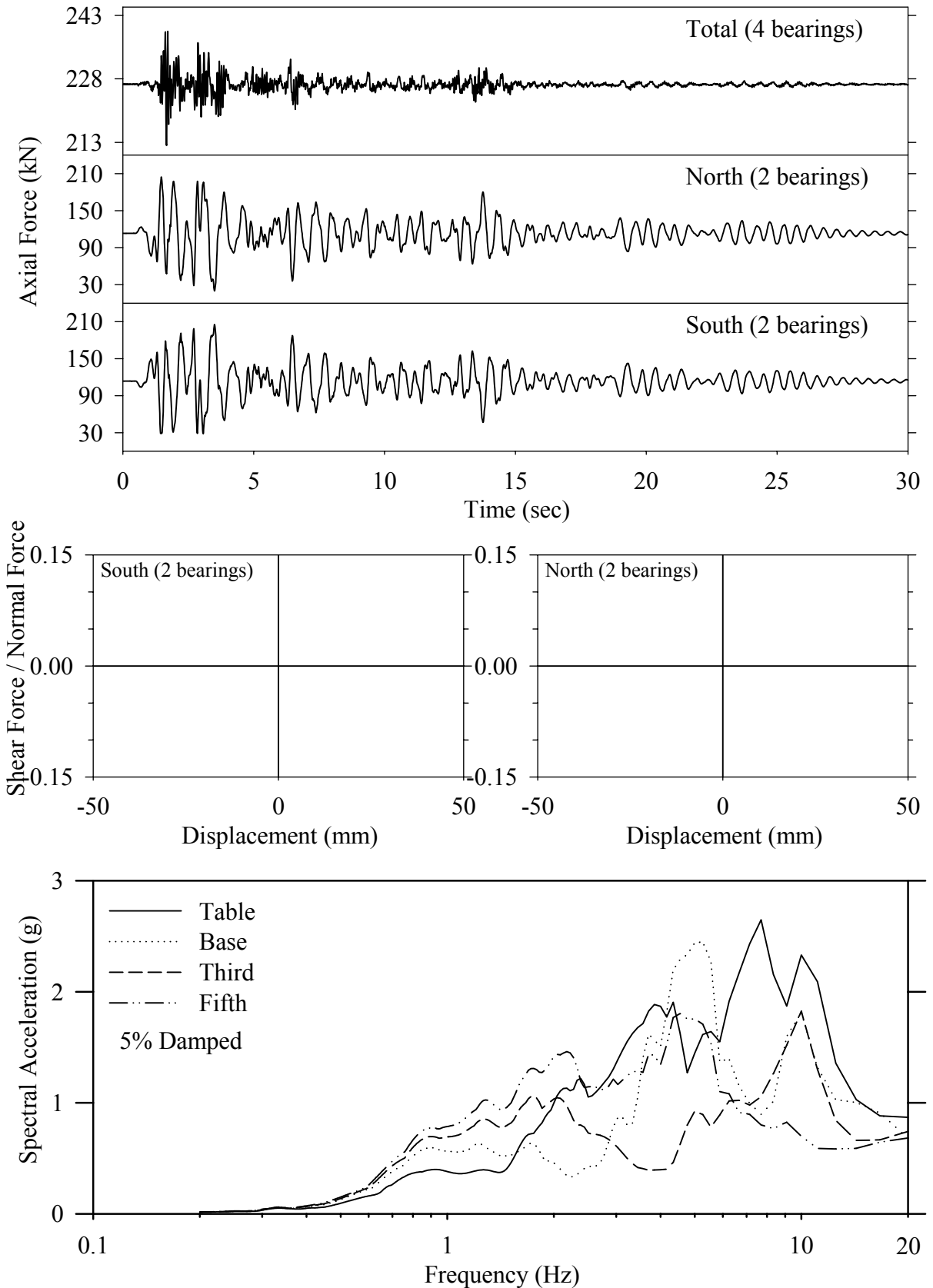


Test LCMFE20.1, El Centro S00E 200%, MF/Lead Core

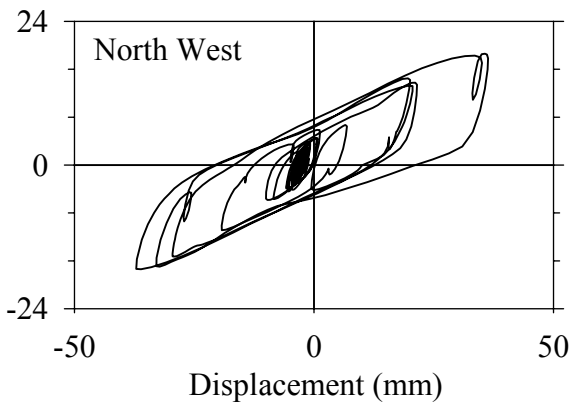
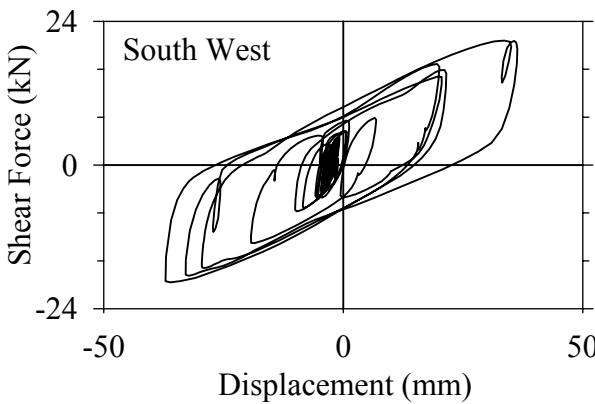
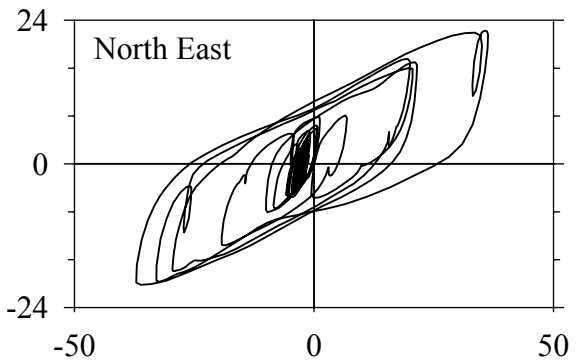
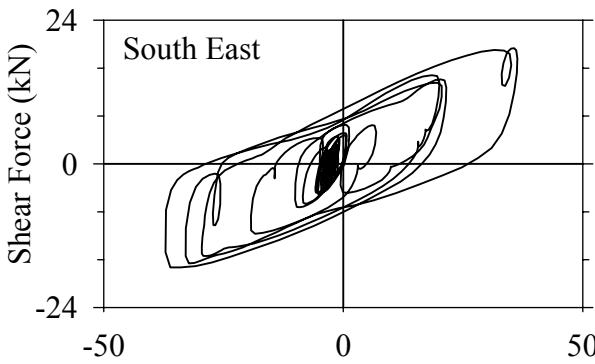
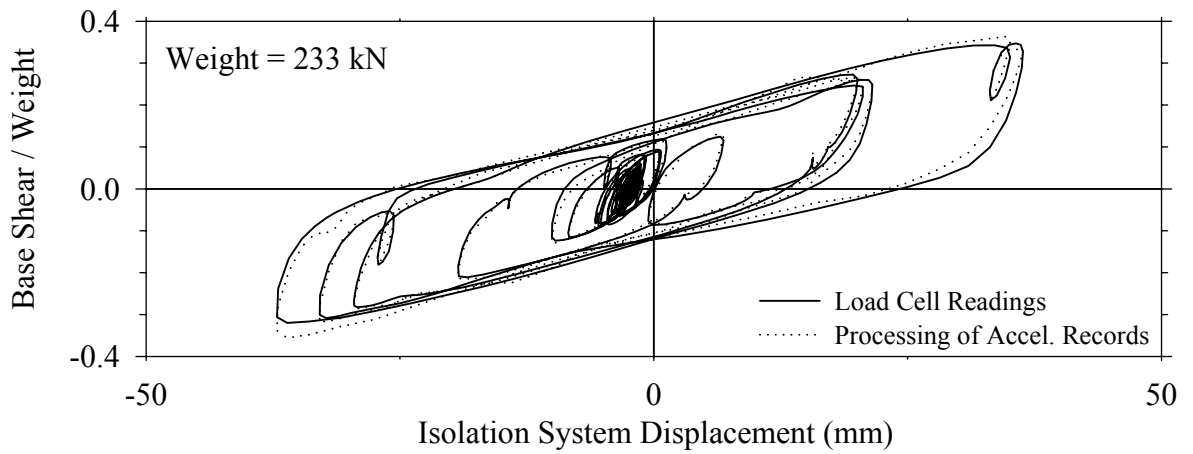
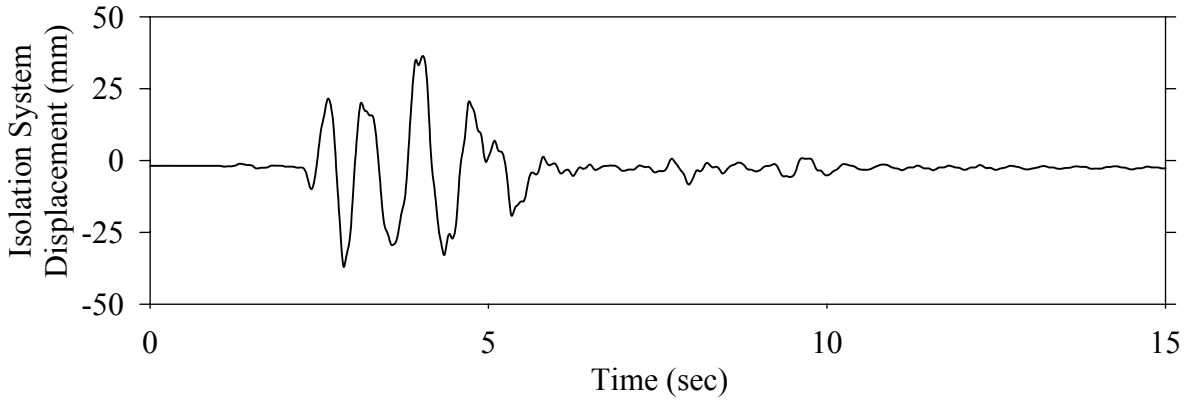




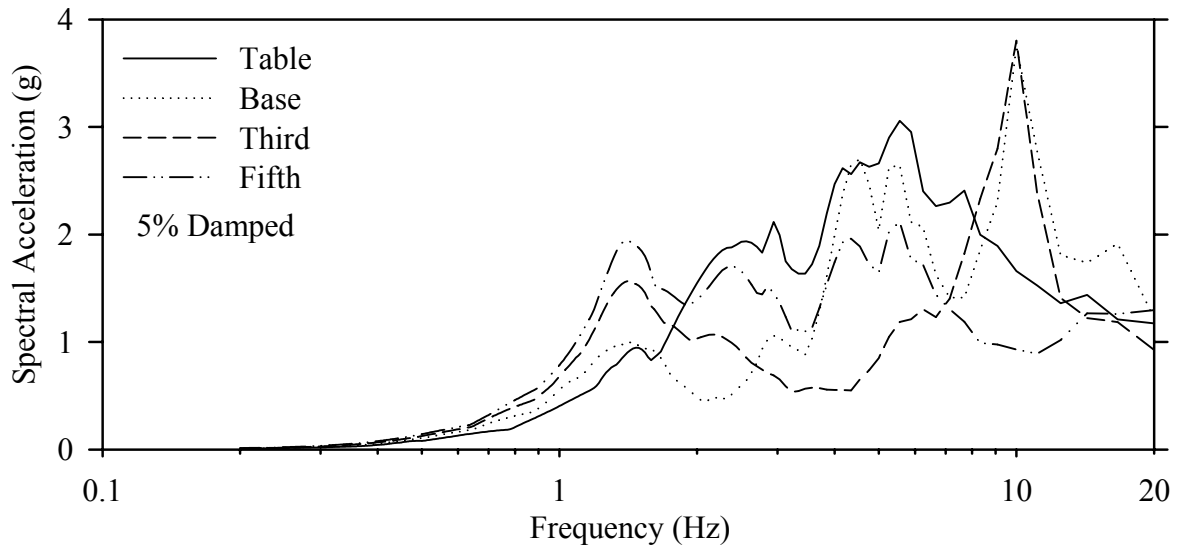
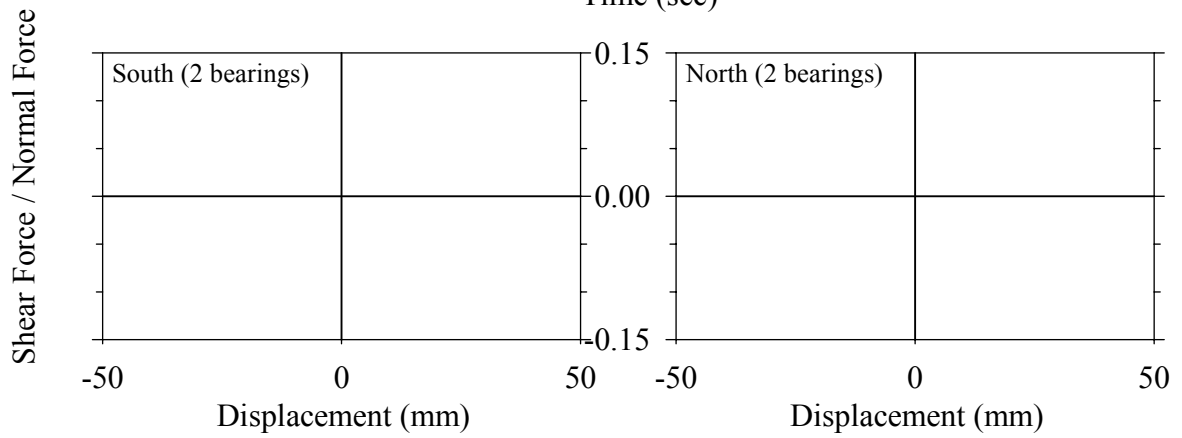
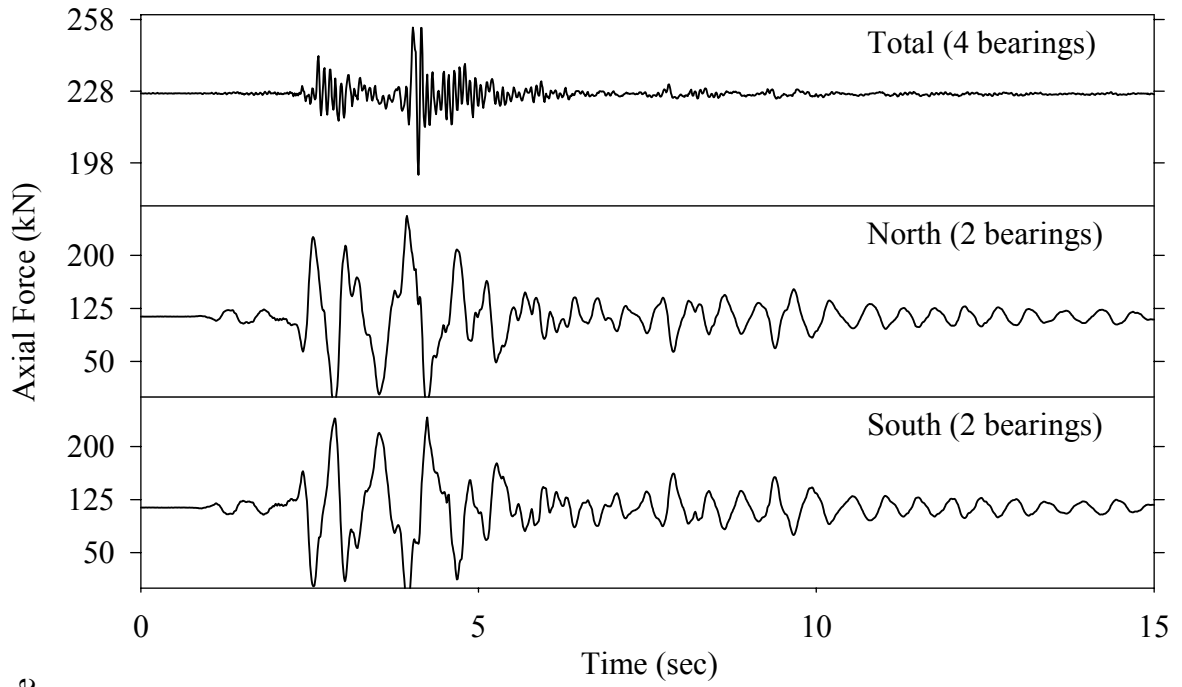
Test LCMFE20.1, El Centro S00E 200%, MF/Lead Core



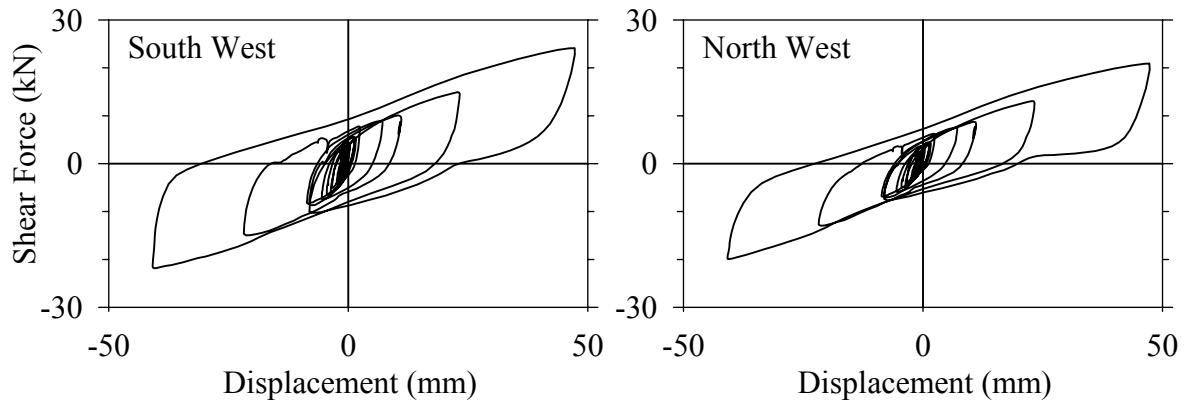
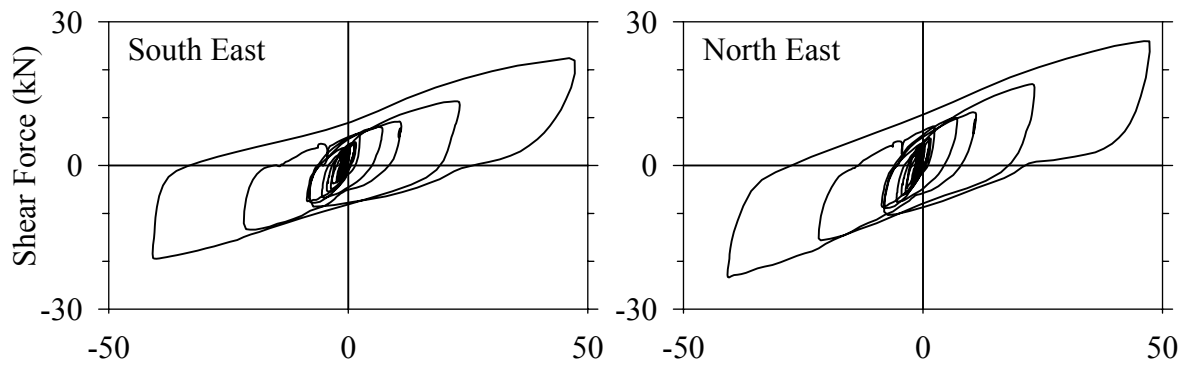
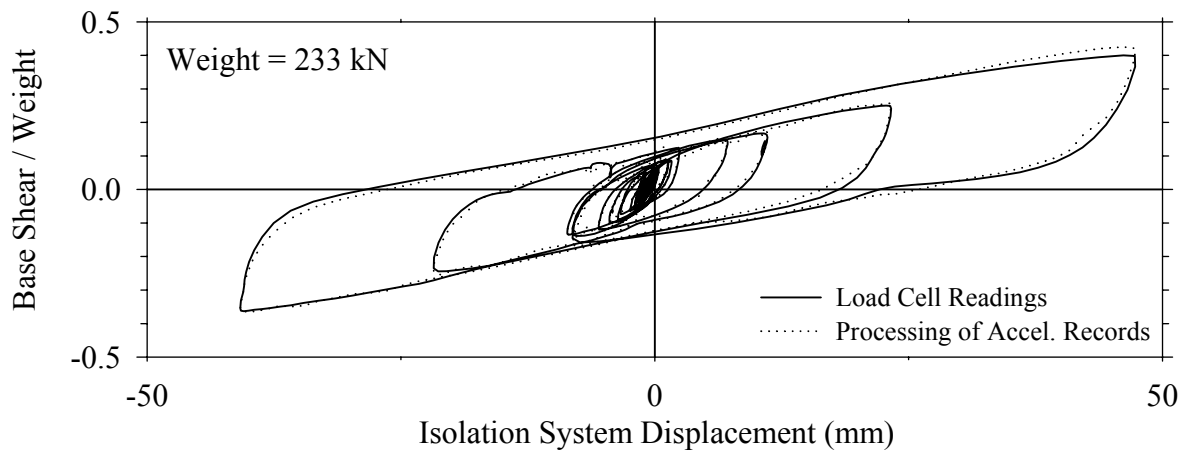
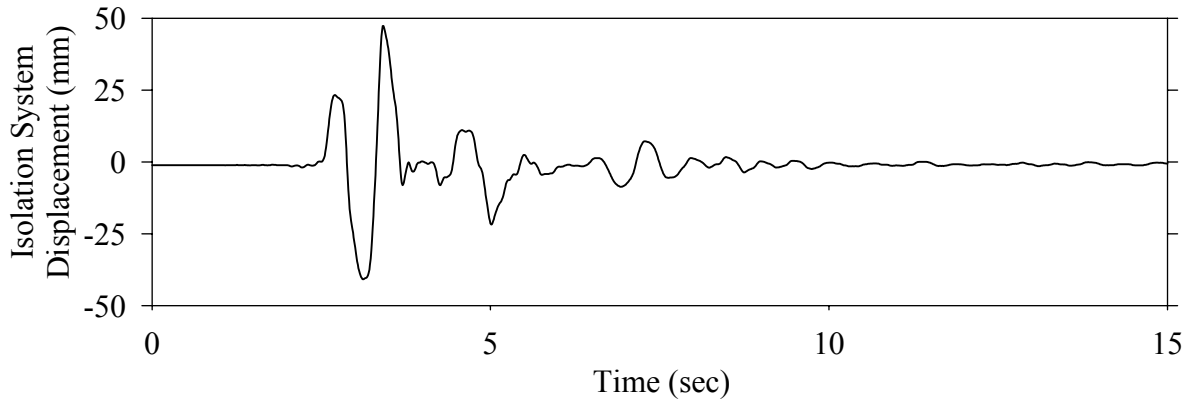
Test LCMFK10.1, Kobe N-S 100%, MF/Lead Core



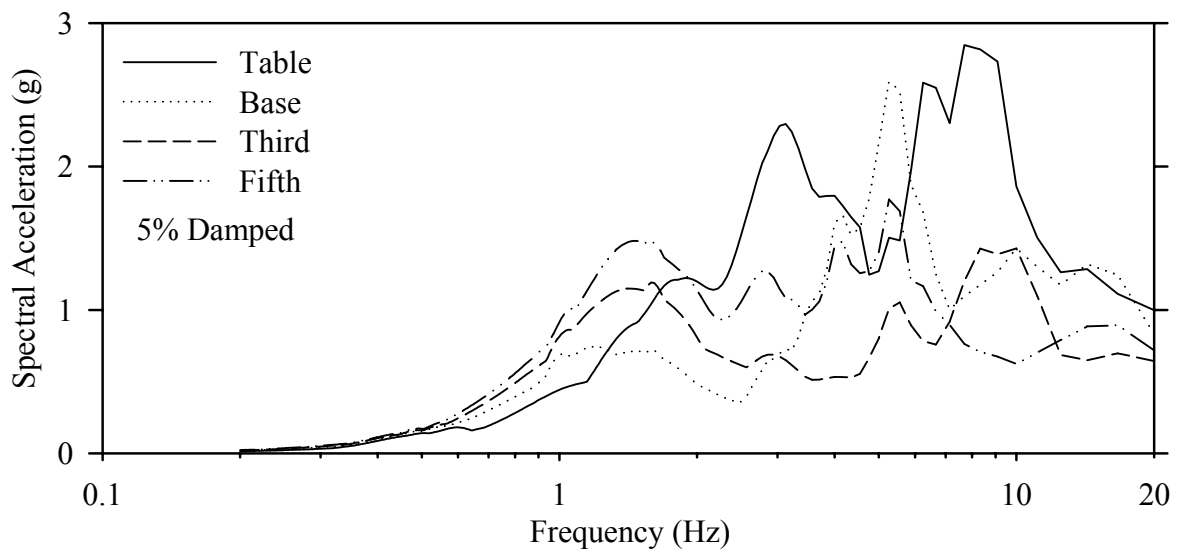
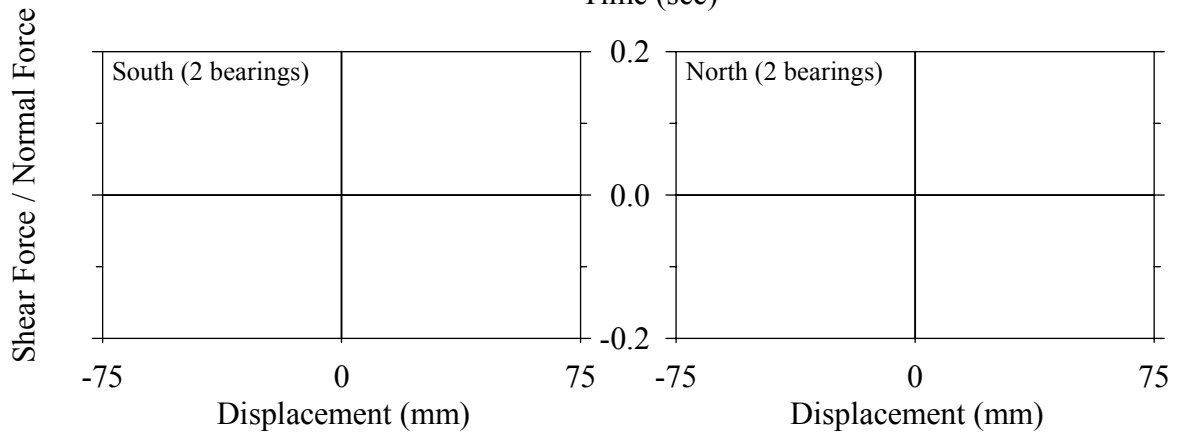
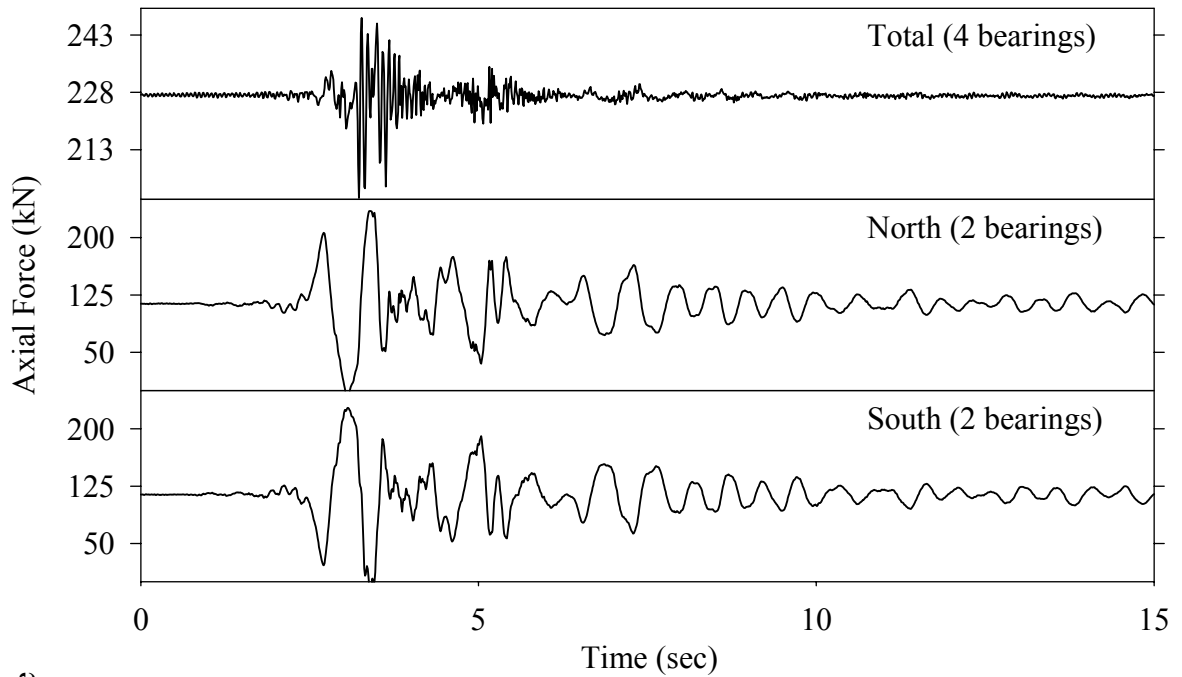
Test LCMFK10.1, Kobe N-S 100%, MF/Lead Core



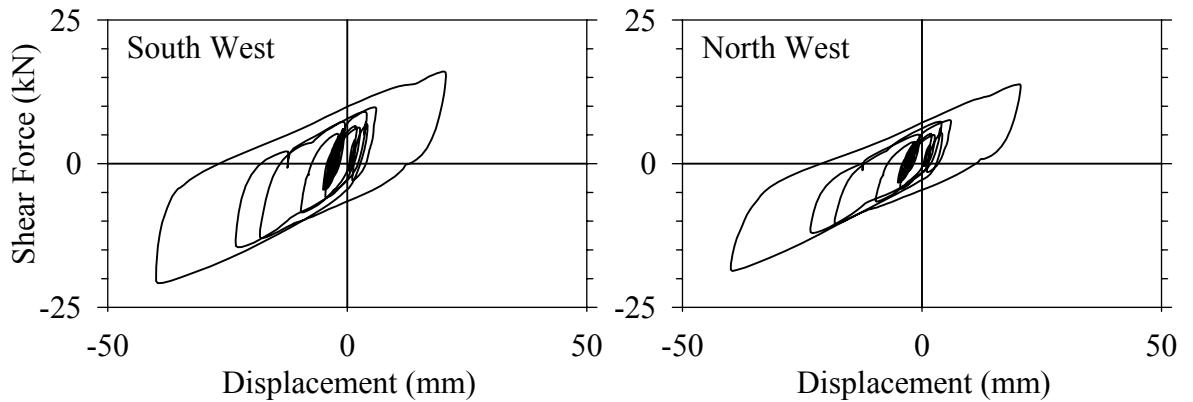
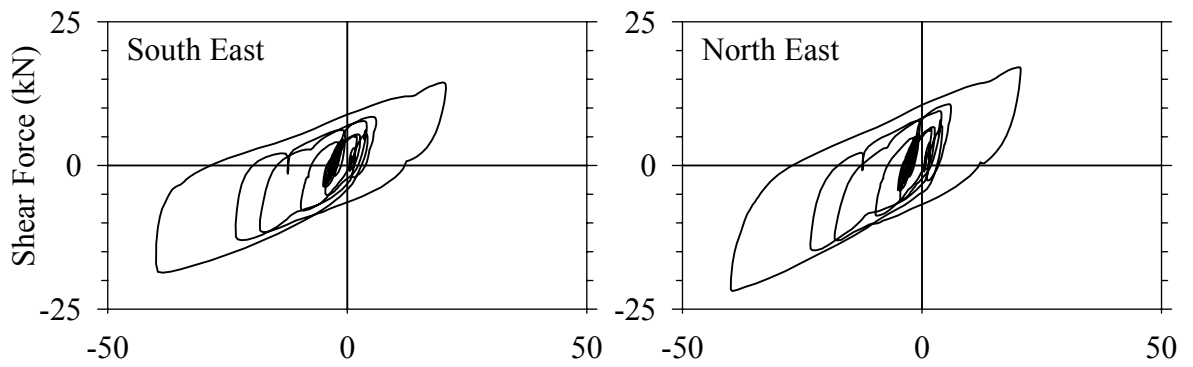
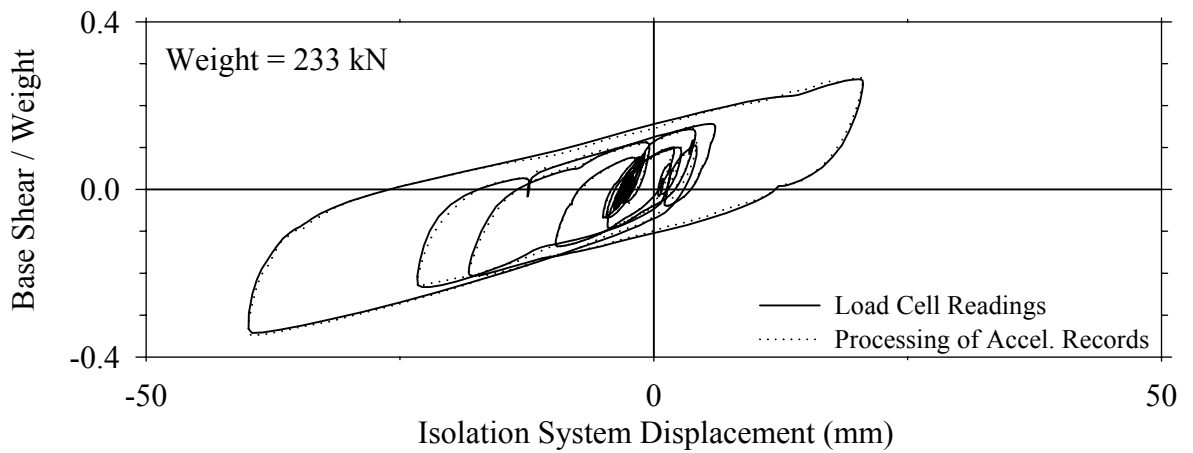
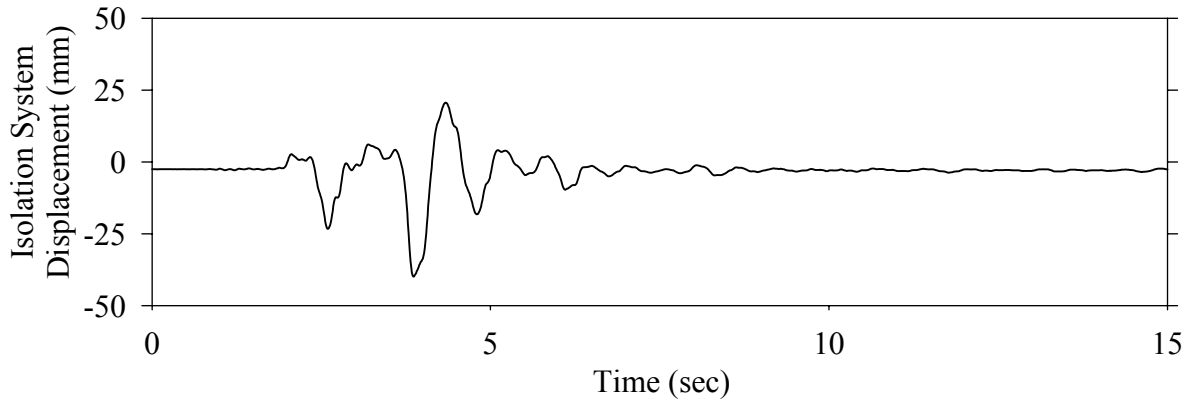
Test LCMFN10.1, Northridge Newhall 360° 100%, MF/Lead Core



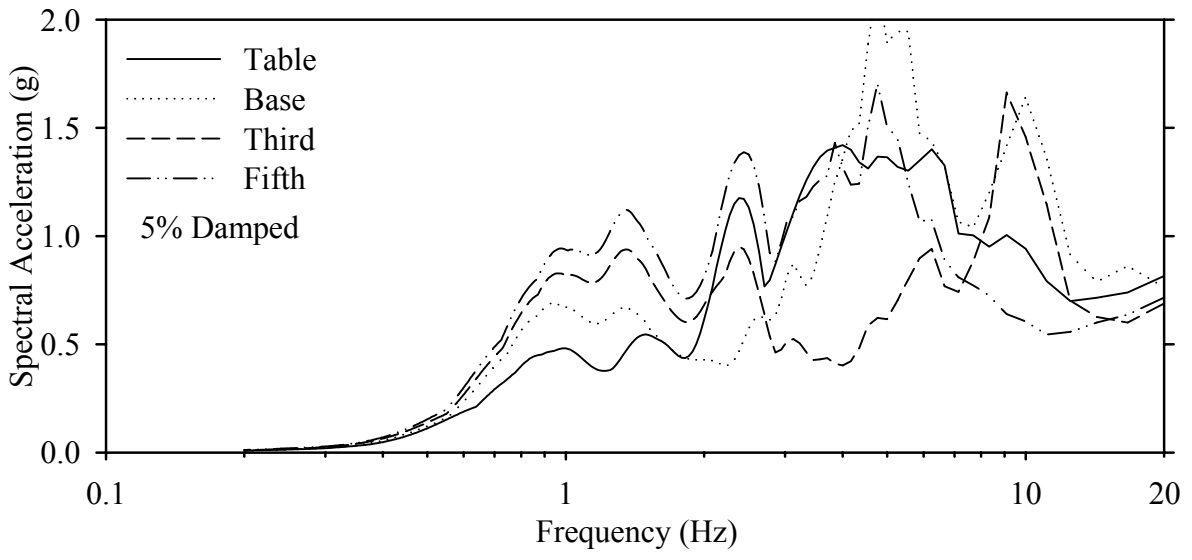
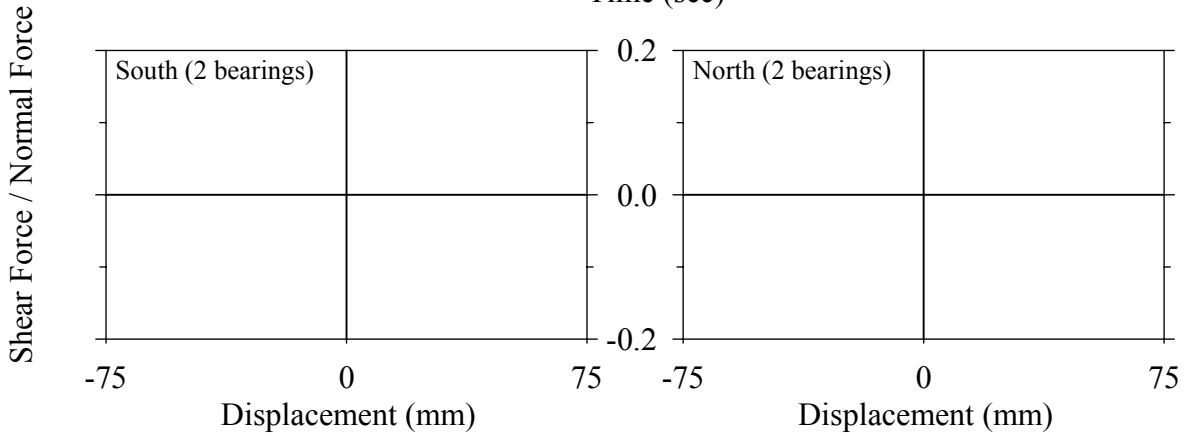
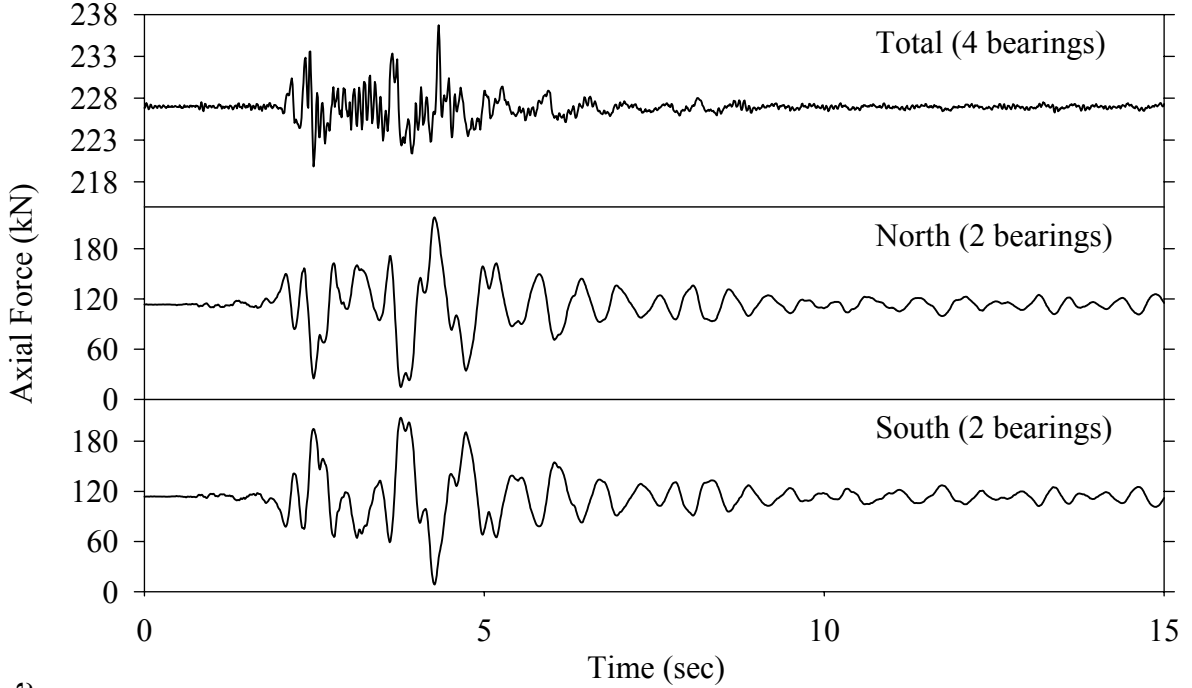
Test LCMFN10.1, Northridge Newhall 360° 100%, MF/Lead Core



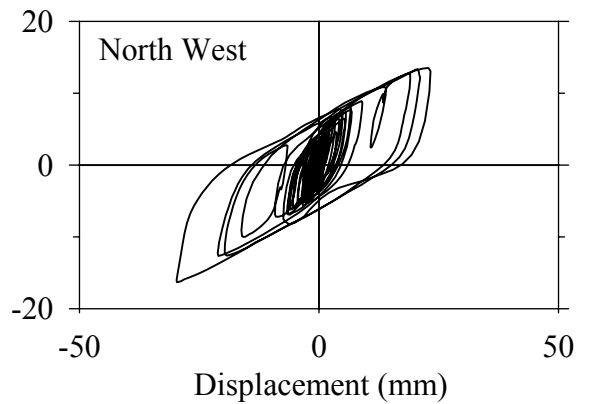
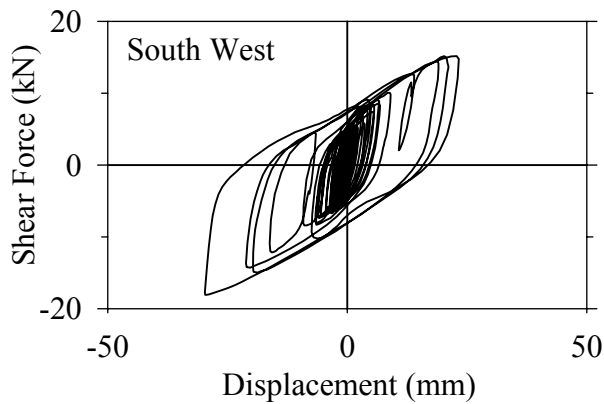
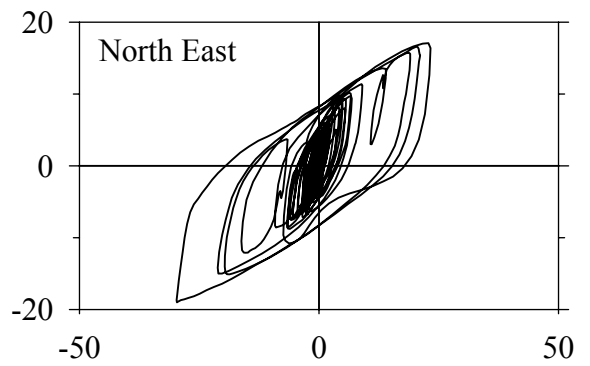
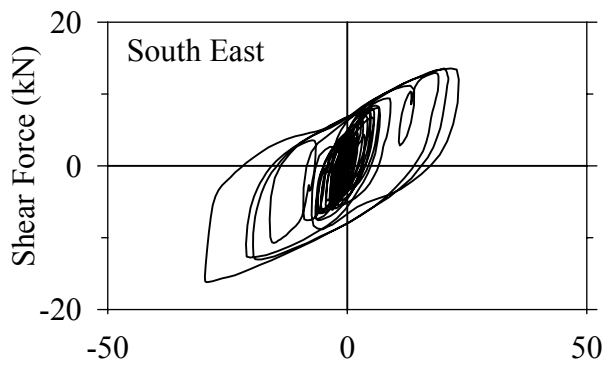
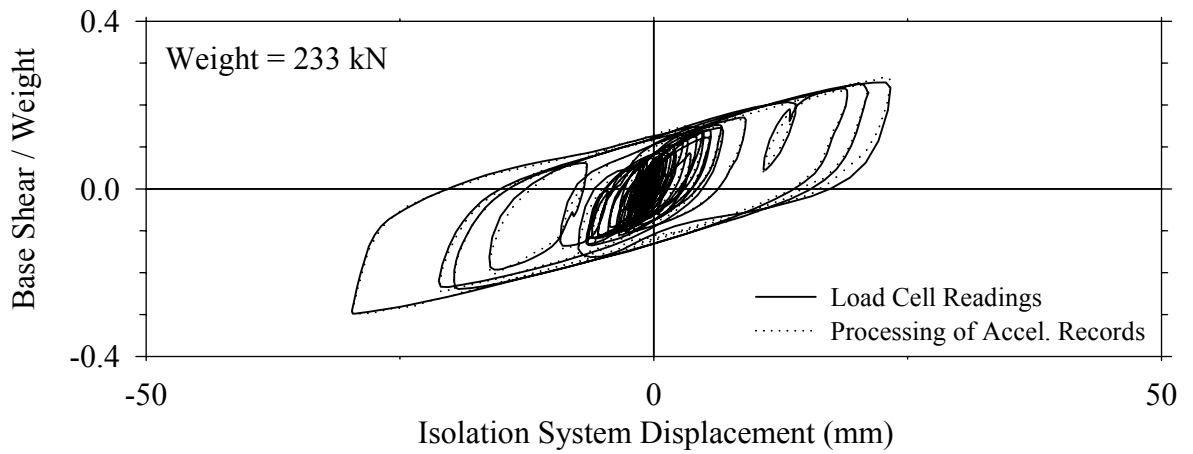
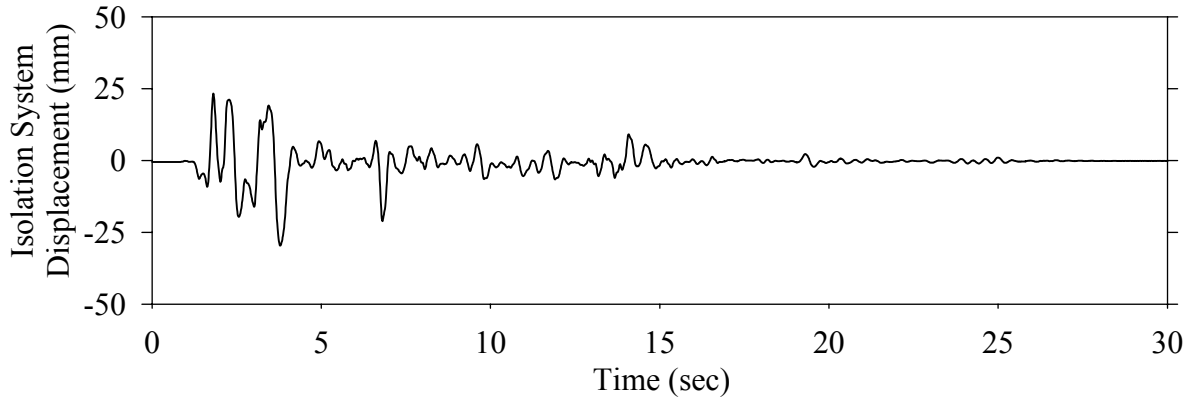
Test LCMFS10.1, Northridge Sylmar 90° 100%, MF/Lead Core



Test LCMFS10.1, Northridge Sylmar 90° 100%, MF/Lead Core

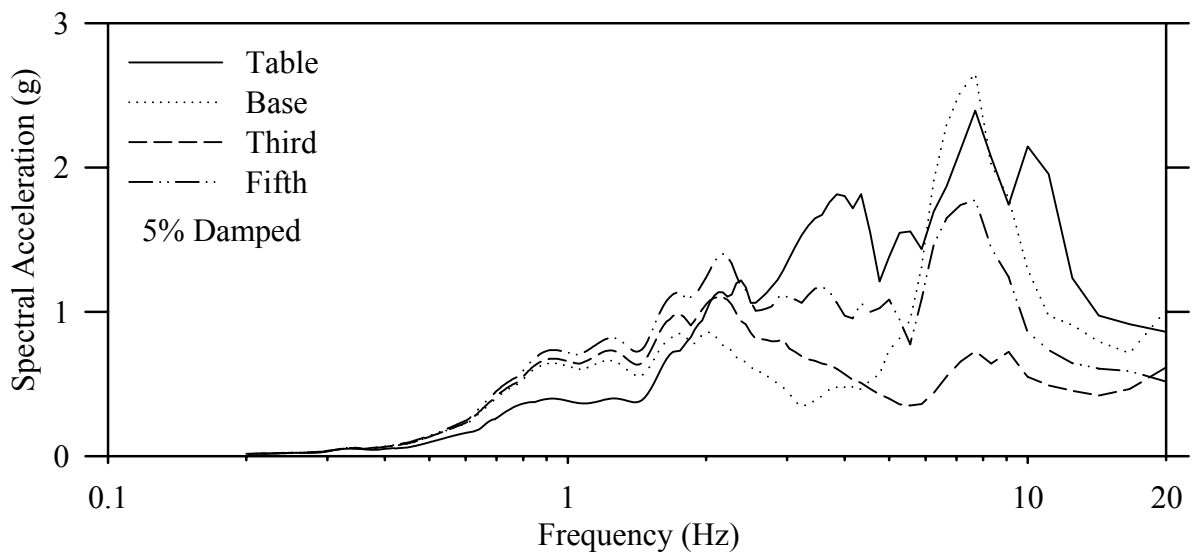
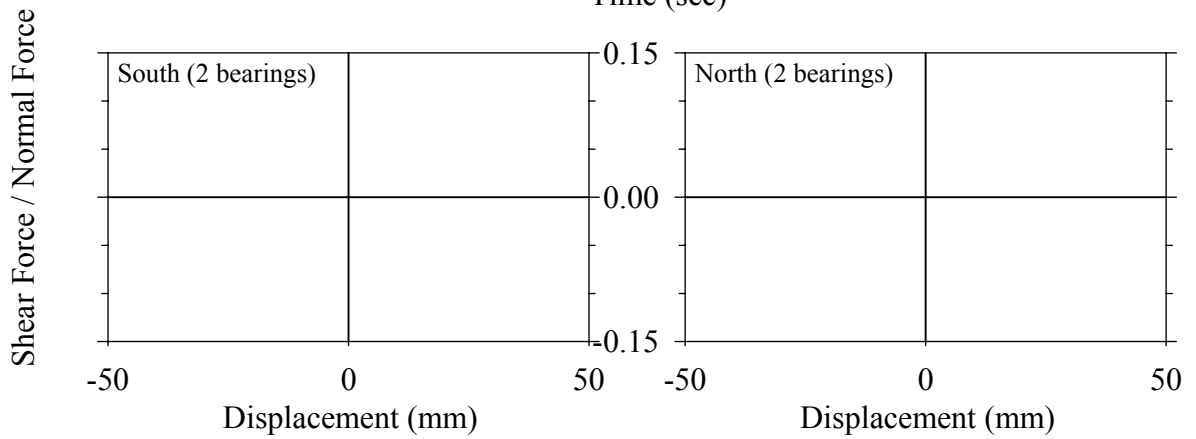
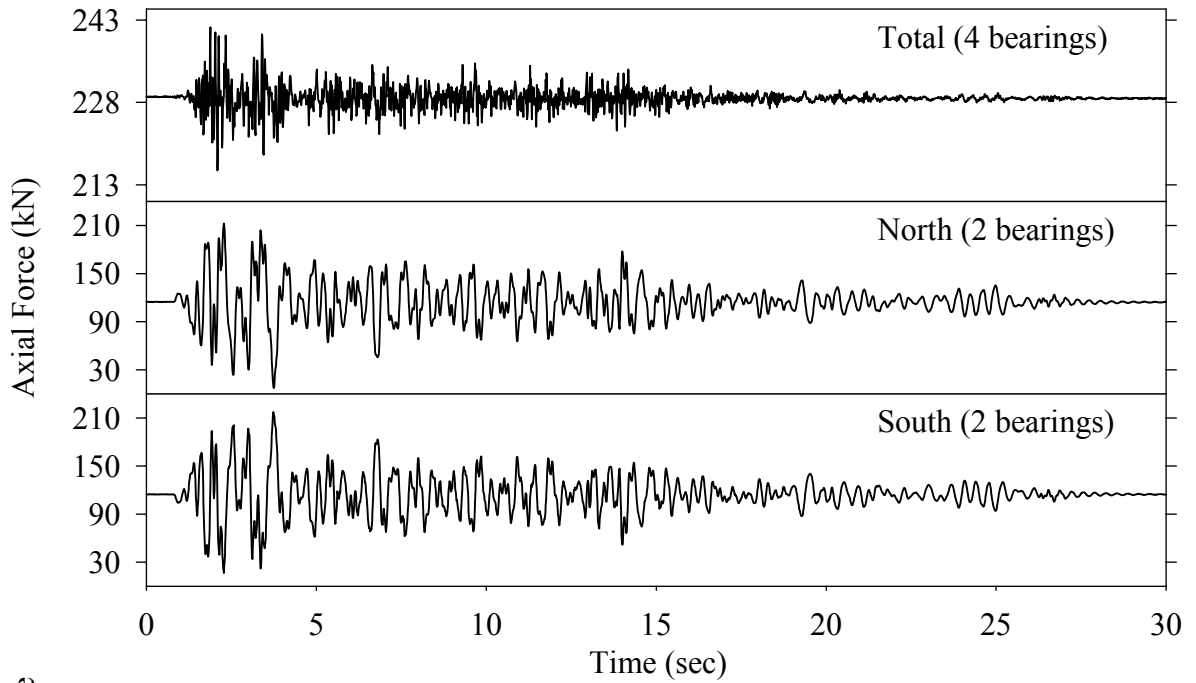


Test LCSBE20.1, El Centro S00E 200%, SB/Lead Core

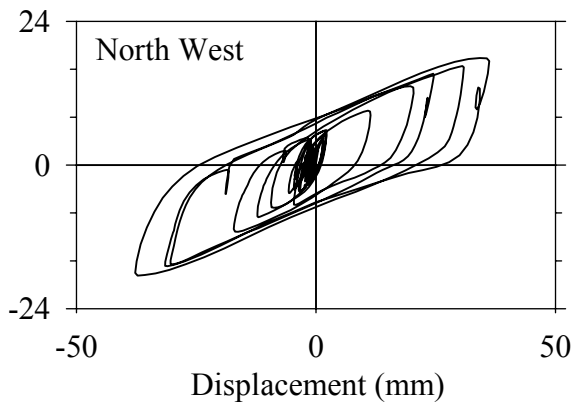
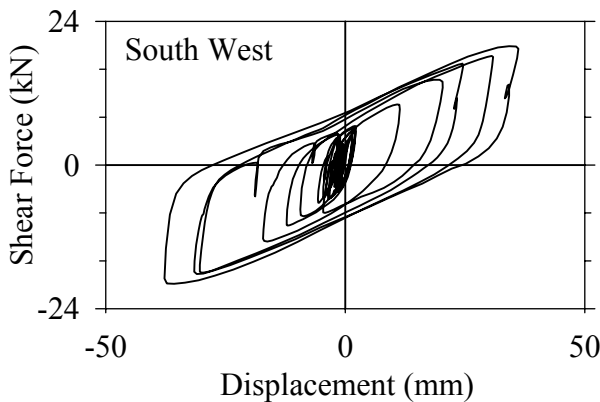
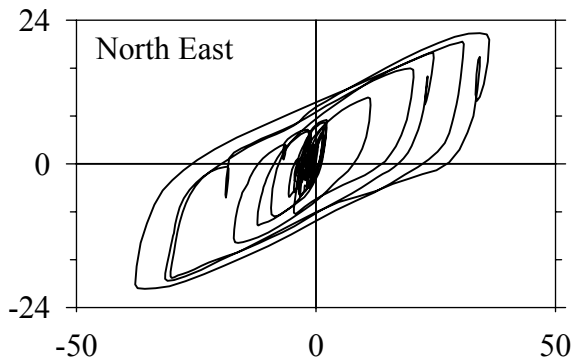
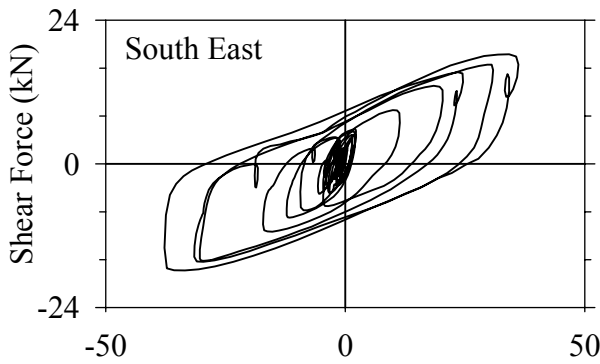
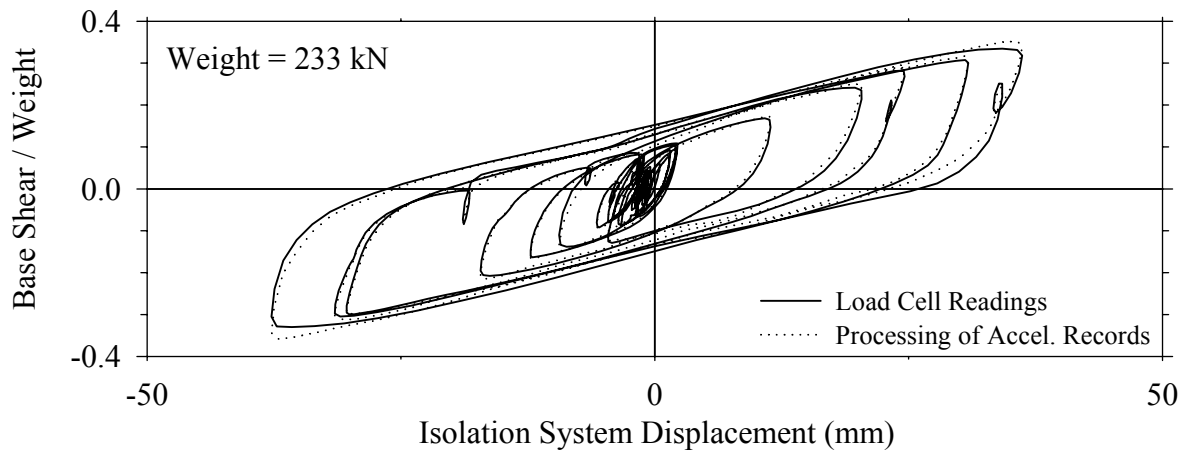
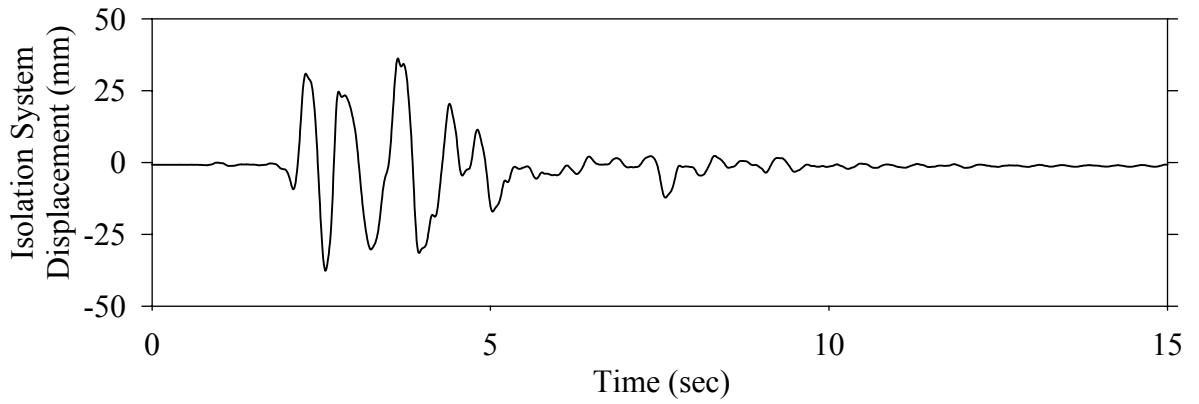




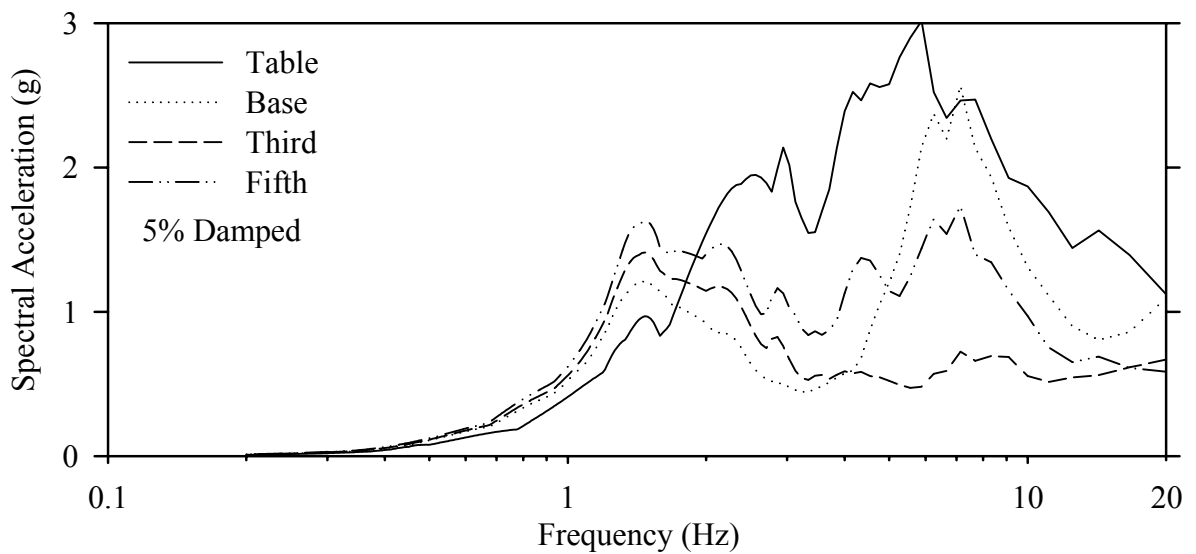
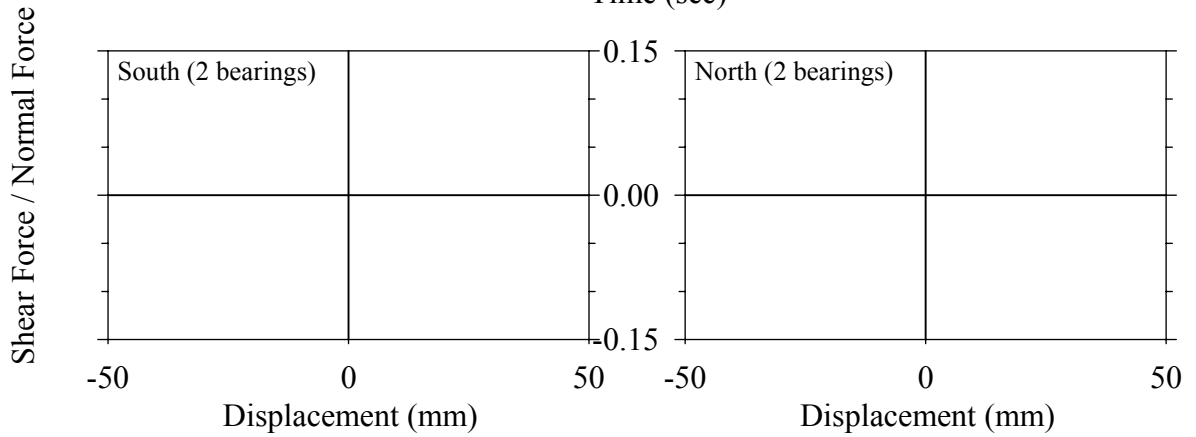
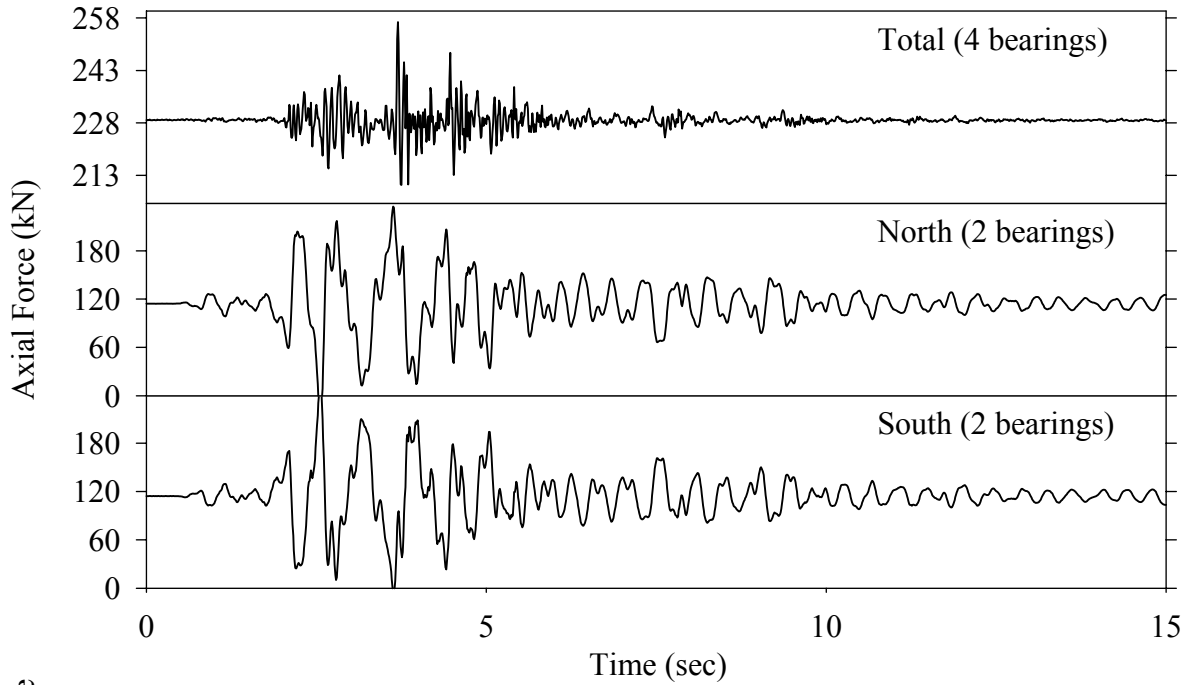
Test LCSBE20.1, El Centro S00E 200%, SB/Lead Core



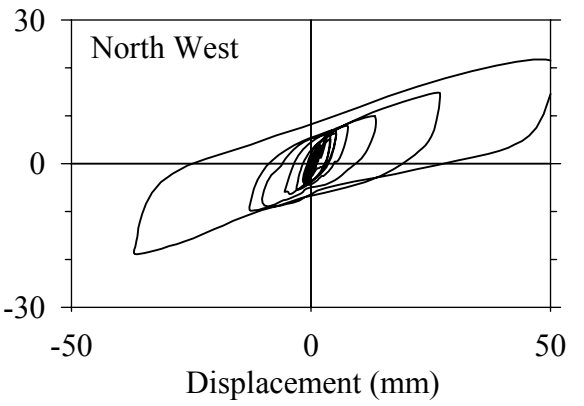
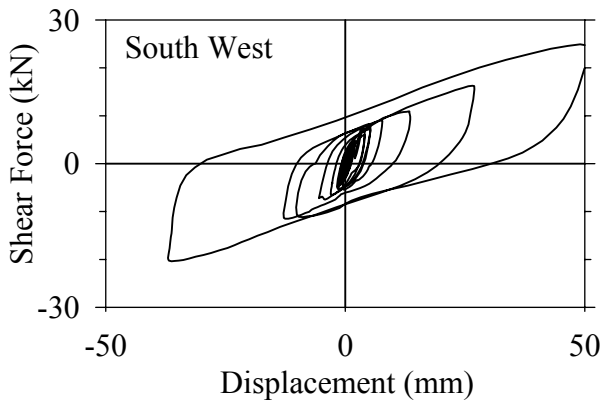
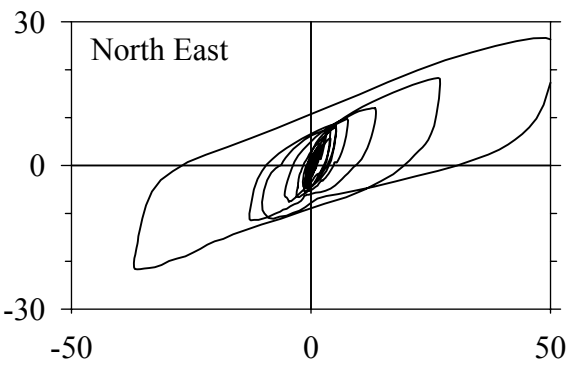
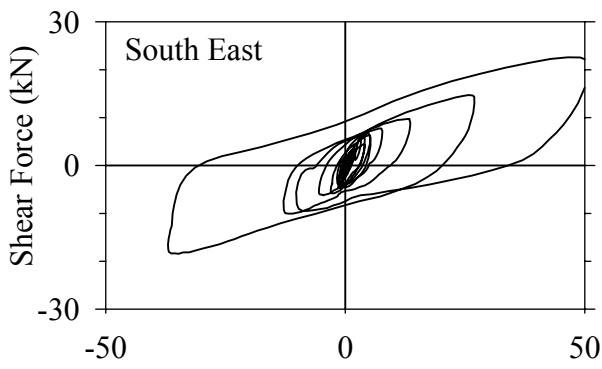
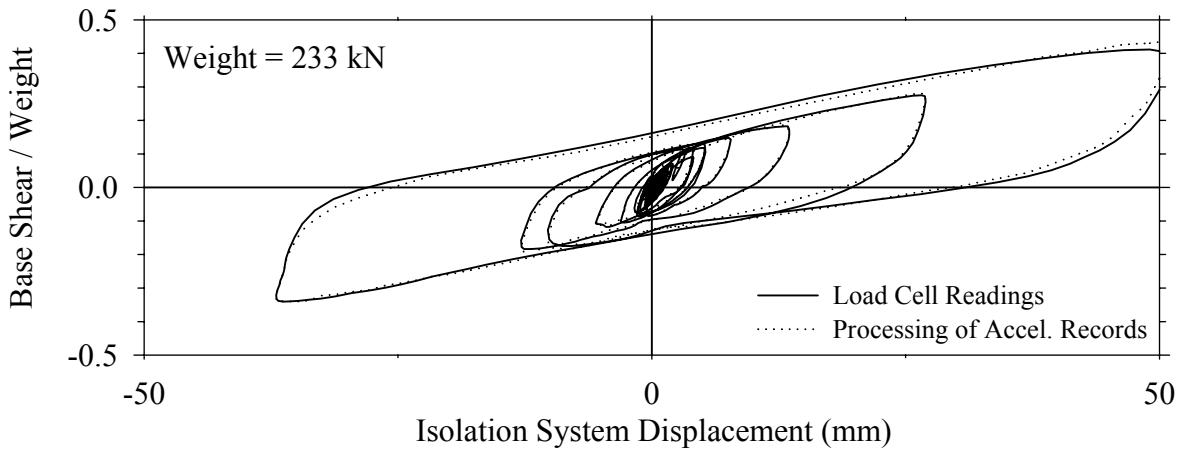
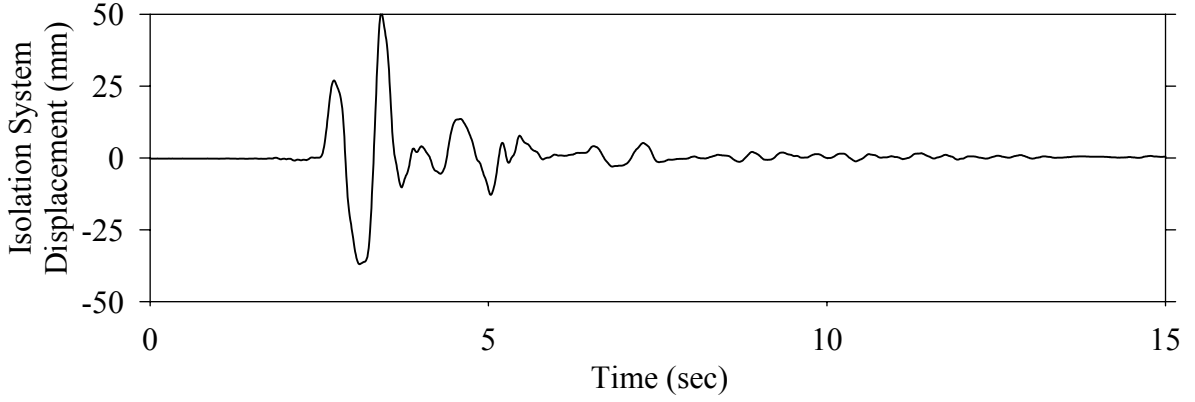
Test LCSBK10.1, Kobe N-S 100%, SB/Lead Core



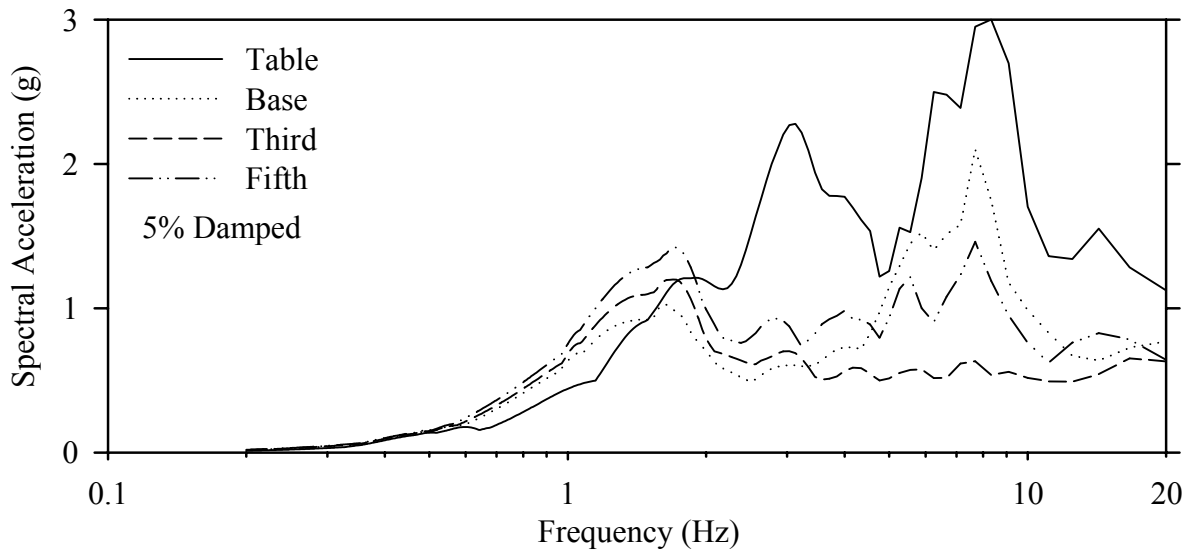
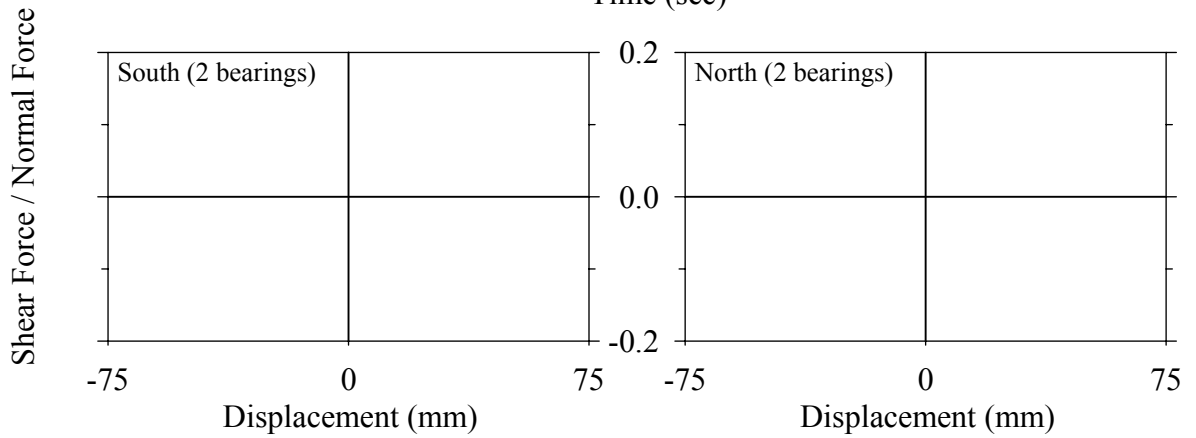
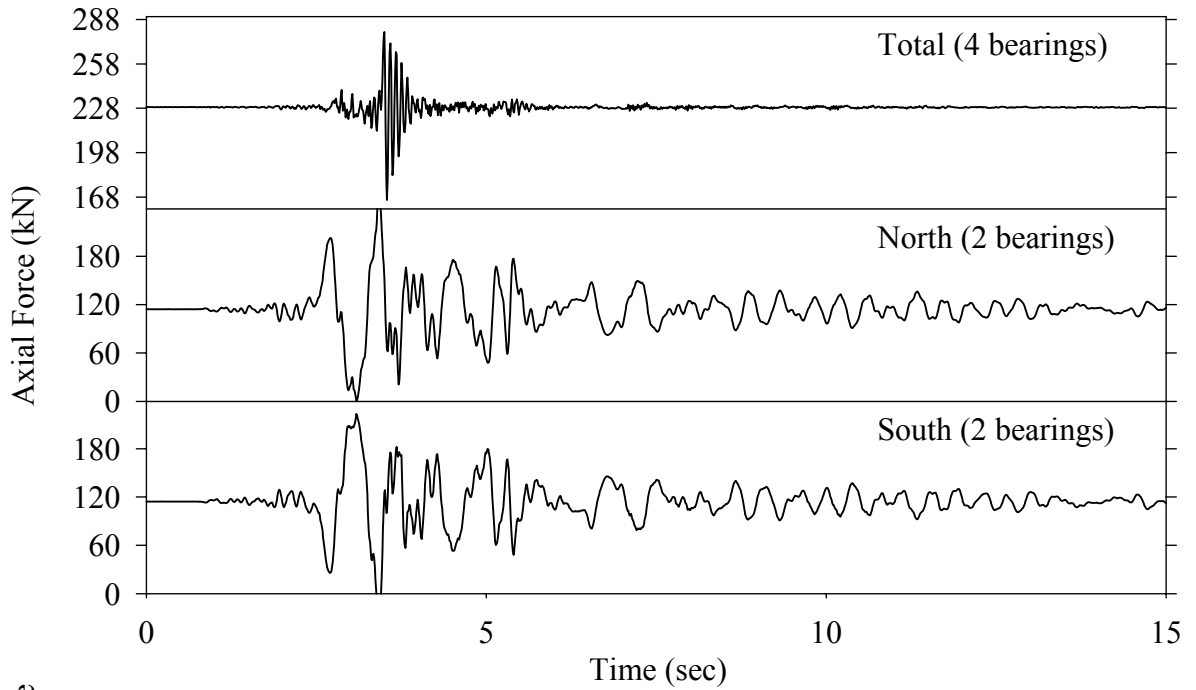
Test LCSBK10.1, Kobe N-S 100%, SB/Lead Core



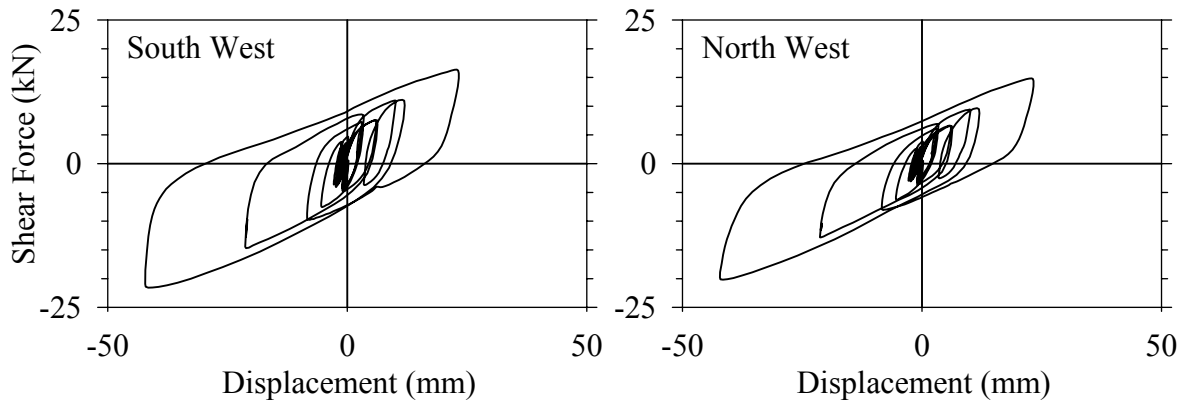
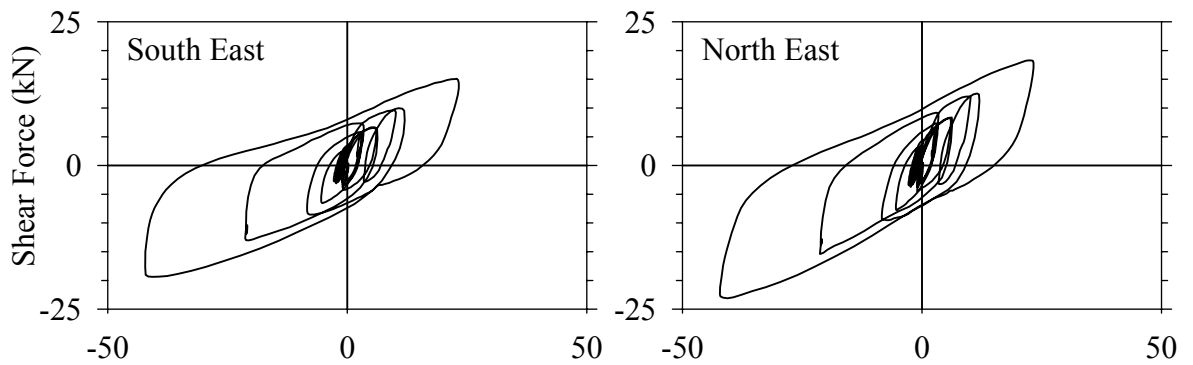
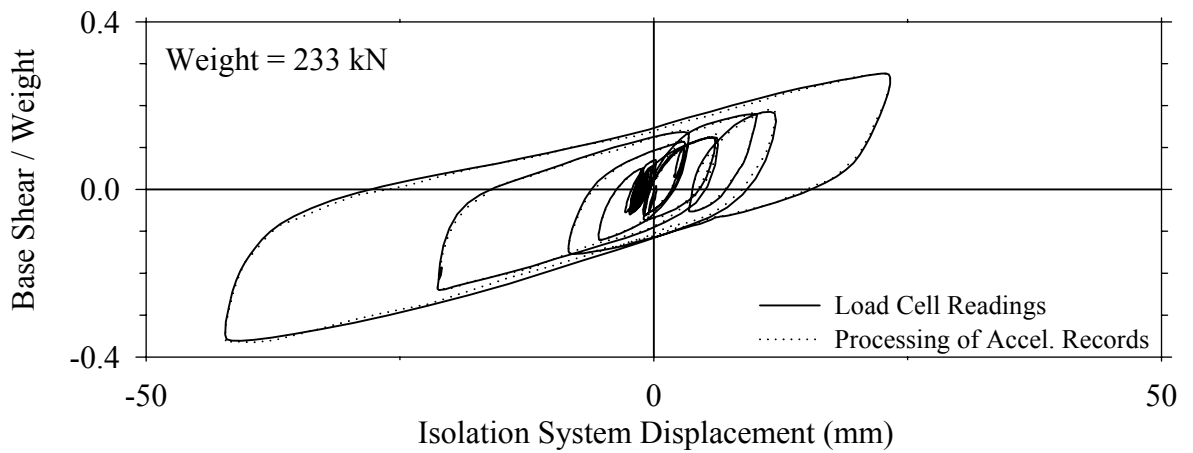
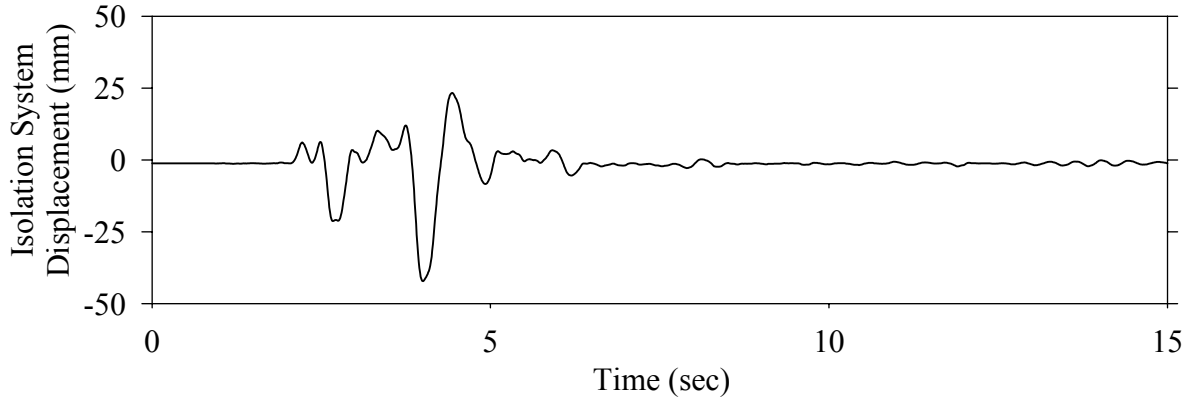
Test LCSBN10.1, Northridge Newhall 360° 100%, SB/Lead Core



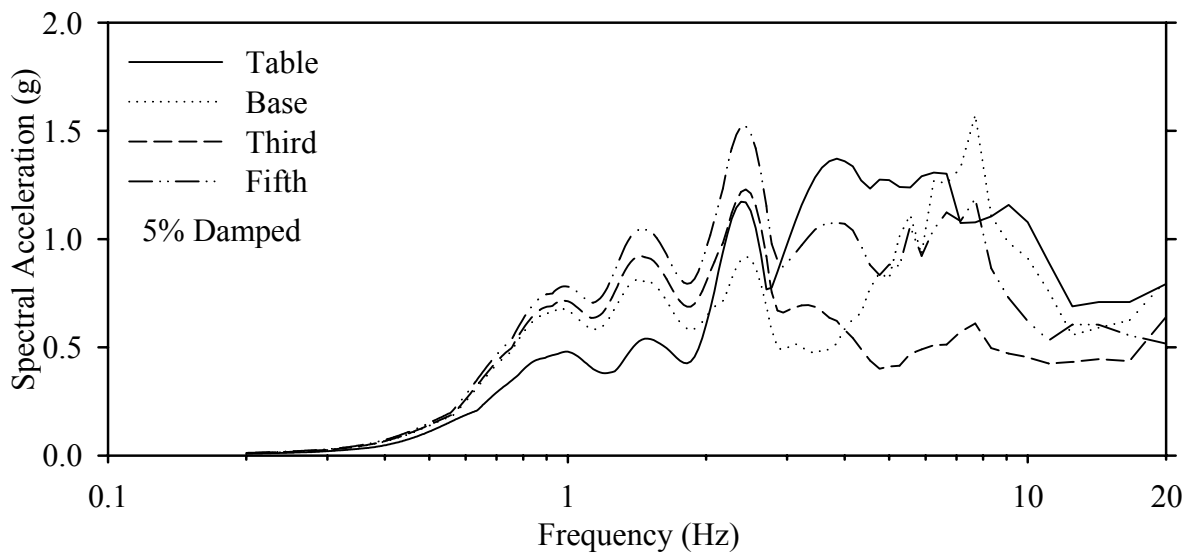
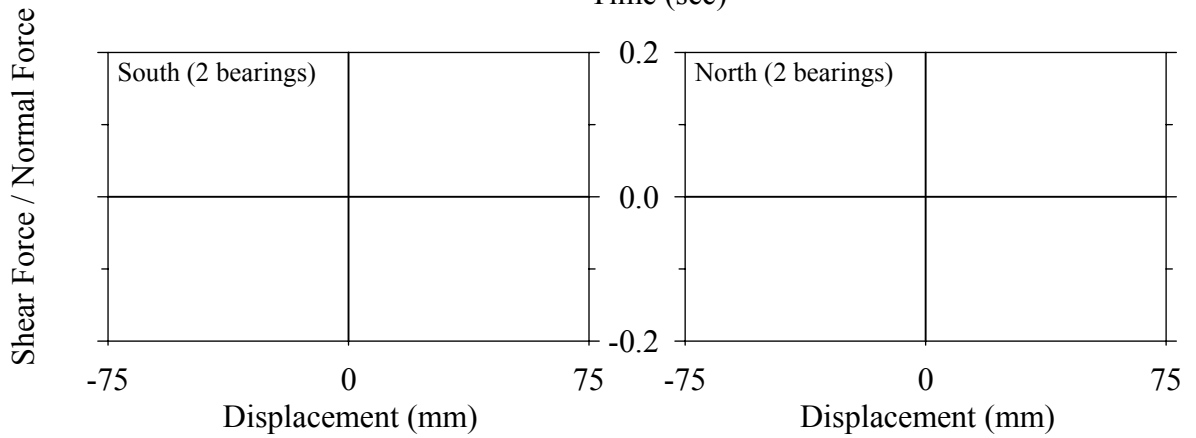
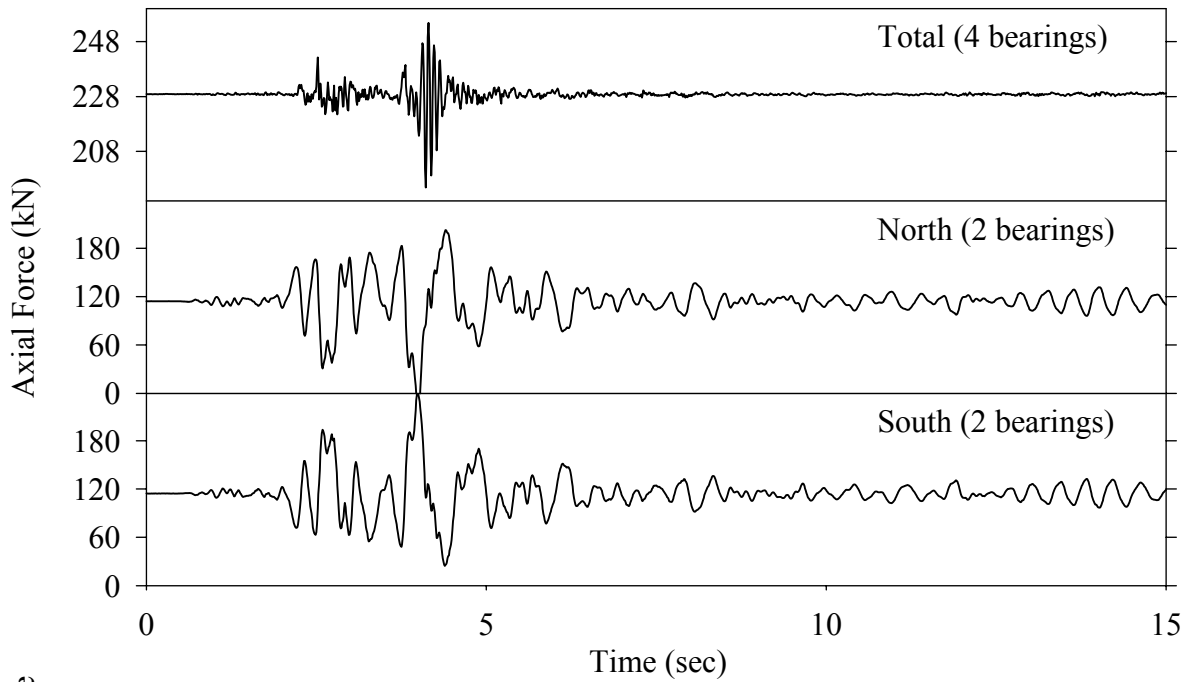
Test LCSBN10.1, Northridge Newhall 360° 100%, SB/Lead Core



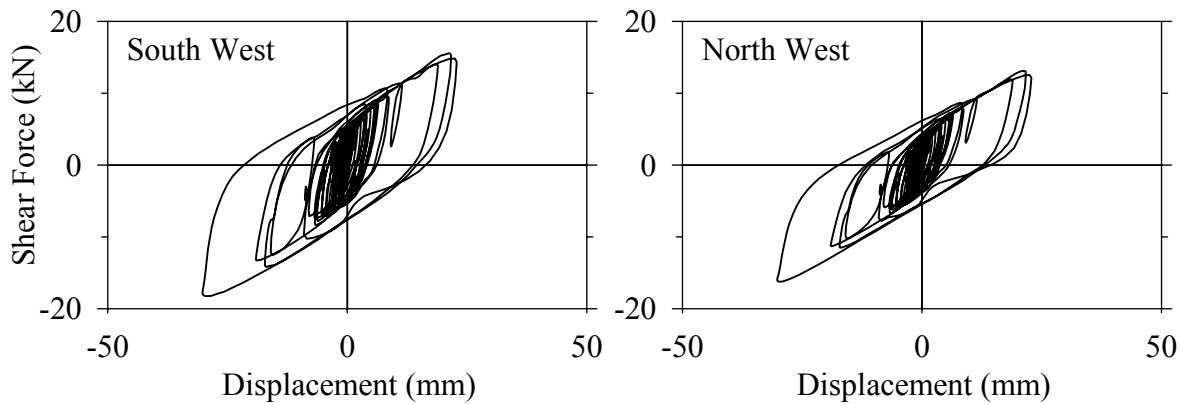
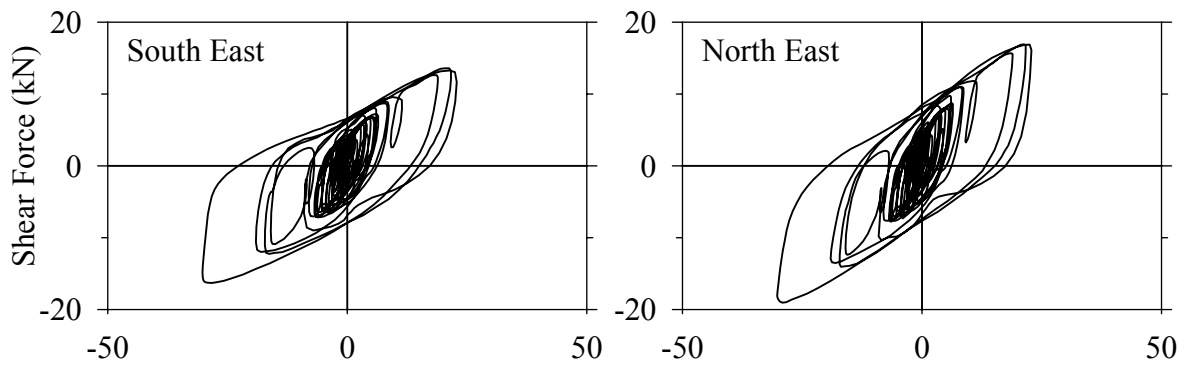
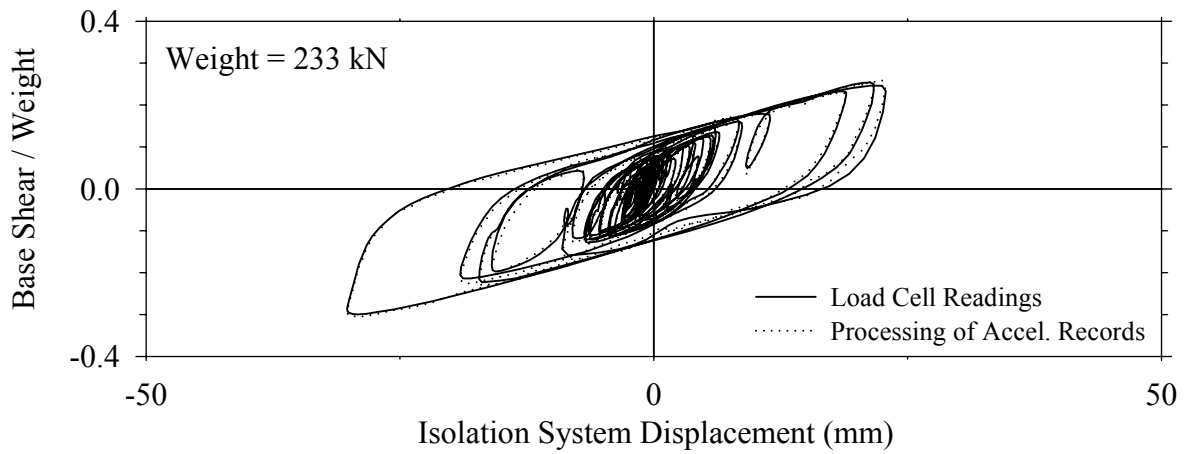
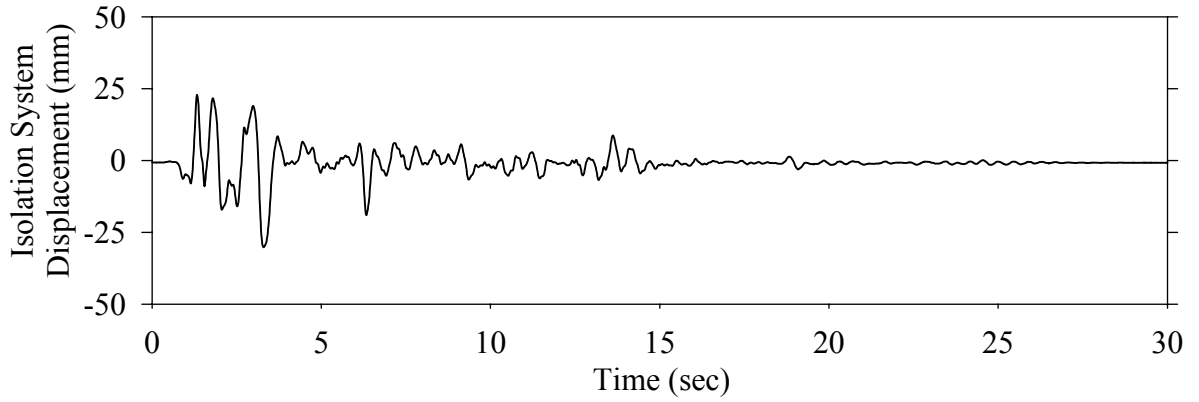
Test LCSBS10.1, Northridge Sylmar 90° 100%, SB/Lead Core



Test LCSBS10.1, Northridge Sylmar 90° 100%, SB/Lead Core

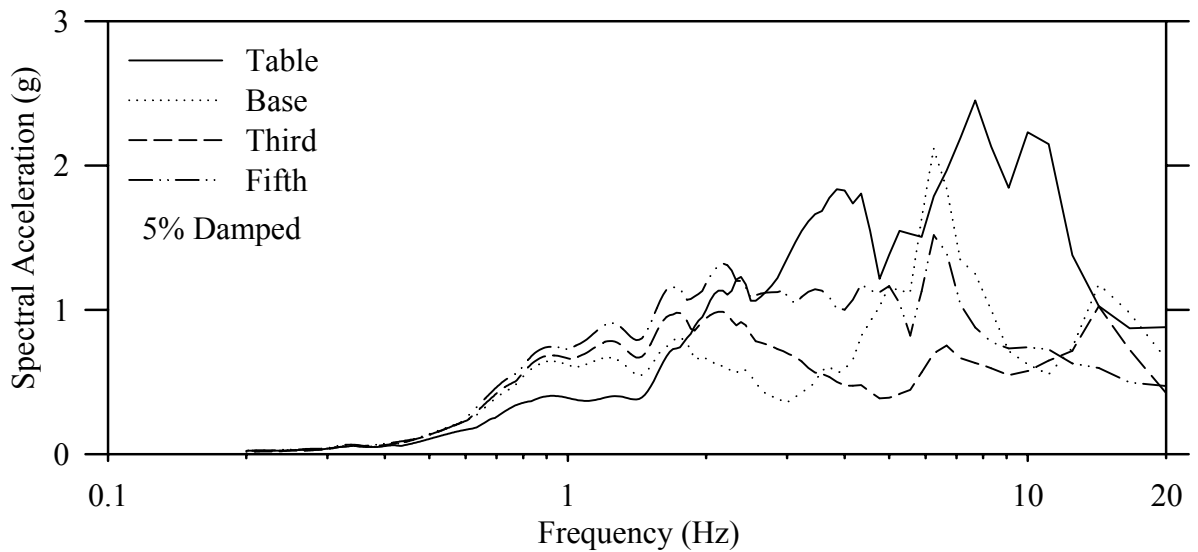
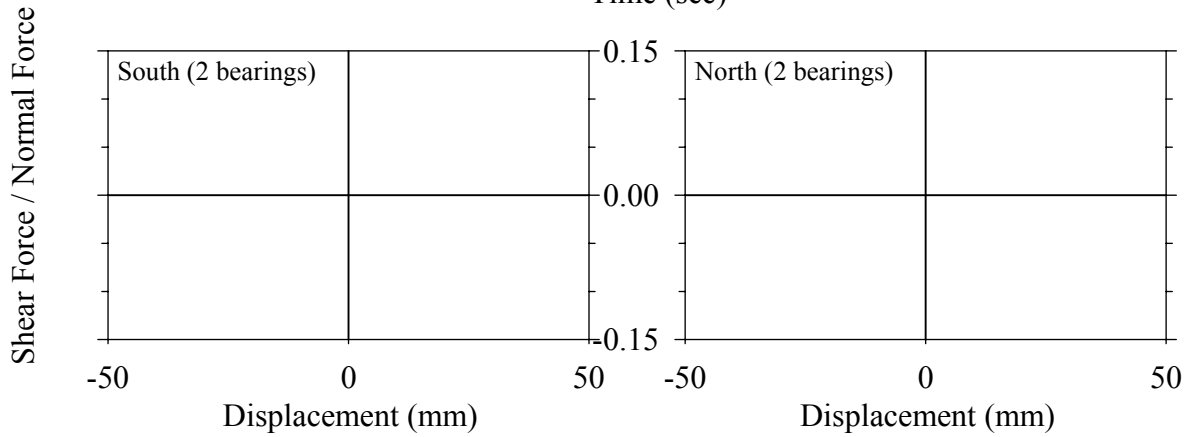
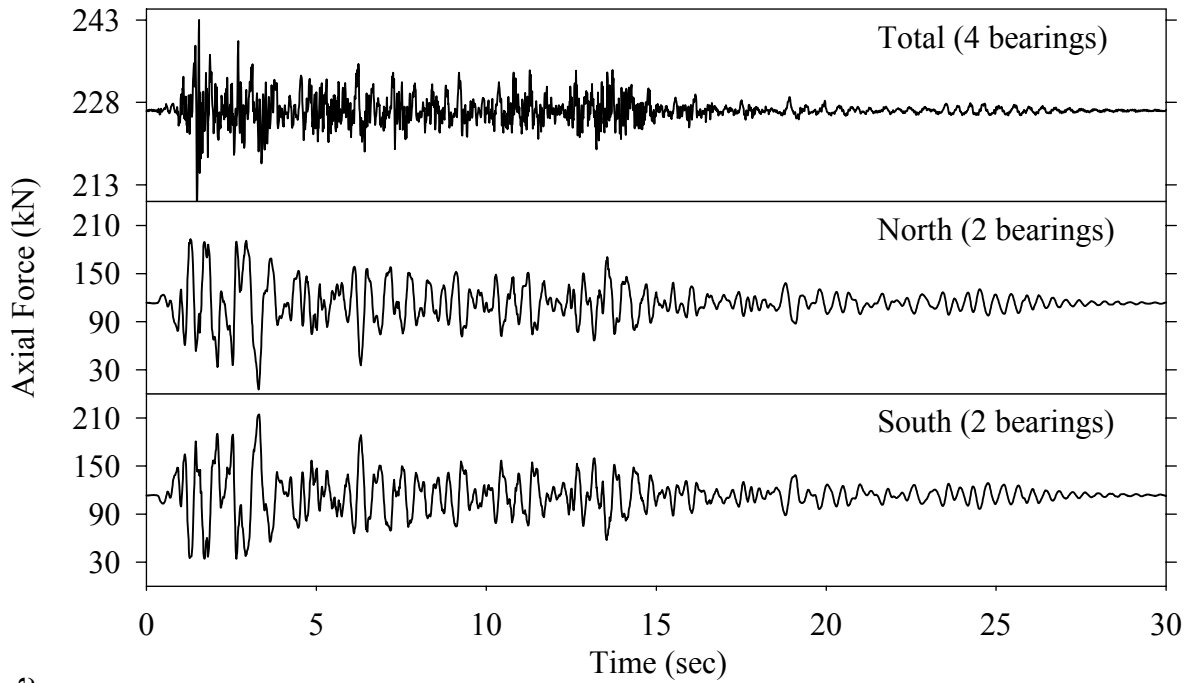


Test LCABE20.1, El Centro S00E 200%, AB/Lead Core

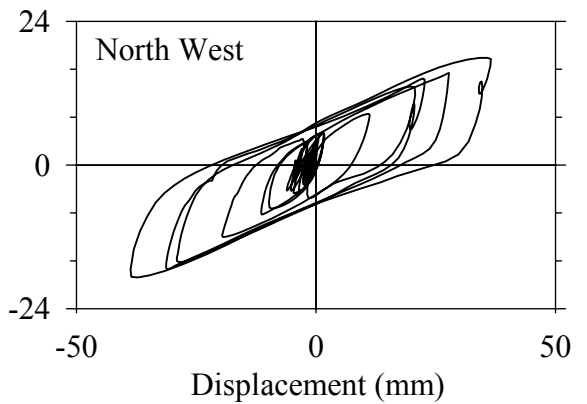
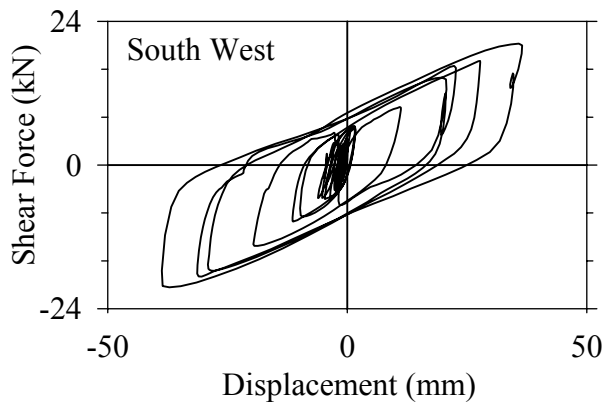
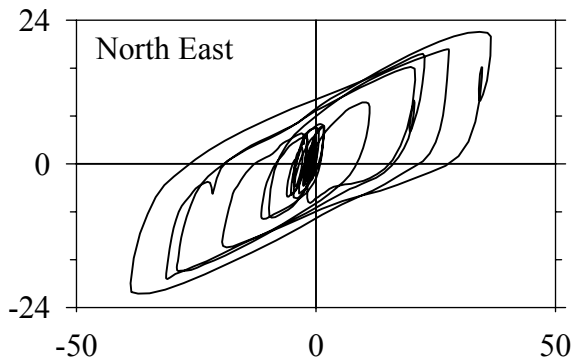
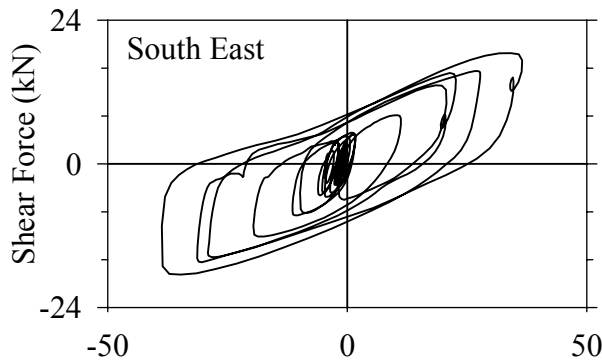
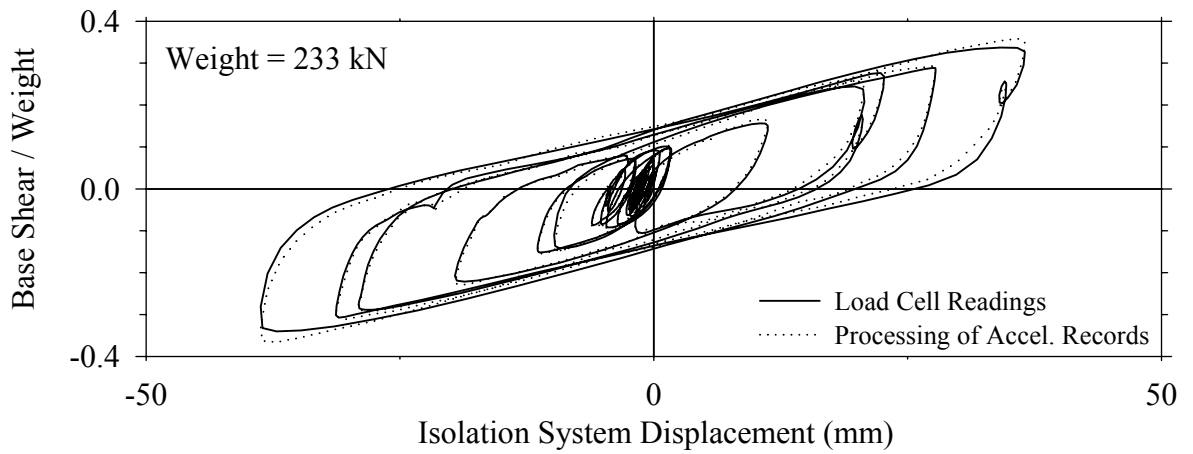
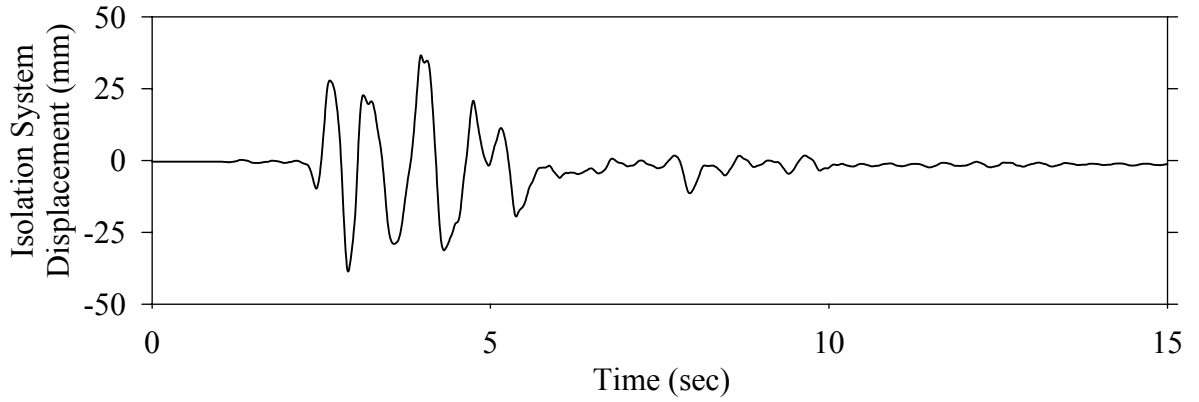




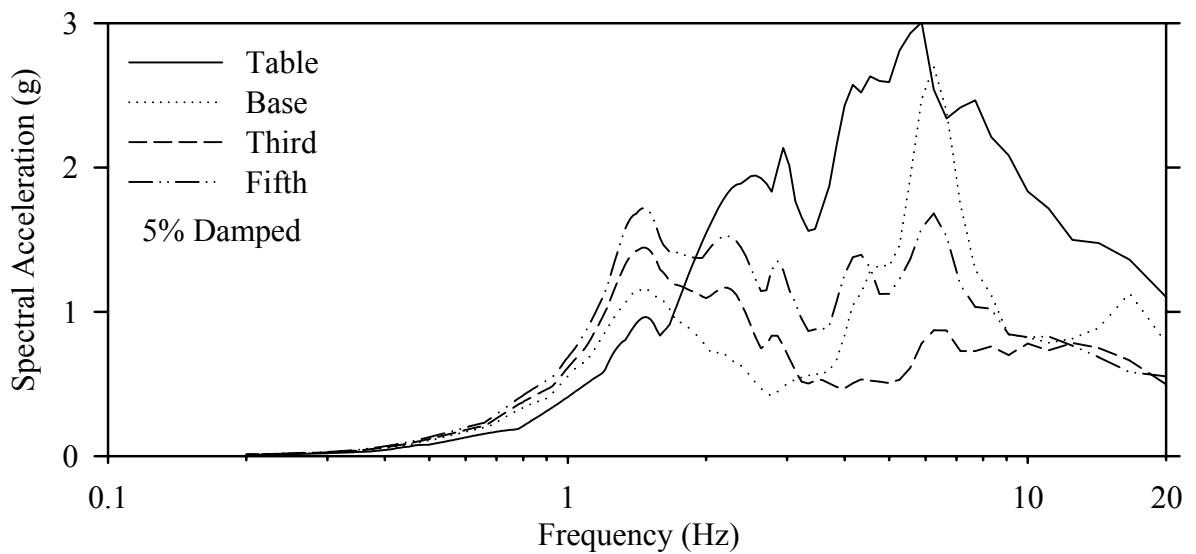
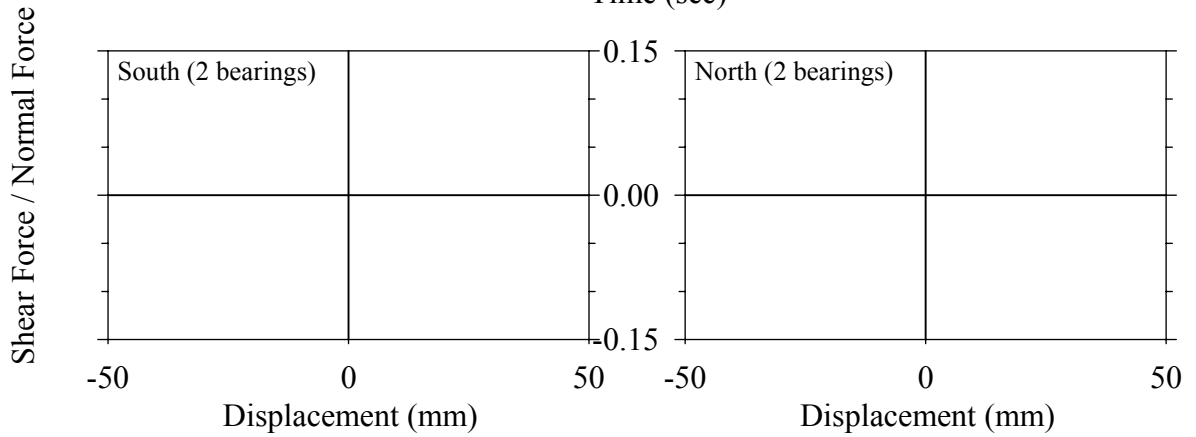
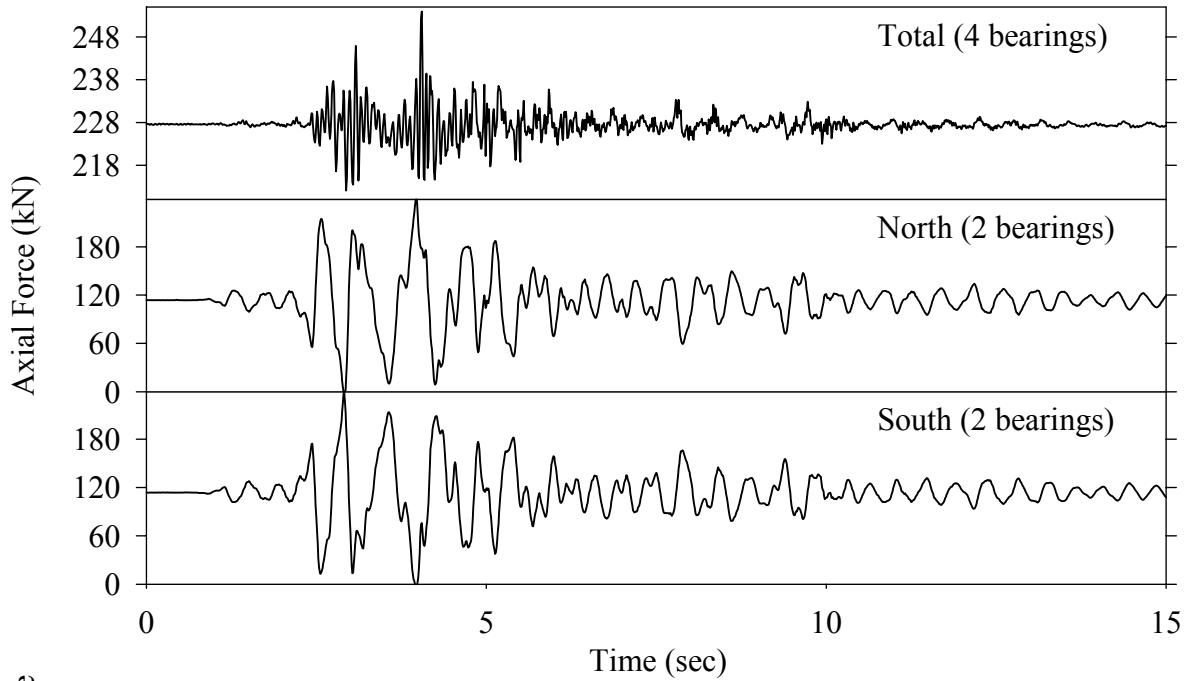
Test LCABE20.1, El Centro S00E 200%, AB/Lead Core



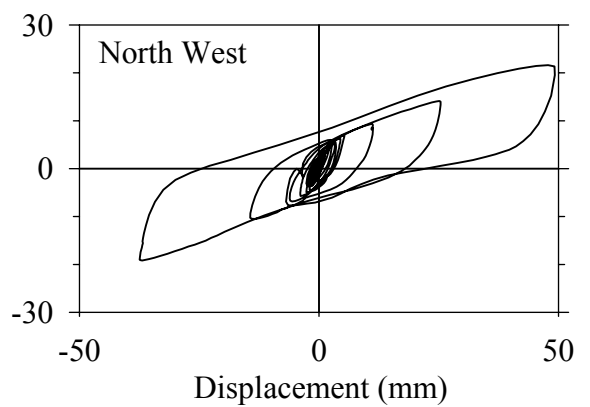
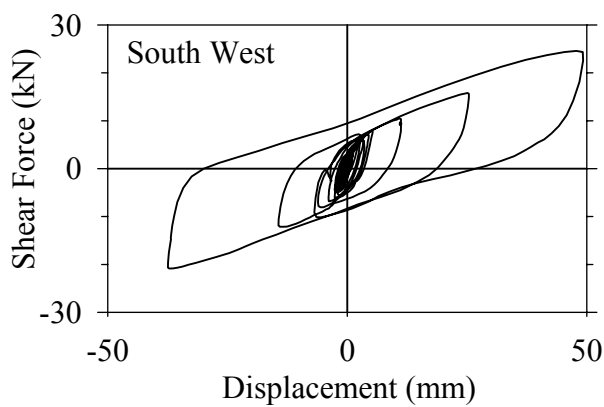
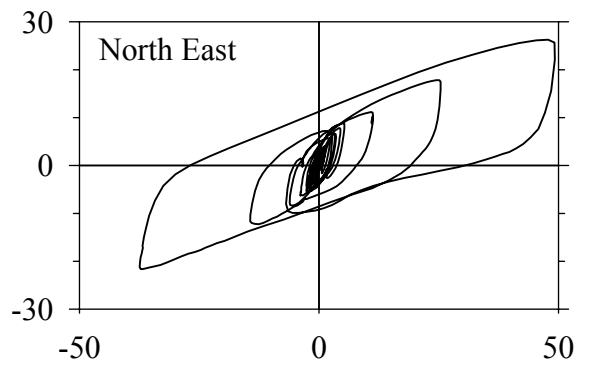
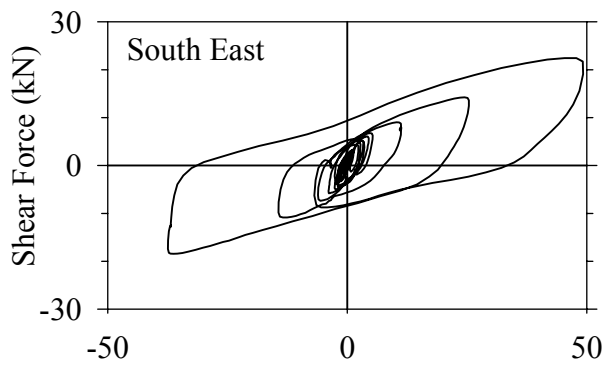
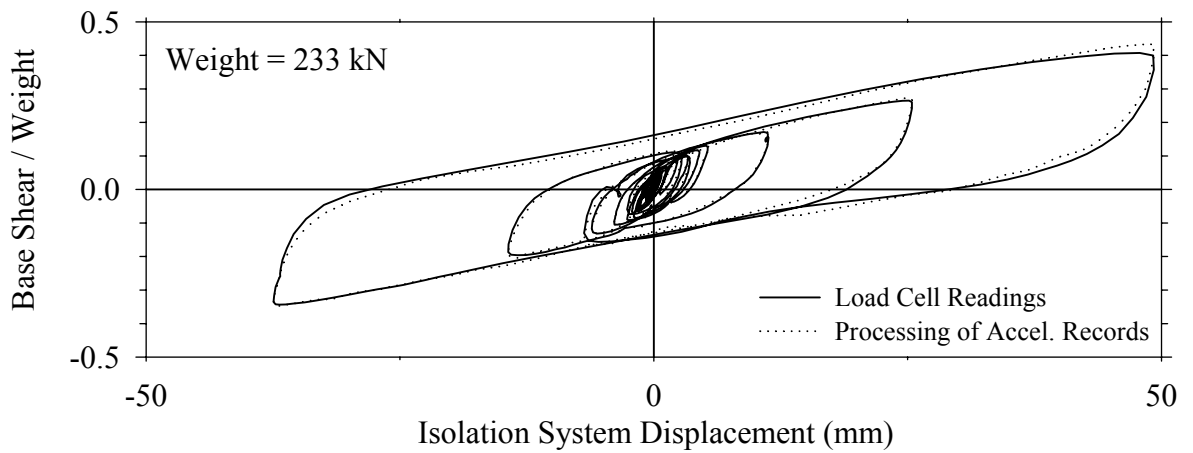
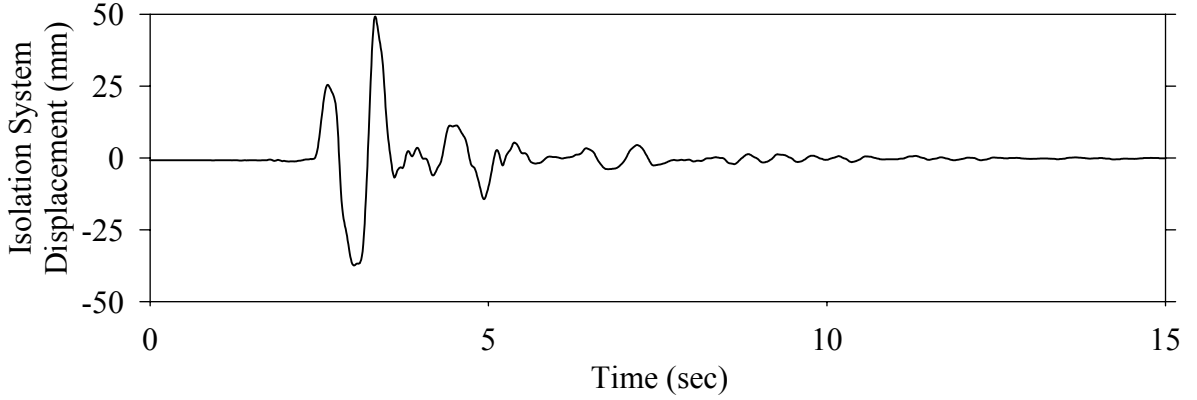
Test LCABK10.1, Kobe N-S 100%, AB/Lead Core



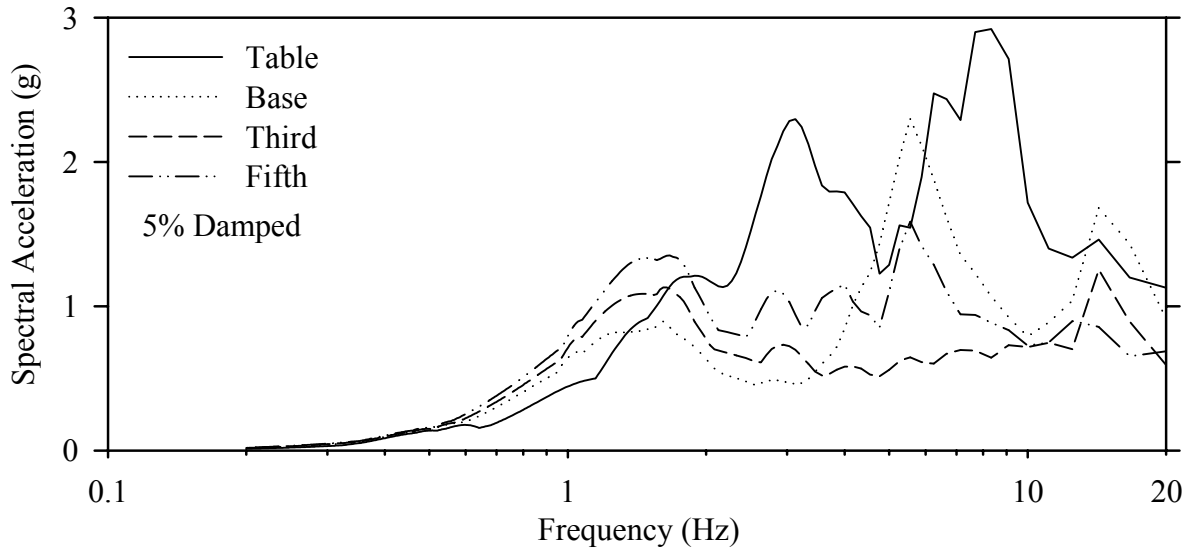
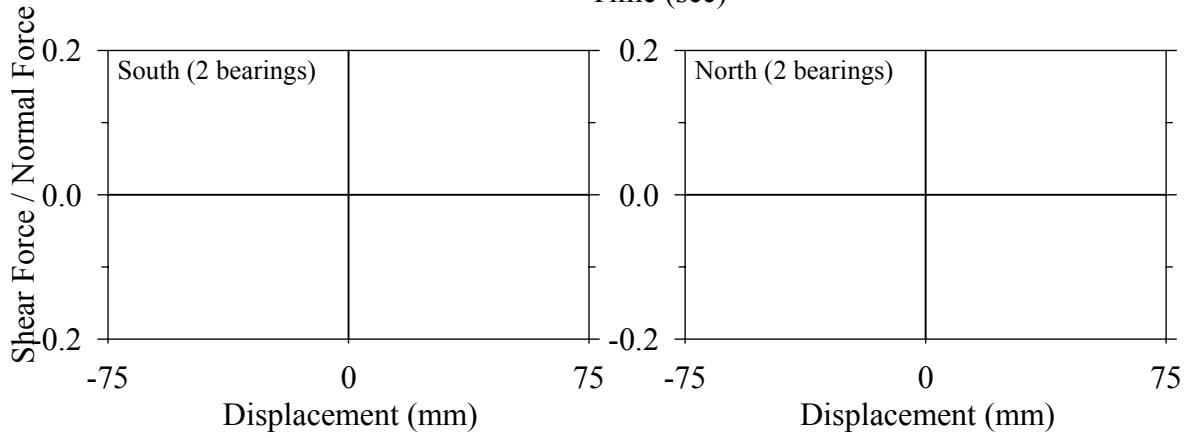
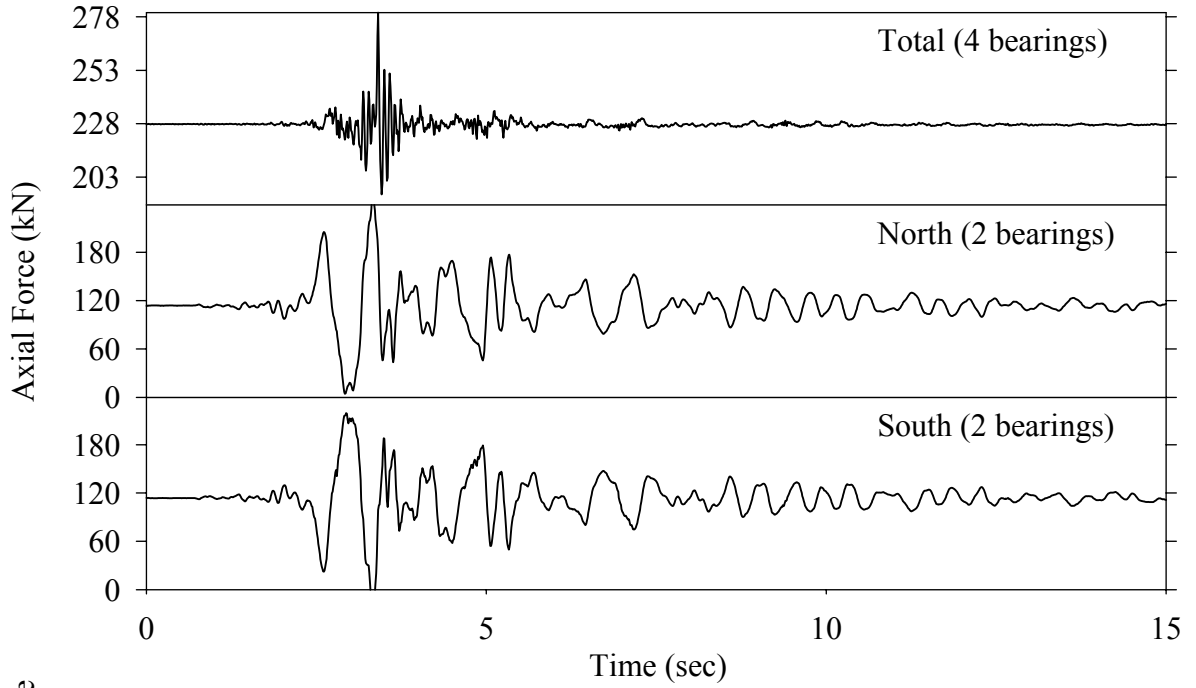
Test LCABK10.1, Kobe N-S 100%, AB/Lead Core



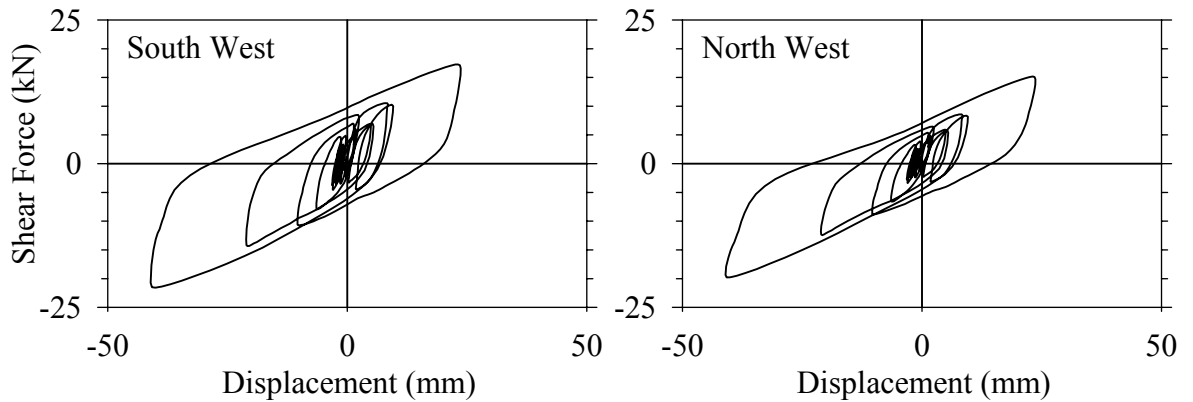
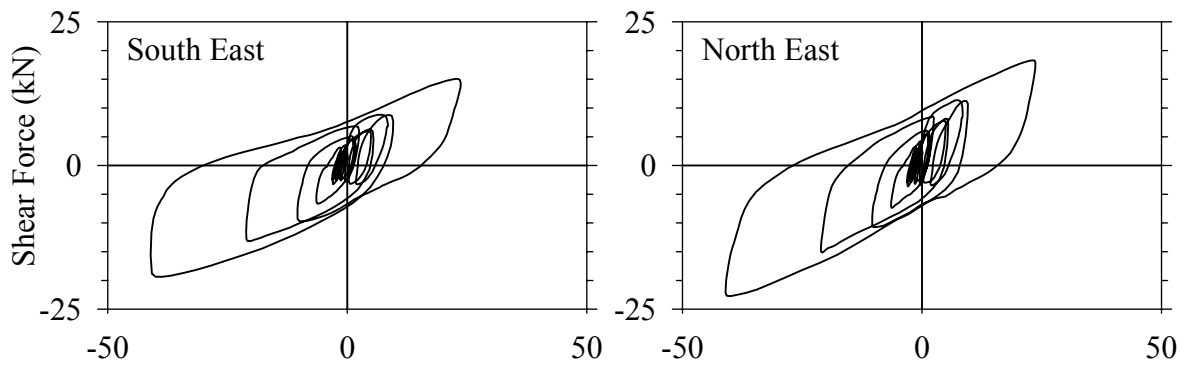
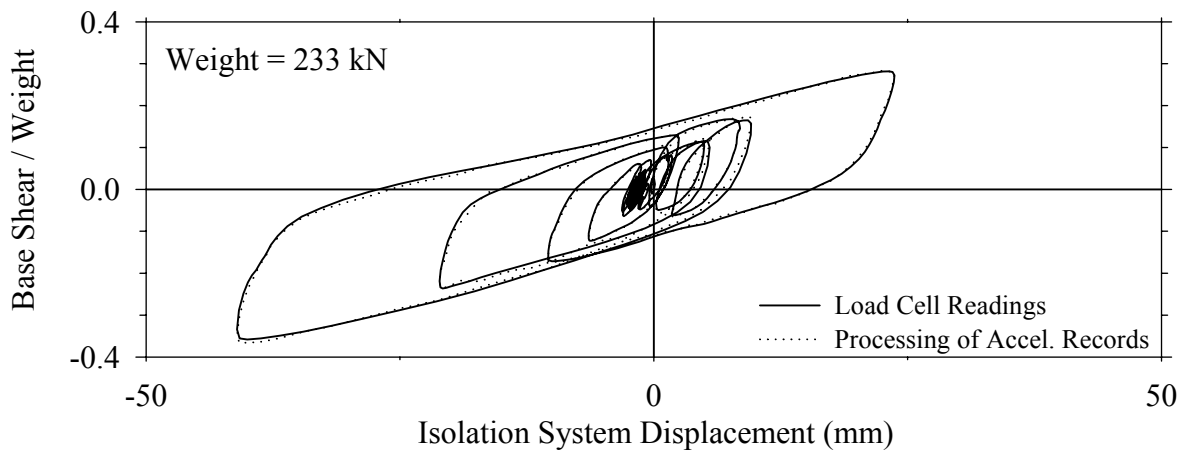
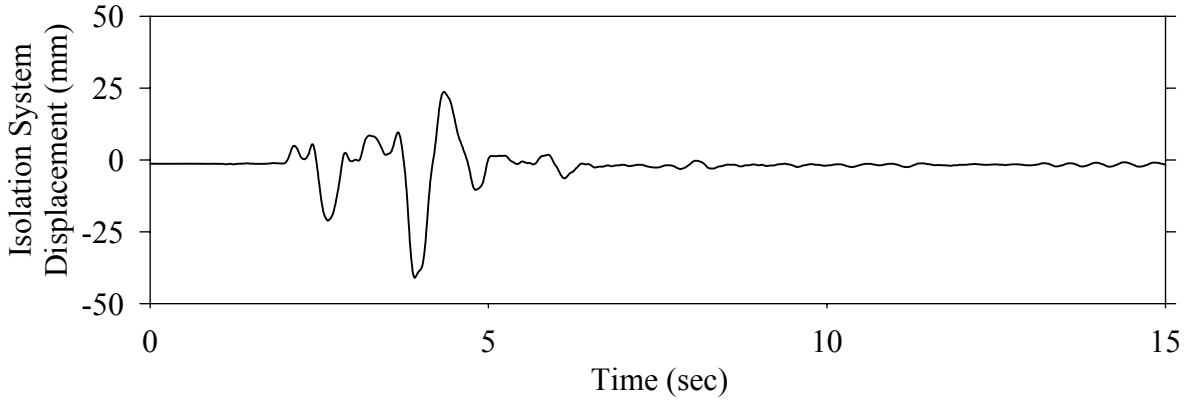
Test LCABN10.1, Northridge Newhall 360° 100%, AB/Lead Core



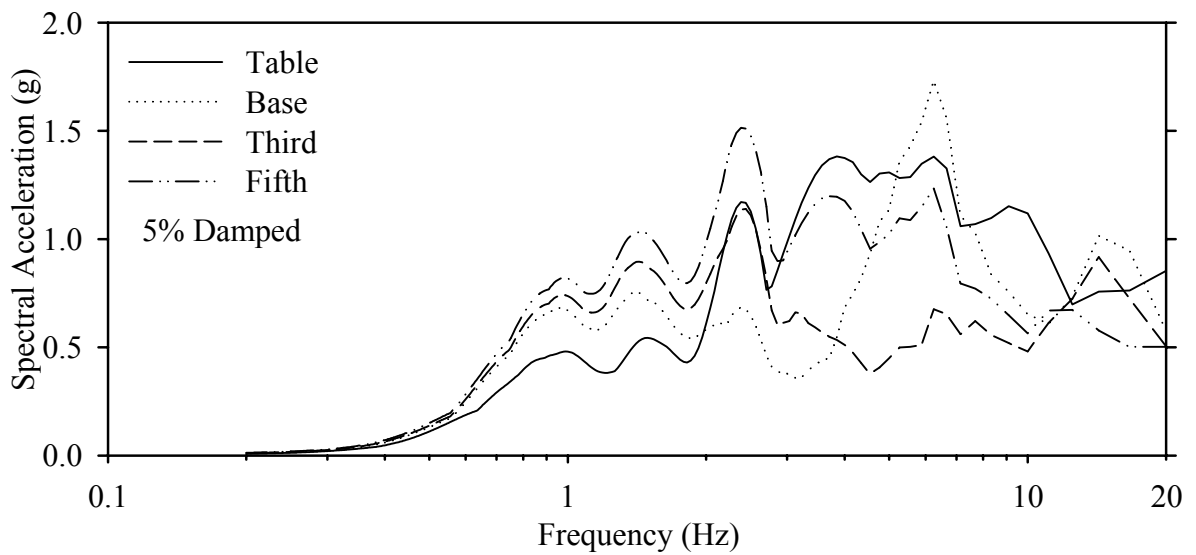
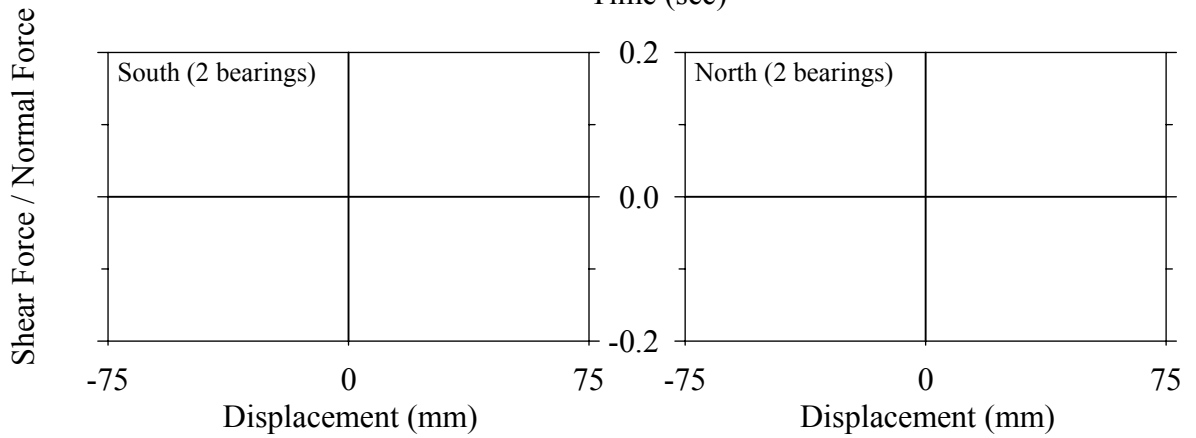
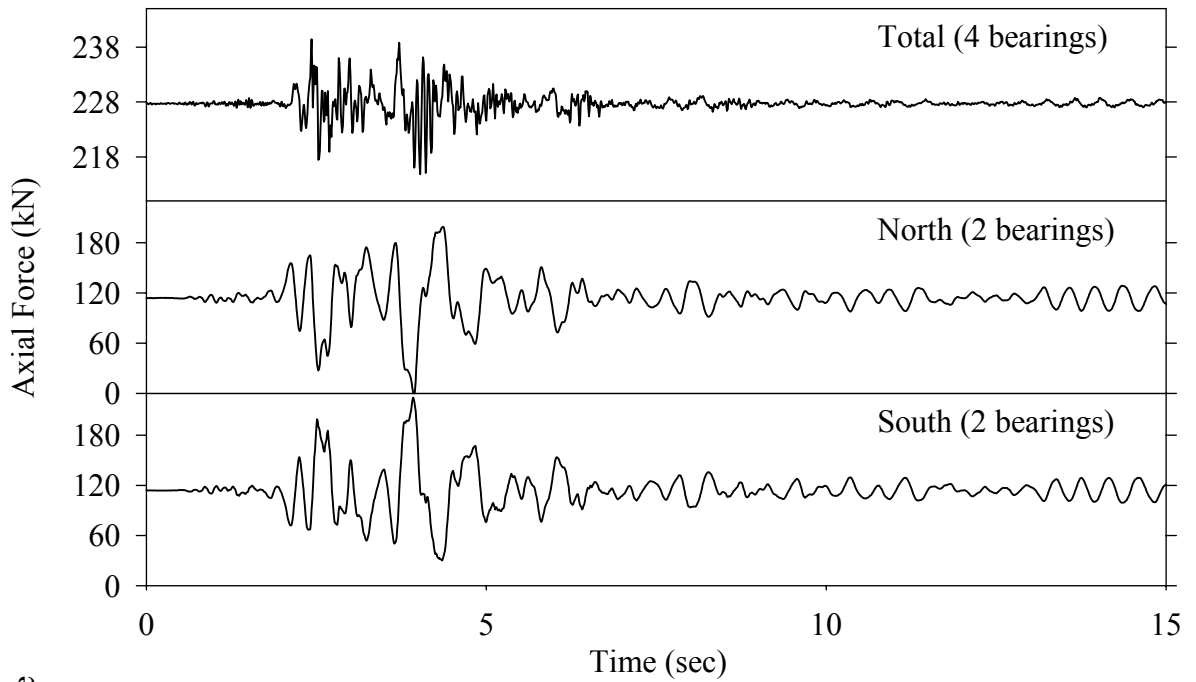
Test LCABN10.1, Northridge Newhall 360° 100%, AB/Lead Core



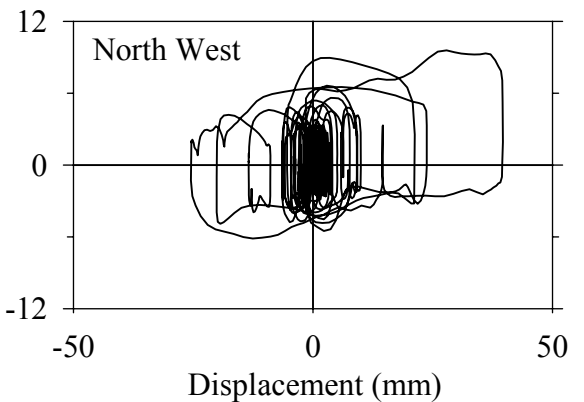
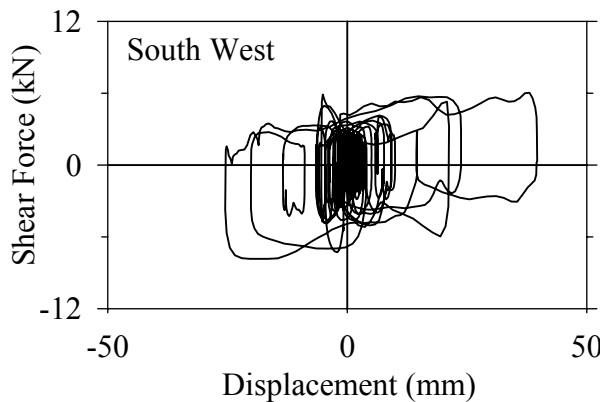
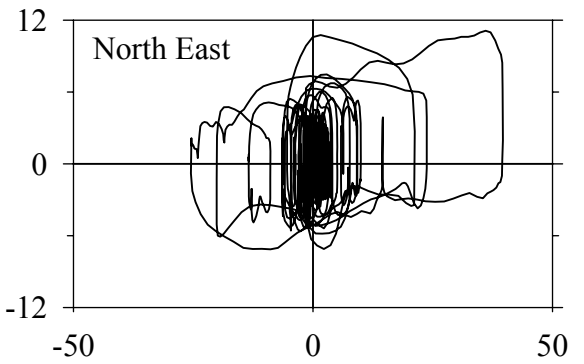
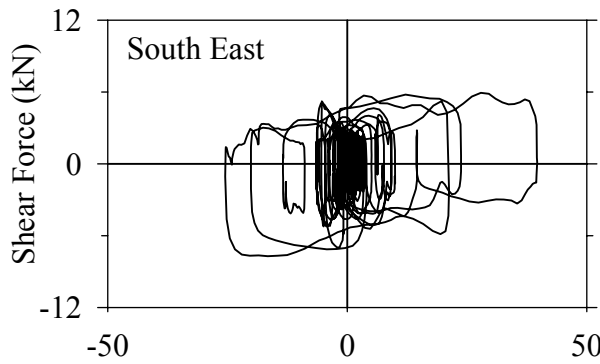
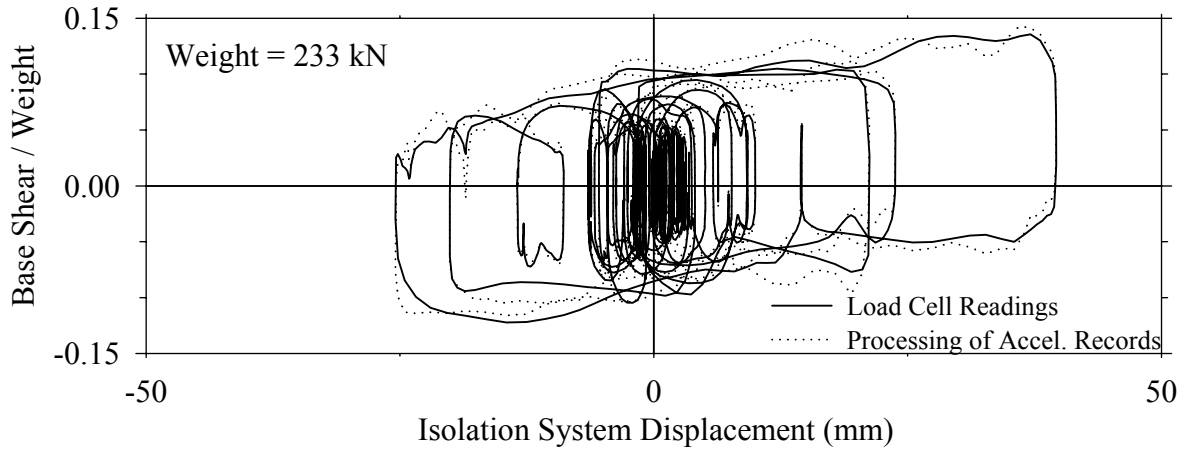
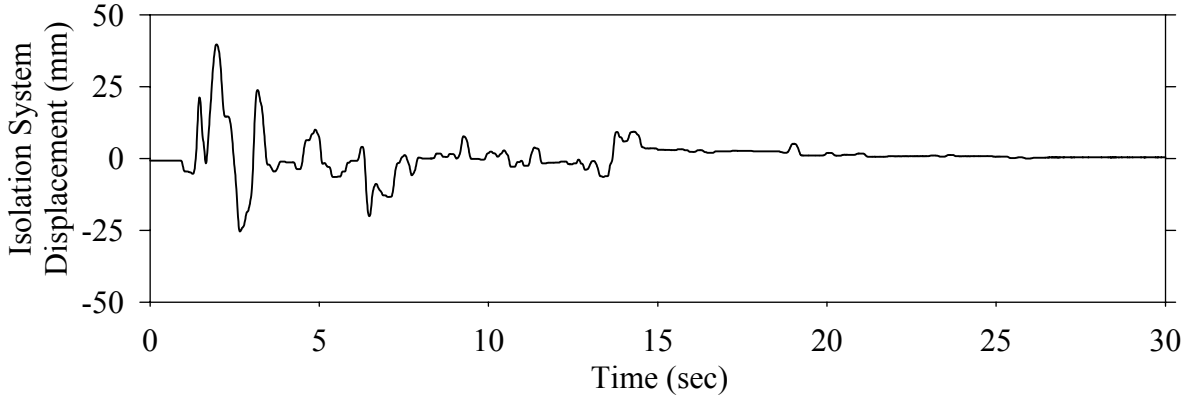
Test LCABS10.1, Northridge Sylmar 90° 100%, AB/Lead Core



Test LCABS10.1, Northridge Sylmar 90° 100%, AB/Lead Core

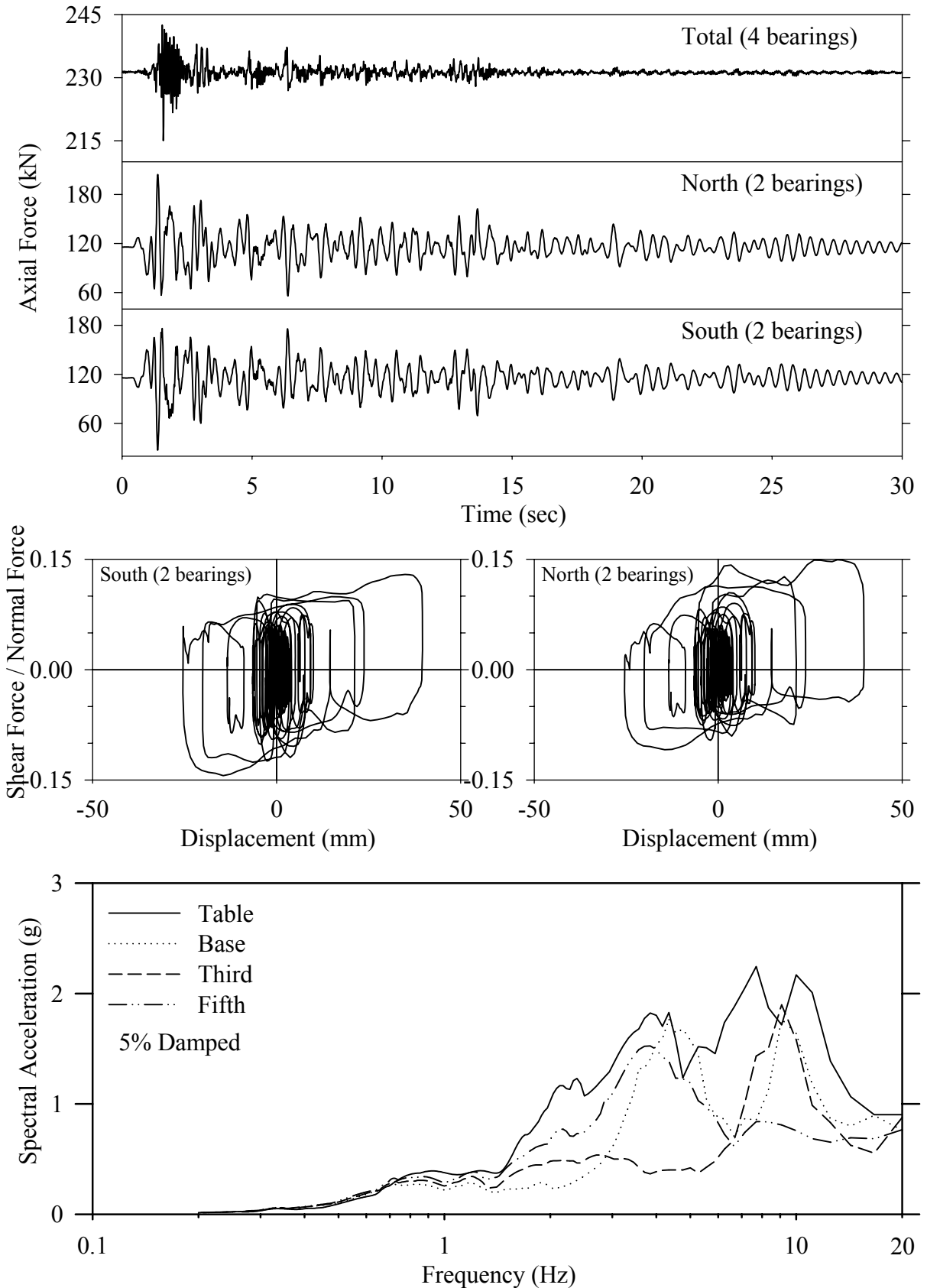


Test FPMFE20.1, El Centro S00E 200%, MF/FPS

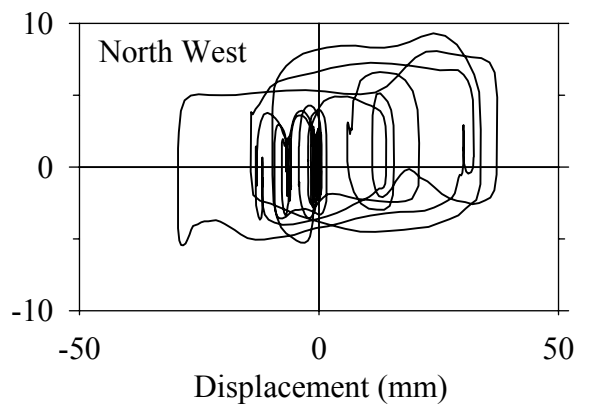
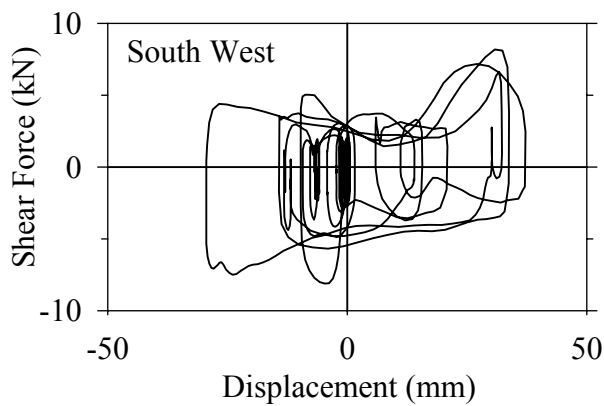
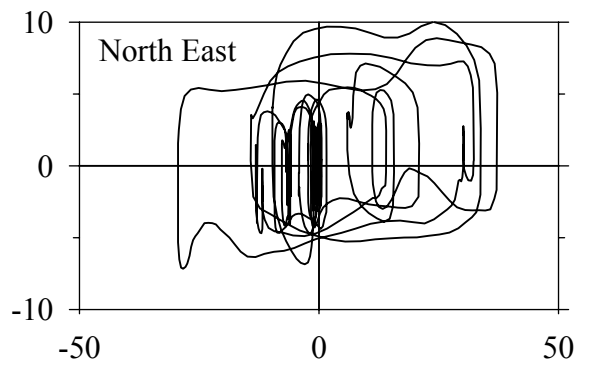
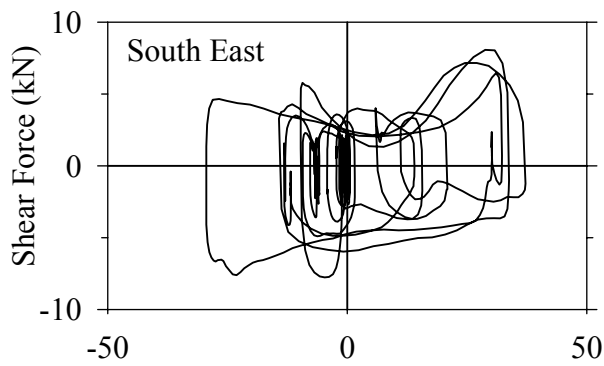
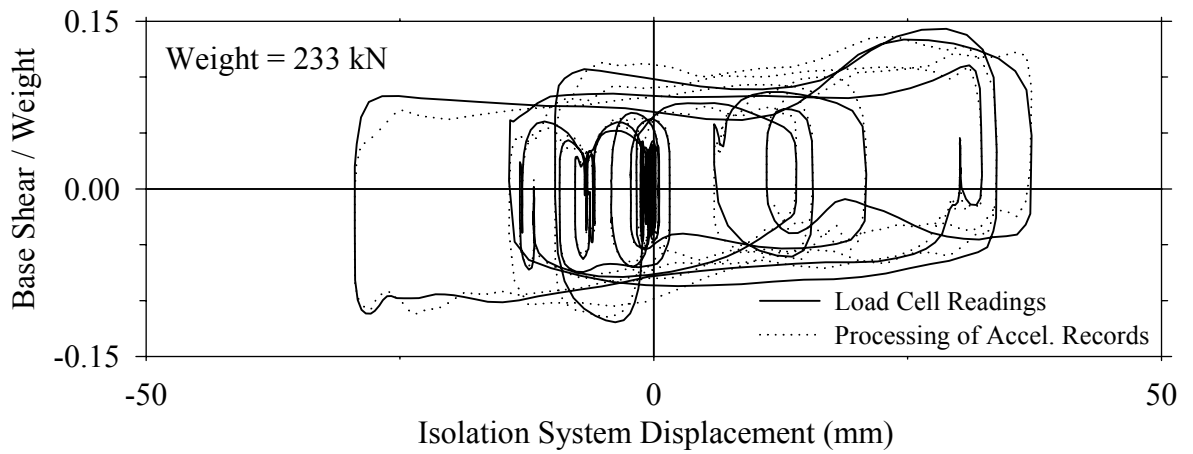
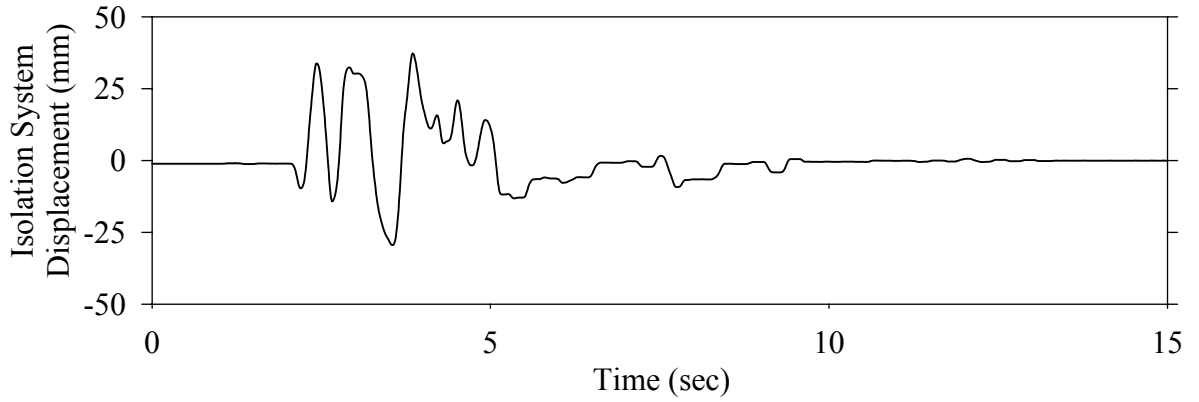




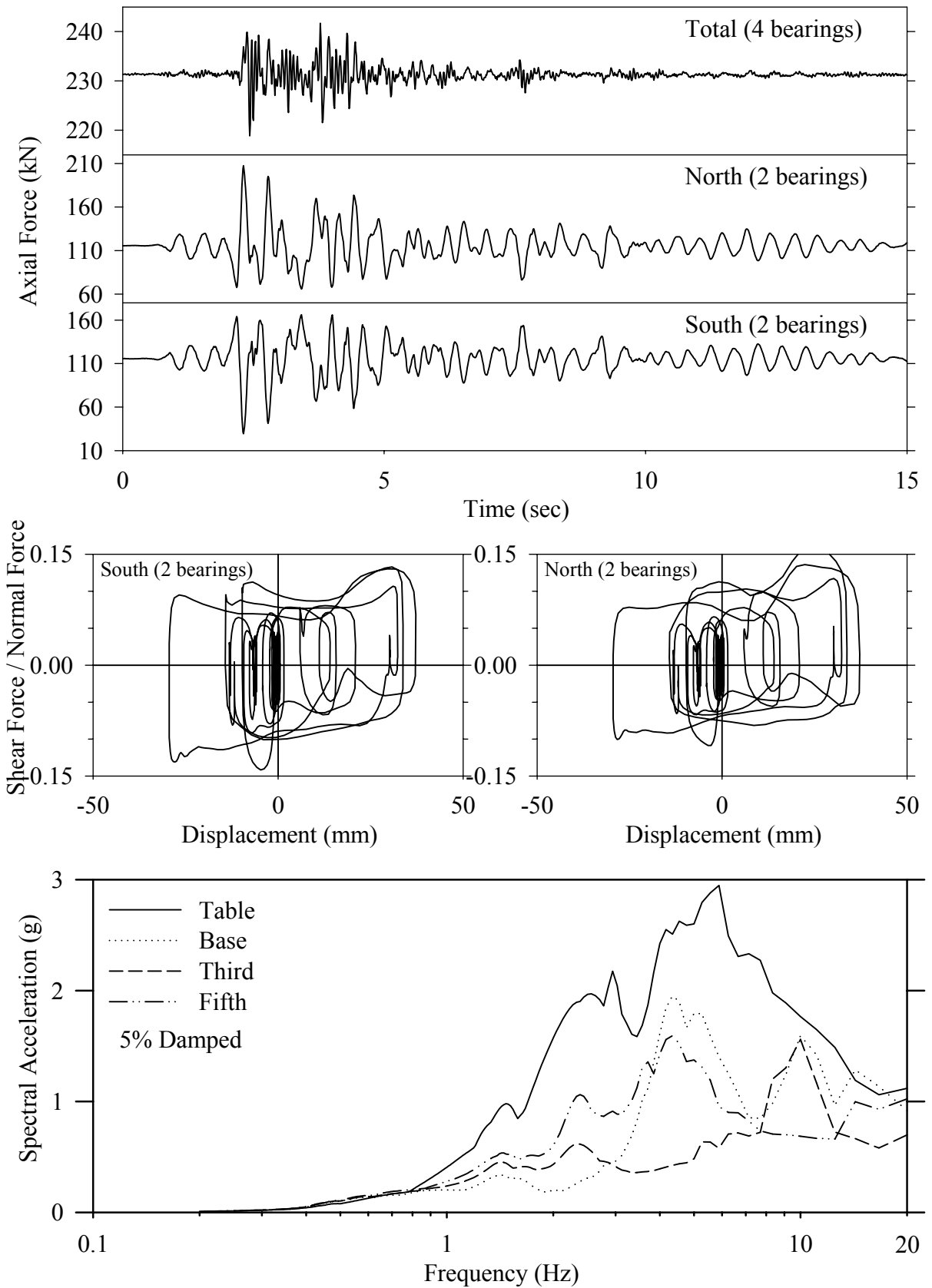
Test FPMFE20.1, El Centro S00E 200%, MF/FPS



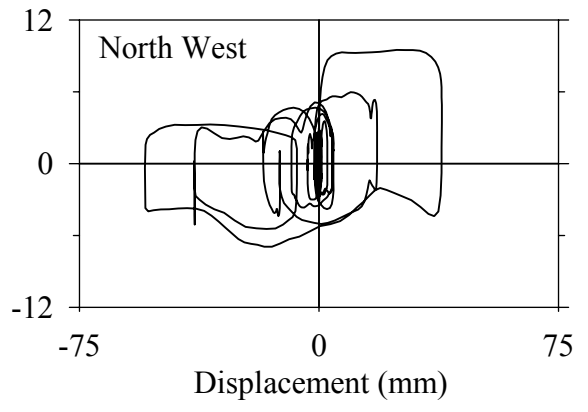
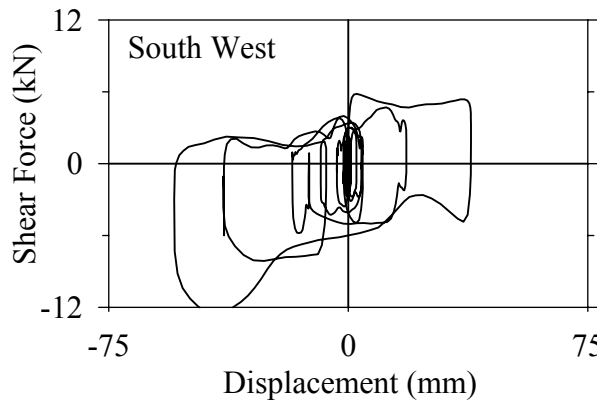
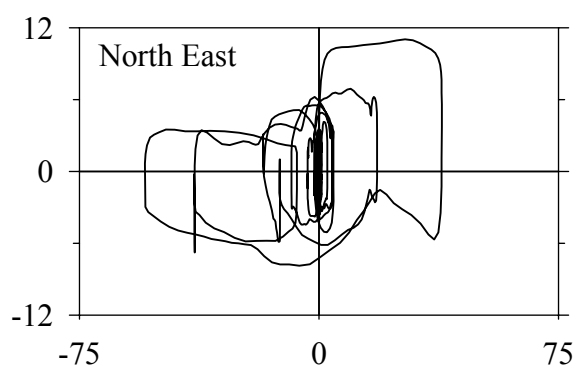
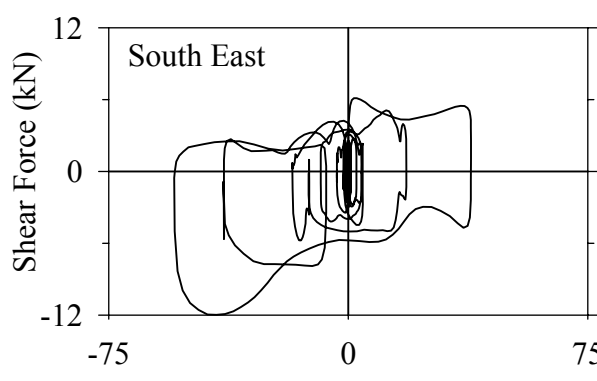
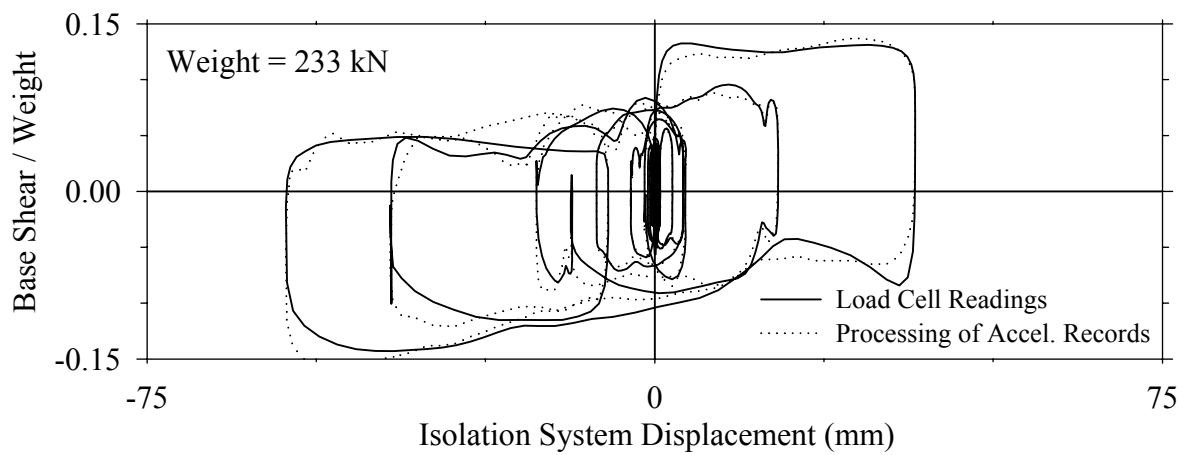
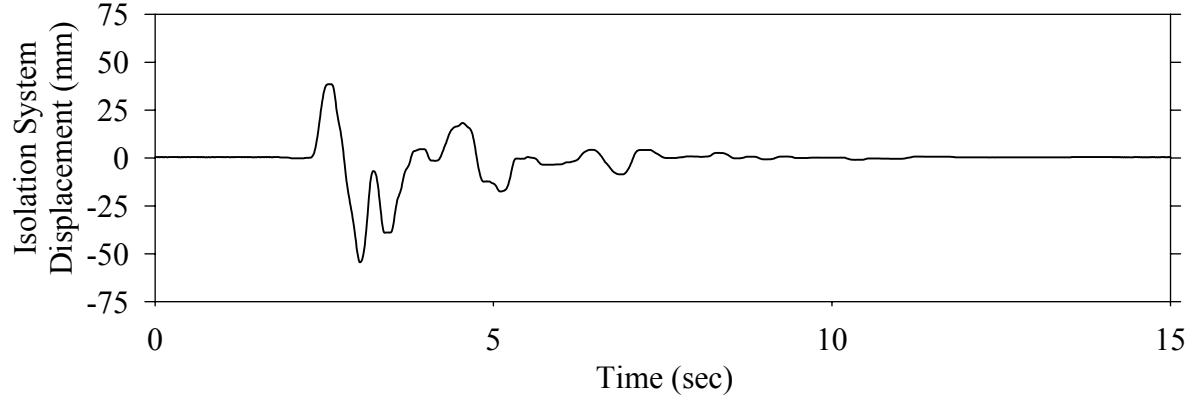
Test FPMFK10.1, Kobe N-S 100%, MF/FPS



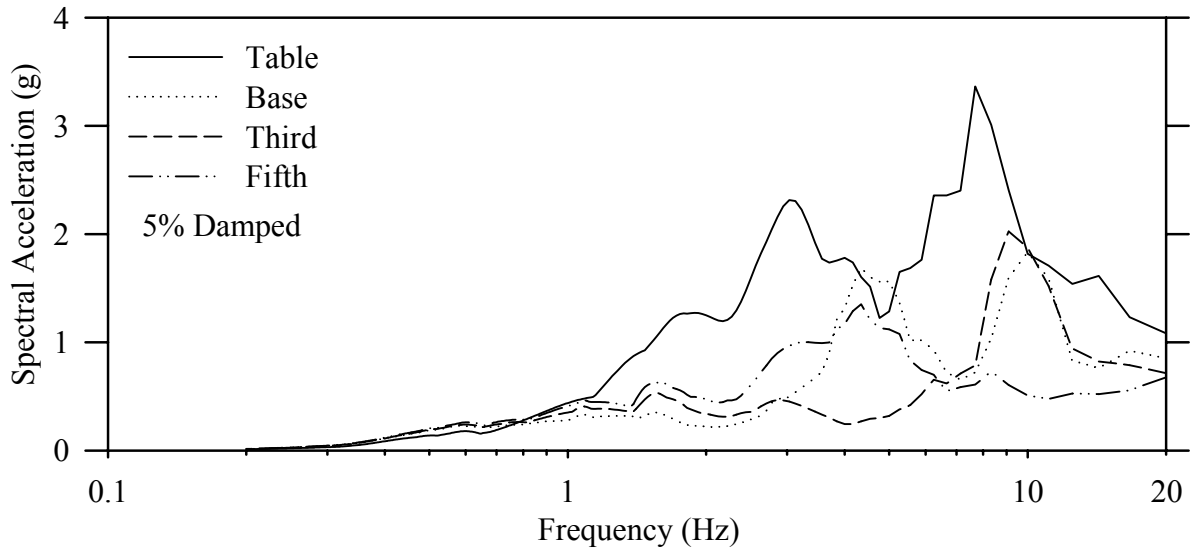
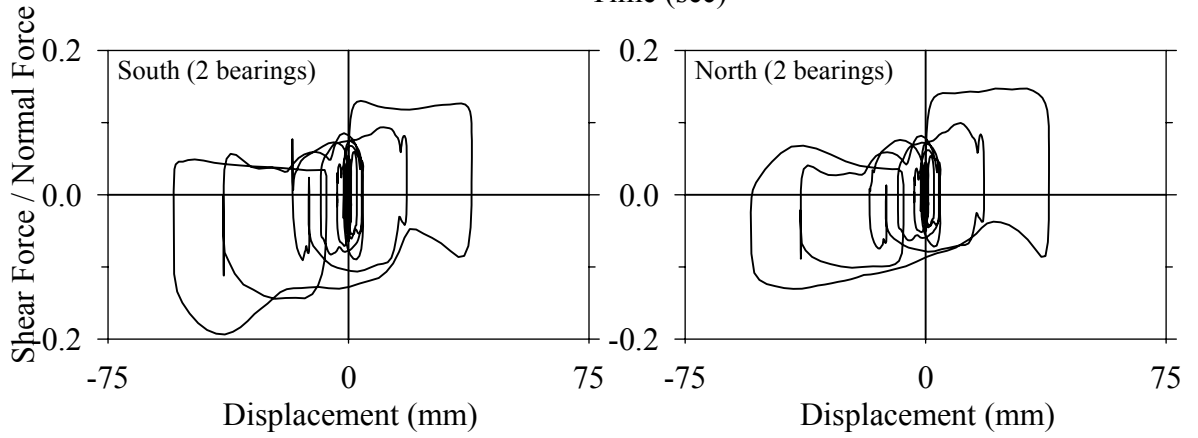
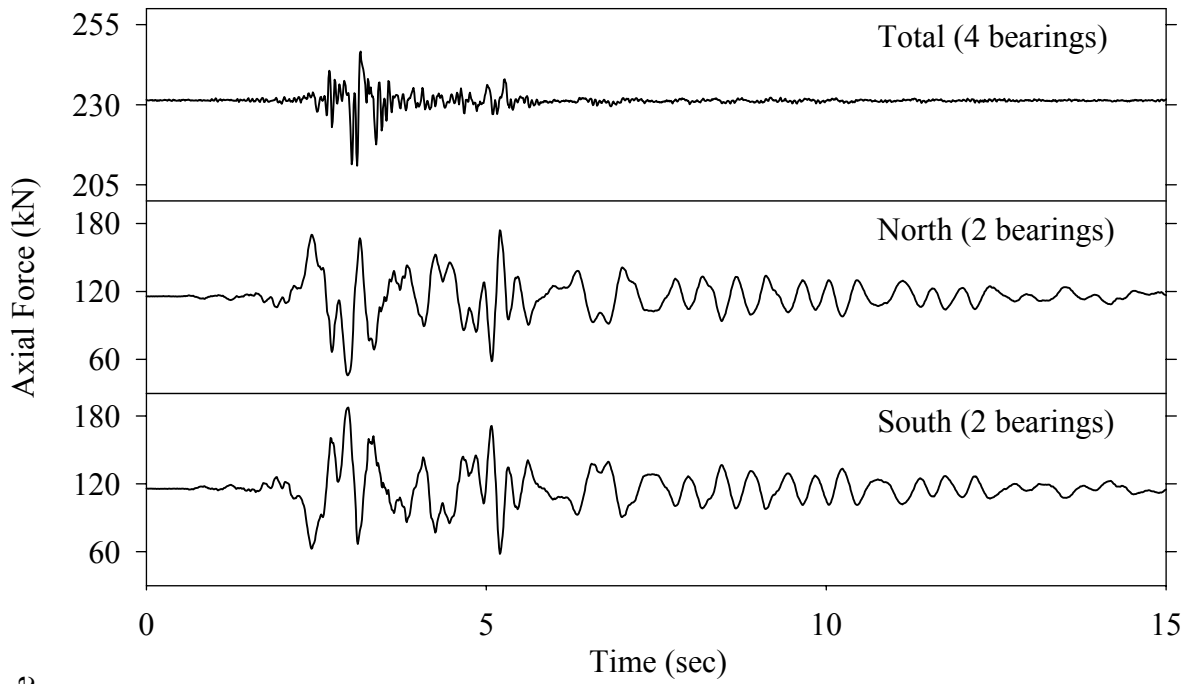
Test FPMFK10.1, Kobe N-S 100%, MF/FPS



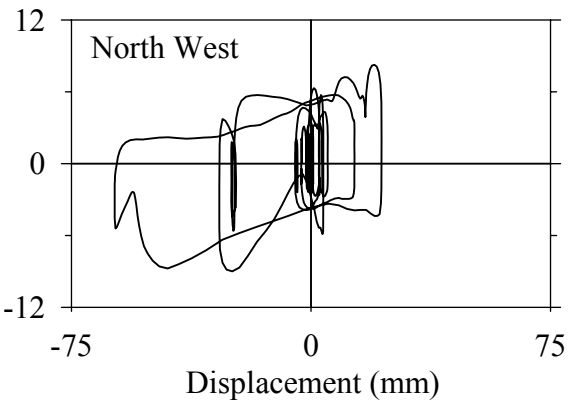
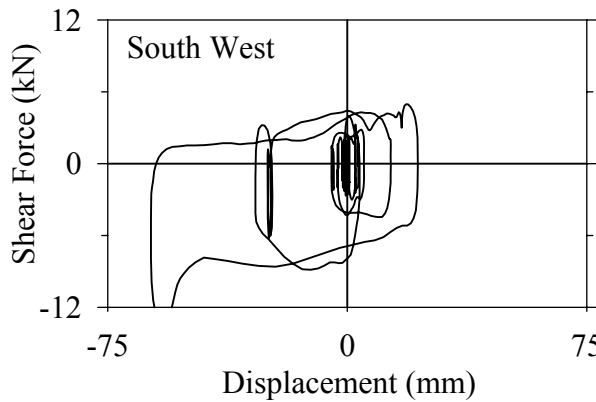
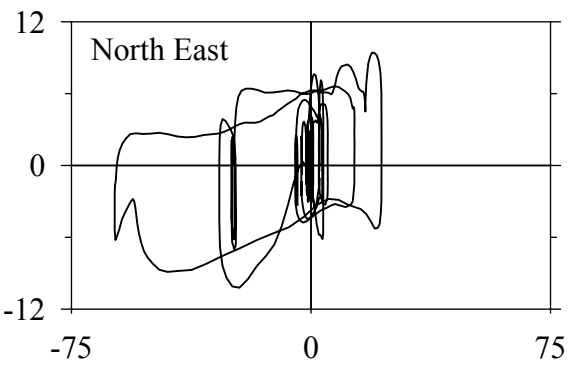
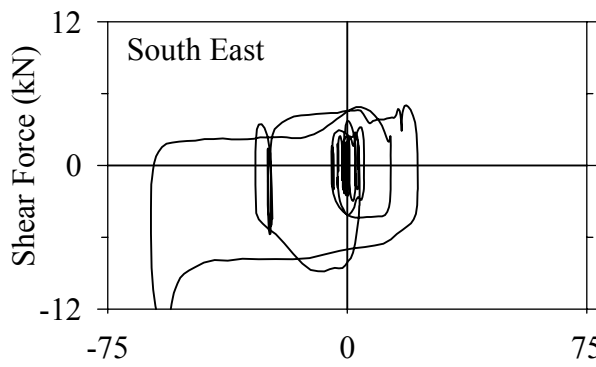
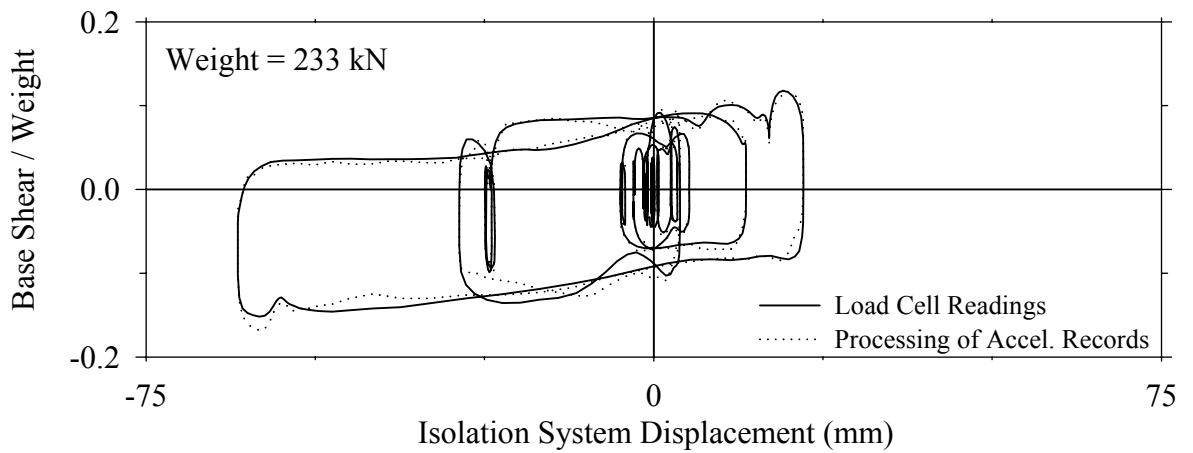
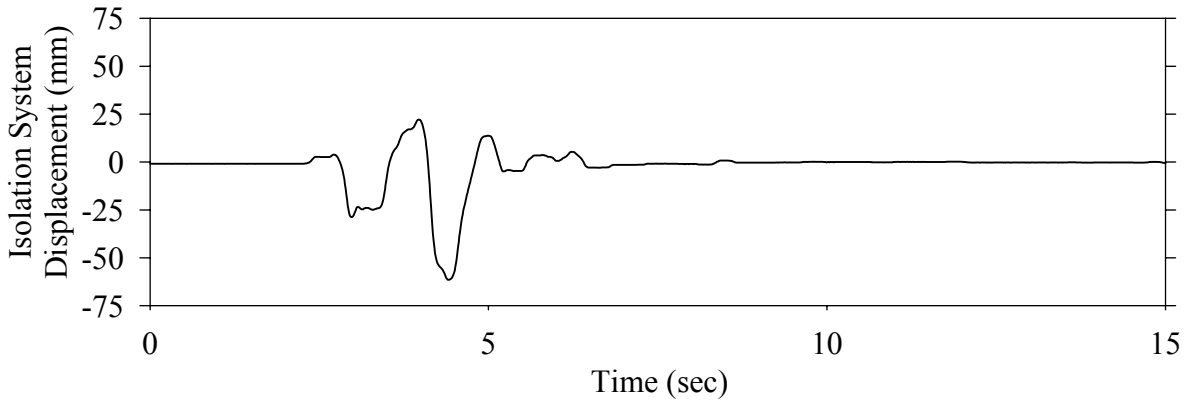
Test FPMFN10.1, Northridge Newhall 360° 100%, MF/FPS



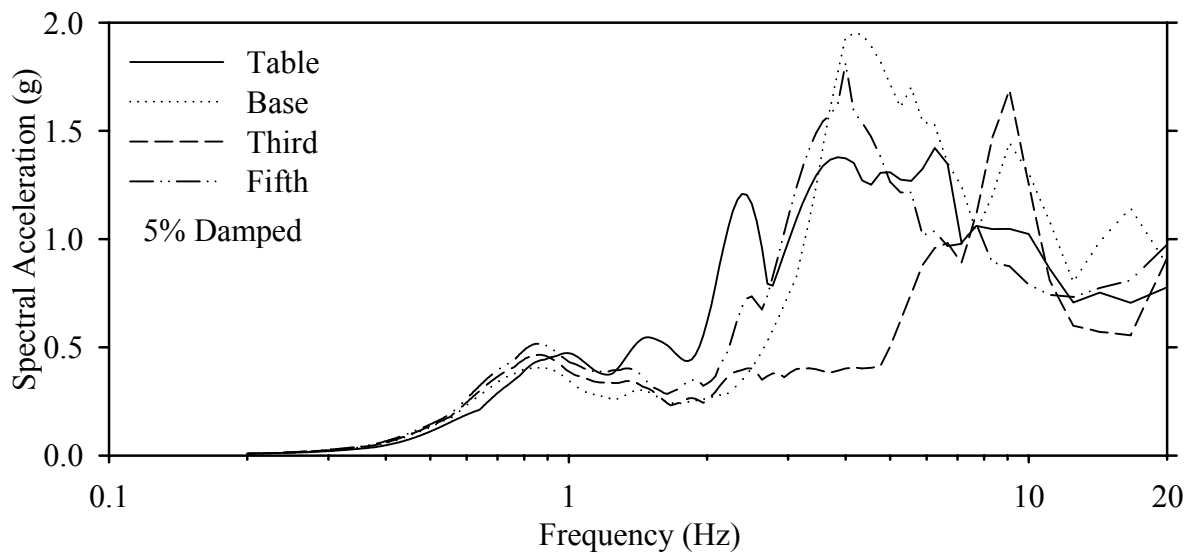
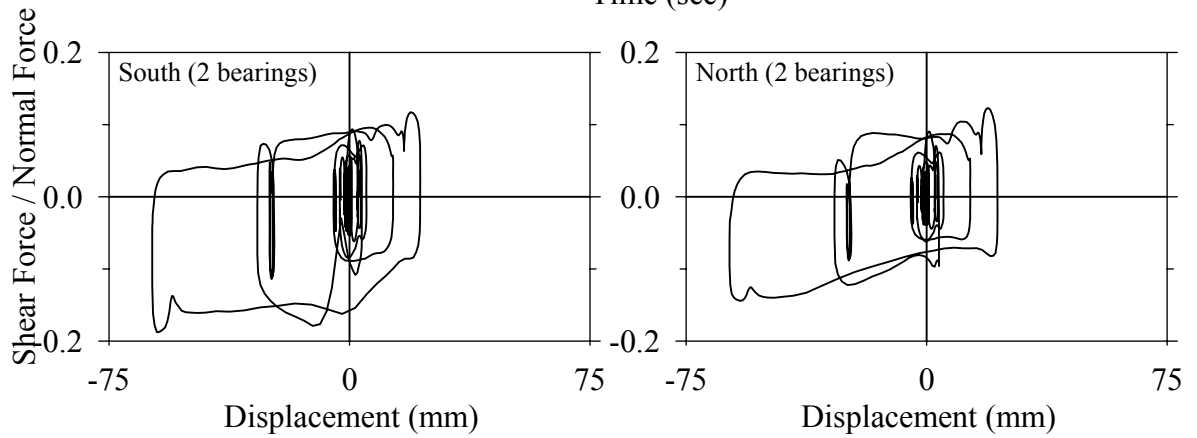
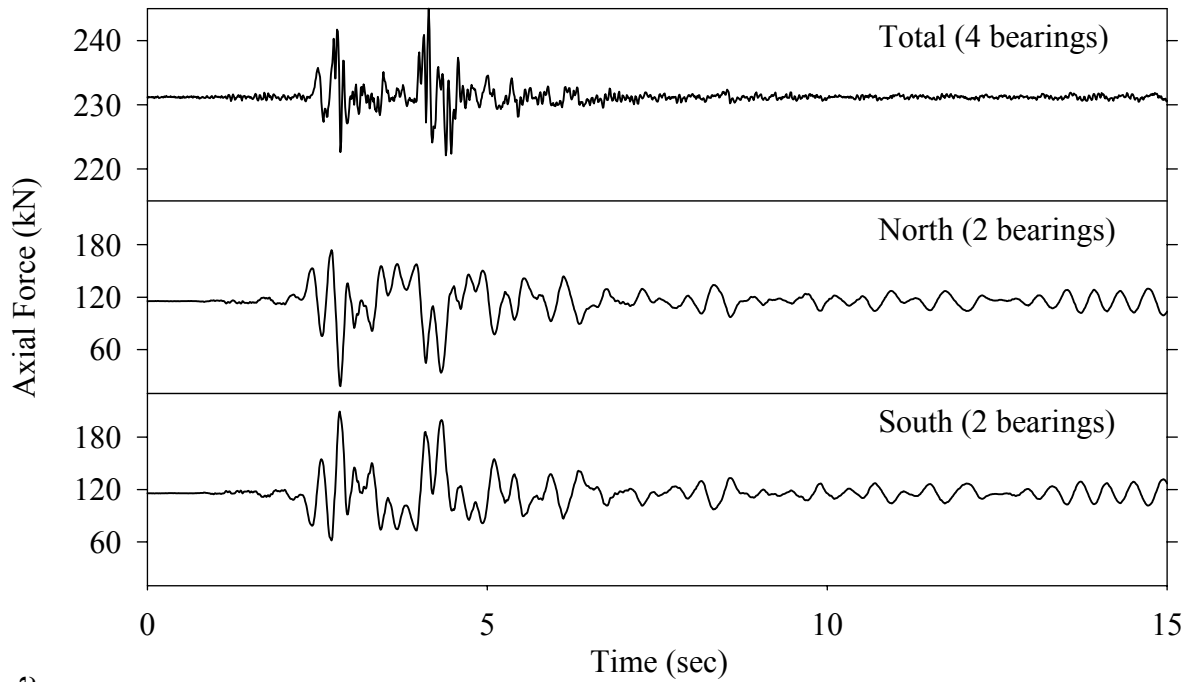
Test FPMFN10.1, Northridge Newhall 360° 100%, MF/FPS



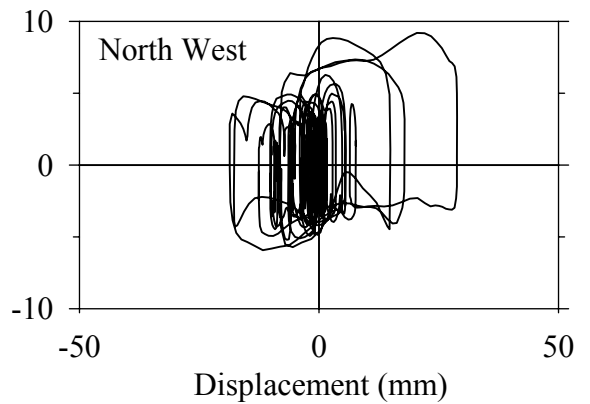
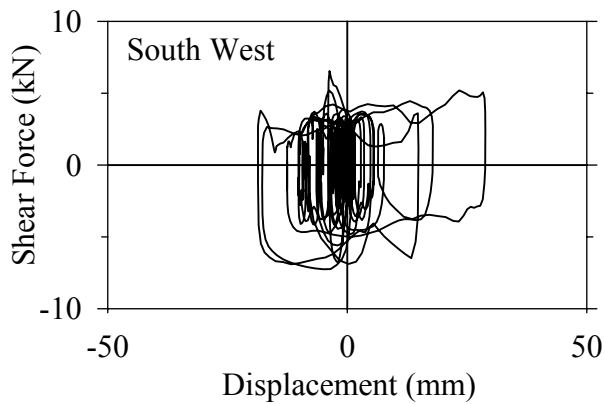
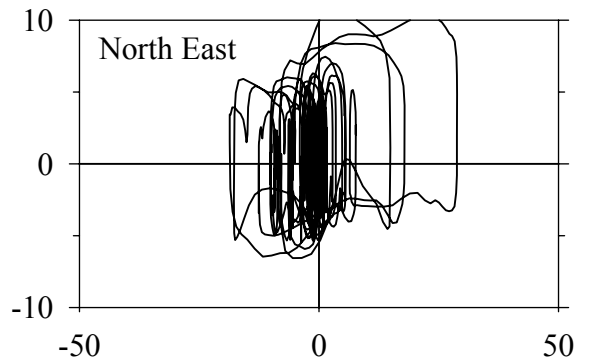
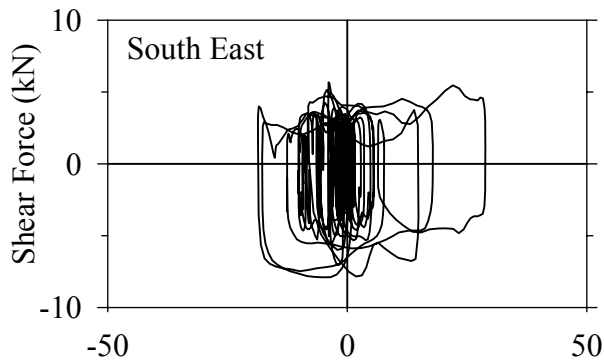
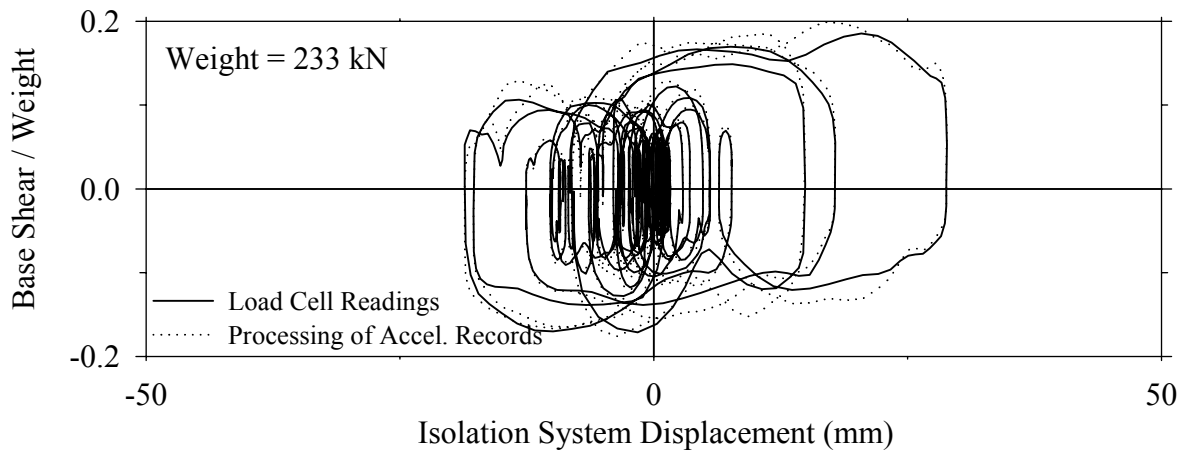
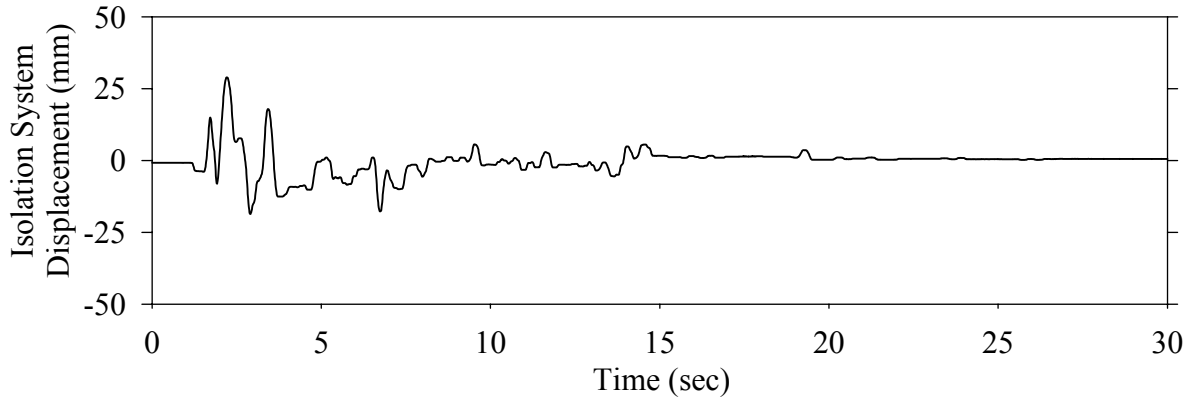
Test FPMFS10.1, Northridge Sylmar 90° 100%, MF/FPS



Test FPMFS10.1, Northridge Sylmar 90° 100%, MF/FPS

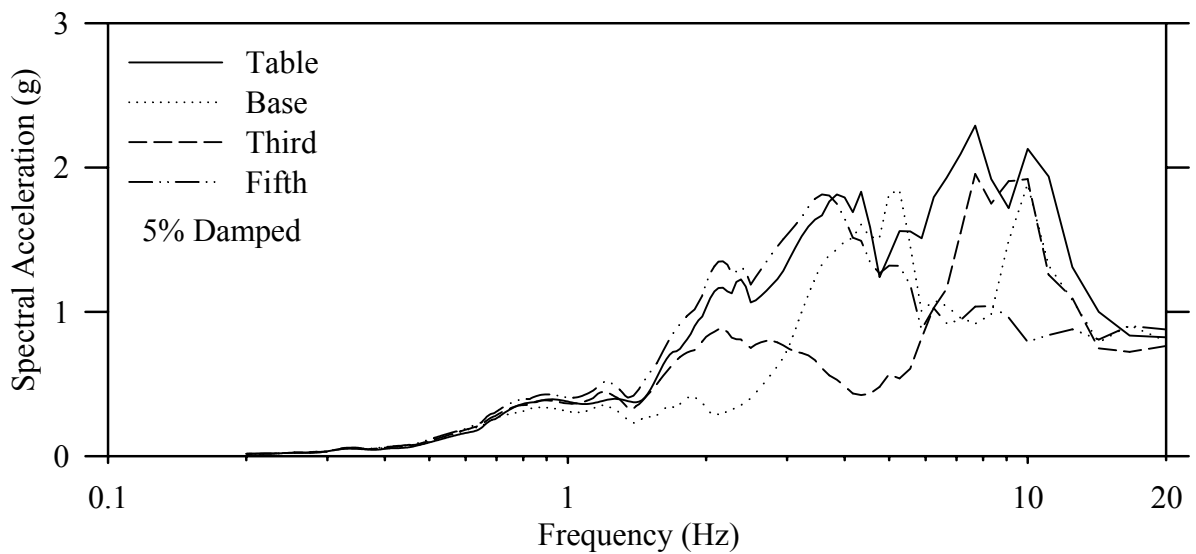
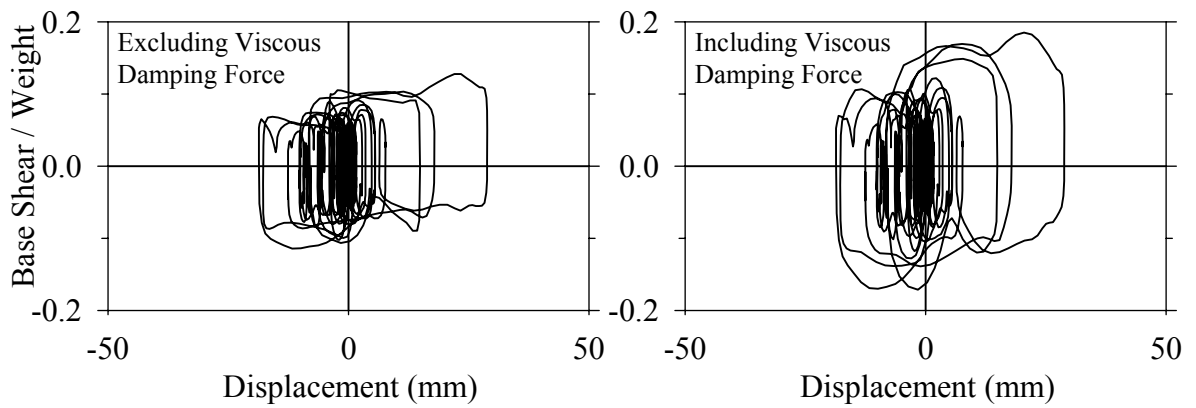
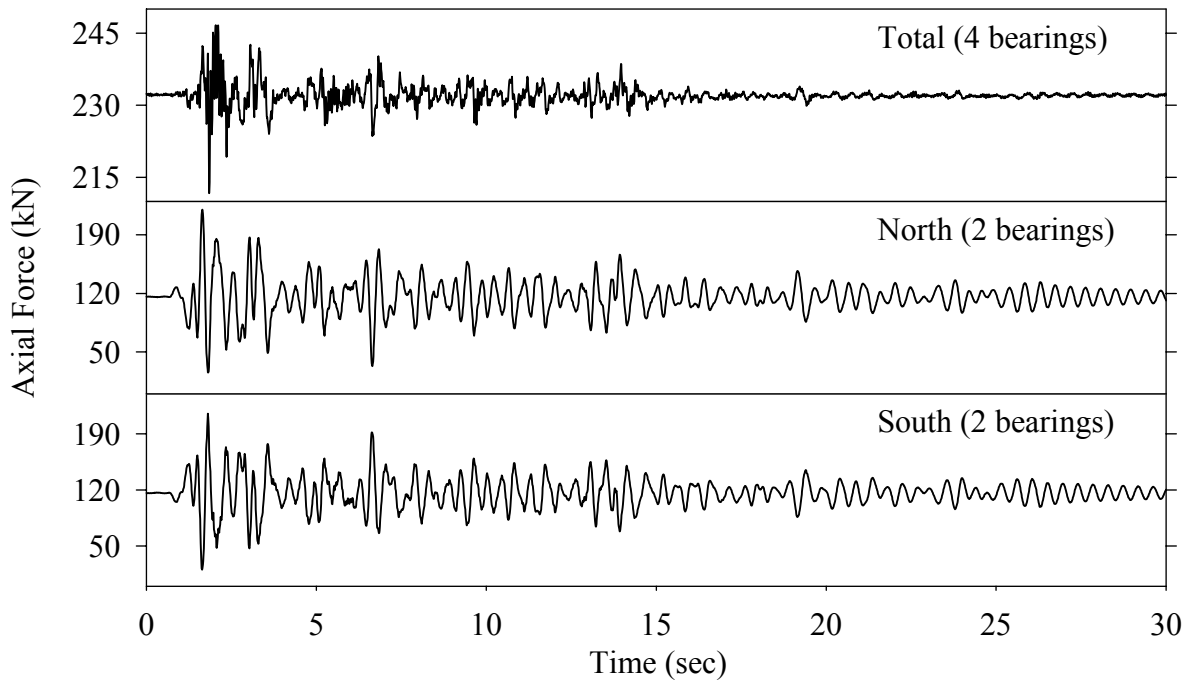


Test FPMLE20.1, El Centro S00E 200%, MF/FPS-LD

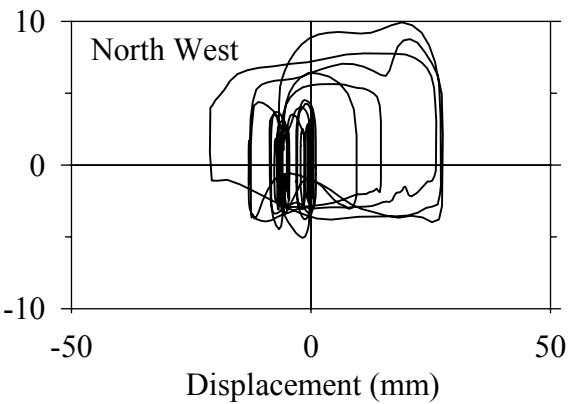
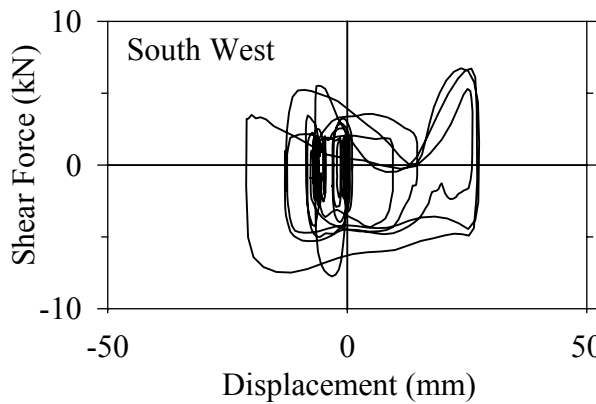
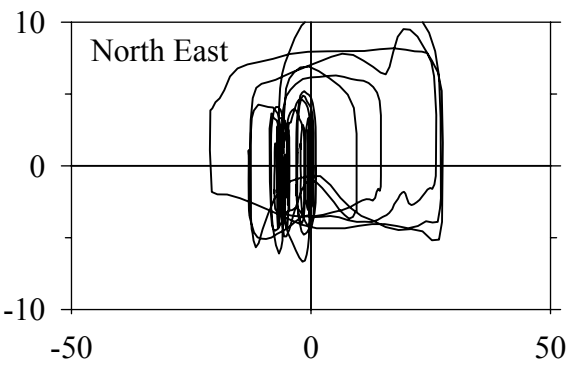
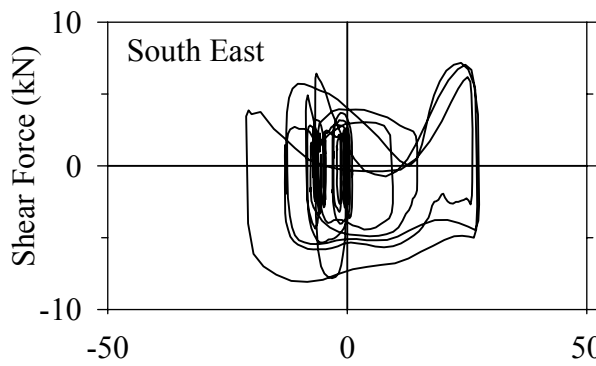
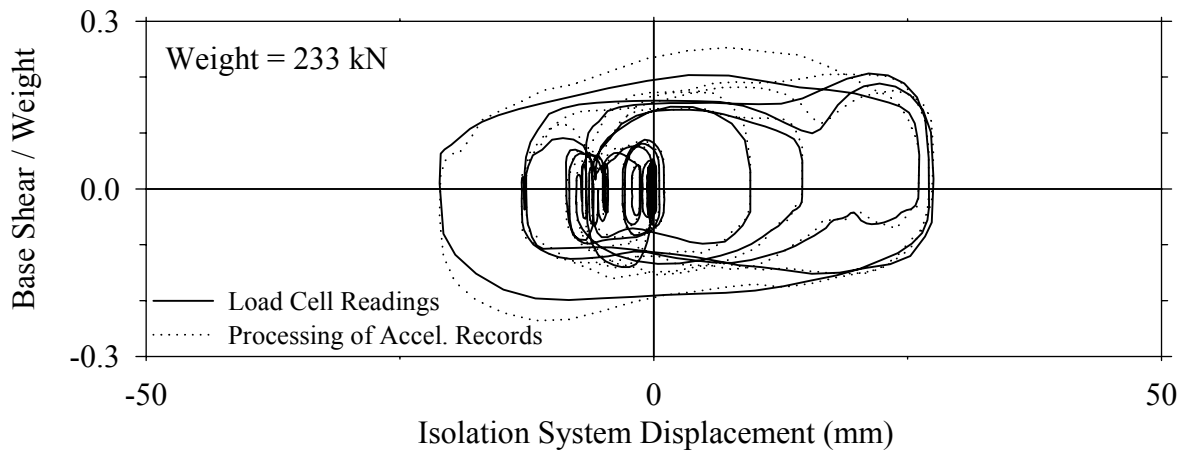
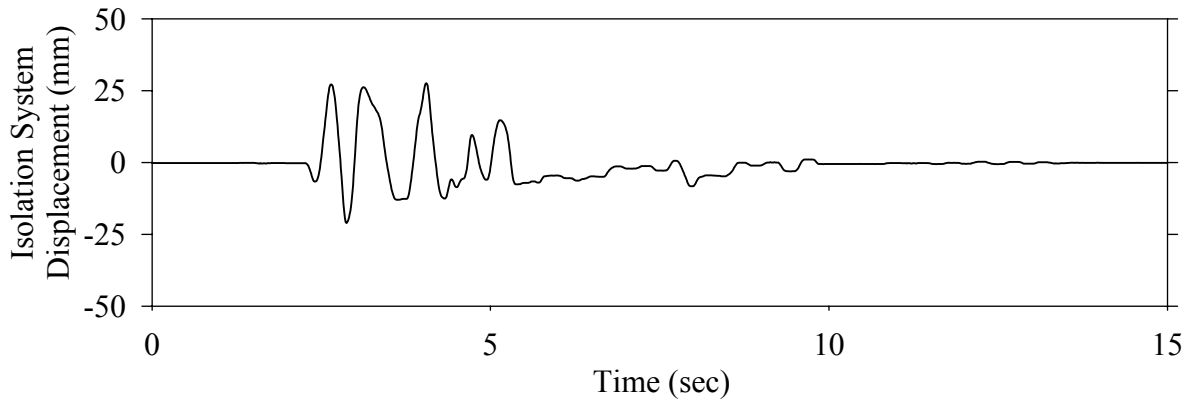




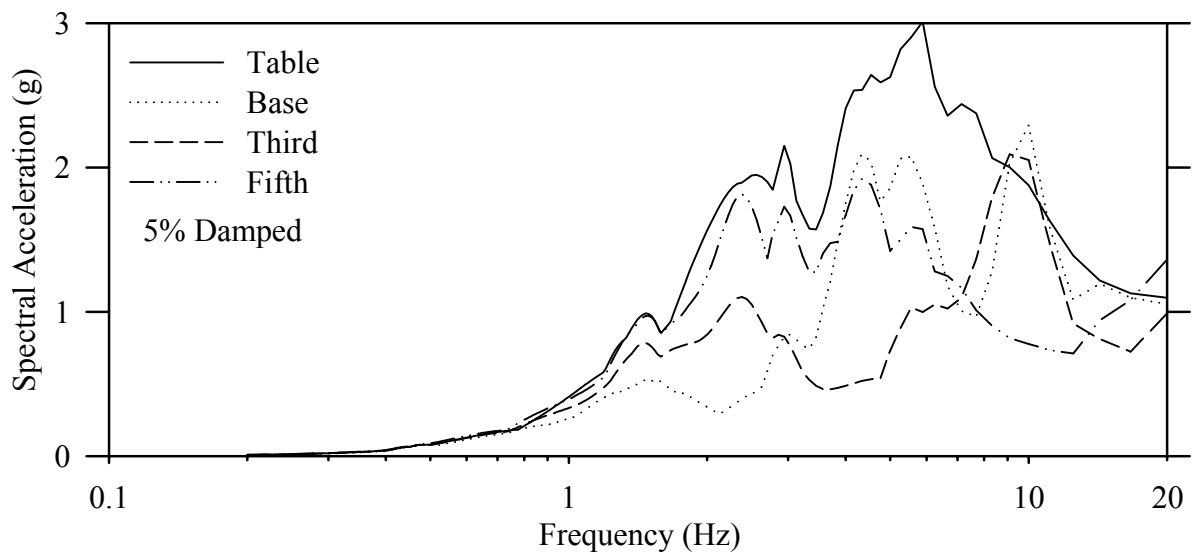
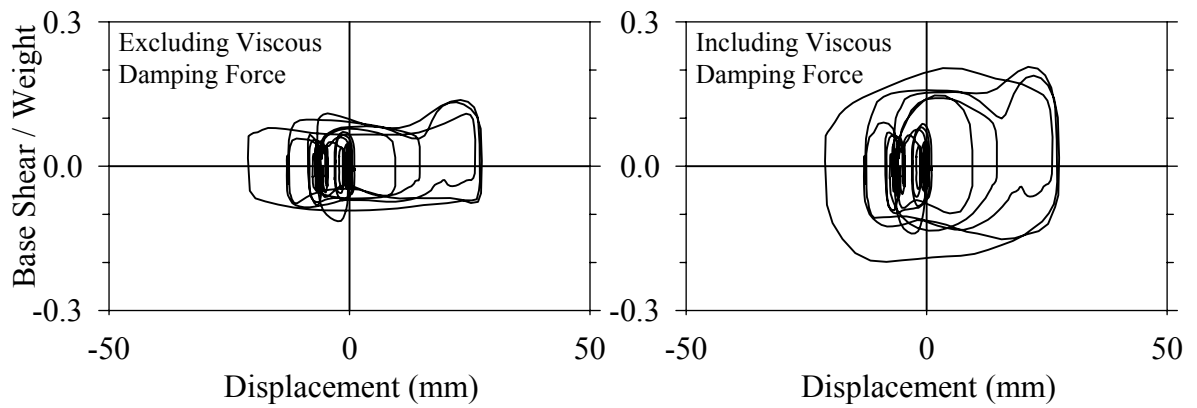
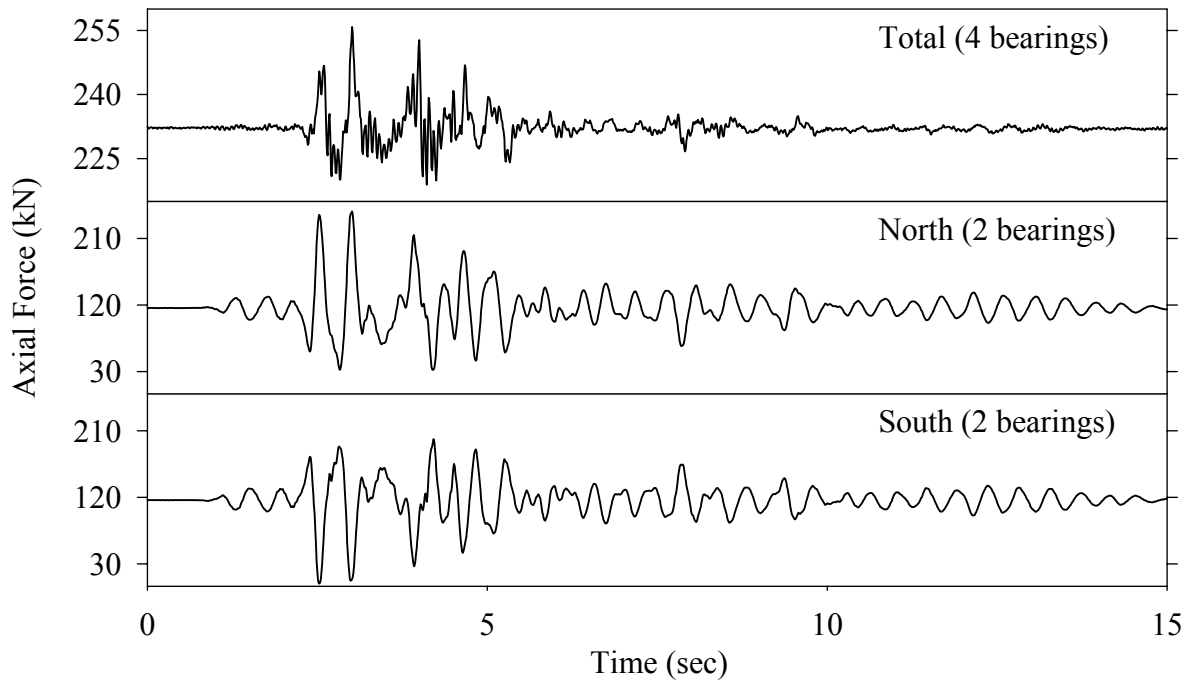
Test FPMLE20.1, El Centro S00E 200%, MF/FPS-LD



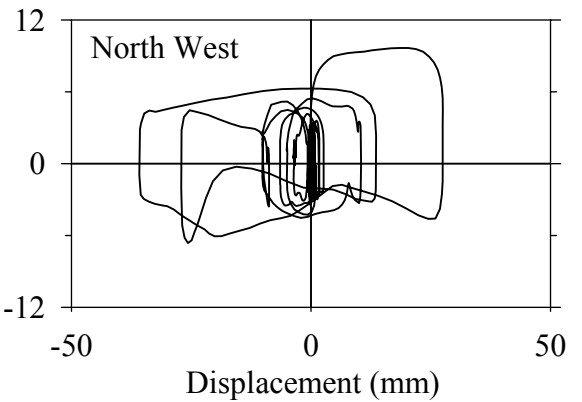
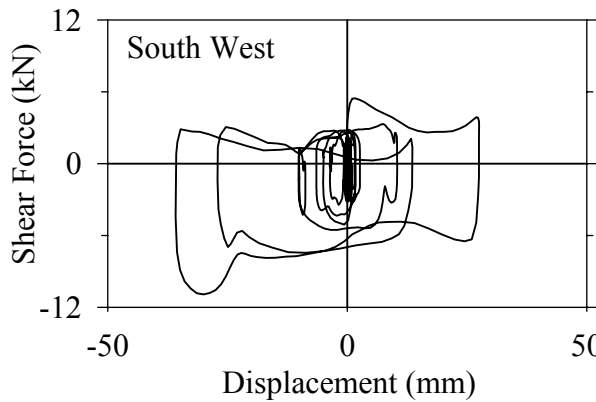
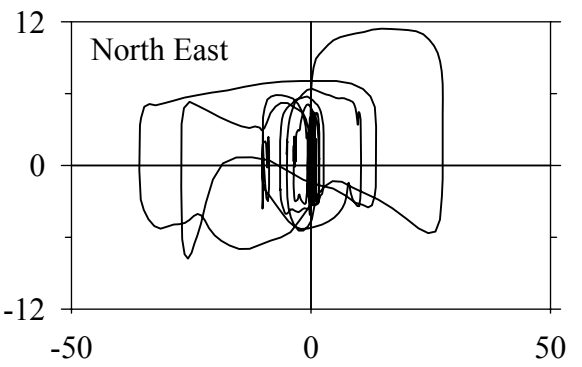
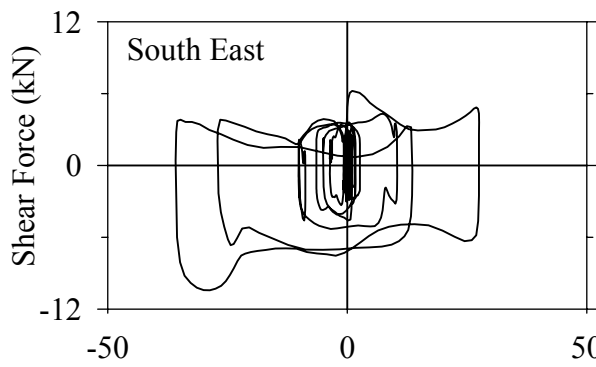
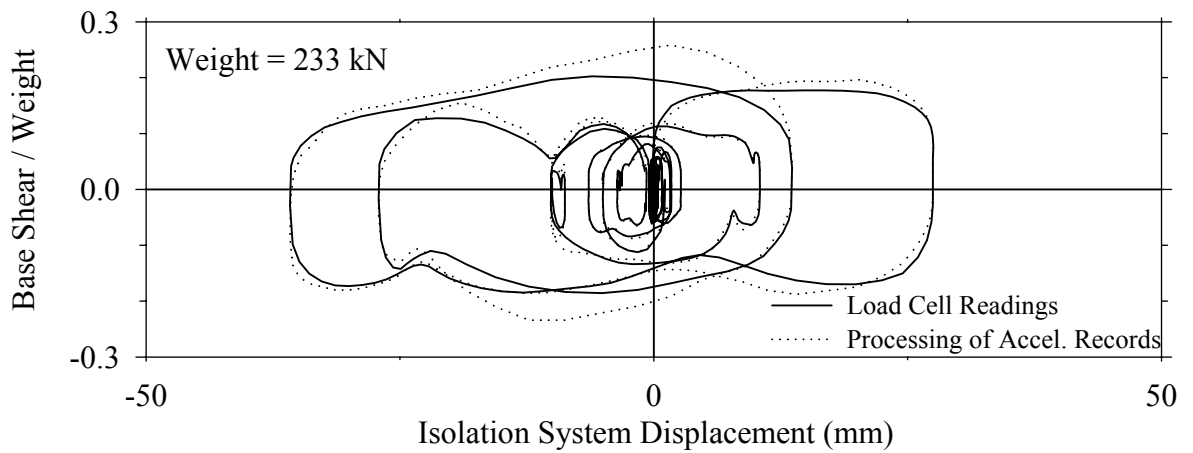
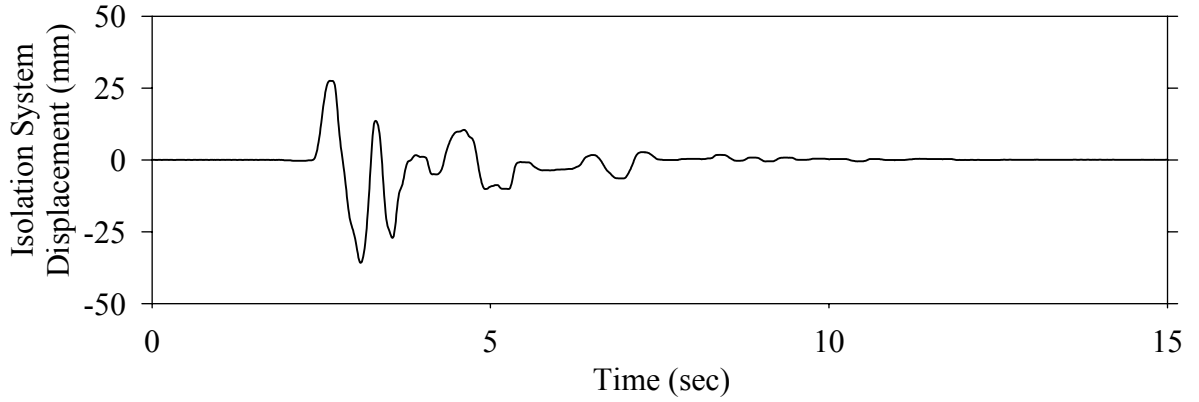
Test FPMLK10.1, Kobe N-S 100%, MF/FPS-LD



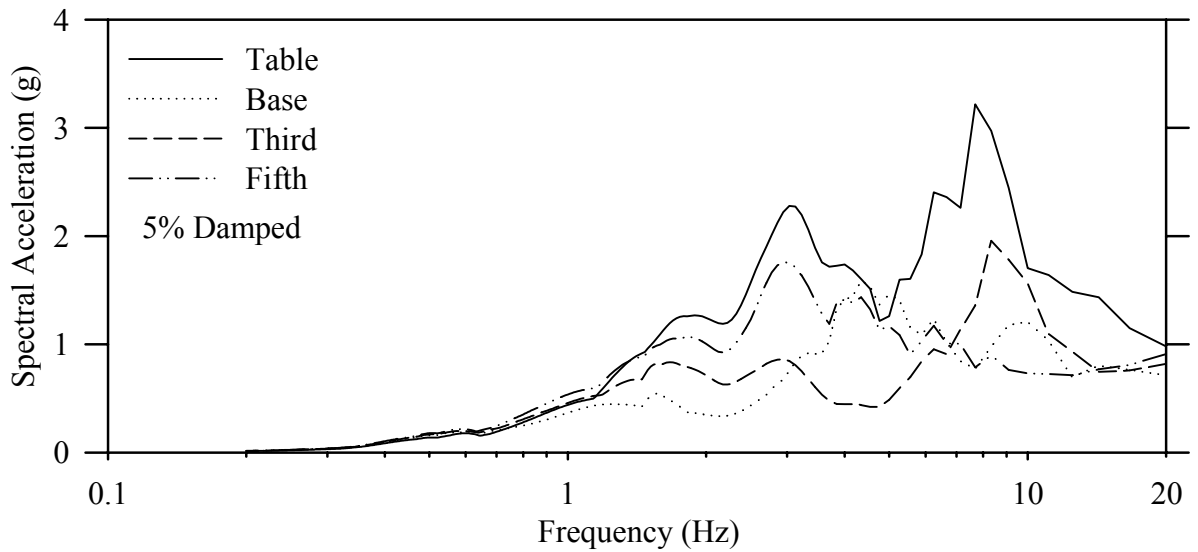
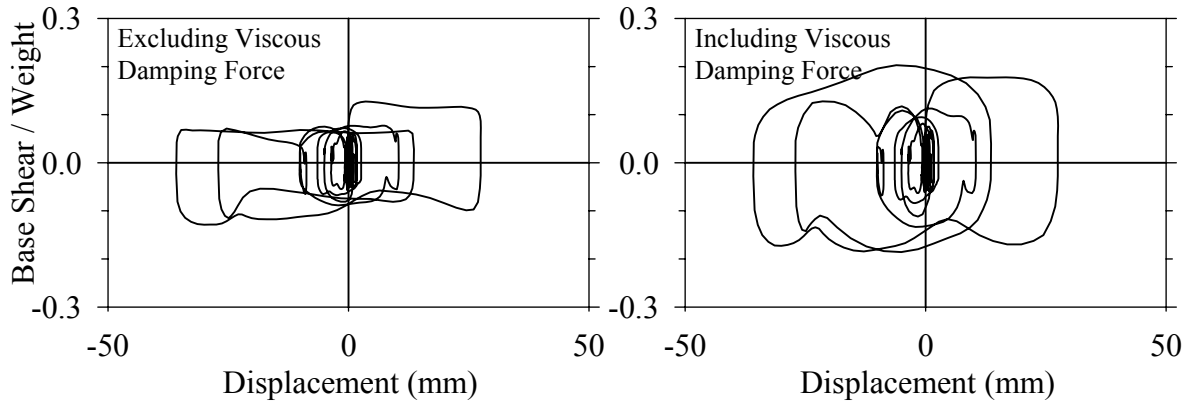
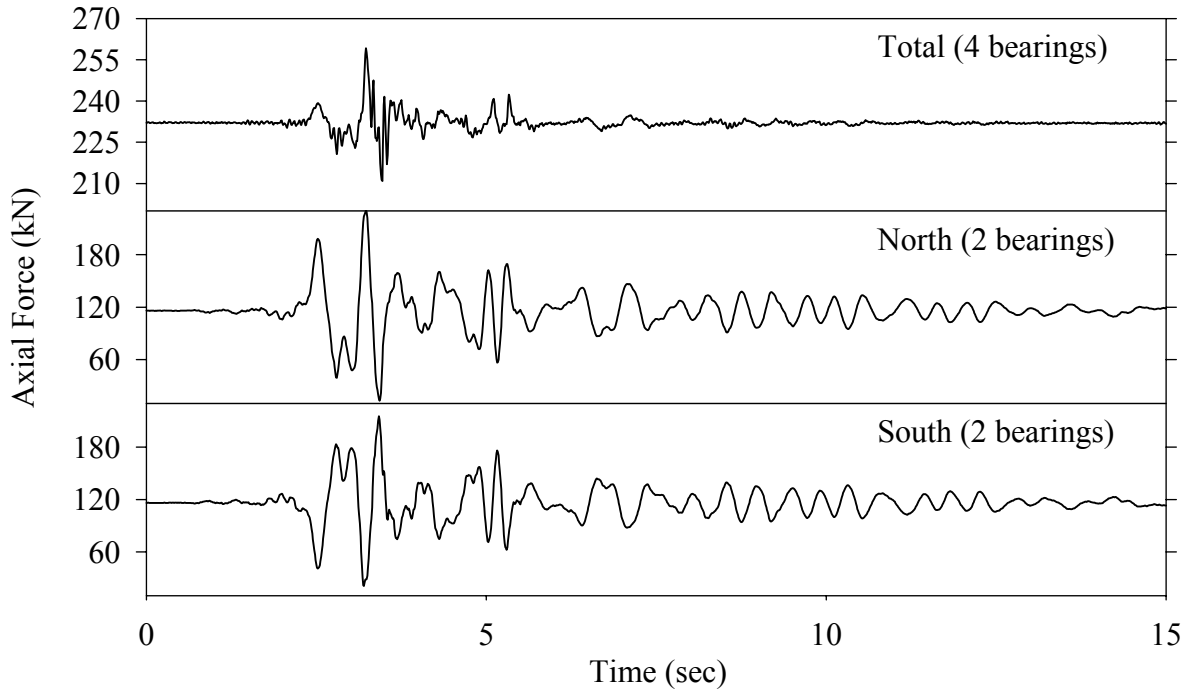
Test FPMLK10.1, Kobe N-S 100%, MF/FPS-LD



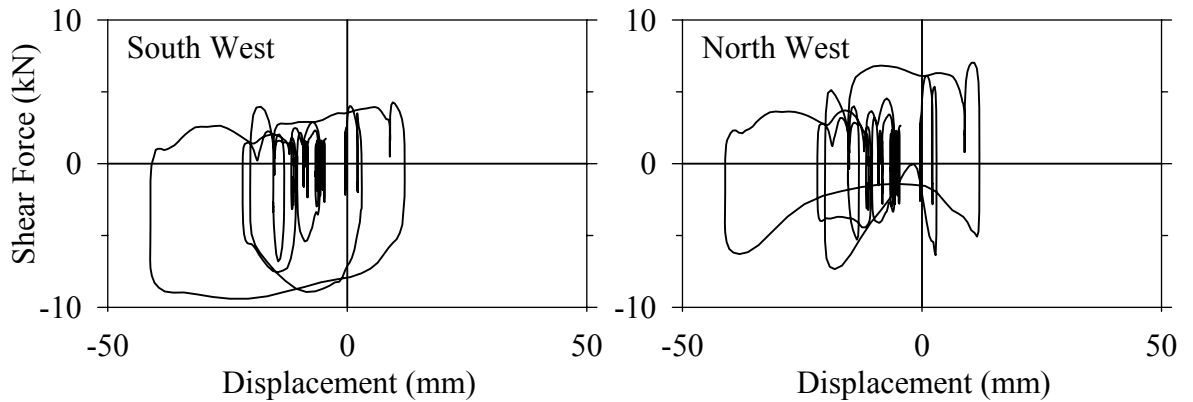
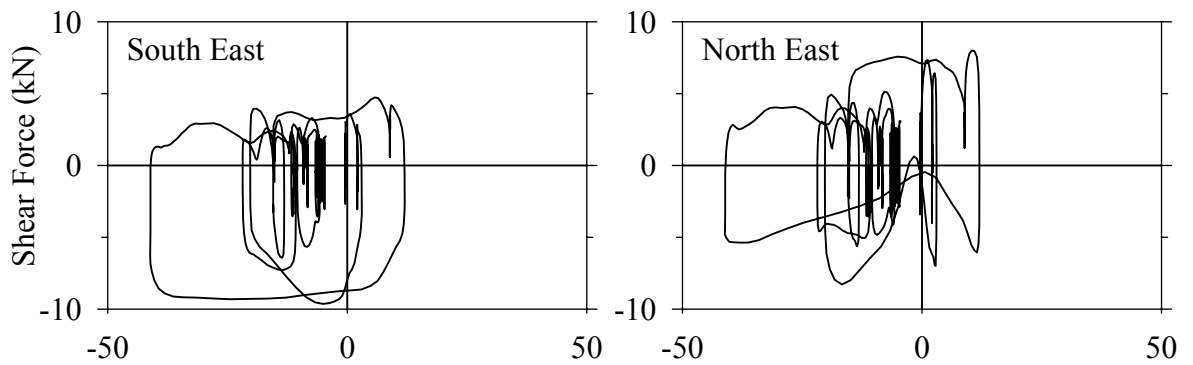
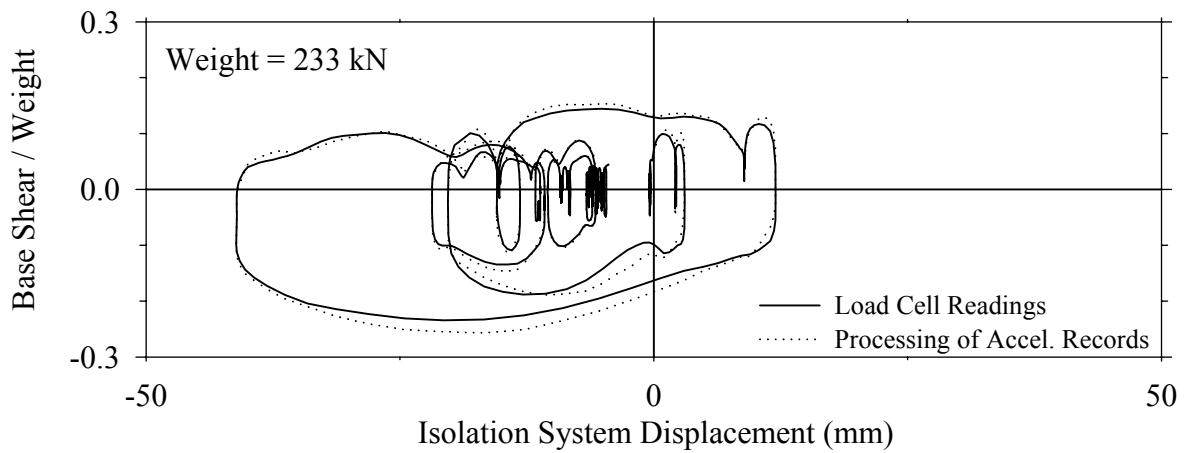
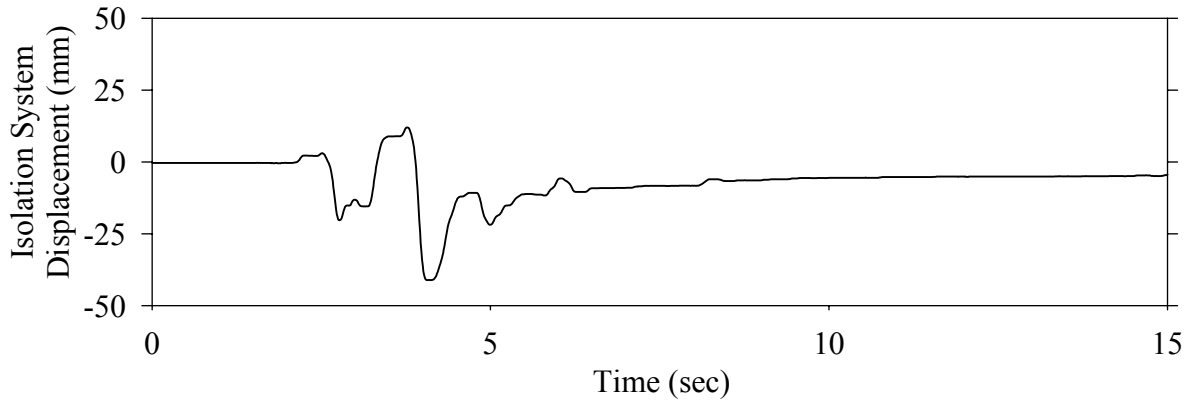
Test FPMLN10.1, Northridge Newhall 360° 100%, MF/FPS-LD



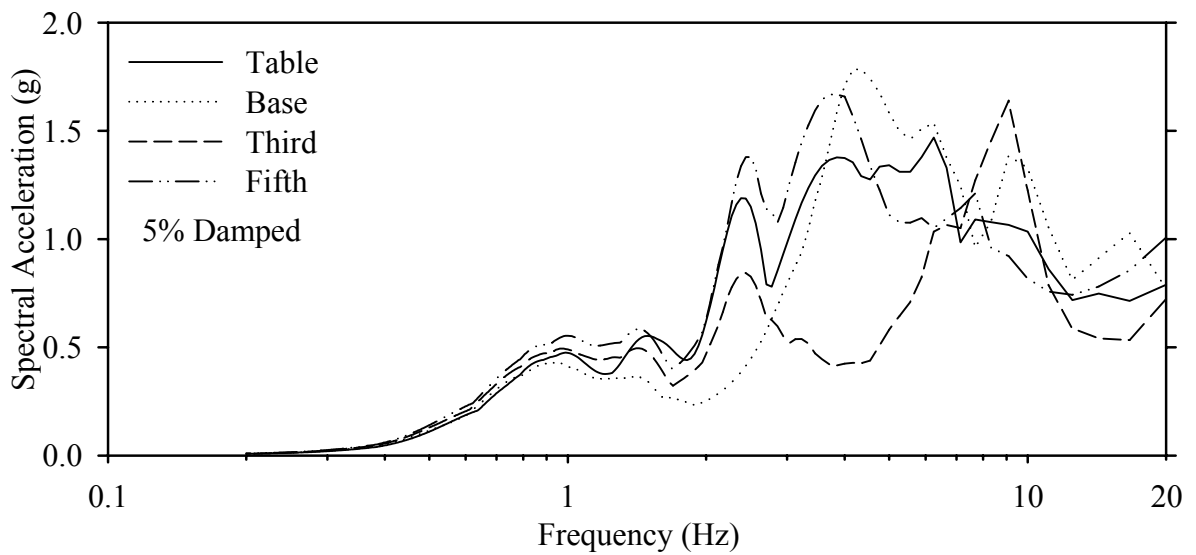
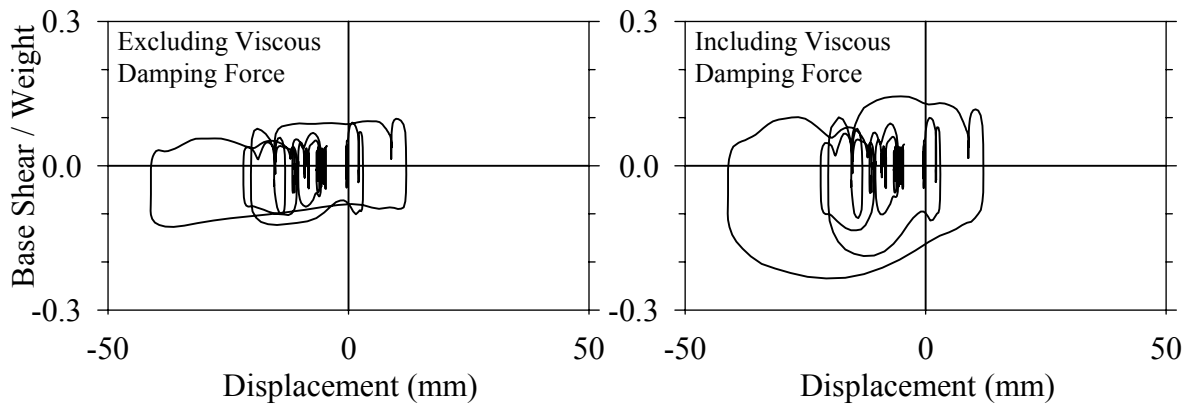
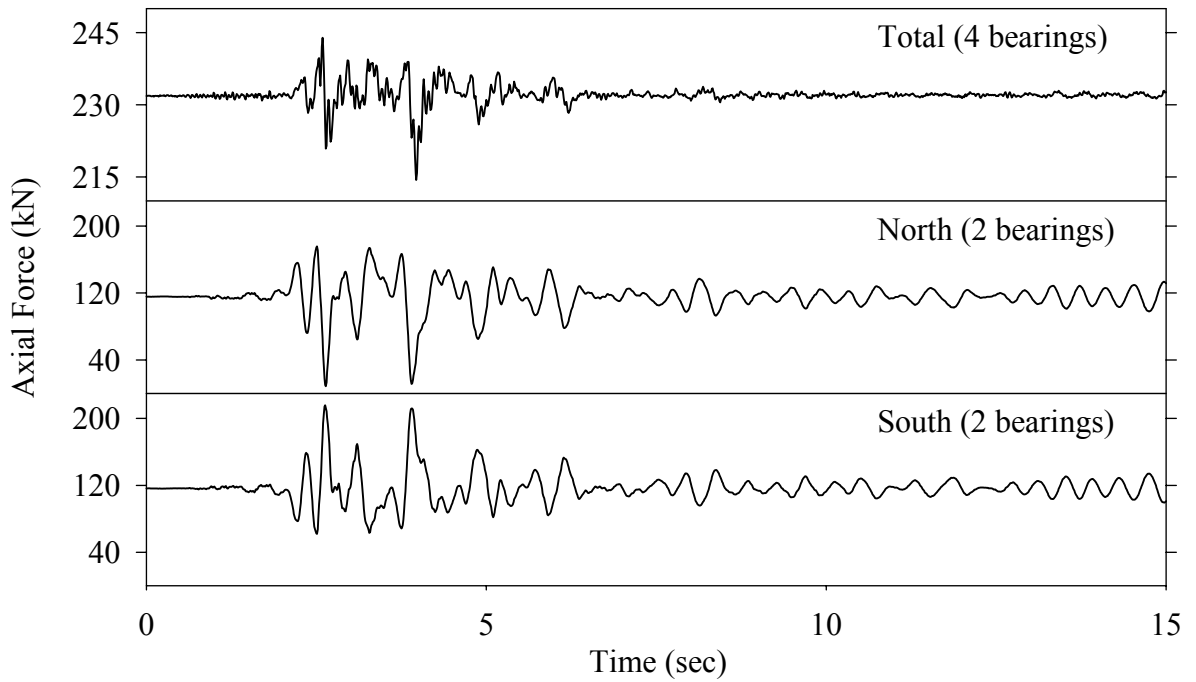
Test FPMLN10.1, Northridge Newhall 360° 100%, MF/FPS-LD



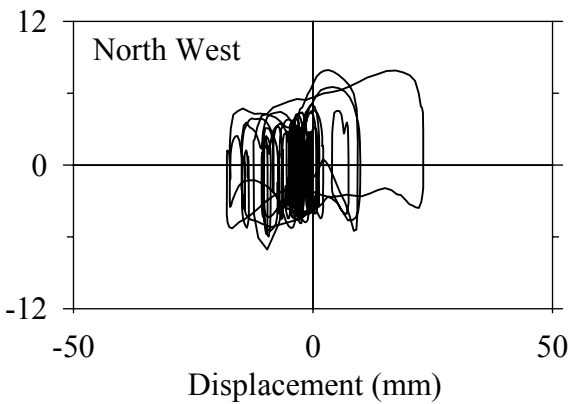
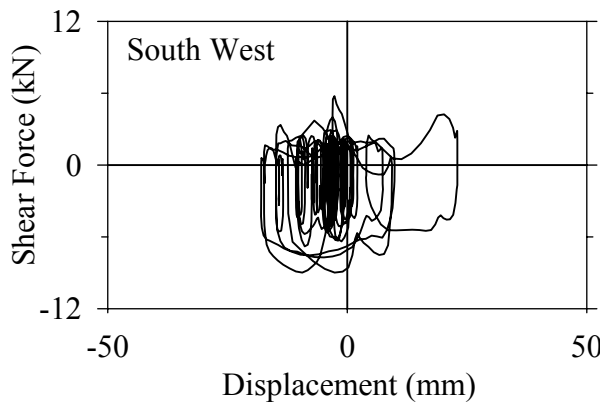
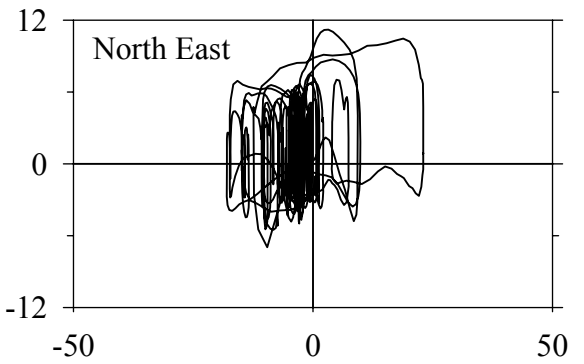
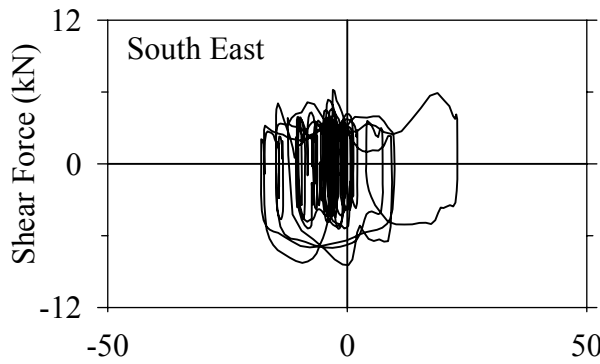
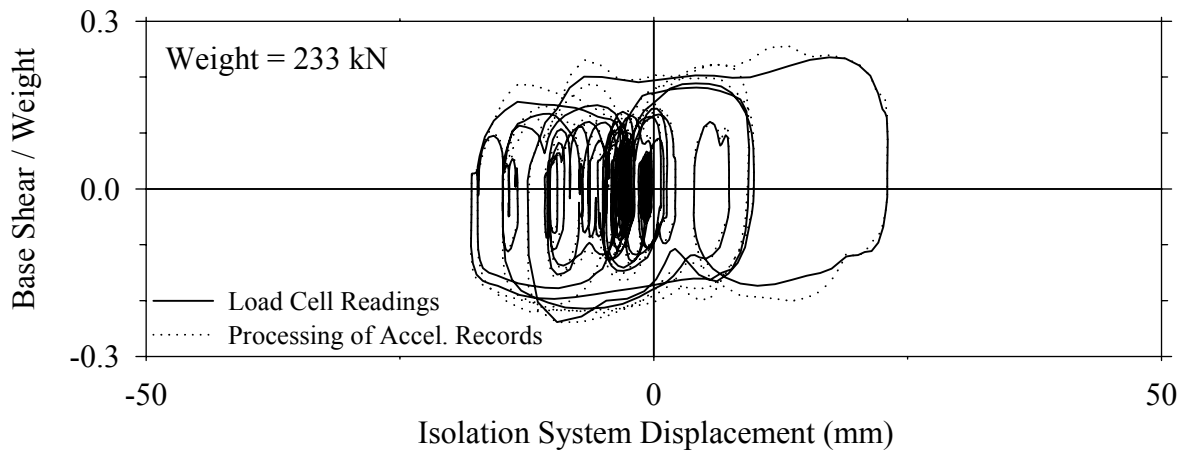
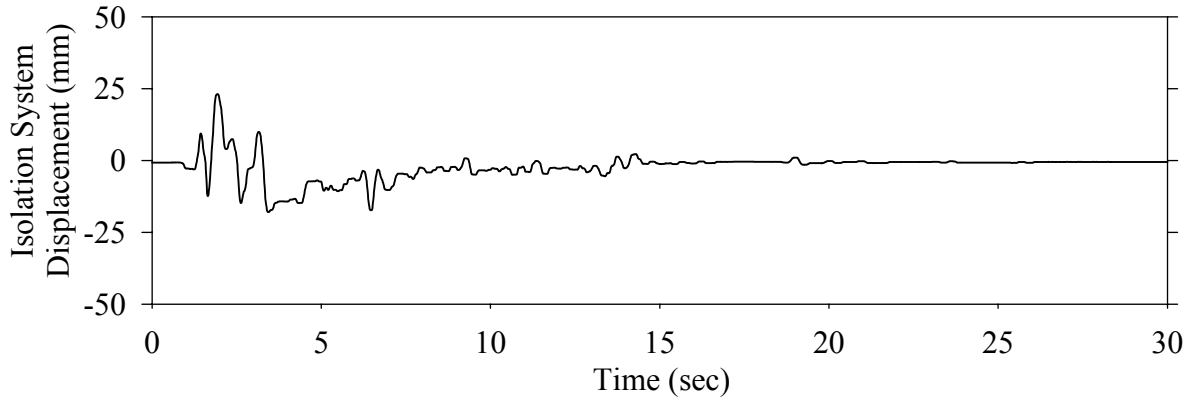
Test FPMLS10.1, Northridge Sylmar 90° 100%, MF/FPS-LD



Test FPMLS10.1, Northridge Sylmar 90° 100%, MF/FPS-LD

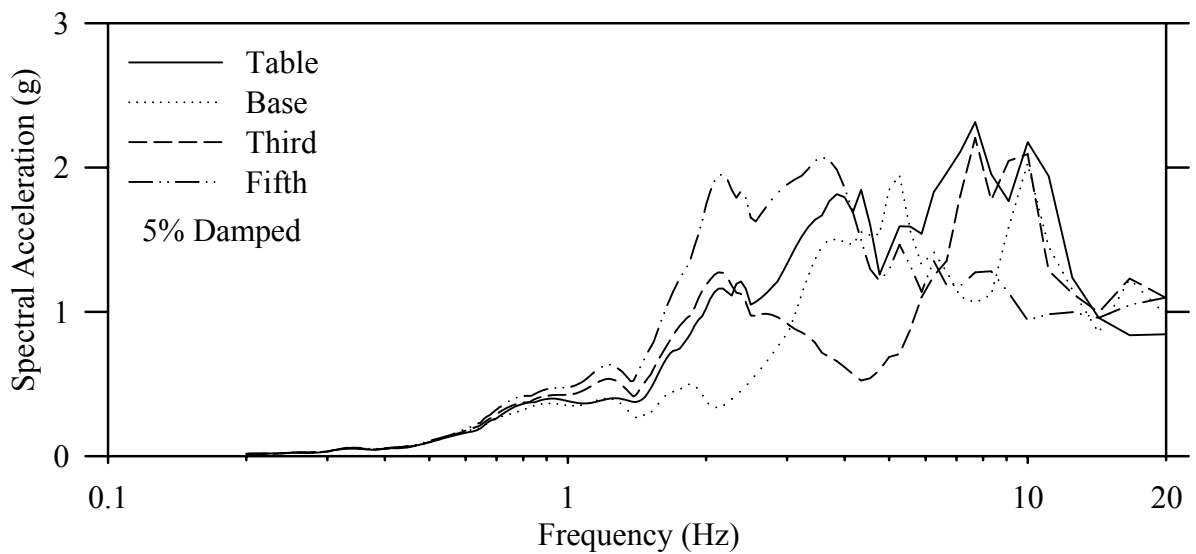
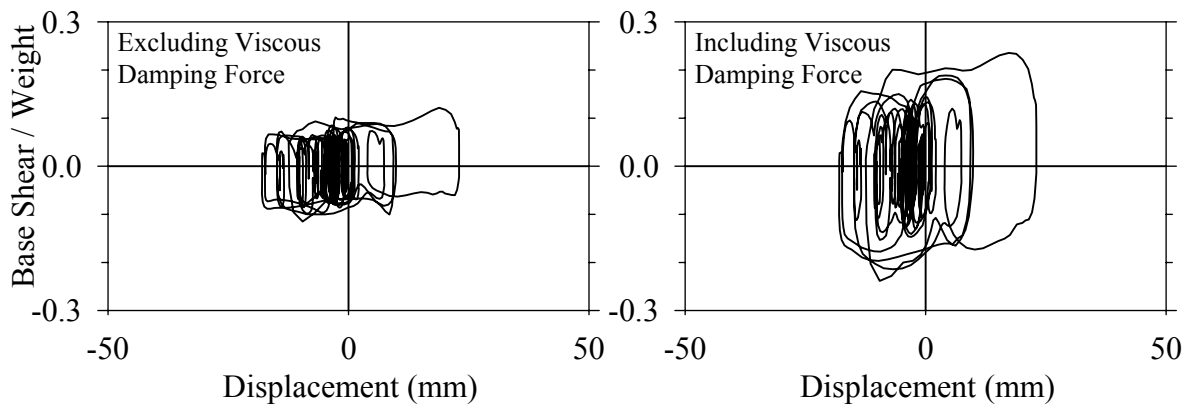
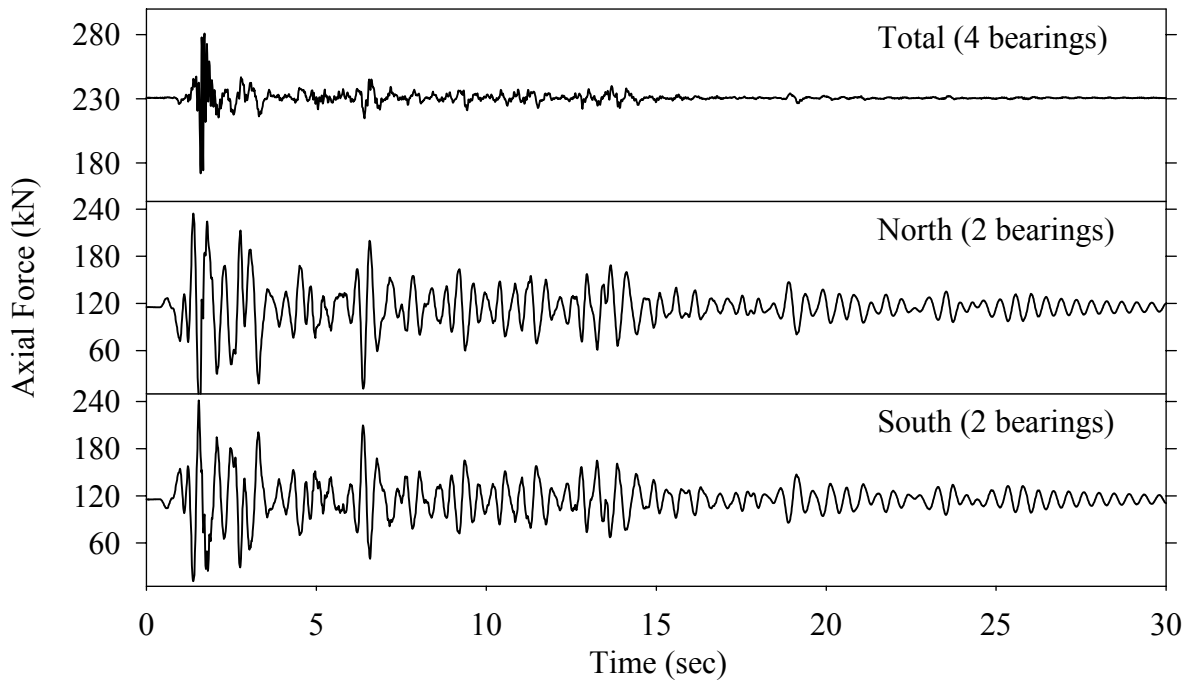


Test FPMNE20.1, El Centro S00E 200%, MF/FPS-NLD

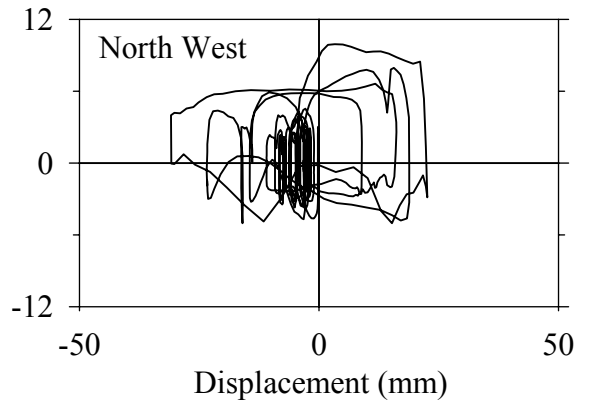
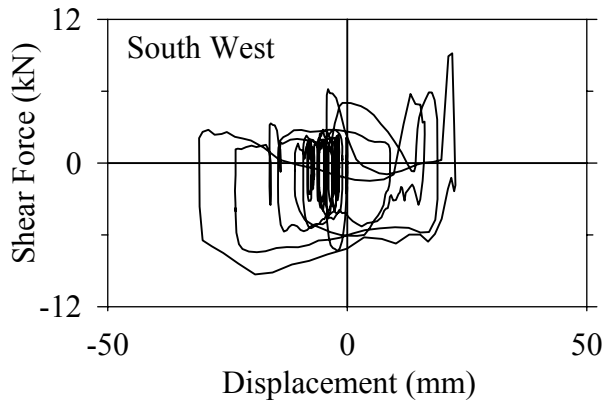
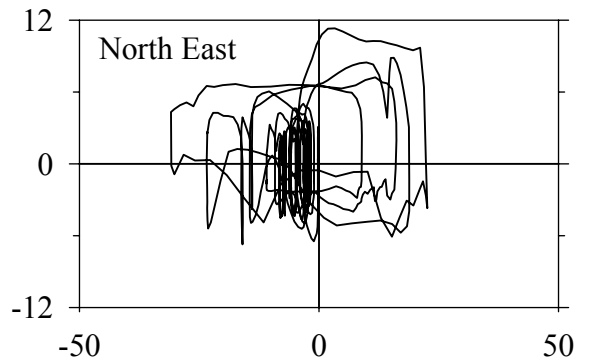
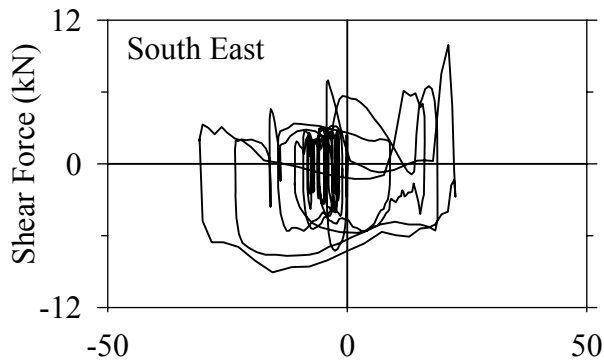
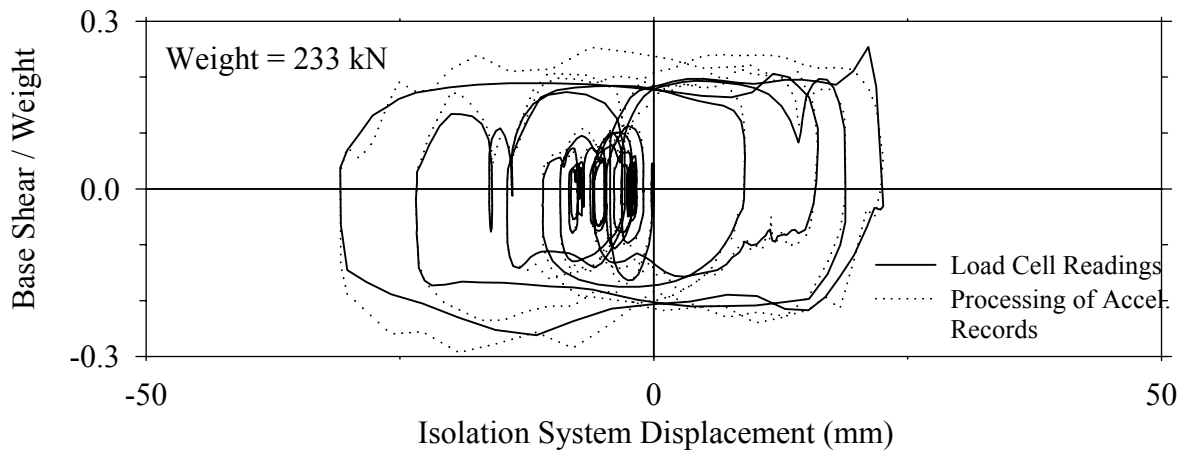
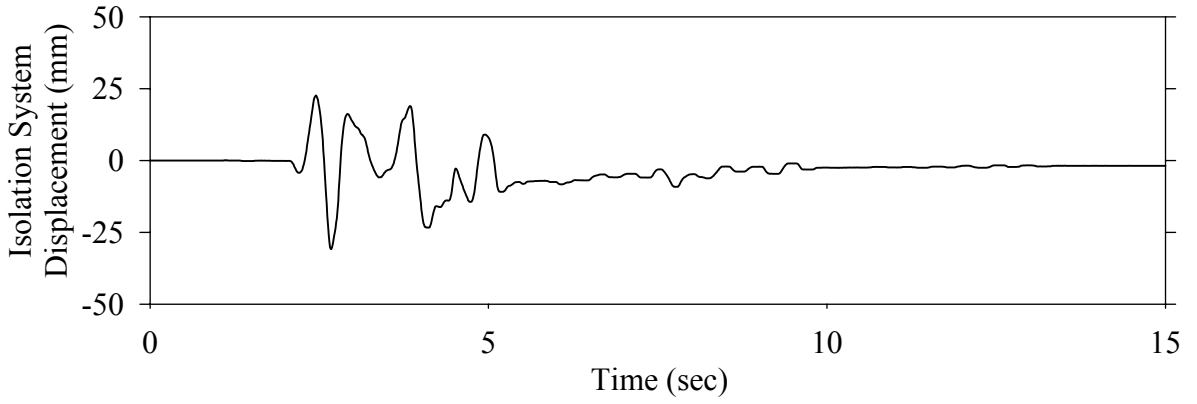




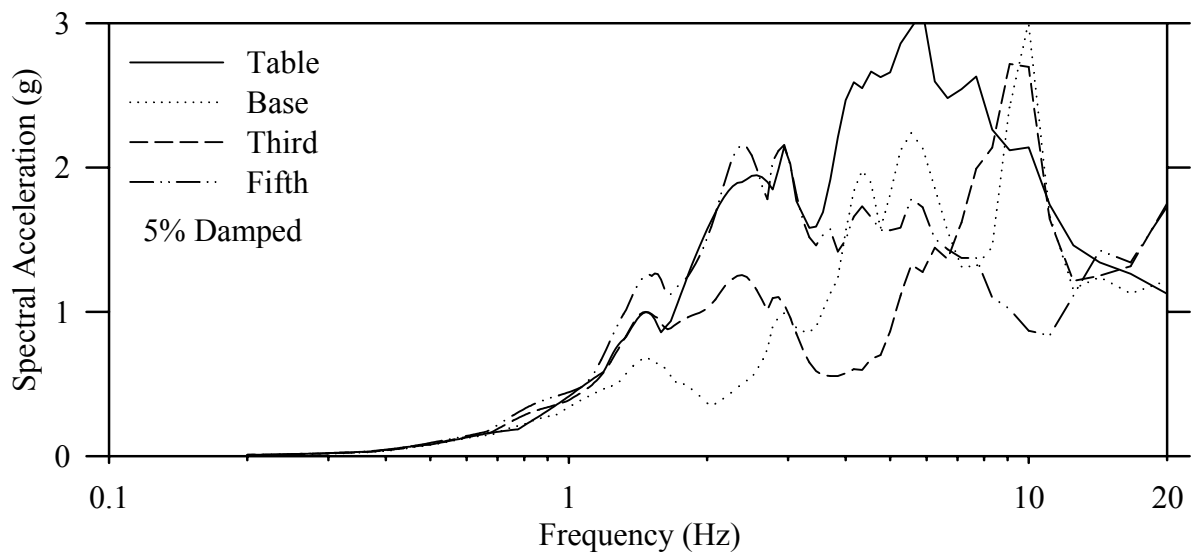
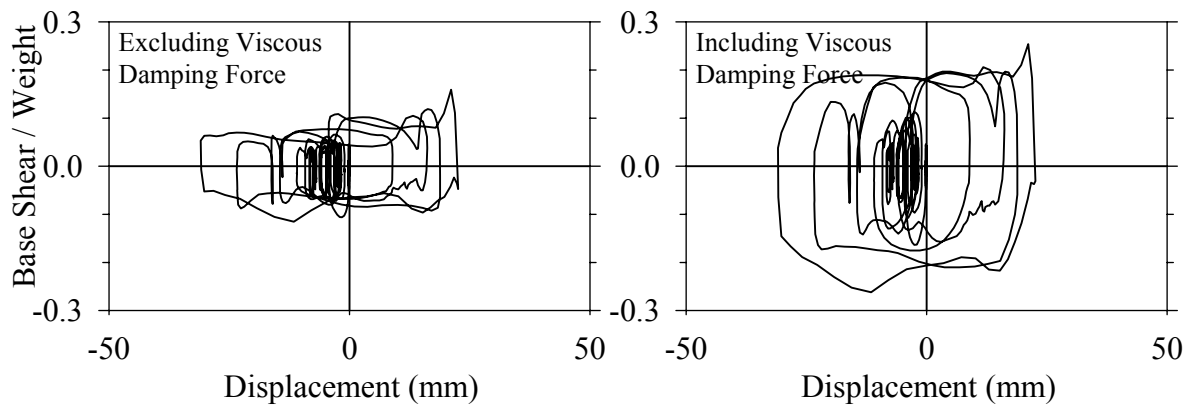
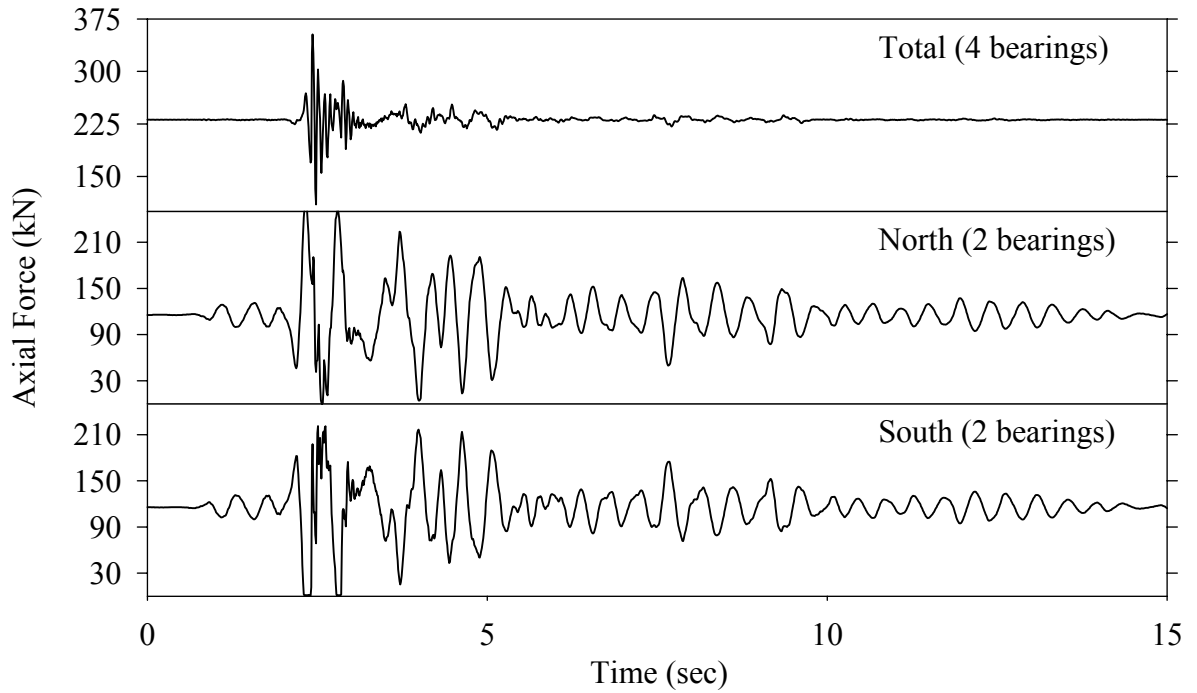
Test FPMNE20.1, El Centro S00E 200%, MF/FPS-NLD



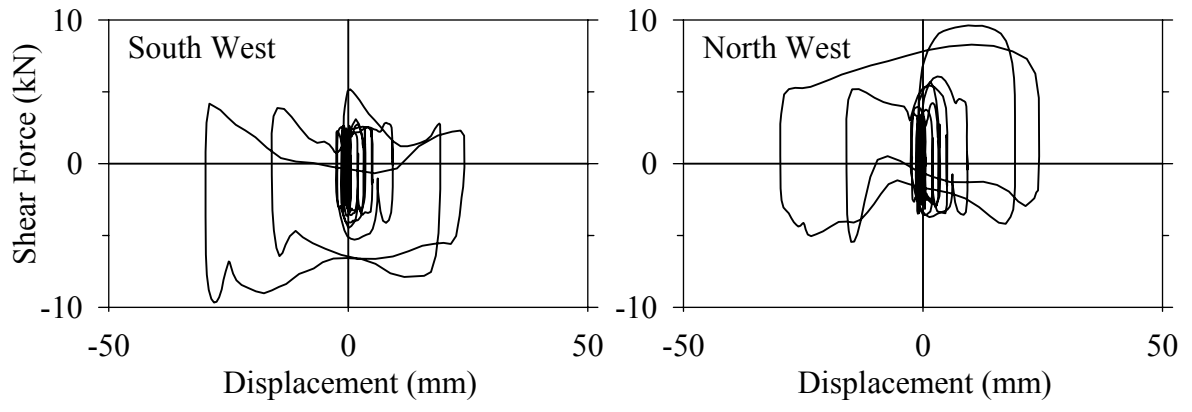
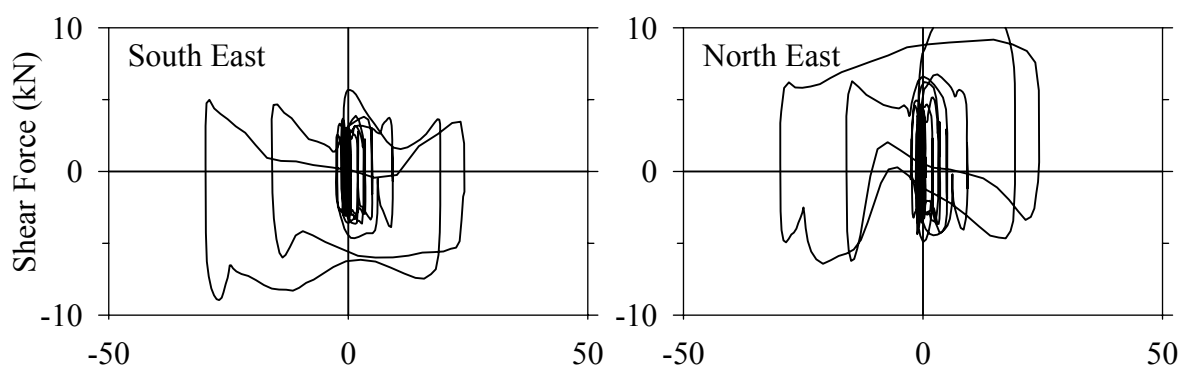
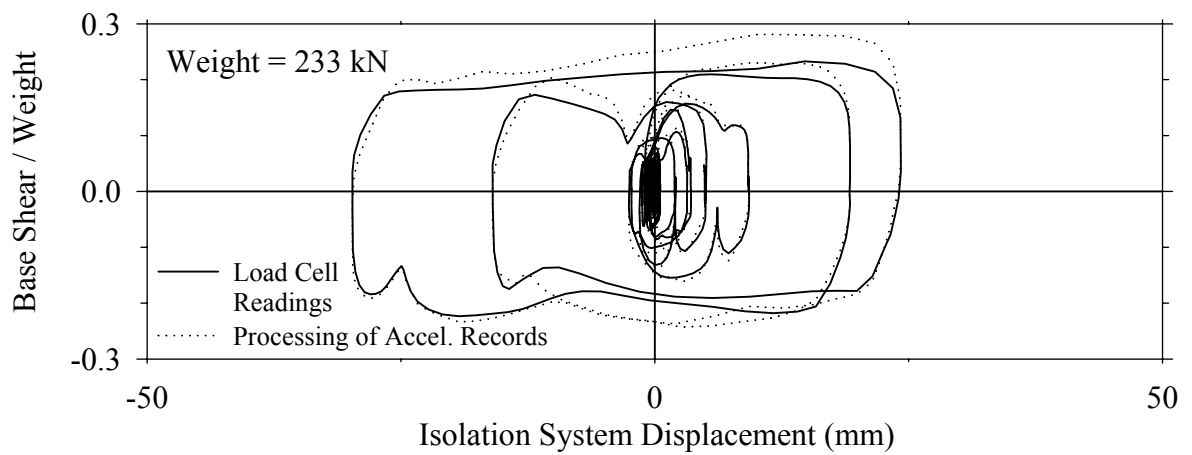
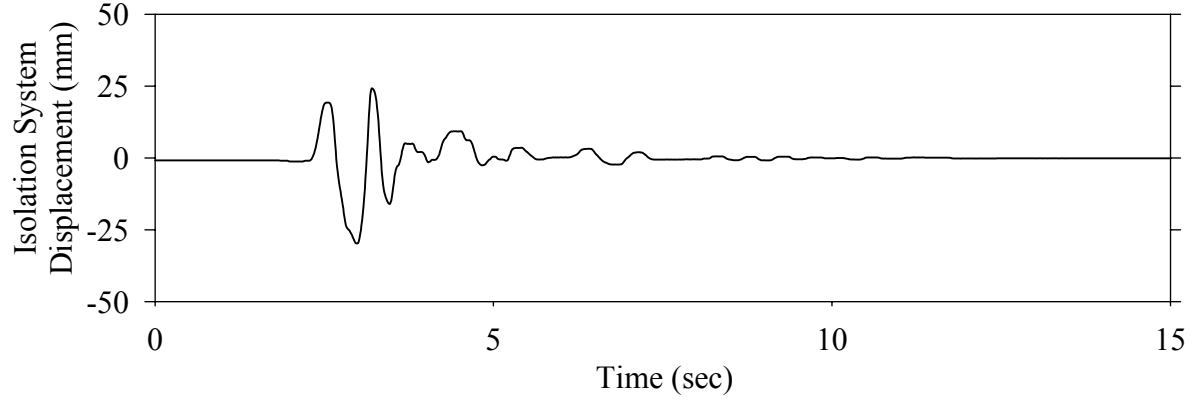
Test FPMNK10.1, Kobe N-S 100%, MF/FPS-NLD



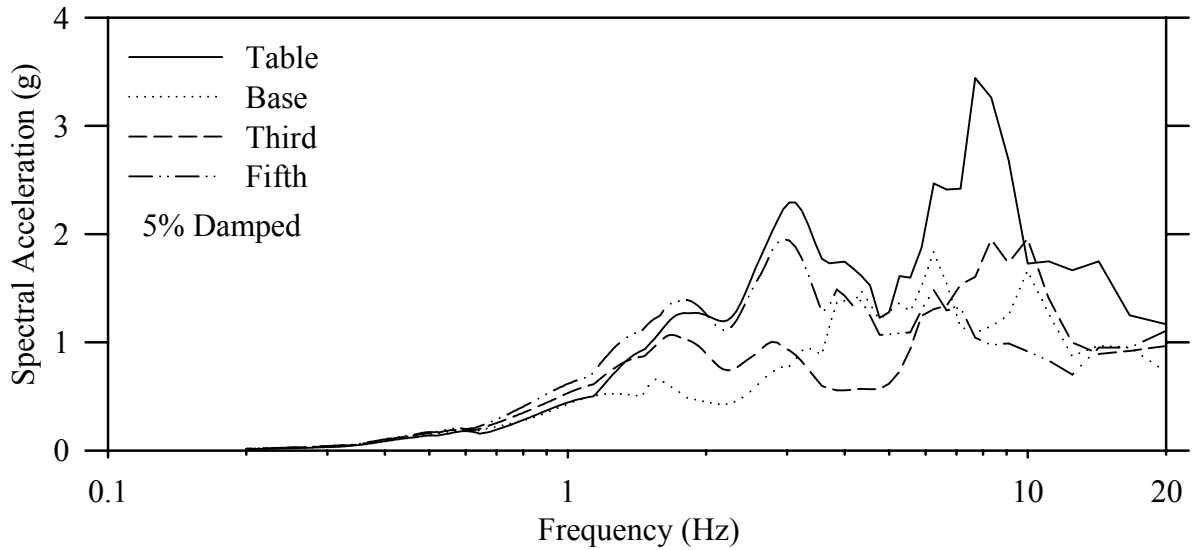
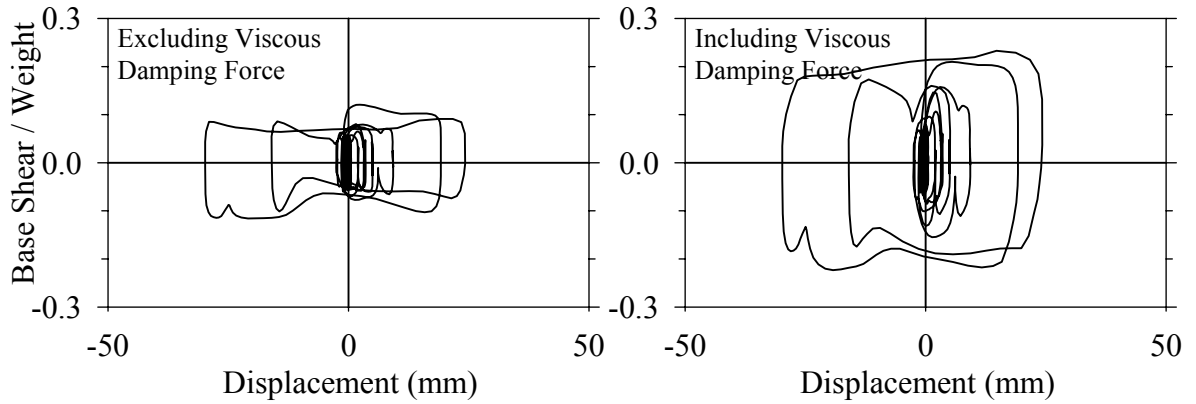
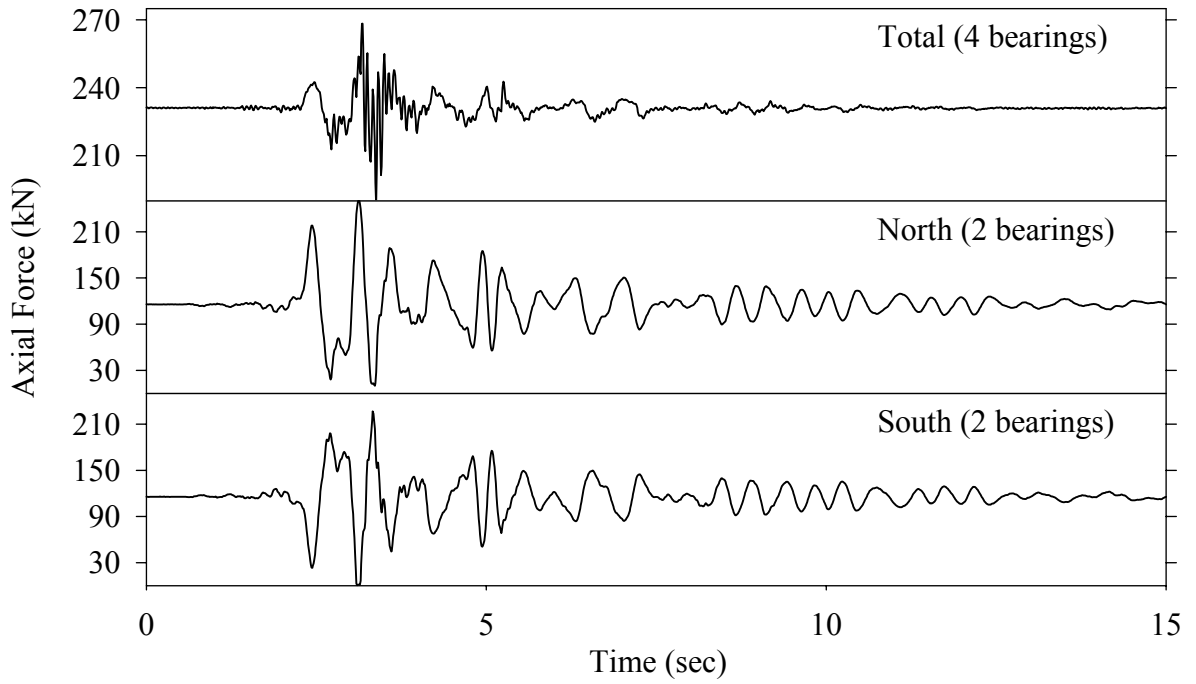
Test FPMNK10.1, Kobe N-S 100%, MF/FPS-NLD



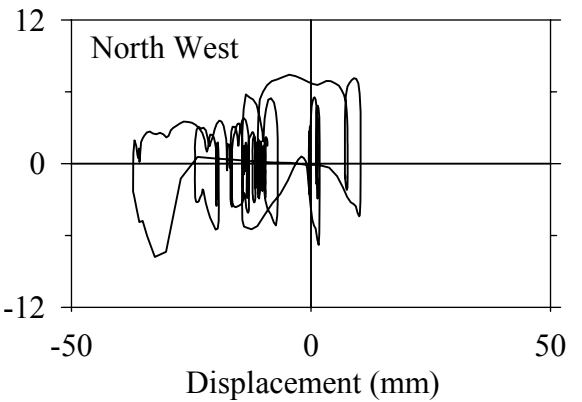
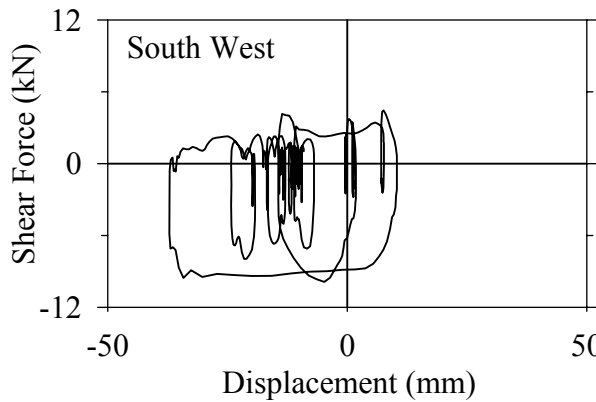
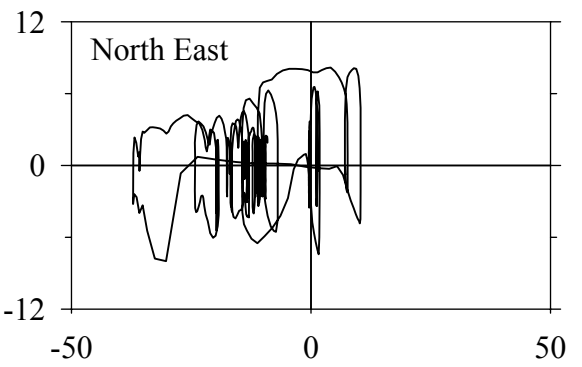
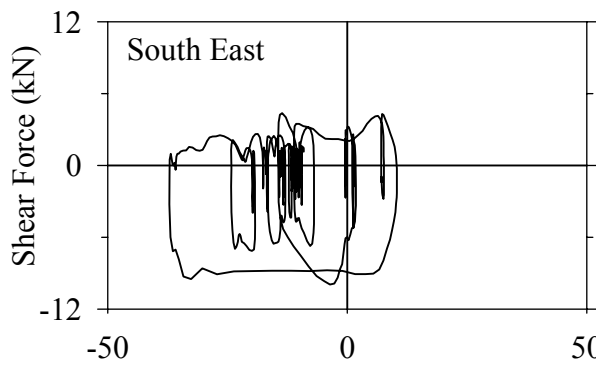
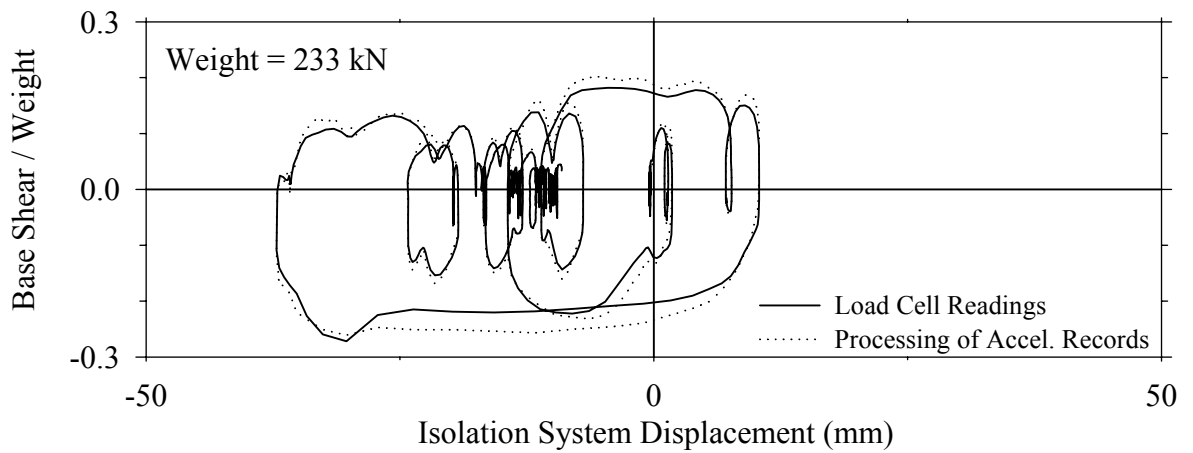
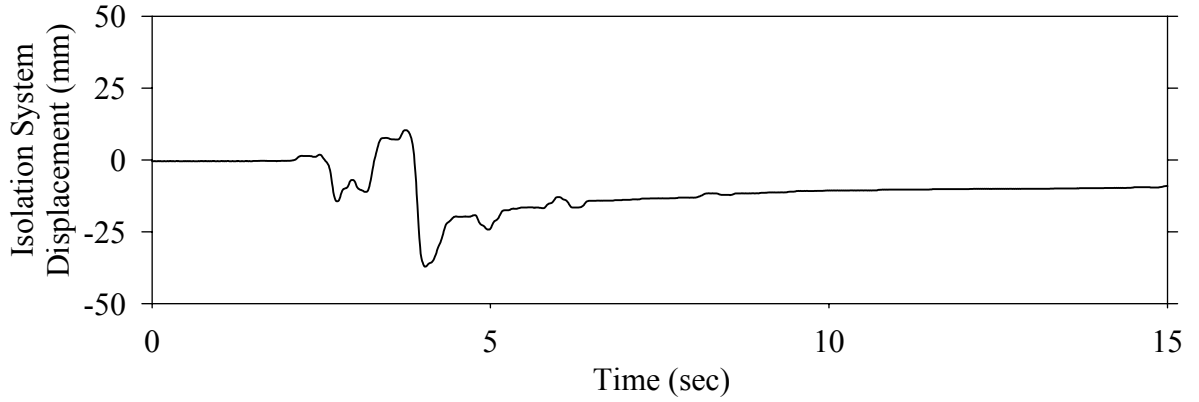
Test FPMNN10.1, Northridge Newhall 360° 100%, MF/FPS-NLD



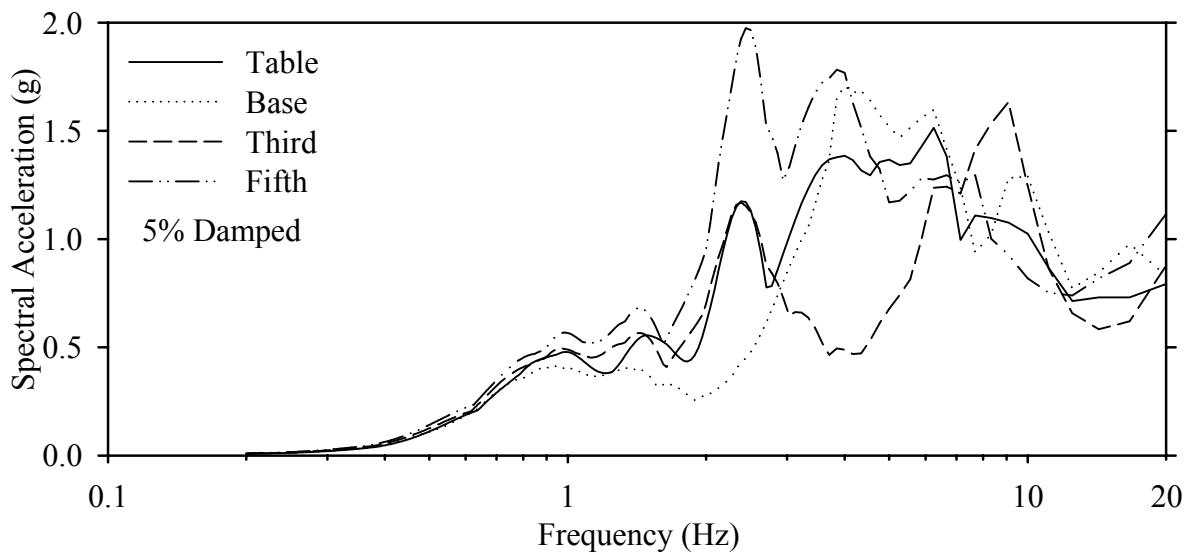
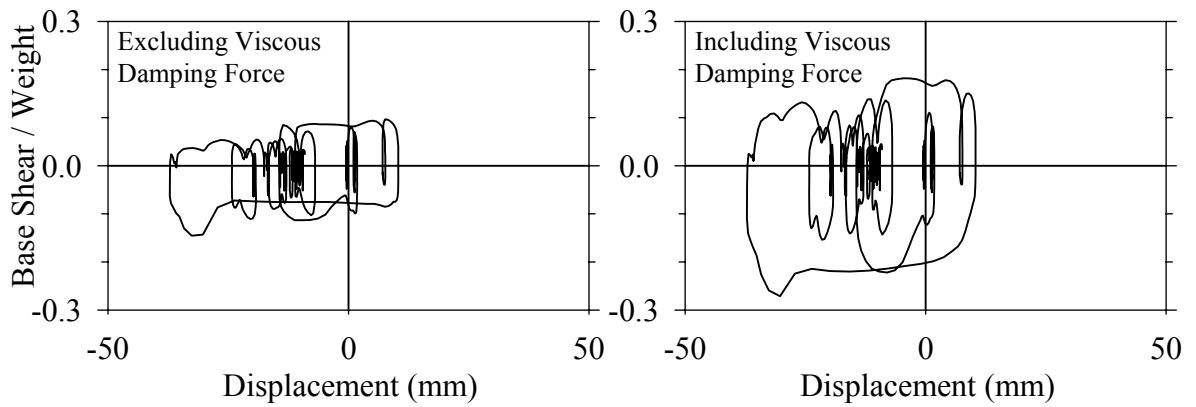
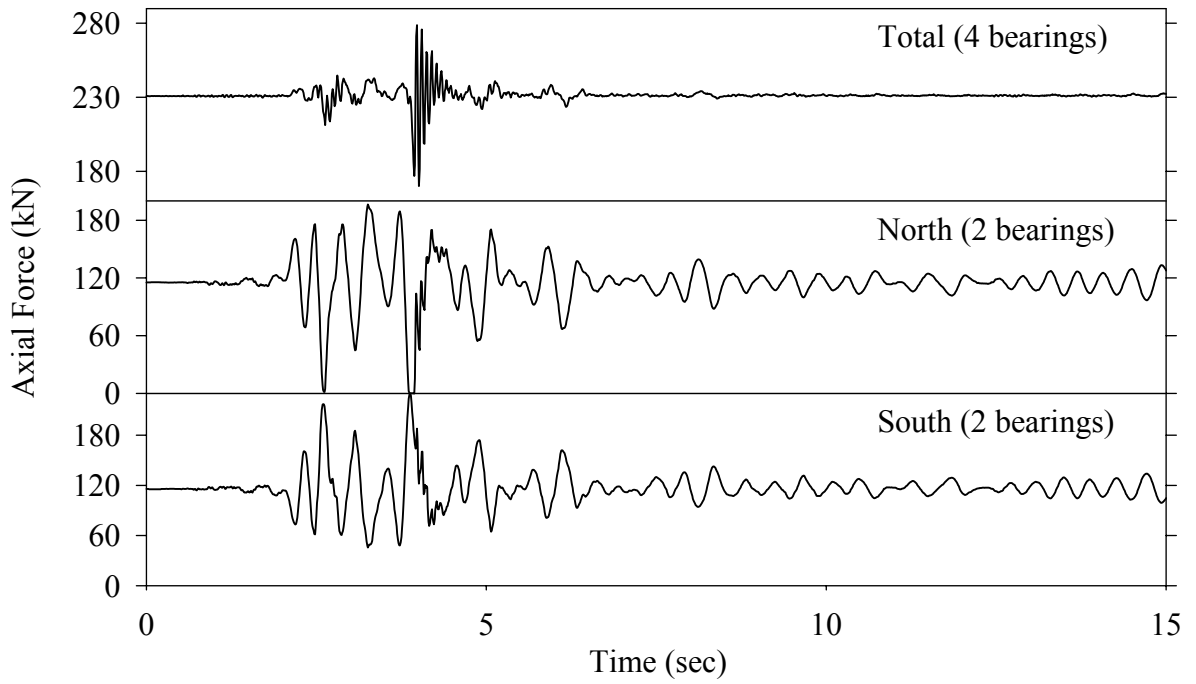
Test FPMNN10.1, Northridge Newhall 360° 100%, MF/FPS-NLD



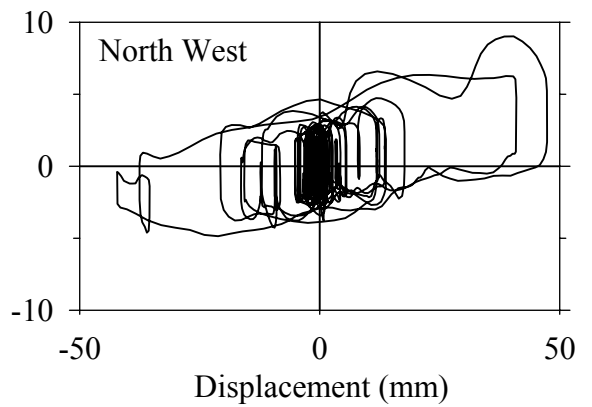
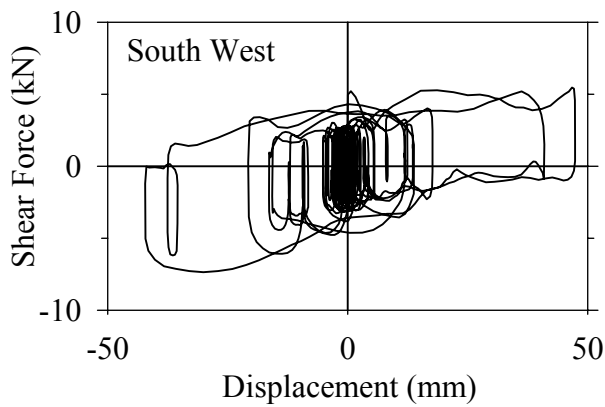
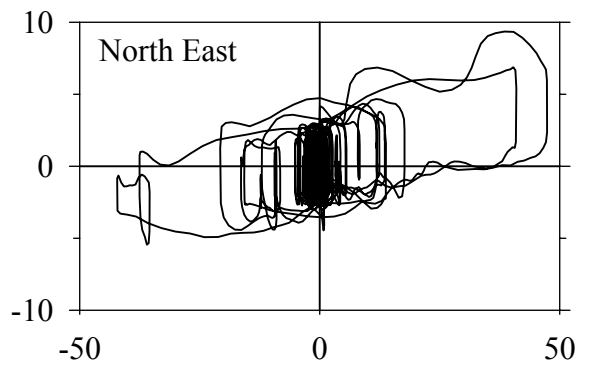
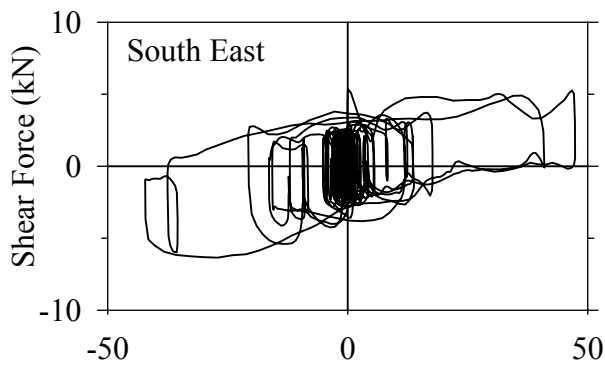
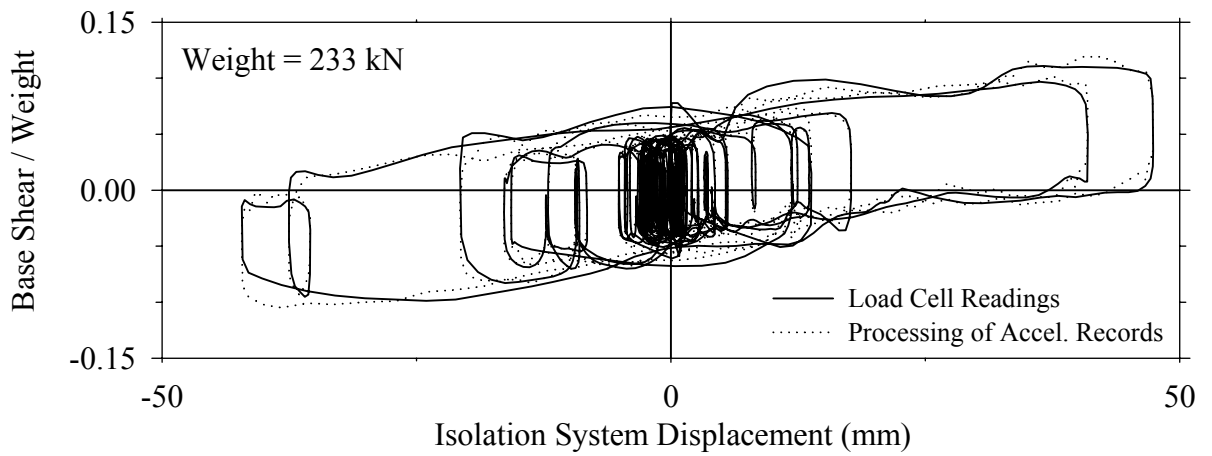
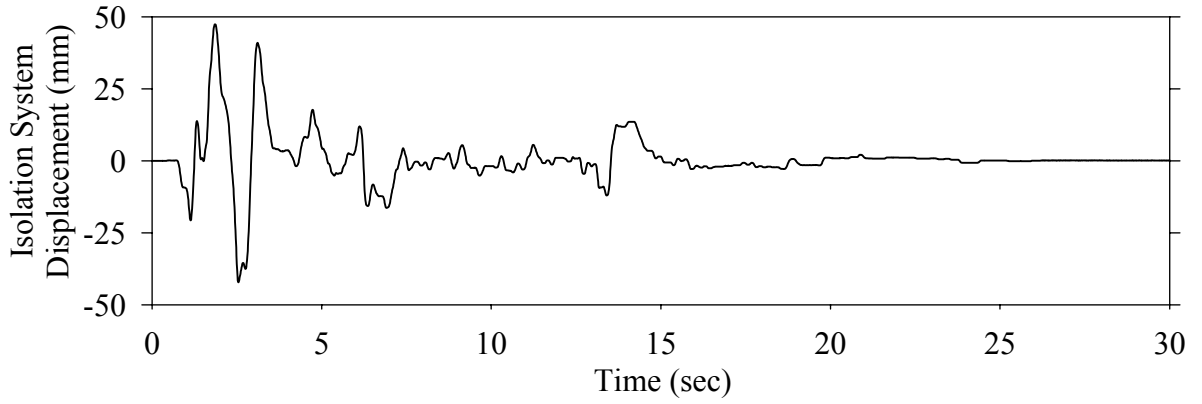
Test FPMNS10.1, Northridge Sylmar 90° 100%, MF/FPS-NLD



Test FPMNS10.1, Northridge Sylmar 90° 100%, MF/FPS-NLD

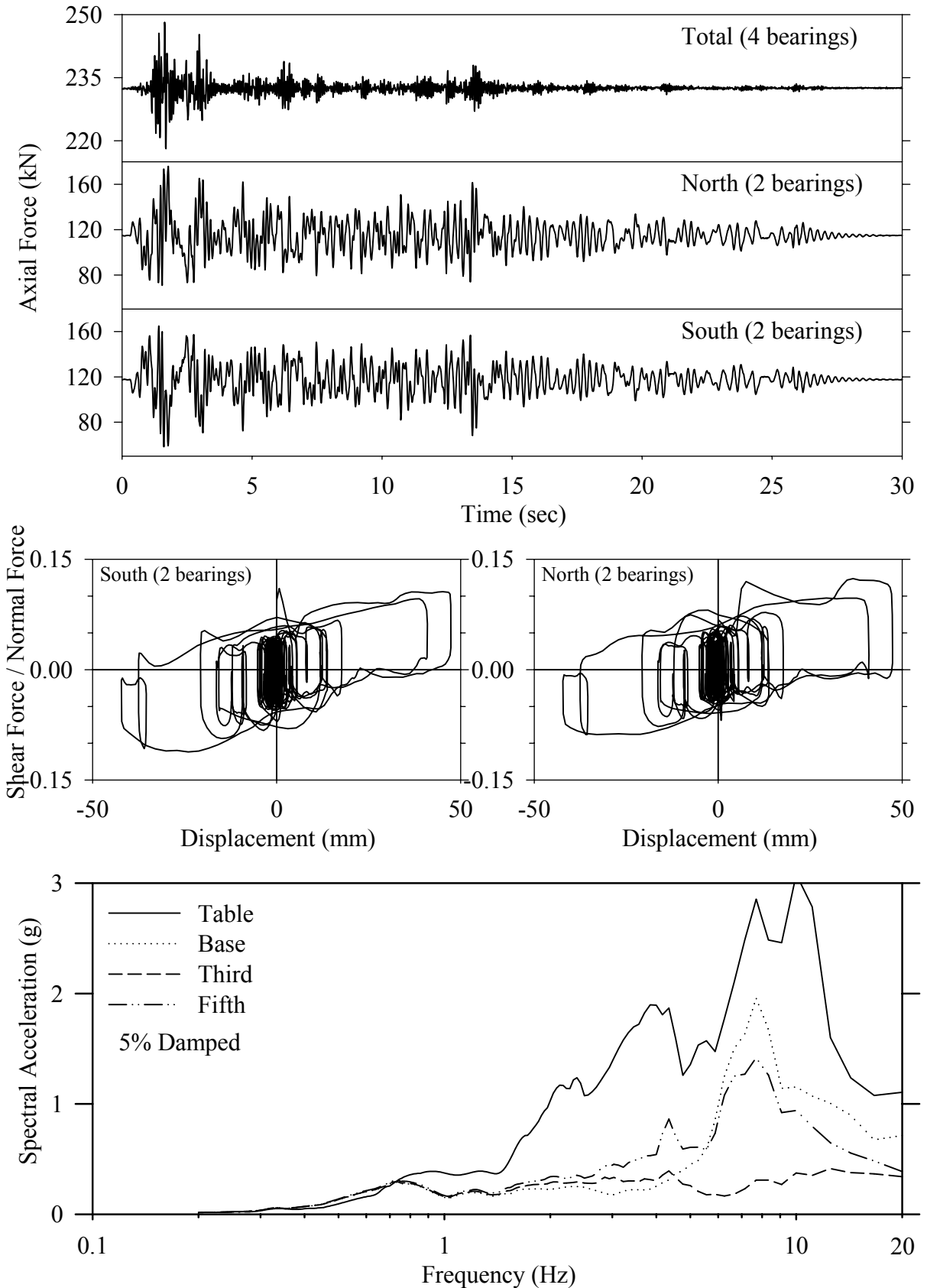


Test FPSBE20.2, El Centro S00E 200% Test 2, SB/FPS

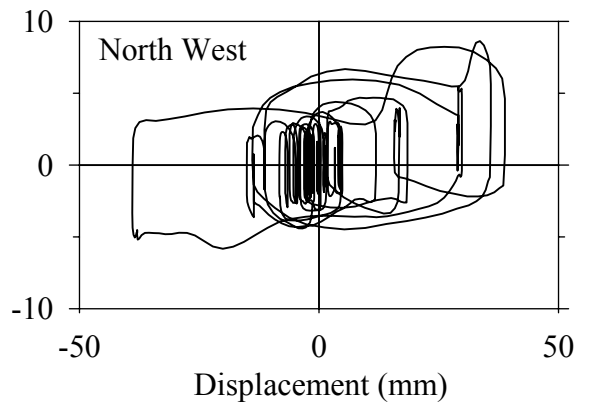
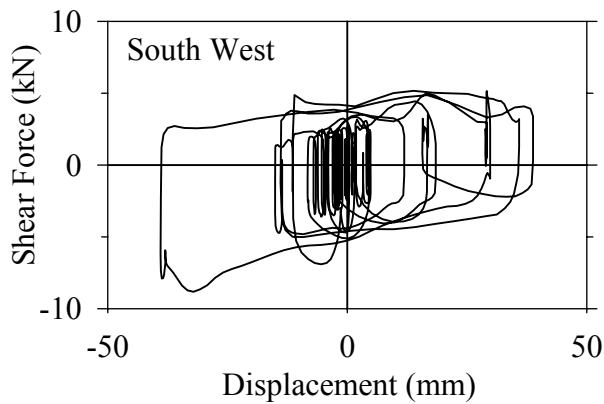
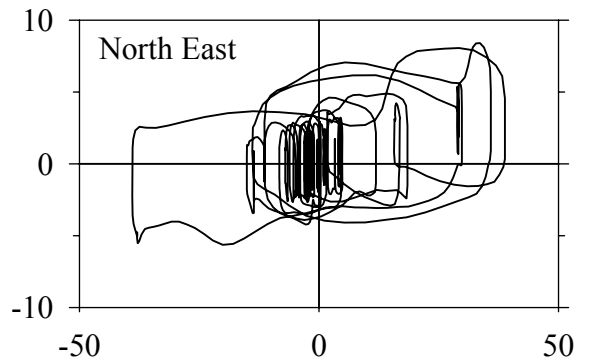
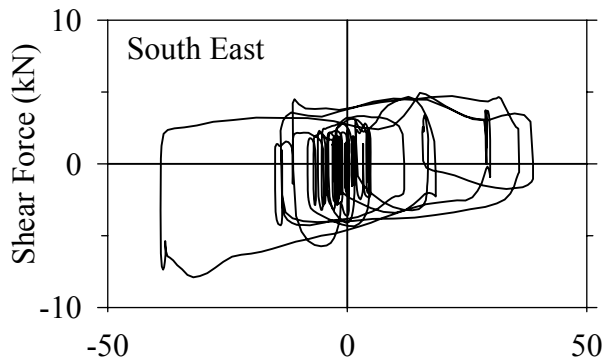
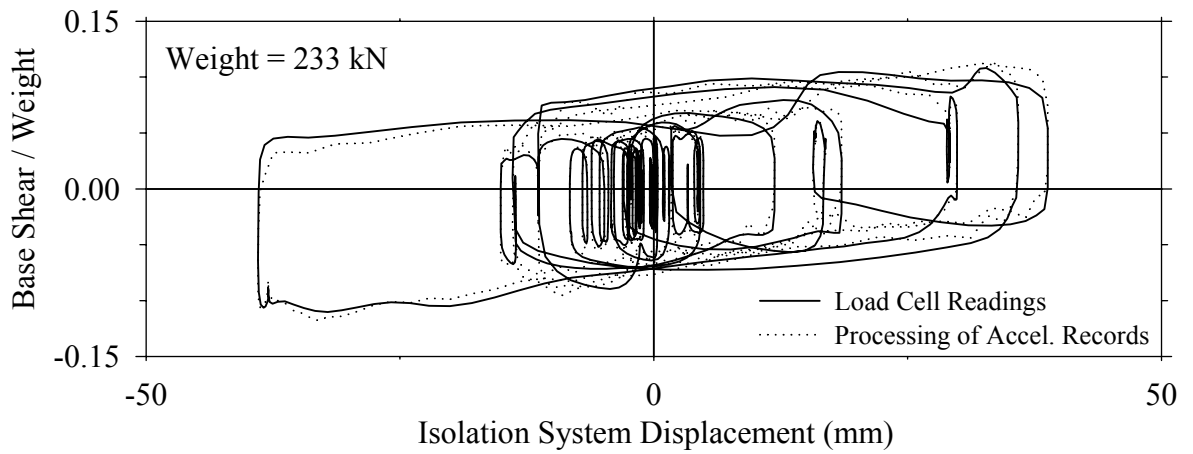
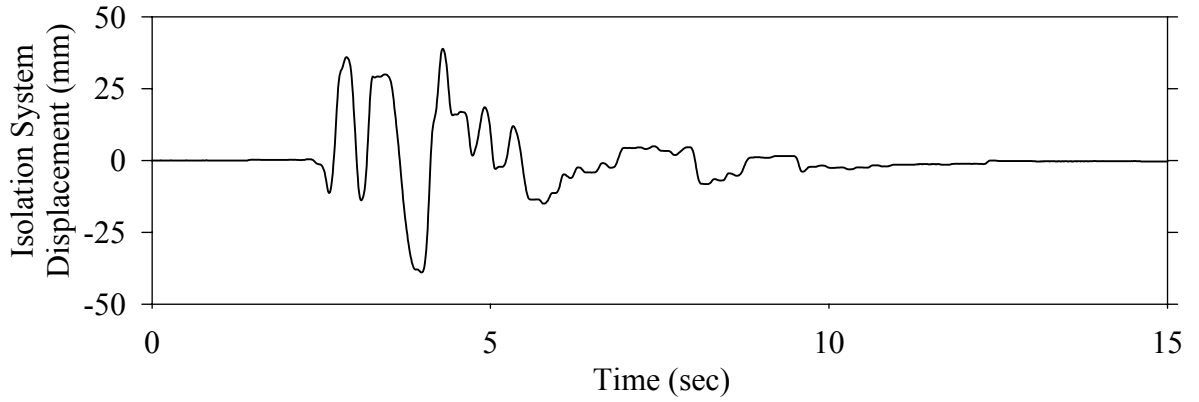




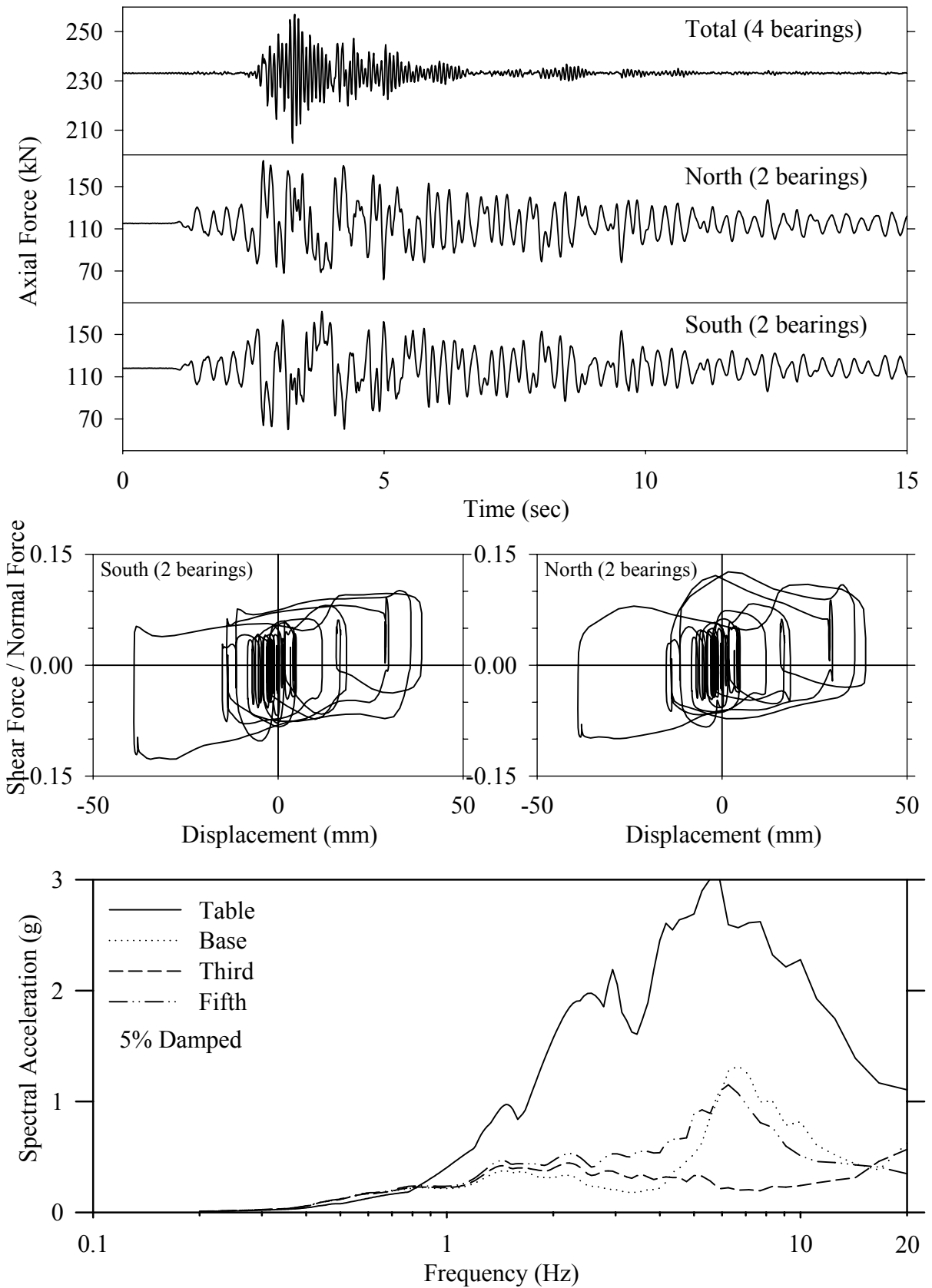
Test FPSBE20.2, El Centro S00E 200% Test 2, SB/FPS



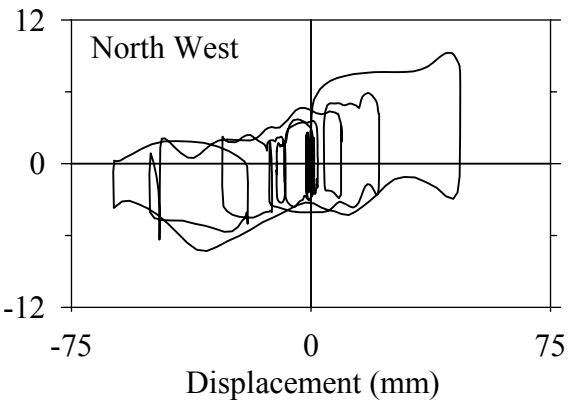
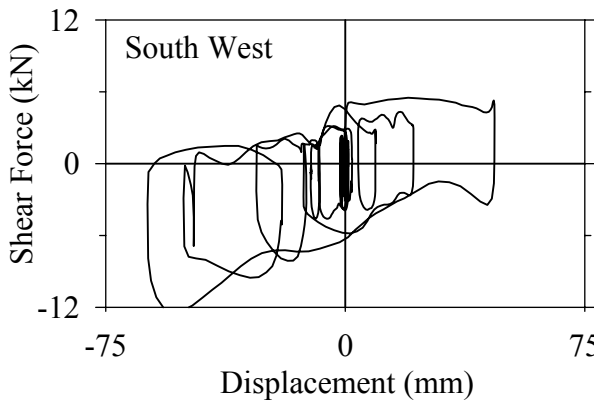
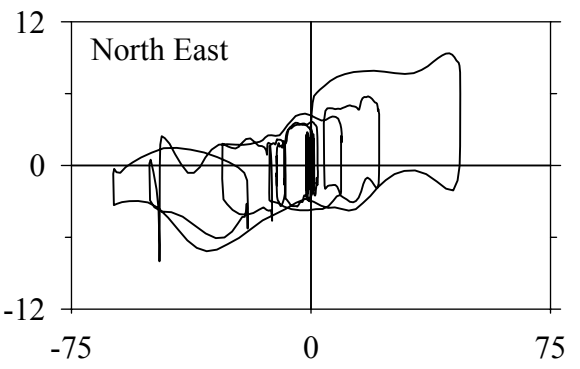
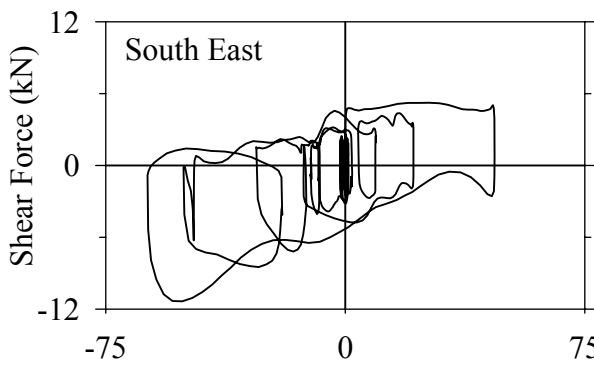
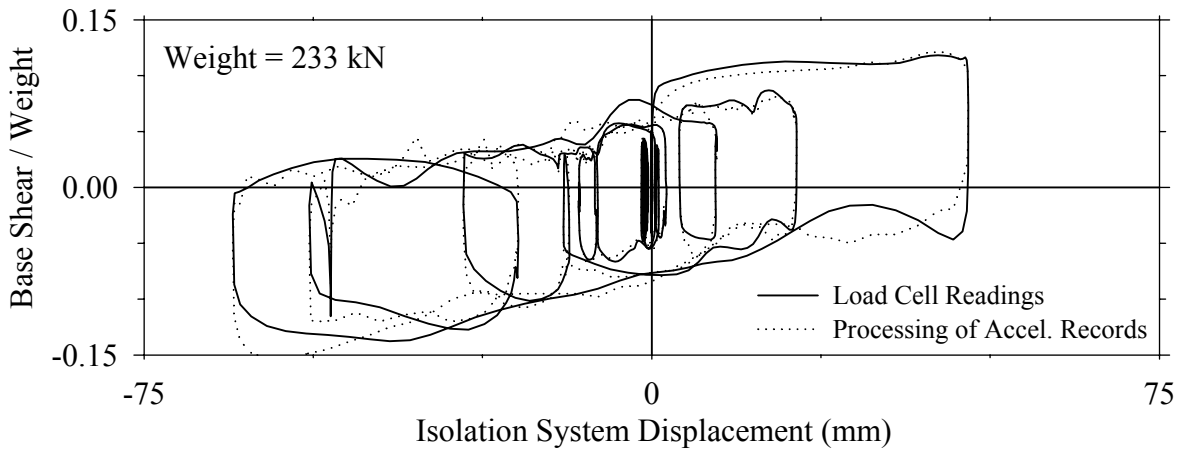
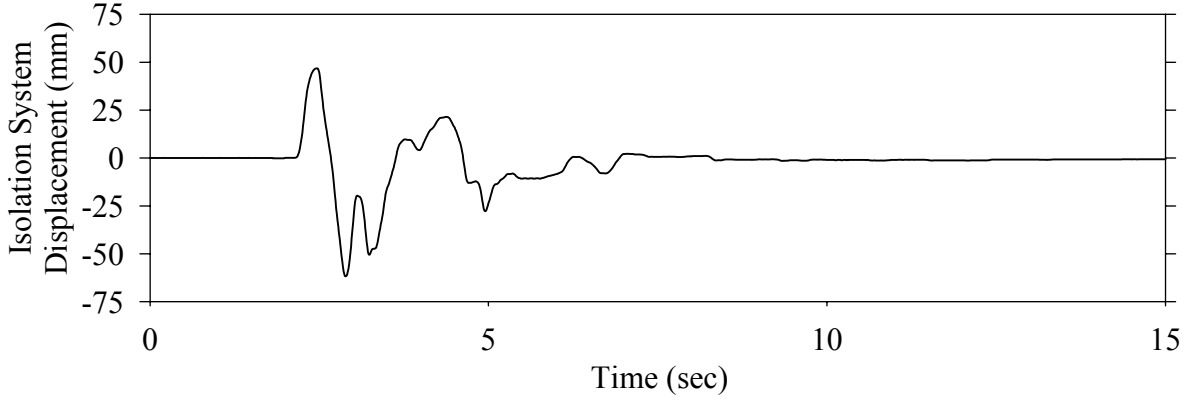
Test FPSBK10.1, Kobe N-S 100%, SB/FPS



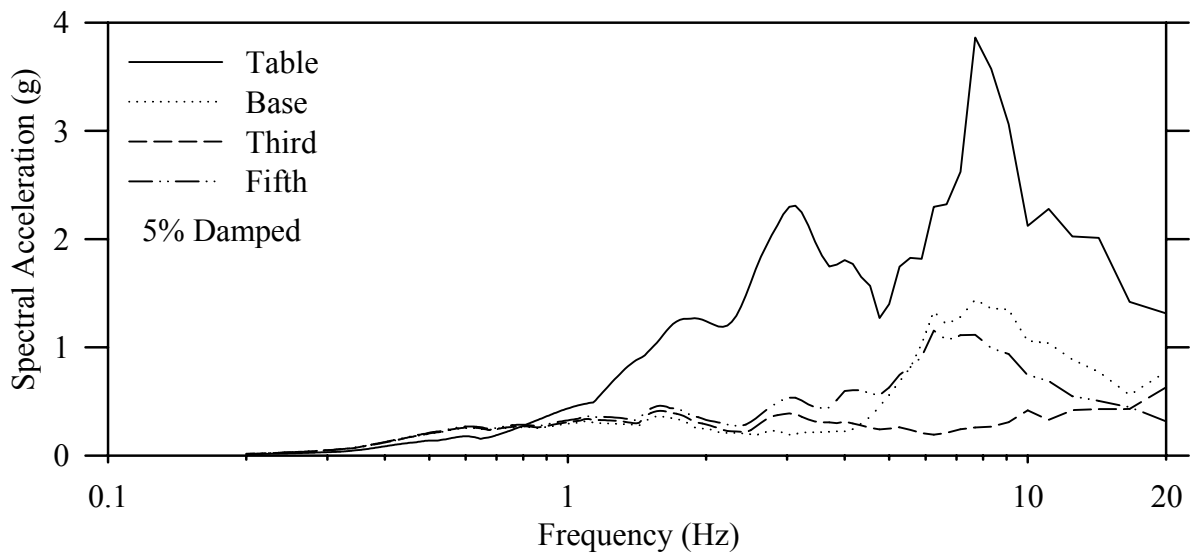
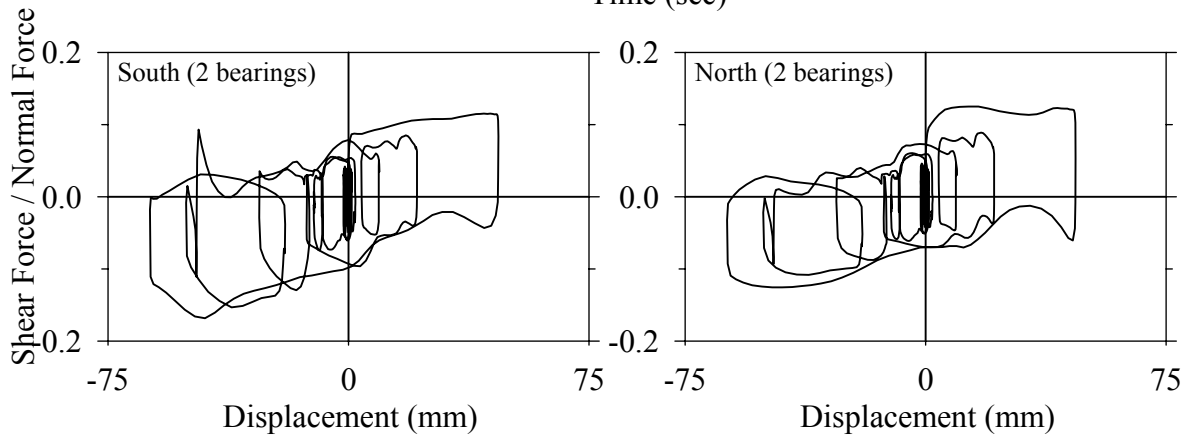
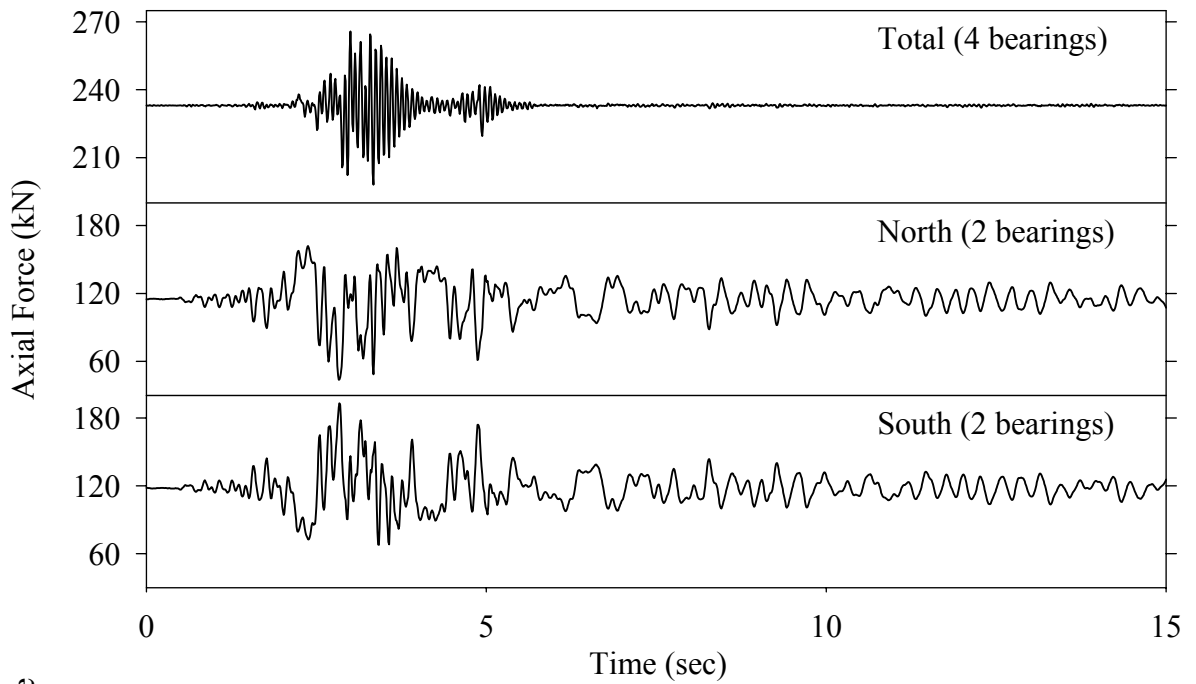
Test FPSBK10.1, Kobe N-S 100%, SB/FPS



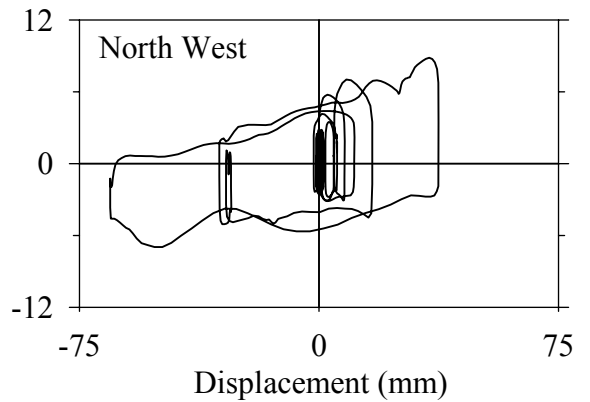
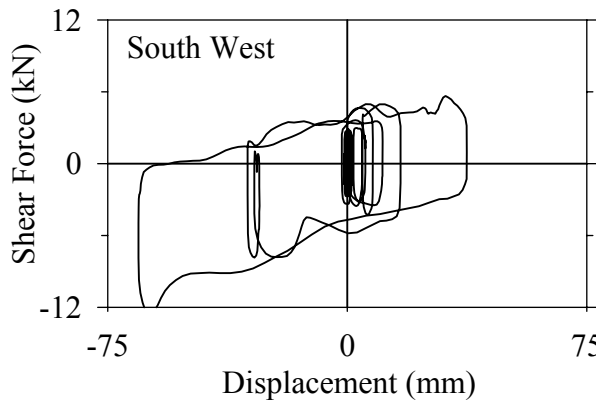
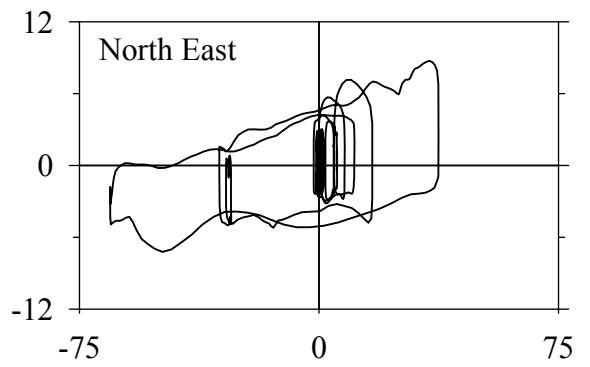
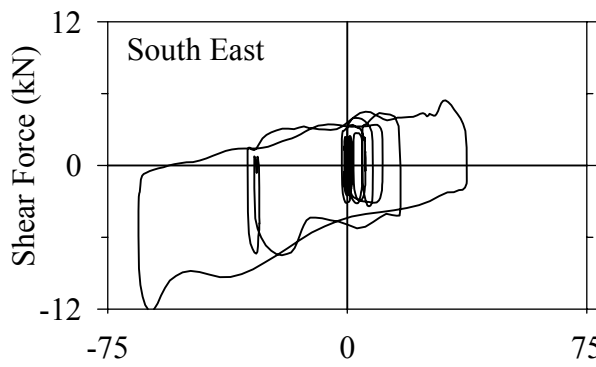
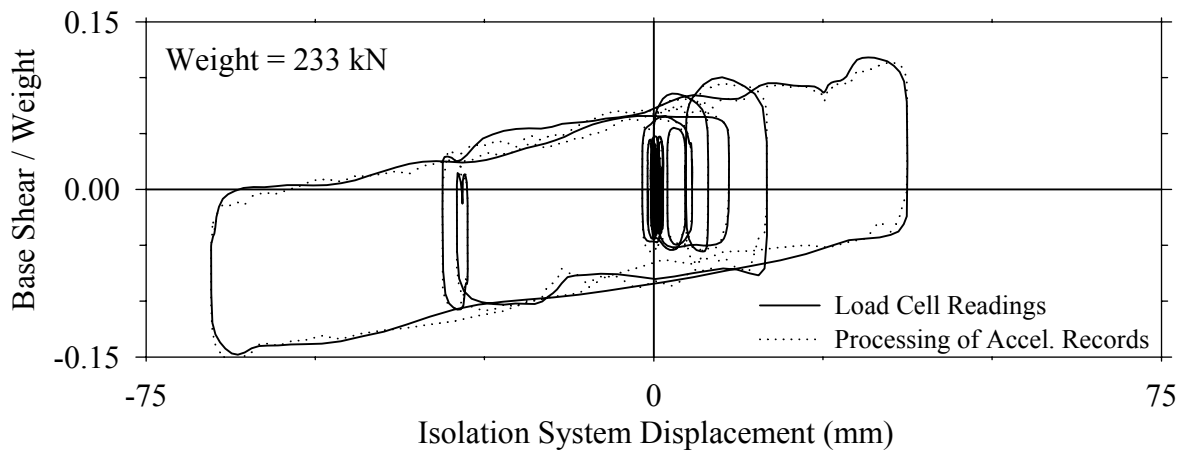
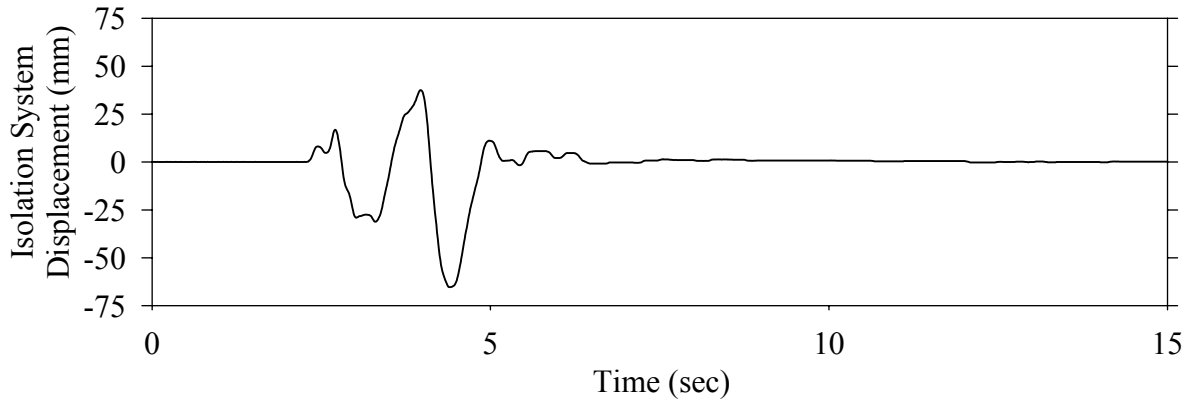
Test FPSBN10.1, Northridge Newhall 360° 100%, SB/FPS



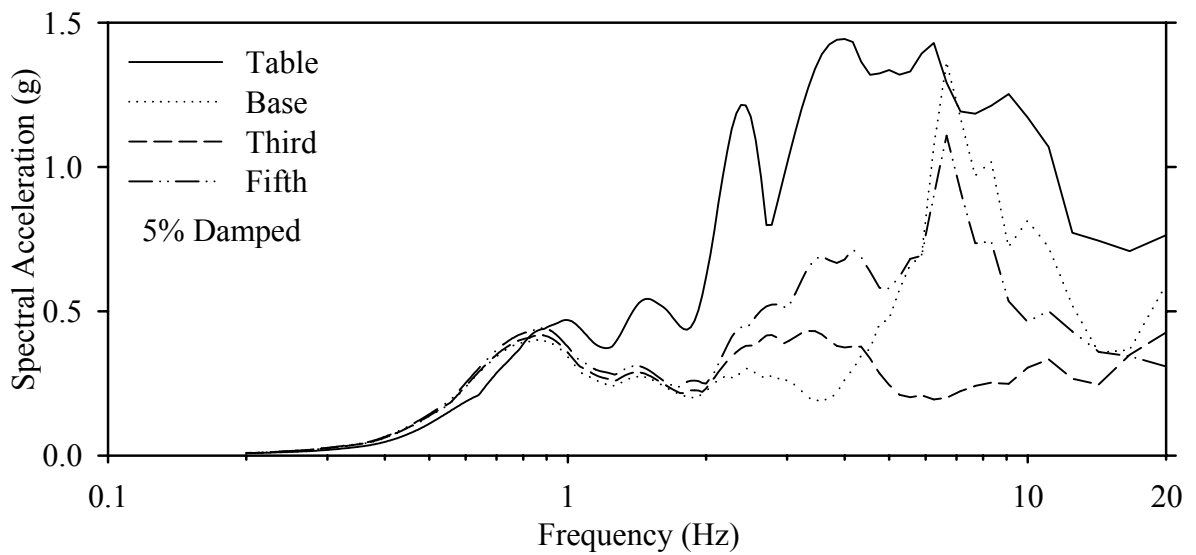
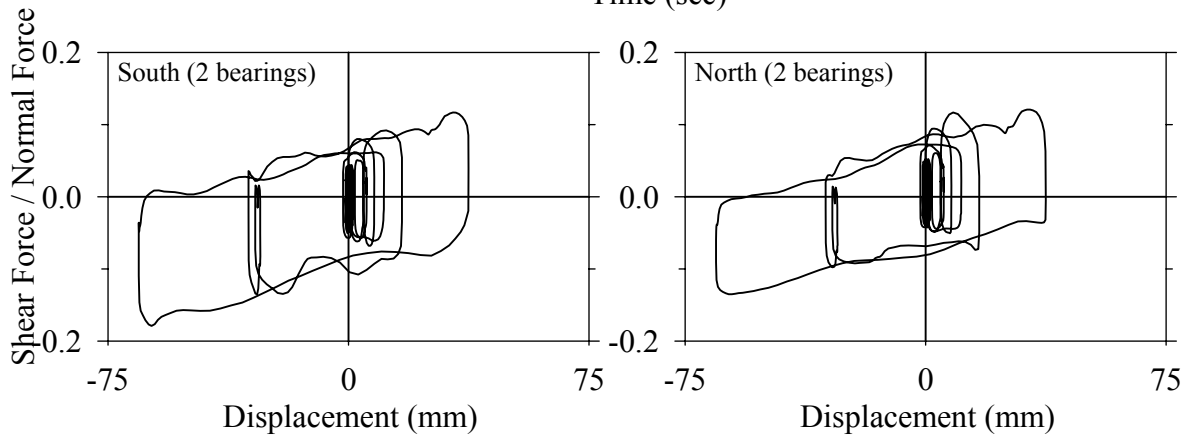
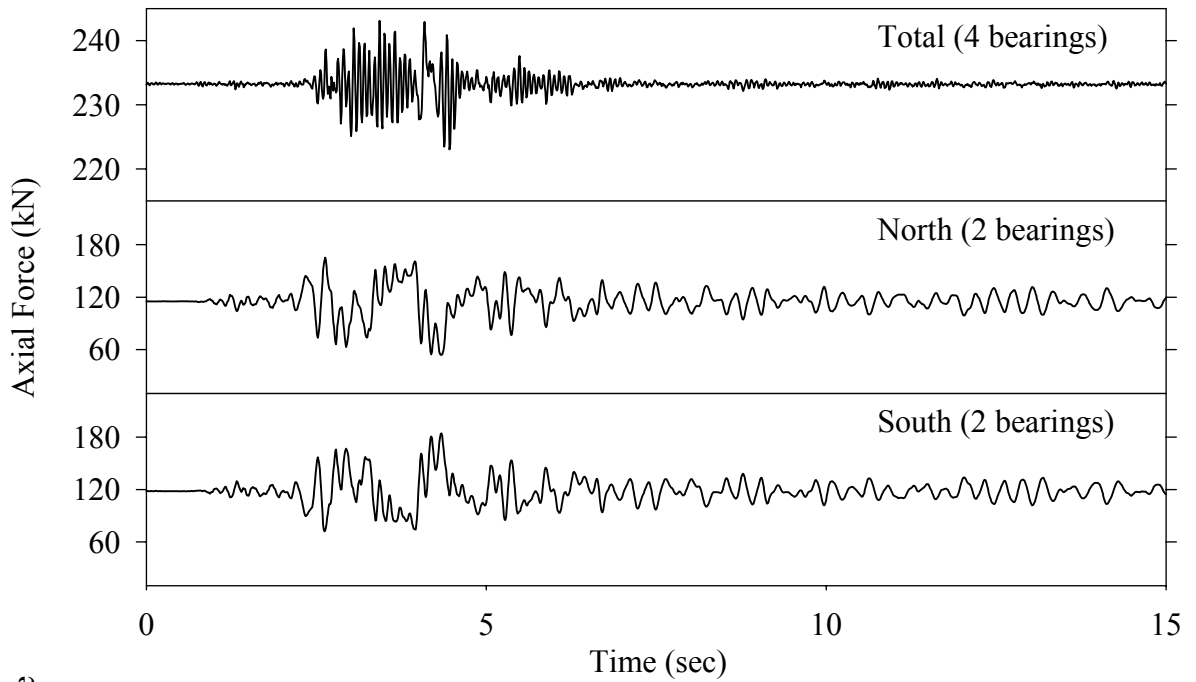
Test FPSBN10.1, Northridge Newhall 360° 100%, SB/FPS



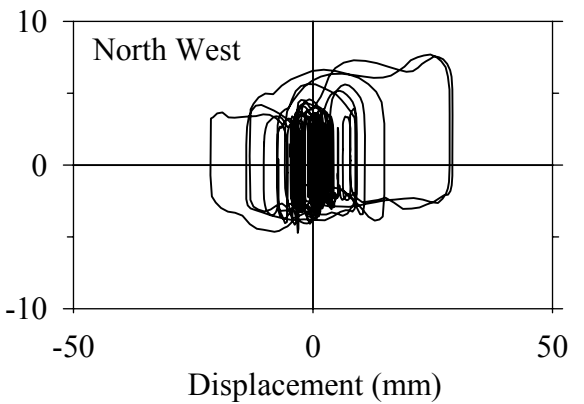
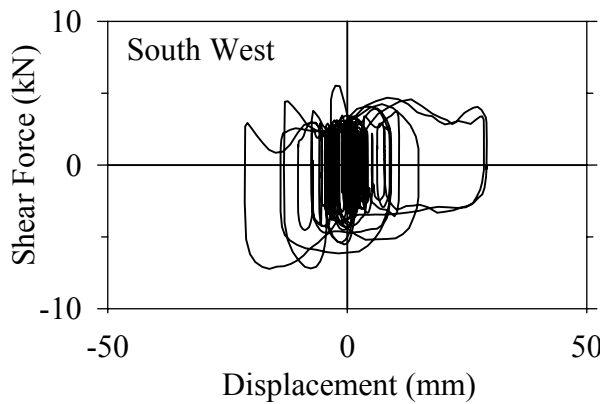
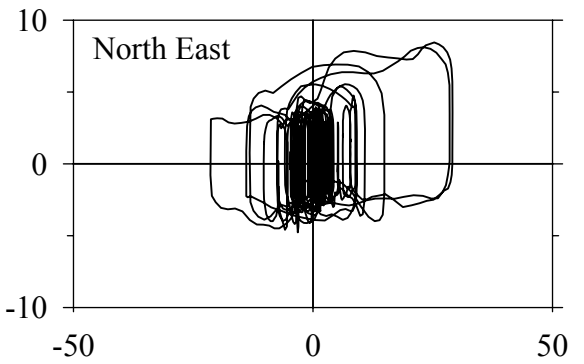
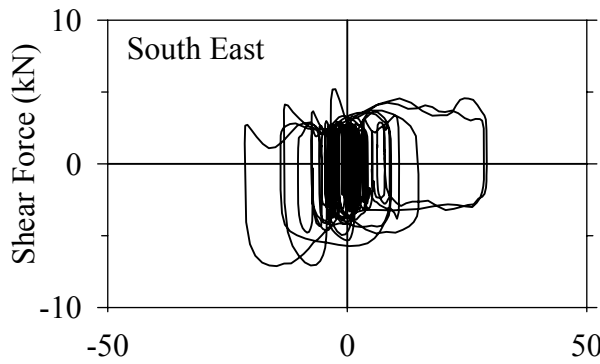
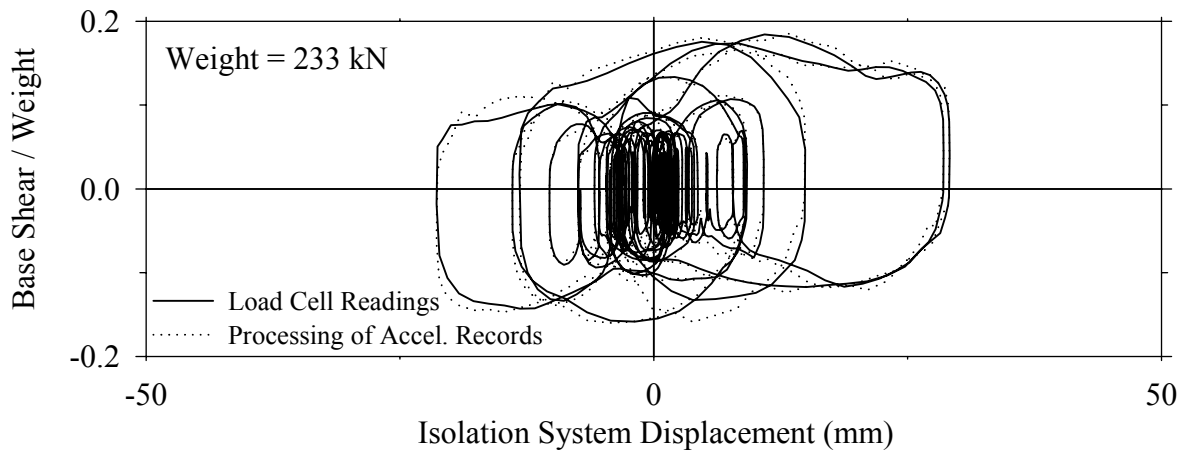
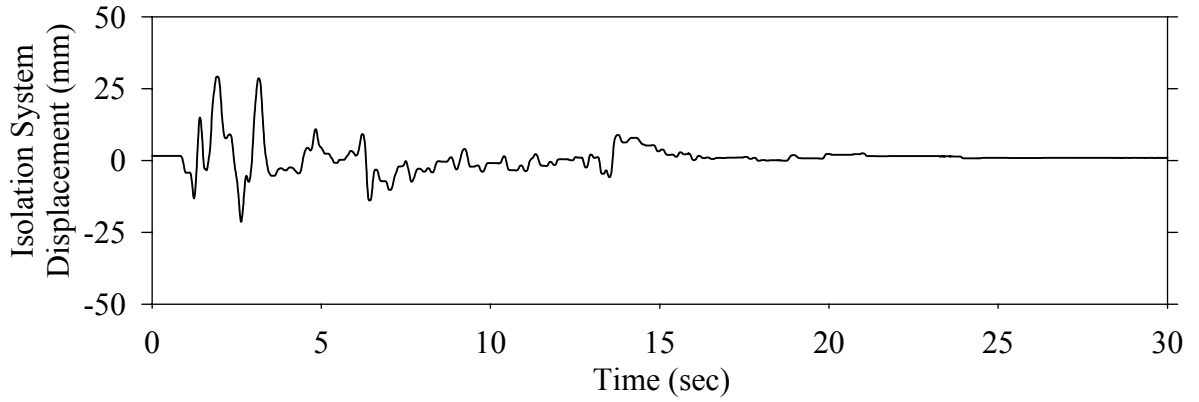
Test FPSBS10.1, Northridge Sylmar 90° 100%, SB/FPS



Test FPSBS10.1, Northridge Sylmar 90° 100%, SB/FPS

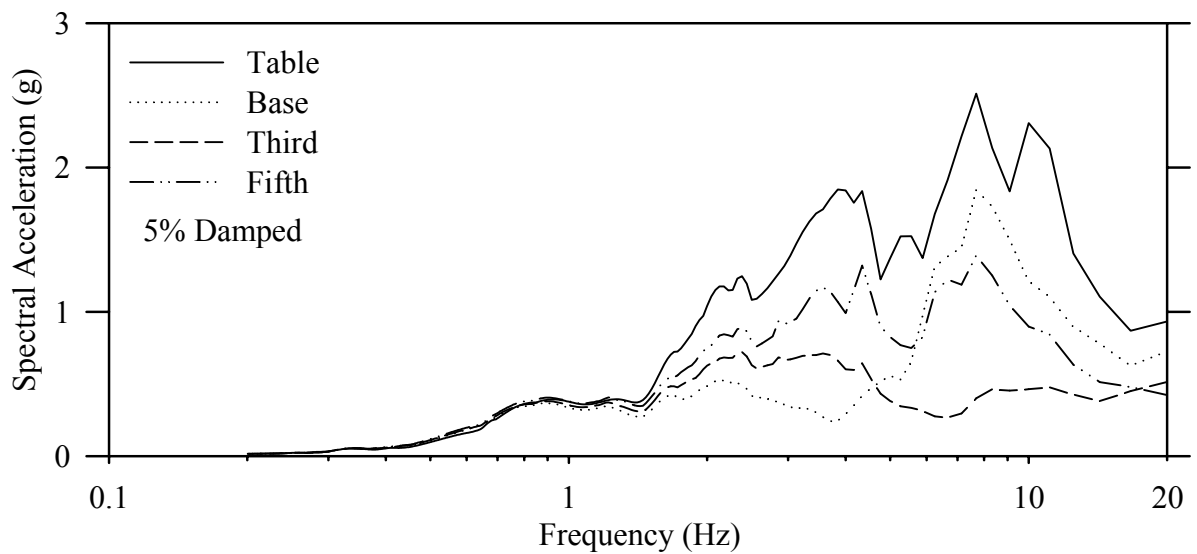
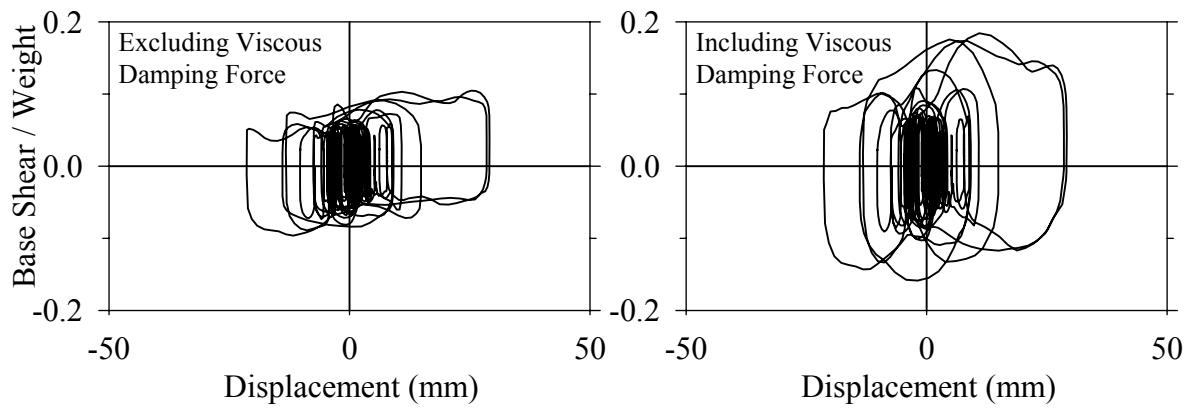
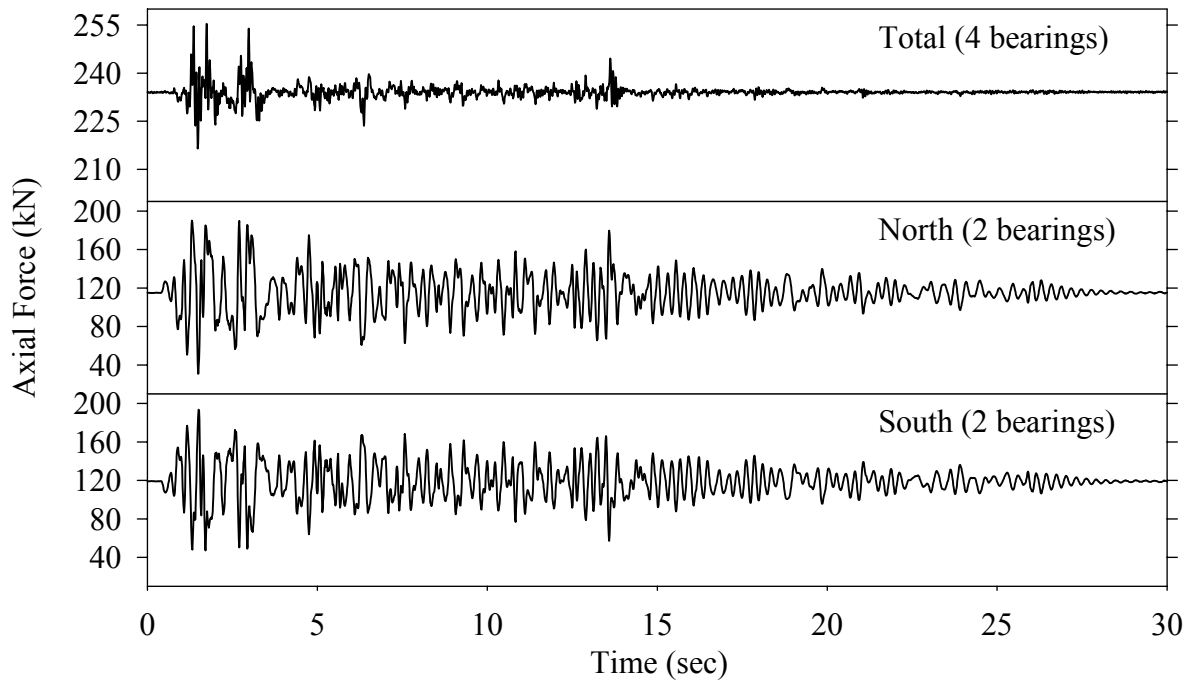


Test FPSLE20.2, El Centro S00E 200% Test 2, SB/FPS-LD

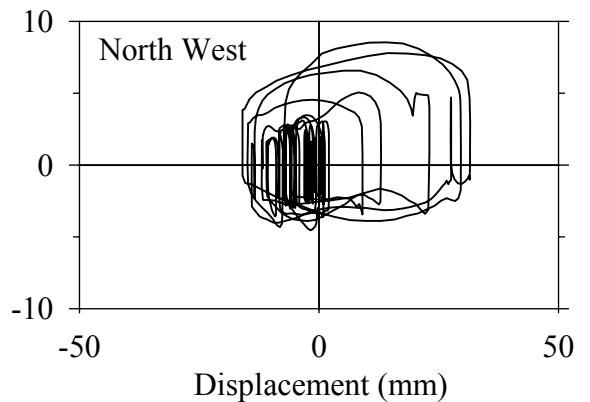
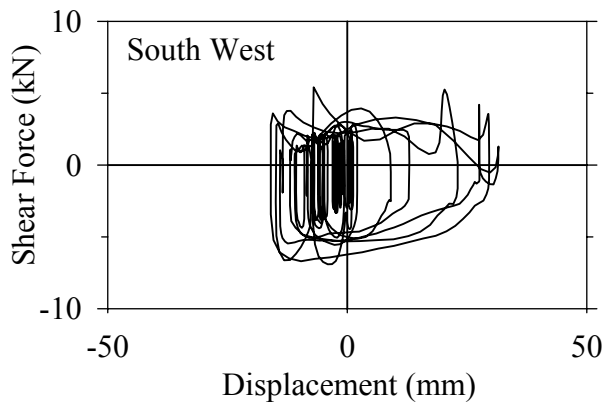
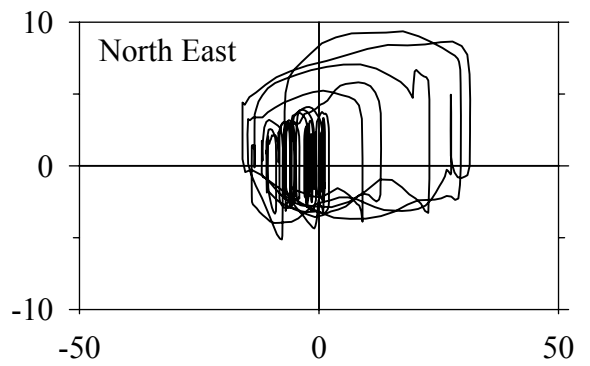
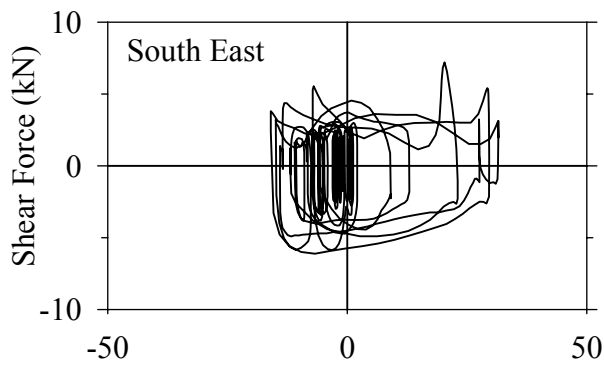
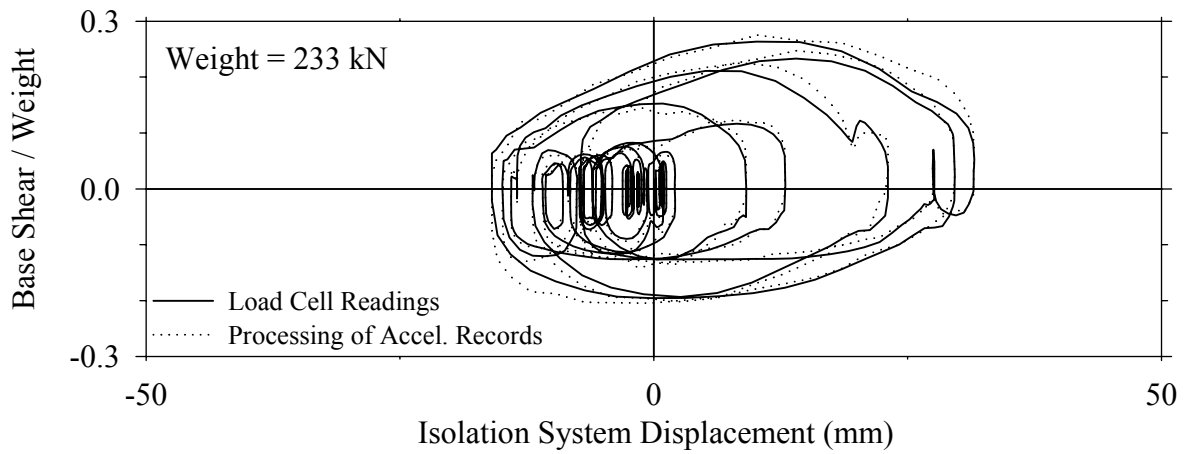
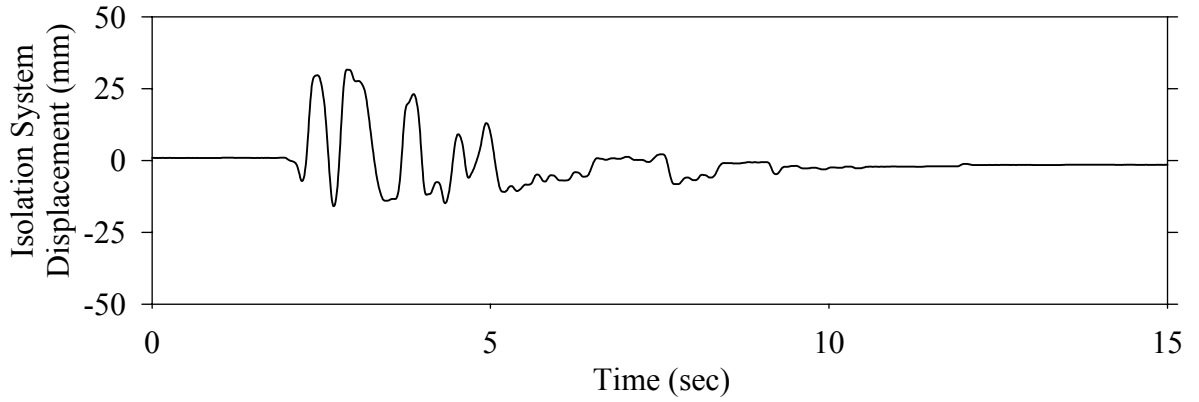




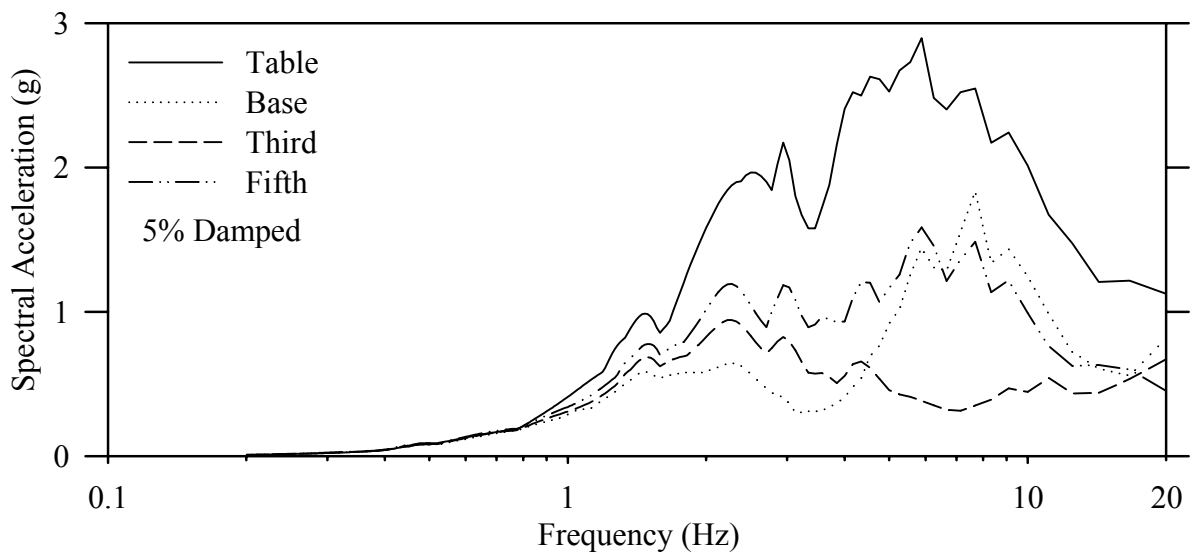
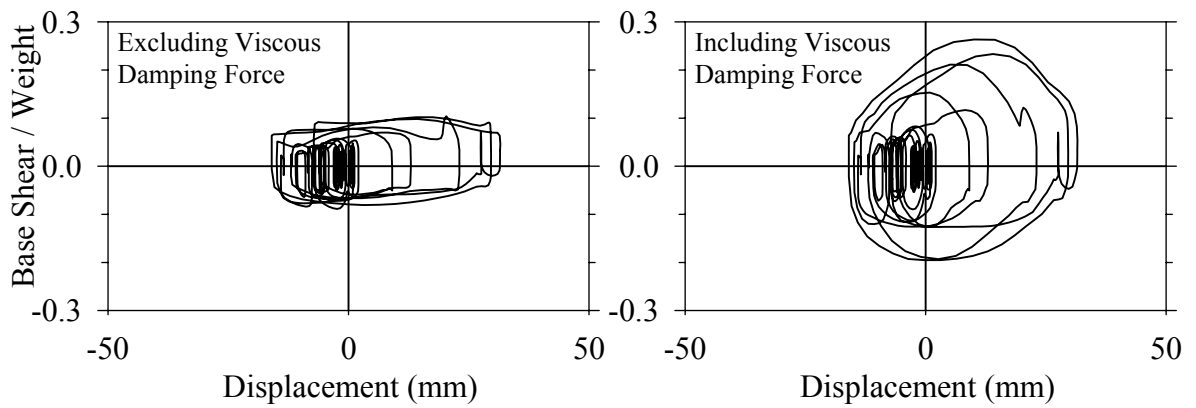
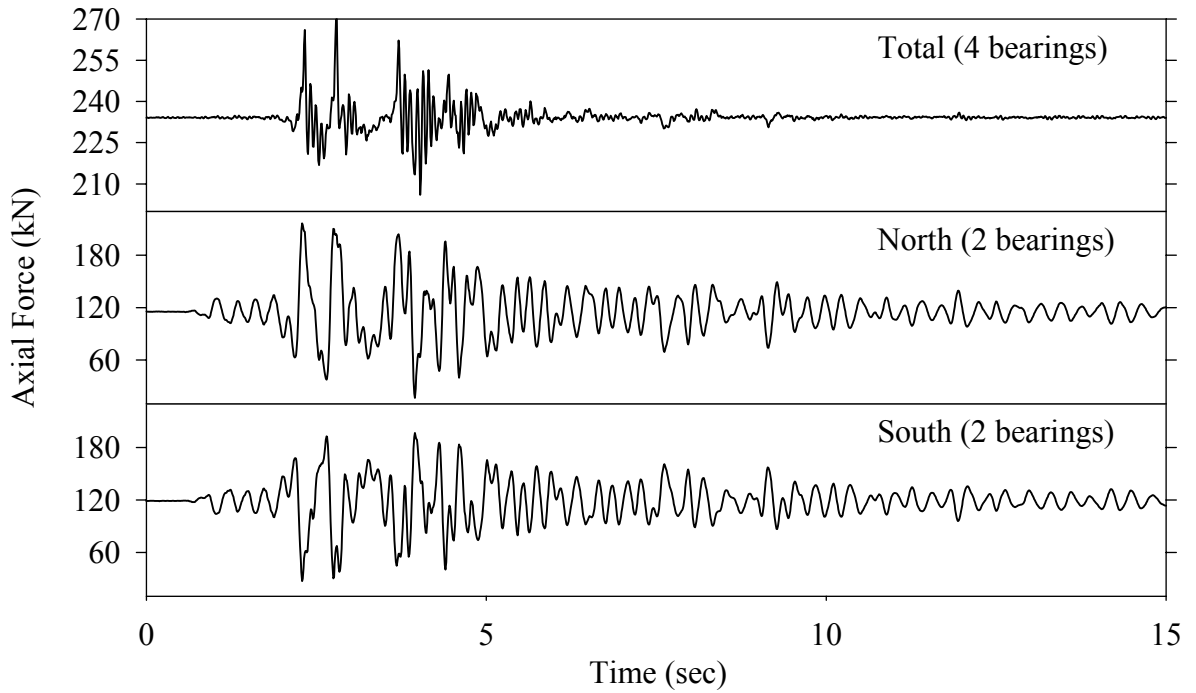
Test FPSLE20.2, El Centro S00E 200% Test 2, SB/FPS-LD



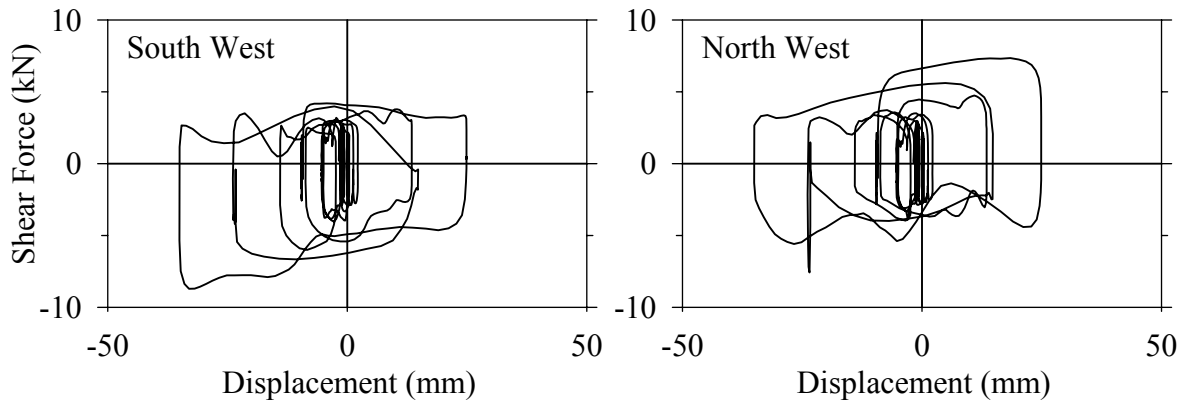
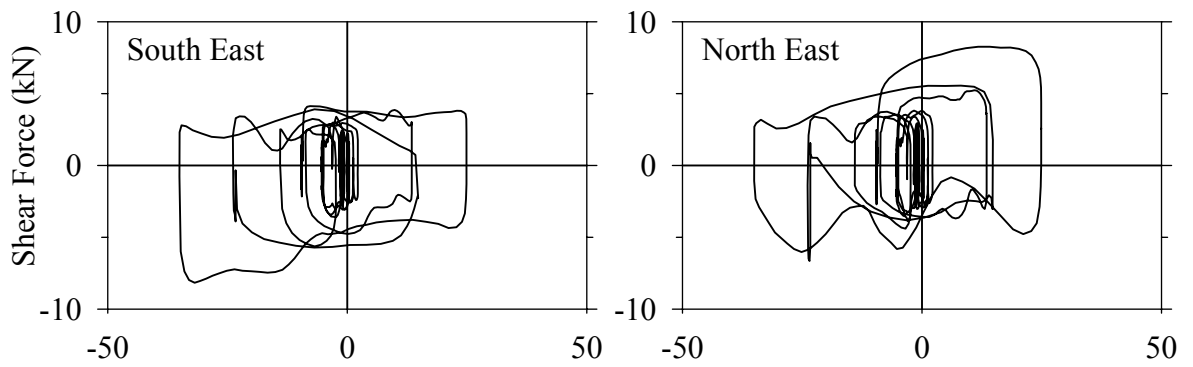
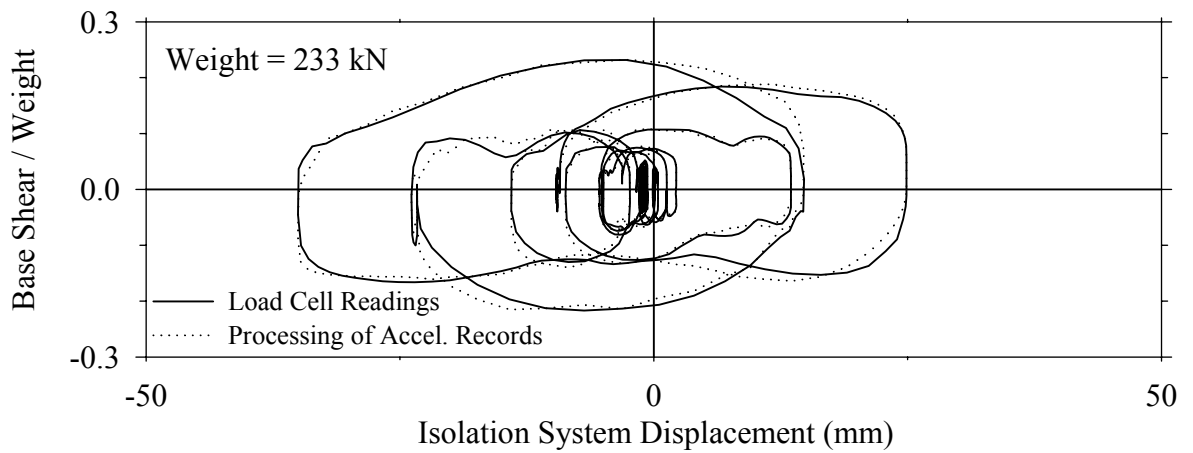
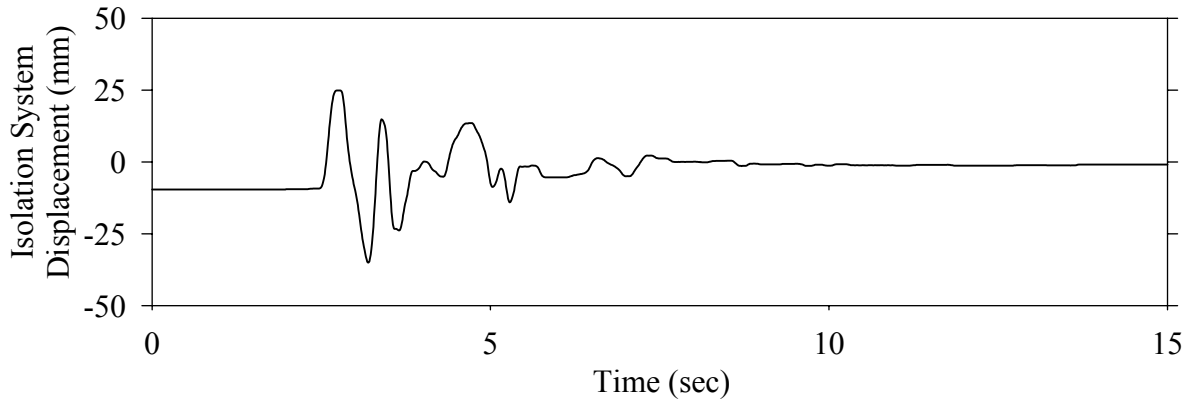
Test FPSLK10.1, Kobe N-S 100%, SB/FPS-LD



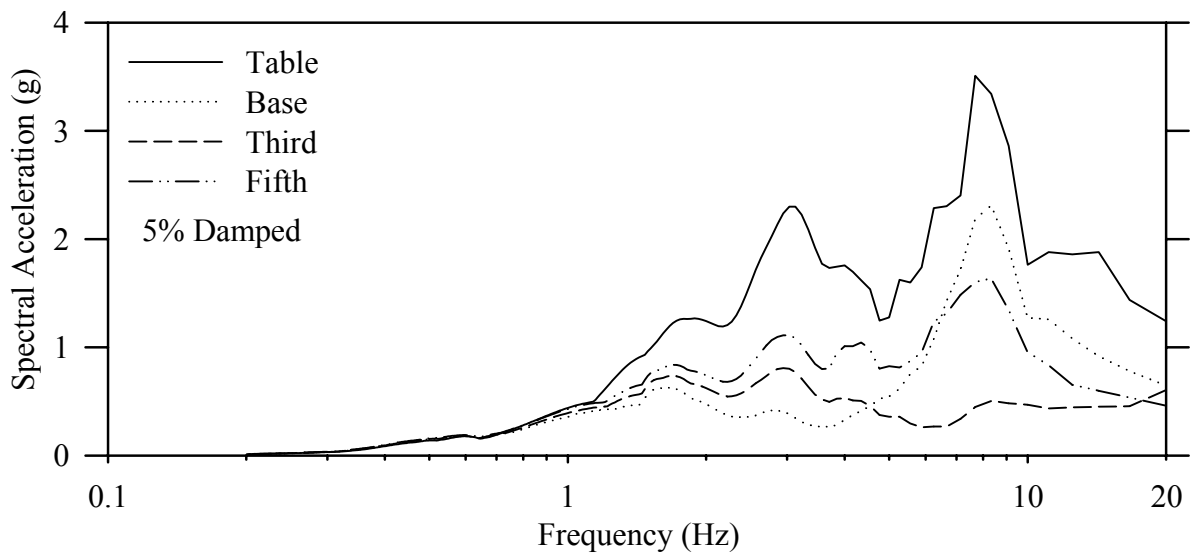
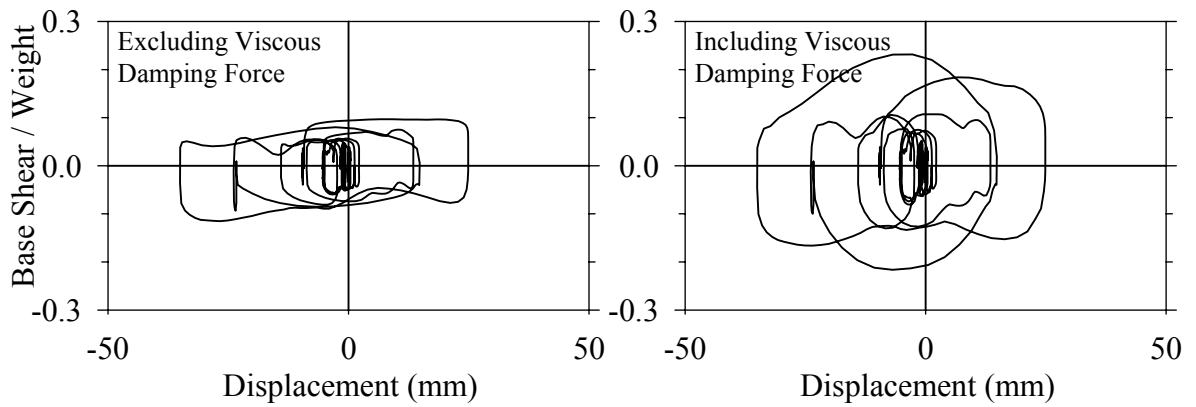
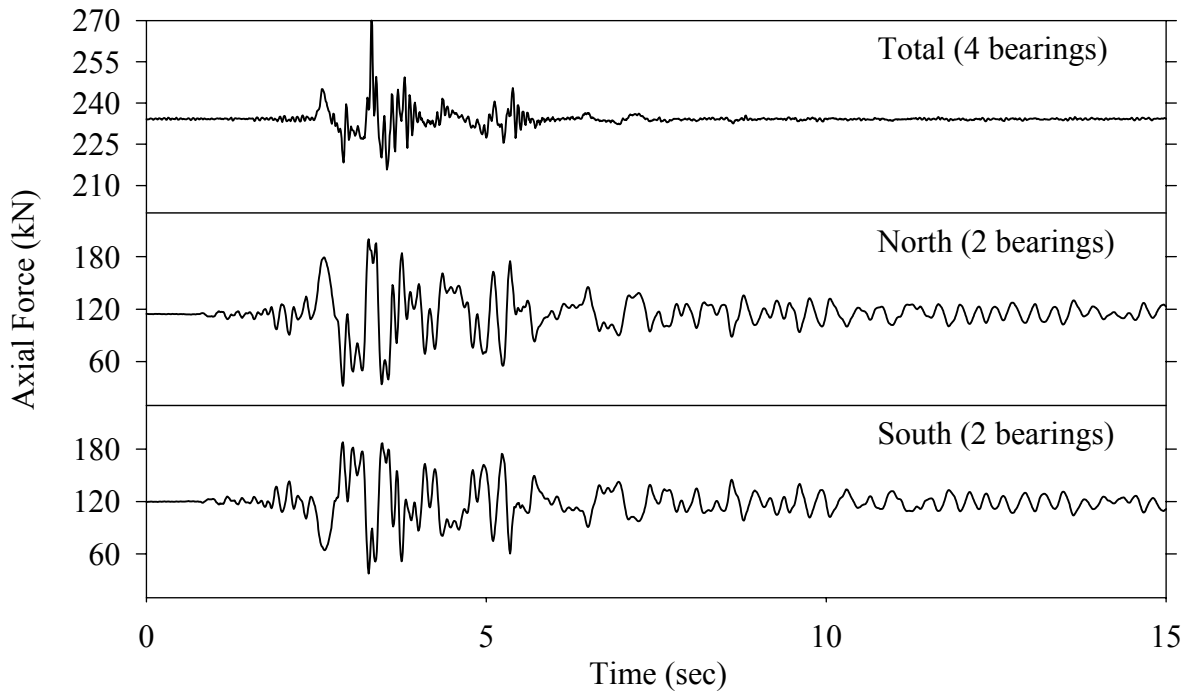
Test FPSLK10.1, Kobe N-S 100%, SB/FPS-LD



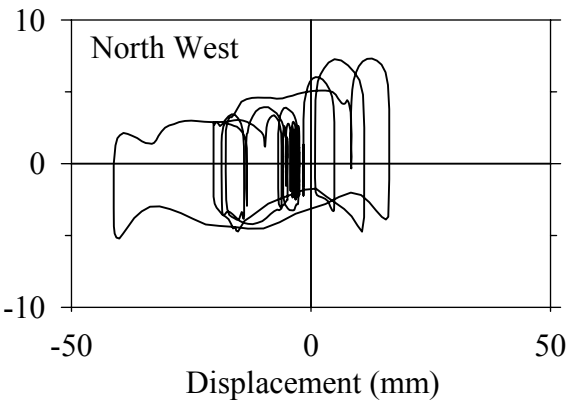
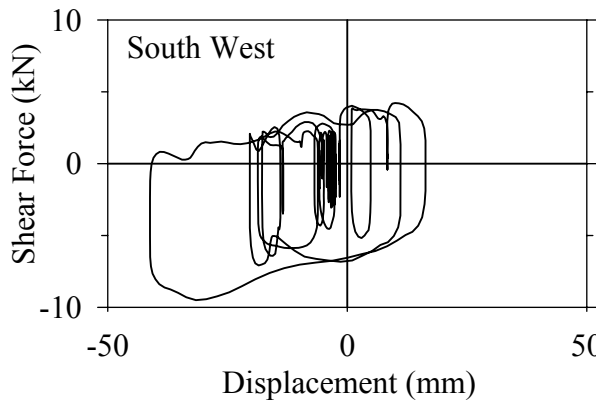
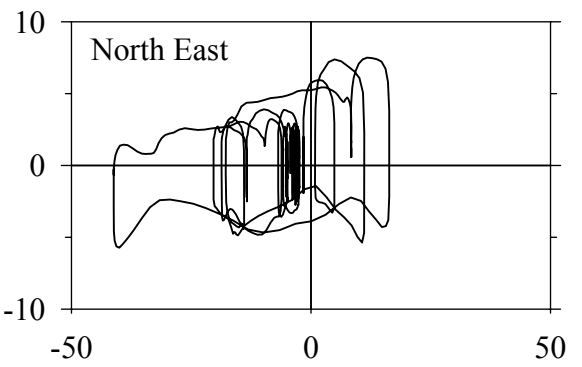
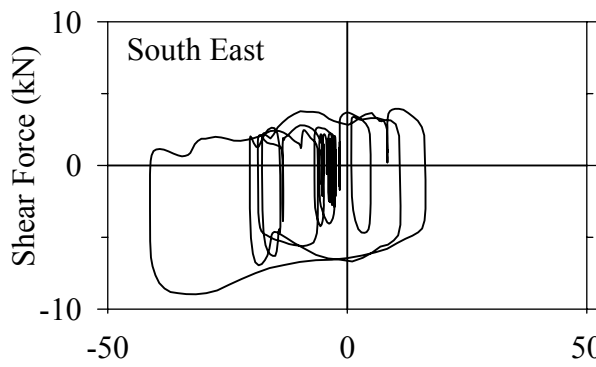
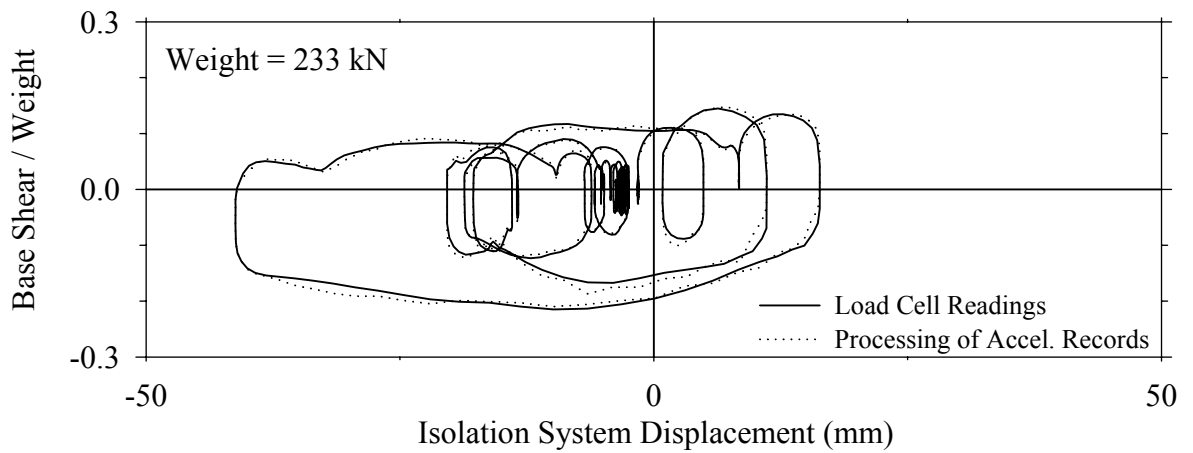
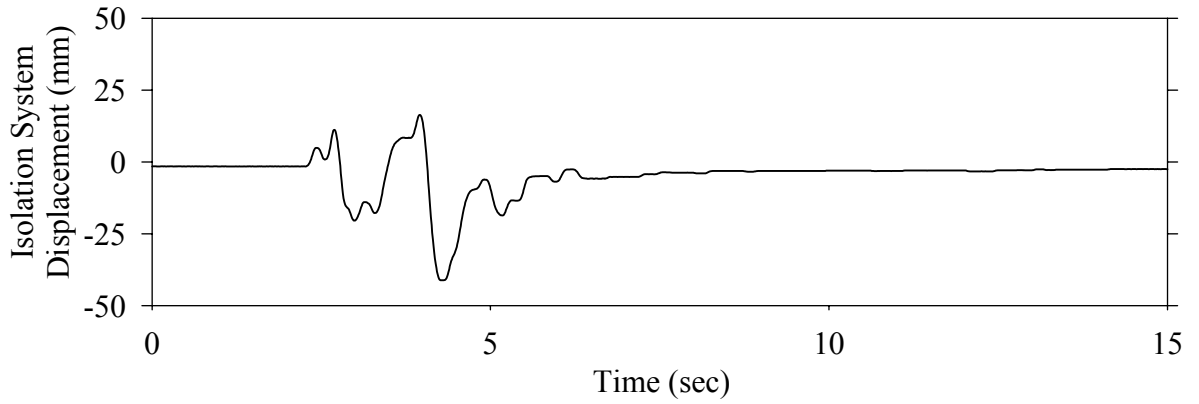
Test FPSLN31.1, Northridge Newhall 360° 100%, SB/FPS-LD



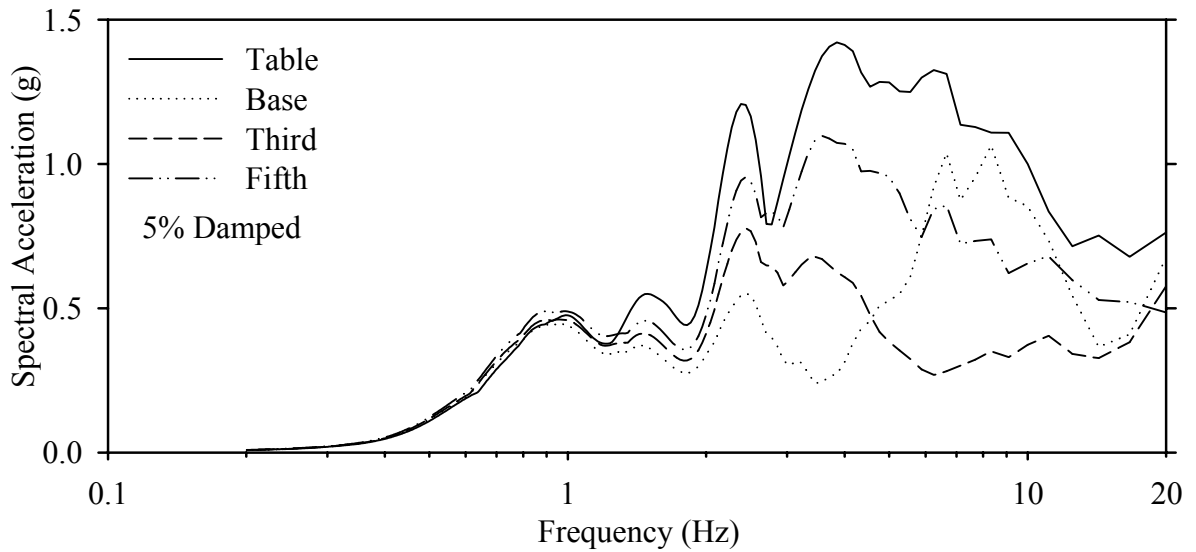
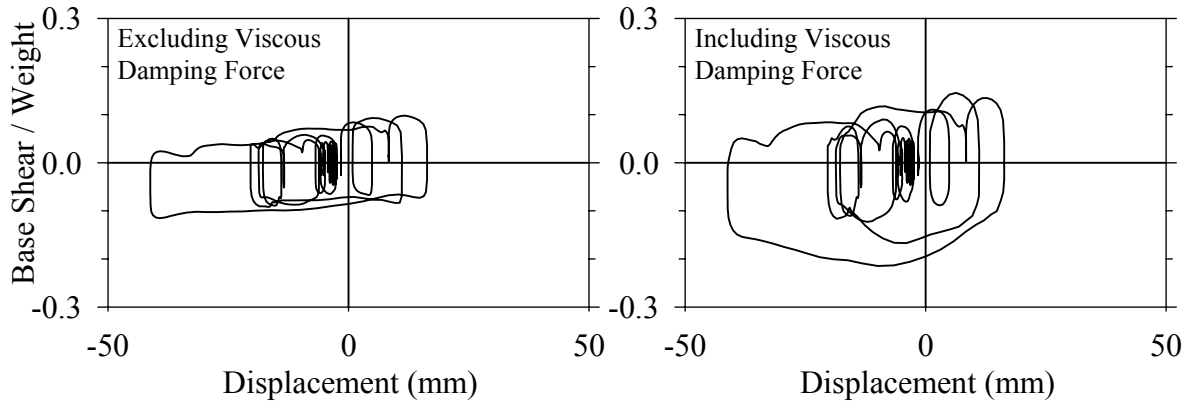
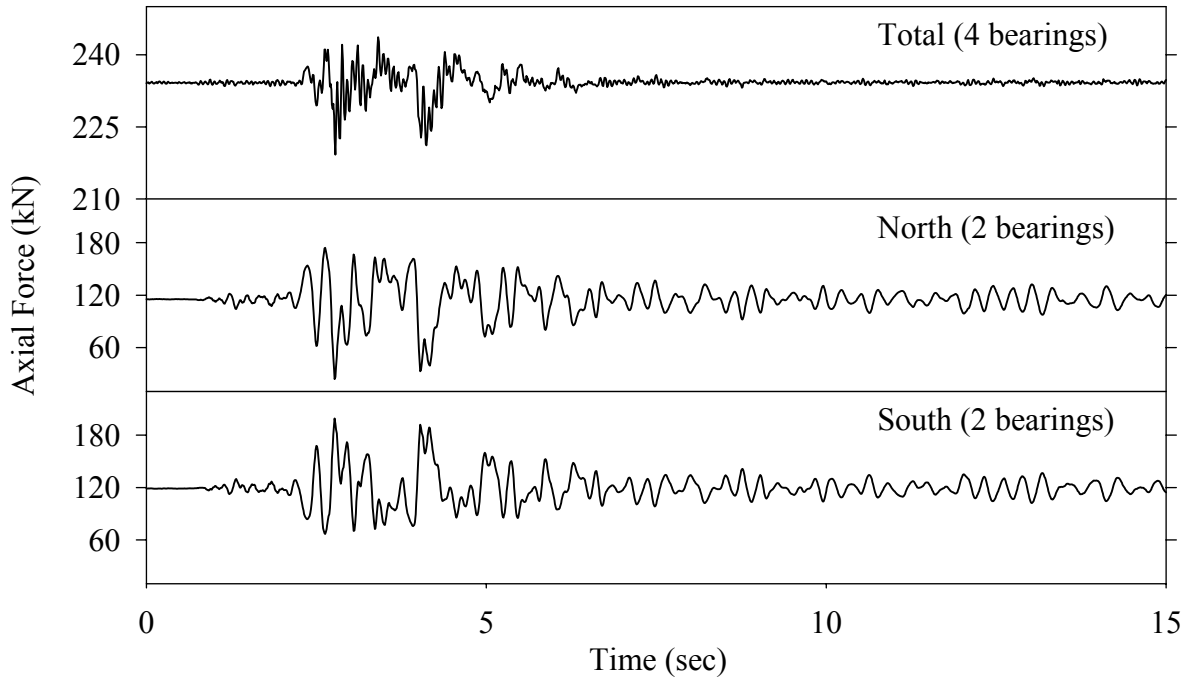
Test FPSLN31.1, Northridge Newhall 360° 100%, SB/FPS-LD



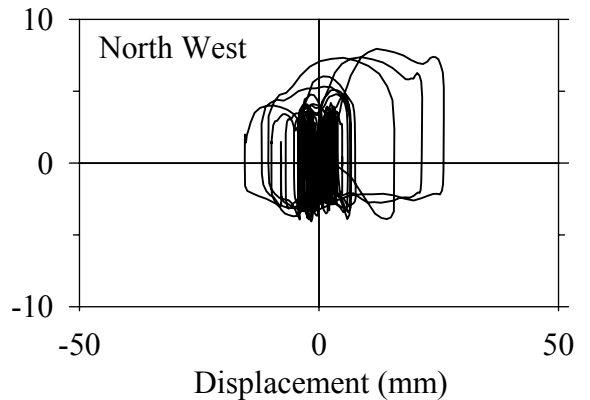
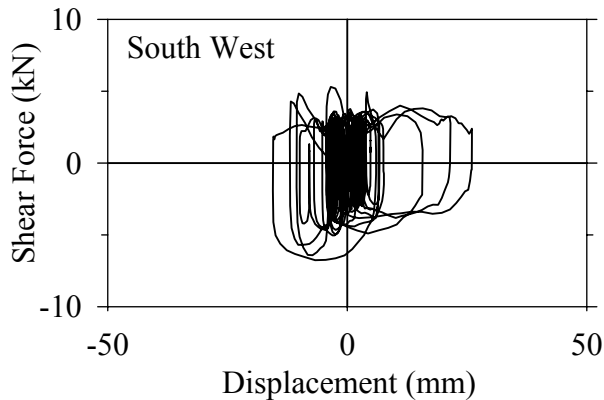
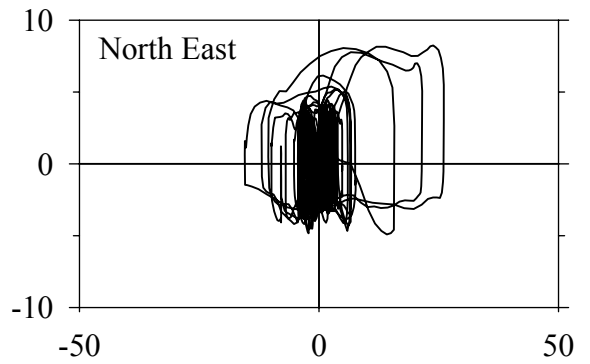
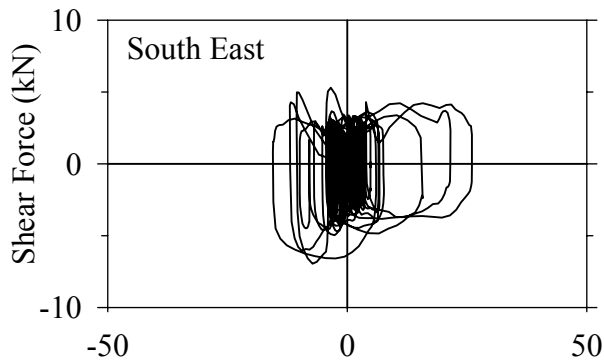
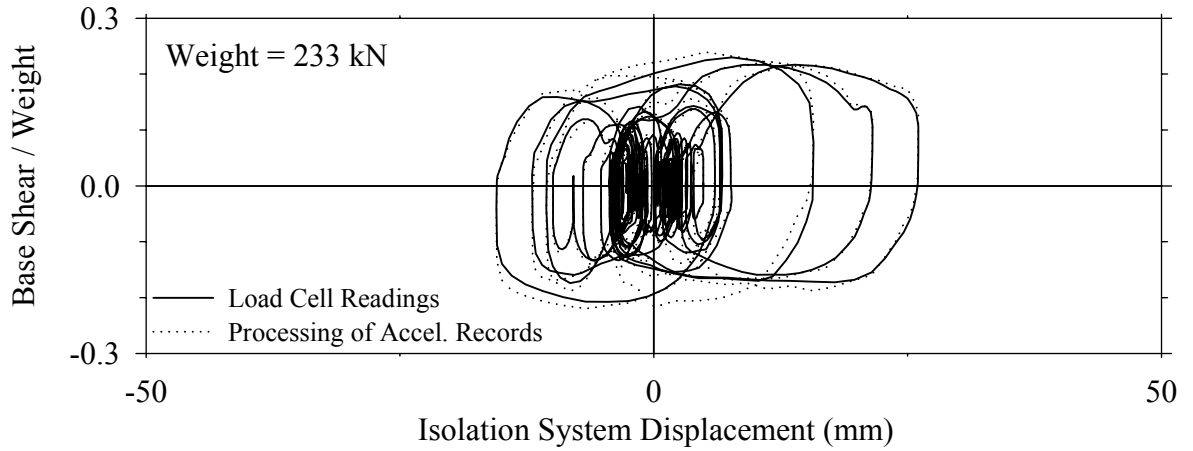
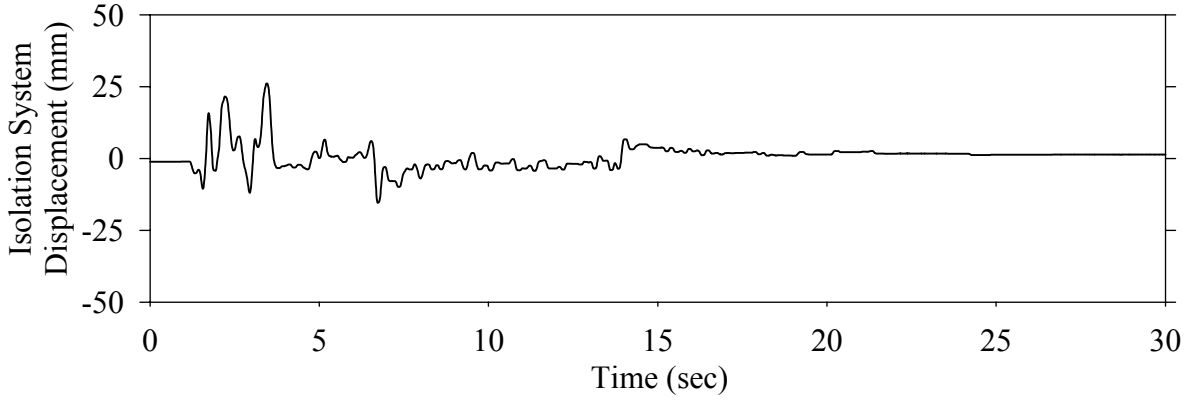
Test FPSLS10.1, Northridge Sylmar 90° 100%, SB/FPS-LD



Test FPSLS10.1, Northridge Sylmar 90° 100%, SB/FPS-LD

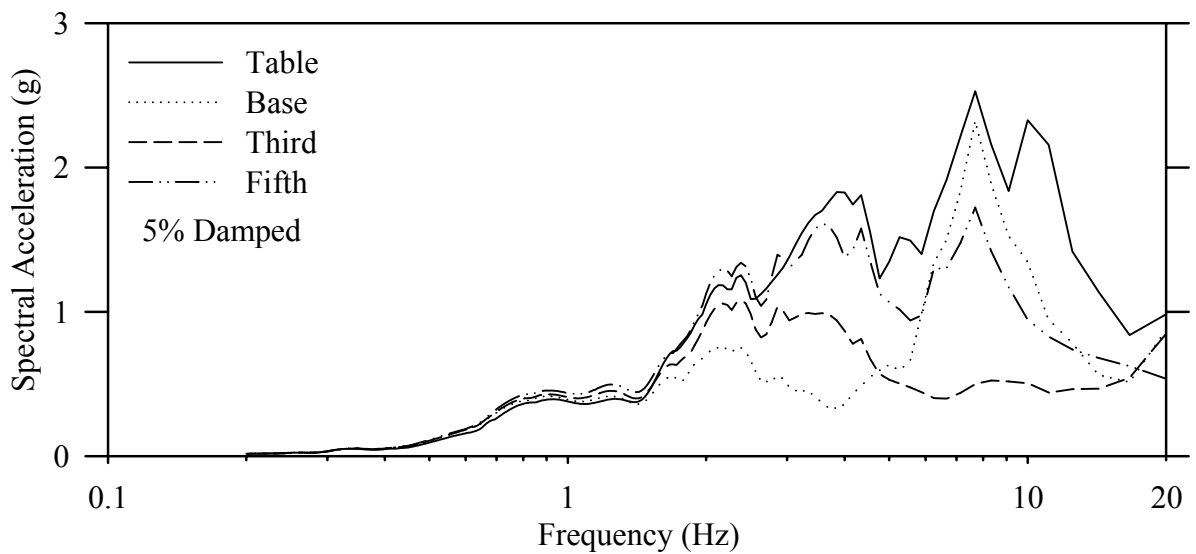
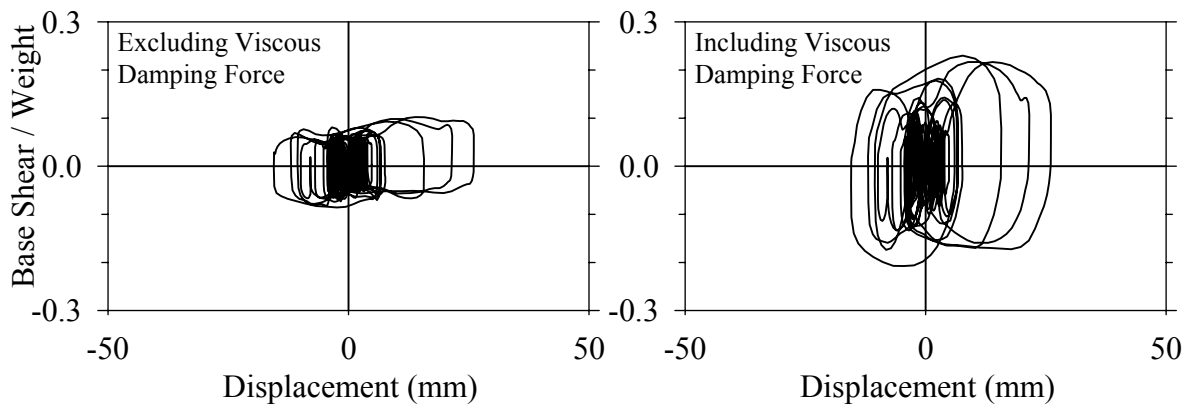
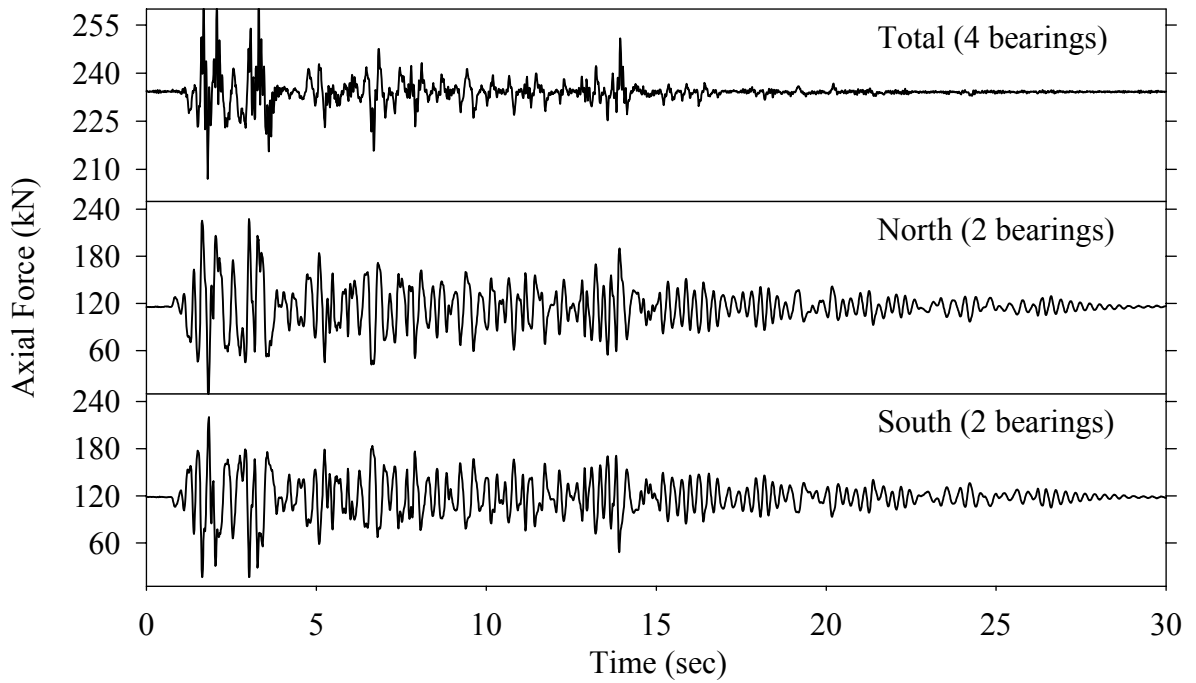


Test FPSNE20.2, El Centro S00E 200% Test 2, SB/FPS-NLD

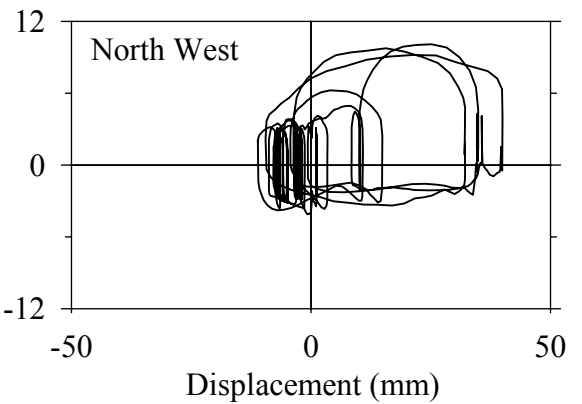
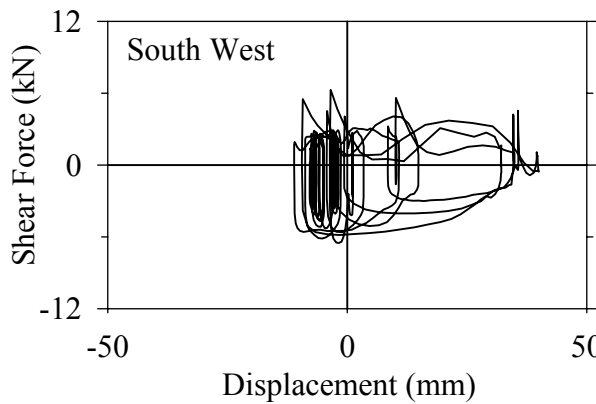
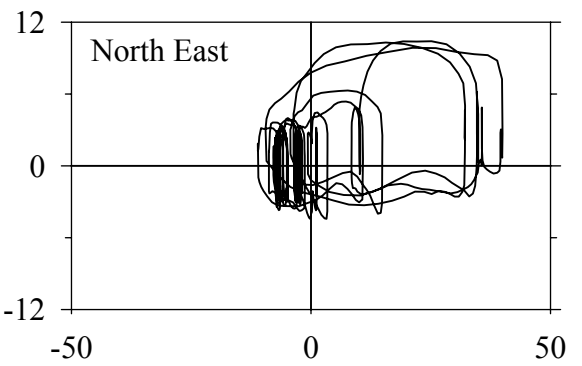
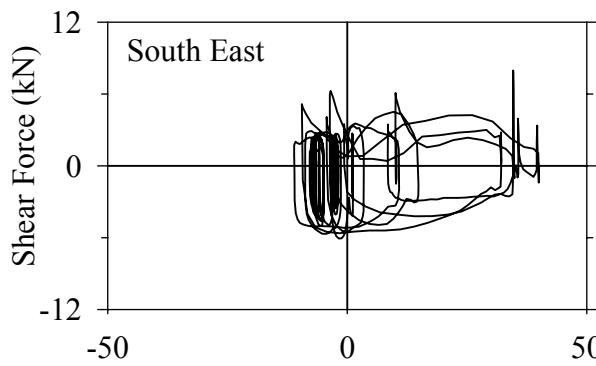
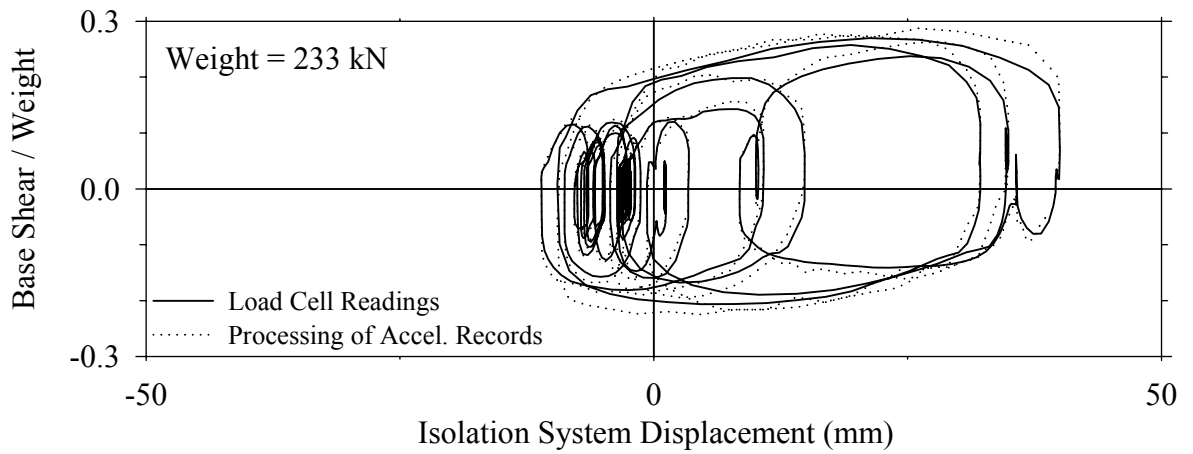
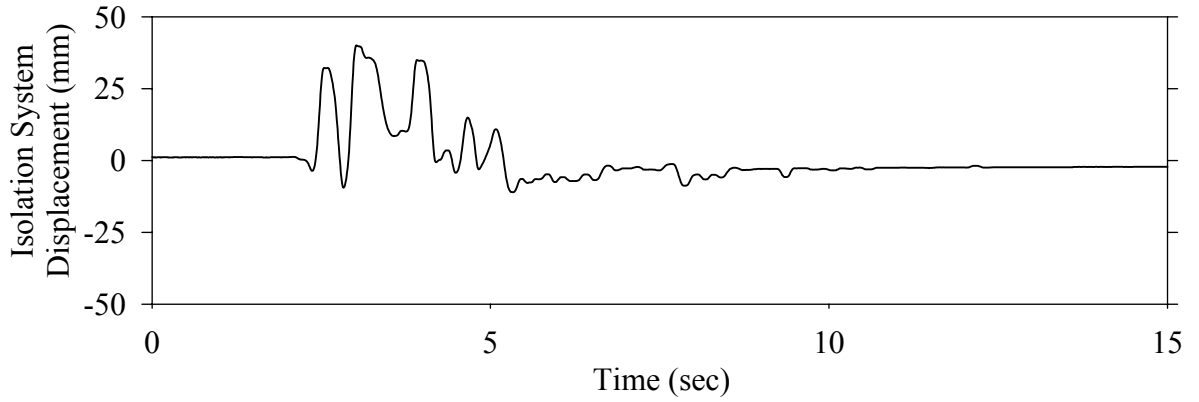




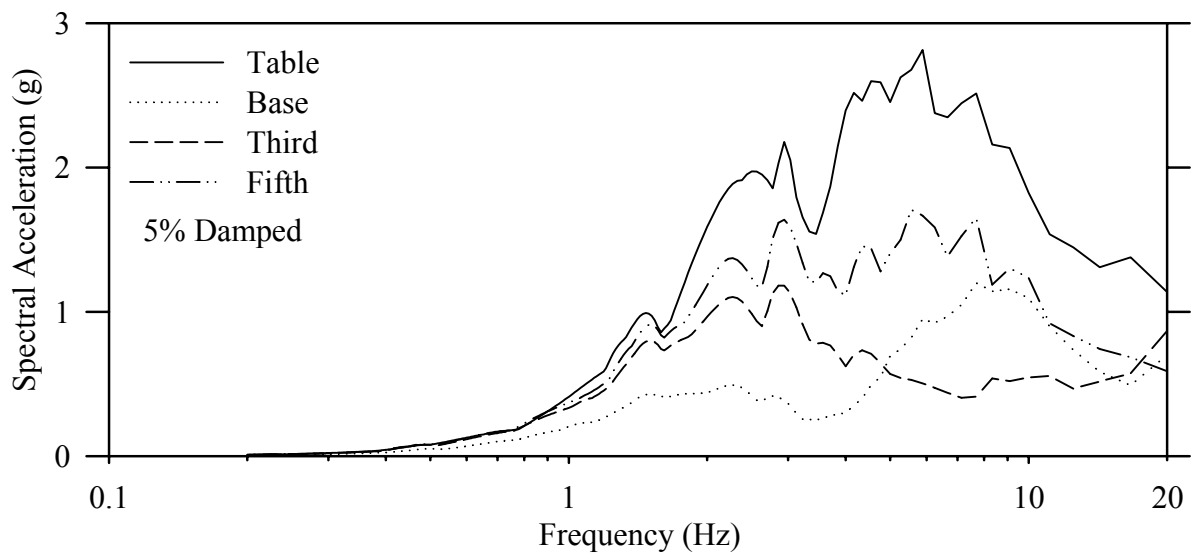
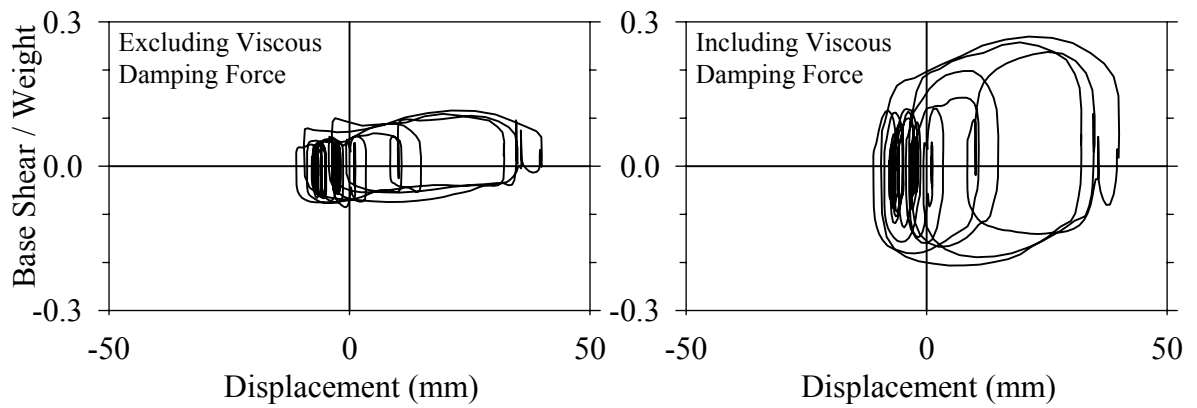
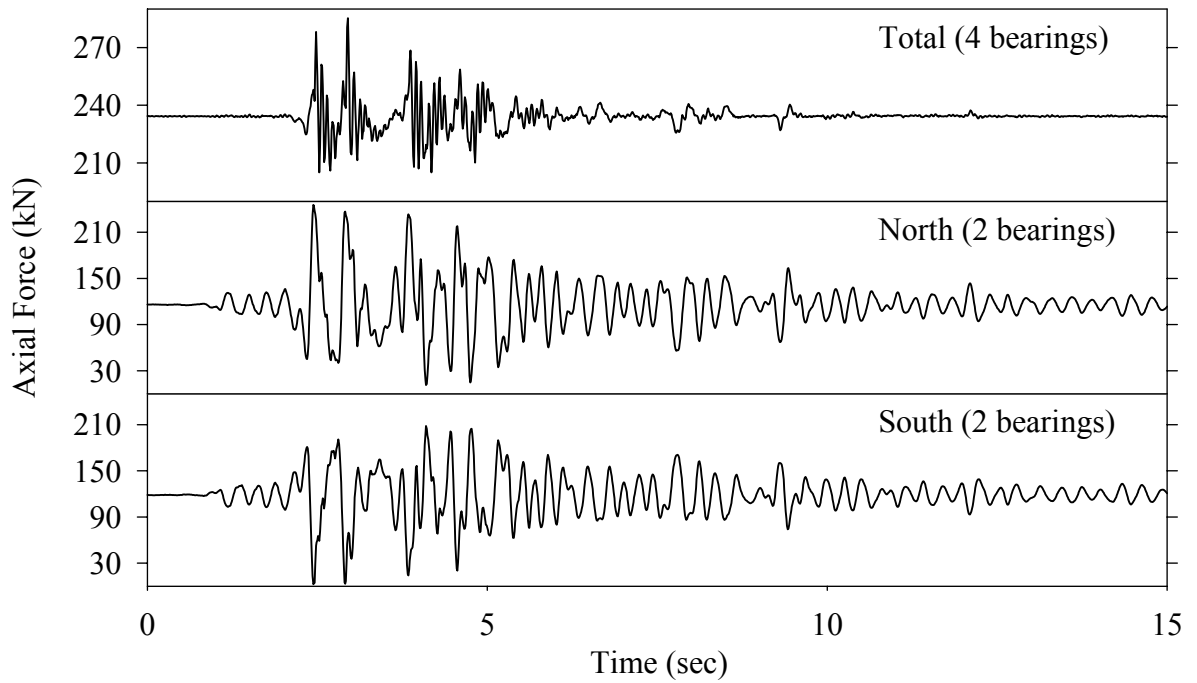
Test FPSNE20.2, El Centro S00E 200% Test 2, SB/FPS-NLD



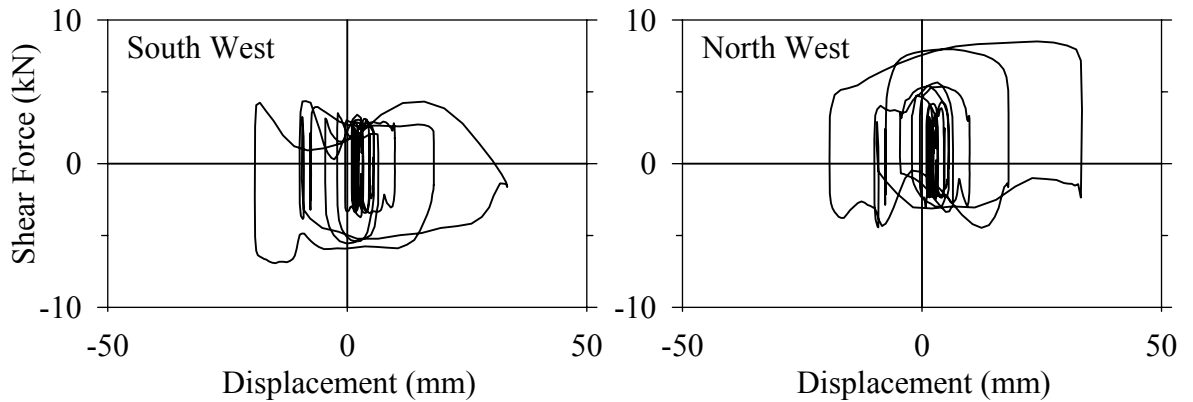
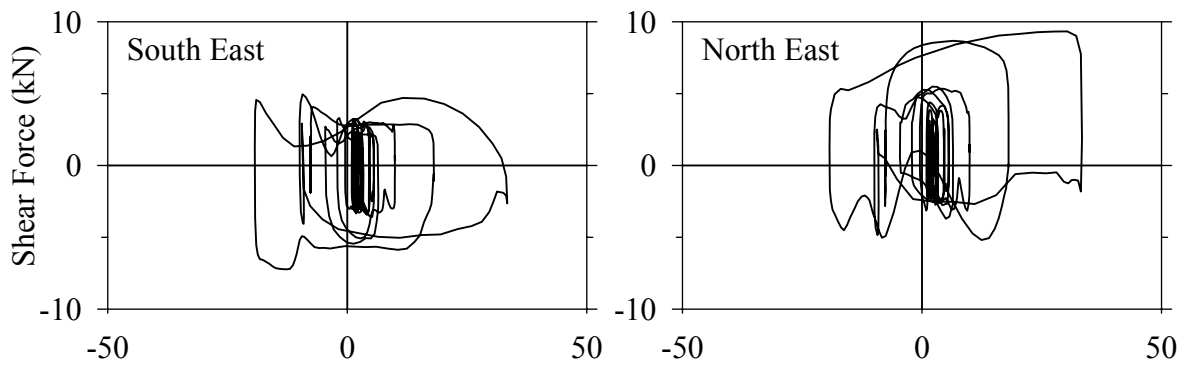
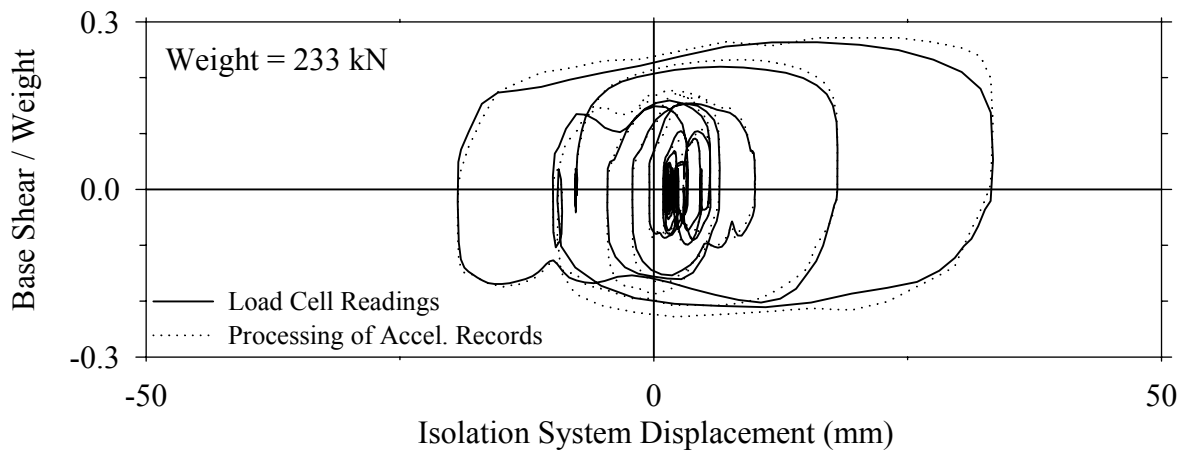
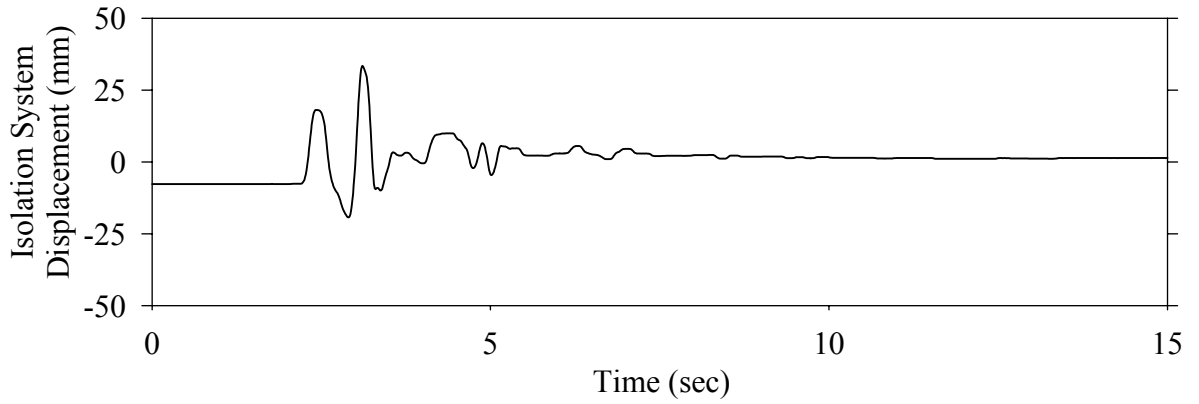
Test FPSNK10.1, Kobe N-S 100%, SB/FPS-NLD



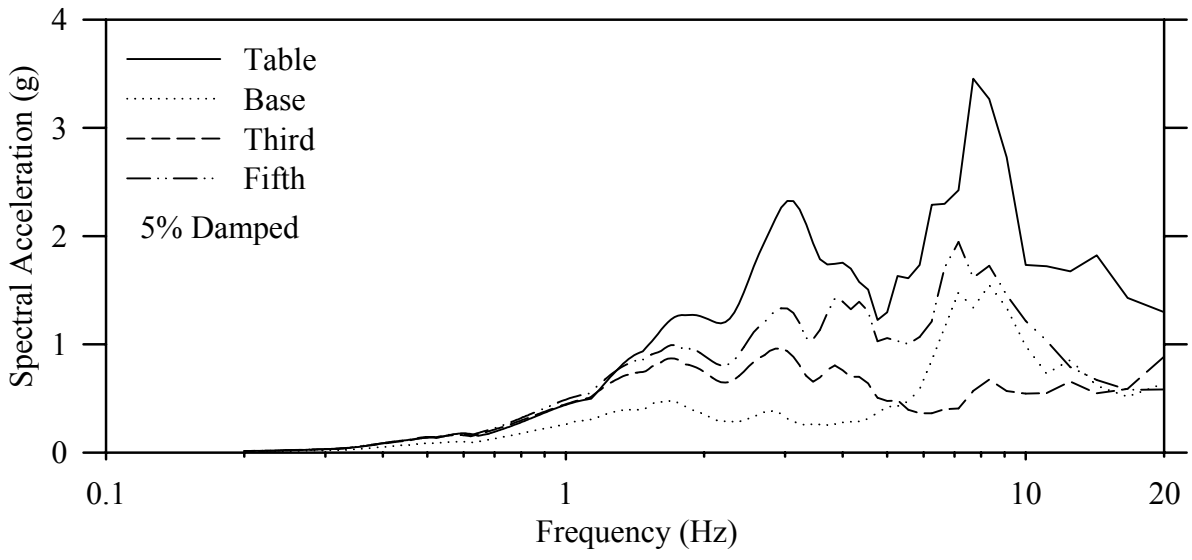
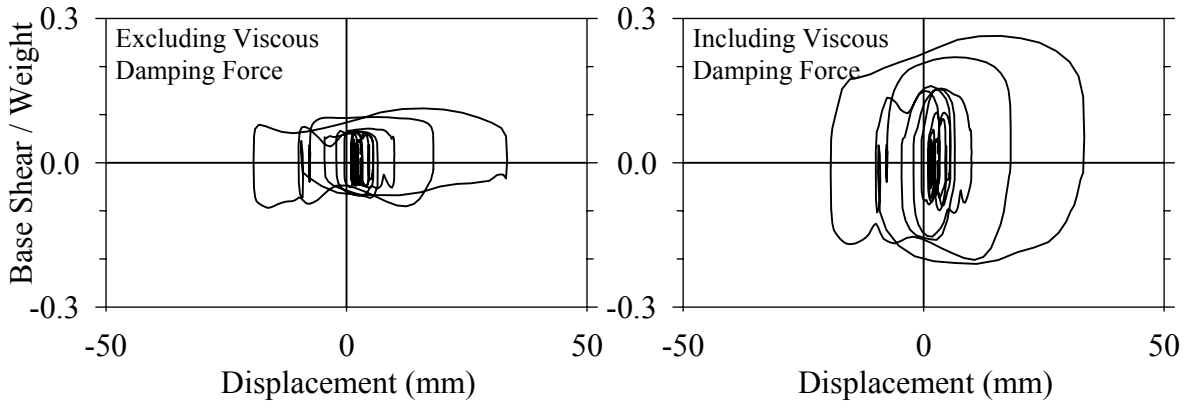
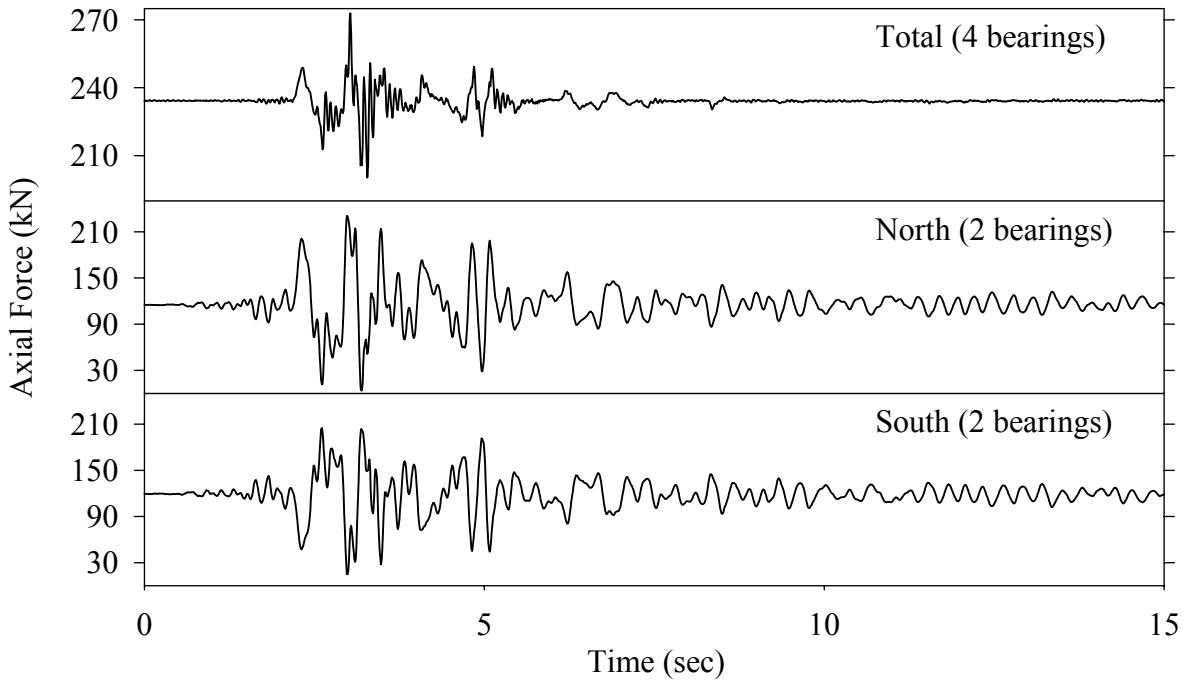
Test FPSNK10.1, Kobe N-S 100%, SB/FPS-NLD



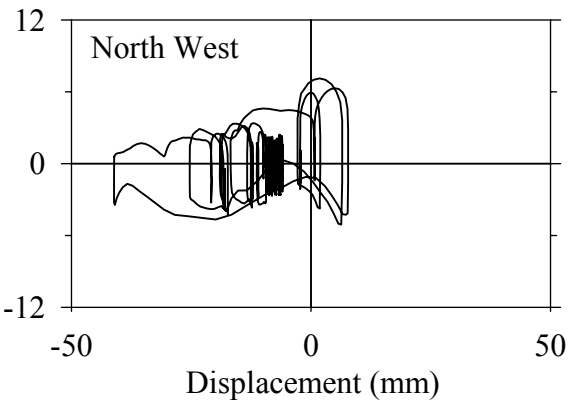
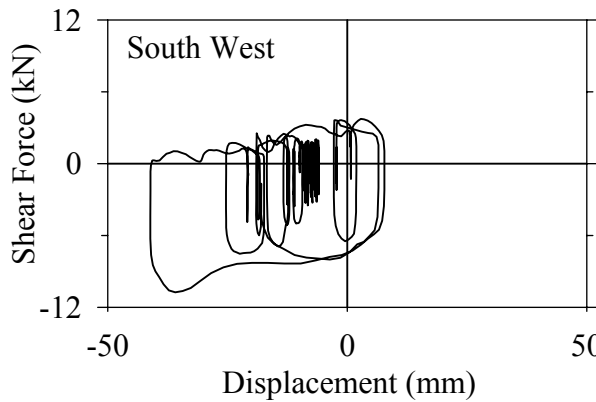
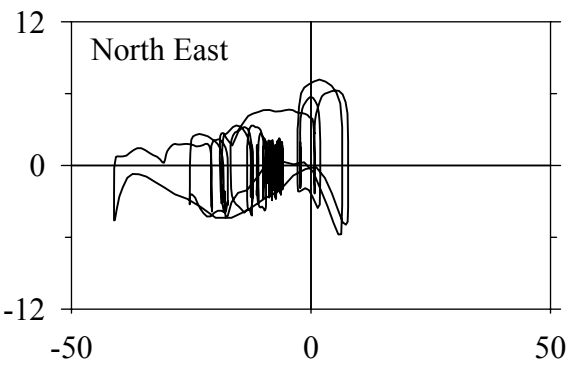
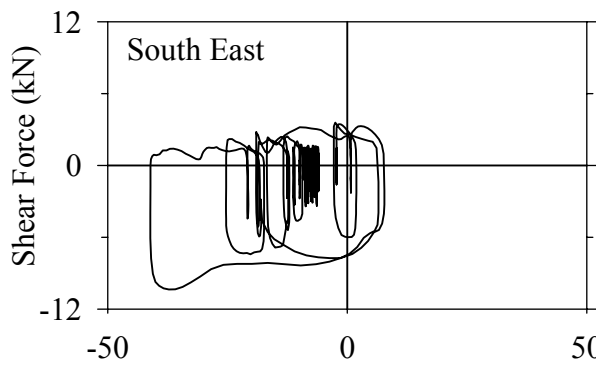
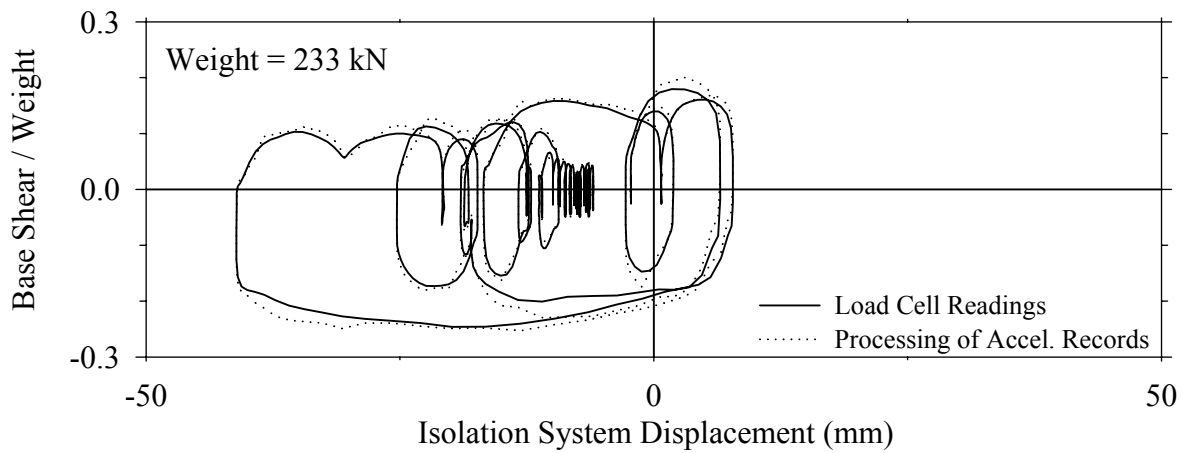
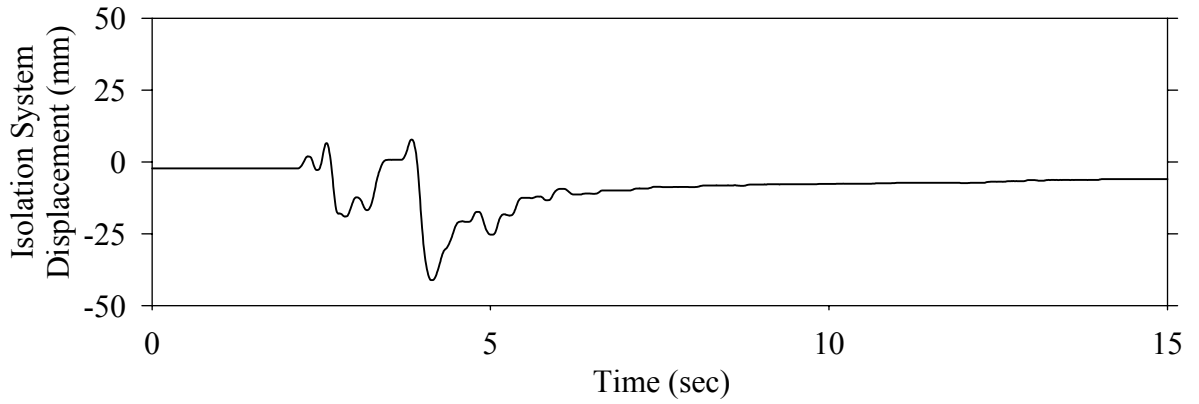
Test FPSNN10.1, Northridge Newhall 360° 100%, SB/FPS-NLD



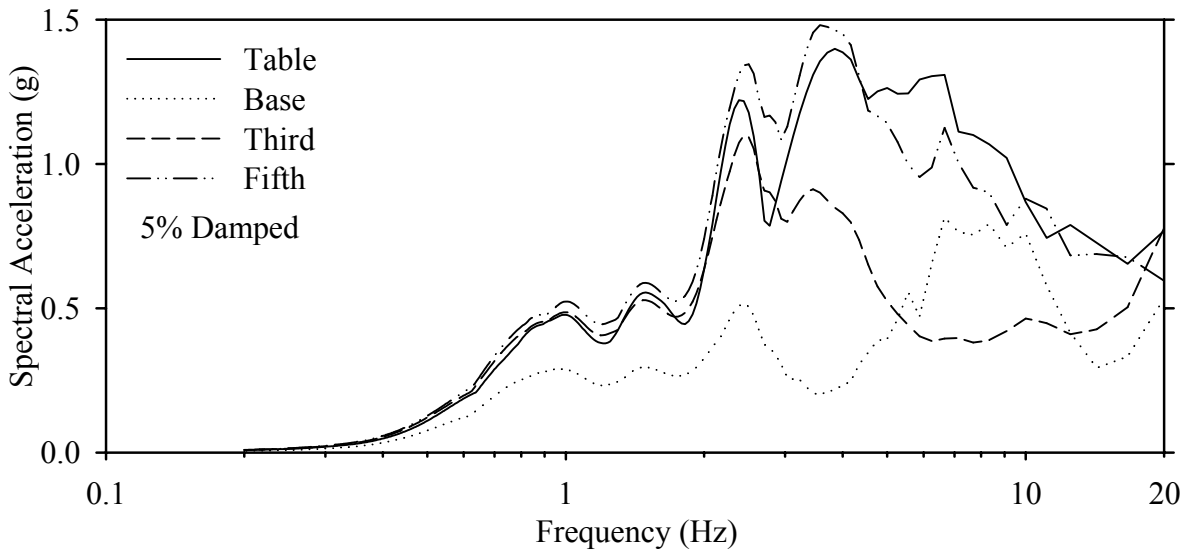
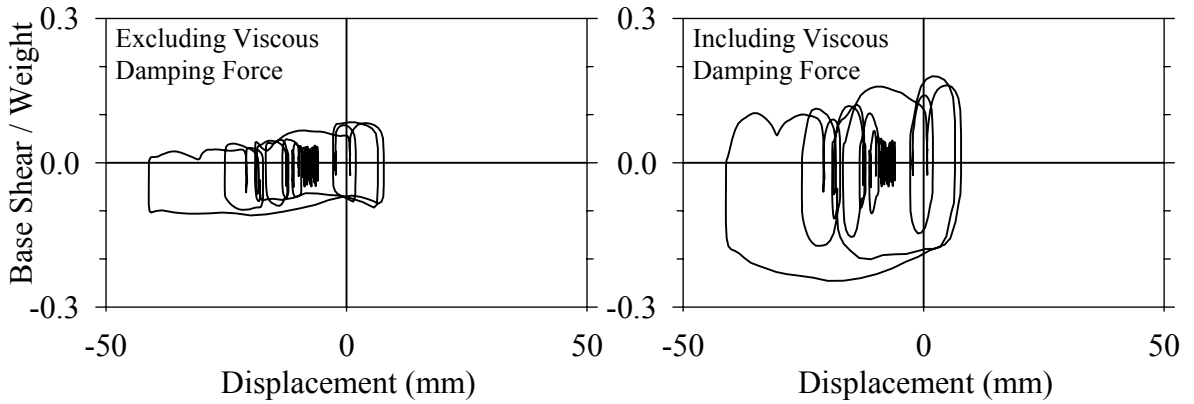
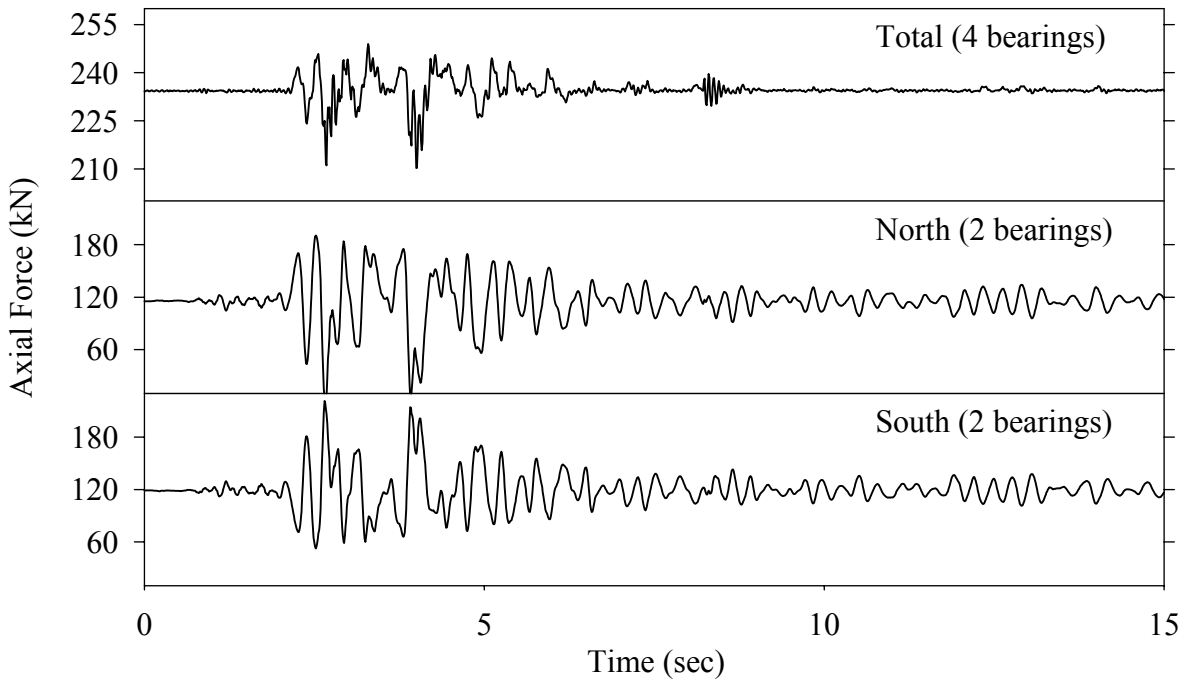
Test FPSNN10.1, Northridge Newhall 360° 100%, SB/FPS-NLD



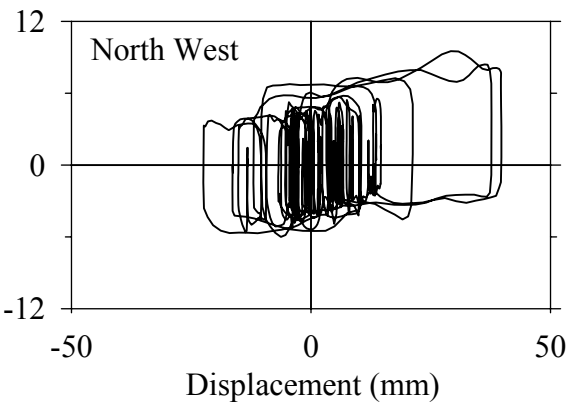
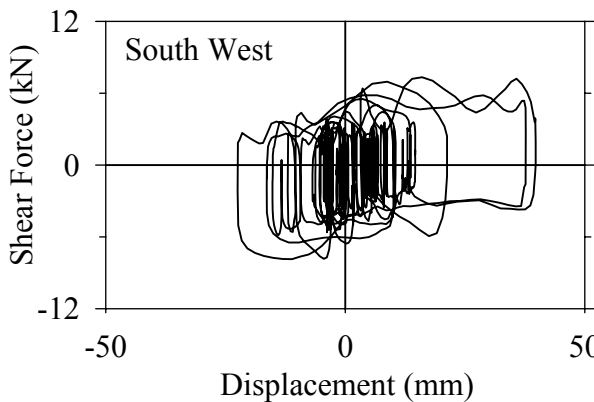
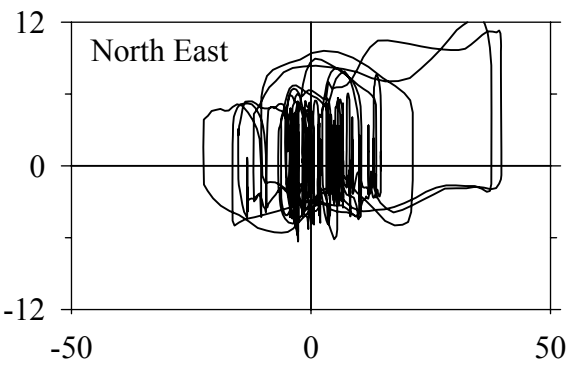
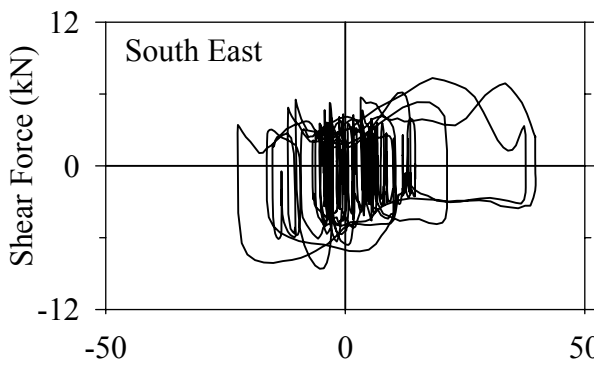
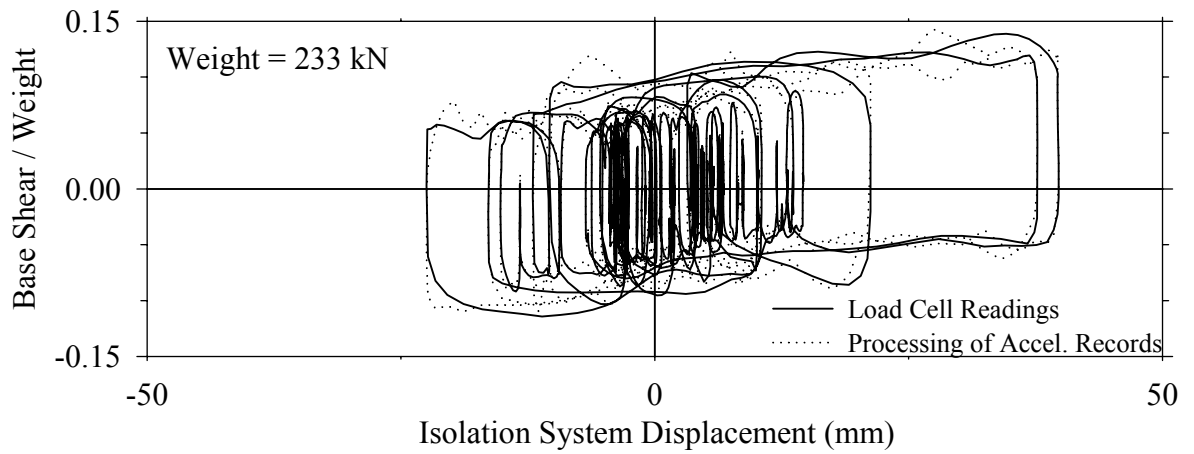
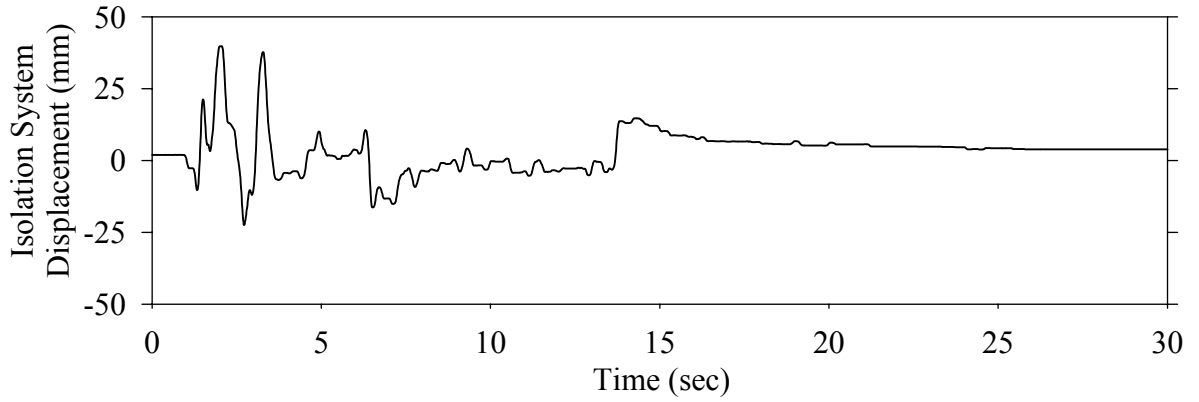
Test FPSNS10.1, Northridge Sylmar 90° 100%, SB/FPS-NLD



Test FPSNS10.1, Northridge Sylmar 90° 100%, SB/FPS-NLD

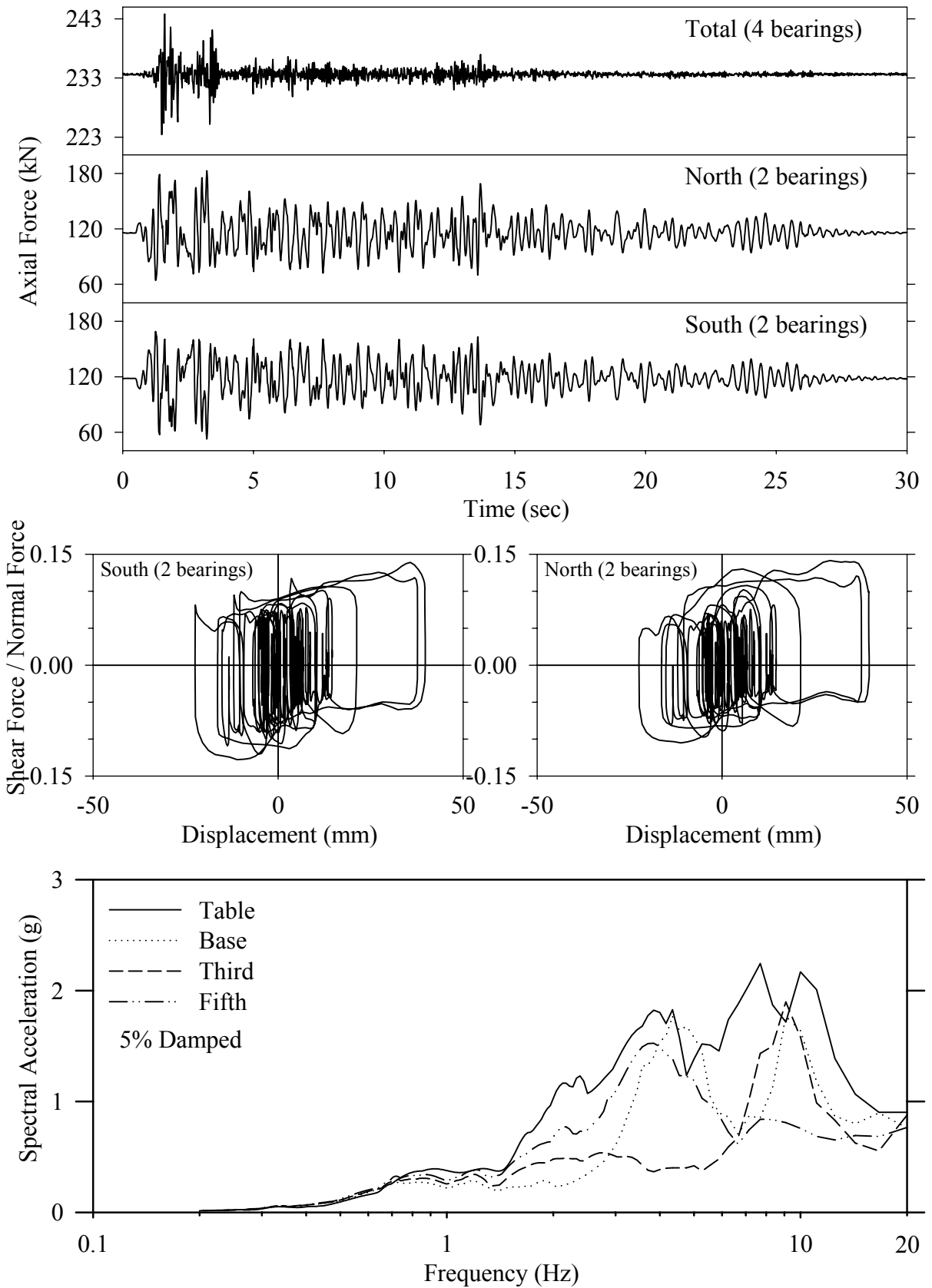


Test FPABE20.1, El Centro S00E 200%, AB/FPS

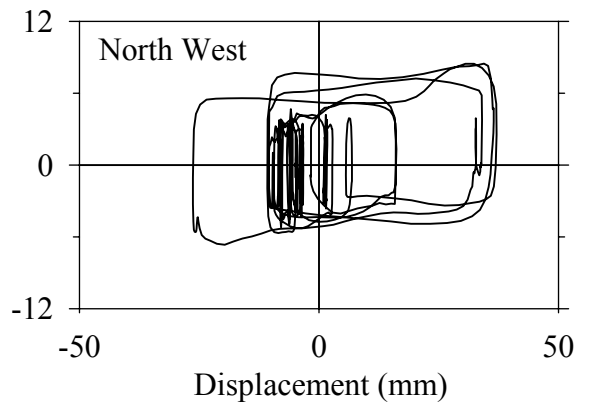
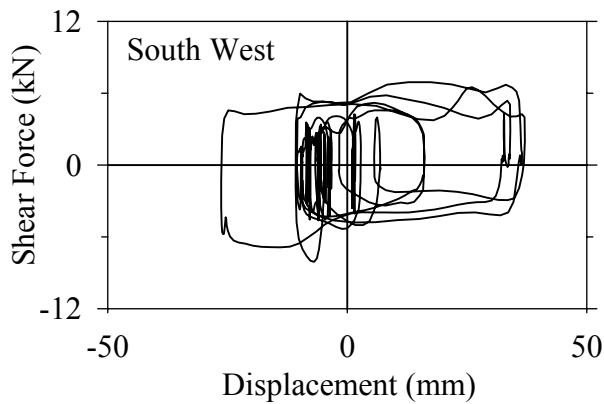
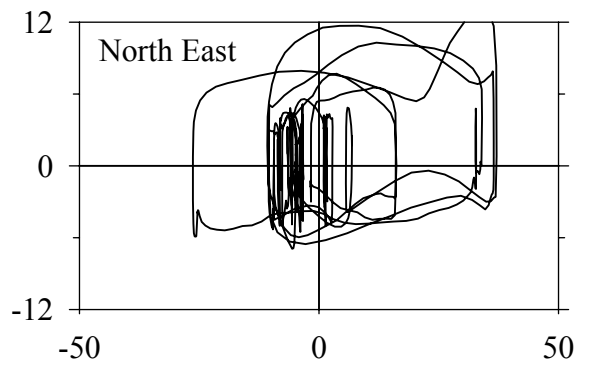
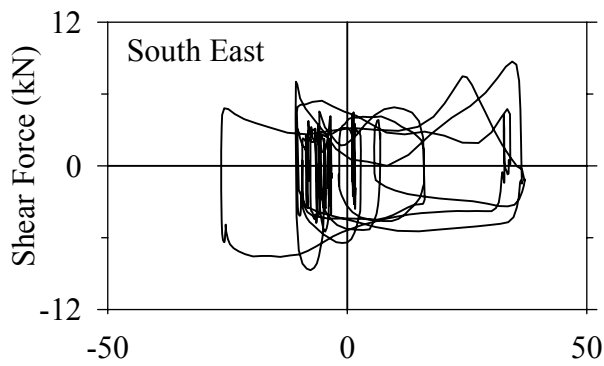
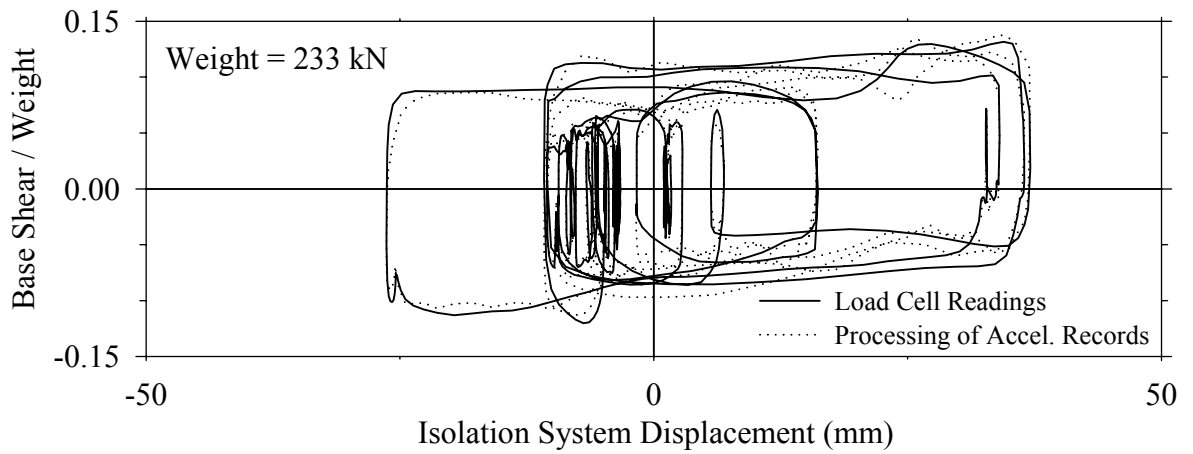
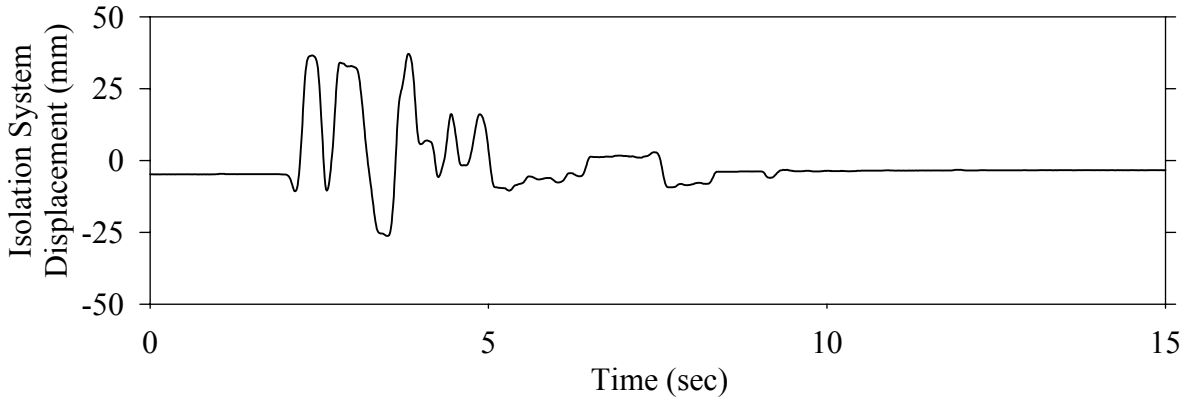




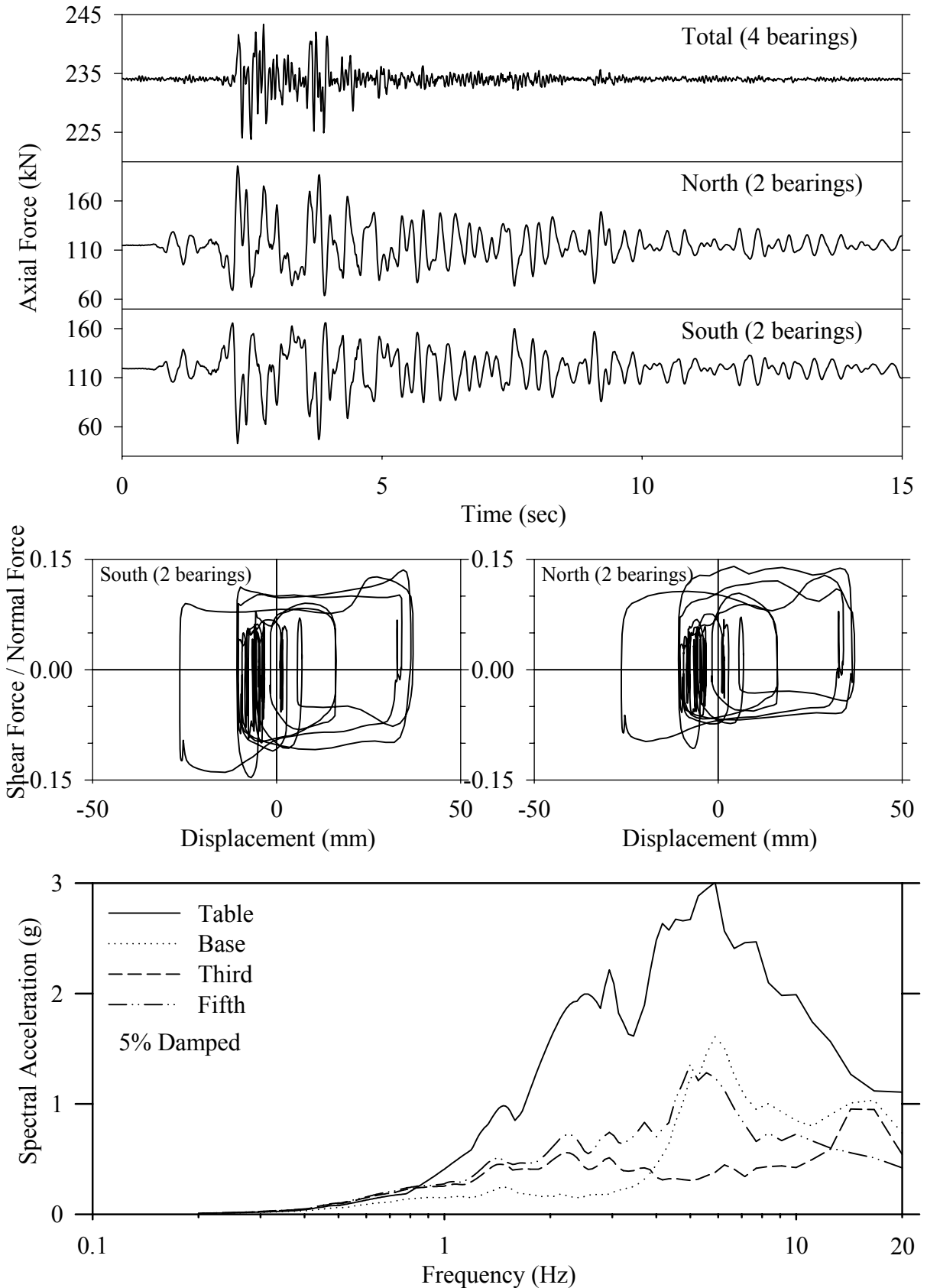
Test FPABE20.1, El Centro S00E 200%, AB/FPS



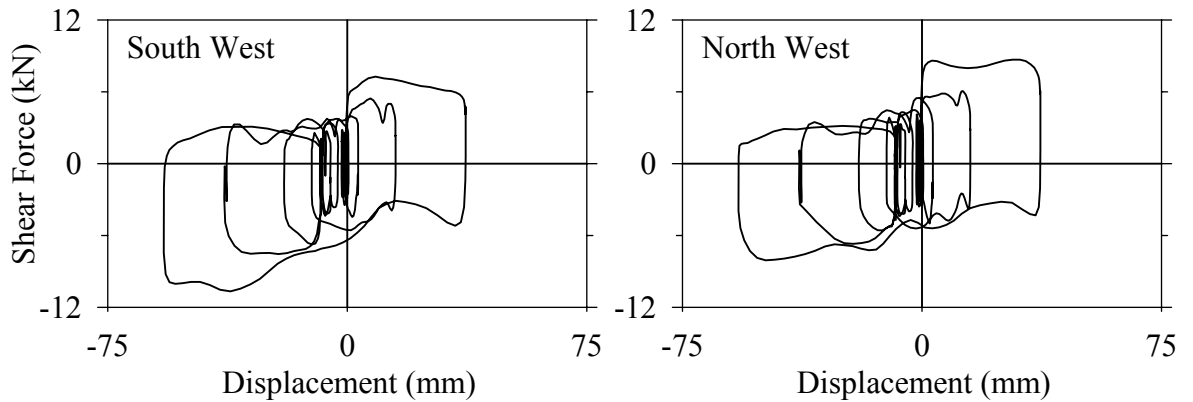
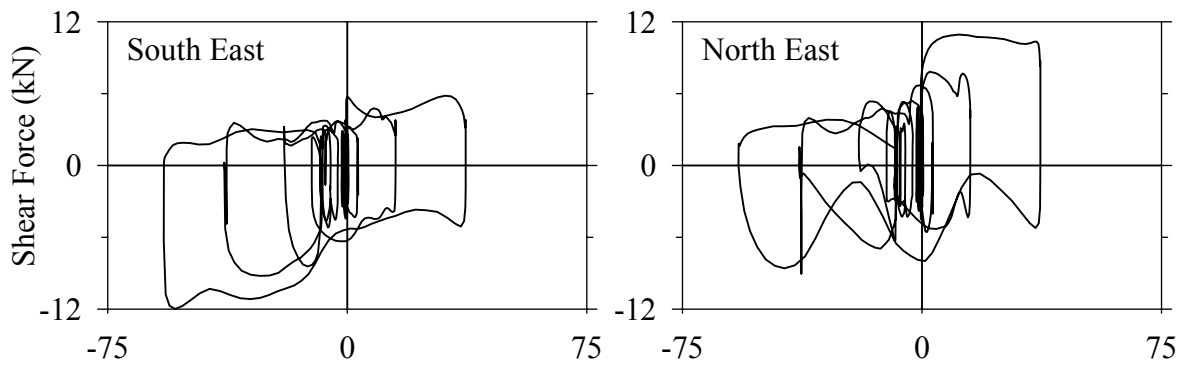
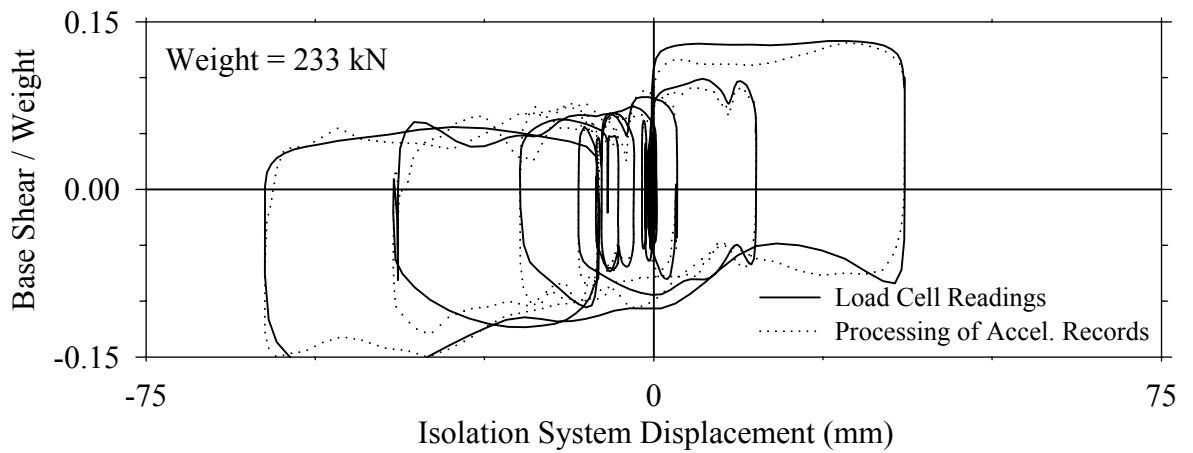
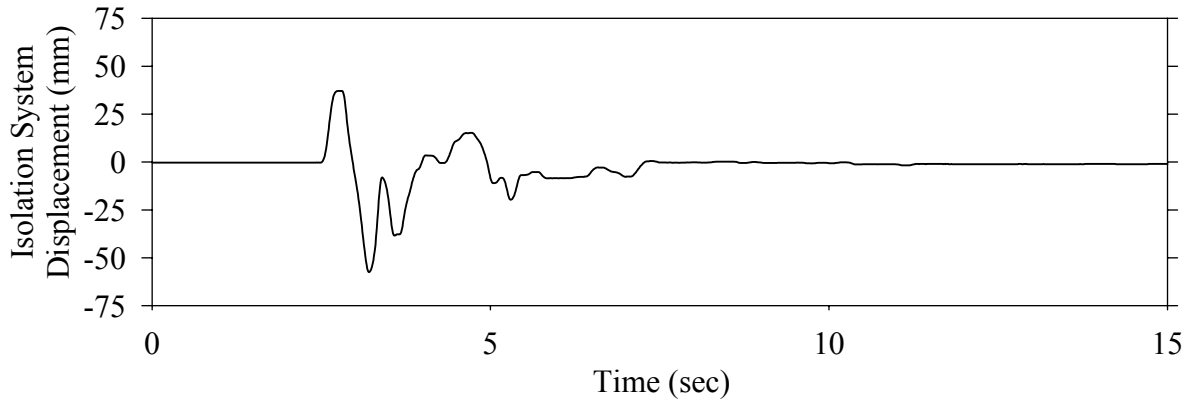
Test FPABK10.1, Kobe N-S 100%, AB/FPS



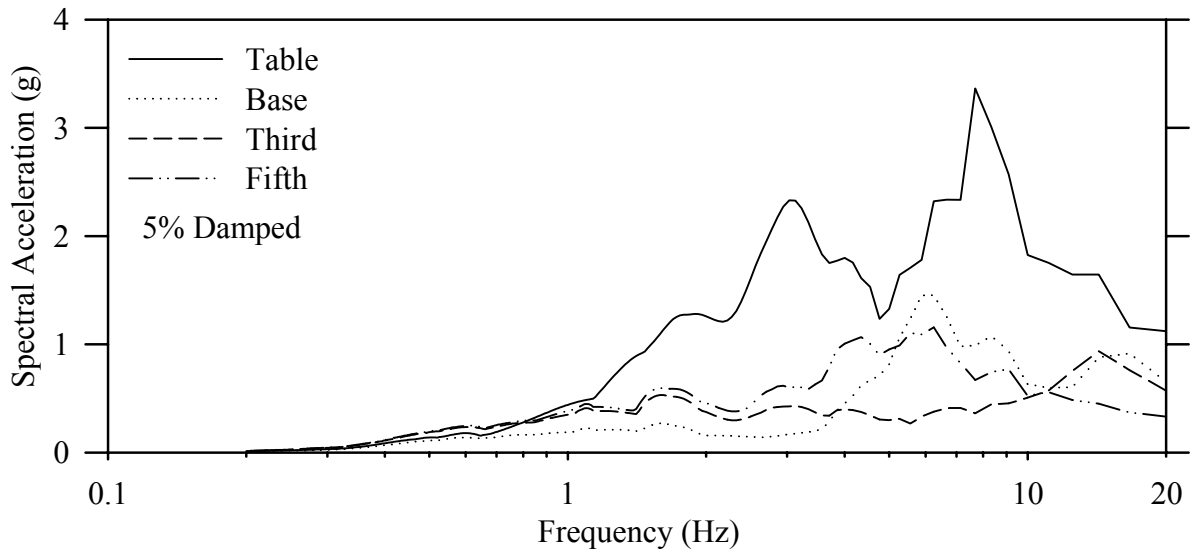
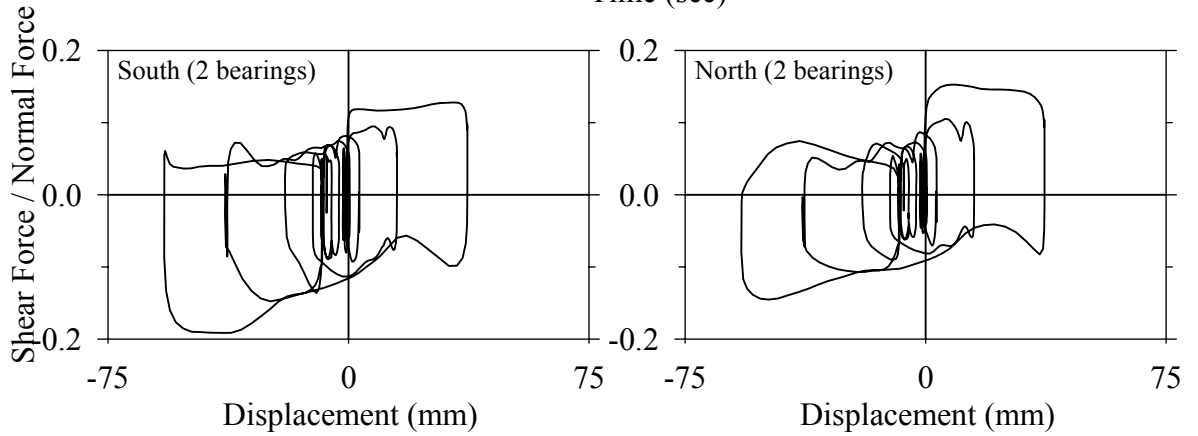
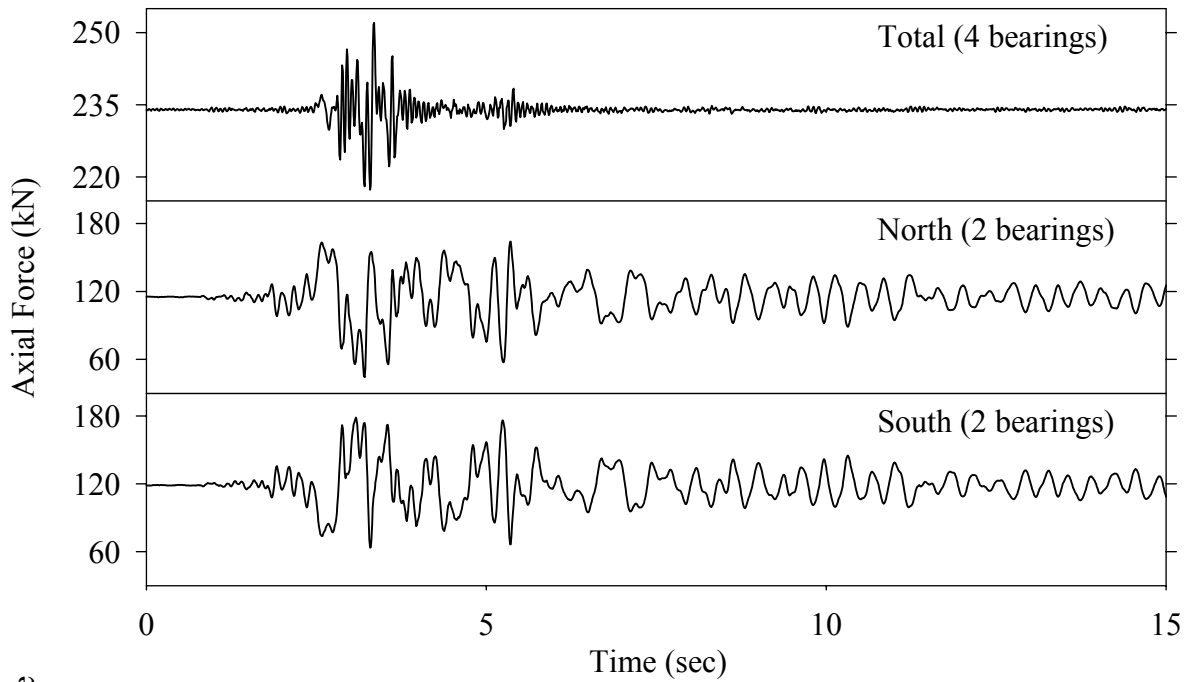
Test FPABK10.1, Kobe N-S 100%, AB/FPS



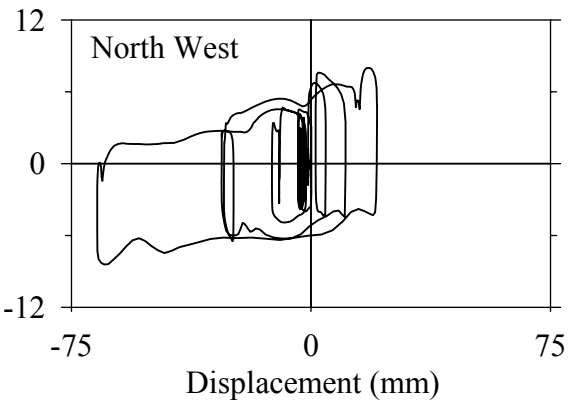
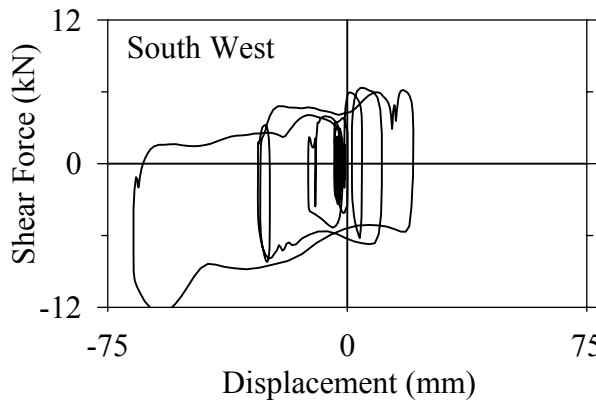
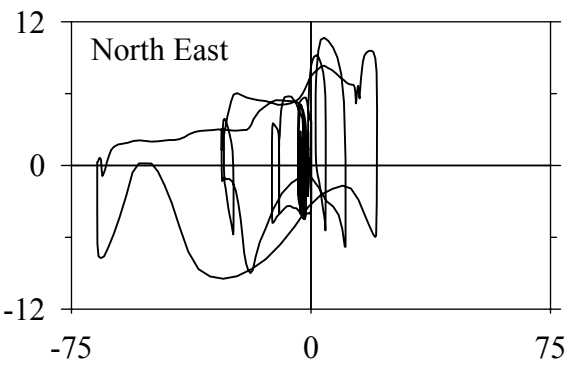
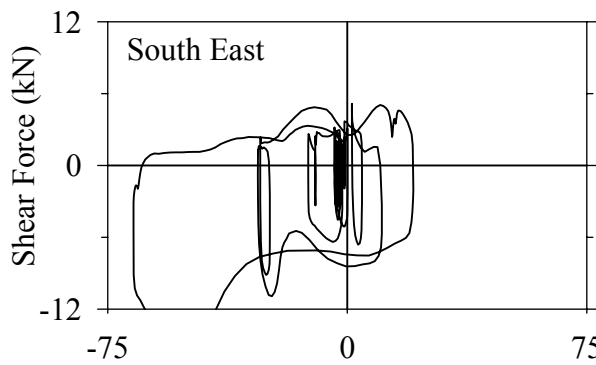
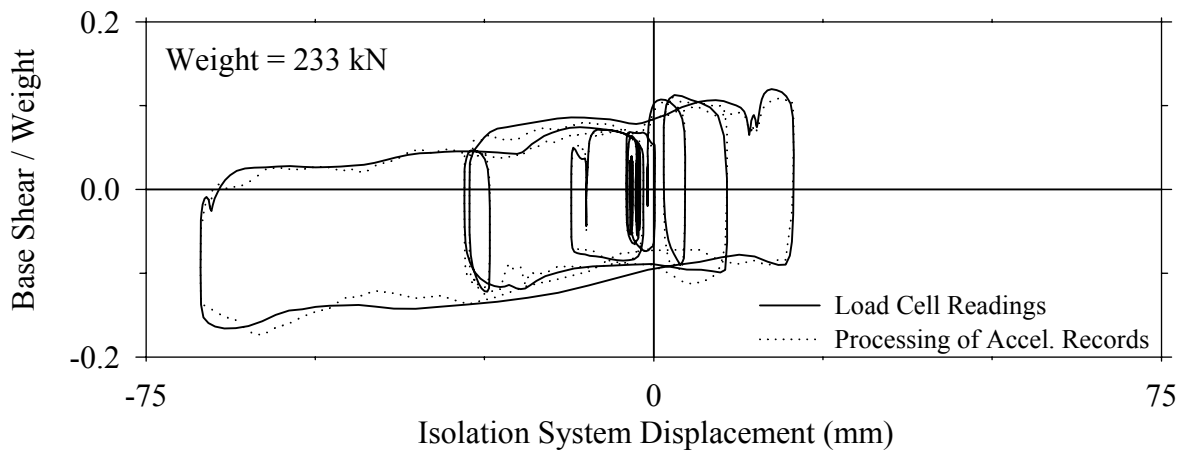
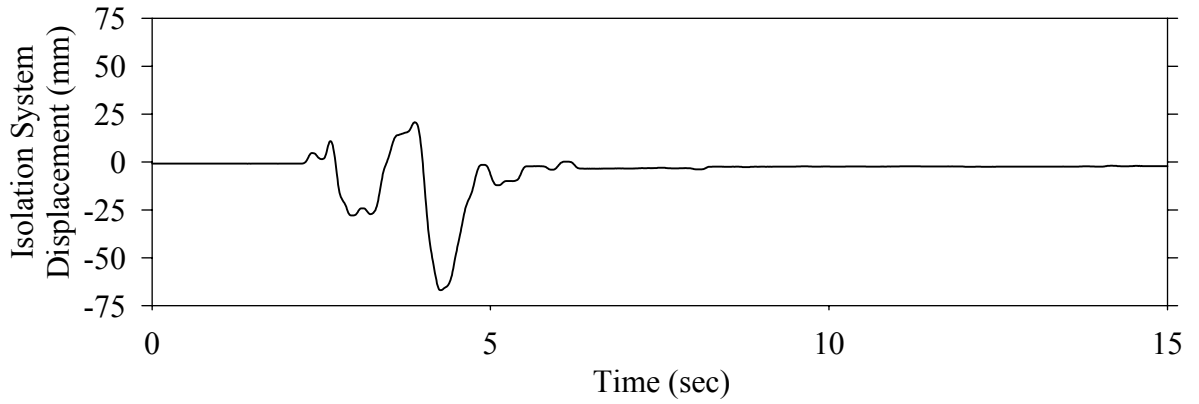
Test FPABN10.1, Northridge Newhall 360° 100%, AB/FPS



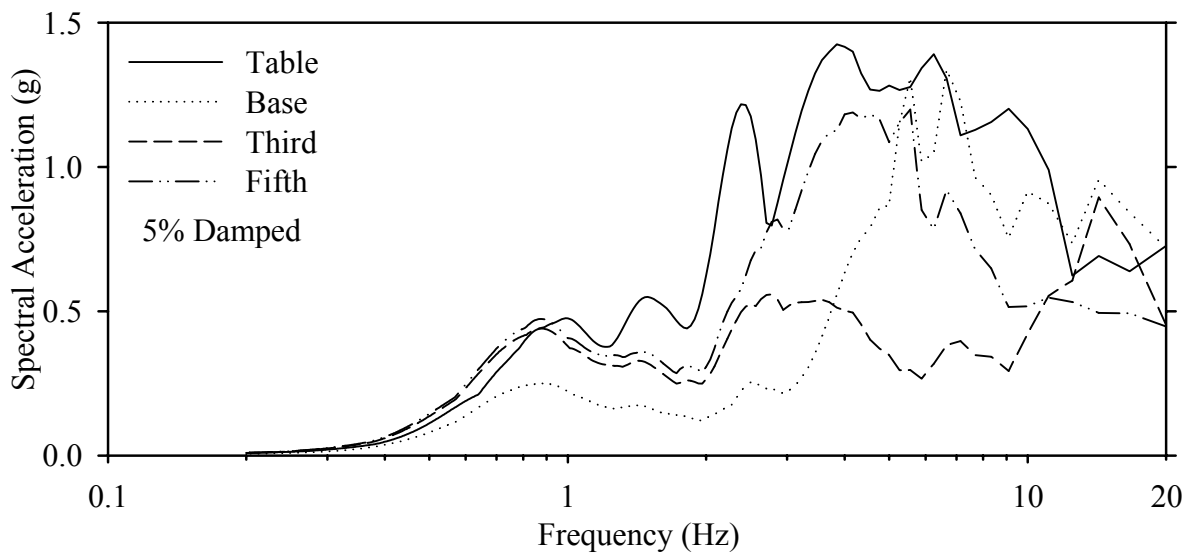
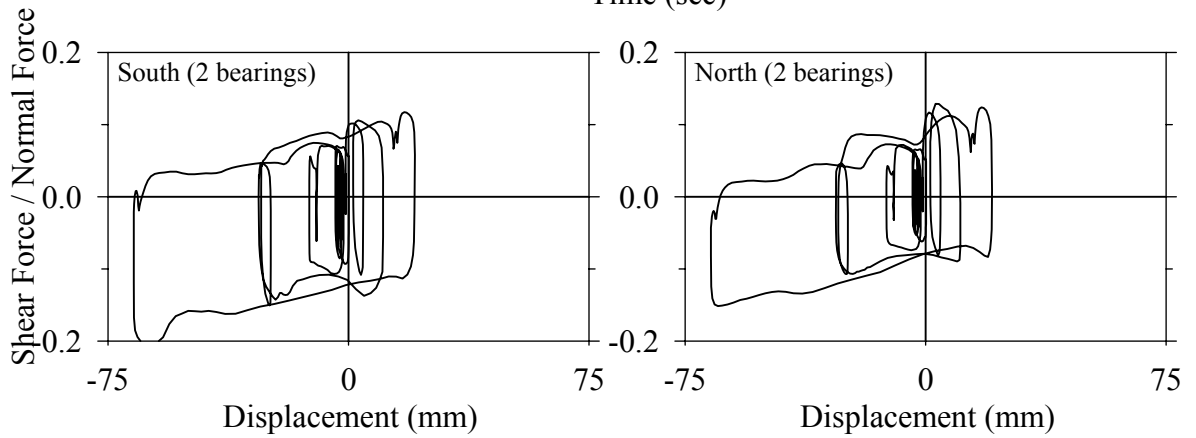
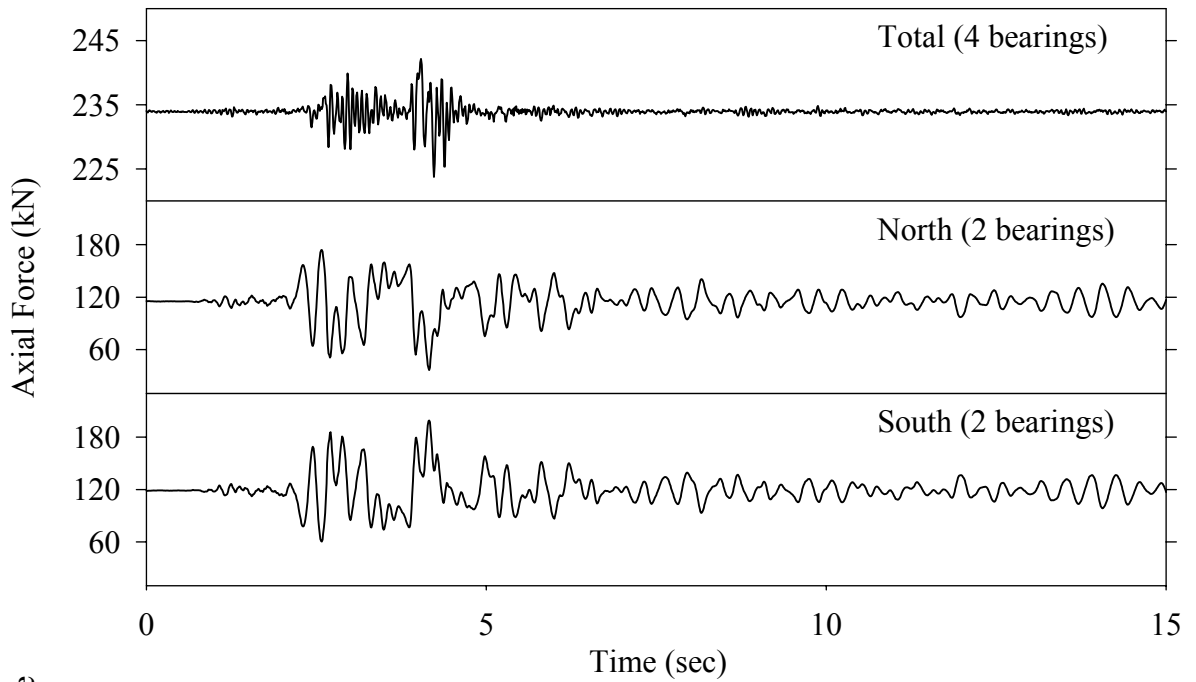
Test FPABN10.1, Northridge Newhall 360° 100%, AB/FPS



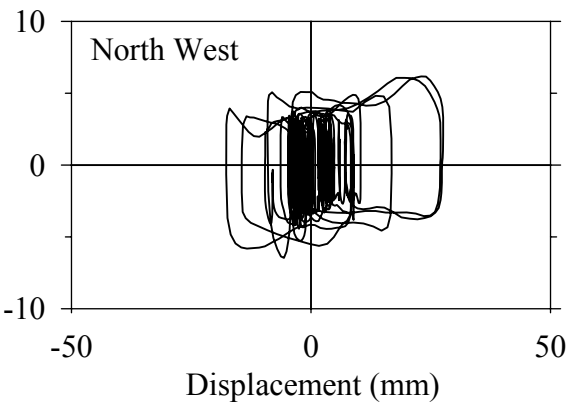
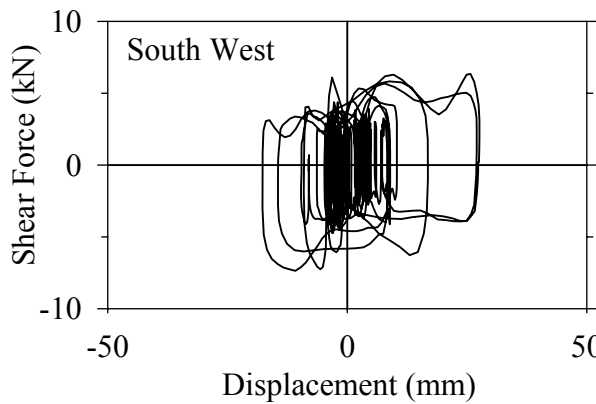
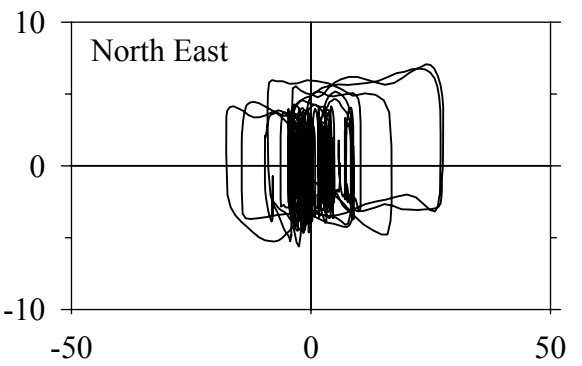
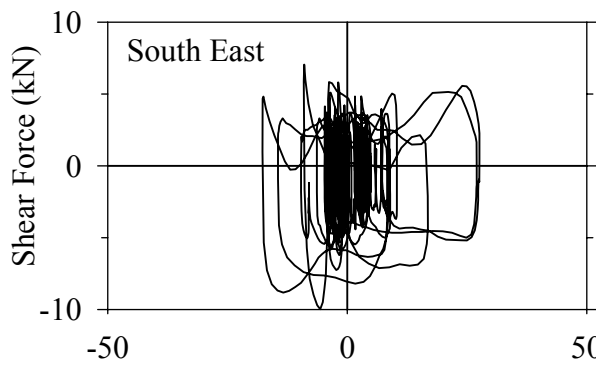
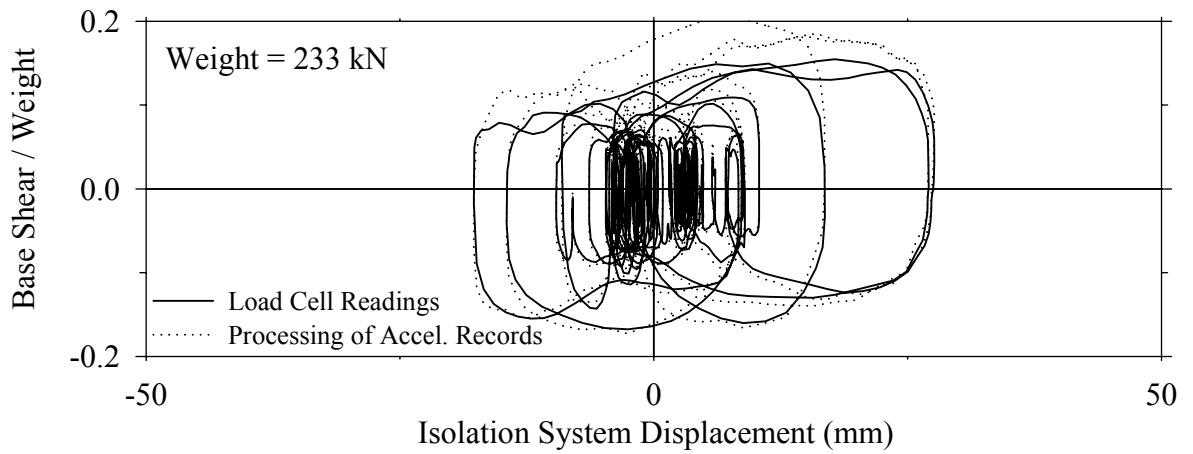
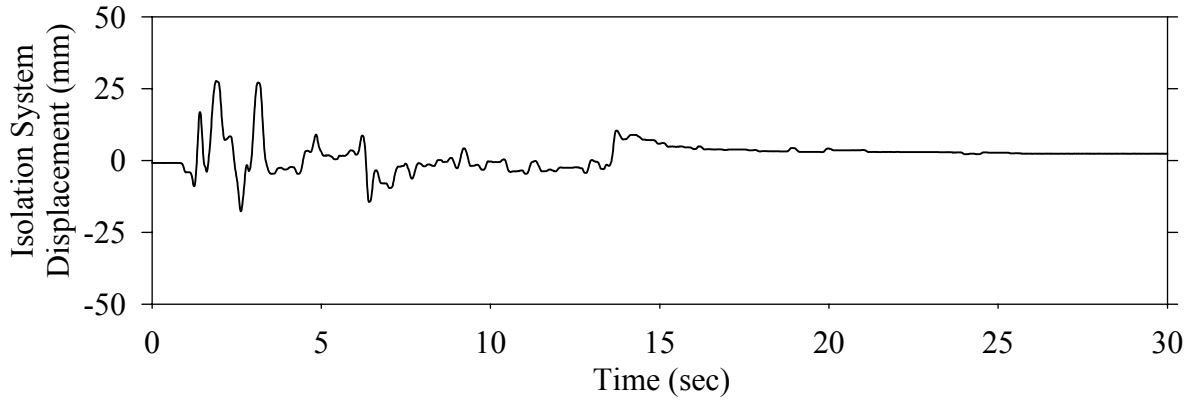
Test FPABS10.1, Northridge Sylmar 90° 100%, AB/FPS



Test FPABS10.1, Northridge Sylmar 90° 100%, AB/FPS

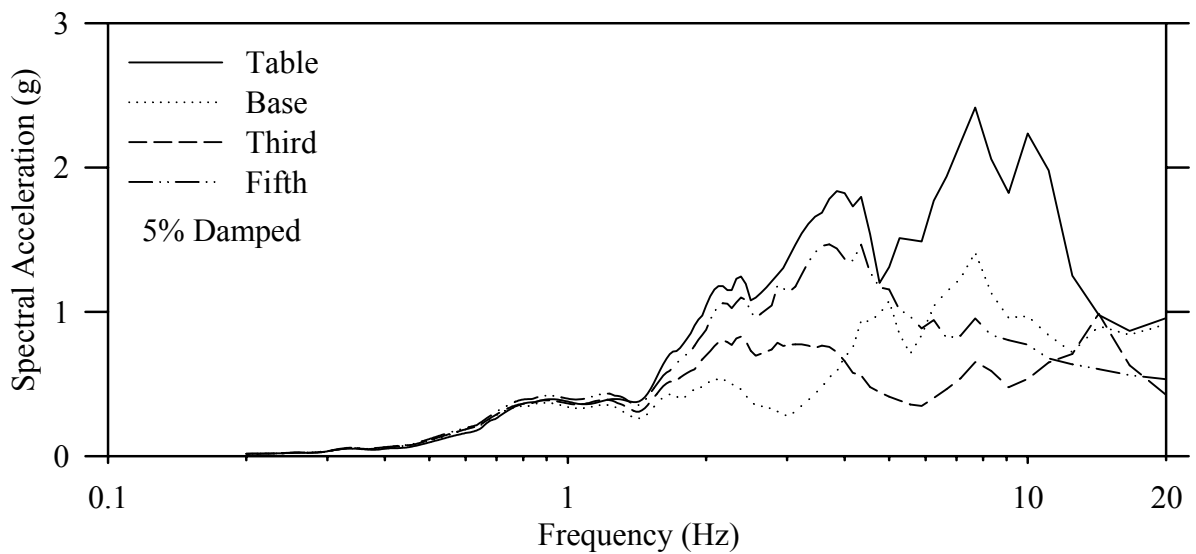
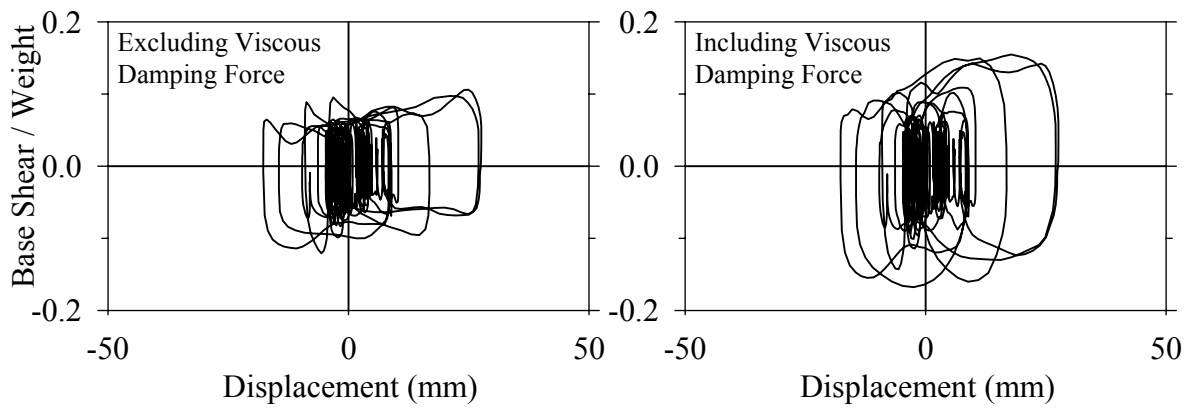
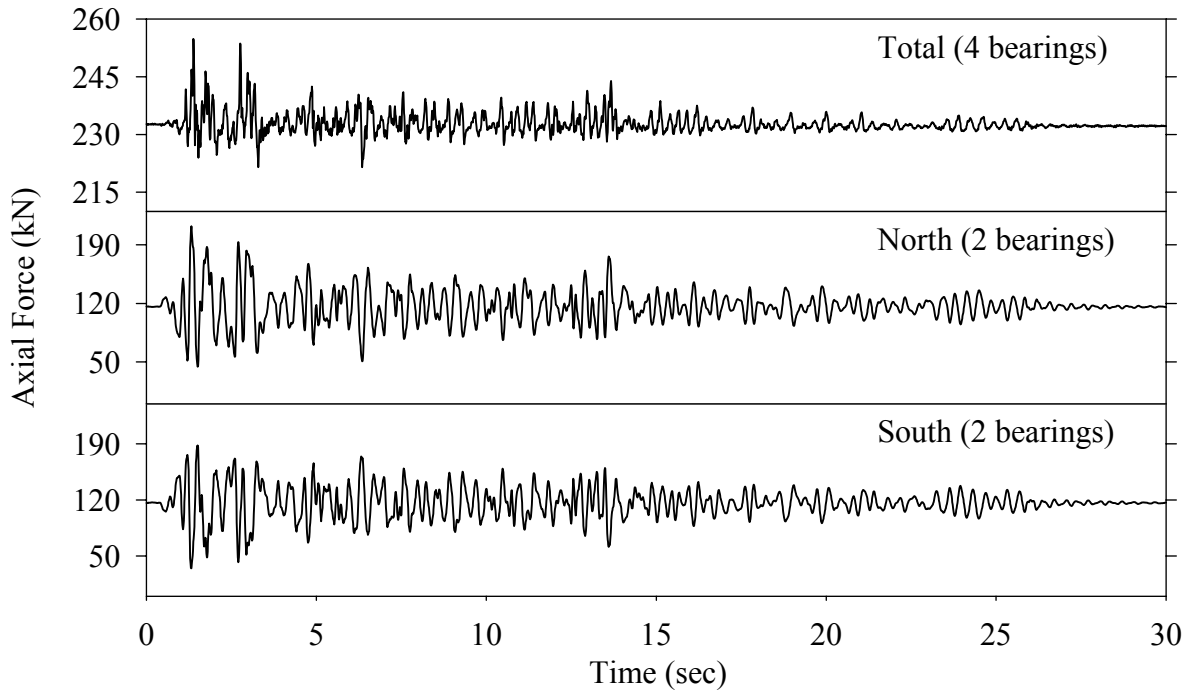


Test FPALE20.2, El Centro S00E 200% Test 2, AB/FPS-LD

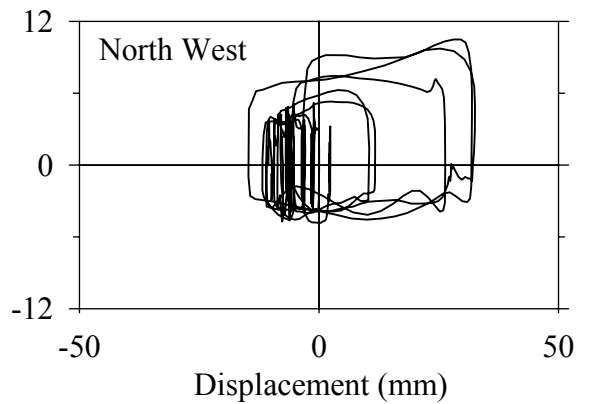
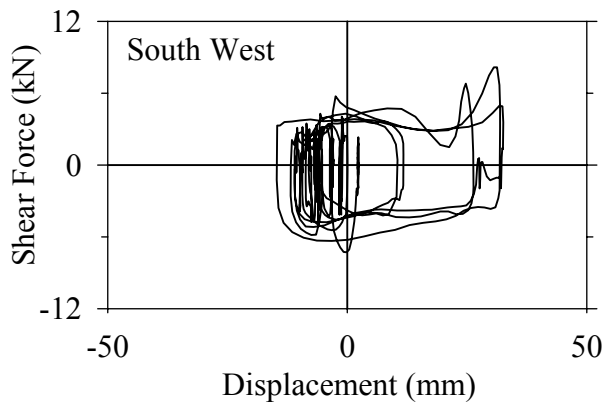
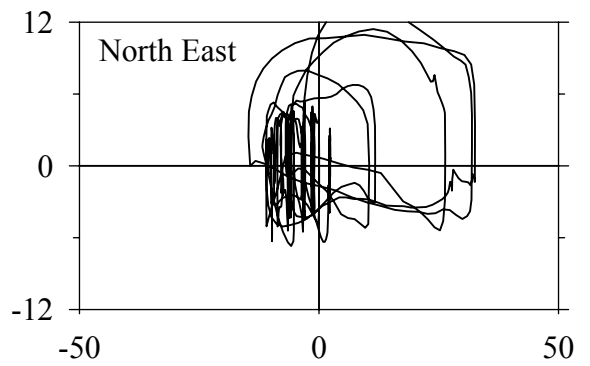
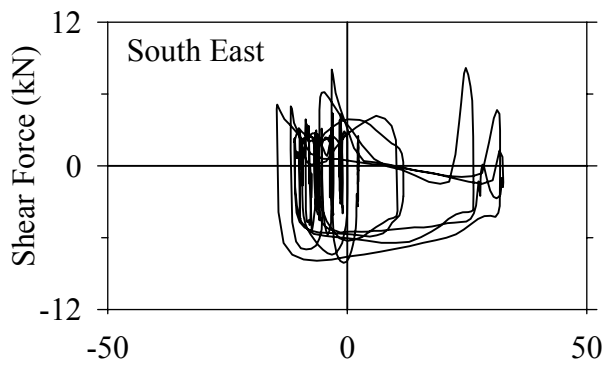
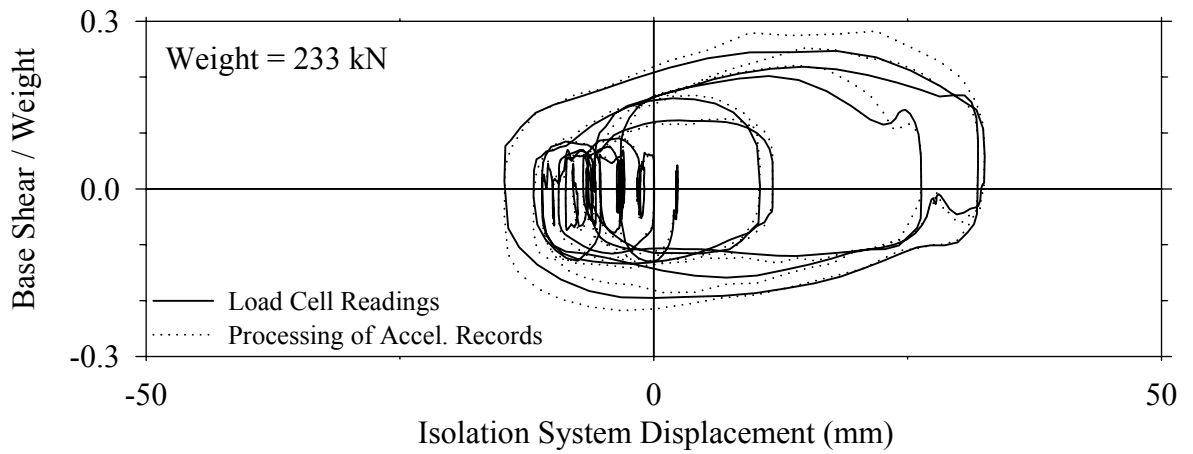
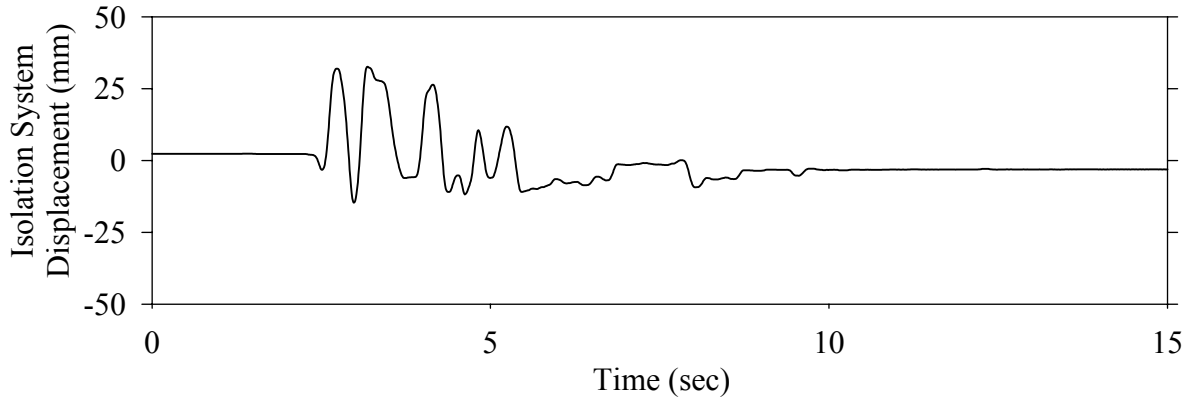




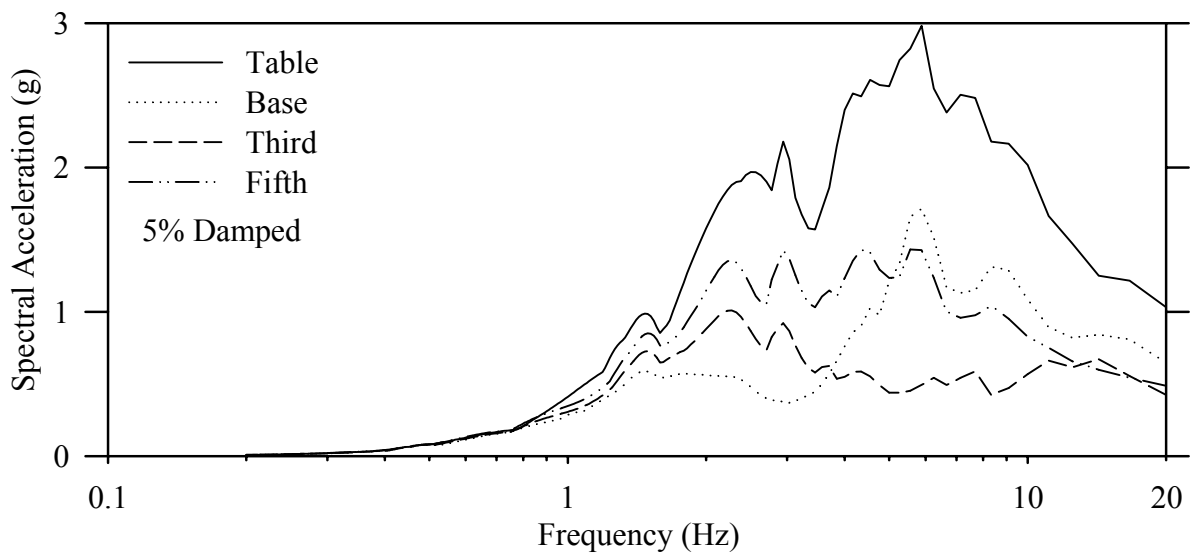
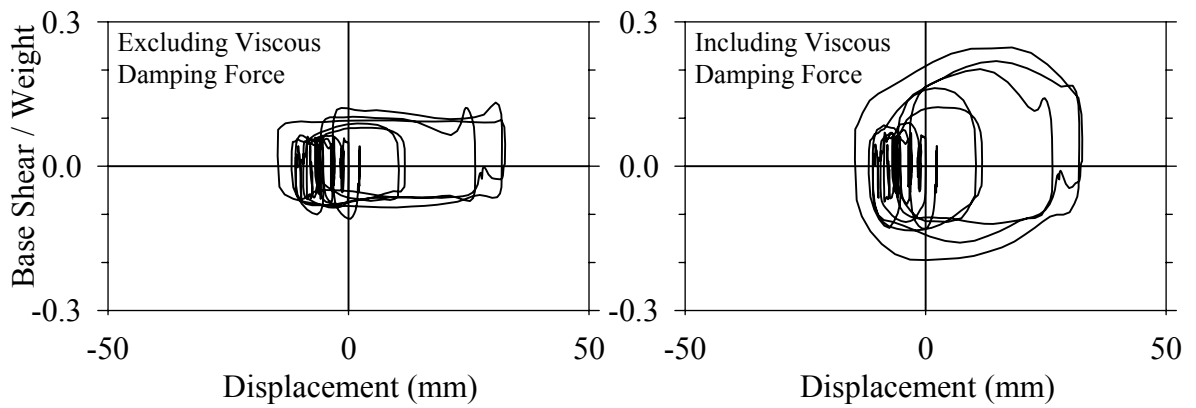
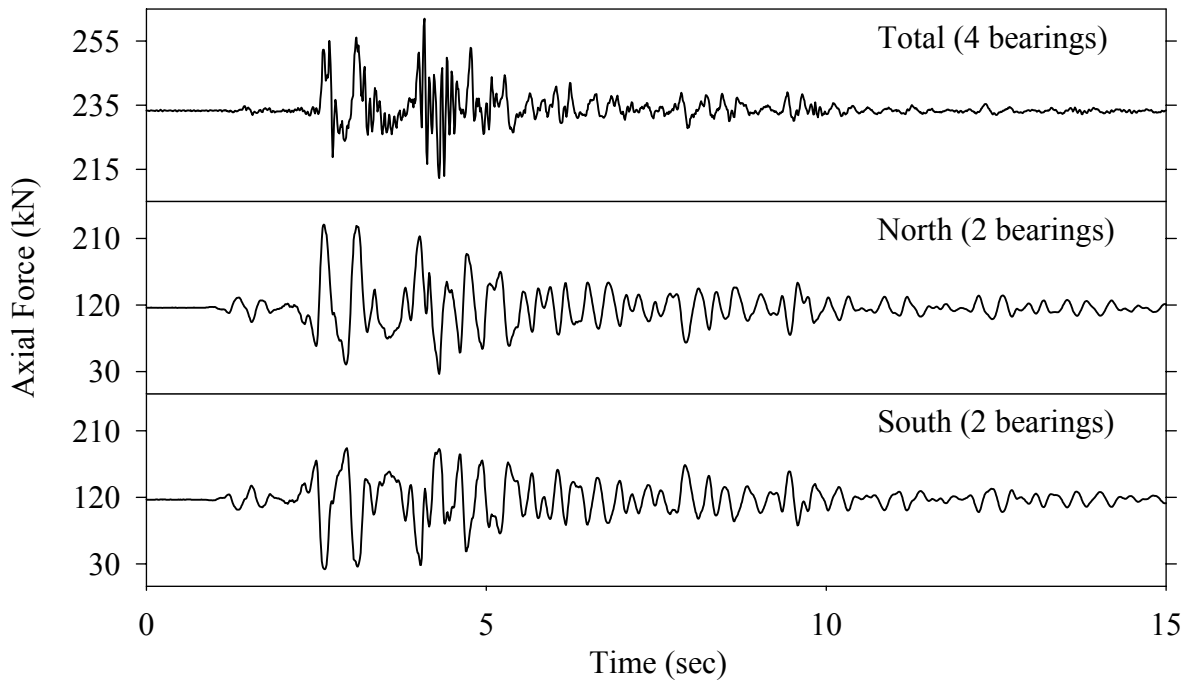
Test FPALE20.2, El Centro S00E 200% Test 2, AB/FPS-LD



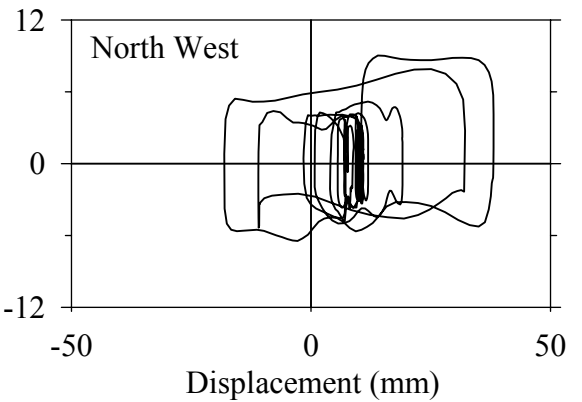
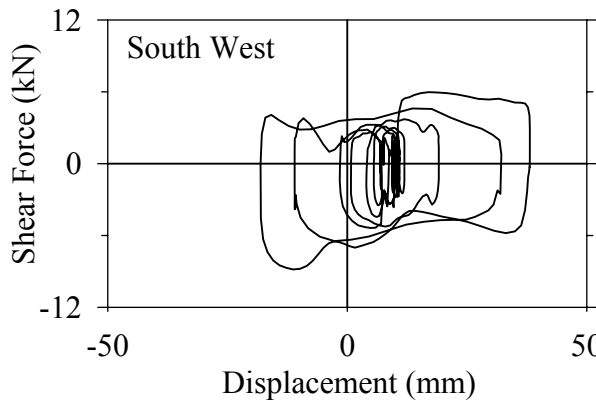
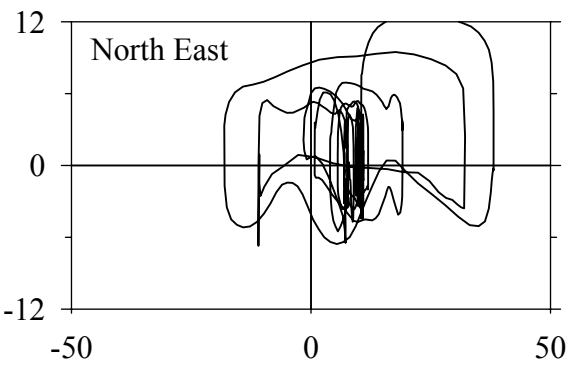
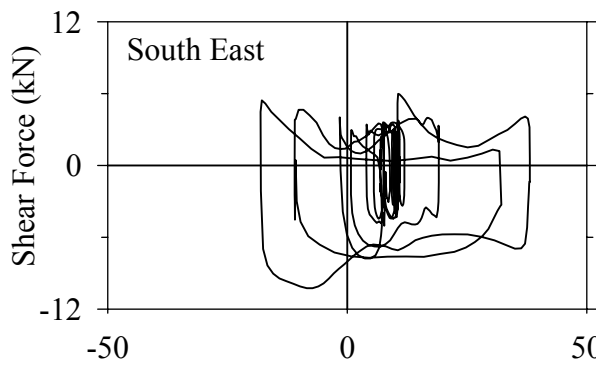
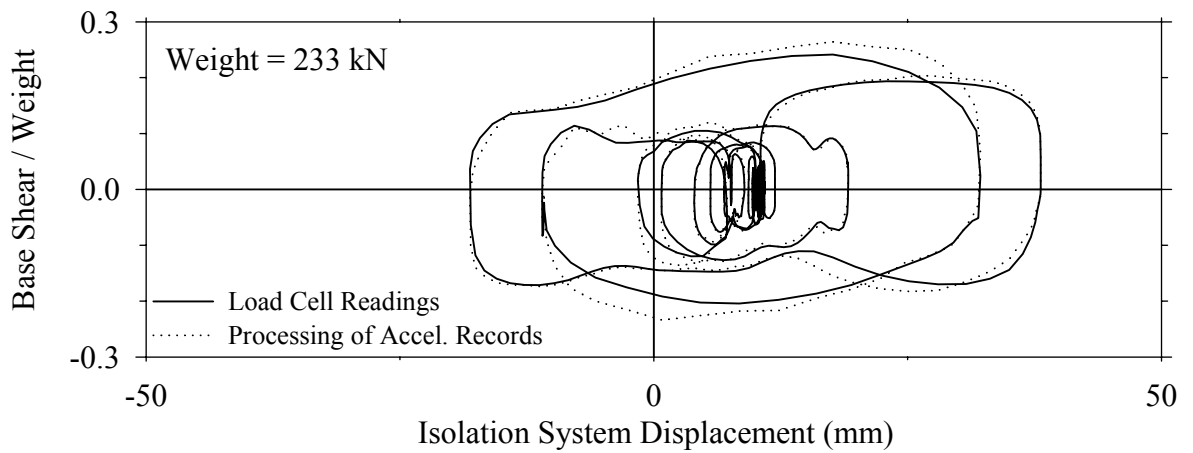
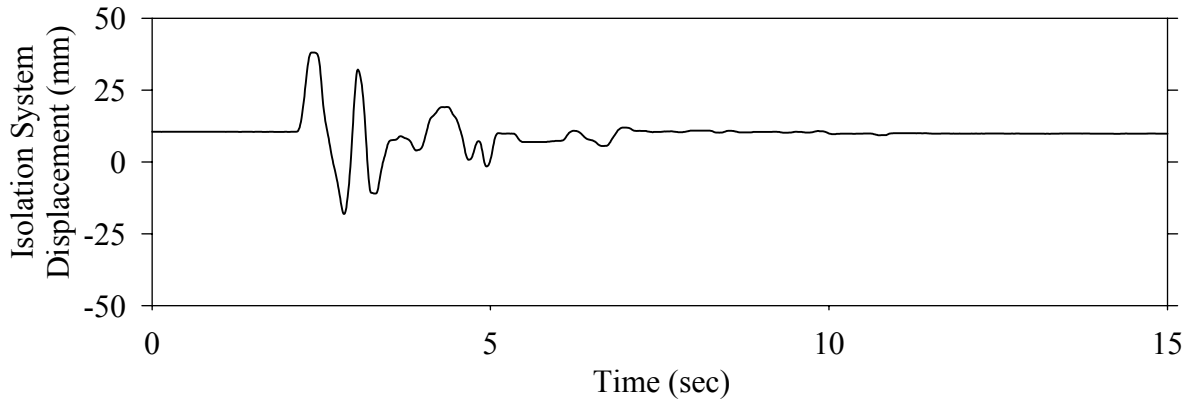
Test FPALK10.2, Kobe N-S 100% Test 2, AB/FPS-LD



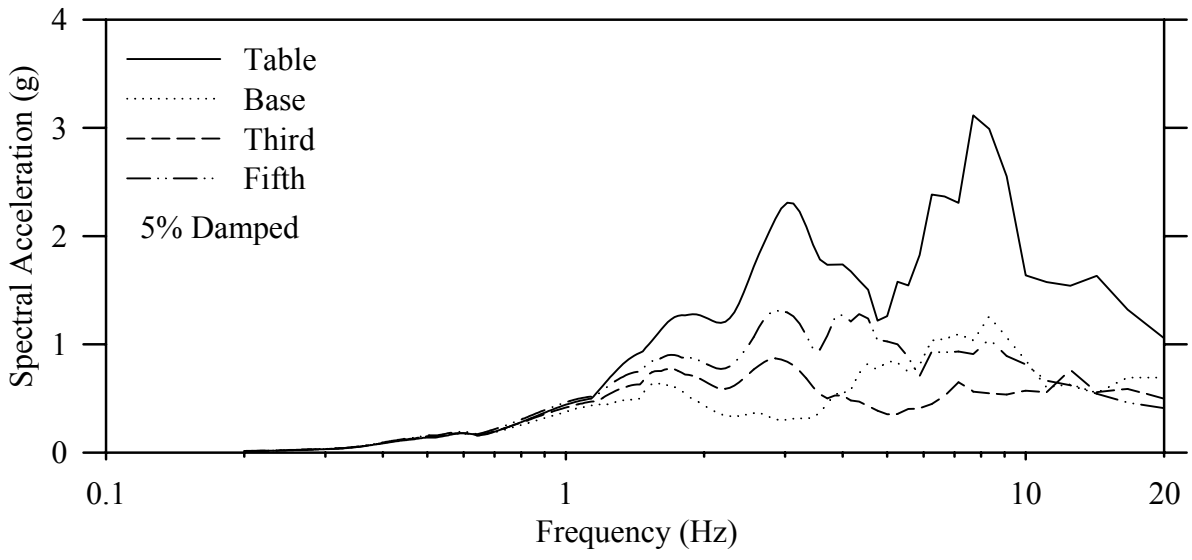
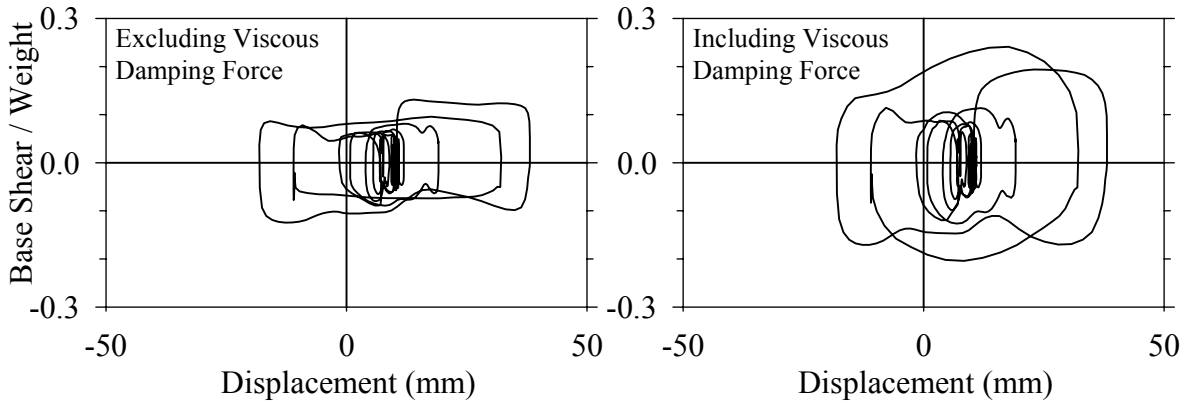
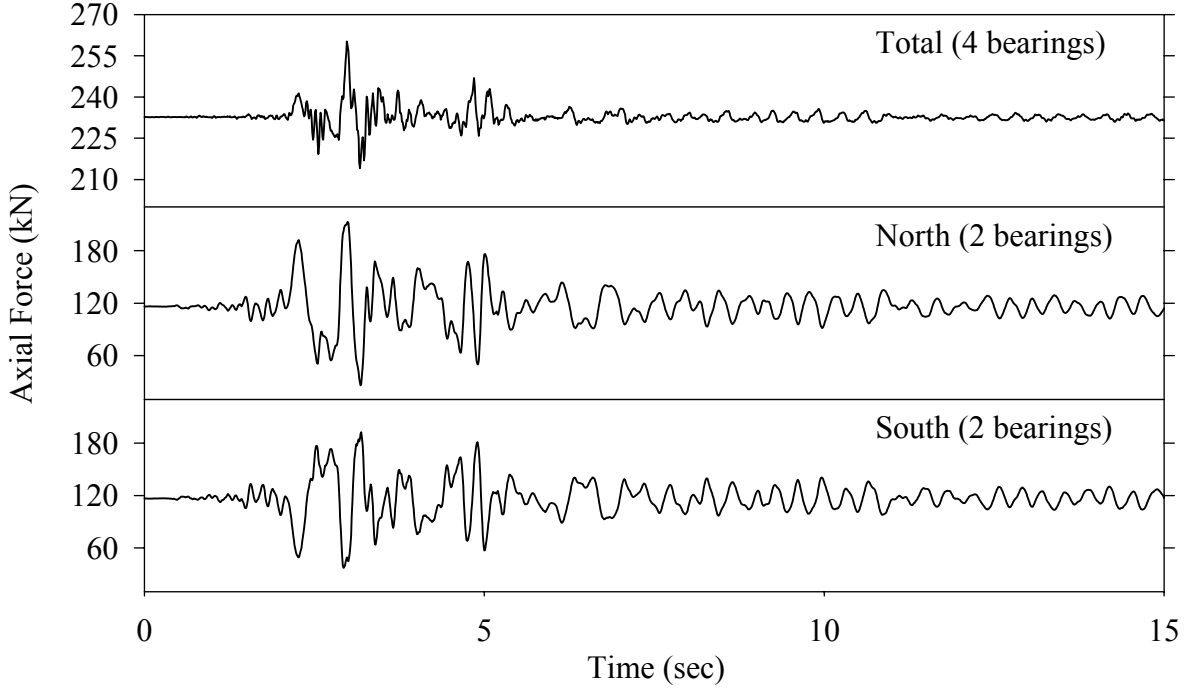
Test FPALK10.2, Kobe N-S 100% Test 2, AB/FPS-LD



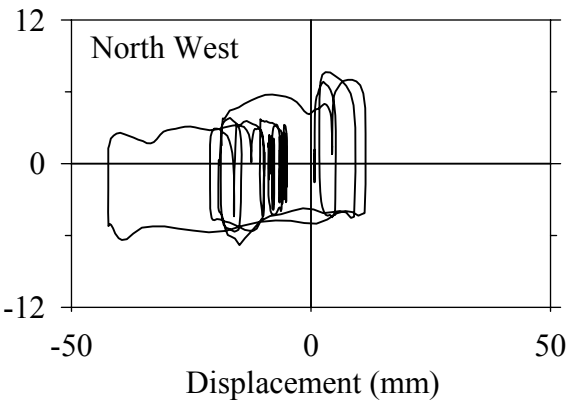
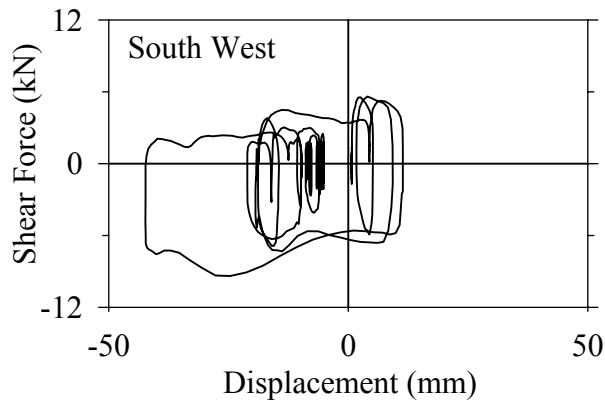
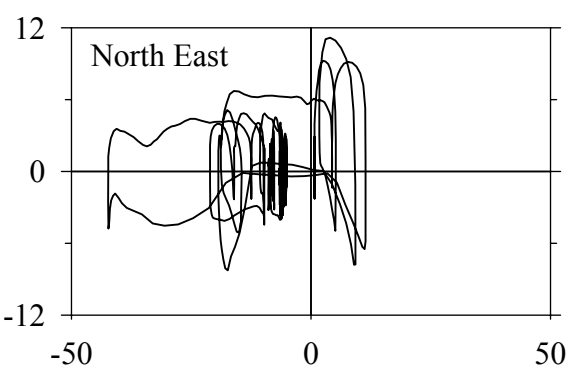
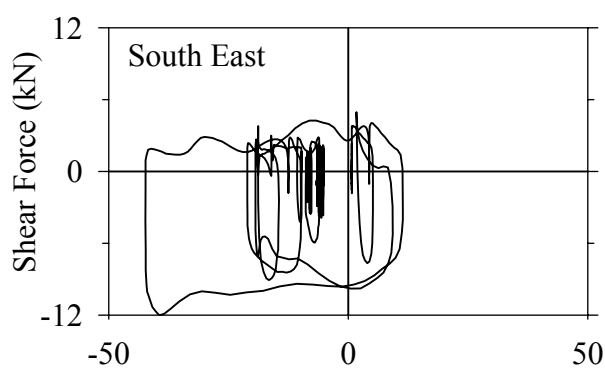
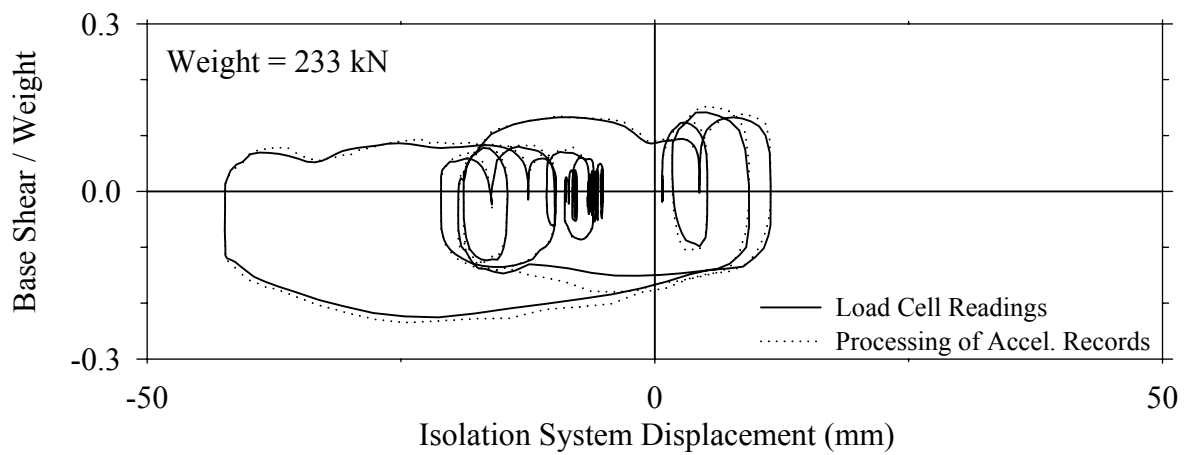
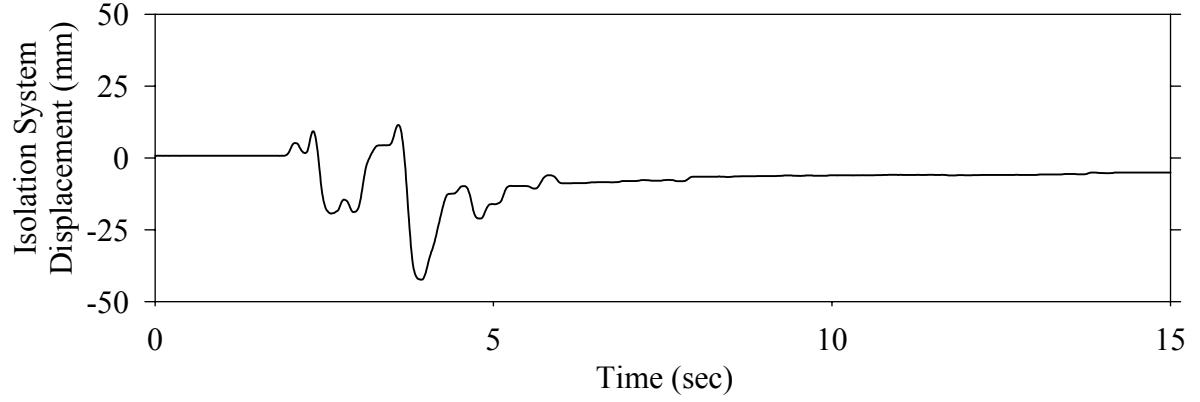
Test FPALN10.1, Northridge Newhall 360° 100%, AB/FPS-LD



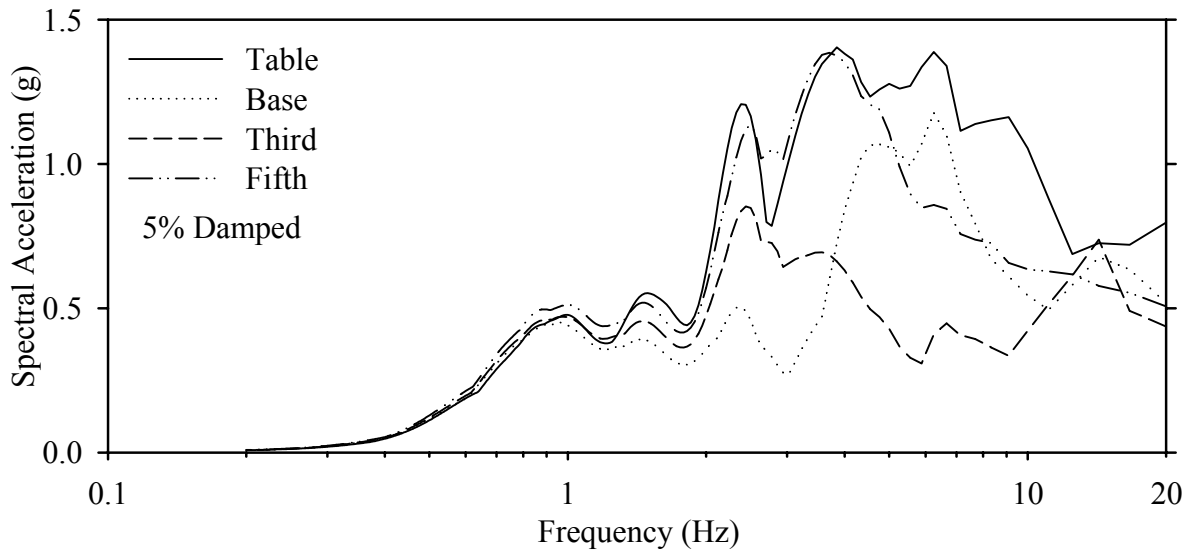
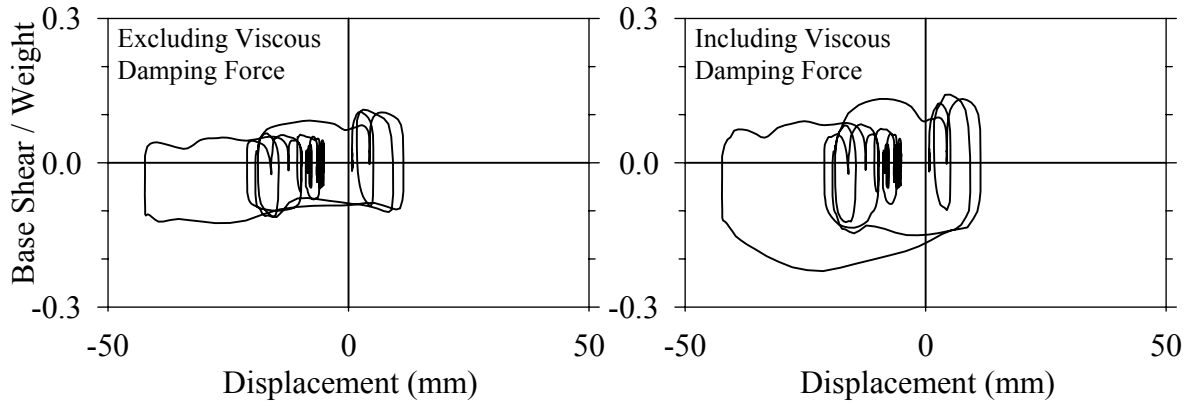
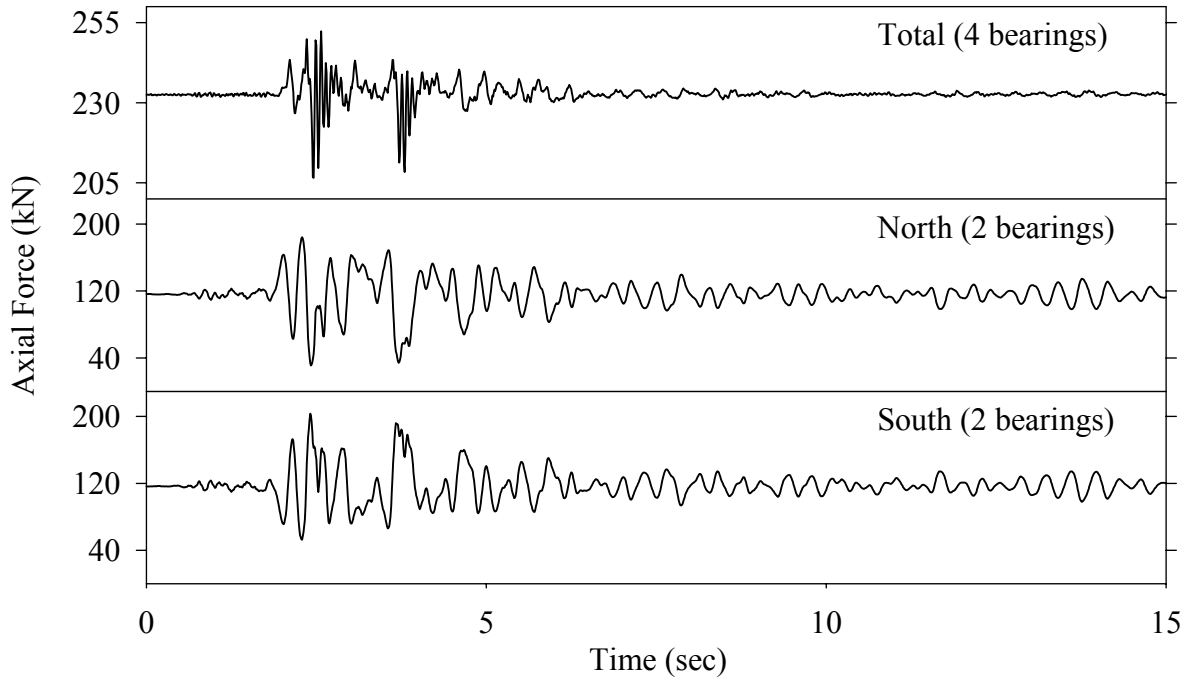
Test FPALN10.1, Northridge Newhall 360° 100%, AB/FPS-LD



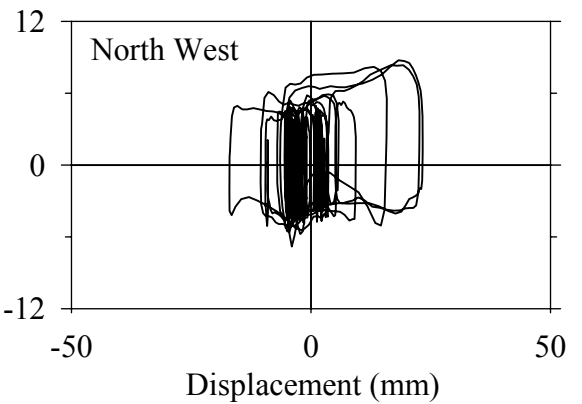
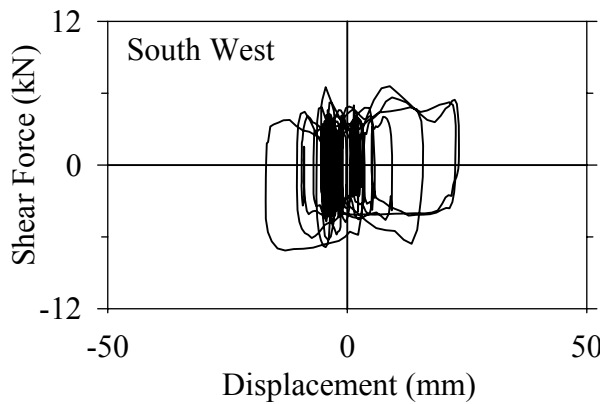
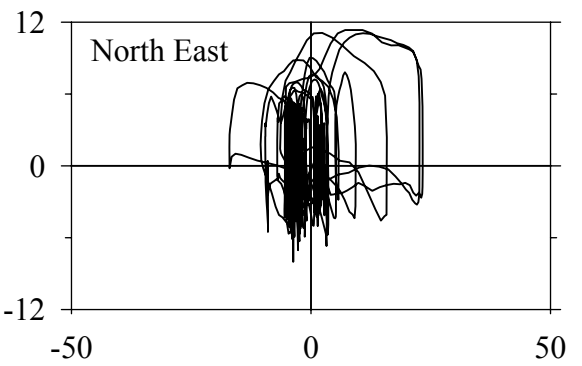
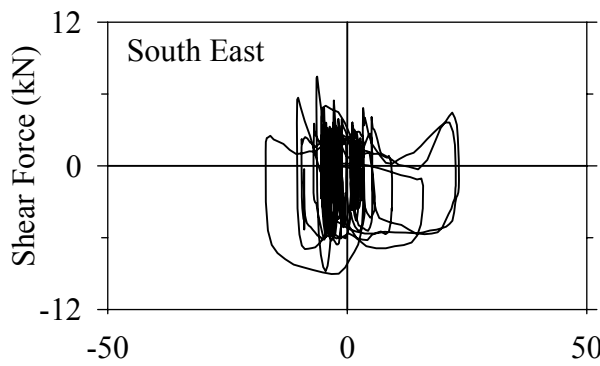
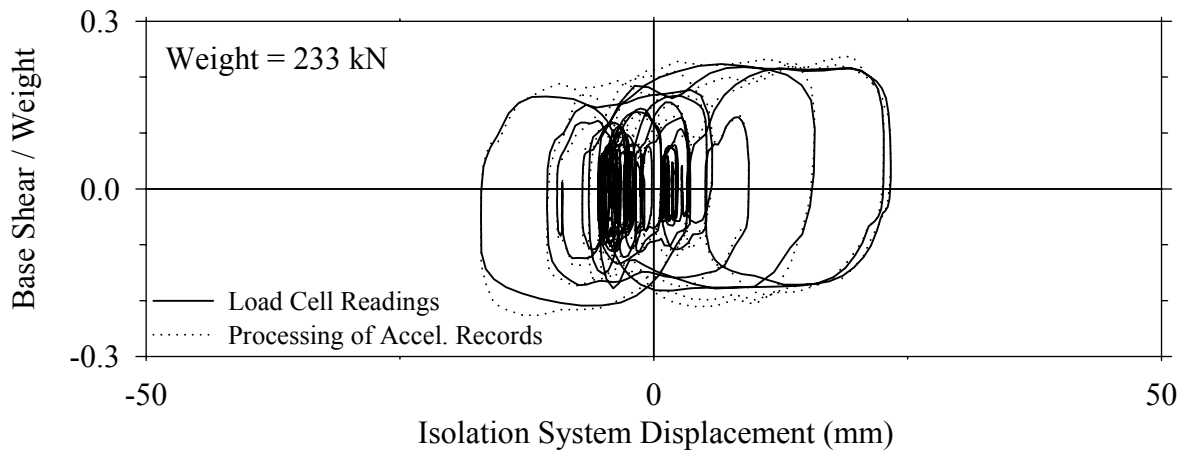
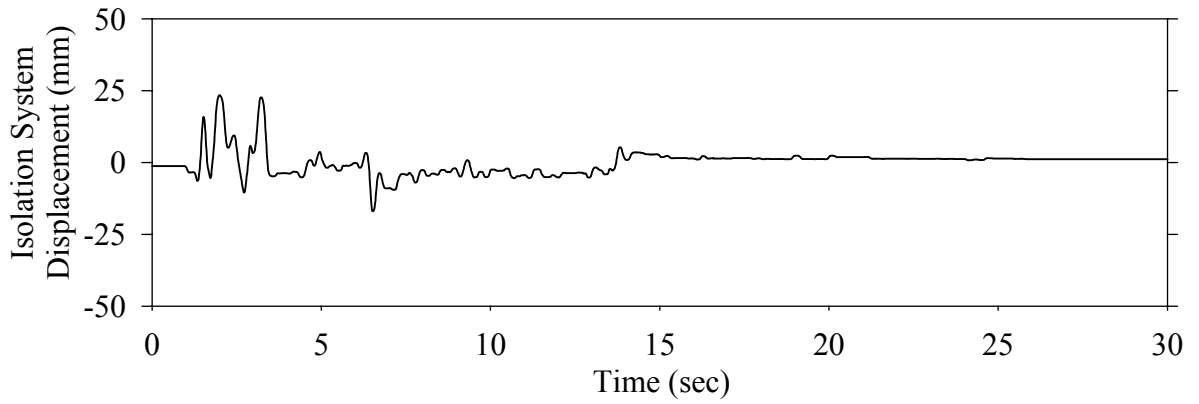
Test FPALS10.1, Northridge Sylmar 90° 100%, AB/FPS-LD



Test FPALS10.1, Northridge Sylmar 90° 100%, AB/FPS-LD

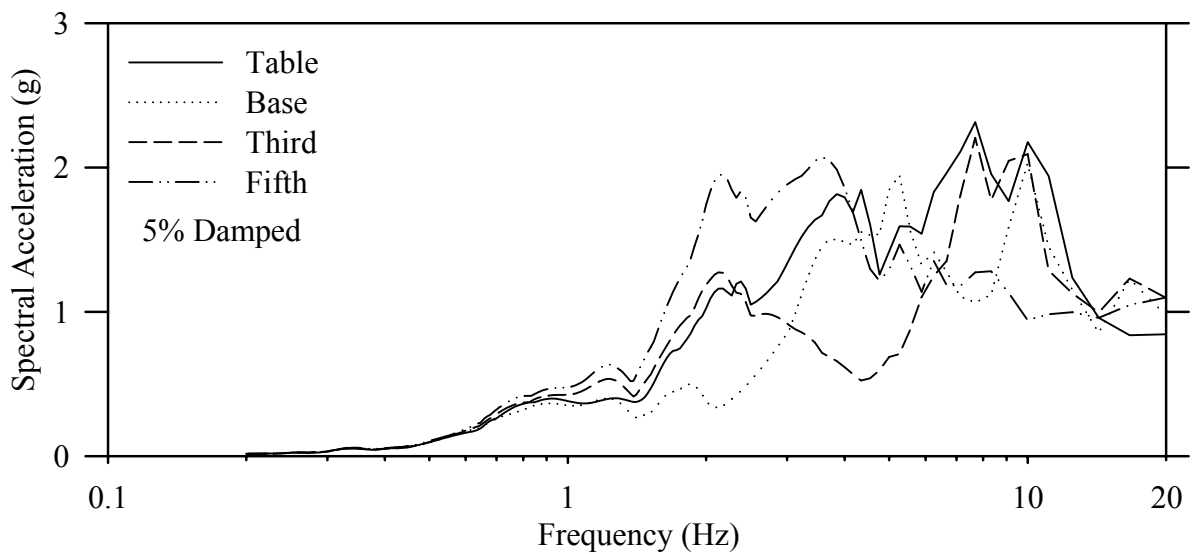
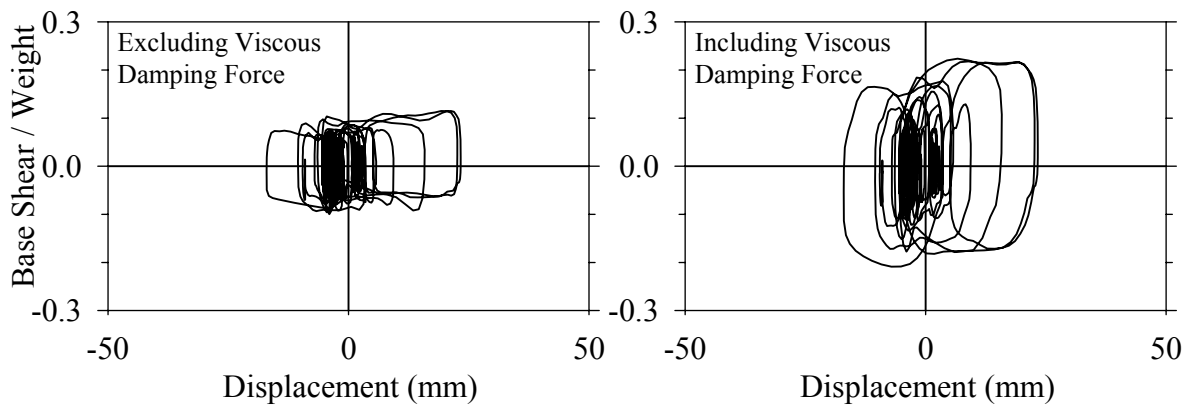
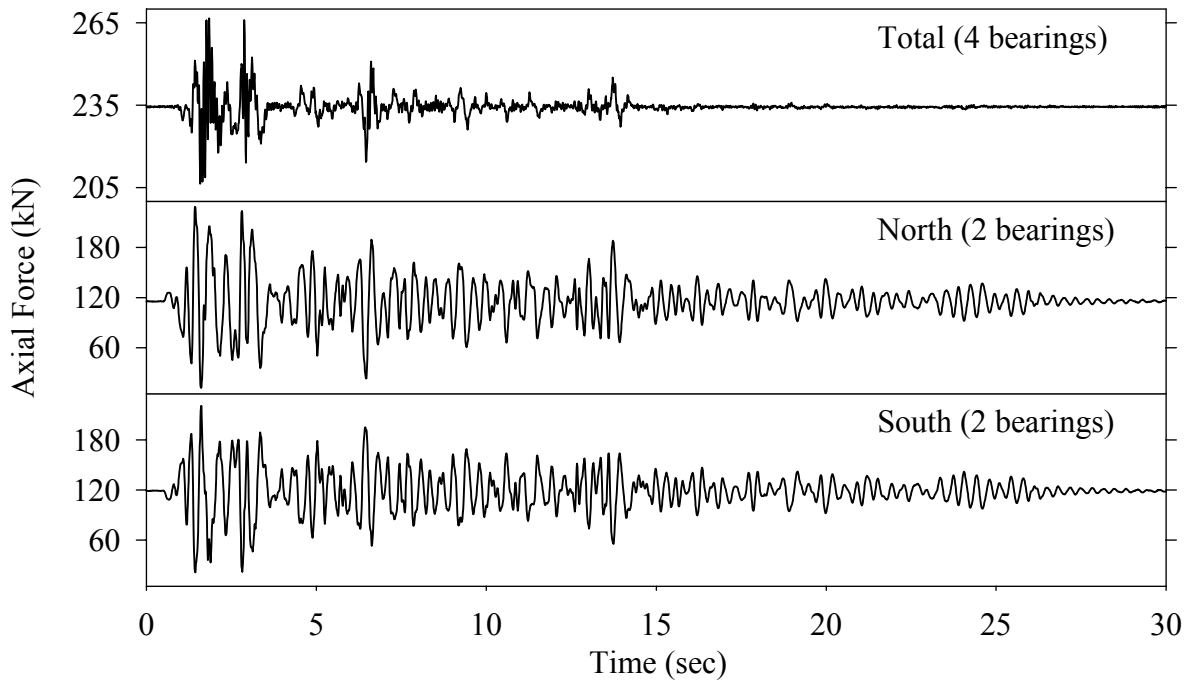


Test FPANE20.1, El Centro S00E 200%, AB/FPS-NLD

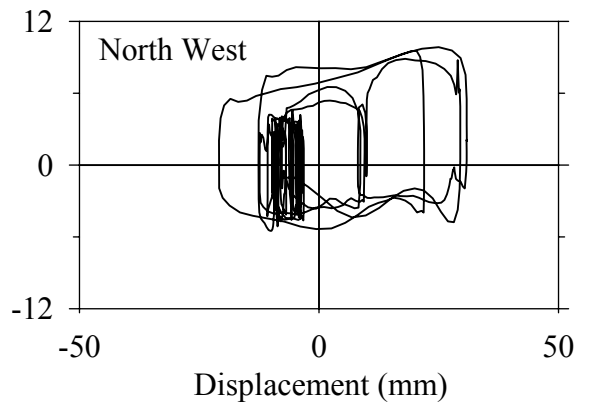
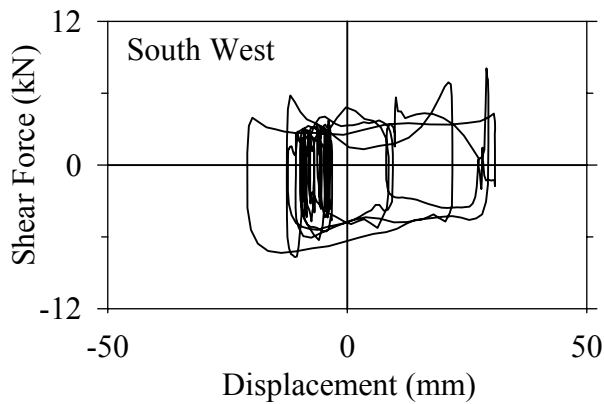
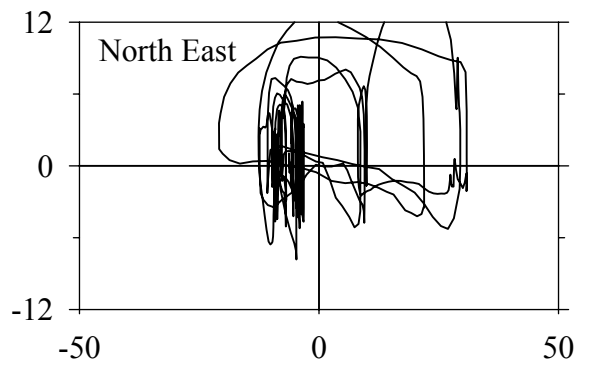
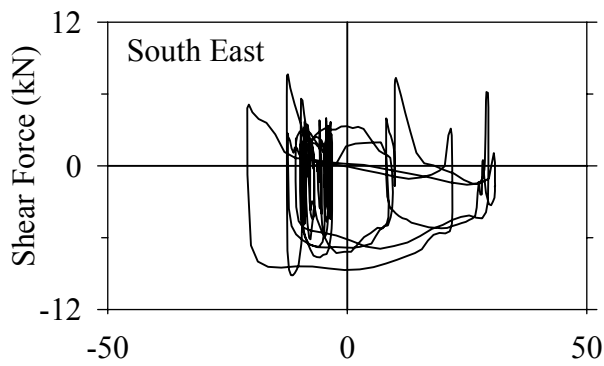
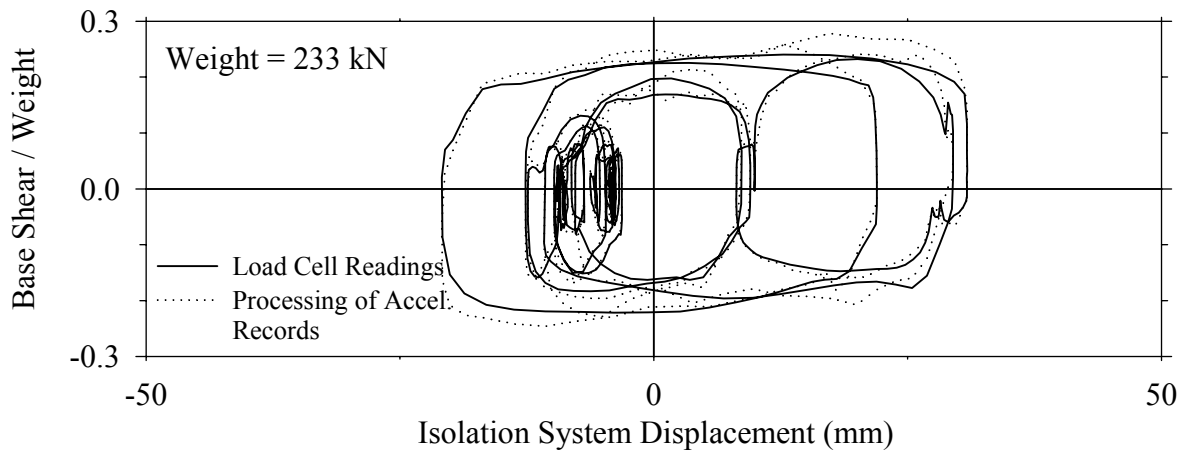
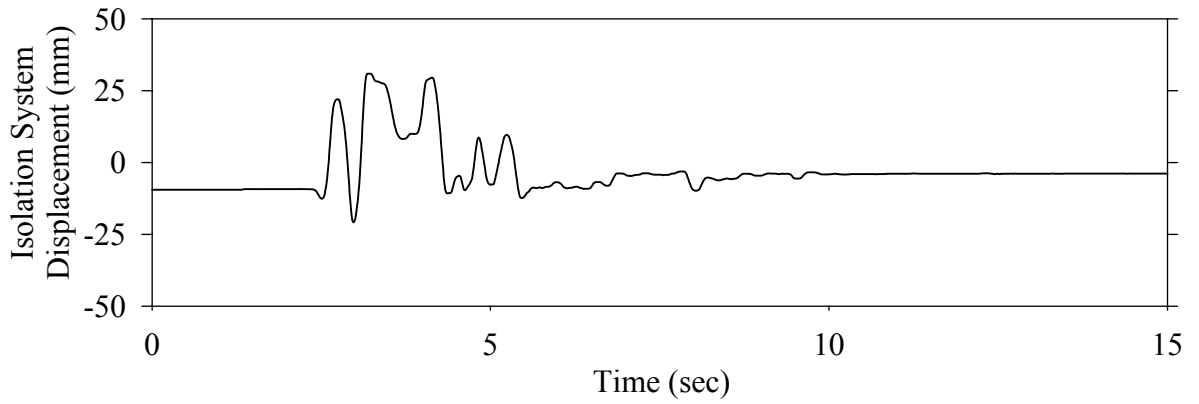




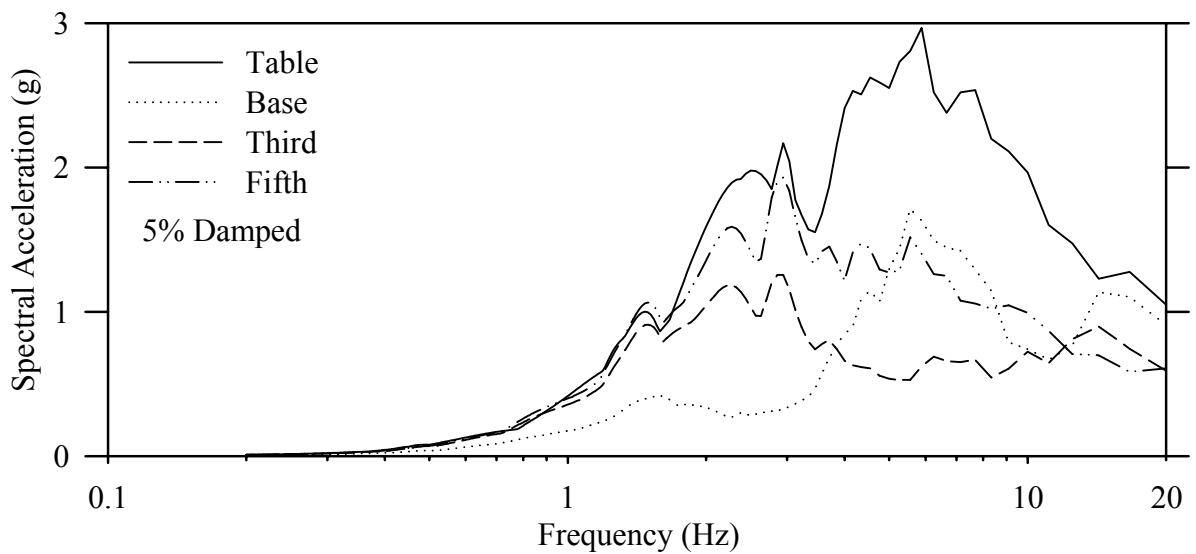
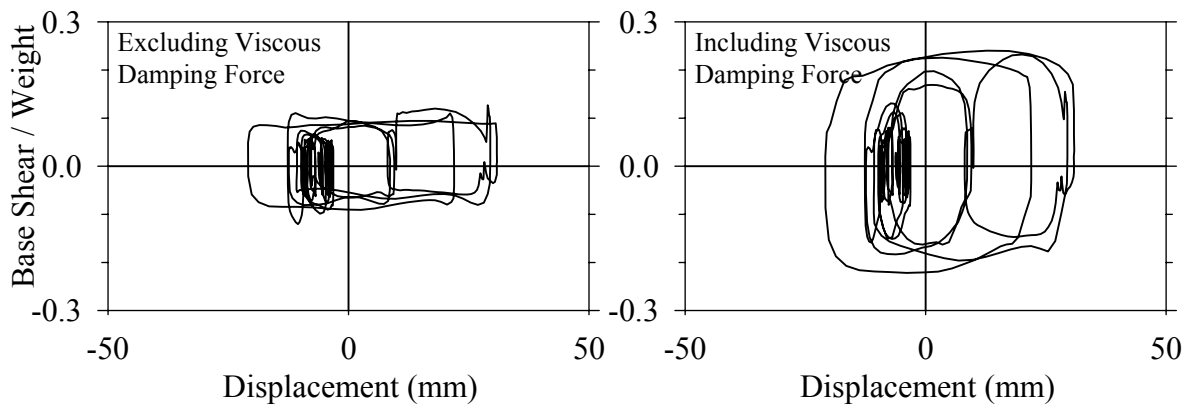
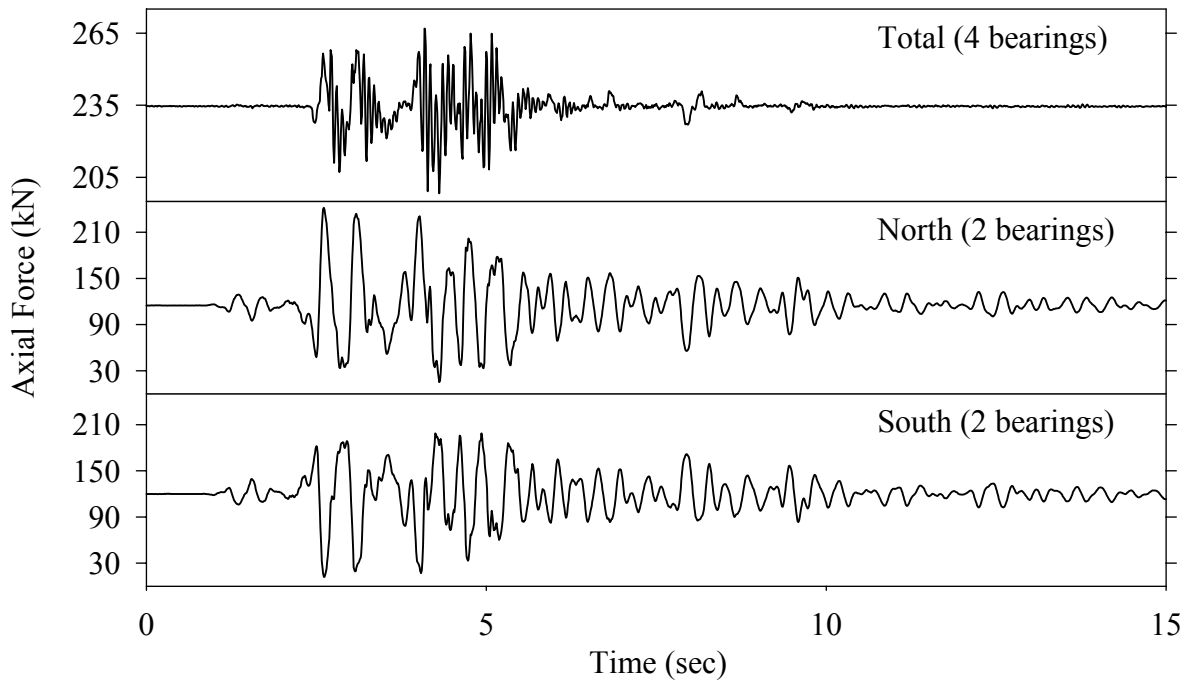
Test FPANE20.1, El Centro S00E 200%, AB/FPS-NLD



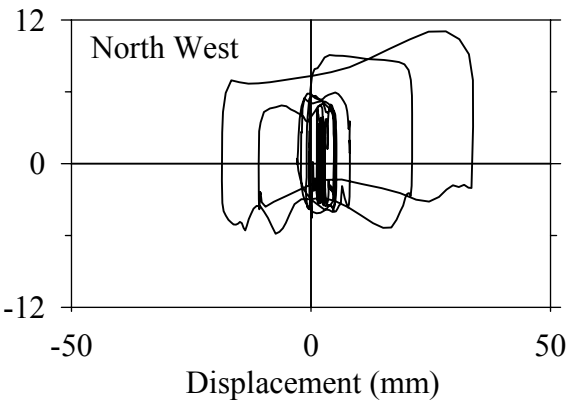
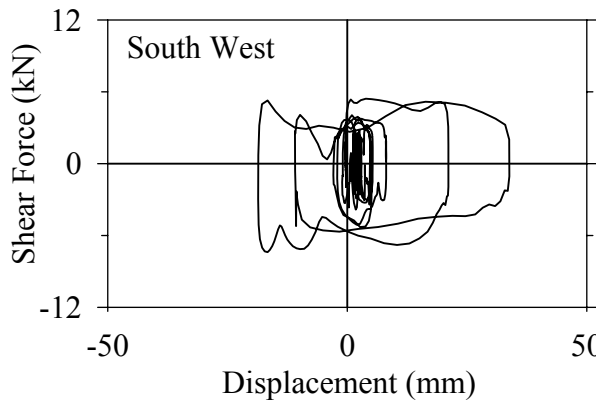
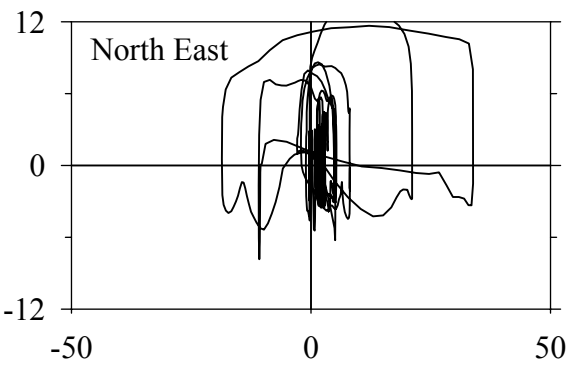
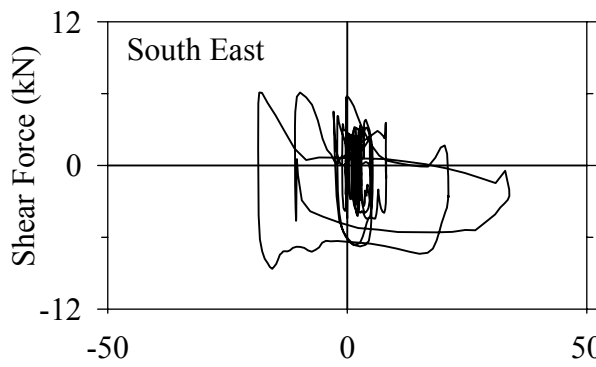
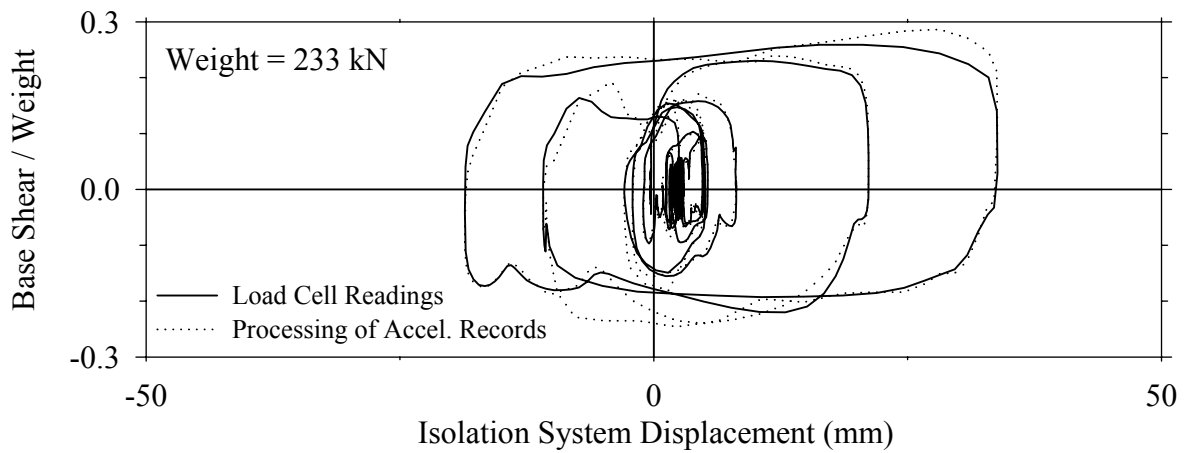
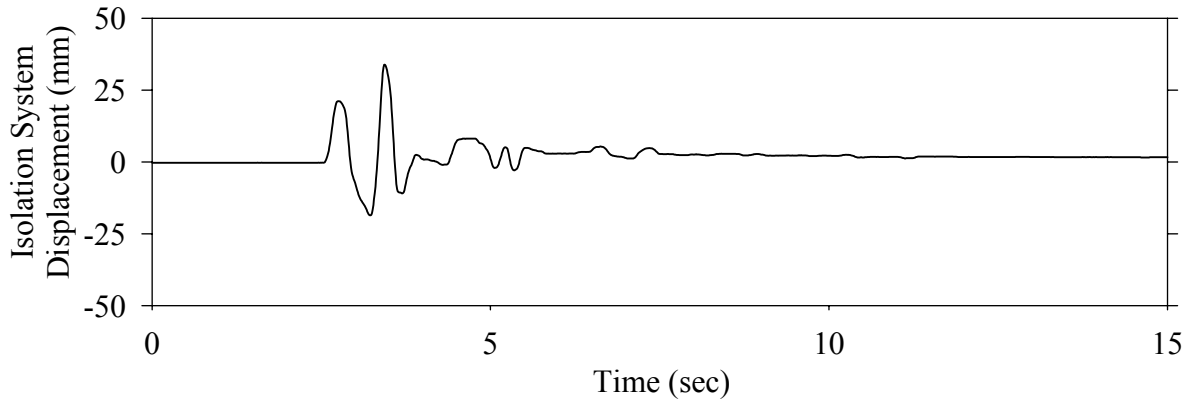
Test FPANK10.1, Kobe N-S 100%, AB/FPS-NLD



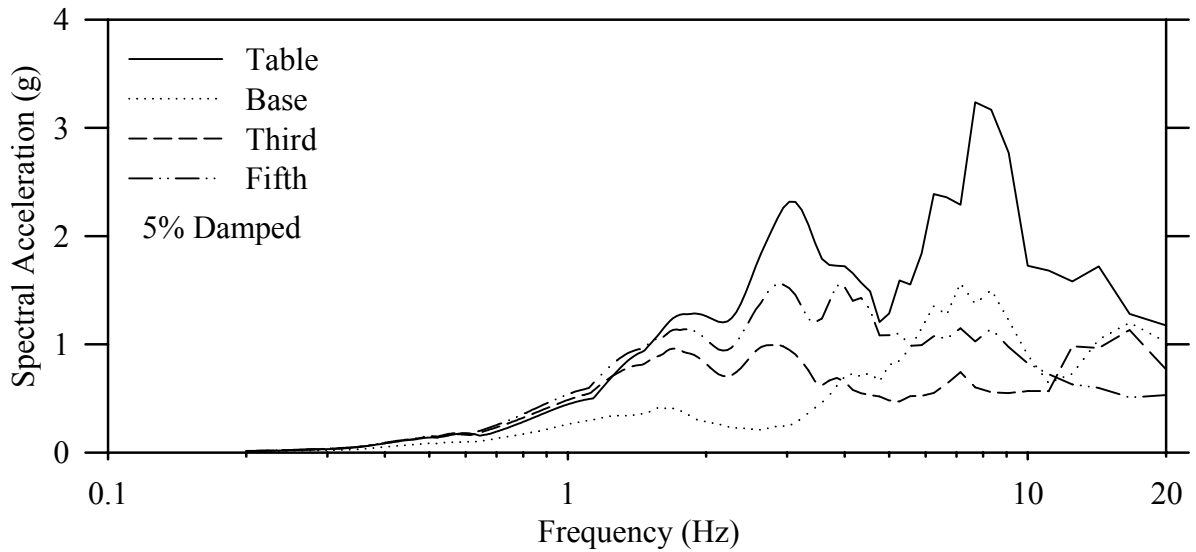
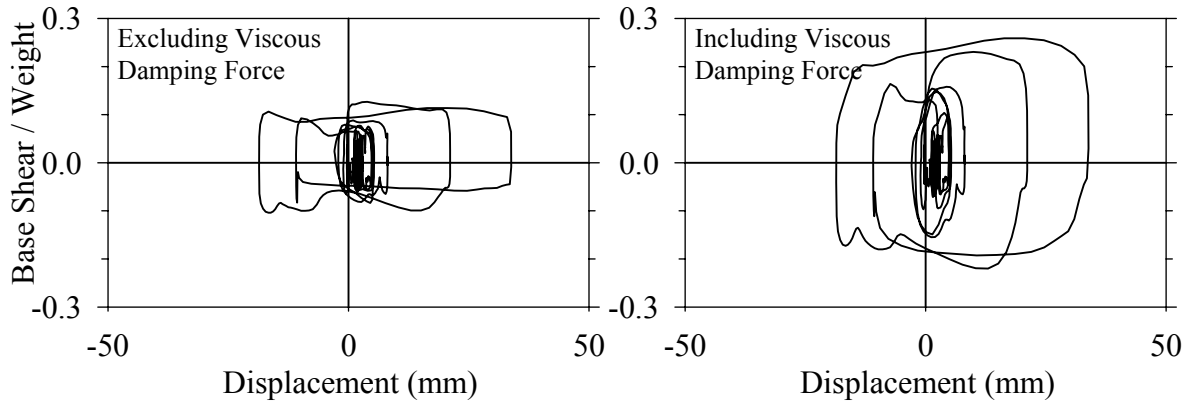
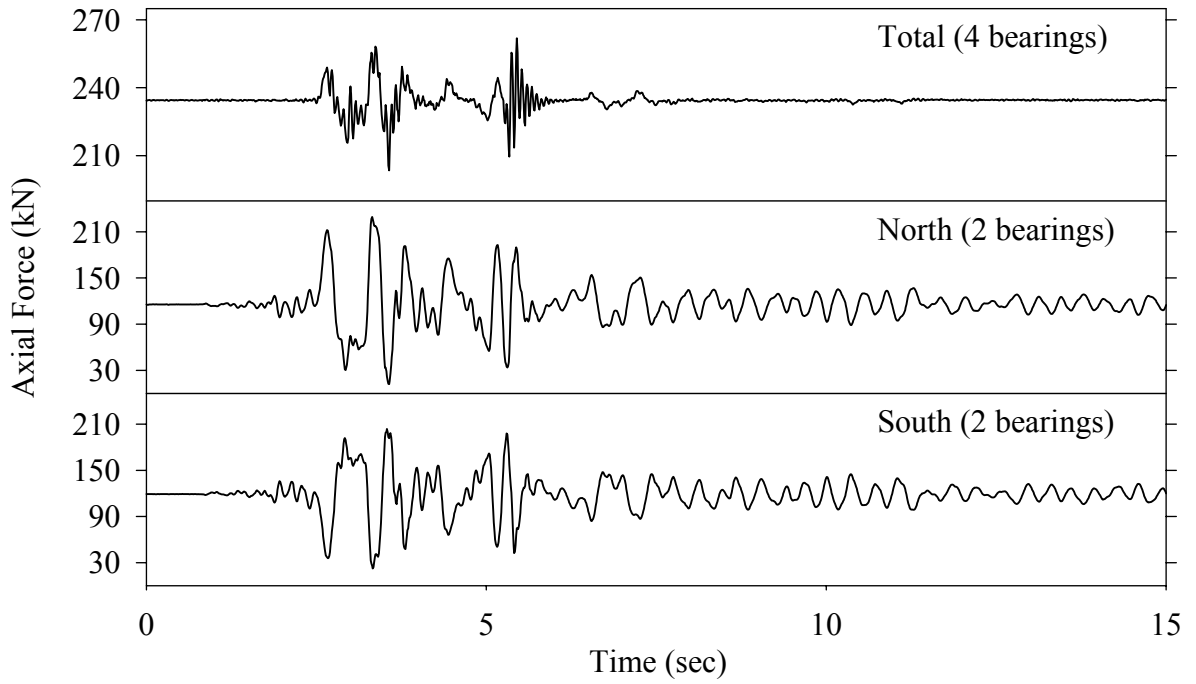
Test FPANK10.1, Kobe N-S 100%, AB/FPS-NLD



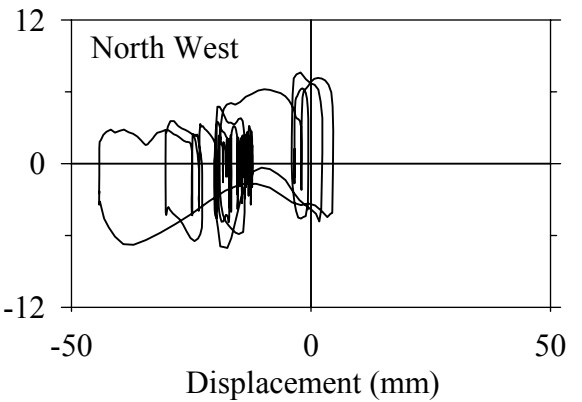
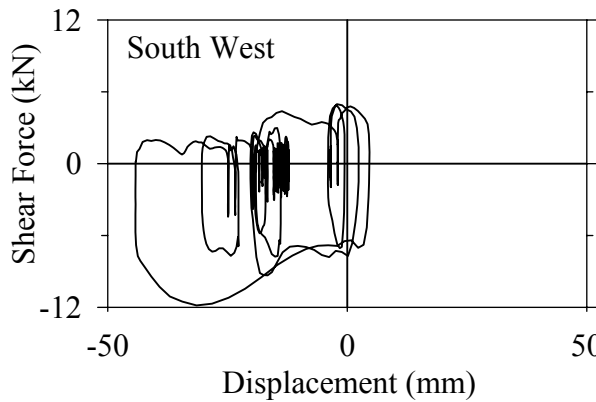
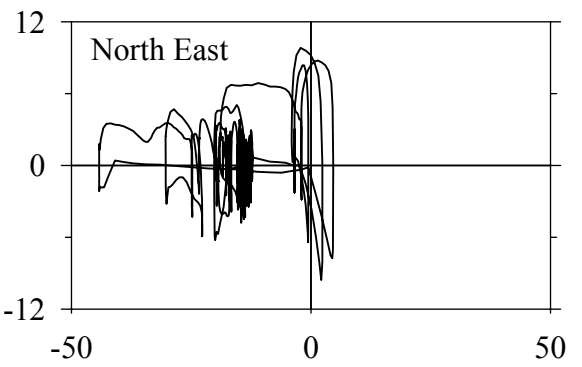
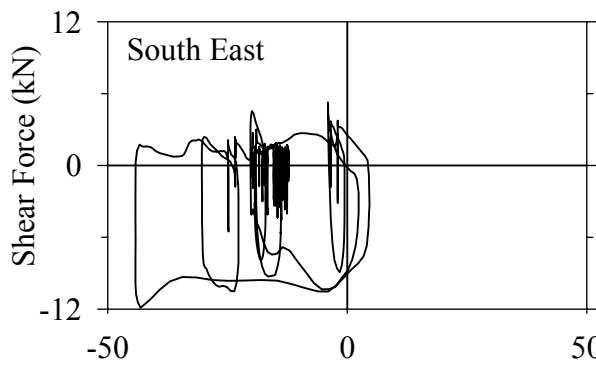
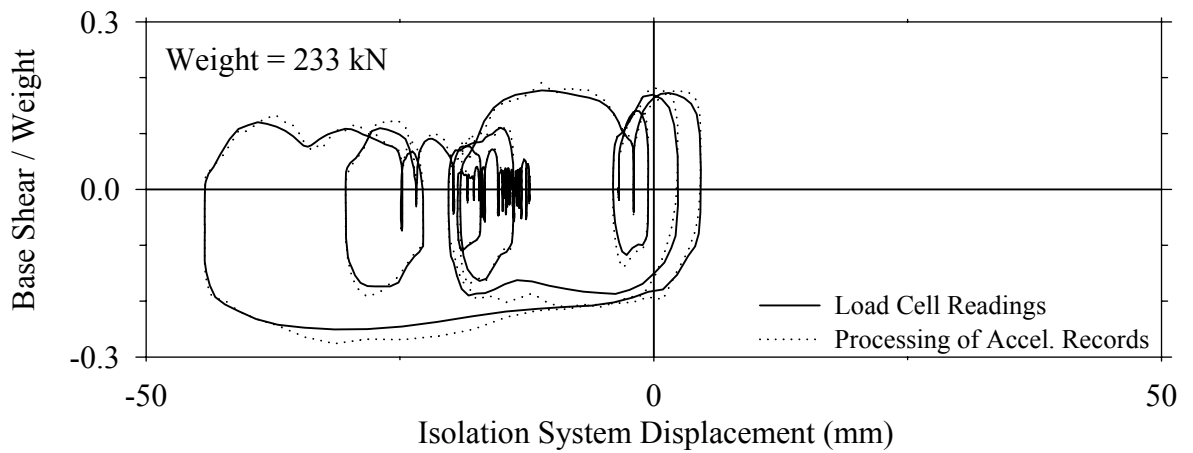
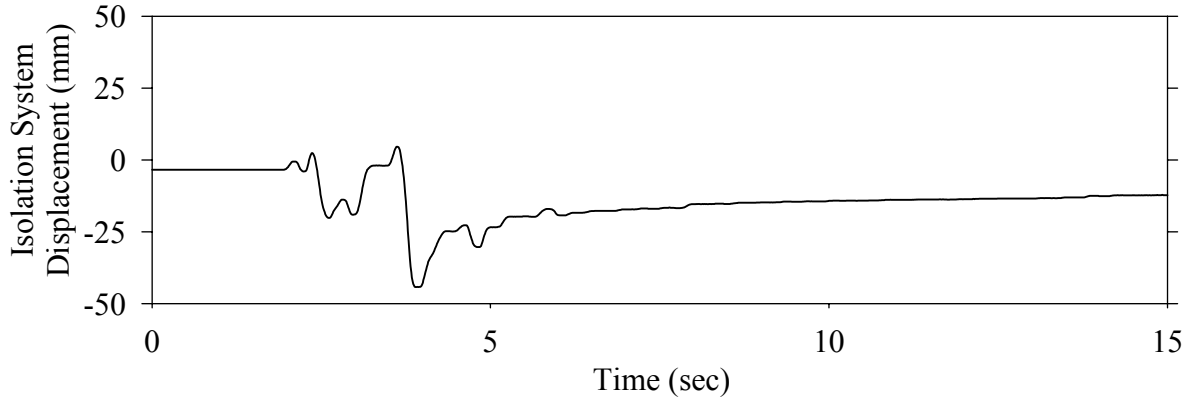
Test FPANN10.1, Northridge Newhall 360° 100%, AB/FPS-NLD



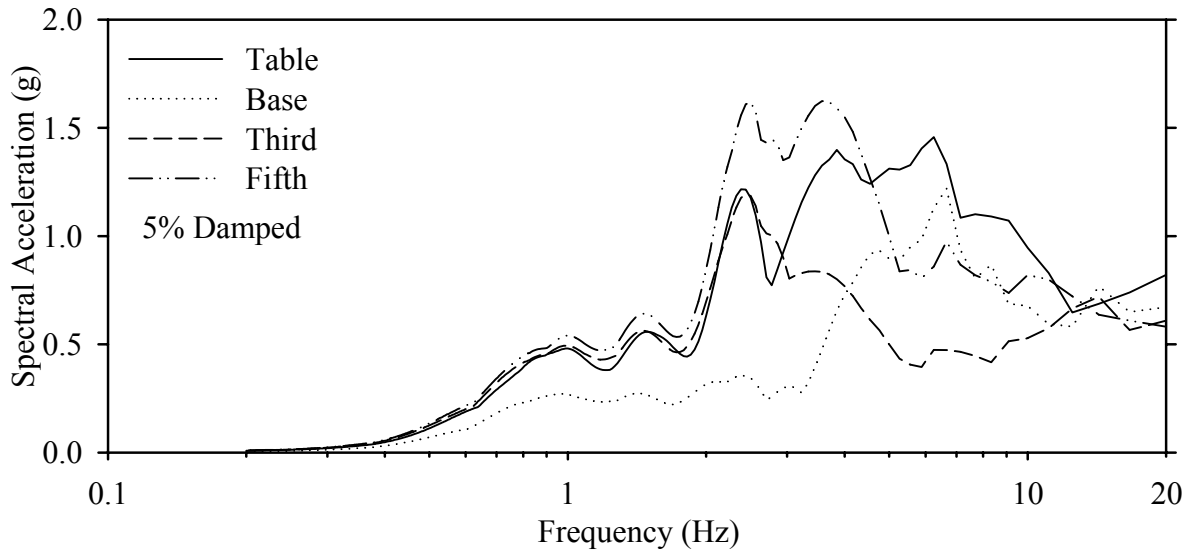
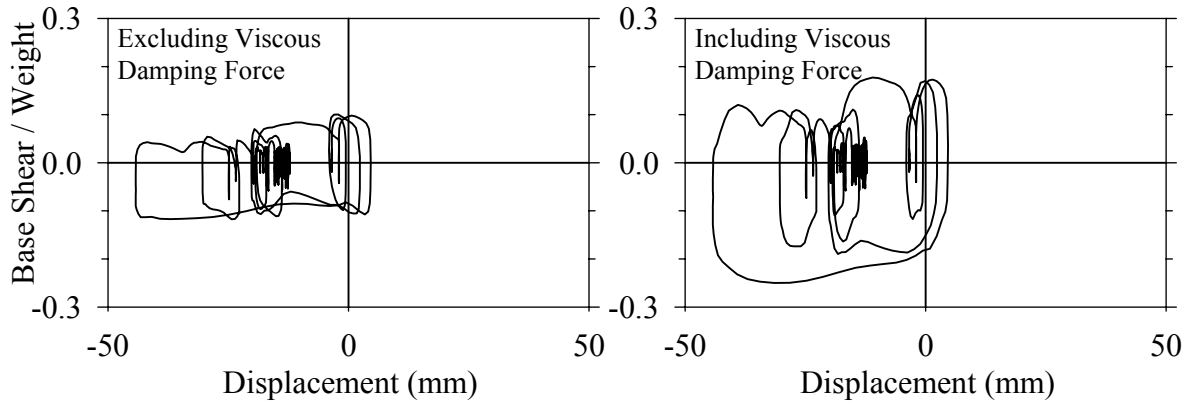
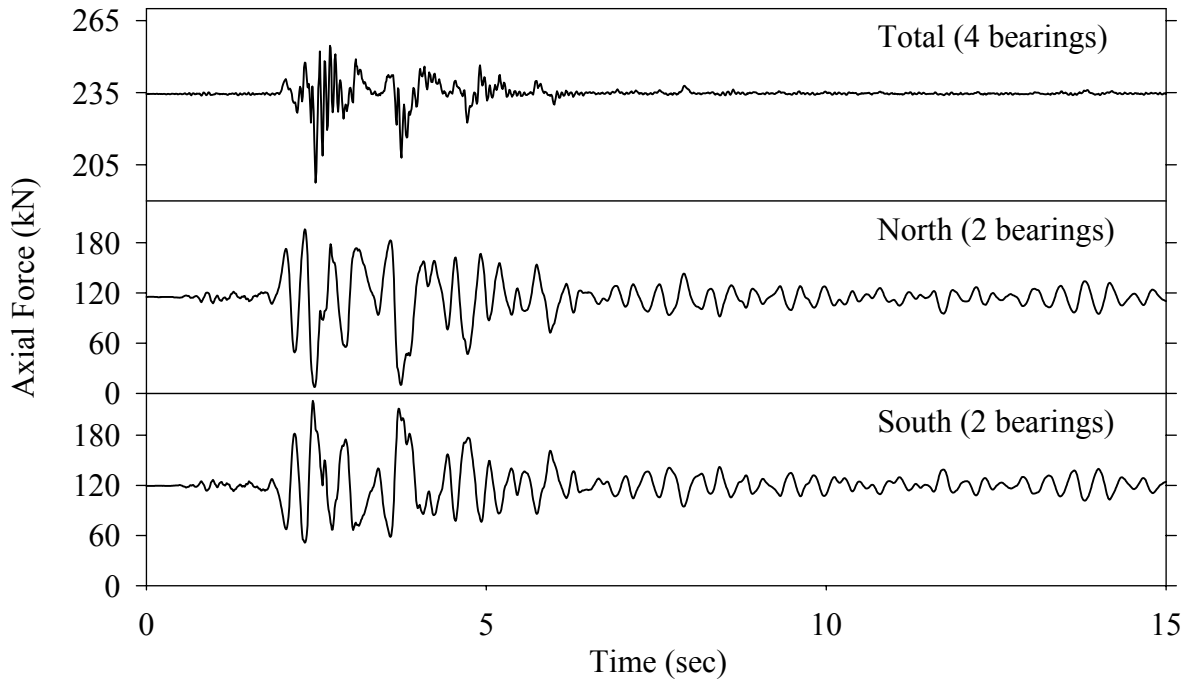
Test FPANN10.1, Northridge Newhall 360° 100%, AB/FPS-NLD



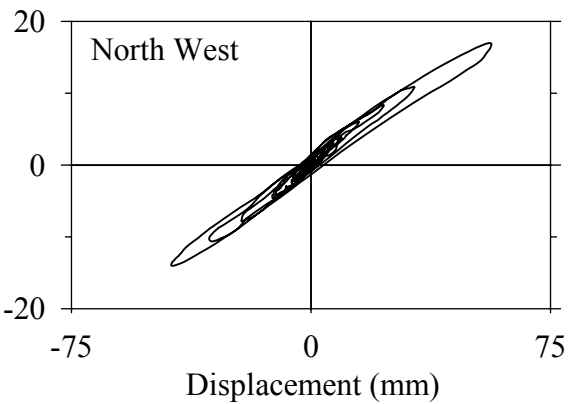
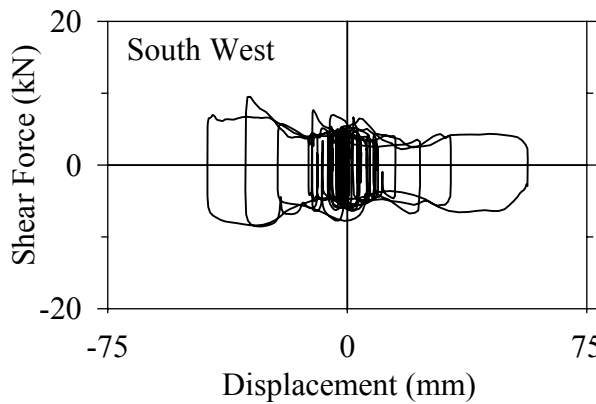
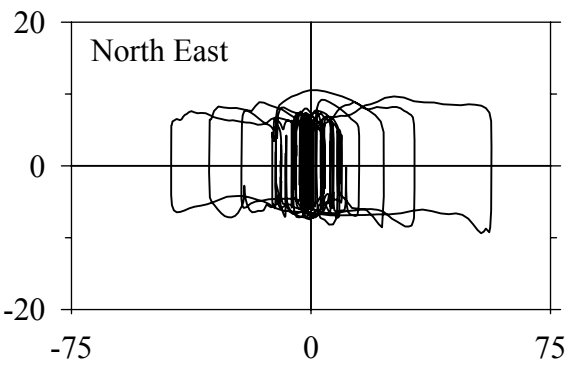
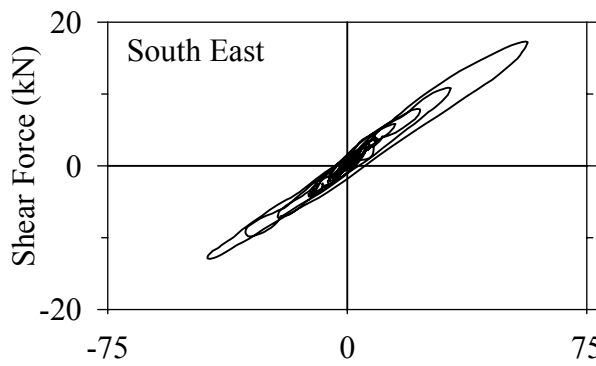
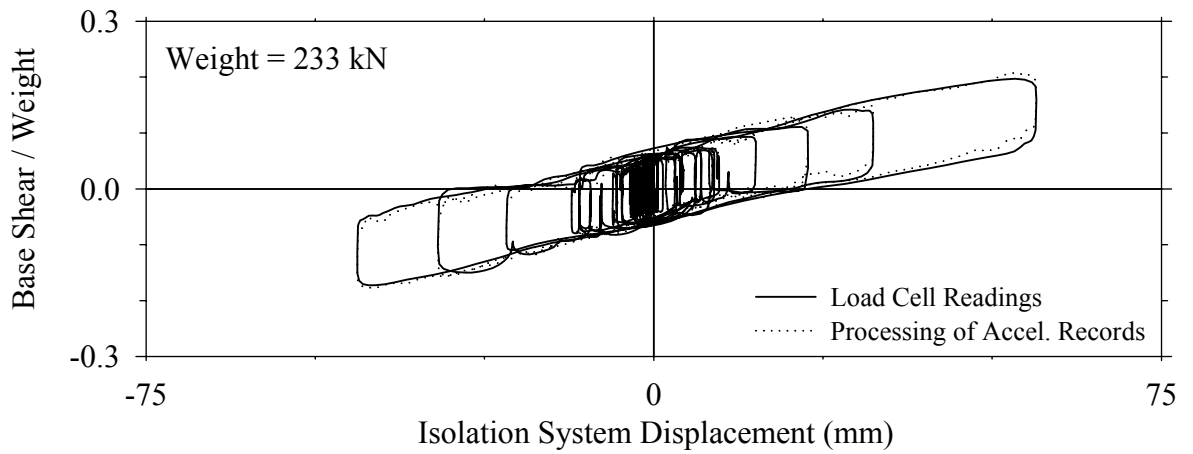
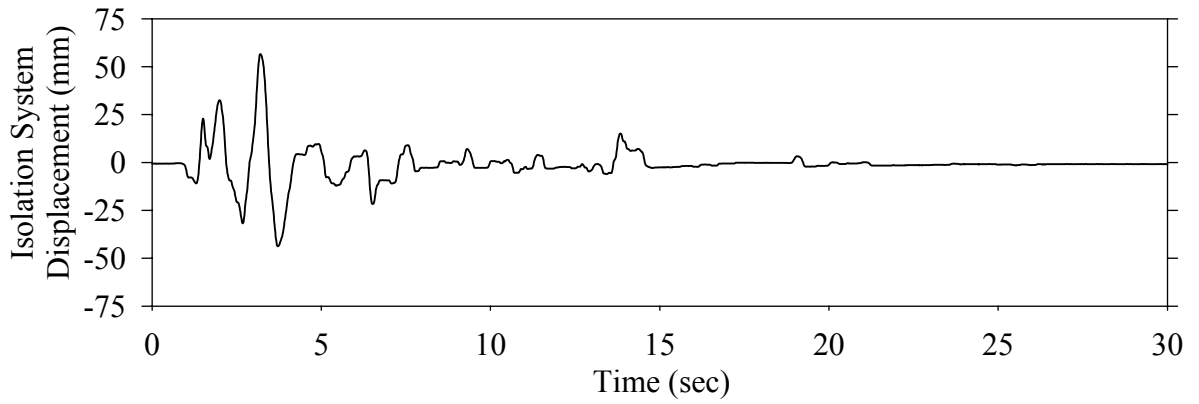
Test FPANS10.1, Northridge Sylmar 90° 100%, AB/FPS-NLD



Test FPANS10.1, Northridge Sylmar 90° 100%, AB/FPS-NLD

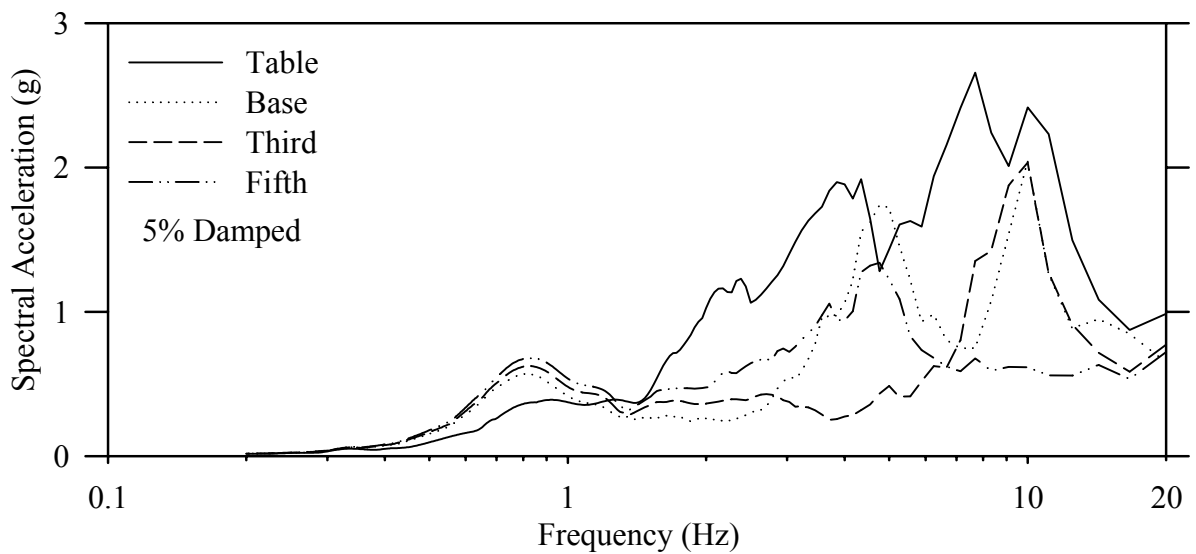
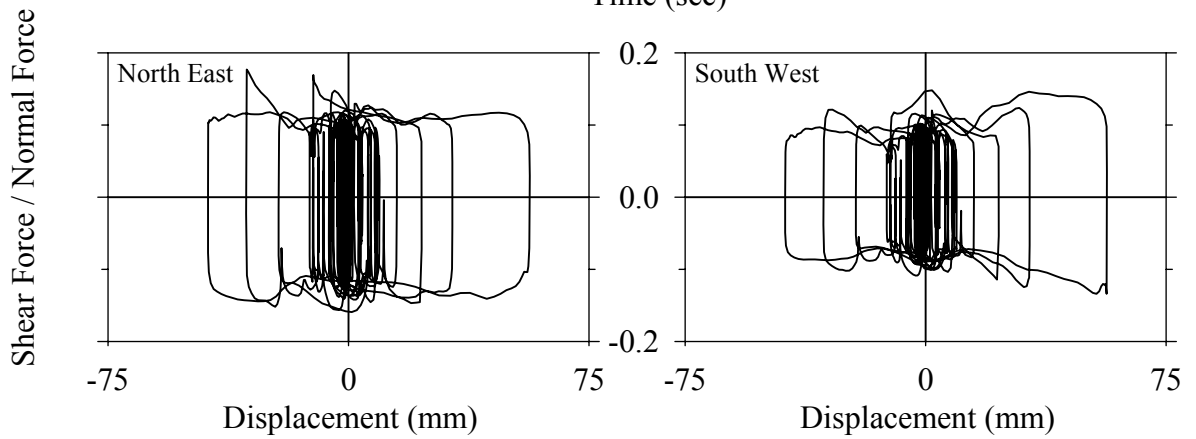
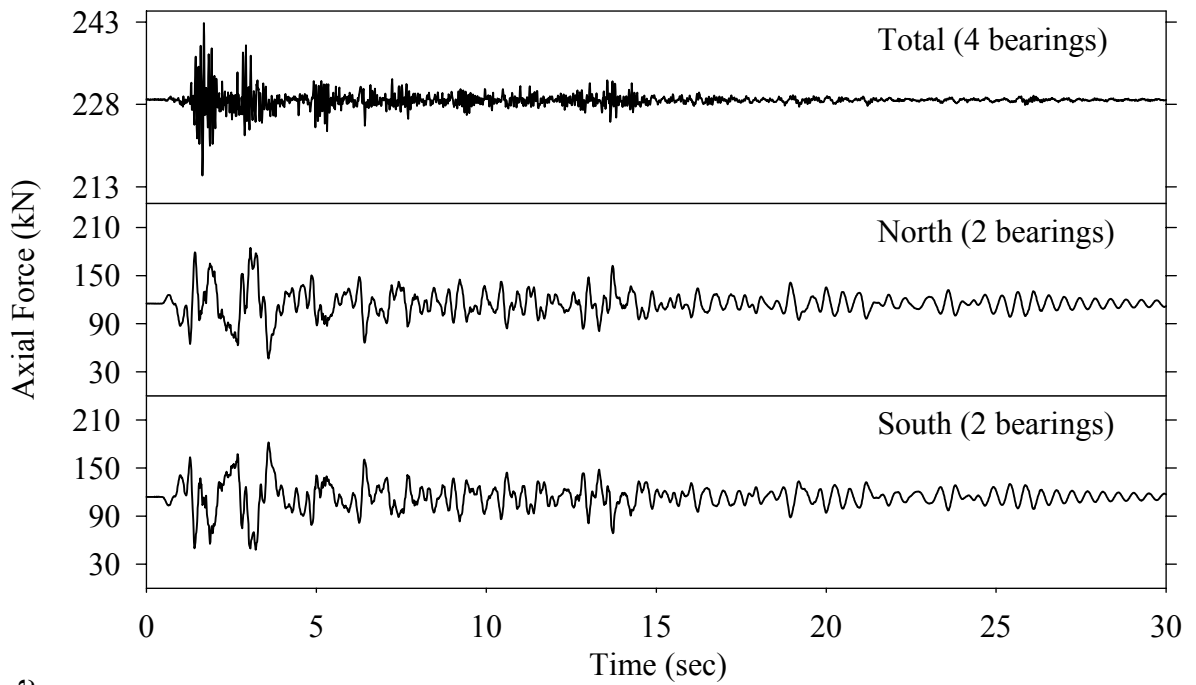


Test EFMFE20.1, El Centro S00E 200%, MF/Flat Sliding + Elastomeric

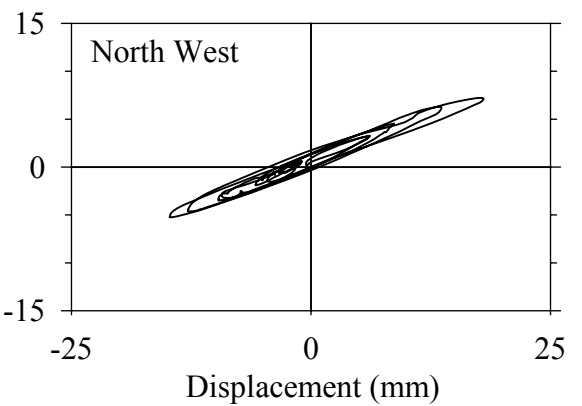
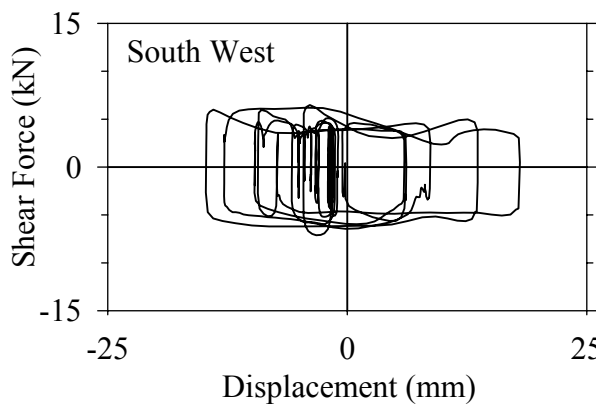
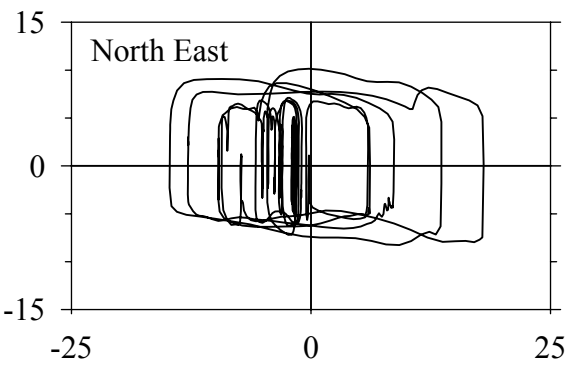
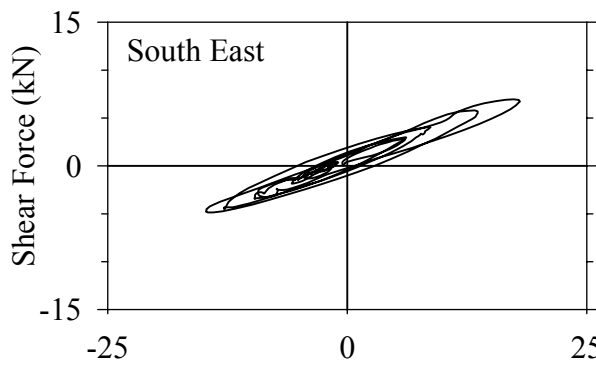
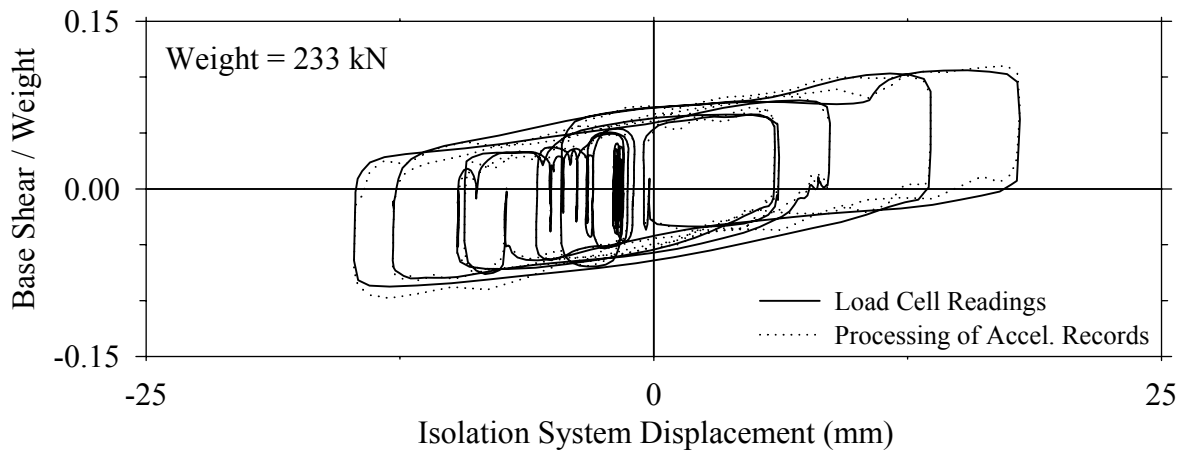
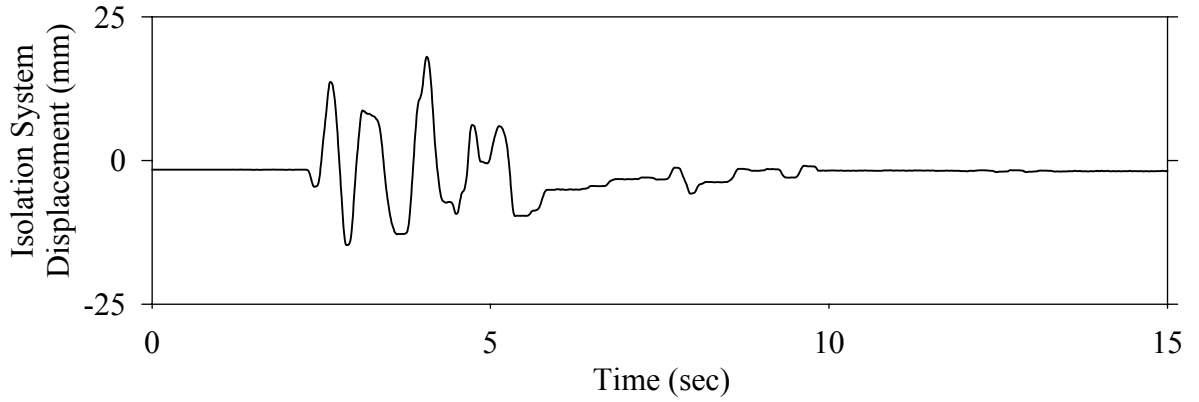




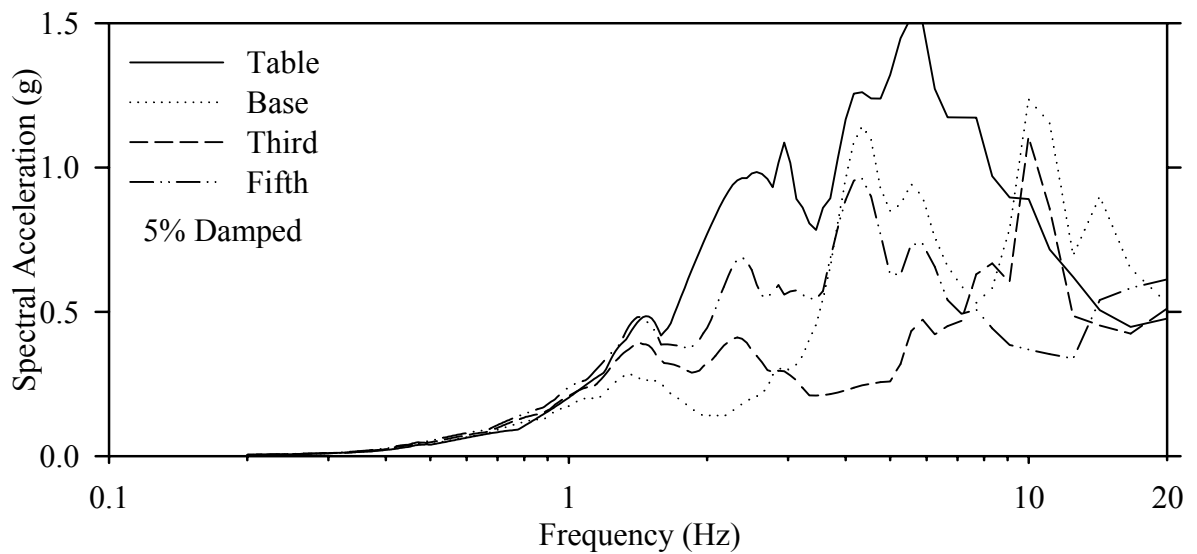
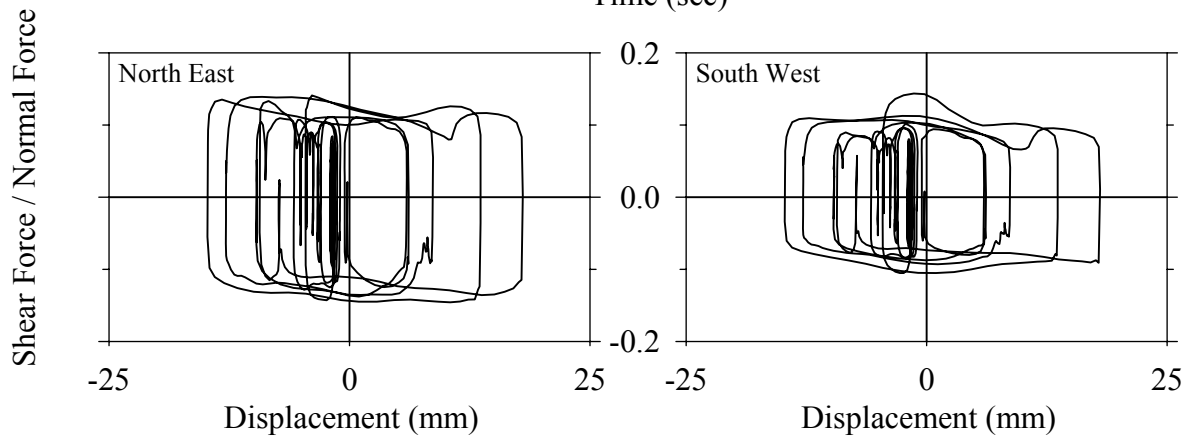
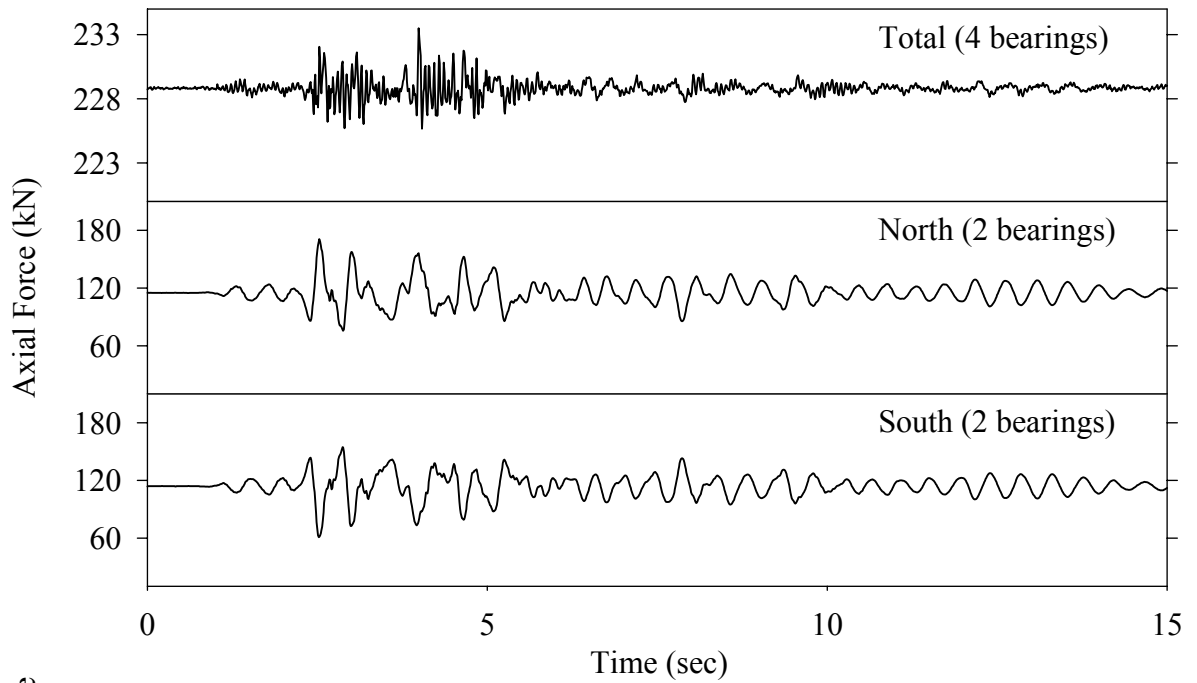
Test EFMFE20.1, El Centro S00E 200%, MF/Flat Sliding + Elastomeric



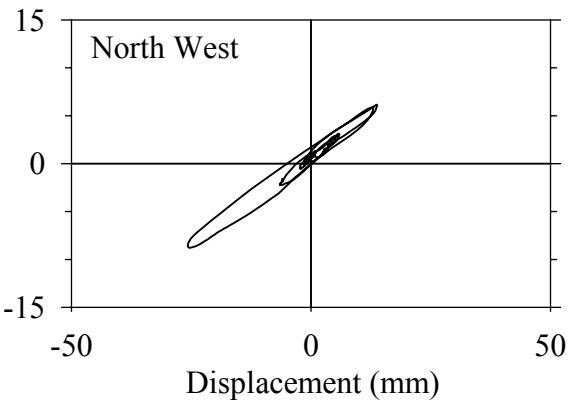
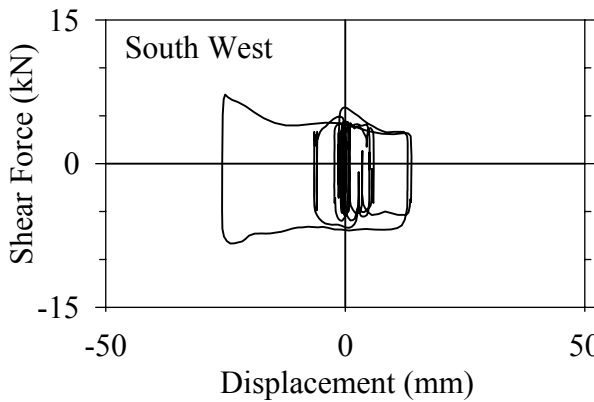
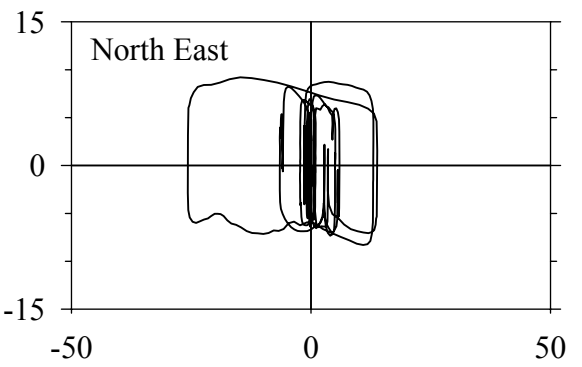
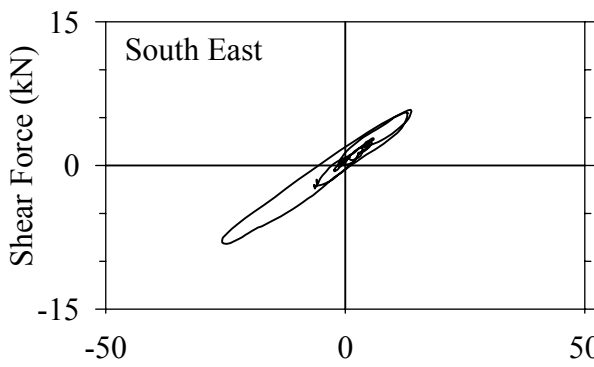
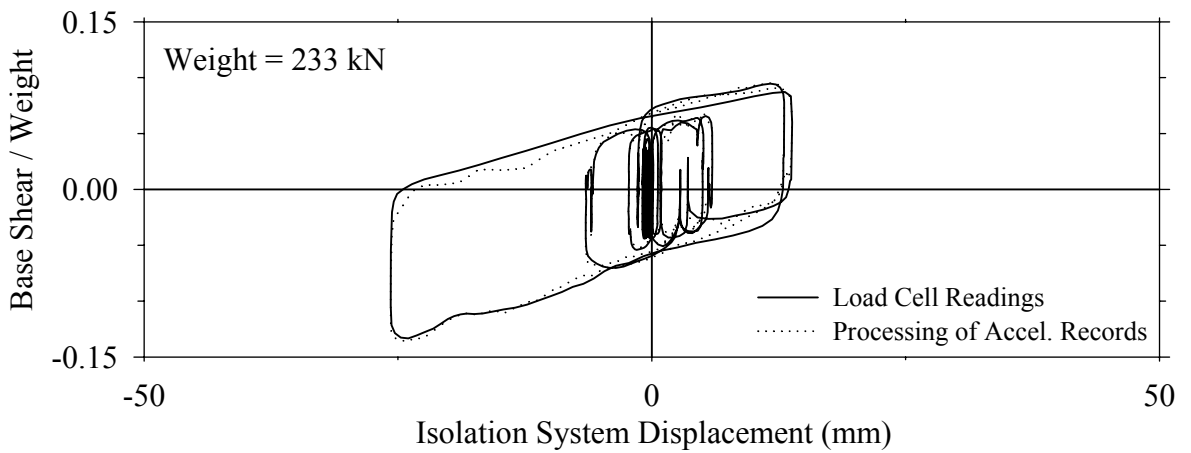
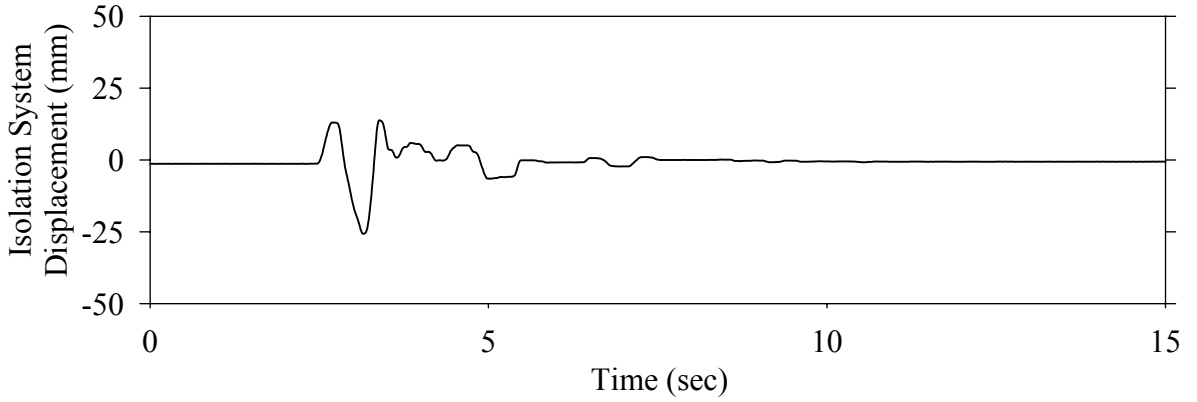
Test EFMFK50.1, Kobe N-S 50%, MF/Flat Sliding + Elastomeric



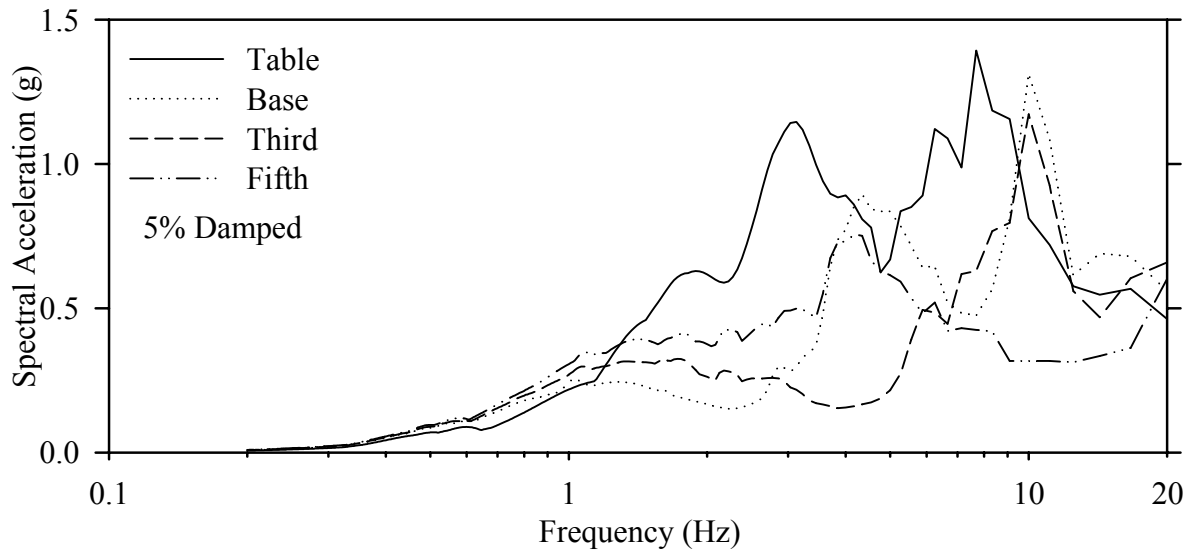
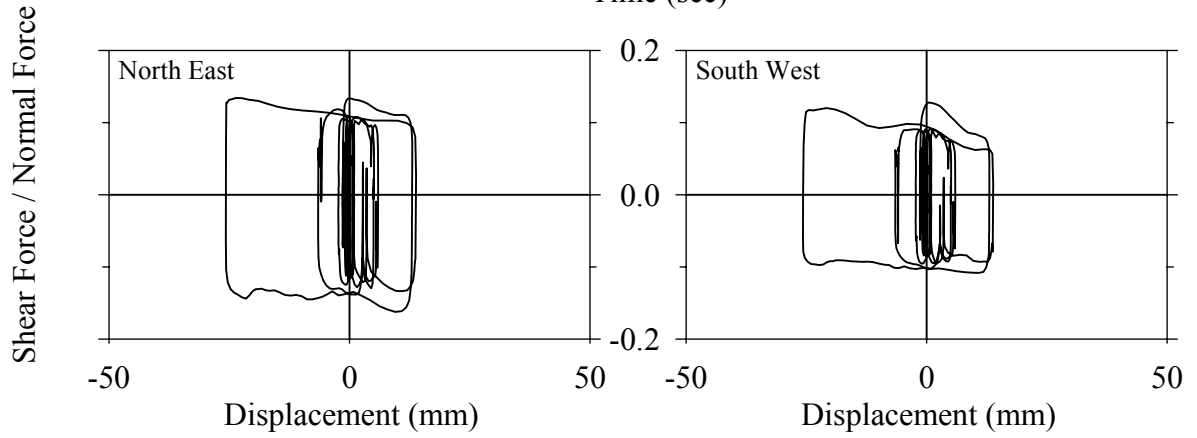
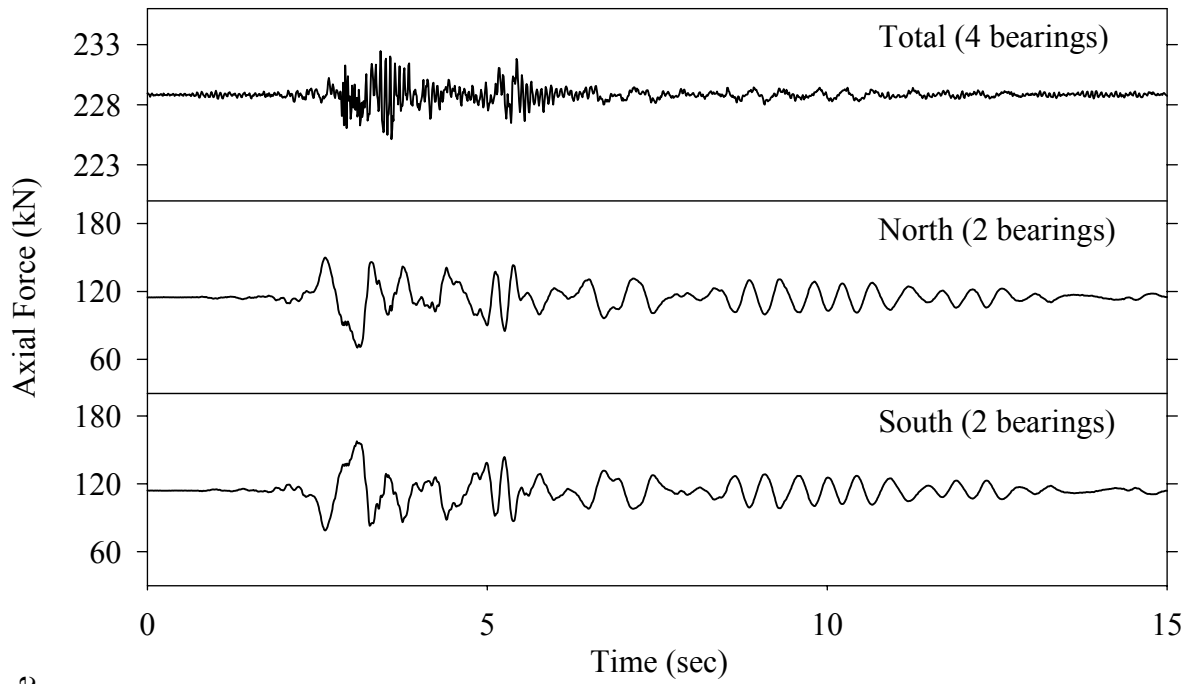
Test EFMFK50.1, Kobe N-S 50%, MF/Flat Sliding + Elastomeric



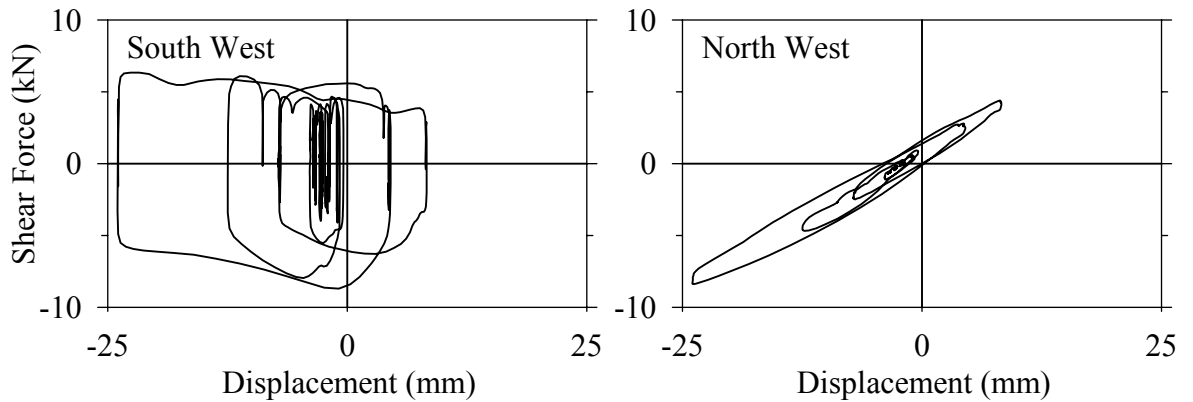
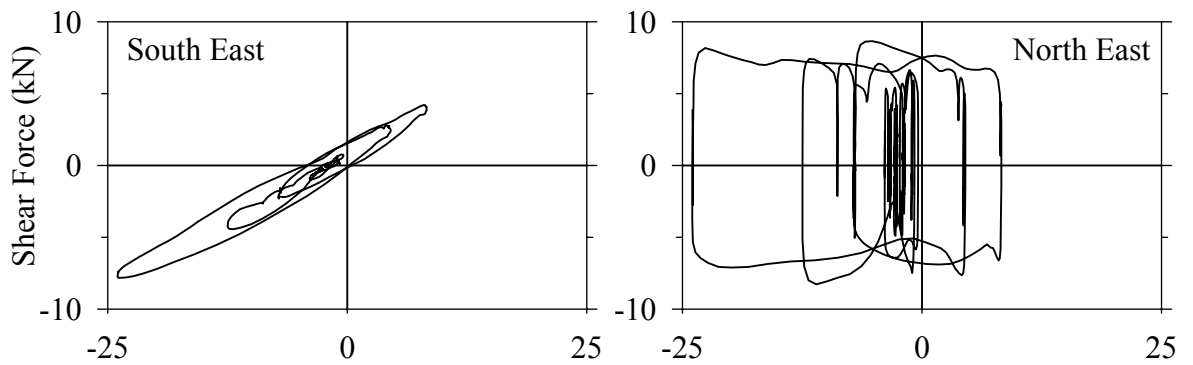
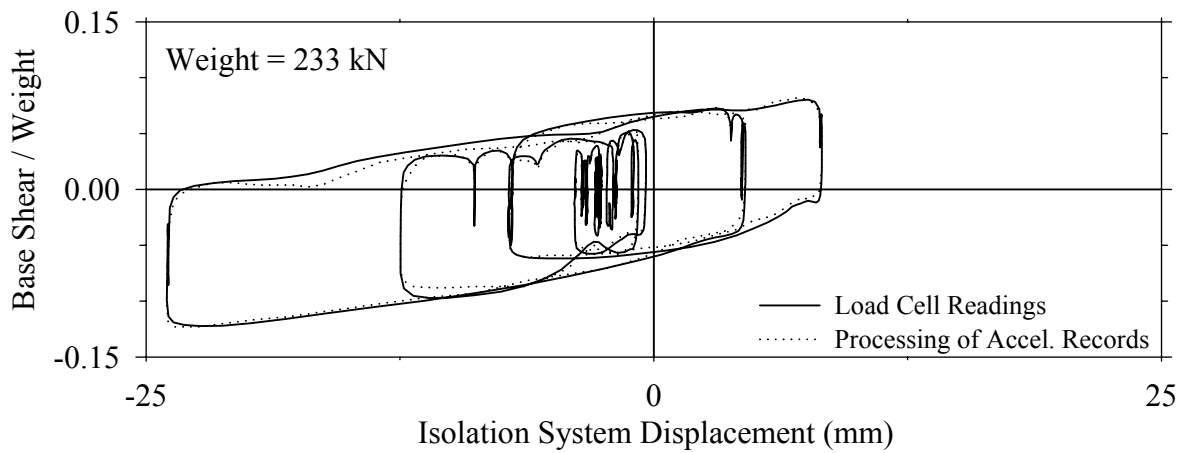
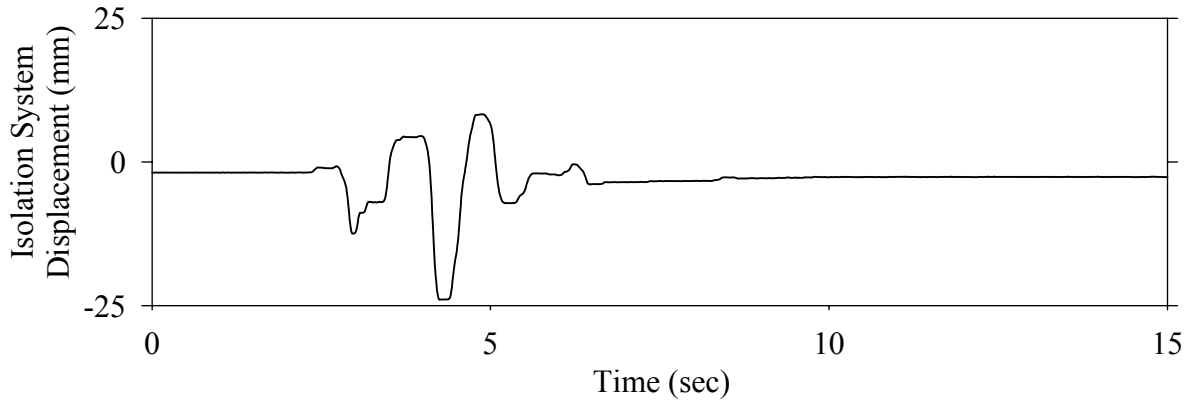
Test EFMFN50.1, Northridge Newhall 360° 50%, MF/Flat Sliding + Elastomeric



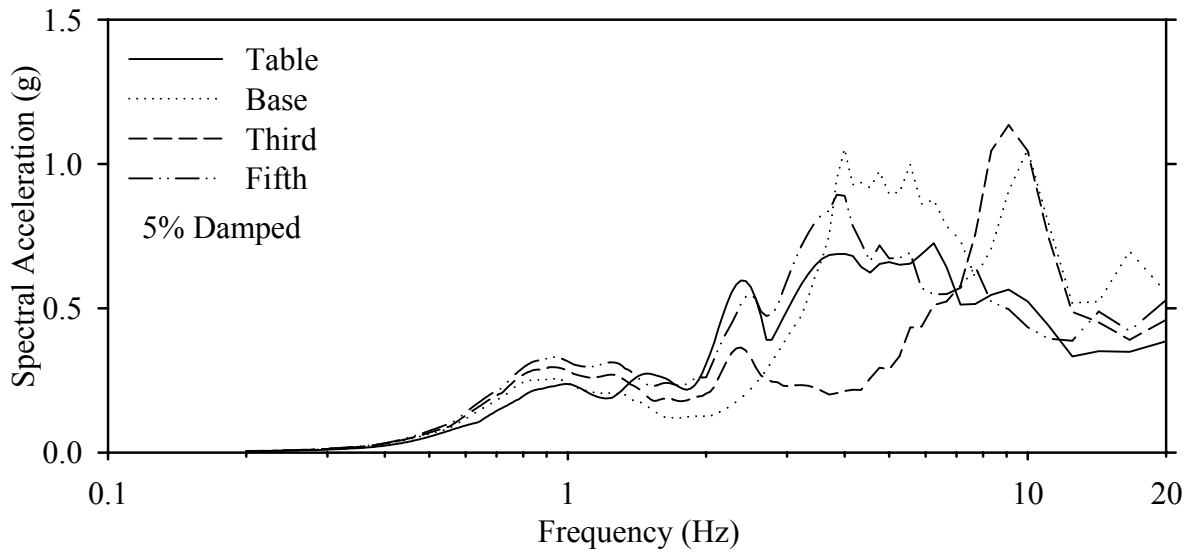
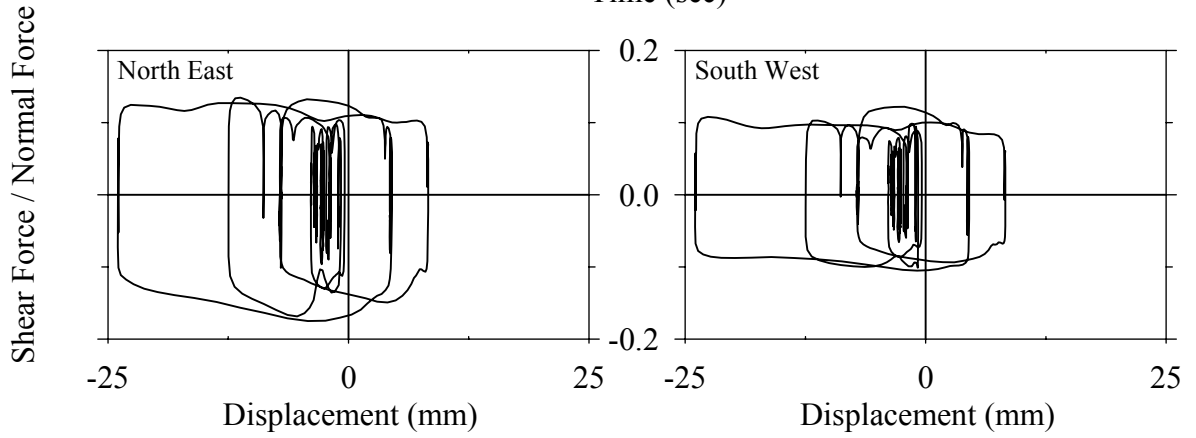
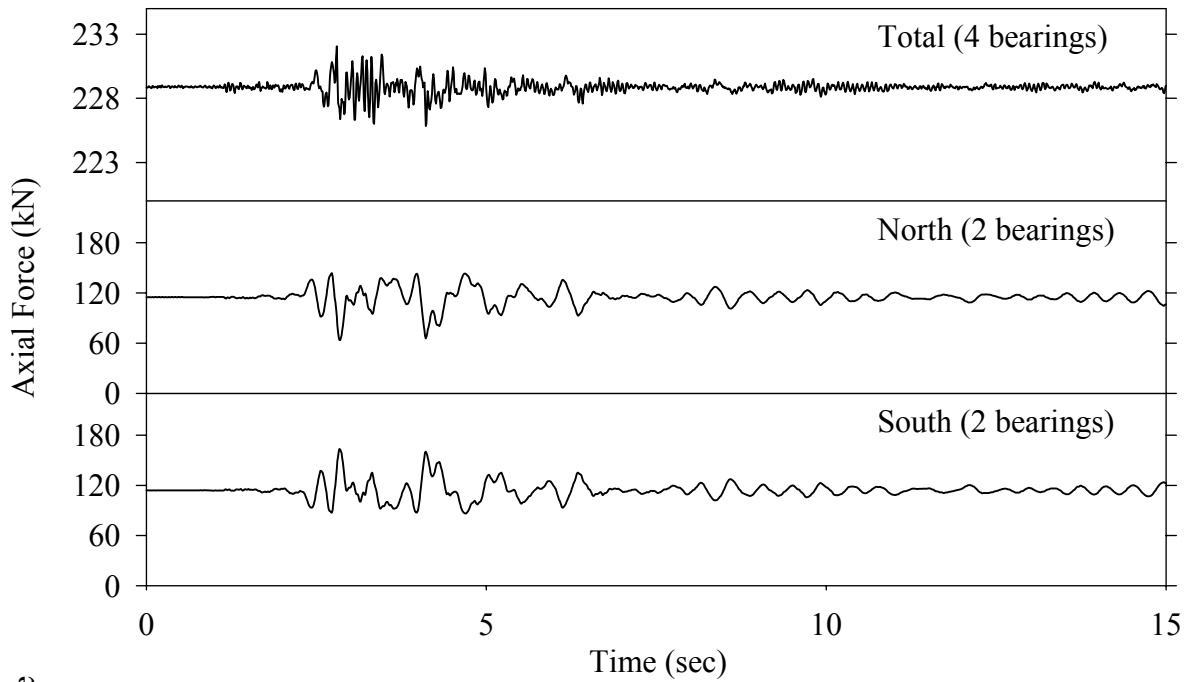
Test EFMFN50.1, Northridge Newhall 360° 50%, MF/Flat Sliding + Elastomeric



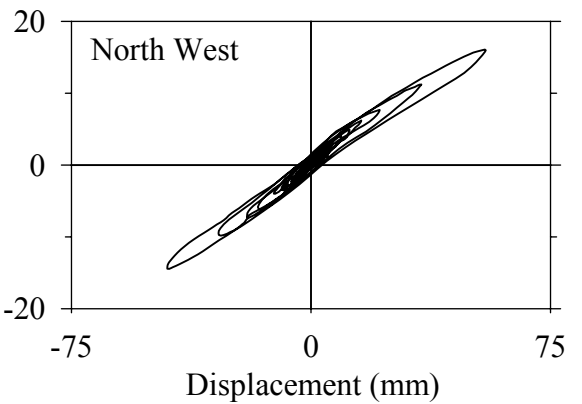
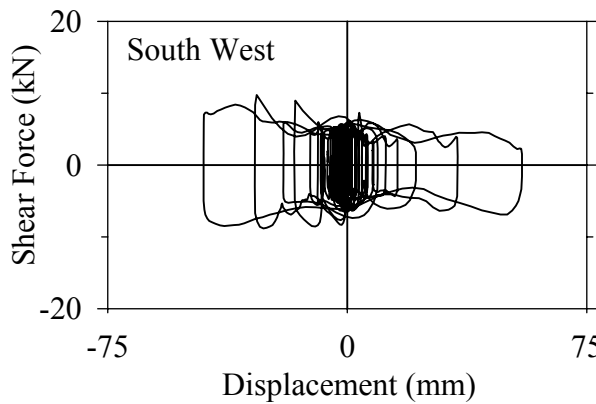
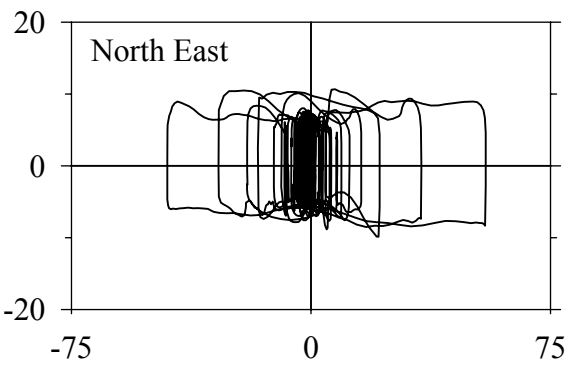
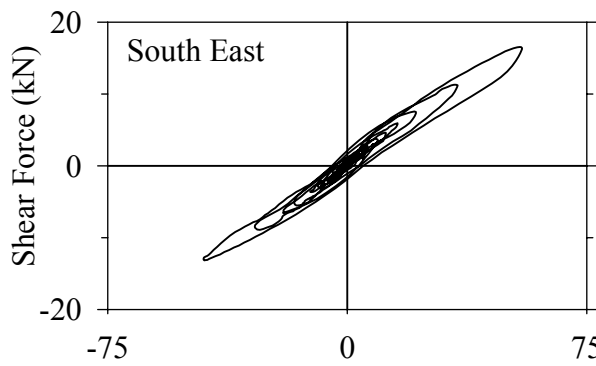
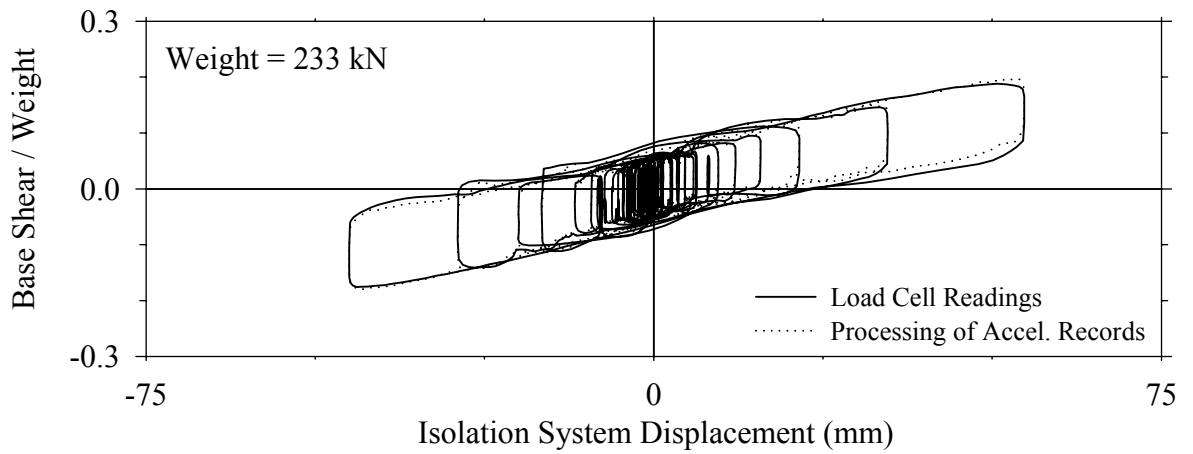
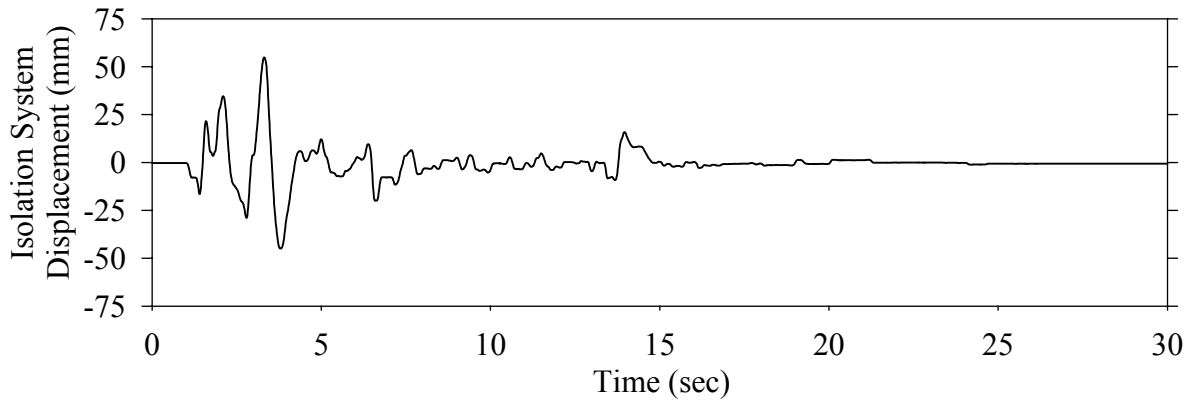
Test EFMFS50.1, Northridge Sylmar 90° 50%, MF/Flat Sliding + Elastomeric



Test EFMFS50.1, Northridge Sylmar 90° 50%, MF/Flat Sliding + Elastomeric

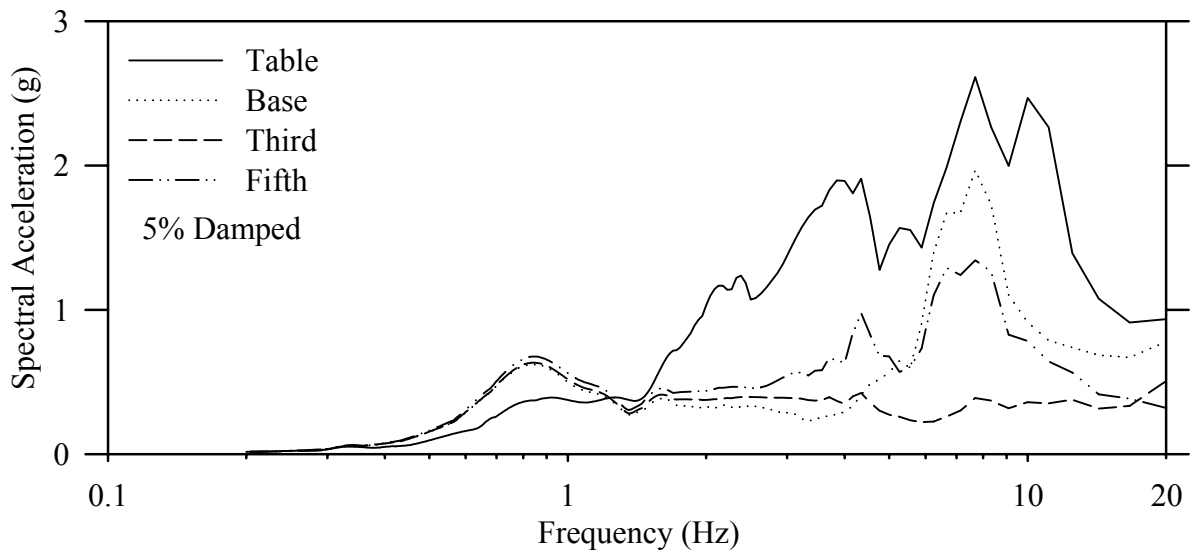
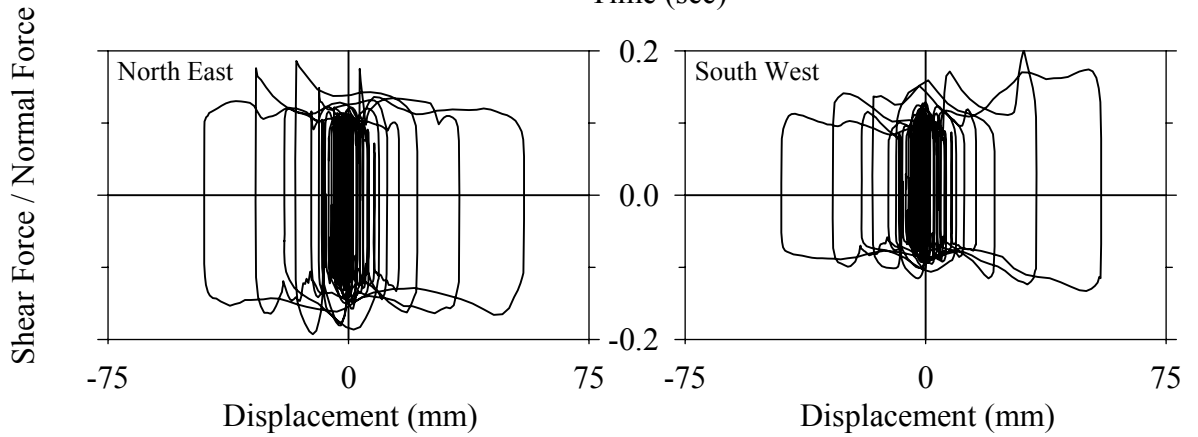
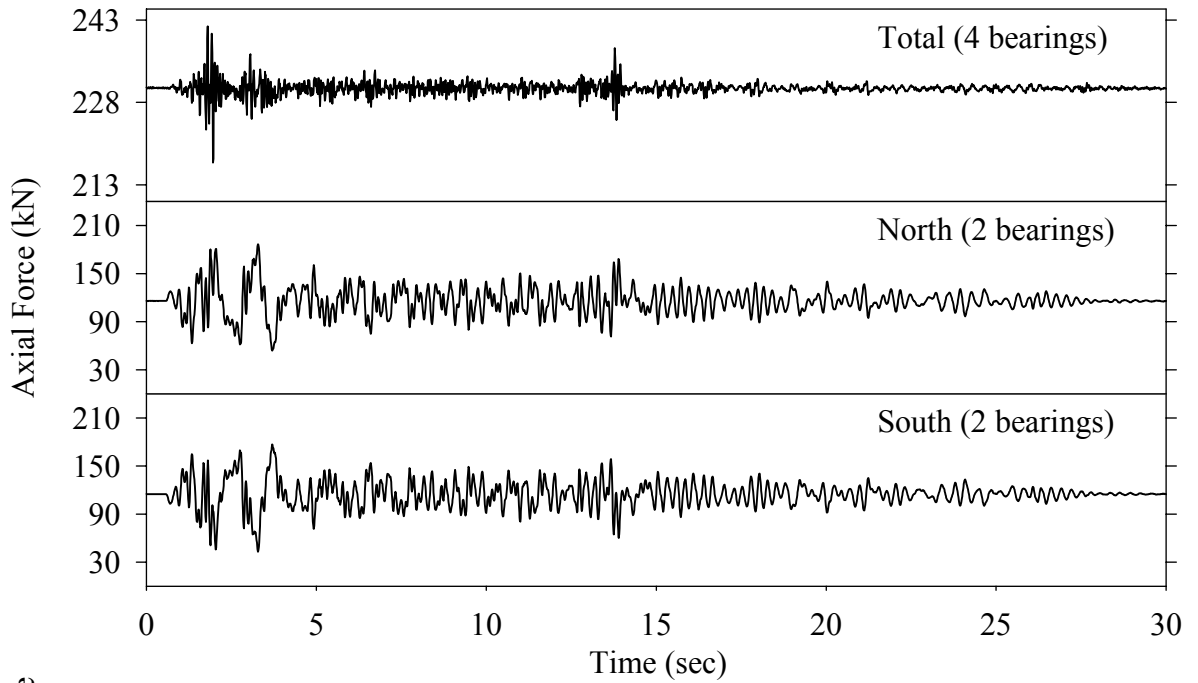


Test EFSBE20.1, El Centro S00E 200%, SB/Flat Sliding + Elastomeric

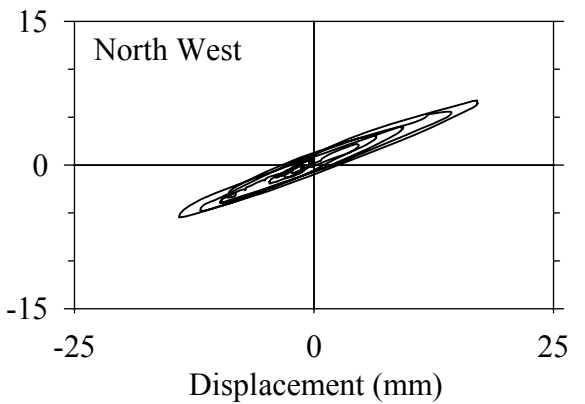
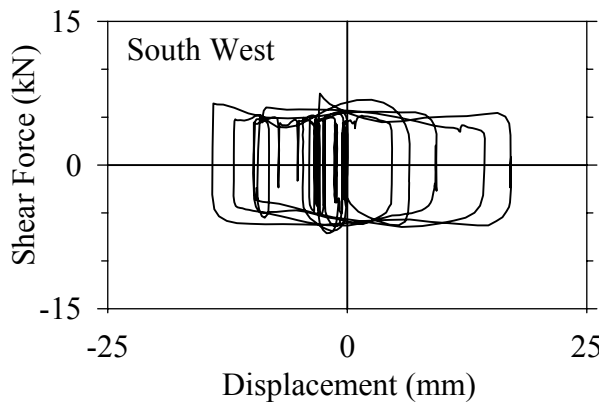
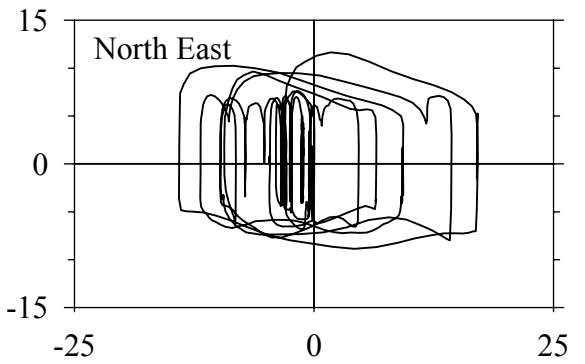
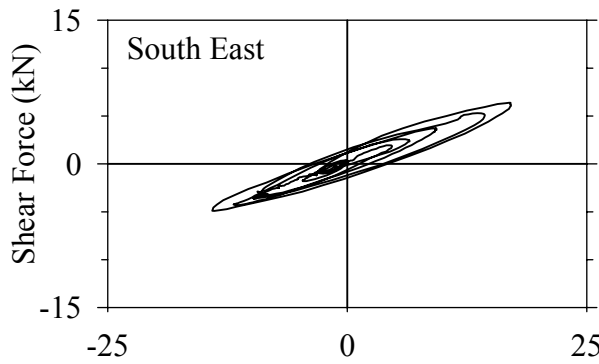
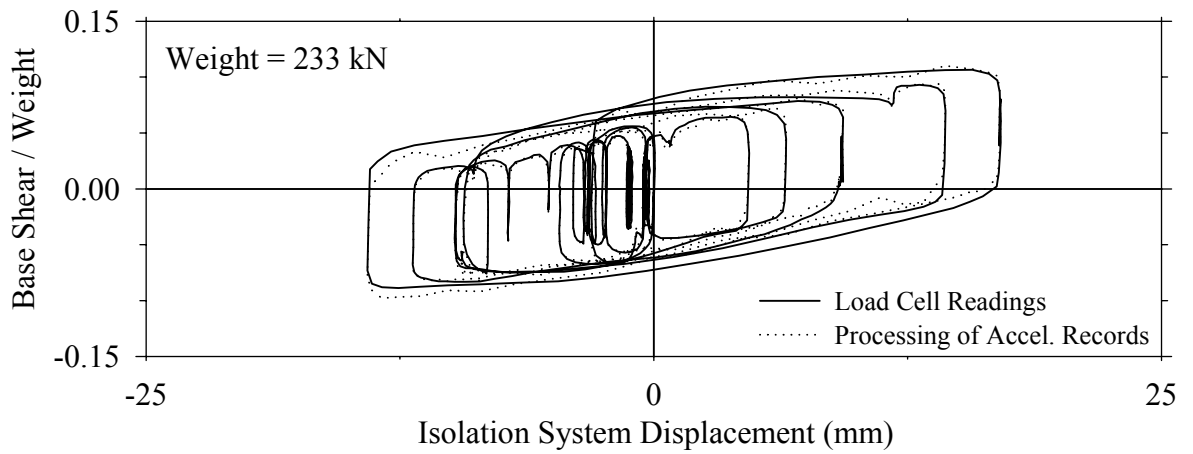
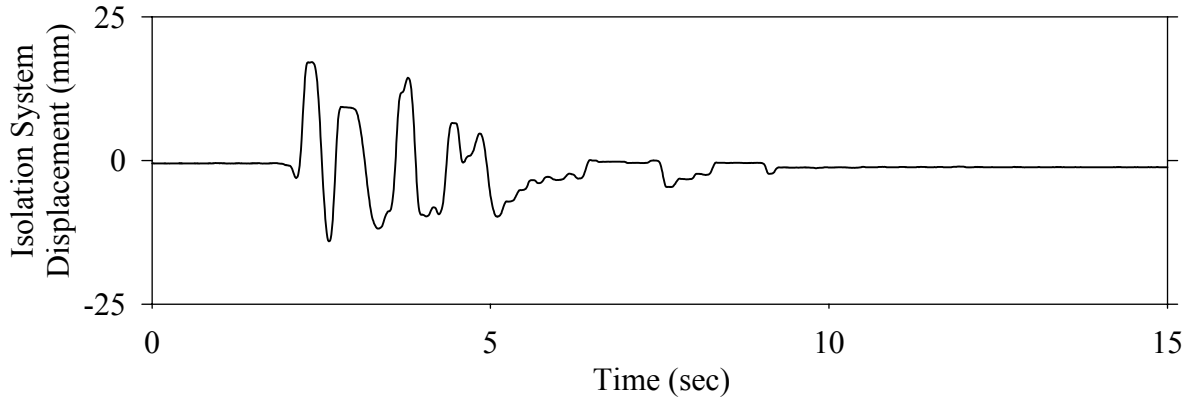




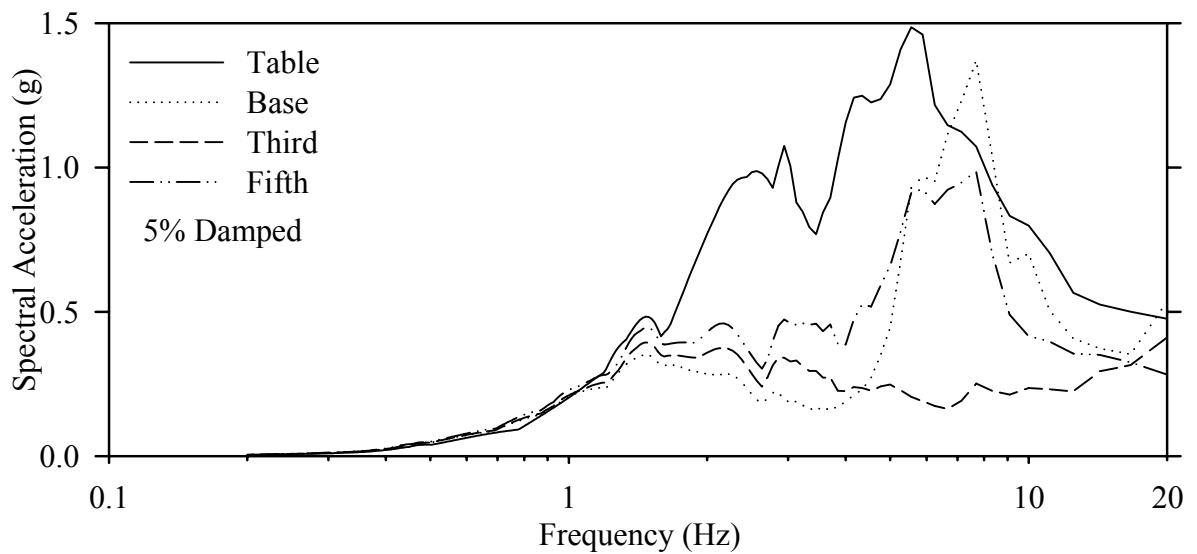
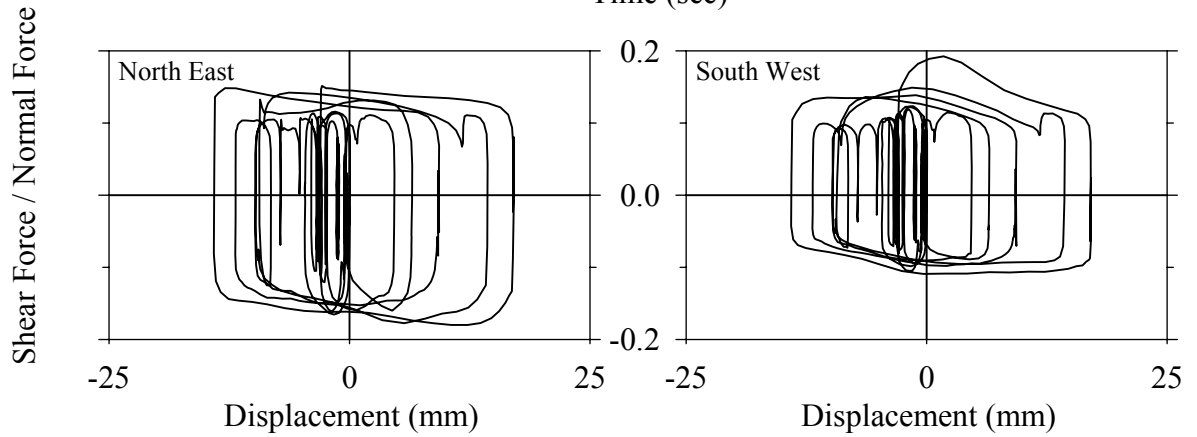
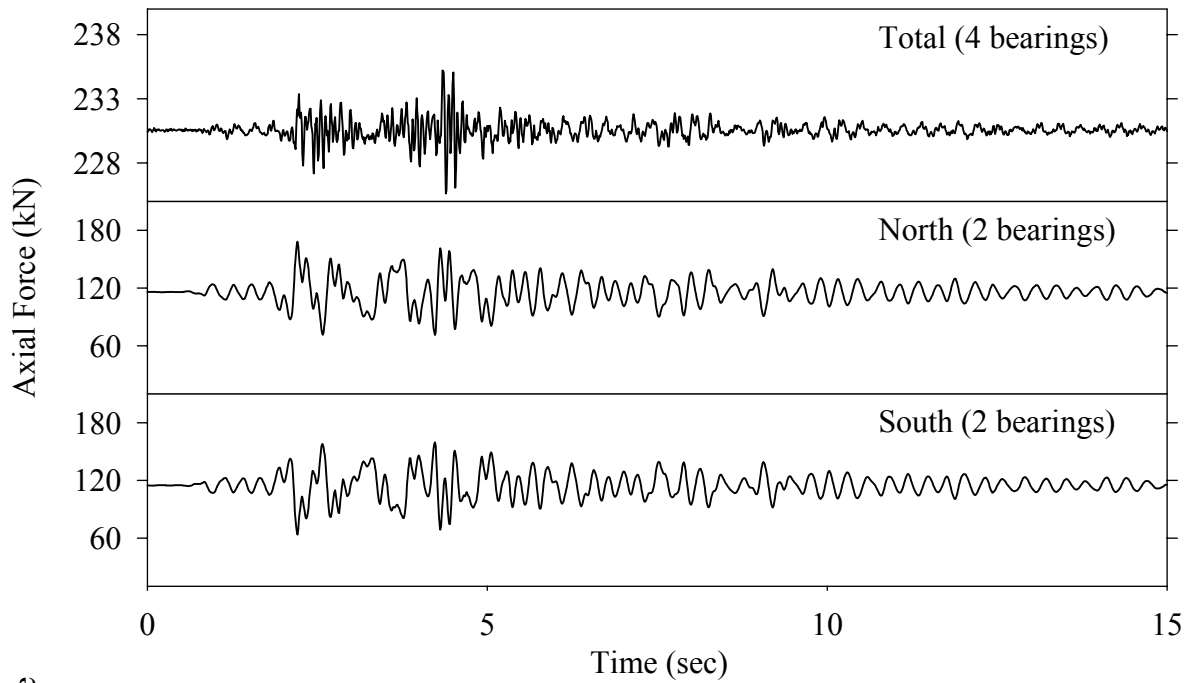
Test EFSBE20.1, El Centro S00E 200%, SB/Flat Sliding + Elastomeric



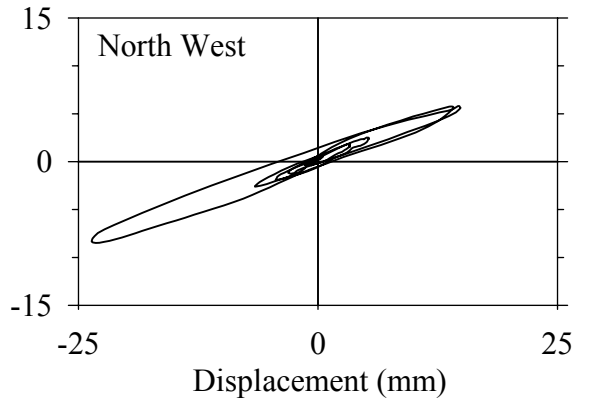
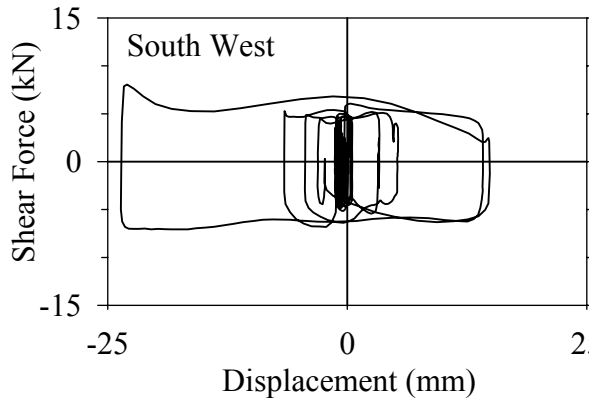
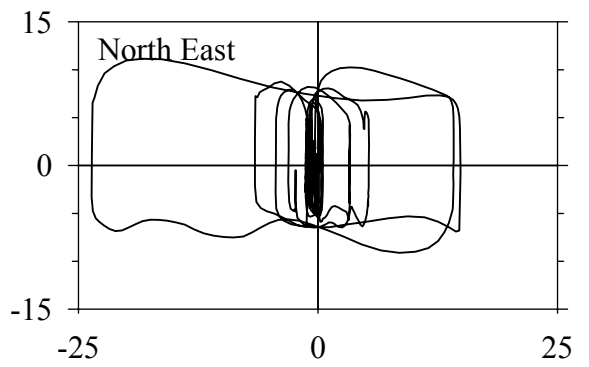
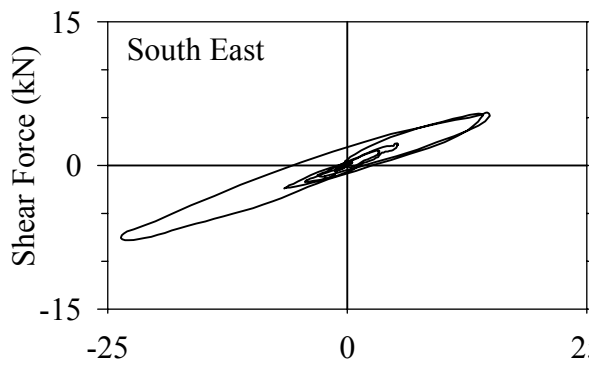
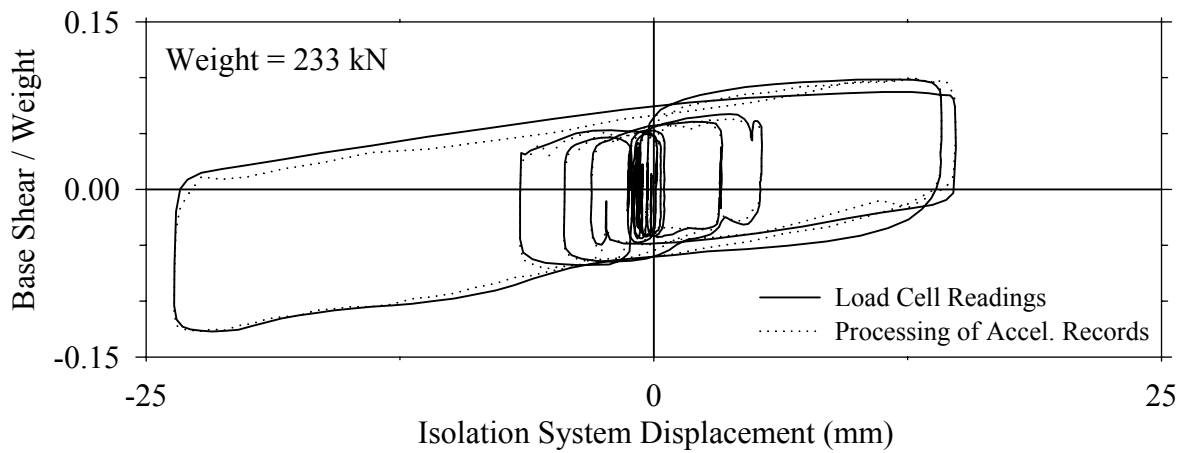
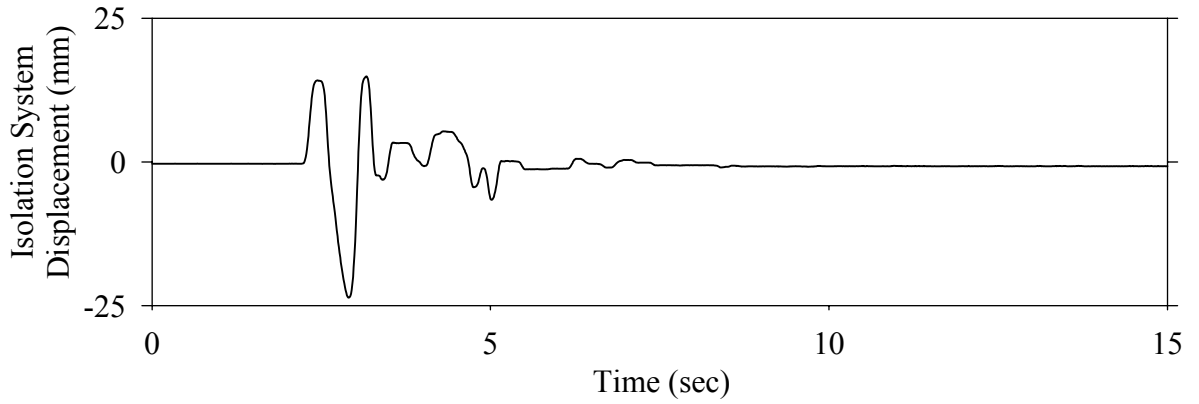
Test EFSBK50.1, Kobe N-S 50%, SB/Flat Sliding + Elastomeric



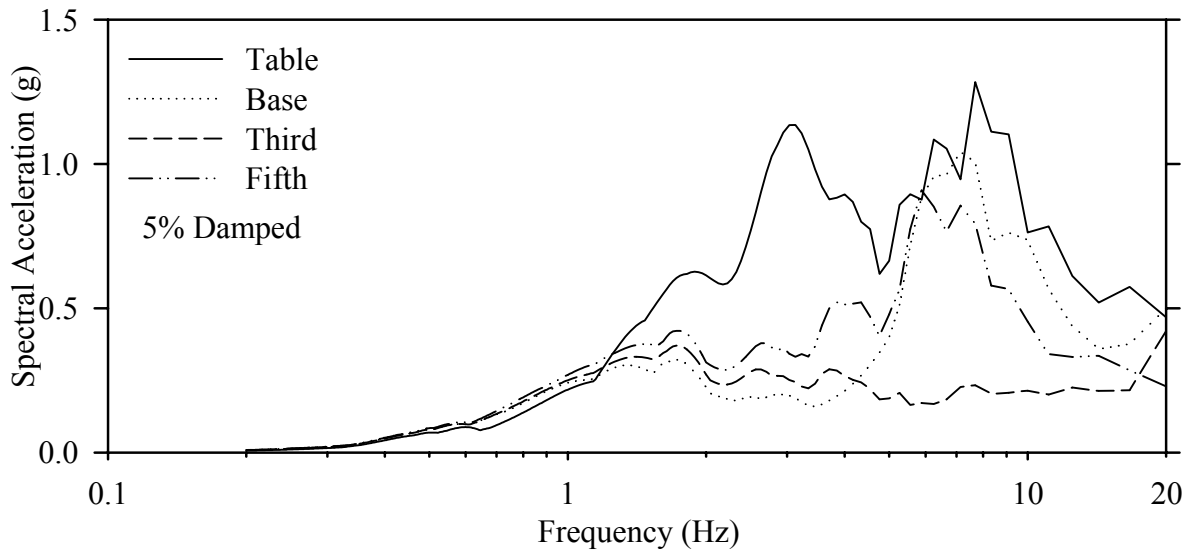
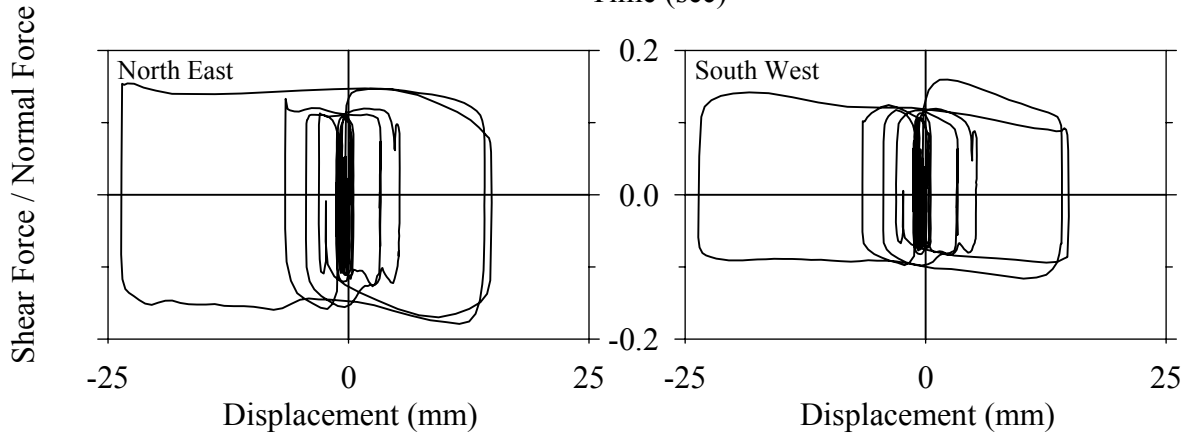
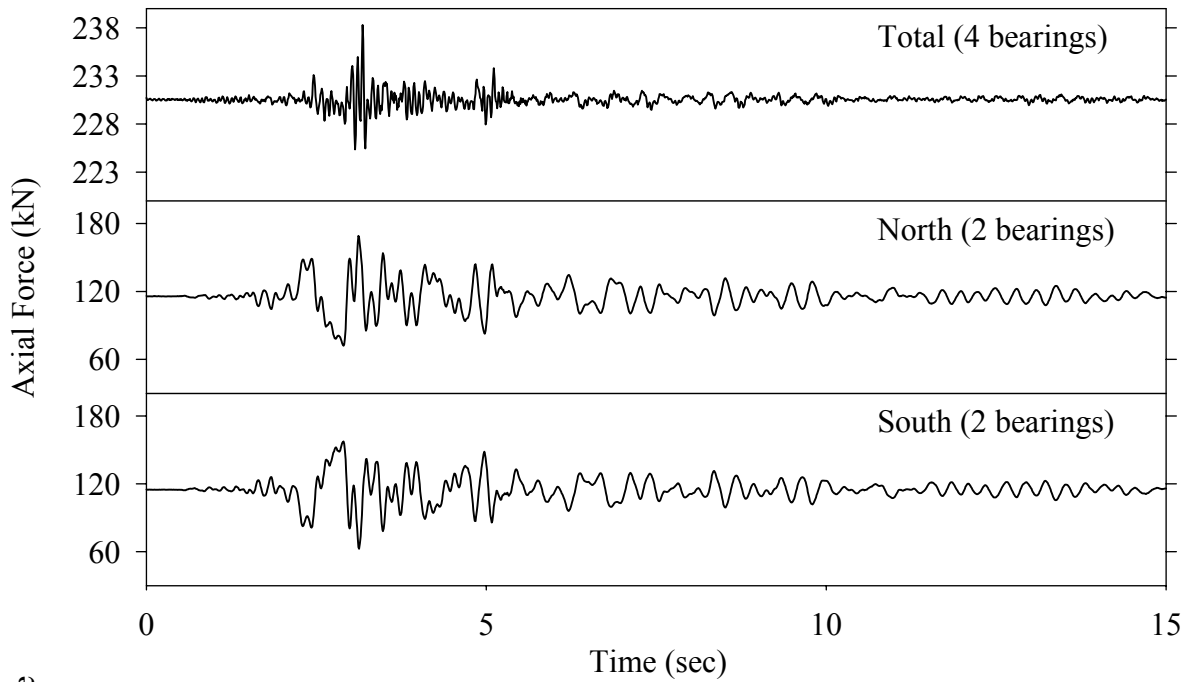
Test EFSBK50.1, Kobe N-S 50%, SB/Flat Sliding + Elastomeric



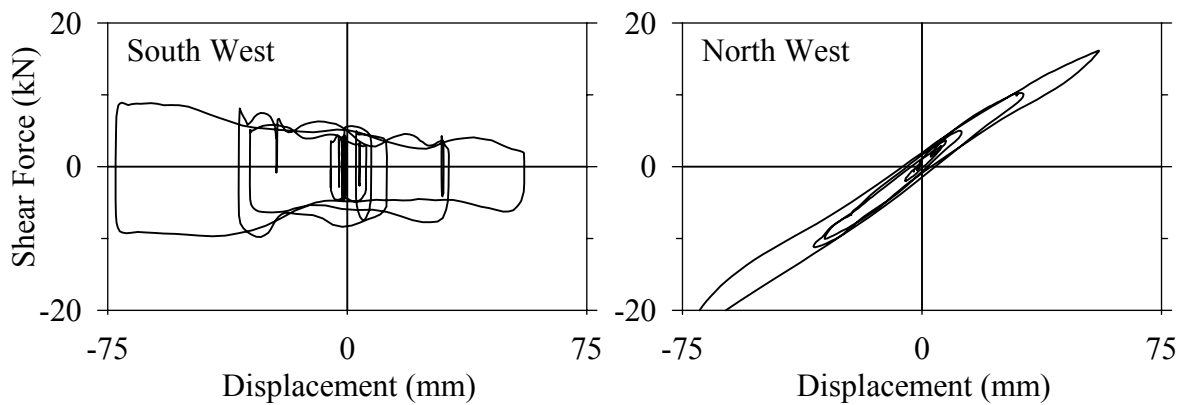
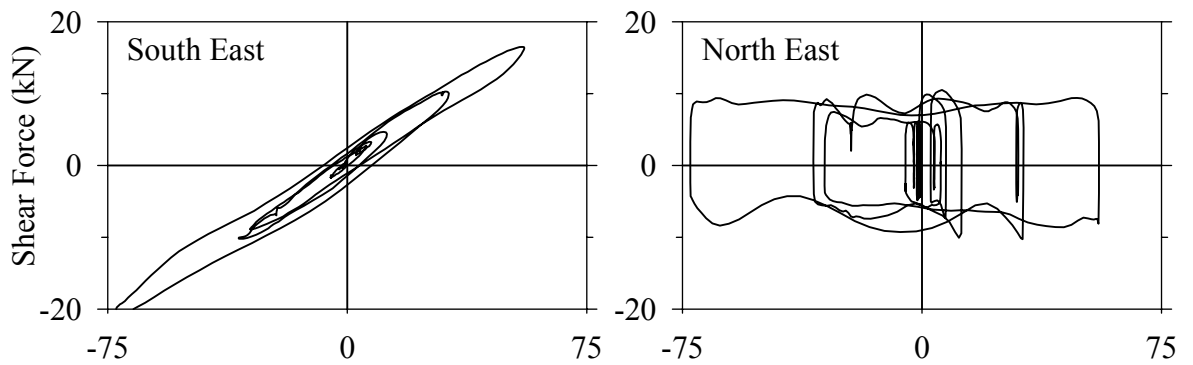
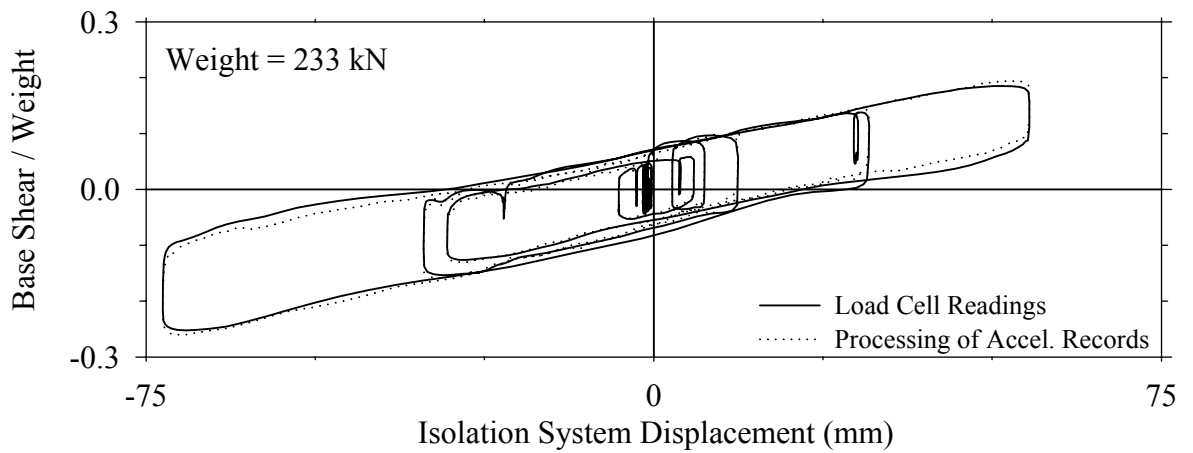
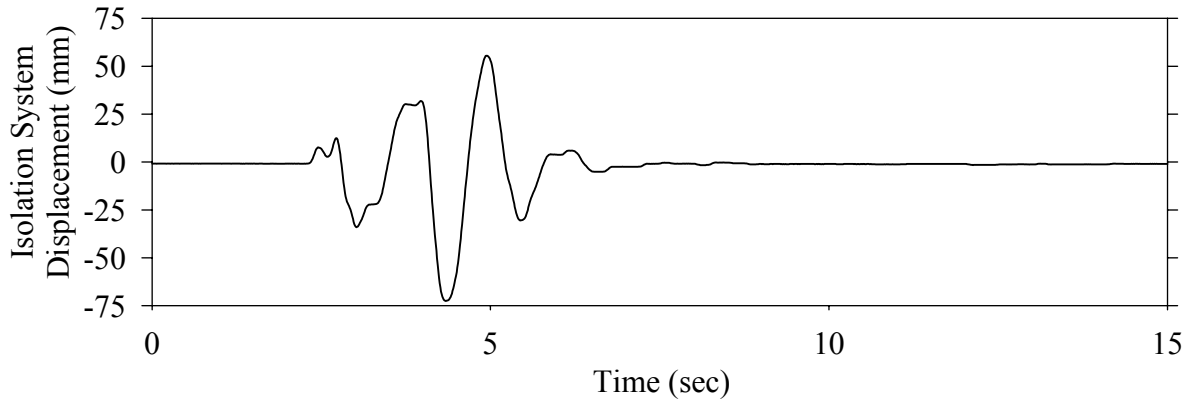
Test EFSBN50.1, Northridge Newhall 360° 50%, SB/Flat Sliding + Elastomeric



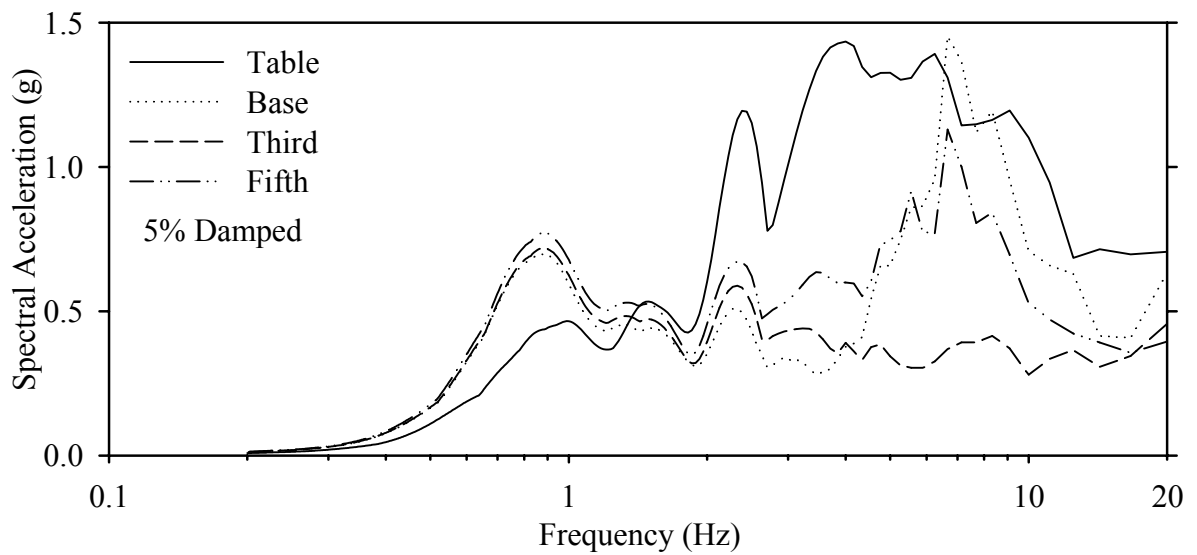
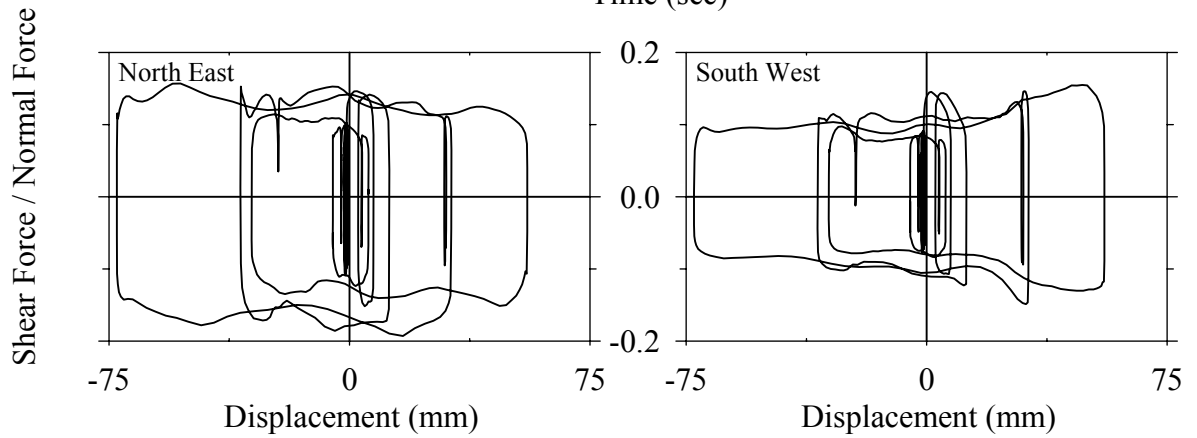
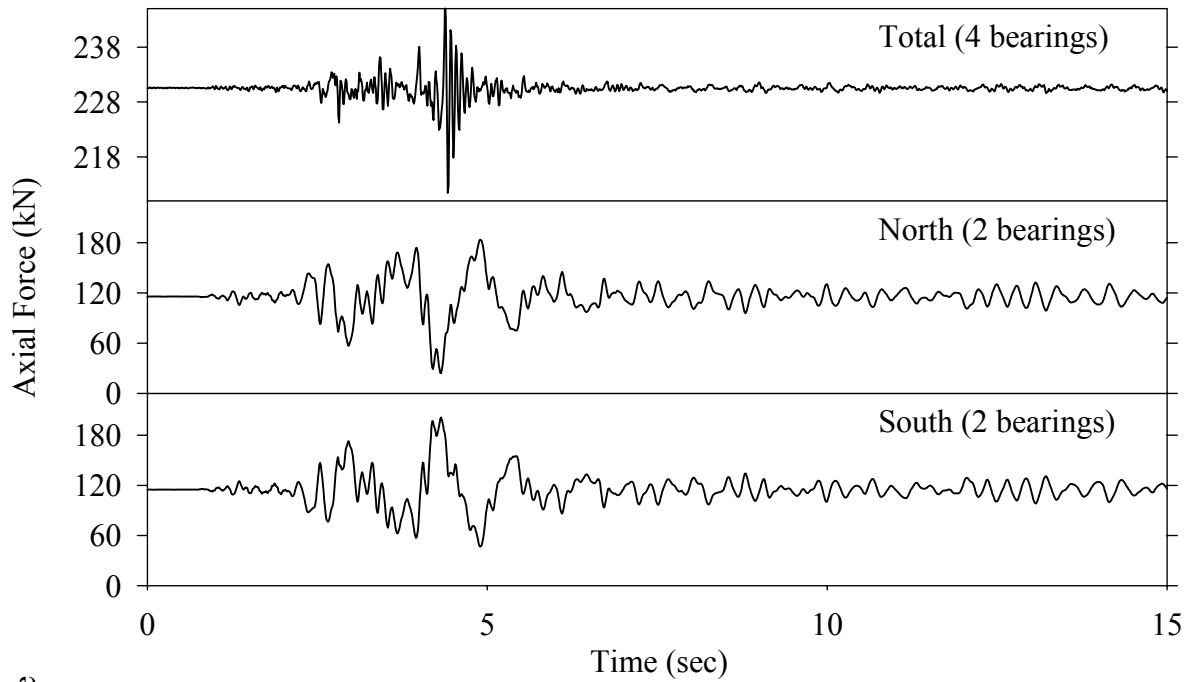
Test EFSBN50.1, Northridge Newhall 360° 50%, SB/Flat Sliding + Elastomeric



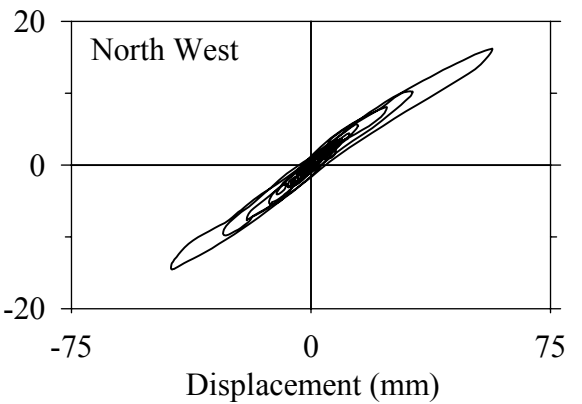
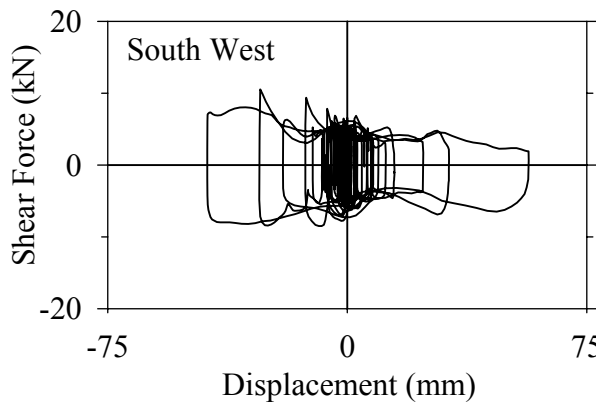
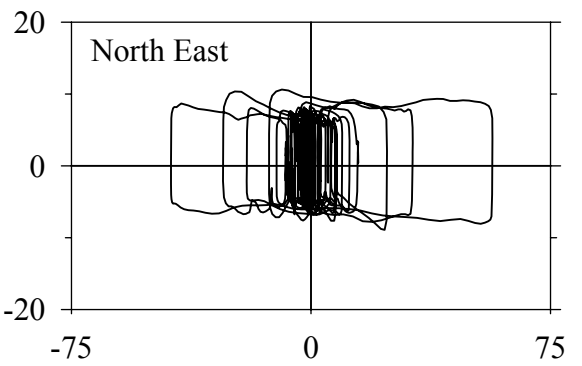
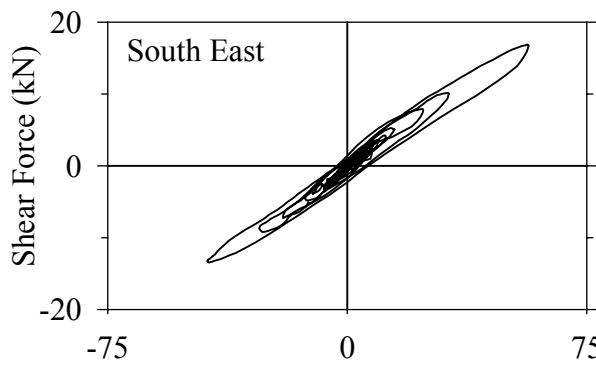
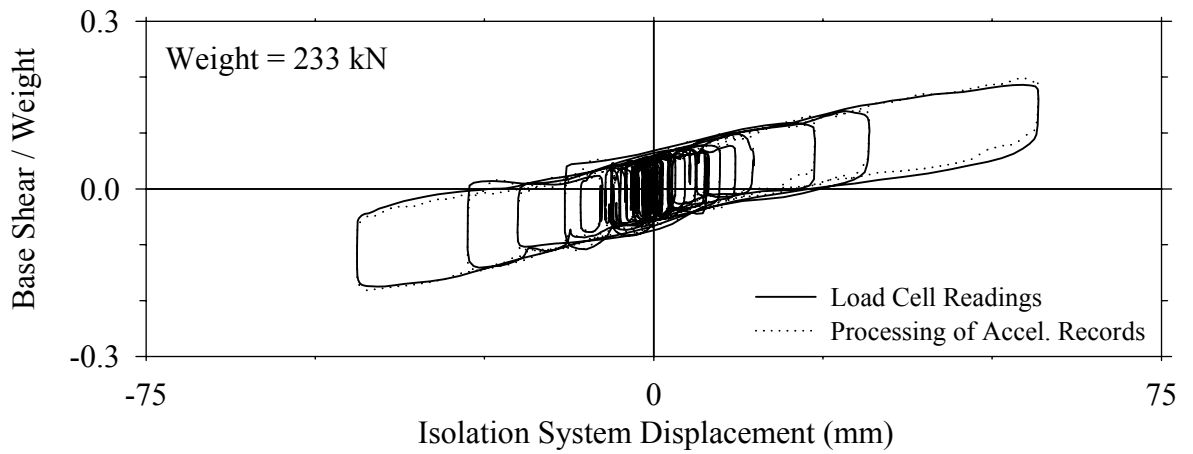
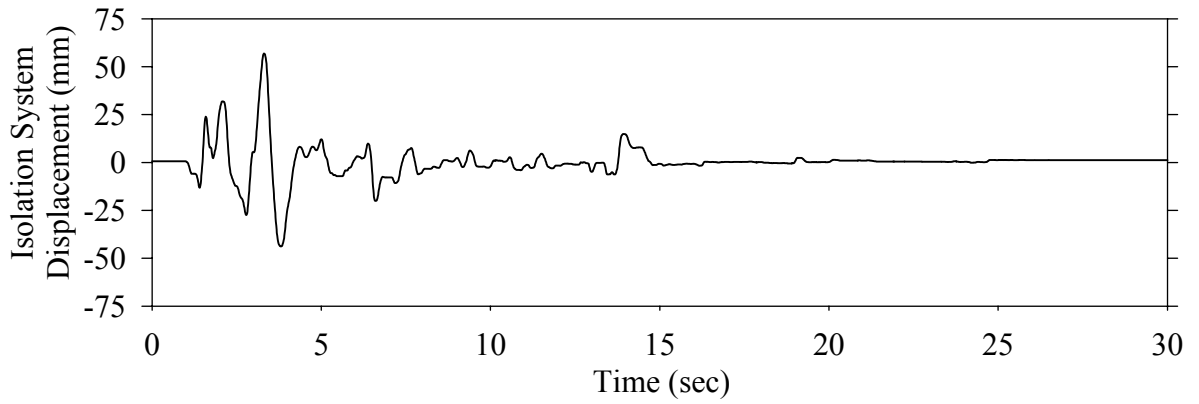
Test EFSBS10.1, Northridge Sylmar 90° 100%, SB/Flat Sliding + Elastomeric



Test EFSBS10.1, Northridge Sylmar 90° 100%, SB/Flat Sliding + Elastomeric

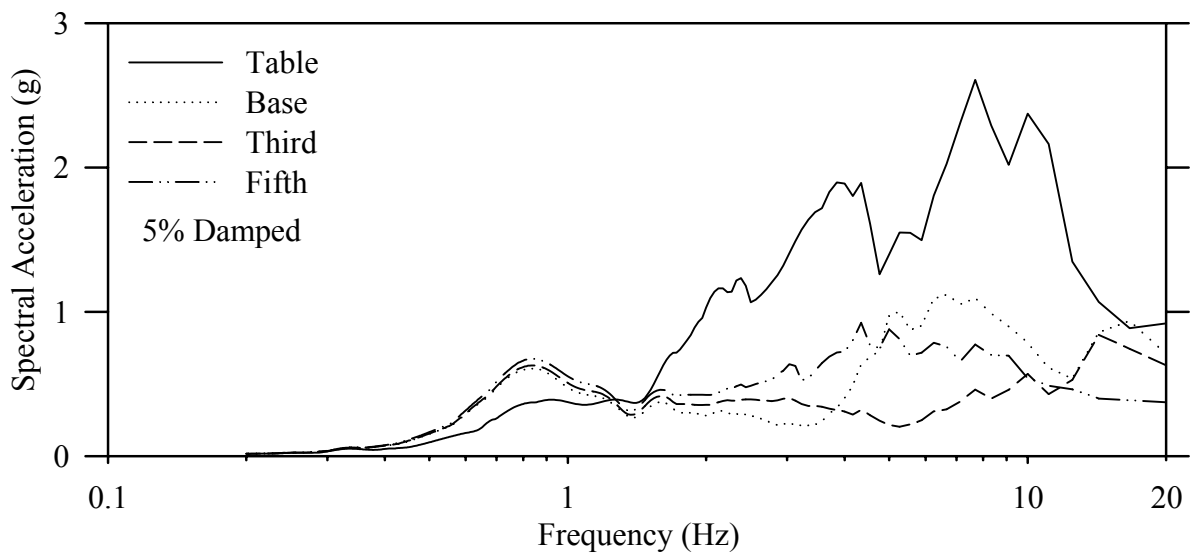
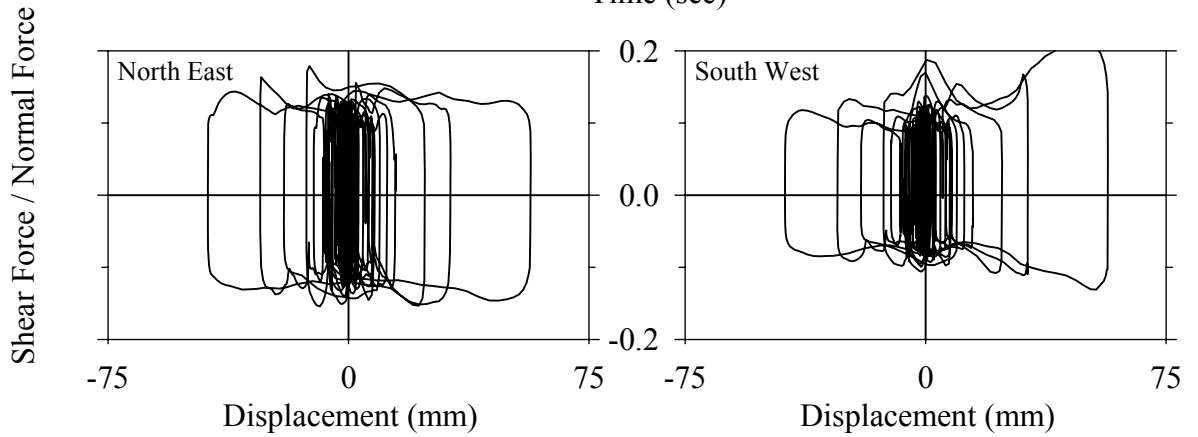
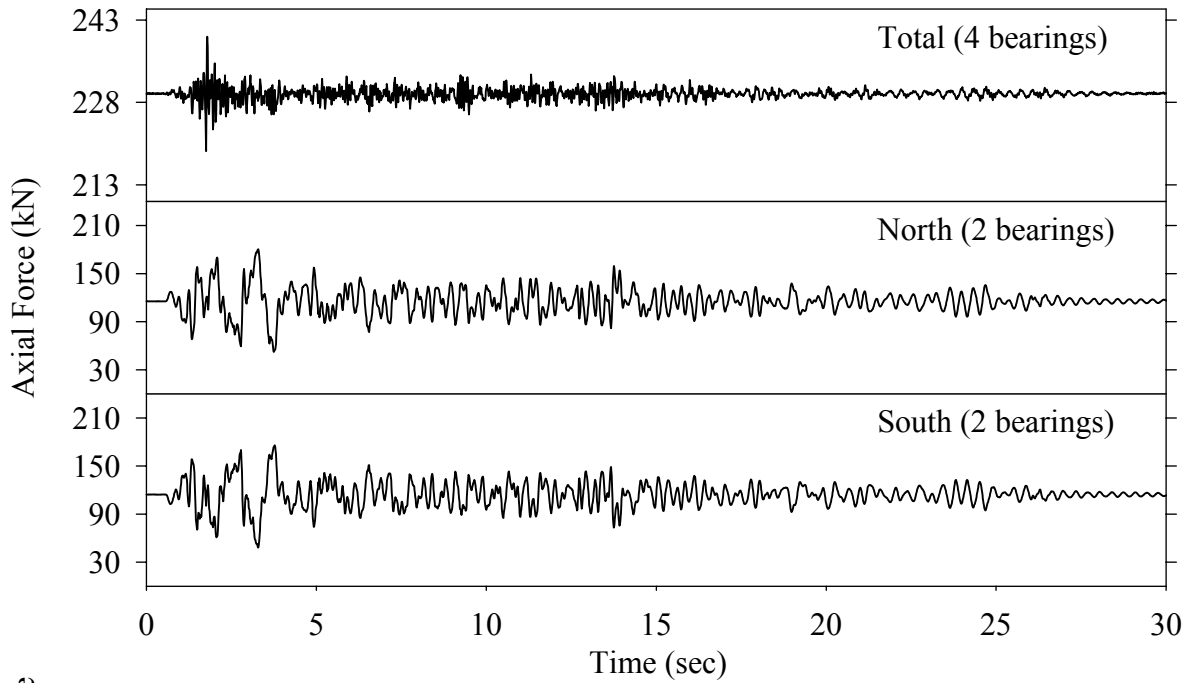


Test EFABE20.1, El Centro S00E 200%, AB/Flat Sliding + Elastomeric

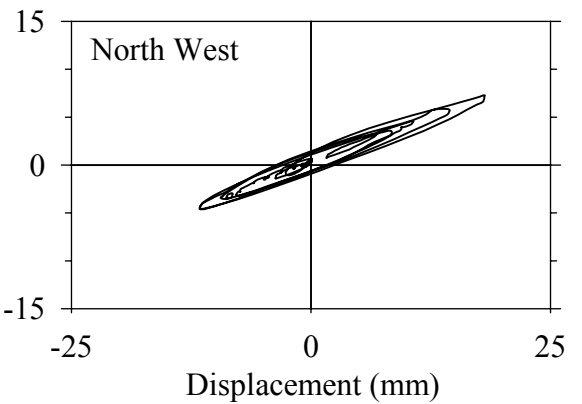
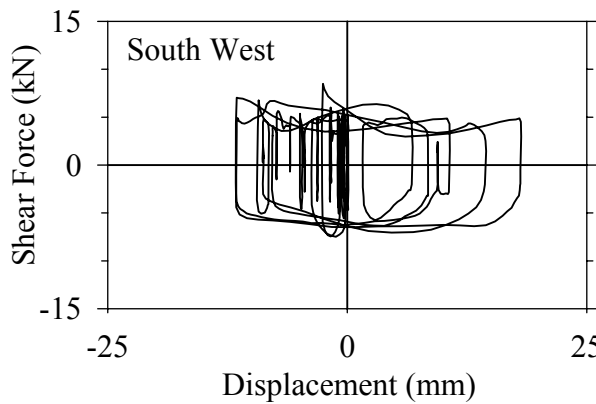
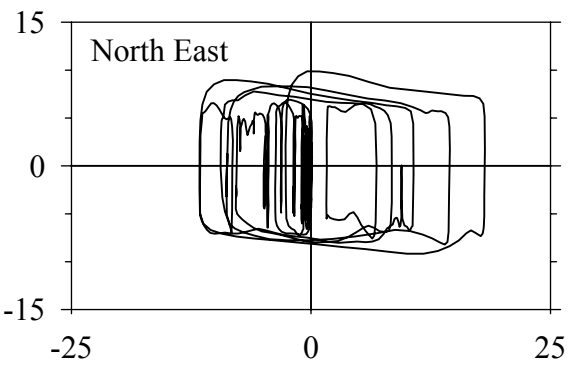
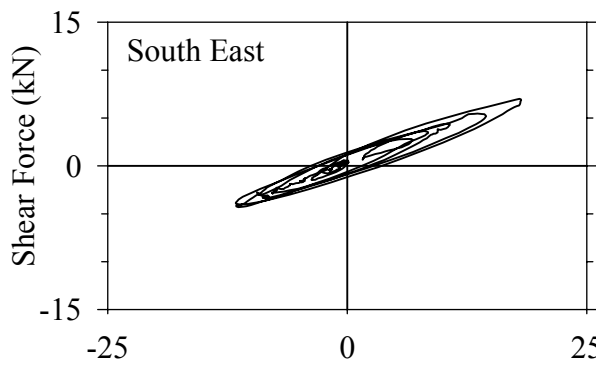
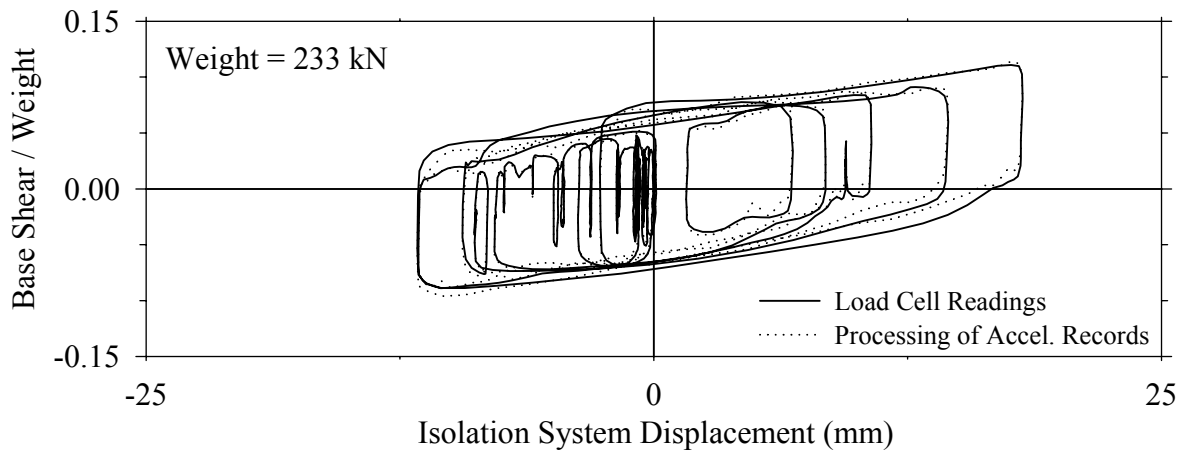
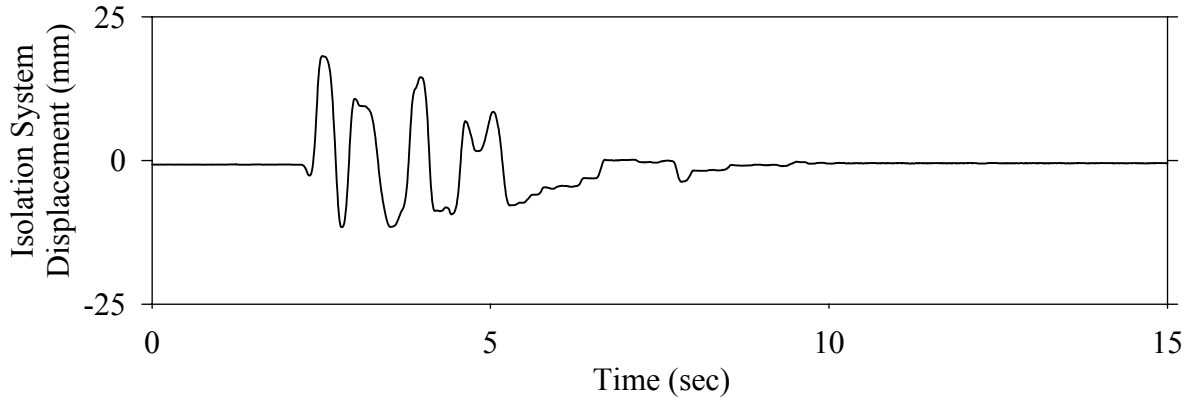




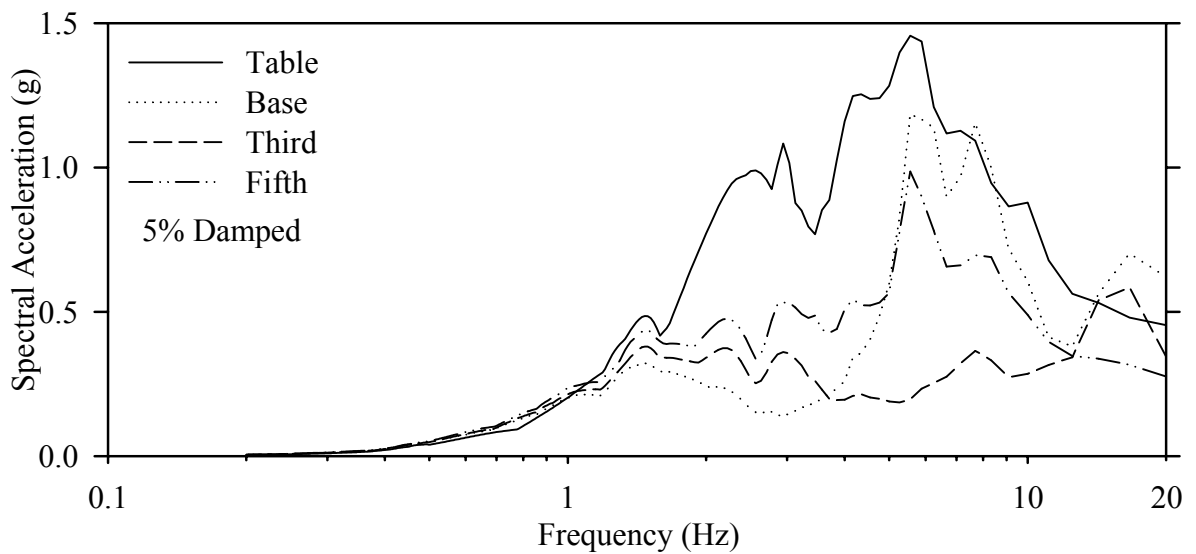
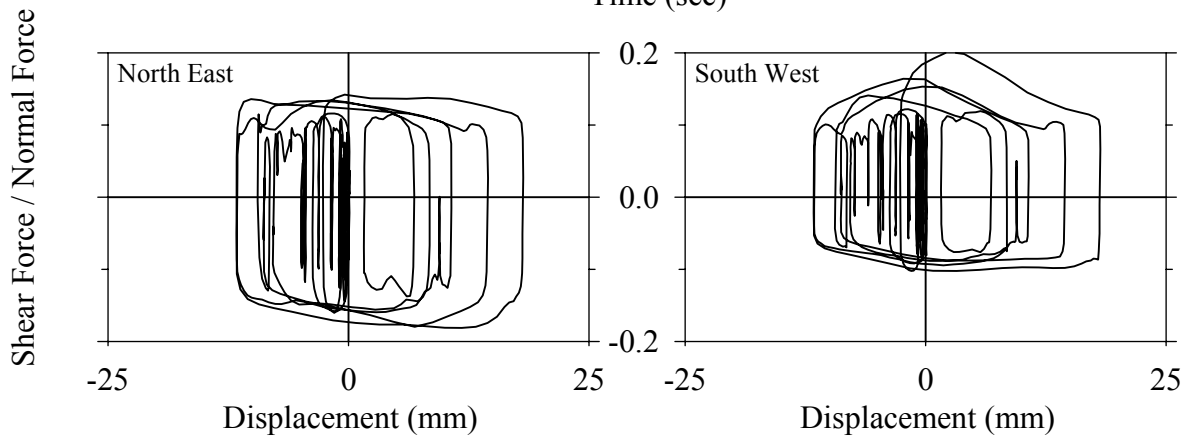
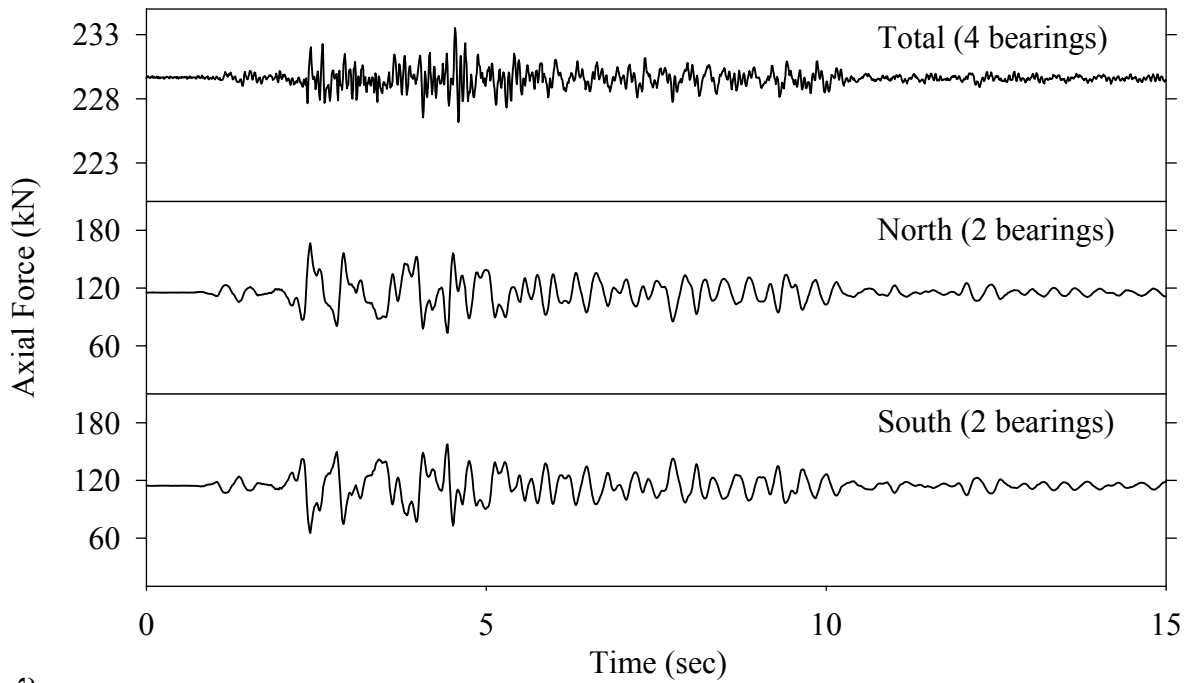
Test EFABE20.1, El Centro S00E 200%, AB/Flat Sliding + Elastomeric



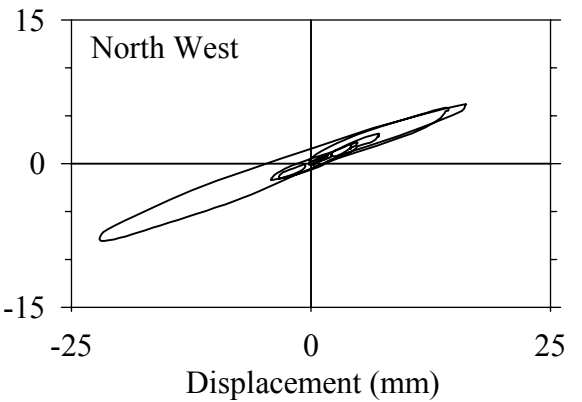
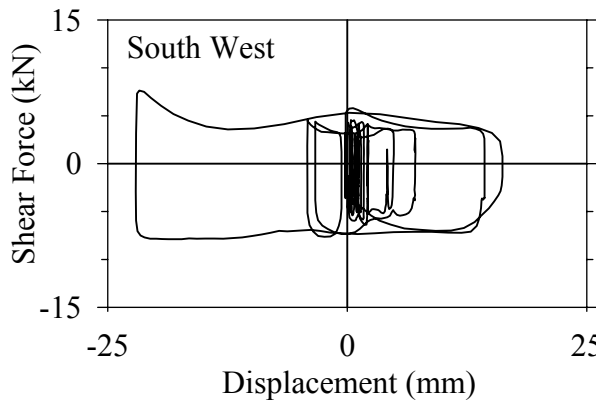
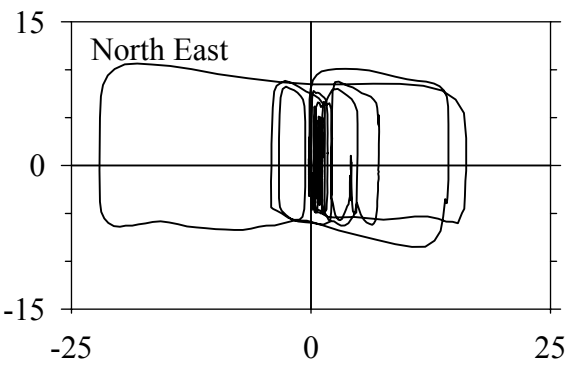
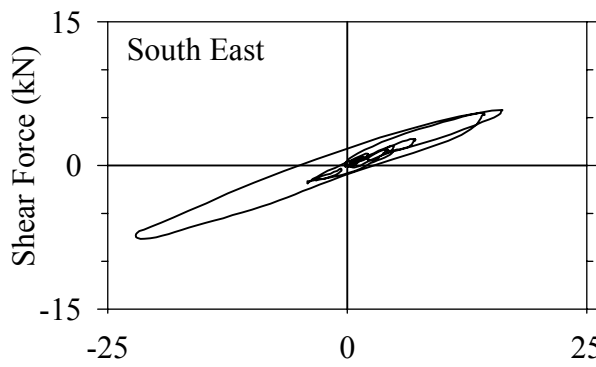
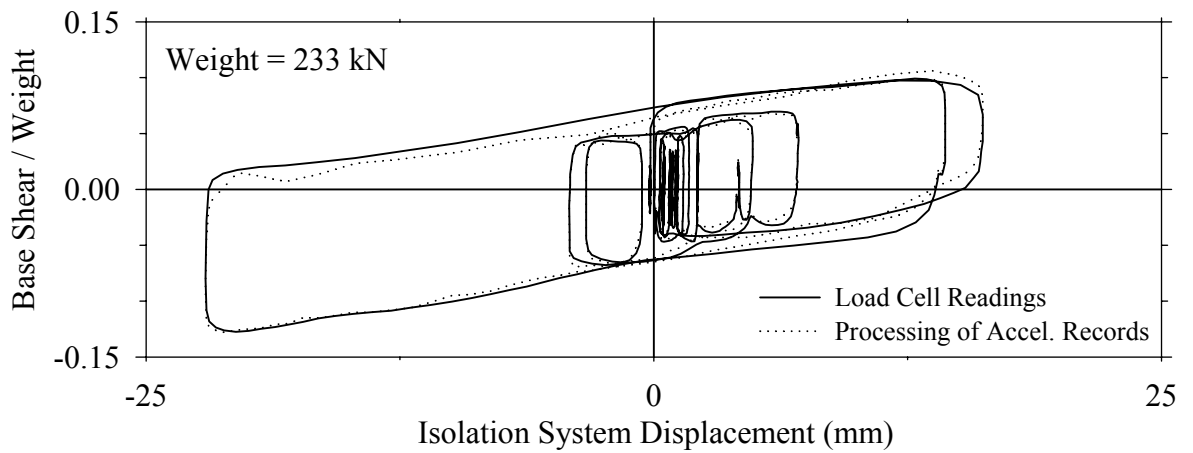
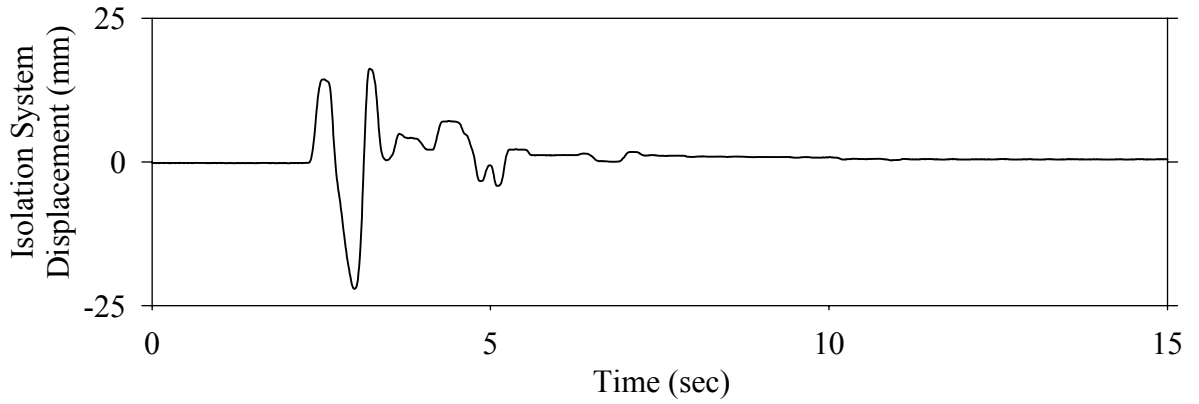
Test EFABK50.1, Kobe N-S 50%, AB/Flat Sliding + Elastomeric



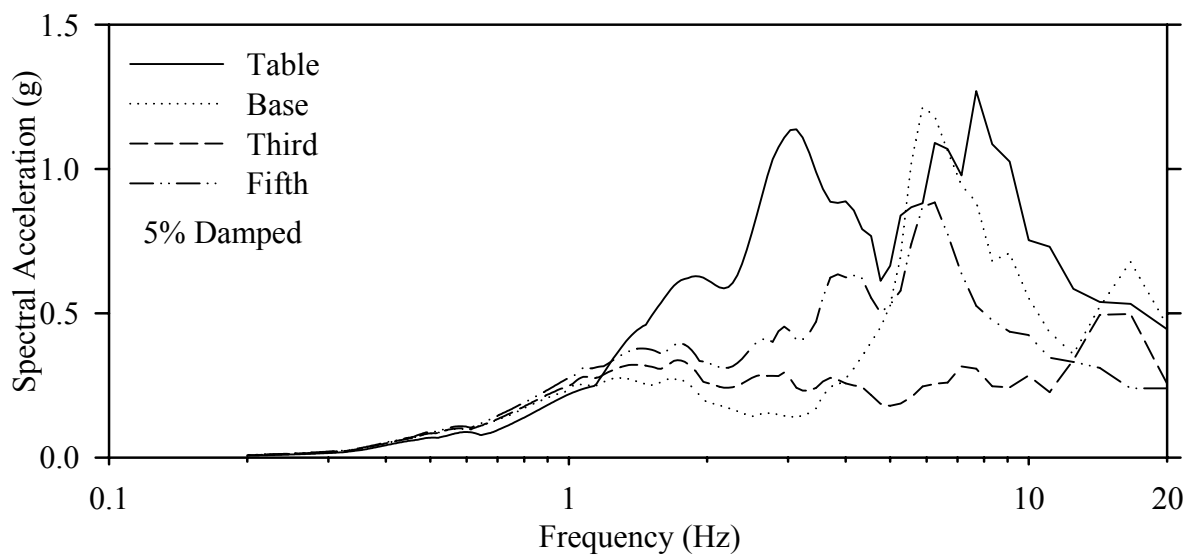
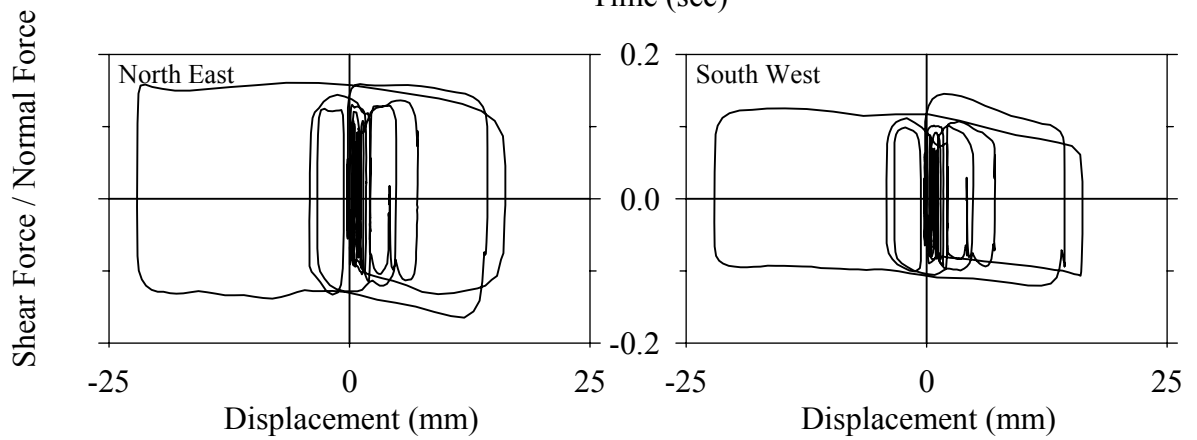
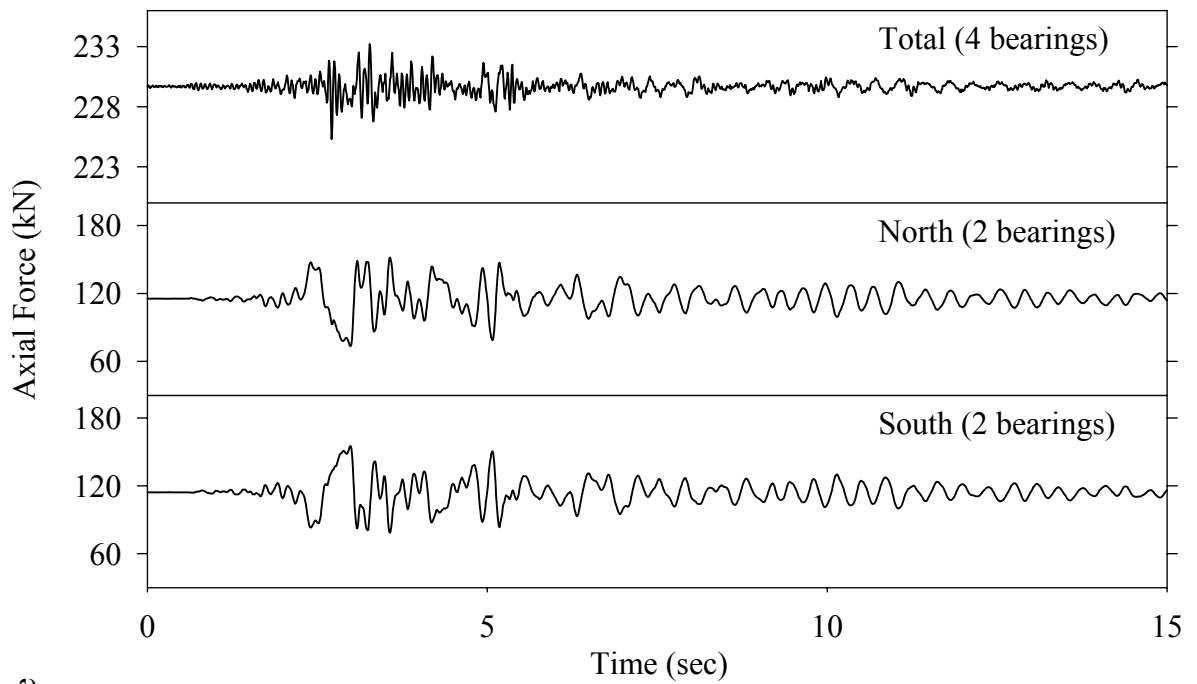
Test EFABK50.1, Kobe N-S 50%, AB/Flat Sliding + Elastomeric



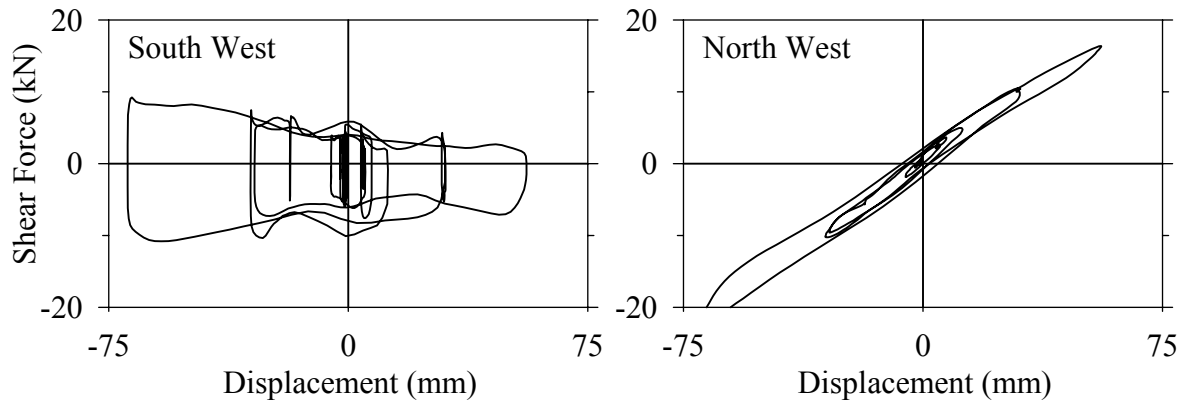
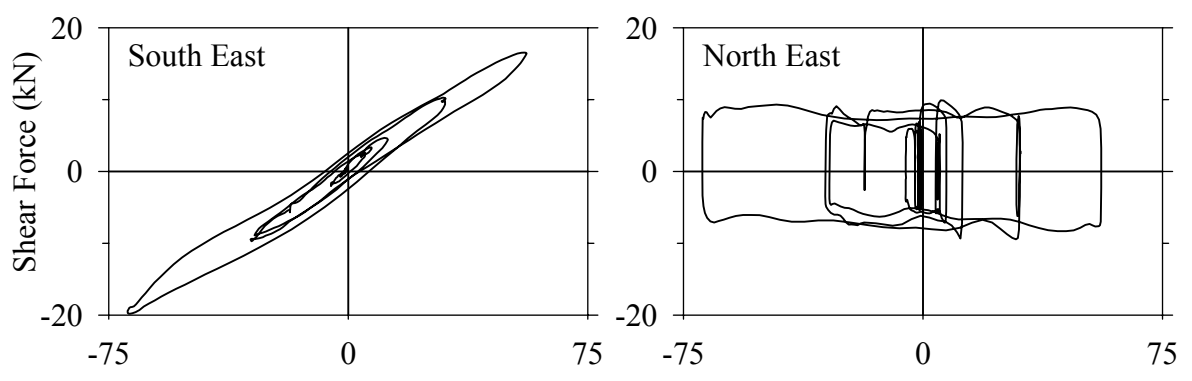
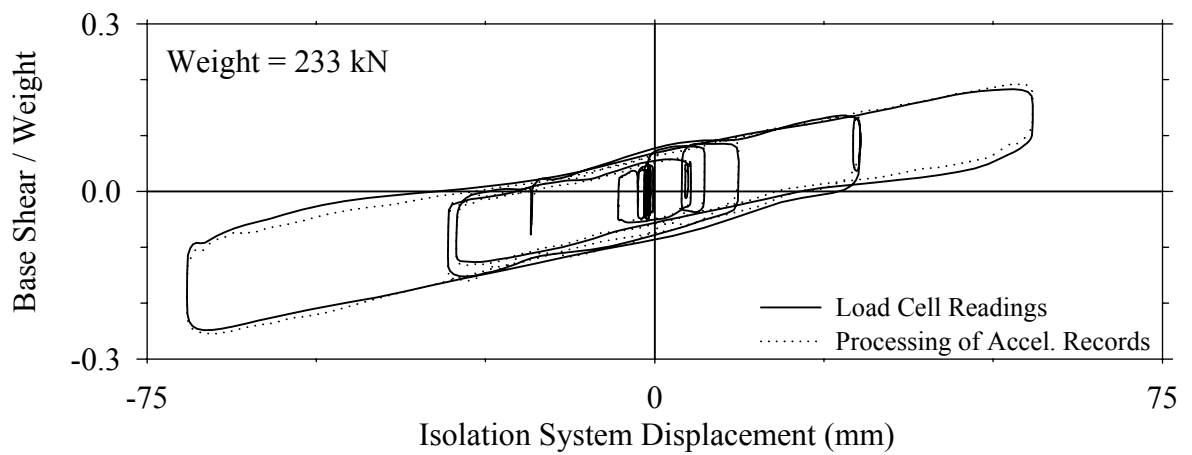
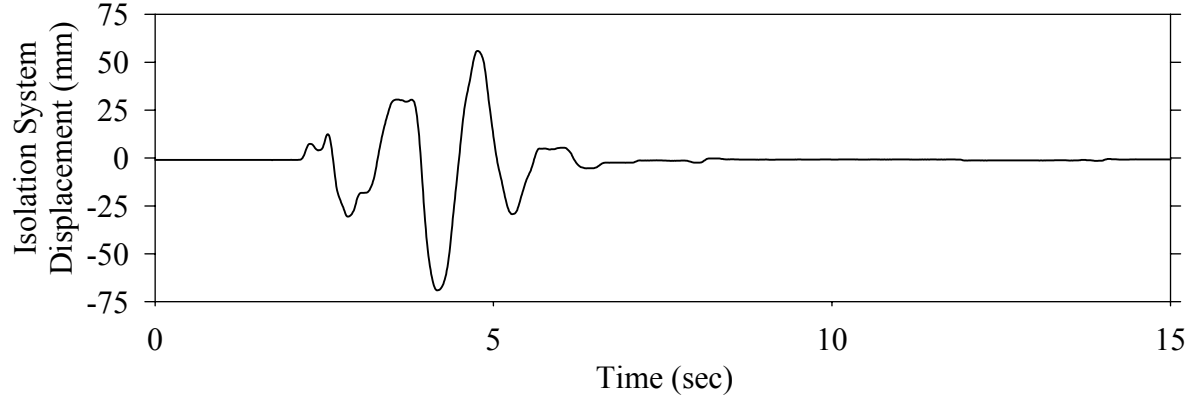
Test EFABN50.1, Northridge Newhall 360° 50%, AB/Flat Sliding + Elastomeric



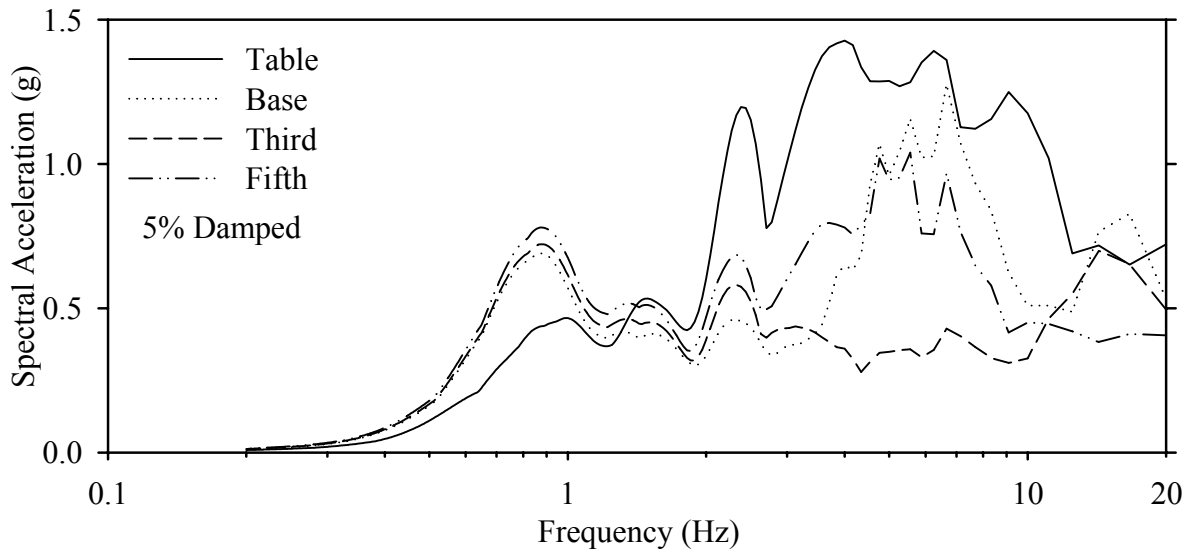
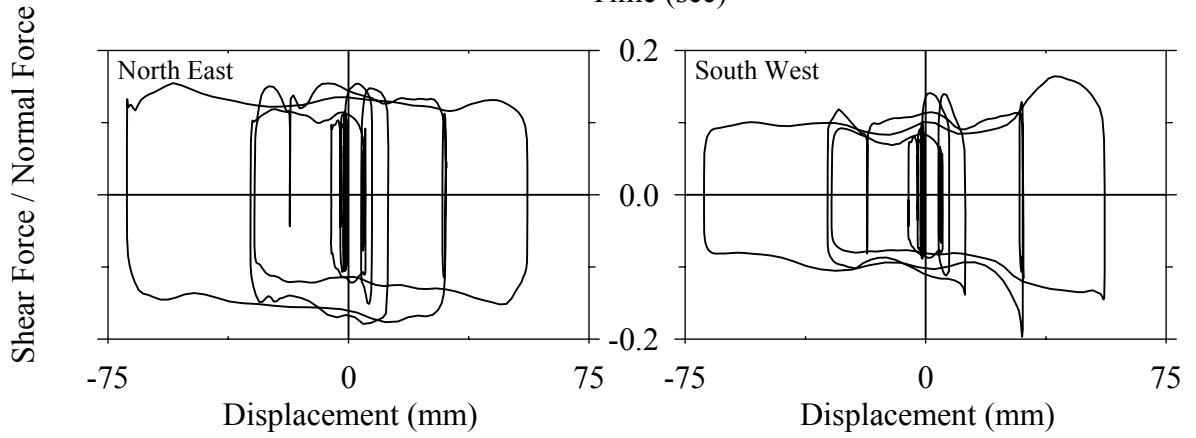
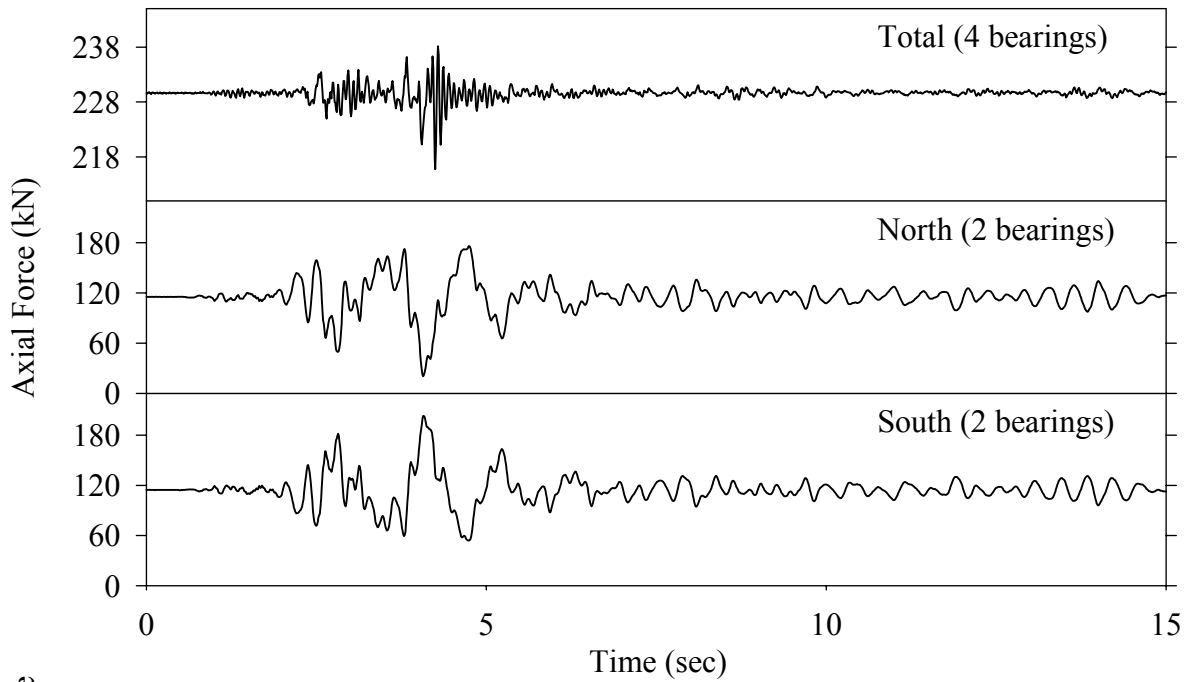
Test EFABN50.1, Northridge Newhall 360° 50%, AB/Flat Sliding + Elastomeric



Test EFABS10.1, Northridge Sylmar 90° 100%, AB/Flat Sliding + Elastomeric



Test EFABS10.1, Northridge Sylmar 90° 100%, AB/Flat Sliding + Elastomeric



**APPENDIX B**

**COMPUTER PROGRAM SAMPLE INPUT FILES**



## SAP2000 MOMENT FRAME

### 6-STORY FPS ISOLATED BUILDING (UPLIFT)

; File C:\Program Files\dissertation work\results\FPS\mf\fpml\fpsmfl.d.\$2k saved 6/26/02  
13:30:17 in Kip-in

#### SYSTEM

DOF=UX,UY,UZ,RX,RY,RZ LENGTH=IN FORCE=Kip LINES=59

#### JOINT

1 X=-72 Y=0 Z=0  
2 X=-72 Y=0 Z=36  
3 X=-72 Y=0 Z=72  
4 X=-72 Y=0 Z=108  
5 X=-72 Y=0 Z=144  
6 X=-72 Y=0 Z=180  
7 X=-72 Y=0 Z=216  
8 X=-24 Y=0 Z=0  
9 X=-24 Y=0 Z=36  
10 X=-24 Y=0 Z=72  
11 X=-24 Y=0 Z=108  
12 X=-24 Y=0 Z=144  
13 X=-24 Y=0 Z=180  
14 X=-24 Y=0 Z=216  
15 X=24 Y=0 Z=0  
16 X=24 Y=0 Z=36  
17 X=24 Y=0 Z=72  
18 X=24 Y=0 Z=108  
19 X=24 Y=0 Z=144  
20 X=24 Y=0 Z=180  
21 X=24 Y=0 Z=216  
22 X=72 Y=0 Z=0  
23 X=72 Y=0 Z=36  
24 X=72 Y=0 Z=72  
25 X=72 Y=0 Z=108  
26 X=72 Y=0 Z=144  
27 X=72 Y=0 Z=180  
28 X=72 Y=0 Z=216  
29 X=-72 Y=0 Z=-14  
30 X=-24 Y=0 Z=-14  
31 X=24 Y=0 Z=-14  
32 X=72 Y=0 Z=-14  
33 X=-48 Y=0 Z=-14  
34 X=48 Y=0 Z=-14  
35 X=-72 Y=0 Z=126

36 X=-24 Y=0 Z=126  
37 X=24 Y=0 Z=126  
38 X=72 Y=0 Z=126  
39 X=-72 Y=48 Z=0  
40 X=-72 Y=48 Z=36  
41 X=-72 Y=48 Z=72  
42 X=-72 Y=48 Z=108  
43 X=-48 Y=0 Z=-40  
44 X=-48 Y=0 Z=-24  
45 X=-72 Y=48 Z=144  
46 X=-72 Y=48 Z=180  
47 X=-72 Y=48 Z=216  
48 X=-24 Y=48 Z=0  
49 X=-24 Y=48 Z=36  
50 X=-24 Y=48 Z=72  
51 X=-24 Y=48 Z=108  
52 X=-24 Y=48 Z=144  
53 X=-24 Y=48 Z=180  
54 X=-24 Y=48 Z=216  
55 X=24 Y=48 Z=0  
56 X=24 Y=48 Z=36  
57 X=24 Y=48 Z=72  
58 X=24 Y=48 Z=108  
59 X=24 Y=48 Z=144  
60 X=24 Y=48 Z=180  
61 X=24 Y=48 Z=216  
62 X=72 Y=48 Z=0  
63 X=72 Y=48 Z=36  
64 X=72 Y=48 Z=72  
65 X=72 Y=48 Z=108  
66 X=72 Y=48 Z=144  
67 X=72 Y=48 Z=180  
68 X=72 Y=48 Z=216  
69 X=-72 Y=48 Z=-14  
70 X=-24 Y=48 Z=-14  
71 X=24 Y=48 Z=-14  
72 X=72 Y=48 Z=-14  
73 X=-48 Y=48 Z=-14  
74 X=48 Y=48 Z=-14  
75 X=-72 Y=48 Z=126  
76 X=-24 Y=48 Z=126  
77 X=24 Y=48 Z=126  
78 X=72 Y=48 Z=126  
79 X=48 Y=0 Z=-40  
80 X=48 Y=0 Z=-24  
81 X=-48 Y=48 Z=-40

82 X=-48 Y=48 Z=-24  
83 X=48 Y=48 Z=-40  
84 X=48 Y=48 Z=-24  
85 X=0 Y=0 Z=-14  
86 X=0 Y=48 Z=-14  
87 X=-29 Y=21 Z=-27  
88 X=-29 Y=27 Z=-27

RESTRAINT

ADD=43 DOF=U1,U2,U3,R1,R2,R3  
ADD=79 DOF=U1,U2,U3,R1,R2,R3  
ADD=81 DOF=U1,U2,U3,R1,R2,R3  
ADD=83 DOF=U1,U2,U3,R1,R2,R3  
ADD=87 DOF=U1,U2,U3  
ADD=88 DOF=U1,U2,U3

PATTERN

NAME=DEFAULT

MASS

ADD=1 U1=.0013 U2=.0013 U3=.0013  
ADD=2 U1=.00167 U2=.00167 U3=.00167 R1=.005 R2=.005 R3=.005  
ADD=3 U1=.00167 U2=.00167 U3=.00167 R1=.005 R2=.005 R3=.005  
ADD=4 U1=.00167 U2=.00167 U3=.00167 R1=.005 R2=.005 R3=.005  
ADD=5 U1=.00167 U2=.00167 U3=.00167 R1=.005 R2=.005 R3=.005  
ADD=6 U1=.00167 U2=.00167 U3=.00167 R1=.005 R2=.005 R3=.005  
ADD=7 U1=.00165 U2=.00165 U3=.00165 R1=.005 R2=.005 R3=.005  
ADD=8 U1=.0026 U2=.0026 U3=.0026  
ADD=9 U1=.00335 U2=.00335 U3=.00335 R1=.01 R2=.01 R3=.01  
ADD=10 U1=.00335 U2=.00335 U3=.00335 R1=.01 R2=.01 R3=.01  
ADD=11 U1=.00335 U2=.00335 U3=.00335 R1=.01 R2=.01 R3=.01  
ADD=12 U1=.00335 U2=.00335 U3=.00335 R1=.01 R2=.01 R3=.01  
ADD=13 U1=.00335 U2=.00335 U3=.00335 R1=.01 R2=.01 R3=.01  
ADD=14 U1=.0033 U2=.0033 U3=.0033 R1=.01 R2=.01 R3=.01  
ADD=15 U1=.0026 U2=.0026 U3=.0026  
ADD=16 U1=.00335 U2=.00335 U3=.00335 R1=.01 R2=.01 R3=.01  
ADD=17 U1=.00335 U2=.00335 U3=.00335 R1=.01 R2=.01 R3=.01  
ADD=18 U1=.00335 U2=.00335 U3=.00335 R1=.01 R2=.01 R3=.01  
ADD=19 U1=.00335 U2=.00335 U3=.00335 R1=.01 R2=.01 R3=.01  
ADD=20 U1=.00335 U2=.00335 U3=.00335 R1=.01 R2=.01 R3=.01  
ADD=21 U1=.0033 U2=.0033 U3=.0033 R1=.01 R2=.01 R3=.01  
ADD=22 U1=.0013 U2=.0013 U3=.0013  
ADD=23 U1=.00167 U2=.00167 U3=.00167 R1=.005 R2=.005 R3=.005  
ADD=24 U1=.00167 U2=.00167 U3=.00167 R1=.005 R2=.005 R3=.005  
ADD=25 U1=.00167 U2=.00167 U3=.00167 R1=.005 R2=.005 R3=.005  
ADD=26 U1=.00167 U2=.00167 U3=.00167 R1=.005 R2=.005 R3=.005

ADD=27 U1=.00167 U2=.00167 U3=.00167 R1=.005 R2=.005 R3=.005  
 ADD=28 U1=.00165 U2=.00165 U3=.00165 R1=.005 R2=.005 R3=.005  
 ADD=39 U1=.0013 U2=.0013 U3=.0013  
 ADD=40 U1=.00167 U2=.00167 U3=.00167 R1=.005 R2=.005 R3=.005  
 ADD=41 U1=.00167 U2=.00167 U3=.00167 R1=.005 R2=.005 R3=.005  
 ADD=42 U1=.00167 U2=.00167 U3=.00167 R1=.005 R2=.005 R3=.005  
 ADD=45 U1=.00167 U2=.00167 U3=.00167 R1=.005 R2=.005 R3=.005  
 ADD=46 U1=.00167 U2=.00167 U3=.00167 R1=.005 R2=.005 R3=.005  
 ADD=47 U1=.00165 U2=.00165 U3=.00165 R1=.005 R2=.005 R3=.005  
 ADD=48 U1=.0026 U2=.0026 U3=.0026  
 ADD=49 U1=.00335 U2=.00335 U3=.00335 R1=.01 R2=.01 R3=.01  
 ADD=50 U1=.00335 U2=.00335 U3=.00335 R1=.01 R2=.01 R3=.01  
 ADD=51 U1=.00335 U2=.00335 U3=.00335 R1=.01 R2=.01 R3=.01  
 ADD=52 U1=.00335 U2=.00335 U3=.00335 R1=.01 R2=.01 R3=.01  
 ADD=53 U1=.00335 U2=.00335 U3=.00335 R1=.01 R2=.01 R3=.01  
 ADD=54 U1=.0033 U2=.0033 U3=.0033 R1=.01 R2=.01 R3=.01  
 ADD=55 U1=.0026 U2=.0026 U3=.0026  
 ADD=56 U1=.00335 U2=.00335 U3=.00335 R1=.01 R2=.01 R3=.01  
 ADD=57 U1=.00335 U2=.00335 U3=.00335 R1=.01 R2=.01 R3=.01  
 ADD=58 U1=.00335 U2=.00335 U3=.00335 R1=.01 R2=.01 R3=.01  
 ADD=59 U1=.00335 U2=.00335 U3=.00335 R1=.01 R2=.01 R3=.01  
 ADD=60 U1=.00335 U2=.00335 U3=.00335 R1=.01 R2=.01 R3=.01  
 ADD=61 U1=.0033 U2=.0033 U3=.0033 R1=.01 R2=.01 R3=.01  
 ADD=62 U1=.0013 U2=.0013 U3=.0013  
 ADD=63 U1=.00167 U2=.00167 U3=.00167 R1=.005 R2=.005 R3=.005  
 ADD=64 U1=.00167 U2=.00167 U3=.00167 R1=.005 R2=.005 R3=.005  
 ADD=65 U1=.00167 U2=.00167 U3=.00167 R1=.005 R2=.005 R3=.005  
 ADD=66 U1=.00167 U2=.00167 U3=.00167 R1=.005 R2=.005 R3=.005  
 ADD=67 U1=.00167 U2=.00167 U3=.00167 R1=.005 R2=.005 R3=.005  
 ADD=68 U1=.00165 U2=.00165 U3=.00165 R1=.005 R2=.005 R3=.005

#### MATERIAL

NAME=STEEL IDES=S  
 T=0 E=29000 U=.3 A=.0000065 FY=36  
 NAME=CONC IDES=C M=2.246377E-07 W=.0000868  
 T=0 E=3600 U=.2 A=.0000055  
 NAME=OTHER IDES=N M=2.246377E-07 W=.0000868  
 T=0 E=3600 U=.2 A=.0000055

#### FRAME SECTION

NAME=FSEC1 MAT=STEEL SH=R T=18,10 A=180 J=3916.671 I=4860,1500  
 AS=150,150  
 NAME=S3X5.7 MAT=STEEL A=1.67 J=.04 I=2.52,455 AS=.51,1.0097  
 S=1.68,390558 Z=1.95,653 R=1.228406,5219723 T=3,2.33,26,17,2.33,26  
 SHN=S3X5.7 DSG=I

NAME=W14X90 MAT=STEEL SH=I T=14.02,14.52,.71,.44,14.52,.71 A=26.1624  
 J=3.707751 I=987.3821,362.3382 AS=6.1688,17.182  
 NAME=W44X285 MAT=STEEL A=419 J=300 I=123000,2450 AS=225.605,174.2  
 S=1117.674,82.98052 Z=1310,135 R=17.13348,2.41811  
 T=44.02,11.81,1.77,1.025,11.81,1.77 SHN=W44X285 DSG=W  
 NAME=L1.5X1.5X1/4 MAT=STEEL A=.688 J=.015 I=.139,.139 AS=.375,.375  
 S=.1340004,.1340004 Z=.242,.242 R=.4494829,.4494829 T=1.5,1.5,.25,.25,0,0  
 SHN=L1.5X1.5X1/4 DSG=L

#### NLPROP

NAME=FPS TYPE=Isolator2  
 DOF=U1 KE=30000 CE=0 K=30000  
 DOF=U2 KE=1.74 CE=0 DJ=5 K=1000 FRICT=.02,.08 RATE=.51 RADIUS=30  
 DOF=U3 KE=1.74 CE=0 DJ=5 K=1000 FRICT=.02,.08 RATE=.51 RADIUS=30  
 NAME=FLATSLIDER TYPE=Isolator2  
 DOF=U1 KE=30000 CE=0 K=30000  
 DOF=U2 KE=1.74 CE=0 DJ=5 K=1000 FRICT=.02,.11 RATE=.51  
 RADIUS=10000  
 DOF=U3 KE=1.74 CE=0 DJ=5 K=1000 FRICT=.02,.11 RATE=.51  
 RADIUS=10000  
 NAME=LEADCORE TYPE=Plastic1  
 DOF=U1 KE=300 CE=.2 K=300 YIELD=100 RATIO=.9 EXP=1  
 DOF=U2 KE=3.6 CE=0 DJ=5 K=30 YIELD=2.4 RATIO=.07 EXP=1  
 DOF=U3 KE=3.6 CE=0 DJ=5 K=30 YIELD=2.4 RATIO=.07 EXP=1  
 NAME=ELASTOMERIC TYPE=Isolator1  
 DOF=U1 KE=550 CE=.39  
 DOF=U2 KE=1.76 CE=0 DJ=5 K=3.14 YIELD=.75 RATIO=.55  
 DOF=U3 KE=1.76 CE=0 DJ=5 K=3.14 YIELD=.75 RATIO=.55  
 NAME=LINEAR TYPE=Damper  
 DOF=U1 KE=0 CE=0 K=10000 C=.3792 CEXP=1  
 NAME=NONLINEAR TYPE=Damper  
 DOF=U1 KE=0 CE=0 K=10000 C=1.8075 CEXP=.397

#### FRAME

1 J=1,2 SEC=S3X5.7 NSEG=2 ANG=0 IOFF=1.5 JOFF=4.5 RIGID=.6  
 2 J=2,3 SEC=S3X5.7 NSEG=2 ANG=0 IOFF=4.5 JOFF=4.5 RIGID=.6  
 3 J=3,4 SEC=S3X5.7 NSEG=2 ANG=0 IOFF=4.5 JOFF=4.5 RIGID=.6  
 4 J=39,40 SEC=S3X5.7 NSEG=2 ANG=0 IOFF=1.5 JOFF=4.5 RIGID=.6  
 5 J=5,6 SEC=S3X5.7 NSEG=2 ANG=0 IOFF=4.5 JOFF=4.5 RIGID=.6  
 6 J=6,7 SEC=S3X5.7 NSEG=2 ANG=0 IOFF=4.5 JOFF=4.5 RIGID=.6  
 7 J=8,9 SEC=S3X5.7 NSEG=2 ANG=0 IOFF=1.5 JOFF=4.5 RIGID=.6  
 8 J=9,10 SEC=S3X5.7 NSEG=2 ANG=0 IOFF=4.5 JOFF=4.5 RIGID=.6  
 9 J=10,11 SEC=S3X5.7 NSEG=2 ANG=0 IOFF=4.5 JOFF=4.5 RIGID=.6  
 10 J=40,41 SEC=S3X5.7 NSEG=2 ANG=0 IOFF=4.5 JOFF=4.5 RIGID=.6  
 11 J=12,13 SEC=S3X5.7 NSEG=2 ANG=0 IOFF=4.5 JOFF=4.5 RIGID=.6

12 J=13,14 SEC=S3X5.7 NSEG=2 ANG=0 IOFF=4.5 JOFF=4.5 RIGID=.6  
13 J=15,16 SEC=S3X5.7 NSEG=2 ANG=0 IOFF=1.5 JOFF=4.5 RIGID=.6  
14 J=16,17 SEC=S3X5.7 NSEG=2 ANG=0 IOFF=4.5 JOFF=4.5 RIGID=.6  
15 J=17,18 SEC=S3X5.7 NSEG=2 ANG=0 IOFF=4.5 JOFF=4.5 RIGID=.6  
16 J=41,42 SEC=S3X5.7 NSEG=2 ANG=0 IOFF=4.5 JOFF=4.5 RIGID=.6  
17 J=19,20 SEC=S3X5.7 NSEG=2 ANG=0 IOFF=4.5 JOFF=4.5 RIGID=.6  
18 J=20,21 SEC=S3X5.7 NSEG=2 ANG=0 IOFF=4.5 JOFF=4.5 RIGID=.6  
19 J=22,23 SEC=S3X5.7 NSEG=2 ANG=0 IOFF=1.5 JOFF=4.5 RIGID=.6  
20 J=23,24 SEC=S3X5.7 NSEG=2 ANG=0 IOFF=4.5 JOFF=4.5 RIGID=.6  
21 J=24,25 SEC=S3X5.7 NSEG=2 ANG=0 IOFF=4.5 JOFF=4.5 RIGID=.6  
22 J=45,46 SEC=S3X5.7 NSEG=2 ANG=0 IOFF=4.5 JOFF=4.5 RIGID=.6  
23 J=26,27 SEC=S3X5.7 NSEG=2 ANG=0 IOFF=4.5 JOFF=4.5 RIGID=.6  
24 J=27,28 SEC=S3X5.7 NSEG=2 ANG=0 IOFF=4.5 JOFF=4.5 RIGID=.6  
25 J=2,9 SEC=S3X5.7 NSEG=4 ANG=0 IOFF=4.5 JOFF=4.5 RIGID=.6  
26 J=3,10 SEC=S3X5.7 NSEG=4 ANG=0 IOFF=4.5 JOFF=4.5 RIGID=.6  
27 J=4,11 SEC=S3X5.7 NSEG=4 ANG=0 IOFF=4.5 JOFF=4.5 RIGID=.6  
28 J=5,12 SEC=S3X5.7 NSEG=4 ANG=0 IOFF=4.5 JOFF=4.5 RIGID=.6  
29 J=6,13 SEC=S3X5.7 NSEG=4 ANG=0 IOFF=4.5 JOFF=4.5 RIGID=.6  
30 J=7,14 SEC=S3X5.7 NSEG=4 ANG=0 IOFF=4.5 JOFF=4.5 RIGID=.6  
31 J=9,16 SEC=S3X5.7 NSEG=4 ANG=0 IOFF=4.5 JOFF=4.5 RIGID=.6  
32 J=10,17 SEC=S3X5.7 NSEG=4 ANG=0 IOFF=4.5 JOFF=4.5 RIGID=.6  
33 J=11,18 SEC=S3X5.7 NSEG=4 ANG=0 IOFF=4.5 JOFF=4.5 RIGID=.6  
34 J=12,19 SEC=S3X5.7 NSEG=4 ANG=0 IOFF=4.5 JOFF=4.5 RIGID=.6  
35 J=13,20 SEC=S3X5.7 NSEG=4 ANG=0 IOFF=4.5 JOFF=4.5 RIGID=.6  
36 J=14,21 SEC=S3X5.7 NSEG=4 ANG=0 IOFF=4.5 JOFF=4.5 RIGID=.6  
37 J=16,23 SEC=S3X5.7 NSEG=4 ANG=0 IOFF=4.5 JOFF=4.5 RIGID=.6  
38 J=17,24 SEC=S3X5.7 NSEG=4 ANG=0 IOFF=4.5 JOFF=4.5 RIGID=.6  
39 J=18,25 SEC=S3X5.7 NSEG=4 ANG=0 IOFF=4.5 JOFF=4.5 RIGID=.6  
40 J=19,26 SEC=S3X5.7 NSEG=4 ANG=0 IOFF=4.5 JOFF=4.5 RIGID=.6  
41 J=20,27 SEC=S3X5.7 NSEG=4 ANG=0 IOFF=4.5 JOFF=4.5 RIGID=.6  
42 J=21,28 SEC=S3X5.7 NSEG=4 ANG=0 IOFF=4.5 JOFF=4.5 RIGID=.6  
43 J=1,29 SEC=W14X90 NSEG=2 ANG=0 JOFF=6 RIGID=.9  
44 J=8,30 SEC=W14X90 NSEG=2 ANG=0 JOFF=6 RIGID=.9  
45 J=15,31 SEC=W14X90 NSEG=2 ANG=0 JOFF=6 RIGID=.9  
46 J=22,32 SEC=W14X90 NSEG=2 ANG=0 JOFF=6 RIGID=.9  
47 J=46,47 SEC=S3X5.7 NSEG=2 ANG=0 IOFF=4.5 JOFF=4.5 RIGID=.6  
49 J=48,49 SEC=S3X5.7 NSEG=2 ANG=0 IOFF=1.5 JOFF=4.5 RIGID=.6  
50 J=29,33 SEC=W14X90 NSEG=4 ANG=0  
51 J=33,30 SEC=W14X90 NSEG=4 ANG=0  
52 J=31,34 SEC=W14X90 NSEG=4 ANG=0  
53 J=34,32 SEC=W14X90 NSEG=4 ANG=0  
54 J=4,35 SEC=S3X5.7 NSEG=2 ANG=0 IOFF=4.5 JOFF=4.5 RIGID=.6  
55 J=35,5 SEC=S3X5.7 NSEG=2 ANG=0 IOFF=4.5 JOFF=4.5 RIGID=.6  
56 J=11,36 SEC=S3X5.7 NSEG=2 ANG=0 IOFF=4.5 JOFF=4.5 RIGID=.6  
57 J=36,12 SEC=S3X5.7 NSEG=2 ANG=0 IOFF=4.5 JOFF=4.5 RIGID=.6  
58 J=18,37 SEC=S3X5.7 NSEG=2 ANG=0 IOFF=4.5 JOFF=4.5 RIGID=.6

59 J=37,19 SEC=S3X5.7 NSEG=2 ANG=0 IOFF=4.5 JOFF=4.5 RIGID=.6  
60 J=25,38 SEC=S3X5.7 NSEG=2 ANG=0 IOFF=4.5 JOFF=4.5 RIGID=.6  
61 J=38,26 SEC=S3X5.7 NSEG=2 ANG=0 IOFF=4.5 JOFF=4.5 RIGID=.6  
62 J=49,50 SEC=S3X5.7 NSEG=2 ANG=0 IOFF=4.5 JOFF=4.5 RIGID=.6  
63 J=50,51 SEC=S3X5.7 NSEG=2 ANG=0 IOFF=4.5 JOFF=4.5 RIGID=.6  
64 J=52,53 SEC=S3X5.7 NSEG=2 ANG=0 IOFF=4.5 JOFF=4.5 RIGID=.6  
65 J=53,54 SEC=S3X5.7 NSEG=2 ANG=0 IOFF=4.5 JOFF=4.5 RIGID=.6  
66 J=55,56 SEC=S3X5.7 NSEG=2 ANG=0 IOFF=1.5 JOFF=4.5 RIGID=.6  
67 J=56,57 SEC=S3X5.7 NSEG=2 ANG=0 IOFF=4.5 JOFF=4.5 RIGID=.6  
68 J=57,58 SEC=S3X5.7 NSEG=2 ANG=0 IOFF=4.5 JOFF=4.5 RIGID=.6  
69 J=59,60 SEC=S3X5.7 NSEG=2 ANG=0 IOFF=4.5 JOFF=4.5 RIGID=.6  
70 J=60,61 SEC=S3X5.7 NSEG=2 ANG=0 IOFF=4.5 JOFF=4.5 RIGID=.6  
71 J=62,63 SEC=S3X5.7 NSEG=2 ANG=0 IOFF=1.5 JOFF=4.5 RIGID=.6  
72 J=63,64 SEC=S3X5.7 NSEG=2 ANG=0 IOFF=4.5 JOFF=4.5 RIGID=.6  
73 J=64,65 SEC=S3X5.7 NSEG=2 ANG=0 IOFF=4.5 JOFF=4.5 RIGID=.6  
74 J=66,67 SEC=S3X5.7 NSEG=2 ANG=0 IOFF=4.5 JOFF=4.5 RIGID=.6  
75 J=67,68 SEC=S3X5.7 NSEG=2 ANG=0 IOFF=4.5 JOFF=4.5 RIGID=.6  
76 J=40,49 SEC=S3X5.7 NSEG=4 ANG=0 IOFF=4.5 JOFF=4.5 RIGID=.6  
77 J=41,50 SEC=S3X5.7 NSEG=4 ANG=0 IOFF=4.5 JOFF=4.5 RIGID=.6  
78 J=42,51 SEC=S3X5.7 NSEG=4 ANG=0 IOFF=4.5 JOFF=4.5 RIGID=.6  
79 J=45,52 SEC=S3X5.7 NSEG=4 ANG=0 IOFF=4.5 JOFF=4.5 RIGID=.6  
80 J=46,53 SEC=S3X5.7 NSEG=4 ANG=0 IOFF=4.5 JOFF=4.5 RIGID=.6  
81 J=47,54 SEC=S3X5.7 NSEG=4 ANG=0 IOFF=4.5 JOFF=4.5 RIGID=.6  
82 J=49,56 SEC=S3X5.7 NSEG=4 ANG=0 IOFF=4.5 JOFF=4.5 RIGID=.6  
83 J=50,57 SEC=S3X5.7 NSEG=4 ANG=0 IOFF=4.5 JOFF=4.5 RIGID=.6  
84 J=51,58 SEC=S3X5.7 NSEG=4 ANG=0 IOFF=4.5 JOFF=4.5 RIGID=.6  
85 J=52,59 SEC=S3X5.7 NSEG=4 ANG=0 IOFF=4.5 JOFF=4.5 RIGID=.6  
86 J=53,60 SEC=S3X5.7 NSEG=4 ANG=0 IOFF=4.5 JOFF=4.5 RIGID=.6  
87 J=54,61 SEC=S3X5.7 NSEG=4 ANG=0 IOFF=4.5 JOFF=4.5 RIGID=.6  
88 J=56,63 SEC=S3X5.7 NSEG=4 ANG=0 IOFF=4.5 JOFF=4.5 RIGID=.6  
89 J=57,64 SEC=S3X5.7 NSEG=4 ANG=0 IOFF=4.5 JOFF=4.5 RIGID=.6  
90 J=58,65 SEC=S3X5.7 NSEG=4 ANG=0 IOFF=4.5 JOFF=4.5 RIGID=.6  
91 J=59,66 SEC=S3X5.7 NSEG=4 ANG=0 IOFF=4.5 JOFF=4.5 RIGID=.6  
92 J=60,67 SEC=S3X5.7 NSEG=4 ANG=0 IOFF=4.5 JOFF=4.5 RIGID=.6  
93 J=61,68 SEC=S3X5.7 NSEG=4 ANG=0 IOFF=4.5 JOFF=4.5 RIGID=.6  
94 J=39,69 SEC=W14X90 NSEG=2 ANG=0 JOFF=6 RIGID=.9  
95 J=48,70 SEC=W14X90 NSEG=2 ANG=0 JOFF=6 RIGID=.9  
96 J=55,71 SEC=W14X90 NSEG=2 ANG=0 JOFF=6 RIGID=.9  
97 J=62,72 SEC=W14X90 NSEG=2 ANG=0 JOFF=6 RIGID=.9  
99 J=69,73 SEC=W14X90 NSEG=4 ANG=0  
100 J=73,70 SEC=W14X90 NSEG=4 ANG=0  
101 J=71,74 SEC=W14X90 NSEG=4 ANG=0  
102 J=74,72 SEC=W14X90 NSEG=4 ANG=0  
103 J=42,75 SEC=S3X5.7 NSEG=2 ANG=0 IOFF=4.5 JOFF=4.5 RIGID=.6  
104 J=75,45 SEC=S3X5.7 NSEG=2 ANG=0 IOFF=4.5 JOFF=4.5 RIGID=.6  
105 J=51,76 SEC=S3X5.7 NSEG=2 ANG=0 IOFF=4.5 JOFF=4.5 RIGID=.6

106 J=76,52 SEC=S3X5.7 NSEG=2 ANG=0 IOFF=4.5 JOFF=4.5 RIGID=.6  
107 J=58,77 SEC=S3X5.7 NSEG=2 ANG=0 IOFF=4.5 JOFF=4.5 RIGID=.6  
108 J=77,59 SEC=S3X5.7 NSEG=2 ANG=0 IOFF=4.5 JOFF=4.5 RIGID=.6  
109 J=65,78 SEC=S3X5.7 NSEG=2 ANG=0 IOFF=4.5 JOFF=4.5 RIGID=.6  
110 J=78,66 SEC=S3X5.7 NSEG=2 ANG=0 IOFF=4.5 JOFF=4.5 RIGID=.6  
111 J=47,7 SEC=S3X5.7 NSEG=4 ANG=0  
112 J=54,14 SEC=S3X5.7 NSEG=4 ANG=0  
113 J=61,21 SEC=S3X5.7 NSEG=4 ANG=0  
114 J=68,28 SEC=S3X5.7 NSEG=4 ANG=0  
115 J=47,14 SEC=L1.5X1.5X1/4 NSEG=4 ANG=0 IREL=R2,R3 JREL=R1,R2,R3  
116 J=54,7 SEC=L1.5X1.5X1/4 NSEG=4 ANG=0 IREL=R2,R3 JREL=R1,R2,R3  
117 J=54,21 SEC=L1.5X1.5X1/4 NSEG=4 ANG=0 IREL=R2,R3 JREL=R1,R2,R3  
118 J=61,14 SEC=L1.5X1.5X1/4 NSEG=4 ANG=0 IREL=R2,R3 JREL=R1,R2,R3  
119 J=61,28 SEC=L1.5X1.5X1/4 NSEG=4 ANG=0 IREL=R2,R3 JREL=R1,R2,R3  
120 J=68,21 SEC=L1.5X1.5X1/4 NSEG=4 ANG=0 IREL=R2,R3 JREL=R1,R2,R3  
121 J=46,6 SEC=S3X5.7 NSEG=4 ANG=0  
122 J=53,13 SEC=S3X5.7 NSEG=4 ANG=0  
123 J=60,20 SEC=S3X5.7 NSEG=4 ANG=0  
124 J=67,27 SEC=S3X5.7 NSEG=4 ANG=0  
125 J=46,13 SEC=L1.5X1.5X1/4 NSEG=4 ANG=0 IREL=R2,R3 JREL=R1,R2,R3  
126 J=53,6 SEC=L1.5X1.5X1/4 NSEG=4 ANG=0 IREL=R2,R3 JREL=R1,R2,R3  
127 J=53,20 SEC=L1.5X1.5X1/4 NSEG=4 ANG=0 IREL=R2,R3 JREL=R1,R2,R3  
128 J=60,13 SEC=L1.5X1.5X1/4 NSEG=4 ANG=0 IREL=R2,R3 JREL=R1,R2,R3  
129 J=60,27 SEC=L1.5X1.5X1/4 NSEG=4 ANG=0 IREL=R2,R3 JREL=R1,R2,R3  
130 J=67,20 SEC=L1.5X1.5X1/4 NSEG=4 ANG=0 IREL=R2,R3 JREL=R1,R2,R3  
131 J=45,5 SEC=S3X5.7 NSEG=4 ANG=0  
132 J=52,12 SEC=S3X5.7 NSEG=4 ANG=0  
133 J=59,19 SEC=S3X5.7 NSEG=4 ANG=0  
134 J=66,26 SEC=S3X5.7 NSEG=4 ANG=0  
135 J=45,12 SEC=L1.5X1.5X1/4 NSEG=4 ANG=0 IREL=R2,R3 JREL=R1,R2,R3  
136 J=52,5 SEC=L1.5X1.5X1/4 NSEG=4 ANG=0 IREL=R2,R3 JREL=R1,R2,R3  
137 J=52,19 SEC=L1.5X1.5X1/4 NSEG=4 ANG=0 IREL=R2,R3 JREL=R1,R2,R3  
138 J=59,12 SEC=L1.5X1.5X1/4 NSEG=4 ANG=0 IREL=R2,R3 JREL=R1,R2,R3  
139 J=59,26 SEC=L1.5X1.5X1/4 NSEG=4 ANG=0 IREL=R2,R3 JREL=R1,R2,R3  
140 J=66,19 SEC=L1.5X1.5X1/4 NSEG=4 ANG=0 IREL=R2,R3 JREL=R1,R2,R3  
141 J=42,4 SEC=S3X5.7 NSEG=4 ANG=0  
142 J=51,11 SEC=S3X5.7 NSEG=4 ANG=0  
143 J=58,18 SEC=S3X5.7 NSEG=4 ANG=0  
144 J=65,25 SEC=S3X5.7 NSEG=4 ANG=0  
145 J=42,11 SEC=L1.5X1.5X1/4 NSEG=4 ANG=0 IREL=R2,R3 JREL=R1,R2,R3  
146 J=51,4 SEC=L1.5X1.5X1/4 NSEG=4 ANG=0 IREL=R2,R3 JREL=R1,R2,R3  
147 J=51,18 SEC=L1.5X1.5X1/4 NSEG=4 ANG=0 IREL=R2,R3 JREL=R1,R2,R3  
148 J=58,11 SEC=L1.5X1.5X1/4 NSEG=4 ANG=0 IREL=R2,R3 JREL=R1,R2,R3  
149 J=58,25 SEC=L1.5X1.5X1/4 NSEG=4 ANG=0 IREL=R2,R3 JREL=R1,R2,R3  
150 J=65,18 SEC=L1.5X1.5X1/4 NSEG=4 ANG=0 IREL=R2,R3 JREL=R1,R2,R3  
151 J=41,3 SEC=S3X5.7 NSEG=4 ANG=0



152 J=50,10 SEC=S3X5.7 NSEG=4 ANG=0  
153 J=57,17 SEC=S3X5.7 NSEG=4 ANG=0  
154 J=64,24 SEC=S3X5.7 NSEG=4 ANG=0  
155 J=41,10 SEC=L1.5X1.5X1/4 NSEG=4 ANG=0 IREL=R2,R3 JREL=R1,R2,R3  
156 J=50,3 SEC=L1.5X1.5X1/4 NSEG=4 ANG=0 IREL=R2,R3 JREL=R1,R2,R3  
157 J=50,17 SEC=L1.5X1.5X1/4 NSEG=4 ANG=0 IREL=R2,R3 JREL=R1,R2,R3  
158 J=57,10 SEC=L1.5X1.5X1/4 NSEG=4 ANG=0 IREL=R2,R3 JREL=R1,R2,R3  
159 J=57,24 SEC=L1.5X1.5X1/4 NSEG=4 ANG=0 IREL=R2,R3 JREL=R1,R2,R3  
160 J=64,17 SEC=L1.5X1.5X1/4 NSEG=4 ANG=0 IREL=R2,R3 JREL=R1,R2,R3  
161 J=40,2 SEC=S3X5.7 NSEG=4 ANG=0  
162 J=49,9 SEC=S3X5.7 NSEG=4 ANG=0  
163 J=56,16 SEC=S3X5.7 NSEG=4 ANG=0  
164 J=63,23 SEC=S3X5.7 NSEG=4 ANG=0  
165 J=40,9 SEC=L1.5X1.5X1/4 NSEG=4 ANG=0 IREL=R2,R3 JREL=R1,R2,R3  
166 J=49,2 SEC=L1.5X1.5X1/4 NSEG=4 ANG=0 IREL=R2,R3 JREL=R1,R2,R3  
167 J=49,16 SEC=L1.5X1.5X1/4 NSEG=4 ANG=0 IREL=R2,R3 JREL=R1,R2,R3  
168 J=56,9 SEC=L1.5X1.5X1/4 NSEG=4 ANG=0 IREL=R2,R3 JREL=R1,R2,R3  
169 J=56,23 SEC=L1.5X1.5X1/4 NSEG=4 ANG=0 IREL=R2,R3 JREL=R1,R2,R3  
170 J=63,16 SEC=L1.5X1.5X1/4 NSEG=4 ANG=0 IREL=R2,R3 JREL=R1,R2,R3  
171 J=7,46 SEC=L1.5X1.5X1/4 NSEG=2 ANG=0 IREL=R2,R3 JREL=R1,R2,R3  
172 J=47,6 SEC=L1.5X1.5X1/4 NSEG=2 ANG=0 IREL=R2,R3 JREL=R1,R2,R3  
173 J=6,45 SEC=L1.5X1.5X1/4 NSEG=2 ANG=0 IREL=R2,R3 JREL=R1,R2,R3  
174 J=46,5 SEC=L1.5X1.5X1/4 NSEG=2 ANG=0 IREL=R2,R3 JREL=R1,R2,R3  
175 J=5,42 SEC=L1.5X1.5X1/4 NSEG=2 ANG=0 IREL=R2,R3 JREL=R1,R2,R3  
176 J=45,4 SEC=L1.5X1.5X1/4 NSEG=2 ANG=0 IREL=R2,R3 JREL=R1,R2,R3  
177 J=4,41 SEC=L1.5X1.5X1/4 NSEG=2 ANG=0 IREL=R2,R3 JREL=R1,R2,R3  
178 J=42,3 SEC=L1.5X1.5X1/4 NSEG=2 ANG=0 IREL=R2,R3 JREL=R1,R2,R3  
179 J=3,40 SEC=L1.5X1.5X1/4 NSEG=2 ANG=0 IREL=R2,R3 JREL=R1,R2,R3  
180 J=41,2 SEC=L1.5X1.5X1/4 NSEG=2 ANG=0 IREL=R2,R3 JREL=R1,R2,R3  
181 J=2,39 SEC=L1.5X1.5X1/4 NSEG=2 ANG=0 IREL=R2,R3 JREL=R1,R2,R3  
182 J=40,1 SEC=L1.5X1.5X1/4 NSEG=2 ANG=0 IREL=R2,R3 JREL=R1,R2,R3  
183 J=30,85 SEC=W14X90 NSEG=4 ANG=0  
184 J=85,31 SEC=W14X90 NSEG=4 ANG=0  
185 J=70,86 SEC=W14X90 NSEG=4 ANG=0  
186 J=86,71 SEC=W14X90 NSEG=4 ANG=0  
195 J=43,44 SEC=W14X90 NSEG=2 ANG=0  
196 J=79,80 SEC=W14X90 NSEG=2 ANG=0  
197 J=81,82 SEC=W14X90 NSEG=2 ANG=0  
198 J=83,84 SEC=W14X90 NSEG=2 ANG=0  
207 J=14,53 SEC=L1.5X1.5X1/4 NSEG=2 ANG=0 IREL=R2,R3 JREL=R1,R2,R3  
208 J=54,13 SEC=L1.5X1.5X1/4 NSEG=2 ANG=0 IREL=R2,R3 JREL=R1,R2,R3  
209 J=13,52 SEC=L1.5X1.5X1/4 NSEG=2 ANG=0 IREL=R2,R3 JREL=R1,R2,R3  
210 J=53,12 SEC=L1.5X1.5X1/4 NSEG=2 ANG=0 IREL=R2,R3 JREL=R1,R2,R3  
211 J=12,51 SEC=L1.5X1.5X1/4 NSEG=2 ANG=0 IREL=R2,R3 JREL=R1,R2,R3  
212 J=52,11 SEC=L1.5X1.5X1/4 NSEG=2 ANG=0 IREL=R2,R3 JREL=R1,R2,R3  
213 J=11,50 SEC=L1.5X1.5X1/4 NSEG=2 ANG=0 IREL=R2,R3 JREL=R1,R2,R3

214 J=51,10 SEC=L1.5X1.5X1/4 NSEG=2 ANG=0 IREL=R2,R3 JREL=R1,R2,R3  
215 J=10,49 SEC=L1.5X1.5X1/4 NSEG=2 ANG=0 IREL=R2,R3 JREL=R1,R2,R3  
216 J=50,9 SEC=L1.5X1.5X1/4 NSEG=2 ANG=0 IREL=R2,R3 JREL=R1,R2,R3  
217 J=9,48 SEC=L1.5X1.5X1/4 NSEG=2 ANG=0 IREL=R2,R3 JREL=R1,R2,R3  
218 J=49,8 SEC=L1.5X1.5X1/4 NSEG=2 ANG=0 IREL=R2,R3 JREL=R1,R2,R3  
219 J=21,60 SEC=L1.5X1.5X1/4 NSEG=2 ANG=0 IREL=R2,R3 JREL=R1,R2,R3  
220 J=61,20 SEC=L1.5X1.5X1/4 NSEG=2 ANG=0 IREL=R2,R3 JREL=R1,R2,R3  
221 J=20,59 SEC=L1.5X1.5X1/4 NSEG=2 ANG=0 IREL=R2,R3 JREL=R1,R2,R3  
222 J=60,19 SEC=L1.5X1.5X1/4 NSEG=2 ANG=0 IREL=R2,R3 JREL=R1,R2,R3  
223 J=19,58 SEC=L1.5X1.5X1/4 NSEG=2 ANG=0 IREL=R2,R3 JREL=R1,R2,R3  
224 J=59,18 SEC=L1.5X1.5X1/4 NSEG=2 ANG=0 IREL=R2,R3 JREL=R1,R2,R3  
225 J=18,57 SEC=L1.5X1.5X1/4 NSEG=2 ANG=0 IREL=R2,R3 JREL=R1,R2,R3  
226 J=58,17 SEC=L1.5X1.5X1/4 NSEG=2 ANG=0 IREL=R2,R3 JREL=R1,R2,R3  
227 J=17,56 SEC=L1.5X1.5X1/4 NSEG=2 ANG=0 IREL=R2,R3 JREL=R1,R2,R3  
228 J=57,16 SEC=L1.5X1.5X1/4 NSEG=2 ANG=0 IREL=R2,R3 JREL=R1,R2,R3  
229 J=16,55 SEC=L1.5X1.5X1/4 NSEG=2 ANG=0 IREL=R2,R3 JREL=R1,R2,R3  
230 J=56,15 SEC=L1.5X1.5X1/4 NSEG=2 ANG=0 IREL=R2,R3 JREL=R1,R2,R3  
231 J=28,67 SEC=L1.5X1.5X1/4 NSEG=2 ANG=0 IREL=R2,R3 JREL=R1,R2,R3  
232 J=68,27 SEC=L1.5X1.5X1/4 NSEG=2 ANG=0 IREL=R2,R3 JREL=R1,R2,R3  
233 J=27,66 SEC=L1.5X1.5X1/4 NSEG=2 ANG=0 IREL=R2,R3 JREL=R1,R2,R3  
234 J=67,26 SEC=L1.5X1.5X1/4 NSEG=2 ANG=0 IREL=R2,R3 JREL=R1,R2,R3  
235 J=26,65 SEC=L1.5X1.5X1/4 NSEG=2 ANG=0 IREL=R2,R3 JREL=R1,R2,R3  
236 J=66,25 SEC=L1.5X1.5X1/4 NSEG=2 ANG=0 IREL=R2,R3 JREL=R1,R2,R3  
237 J=25,64 SEC=L1.5X1.5X1/4 NSEG=2 ANG=0 IREL=R2,R3 JREL=R1,R2,R3  
238 J=65,24 SEC=L1.5X1.5X1/4 NSEG=2 ANG=0 IREL=R2,R3 JREL=R1,R2,R3  
239 J=24,63 SEC=L1.5X1.5X1/4 NSEG=2 ANG=0 IREL=R2,R3 JREL=R1,R2,R3  
240 J=64,23 SEC=L1.5X1.5X1/4 NSEG=2 ANG=0 IREL=R2,R3 JREL=R1,R2,R3  
241 J=23,62 SEC=L1.5X1.5X1/4 NSEG=2 ANG=0 IREL=R2,R3 JREL=R1,R2,R3  
242 J=63,22 SEC=L1.5X1.5X1/4 NSEG=2 ANG=0 IREL=R2,R3 JREL=R1,R2,R3  
243 J=73,33 SEC=W14X90 NSEG=4 ANG=0  
244 J=70,30 SEC=W14X90 NSEG=4 ANG=0  
245 J=71,31 SEC=W14X90 NSEG=4 ANG=0  
246 J=74,34 SEC=W14X90 NSEG=4 ANG=0

#### NLLINK

1 J=85,87 NLP=LINEAR ANG=0  
2 J=86,88 NLP=LINEAR ANG=0  
3 J=44,33 NLP=FPS ANG=0  
4 J=80,34 NLP=FPS ANG=0  
6 J=82,73 NLP=FPS ANG=0  
8 J=84,74 NLP=FPS ANG=0

#### LOAD

NAME=WEIGHT SW=1 CSYS=0

#### MODE

TYPE=EIGEN N=20 TOL=.00001 RESMASS=Y

FUNCTION

NAME=RAMP5 NPL=1 PRINT=Y

0 0

5 .5

10 1

NAME=NEWHALL DT=0 NPL=1 PRINT=Y FILE=newh100.txt

NAME=KOBE DT=0 NPL=1 PRINT=Y FILE=kobe100.txt

NAME=SYLMAR DT=0 NPL=1 PRINT=Y FILE=sylm100.txt

NAME=ELCENTRO DT=0 NPL=1 PRINT=Y FILE=elcen200.txt

HISTORY

NAME=RAMPIT TYPE=NON NSTEP=2000 DT=.01 DAMP=.99 FTOL=.00001  
ETOL=.00001 DTMAX=.005 DTMIN=5E-12

ACC=U3 FUNC=RAMP5 SF=386.22 AT=0

NAME=NEWHAL TYPE=NON NSTEP=1500 DT=.01 DAMP=.02 PREV=RAMPIT  
DTMAX=.005 DTMIN=5E-12

MODE=1 DAMP=.04

MODE=2 DAMP=.04

MODE=3 DAMP=.04

ACC=U1 ANG=0 FUNC=NEWHALL SF=-386.22 AT=0

NAME=ELCENTRO TYPE=NON NSTEP=3000 DT=.01 DAMP=.02  
PREV=RAMPIT DTMAX=.005 DTMIN=5E-11

MODE=1 DAMP=.04

MODE=2 DAMP=.04

MODE=3 DAMP=.04

ACC=U1 ANG=0 FUNC=ELCENTRO SF=-386.22 AT=0

NAME=KOBE TYPE=NON NSTEP=1500 DT=.01 DAMP=.02 PREV=RAMPIT  
DTMAX=.005 DTMIN=5E-11

MODE=1 DAMP=.04

MODE=2 DAMP=.04

MODE=3 DAMP=.04

ACC=U1 ANG=0 FUNC=KOBE SF=-386.22 AT=0

NAME=SYLMAR TYPE=NON NSTEP=1500 DT=.01 DAMP=.02 PREV=RAMPIT  
DTMAX=.005 DTMIN=5E-11

MODE=1 DAMP=.04

MODE=2 DAMP=.04

MODE=3 DAMP=.04

ACC=U1 ANG=0 FUNC=SYLMAR SF=-386.22 AT=0

COMBO

NAME=DSTL1

LOAD=WEIGHT SF=1

NAME=DSTL2

LOAD=WEIGHT SF=1

OUTPUT

; No Output Requested

END

; The following data is used for graphics, design and pushover analysis.  
; If changes are made to the analysis data above, then the following data  
; should be checked for consistency.

SAP2000 V7.44 SUPPLEMENTAL DATA

GRID GLOBAL X "1" -72

GRID GLOBAL X "2" -48

GRID GLOBAL X "3" -36

GRID GLOBAL X "4" -29

GRID GLOBAL X "5" -24

GRID GLOBAL X "6" 0

GRID GLOBAL X "7" 24

GRID GLOBAL X "8" 48

GRID GLOBAL X "9" 60

GRID GLOBAL X "10" 72

GRID GLOBAL Y "11" 0

GRID GLOBAL Y "12" 21

GRID GLOBAL Y "13" 27

GRID GLOBAL Y "14" 48

GRID GLOBAL Z "15" -40

GRID GLOBAL Z "16" -27

GRID GLOBAL Z "17" -24

GRID GLOBAL Z "18" -14

GRID GLOBAL Z "19" -7

GRID GLOBAL Z "20" 0

GRID GLOBAL Z "21" 36

GRID GLOBAL Z "22" 72

GRID GLOBAL Z "23" 108

GRID GLOBAL Z "24" 144

GRID GLOBAL Z "25" 180

GRID GLOBAL Z "26" 216

MATERIAL STEEL FY 36

MATERIAL CONC FYREBAR 60 FYSHEAR 40 FC 4 FCSHEAR 4

FRAMESECTION W44X285 A 83.8 MFA 5 J 60 MFJ 5 I33 24600 MFI33 5 I22 490  
MFI22 5 AS2 45.121 MFAS2 5 AS3 34.84 MFAS3 5

STATICLOAD WEIGHT TYPE DEAD

COMBO DSTL1 DESIGN STEEL

COMBO DSTL2 DESIGN STEEL

END SUPPLEMENTAL DATA

### 3D-BASIS-ME MOMENT FRAME FPS WITH NONLINEAR DAMPERS

4 FPS bearings 6 story mf- CONSTANT NORMAL LOAD

in	Kips/in*sec <sup>2</sup>				secs
2 1 6 4	386.22				
6 6					
0.00001	.001	600	100000	1	
0.5	0.25				
1	0.01	3000	0	386.22	
215.9	2147.2	6693.	14656.	25691.	37147.
-4.031	0.001	0.001	-3.73	0.001	0.001
-3.212	0.001	0.001	-2.507	0.001	0.001
-1.65	0.001	0.001	-0.73	0.001	0.001
3.77	0.001	0.001	1.59	0.001	0.001
-1.33	0.001	0.001	-3.5	0.001	0.001
-3.823	0.001	0.001	-2.136	0.001	0.001
-3.24	0.001	0.001	1.37	0.001	0.001
3.893	0.001	0.001	1.176	0.001	0.001
-3.157	0.001	0.001	-3.33	0.001	0.001
2.49	0.001	0.001	-3.49	0.001	0.001
-1.18	0.001	0.001	3.84	0.001	0.001
0.08	0.001	0.001	-3.94	0.001	0.001
1.574	0.001	0.001	-3.724	0.001	0.001
3.0	0.001	0.001	0.29	0.001	0.001
-3.31	0.001	0.001	3.67	0.001	0.001
-0.77	0.001	0.001	2.315	0.001	0.001
-3.52	0.001	0.001	3.91	0.001	0.001
-3.43	0.001	0.001	2.246	0.001	0.001
0.0198	0.02	0.02	0.02	0.02	0.02
100.	100.	100.	100.	100.	100.
0.04	0.02	0.02	0.02	0.02	0.02
0.0001	0.0001				
0.0001	0.0001				
0.0001	0.0001				
0.0001	0.0001				
0.0001	0.0001				
0.0001	0.0001				
216.0	180.0	144.0	108.0	72.0	36.0
1.74	1.74	0	0	0	0
0.0154	75.				
0.01	0.01	0.1	0	0	
-48.0	24.0				
-48.0	-24.0				
48.0	24.0				
48.0	-24.0				
0.0	24.0				

```

0.0   -24.0
3     4
0.08 0.08 0.02 0.02 0.51 0.51 0.001 0.001 13.1
3     4
0.08 0.08 0.02 0.02 0.51 0.51 0.001 0.001 13.1
3     4
0.08 0.08 0.02 0.02 0.51 0.51 0.001 0.001 13.1
3     4
0.08 0.08 0.02 0.02 0.51 0.51 0.001 0.001 13.1
1     2
1.51  0.397
1     2
1.51  0.397
1 1000 0
1 2 3 4
1
0 0

```

### 3D-BASIS-ME MOMENT FRAME ELASTOMERIC WITH LINEAR DAMPERS

4 FPS bearings 6 story mf- CONSTANT NORMAL LOAD

```

in          Kips/in*sec^2      secs
2 1 6 4 386.22
6 6
0.00001 .001 600 100000 1
0.5 0.25
1 0.01 3000 0 386.22
215.9 2147.2 6693. 14656. 25691. 37147.
-4.031 0.001 0.001 -3.73 0.001 0.001
-3.212 0.001 0.001 -2.507 0.001 0.001
-1.65 0.001 0.001 -0.73 0.001 0.001
3.77 0.001 0.001 1.59 0.001 0.001
-1.33 0.001 0.001 -3.5 0.001 0.001
-3.823 0.001 0.001 -2.136 0.001 0.001
-3.24 0.001 0.001 1.37 0.001 0.001
3.893 0.001 0.001 1.176 0.001 0.001
-3.157 0.001 0.001 -3.33 0.001 0.001
2.49 0.001 0.001 -3.49 0.001 0.001
-1.18 0.001 0.001 3.84 0.001 0.001
0.08 0.001 0.001 -3.94 0.001 0.001
1.574 0.001 0.001 -3.724 0.001 0.001
3.0 0.001 0.001 0.29 0.001 0.001
-3.31 0.001 0.001 3.67 0.001 0.001
-0.77 0.001 0.001 2.315 0.001 0.001
-3.52 0.001 0.001 3.91 0.001 0.001
-3.43 0.001 0.001 2.246 0.001 0.001

```

0.0198 0.02 0.02 0.02 0.02 0.02  
 100. 100. 100. 100. 100. 100.  
 0.04 0.02 0.02 0.02 0.02 0.02  
 0.0001 0.0001  
 0.0001 0.0001  
 0.0001 0.0001  
 0.0001 0.0001  
 0.0001 0.0001  
 0.0001 0.0001  
 0.0001 0.0001  
 216.0 180.0 144.0 108.0 72.0 36.0 0.0  
 1.74 1.74 0 0 0  
 0.0154 75.  
 0.04 0.04 0.1 0 0  
 -48.0 24.0  
 -48.0 -24.0  
 48.0 24.0  
 48.0 -24.0  
 0.0 24.0  
 0.0 -24.0  
 3 7  
 0.3 2.0 1.5 .82 .825 .2  
 3 7  
 0.3 2.0 1.5 .82 .825 .2  
 3 7  
 0.3 2.0 1.5 .82 .825 .2  
 3 7  
 0.3 2.0 1.5 .82 .825 .2  
 1 2  
 0.23 1.0  
 1 2  
 0.23 1.0  
 1 1000 0  
 1 2 3 4  
 1  
 0 0

## **APPENDIX C**

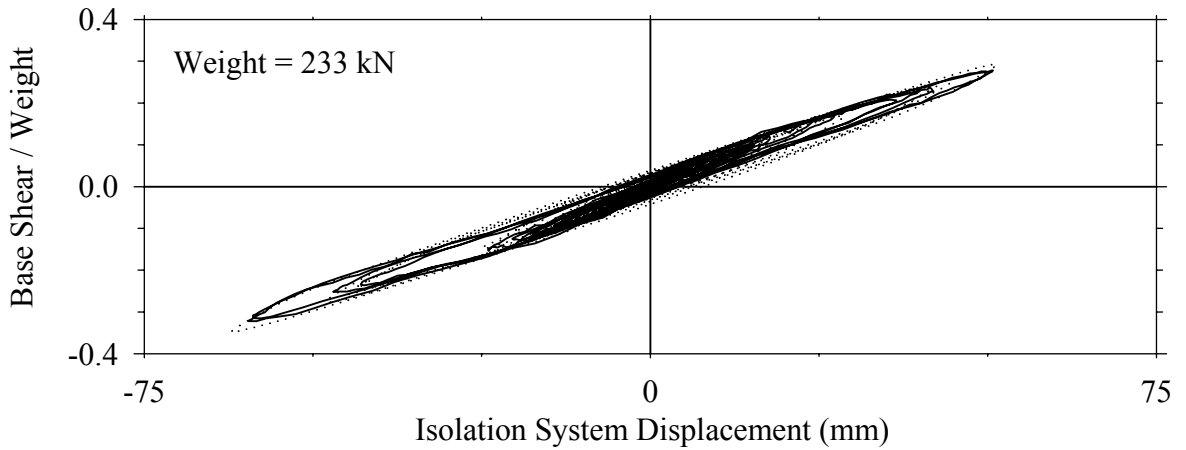
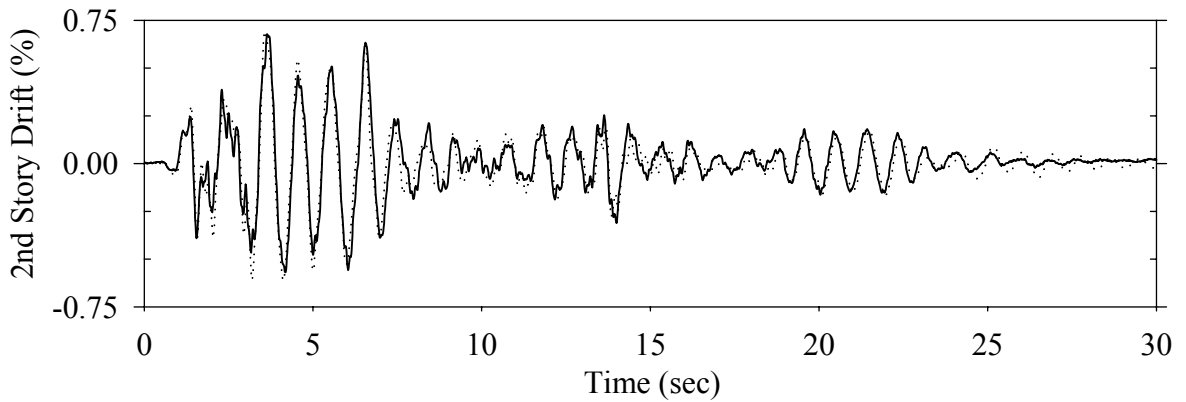
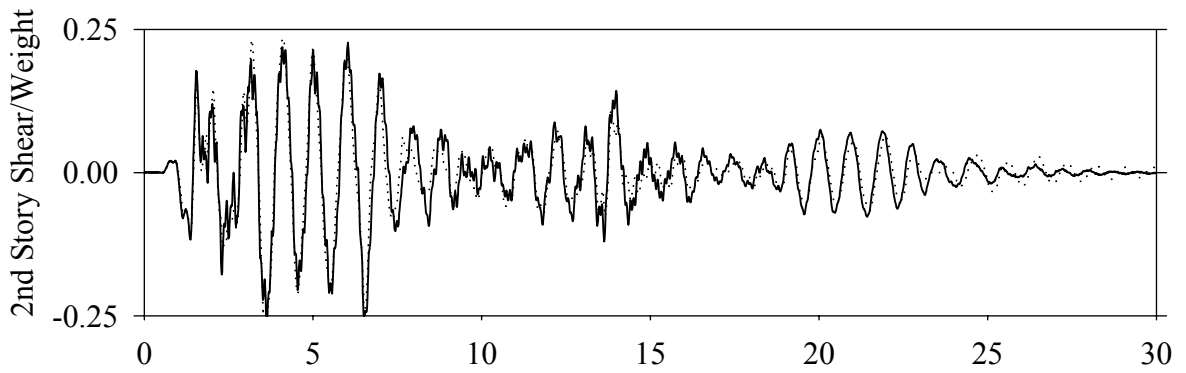
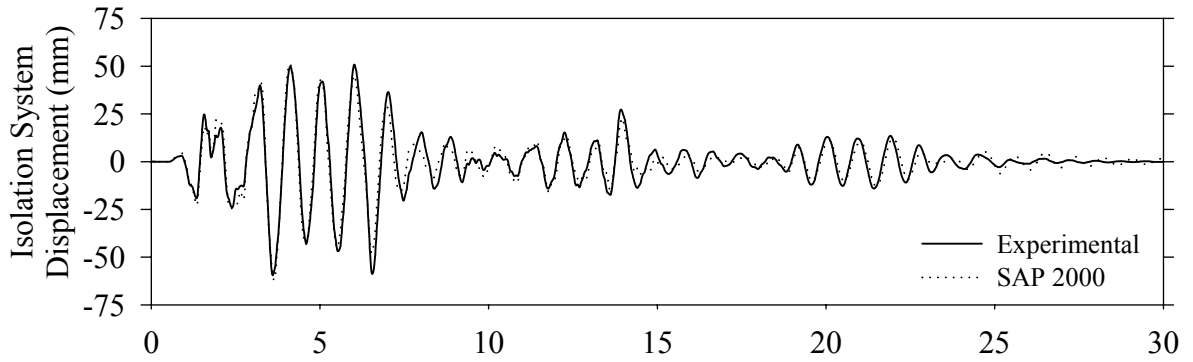
### **ANALYTICAL (SAP2000) vs. EXPERIMENTAL RESPONSE**



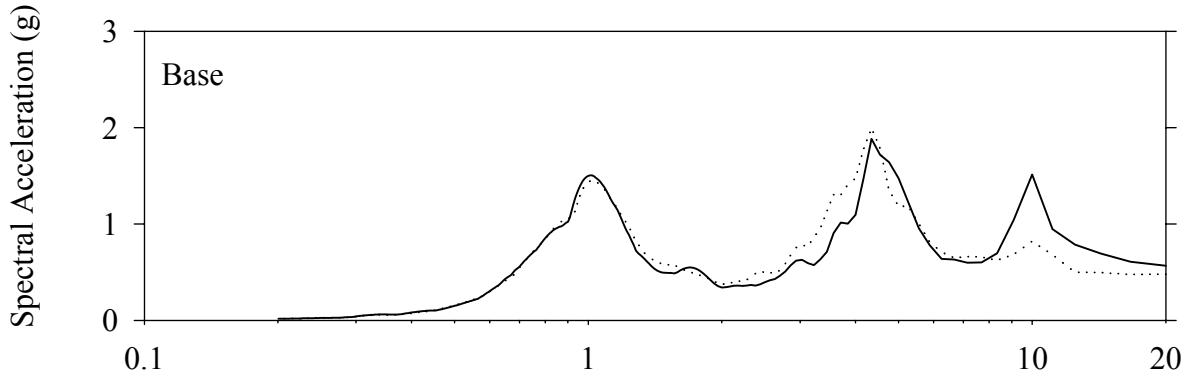
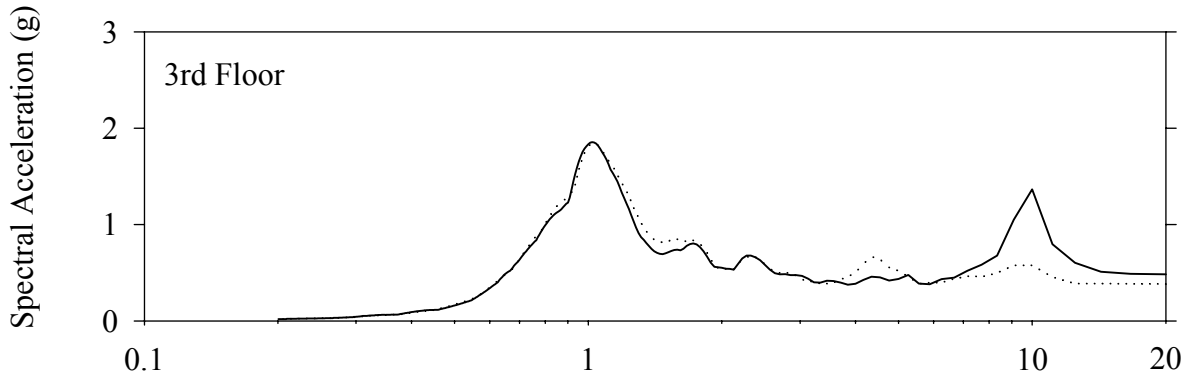
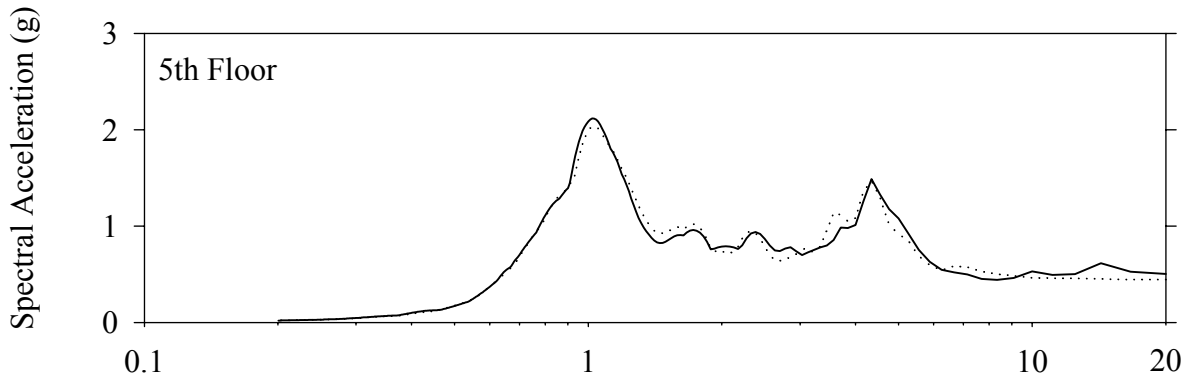
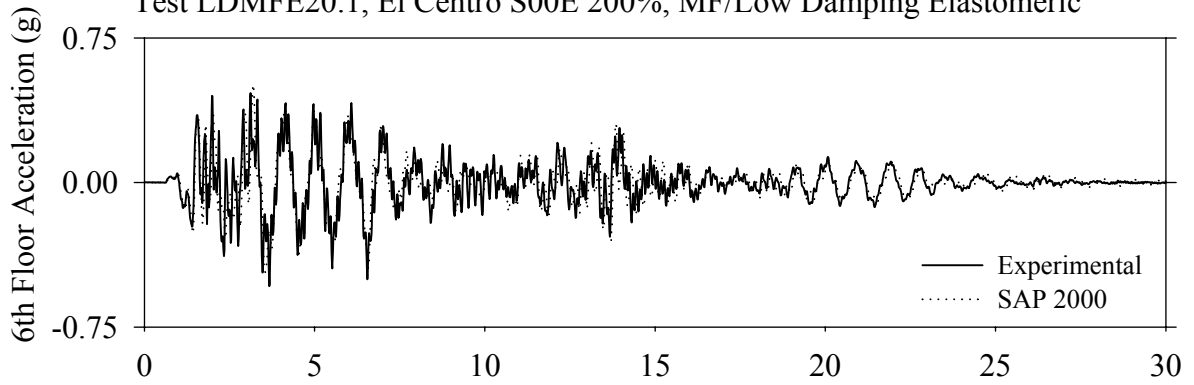
This appendix presents results in graphical form for four excitations of each configuration tested. The presented results include:

1. Isolation system displacement history.
2. Second story shear divided by weight time history.
3. Second story drift divided by story height time history.
4. Base shear divided by weight versus isolation system displacement loop.
5. Sixth floor total acceleration time history.
6. The 5% damped spectra calculated from the recorded acceleration time histories of the 5<sup>th</sup> floor in the range from 0 to 20 Hz.
7. The 5% damped spectra calculated from the recorded acceleration time histories of the 3<sup>rd</sup> floor in the range from 0 to 20 Hz.
8. The 5% damped spectra calculated from the recorded acceleration time histories of the base in the range from 0 to 20 Hz.

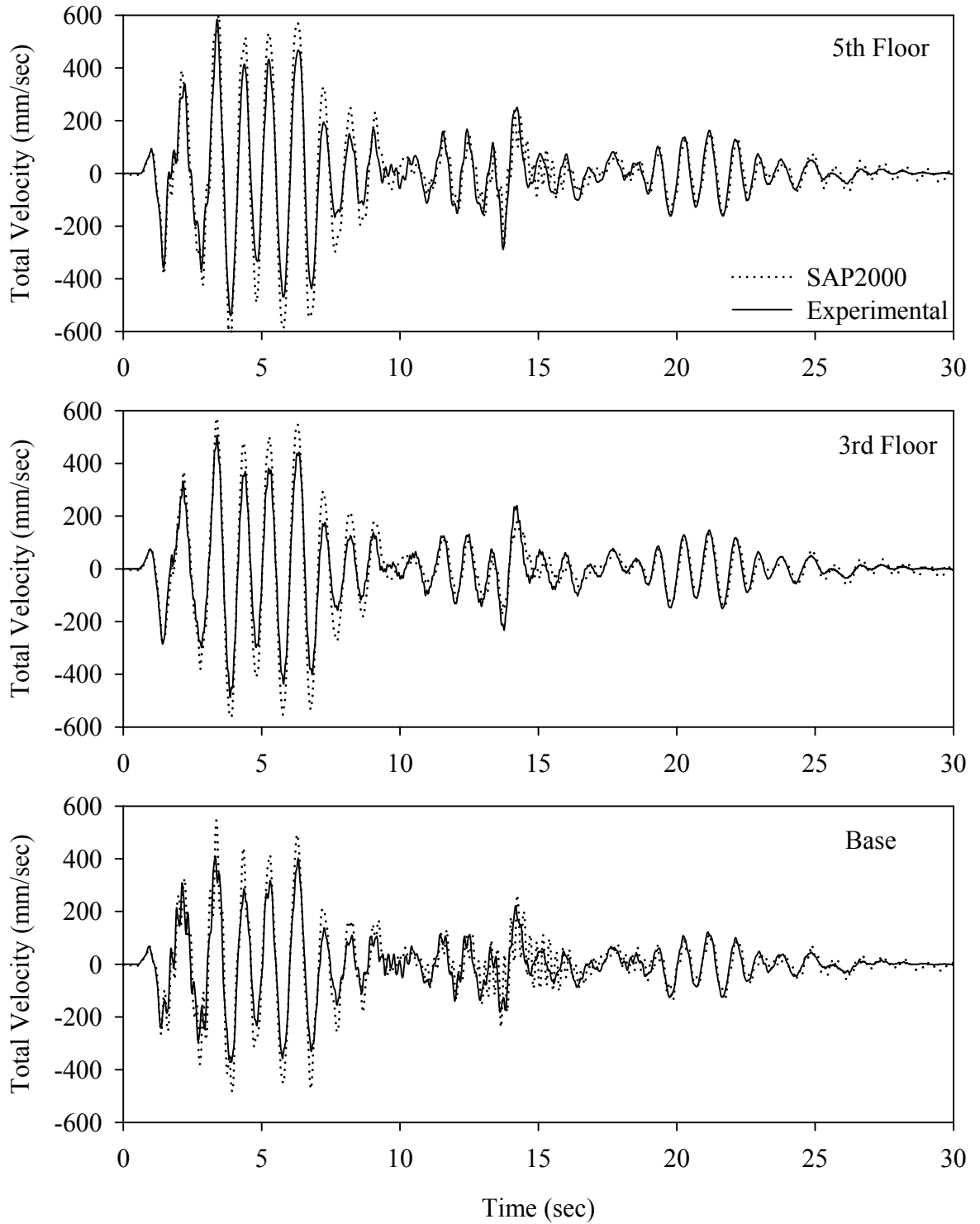
Test LDMFE20.1, El Centro S00E 200%, MF/Low Damping Elastomeric



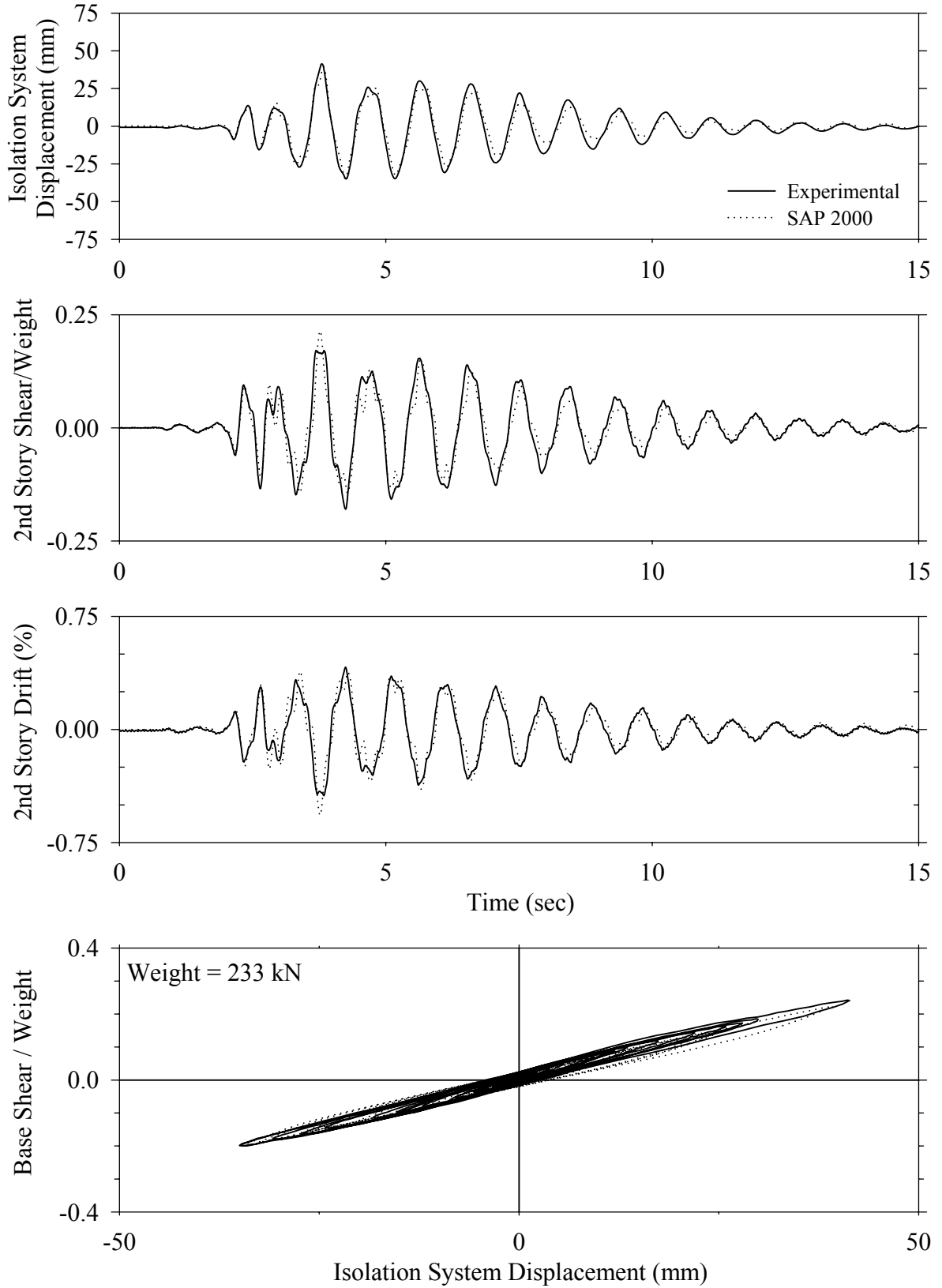
Test LDMFE20.1, El Centro S00E 200%, MF/Low Damping Elastomeric



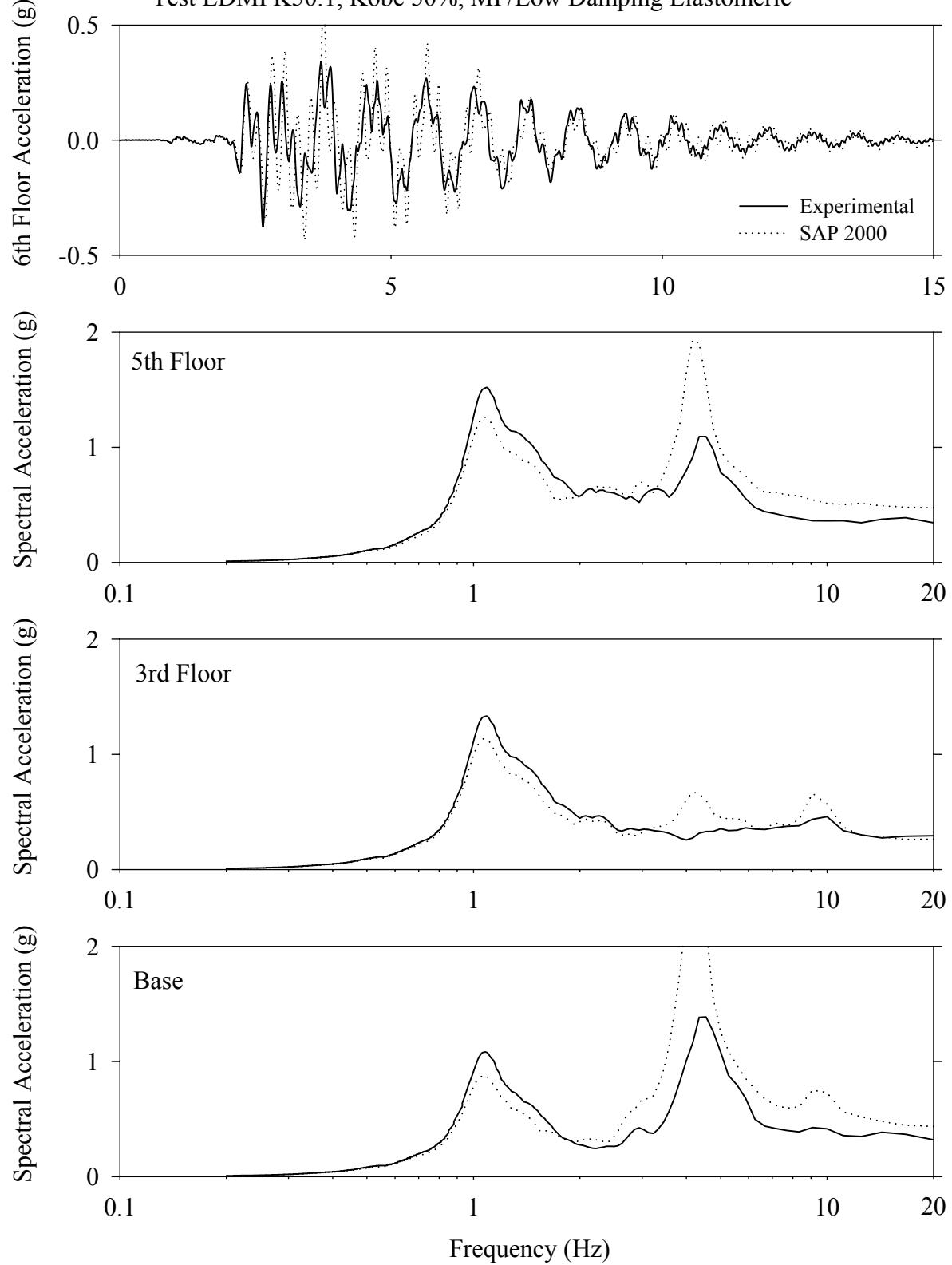
Test LDMFE20.1, El Centro S00E 200%, MF/Low Damping Elastomeric



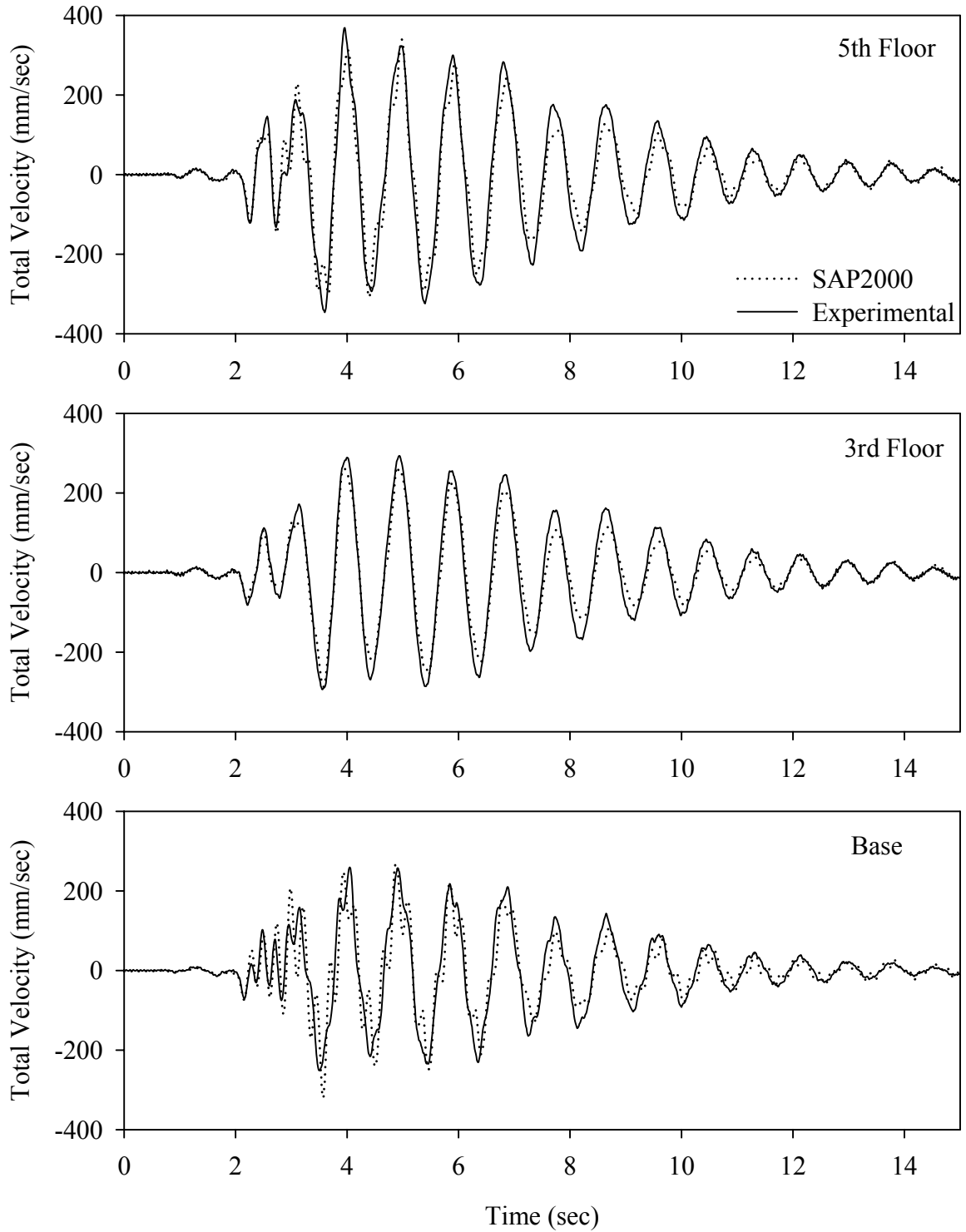
Test LDMFK50.1, Kobe 50%, MF/Low Damping Elastomeric



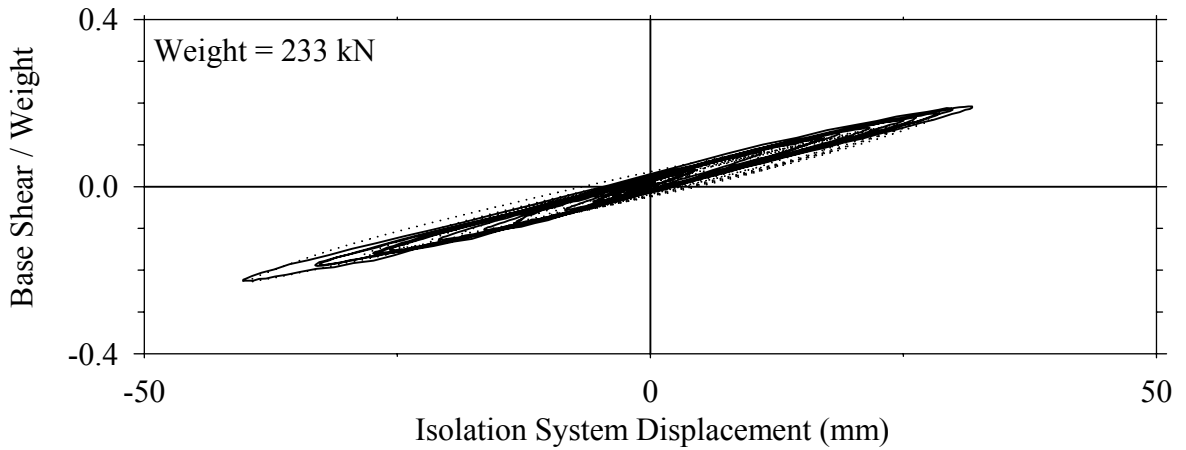
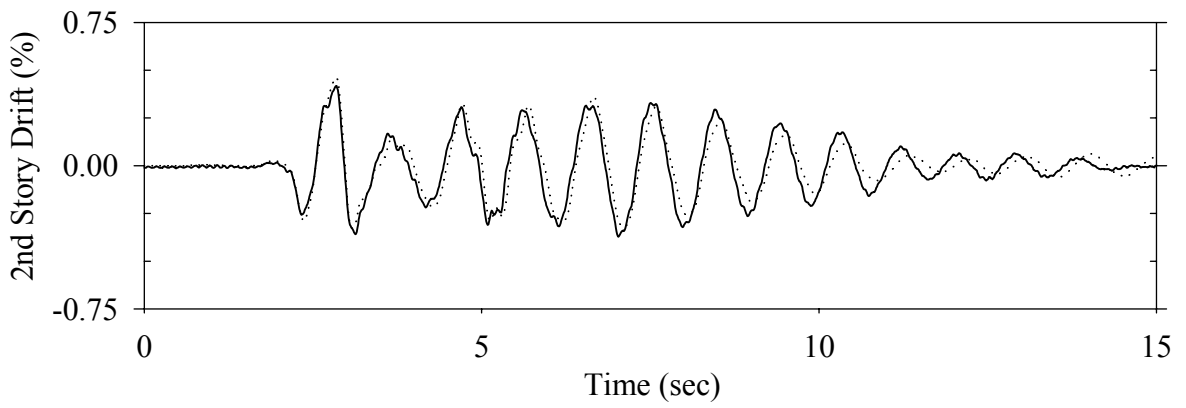
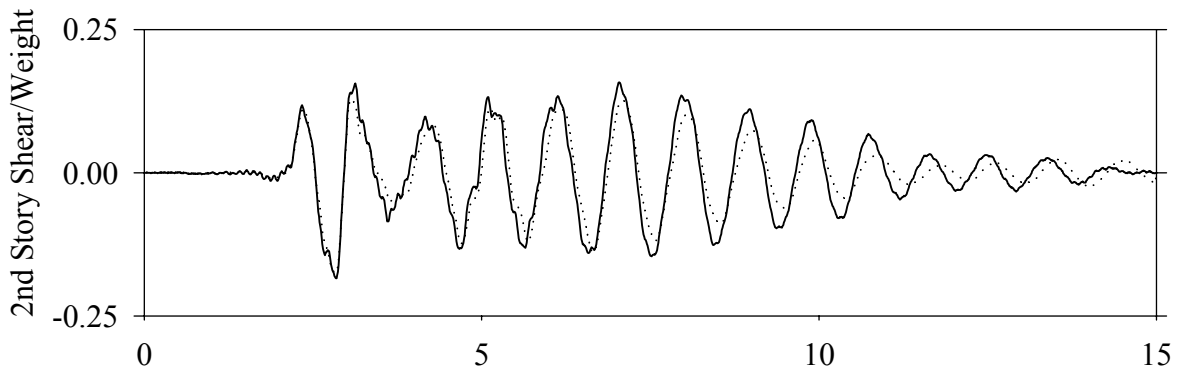
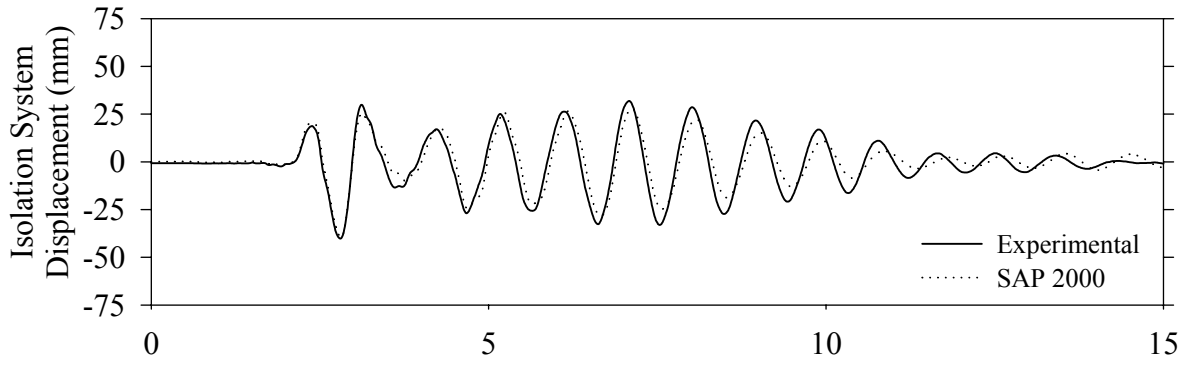
Test LDMFK50.1, Kobe 50%, MF/Low Damping Elastomeric



Test LDMFK50.1, Kobe 50%, MF/Low Damping Elastomeric

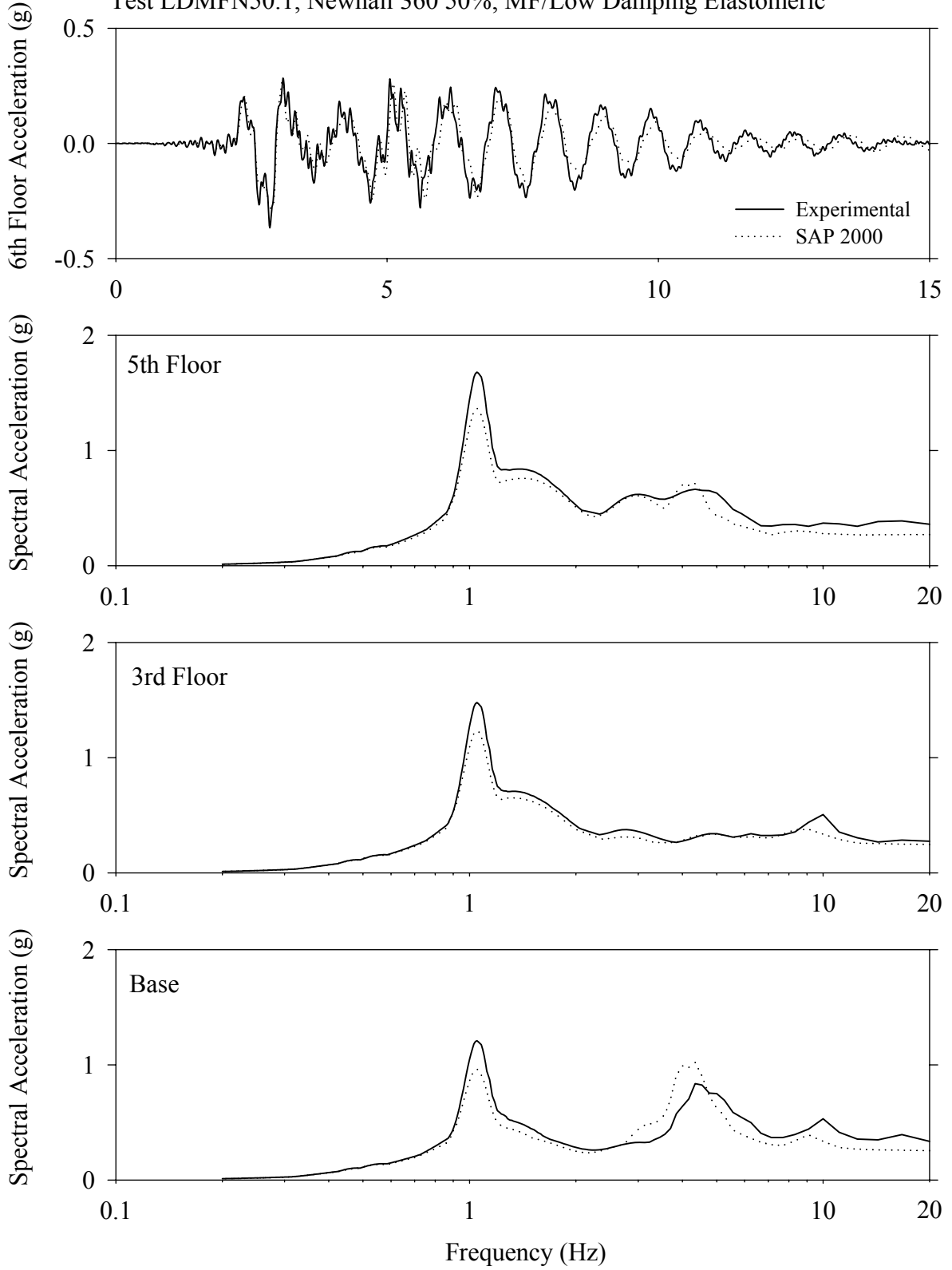


Test LDMFN50.1, Newhall 360 50%, MF/Low Damping Elastomeric

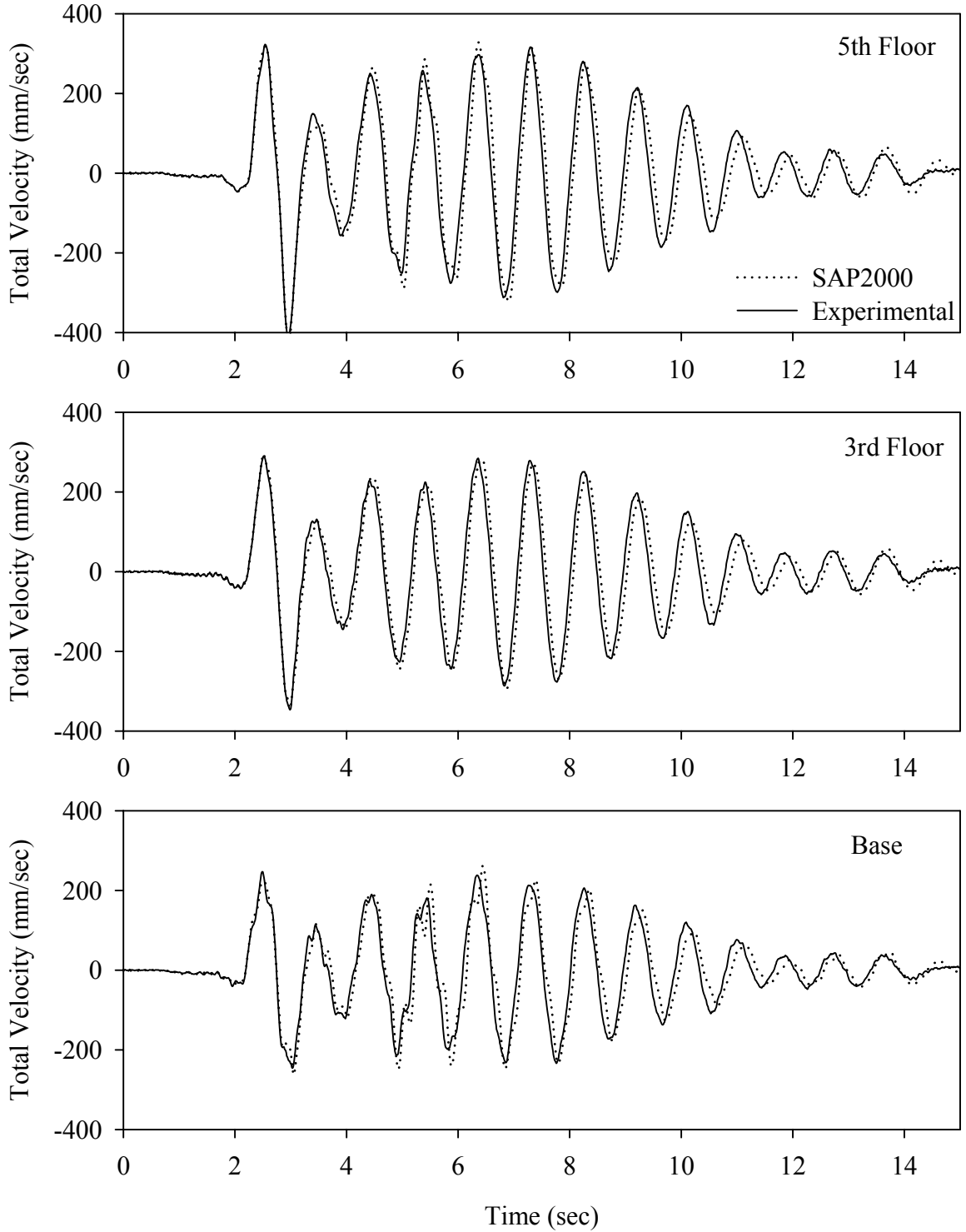




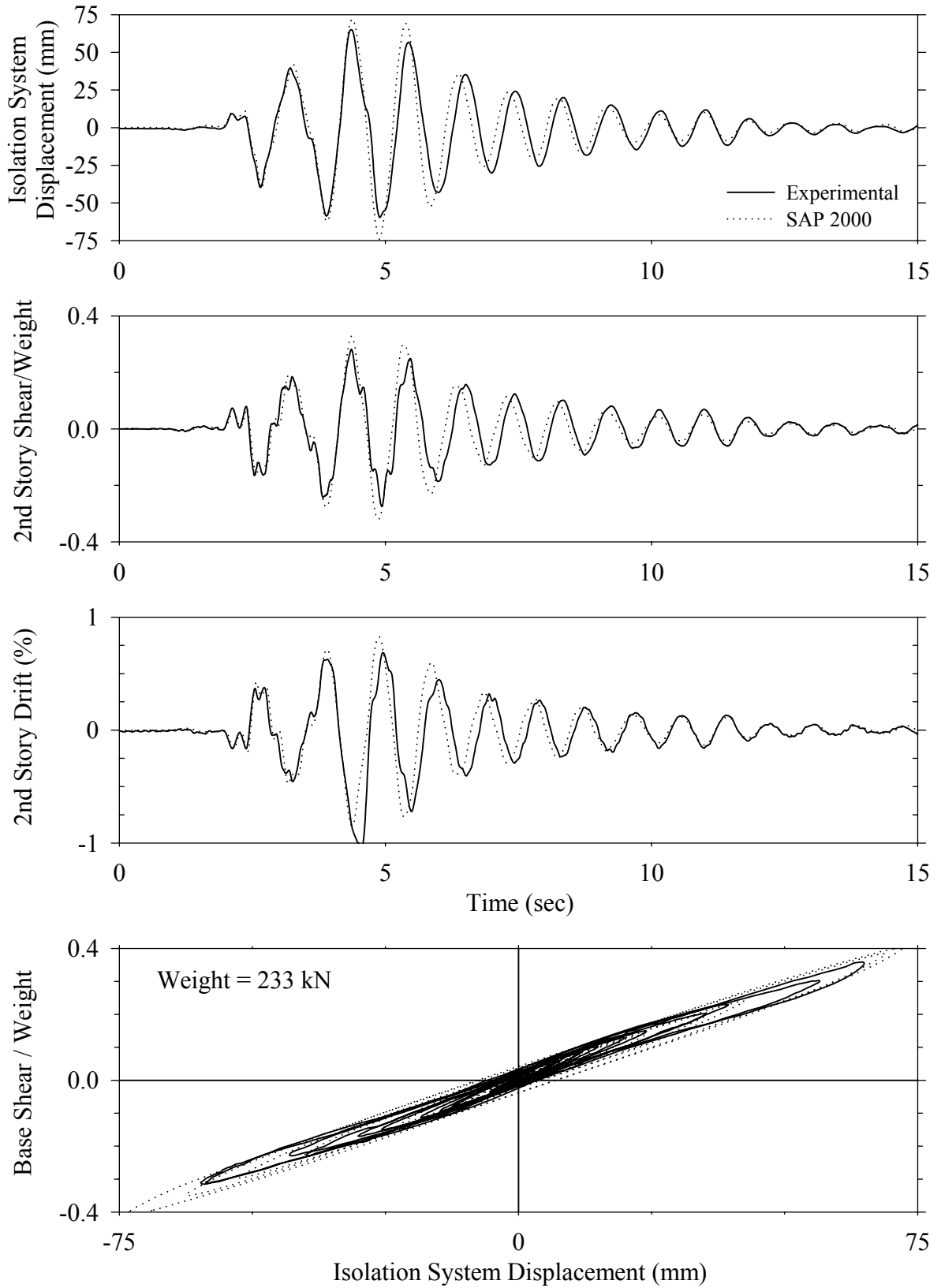
Test LDMFN50.1, Newhall 360 50%, MF/Low Damping Elastomeric



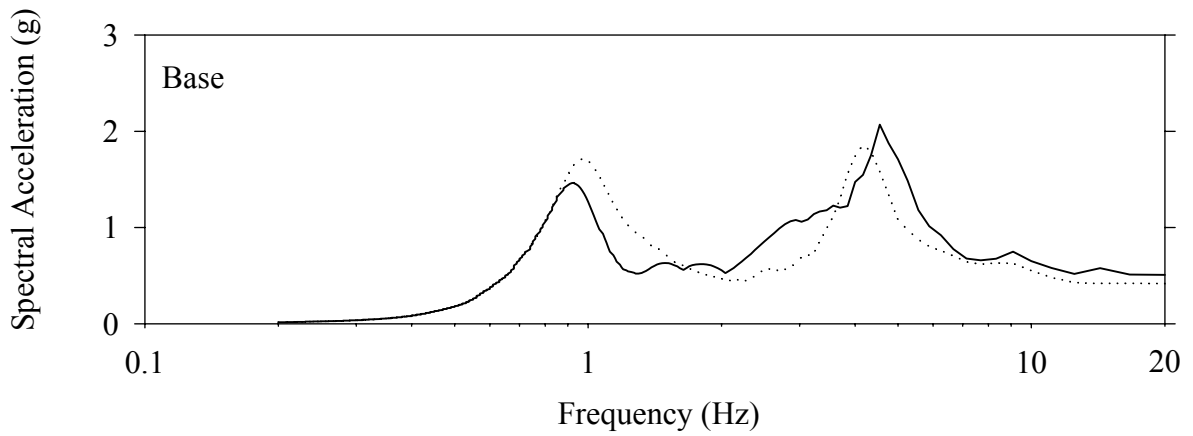
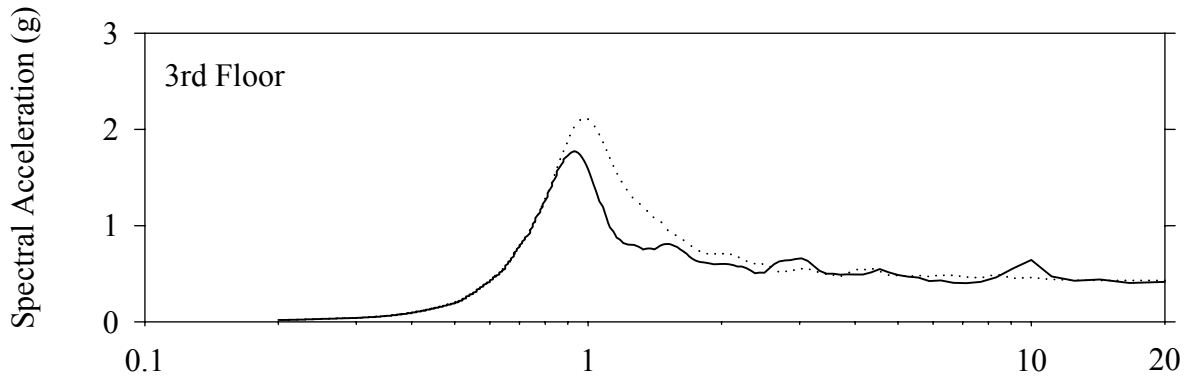
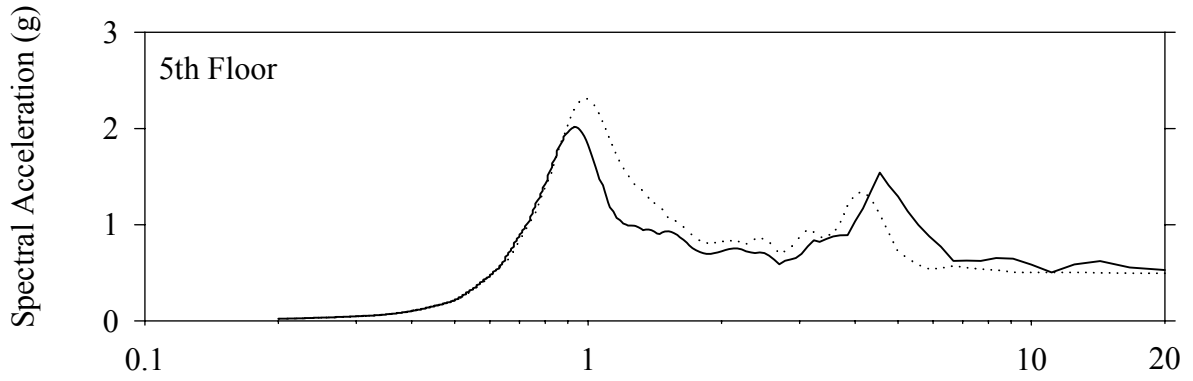
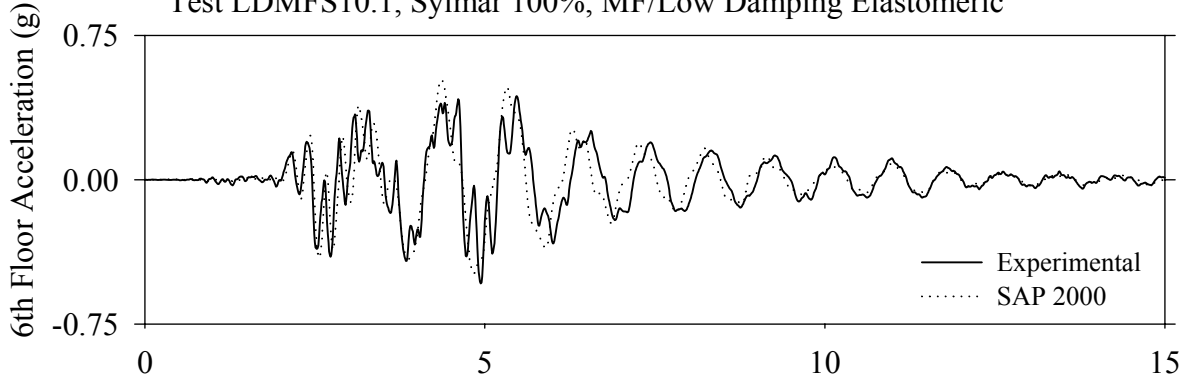
Test LDMFN50.1, Newhall 360 50%, MF/Low Damping Elastomeric



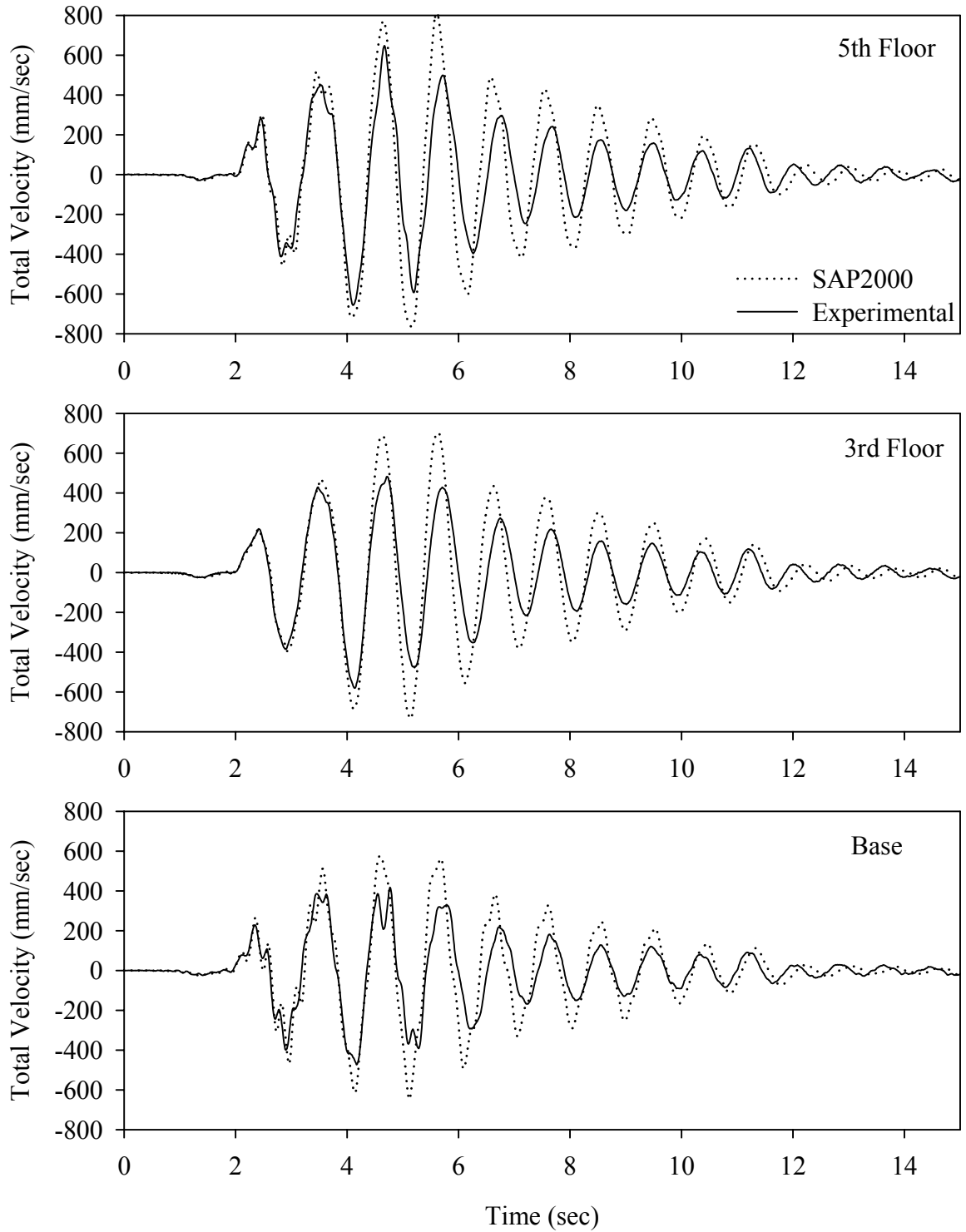
Test LDMFS10.1, Sylmar 100%, MF/Low Damping Elastomeric



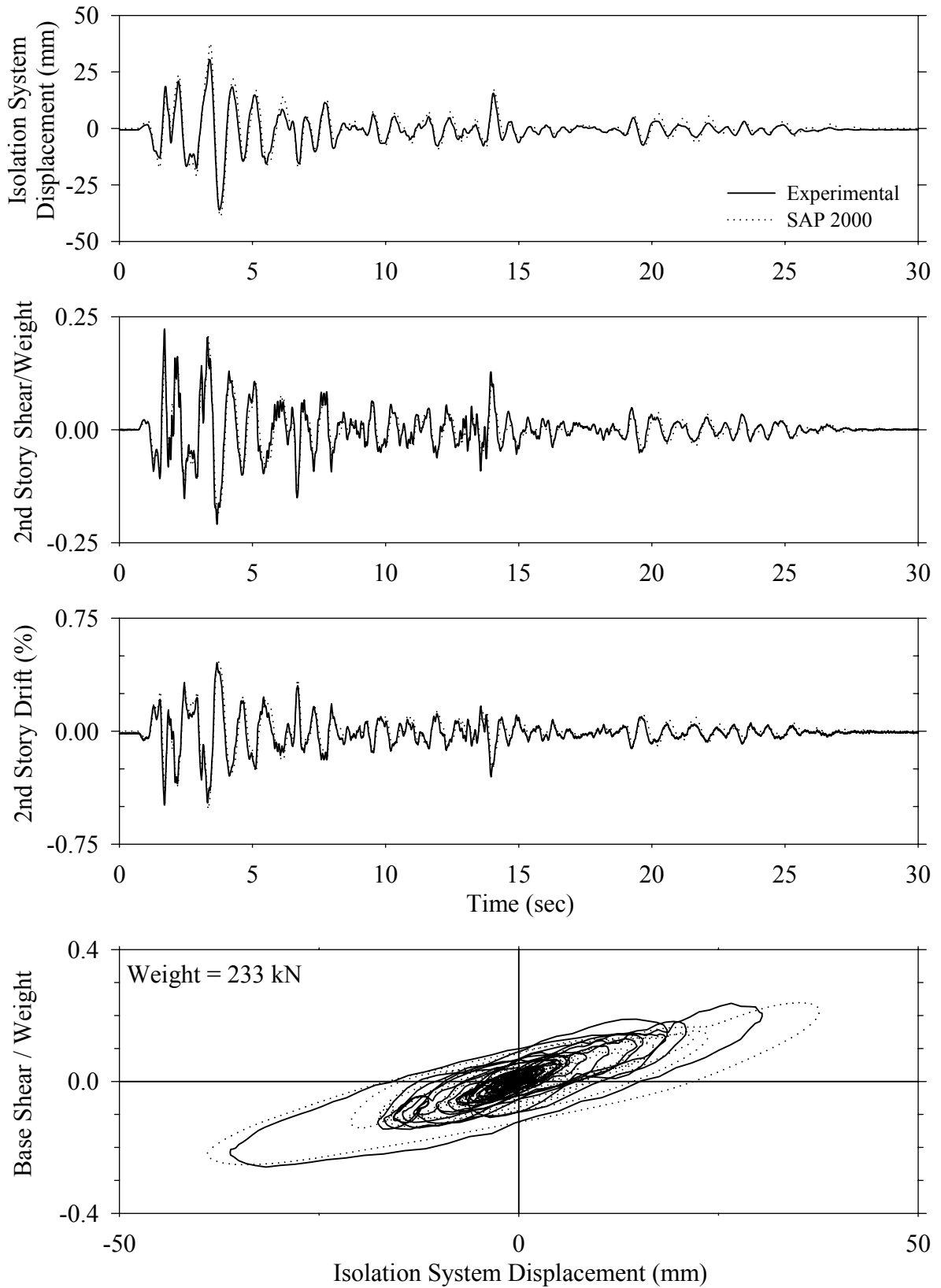
Test LDMFS10.1, Sylmar 100%, MF/Low Damping Elastomeric



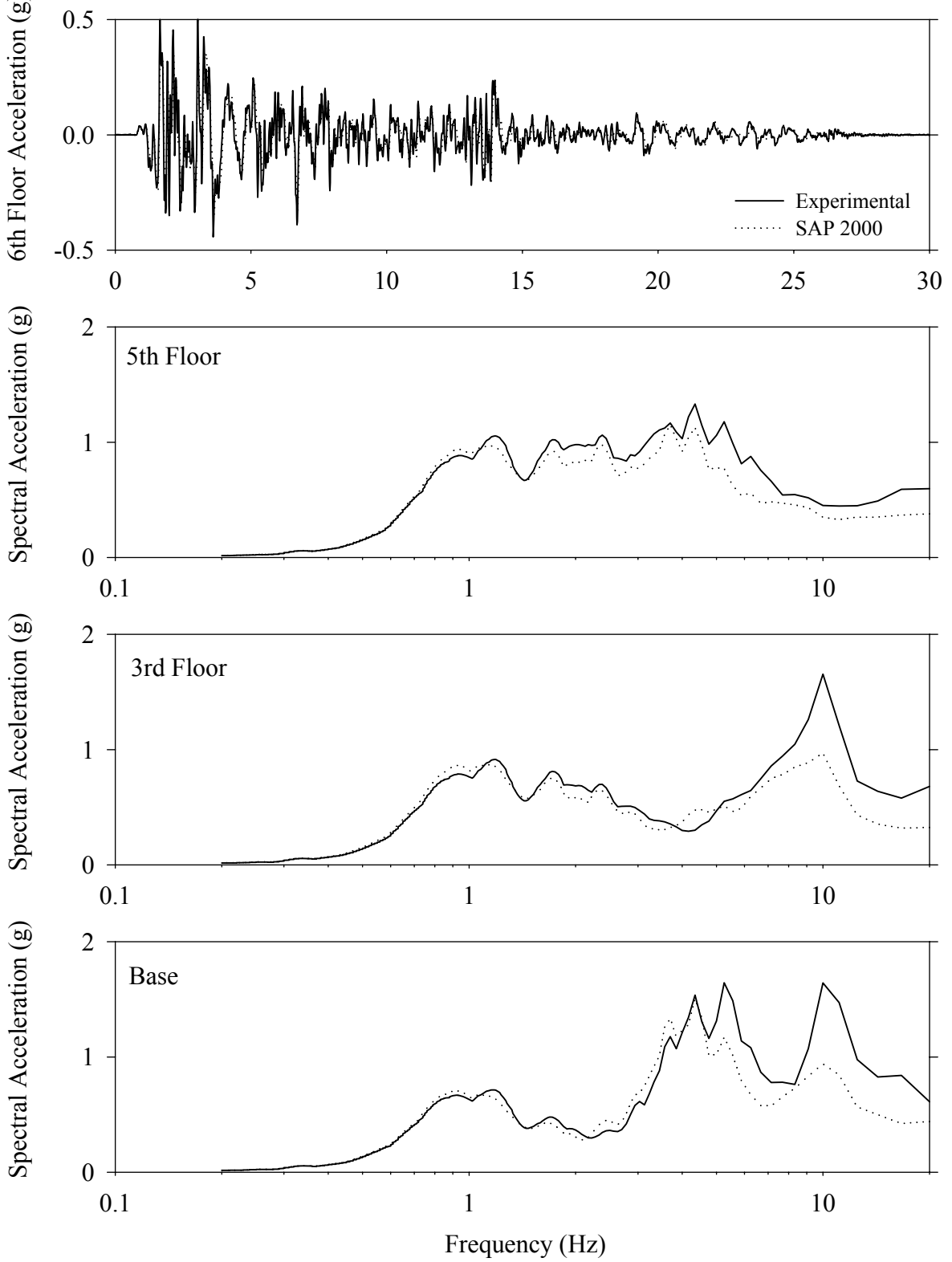
Test LDMFS10.1, Sylmar 100%, MF/Low Damping Elastomeric



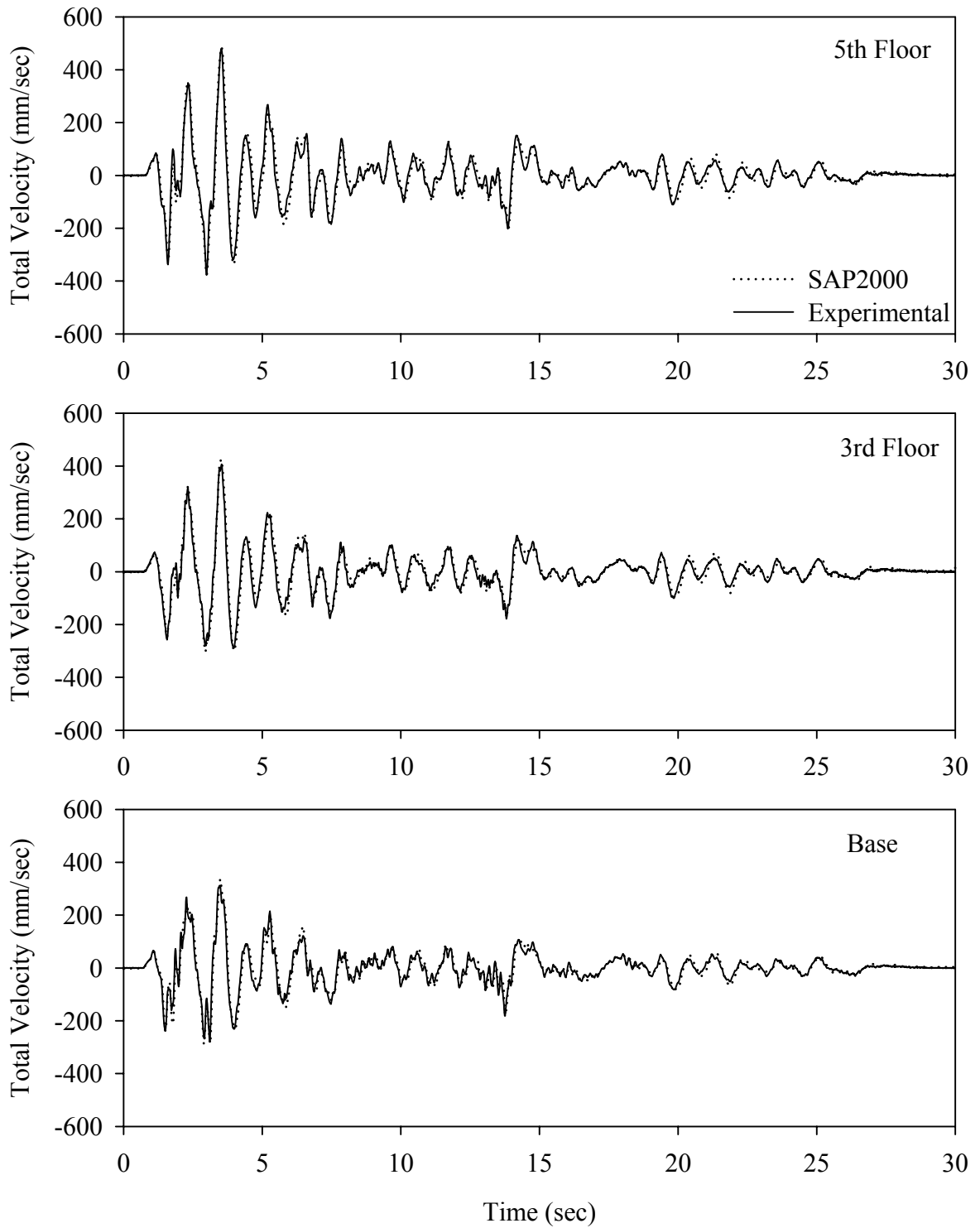
Test LDMLE20.1, El Centro S00E 200%, MF/Low Damping Elastomeric with Linear Dampers



Test LDMLE20.1, El Centro S00E 200%, MF/Low Damping Elastomeric with Linear Dampers

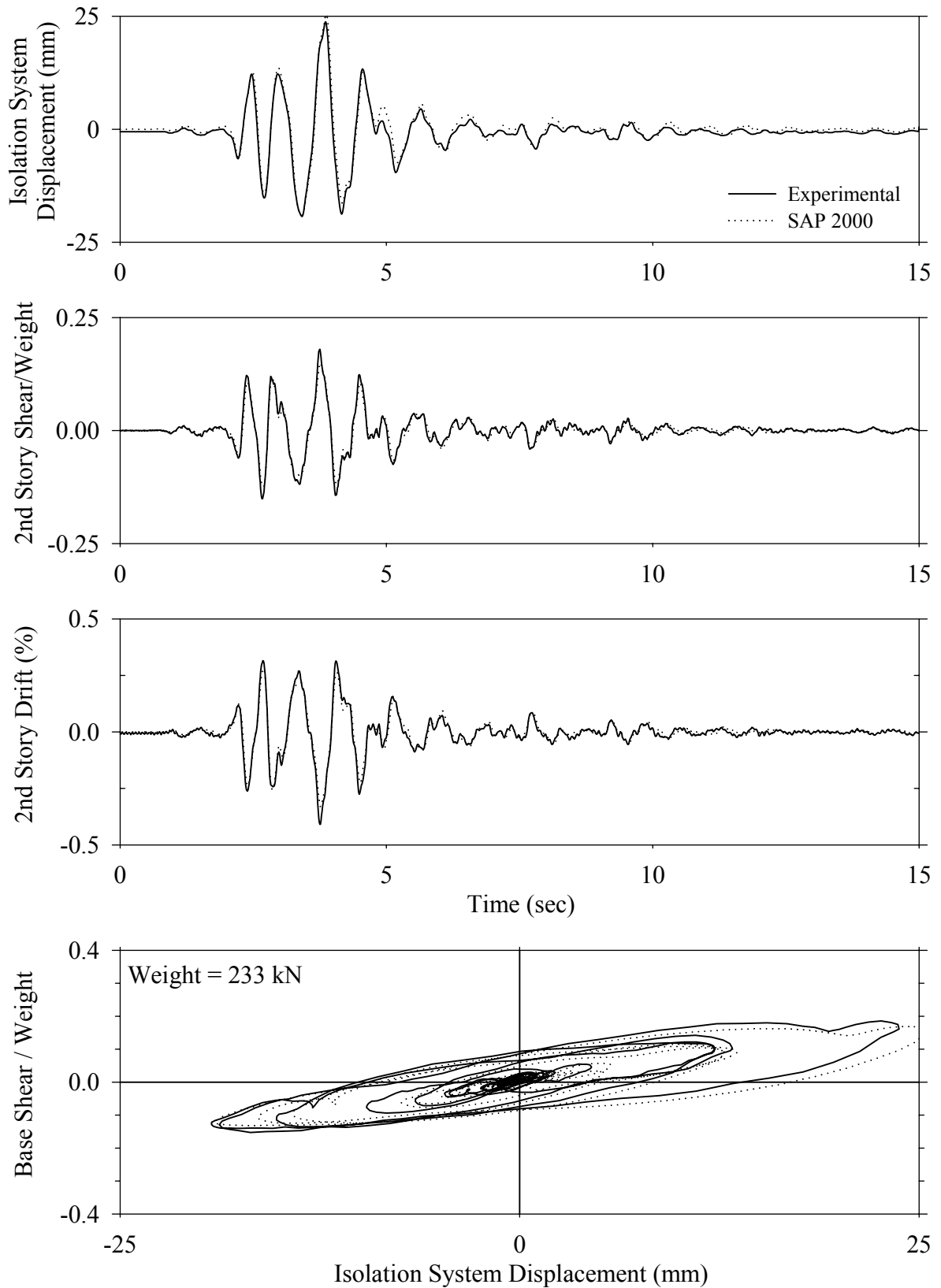


Test LDMLE20.1, El Centro S00E 200%, MF/Low Damping Elastomeric with Linear Dampers

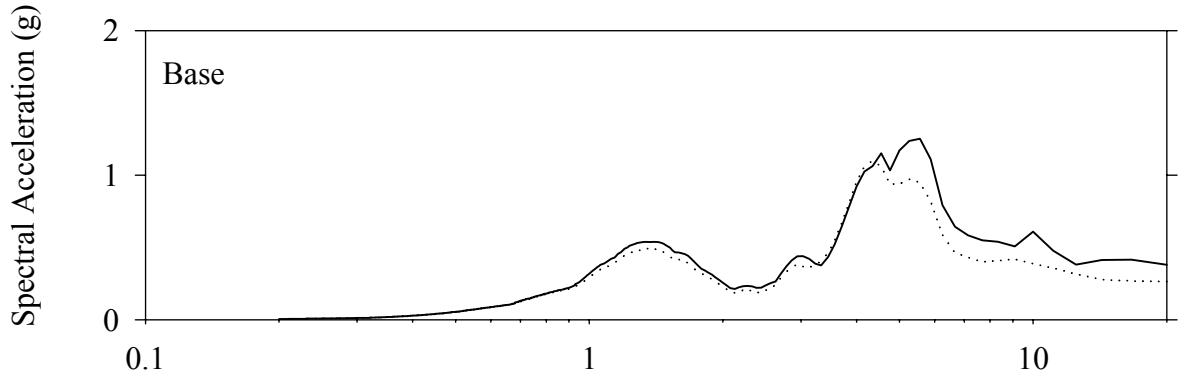
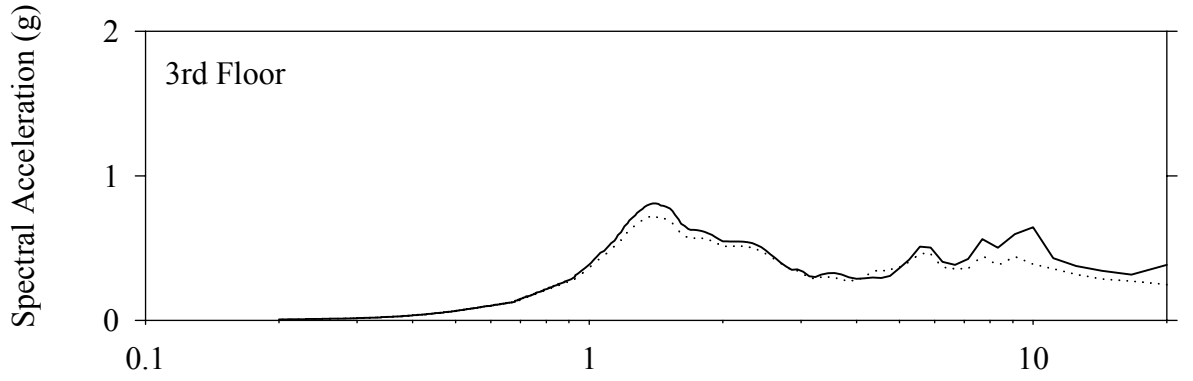
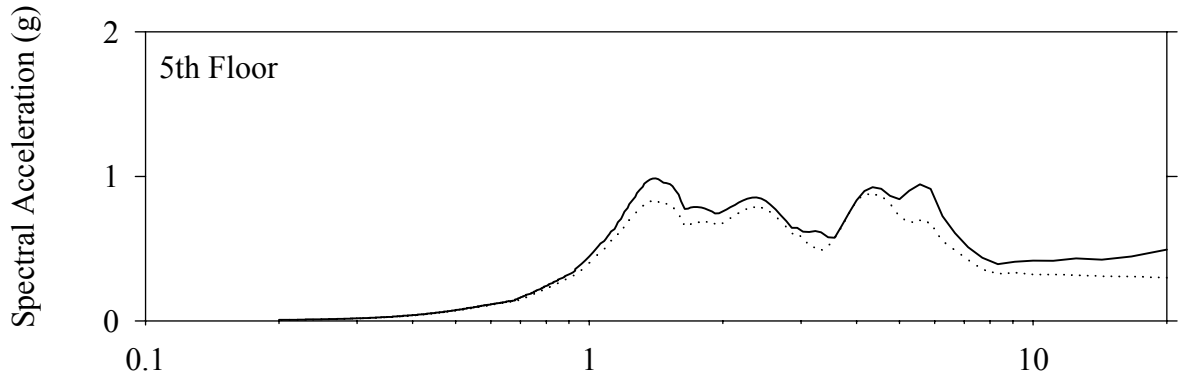
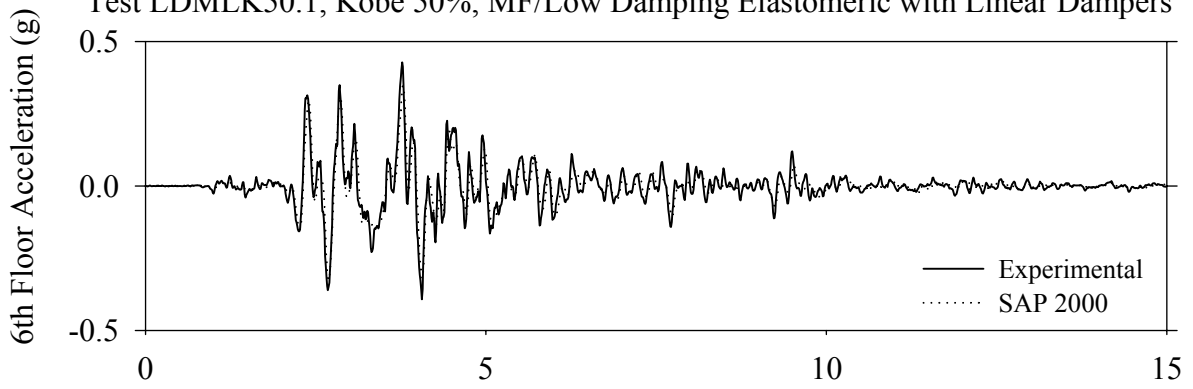




Test LDMLK50.1, Kobe 50%, MF/Low Damping Elastomeric with Linear Dampers

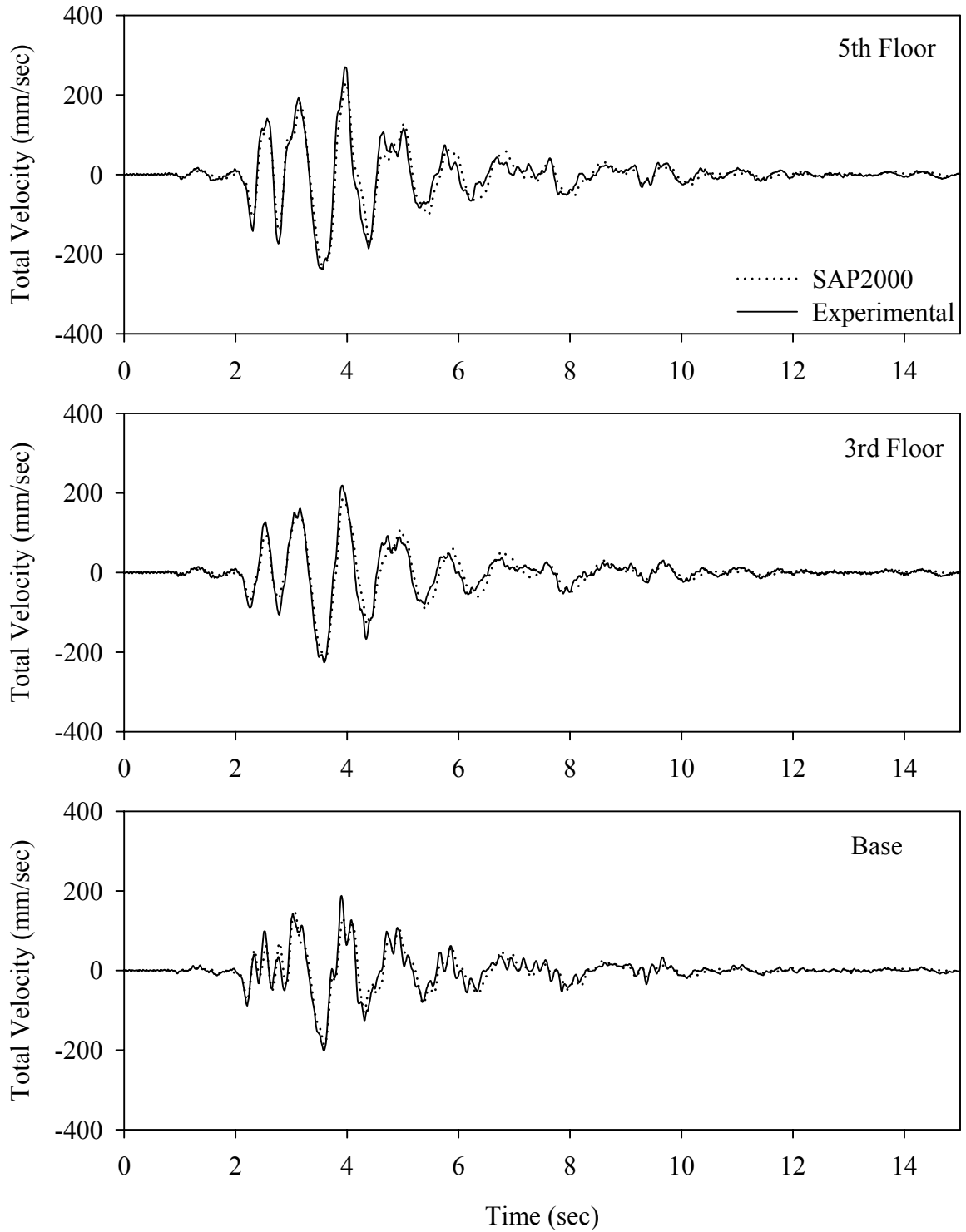


Test LDMLK50.1, Kobe 50%, MF/Low Damping Elastomeric with Linear Dampers

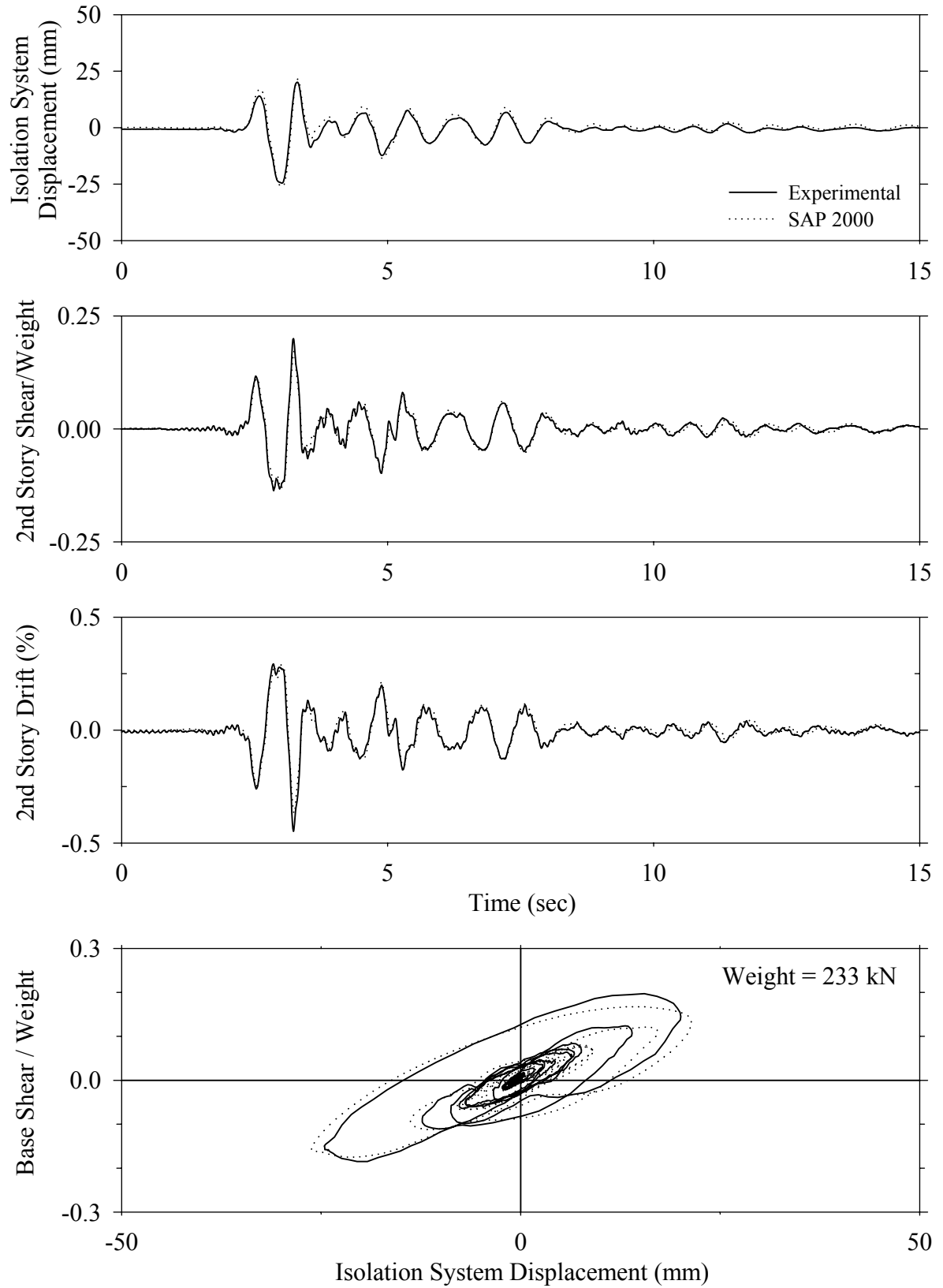


Frequency (Hz)

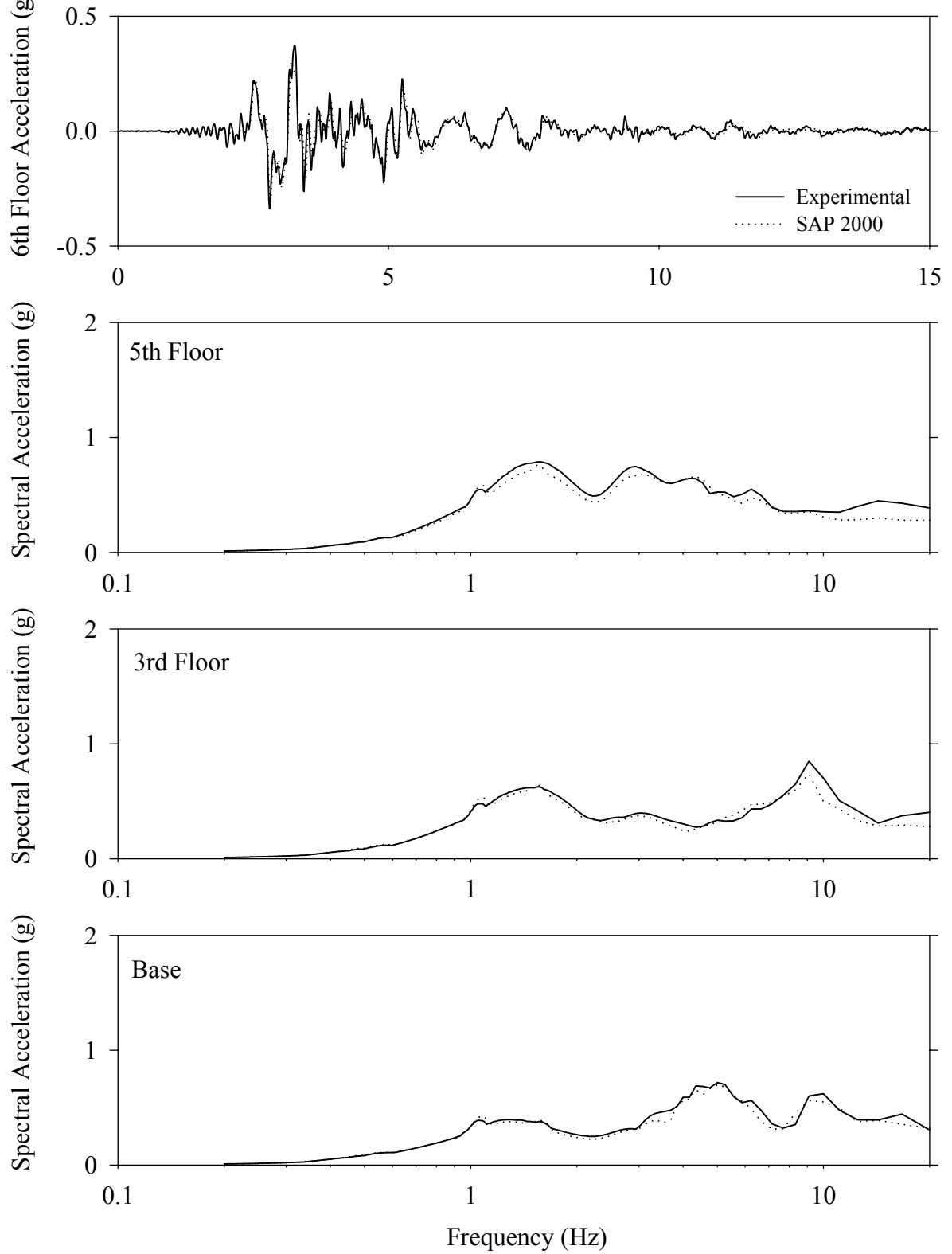
Test LDMLK50.1, Kobe 50%, MF/Low Damping Elastomeric with Linear Dampers



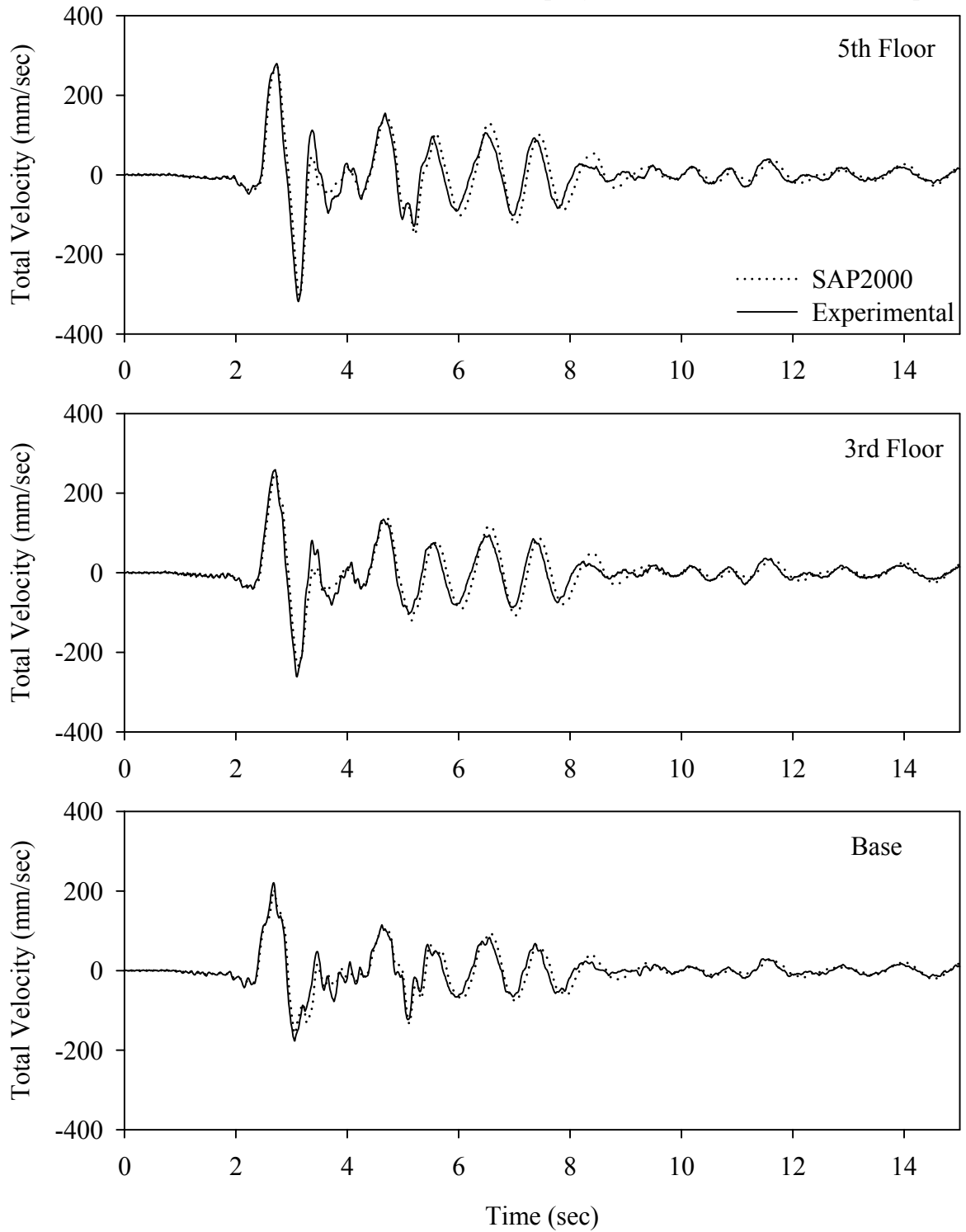
Test LDMLN50.1, Newhall 360 50%, MF/Low Damping Elastomeric with Linear Dampers



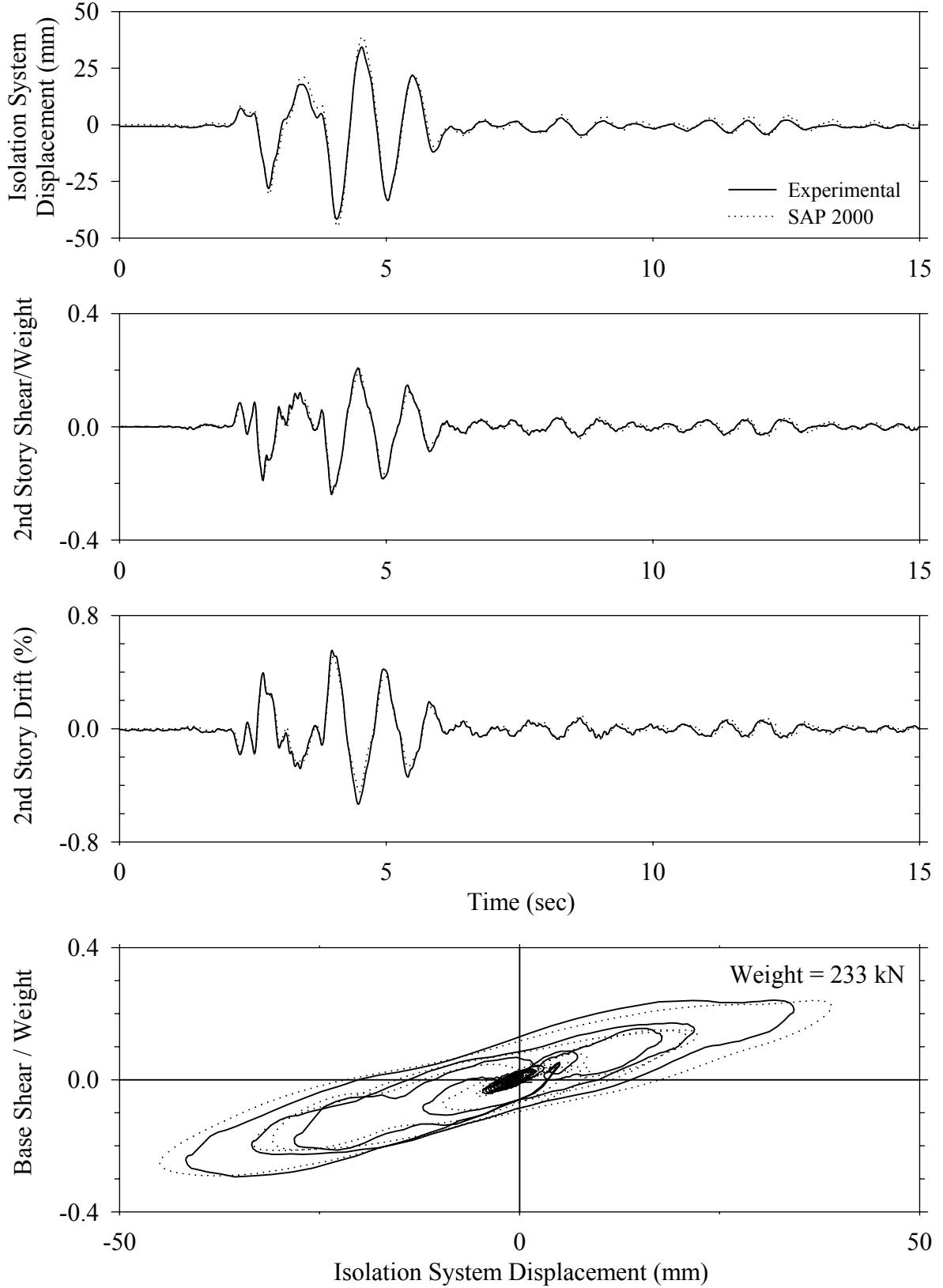
Test LDMLN50.1, Newhall 360 50%, MF/Low Damping Elastomeric with Linear Dampers



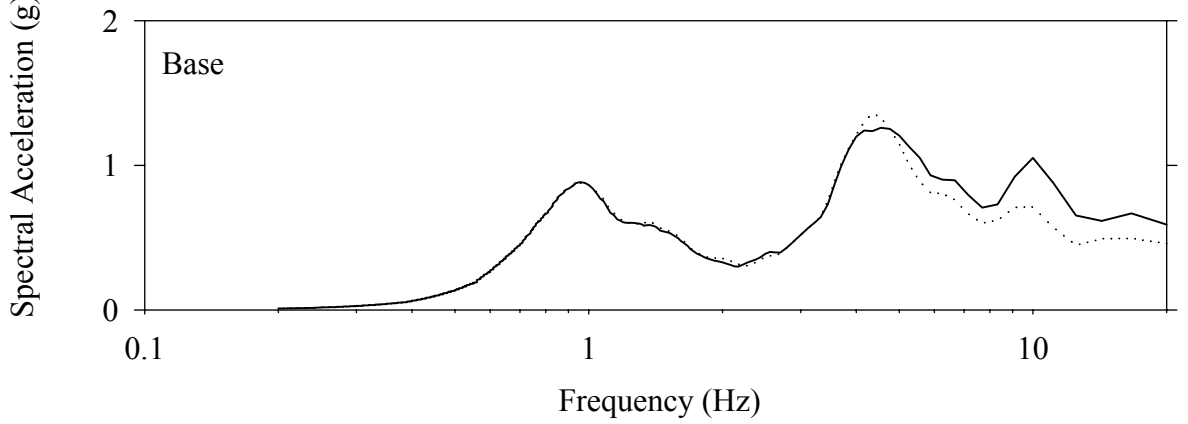
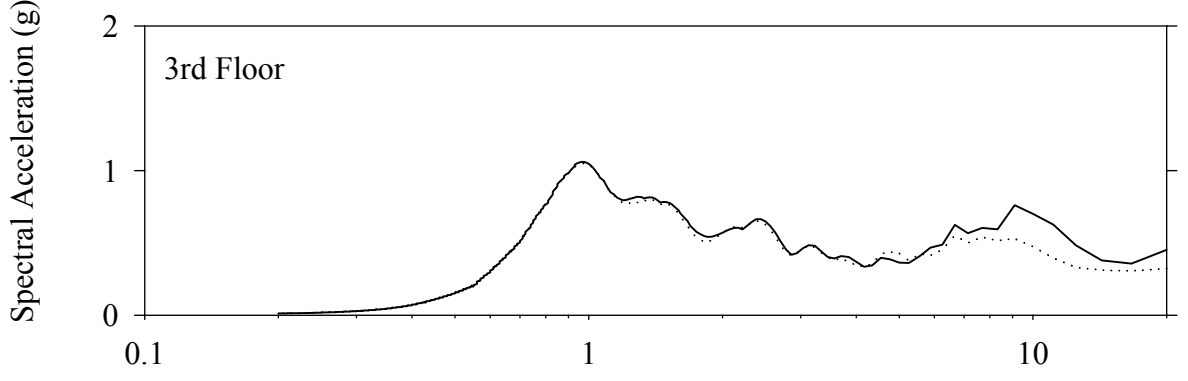
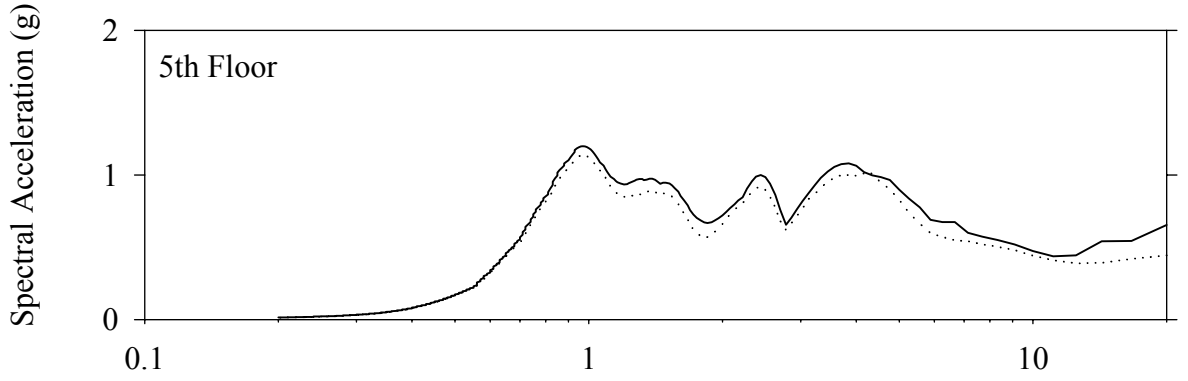
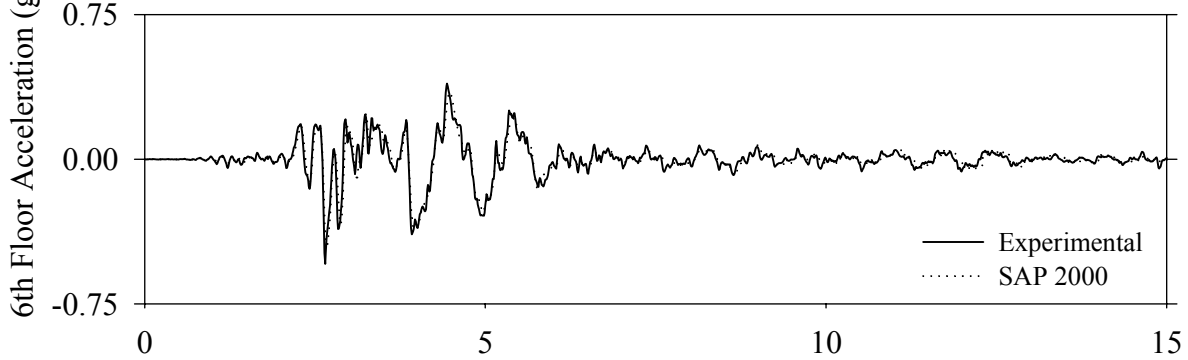
Test LDMLN50.1, Newhall 360 50%, MF/Low Damping Elastomeric with Linear Dampers



Test LDMLS10.1, Sylmar 100%, MF/Low Damping Elastomeric with Linear Dampers

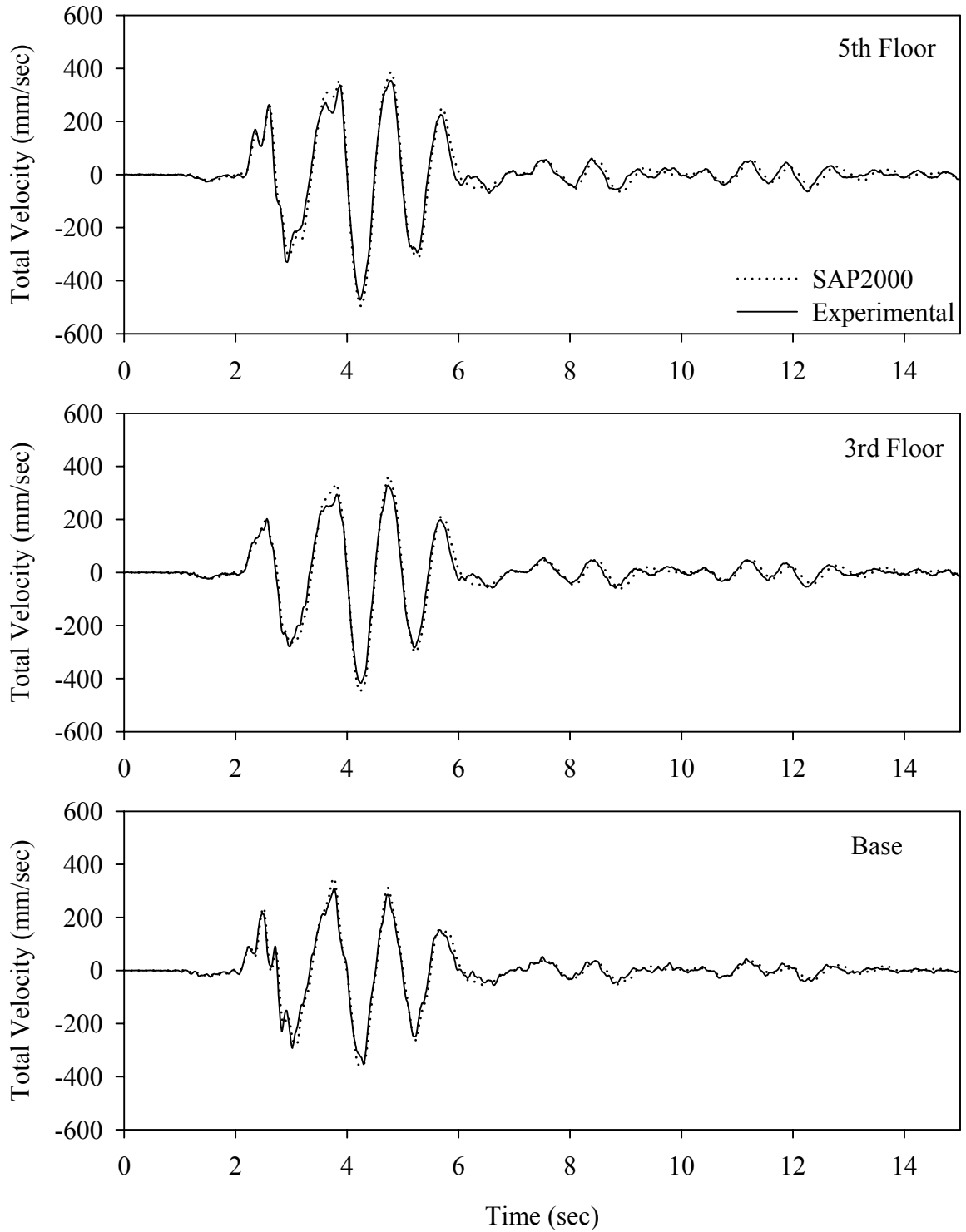


Test LDMLS10.1, Sylmar 100%, MF/Low Damping Elastomeric with Linear Dampers

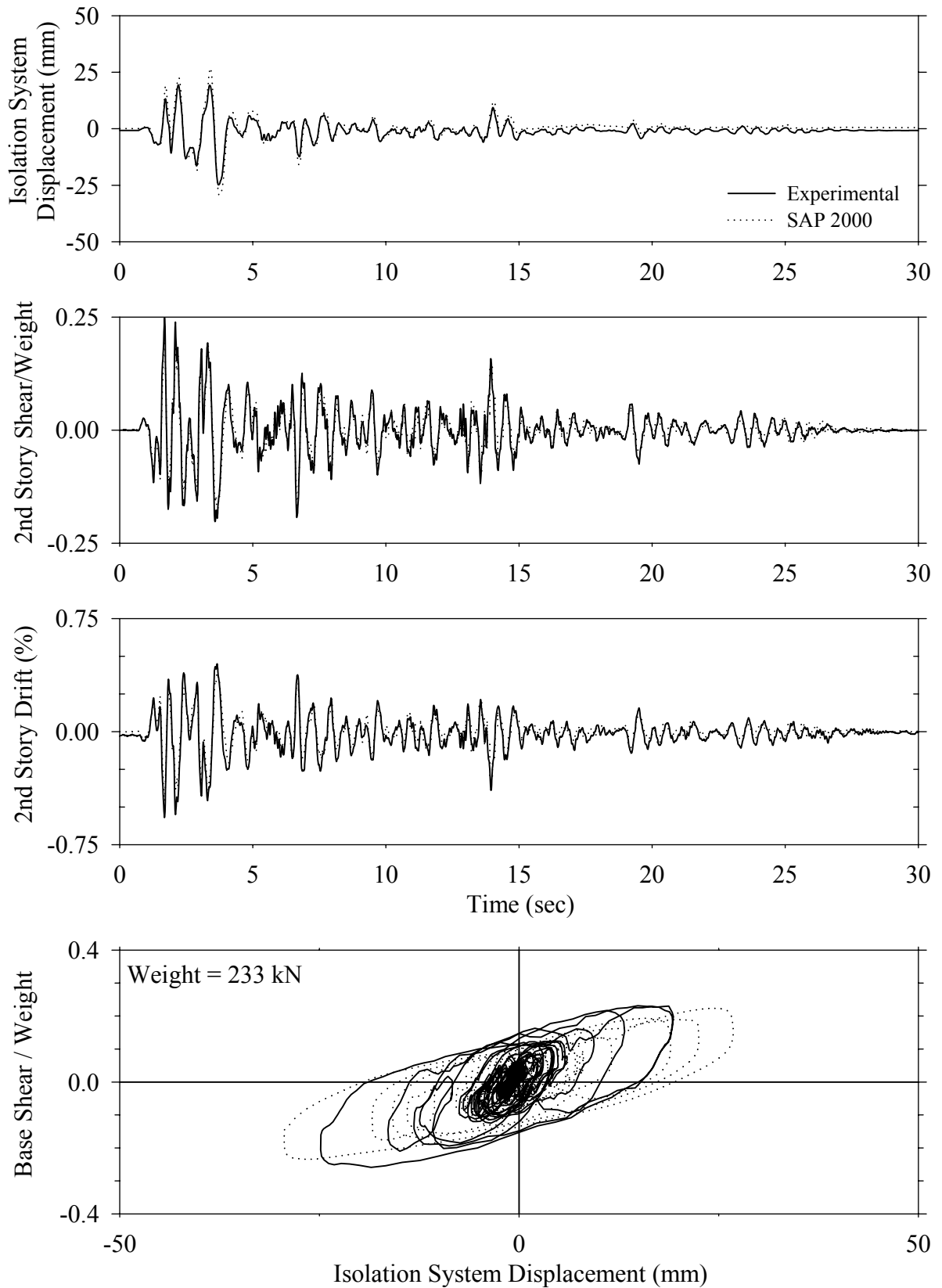




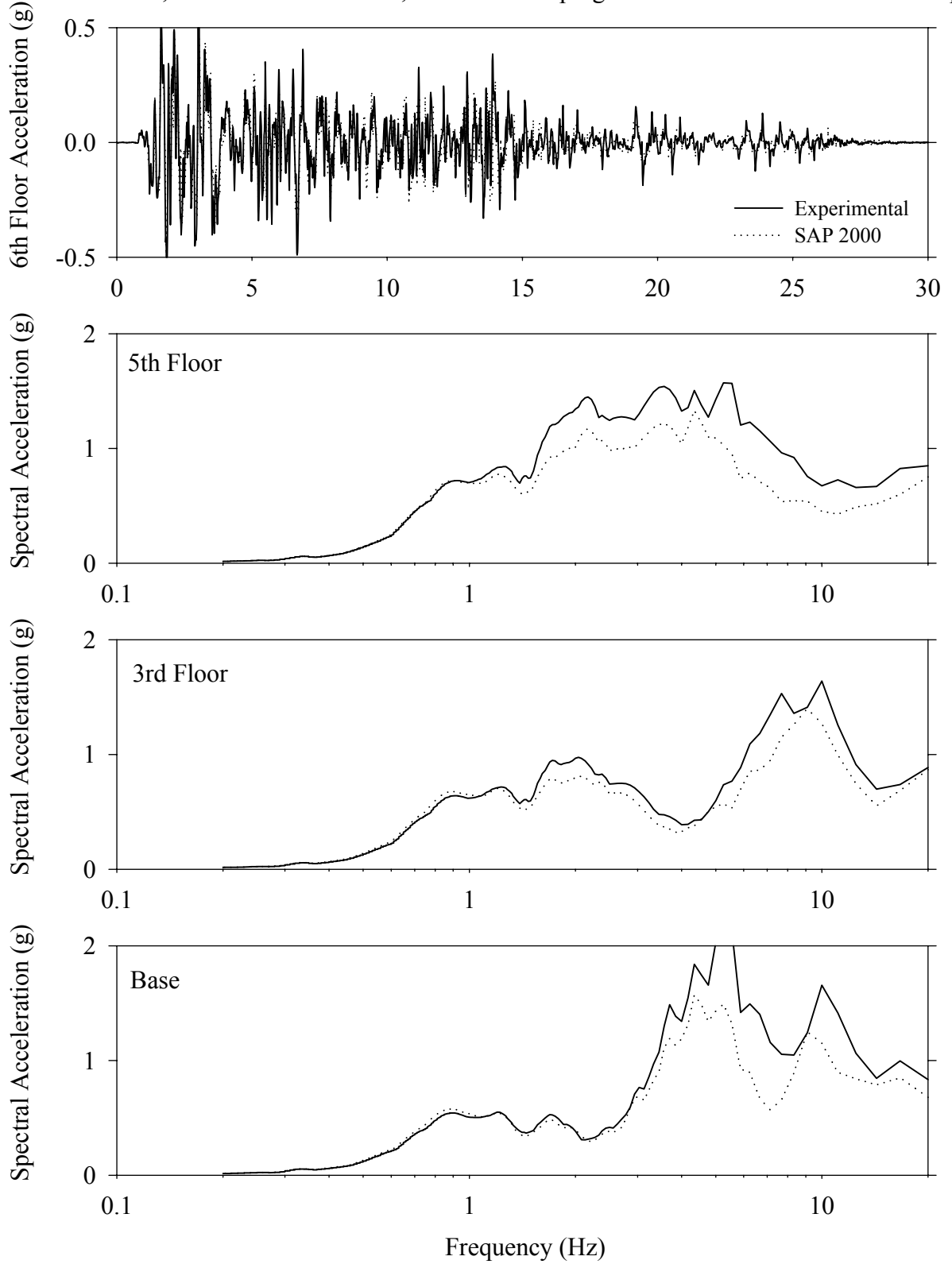
Test LDMLS10.1, Sylmar 100%, MF/Low Damping Elastomeric with Linear Dampers



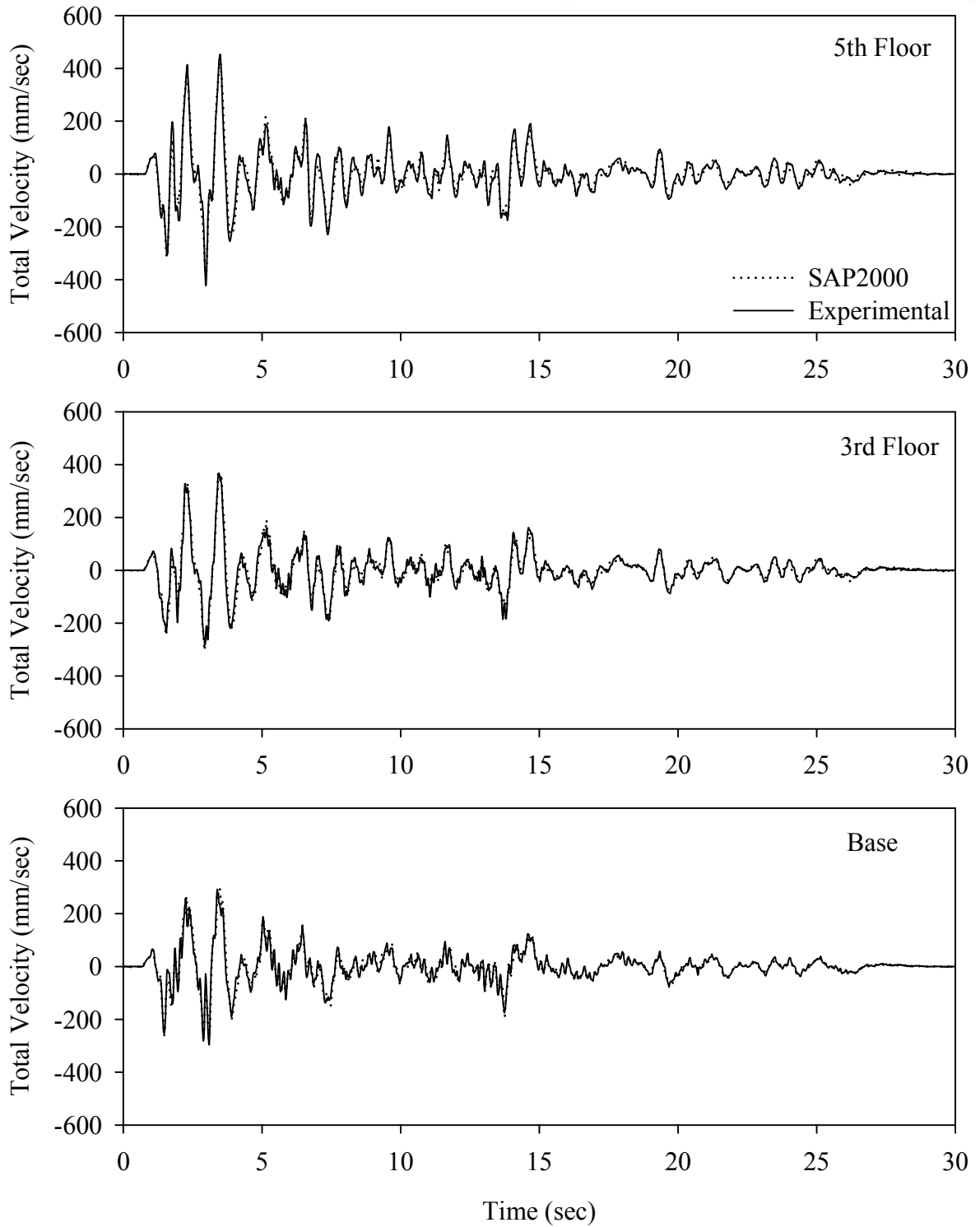
Test LDMNE20.1, El Centro S00E 200%, MF/Low Damping Elastomeric with Nonlinear Dampers



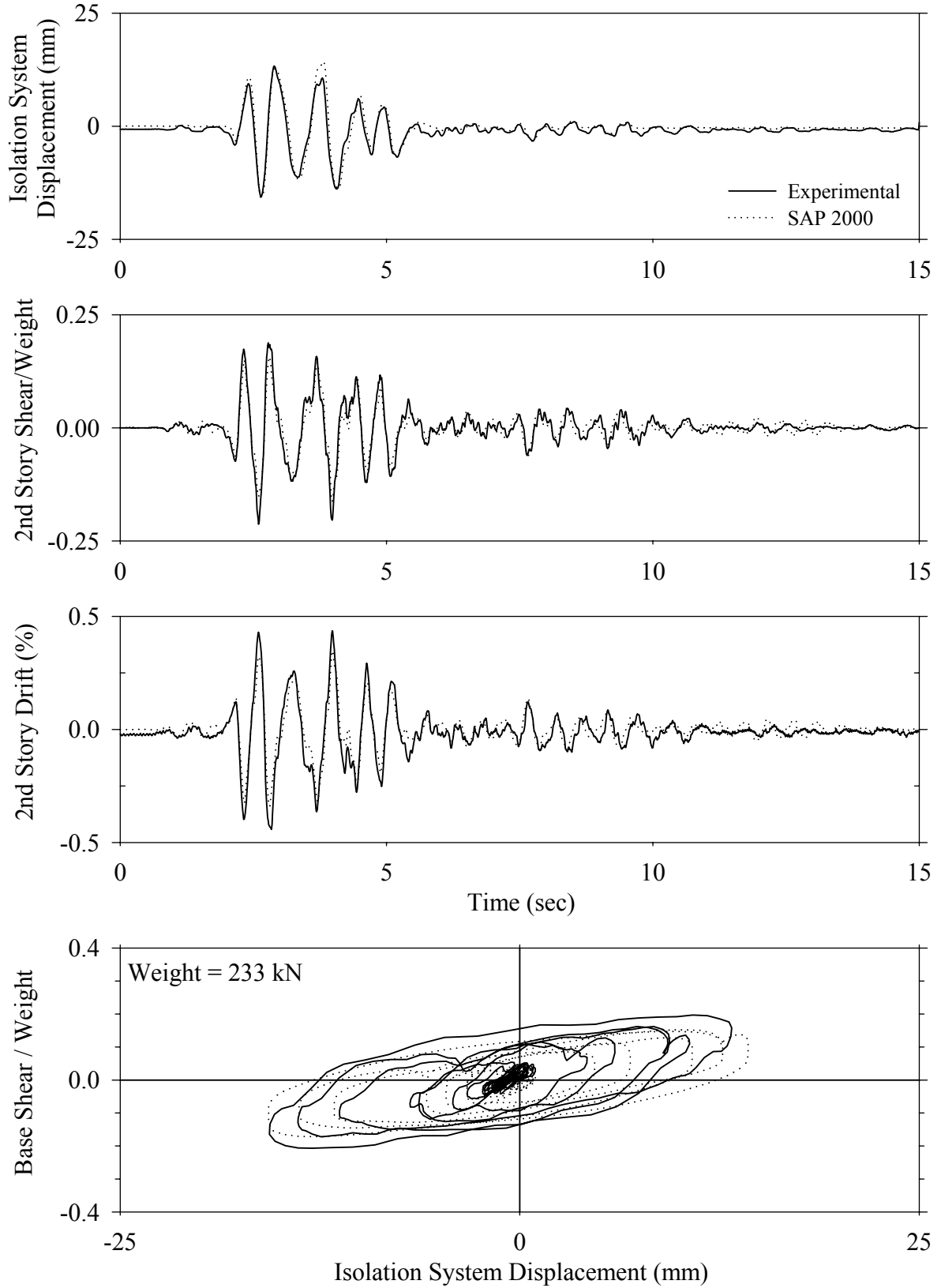
Test LDMNE20.1, El Centro S00E 200%, MF/Low Damping Elastomeric with Nonlinear Dampers



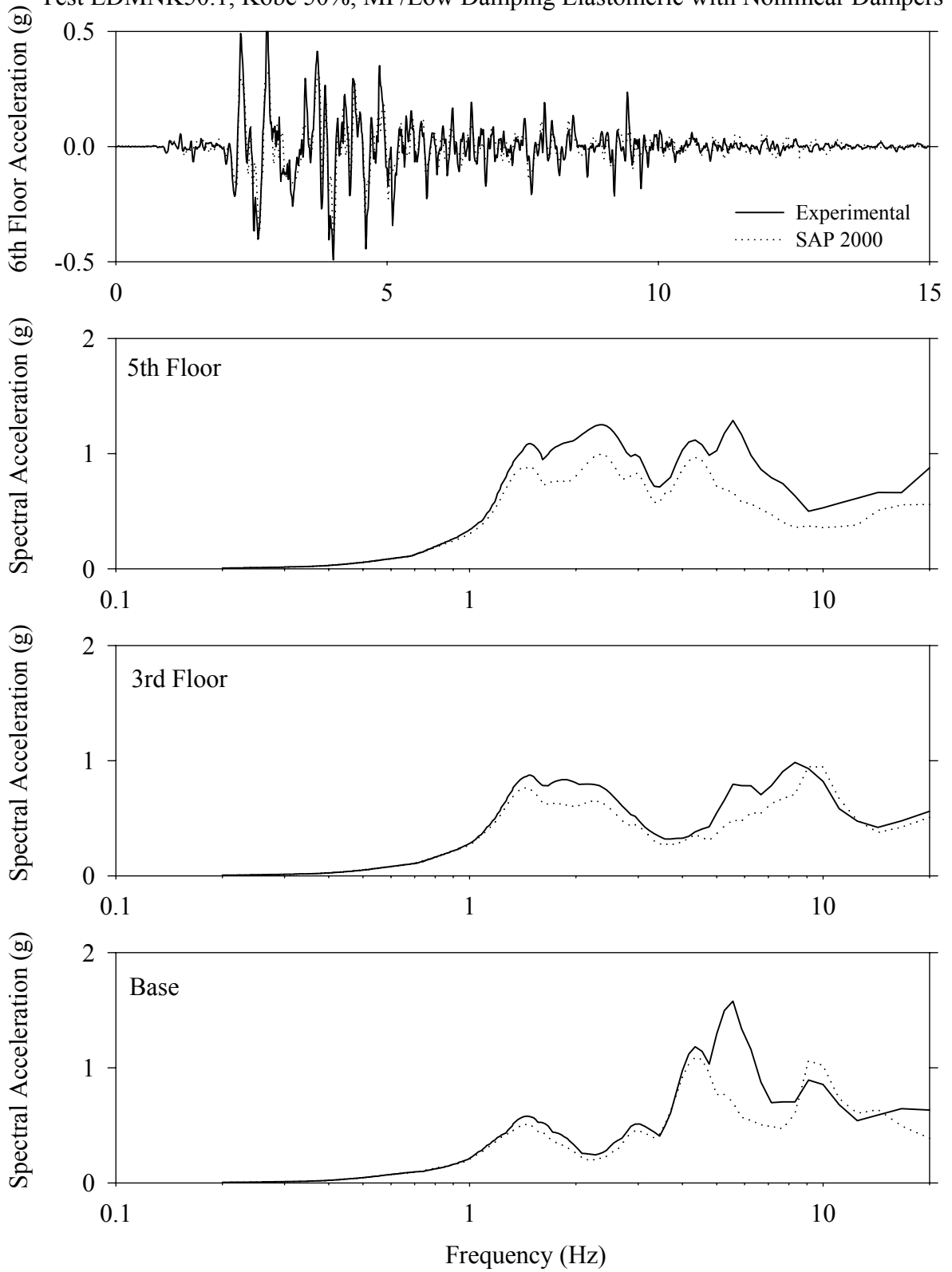
Test LDMNE20.1, El Centro S00E 200%, MF/Low Damping Elastomeric with Nonlinear Dampers



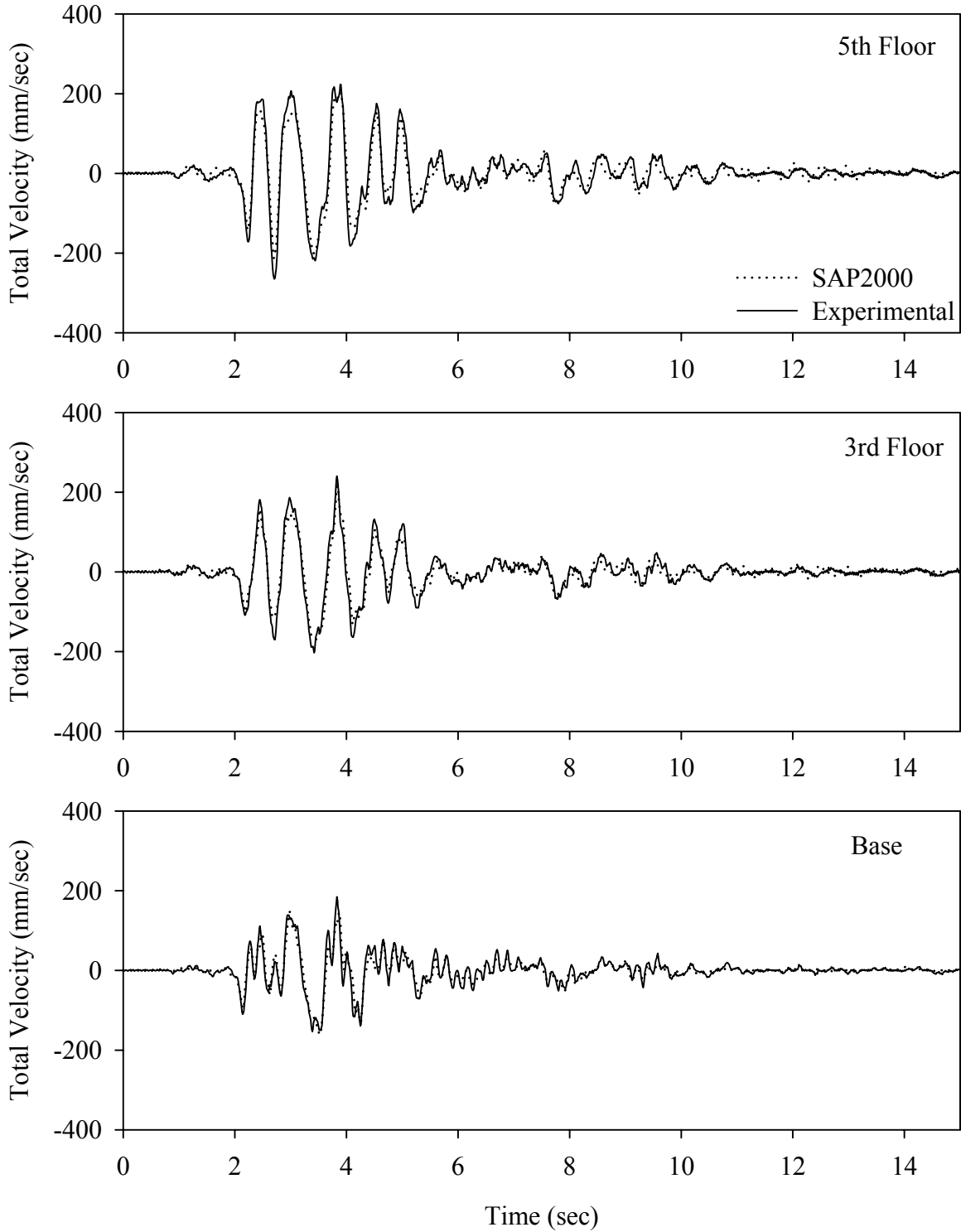
Test LDMNK50.1, Kobe 50%, MF/Low Damping Elastomeric with Nonlinear Dampers



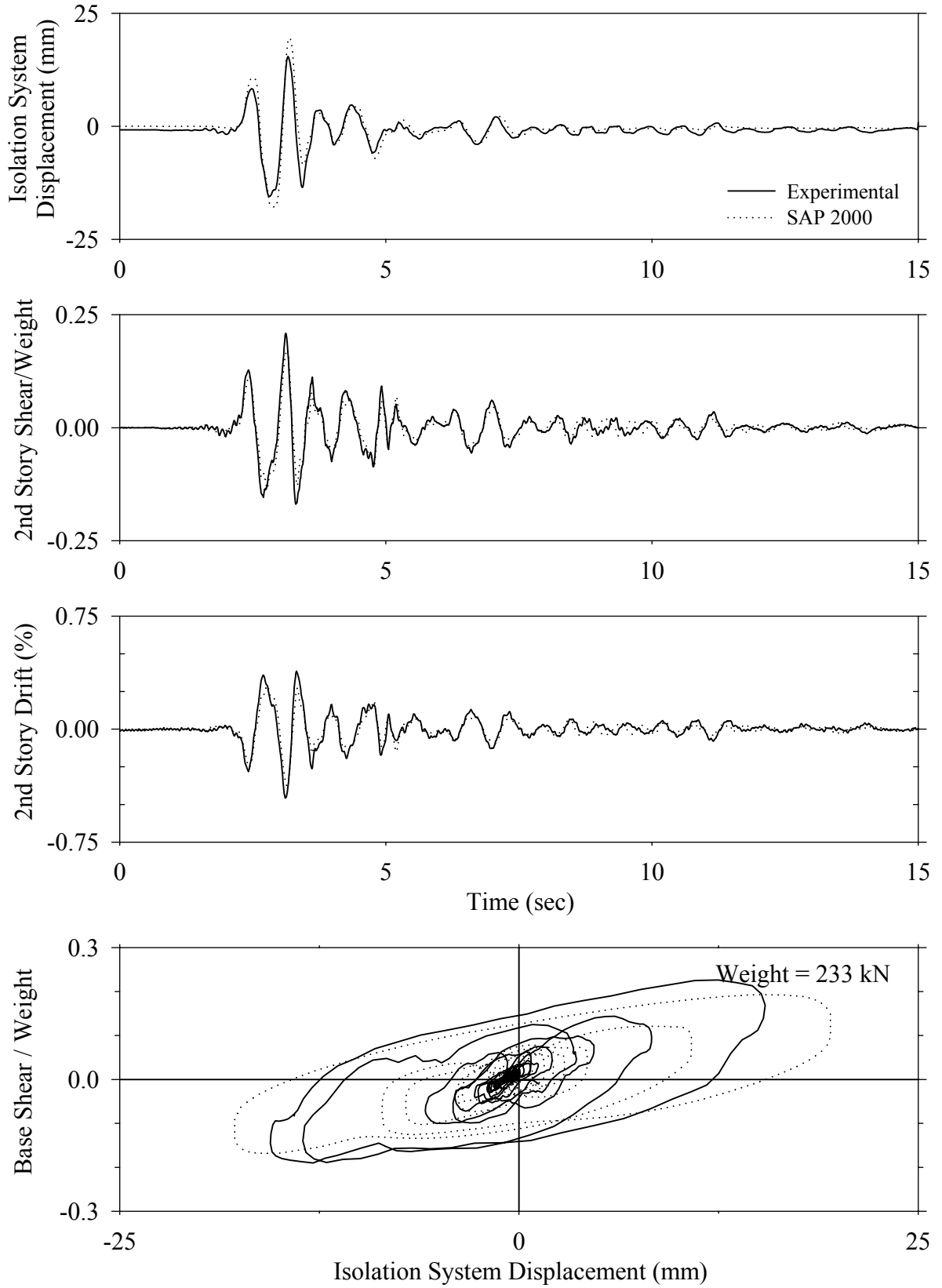
Test LDMNK50.1, Kobe 50%, MF/Low Damping Elastomeric with Nonlinear Dampers



Test LDMNK50.1, Kobe 50%, MF/Low Damping Elastomeric with Nonlinear Dampers

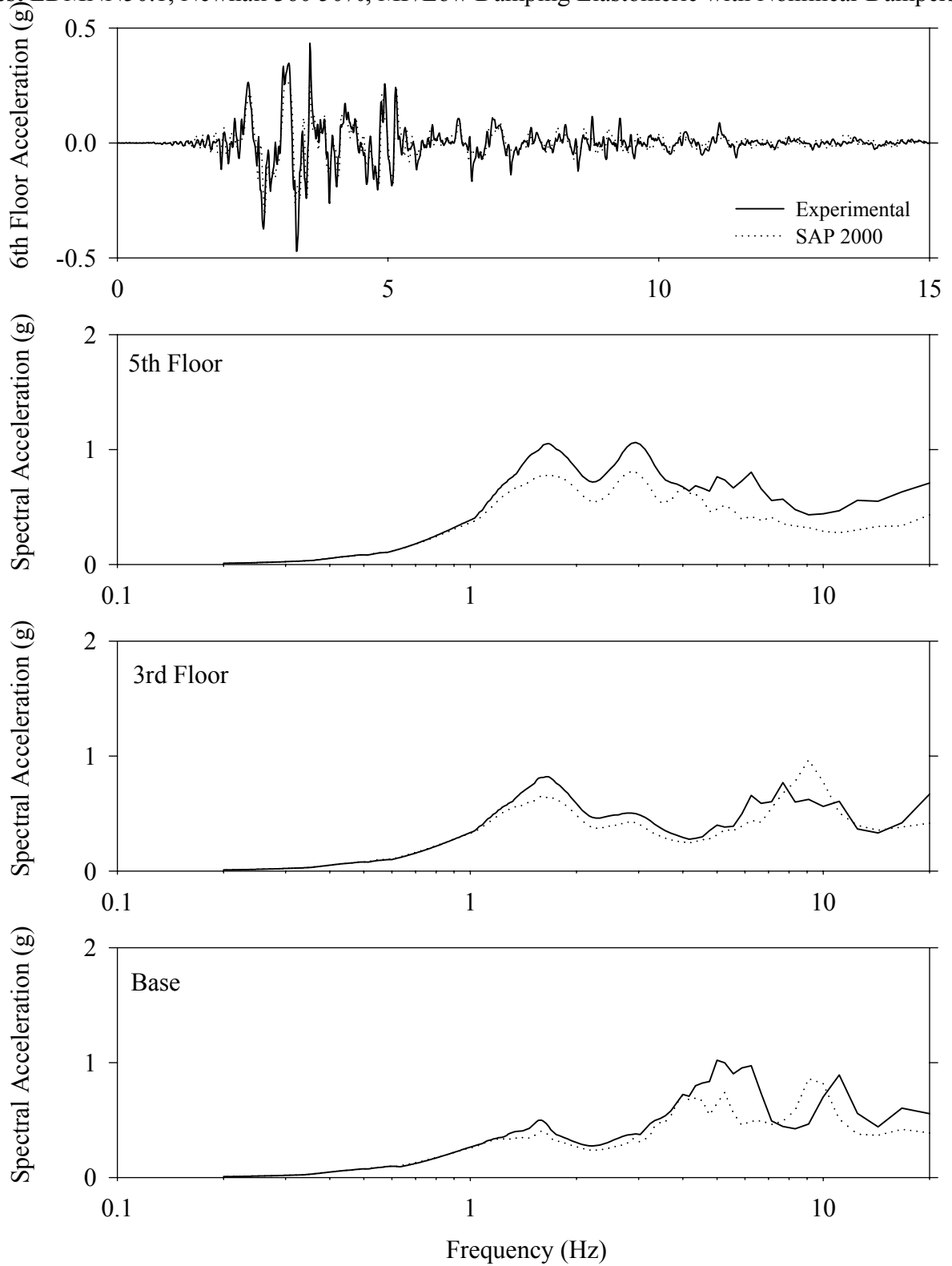


Test LDMNN50.1, Newhall 360 50%, MF/Low Damping Elastomeric with Nonlinear Dampers

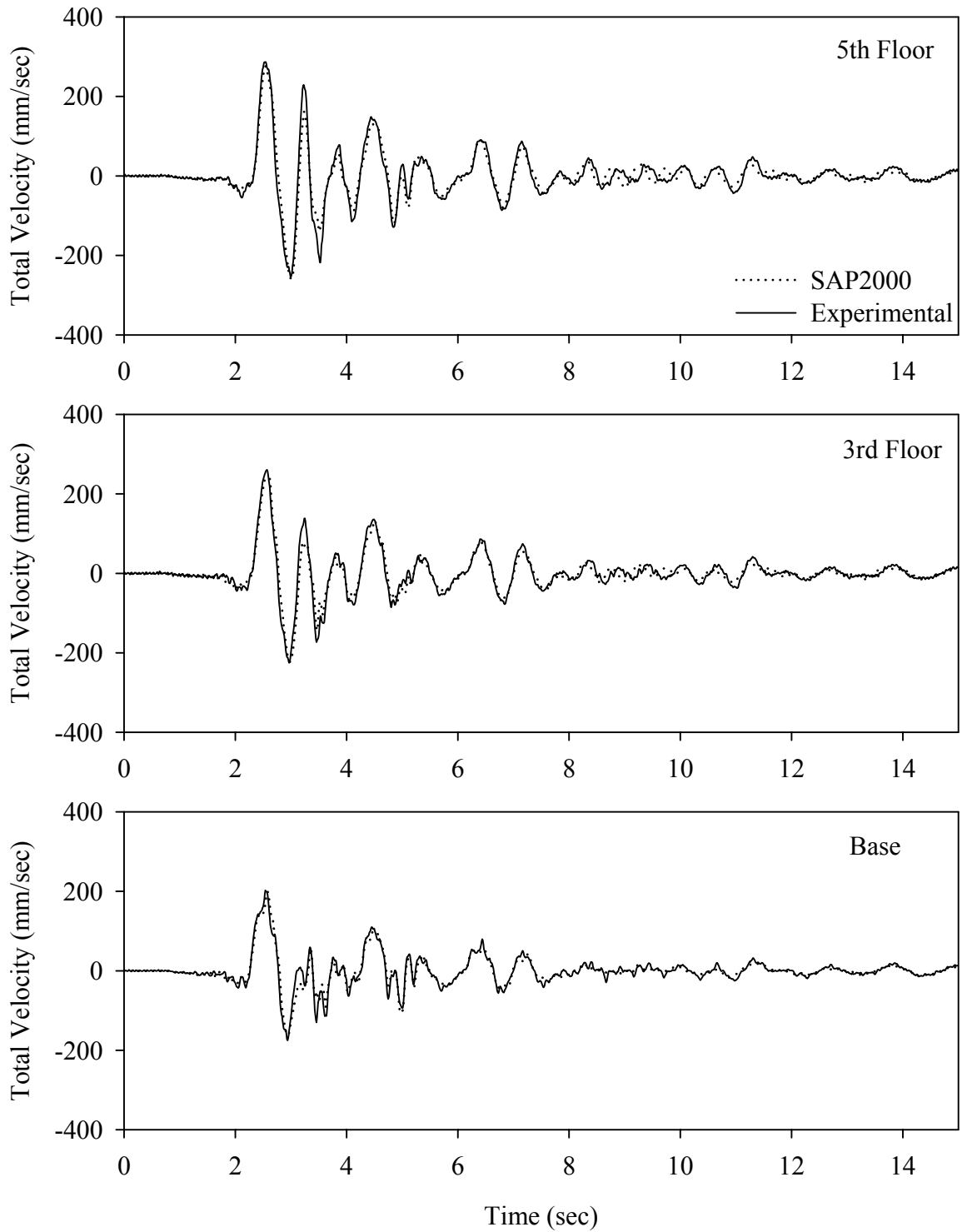




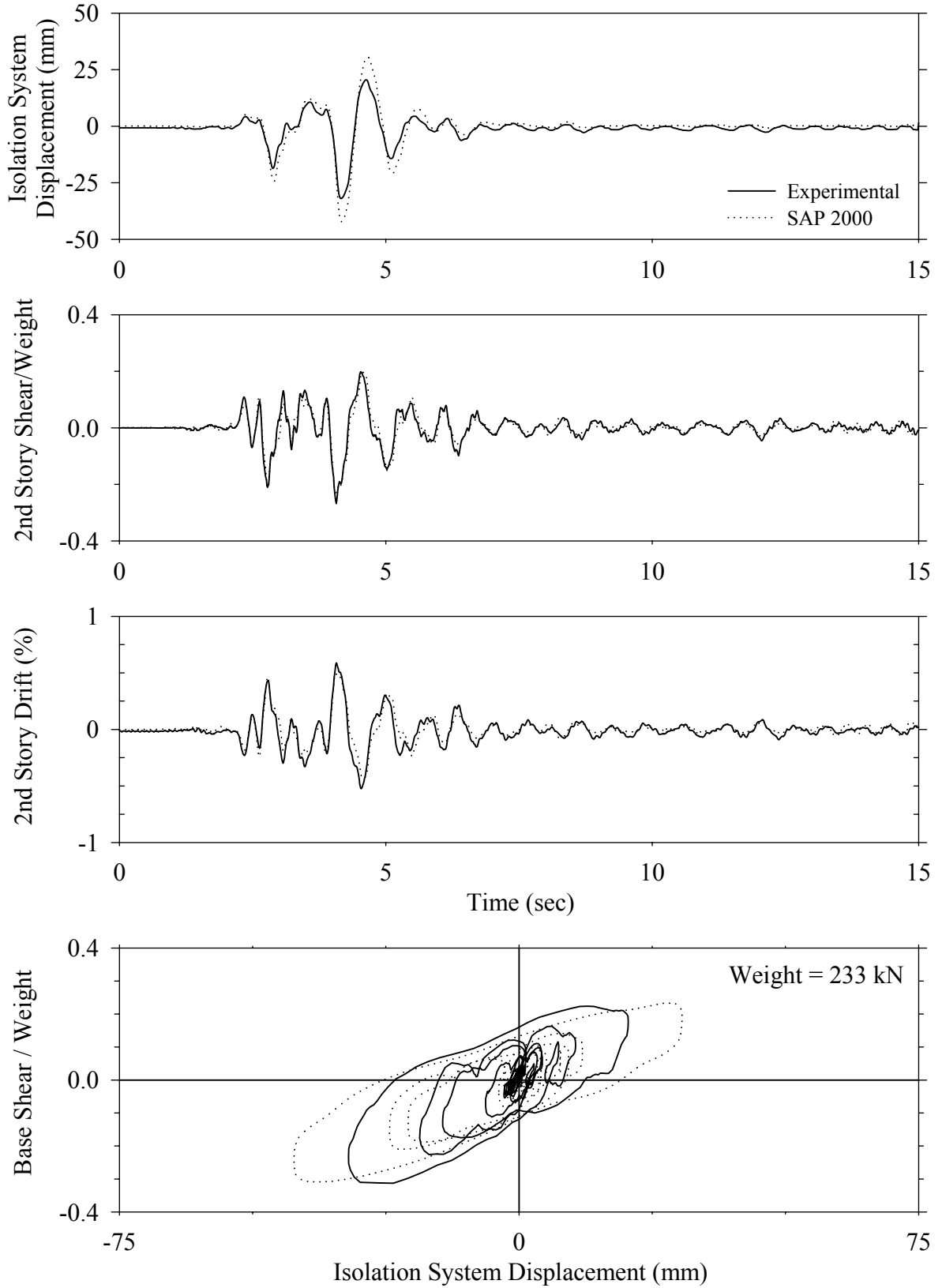
Test LDMNN50.1, Newhall 360 50%, MF/Low Damping Elastomeric with Nonlinear Dampers



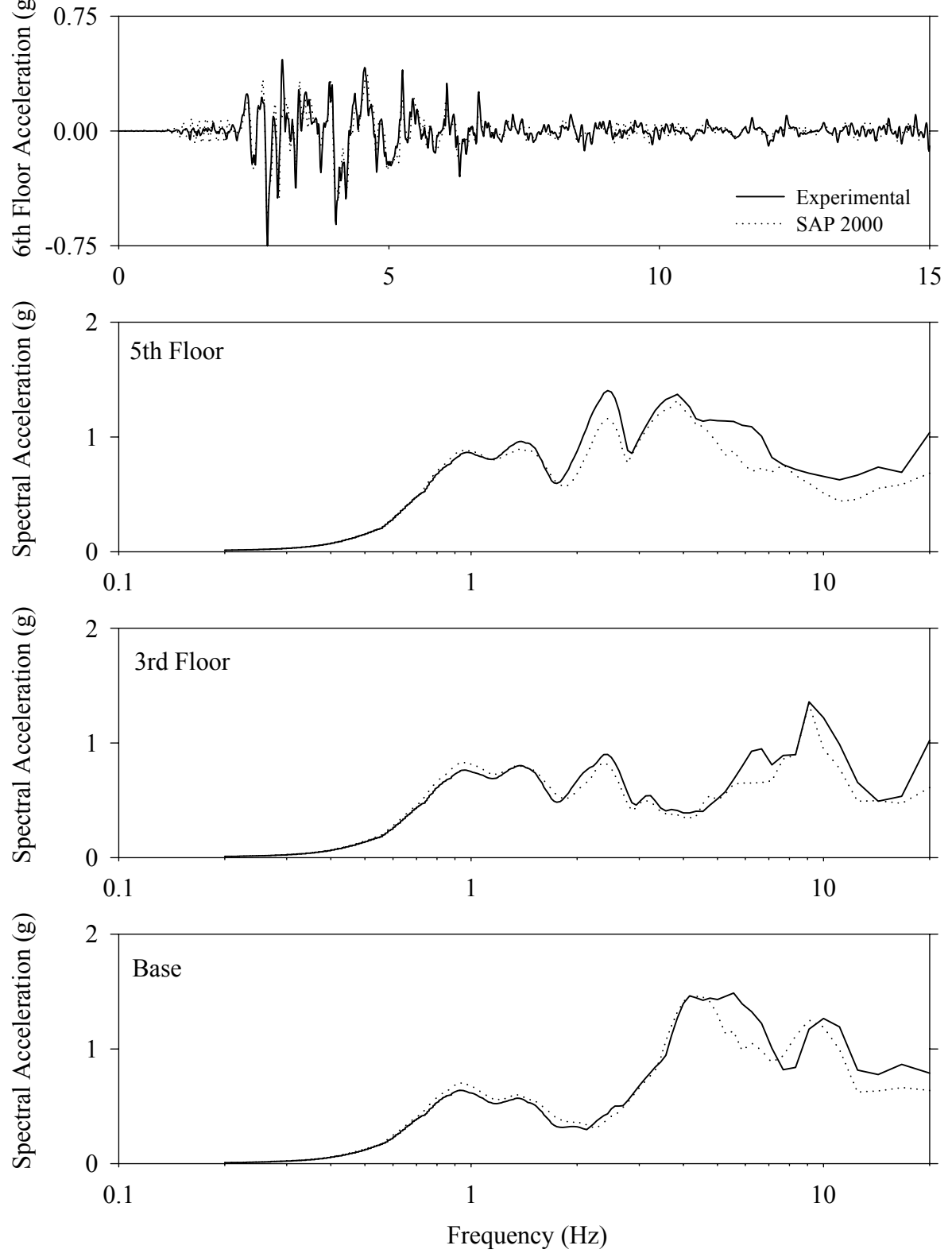
Test LDMNN50.1, Newhall 360 50%, MF/Low Damping Elastomeric with Nonlinear Dampers



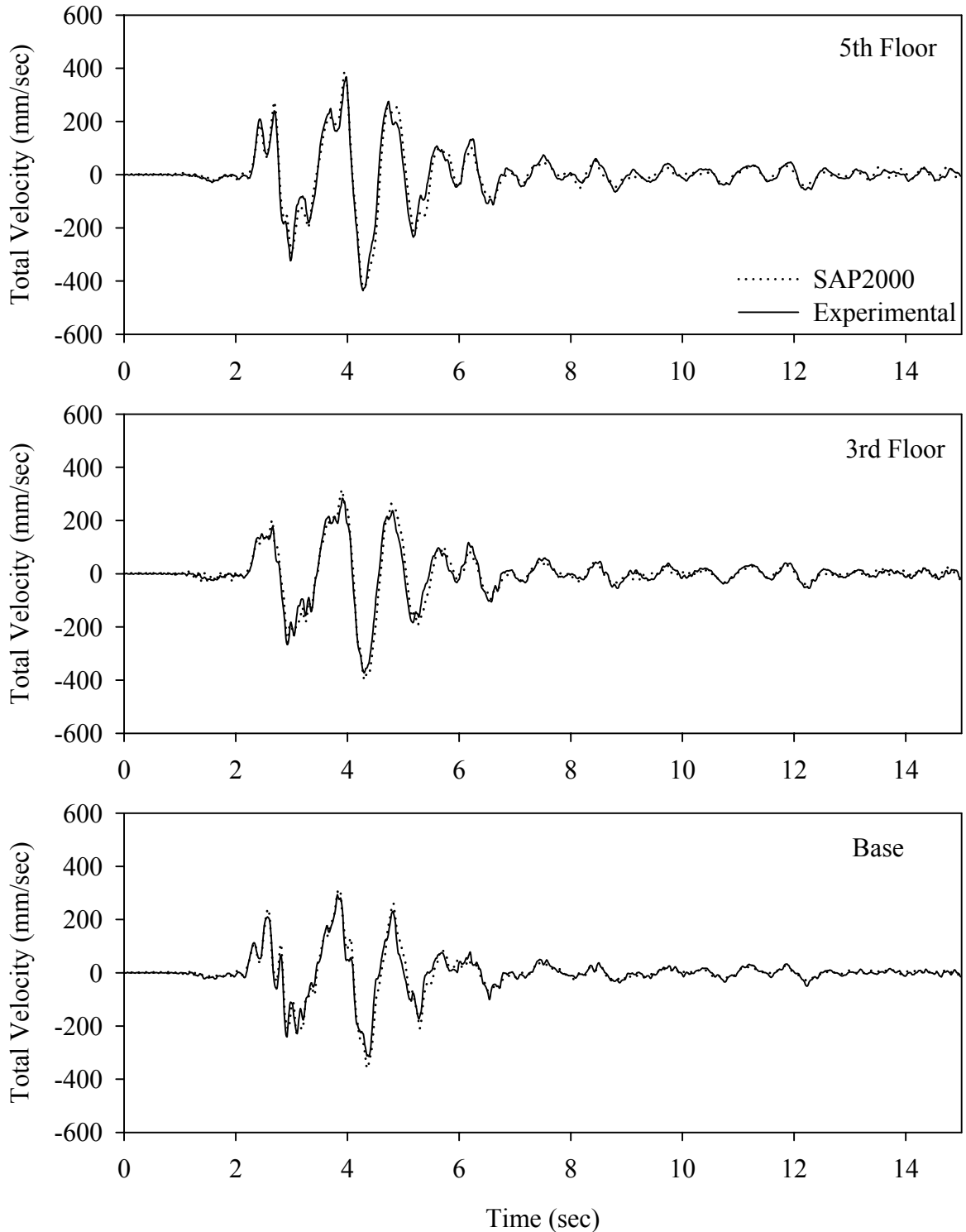
Test LDMNS10.1, Sylmar 100%, MF/Low Damping Elastomeric with Nonlinear Dampers



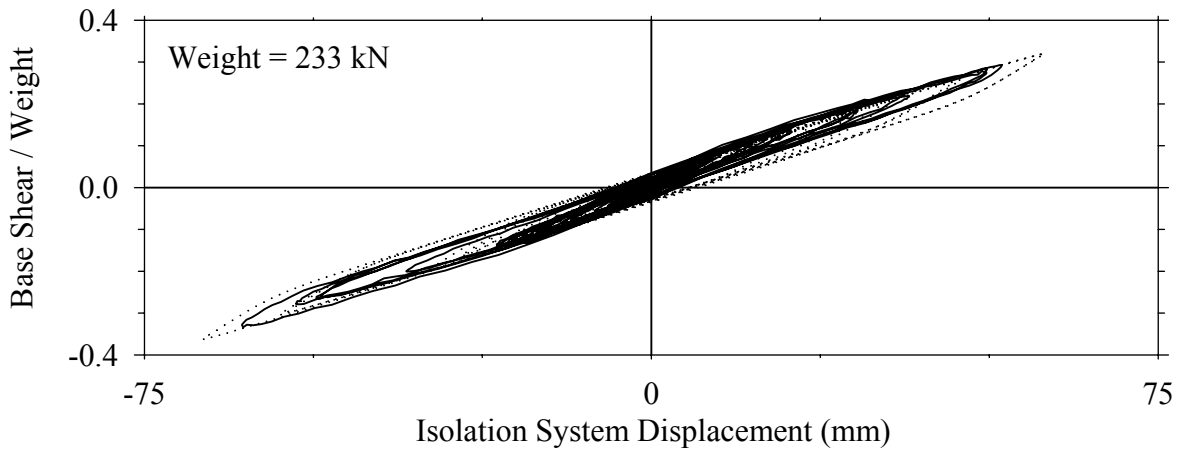
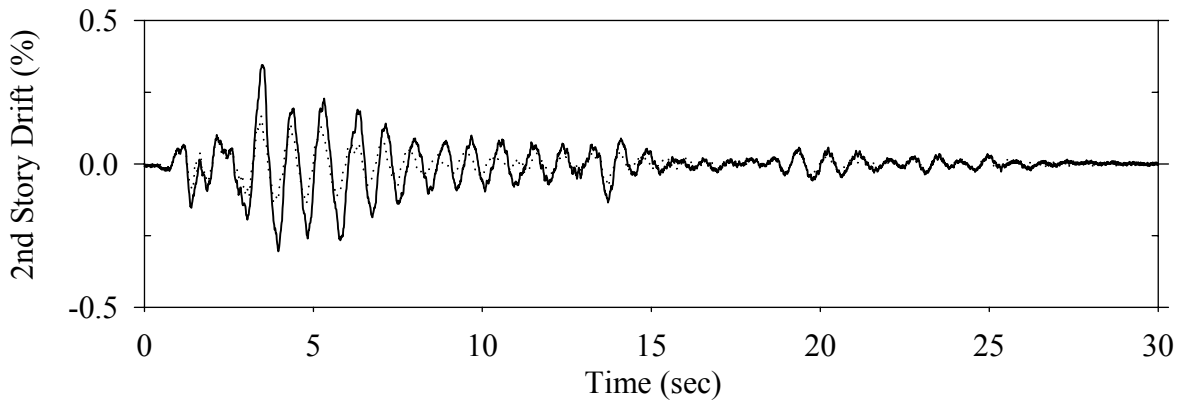
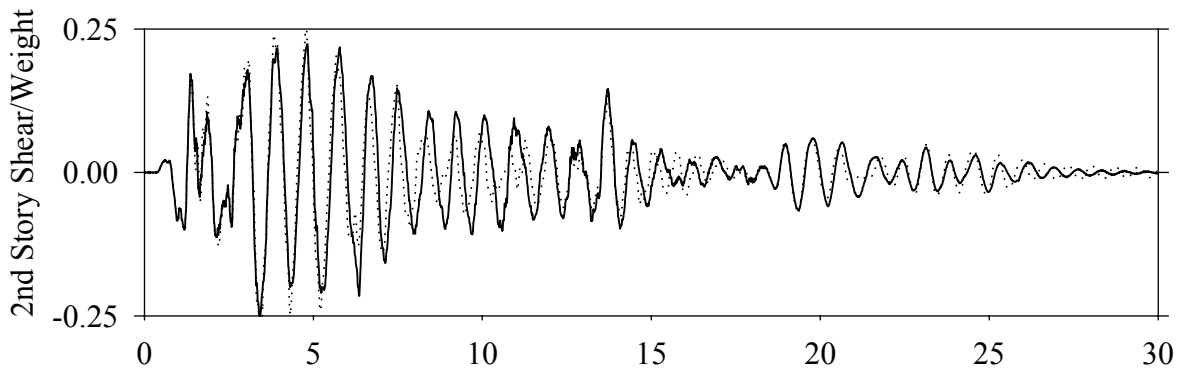
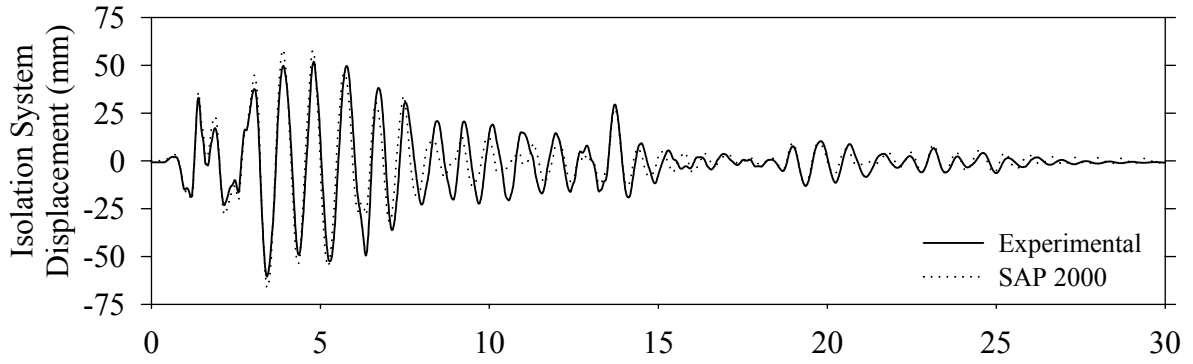
Test LDMNS10.1, Sylmar 100%, MF/Low Damping Elastomeric with Nonlinear Dampers



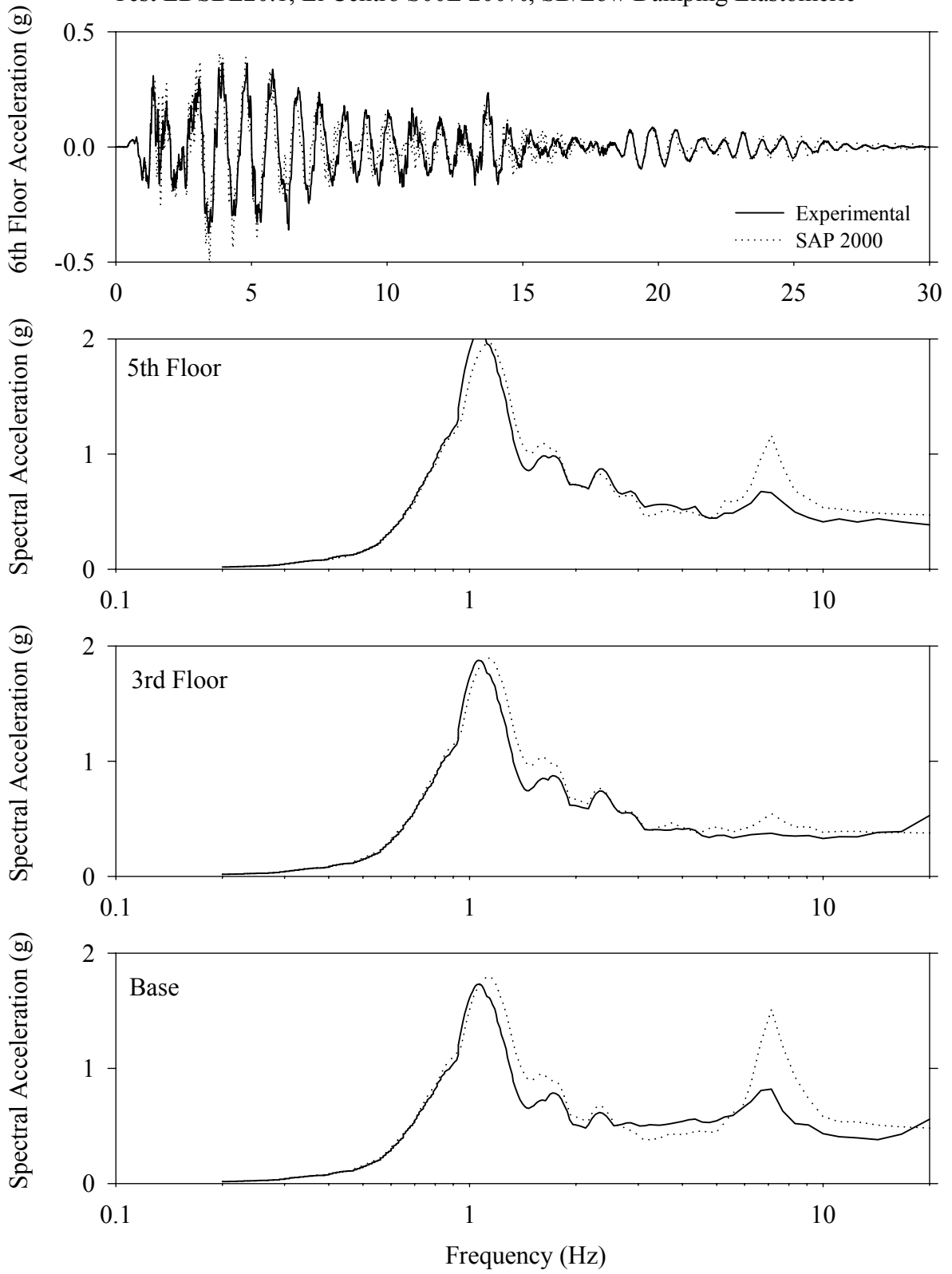
Test LDMNS10.1, Sylmar 100%, MF/Low Damping Elastomeric with Nonlinear Dampers



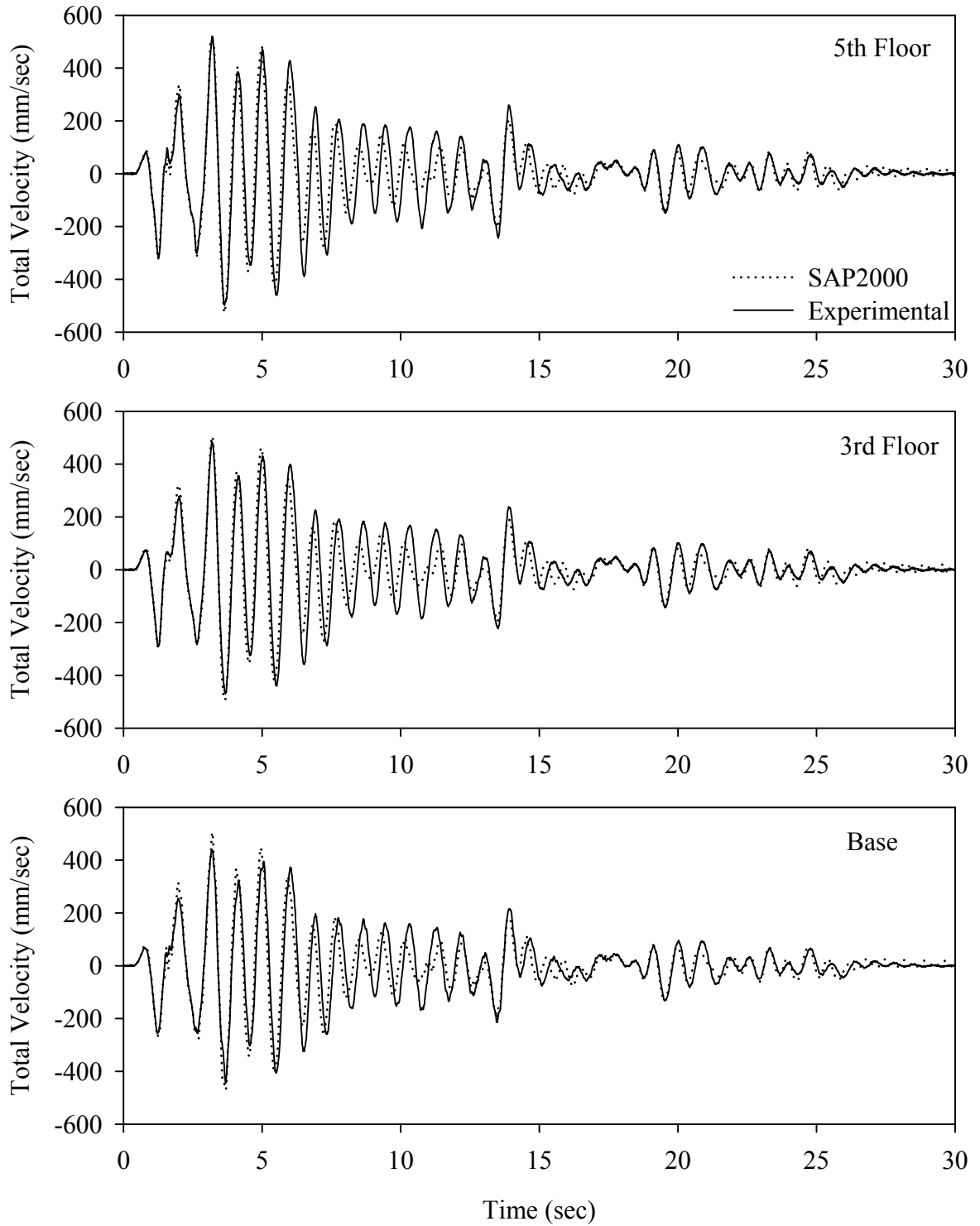
Test LDSBE20.1, El Centro S00E 200%, SB/Low Damping Elastomeric



Test LDSBE20.1, El Centro S00E 200%, SB/Low Damping Elastomeric

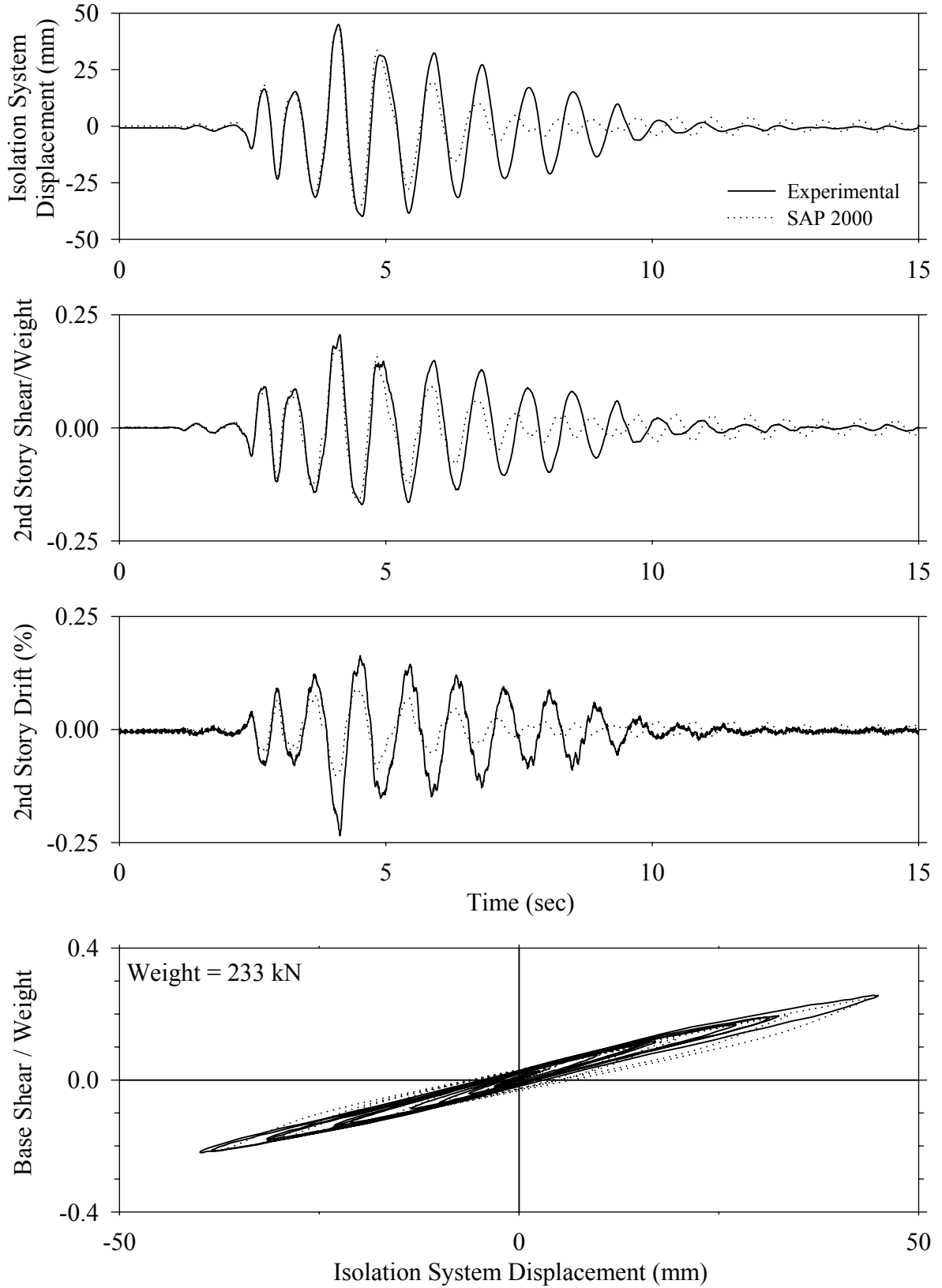


Test LDSBE20.1, El Centro S00E 200%, SB/Low Damping Elastomeric

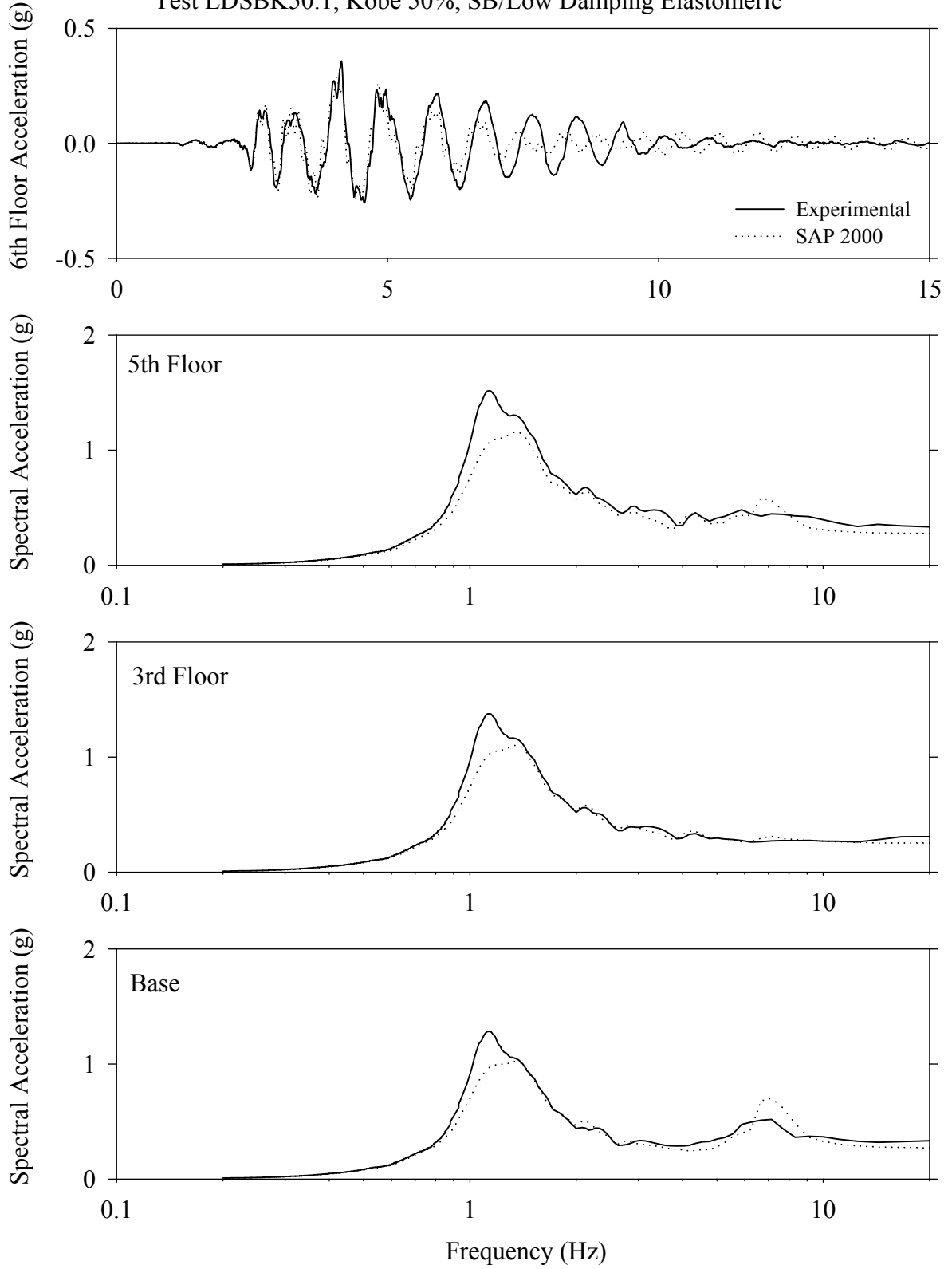




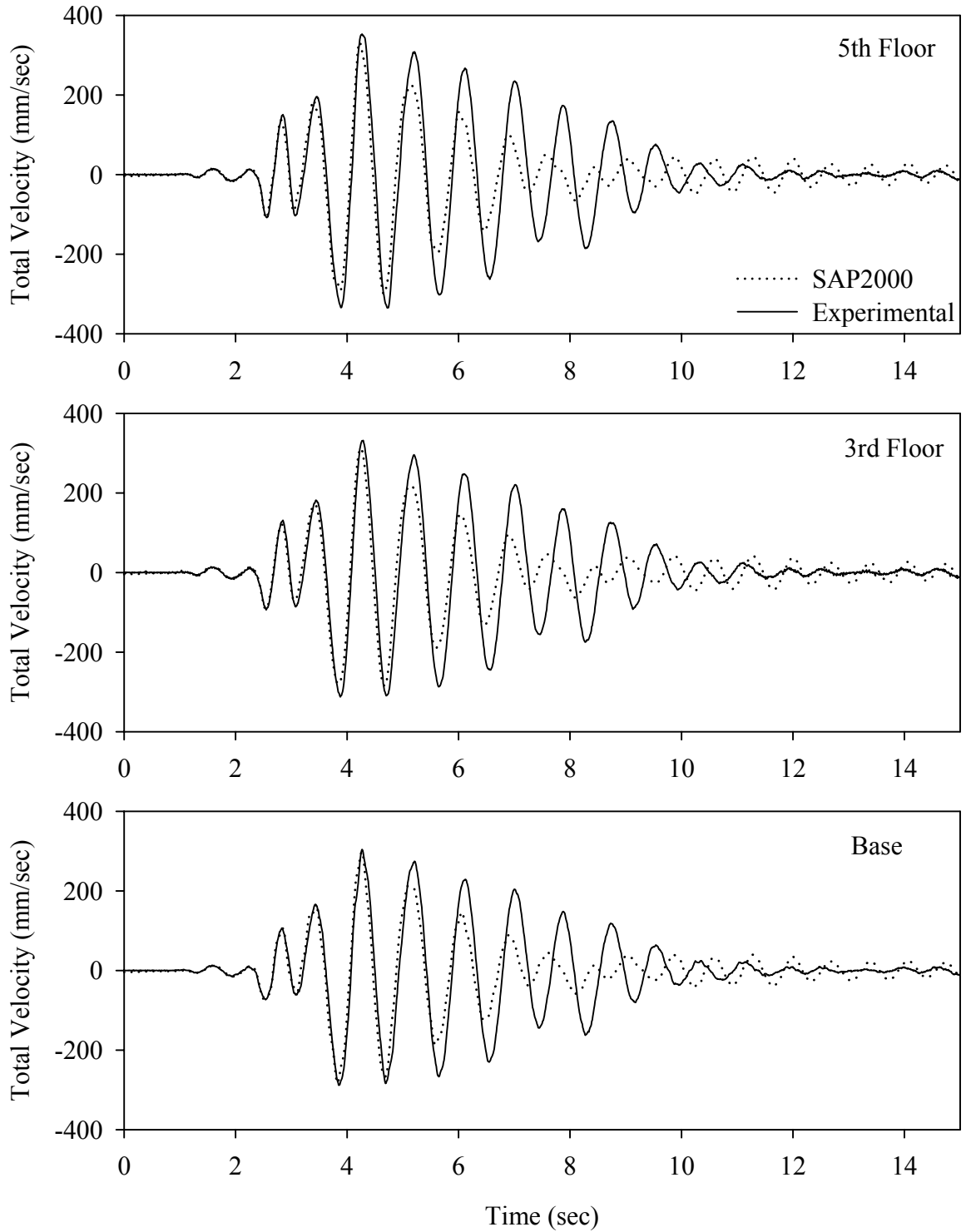
Test LDSBK50.1, Kobe 50%, SB/Low Damping Elastomeric



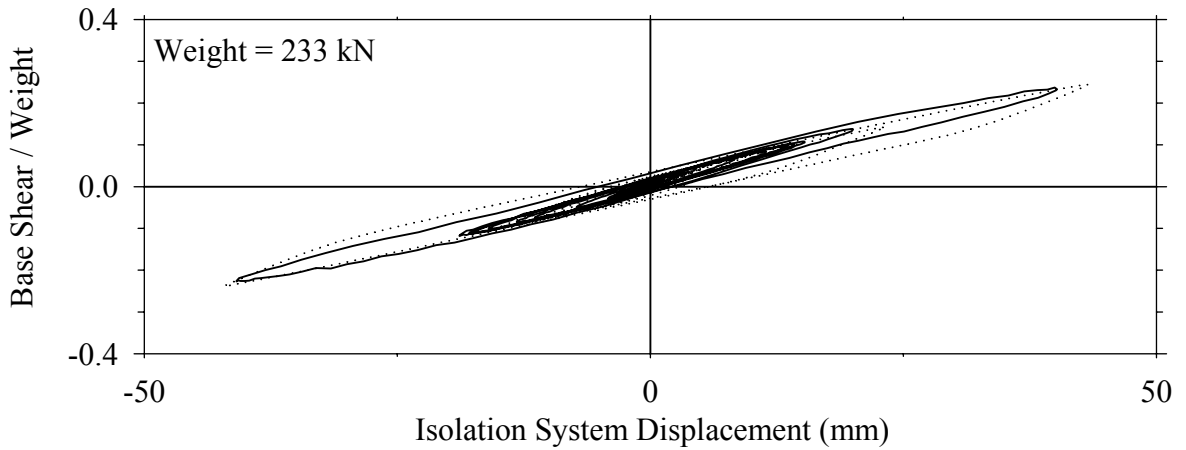
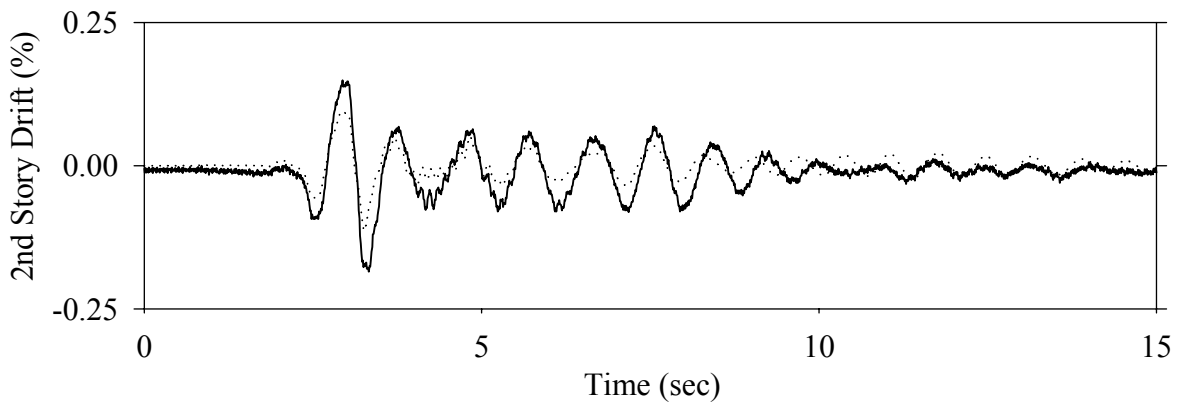
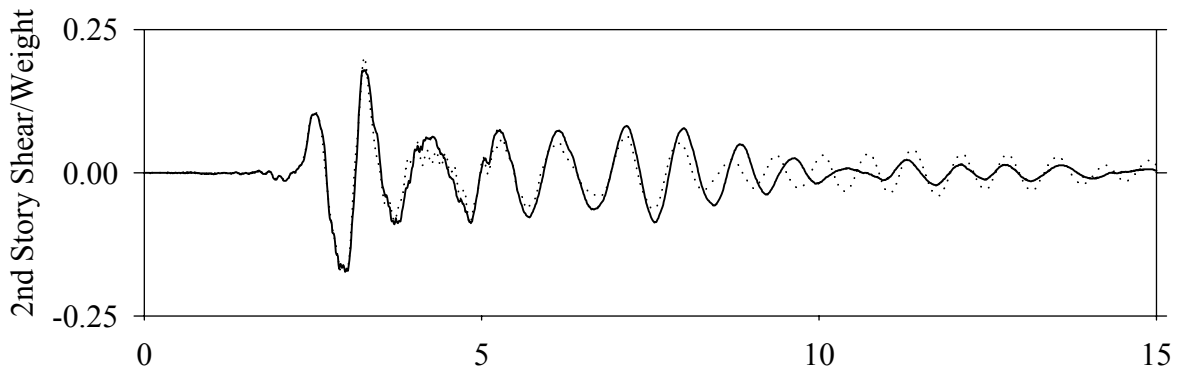
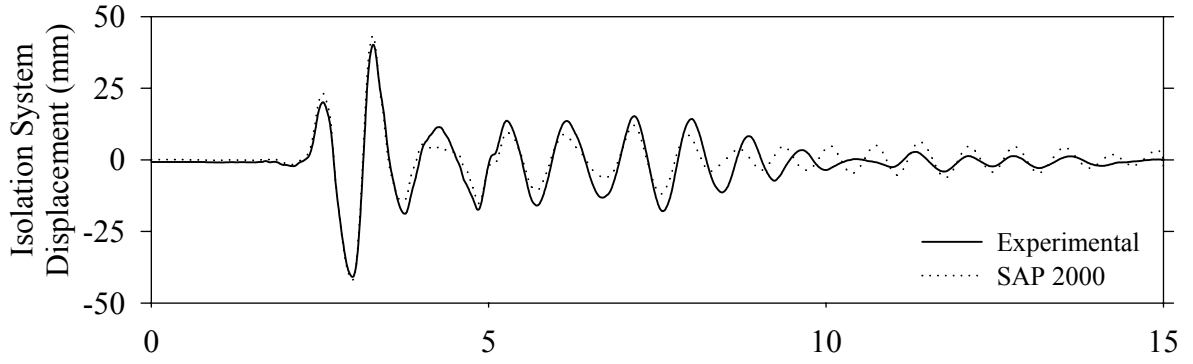
Test LDSBK50.1, Kobe 50%, SB/Low Damping Elastomeric



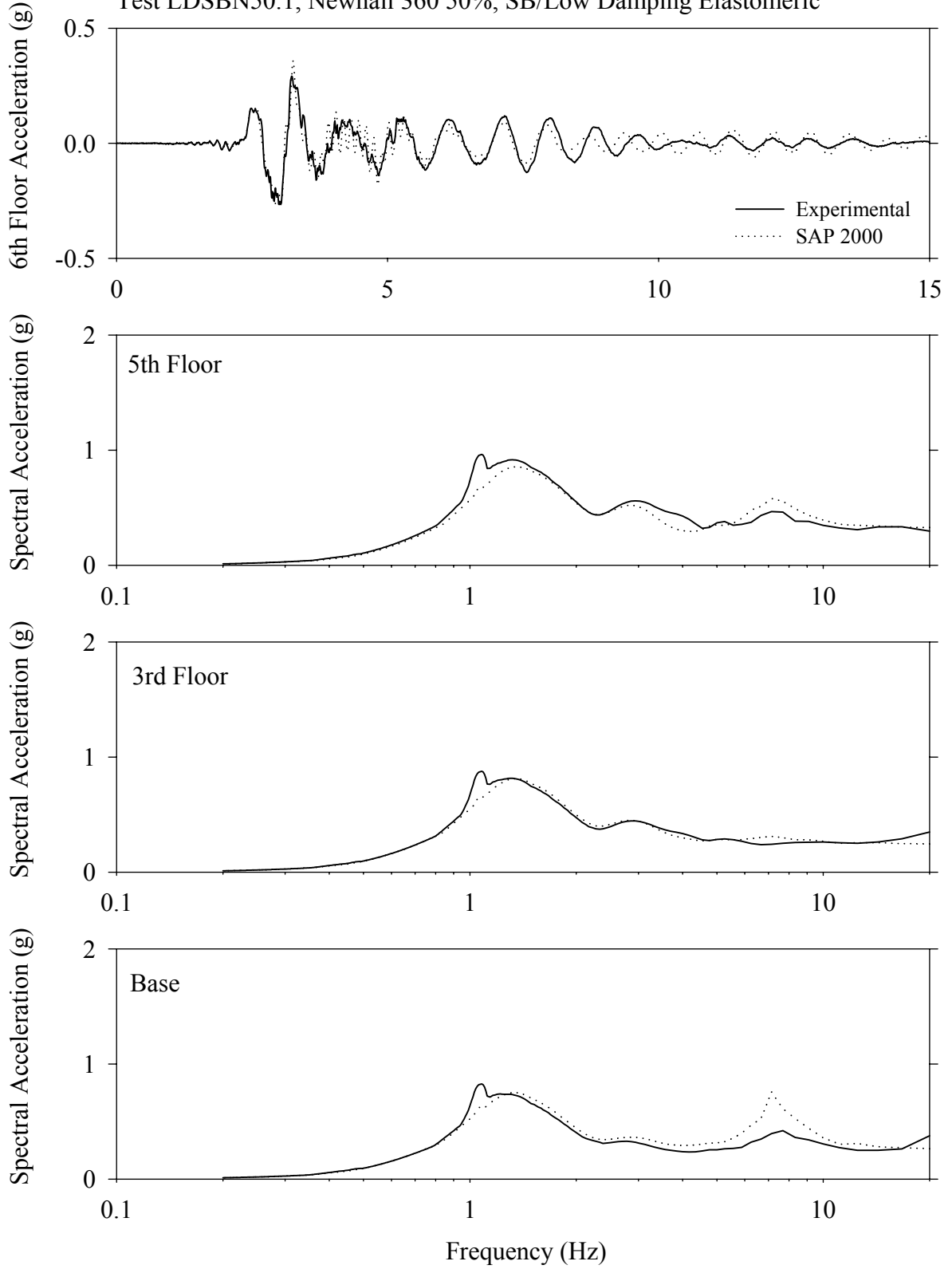
Test LDSBK50.1, Kobe 50%, SB/Low Damping Elastomeric



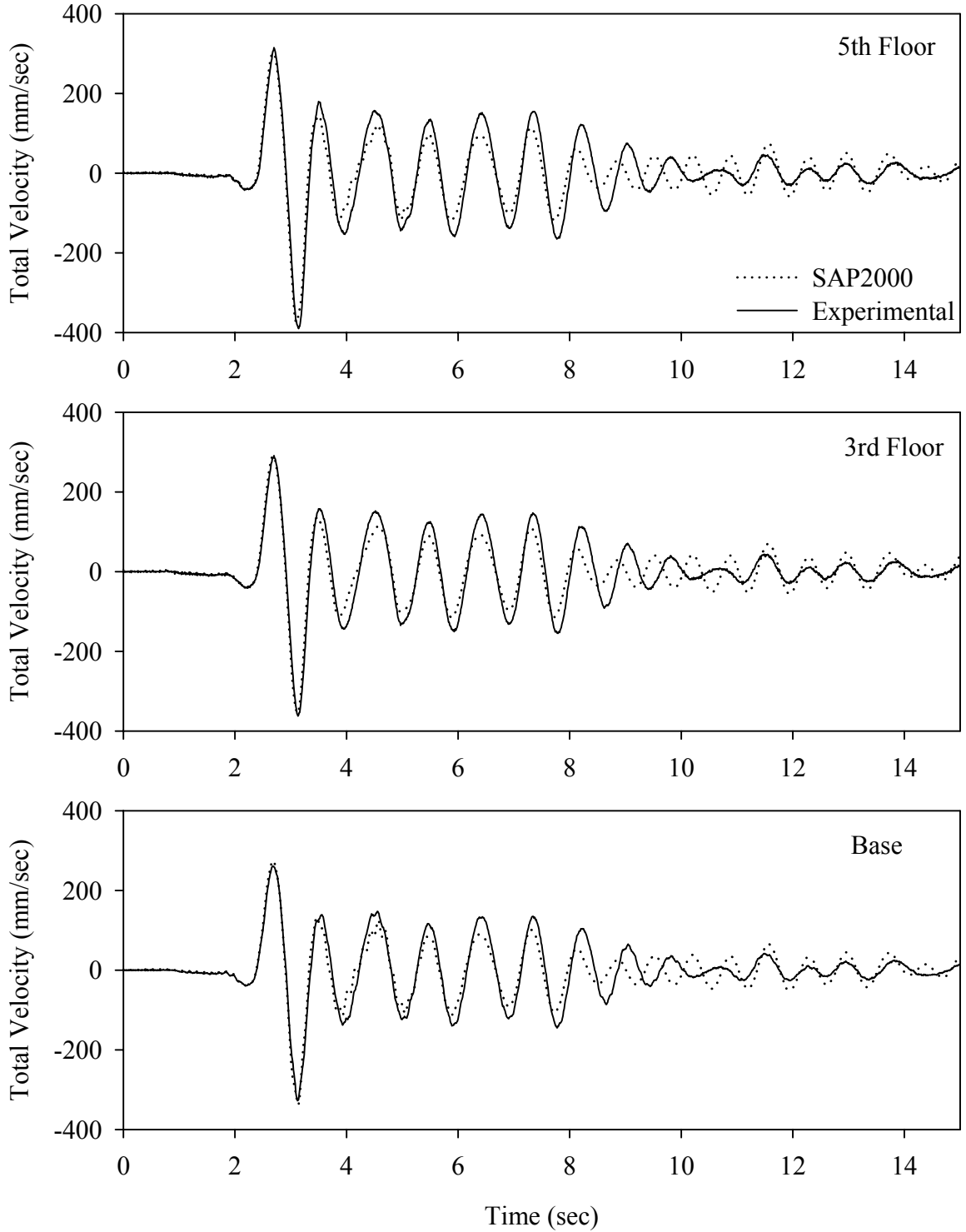
Test LDSBN50.1, Newhall 360 50%, SB/Low Damping Elastomeric



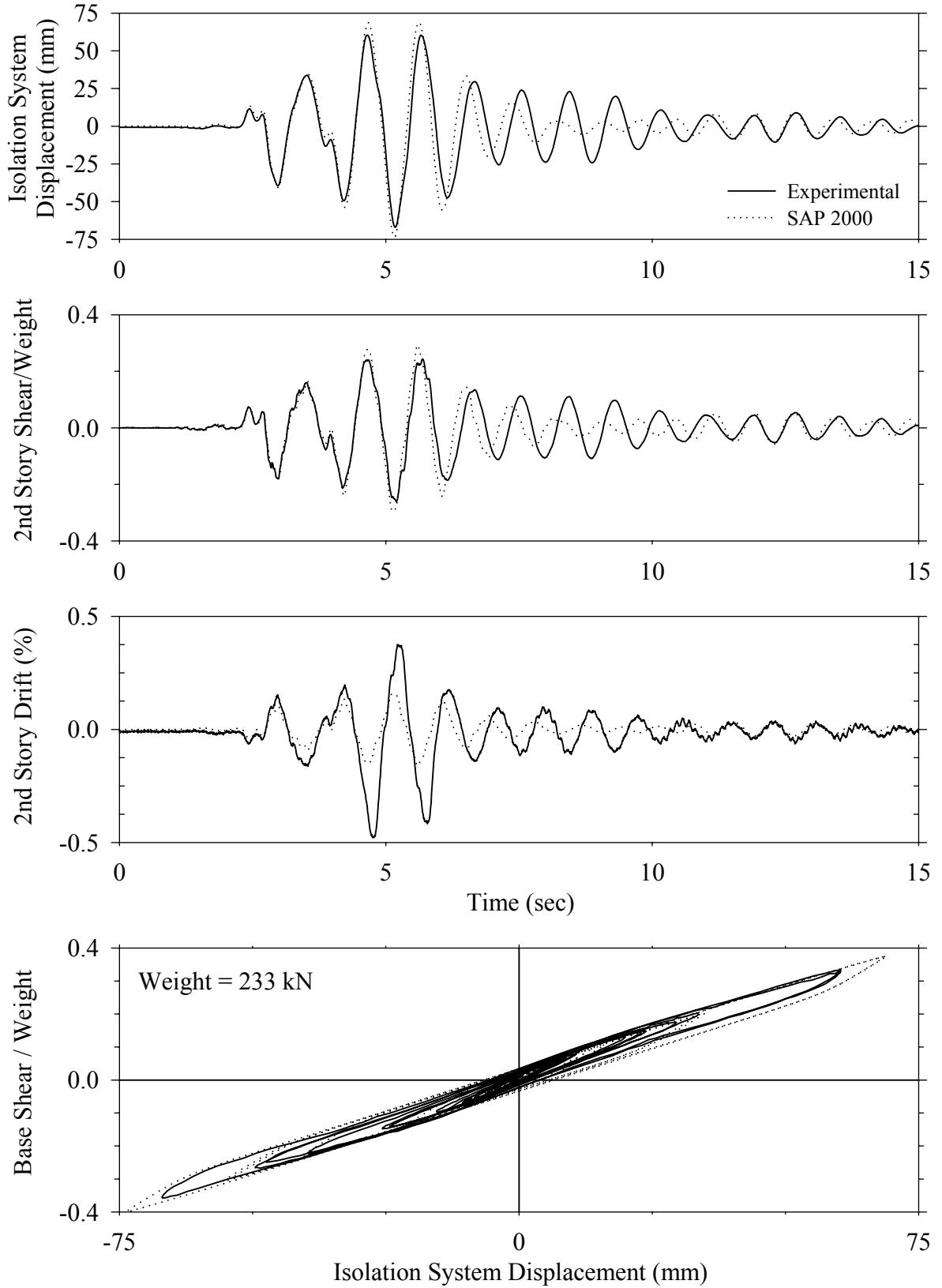
Test LDSBN50.1, Newhall 360 50%, SB/Low Damping Elastomeric



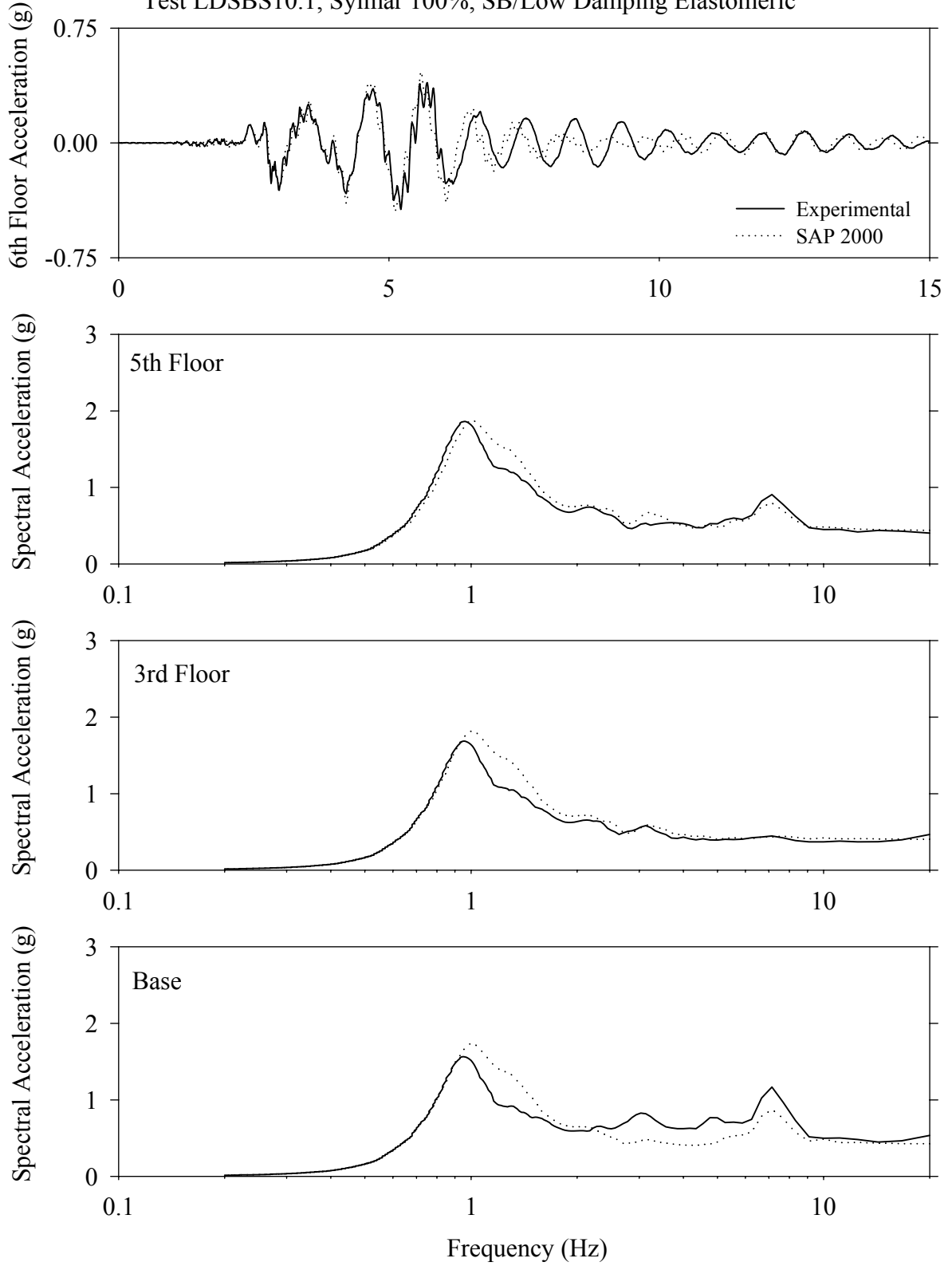
Test LDSBN50.1, Newhall 360 50%, SB/Low Damping Elastomeric



Test LDSBS10.1, Sylmar 100%, SB/Low Damping Elastomeric

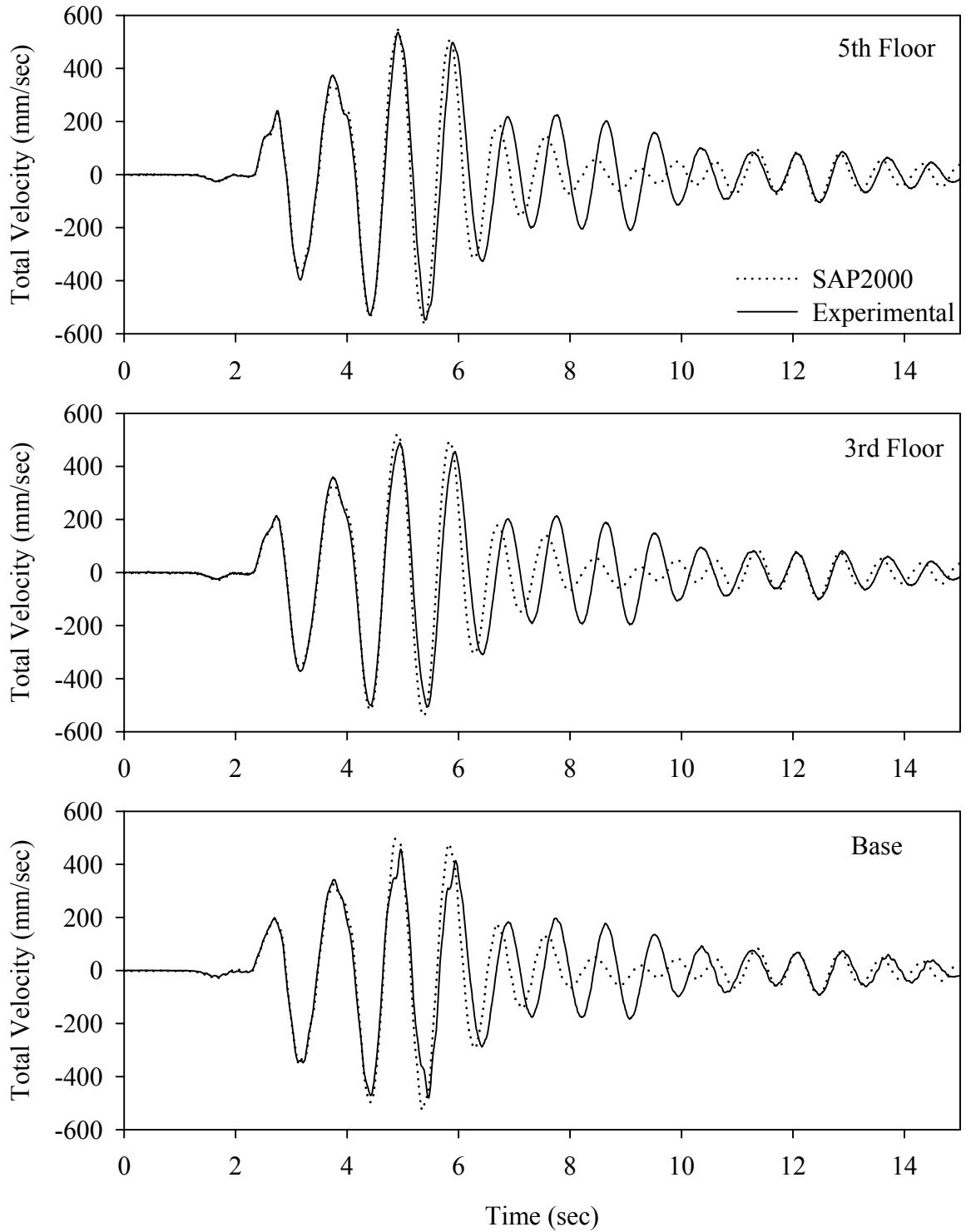


Test LDSBS10.1, Sylmar 100%, SB/Low Damping Elastomeric

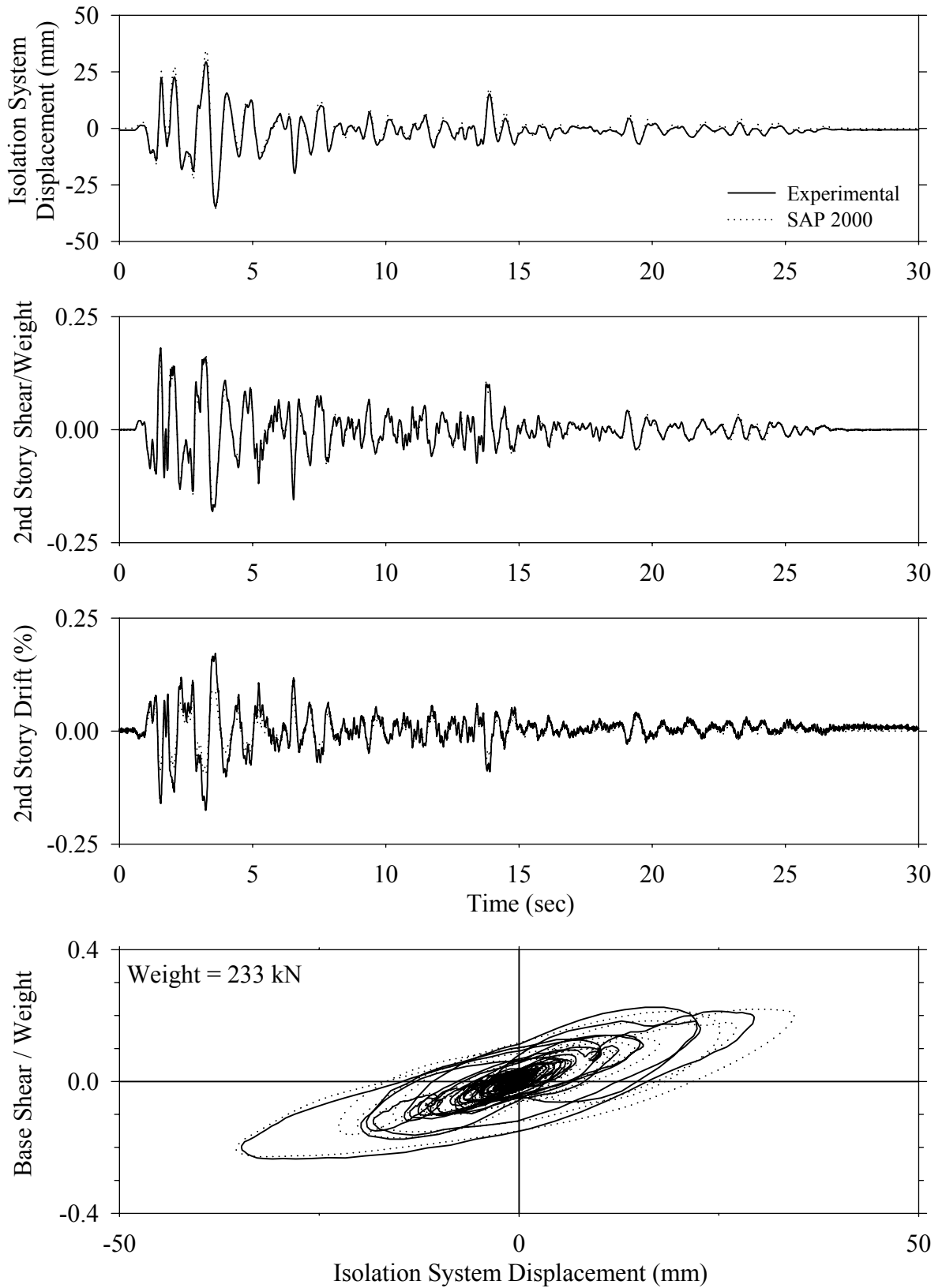




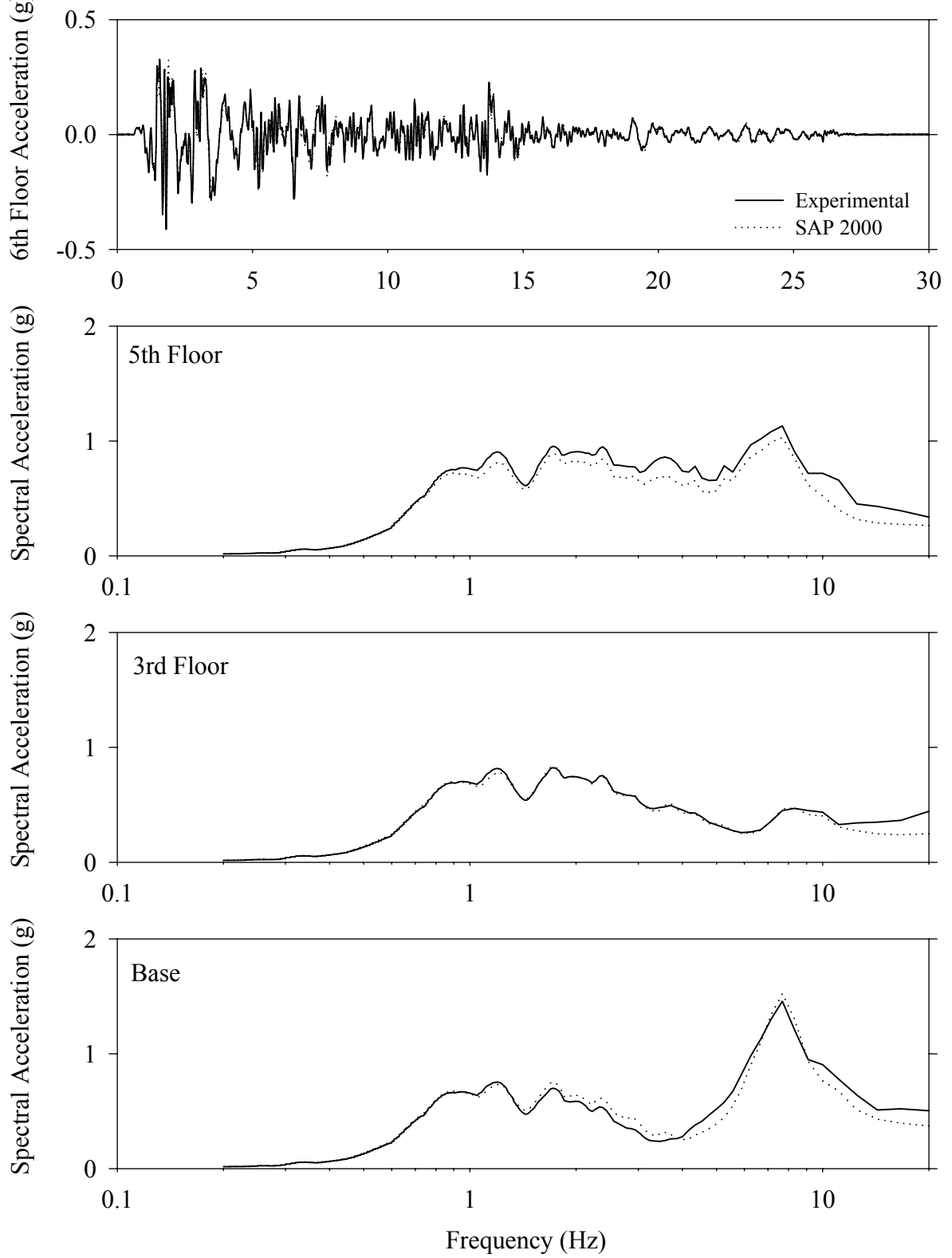
Test LDSBS10.1, Sylmar 100%, SB/Low Damping Elastomeric



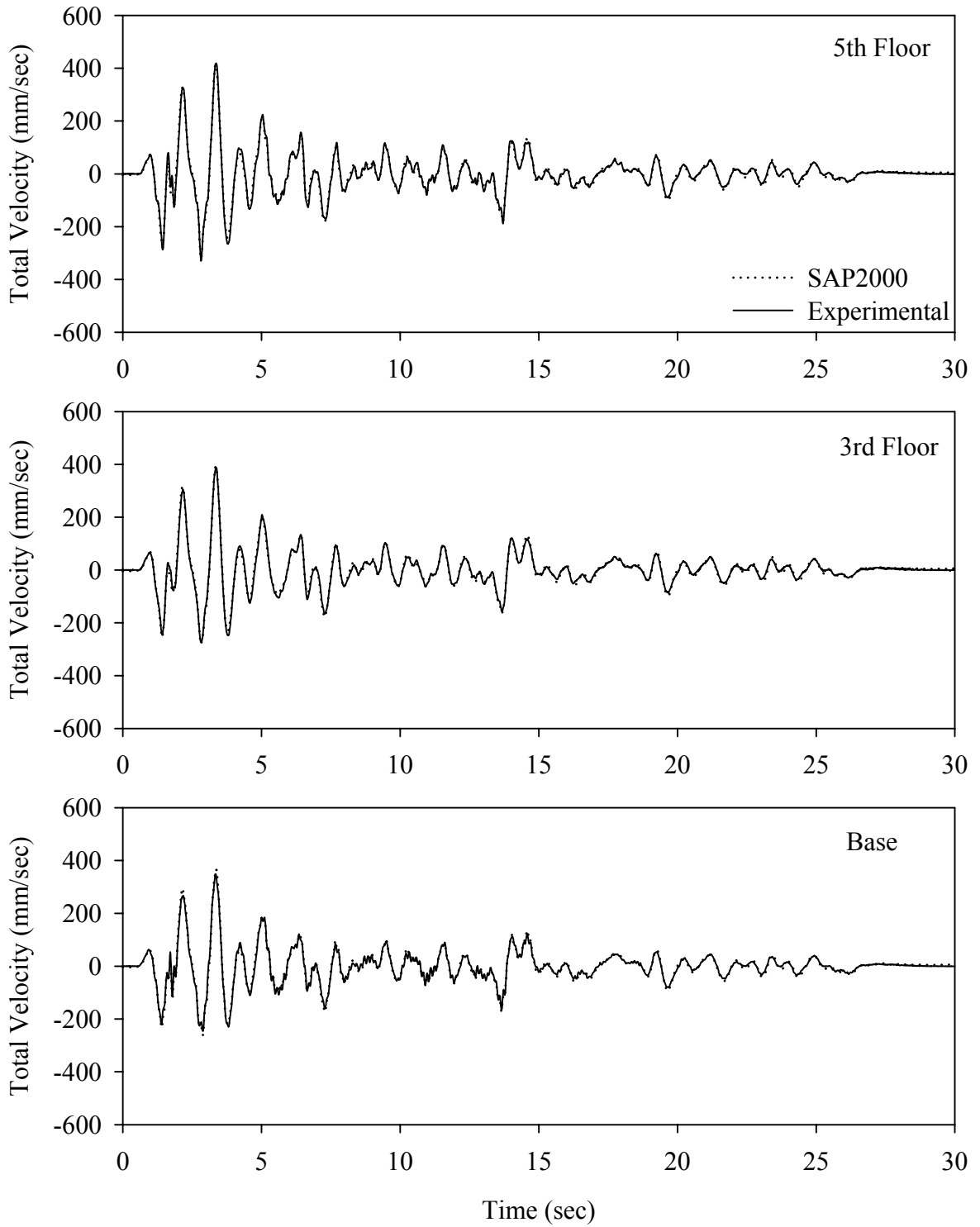
Test LDSLE20.1, El Centro S00E 200%, SB/Low Damping Elastomeric with Linear Dampers



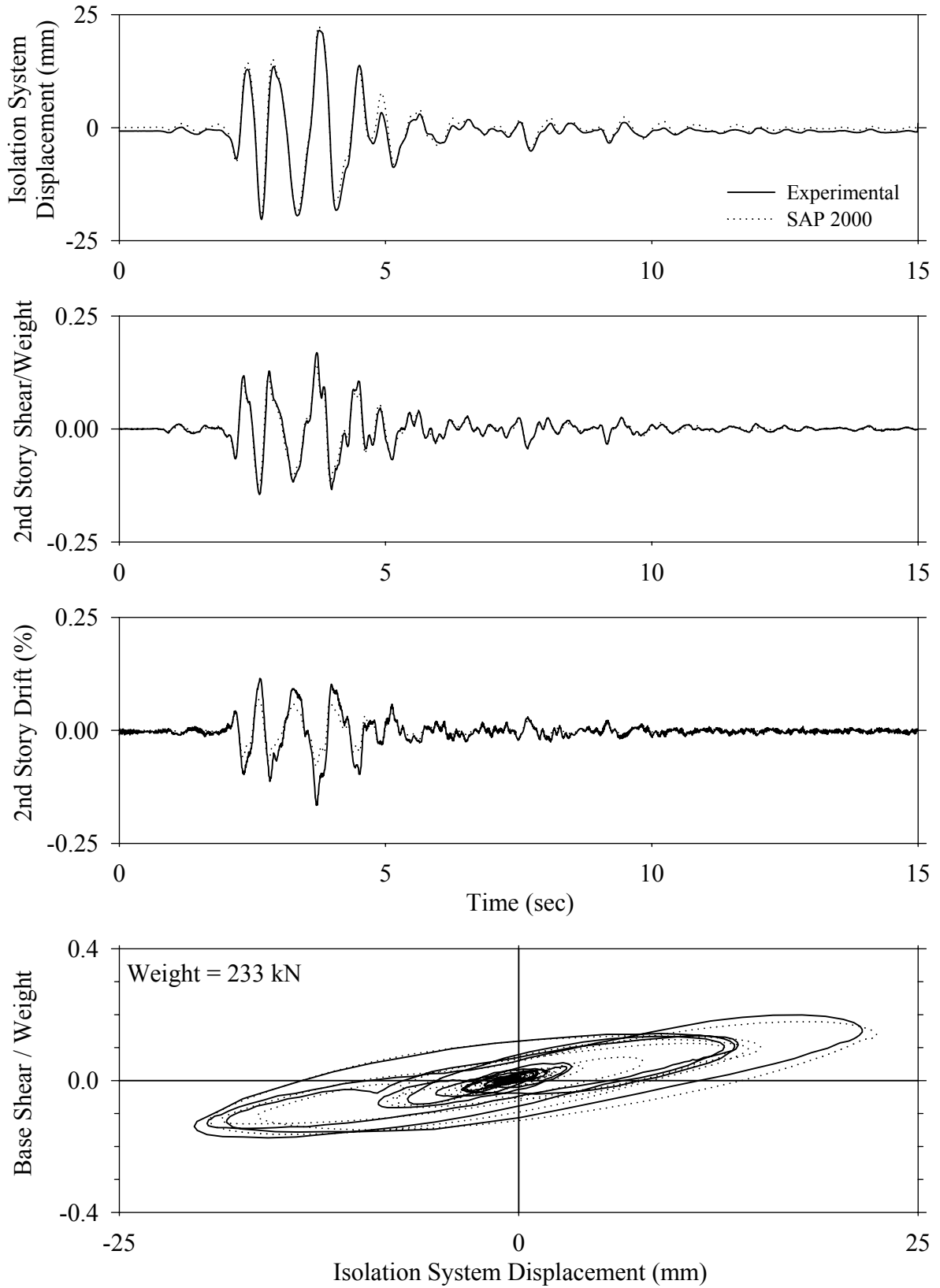
Test LDSLE20.1, El Centro S00E 200%, SB/Low Damping Elastomeric with Linear Dampers



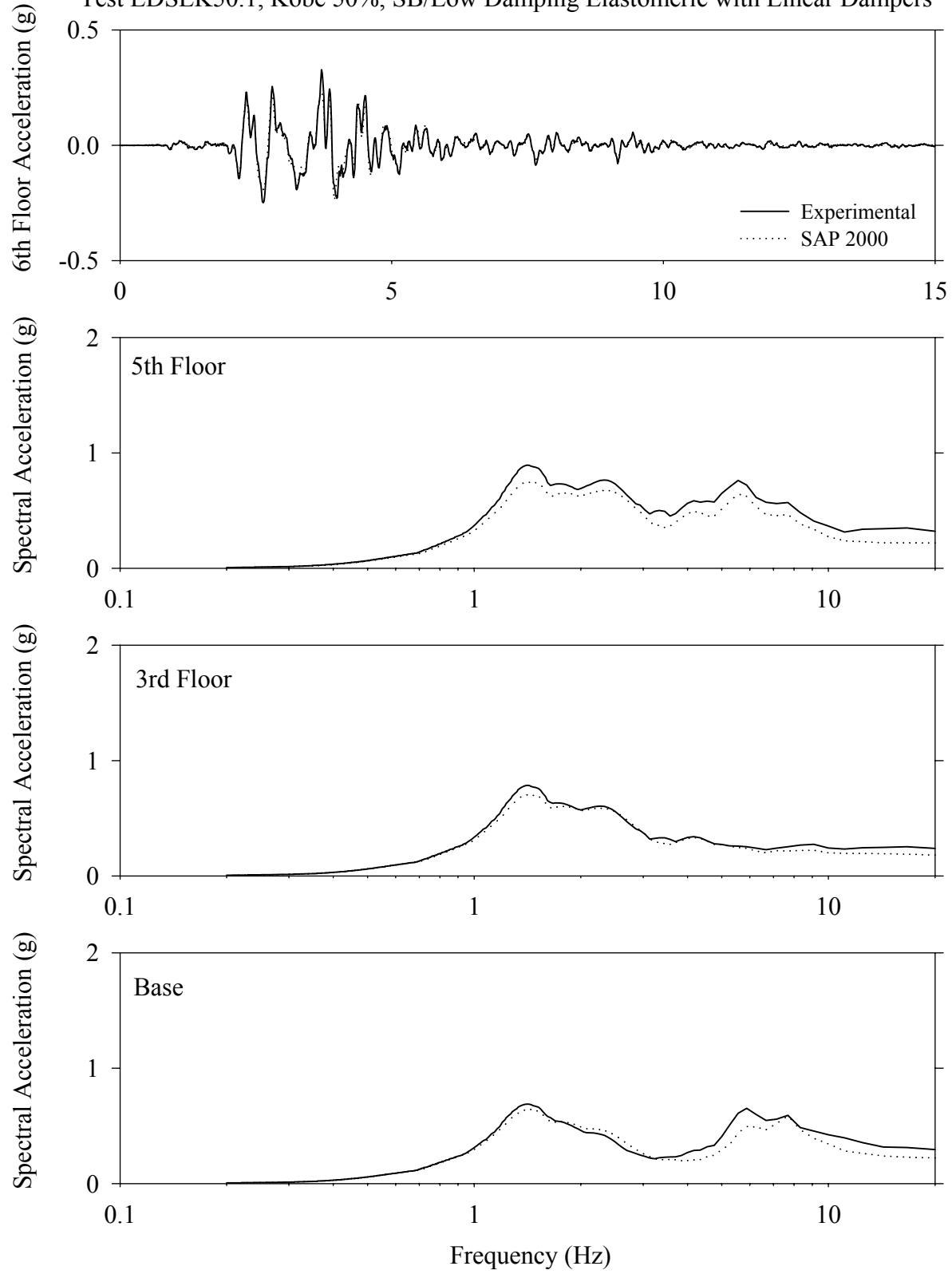
Test LDSLE20.1, El Centro S00E 200%, SB/Low Damping Elastomeric with Linear Dampers



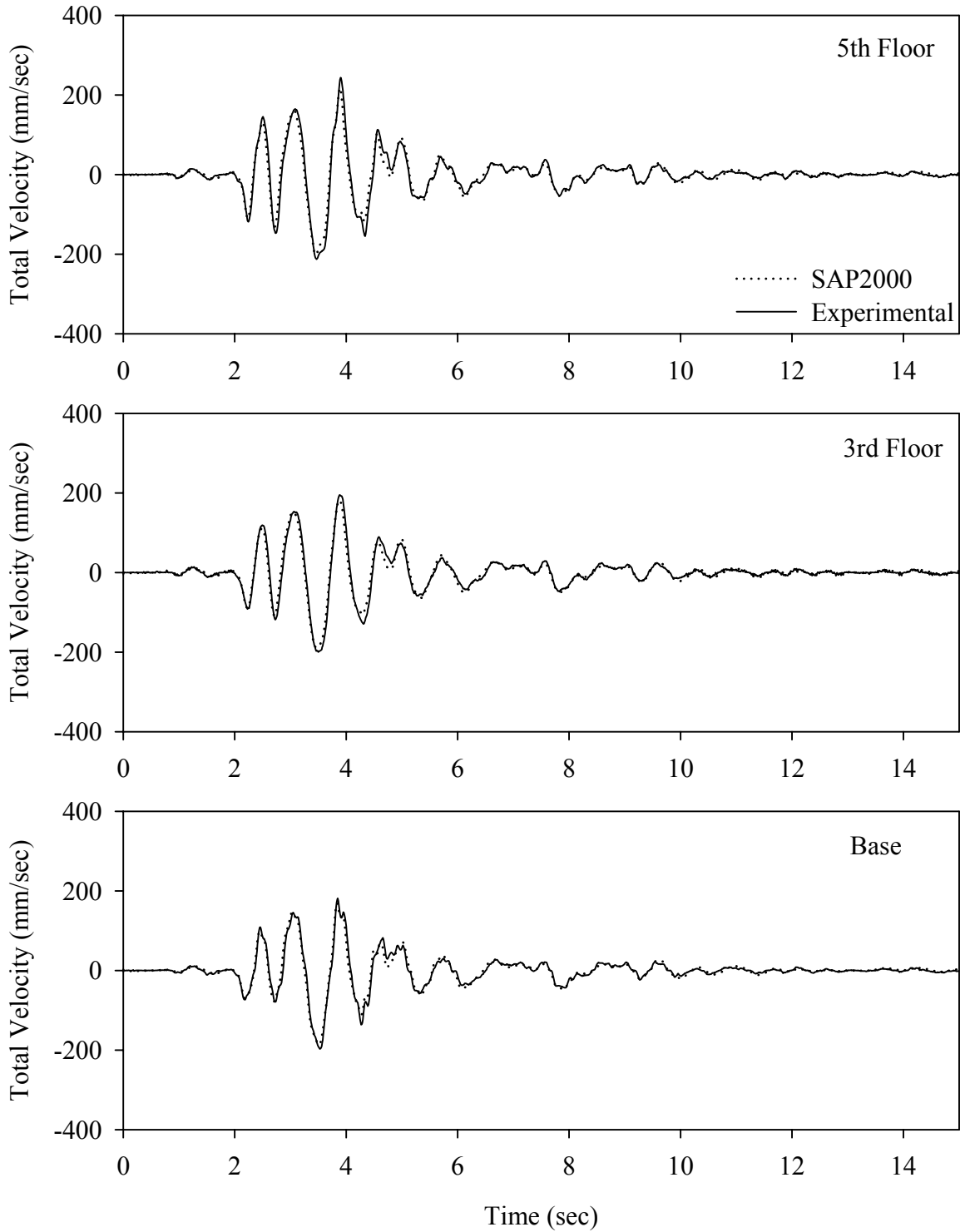
Test LDSLK50.1, Kobe 50%, SB/Low Damping Elastomeric with Linear Dampers



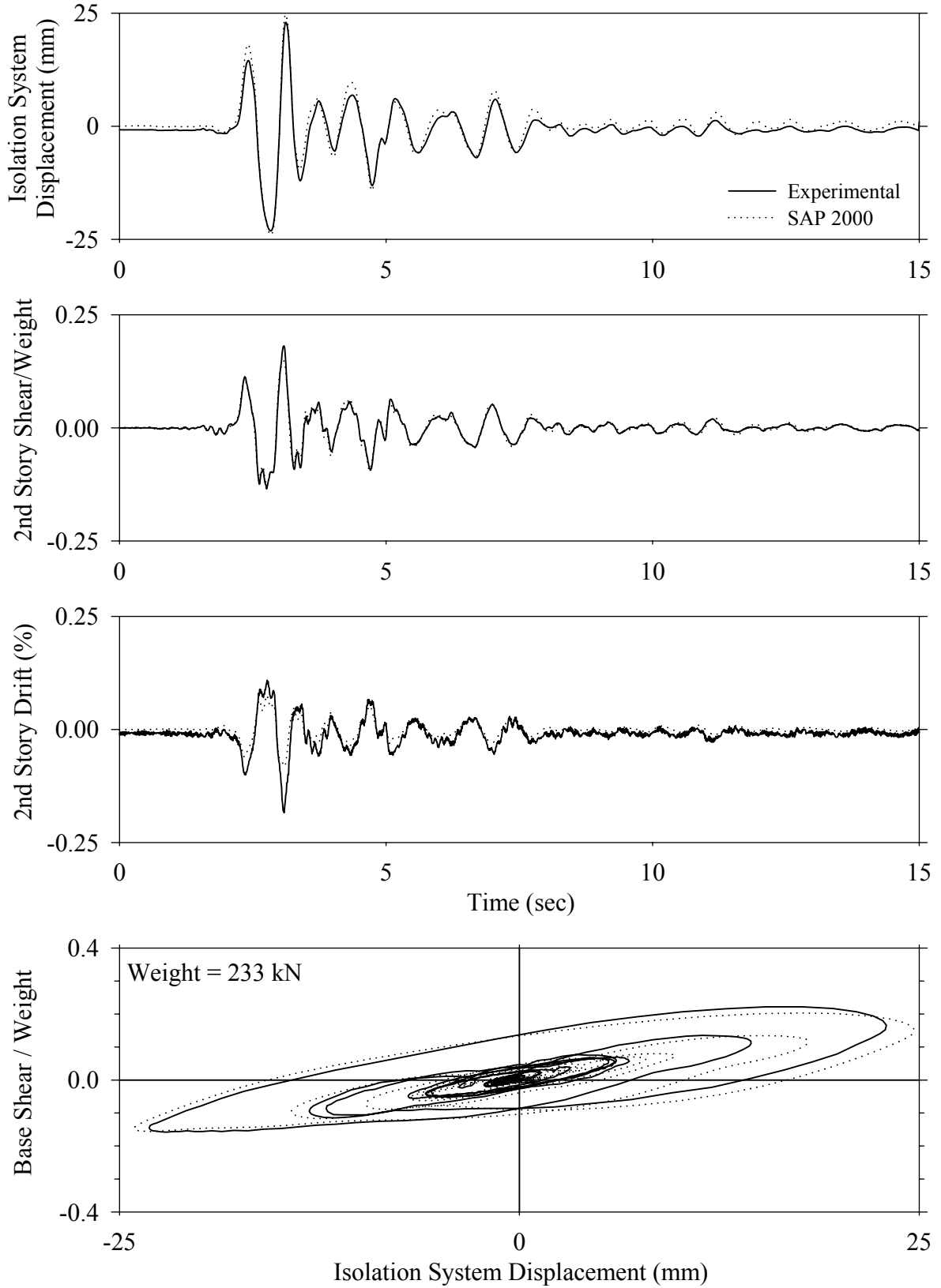
Test LDSLK50.1, Kobe 50%, SB/Low Damping Elastomeric with Linear Dampers



Test LDSLK50.1, Kobe 50%, SB/Low Damping Elastomeric with Linear Dampers

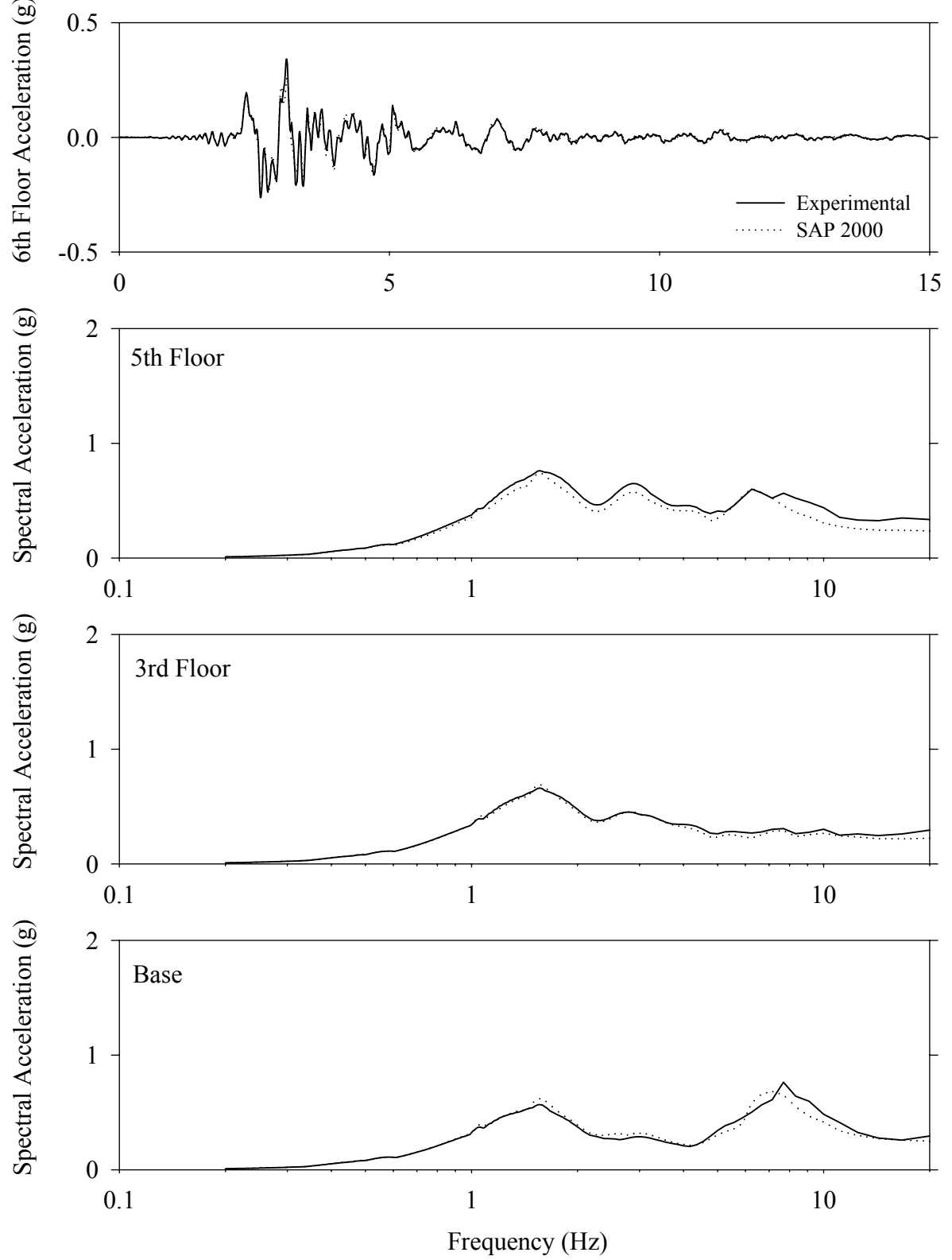


Test LDSLN50.1, Newhall 360 50%, SB/Low Damping Elastomeric with Linear Dampers

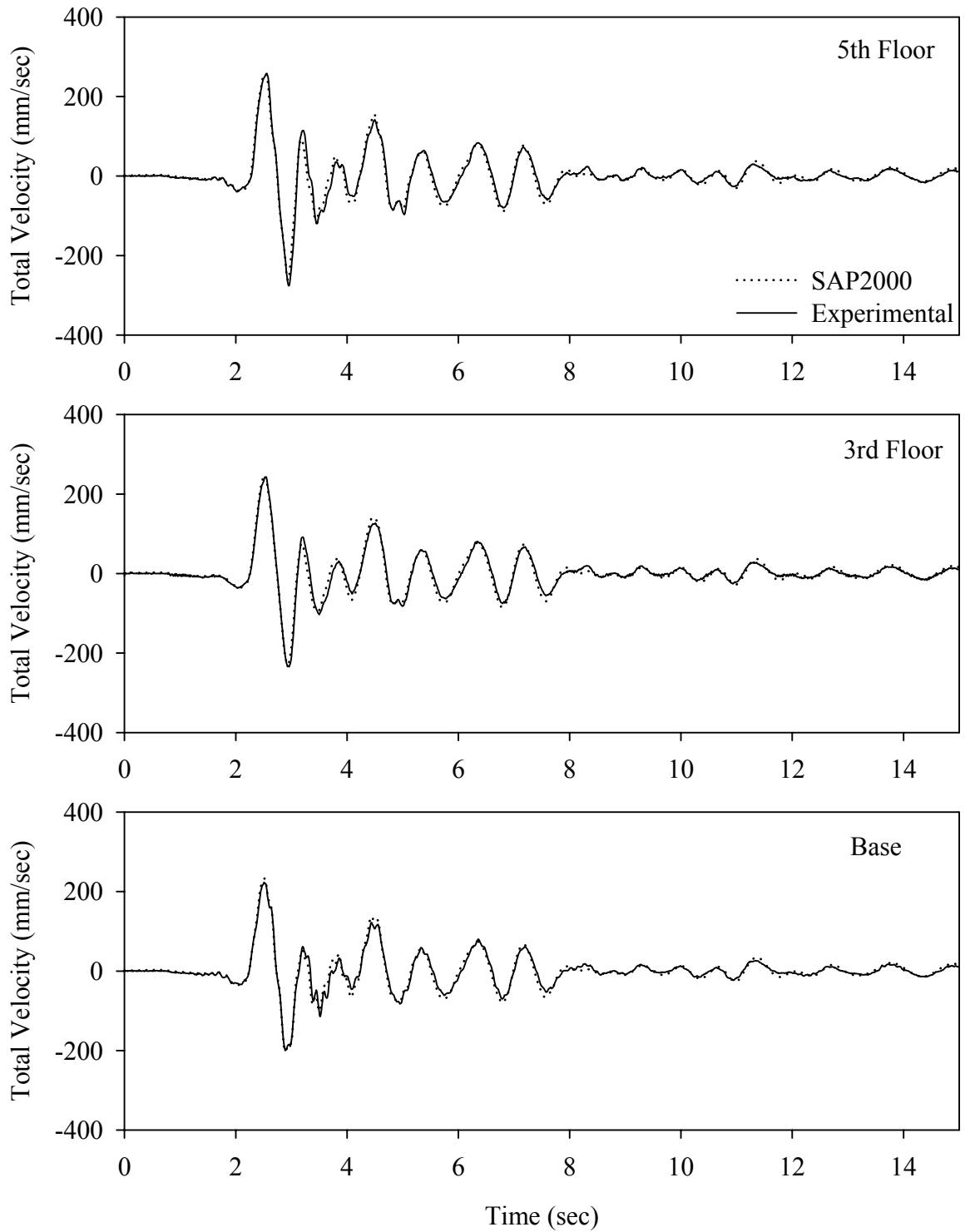




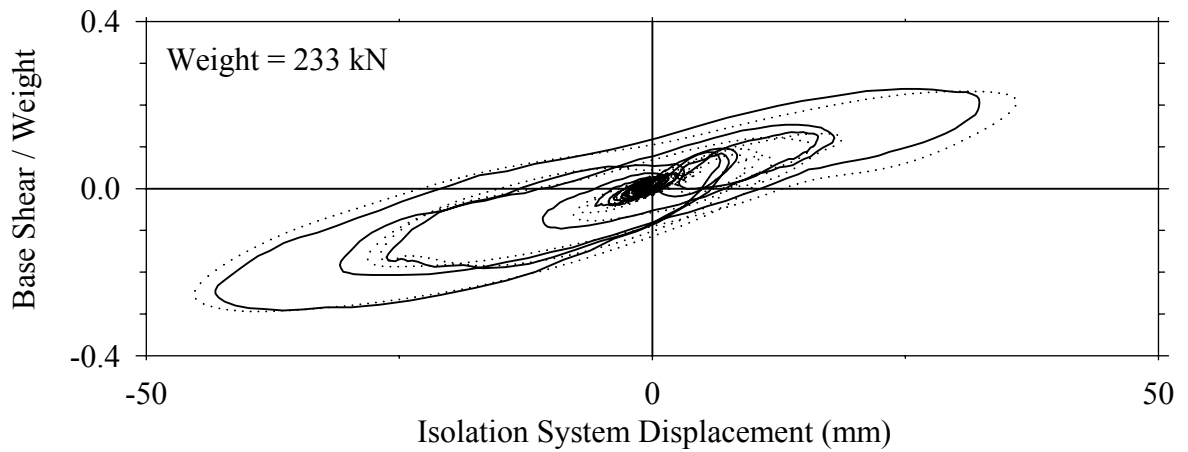
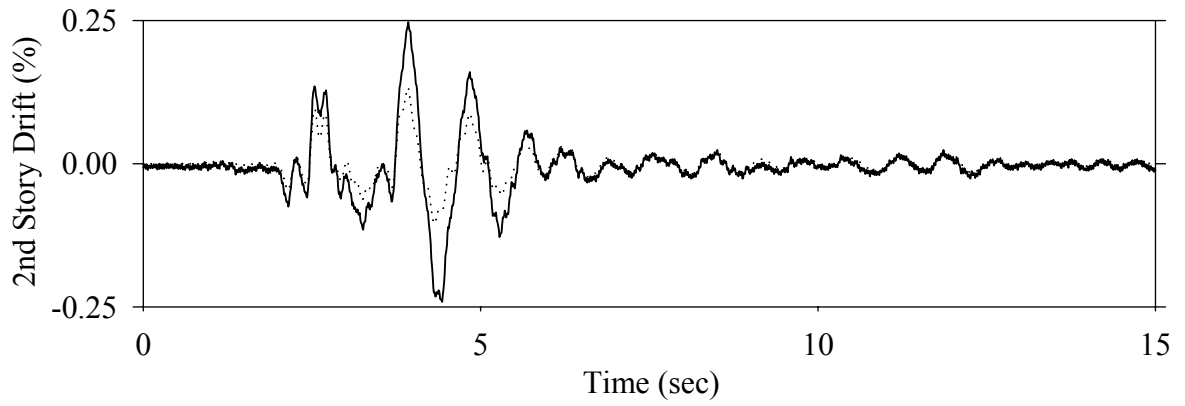
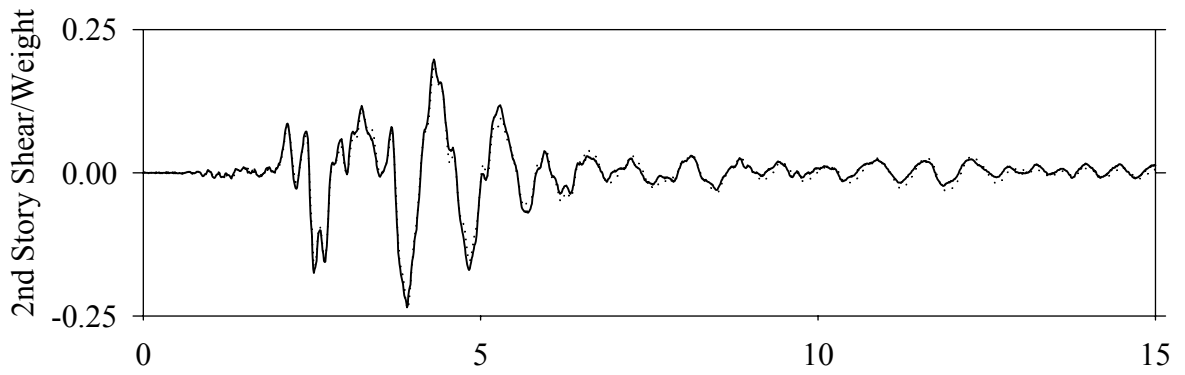
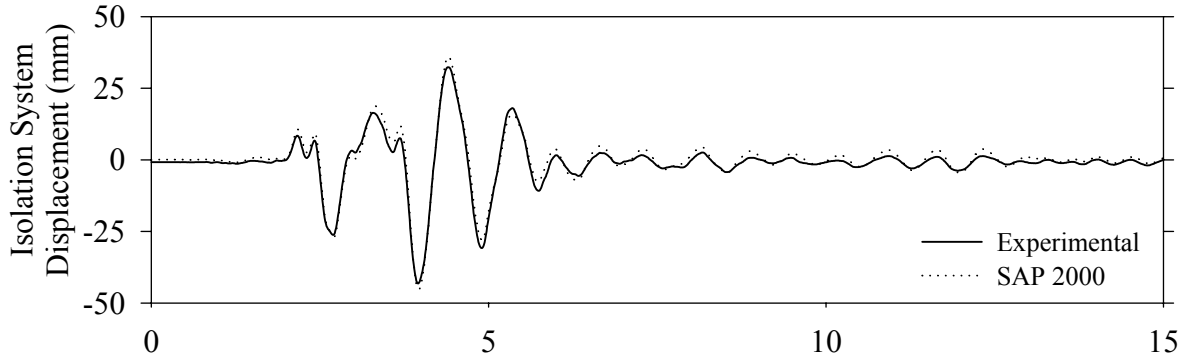
Test LDSLN50.1, Newhall 360 50%, SB/Low Damping Elastomeric with Linear Dampers



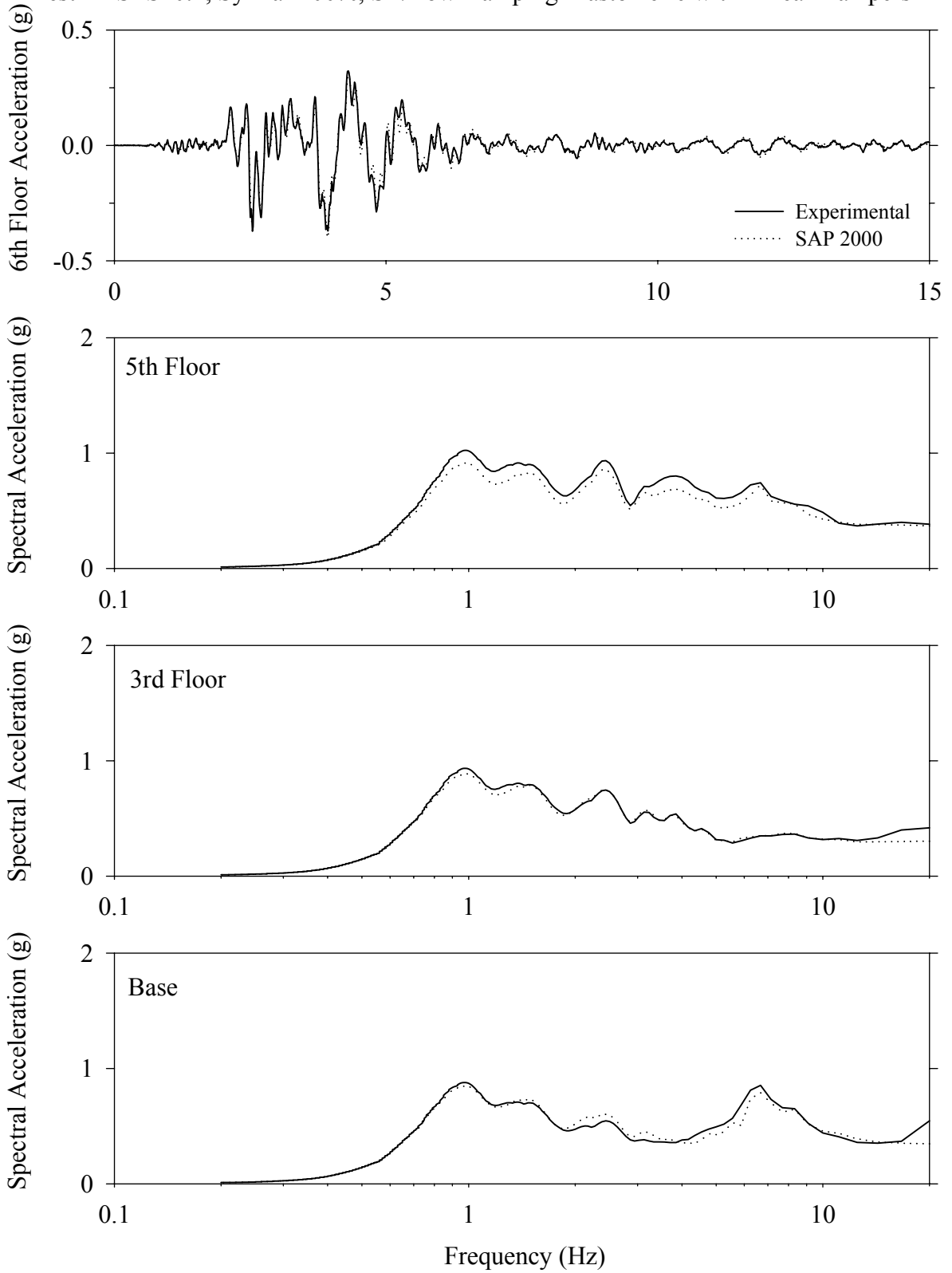
Test LDSLN50.1, Newhall 360 50%, SB/Low Damping Elastomeric with Linear Dampers



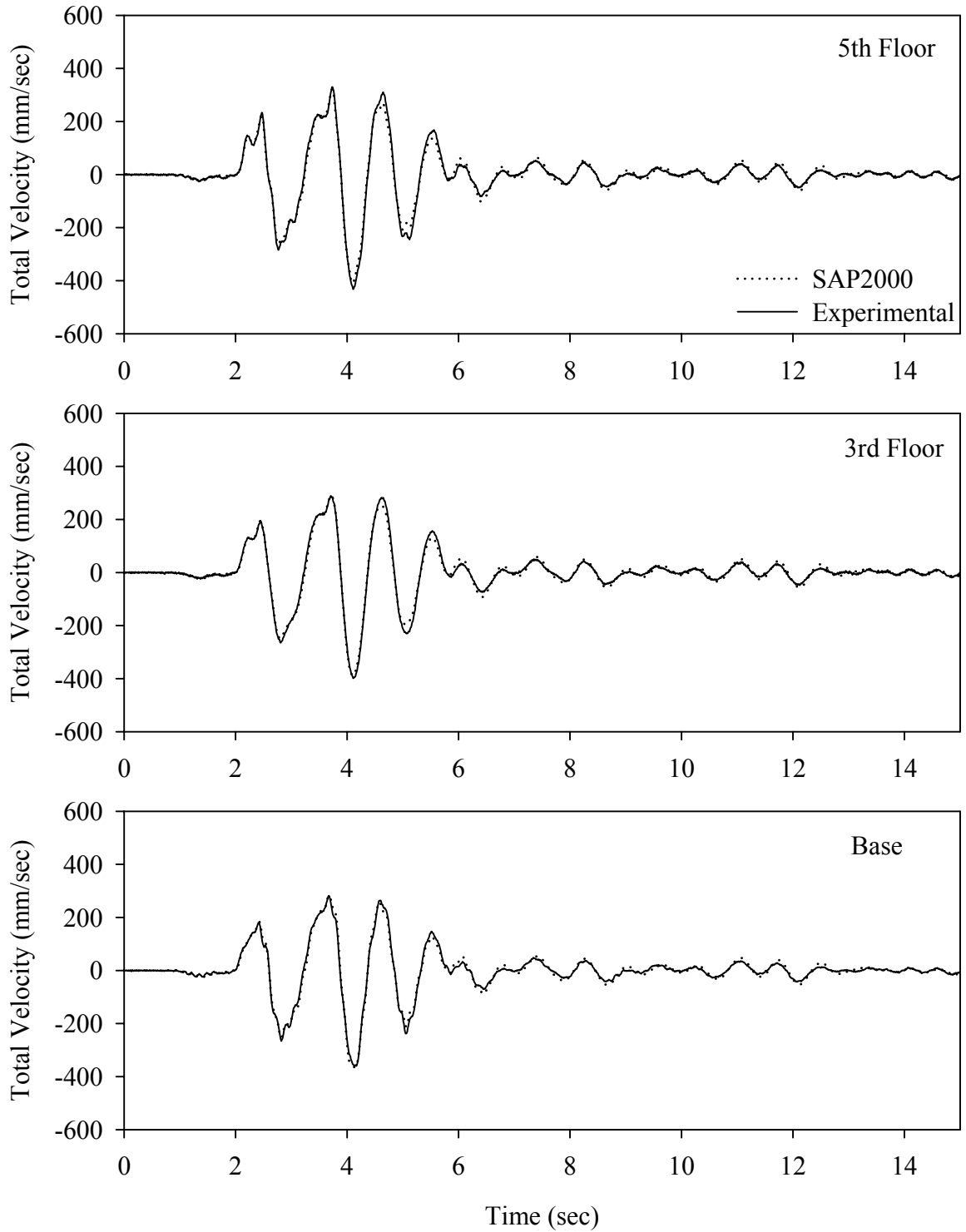
Test LDSLS10.1, Sylmar 100%, SB/Low Damping Elastomeric with Linear Dampers



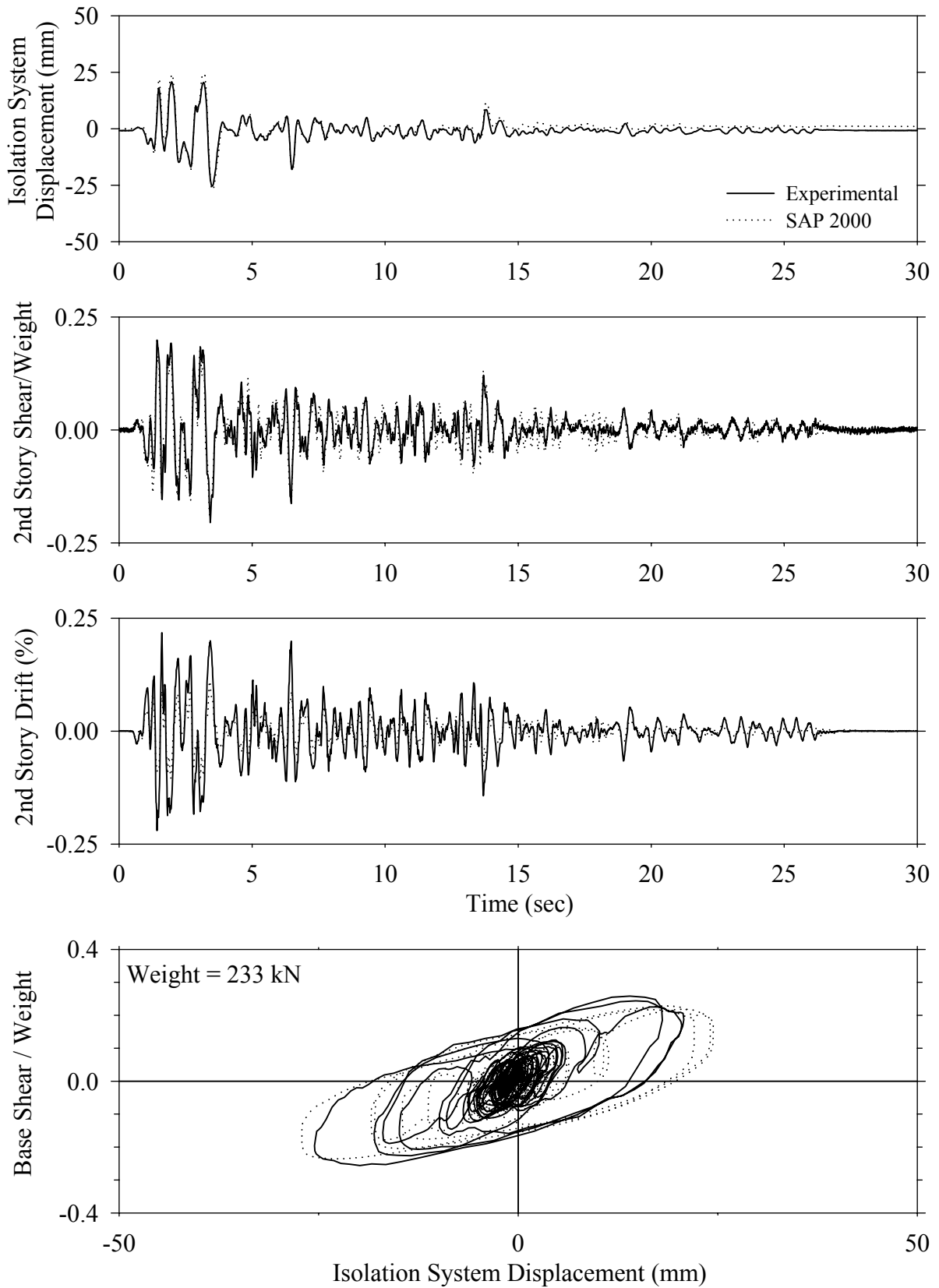
Test LDSLS10.1, Sylmar 100%, SB/Low Damping Elastomeric with Linear Dampers



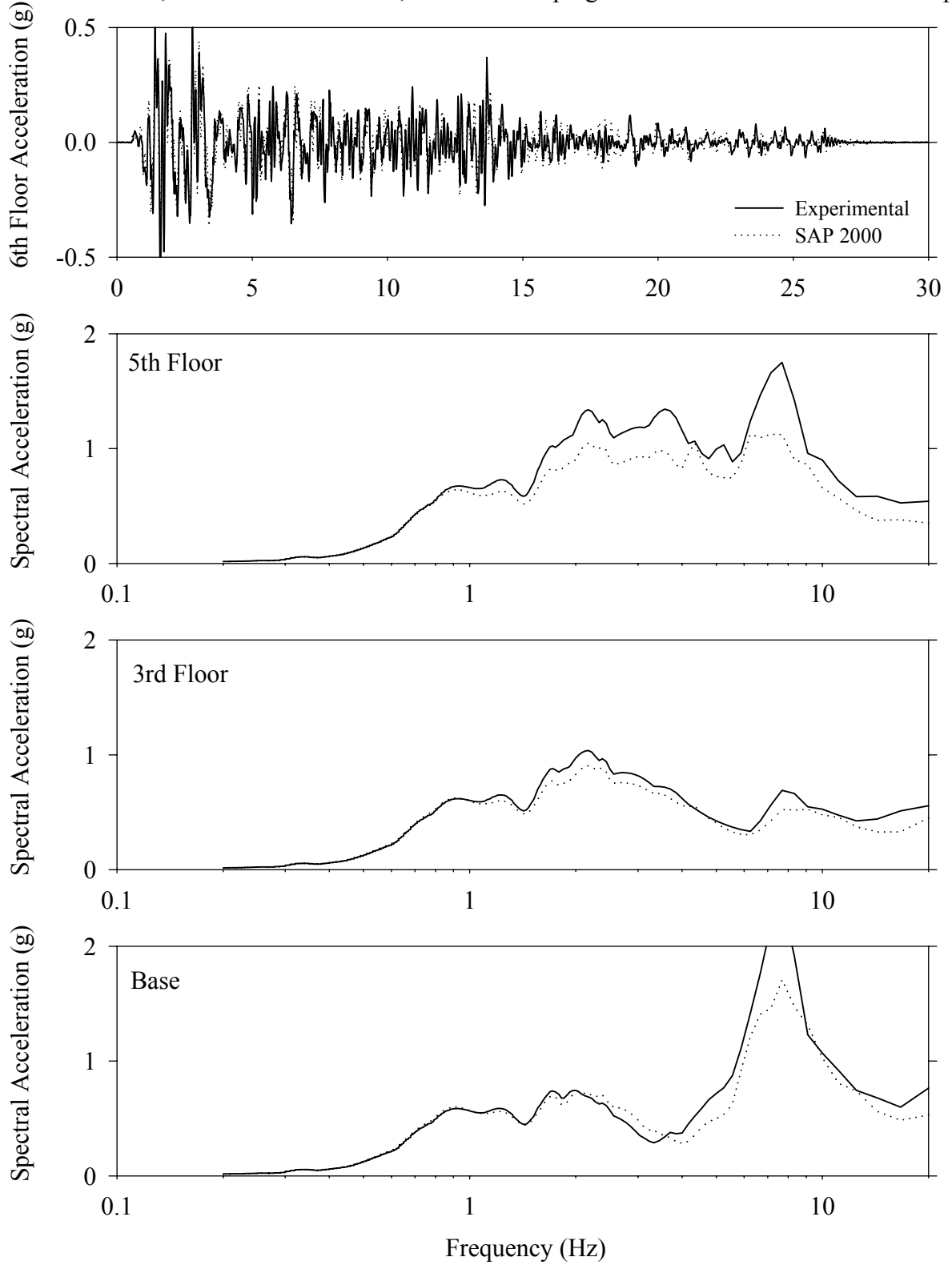
Test LDSLS10.1, Sylmar 100%, SB/Low Damping Elastomeric with Linear Dampers



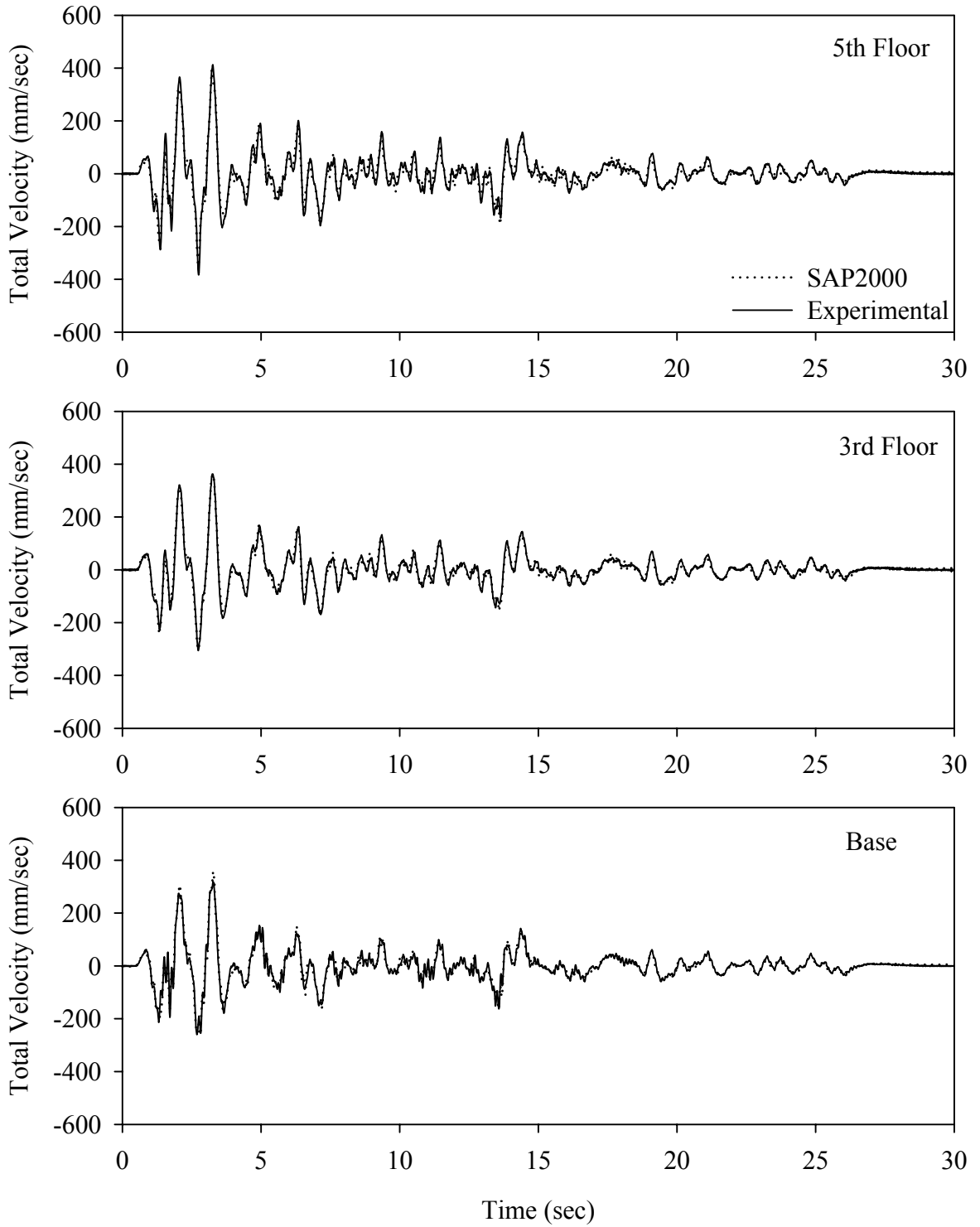
Test LDSNE20.1, El Centro S00E 200%, SB/Low Damping Elastomeric with Nonlinear Dampers



Test LDSNE20.1, El Centro S00E 200%, SB/Low Damping Elastomeric with Nonlinear Dampers

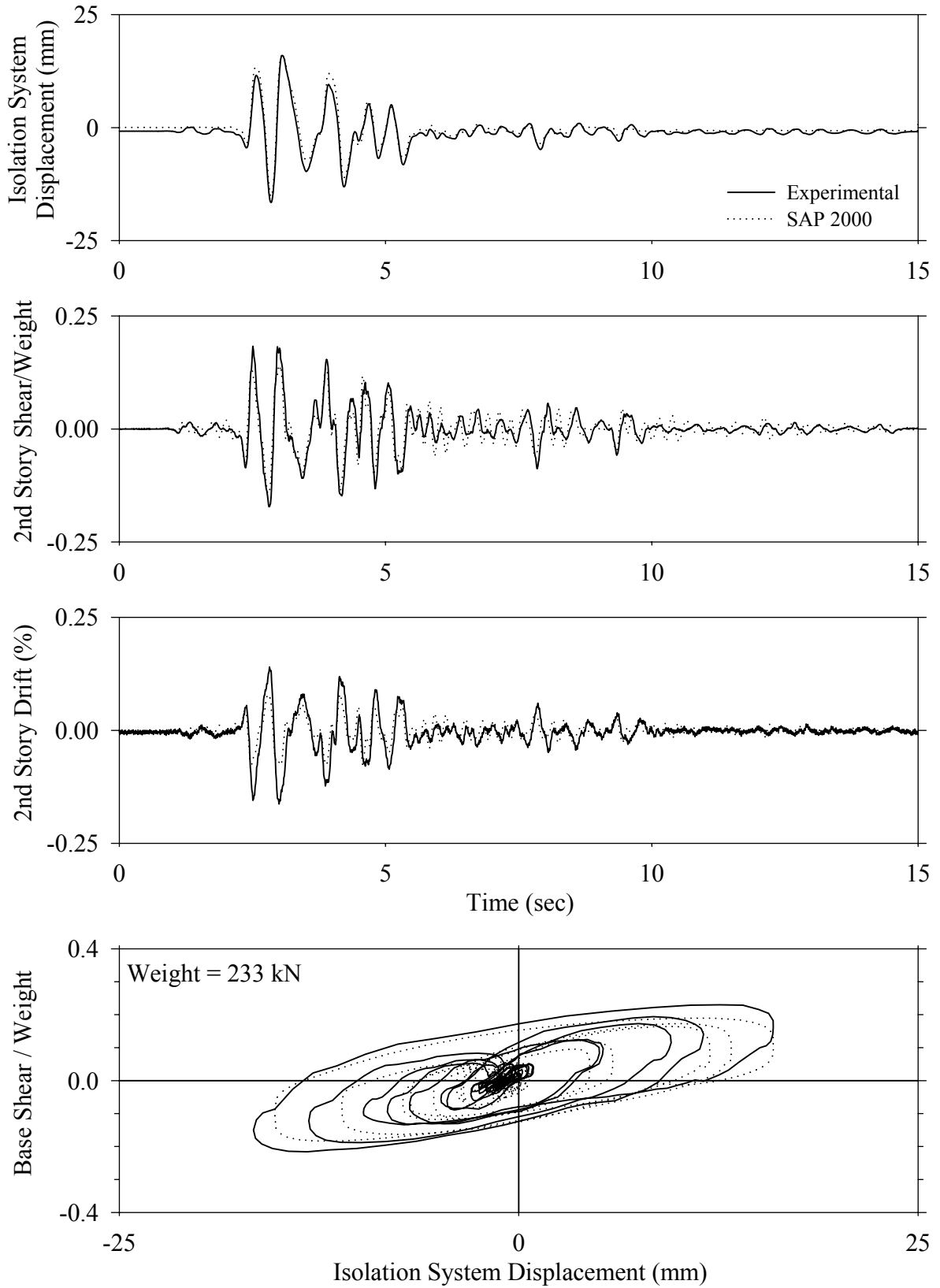


Test LDSNE20.1, El Centro S00E 200%, SB/Low Damping Elastomeric with Nonlinear Dampers

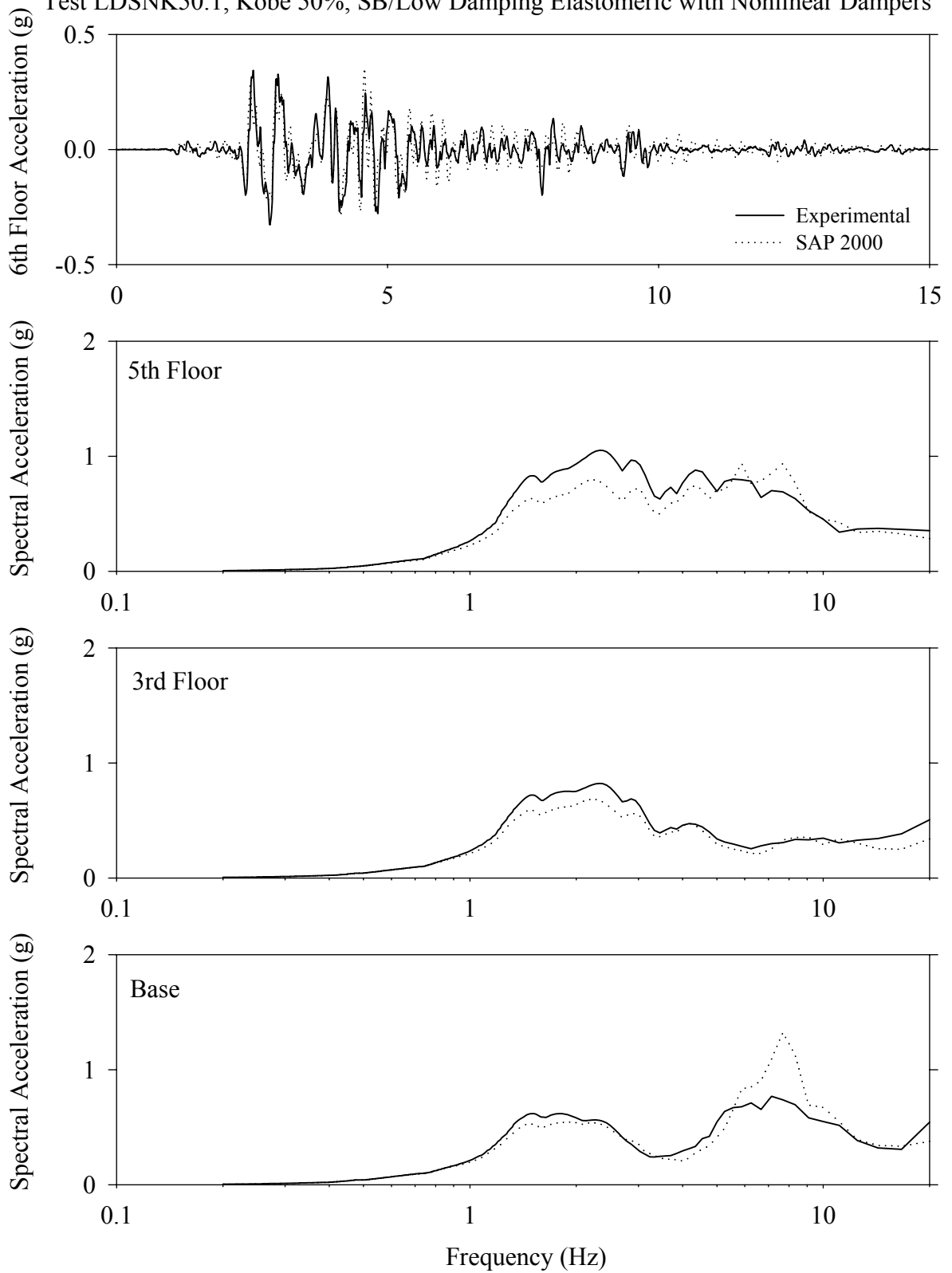




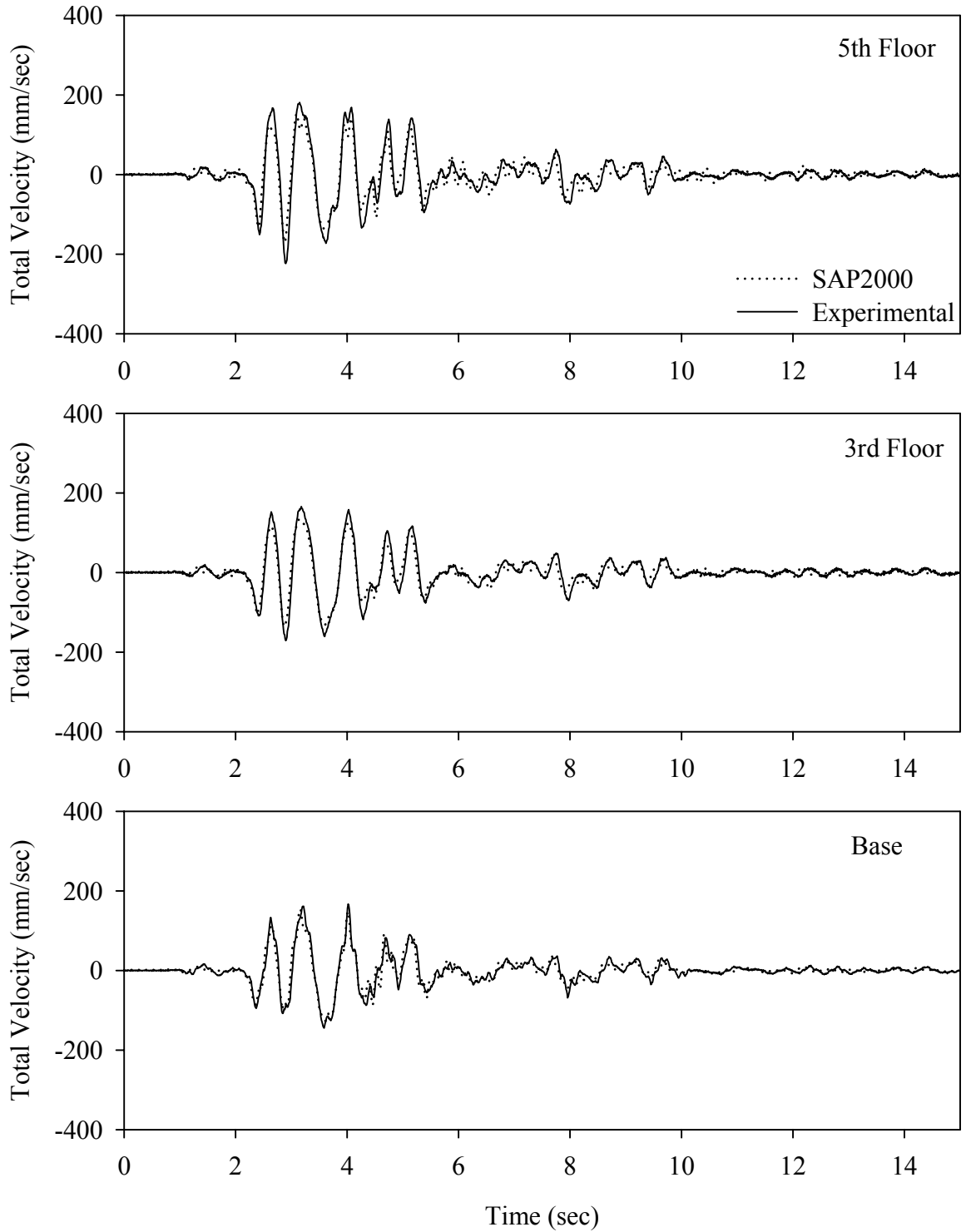
Test LDSNK50.1, Kobe 50%, SB/Low Damping Elastomeric with Nonlinear Dampers



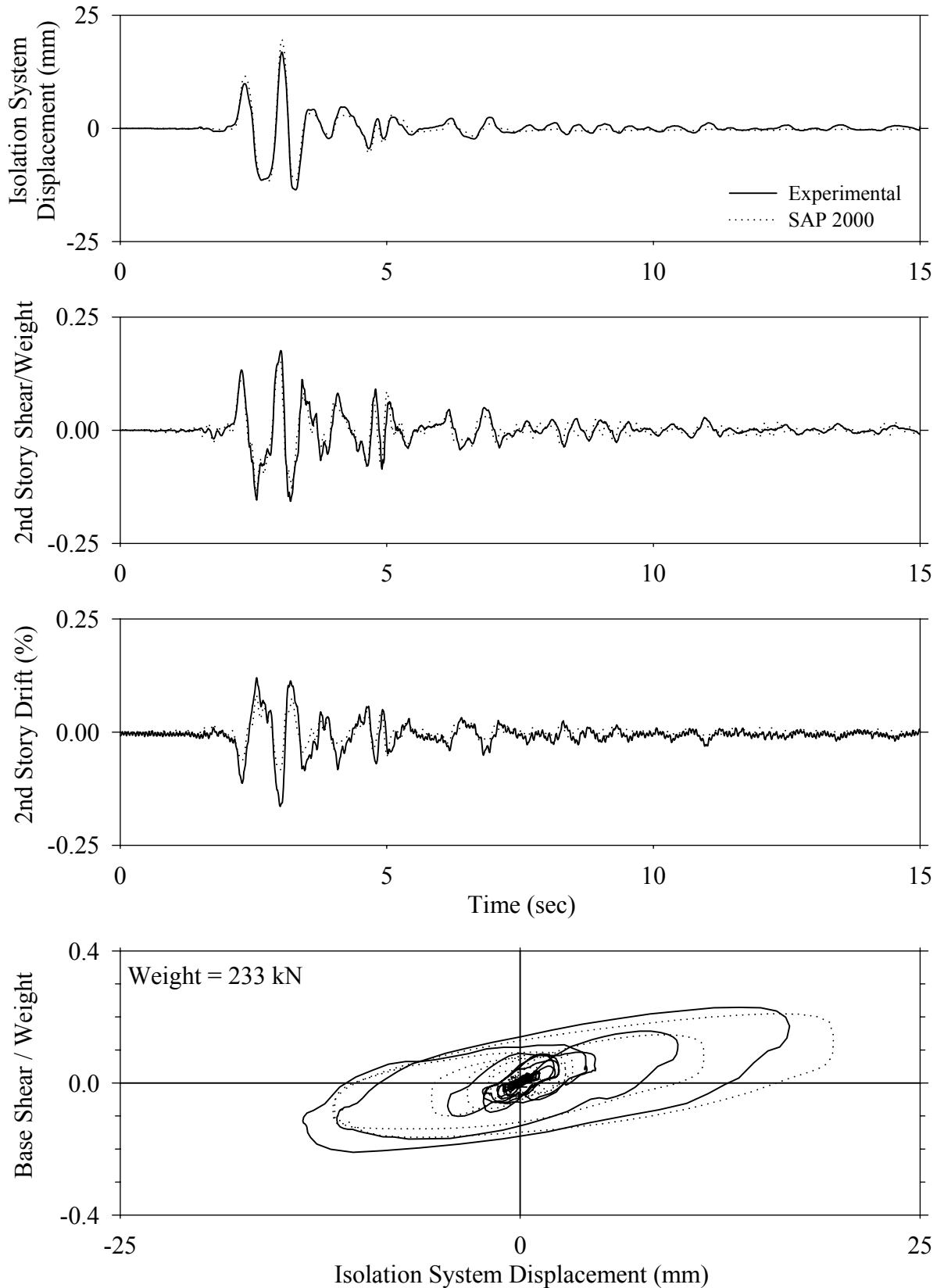
Test LDSNK50.1, Kobe 50%, SB/Low Damping Elastomeric with Nonlinear Dampers



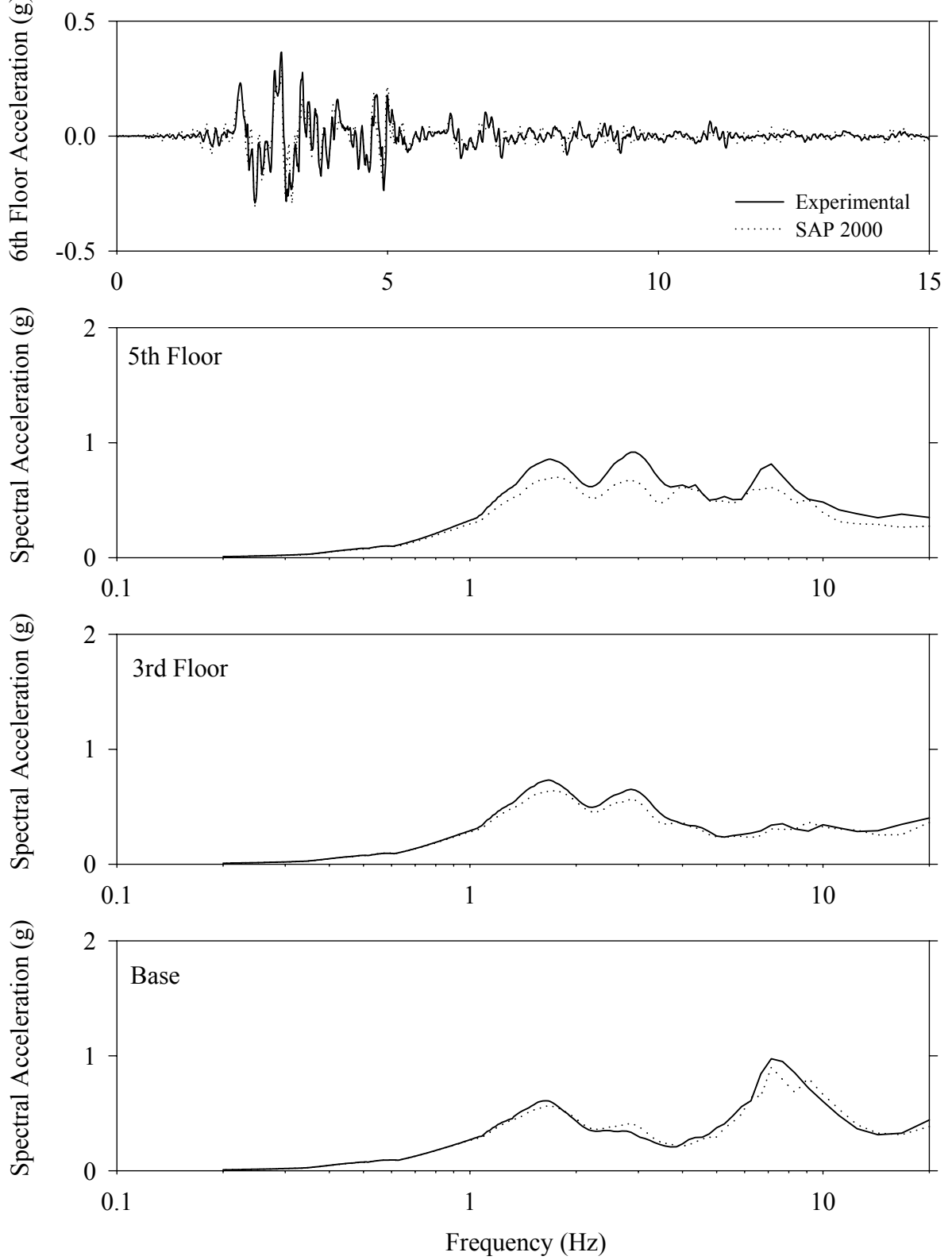
Test LDSNK50.1, Kobe 50%, SB/Low Damping Elastomeric with Nonlinear Dampers



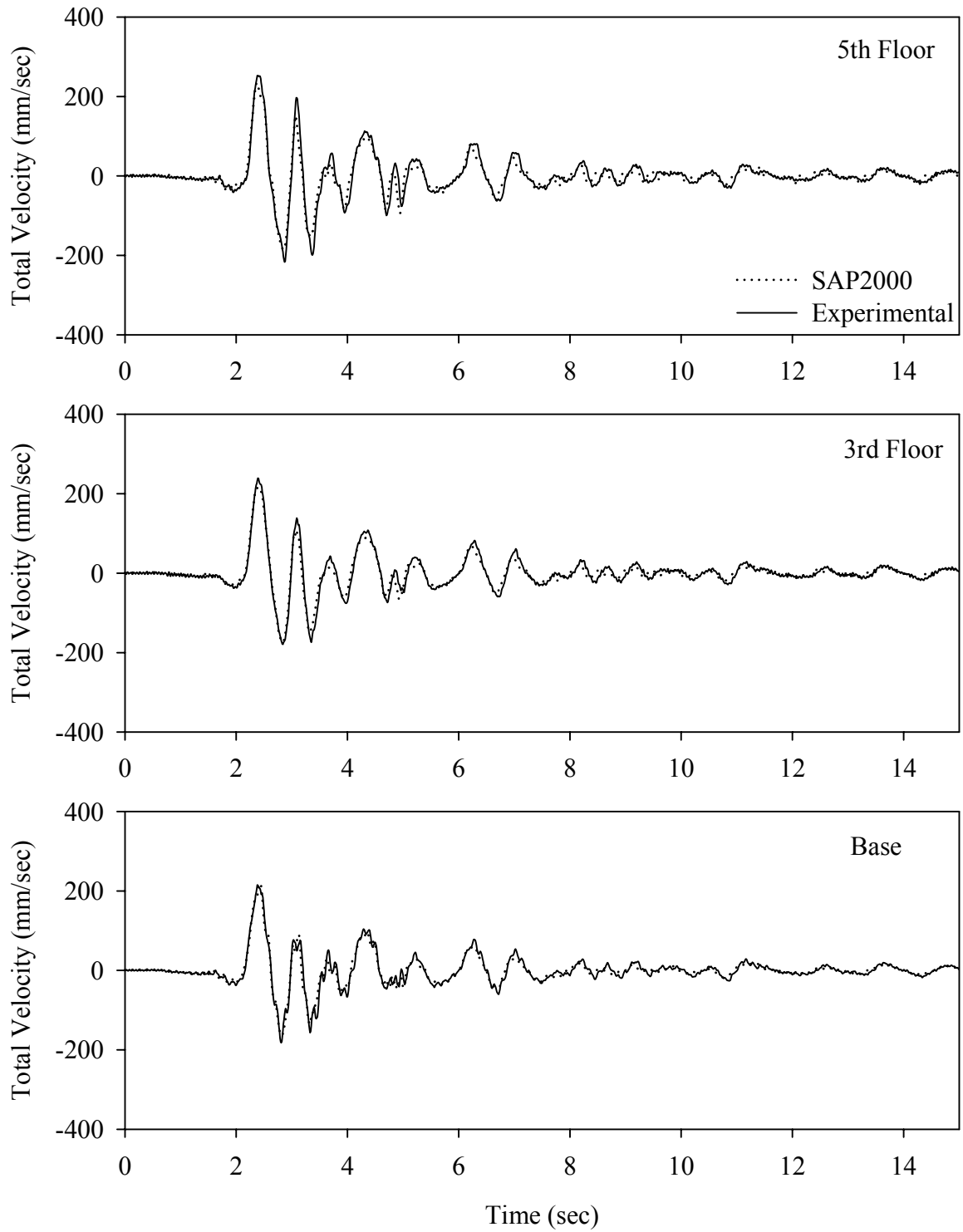
Test LDSNN50.1, Newhall 360 50%, SB/Low Damping Elastomeric with Nonlinear Dampers



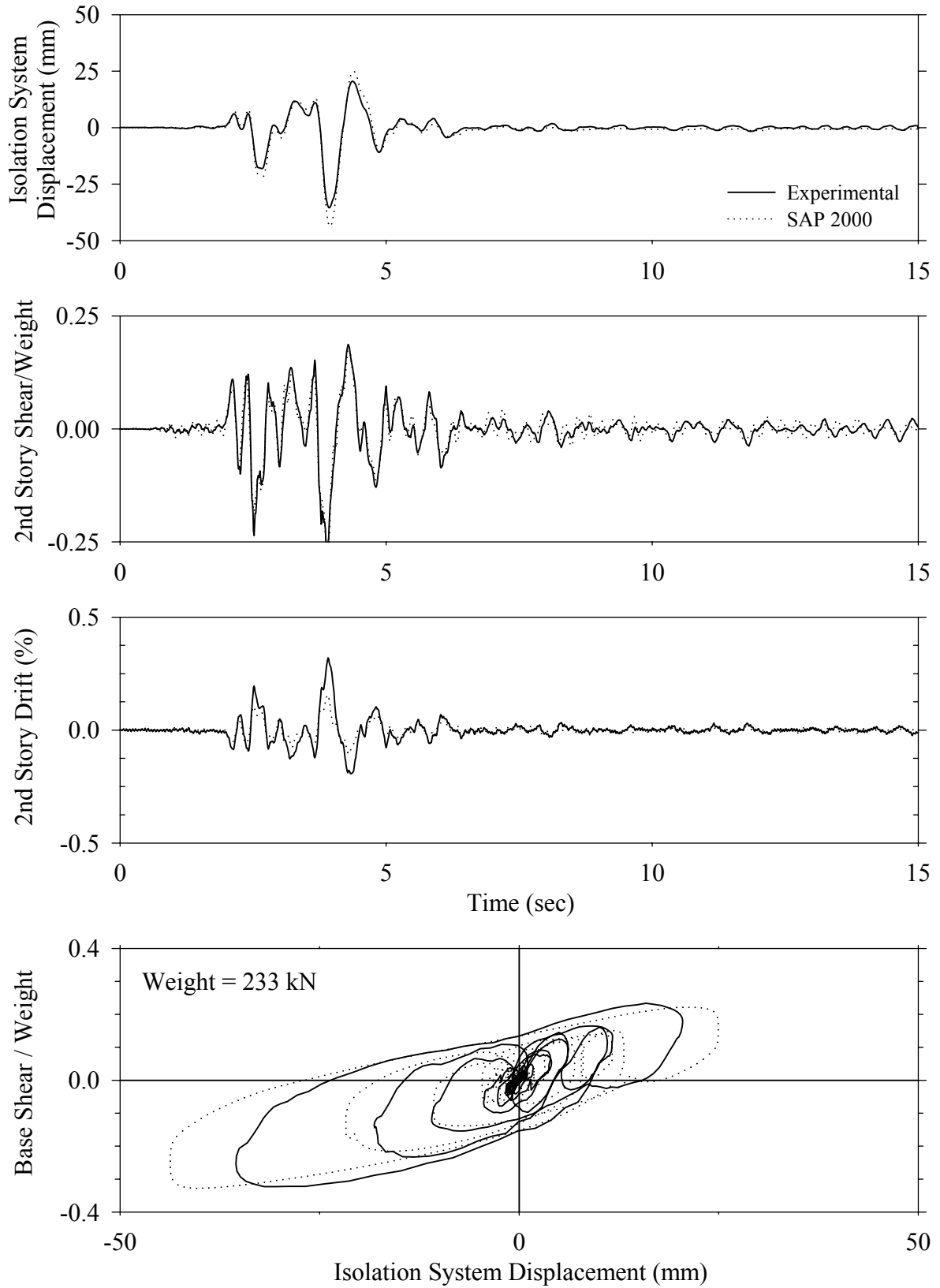
Test LDSNN50.1, Newhall 360 50%, SB/Low Damping Elastomeric with Nonlinear Dampers



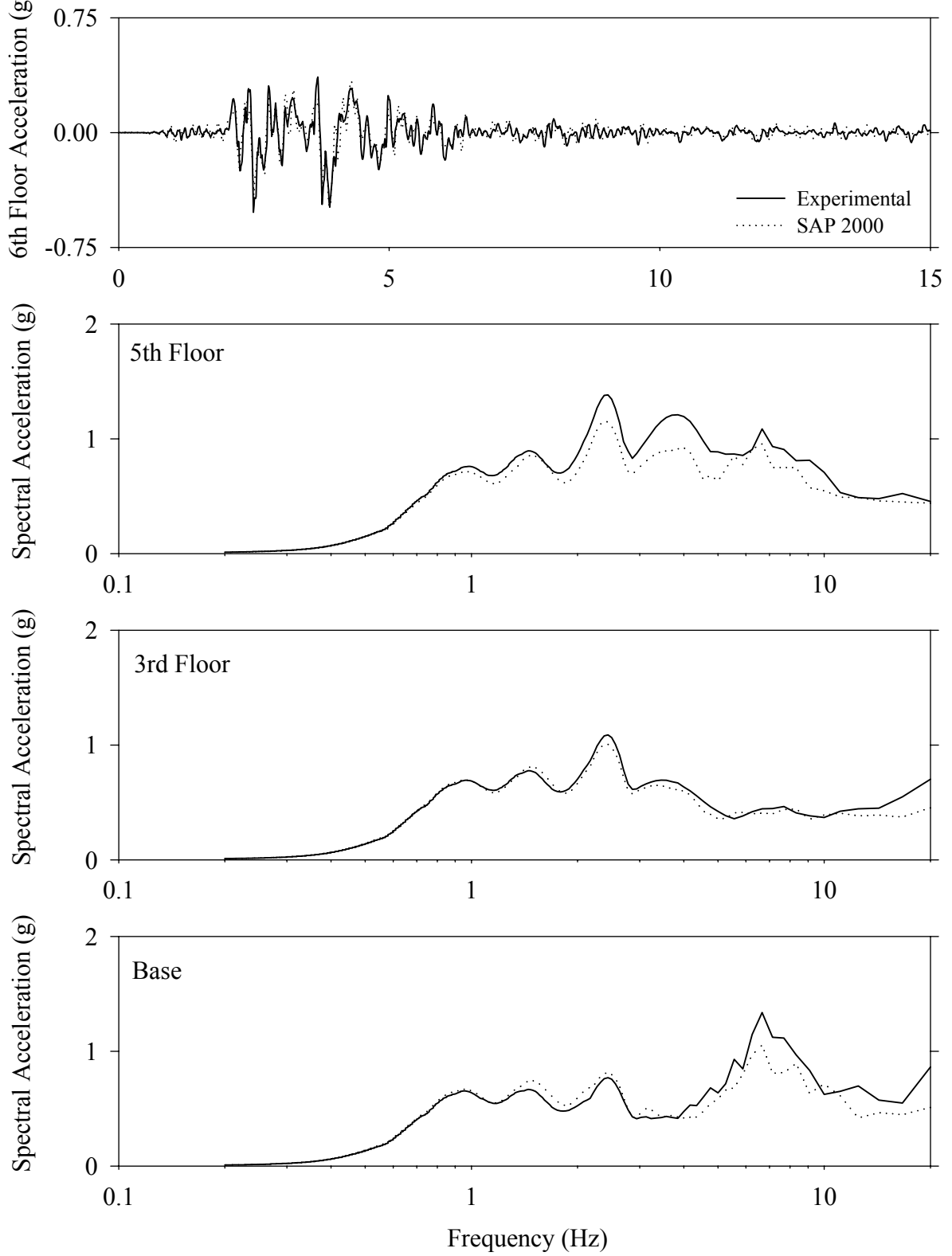
Test LDSNN50.1, Newhall 360 50%, SB/Low Damping Elastomeric with Nonlinear Dampers



Test LDSNS10.1, Sylmar 100%, SB/Low Damping Elastomeric with Nonlinear Dampers

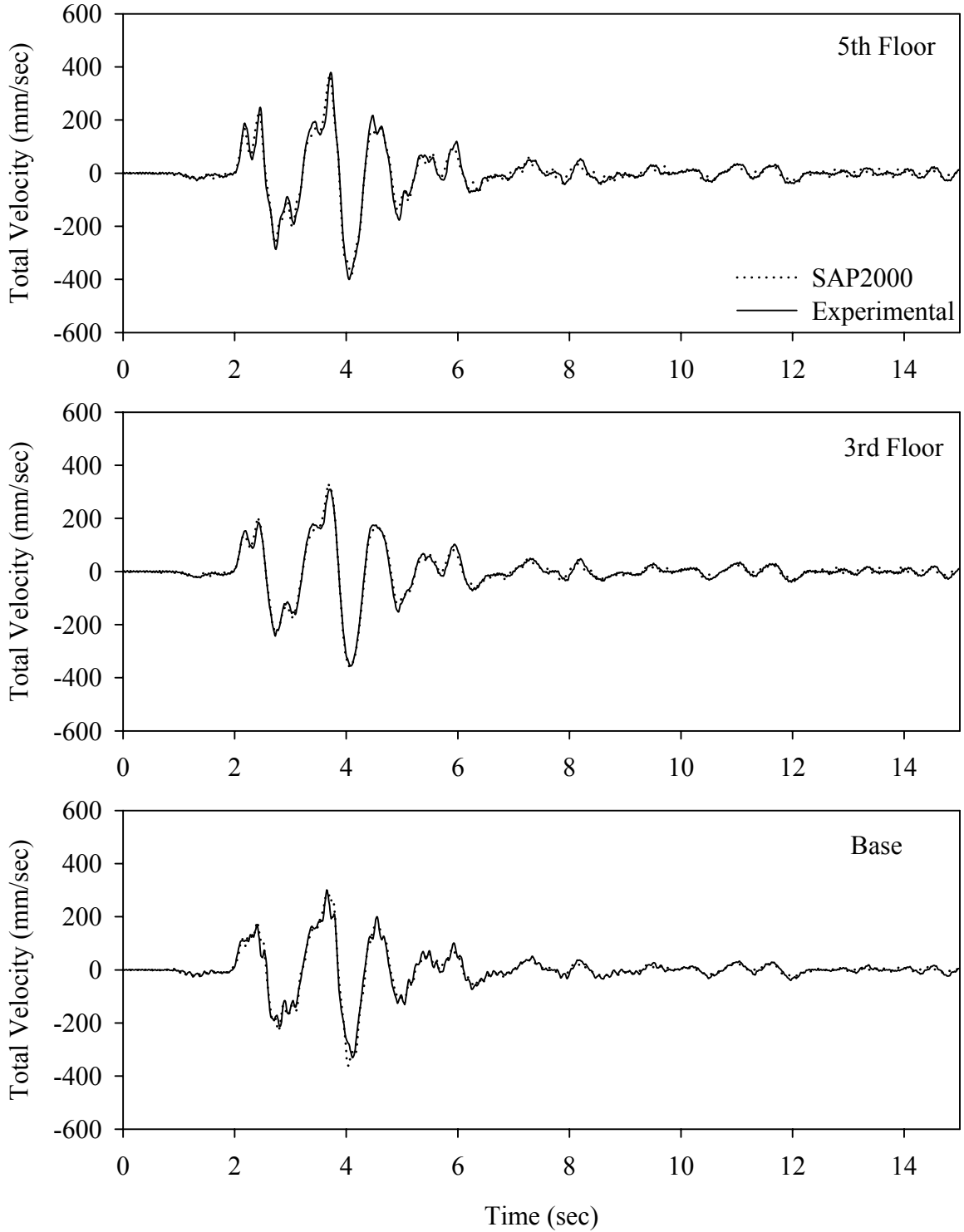


Test LDSNS10.1, Sylmar 100%, SB/Low Damping Elastomeric with Nonlinear Dampers

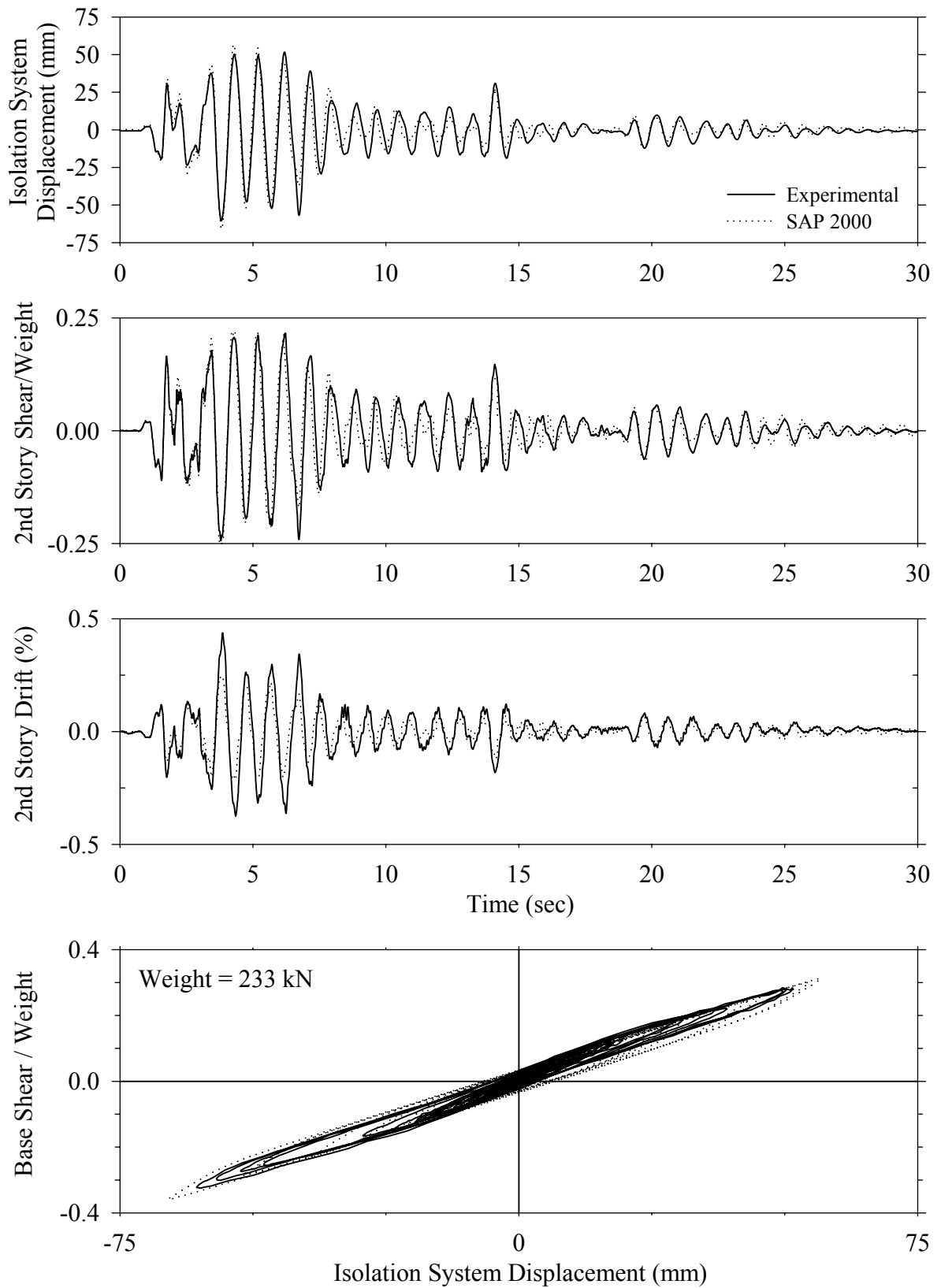




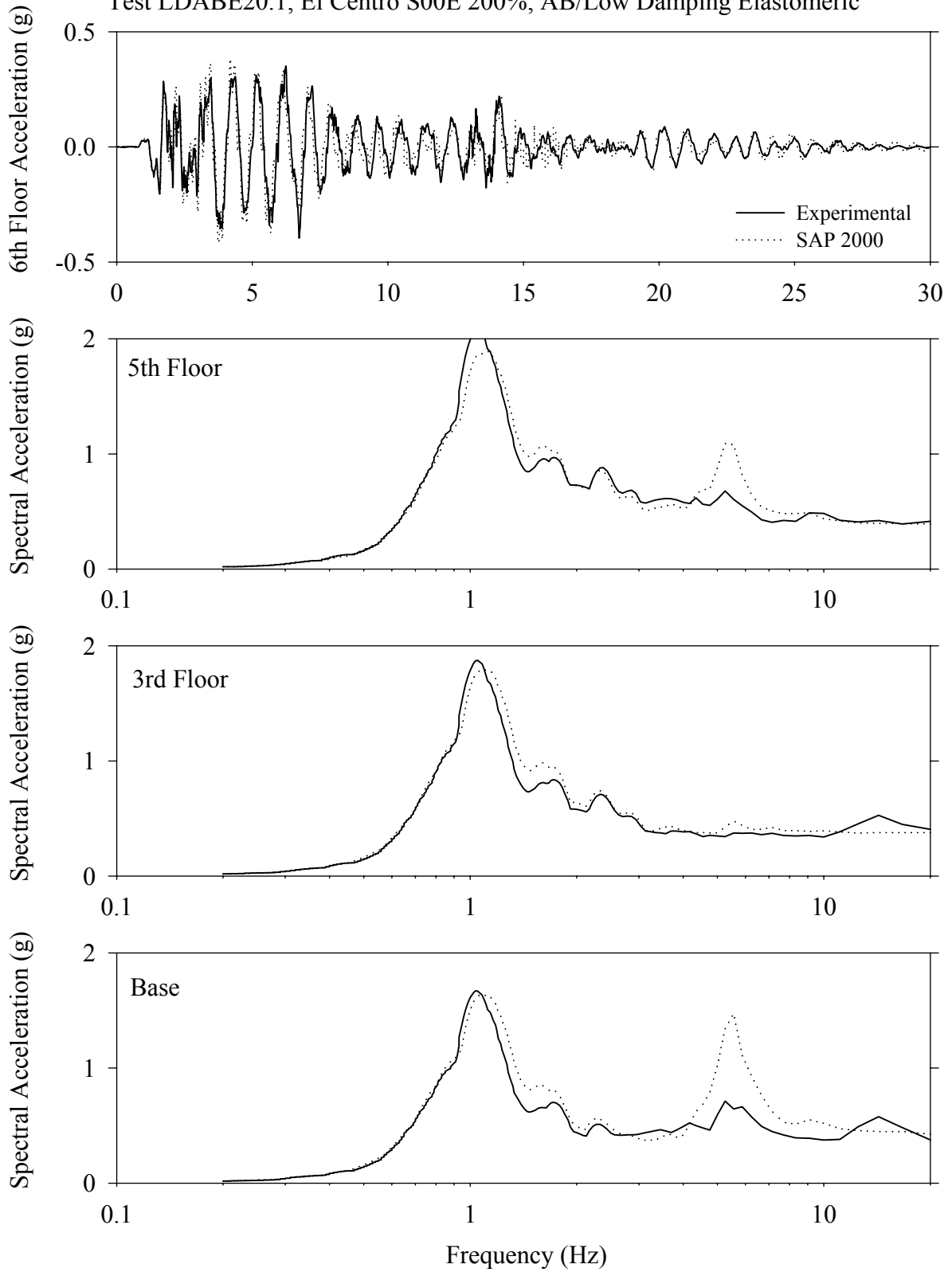
Test LDSNS10.1, Sylmar 100%, SB/Low Damping Elastomeric with Nonlinear Dampers



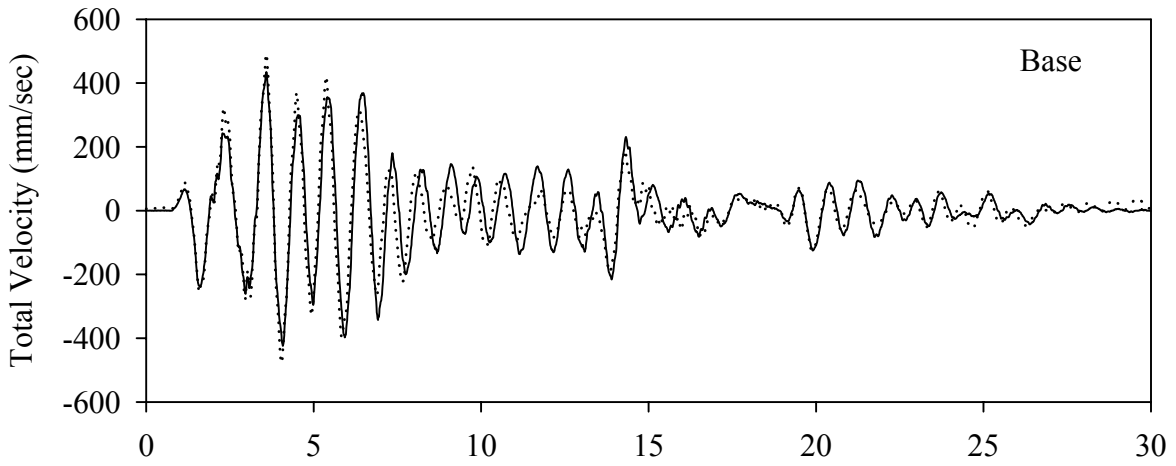
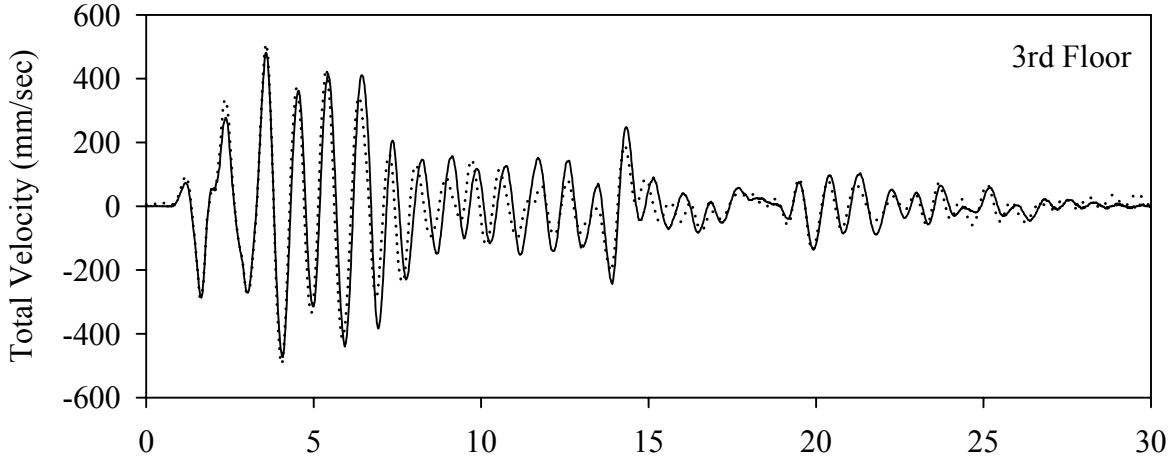
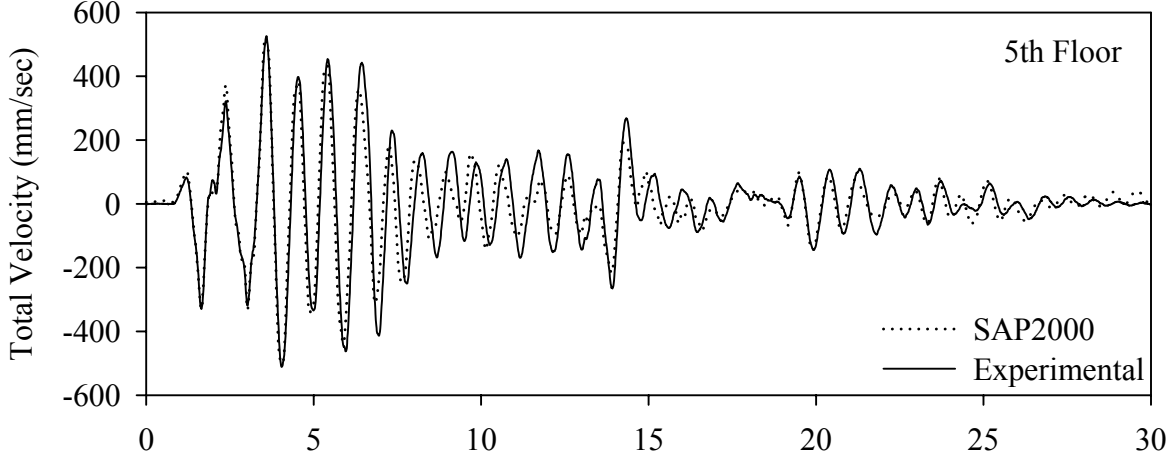
Test LDABE20.1, El Centro S00E 200%, AB/Low Damping Elastomeric



Test LDABE20.1, El Centro S00E 200%, AB/Low Damping Elastomeric

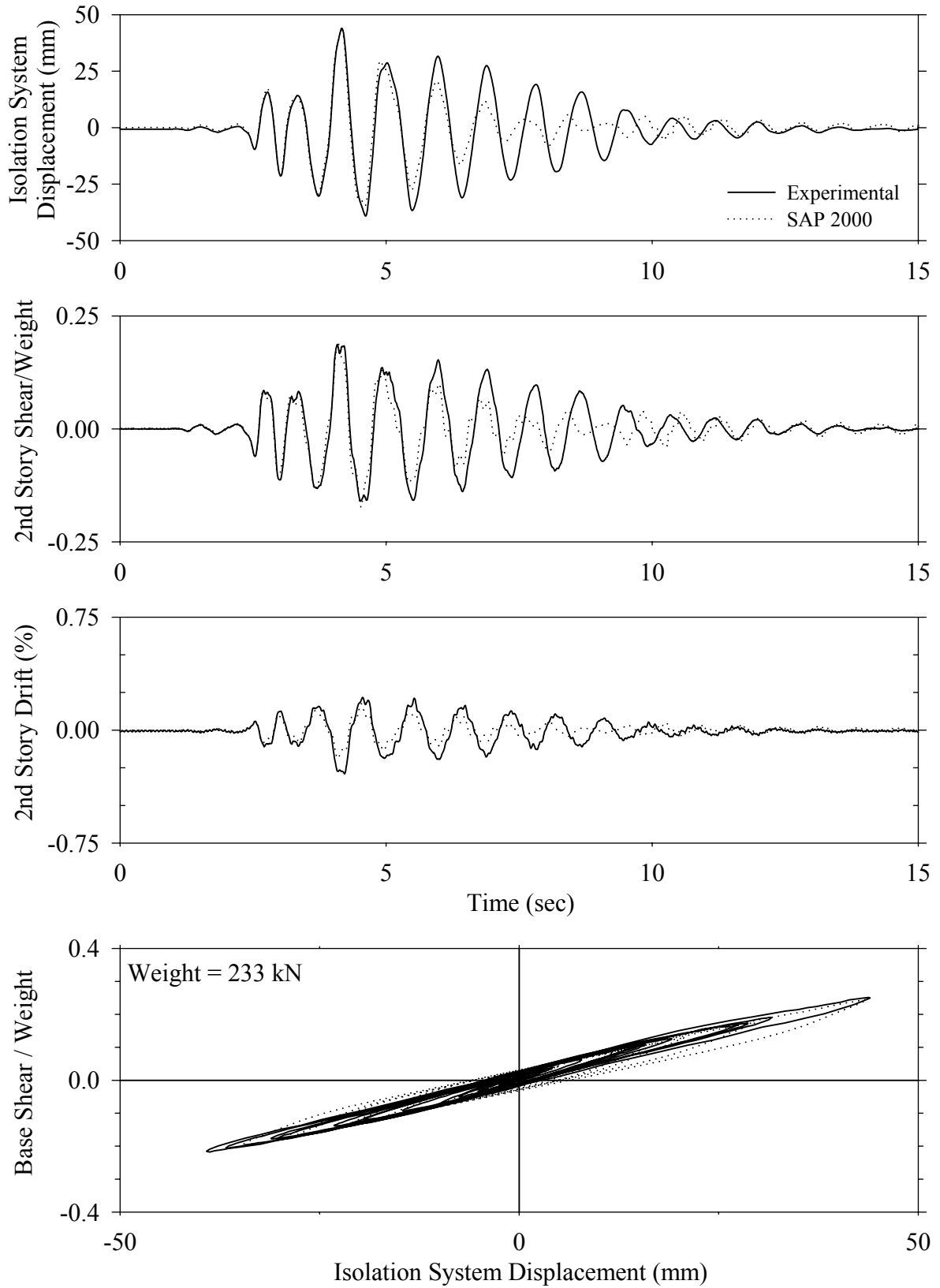


Test LDABE20.1, El Centro S00E 200%, AB/Low Damping Elastomeric

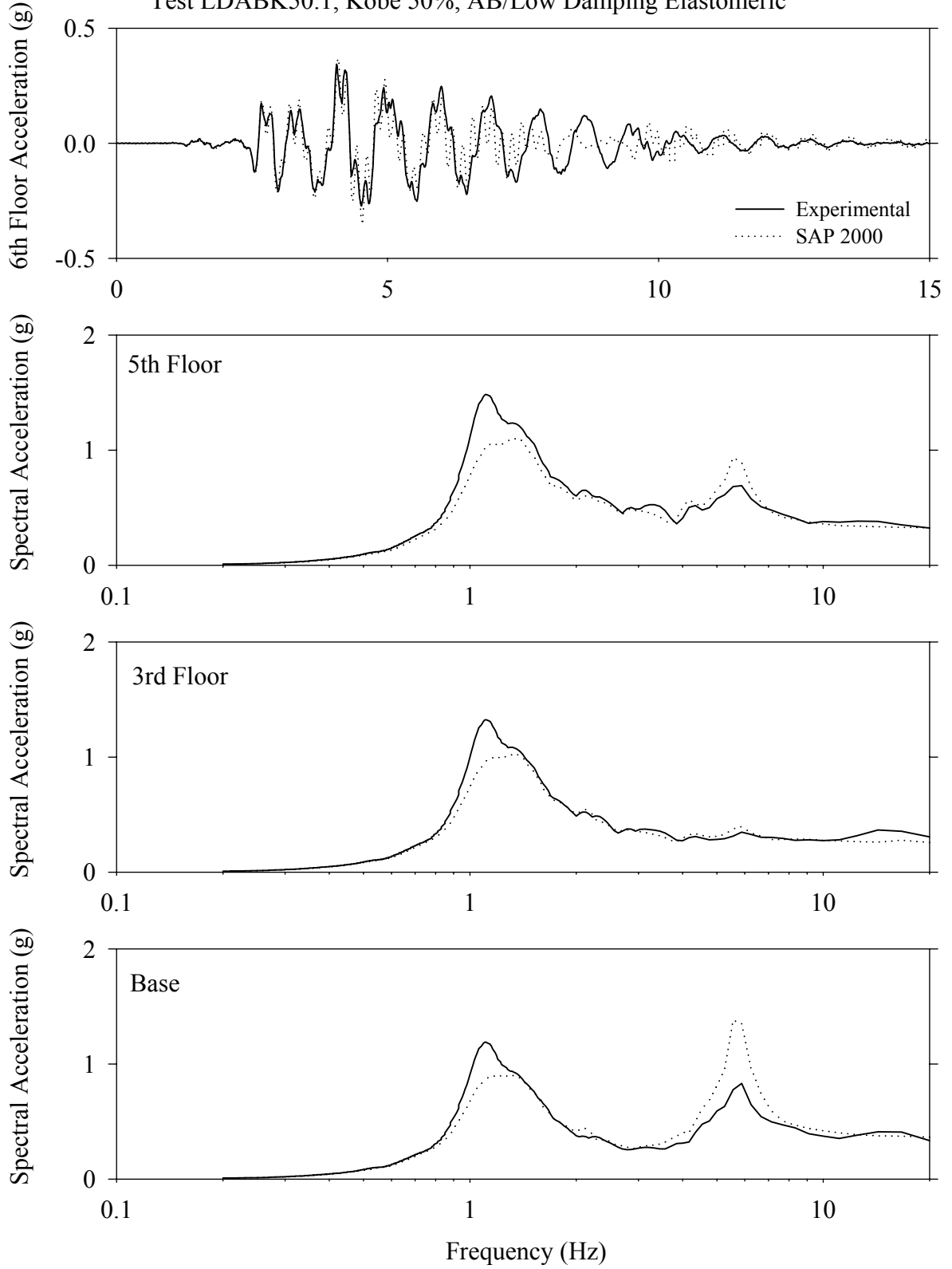


Time (sec)

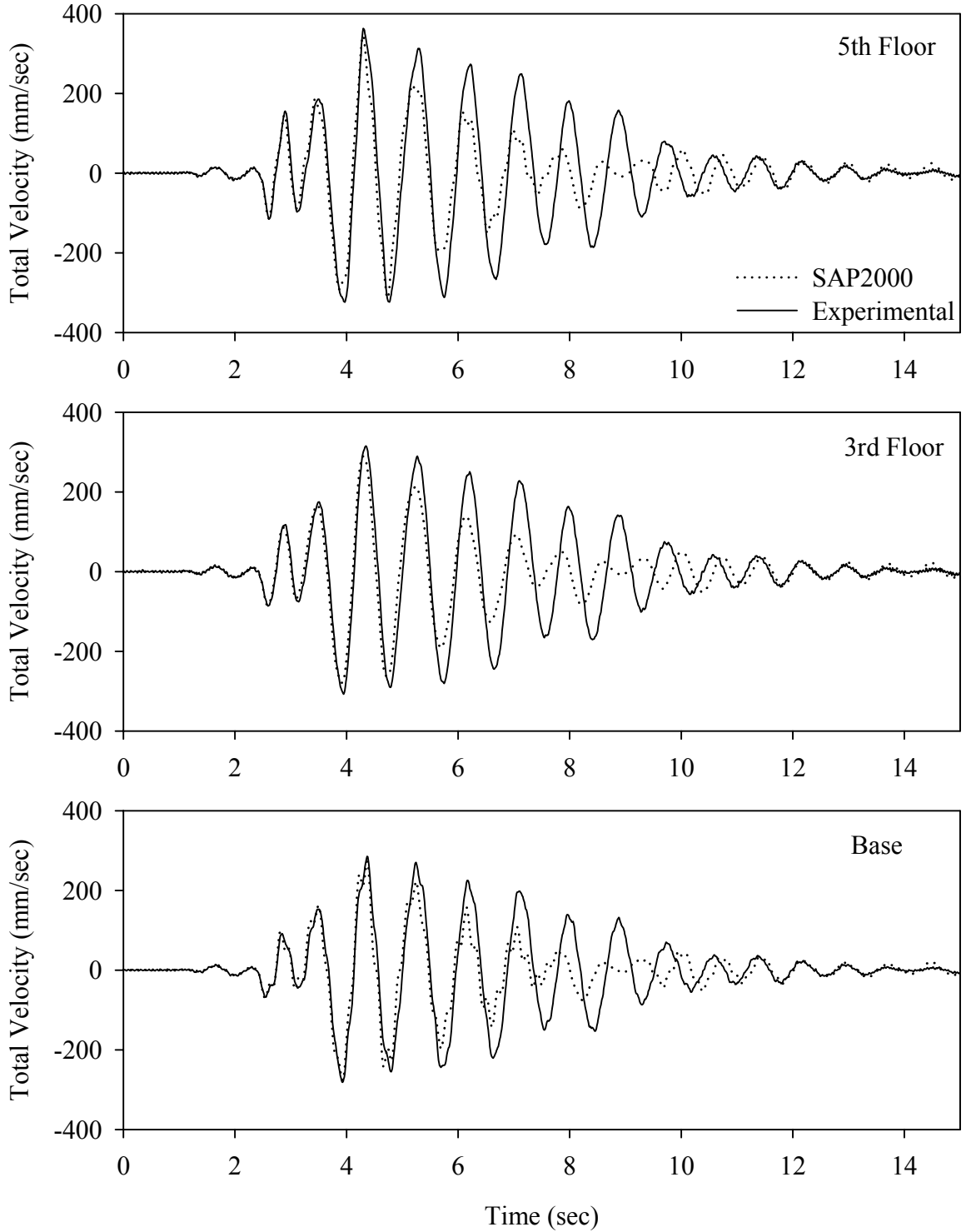
Test LDABK50.1, Kobe 50%, AB/Low Damping Elastomeric



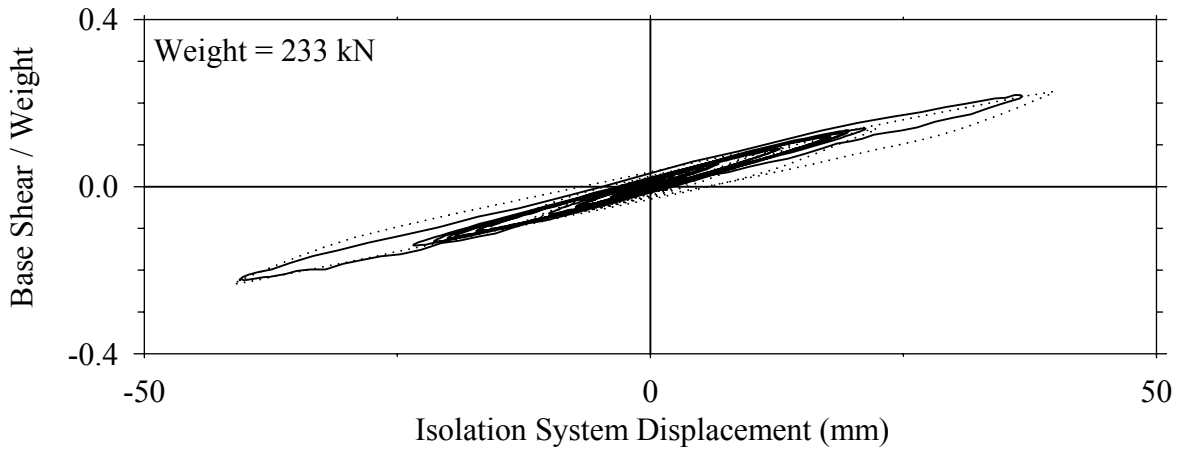
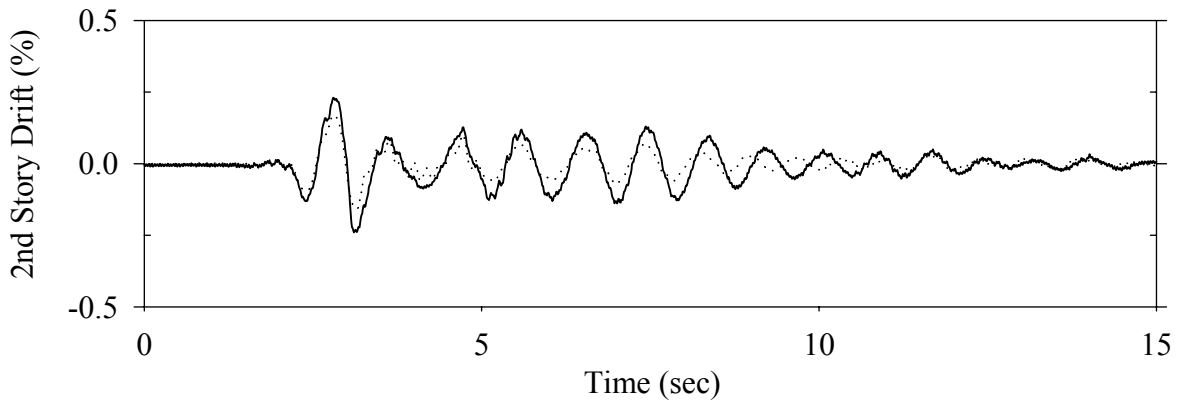
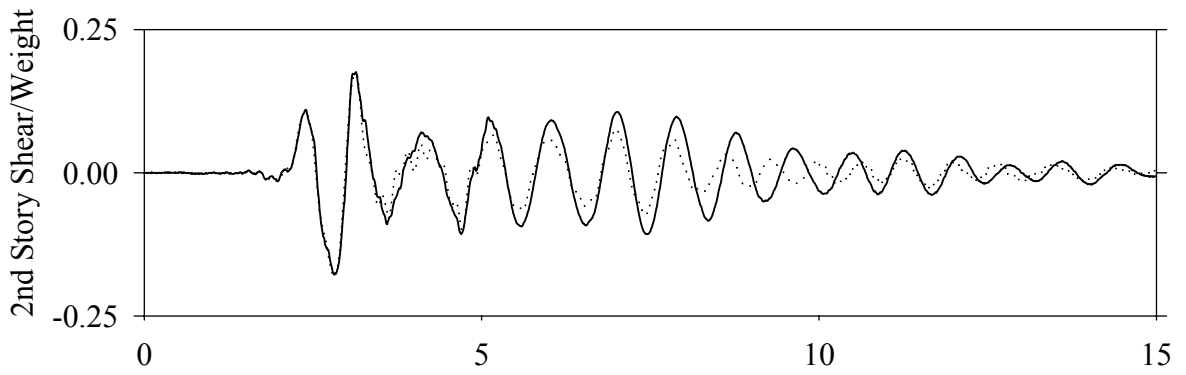
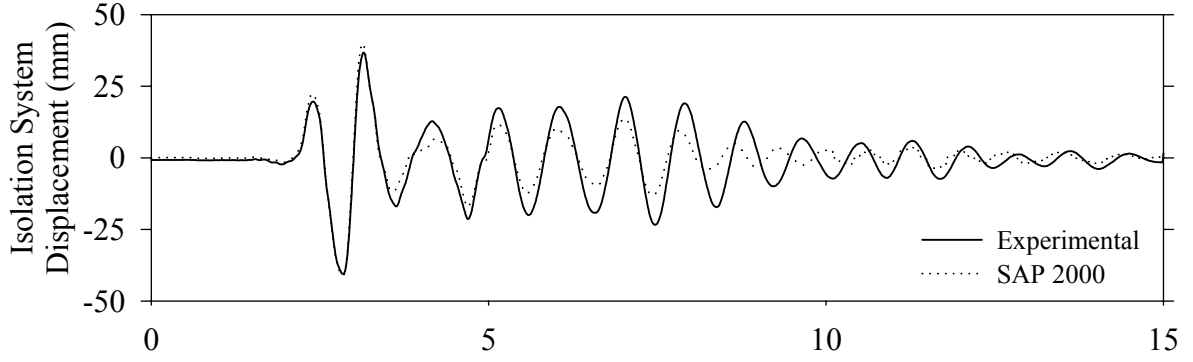
Test LDABK50.1, Kobe 50%, AB/Low Damping Elastomeric



Test LDABK50.1, Kobe 50%, AB/Low Damping Elastomeric

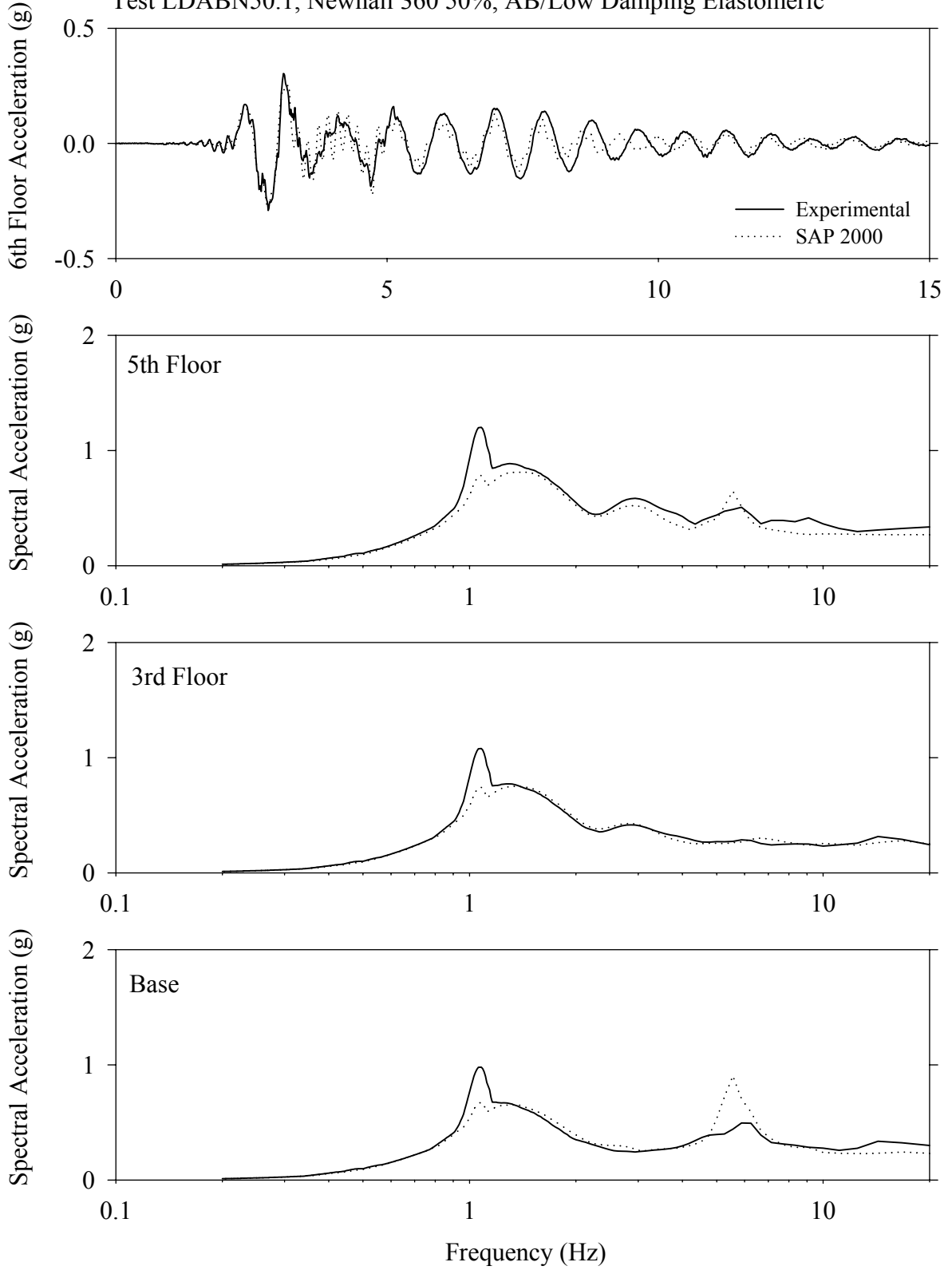


Test LDABN50.1, Newhall 360 50%, AB/Low Damping Elastomeric

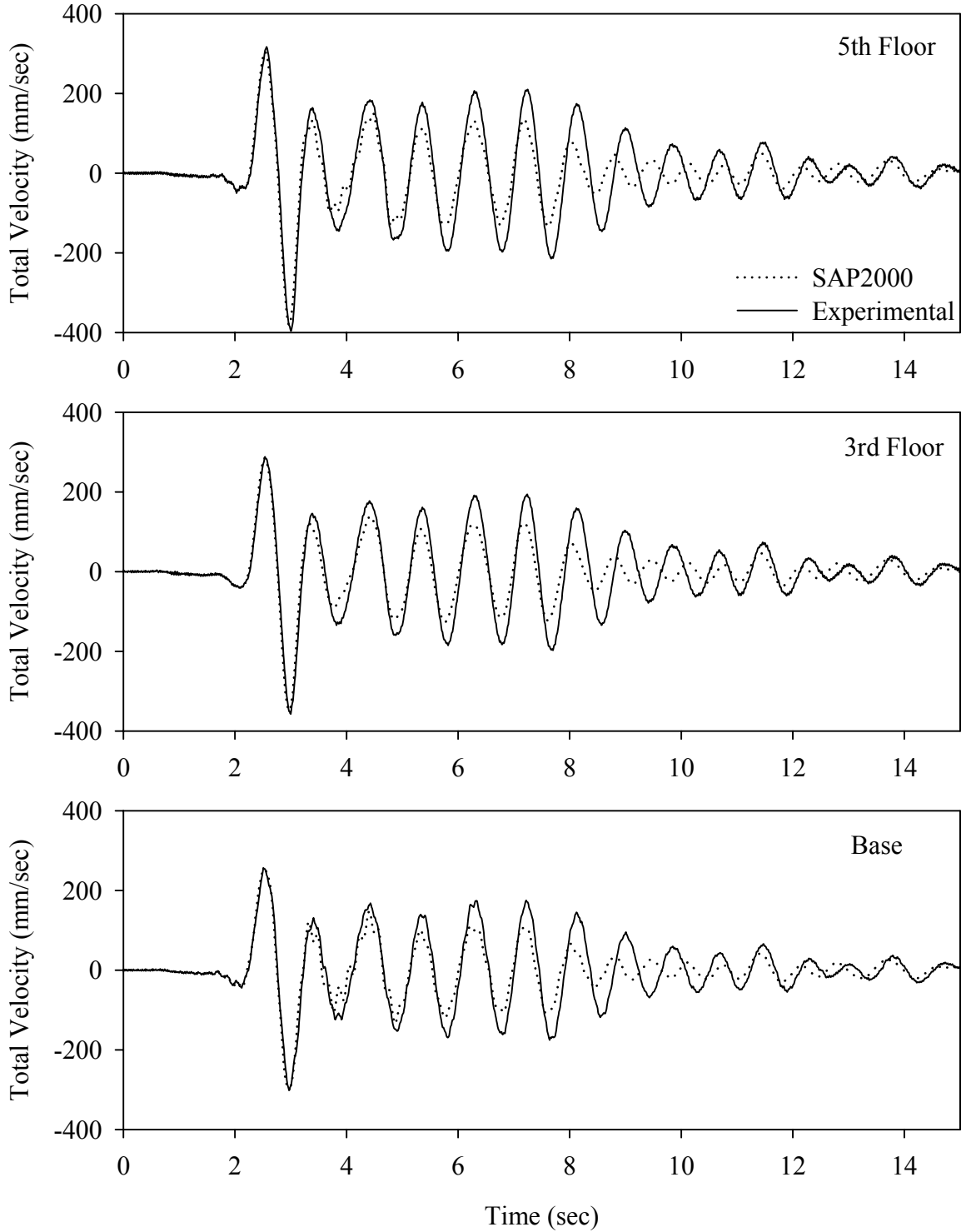




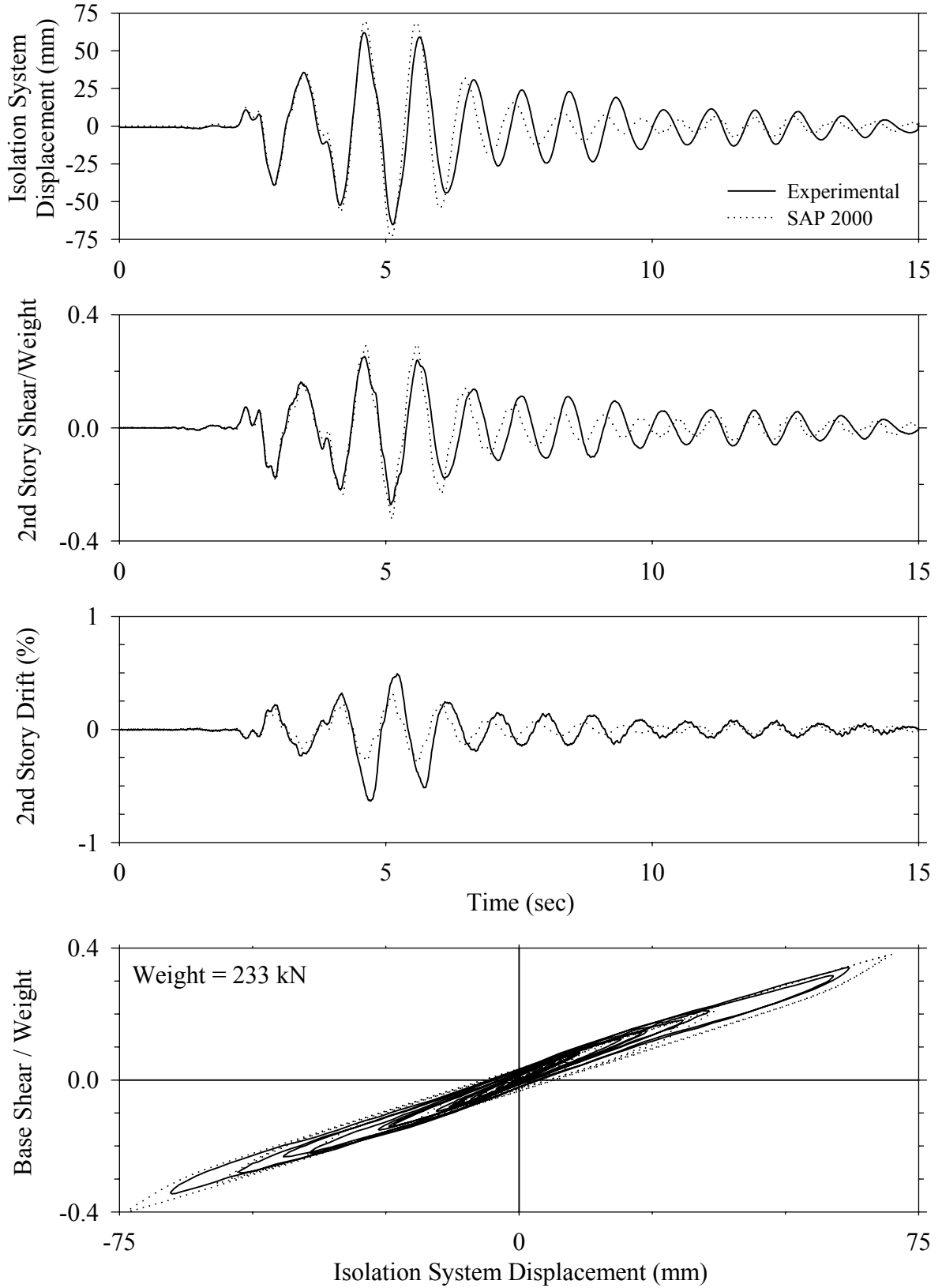
Test LDABN50.1, Newhall 360 50%, AB/Low Damping Elastomeric



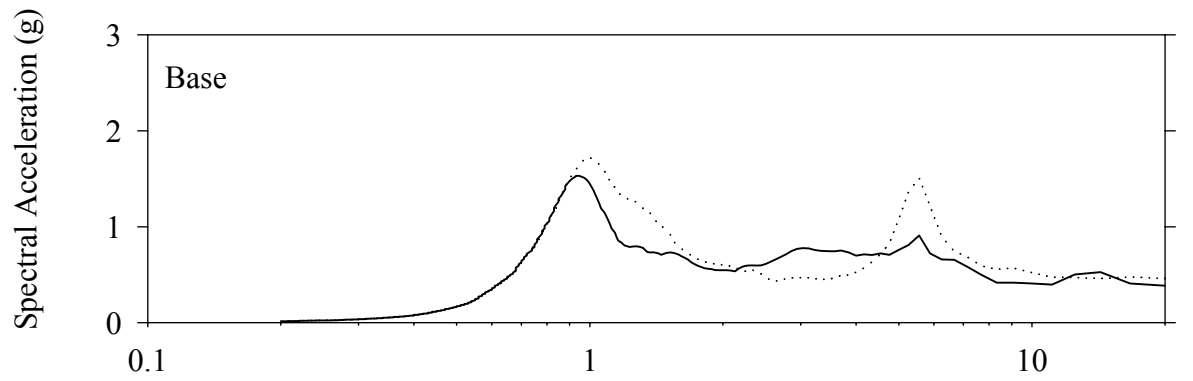
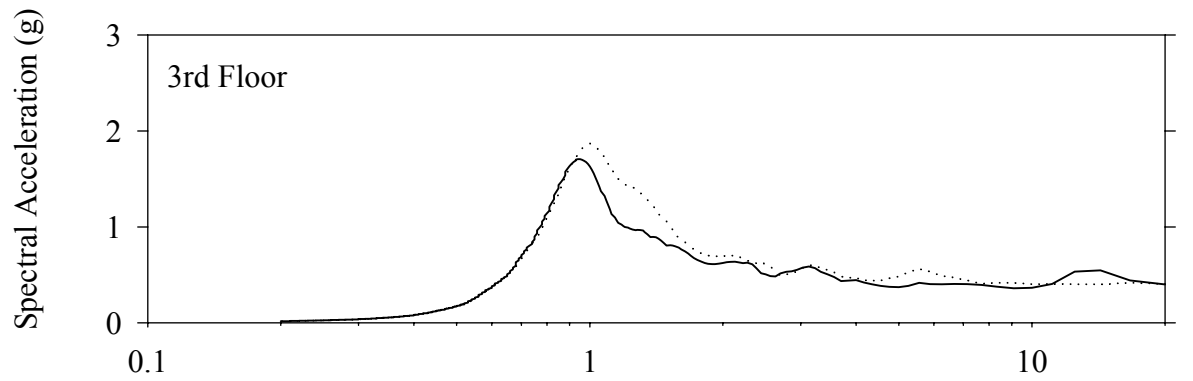
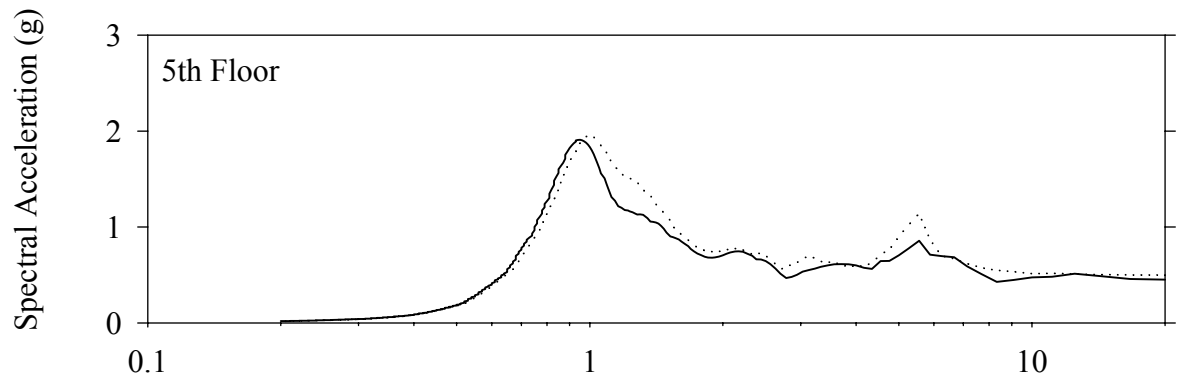
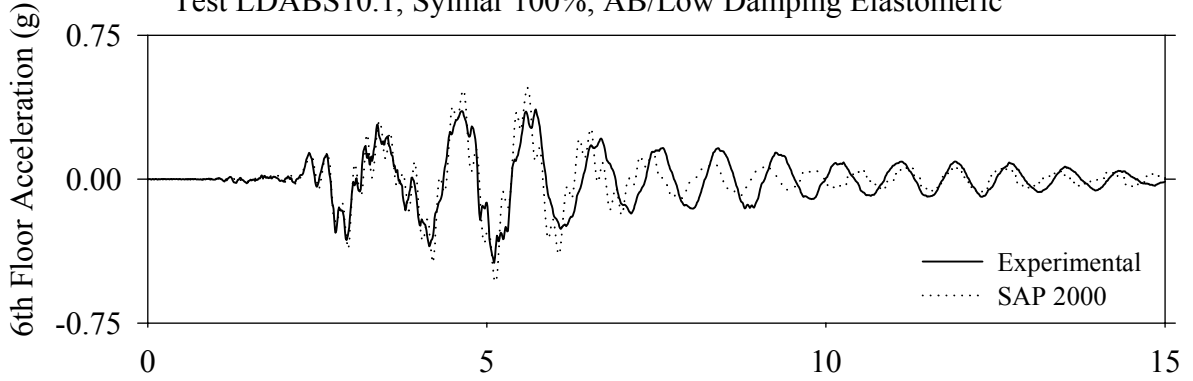
Test LDABN50.1, Newhall 360 50%, AB/Low Damping Elastomeric



Test LDABS10.1, Sylmar 100%, AB/Low Damping Elastomeric

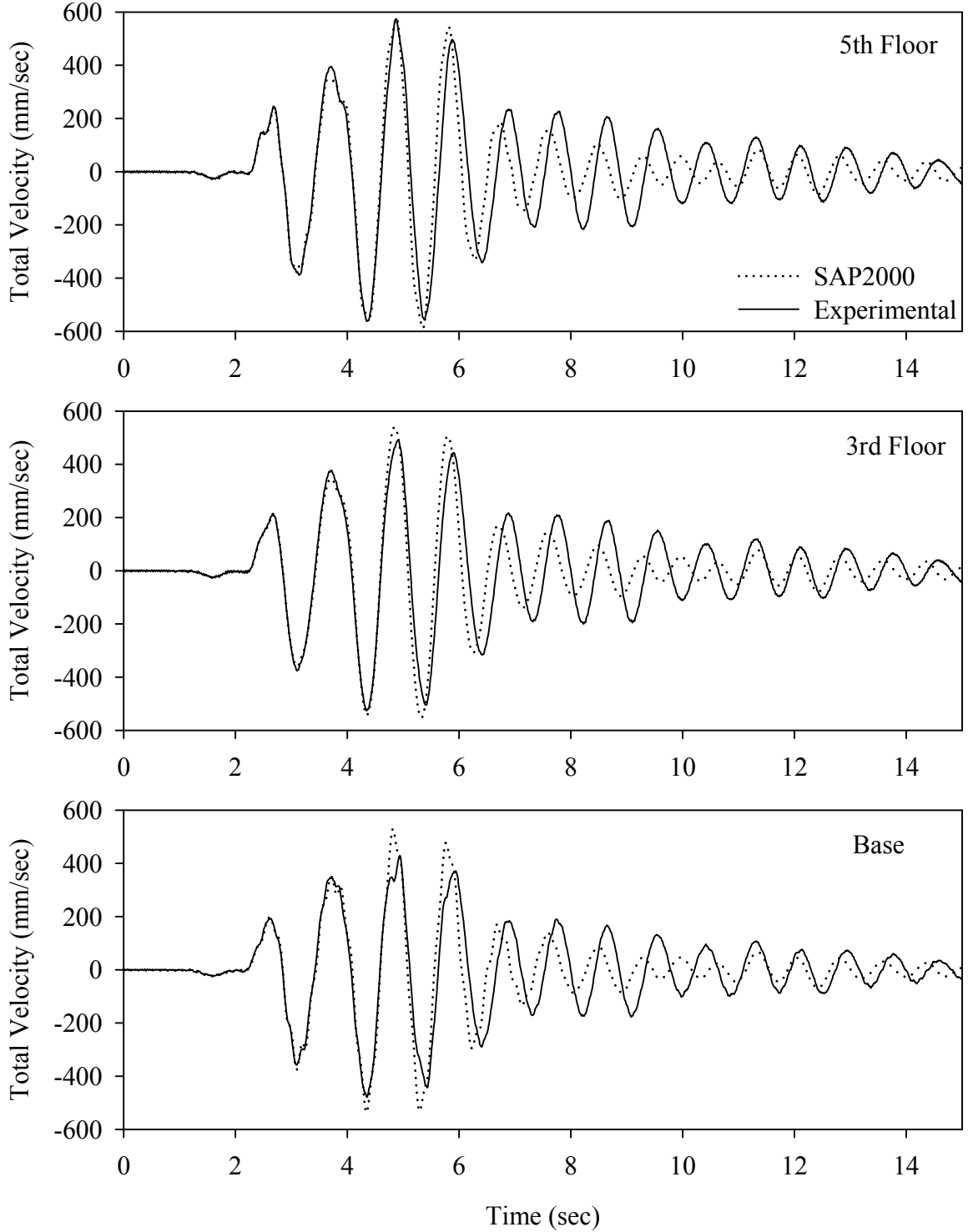


Test LDABS10.1, Sylmar 100%, AB/Low Damping Elastomeric

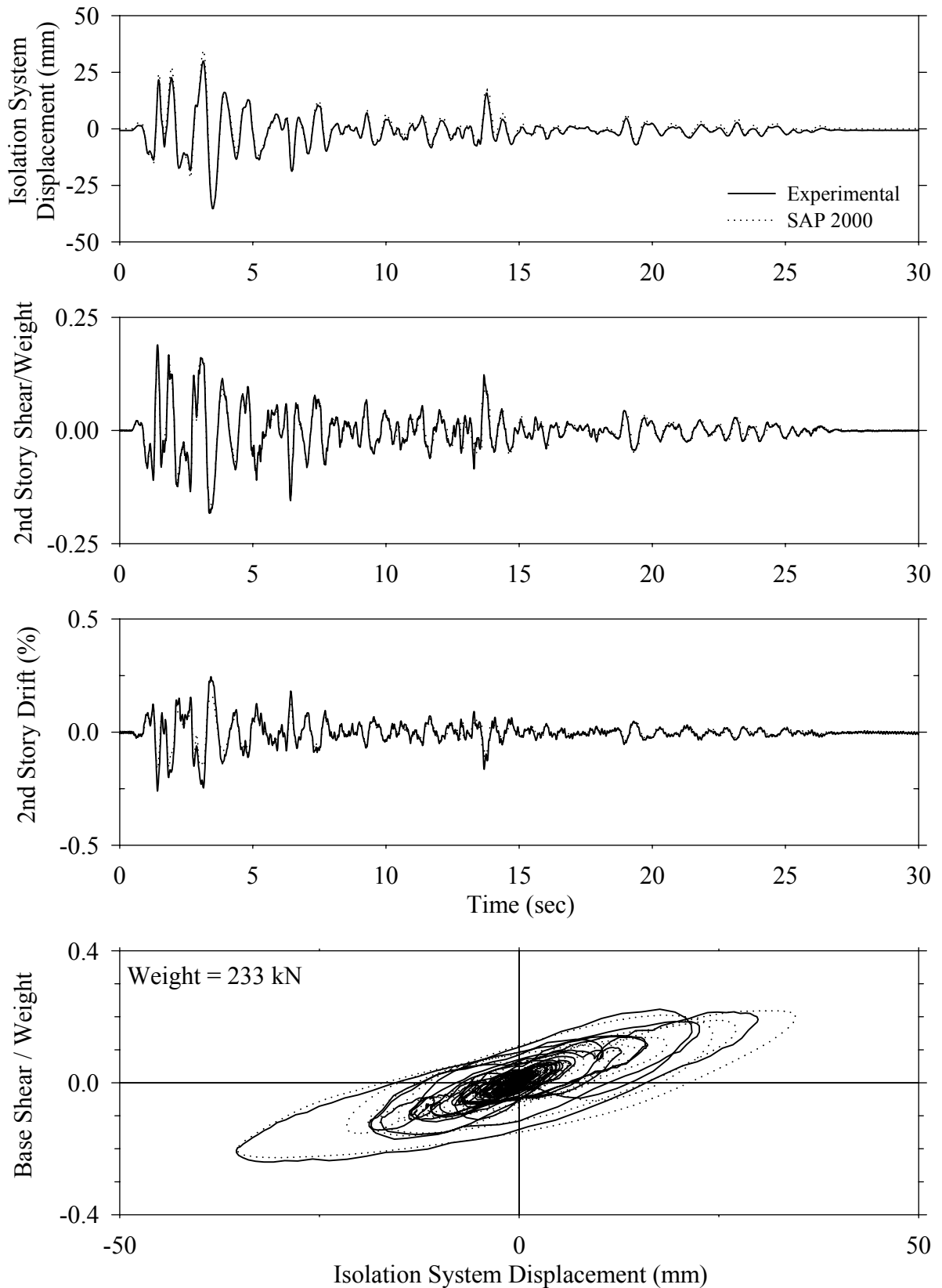


Frequency (Hz)

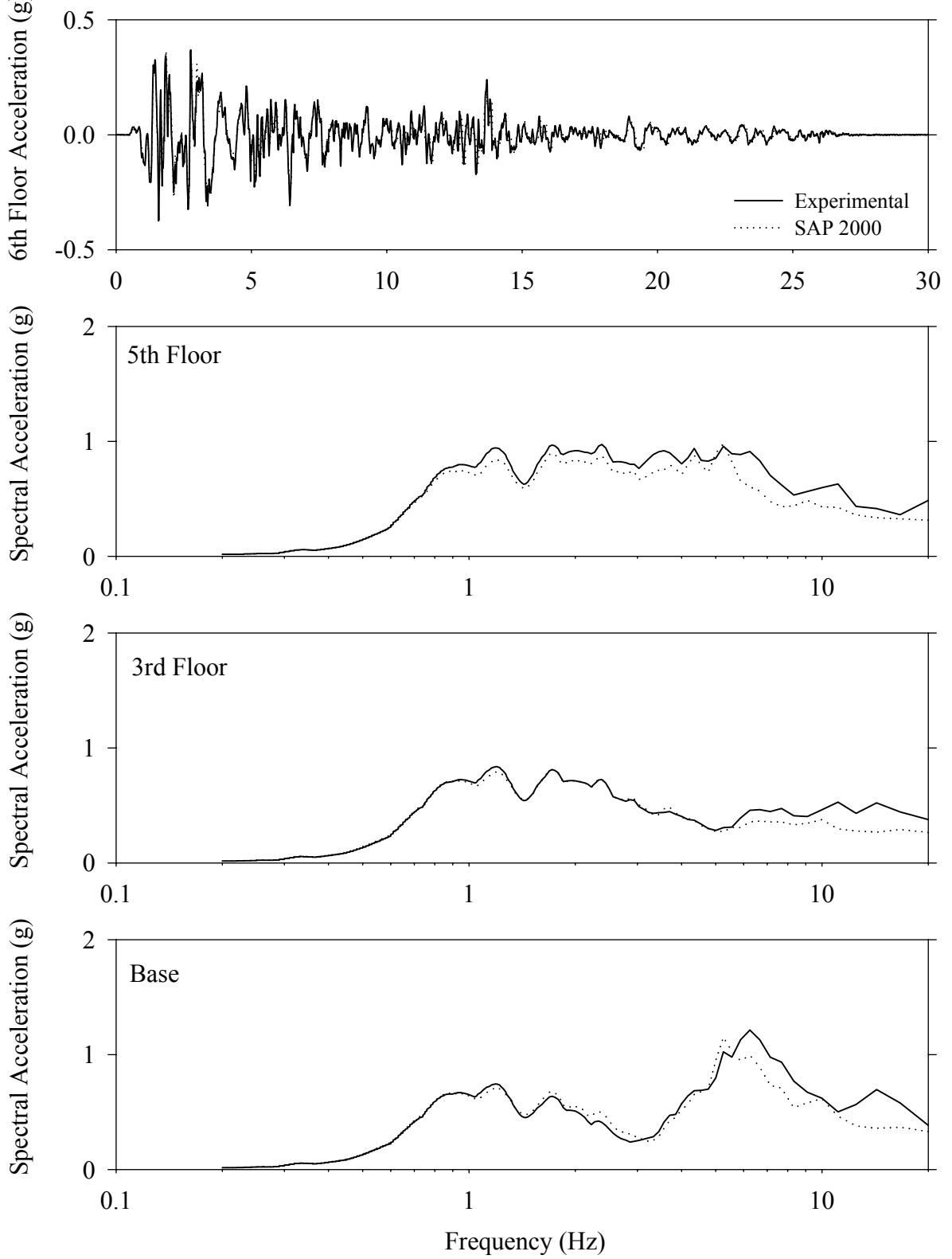
Test LDABS10.1, Sylmar 100%, AB/Low Damping Elastomeric



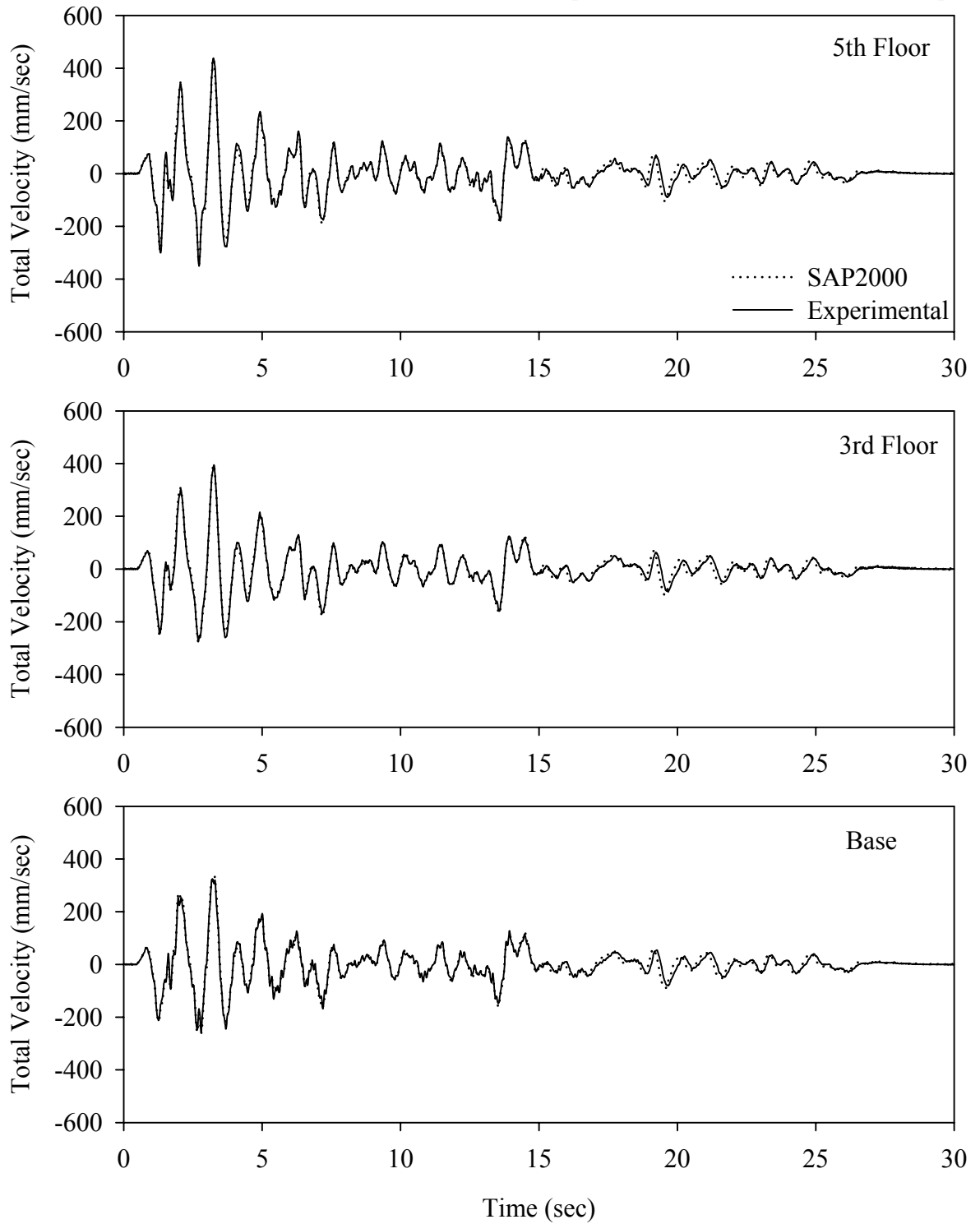
Test LDALE20.1, El Centro S00E 200%, AB/Low Damping Elastomeric with Linear Dampers



Test LDALE20.1, El Centro S00E 200%, AB/Low Damping Elastomeric with Linear Dampers

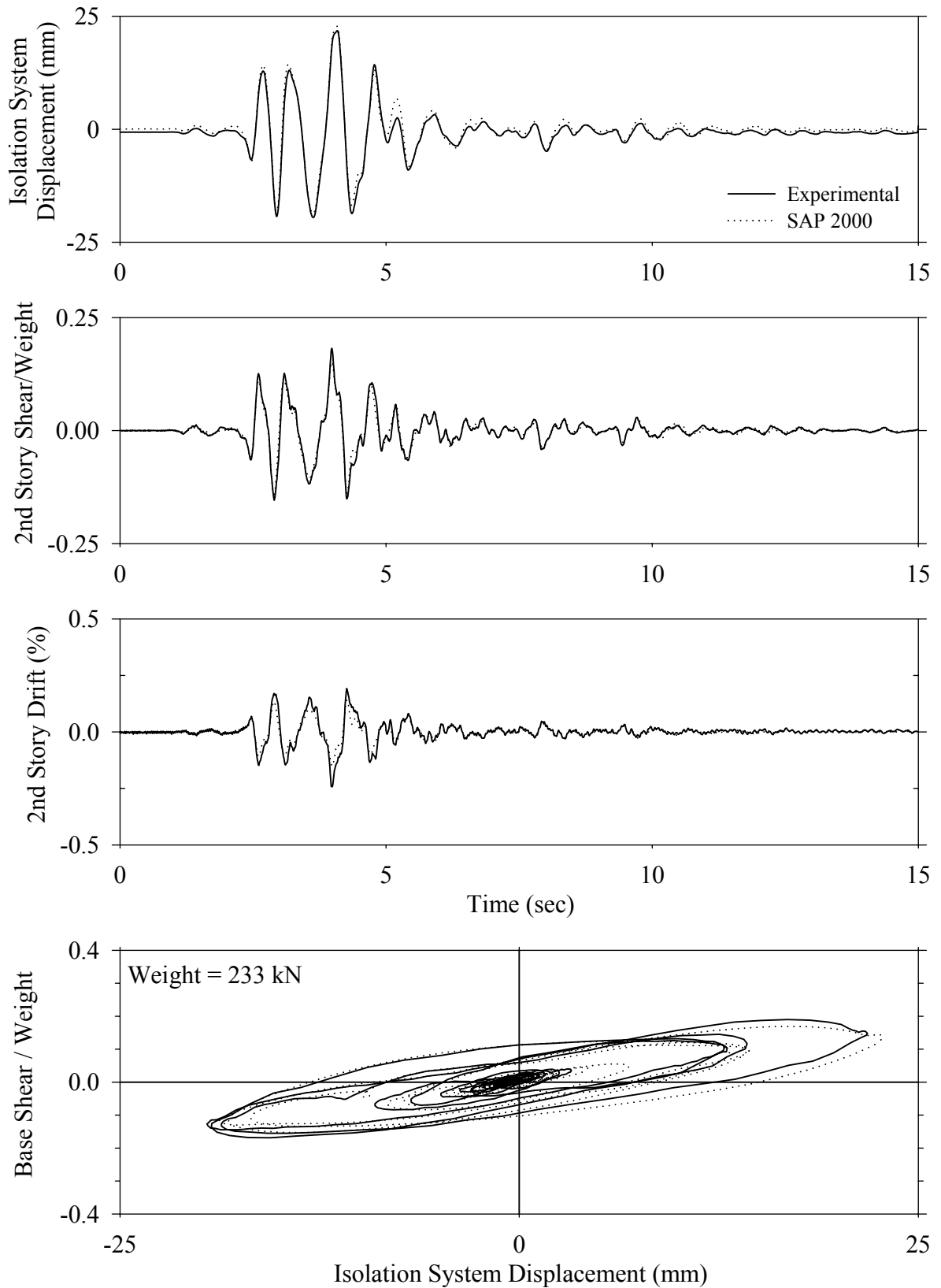


Test LDALE20.1, El Centro S00E 200%, AB/Low Damping Elastomeric with Linear Dampers

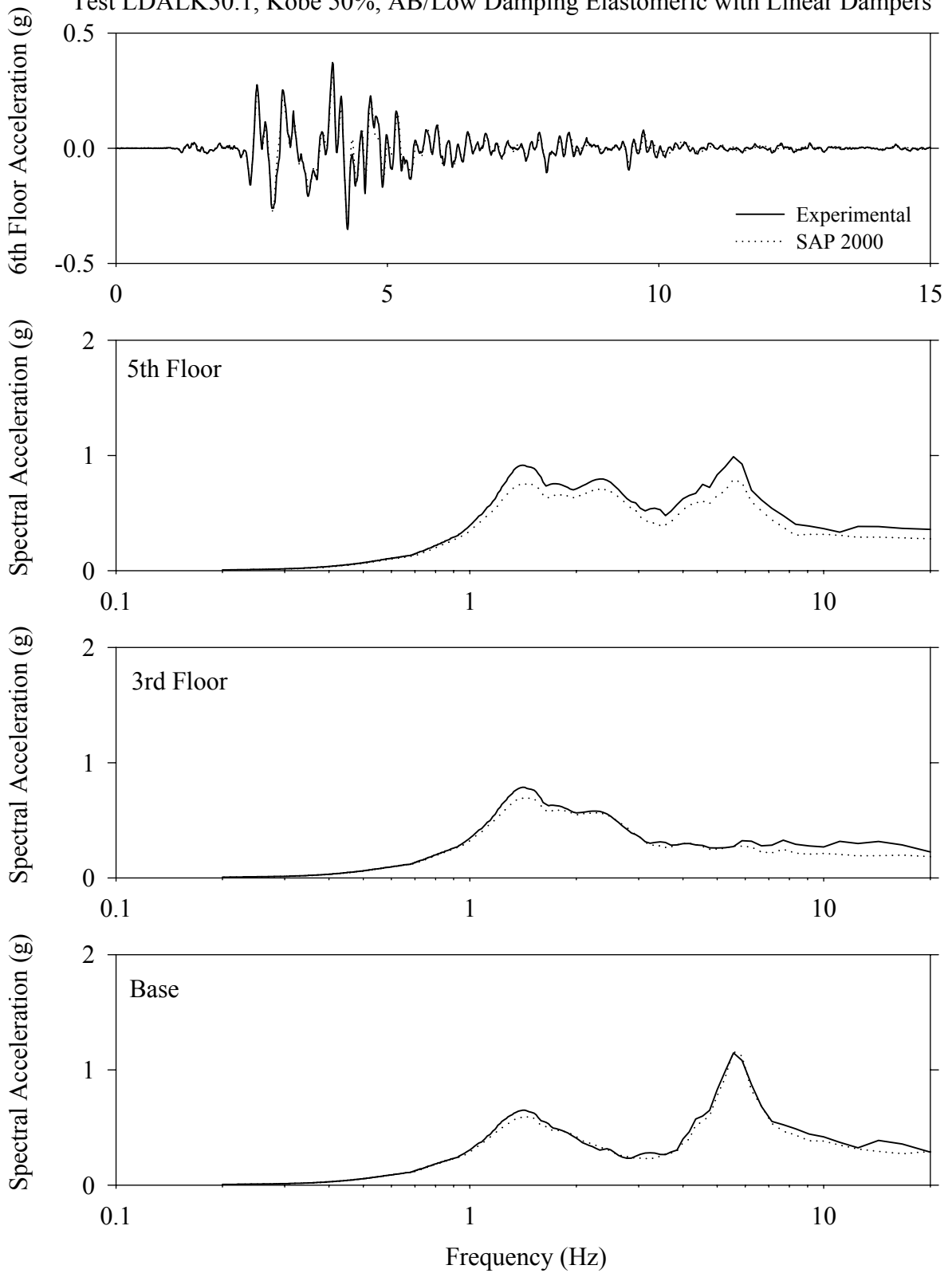




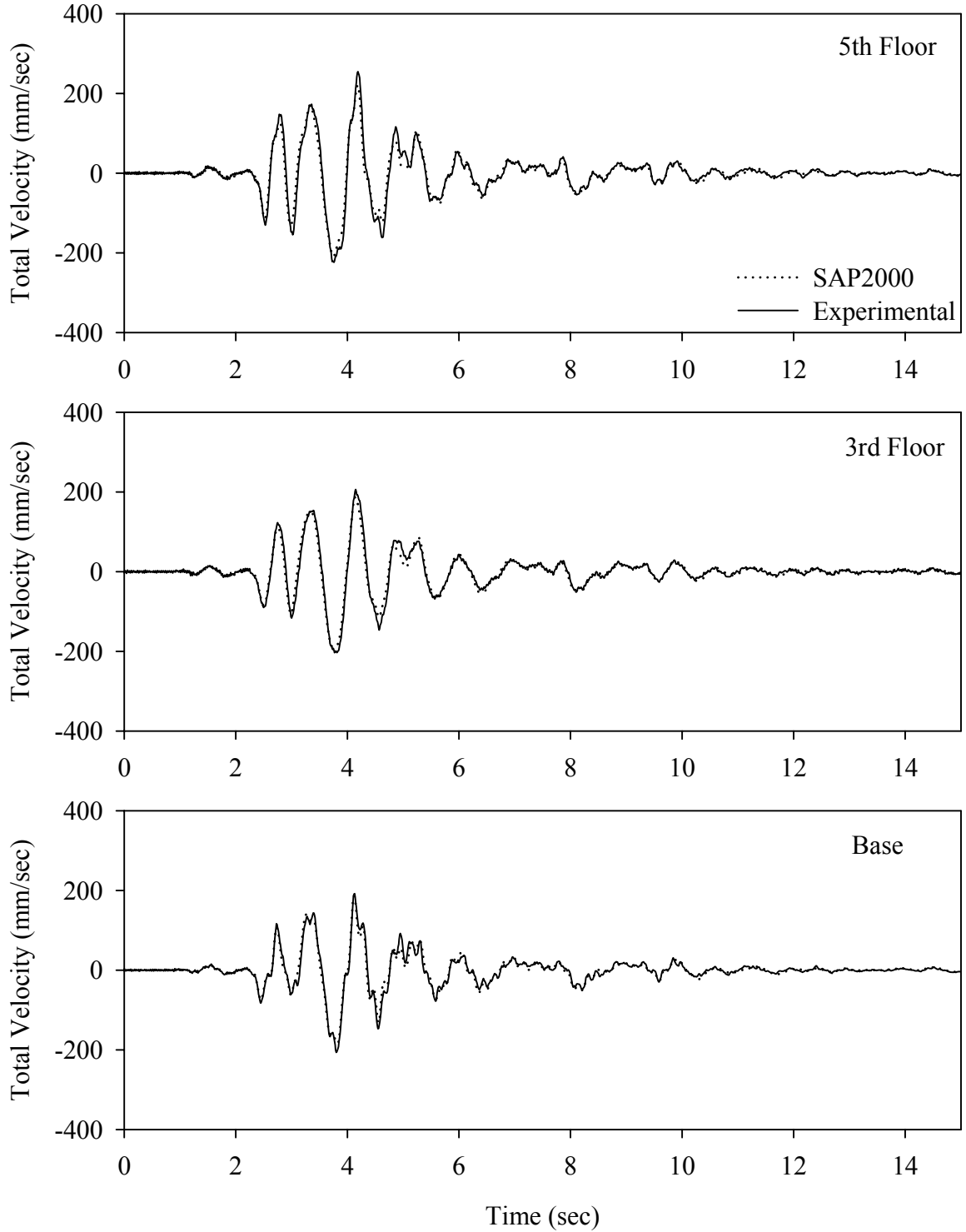
Test LDALK50.1, Kobe 50%, AB/Low Damping Elastomeric with Linear Dampers



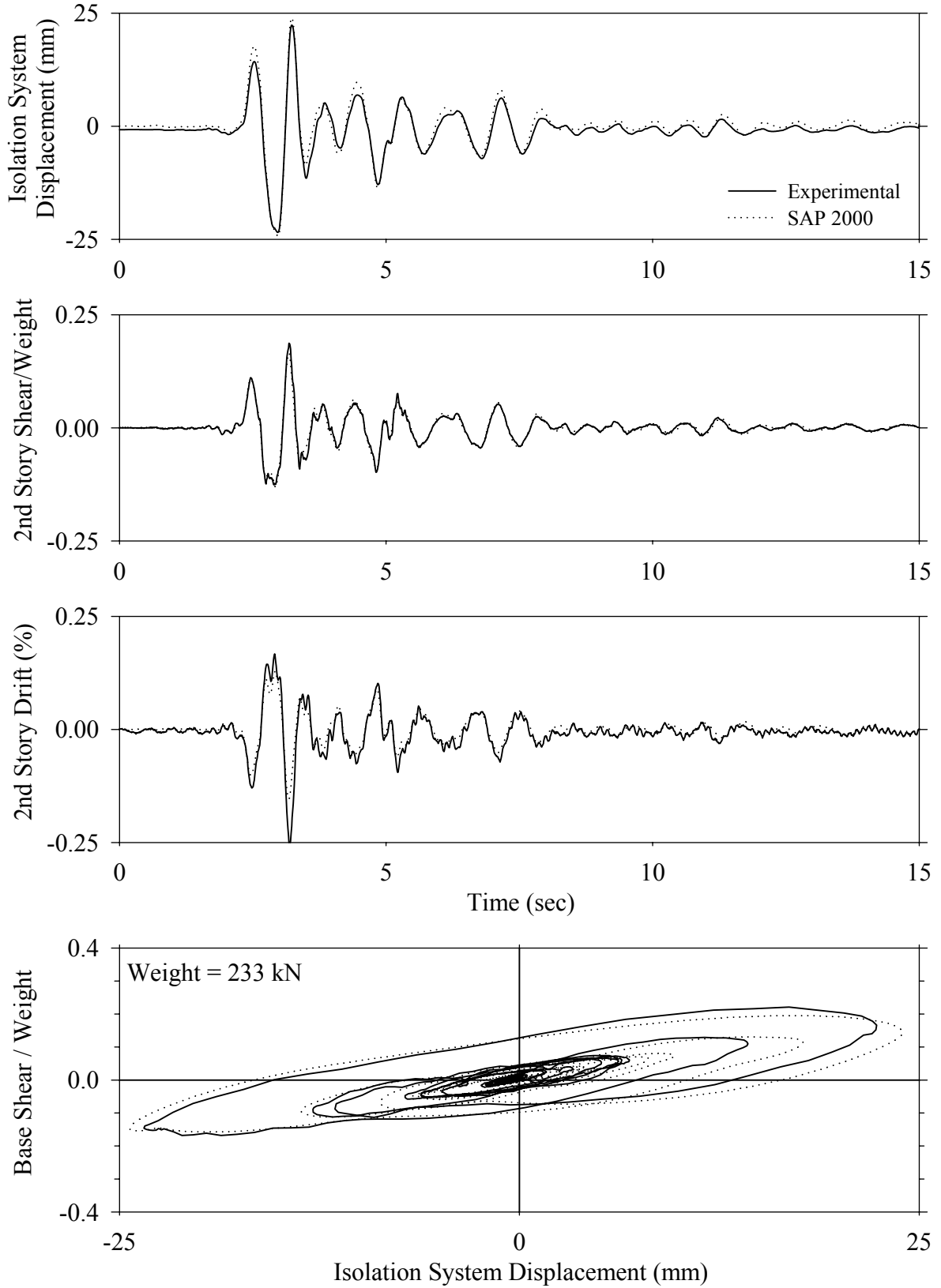
Test LDALK50.1, Kobe 50%, AB/Low Damping Elastomeric with Linear Dampers



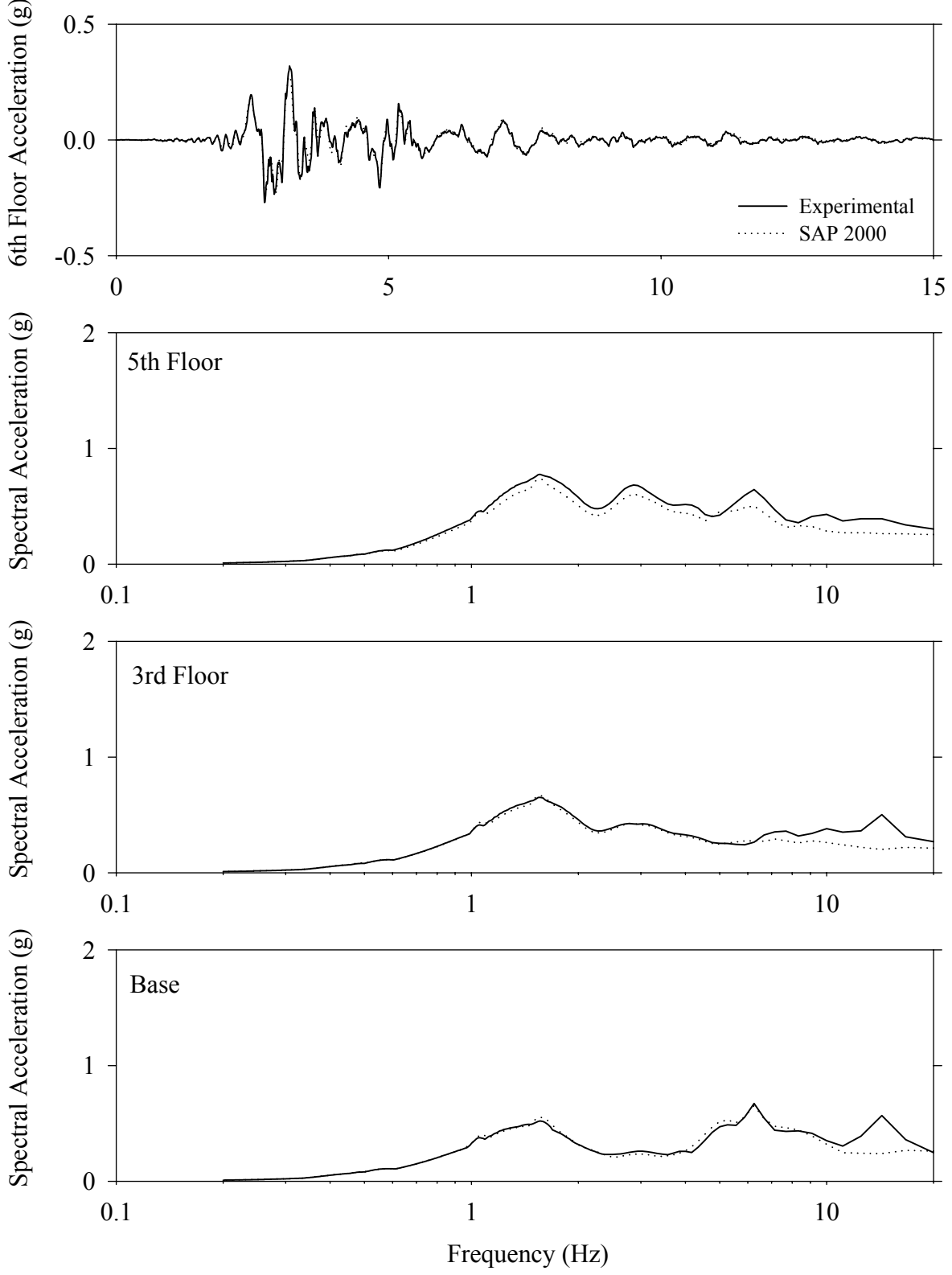
Test LDALK50.1, Kobe 50%, AB/Low Damping Elastomeric with Linear Dampers



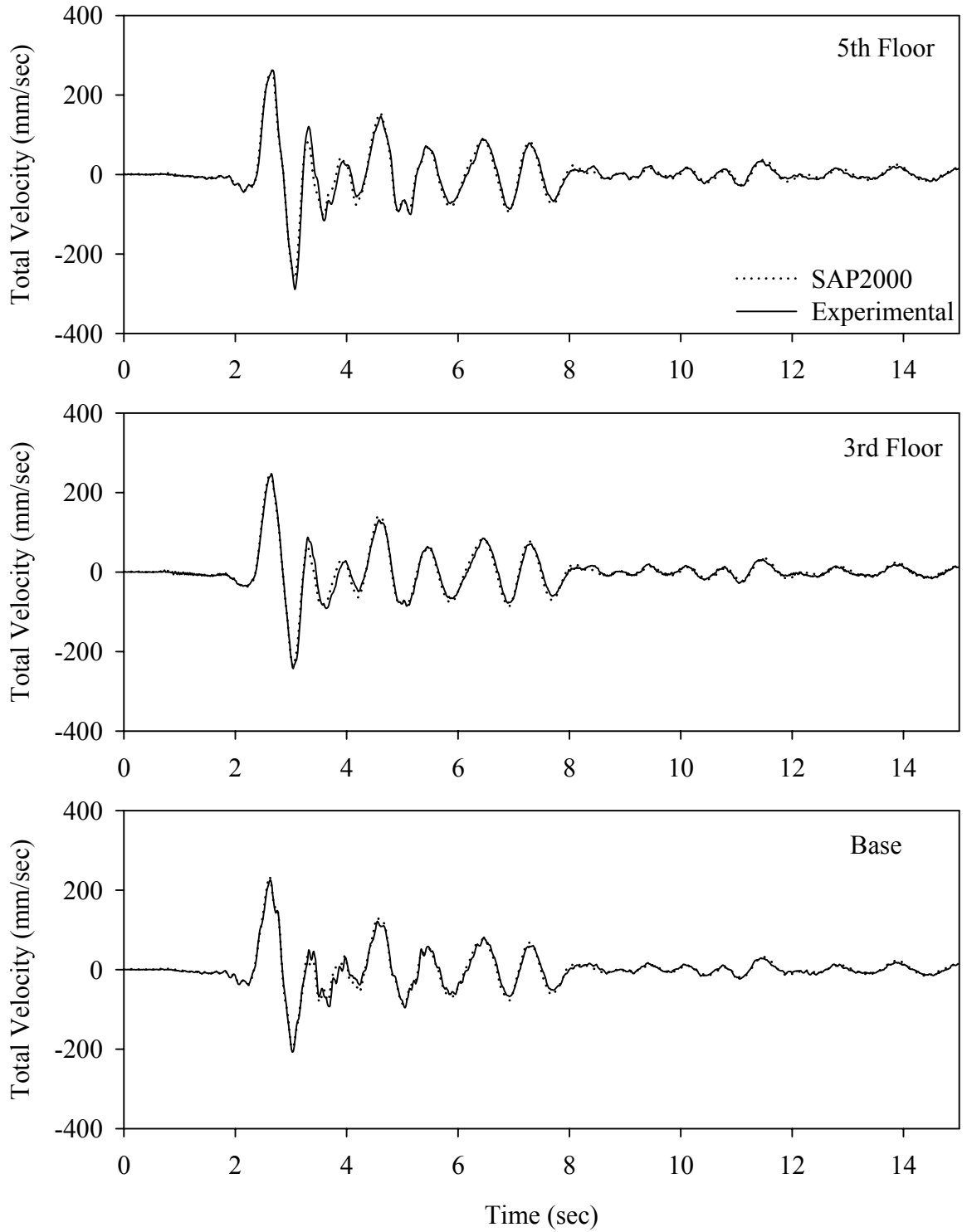
Test LDALN50.1, Newhall 360 50%, AB/Low Damping Elastomeric with Linear Dampers



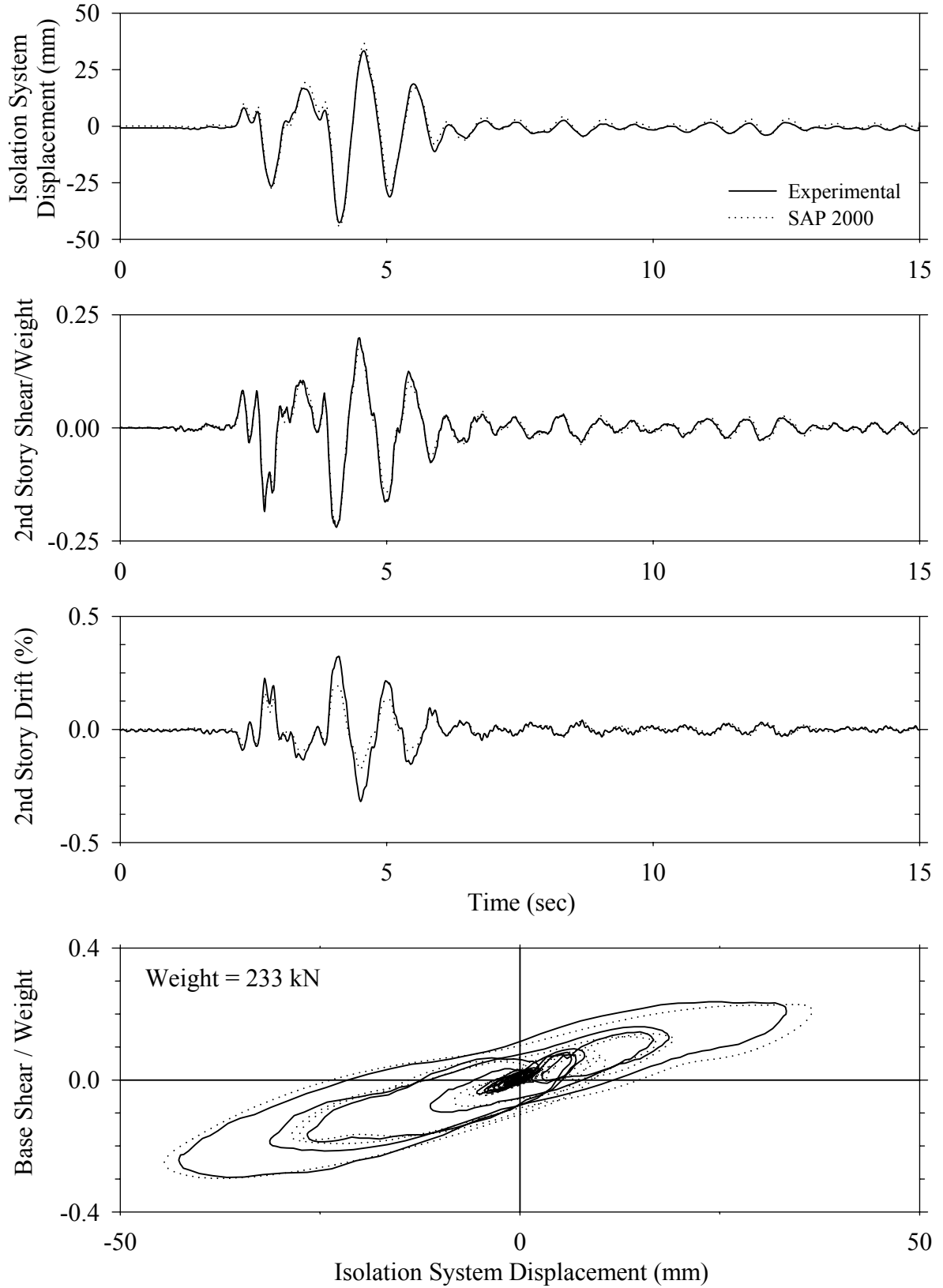
Test LDALN50.1, Newhall 360 50%, AB/Low Damping Elastomeric with Linear Dampers



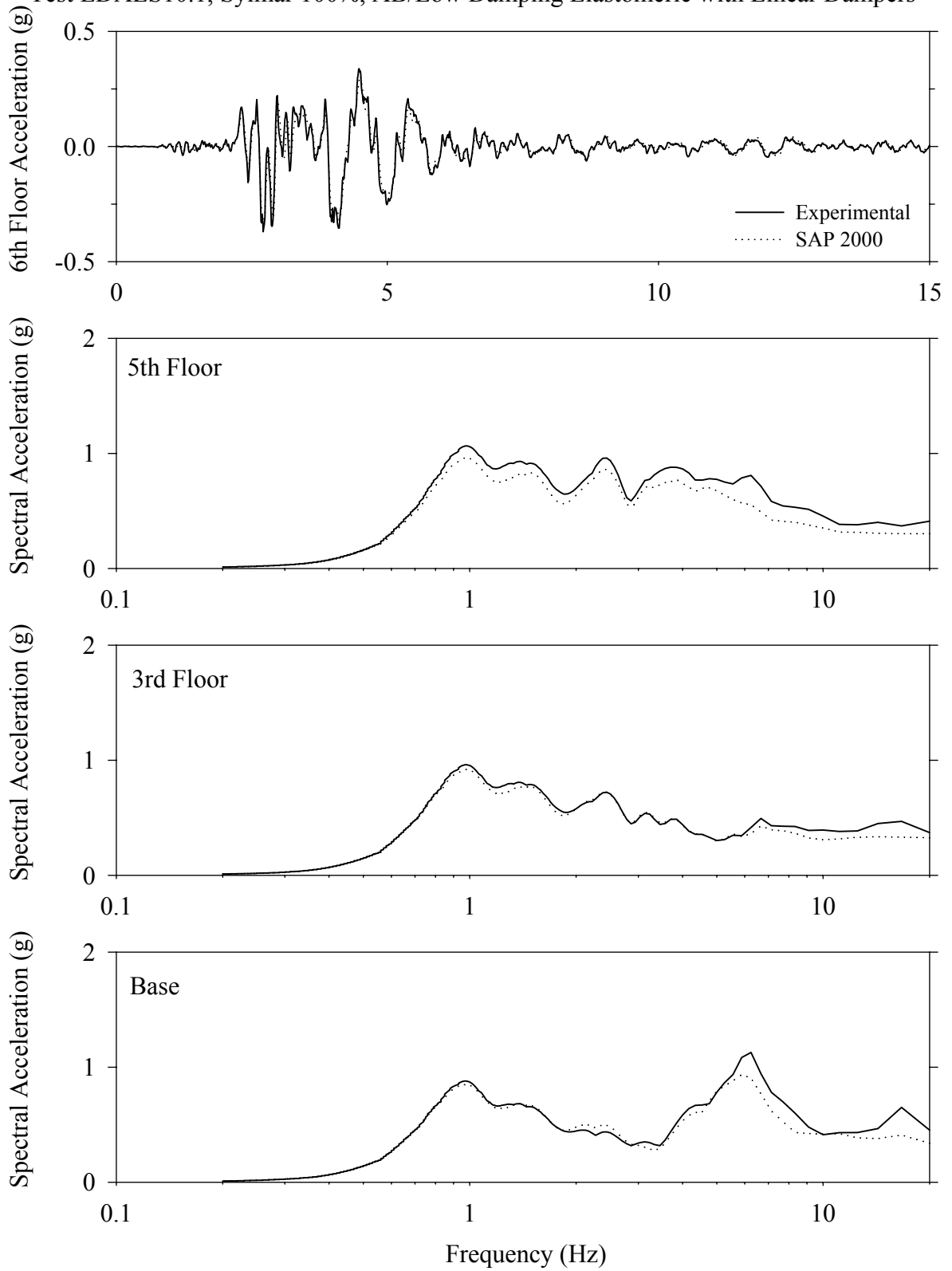
Test LDALN50.1, Newhall 360 50%, AB/Low Damping Elastomeric with Linear Dampers



Test LDALS10.1, Sylmar 100%, AB/Low Damping Elastomeric with Linear Dampers

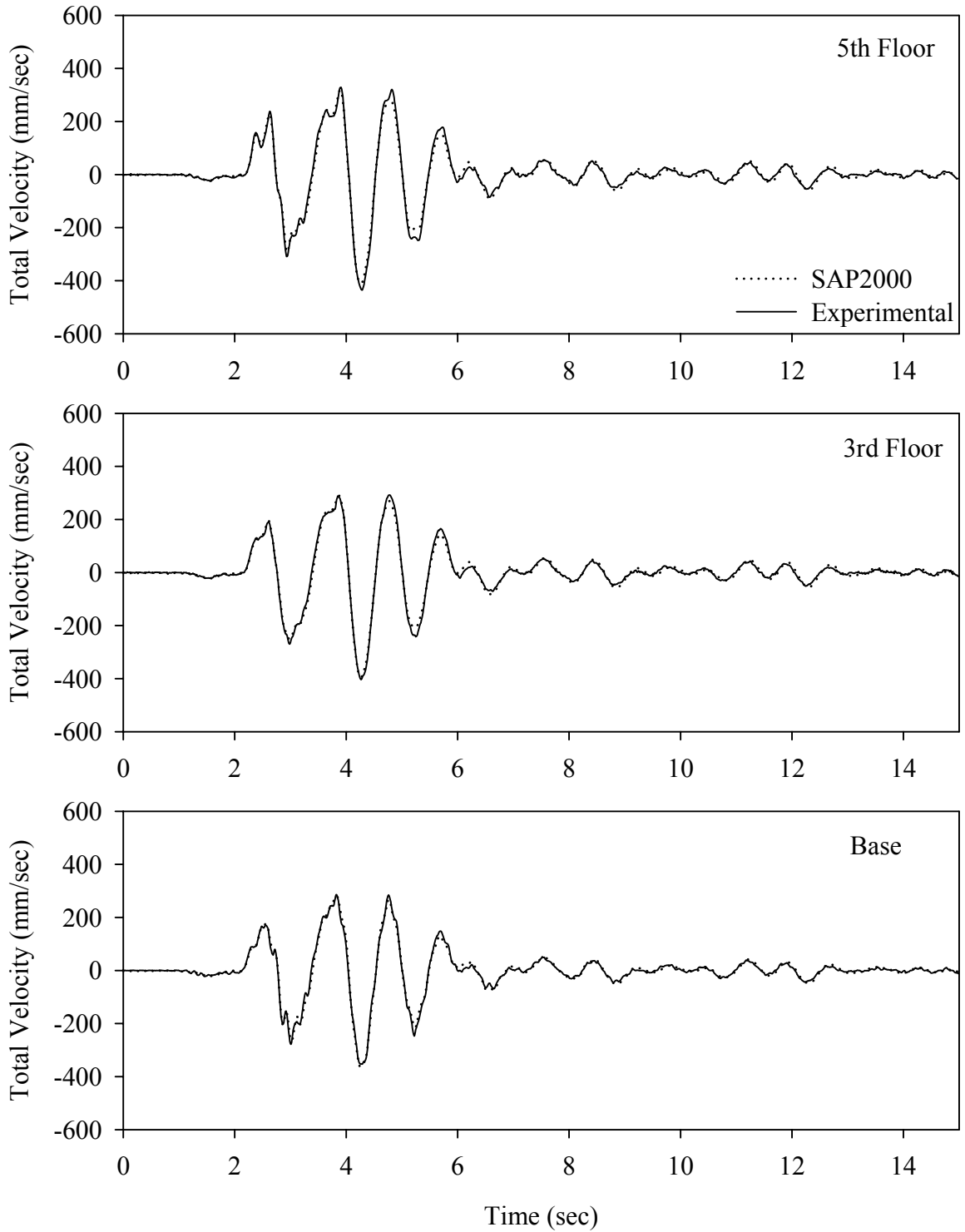


Test LDALS10.1, Sylmar 100%, AB/Low Damping Elastomeric with Linear Dampers

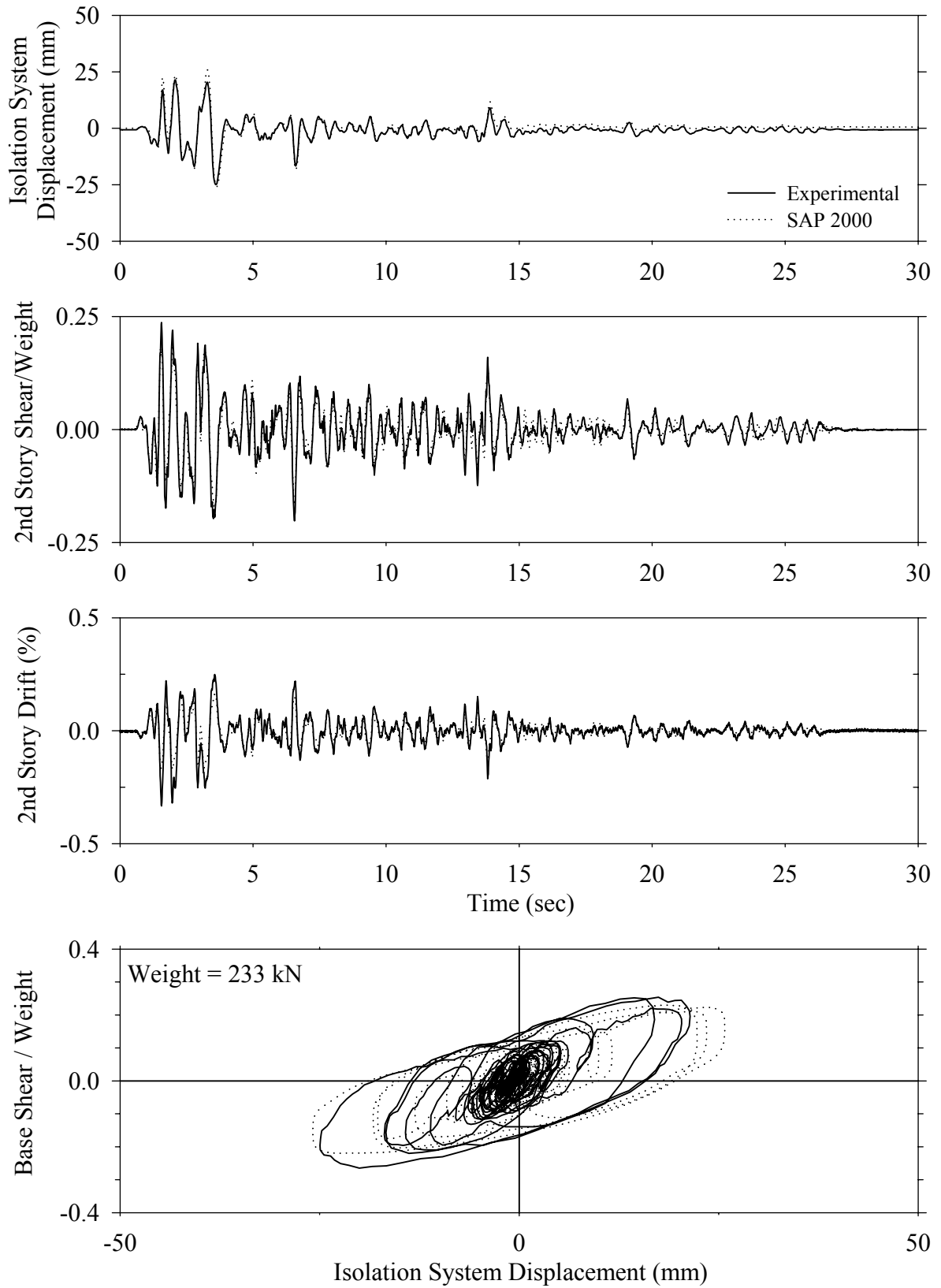




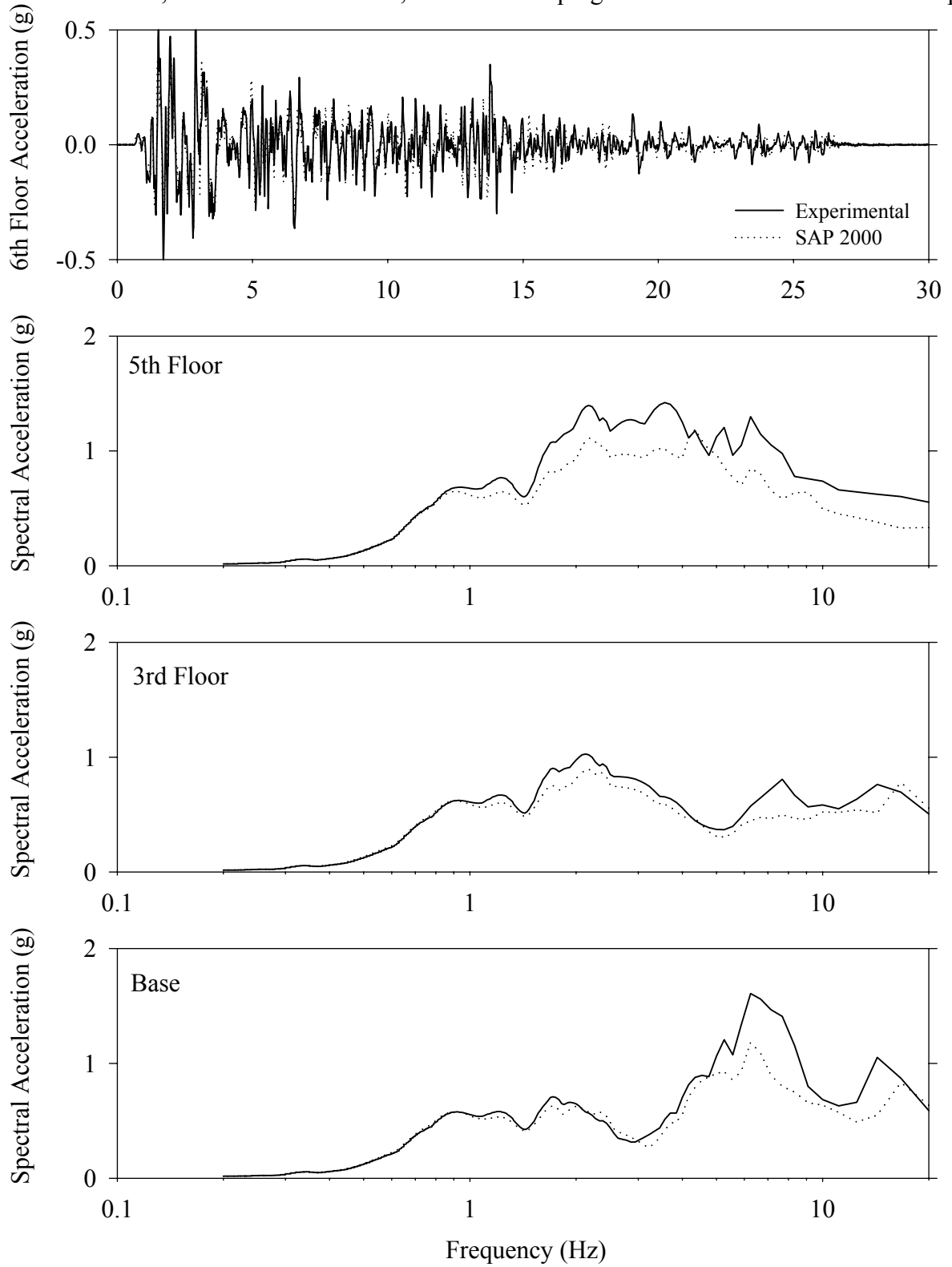
Test LDALS10.1, Sylmar 100%, AB/Low Damping Elastomeric with Linear Dampers



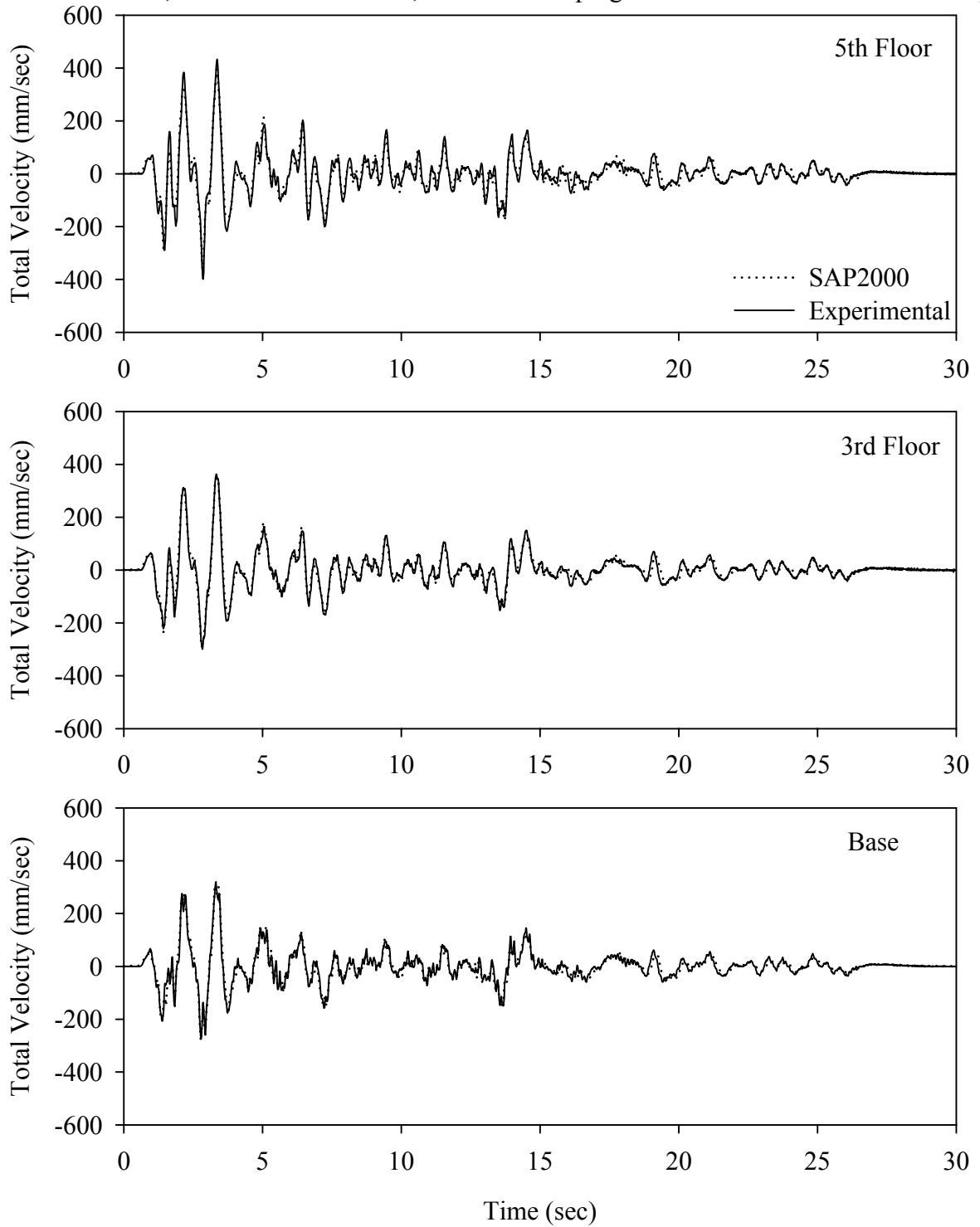
Test LDANE20.1, El Centro S00E 200%, AB/Low Damping Elastomeric with Nonlinear Dampers



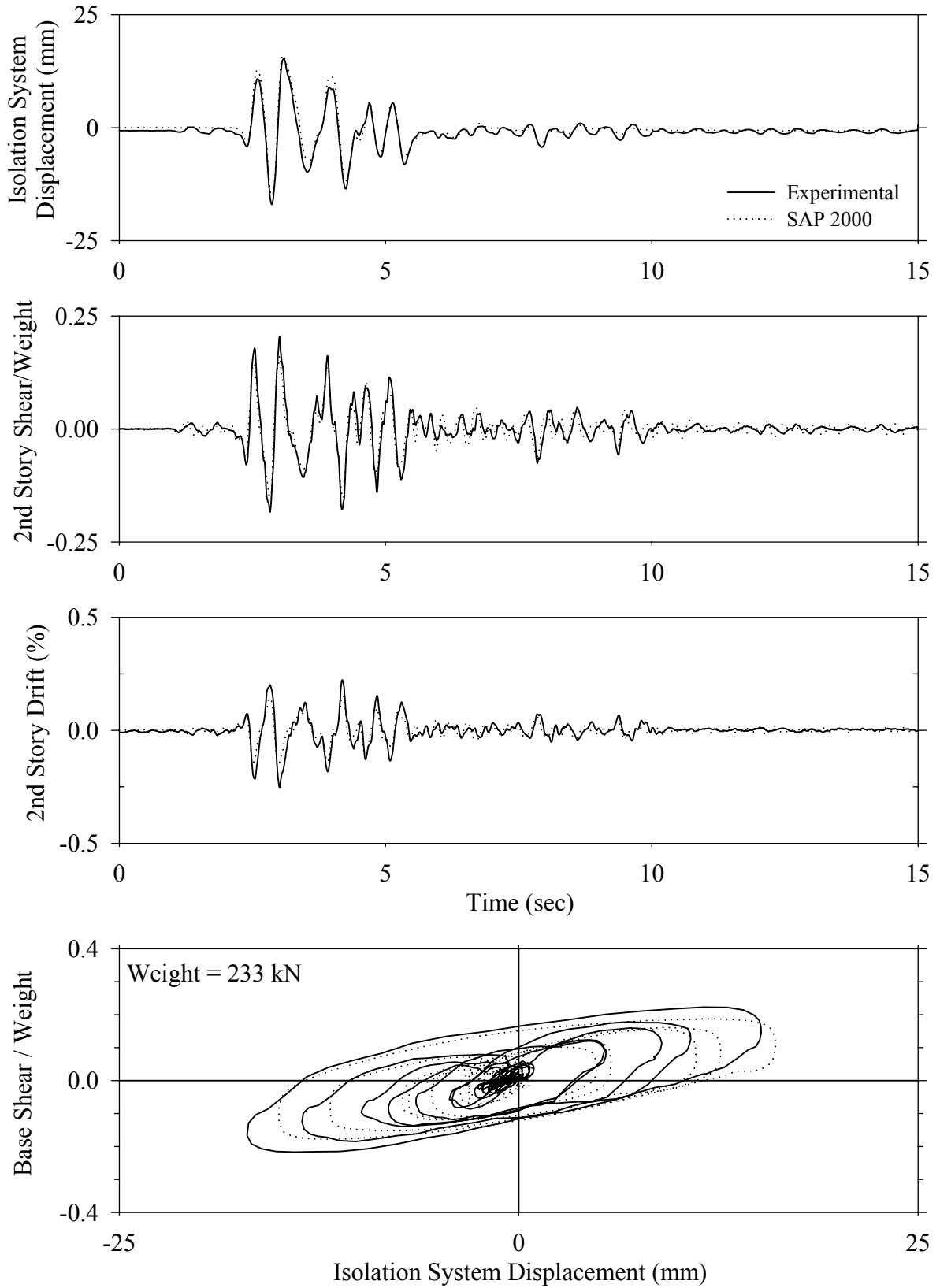
Test LDANE20.1, El Centro S00E 200%, AB/Low Damping Elastomeric with Nonlinear Dampers



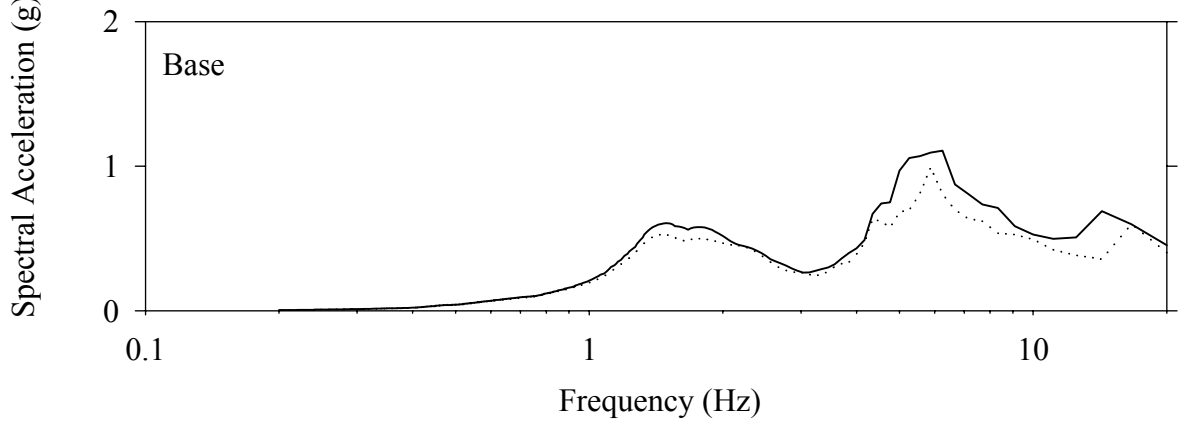
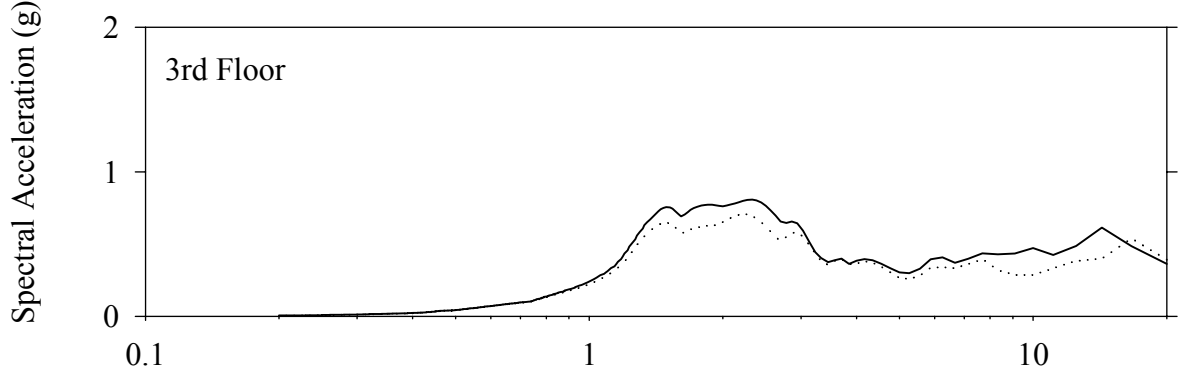
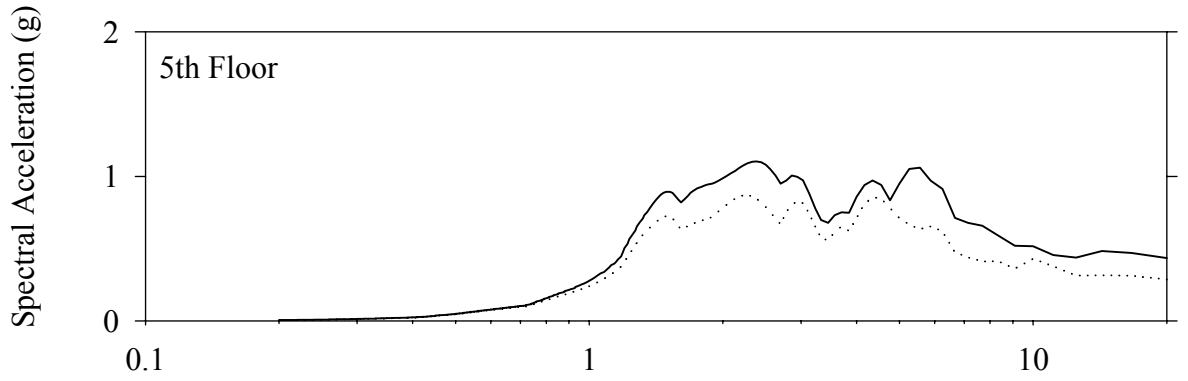
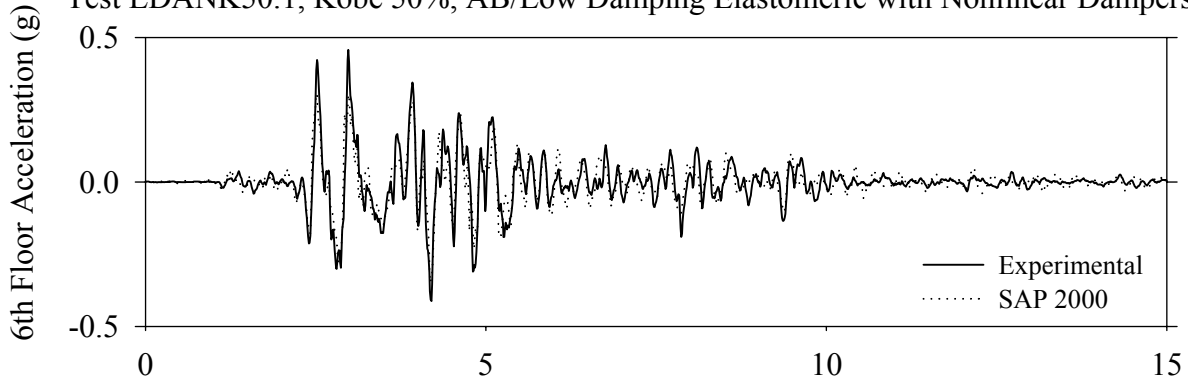
Test LDANE20.1, El Centro S00E 200%, AB/Low Damping Elastomeric with Nonlinear Dampers



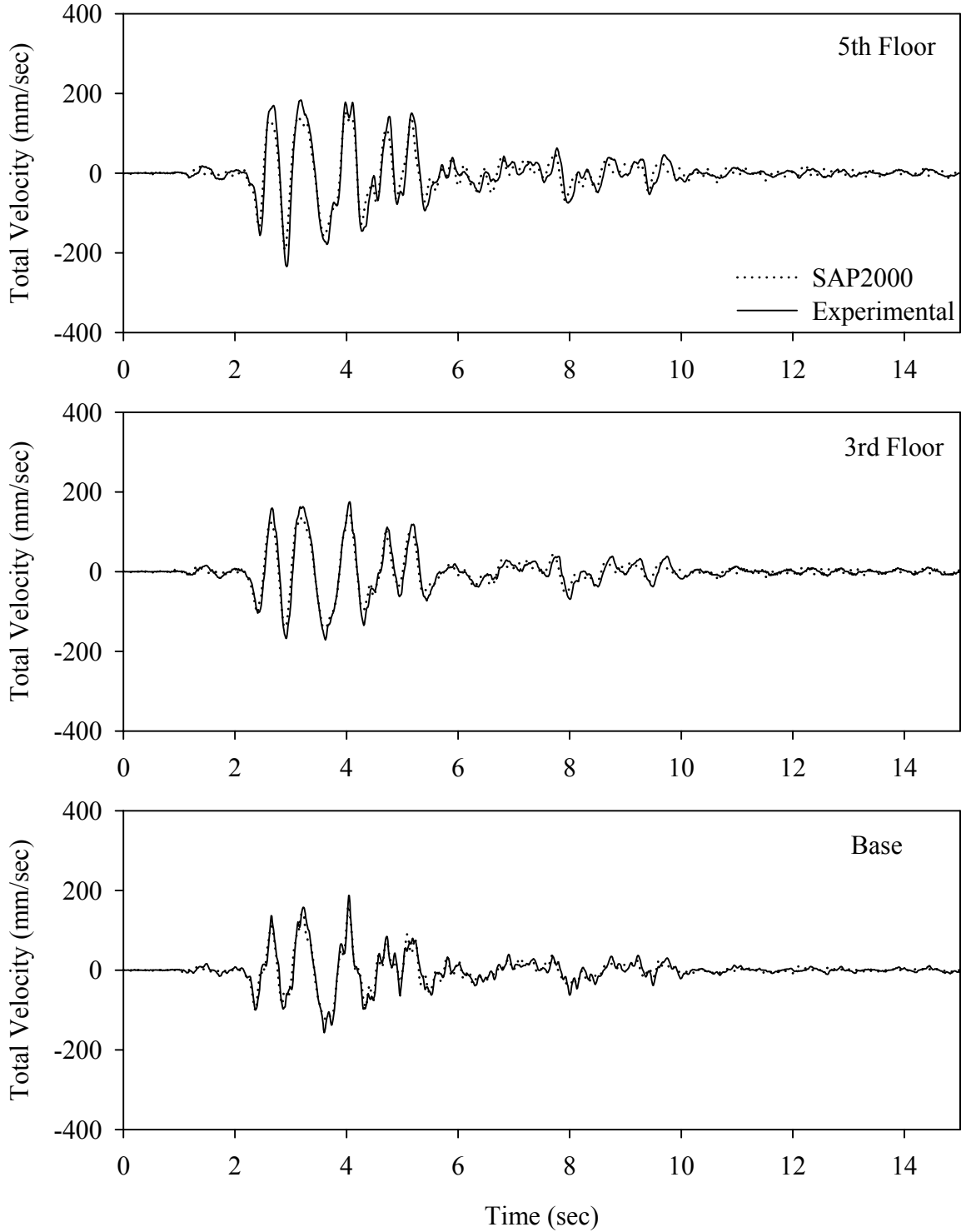
Test LDANK50.1, Kobe 50%, AB/Low Damping Elastomeric with Nonlinear Dampers



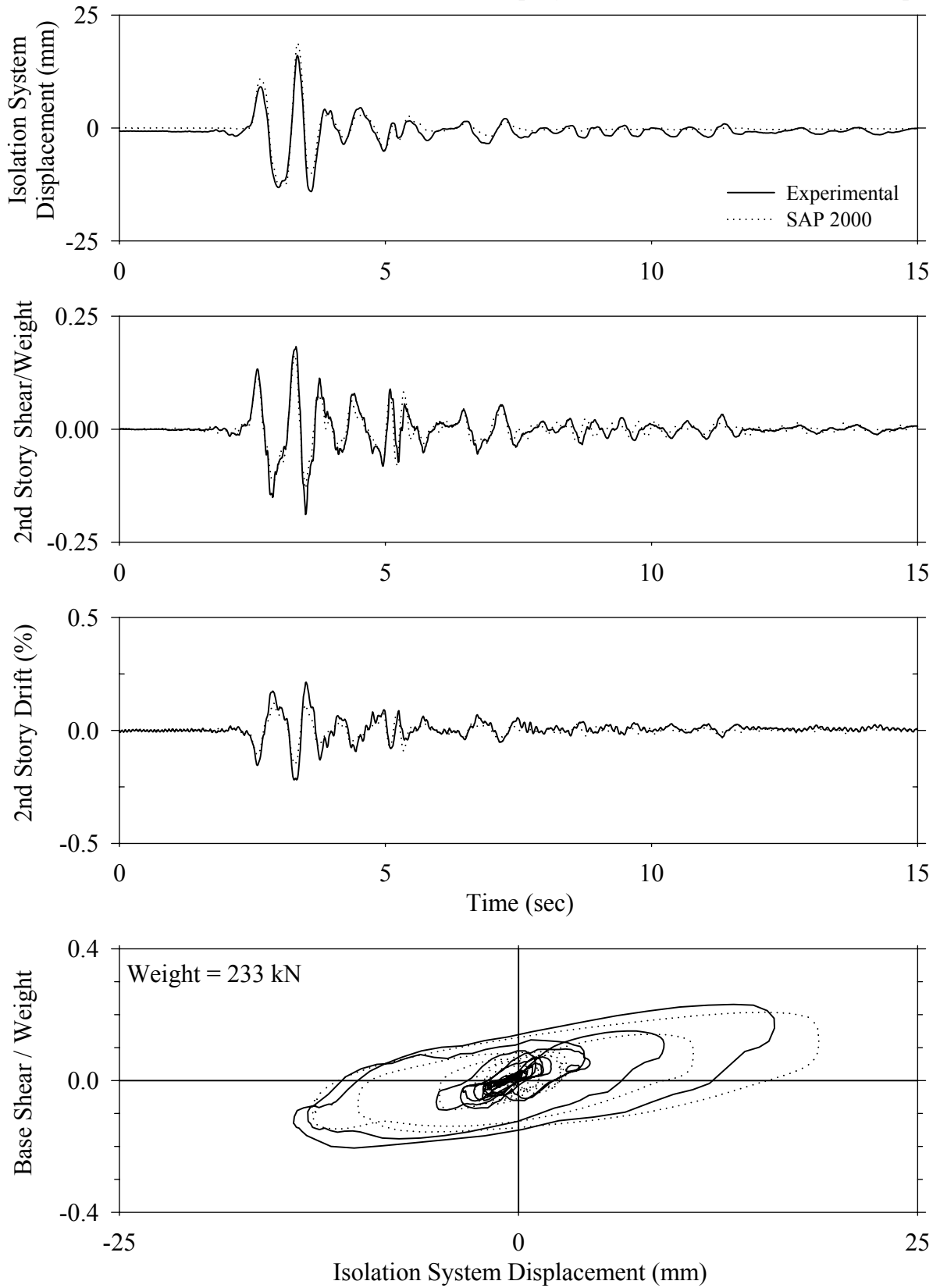
Test LDANK50.1, Kobe 50%, AB/Low Damping Elastomeric with Nonlinear Dampers



Test LDANK50.1, Kobe 50%, AB/Low Damping Elastomeric with Nonlinear Dampers

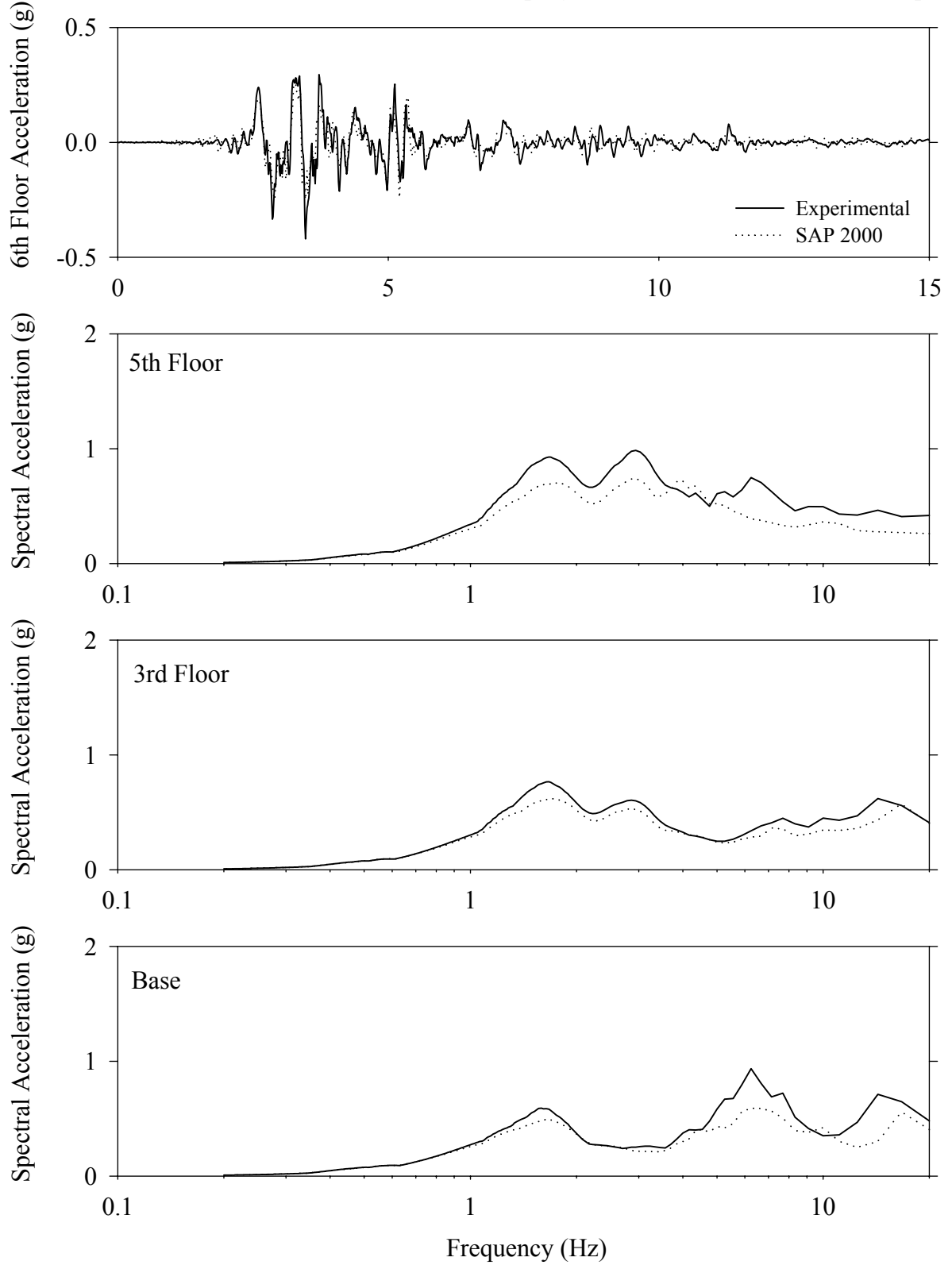


Test LDANN50.1, Newhall 360 50%, AB/Low Damping Elastomeric with Nonlinear Dampers

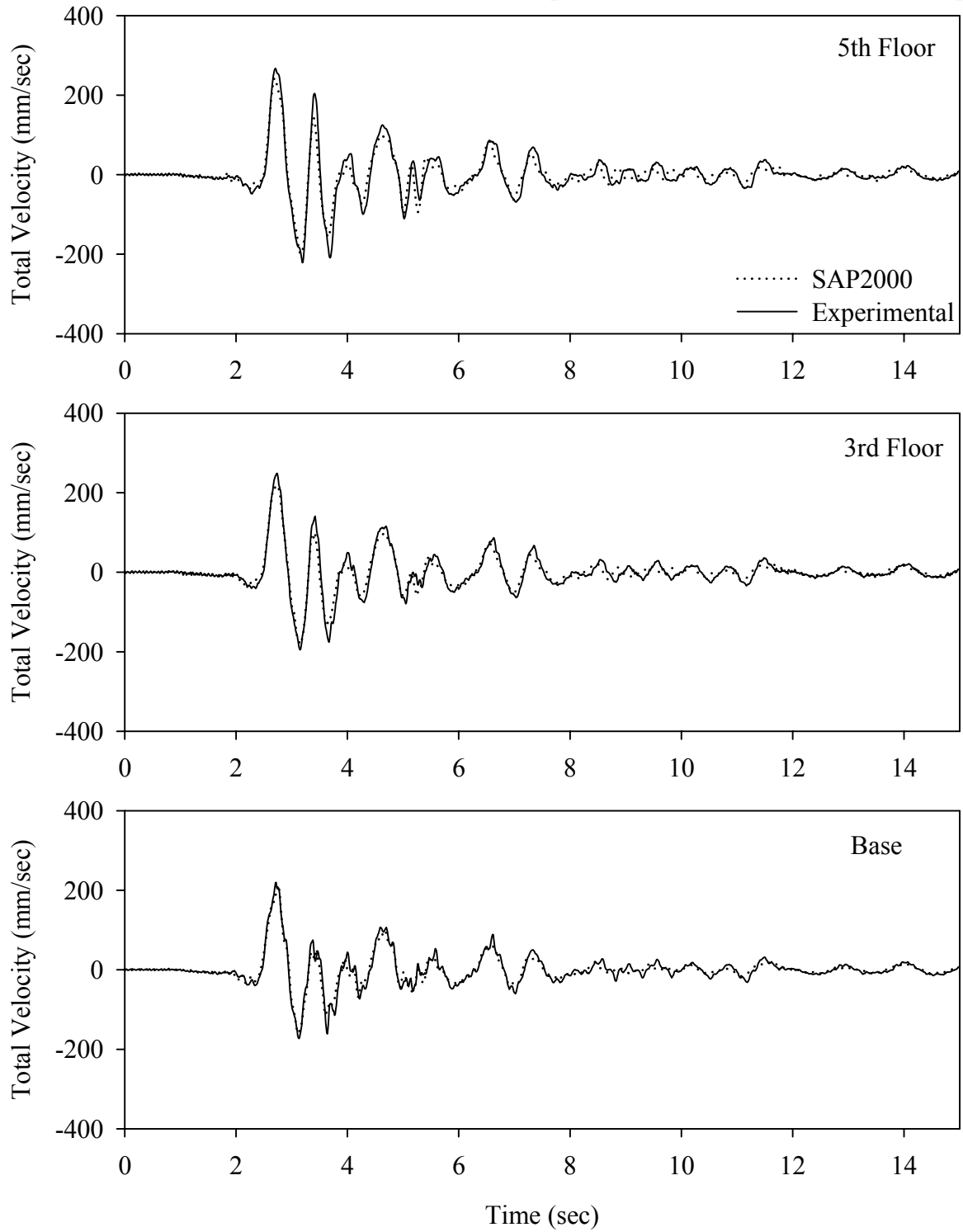




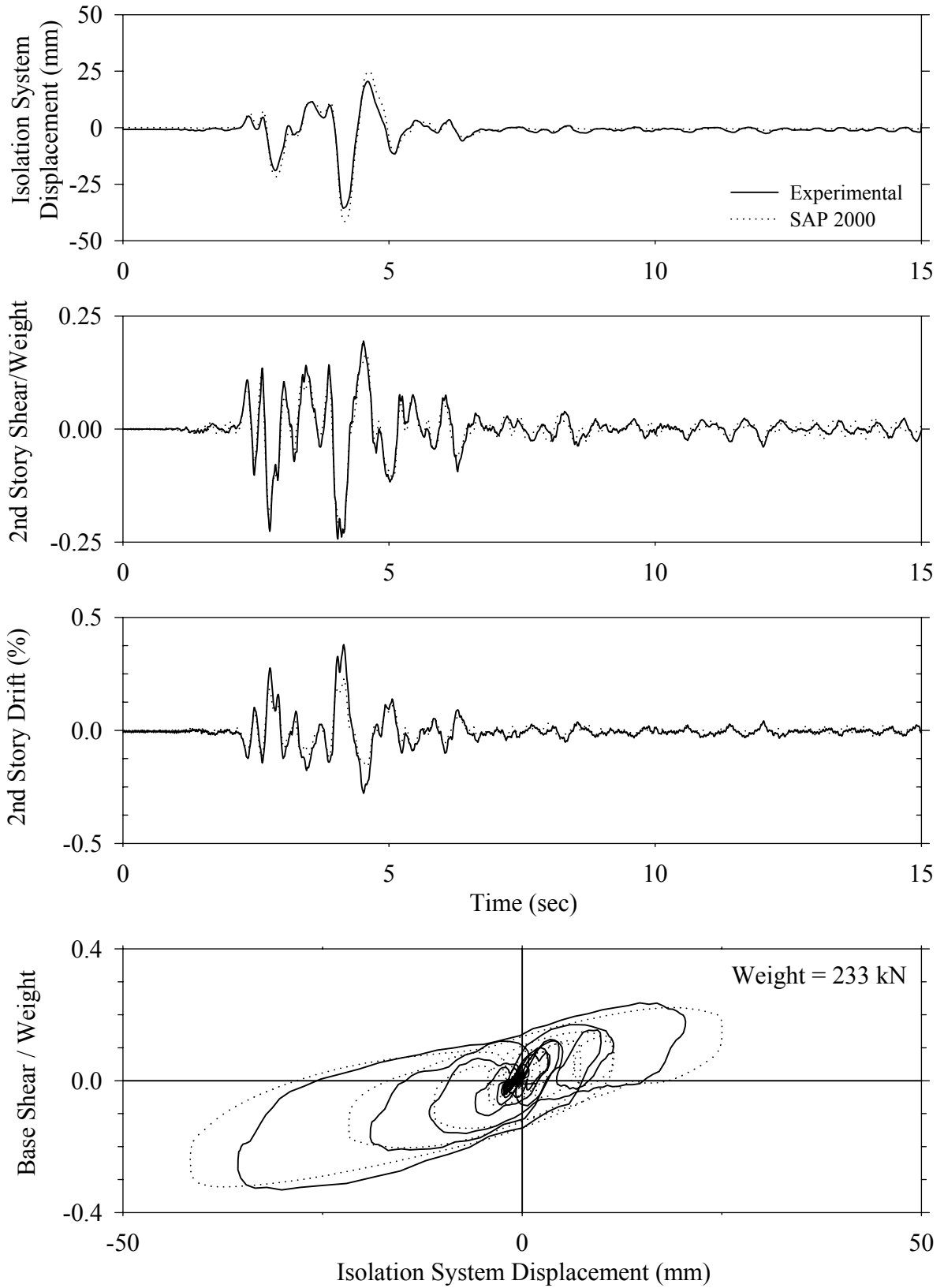
Test LDANN50.1, Newhall 360 50%, AB/Low Damping Elastomeric with Nonlinear Dampers



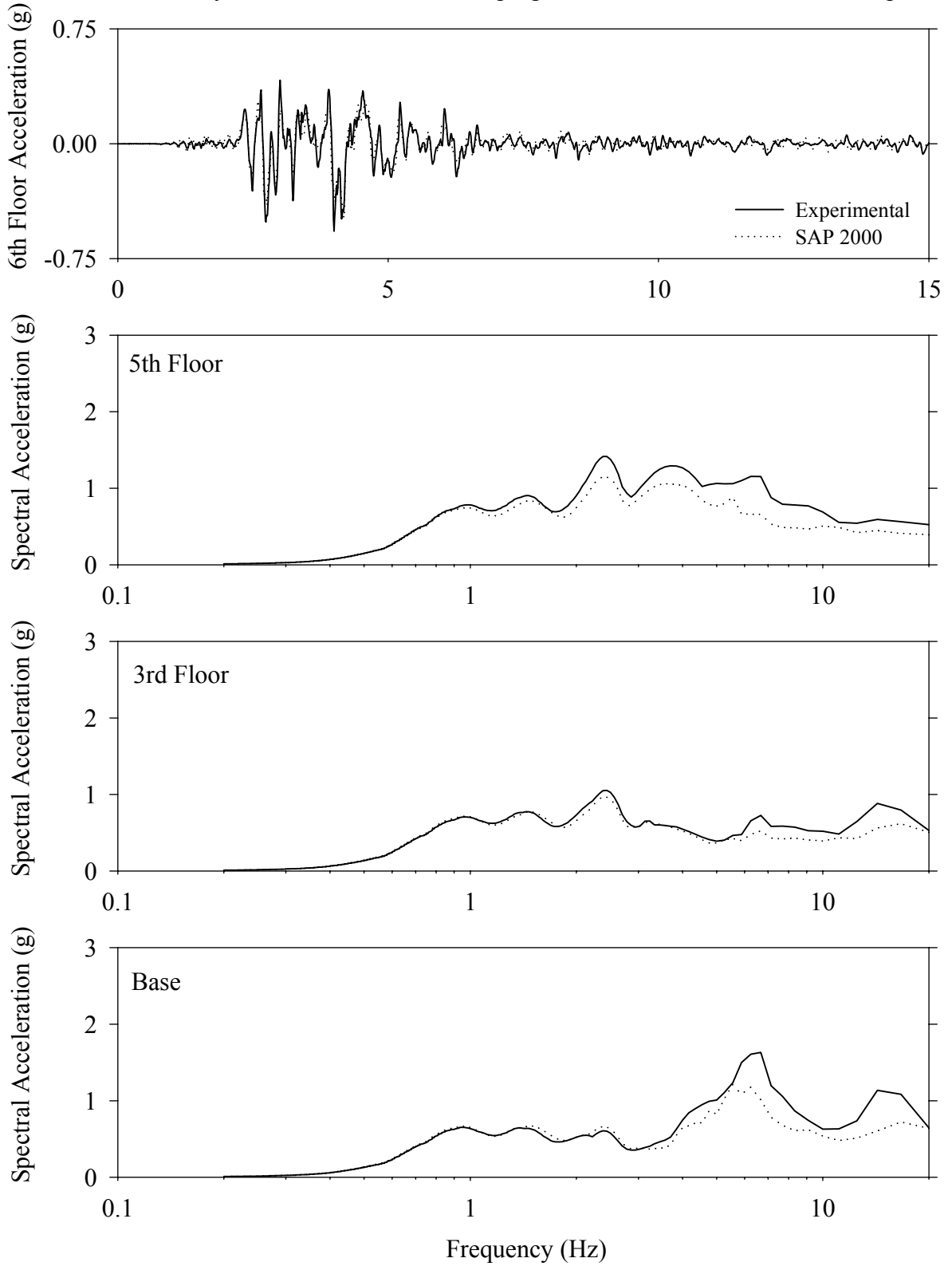
Test LDANN50.1, Newhall 360 50%, AB/Low Damping Elastomeric with Nonlinear Dampers



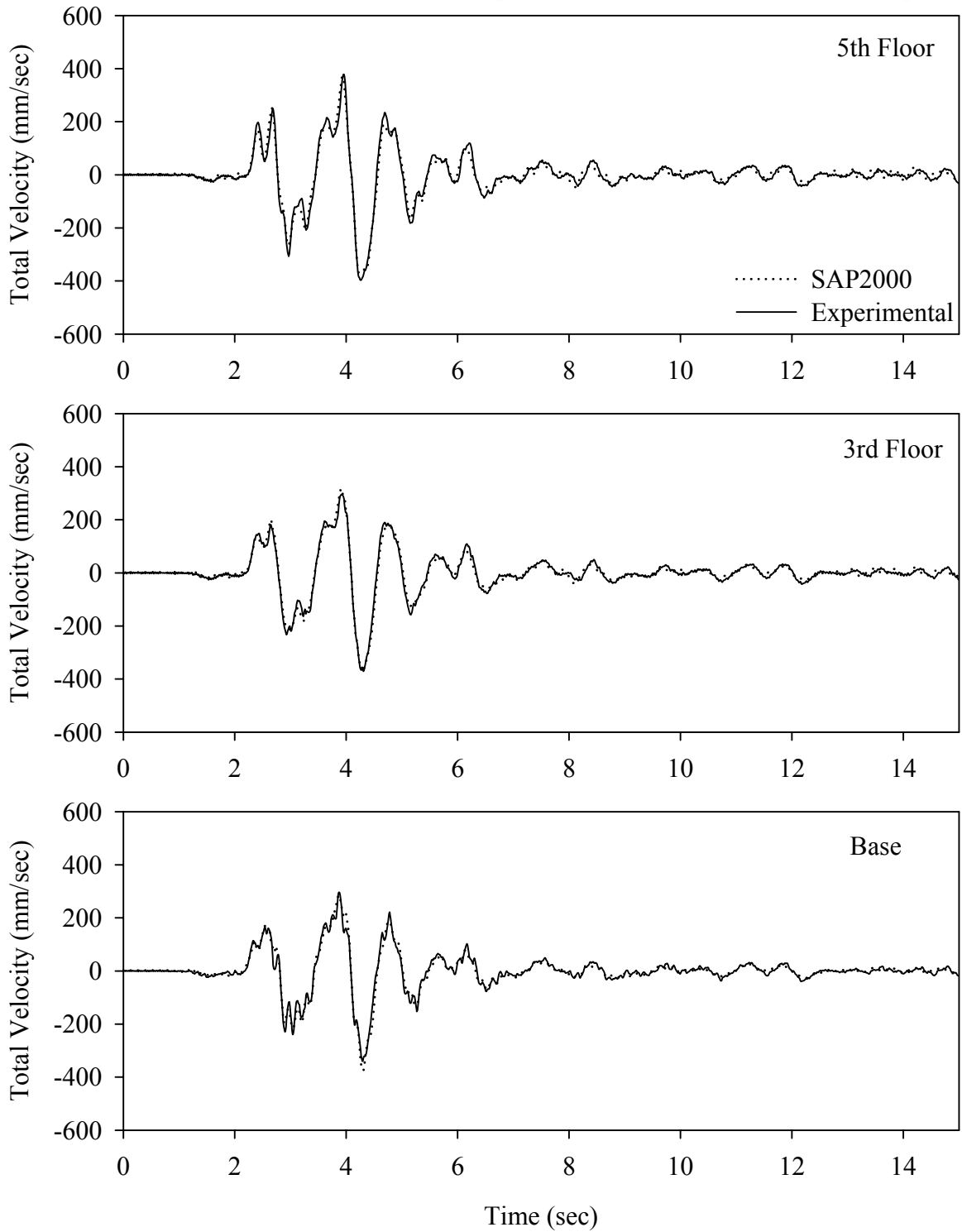
Test LDANS10.1, Sylmar 100%, AB/Low Damping Elastomeric with Nonlinear Dampers



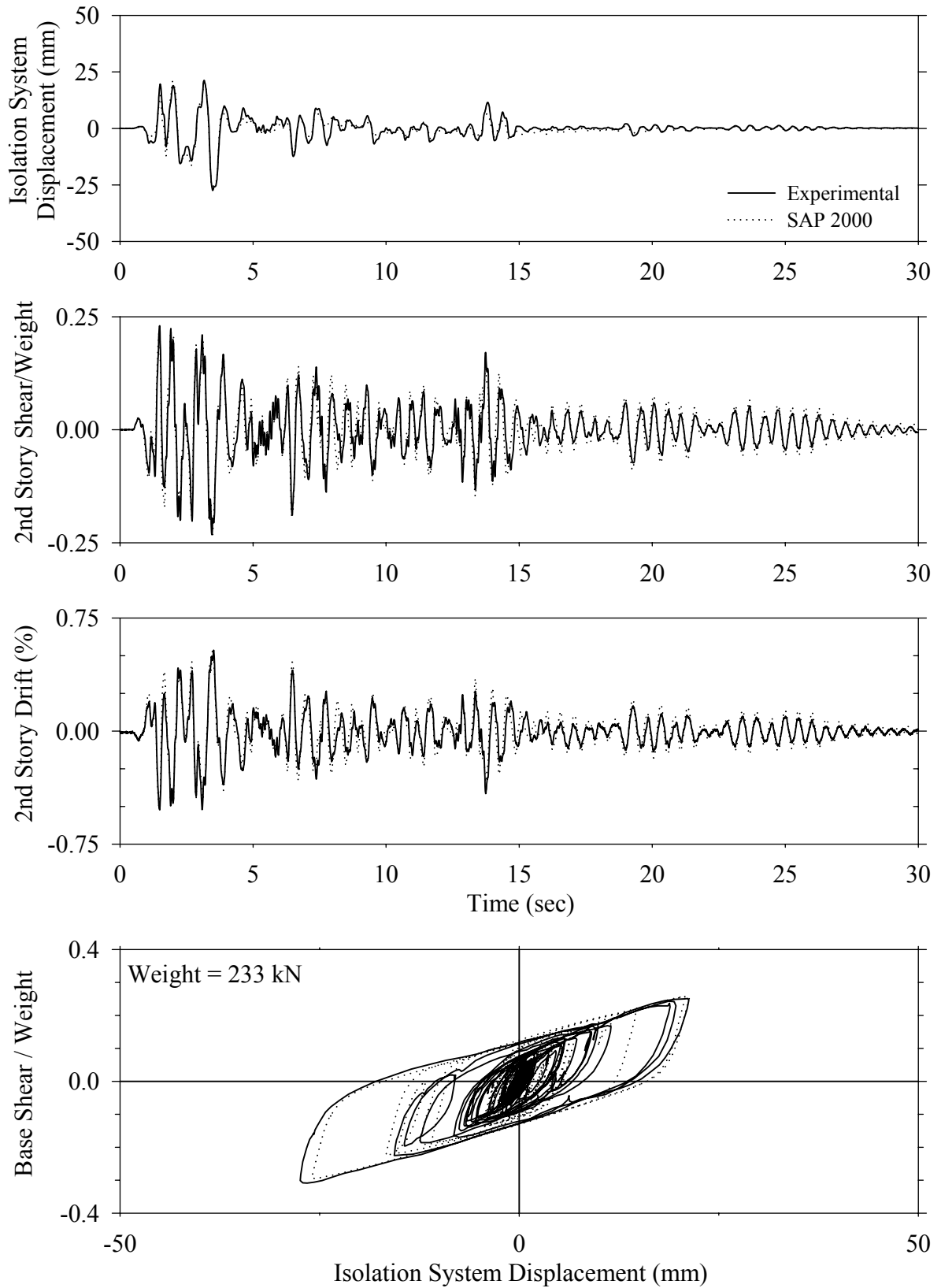
Test LDANS10.1, Sylmar 100%, AB/Low Damping Elastomeric with Nonlinear Dampers



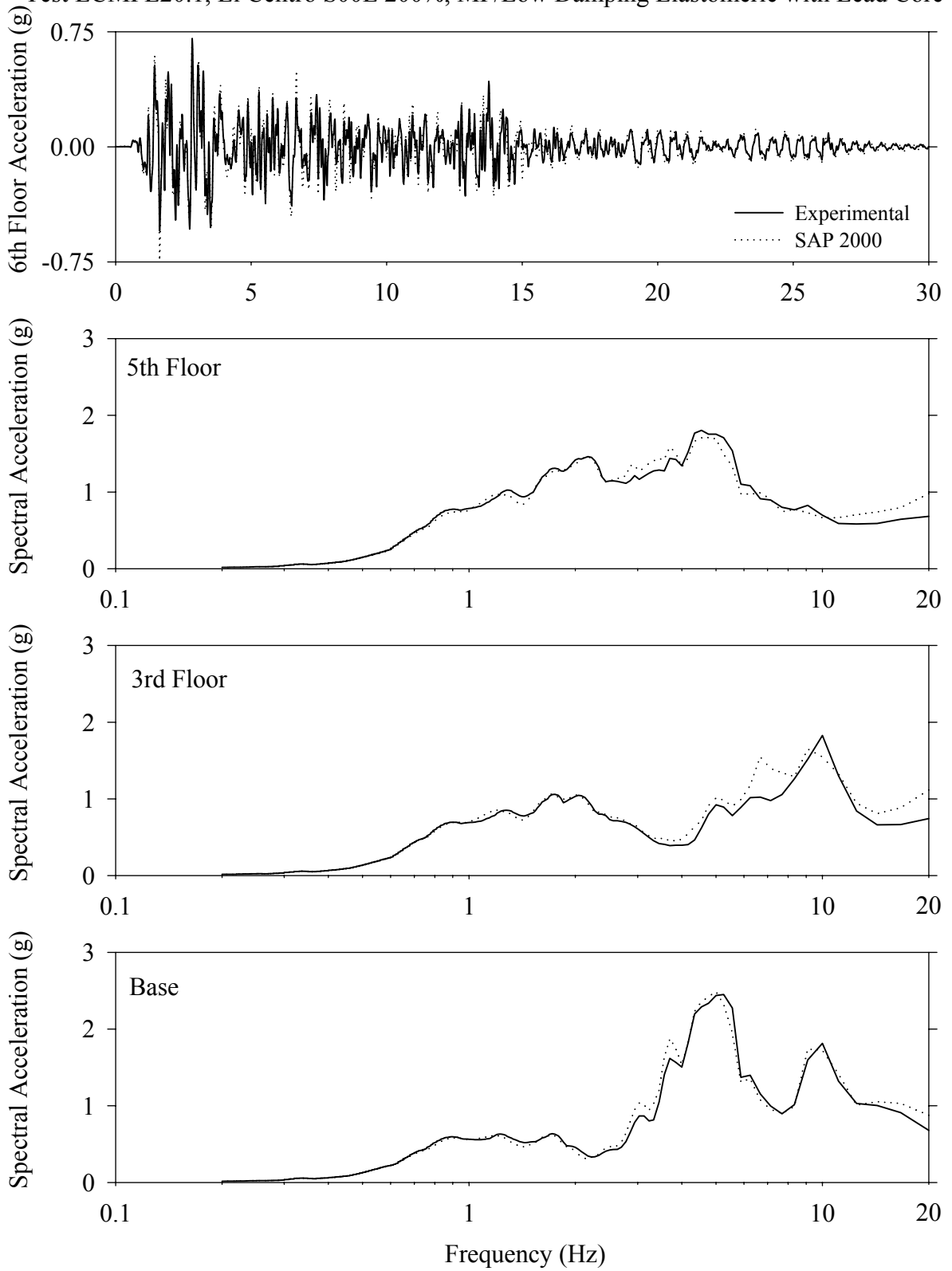
Test LDANS10.1, Sylmar 100%, AB/Low Damping Elastomeric with Nonlinear Dampers



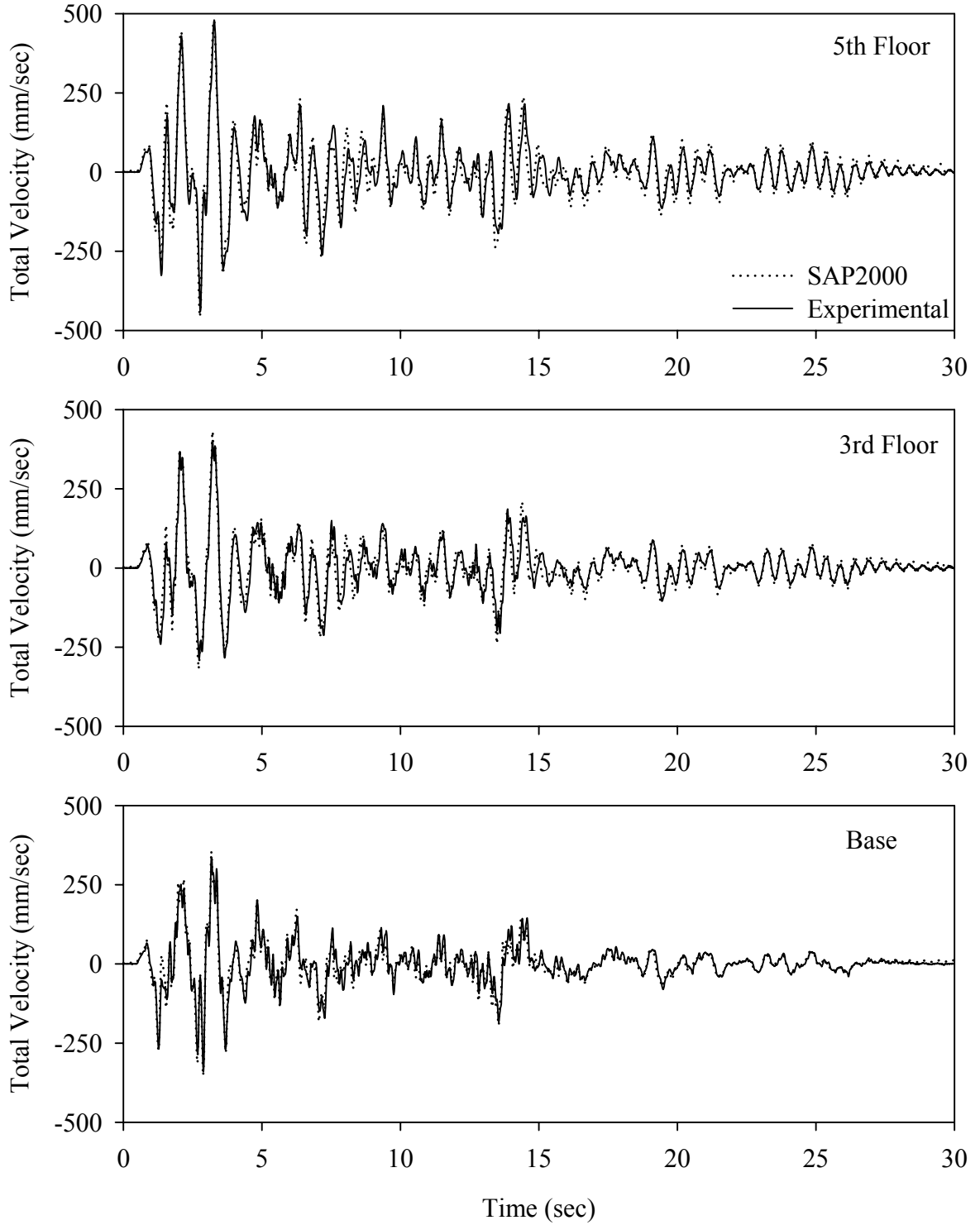
Test LCMFE20.1, El Centro S00E 200%, MF/Low Damping Elastomeric with Lead Core



Test LCMFE20.1, El Centro S00E 200%, MF/Low Damping Elastomeric with Lead Core

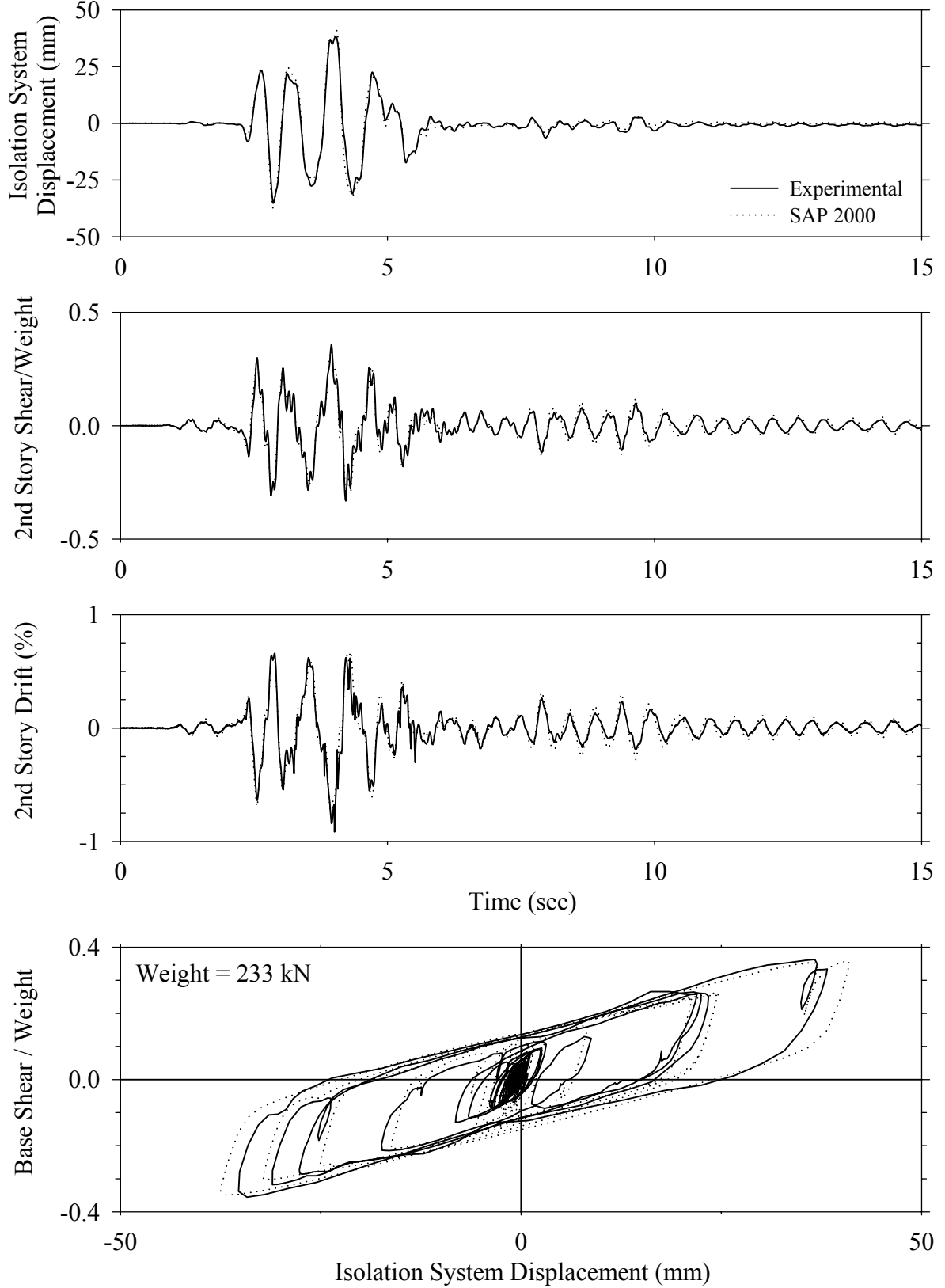


Test LCMFE20.1, El Centro S00E 200%, MF/Low Damping Elastomeric with Lead Core

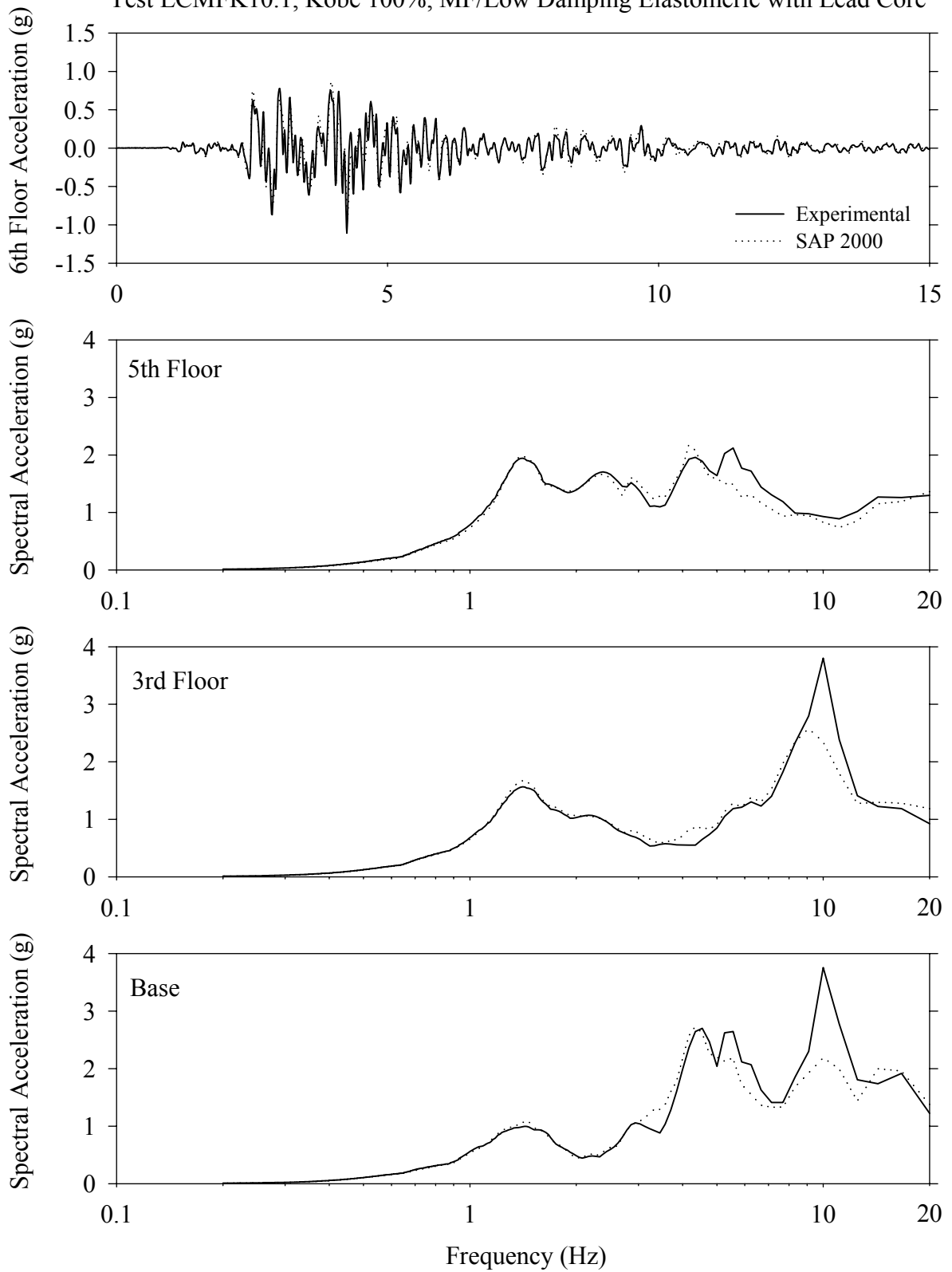




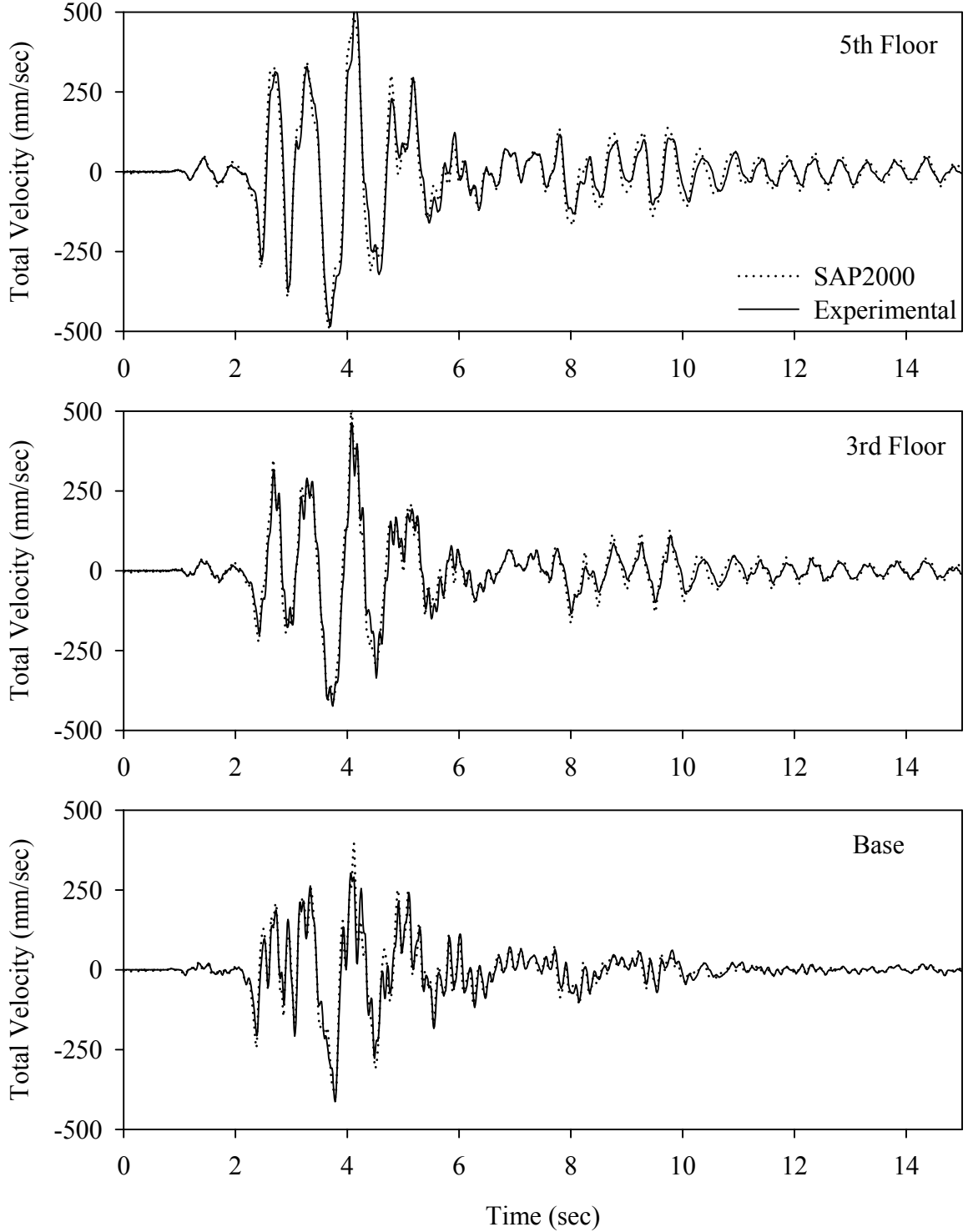
Test LCMFK10.1, Kobe 100%, MF/Low Damping Elastomeric with Lead Core



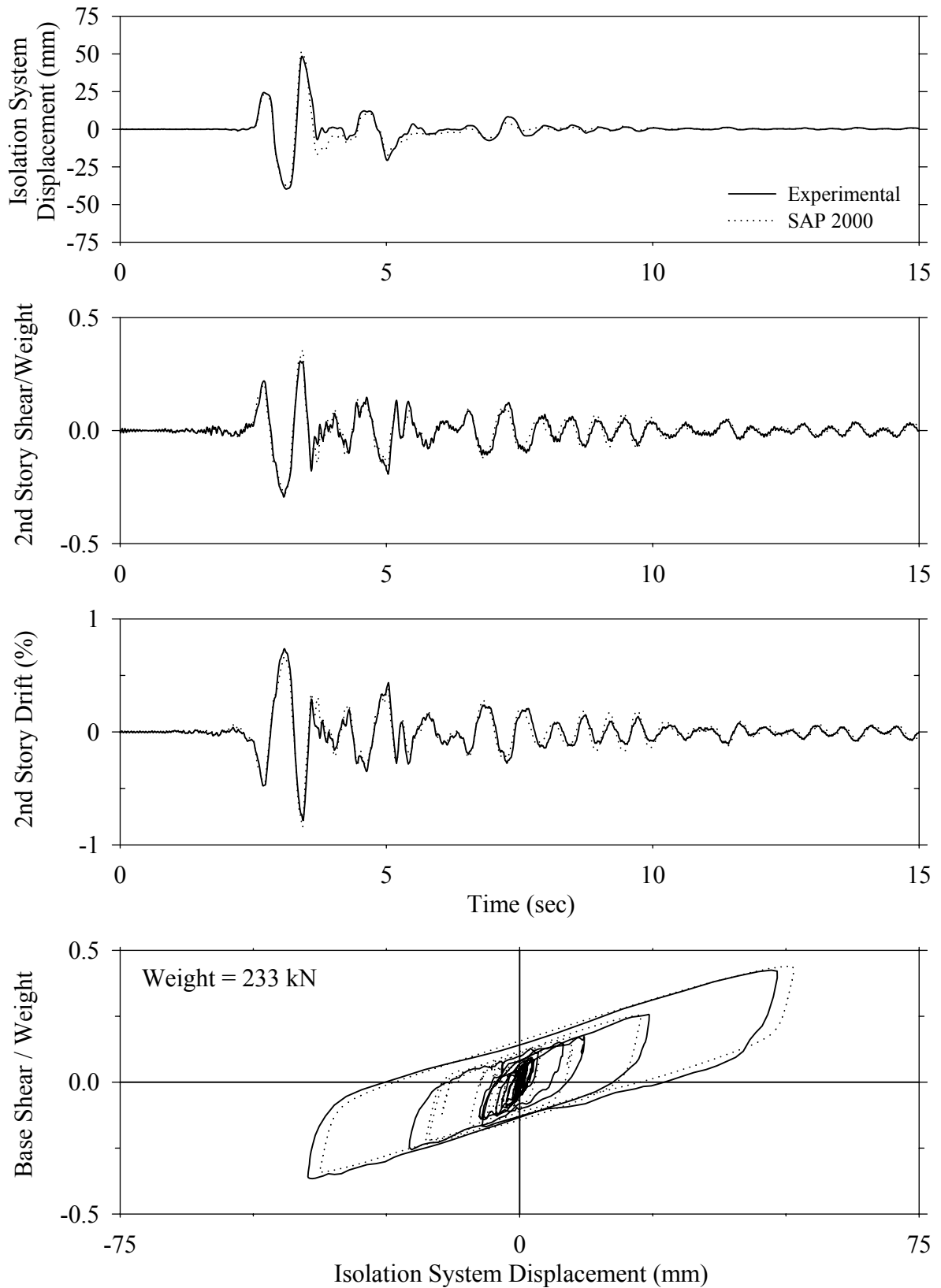
Test LCMFK10.1, Kobe 100%, MF/Low Damping Elastomeric with Lead Core

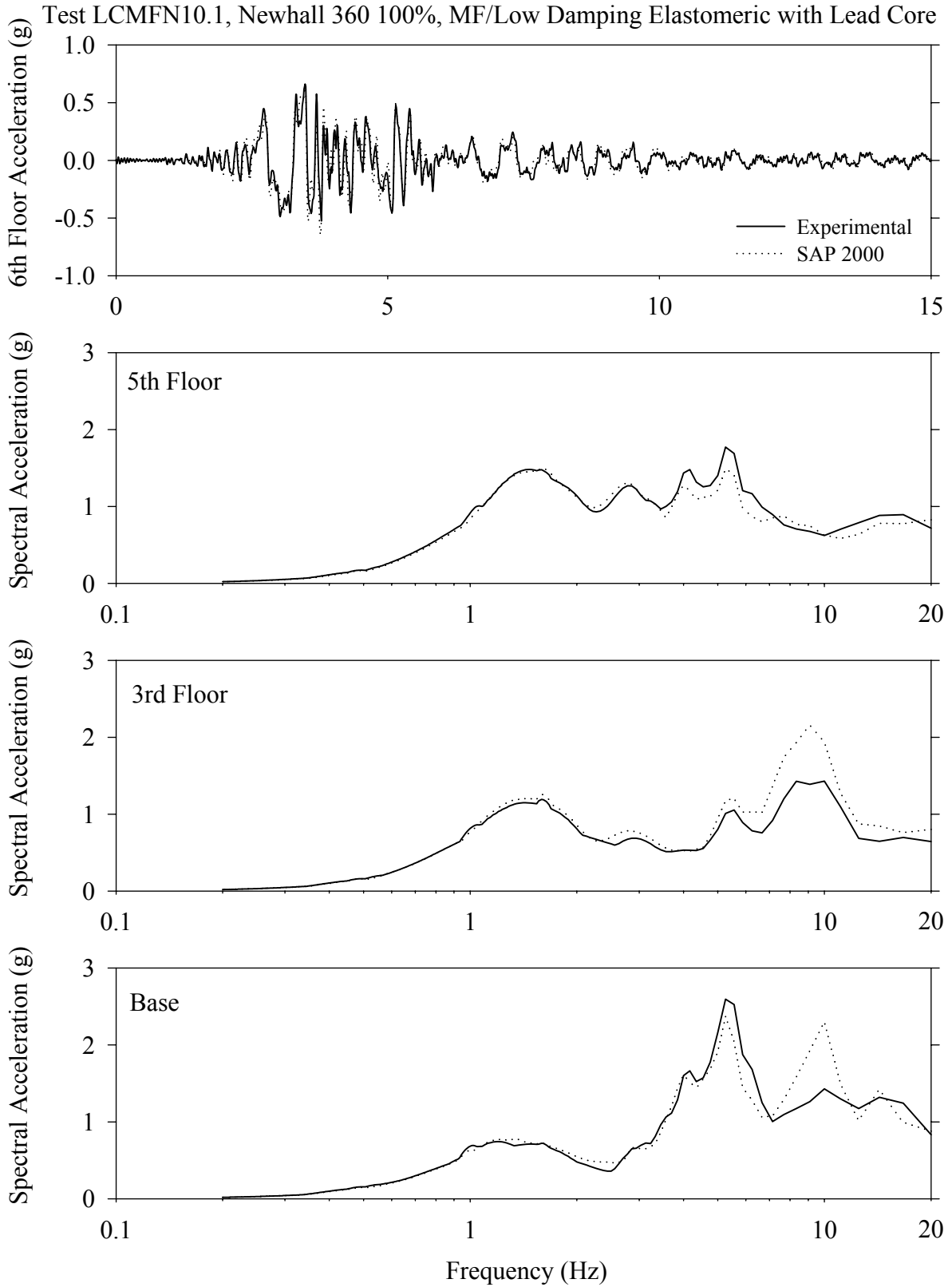


Test LCMFK10.1, Kobe 100%, MF/Low Damping Elastomeric with Lead Core

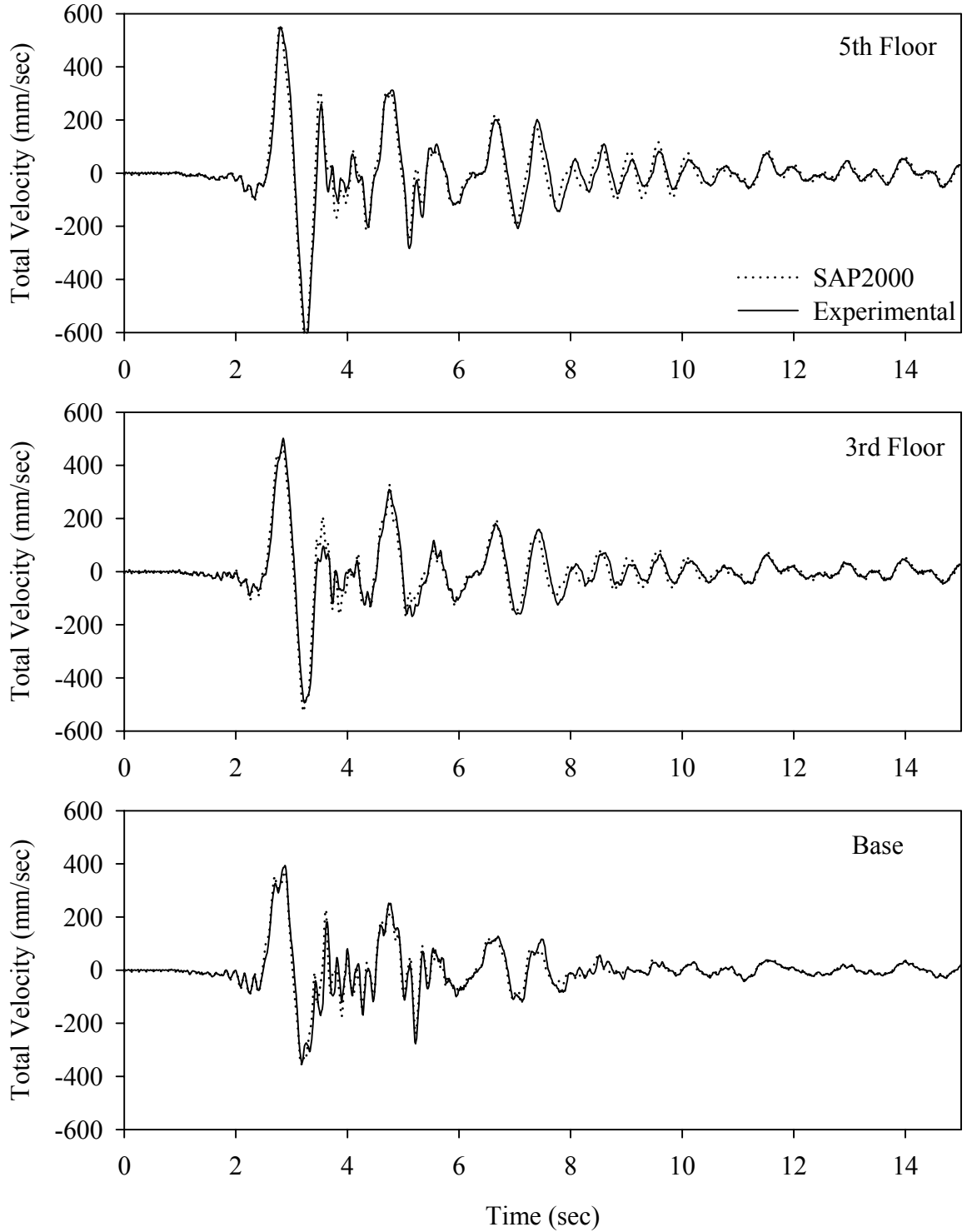


Test LCMFN10.1, Newhall 360 100%, MF/Low Damping Elastomeric with Lead Core

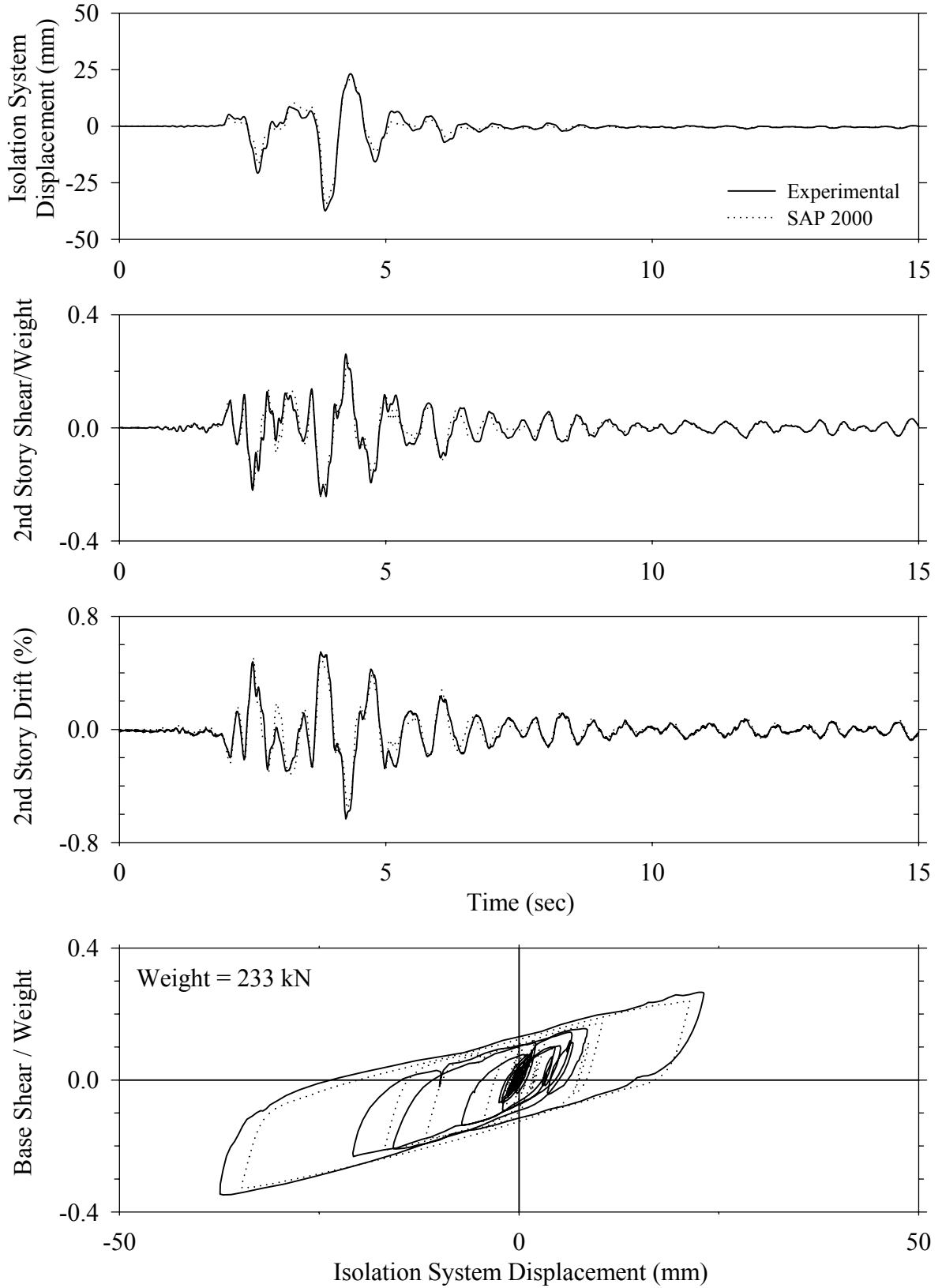




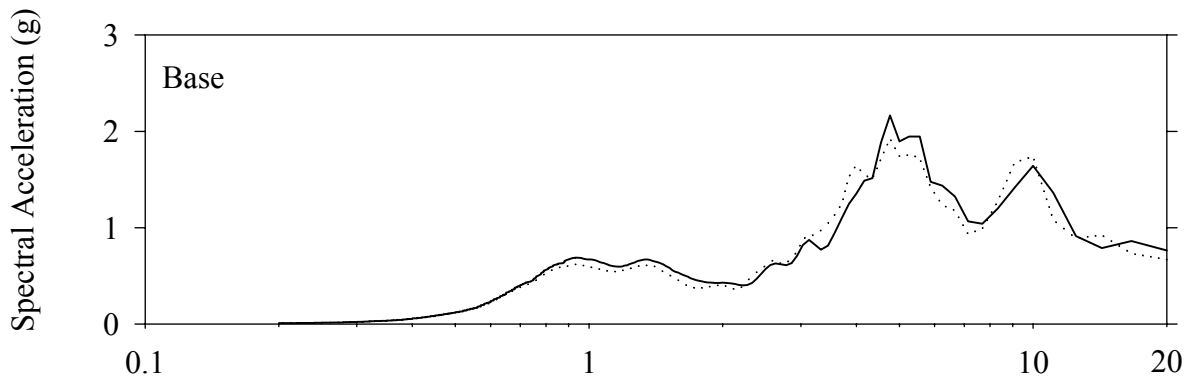
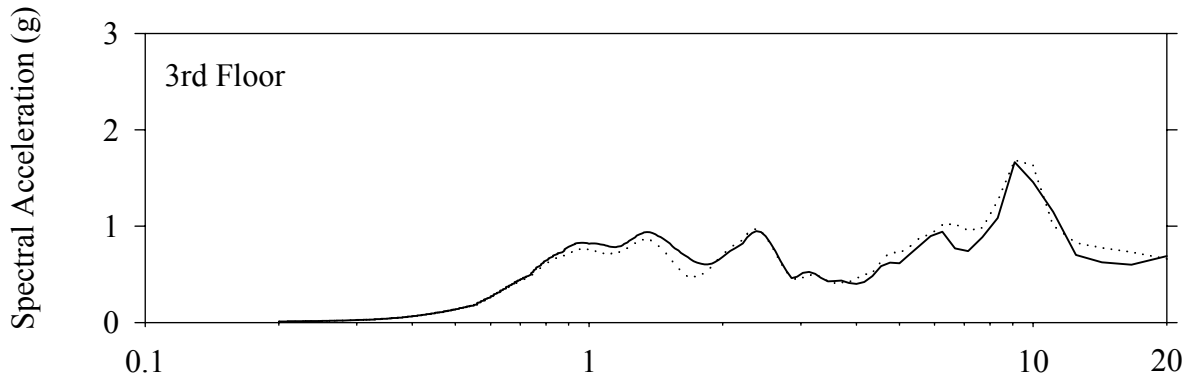
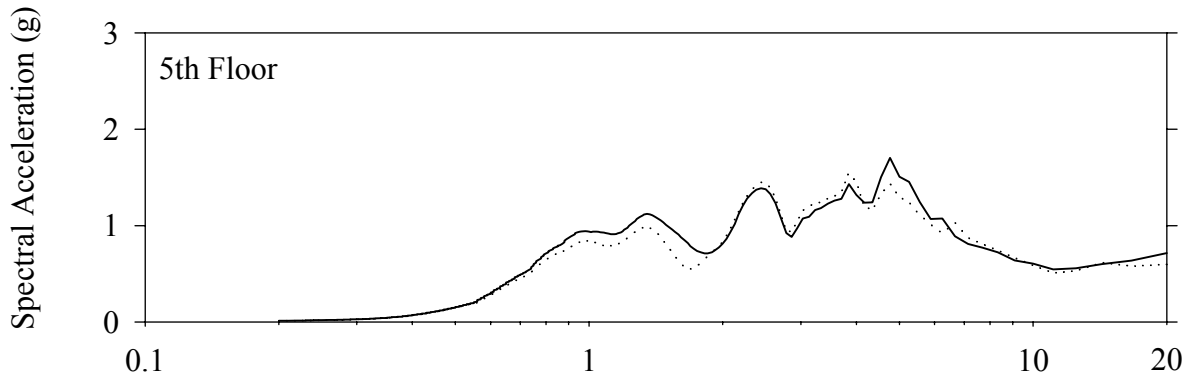
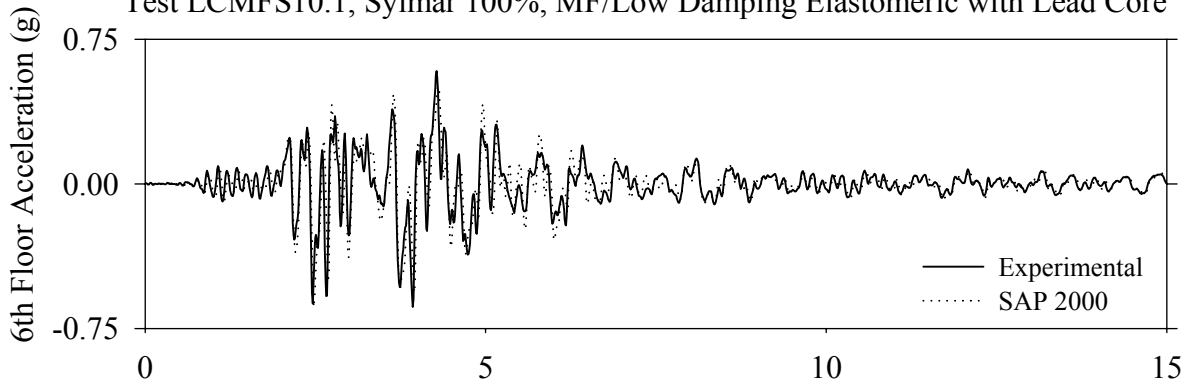
Test LCMFN10.1, Newhall 360 100%, MF/Low Damping Elastomeric with Lead Core



Test LCMFS10.1, Sylmar 100%, MF/Low Damping Elastomeric with Lead Core

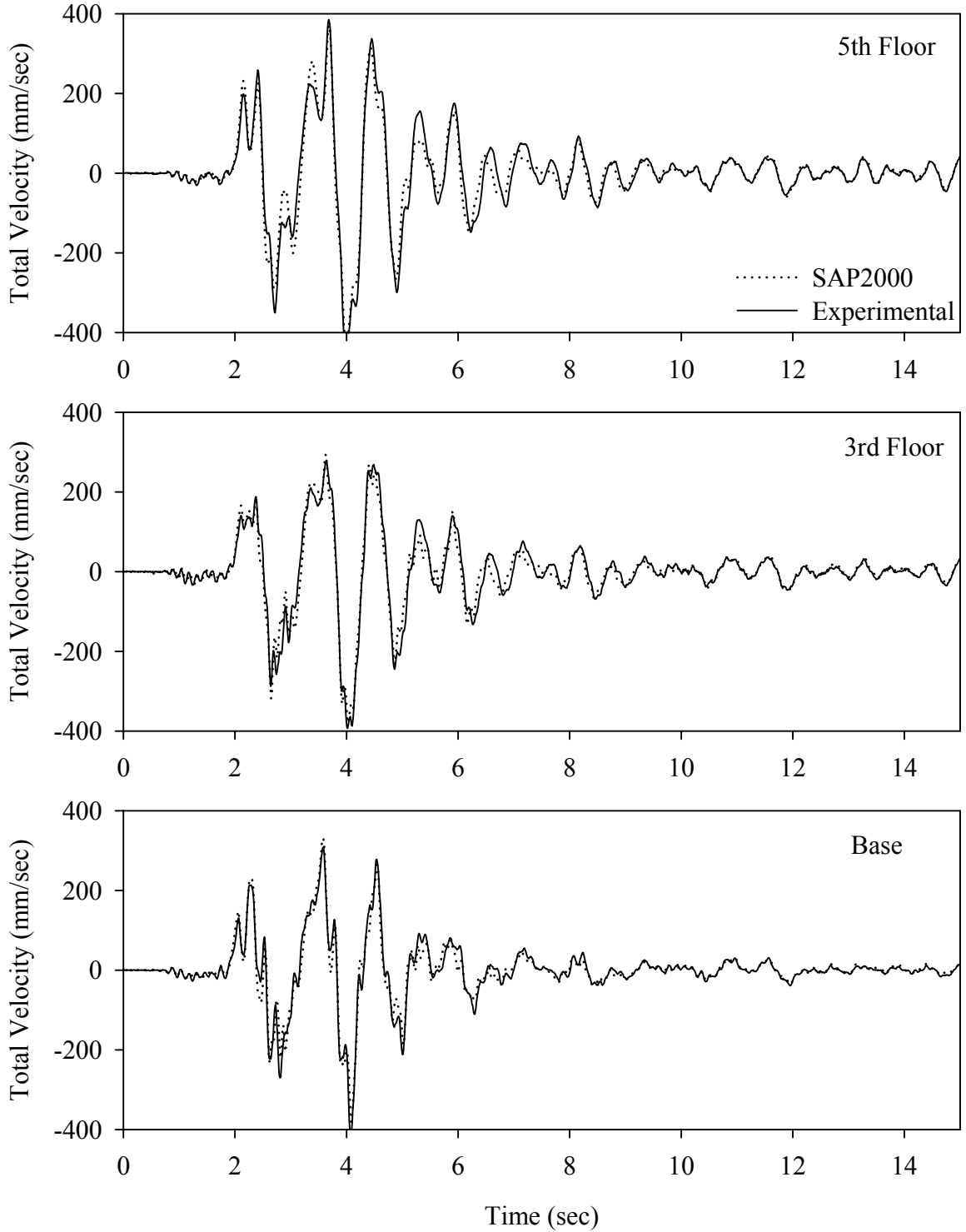


Test LCMFS10.1, Sylmar 100%, MF/Low Damping Elastomeric with Lead Core

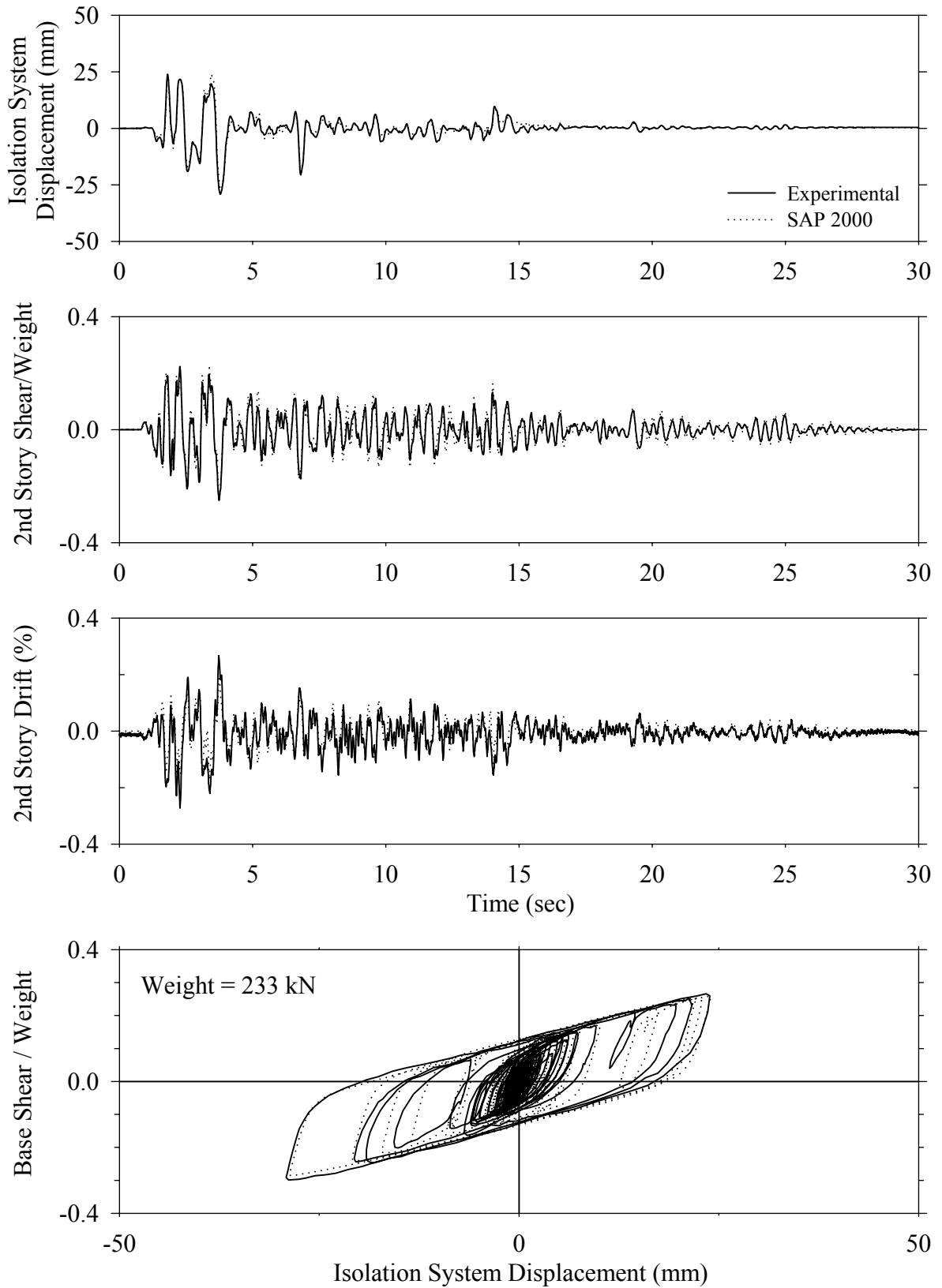




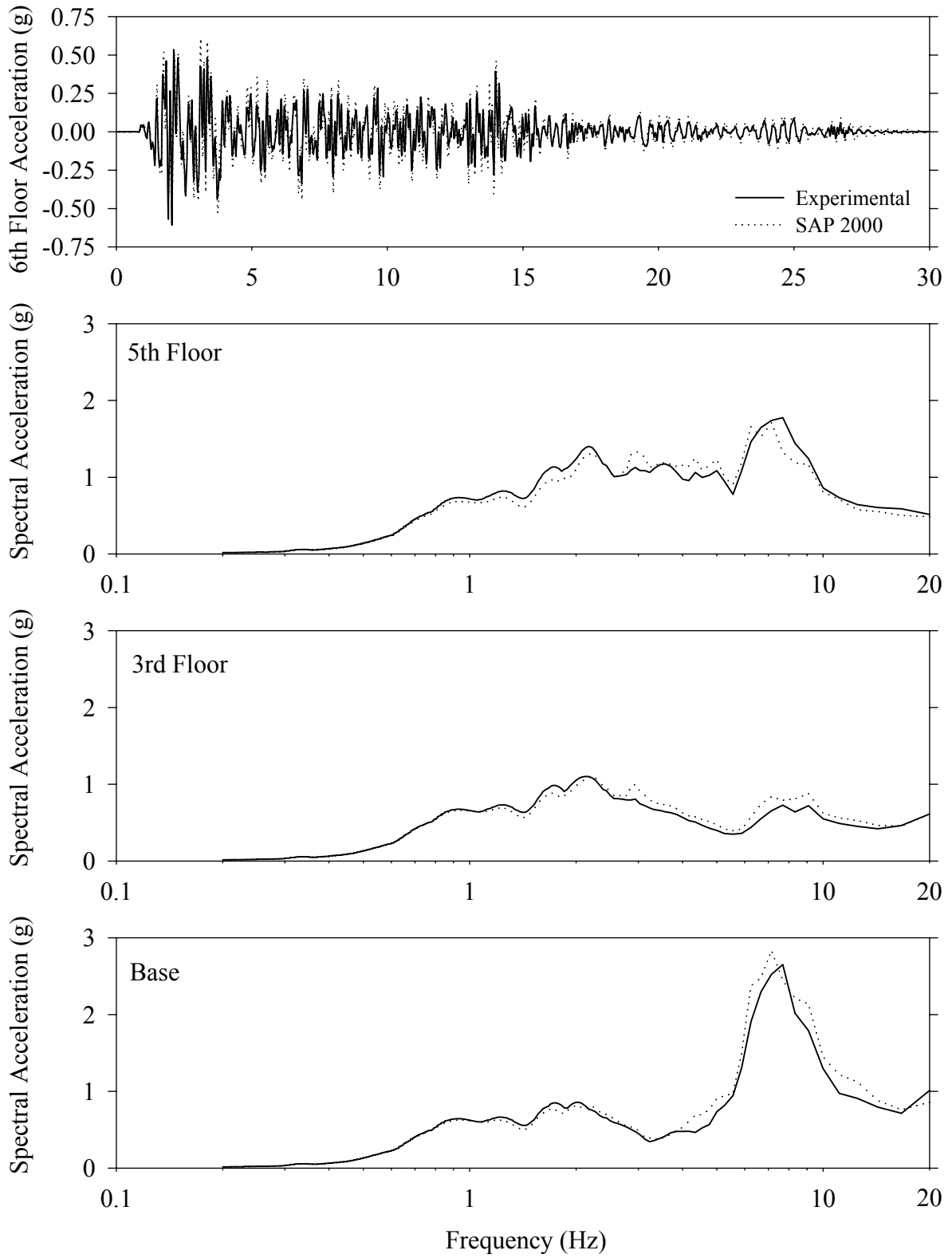
Test LCMFS10.1, Sylmar 100%, MF/Low Damping Elastomeric with Lead Core



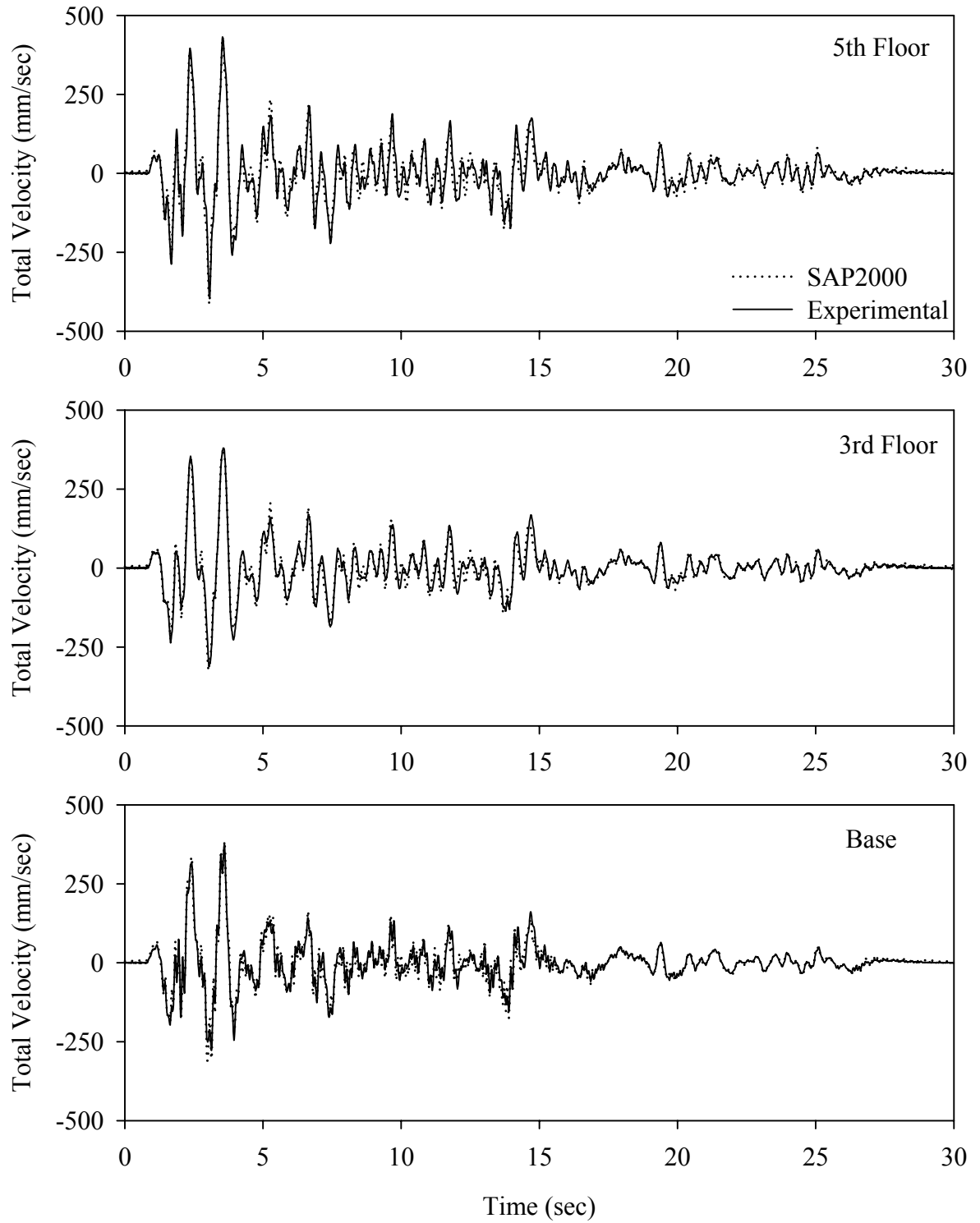
Test LCSBE20.1, El Centro S00E 200%, SB/Low Damping Elastomeric with Lead Core



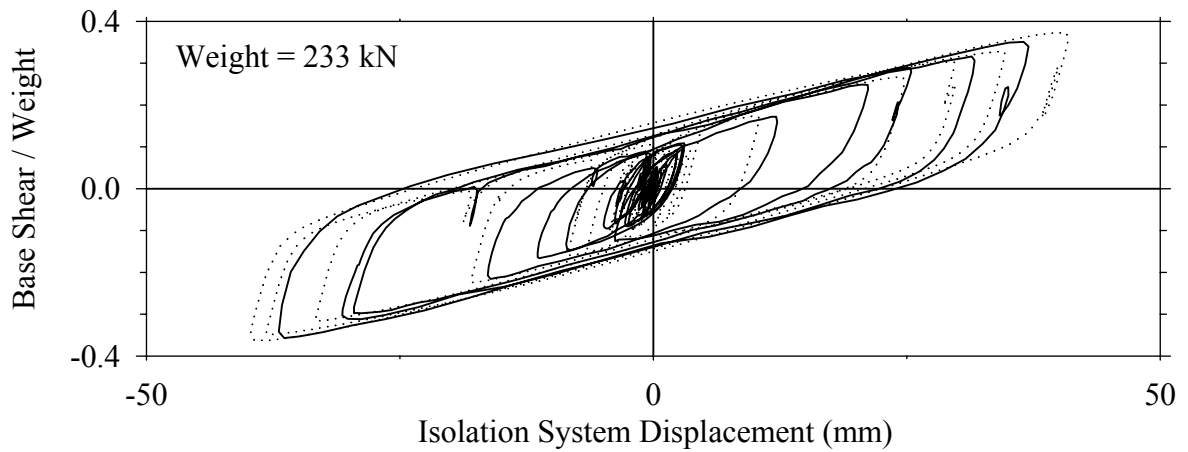
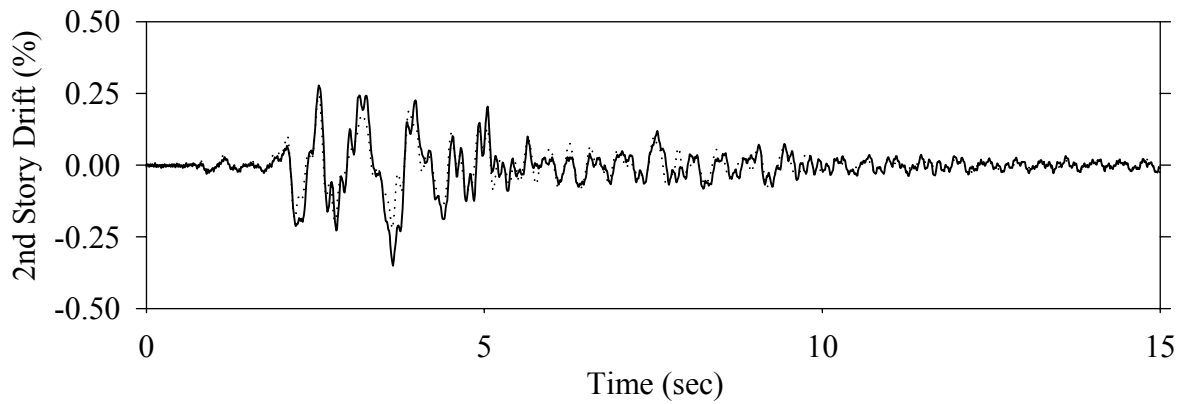
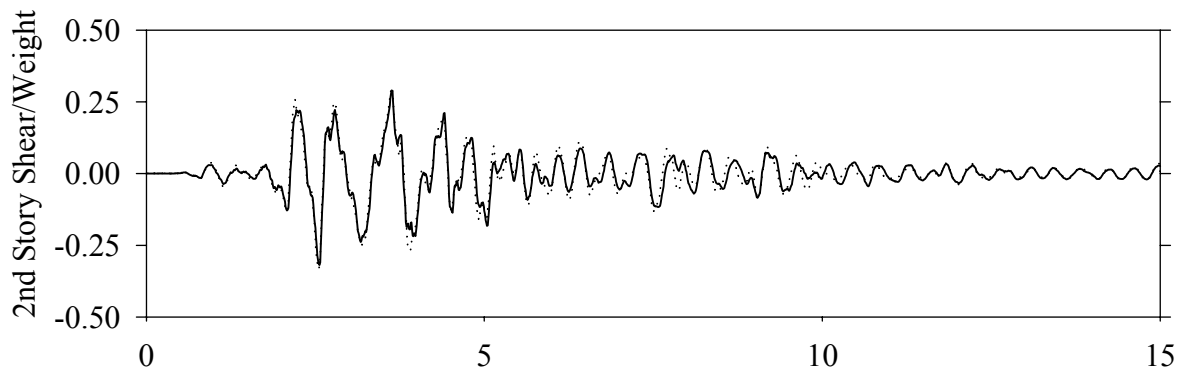
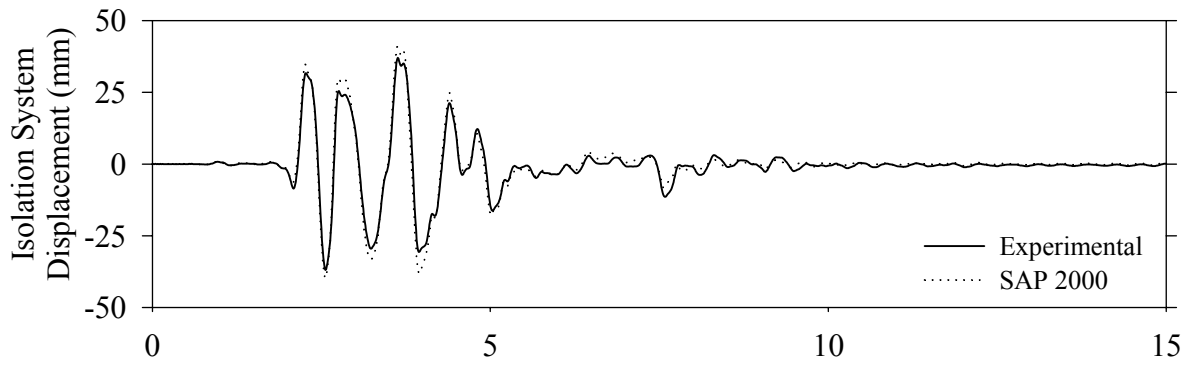
Test LCSBE20.1, El Centro S00E 200%, SB/Low Damping Elastomeric with Lead Core



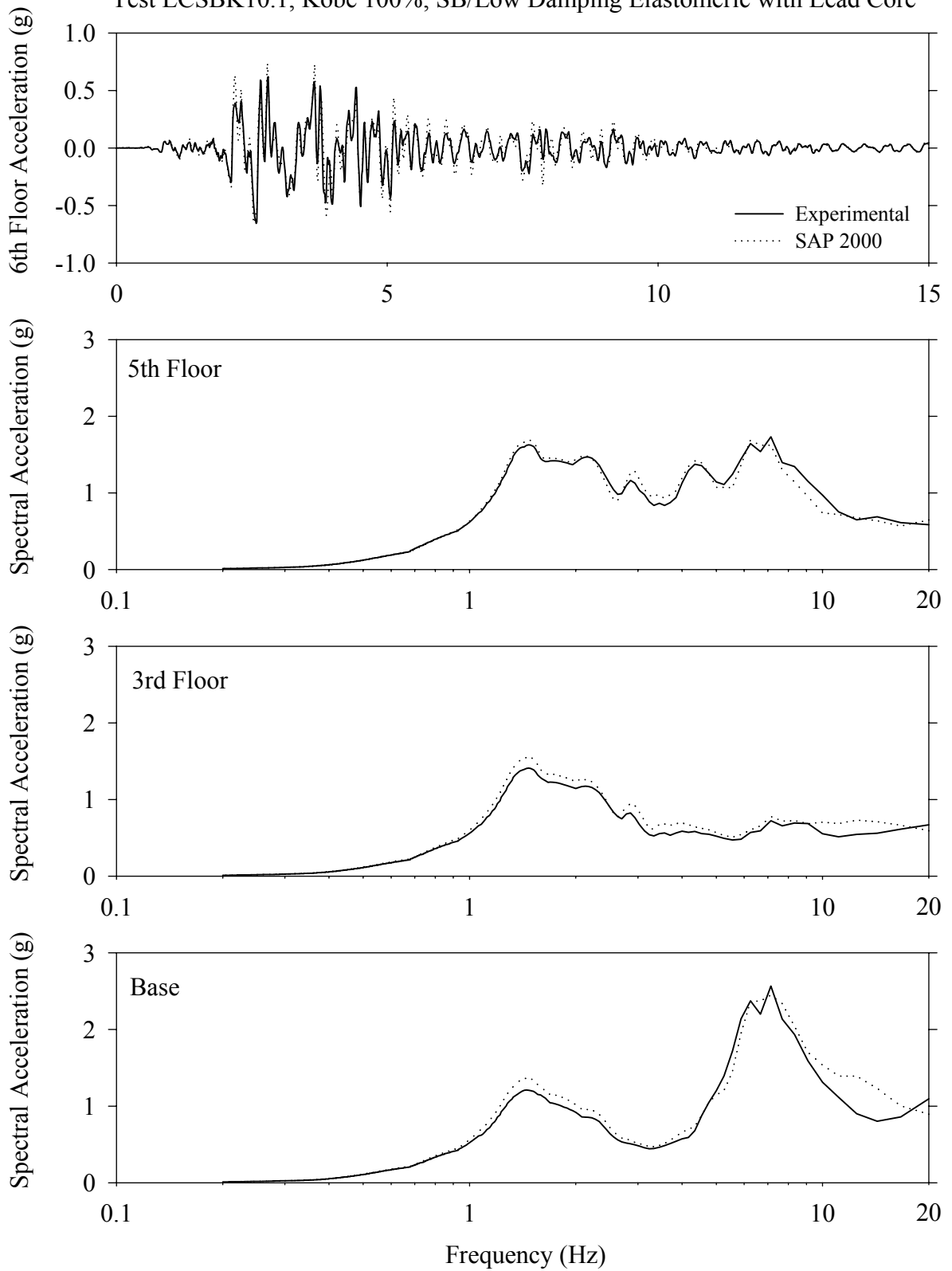
Test LCSBE20.1, El Centro S00E 200%, SB/Low Damping Elastomeric with Lead Core



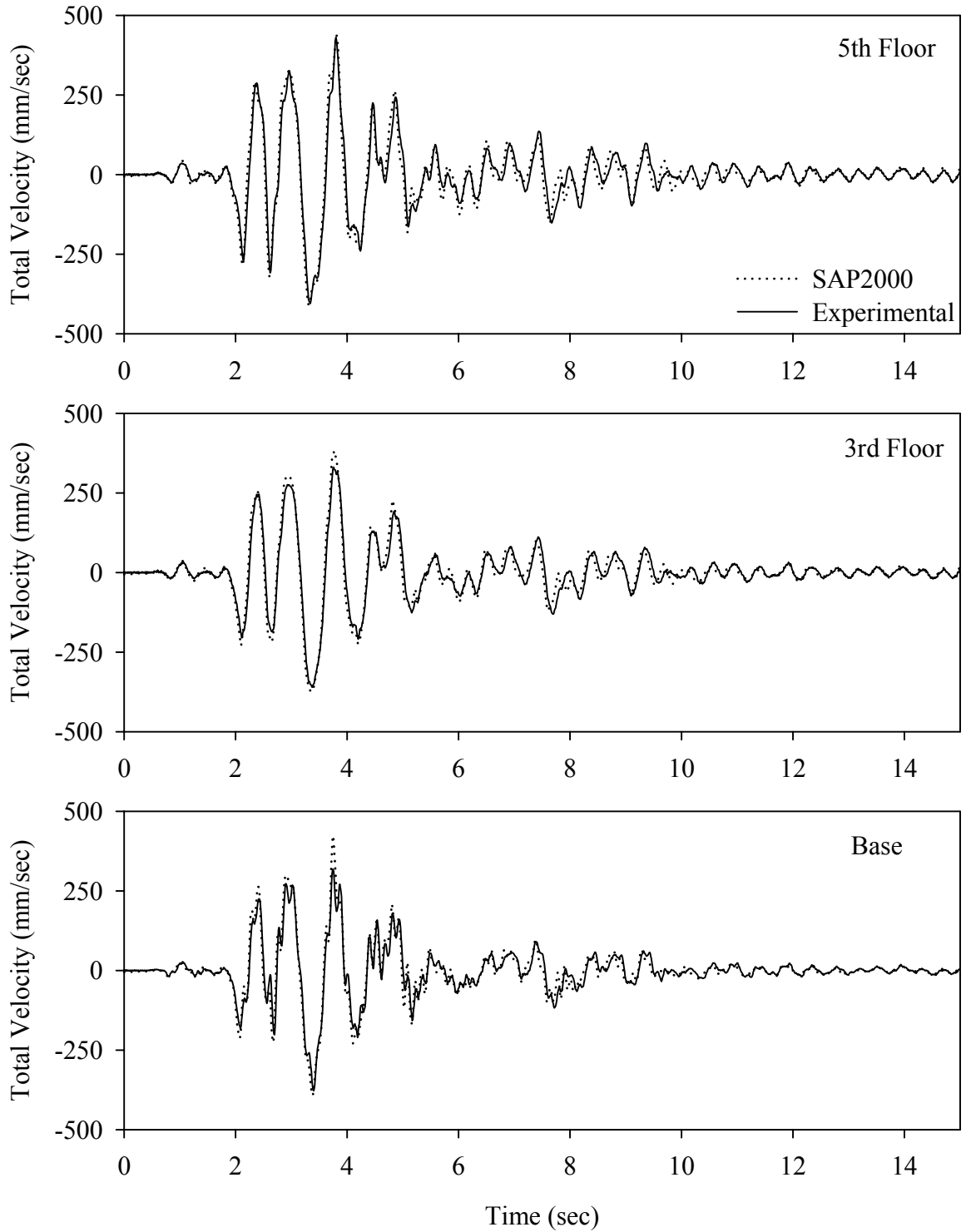
Test LCSBK10.1, Kobe 100%, SB/Low Damping Elastomeric with Lead Core



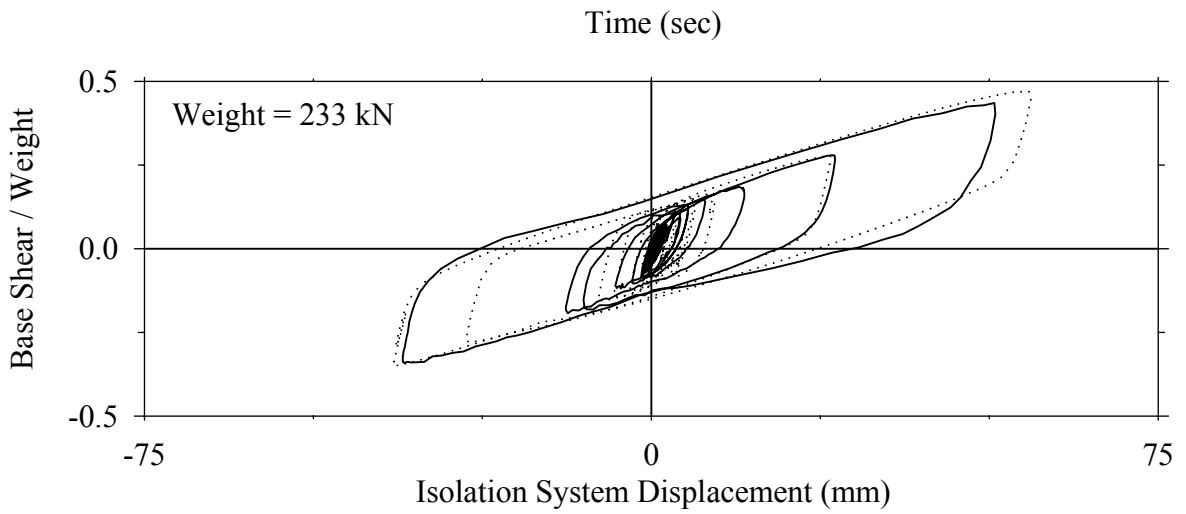
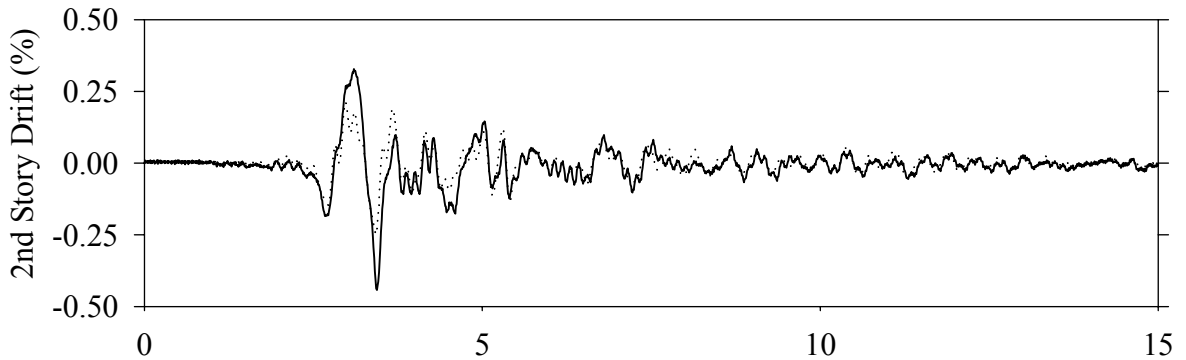
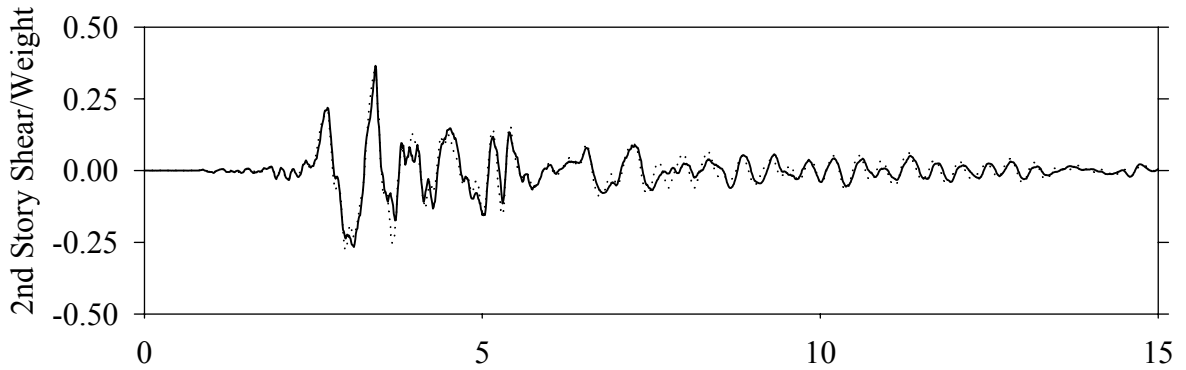
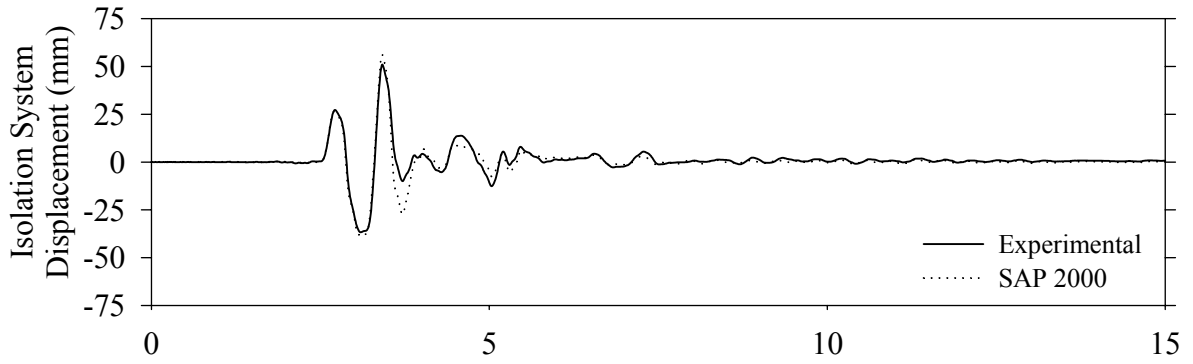
Test LCSBK10.1, Kobe 100%, SB/Low Damping Elastomeric with Lead Core



Test LCSBK10.1, Kobe 100%, SB/Low Damping Elastomeric with Lead Core

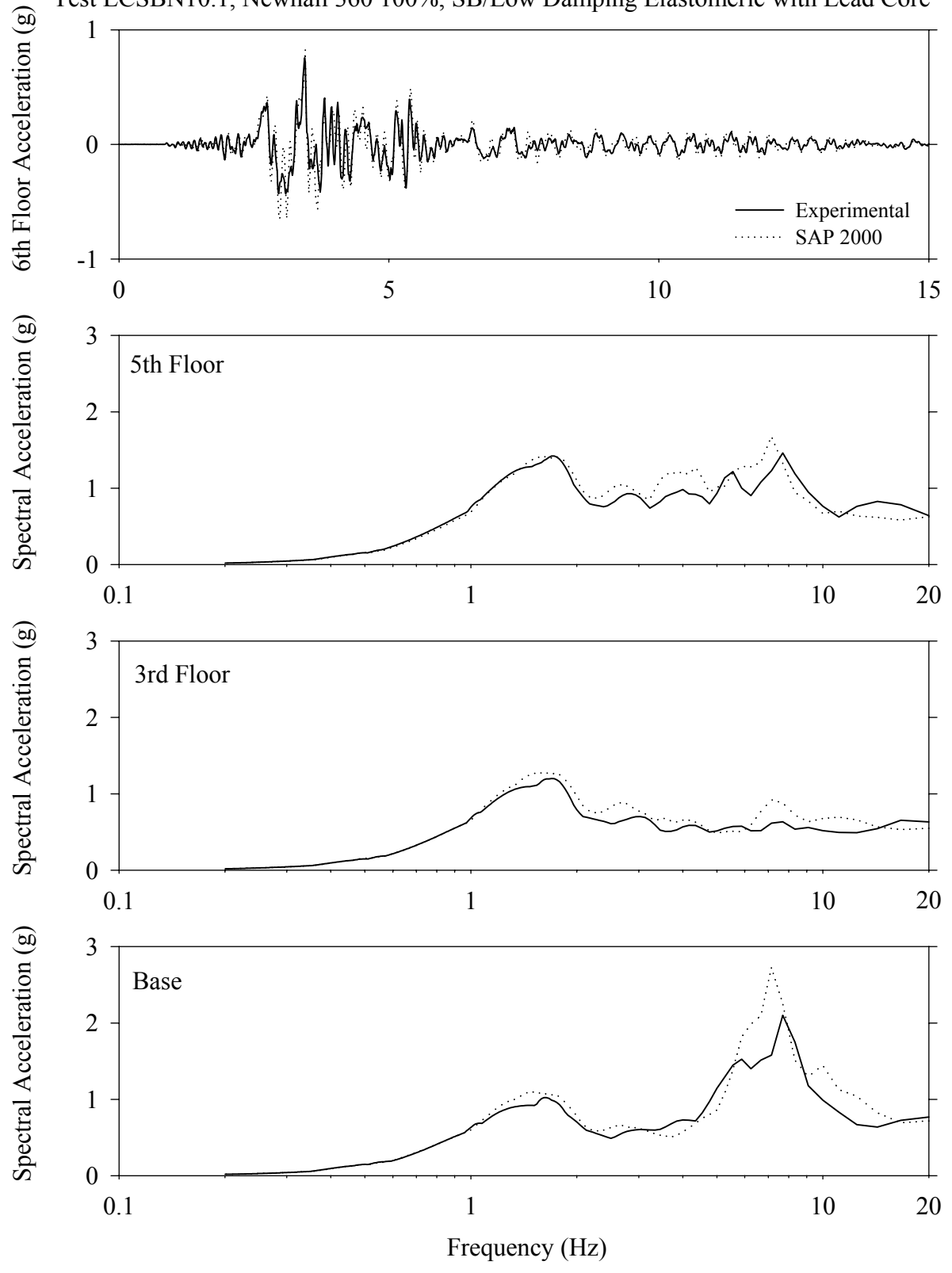


Test LCSBN10.1, Newhall 360 100%, SB/Low Damping Elastomeric with Lead Core

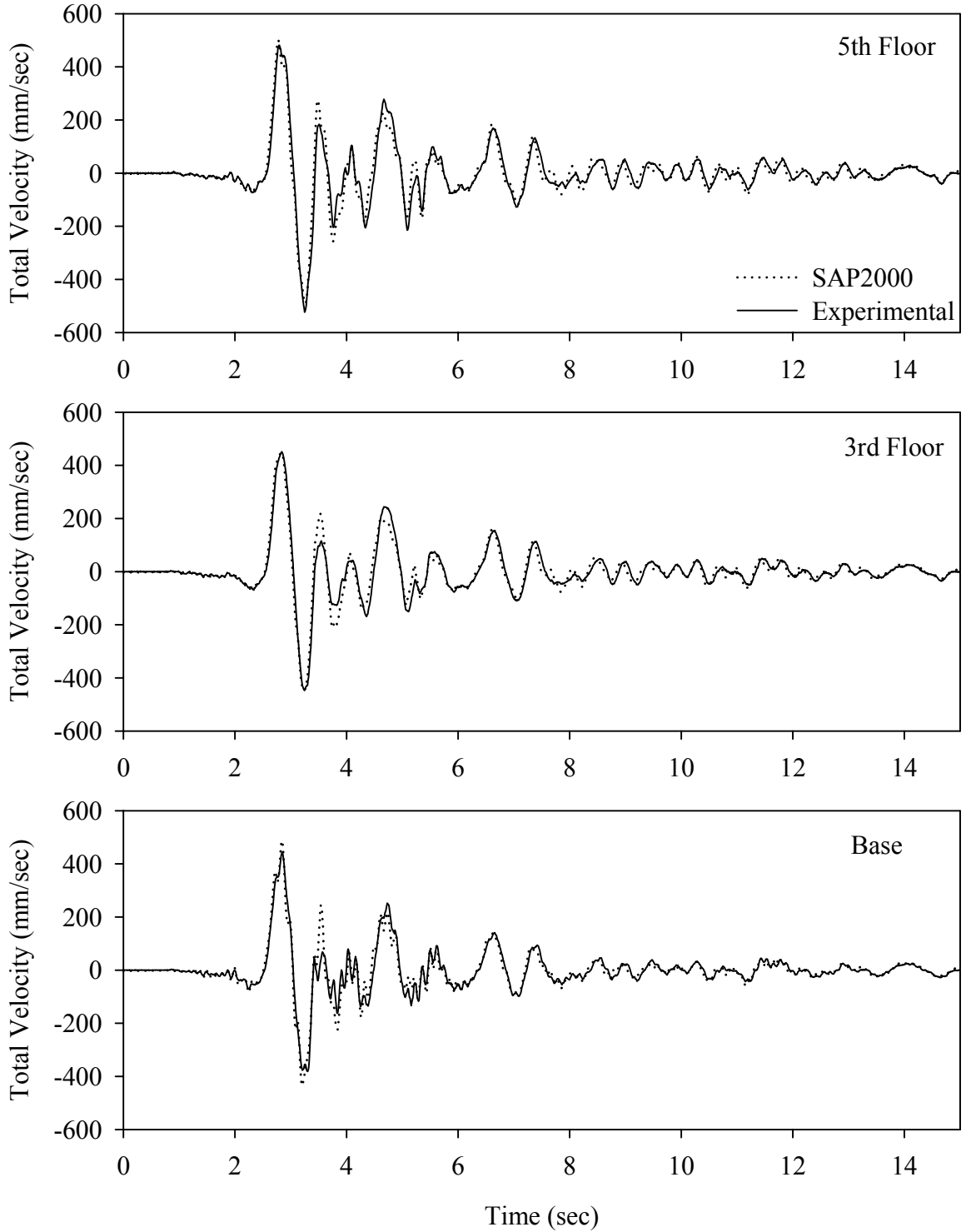




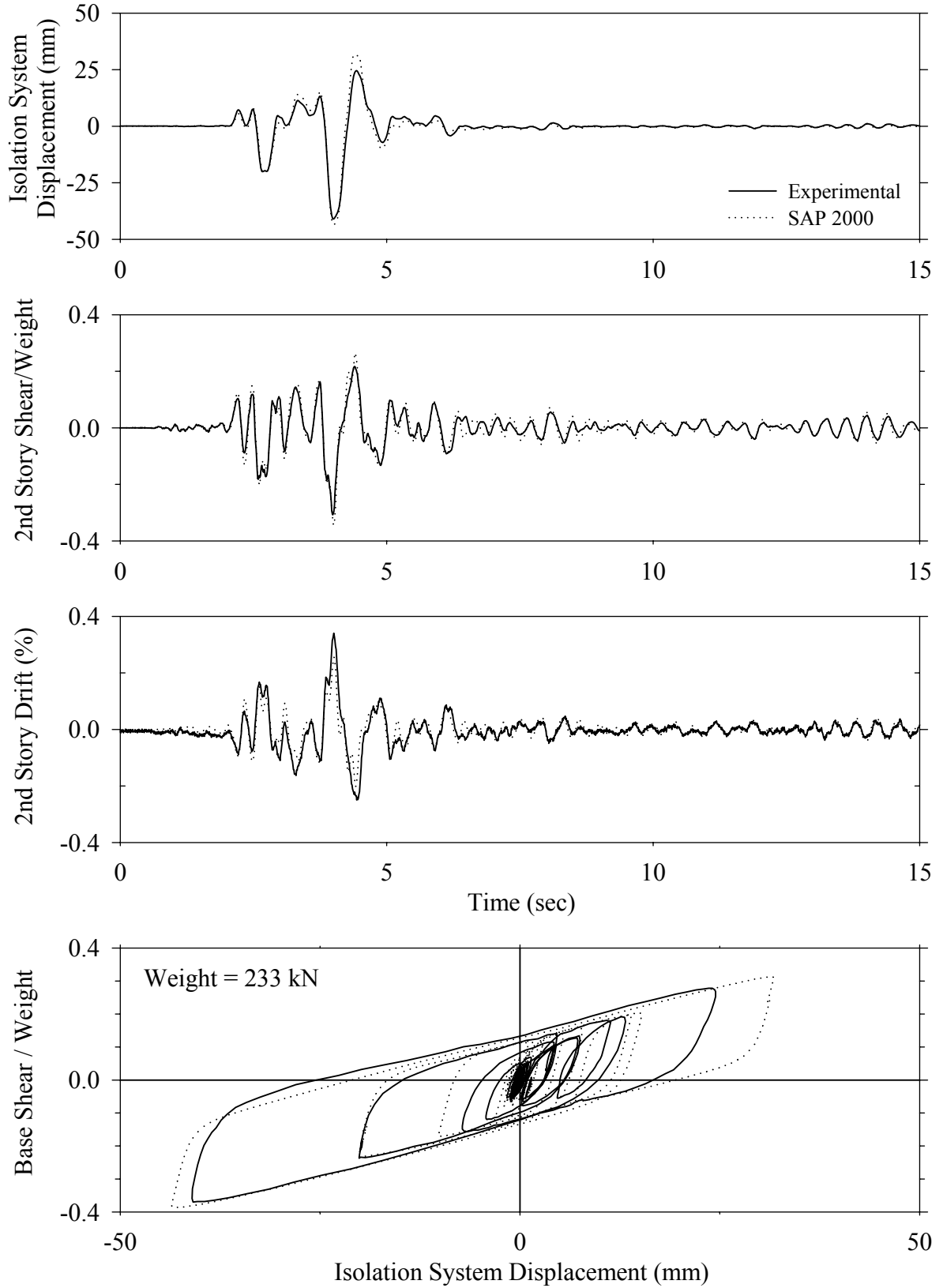
Test LCSBN10.1, Newhall 360 100%, SB/Low Damping Elastomeric with Lead Core



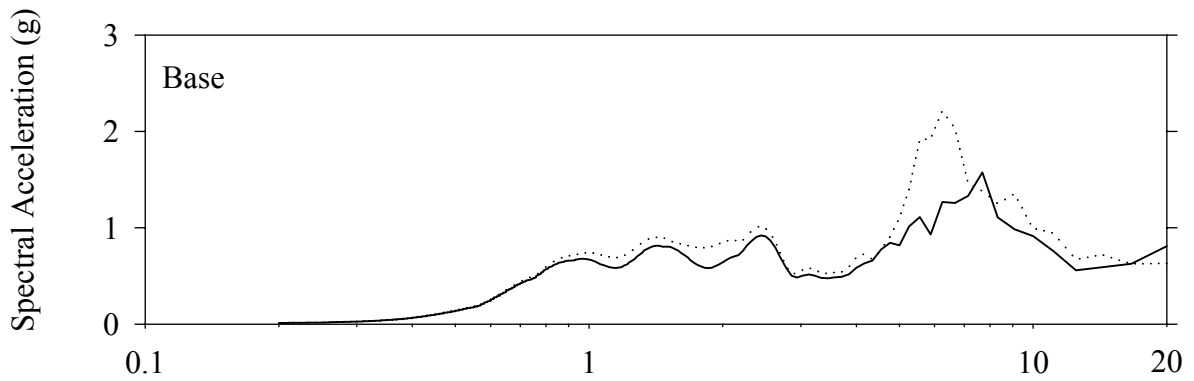
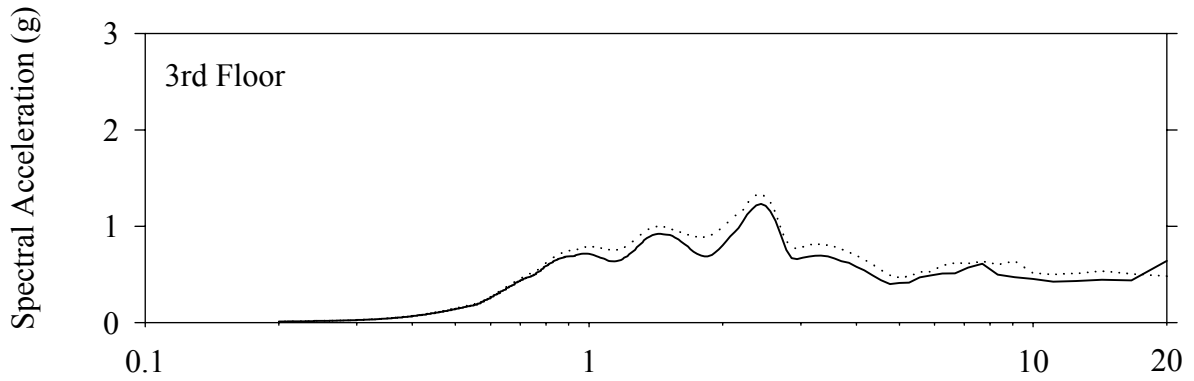
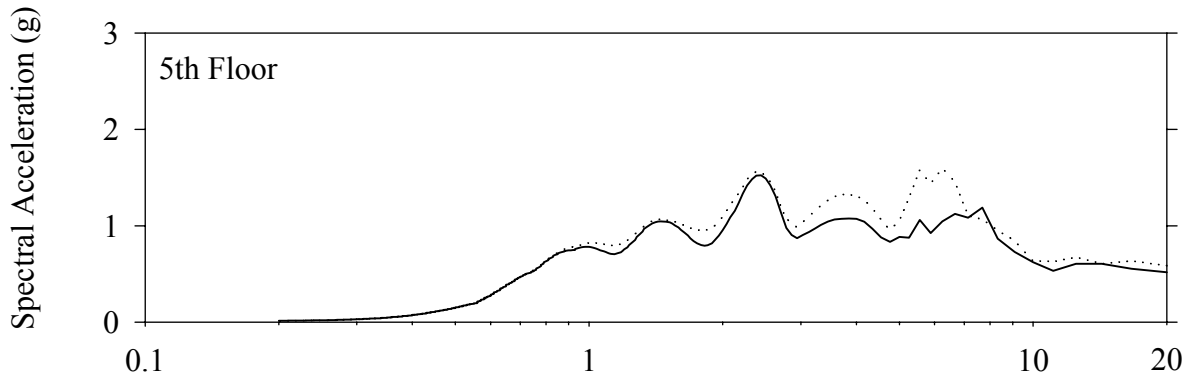
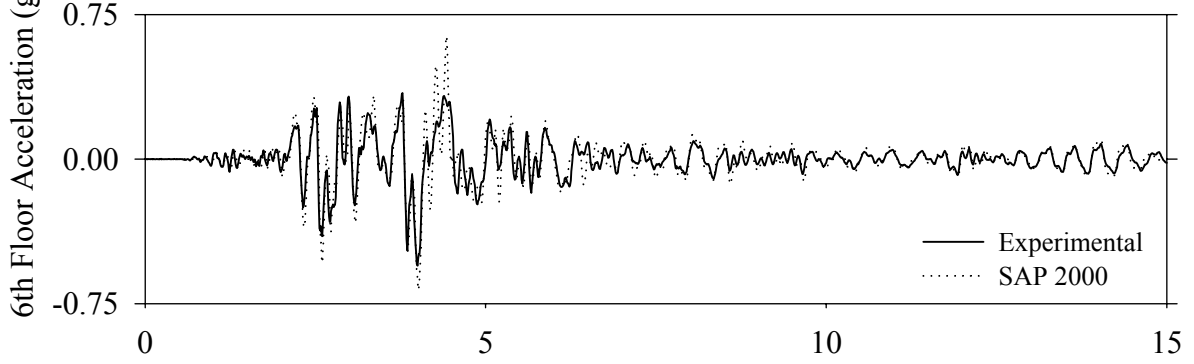
Test LCSBN10.1, Newhall 360 100%, SB/Low Damping Elastomeric with Lead Core



Test LCSBS10.1, Sylmar 100%, SB/Low Damping Elastomeric with Lead Core

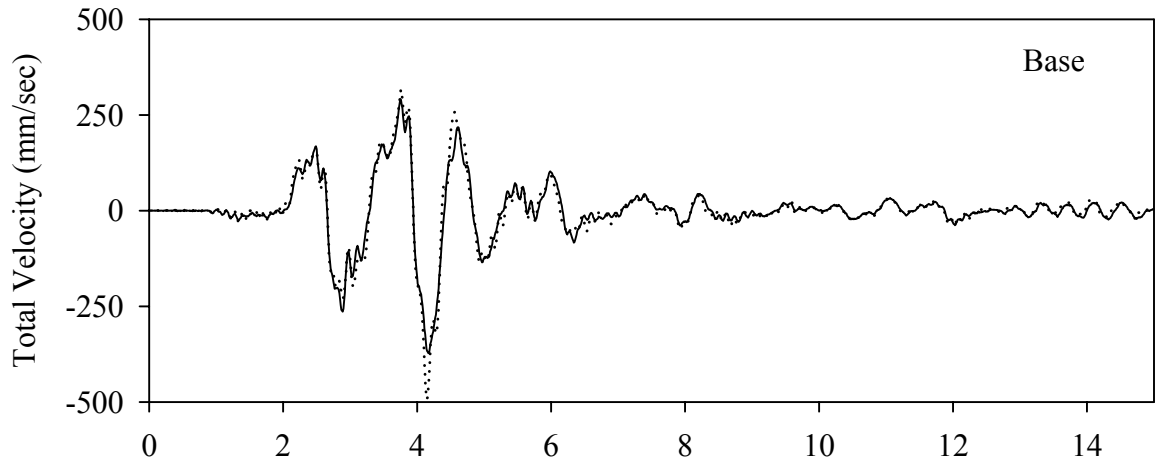
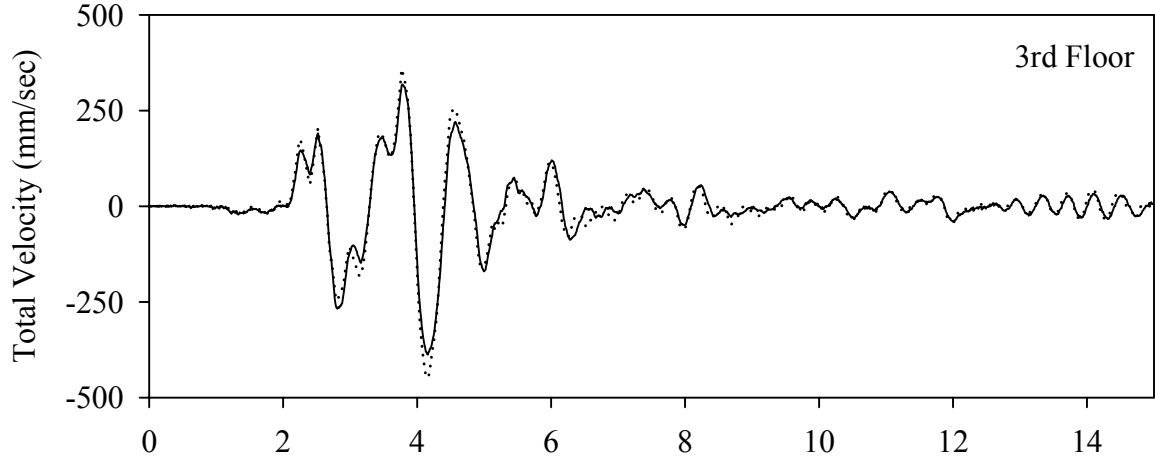
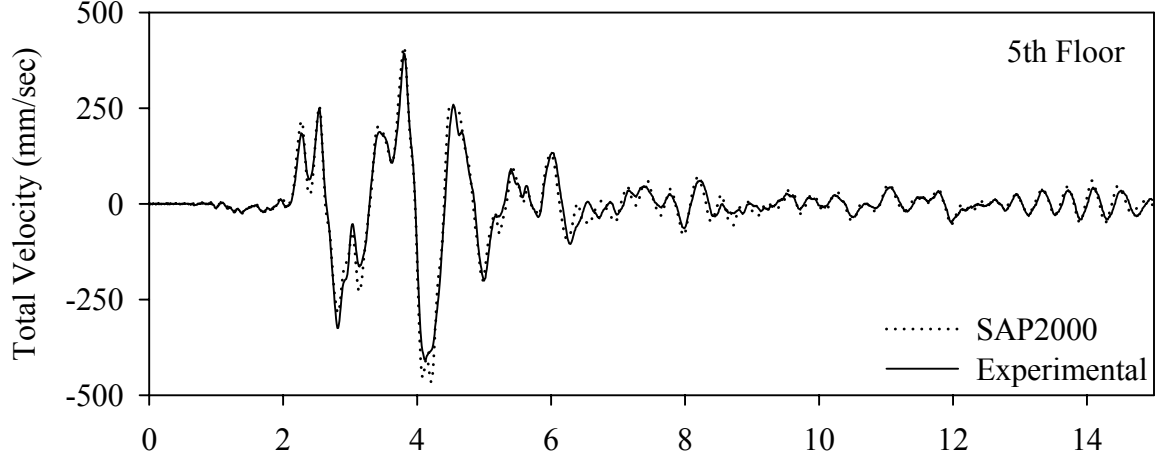


Test LCSBS10.1, Sylmar 100%, SB/Low Damping Elastomeric with Lead Core



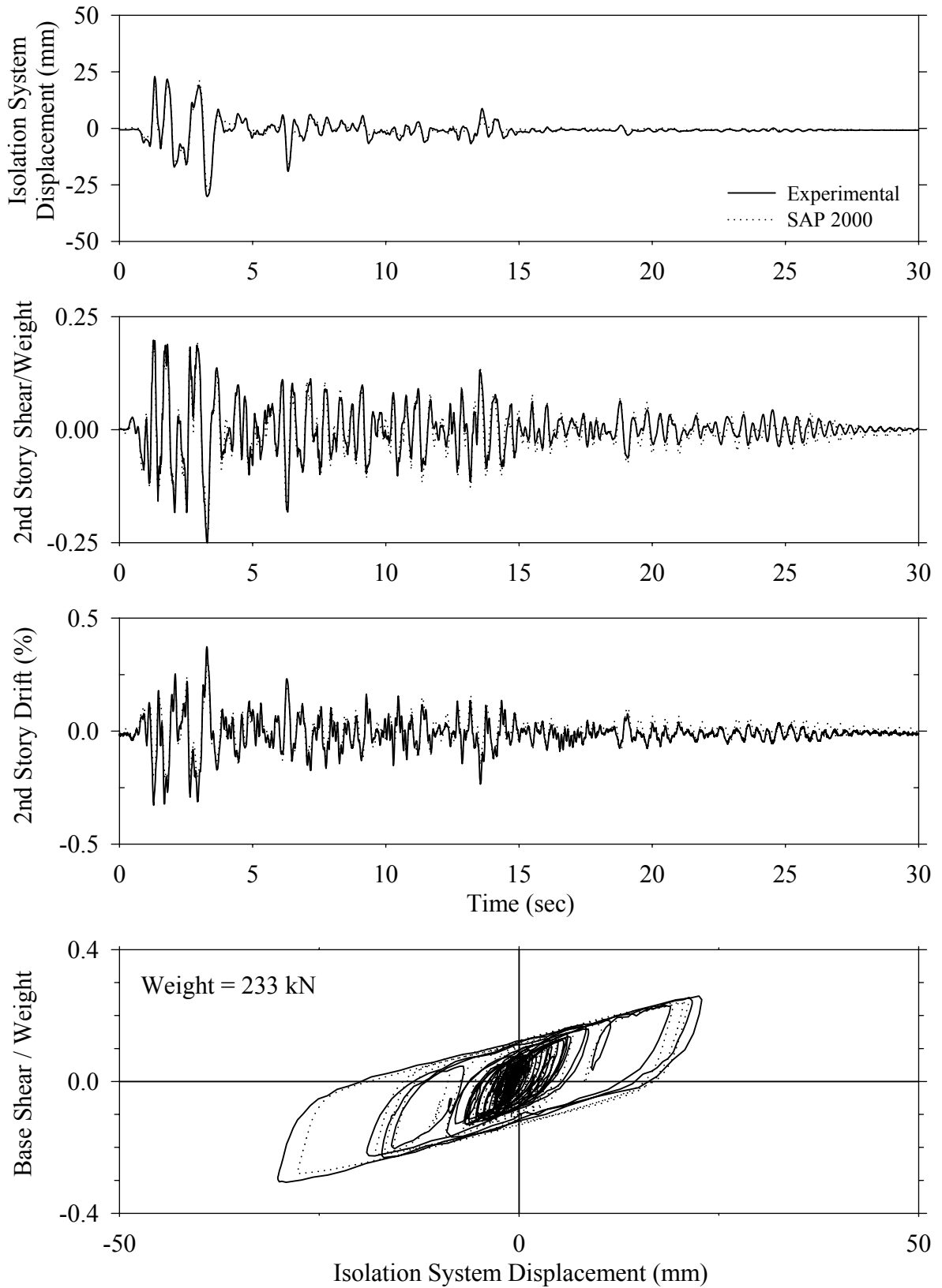
Frequency (Hz)

Test LCSBS10.1, Sylmar 100%, SB/Low Damping Elastomeric with Lead Core

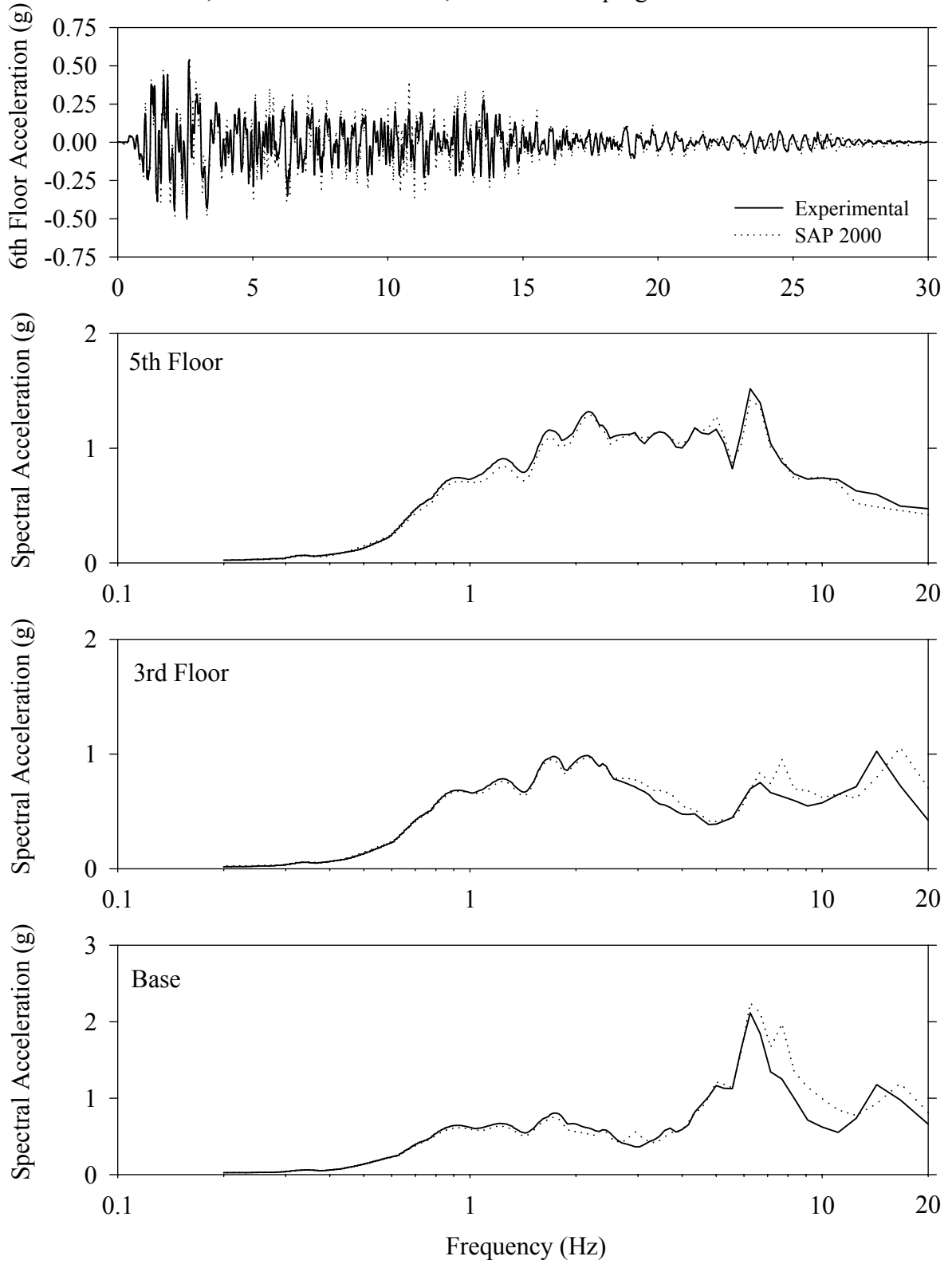


Time (sec)

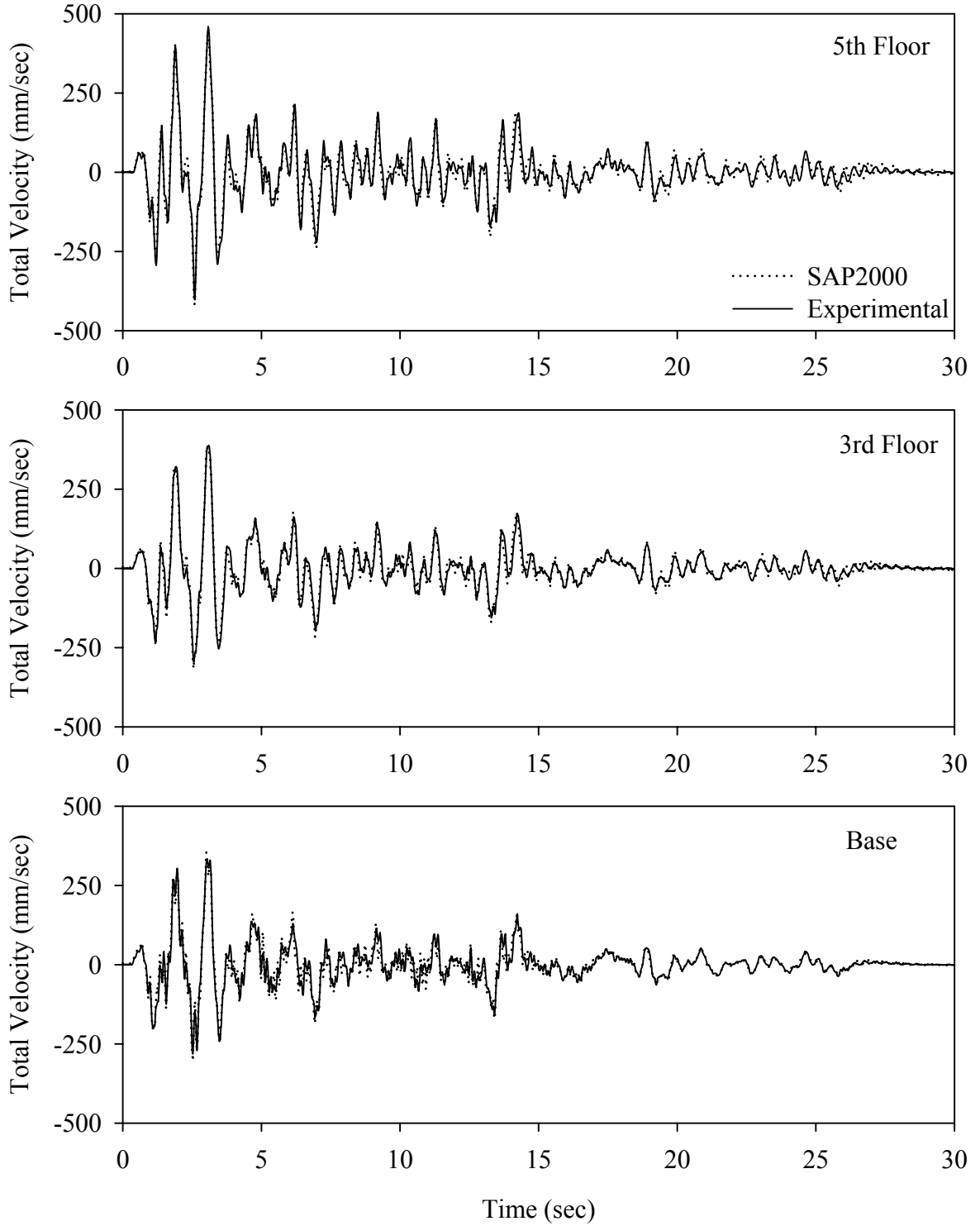
Test LCABE20.1, El Centro S00E 200%, AB/Low Damping Elastomeric with Lead Core



Test LCABE20.1, El Centro S00E 200%, AB/Low Damping Elastomeric with Lead Core

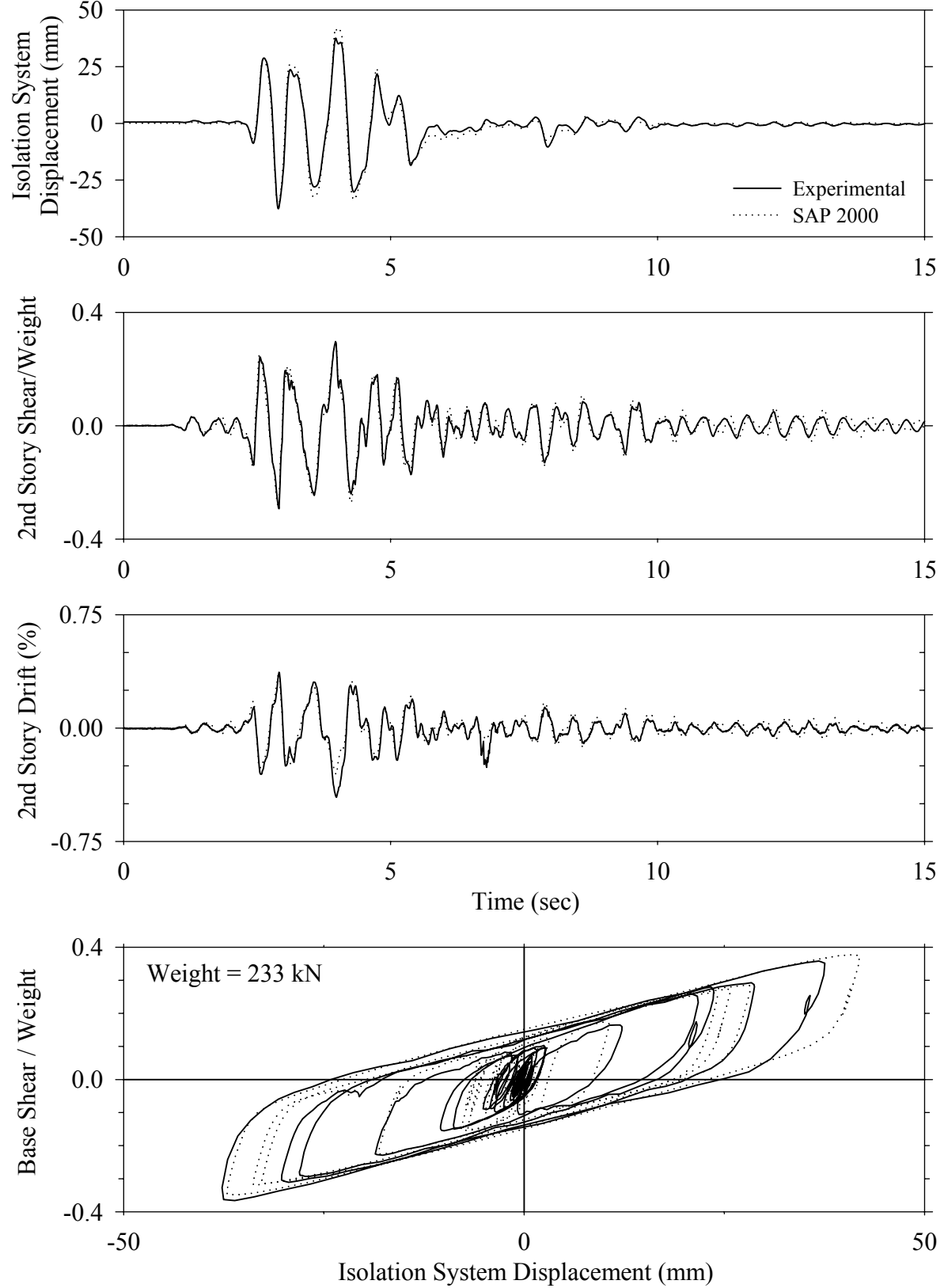


Test LCABE20.1, El Centro S00E 200%, AB/Low Damping Elastomeric with Lead Core

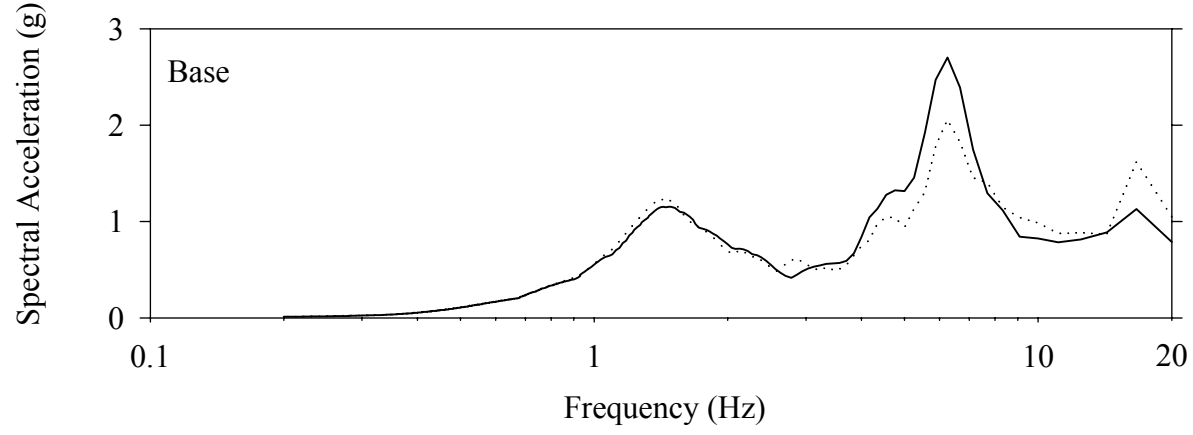
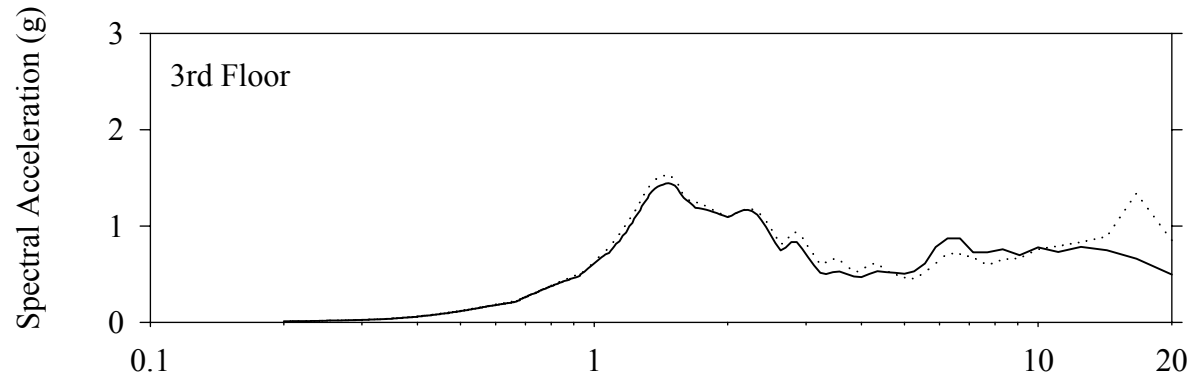
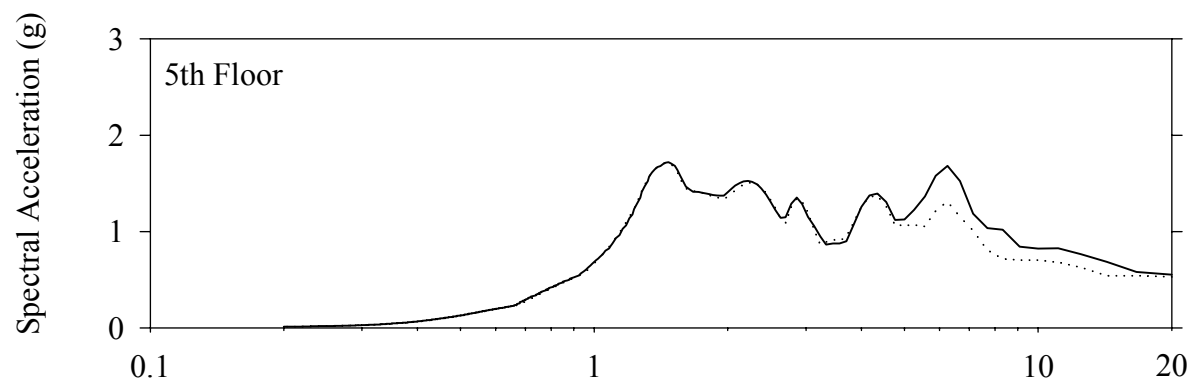
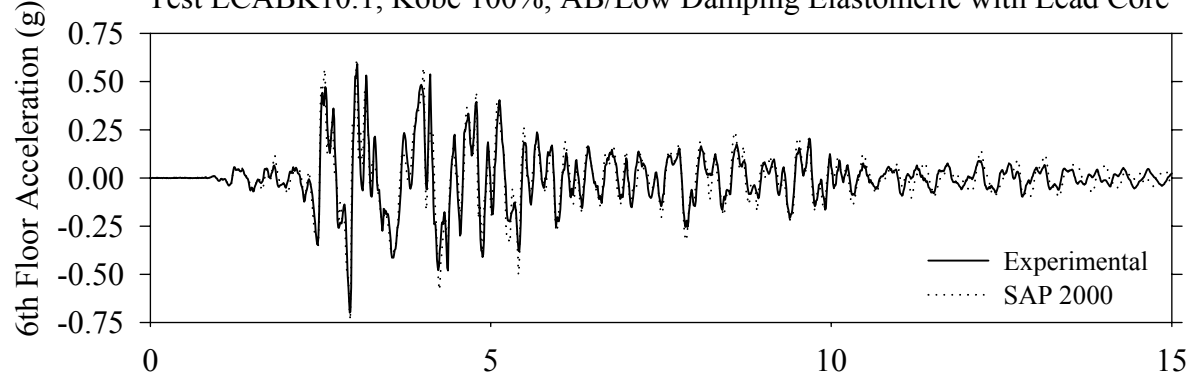




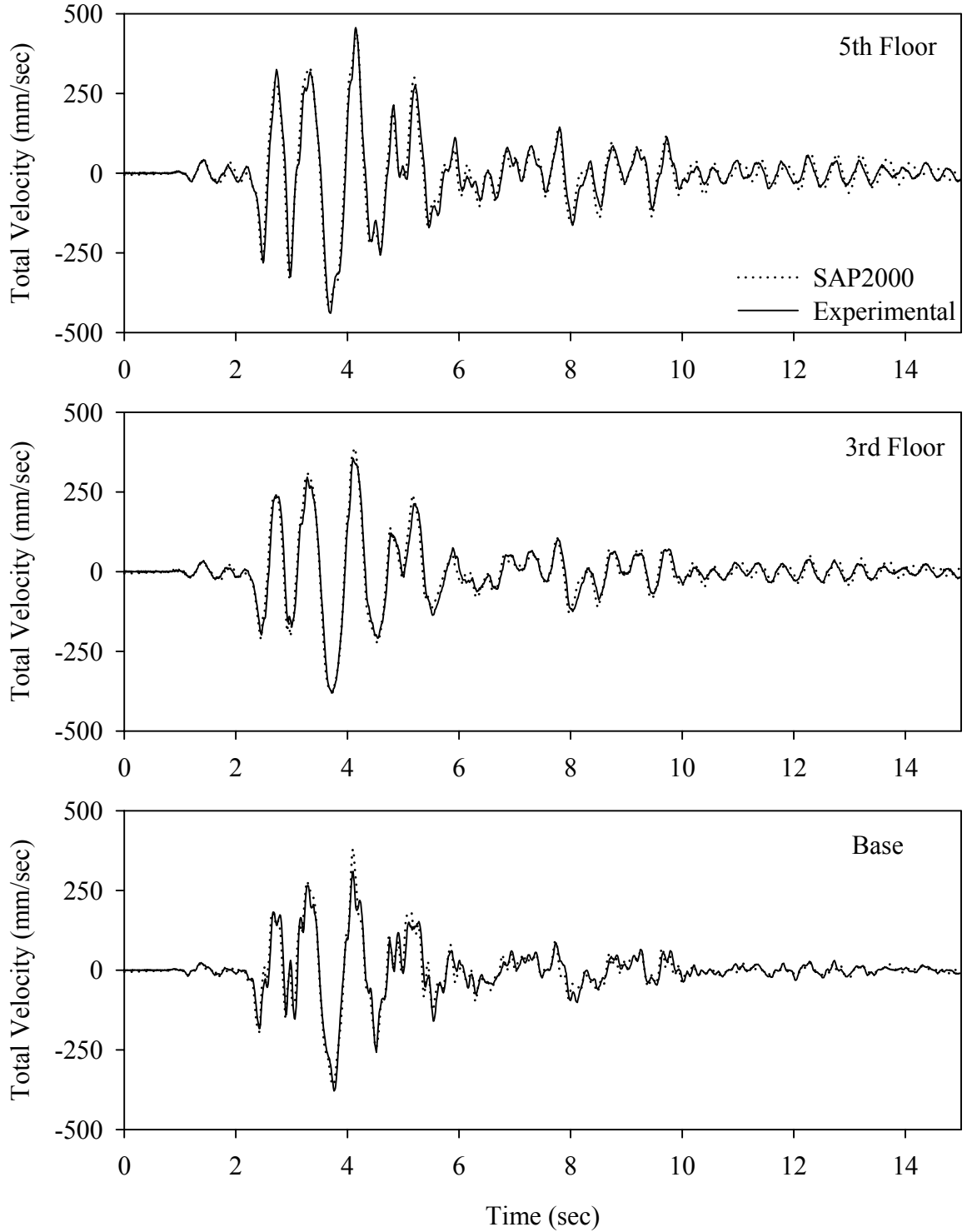
Test LCABK10.1, Kobe 100%, AB/Low Damping Elastomeric with Lead Core



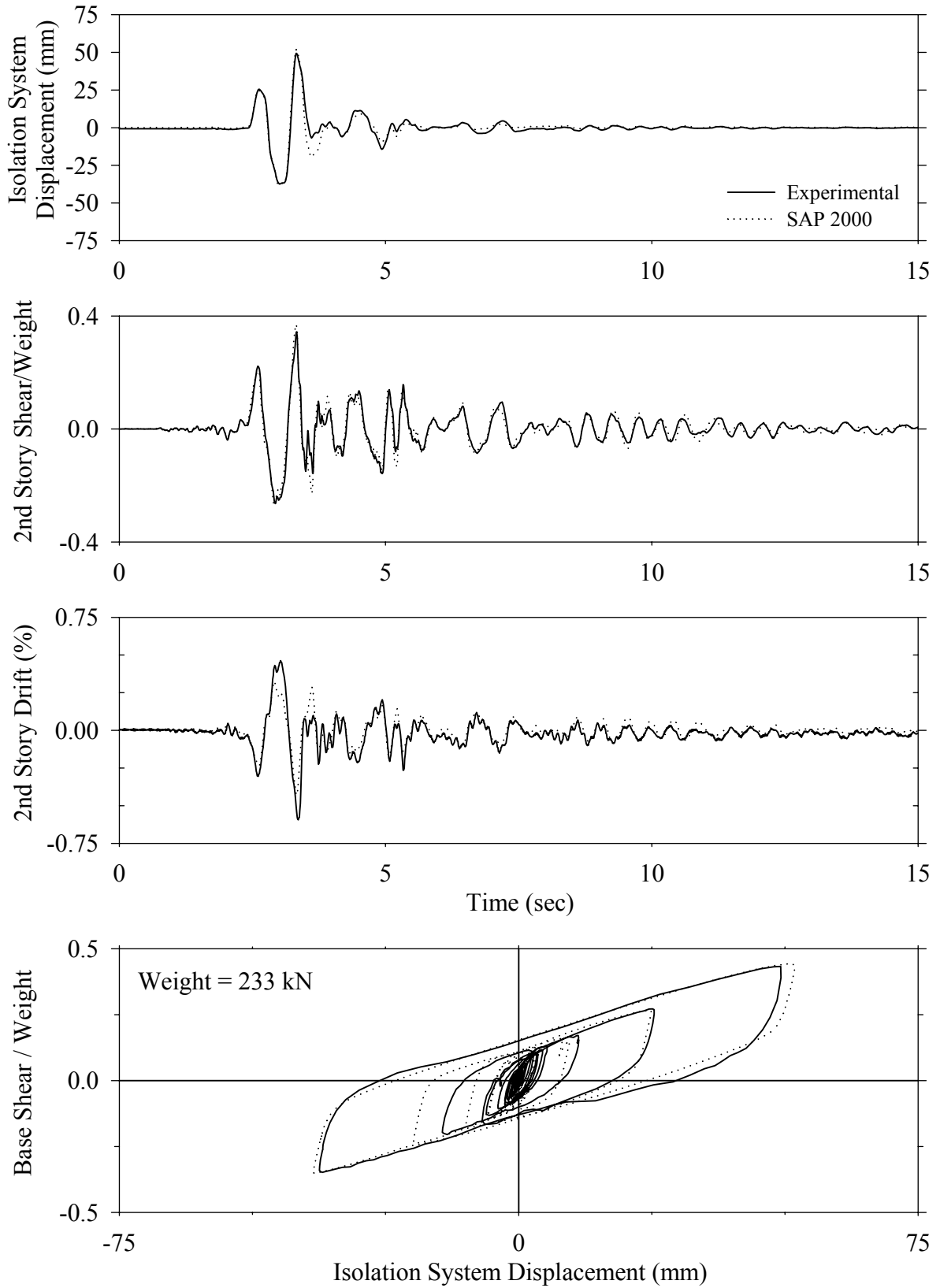
Test LCABK10.1, Kobe 100%, AB/Low Damping Elastomeric with Lead Core



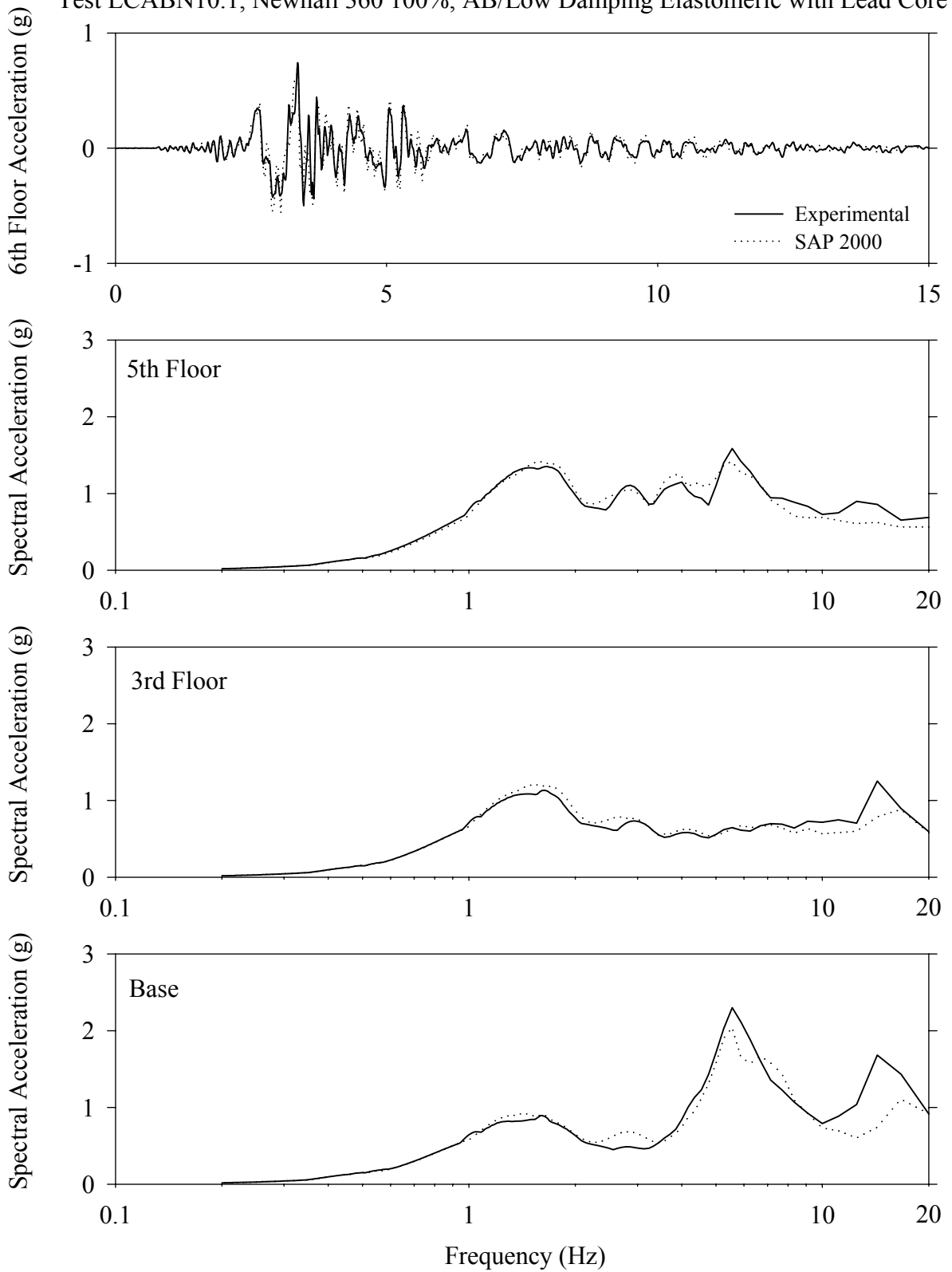
Test LCABK10.1, Kobe 100%, AB/Low Damping Elastomeric with Lead Core



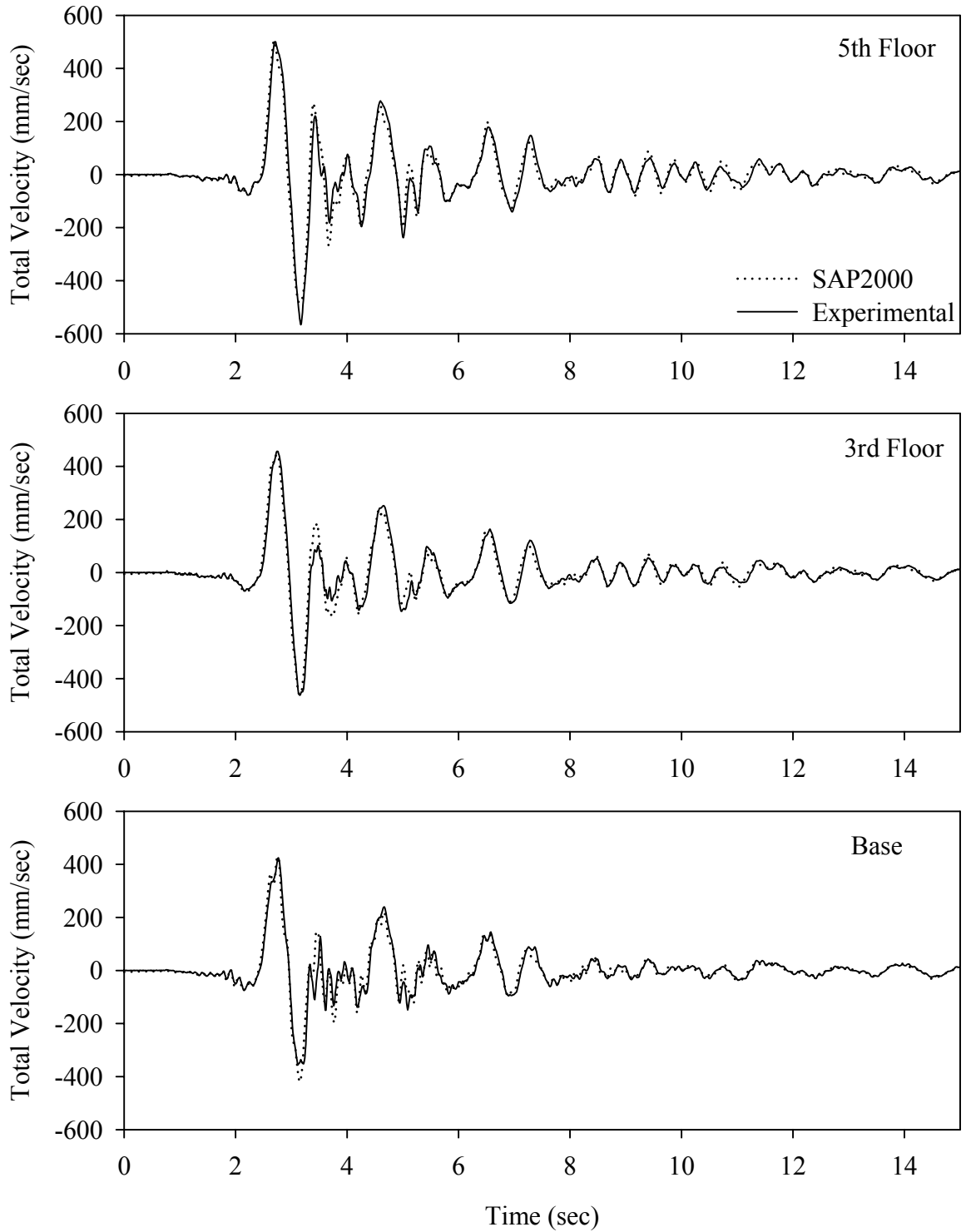
Test LCABN10.1, Newhall 360 100%, AB/Low Damping Elastomeric with Lead Core



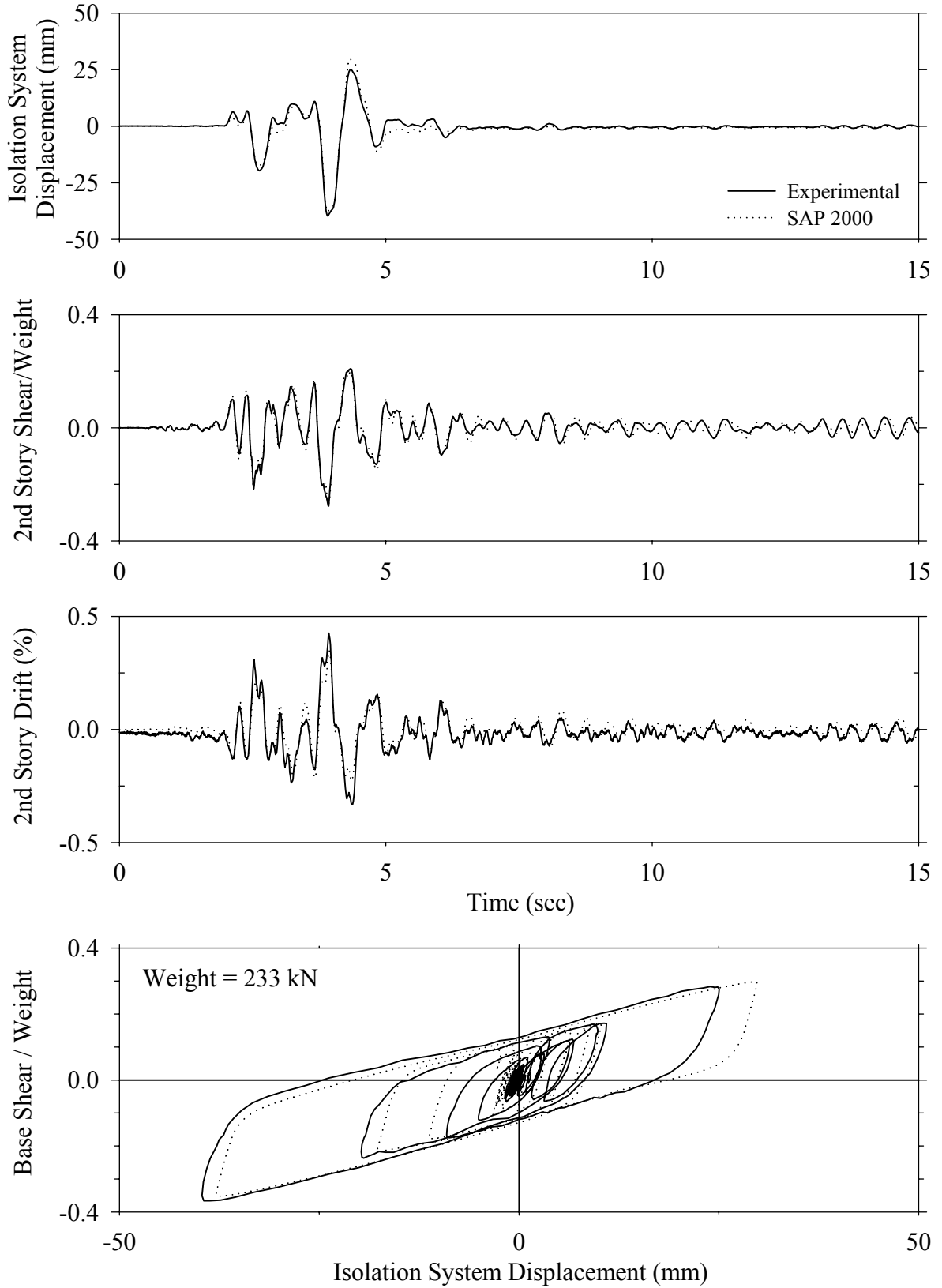
Test LCABN10.1, Newhall 360 100%, AB/Low Damping Elastomeric with Lead Core



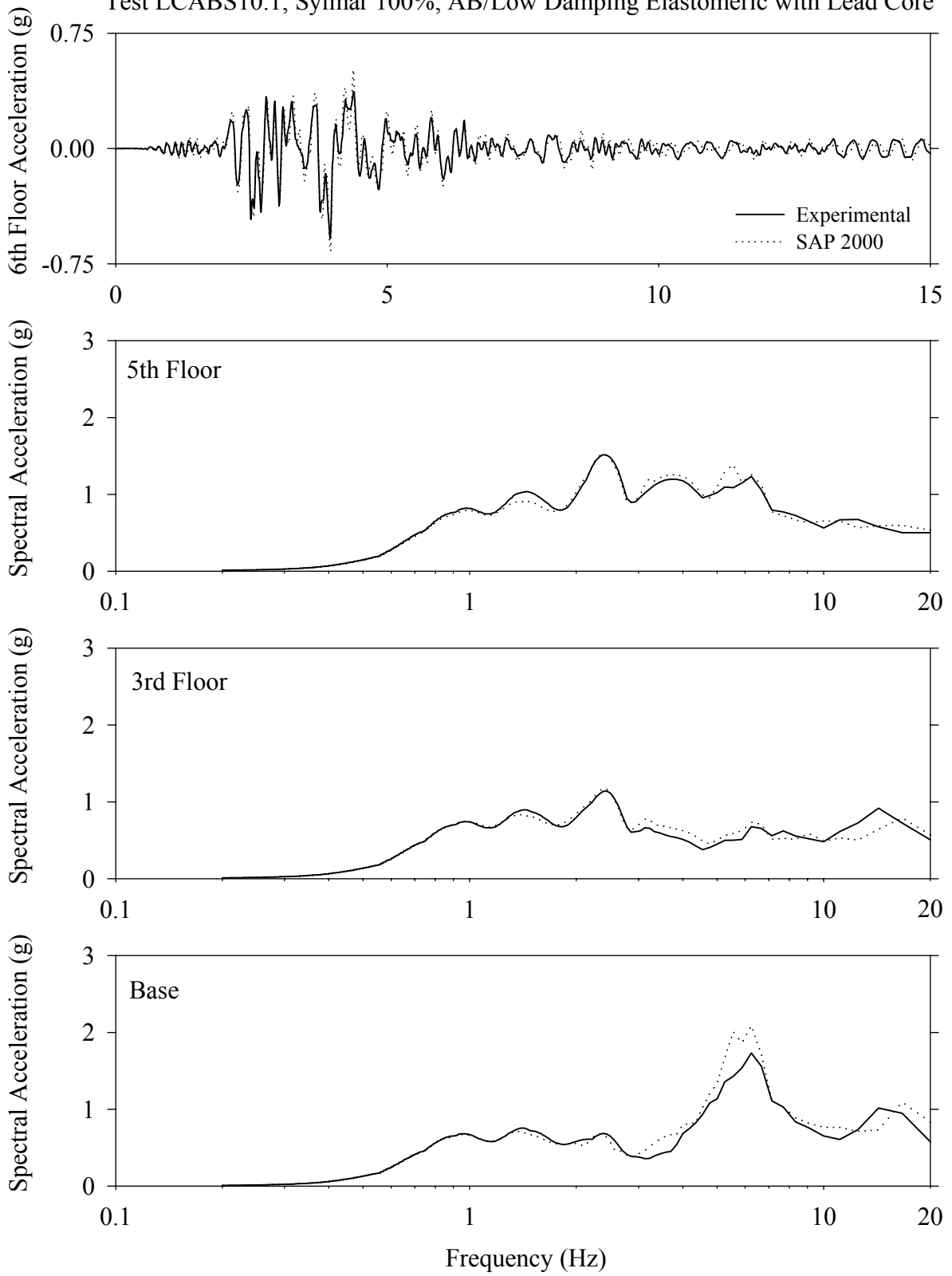
Test LCABN10.1, Newhall 360 100%, AB/Low Damping Elastomeric with Lead Core



Test LCABS10.1, Sylmar 100%, AB/Low Damping Elastomeric with Lead Core

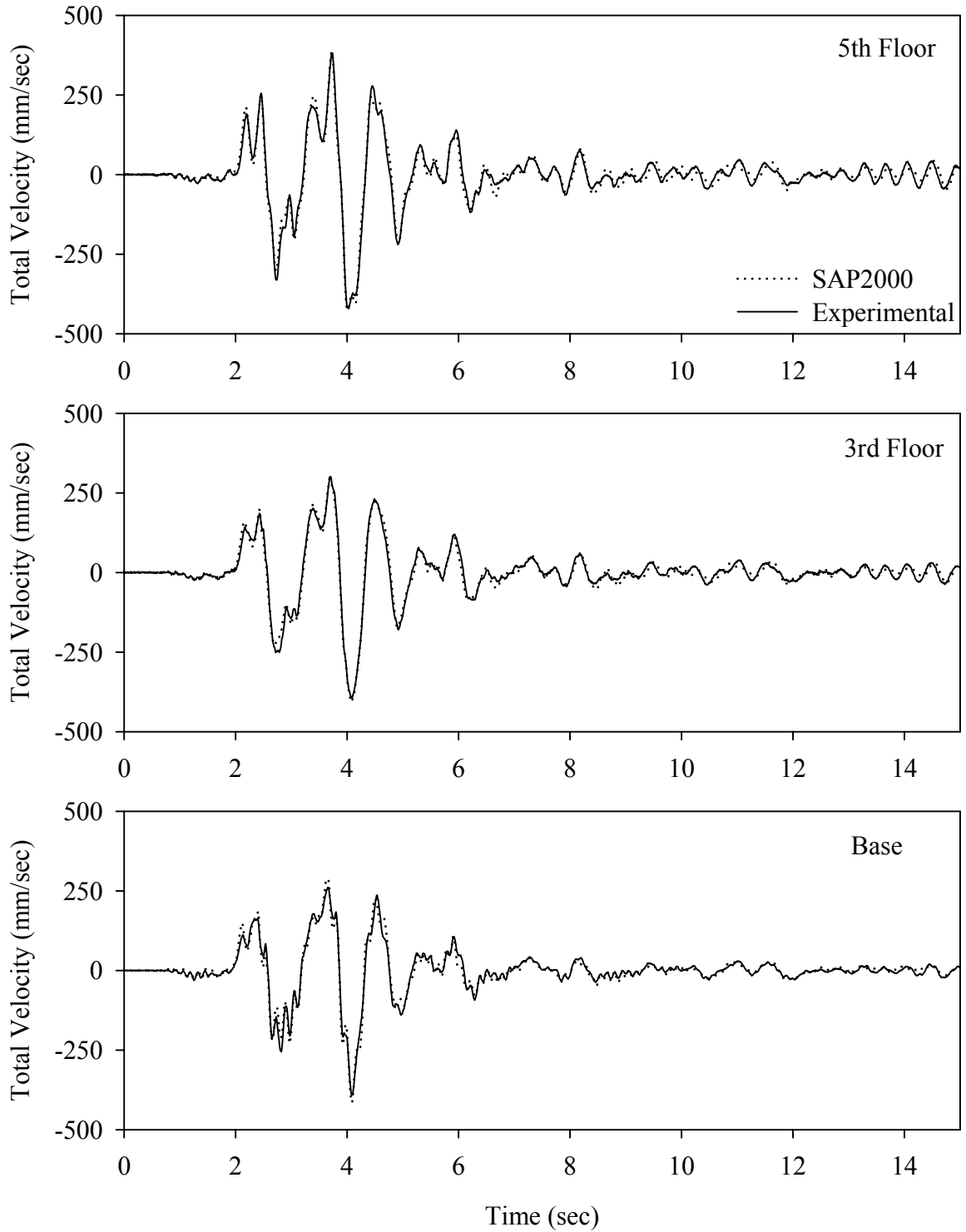


Test LCABS10.1, Sylmar 100%, AB/Low Damping Elastomeric with Lead Core

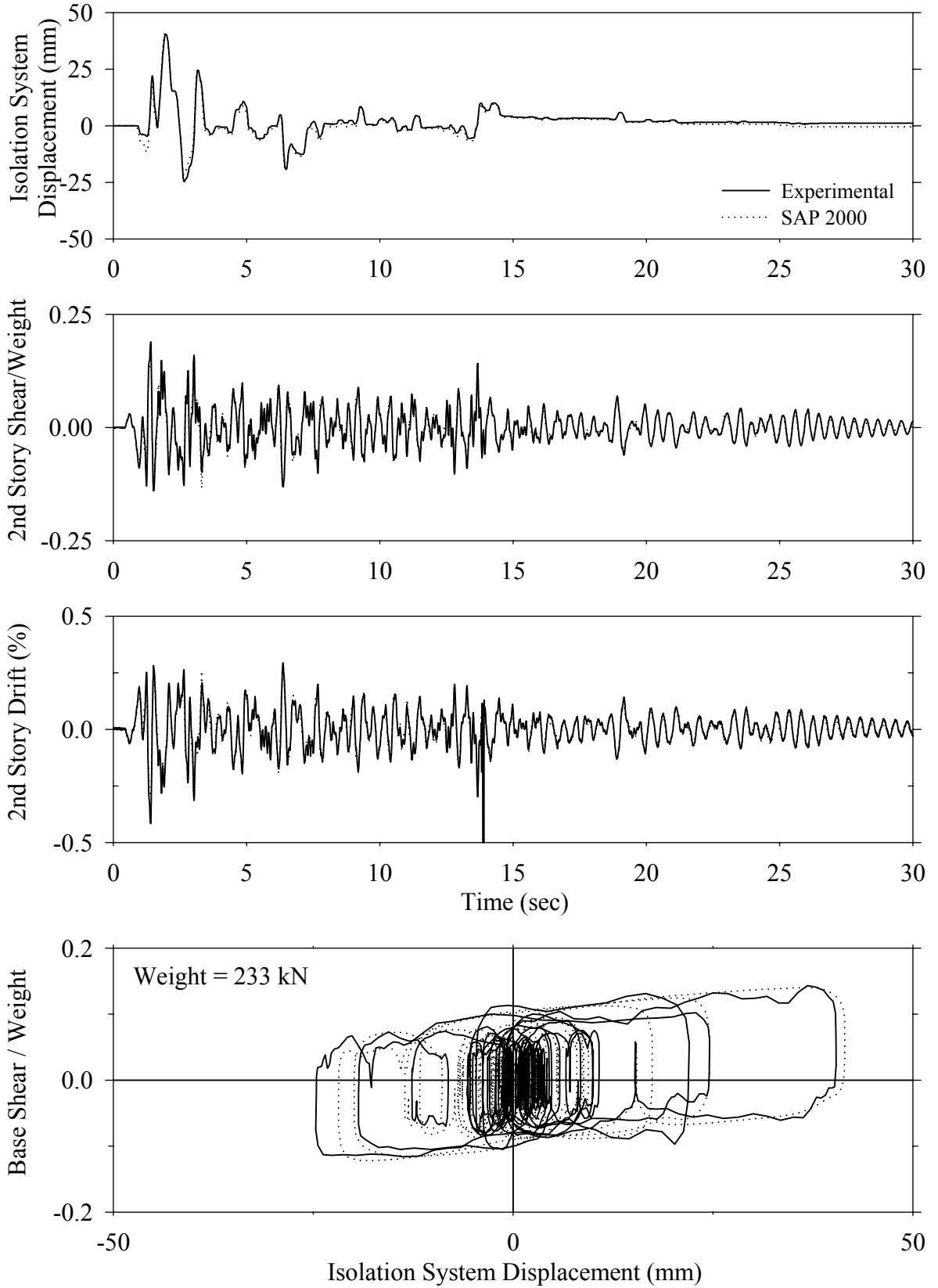




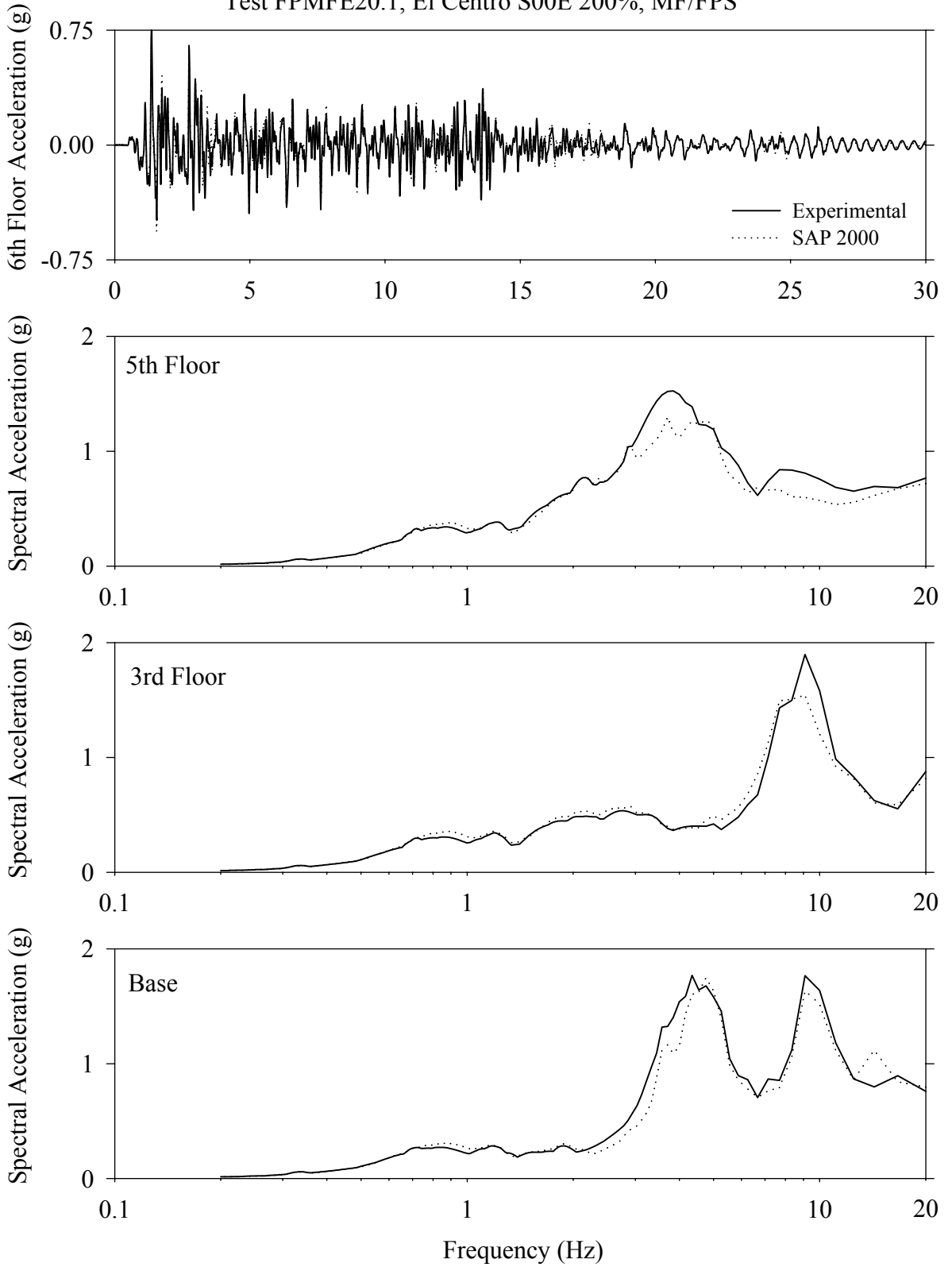
Test LCABS10.1, Sylmar 100%, AB/Low Damping Elastomeric with Lead Core



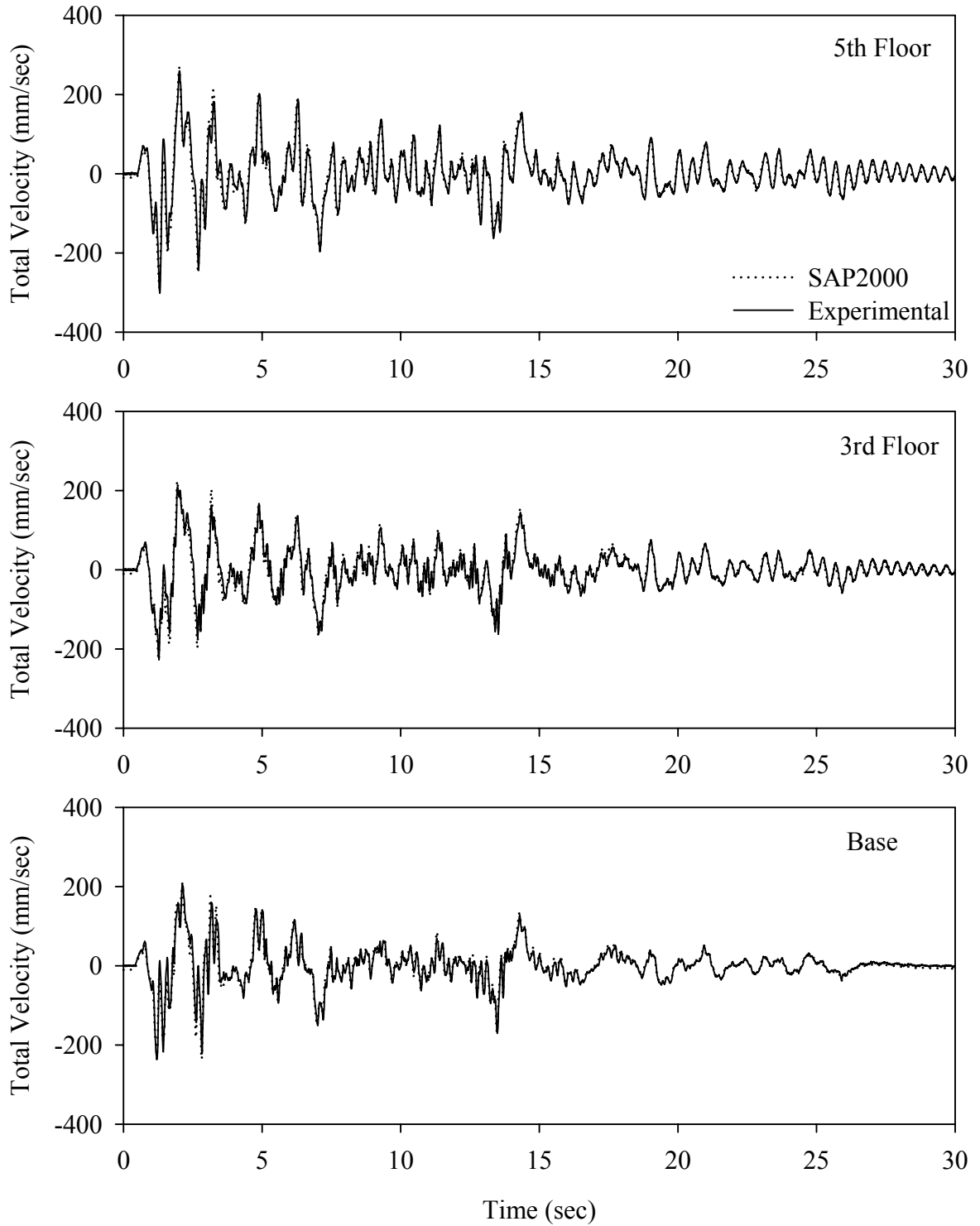
Test FPMFE20.1, El Centro S00E 200%, MF/FPS



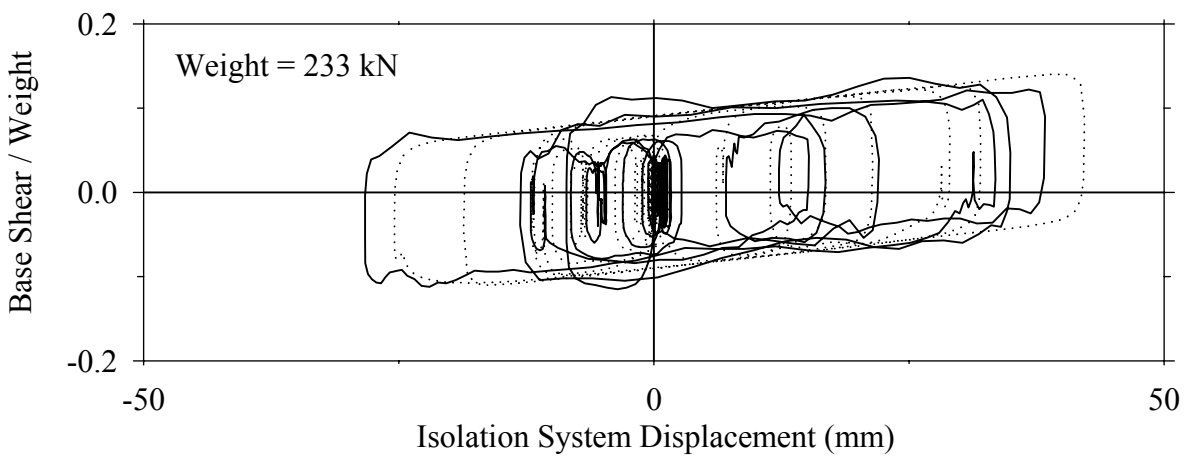
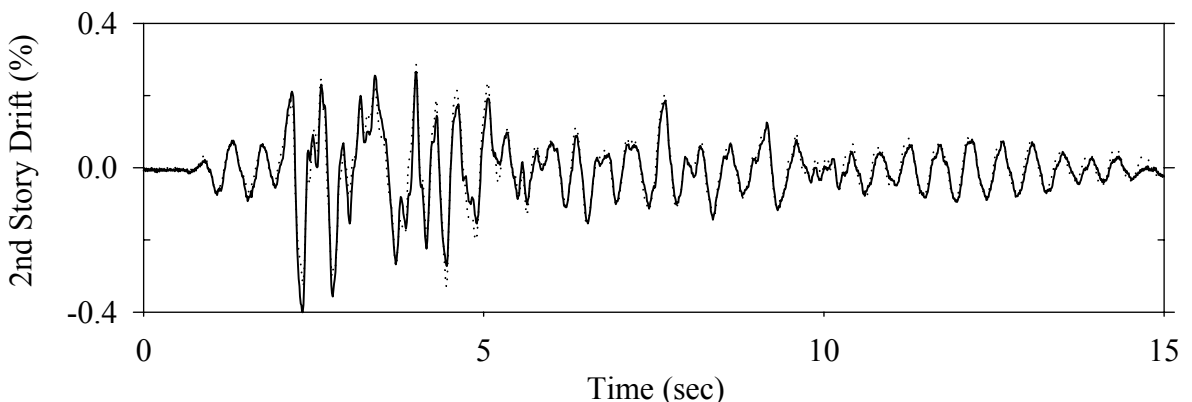
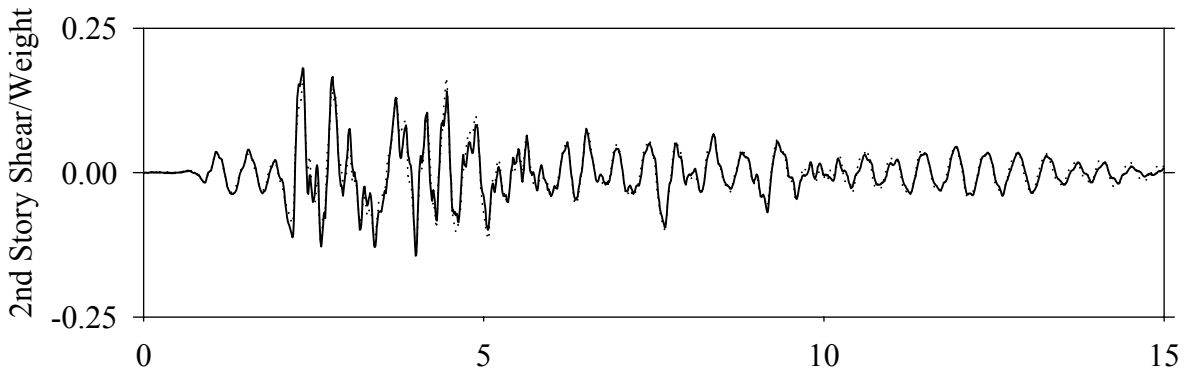
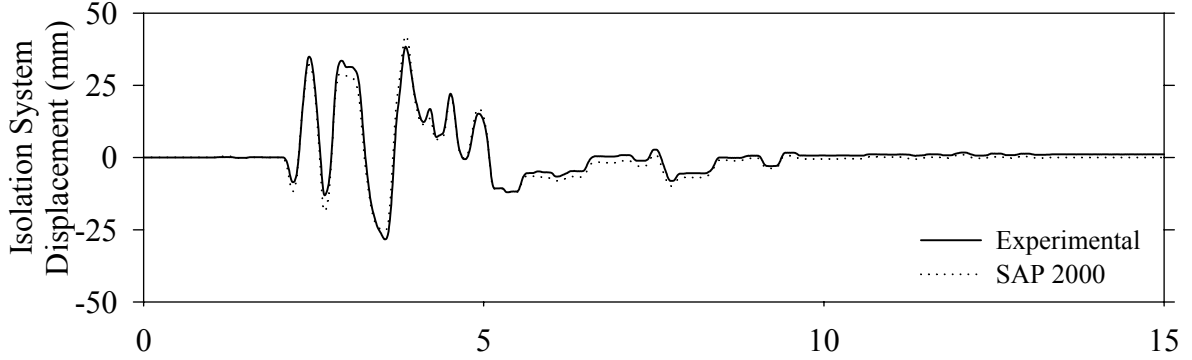
Test FPMFE20.1, El Centro S00E 200%, MF/FPS



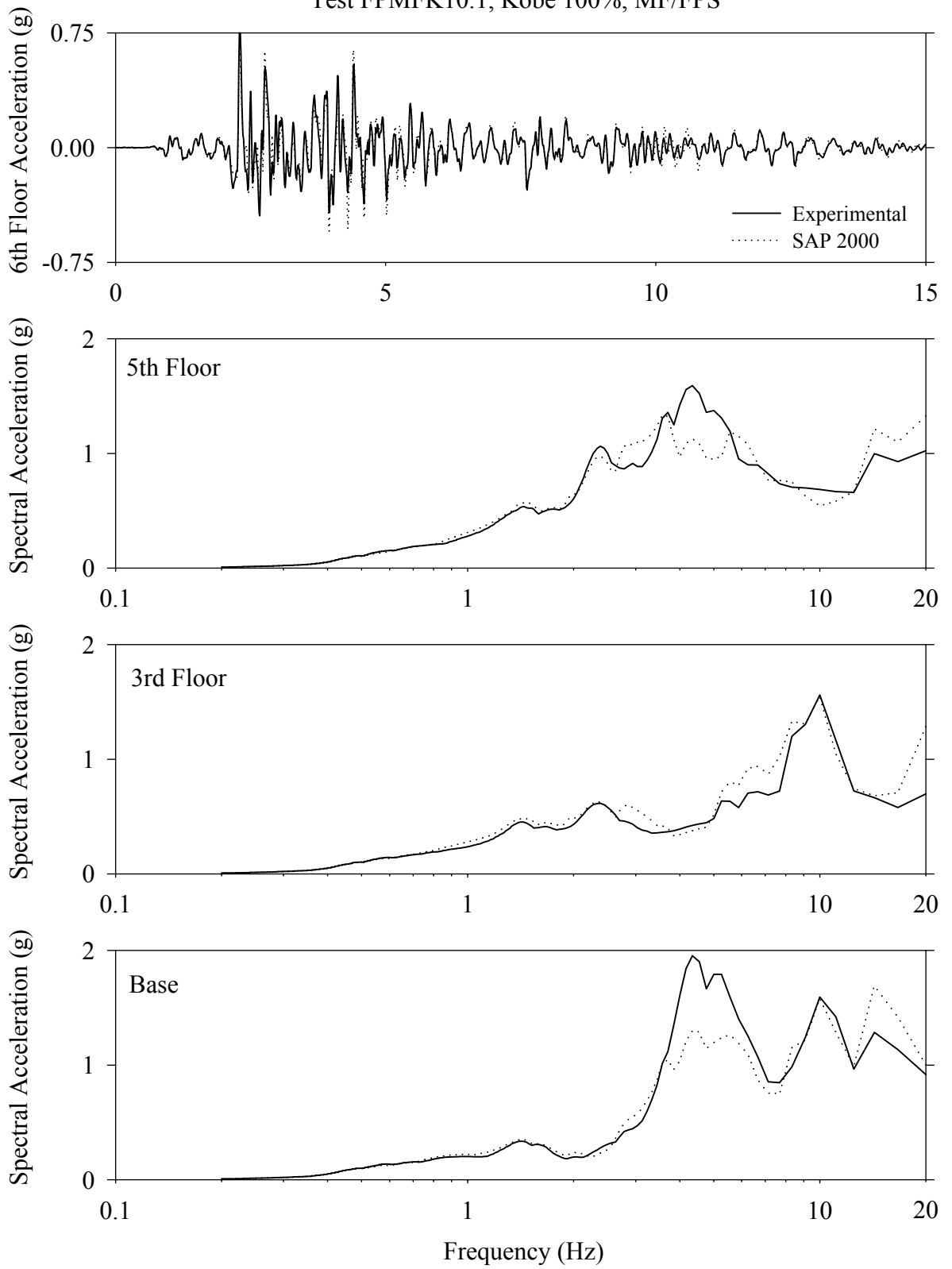
Test FPMFE20.1, El Centro S00E 200%, MF/FPS



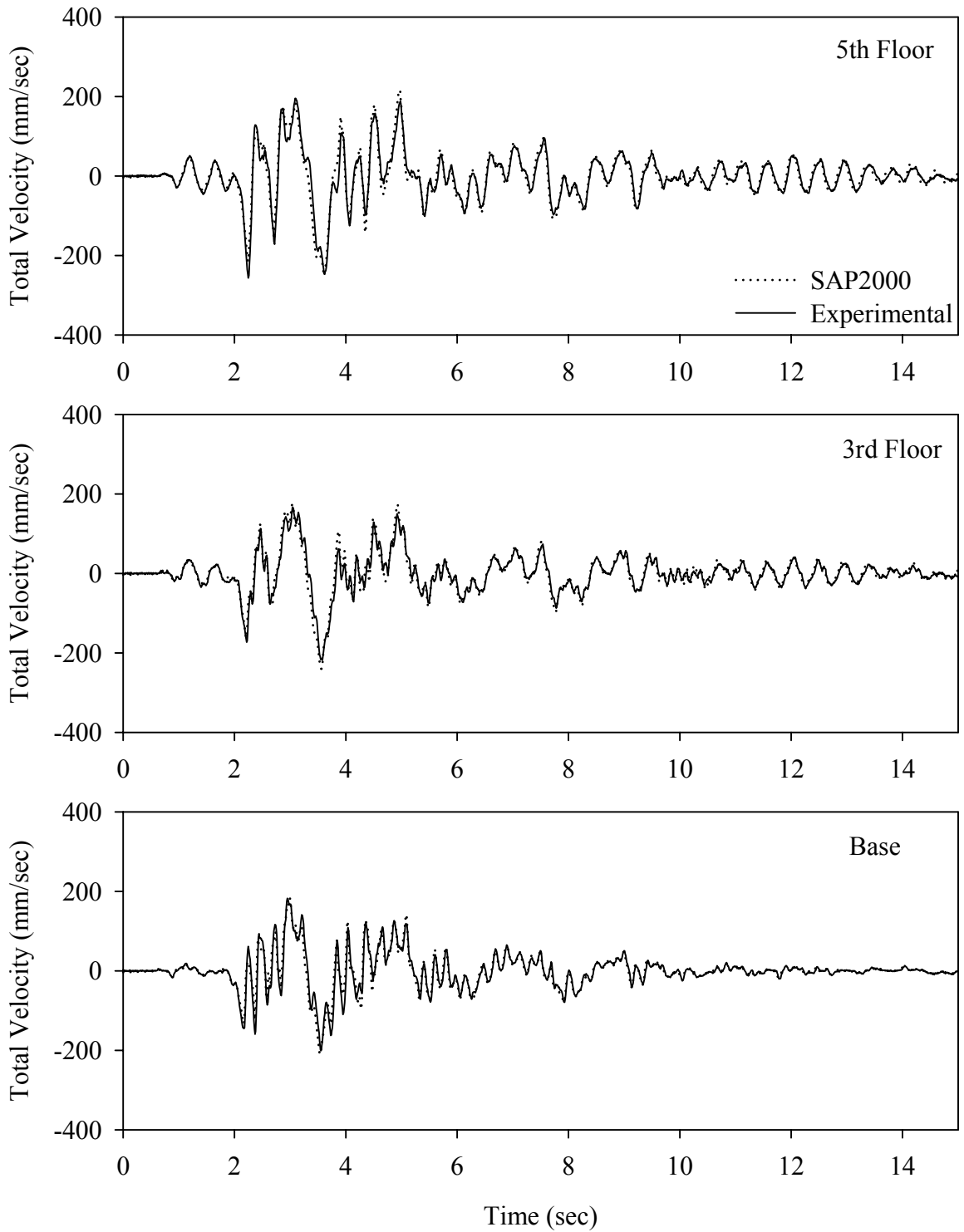
Test FPMFK10.1, Kobe 100%, MF/FPS



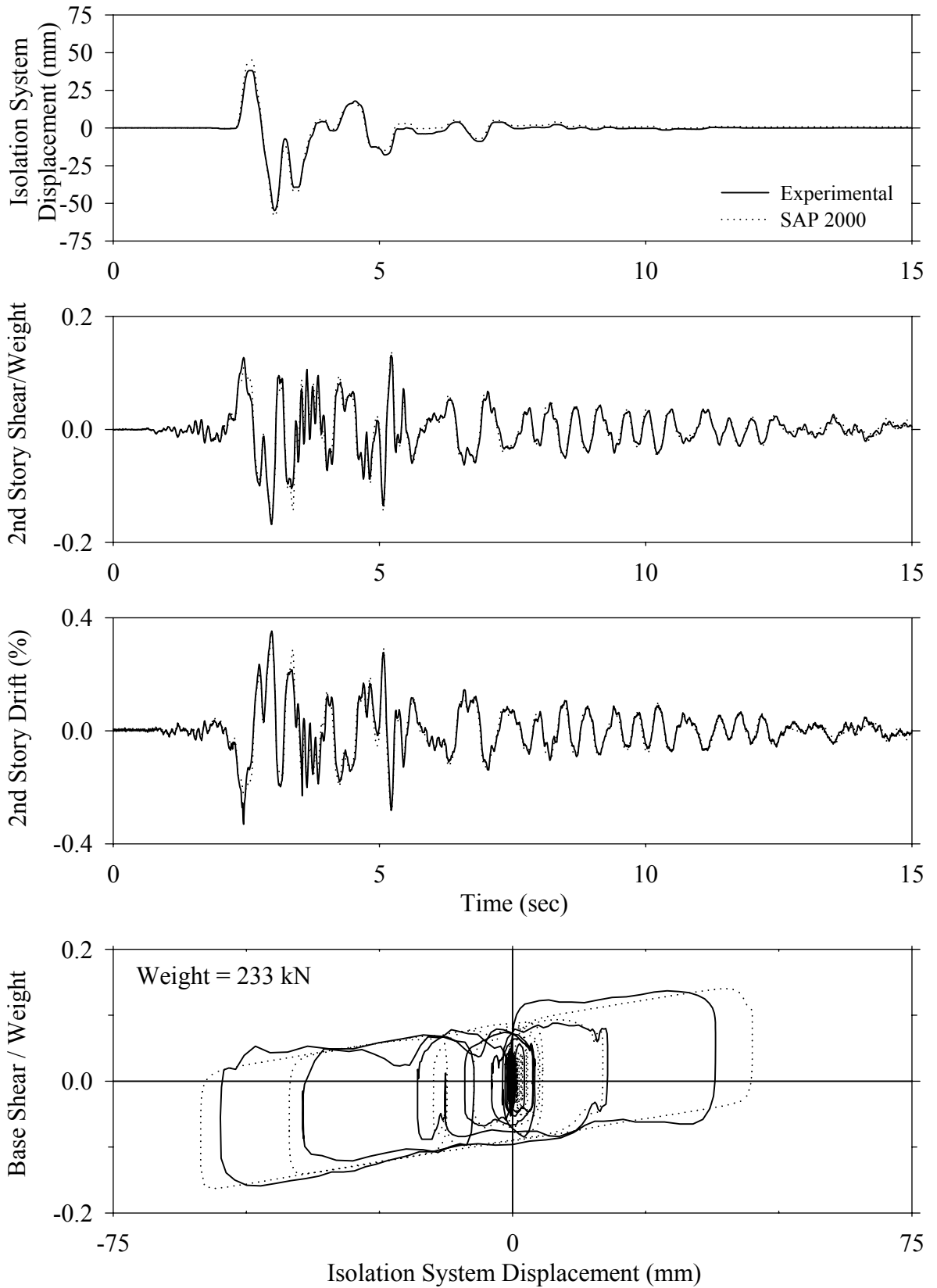
Test FPMFK10.1, Kobe 100%, MF/FPS



Test FPMFK10.1, Kobe 100%, MF/FPS

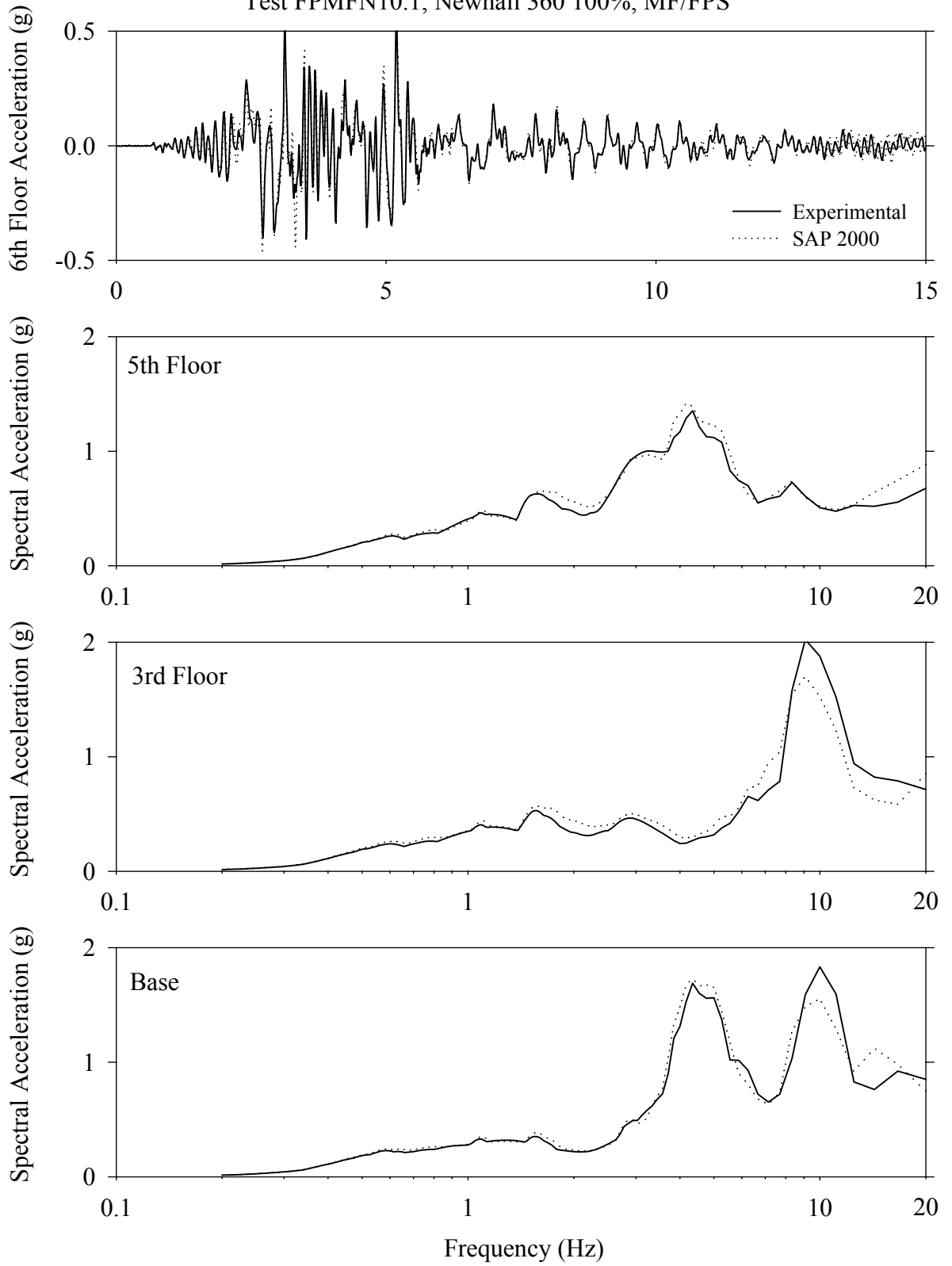


Test FPMFN10.1, Newhall 360 100%, MF/FPS

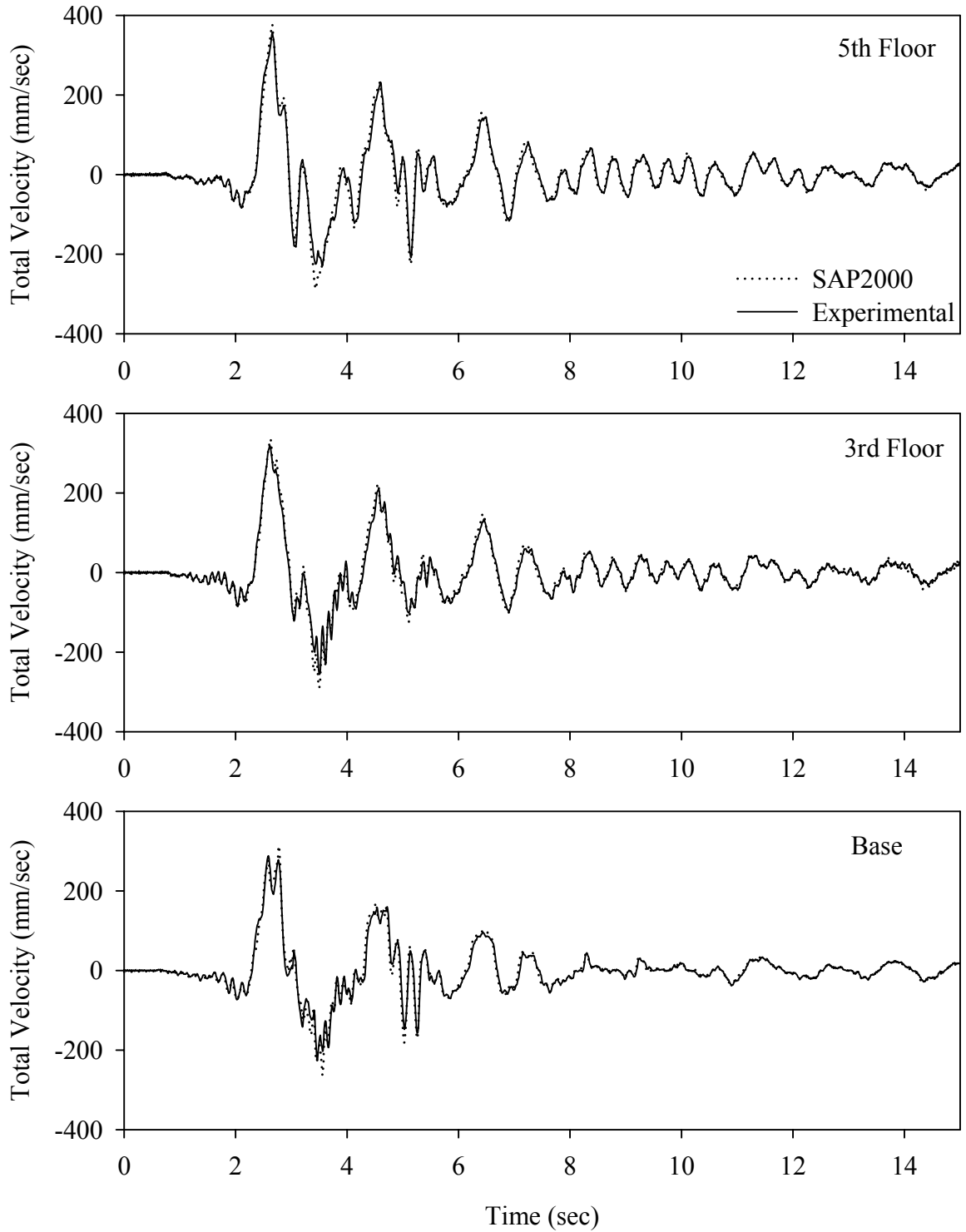




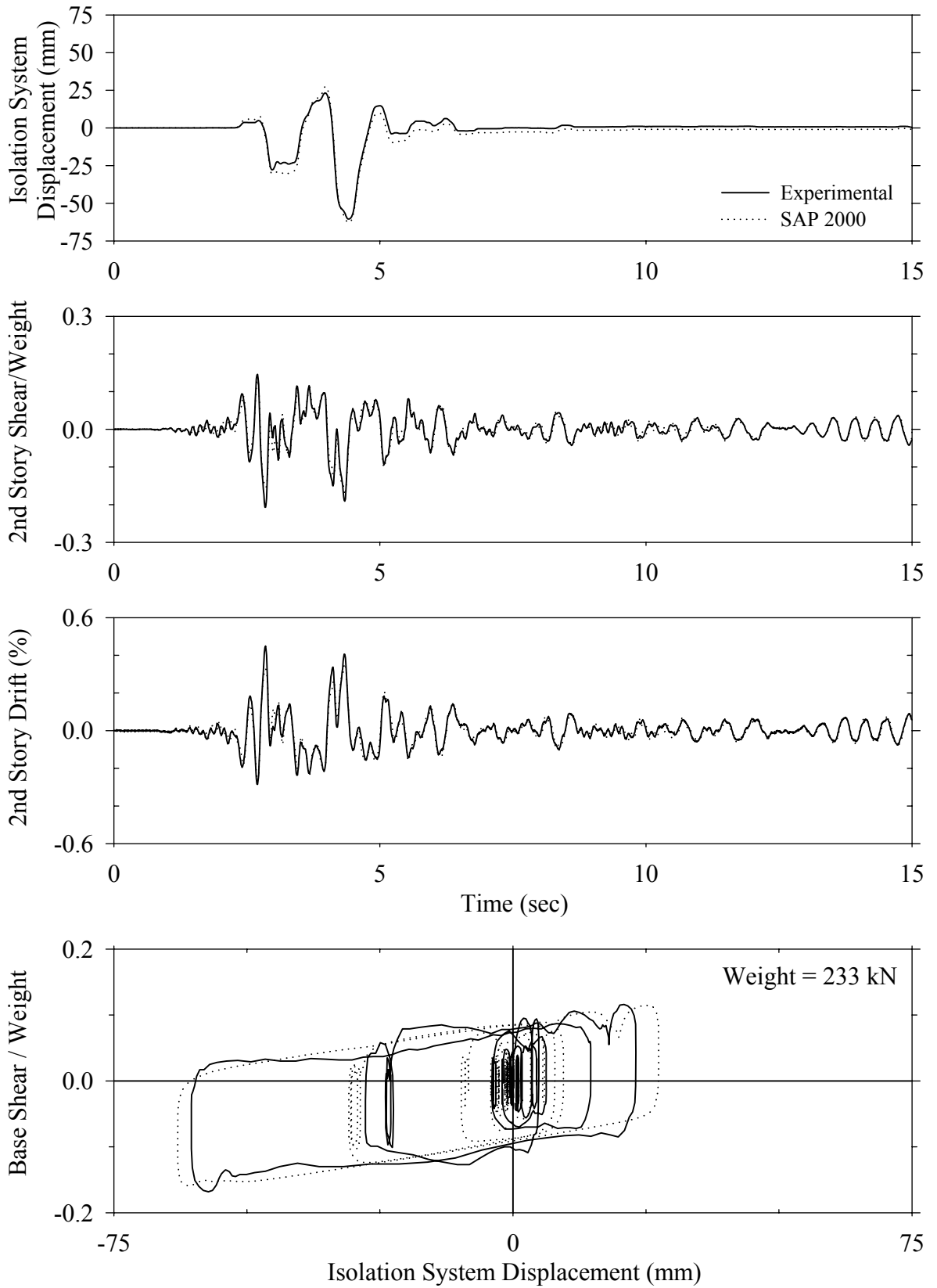
Test FPMFN10.1, Newhall 360 100%, MF/FPS



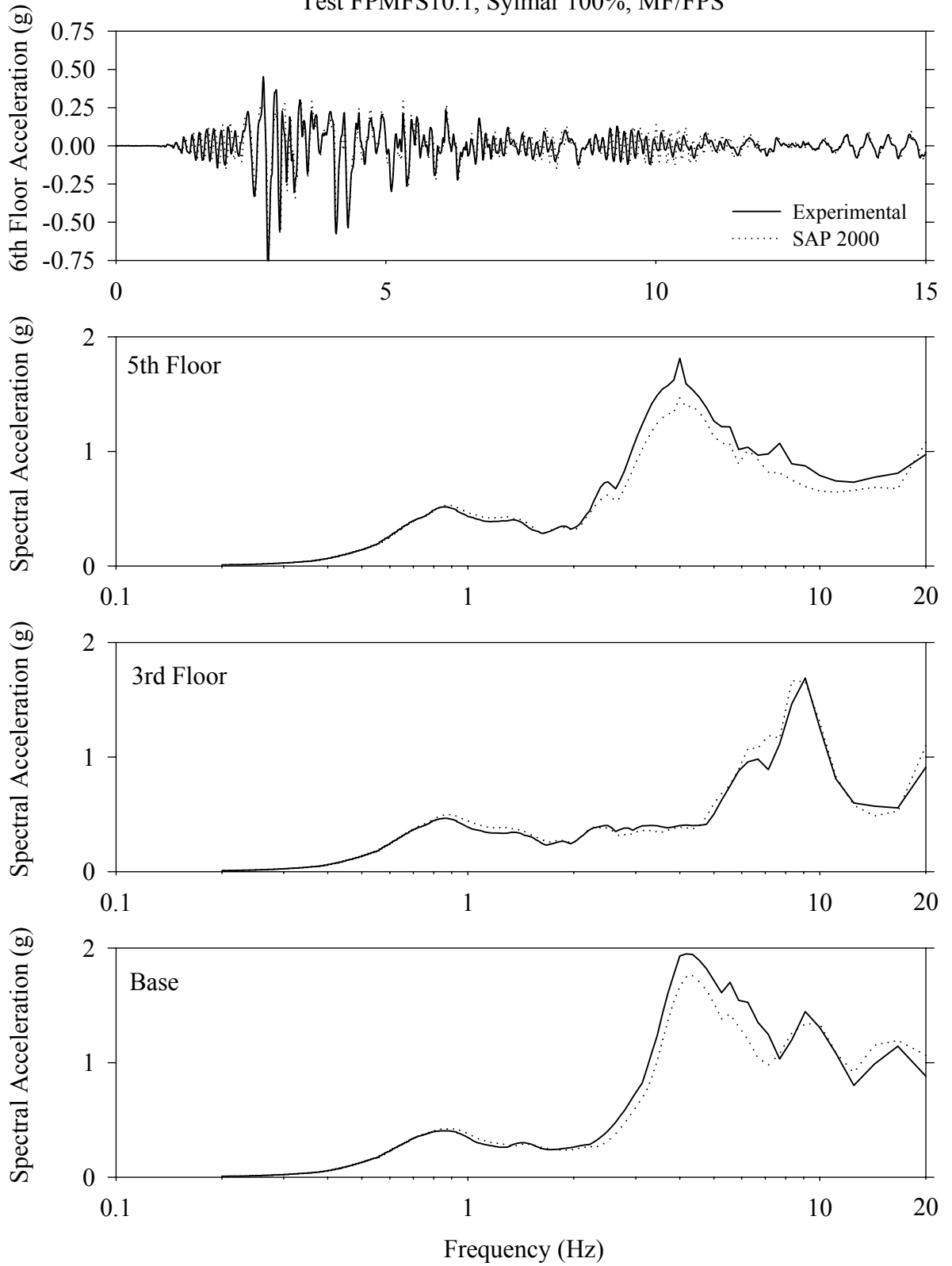
Test FPMFN10.1, Newhall 360 100%, MF/FPS



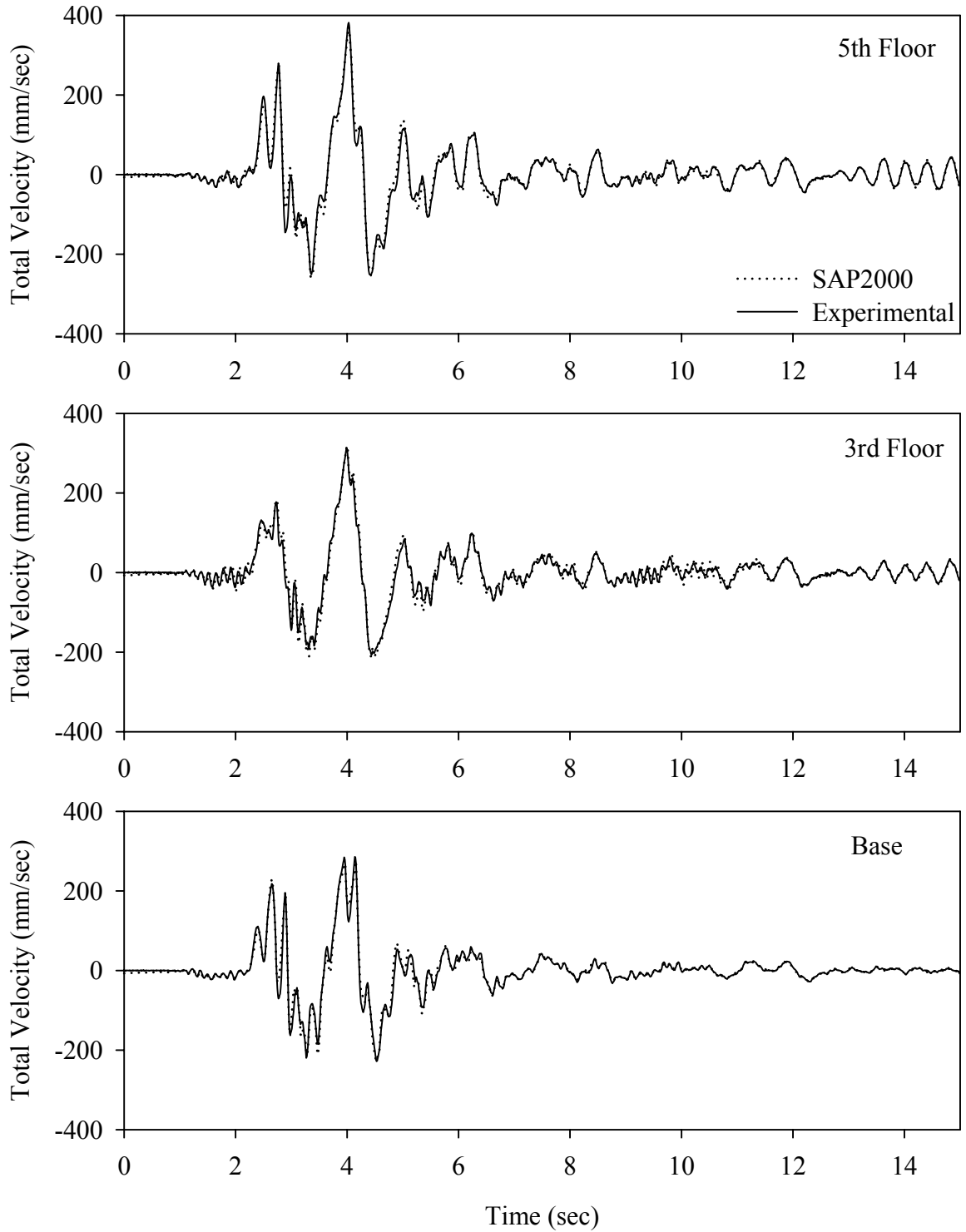
Test FPMFS10.1, Sylmar 100%, MF/FPS



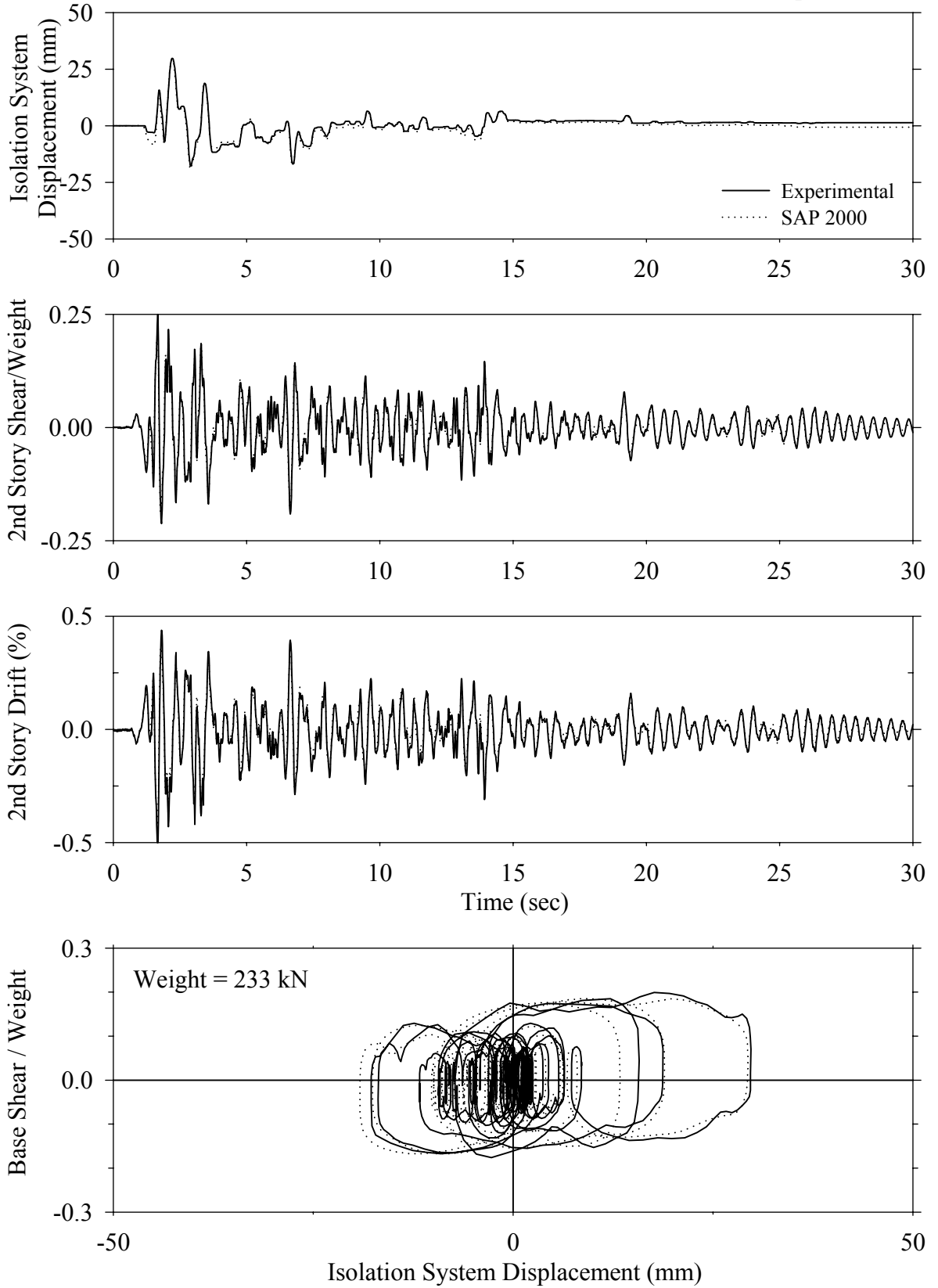
Test FPMFS10.1, Sylmar 100%, MF/FPS



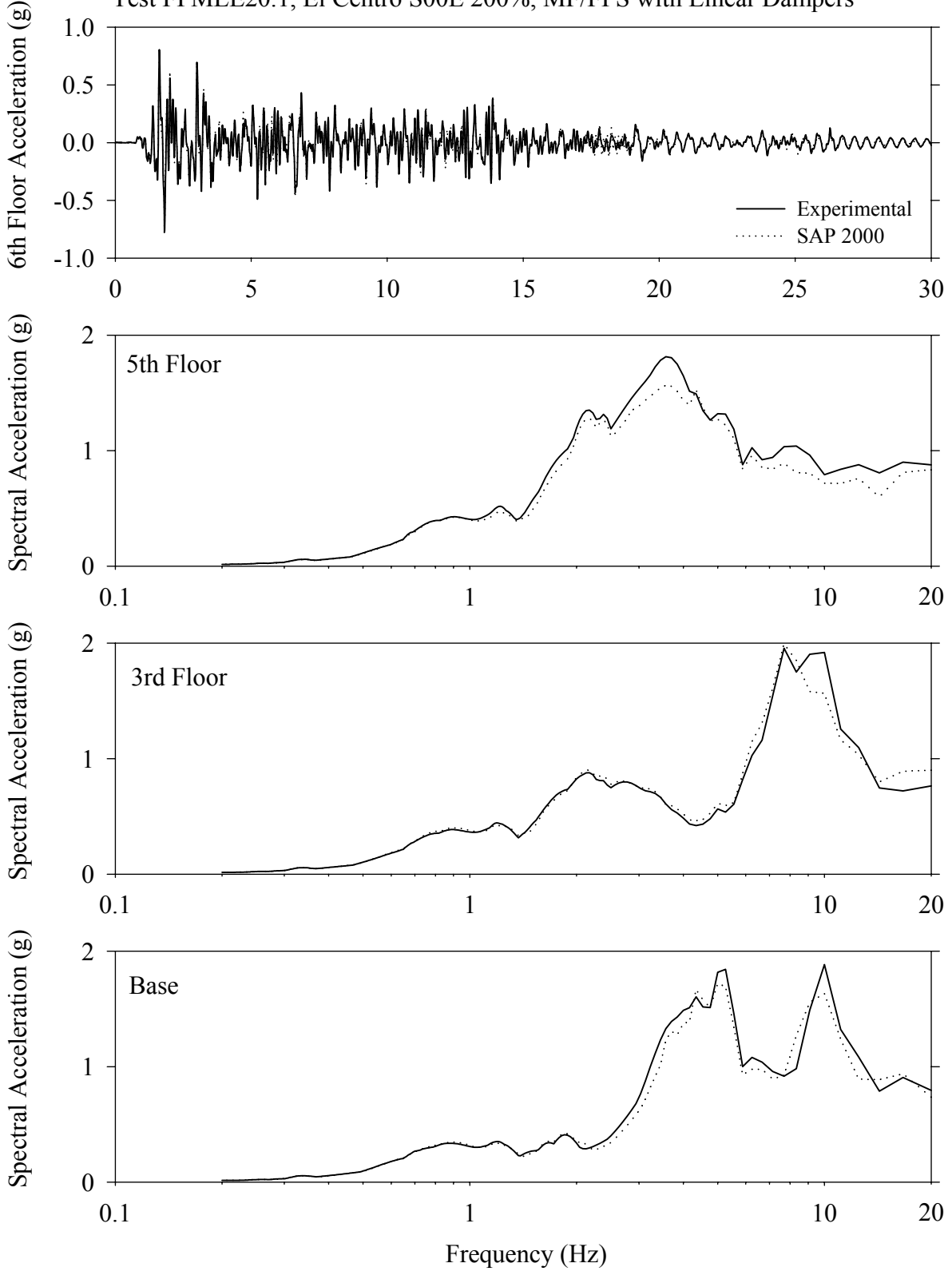
Test FPMFS10.1, Sylmar 100%, MF/FPS



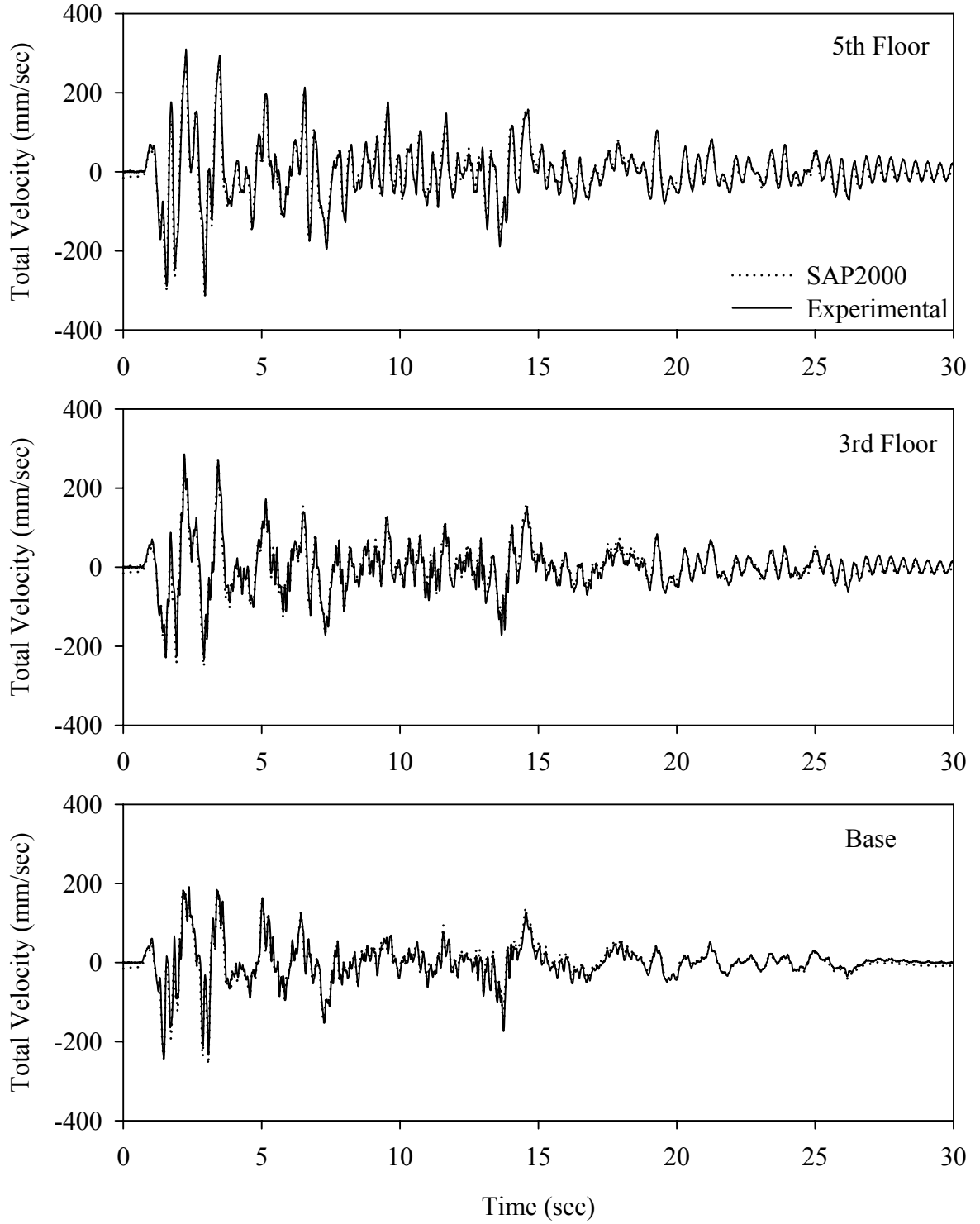
Test FPMLE20.1, El Centro S00E 200%, MF/FPS with Linear Dampers



Test FPMLE20.1, El Centro S00E 200%, MF/FPS with Linear Dampers

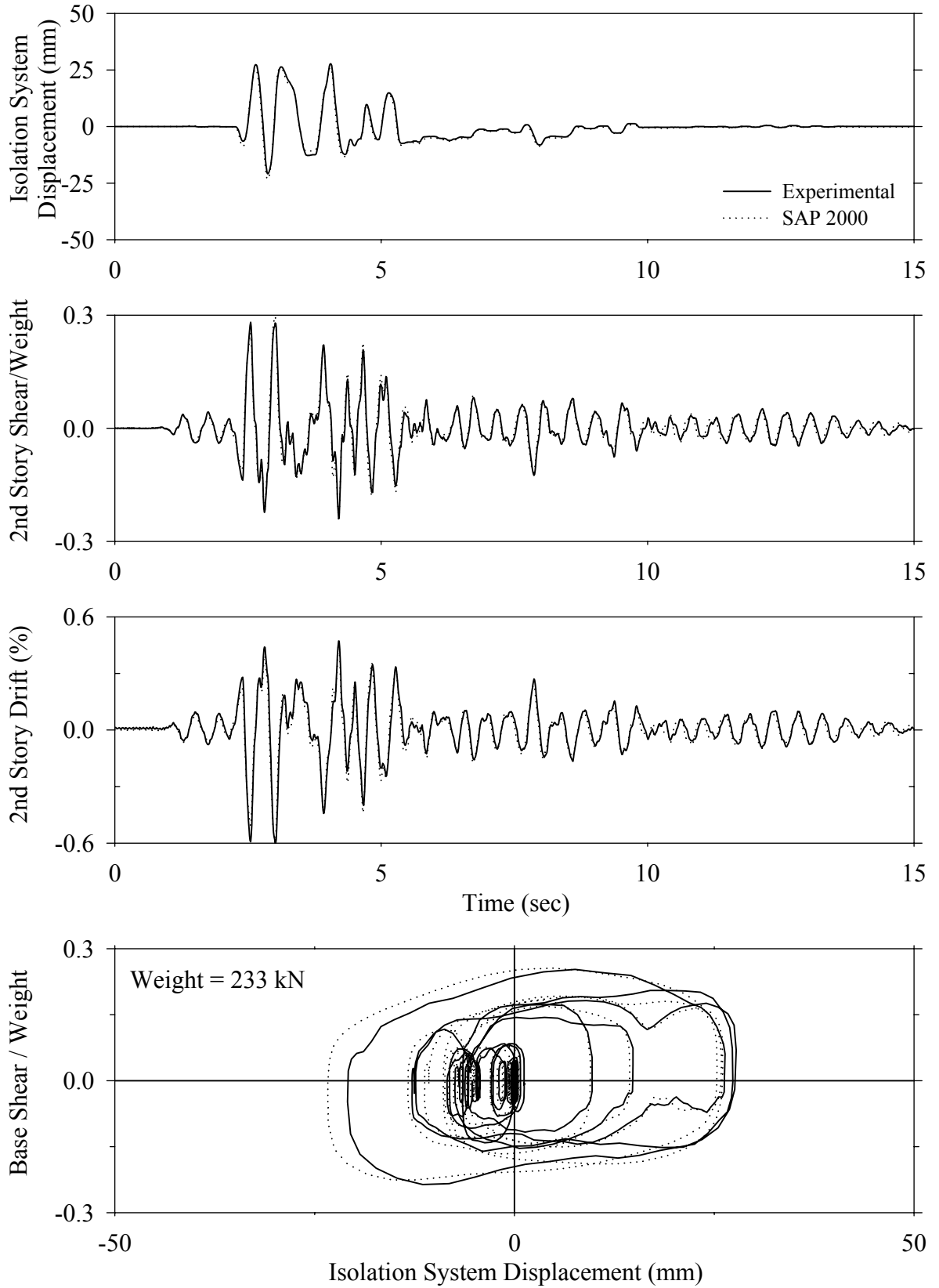


Test FPMLE20.1, El Centro S00E 200%, MF/FPS with Linear Dampers

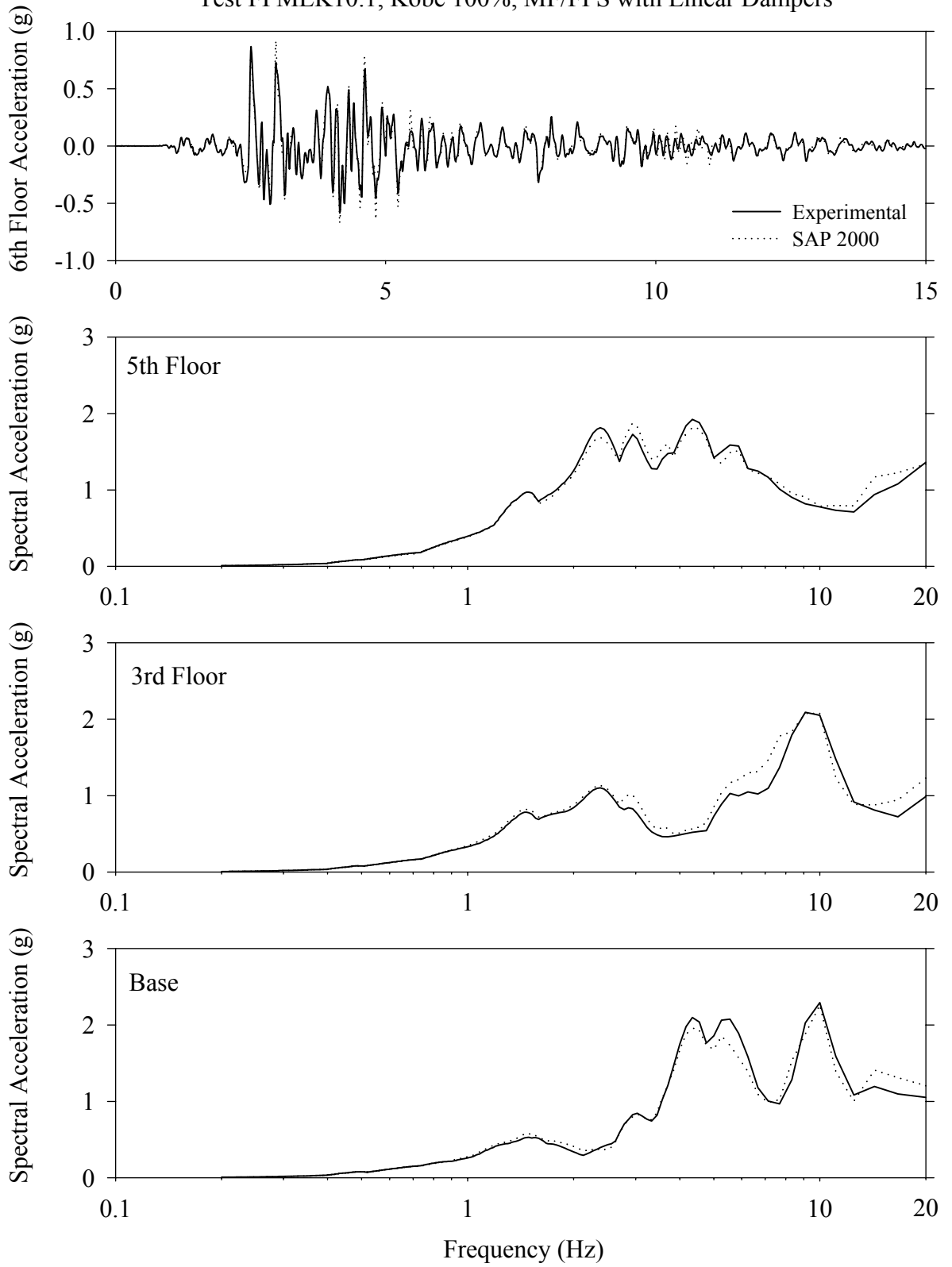




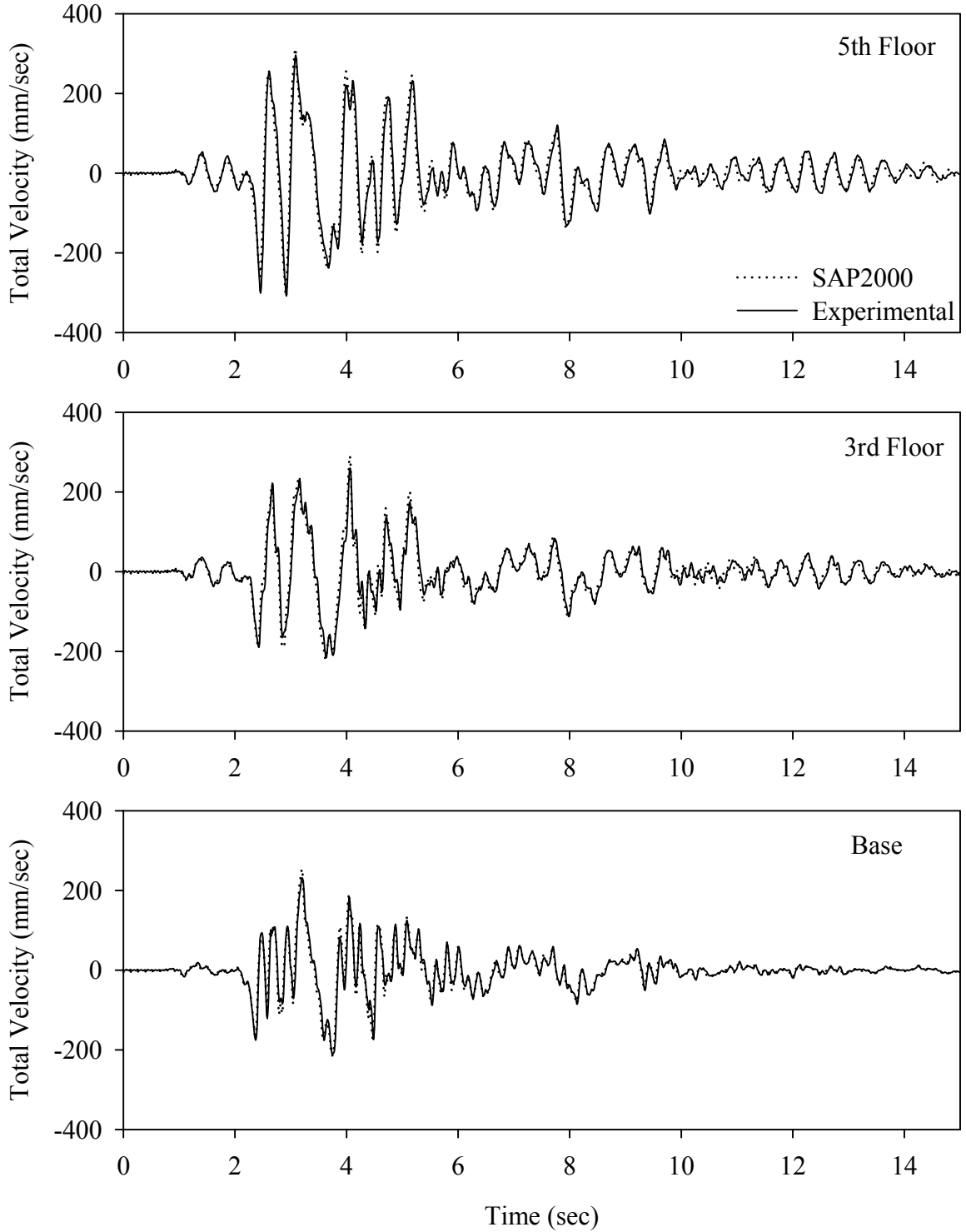
Test FPMLK10.1, Kobe 100%, MF/FPS with Linear Dampers



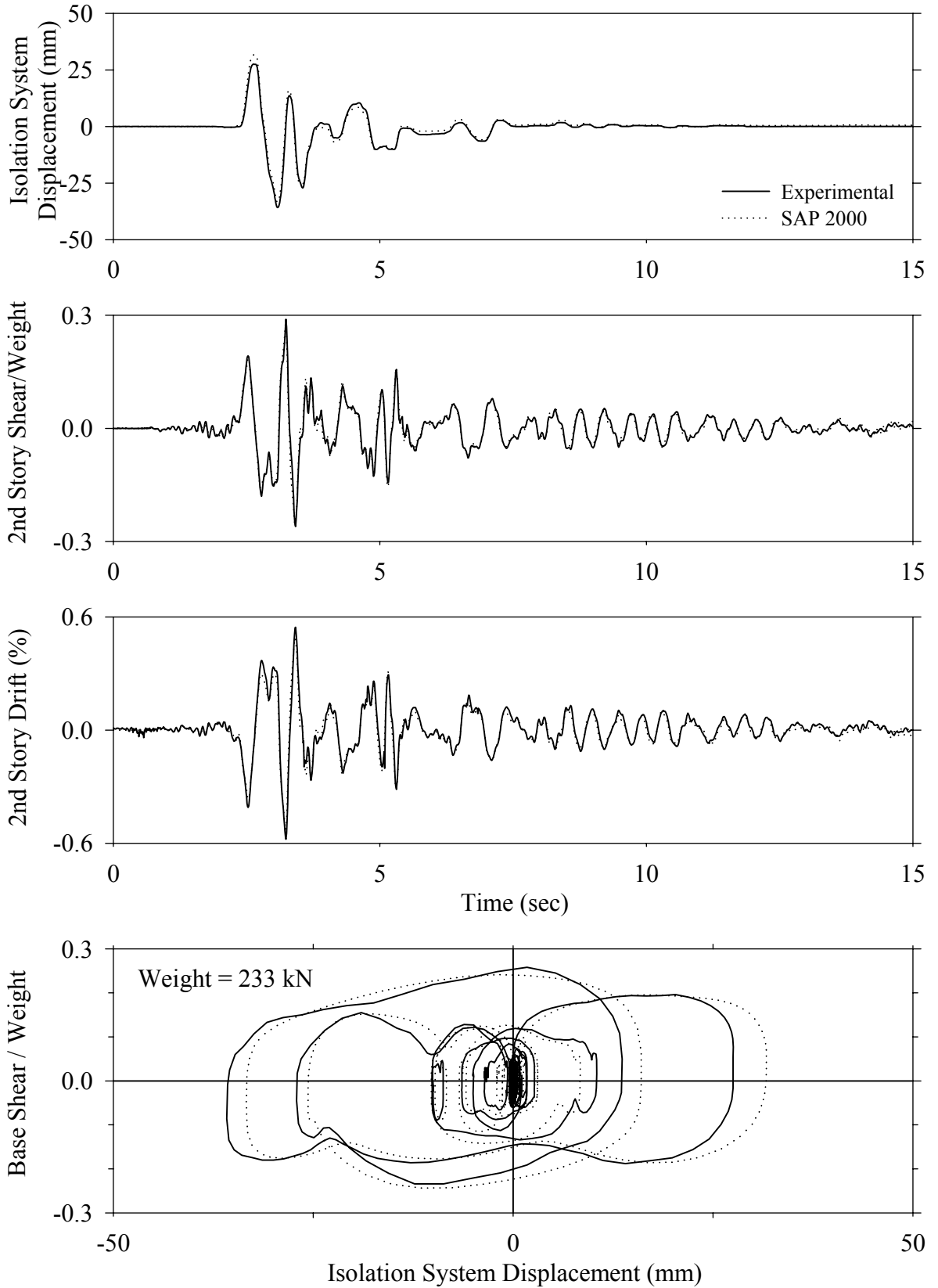
Test FPMLK10.1, Kobe 100%, MF/FPS with Linear Dampers



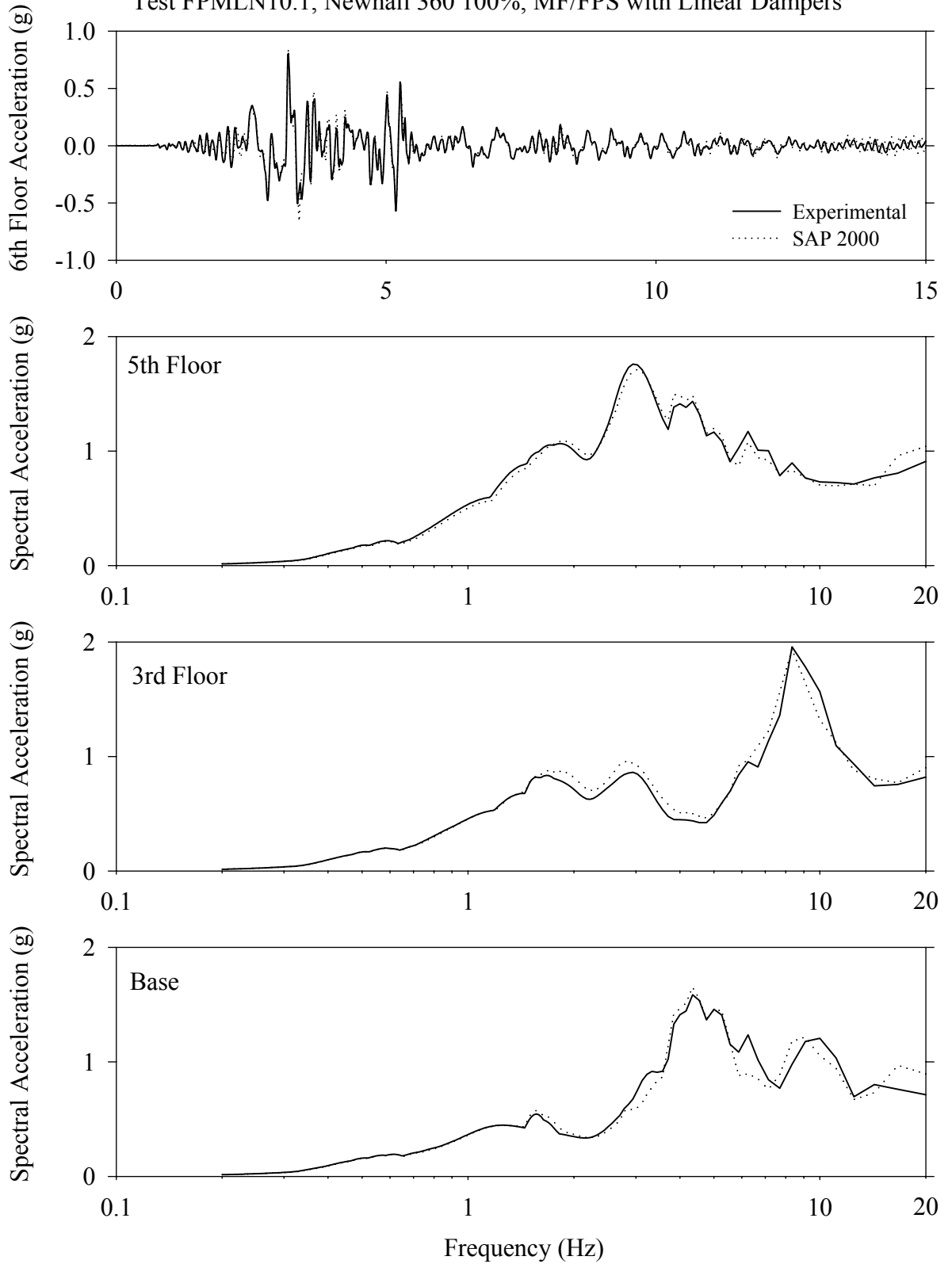
Test FPMLK10.1, Kobe 100%, MF/FPS with Linear Dampers



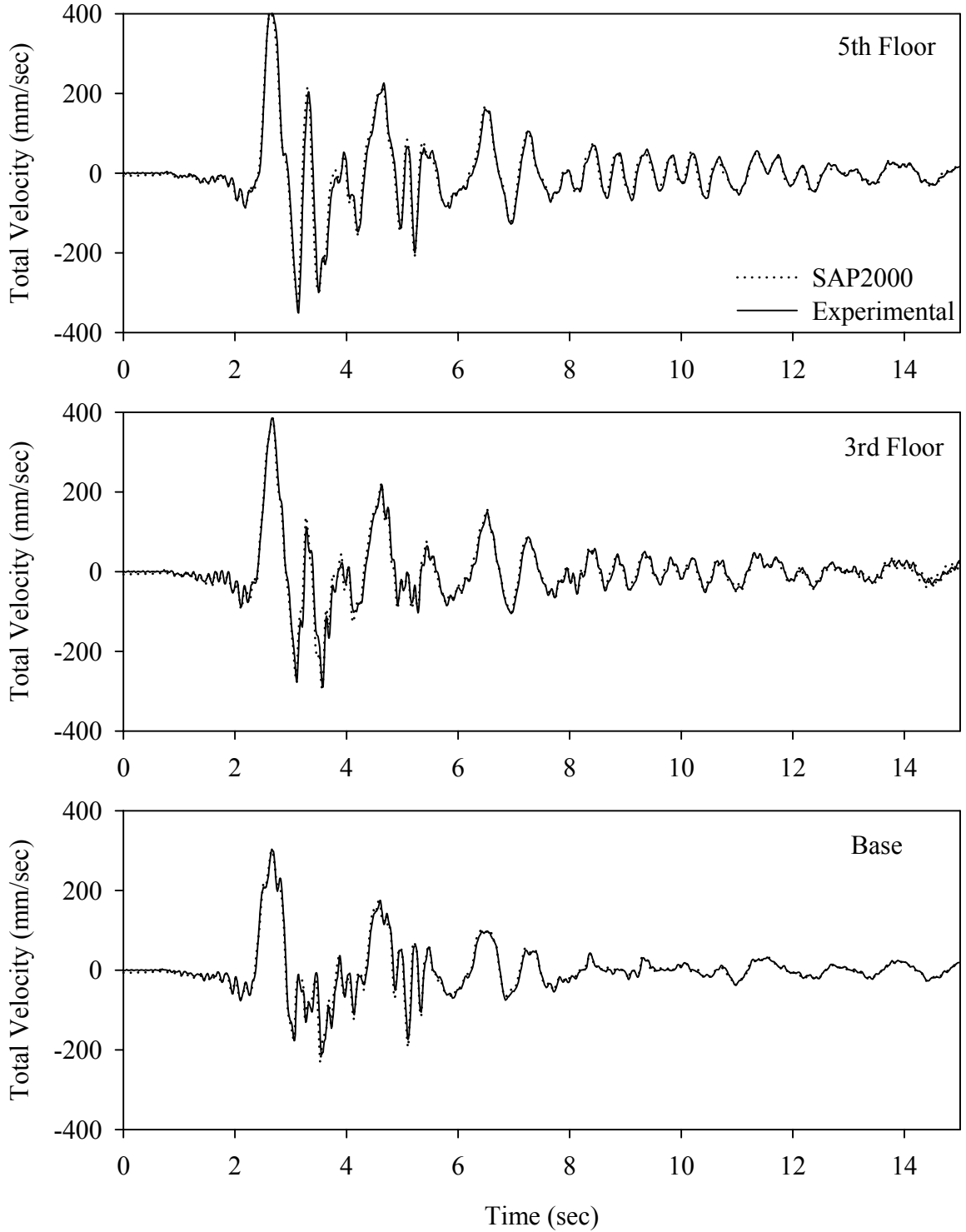
Test FPMLN10.1, Newhall 360 100%, MF/FPS with Linear Dampers



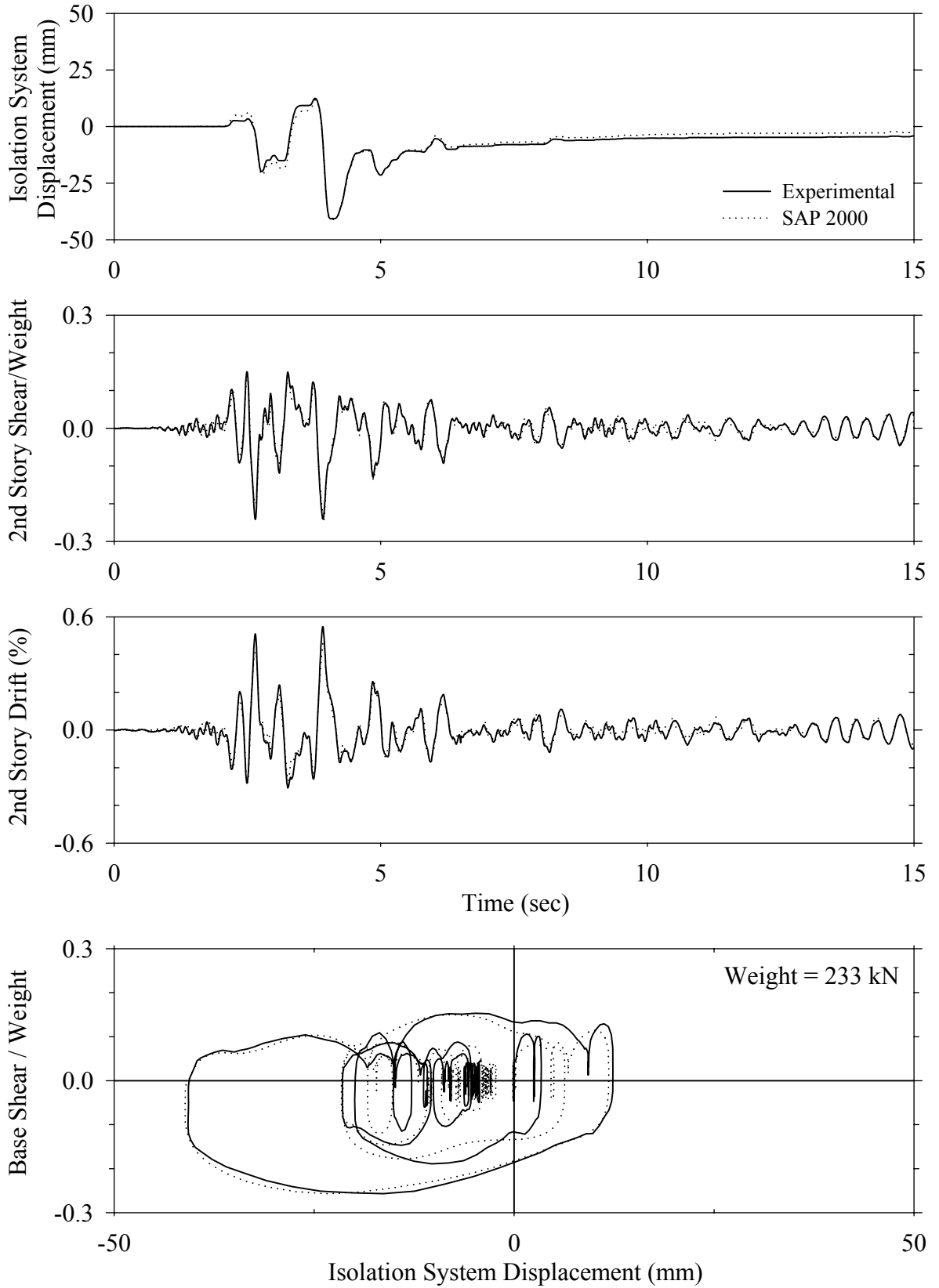
Test FPMLN10.1, Newhall 360 100%, MF/FPS with Linear Dampers



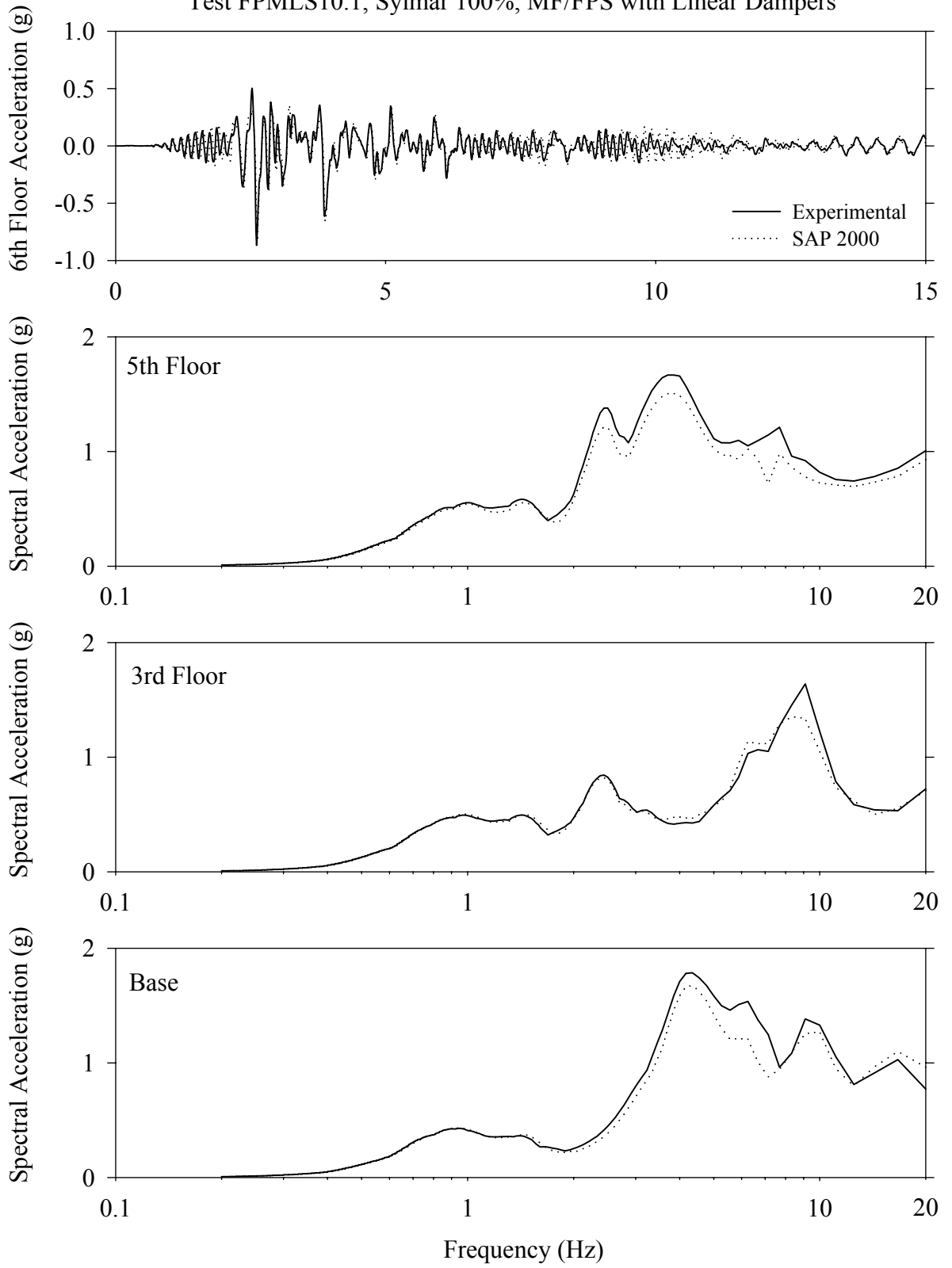
Test FPMLN10.1, Newhall 360 100%, MF/FPS with Linear Dampers



Test FPMLS10.1, Sylmar 100%, MF/FPS with Linear Dampers

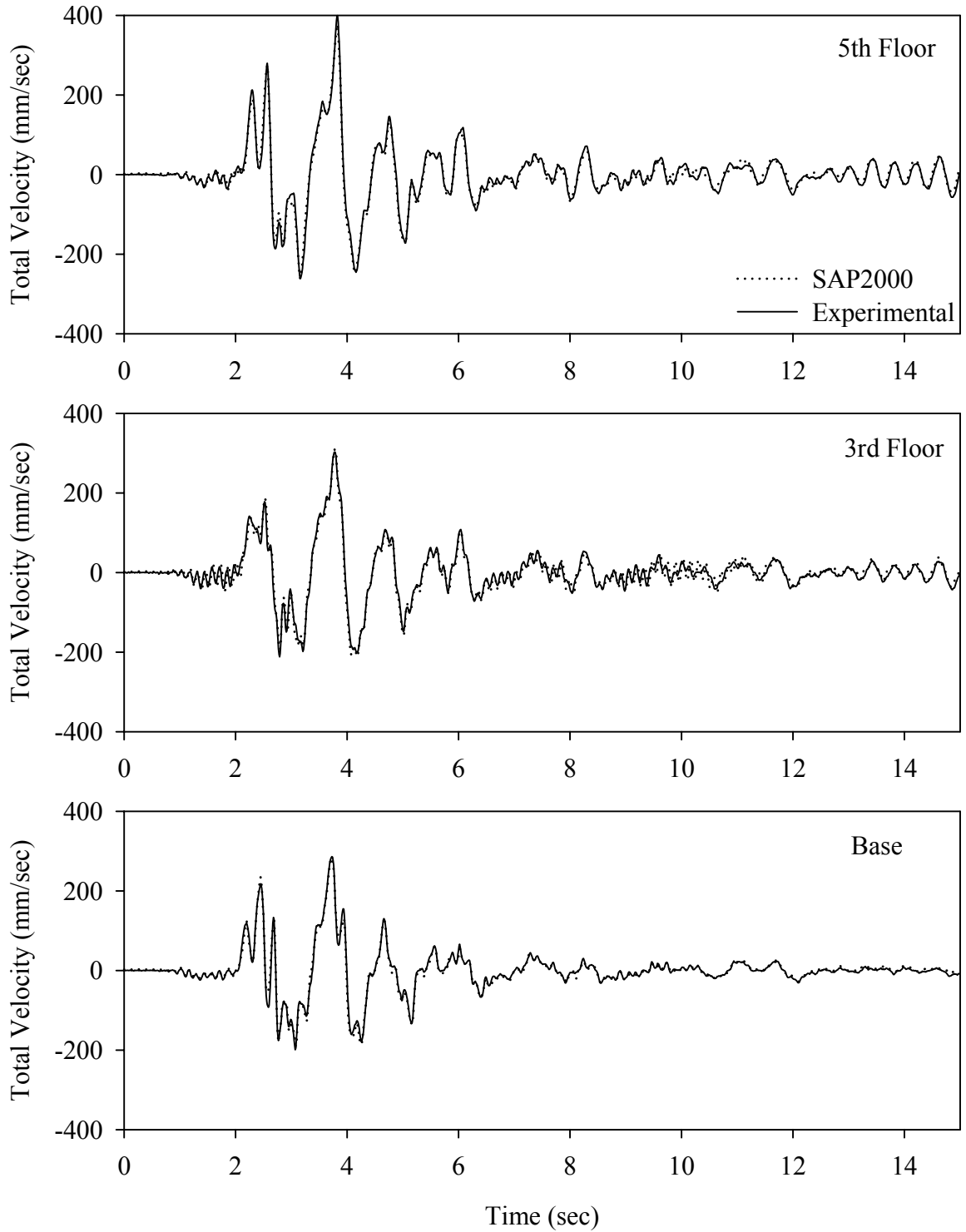


Test FPMLS10.1, Sylmar 100%, MF/FPS with Linear Dampers

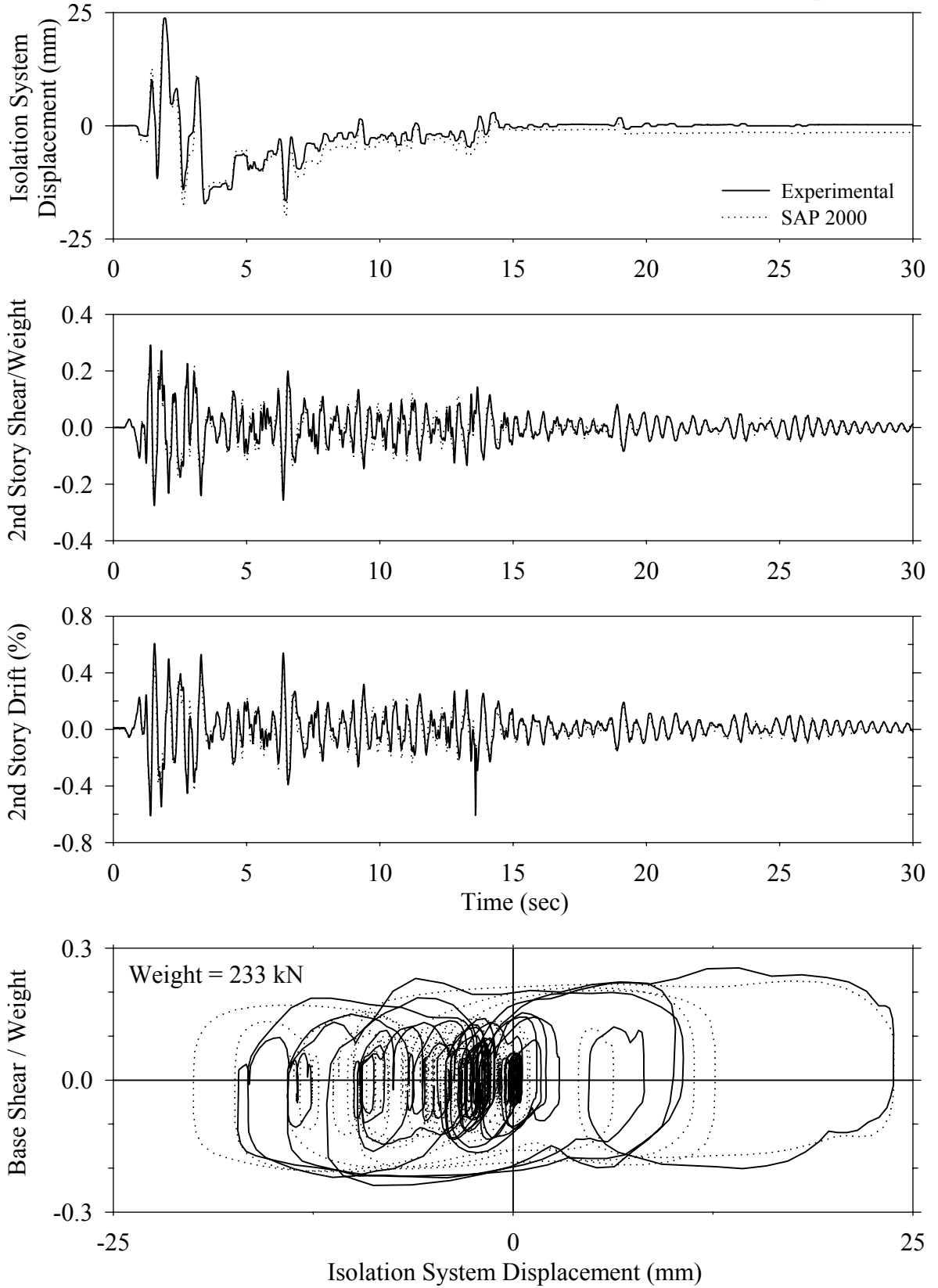




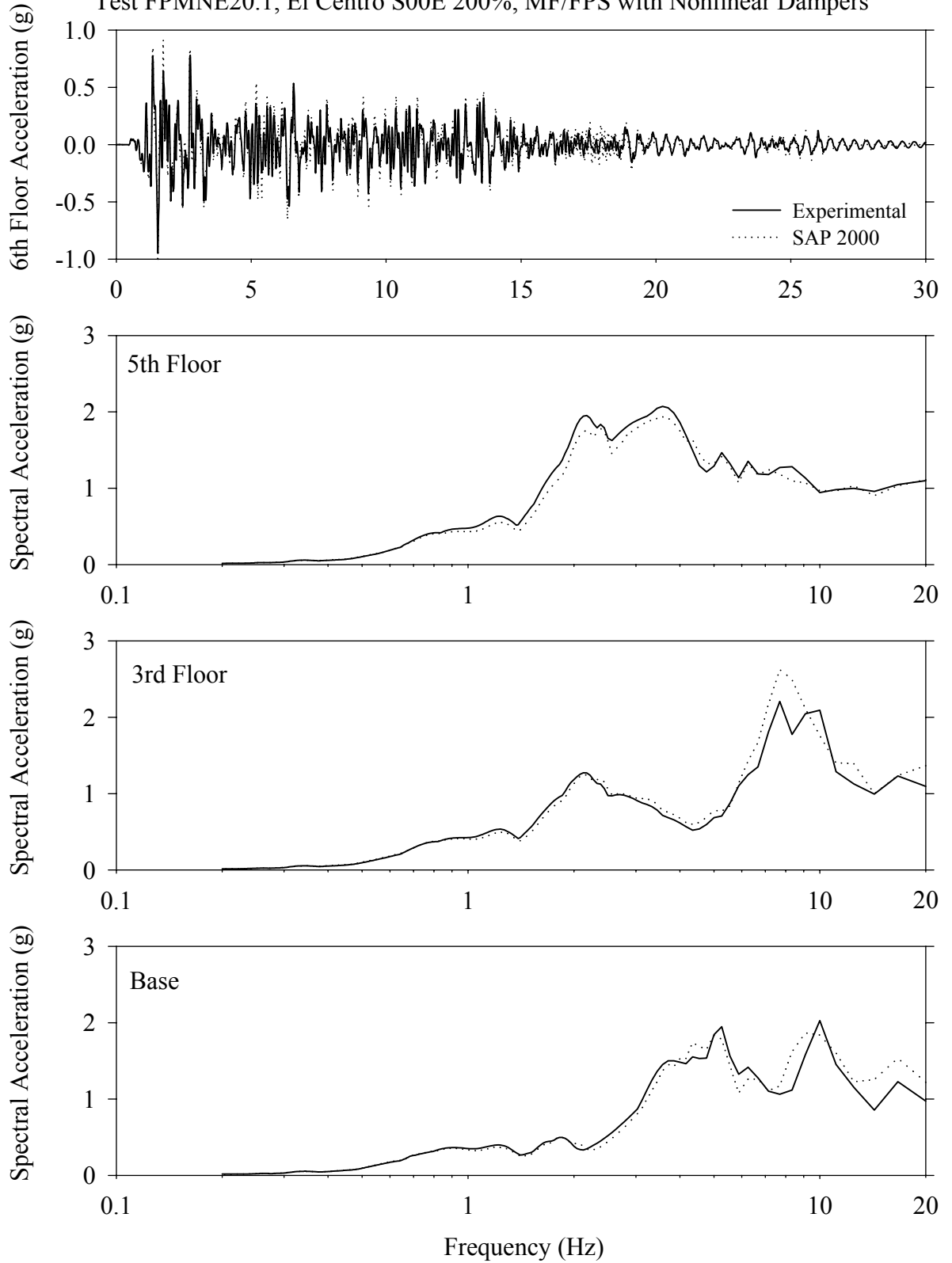
Test FPMLS10.1, Sylmar 100%, MF/FPS with Linear Dampers



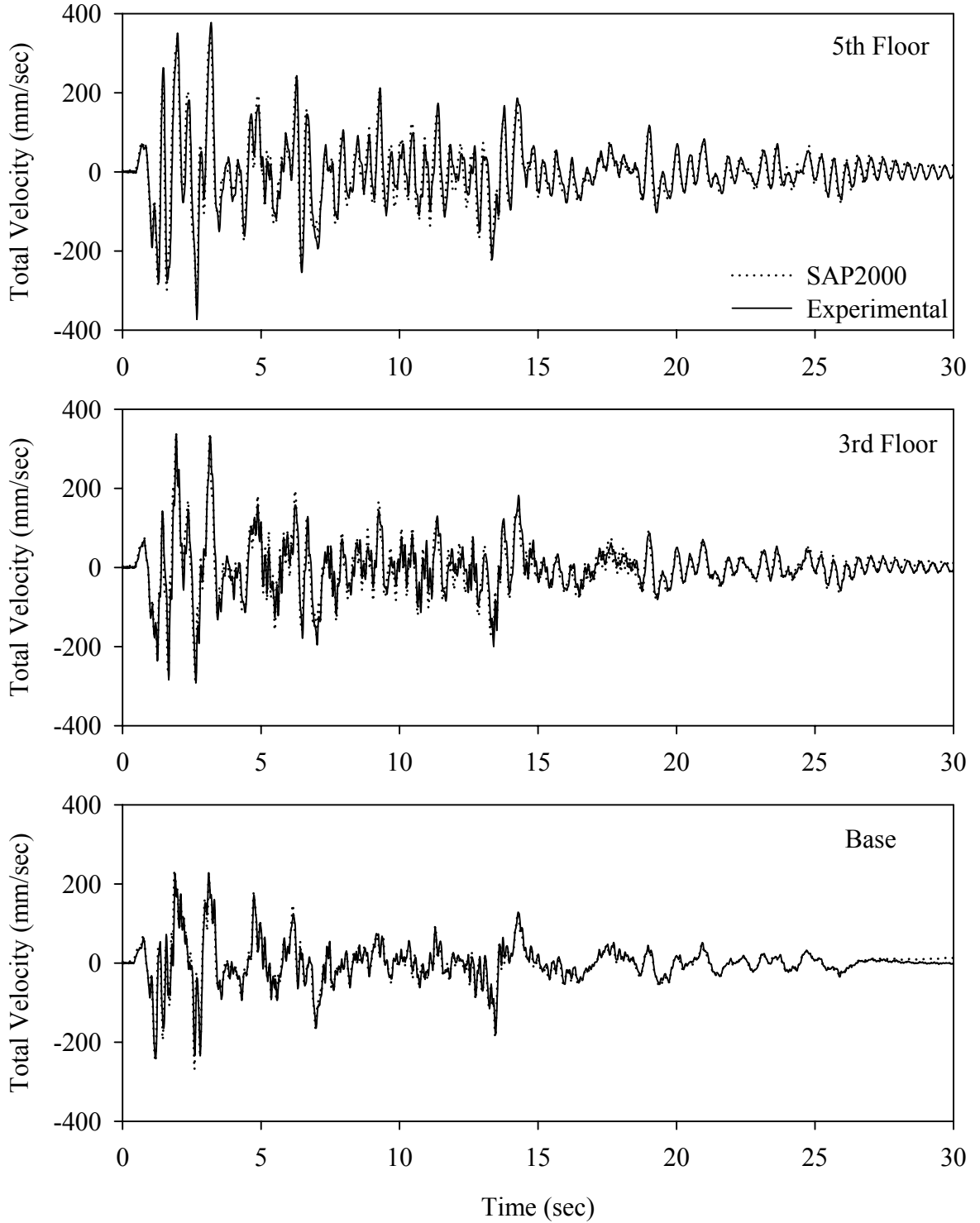
Test FPMNE20.1, El Centro S00E 200%, MF/FPS with Nonlinear Dampers



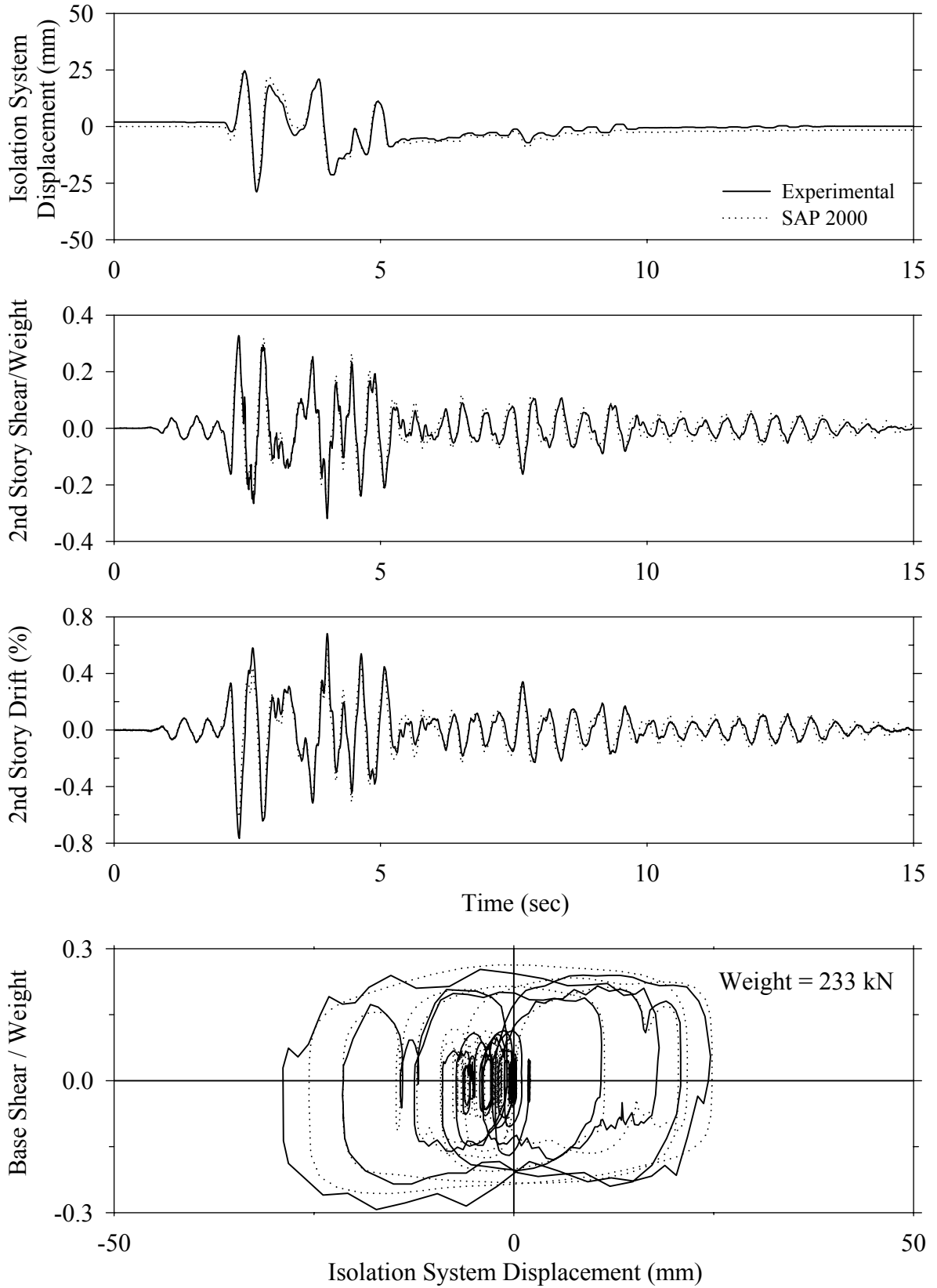
Test FPMNE20.1, El Centro S00E 200%, MF/FPS with Nonlinear Dampers



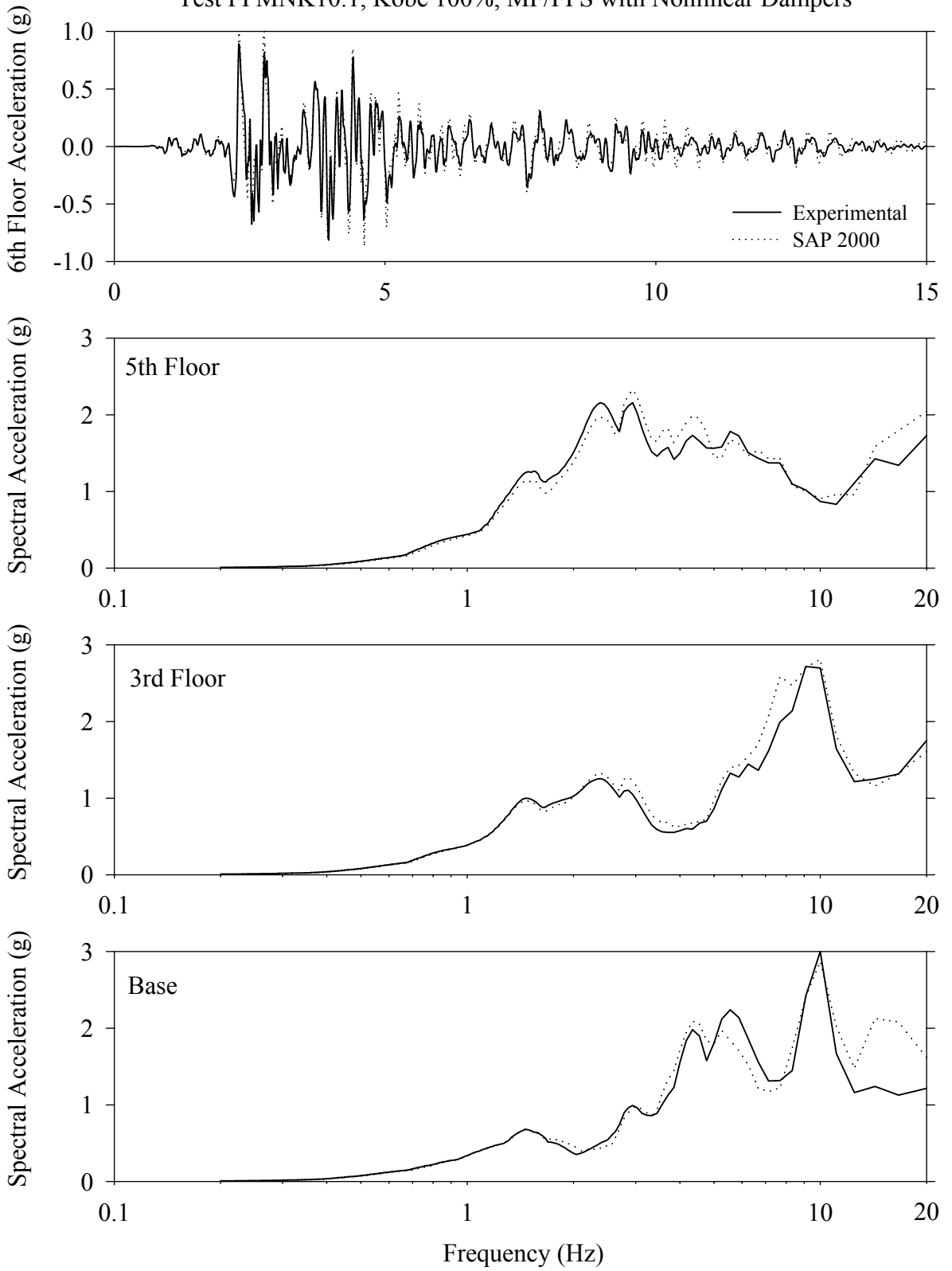
Test FPMNE20.1, El Centro S00E 200%, MF/FPS with Nonlinear Dampers



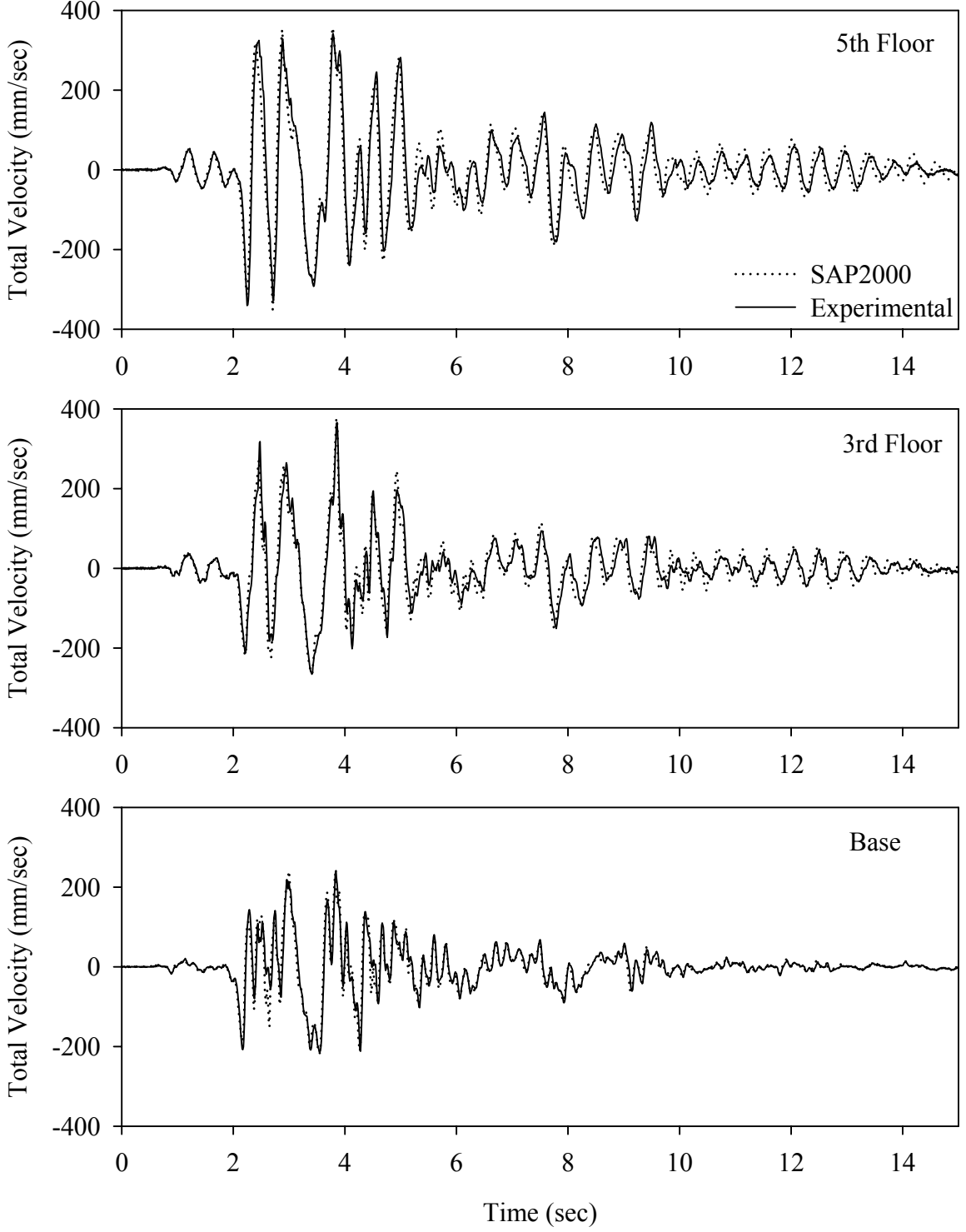
Test FPMNK10.1, Kobe 100%, MF/FPS with Nonlinear Dampers



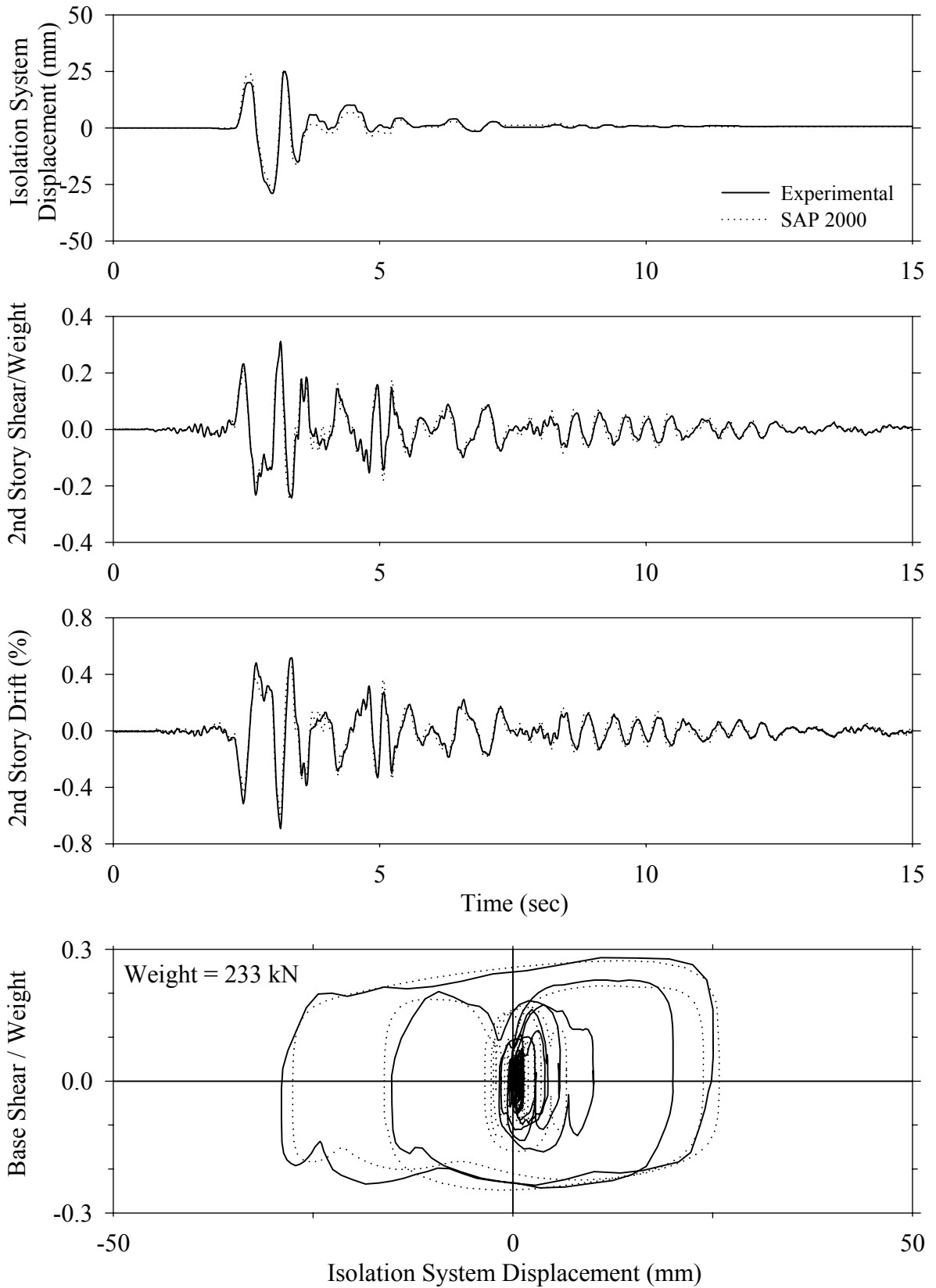
Test FPMNK10.1, Kobe 100%, MF/FPS with Nonlinear Dampers



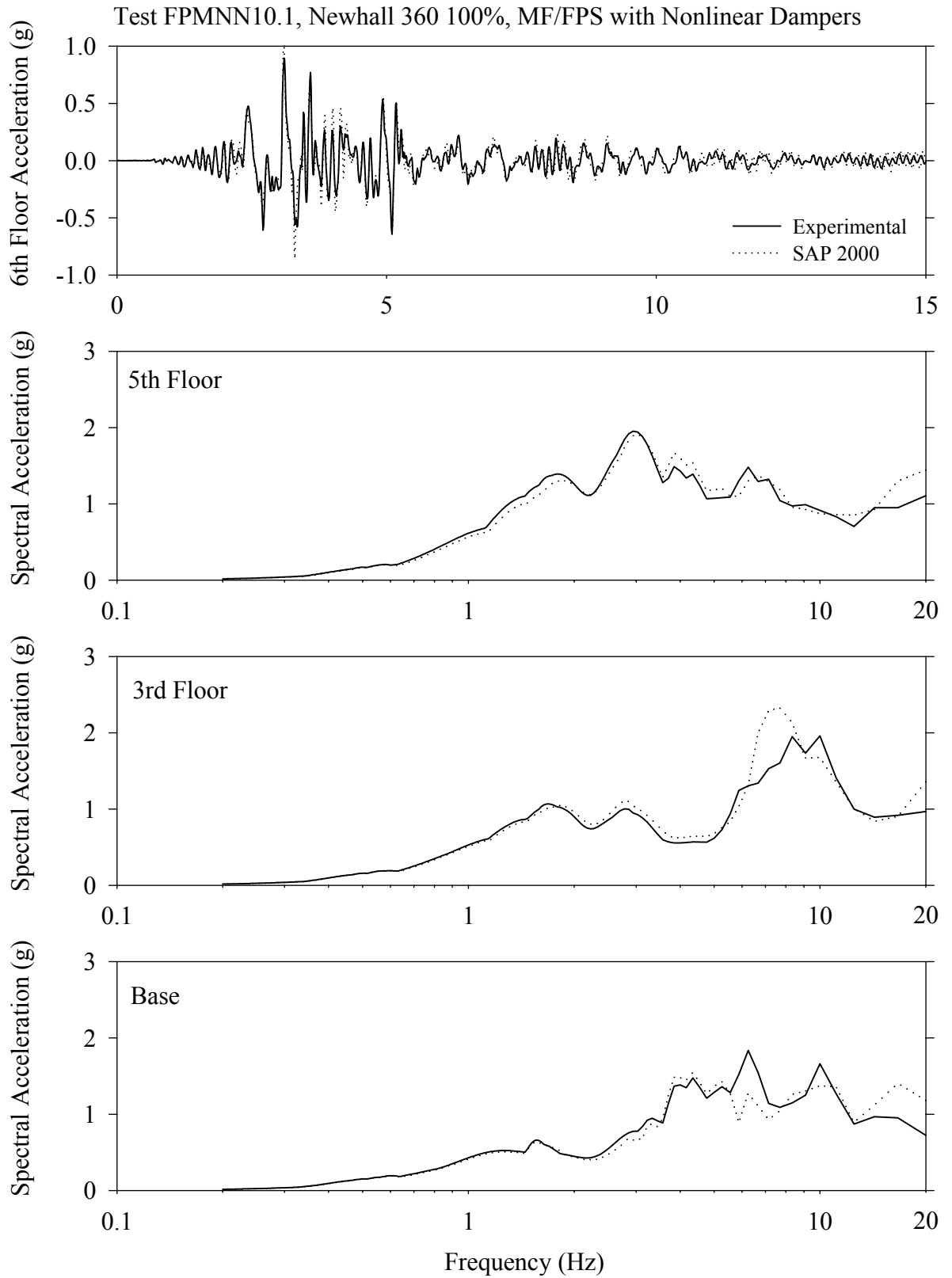
Test FPMNK10.1, Kobe 100%, MF/FPS with Nonlinear Dampers



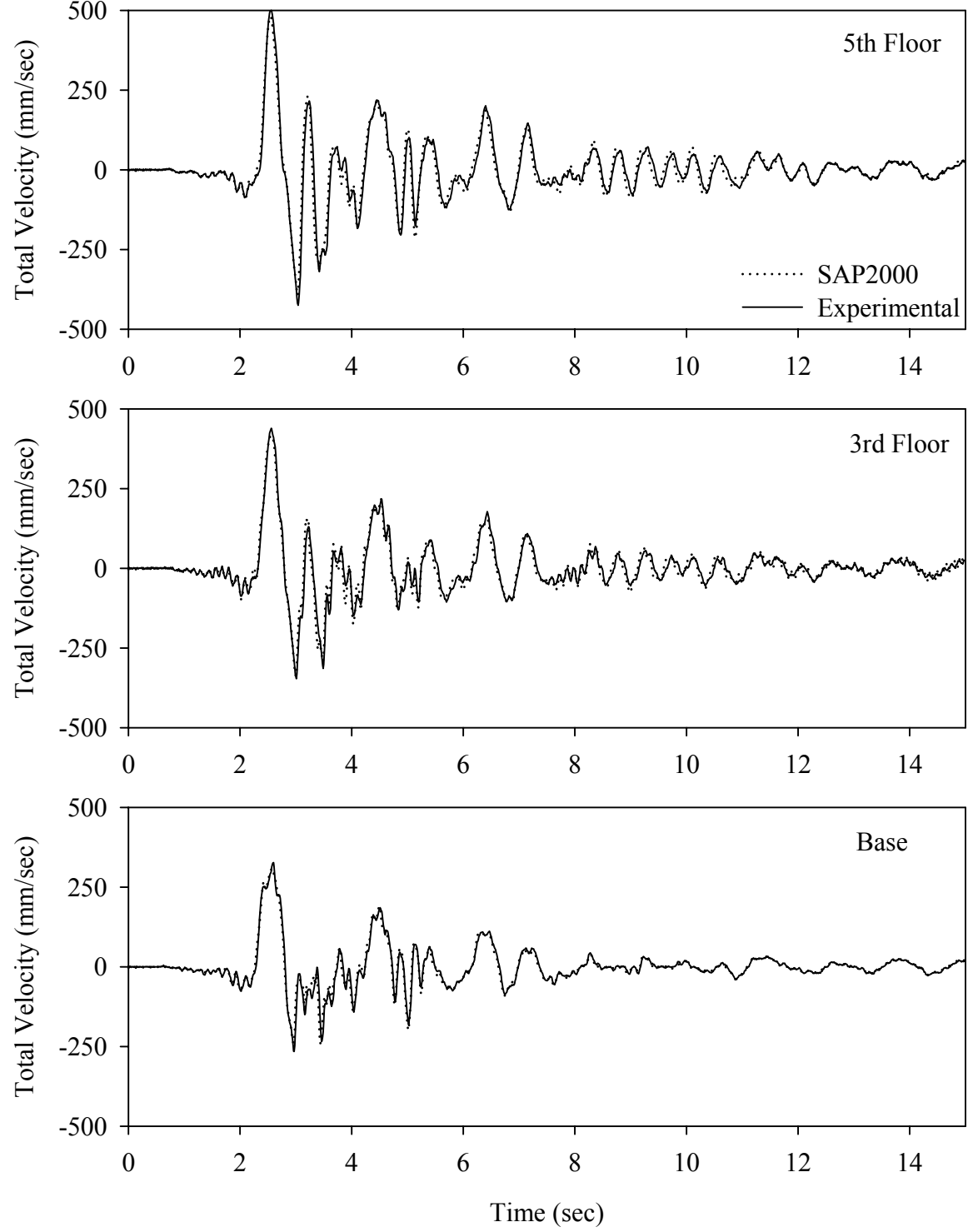
Test FPMNN10.1, Newhall 360 100%, MF/FPS with Nonlinear Dampers



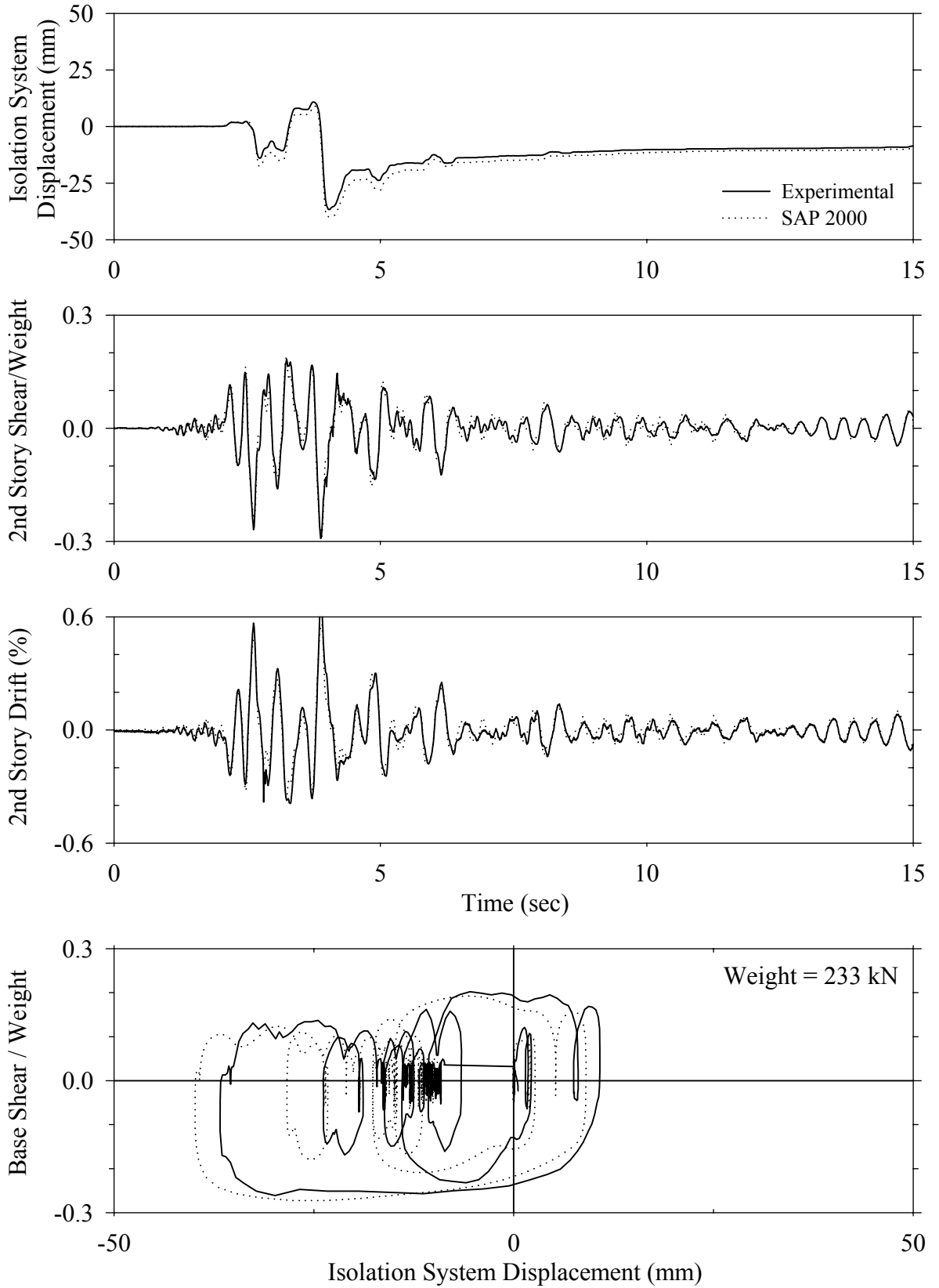




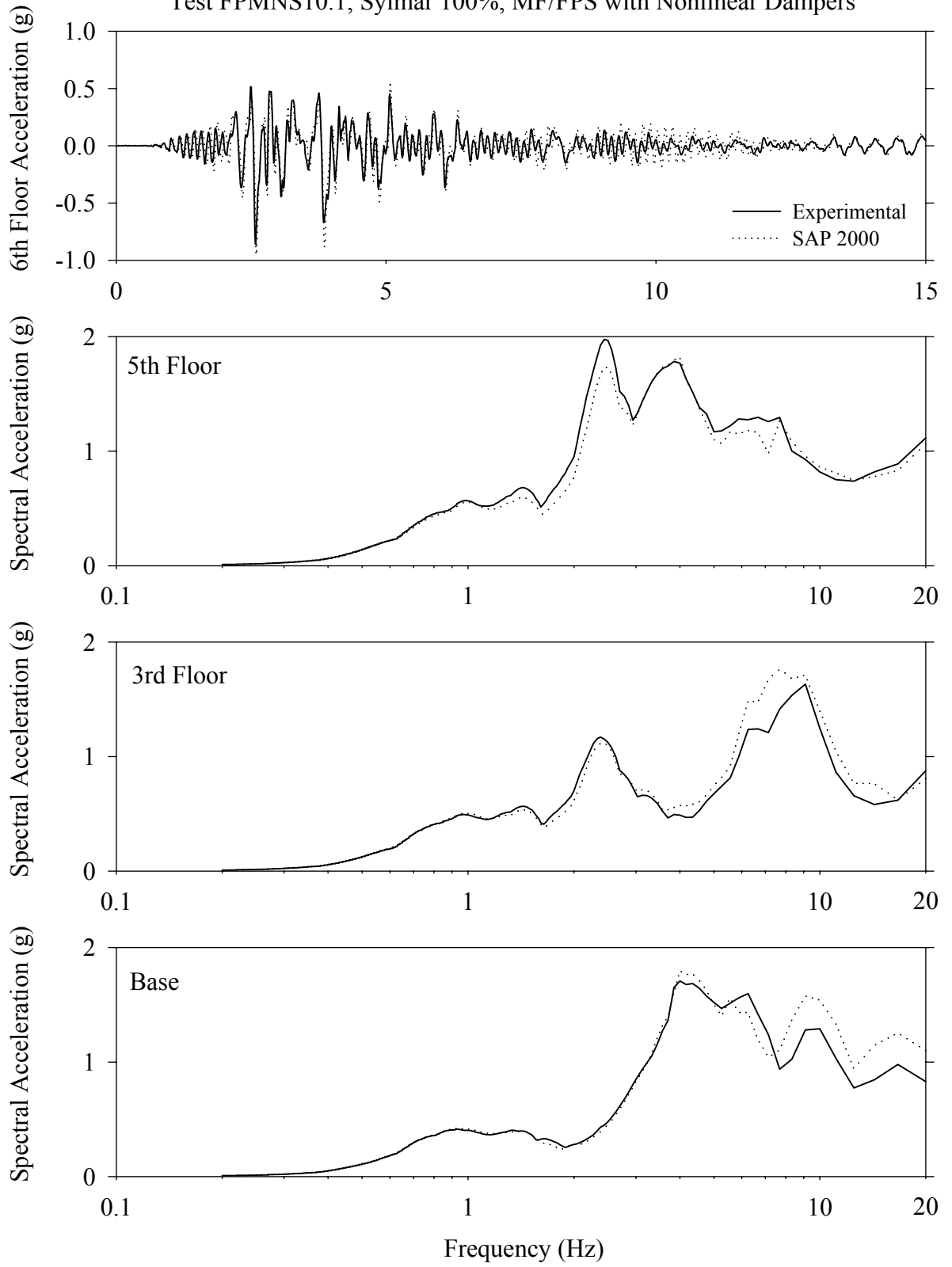
Test FPMNN10.1, Newhall 360 100%, MF/FPS with Nonlinear Dampers



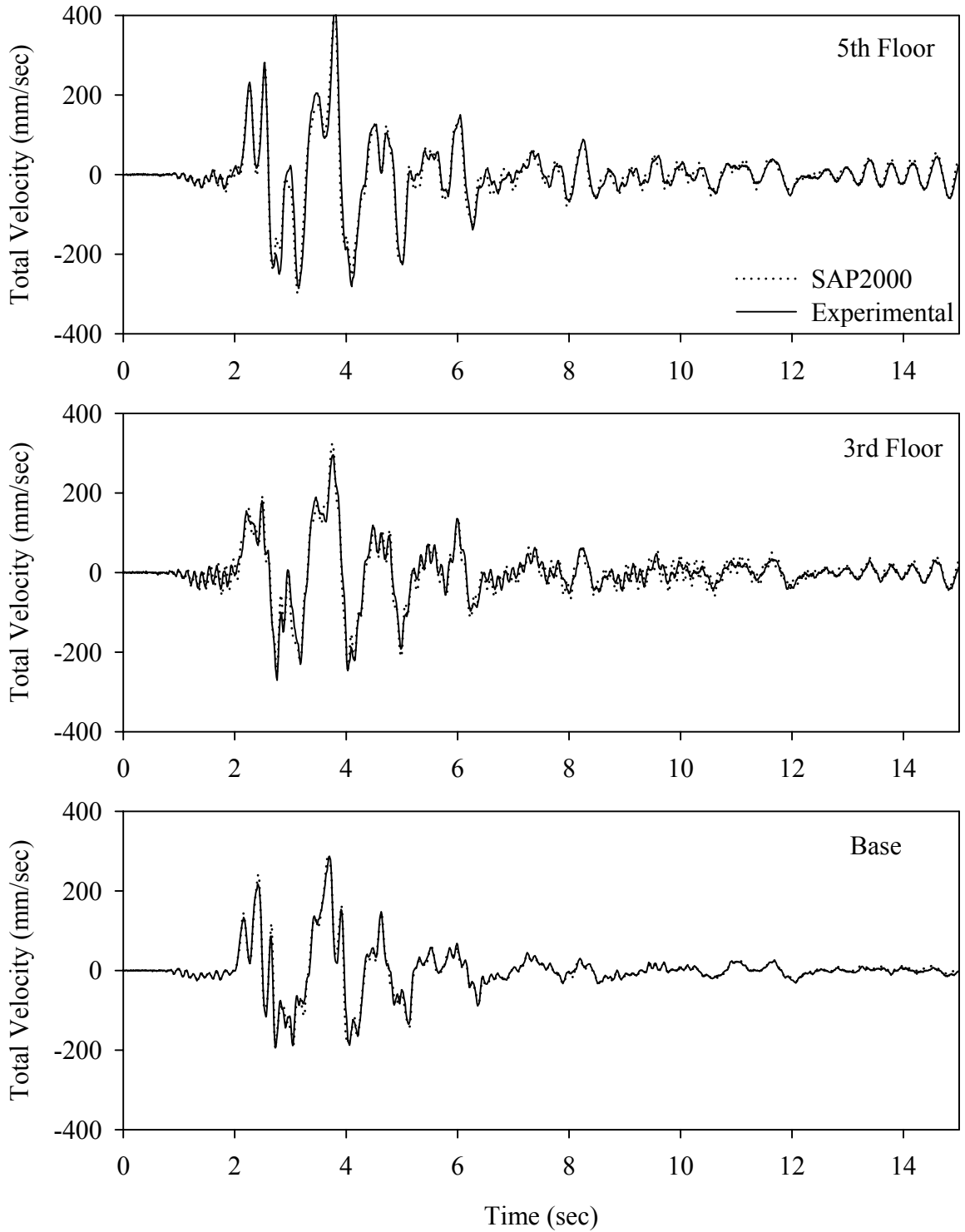
Test FPMNS10.1, Sylmar 100%, MF/FPS with Nonlinear Dampers



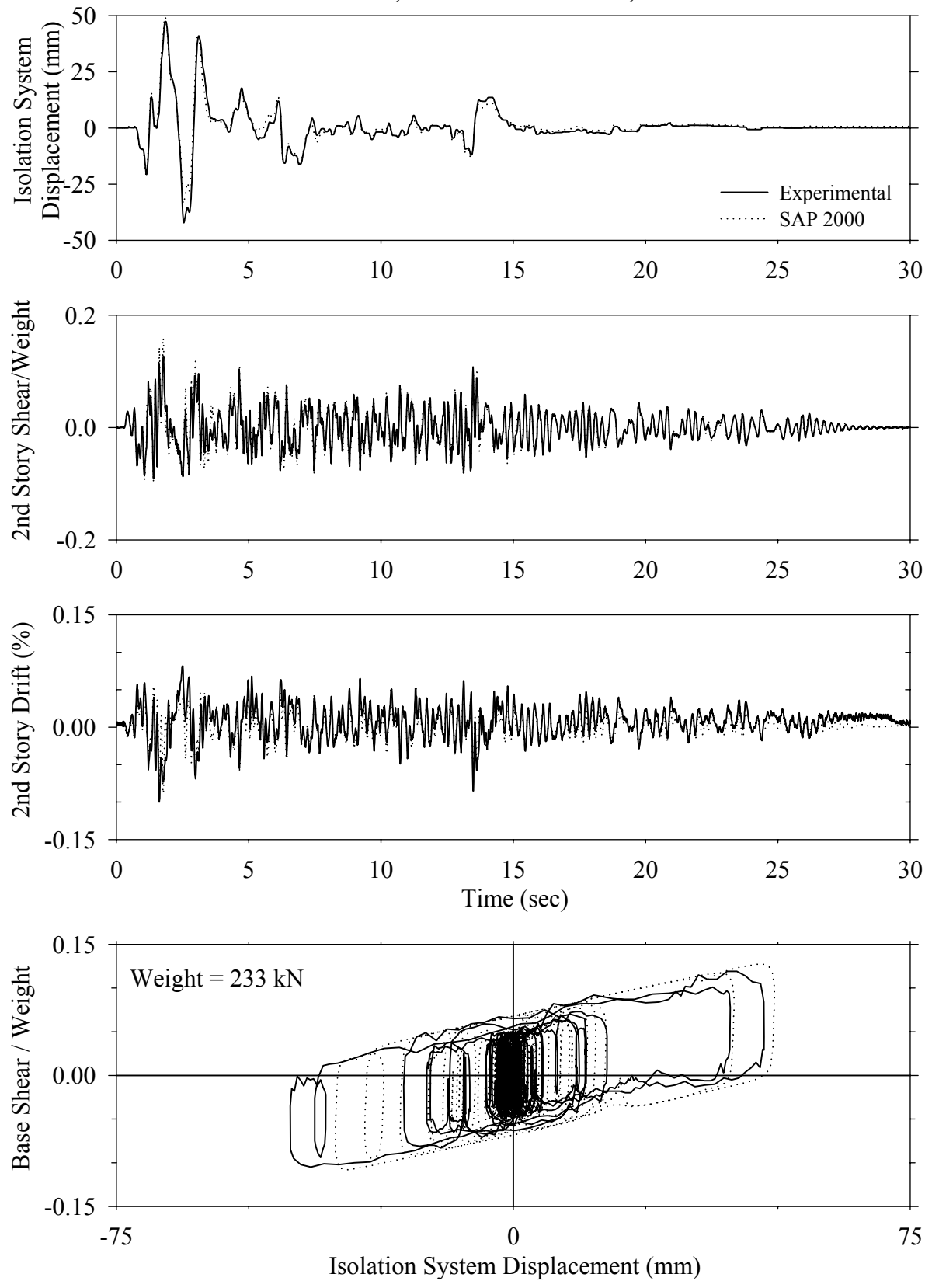
Test FPMNS10.1, Sylmar 100%, MF/FPS with Nonlinear Dampers



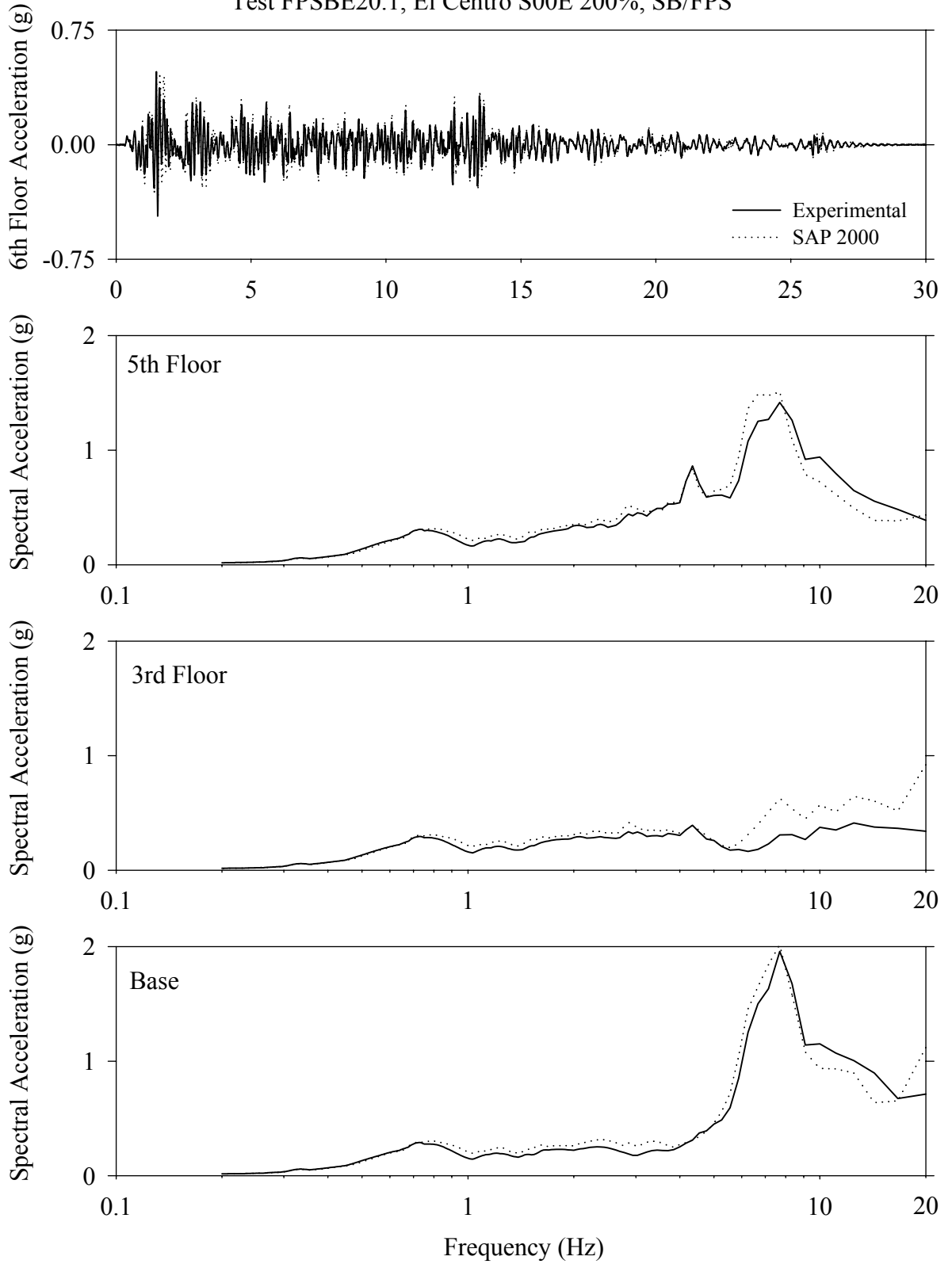
Test FPMNS10.1, Sylmar 100%, MF/FPS with Nonlinear Dampers



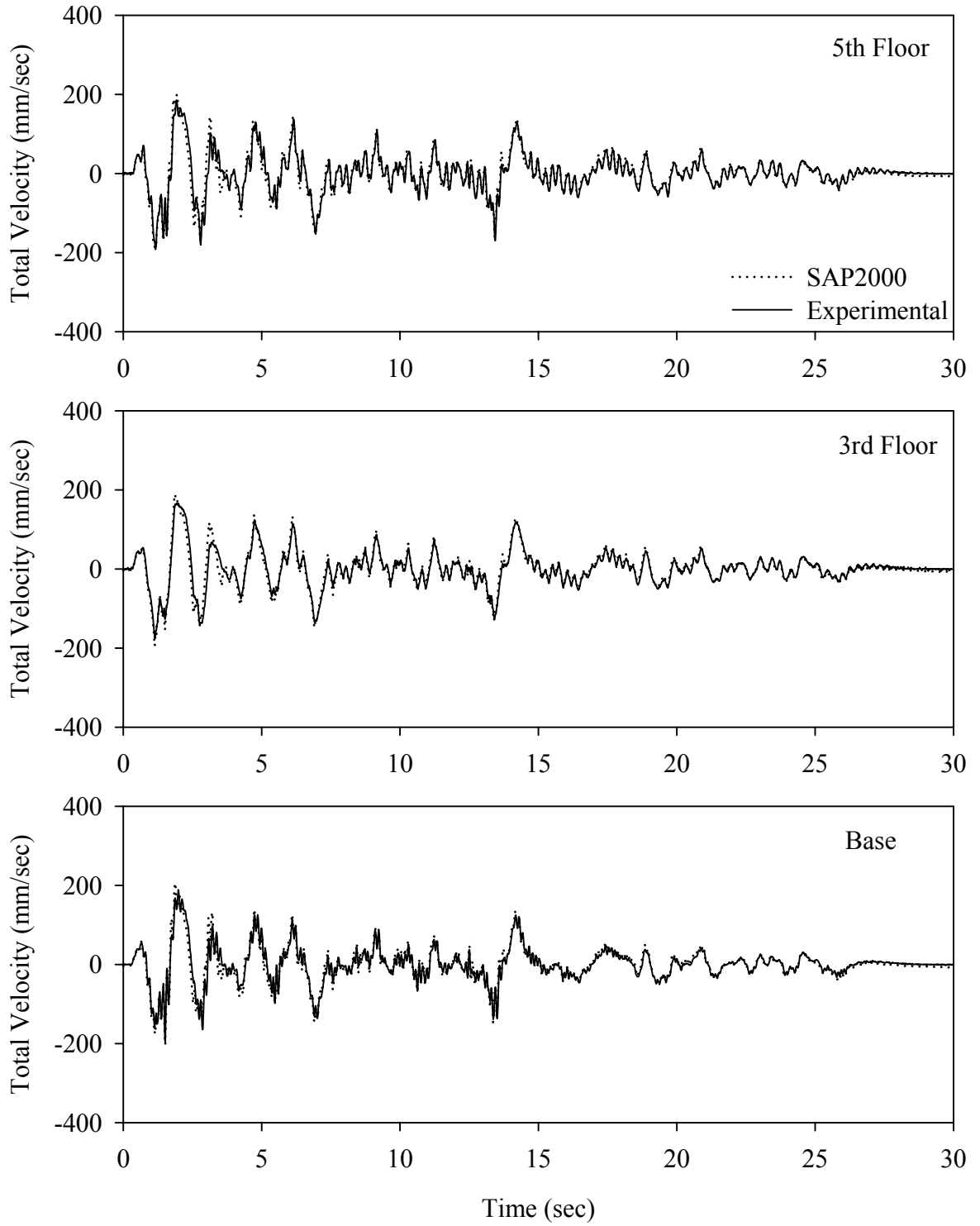
Test FPSBE20.1, El Centro S00E 200%, SB/FPS



Test FPSBE20.1, El Centro S00E 200%, SB/FPS

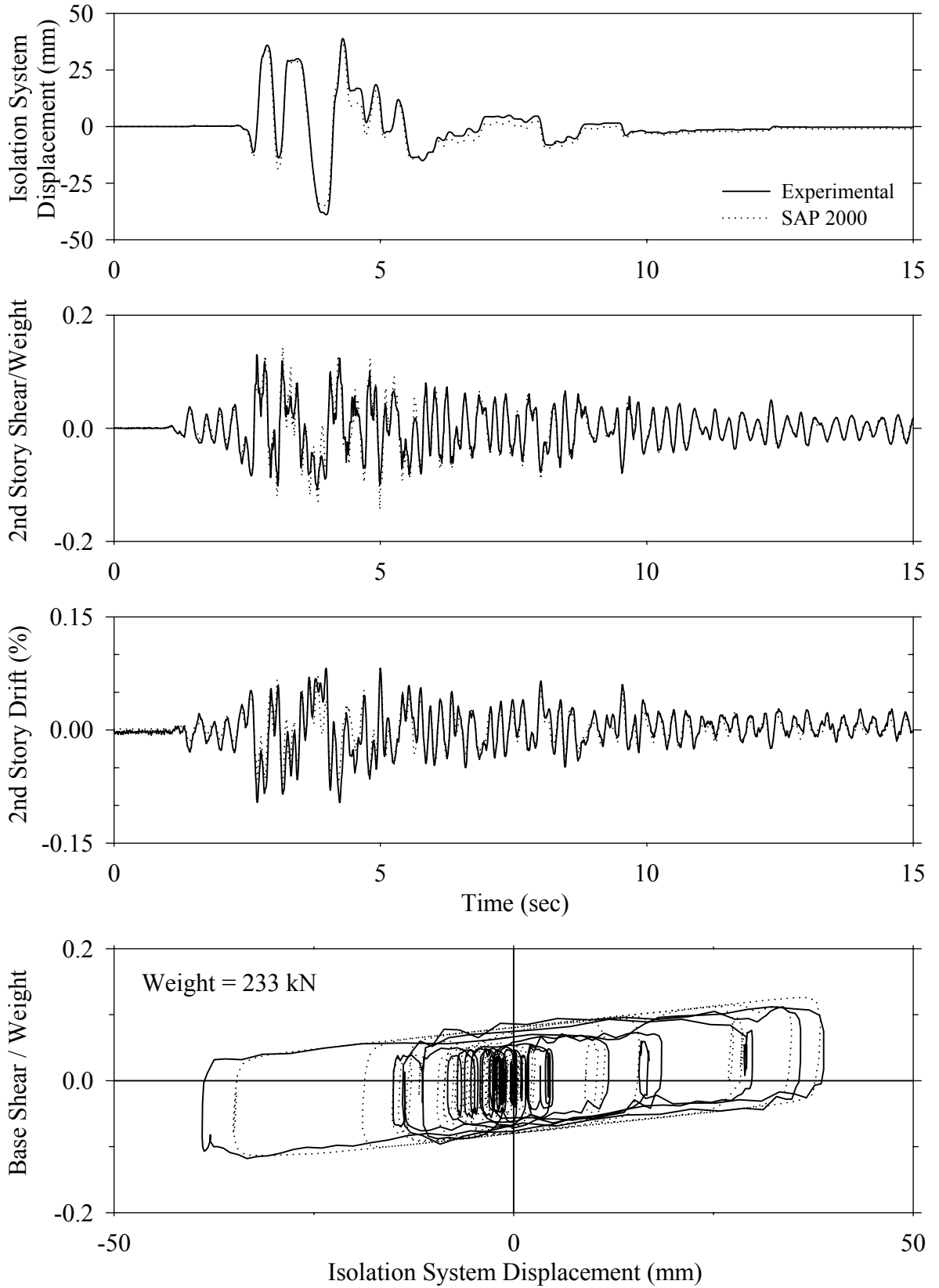


Test FPSBE20.1, El Centro S00E 200%, SB/FPS

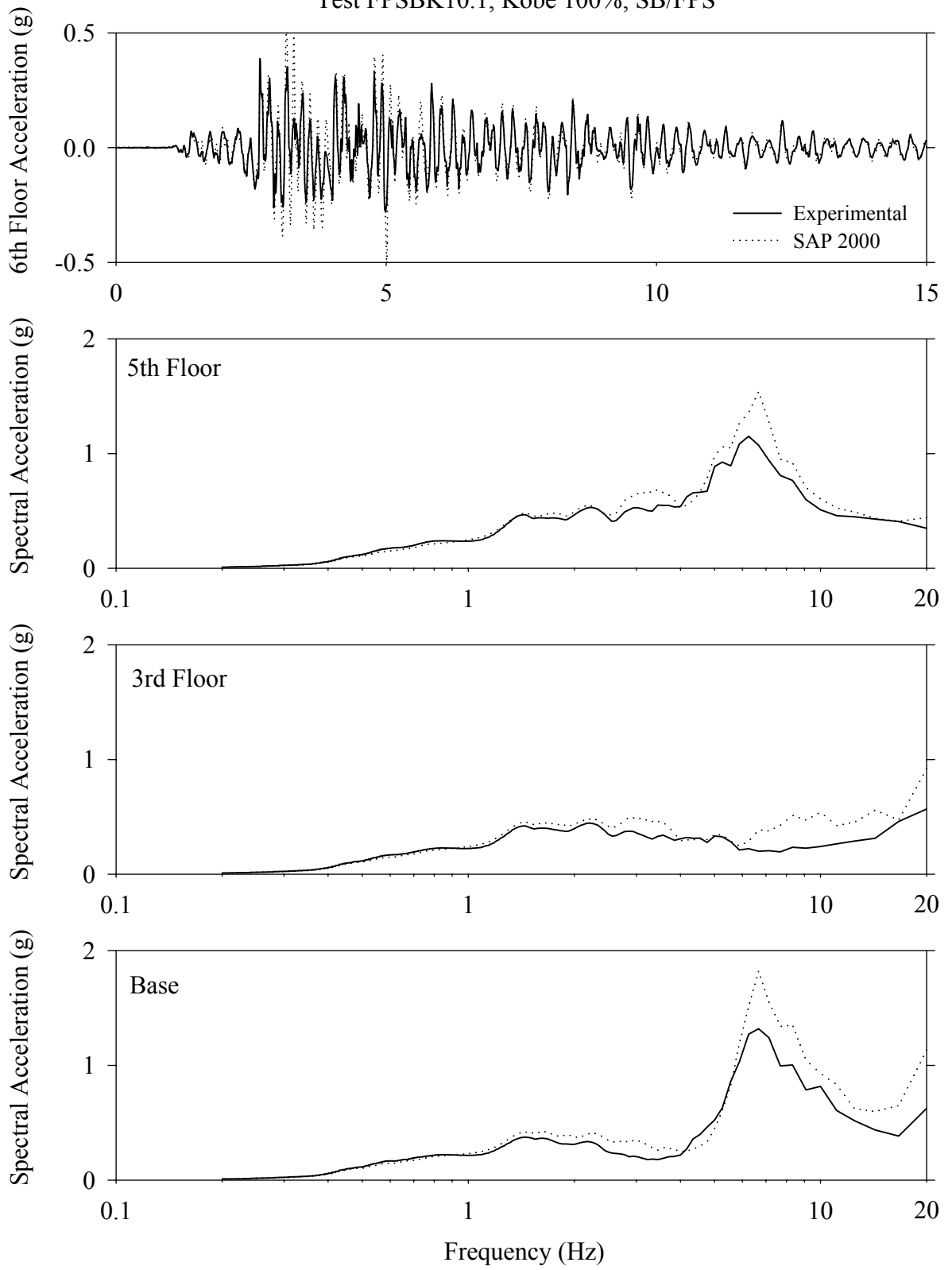




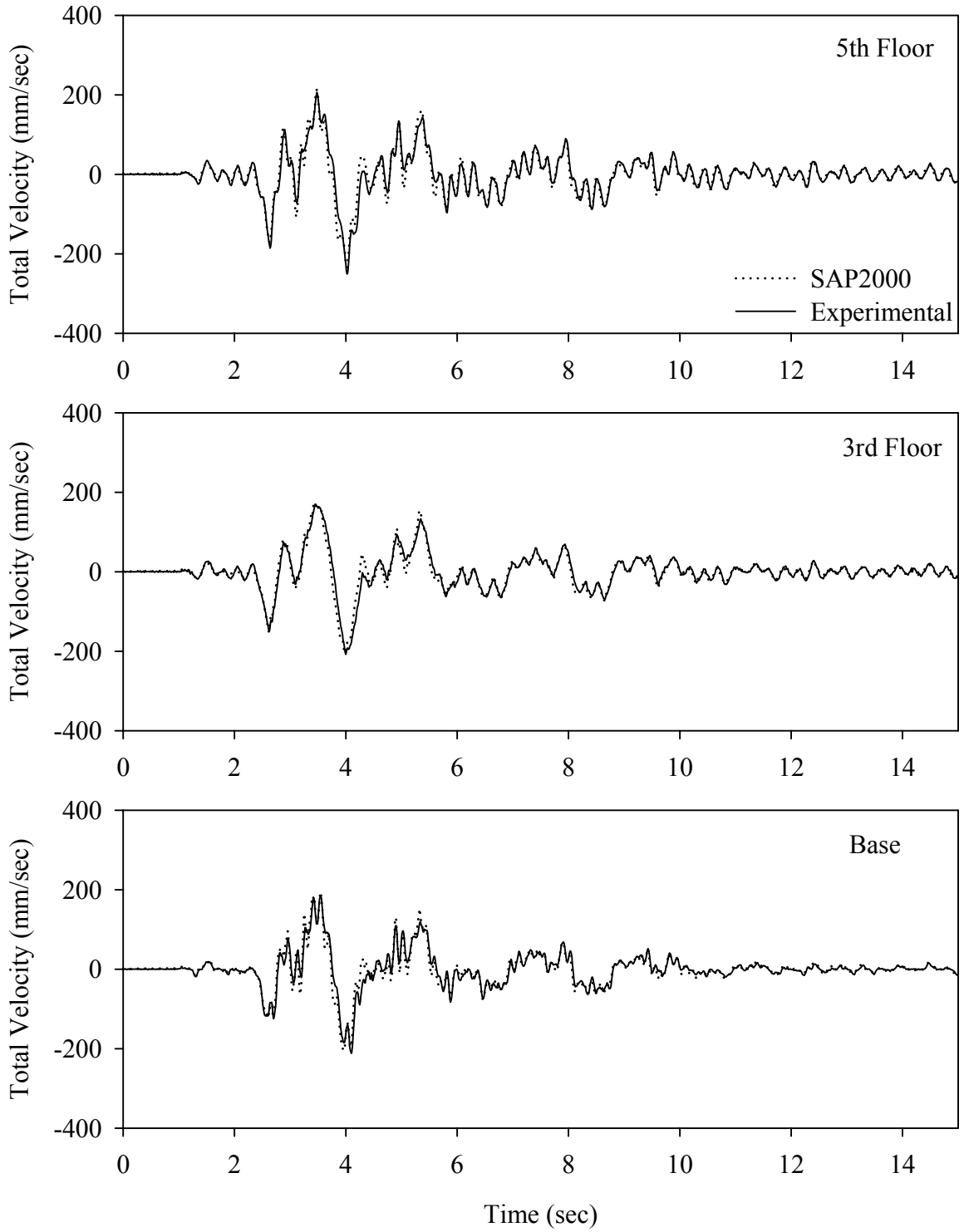
Test FPSBK10.1, Kobe 100%, SB/FPS



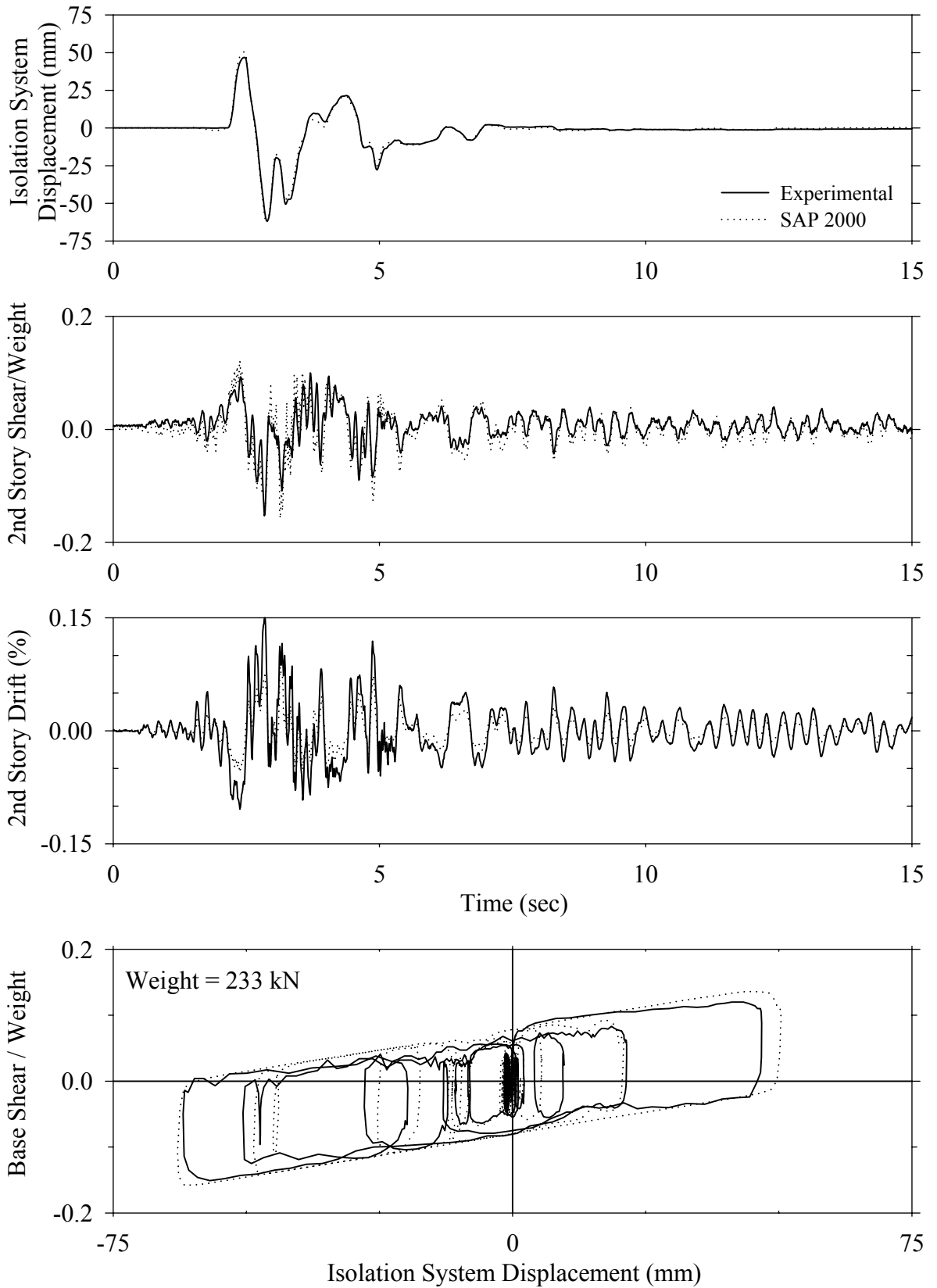
Test FPSBK10.1, Kobe 100%, SB/FPS



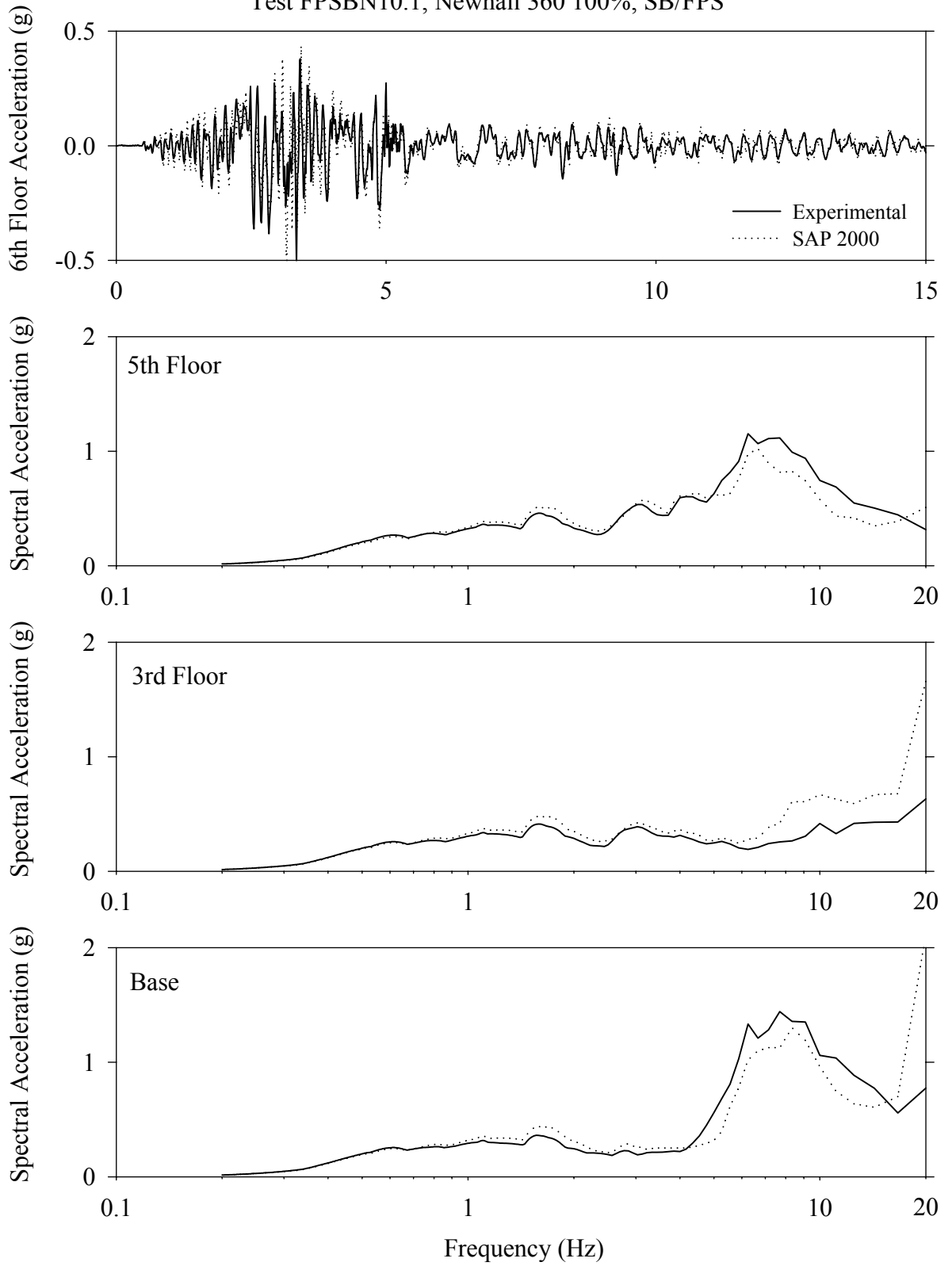
Test FPSBK10.1, Kobe 100%, SB/FPS



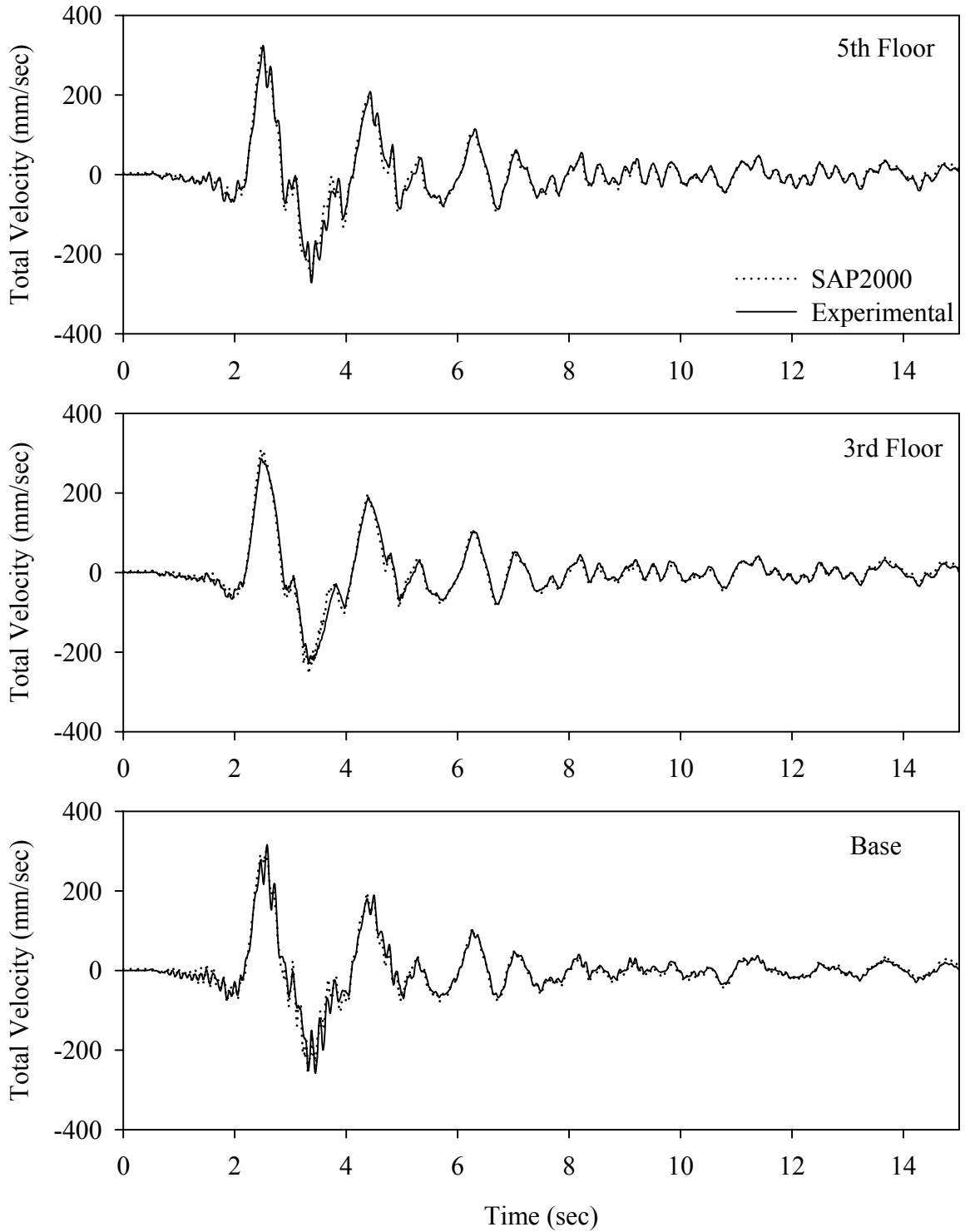
Test FPSBN10.1, Newhall 360 100%, SB/FPS



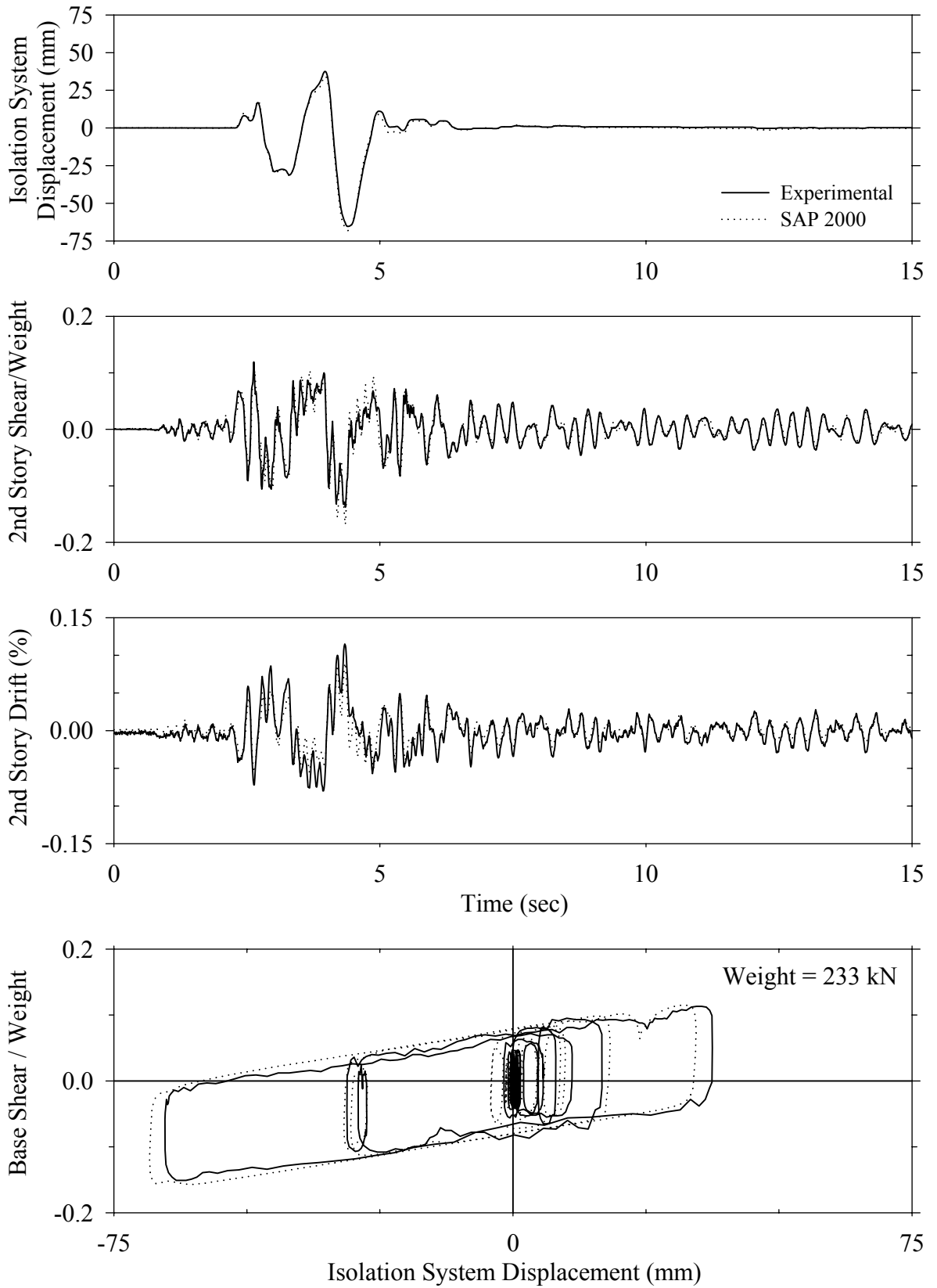
Test FPSBN10.1, Newhall 360 100%, SB/FPS



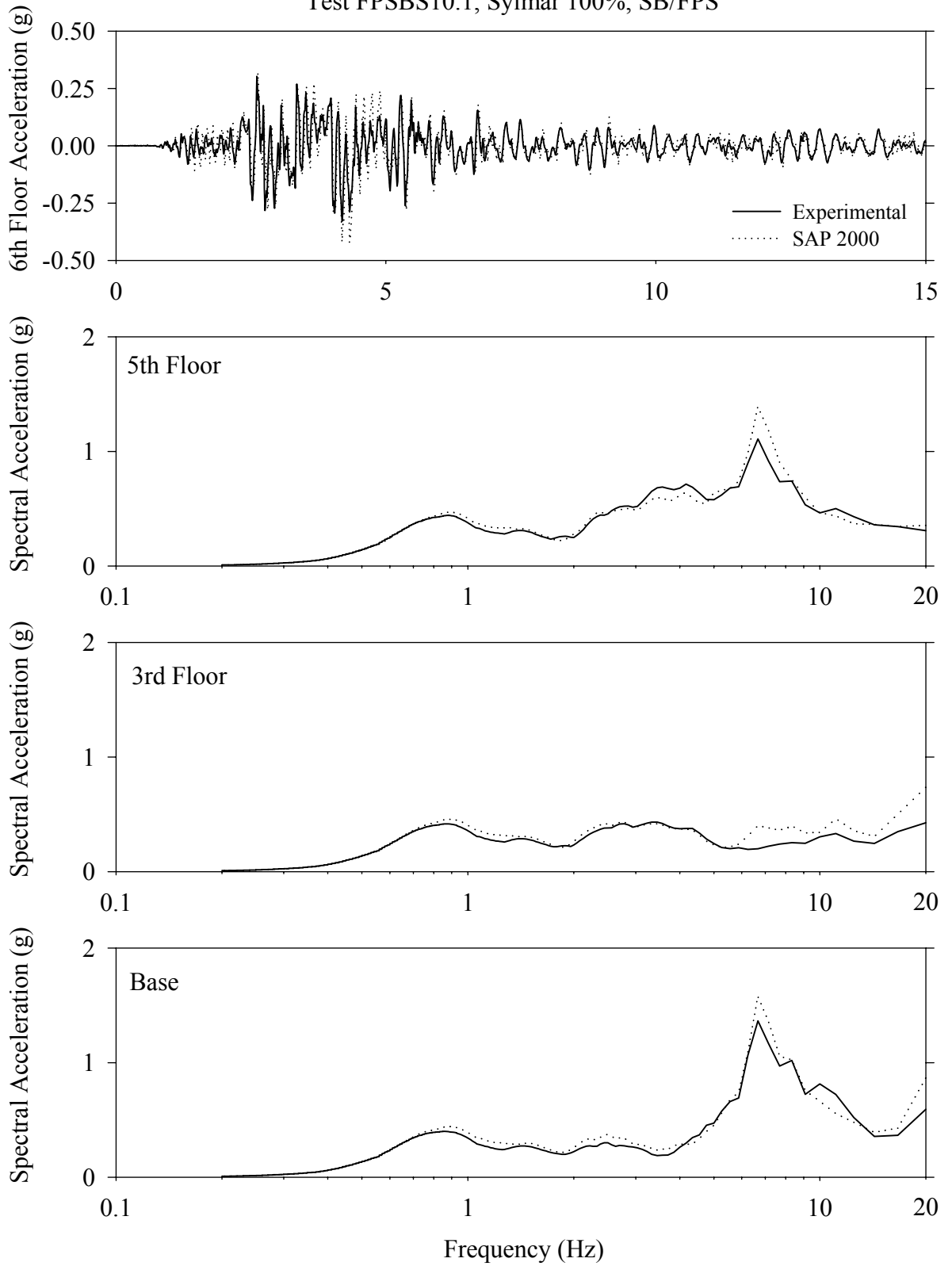
Test FPSBN10.1, Newhall 360 100%, SB/FPS



Test FPSBS10.1, Sylmar 100%, SB/FPS

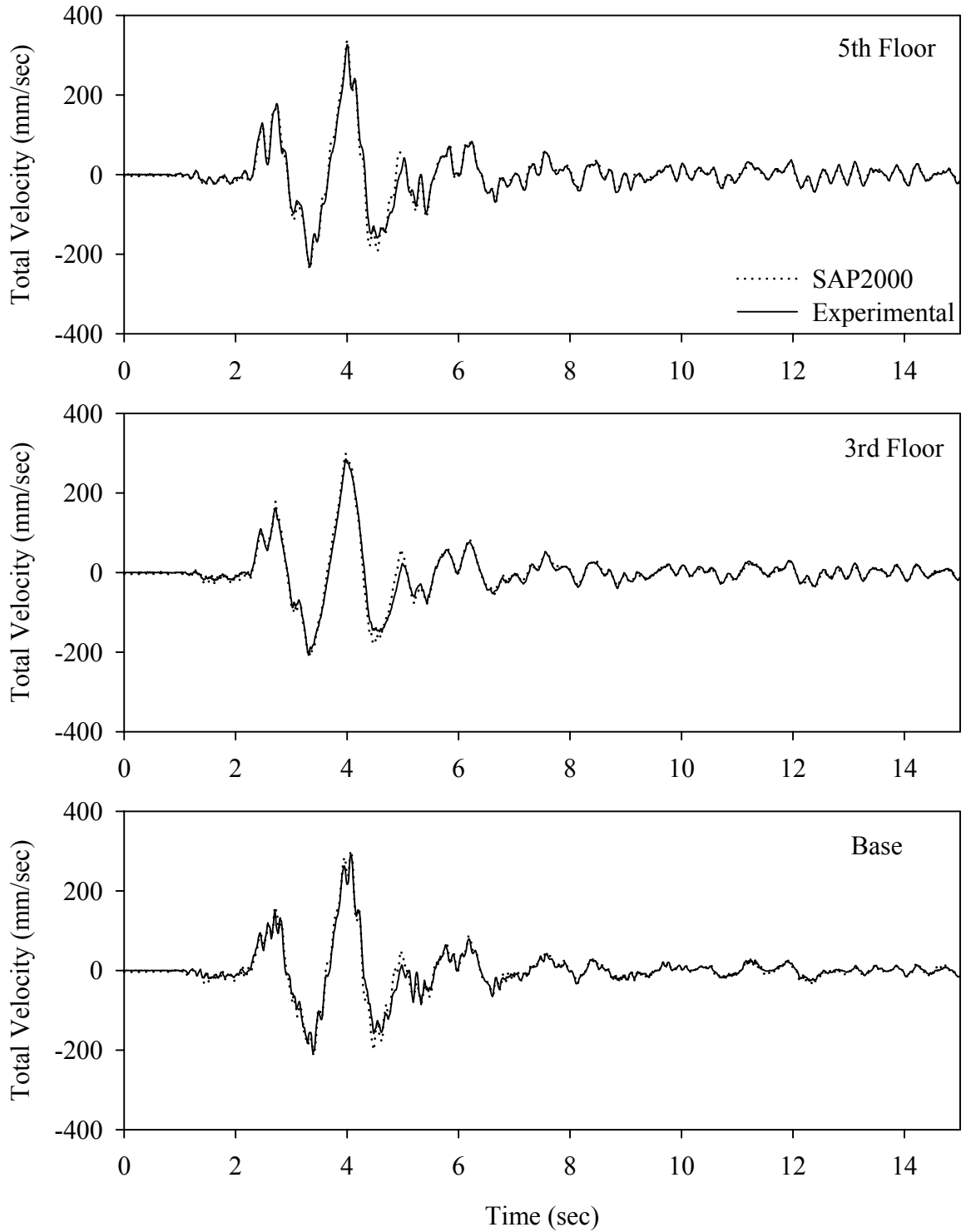


Test FPSBS10.1, Sylmar 100%, SB/FPS

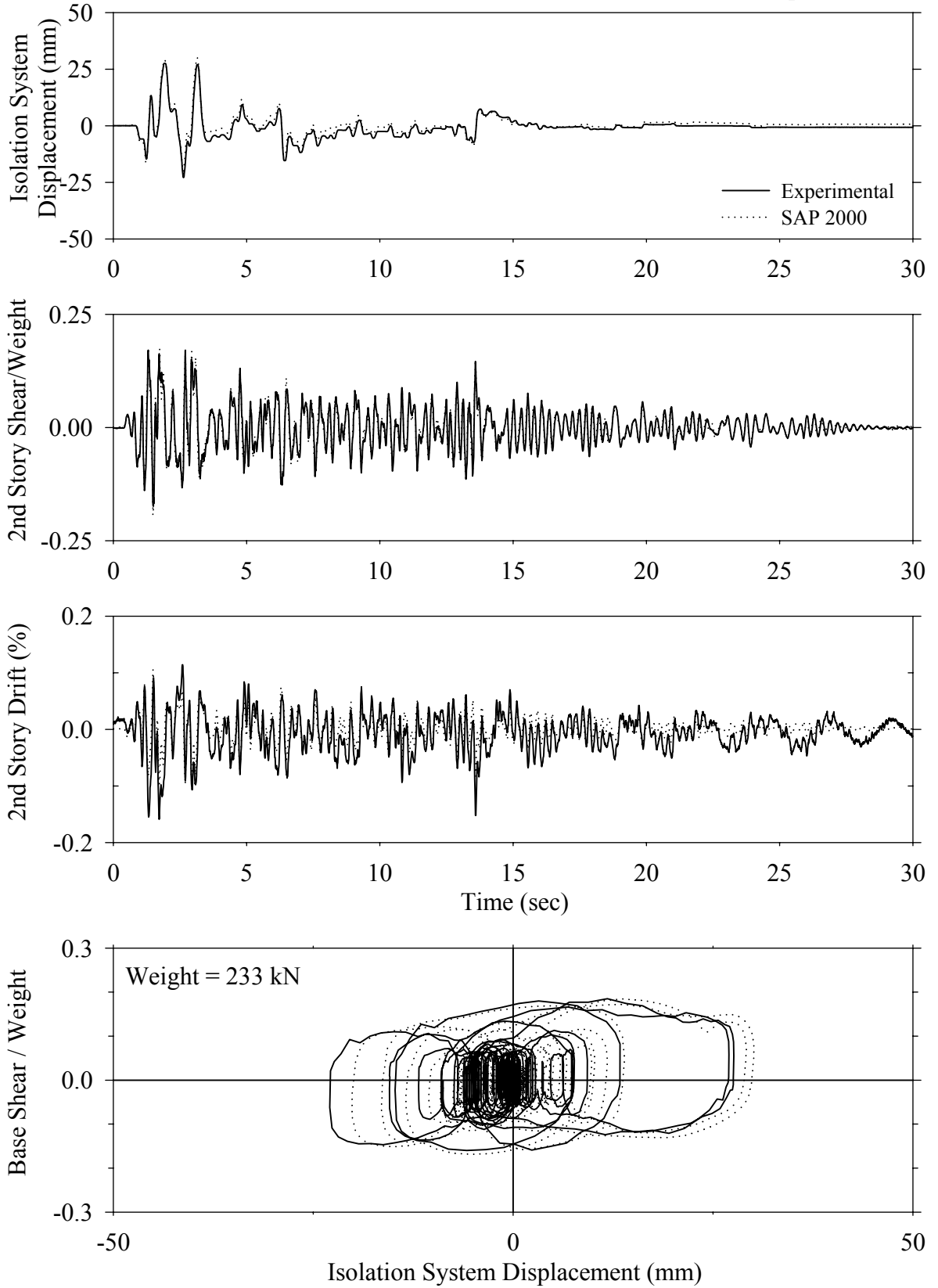




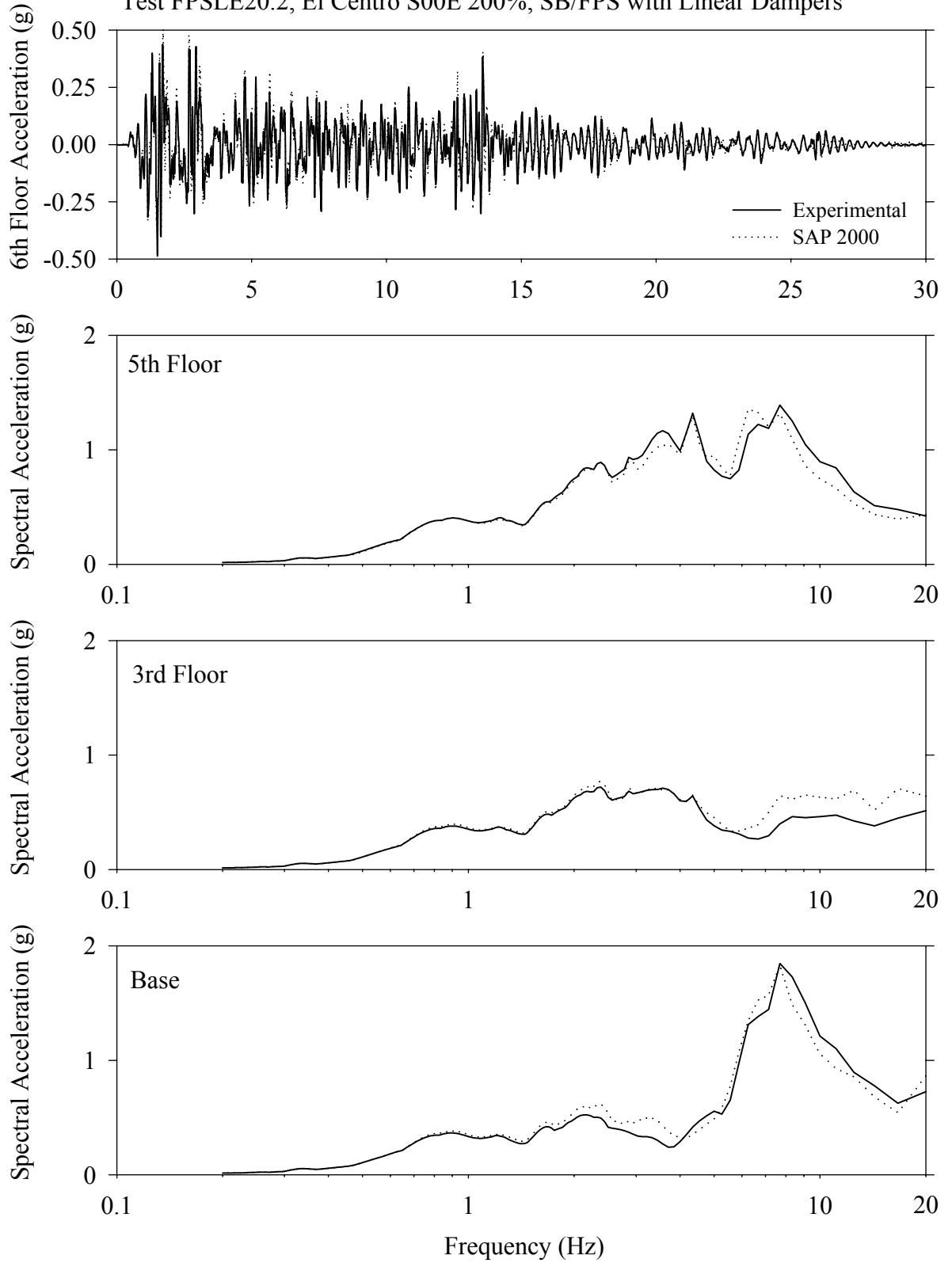
Test FPSBS10.1, Sylmar 100%, SB/FPS



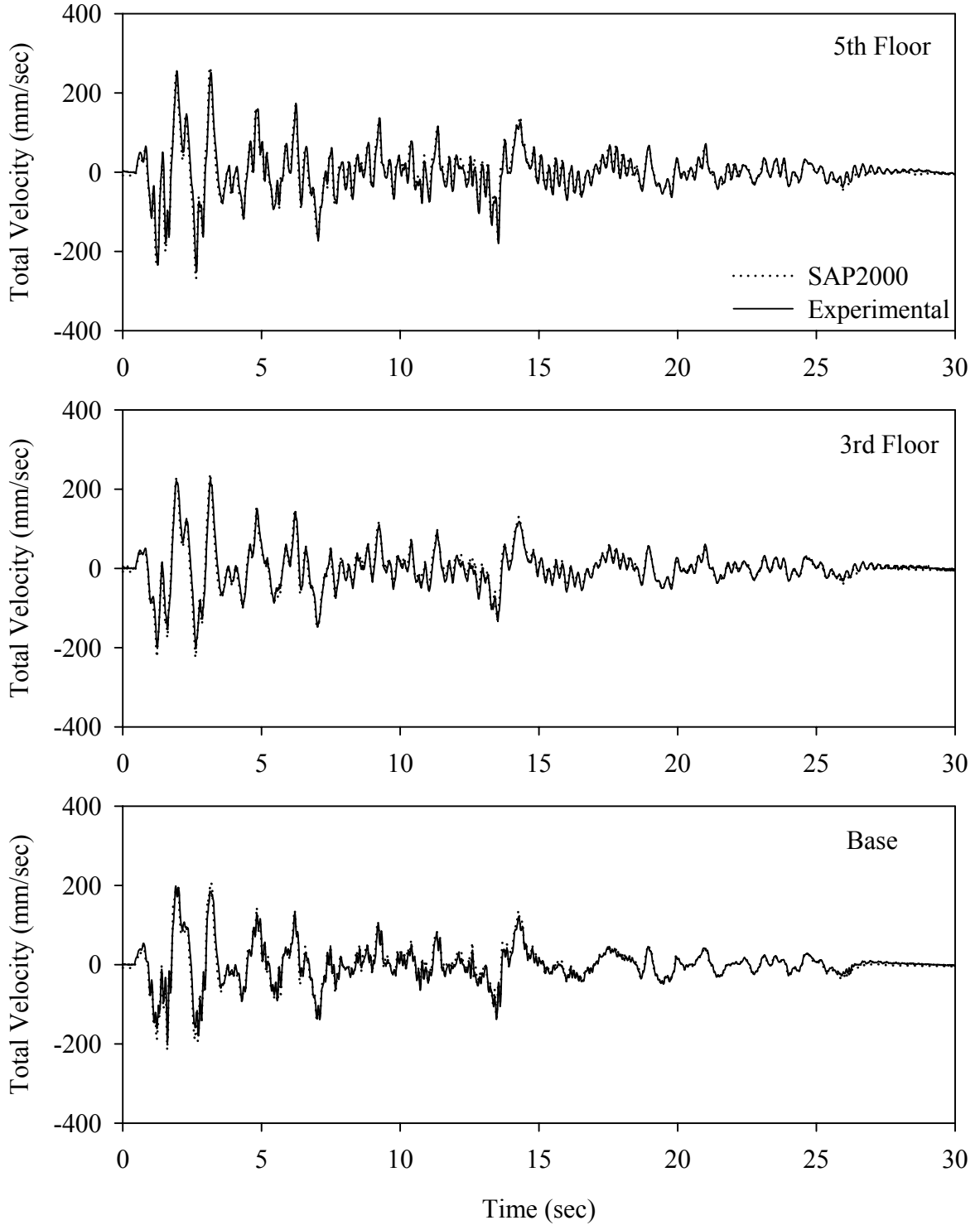
Test FPSLE20.2, El Centro S00E 200%, SB/FPS with Linear Dampers



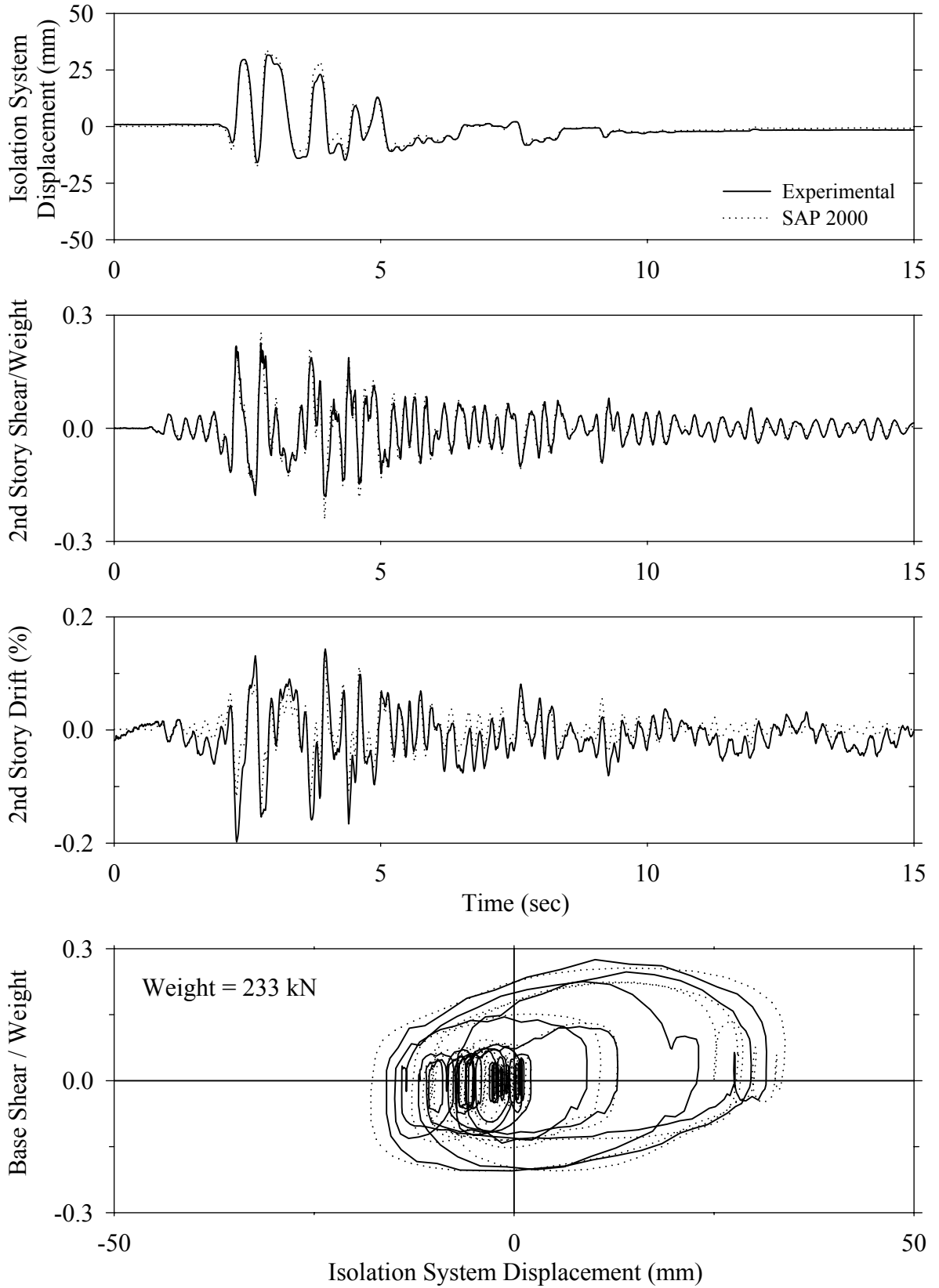
Test FPSLE20.2, El Centro S00E 200%, SB/FPS with Linear Dampers



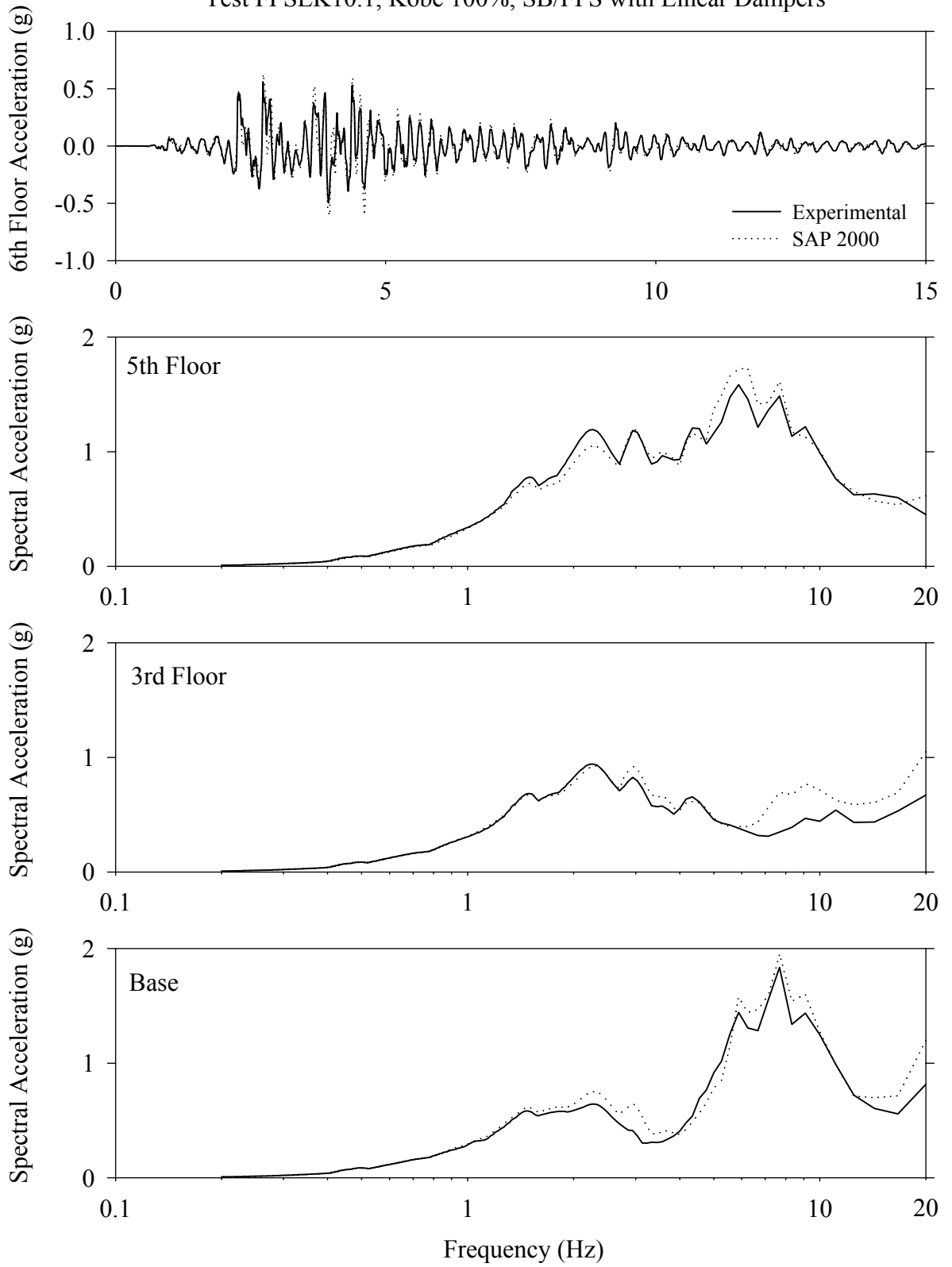
Test FPSLE20.1, El Centro S00E 200%, SB/FPS with Linear Dampers



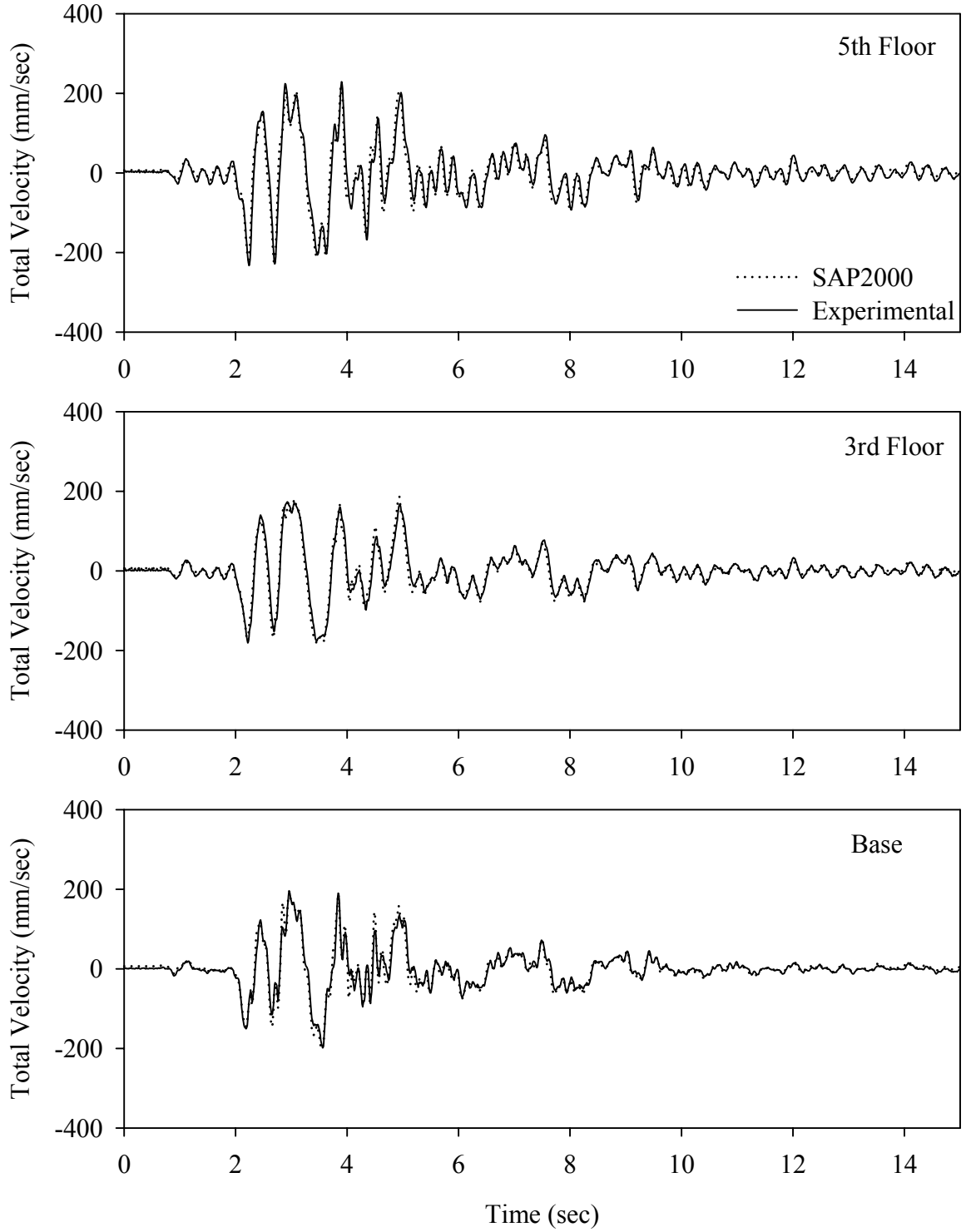
Test FPSLK10.1, Kobe 100%, SB/FPS with Linear Dampers



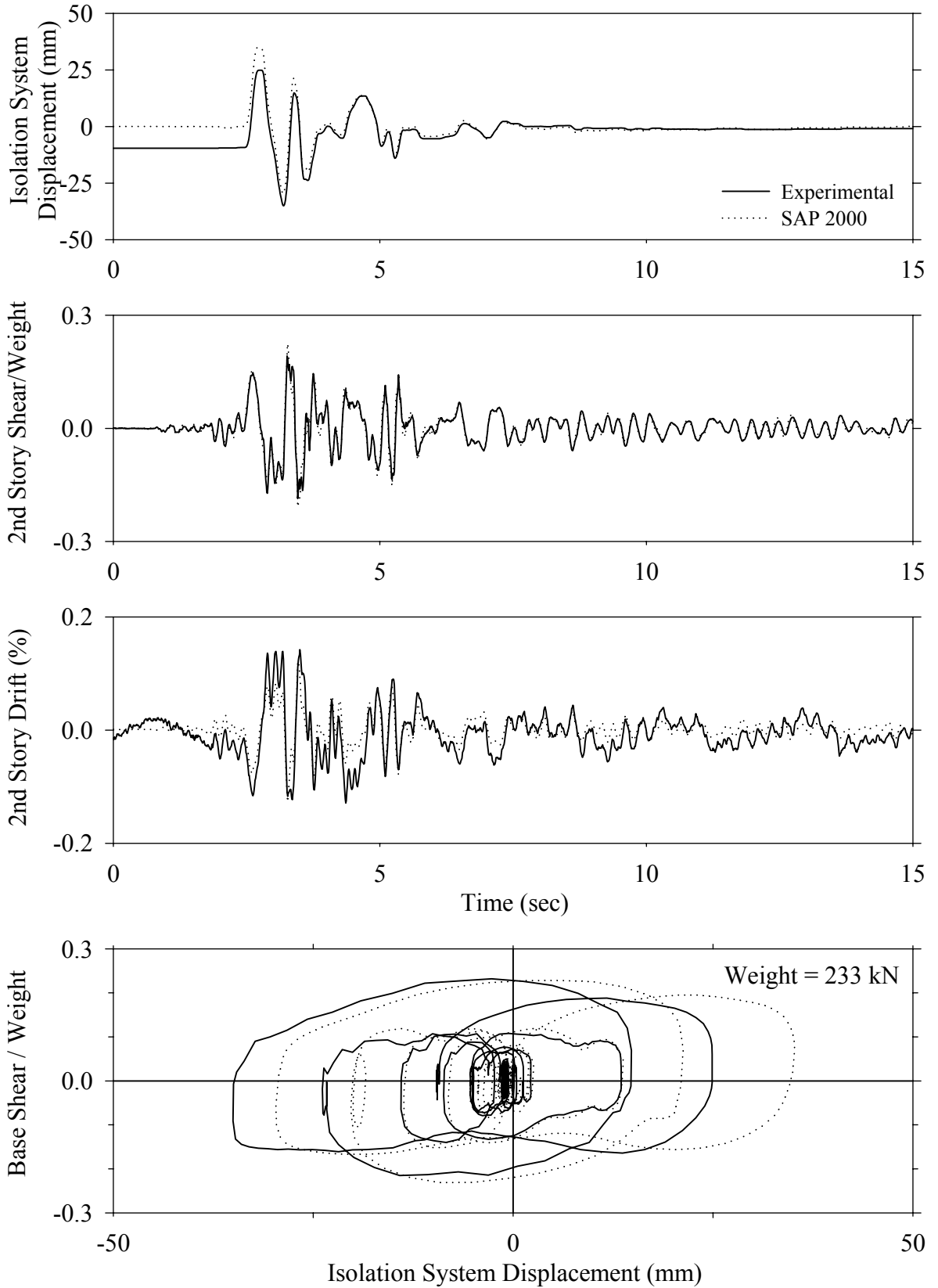
Test FPSLK10.1, Kobe 100%, SB/FPS with Linear Dampers



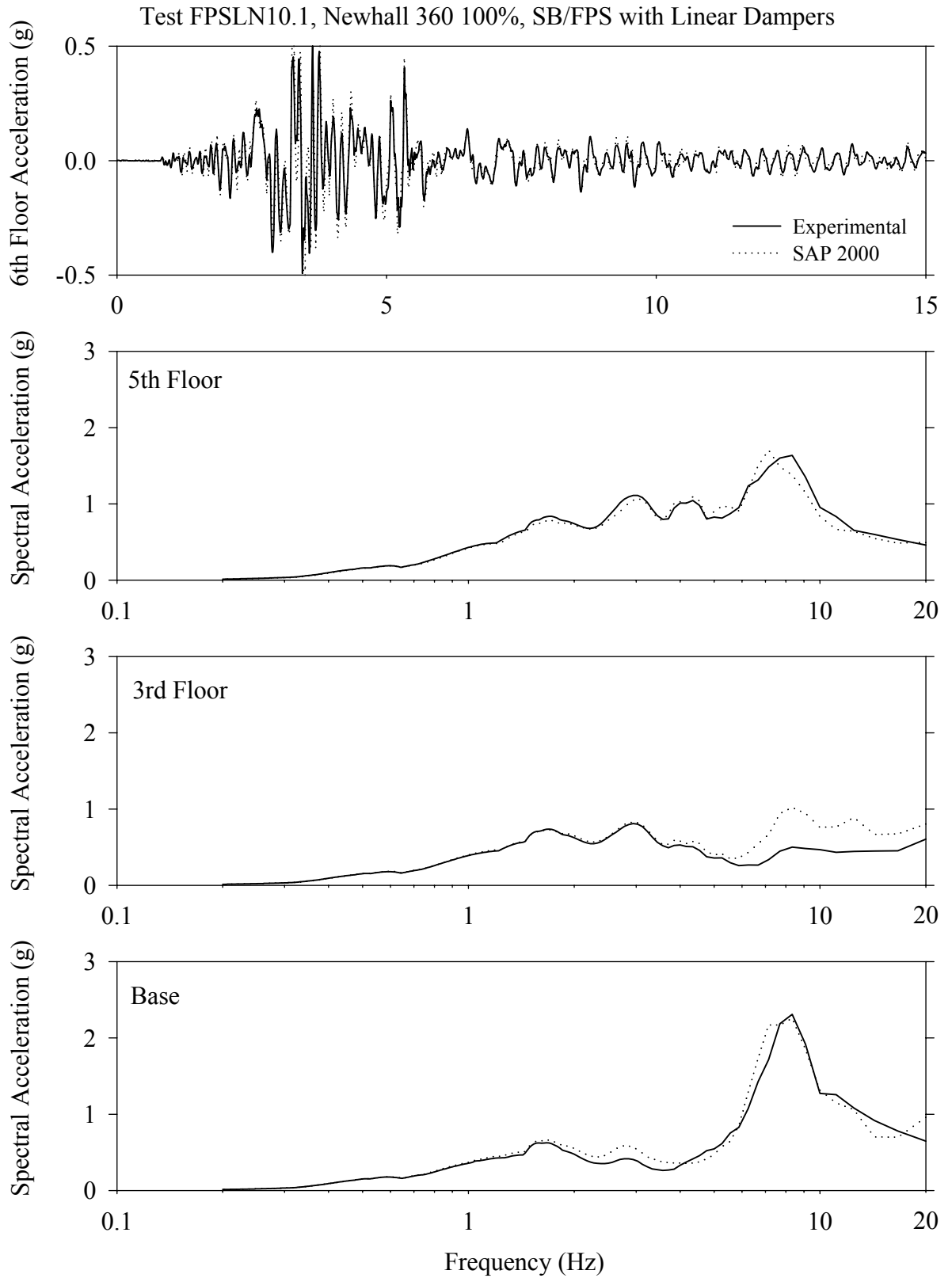
Test FPSLK10.1, Kobe 100%, SB/FPS with Linear Dampers



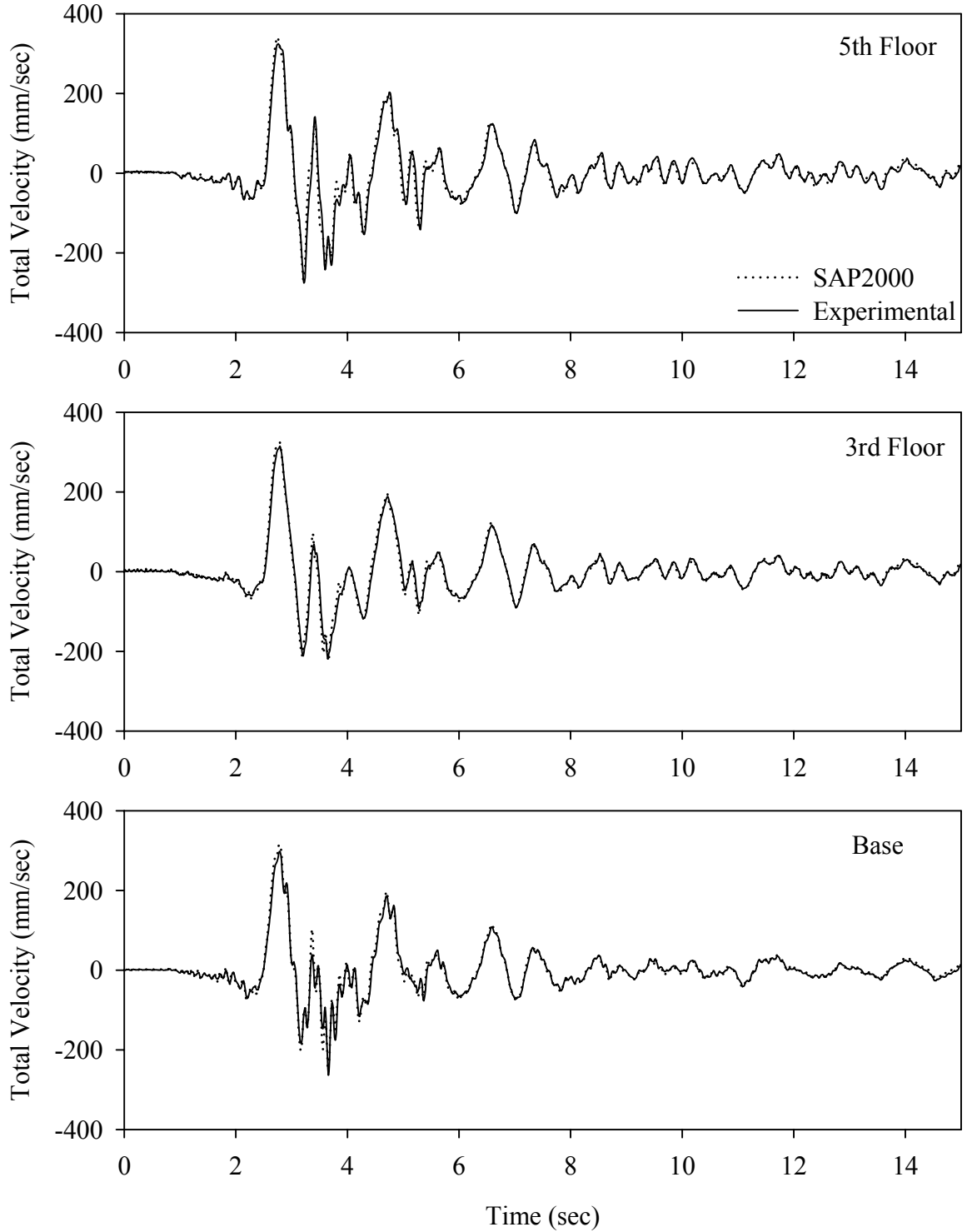
Test FPSLN10.1, Newhall 360 100%, SB/FPS with Linear Dampers



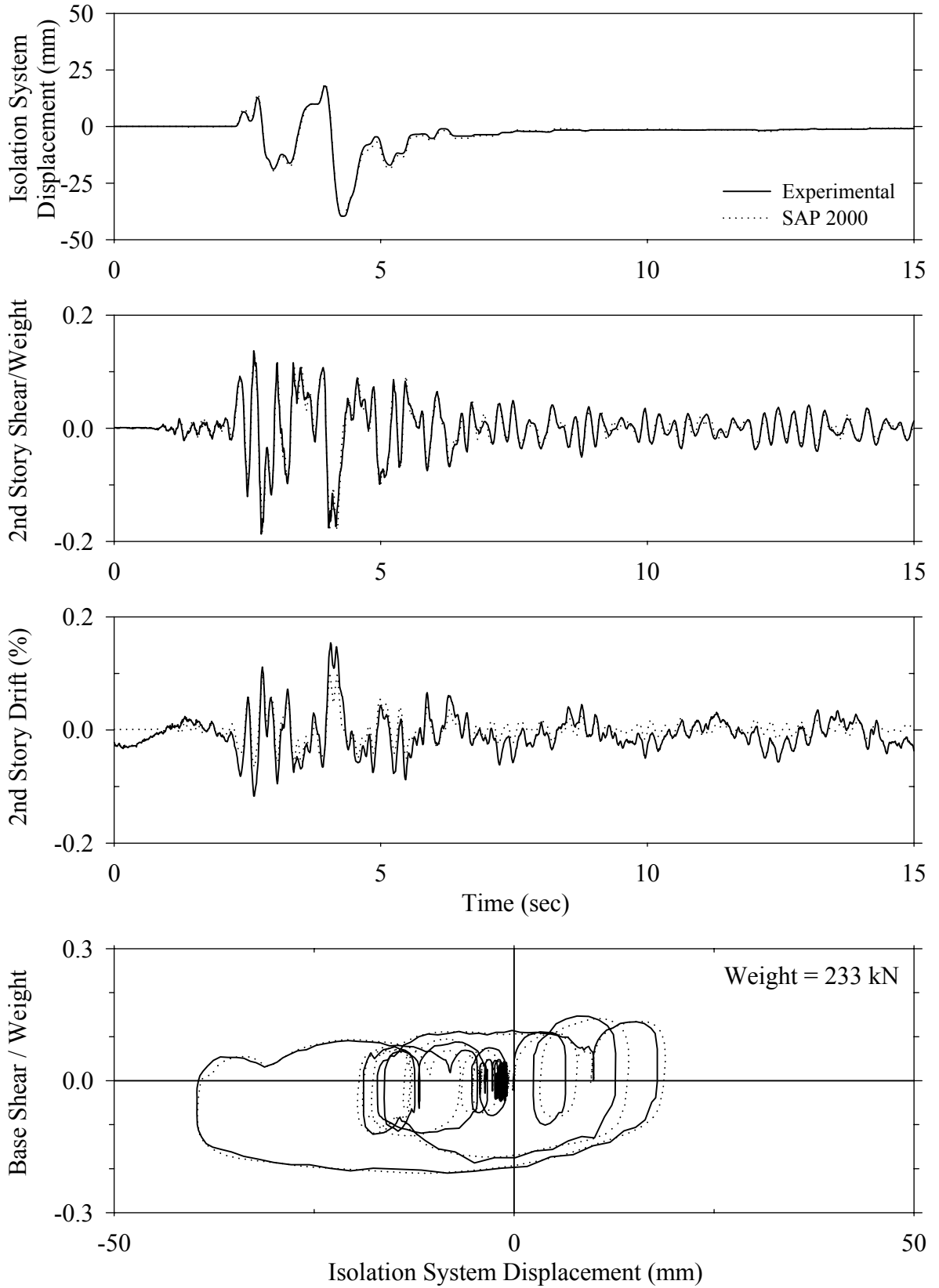




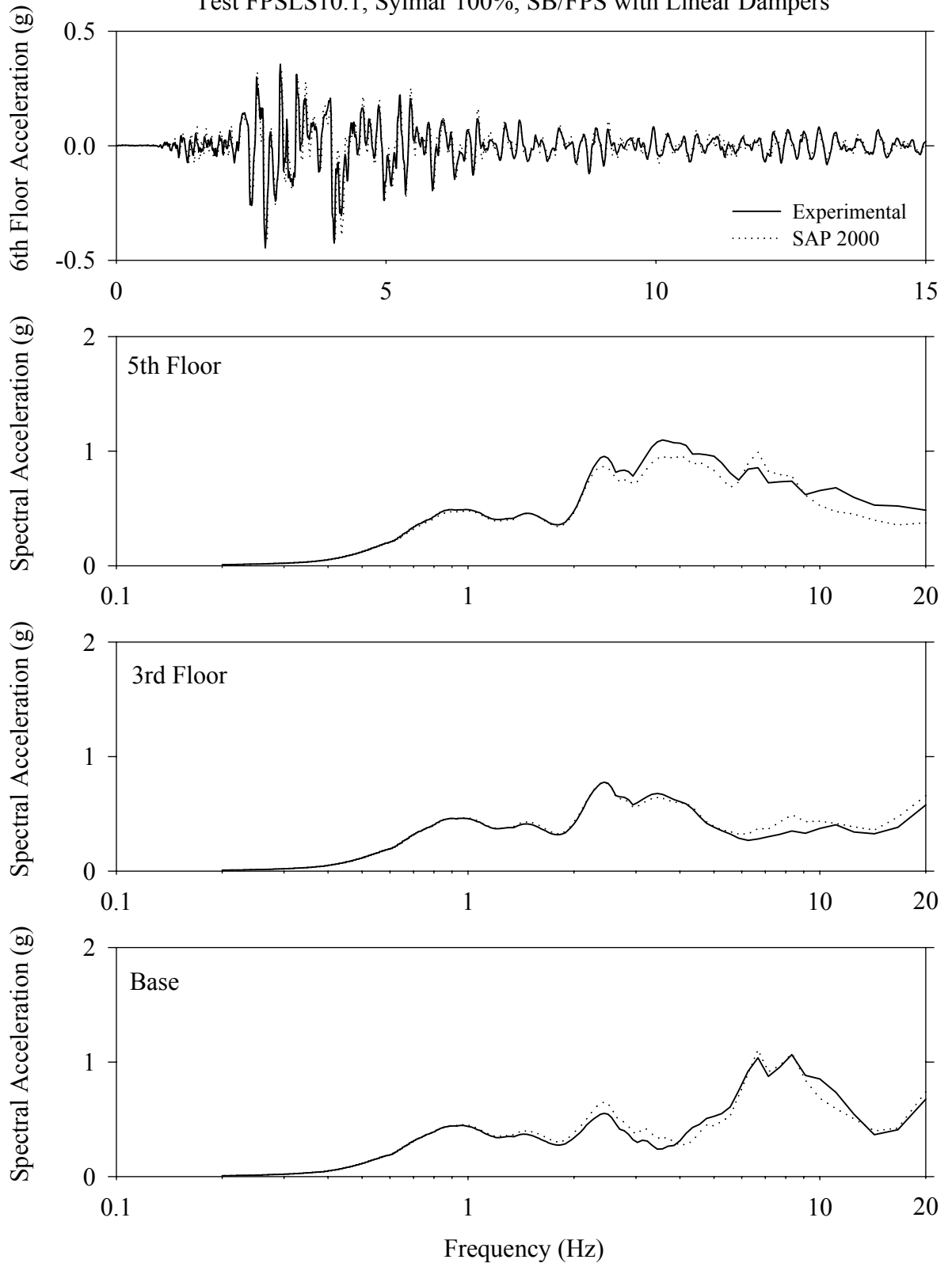
Test FPSLN10.1, Newhall 360 100%, SB/FPS with Linear Dampers



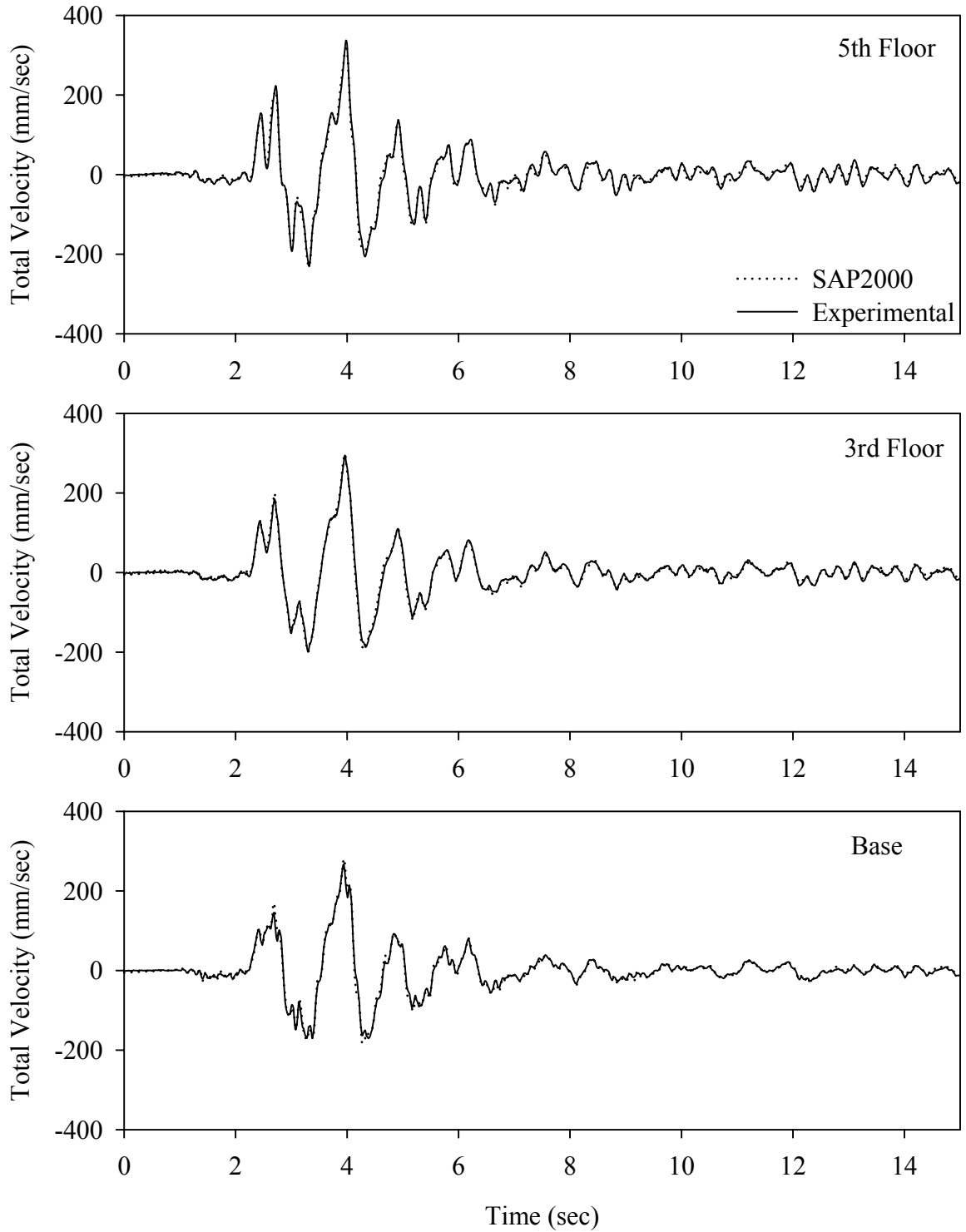
Test FPSLS10.1, Sylmar 100%, SB/FPS with Linear Dampers



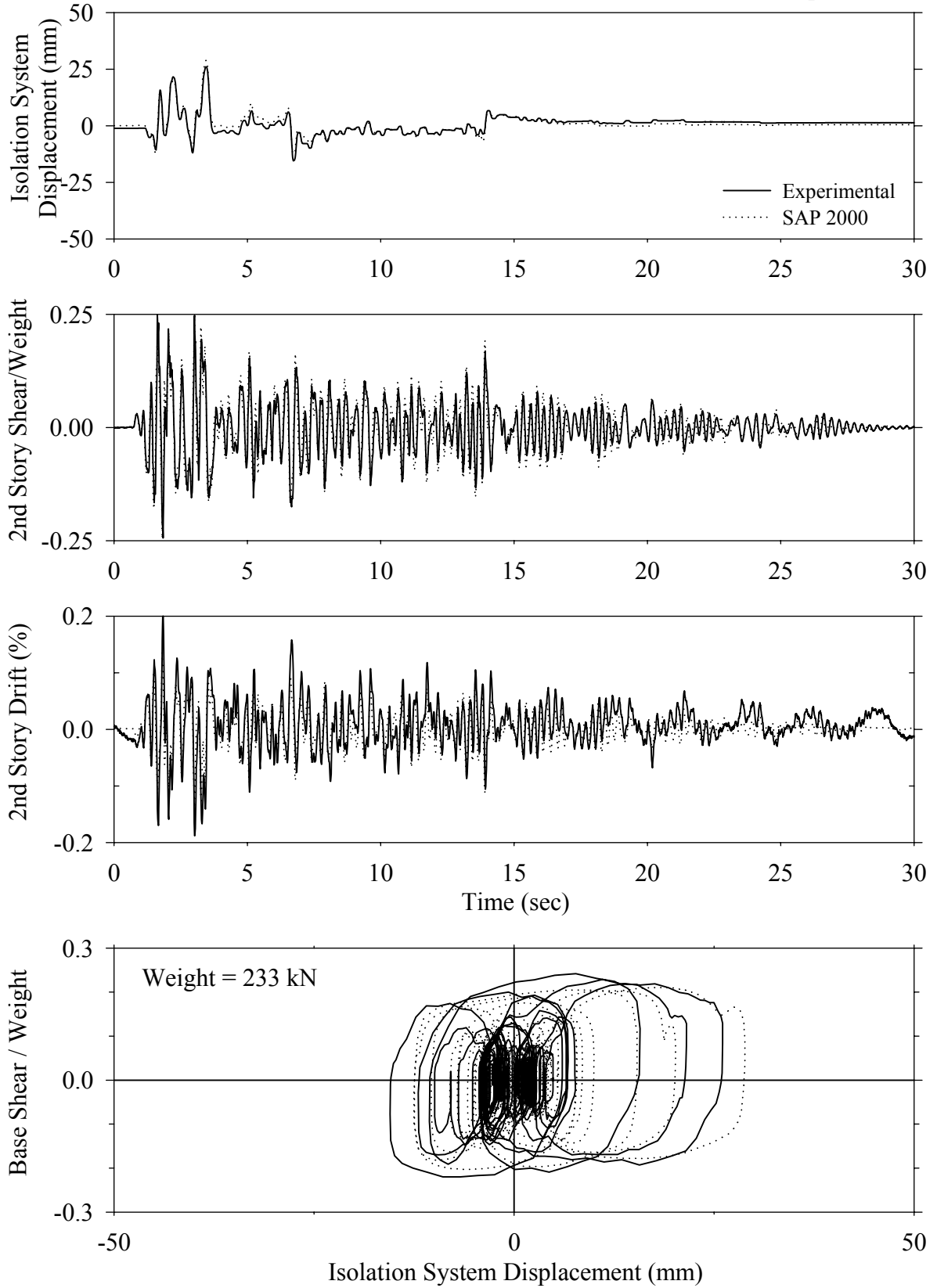
Test FPSLS10.1, Sylmar 100%, SB/FPS with Linear Dampers



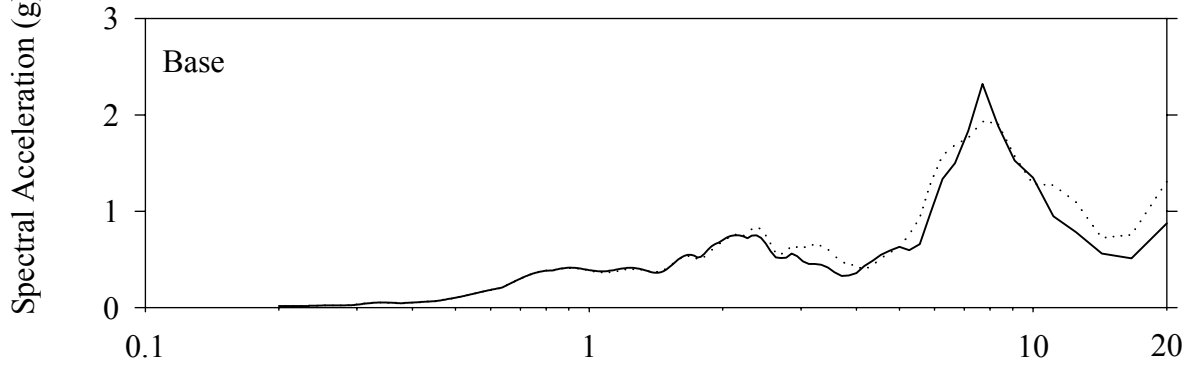
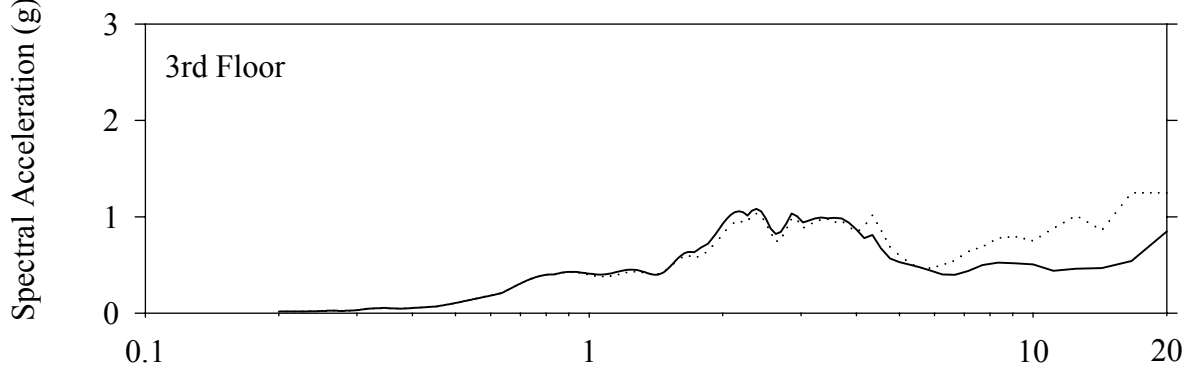
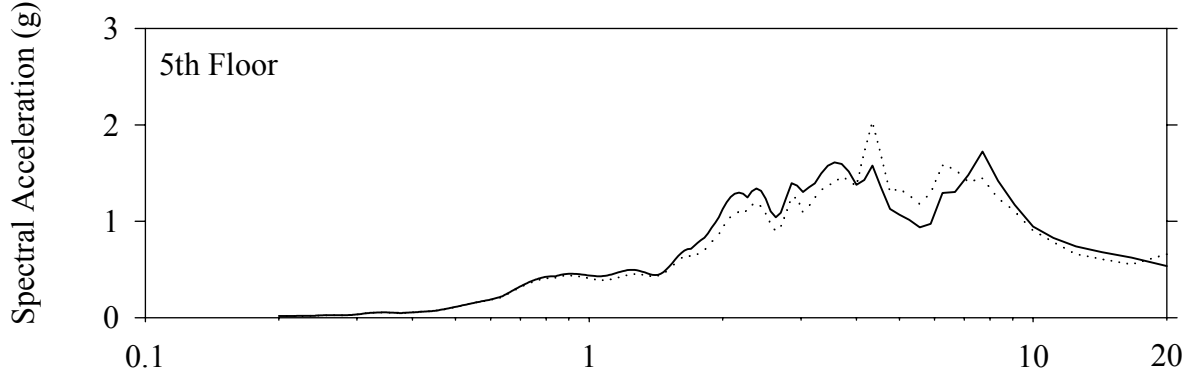
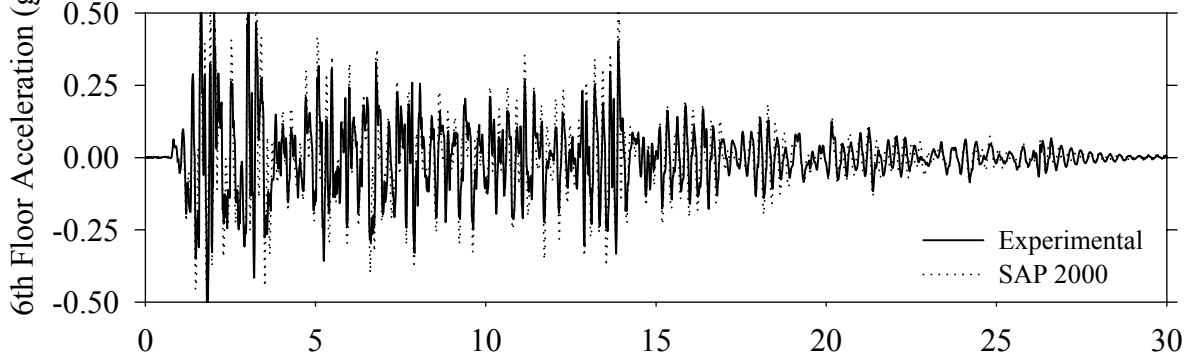
Test FPSLS10.1, Sylmar 100%, SB/FPS with Linear Dampers



Test FPSNE20.2, El Centro S00E 200%, SB/FPS with Nonlinear Dampers

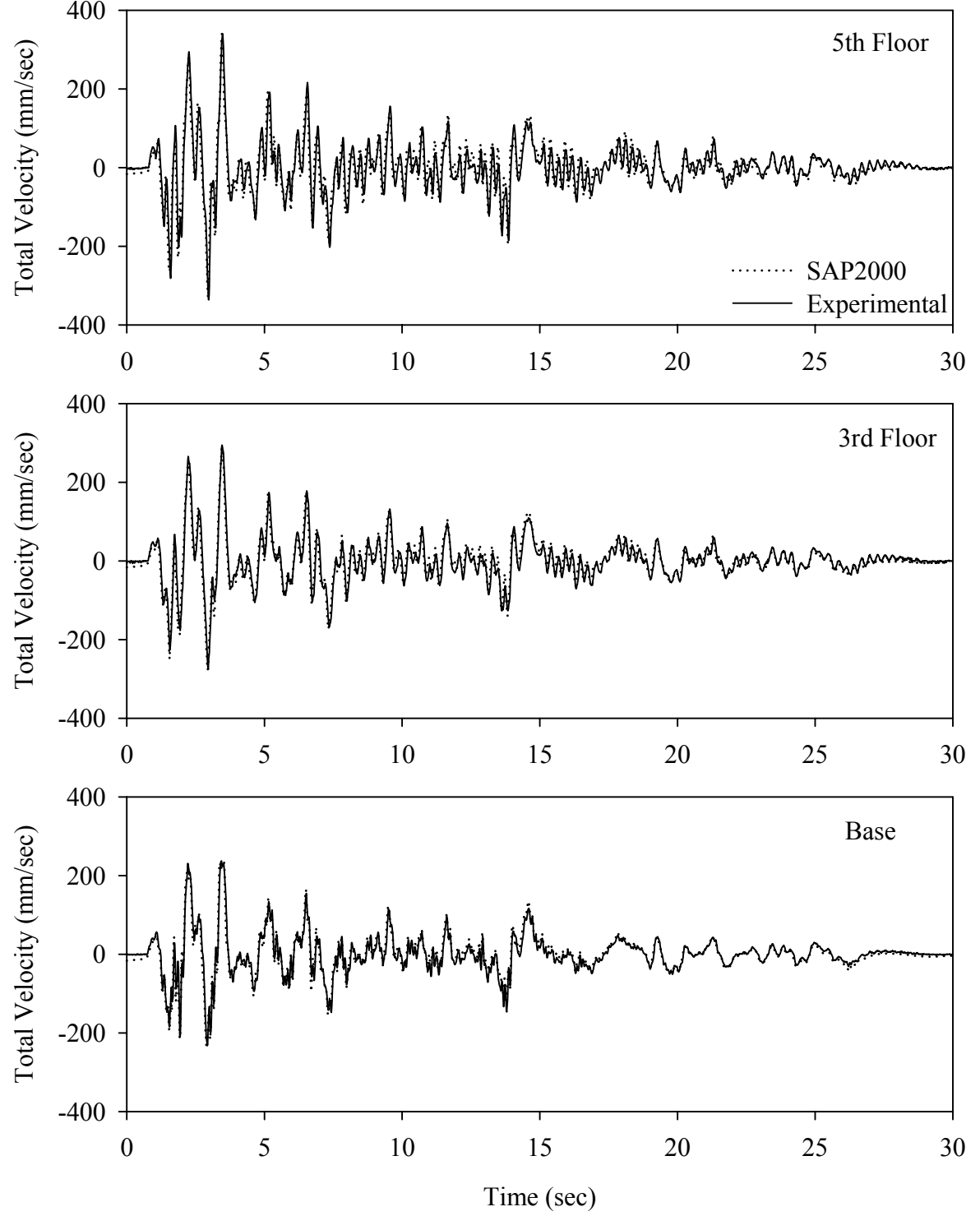


Test FPSNE20.2, El Centro S00E 200%, SB/FPS with Nonlinear Dampers



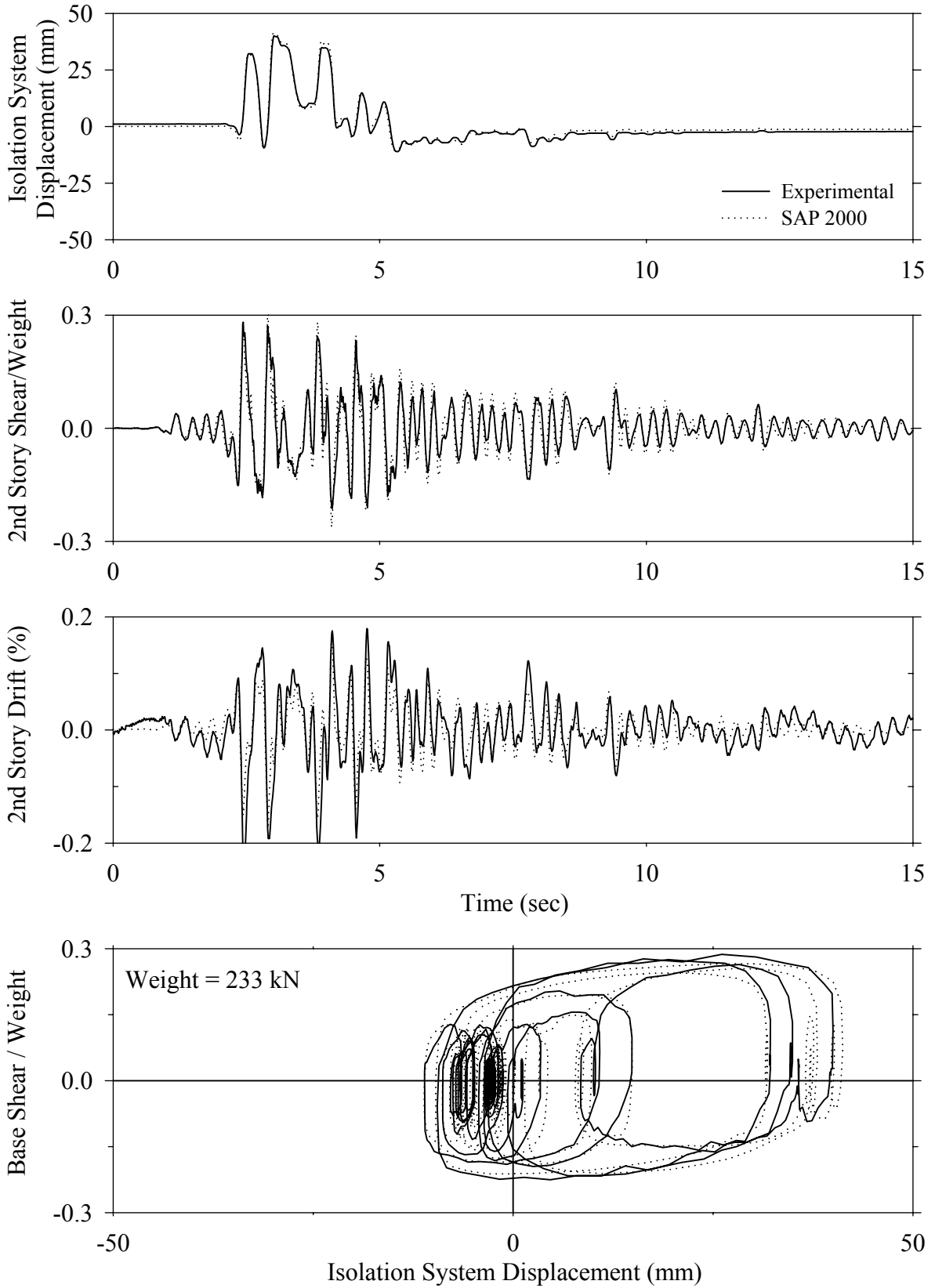
Frequency (Hz)

Test FPSNE20.1, El Centro S00E 200%, SB/FPS with Nonlinear Dampers

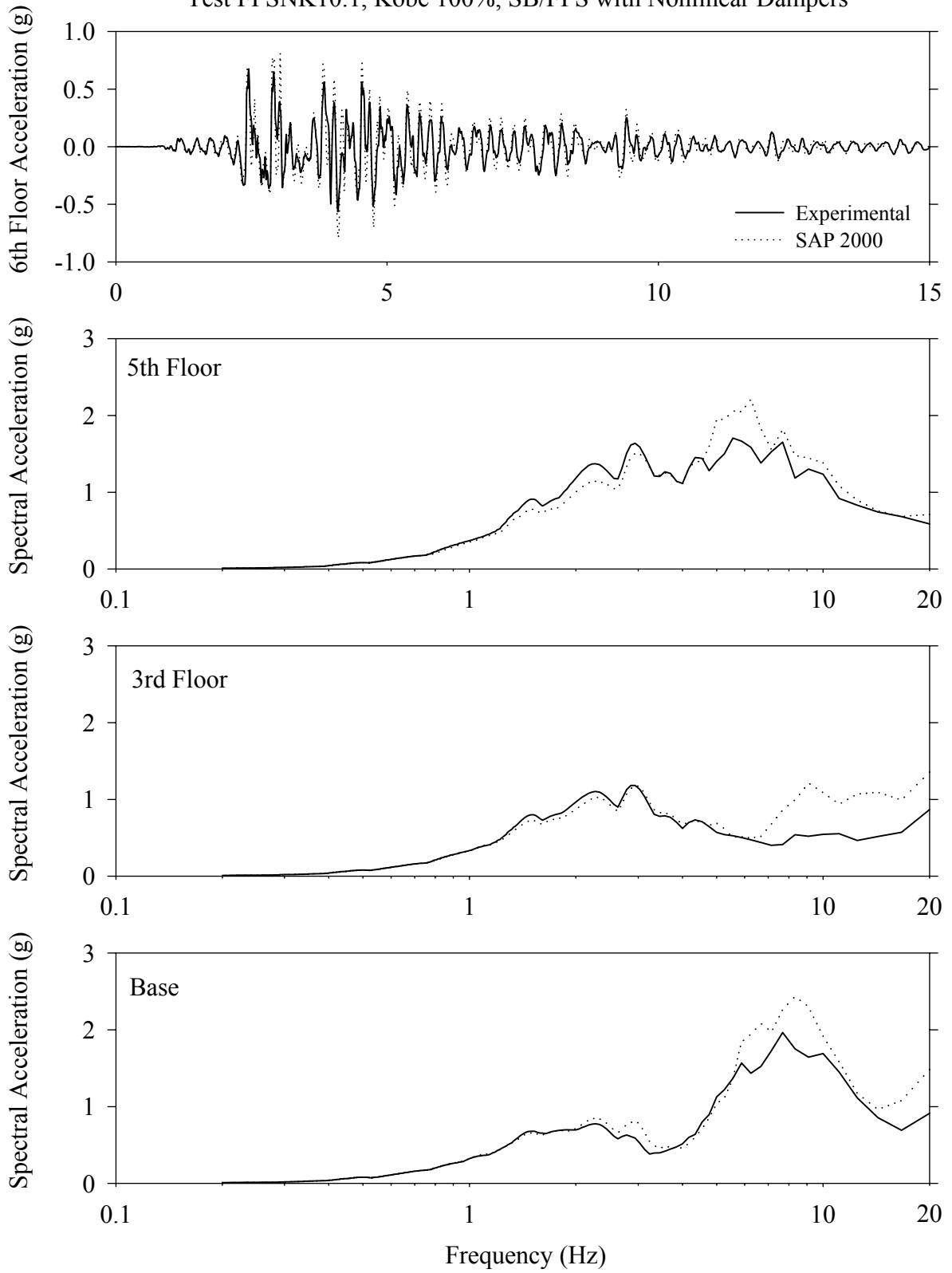




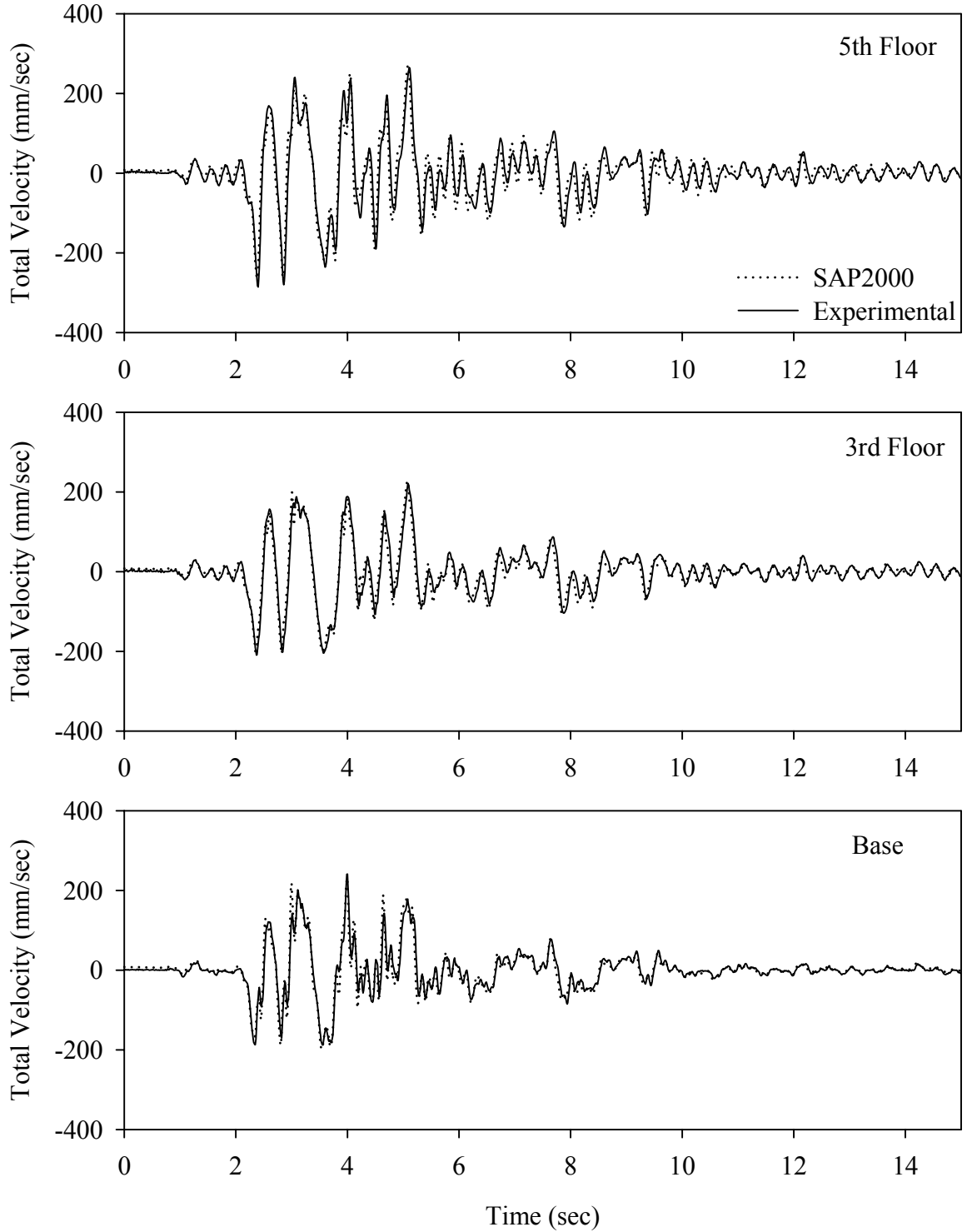
Test FPSNK10.1, Kobe 100%, SB/FPS with Nonlinear Dampers



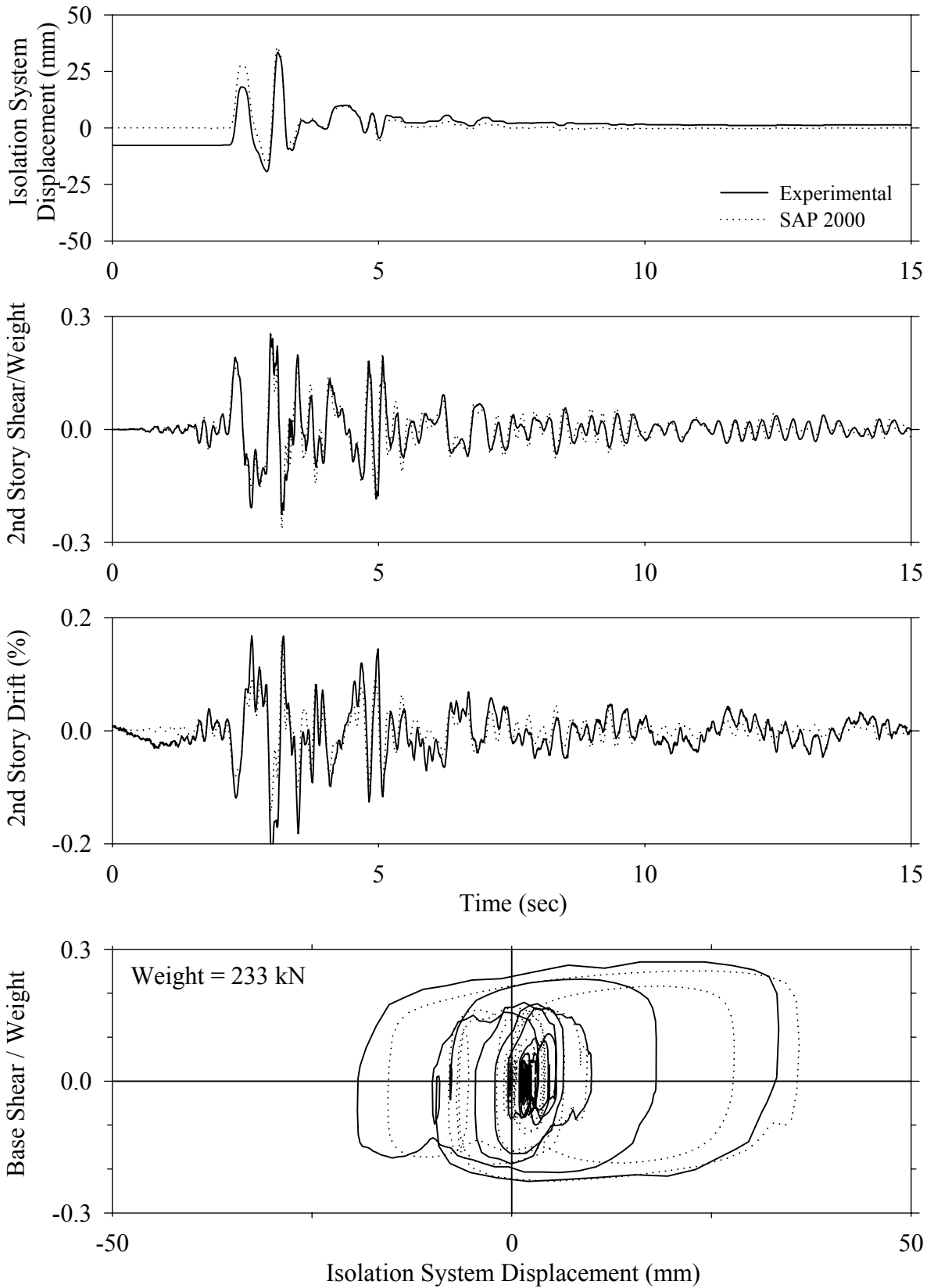
Test FPSNK10.1, Kobe 100%, SB/FPS with Nonlinear Dampers



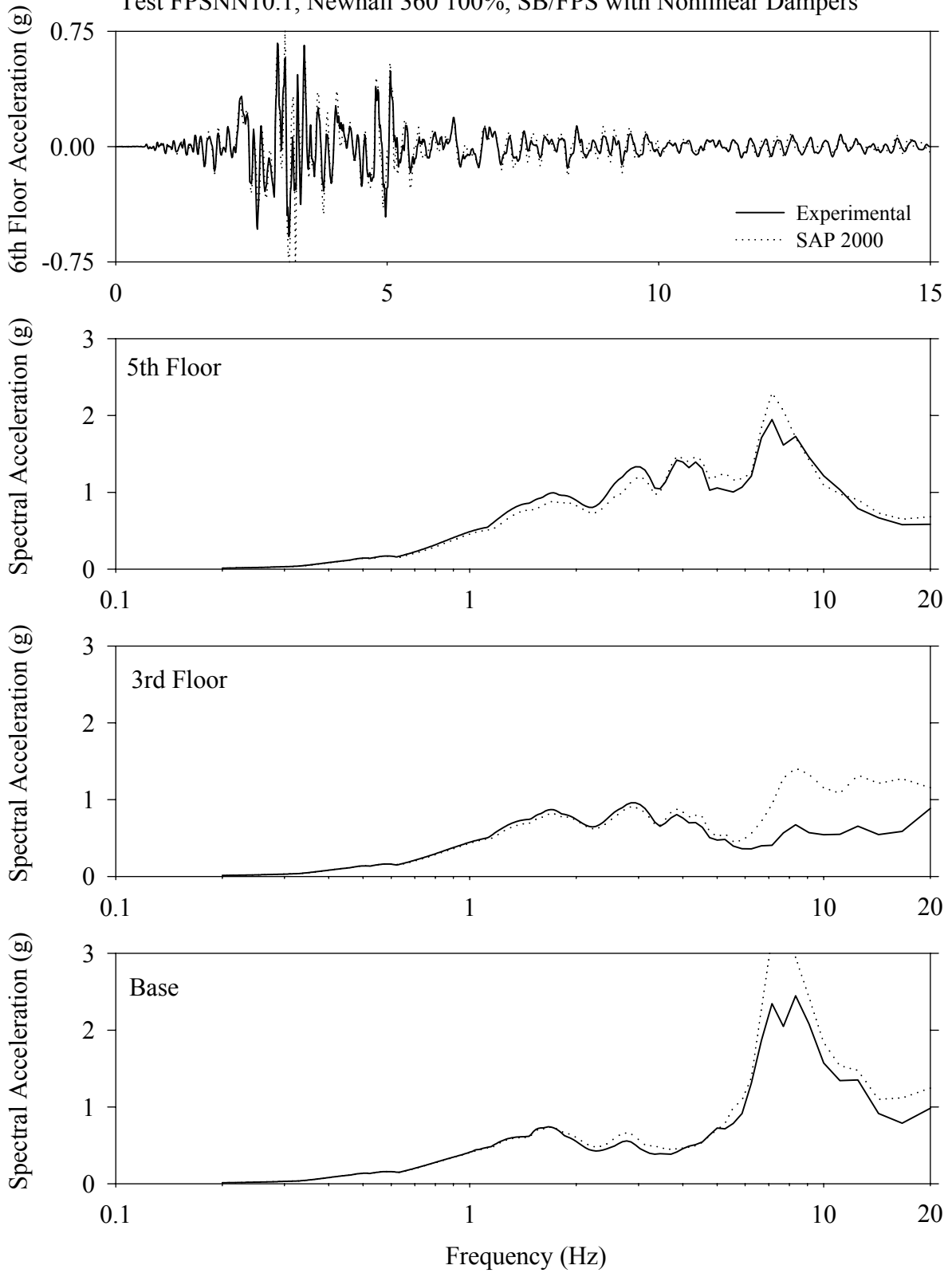
Test FPSNK10.1, Kobe 100%, SB/FPS with Nonlinear Dampers



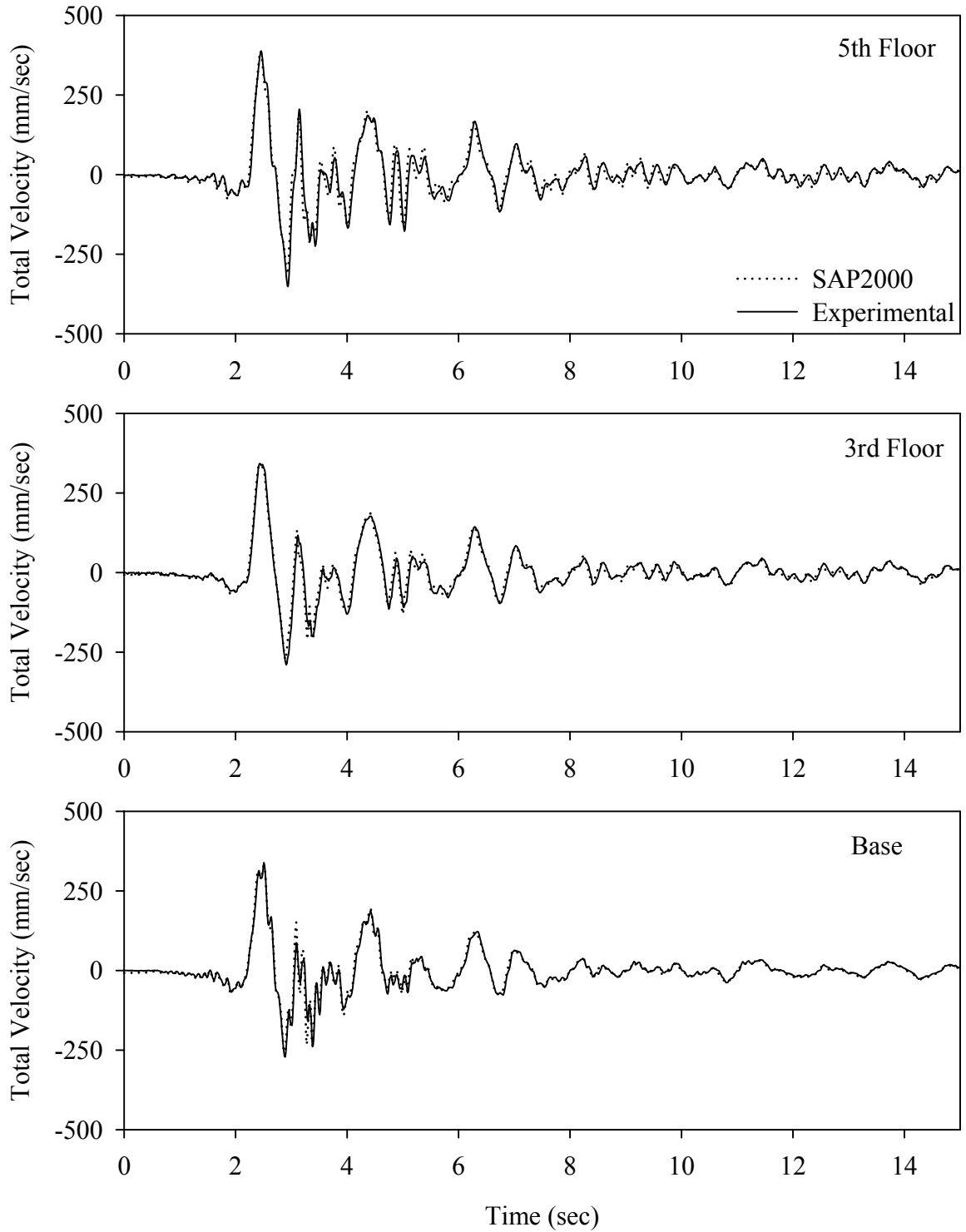
Test FPSNN10.1, Newhall 360 100%, SB/FPS with Nonlinear Dampers



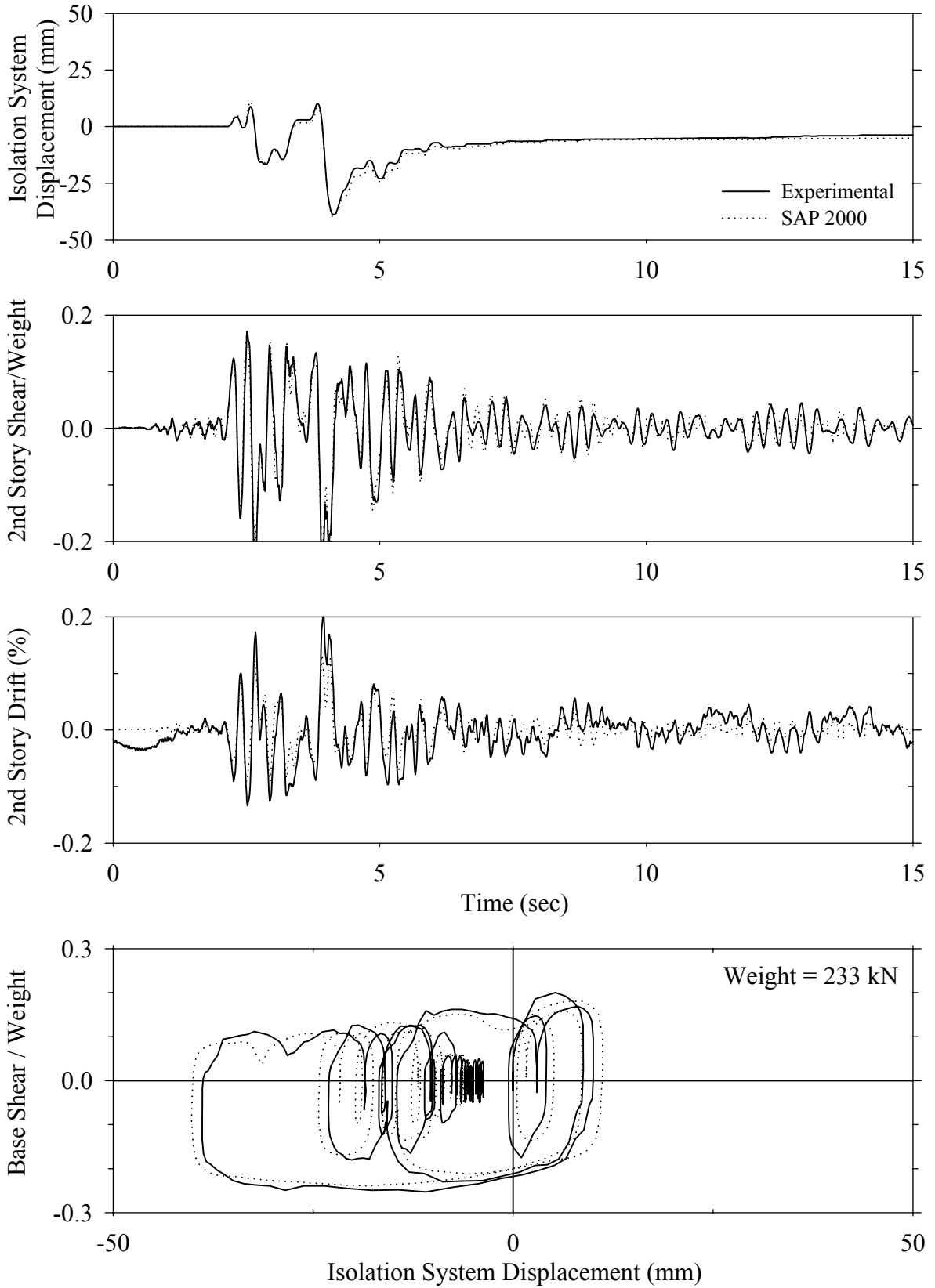
Test FPSNN10.1, Newhall 360 100%, SB/FPS with Nonlinear Dampers



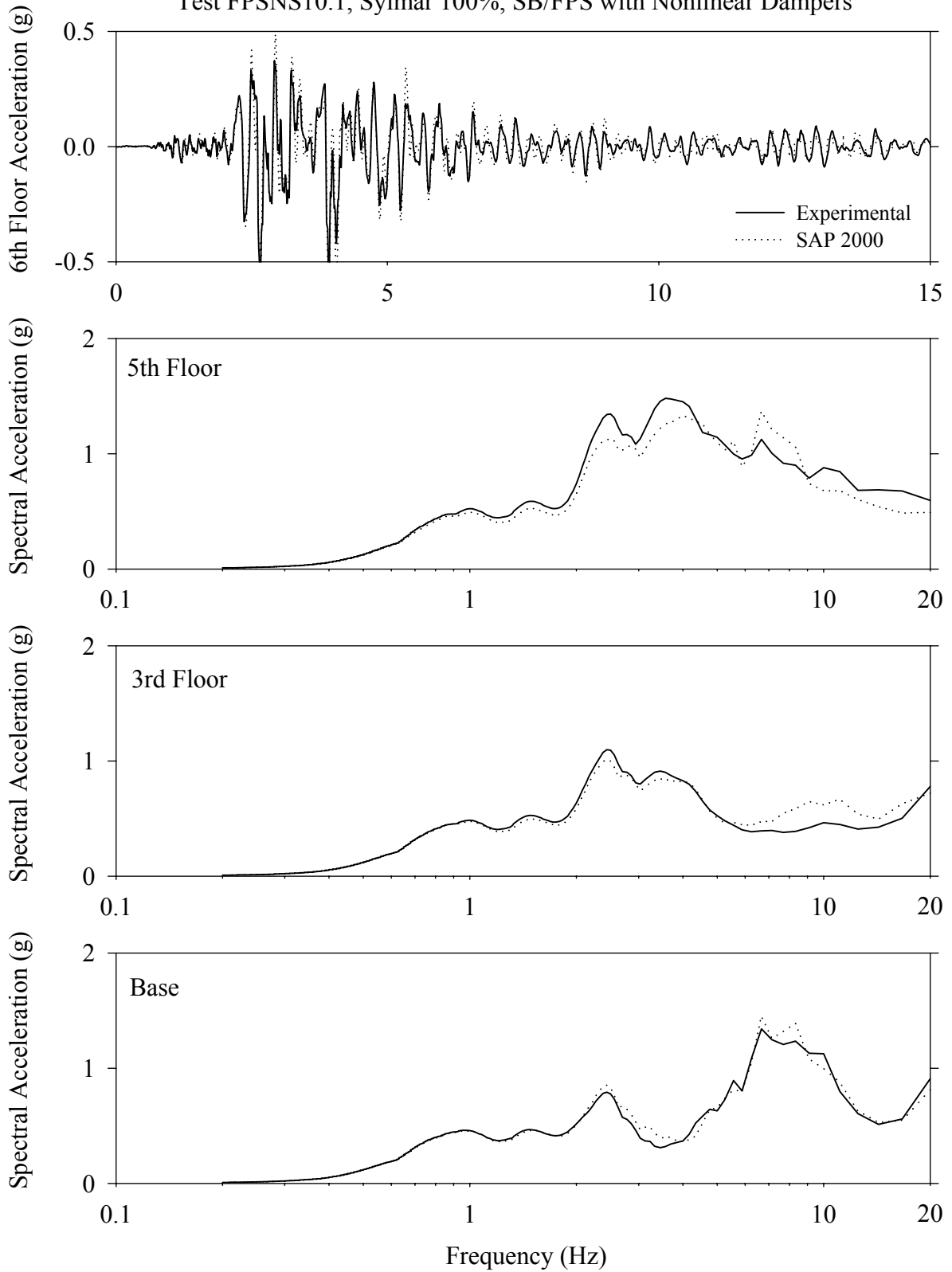
Test FPSNN10.1, Newhall 360 100%, SB/FPS with Nonlinear Dampers



Test FPSNS10.1, Sylmar 100%, SB/FPS with Nonlinear Dampers

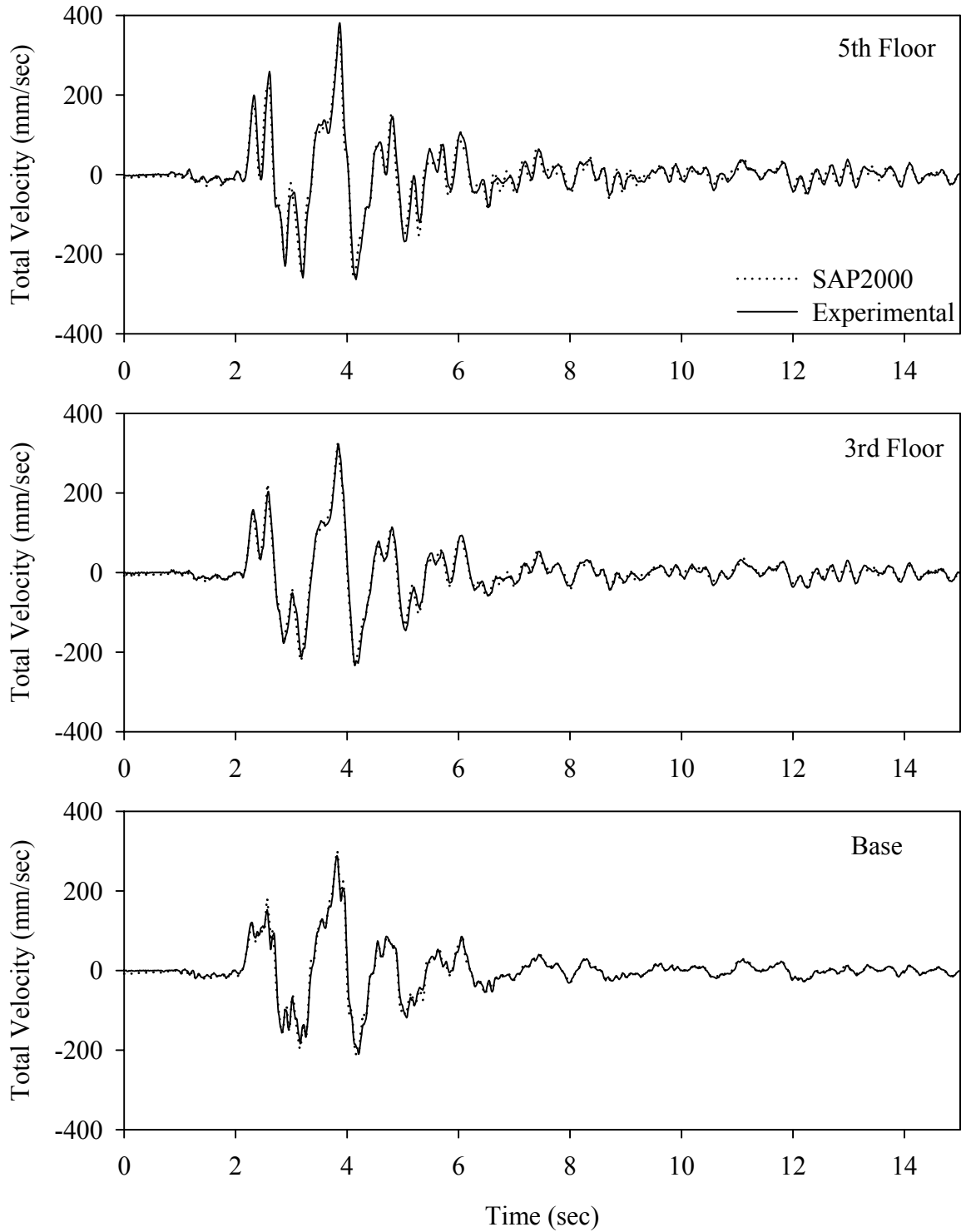


Test FPSNS10.1, Sylmar 100%, SB/FPS with Nonlinear Dampers

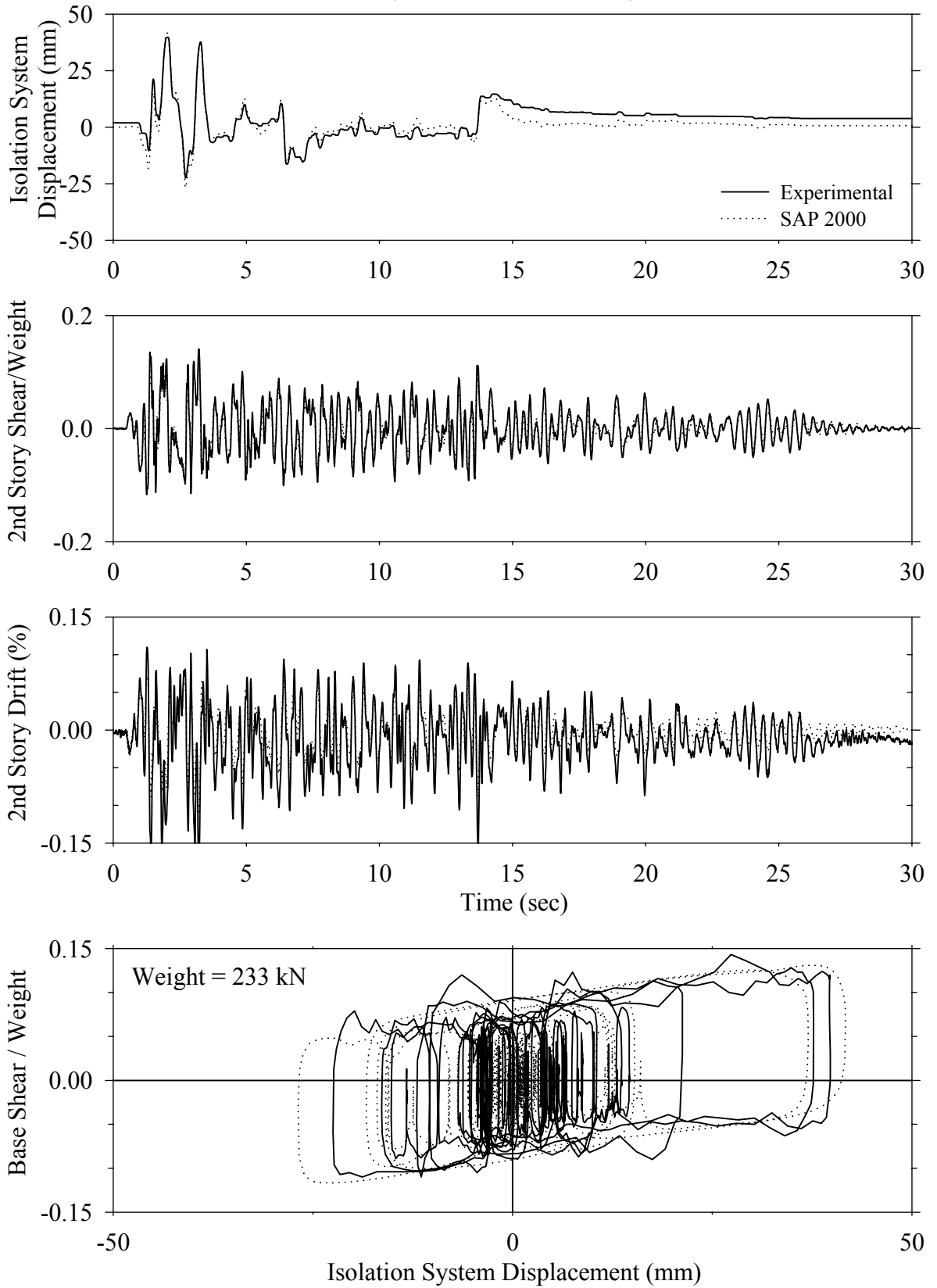




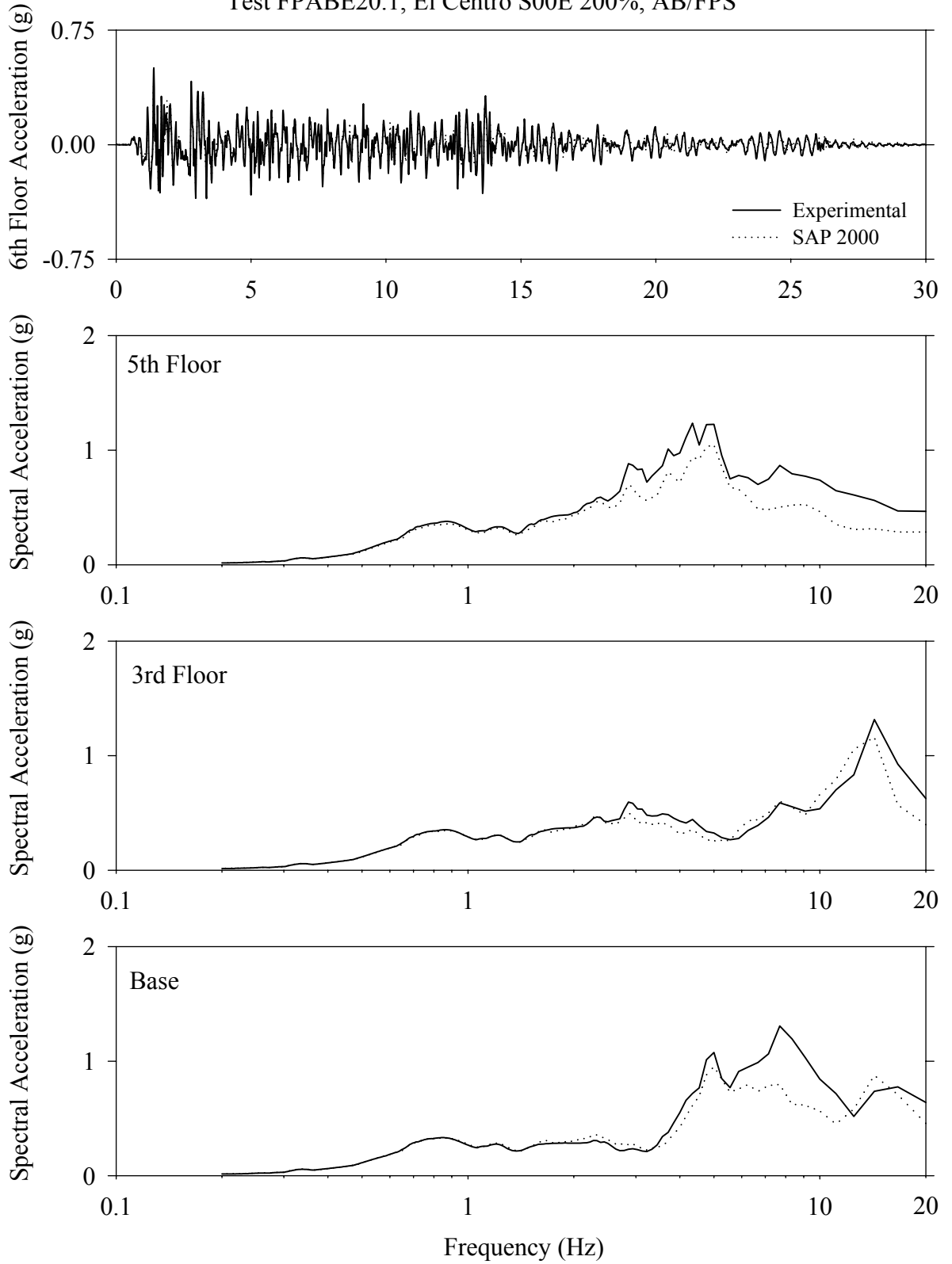
Test FPSNS10.1, Sylmar 100%, SB/FPS with Nonlinear Dampers



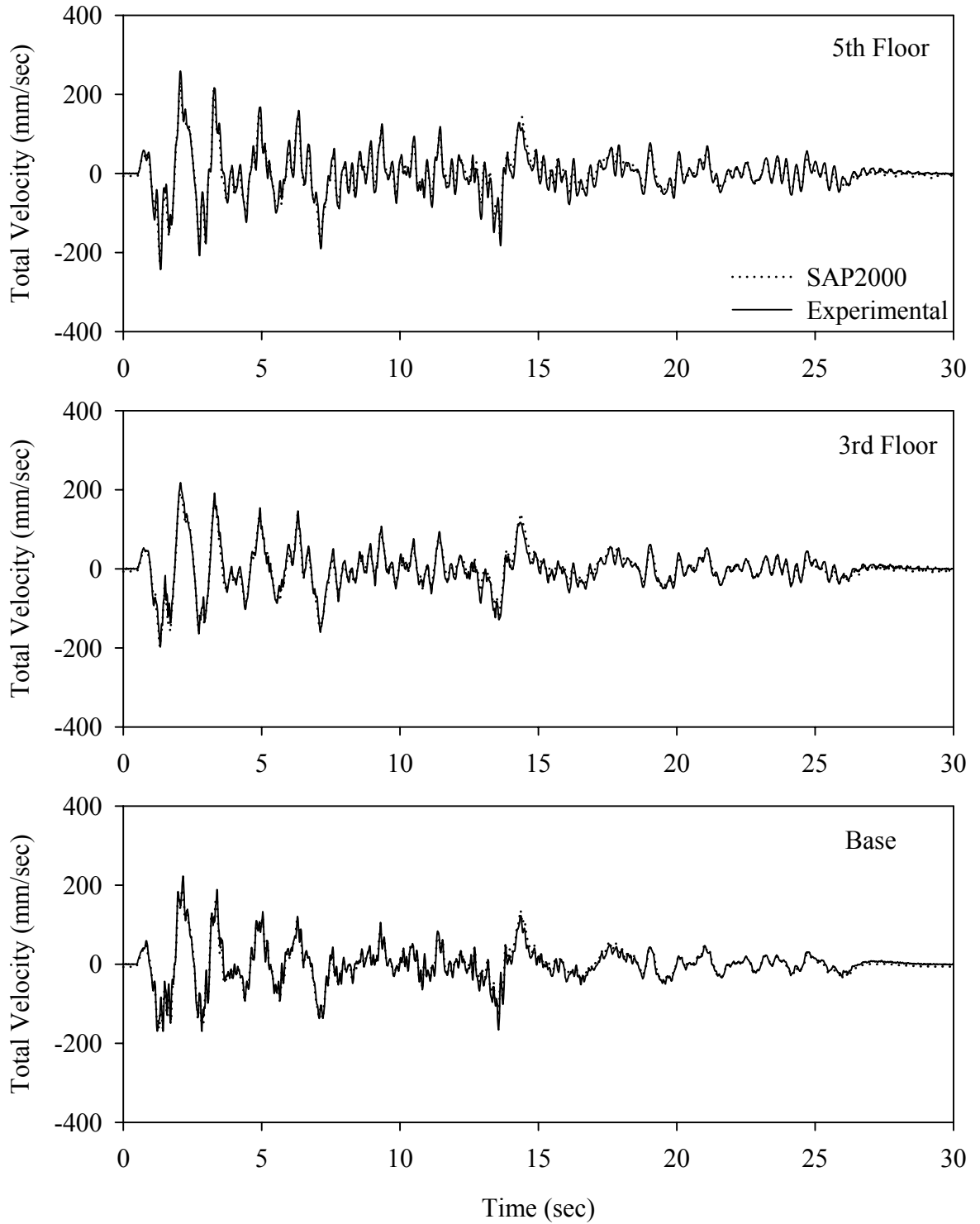
Test FPABE20.1, El Centro S00E 200%, AB/FPS



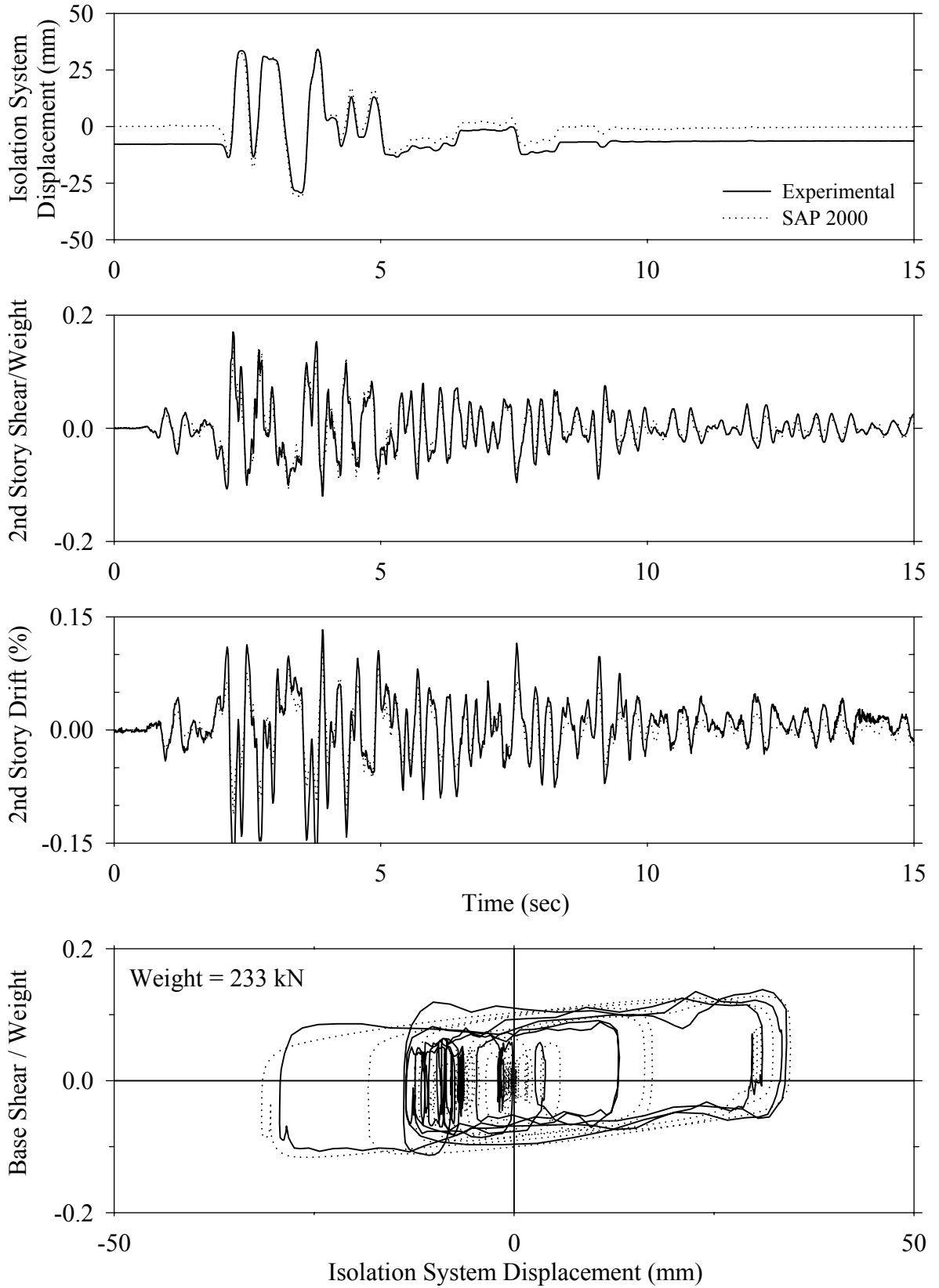
Test FPABE20.1, El Centro S00E 200%, AB/FPS



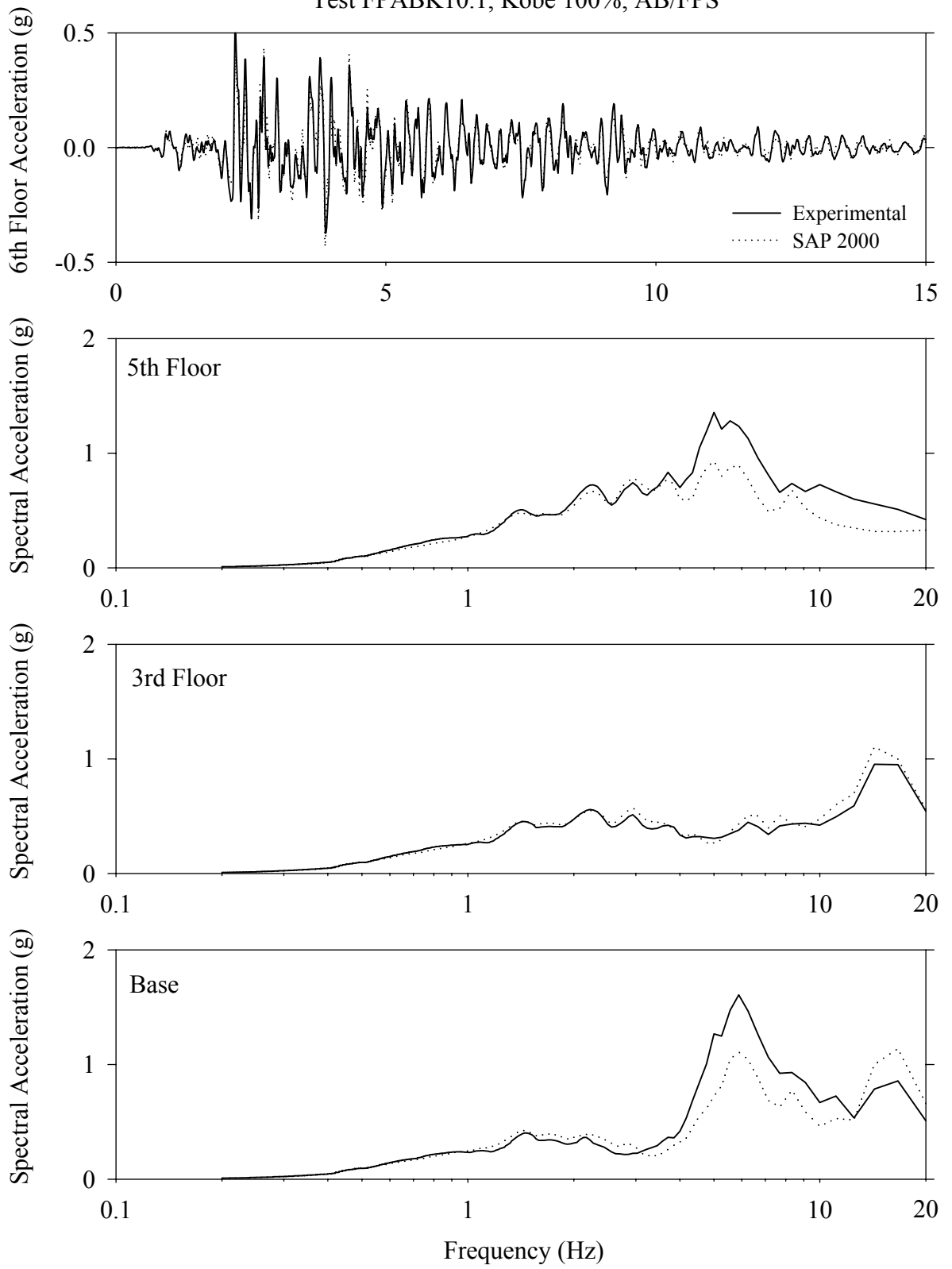
Test FPABE20.1, El Centro S00E 200%, AB/FPS



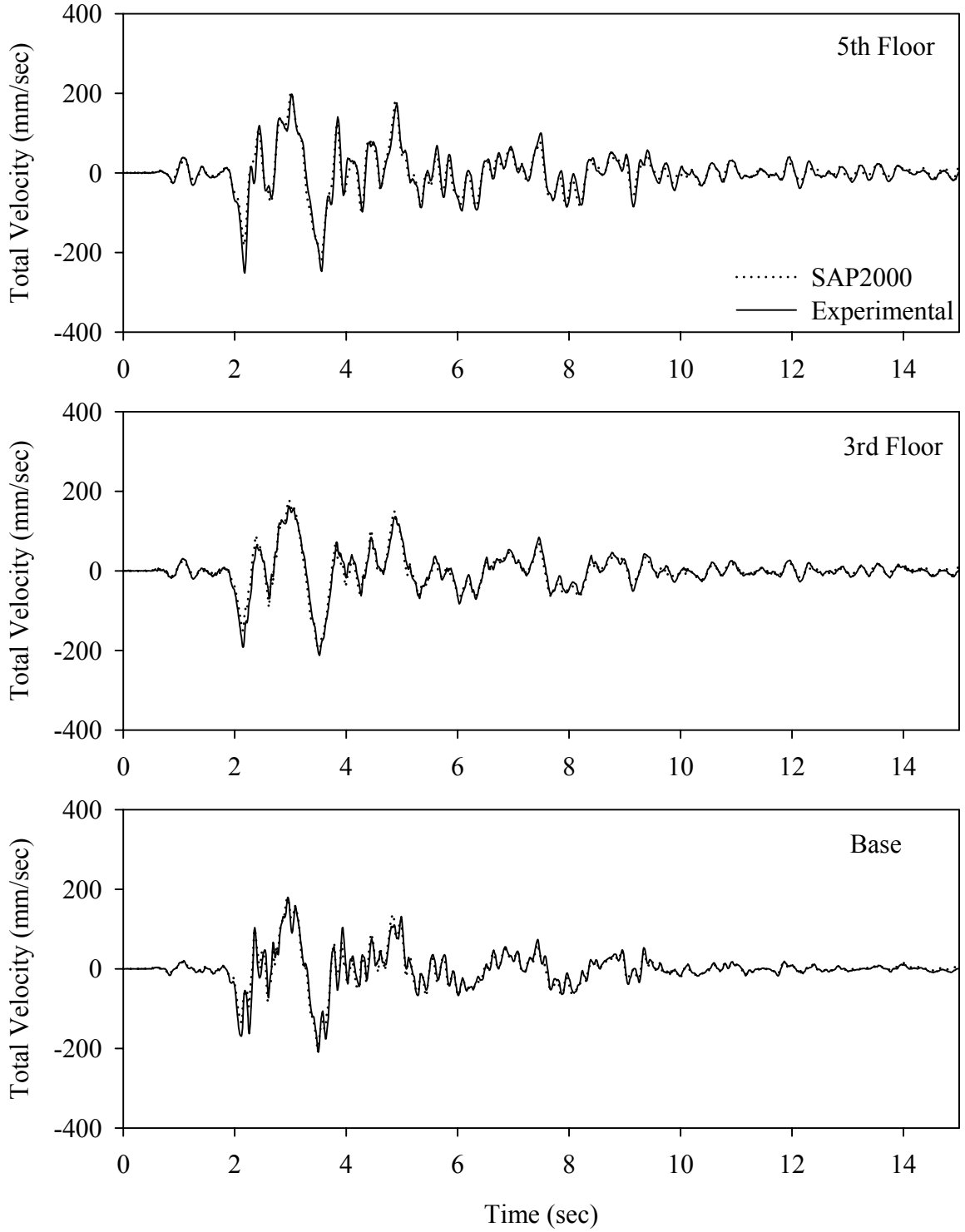
Test FPABK10.1, Kobe 100%, AB/FPS



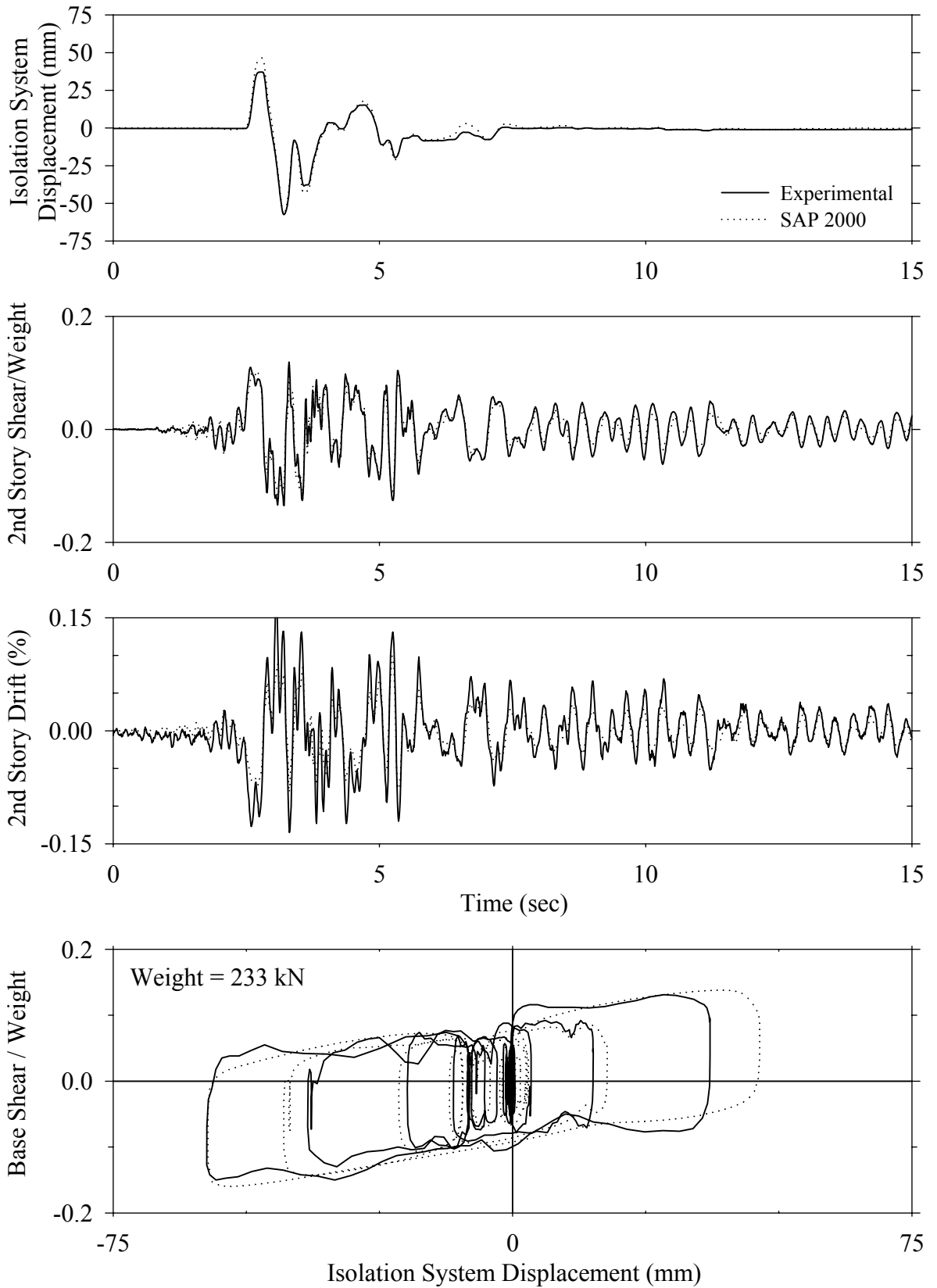
Test FPABK10.1, Kobe 100%, AB/FPS



Test FPABK10.1, Kobe 100%, AB/FPS

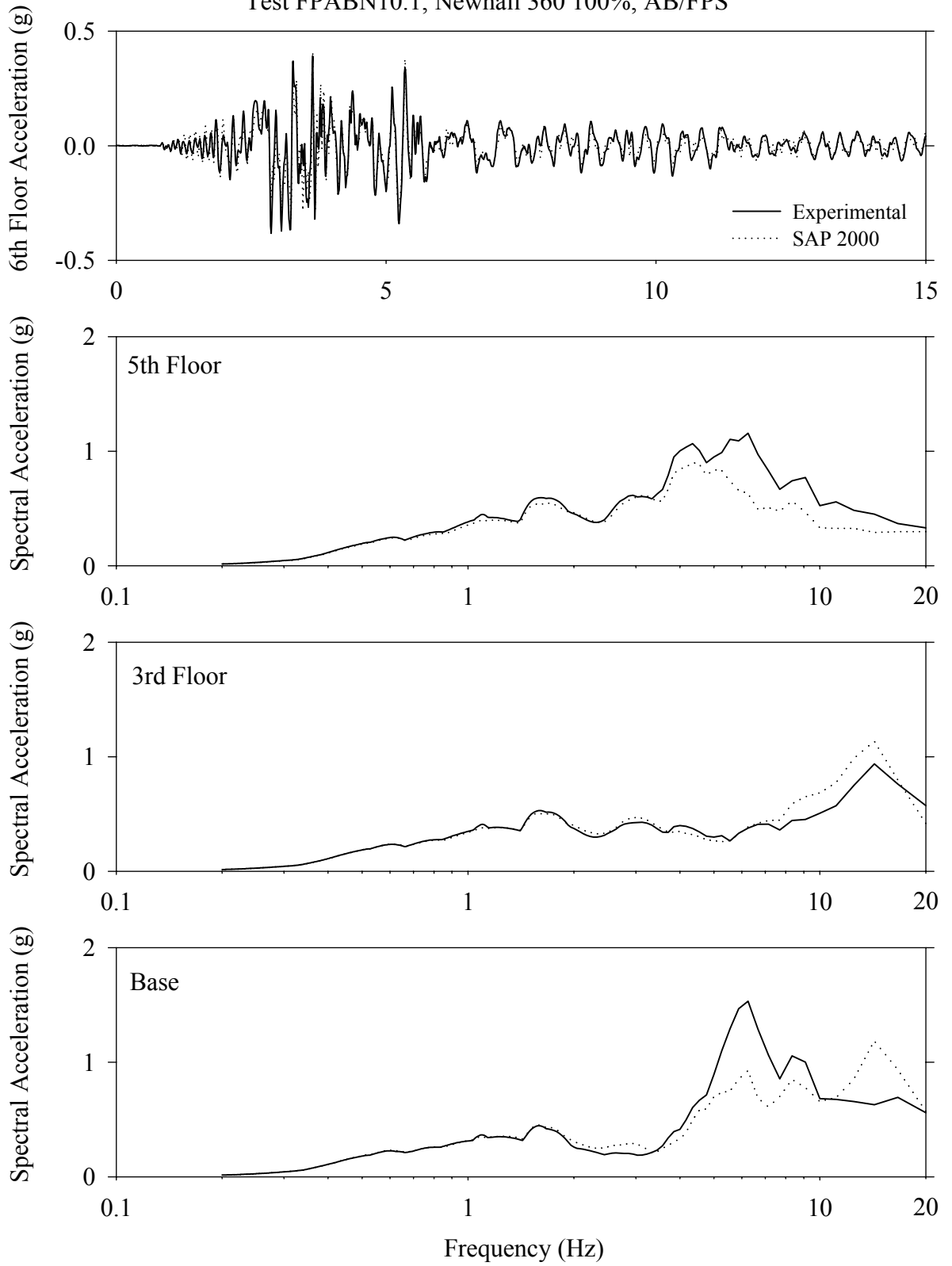


Test FPABN10.1, Newhall 360 100%, AB/FPS

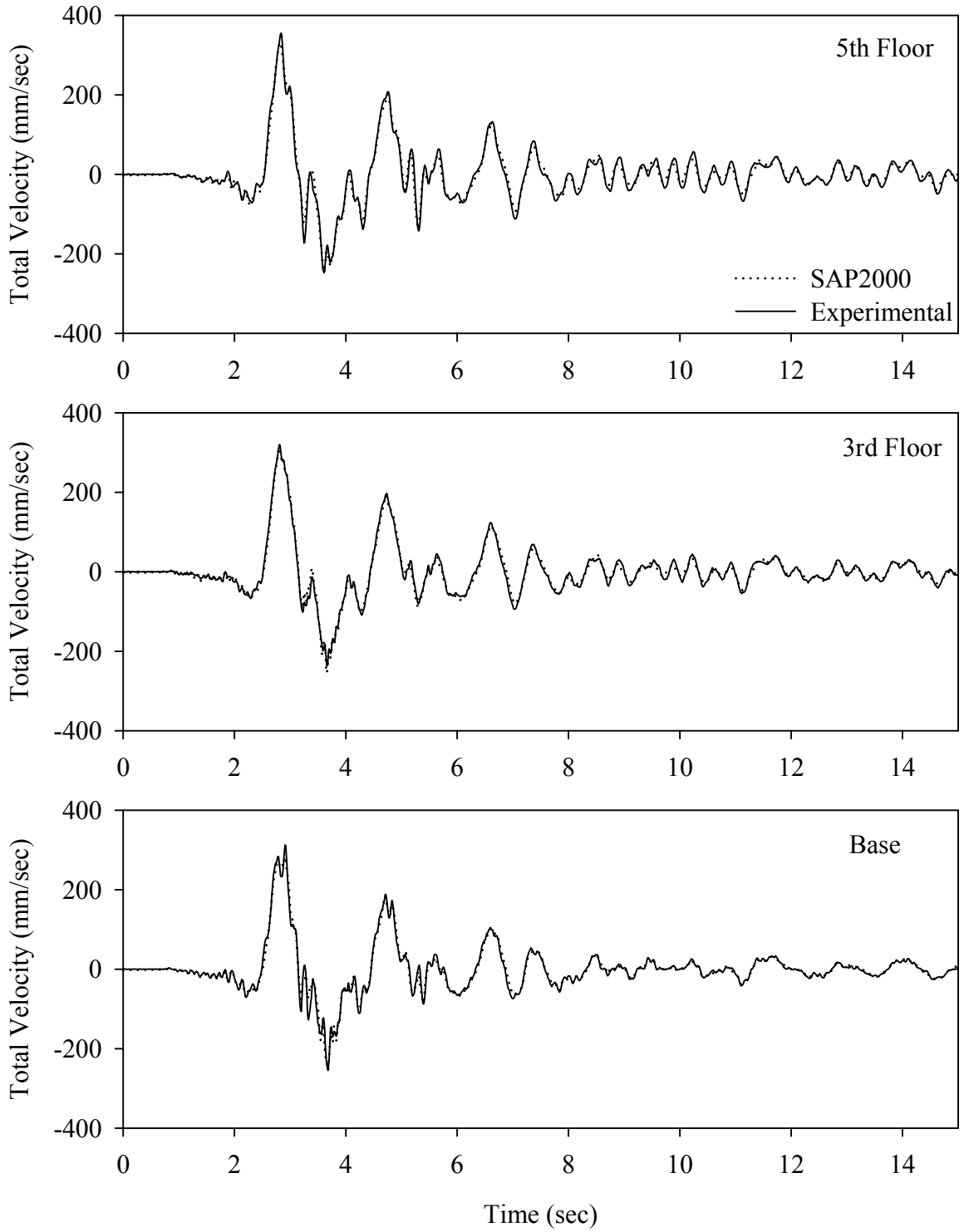




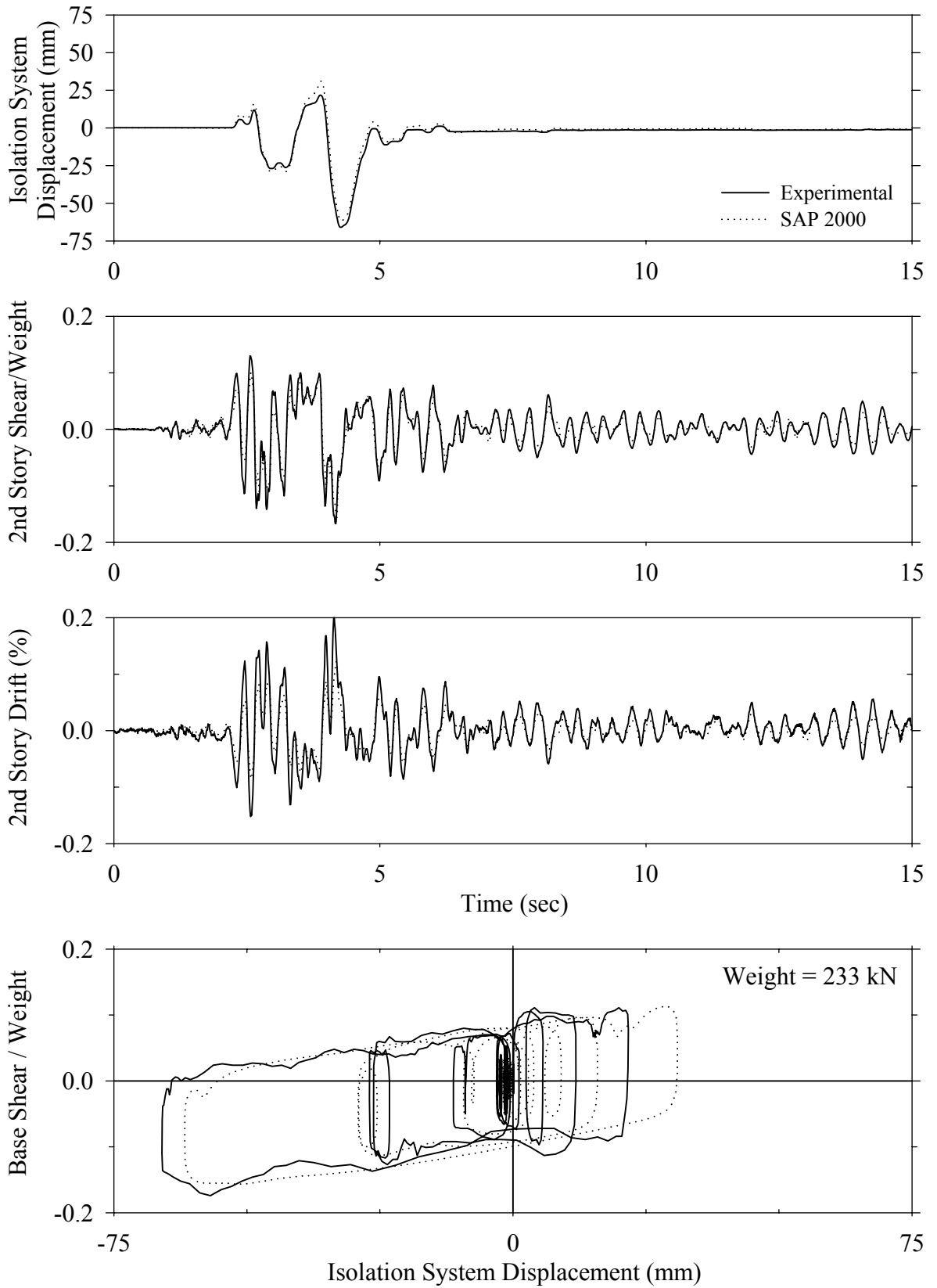
Test FPABN10.1, Newhall 360 100%, AB/FPS



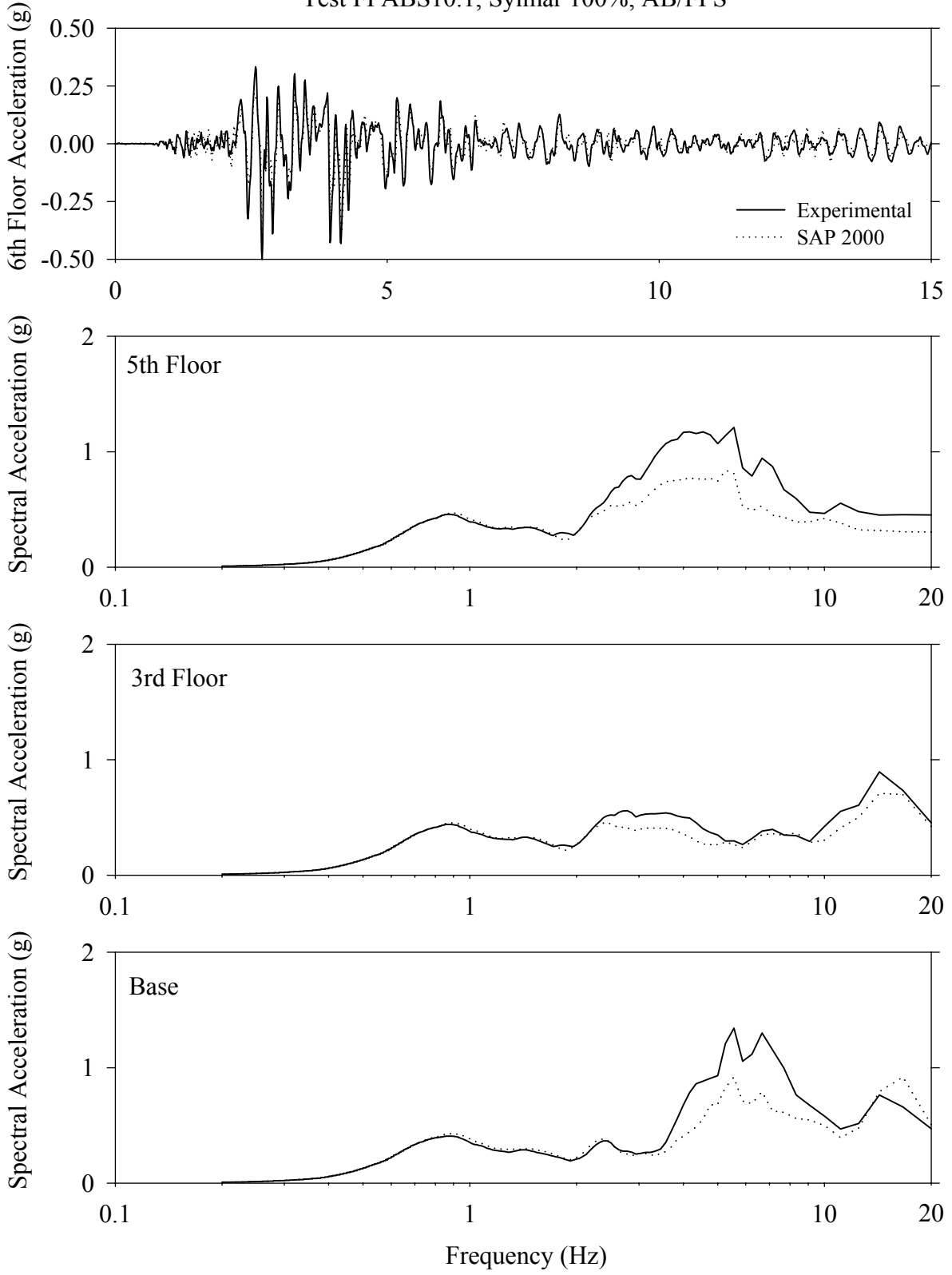
Test FPABN10.1, Newhall 360 100%, AB/FPS



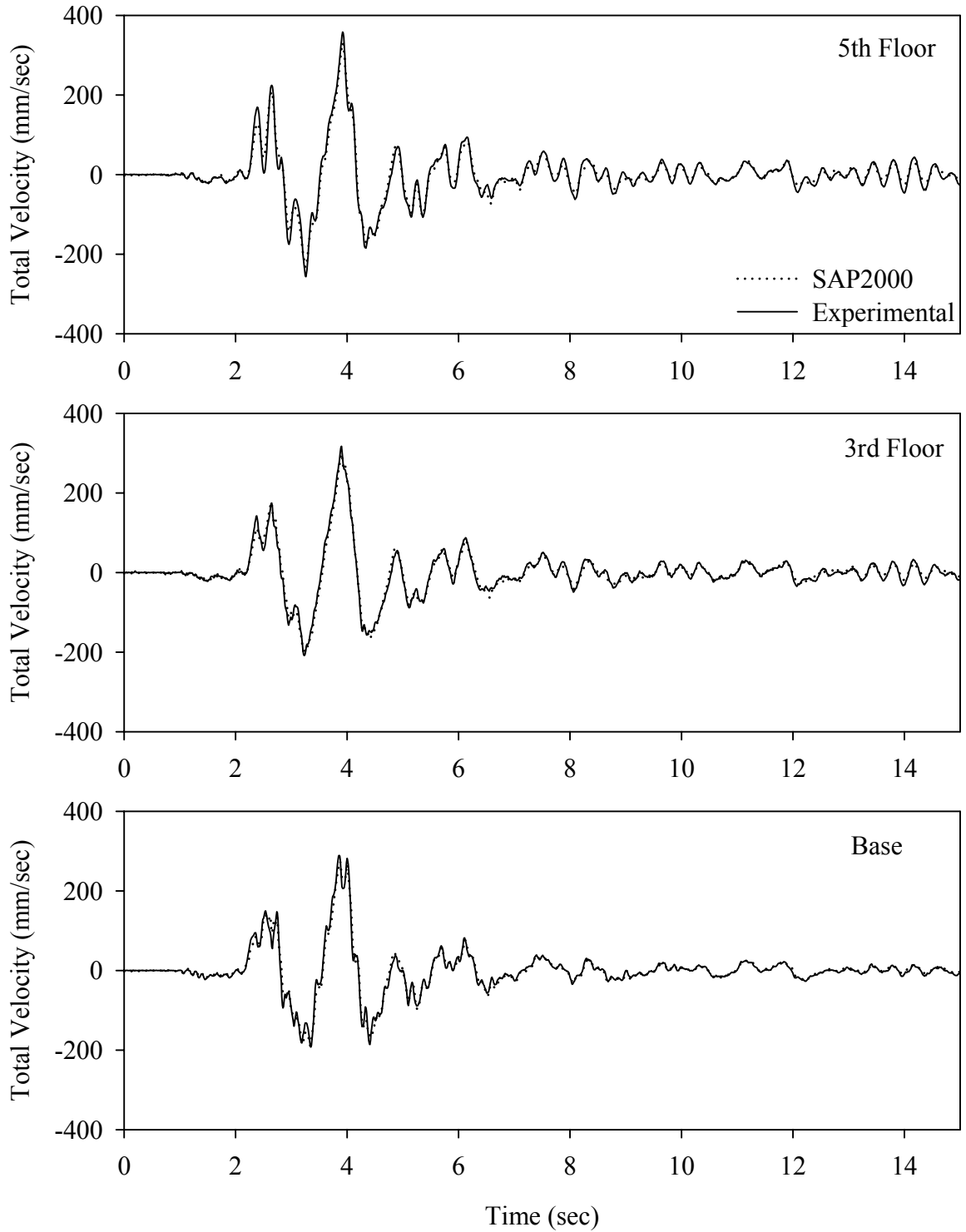
Test FPABS10.1, Sylmar 100%, AB/FPS



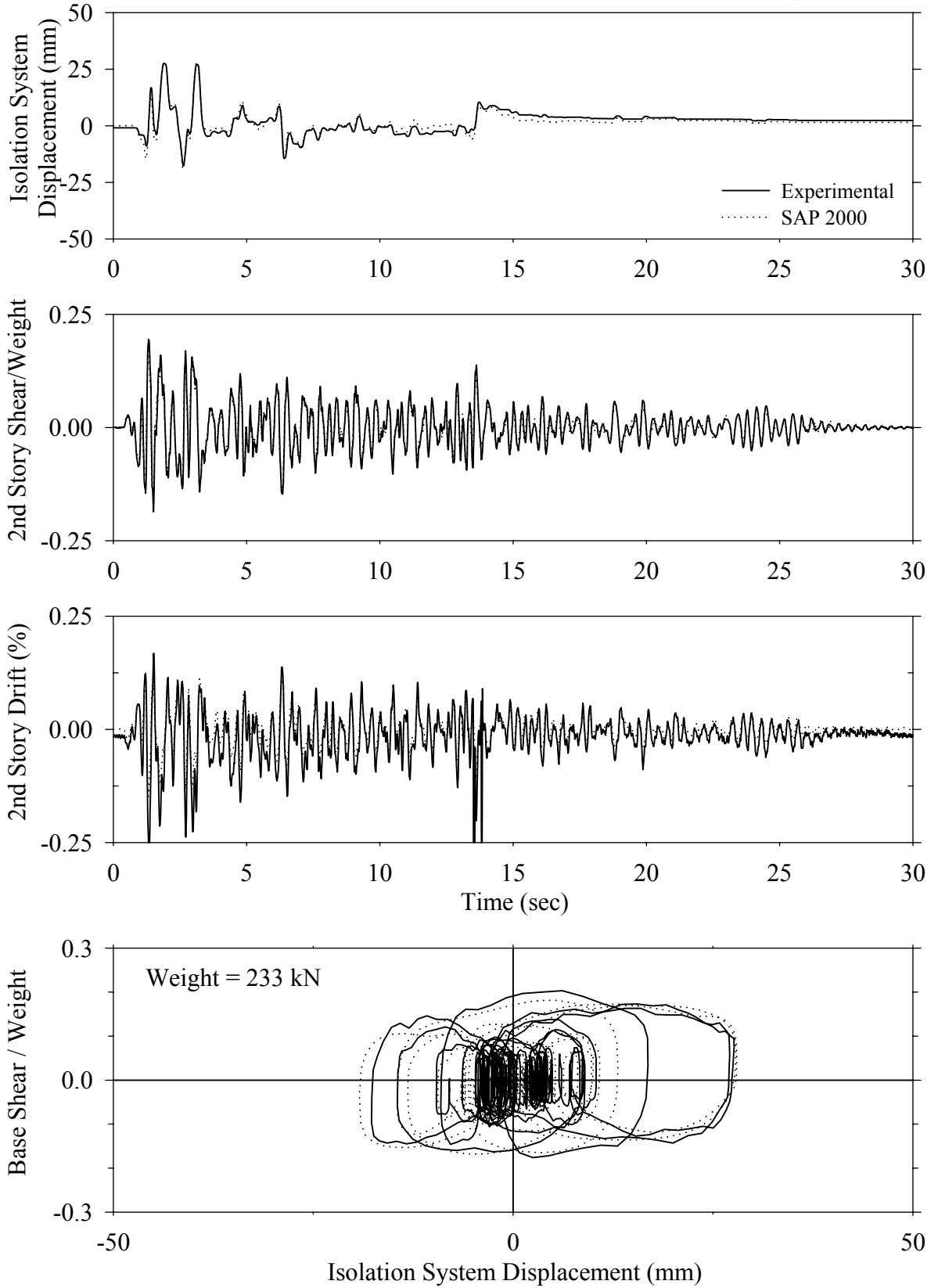
Test FPABS10.1, Sylmar 100%, AB/FPS



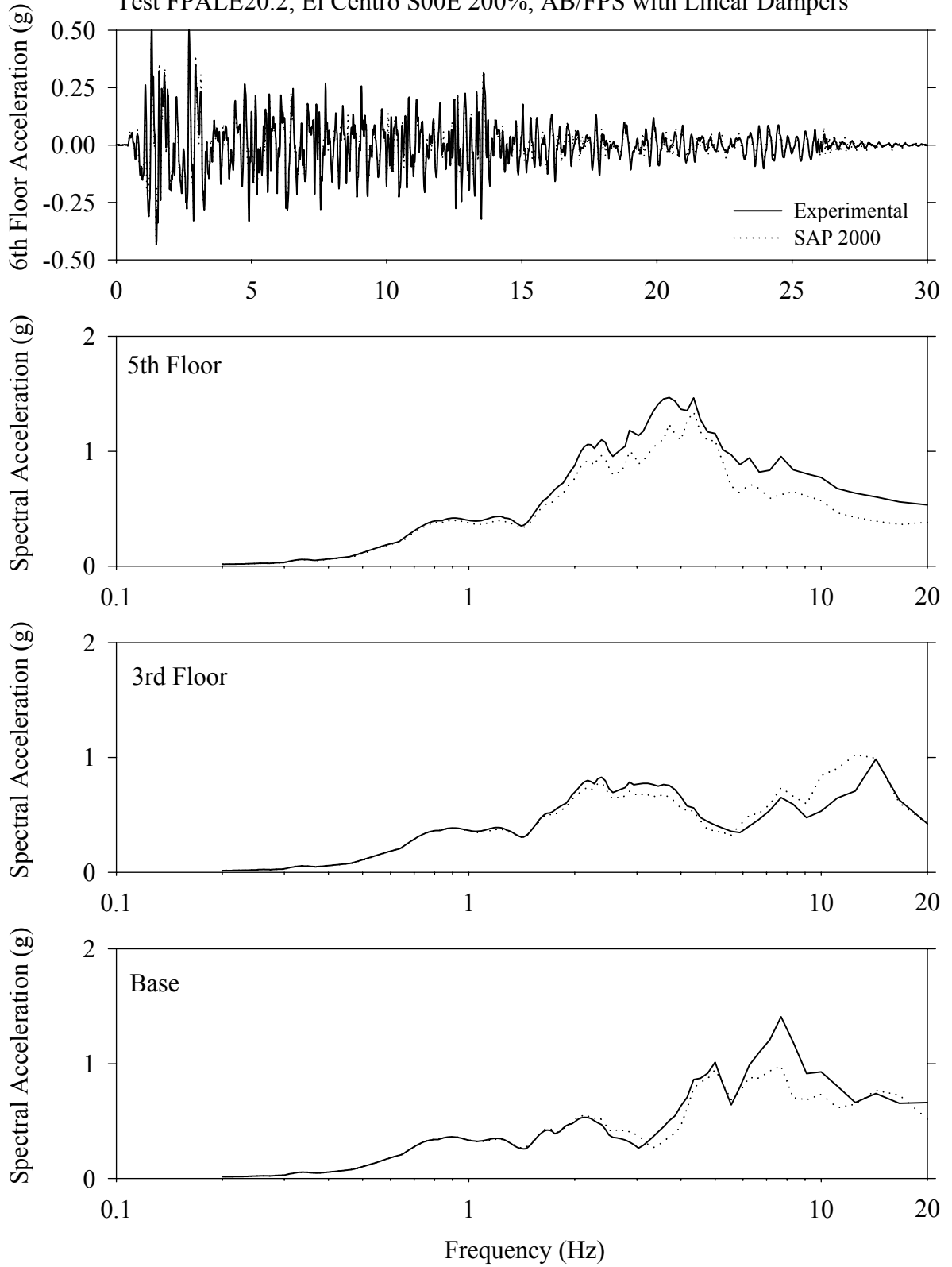
Test FPABS10.1, Sylmar 100%, AB/FPS



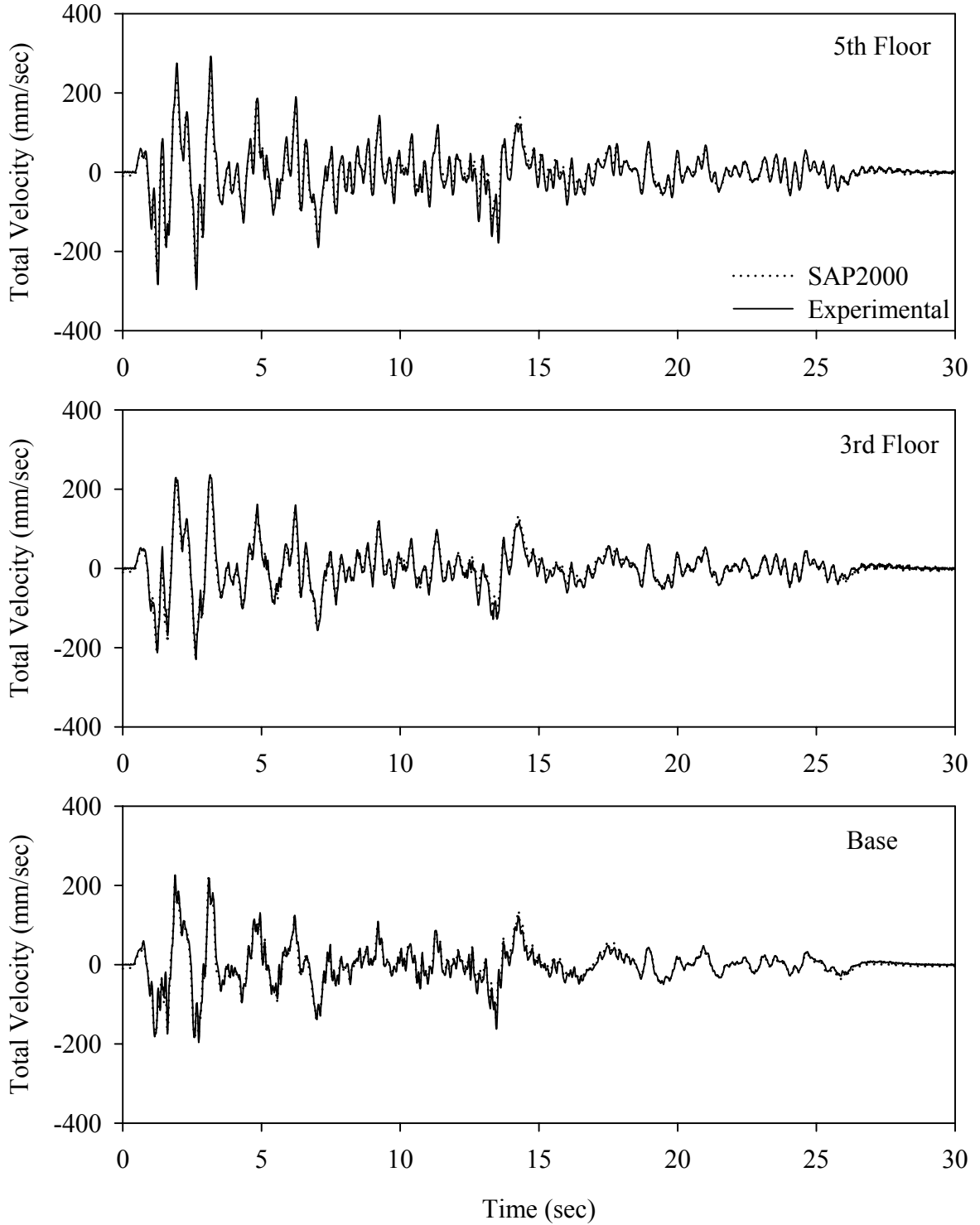
Test FPALE20.2, El Centro S00E 200%, AB/FPS with Linear Dampers



Test FPALE20.2, El Centro S00E 200%, AB/FPS with Linear Dampers

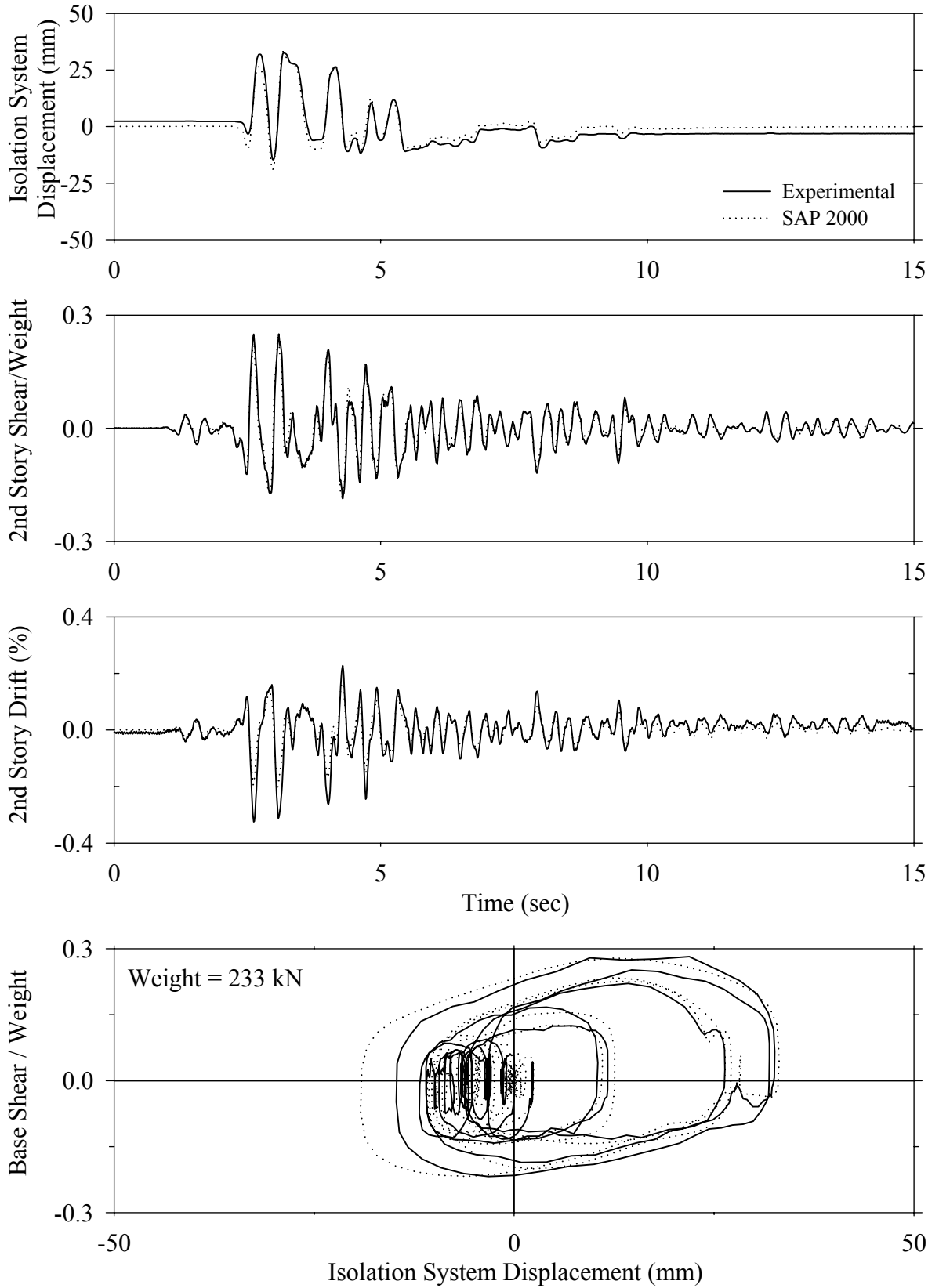


Test FPALE20.1, El Centro S00E 200%, AB/FPS with Linear Dampers

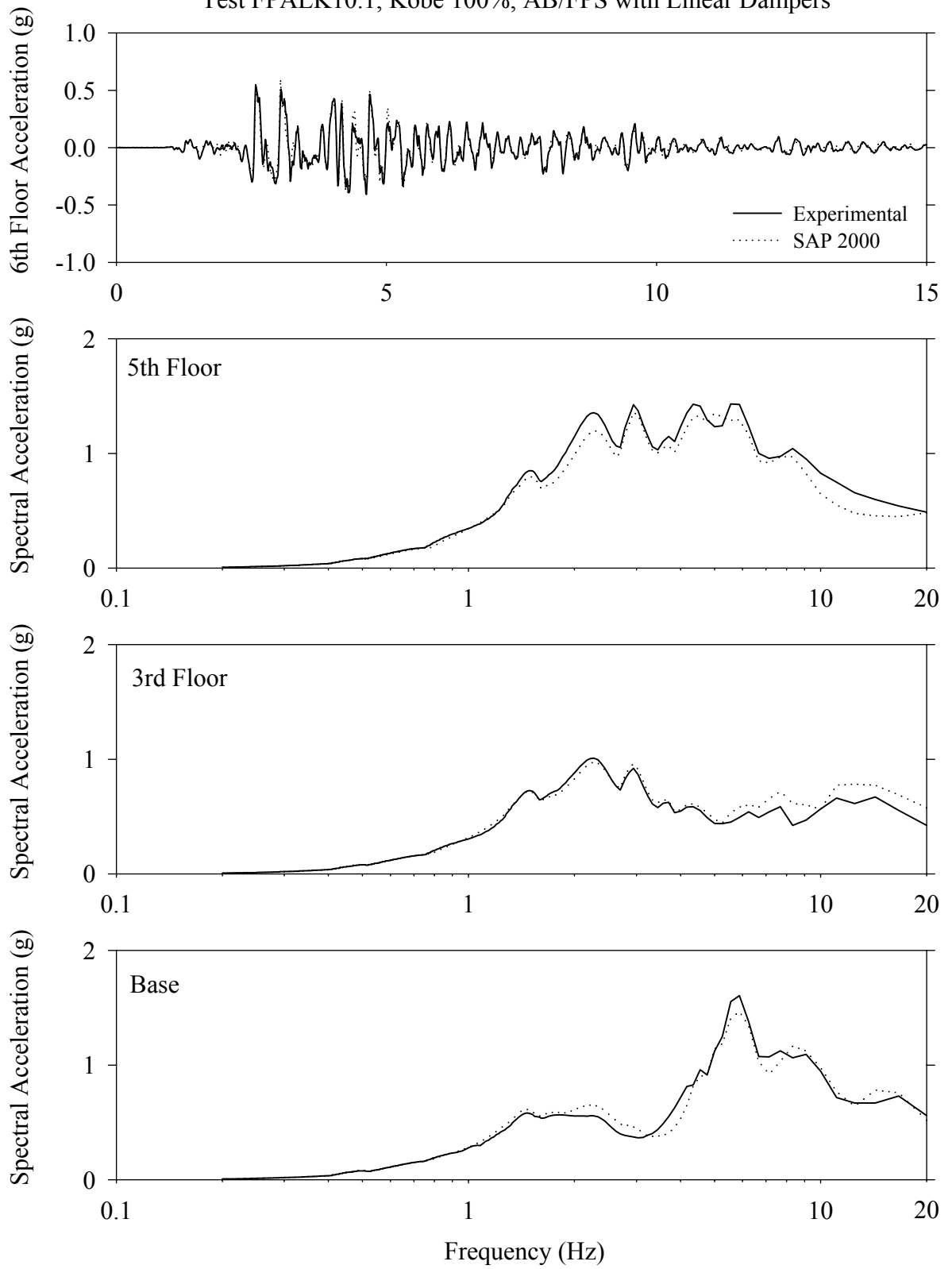




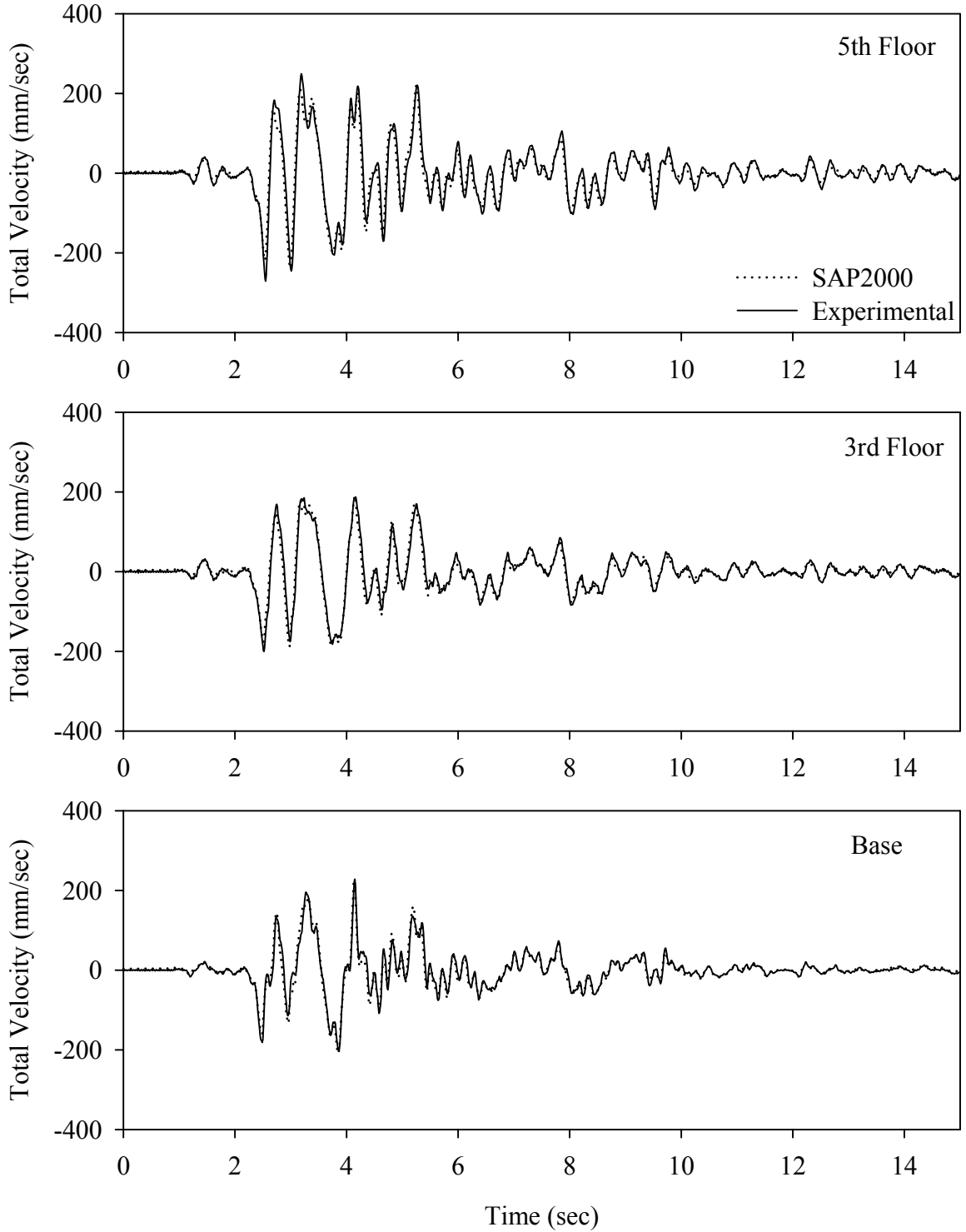
Test FPALK10.1, Kobe 100%, AB/FPS with Linear Dampers



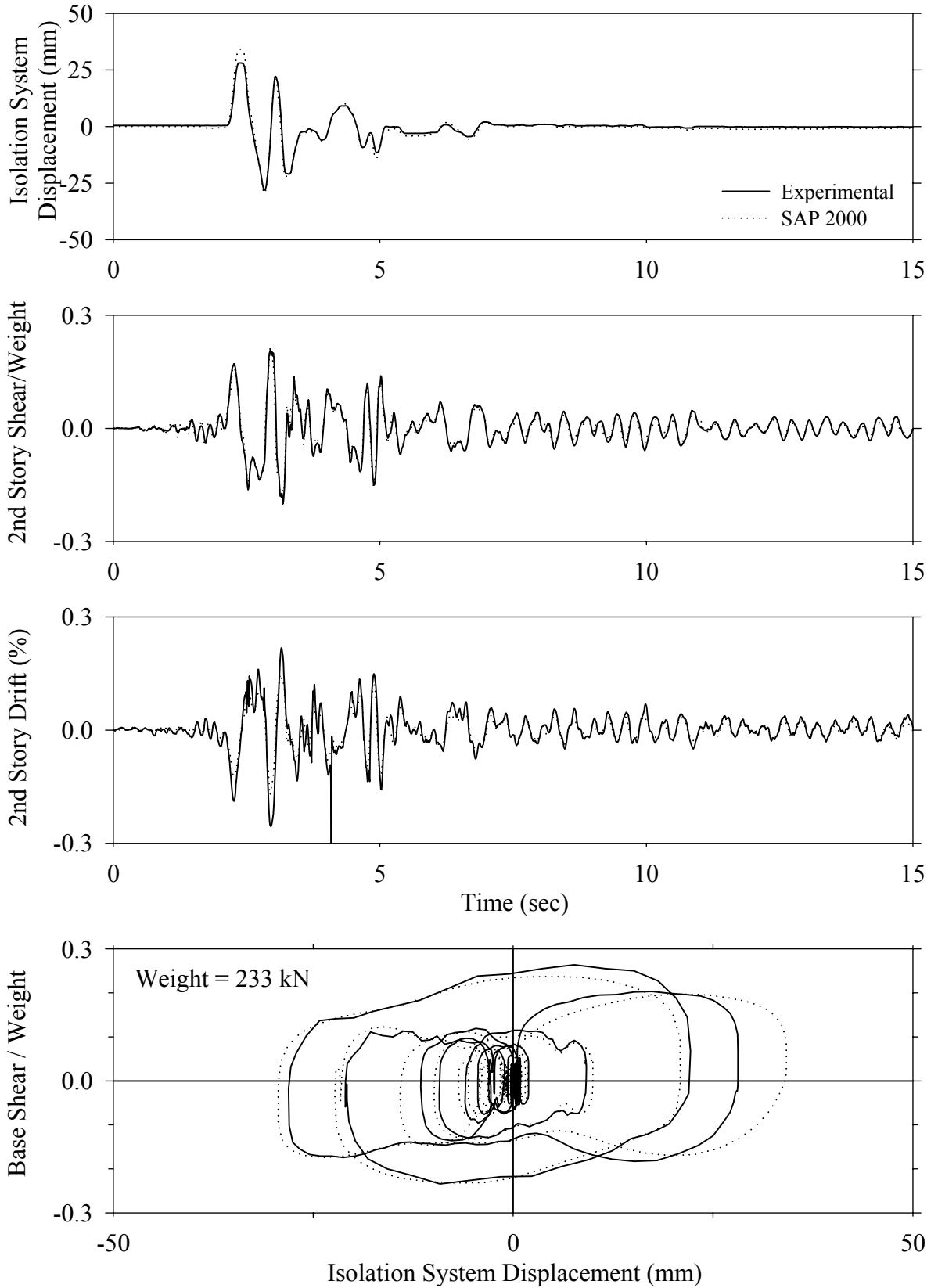
Test FPALK10.1, Kobe 100%, AB/FPS with Linear Dampers



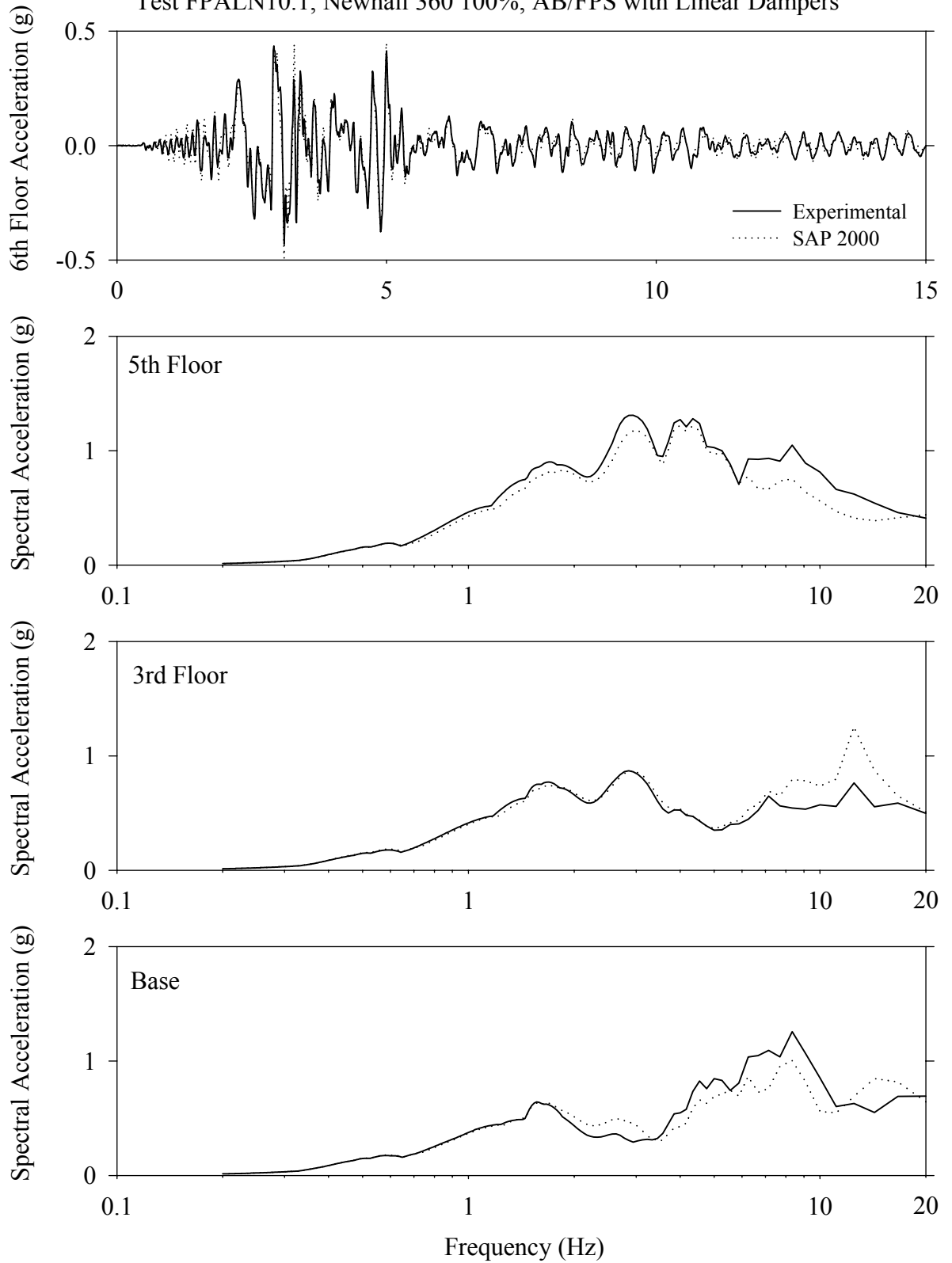
Test FPALK10.1, Kobe 100%, AB/FPS with Linear Dampers



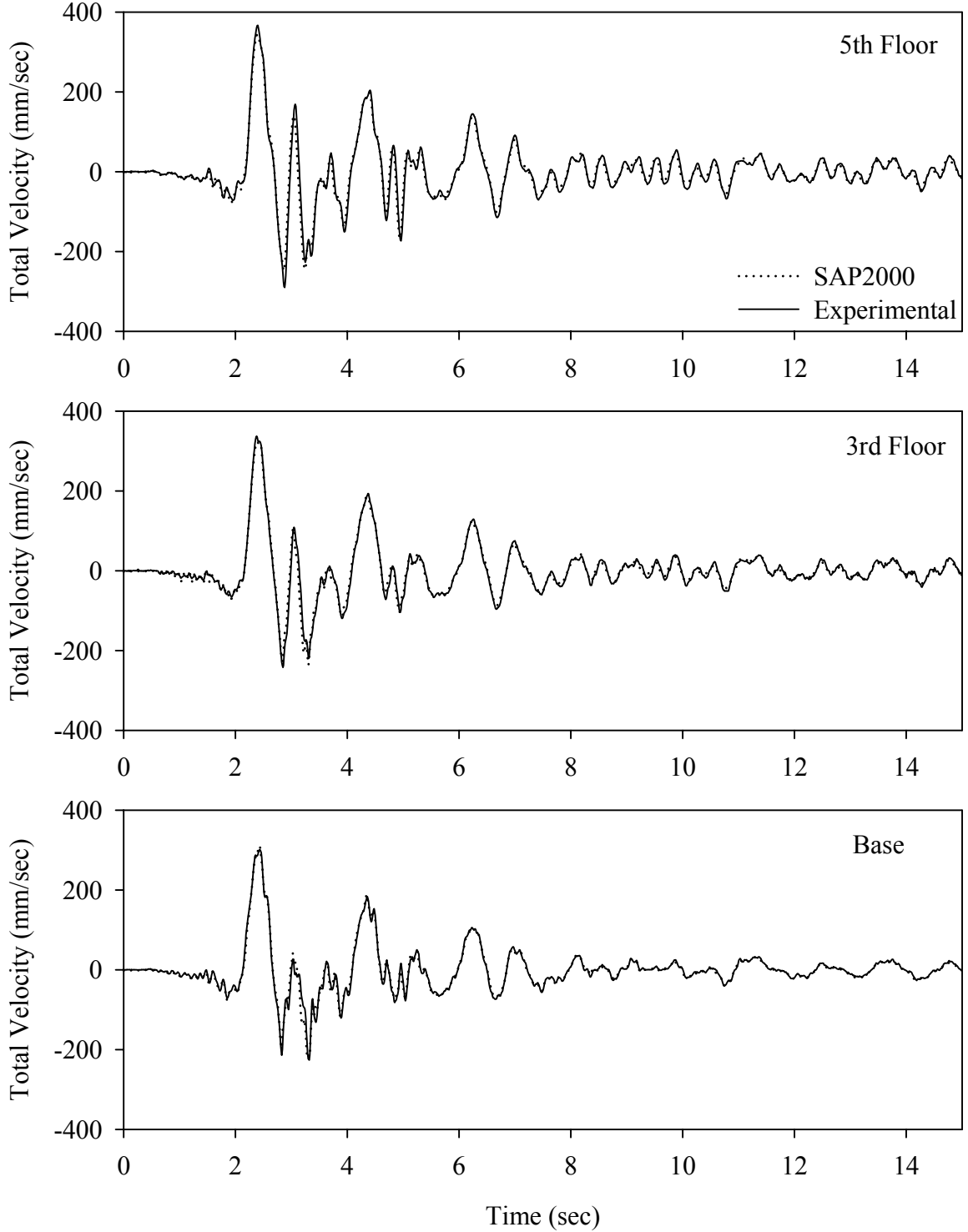
Test FPALN10.1, Newhall 360 100%, AB/FPS with Linear Dampers



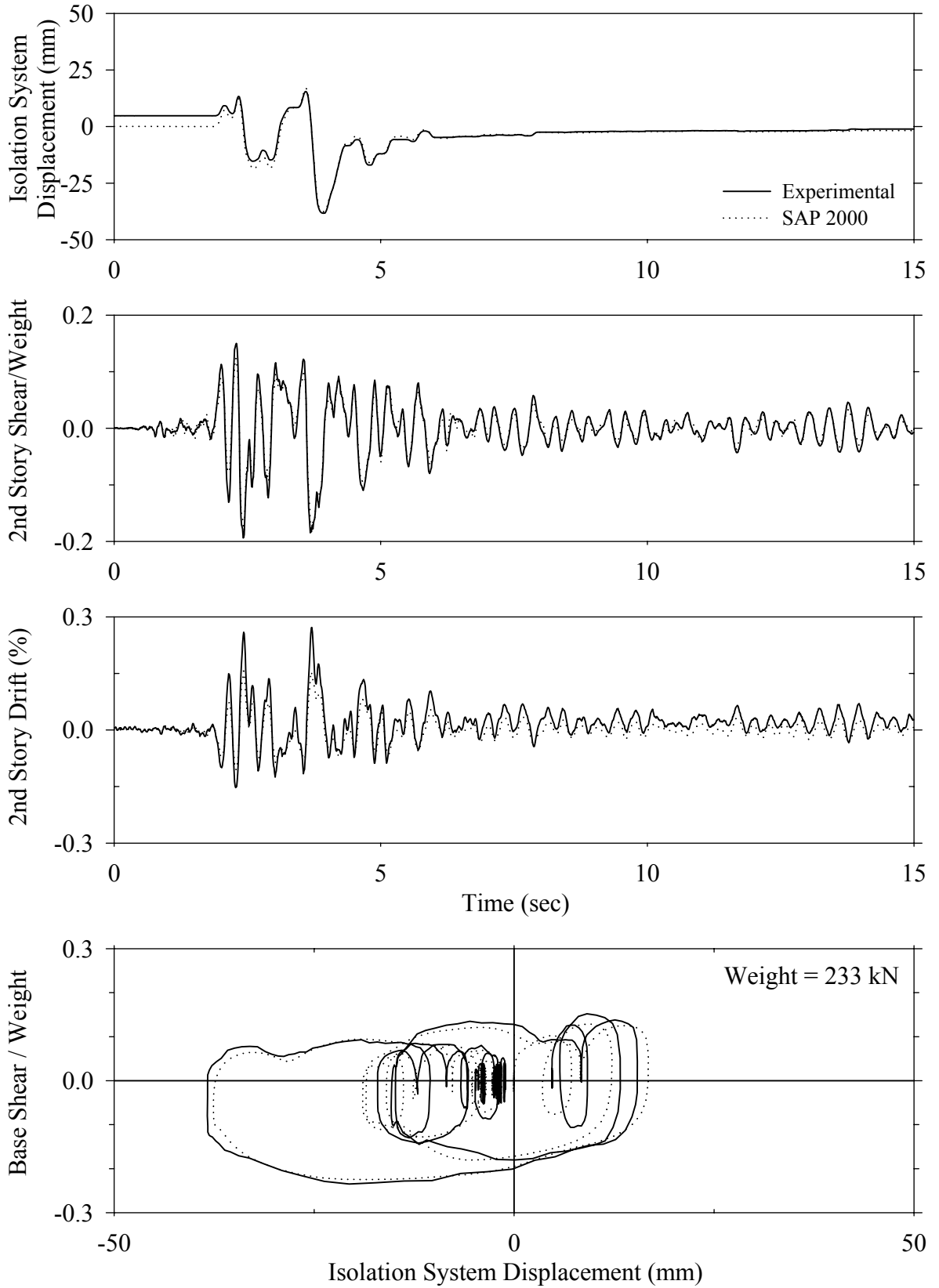
Test FPALN10.1, Newhall 360 100%, AB/FPS with Linear Dampers



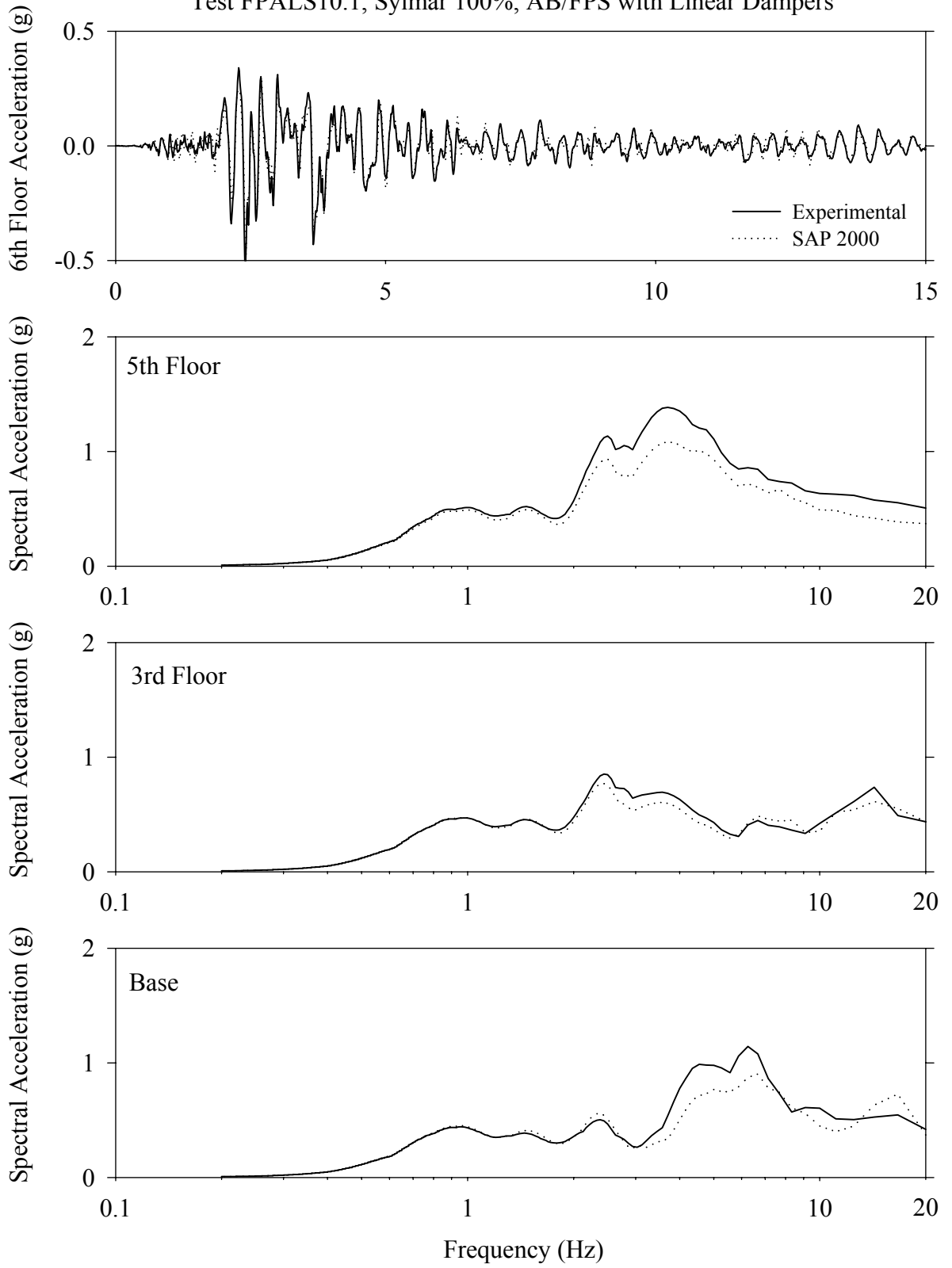
Test FPALN10.1, Newhall 360 100%, AB/FPS with Linear Dampers



Test FPALS10.1, Sylmar 100%, AB/FPS with Linear Dampers

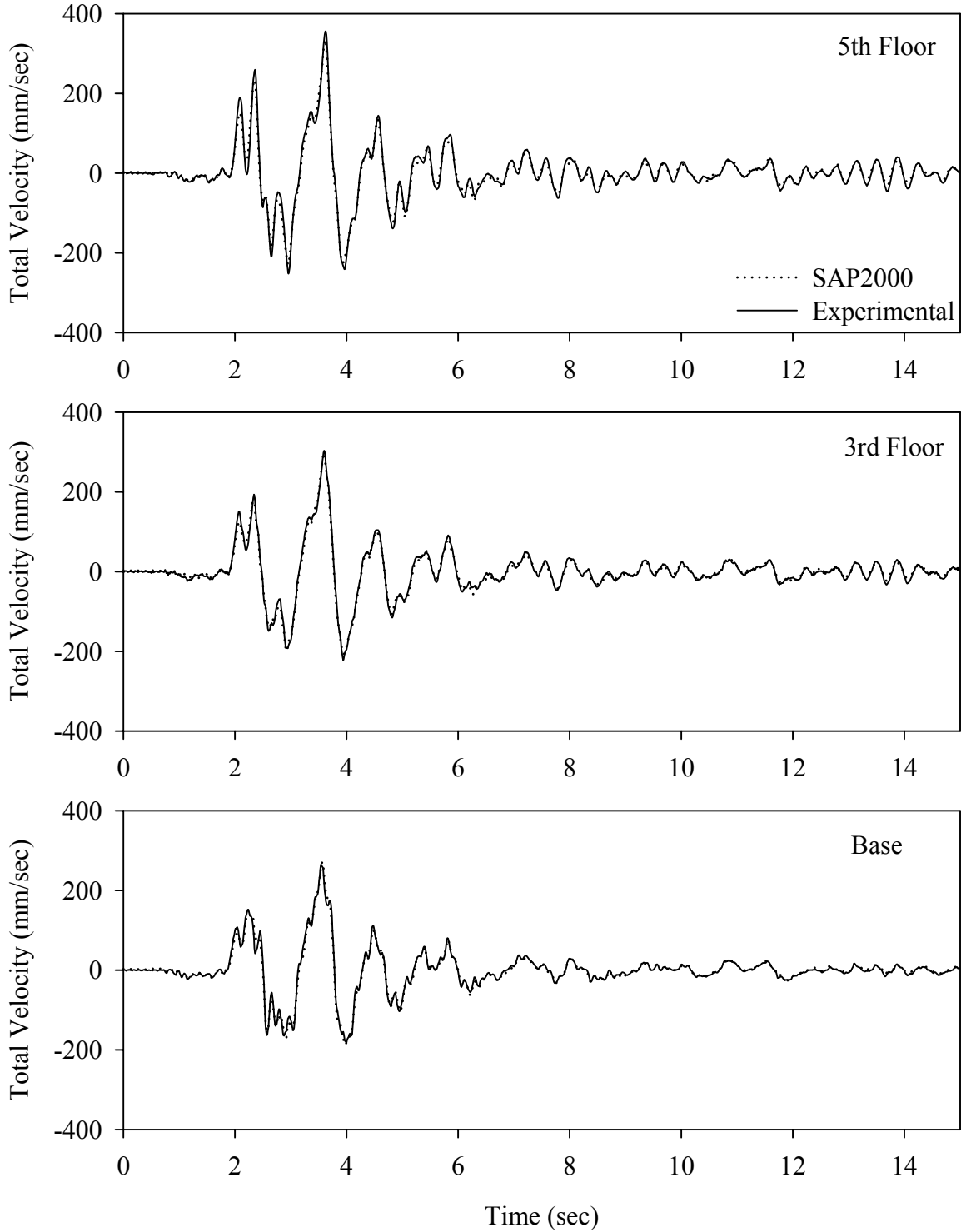


Test FPALS10.1, Sylmar 100%, AB/FPS with Linear Dampers

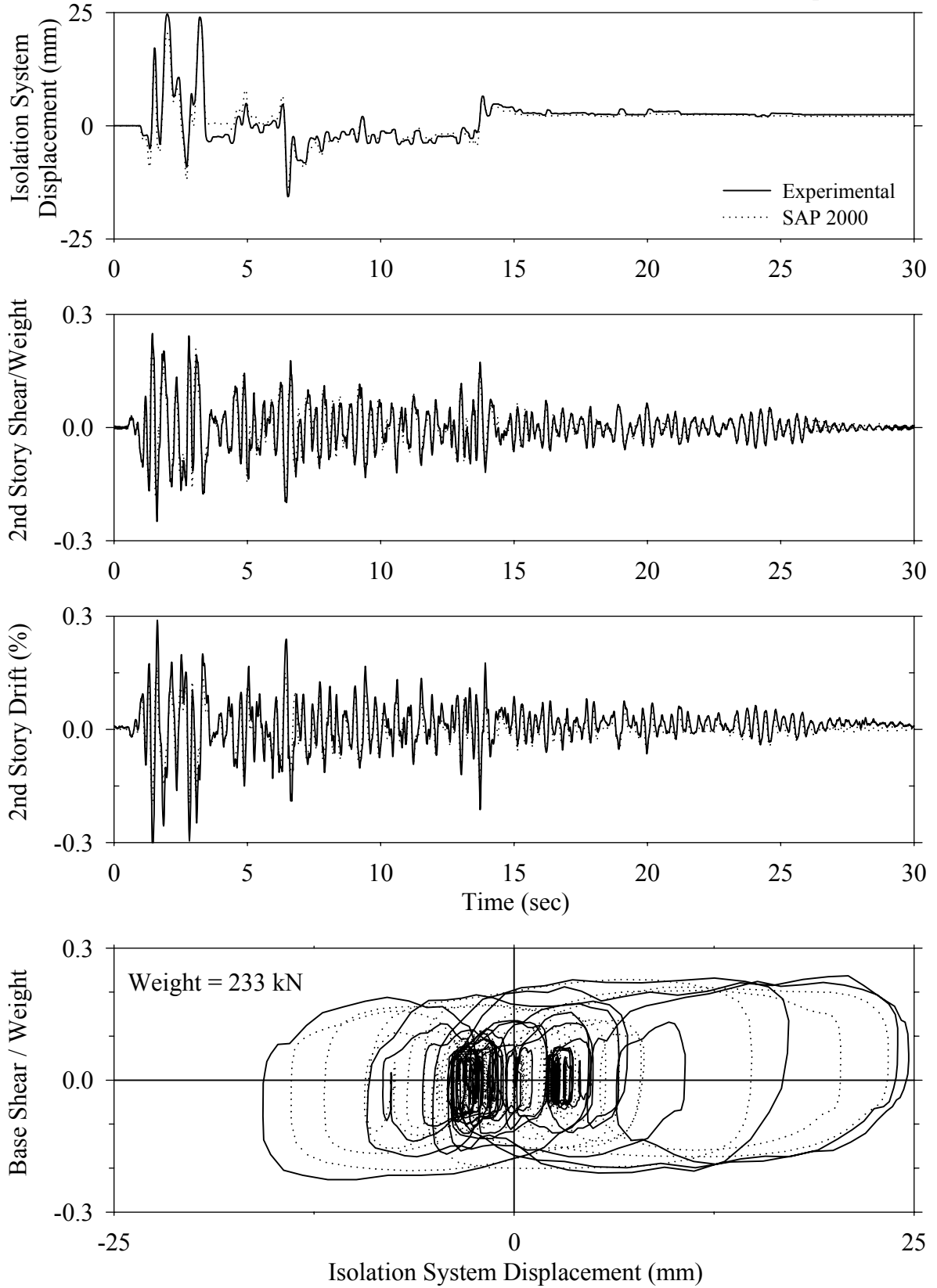




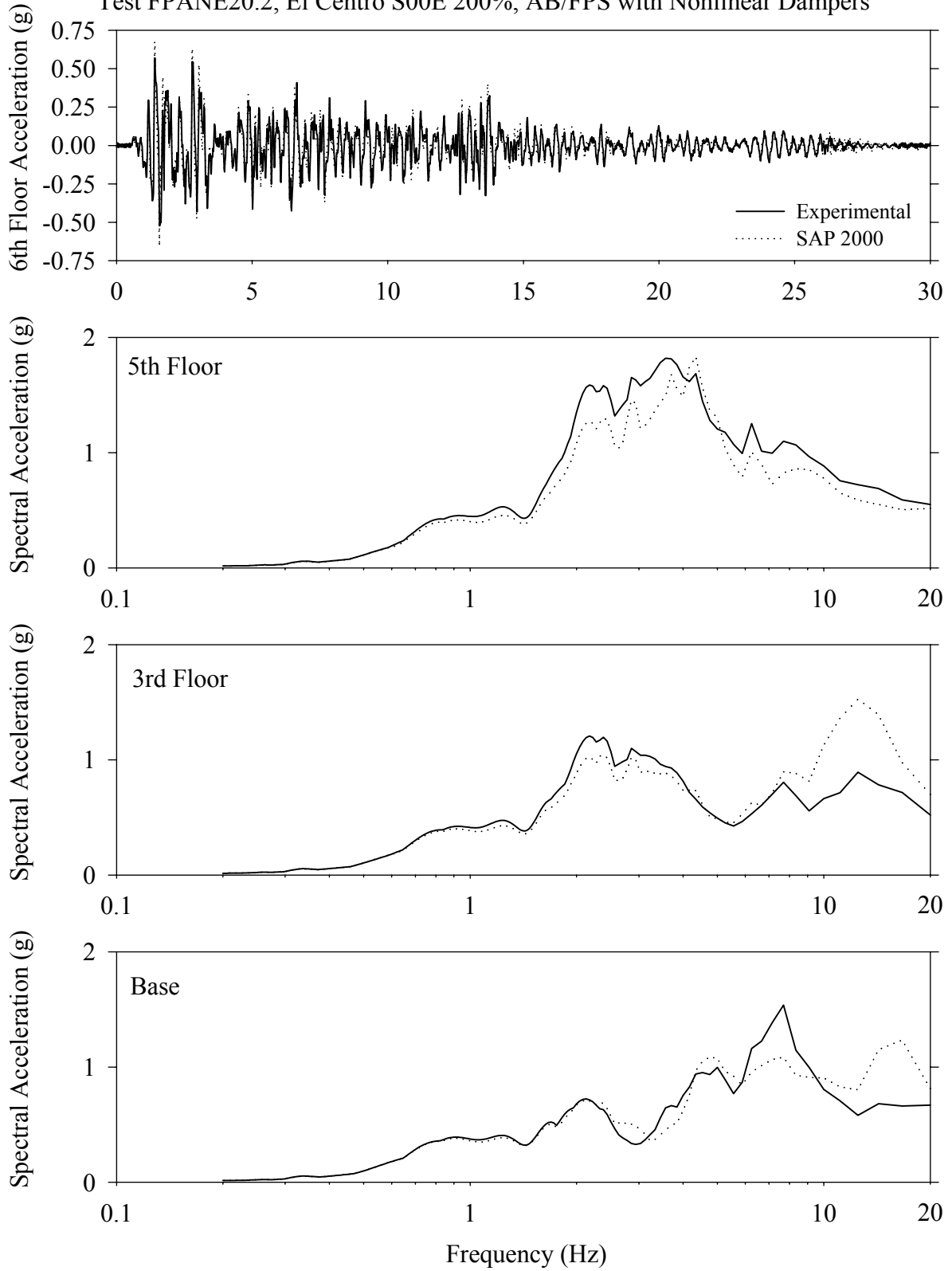
Test FPALS10.1, Sylmar 100%, AB/FPS with Linear Dampers



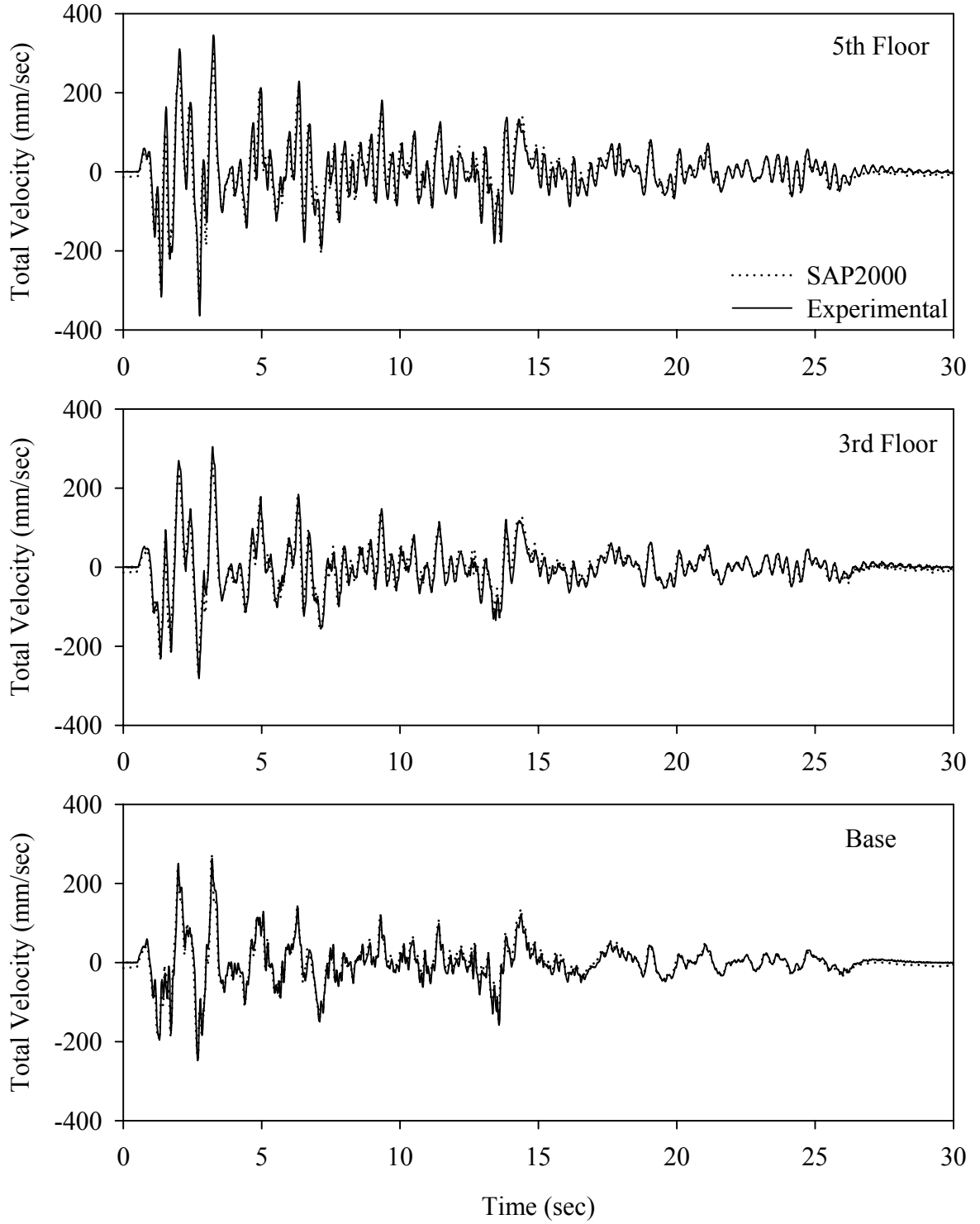
Test FPANE20.2, El Centro S00E 200%, AB/FPS with Nonlinear Dampers



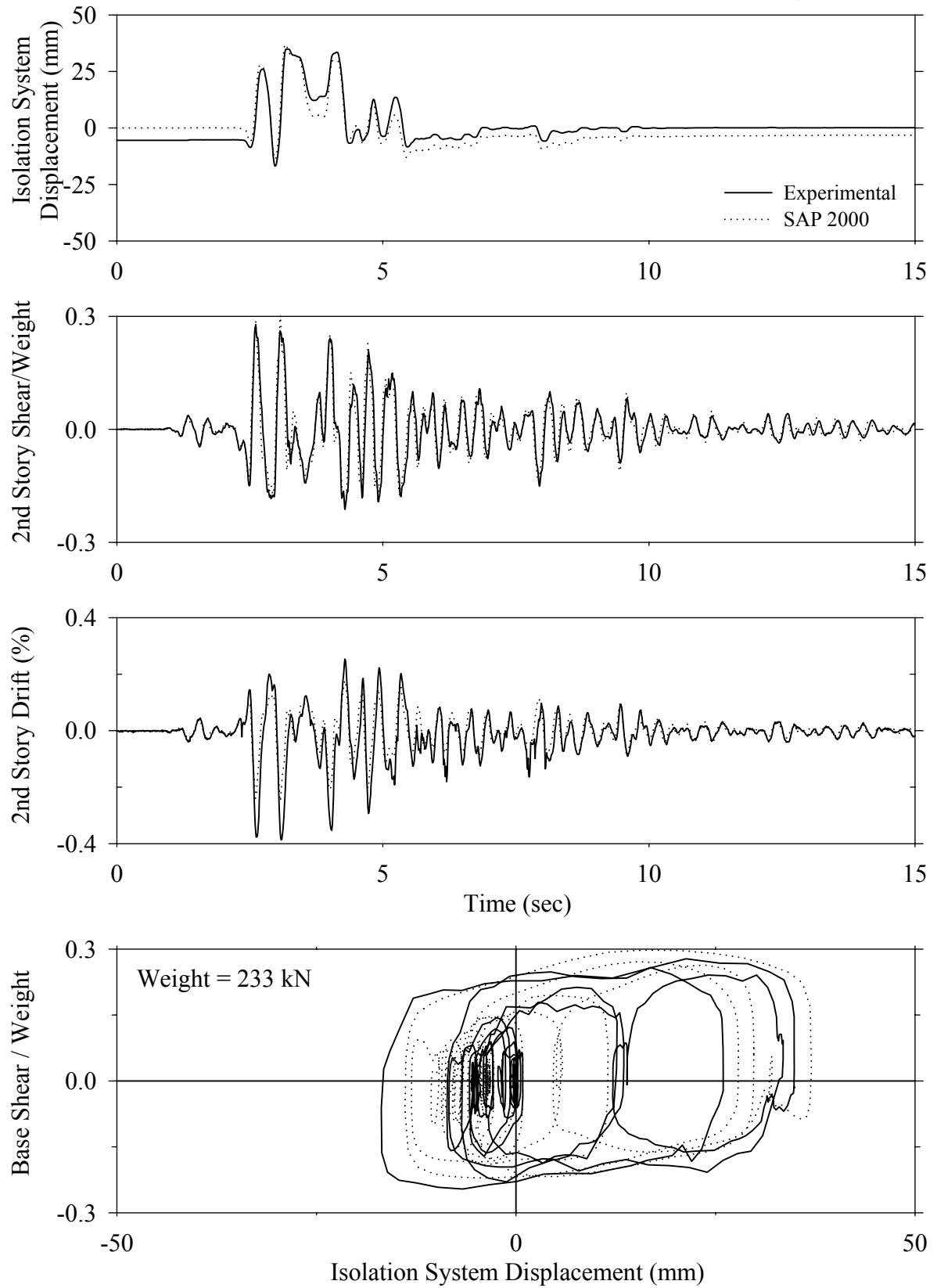
Test FPANE20.2, El Centro S00E 200%, AB/FPS with Nonlinear Dampers



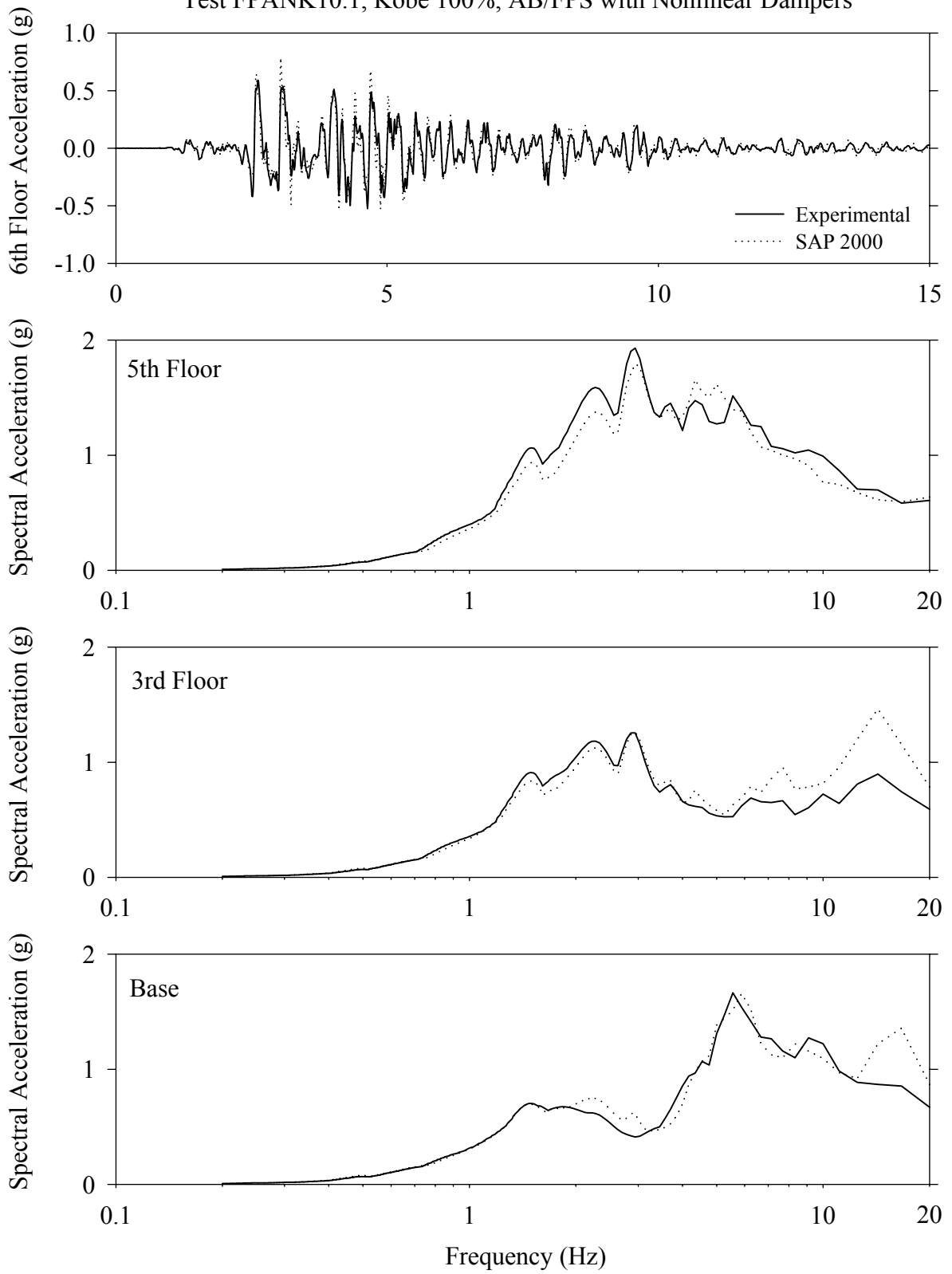
Test FPANE20.1, El Centro S00E 200%, AB/FPS with Nonlinear Dampers



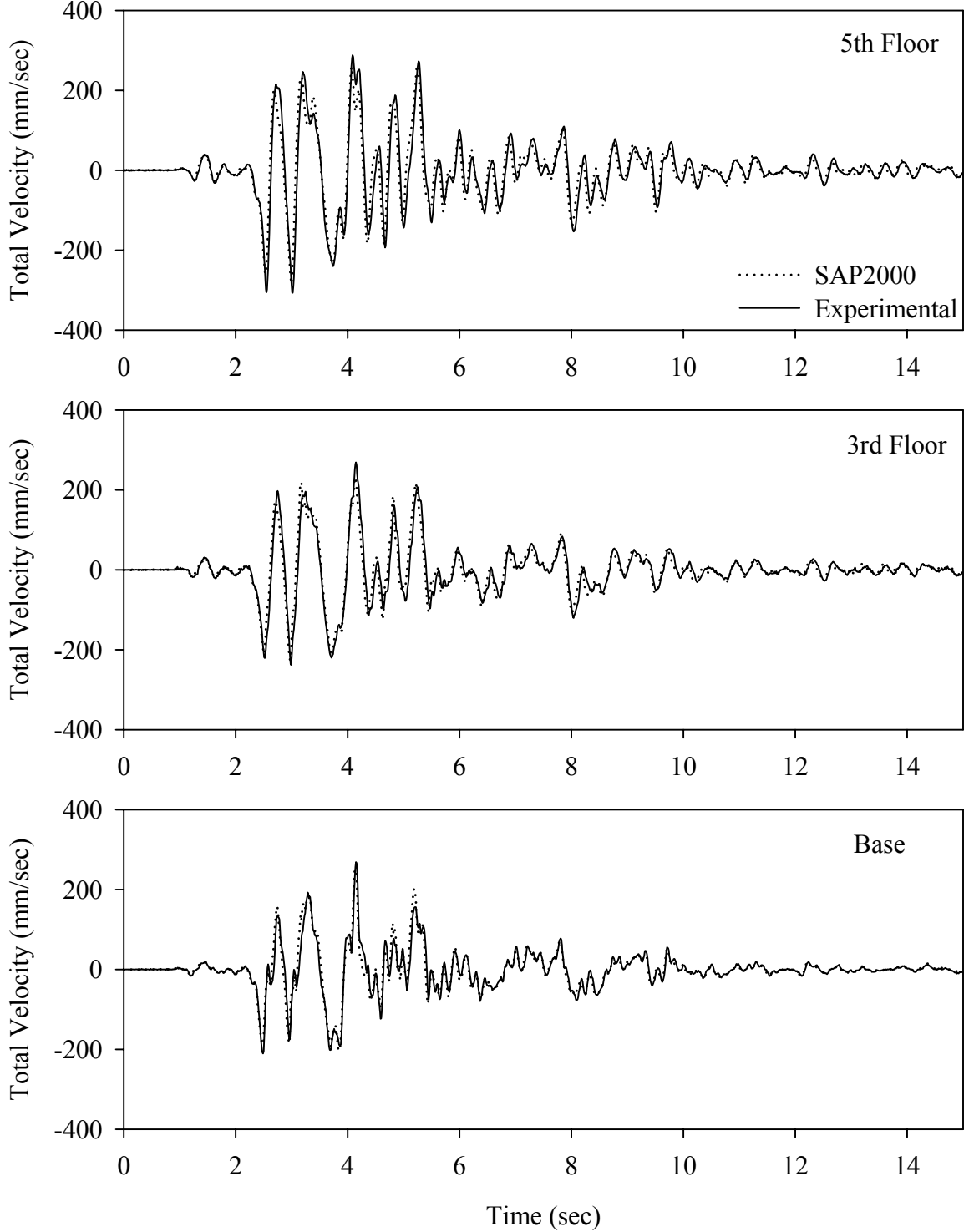
Test FPANK10.1, Kobe 100%, AB/FPS with Nonlinear Dampers



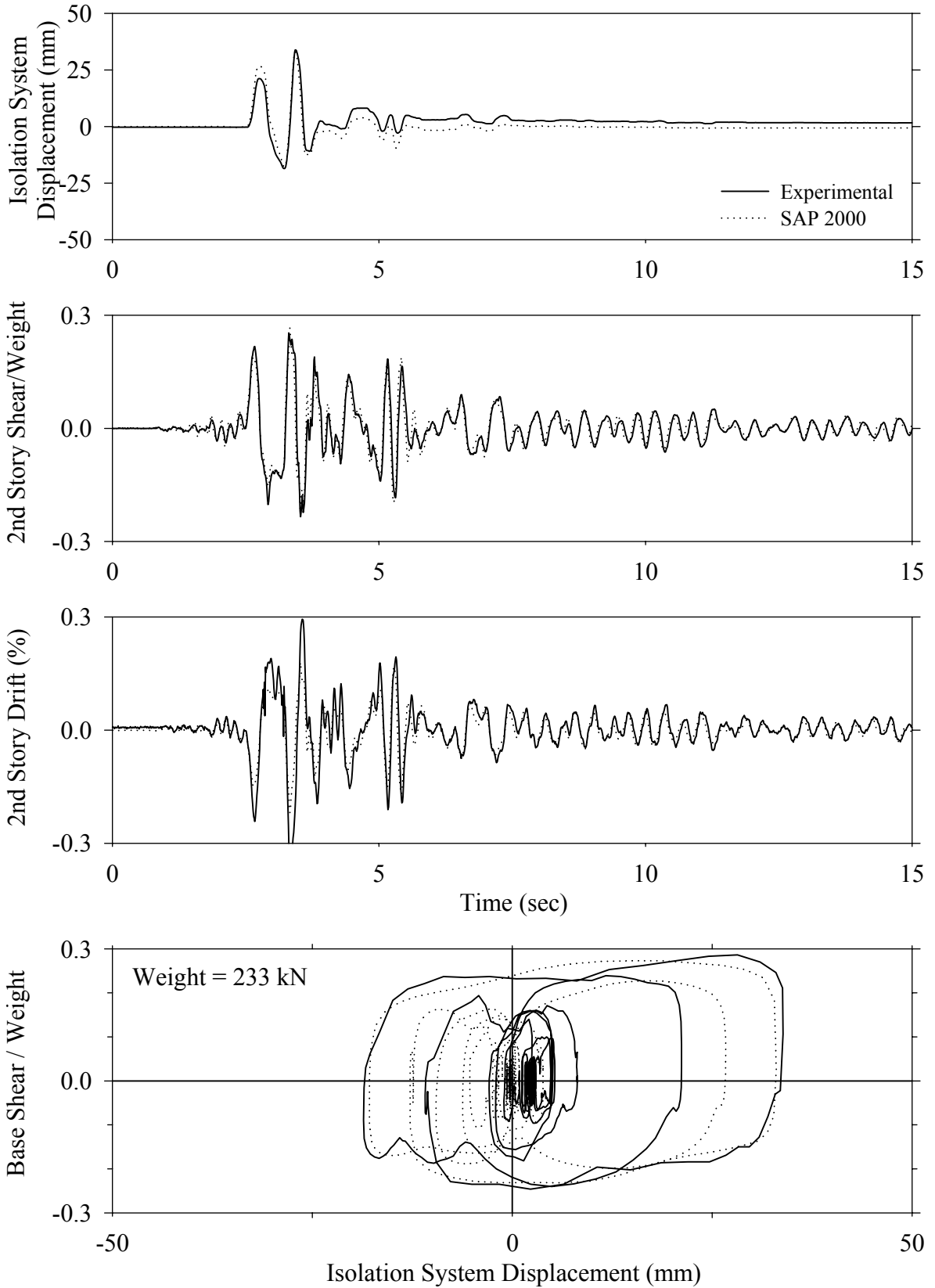
Test FPANK10.1, Kobe 100%, AB/FPS with Nonlinear Dampers



Test FPANK10.1, Kobe 100%, AB/FPS with Nonlinear Dampers

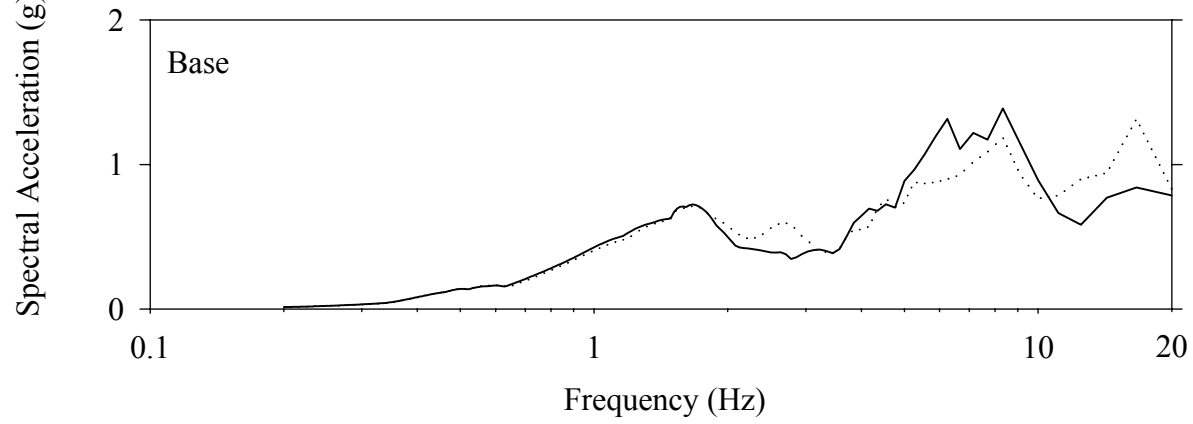
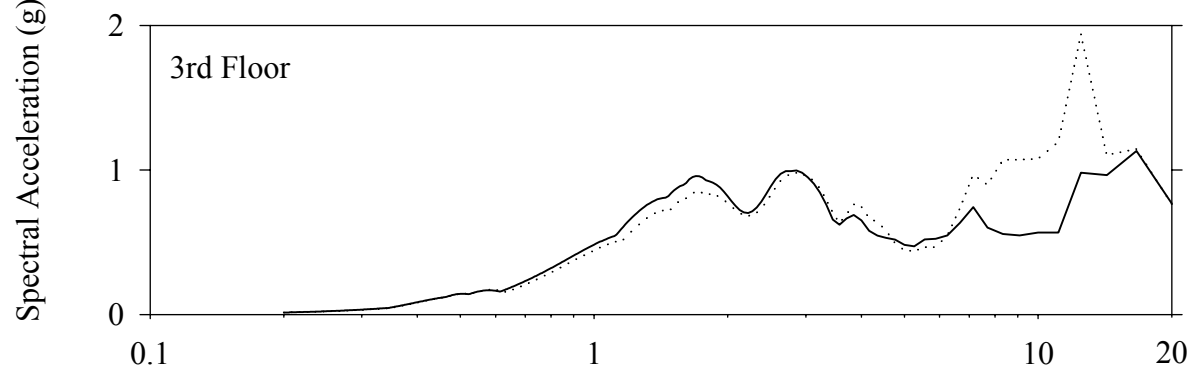
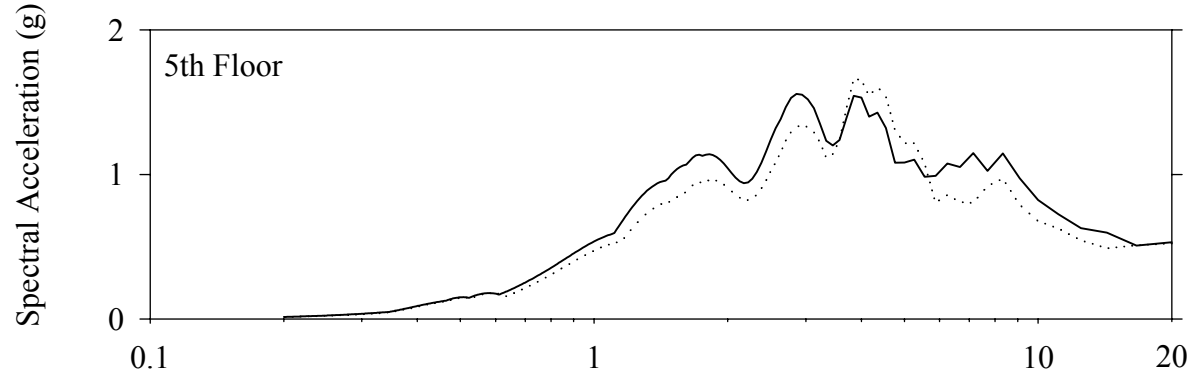
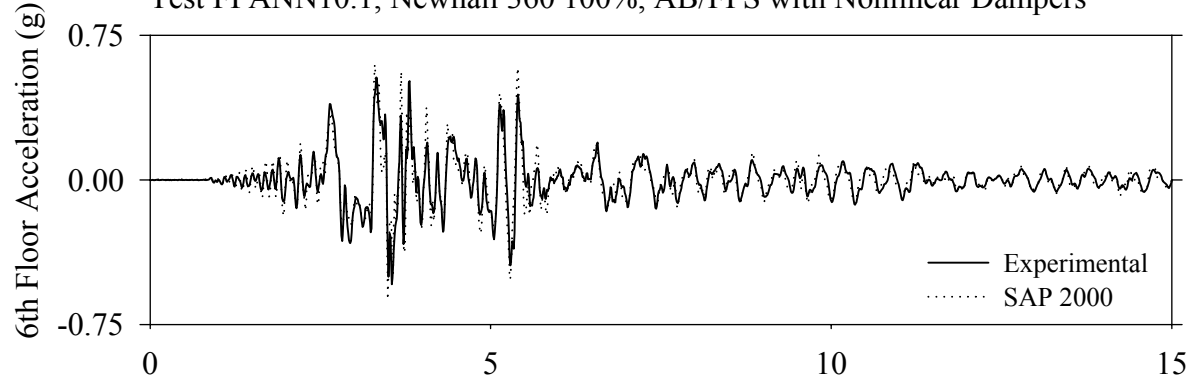


Test FPANN10.1, Newhall 360 100%, AB/FPS with Nonlinear Dampers

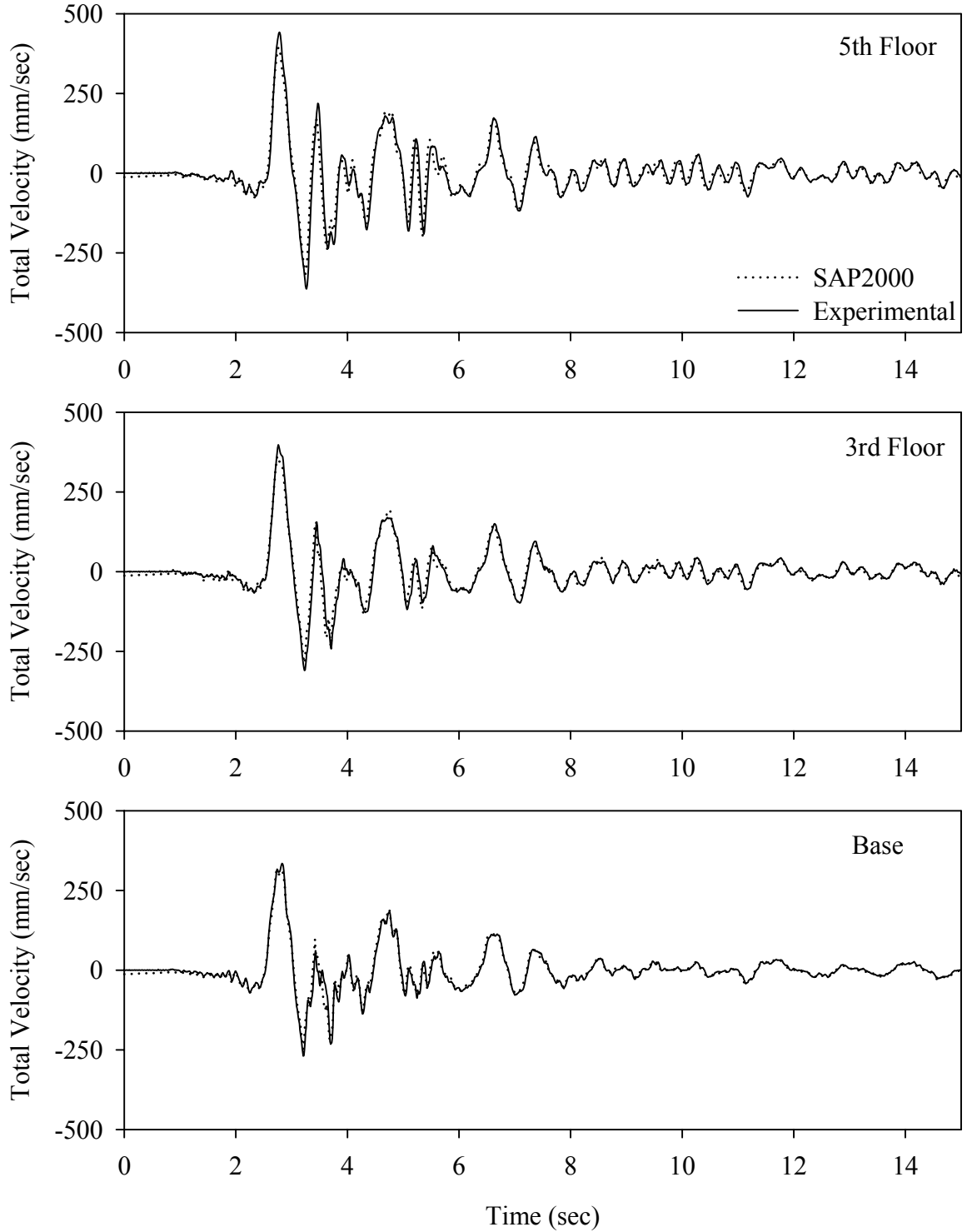




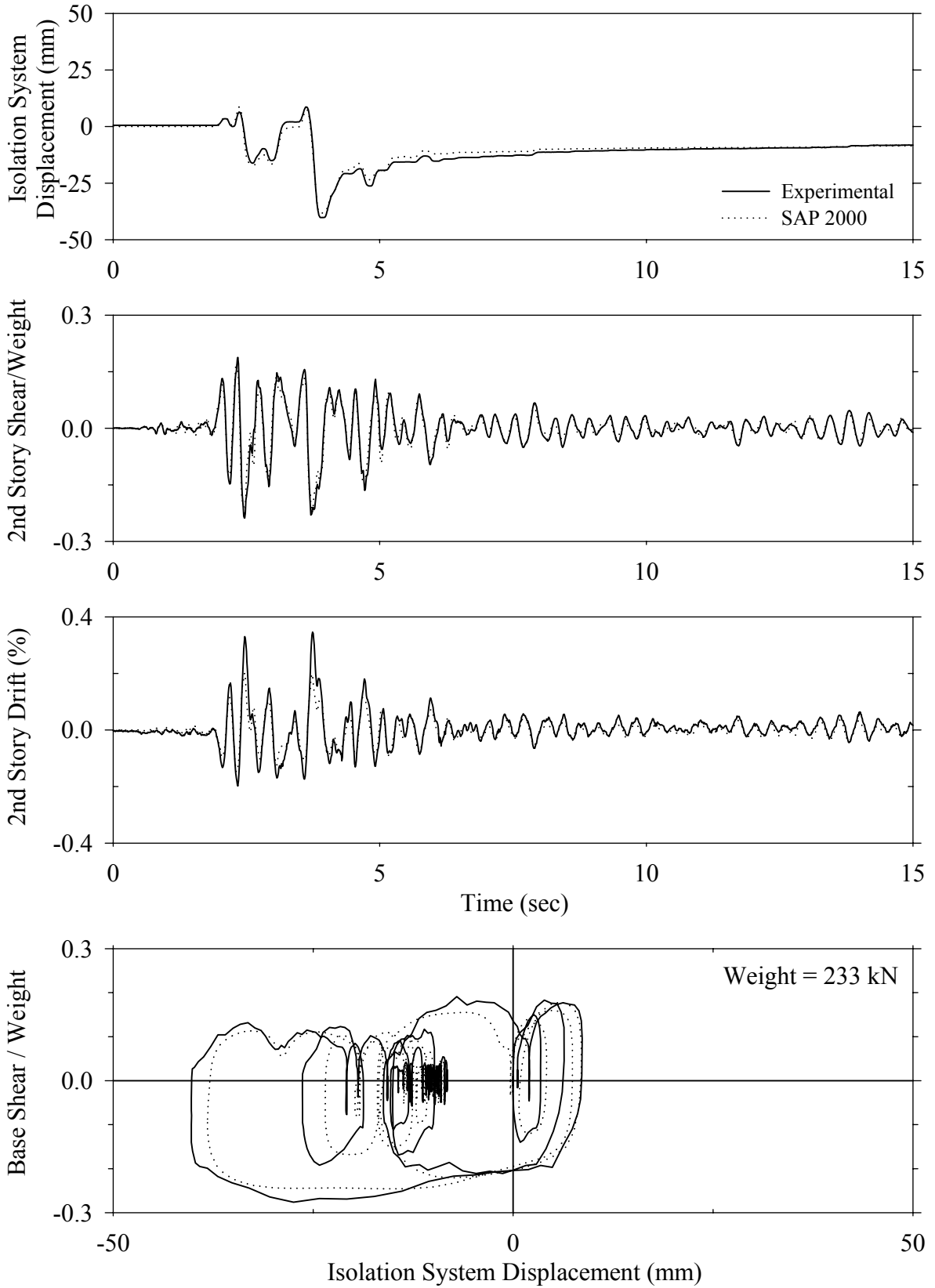
Test FPANN10.1, Newhall 360 100%, AB/FPS with Nonlinear Dampers



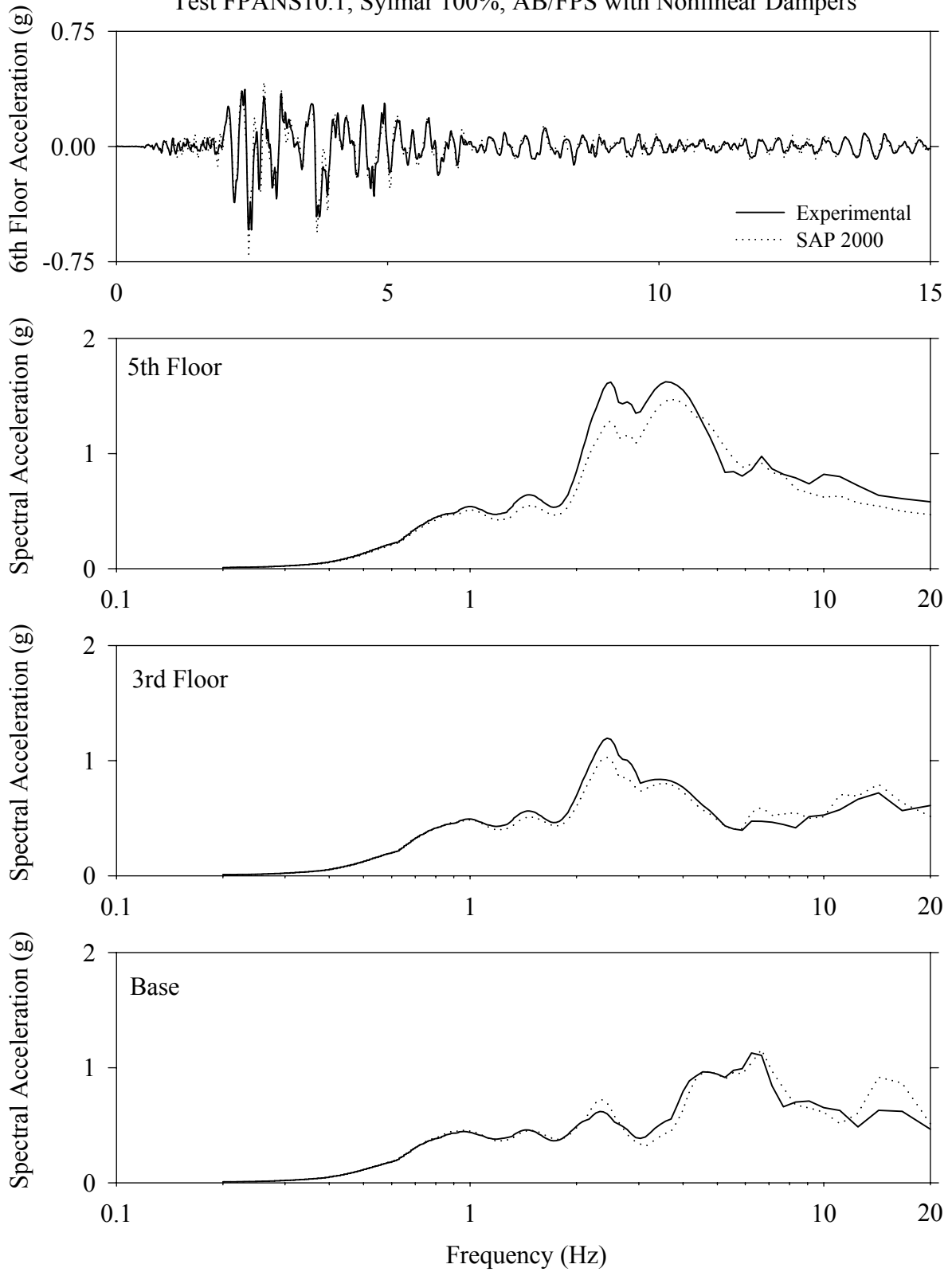
Test FPANN10.1, Newhall 360 100%, AB/FPS with Nonlinear Dampers



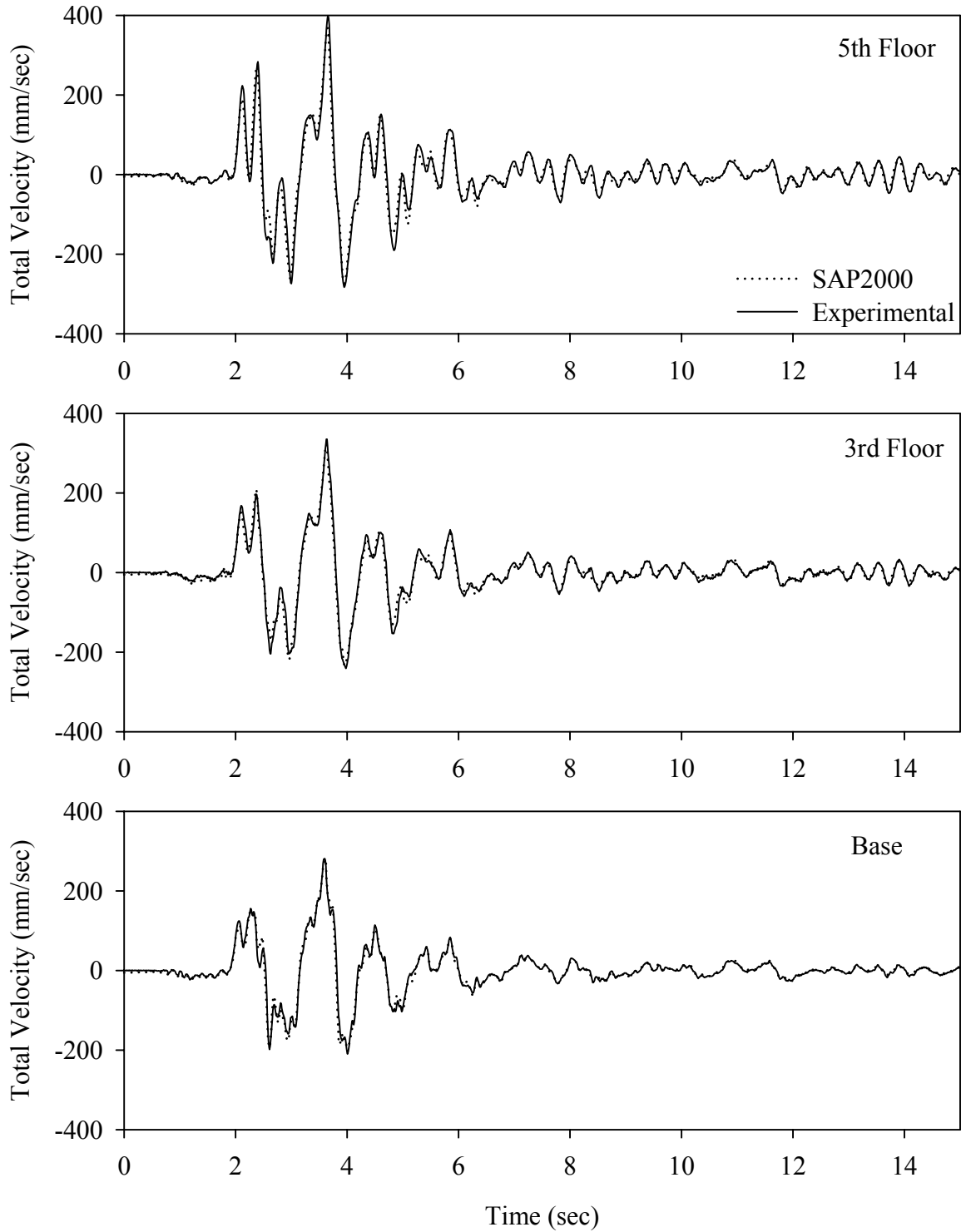
Test FPANS10.1, Sylmar 100%, AB/FPS with Nonlinear Dampers



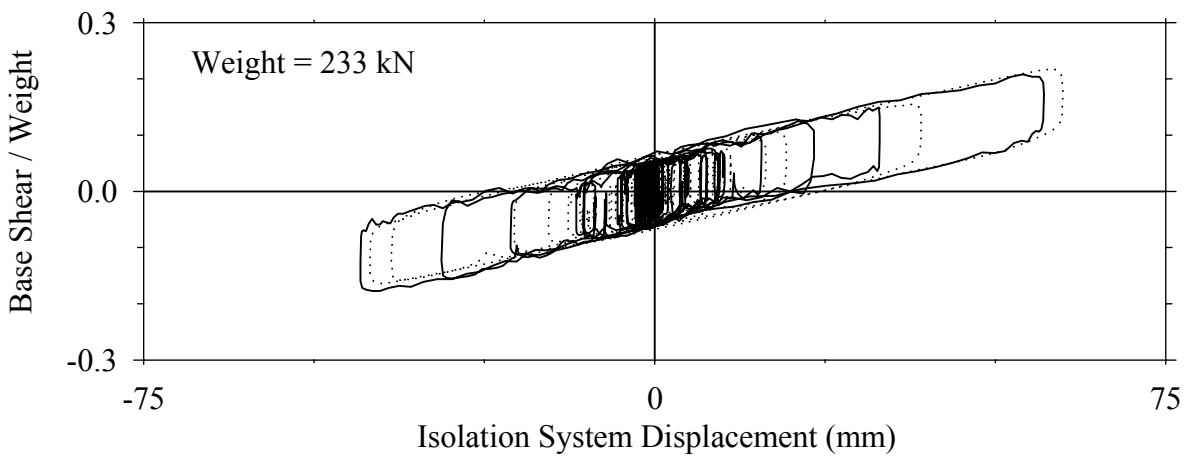
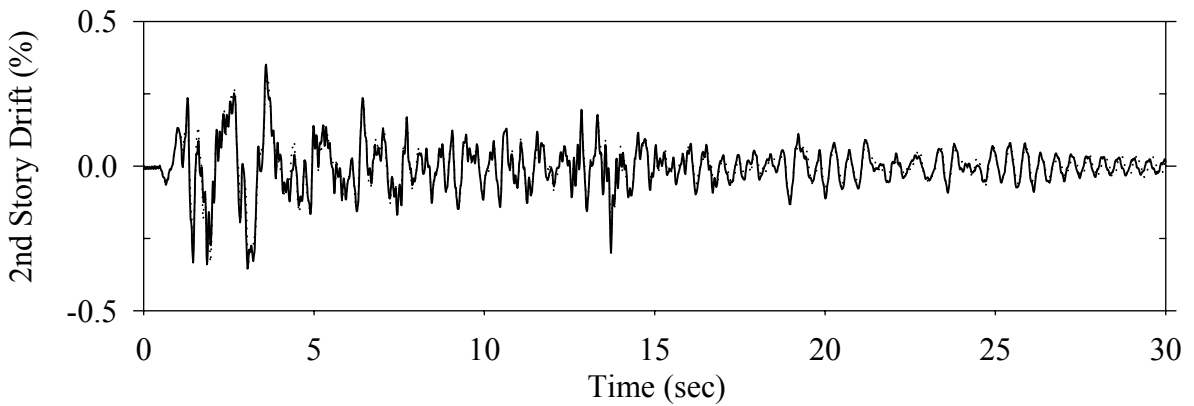
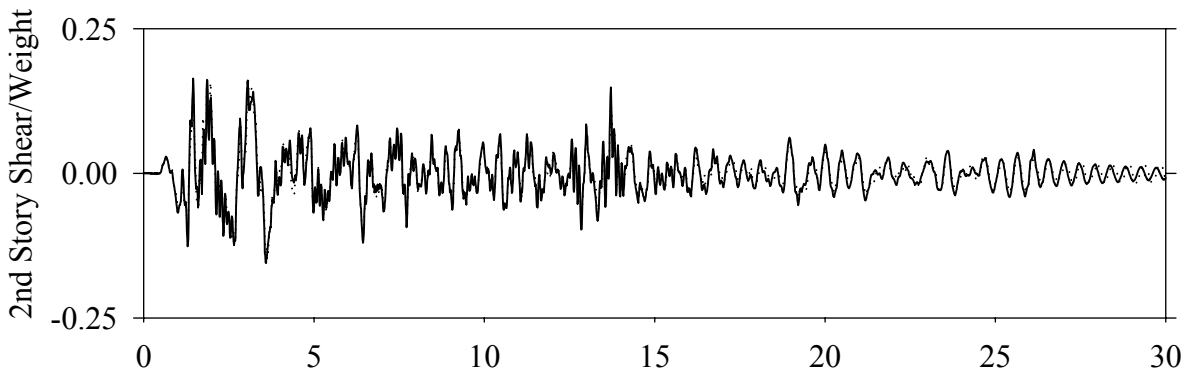
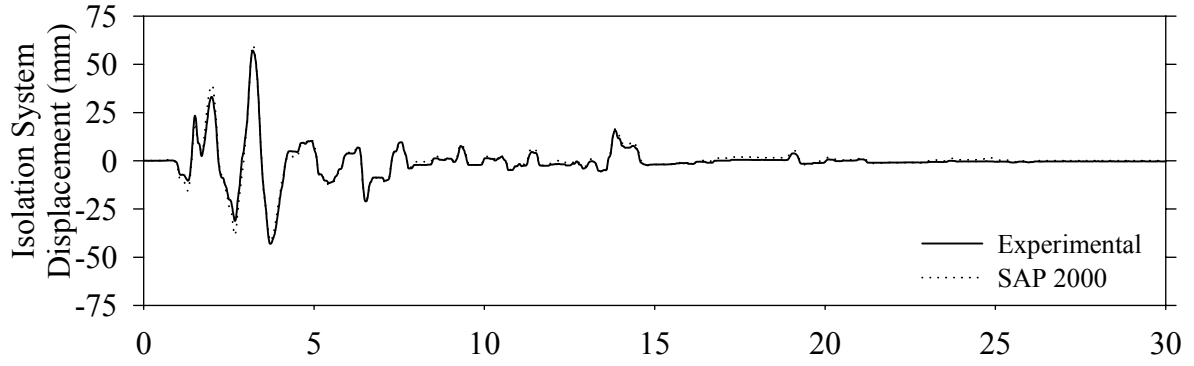
Test FPANS10.1, Sylmar 100%, AB/FPS with Nonlinear Dampers



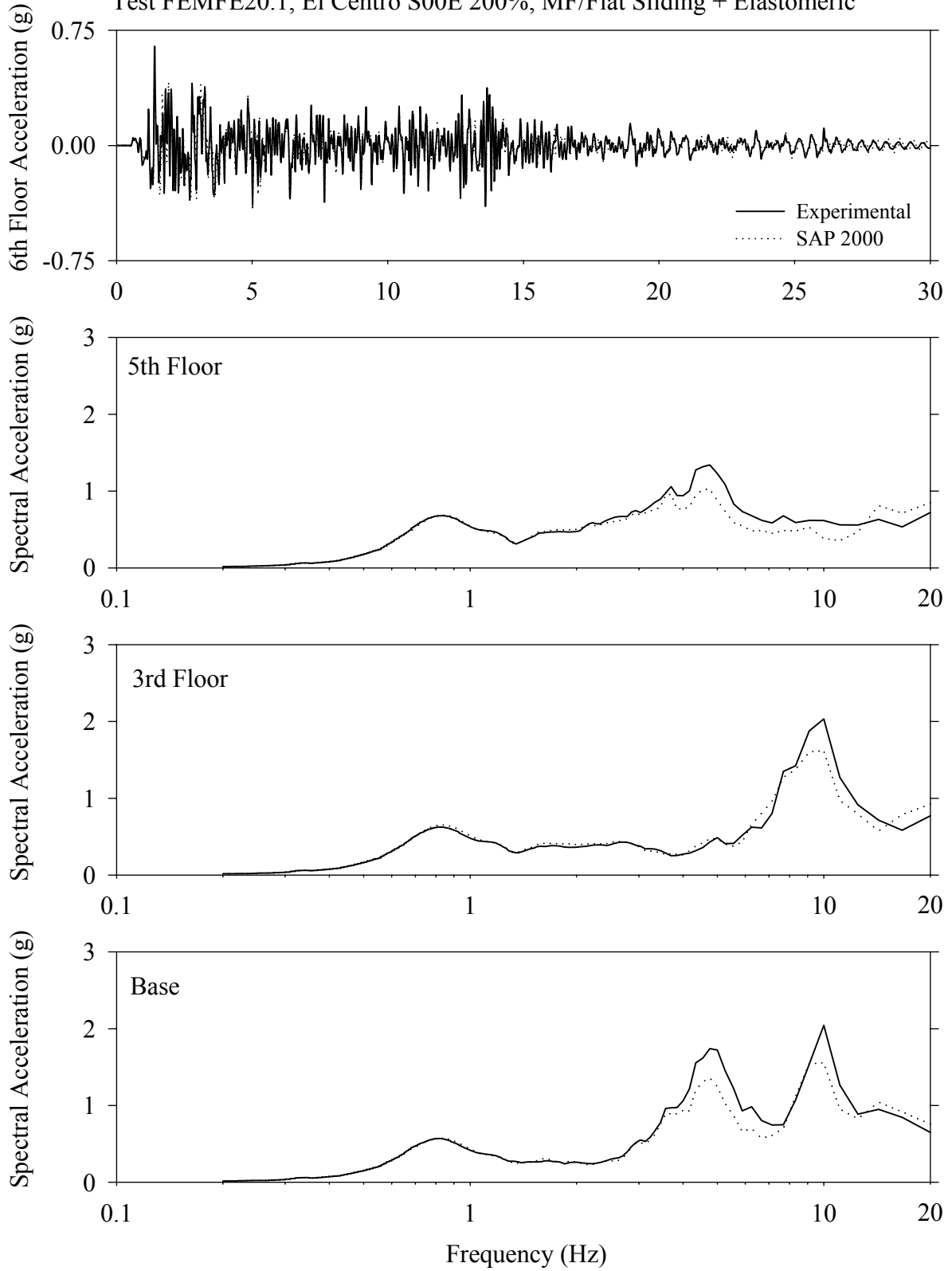
Test FPANS10.1, Sylmar 100%, AB/FPS with Nonlinear Dampers



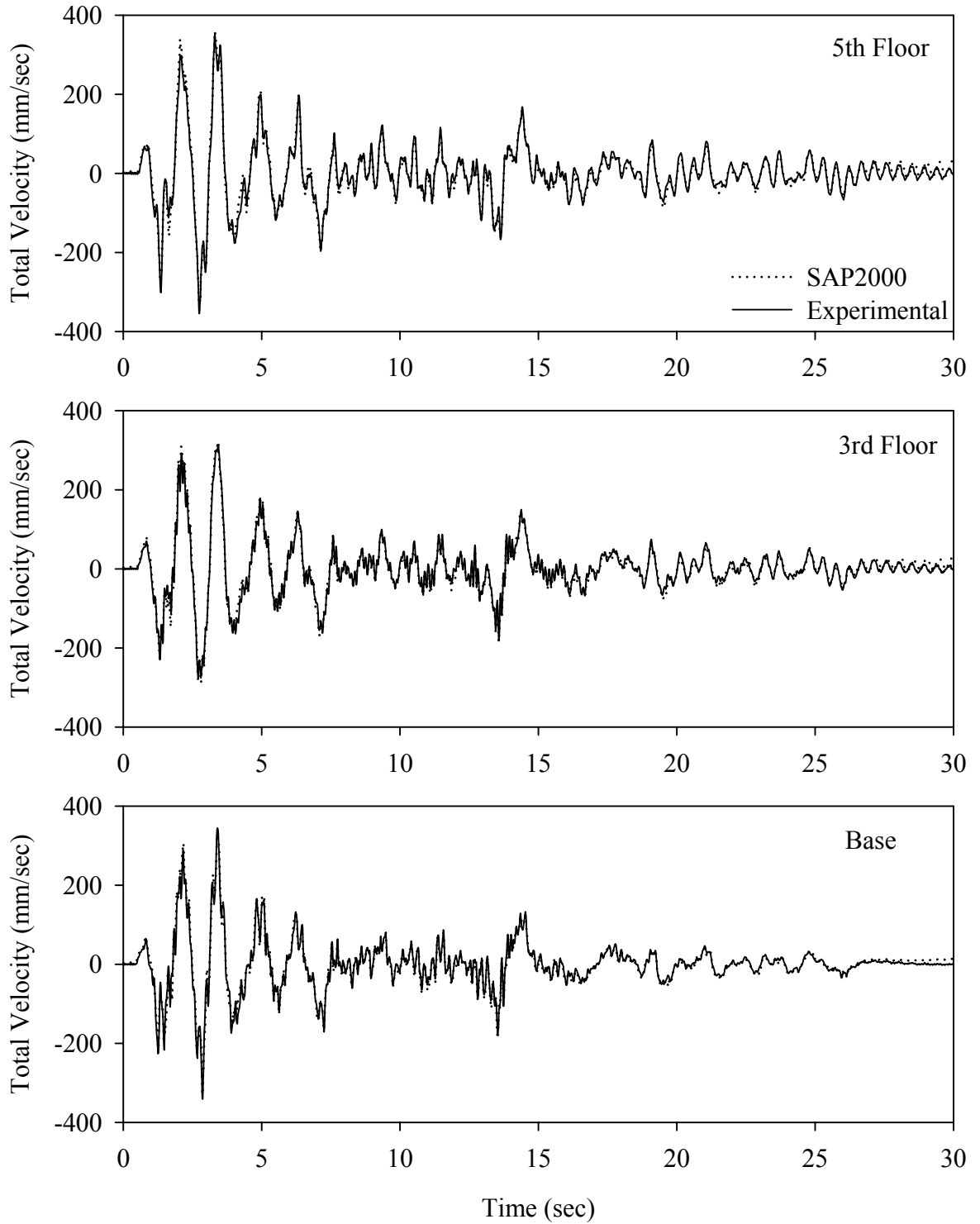
Test FEMFE20.1, El Centro S00E 200%, MF/Flat Sliding + Elastomeric



Test FEMFE20.1, El Centro S00E 200%, MF/Flat Sliding + Elastomeric

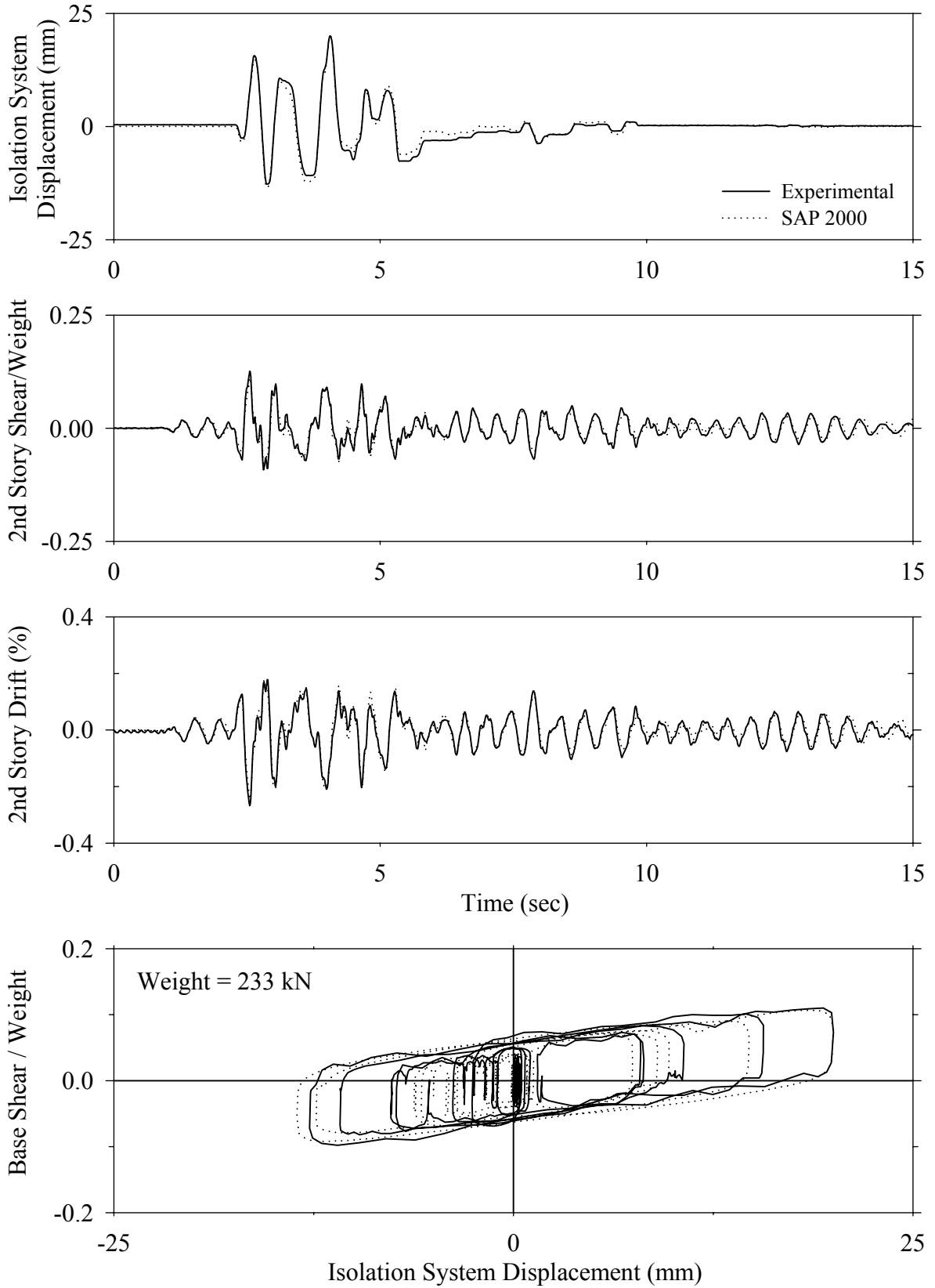


Test FEMFE20.1, El Centro S00E 200%, MF/Flat Sliding + Elastomeric

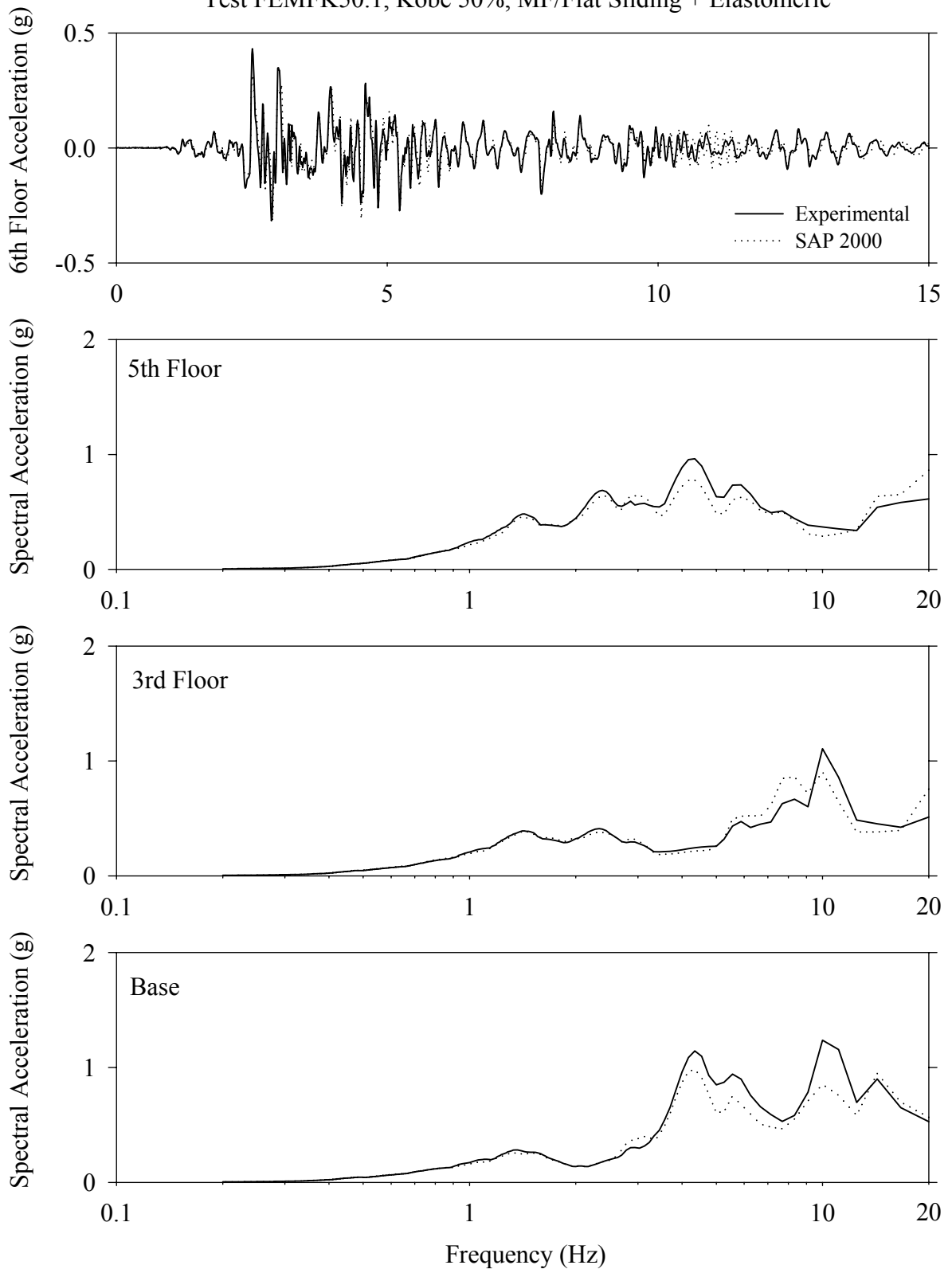




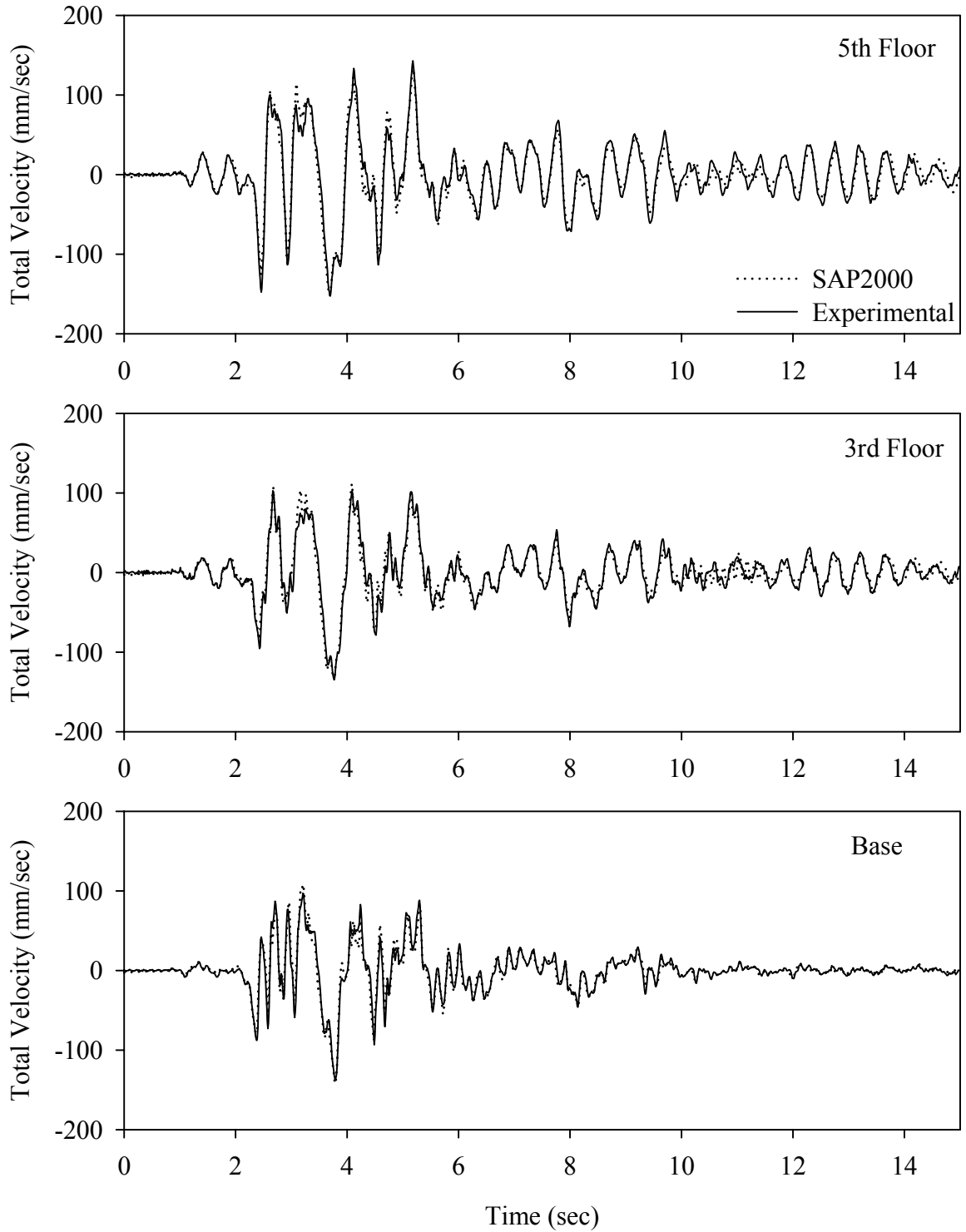
Test FEMFK50.1, Kobe 50%, MF/Flat Sliding + Elastomeric



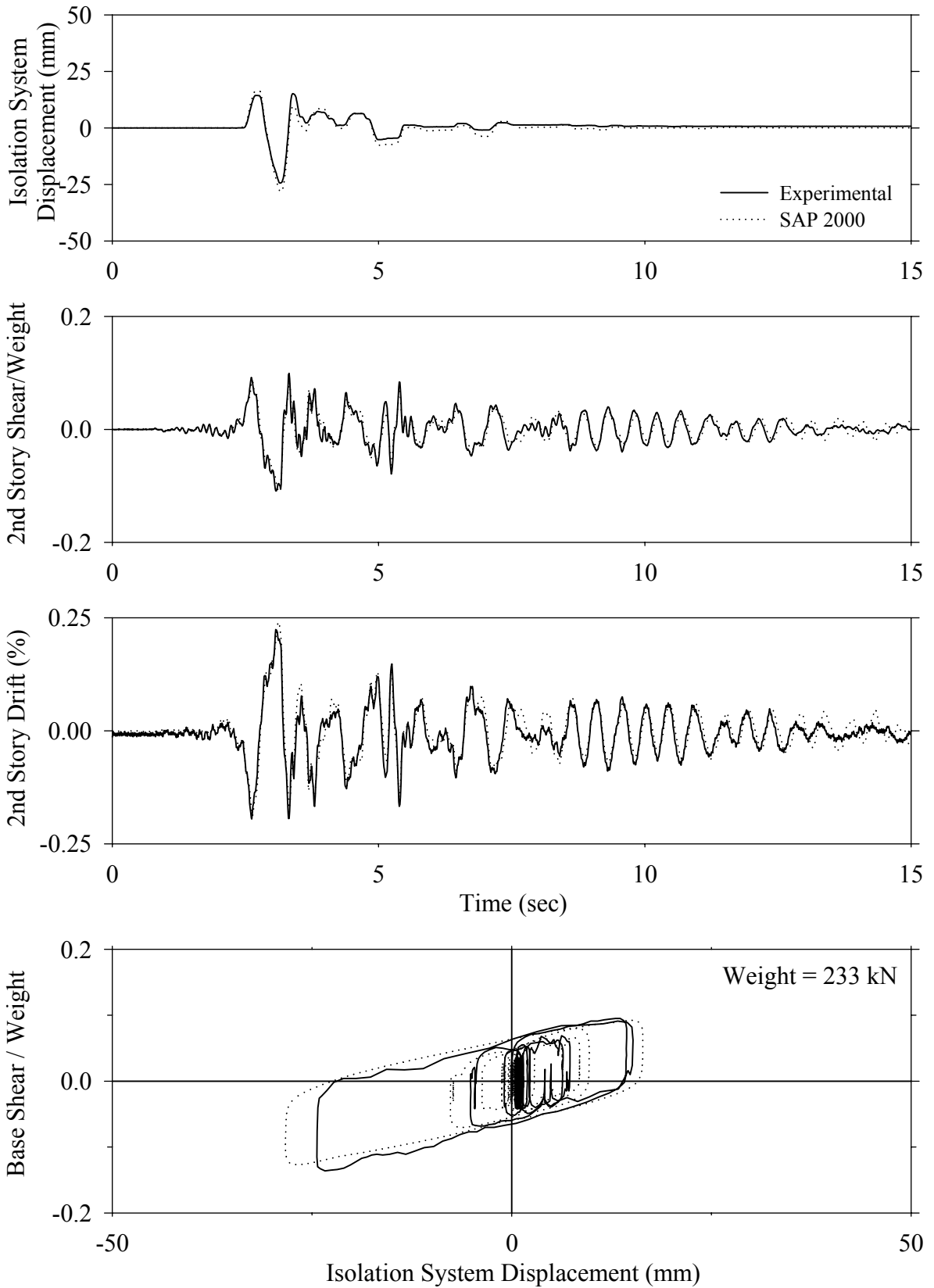
Test FEMFK50.1, Kobe 50%, MF/Flat Sliding + Elastomeric



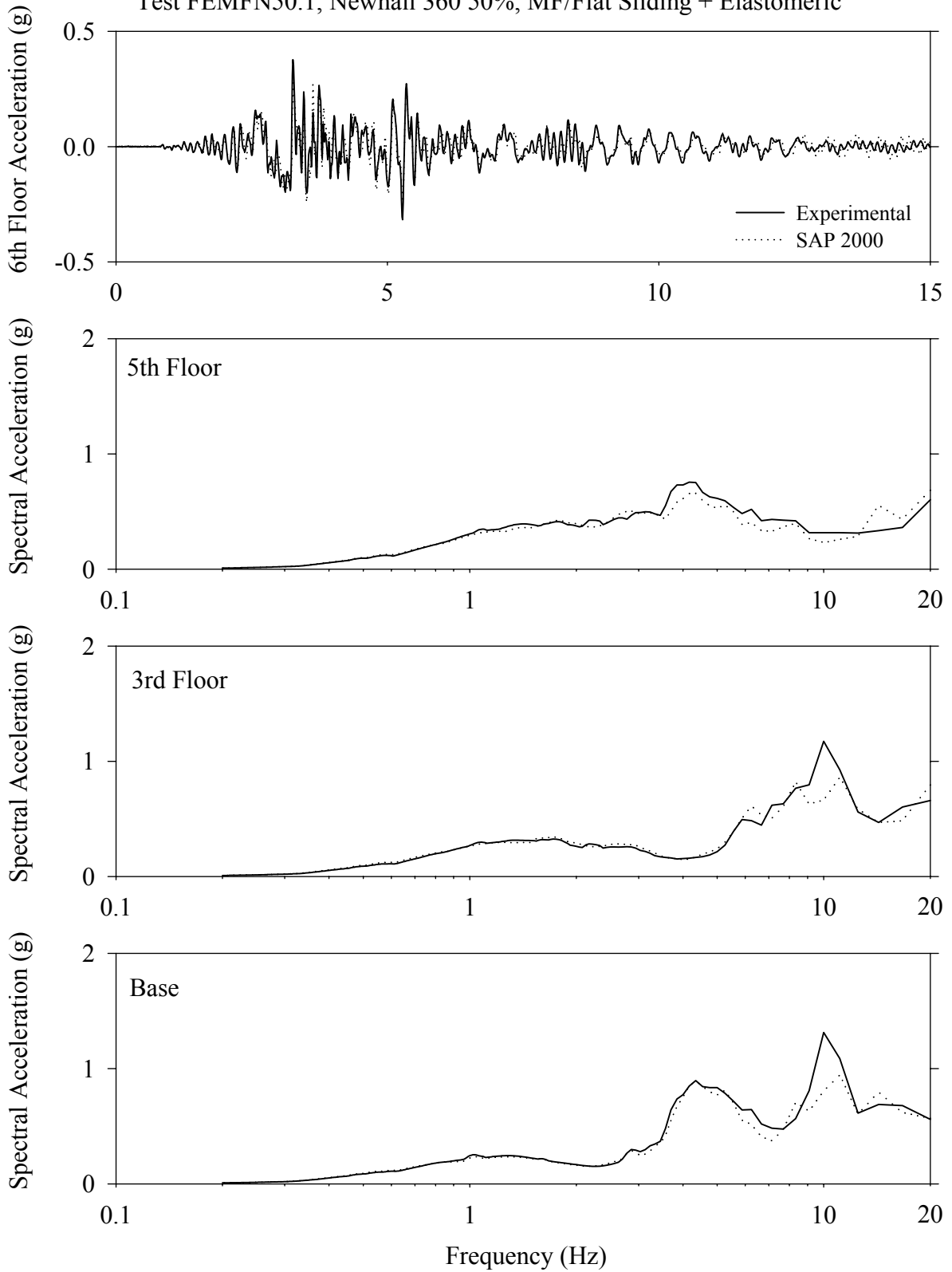
Test FEMFK50.1, Kobe 50%, MF/Flat Sliding + Elastomeric



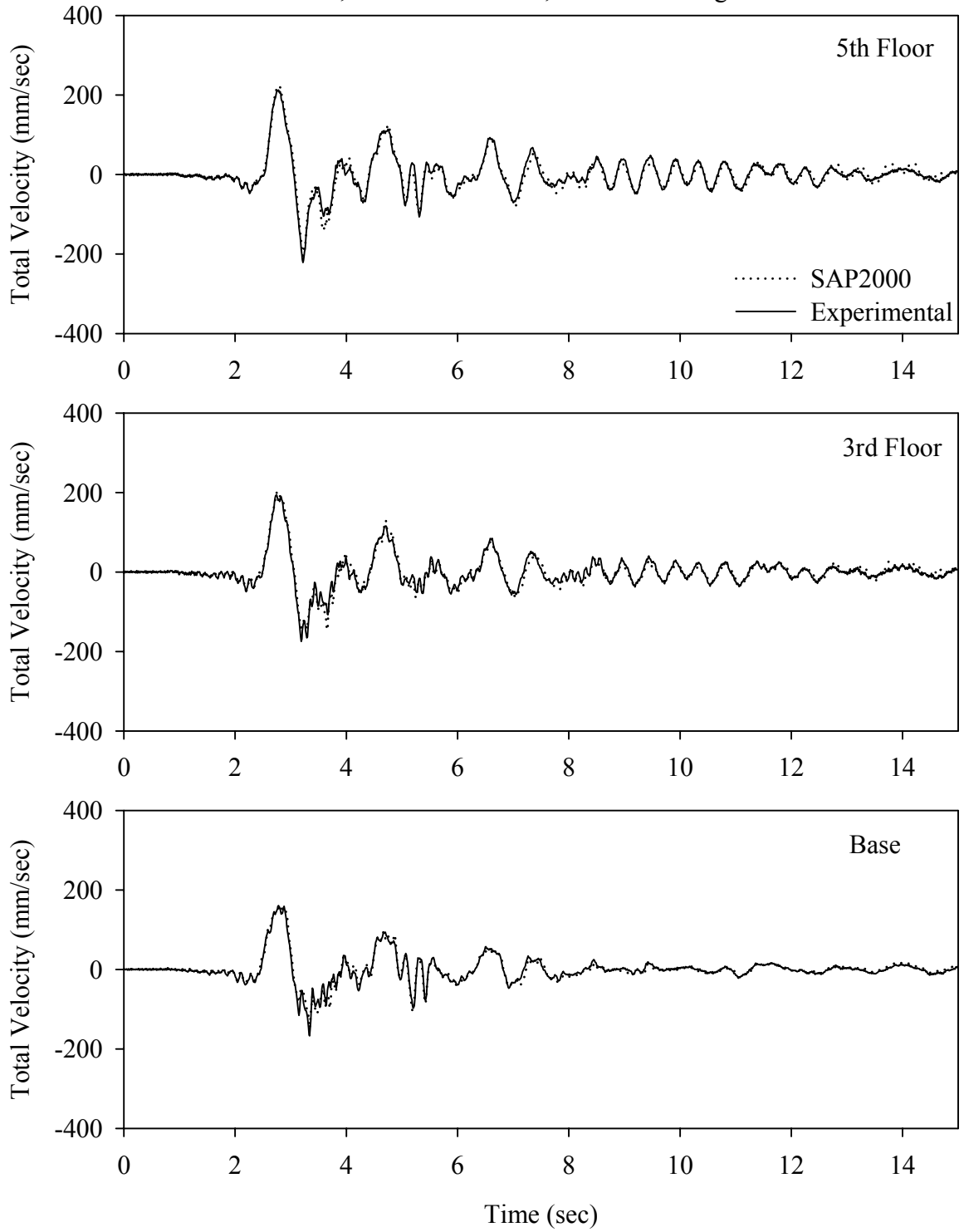
Test FEMFN50.1, Newhall 360 50%, MF/Flat Sliding + Elastomeric



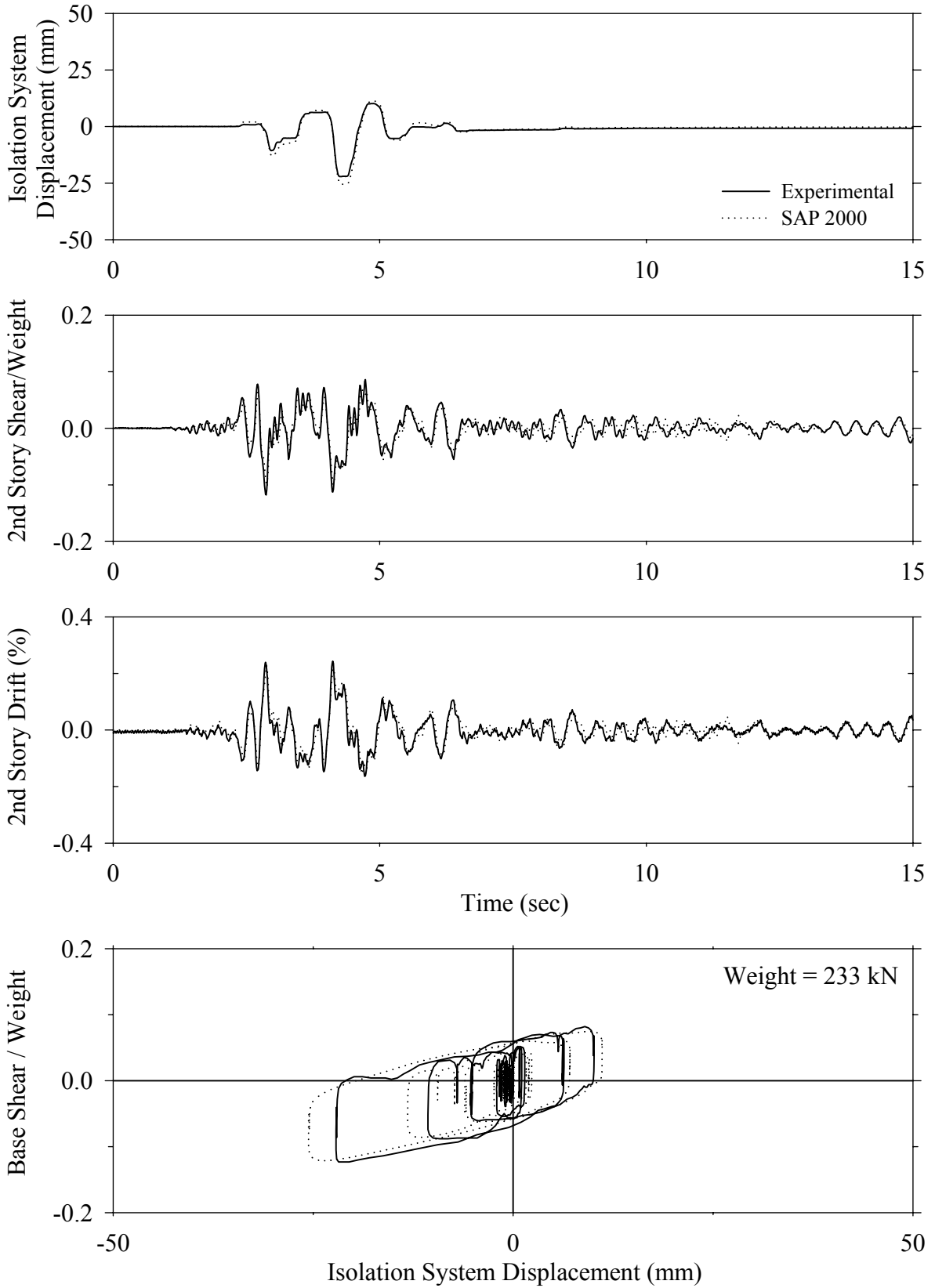
Test FEMFN50.1, Newhall 360 50%, MF/Flat Sliding + Elastomeric



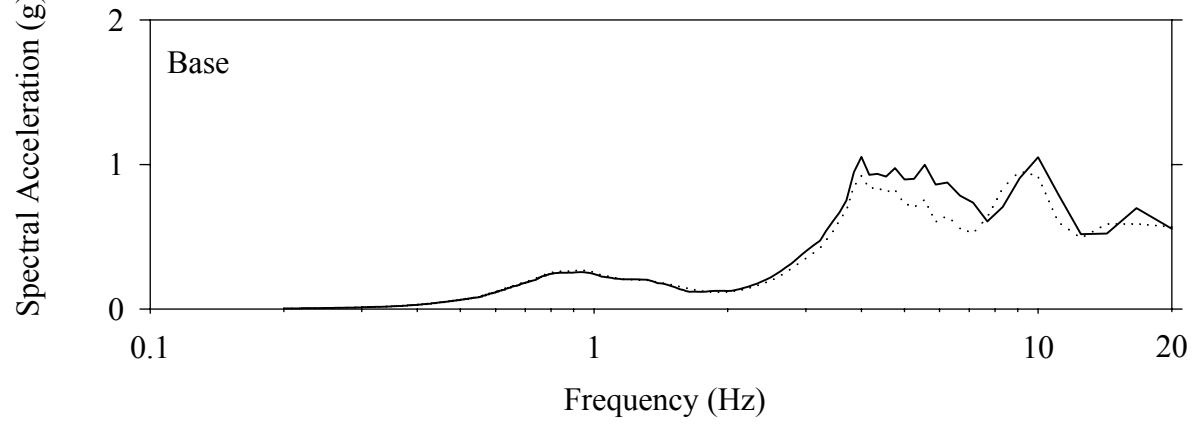
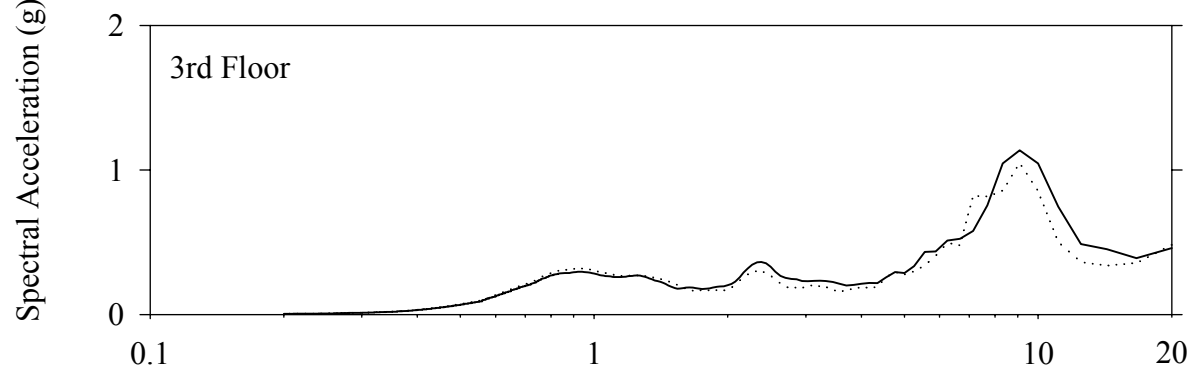
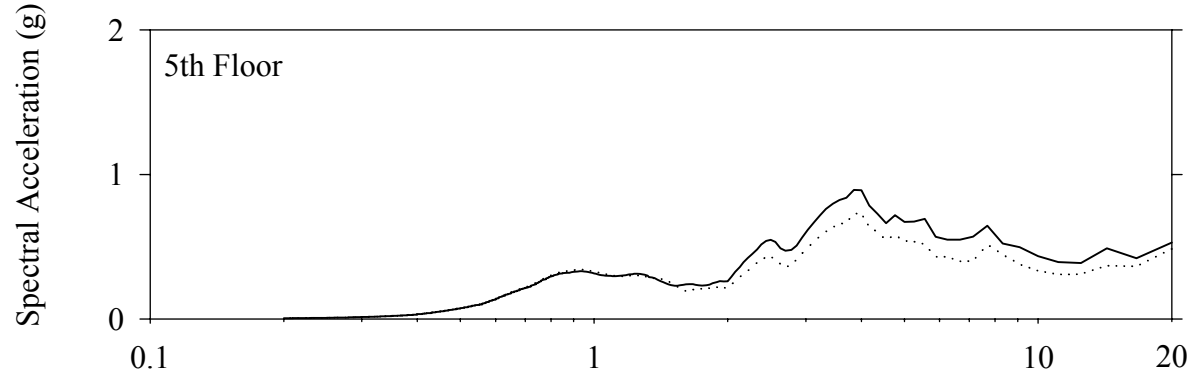
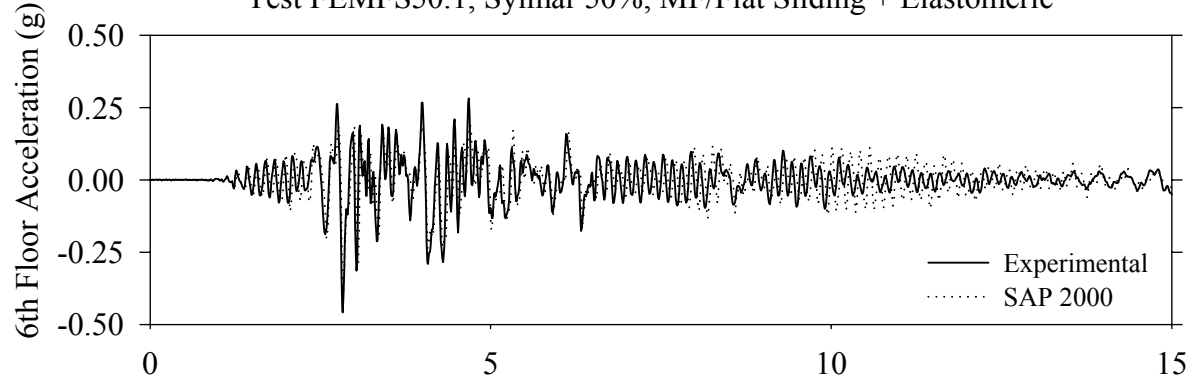
Test FEMFN50.1, Newhall 360 50%, MF/Flat Sliding + Elastomeric



Test FEMFS50.1, Sylmar 50%, MF/Flat Sliding + Elastomeric

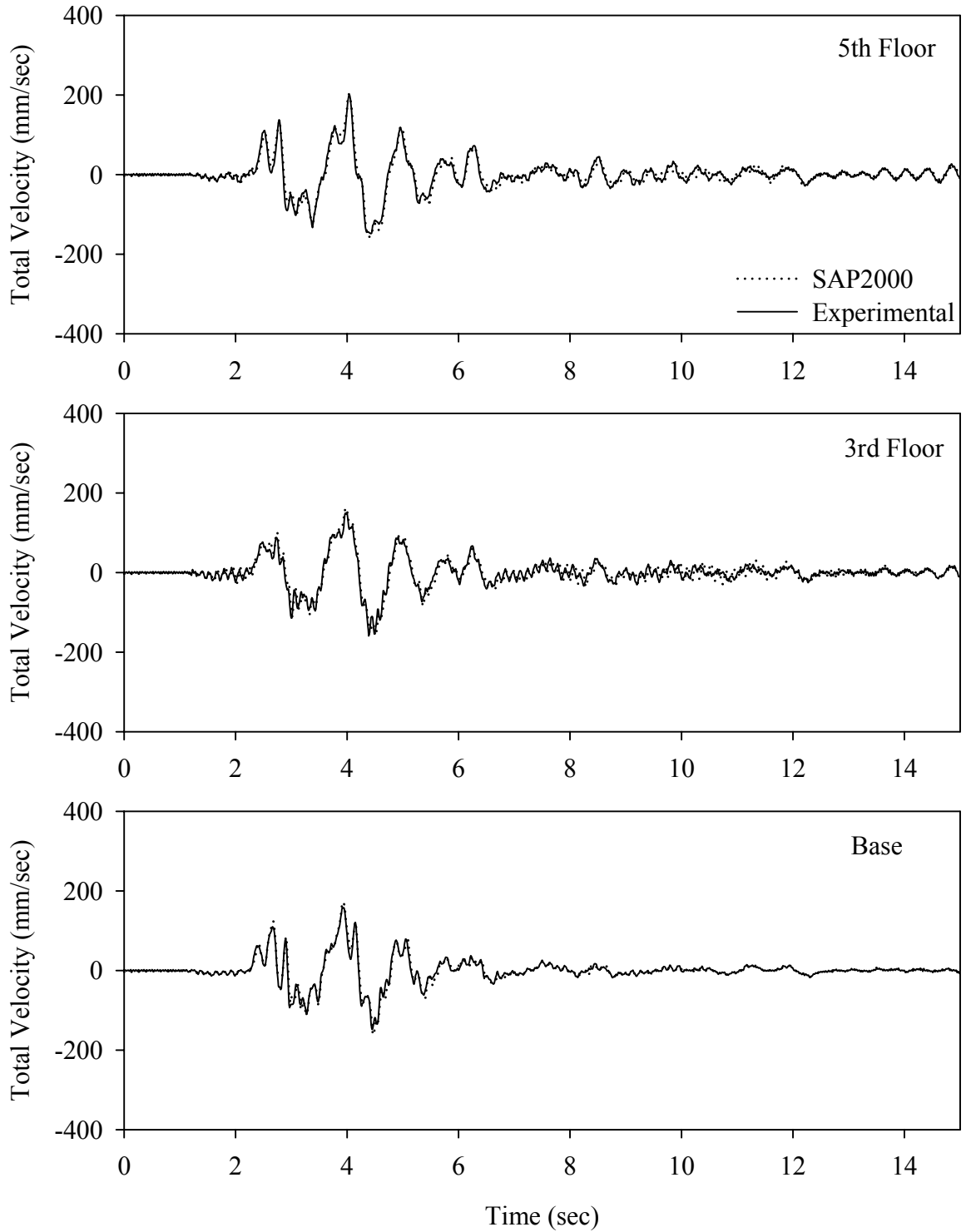


Test FEMFS50.1, Sylmar 50%, MF/Flat Sliding + Elastomeric

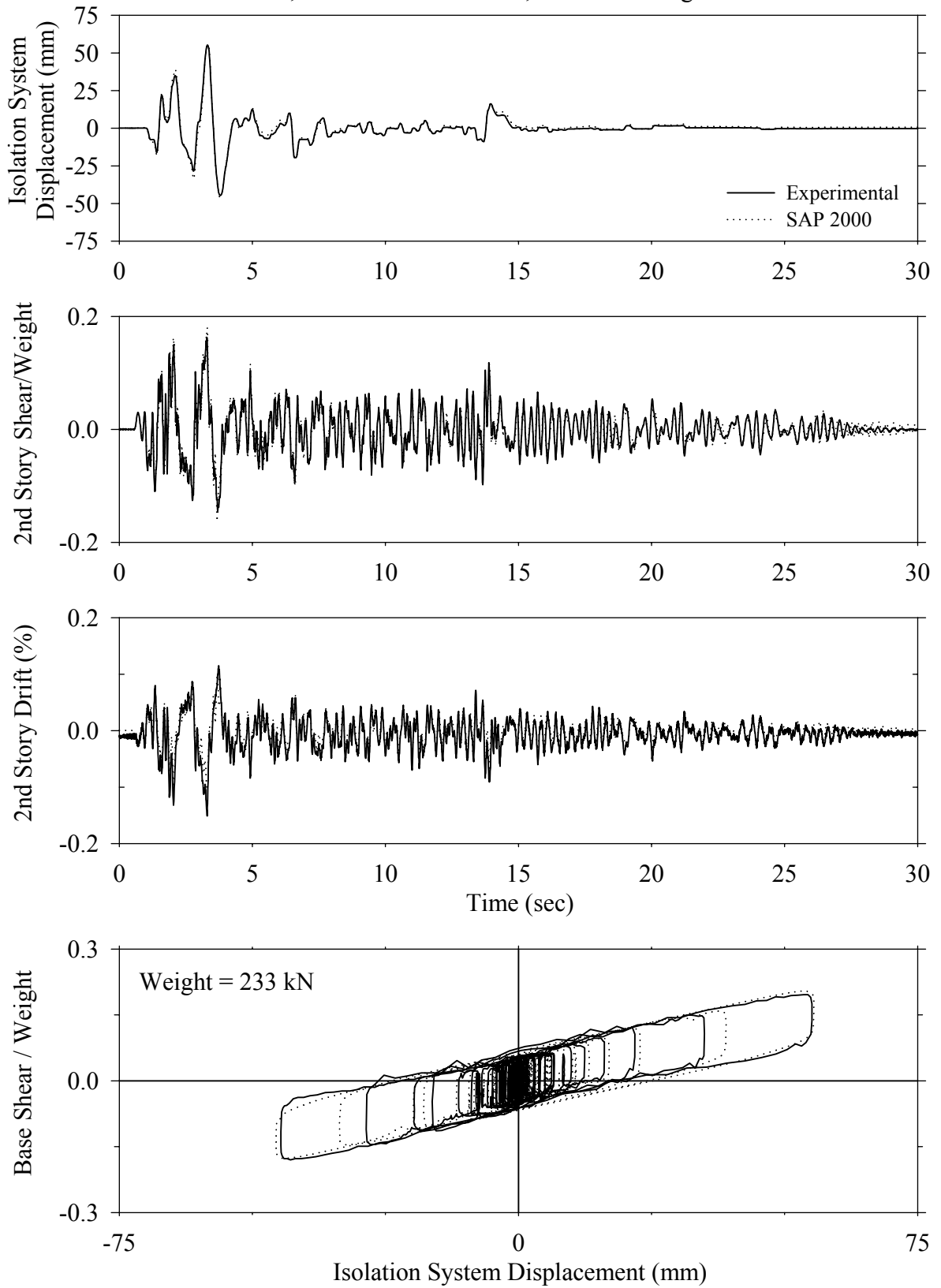




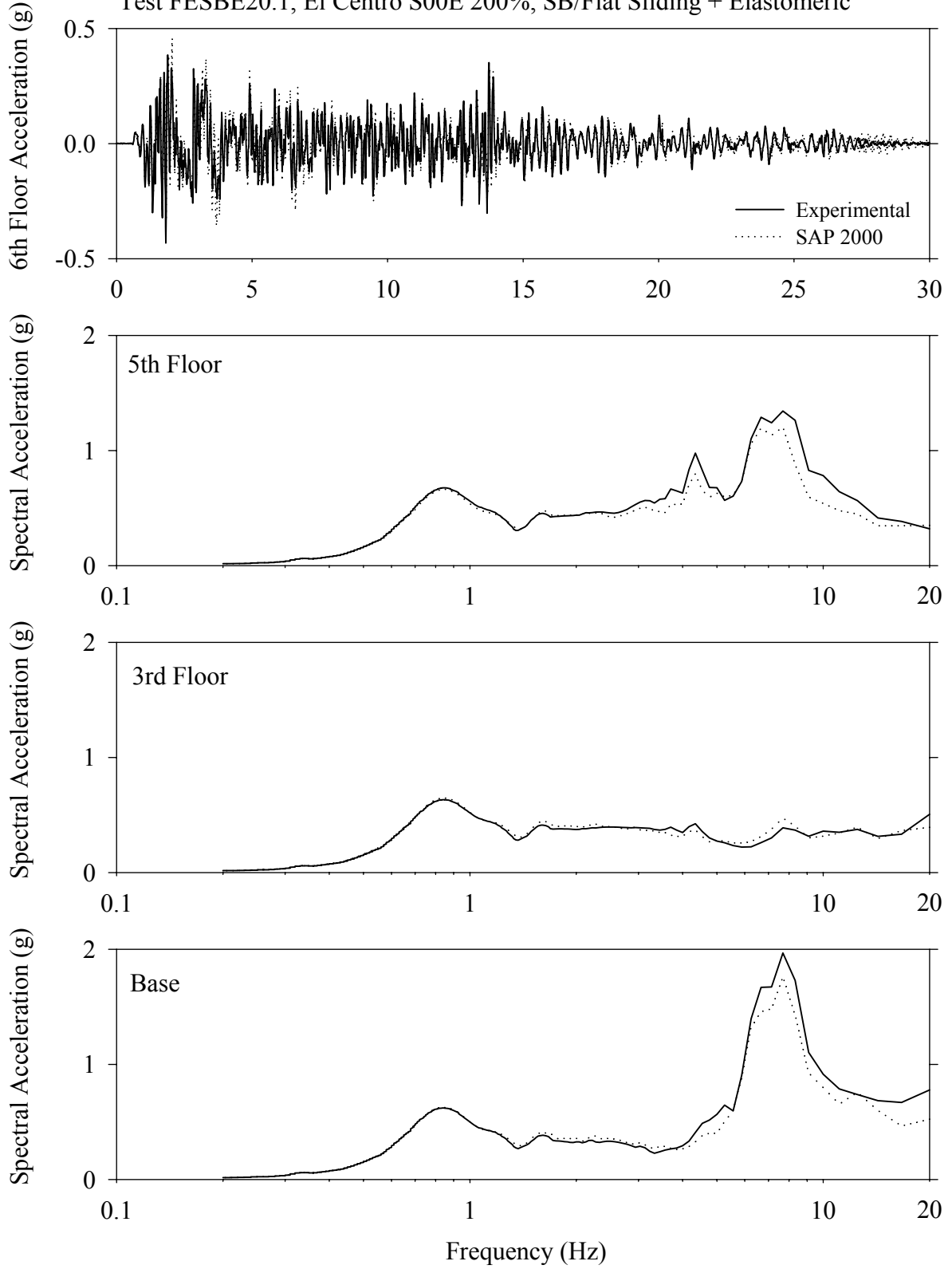
Test FEMFS50.1, Sylmar 50%, MF/Flat Sliding + Elastomeric



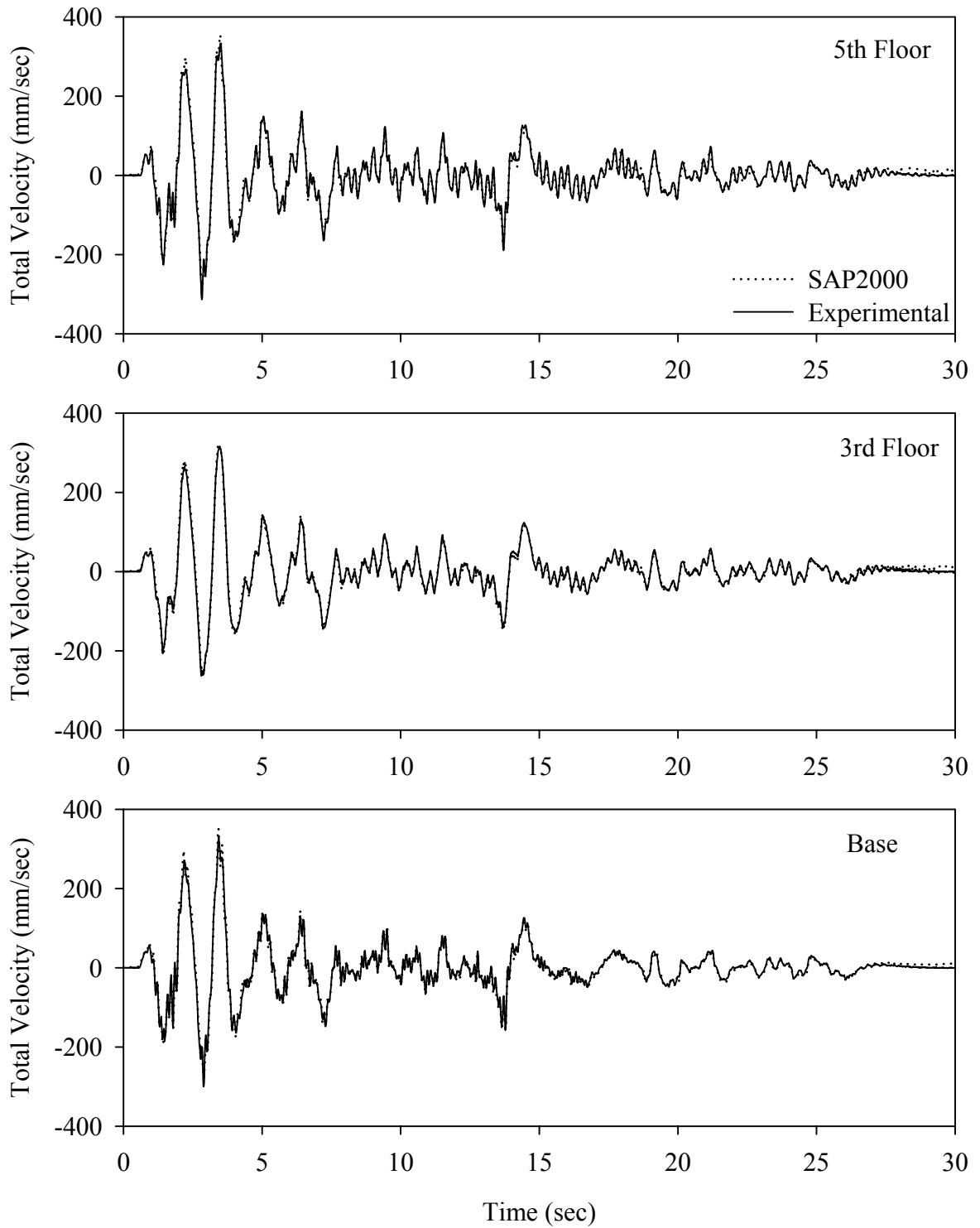
Test FESBE20.1, El Centro S00E 200%, SB/Flat Sliding + Elastomeric



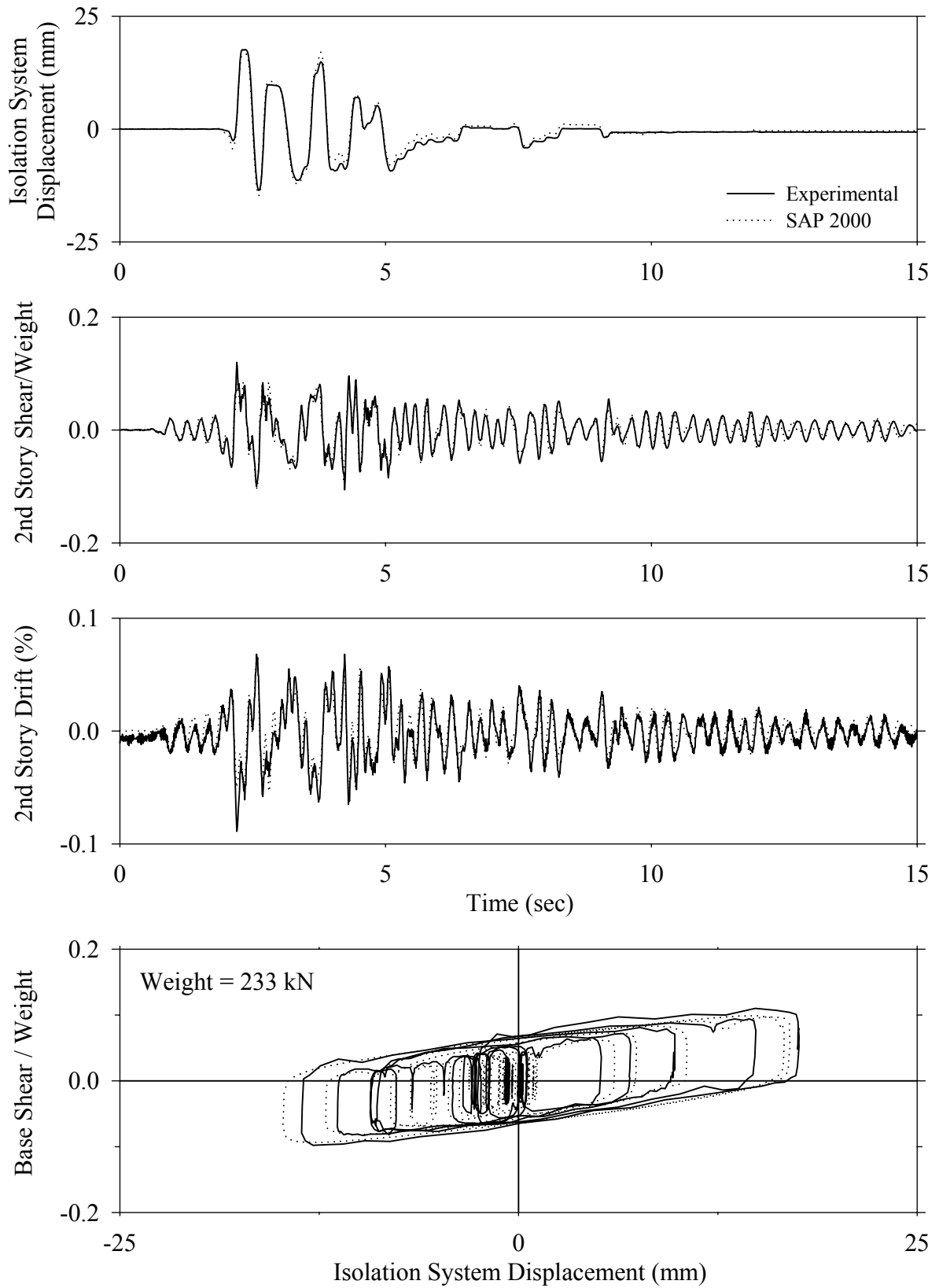
Test FESBE20.1, El Centro S00E 200%, SB/Flat Sliding + Elastomeric



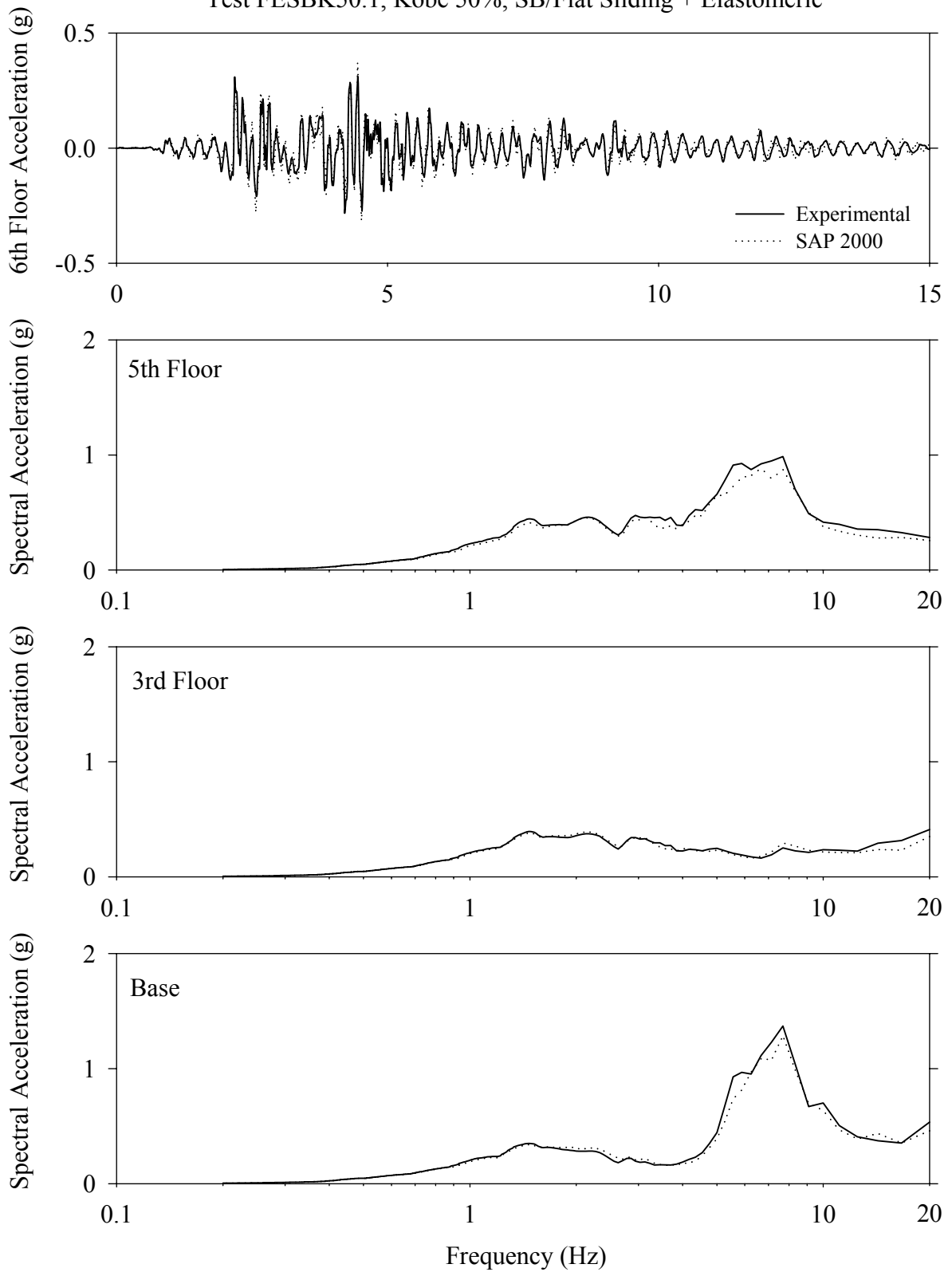
Test FESBE20.1, El Centro S00E 200%, SB/Flat Sliding + Elastomeric



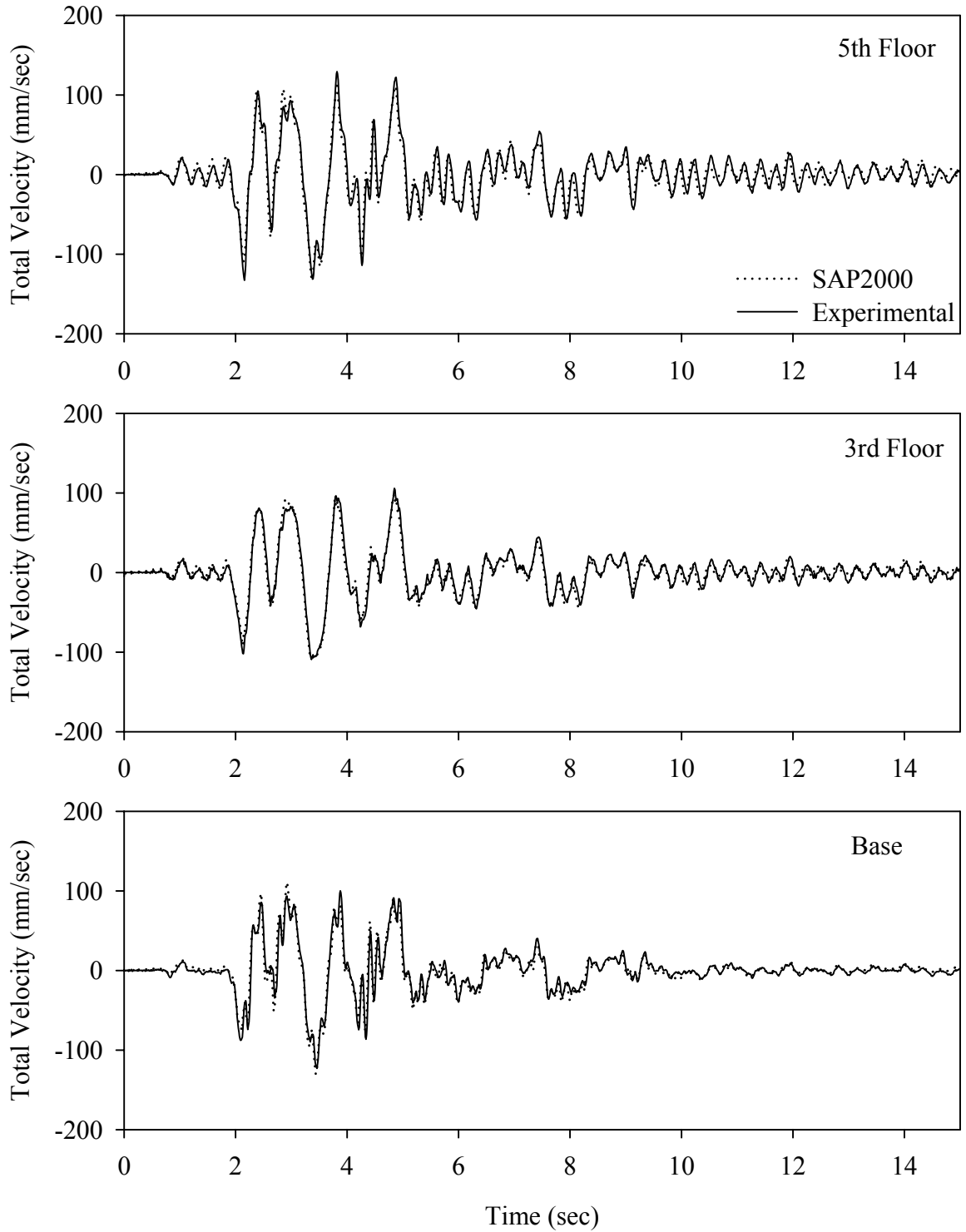
Test FESBK50.1, Kobe 50%, SB/Flat Sliding + Elastomeric



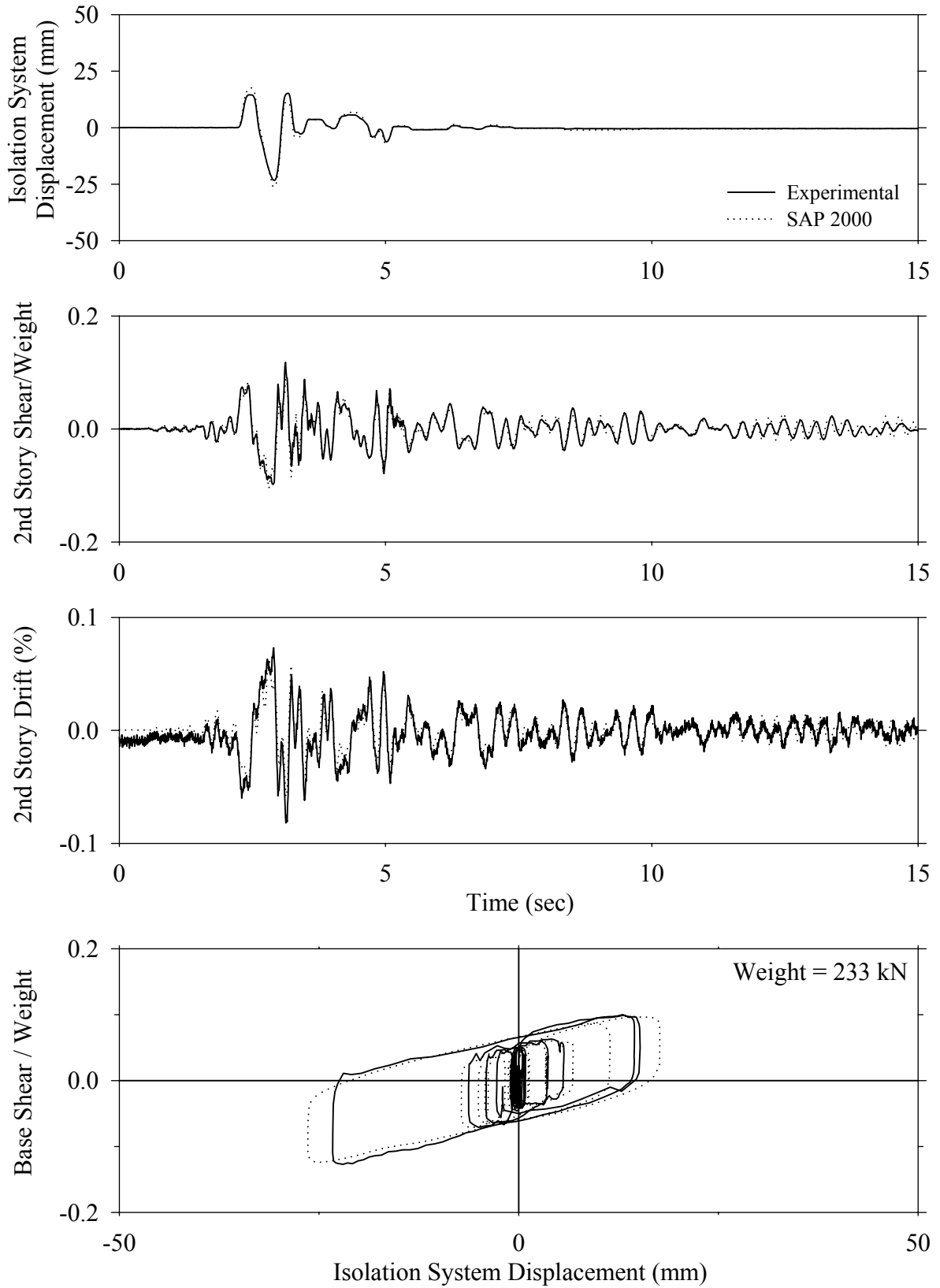
Test FESBK50.1, Kobe 50%, SB/Flat Sliding + Elastomeric



Test FESBK50.1, Kobe 50%, SB/Flat Sliding + Elastomeric

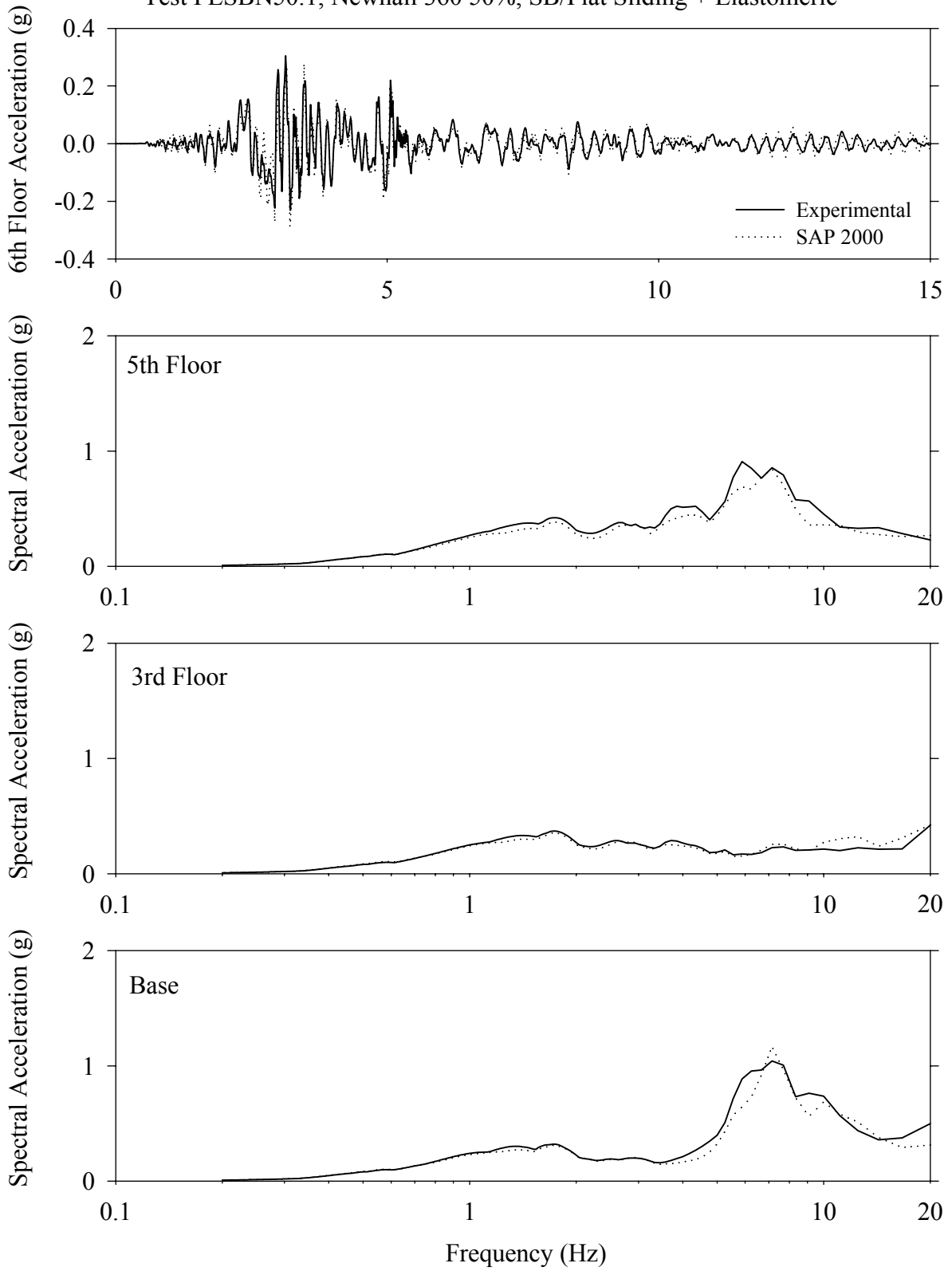


Test FESBN50.1, Newhall 360 50%, SB/Flat Sliding + Elastomeric

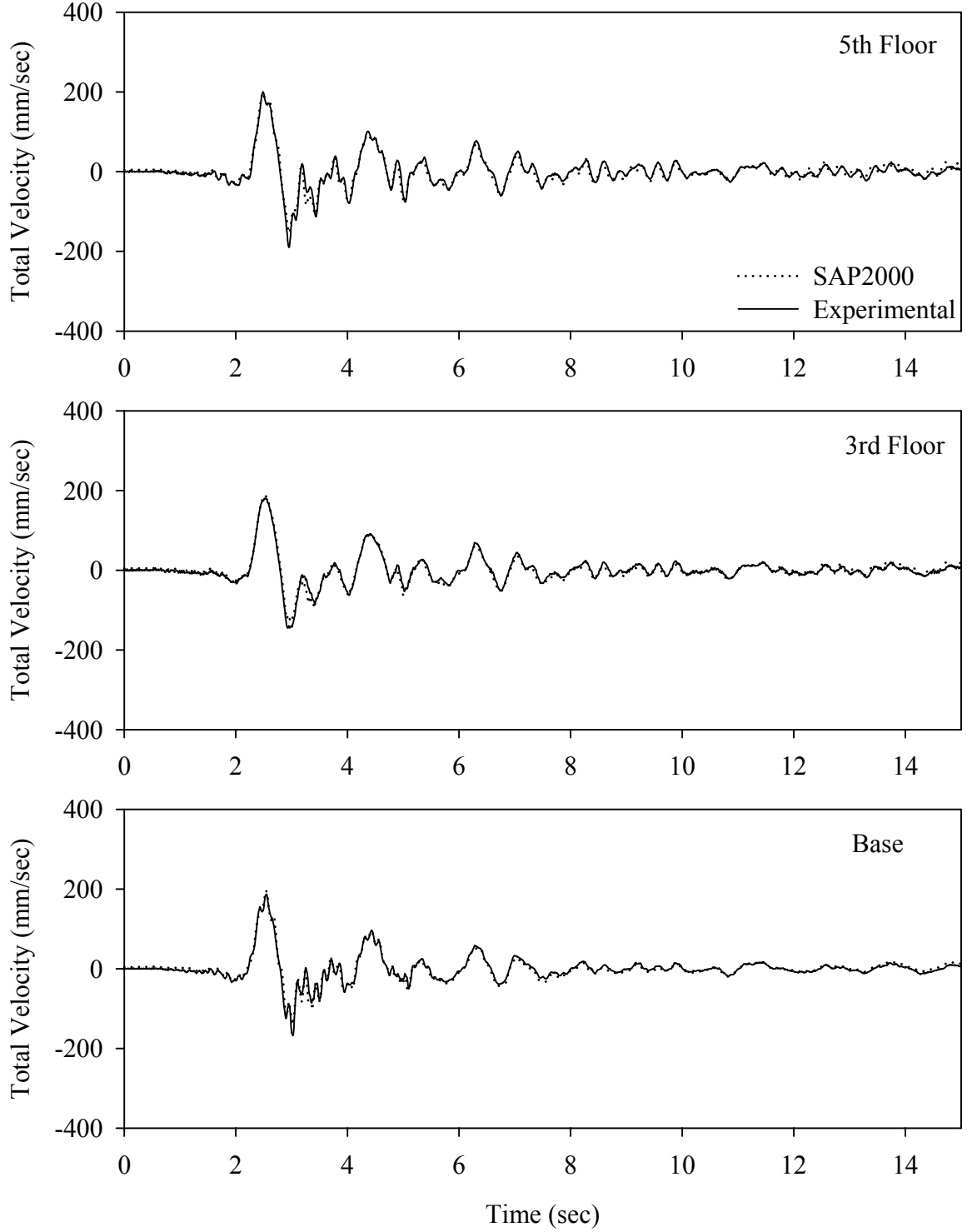




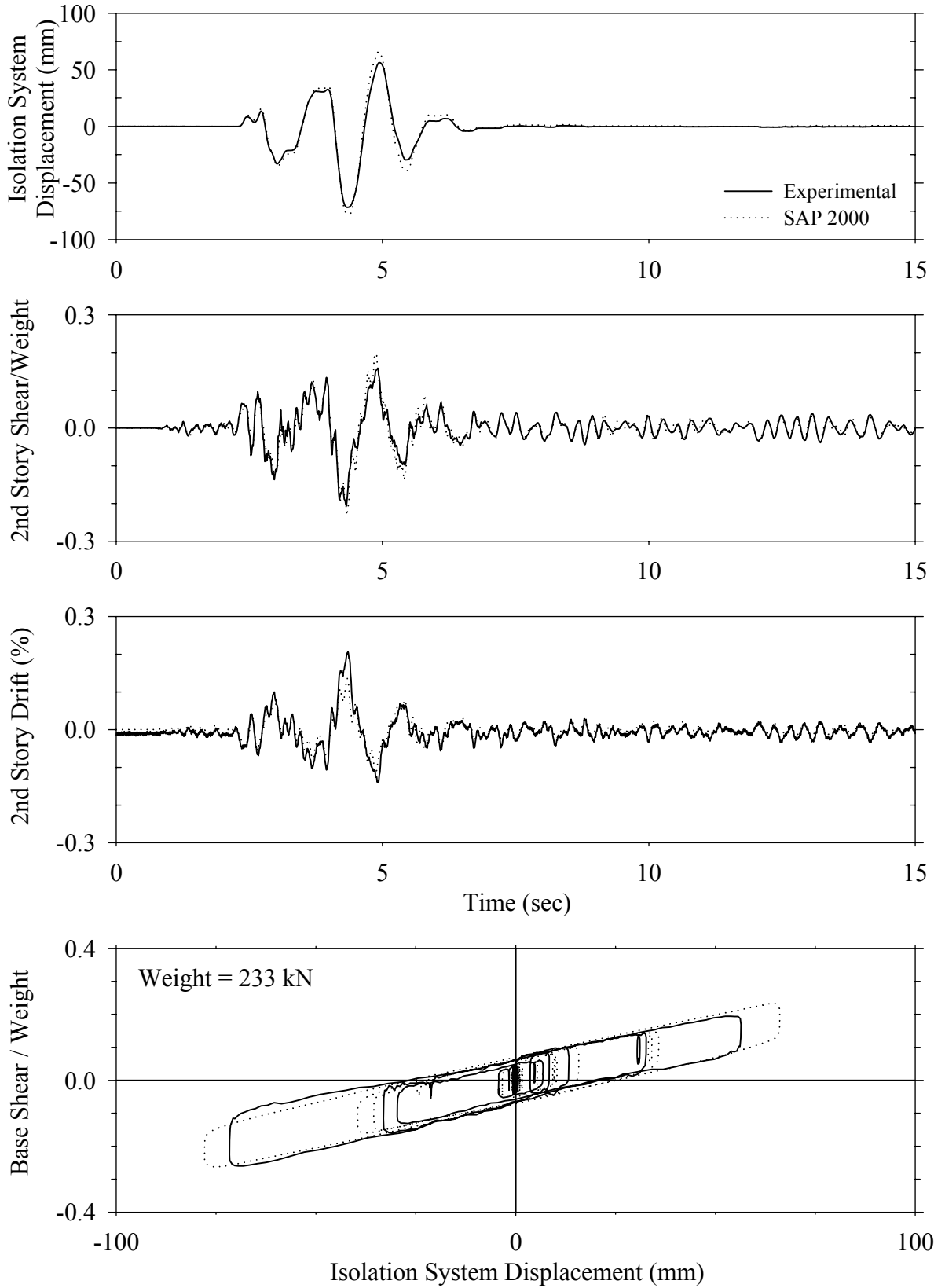
Test FESBN50.1, Newhall 360 50%, SB/Flat Sliding + Elastomeric



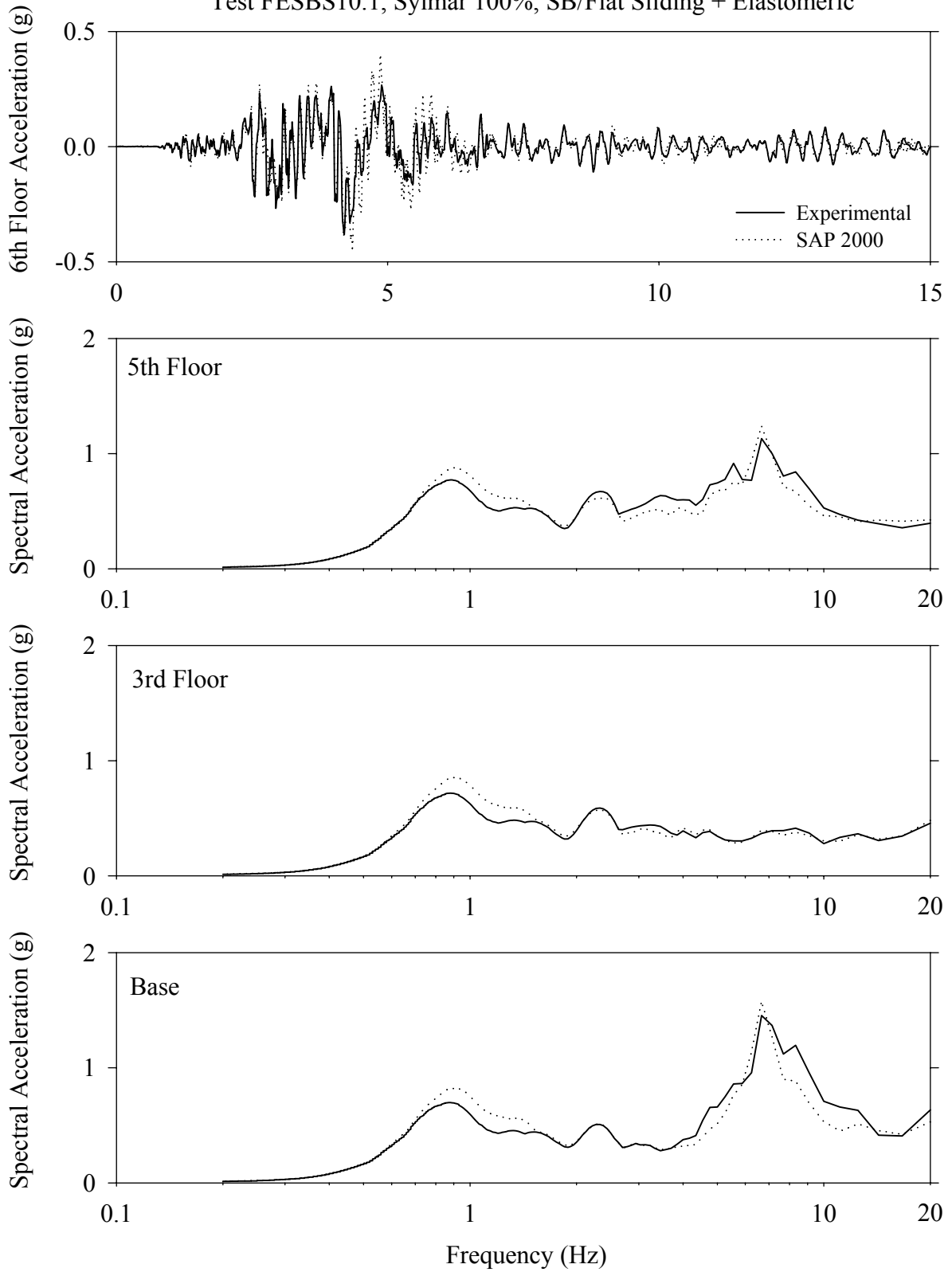
Test FESBN50.1, Newhall 360 50%, SB/Flat Sliding + Elastomeric



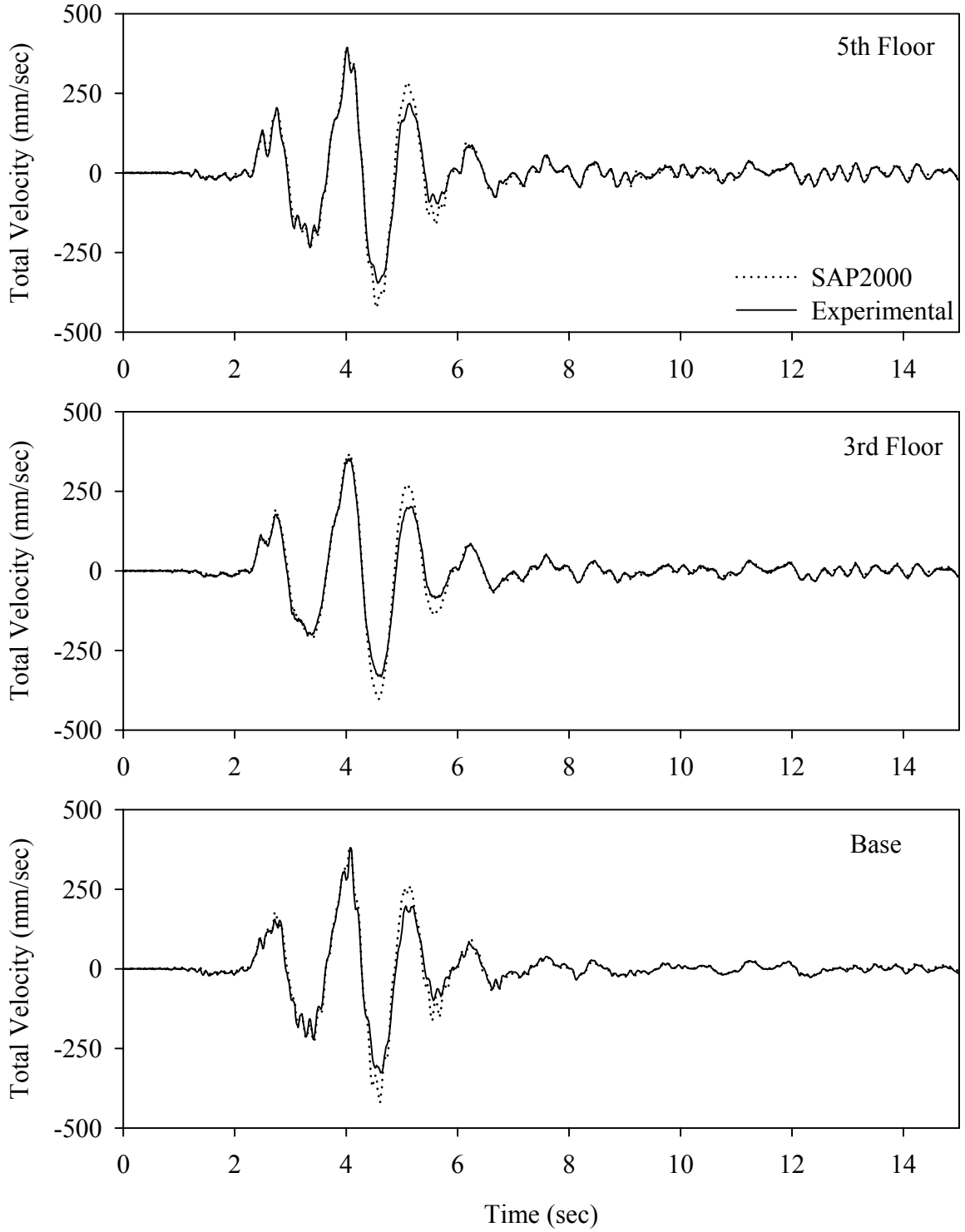
Test FESBS10.1, Sylmar 100%, SB/Flat Sliding + Elastomeric



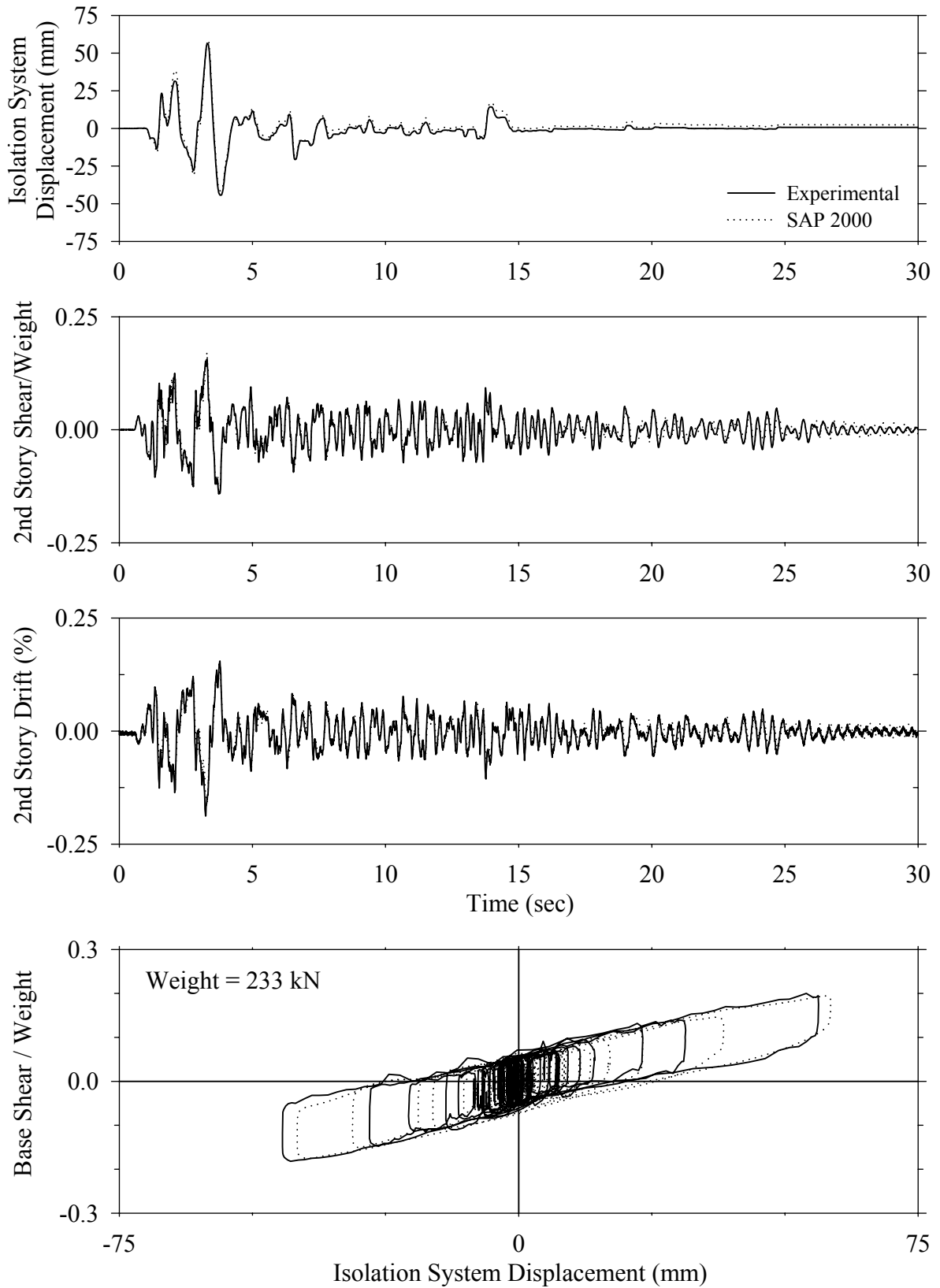
Test FESBS10.1, Sylmar 100%, SB/Flat Sliding + Elastomeric



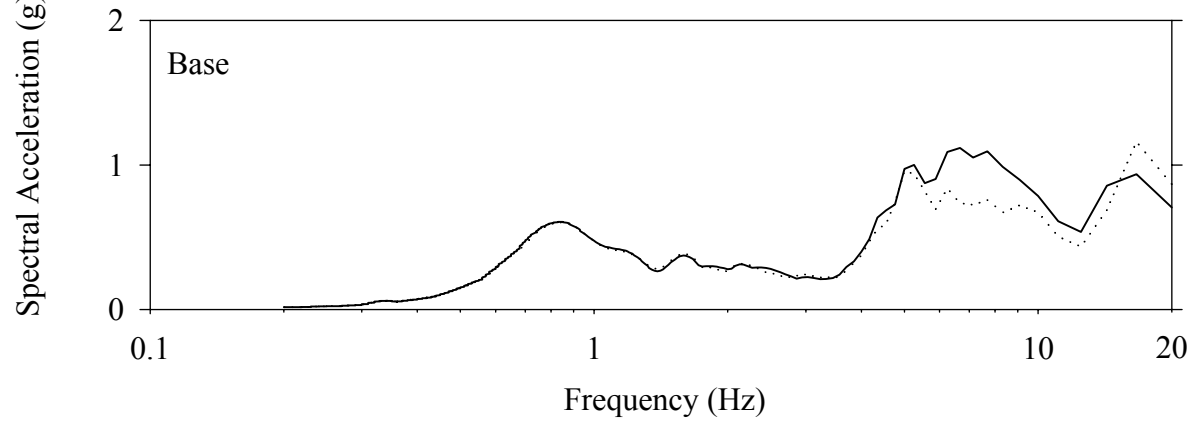
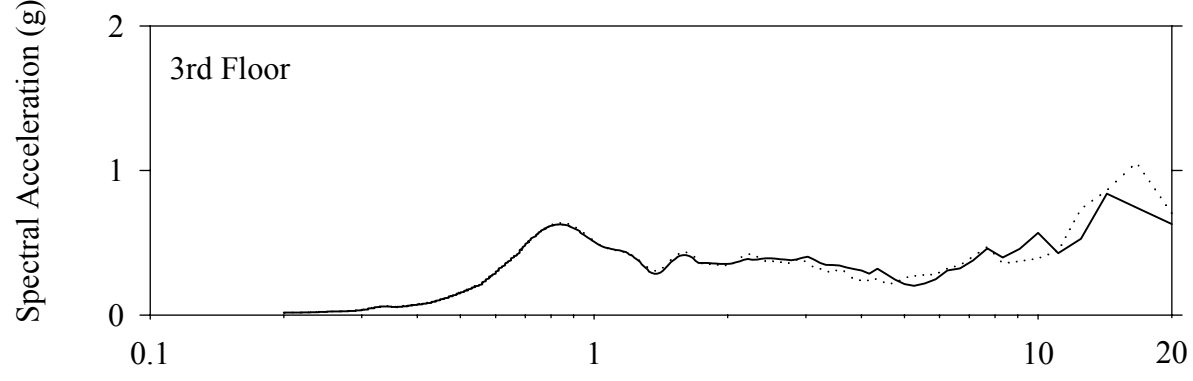
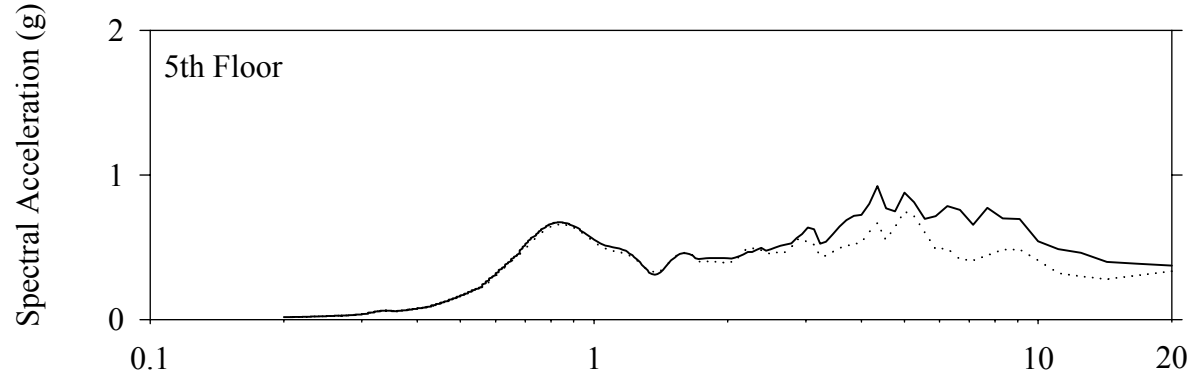
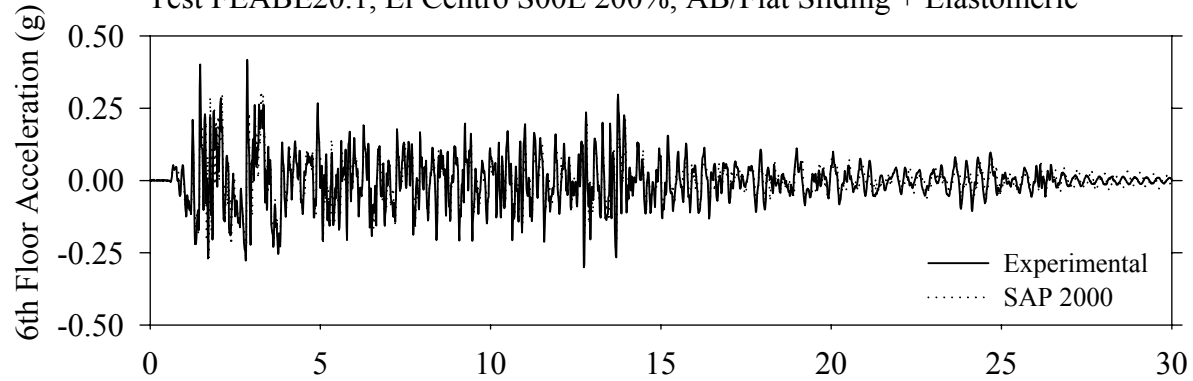
Test FESBS10.1, Sylmar 100%, SB/Flat Sliding + Elastomeric



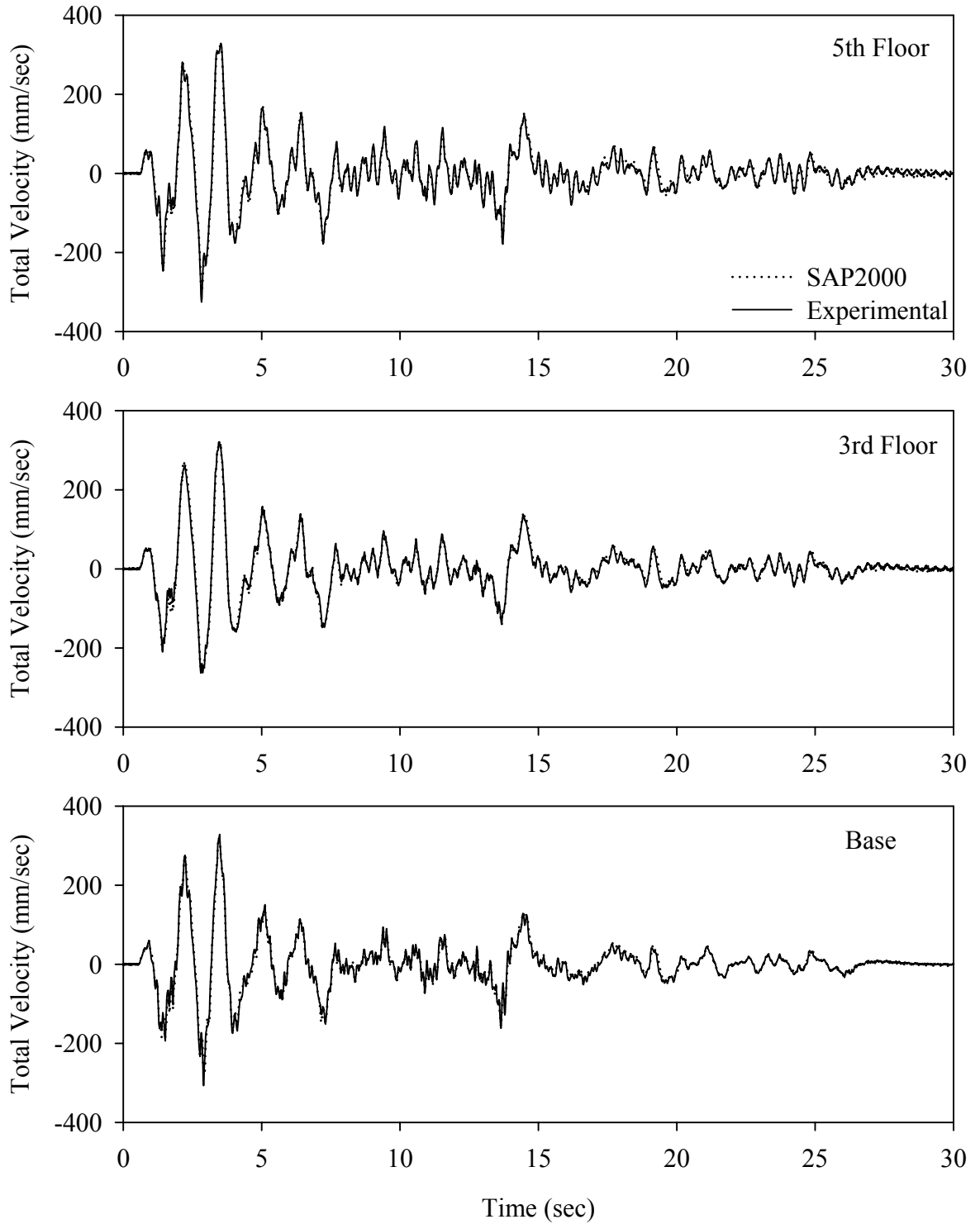
Test FEABE20.1, El Centro S00E 200%, AB/Flat Sliding + Elastomeric



Test FEABE20.1, El Centro S00E 200%, AB/Flat Sliding + Elastomeric

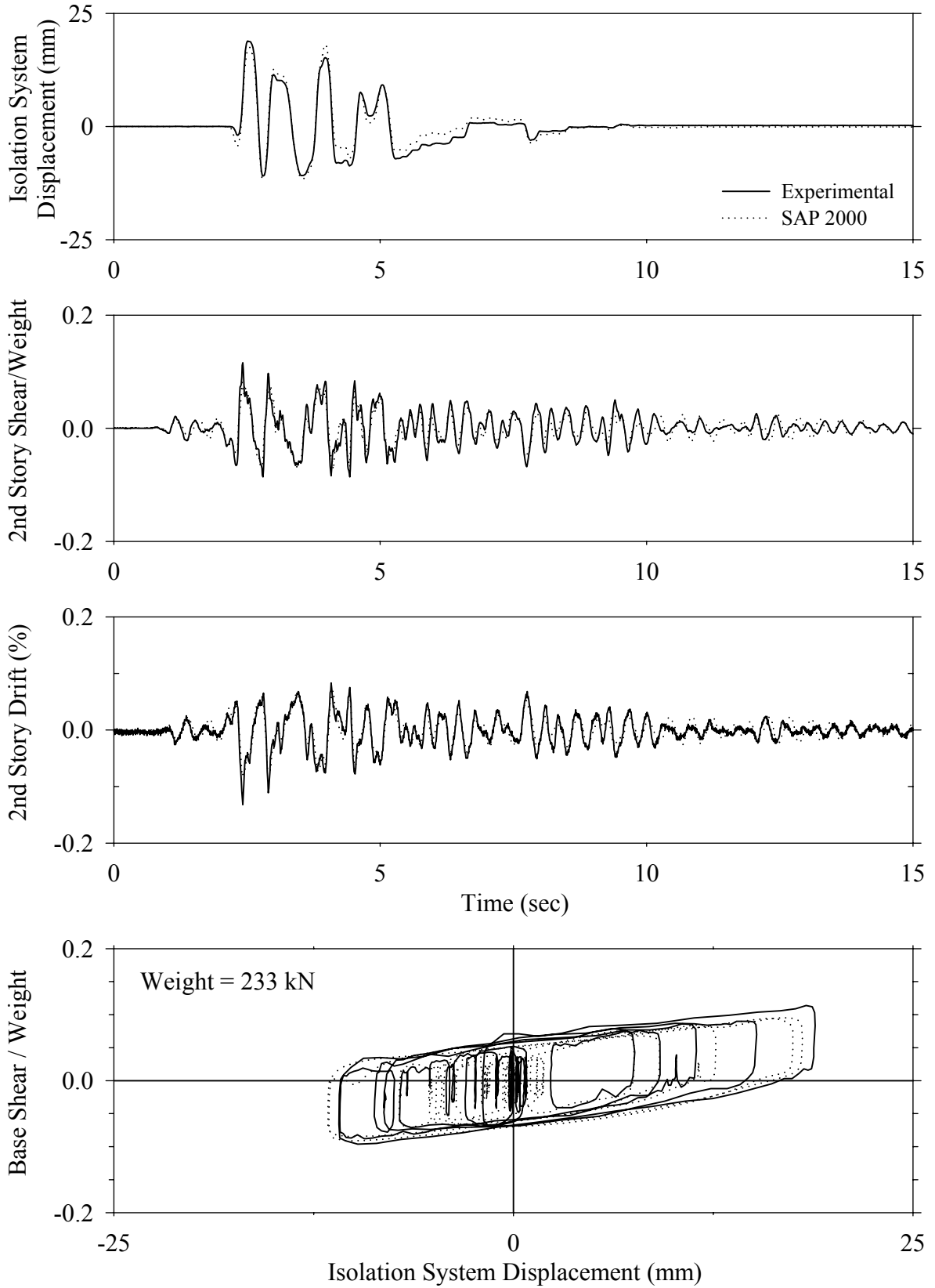


Test FEABE20.1, El Centro S00E 200%, AB/Flat Sliding + Elastomeric

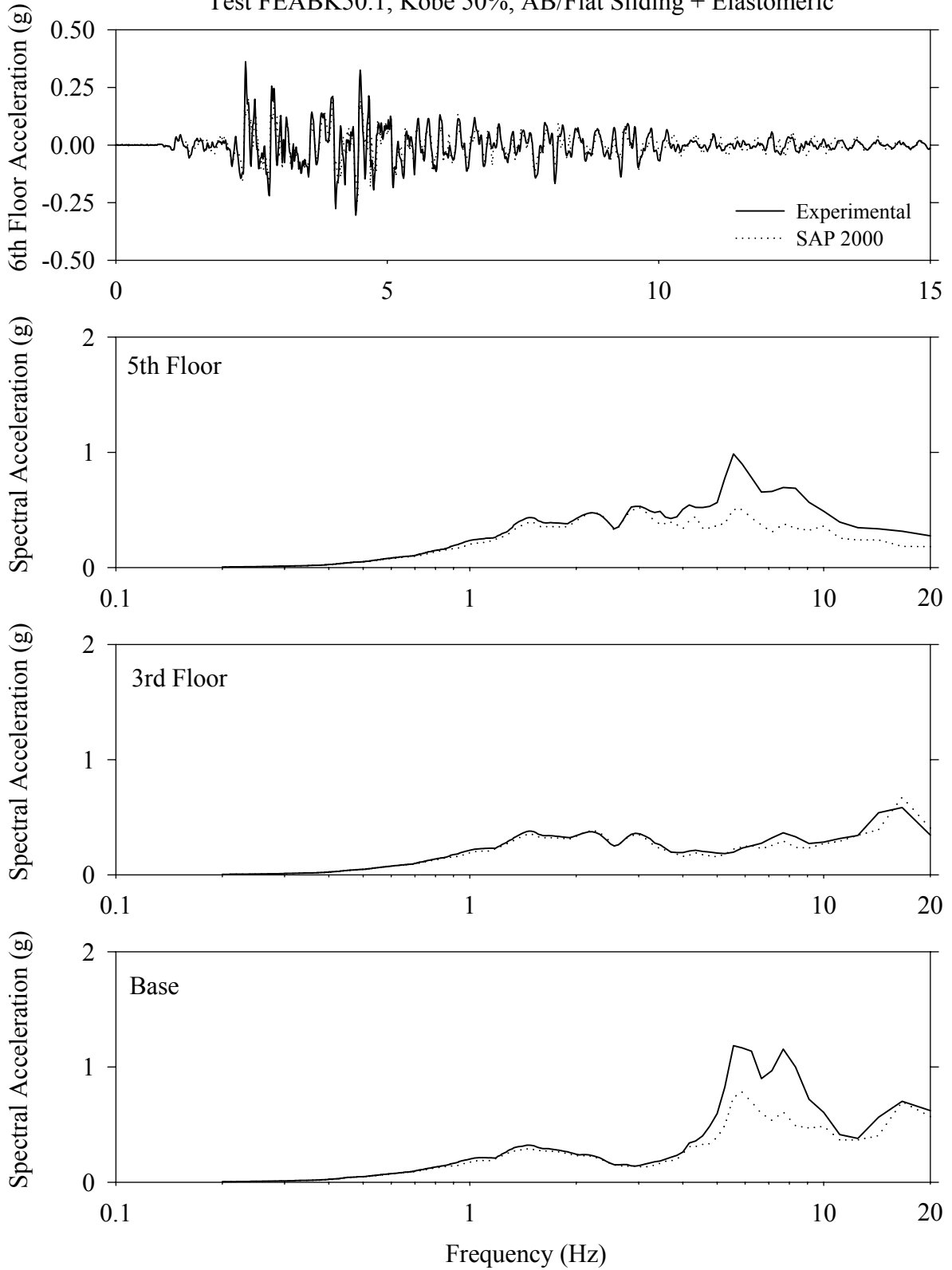




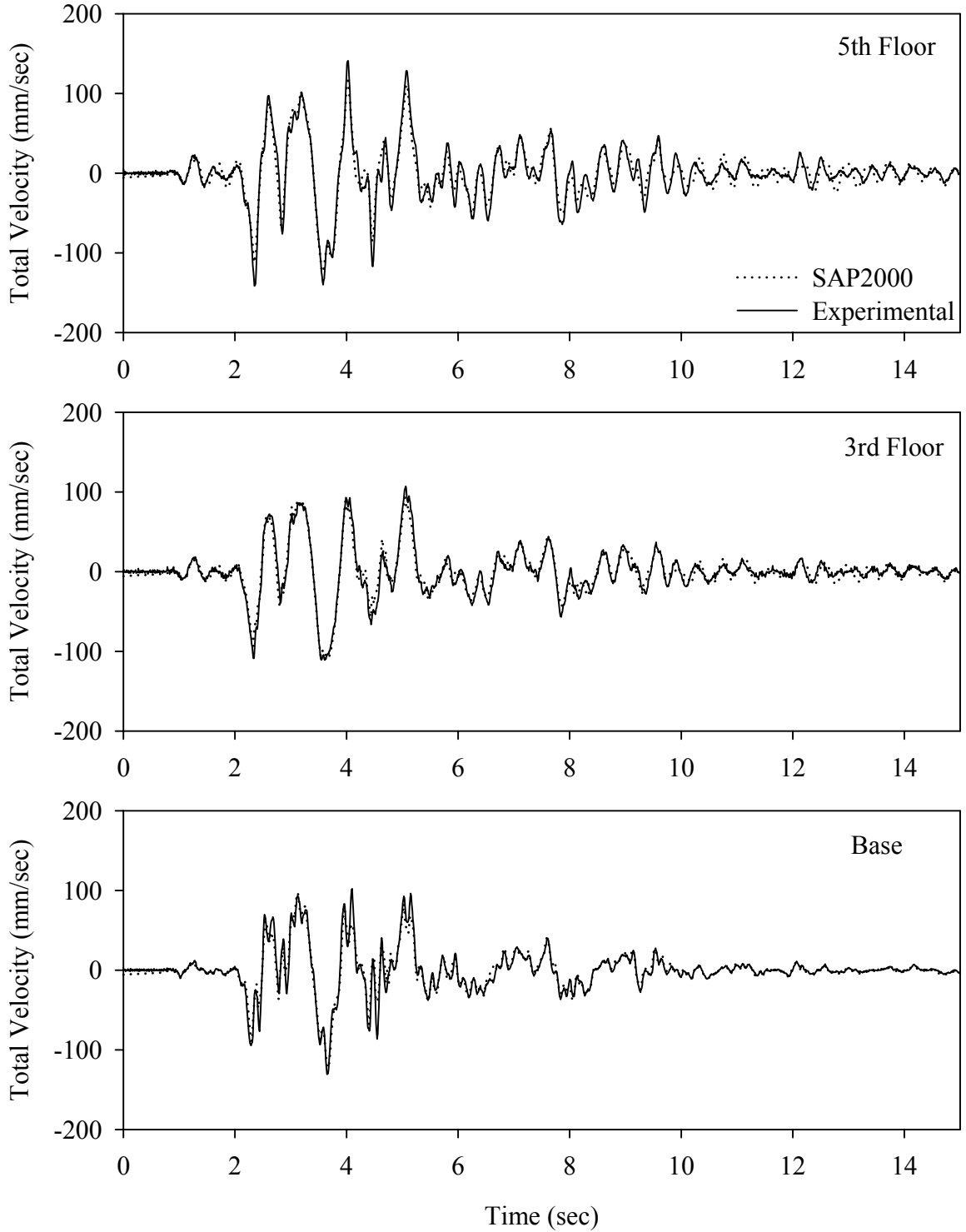
Test FEABK50.1, Kobe 50%, AB/Flat Sliding + Elastomeric



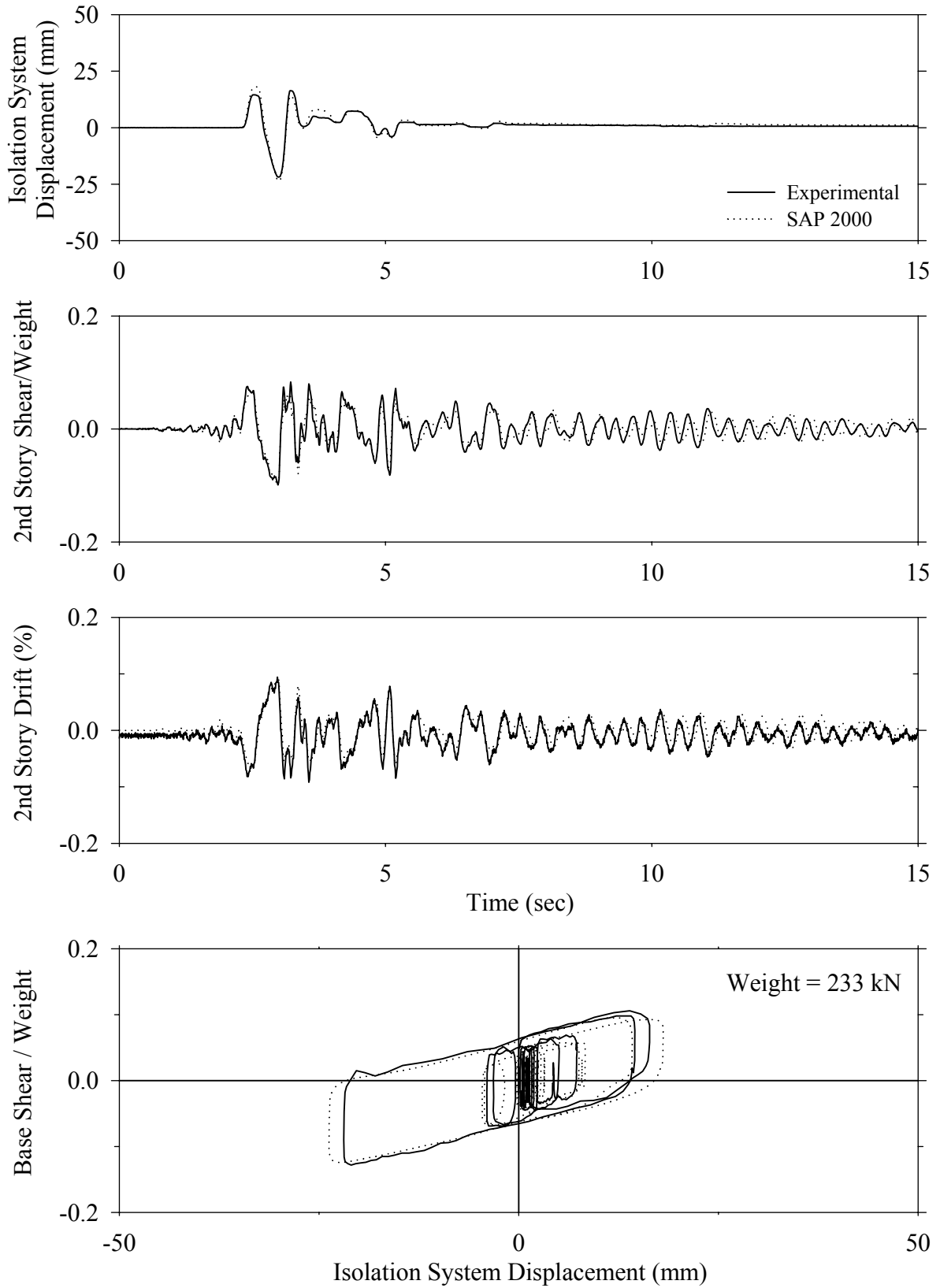
Test FEABK50.1, Kobe 50%, AB/Flat Sliding + Elastomeric



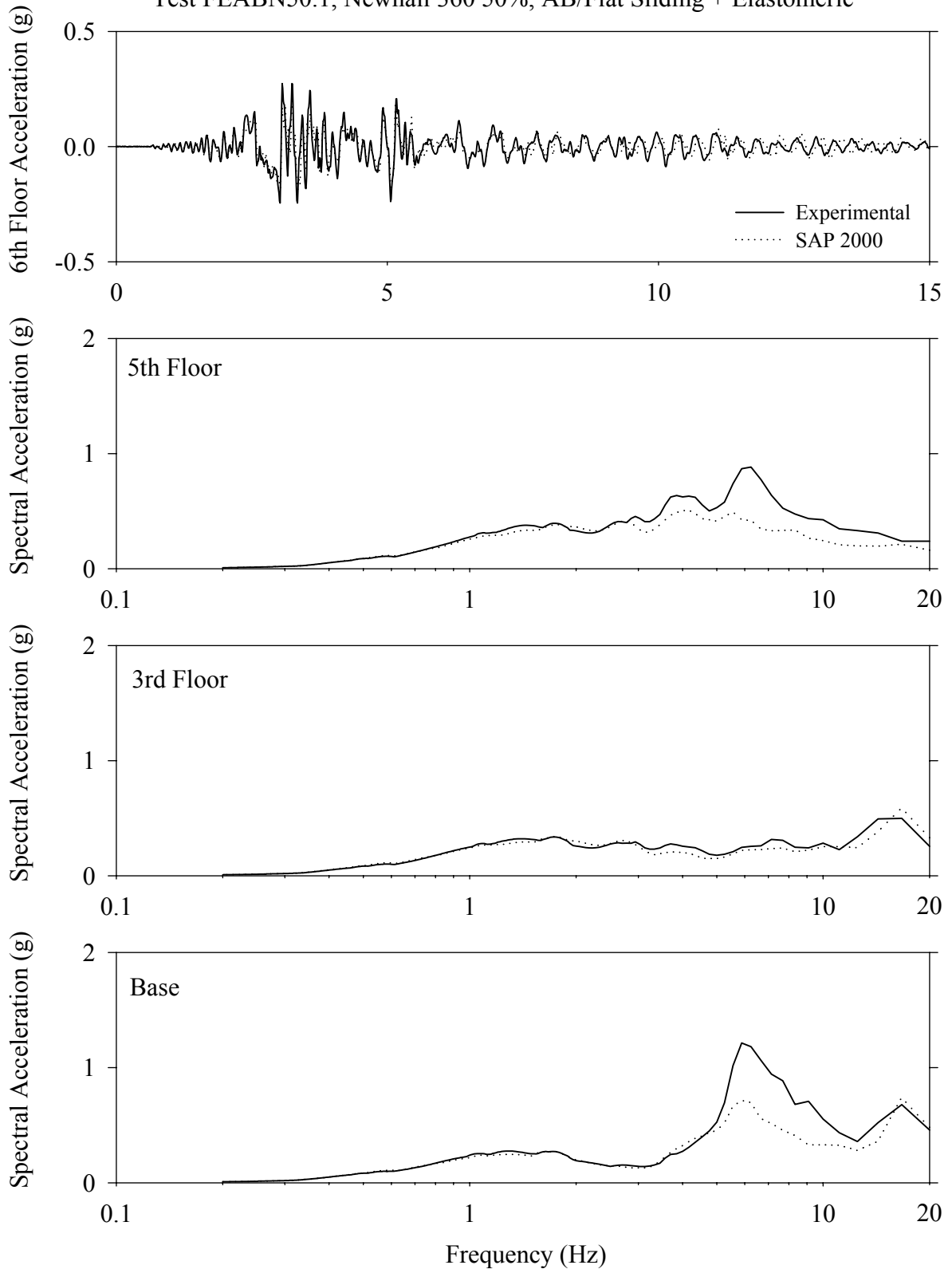
Test FEABK50.1, Kobe 50%, AB/Flat Sliding + Elastomeric



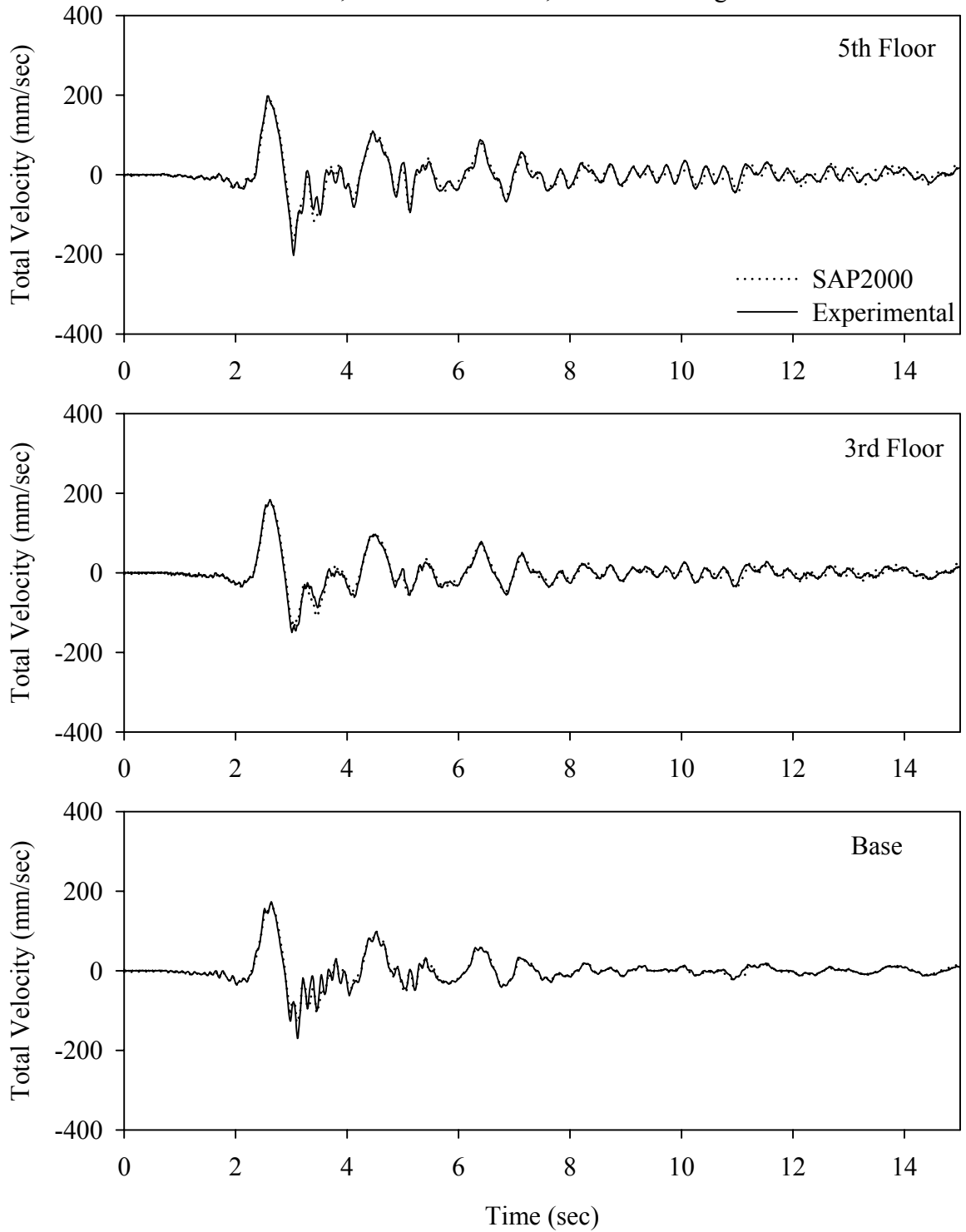
Test FEABN50.1, Newhall 360 50%, AB/Flat Sliding + Elastomeric



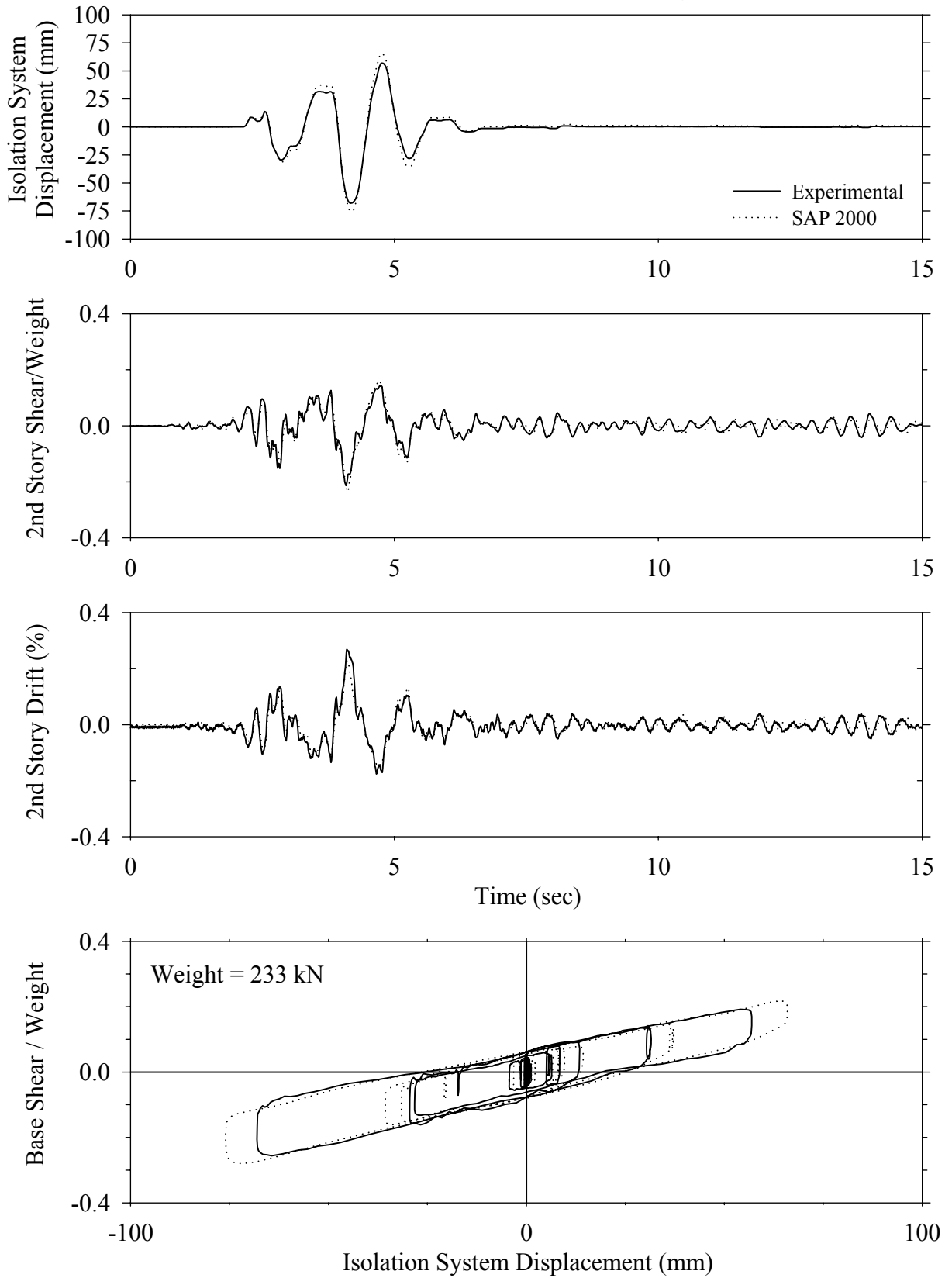
Test FEABN50.1, Newhall 360 50%, AB/Flat Sliding + Elastomeric



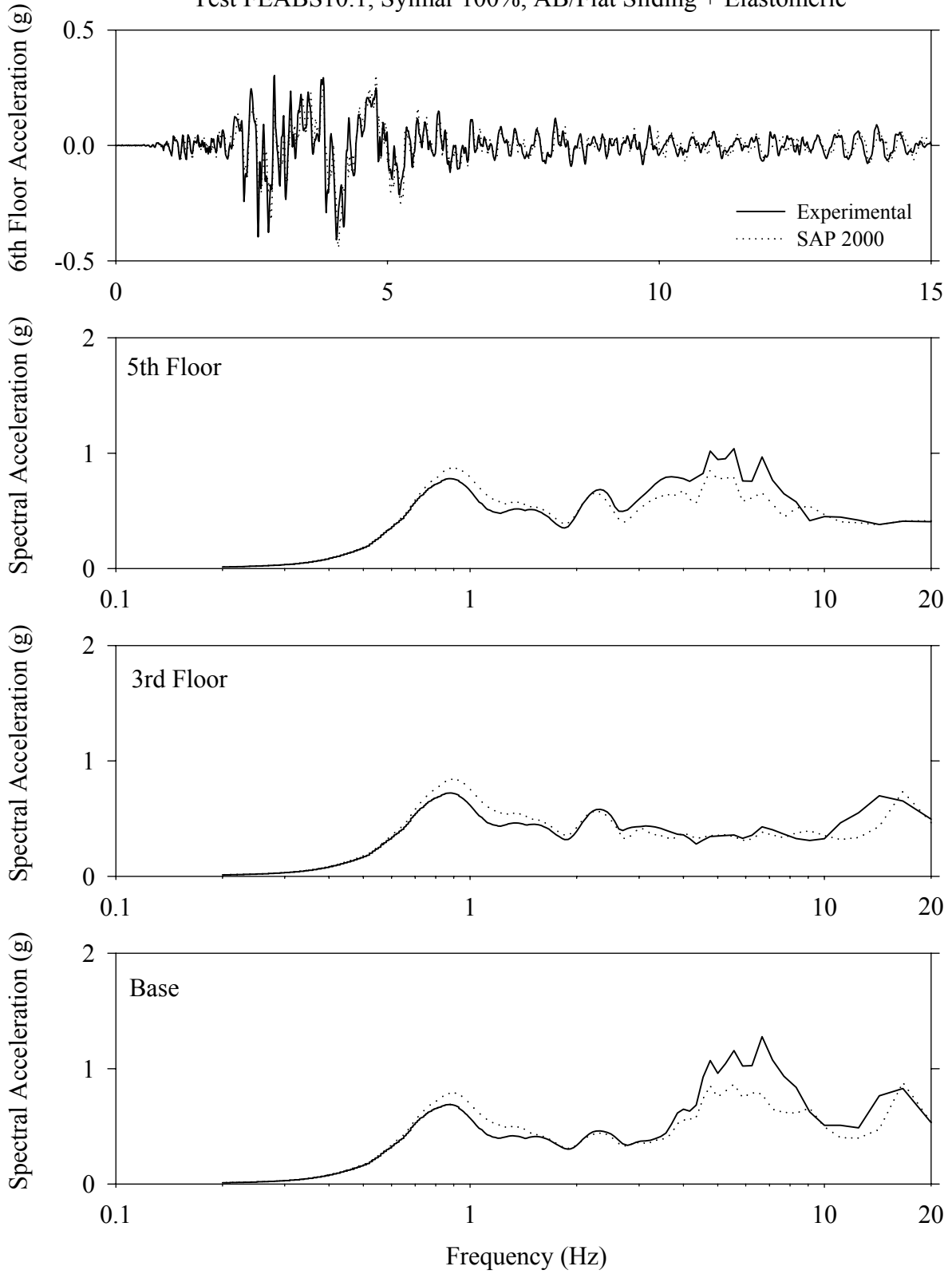
Test FEABN50.1, Newhall 360 50%, AB/Flat Sliding + Elastomeric



Test FEABS10.1, Sylmar 100%, AB/Flat Sliding + Elastomeric

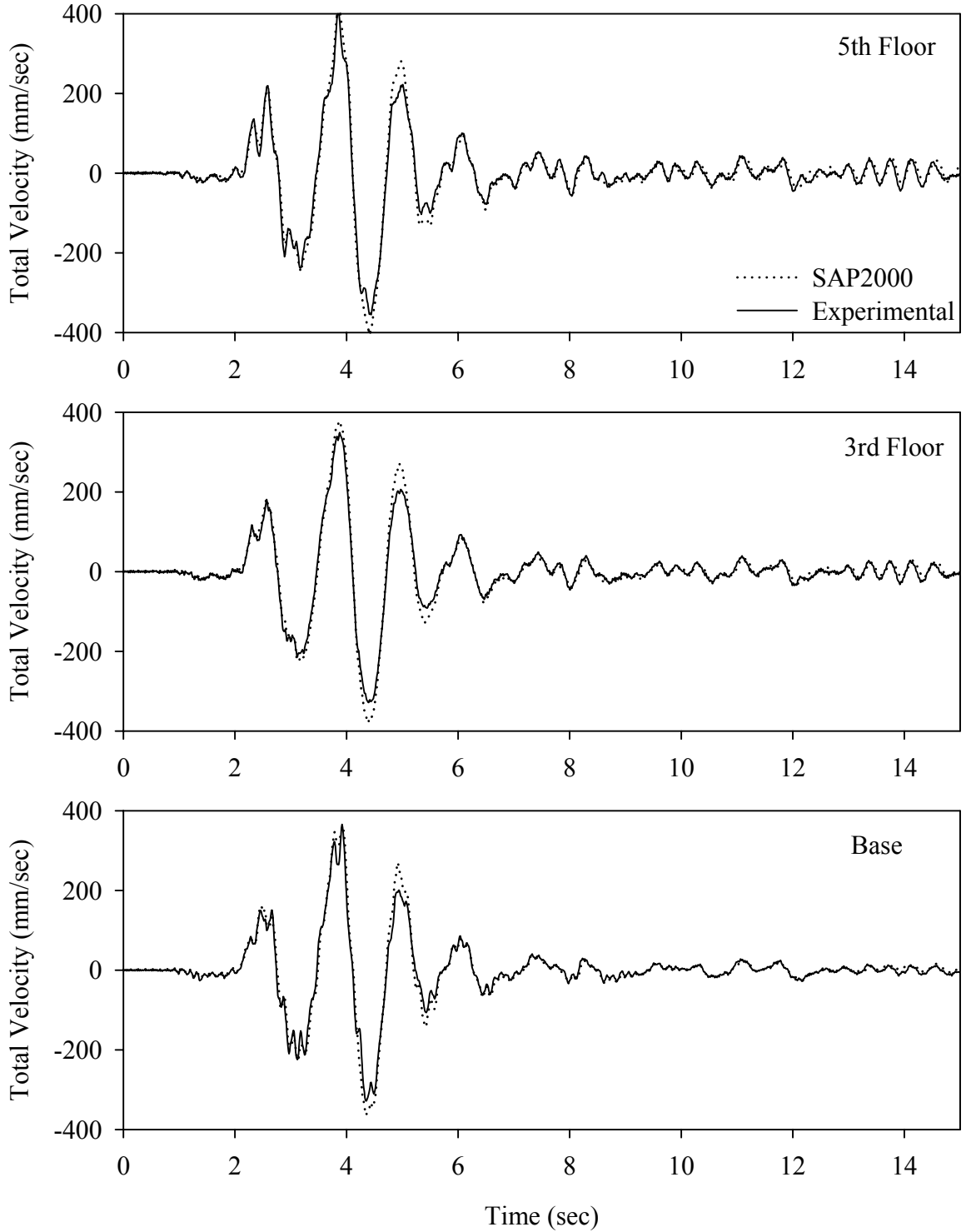


Test FEABS10.1, Sylmar 100%, AB/Flat Sliding + Elastomeric





Test FEABS10.1, Sylmar 100%, AB/Flat Sliding + Elastomeric



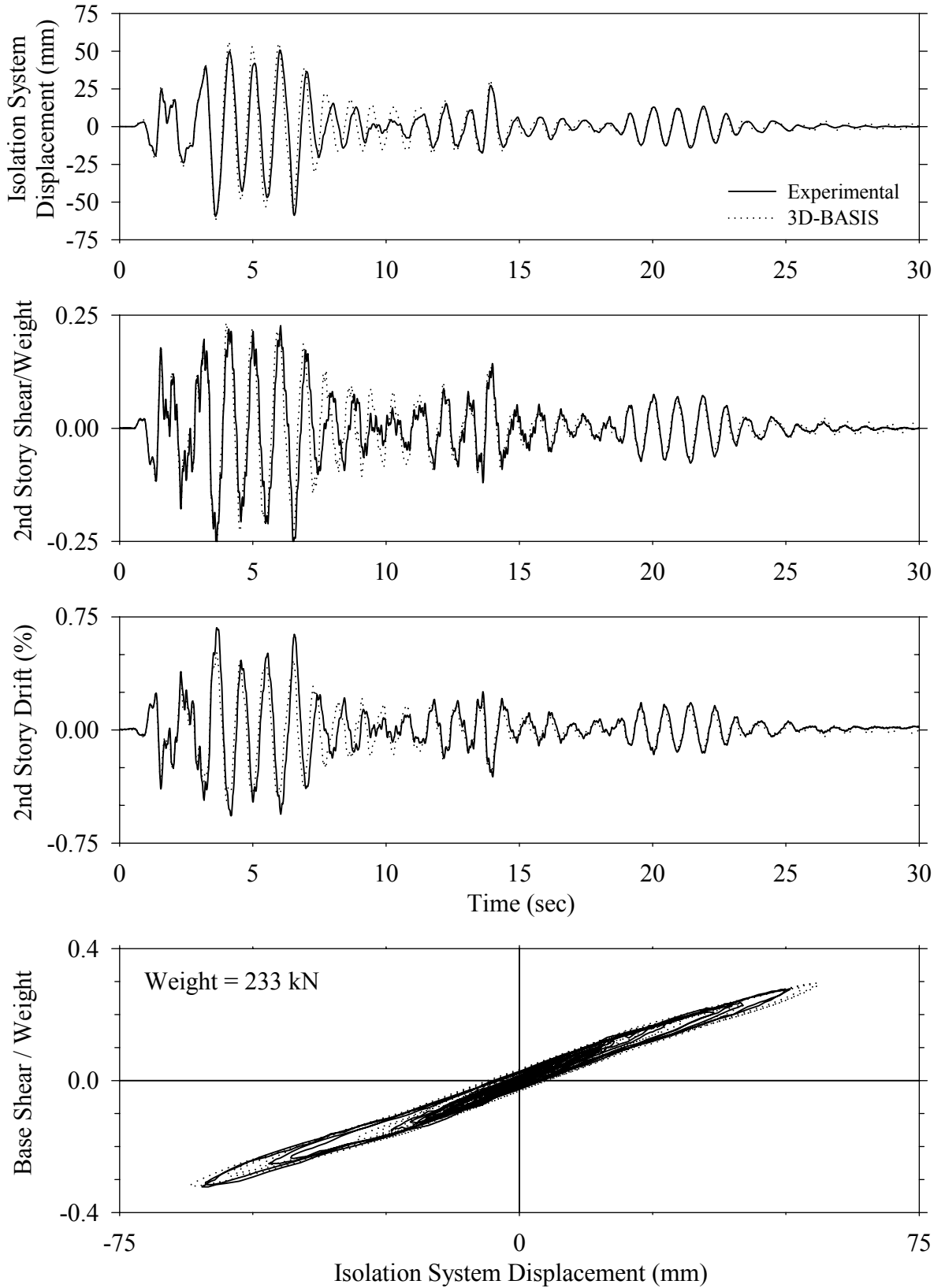
## **APPENDIX D**

### **ANALYTICAL (3D-BASIS-ME) vs. EXPERIMENTAL RESPONSE**

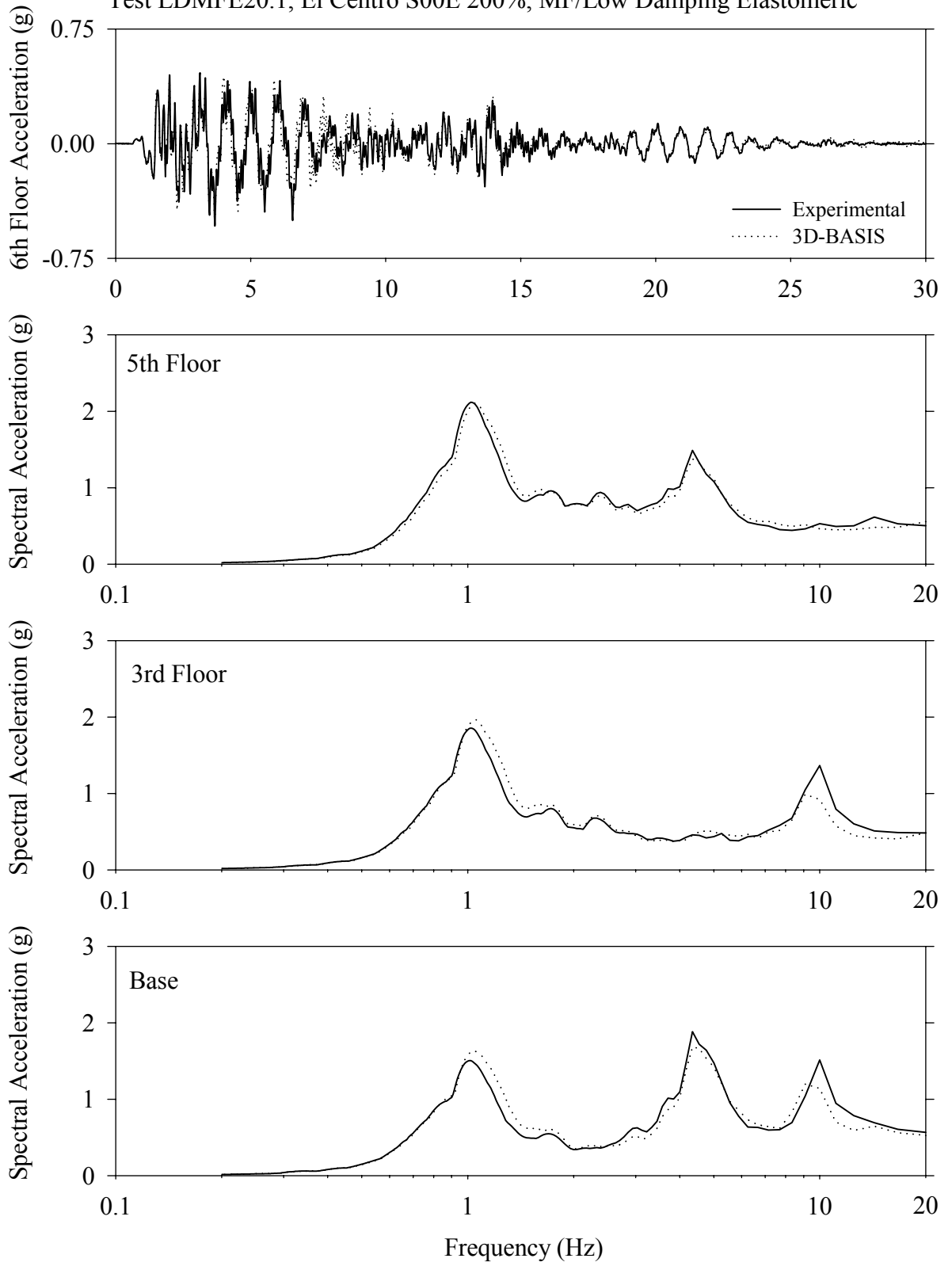
This appendix presents results in graphical form for four excitations of each configuration tested. The presented results include:

1. Isolation system displacement history.
2. Second story shear divided by weight time history.
3. Second story drift divided by story height time history.
4. Base shear divided by weight versus isolation system displacement loop.
5. Sixth floor total acceleration time history.
6. The 5% damped spectra calculated from the recorded acceleration time histories of the 5<sup>th</sup> floor in the range from 0 to 20 Hz.
7. The 5% damped spectra calculated from the recorded acceleration time histories of the 3<sup>rd</sup> floor in the range from 0 to 20 Hz.
8. The 5% damped spectra calculated from the recorded acceleration time histories of the base in the range from 0 to 20 Hz.

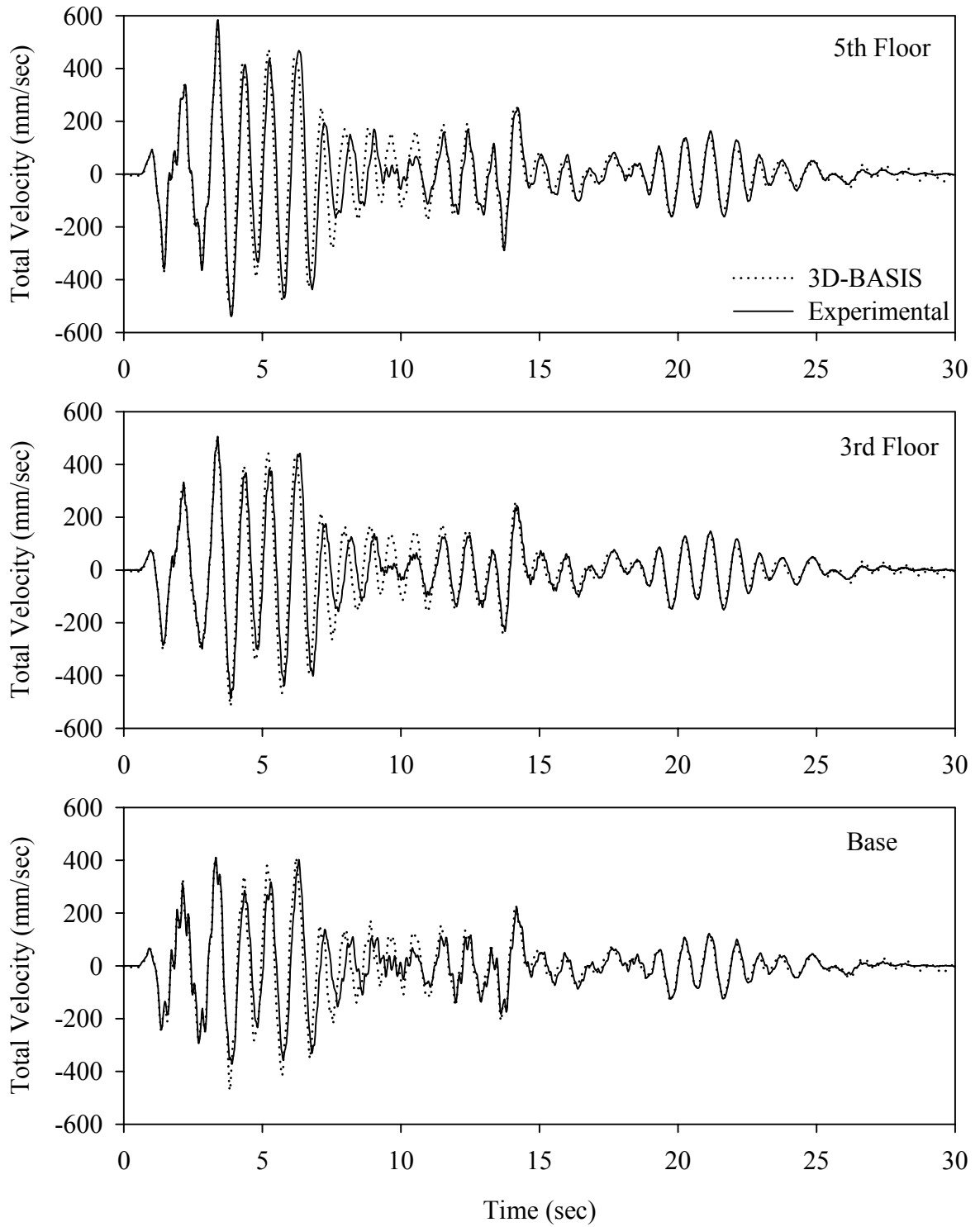
Test LDMFE20.1, El Centro S00E 200%, MF/Low Damping Elastomeric



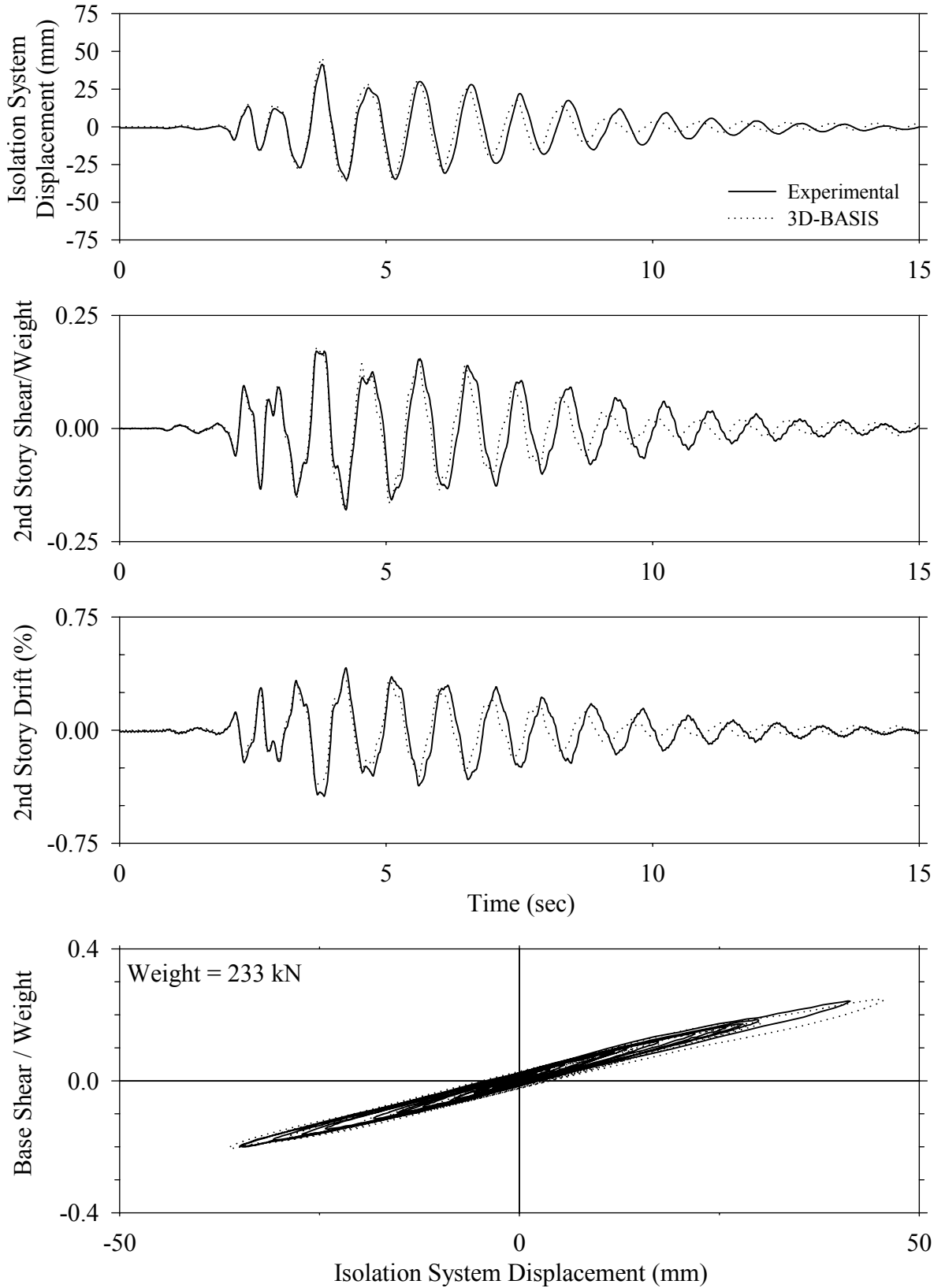
Test LDMFE20.1, El Centro S00E 200%, MF/Low Damping Elastomeric



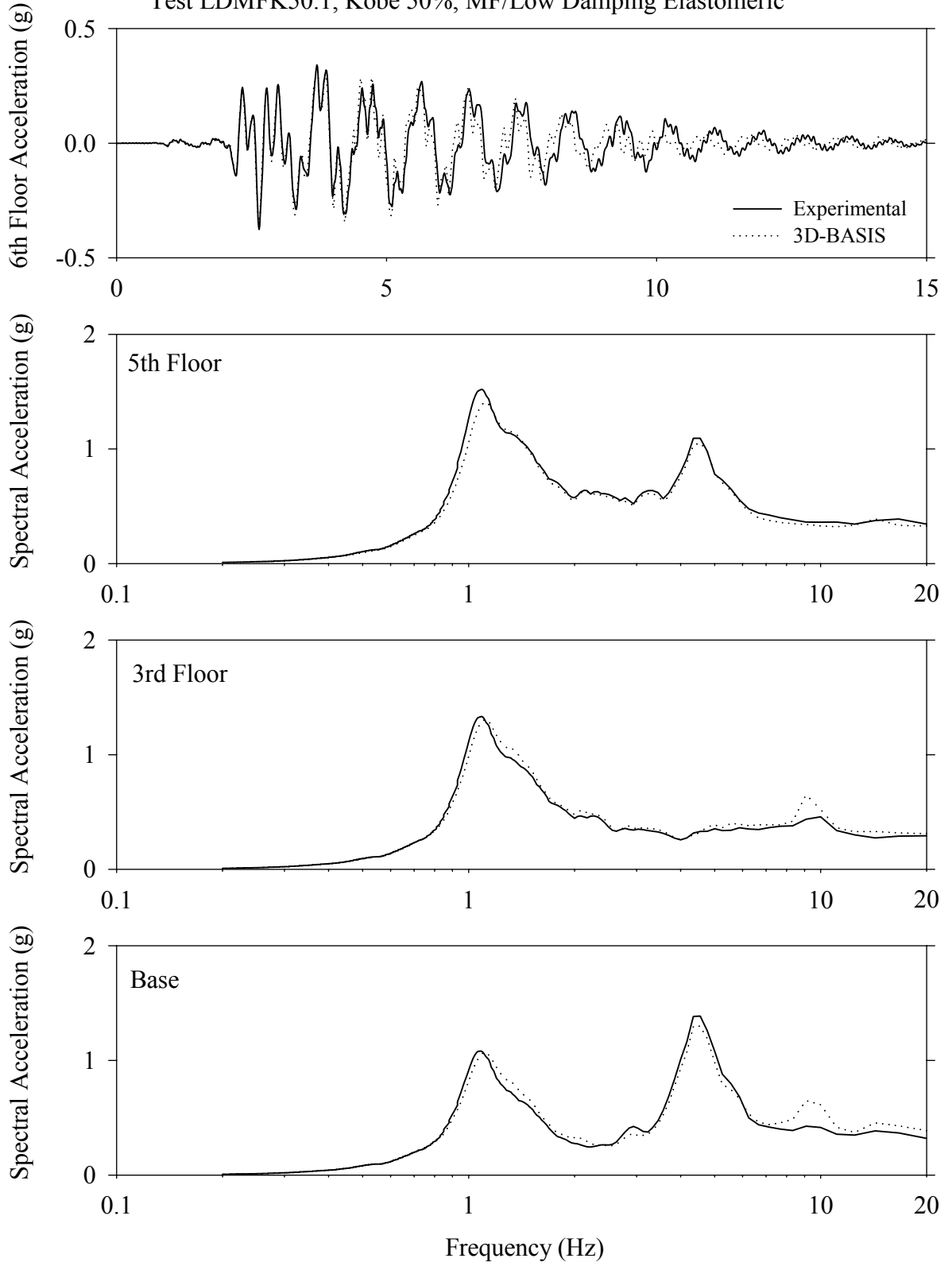
Test LDMFE20.1, El Centro S00E 200%, MF/Low Damping Elastomeric



Test LDMFK50.1, Kobe 50%, MF/Low Damping Elastomeric

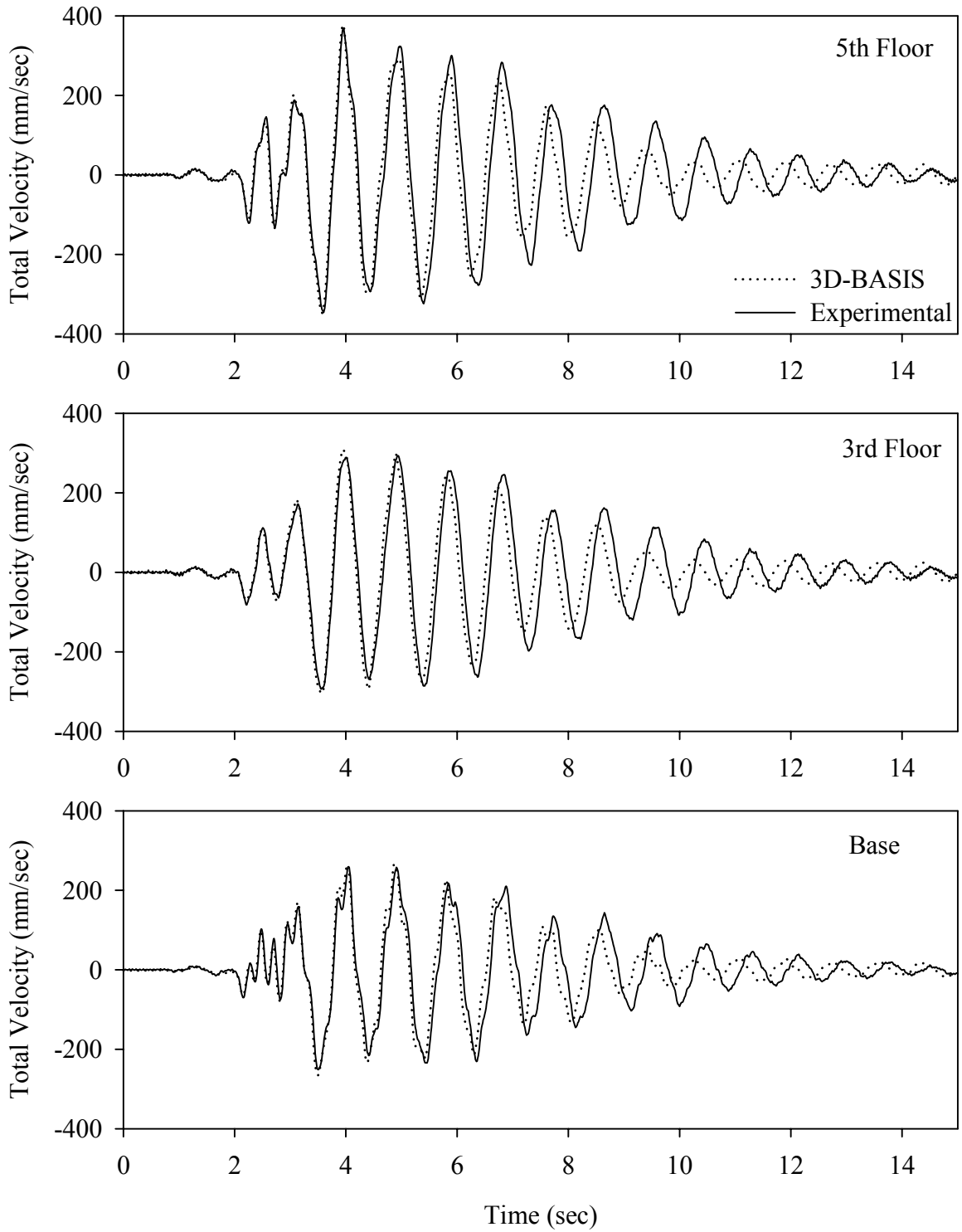


Test LDMFK50.1, Kobe 50%, MF/Low Damping Elastomeric

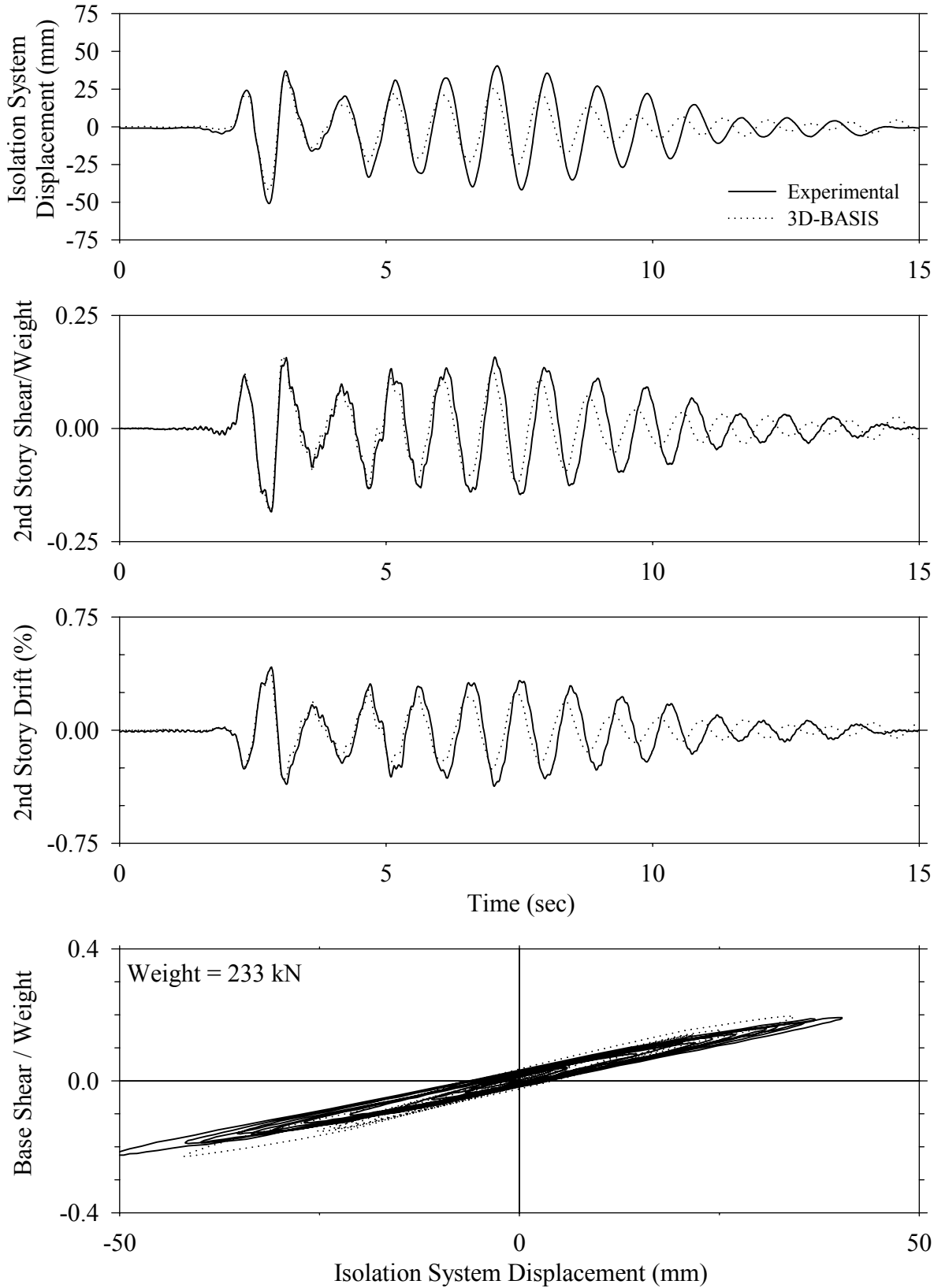




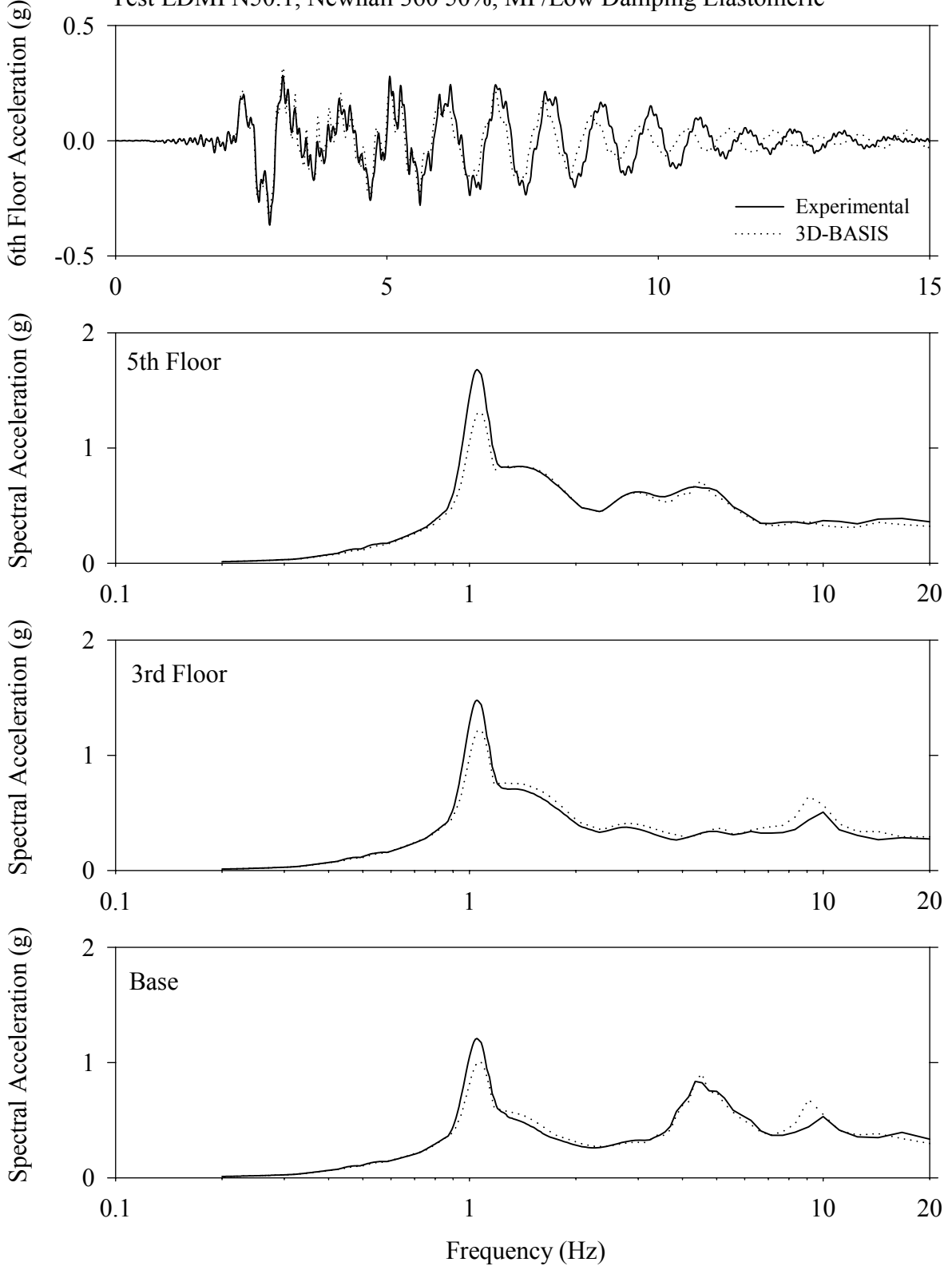
Test LDMFK50.1, Kobe 50%, MF/Low Damping Elastomeric



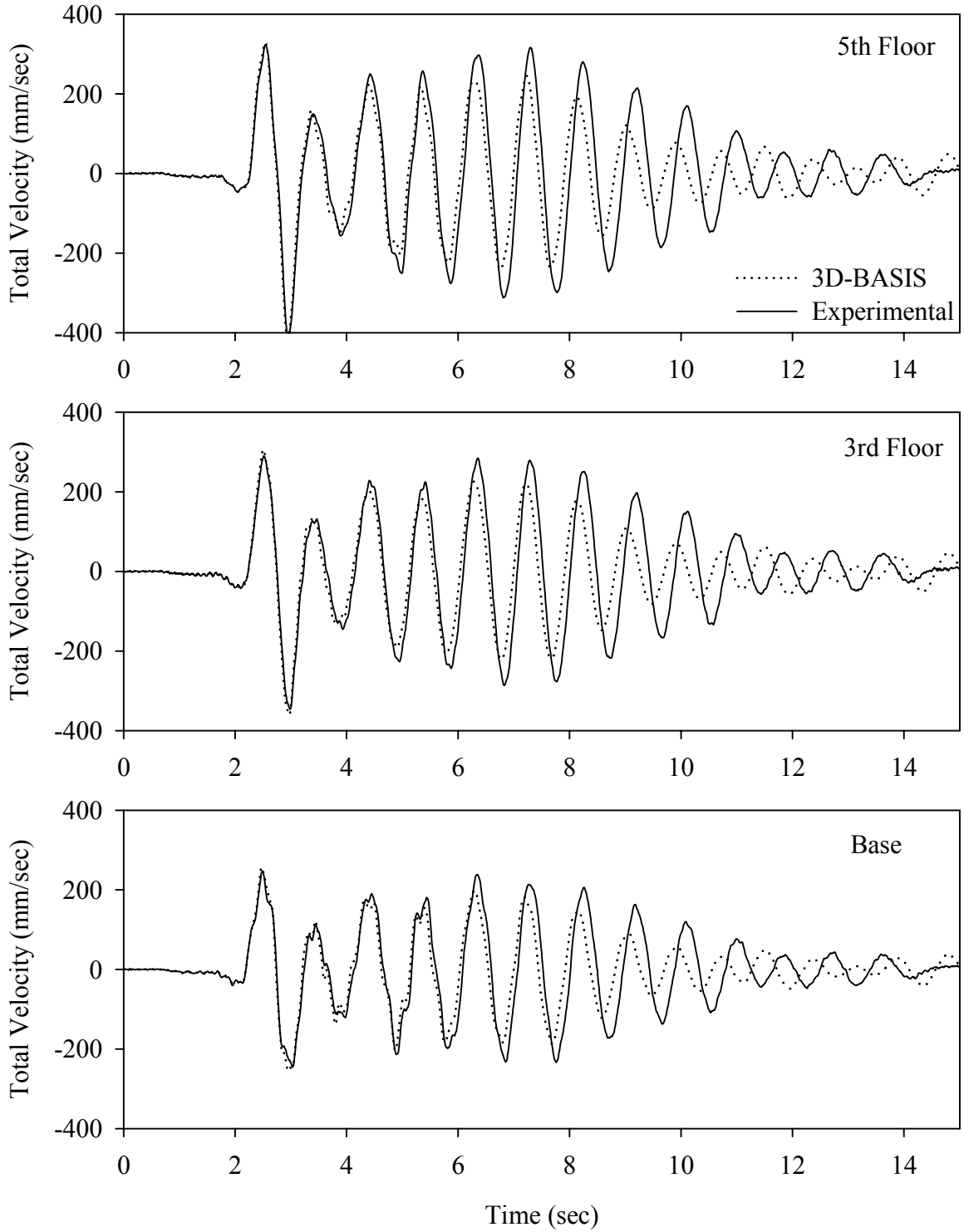
Test LDMFN50.1, Newhall 360 50%, MF/Low Damping Elastomeric



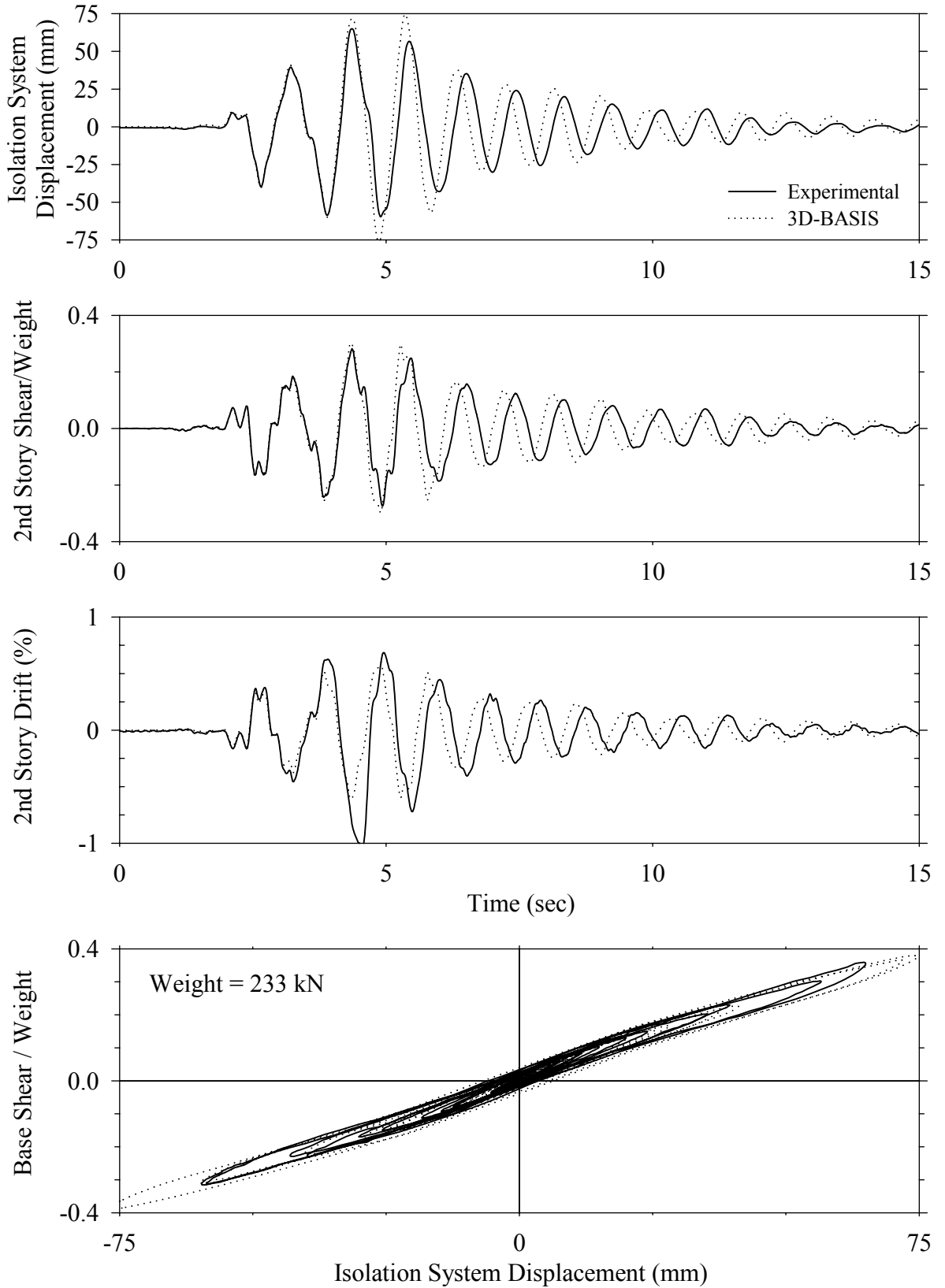
Test LDMFN50.1, Newhall 360 50%, MF/Low Damping Elastomeric



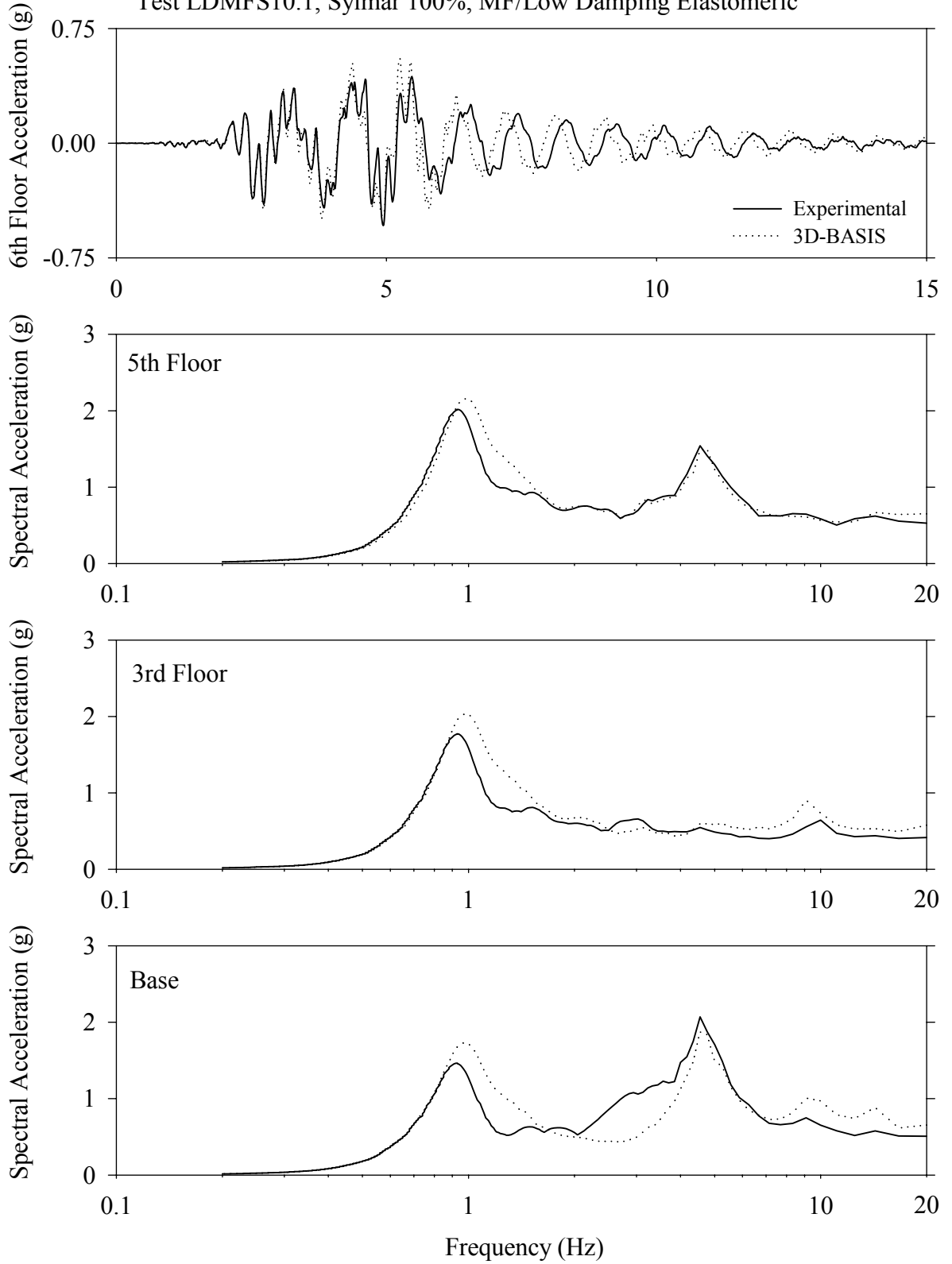
Test LDMFN50.1, Newhall 360 50%, MF/Low Damping Elastomeric



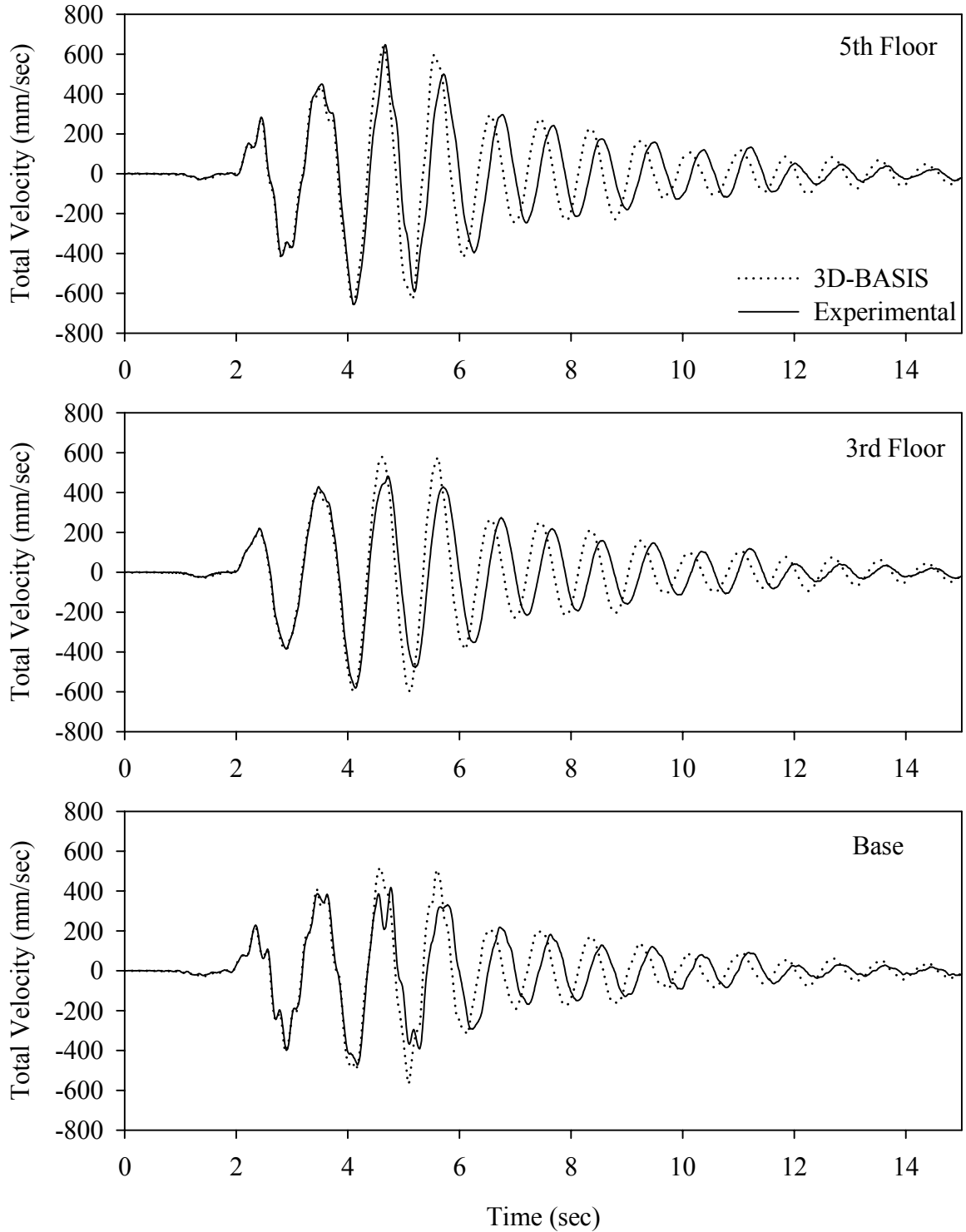
Test LDMFS10.1, Sylmar 100%, MF/Low Damping Elastomeric



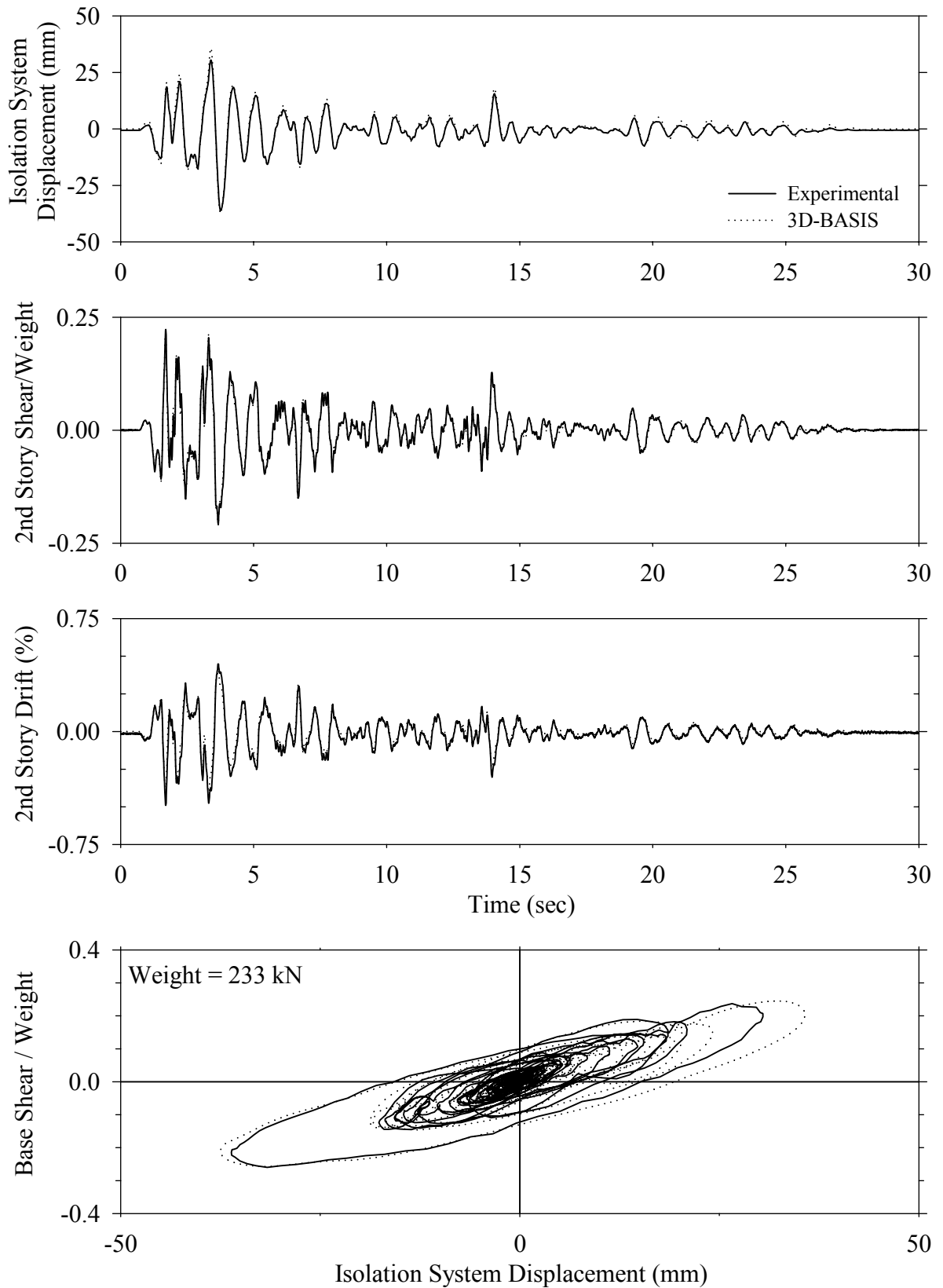
Test LDMFS10.1, Sylmar 100%, MF/Low Damping Elastomeric



Test LDMFS10.1, Sylmar 100%, MF/Low Damping Elastomeric

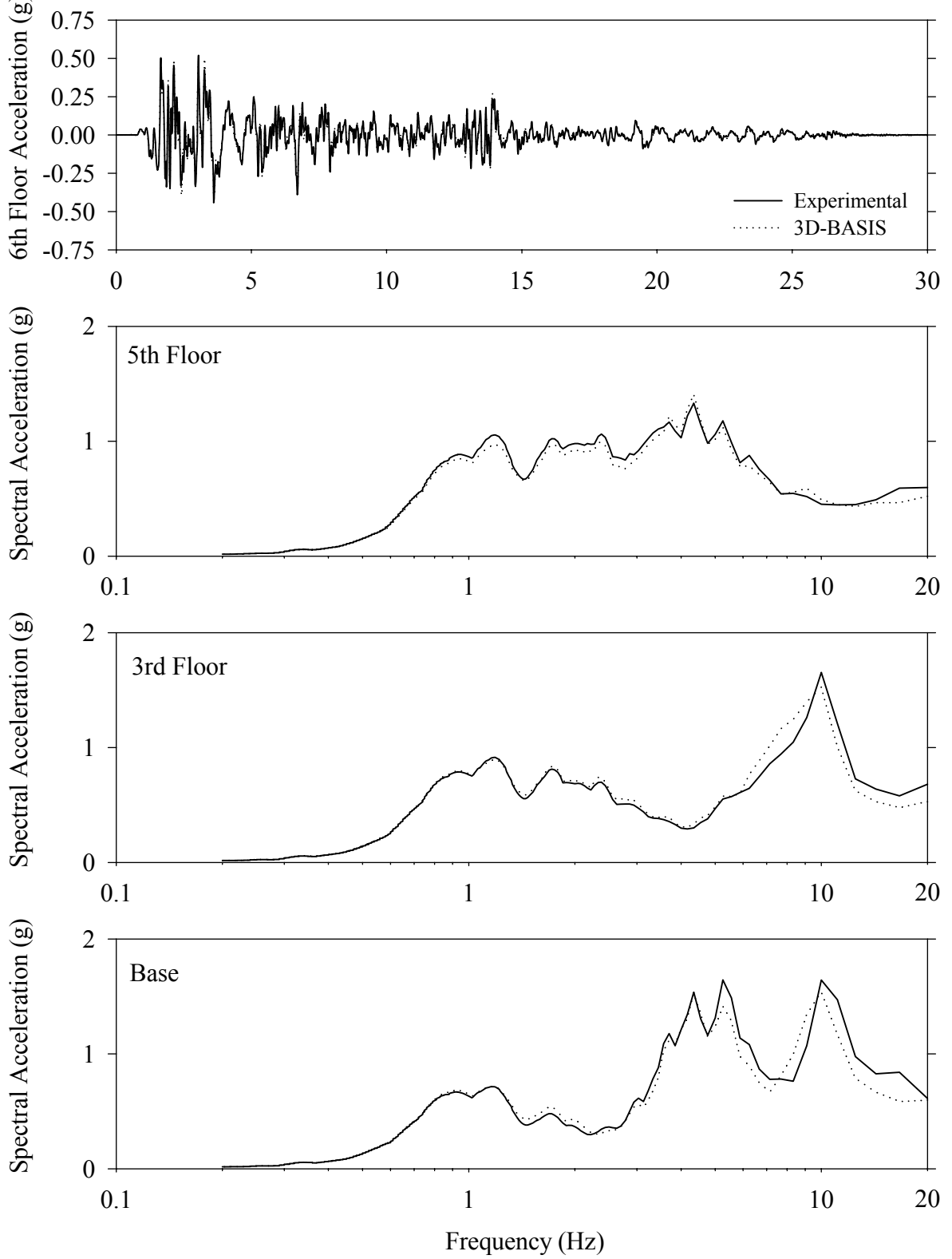


Test LDMLE20.1, El Centro S00E 200%, MF/Low Damping Elastomeric with Linear Dampers

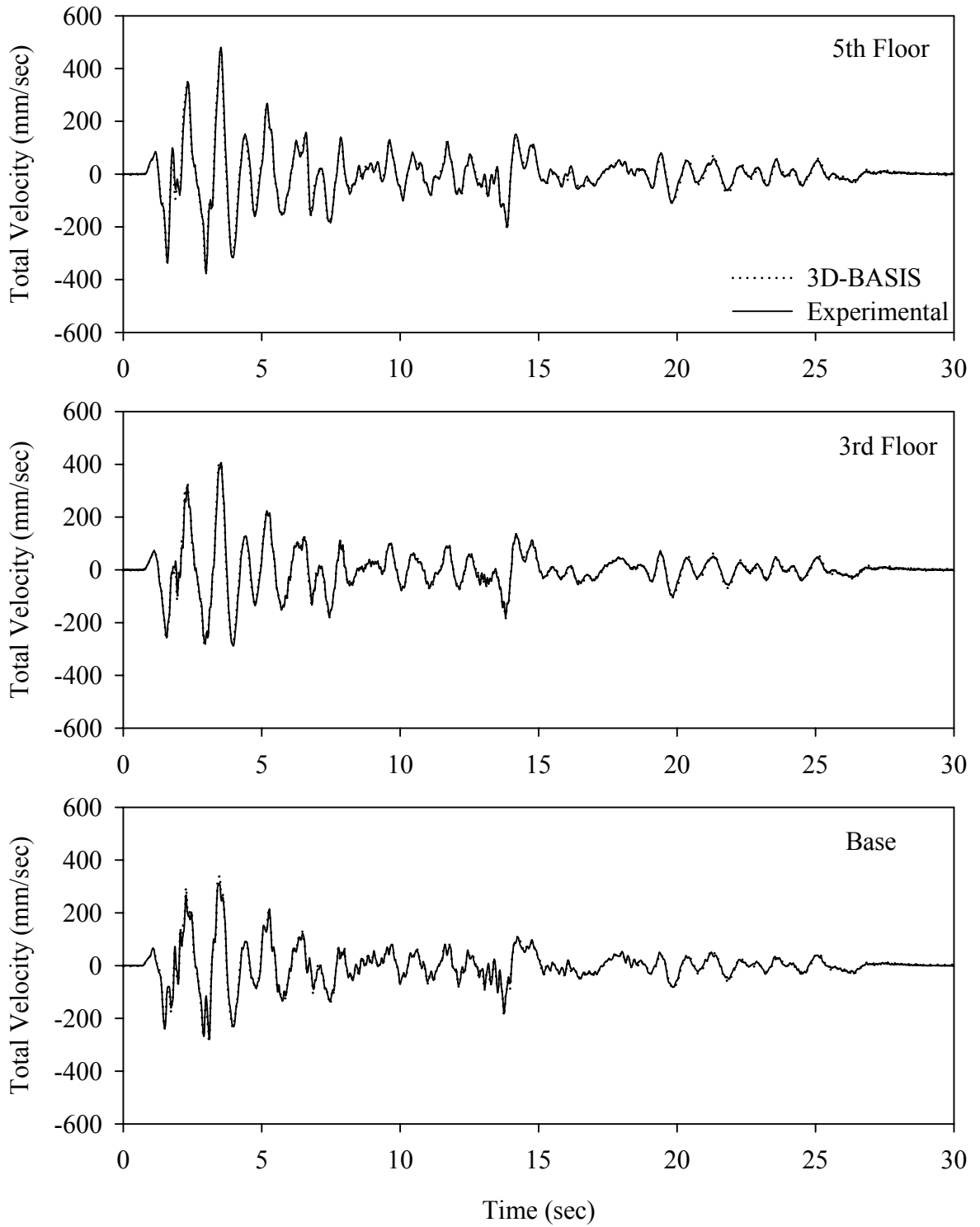




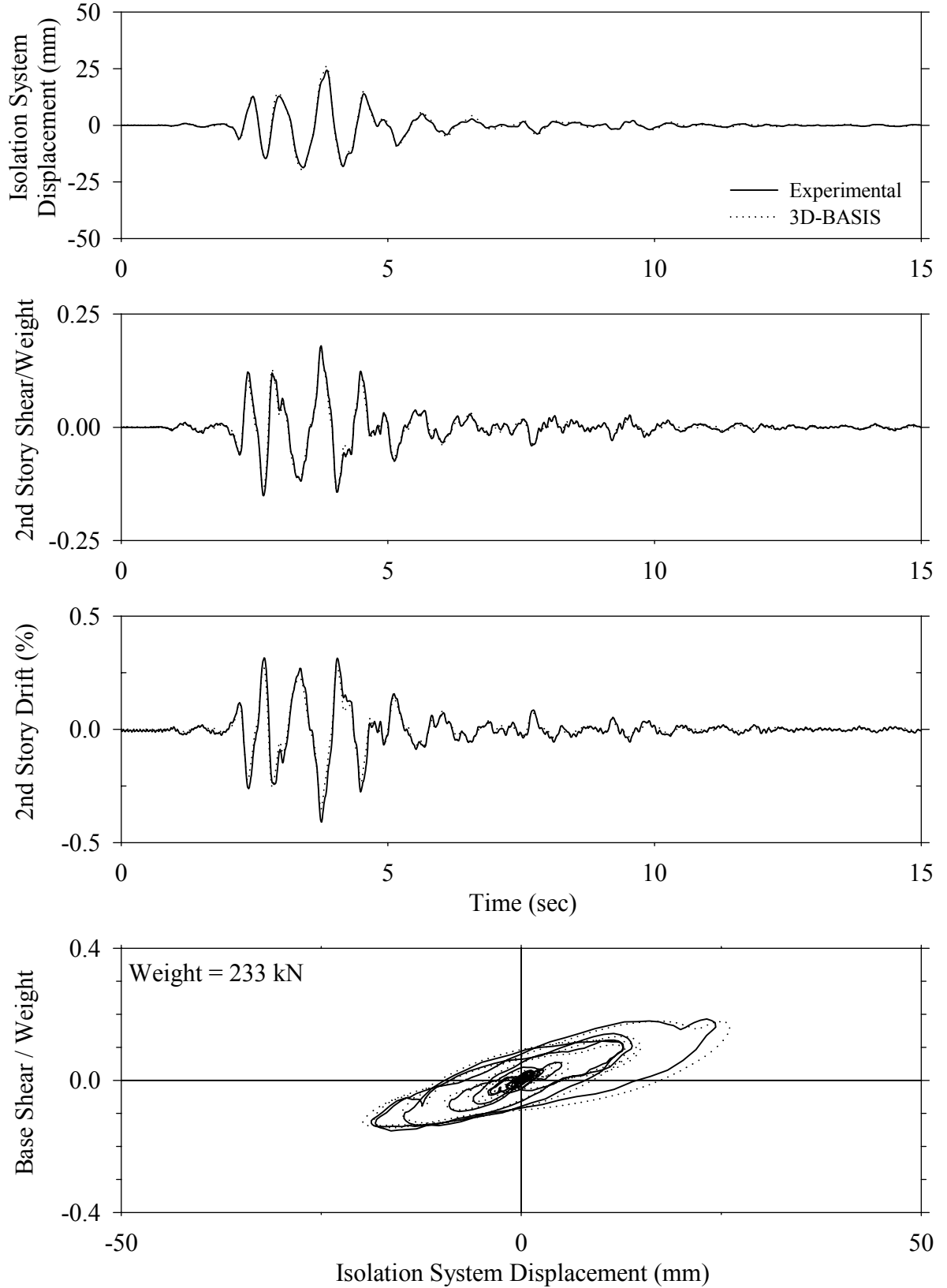
Test LDMLE20.1, El Centro S00E 200%, MF/Low Damping Elastomeric with Linear Dampers



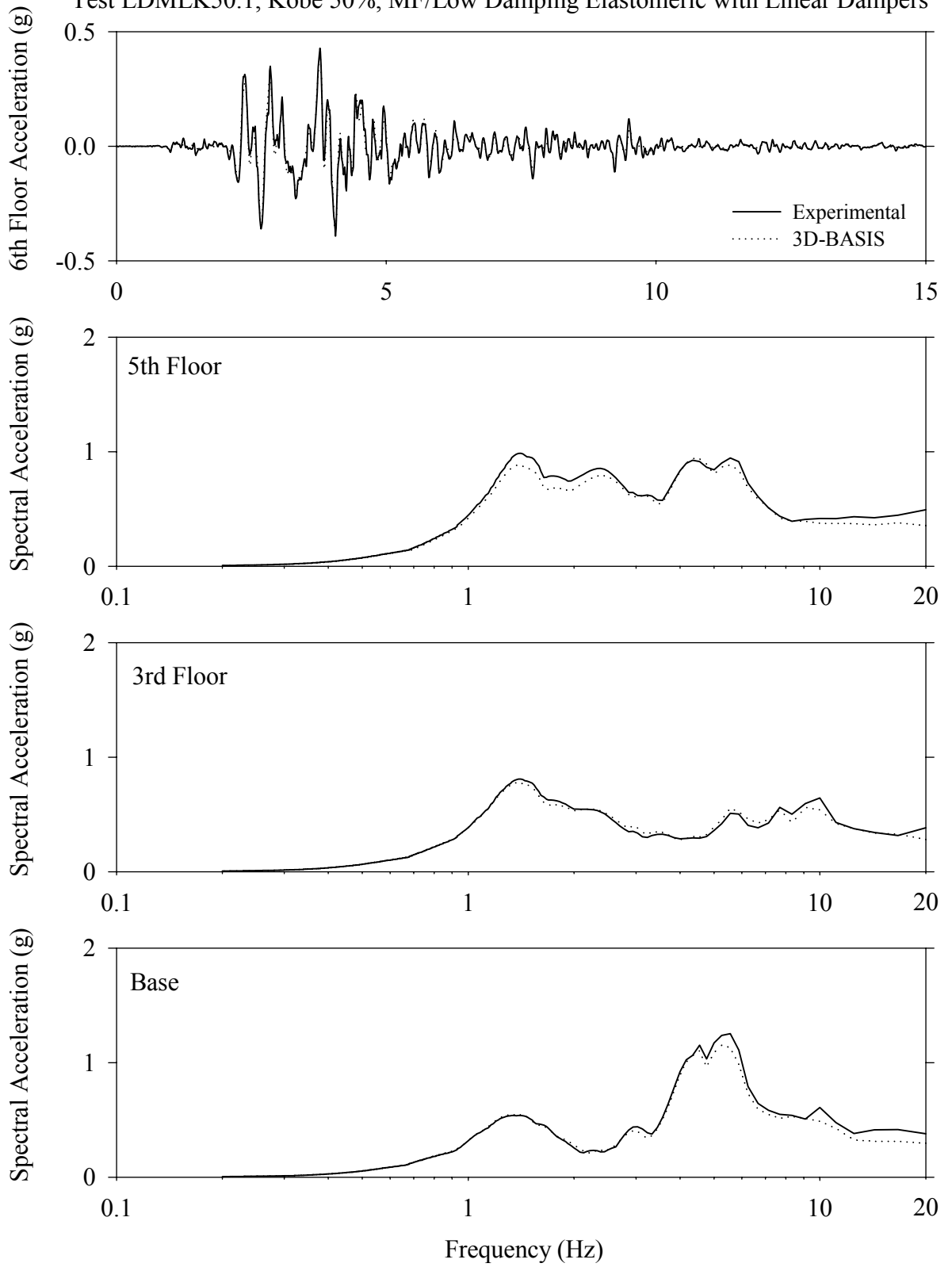
Test LDMLE20.1, El Centro S00E 200%, MF/Low Damping Elastomeric with Linear Dampers



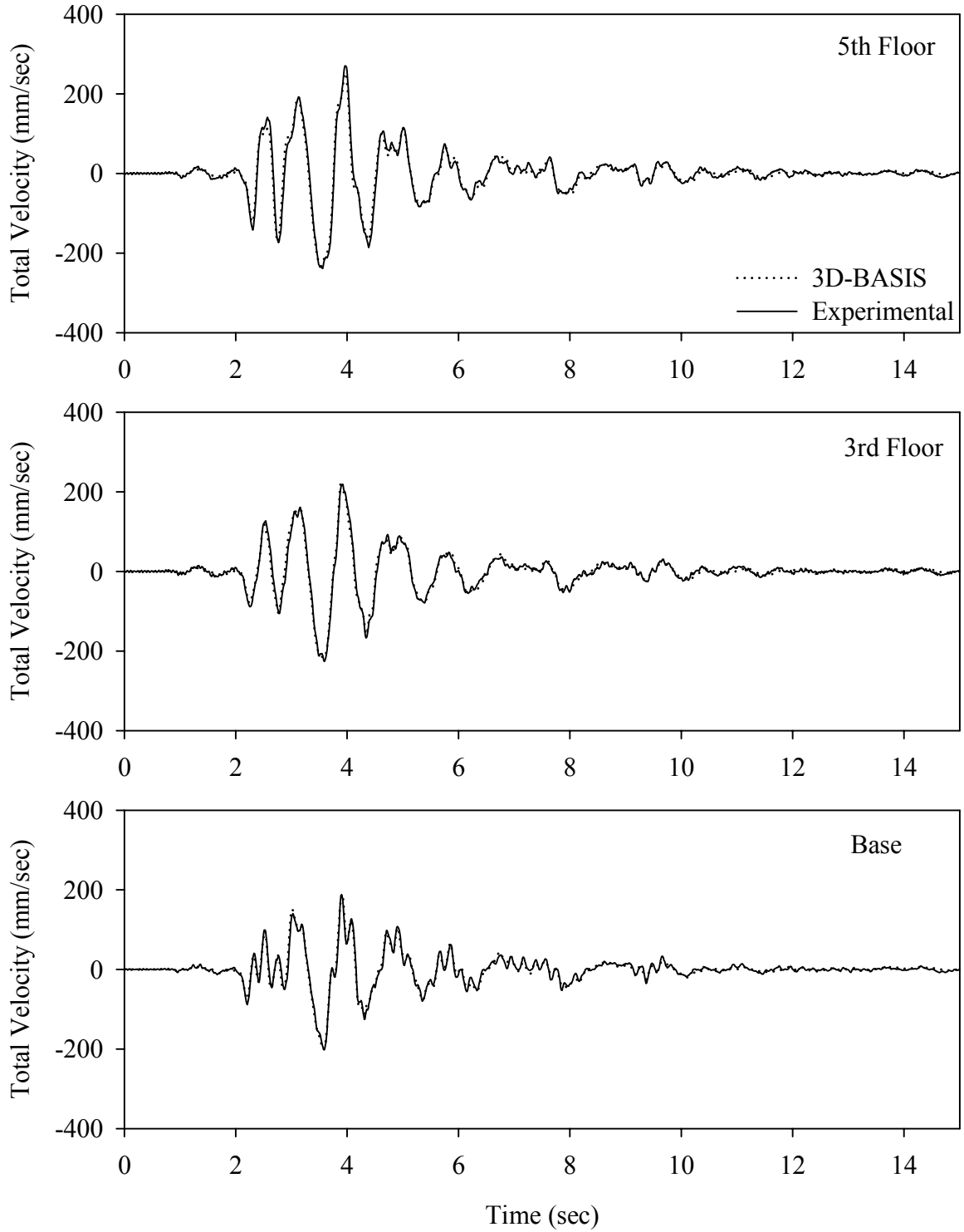
Test LDMLK50.1, Kobe 50%, MF/Low Damping Elastomeric with Linear Dampers



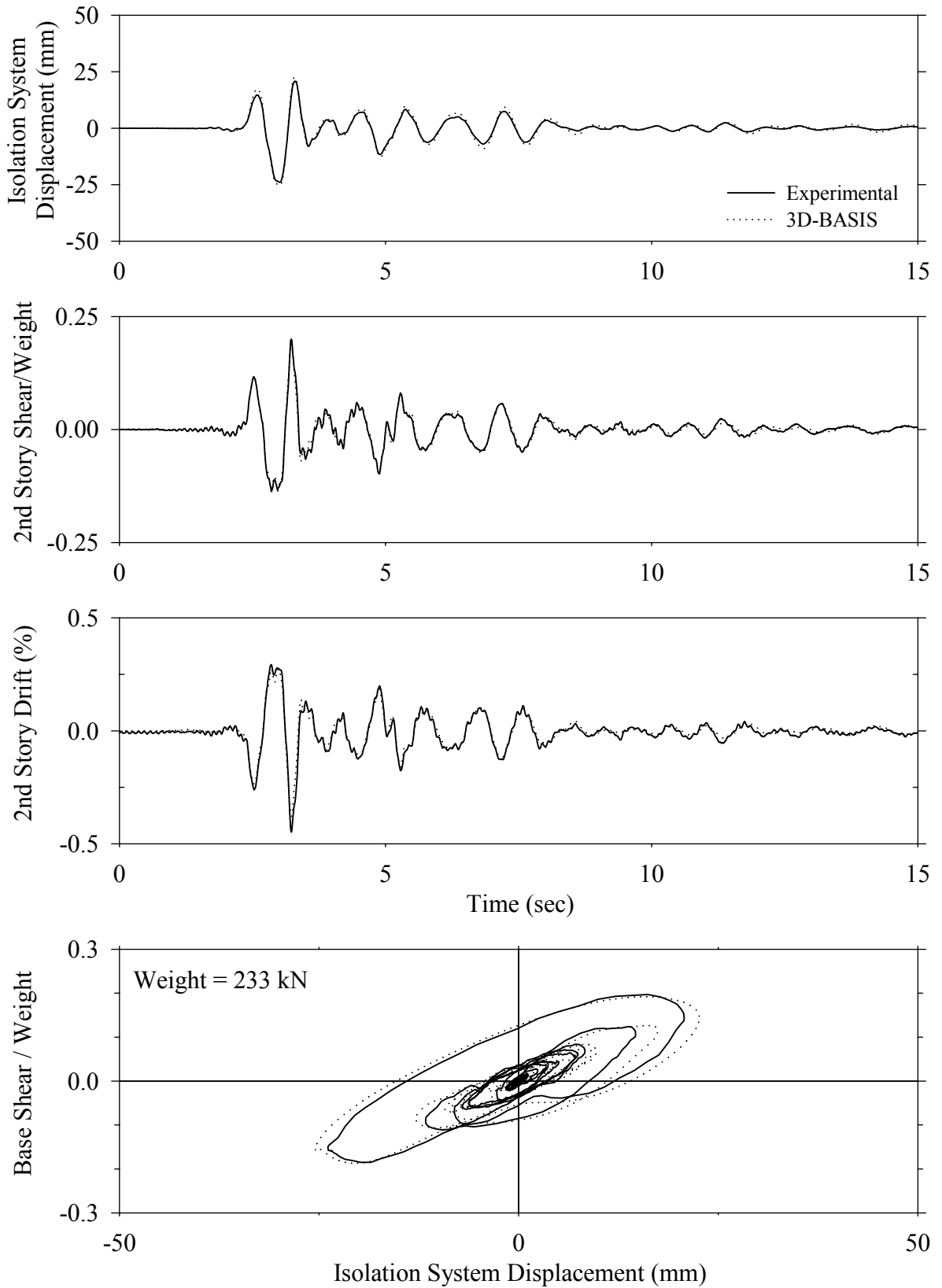
Test LDMLK50.1, Kobe 50%, MF/Low Damping Elastomeric with Linear Dampers



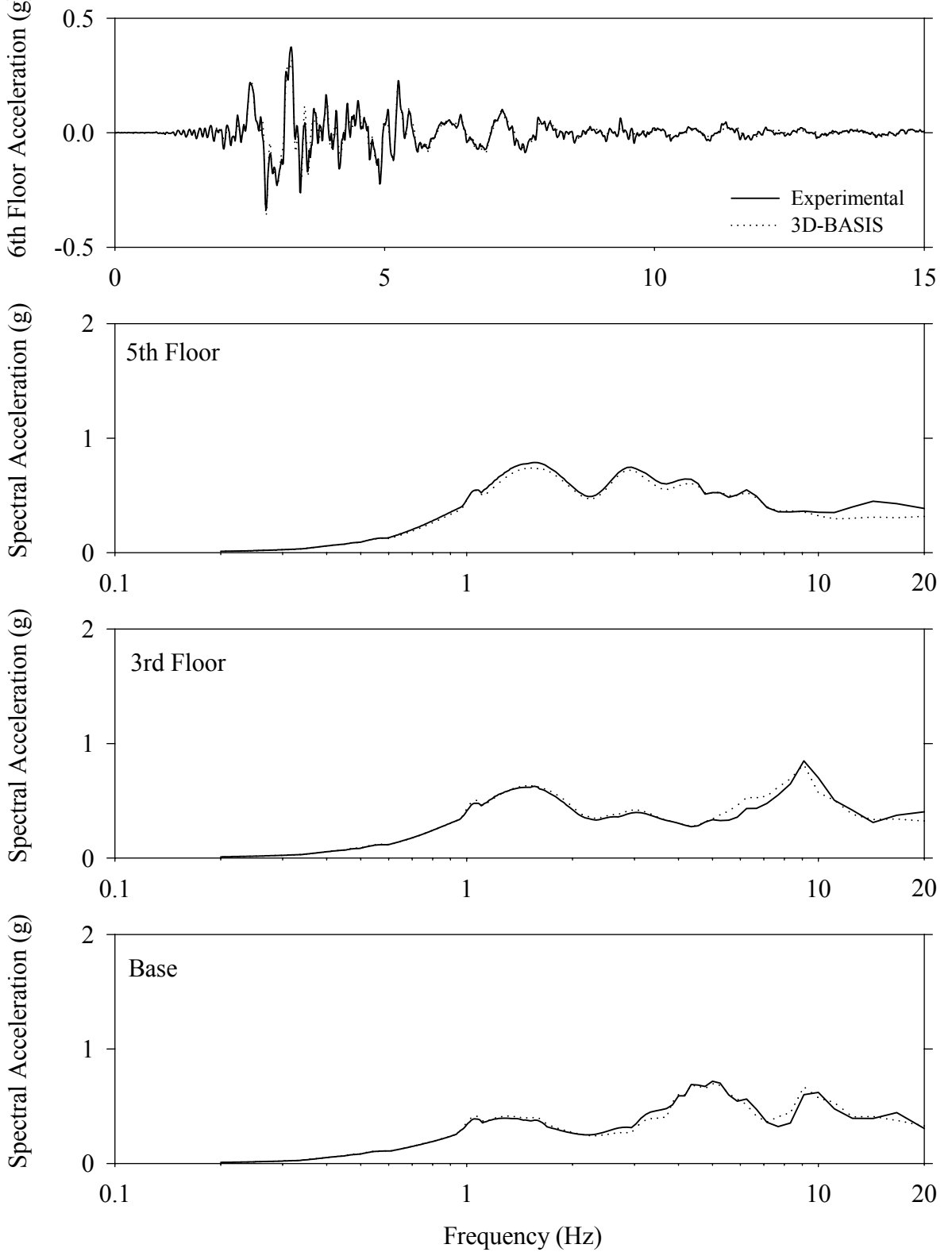
Test LDMLK50.1, Kobe 50%, MF/Low Damping Elastomeric with Linear Dampers



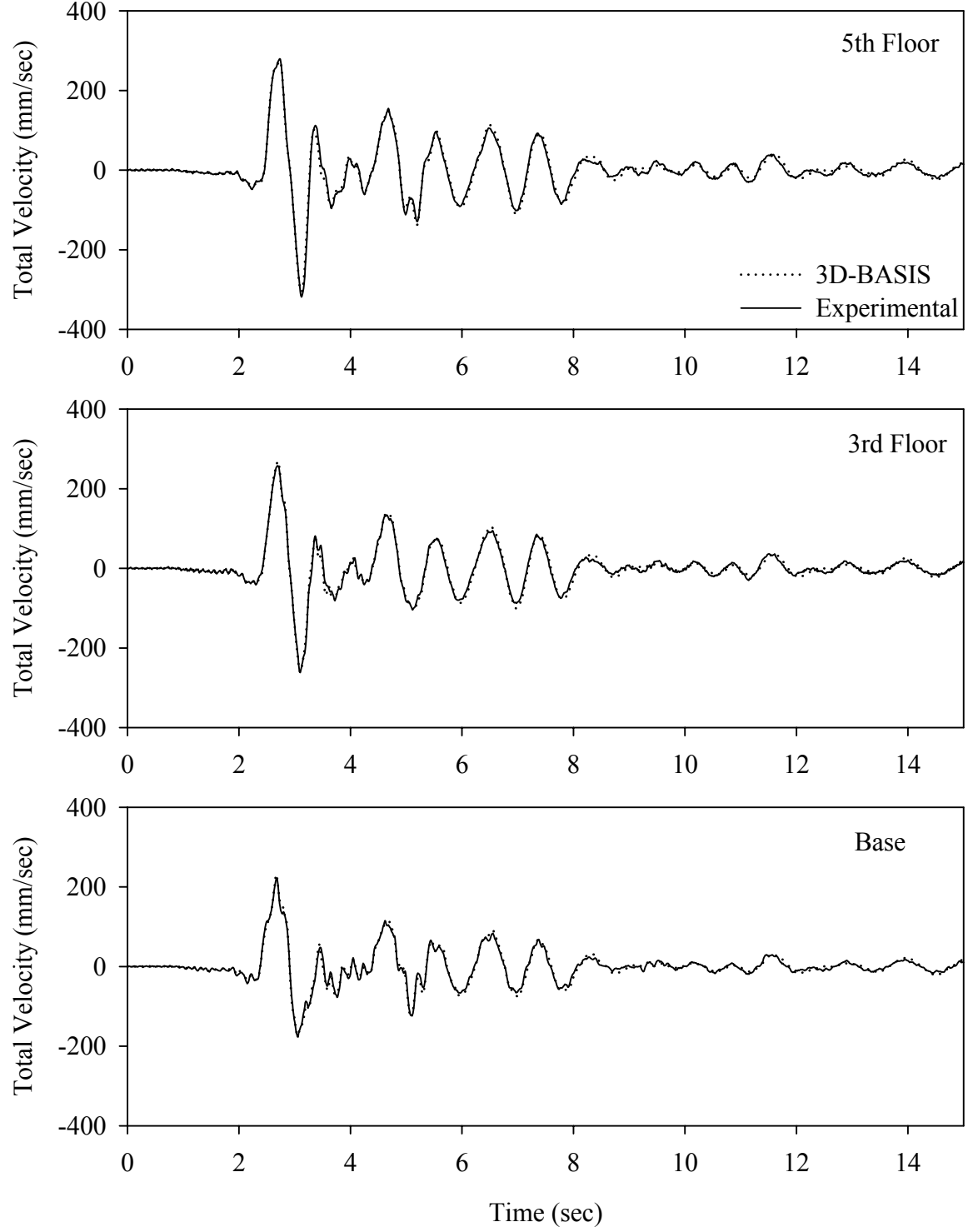
Test LDMLN50.1, Newhall 360 50%, MF/Low Damping Elastomeric with Linear Dampers



Test LDMLN50.1, Newhall 360 50%, MF/Low Damping Elastomeric with Linear Dampers

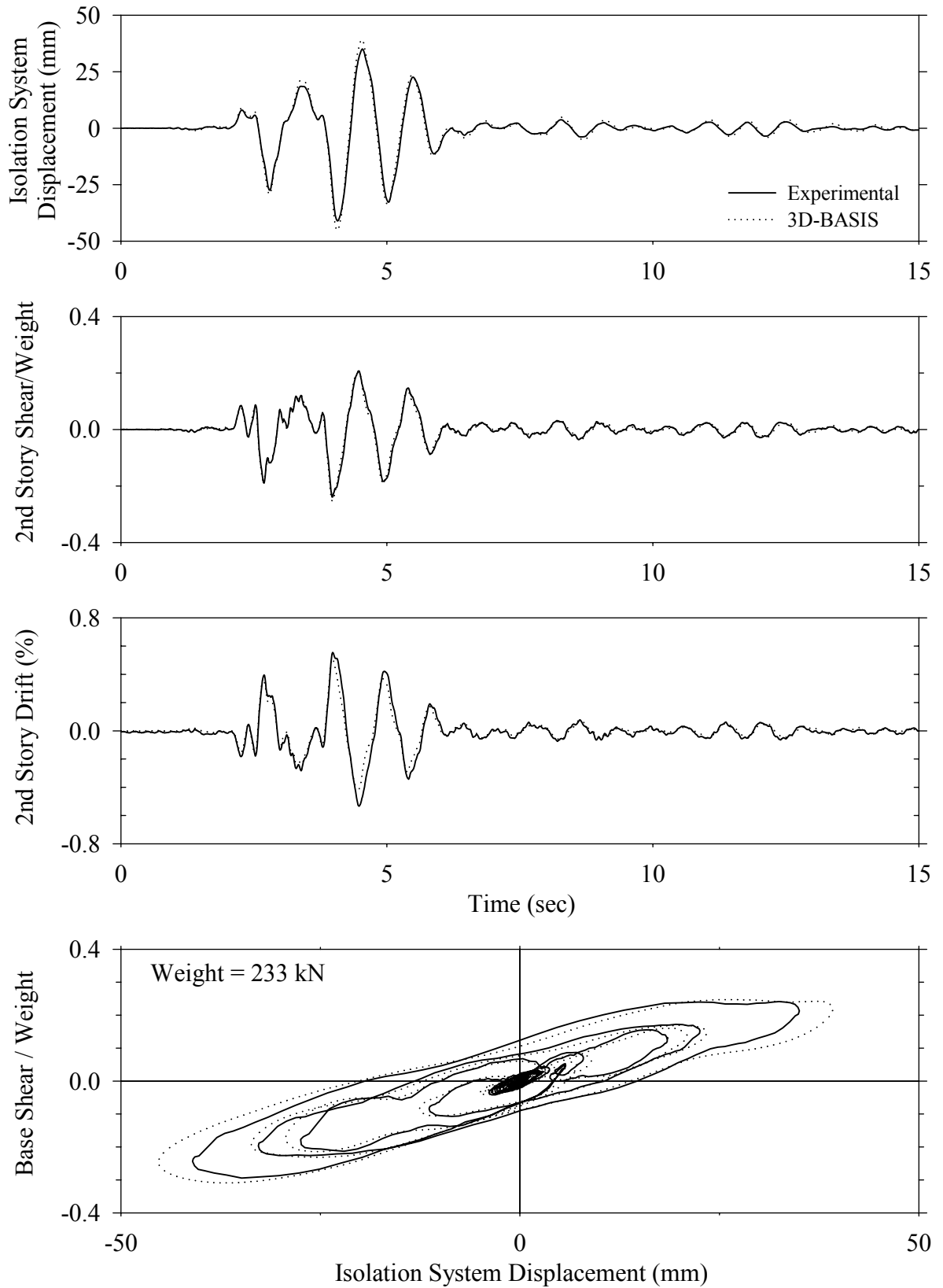


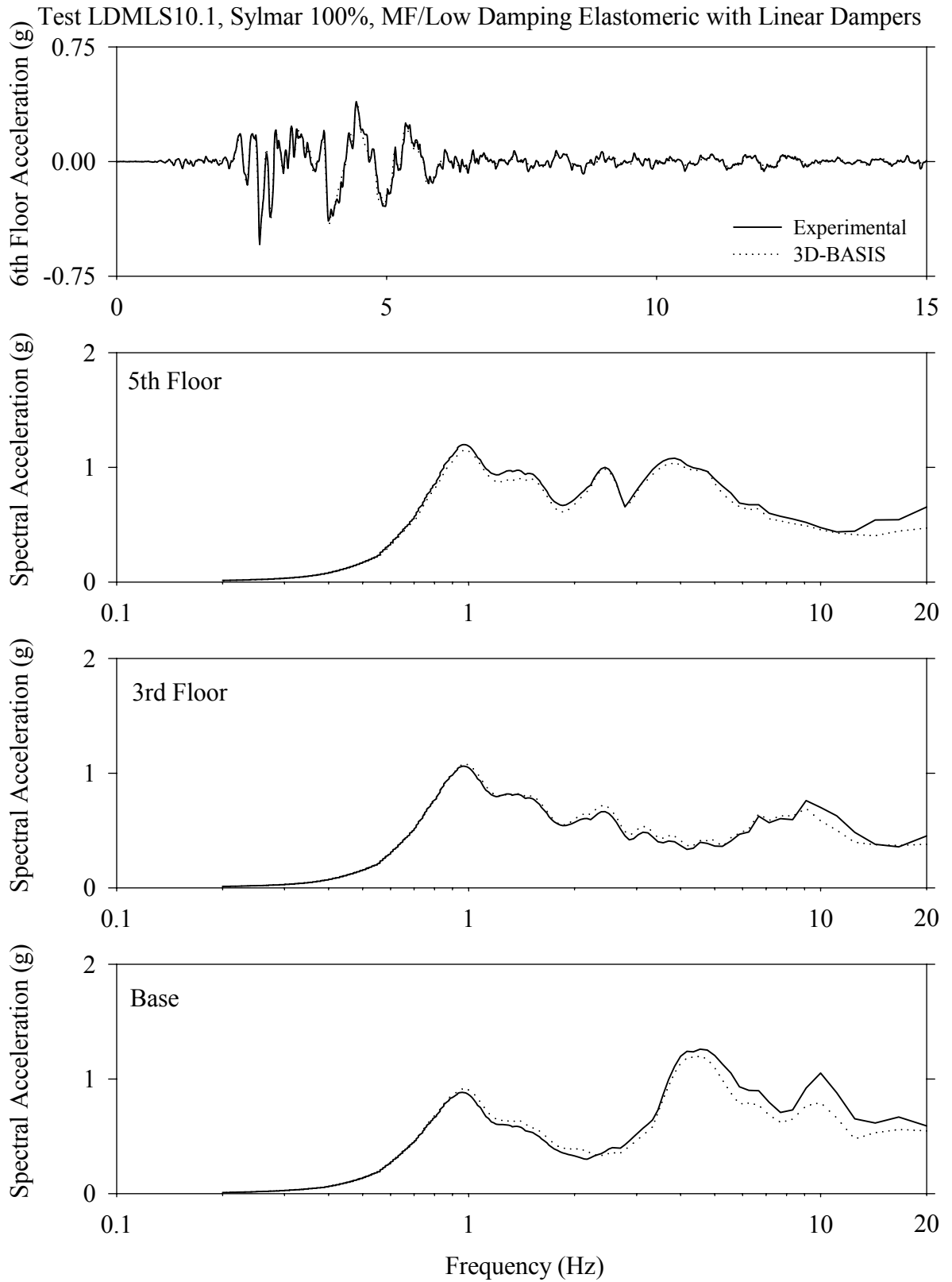
Test LDMLN50.1, Newhall 360 50%, MF/Low Damping Elastomeric with Linear Dampers



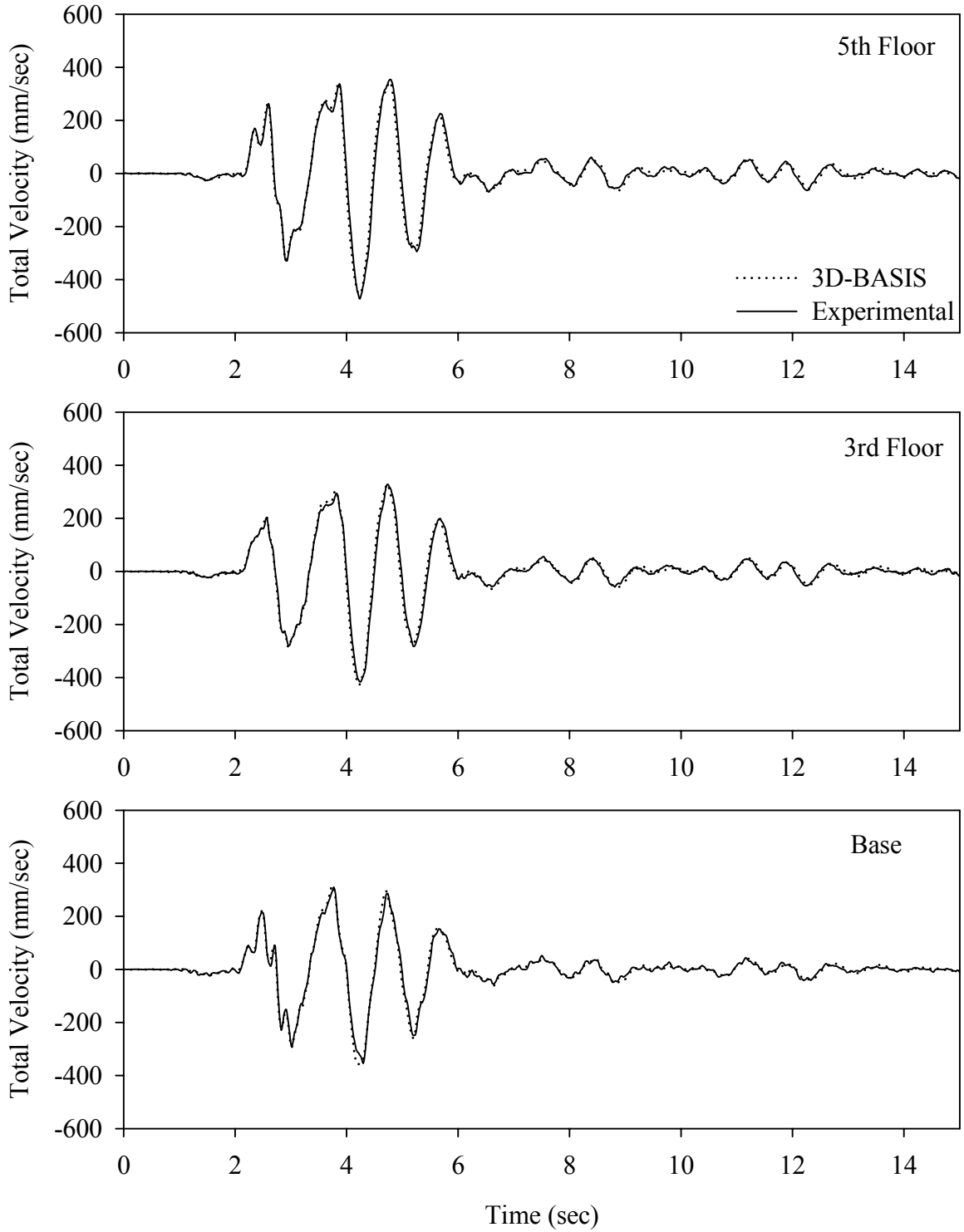


Test LDMLS10.1, Sylmar 100%, MF/Low Damping Elastomeric with Linear Dampers

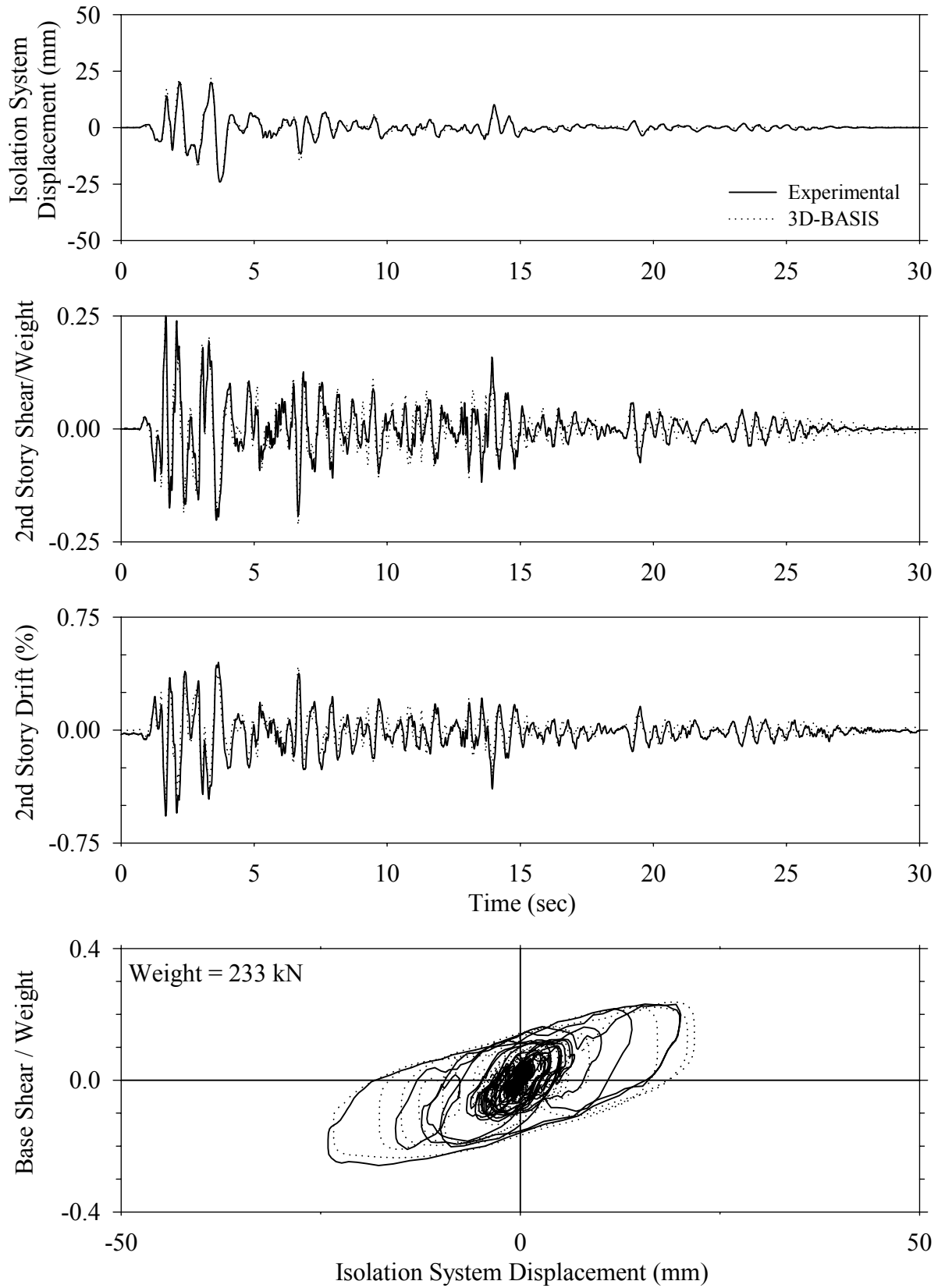




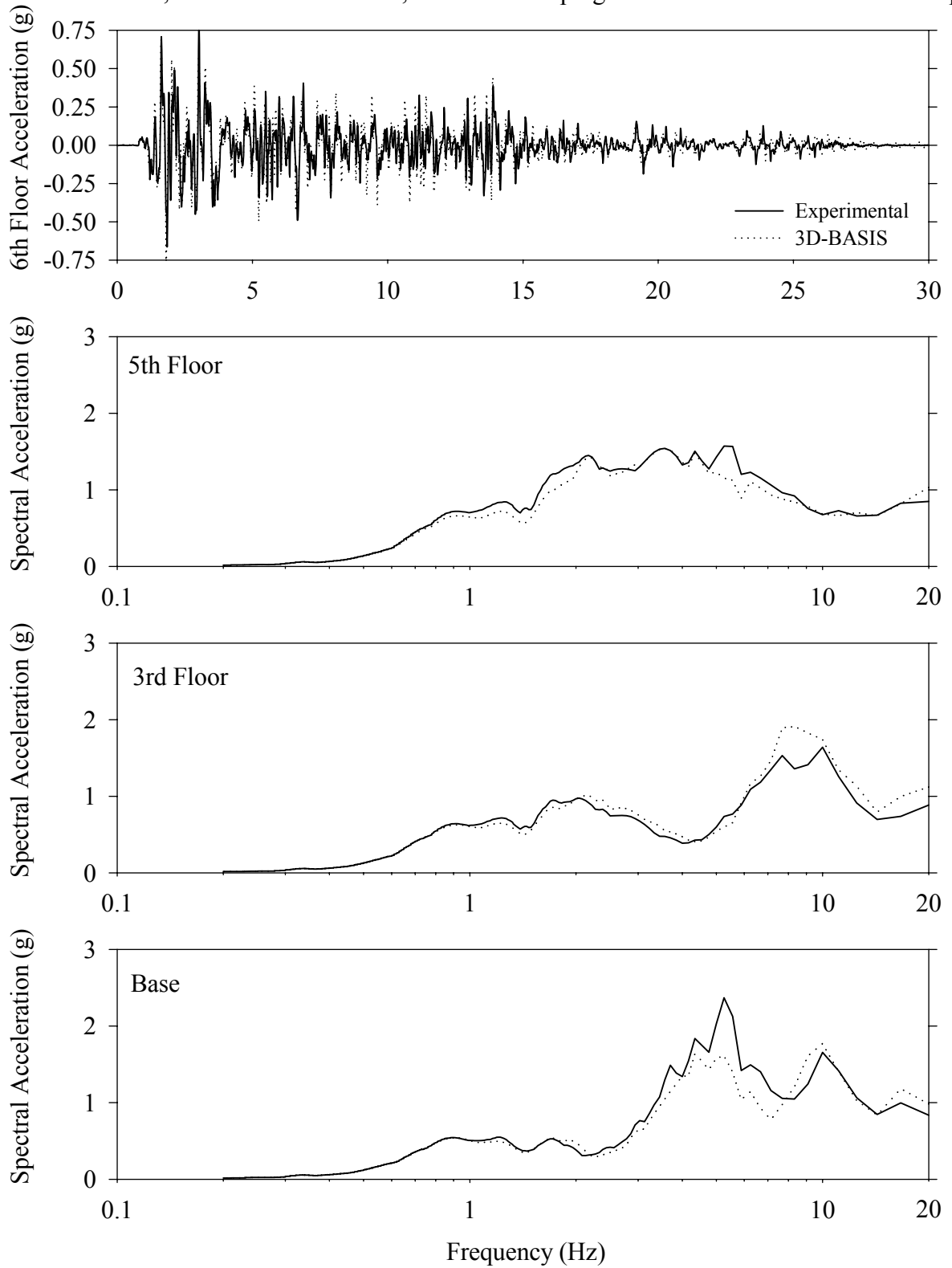
Test LDMLS10.1, Sylmar 100%, MF/Low Damping Elastomeric with Linear Dampers



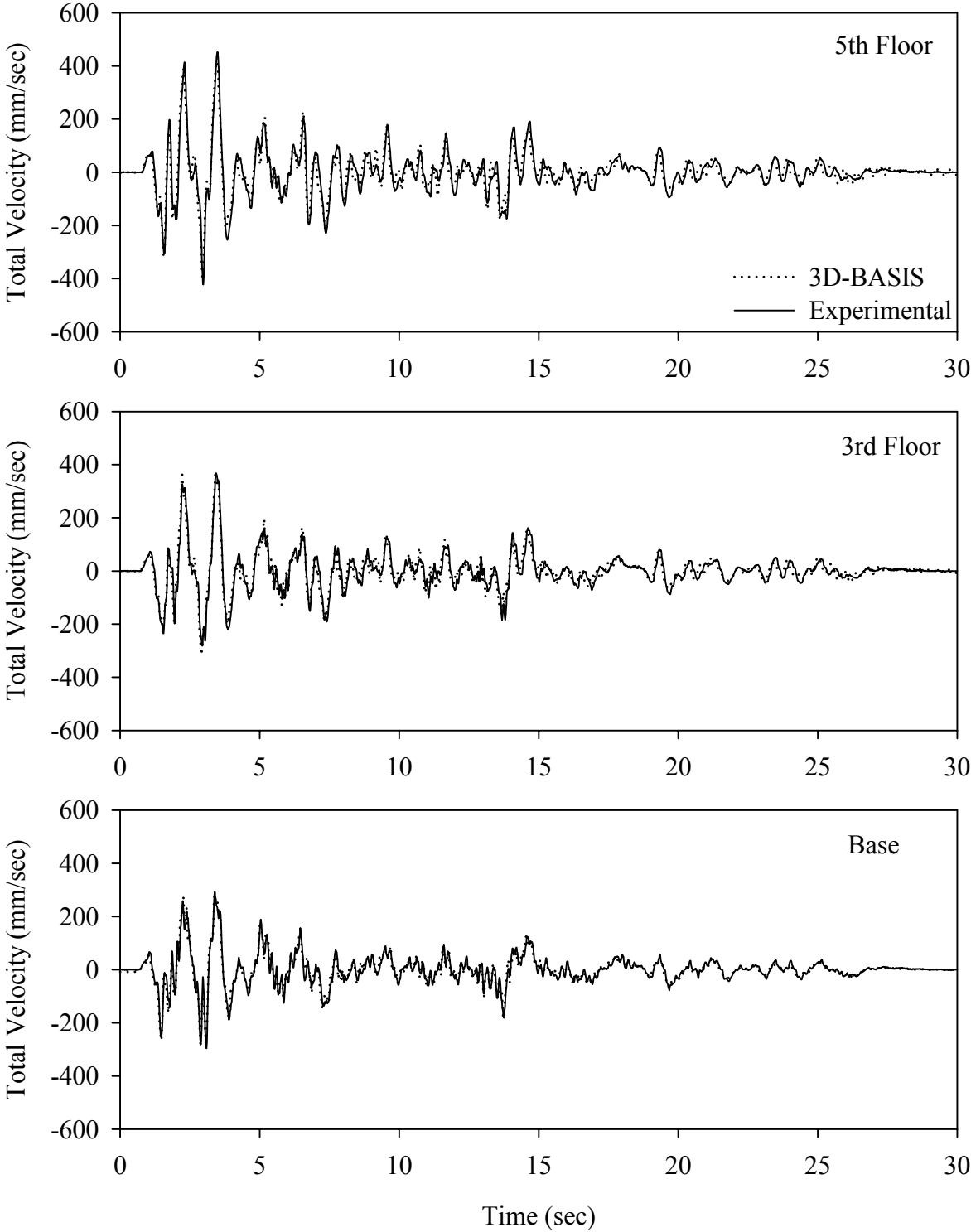
Test LDMNE20.1, El Centro S00E 200%, MF/Low Damping Elastomeric with Nonlinear Dampers



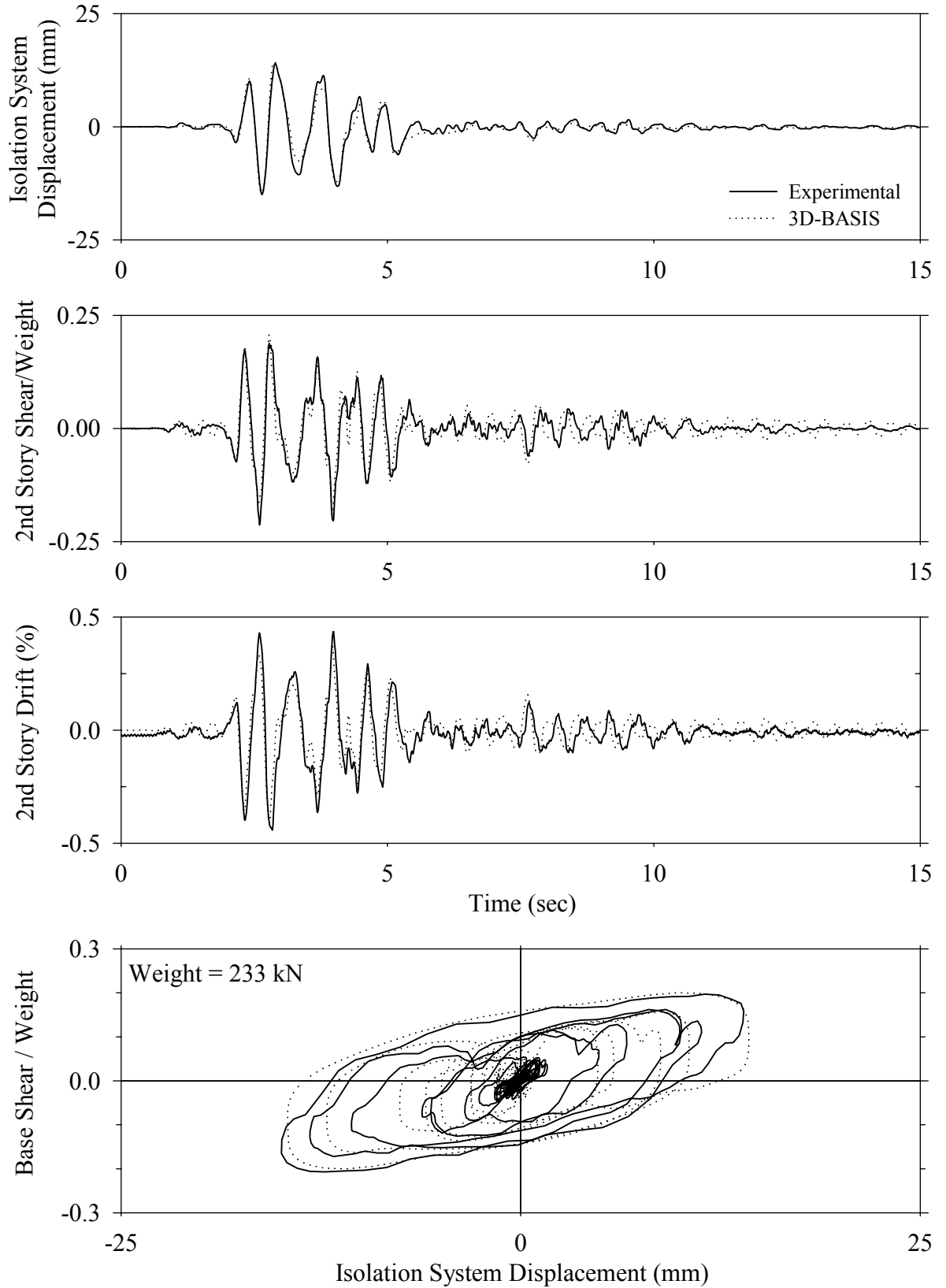
Test LDMNE20.1, El Centro S00E 200%, MF/Low Damping Elastomeric with Nonlinear Dampers



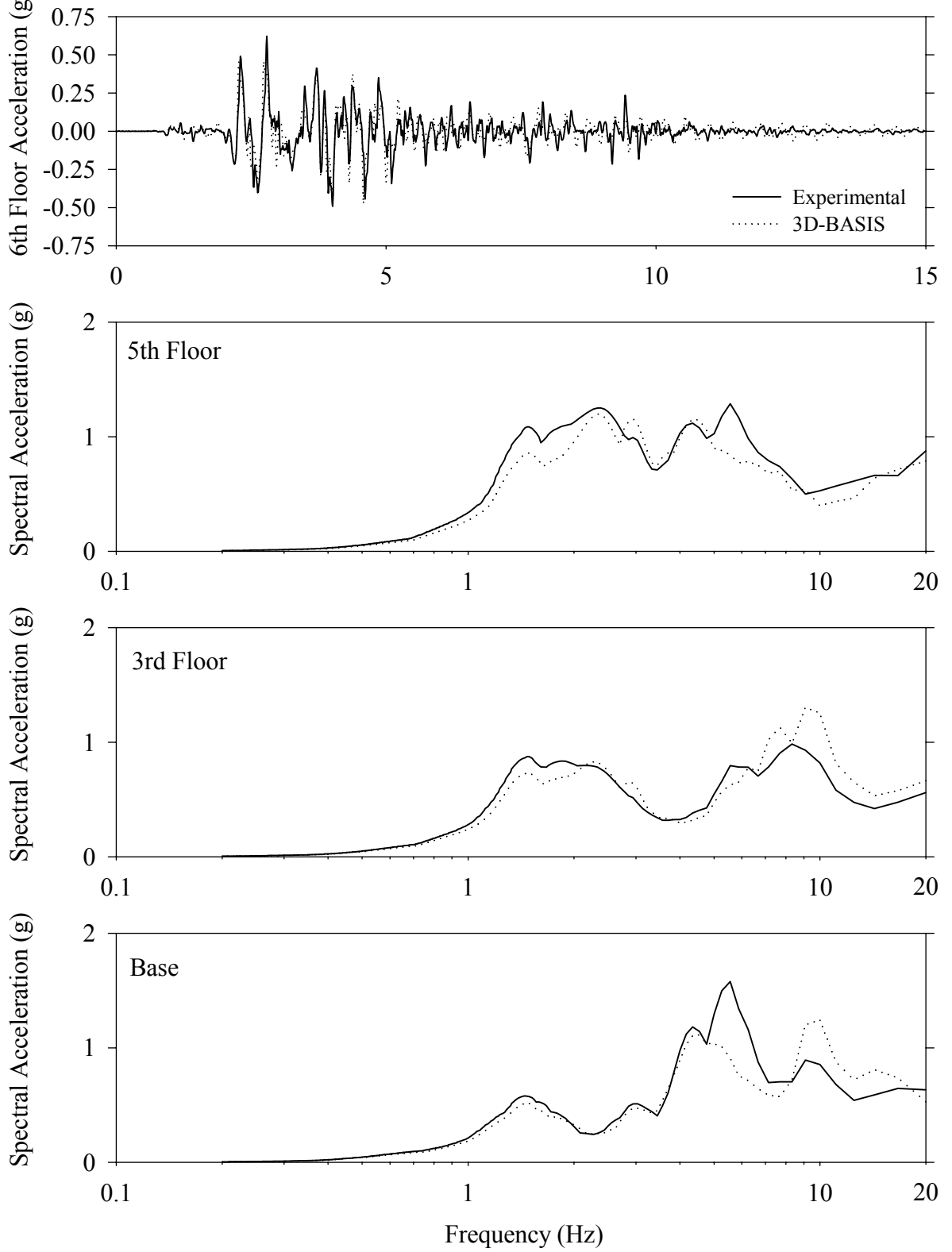
Test LDMNE20.1, El Centro S00E 200%, MF/Low Damping Elastomeric with Nonlinear Dampers



Test LDMNK50.1, Kobe 50%, MF/Low Damping Elastomeric with Nonlinear Dampers

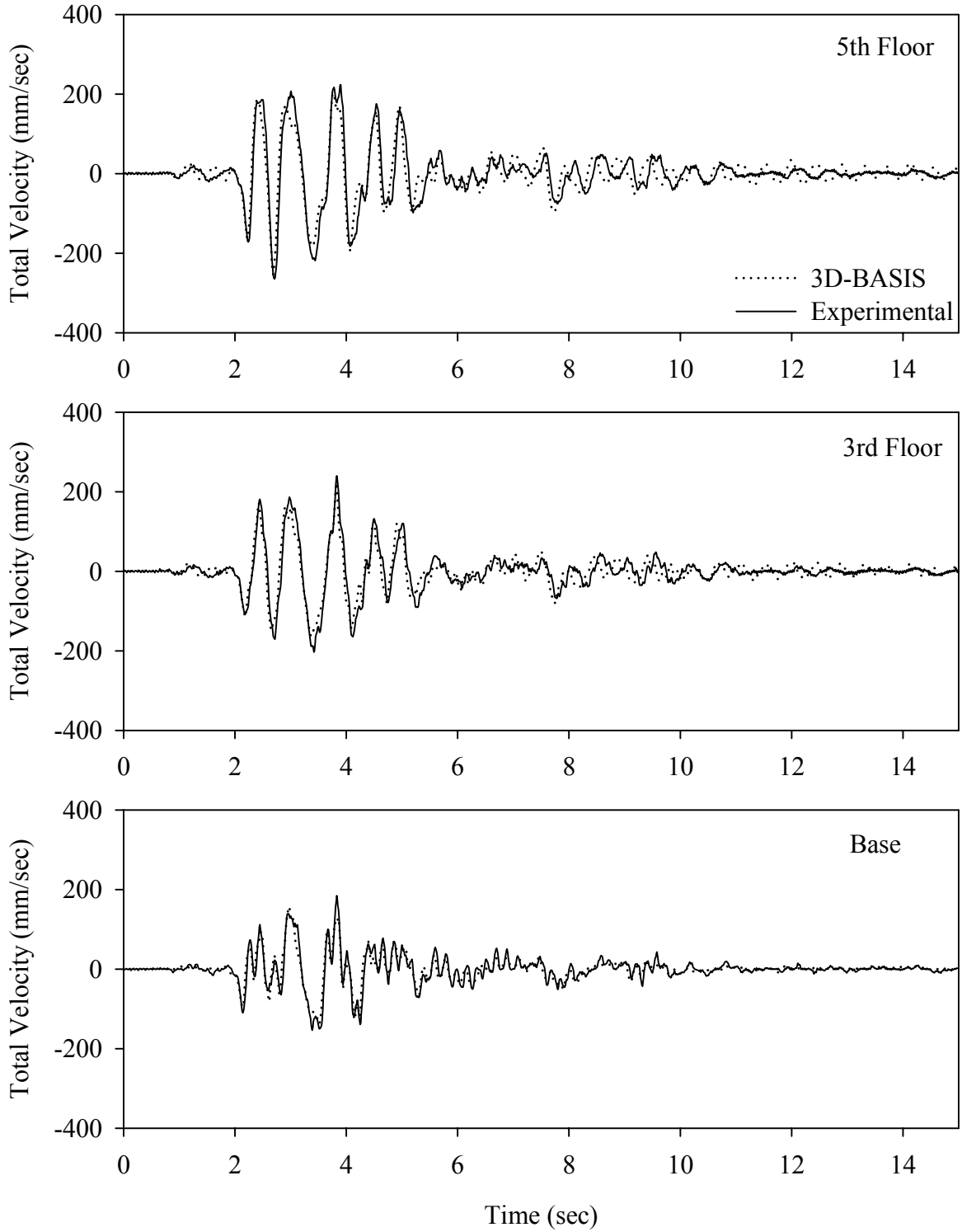


Test LDMNK50.1, Kobe 50%, MF/Low Damping Elastomeric with Nonlinear Dampers

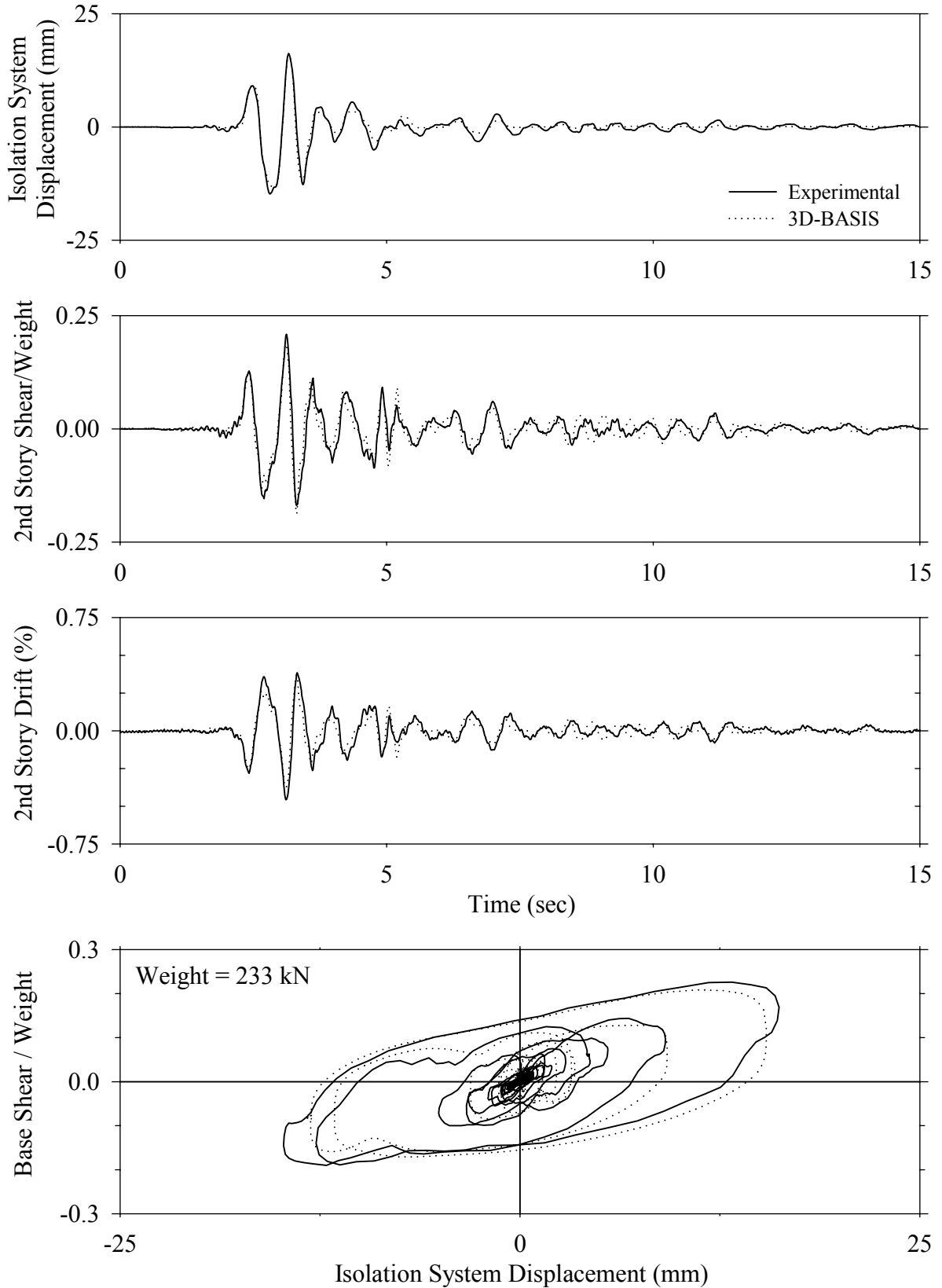




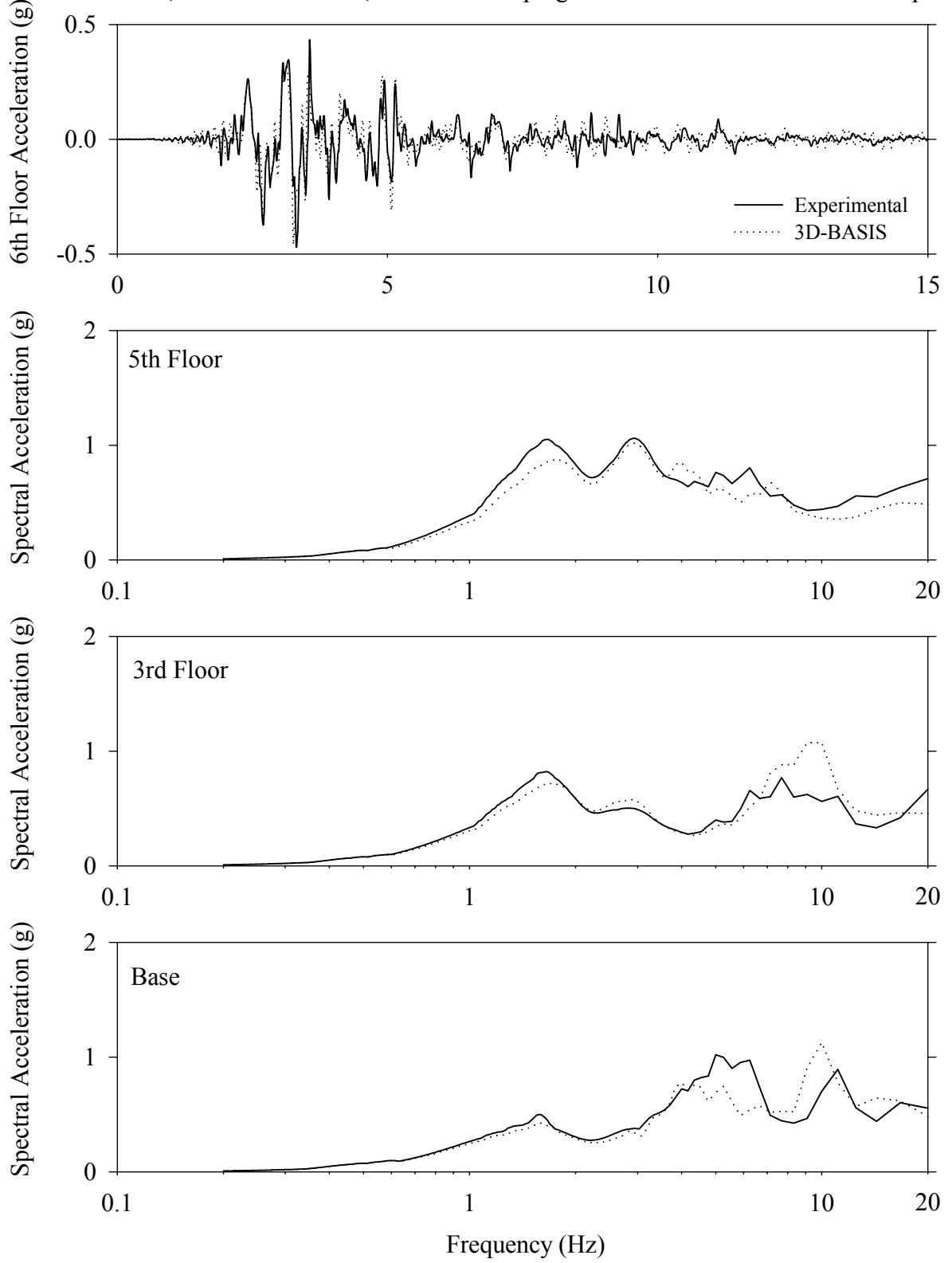
Test LDMNK50.1, Kobe 50%, MF/Low Damping Elastomeric with Nonlinear Dampers



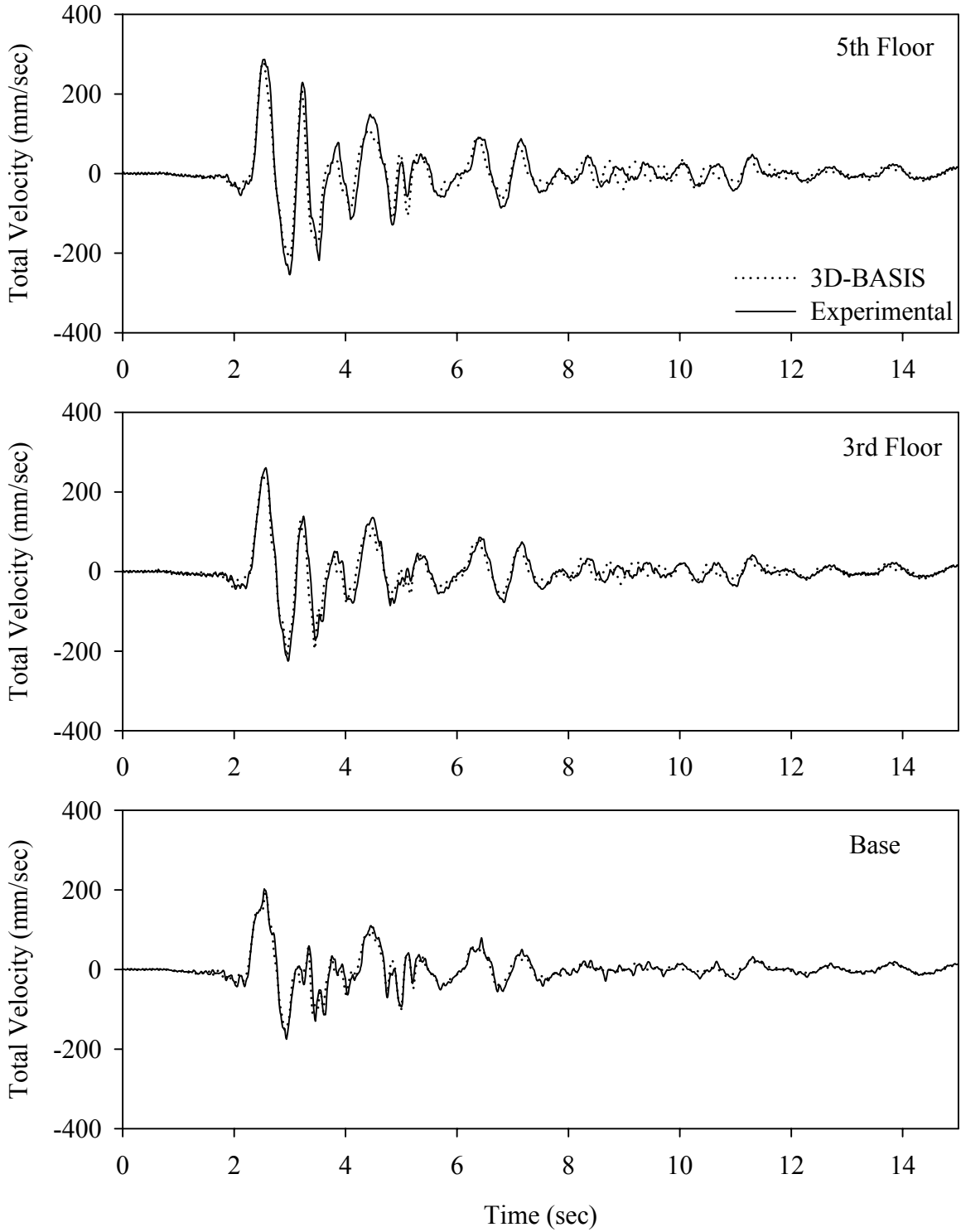
Test LDMNN50.1, Newhall 360 50%, MF/Low Damping Elastomeric with Nonlinear Dampers



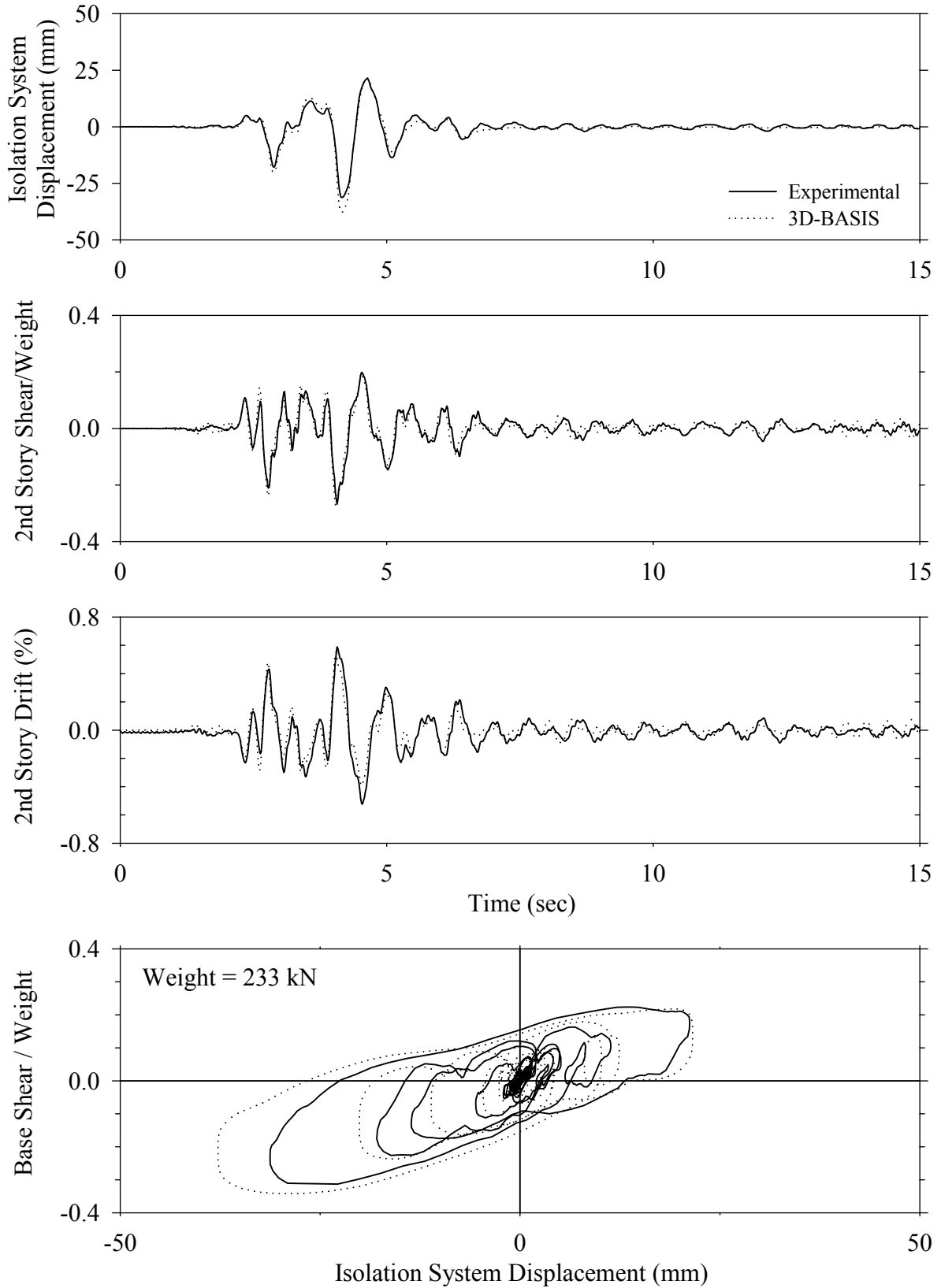
Test LDMNN50.1, Newhall 360 50%, MF/Low Damping Elastomeric with Nonlinear Dampers



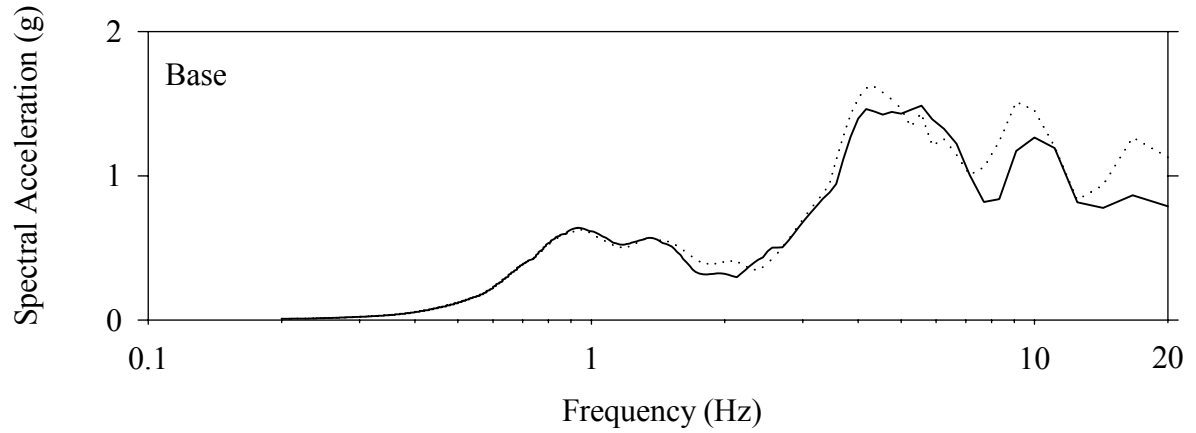
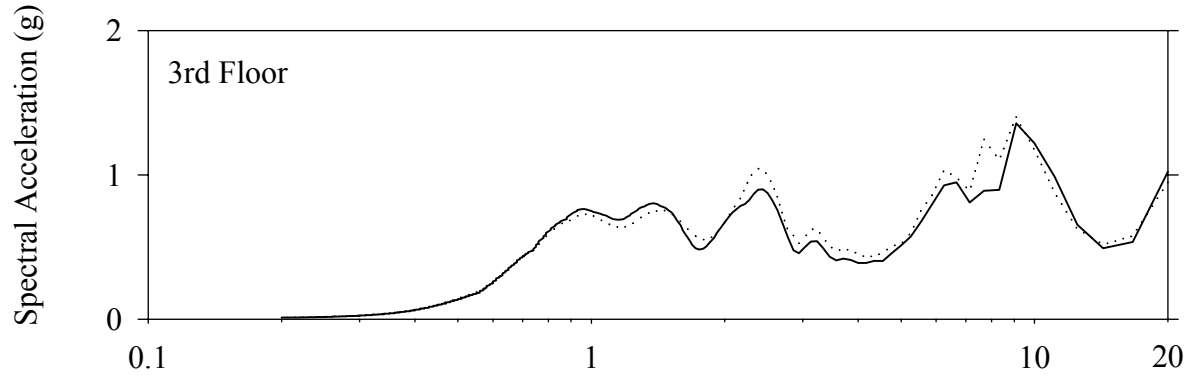
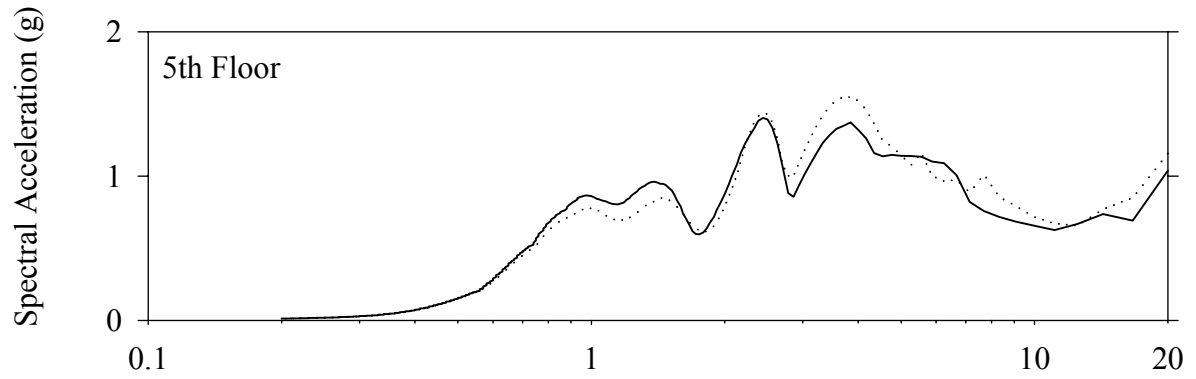
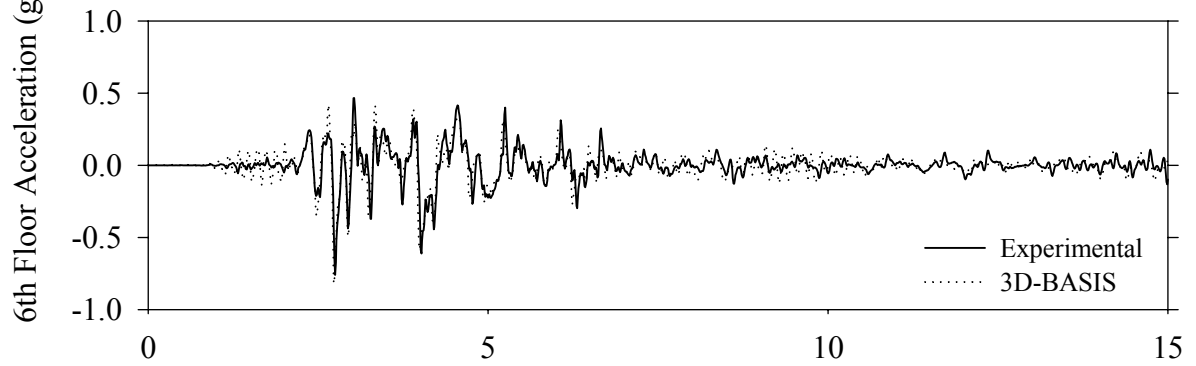
Test LDMNN50.1, Newhall 360 50%, MF/Low Damping Elastomeric with Nonlinear Dampers



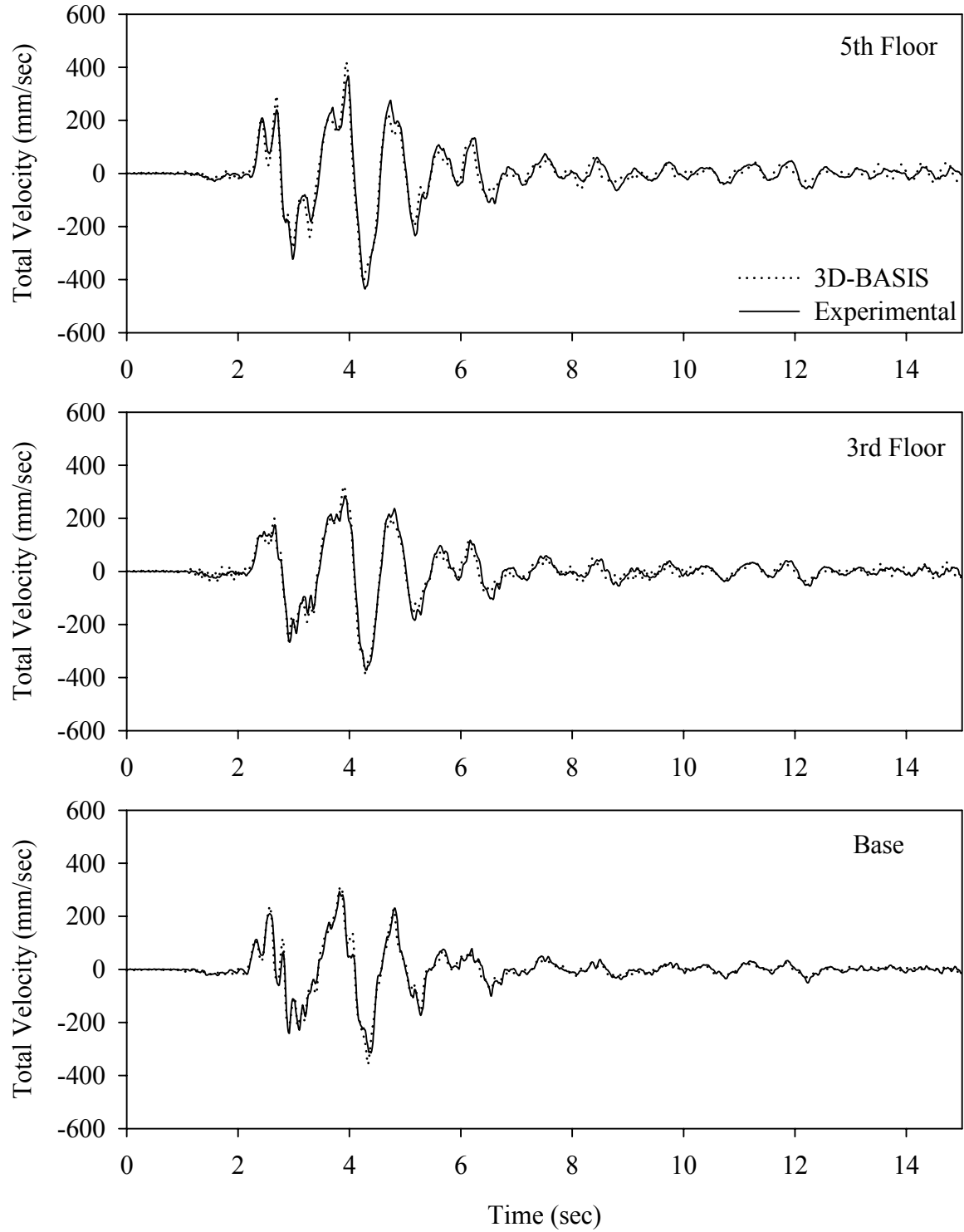
Test LDMNS10.1, Sylmar 100%, MF/Low Damping Elastomeric with Nonlinear Dampers



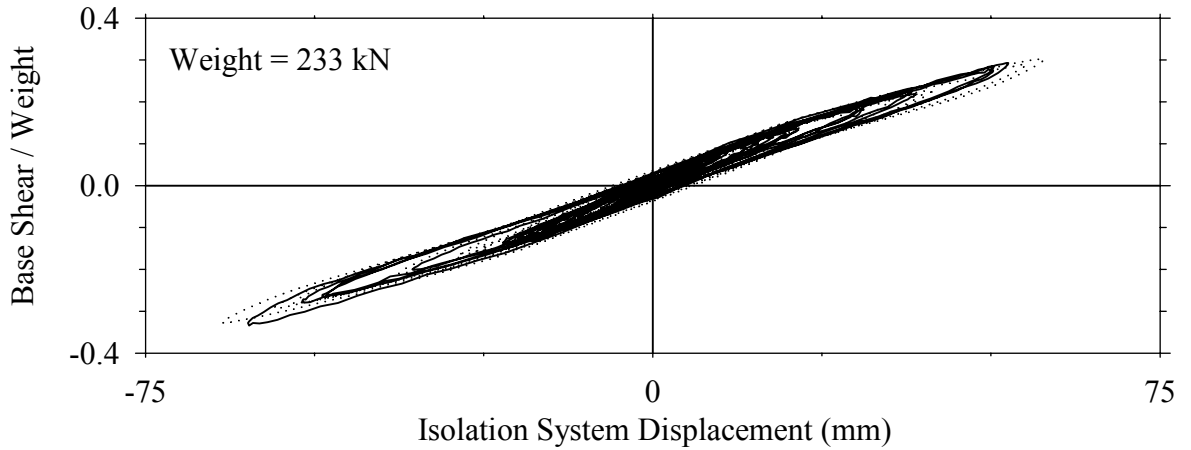
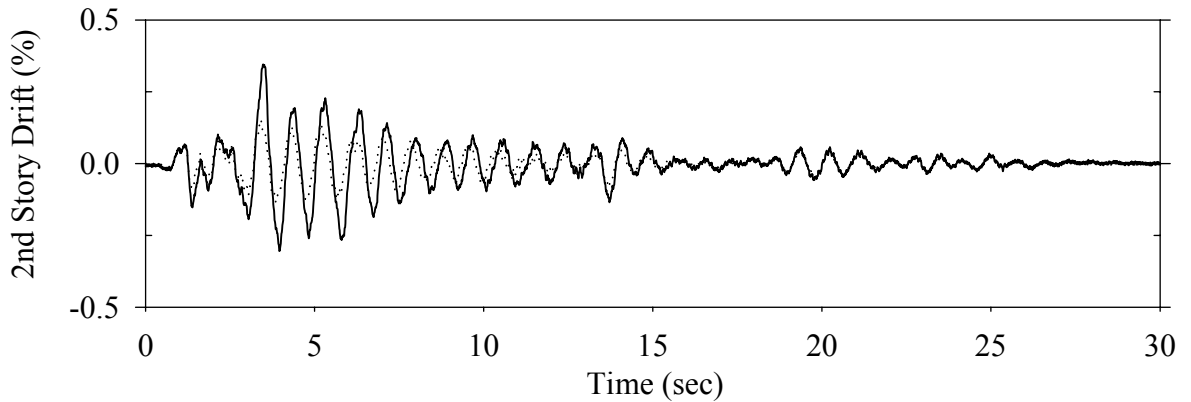
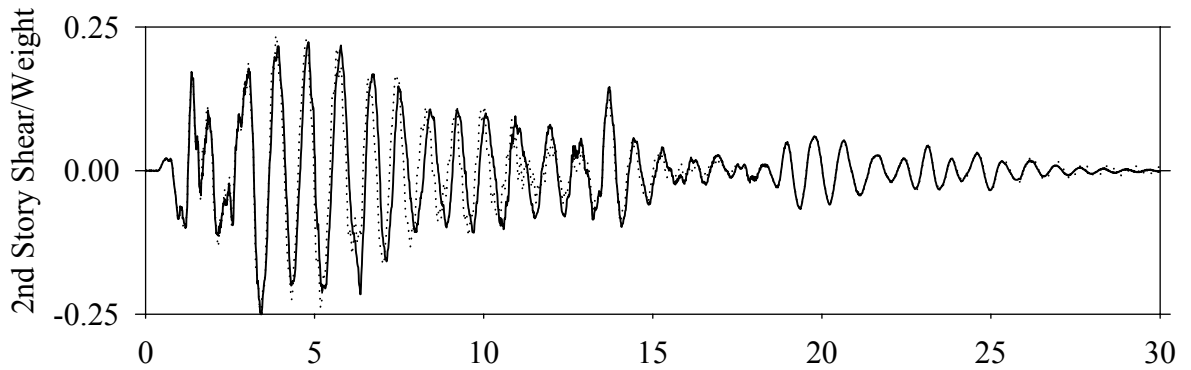
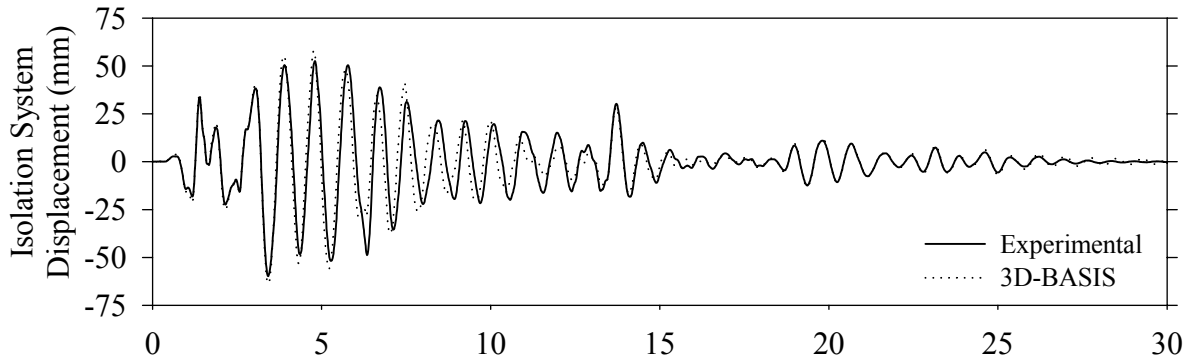
Test LDMNS10.1, Sylmar 100%, MF/Low Damping Elastomeric with Nonlinear Dampers



Test LDMNS10.1, Sylmar 100%, MF/Low Damping Elastomeric with Nonlinear Dampers

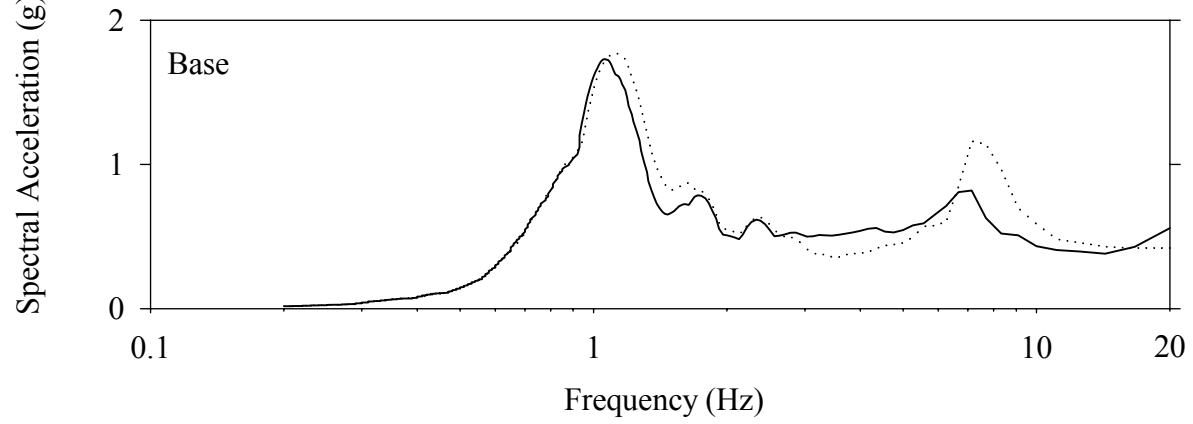
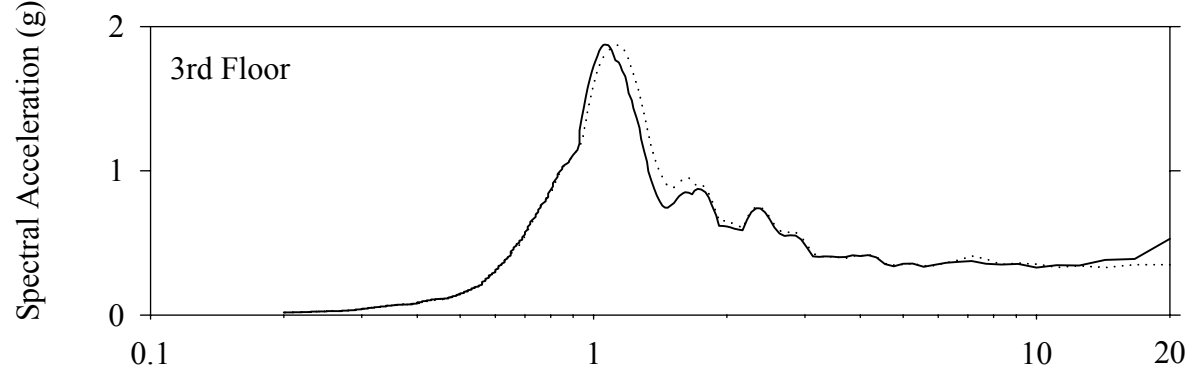
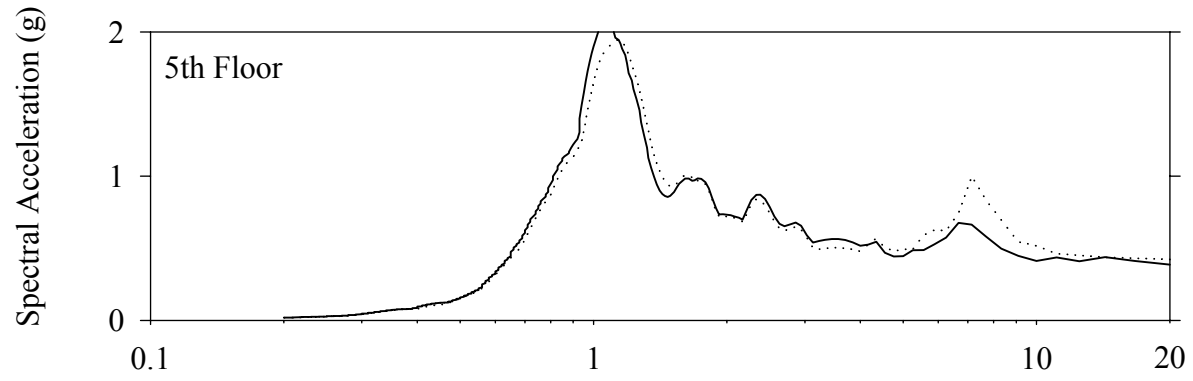
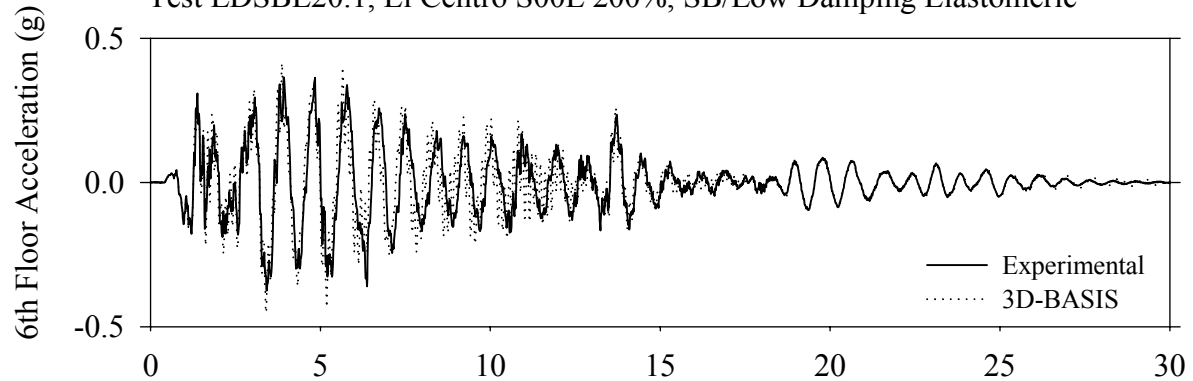


Test LDSBE20.1, El Centro S00E 200%, SB/Low Damping Elastomeric

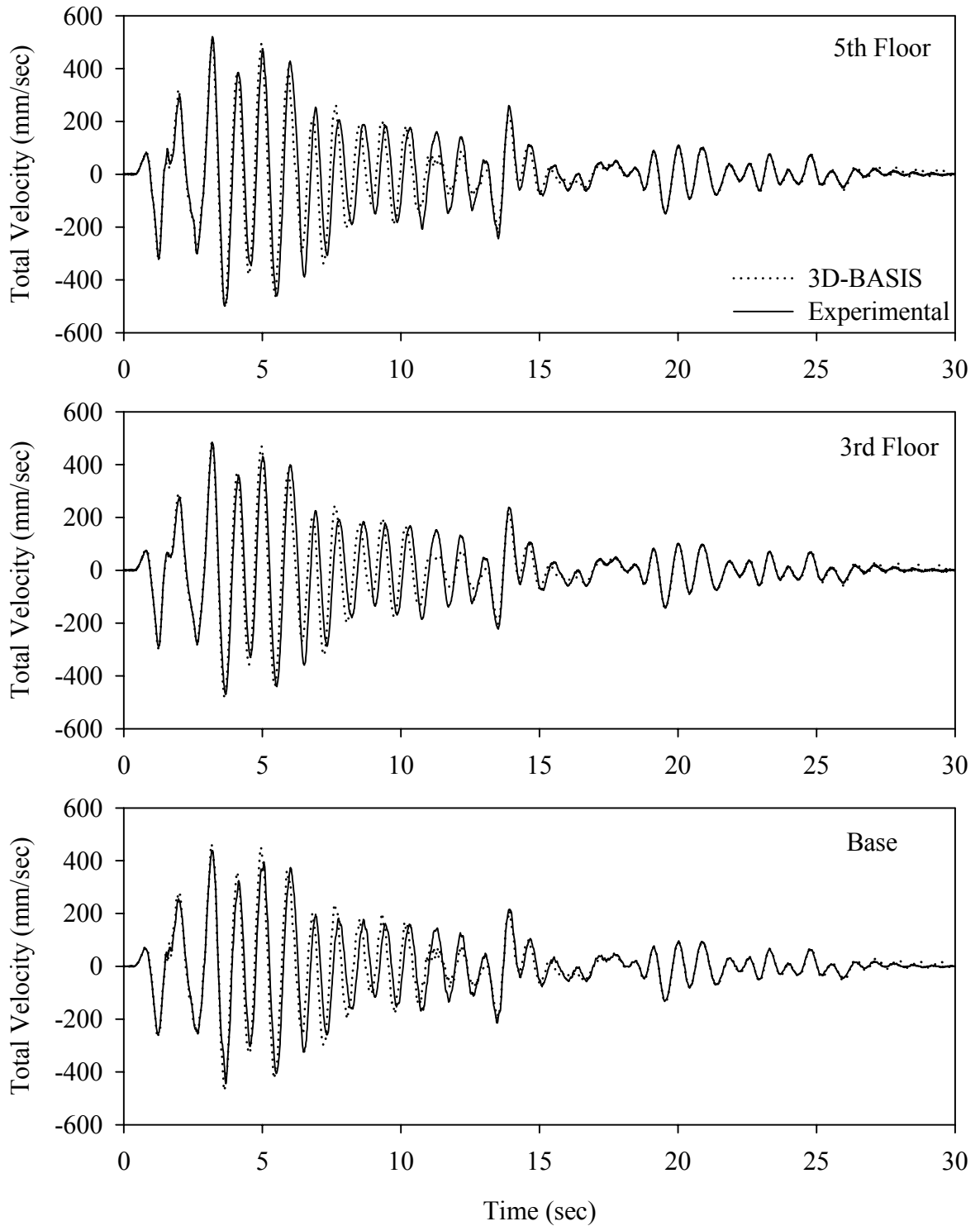




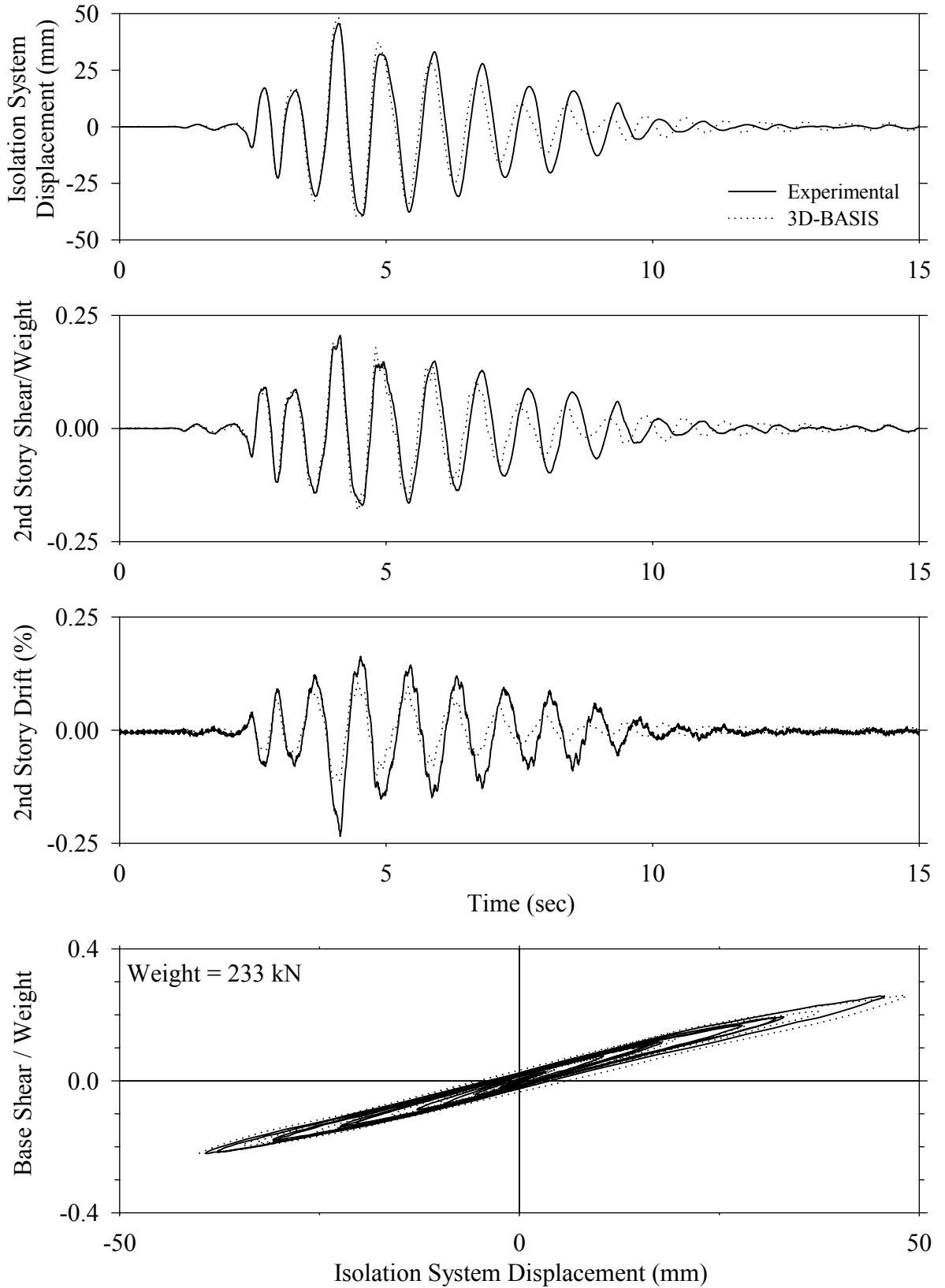
Test LDSBE20.1, El Centro S00E 200%, SB/Low Damping Elastomeric



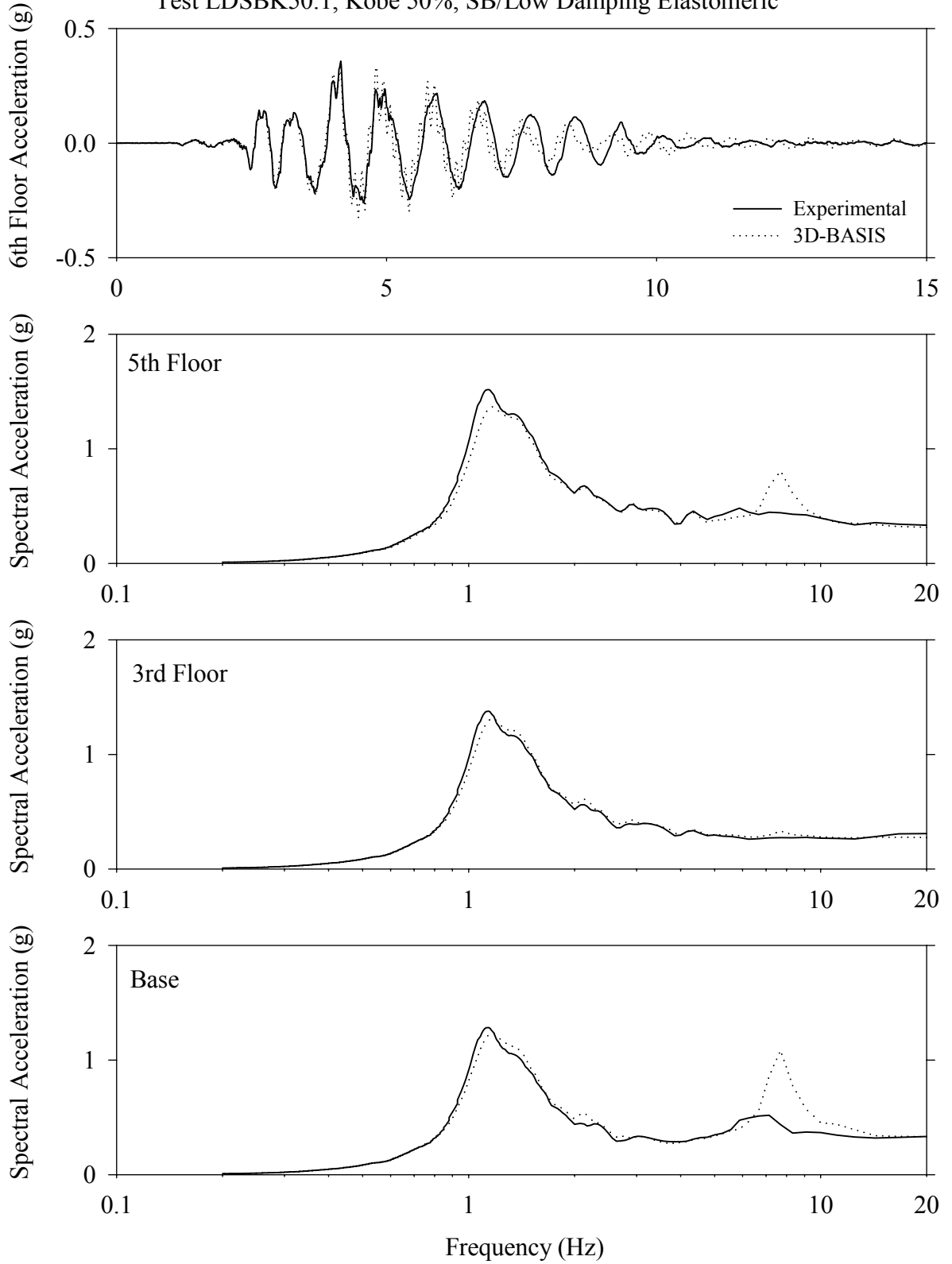
Test LDSBE20.1, El Centro S00E 200%, SB/Low Damping Elastomeric



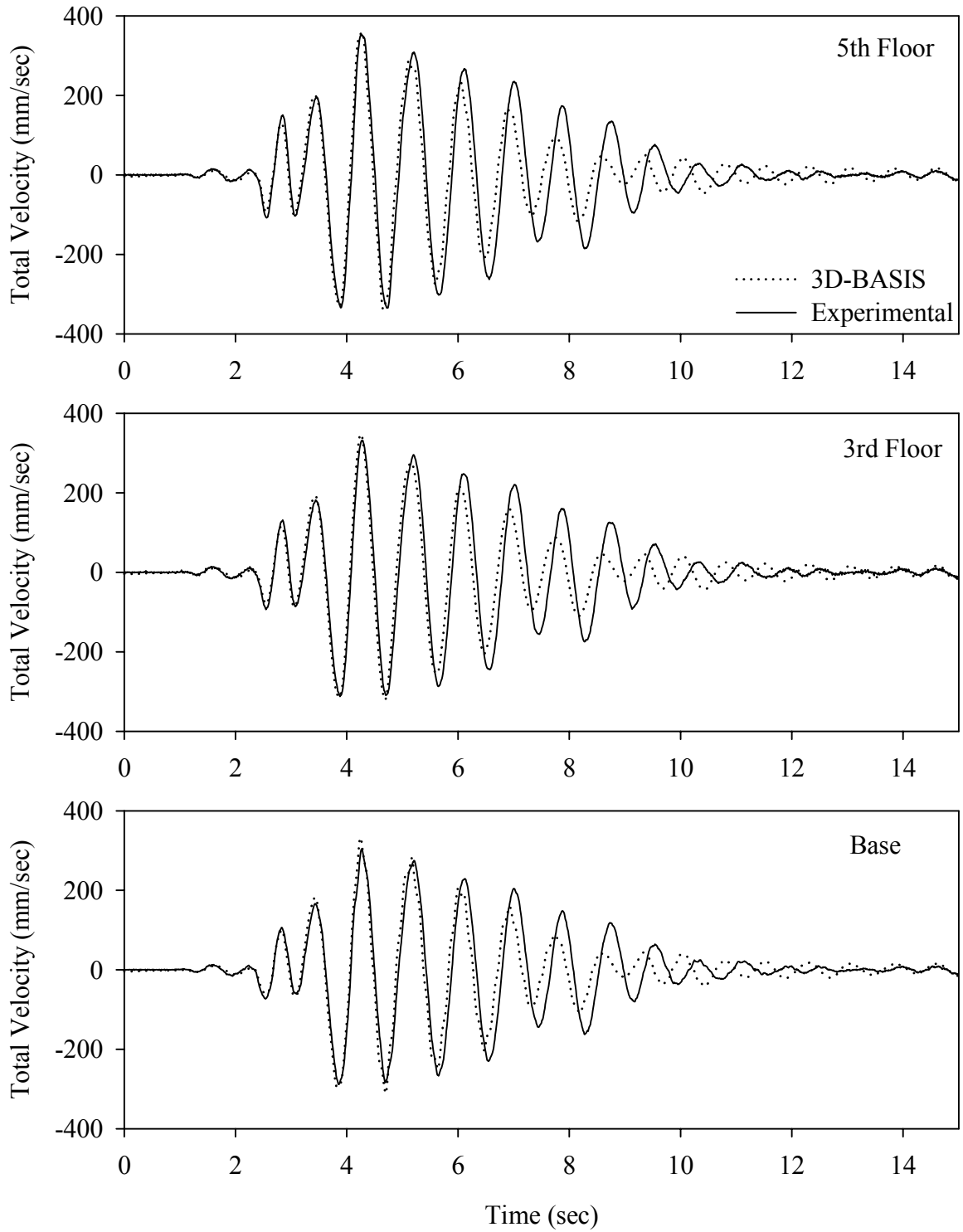
Test LDSBK50.1, Kobe 50%, SB/Low Damping Elastomeric



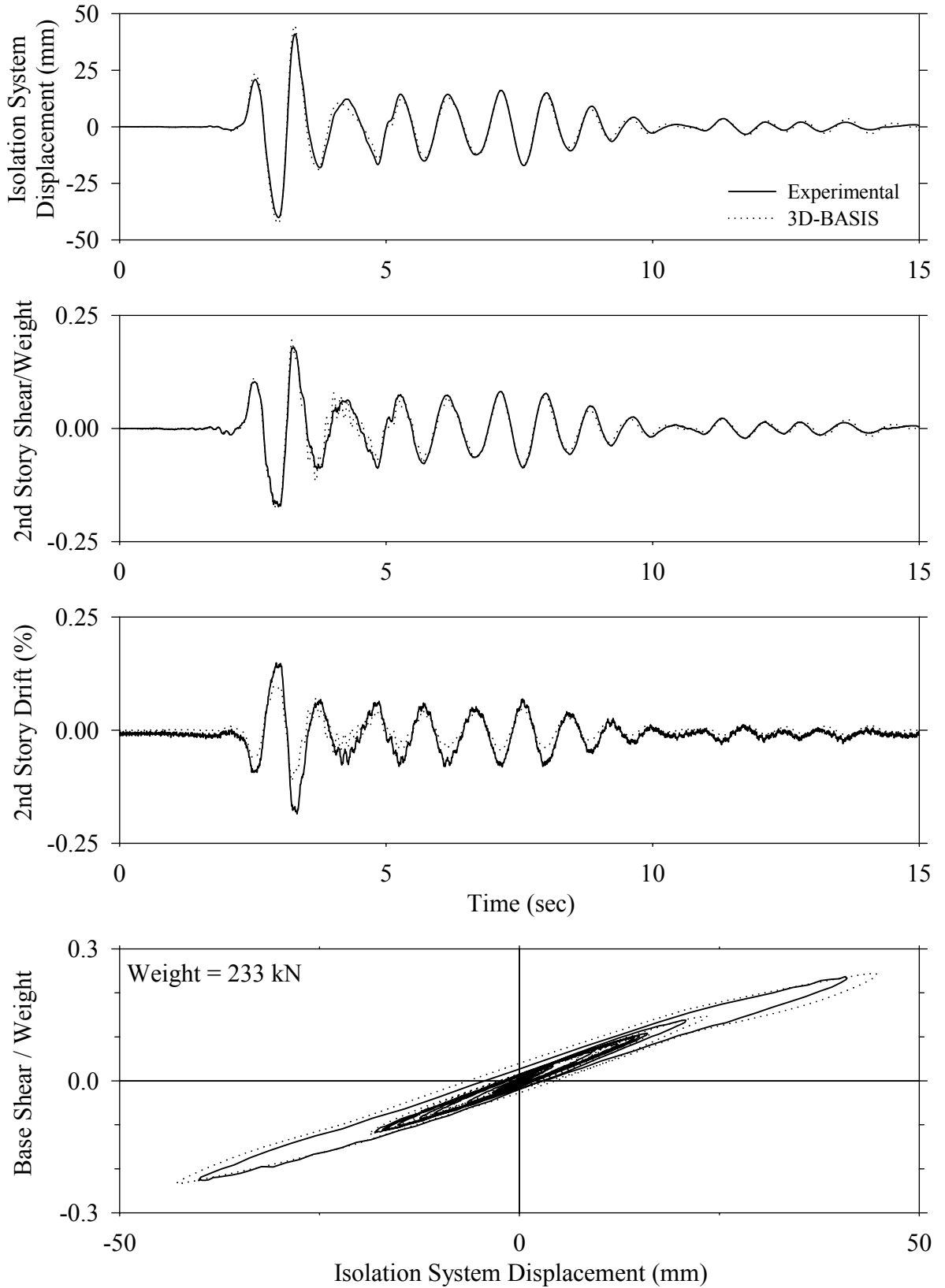
Test LDSBK50.1, Kobe 50%, SB/Low Damping Elastomeric



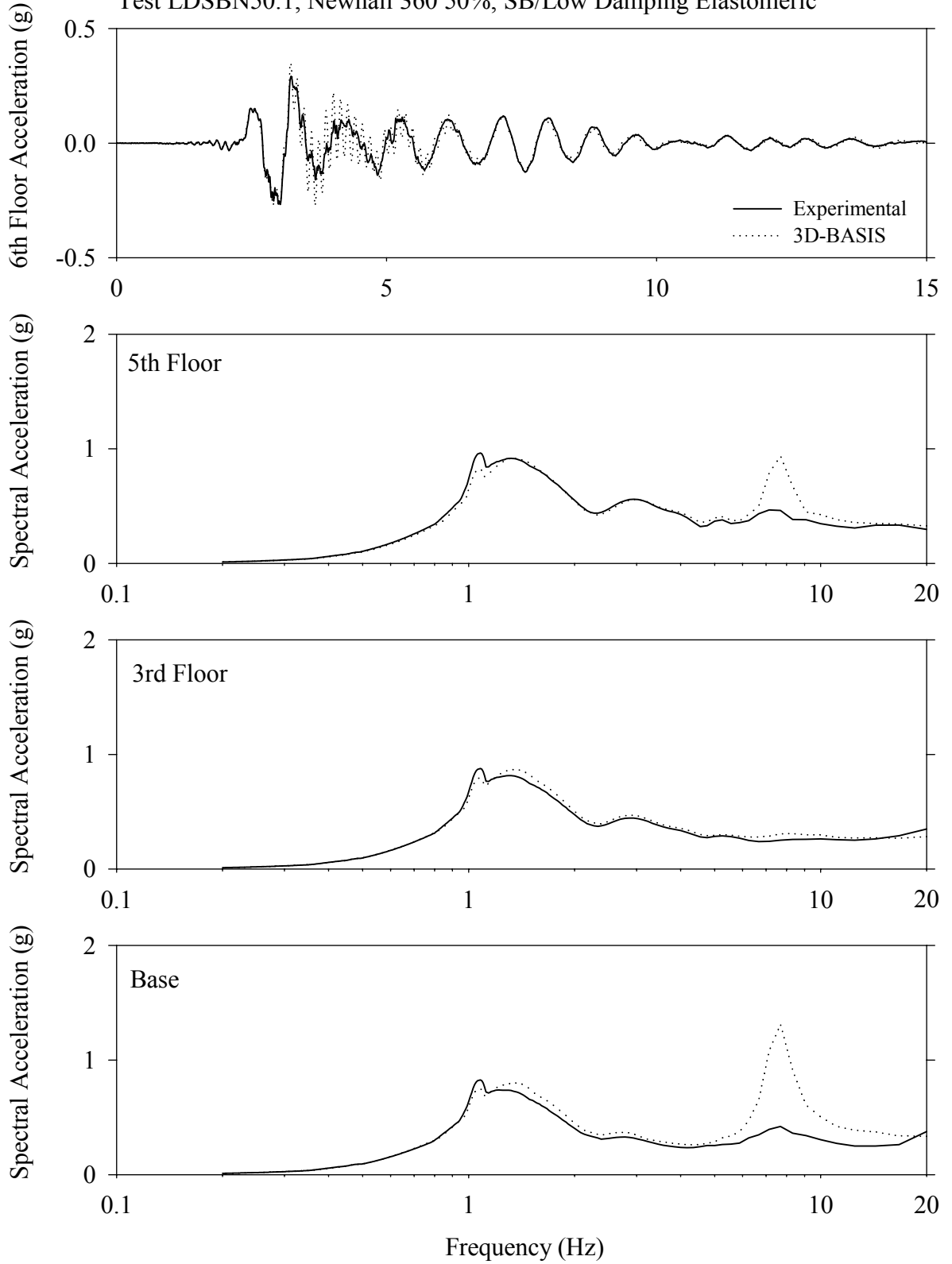
Test LDSBK50.1, Kobe 50%, SB/Low Damping Elastomeric



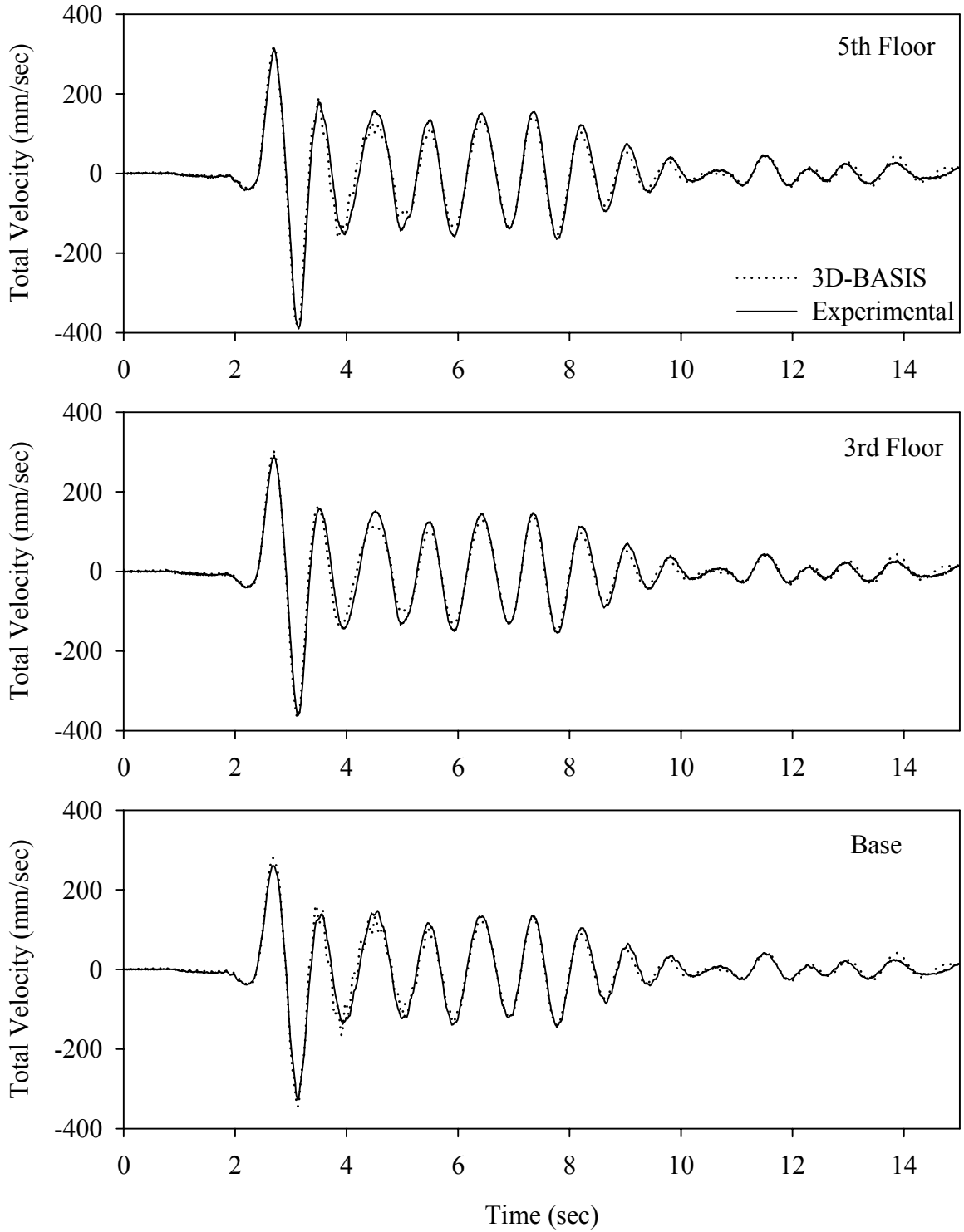
Test LDSBN50.1, Newhall 360 50%, SB/Low Damping Elastomeric



Test LDSBN50.1, Newhall 360 50%, SB/Low Damping Elastomeric

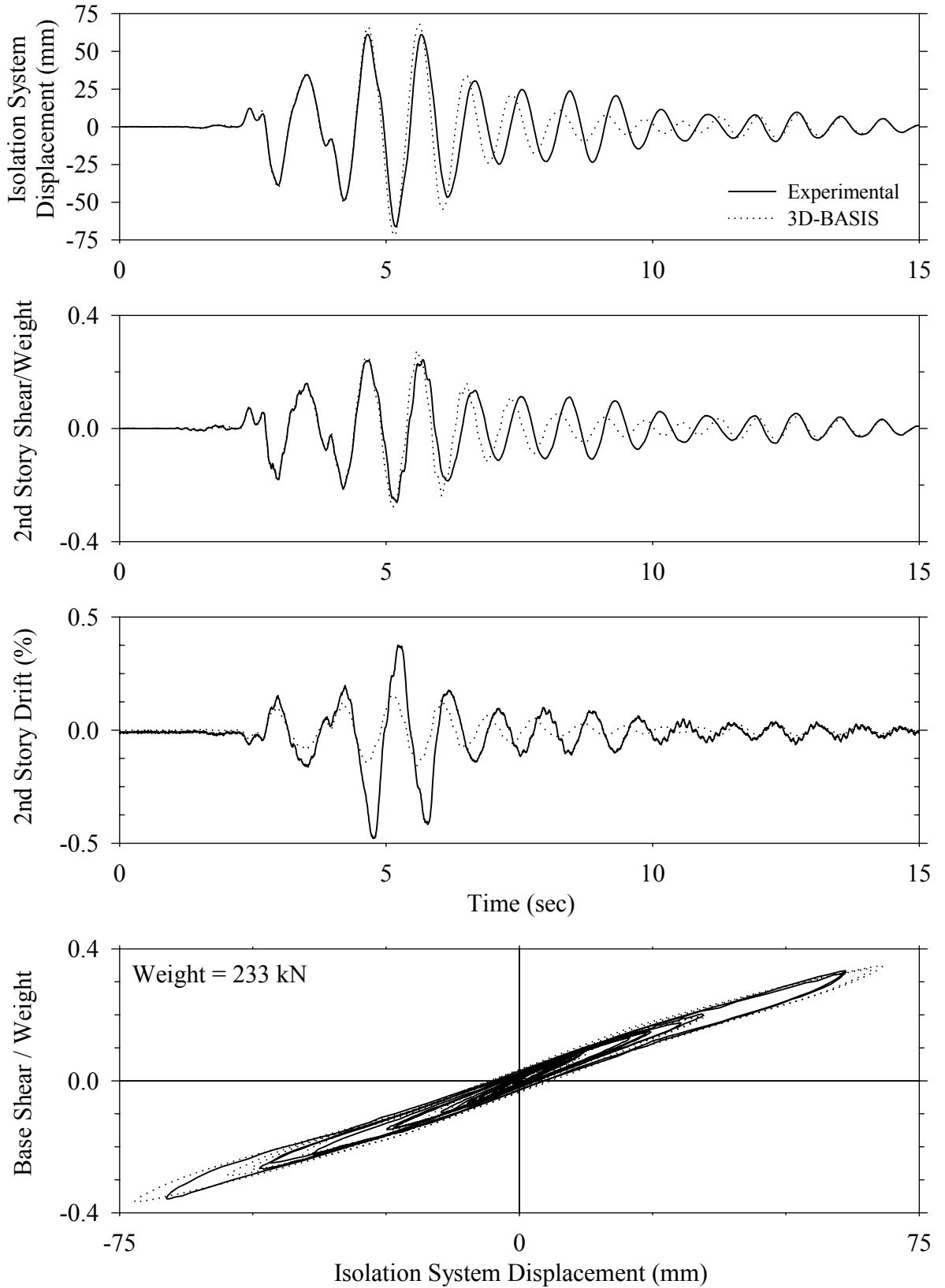


Test LDSBN50.1, Newhall 360 50%, SB/Low Damping Elastomeric

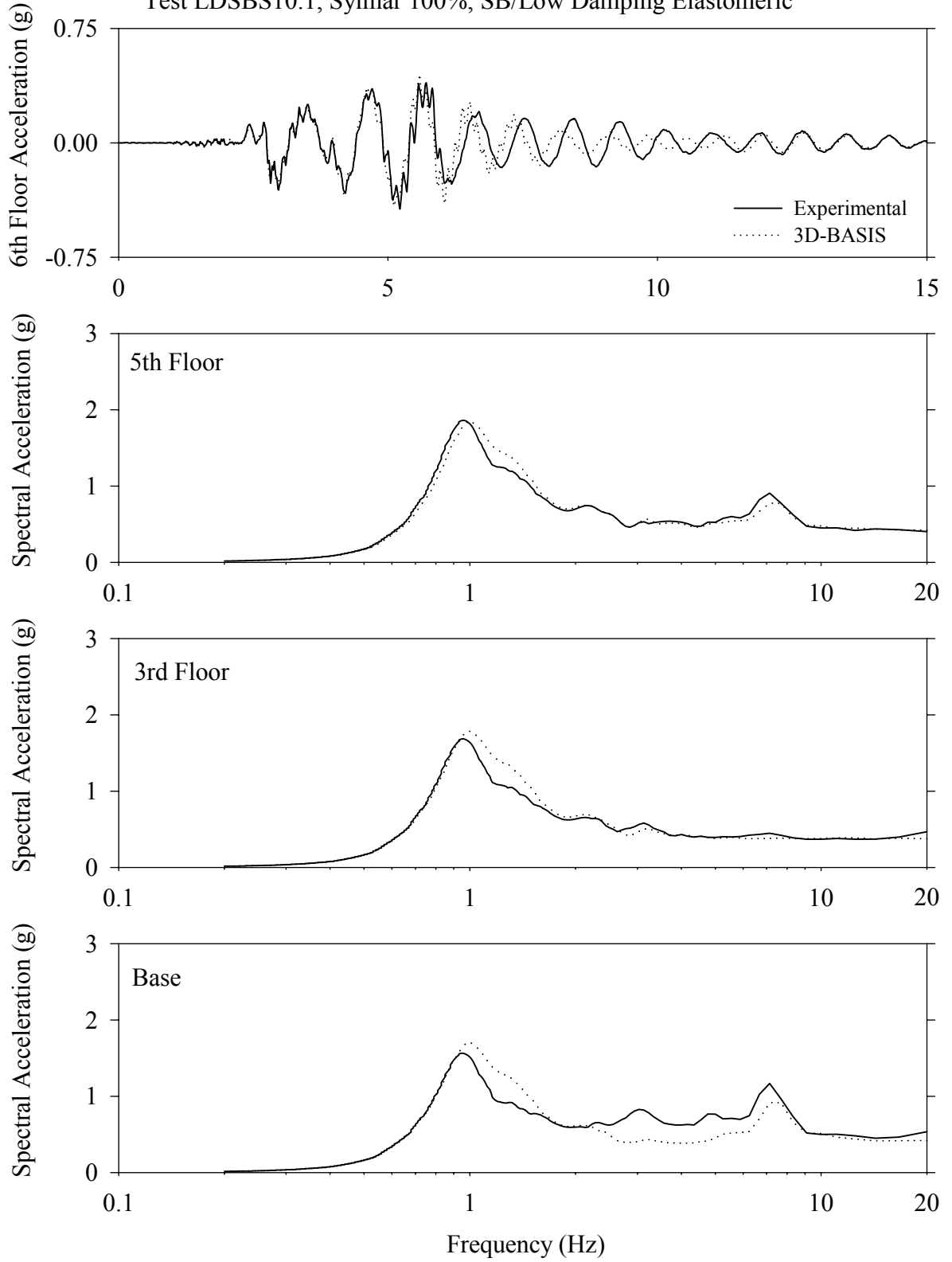




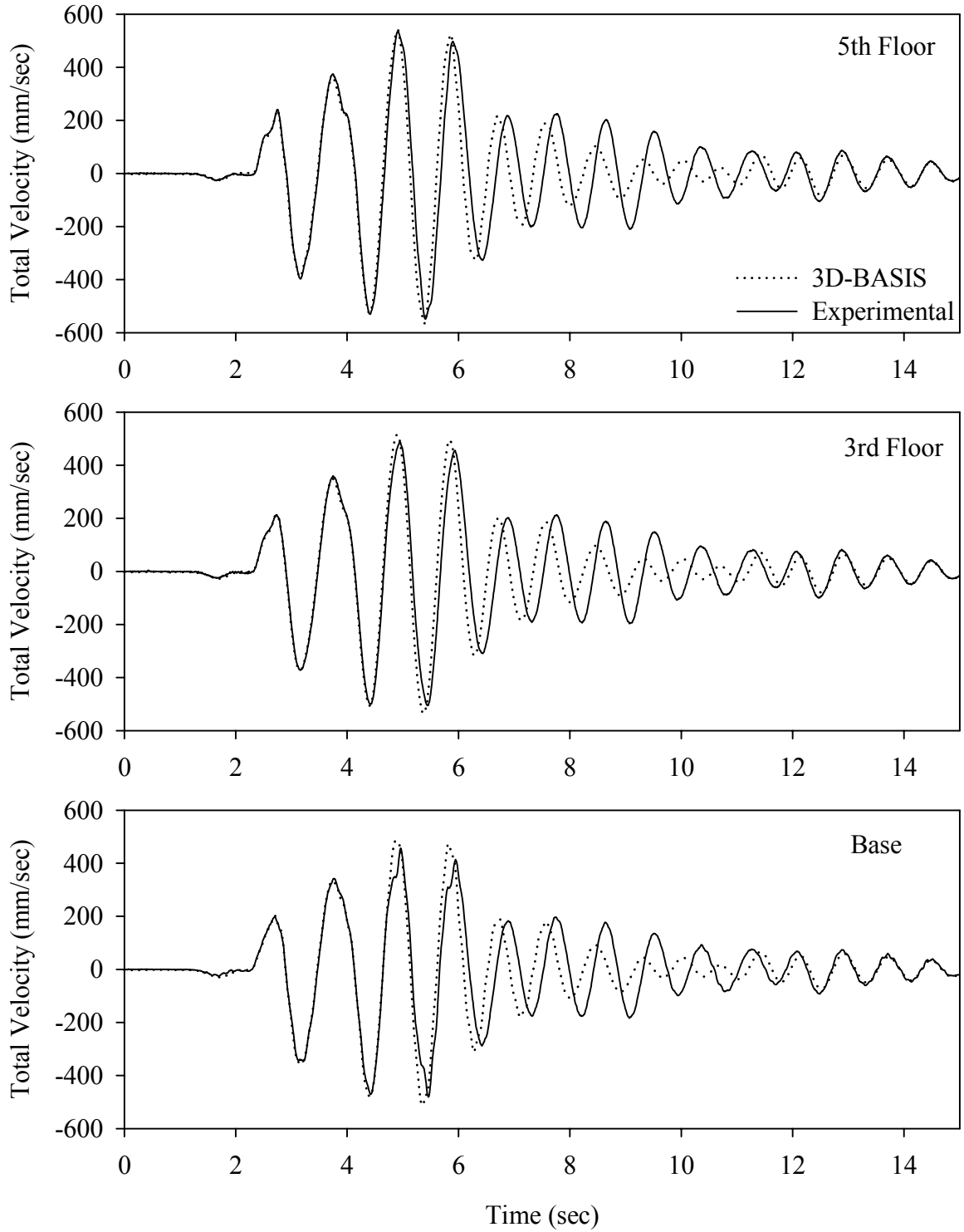
Test LDSBS10.1, Sylmar 100%, SB/Low Damping Elastomeric



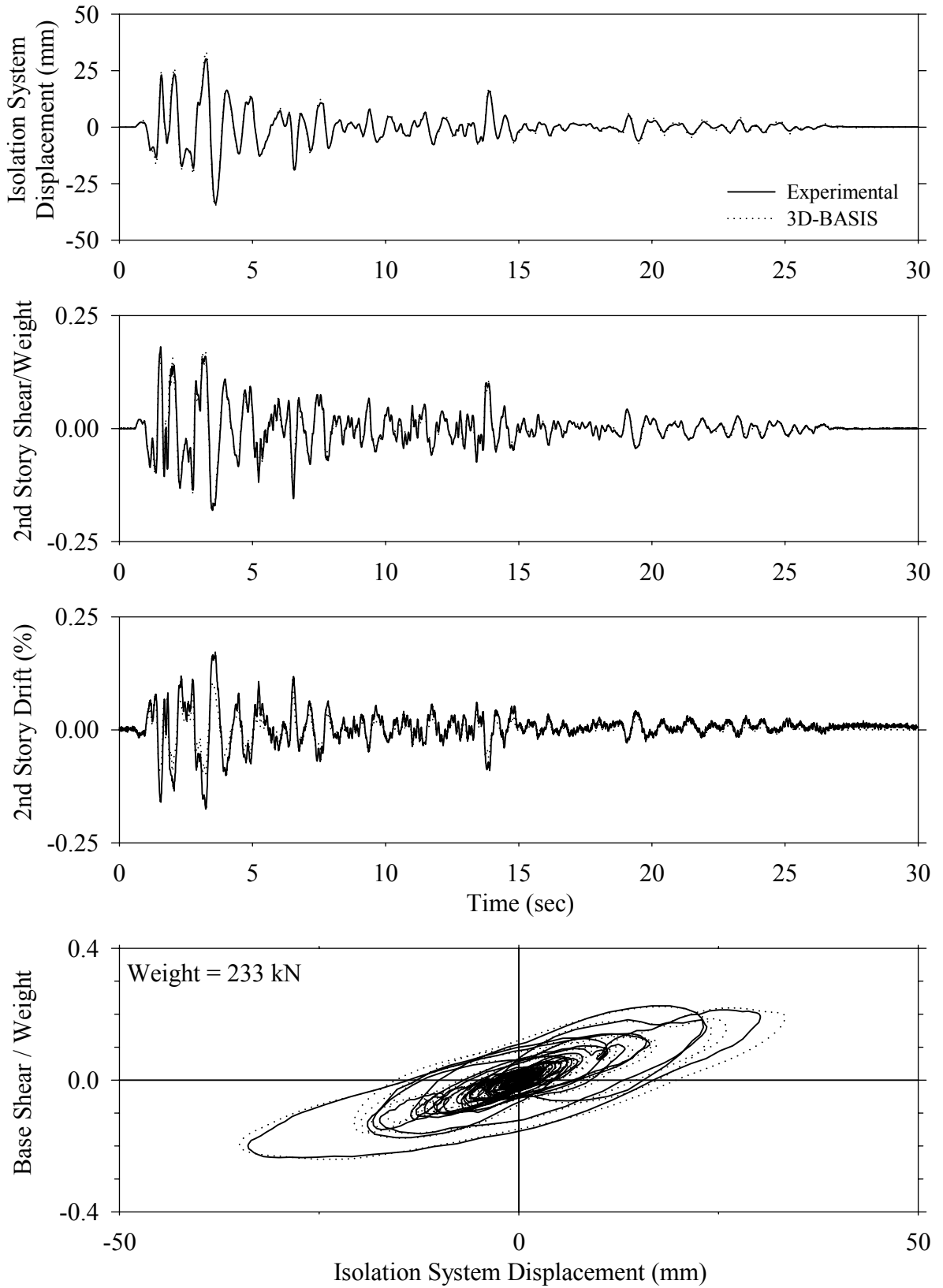
Test LDSBS10.1, Sylmar 100%, SB/Low Damping Elastomeric



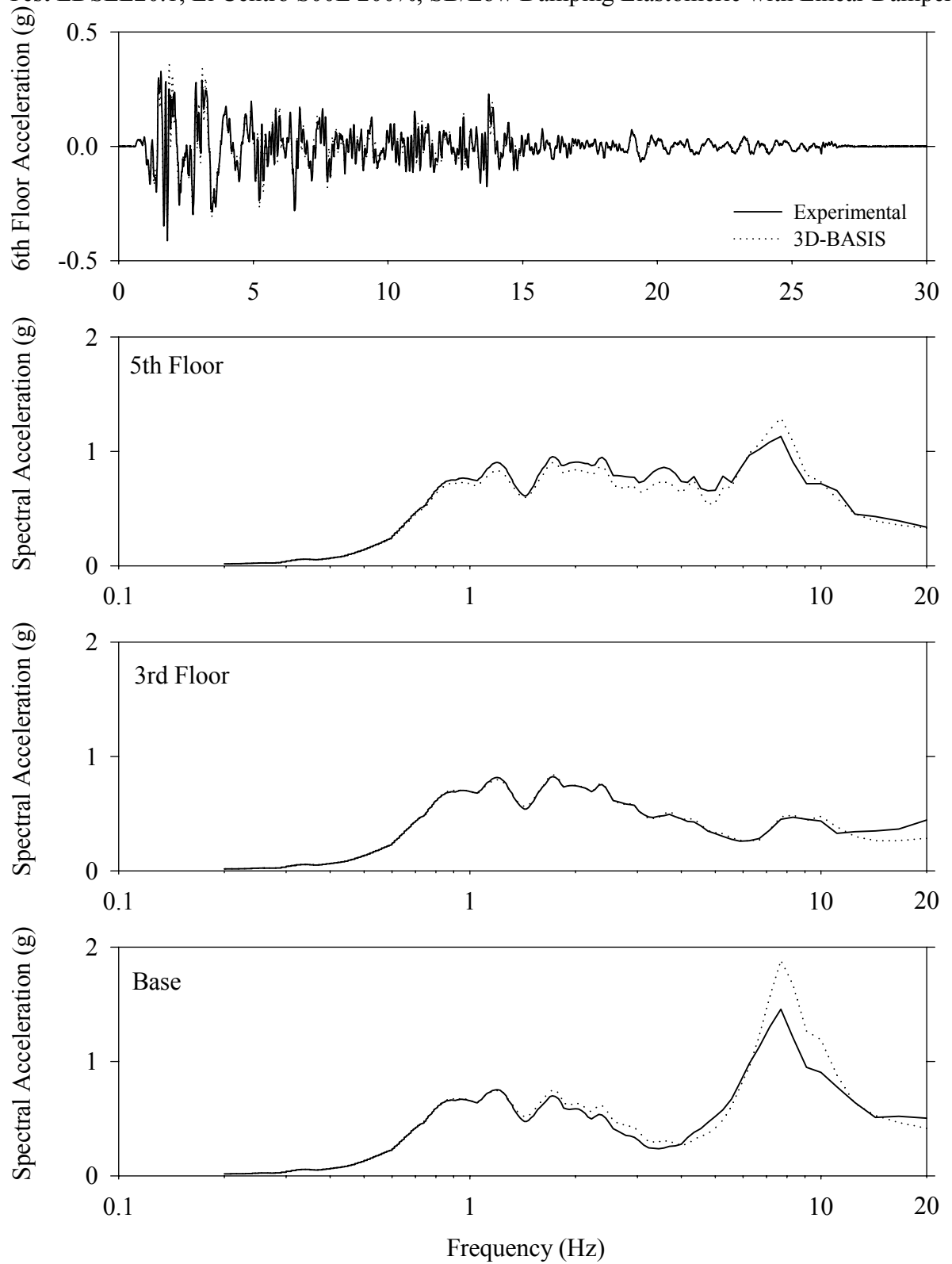
Test LDSBS10.1, Sylmar 100%, SB/Low Damping Elastomeric



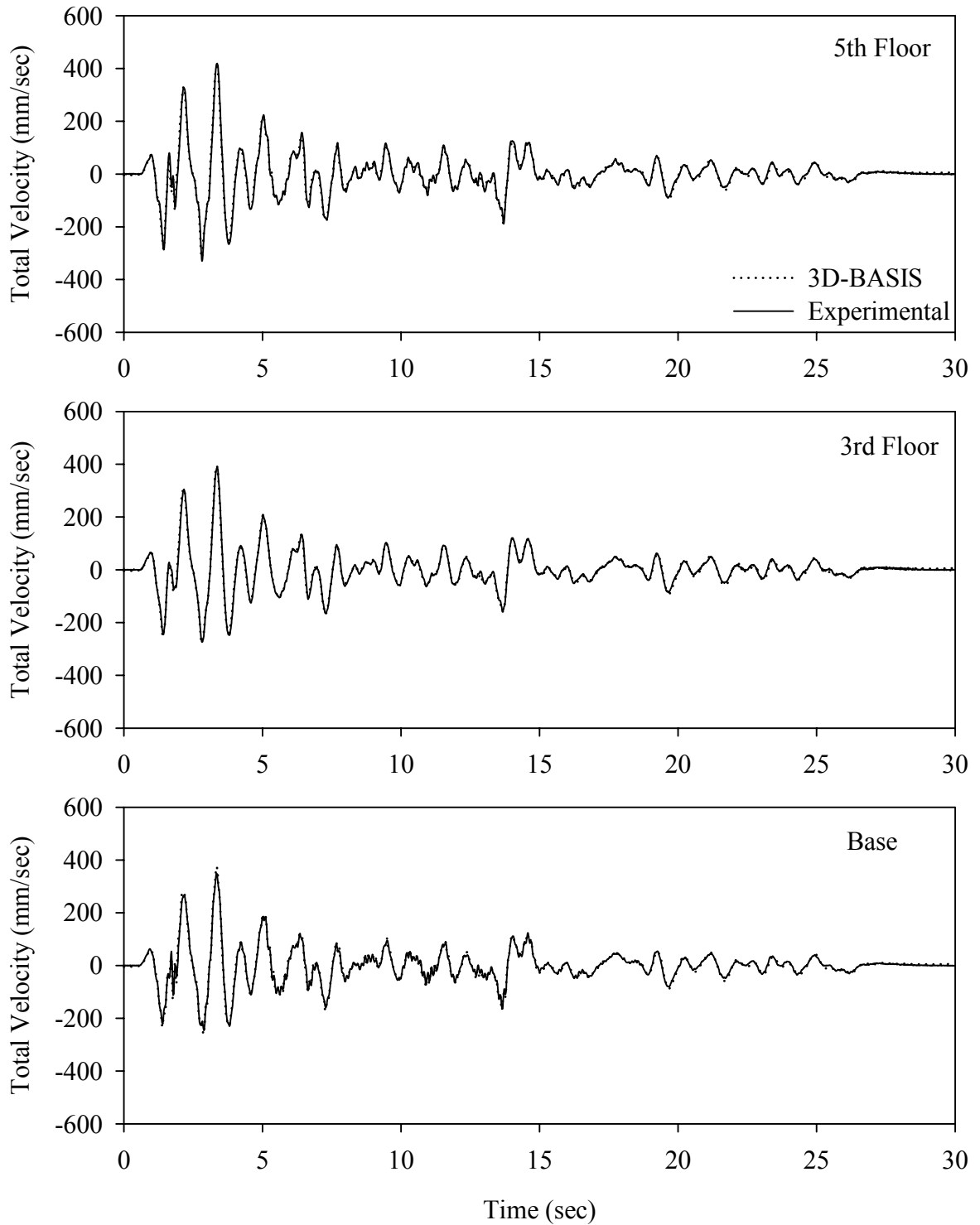
Test LDSLE20.1, El Centro S00E 200%, SB/Low Damping Elastomeric with Linear Dampers



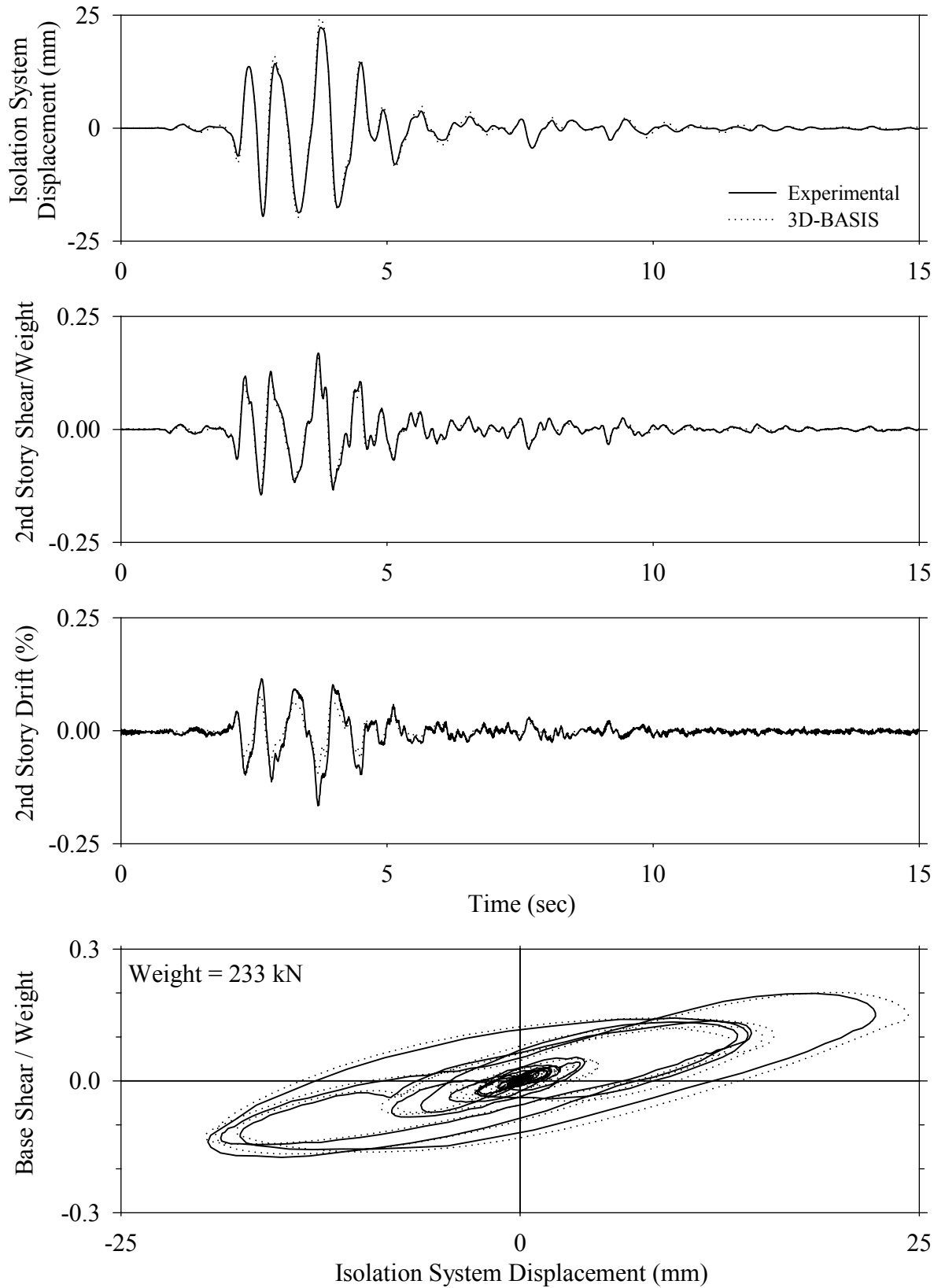
Test LDSLE20.1, El Centro S00E 200%, SB/Low Damping Elastomeric with Linear Dampers



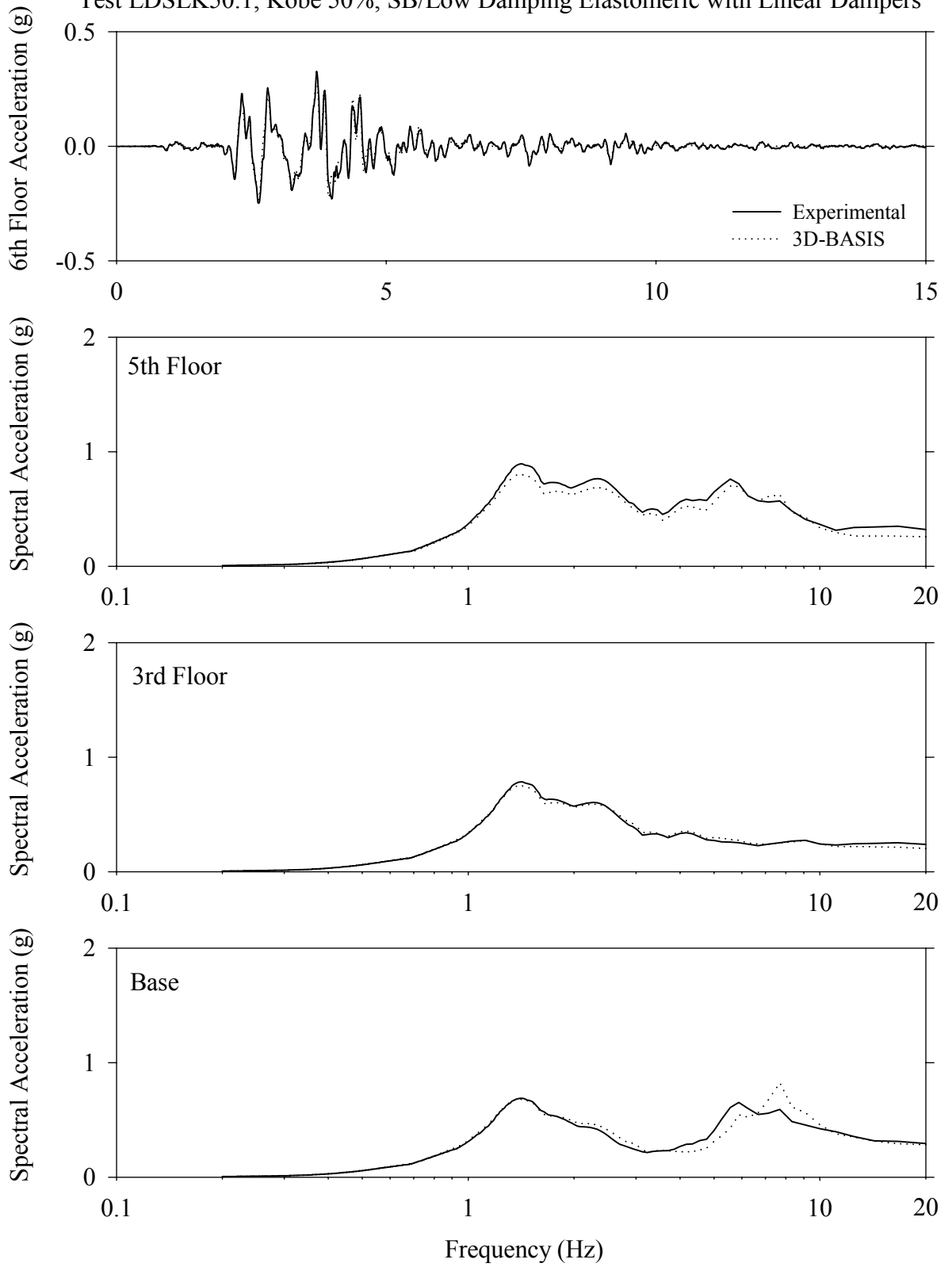
Test LDSLE20.1, El Centro S00E 200%, SB/Low Damping Elastomeric with Linear Dampers



Test LDSLK50.1, Kobe 50%, SB/Low Damping Elastomeric with Linear Dampers

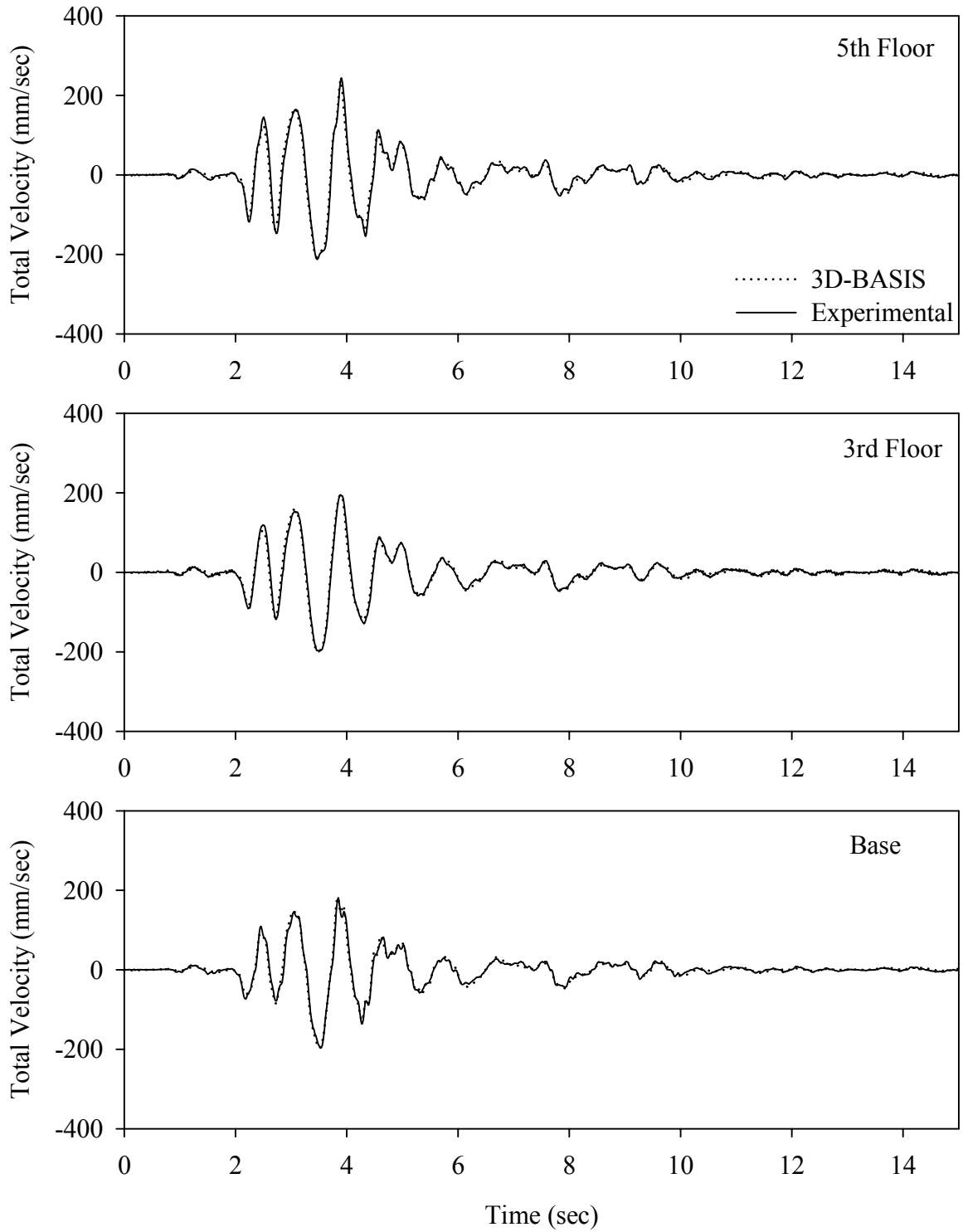


Test LDSLK50.1, Kobe 50%, SB/Low Damping Elastomeric with Linear Dampers

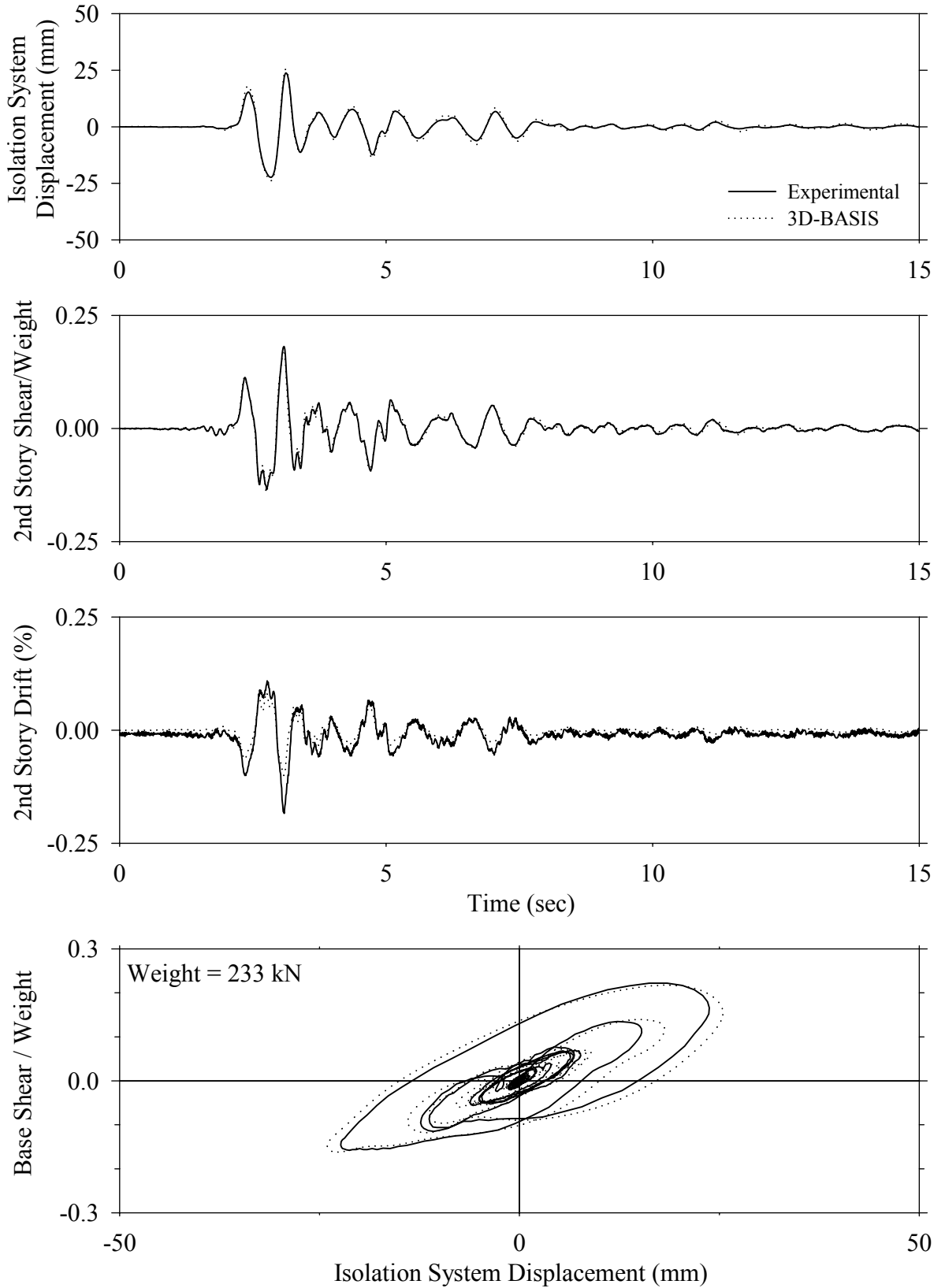




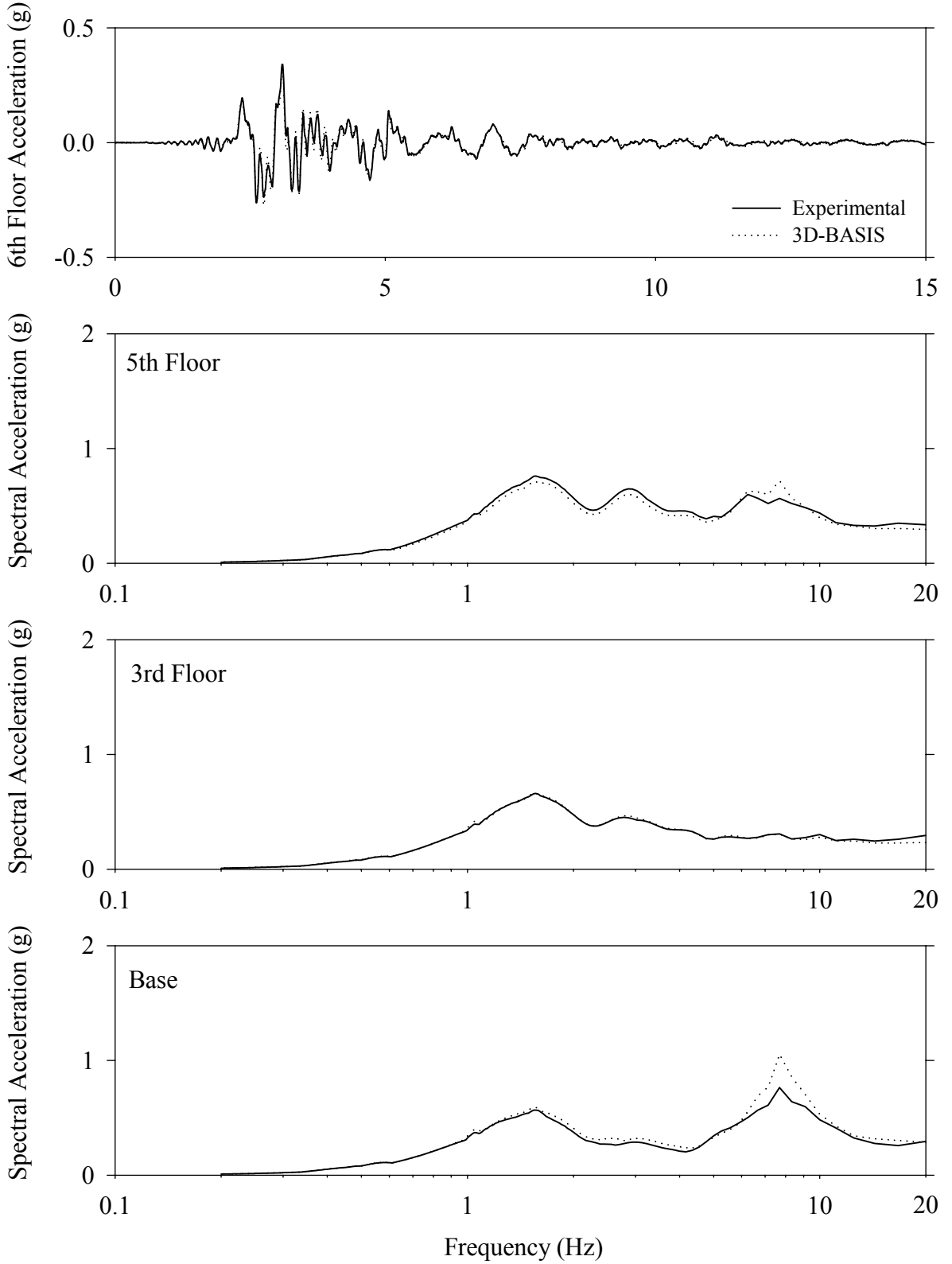
Test LDSLK50.1, Kobe 50%, SB/Low Damping Elastomeric with Linear Dampers



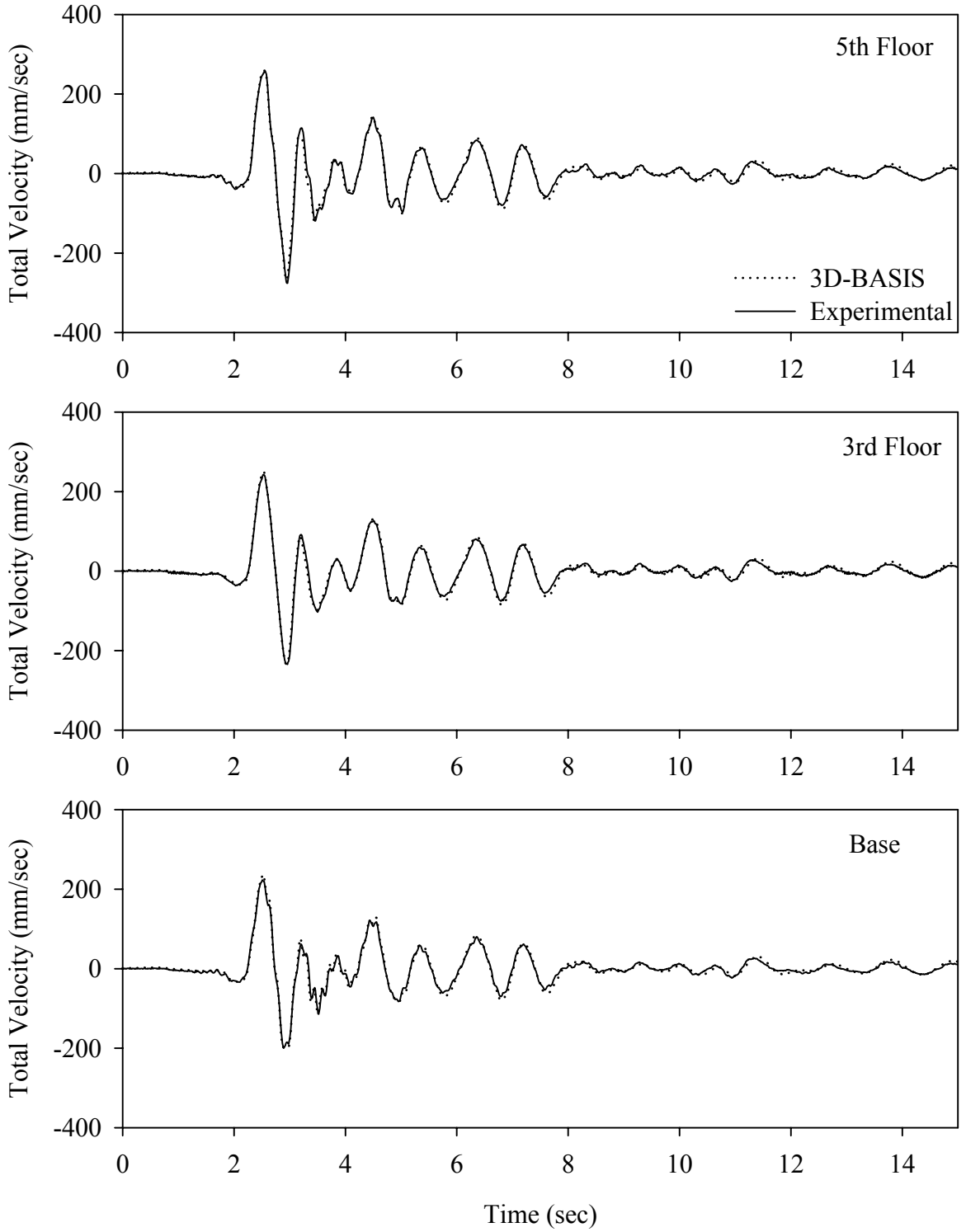
Test LDSLN50.1, Newhall 360 50%, SB/Low Damping Elastomeric with Linear Dampers



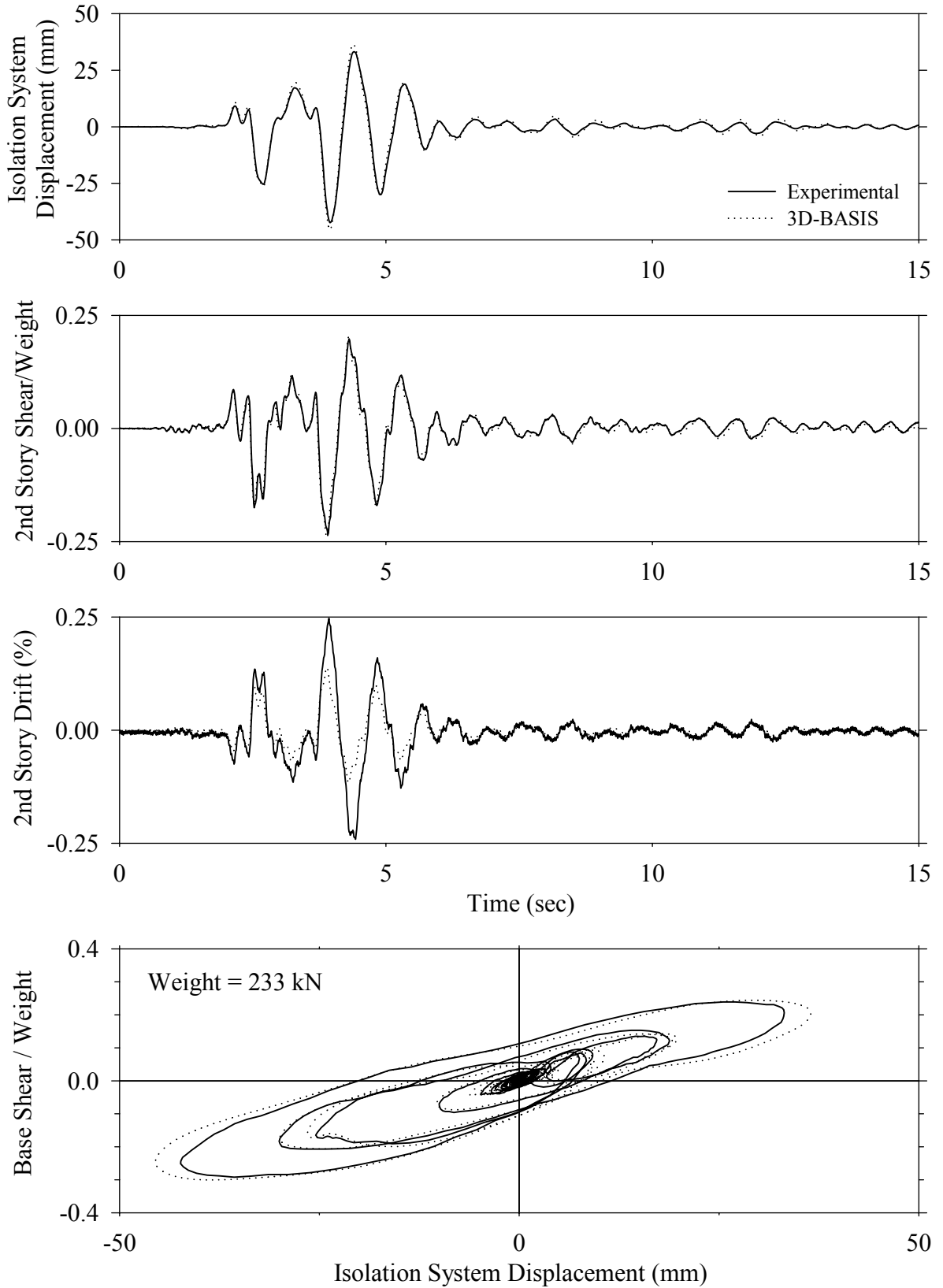
Test LDSLN50.1, Newhall 360 50%, SB/Low Damping Elastomeric with Linear Dampers



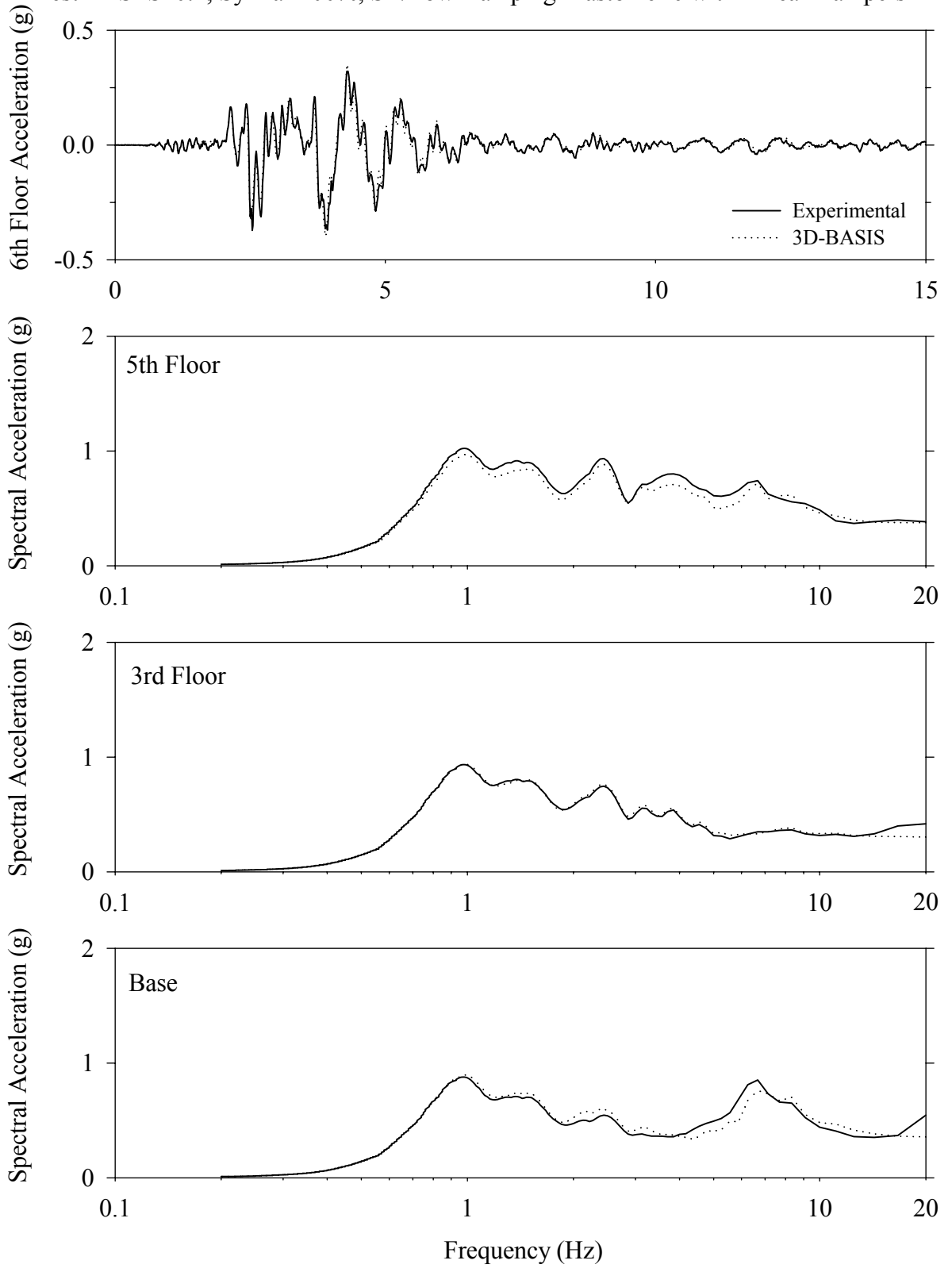
Test LDSLN50.1, Newhall 360 50%, SB/Low Damping Elastomeric with Linear Dampers



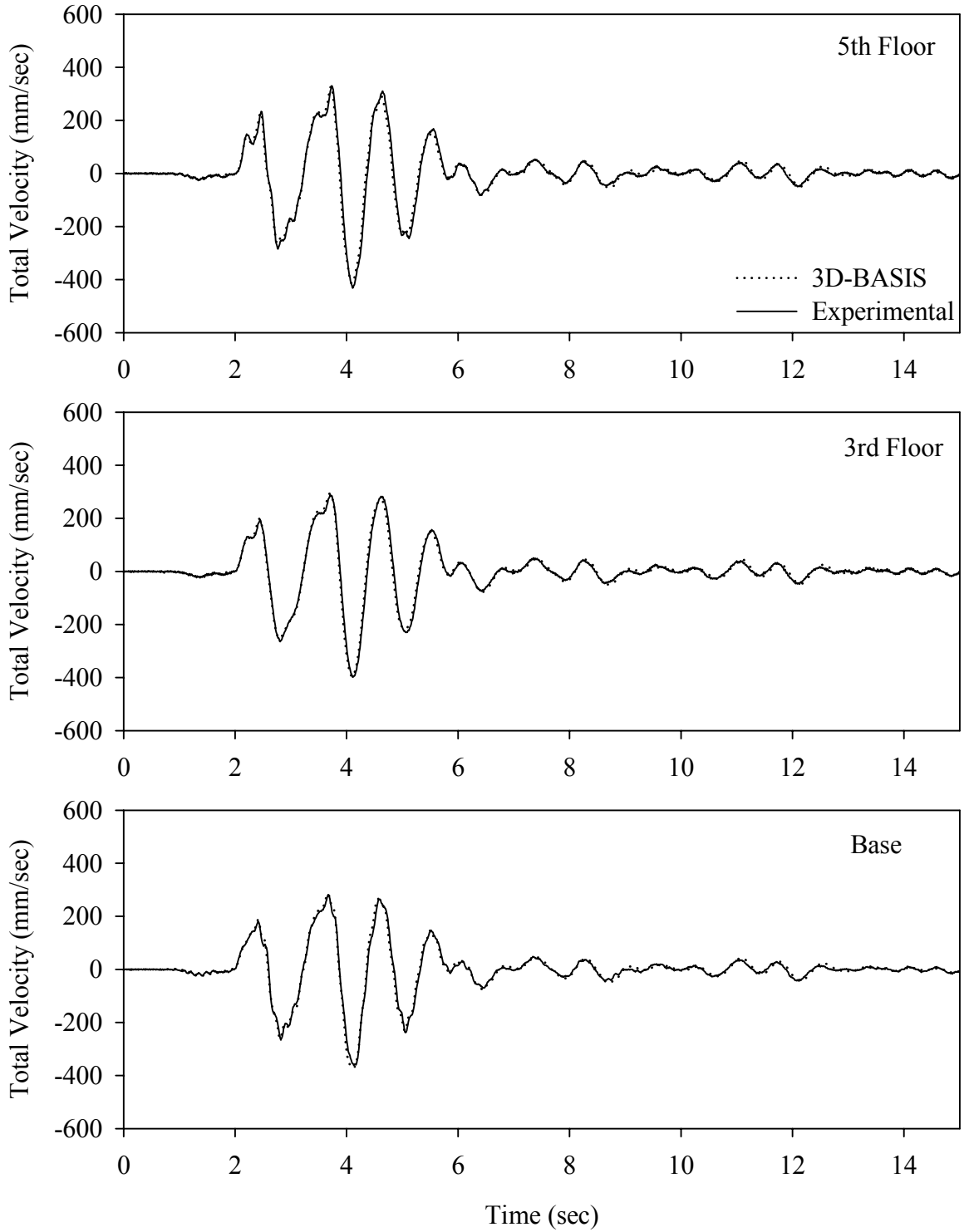
Test LDSLS10.1, Sylmar 100%, SB/Low Damping Elastomeric with Linear Dampers



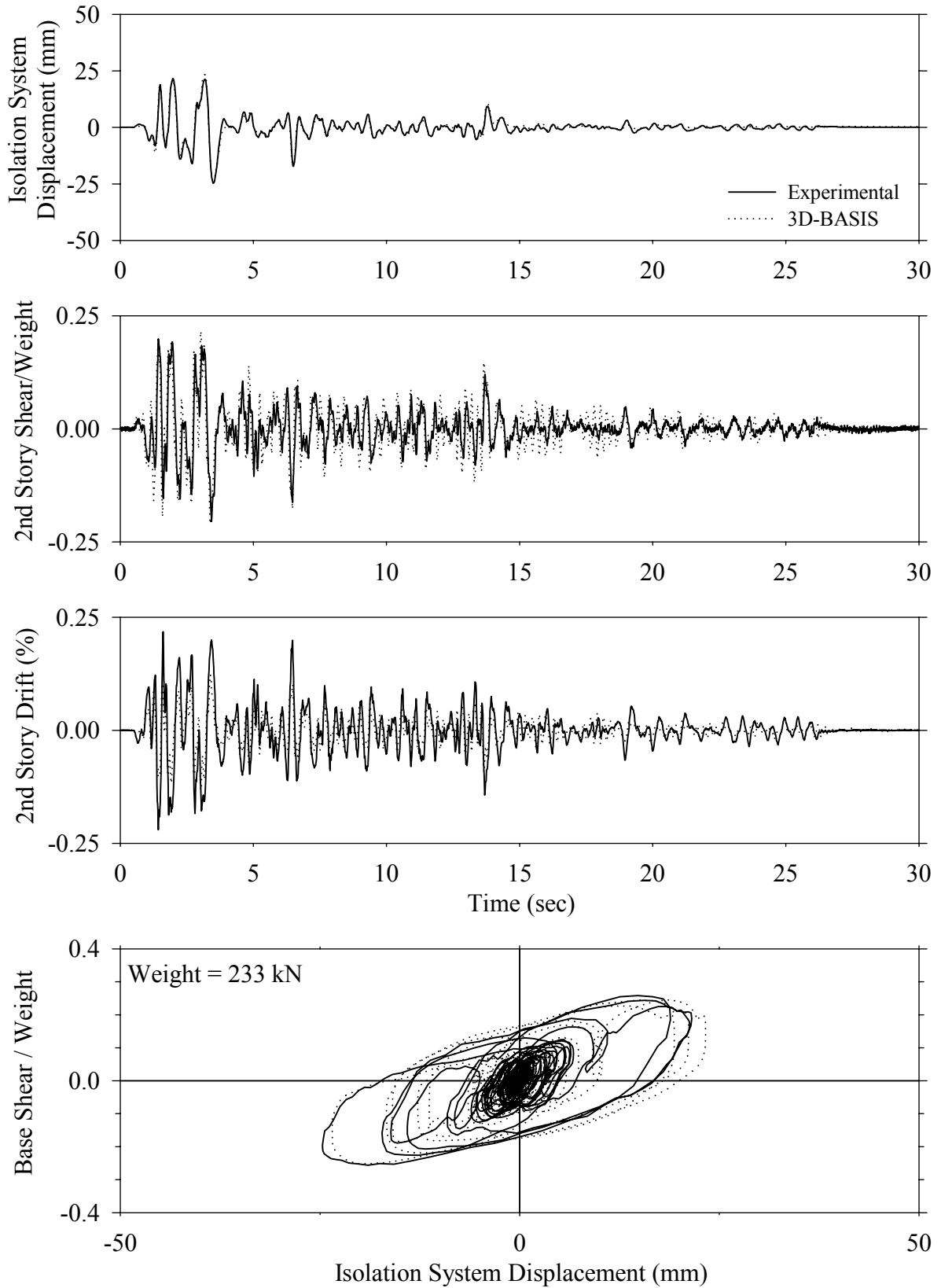
Test LDSLS10.1, Sylmar 100%, SB/Low Damping Elastomeric with Linear Dampers



Test LDSLS10.1, Sylmar 100%, SB/Low Damping Elastomeric with Linear Dampers

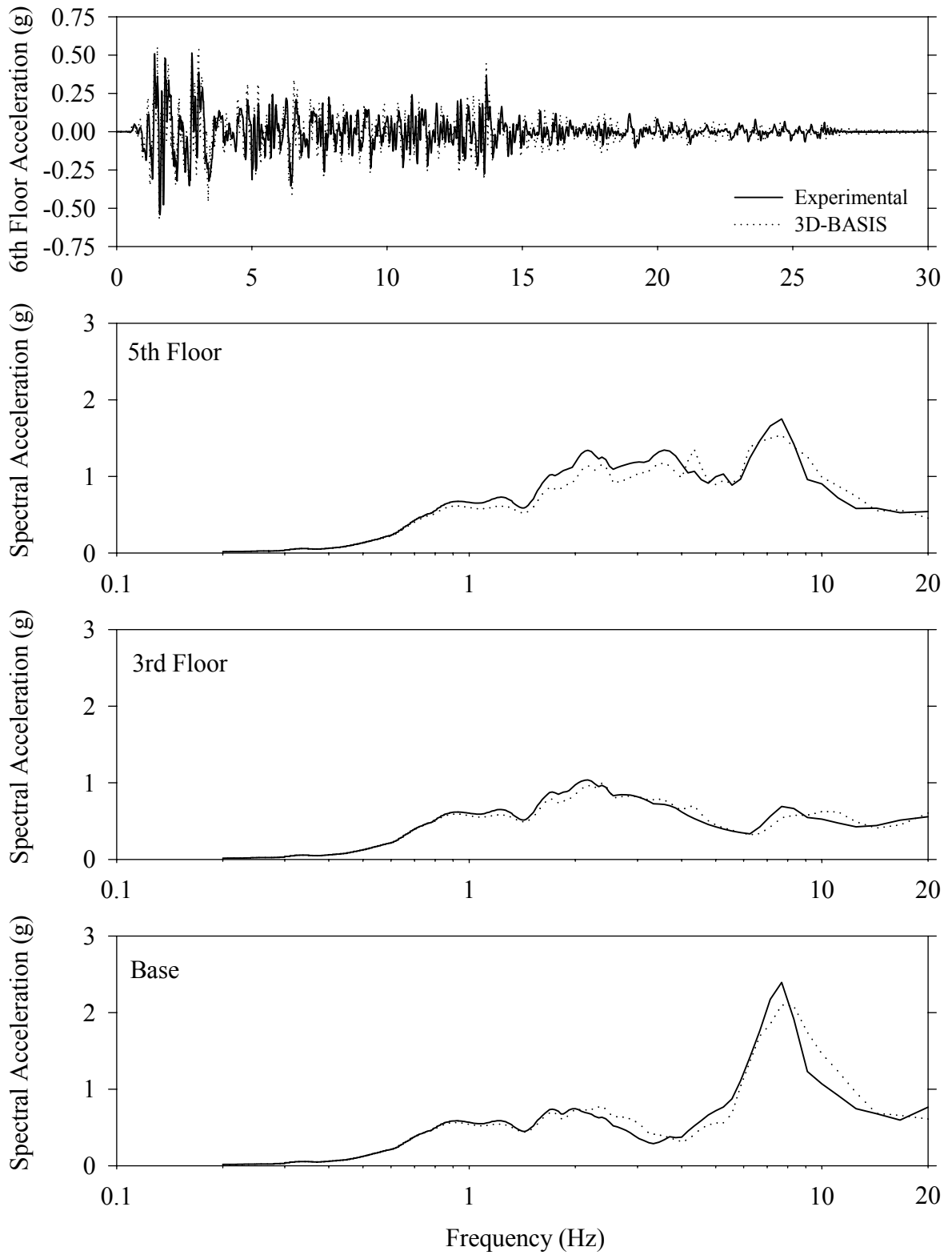


Test LDSNE20.1, El Centro S00E 200%, SB/Low Damping Elastomeric with Nonlinear Dampers

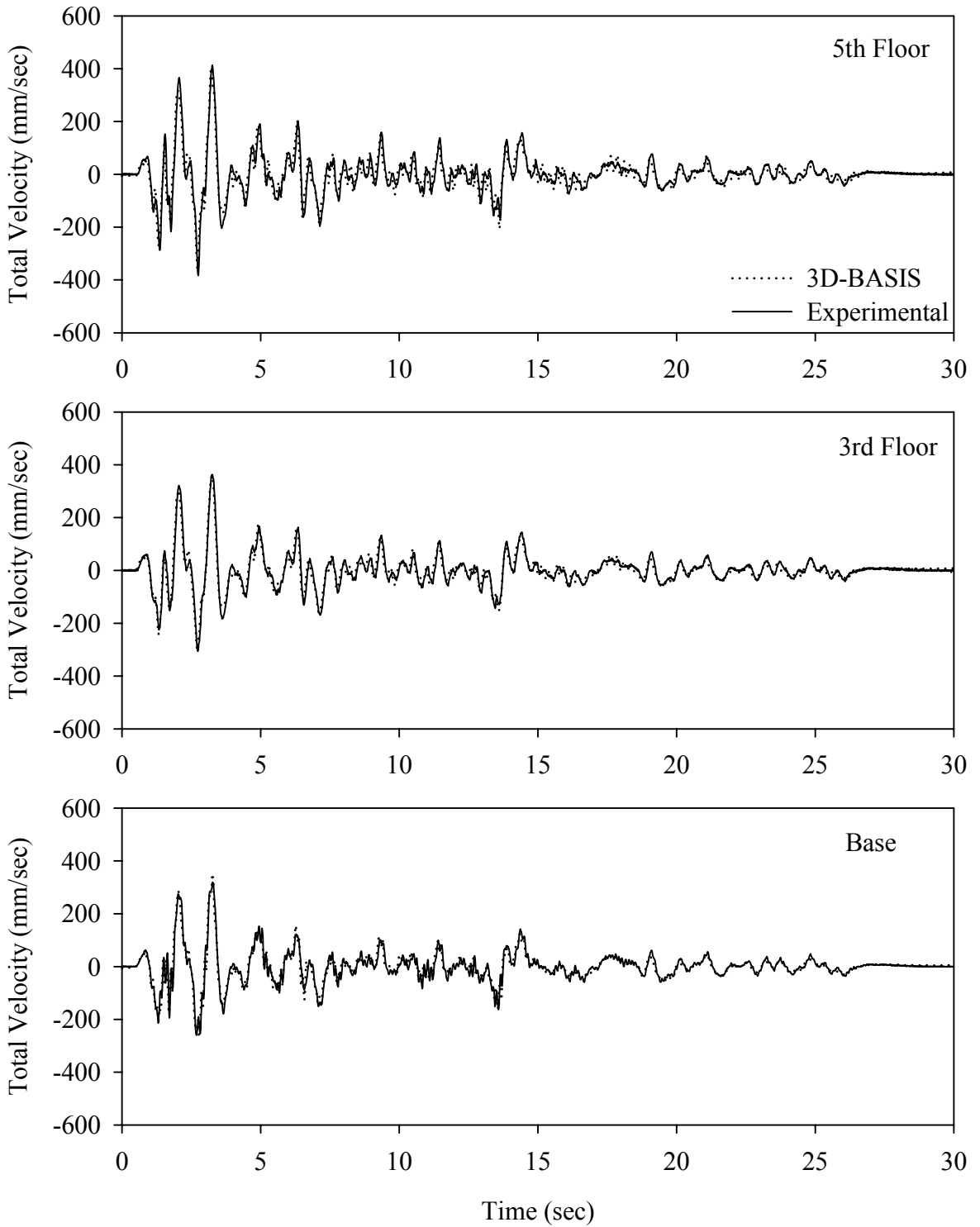




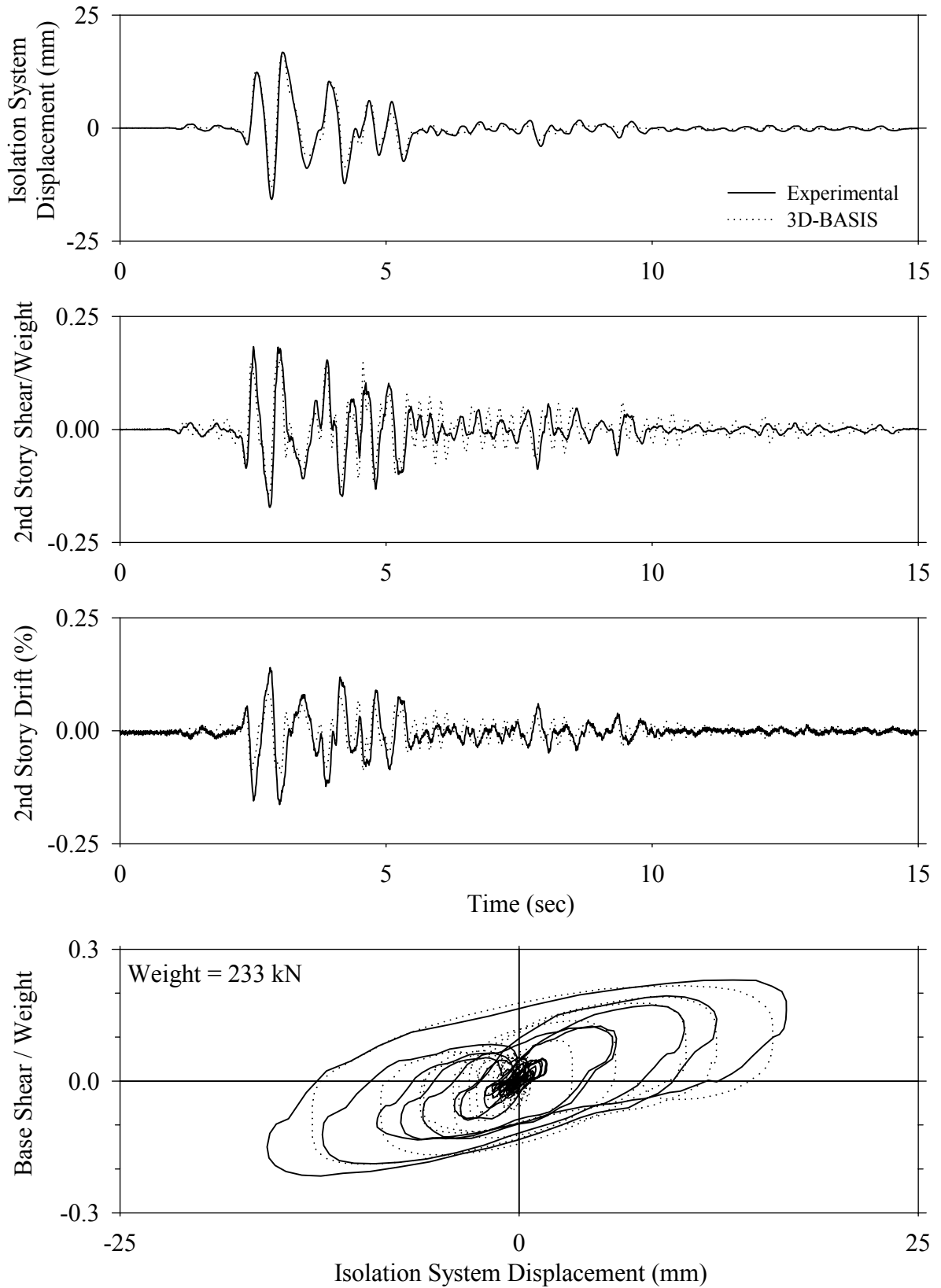
Test LDSNE20.1, El Centro S00E 200%, SB/Low Damping Elastomeric with Nonlinear Dampers



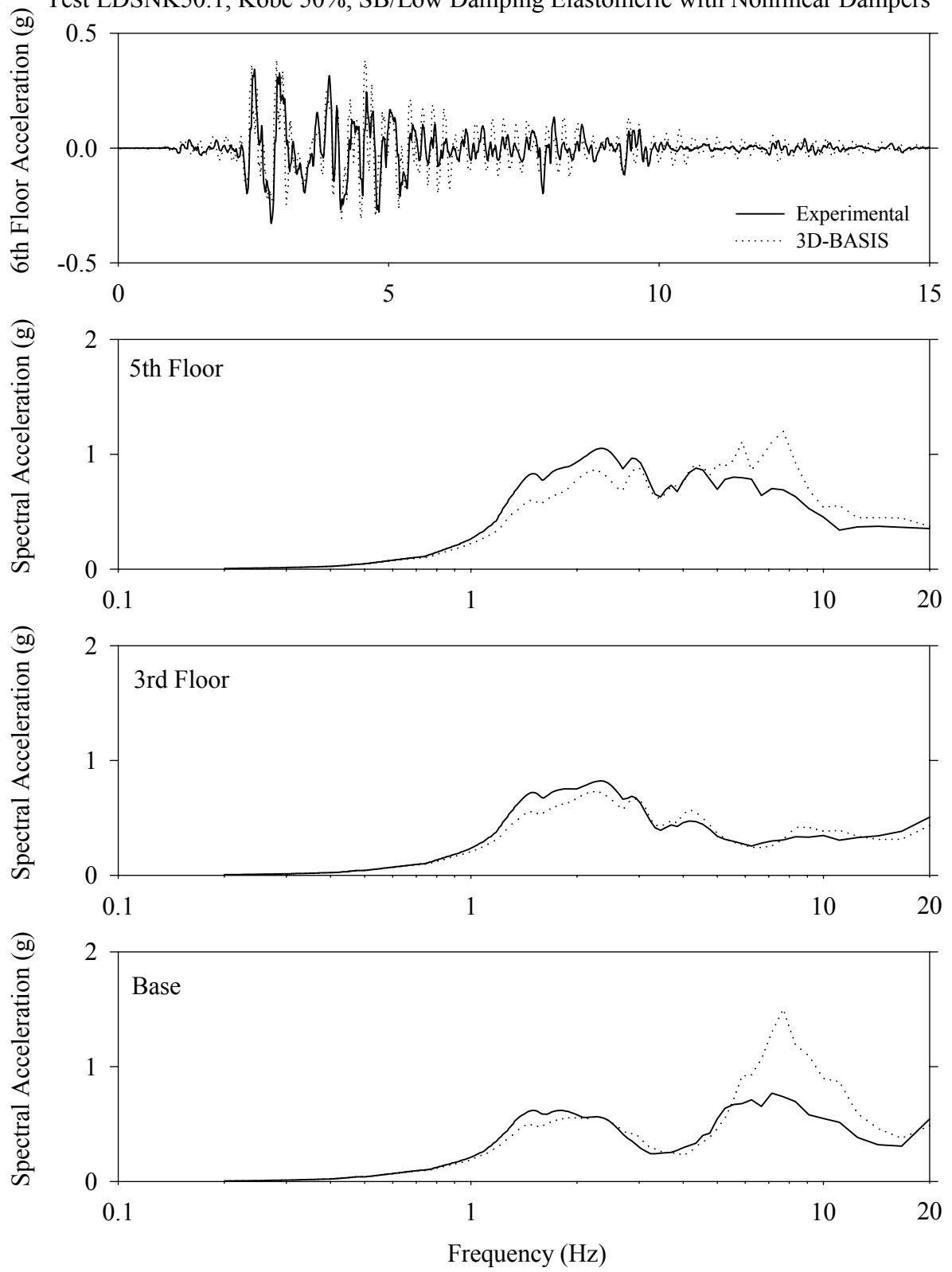
Test LDSNE20.1, El Centro S00E 200%, SB/Low Damping Elastomeric with Nonlinear Dampers



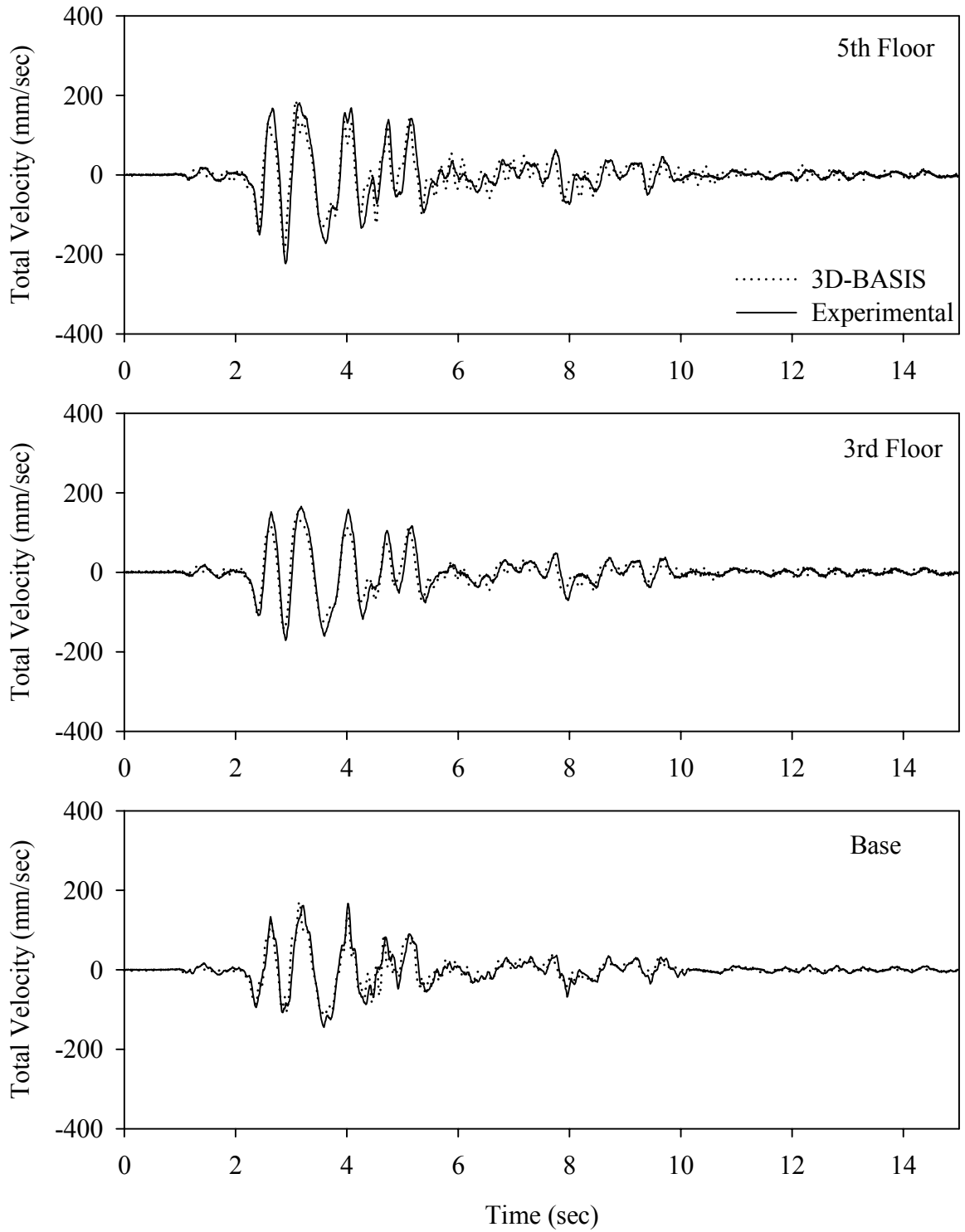
Test LDSNK50.1, Kobe 50%, SB/Low Damping Elastomeric with Nonlinear Dampers



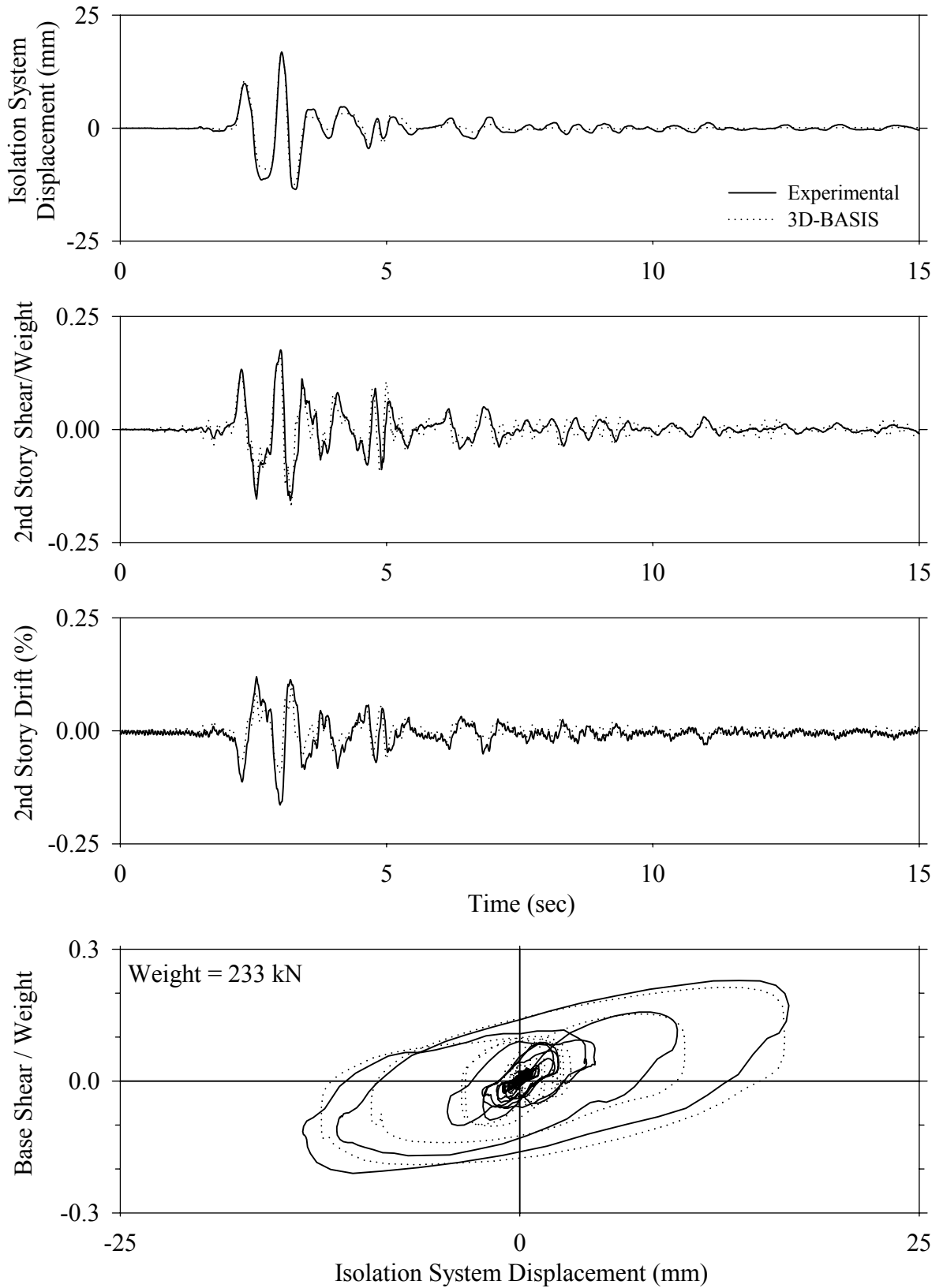
Test LDSNK50.1, Kobe 50%, SB/Low Damping Elastomeric with Nonlinear Dampers



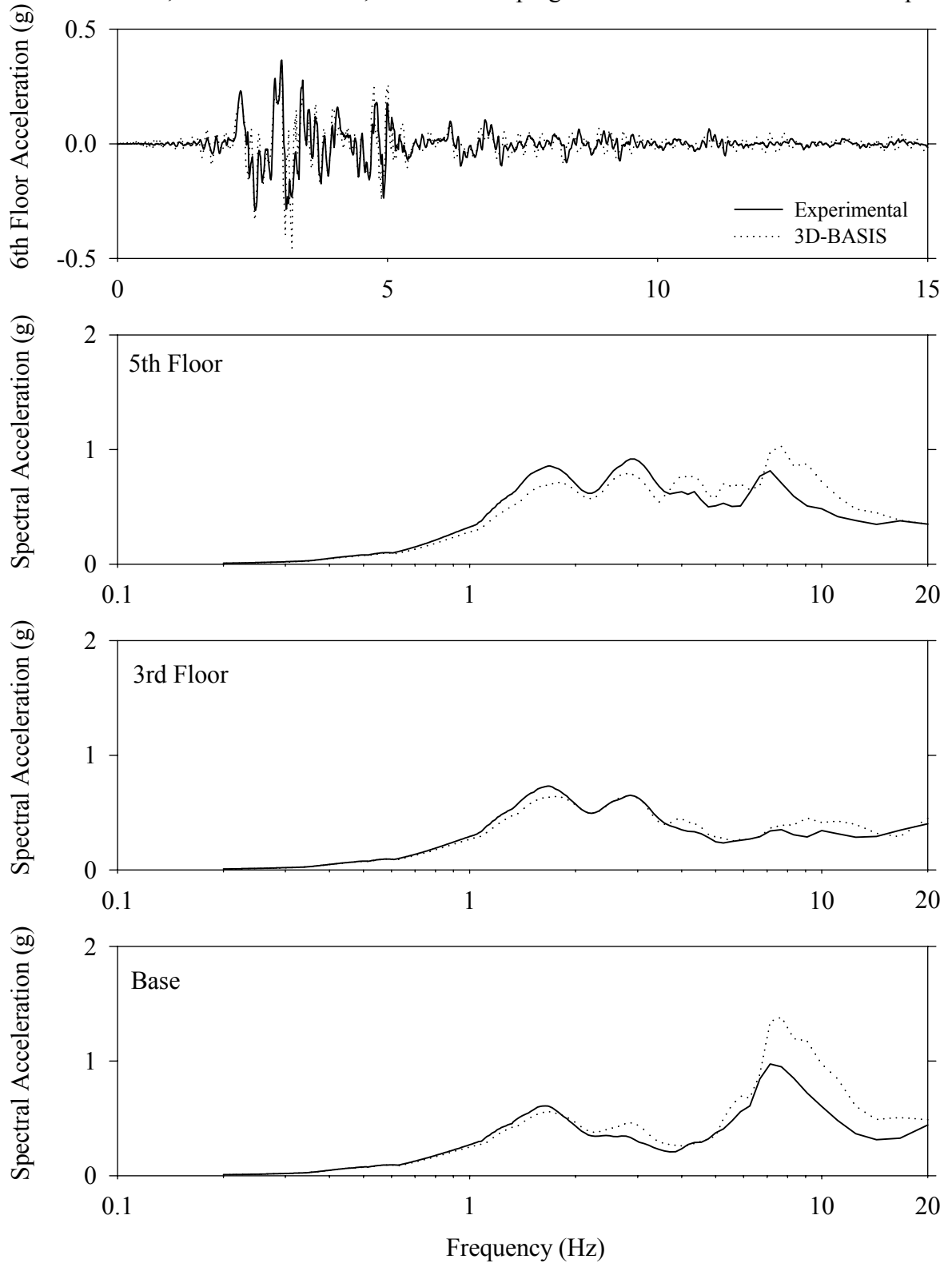
Test LDSNK50.1, Kobe 50%, SB/Low Damping Elastomeric with Nonlinear Dampers



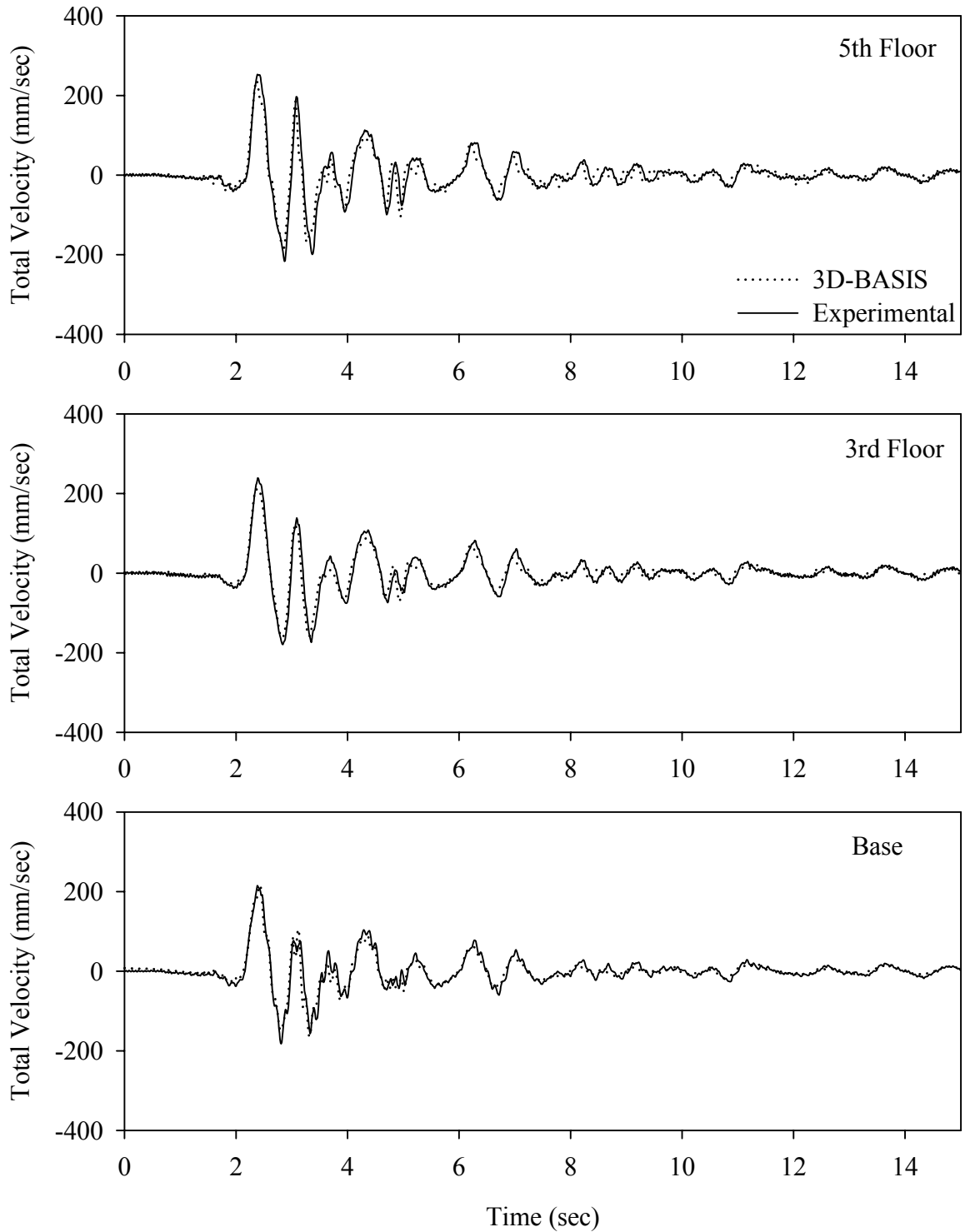
Test LDSNN50.1, Newhall 360 50%, SB/Low Damping Elastomeric with Nonlinear Dampers



Test LDSNN50.1, Newhall 360 50%, SB/Low Damping Elastomeric with Nonlinear Dampers

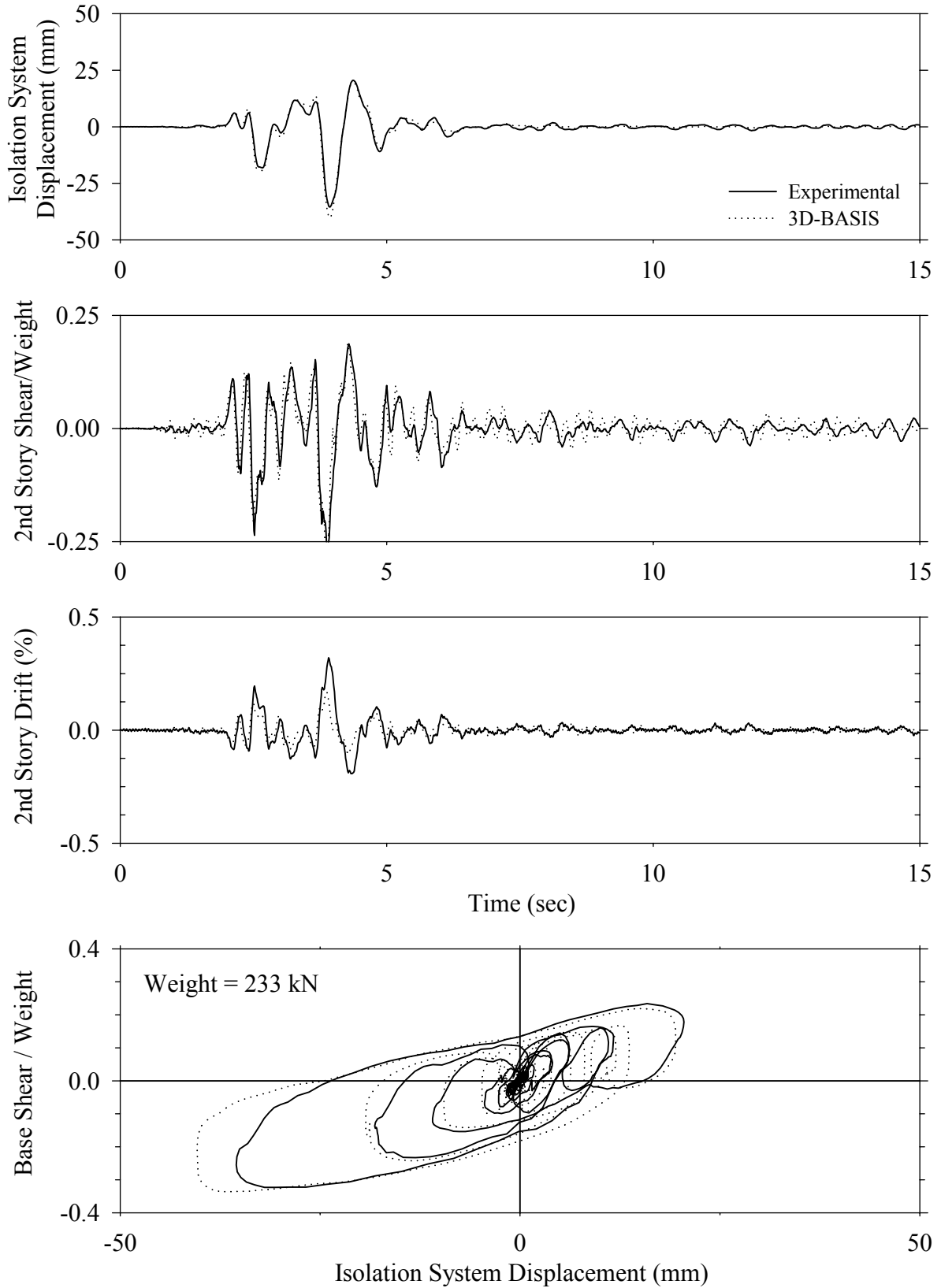


Test LDSNN50.1, Newhall 360 50%, SB/Low Damping Elastomeric with Nonlinear Dampers

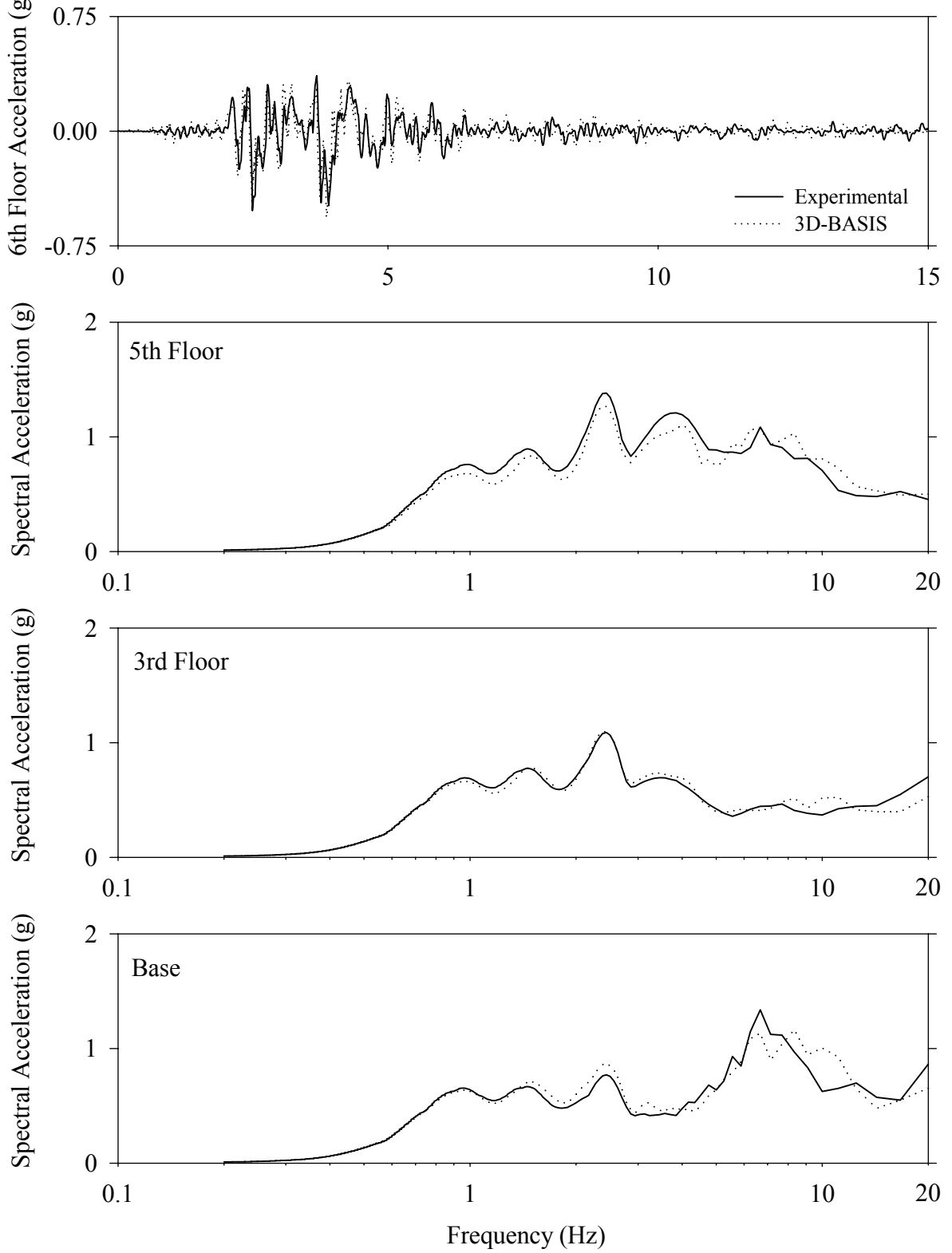




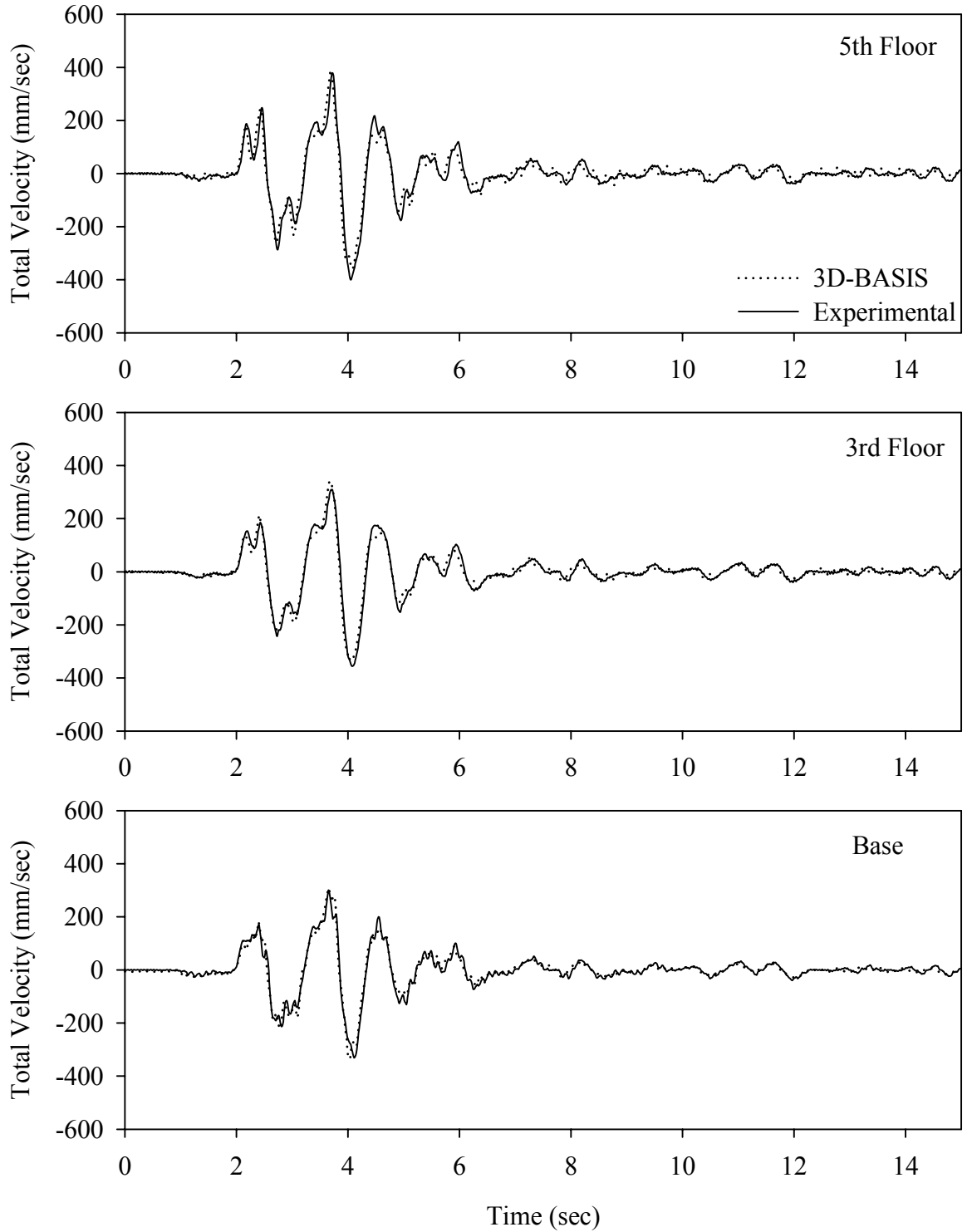
Test LDSNS10.1, Sylmar 100%, SB/Low Damping Elastomeric with Nonlinear Dampers



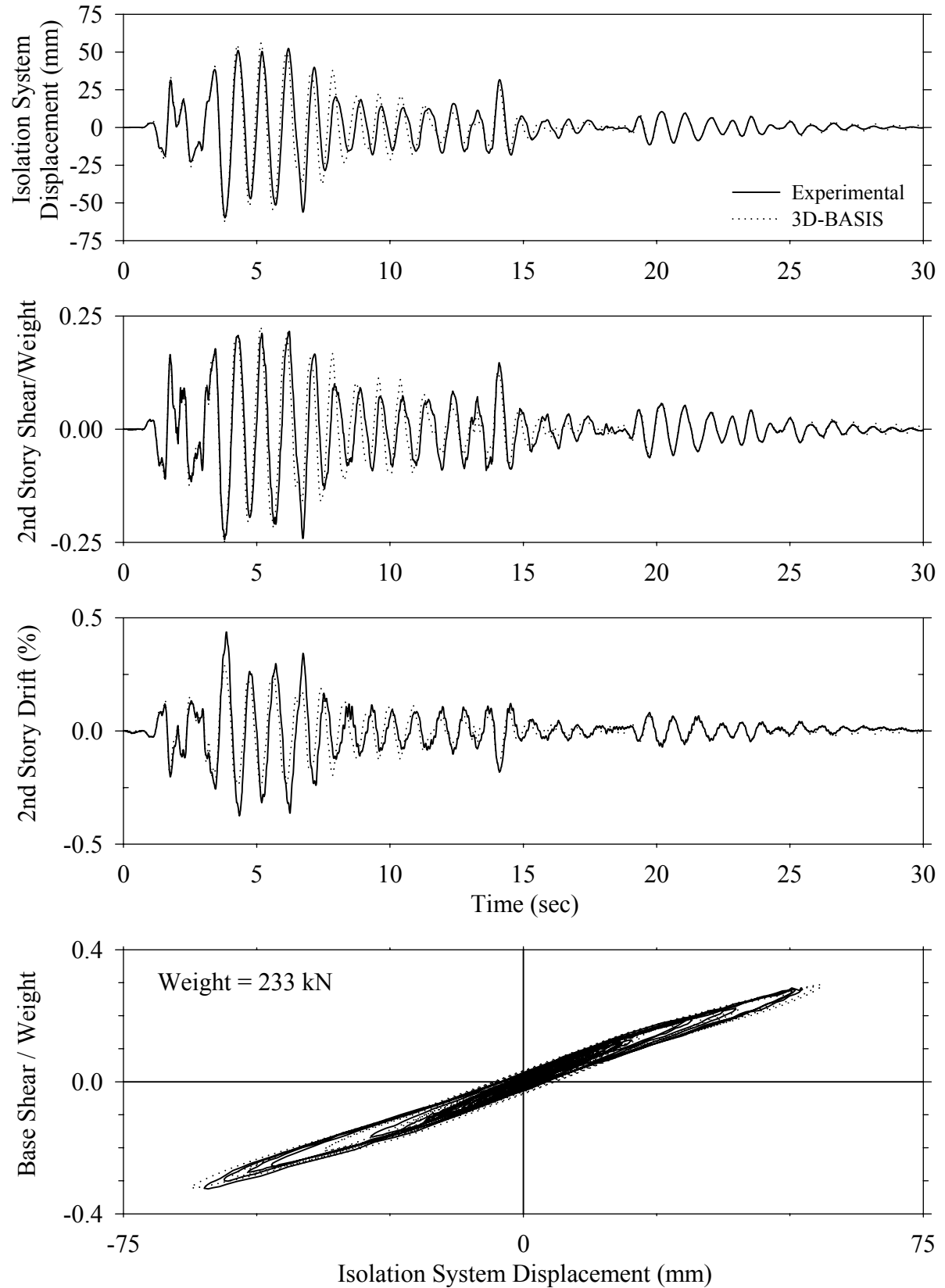
Test LDSNS10.1, Sylmar 100%, SB/Low Damping Elastomeric with Nonlinear Dampers



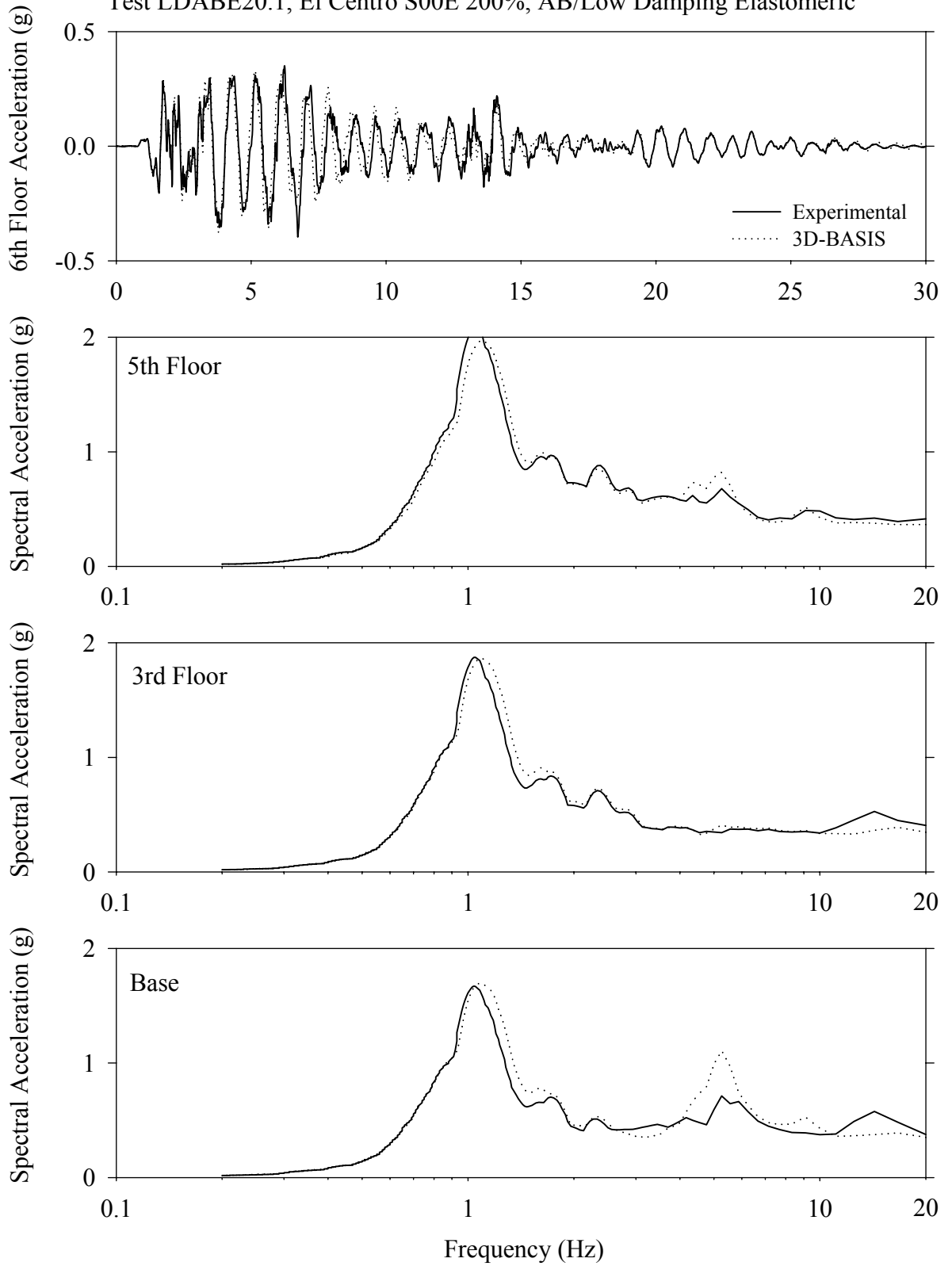
Test LDSNS10.1, Sylmar 100%, SB/Low Damping Elastomeric with Nonlinear Dampers



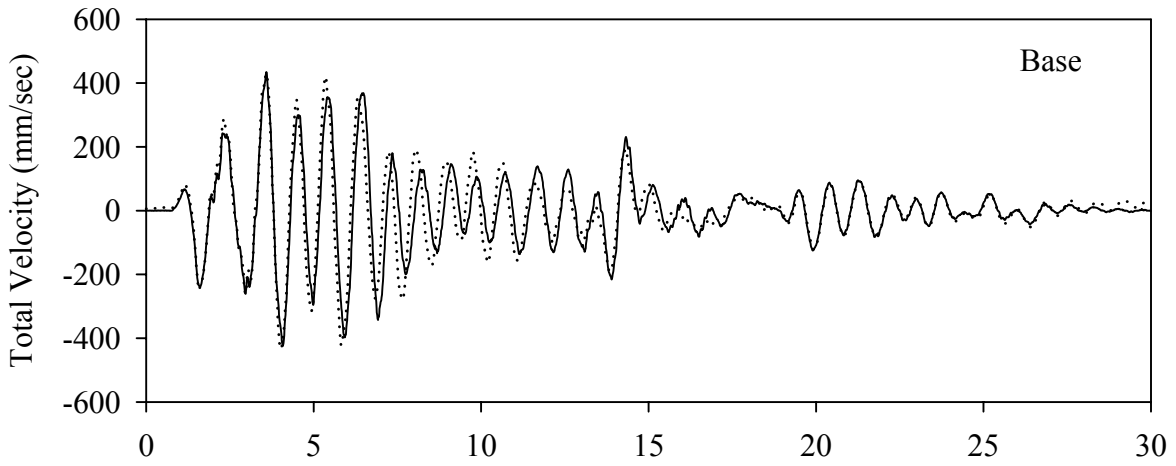
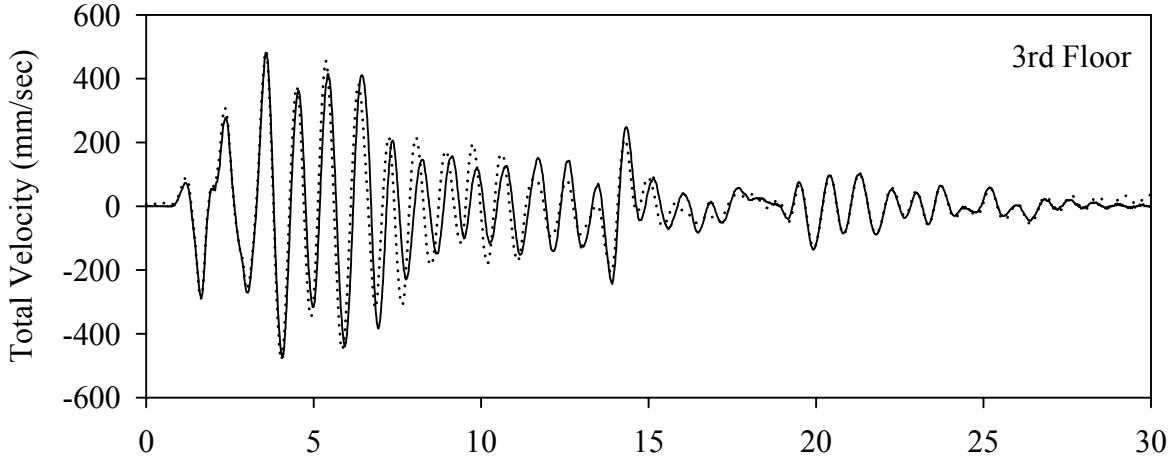
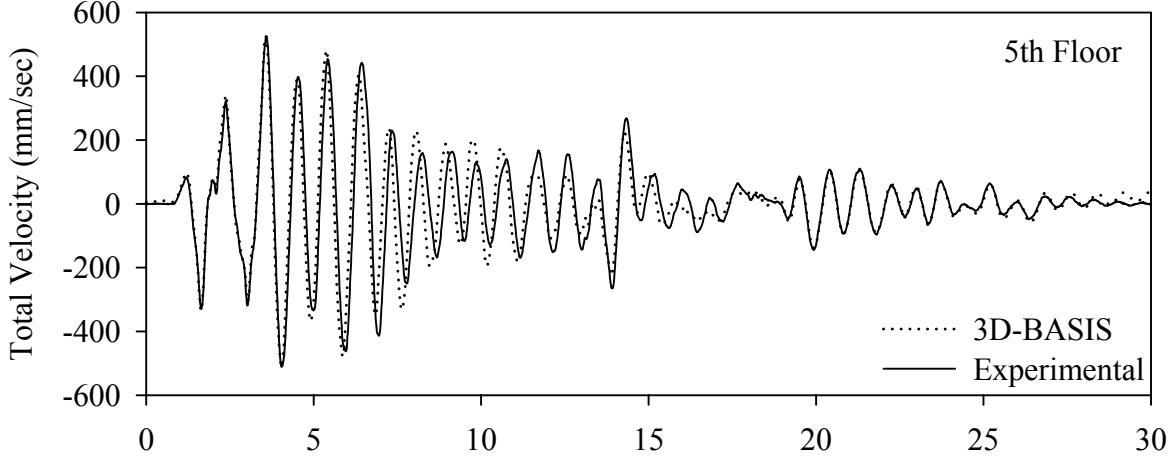
Test LDABE20.1, El Centro S00E 200%, AB/Low Damping Elastomeric



Test LDABE20.1, El Centro S00E 200%, AB/Low Damping Elastomeric

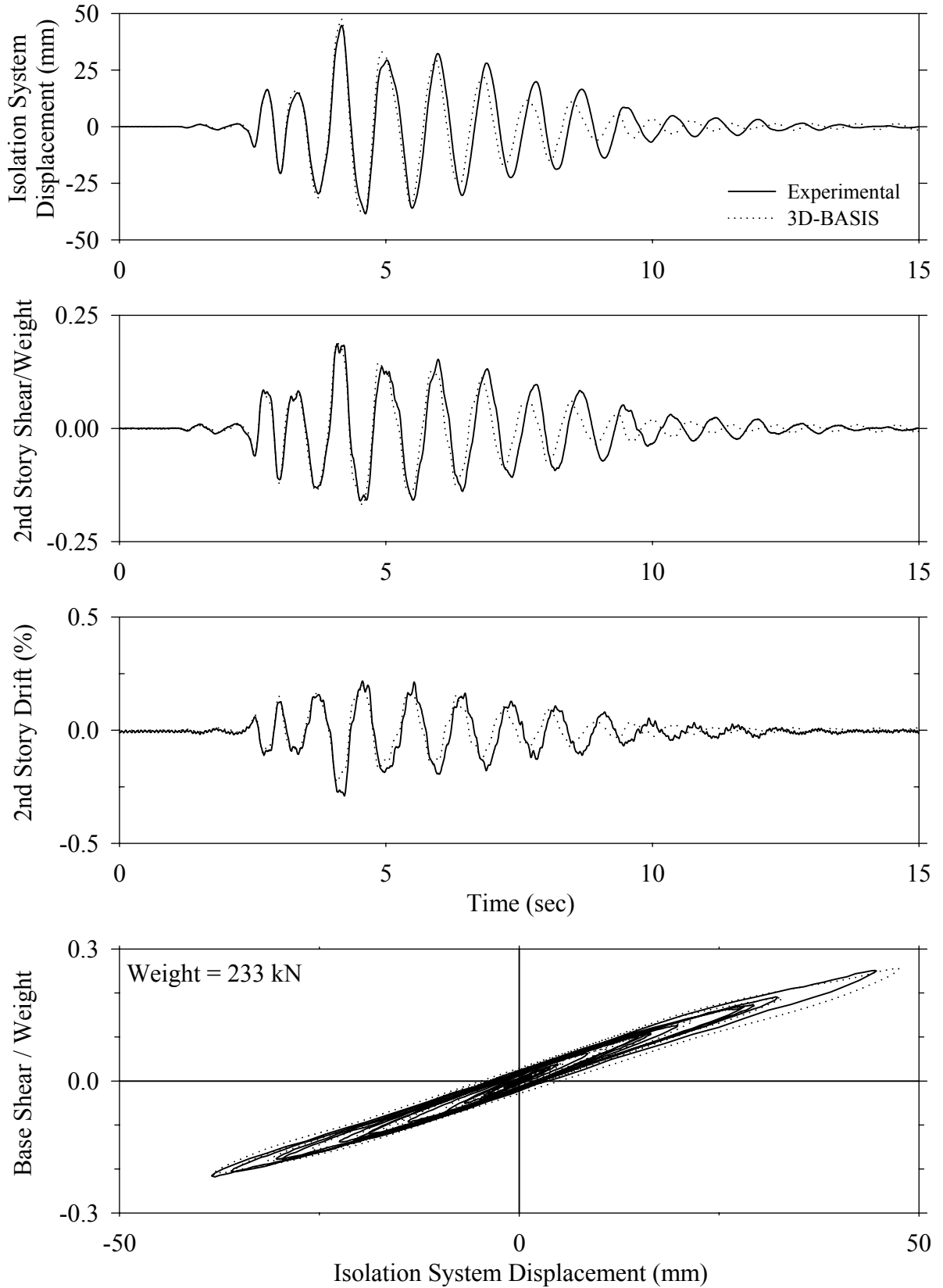


Test LDABE20.1, El Centro S00E 200%, AB/Low Damping Elastomeric

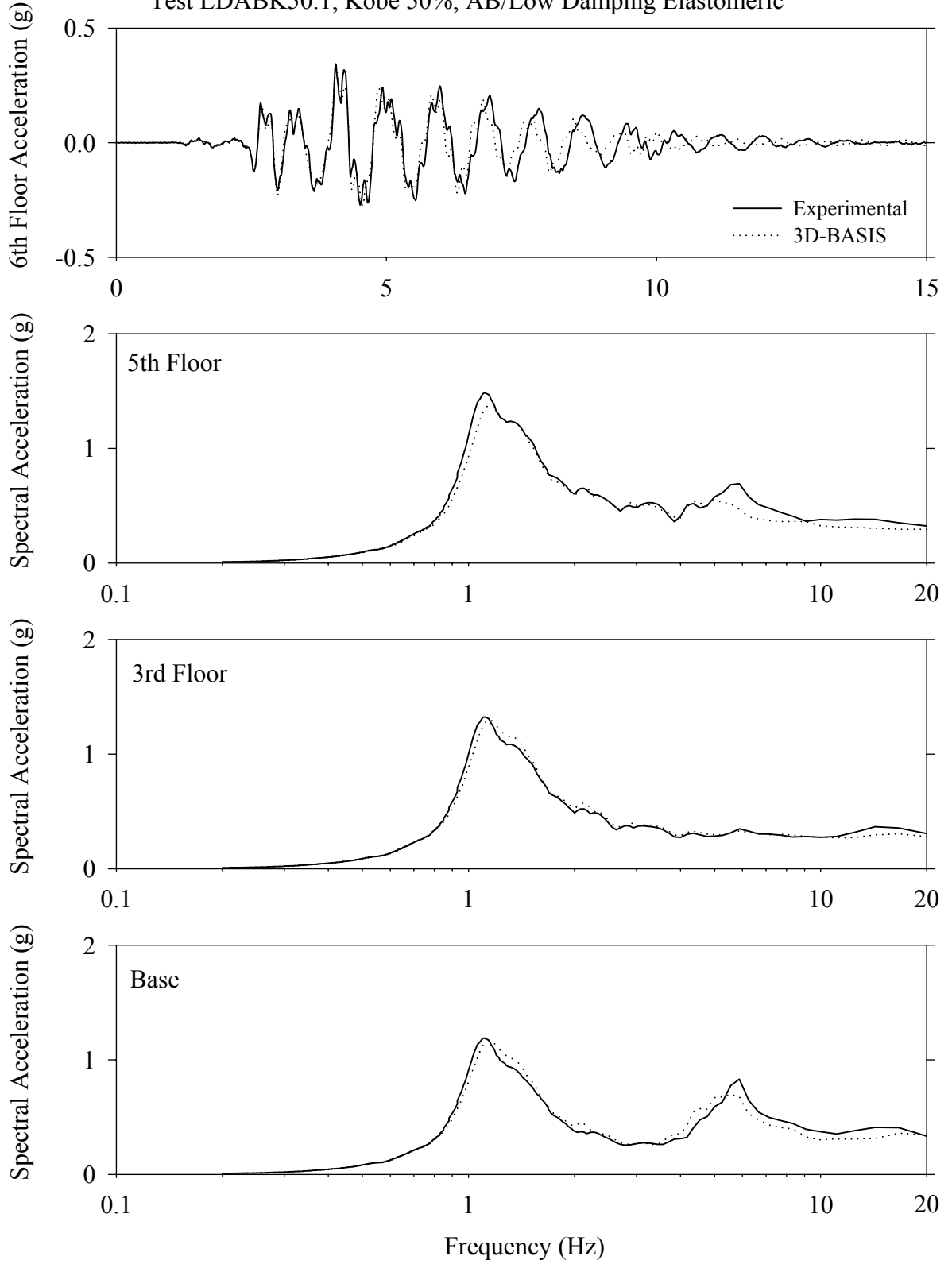


Time (sec)

Test LDABK50.1, Kobe 50%, AB/Low Damping Elastomeric

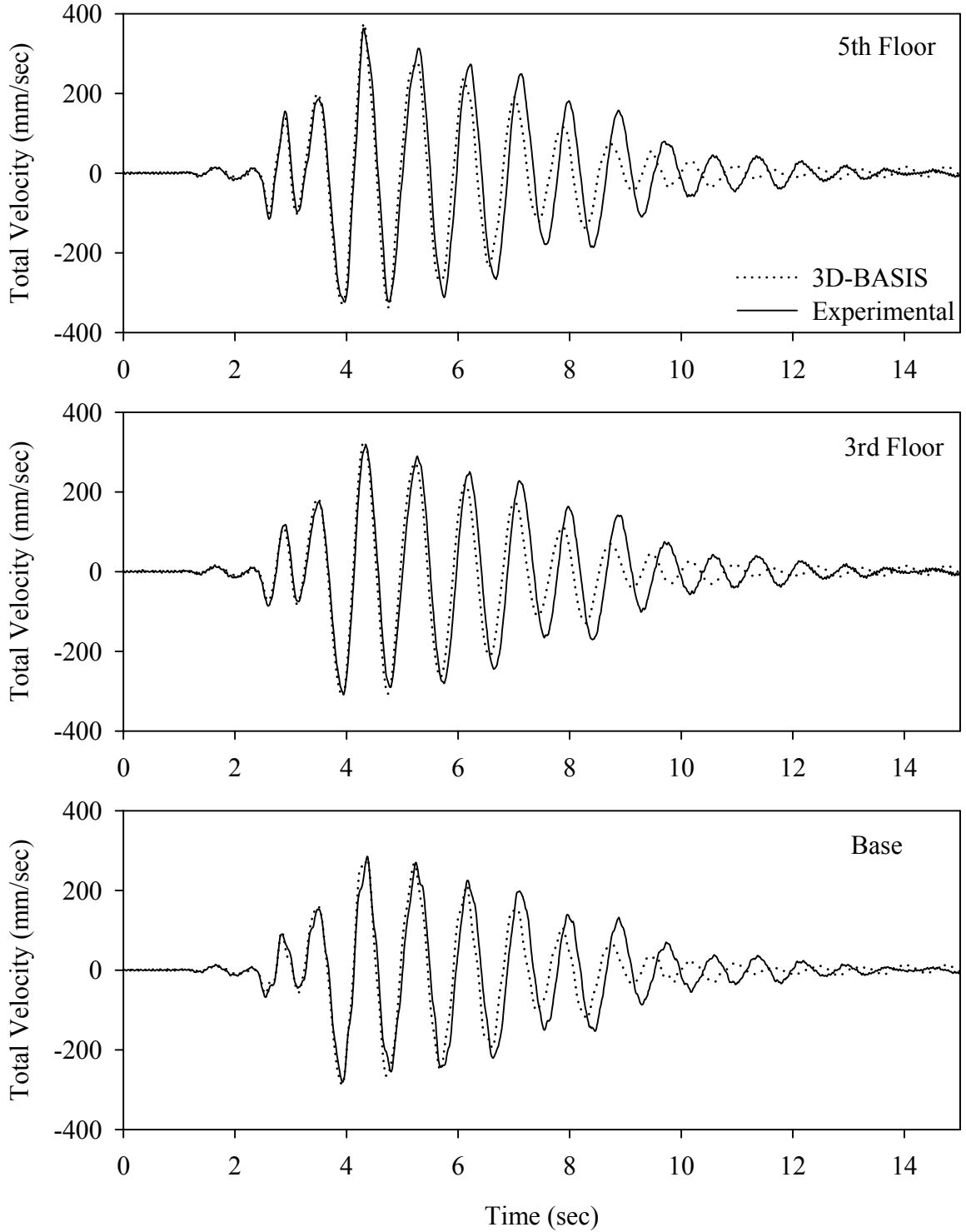


Test LDABK50.1, Kobe 50%, AB/Low Damping Elastomeric

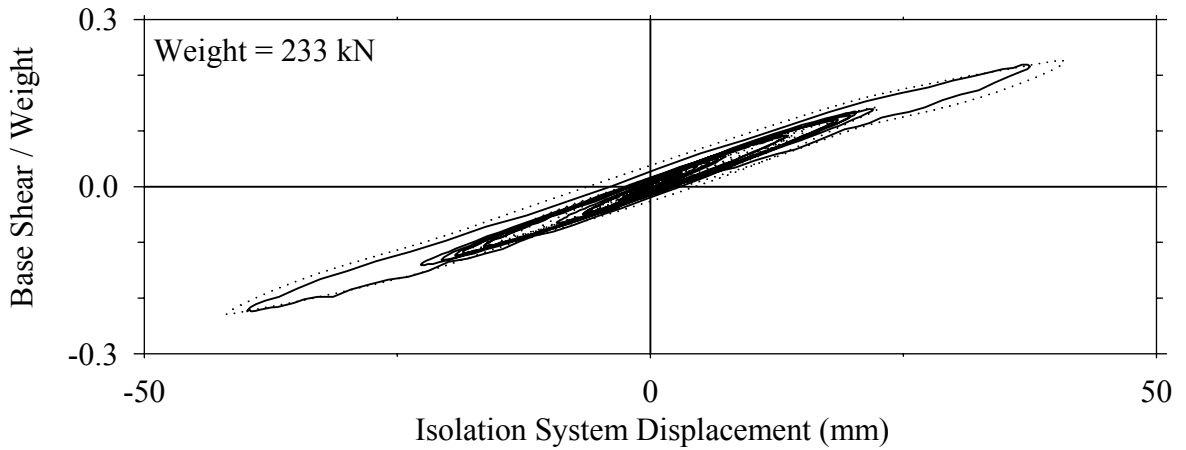
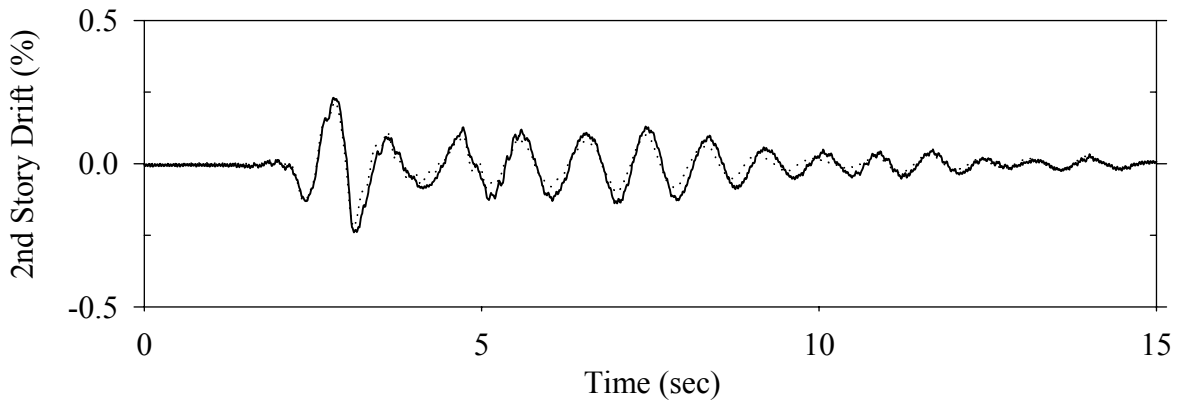
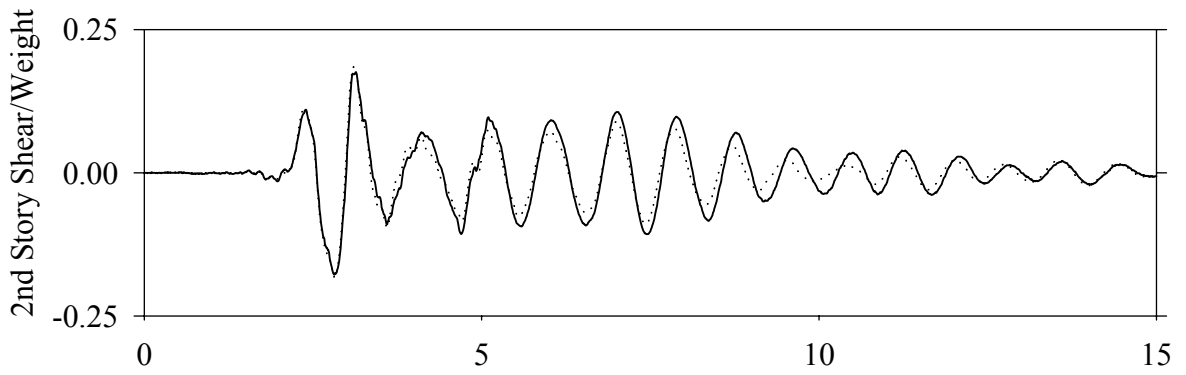
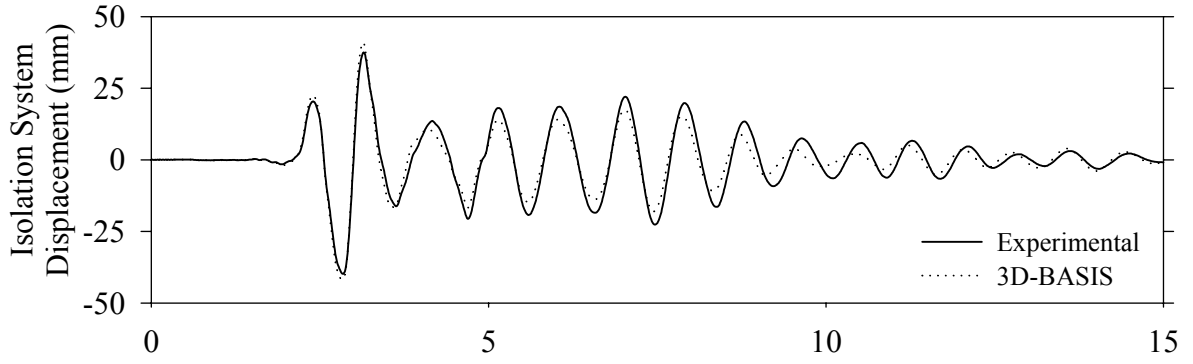




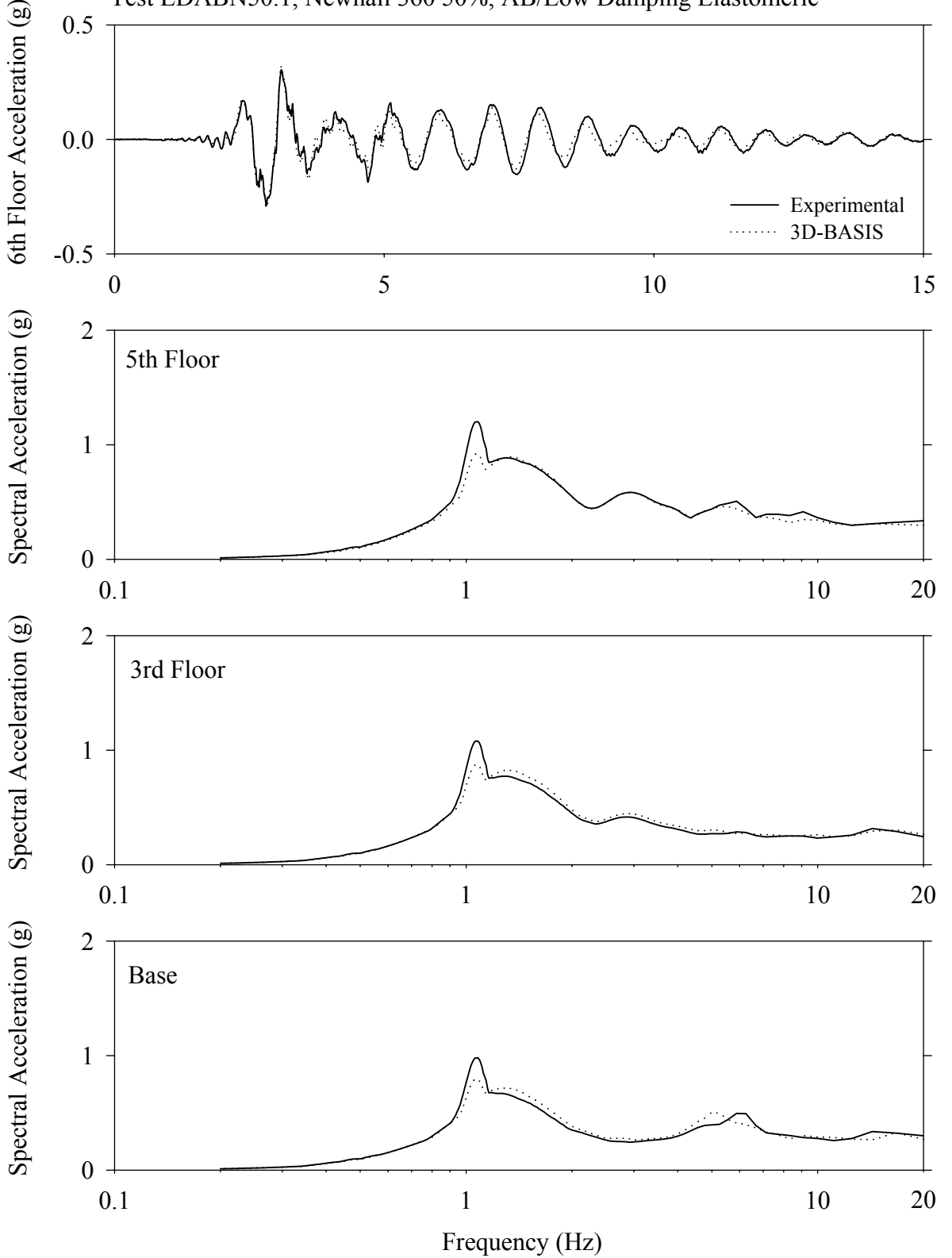
Test LDABK50.1, Kobe 50%, AB/Low Damping Elastomeric



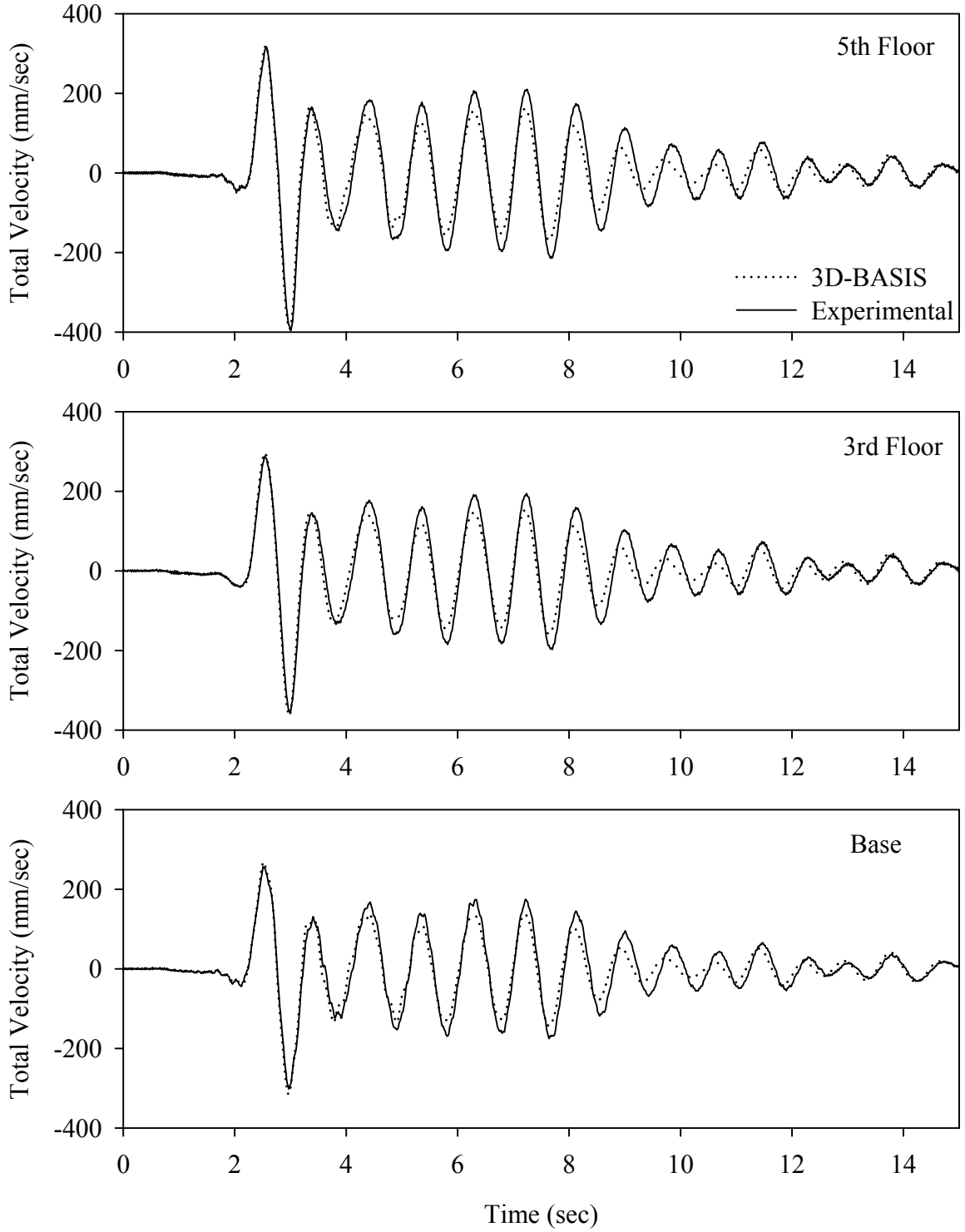
Test LDABN50.1, Newhall 360 50%, AB/Low Damping Elastomeric



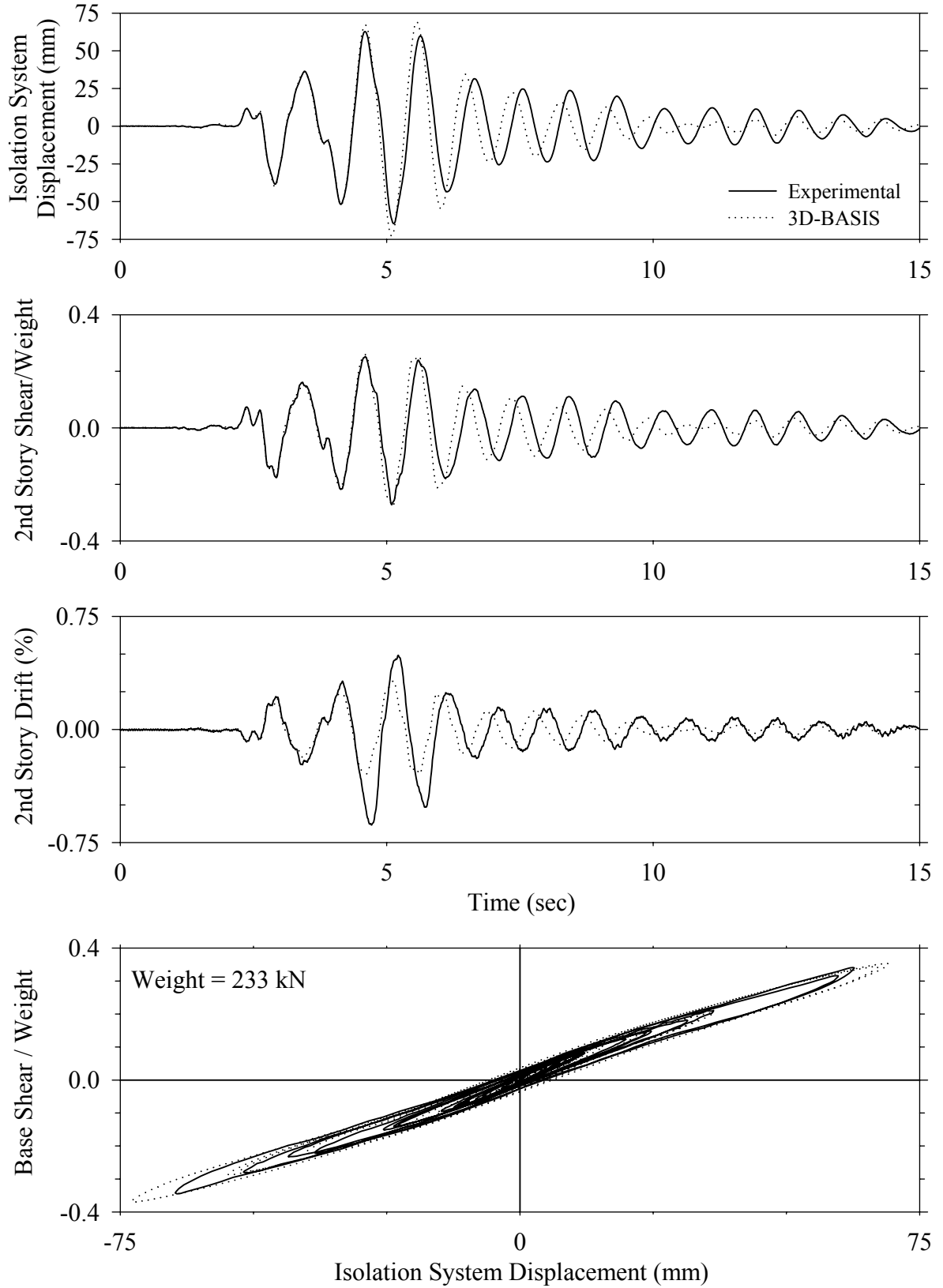
Test LDABN50.1, Newhall 360 50%, AB/Low Damping Elastomeric



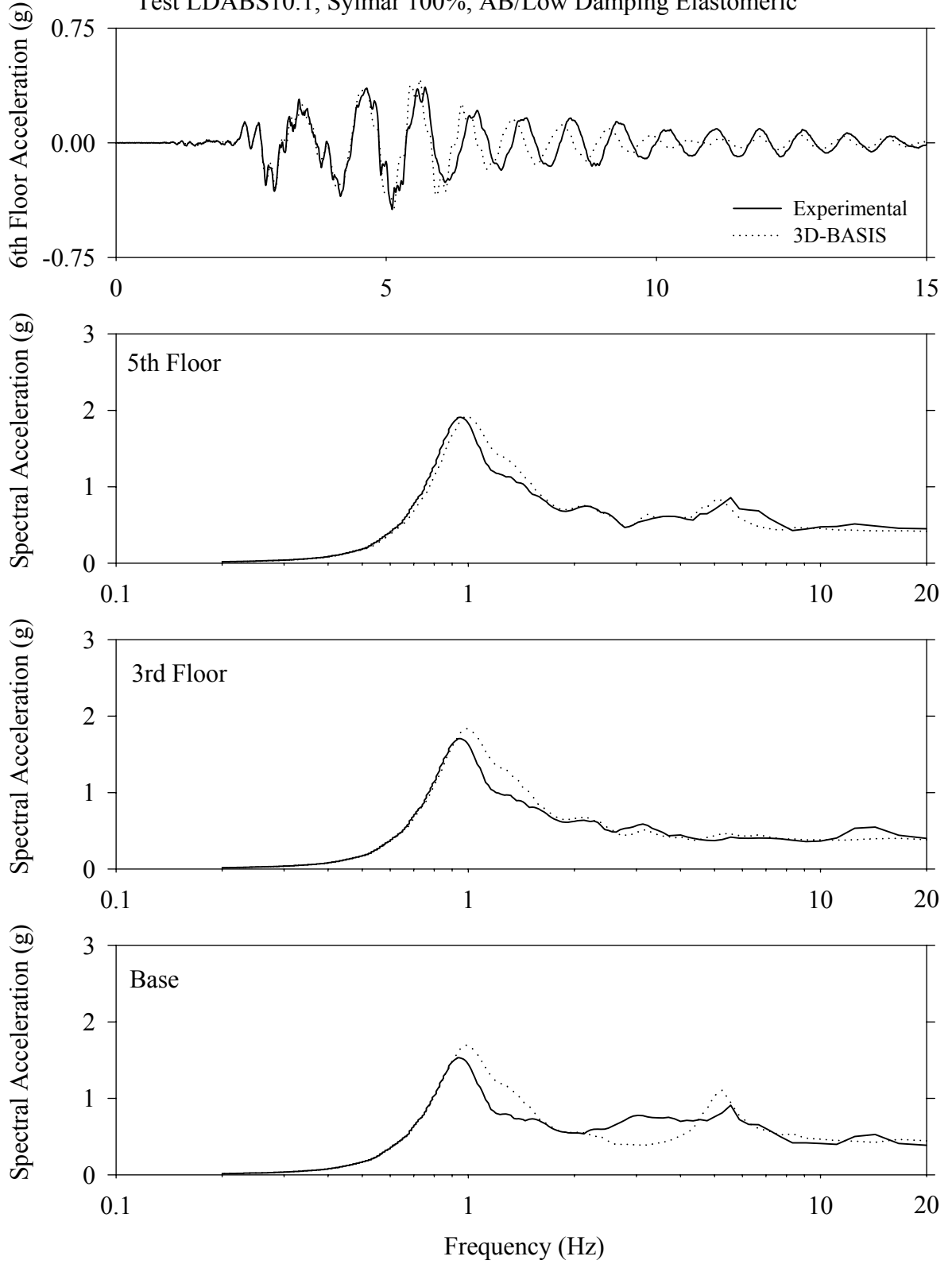
Test LDABN50.1, Newhall 360 50%, AB/Low Damping Elastomeric



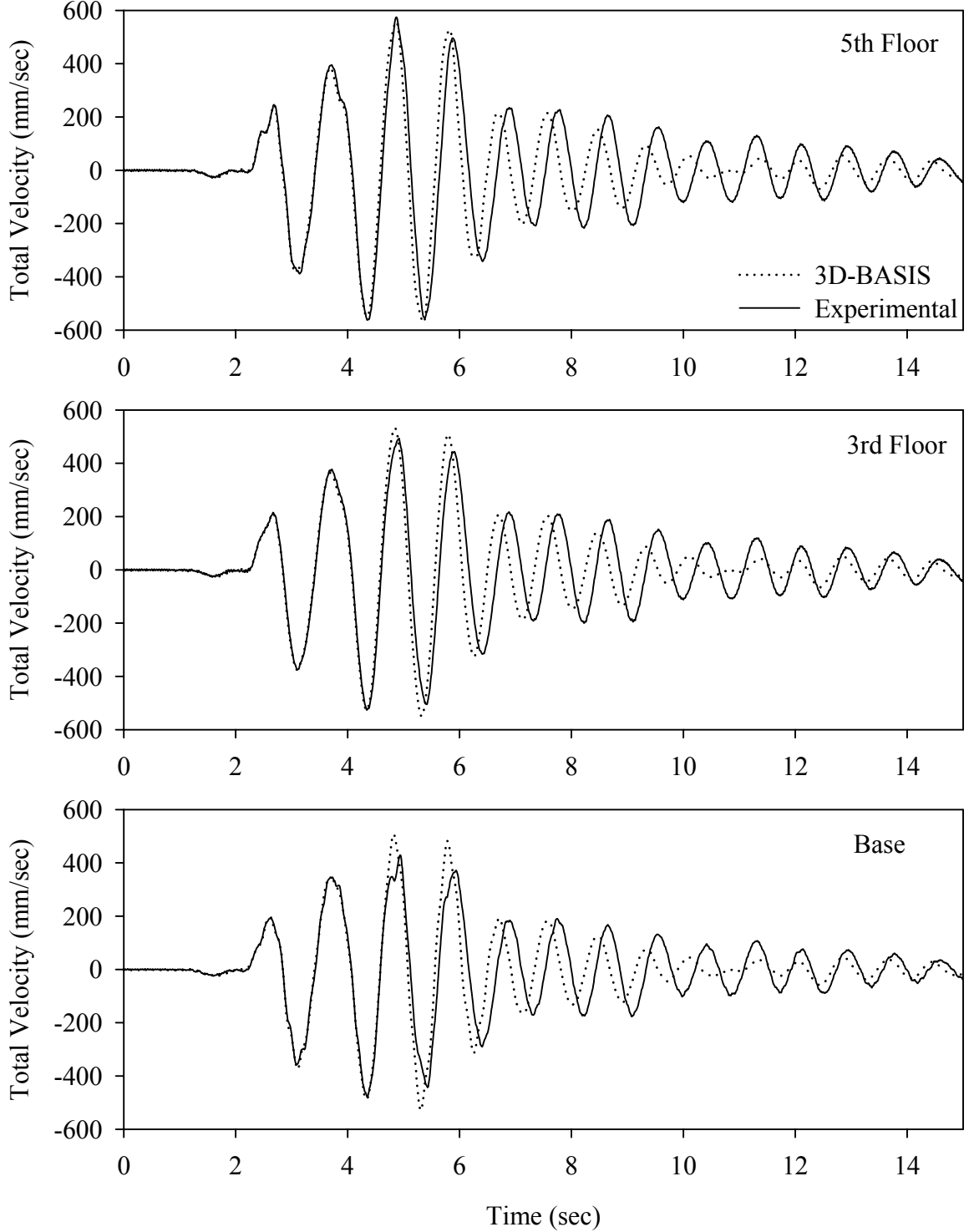
Test LDABS10.1, Sylmar 100%, AB/Low Damping Elastomeric



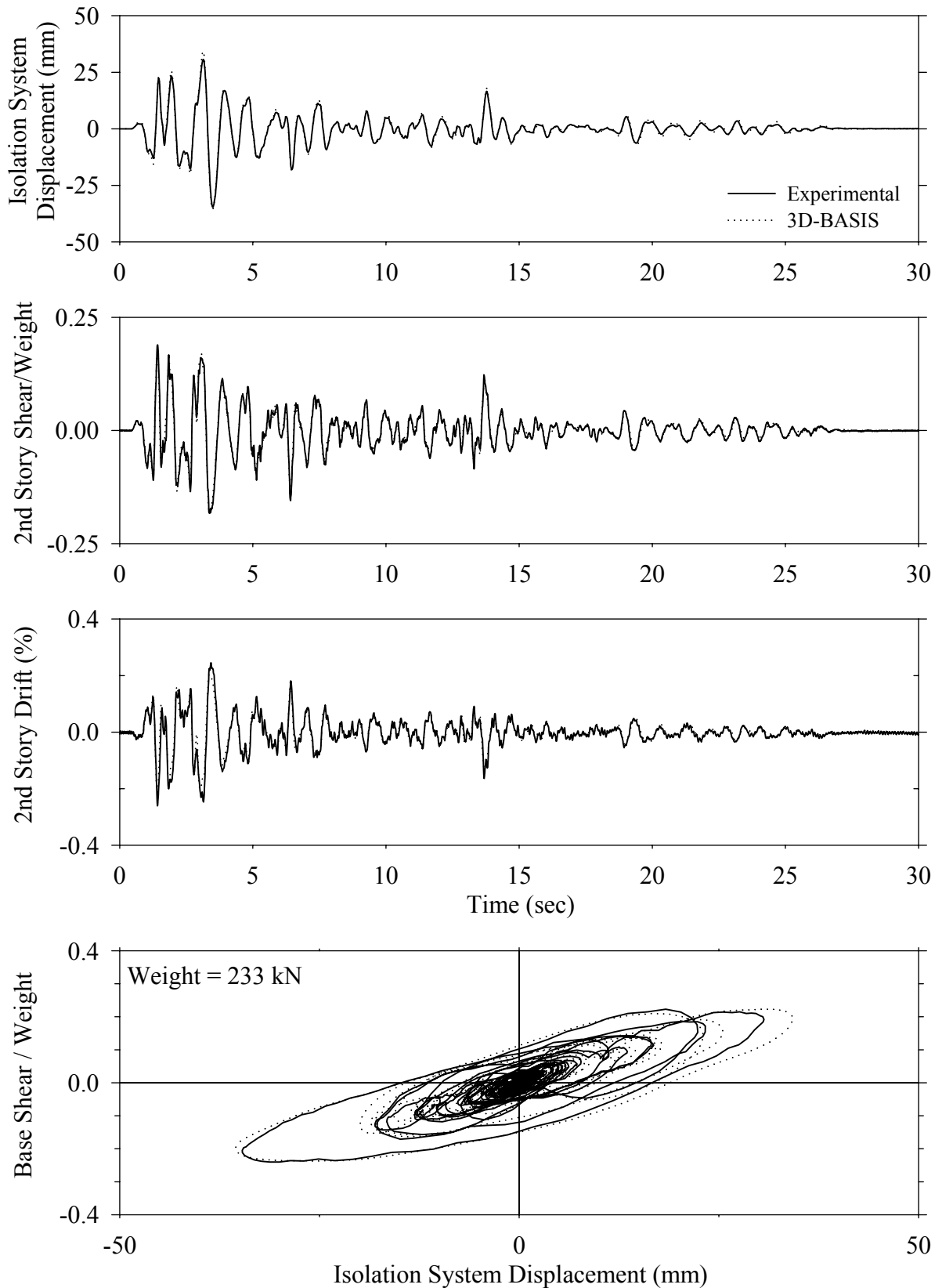
Test LDABS10.1, Sylmar 100%, AB/Low Damping Elastomeric



Test LDABS10.1, Sylmar 100%, AB/Low Damping Elastomeric

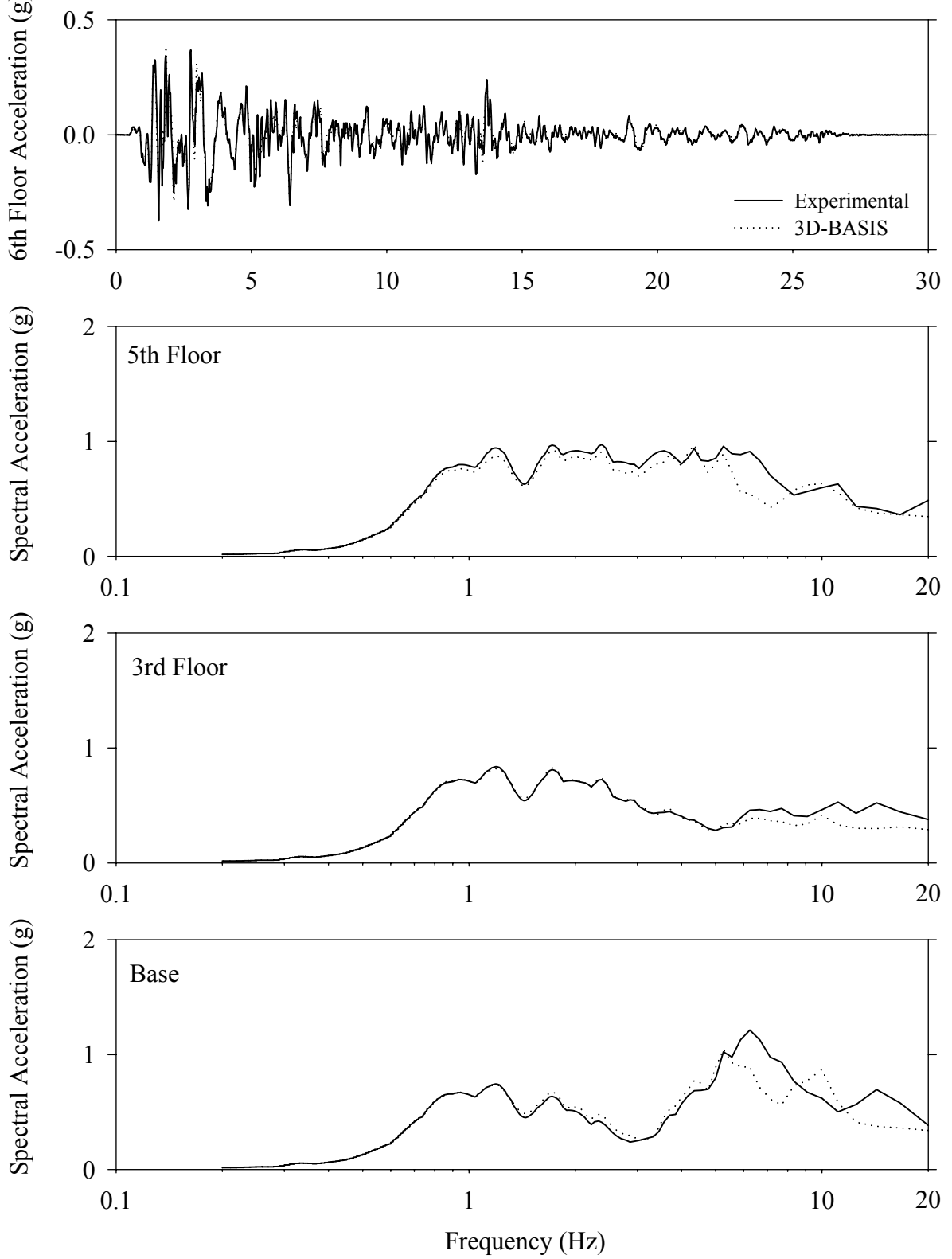


Test LDALE20.1, El Centro S00E 200%, AB/Low Damping Elastomeric with Linear Dampers

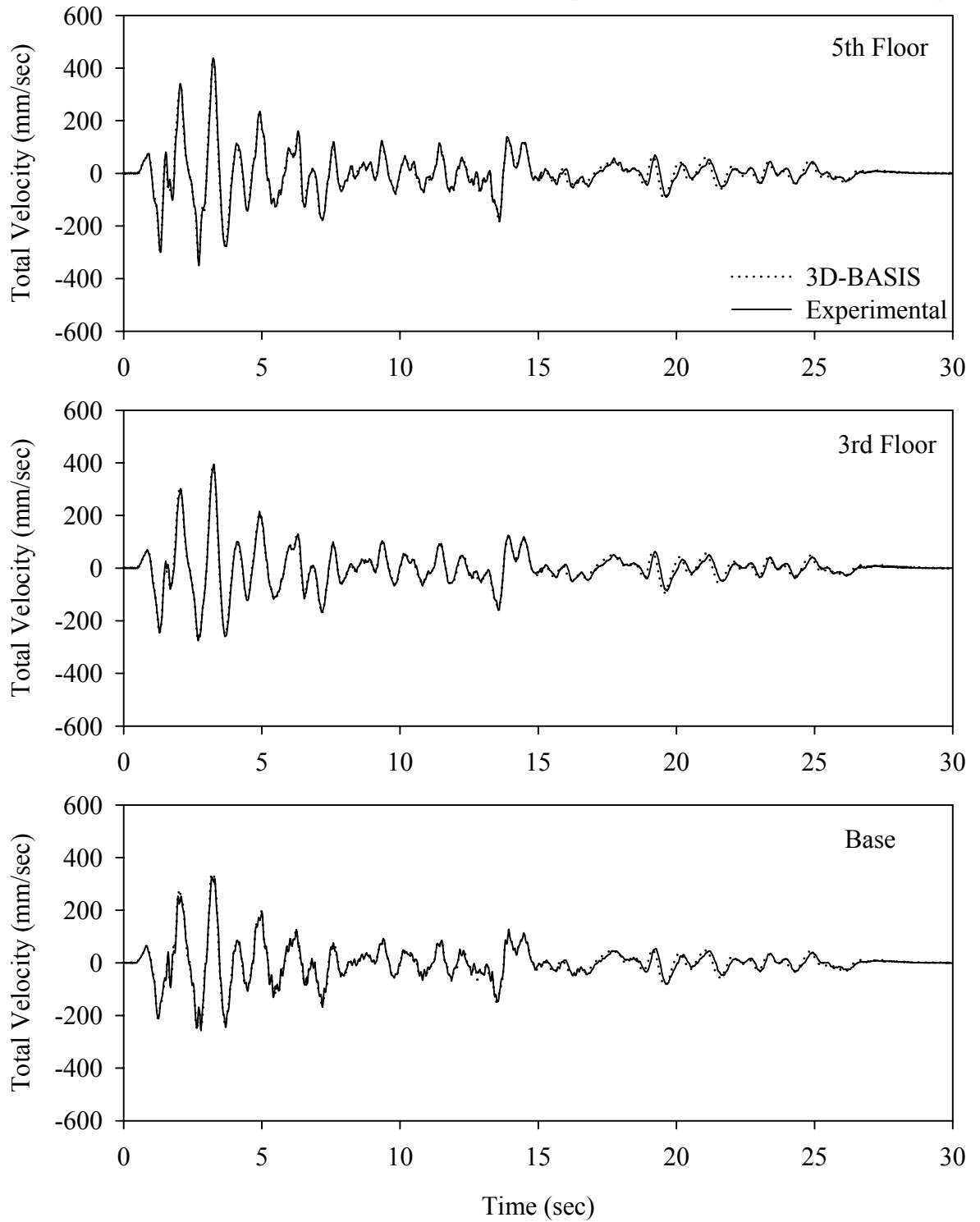




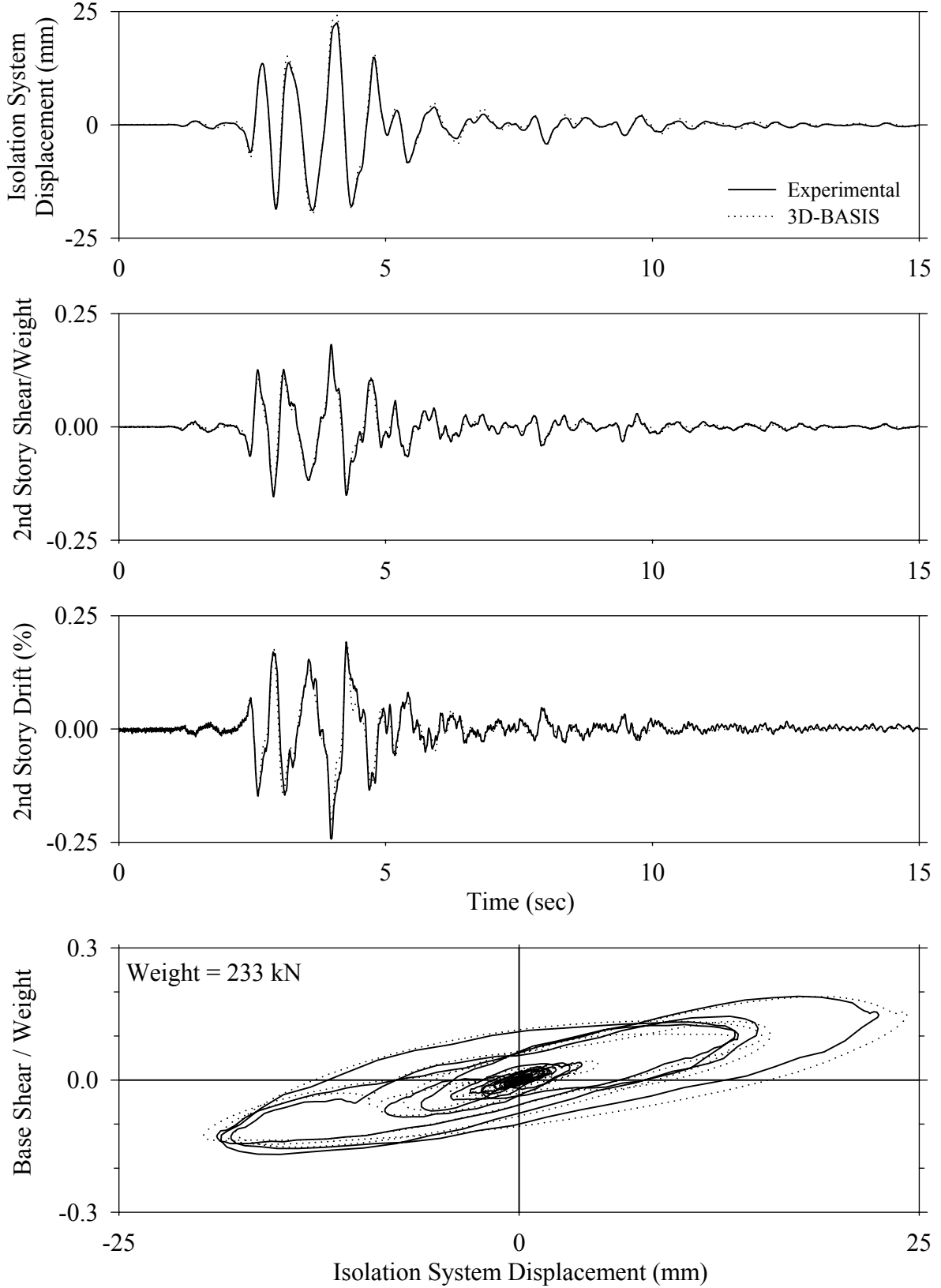
Test LDALE20.1, El Centro S00E 200%, AB/Low Damping Elastomeric with Linear Dampers



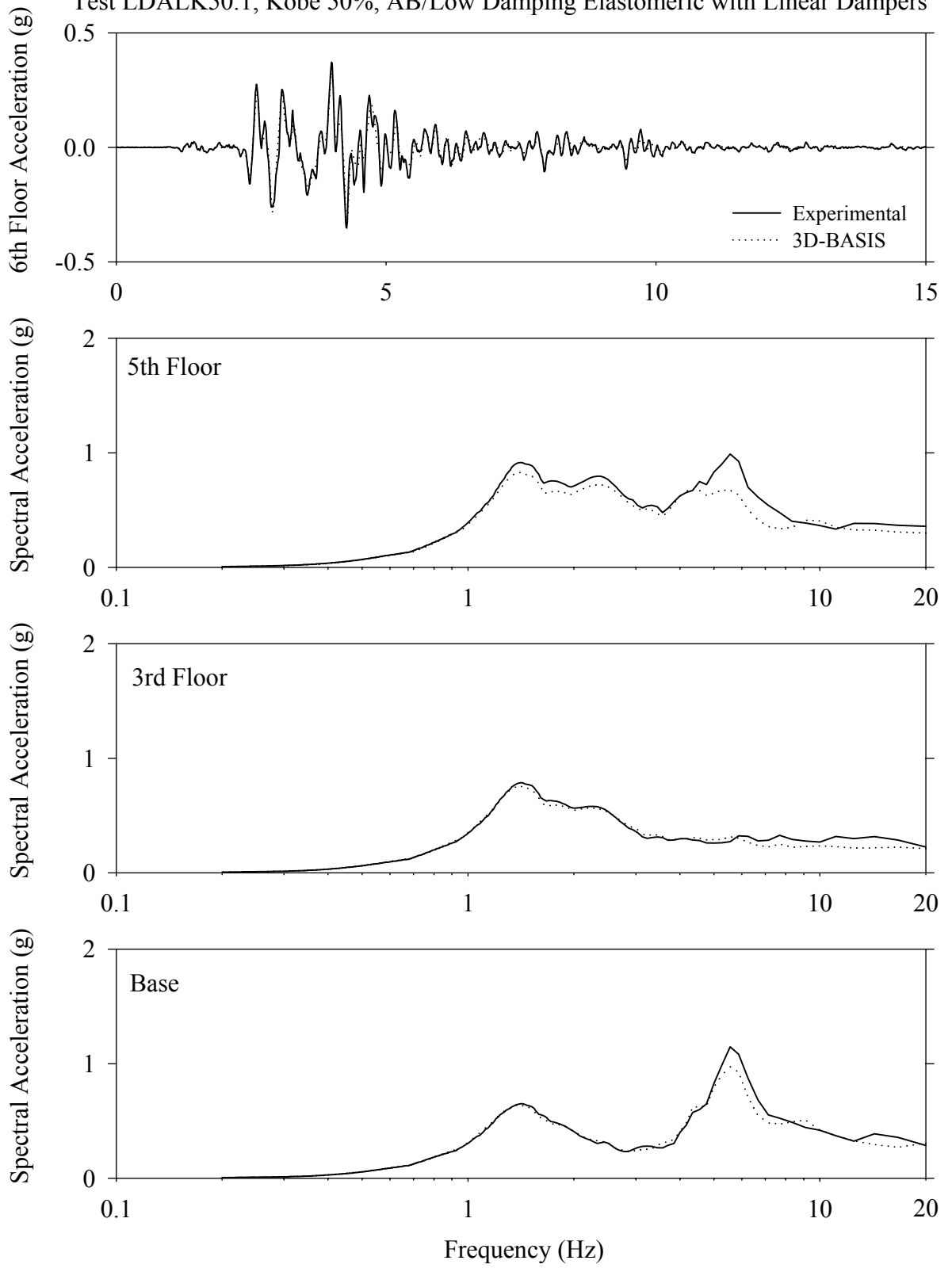
Test LDALE20.1, El Centro S00E 200%, AB/Low Damping Elastomeric with Linear Dampers



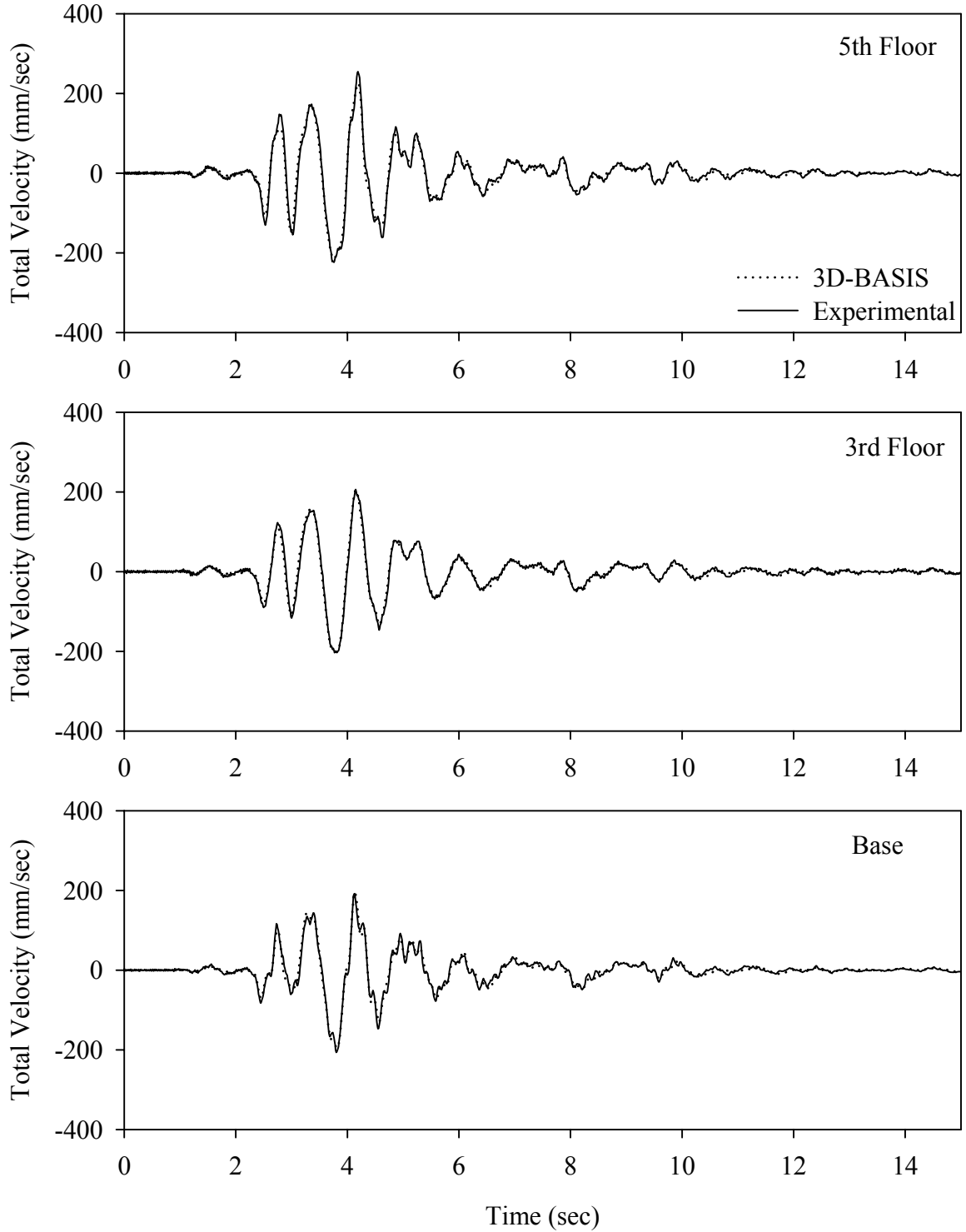
Test LDALK50.1, Kobe 50%, AB/Low Damping Elastomeric with Linear Dampers



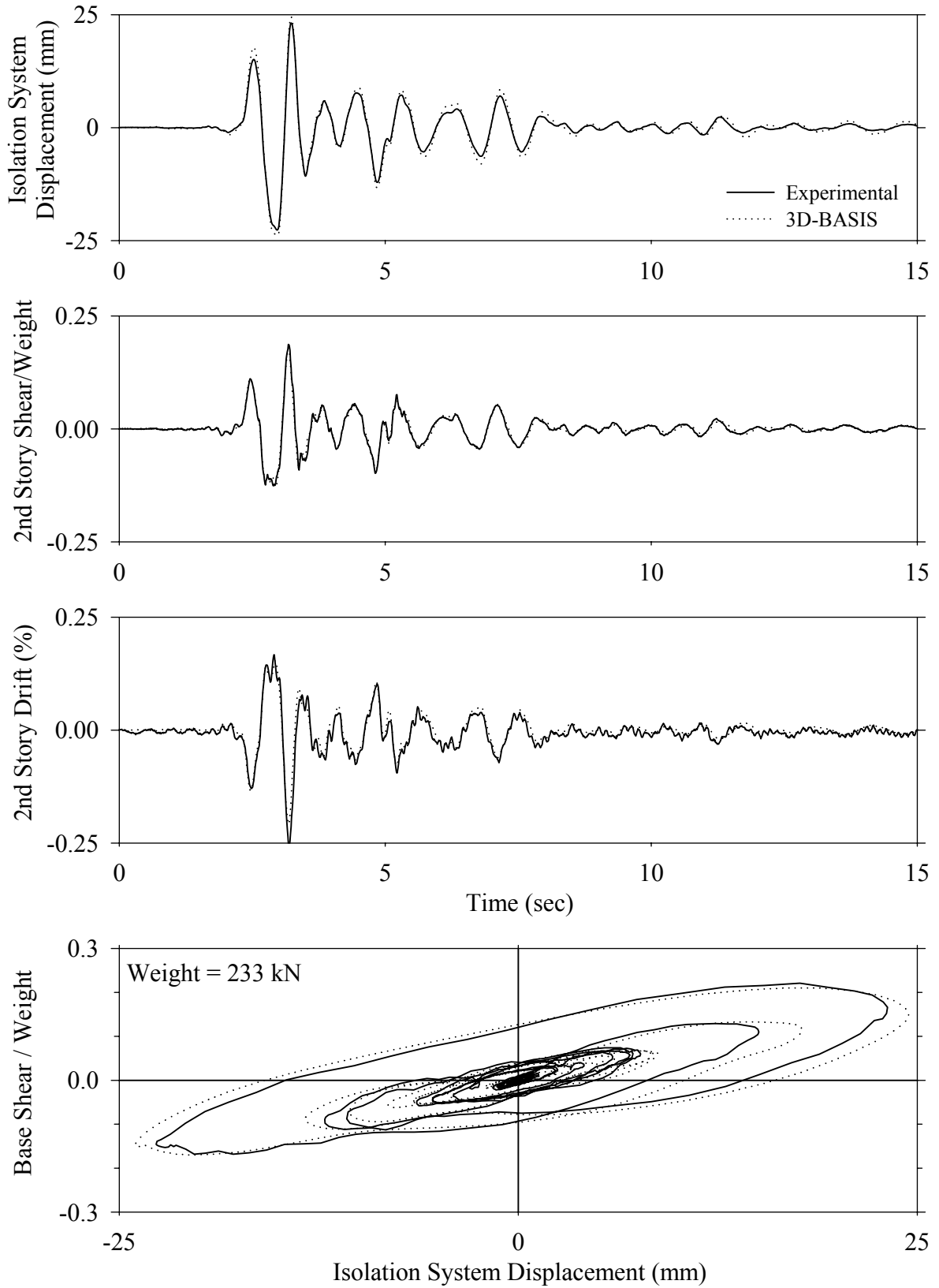
Test LDALK50.1, Kobe 50%, AB/Low Damping Elastomeric with Linear Dampers



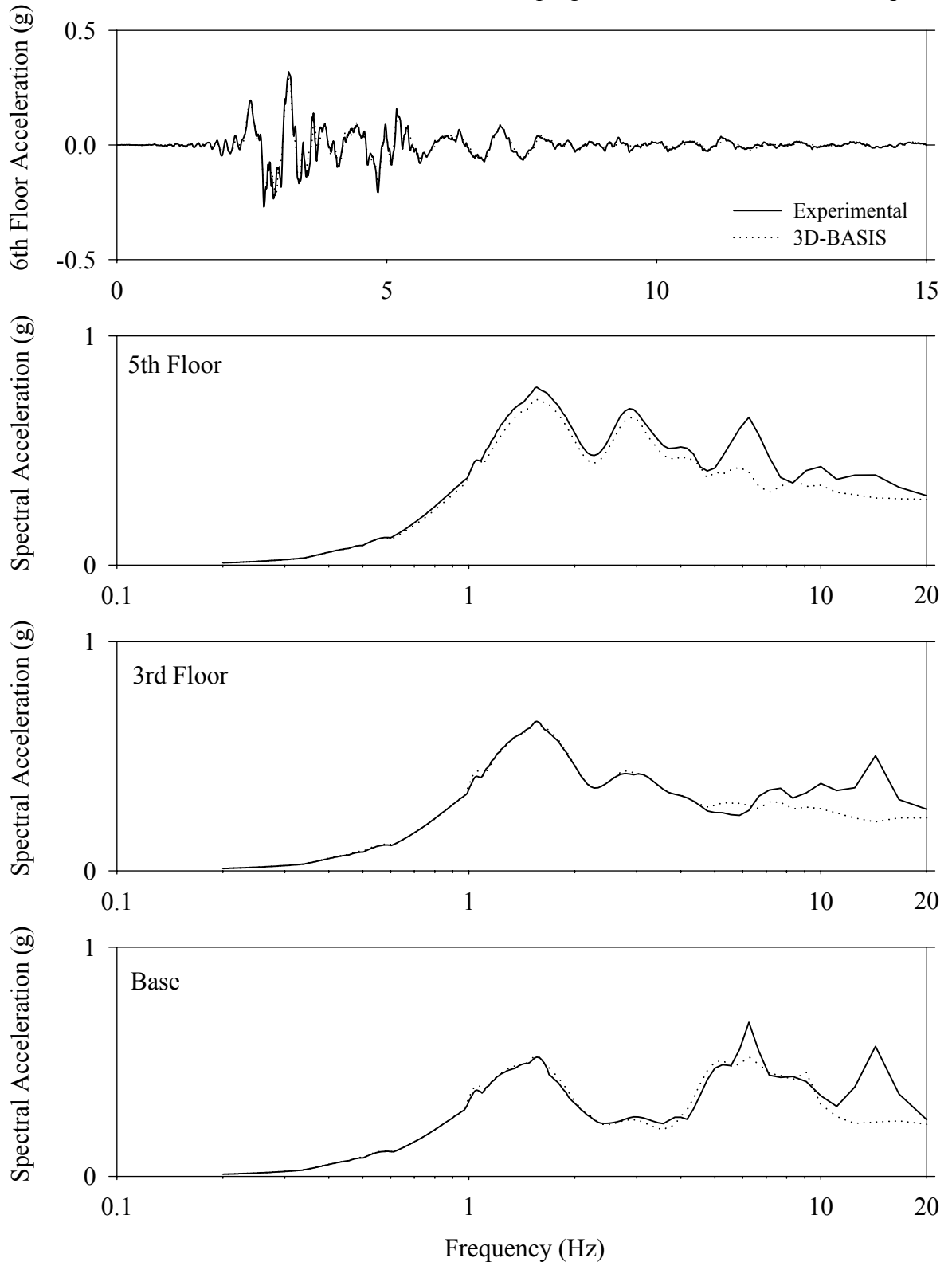
Test LDALK50.1, Kobe 50%, AB/Low Damping Elastomeric with Linear Dampers



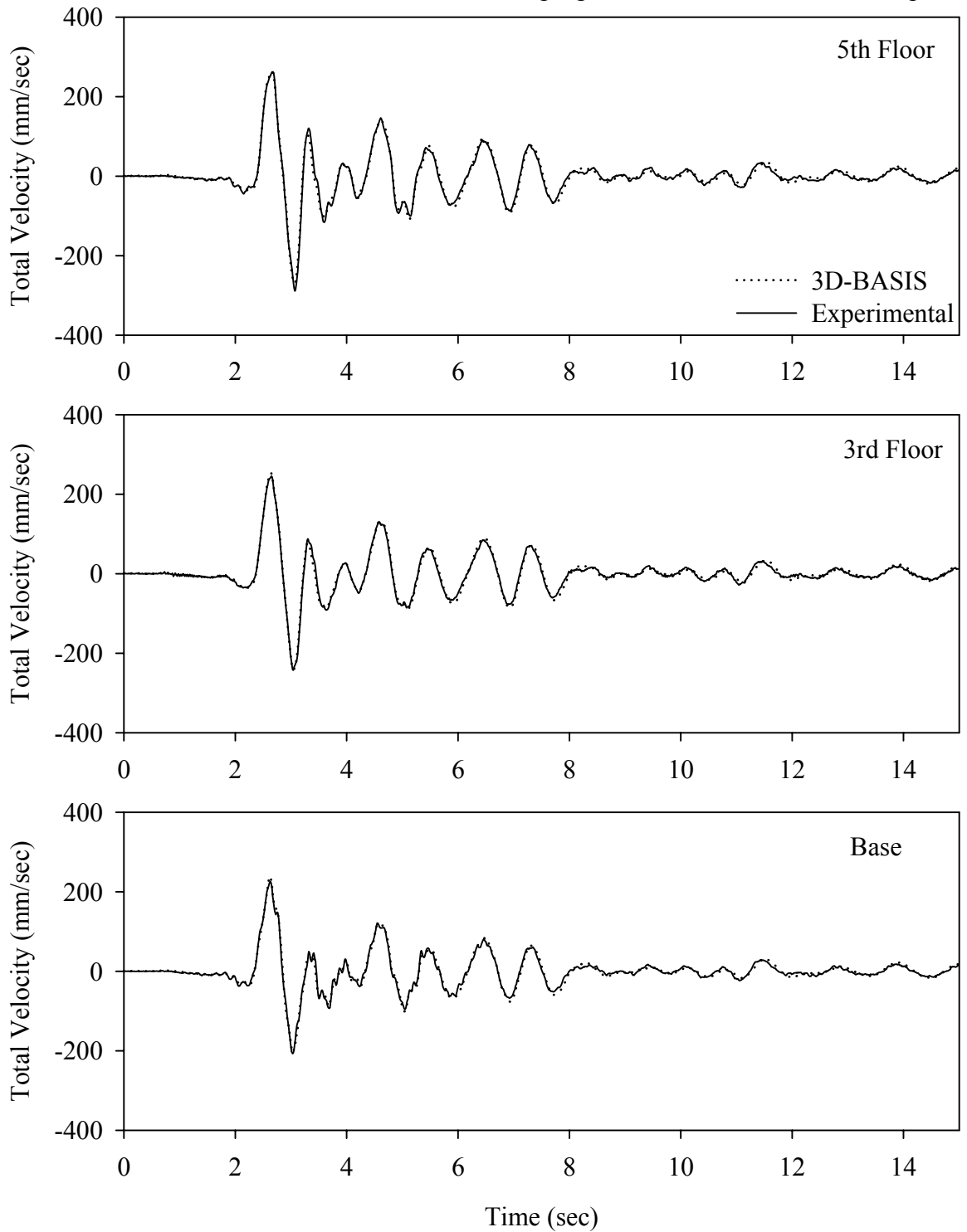
Test LDALN50.1, Newhall 360 50%, AB/Low Damping Elastomeric with Linear Dampers



Test LDALN50.1, Newhall 360 50%, AB/Low Damping Elastomeric with Linear Dampers

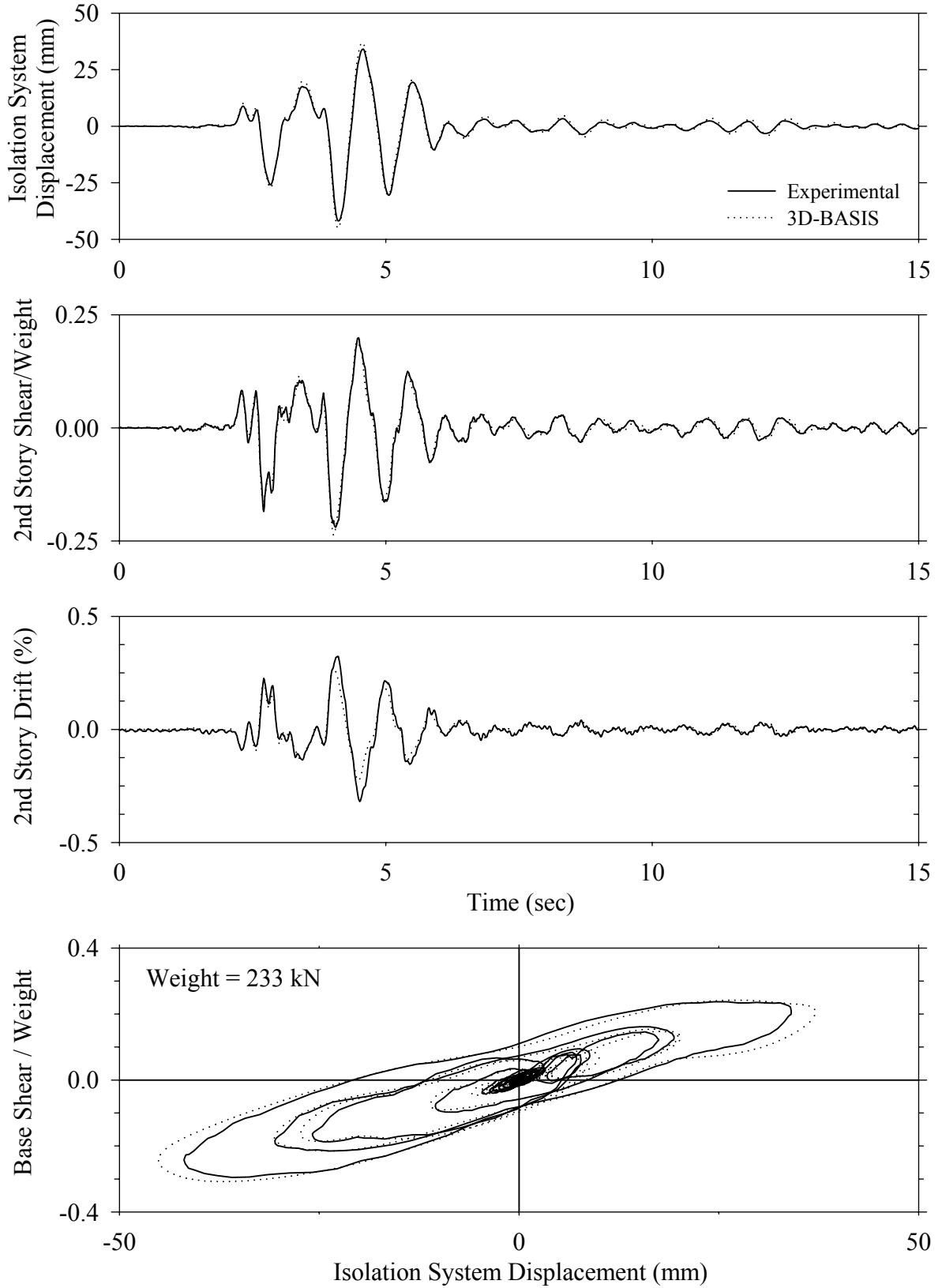


Test LDALN50.1, Newhall 360 50%, AB/Low Damping Elastomeric with Linear Dampers

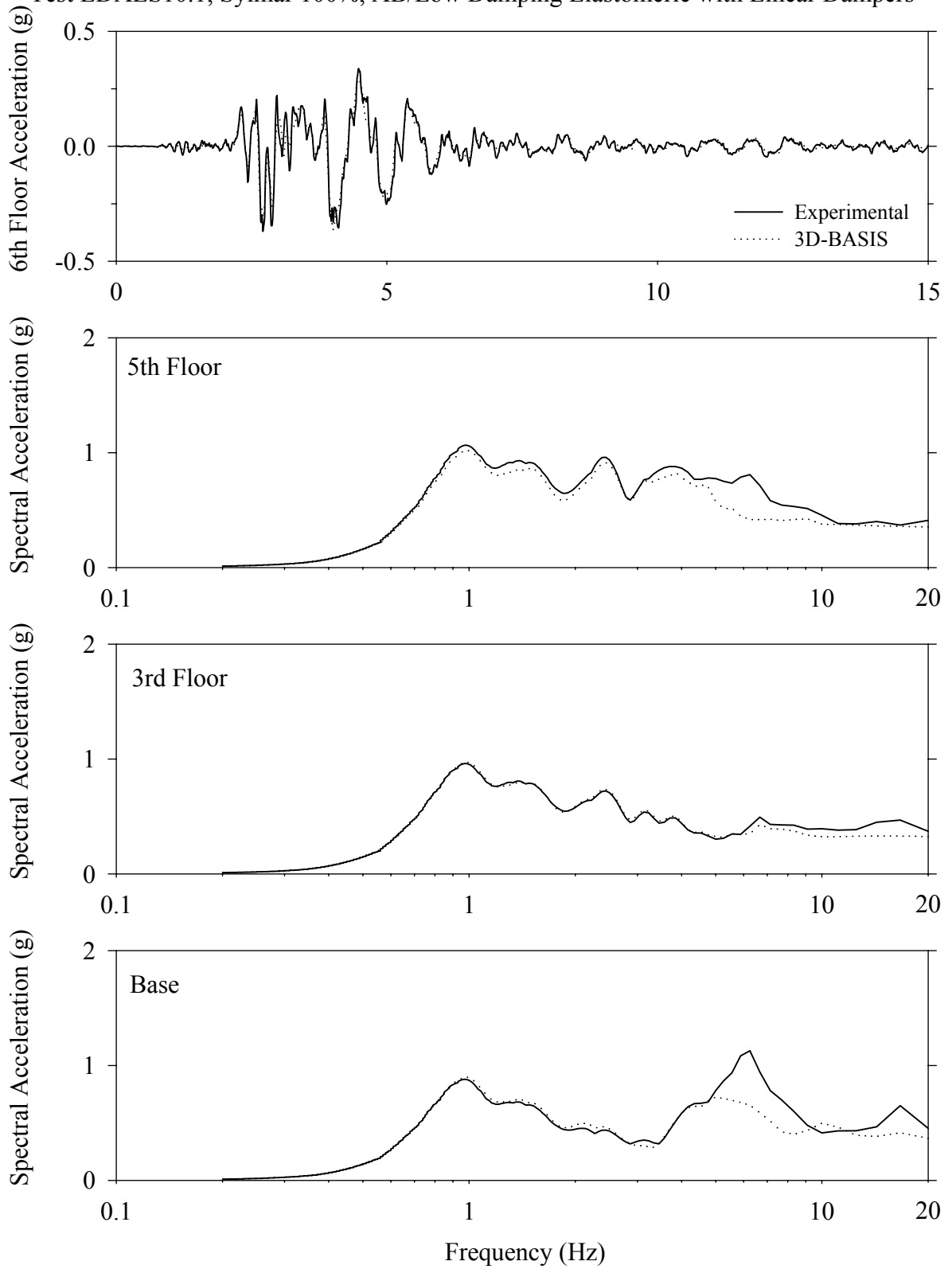




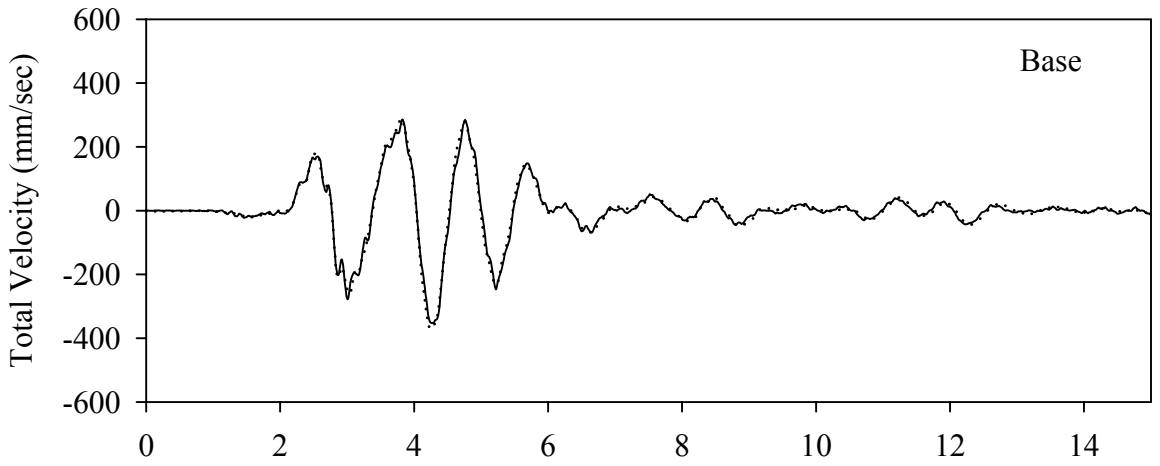
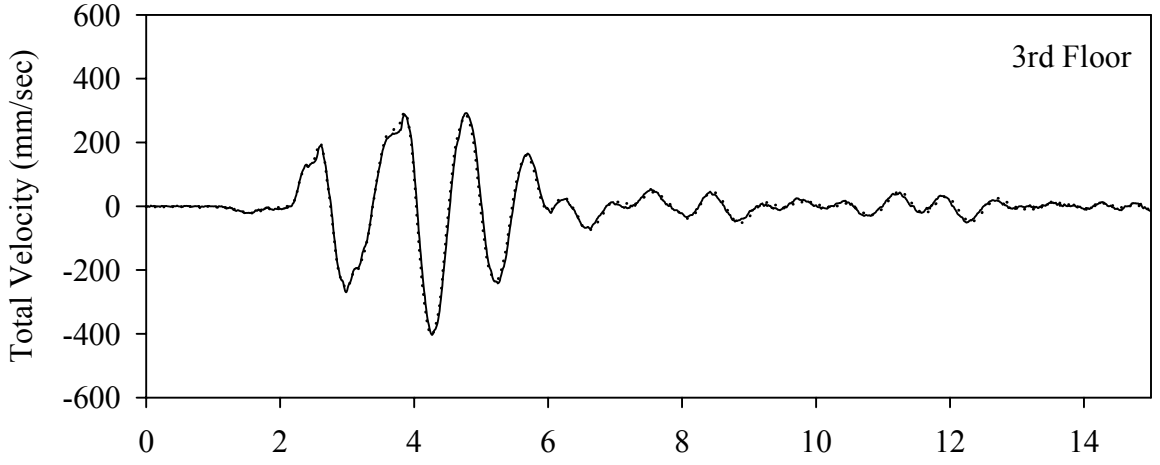
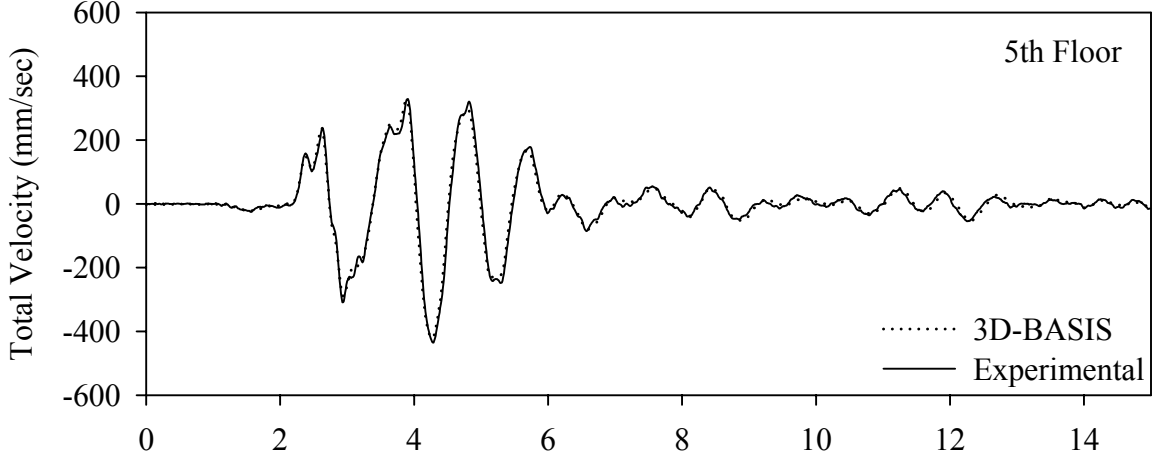
Test LDALS10.1, Sylmar 100%, AB/Low Damping Elastomeric with Linear Dampers



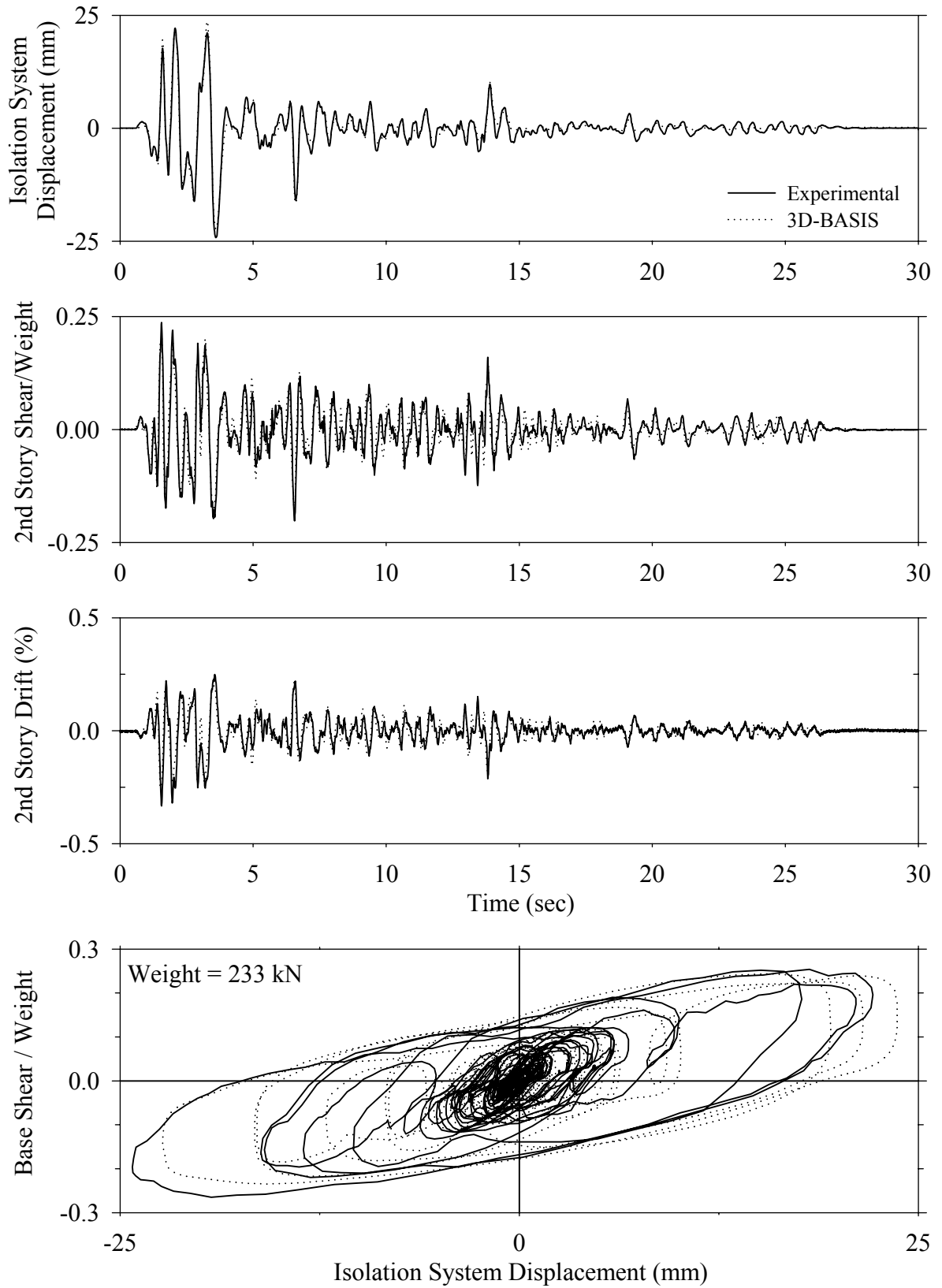
Test LDALS10.1, Sylmar 100%, AB/Low Damping Elastomeric with Linear Dampers



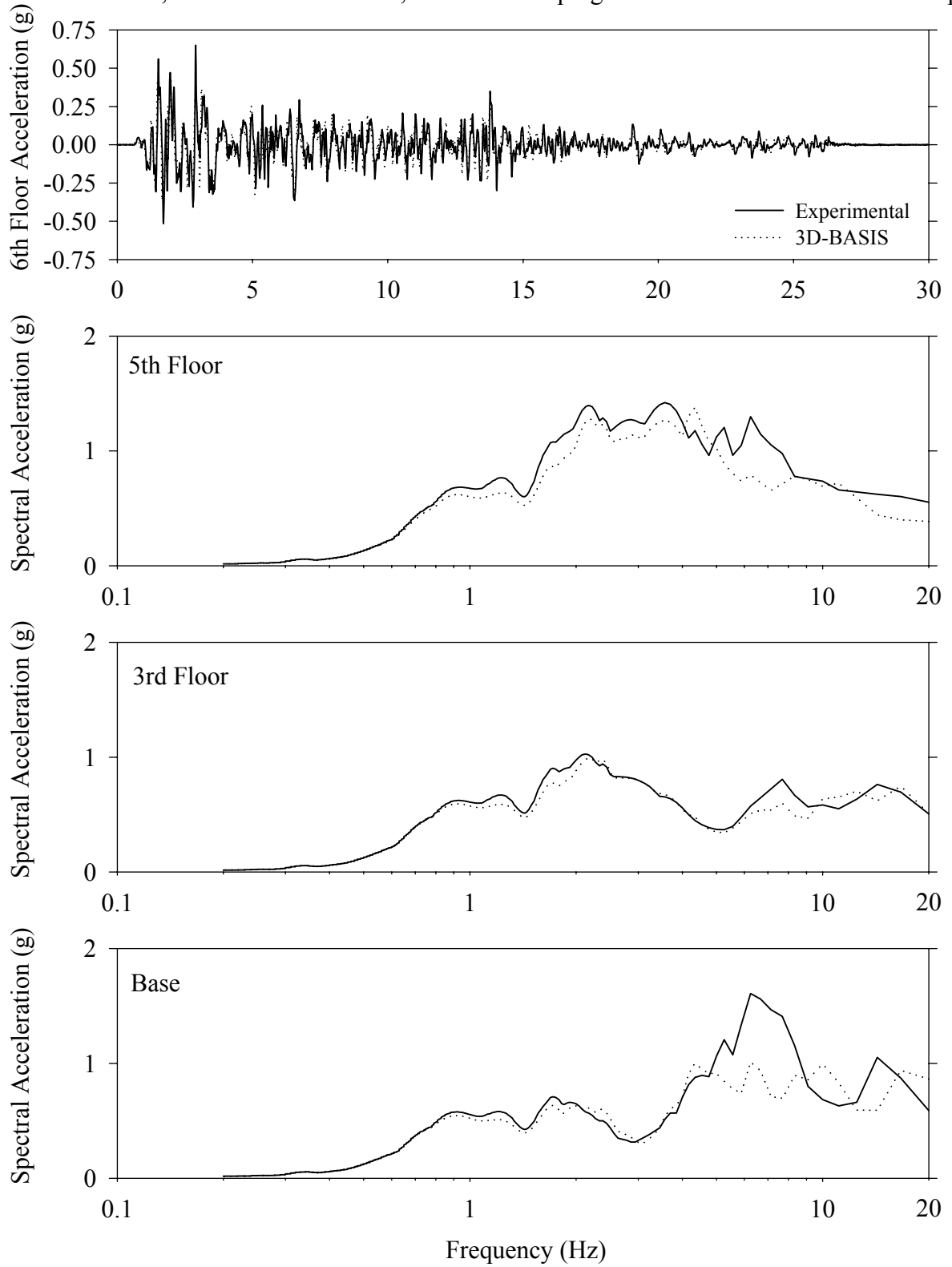
Test LDALS10.1, Sylmar 100%, AB/Low Damping Elastomeric with Linear Dampers



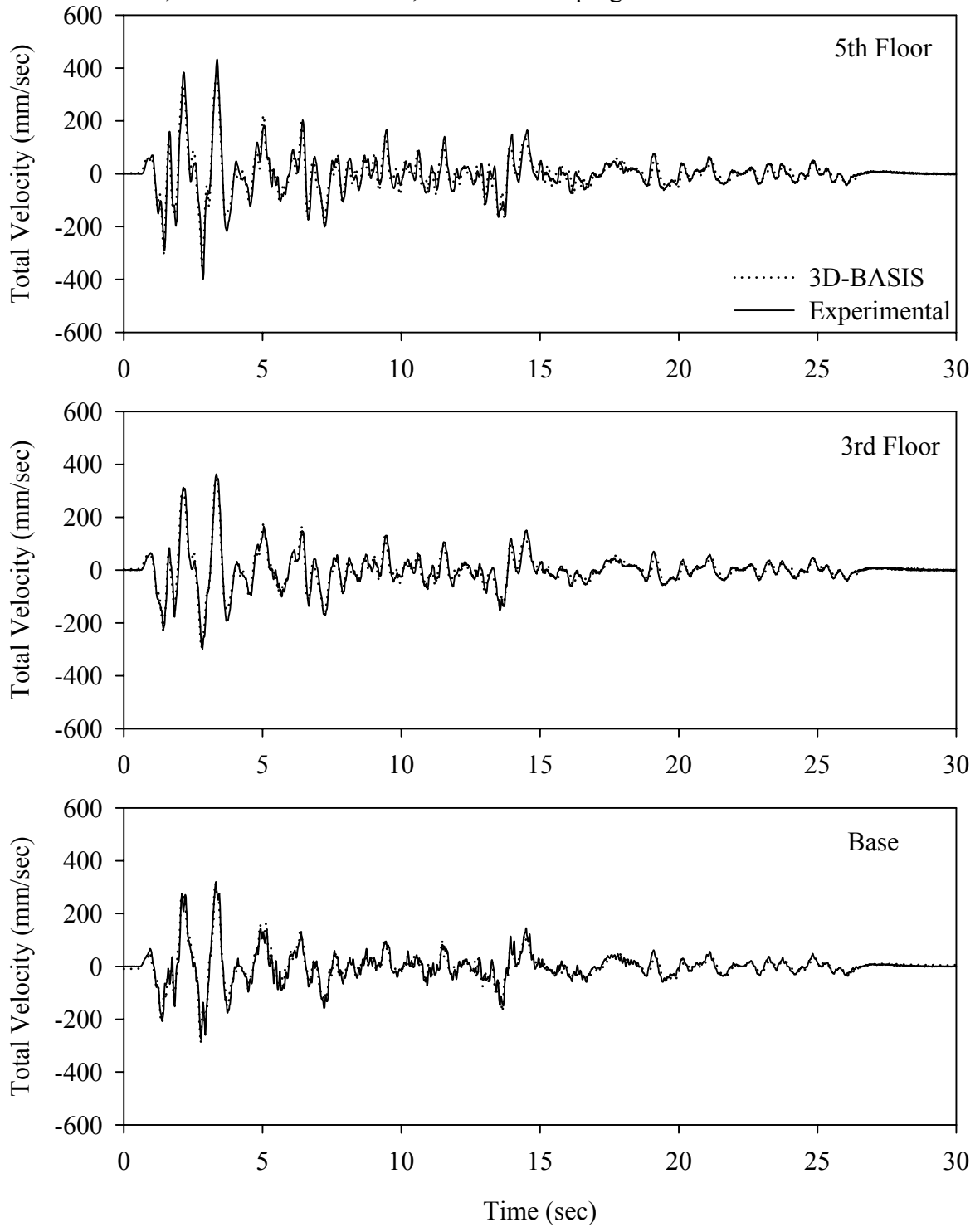
Test LDANE20.1, El Centro S00E 200%, AB/Low Damping Elastomeric with Nonlinear Dampers



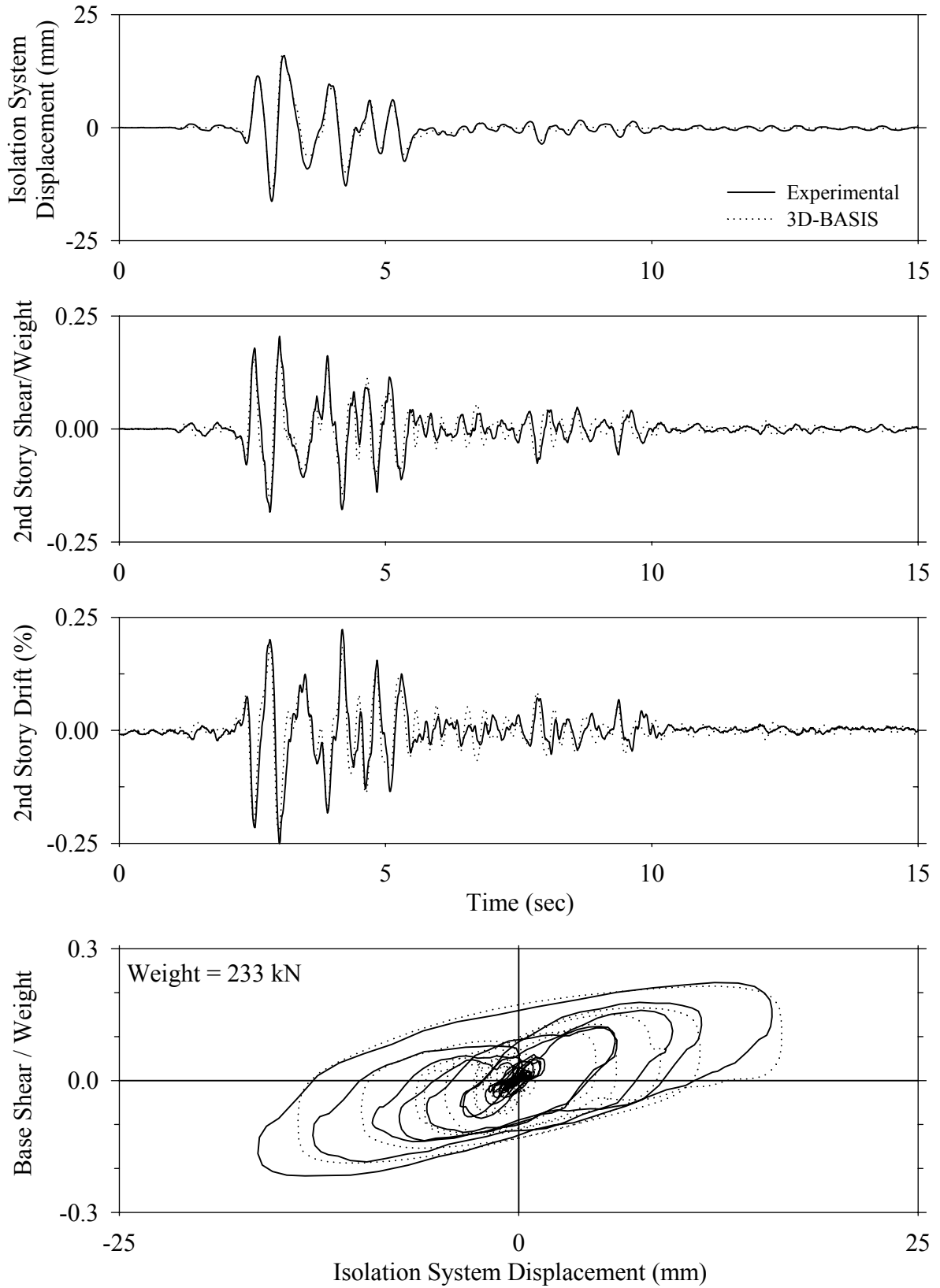
Test LDANE20.1, El Centro S00E 200%, AB/Low Damping Elastomeric with Nonlinear Dampers



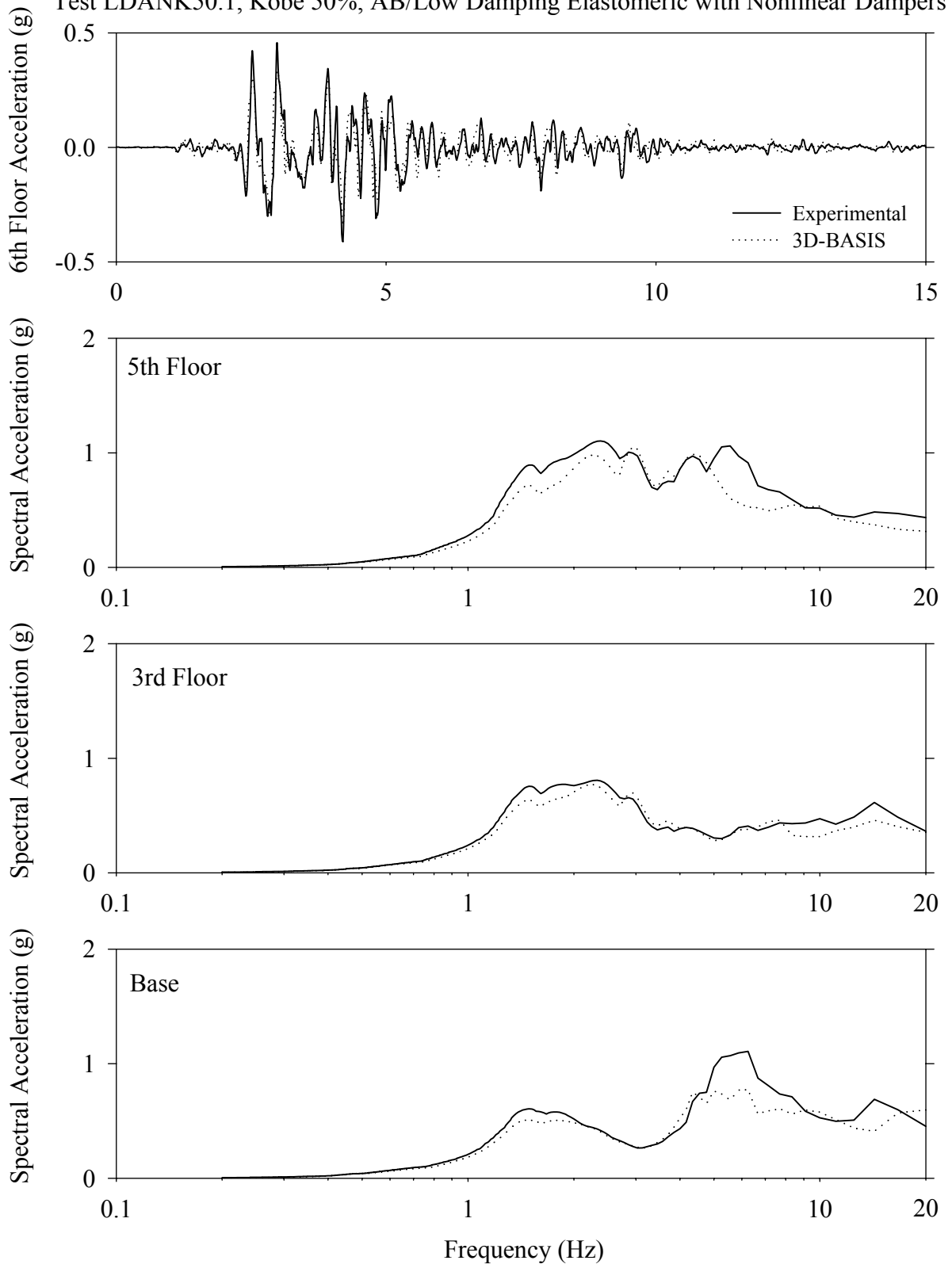
Test LDANE20.1, El Centro S00E 200%, AB/Low Damping Elastomeric with Nonlinear Dampers



Test LDANK50.1, Kobe 50%, AB/Low Damping Elastomeric with Nonlinear Dampers

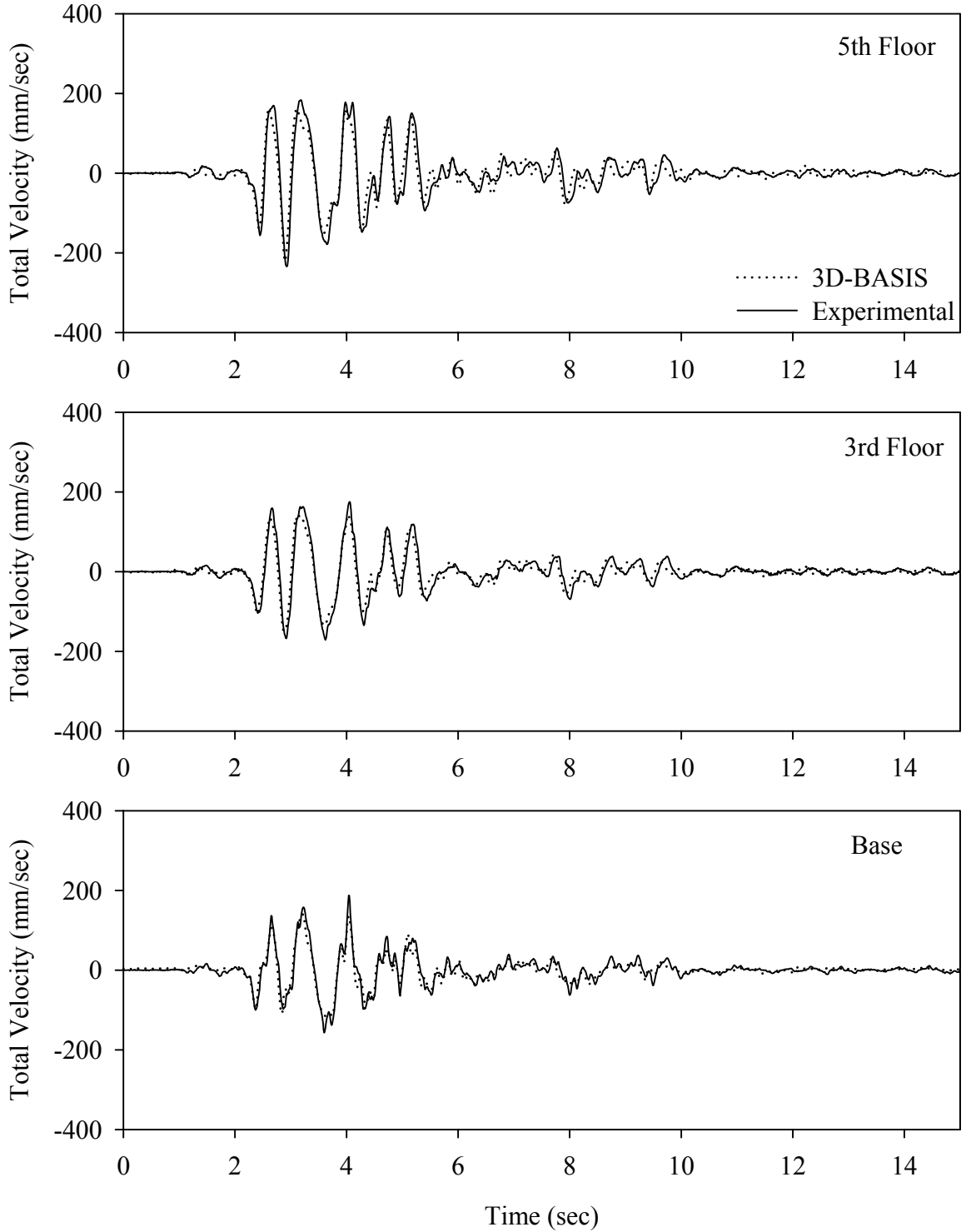


Test LDANK50.1, Kobe 50%, AB/Low Damping Elastomeric with Nonlinear Dampers

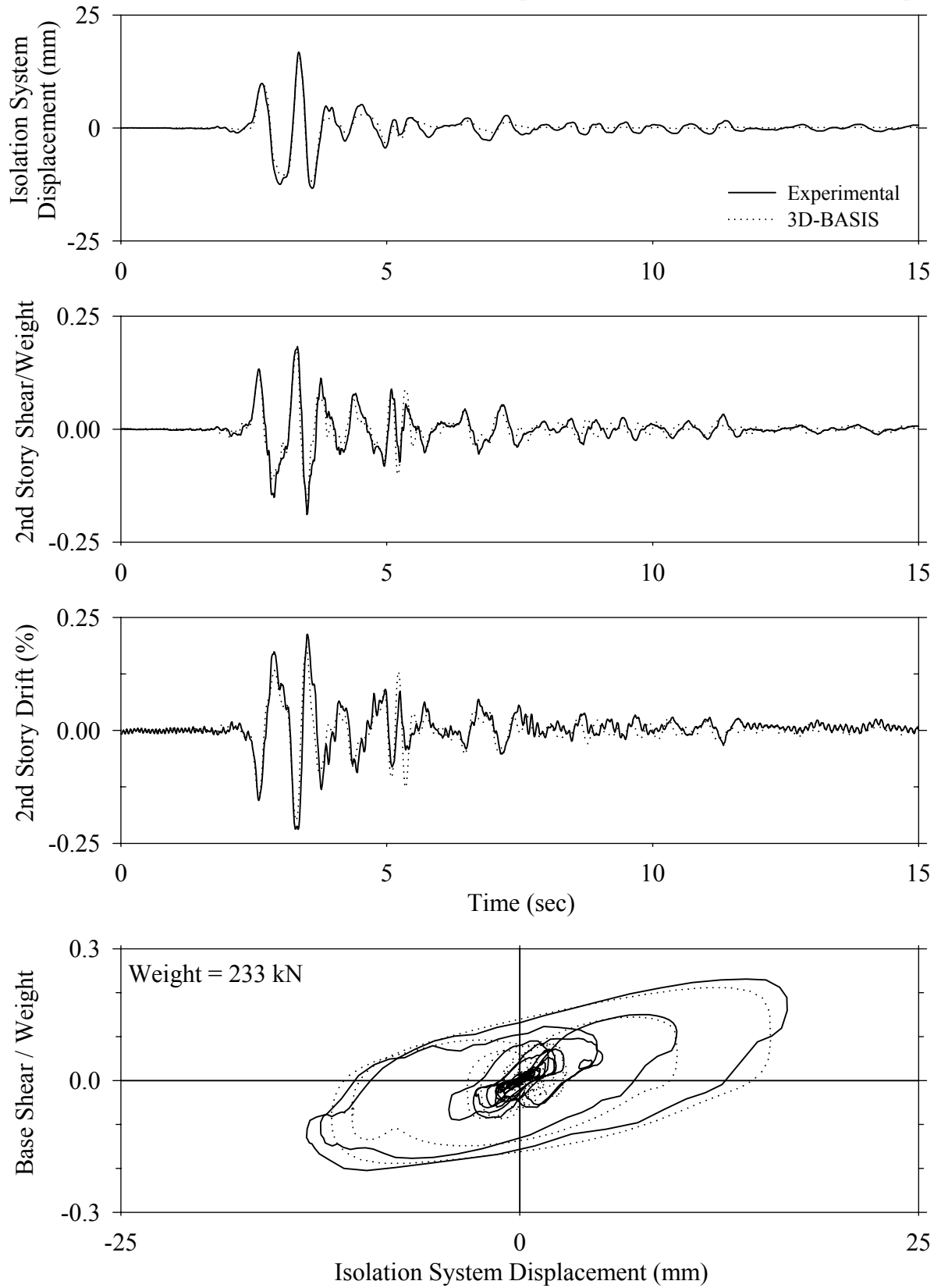




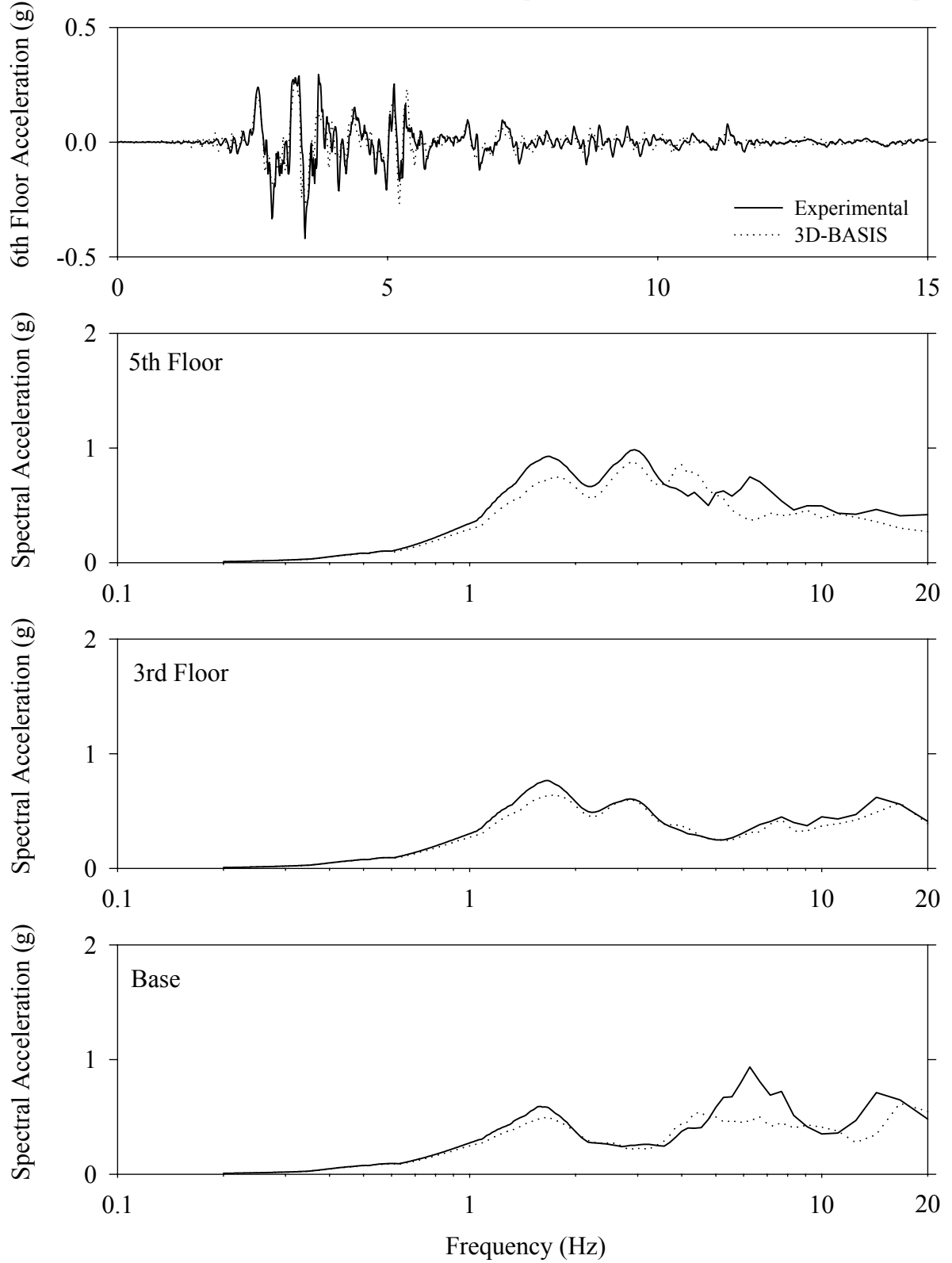
Test LDANK50.1, Kobe 50%, AB/Low Damping Elastomeric with Nonlinear Dampers



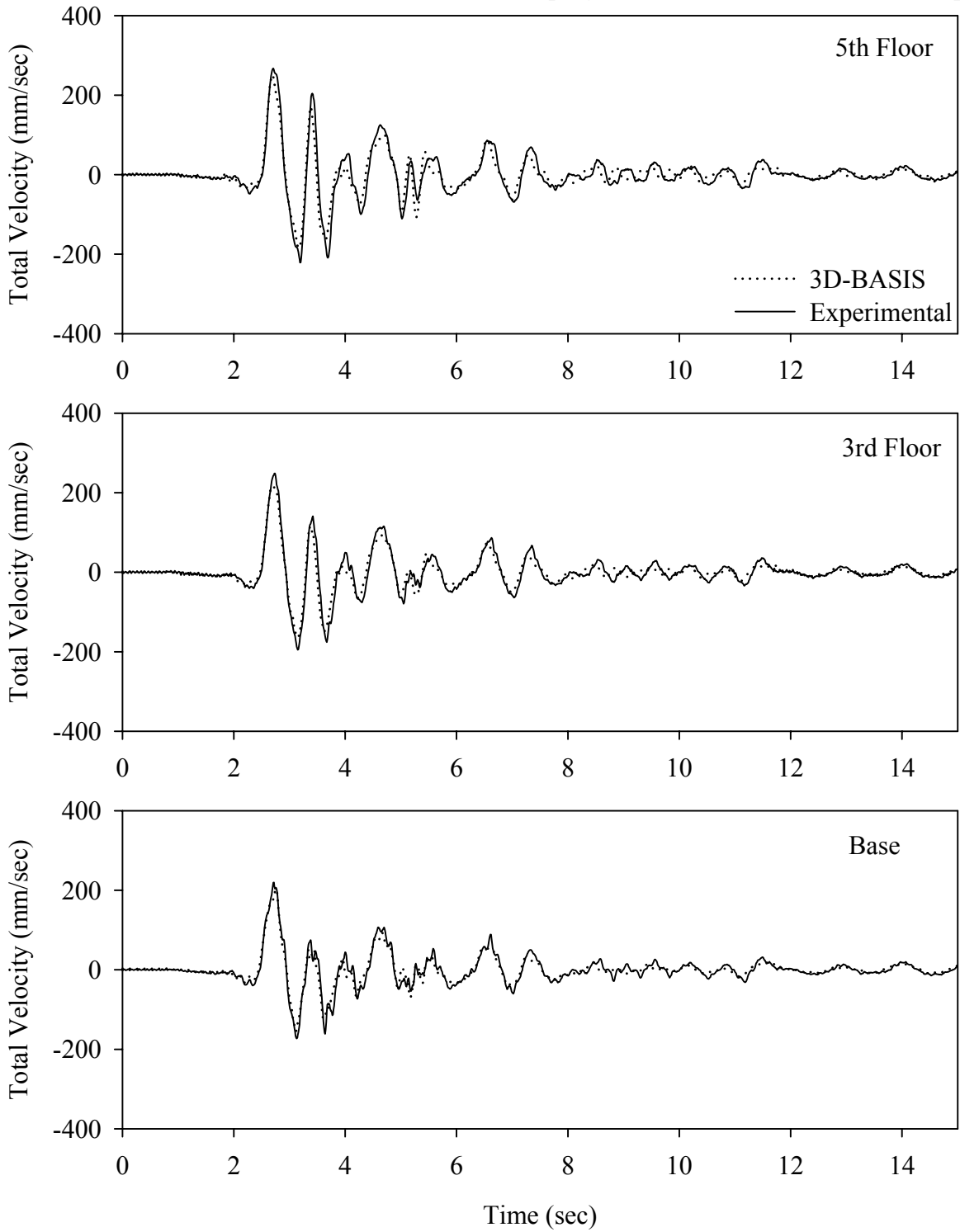
Test LDANN50.1, Newhall 360 50%, AB/Low Damping Elastomeric with Nonlinear Dampers



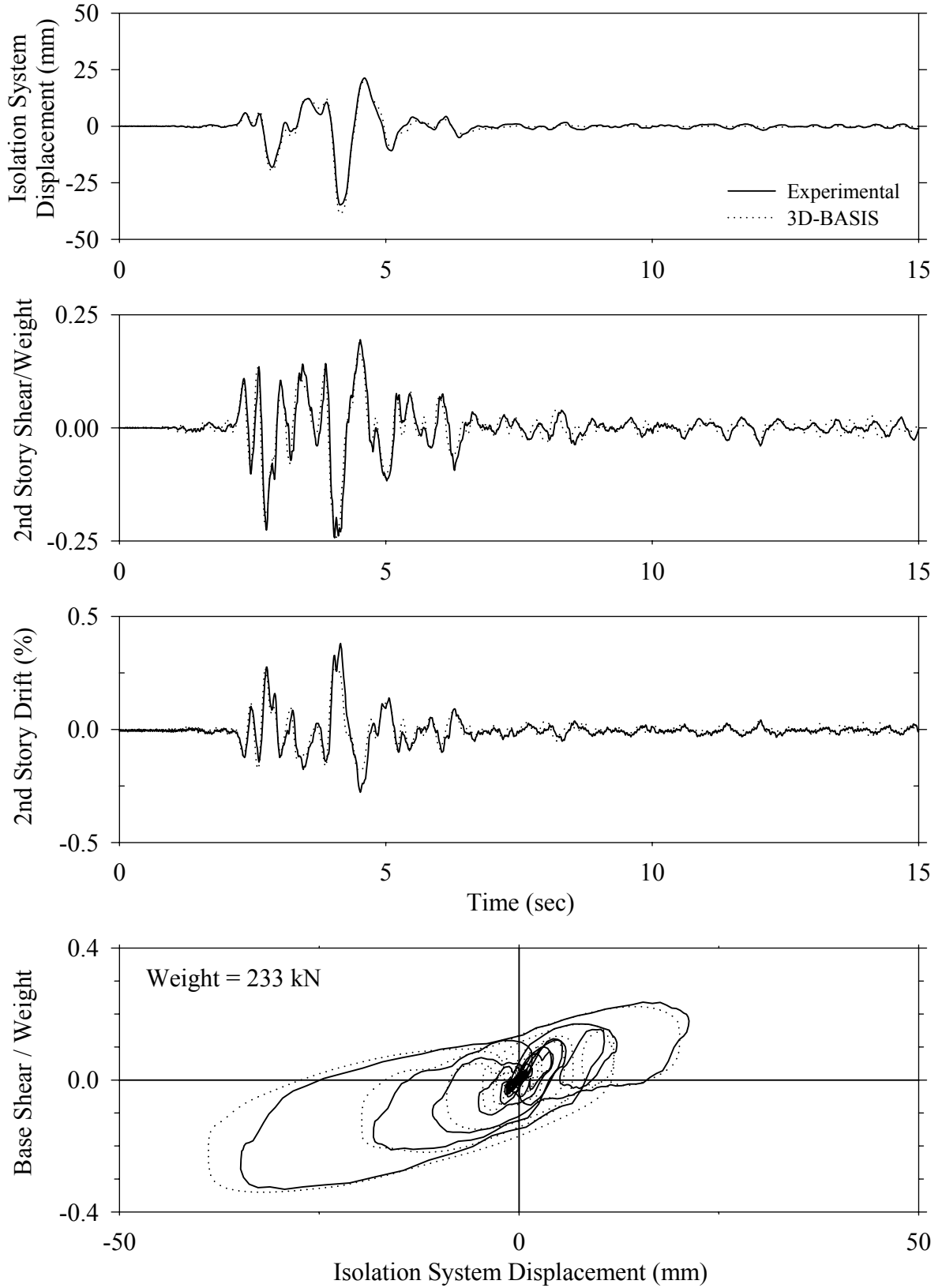
Test LDANN50.1, Newhall 360 50%, AB/Low Damping Elastomeric with Nonlinear Dampers



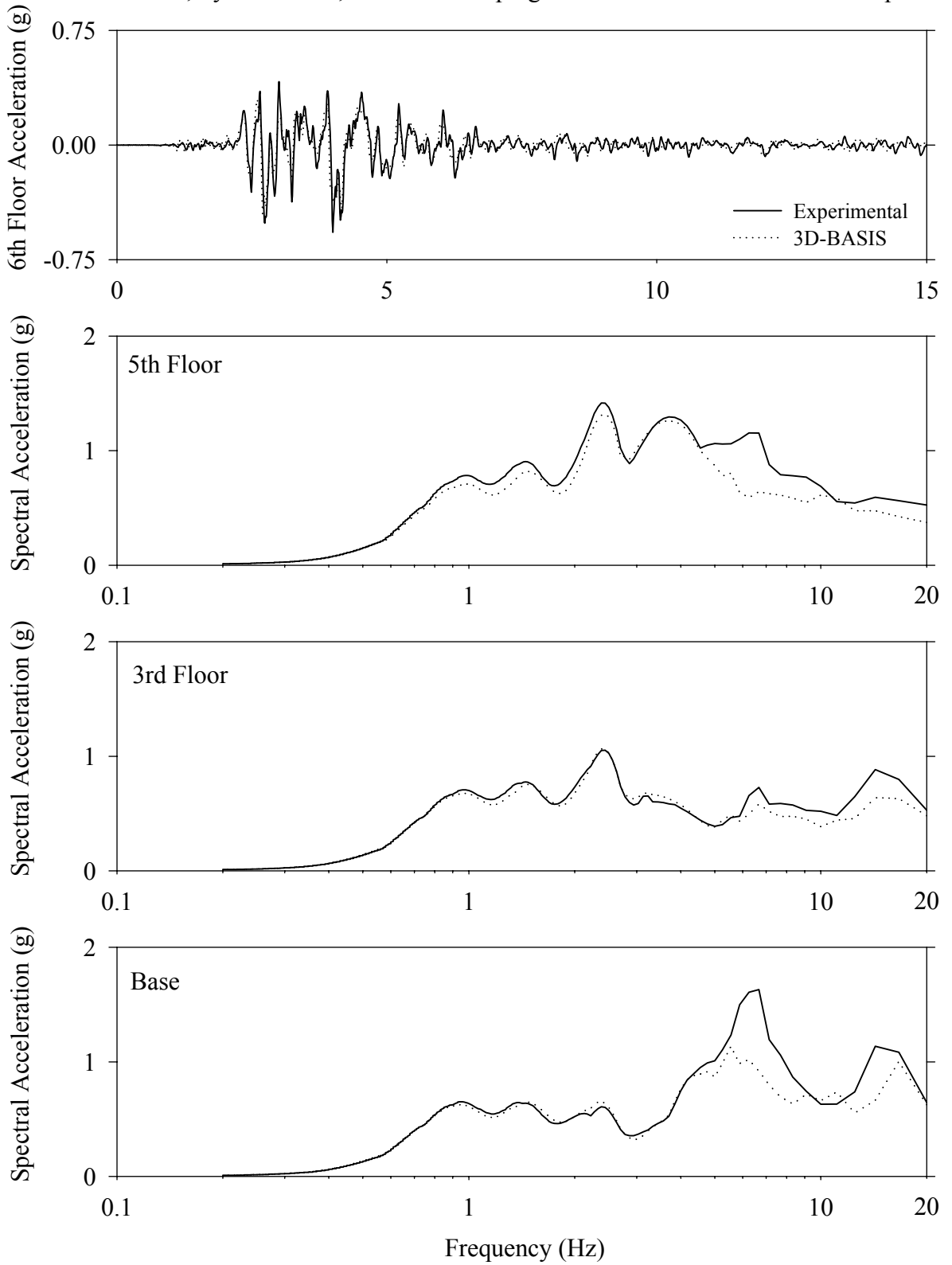
Test LDANN50.1, Newhall 360 50%, AB/Low Damping Elastomeric with Nonlinear Dampers



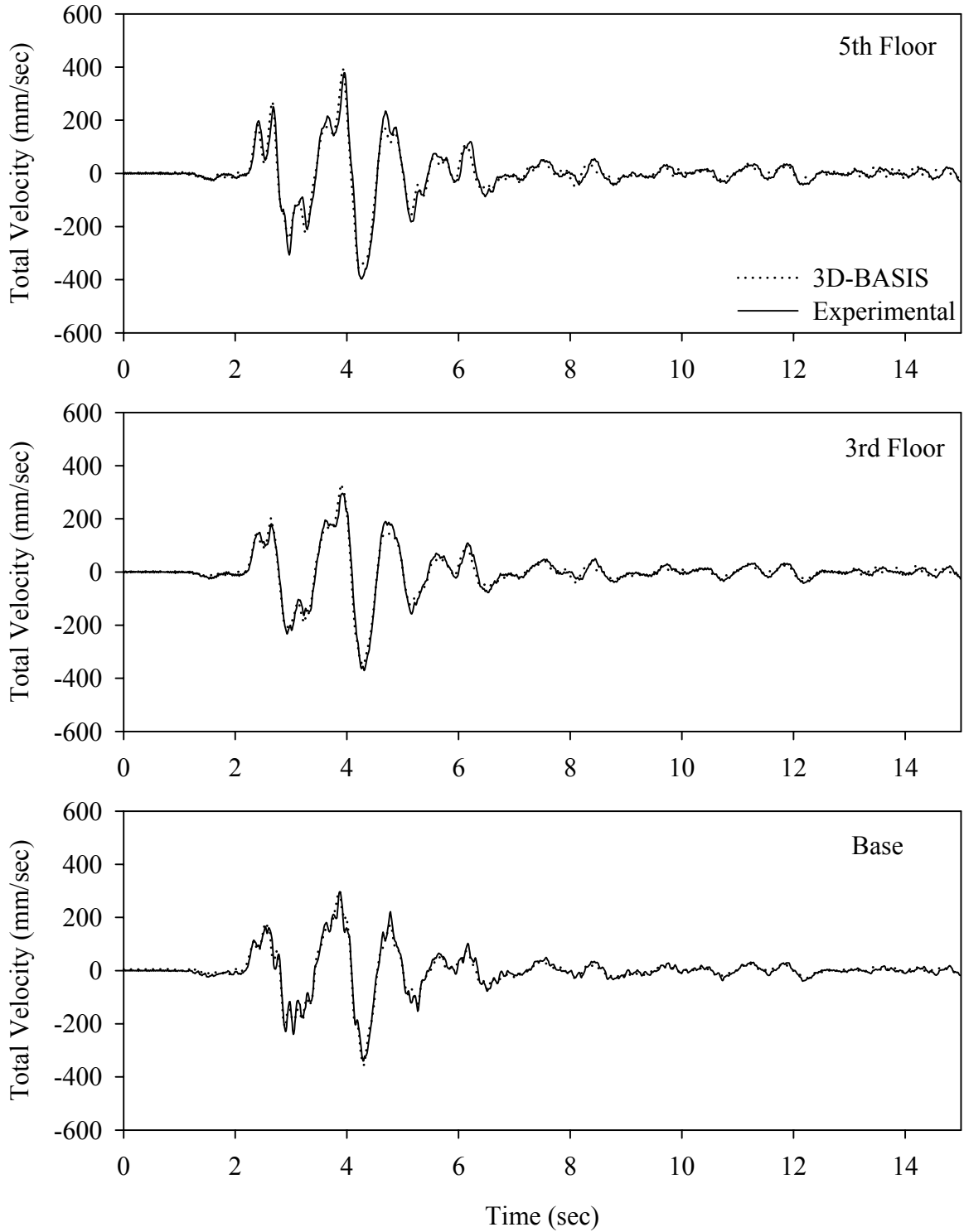
Test LDANS10.1, Sylmar 100%, AB/Low Damping Elastomeric with Nonlinear Dampers



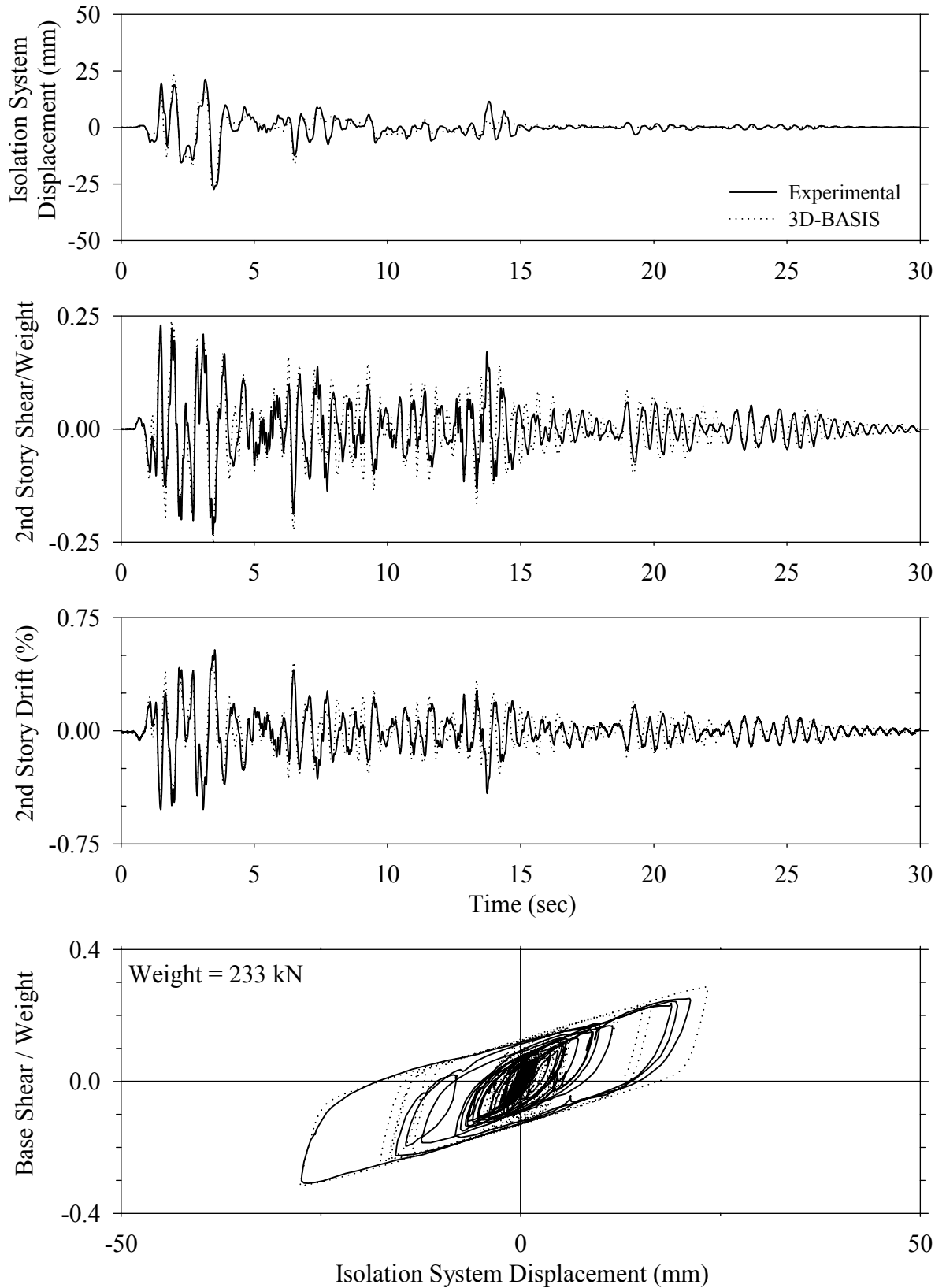
Test LDANS10.1, Sylmar 100%, AB/Low Damping Elastomeric with Nonlinear Dampers



Test LDANS10.1, Sylmar 100%, AB/Low Damping Elastomeric with Nonlinear Dampers

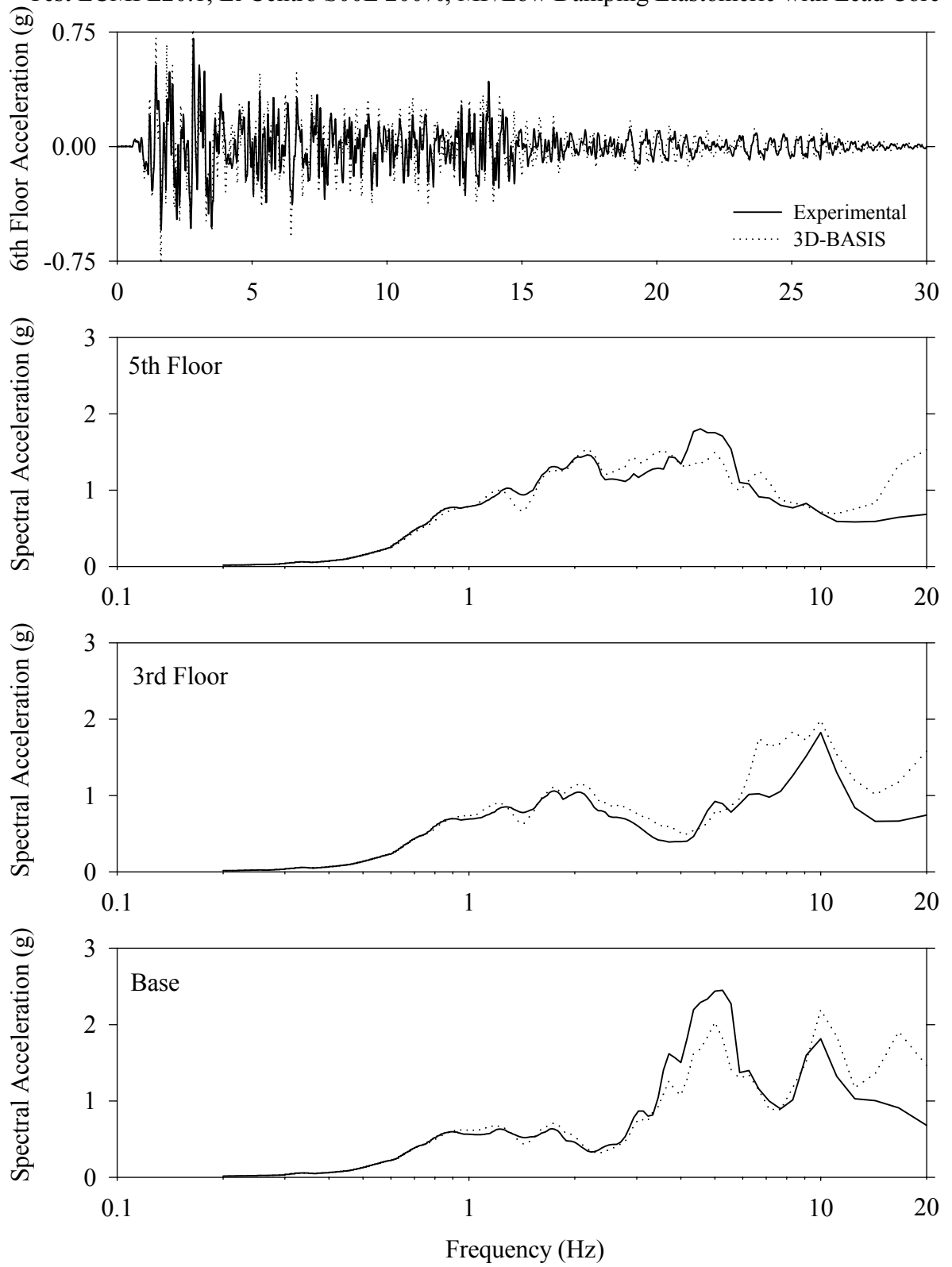


Test LCMFE20.1, El Centro S00E 200%, MF/Low Damping Elastomeric with Lead Core

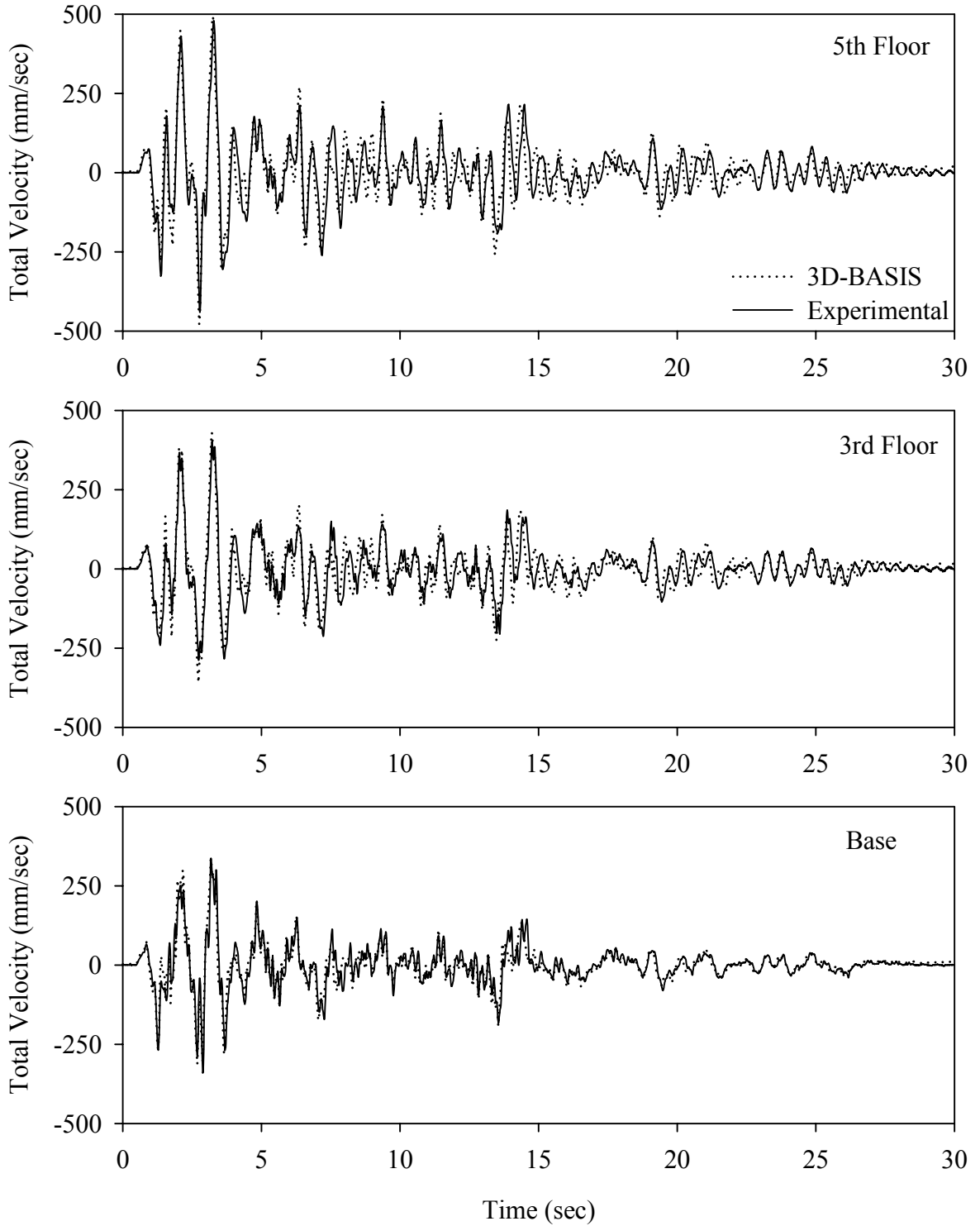




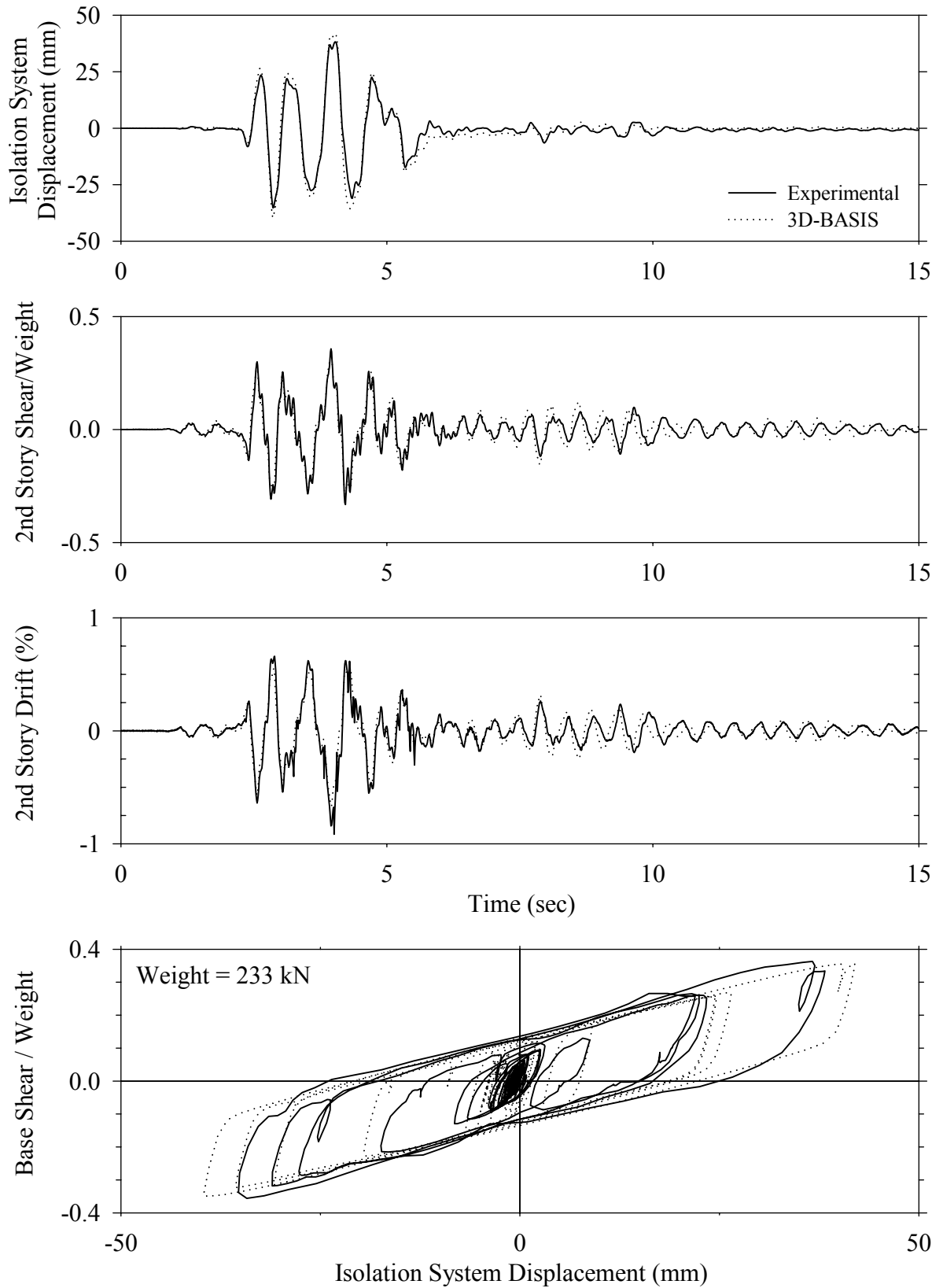
Test LCMFE20.1, El Centro S00E 200%, MF/Low Damping Elastomeric with Lead Core



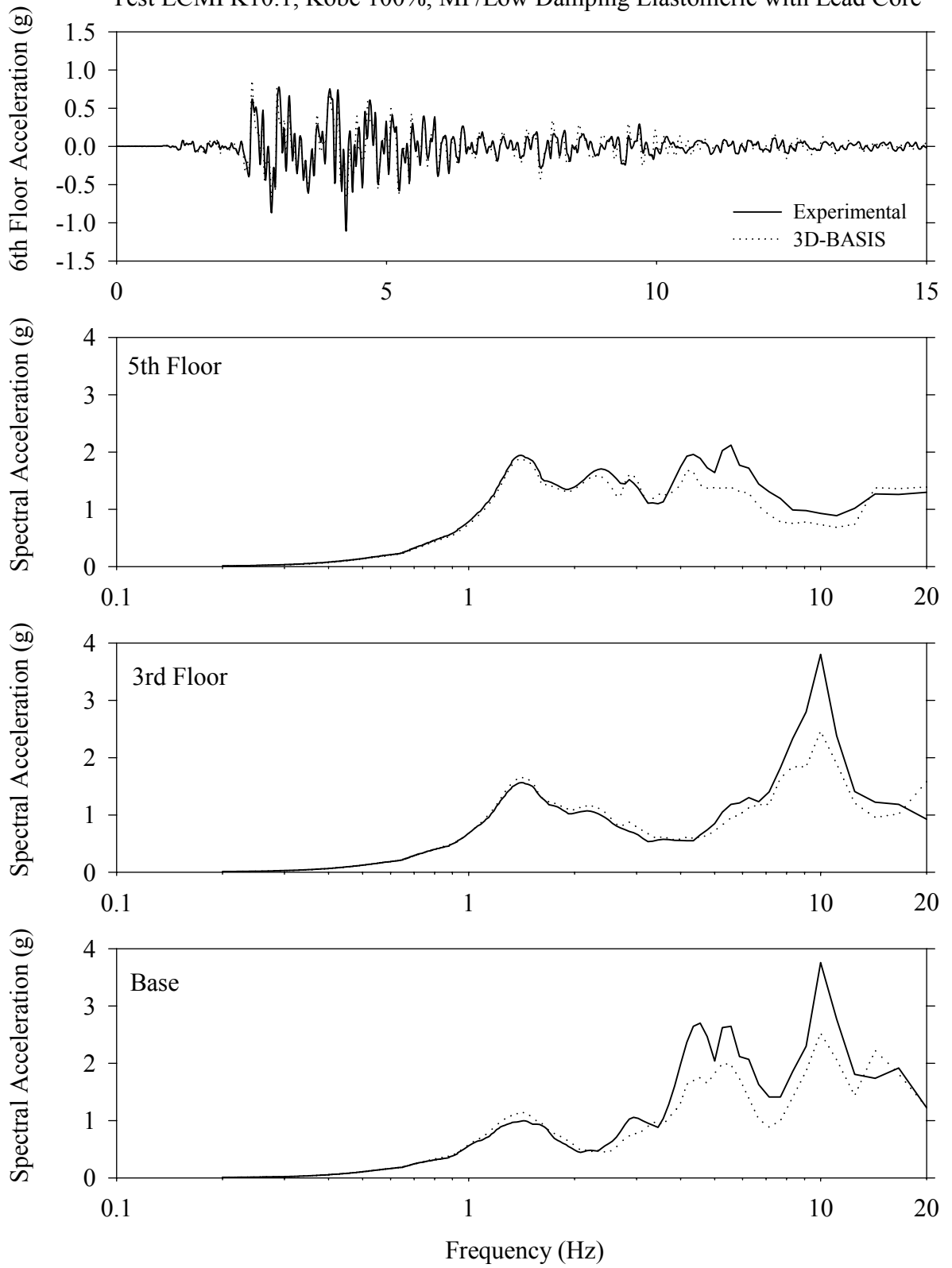
Test LCMFE20.1, El Centro S00E 200%, MF/Low Damping Elastomeric with Lead Core



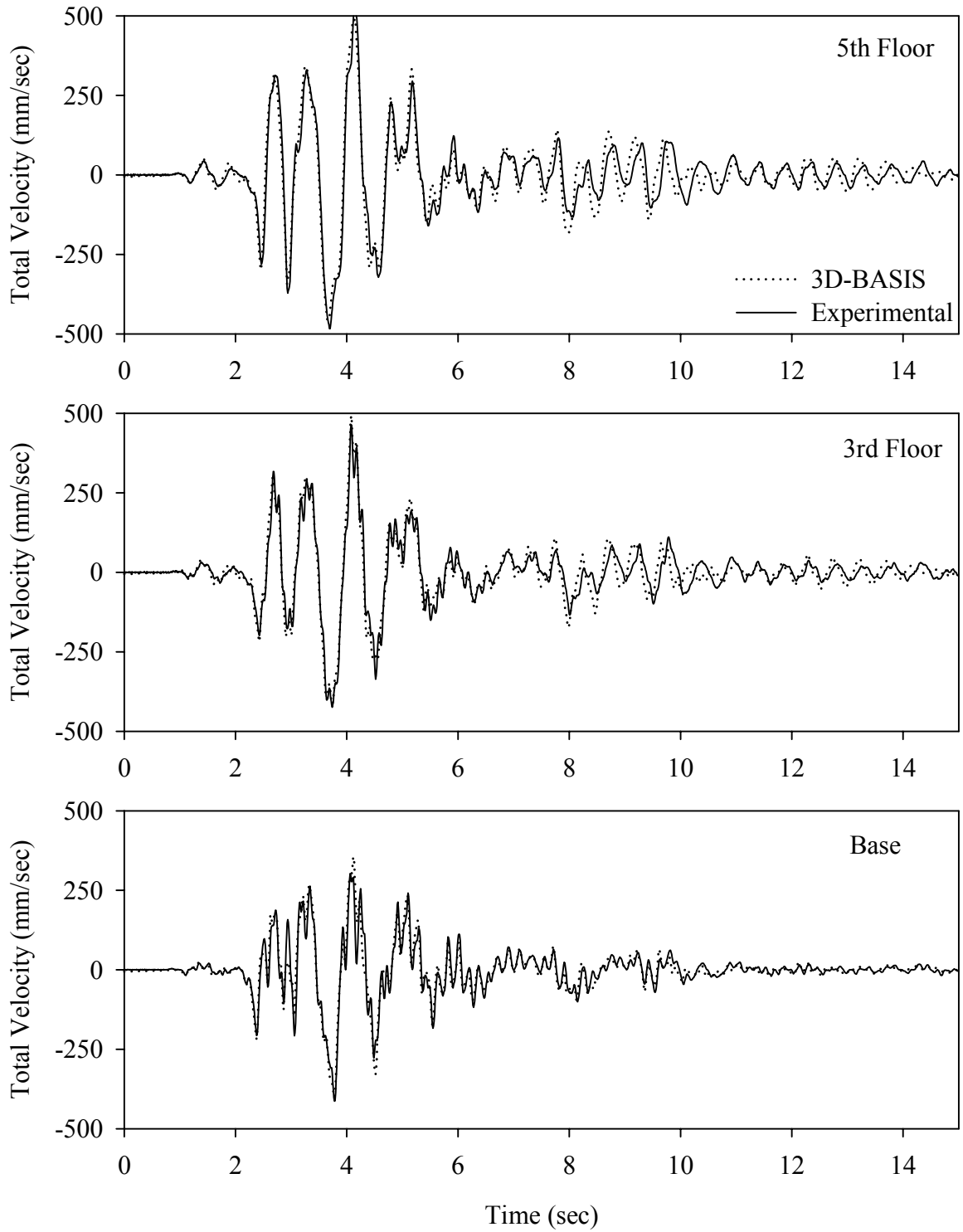
Test LCMFK10.1, Kobe 100%, MF/Low Damping Elastomeric with Lead Core



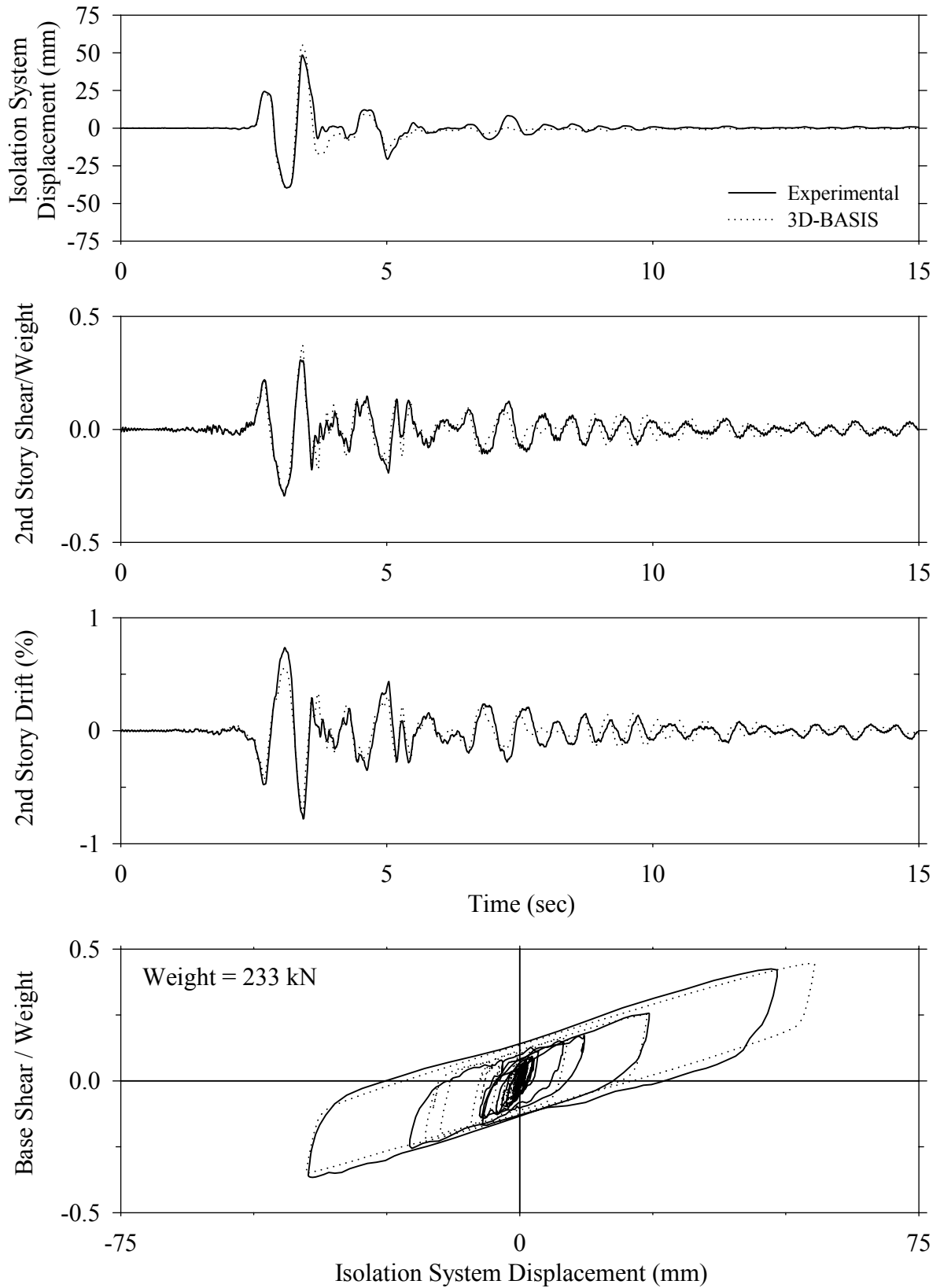
Test LCMFK10.1, Kobe 100%, MF/Low Damping Elastomeric with Lead Core



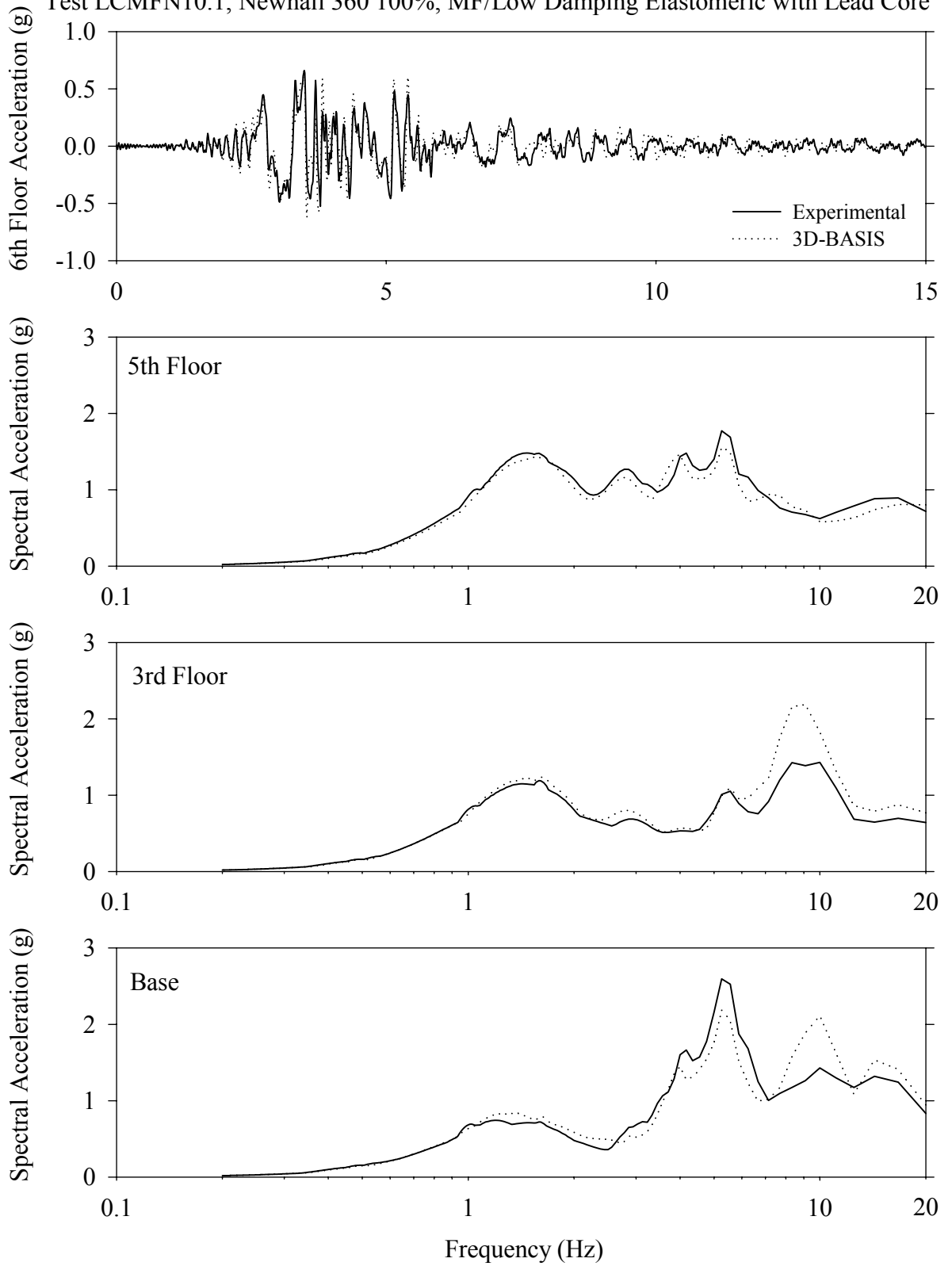
Test LCMFK10.1, Kobe 100%, MF/Low Damping Elastomeric with Lead Core



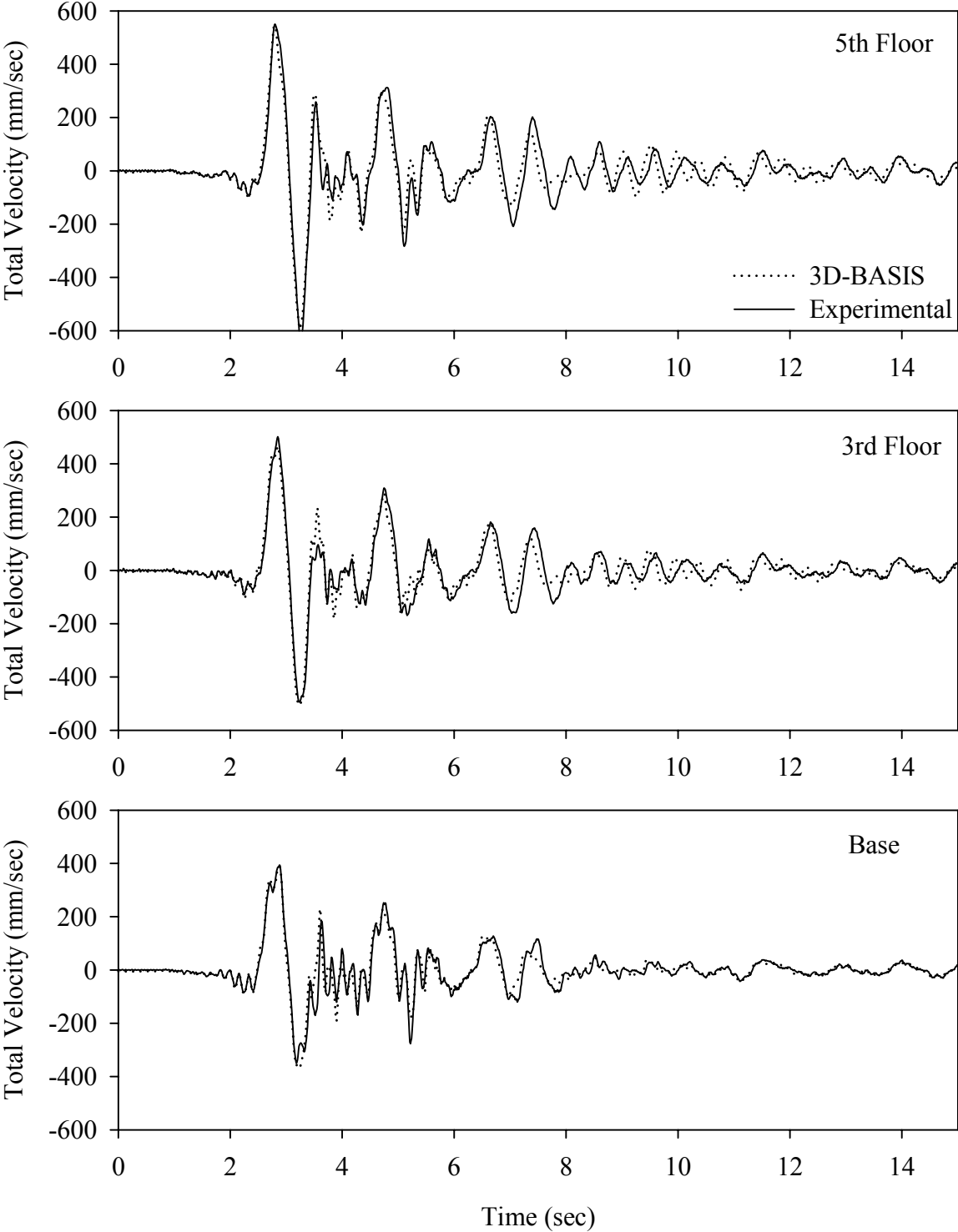
Test LCMFN10.1, Newhall 360 100%, MF/Low Damping Elastomeric with Lead Core



Test LCMFN10.1, Newhall 360 100%, MF/Low Damping Elastomeric with Lead Core

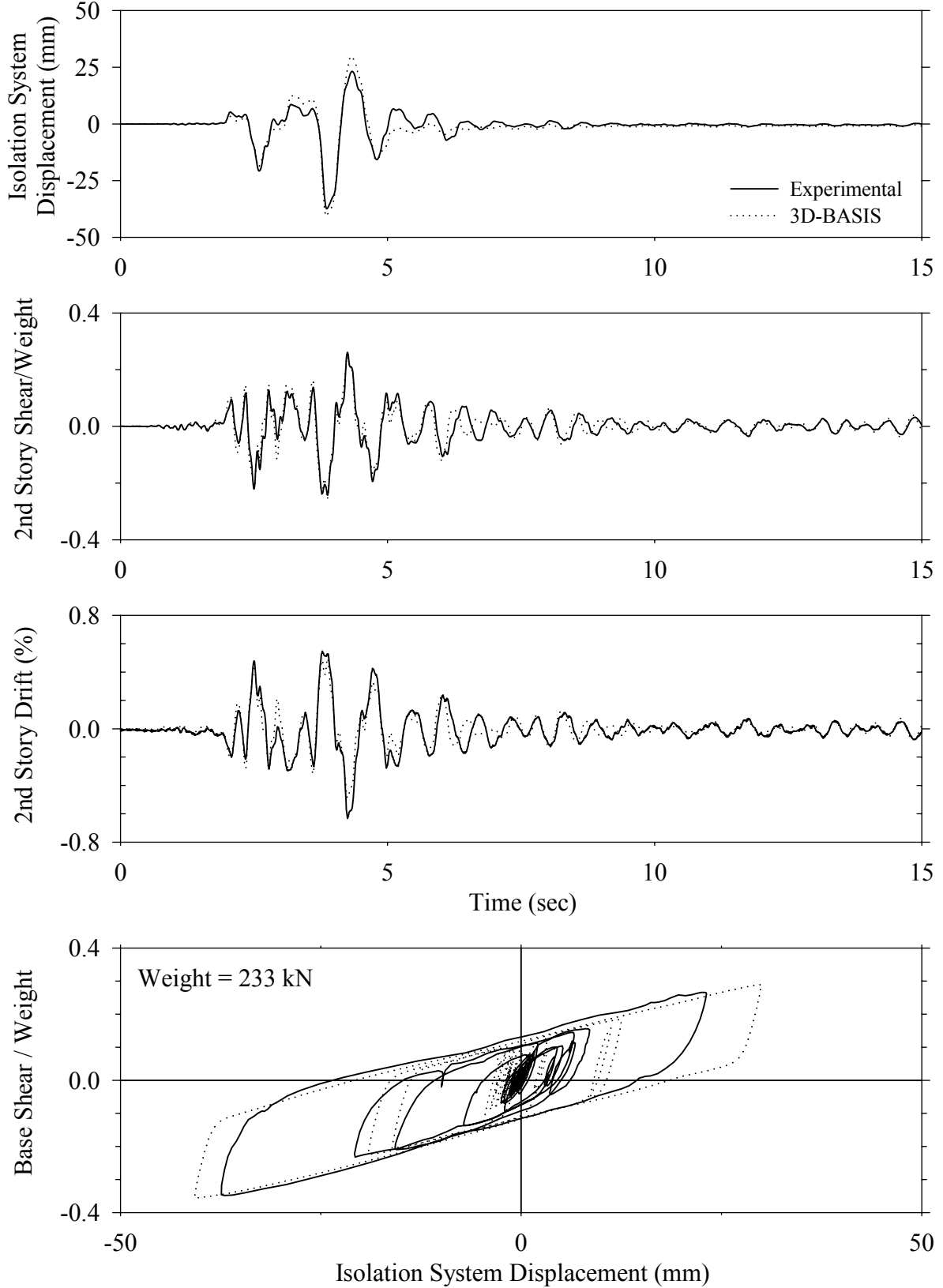


Test LCMFN10.1, Newhall 360 100%, MF/Low Damping Elastomeric with Lead Core

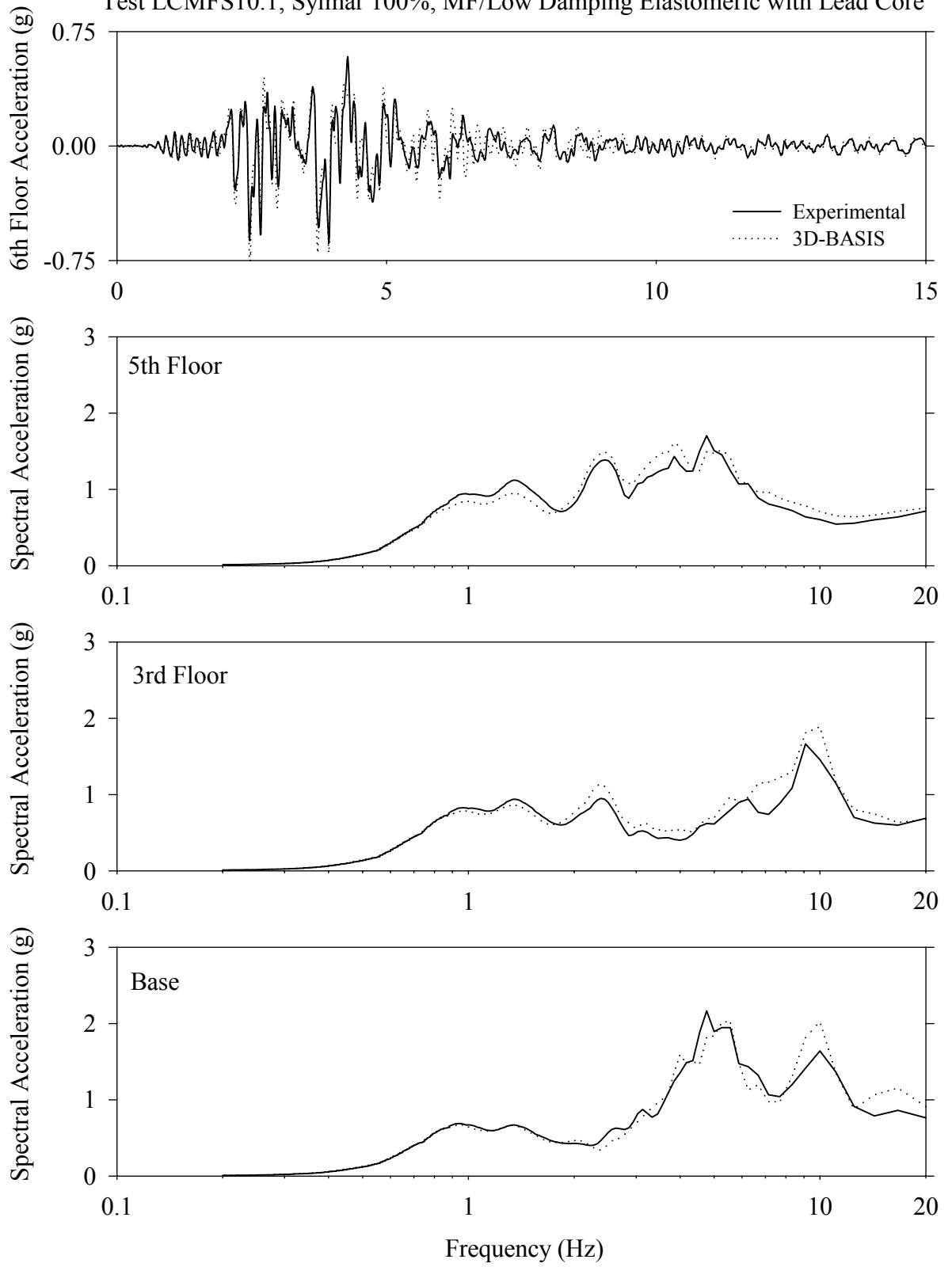




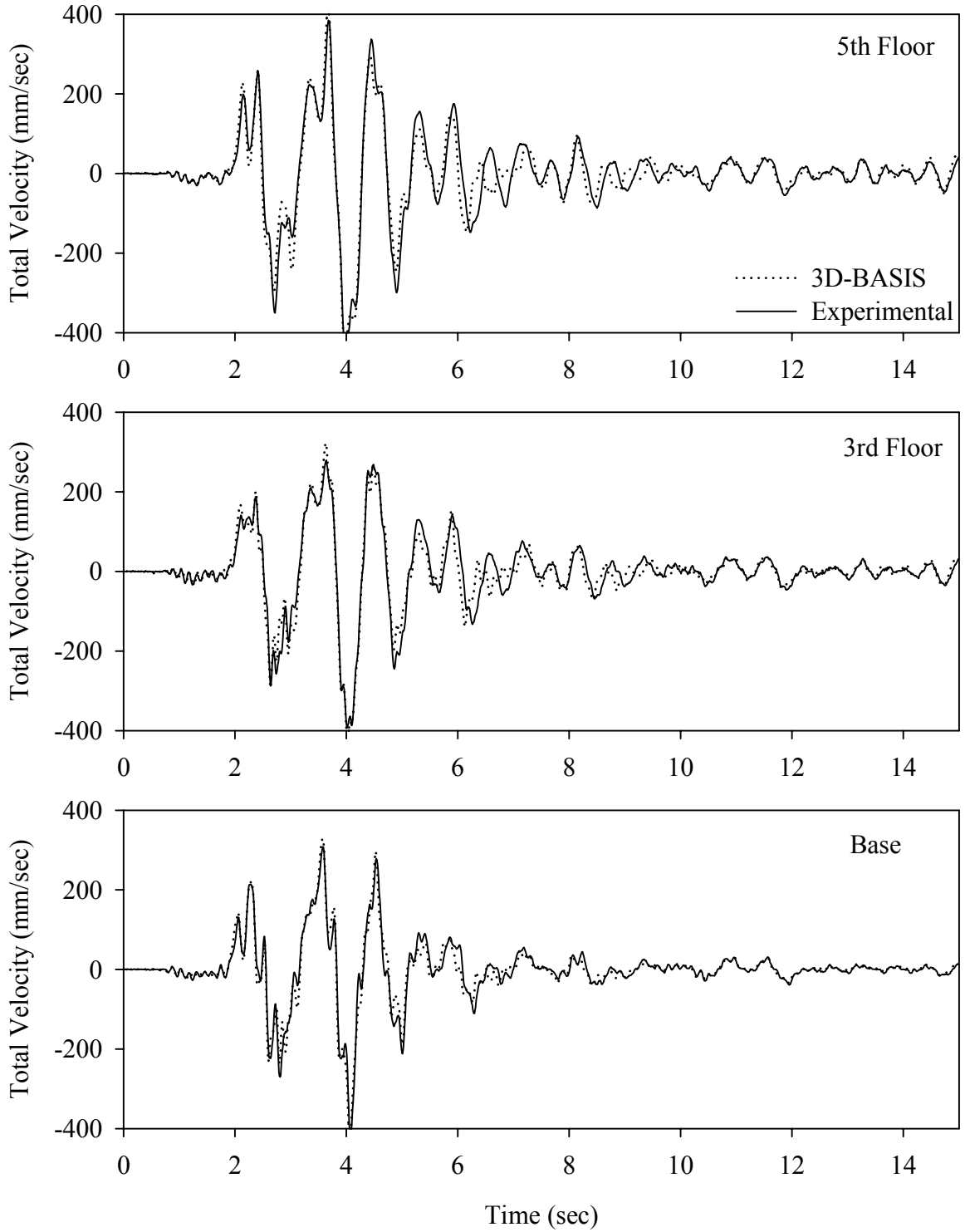
Test LCMFS10.1, Sylmar 100%, MF/Low Damping Elastomeric with Lead Core



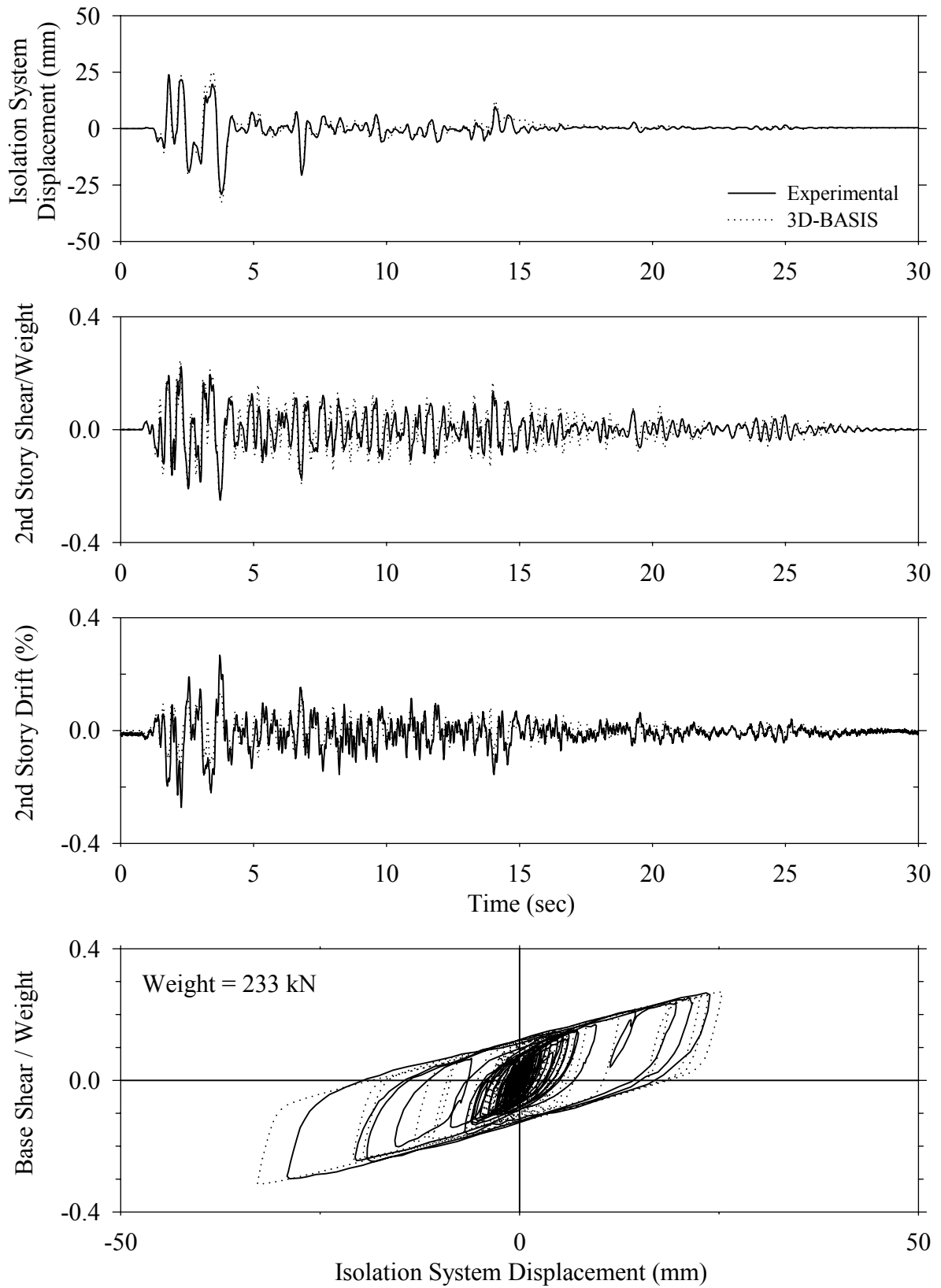
Test LCMFS10.1, Sylmar 100%, MF/Low Damping Elastomeric with Lead Core



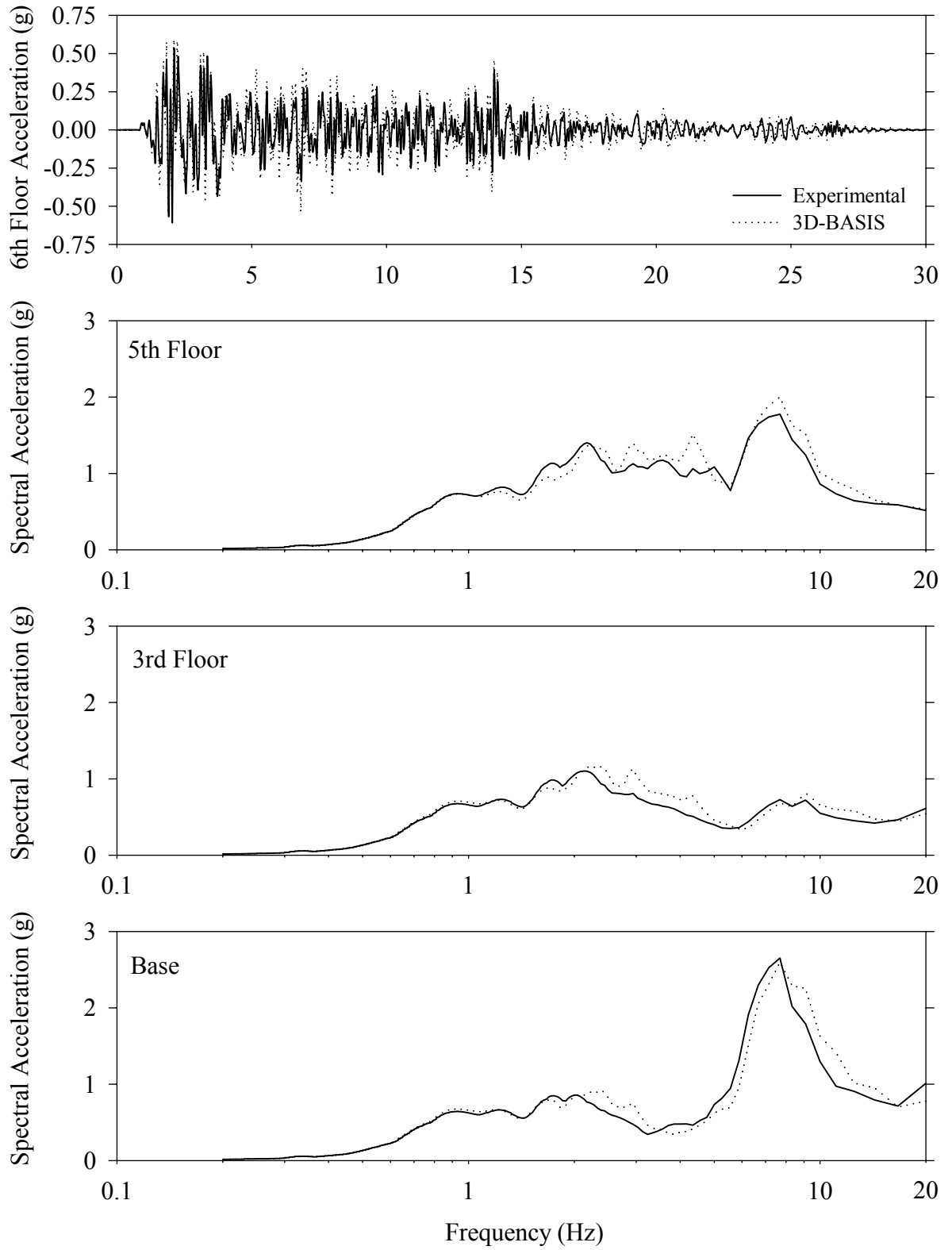
Test LCMFS10.1, Sylmar 100%, MF/Low Damping Elastomeric with Lead Core



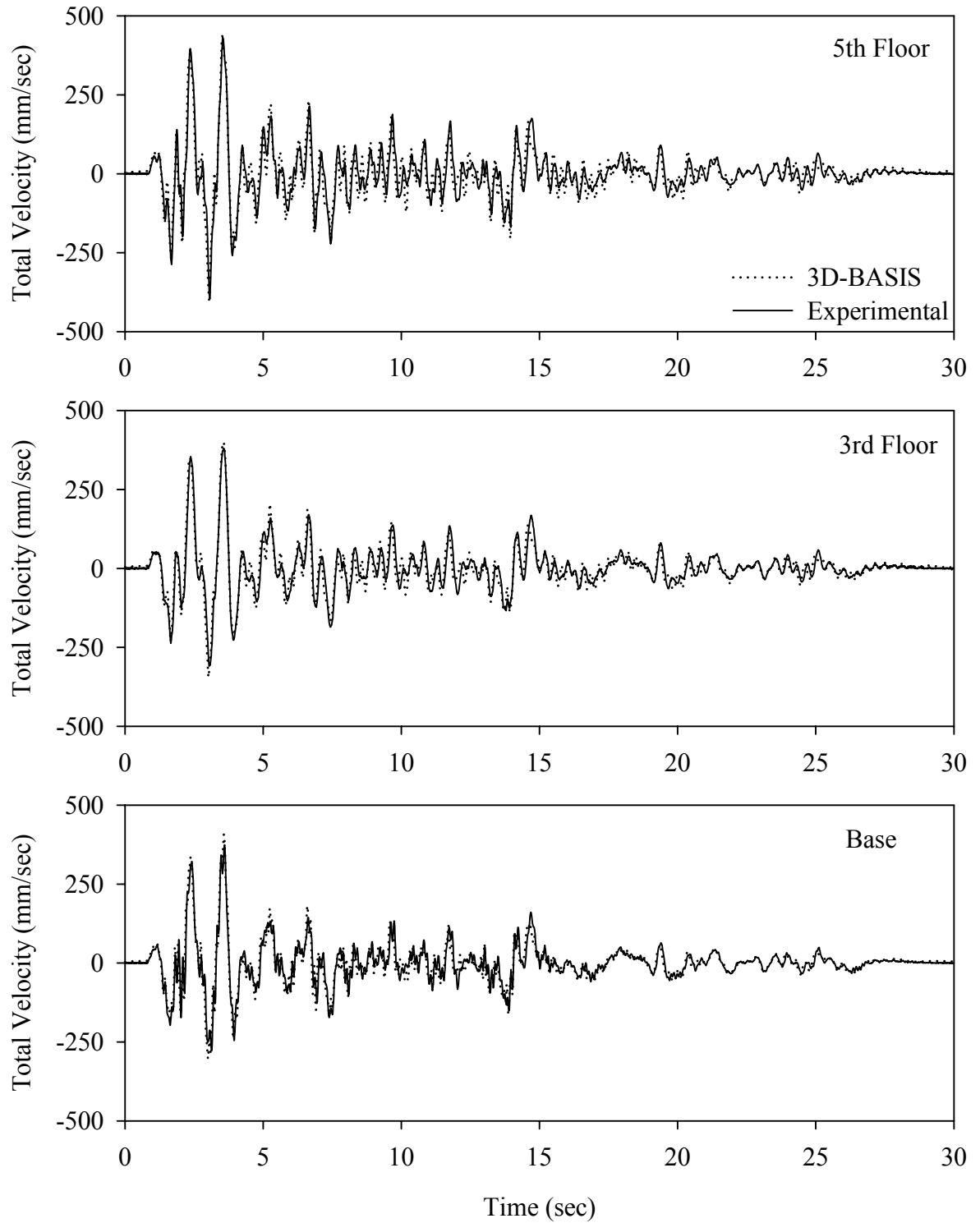
Test LCSBE20.1, El Centro S00E 200%, SB/Low Damping Elastomeric with Lead Core



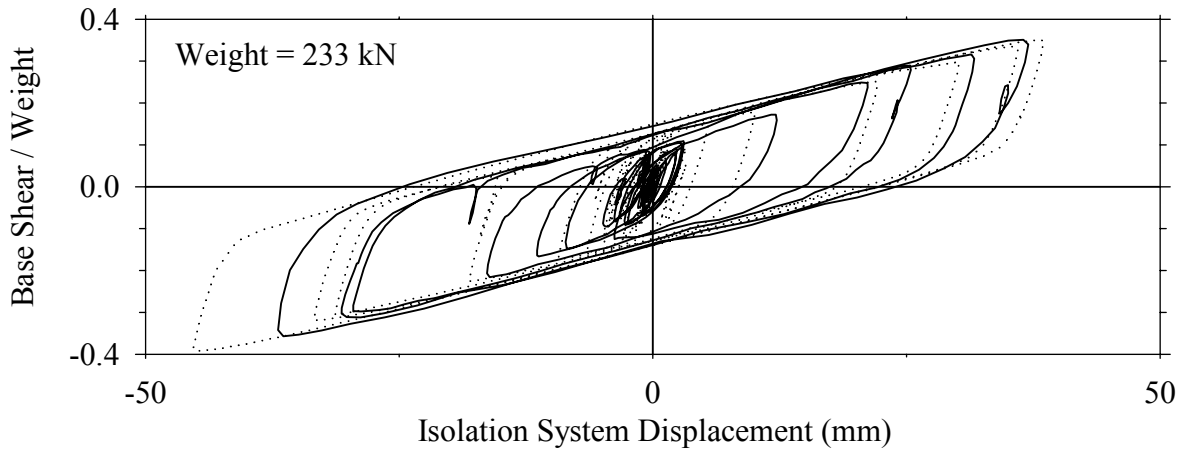
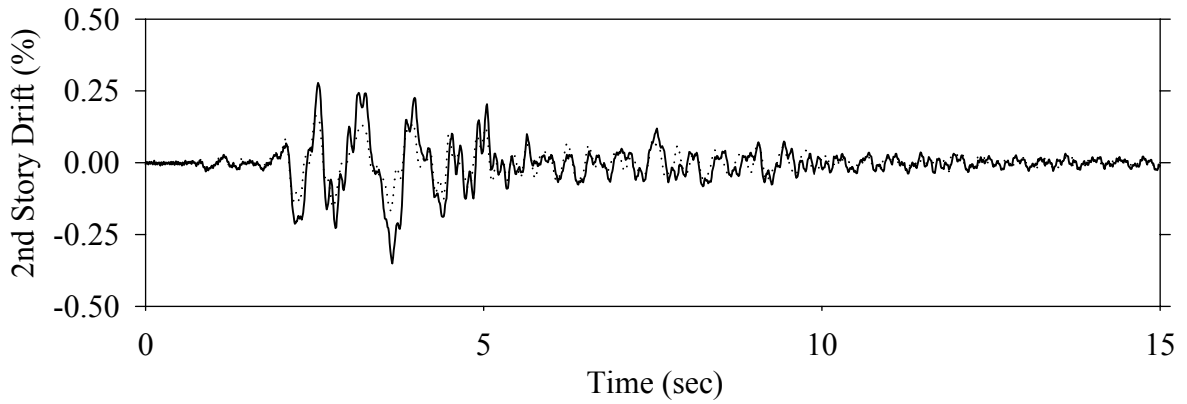
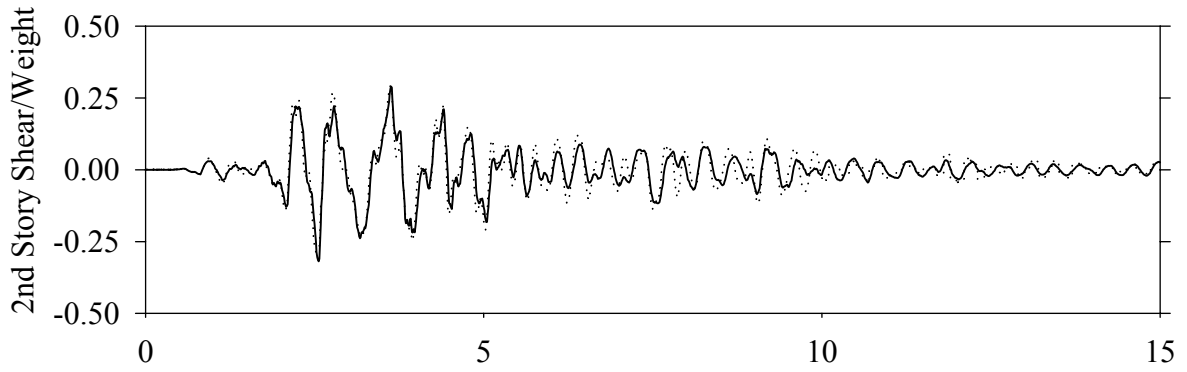
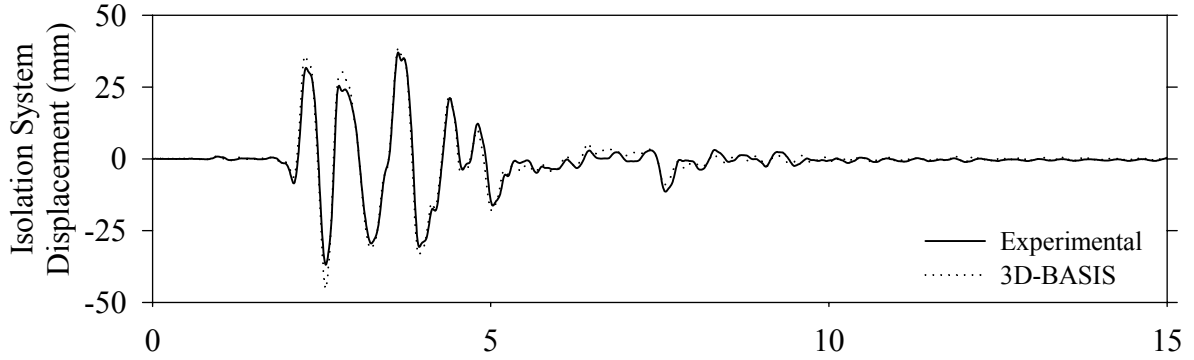
Test LCSBE20.1, El Centro S00E 200%, SB/Low Damping Elastomeric with Lead Core



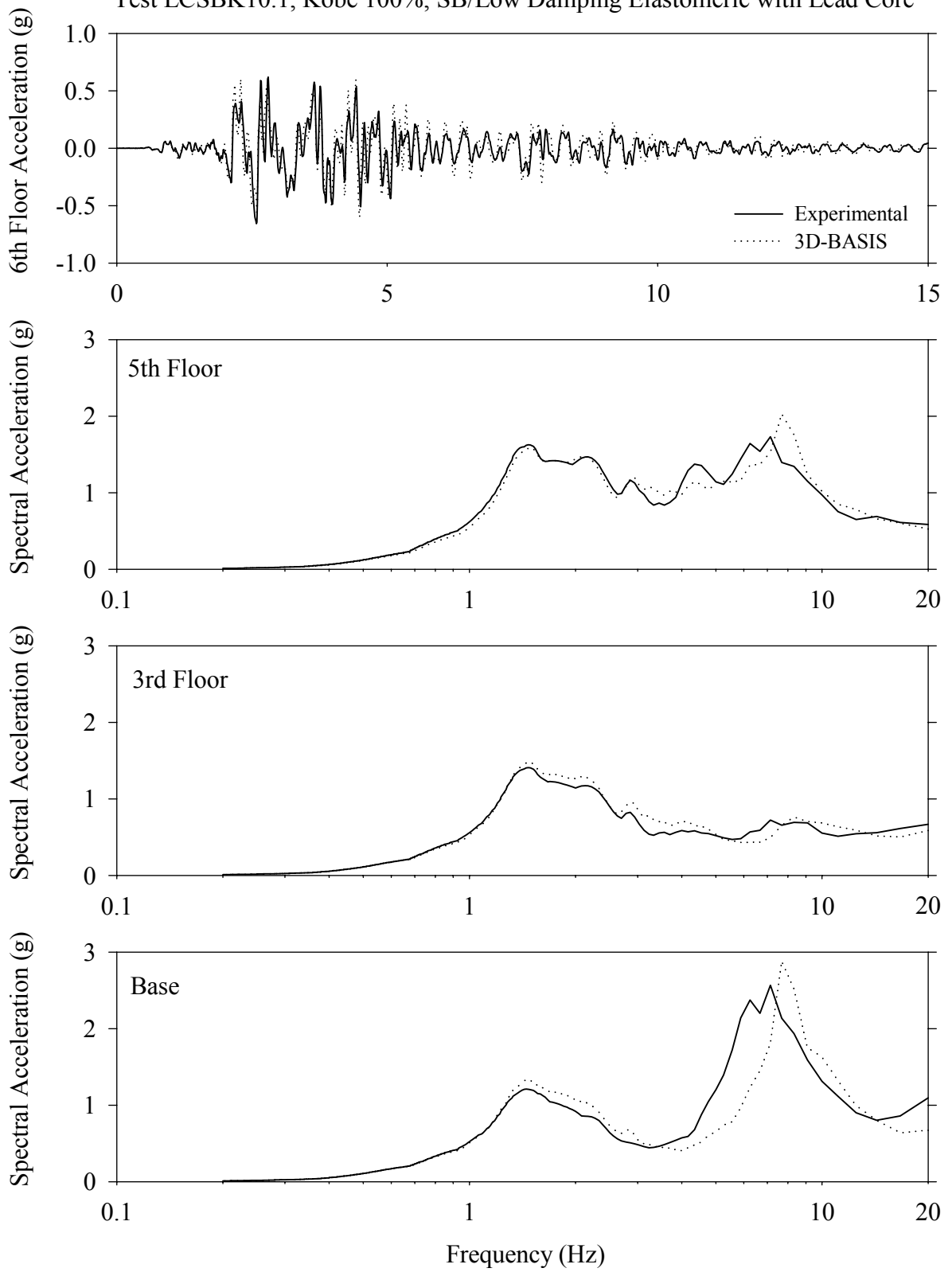
Test LCSBE20.1, El Centro S00E 200%, SB/Low Damping Elastomeric with Lead Core



Test LCSBK10.1, Kobe 100%, SB/Low Damping Elastomeric with Lead Core

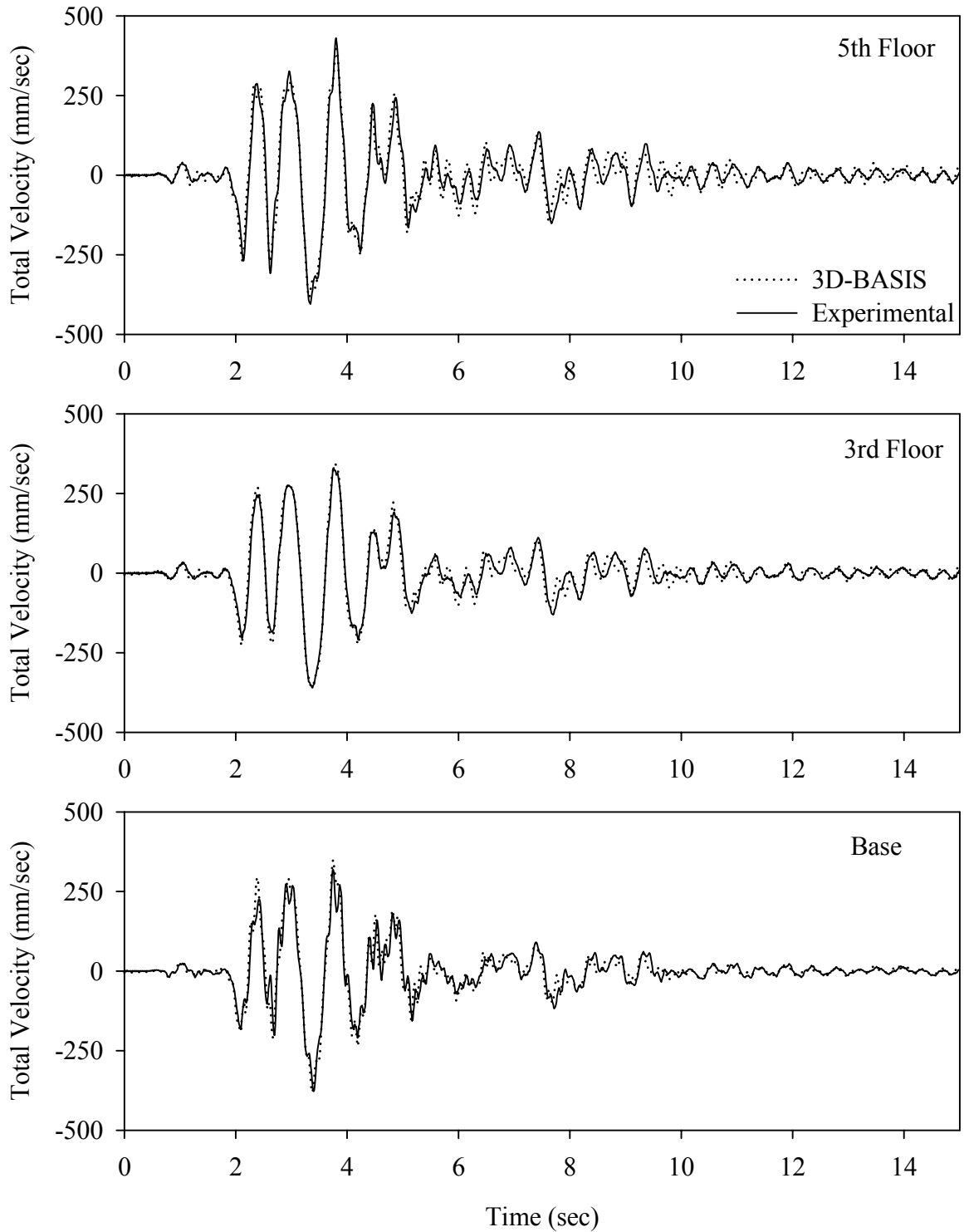


Test LCSBK10.1, Kobe 100%, SB/Low Damping Elastomeric with Lead Core

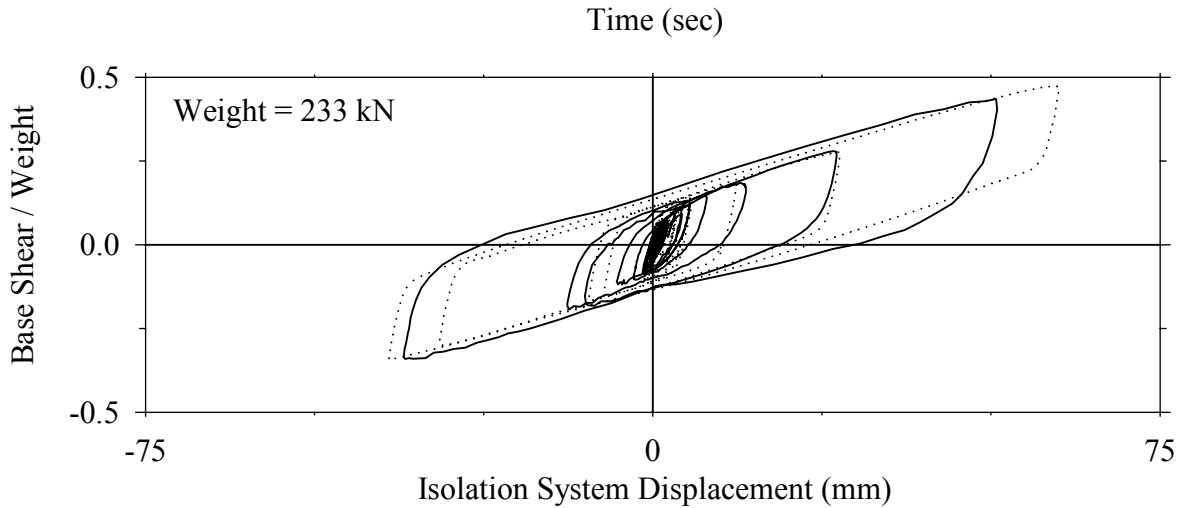
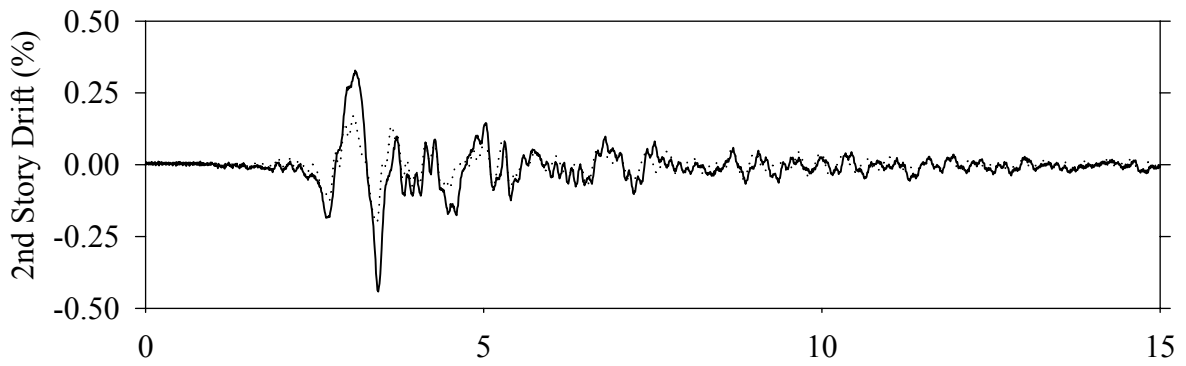
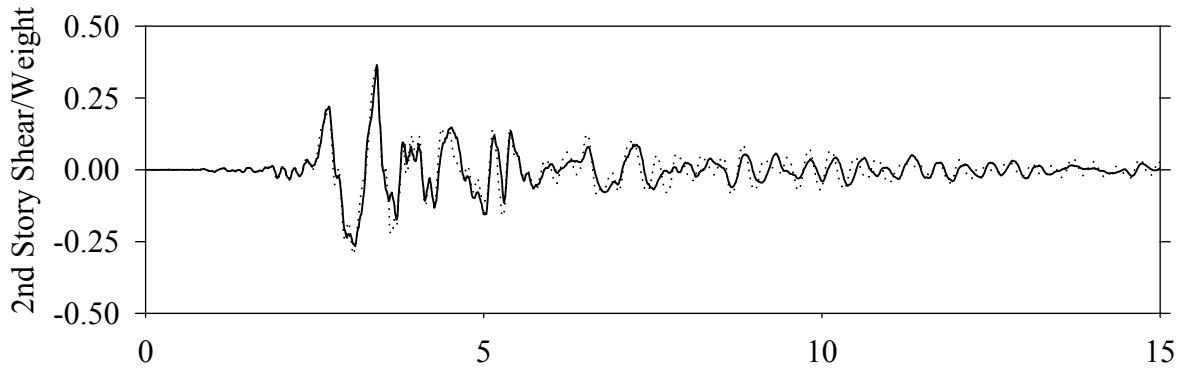
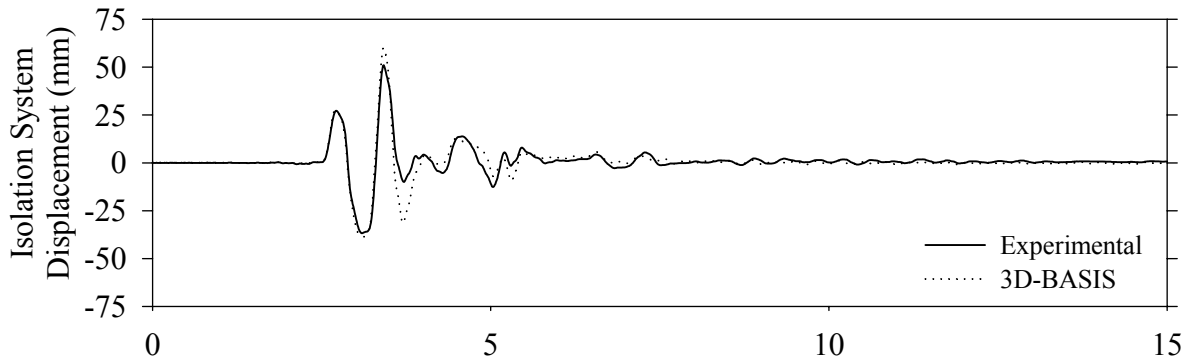




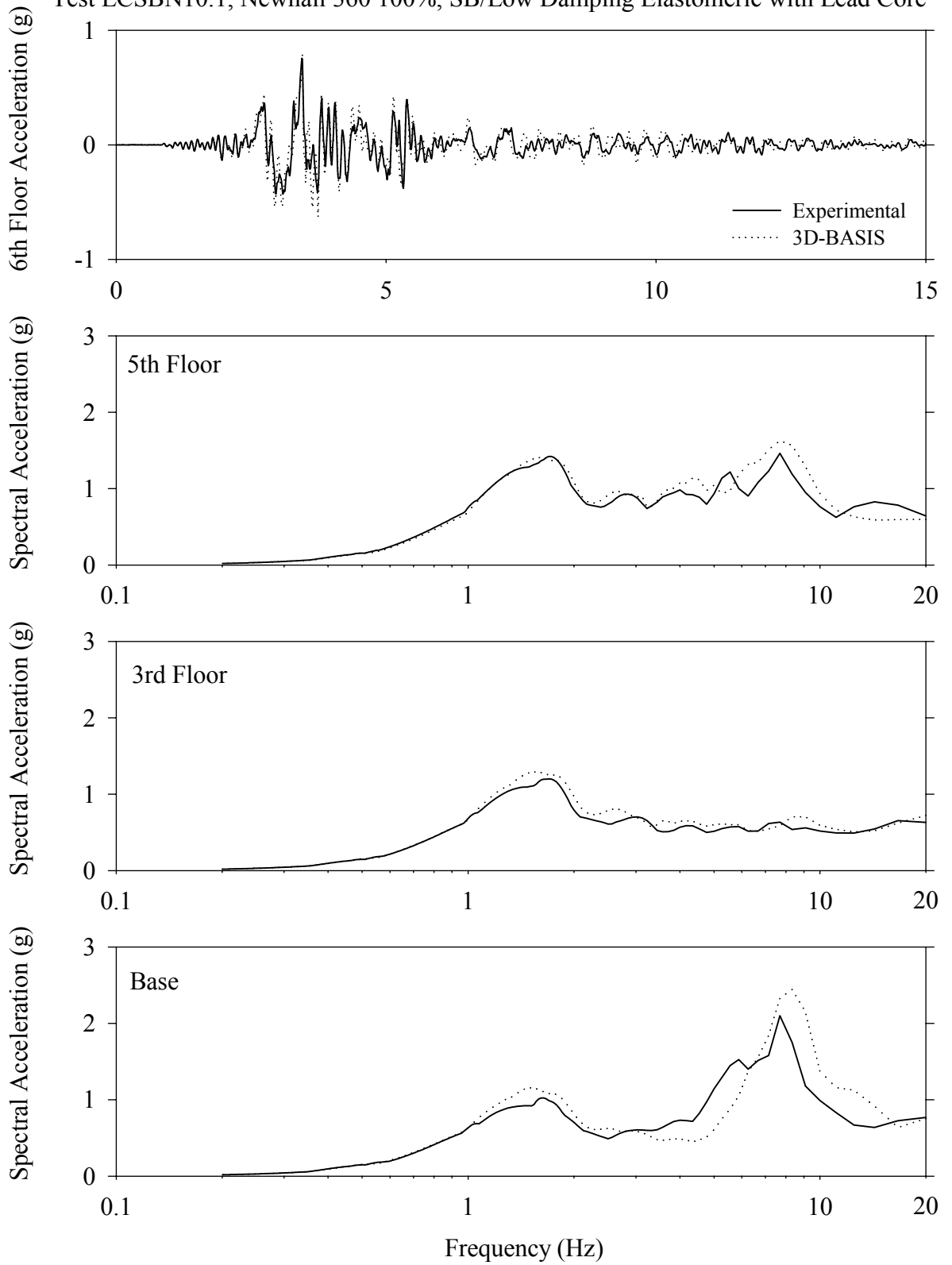
Test LCSBK10.1, Kobe 100%, SB/Low Damping Elastomeric with Lead Core



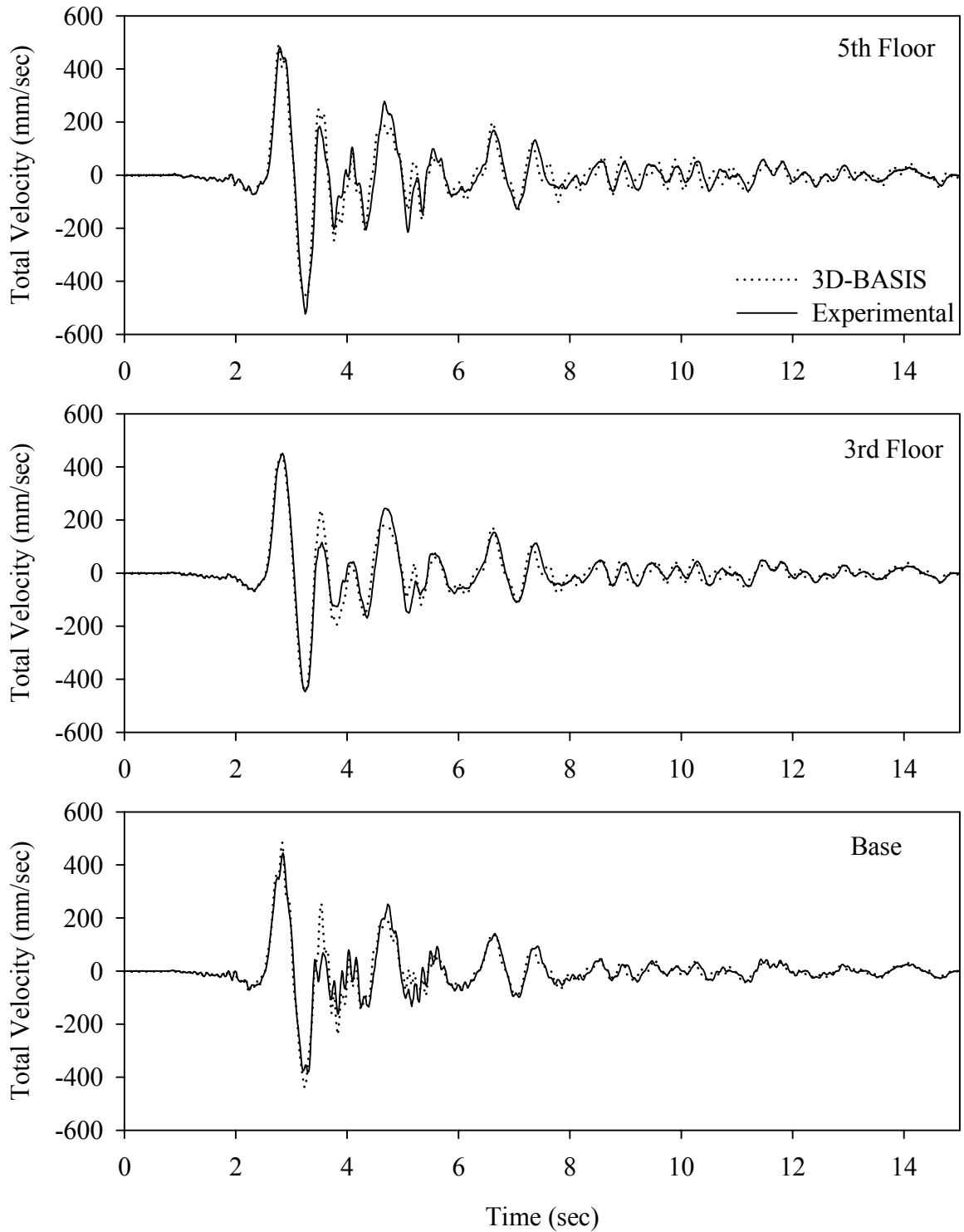
Test LDSBN10.1, Newhall 360 100%, SB/Low Damping Elastomeric with Lead Core



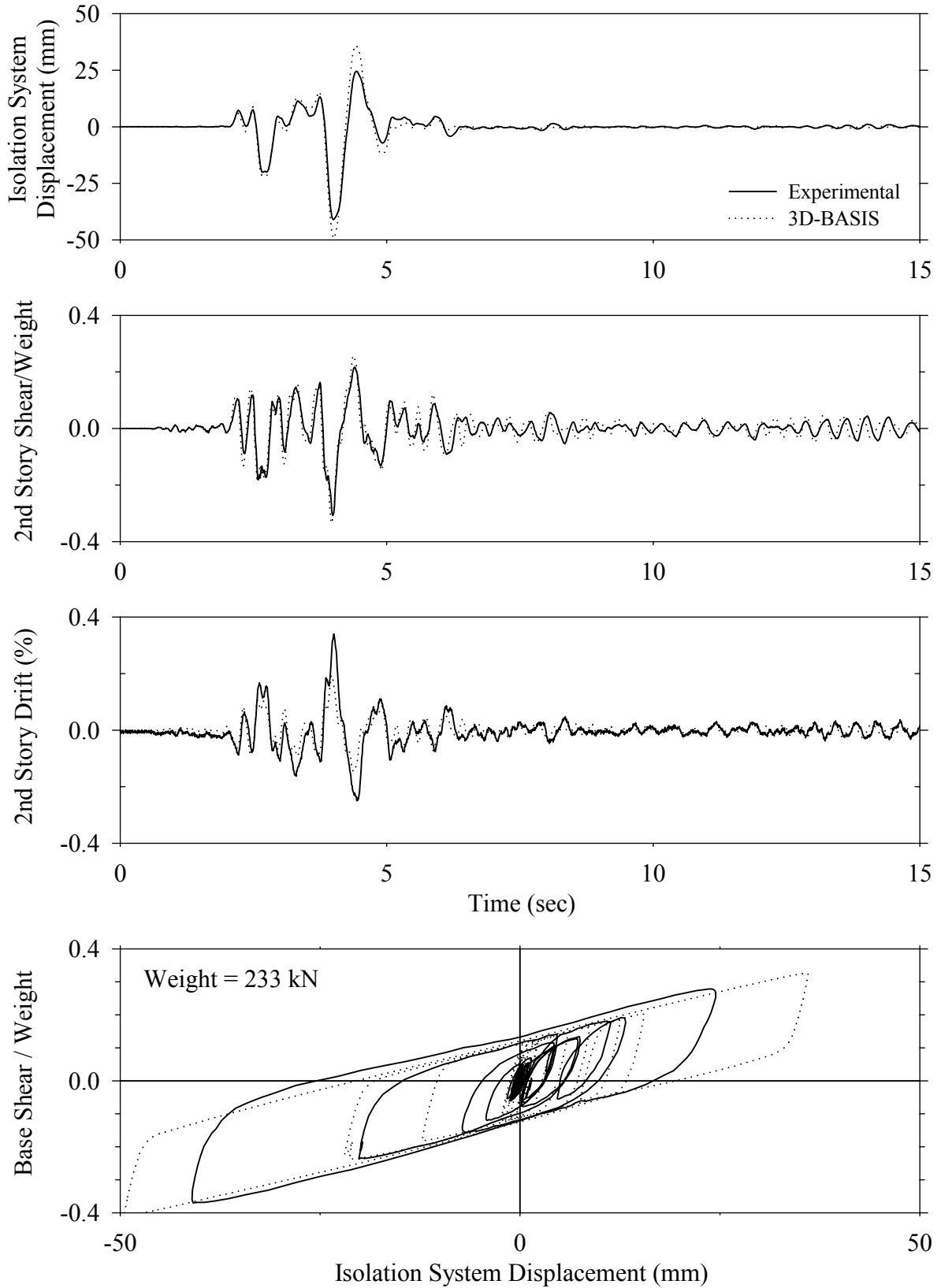
Test LCSBN10.1, Newhall 360 100%, SB/Low Damping Elastomeric with Lead Core



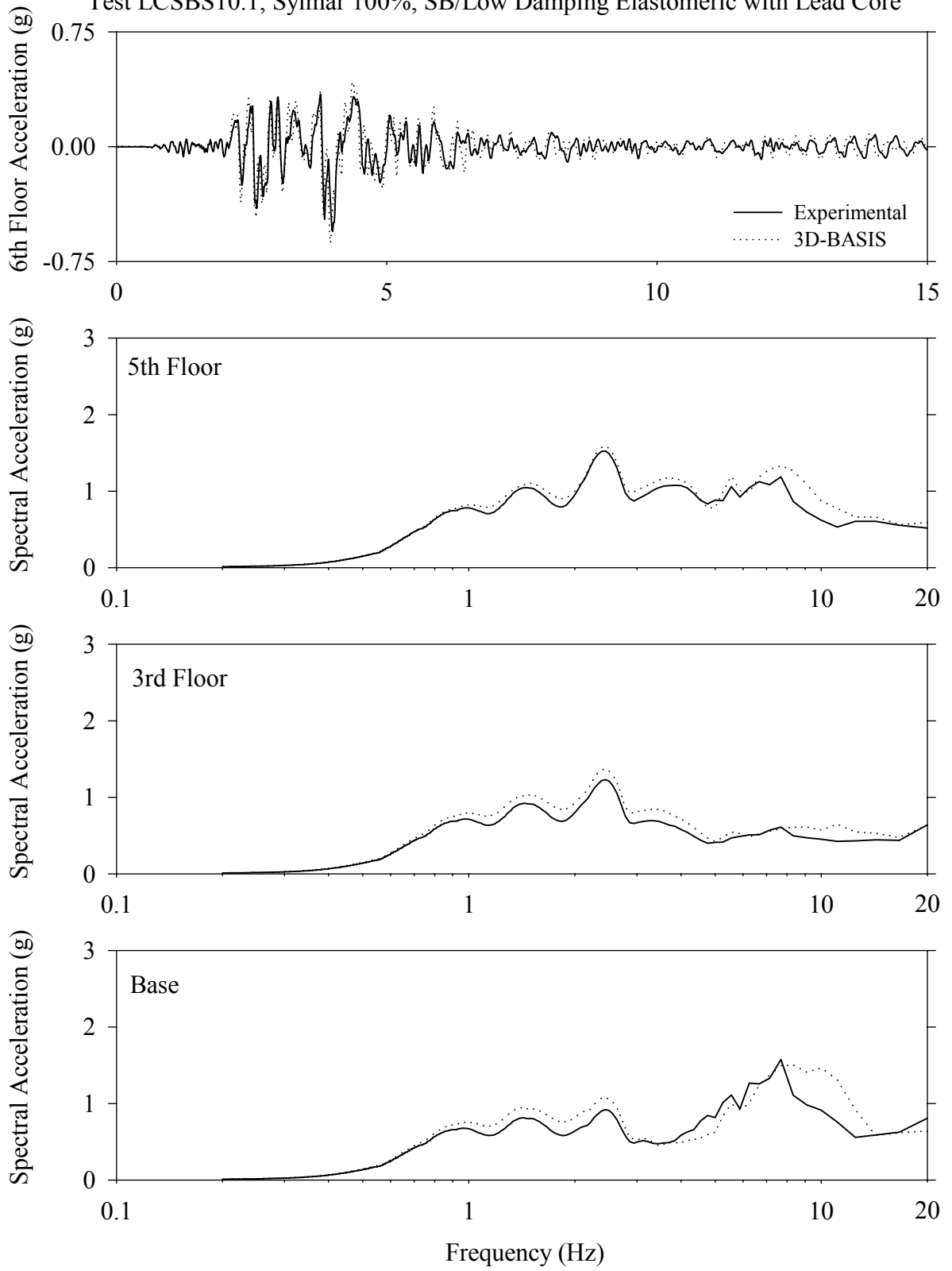
Test LCSBN10.1, Newhall 360 100%, SB/Low Damping Elastomeric with Lead Core



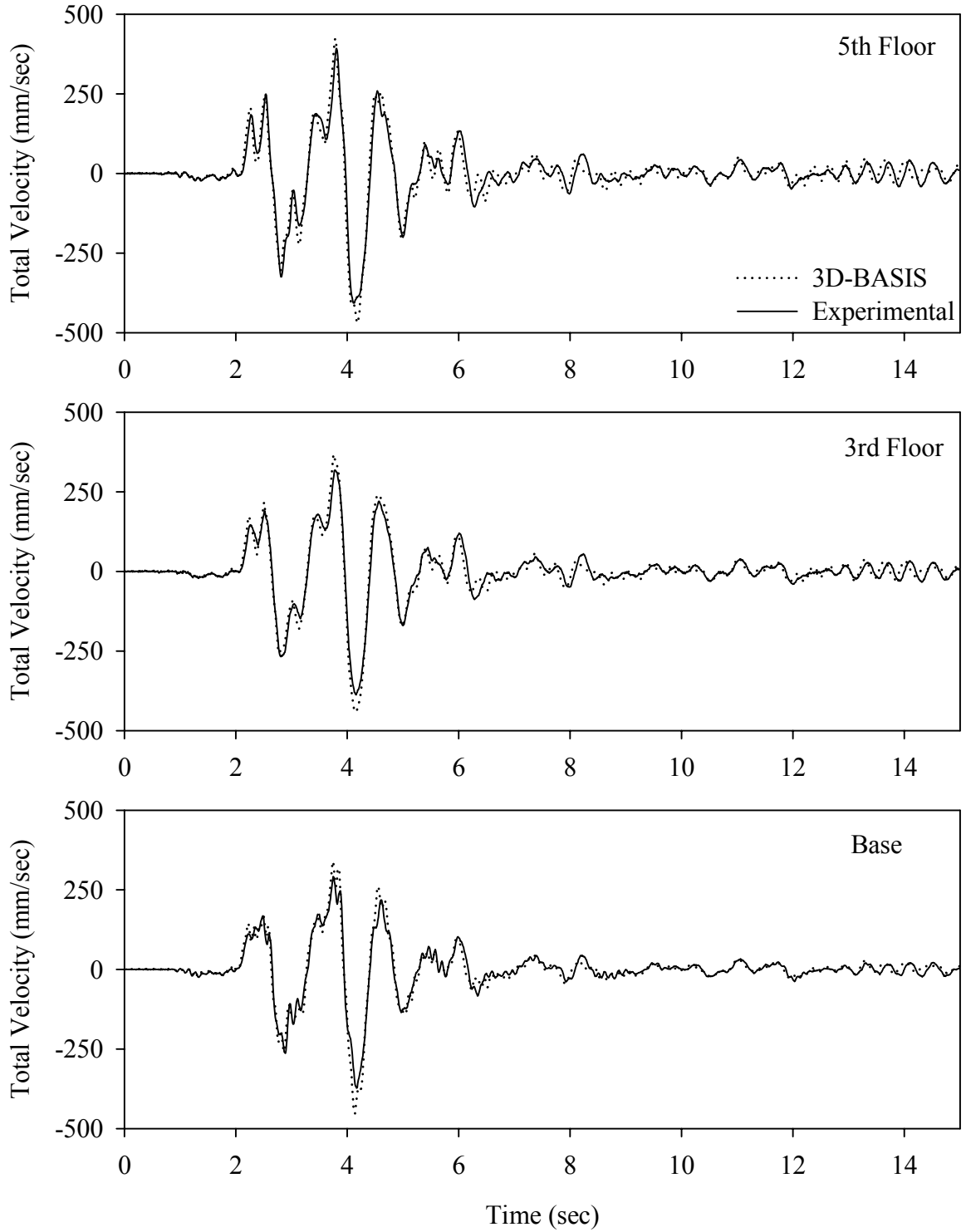
Test LCSBS10.1, Sylmar 100%, SB/Low Damping Elastomeric with Lead Core



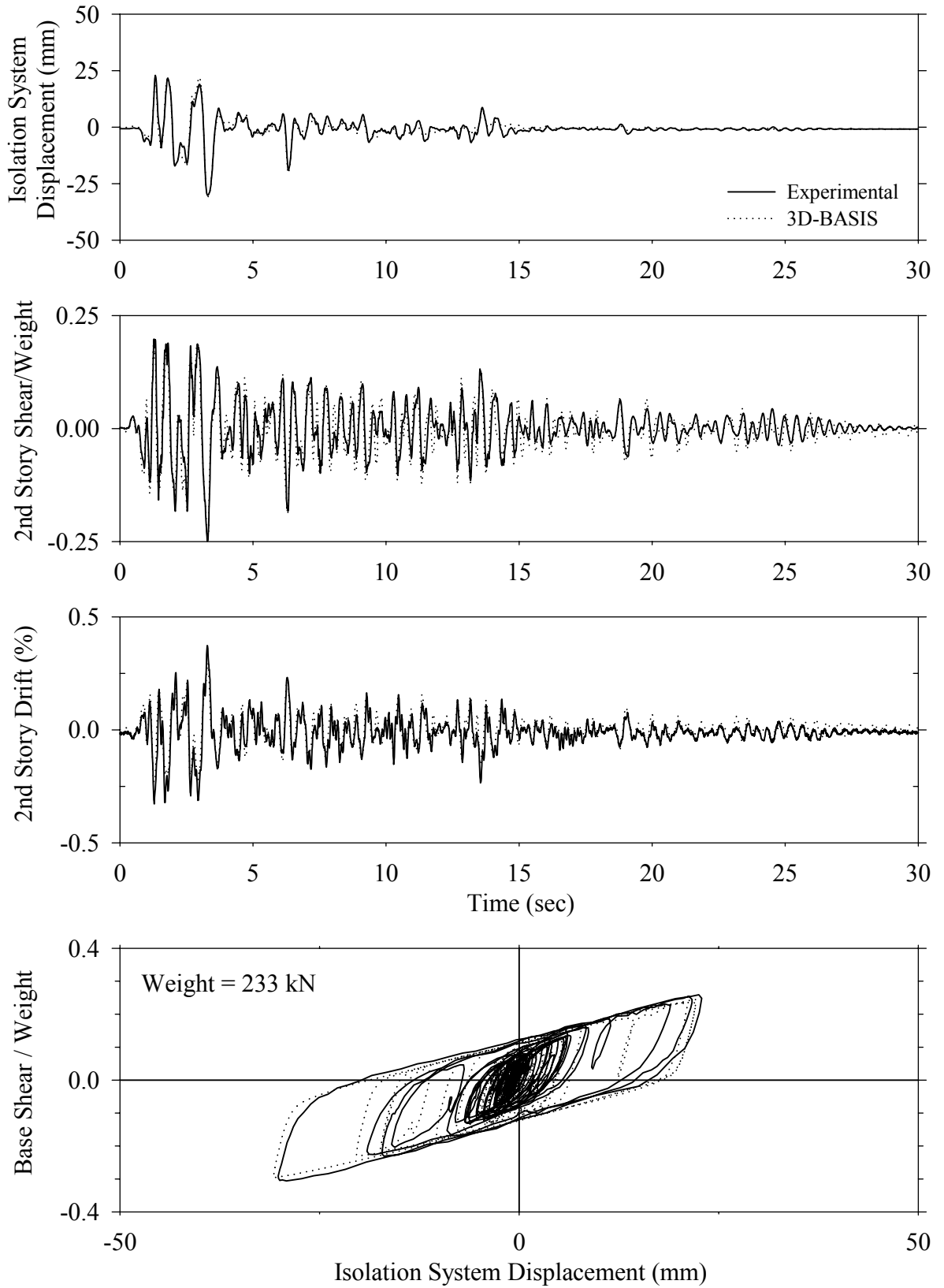
Test LCSBS10.1, Sylmar 100%, SB/Low Damping Elastomeric with Lead Core



Test LCSBS10.1, Sylmar 100%, SB/Low Damping Elastomeric with Lead Core

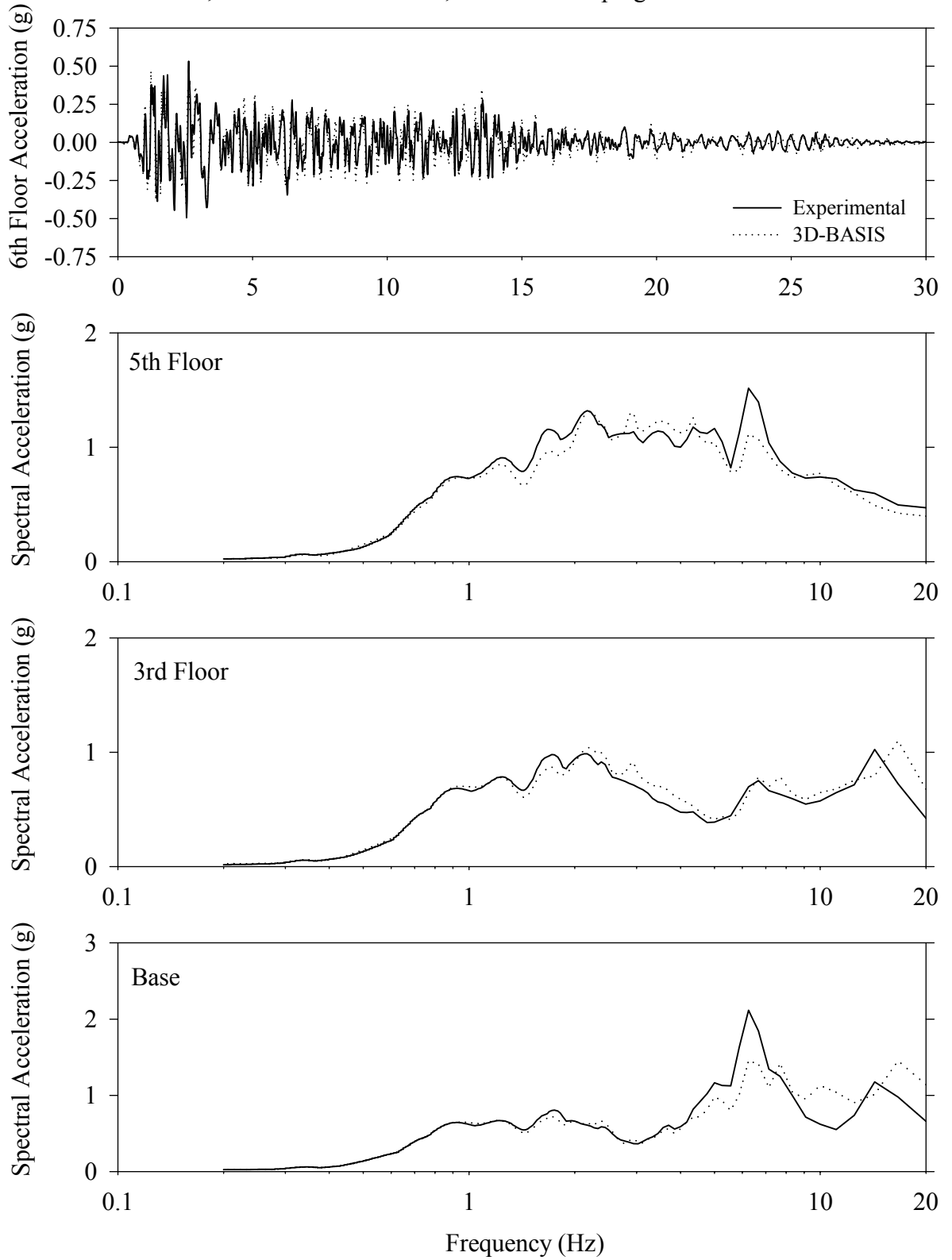


Test LCABE20.1, El Centro S00E 200%, AB/Low Damping Elastomeric with Lead Core

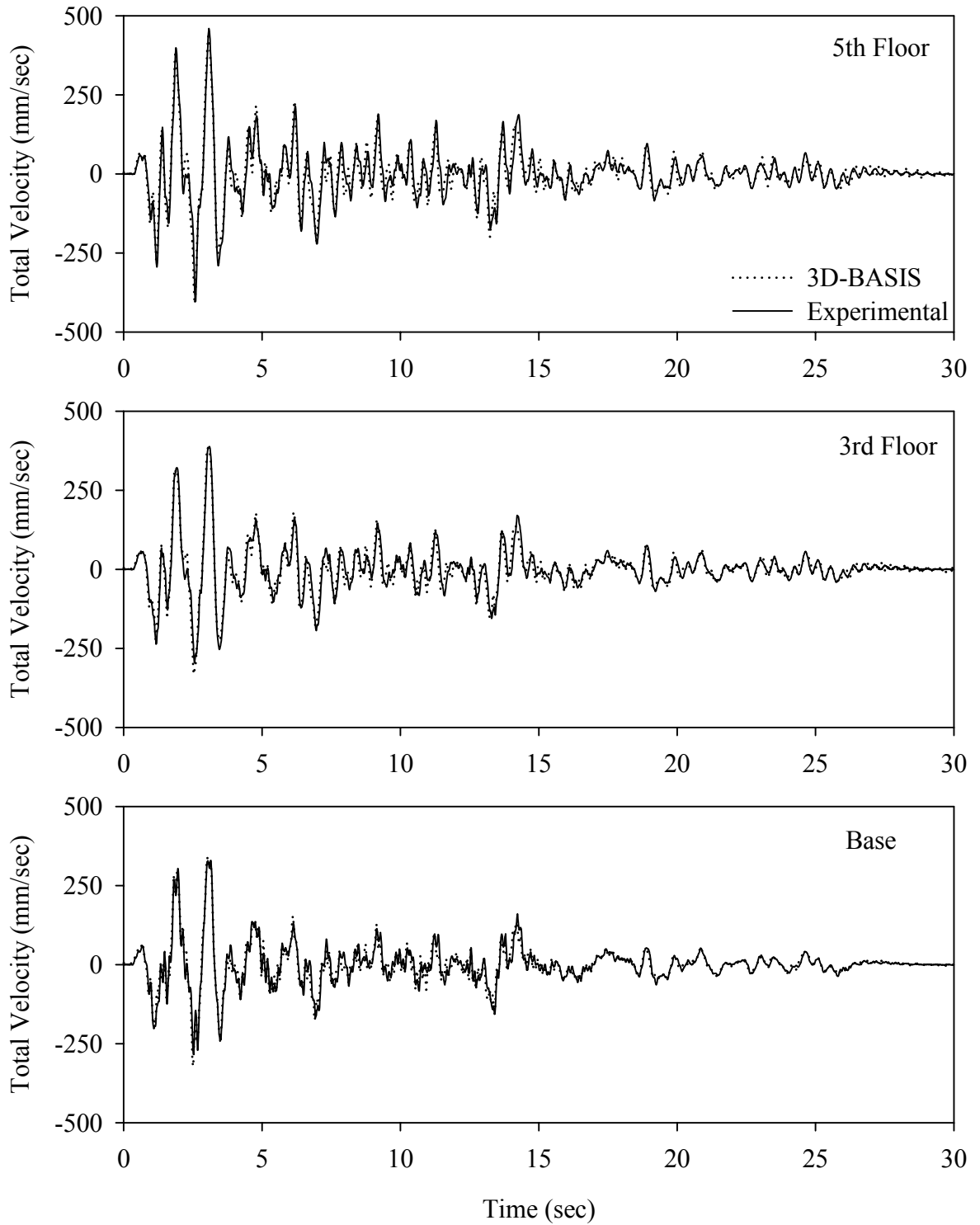




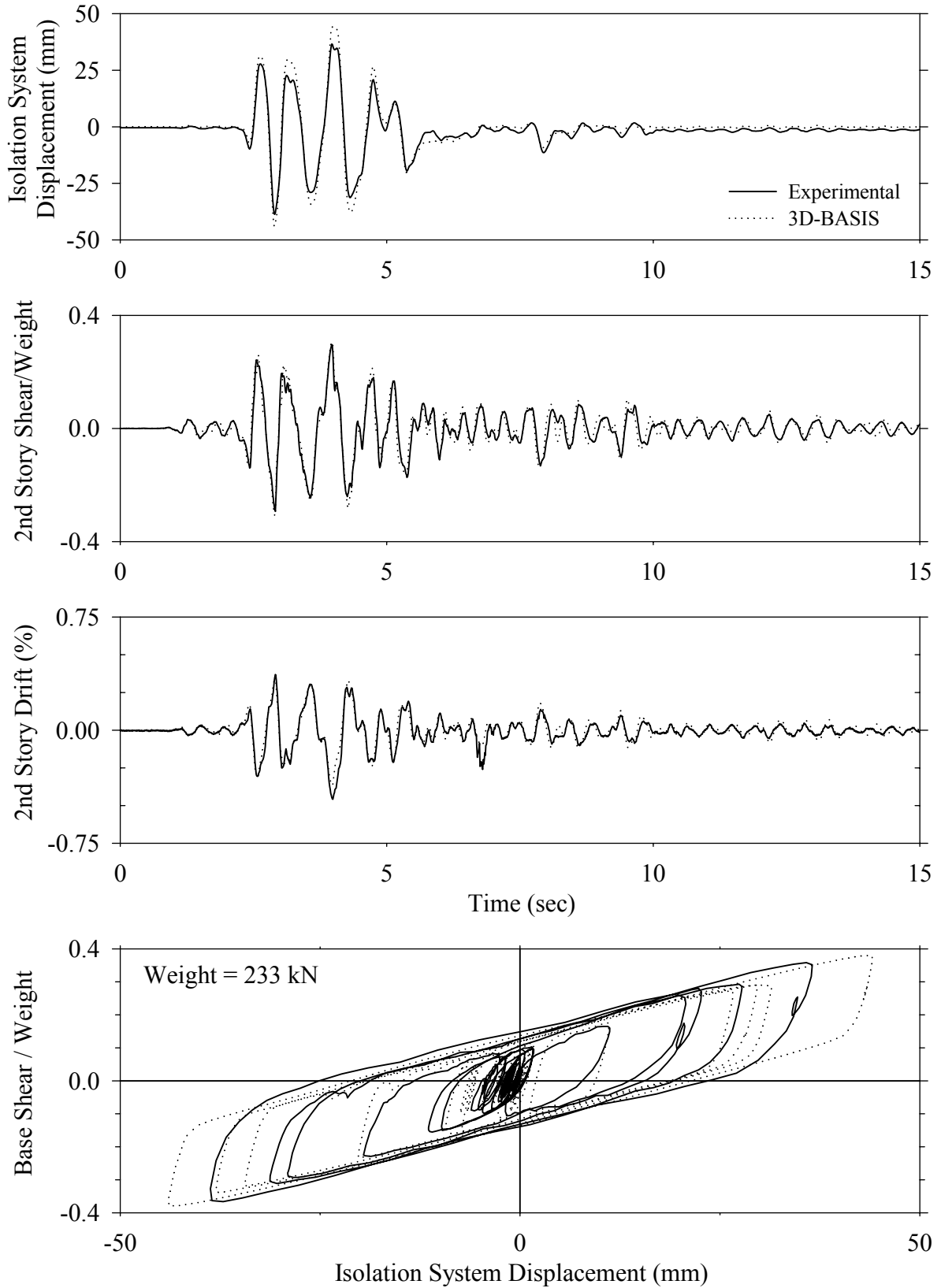
Test LCABE20.1, El Centro S00E 200%, AB/Low Damping Elastomeric with Lead Core



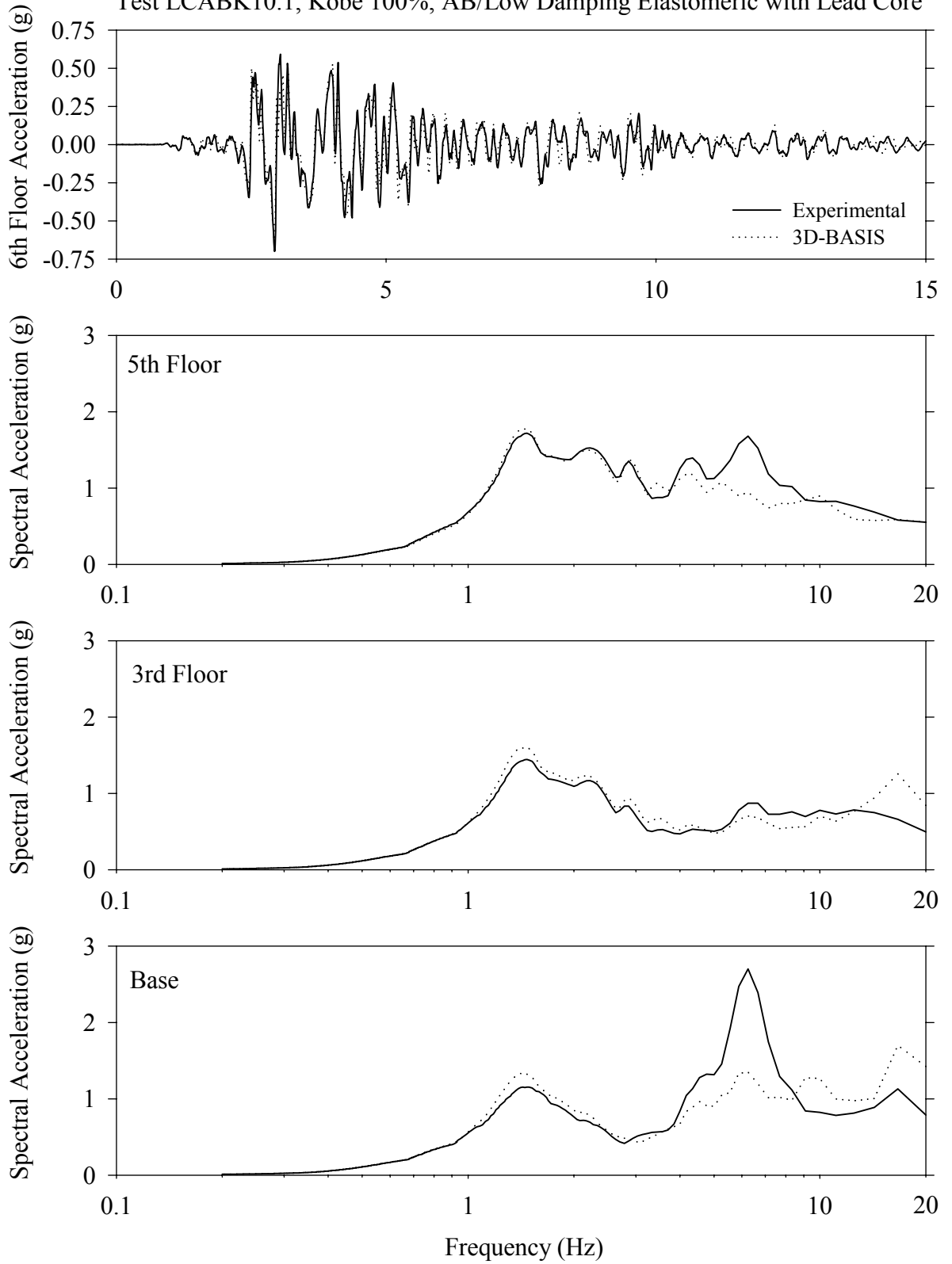
Test LCABE20.1, El Centro S00E 200%, AB/Low Damping Elastomeric with Lead Core



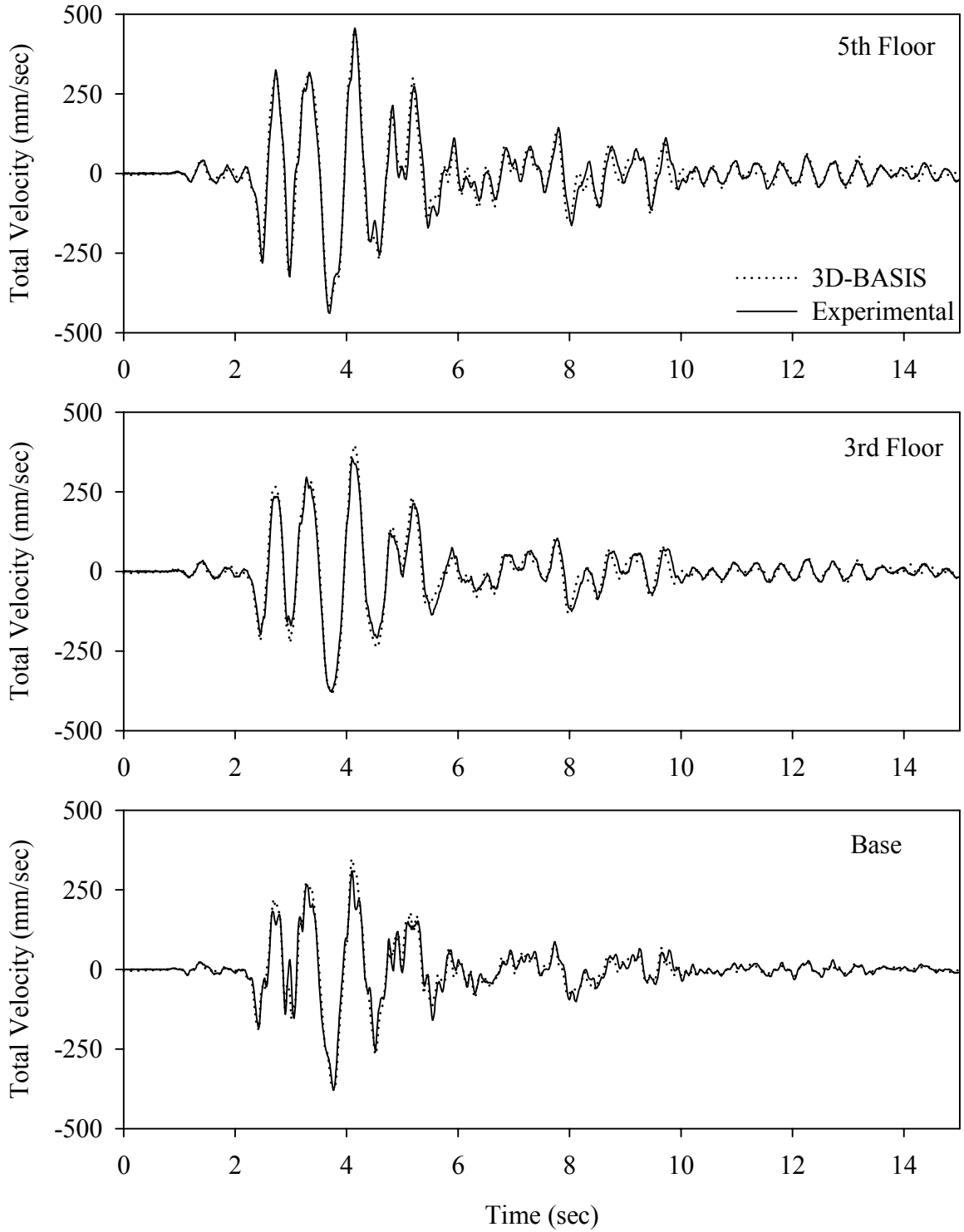
Test LCABK10.1, Kobe 100%, AB/Low Damping Elastomeric with Lead Core



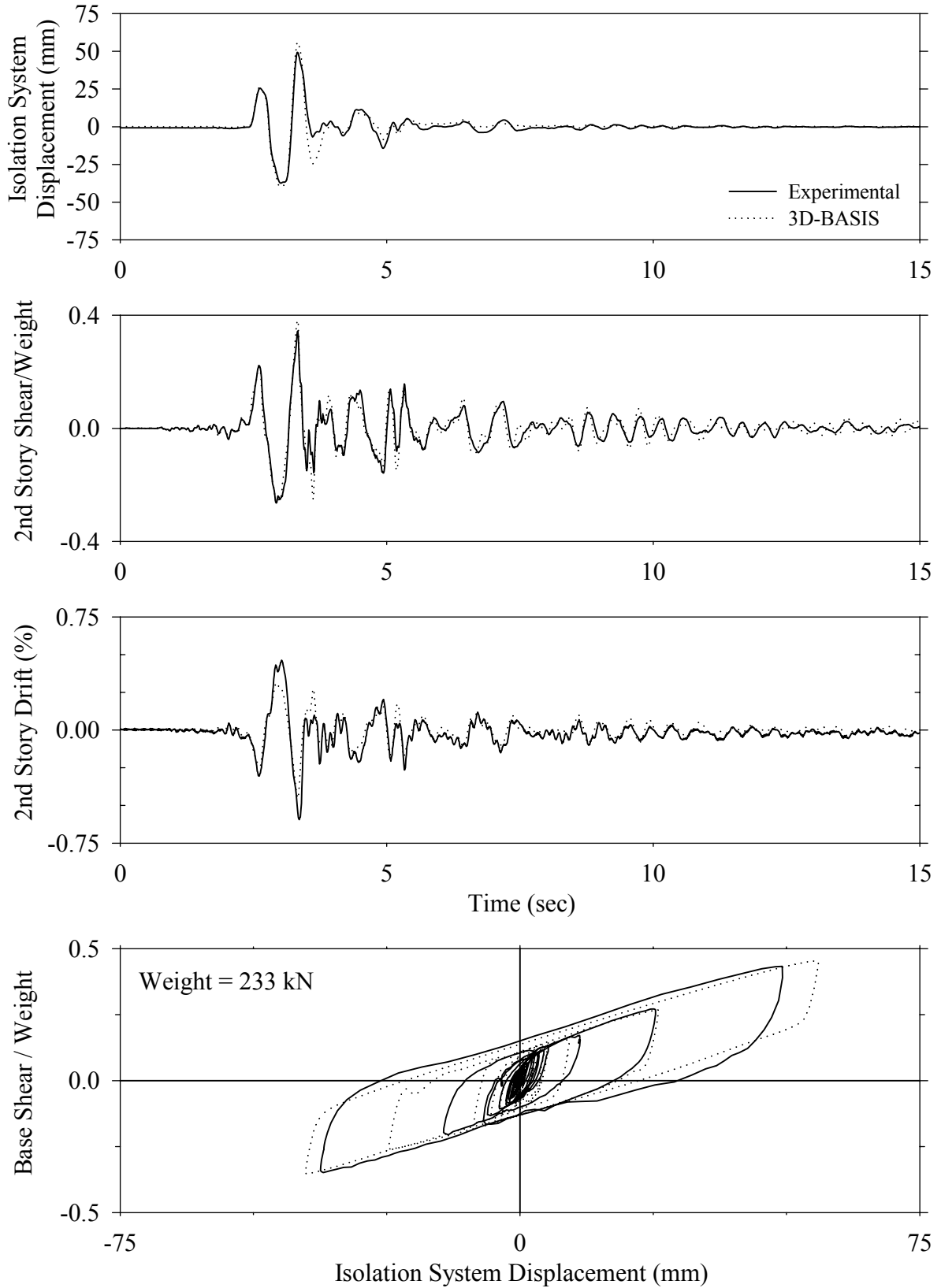
Test LCABK10.1, Kobe 100%, AB/Low Damping Elastomeric with Lead Core



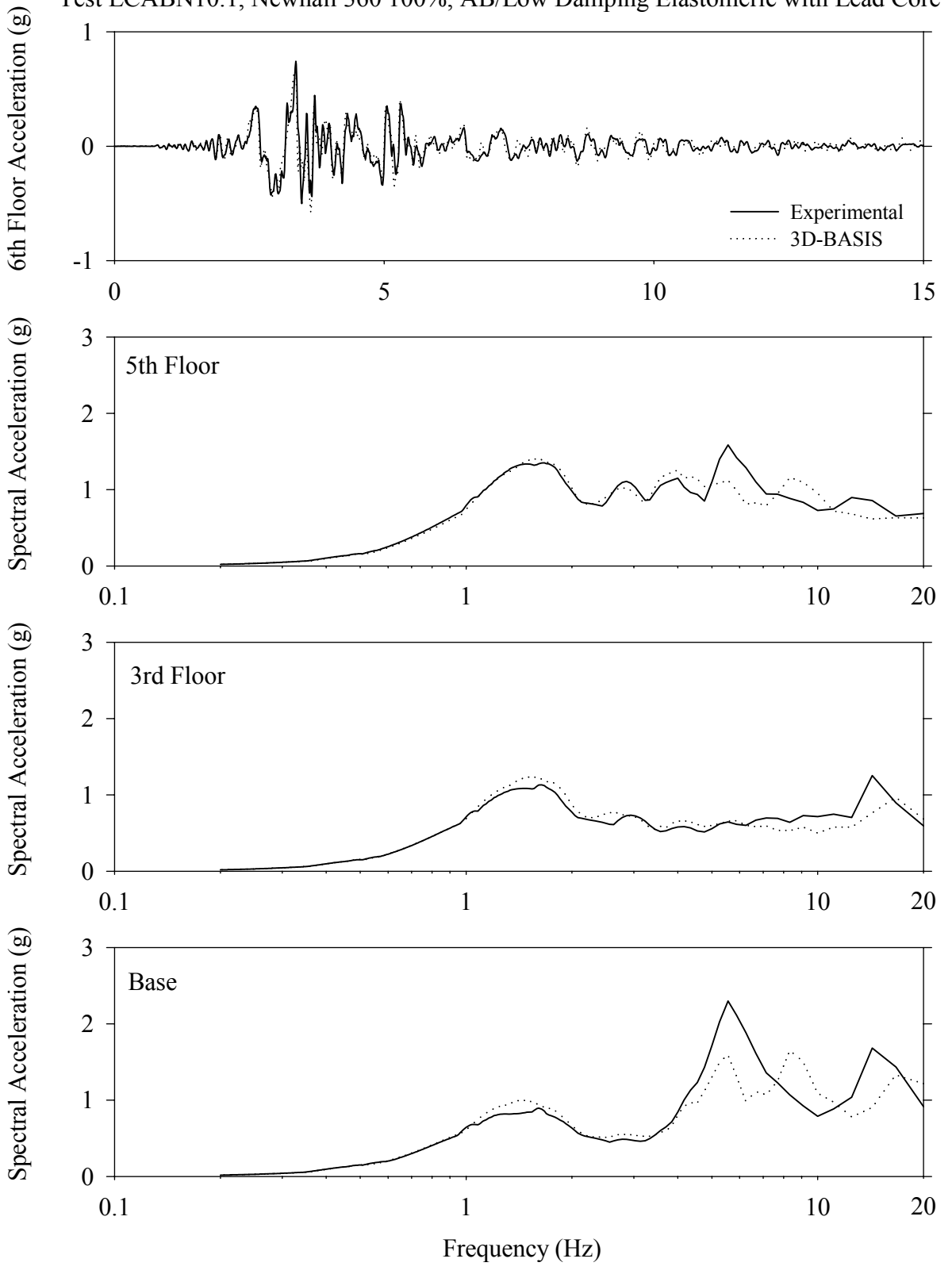
Test LCABK10.1, Kobe 100%, AB/Low Damping Elastomeric with Lead Core



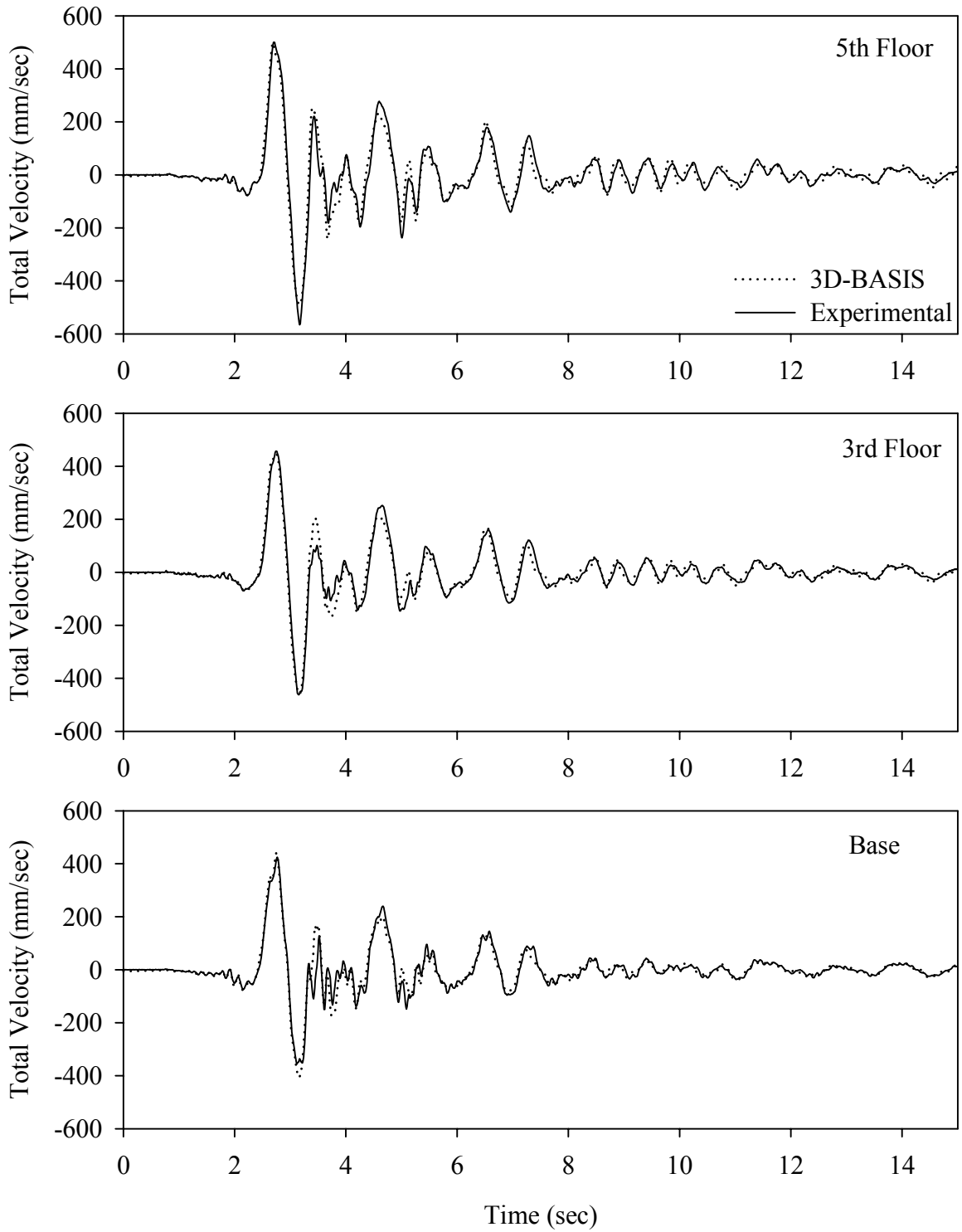
Test LCABN10.1, Newhall 360 100%, AB/Low Damping Elastomeric with Lead Core



Test LCABN10.1, Newhall 360 100%, AB/Low Damping Elastomeric with Lead Core

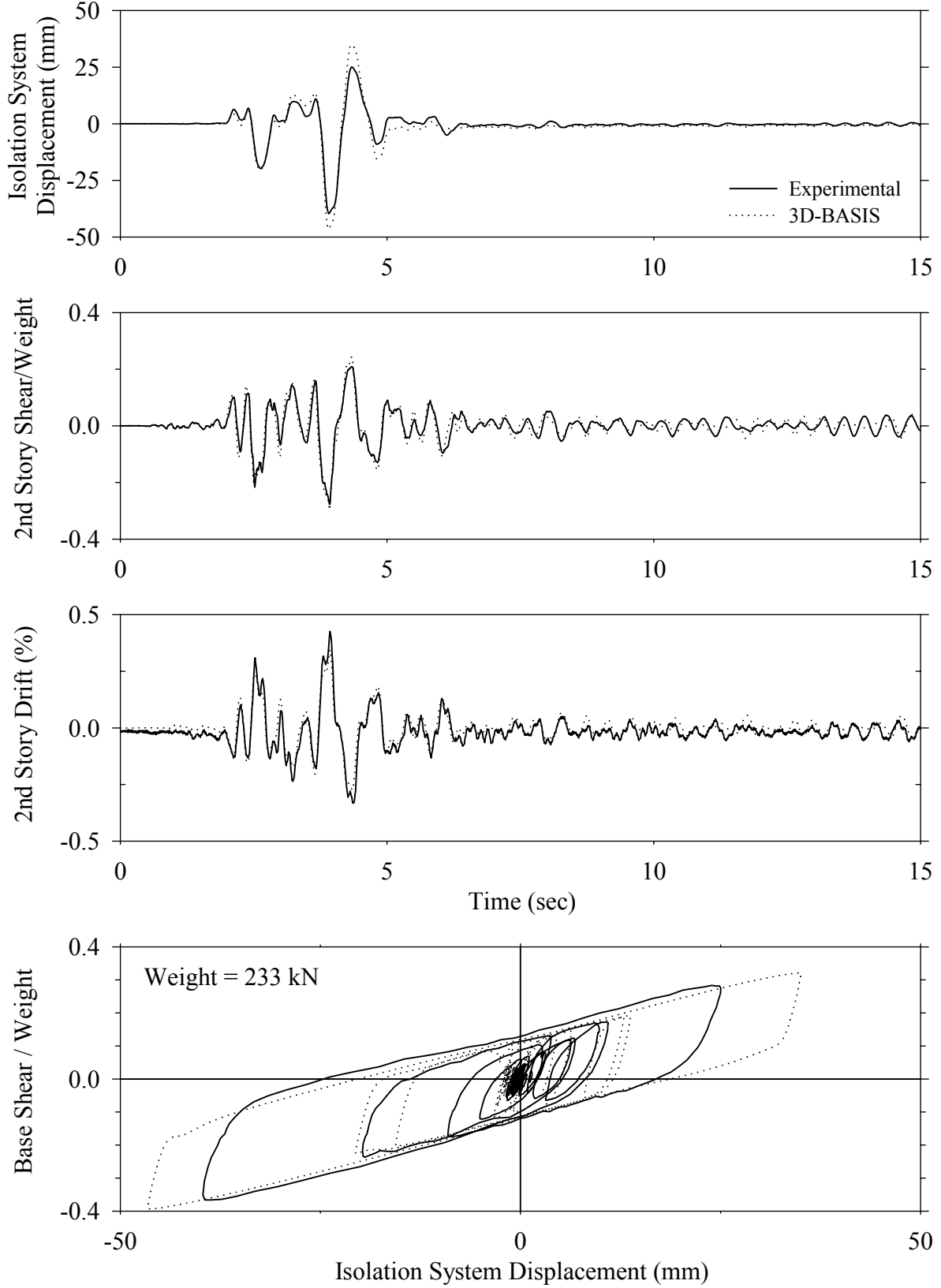


Test LCABN10.1, Newhall 360 100%, AB/Low Damping Elastomeric with Lead Core

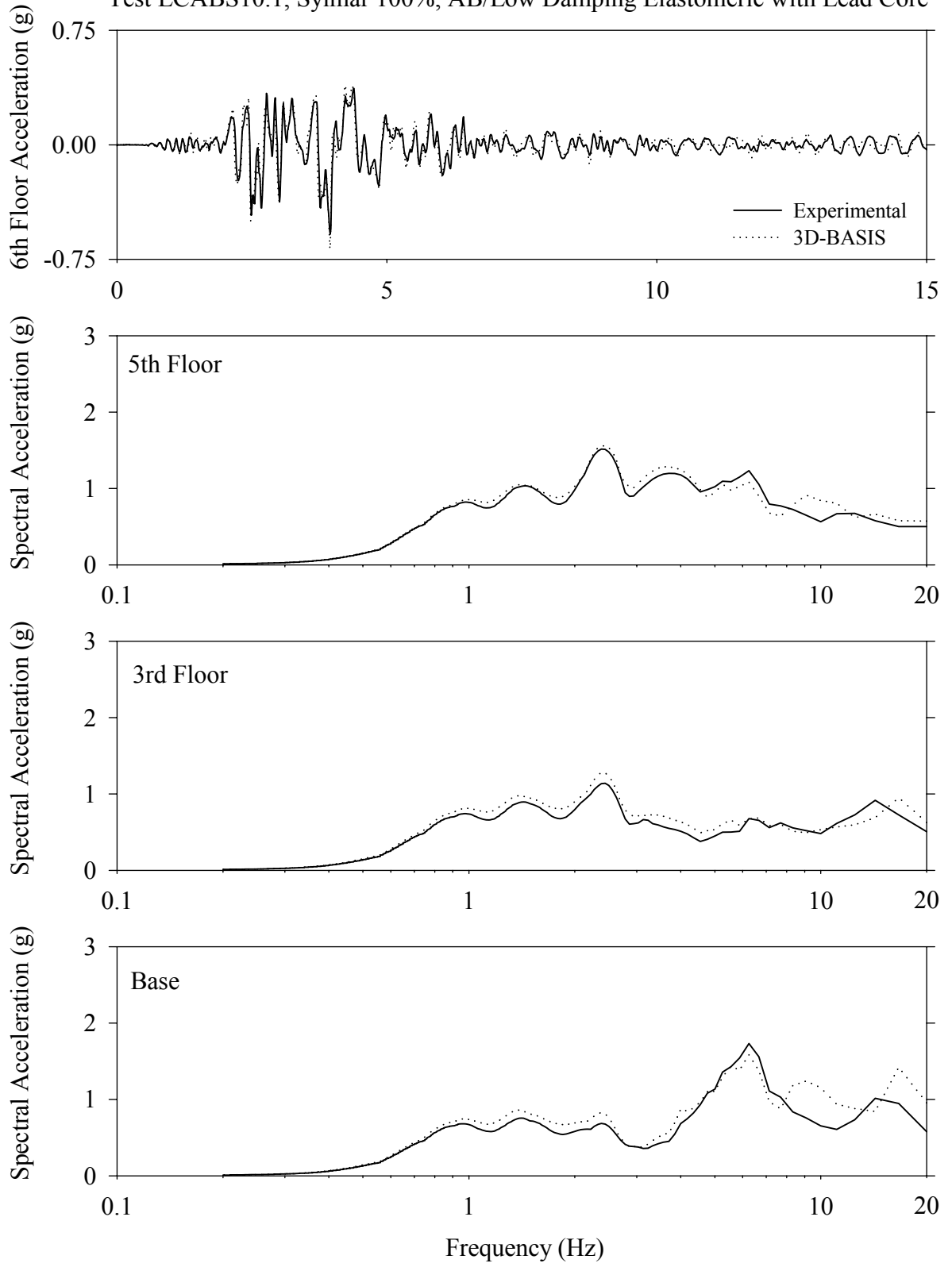




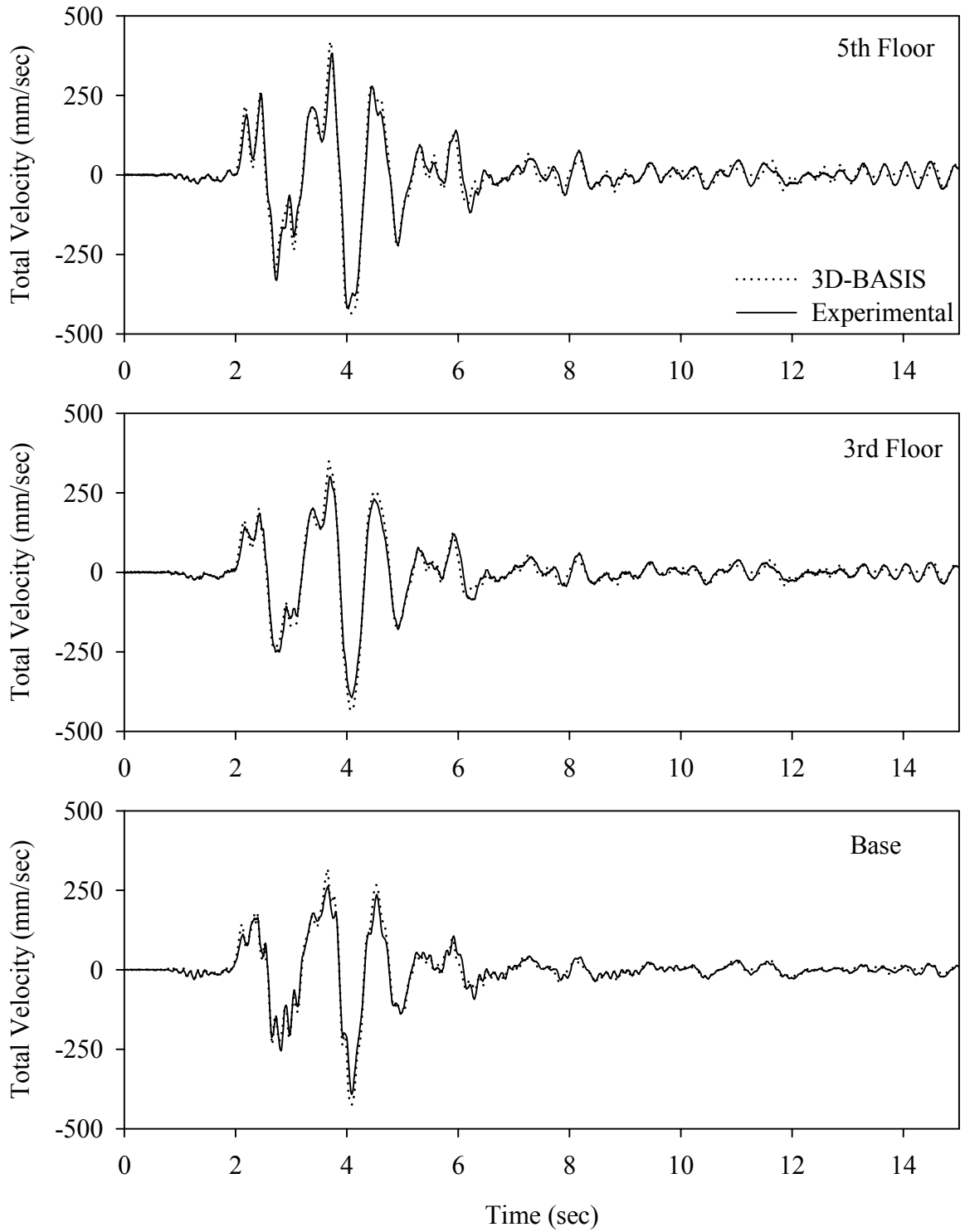
Test LCABS10.1, Sylmar 100%, AB/Low Damping Elastomeric with Lead Core



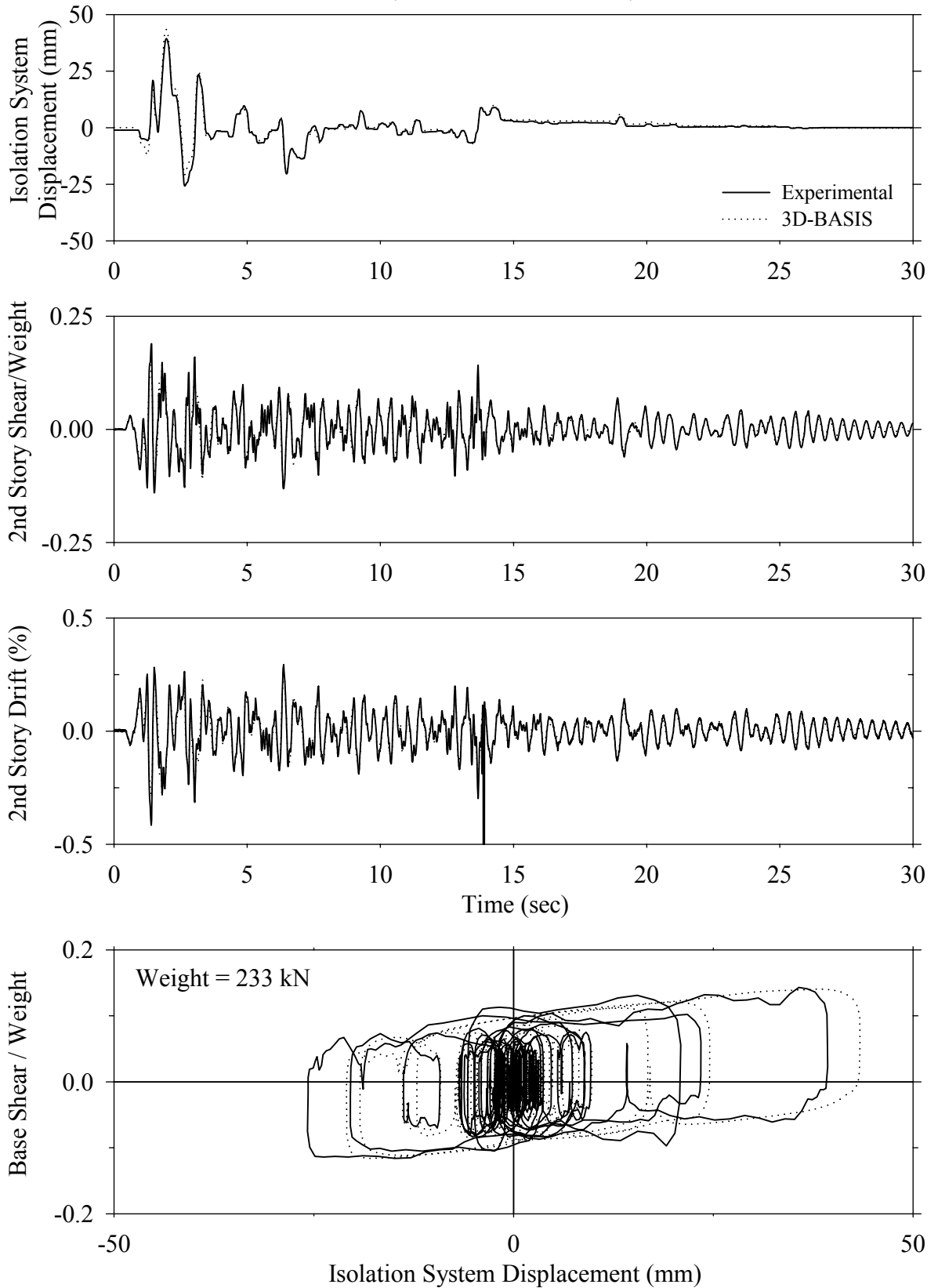
Test LCABS10.1, Sylmar 100%, AB/Low Damping Elastomeric with Lead Core



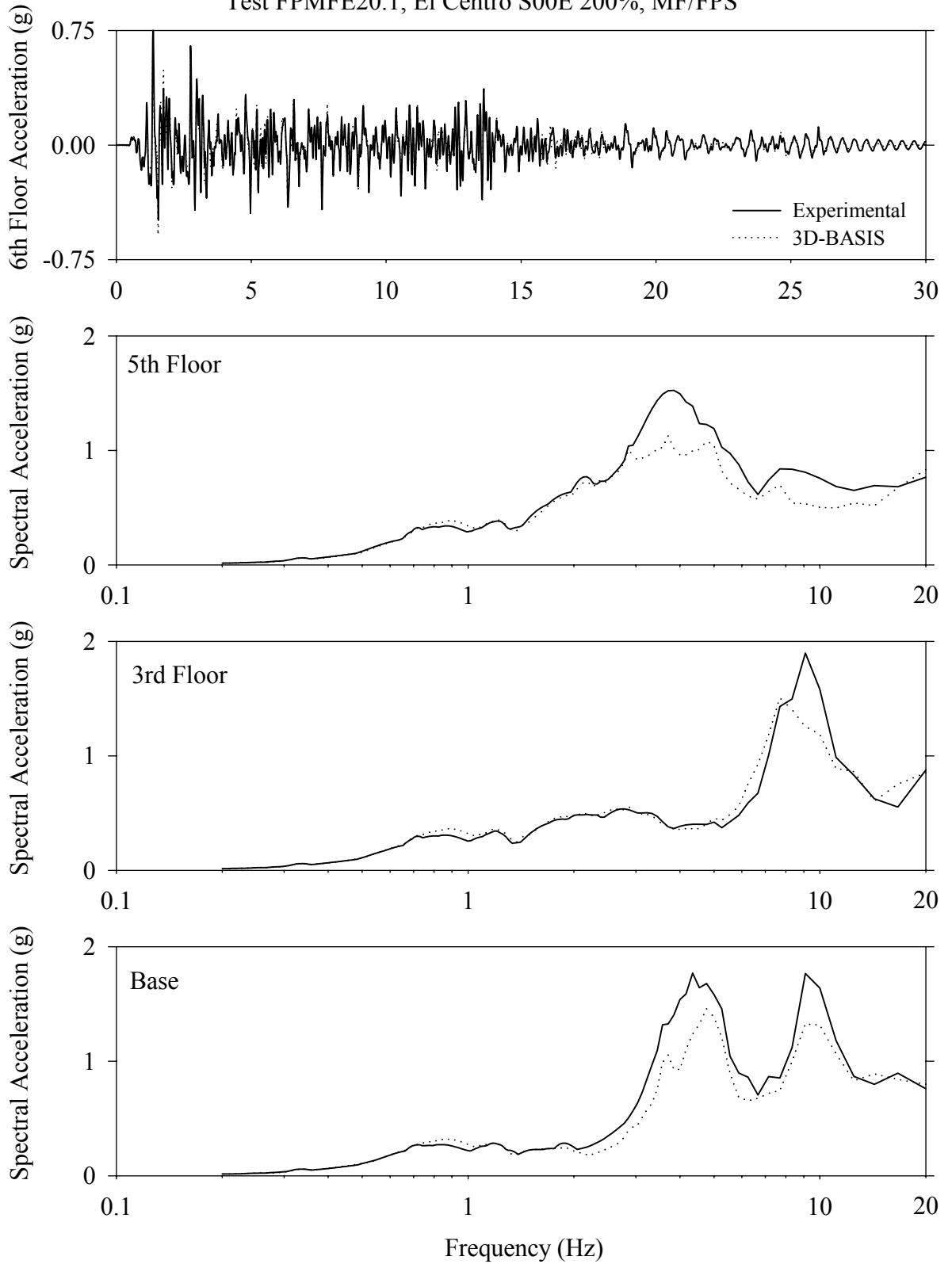
Test LCABS10.1, Sylmar 100%, AB/Low Damping Elastomeric with Lead Core



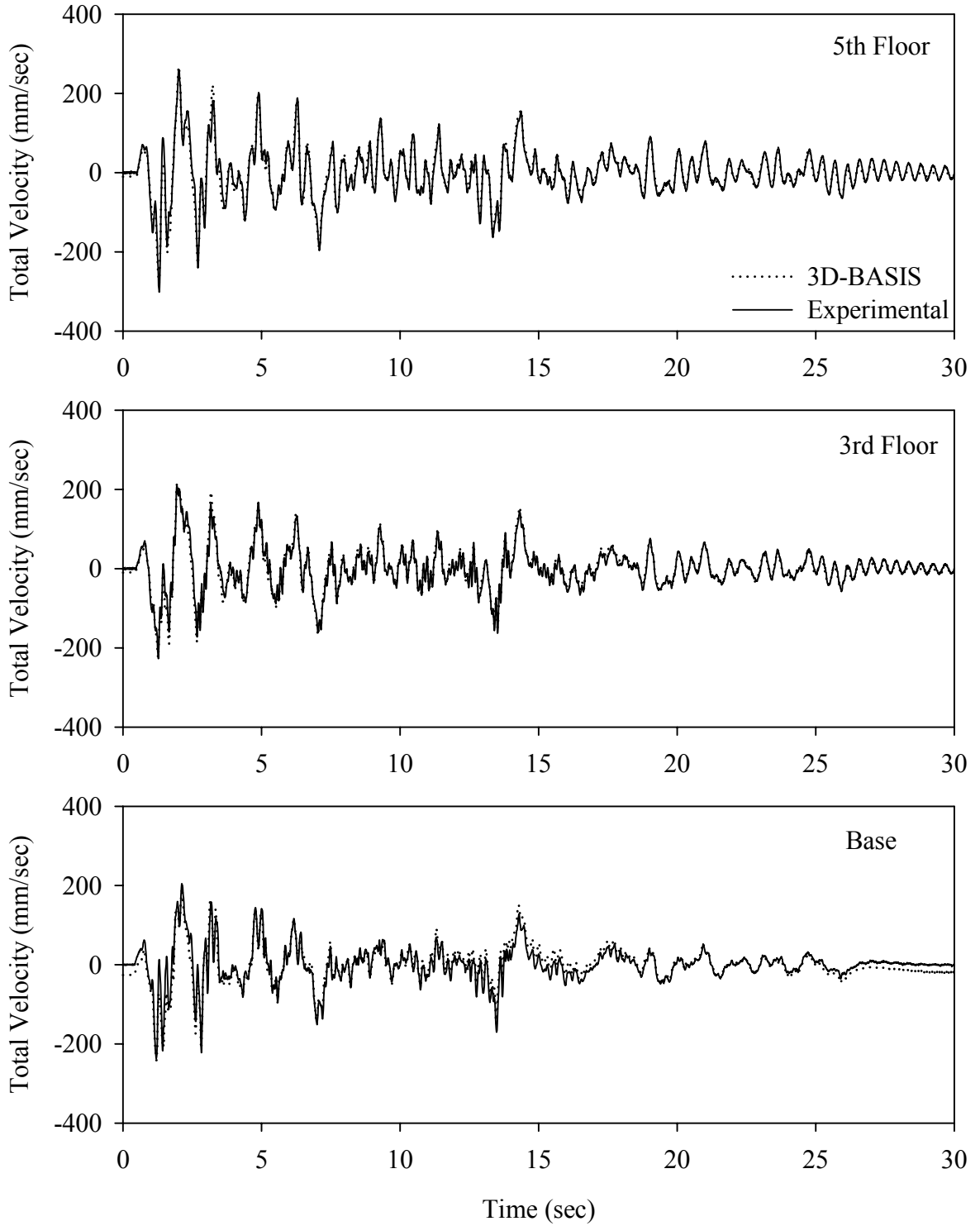
Test FPMFE20.1, El Centro S00E 200%, MF/FPS



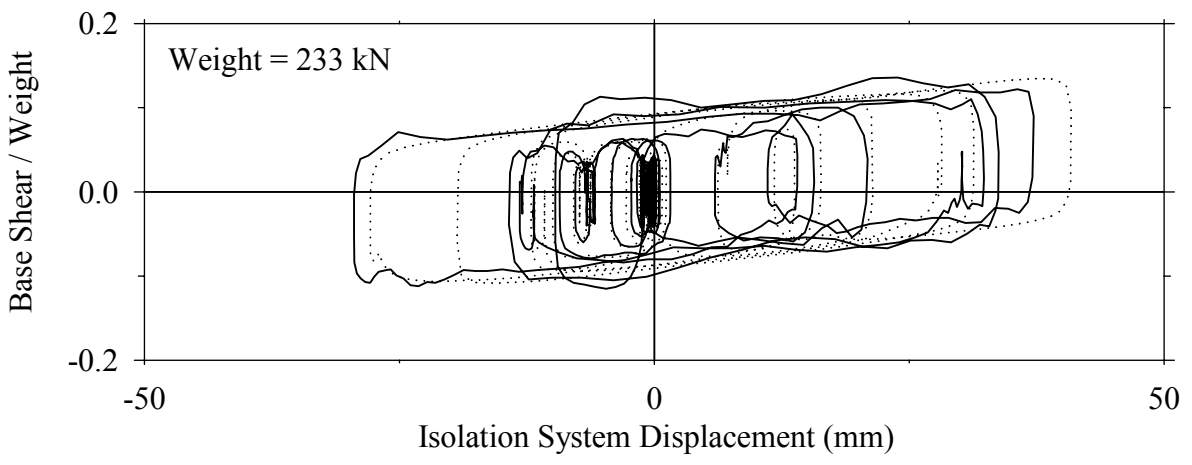
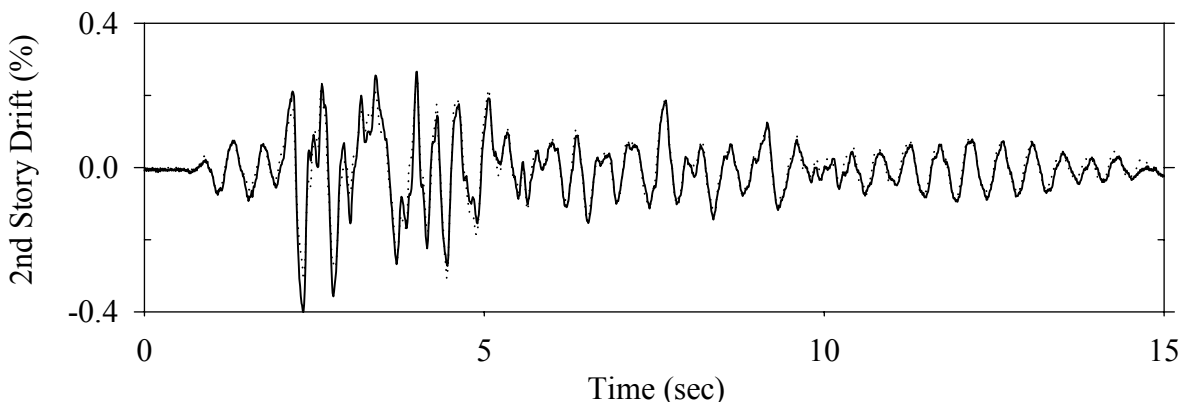
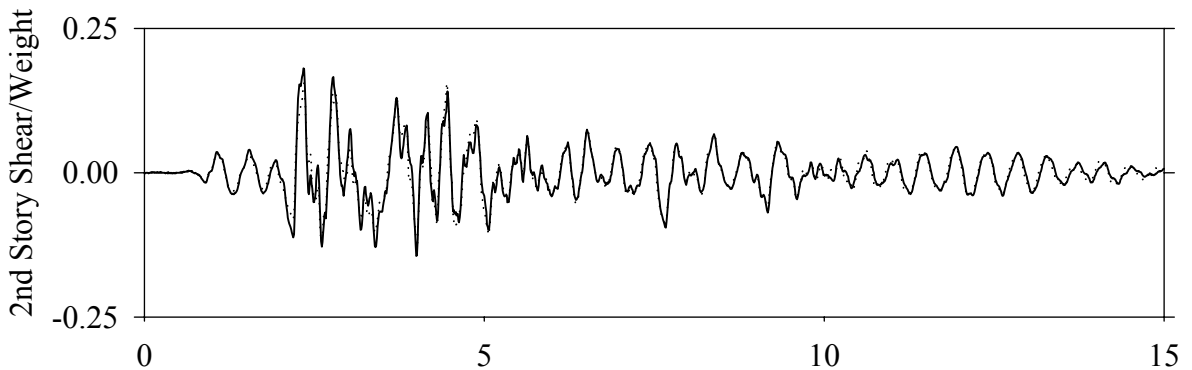
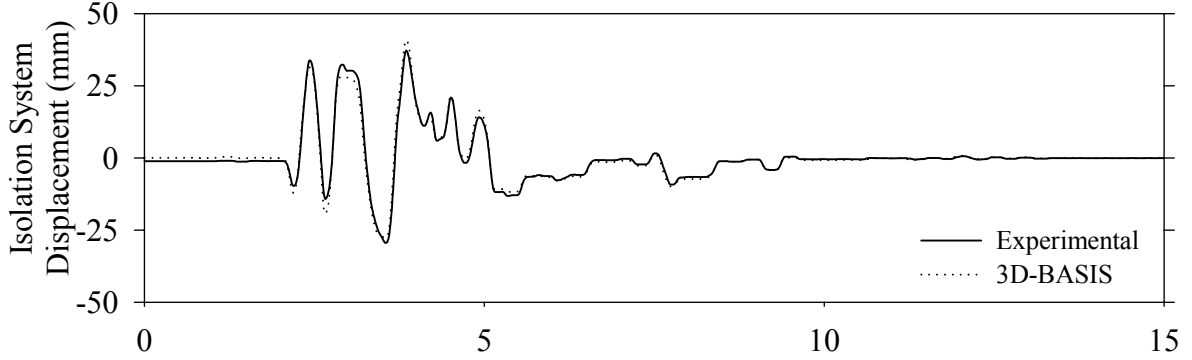
Test FPMFE20.1, El Centro S00E 200%, MF/FPS



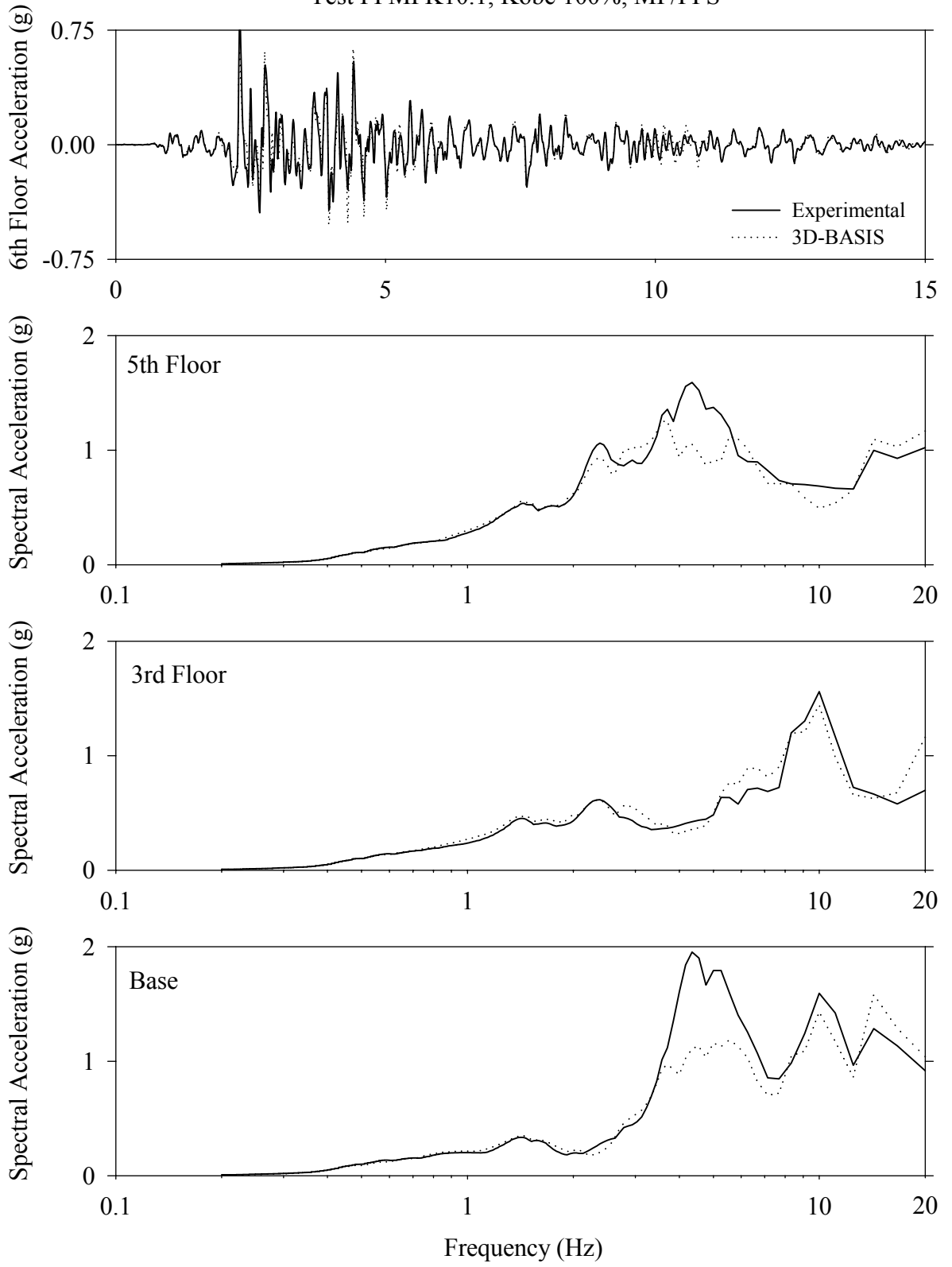
Test FPMFE20.1, El Centro S00E 200%, MF/FPS



Test FPMFK10.1, Kobe 100%, MF/FPS

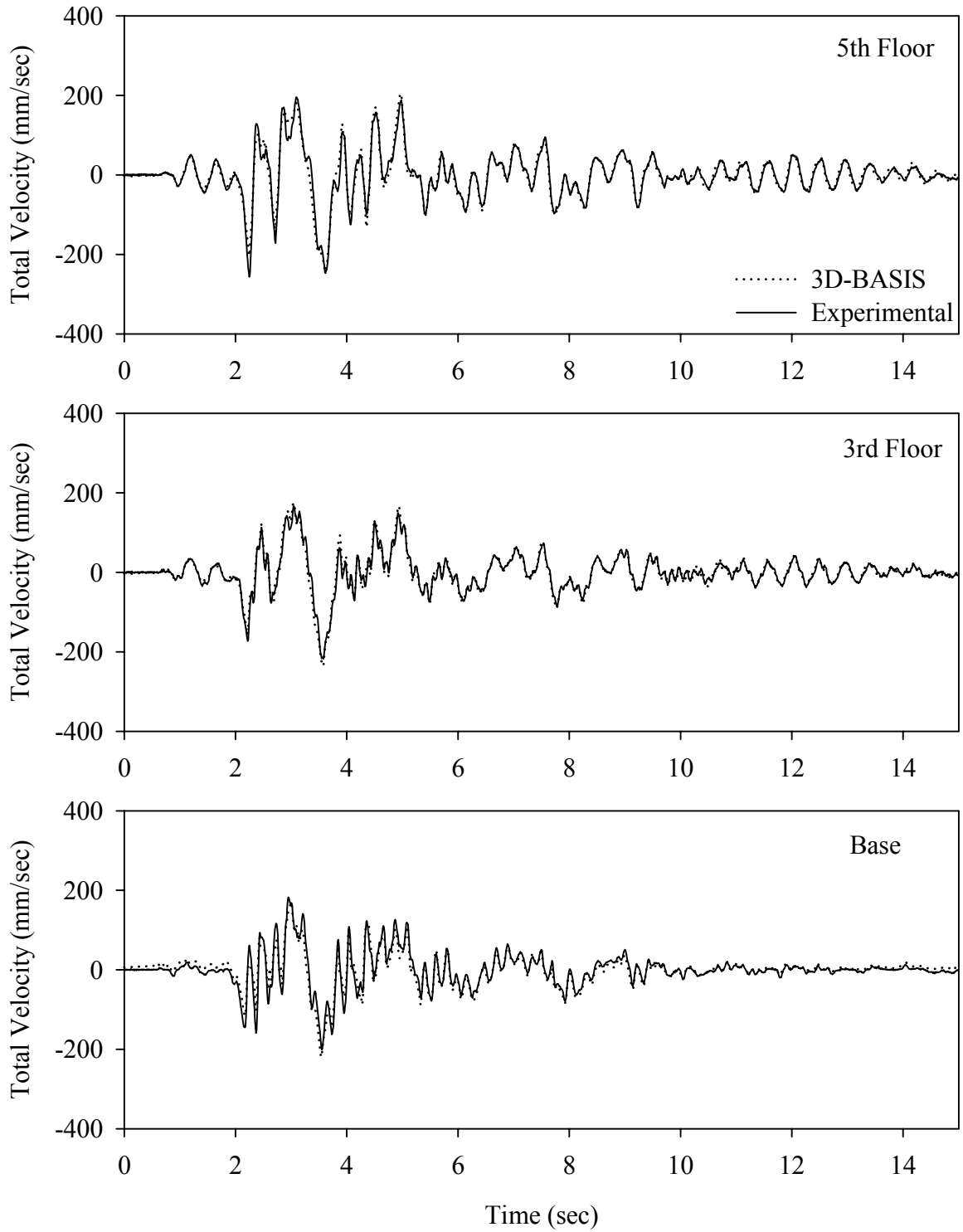


Test FPMFK10.1, Kobe 100%, MF/FPS

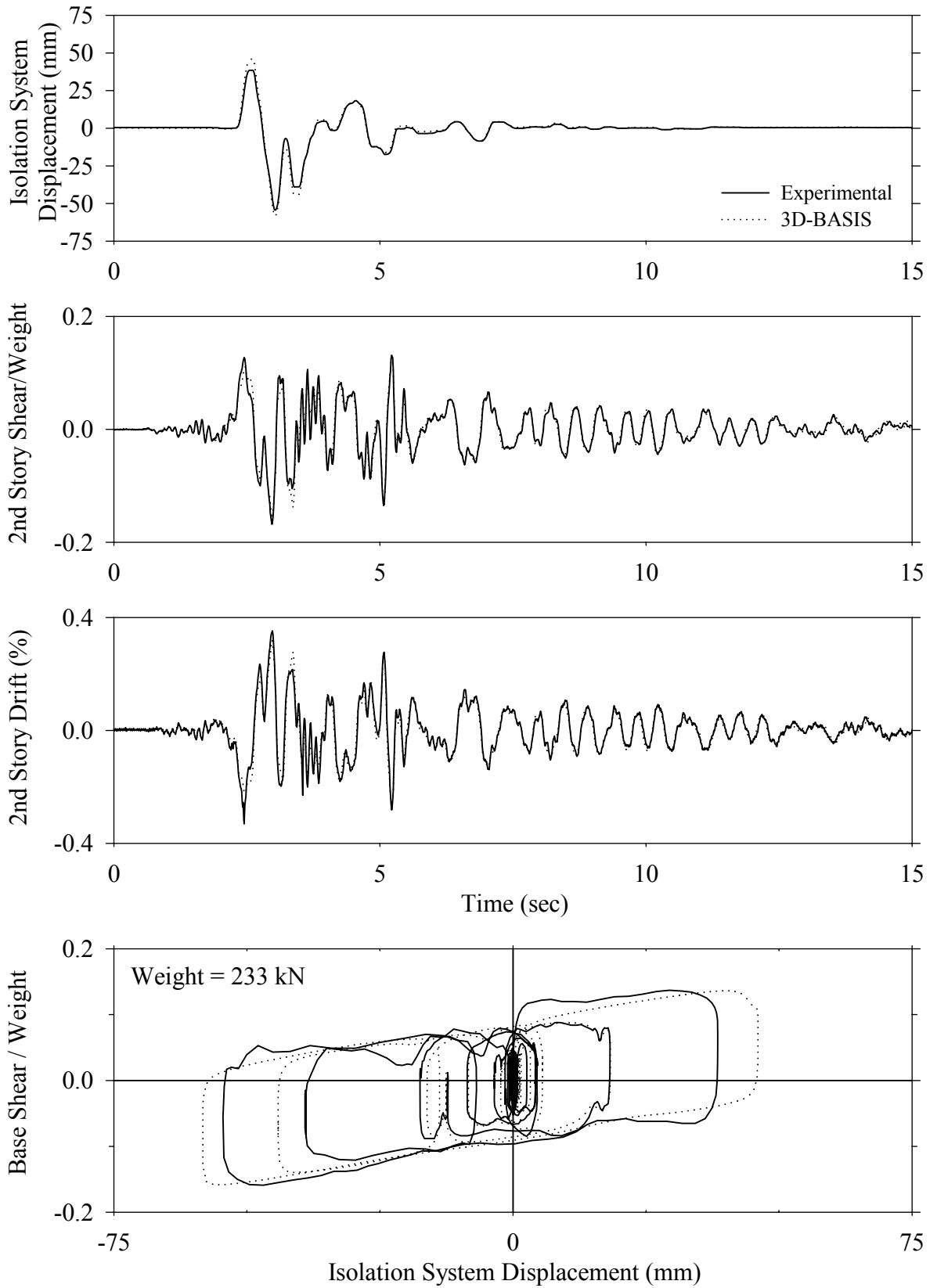




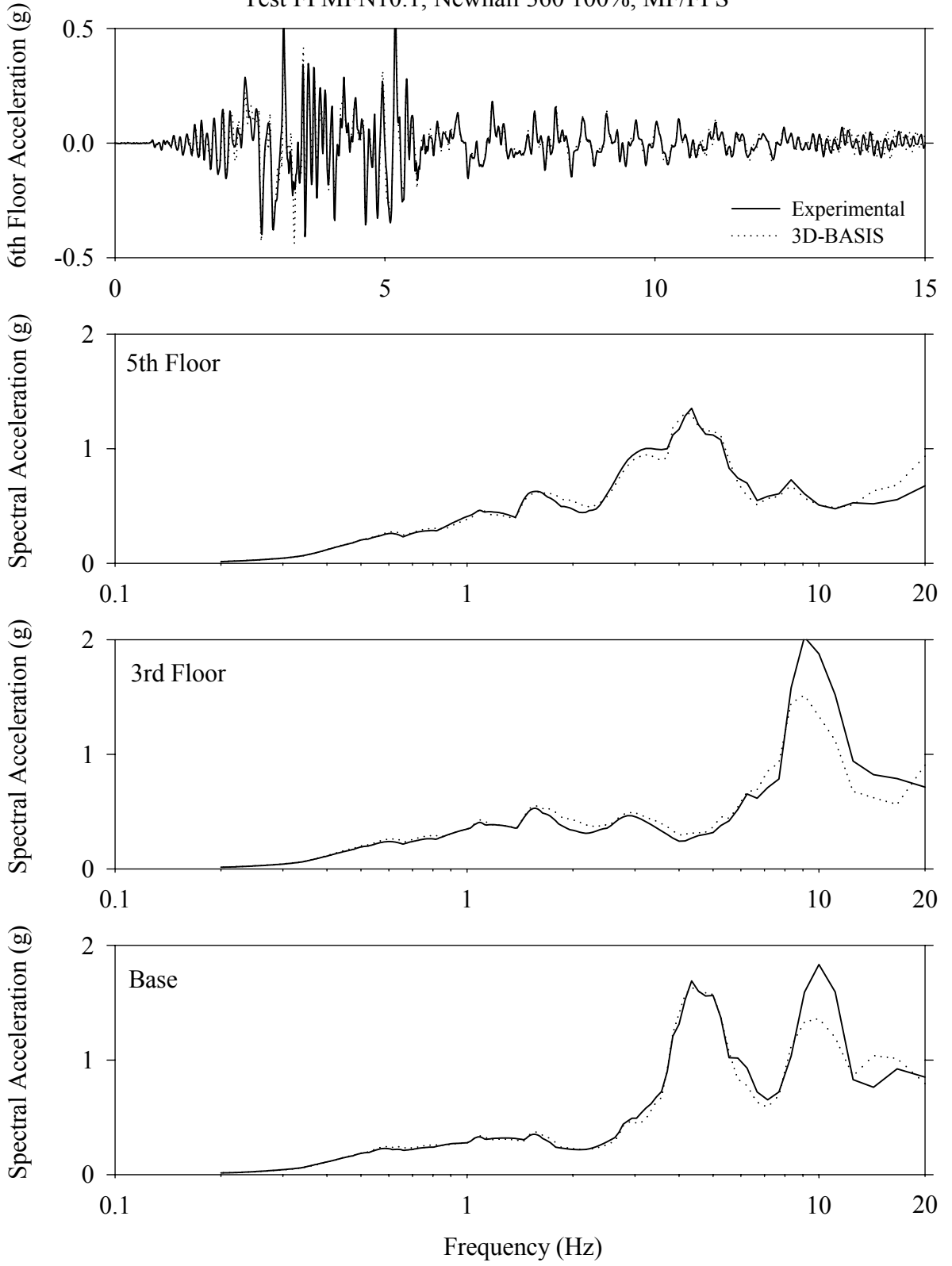
Test FPMFK10.1, Kobe 100%, MF/FPS



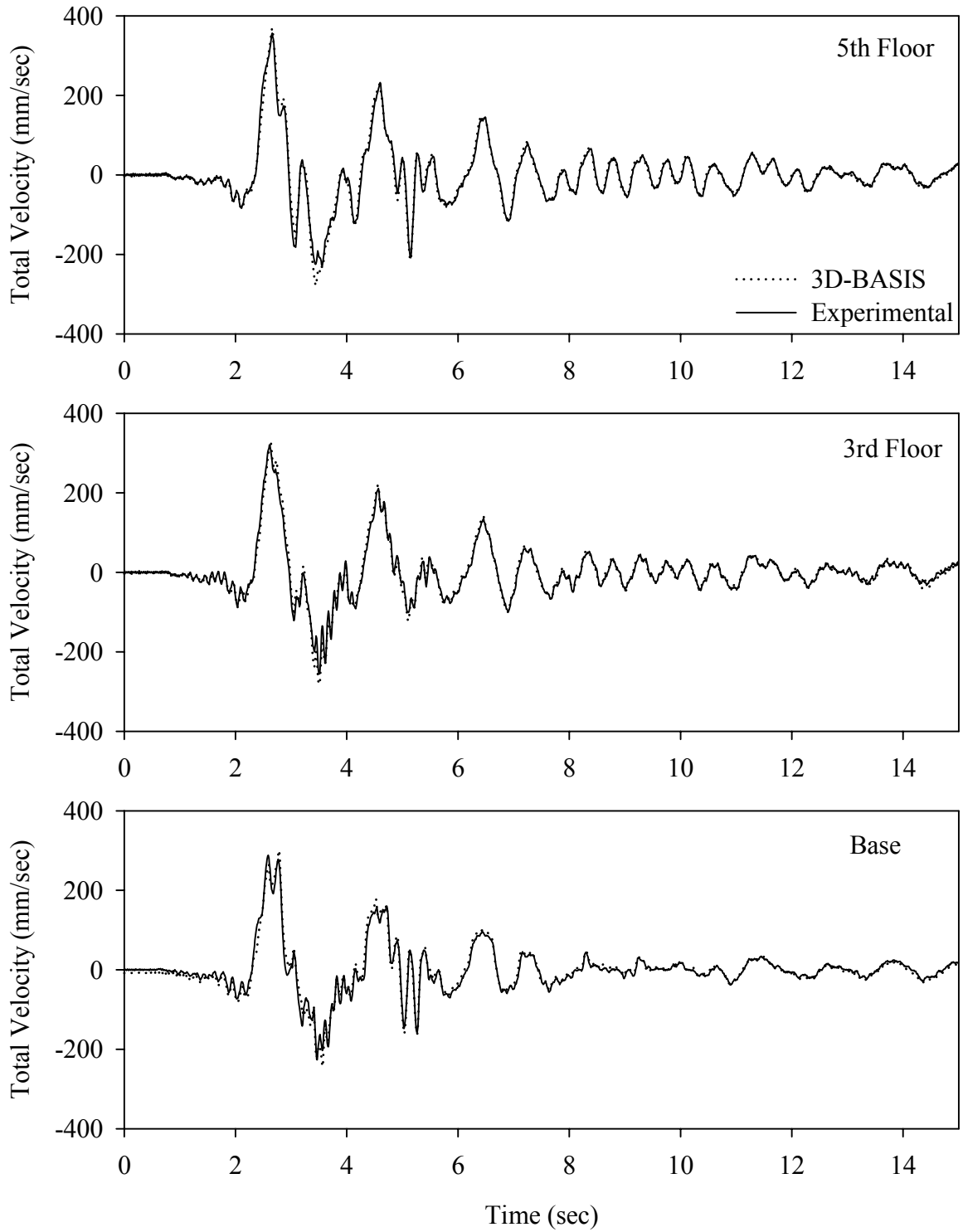
Test FPMFN10.1, Newhall 360 100%, MF/FPS



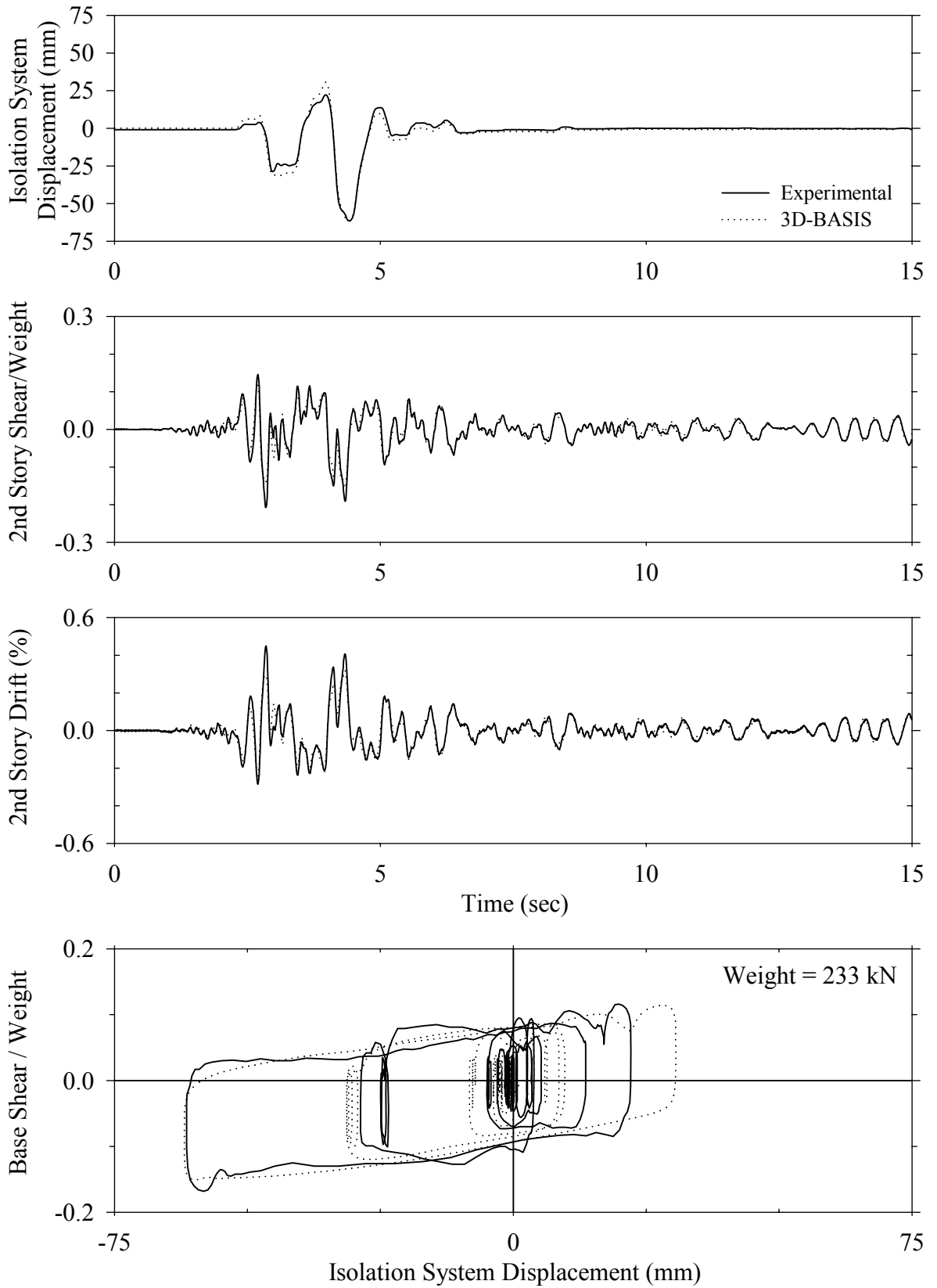
Test FPMFN10.1, Newhall 360 100%, MF/FPS



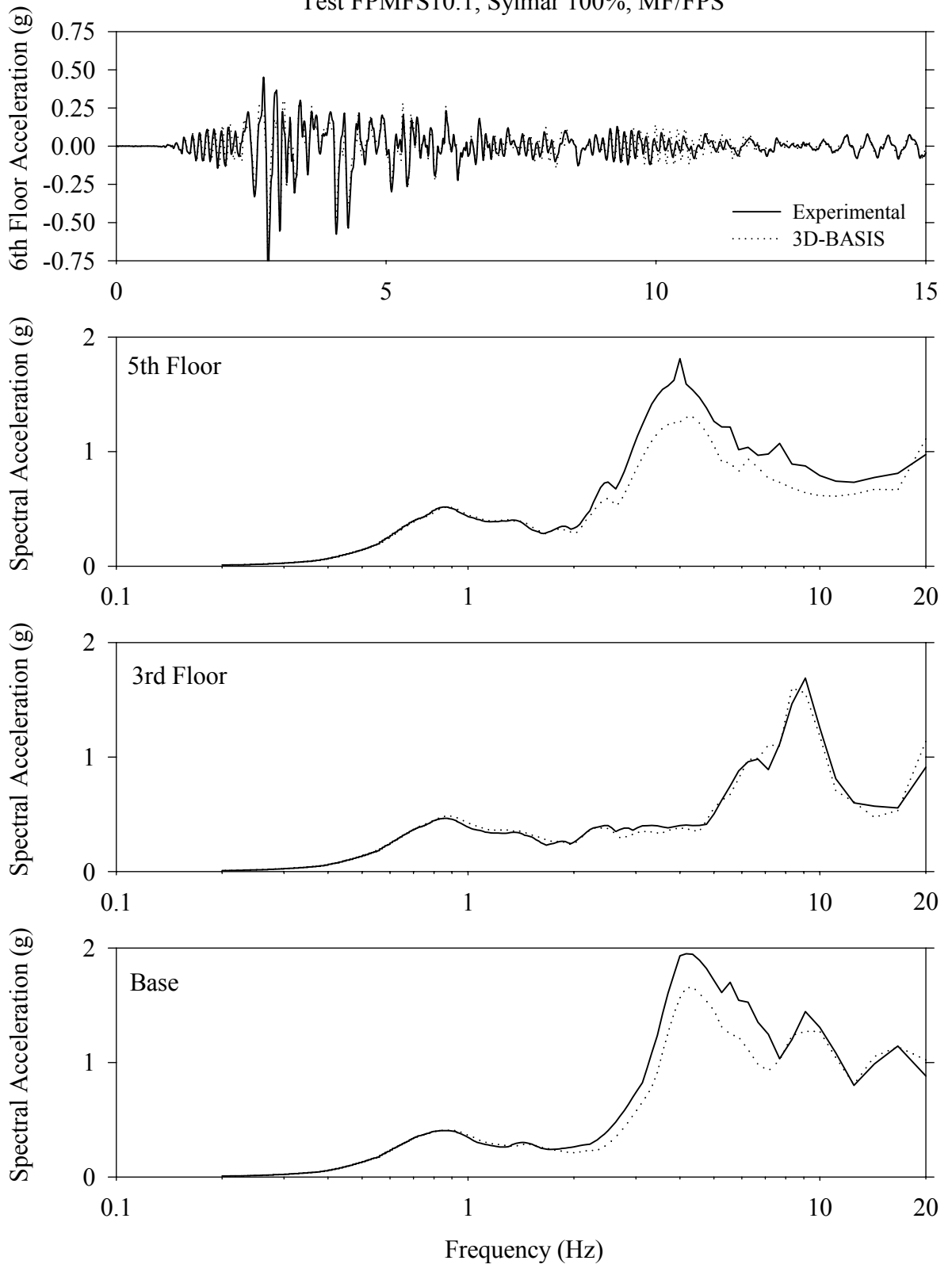
Test FPMFN10.1, Newhall 360 100%, MF/FPS



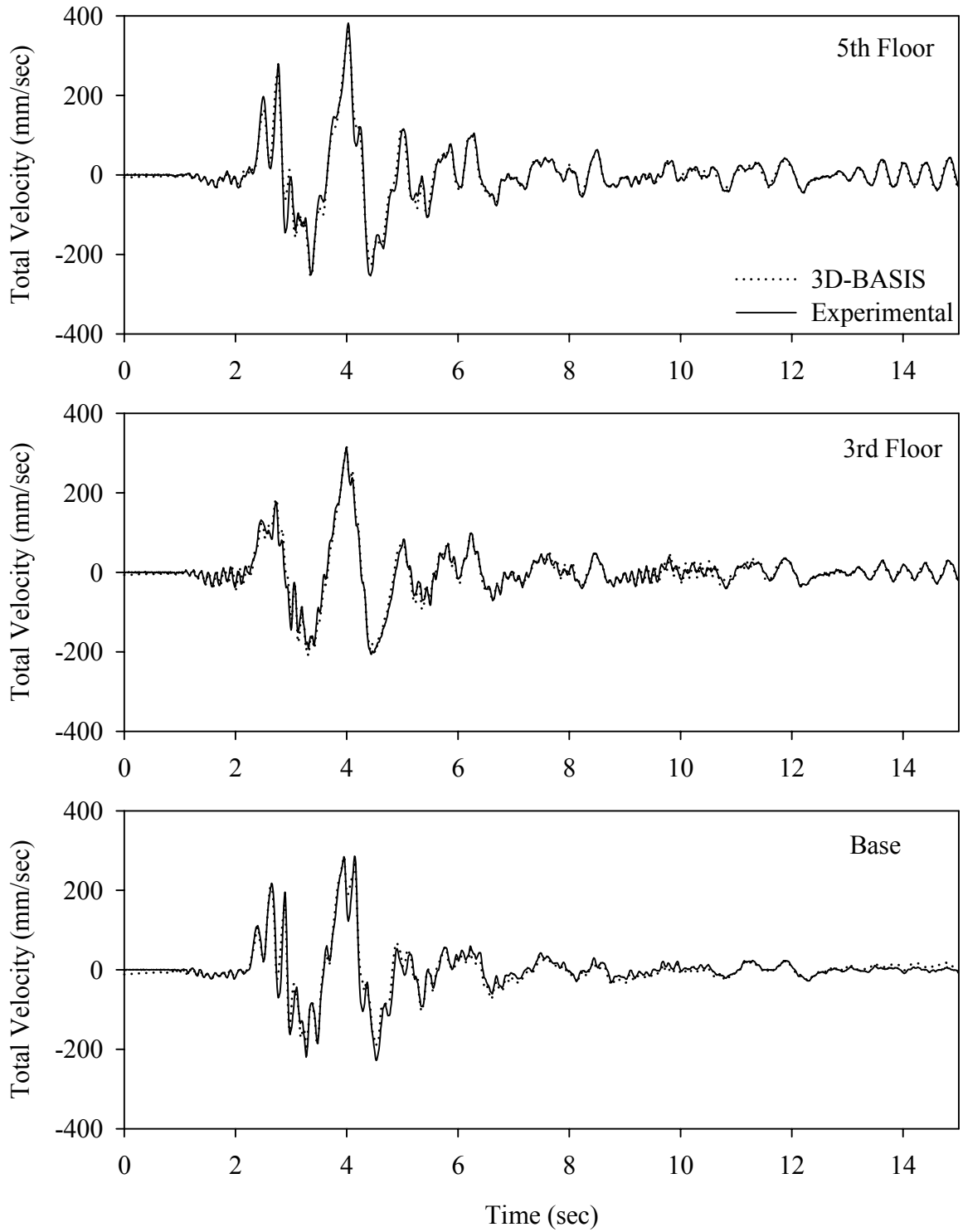
Test FPMFS10.1, Sylmar 100%, MF/FPS



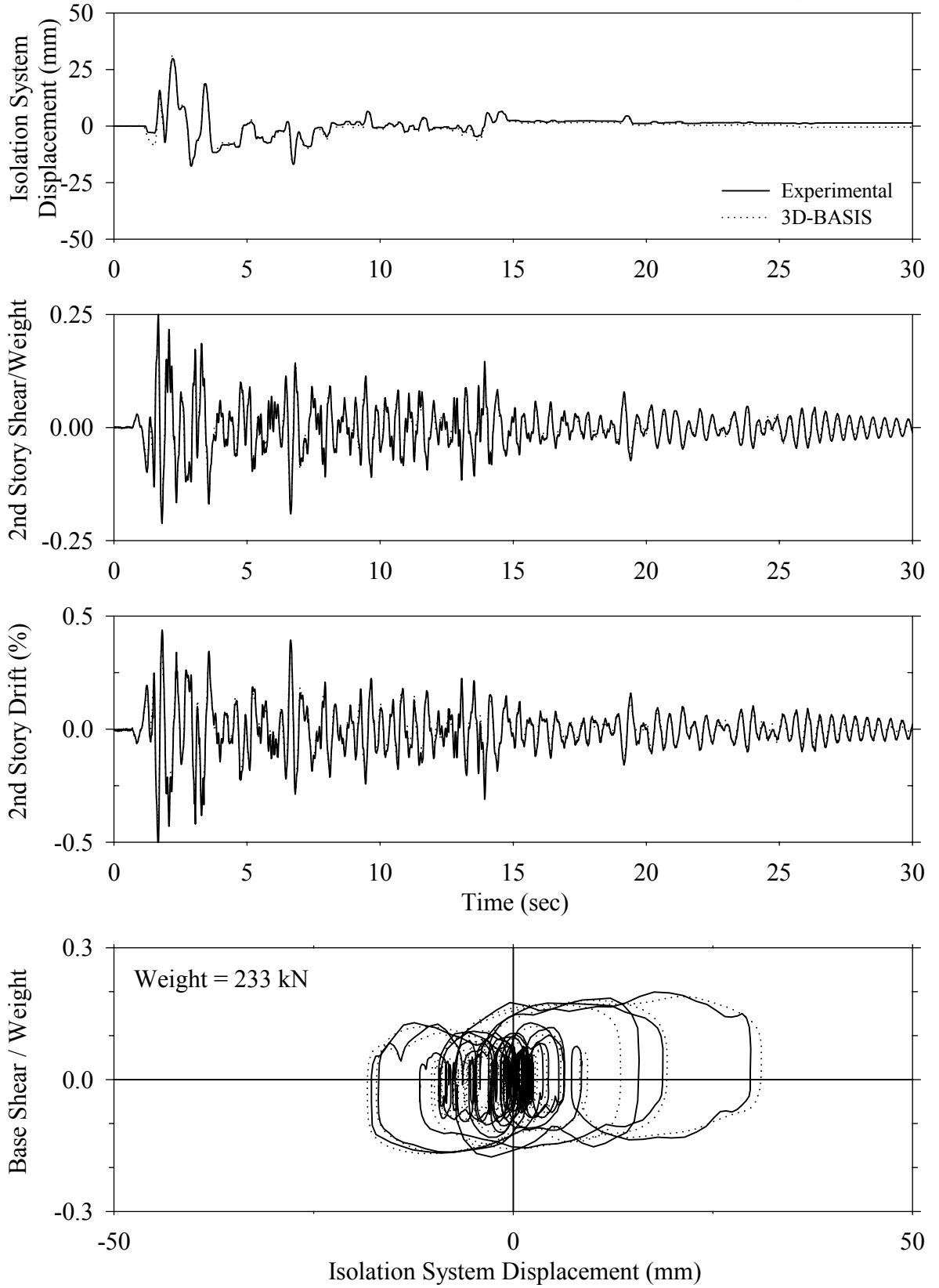
Test FPMFS10.1, Sylmar 100%, MF/FPS



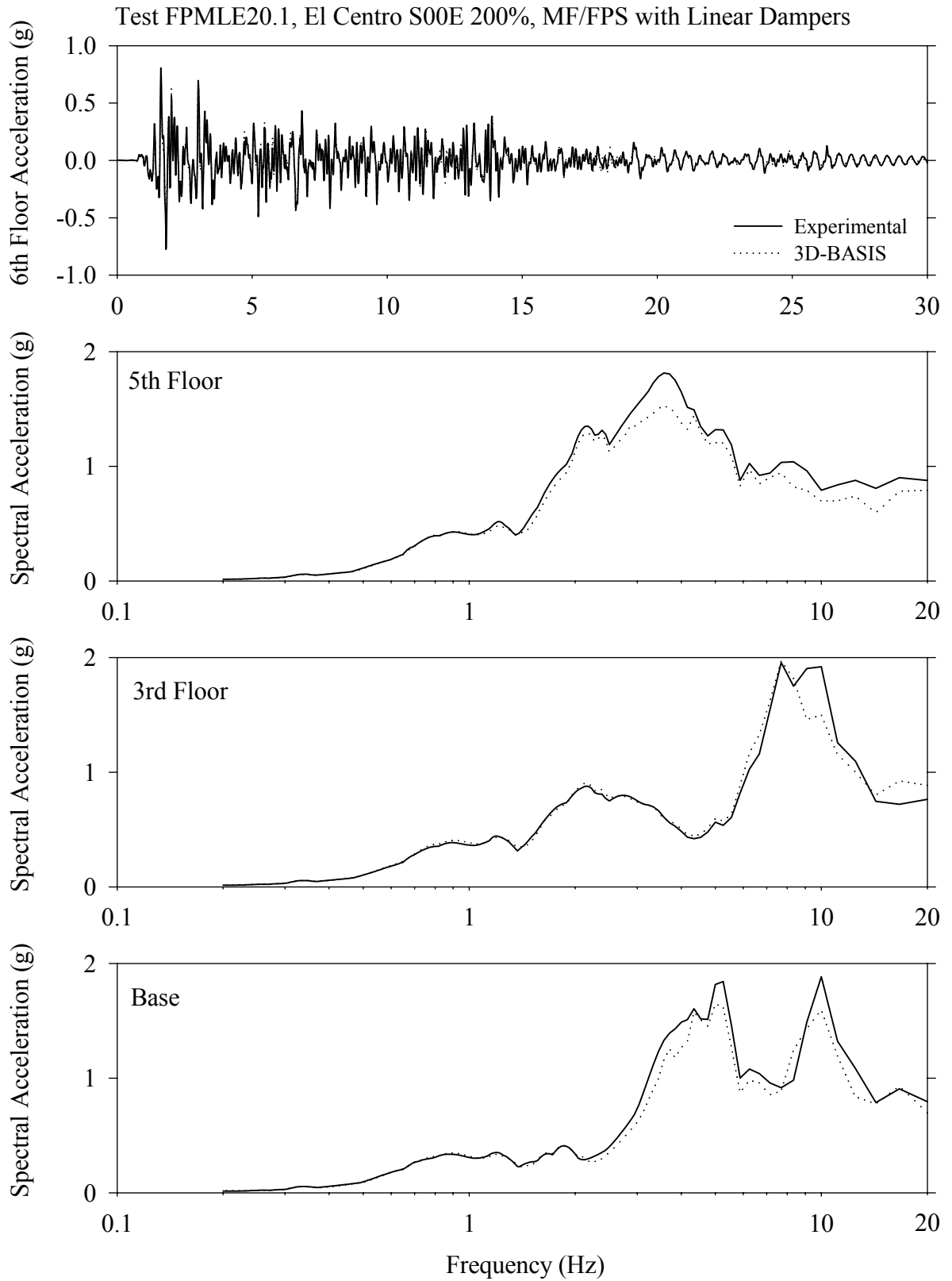
Test FPMFS10.1, Sylmar 100%, MF/FPS



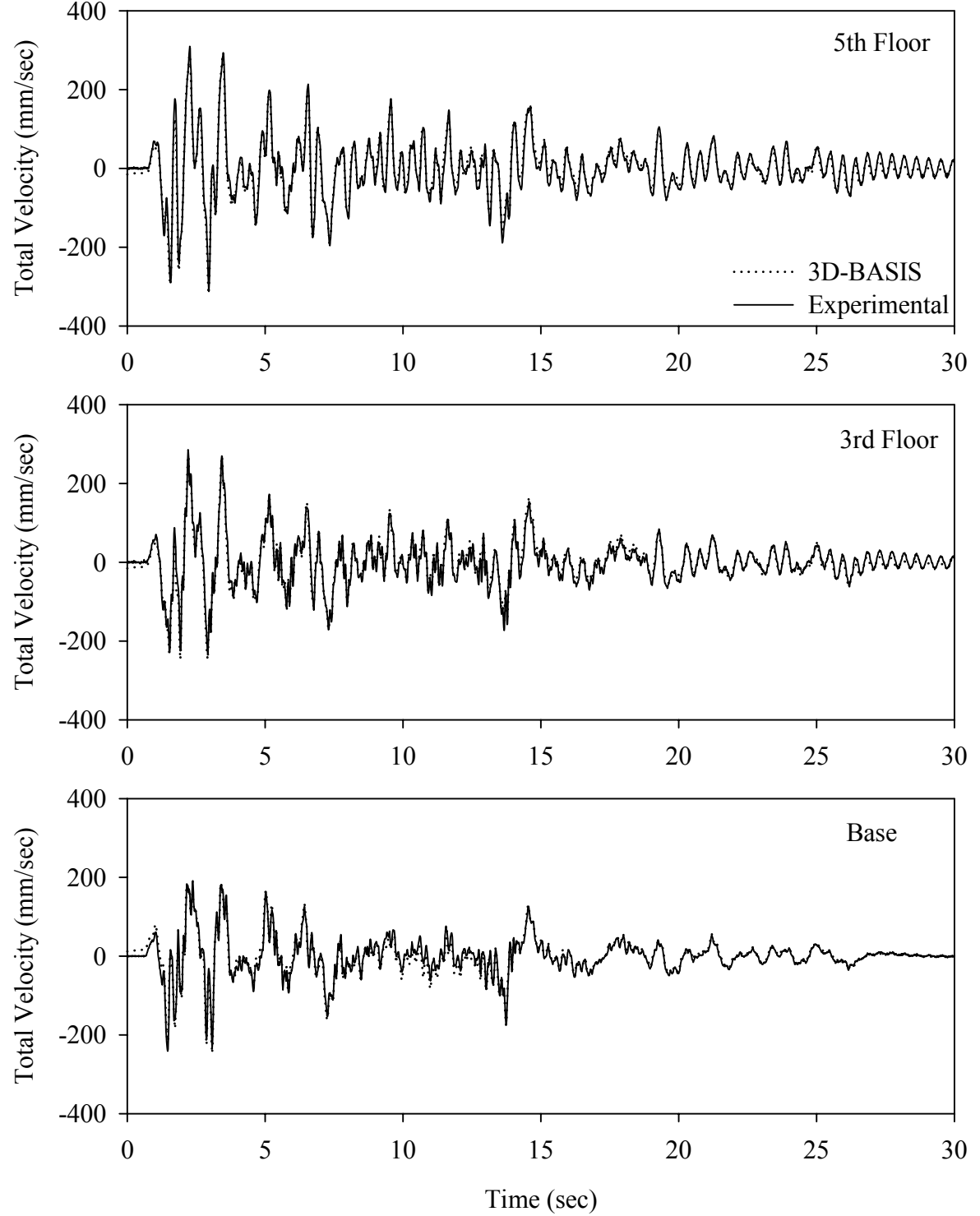
Test FPMLE20.1, El Centro S00E 200%, MF/FPS with Linear Dampers



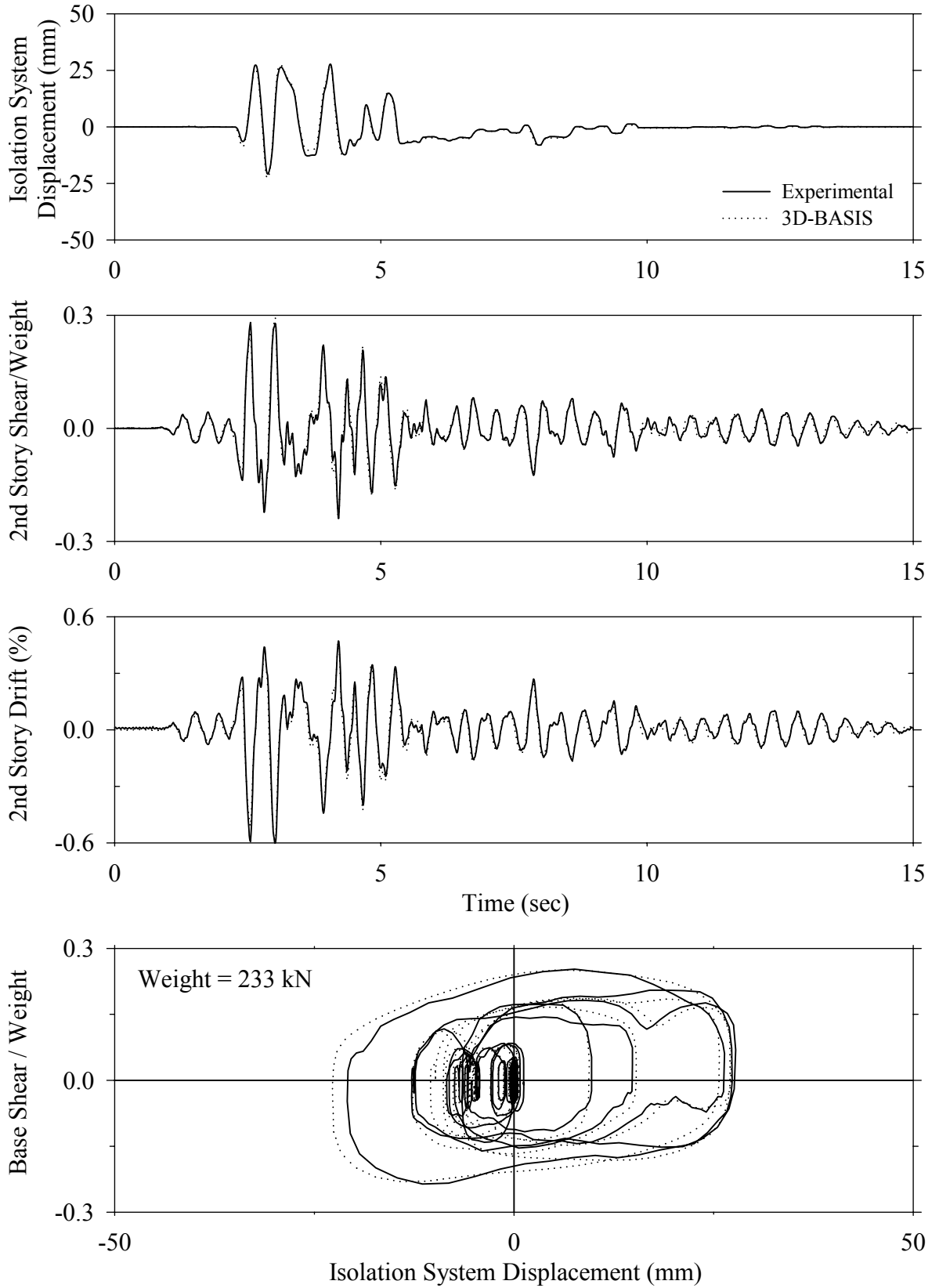




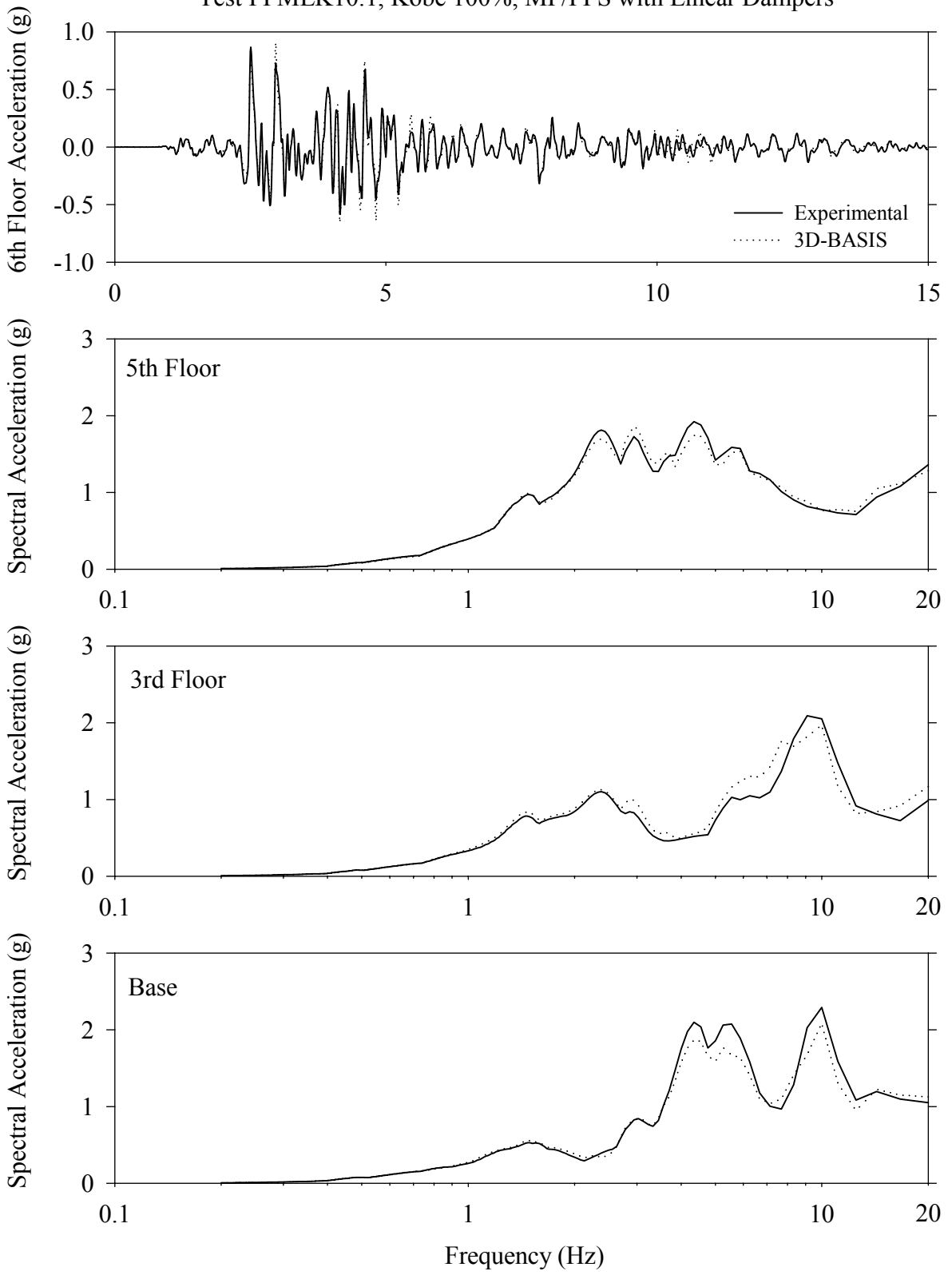
Test FPMLE20.1, El Centro S00E 200%, MF/FPS with Linear Dampers



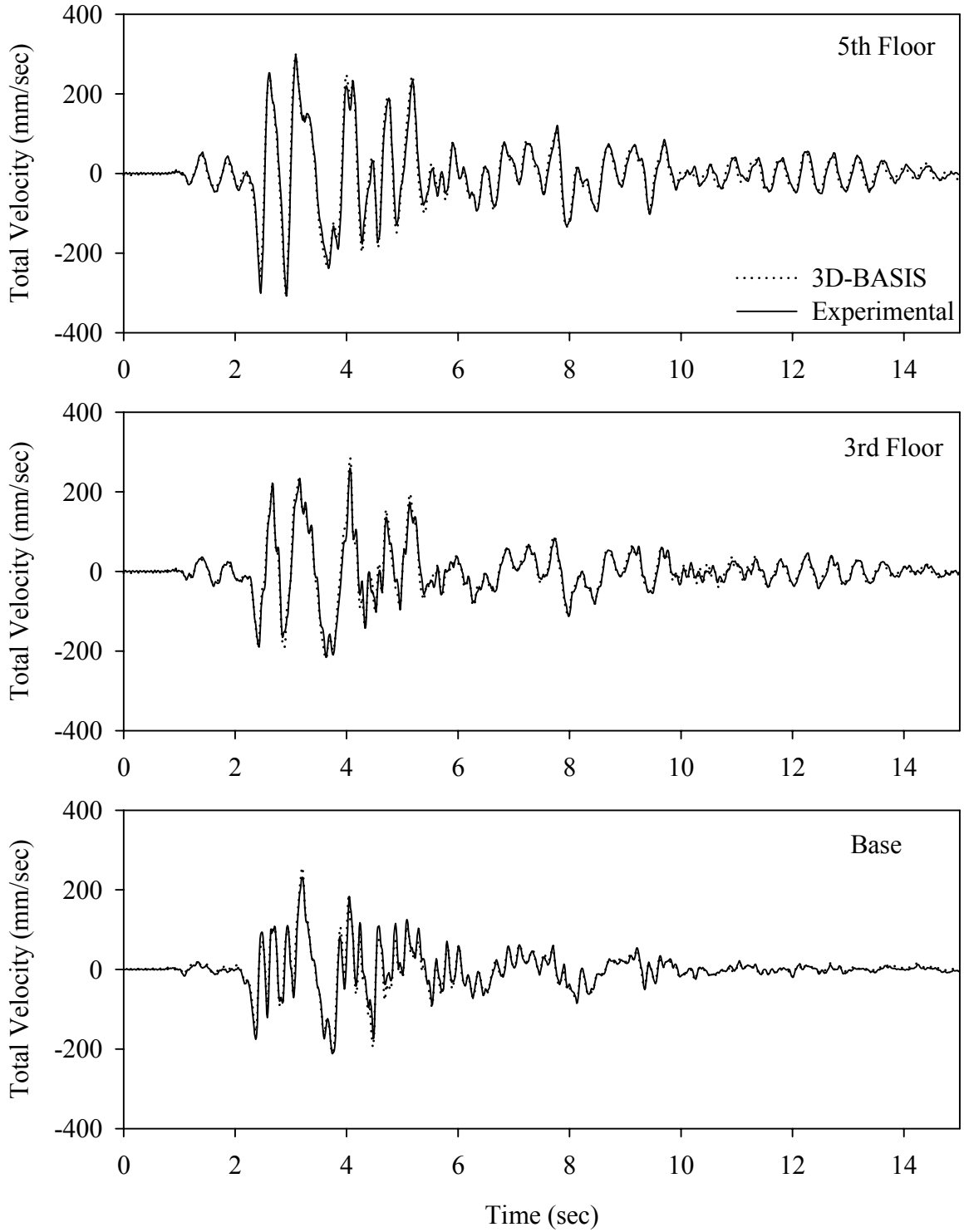
Test FPMLK10.1, Kobe 100%, MF/FPS with Linear Dampers



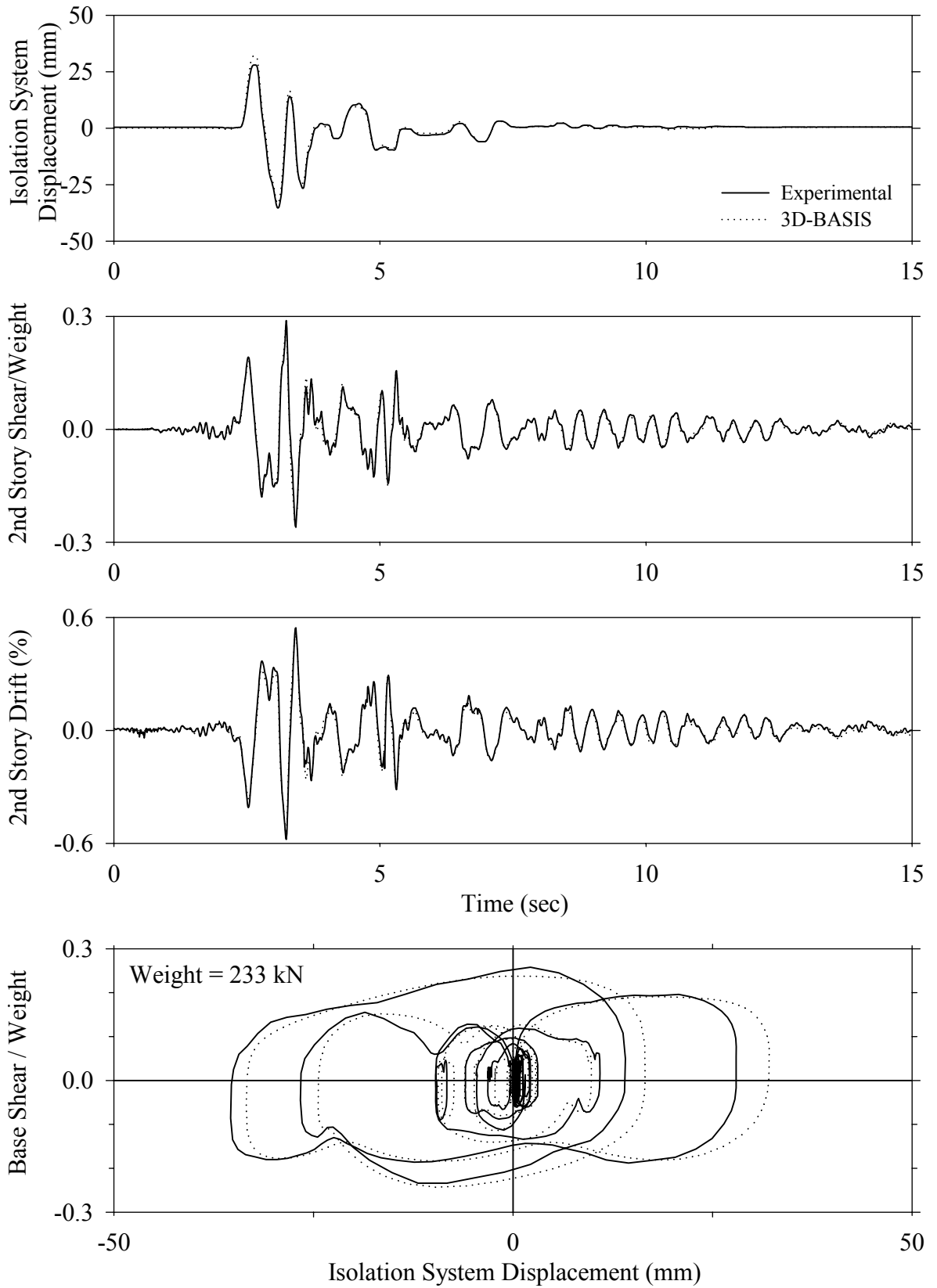
Test FPMLK10.1, Kobe 100%, MF/FPS with Linear Dampers



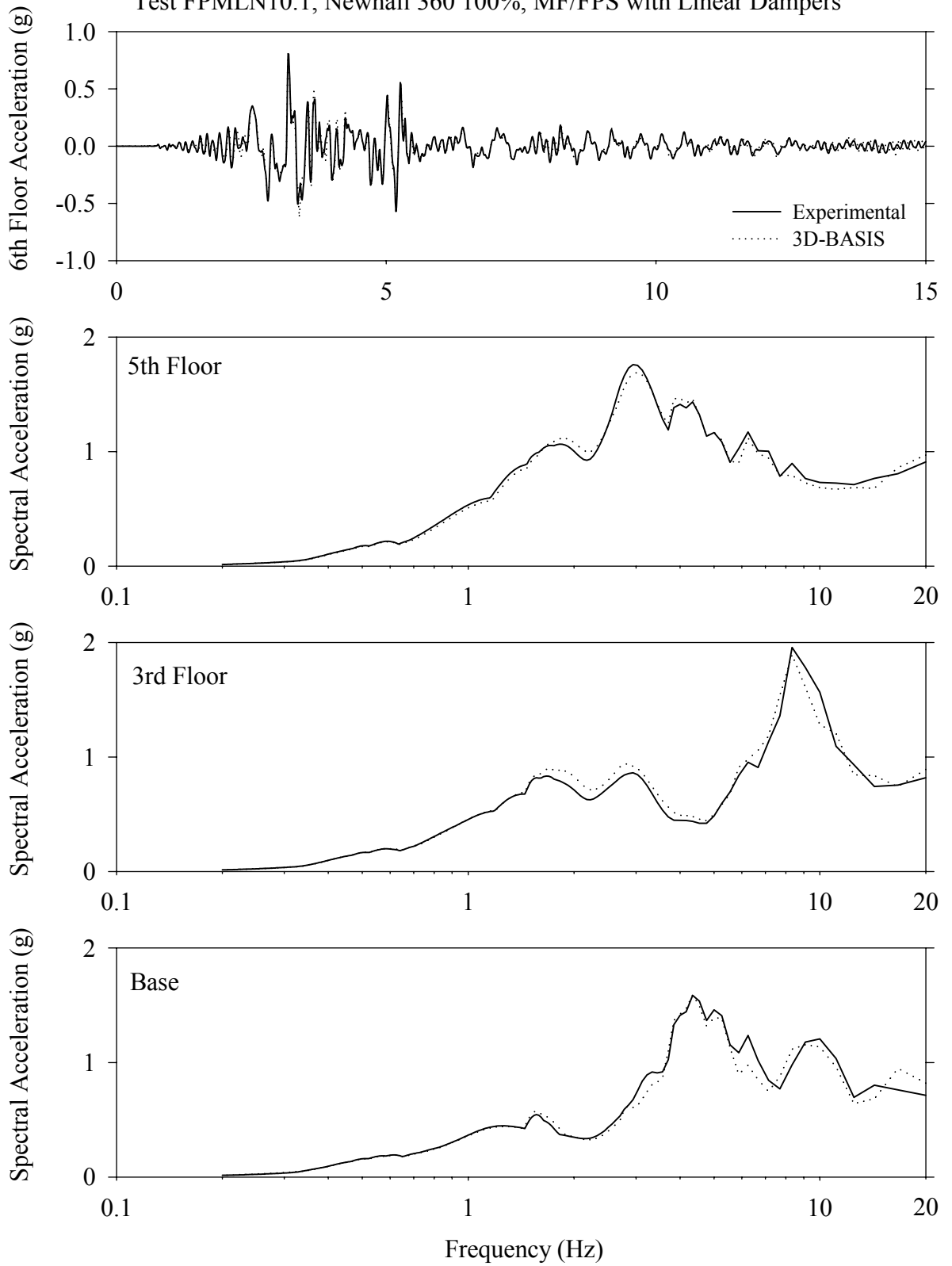
Test FPMLK10.1, Kobe 100%, MF/FPS with Linear Dampers



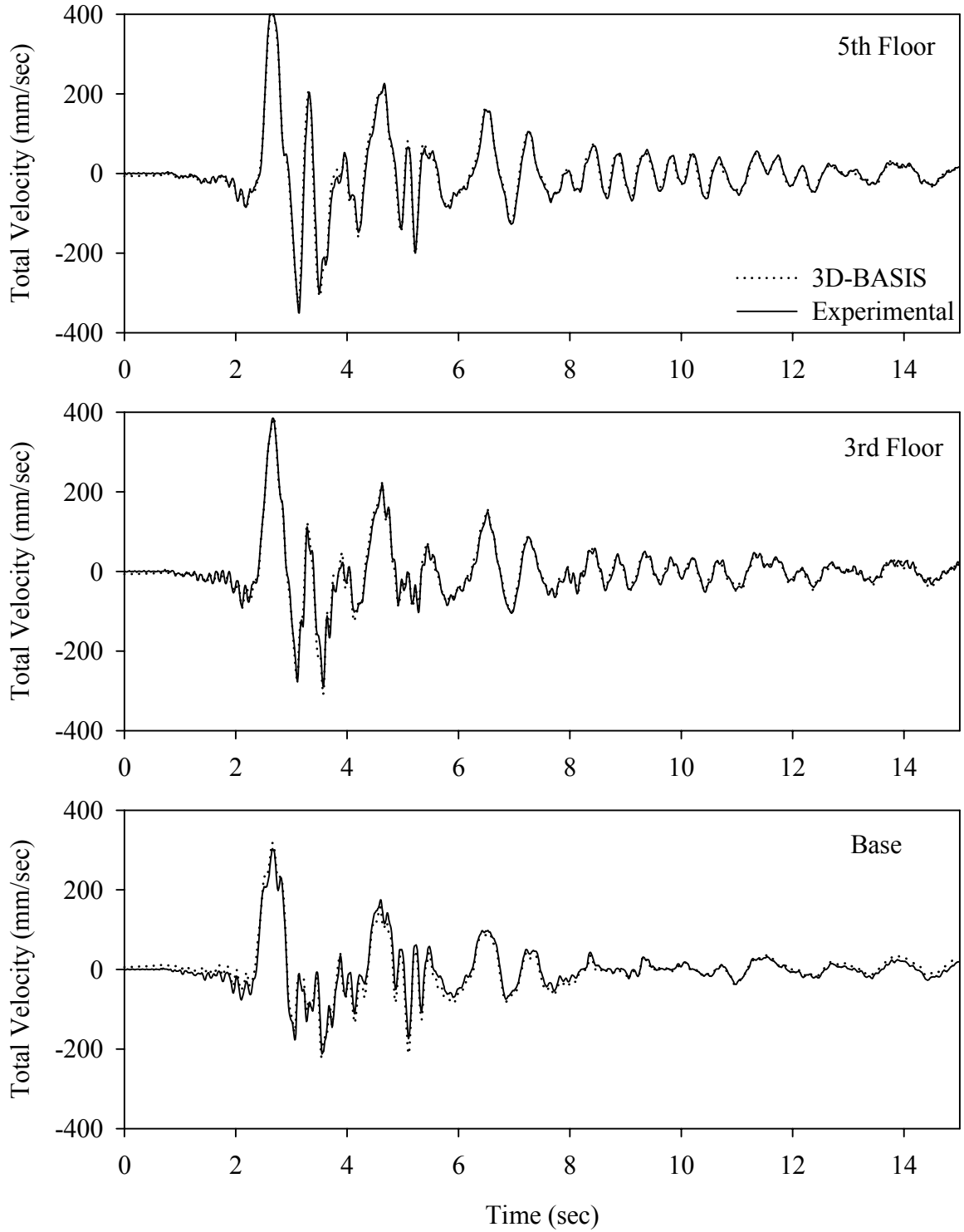
Test FPMLN10.1, Newhall 360 100%, MF/FPS with Linear Dampers



Test FPMLN10.1, Newhall 360 100%, MF/FPS with Linear Dampers

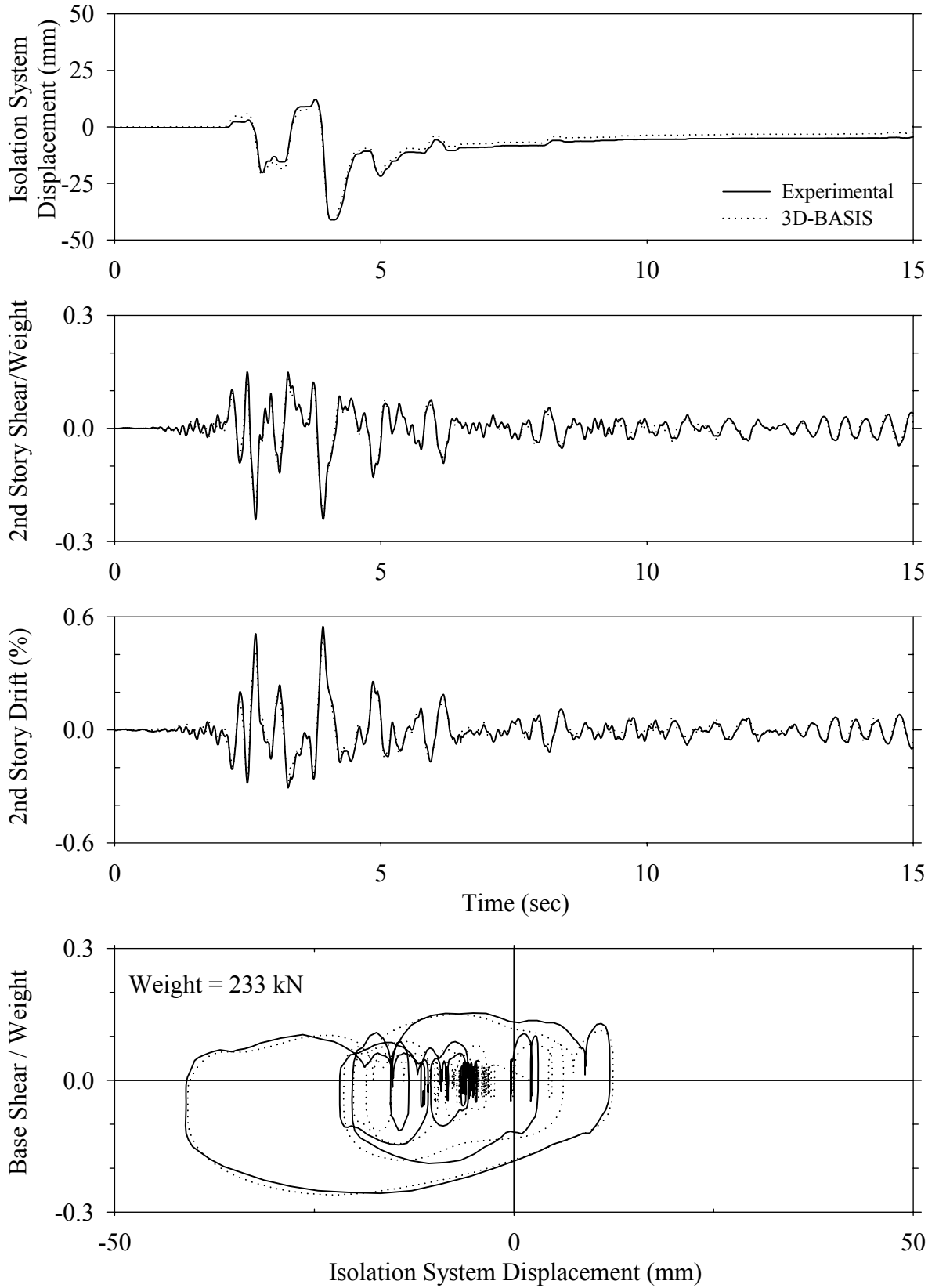


Test FPMLN10.1, Newhall 360 100%, MF/FPS with Linear Dampers

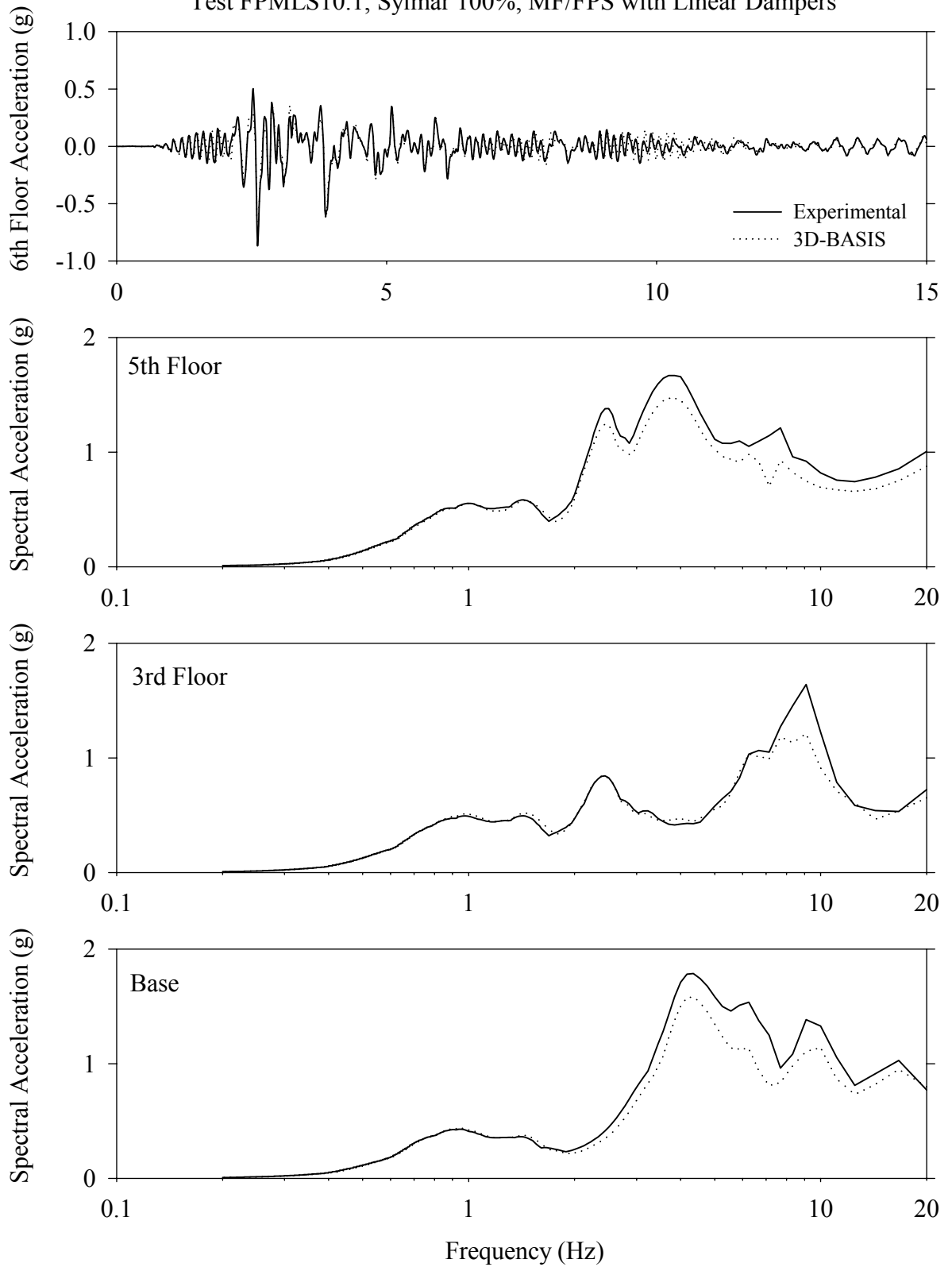




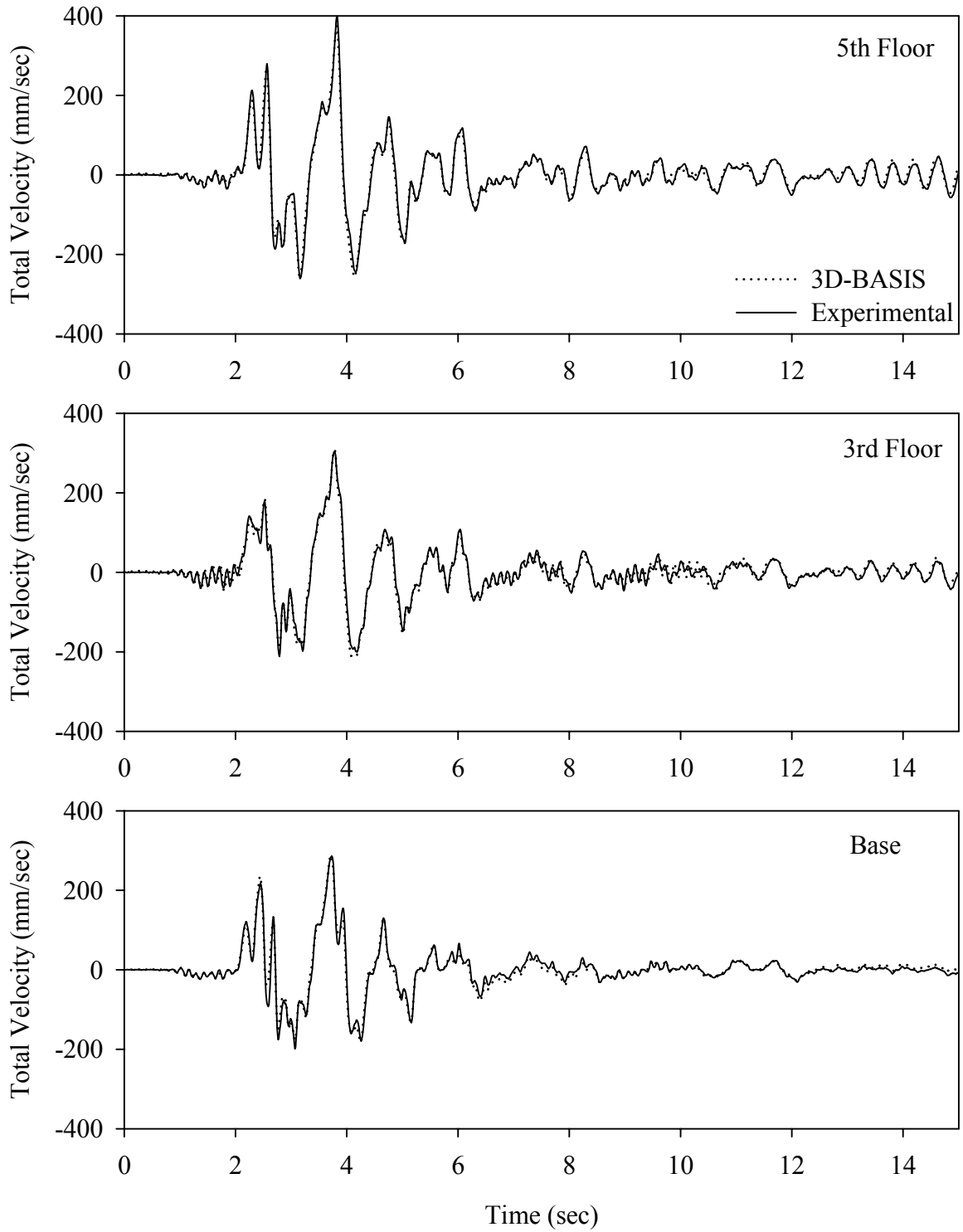
Test FPMLS10.1, Sylmar 100%, MF/FPS with Linear Dampers



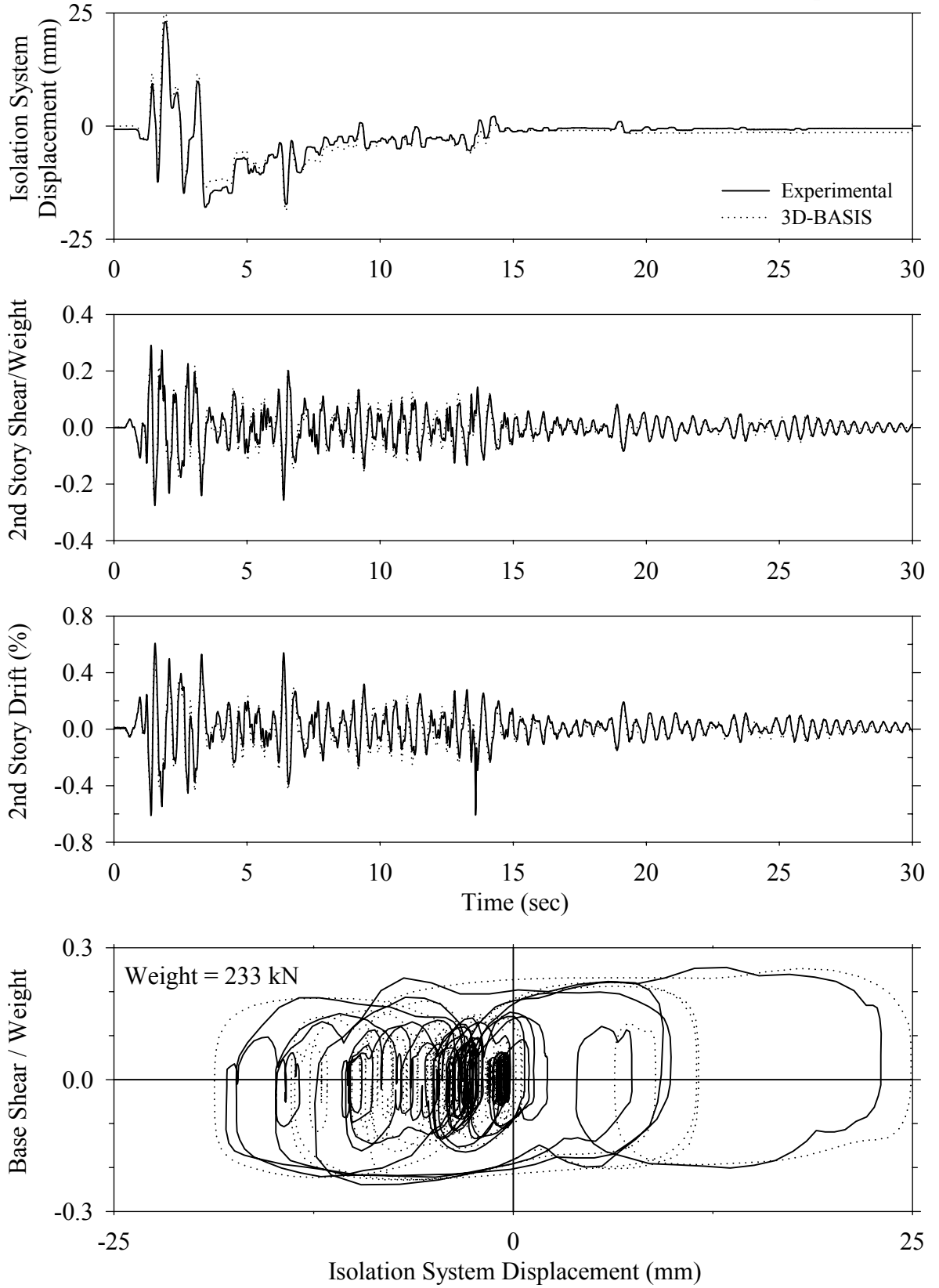
Test FPMLS10.1, Sylmar 100%, MF/FPS with Linear Dampers



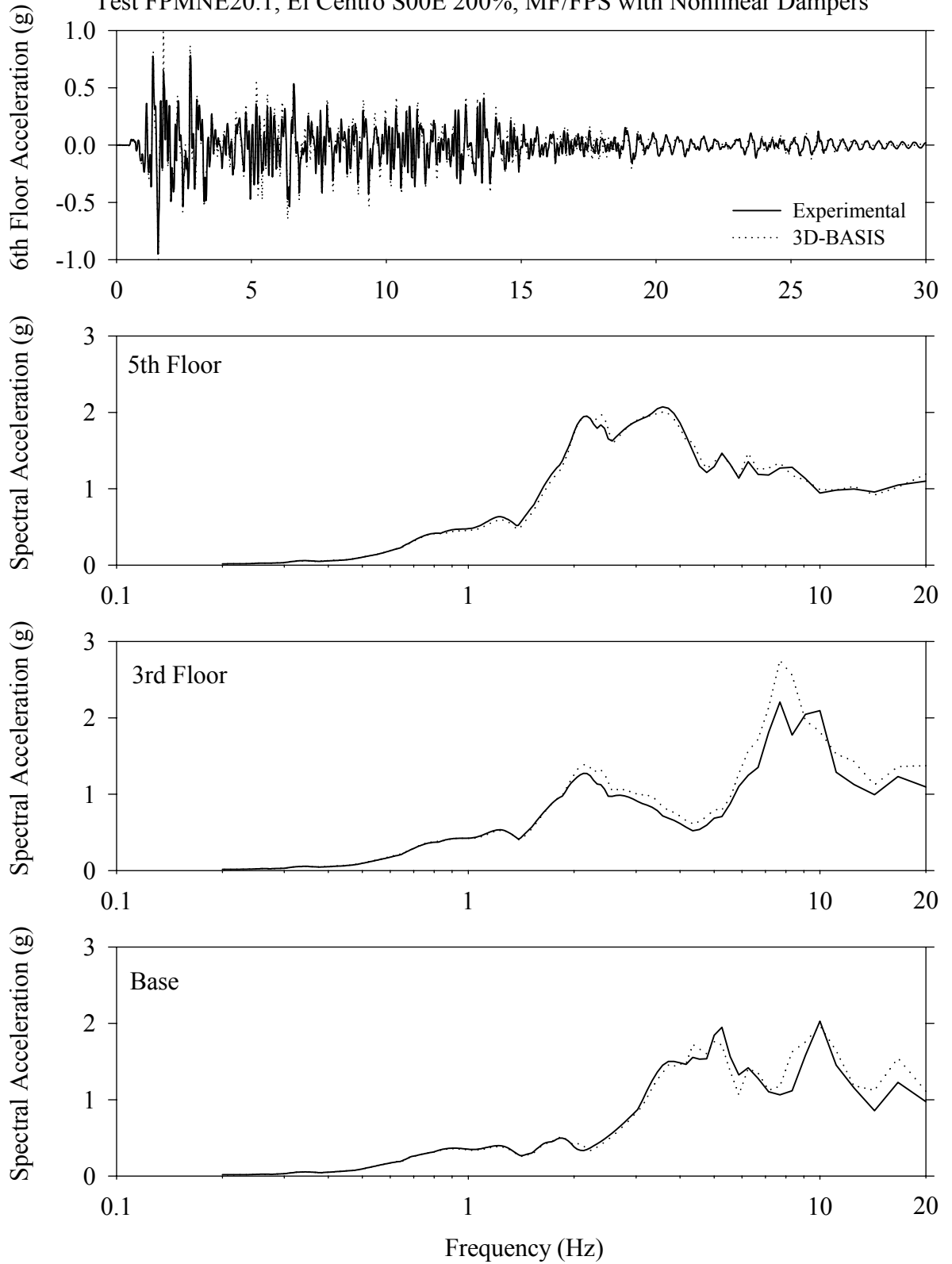
Test FPMLS10.1, Sylmar 100%, MF/FPS with Linear Dampers



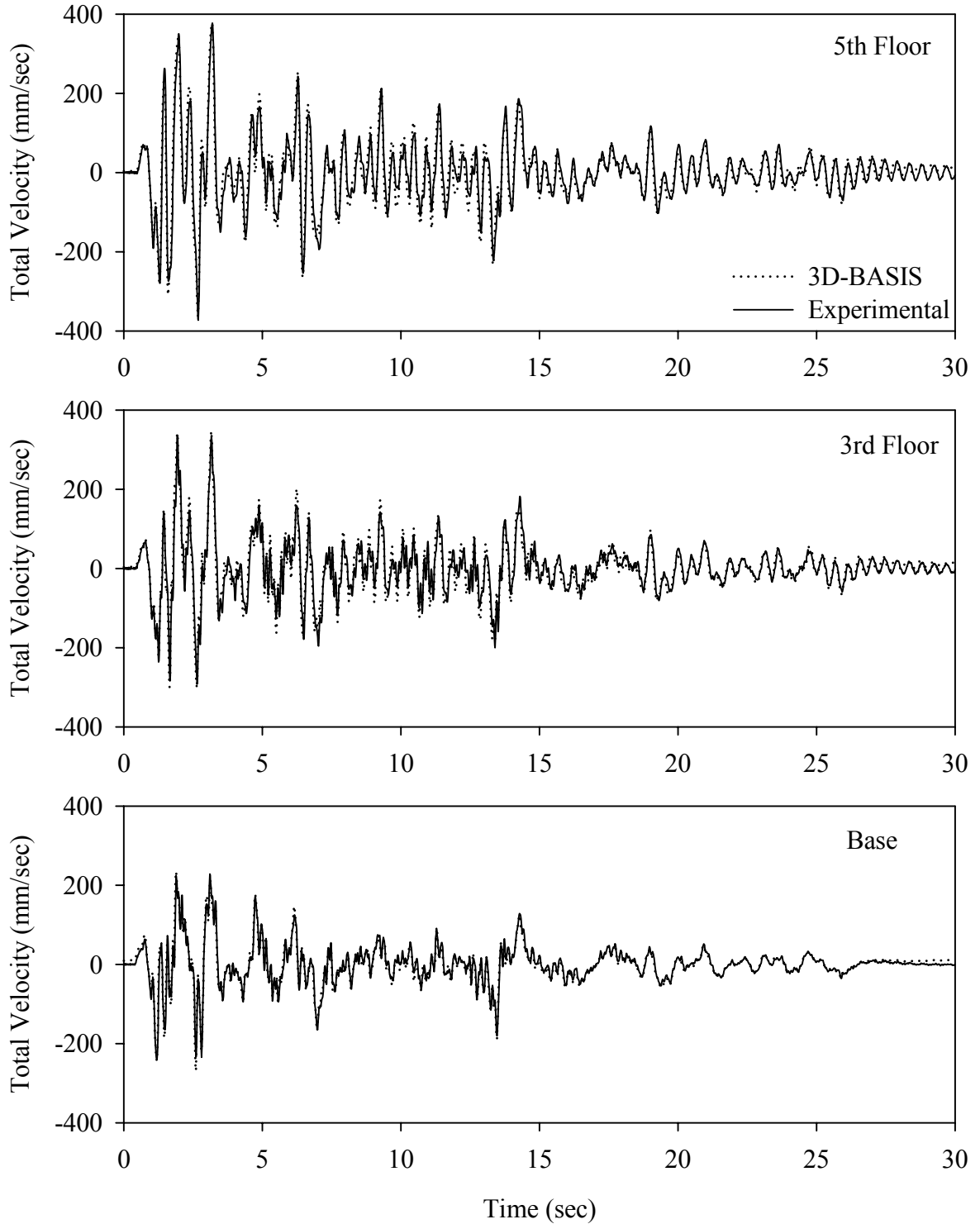
Test FPMNE20.1, El Centro S00E 200%, MF/FPS with Nonlinear Dampers



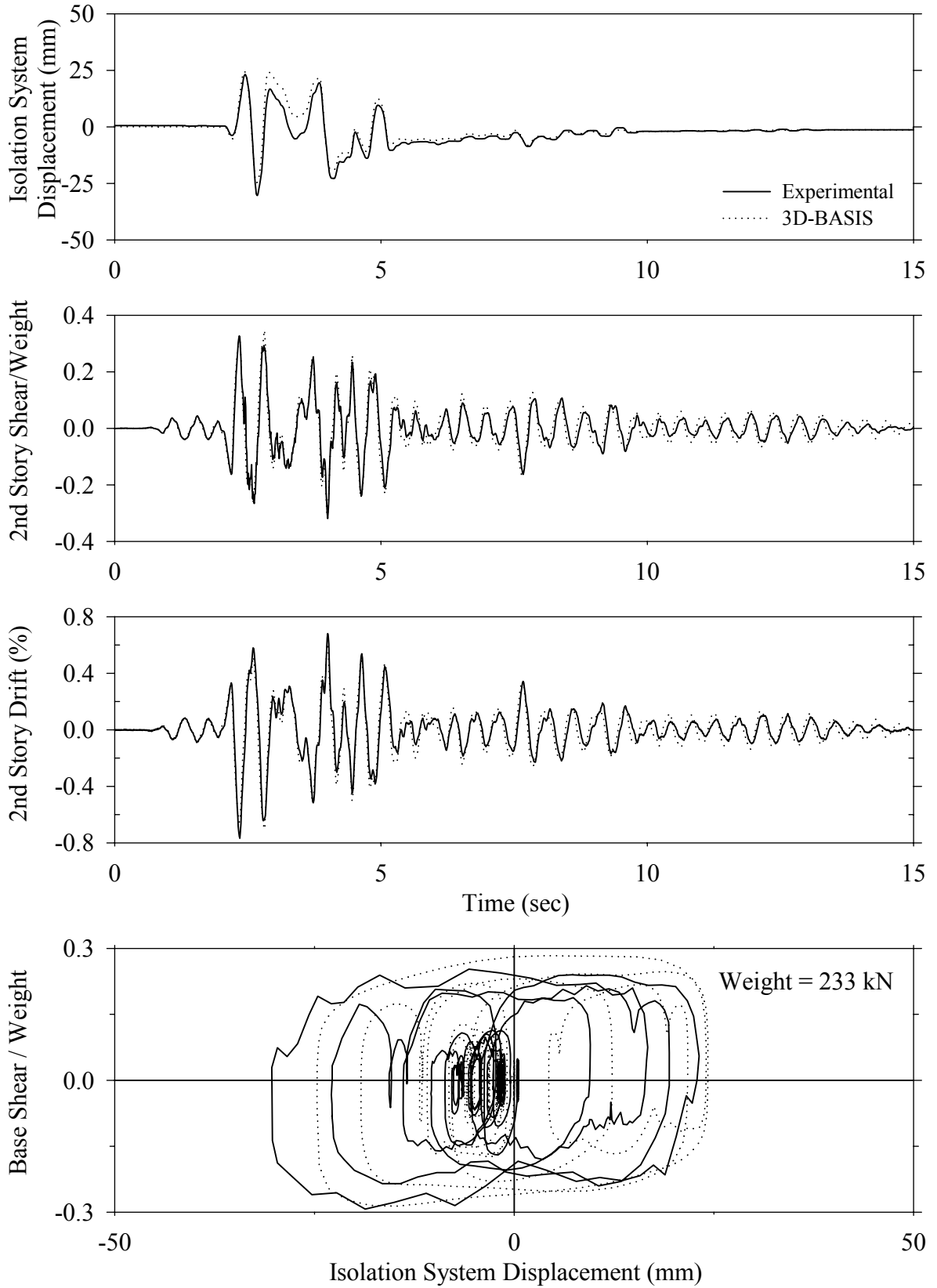
Test FPMNE20.1, El Centro S00E 200%, MF/FPS with Nonlinear Dampers



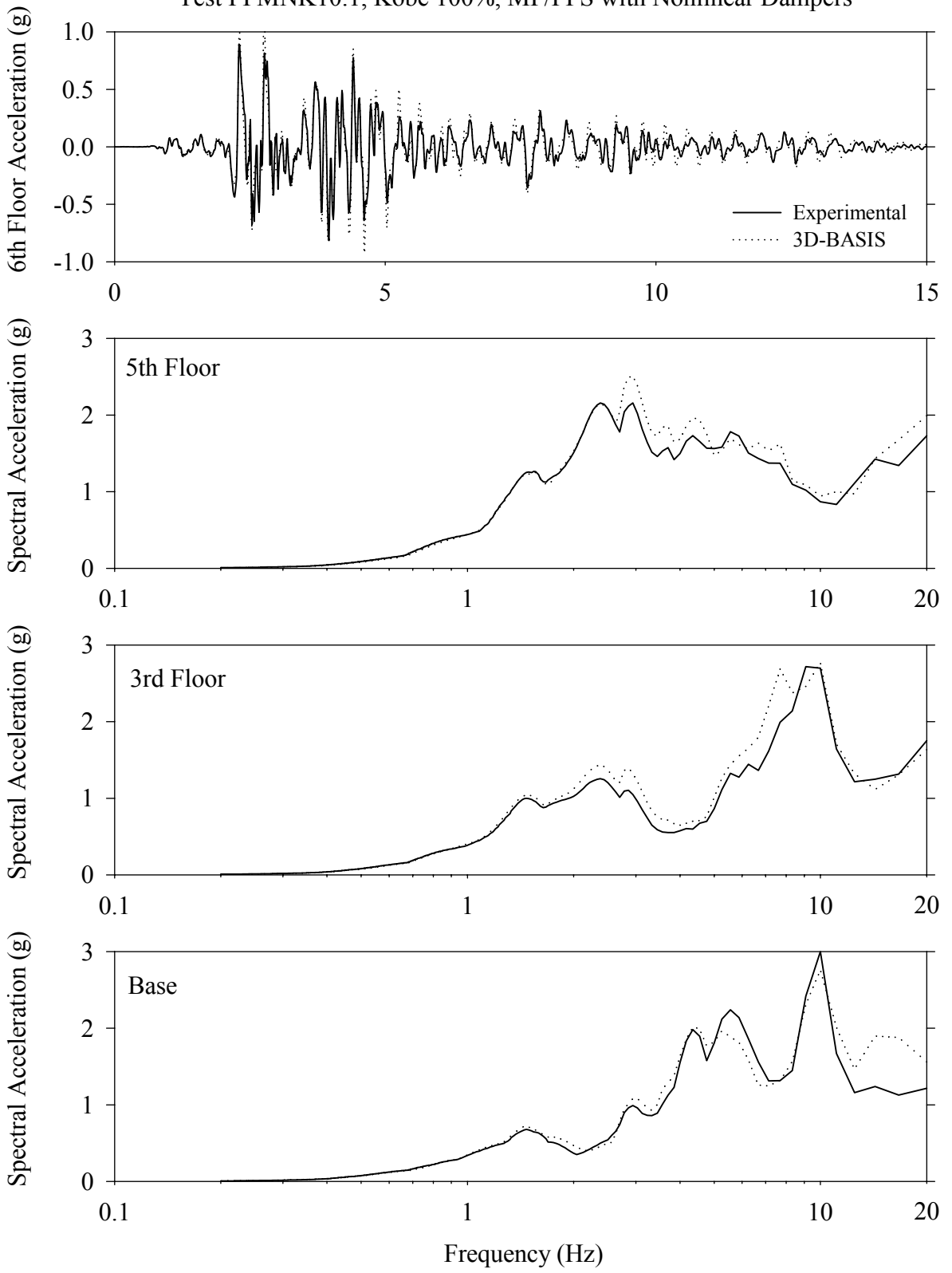
Test FPMNE20.1, El Centro S00E 200%, MF/FPS with Nonlinear Dampers



Test FPMNK10.1, Kobe 100%, MF/FPS with Nonlinear Dampers

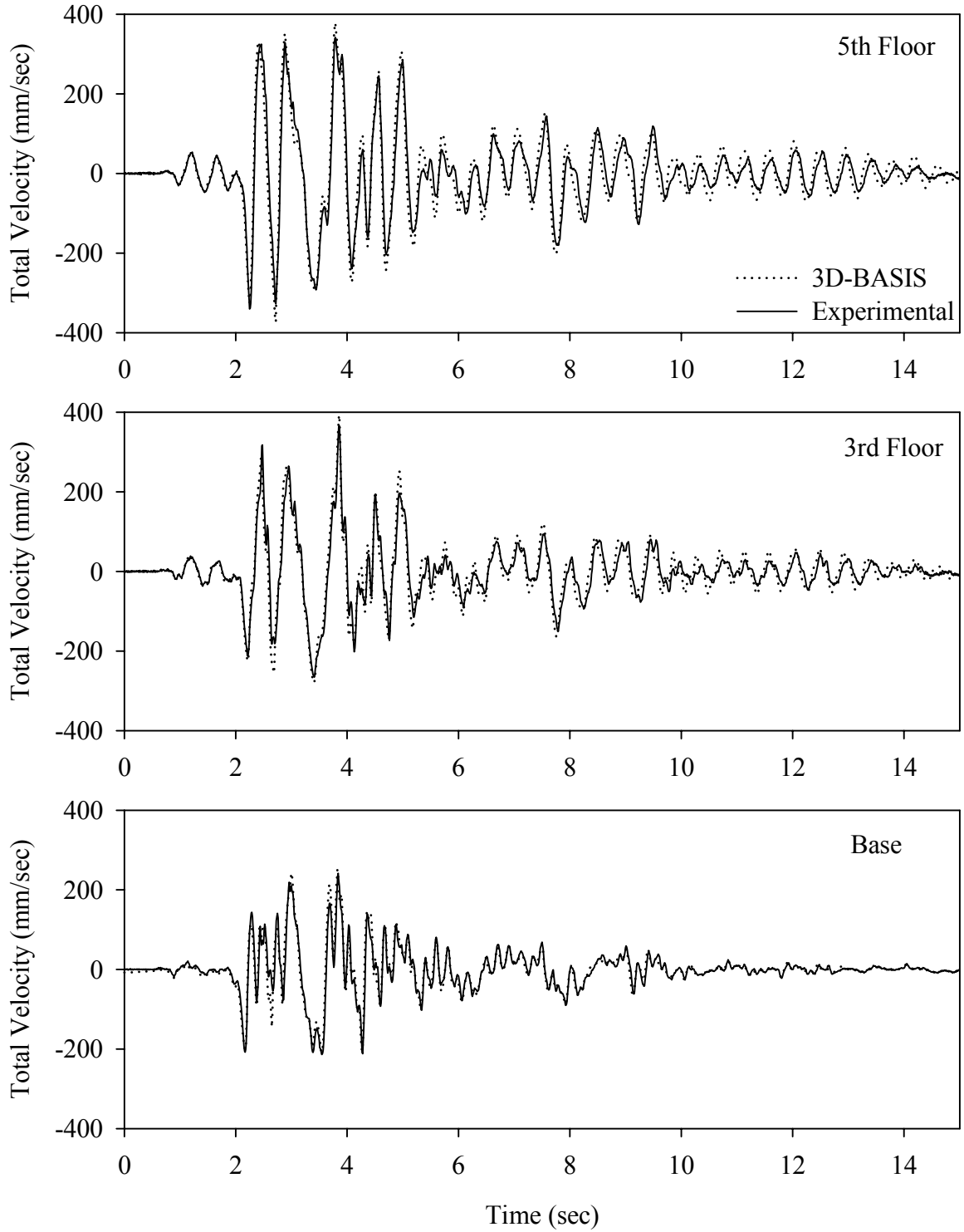


Test FPMNK10.1, Kobe 100%, MF/FPS with Nonlinear Dampers

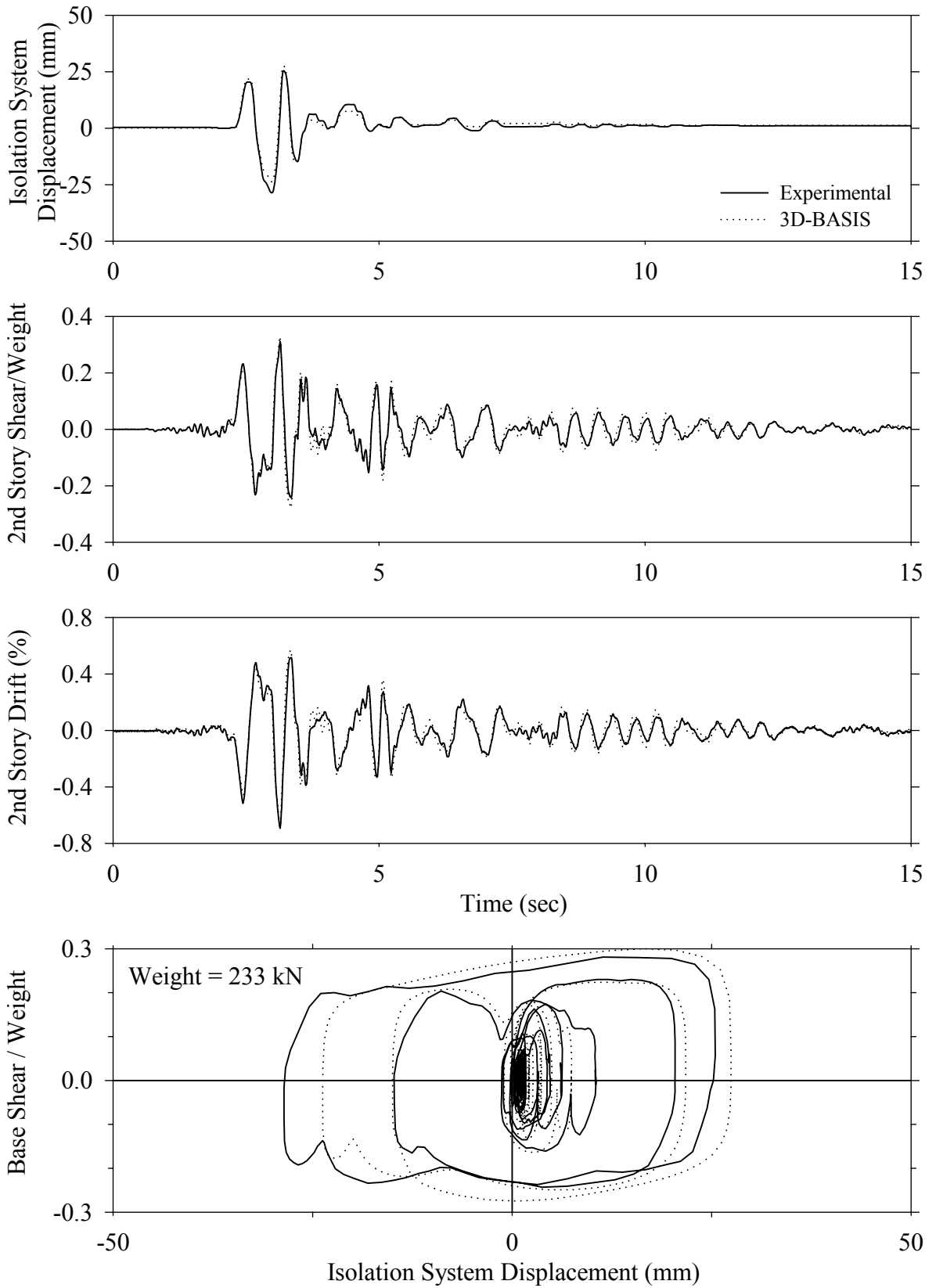




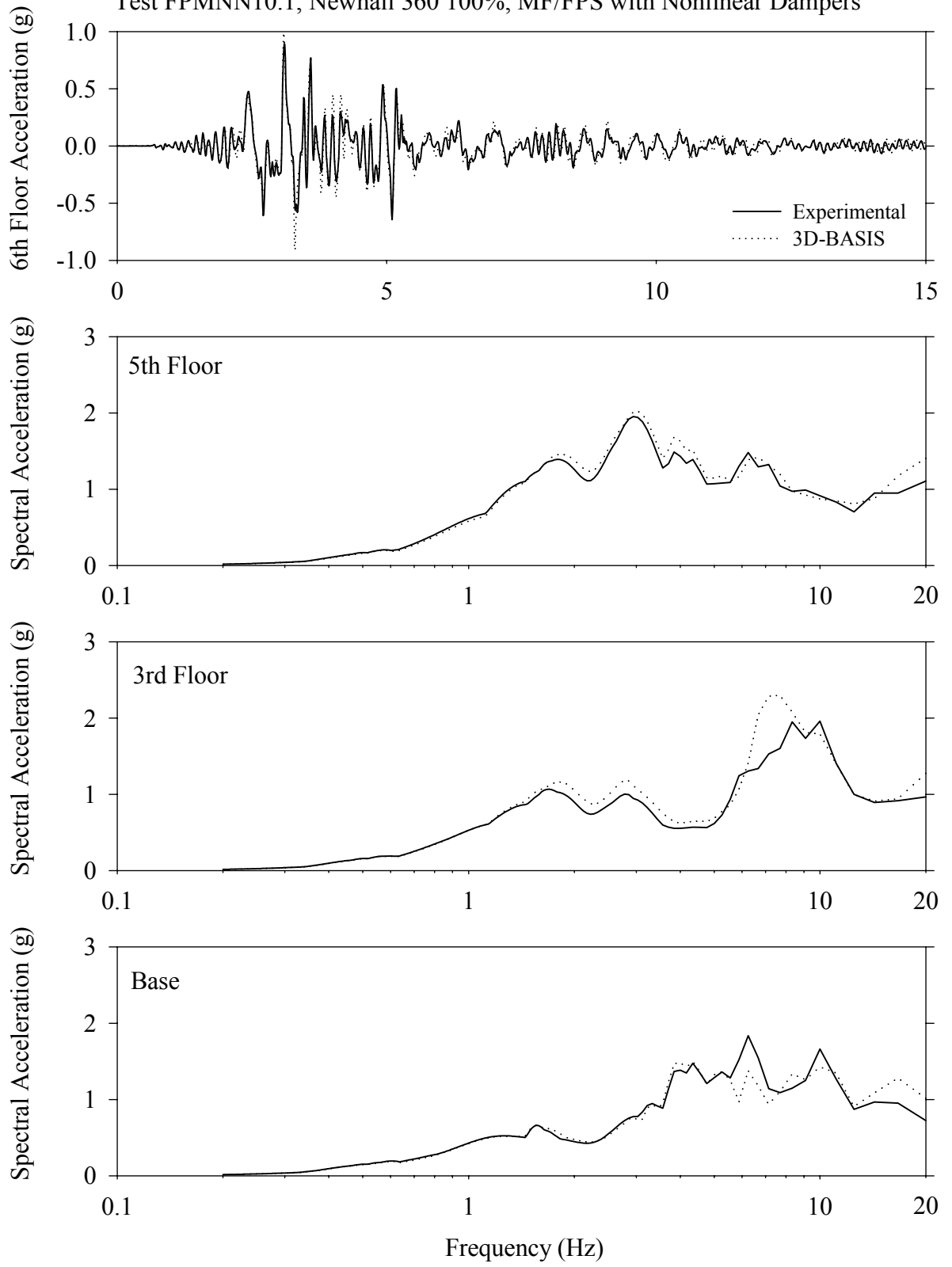
Test FPMNK10.1, Kobe 100%, MF/FPS with Nonlinear Dampers



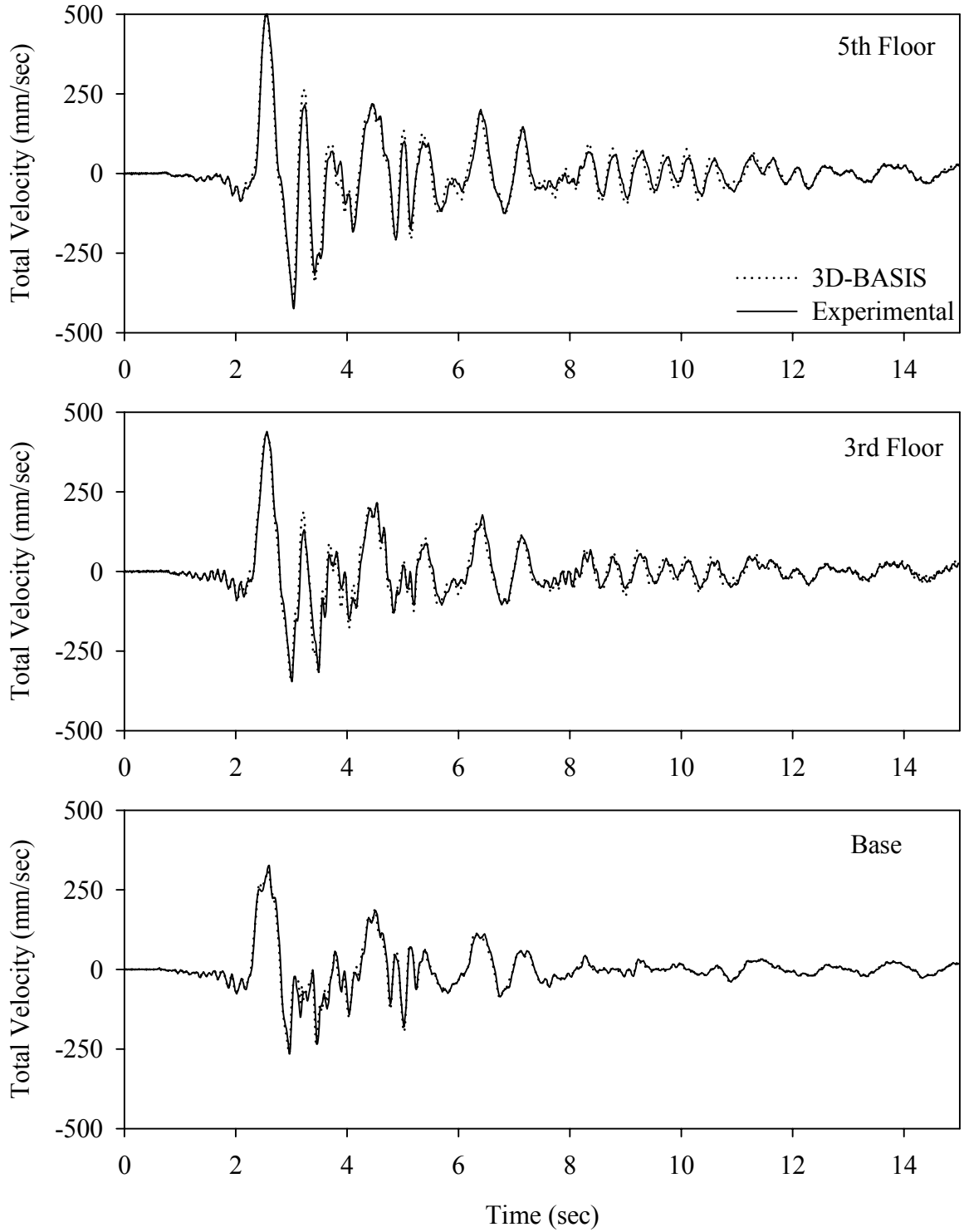
Test FPMNN10.1, Newhall 360 100%, MF/FPS with Nonlinear Dampers



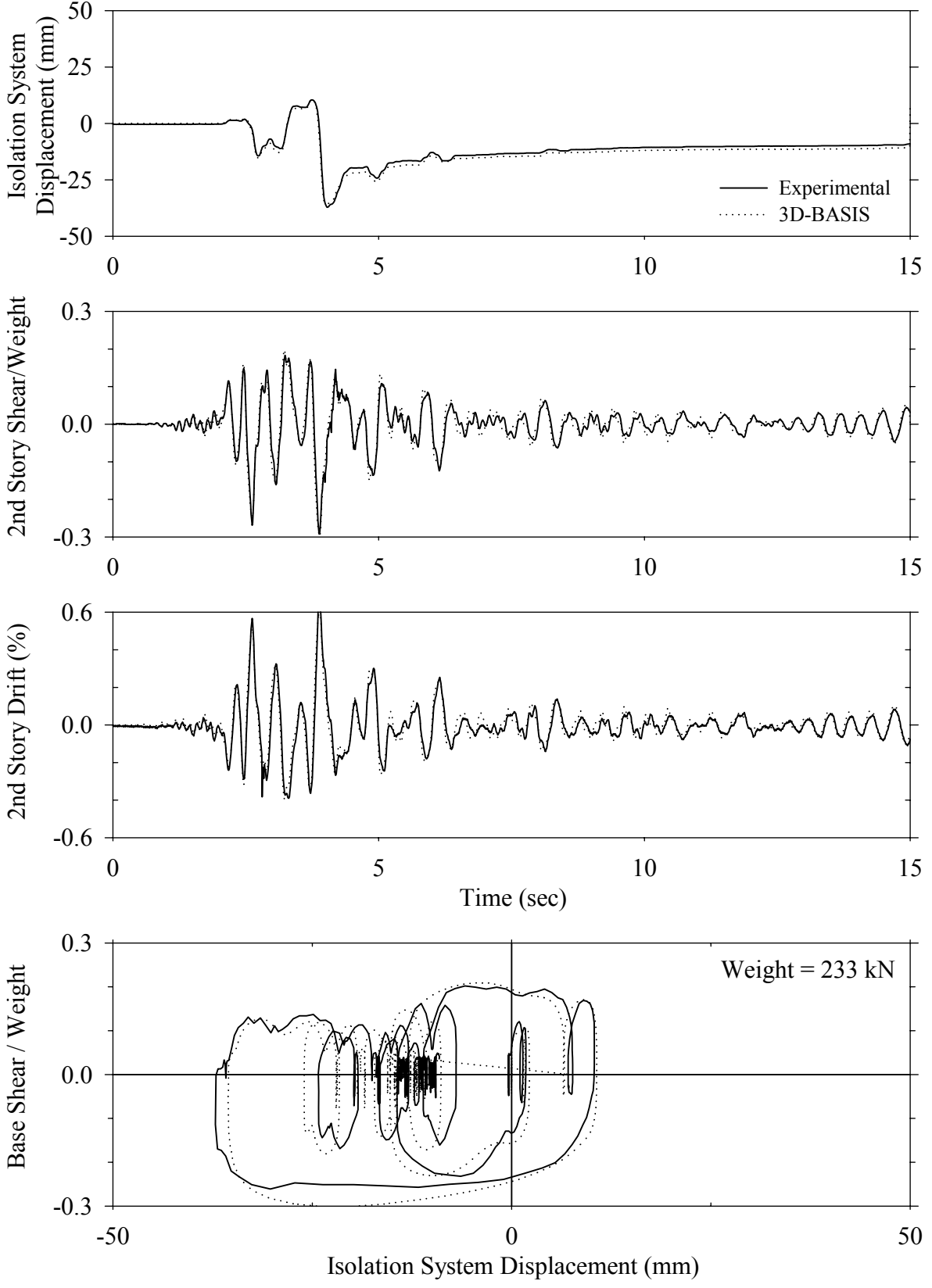
Test FPMNN10.1, Newhall 360 100%, MF/FPS with Nonlinear Dampers



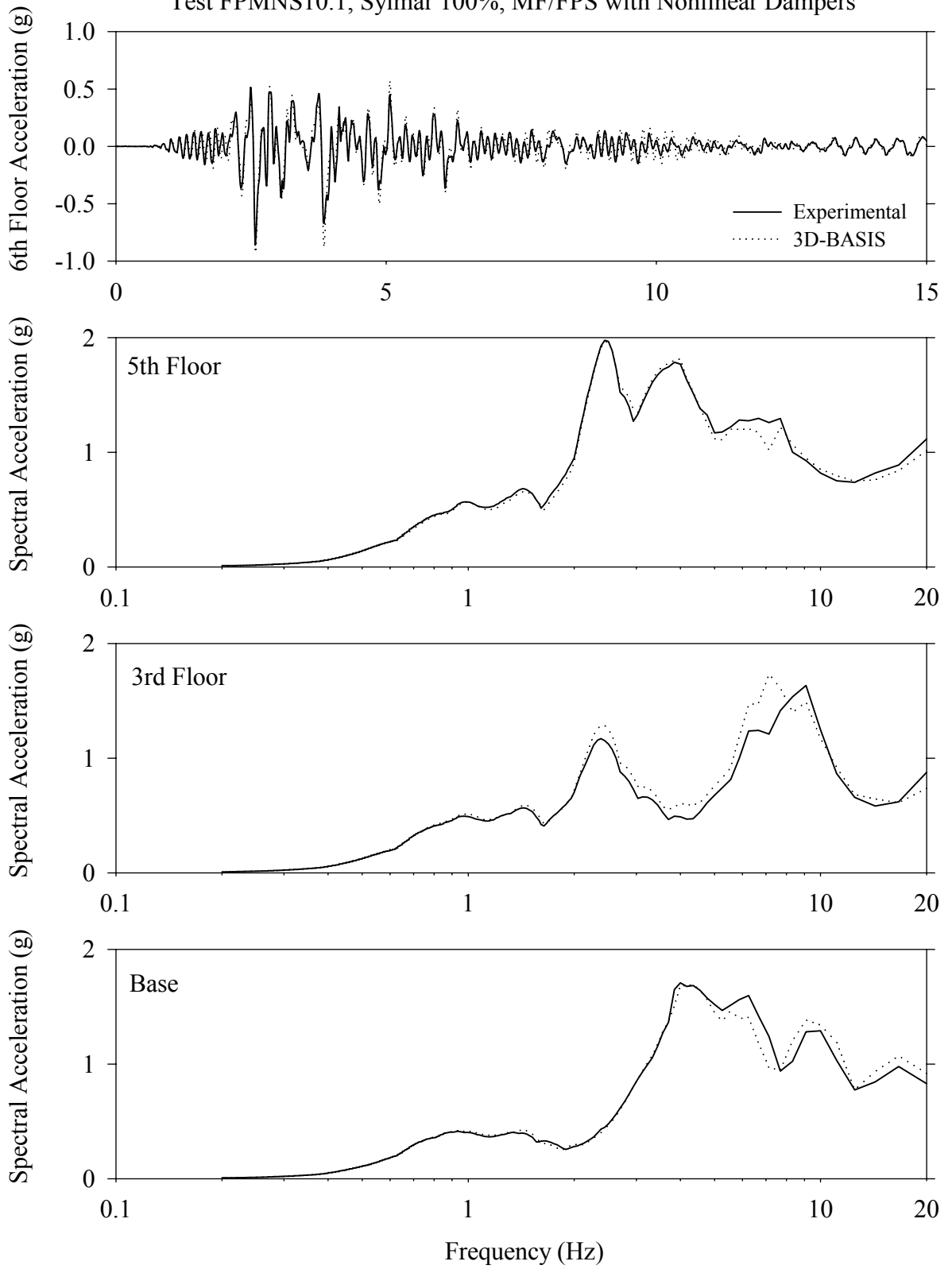
Test FPMNN10.1, Newhall 360 100%, MF/FPS with Nonlinear Dampers



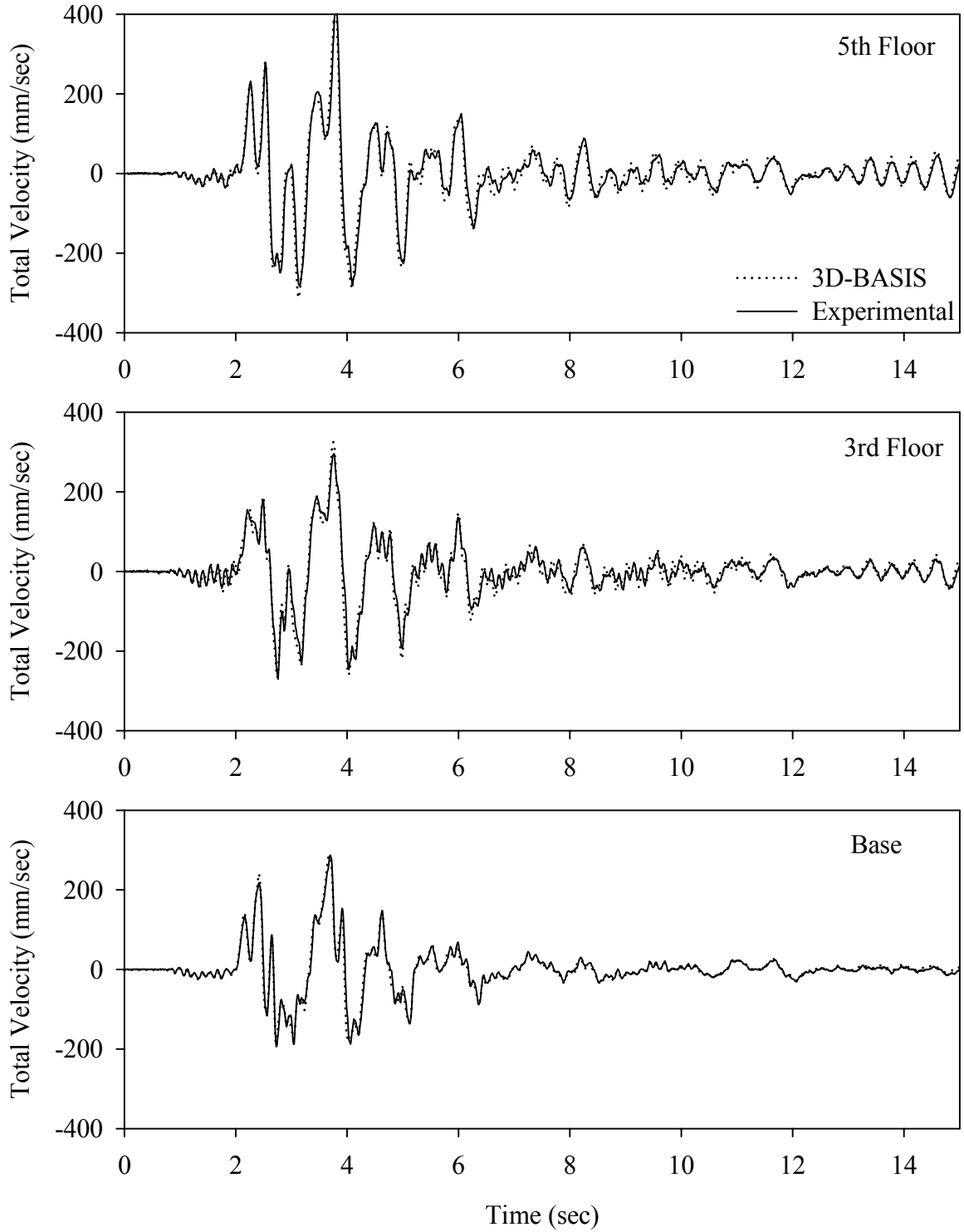
Test FPMNS10.1, Sylmar 100%, MF/FPS with Nonlinear Dampers



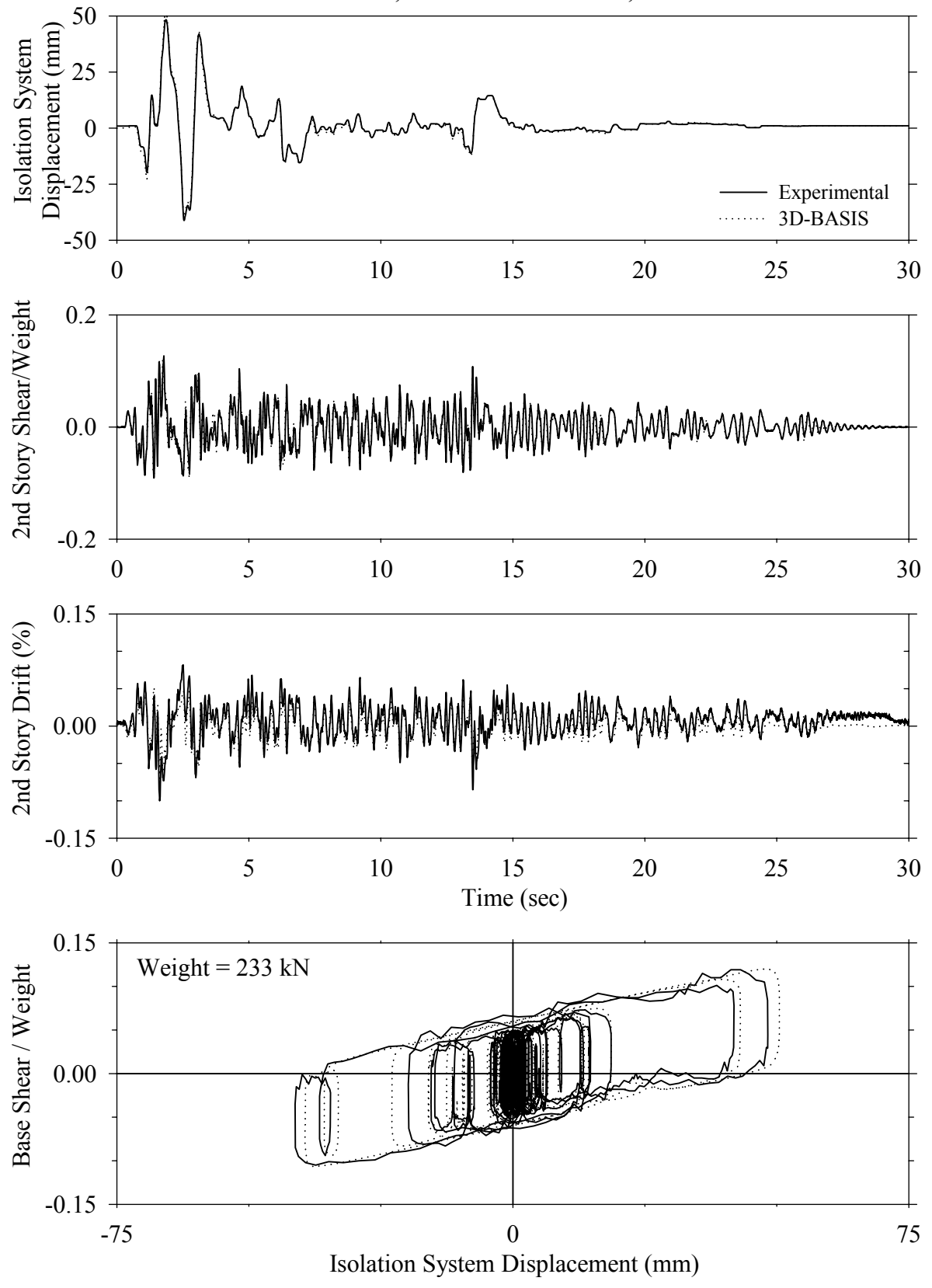
Test FPMNS10.1, Sylmar 100%, MF/FPS with Nonlinear Dampers



Test FPMNS10.1, Sylmar 100%, MF/FPS with Nonlinear Dampers

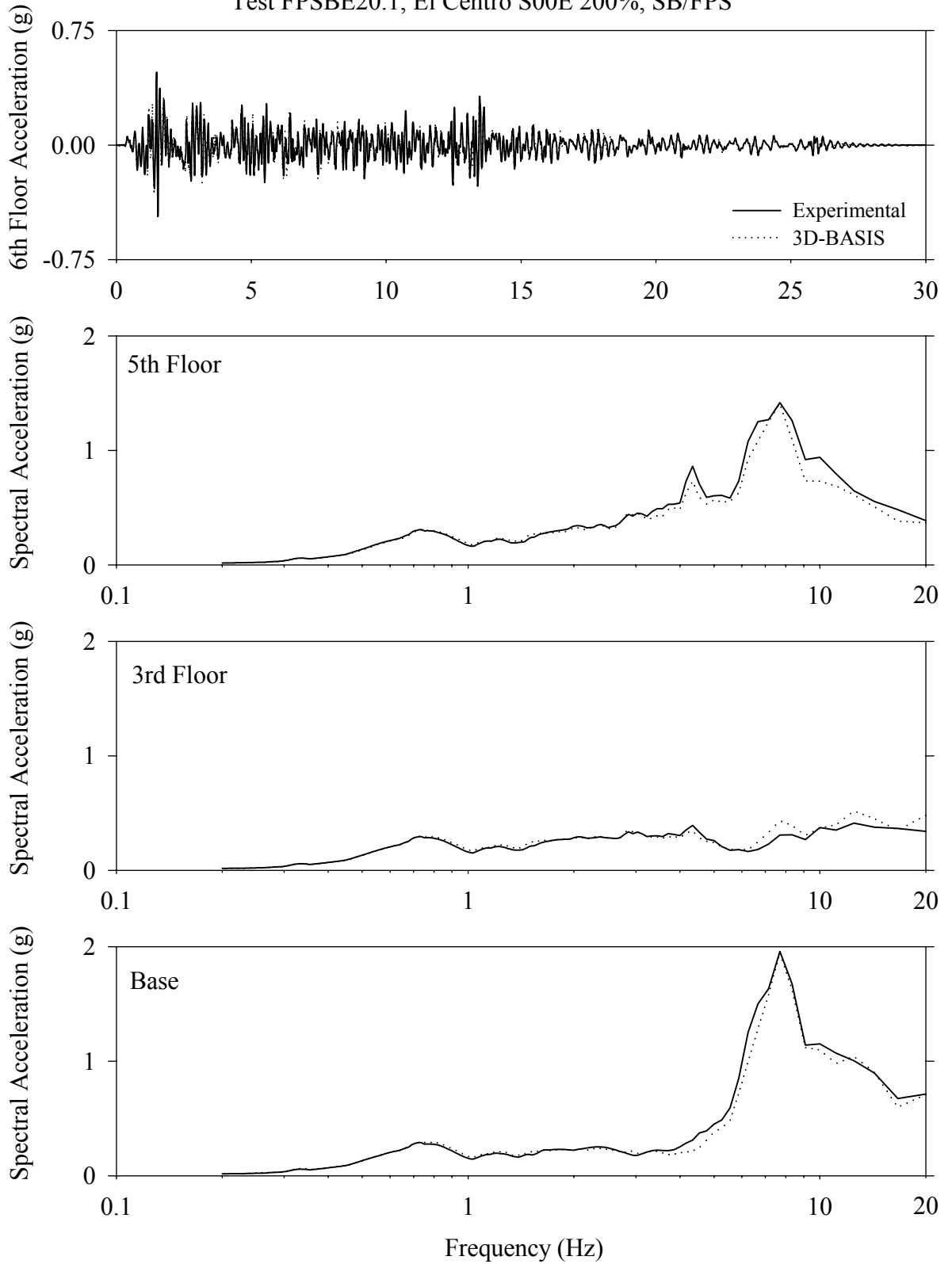


Test FPSBE20.1, El Centro S00E 200%, SB/FPS

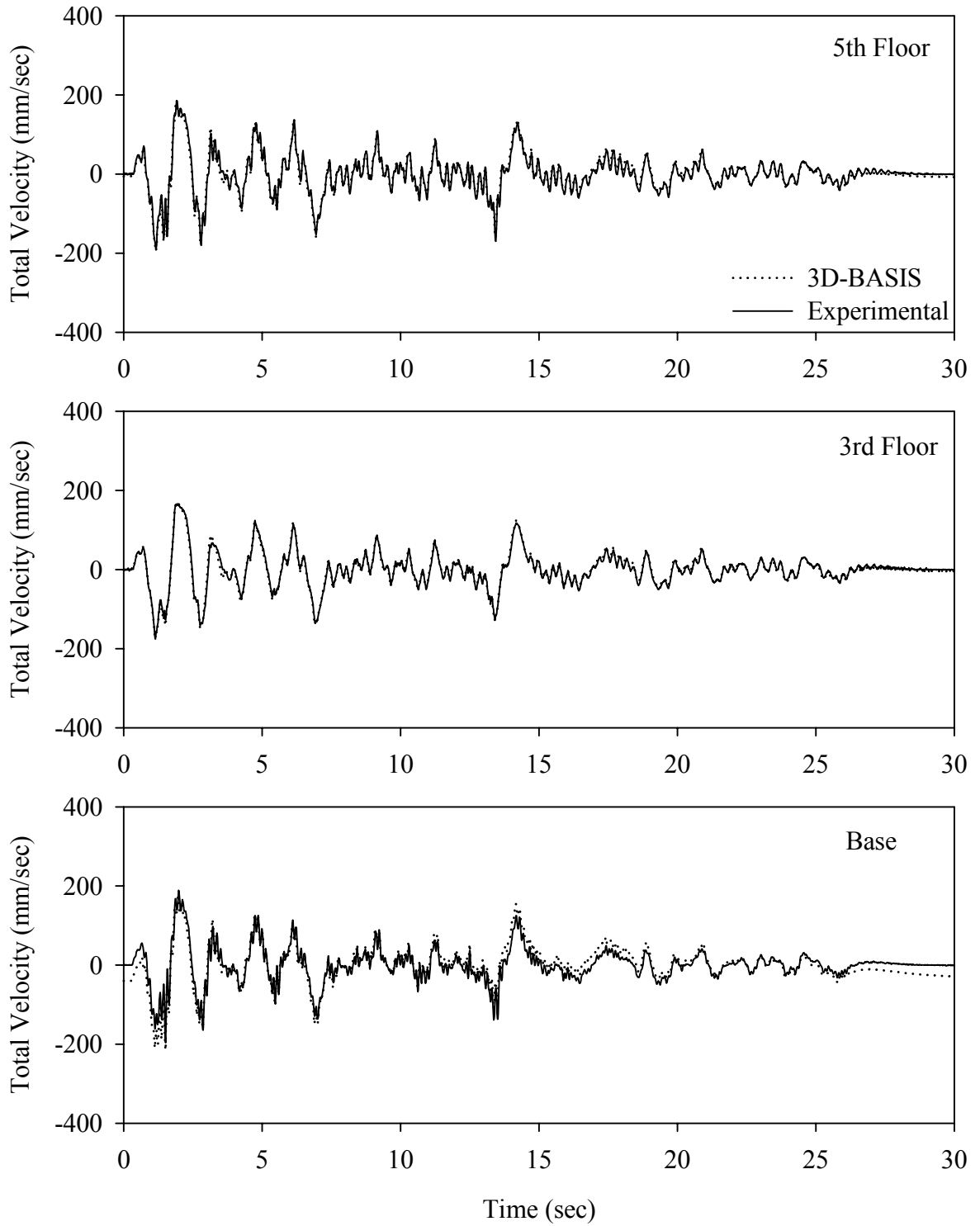




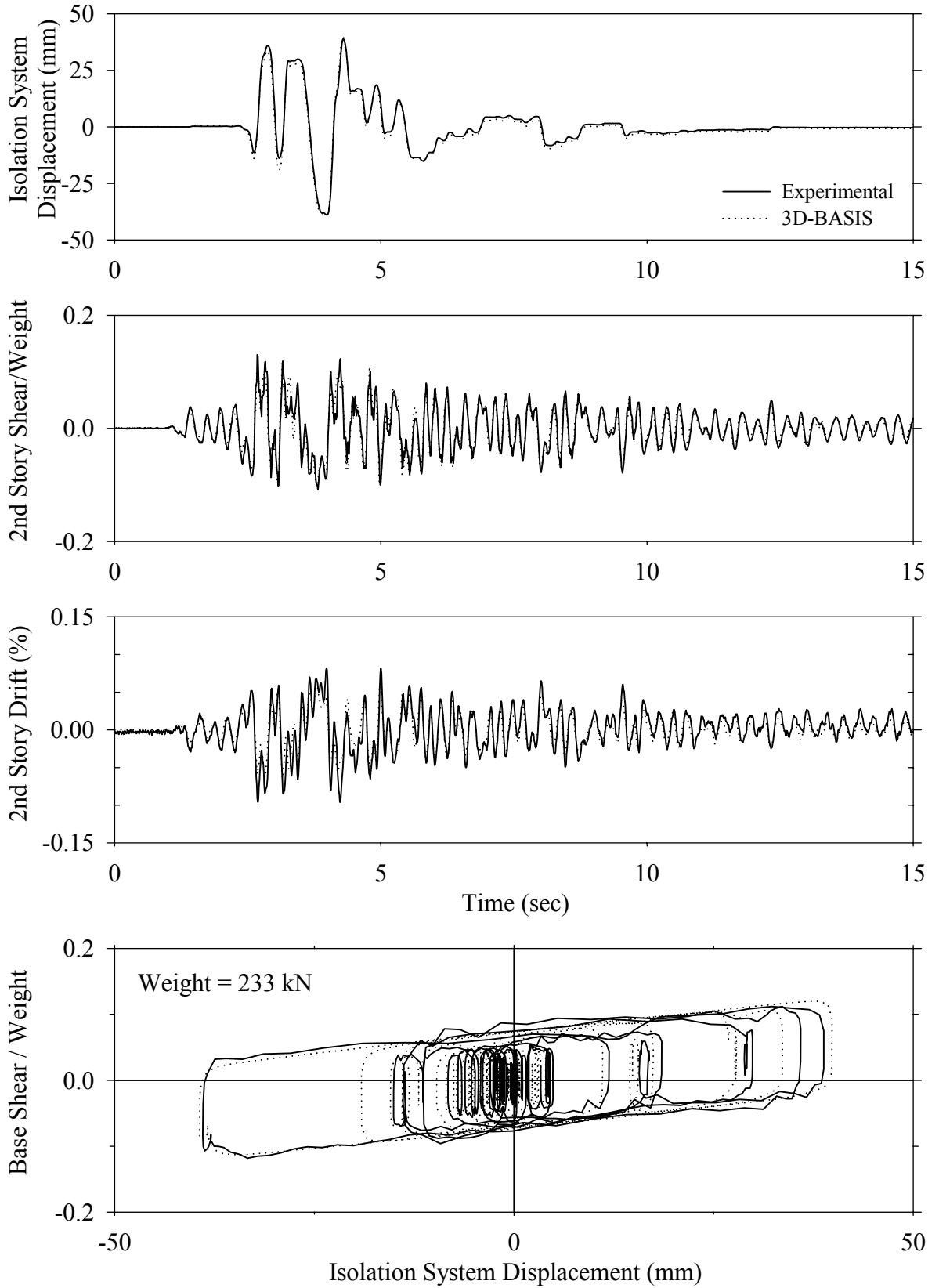
Test FPSBE20.1, El Centro S00E 200%, SB/FPS



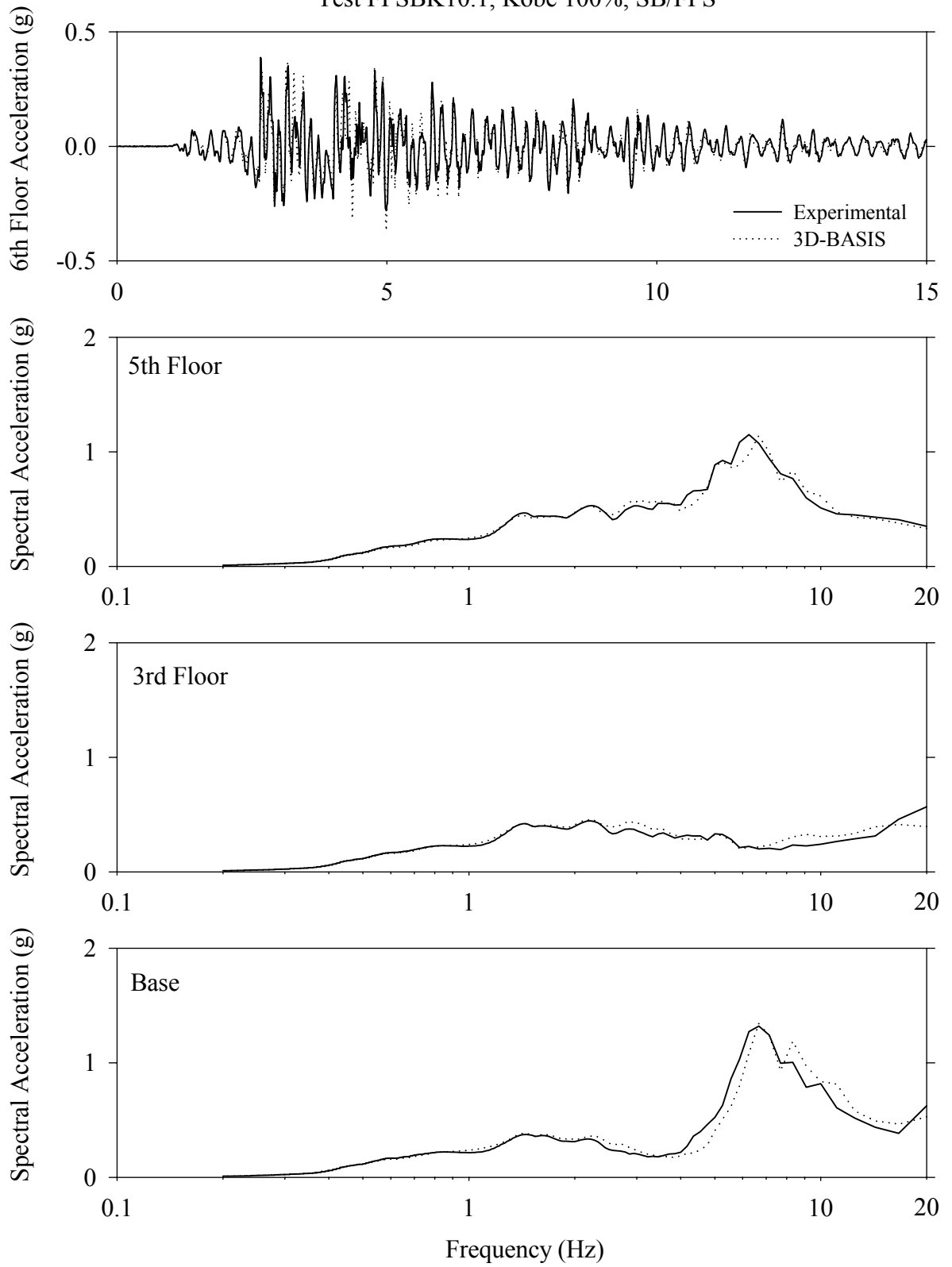
Test FPSBE20.1, El Centro S00E 200%, SB/FPS



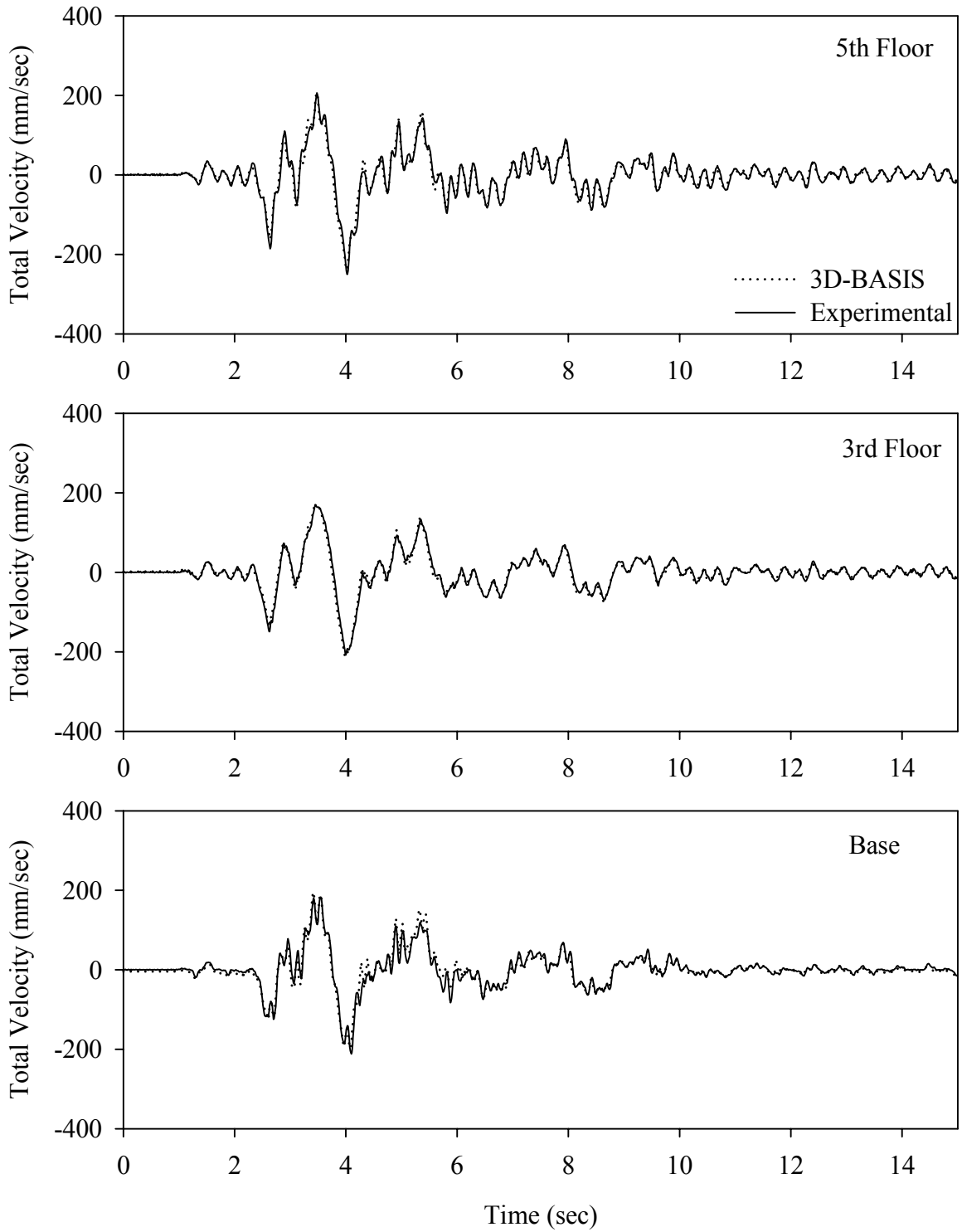
Test FPSBK10.1, Kobe 100%, SB/FPS



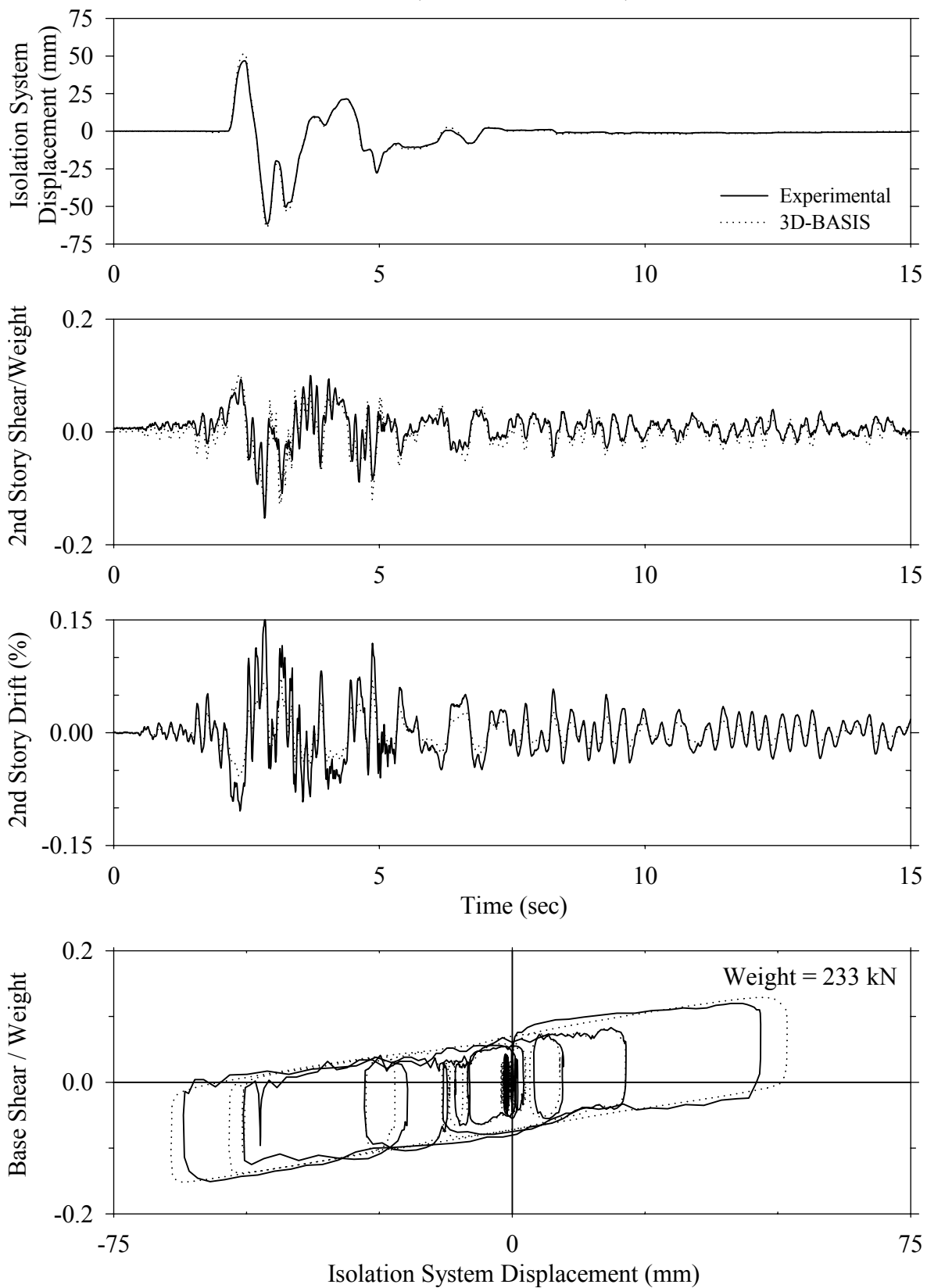
Test FPSBK10.1, Kobe 100%, SB/FPS



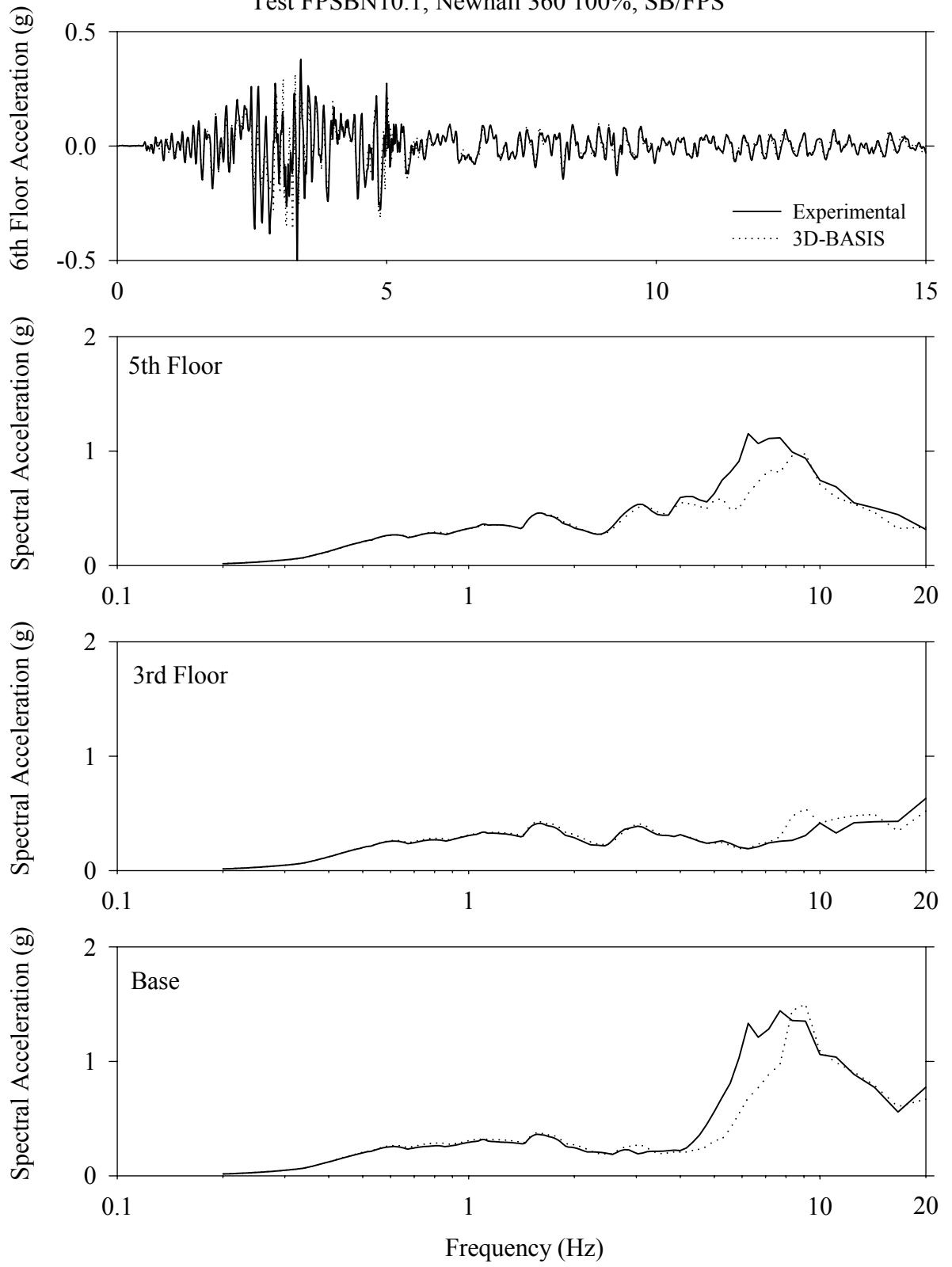
Test FPSBK10.1, Kobe 100%, SB/FPS



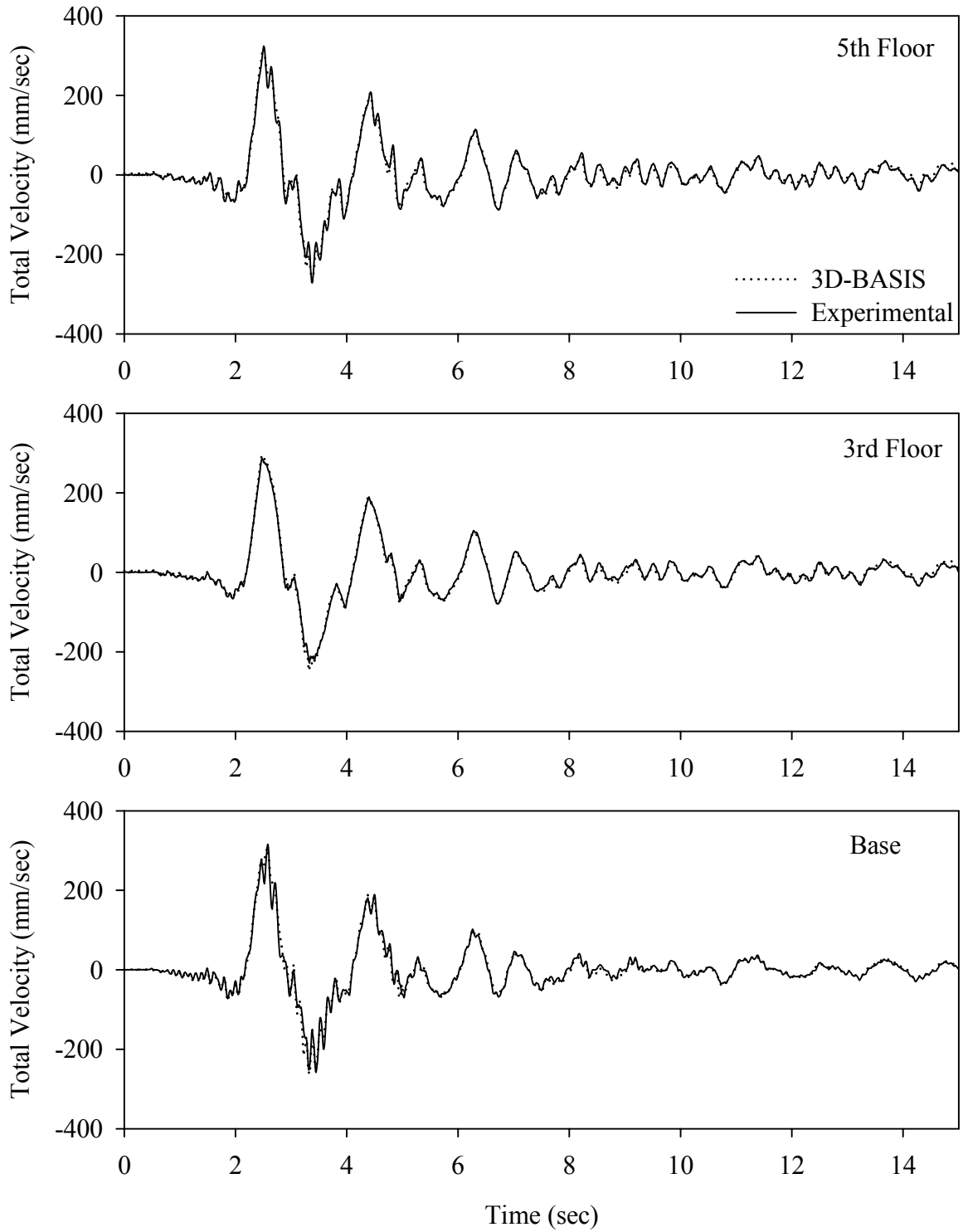
Test FPSBN10.1, Newhall 360 100%, SB/FPS



Test FPSBN10.1, Newhall 360 100%, SB/FPS

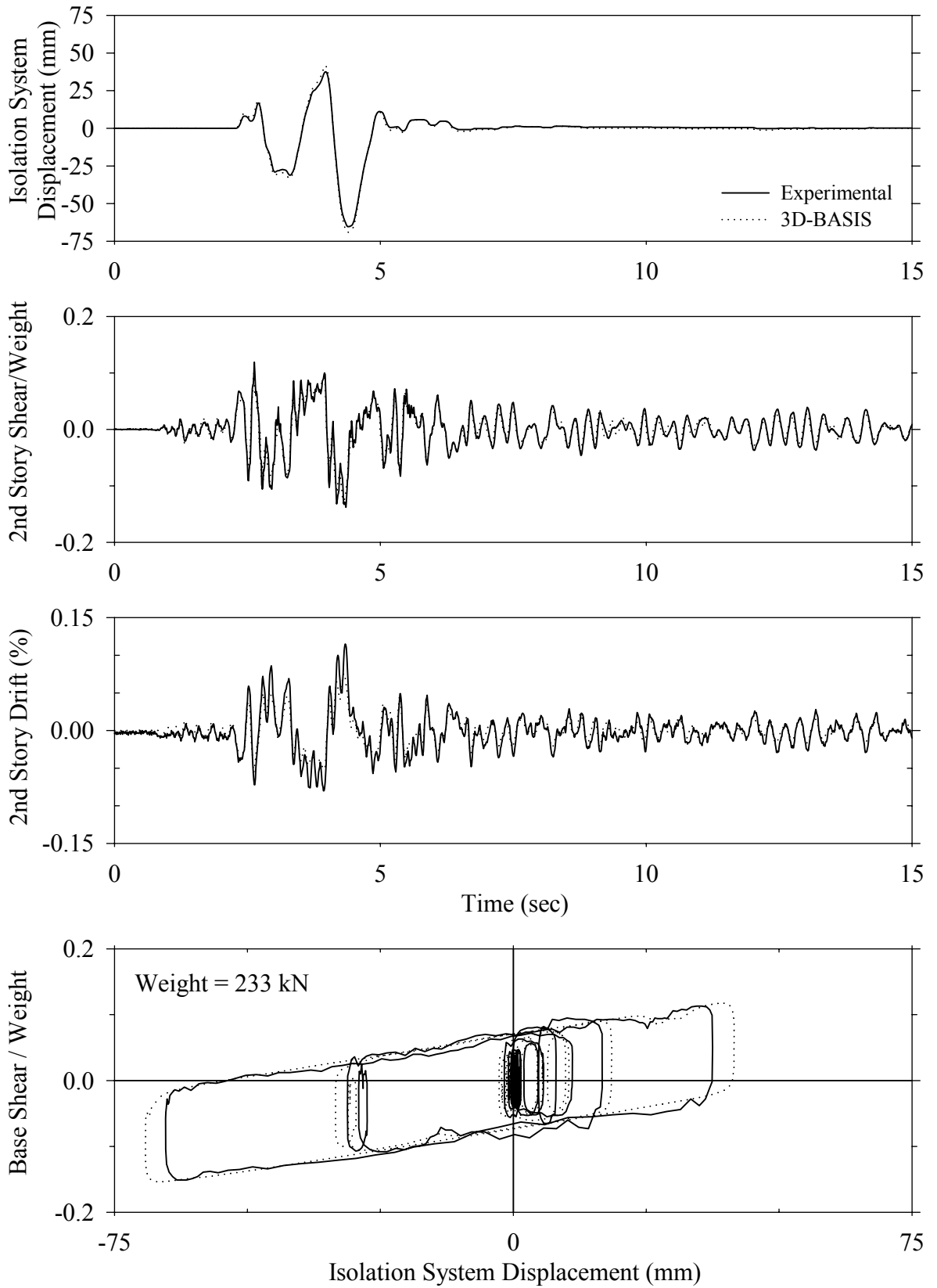


Test FPSBN10.1, Newhall 360 100%, SB/FPS

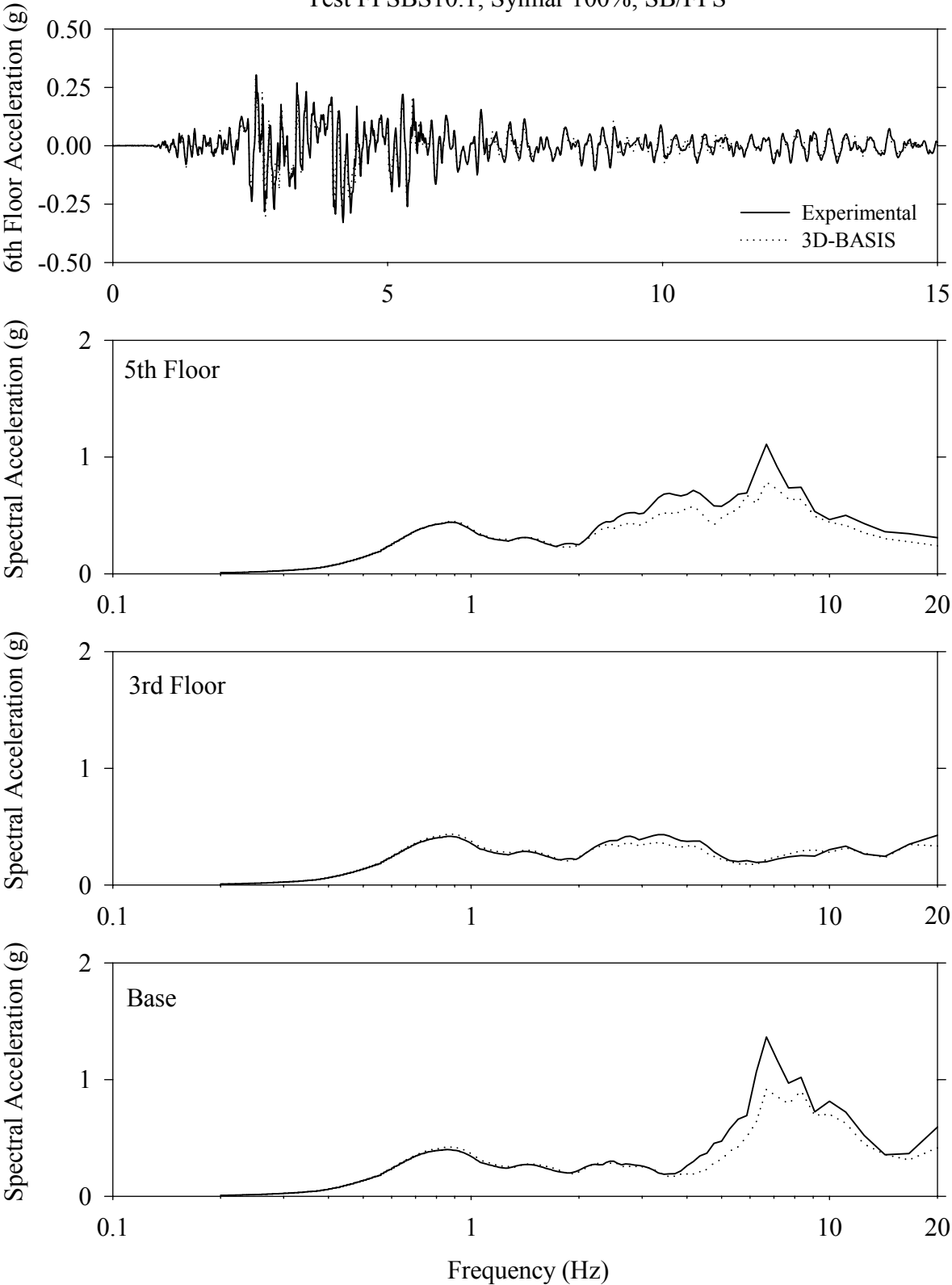




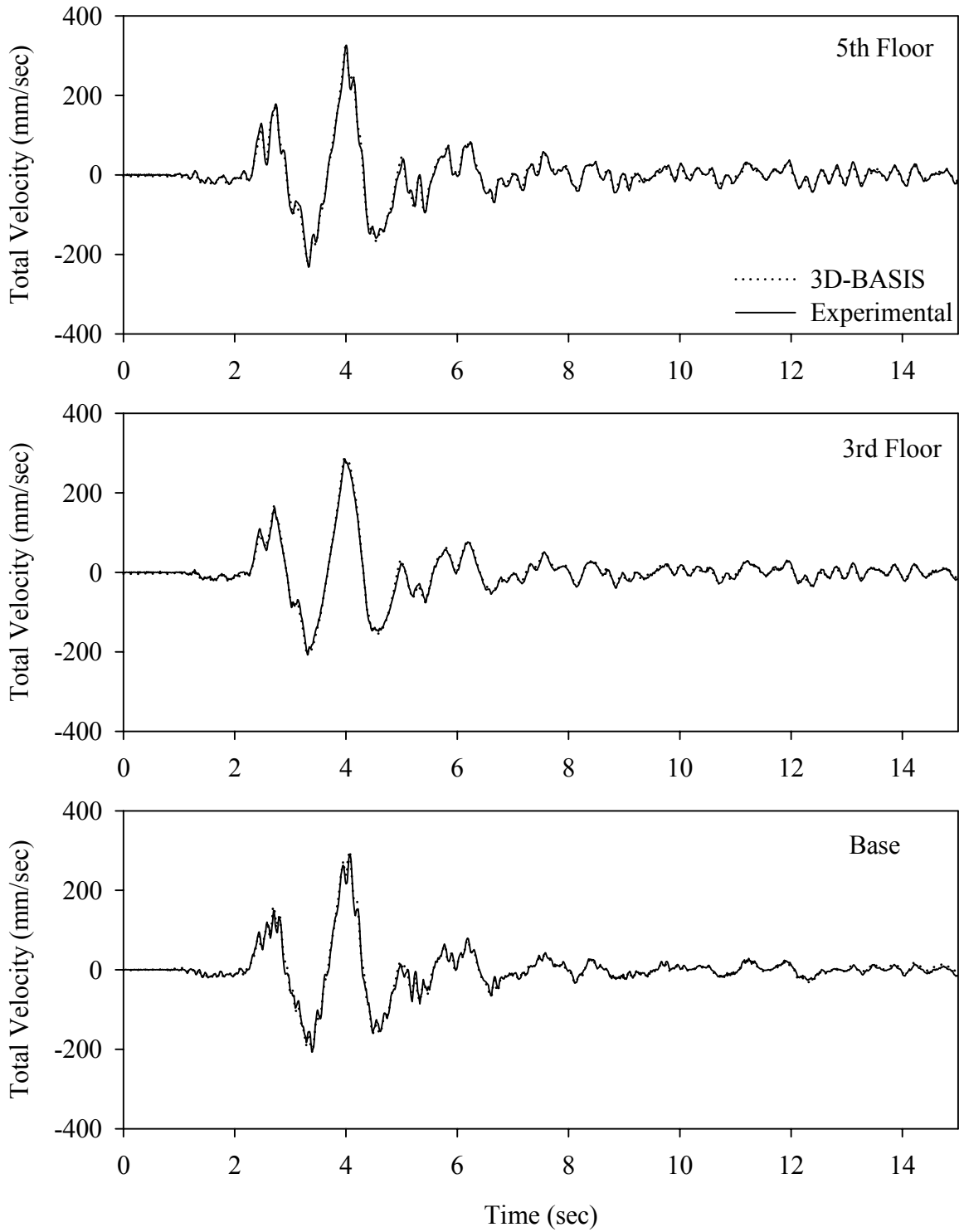
Test FPSBS10.1, Sylmar 100%, SB/FPS



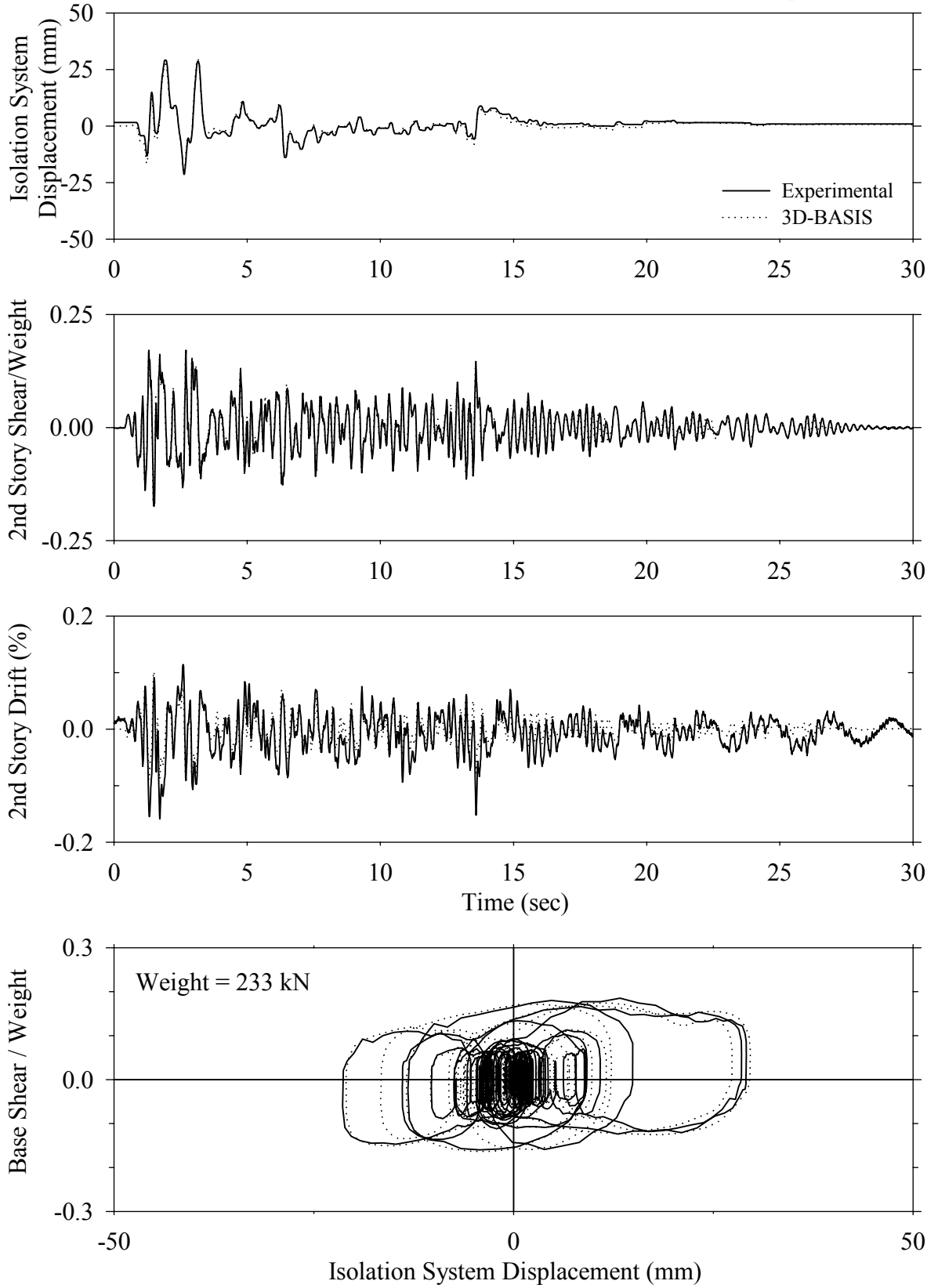
Test FPSBS10.1, Sylmar 100%, SB/FPS



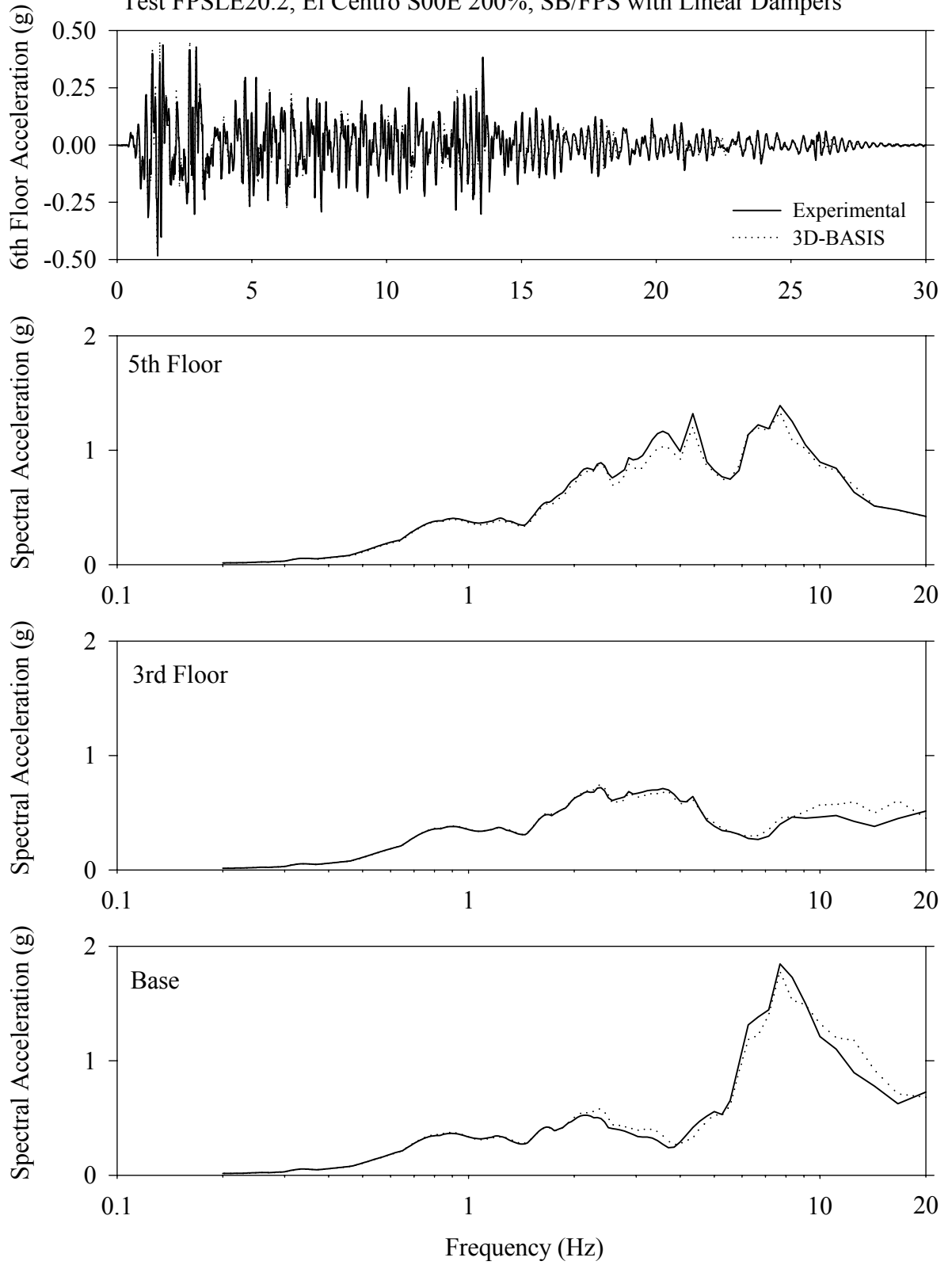
Test FPSBS10.1, Sylmar 100%, SB/FPS



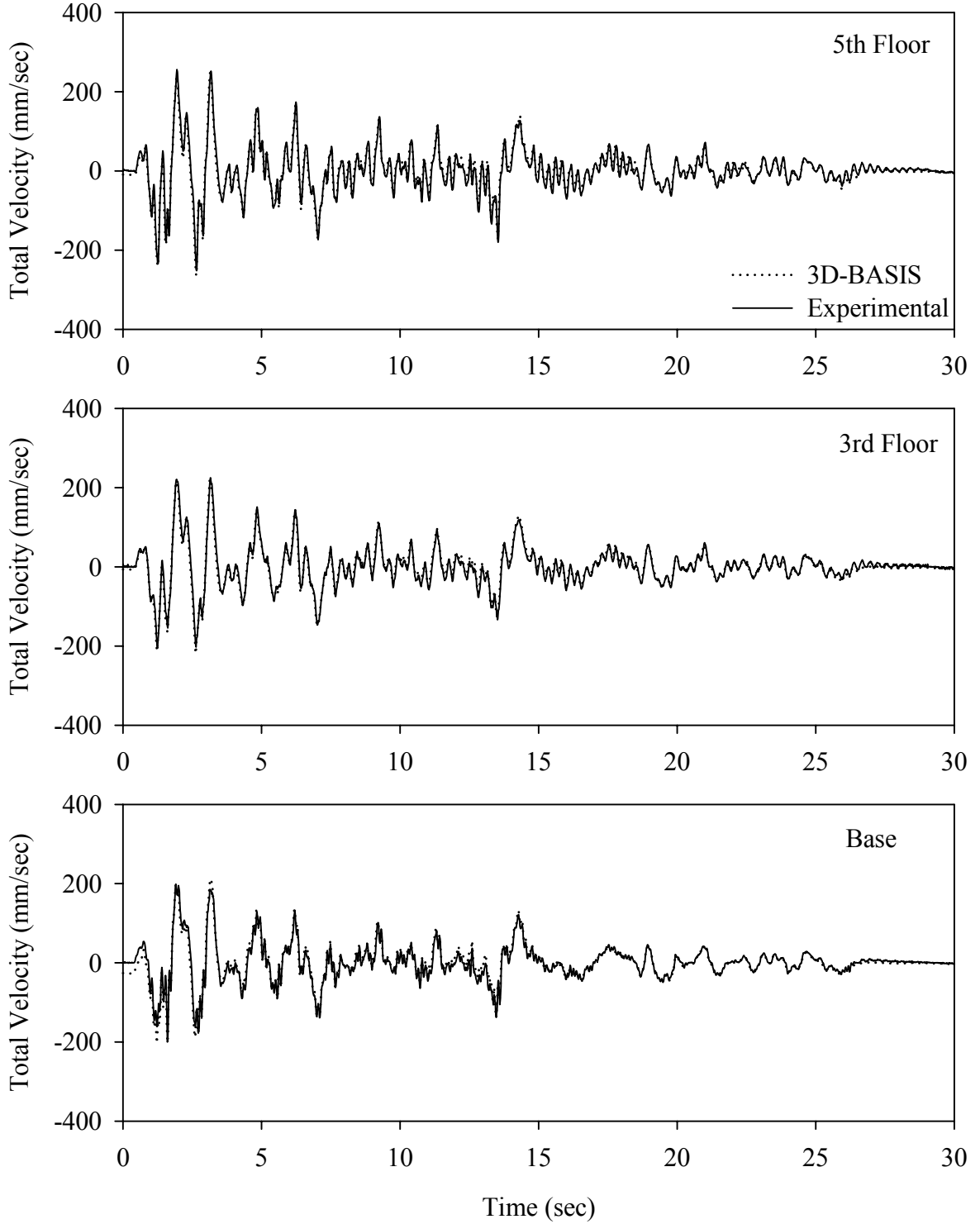
Test FPSLE20.2, El Centro S00E 200%, SB/FPS with Linear Dampers



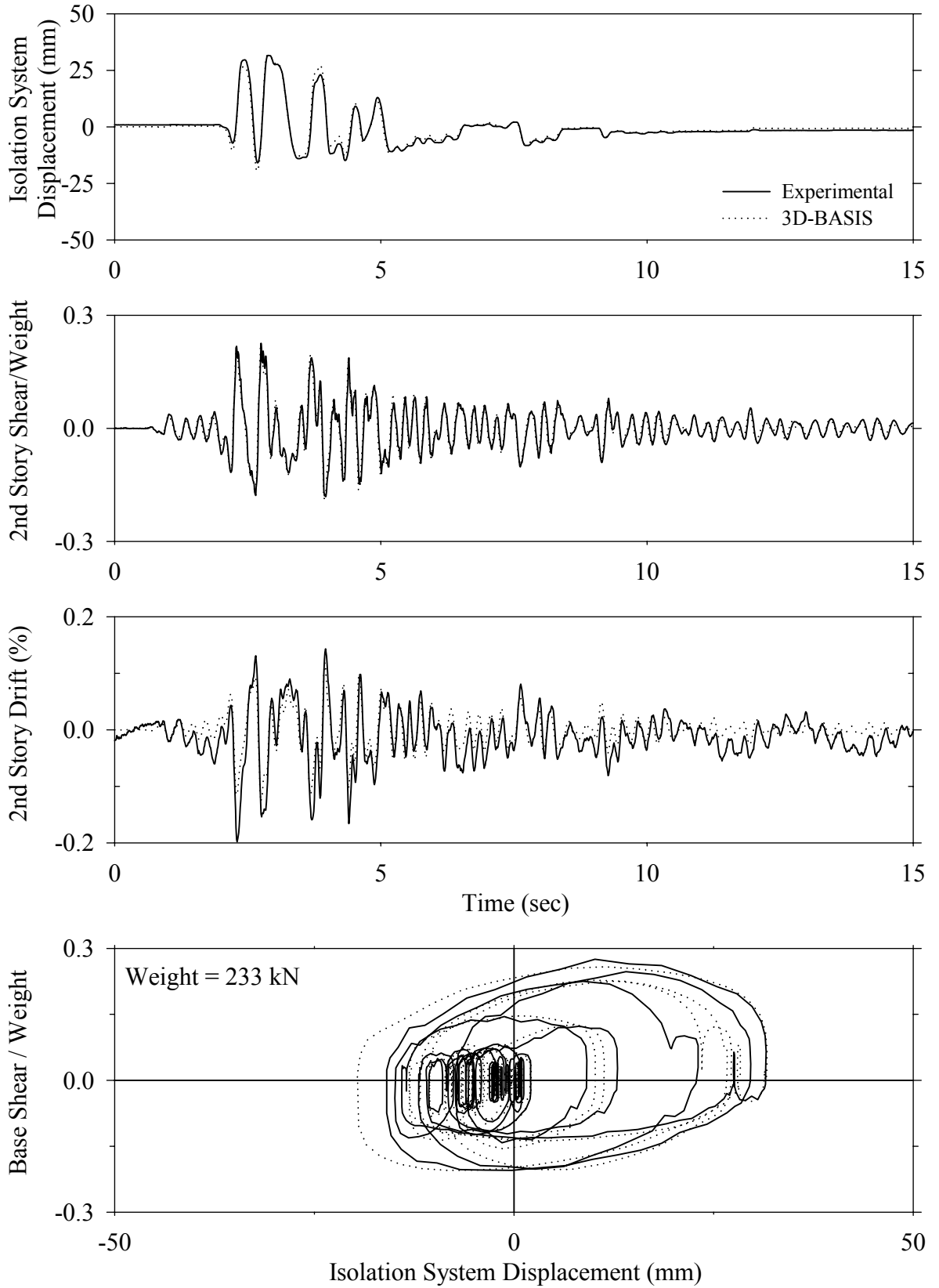
Test FPSLE20.2, El Centro S00E 200%, SB/FPS with Linear Dampers



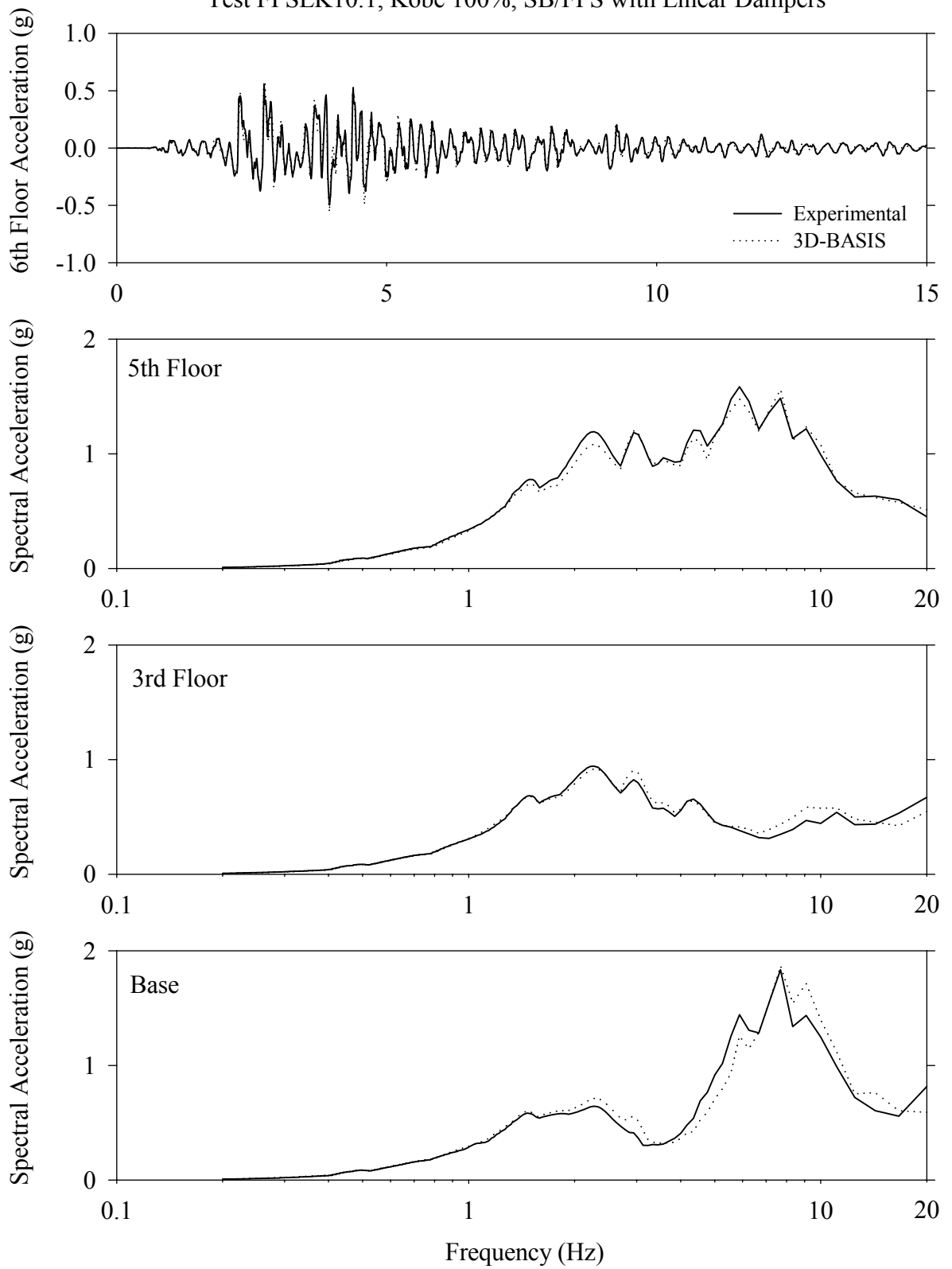
Test FPSLE20.1, El Centro S00E 200%, SB/FPS with Linear Dampers



Test FPSLK10.1, Kobe 100%, SB/FPS with Linear Dampers

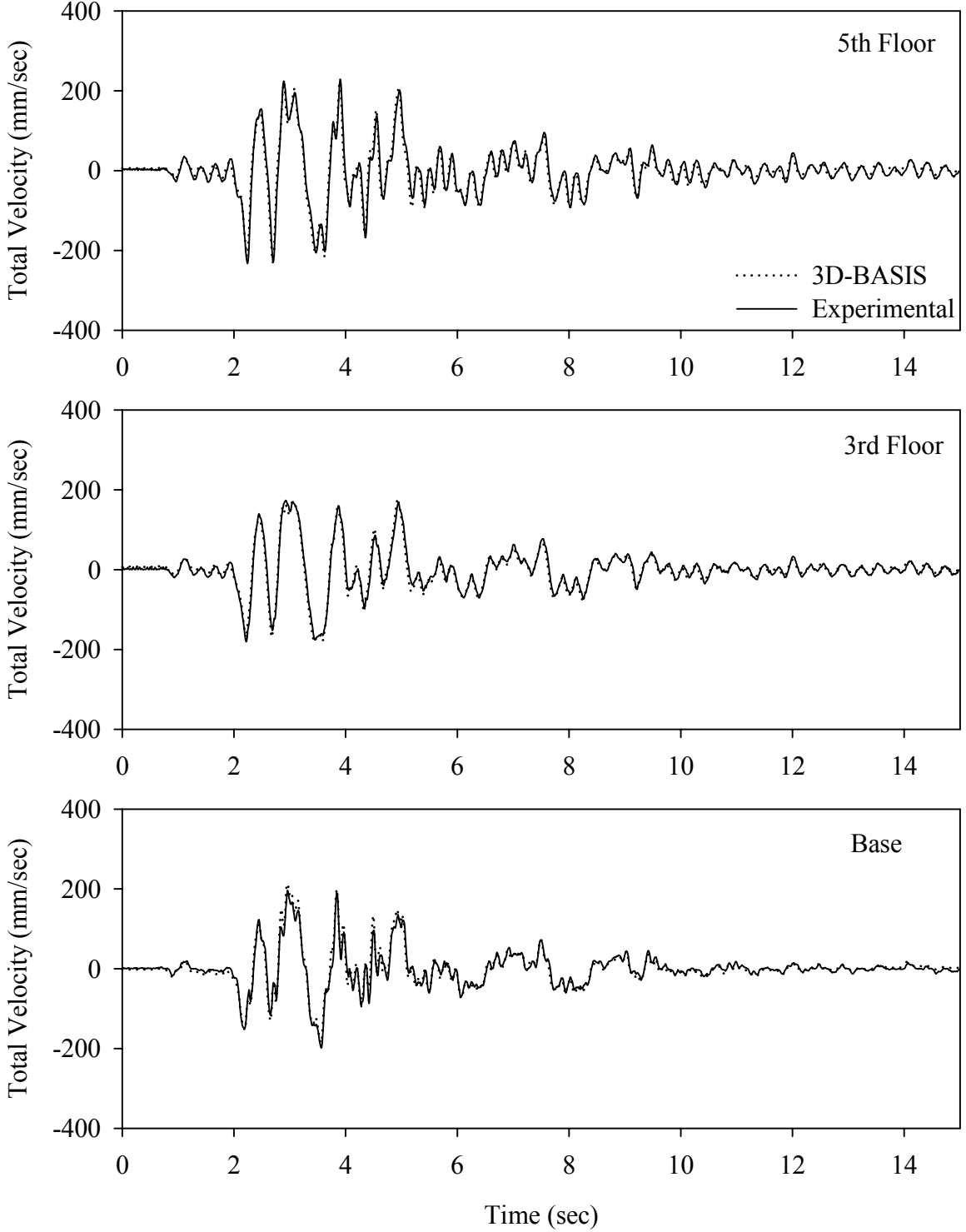


Test FPSLK10.1, Kobe 100%, SB/FPS with Linear Dampers

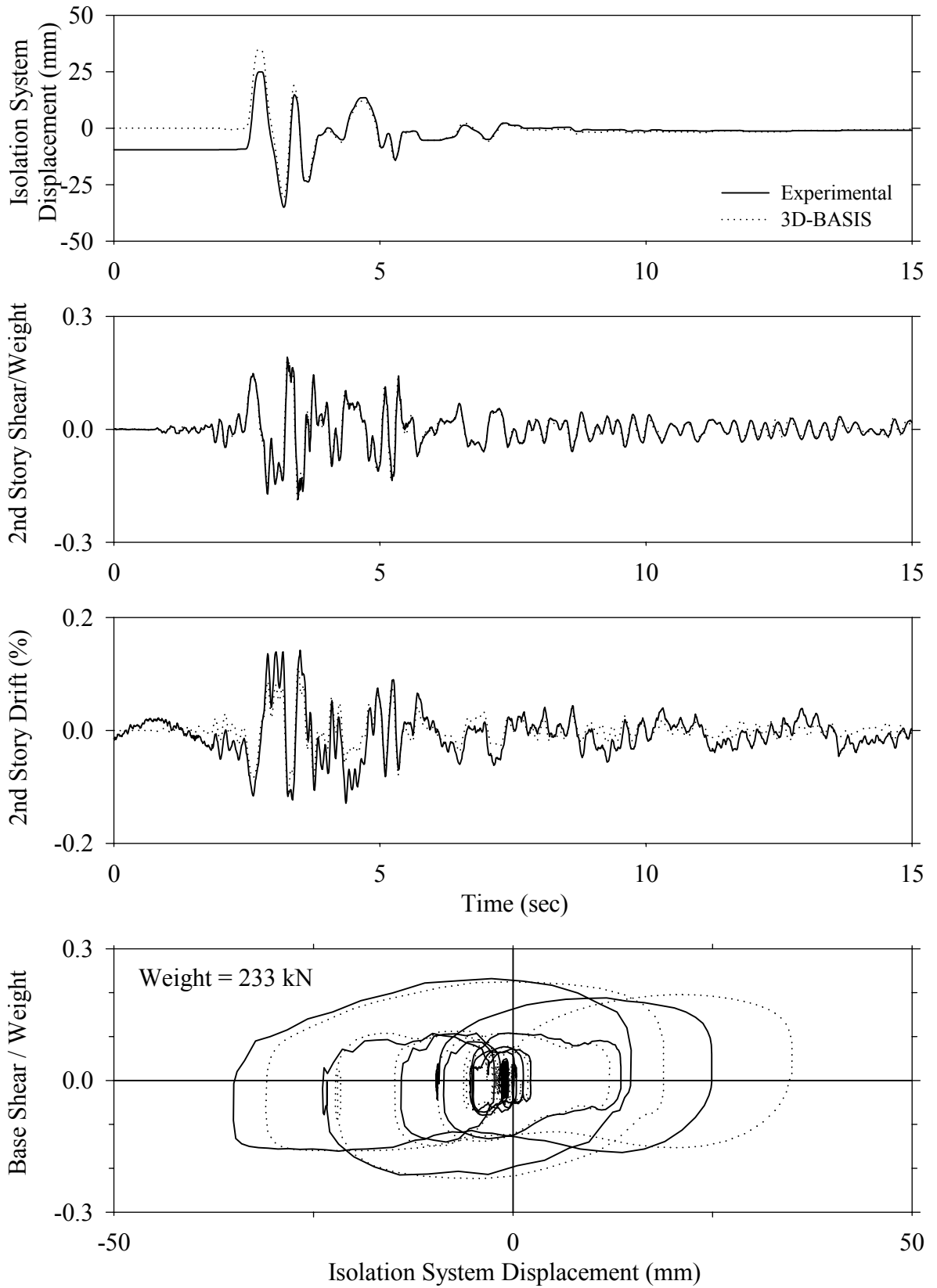


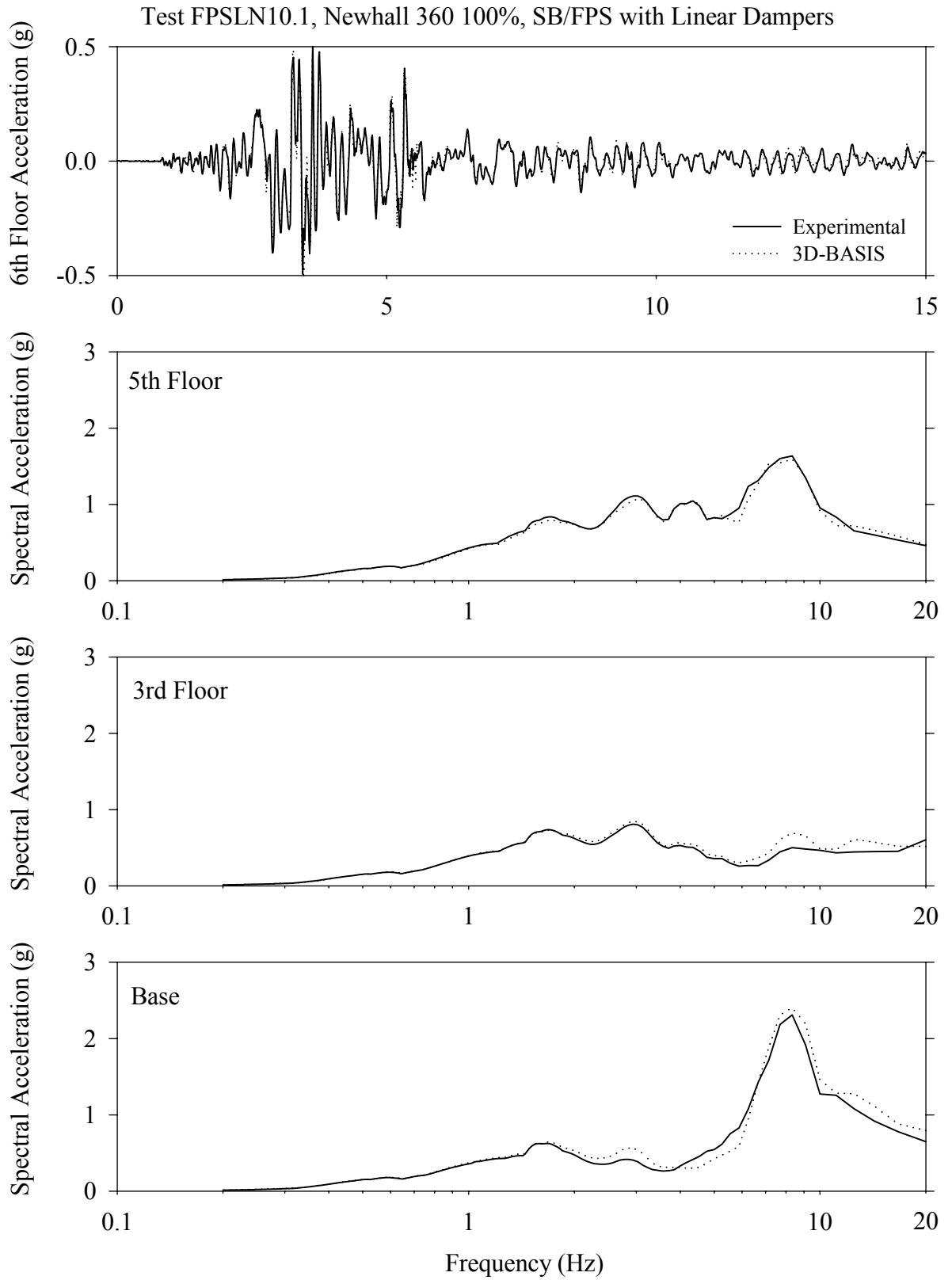


Test FPSLK10.1, Kobe 100%, SB/FPS with Linear Dampers

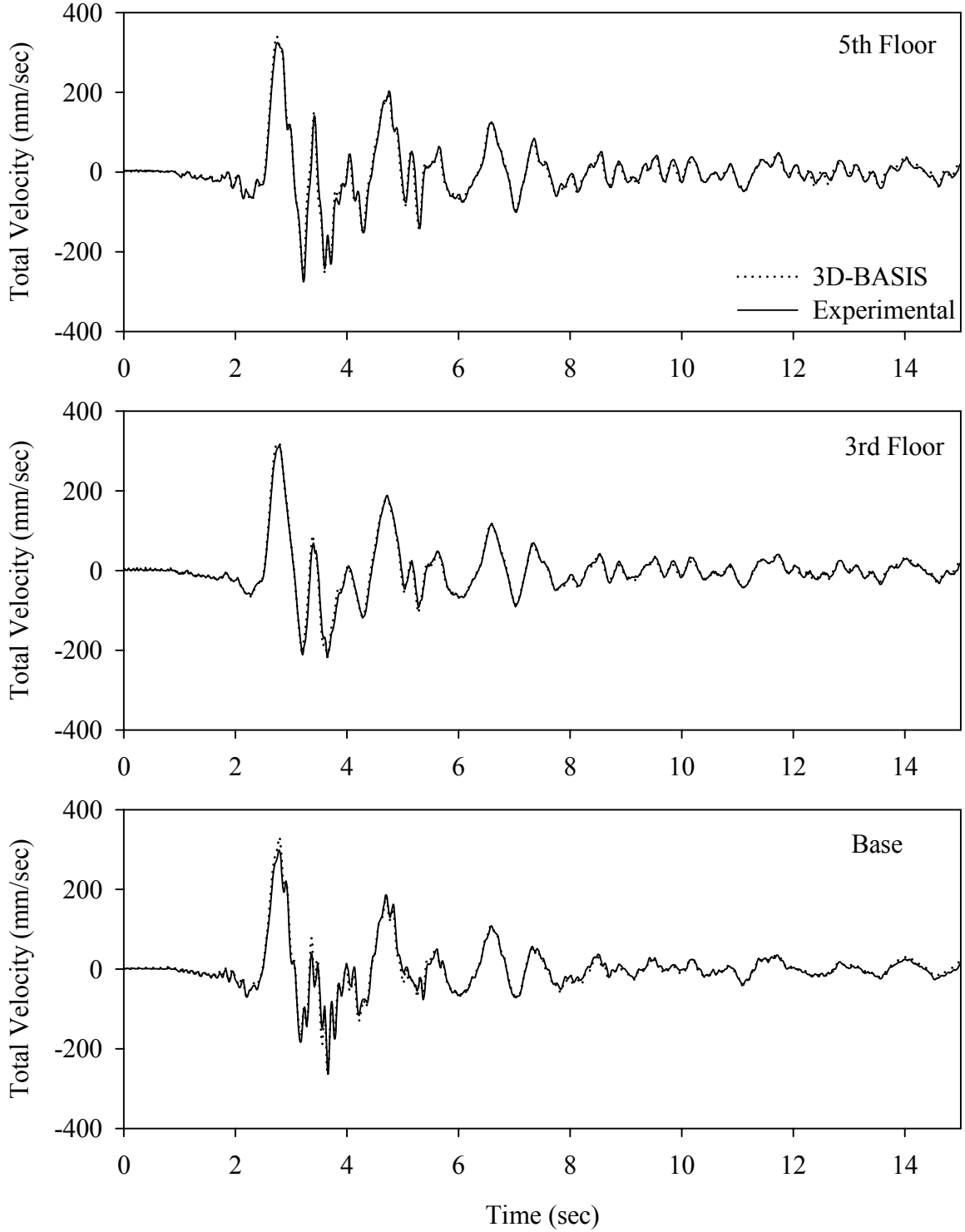


Test FPSLN10.1, Newhall 360 100%, SB/FPS with Linear Dampers

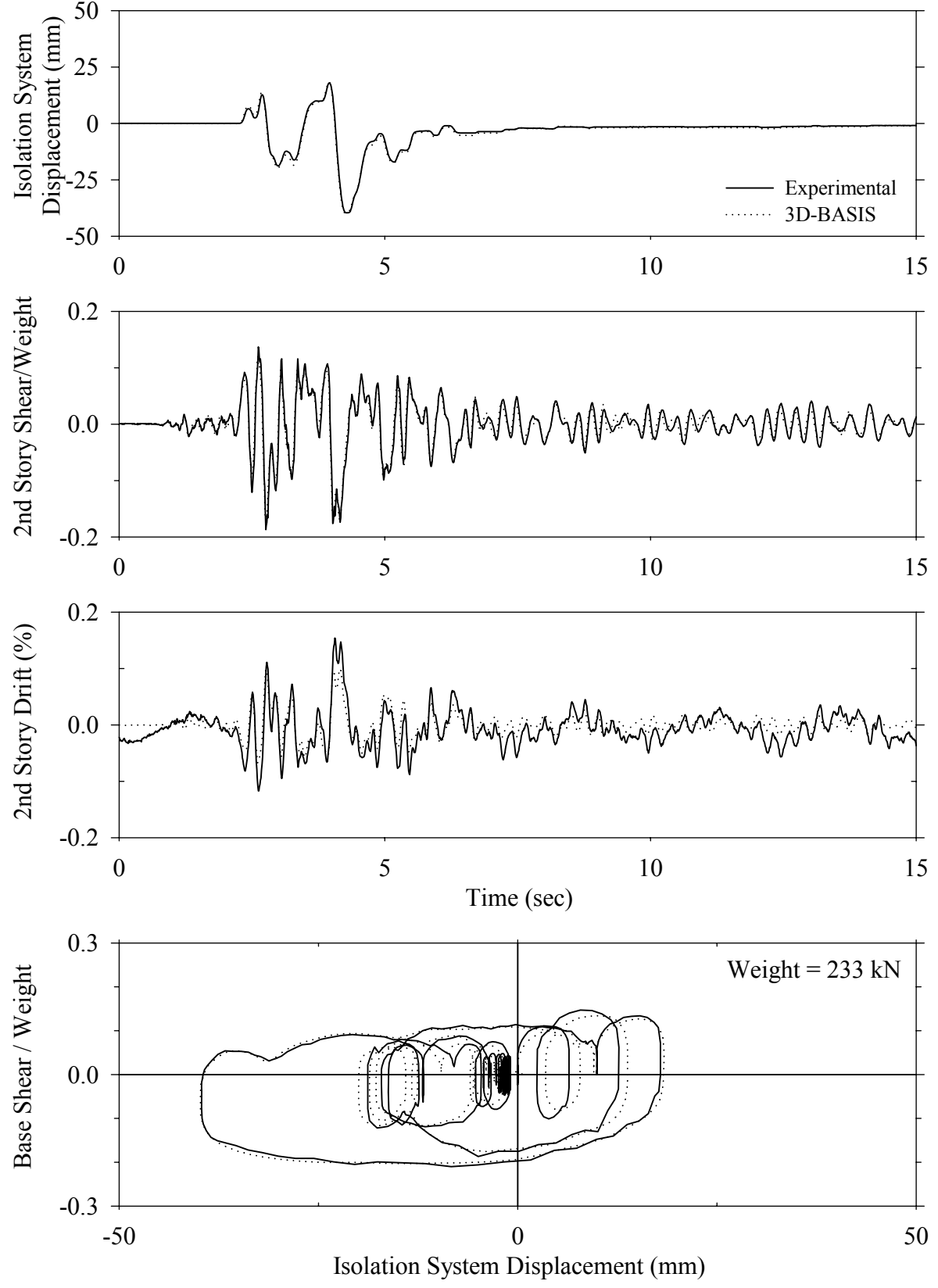




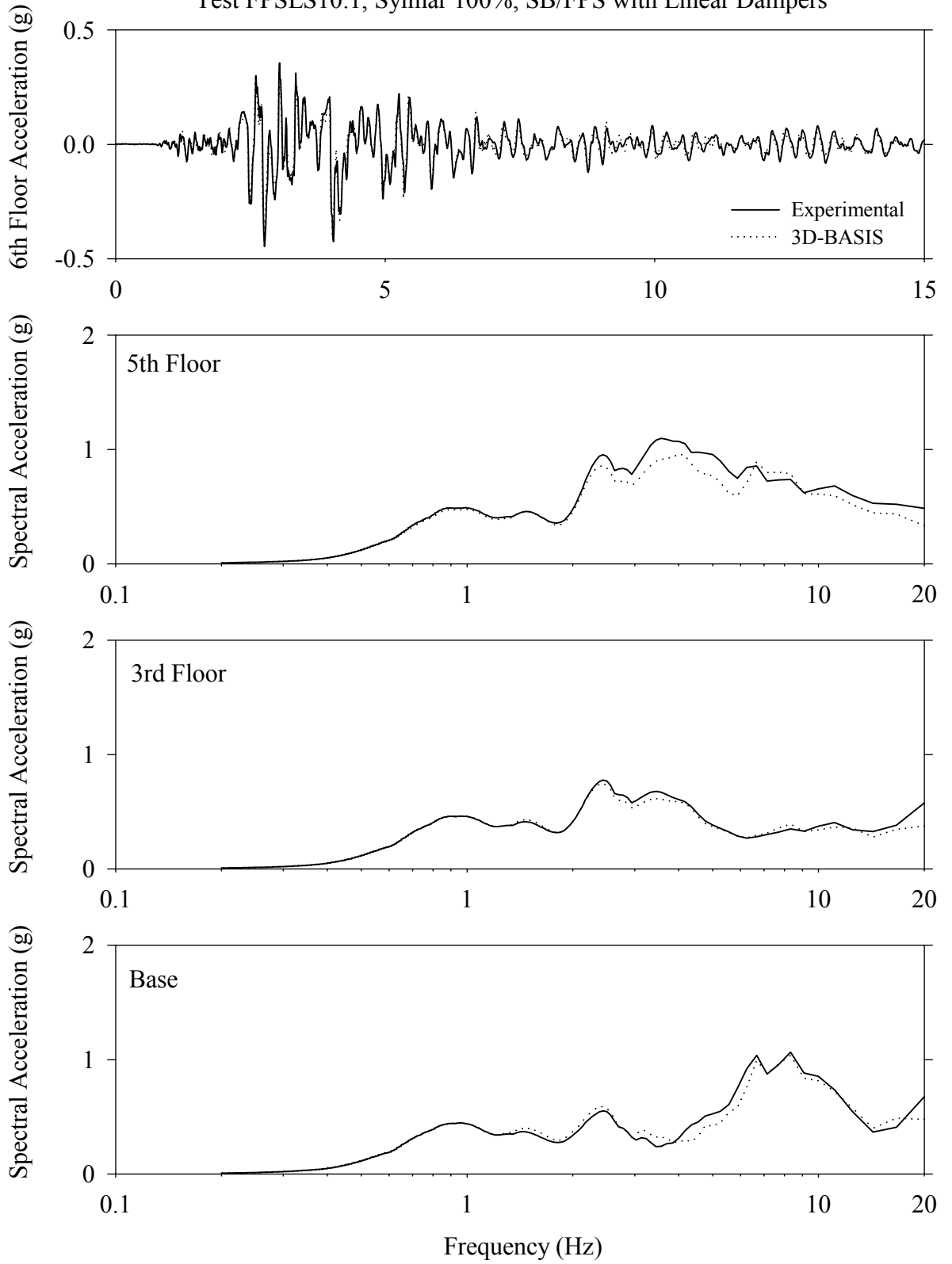
Test FPSLN10.1, Newhall 360 100%, SB/FPS with Linear Dampers



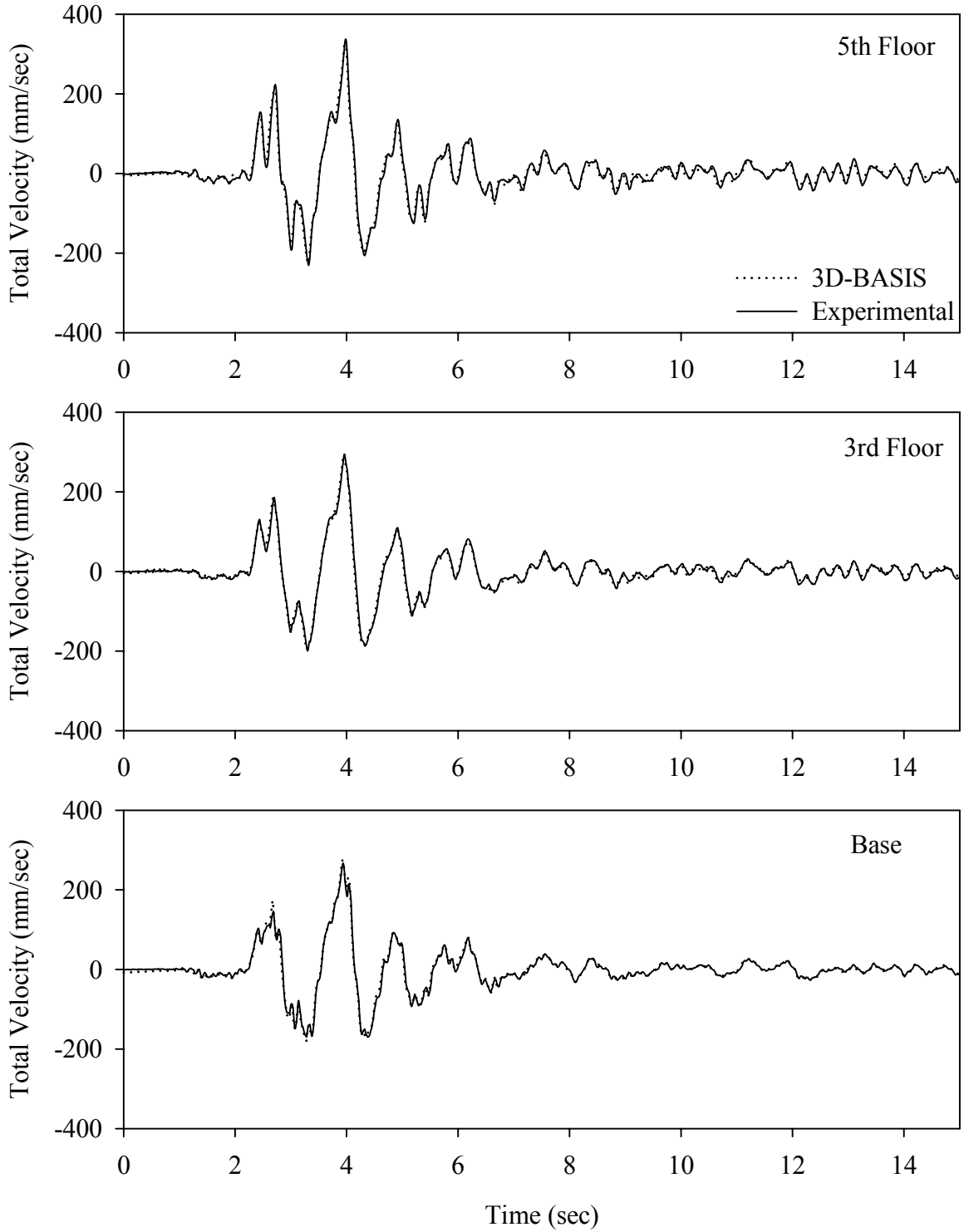
Test FPSLS10.1, Sylmar 100%, SB/FPS with Linear Dampers



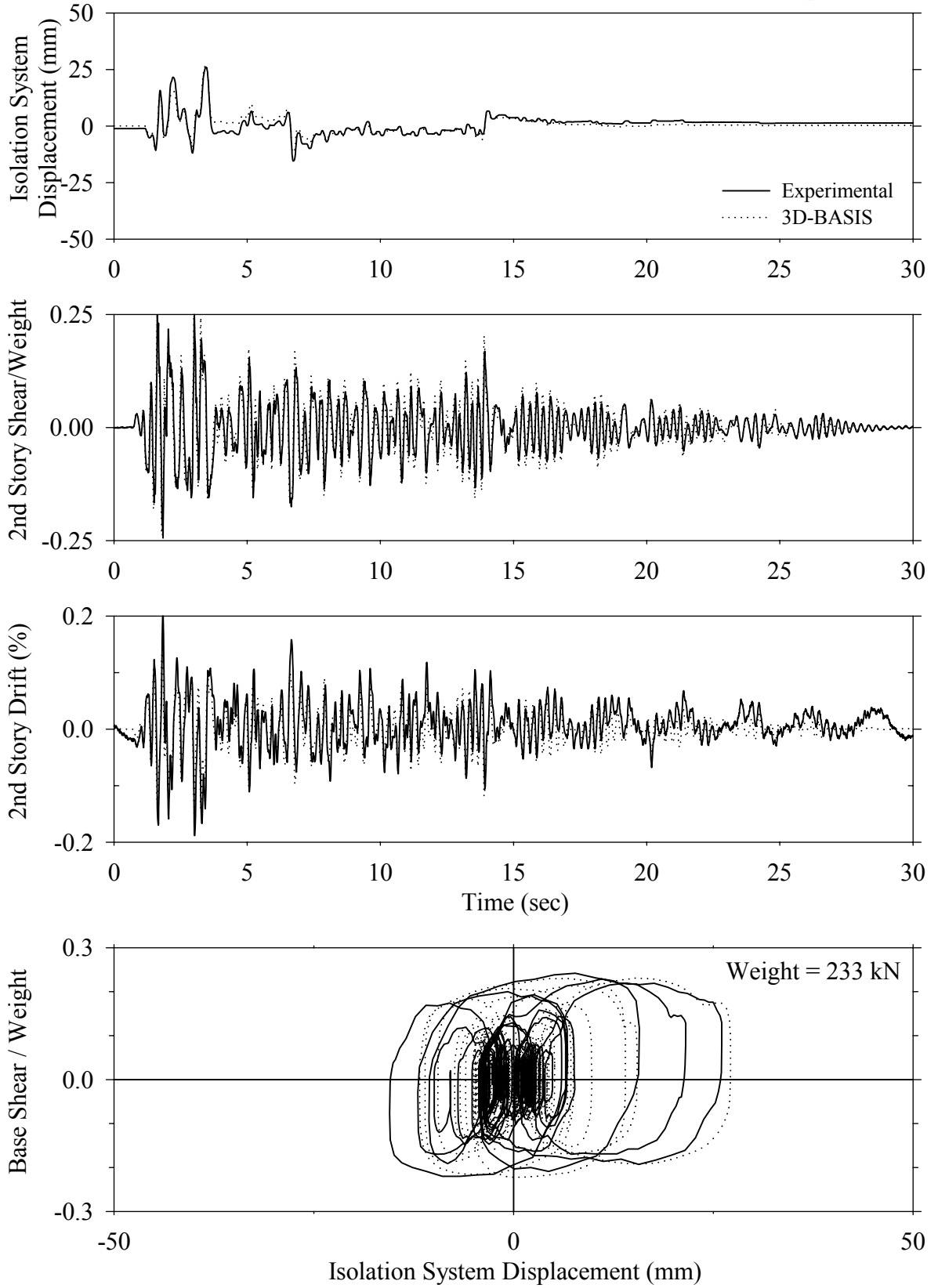
Test FPSLS10.1, Sylmar 100%, SB/FPS with Linear Dampers



Test FPSLS10.1, Sylmar 100%, SB/FPS with Linear Dampers

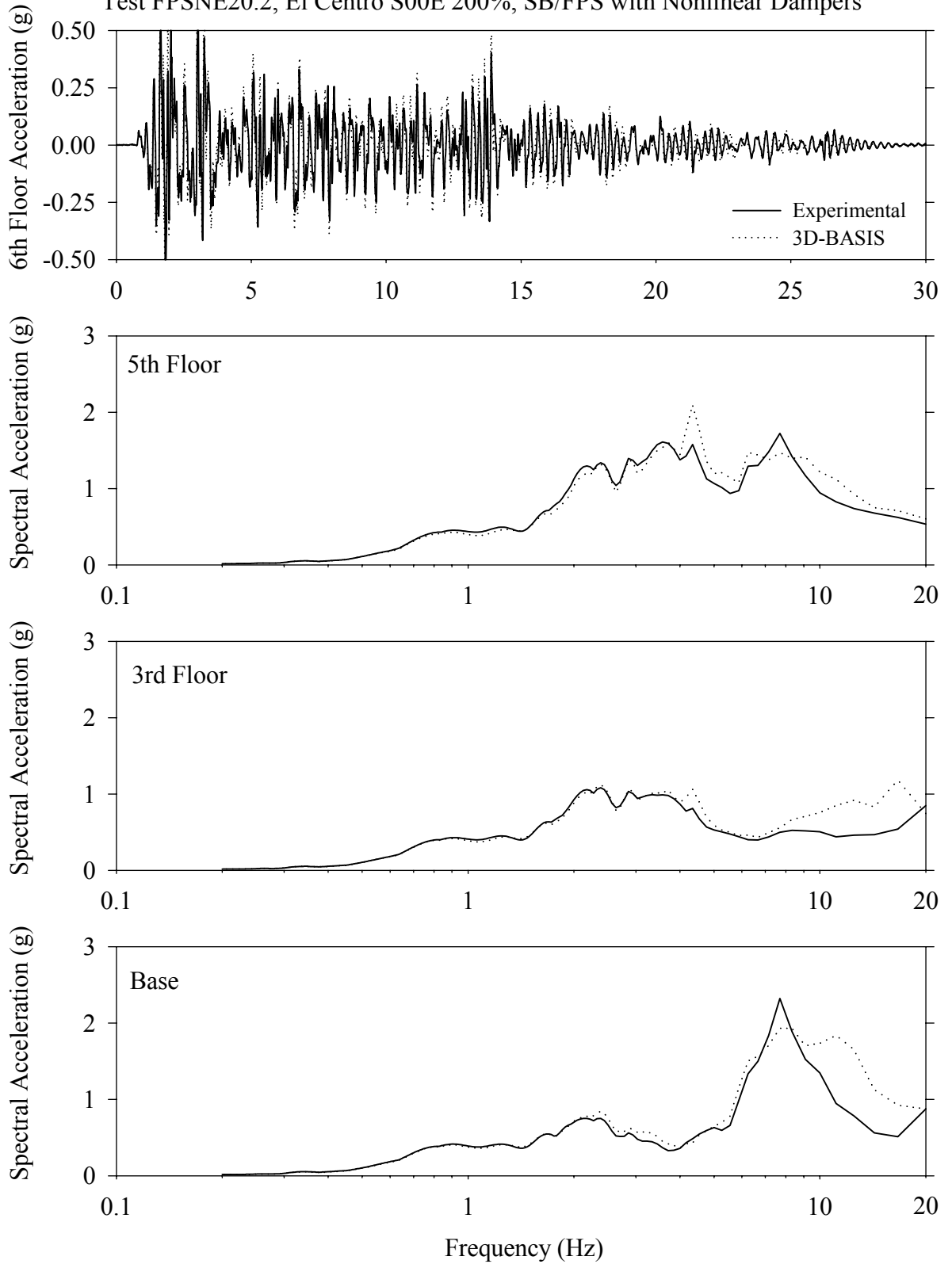


Test FPSNE20.2, El Centro S00E 200%, SB/FPS with Nonlinear Dampers

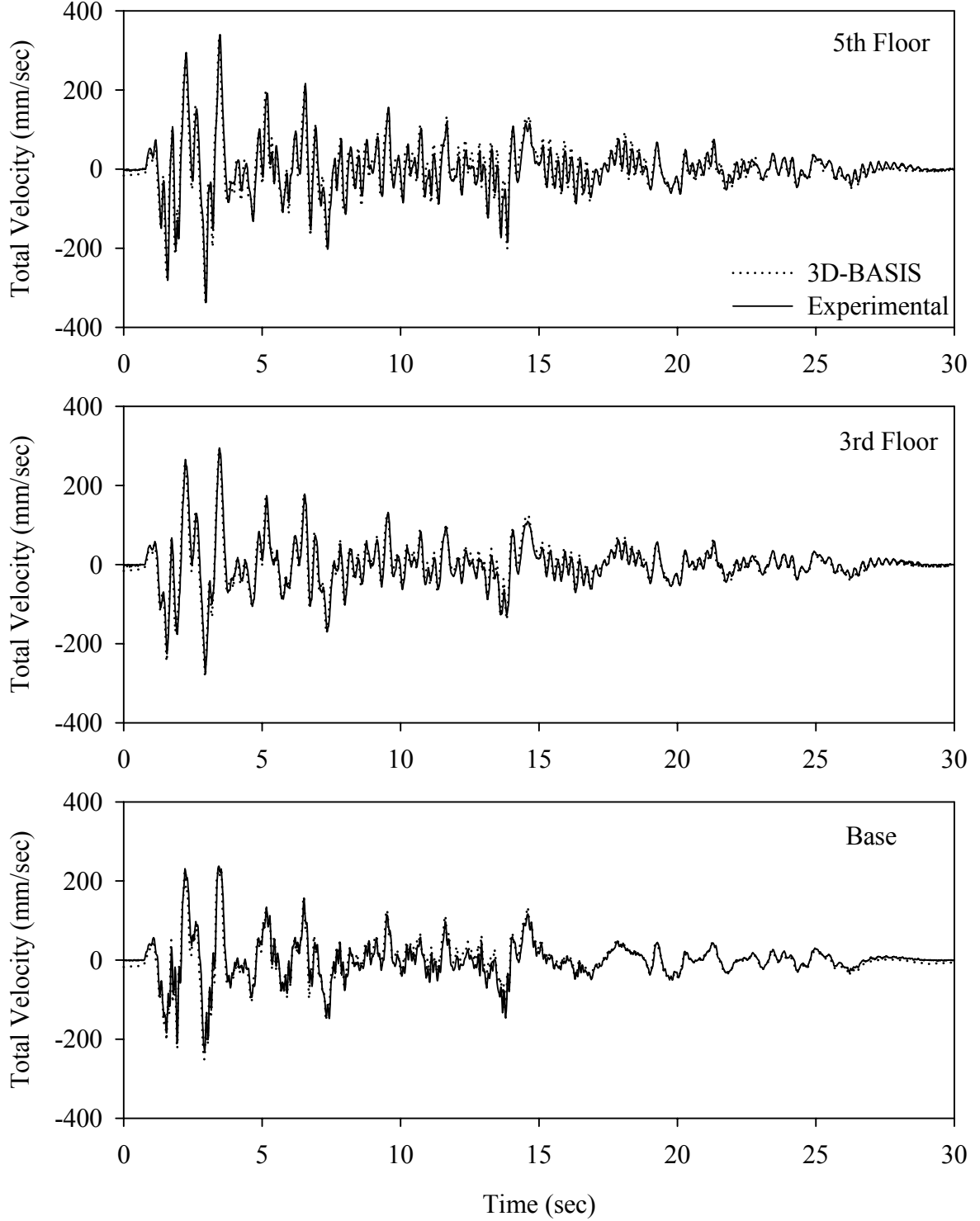




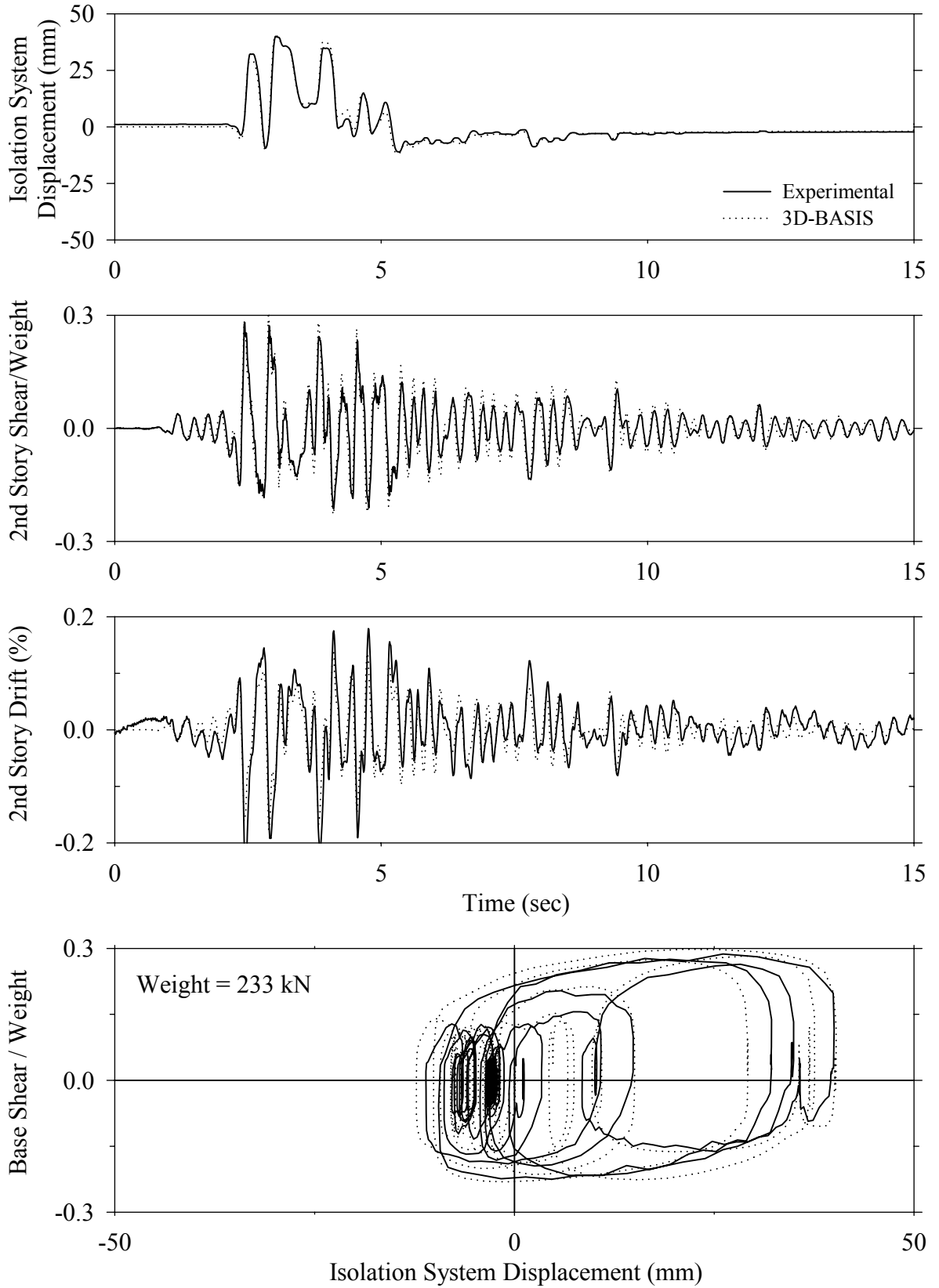
Test FPSNE20.2, El Centro S00E 200%, SB/FPS with Nonlinear Dampers



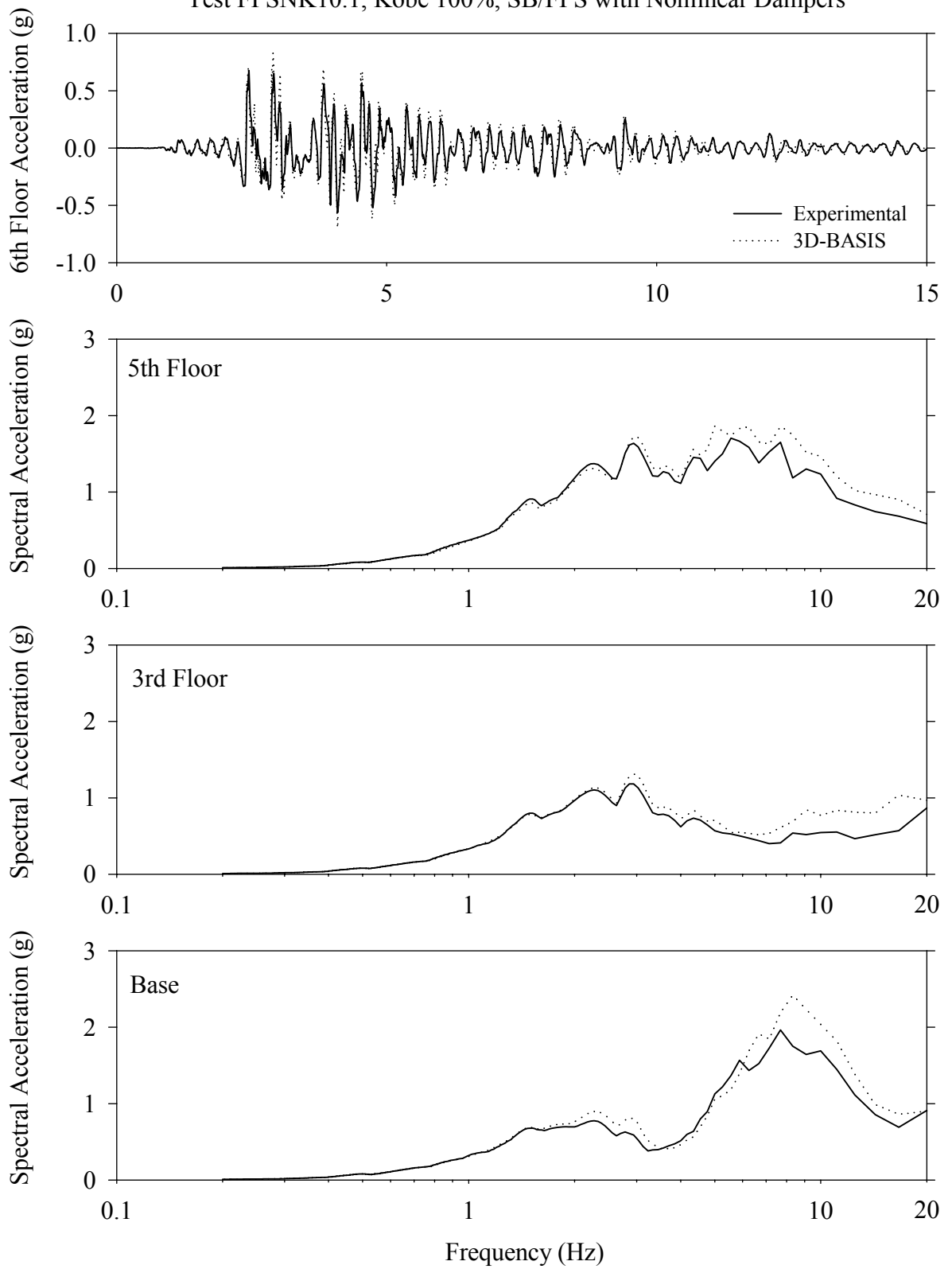
Test FPSNE20.1, El Centro S00E 200%, SB/FPS with Nonlinear Dampers



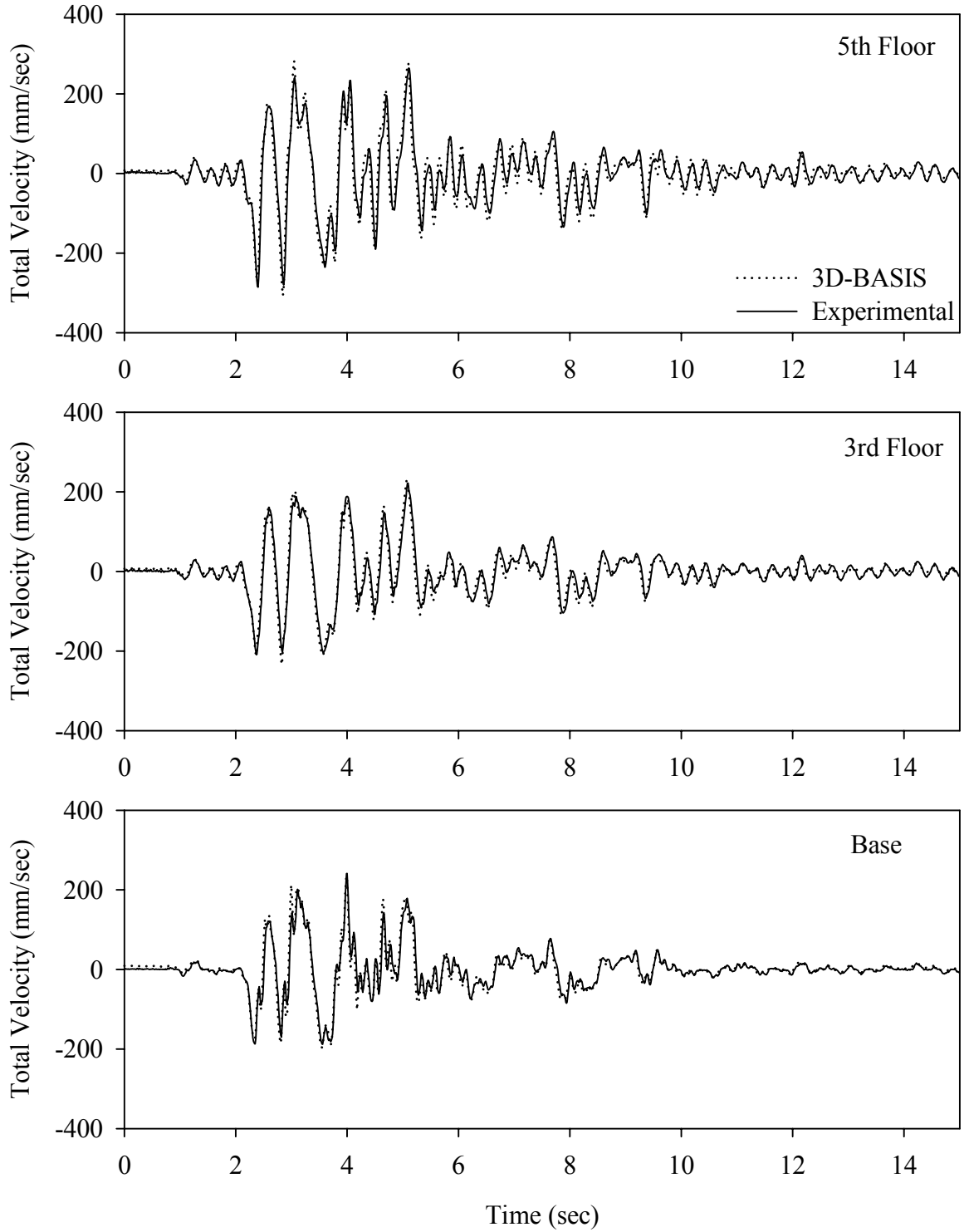
Test FPSNK10.1, Kobe 100%, SB/FPS with Nonlinear Dampers



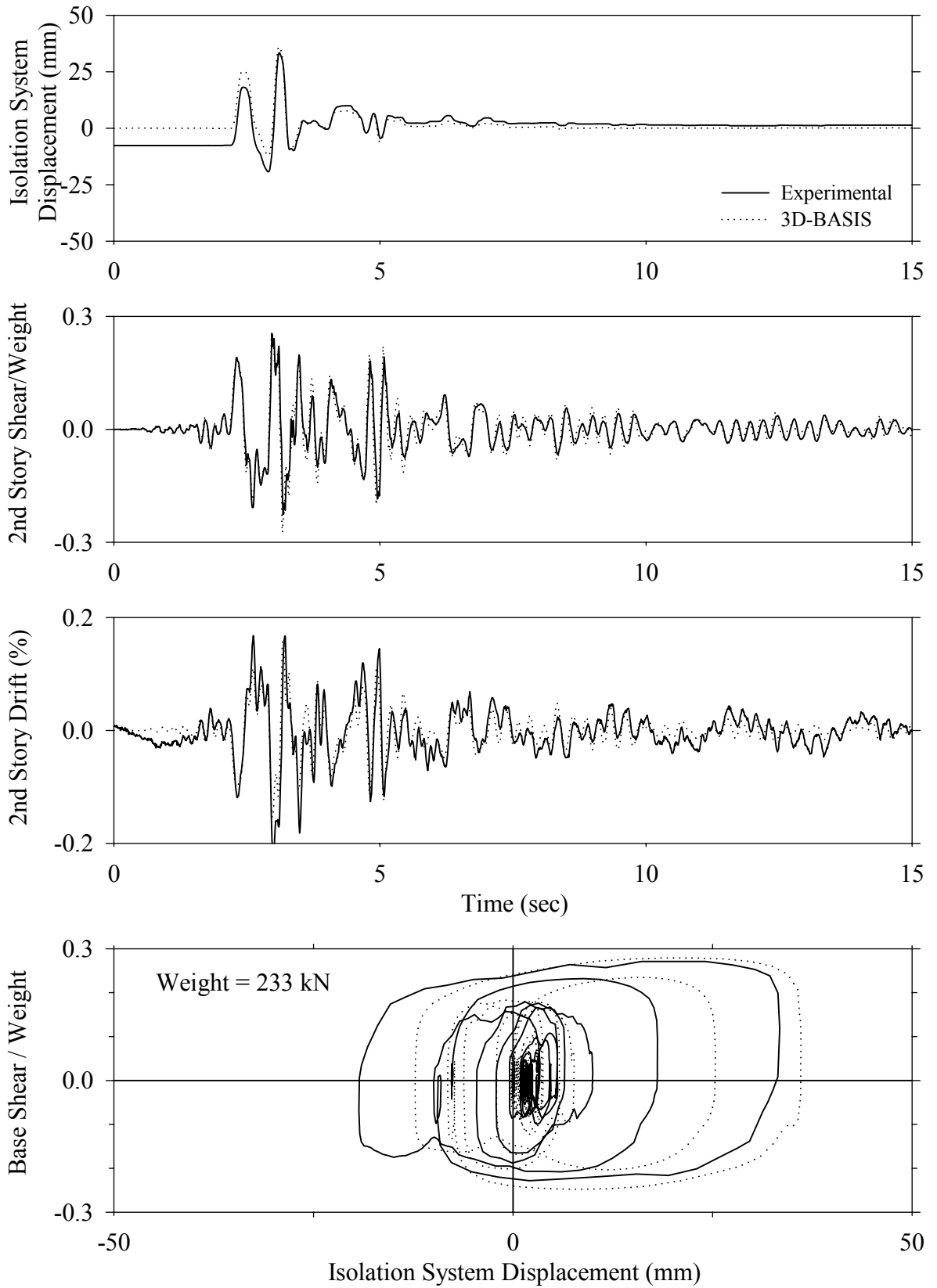
Test FPSNK10.1, Kobe 100%, SB/FPS with Nonlinear Dampers



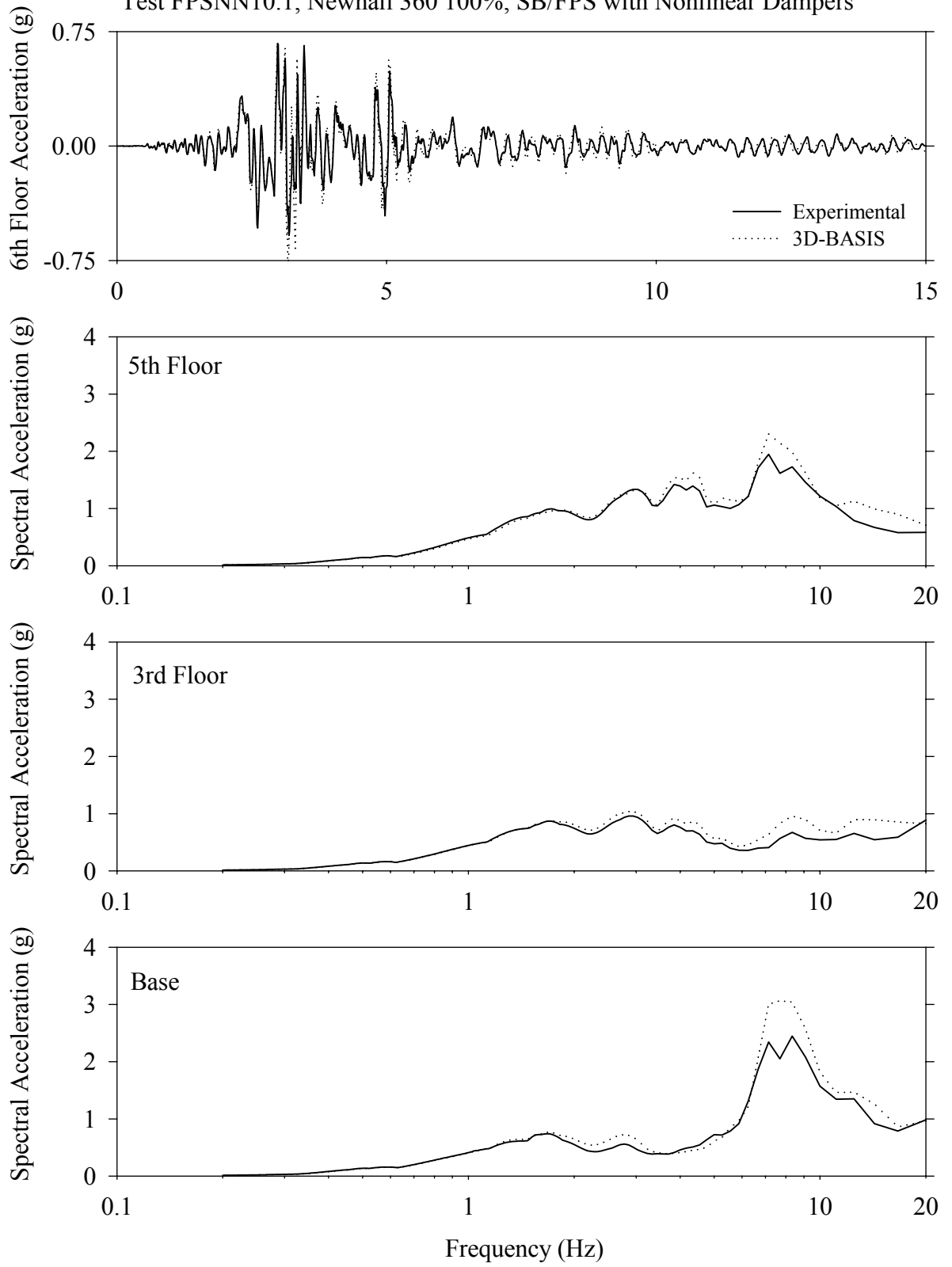
Test FPSNK10.1, Kobe 100%, SB/FPS with Nonlinear Dampers



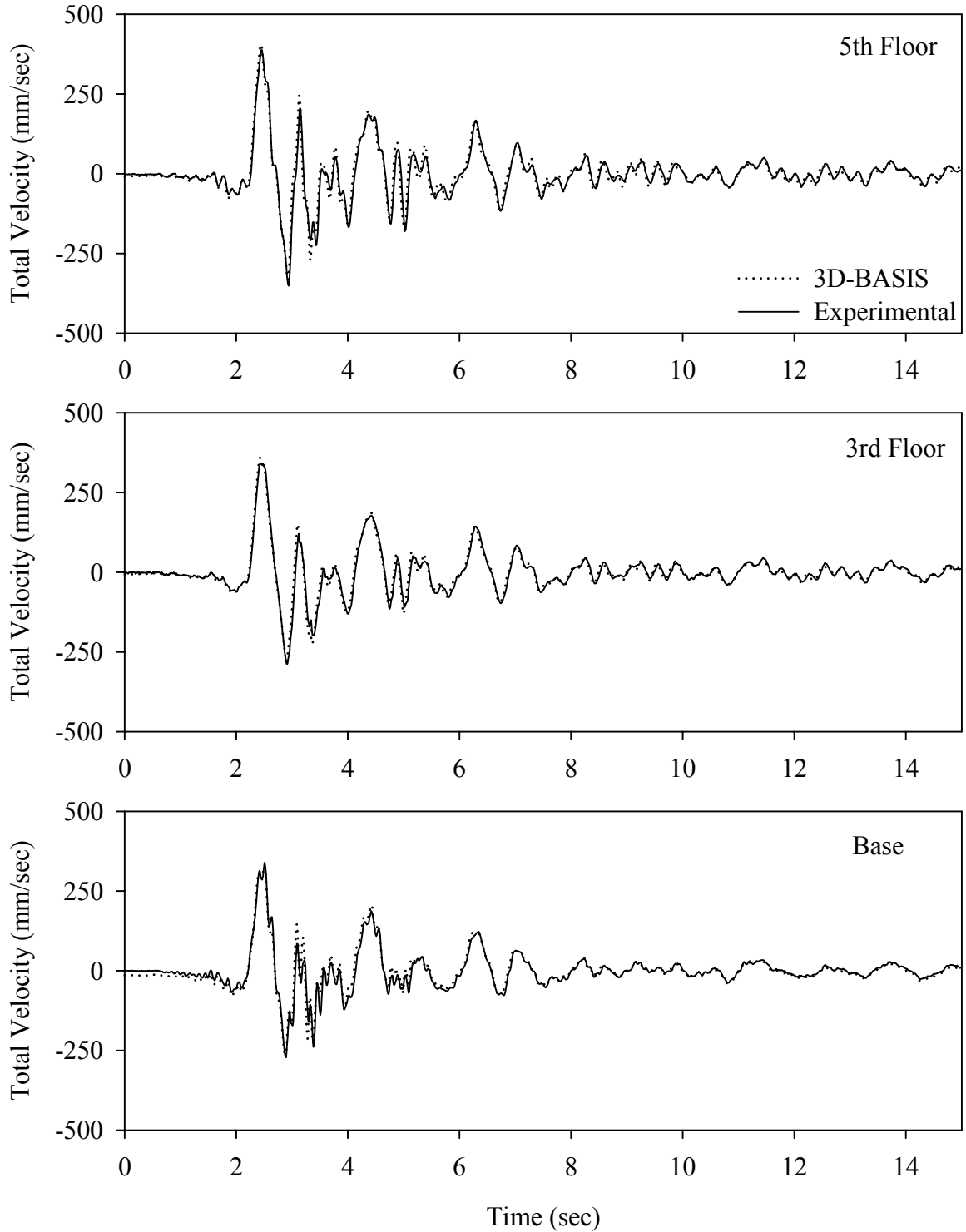
Test FPSNN10.1, Newhall 360 100%, SB/FPS with Nonlinear Dampers



Test FPSNN10.1, Newhall 360 100%, SB/FPS with Nonlinear Dampers

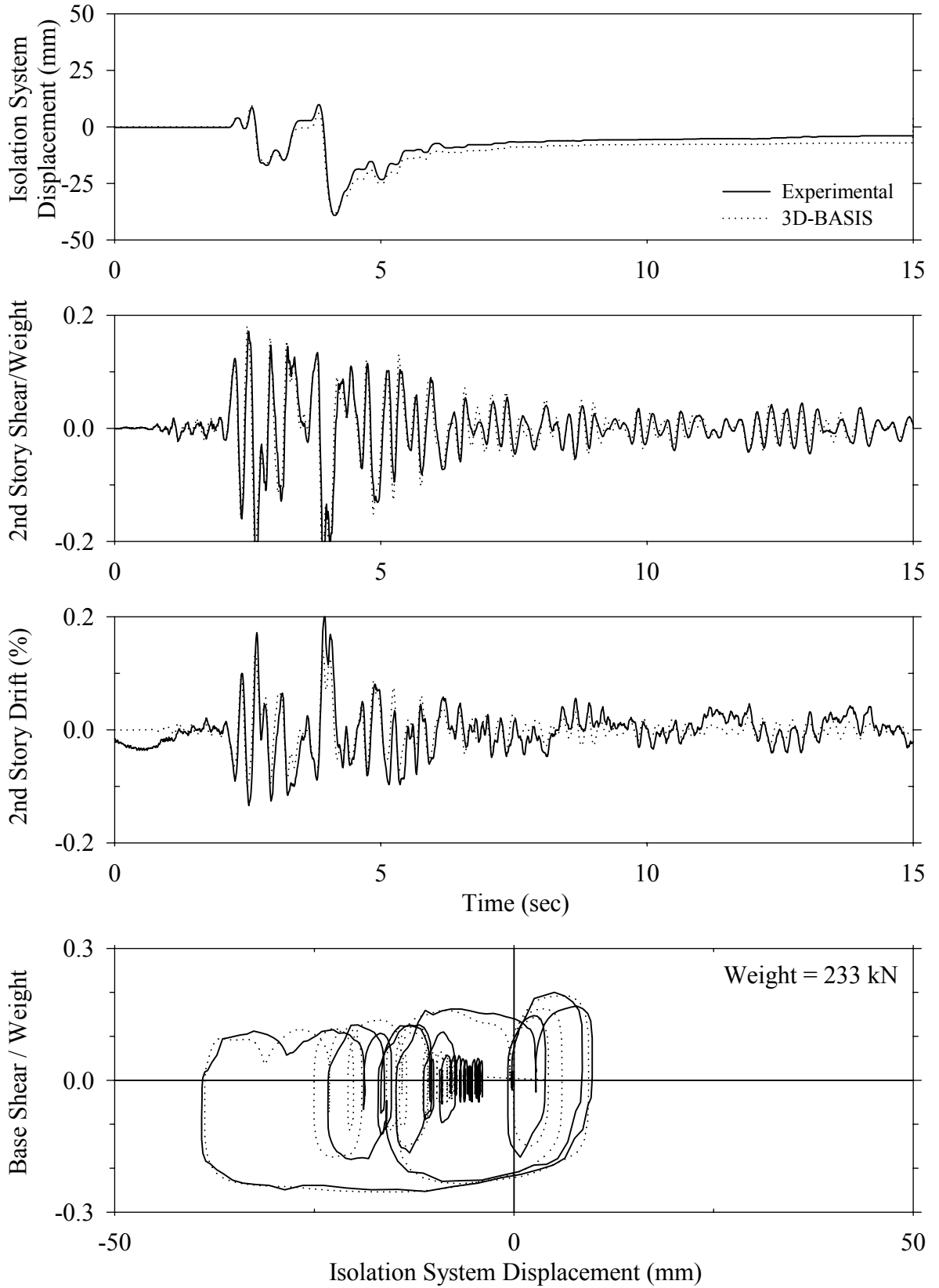


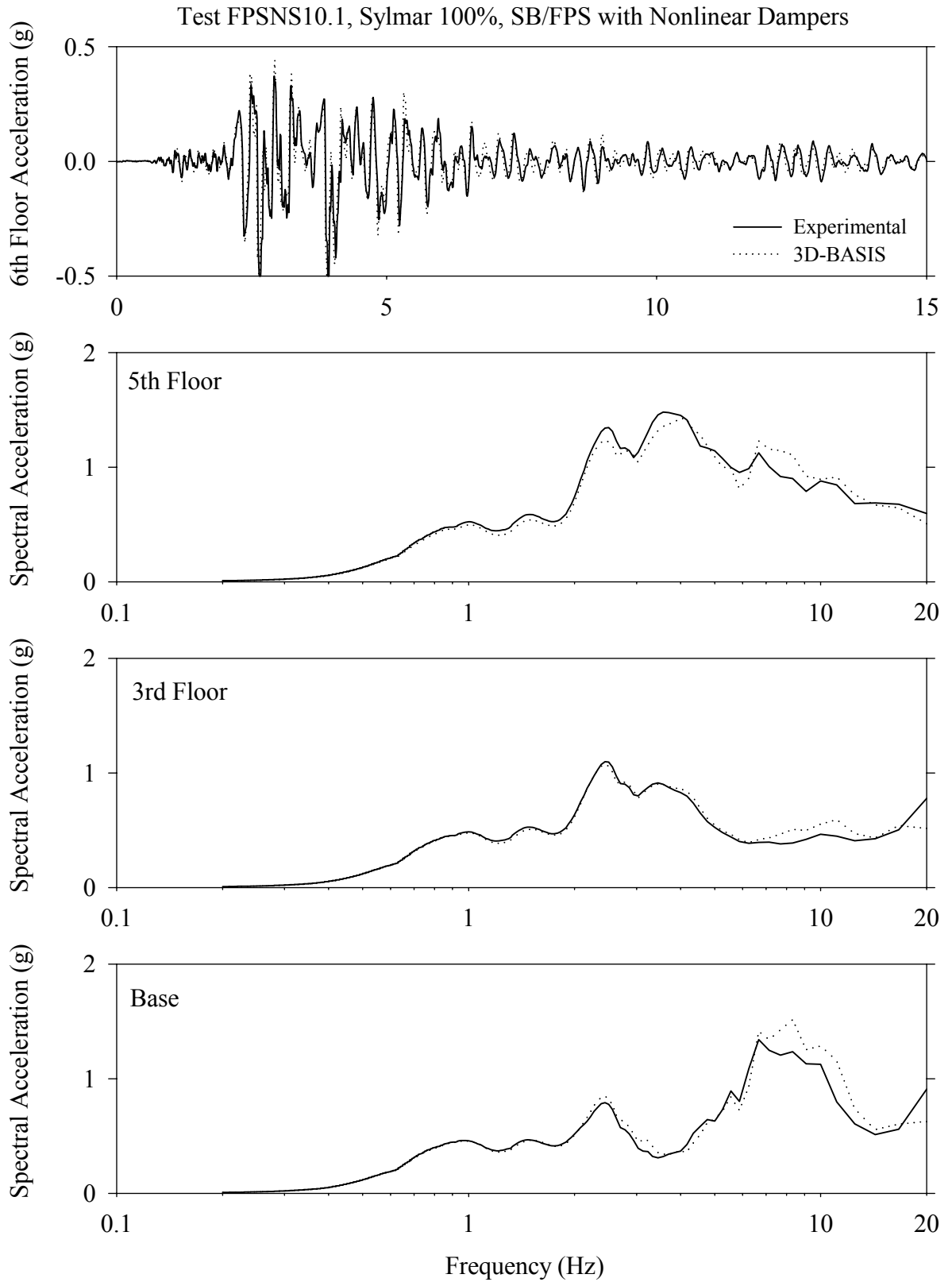
Test FPSNN10.1, Newhall 360 100%, SB/FPS with Nonlinear Dampers



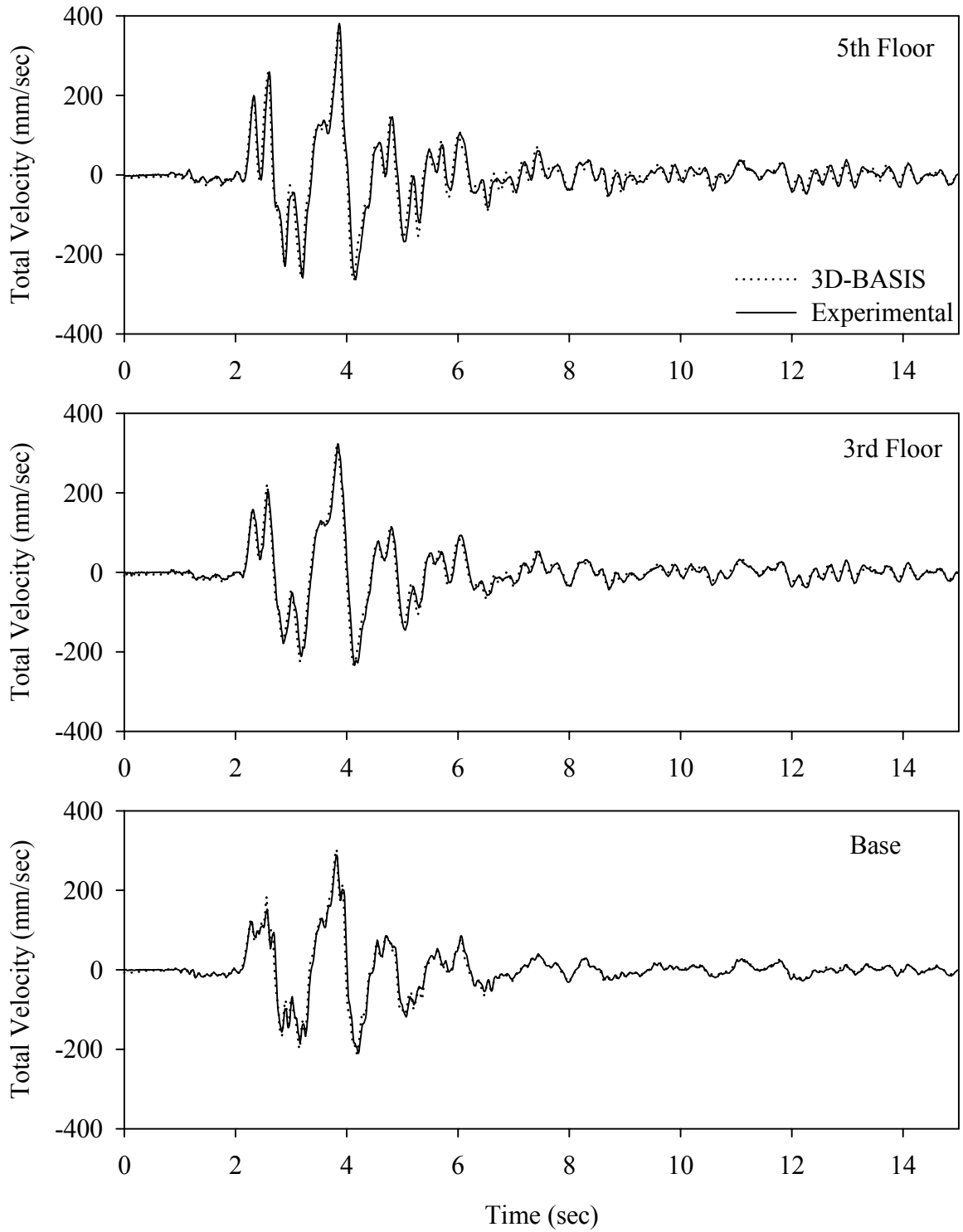


Test FPSNS10.1, Sylmar 100%, SB/FPS with Nonlinear Dampers

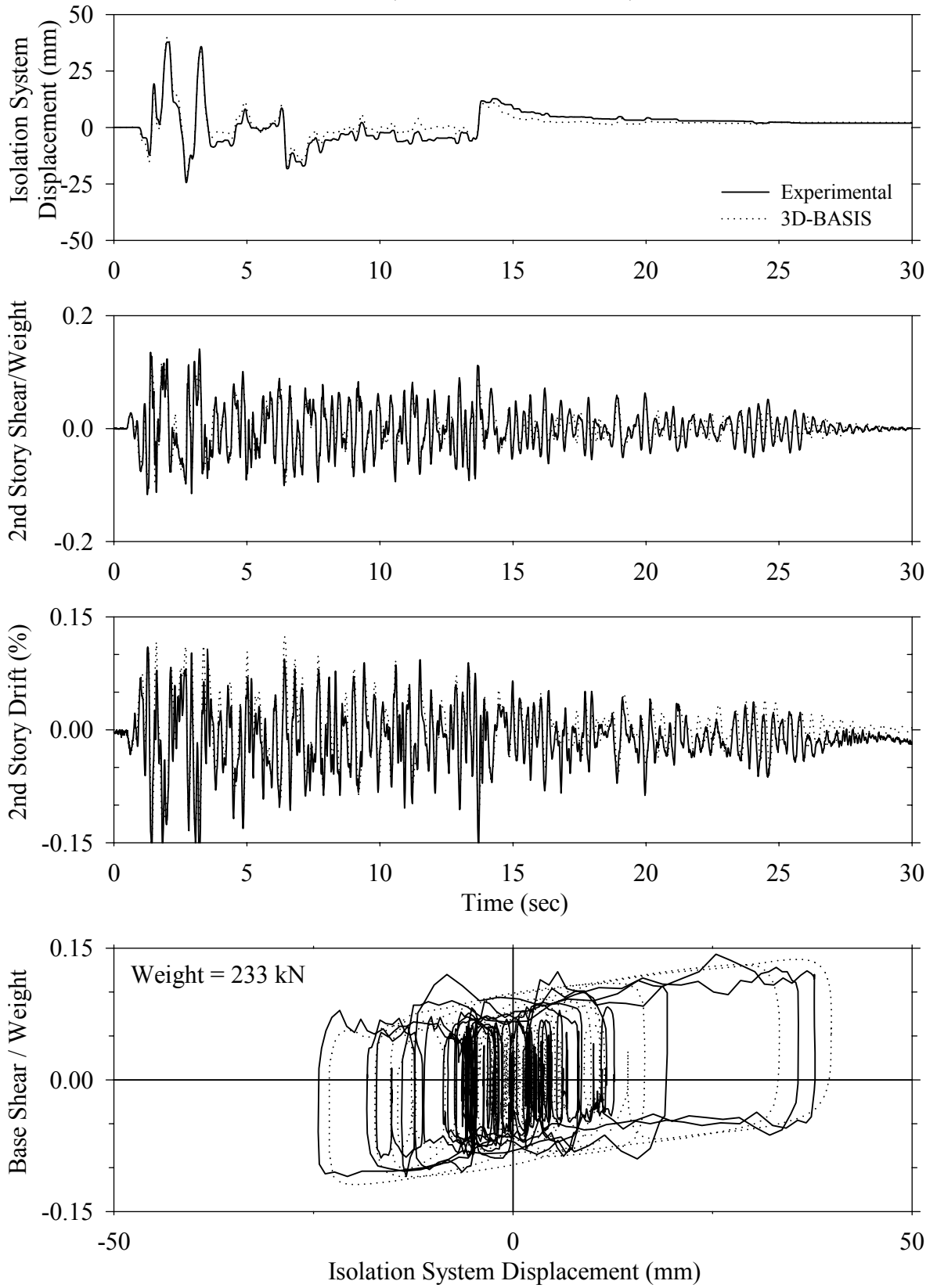




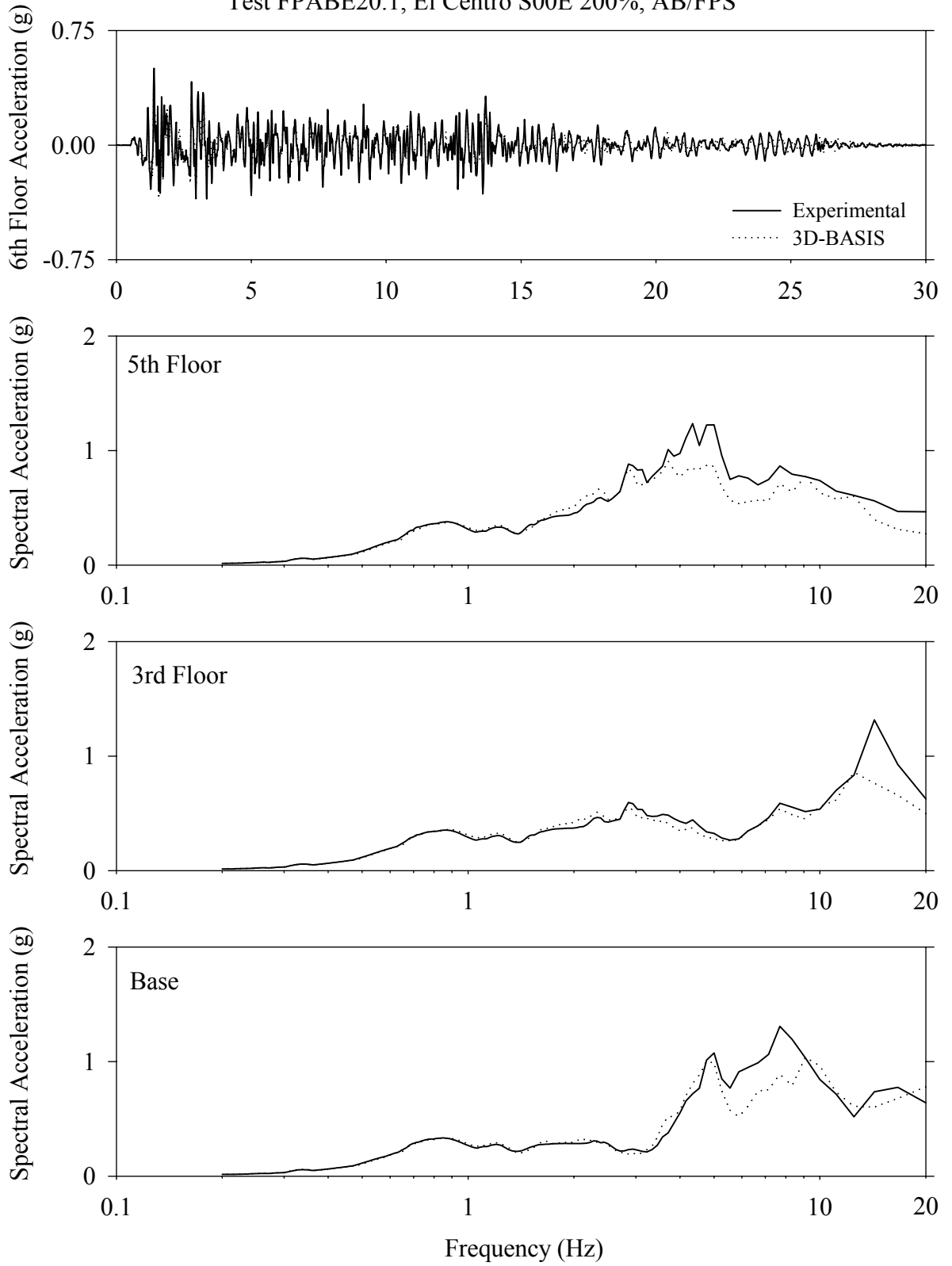
Test FPSNS10.1, Sylmar 100%, SB/FPS with Nonlinear Dampers



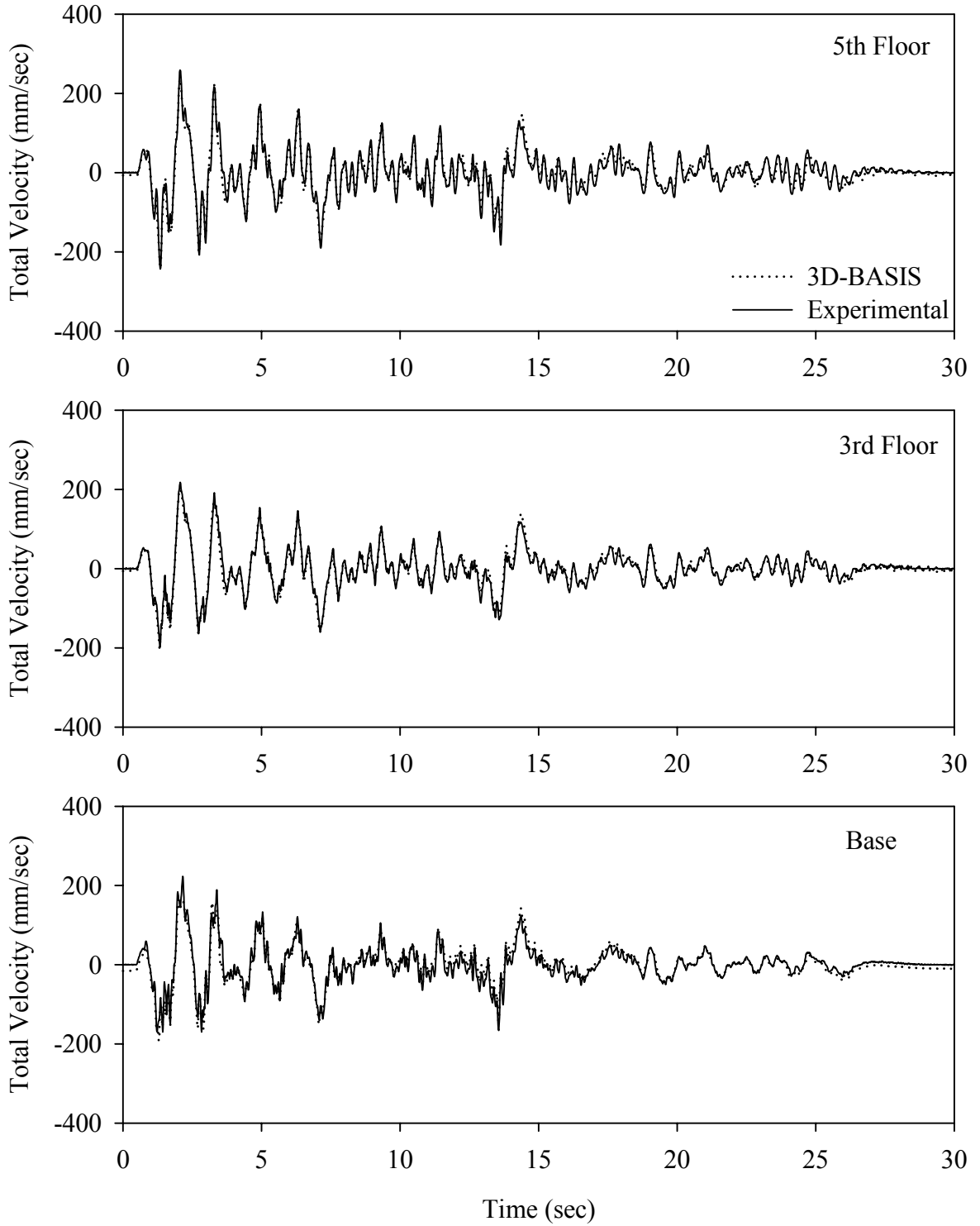
Test FPABE20.1, El Centro S00E 200%, AB/FPS



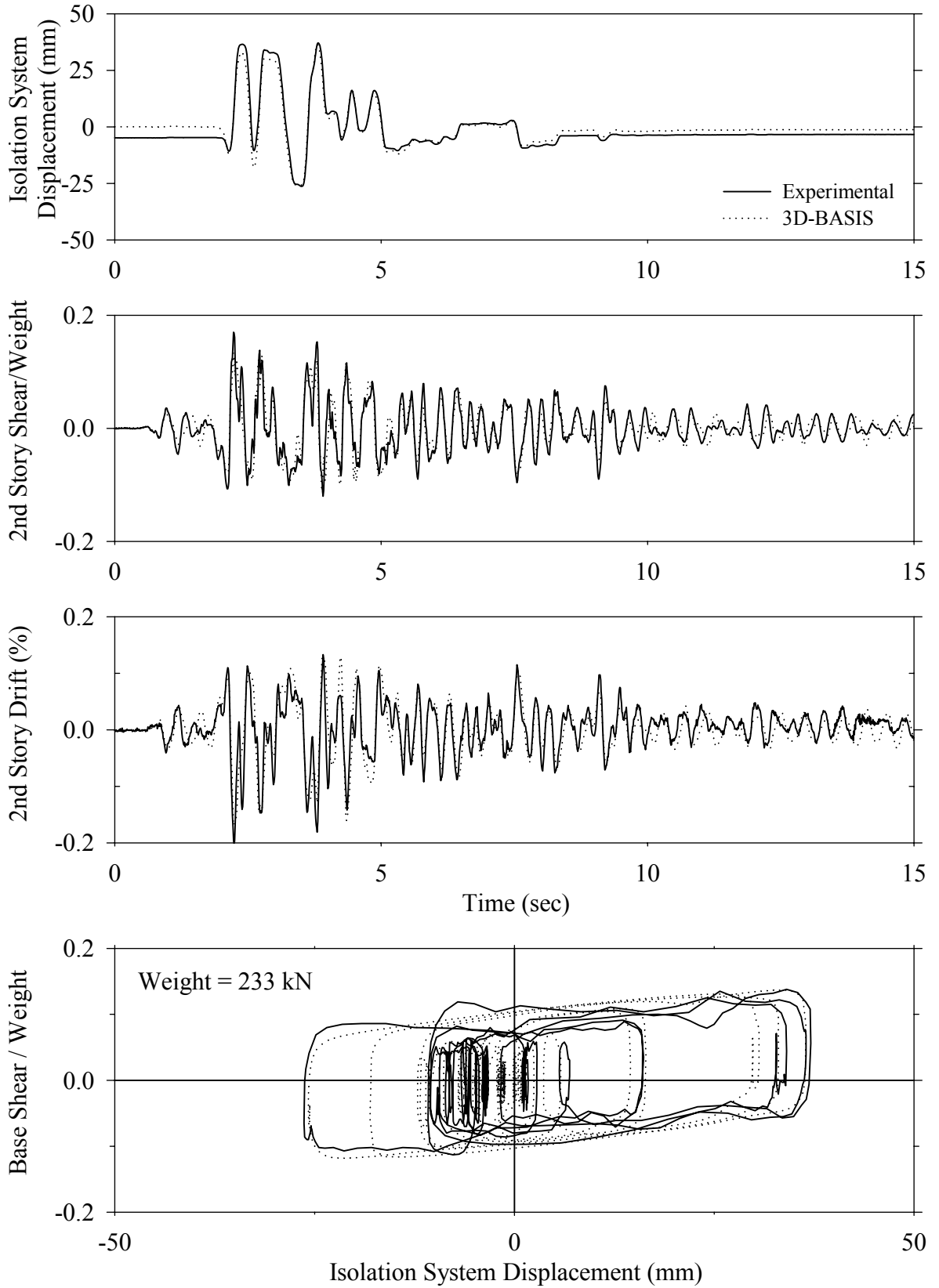
Test FPABE20.1, El Centro S00E 200%, AB/FPS



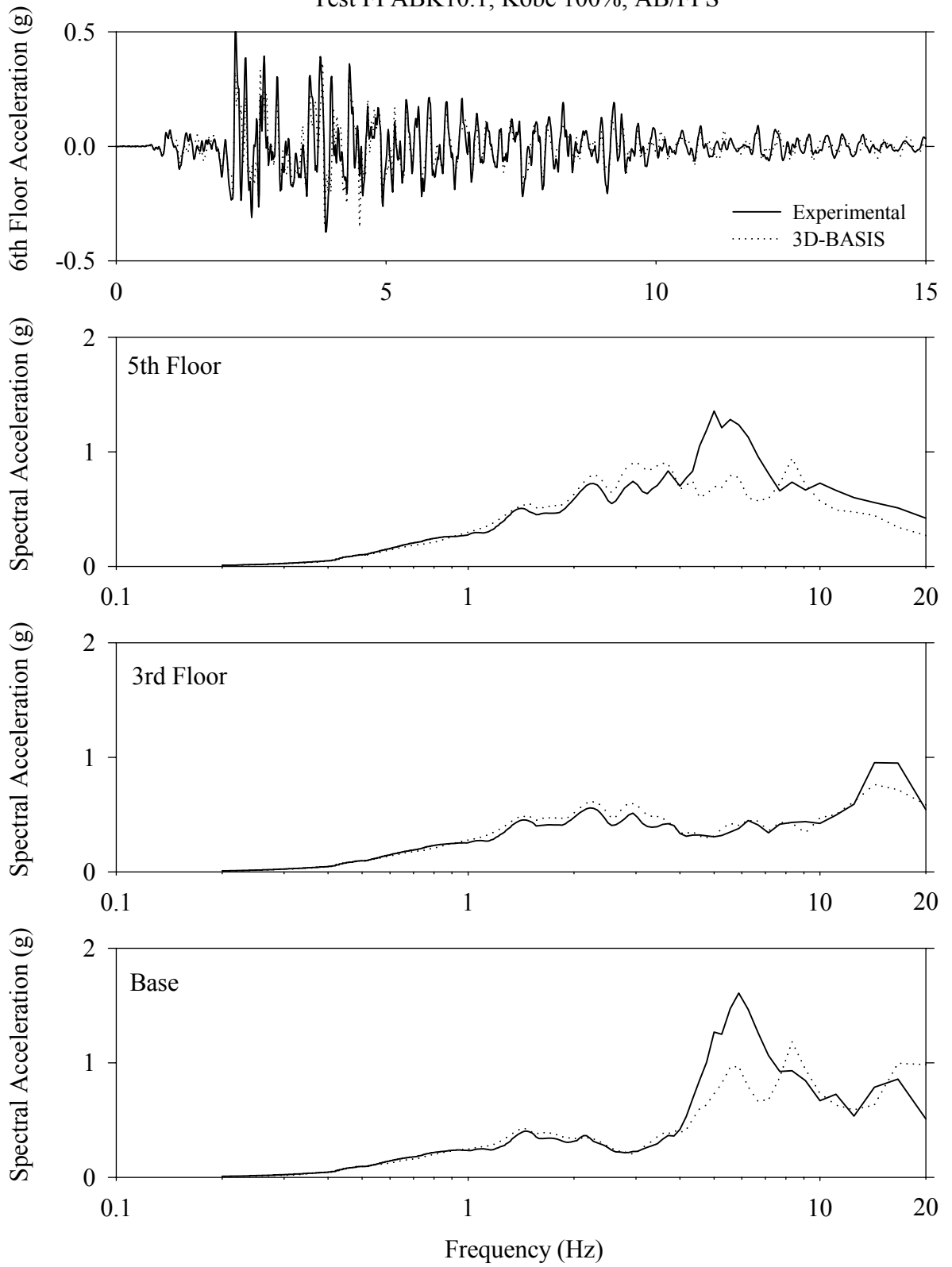
Test FPABE20.1, El Centro S00E 200%, AB/FPS



Test FPABK10.1, Kobe 100%, AB/FPS

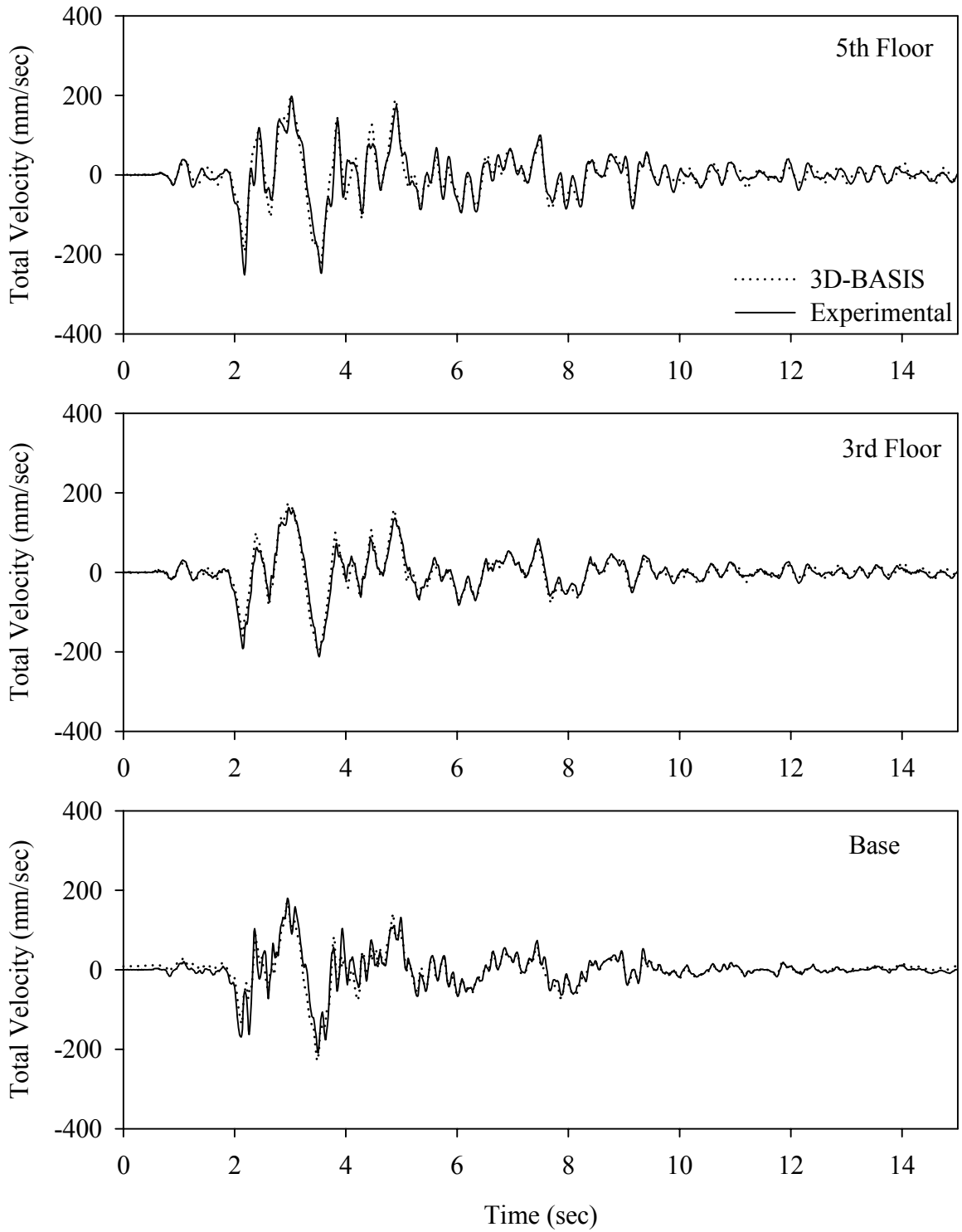


Test FPABK10.1, Kobe 100%, AB/FPS

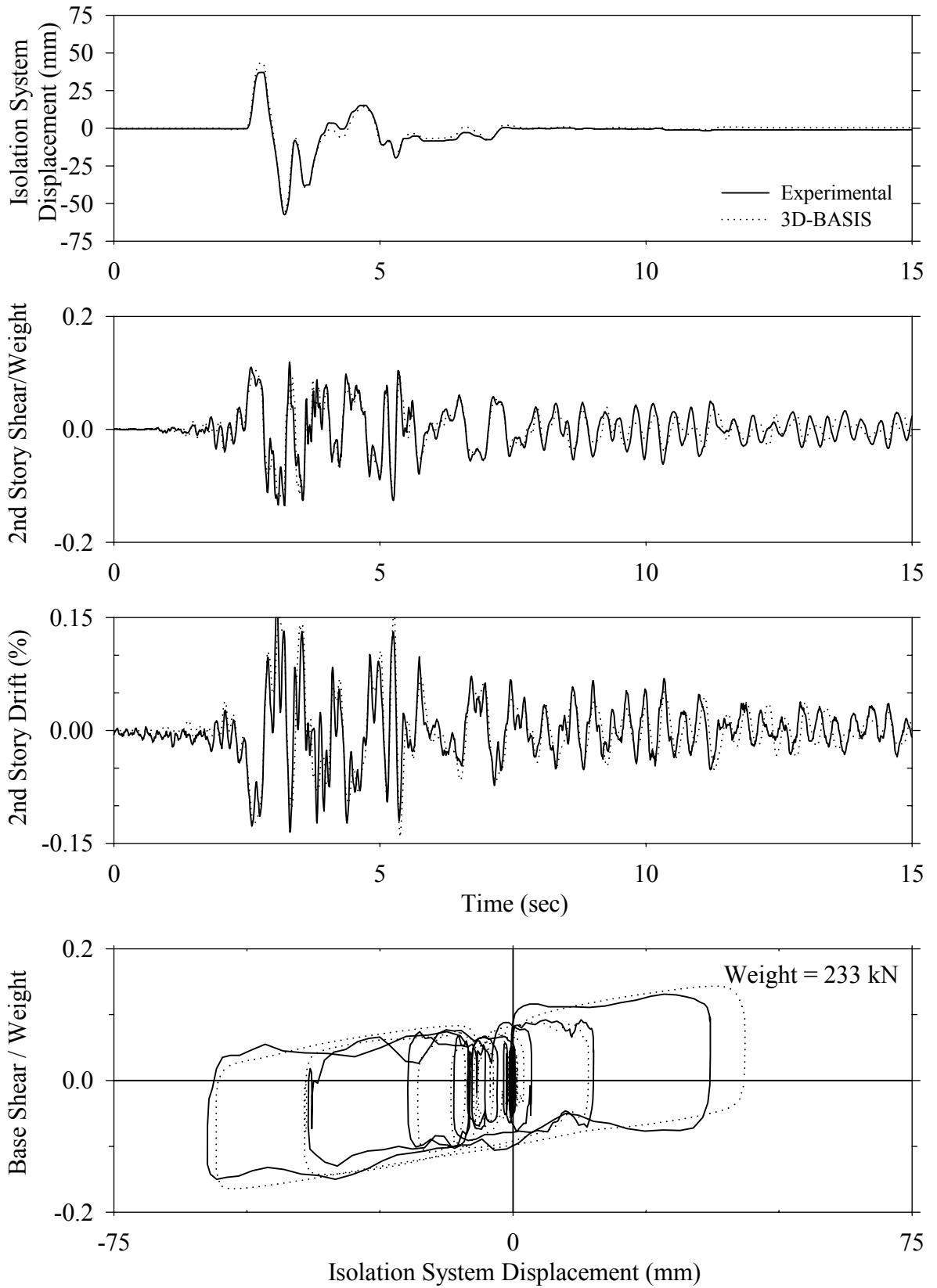




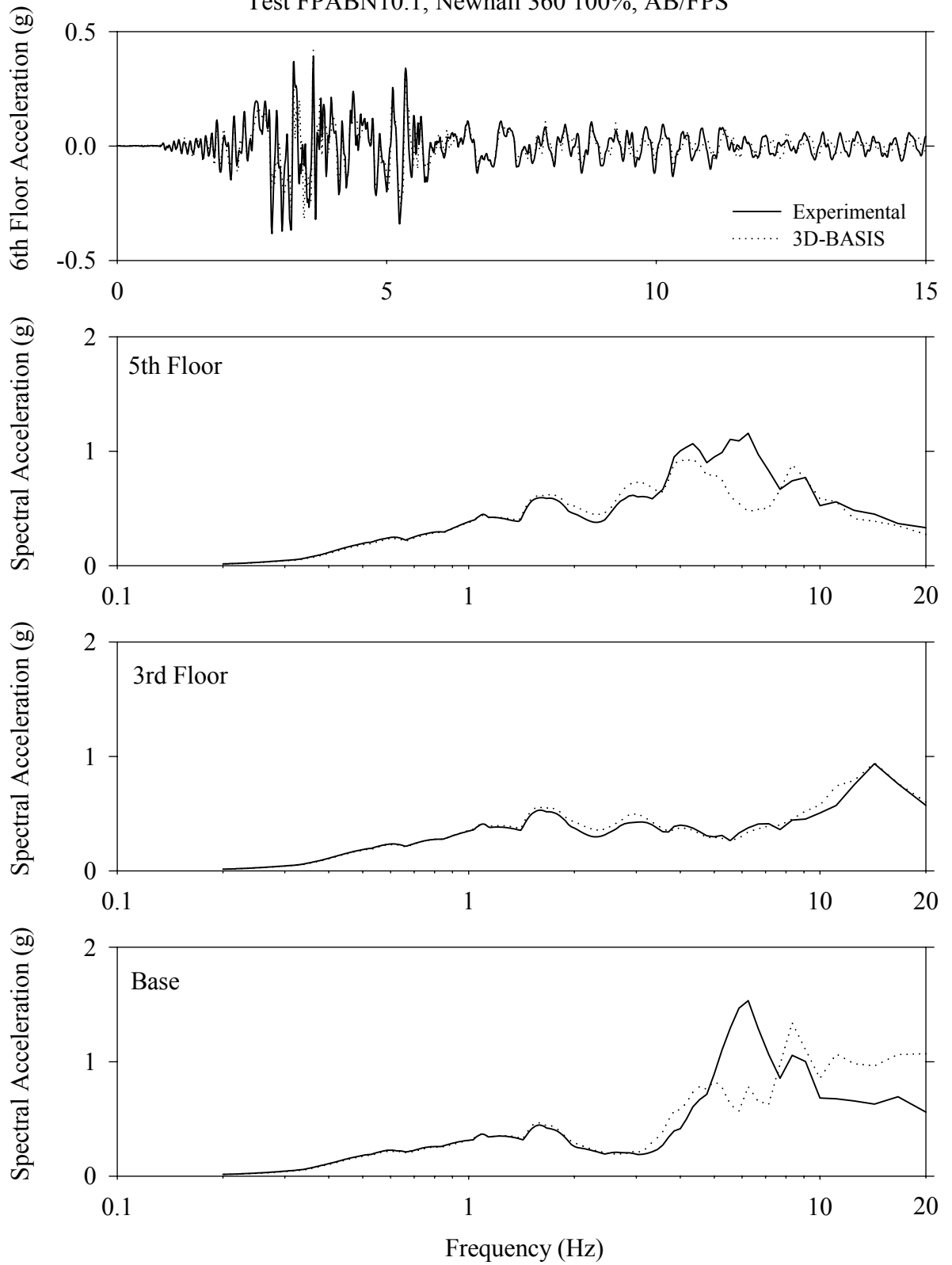
Test FPABK10.1, Kobe 100%, AB/FPS



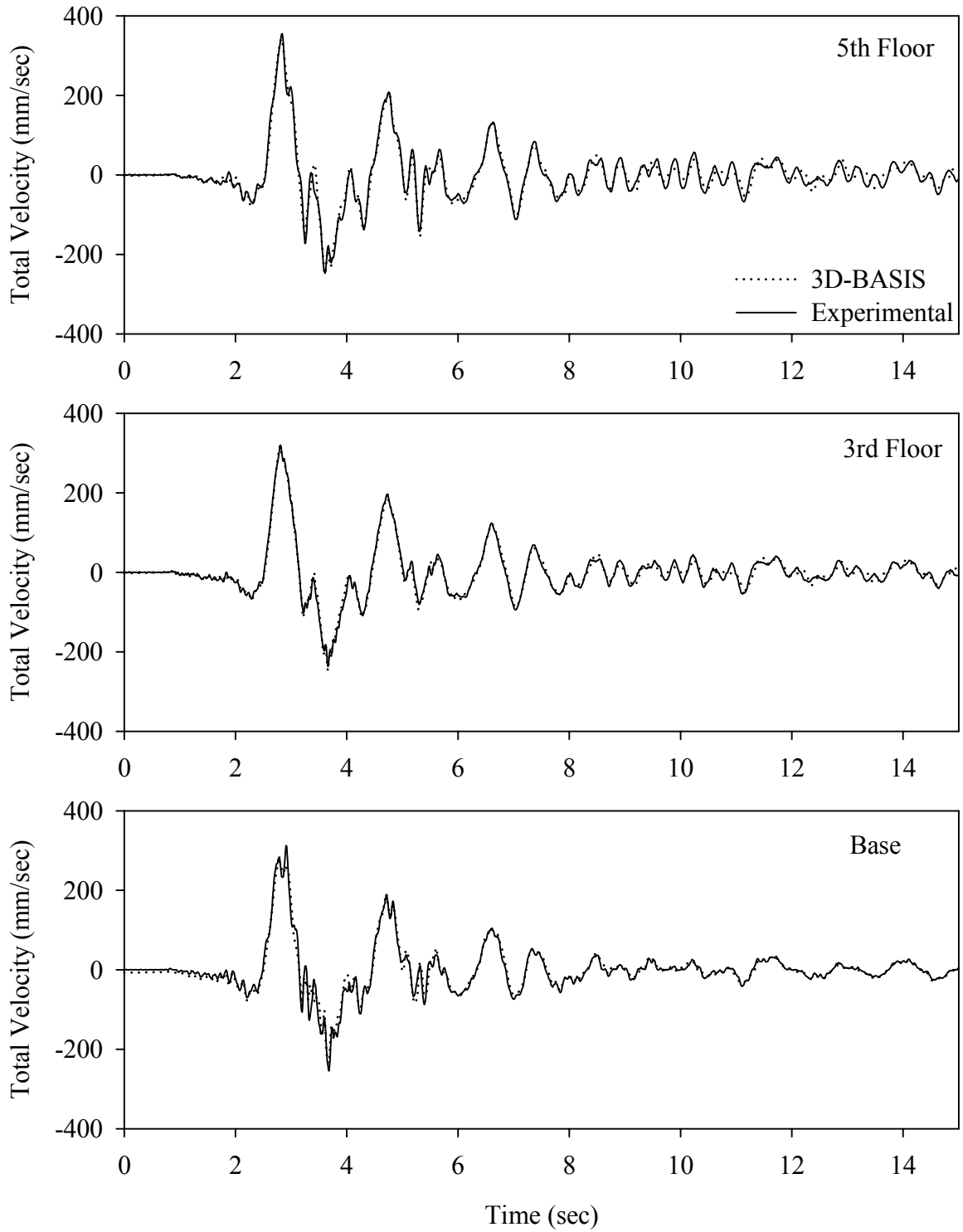
Test FPABN10.1, Newhall 360 100%, AB/FPS



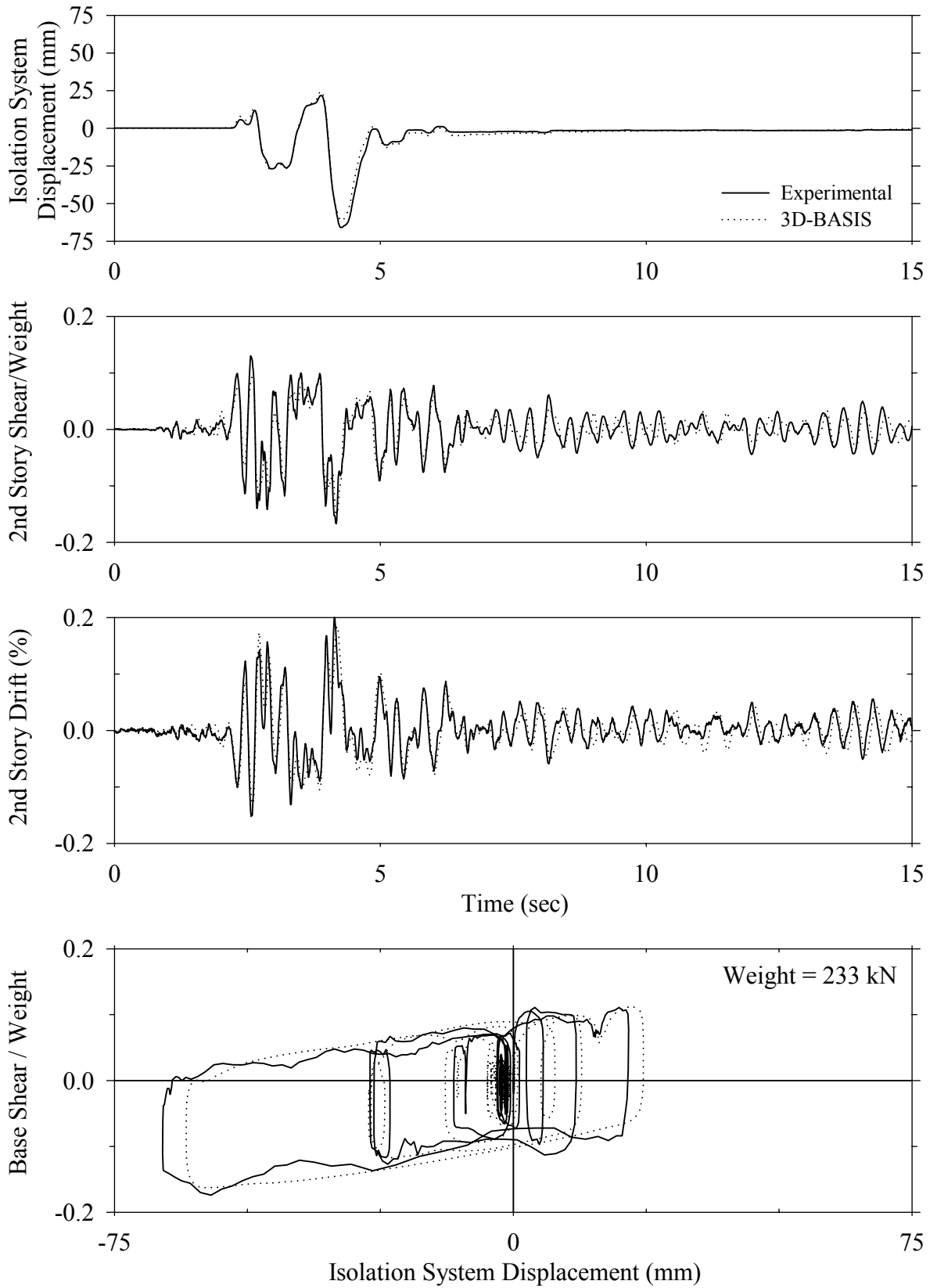
Test FPABN10.1, Newhall 360 100%, AB/FPS



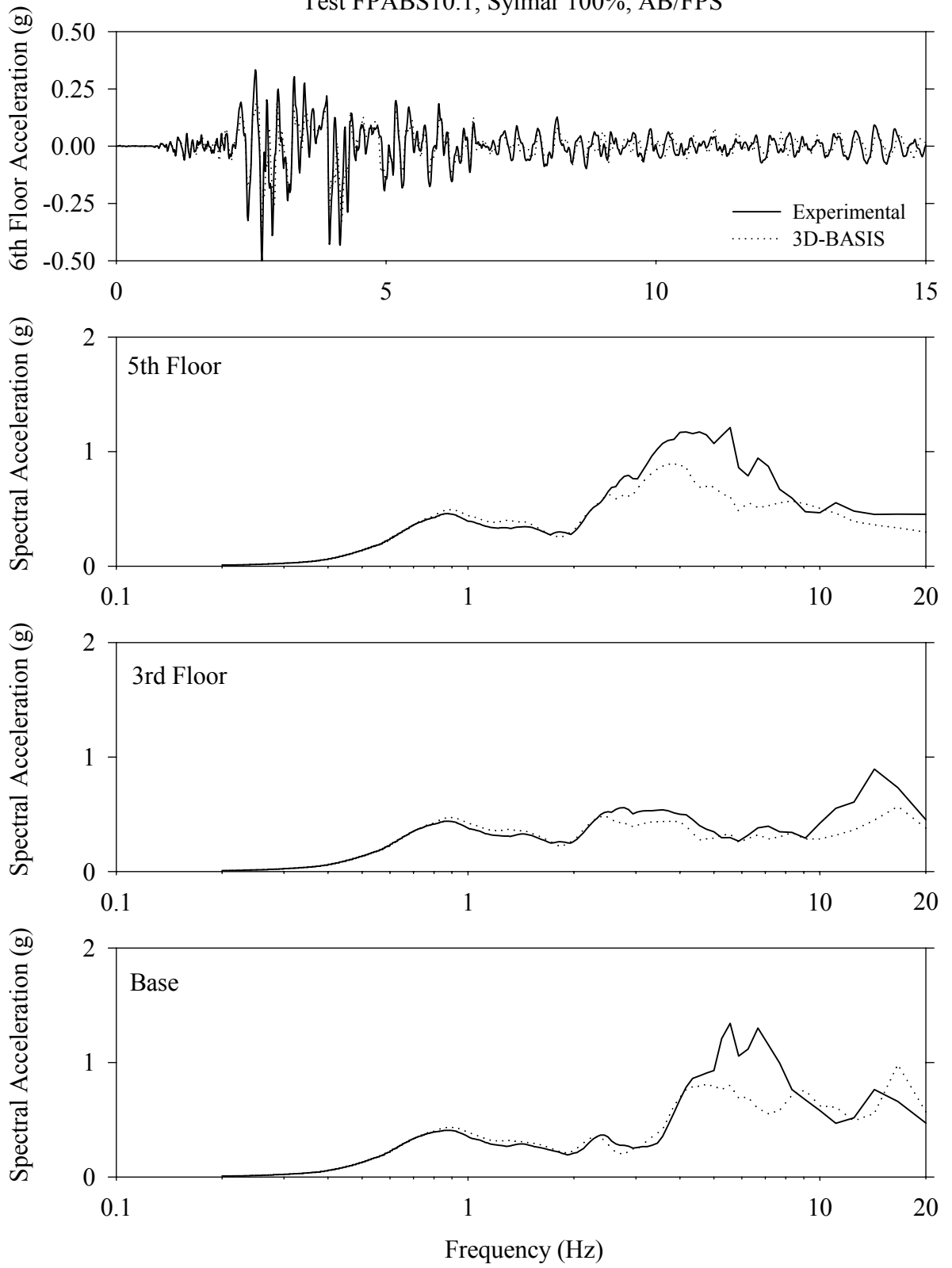
Test FPABN10.1, Newhall 360 100%, AB/FPS



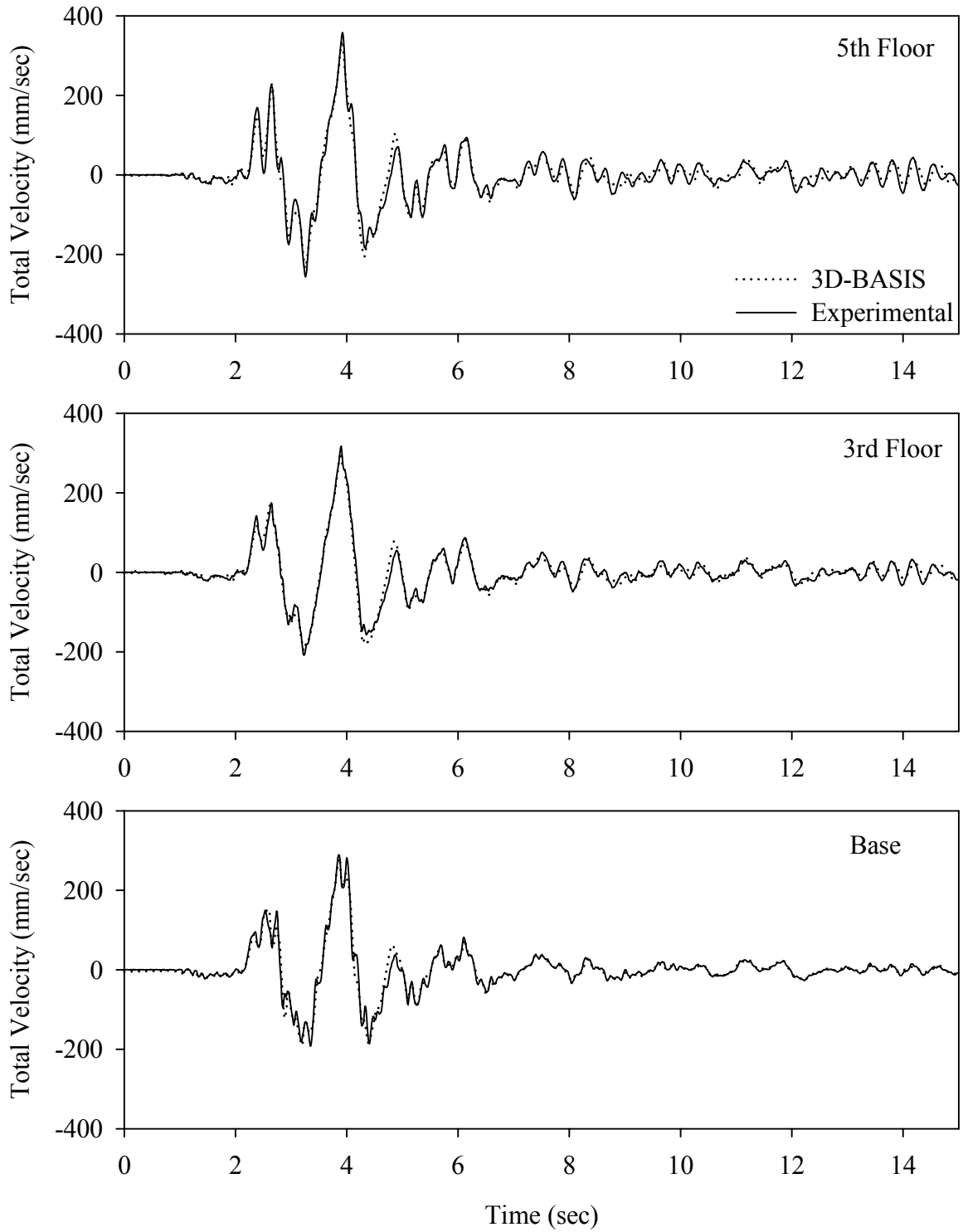
Test FPABS10.1, Sylmar 100%, AB/FPS



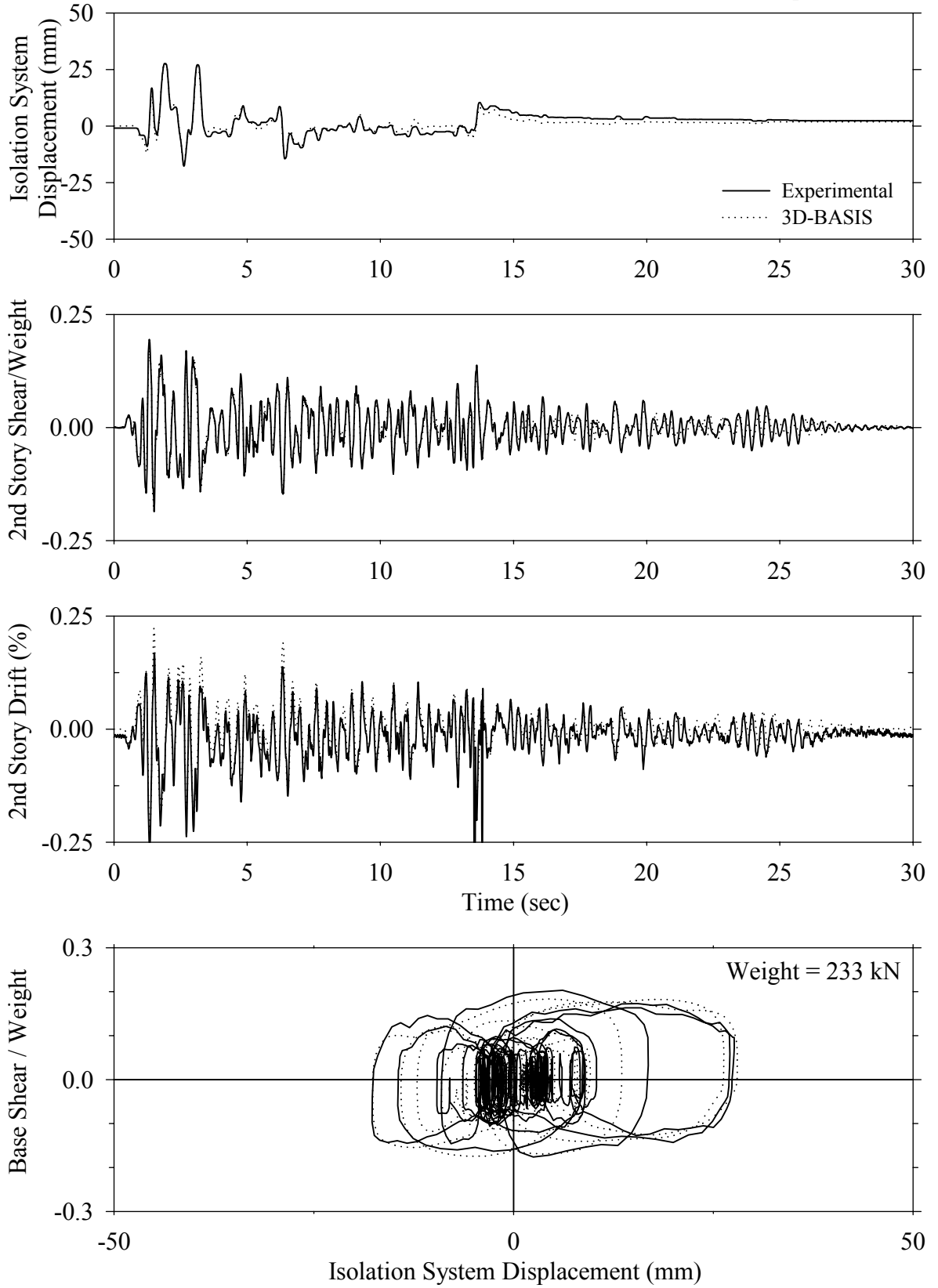
Test FPABS10.1, Sylmar 100%, AB/FPS



Test FPABS10.1, Sylmar 100%, AB/FPS

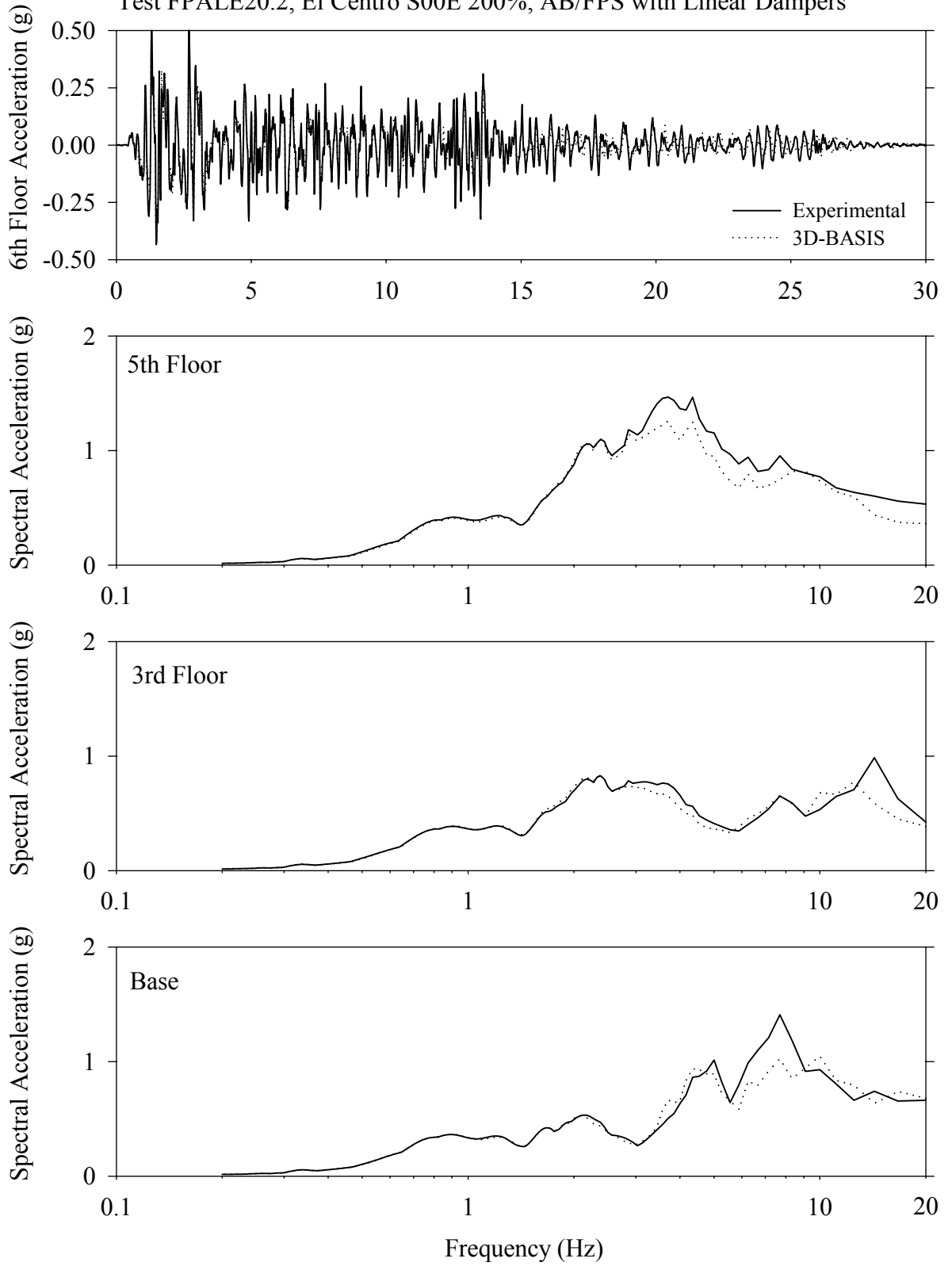


Test FPALE20.2, El Centro S00E 200%, AB/FPS with Linear Dampers

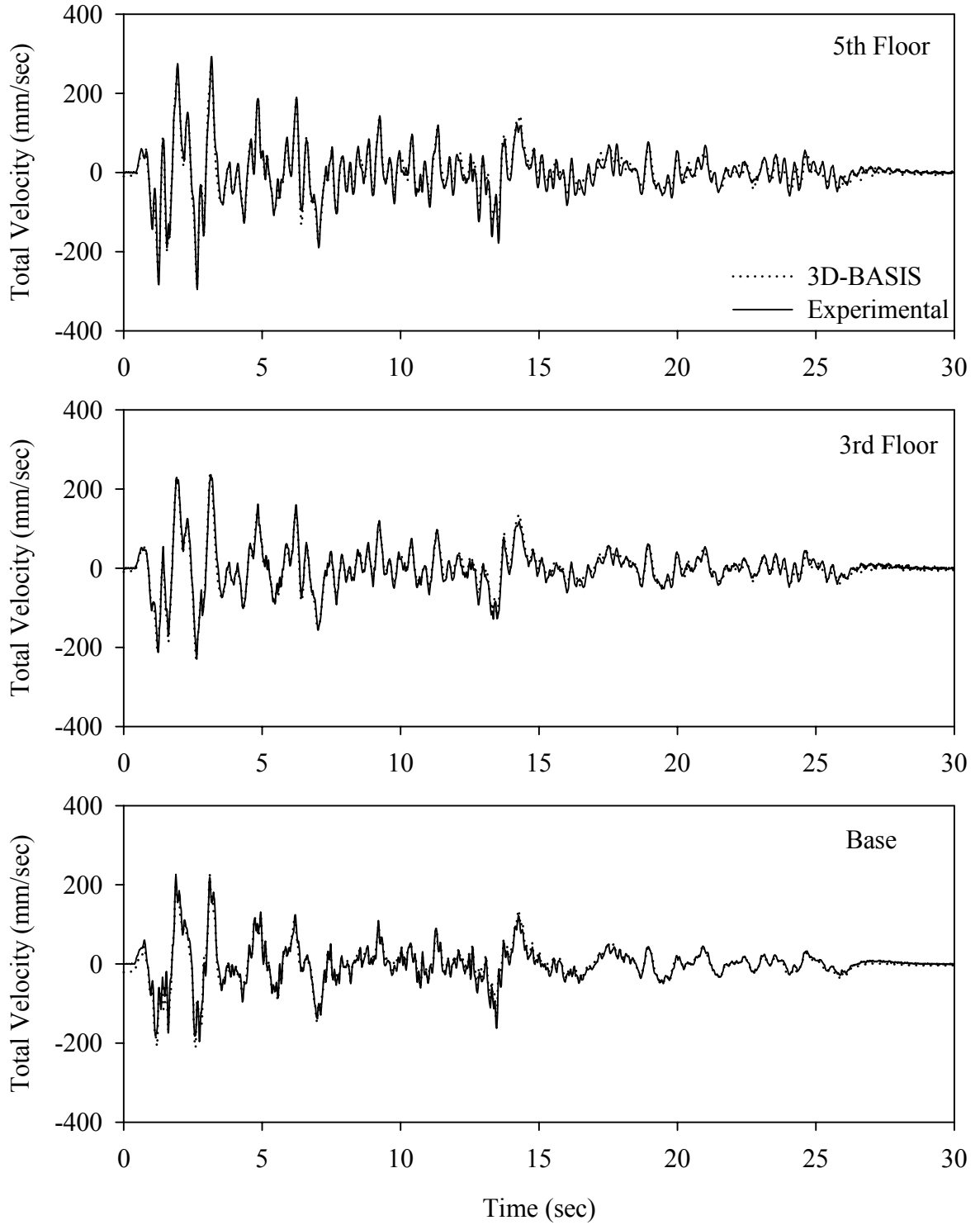




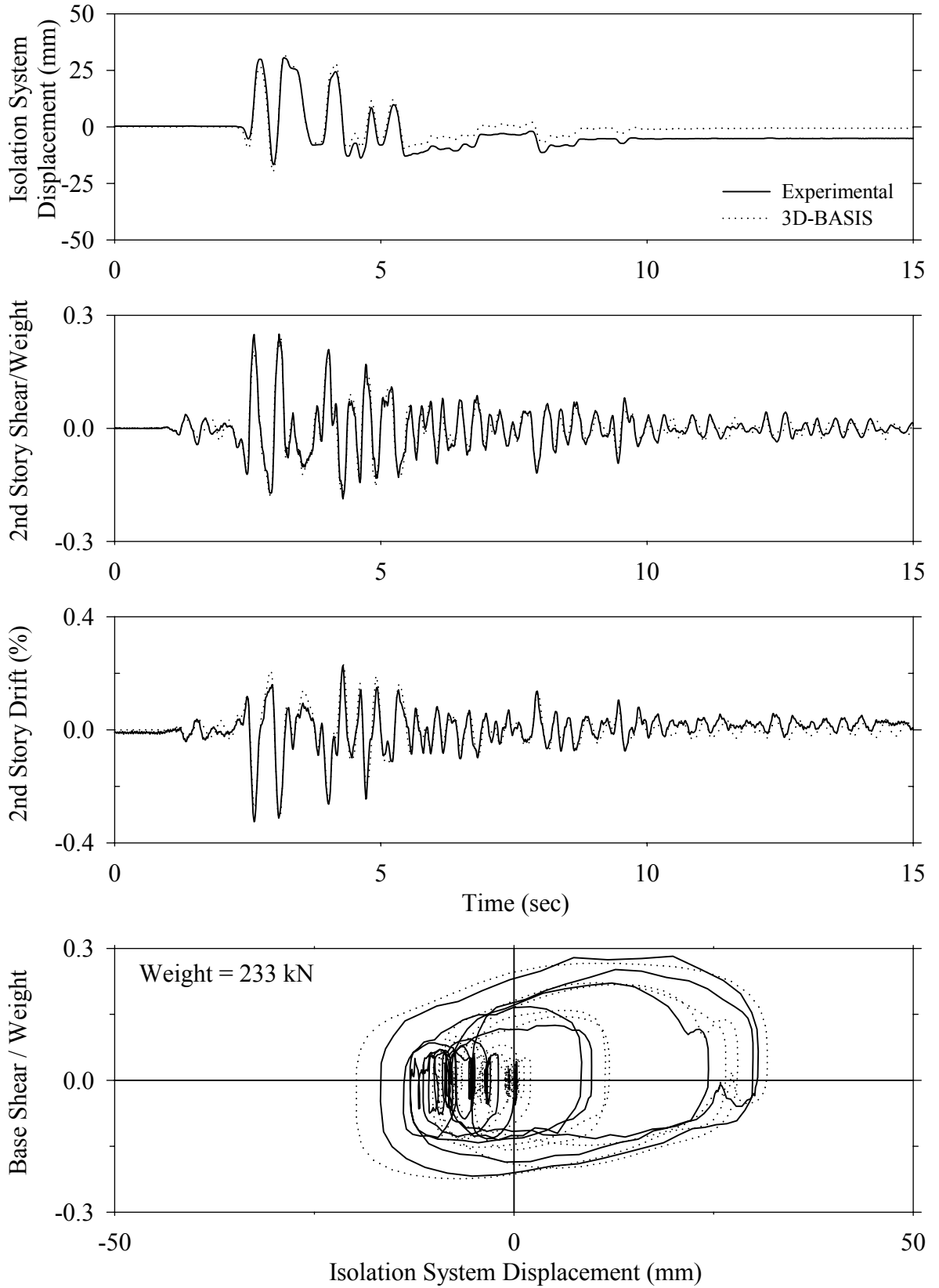
Test FPALE20.2, El Centro S00E 200%, AB/FPS with Linear Dampers



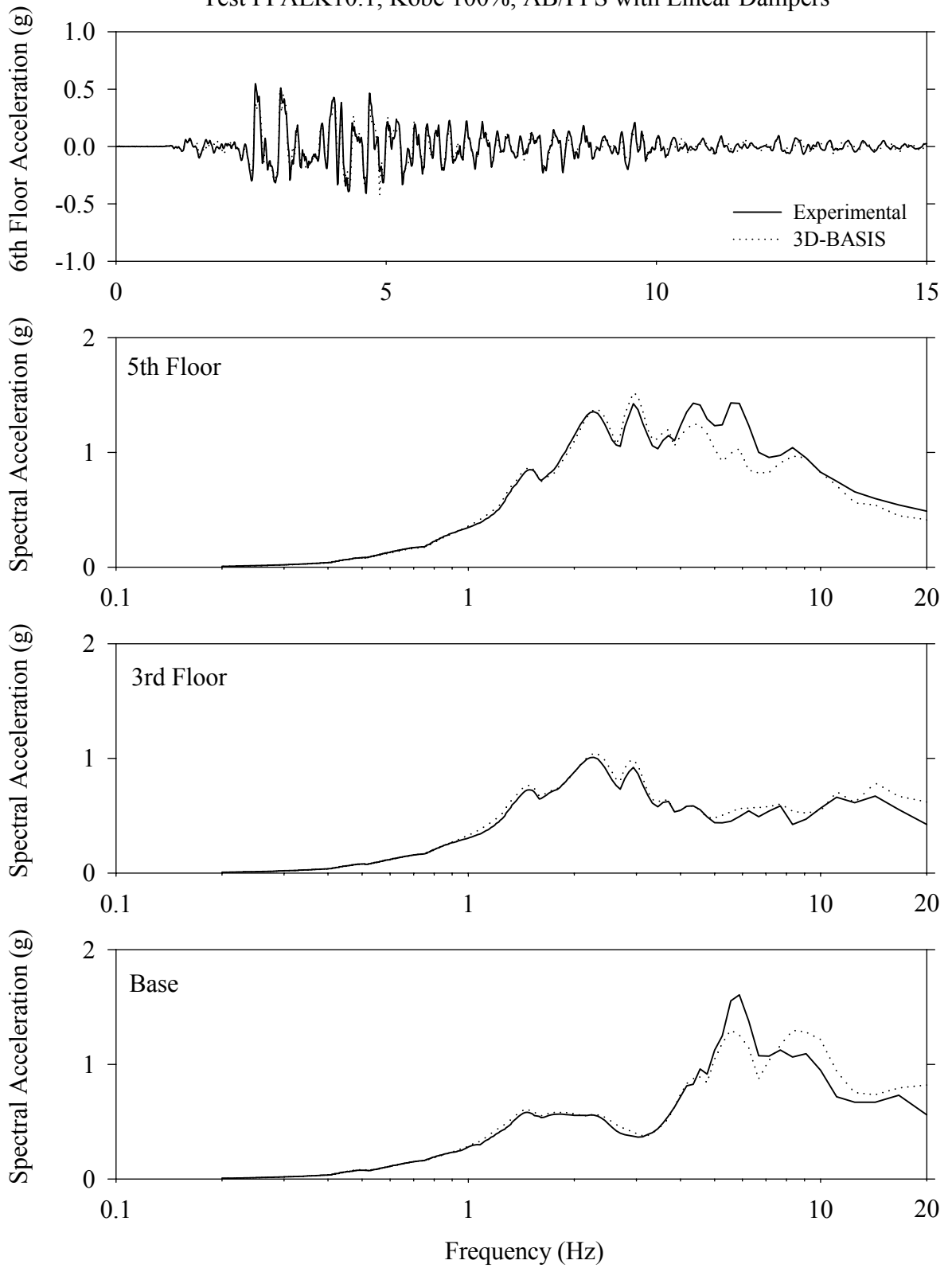
Test FPALE20.1, El Centro S00E 200%, AB/FPS with Linear Dampers



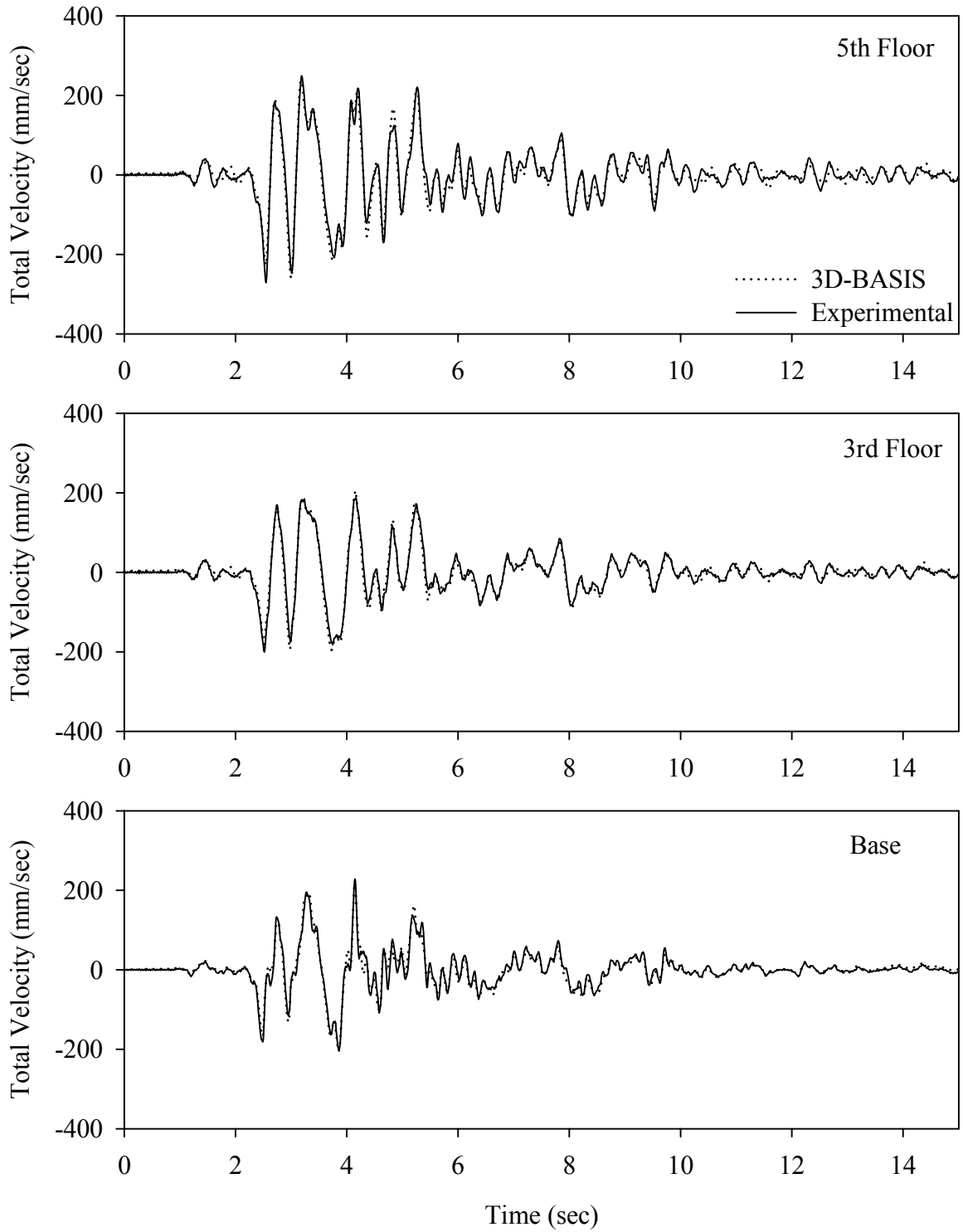
Test FPALK10.1, Kobe 100%, AB/FPS with Linear Dampers



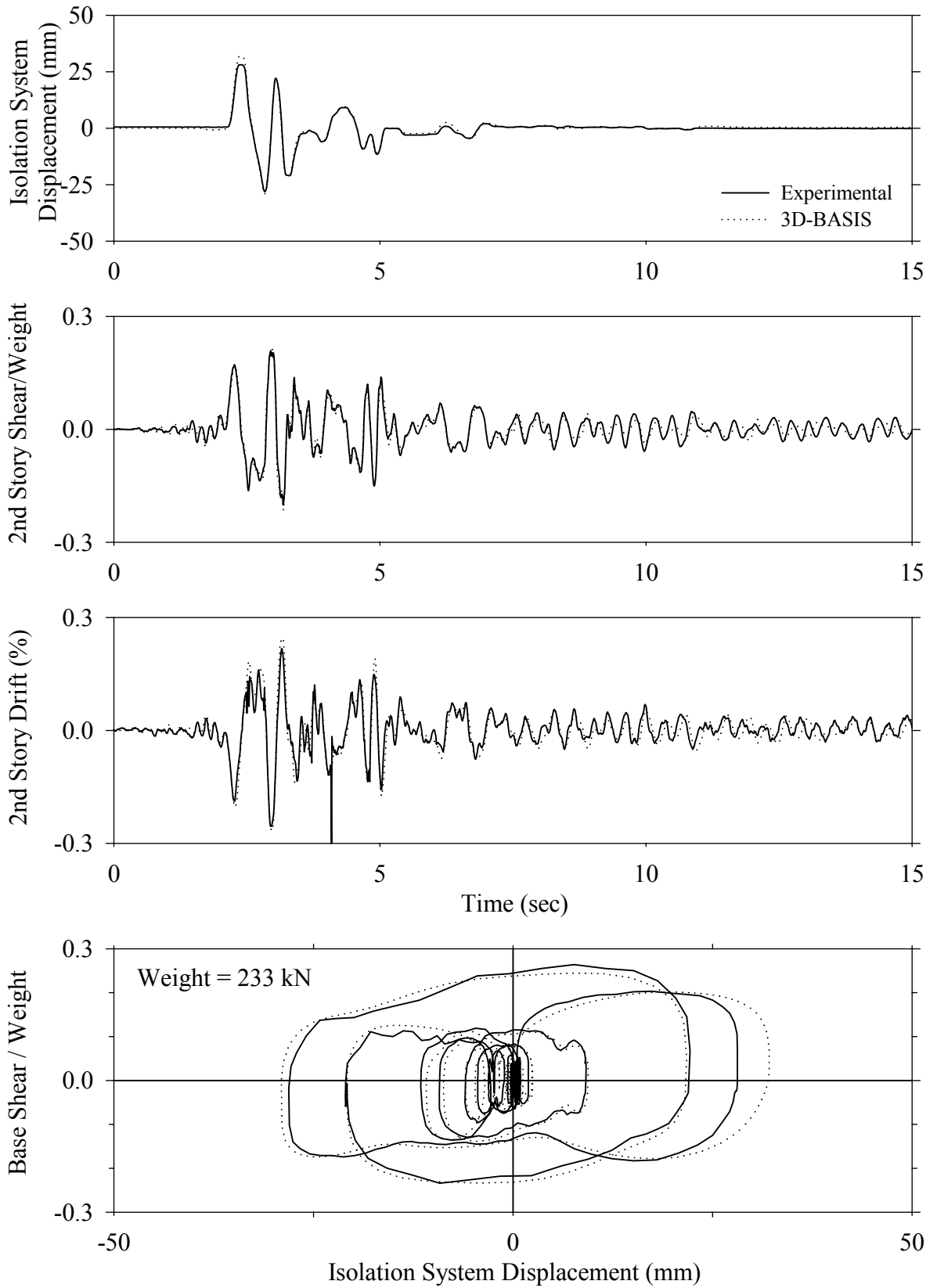
Test FPALK10.1, Kobe 100%, AB/FPS with Linear Dampers



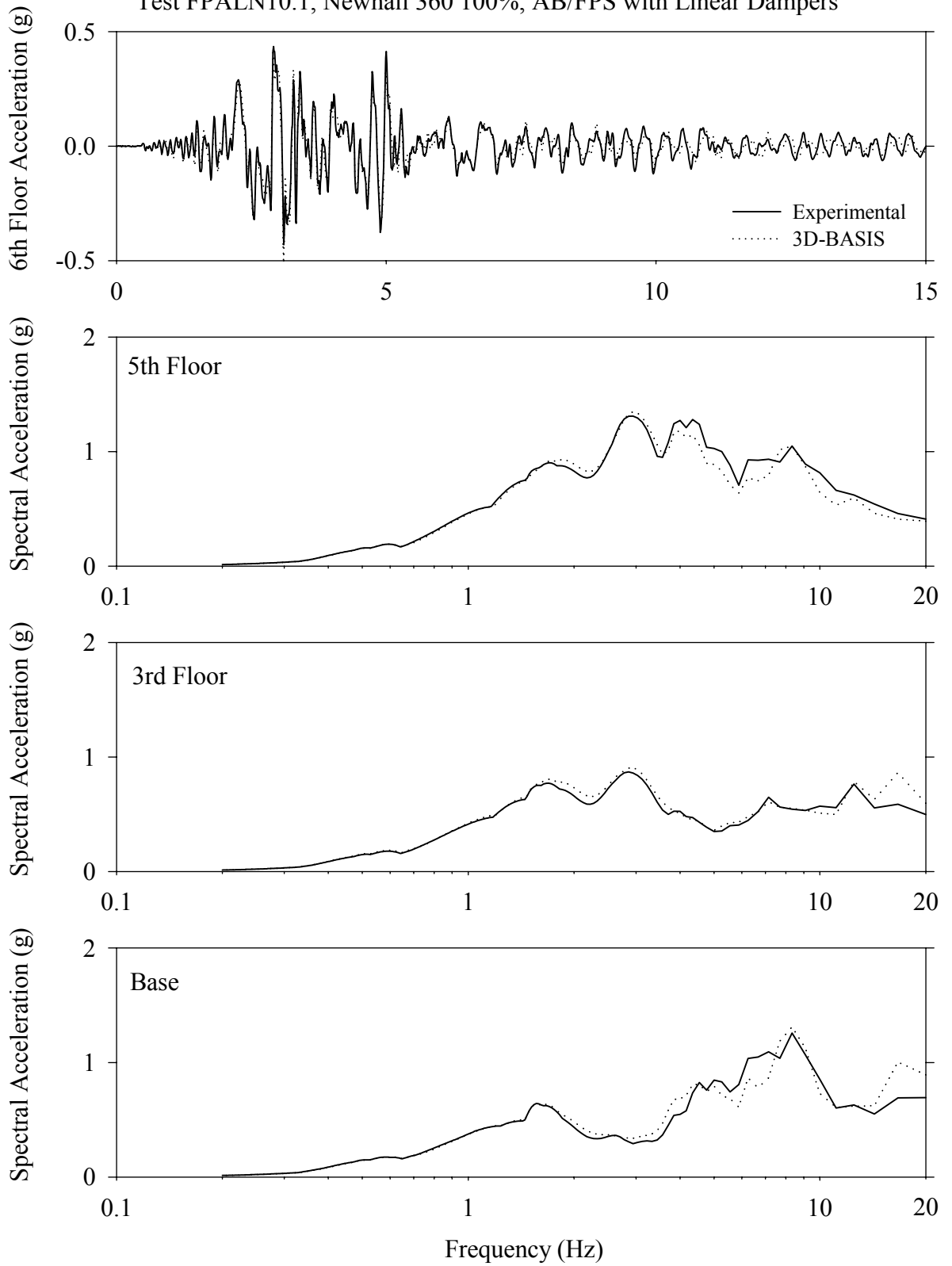
Test FPALK10.1, Kobe 100%, AB/FPS with Linear Dampers



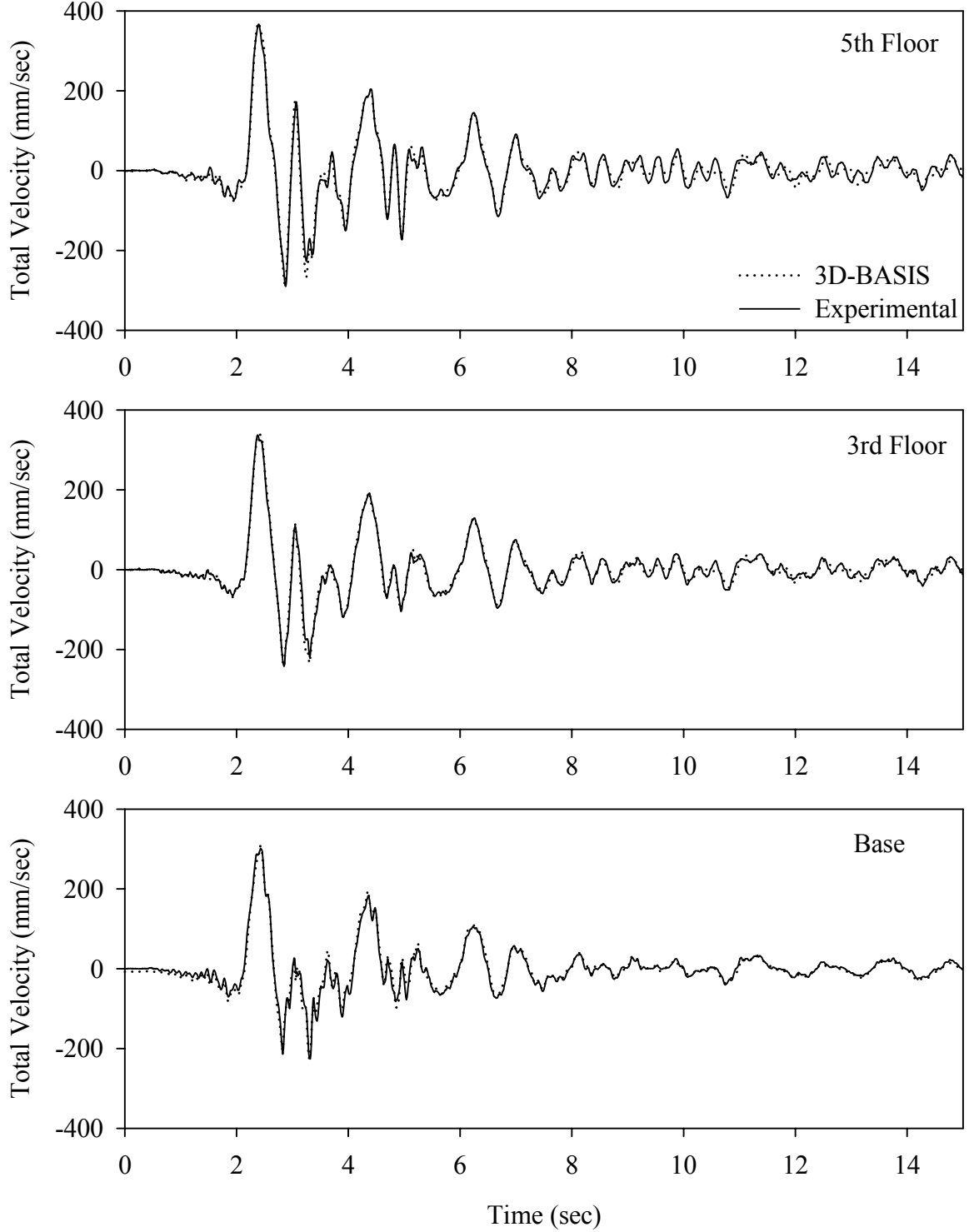
Test FPALN10.1, Newhall 360 100%, AB/FPS with Linear Dampers



Test FPALN10.1, Newhall 360 100%, AB/FPS with Linear Dampers

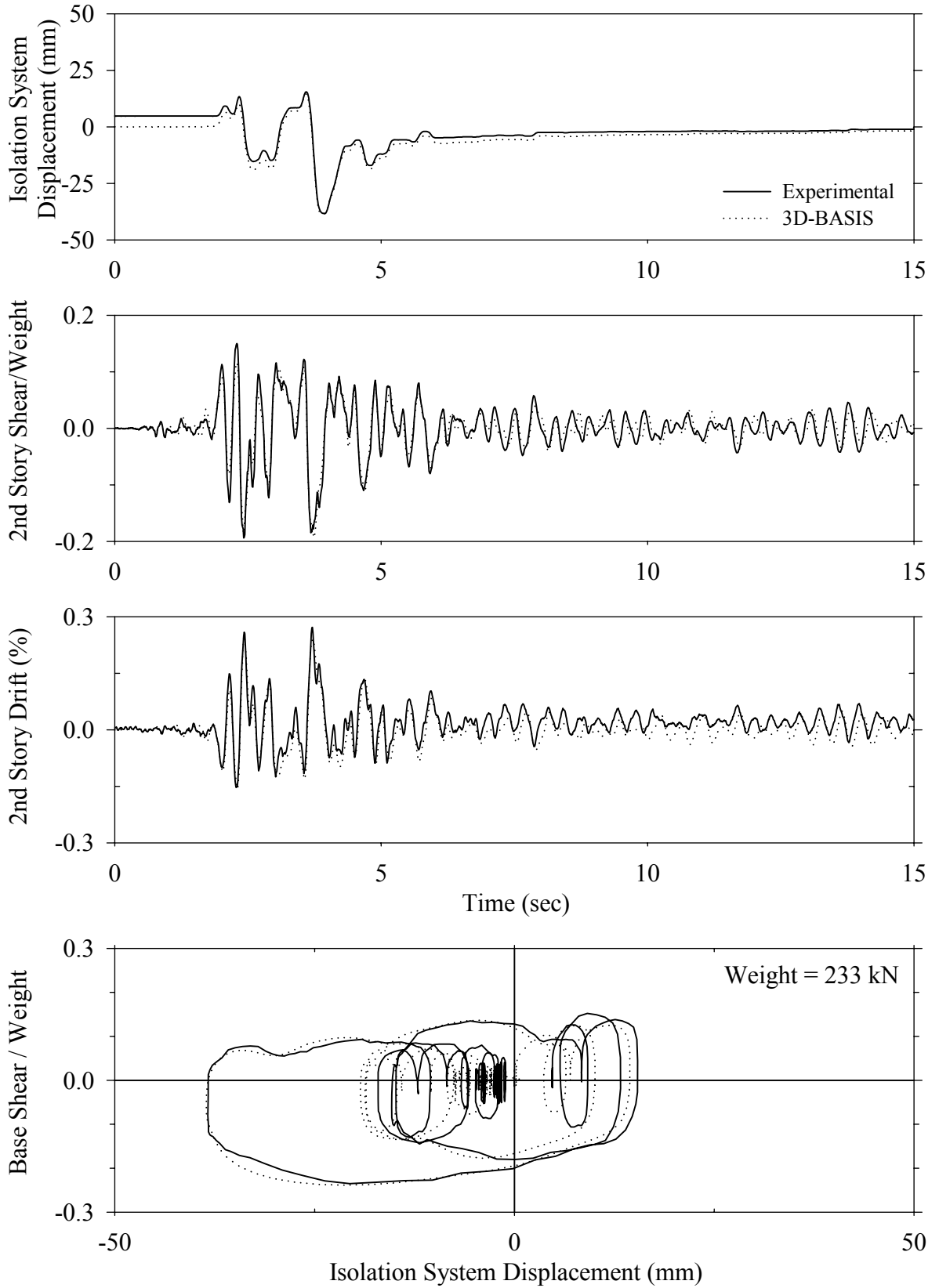


Test FPALN10.1, Newhall 360 100%, AB/FPS with Linear Dampers

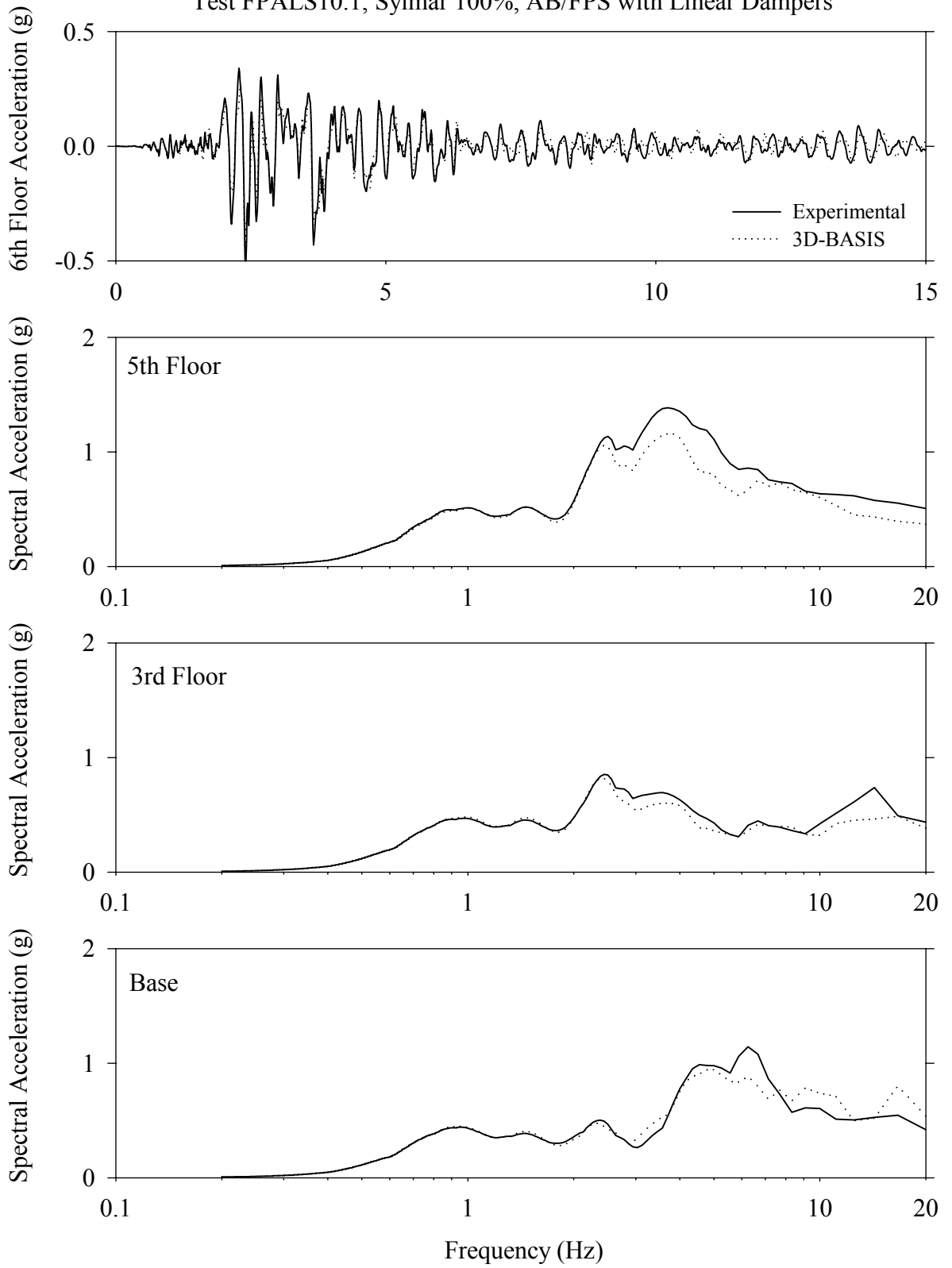




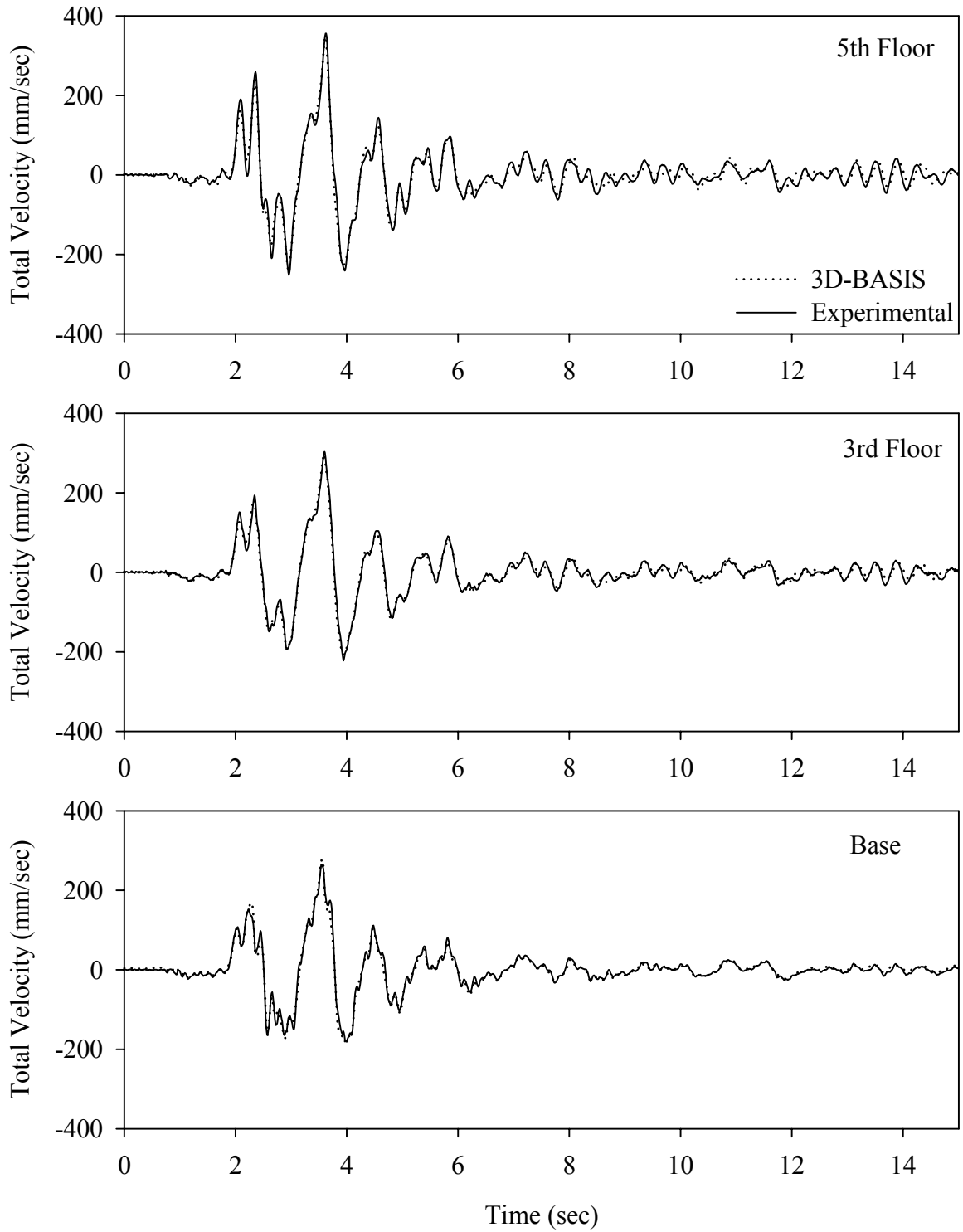
Test FPALS10.1, Sylmar 100%, AB/FPS with Linear Dampers



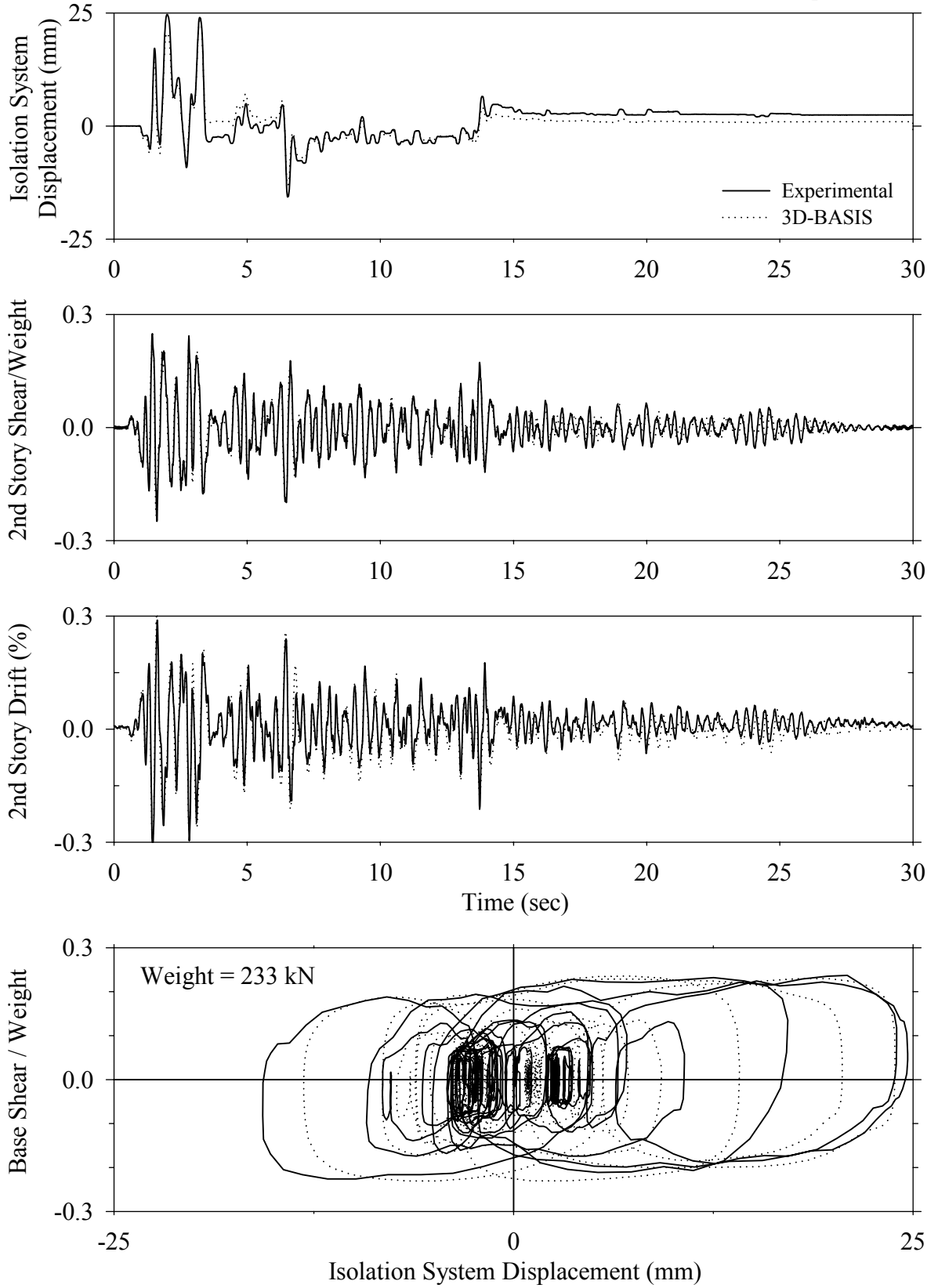
Test FPALS10.1, Sylmar 100%, AB/FPS with Linear Dampers



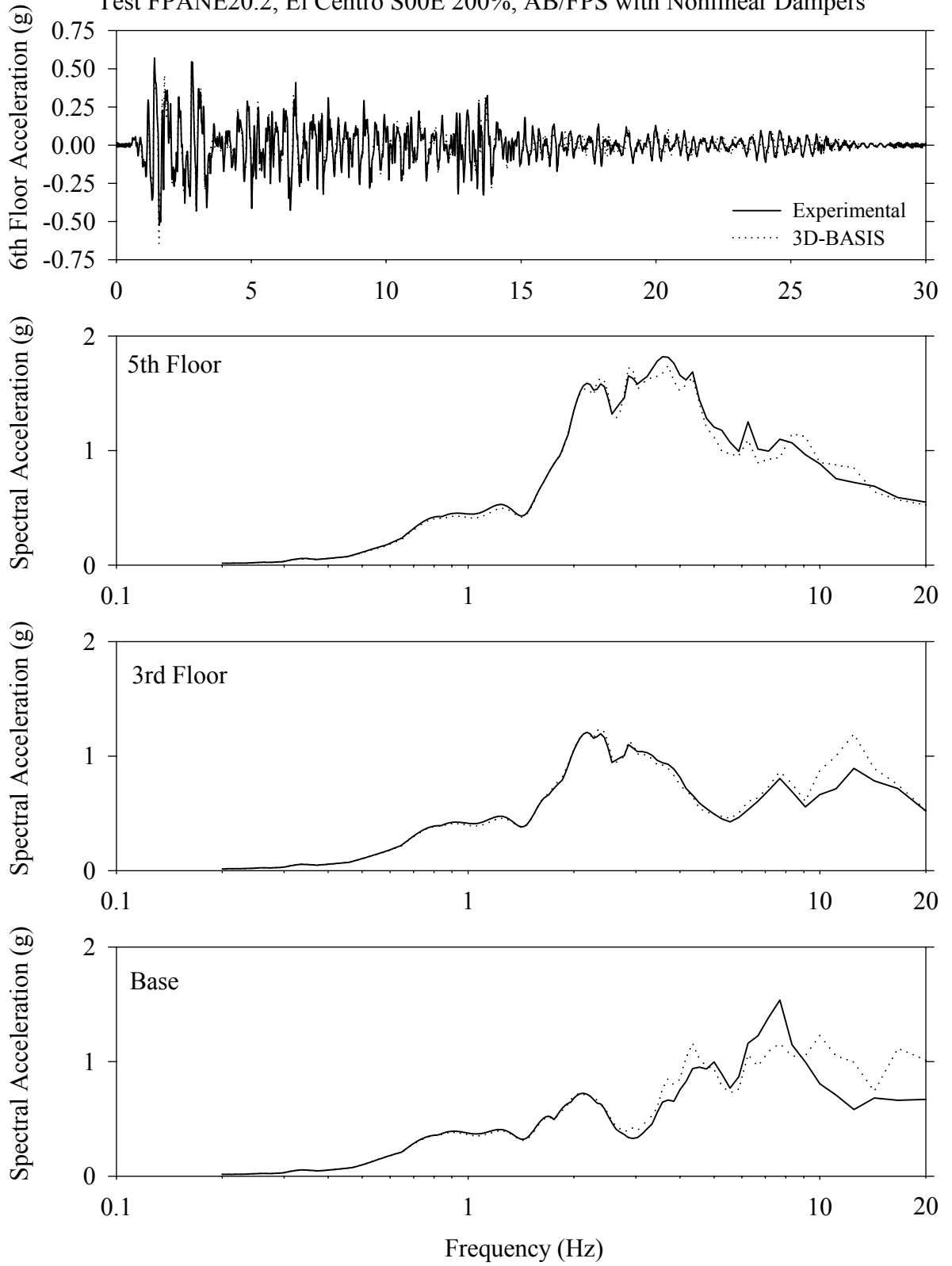
Test FPALS10.1, Sylmar 100%, AB/FPS with Linear Dampers



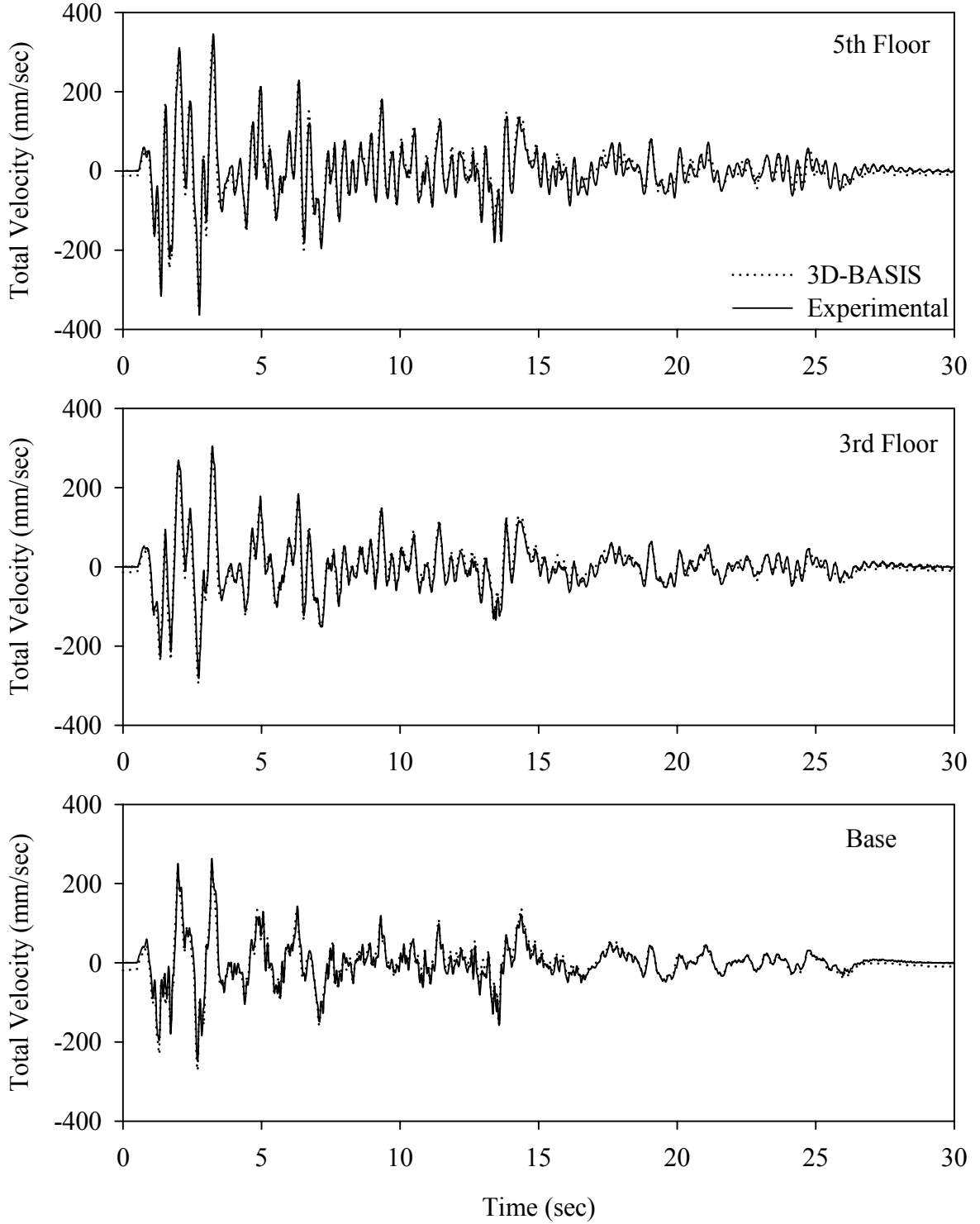
Test FPANE20.2, El Centro S00E 200%, AB/FPS with Nonlinear Dampers



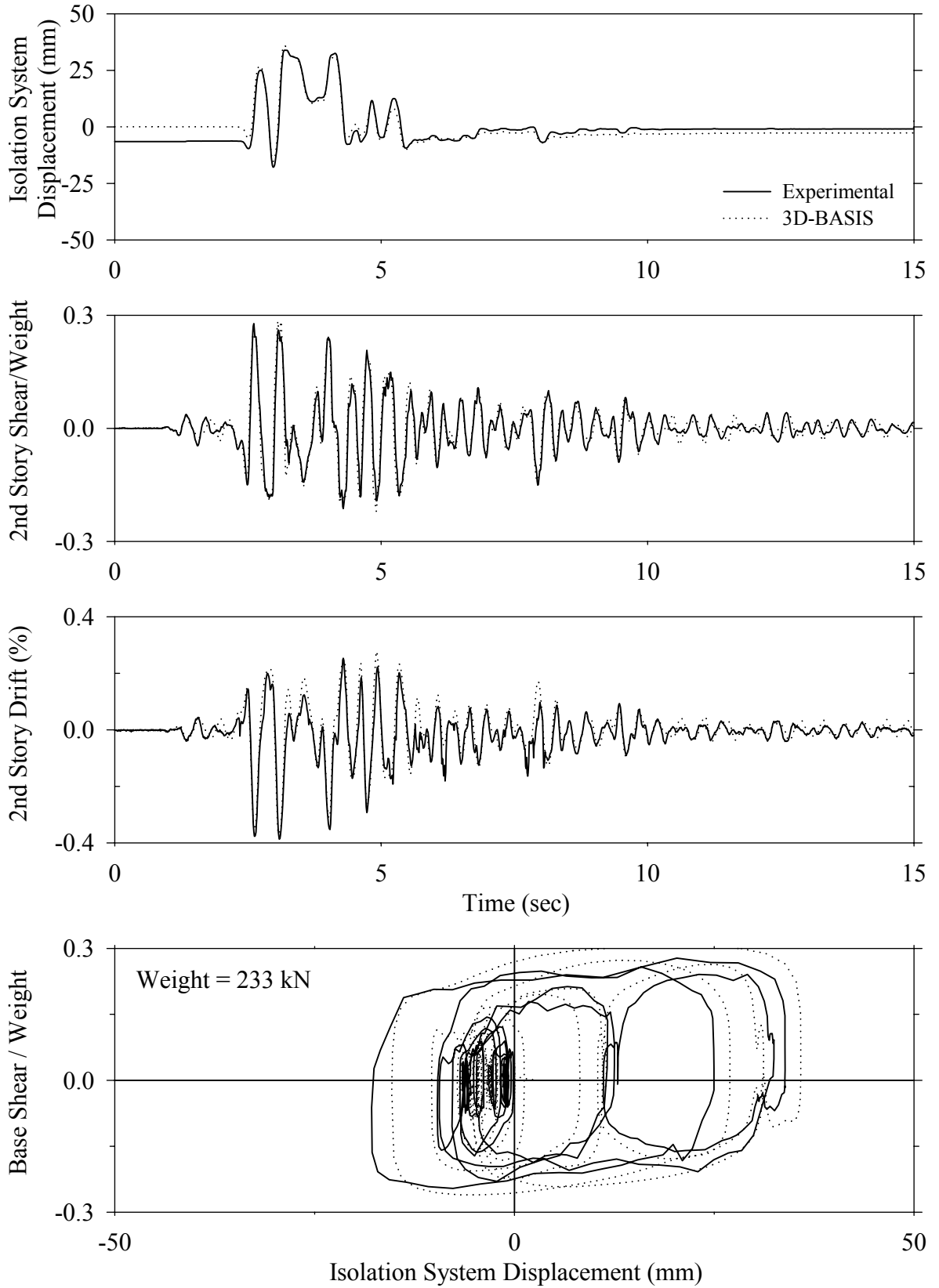
Test FPANE20.2, El Centro S00E 200%, AB/FPS with Nonlinear Dampers



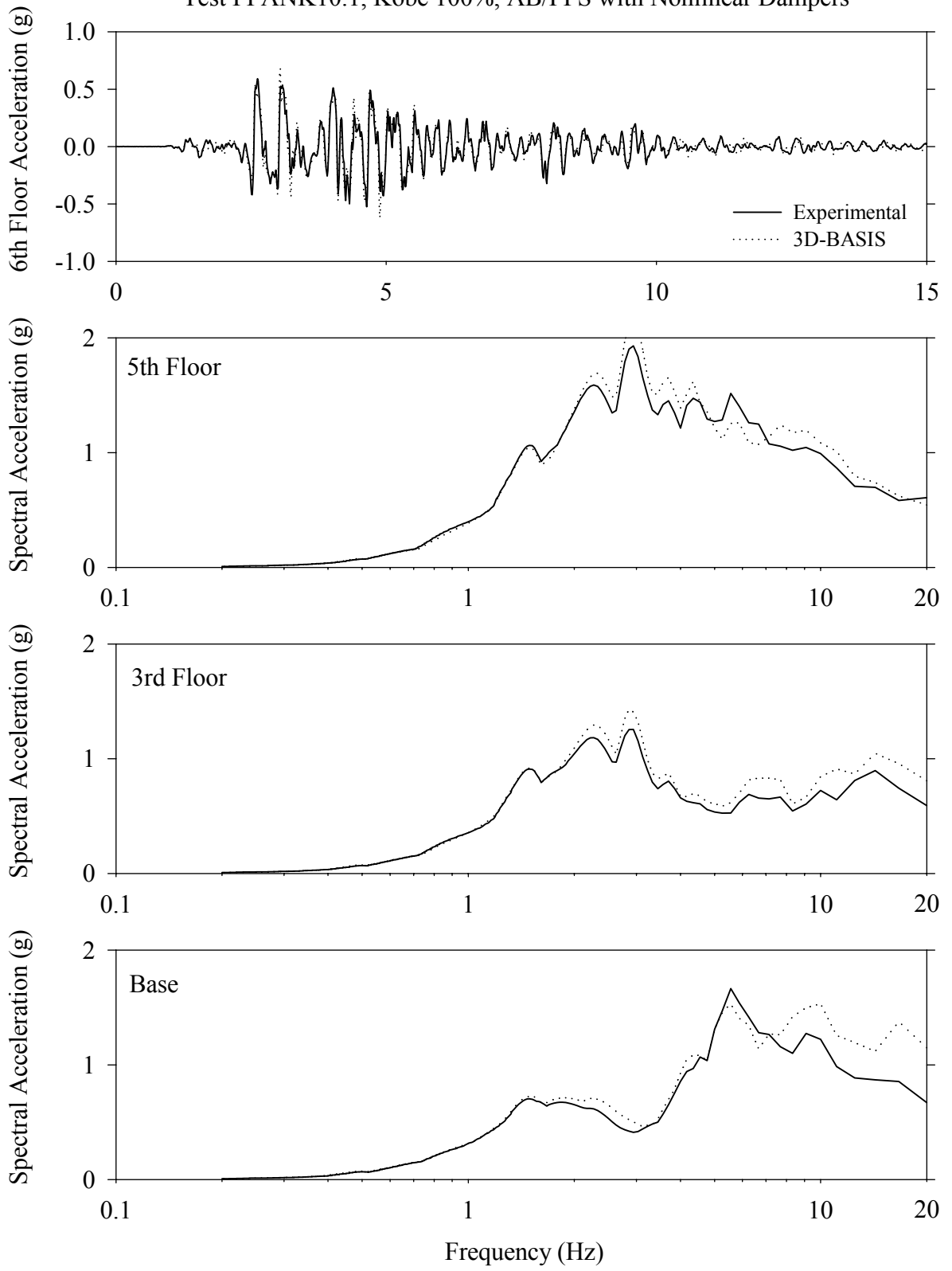
Test FPANE20.1, El Centro S00E 200%, AB/FPS with Nonlinear Dampers



Test FPANK10.1, Kobe 100%, AB/FPS with Nonlinear Dampers

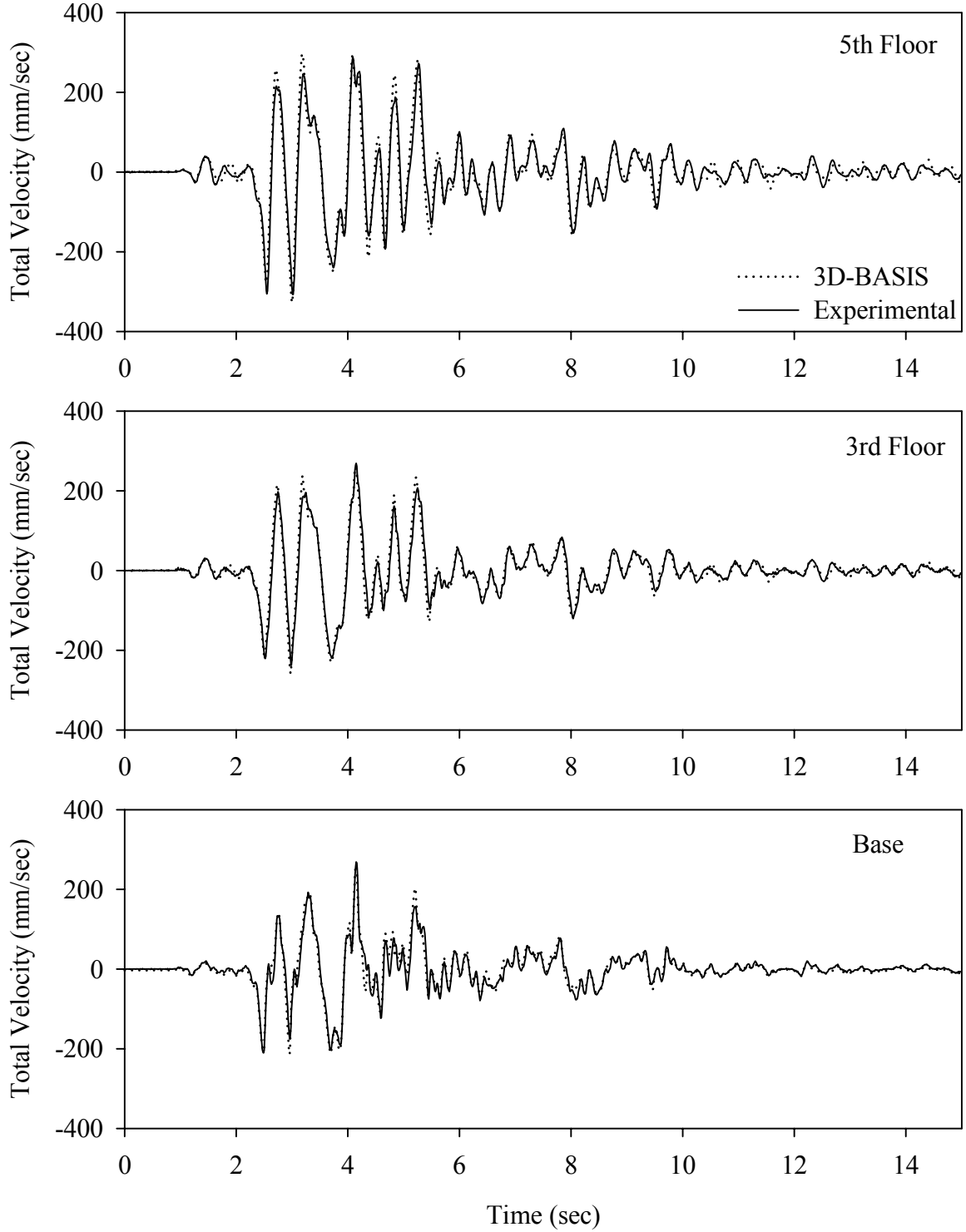


Test FPANK10.1, Kobe 100%, AB/FPS with Nonlinear Dampers

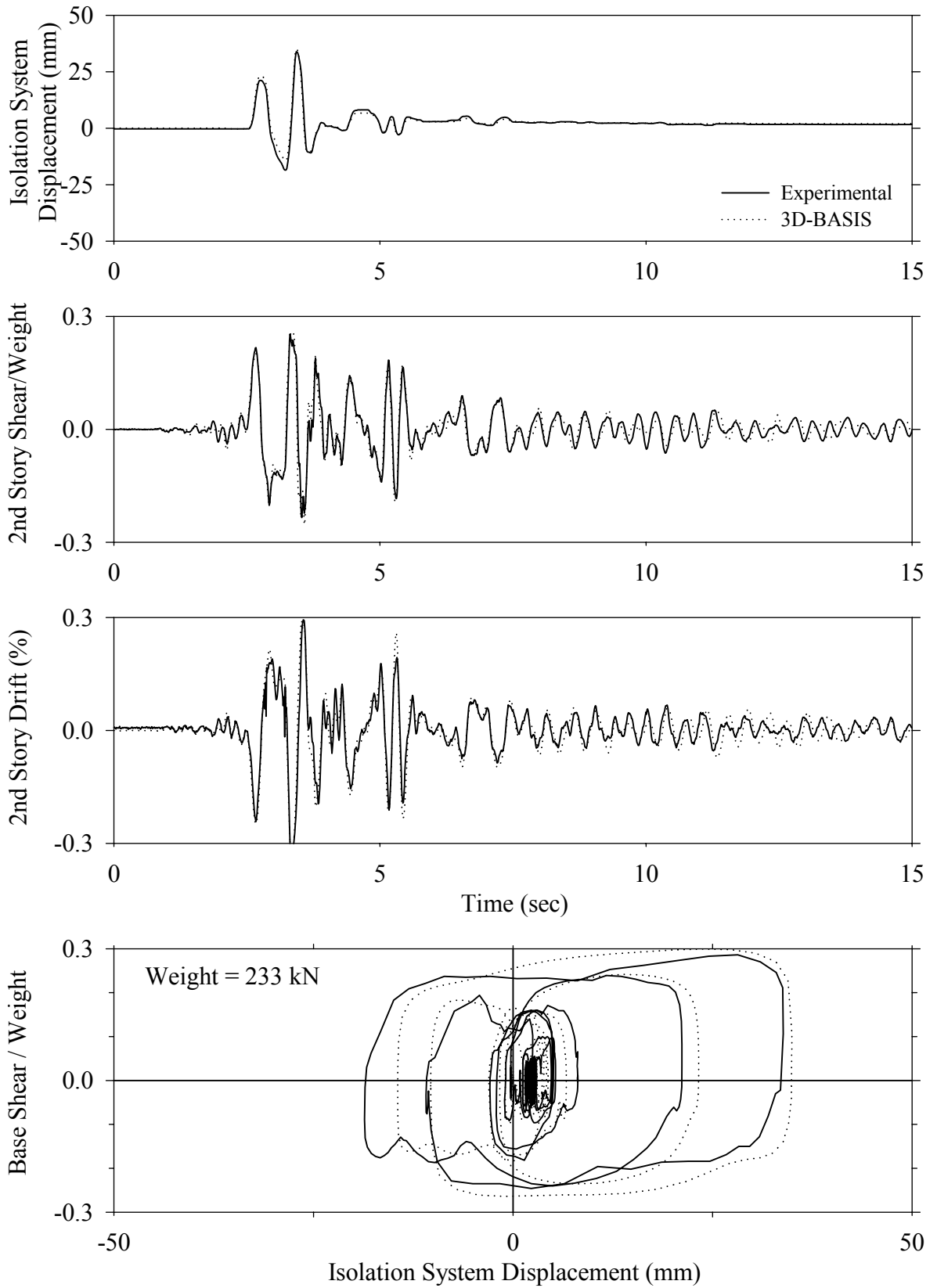




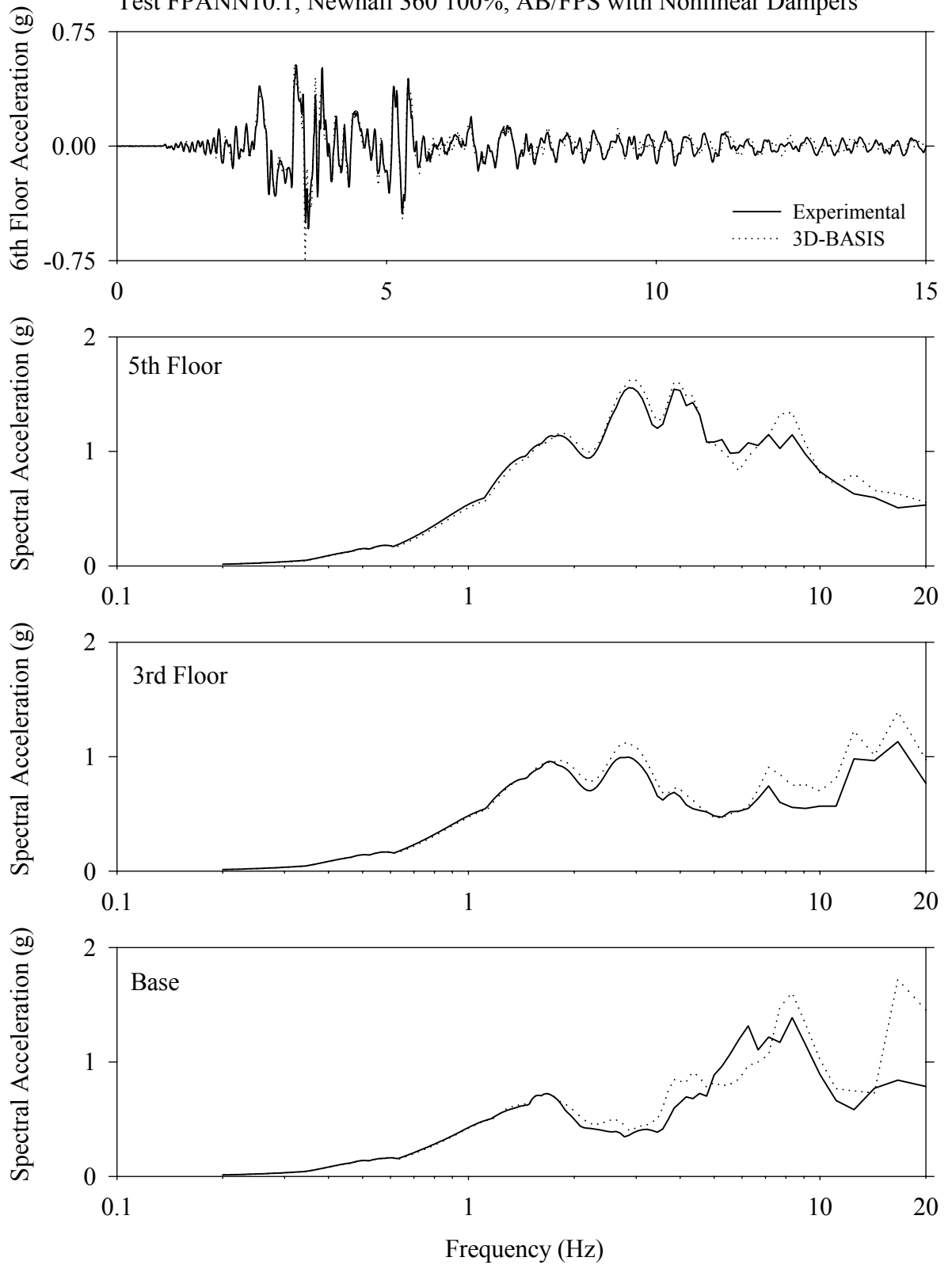
Test FPANK10.1, Kobe 100%, AB/FPS with Nonlinear Dampers



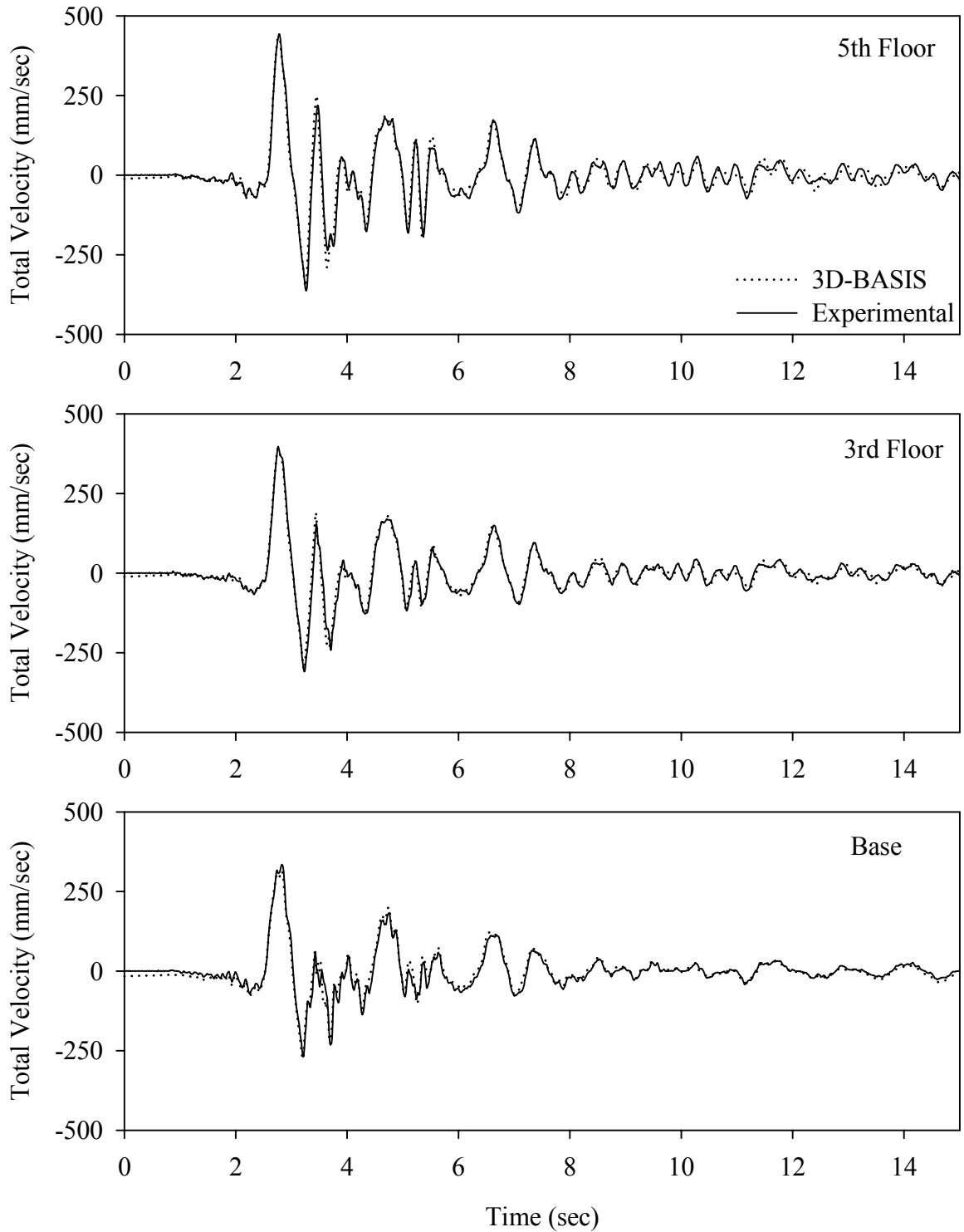
Test FPANN10.1, Newhall 360 100%, AB/FPS with Nonlinear Dampers



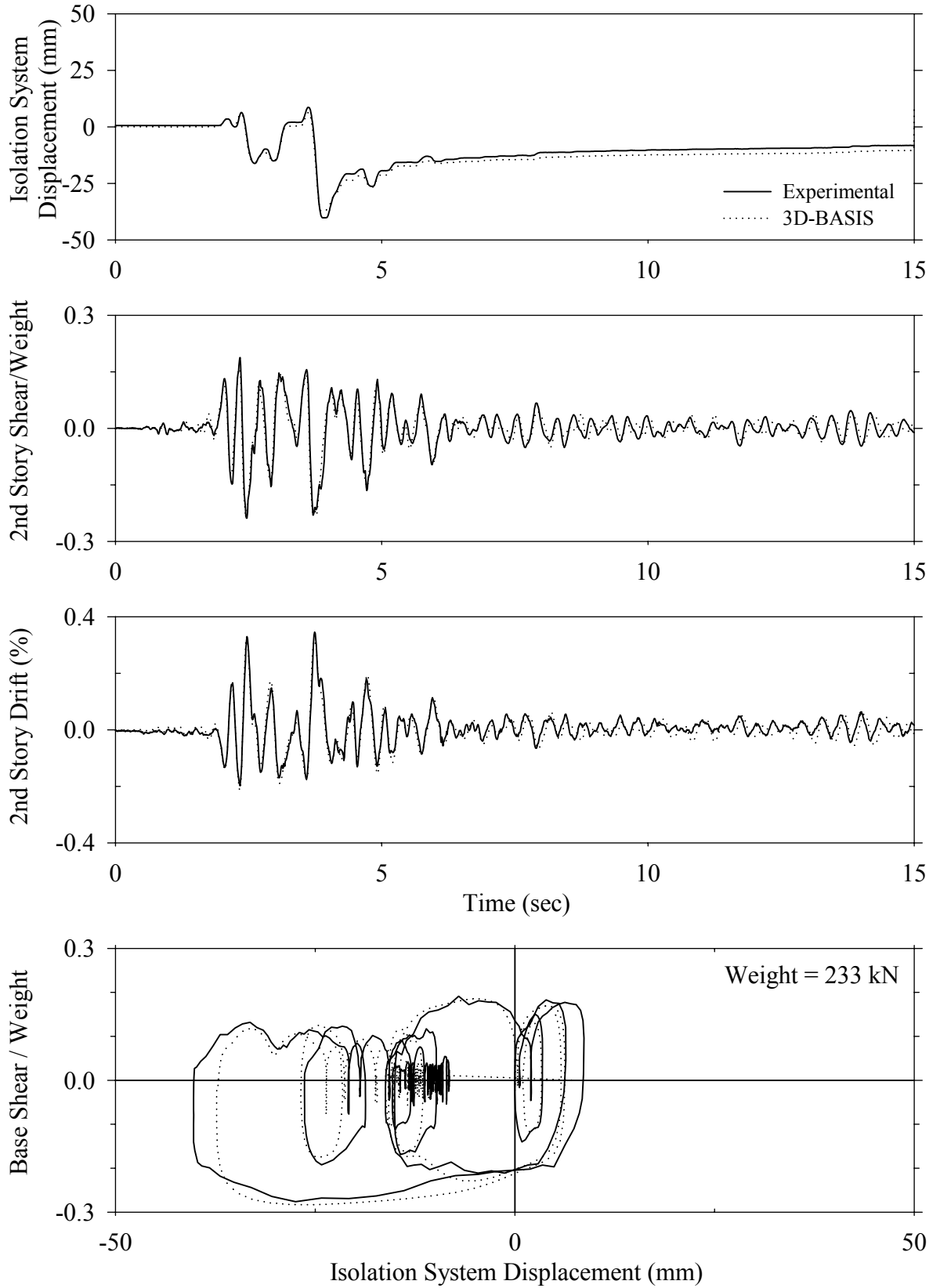
Test FPANN10.1, Newhall 360 100%, AB/FPS with Nonlinear Dampers



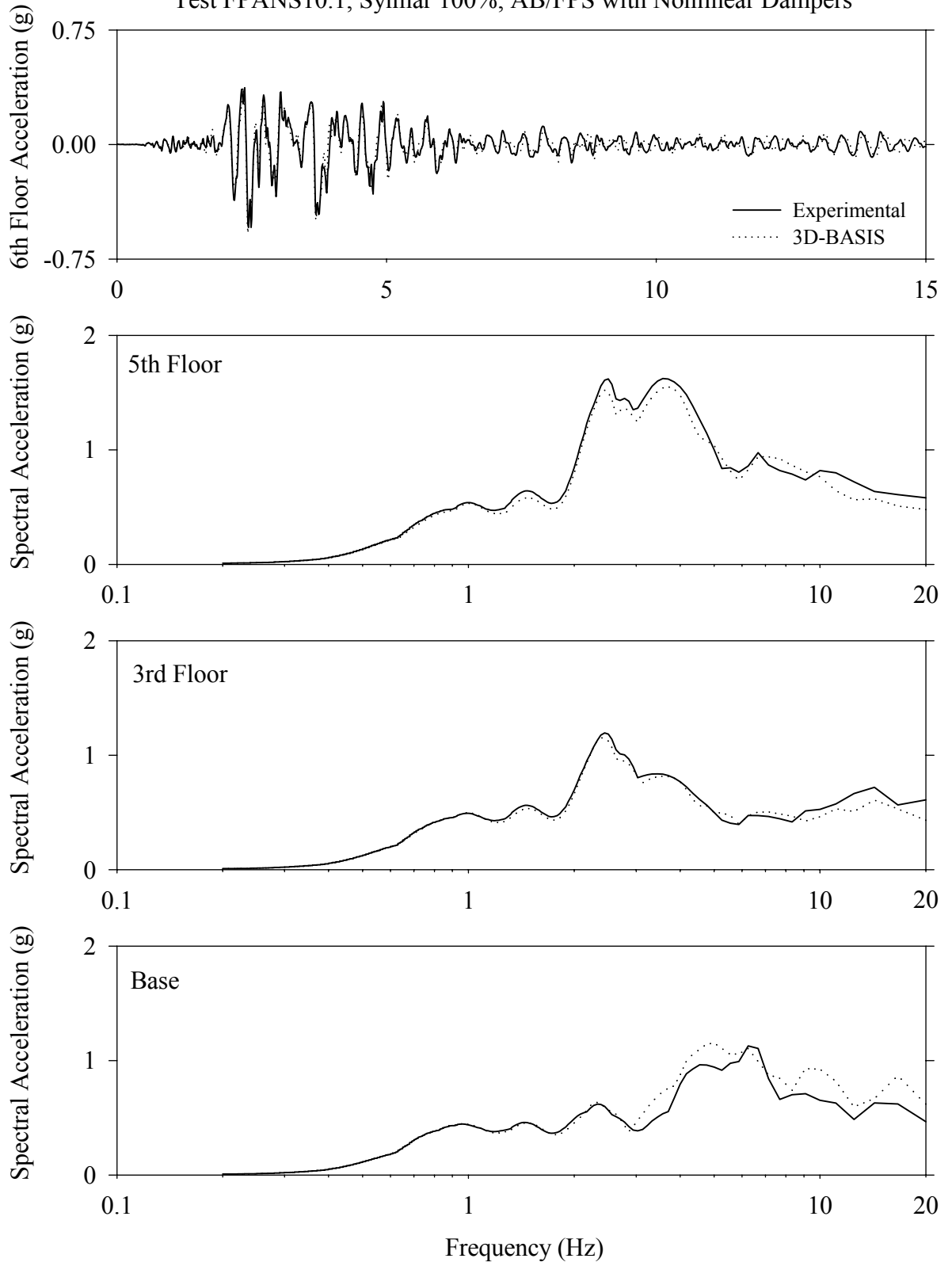
Test FPANN10.1, Newhall 360 100%, AB/FPS with Nonlinear Dampers



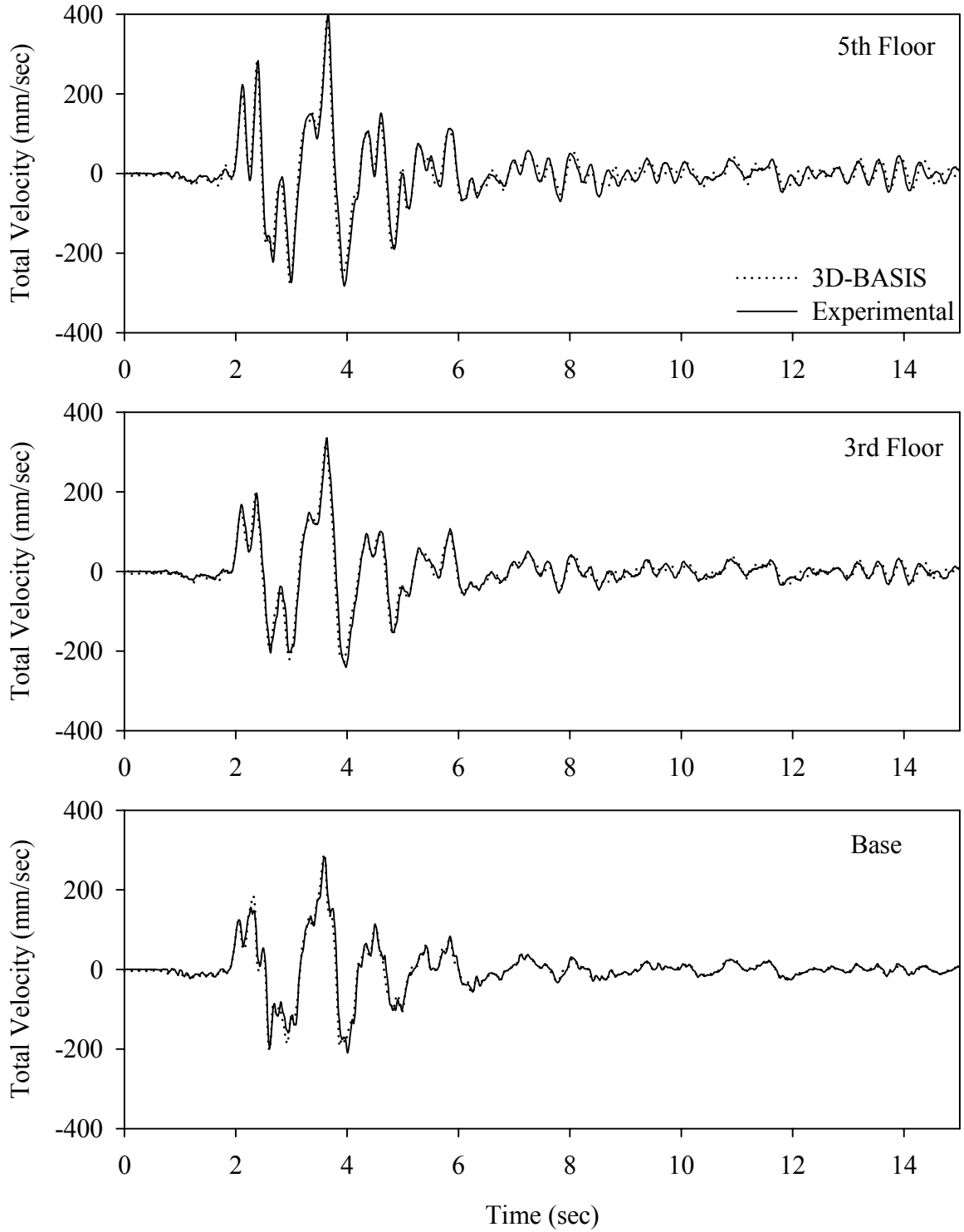
Test FPANS10.1, Sylmar 100%, AB/FPS with Nonlinear Dampers



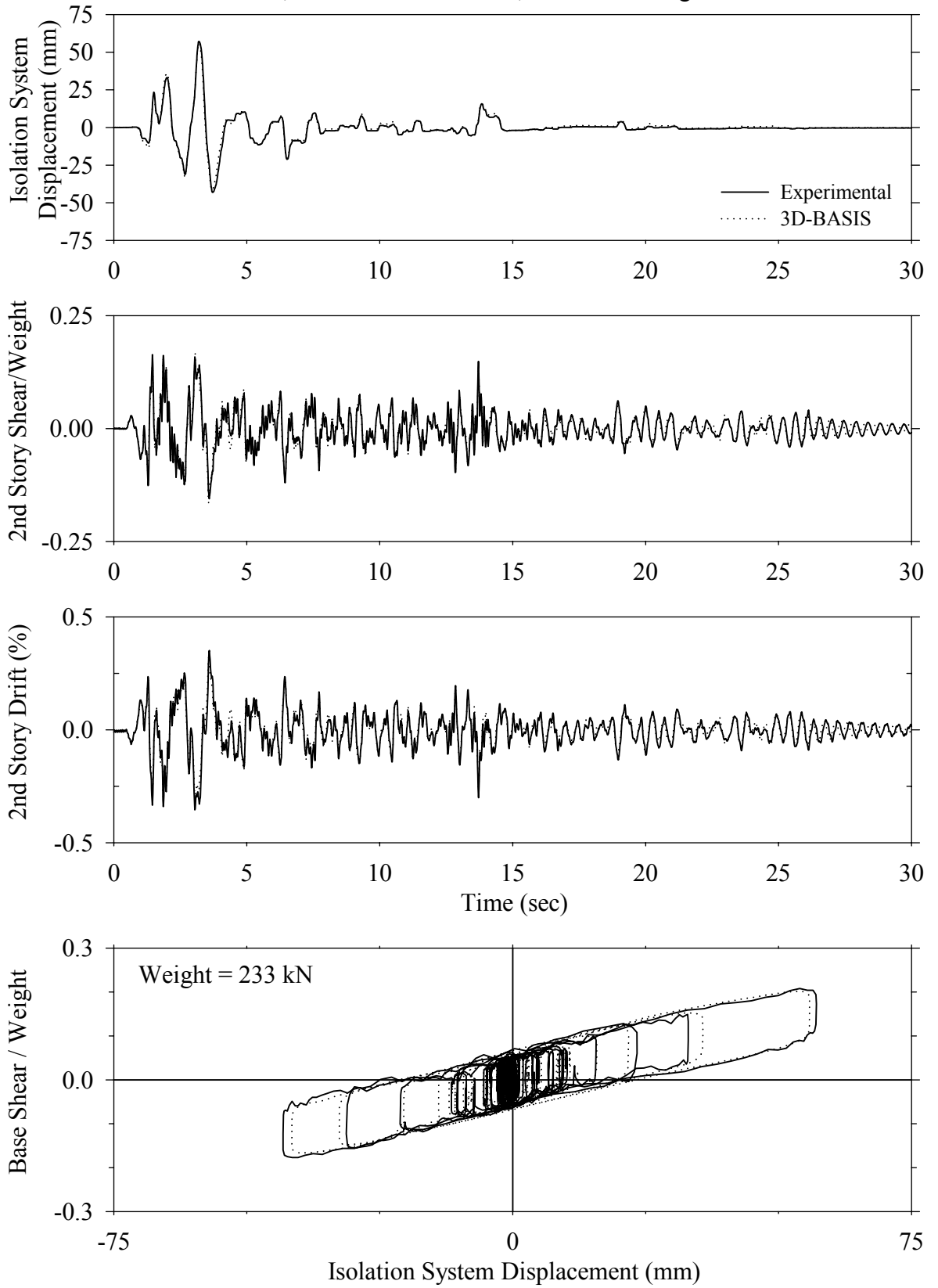
Test FPANS10.1, Sylmar 100%, AB/FPS with Nonlinear Dampers



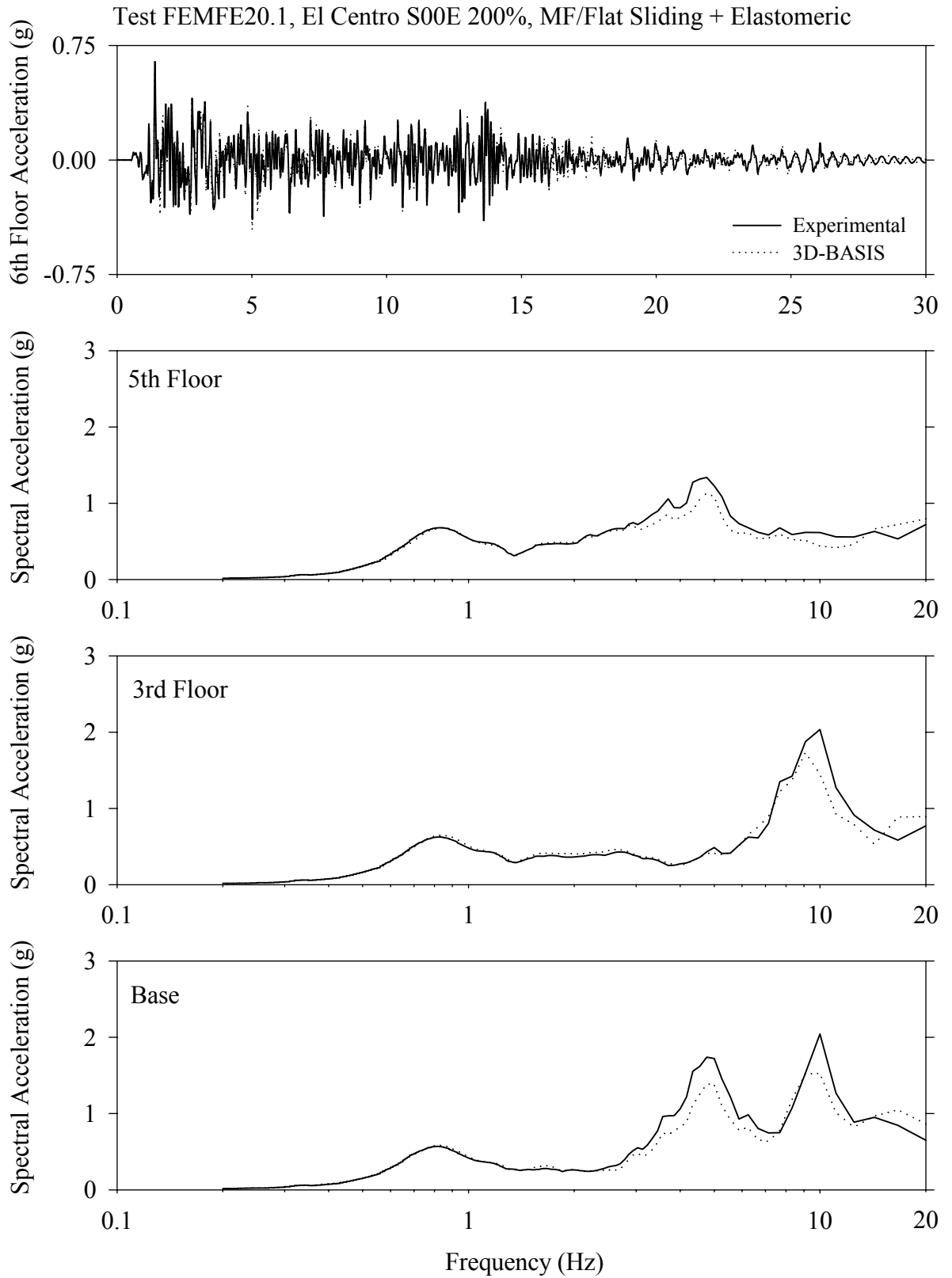
Test FPANS10.1, Sylmar 100%, AB/FPS with Nonlinear Dampers



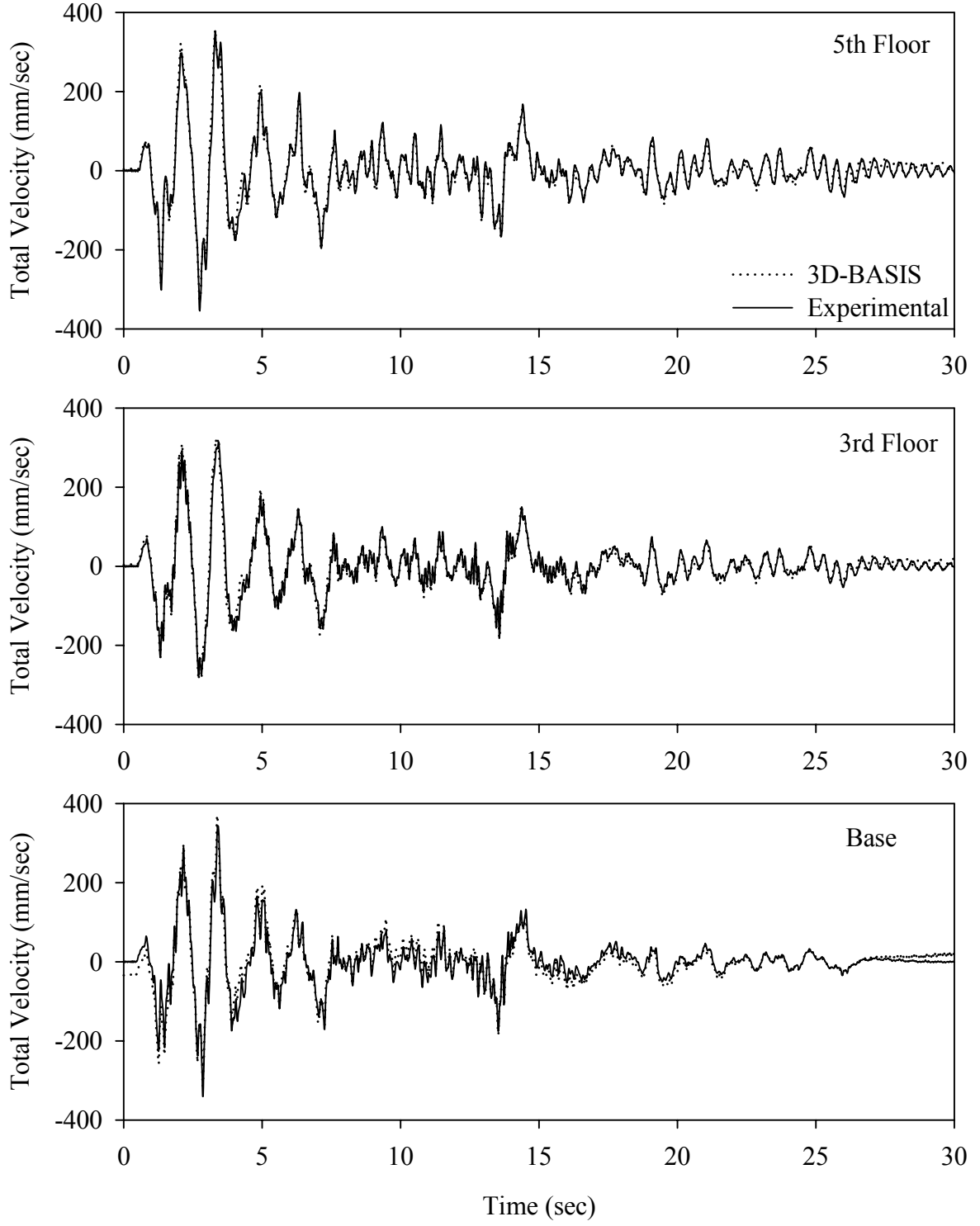
Test FEMFE20.1, El Centro S00E 200%, MF/Flat Sliding + Elastomeric



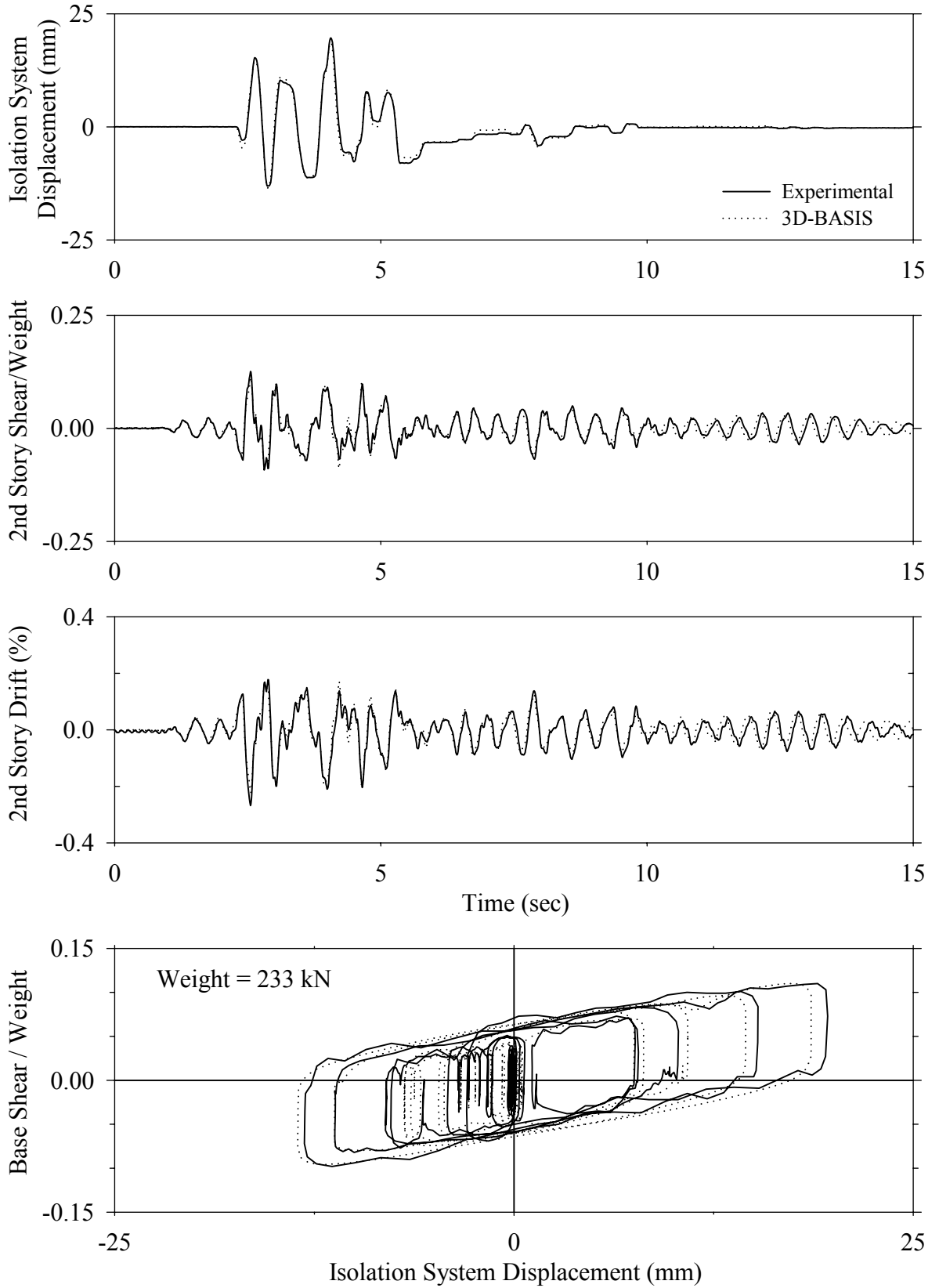




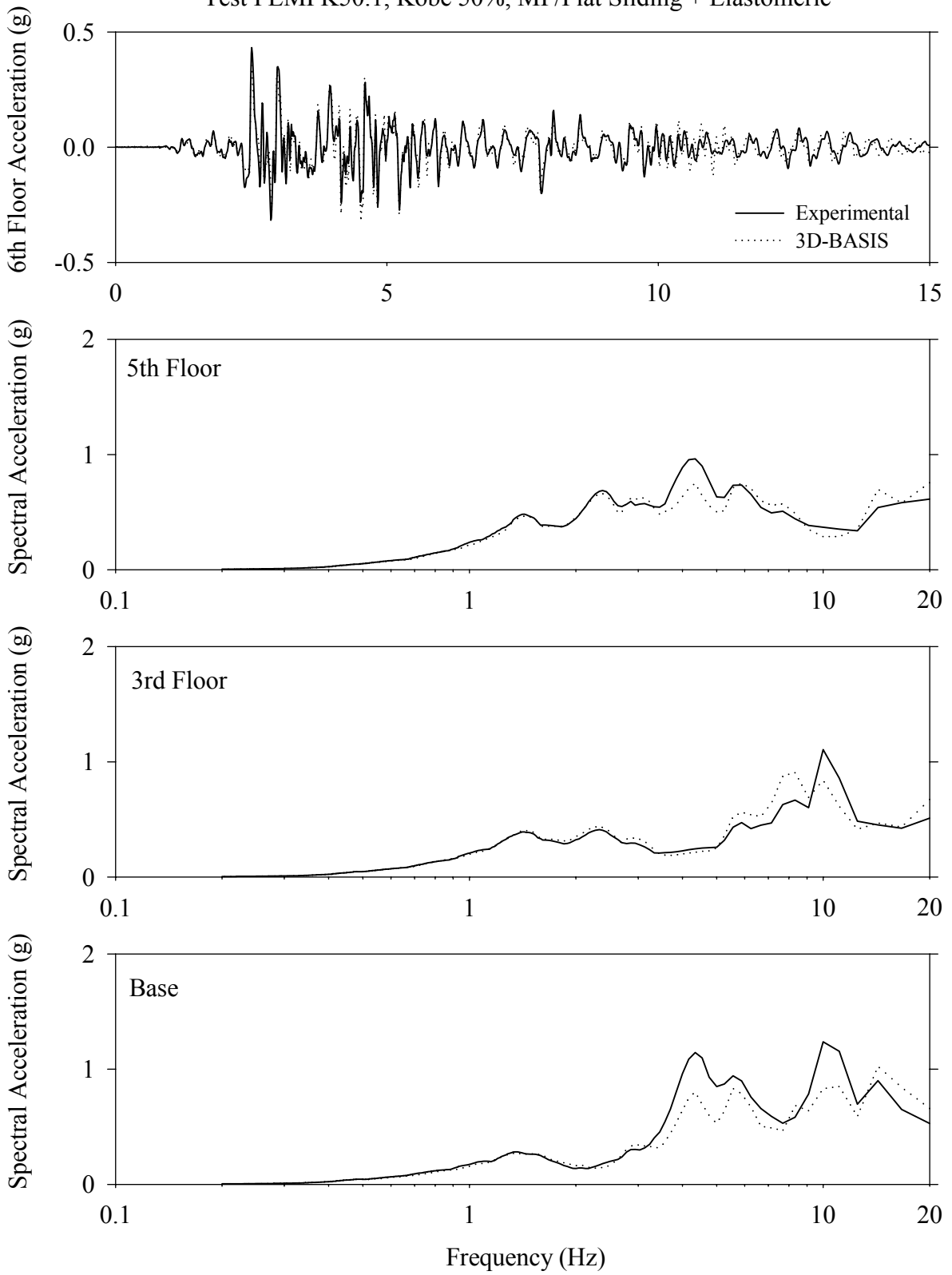
Test FEMFE20.1, El Centro S00E 200%, MF/Flat Sliding + Elastomeric



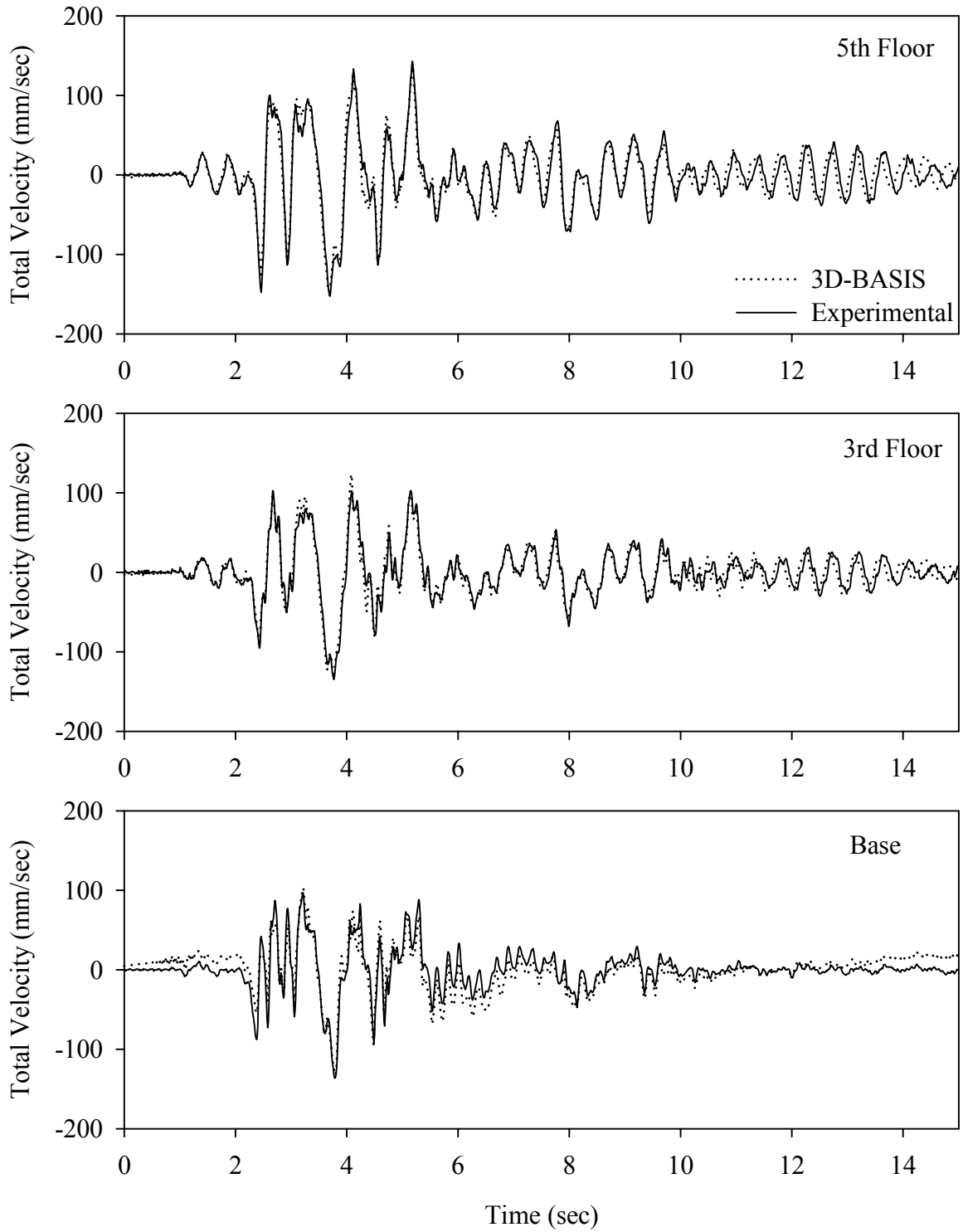
Test FEMFK50.1, Kobe 50%, MF/Flat Sliding + Elastomeric



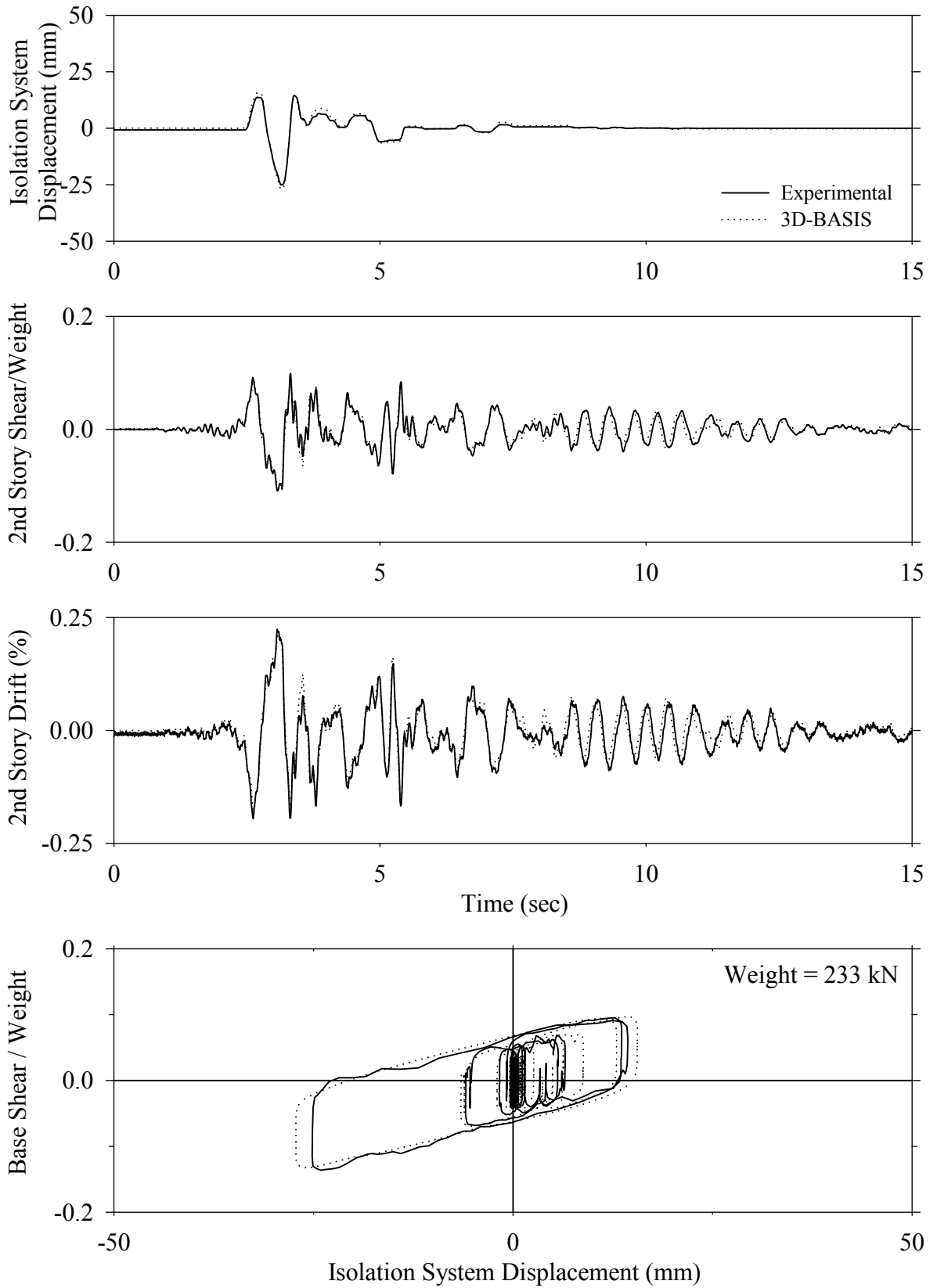
Test FEMFK50.1, Kobe 50%, MF/Flat Sliding + Elastomeric

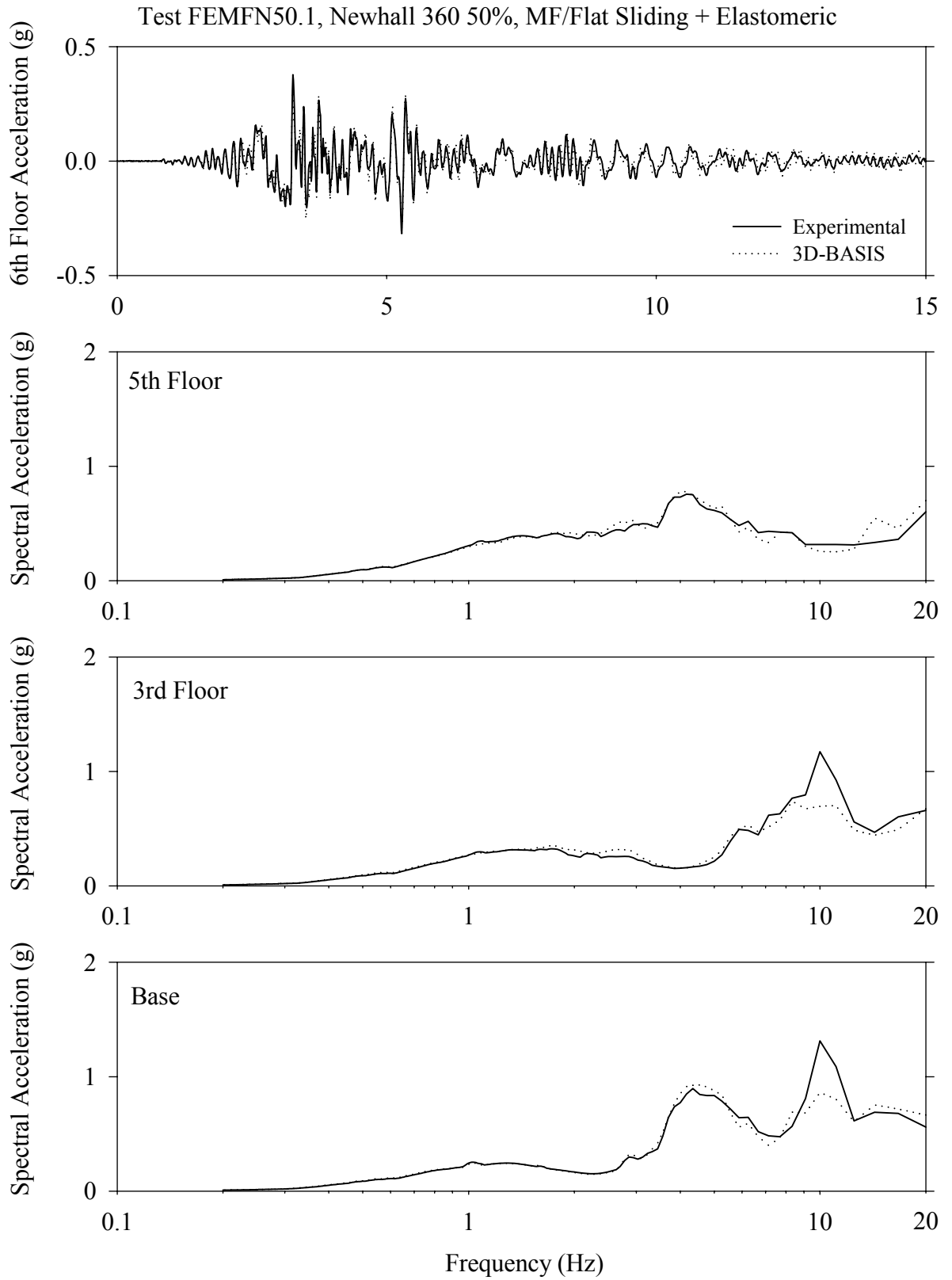


Test FEMFK50.1, Kobe 50%, MF/Flat Sliding + Elastomeric

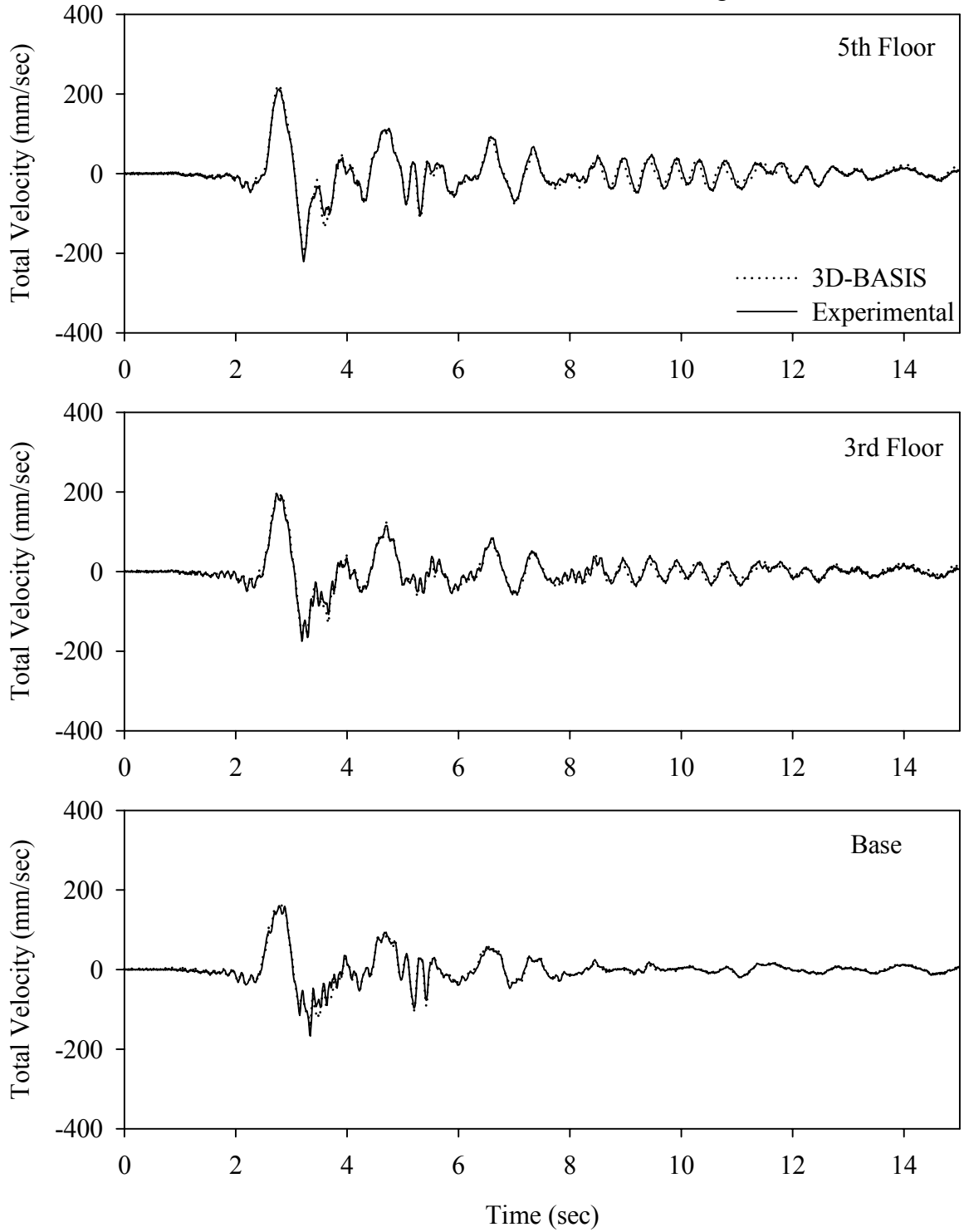


Test FEMFN50.1, Newhall 360 50%, MF/Flat Sliding + Elastomeric



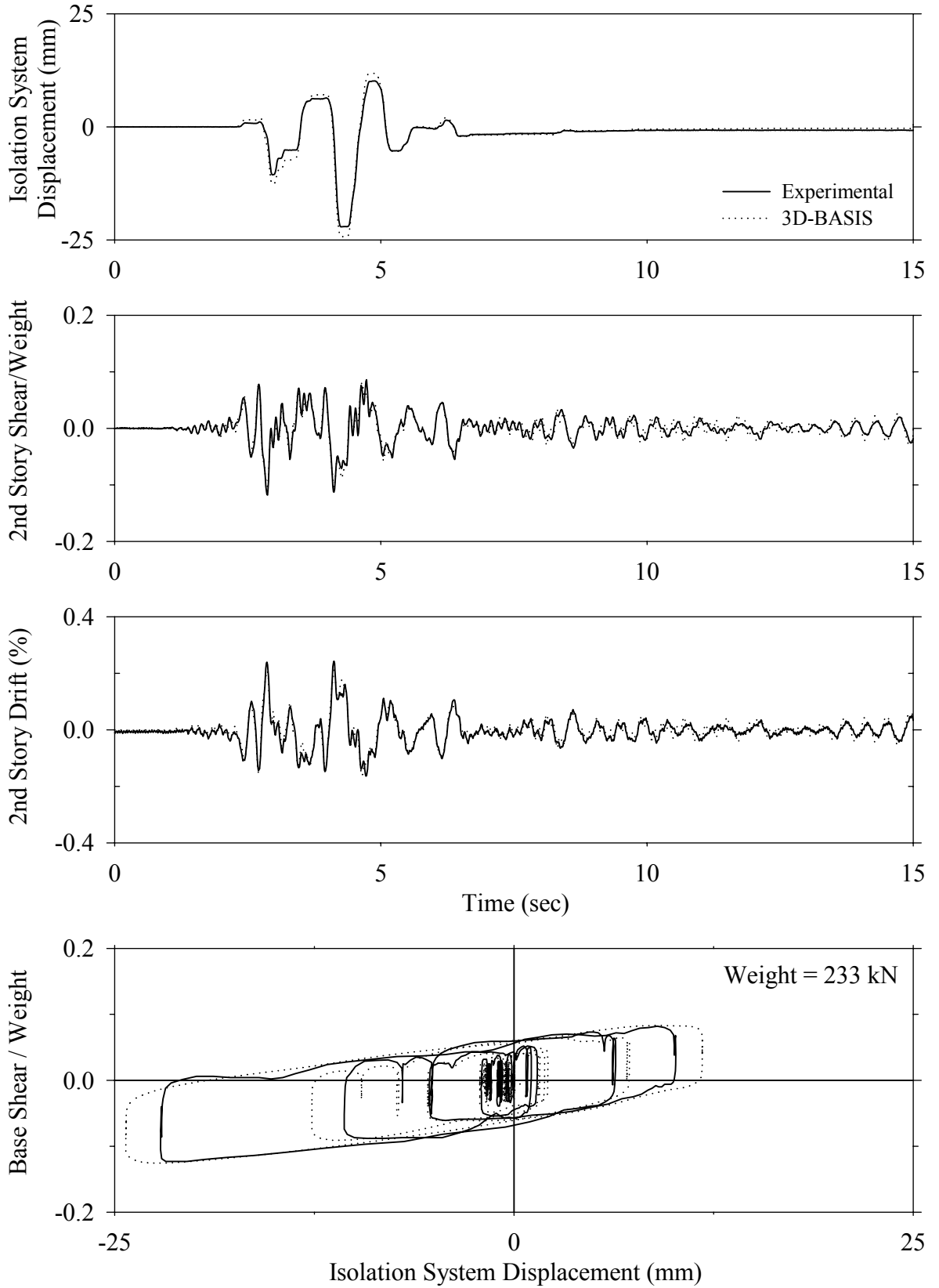


Test FEMFN50.1, Newhall 360 50%, MF/Flat Sliding + Elastomeric

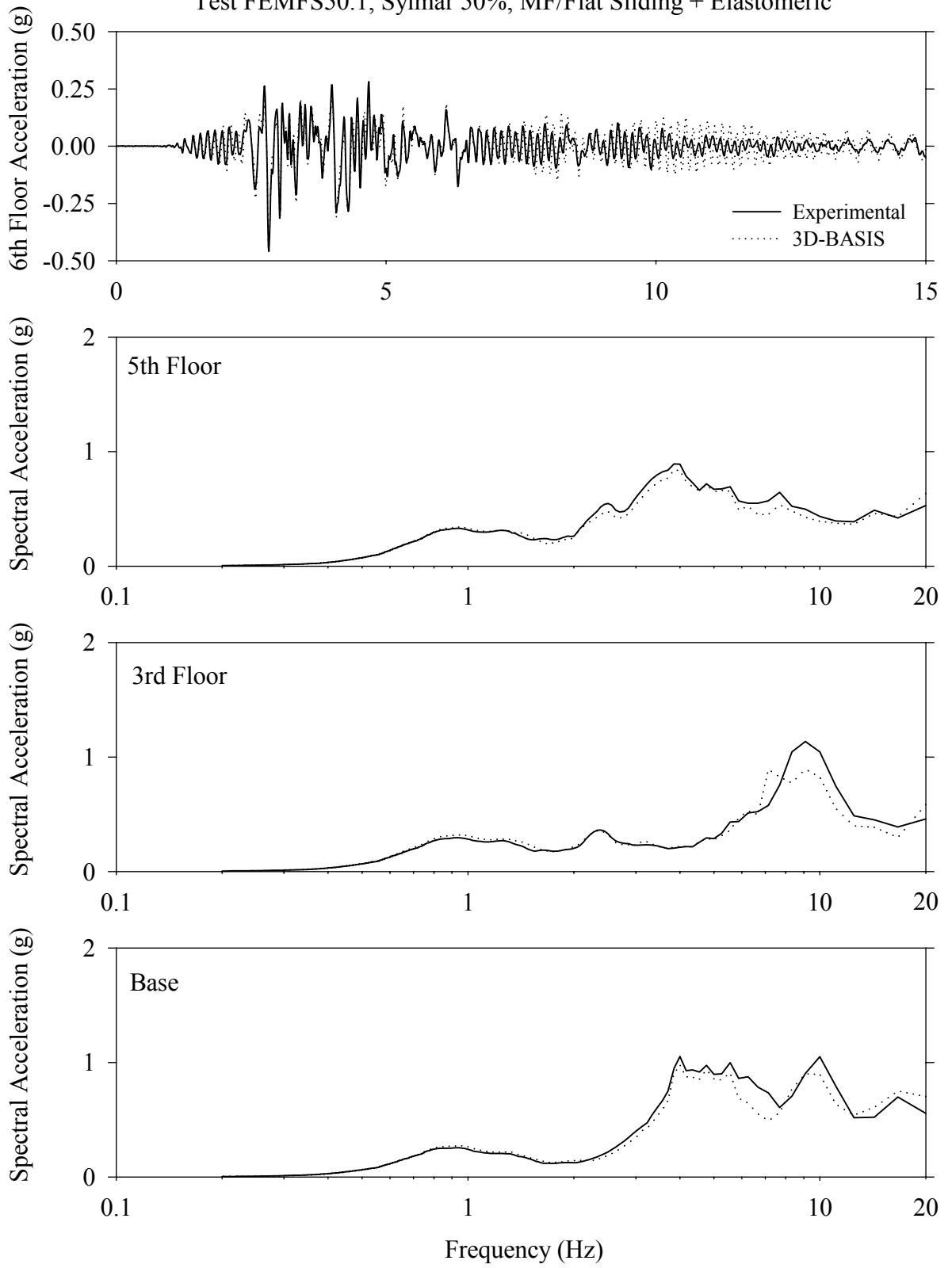




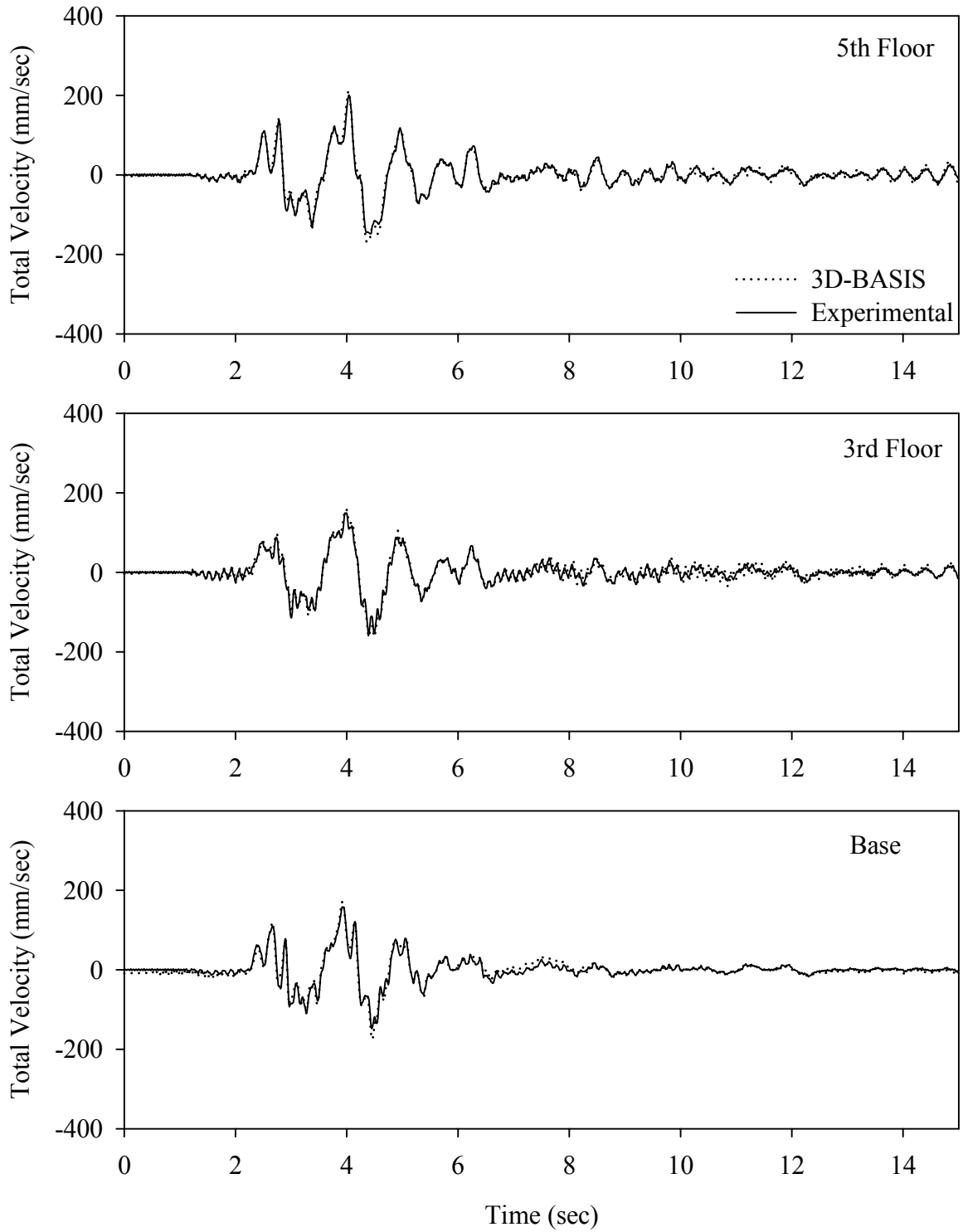
Test FEMFS50.1, Sylmar 50%, MF/Flat Sliding + Elastomeric



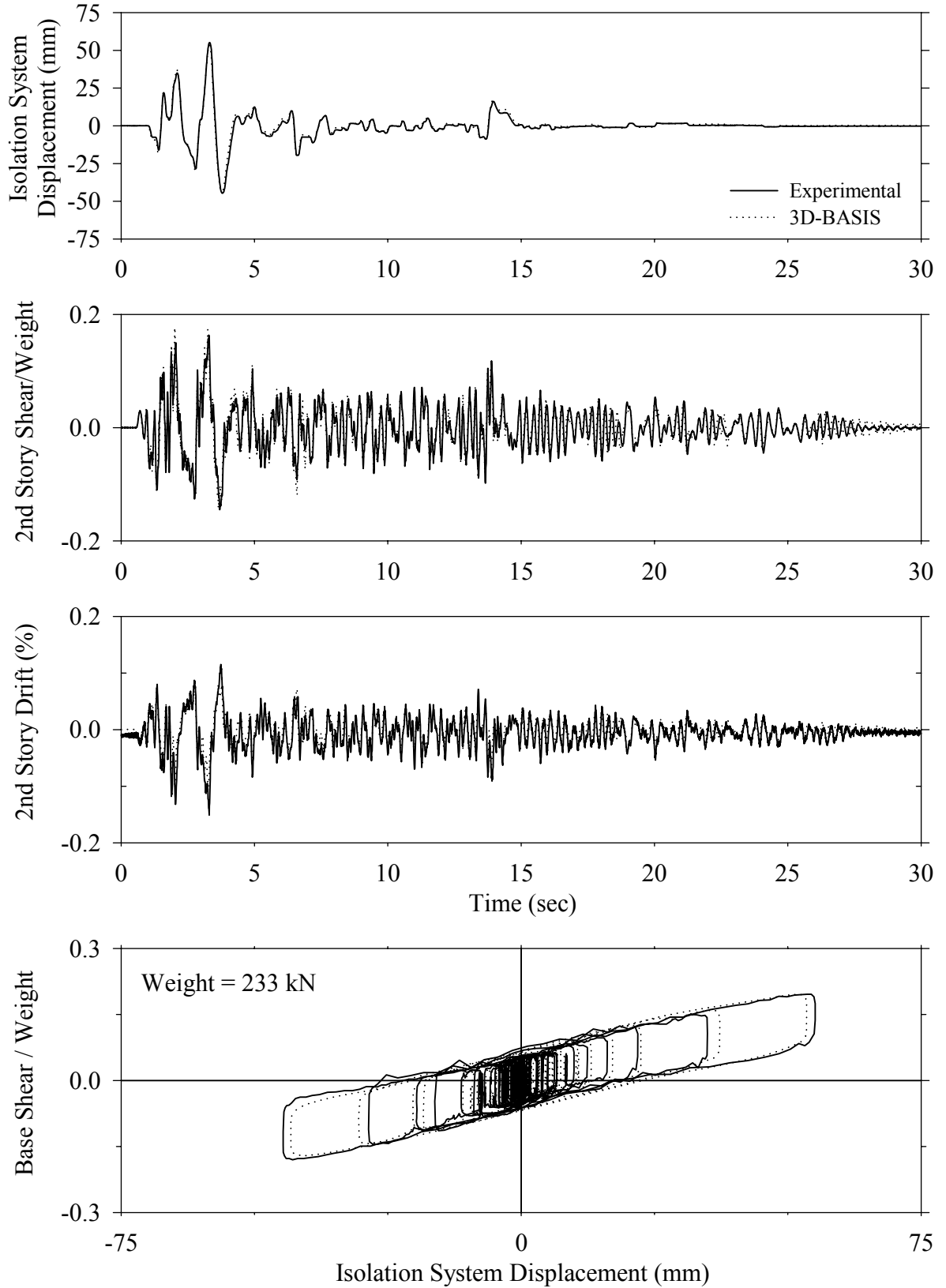
Test FEMFS50.1, Sylmar 50%, MF/Flat Sliding + Elastomeric

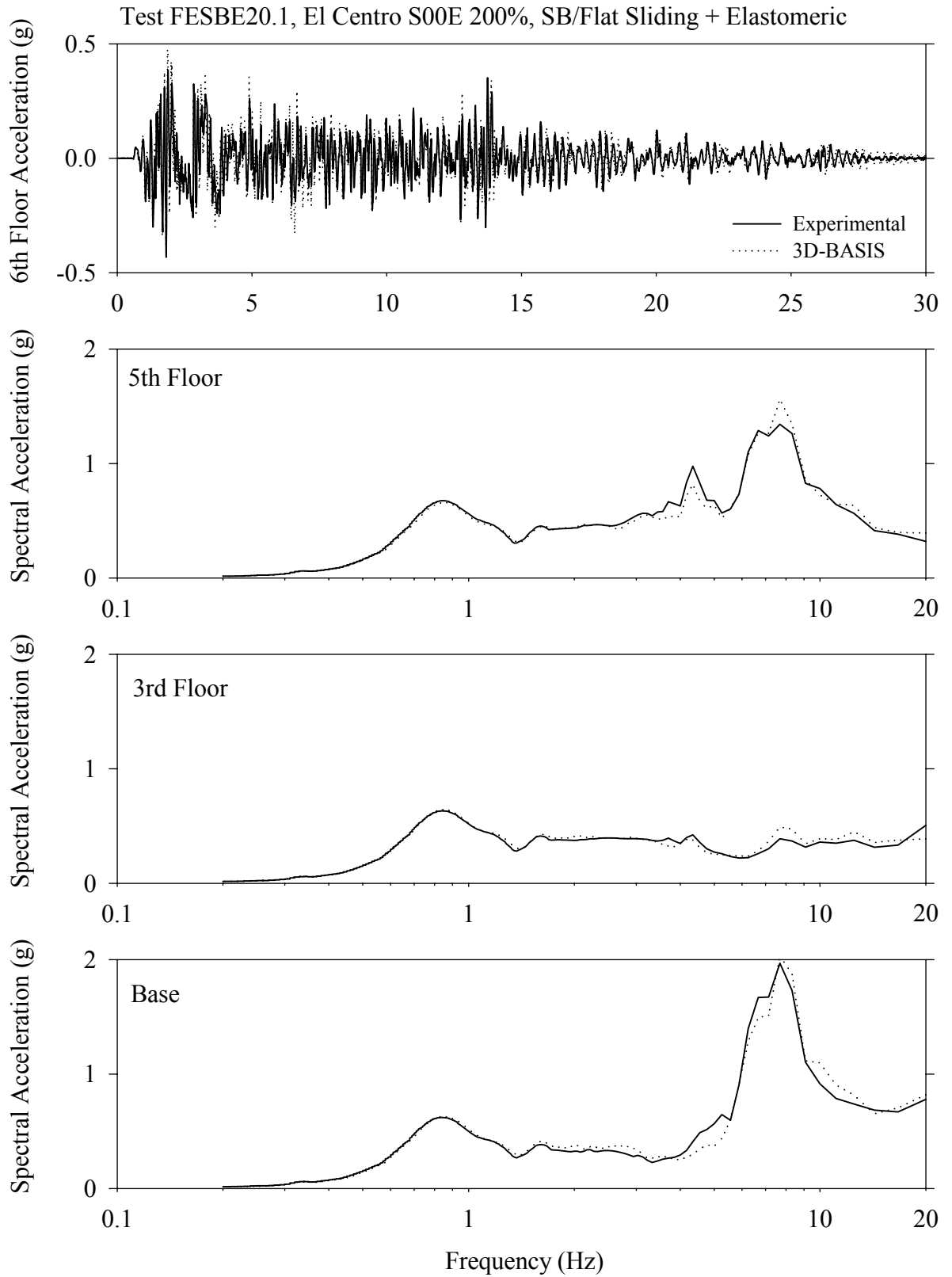


Test FEMFS50.1, Sylmar 50%, MF/Flat Sliding + Elastomeric

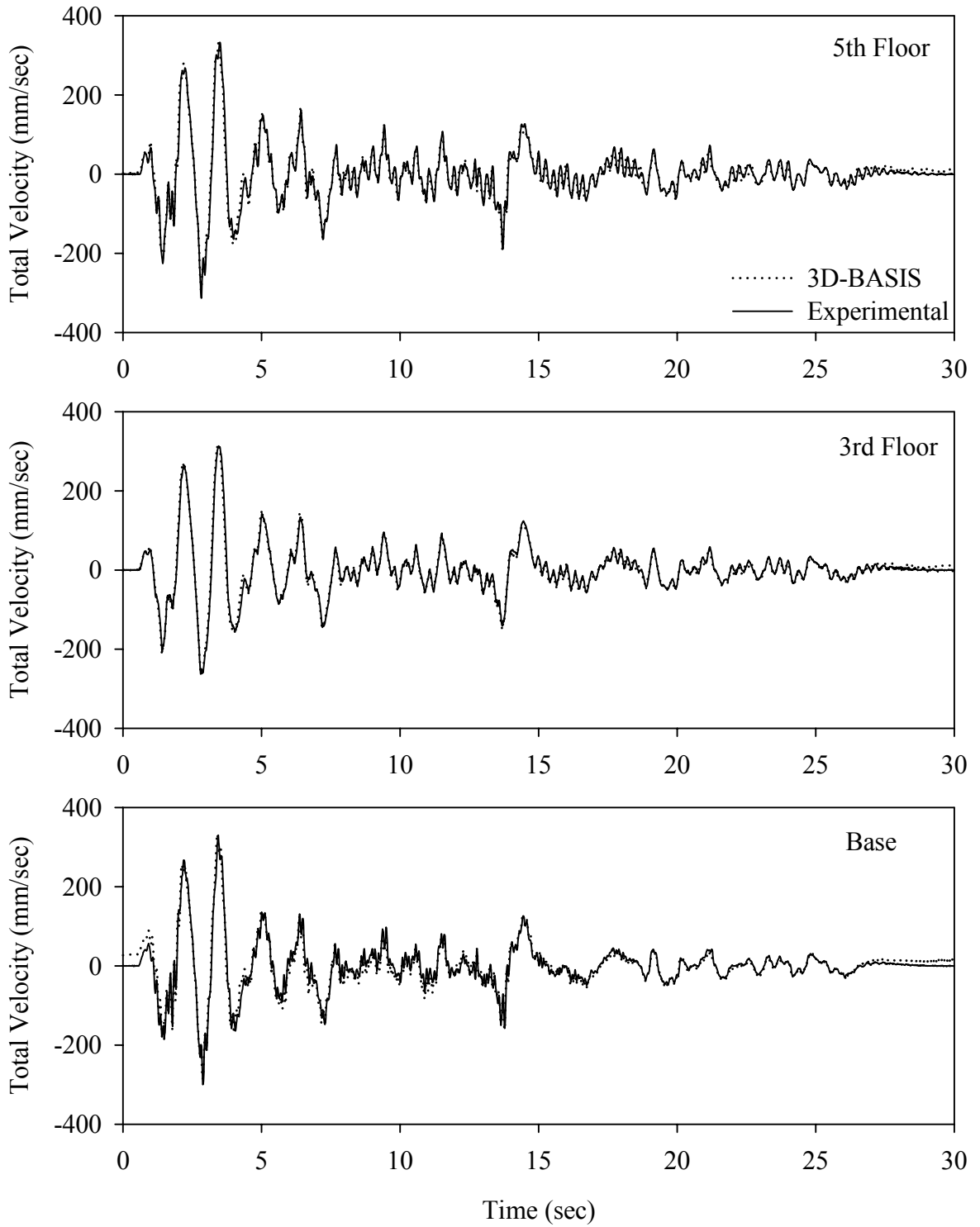


Test FESBE20.1, El Centro S00E 200%, SB/Flat Sliding + Elastomeric

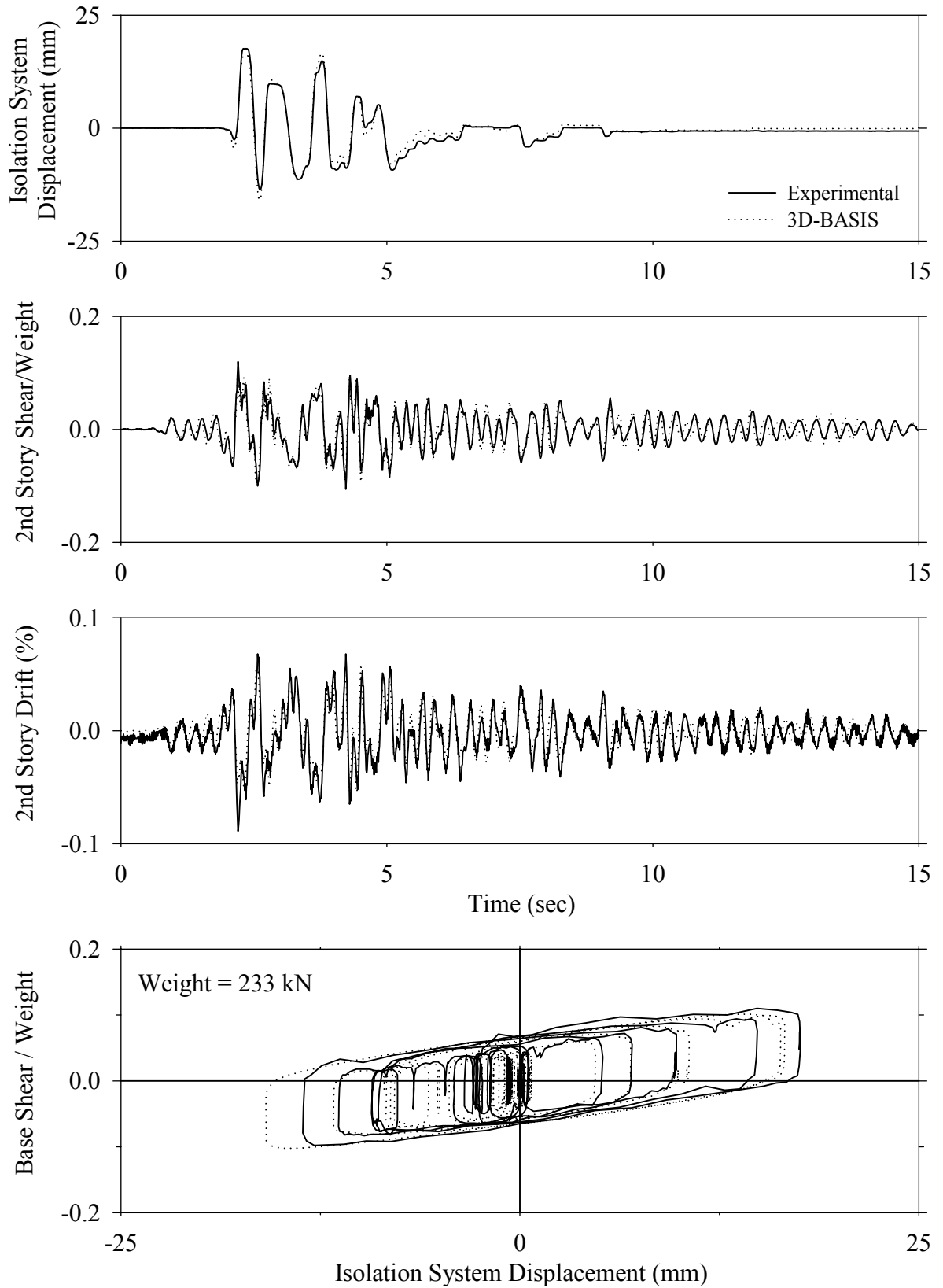




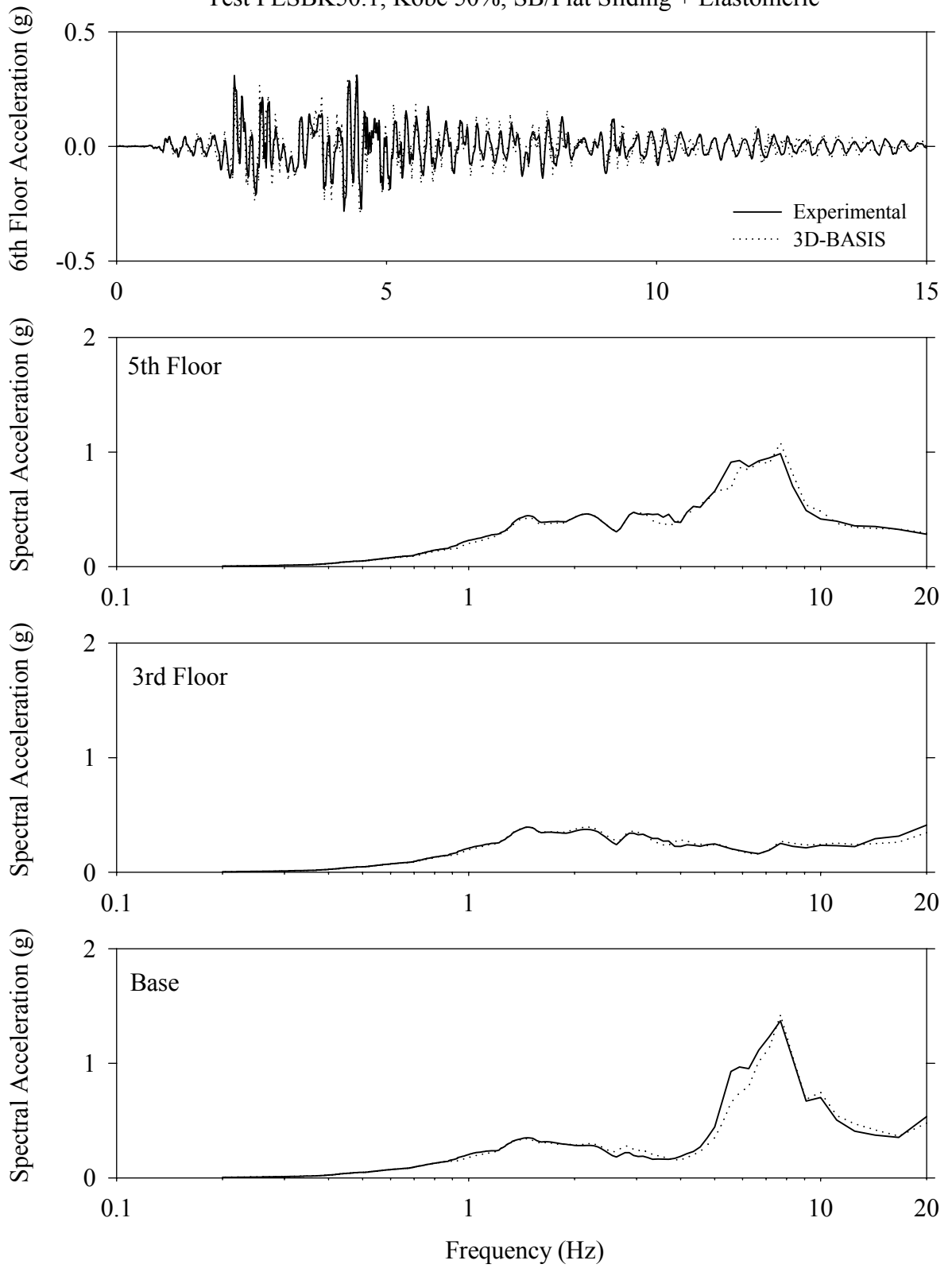
Test FESBE20.1, El Centro S00E 200%, SB/Flat Sliding + Elastomeric



Test FESBK50.1, Kobe 50%, SB/Flat Sliding + Elastomeric

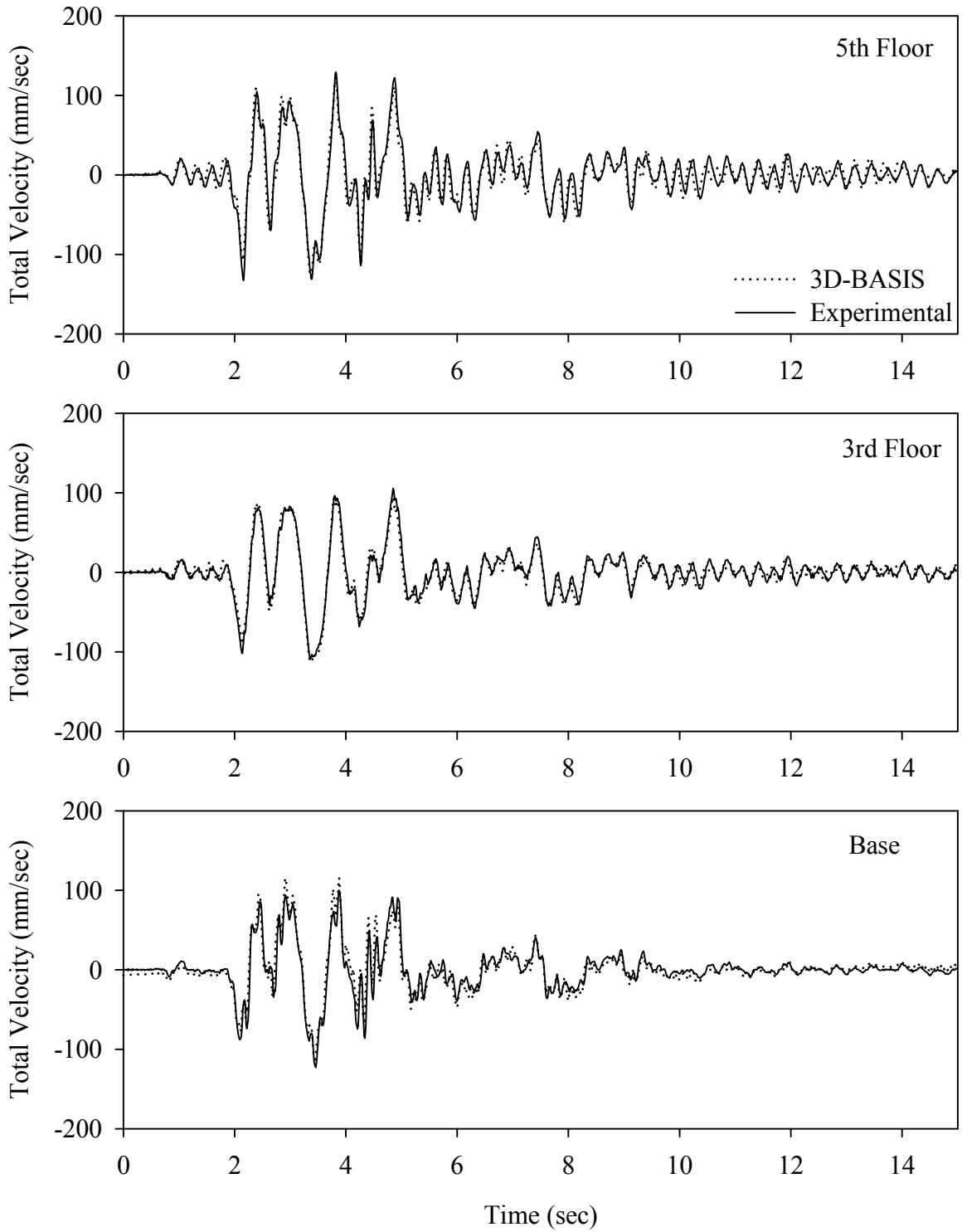


Test FESBK50.1, Kobe 50%, SB/Flat Sliding + Elastomeric

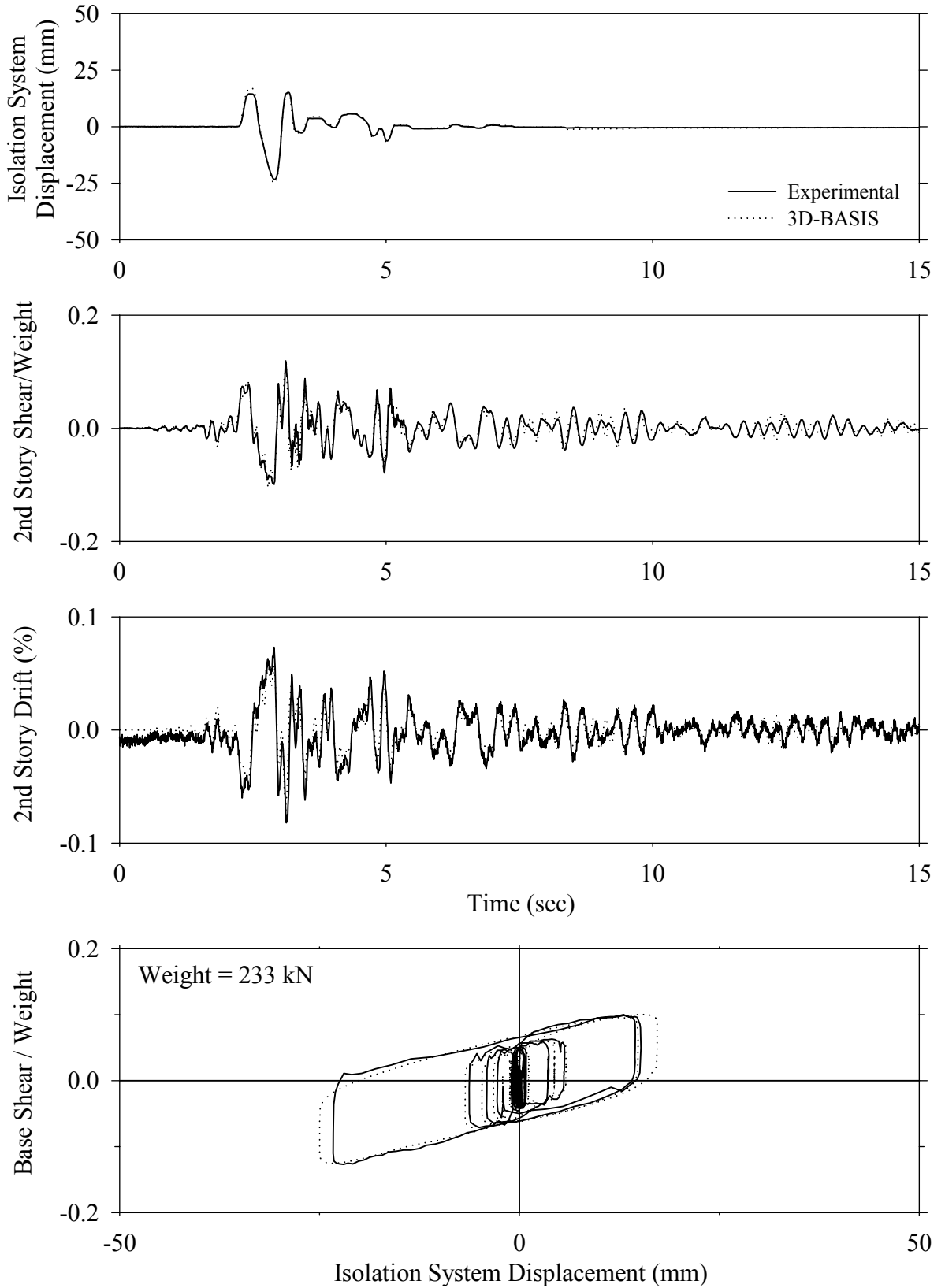




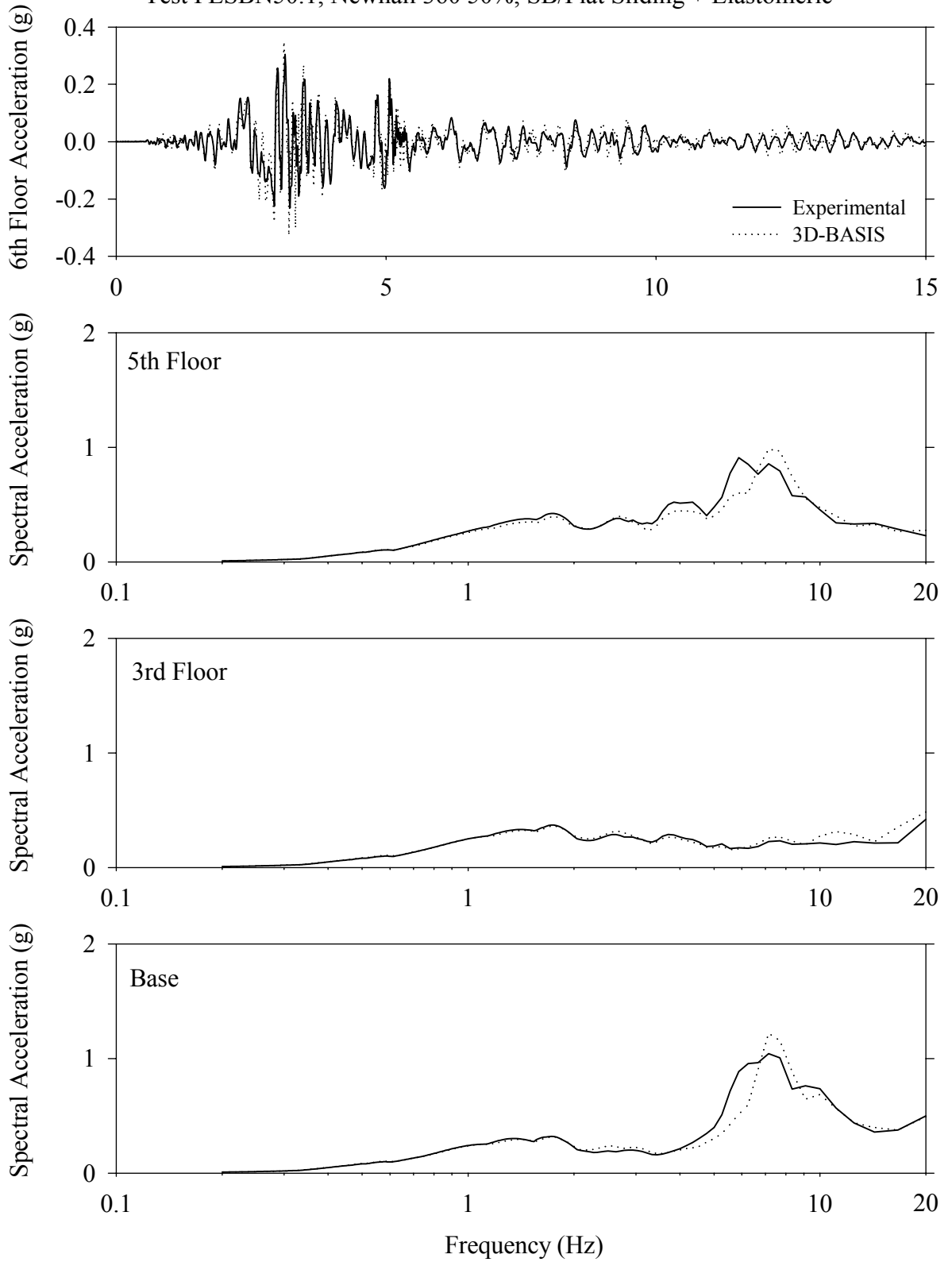
Test FESBK50.1, Kobe 50%, SB/Flat Sliding + Elastomeric



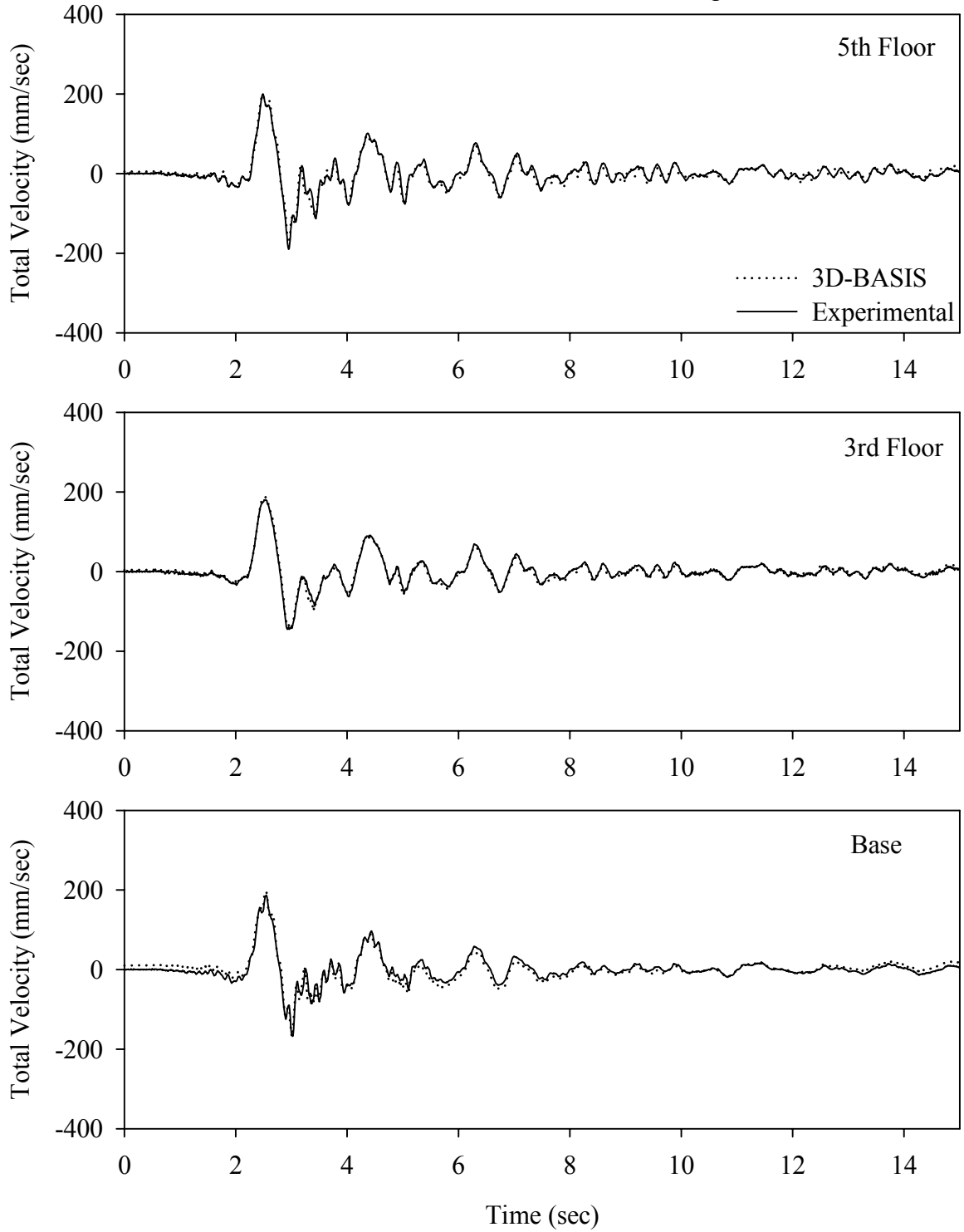
Test FESBN50.1, Newhall 360 50%, SB/Flat Sliding + Elastomeric



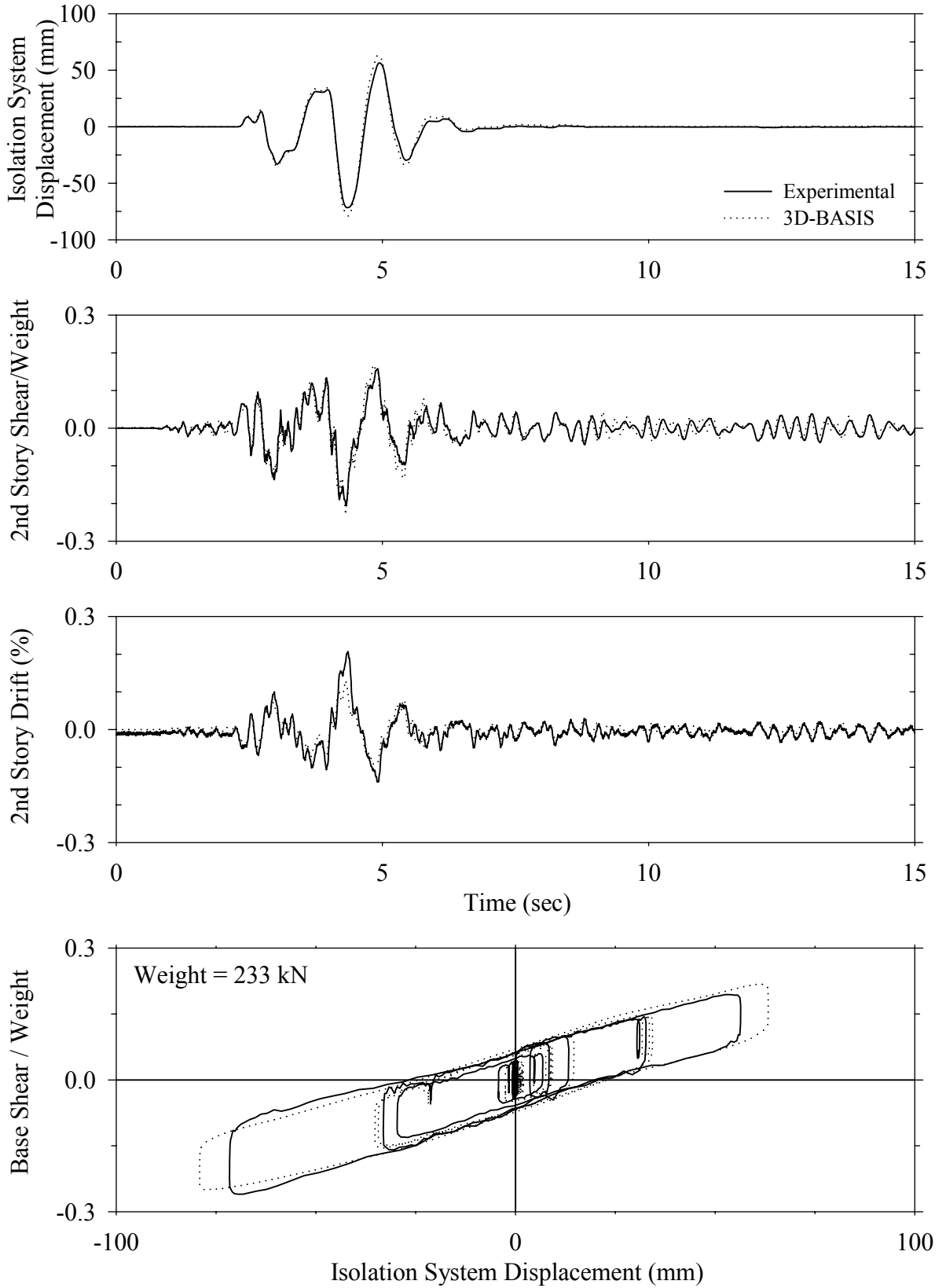
Test FESBN50.1, Newhall 360 50%, SB/Flat Sliding + Elastomeric



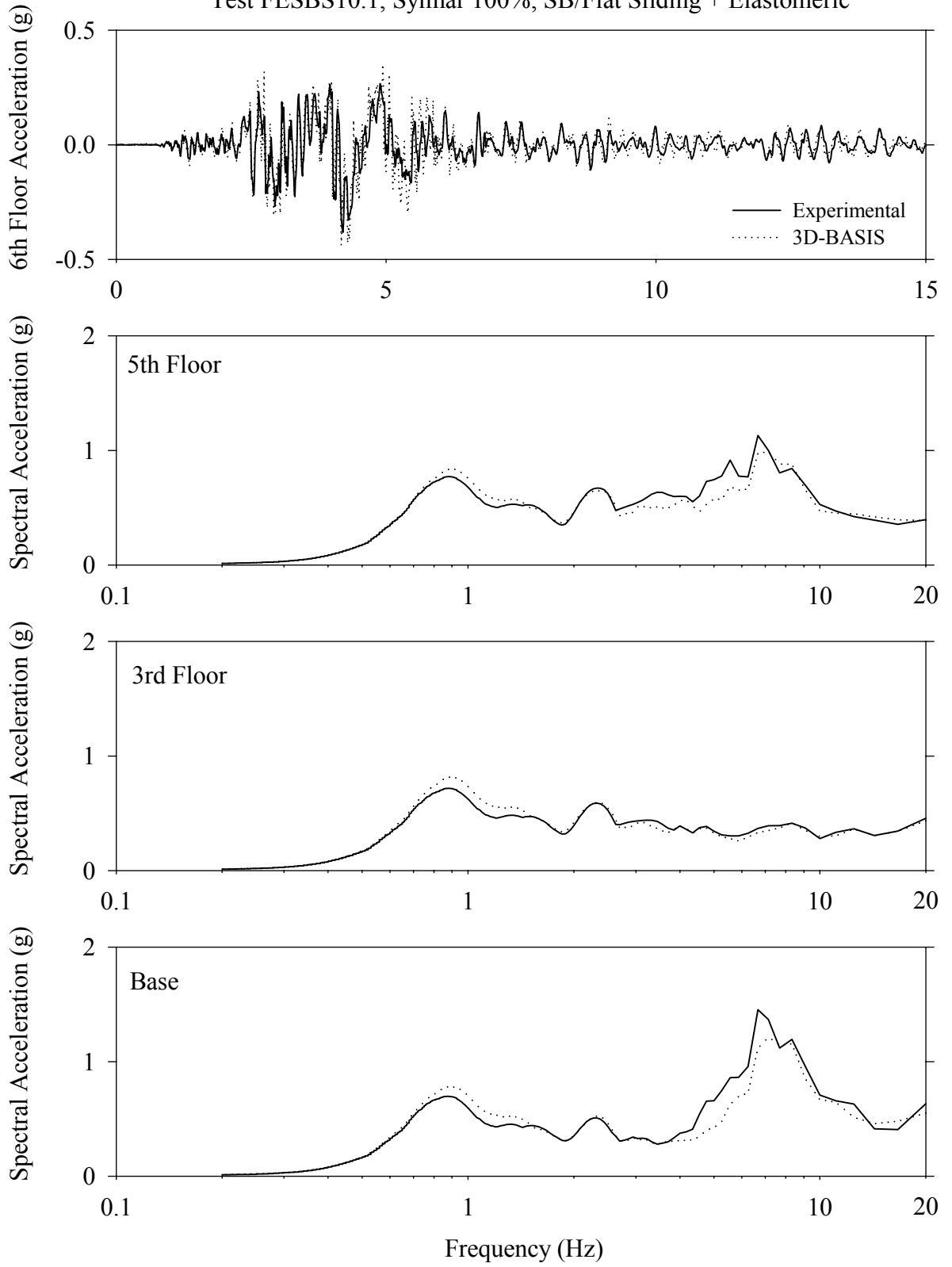
Test FESBN50.1, Newhall 360 50%, SB/Flat Sliding + Elastomeric



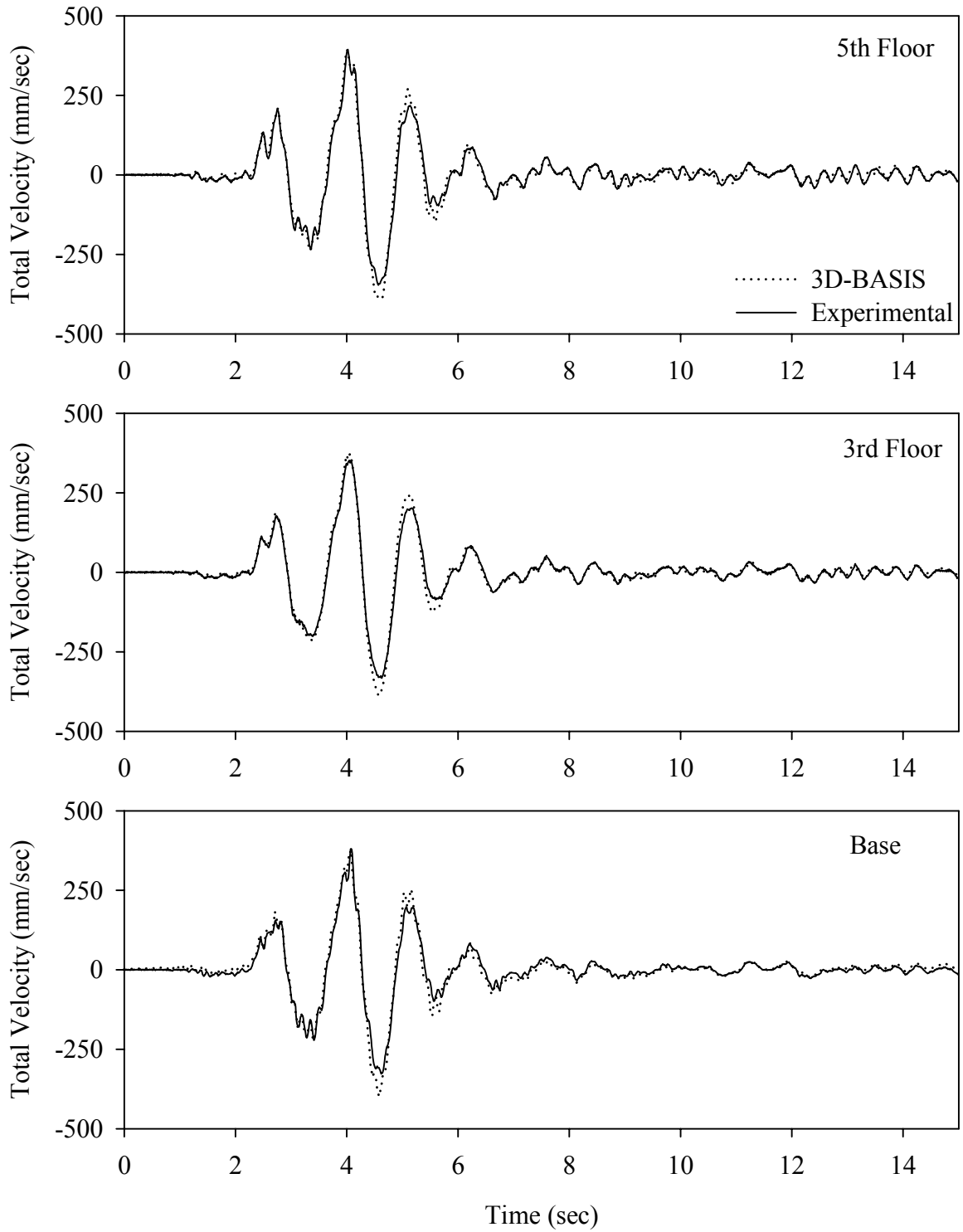
Test FESBS10.1, Sylmar 100%, SB/Flat Sliding + Elastomeric



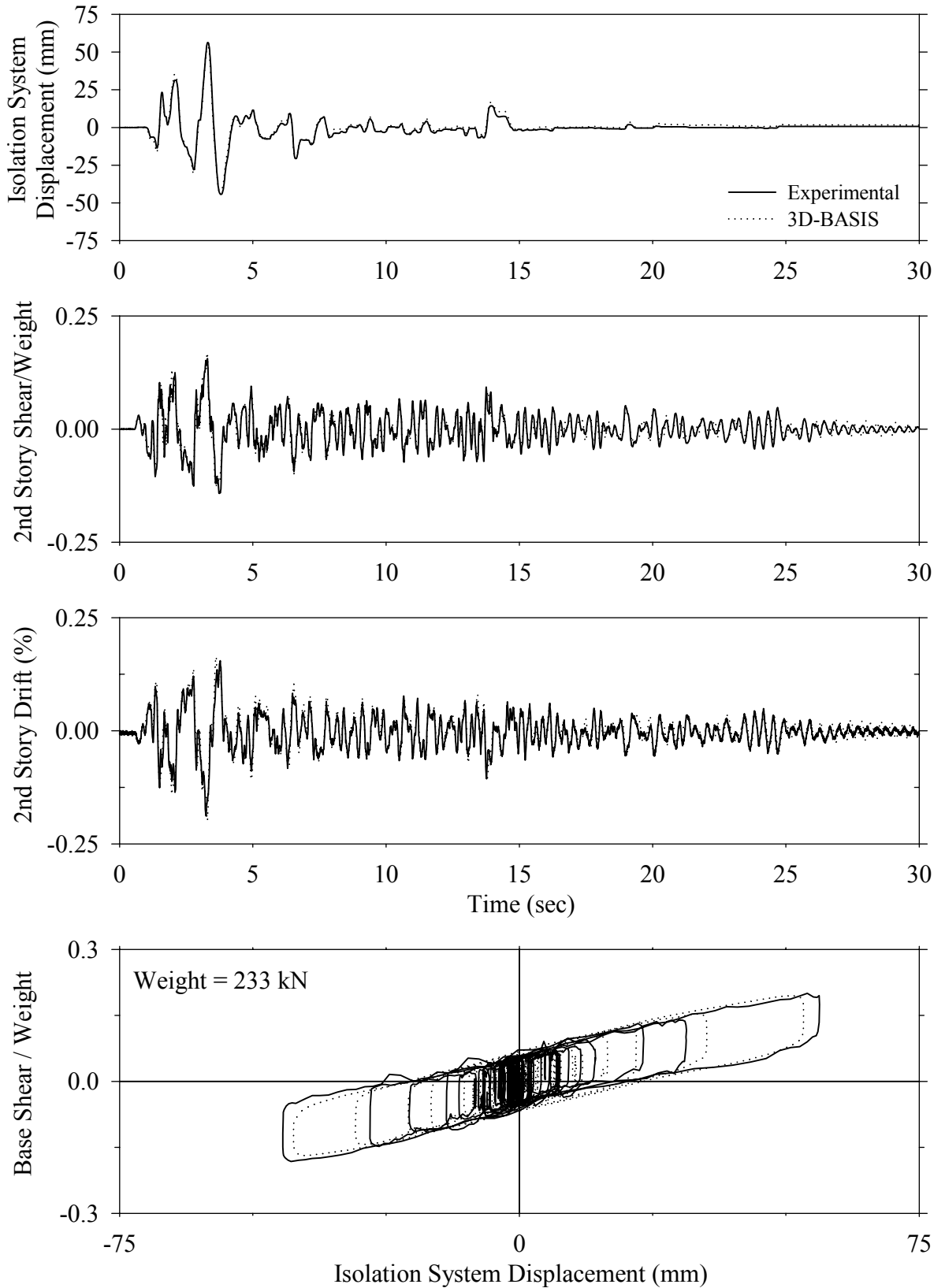
Test FESBS10.1, Sylmar 100%, SB/Flat Sliding + Elastomeric



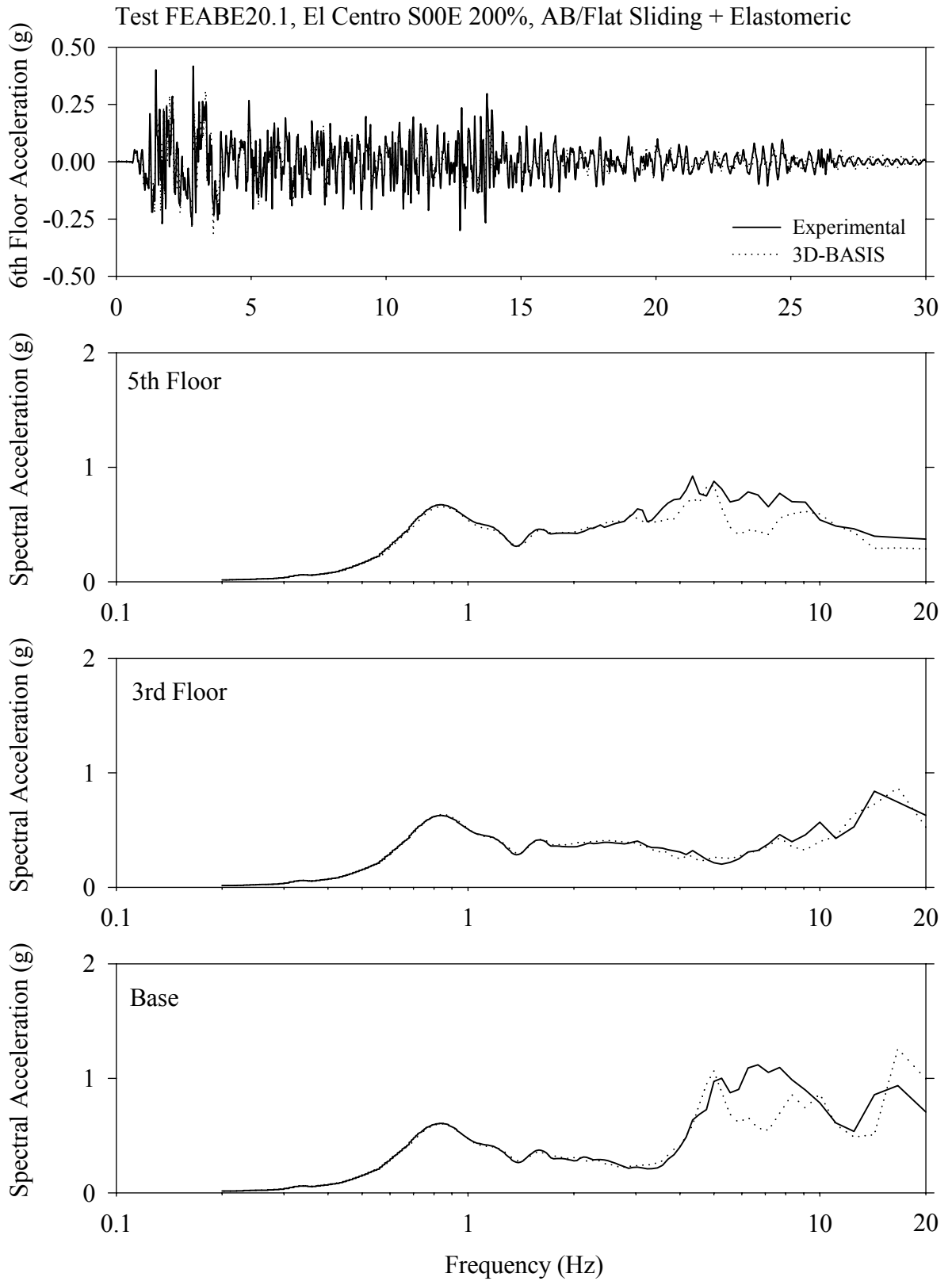
Test FESBS10.1, Sylmar 100%, SB/Flat Sliding + Elastomeric



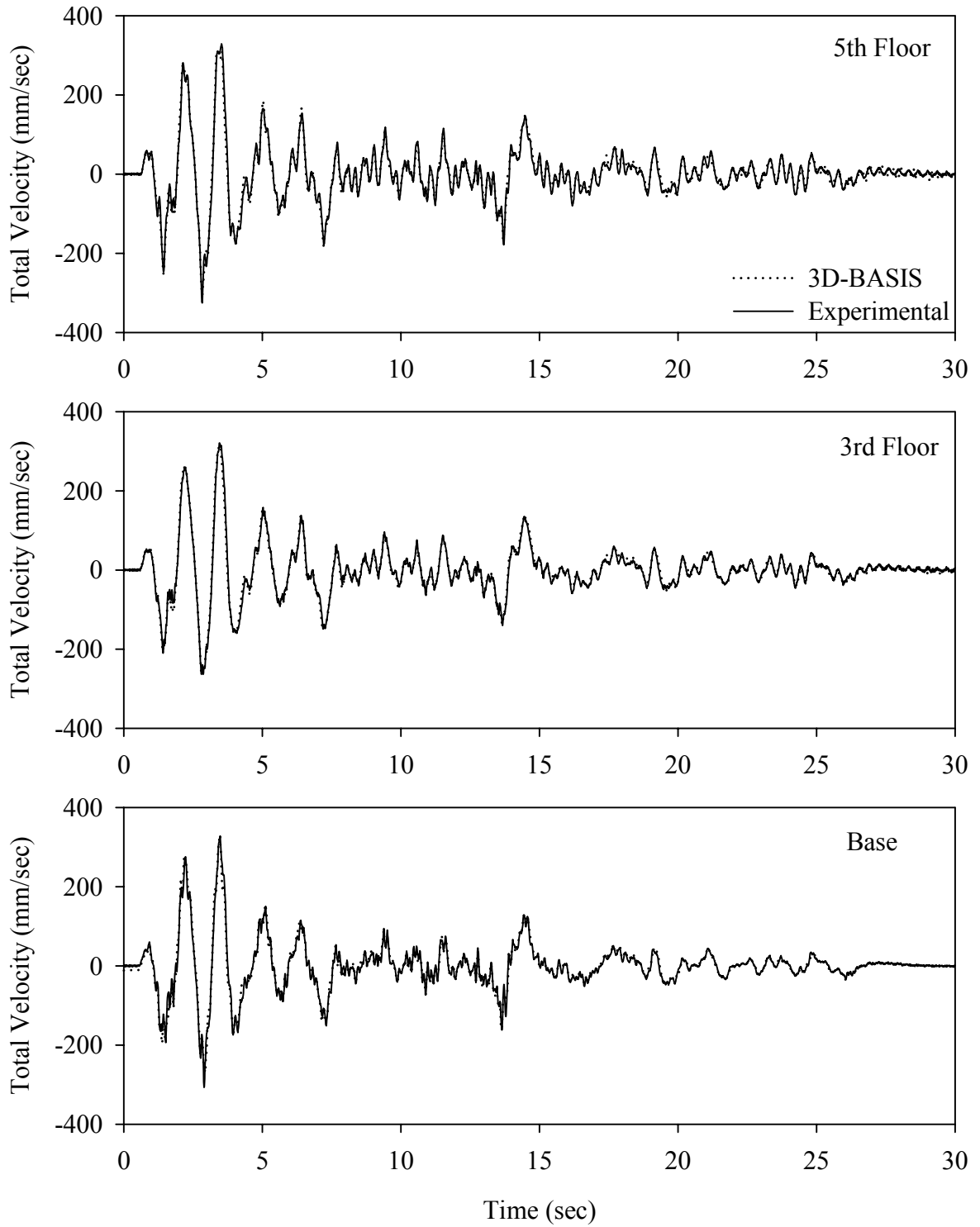
Test FEABE20.1, El Centro S00E 200%, AB/Flat Sliding + Elastomeric



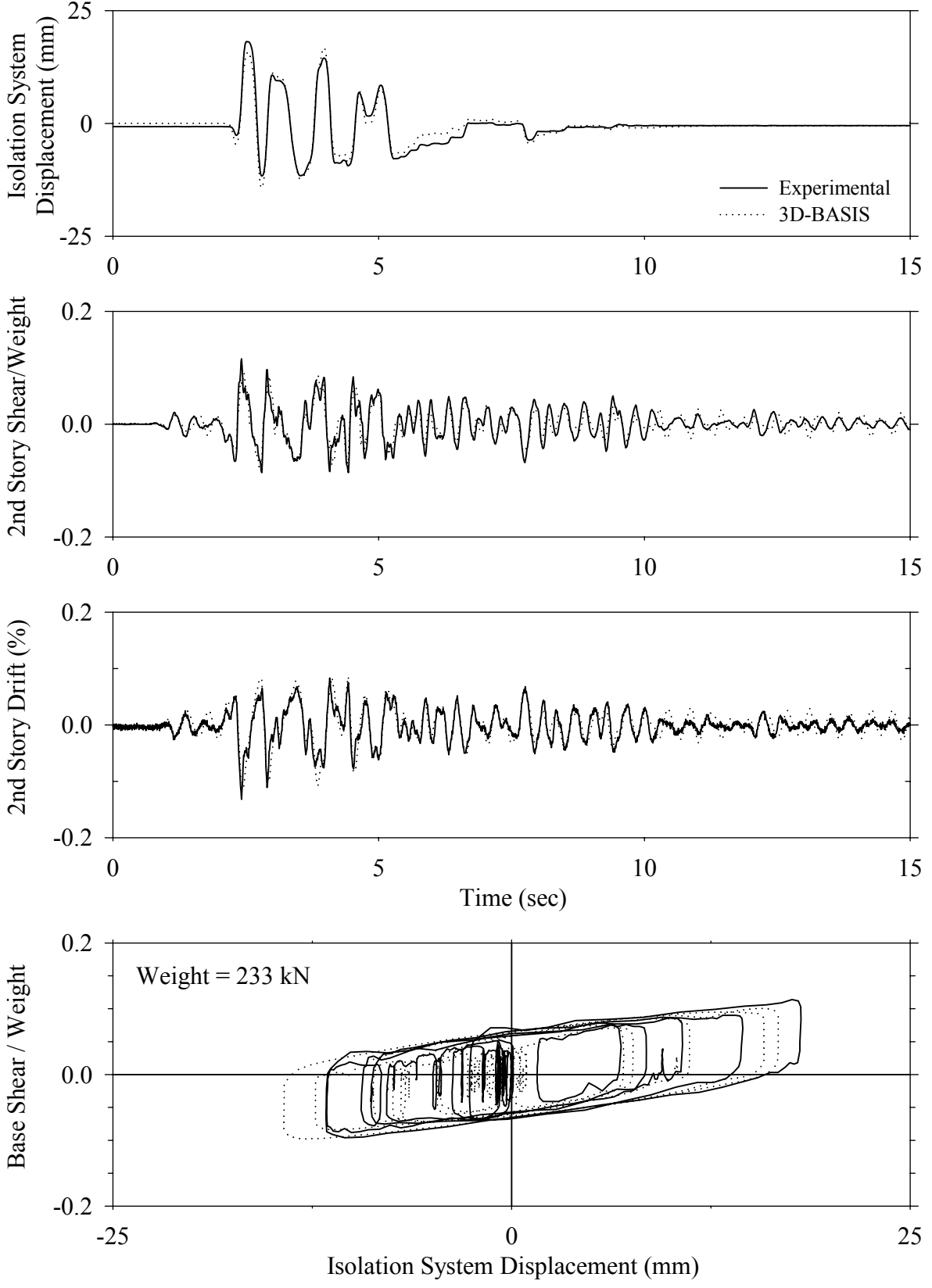




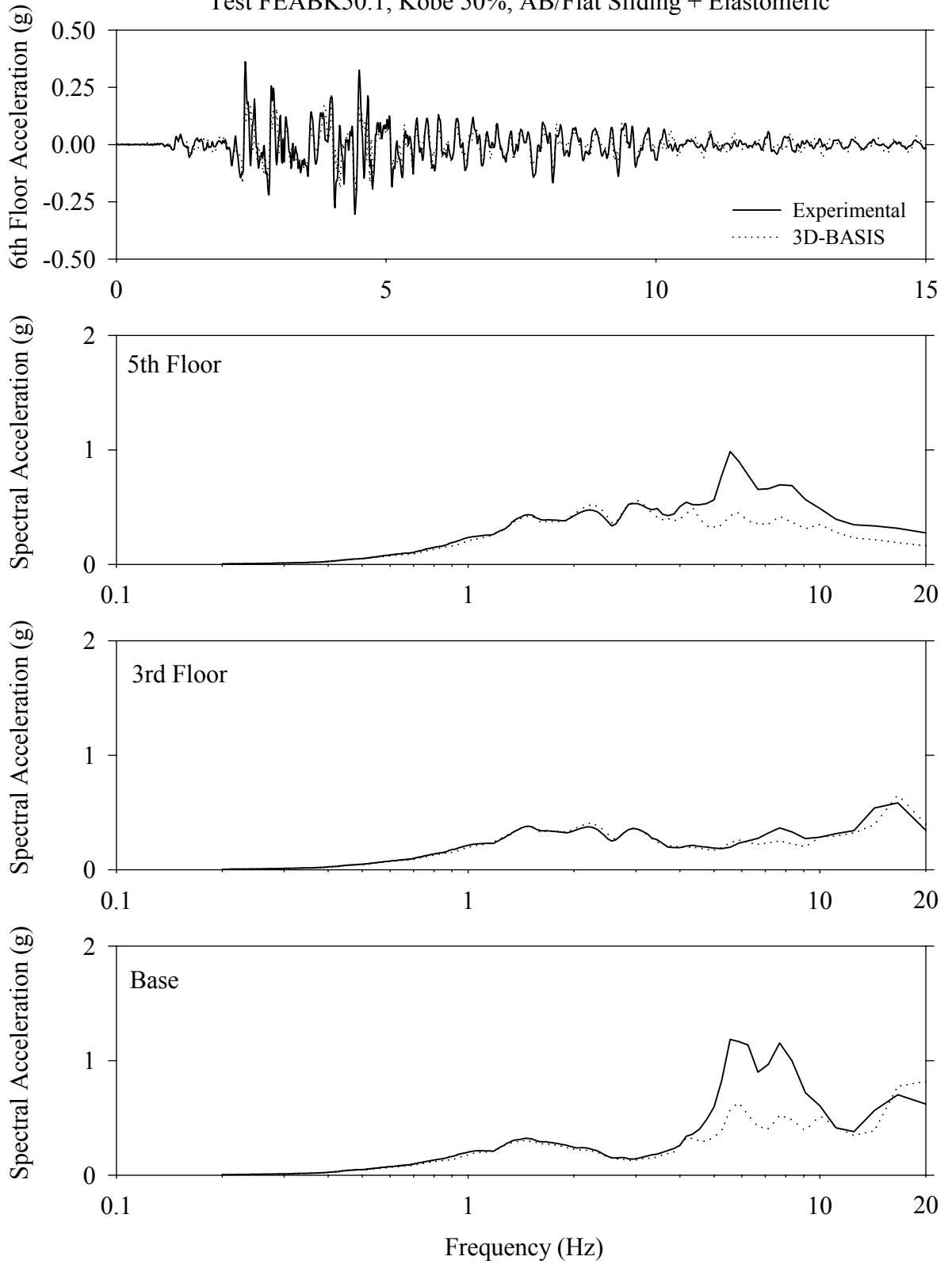
Test FEABE20.1, El Centro S00E 200%, AB/Flat Sliding + Elastomeric



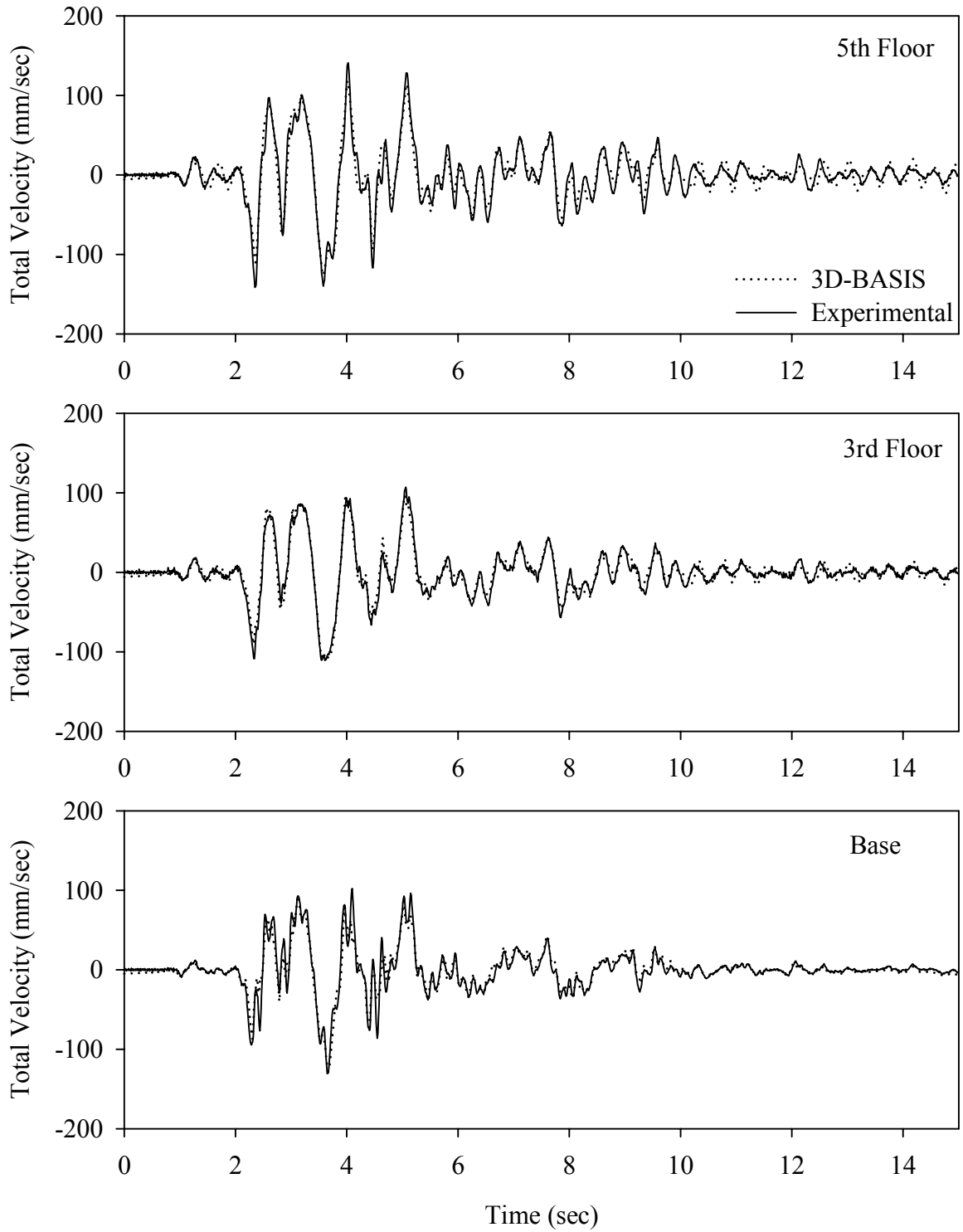
Test FEABK50.1, Kobe 50%, AB/Flat Sliding + Elastomeric



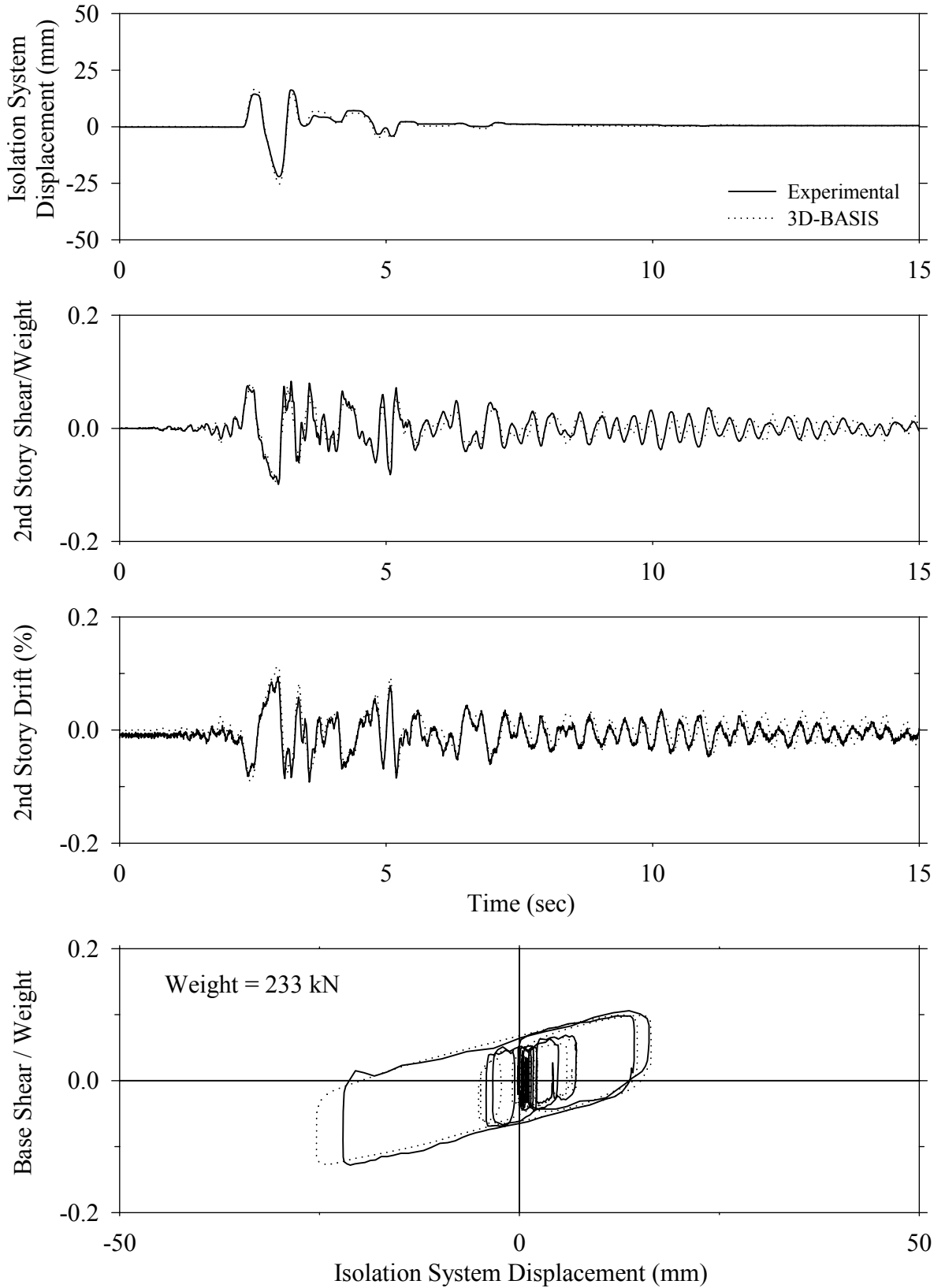
Test FEABK50.1, Kobe 50%, AB/Flat Sliding + Elastomeric



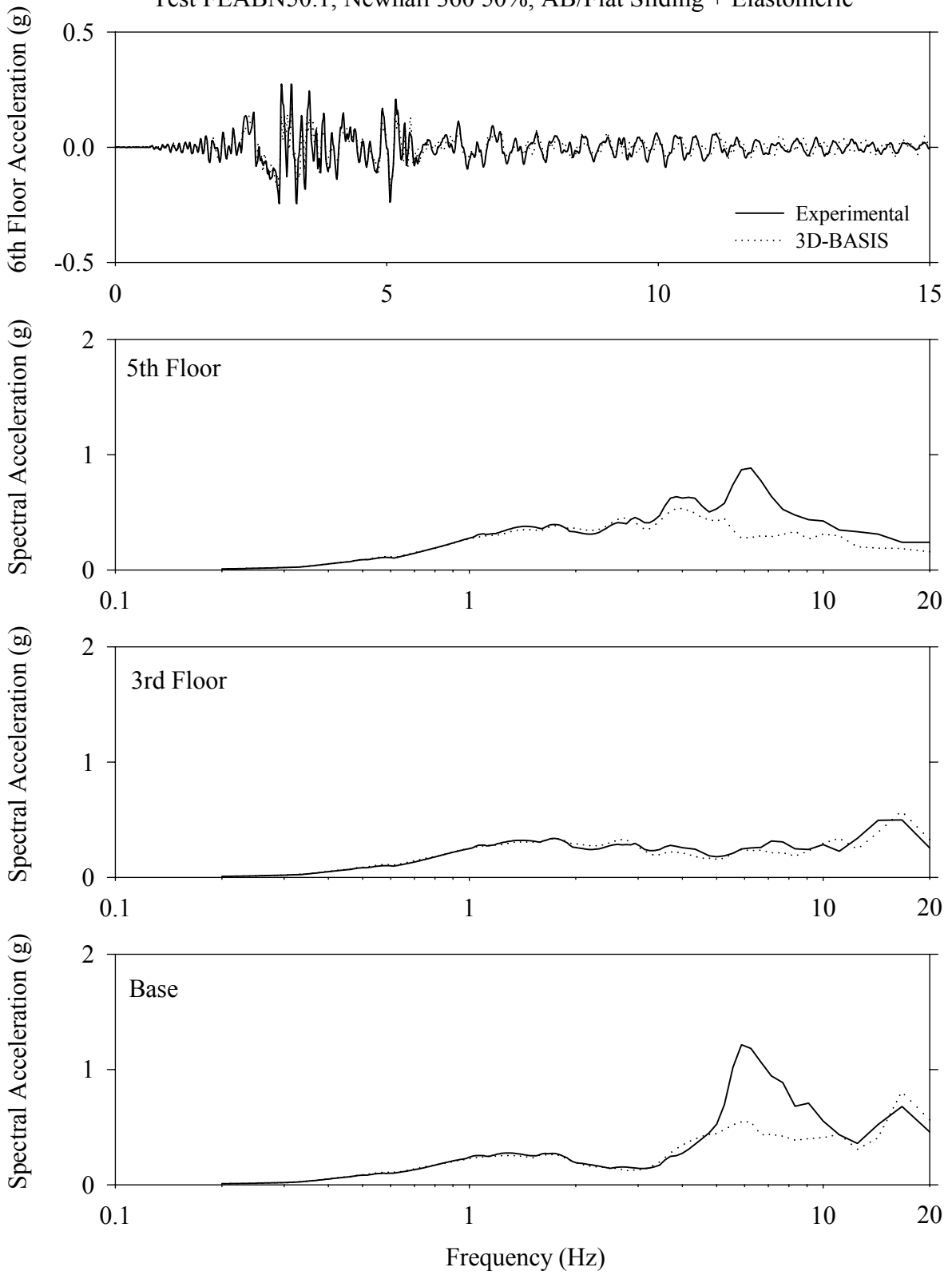
Test FEABK50.1, Kobe 50%, AB/Flat Sliding + Elastomeric



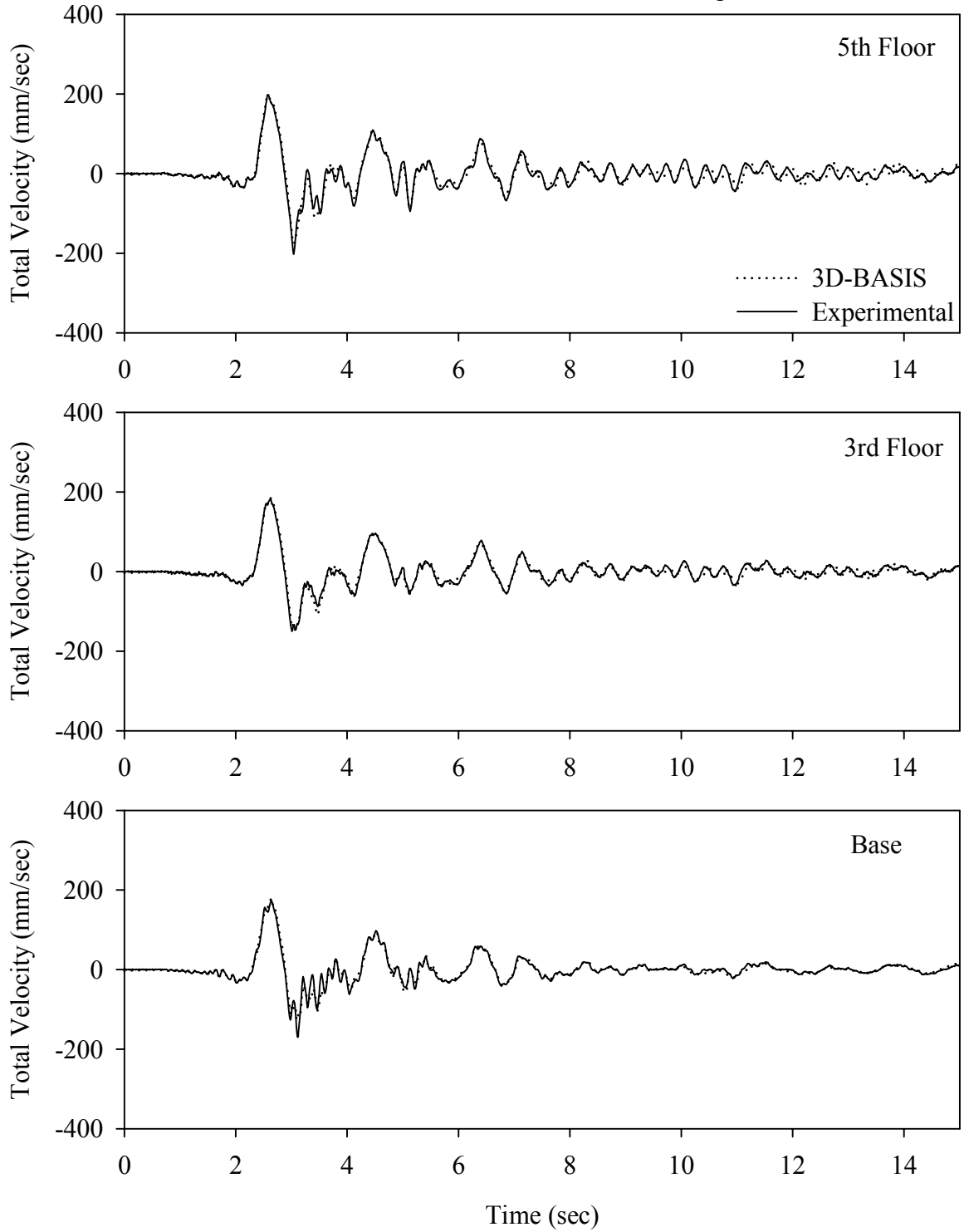
Test FEABN50.1, Newhall 360 50%, AB/Flat Sliding + Elastomeric



Test FEABN50.1, Newhall 360 50%, AB/Flat Sliding + Elastomeric

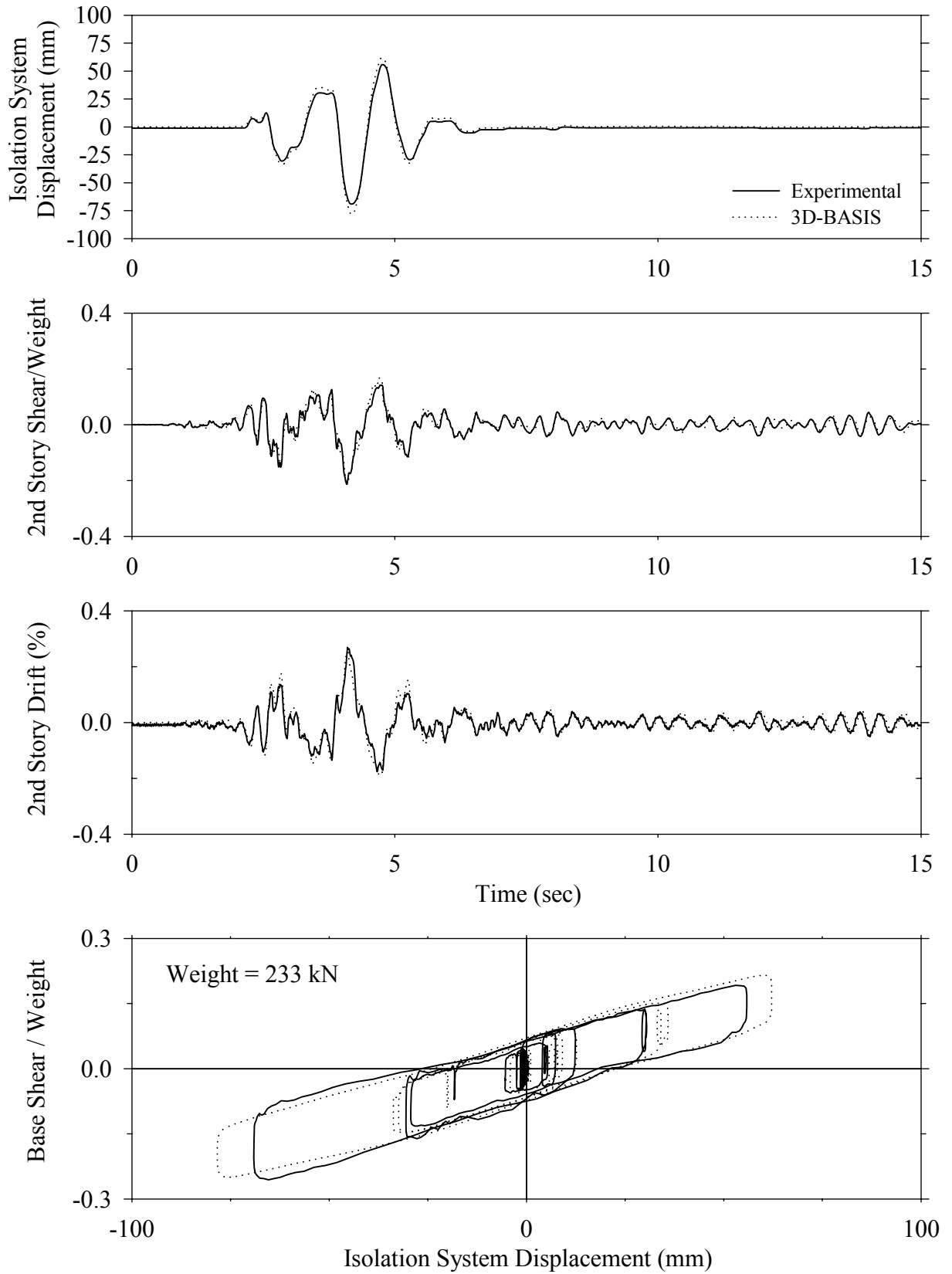


Test FEABN50.1, Newhall 360 50%, AB/Flat Sliding + Elastomeric

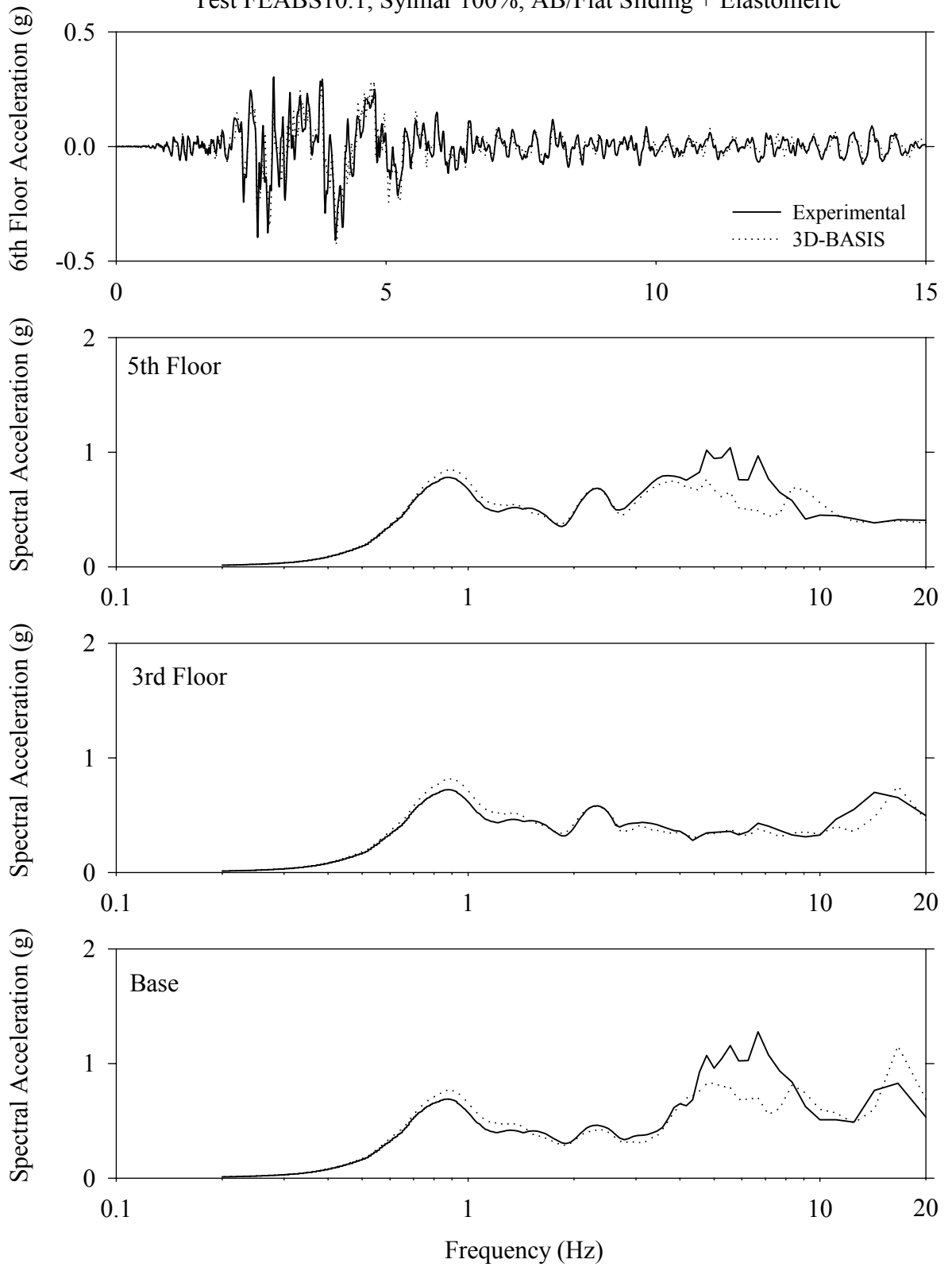




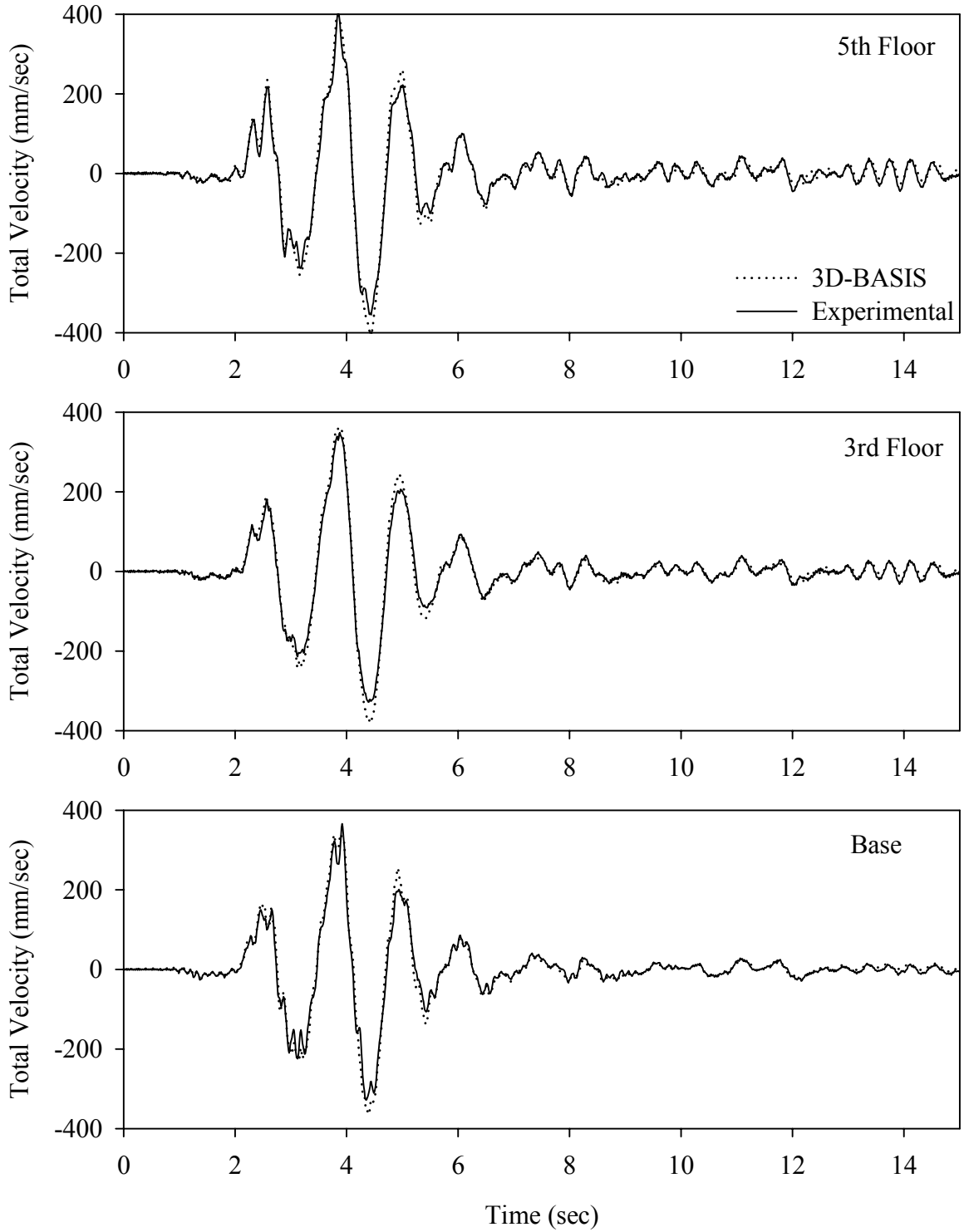
Test FEABS10.1, Sylmar 100%, AB/Flat Sliding + Elastomeric



Test FEABS10.1, Sylmar 100%, AB/Flat Sliding + Elastomeric



Test FEABS10.1, Sylmar 100%, AB/Flat Sliding + Elastomeric



# MCEER

University at Buffalo, State University of New York  
Red Jacket Quadrangle ■ Buffalo, New York 14261  
Phone: (716) 645-3391 ■ Fax: (716) 645-3399  
E-mail: [mceer@mceermail.buffalo.edu](mailto:mceer@mceermail.buffalo.edu) ■ WWW Site <http://mceer.buffalo.edu>



University at Buffalo *The State University of New York*

ISSN 1520-295X